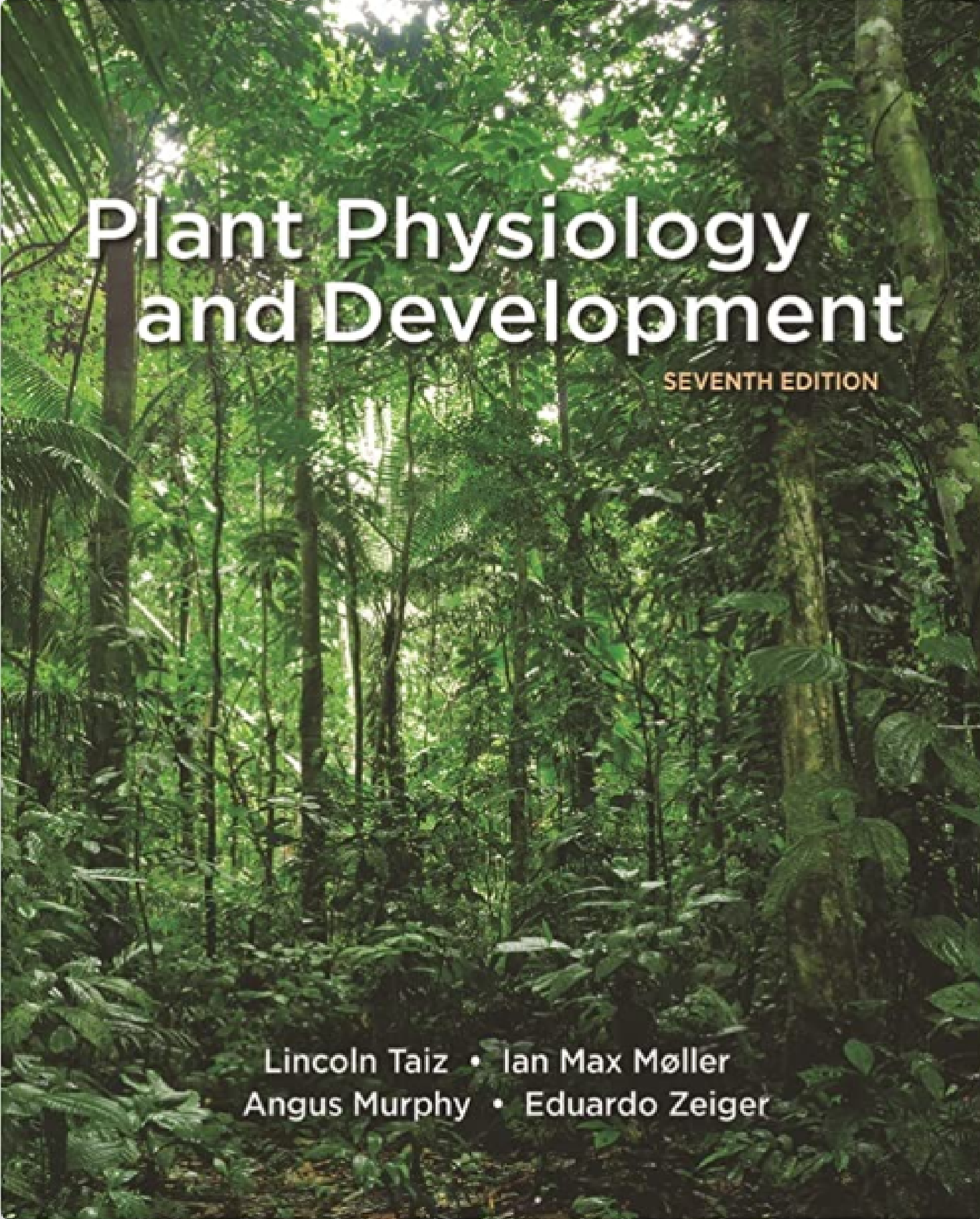

Plant Physiology
and Development
SEVENTH EDITION
Lincoln Taiz • Ian Max Møller
Angus Murphy • Eduardo Zeiger

Plant Physiology and Development

SEVENTH EDITION

00_Taiz7e-FM.indd 1 5/2/22 2:04 PM



00_Taiz7e-FM.indd 2 5/2/22 2:04 PM

Plant Physiology and Development

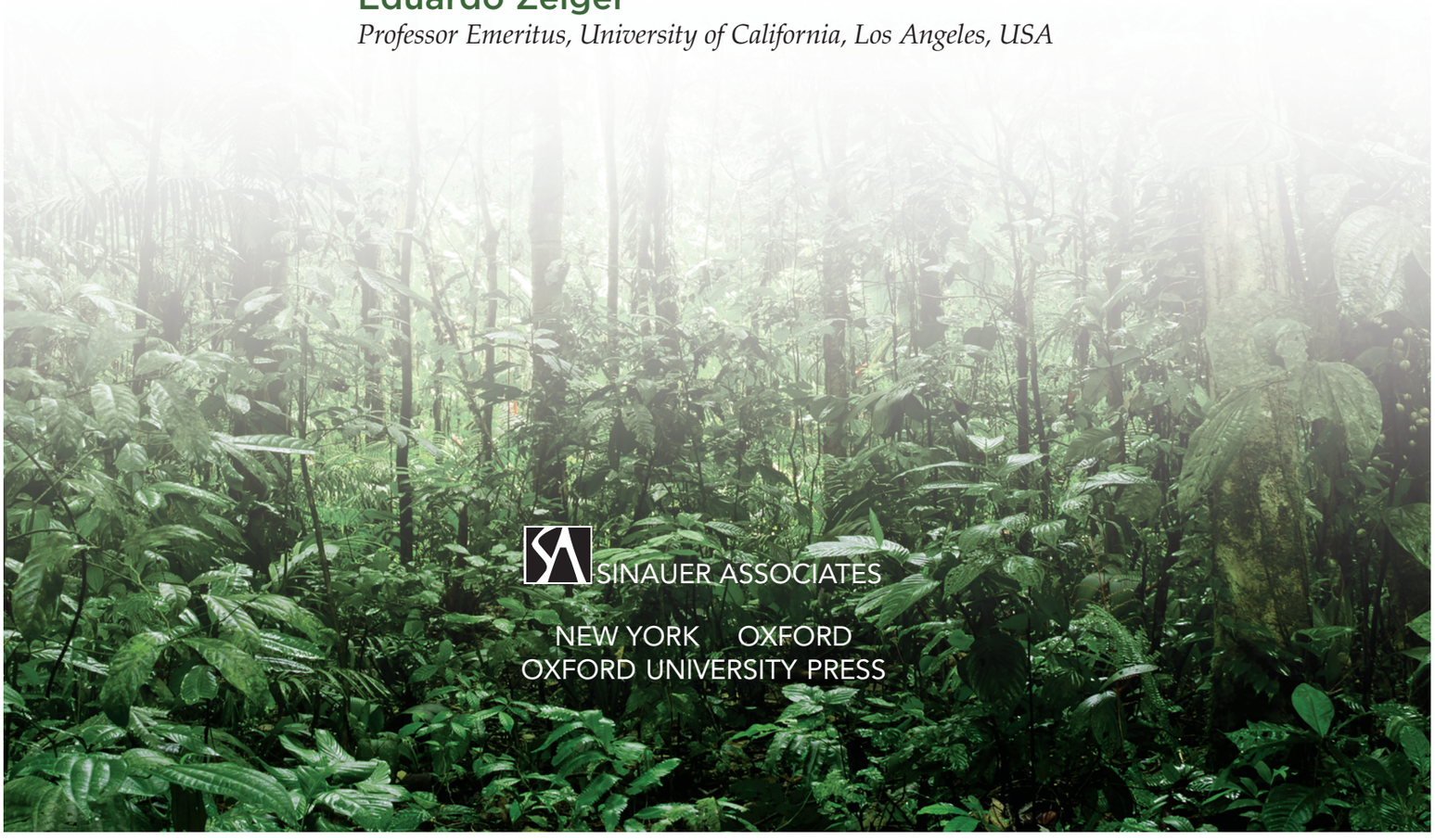
SEVENTH EDITION

Lincoln Taiz
Professor Emeritus, University of California, Santa Cruz, USA

Ian Max Møller
Professor Emeritus, Aarhus University, Denmark

Angus Murphy
Professor, University of Maryland, USA

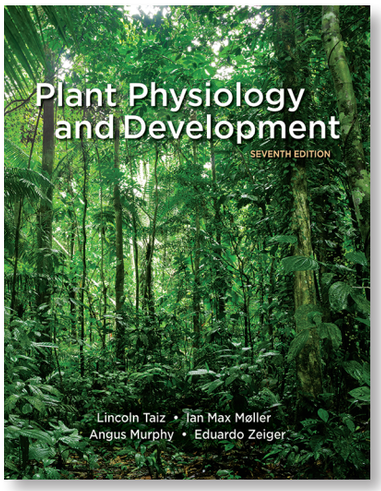
Eduardo Zeiger
Professor Emeritus, University of California, Los Angeles, USA



SINAUER ASSOCIATES

NEW YORK OXFORD
OXFORD UNIVERSITY PRESS

00_Taiz7e-FM.indd 3 5/2/22 2:04 PM



On the Cover: Yasuní National Park in the Amazon rainforest, Ecuador, may be one of the most biodiverse places on Earth. © Fotos593/Shutterstock

Oxford University Press is a department of the University of Oxford. It furthers the University's objective of excellence in research, scholarship, and education by publishing worldwide. Oxford is a registered trade mark of Oxford University Press in the UK and certain other countries.

Published in the United States of America by Oxford University Press
198 Madison Avenue, New York, NY 10016, United States of America

© 2023, 2015, 2010, 2006, 2002, 1998, 1991 Oxford University Press
Sinauer Associates is an imprint of Oxford University Press.

For titles covered by Section 112 of the US Higher Education Opportunity Act, please visit www.oup.com/us/he for the latest information about pricing and alternate formats.

All rights reserved. No part of this publication may be reproduced, stored in a retrieval system, or transmitted, in any form or by any means, without the prior permission in writing of Oxford University Press, or as expressly permitted by law, by license, or under terms agreed with the appropriate reproduction rights organization. Inquiries concerning reproduction outside the scope of the above should be sent to the Rights Department, Oxford University Press, at the address above.

You must not circulate this work in any other form and you must impose this same condition on any acquirer.

Address editorial correspondence to:
Sinauer Associates
23 Plumtree Road
Sunderland, MA 01375 USA

Notice of Trademarks
Throughout this book trademark names may have been used, and in some instances, depicted. In lieu of appending the trademark symbol to each occurrence, the authors and publisher state that these trademarks are used in an editorial fashion, to the benefit of the trademark owners, and with no intent to infringe upon the trademarks. Every effort has been made to determine and contact copyright holders. In the case of any omissions, the publisher will be pleased to make suitable acknowledgement in future editions.

Library of Congress Cataloging-in-Publication Data
Names: Taiz, Lincoln, editor. | Møller, I. M. (Ian Max), editor. | Murphy, Angus S., editor. | Zeiger, Eduardo, editor.

Title: Plant physiology and development / Lincoln Taiz, Ian Max Møller, Angus Murphy, Eduardo Zeiger.

Description: Seventh edition. | New York, NY : Sinauer Associates : Oxford University Press, [2022] | Includes bibliographical references and index. | Summary: "Plant Physiology and Development incorporates the latest advances in plant biology, making it the most authoritative and widely used upper-division plant biology textbook. Up-to-date, comprehensive, and meticulously illustrated, the improved integration of developmental material throughout the text ensures that Plant Physiology and Development provides the best educational foundation possible for the next generation of plant biologists"-- Provided by publisher.

Identifiers: LCCN 2021050436 (print) | LCCN 2021050437 (ebook) | ISBN 9780197577240 (hardback) | ISBN 9780197614235 | ISBN 9780197614228 (epub)

Subjects: LCSH: Plant physiology. | Plants--Development.

Classification: LCC QK711.2 .T35 2022 (print) | LCC QK711.2 (ebook) | DDC 571.2--dc23/eng/20211027

LC record available at https://lccn.loc.gov/2021050436

LC ebook record available at https://lccn.loc.gov/2021050437

9 8 7 6 5 4 3 2 1
Printed in the United States of America

Brief Table of Contents

UNIT I Structure and Information Systems of Plant Cells 1

CHAPTER 1 **Plant and Cell Architecture 3**
CHAPTER 2 **Cell Walls: Structure, Formation, and Expansion 45**
CHAPTER 3 **Genome Structure and Gene Expression 73**
CHAPTER 4 **Signals and Signal Transduction 103**

UNIT II Transport and Translocation of Water and Solutes 151

CHAPTER 5 **Water and Plant Cells 153**
CHAPTER 6 **Water Balance of Plants 169**
CHAPTER 7 **Mineral Nutrition 189**
CHAPTER 8 **Solute Transport 217**

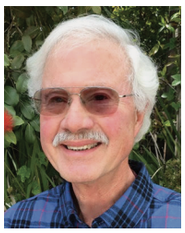
UNIT III Biochemistry and Metabolism 245

CHAPTER 9 **Photosynthesis: The Light Reactions 247**
CHAPTER 10 **Photosynthesis: The Carbon Reactions 281**
CHAPTER 11 **Photosynthesis: Physiological and Ecological Considerations 321**
CHAPTER 12 **Translocation in the Phloem 345**
CHAPTER 13 **Respiration and Lipid Metabolism 379**
CHAPTER 14 **Assimilation of Inorganic Nutrients 417**
CHAPTER 15 **Abiotic Stress 443**

UNIT IV Growth and Development 473

CHAPTER 16 **Signals from Sunlight 475**
CHAPTER 17 **Seed Dormancy, Germination, and Seedling Establishment 505**
CHAPTER 18 **Vegetative Growth and Organogenesis: Primary Growth of the Plant Axis 541**
CHAPTER 19 **Vegetative Growth and Organogenesis: Branching and Secondary Growth 567**
CHAPTER 20 **The Control of Flowering and Floral Development 591**
CHAPTER 21 **Sexual Reproduction: From Gametes to Fruits 625**
CHAPTER 22 **Embryogenesis: The Origin of Plant Architecture 669**
CHAPTER 23 **Plant Senescence and Developmental Cell Death 691**
CHAPTER 24 **Biotic Interactions 721**

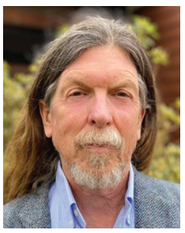
Editors



Lincoln Taiz is Professor Emeritus of Molecular, Cellular, and Developmental Biology at the University of California, Santa Cruz. He received his Ph.D. degree in Botany from the University of California, Berkeley. Dr. Taiz's primary research focus has been on the structure, function, and evolution of vacuolar H^+-ATPases. Other research interests include plant hormone transport and activity, cell wall mechanical properties, and heavy metal toxicity. Dr. Taiz is also the co-author with Lee Taiz of a popular science book on the discovery and denial of sex in plants, called *Flora Unveiled*.



Ian Max Møller is Professor Emeritus of Molecular Biology and Genetics at Aarhus University, Denmark. He received his Ph.D. in Plant Biochemistry from Imperial College, London, UK after which he worked at Lund University, Sweden for 20 years before returning to Denmark. He has investigated plant mitochondria throughout his career and his current interests include proteomics, oxidative stress, and post-translational modification of proteins as a regulatory mechanism. (Chapter 13)



Angus Murphy is a Professor of Plant Science and Landscape Architecture at the University of Maryland. He received a Ph.D. at the University of California, Santa Cruz. His research explores the transport and metabolism of plant hormones and their role in development and environmental responses. Much of that research is focused on the functions of ATP Binding Cassette transporters and other proteins that are clustered in ordered membrane nanodomains. (Chapters 1 and 4)

Editor Emeritus



Eduardo Zeiger is Professor Emeritus of Biology at the University of California, Los Angeles. He received a Ph.D. in Plant Genetics at the University of California, Davis. His research interests include stomatal function, the sensory transduction of blue-light responses, and the study of stomatal acclimations associated with increases in crop yields.

Principle Contributors



Andreas Blennow is Professor of Starch Biotechnology at the University of Copenhagen, Denmark. He received his Ph.D. in Biochemistry at Lund University, Sweden. His research activities span polysaccharide, especially starch, structure and functionality, metabolism, and crop engineering. (Chapter 10)



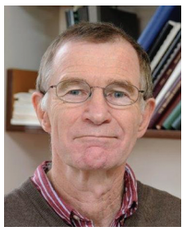
Eduardo Blumwald is a Distinguished Professor of Cell Biology and the Will W. Lester Endowed Chair at the Department of Plant Sciences, University of California at Davis. He received his Ph.D. in Bioenergetics from the Hebrew University of Jerusalem. His research focuses on the adaptation of plants to environmental stress, the cellular/molecular bases of fruit quality and engineering nitrogen-fixation in cereals. (Chapter 15)



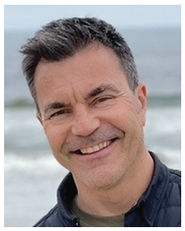
Federica Brandizzi is a University Distinguished Professor and MSU Foundation Professor of Plant Biology at Michigan State University. She obtained her Ph.D. in Cellular and Molecular Biology at the University of Rome, Italy. She pursued her post-doctoral training at the University of Oxford and Oxford Brookes University in the UK, working on the biology of plant endomembranes. The focus of her research is the fundamental mechanisms underlying the morphological and functional identity of the organelles of the plant secretory pathway in model dicot and monocot species in physiological growth and in stress, applying such knowledge to improve economically relevant crops. (Chapter 1)



Siobhan A. Braybrook is an Assistant Professor of Molecular, Cell and Developmental Biology at the University of California, Los Angeles. She received a Ph.D. in Plant Molecular Biology from the University of California, Davis. She is also a member of the California Nanosystems Institute, the Molecular Biology Institute, and the Center for the Study of Women at UCLA. (Chapter 2)



John J. Browse is a Professor in the Institute of Biological Chemistry at Washington State University. He received his Ph.D. from the University of Auckland, New Zealand. Dr. Browse's research interests include the biochemistry of lipid metabolism and the responses of plants to low temperatures. (Chapter 13)



John M. Christie is Professor of Photobiology at the Institute of Molecular Cell and Systems Biology at the University of Glasgow. His research interests center on using diverse approaches, ranging from biophysical to physiological, to understand how photosensory systems operate to shape plant growth and development. His research has resulted in major advances in the field of photobiology, including the identification of the long sought-after photoreceptor for phototropism and more recently the elusive plant UV-B photoreceptor. His work also extends to developing new optogenetic tools to non-invasively track bacterial and viral infections and control neural processes by using light. (Chapter 16)



Asaph B. Cousins is a Professor in the School of Biological Sciences at Washington State University. Dr. Cousins received his B.S. in Botany from California State University-Chico and obtained his Ph.D. in plant biology from Arizona State University. His research focuses on determining leaf biochemical and structural mechanisms influencing photosynthetic efficiency in diverse C_4 grasses, key C_4 biofuel and crop species, and in the C_3 plant rice engineered with C_4 traits. (Chapters 10 and 11)



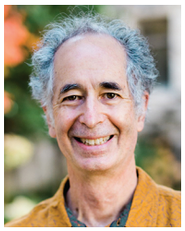
José Feijó is a Professor in the Department of Cell Biology and Molecular Genetics at the University of Maryland. His research includes working on the biophysical basis of cell-cell communication during sexual reproduction of mosses and angiosperms. (Chapter 21)



Simon Gilroy is a Professor in the Department of Botany at the University of Wisconsin-Madison. He received his Ph.D. in Plant Biochemistry at the University of Edinburgh and completed post-doctoral research at the University of California, Berkeley before taking a faulty position at the Pennsylvania State University and then moving to his current position in Wisconsin in 2007. His research focuses on defining the signaling networks used by plants to respond to environmental stimuli and on how plants react to growing in space. (Chapter 24)



N. Michele Holbrook is a Professor in the Department of Organismic and Evolutionary Biology at Harvard University. She received her Ph.D. from Stanford University. Dr. Holbrook's research group focuses on water relations and long-distance transport through xylem and phloem. (Chapters 5 and 6)



Roger W. Innes holds the Class of 1954 Professorship in Biology at Indiana University-Bloomington, and currently directs IUB's Electron Microscopy Center. He received his Ph.D. in Molecular, Cellular, and Developmental Biology at the University of Colorado-Boulder and completed post-doctoral research at the University of California, Berkeley, where he helped develop Arabidopsis as a model system for studying molecular plant-microbe interactions. He is an elected fellow of the American Association for the Advancement of Science and the American Academy of Microbiology. (Chapter 24)



Alexander Jones is a Group Leader at Sainsbury Laboratory, Cambridge University, UK. He received his Ph.D. at the University of California, Berkeley and received postdoctoral training in Plant Biology at the Carnegie Institution at Stanford University. His interest is in the way plant hormones coordinate cellular activities in service of overall plant physiology and development. Today, his group engineers novel tools to detect and perturb plant hormones to bring cellular hormone dynamics into sharper focus. (Chapters 18 and 19)



David M. Kramer is a Professor in the Department of Biochemistry and Molecular Biology and the MSU-DOE Plant Research Laboratory at Michigan State University. He received his Ph.D. in Biophysics from University of Illinois at Urbana-Champaign. His research focuses on how the energy transduction machinery of photosynthesis functions in living organisms and how it is impacted by dynamic environmental conditions. (Chapter 9)



June M. Kwak is a Professor in the Department of New Biology at DGIST in South Korea. He received his Ph.D. from POSTECH, South Korea. His research focuses on cellular signaling networks and the flexibility of developmental programs. (Chapter 23)



Pyung Ok Lim is a Professor in the Department of New Biology at DGIST in the Republic of Korea. She received her Ph.D. from Michigan State University. Her current research focuses on the regulatory mechanisms that underlie plant senescence and the interaction between the circadian clock and leaf aging. (Chapter 23)



Zhongchi Liu is a Professor at the University of Maryland, College Park. Her research focuses on the developmental mechanisms of wild diploid strawberry *Fragaria vesca*. (Chapter 21)



Andreas Madlung is a Professor in the Department of Biology at the University of Puget Sound. He received a Ph.D. in Molecular and Cellular Biology from Oregon State University. Research in his laboratory addresses the influence of genome structure on plant development and evolution, as well as phytochrome-mediated plant responses to light. (Chapter 3)



Ron Mittler is a Professor in the Division of Plant Sciences and Technology, and in the Department of Surgery, at the University of Missouri, Columbia. He received his Ph.D. in Biochemistry at Rutgers University. His research is focused on reactive oxygen species metabolism and signaling in plant and animal cells, systemic responses of plants to stress, cancer biology, and stress combination. (Chapter 15)



Sofía Otero is a Scientific Evidence Officer at the Science and Technology Office of the Congress of Deputies in Spain. She received her Ph.D. from the Universidad Autonoma de Madrid and postdoctoral training in the Sainsbury Laboratory at the University of Cambridge. Her research interests pivoted on uncovering mechanisms determining cell identity in root development and omics technologies. Sofía is also passionate

about science education and has served as college lecturer at Newnham College and assistant features editor for *The Plant Cell*. (Chapter 19)



Wendy A. Peer is an Associate Professor of Plant Biology and Chemical Ecology in the Department of Environmental Science and Technology. She received her Ph.D. at the University of California, Santa Cruz. Wendy Peer's research focuses on developmental, biotic, and abiotic interactions that affect seedling establishment and on identifying novel applications of microbial pairing with plant-based foods to enhance food quality and nutrition. (Chapter 17)



Yiping Qi is a Professor at Department of Plant Science and Landscape Architecture at University of Maryland, College Park. He received a Ph.D. in Plant Biology from University of Minnesota. His lab works on plant genome engineering and synthetic biology. He is interested in developing and improving tools for editing plant genome, fine-tuning plant transcriptome, detecting plant pathogens and sensing environmental stresses. Through collaboration with other scientists, his long-term goal is to conduct translational research for breeding and engineering better crops to reduce carbon emissions and ensure global food and nutrition security. (Chapter 3)



Simona Radutoiu is an Associate Professor at the Department of Molecular Biology and Genetics, Aarhus University, Denmark. She has a Ph.D. in Plant Physiology from University of Agronomy, Bucharest, Romania. Her research focuses on signaling in plant symbiosis with nitrogen-fixing bacteria and root microbiota establishment. (Chapter 14)



Allan G. Rasmusson is Professor in Plant Physiology at Lund University in Sweden. He received his Ph.D. in Plant Physiology at Lund University and made a postdoc at IGF Berlin. His current research centers on the cell biology of plant biostimulation and metabolic redox control. (Chapter 13)



Nidhi Rawat is an Associate Professor of Plant Pathology at the University of Maryland. She received her Ph.D. from the Indian Institute of Technology, Roorkee. Her research identifies plant defense genes that provide resistance to fungal pathogens. That work includes elucidation of molecular plant defense mechanisms and improvement of cereal grain varieties under increased pathogen pressure associated with climate change. (Chapter 3)



Sarah Robinson is a Group Leader at the Sainsbury Laboratory, University of Cambridge, UK and a Royal Society University Research Fellow. She received her Ph.D. in Plant Biology at the John Innes Centre before undertaking postdoctoral research at the University of Bern, Switzerland. Her lab takes an interdisciplinary approach to understanding plant development, with a particular focus on the role of mechanical stress. (Chapters 18 and 19)



Alexander Schulz is Professor of Cell Biology and Bioimaging at University of Copenhagen, Copenhagen, Denmark. He received his Ph.D. from the University of Heidelberg, Germany. His research interests center around structure, function and regeneration of the phloem of angio-sperms and gymnosperms, including the plasmodesmatal and apoplastic transport to and from the phloem. (Chapter 12)



Claus Schwechheimer is a Professor of Plant Systems Biology at the Technical University of Munich, Germany. He received a Ph.D. from the University of East Anglia in the UK. He is interested in understanding the molecular mechanisms underlying the mode of action of the phytohormones auxin and gibberellin in plant development. His lab currently investigates protein kinases in the regulation of PIN auxin transporters and GATA transcription factors in the regulation of primary metabolism and plant growth. Claus Schwechheimer is also coordinator of the research network "Molecular mechanisms regulating yield and yield stability in plants." (Chapter 4)



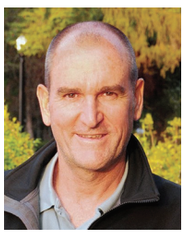
Young Hun Song is an Associate Professor in the Department of Agricultural Biotechnology at Seoul National University in Seoul, Korea. He received a Ph.D. from Gyeongsang National University in Korea in 2008. (Chapter 20)



Vijay Tiwari is an Assistant Professor of Cereal Crops Genomics at the University of Maryland. He received his Ph.D. from the Indian Institute of Technology, Roorkee. His research focus is on the use of advanced molecular genetic tools to accelerate the identification and deployment of genetic traits that improve the yields, nutrient utilization, and resilience of cereal food crops. (Chapter 3)



Yi-Fang Tsay is a Distinguished Research Fellow at the Institute of Molecular Biology, Academia Sinica, Taiwan. She has a Ph.D. in Biology from Carnegie-Mellon University, Pittsburgh, PA, USA. Her research focuses on nitrate transport, signaling, and utilization efficiency. (Chapter 14)



Michael Udvardi is Professor of Legume Genomics at The University of Queensland in Brisbane, Australia. He received his Ph.D. in Plant Biochemistry at The Australian National University. His research focuses on symbiotic nitrogen fixation in legumes and genomic approaches to crop improvement. (Chapter 7)



John M. Ward is a Professor in the Department of Plant and Microbial Biology at the University of Minnesota Twin Cities. He received a Ph.D. in Botany from the University of Maryland. His research focuses on the function of proton-coupled transporters for metabolites and nutrients. (Chapters 7 and 8)



Dolf Weijers is Professor and Chair of Biochemistry at Wageningen University (the Netherlands). His research focuses on understanding the biochemical and cellular principles regulating plant development and its evolution, in which the Arabidopsis embryo is frequently used as a model system. (Chapter 22)



Christopher D. Whitewoods is a Career Development Fellow at Sainsbury Laboratory, Cambridge University, UK, where he investigates how plants pattern themselves in three dimensions. He received his Ph.D. in Plant Development from the University of Cambridge. (Chapter 18)



Hye Ryun Woo is an Associate Professor in the Department of New Biology at DGIST in the Republic of Korea. She received her Ph.D. from POSTECH, the Republic of Korea. Her current research centers on understanding the molecular genetic mechanisms underlying leaf growth and senescence. (Chapter 23)

Preface

We are excited and honored to present to the plant biology community a new edition of *Plant Physiology and Development*. As in previous editions, our overarching goal for the Seventh Edition has been to provide students with a thorough grounding in the principles of plant physiology and development, as well as a solid grasp of the most important cutting edge research findings. Our goal with each edition is to integrate historical continuity and recent research breakthroughs into a seamless whole.

The Seventh Edition also addresses a new temporal element—the *future* of plant biology. It is no longer controversial to state that human civilization has become unsustainable. The extraction and combustion of fossil fuels, release of manufacturing byproducts, intensive animal farming, and destruction of tropical and boreal ecosystems have, according to the National Oceanic and Atmospheric Administration (NOAA), produced the greatest accumulation of atmospheric greenhouse gases since the Mid-Pliocene Warm Period, 3.6 million years ago. This process, which began during the Industrial Revolution in the early 19th century, and which was greatly accelerated in the mid-20th century, has raised the average surface temperatures a full 1°C above the preindustrial average. This seemingly small temperature rise is occurring so rapidly that it is taking a toll on the world's biodiversity.

Many scientists believe we have now left the relatively stable climate of the Holocene epoch and have entered a dangerous new geological epoch, the Anthropocene, which is characterized by human domination of the biosphere and perturbation of various geochemical cycles of the Earth system. The dire situation was summed up by António Guterres, the Secretary-General of the United Nations, in his presentation of the 2022 Sixth Assessment Report of the Intergovernmental Panel on Climate Change (IPCC):

> *The jury has reached a verdict. And it is damning… We are on a fast track to climate disaster. Major cities under water. Unprecedented heatwaves. Terrifying storms. Widespread water shortages. The extinction of a million species of plants and animals. This is not fiction or exaggeration. It is what science tells us will result from our current energy policies.*

Mitigation of climate change, preservation of ecosystems, and adaptation of crop systems to prevent mass hunger will require an international interdisciplinary effort of enormous proportions, and plant biology will be right at the center of the action. As primary producers, plants provide habitat and food for the rest of the biosphere. Knowledge of the fundamentals of plant physiology will therefore be required to achieve meaningful interventions in key ecosystems. Highly variable and shifting extreme weather patterns are expected to disrupt global crop production. Development and adoption of adaptive approaches to achieve low-input sustainable agriculture are now inescapable priorities.

Above all, plants will play a central role in the achievement of global net zero carbon emissions. Ever since the Great Oxygenation Event ~2.4 billion years ago, the photosynthetic activity of plants, algae, and cyanobacteria has been regulating the planet's temperature by drawing down and sequestering atmospheric CO_2. Efforts to achieve improved photosynthetic efficiency, carbon sequestration, and nutrient utilization are just a few of the many research areas where plant scientists are already making an impact. It is our hope that students who study plant physiology and development will become key contributors to efforts to use the knowledge of plant growth and function to create new solutions to rescue our planet.

Organization

The Seventh Edition of *Plant Physiology and Development* continues efforts within the plant biology community to integrate plant physiology and development as complementary and inseparable areas of learning in a coherent text that provides a comprehensive understanding of plant processes for upper-level undergraduate and graduate students. With the availability of *Fundamentals of Plant Physiology*, a comprehensive and rigorous textbook generated by the same authors and aimed at undergraduate classes with outcomes that include less molecular genetics and biochemistry, *Plant Physiology and Development* can focus on a student audience where these areas of expertise are important learning outcomes for classes and curricula.

The text is organized in four units to provide scaffolded learning as students move through the material.

- A new four-chapter Introductory Unit I, Structure and Information Systems of Plant Cells, has been implemented to ensure all students begin with a common starting point. Unit I is also organized in a manner that allows the chapters to be used as reference material as students engage with the topics of subsequent chapters. This major restructuring also enables modernization of the teaching of traditional physiological topics by introducing genomics, molecular genetics, genome editing, and the basic concepts of signal transduction at the outset of the course. All four chapters provide important insights into processes and structures that are unique to plants.
- Unit II describes Transport and Translocation of Water and Solutes in an updated format that enhances student comprehension of basic physiological principles.

- Unit III describes Biochemistry and Metabolism to provide students with a clear understanding of these processes in plants. The last chapter of this section (Chapter 15: Abiotic Stress) describes stress responses in a context that integrates the subjects learned in the preceding chapters to enhance overall comprehension before proceeding to the detailed study of developmental processes.
- Unit IV focuses on plant Growth and Development. This unit takes the reader through the stages of plant development and culminates with an integrative final chapter (Chapter 24) that describes Biotic Interactions.

New to This Edition

- Inclusion of highlight boxes that address climate change and biotechnology topics that are relevant to plant physiology.
- Chapter 15: Abiotic Stress has been brought forward to serve as a tool to assist students in integration of the concepts learned in the first three units of the text
- The subject of Vegetative Growth and Organogenesis is now addressed in two chapters. Chapter 18: Vegetative Growth of the Primary Axis focuses on meristems and primary root, shoot, and leaf development. Chapter 19: Vegetative Growth and Organogenesis: Branching and Secondary Growth includes updated sections describing the development of root architecture, cambial function, and epicormic branching.
- The subject of Embryogenesis is now addressed in Chapter 22, which immediately follows Chapter 21: Sexual Reproduction: From Gametes to Fruits. This placement allows the subject to be taught together with fertilization and seed development or before Chapter 17: Seed Dormancy, Germination, and Seedling Establishment.
- Chapter 24: Biotic Interactions has been reformulated to better integrate the concepts of Development with the first three units of the text. New material on plant responses to herbivory and pathogens has been extensively incorporated into the chapter.
- In addition to topical boxes in the chapters, Web Topics and Essays have been extensively updated to reflect new developments and to highlight plant breeding/biotechnology and the impacts of climate change. The Web material amplifies the theme of integrative approaches to solve global problems in food production, renewable energy, and environmental sustainability.
- Continues to include the most recent and important developments in plant science at a level of complexity that is appropriate for third- and fourth-year undergraduate plant physiology classes.
- Advanced genomics, molecular assisted breeding, and plant genome engineering with CRISPR and similar tools are presented by leaders in the field.
- Conservative nomenclature for genes, gene products, mutants, and epigenetic factors has been standardized throughout the text.
- Concise Suggested Readings are included at the end of each chapter and links to a more extensive online bibliography. Web Topics and Web Essays include associated references. New chapter authors, who are leaders in their respective fields, bring an enhanced sense of relevance to the material presented.

Acknowledgments

This Seventh Edition of *Plant Physiology and Development* is truly a product of efforts from the plant science community. First and foremost, we thank the many talented new and continuing chapter authors whose commitment to excellence in higher education and belief in the text motivated them to take time off from their busy schedules to update and, in some cases, rewrite and reorganize, chapters related to their fields of specialization. In addition, we want to acknowledge the hundreds of colleagues who have provided expertise, information, and criticism of the material presented in the text. The American Society of Plant Biologists and the Society for Experimental Biology provided platforms for discussion and outreach for this project, for which we are grateful. In addition, we especially want to thank Dr. Wendy Peer for her contributions to the overall development of the Seventh Edition and for organizing and compiling the Learning Objectives and Self-Assessment Quizzes for the enhanced e-book.

Finally, we wish to express our gratitude to the entire production team at Oxford University Press/Sinauer Associates for all their encouragement and guidance throughout the lengthy process of organizing, writing, and producing the Seventh Edition: Joan Kalkut, our Editor, provided steady leadership throughout; Linnea Duley, our Production Editor, shepherded each chapter through the production phase from start to finish; Editorial Assistant Arthur Pero organized files throughout the revision process and handled our contracts; Dr. Laura Green made many helpful suggestions that improved the organizational logic and clarity of the chapters; Elizabeth Pierson, our copyeditor, deserves much of the credit for the consistency and clarity of the writing style throughout the text; Donna DiCarlo and Meg Clark, Production Specialists, crafted the fresh book design and page layouts; and finally Elizabeth Morales, the outstanding scientific illustrator, provided continuity with previous editions. Last, but certainly not least, we wish to recognize and salute our "editor emeritus" Eduardo Zeiger's enormous contributions to previous editions of the text, including its original conception and multi-author format.

Ian Max Møller, Slagelse, Denmark
Angus Murphy, College Park, MD, USA
Lincoln Taiz, Santa Cruz, CA, USA
April 2022

ACCESSIBLE COLOR CONTENT

Every opportunity has been taken to ensure that the content herein is fully accessible to those who have difficulty perceiving color. Exceptions are cases where the colors provided are expressly required because of the purpose of the illustration.

Reviewers

Rick Amasino
University of Wisconsin

Tom Beeckman
Ghent University

Phillip Benfey
Duke University

Eva Benková
Institute of Science and Technology, Austria

Frederic Berger
Gregor Mendel Institute, Austria

Brad Binder
University of Tennessee, Knoxville

Joshua Blakeslee
The Ohio State University

Michael Blatt
University of Glasgow

Caren Chang
University of Maryland

Karen K. Christensen-Dalsgaard
MacEwan University

Gary D. Coleman
University of Maryland

Daniel Cosgrove
Pennsylvania State University

Custodio de Oliveira Nunes
University of Maryland

Annie Deslauriers
Université du Québec à Chicoutimi

José Díaz Varela
Universidade da Coruña

Christian Fankhauser
Université de Lausanne

Ted Farmer
Université de Lausanne

Duarte Figueiredo
Max Planck Institute for Molecular Biology, Potsdam

Henrik Flyvbjerg
Technical University of Denmark

Vernonica Franklin-Tong
University of Birmingham

Susheng Gan
Cornell University

Larry Griffing
Texas A&M University

Paul Guy
University of Otago

Chris Hawes
Oxford Brookes University

Rainer Hedrich
Universität Würzburg

Yrjö Helariutta
University of Cambridge

Maria Janssen
Enza Zaden

Poul Erik Jensen
University of Copenhagen

Lothar Kalmbach
University of Cambridge

Joseph Kieber
University of North Carolina

Yeh Kuo-Chen
Academia Sinica

Hans Lambers
The University of Western Australia

David Macherel
University of Angers

Teun Munnik
University of Amsterdam

June Nasrallah
Cornell University

Michael Broberg Palmgren
University of Copenhagen

Jarmila Pitterman
University of California, Santa Cruz

William Plaxton
Queens University

Subramanian Sankaranarayanan
Nagoya University

Eric Schaller
Dartmouth University

Julian Schroeder
University of California, San Diego

Robert Sharwood
Western Sydney University

Joe H. Sullivan
University of Maryland

Miltos Tsiantis
Max Planck Institute for Plant Breeding Research, Cologne

Thomas Vogelmann
University of Vermont

Olga Voronova Komarov
Botanical Institute, Russian Academy of Sciences

Danielle Way
University of Western Ontario

Shunyuan Xiao
University of Maryland

Viktor Žárský
Charles University, Prague

00_Taiz7e-FM.indd 13 5/2/22 2:04 PM

Digital Resources

Plant Physiology and Development, SEVENTH EDITION

For the Student

(Available at oup.com/he/taiz7e)

The *Plant Physiology and Development*, Seventh Edition student website supplements the coverage provided in the textbook with additional and more advanced material on current research and selected topics of interest. In-text references to Web Topics and Essays are included throughout the textbook, and the end of each chapter includes a complete list of Topics and Essays for that chapter. The site includes the following:

- **Web Topics**: Additional coverage of selected topics
- **Web Essays**: Articles on cutting-edge research, written by the researchers themselves
- **Flashcards**: Help students master the hundreds of new terms introduced in the textbook
- **Study Questions**: A set of short-answer questions for each chapter
- **References**: A set of chapter-specific references
- **Web Appendices**: Four complete appendices are available online:
  - Web Appendix 1: *Energy and Enzymes*
  - Web Appendix 2: *Kinematic Analysis of Plant Growth*
  - Web Appendix 3: *Hormone Biosynthetic Pathways*
  - Web Appendix 4: *Specialized Metabolites*

For the Instructor

(Available at oup.com/he/taiz7e)

Instructors using *Plant Physiology and Development*, Seventh Edition, have access to a collection of PowerPoint resources from the textbook for use in preparing lectures and other course materials. All the figures and tables from each chapter have been reformatted and optimized for exceptional image quality when projected in class.

Flexible Options

Enhanced E-Book
(ISBN 978-0-19761-422-8)

Ideal for self-study, the *Plant Physiology and Development*, Seventh Edition, enhanced e-book delivers the full suite of digital resources in a format independent from any courseware or learning management system platform, making the online resources more accessible for students. The enhanced e-book is available via RedShelf, VitalSource, and other leading higher education e-book vendors and includes the following student resources:

- **NEW Learning Objectives**: Outline the important takeaways of every major section
- **NEW Self-Assessment Quizzes**: A brief quiz following each major section allows students to gauge their understanding of key concepts before proceeding
- **Web Topics**: Additional coverage of selected topics
- **Web Essays**: Articles on cutting-edge research, written by the researchers themselves
- **Flashcards**: Help students master the hundreds of new terms introduced in the textbook
- **Web Appendices**: Four complete appendices (see list in Student Resources)

Loose-Leaf Textbook
(ISBN 978-0-19761-423-5)

Plant Physiology and Development is available in a three-hole punched, loose-leaf format. Students can take just the sections they need to class and can easily integrate instructor material with the text.

Table of Contents

UNIT I Structure and Information Systems of Plant Cells 1

CHAPTER 1
Plant and Cell Architecture 3

1.1 Plant Life Processes: Unifying Principles 4
- Plant life cycles alternate between diploid and haploid generations 5

1.2 Overview of Plant Structure 7
- Plant cells are surrounded by rigid cell walls 7
- Plasmodesmata allow the free movement of molecules between cells 7
- New cells originate in dividing tissues called meristems 10

1.3 Plant Tissue Types 10
- Dermal tissues cover the surfaces of plants 11
- Ground tissues form the bodies of plants 12
- Vascular tissues form transport networks between different parts of the plant 14

1.4 Plant Cell Compartments 15
- Biological membranes are lipid bilayers that contain proteins 15

1.5 The Nucleus 18
- Gene expression involves transcription, translation, and protein processing 20
- Posttranslational modification of proteins determines their location, activity, and longevity 22

1.6 The Endomembrane System 23
- The endoplasmic reticulum is a network of internal membranes 23
- Cell wall matrix polysaccharides, secretory proteins and glycoproteins are processed in the Golgi apparatus 24
- The plasma membrane has specialized regions involved in membrane recycling 26
- Vacuoles have diverse functions in plant cells 27
- Oil bodies are lipid-storing organelles 28
- Peroxisomes play specialized metabolic roles in leaves and seeds 28

1.7 Independently Dividing Semiautonomous Organelles 29
- Proplastids mature into specialized plastids in different plant tissues 30
- Plastidial and mitochondrial division are independent of nuclear division in land plants 31

1.8 The Plant Cytoskeleton 32
- The plant cytoskeleton consists of microtubules and microfilaments 32
- Actin, tubulin, and their polymers are in constant flux in the living cell 32
- Microtubules are dynamic cylinders 34
- Cytoskeletal motor proteins mediate cytoplasmic streaming and directed organelle movement 34

1.9 Cell Cycle Regulation 36
- Each phase of the cell cycle has a specific set of biochemical and cellular activities 36
- The cell cycle is regulated by cyclins and cyclin-dependent kinases 38
- Mitosis and cytokinesis involve both microtubules and the endomembrane system 38

CHAPTER 2
Cell Walls: Structure, Formation, and Expansion 45

2.1 Overview of Plant Cell Wall Functions and Structures 46
- Plant cell walls vary in structure and function 46
- Components differ for primary and secondary cell walls 48
- Cellulose microfibrils have an ordered structure and are synthesized at the plasma membrane 50
- Matrix polysaccharides are delivered to the wall via vesicles 53
- Hemicelluloses are matrix polysaccharides that bind to cellulose 54
- Pectins are hydrophilic gel-forming components of the primary cell wall 54

2.2 The Dynamic Primary Cell Wall 58
- Primary cell walls are continually assembled during cell growth 58

2.3 Mechanisms of Cell Expansion 58
- Microfibril orientation influences growth directionality of cells with diffuse growth 59
- Microfibril orientation in the multilayered cell wall changes over time 60
- Cortical microtubules influence the orientation of newly deposited microfibrils 60

Many factors influence the extent and rate of cell growth 62
Stress relaxation of the cell wall drives water uptake and cell expansion 62
Leaf epidermal pavement cells provide a model for regulated cell wall expansion 63
Acid-induced growth and wall stress relaxation are mediated by expansins 63
Cell wall models are hypotheses about how molecular components fit together to make a functional wall 64
Many structural changes accompany the cessation of wall expansion 65

2.4 Secondary Cell Wall Structure and Function 66
Secondary cell walls are rich in cellulose and hemicellulose and often have a hierarchical organization 67
Lignification transforms the SCW into a hydrophobic structure resistant to deconstruction 67

CHAPTER 3
Genome Structure and Gene Expression 73

3.1 Nuclear Genome Organization 73
The nuclear genome is packaged into chromatin 74
Centromeres, telomeres, and nucleolar organizer regions contain repetitive sequences 74
Transposons are mobile sequences within the genome 75
Chromosome organization is not random in the interphase nucleus 76
Meiosis halves the number of chromosomes and allows for the recombination of alleles 76
Polyploids contain multiple copies of the entire genome 78

3.2 Plant Cytoplasmic Genomes: Mitochondria and Plastids 80

3.3 Transcriptional Regulation of Nuclear Gene Expression 81
RNA polymerase II binds to the promoter region of most protein-coding genes 81
Conserved nucleotide sequences signal transcriptional termination and polyadenylation 84
Epigenetic modifications help determine gene activity 84

3.4 Posttranscriptional Regulation of Nuclear Gene Expression 86
All RNA molecules are subject to decay 86
Noncoding RNAs regulate mRNA activity via the RNA interference (RNAi) pathway 86

3.5 Tools for Studying Gene Function 90
Mutant analysis can help elucidate gene function 90
BOX 3.1 Genetic Traits from Wild Grasses Are Used to Make Grain Crops More Resilient to Climate Change and Global Pathogen Threats 91
Molecular techniques can measure the activity of genes 92
Gene fusions can create reporter genes 92

3.6 Genetic Modification of Plants 93

3.7 Editing Plant Genomes 95
Sequence-specific nucleases induce targeted mutations 95
Gene editing can lead to precise gene replacement 97
Base editing can be used as an alternative to homology-directed repair 97
Prime editing uses an RNA repair template and reverse transcription 99

3.8 Engineering Crop Plants 99
Transgenes can confer resistance to herbicides or plant pests 99
Genetic engineering of plants remains controversial 100

CHAPTER 4
Signals and Signal Transduction 103

4.1 Temporal and Spatial Aspects of Signaling 104

4.2 Signal Perception and Amplification 105
Receptors are located throughout the cell and are conserved across kingdoms 105
Signals must be amplified intracellularly to regulate their target molecules 106
Evolutionarily conserved MAP kinases amplify cellular signals 107
Evolutionarily conserved kinases regulate programmed and plastic plant development 107
Extracellular signals are perceived and transmitted by receptor-like kinases 108
Phosphatases are the "off switch" of protein phosphorylation 109
Other protein modifications can reconfigure cellular processes 109
Ca^{2+} is the most ubiquitous second messenger in plants and other eukaryotes 109
Changes in the cytosolic or cell wall pH can serve as second messengers for hormonal and stress responses 110
Reactive oxygen species act as second messengers mediating both environmental and developmental signals 111
Lipid signaling molecules act as second messengers that regulate a variety of cellular processes 111

4.3 Hormones and Plant Development 113
Auxin was discovered in early studies of coleoptile bending during phototropism 114
Gibberellins promote stem growth and were discovered in relation to the "foolish seedling disease" of rice 114
Cytokinins were discovered as cell division–promoting factors in tissue-culture experiments 116
Ethylene is a gaseous hormone that promotes fruit ripening and other developmental processes 117
Abscisic acid regulates seed maturation and stomatal closure in response to water stress 117
Brassinosteroids regulate photomorphogenesis, germination, and other developmental processes 118
Strigolactones suppress branching and promote rhizosphere interactions 118

4.4 Phytohormone Metabolism and Homeostasis 119

Indole-3-pyruvate is the primary intermediate in auxin biosynthesis 119

Gibberellins are synthesized by oxidation of the diterpene ent-kaurene 121

Cytokinins are adenine derivatives with isoprene side chains 123

Ethylene is synthesized from methionine via the intermediate ACC 124

Abscisic acid is synthesized from a carotenoid intermediate 125

Brassinosteroids are derived from the sterol campesterol 126

Strigolactones are synthesized from β-carotene 127

4.5 Movement of Hormones within the Plant 127

Plant polarity is maintained by polar auxin streams 128

Auxin transport is regulated by multiple mechanisms 131

4.6 Hormonal Signaling Pathways 132

The cytokinin and ethylene signal transduction pathways are derived from the bacterial two-component regulatory system 132

Receptor-like kinases mediate brassinosteroid and certain auxin signaling pathways 136

The core ABA signaling components include phosphatases and kinases 136

Plant hormone signaling pathways generally employ negative regulation 139

Several plant hormone receptors include components of the ubiquitination machinery and mediate signaling via protein degradation 139

Plants have evolved mechanisms for switching off or attenuating signaling responses 143

The cellular response output to a signal is often tissue-specific 144

Hormone responses are modulated by other endogenous molecules 144

Plants use electrical signaling for communication between tissues 146

Cross-regulation allows signal transduction pathways to be integrated 147

UNIT II Transport and Translocation of Water and Solutes 151

CHAPTER 5
Water and Plant Cells 153

5.1 Water in Plant Life 153

5.2 The Structure and Properties of Water 154

Water is a polar molecule that forms hydrogen bonds 154

Water is an excellent solvent 154

Water has distinctive thermal properties relative to its size 155

Water has a high surface tension 155

Water has a high tensile strength 156

5.3 Diffusion and Osmosis 157

Diffusion is the net movement of molecules by random thermal agitation 157

Diffusion is most effective over short distances 158

Osmosis describes the net movement of water across a selectively permeable barrier 159

5.4 Water Potential 159

The chemical potential of water represents the free-energy status of water 159

Three major factors contribute to water potential 159

Water potentials can be measured 160

5.5 Water Potential of Plant Cells 161

Water enters the cell along a water potential gradient 161

Water can also leave the cell in response to a water potential gradient 162

Water potential and its components vary with growth conditions and location within the plant 163

5.6 Cell Wall and Membrane Properties 163

Small changes in plant cell volume cause large changes in turgor pressure 163

The rate at which cells gain or lose water is influenced by plasma membrane hydraulic conductivity 164

Aquaporins facilitate the movement of water across membranes 165

5.7 Plant Water Status 166

Physiological processes are affected by plant water status 166

Solute accumulation helps cells maintain turgor and volume 166

CHAPTER 6
Water Balance of Plants 169

6.1 Water in the Soil 169

Soil water potential is affected by solutes, surface tension, and gravity 170

Water moves through the soil by bulk flow 171

6.2 Water Absorption by Roots 171

Water moves in the root via the apoplast, symplasm, and transmembrane pathways 172

Solute accumulation in the xylem can generate "root pressure" 174

6.3 Water Transport through the Xylem 174

The xylem consists of two types of transport cells 174

Water moves through the xylem by pressure-driven bulk flow 176
Water movement through the xylem requires a smaller pressure gradient than movement through living cells 177
What pressure difference is needed to lift water 100 meters to a treetop? 177
The cohesion–tension theory explains water transport in the xylem 178
Xylem transport of water in trees faces physical challenges 178
Plants have several mechanisms to overcome losses of xylem conductivity caused by embolism 180

6.4 Water Movement from the Leaf to the Atmosphere 181

Leaves have a large hydraulic resistance 181
The driving force for transpiration is the difference in water vapor concentration 182
Water loss is also affected by the pathway resistances 182
Stomatal control couples leaf transpiration to leaf photosynthesis 183
The cell walls of guard cells have specialized features 183
Changes in guard cell turgor pressure cause stomata to open and close 184
Internal and external signals regulate the osmotic balance of guard cells 185
The transpiration ratio measures the relationship between water loss and carbon gain 186

6.5 Overview: The Soil–Plant–Atmosphere Continuum 186

CHAPTER 7
Mineral Nutrition 189

BOX 7.1 Nitrogen Fertilizers and Climate Change 190

7.1 Essential Nutrients, Deficiencies, and Plant Disorders 191

Special techniques are used in nutritional studies 193
Nutrient solutions can sustain rapid plant growth 194
Mineral deficiencies disrupt plant metabolism and function 195
Plant tissue analysis reveals mineral deficiencies 199
BOX 7.2 Ionomics: A Powerful Approach to Study Mineral Nutrition 200

7.2 Treating Nutritional Deficiencies 201

Crop yields can be improved by the addition of fertilizers 201
Some mineral nutrients can be absorbed by leaves 202

7.3 Soil, Roots, and Microbes 202

Negatively charged soil particles affect the adsorption of mineral nutrients 202
Soil pH affects nutrient availability, soil microbes, and root growth 204
Excess mineral ions in the soil limit plant growth 204
Some plants develop extensive root systems 205
Root systems differ in form but are based on common structures 205
Different areas of the root absorb mineral ions differently 207
Nutrient availability influences root growth and development 208
Mycorrhizal symbioses facilitate nutrient uptake by roots 210
Nutrients move between mycorrhizal fungi and root cells 213

CHAPTER 8
Solute Transport 217

8.1 Passive and Active Transport 218

8.2 Transport of Ions across Membrane Barriers 219

Different diffusion rates for cations and anions produce diffusion potentials 220
How does membrane potential relate to ion distribution? 220
The Nernst equation distinguishes between active and passive transport 221
Proton transport is a major determinant of the membrane potential 222

8.3 Membrane Transport Processes 223

Channels enhance diffusion across membranes 224
Carriers bind and transport specific substances 226
Primary active transport requires energy 226
Secondary active transport is driven by ion gradients 226
Kinetic analyses can elucidate transport mechanisms 228

8.4 Membrane Transport Proteins 228

Genes encoding many transporters have been identified 230
Transporters exist for diverse nitrogen-containing compounds 230
Cation transporters are diverse 231
Anion transporters have been identified 233
Transporters for metal and metalloid ions transport essential micronutrients 234
Aquaporins have diverse functions 235
Plasma membrane H^+-ATPases are highly regulated P-type ATPases 236
The tonoplast H^+-ATPase drives solute accumulation in vacuoles 237
H^+-pyrophosphatases and P-type H^+-ATPases also pump protons at the tonoplast 238

8.5 Transport in Stomatal Guard Cells 238

Blue light induces stomatal opening 239
Abscisic acid and high CO_2 induce stomatal closing 240

8.6 Ion Transport in Roots 240

Solutes move through both apoplast and symplasm 240
Ions cross both symplasm and apoplast 241
Xylem parenchyma cells participate in xylem loading 242

UNIT III Biochemistry and Metabolism 245

CHAPTER 9
Photosynthesis: The Light Reactions 247

9.1 Photosynthesis in Green Plants 247

9.2 General Concepts 248

Light consists of photons with characteristic energies 248

Absorption of photosynthetically active light changes the electronic states of chlorophylls 248

Photosynthetic pigments absorb the light that powers photosynthesis 250

9.3 Key Experiments in Understanding Photosynthesis 252

Action spectra relate light absorption to photosynthetic activity 252

Photosynthesis takes place in complexes containing light-harvesting antennas and photochemical reaction centers 253

The chemical reaction of photosynthesis is driven by light 254

Light drives the reduction of $NADP^+$ and the formation of ATP 254

Oxygen-evolving organisms have two photosystems that operate in series 255

9.4 Organization of the Photosynthetic Apparatus 256

The chloroplast is the site of photosynthesis 256

Thylakoids contain integral membrane proteins 257

Photosystems I and II are spatially separated in the thylakoid membrane 257

Anoxygenic photosynthetic bacteria have a single reaction center 259

9.5 Organization of Light-Absorbing Antenna Systems 259

Antenna systems contain chlorophyll and are membrane-associated 259

The antenna funnels energy to the reaction center 260

Many antenna pigment–protein complexes have a common structural motif 260

9.6 Mechanisms of Electron Transport 261

Electrons from chlorophyll travel through the carriers organized in the Z scheme 261

Energy is captured when an excited chlorophyll reduces an electron acceptor molecule 263

The reaction center chlorophylls of the two photosystems absorb at different wavelengths 264

The PSII reaction center is a multi-subunit pigment–protein complex 264

Water is oxidized to oxygen by PSII 264

Pheophytin and two quinones accept electrons from PSII 265

Electron flow through the cytochrome b_6f complex also transports protons 266

Plastocyanin carries electrons between the cytochrome b_6f complex and photosystem I 268

The PSI reaction center oxidizes PC and reduces ferredoxin, which transfers electrons to $NADP^+$ 268

Some herbicides block photosynthetic electron flow 269

9.7 Proton Transport and ATP Synthesis in the Chloroplast 270

Cyclic electron flow augments the output of ATP to balance the chloroplast energy budget 272

9.8 Repair and Regulation of the Photosynthetic Machinery 273

Carotenoids serve as photoprotective agents 273

Some xanthophylls also participate in energy dissipation 274

The PSII reaction center is easily damaged and rapidly repaired 274

Thylakoid stacking permits energy partitioning between the photosystems 275

9.9 Genetics, Assembly, and Evolution of Photosynthetic Systems 275

Chloroplast genes exhibit non-Mendelian patterns of inheritance 275

Most chloroplast proteins are imported from the cytoplasm 275

The biosynthesis and breakdown of chlorophyll are complex pathways 276

Complex photosynthetic organisms have evolved from simpler forms 276

CHAPTER 10
Photosynthesis: The Carbon Reactions 281

10.1 The Calvin–Benson Cycle 282

The Calvin–Benson cycle has three phases: carboxylation, reduction, and regeneration 282

The fixation of CO_2 via carboxylation of ribulose 1,5-bisphosphate and the reduction of 3-phosphoglycerate yield triose phosphates 283

The regeneration of ribulose 1,5-bisphosphate ensures the continuous assimilation of CO_2 284

An induction period precedes the steady state of photosynthetic CO_2 assimilation 285

Many mechanisms regulate the Calvin–Benson cycle 286

Rubisco activase regulates the catalytic activity of Rubisco 287

Light regulates the Calvin–Benson cycle via the ferredoxin–thioredoxin system 288

Light-dependent ion movements modulate enzymes of the Calvin–Benson cycle 289

Light controls the assembly of chloroplast enzymes into supramolecular complexes 289

10.2 The Oxygenation Reaction of Rubisco and Photorespiration 290

The oxygenation of ribulose 1,5-bisphosphate sets in motion photorespiration 291

Photorespiration is linked to the photosynthetic electron transport system 295

Enzymes of plant photorespiration derive from different ancestors 295

BOX 10.1 Production of Biomass May Be Enhanced by Engineering Photorespiration 296

Photorespiration interacts with many metabolic pathways 296

10.3 Inorganic Carbon–Concentrating Mechanisms 297

10.4 Inorganic Carbon–Concentrating Mechanisms: C_4 Photosynthetic Carbon Fixation 297

Malate and aspartate are the primary carboxylation products of the C_4 cycle 298

Kranz-type C_4 plants assimilate CO_2 by the concerted action of two different types of cells 299

The C_4 subtypes use different mechanisms to decarboxylate four-carbon acids transported to bundle sheath cells 301

Bundle sheath cells and mesophyll cells exhibit anatomical and biochemical differences 301

The C_4 cycle also concentrates CO_2 in single cells 302

Light regulates the activity of key C_4 enzymes 302

Photosynthetic assimilation of CO_2 in C_4 plants requires more transport processes than in C_3 plants 302

In hot, dry climates, the C_4 cycle reduces photorespiration 303

10.5 Inorganic Carbon–Concentrating Mechanisms: Crassulacean Acid Metabolism (CAM) 303

Different mechanisms regulate C_4 PEPCase and CAM PEPCase 305

CAM is a versatile mechanism sensitive to environmental stimuli 305

10.6 Accumulation and Partitioning of Photosynthates—Starch and Sucrose 305

10.7 Formation and Mobilization of Chloroplast Starch 306

Chloroplast stroma accumulates starch as insoluble granules during the day 307

Starch degradation at night requires the phosphorylation of amylopectin 310

The export of maltose prevails in the nocturnal breakdown of transitory starch 310

The synthesis and degradation of the starch granule are regulated by multiple mechanisms 311

10.8 Sucrose Biosynthesis and Signaling 312

Triose phosphates from the Calvin–Benson cycle build up the cytosolic pool of three important hexose phosphates in the light 312

Fructose 2,6-bisphosphate regulates the hexose phosphate pool in the light 314

Sucrose is continuously synthesized in the cytosol 314

Sucrose plays only a minor role in stomatal regulation 316

CHAPTER 11
Photosynthesis: Physiological and Ecological Considerations 321

11.1 Photosynthesis Is Influenced by Leaf Properties 322

Leaf anatomy and canopy structure optimize light absorption 323

Leaf angle and leaf movement can control light absorption 325

Leaves acclimate to sun and shade environments 325

11.2 Effects of Light on Photosynthesis in the Intact Leaf 326

Photosynthetic light-response curves reveal differences in leaf properties 326

Leaves must dissipate excess light energy as heat 328

Absorption of too much light can lead to photoinhibition 330

11.3 Effects of Temperature on Photosynthesis in the Intact Leaf 331

Leaves must dissipate vast quantities of heat 331

There is an optimal temperature for photosynthesis 332

Photosynthesis is sensitive to both high and low temperatures 332

Photosynthetic efficiency is temperature-sensitive 333

11.4 Effects of Carbon Dioxide on Photosynthesis in the Intact Leaf 334

Atmospheric CO_2 concentration keeps rising 334

CO_2 diffusion to the chloroplast is essential to photosynthesis 334

CO_2 supply imposes limitations on photosynthesis 336

How will photosynthesis and respiration change in the future under elevated CO_2 conditions? 338

11.5 Stable Isotopes Record Photosynthetic Properties 340

How do we measure the stable carbon isotopes of plants? 340

Why does the carbon isotope ratio vary in plants? 341

CHAPTER 12
Translocation in the Phloem 345

12.1 Patterns of Translocation: Source to Sink 346

12.2 Pathways of Translocation 347

Sugar is translocated in phloem sieve elements 347

Mature sieve elements are living cells specialized for translocation 347

Large pores in cell walls are the prominent feature of sieve elements 348

Companion cells aid the highly specialized sieve elements 350

12.3 Phloem Loading 351

Phloem loading can occur via the apoplast or symplasm 351

Apoplastic loading is characteristic of many herbaceous species 352

Sucrose loading in the apoplastic pathway requires metabolic energy 352

Phloem loading in the apoplastic pathway involves a sucrose–H^+ symporter 353

Transfer cells are companion cells that are specialized for membrane transport 353

Phloem loading is symplasmic in some species 354

The oligomer-trapping model explains symplasmic loading in plants with intermediary-type companion cells 354

Phloem loading is passive in several tree species 355

The type of phloem loading is correlated with several significant characteristics 356

12.4 Long-Distance Transport: A Pressure-Driven Mechanism 357

Mass transfer is much faster than diffusion 357

The pressure-flow model is a passive mechanism for phloem transport 357

The pressure is osmotically generated 357

Some predictions of pressure flow have been confirmed, while others require further experimentation 359

Functional sieve plate pores appear to be open channels 359

Are the pressure gradients in the sieve elements sufficient to drive phloem transport in trees? 360

Modified models for translocation by mass flow have been suggested 361

Does translocation in gymnosperms involve a different mechanism? 361

12.5 Materials Translocated in the Phloem 361

Sugars are translocated in a nonreducing form 362

Other small organic solutes are translocated in the phloem 362

Phloem-mobile macromolecules often originate in companion cells 364

Damaged sieve elements are sealed off 364

12.6 Phloem Unloading and Sink-to-Source Transition 365

Phloem unloading and short-distance transport can occur via symplasmic or apoplastic pathways 366

Symplasmic unloading supplies growing vegetative sinks 366

Symplasmic unloading is passive but depends on energy consumption in the sink 367

Import into seeds, fruits, and storage organs often involves an apoplastic step 367

Apoplastic import is active and requires metabolic energy 368

The transition of a leaf from sink to source is gradual 369

12.7 Photosynthate Distribution: Allocation and Partitioning 371

Allocation includes storage, utilization, and transport 371

Source leaves regulate allocation 371

Various sinks partition transport sugars 372

Sink tissues compete for available translocated photosynthate 372

Sink strength depends on sink size and activity 372

The source adjusts over the long term to changes in the source-to-sink ratio 373

12.8 Transport of Signaling Molecules 373

Turgor pressure and chemical signals coordinate source and sink activities 374

Mobile RNAs function as signal molecules in the phloem to regulate growth and development 374

Mobile proteins also function as signal molecules to regulate growth and development 375

Plasmodesmata function in phloem signaling 375

BOX 12.1 Relevance of Phloem Translocation and Signaling for Climate Change and Biotechnology 376

CHAPTER 13
Respiration and Lipid Metabolism 379

13.1 Overview of Plant Respiration 379

13.2 Glycolysis 382

Glycolysis metabolizes carbohydrates from several sources 382

The energy-conserving phase of glycolysis produces pyruvate, ATP, and NADH 384

Plants have alternative glycolytic reactions 385

In the absence of oxygen, fermentation regenerates the NAD^+ needed for glycolytic ATP production 385

13.3 The Oxidative Pentose Phosphate Pathway 386

The oxidative pentose phosphate pathway produces NADPH and biosynthetic intermediates 386

The oxidative pentose phosphate pathway is controlled by cellular redox status 388

13.4 The Tricarboxylic Acid Cycle 388

Mitochondria are semiautonomous organelles 388

Pyruvate enters the mitochondrion and is oxidized via the TCA cycle 389

The TCA cycle of plants has unique features 391

13.5 Oxidative Phosphorylation 391

The electron transport chain catalyzes a flow of electrons from NADH to O_2 392

The electron transport chain has supplementary branches 393

ATP synthesis in the mitochondrion is coupled to electron transport 394

Transporters exchange substrates and products 396

Aerobic respiration yields about 60 molecules of ATP per molecule of sucrose 396

Several subunits of respiratory complexes are encoded by the mitochondrial genome 396

Plants have several mechanisms that lower the ATP yield 398

Respiration is an integral part of a redox and biosynthesis network 400
Respiration is controlled at multiple levels 401

13.6 Respiration in Intact Plants and Tissues 402

Plants respire roughly half of the daily photosynthetic yield 402
Respiratory processes operate during photosynthesis 403
Different tissues and organs respire at different rates 403
BOX 13.1 Modifying Respiration for Future Needs 404
Environmental factors alter respiration rates 404

13.7 Lipid Metabolism 405

Fats and oils store large amounts of energy 405
Triacylglycerols are stored in oil bodies 406
BOX 13.2 Biotechnology of Lipids in a Changing World 407
Polar glycerolipids are the main structural lipids in membranes 407
Fatty acid biosynthesis consists of cycles of two-carbon addition 407
Glycerolipids are synthesized in the plastids and the ER 410
Lipid composition influences membrane function 411
Membrane lipids are precursors of important signaling compounds 411
Storage lipids are converted into carbohydrates in germinating seeds 411

CHAPTER 14
Assimilation of Inorganic Nutrients 417

14.1 Nitrogen in the Environment 418

Nitrogen passes through several forms in a biogeochemical cycle 418
Unassimilated ammonium or nitrate may be dangerous 419

14.2 Nitrate Assimilation 420

Many factors regulate nitrate reductase 421
Nitrite reductase converts nitrite to ammonium 421
Both roots and shoots assimilate nitrate 422
Nitrate can be transported in both xylem and phloem 422
Transceptor contributes to nitrate signaling 423

14.3 Ammonium Assimilation 424

Converting ammonium to amino acids requires two enzymes 424
Ammonium can be assimilated via an alternative pathway 426
Transamination reactions transfer nitrogen 426
Asparagine and glutamine link carbon and nitrogen metabolism 426

14.4 Amino Acid Biosynthesis 426

14.5 Biological Nitrogen Fixation 427

Free-living and symbiotic bacteria fix nitrogen 428
Nitrogen fixation requires microanaerobic or anaerobic conditions 429
BOX 14.1 Challenges and Solutions for Solving Nitrogen Deficiency in Future Agriculture 430
Symbiotic nitrogen fixation occurs in specialized structures 430
Establishing symbiosis requires an exchange of signals 431
Nod factors produced by bacteria act as signals for symbiosis 431
Nodule formation involves phytohormones 432
The nitrogenase enzyme complex fixes N_2 434
Amides and ureides are the transported forms of nitrogen 435

14.6 Sulfur Assimilation 435

Sulfate is the form of sulfur transported into plants 435
Sulfate assimilation requires the reduction of sulfate to cysteine 436
Sulfate assimilation occurs mostly in leaves 438
Methionine is synthesized from cysteine 438

14.7 Phosphate Assimilation 438

miRNAs contribute to phosphate and sulfate signaling 438

14.8 Oxygen Assimilation 439

14.9 The Energetics of Nutrient Assimilation 439

CHAPTER 15
Abiotic Stress 443

15.1 Defining Plant Stress 444

Physiological adjustment to abiotic stress involves trade-offs between vegetative and reproductive development 445

15.2 Acclimation and Adaptation 445

Adaptation to stress involves genetic modification over many generations 445
Acclimation allows plants to respond to environmental fluctuations 446

15.3 Environmental Factors and Their Biological Impacts on Plants 446

Water deficit decreases turgor pressure, increases ion toxicity, and inhibits photosynthesis 447
Temperature stress affects a broad spectrum of physiological processes 447
Flooding results in anaerobic stress to the root 448
Salinity stress has both osmotic and cytotoxic effects 449
During freezing stress, extracellular ice crystal formation causes cell dehydration 449
Heavy metals can both mimic essential mineral nutrients and generate ROS 449
Ozone and ultraviolet light generate ROS that cause lesions and induce PCD 450
Combinations of abiotic stresses can induce unique signaling and metabolic pathways 450

Interactions occur between abiotic and biotic stresses 451
Sequential exposure to different abiotic stresses sometimes confers cross-protection 451
Beneficial microbes can improve plant tolerance to abiotic stress 451

15.4 Stress-Sensing Mechanisms in Plants 452

Early-acting stress sensors provide the initial signal for the stress response 452

15.5 Signaling Pathways Activated in Response to Abiotic Stress 453

The signaling intermediates of many stress-response pathways can interact 453
Acclimation to stress involves transcriptional regulatory networks called regulons 455
Chloroplasts and mitochondria respond to abiotic stress by sending stress signals to the nucleus 456
Plant-wide waves of Ca^{2+} and ROS mediate systemic acquired acclimation 456
Epigenetic mechanisms, retrotransposons, and small RNAs provide additional protection against stress 456
Hormonal interactions regulate abiotic stress responses 459

15.6 Physiological and Developmental Mechanisms That Protect Plants against Abiotic Stress 460

Plants adjust osmotically to drying soils by accumulating solutes 460
Submerged organs develop aerenchyma tissue in response to hypoxia 461
Antioxidants and ROS-scavenging pathways protect cells from oxidative stress 462
Molecular chaperones and molecular shields protect proteins and membranes during abiotic stress 462
Plants can alter their membrane lipids in response to temperature and other abiotic stresses 463
Exclusion and internal tolerance mechanisms allow plants to cope with toxic ions 464
Phytochelatins and other chelators contribute to internal tolerance of toxic metal ions 465
Plants use cryoprotectant molecules and antifreeze proteins to prevent ice crystal formation 466
ABA signaling during water stress causes the massive efflux of K^+ and anions from guard cells 466
Plants can alter their morphology in response to abiotic stress 467
The process of recovery from stress can be dangerous to the plant and requires a coordinated adjustment of plant metabolism and physiology 469

UNIT IV Growth and Development 473

CHAPTER 16
Signals from Sunlight 475

16.1 Plant Photoreceptors 476

Photoresponses are driven by light quality or spectral properties of the energy absorbed 477
Plants responses to light can be distinguished by the amount of light required 478

16.2 Phytochromes 480

Phytochrome is the primary photoreceptor for red and far-red light 480
Phytochrome can interconvert between Pr and Pfr forms 480
Pfr is the physiologically active form of phytochrome 481
The phytochrome chromophore and protein both undergo conformational changes in response to red light 481
Pfr is partitioned between the cytosol and the nucleus 483

16.3 Phytochrome Responses 484

Phytochrome responses vary in lag time and escape time 484
Phytochrome responses fall into three main categories based on the amount of light required 484
Phytochrome A mediates responses to continuous far-red light 486
Phytochrome B mediates responses to continuous red or white light 486
Roles for phytochromes C, D, and E are emerging 486

16.4 Phytochrome Signaling Pathways 487

Phytochrome regulates membrane potentials and ion fluxes 487
Phytochrome regulates gene expression 487
Phytochrome interacting factors (PIFs) act early in signaling 488
Phytochrome signaling involves protein phosphorylation and dephosphorylation 488
Phytochrome-induced photomorphogenesis involves protein degradation 489

16.5 Blue-Light Responses and Photoreceptors 490

Blue-light responses have characteristic kinetics and lag times 490

16.6 Cryptochromes 491

The activated FAD chromophore of cryptochrome causes a conformational change in the protein 491
cry1 and cry2 have different developmental effects 492
Nuclear cryptochromes inhibit COP1-induced protein degradation 493
Cryptochrome can also bind to transcriptional regulators directly 493

16.7 Interactions of Cryptochrome with Other Photoreceptors 493

Stem elongation is inhibited by both red and blue photoreceptors 493

Phytochrome interacts with cryptochrome to regulate flowering 494

The circadian clock is regulated by multiple aspects of light 494

16.8 Phototropins 495

Blue light induces changes in FMN absorption maxima associated with conformation changes 495

The LOV2 domain is primarily responsible for kinase activation in response to blue light 496

Blue light induces a conformational change that "uncages" the kinase domain of phototropin and leads to autophosphorylation 496

Phototropins trigger plant movements that enhance light use 496

Blue light initiates stomatal opening via activation of the plasma membrane H^+-ATPase 498

16.9 Responses to Ultraviolet Radiation 500

CHAPTER 17
Seed Dormancy, Germination, and Seedling Establishment 505

17.1 Seed Structure 506

Seed anatomy varies widely among different plant groups 506

17.2 Seed Dormancy 508

There are two basic types of seed dormancy mechanisms: exogenous and endogenous 508

Non-dormant seeds can exhibit vivipary and precocious germination 509

The ABA:GA ratio is the primary determinant of embryonic seed dormancy 510

17.3 Release from Dormancy 511

Light is an important signal that breaks dormancy in small seeds 511

Some seeds require either chilling or after-ripening to break dormancy 511

Seed dormancy can be broken by various chemical compounds 512

17.4 Seed Germination 512

Germination and postgermination can be divided into three phases corresponding to the phases of water uptake 513

17.5 Mobilization of Stored Reserves 514

Cereal seeds are a model for understanding starch mobilization 515

Legume seeds are a model for understanding protein mobilization 516

Oilseeds are a model for understanding lipid remobilization 517

17.6 Seedling Growth and Establishment 517

The development of emerging seedlings is strongly influenced by light 517

Gibberellins and brassinosteroids both suppress photomorphogenesis in darkness 518

Hook opening is regulated by phytochrome, auxin, and ethylene 519

Vascular differentiation begins during seedling emergence 520

The root tip has specialized cells 520

Ethylene and other hormones regulate root hair development 521

17.7 Differential Growth Enables Successful Seedling Establishment 522

Ethylene affects microtubule orientation and induces lateral cell expansion 523

Auxin promotes growth in stems and coleoptiles, while inhibiting growth in roots 524

The minimum lag time for auxin-induced elongation is 10 minutes 525

Auxin-induced proton extrusion loosens the cell wall 526

17.8 Tropisms: Growth in Response to Directional Stimuli 526

Gravitropism involves the lateral redistribution of auxin 526

The gravitropic stimulus perturbs the symmetric movements of auxin 526

Gravity perception is triggered by the sedimentation of amyloplasts 529

Gravity sensing may involve pH and calcium ions (Ca^{2+}) as second messengers 532

Thigmotropism involves signaling by Ca^{2+}, pH, and reactive oxygen species 533

Hydrotropism involves ABA signaling and asymmetric cytokinin responses 534

Phototropins are the light receptors involved in phototropism 535

Phototropism is mediated by the lateral redistribution of auxin 535

Shoot phototropism occurs in a series of steps 536

CHAPTER 18
Vegetative Growth and Organogenesis: Primary Growth of the Plant Axis 541

18.1 Meristematic Tissues: Foundations for Indeterminate Growth 541

The root and shoot apical meristems use similar strategies to enable indeterminate growth 542

18.2 The Root Apical Meristem 542

The root tip has four developmental zones 542

The origin of different root tissues can be traced to specific initial cells 543

Auxin and cytokinin contribute to the maintenance and function of the RAM 543

18.3 The Shoot Apical Meristem 545

The shoot apical meristem has distinct zones and layers 545

A combination of positive and negative interactions determines apical meristem size 546

KNOX class homeodomain transcription factors help maintain proliferation in the SAM through regulation of cytokinin and GA concentrations 547
Localized auxin accumulation promotes leaf initiation 547
Axillary meristems form in the axils of leaf primordia 548

18.4 Leaf Development 549
Growth determines leaf shape 551

18.5 The Establishment of Leaf Polarity 551
A signal from the SAM initiates adaxial–abaxial polarity 551
Antagonism between sets of transcription factors determines adaxial–abaxial leaf polarity 552
MYB transcription factors, HD-ZIP III proteins, and *KNOX1* repression promote adaxial identity 552
Abaxial identity is determined by auxin, KANADI, and YABBY 552
Blade outgrowth is auxin dependent and regulated by the YABBY and WOX genes 553
Leaf proximal–distal polarity also depends on specific gene expression 553
In compound leaves, de-repression of the *KNOX1* gene promotes leaflet formation 554

18.6 Differentiation of Epidermal Cell Types 555
Guard cell identity is determined by a specialized epidermal lineage 555
Two groups of bHLH transcription factors govern stomatal cell identity transitions 556
Cell-to-cell peptide signals regulate stomatal patterning 557
Intrinsic polarity in the stomatal lineage aids stomatal spacing 557
Environmental factors also regulate stomatal density 558
Stomata development in monocots involves some genes that are orthologous to those in Arabidopsis 558

18.7 Venation Patterns in Leaves 559
The primary leaf vein is initiated discontinuously from the preexisting vascular system 560
Auxin canalization initiates development of the leaf trace 560
Basipetal auxin transport from the L1 layer of the leaf primordium initiates development of the leaf trace procambium 561
The existing vasculature guides the growth of the leaf trace 562
Vascular development proceeds from procambium differentiation 562
Higher-order leaf veins differentiate in a predictable hierarchical order 562
Auxin regulates higher-order vein formation and patterning 563

CHAPTER 19
Vegetative Growth and Organogenesis: Branching and Secondary Growth 567

19.1 Shoot Branching and Architecture 568
Auxin, cytokinins, and strigolactones regulate axillary bud outgrowth 569
Auxin from the shoot tip maintains apical dominance 569
Strigolactones act locally to repress axillary bud growth 571
Cytokinins antagonize the effects of strigolactones 571
Integration of environmental and hormonal branching signals is required for plant fitness 572
Axillary bud dormancy is affected by season, position, and age factors 572

19.2 Root Branching and Architecture 573
Lateral root primordia arise from the xylem pole pericycle cells 573
Lateral root formation can be divided into four distinct stages 574
Lateral root founder cells undergo asymmetric cell divisions to initiate formation of lateral root primordia 576
Monocots and eudicots differ in their predominant root types 576
Transcription factors regulate the gravitropic setpoint angles of lateral roots and shoots 577
Plants can modify their root system architecture to optimize water and nutrient uptake 578

19.3 Secondary Growth 578
Two types of lateral meristems are involved in secondary growth 578
The vascular cambium produces secondary xylem and phloem 579
Mobile transcription factors pre-pattern the vascular cambium 580
The gene networks that control secondary meristems share similarities and differences with those that control the apical meristems 582
Several phytohormones regulate vascular cambium activity and differentiation of secondary xylem and phloem 584
The cork cambium gives rise to the outer corky layer called the periderm 585
Bark has diverse protective and storage functions 586
Epicormic buds covered by bark can sprout after forest fires 586

CHAPTER 20
The Control of Flowering and Floral Development 591

20.1 Floral Evocation: Integrating Environmental Cues 591

20.2 The Shoot Apex and Phase Changes 592
Plants progress through three developmental phases 592
Juvenile tissues are produced first and are located at the base of the shoot 592
Phase changes can be influenced by nutrients, gibberellins, and other signals 593

20.3 Circadian Rhythms: The Clock Within 594
Circadian rhythms exhibit characteristic features 595
Phase shifting adjusts circadian rhythms to different day–night cycles 597
Phytochromes and cryptochromes entrain the clock 597

20.4 Photoperiodism: Monitoring Day Length 597

Plants can be classified according to their photoperiodic responses 597

The leaf is the site of perception of the photoperiodic signal 599

The length of the night is important for floral induction 599

Night breaks can cancel the effect of the dark period 600

Photoperiodic timekeeping during the night depends on a circadian clock 601

The external coincidence model is based on oscillating light sensitivity 602

The coincidence of CONSTANS expression and light promotes flowering in LDPs 602

SDPs use a coincidence mechanism to inhibit flowering in long days 603

BOX 20.1 Refining Molecular Mechanisms of Photoperiodic Flowering Happening in Natural Environments 604

Phytochrome is the primary photoreceptor in photoperiodism 605

A blue-light photoreceptor regulates flowering in some LDPs 606

20.5 Long-Distance Signaling Involved in Flowering 606

Grafting studies provided the first evidence for a transmissible floral stimulus 607

Florigen is translocated in the phloem 608

20.6 The Identification of Florigen 608

The Arabidopsis protein FLOWERING LOCUS T (FT) is florigen 608

20.7 Vernalization: Promoting Flowering with Cold 610

Vernalization results in competence to flower at the shoot apical meristem 610

Vernalization can involve epigenetic changes in gene expression 611

A range of vernalization pathways may have evolved 612

20.8 Multiple Pathways Involved in Flowering 612

Gibberellins and ethylene can induce flowering 612

The transition to flowering involves multiple factors and pathways 613

20.9 Floral Meristems and Floral Organ Development 613

The shoot apical meristem in Arabidopsis changes with development 613

The four different types of floral organs are initiated as separate whorls 614

Two major categories of genes regulate floral development 615

Floral meristem identity genes regulate meristem function 615

Homeotic mutations led to the identification of floral organ identity genes 616

The ABC model partially explains the determination of floral organ identity 617

Arabidopsis Class E genes are required for the activities of the A, B, and C genes 618

According to the Quartet Model, floral organ identity is regulated by tetrameric complexes of the ABCE proteins 619

Class D genes are required for ovule formation 620

Floral asymmetry in flowers is regulated by gene expression 620

CHAPTER 21
Sexual Reproduction: From Gametes to Fruits 625

21.1 Development of the Male and Female Gametophyte Generations 625

21.2 Formation of Male Gametophytes in the Stamen 627

Pollen grain formation occurs in two successive stages 627

The multilayered pollen cell wall is surprisingly complex 629

21.3 Female Gametophyte Development in the Ovule 630

The Arabidopsis gynoecium is an important model system for studying ovule development 631

The vast majority of angiosperms exhibit Polygonum-type embryo sac development 632

Functional megaspores undergo a series of free nuclear mitotic divisions followed by cellularization 632

21.4 Pollination and Fertilization in Flowering Plants 633

The progamic phase includes everything from pollen landing and tube growth to the fusion of sperm and egg 633

Adhesion and hydration of a pollen grain on a compatible flower depend on recognition between pollen and stigma surfaces 634

Ca^{2+}-triggered polarization of the pollen grain precedes tube formation 635

Pollen tubes grow by tip growth 636

Receptor-like kinases are thought to regulate the ROP1 GTPase switch, a master regulator of tip growth 638

Pollen tube tip growth in the pistil is guided by both physical and chemical cues 638

Style tissue may condition pollen tubes to grow toward the embryo sac 639

Synergid cells release chemoattractants that guide pollen tube growth to the micropyle 640

Double fertilization occurs in three distinct stages 641

21.5 Selfing versus Outcrossing 642

Hermaphroditic and monoecious species have evolved floral features to ensure outcrossing 642

Cytoplasmic male sterility (CMS) occurs in the wild and is of great utility in agriculture 642

Self-incompatibility (SI) is the primary mechanism that enforces outcrossing in angiosperms 643

Two distinct genetic mechanisms govern self-incompatibility 644
The Brassicaceae sporophytic SI system is mediated by S locus–encoded receptors and ligands 645
Cytotoxic S-RNases and F-box proteins determine gametophytic self-incompatibility (GSI) 645

21.6 Apomixis: Asexual Reproduction by Seed 647
Apomixis is not an evolutionary dead end 647

21.7 Endosperm Development 647
Cellularization of coenocytic endosperm in Arabidopsis progresses from the micropylar to the chalazal region 648
Cellularization of the coenocytic endosperm of cereals progresses centripetally 649
Endosperm development and embryogenesis can occur autonomously 650
Many of the genes that control endosperm development are differentially expressed maternal or paternal genes 651
Cells of the starchy endosperm and aleurone layer follow divergent developmental pathways 652

21.8 Seed Coat Development 652
Seed coat development appears to be regulated by the endosperm 652

21.9 Seed Maturation and Desiccation Tolerance 653
Seed filling and desiccation tolerance phases overlap in most species 654
The acquisition of desiccation tolerance involves many metabolic pathways 654
During the acquisition of desiccation tolerance, the cells of the embryo acquire a glassy state 655
LEA proteins and nonreducing sugars have been implicated in seed desiccation tolerance 655
Abscisic acid plays a key role in seed maturation 655
Coat-imposed dormancy is correlated with long-term seed viability 655

21.10 Fruit Development and Ripening 656
The phytohormones auxin and gibberellic acid (GA) regulate fruit set and parthenocarpy 656
Specific transcription factors regulate the development of the dehiscence zone 658
Tomato is an important model system for studying fleshy fruit development 659
Fleshy fruits undergo ripening 660
Ripening involves changes in the color of fruit 660
Fruit softening involves the coordinated action of many cell wall–degrading enzymes 661
Taste and flavor reflect changes in acids, sugars, aroma, and other compounds 661
The causal link between ethylene and ripening was demonstrated in transgenic and mutant tomatoes 662
Climacteric and non-climacteric fruit differ in their ethylene responses 662
The ripening process is transcriptionally regulated 663
Studying the molecular mechanism of ripening can have commercial applications 664

CHAPTER 22
Embryogenesis: The Origin of Plant Architecture 669

22.1 Embryogenesis in Monocots and Eudicots 670
Embryogenesis differs between monocots and eudicots, but also shares common features 670

22.2 Establishment of Apical–Basal Polarity 672
Apical–basal polarity is established early in embryogenesis 672
Zygote polarization can be studied using live imaging 673

22.3 Mechanisms Guiding Embryogenesis 676
Intercellular signaling processes play key roles in guiding position-dependent development 677
Cell-cell communication during early embryo development may be regulated by plasmodesmata 677
Mutant analyses have identified genes for signaling processes that are essential for embryo organization 678

22.4 Auxin Signaling During Embryogenesis 680
Spatial patterns of auxin accumulation regulate key developmental events 680
The GNOM protein establishes a polar distribution of PIN auxin efflux proteins 681
MONOPTEROS encodes a transcription factor that is activated by auxin 681

22.5 Radial Patterning During Embryogenesis 682
Procambial precursors for the vascular stele lie at the center of the radial axis 683
The differentiation of cortical and endodermal cells involves the intercellular movement of a transcription factor 684

22.6 Formation of the Root and Shoot Apical Meristems 686
Root formation involves *MONOPTEROS* and other auxin-regulated transcription factors 686
Shoot formation requires HD-ZIP III, *SHOOT MERISTEMLESS*, and *WUSCHEL* genes 687
Plants can initiate embryogenesis in multiple types of cells 687

CHAPTER 23
Plant Senescence and Developmental Cell Death 691

23.1 Programmed Cell Death 692
Distinct types of PCD occur in plants 693
Developmental PCD and pathogen-triggered PCD involve distinct processes 693
The autophagy pathway captures and degrades cellular constituents within lytic compartments 693
Autophagy plays a dual role in the regulation of plant PCD 695
Autophagy is required for nutrient recycling during plant senescence 696

23.2 The Leaf Senescence Syndrome 696

Leaf senescence may be sequential, seasonal, or stress-induced 697

Leaves undergo massive structural and biochemical changes during leaf senescence 698

The autolysis of chloroplast proteins occurs in multiple compartments 698

The STAY-GREEN (SGR) protein is required for both LHCP II protein recycling and chlorophyll catabolism 699

23.3 Regulation of Leaf Senescence: A Multi-Layered Network 700

Leaf senescence depends on the comprehensive regulation of pathways that respond to endogenous and environmental factors 701

Plant hormones and other signaling agents can act as positive or negative regulators of leaf senescence 706

Positive senescence regulators 707

Negative senescence regulators 708

23.4 Abscission 709

Organ abscission is regulated by developmental and environmental cues 711

23.5 Whole-Plant Senescence 713

Angiosperm life cycles may be annual, biennial, or perennial 714

Whole-plant senescence differs from aging in animals 714

The determinacy of shoot apical meristems is developmentally regulated 715

Nutrient redistribution may trigger senescence in monocarpic plants 716

The productivity of tall trees continues to increase right up to the onset of senescence 716

CHAPTER 24
Biotic Interactions 721

24.1 Plant Interactions with Beneficial Microorganisms 723

Nod factors are recognized by the Nod factor receptor (NFR) in legumes 723

Arbuscular mycorrhizal associations and nitrogen-fixing symbioses involve related signaling pathways 723

Rhizobacteria can increase nutrient availability, stimulate root branching, and protect against pathogens 725

24.2 Herbivore Interactions That Harm Plants 725

Mechanical barriers provide a first line of defense against insect pests and pathogens 726

Plant specialized metabolites can deter insect herbivores 728

Plants store constitutive toxic compounds in specialized structures 728

Plants often store defense chemicals as nontoxic water-soluble sugar conjugates in the vacuole 730

24.3 Inducible Defense Responses to Insect Herbivores 732

Plants can recognize specific components of insect saliva 733

Ca^{2+} signaling and activation of the MAP kinase pathway are early events associated with insect herbivory 734

Jasmonate activates defense responses against insect herbivores 734

Jasmonate acts through a conserved ubiquitin ligase signaling mechanism 735

Hormonal interactions contribute to plant–insect herbivore interactions 735

JA initiates the production of defense proteins that inhibit herbivore digestion 736

Herbivore damage induces systemic defenses 736

Glutamate receptor-like (GLR) genes are required for long-distance electrical signaling during herbivory 737

Herbivore-induced volatiles can repel herbivores and attract natural enemies 738

Herbivore-induced volatiles can serve as long-distance signals between plants 739

Herbivore-induced volatiles can also act as systemic signals within a plant 739

Defense responses to herbivores and pathogens are regulated by circadian rhythms 739

Insects have evolved mechanisms to defeat plant defenses 741

24.4 Plant Defenses against Pathogens 741

Microbial pathogens have evolved various strategies to invade host plants 741

Pathogens produce effector molecules that aid in the colonization of their plant host cells 742

Plants can detect pathogens through perception of pathogen-derived "danger signals" 743

R genes provide resistance to individual pathogens by recognizing strain-specific effectors 744

The hypersensitive response is a common defense against pathogens 745

A single encounter with a pathogen may increase resistance to future attacks 746

The main components of the salicylic acid signaling pathway have been identified 746

Phytoalexins with antimicrobial activity accumulate after pathogen attack 747

RNA interference plays a central role in antiviral immune responses in plants 747

Some plant parasitic nematodes form specific associations through the formation of distinct feeding structures 748

Plants compete with other plants by secreting allelopathic specialized metabolites into the soil 749

Some plants are parasites of other plants 749

Glossary G–1

Illustration Credits IC–1

Index I–1



LAURA_VN/Shutterstock

UNIT I

Structure and Information Systems of Plant Cells

CHAPTER 1 **Plant and Cell Architecture**

CHAPTER 2 **Cell Walls: Structure, Formation, and Expansion**

CHAPTER 3 **Genome Structure and Gene Expression**

CHAPTER 4 **Signals and Signal Transduction**

01_Taiz7e-Ch01.indd 1 4/29/22 9:40 AM



01_Taiz7e-Ch01.indd 2 4/29/22 9:40 AM

1 Plant and Cell Architecture



LAURA_VN/Shutterstock

Plant physiology is the study of plant *processes*—how plants grow, develop, and function as they interact with their physical (abiotic) and living (biotic) environments. Although this book will emphasize the physiological, biochemical, and molecular functions of plants, it is important to recognize that, whether we are talking about gas exchange in the leaf, water conduction in the xylem, photosynthesis in the chloroplast, ion transport across membranes, signal transduction pathways involving light and hormones, or gene expression during development, all of these functions depend entirely on structures.

Function derives from structures interacting at every level of scale. It occurs when tiny molecules recognize and bind each other to produce a complex with new functions. It occurs as a new leaf unfolds, as cells and tissues interact during the process of plant development. It occurs when huge organisms shade, nourish, or mate with each other. At every level, from molecules to organisms, structure and function represent different frames of reference of a biological unity.

The fundamental organizational unit of plants, and of all living organisms, is the cell. The term *cell* is derived from the Latin *cella*, meaning "storeroom" or "chamber." It was first used in biology in 1665 by the English scientist Robert Hooke to describe the individual units of the honeycomb-like structure he observed in cork under a compound microscope. The cork "cells" Hooke observed were actually the empty lumens of dead cells surrounded by cell walls, but the term is an apt one, because cells are the basic building blocks that define plant structure.

Moving outward from the cell, groups of specialized cells form specific tissues, and specific tissues arranged in particular patterns are the basis of three-dimensional organs. Just as plant anatomy, the study of the macroscopic arrangements of cells and tissues within organs, received its initial impetus from improvements to the light microscope in the seventeenth century, so plant cell biology, the study of the interior of cells, was stimulated by the first application of the electron microscope to biological material in the mid-twentieth century. Subsequent improvements in

microscopy and molecular biology have revealed astonishing variety and dynamics in the components that make up cells—the organelles, whose combined activities are required for the wide range of cellular and physiological functions that characterize biological organisms.

This chapter provides an overview of the basic anatomy and cell biology of plants, from the macroscopic structure of organs and tissues to the microscopic ultrastructure of cellular organelles. Subsequent chapters will treat these structures in greater detail from the perspective of their physiological and developmental functions at different stages of the plant life cycle.

1.1 Plant Life Processes: Unifying Principles

The spectacular diversity of plant size and form is familiar to everyone. Plants range in height from less than 1 cm to more than 100 m. Plant morphology, or form, is also surprisingly diverse. At first glance, the tiny plant duckweed (*Lemna*) seems to have little in common with a giant saguaro cactus or a redwood tree. No single plant shows the entire spectrum of adaptations to the range of environments that plants occupy on Earth, so plant physiologists often study **model organisms**, plants with short generation times and small **genomes** (the sum of their genetic information) (see **WEB TOPIC 1.1**). These models are useful because all plants, regardless of their specific adaptations, carry out fundamentally similar processes and are based on the same architectural plan.

We can summarize the major unifying principles of plants as follows:

- As Earth's primary producers, plants and green algae are the ultimate solar energy collectors. They harvest the energy of sunlight by converting light energy to chemical energy, which they store in bonds formed when they synthesize carbohydrates from carbon dioxide and water.
- Other than certain reproductive cells, land plants do not move from place to place; they are sessile. As a substitute for motility, they have evolved the ability to grow toward essential resources, such as light, water, and mineral nutrients, throughout their life span.
- Plants are structurally reinforced to support their mass as they grow toward sunlight against the pull of gravity.
- Plants have mechanisms for moving water and minerals from the soil to the sites of photosynthesis and growth, as well as mechanisms for moving the products of photosynthesis to nonphotosynthetic organs and tissues.
- Plants lose water continuously by evaporation and have evolved mechanisms for avoiding desiccation.
- Plants develop from embryos that derive nutrients from the mother plant, and these additional food stores facilitate the production of large self-supporting structures on land.

Based on these principles, we can generally define terrestrial plants as sessile, multicellular organisms derived from embryos, adapted to land, and able to convert carbon dioxide into complex organic compounds through the process of photosynthesis. This broad definition includes a wide spectrum of organisms, from the hornworts to the flowering plants, as illustrated in the diagram, or cladogram, depicting evolutionary lineage as branches, or clades, on a tree (**Figure 1.1**). Plants share with (mostly aquatic) green algae the primitive trait that is so important for photosynthesis in both clades: Their chloroplasts contain the pigments chlorophyll *a* and *b* and β-carotene. **Land plants**, or **embryophytes**, share the evolutionarily derived traits for surviving on land that are absent in the algae. Land plants include the **nonvascular plants**, or **bryophytes** (hornworts, mosses, and liverworts), and the **vascular plants**, or **tracheophytes**, which evolved from a common ancestor. The vascular plants consist of the **non-seed plants** (ferns and their relatives) and the **seed plants** (gymnosperms and angiosperms).[1]

Because plants have many agricultural, industrial, timber, and medical uses, as well as an overwhelming dominance in terrestrial ecosystems, most research in plant biology has focused on the plants that have evolved in the last 300 million years, the seed plants (see Figure 1.1). The **gymnosperms** (from the Greek for "naked seed") include the conifers, cycads, ginkgo, and gnetophytes (which include *Ephedra*, a popular medicinal plant). About 800 species of gymnosperms are known. The largest group of gymnosperms is the **conifers** ("cone-bearers"), which include such commercially important forest trees as pine, fir, spruce, and redwood. The **angiosperms** (from the Greek for "vessel seed") evolved about 183 million years ago and include three major groups: the **monocots**, **eudicots**, and so-called basal angiosperms, which include the Magnolia family and its relatives. Except in the great coniferous forests of Canada, Alaska, and northern Eurasia, angiosperms dominate the landscape. About 370,000 species are known, with an additional 17,000 undescribed species predicted by taxonomists using computer models. (A discussion of plant taxonomic systems is found in **WEB TOPIC 1.2**.) Most of the predicted species are imperiled because they occur primarily in regions of rich biodiversity where habitat destruction is common. The major anatomical innovation of the angiosperms is the flower; hence, they are referred to as **flowering plants**.

[1] Aquatic grasses are classified as land plants, as they are angiosperms that are evolutionarily adapted to periodic or continuous submersion in water.

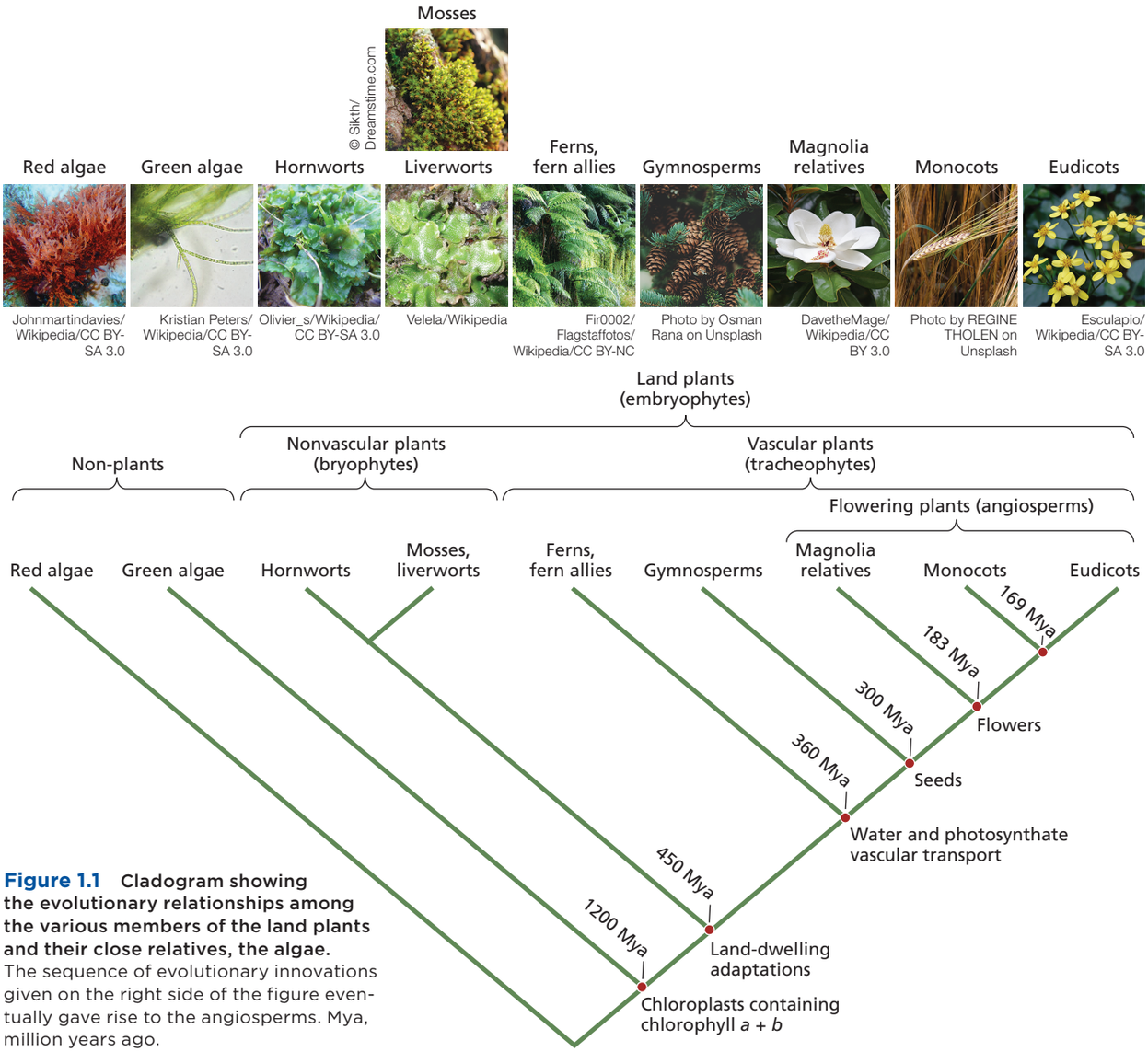


Figure 1.1 **Cladogram showing the evolutionary relationships among the various members of the land plants and their close relatives, the algae.** The sequence of evolutionary innovations given on the right side of the figure eventually gave rise to the angiosperms. Mya, million years ago.

Plant life cycles alternate between diploid and haploid generations

Plants, unlike animals, alternate between two distinct multicellular generations to complete their life cycle. This is called **alternation of generations**. One generation has **diploid** cells, cells with two copies of each chromosome and abbreviated as having **2N** chromosomes, and the other generation has **haploid** cells, cells with only one copy of each chromosome, abbreviated as **1N**. Each of these multicellular generations may be more or less physically and metabolically dependent on the other, depending on their evolutionary grouping.

When diploid (2*N*) animals, as represented by humans on the inner cycle in **Figure 1.2**, produce haploid **gametes**, egg (1*N*) and sperm (1*N*), they do so directly by the process of **meiosis**, cell division resulting in a reduction of the number of chromosomes from 2*N* to 1*N*. In contrast, the products of meiosis in diploid plants are **spores**, and diploid plant forms are therefore called **sporophytes**. Each spore is capable of undergoing **mitosis**, cell division that doesn't change the number of chromosomes in the daughter cells, to form a new haploid multicellular individual, the **gametophyte**, as shown by the outer cycles in Figure 1.2. The haploid gametophytes produce gametes, egg and sperm, by simple mitosis, whereas haploid gametes in animals are produced by meiosis. Once the haploid gametes fuse and **fertilization** takes place to create the 2*N* zygote, the life cycles of animals and plants are similar (see Figure 1.2). The 2*N* zygote undergoes a series of

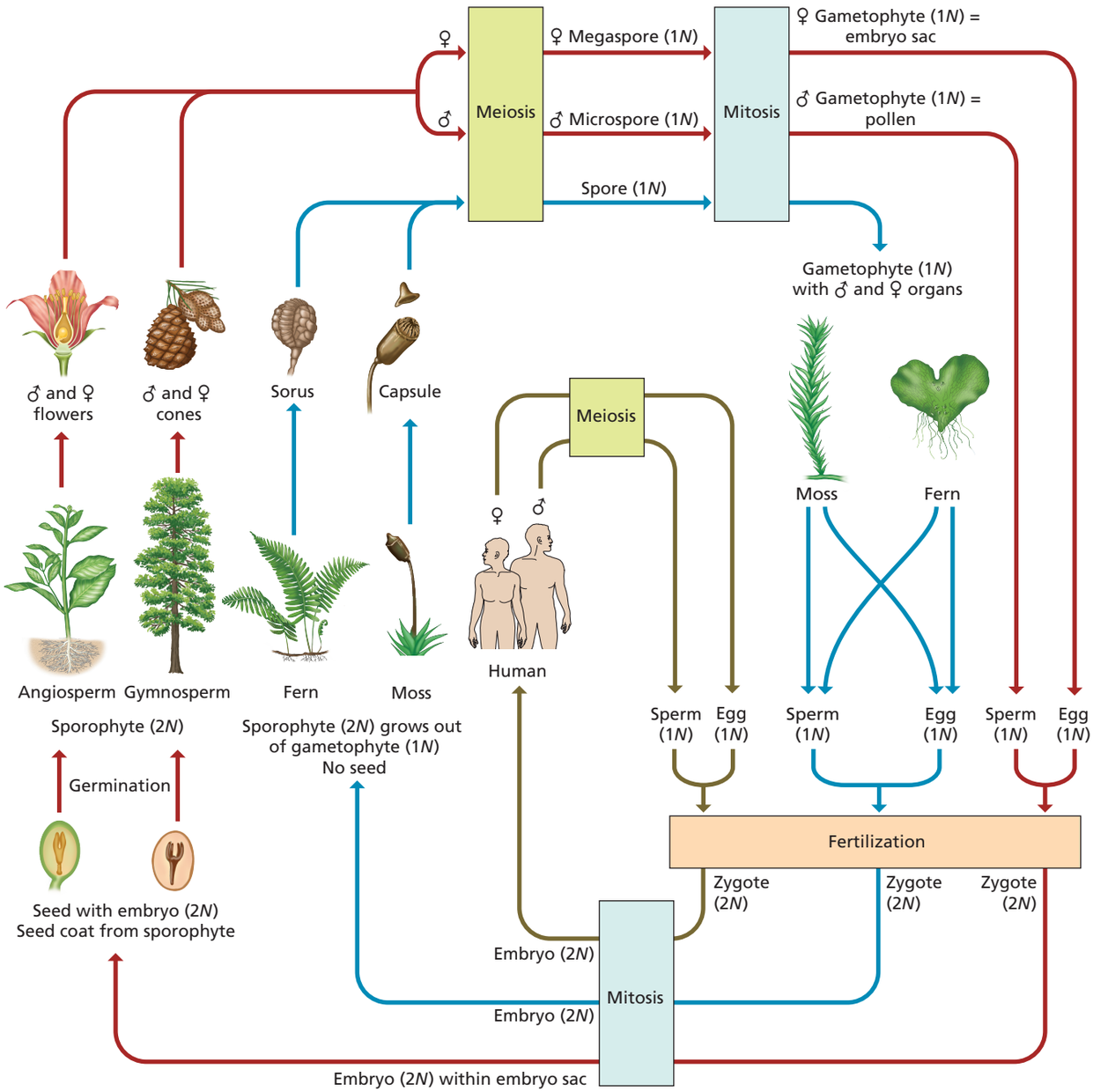


Figure 1.2 **Diagram of the generalized life cycles of plants and animals.** In contrast to animals, plants exhibit alternation of generations. Rather than producing gametes directly by meiosis as animals do, plants produce vegetative spores by meiosis. These 1*N* (haploid) spores divide to produce a second multicellular individual called the gametophyte. The gametophyte then produces gametes (sperm and egg) by mitosis. Following fertilization, the resulting 2*N* (diploid) zygote develops into the mature sporophyte generation, and the cycle begins again (see Chapter 21 for details).

mitotic divisions to produce the embryo, which eventually grows into the mature diploid adult.

Thus, all plant life cycles encompass two separate generations: the diploid, spore-producing **sporophyte generation** and the haploid, gamete-producing **gametophyte generation**. A line drawn between fertilization and meiosis divides these two separate stages of the generalized plant life cycle (see Figure 1.2). Increasing the number of mitoses between fertilization and meiosis increases the size of the sporophyte generation and the number of spores that can be produced. Having more spores per fertilization event could compensate for low

fertility when water becomes scarce on land. This could explain the marked tendency for the increase in size of the sporophyte generation, relative to the gametophyte generation, during the evolution of plants.

The sporophyte generation is dominant in the seed plants, the gymnosperms and angiosperms, and gives rise to different spores: the **megaspores**, which develop into the female gametophyte, and the **microspores**, which develop into the male gametophyte (see Figure 1.2). The way the resulting male and female gametophytes are separated is quite diverse. In angiosperms, a single individual in a **monoecious** (from the Greek for "one house") species has flowers that produce both male and female gametophytes; both can occur in the single "perfect" flower as in tulips, or they can occur in separate male (staminate) and female (pistillate) flowers as in maize (corn; *Zea mays*). If male and female flowers occur on separate individuals, as in willow or poplar trees, then the species is **dioecious** (from the Greek for "two houses"). In gymnosperms, ginkos and cycads are dioecious, while conifers are monoecious. Conifers produce female cones, **megastrobili** (from the Greek for "large cones"; singular *megastrobilus*), usually higher up on the plant than the male cones, **microstrobili** (from the Greek for "small cones"; singular *microstrobilus*). Both megaspores and microspores produce gametophytes with only a few cells, compared with the sporophyte. The processes of gametophyte development are discussed in detail in Chapter 21.

1.2 Overview of Plant Structure

Despite their apparent diversity, all seed plants have the same basic body plan (**Figure 1.3**). The vegetative body comprises three organs—the stem, the root, and the leaves—each with a different direction, or polarity, of growth. The **stem** grows upward and supports the aboveground part of the plant. The **root**, which anchors the plant and absorbs nutrients and water, grows down below the ground. The **leaves**, whose primary function is photosynthesis, grow out laterally from the stem at the **nodes**. Variations in leaf arrangement (**phyllotaxis**) can give rise to many different forms of **shoots**, the term for the leaves and stem together. For example, leaf nodes can spiral around the stem, rotating by a fixed angle between each **internode** (the region between two nodes). Alternatively, leaves can arise oppositely or alternating on either side of the stem.

Organ position and shape are defined by directional patterns of growth that are determined by regulated cell division and expansion. The polarity of growth of the **primary plant axis** (the main stem and taproot) is vertical, whereas the typical leaf grows laterally at the margins to produce the flattened **leaf blade**. The **adaxial** (upper) surface of the leaf faces toward the stem, and the **abaxial** (lower) leaf surface faces away from the stem (see Figure 1.3). The growth polarities of the organs are adapted to their functions: Leaves function in light absorption, stems elongate to lift the leaves toward sunlight, and roots elongate in search of water and nutrients from the soil. The cellular component that directly determines growth polarity in plants is the cell wall.

Plant cells are surrounded by rigid cell walls

The outer lipidic fluid boundary of the living cytoplasm of plant cells is the **plasma membrane** (also called **plasmalemma**), similar to the situation in animals, fungi, and bacteria. Within the plasma membrane, the highly crowded internal collection of hydrated ions, small and large molecules, organelles, and cytoskeletal components apart from the nucleus is called the **cytoplasm**. The liquid portion of the cytoplasm that can be physically separated from insoluble macromolecules, organelles, small compartments referred to as vesicles, and ribosomes is referred to as the **cytosol**. The internal compartment of the membrane-enclosed nucleus in eukaryotes is the nucleoplasm. The large internal compartment in most plant cells known as the **vacuole** is generally considered distinct from the cytoplasm as well, as it contains a less dense solution containing molecules and hydrolyzing enzymes. However, plant cells, unlike animal cells, are further enclosed by a rigid **cell wall** (**Figure 1.4**). Because of the absence of cell walls in animals, embryonic cells are able to migrate from one location to another; developing tissues and organs may thus contain cells that originated in different parts of the organism. In plants such cell migrations are prevented, because each walled cell is cemented to its neighbors by a **middle lamella**. As a consequence, plant development, unlike animal development, depends solely on patterns of cell division and cell enlargement.

Plant cells have two types of walls: primary and secondary (see Figure 1.4A). **Primary cell walls** are typically thin (less than 1 μm) and are characteristic of young, growing cells. **Secondary cell walls** are thicker and stronger than primary walls and are deposited on the inner surface of the primary wall after most cell enlargement has ended. Secondary cell walls owe their strength and toughness to **lignin**, a brittle, gluelike material (see Chapter 2). The evolution of lignified secondary cell walls provided plants with the structural reinforcement necessary to grow vertically above the soil and to colonize the land. Bryophytes, which lack lignified cell walls, are unable to grow more than a few centimeters above the ground.

Plasmodesmata allow the free movement of molecules between cells

The cytoplasm of neighboring cells is usually connected by **plasmodesmata** (singular *plasmodesma*), tubular

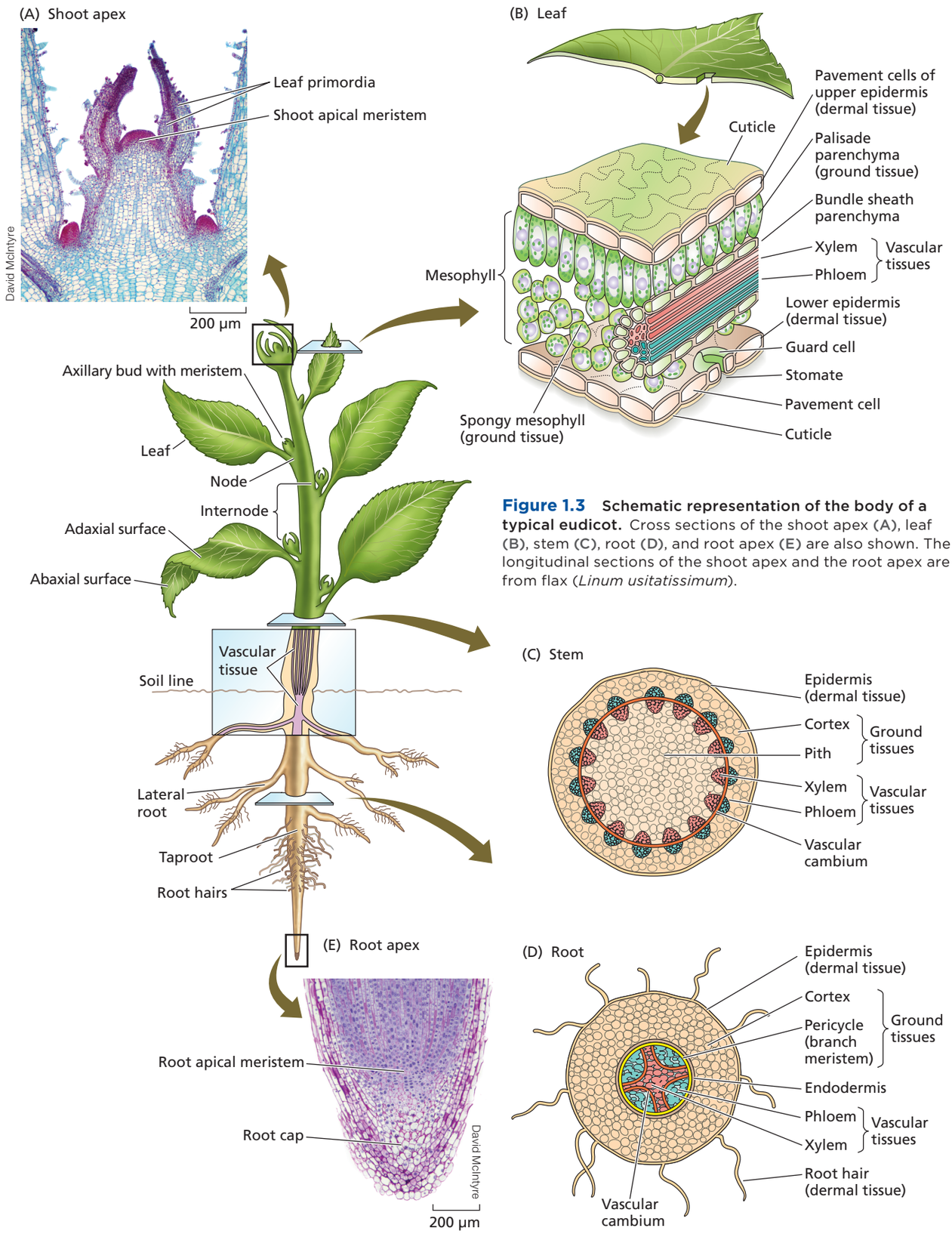


Figure 1.3 Schematic representation of the body of a typical eudicot. Cross sections of the shoot apex **(A)**, leaf **(B)**, stem **(C)**, root **(D)**, and root apex **(E)** are also shown. The longitudinal sections of the shoot apex and the root apex are from flax (*Linum usitatissimum*).

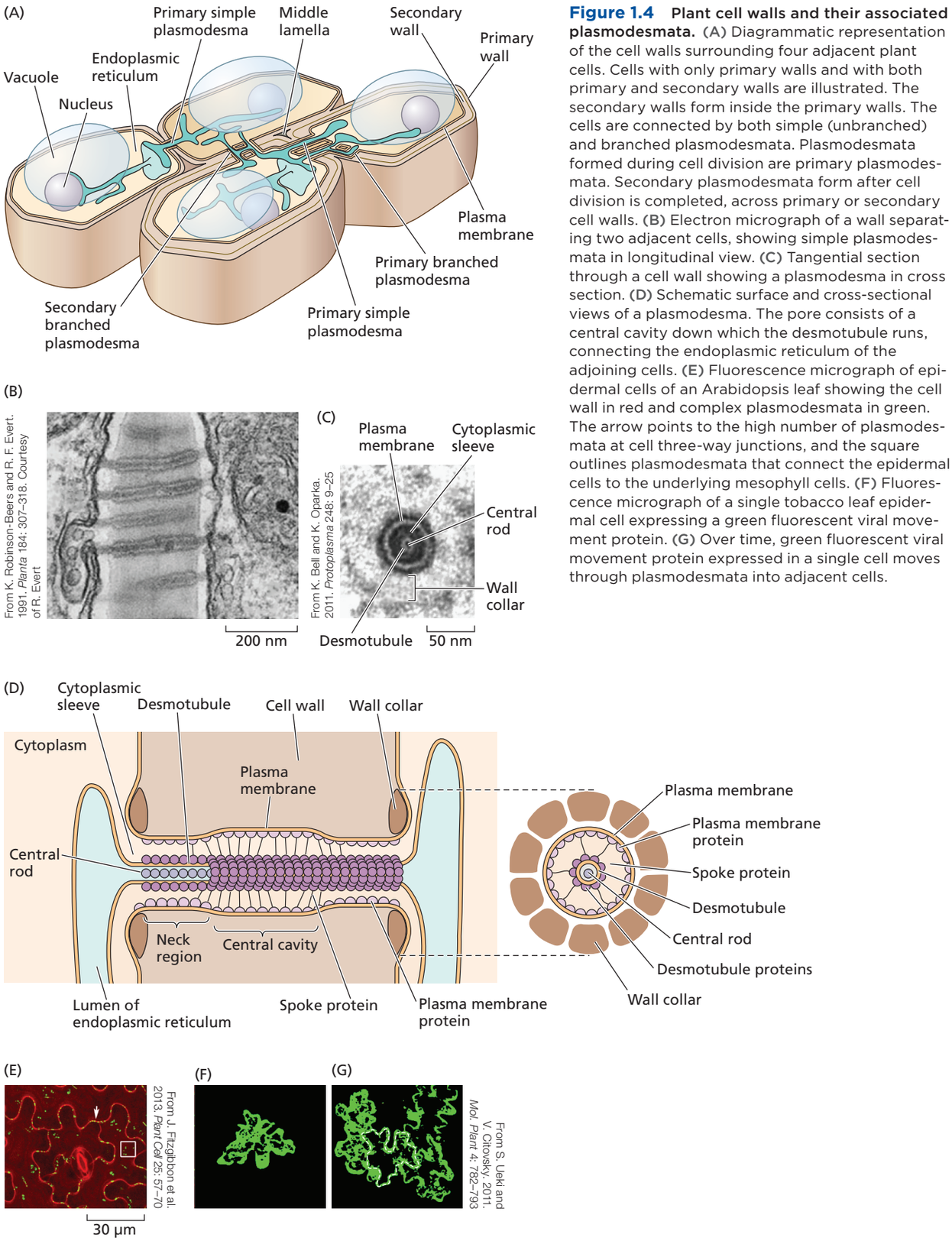


Figure 1.4 Plant cell walls and their associated plasmodesmata. **(A)** Diagrammatic representation of the cell walls surrounding four adjacent plant cells. Cells with only primary walls and with both primary and secondary walls are illustrated. The secondary walls form inside the primary walls. The cells are connected by both simple (unbranched) and branched plasmodesmata. Plasmodesmata formed during cell division are primary plasmodesmata. Secondary plasmodesmata form after cell division is completed, across primary or secondary cell walls. **(B)** Electron micrograph of a wall separating two adjacent cells, showing simple plasmodesmata in longitudinal view. **(C)** Tangential section through a cell wall showing a plasmodesma in cross section. **(D)** Schematic surface and cross-sectional views of a plasmodesma. The pore consists of a central cavity down which the desmotubule runs, connecting the endoplasmic reticulum of the adjoining cells. **(E)** Fluorescence micrograph of epidermal cells of an Arabidopsis leaf showing the cell wall in red and complex plasmodesmata in green. The arrow points to the high number of plasmodesmata at cell three-way junctions, and the square outlines plasmodesmata that connect the epidermal cells to the underlying mesophyll cells. **(F)** Fluorescence micrograph of a single tobacco leaf epidermal cell expressing a green fluorescent viral movement protein. **(G)** Over time, green fluorescent viral movement protein expressed in a single cell moves through plasmodesmata into adjacent cells.

structures 40 to 50 nm in diameter and formed by the connected membranes of adjacent cells (see Figure 1.4). Plasmodesmata facilitate intercellular movement of proteins, nucleic acids, and other macromolecular signals that coordinate developmental processes among plant cells. Primary plasmodesmata are formed during cell division. Secondary plasmodesmata are formed after cells have divided. The core of each plasmodesma is the *desmotubule*, which is an endomembrane structure derived from both adjoining cells. Plant cells interconnected in this way form a continuous cytoplasmic space referred to as the **symplasm**,[2] and transport of small molecules through plasmodesmata is called **symplasmic transport** (see Chapters 6 and 8). Transport through the permeable cell wall space outside the cells (the **apoplast**) is called **apoplastic transport**. Both forms of transport are important in the vascular system of plants (see Chapter 8).

The symplasm can transport water, solutes, and macromolecules between cells without crossing the plasma membrane. However, there is a restriction on the size of molecules that can be transported via the symplasm; this restriction is called the **size exclusion limit**, and it varies with cell type, environment, and developmental stage. The transport can be followed by studying the movement of fluorescently labeled proteins or dyes between cells. The movement through plasmodesmata (see Figure 1.4) is regulated, or gated, by deposition (closing) or degradation (opening) of callose within the plasmodesmatal opening. Systemic spread of plant viruses that are introduced by feeding insects usually involves symplastic movement after expansion of the size exclusion limit by *viral movement proteins* (see Chapter 24).

New cells originate in dividing tissues called meristems

Plant growth is concentrated in localized regions of cell division called **meristems**. Most nuclear divisions (mitosis) and cell divisions (cytokinesis) occur in these meristematic regions. In a young plant, the most active meristems are the **apical meristems**, located at the tips of the stem and the root (see Figure 1.3A and E). The phase of plant development that gives rise to new organs and to the basic plant form is called **primary growth**, which gives rise to the **primary plant body**. Primary growth results from the activity of apical meristems. Cell division in the meristem produces cuboidal cells about 10 μm on each edge. Division is followed by progressive cell expansion, and cells typically elongate to become much longer than they are wide (30–100 μm long, 10–25 μm wide—about half the width of a baby's fine hair and about 50 times the width of a typical bacterium). The increase in length produced by primary growth amplifies the plant's axial (top-to-bottom) polarity, which is established in the embryo.

Meristematic tissue is also found along the length of the root and shoot. **Axillary buds** are meristems that develop at the node in the leaf axil—the region between the leaf and the shoot. Axillary buds become the apical meristems of branches. The branches of roots, the **lateral roots**, arise from meristematic cells in the **pericycle**, or root branch meristem (see Figure 1.3D). This meristematic tissue then becomes the apical meristem of the lateral root.

Another set of meristematic cells, the **cambium**, gives rise to **secondary growth**, which produces an increase in width or diameter of plants, having radial (inside-to-outside) polarity (**Figure 1.5**). The cambial layer that produces wood is called the **vascular cambium**. This meristem arises in the vascular system, between the xylem and the phloem of the primary plant body. The cells of the vascular cambium divide longitudinally to produce derivatives toward the inside or the outside of the stem or root. They also divide transversely to produce **rays** that transmit material radially outward. The inside derivatives differentiate into **secondary xylem**, which conducts water and nutrients from the soil upward to other plant organs. In temperate climates, summer wood is darker and denser than spring wood; alternating layers of summer and spring wood form annual rings. The vascular cambium derivatives displaced toward the outside of the secondary stem or root give rise to **secondary phloem**, which, like primary phloem, conducts the products of photosynthesis downward from the leaves to other organs of the plant. The associated **phloem fibers** add tensile strength to the stem, as do all fibers (see Figure 1.9).

Finally, the **cork cambium**, or **phellogen**, is the cambial layer that produces the protective **periderm** (see Figure 1.5) on the outside of woody plants. The cork cambium typically arises each year within the secondary phloem. The production of layers of water-resistant cork cells by the cork cambium isolates the outer primary tissues of the stem or root from their water supply, the xylem, causing them to shrivel and die. The **bark** of a woody plant is the collective term for several tissues—the secondary phloem, secondary phloem fibers, cortex (in stems), pericycle (in roots), and periderm—that can be peeled off as a unit at the soft layer of vascular cambium.

1.3 Plant Tissue Types

Three major tissue systems are present in all plant organs: dermal tissue, ground tissue, and vascular tissue (see Figure 1.3 B–D). **Dermal tissue** forms the outer protective layer of the plant and is called the **epidermis** in the primary plant body. **Ground tissue** fills out the three-dimensional bulk of the plant and includes the **pith** and **cortex** of primary stems and roots, and the **mesophyll** in leaves. **Vascular tissue** consists of two

[2] The cytoplasm that is connected via plasmodesmata is sometimes referred to as the *symplast*.

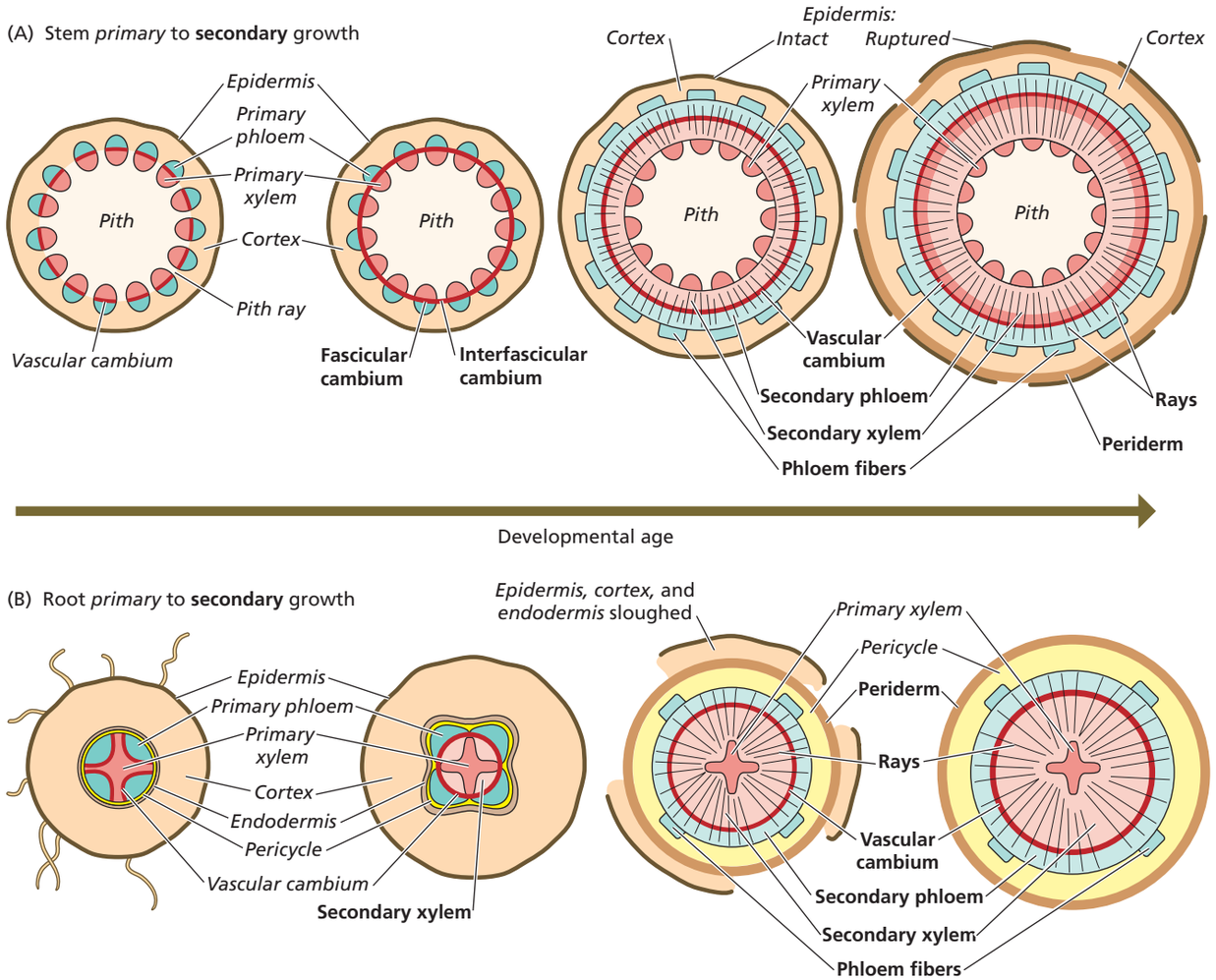


Figure 1.5 **Secondary growth in stems and roots.** Primary growth is labeled in italic text, secondary growth in bold. **(A)** Stem primary to secondary growth. The vascular cambium starts as separated growth regions in the vascular bundles, or fascia, of primary xylem and phloem. As the plant grows, the bundled, fascicular cambium becomes connected by interfascicular cambium between the bundles. Once the vascular cambium forms a continuous ring, it divides inward to generate secondary xylem and divides outward to generate the secondary phloem. Regions in the cortex develop into phloem fibers and the periderm, which contains the phellogen, or cork cambium, and the outer phelloderm. With growth, the epidermis ruptures and rays connect the inner and outer vasculature. **(B)** Root primary to secondary growth. The central vascular cylinder contains the primary phloem and primary xylem. As in the stem, the vascular cambium becomes connected and grows outward, generating secondary phloem and rays. As roots increase in girth, the pericycle generates the root periderm, while the outer epidermis, cortex, and endodermis are sloughed off. The pericycle produces the phloem fibers and rays as well as lateral roots (not shown). The vascular cambium produces secondary phloem and rings of secondary xylem.

types of tissues: **xylem** and **phloem**, each of which consists of conducting cells, generalized parenchyma cells, and thick-walled fibers.

Dermal tissues cover the surfaces of plants

Three examples of leaf dermal cells are shown in **Figure 1.6**. Leaves have an upper and lower epidermis with different cell types in each (see Figure 1.6A). The epidermis includes the pavement cells, which are puzzle-piece shaped in many flowering plants (see Figure 1.6B). In Arabidopsis, pavement cells are the only cells in evidence on a seed leaf (cotyledon), but the epidermis of the true leaves differentiates into more cell types, becoming covered in three-pronged leaf hairs (trichomes) (see Figure 1.6C). Many plants have relatively few chloroplasts in the epidermal tissue of true leaves, perhaps because chloroplast division is shut down. The exception to this is the guard cells—the amazing cells that form the "lips"

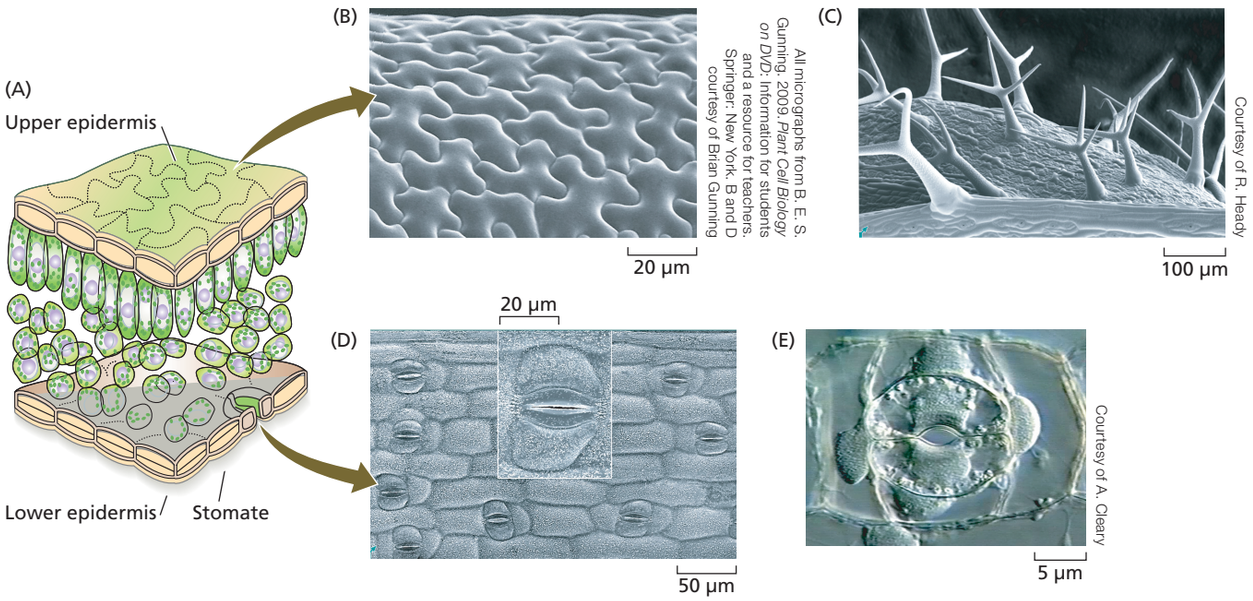


Figure 1.6 Dermal tissue of the leaf of a typical eudicot plant. **(A)** Generalized view of leaf structure. **(B)** Scanning electron micrograph of the epidermal cells of a *Galium aparine* leaf showing the puzzle-piece arrangement of pavement cells in the epidermis. **(C)** Scanning electron micrograph of an epidermis of a true leaf of Arabidopsis. The three-branched trichomes arise from a field of pavement cells and guard cell complexes. **(D)** Scanning electron micrograph with a slightly higher magnification inset of the stomatal complexes in a *Tradescantia* sepal. **(E)** Light micrograph of the stomatal complex of the *Tradescantia* sepal. (All micrographs from B. E. S. Gunning. 2009. *Plant Cell Biology on DVD: Information for students and a resource for teachers*. Springer, New York.)

of the mouths, or stomata, of the leaf (see Figure 1.6D and E)—which contain many chloroplasts. Once made, guard cells become cytoplasmically isolated from the rest of the leaf during the last cell division that forms them and have no plasmodesmata. As we will describe in Chapter 15, the guard cell plasma membrane is quite dynamic, with endocytosis regulating the abundance of ion-regulating K^+ channels on the cell surface. In roots, root hairs differentiate from the epidermis.

Ground tissues form the bodies of plants

The leaf has ground tissue of two different types: the upper elongated *palisade mesophyll* and the irregularly shaped *spongy mesophyll* (**Figure 1.7**). The spongy mesophyll has large air spaces between the cells—they are not cemented all around their periphery with middle lamellae. This allows exchange of gases (carbon dioxide and oxygen) through the air spaces of the leaf during photosynthesis and respiration. Both cell types have many chloroplasts (see Figure 1.7), usually oriented at the cell periphery but able to move in response to light cues perceived by photoreceptors (see Chapter 16).

Mesophyll cells of the leaf can differentiate into a variety of other cell types, and mesophyll is therefore considered a form of **parenchyma**, a ground tissue with thin primary walls (see Figure 1.7). Parenchyma has the capacity to continue division and can differentiate into a variety of

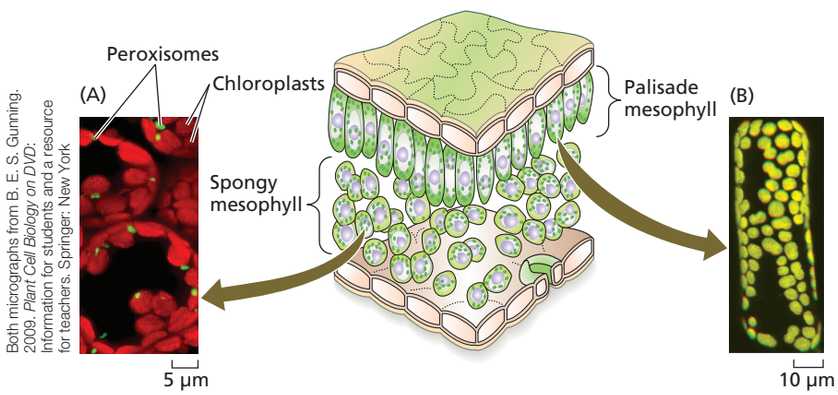


Figure 1.7 Spongy mesophyll and palisade cells in the leaf. **(A)** Fluorescence micrograph of spongy mesophyll cells showing peroxisomes (green) and chloroplasts (red). **(B)** Three-dimensional stereo view of chloroplast distribution in a palisade cell of a leaf. (All micrographs from B. E. S. Gunning. 2009. *Plant Cell Biology on DVD: Information for students and a resource for teachers*. Springer, New York.)

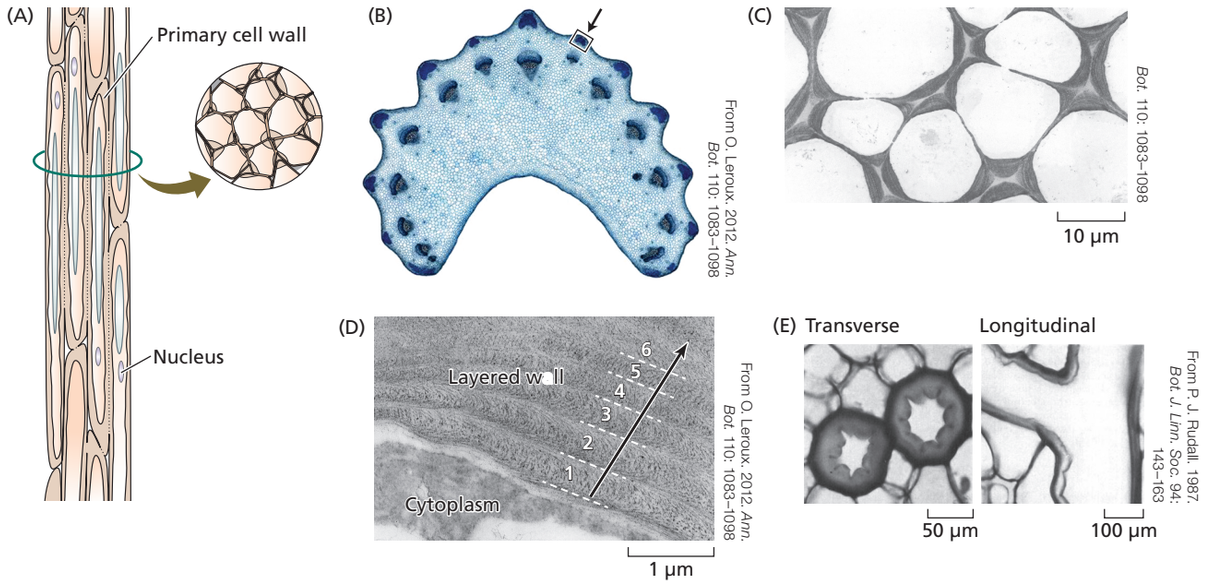


Figure 1.8 **Ground tissue with thick primary walls.** **(A)** Diagram of the collenchyma of celery in longitudinal view and cross section. **(B)** Light micrograph cross section of celery showing collenchyma clusters. The arrow shows a region enriched in collenchyma. **(C)** Electron micrograph of a cross section of celery collenchyma. **(D)** Electron micrograph showing the layered primary wall of the collenchyma of celery. The arrow crosses six layers of primary cell wall. **(E)** Light micrographs of transverse and longitudinal sections of a *Euphorbia* laticifer showing thickened primary walls.

other ground tissues and vascular tissues, after being produced by meristems. For example, parenchyma can differentiate into ground tissue that has thickened primary walls which can nevertheless continue to elongate (**Figure 1.8**). **Collenchyma** (e.g., as in the ribs of celery stalks) has very thick, layered walls (see Figure 1.8A–D) and a tasty crunch! The **laticifers** that carry the milky white latex in rubber trees, poppy plants, leaf-lettuce, and dandelions have irregularly thickened primary walls and continue to elongate (see Figure 1.8E).

Parenchyma can also differentiate into the **schlerenchyma**, which has thick secondary walls (**Figure 1.9**). *Sclereids* come from parenchyma in leaves, fruit (e.g., pear), and flowers (e.g., camellia; see Figure 1.9B). They often have an irregularly branched shape (see Figure 1.9B). Their development in some tissues is dependent on their exposure to environmental stress, such as wind and rain. **Fibers** develop from parenchyma and form elongated support structures with thickened secondary walls both in ground tissue (see Figure 1.9C) and in vascular tissues (see the phloem fibers in Figure 1.5). They can elongate into the longest cells of higher plants; for example, individual fiber cells of the *Ramie* plant can be 25 cm long! Because the walls are hardened with lignin after elongation, the cells have very high tensile strength, and it is no wonder that humans and wild animals make extensive use of such fibers, called bast fibers.

The presence of fibers in both ground and vascular tissues brings up the topic of how the different tissues are separated. In the stem, the vascular cylinder can be filled with ground tissue including parenchymal cells referred to as *pith*, in addition to the vascular tissue (see Figure 1.5A). In the root, the ground tissue is between the dermal tissue and the vascular tissue and is called the root *cortex* (see Figure 1.5B). The boundary between the

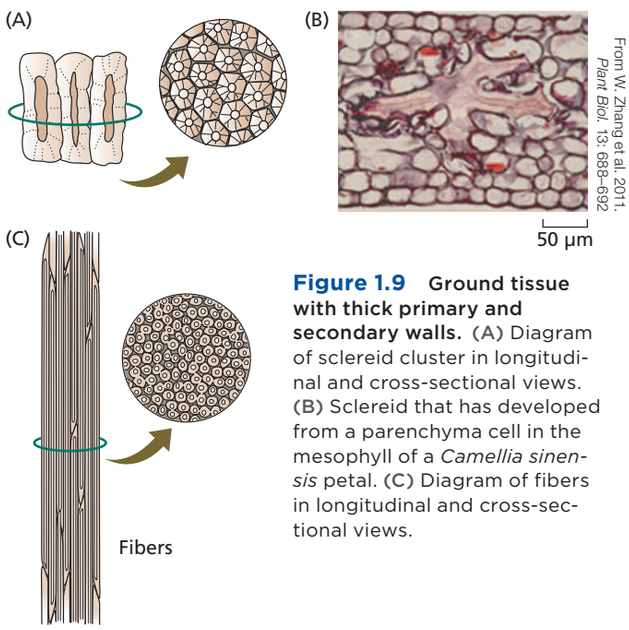


Figure 1.9 **Ground tissue with thick primary and secondary walls.** **(A)** Diagram of sclereid cluster in longitudinal and cross-sectional views. **(B)** Sclereid that has developed from a parenchyma cell in the mesophyll of a *Camellia sinensis* petal. **(C)** Diagram of fibers in longitudinal and cross-sectional views.

cortex and the vascular tissue is a specialized cell type called the **endodermis**, which has a lignin-impregnated **Casparian strip**. As we will describe in Chapter 6, the Casparian strip contributes to the separation of the cortical apoplast from the apoplast of the vascular tissue.

Vascular tissues form transport networks between different parts of the plant

Phloem cells, which conduct the products of photosynthesis from the leaves to roots, flowers, and fruits (see Chapter 12), are living at maturity and have nonlignified cell walls. They include **sieve cells** in gymnosperms, and **sieve tube elements**—which stack to form **sieve tubes**—in angiosperms (**Figure 1.10**). Specialized proteins are made in the phloem cells, such as the P-protein (see Figure 1.10B). The P-protein network forms a reticulum centered on the cross-walls, or sieve plates (see Figure 1.10B and C). Plasmodesmata can be seen in tangential sections of the forming sieve plate (see Figure 1.10C). As with other plasmodesmatal arrays,

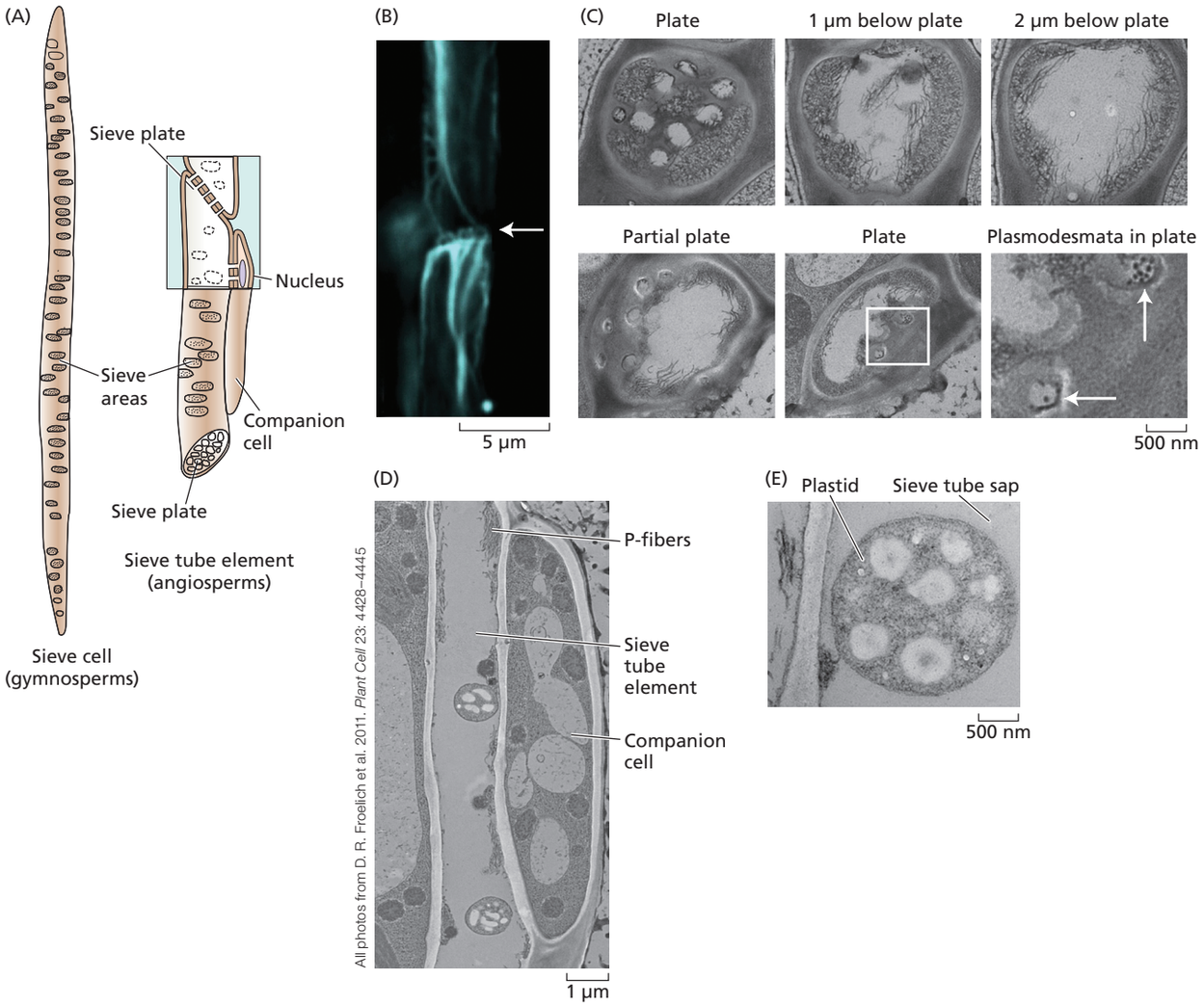


Figure 1.10 **Phloem.** **(A)** Diagram of phloem sieve cells from gymnosperms and a sieve tube element from angiosperms. **(B)** Fluorescence micrograph of the P-protein (SERB2; blue) in a mature living sieve tube element. The arrow indicates the sieve plate. **(C)** Cross sections of a sieve plate of Arabidopsis. Top row: Serial sections through a sieve plate in 1-µm steps. There are several open pores in the center of the plate (left panel), then the clear lumen appears, with dark, fibrous P-protein around the periphery (middle and right panels). Bottom row: When the sieve tube element is sectioned at an angle to the plate, multiple open pores are revealed (left and middle panels), some of which contain multiple plasmodesmata (white arrows in the right panel, which is a higher magnification of the boxed area in the middle panel). **(D)** Electron micrograph of a sieve tube element and a companion cell. Note the fibrillar P-protein aggregates. **(E)** Specifically differentiated plastid in a mature sieve tube element in direct contact with sieve tube sap.

callose is desposited at the sieve plate. The living sieve tube element is connected by plasmodesmata fields, or sieve areas, to adjacent cells, **companion cells** (in angiosperms) and **albuminous cells** (in gymnosperms). Also associated with phloem in some plants are fibers and storage parenchyma.

The xylem cells that conduct water and minerals from the root are nonliving at maturity and known as **tracheary elements**, consist of **tracheids** (found in all vascular plants) and shorter **vessel elements** (found mostly in angiosperms) (**Figure 1.11**). Vessel elements stack end to end to form wide (up to 0.7 mm) columns called **vessels**. Protoxylem cells with primary walls begin to differentiate into mature tracheary elements by laying down secondary cell walls with spiral bands of cellulose and strengthened with lignin. Once elongation has stopped, the top and bottom end walls develop large perforations. On the side walls, secondary walls continue to thicken, except in areas containing pits, which start as plasmodesmata fields and ultimately become channels through the walls shared between adjacent cells. The cells of the tracheids and vessels die, undergoing a process called programmed cell death (see Chapter 23), leaving behind the hardened bundle of vessels made by the secondary walls and connected side to side by pits. The pits are important because flow through these narrow vessels depends on having a continuous liquid stream (see Chapters 2 and 6). If an air bubble, or embolism, forms in a vessel element or tracheid, the stream can be diverted around the embolism through the pits into adjacent cells.

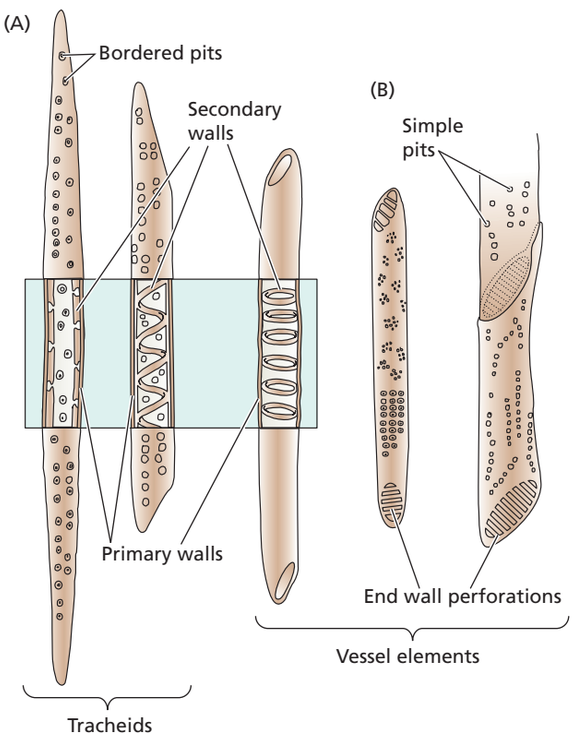


Figure 1.11 **Xylem.** (A) Diagram of two tracheids and a vessel element. The cutaway views (in the blue window) reveal thickenings of secondary wall in spiral (helical) and annular (ring-shaped) arrangements. (B) Diagram of two vessel elements, showing pits (bordered in tracheids, simple in vessel elements) and end wall perforations.

1.4 Plant Cell Compartments

All plant cells have the same basic organization: They contain cytoplasm, a nucleus, and other organelles, all enclosed by the plasma membrane and cell wall (**Figure 1.12**). All plant cells *begin* with a similar complement of organelles. Organelles fall into two main categories based on how they arise:

1. *The endomembrane system and peroxisomes*: the endoplasmic reticulum, nuclear envelope (which encapsulates the nucleus), Golgi apparatus, *trans* Golgi network, vacuole, and endosomes (smaller endomembrane compartments). Other organelles derived from the endomembrane system include oil bodies, peroxisomes, and specialized peroxisomes called glyoxysomes that function in lipid storage and carbon metabolism in seeds and leaves. With the exception of some peroxisomes, components of the endomembrane system are not formed by semiautonomous processes. The endomembrane system plays a central role in secretory processes, cell signaling, specialized metabolite and hormone production, membrane recycling, the cell cycle, and cell expansion.
2. *Semiautonomous (independently dividing) organelles of endosymbiotic origin*: plastids and mitochondria. These organelles function in energy metabolism and storage, and synthesize a wide range of metabolites used in the biosynthesis of all cell components.

Because all of these cellular organelles are membranous compartments, we'll begin by describing membrane structure and function.

Biological membranes are lipid bilayers that contain proteins

All cells are enclosed in a membrane that serves as their outer boundary, separating the cytoplasm from the external environment. This plasma membrane allows the cell to take up and retain certain substances while excluding others. Various transport proteins embedded in the plasma membrane are responsible for this selective traffic of solutes—water-soluble ions and small, uncharged molecules—across the membrane. The accumulation or expulsion of ions or molecules in the cytoplasm through the

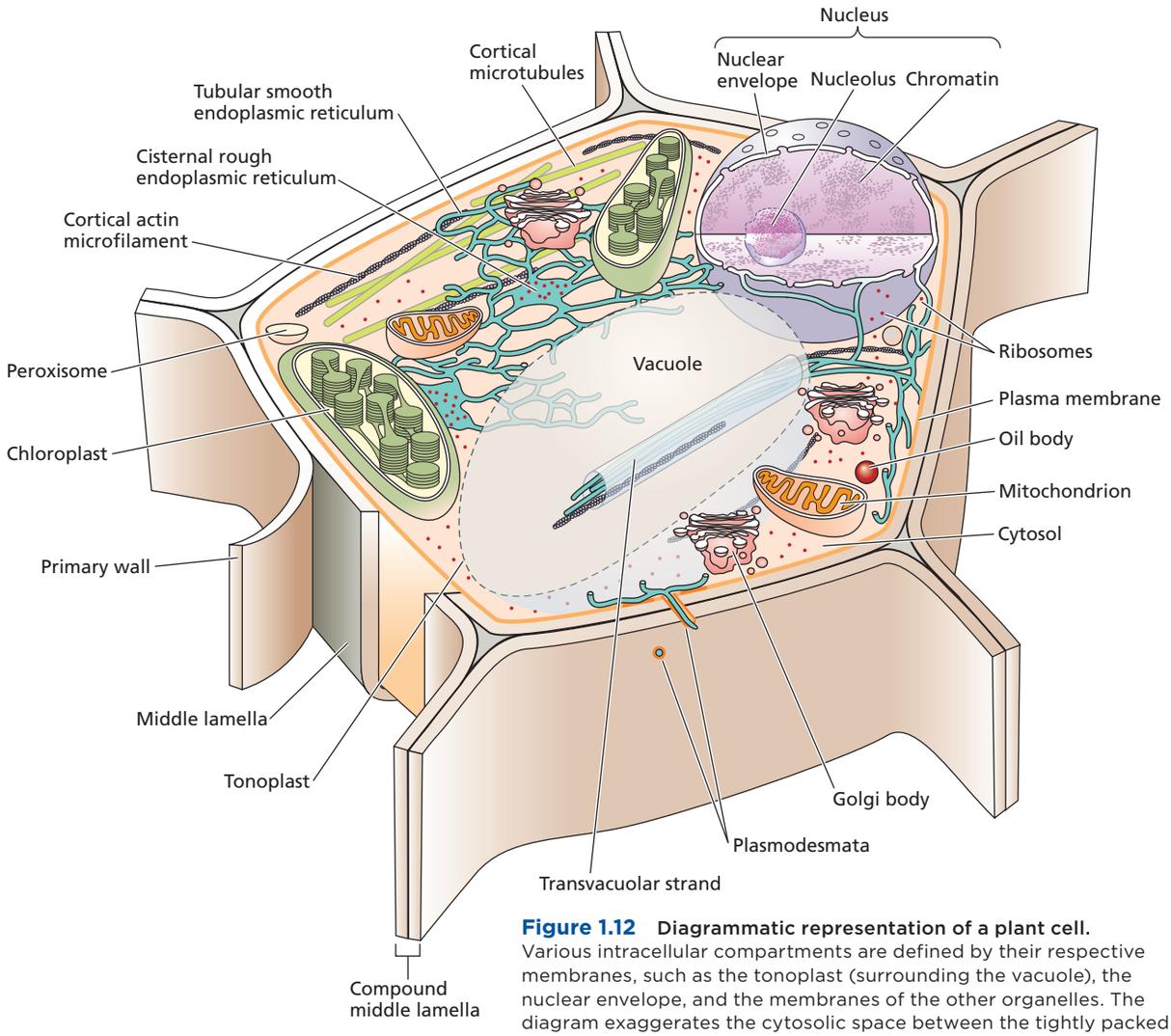


Figure 1.12 **Diagrammatic representation of a plant cell.** Various intracellular compartments are defined by their respective membranes, such as the tonoplast (surrounding the vacuole), the nuclear envelope, and the membranes of the other organelles. The diagram exaggerates the cytosolic space between the tightly packed cytoplasmic compartments.

action of transport proteins consumes metabolic energy. In eukaryotic cells, membranes enshroud the genetic material, delimit the boundaries of other specialized internal organelles of the cell, and regulate the fluxes of ions and metabolites into and out of these compartments.

Biological membranes consist of a double layer (*bilayer*) of lipids in which proteins are embedded in what is referred to as a **fluid mosaic** (**Figure 1.13**). Membrane proteins are embedded in the bilayer and may move laterally depending on the fluidity of their membrane environment. Heterogeneity of the membrane mosaic results from interactions between membrane lipids and proteins as they interact with the cytoskeleton and cell wall. Each layer of the bilayer is called a *leaflet*. In most membranes, proteins make up about half of the membrane's mass. However, the composition of the lipid components and the properties of the proteins vary from membrane to membrane, conferring on each membrane its unique functional characteristics.

LIPIDS The most prominent membrane lipids found in plants are phospholipids, a class of lipids in which two fatty acids are covalently linked to glycerol, which is covalently linked to a phosphate group. Attached to the phosphate group in the phospholipid is a variable component, called the *head group*, such as choline, glycerol, or inositol (see Figure 1.13B). The nonpolar hydrocarbon chains of the fatty acids form a region that is hydrophobic—that is, that excludes water. In contrast to the fatty acids, the head groups are highly polar; consequently, phospholipid molecules display both hydrophilic and hydrophobic properties (i.e., they are *amphipathic*). The fatty acid chains vary

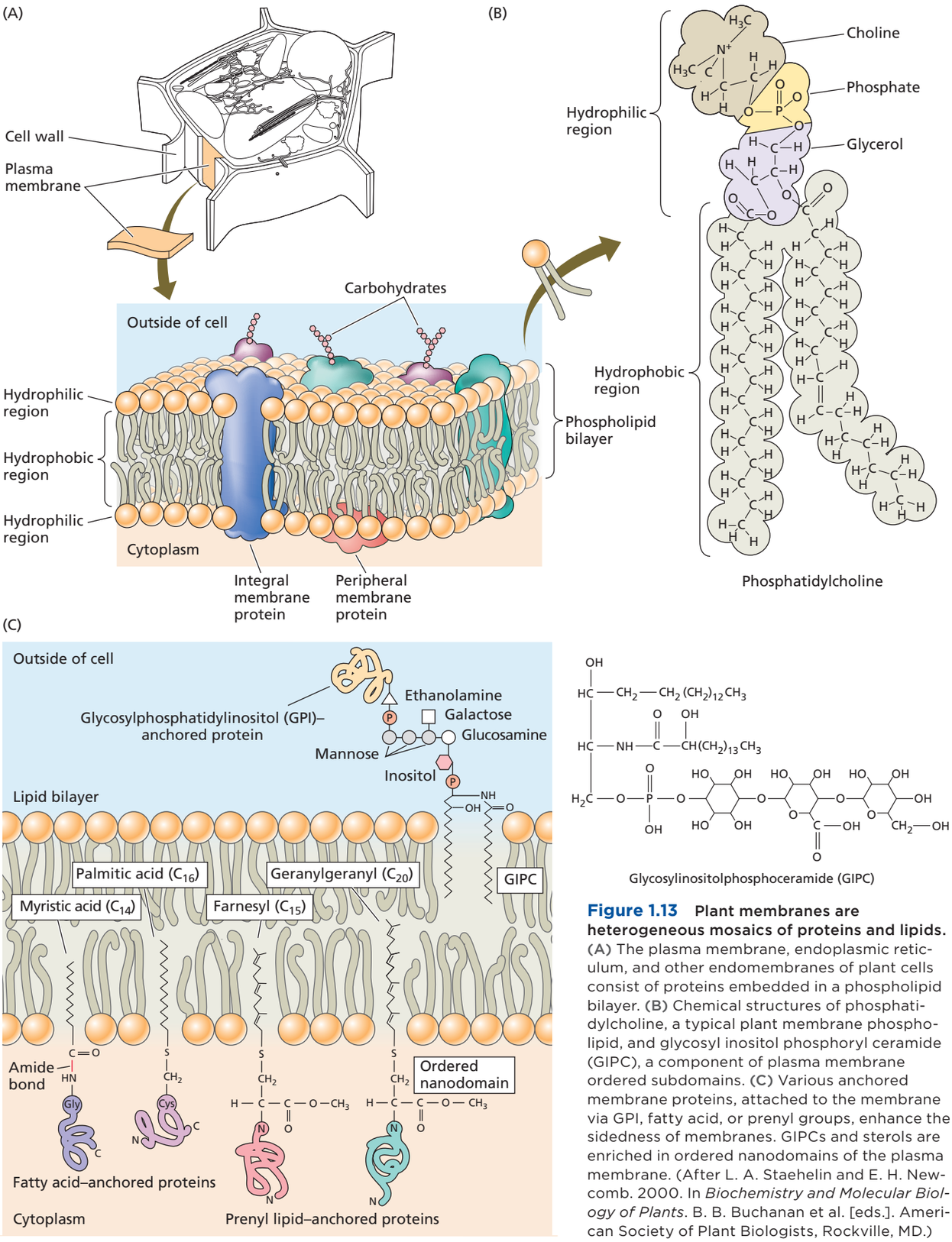


Figure 1.13 **Plant membranes are heterogeneous mosaics of proteins and lipids.** **(A)** The plasma membrane, endoplasmic reticulum, and other endomembranes of plant cells consist of proteins embedded in a phospholipid bilayer. **(B)** Chemical structures of phosphatidylcholine, a typical plant membrane phospholipid, and glycosyl inositol phosphoryl ceramide (GIPC), a component of plasma membrane ordered subdomains. **(C)** Various anchored membrane proteins, attached to the membrane via GPI, fatty acid, or prenyl groups, enhance the sidedness of membranes. GIPCs and sterols are enriched in ordered nanodomains of the plasma membrane. (After L. A. Staehelin and E. H. Newcomb. 2000. In *Biochemistry and Molecular Biology of Plants*. B. B. Buchanan et al. [eds.]. American Society of Plant Biologists, Rockville, MD.)

in length but usually consist of 16 to 24 carbons. If the carbons are linked by single bonds, the fatty acid chain is *saturated* (with hydrogen atoms), but if the chain includes one or more double bonds, it is *unsaturated*.

Double bonds in a fatty acid chain create a kink in the chain that prevents tight packing of the phospholipids in the bilayer (i.e., the bonds adopt a kinked *cis* configuration, as opposed to an unkinked *trans* configuration). The kinks promote membrane fluidity, which is critical for many membrane functions. Various phospholipids are distributed asymmetrically across the plasma membrane, giving the membrane sidedness; in terms of phospholipid composition, the outside leaflet of the plasma membrane that faces the outside of the cell is different from the inside leaflet that faces the cytoplasm. Turnover of membrane lipids is generally more rapid than that of membrane proteins.

In some membranes (particularly the plasma membrane), higher concentrations of sterols such as sitosterol and stigmasterol reduce the fluidity of membrane regions, resulting in the formation of relatively stable rigid lipid subdomains within the membrane. Glycosyl inositol phosphoryl ceramide (GIPC; see Figure 1.13B) and glycosylceramide, known collectively as *sphingolipids*, are relatively hydrophobic lipids that limit lateral diffusion of proteins within the lipid phase, thereby stabilizing lipid-ordered *nanodomains* that are important for clustering of signaling and transport protein complexes.

The membranes of plastids, the group of membrane-bound organelles to which chloroplasts belong (see Section 1.7), are unique in that their lipid component consists almost entirely of glycosylglycerides, the glycosyl polar head groups of which are galactose derivatives. These galactolipids are derived from a common ancestor with cyanobacteria.

PROTEINS The proteins associated with the lipid bilayer are of two main types: integral and peripheral.

Integral membrane proteins are embedded in the lipid bilayer (see Figure 1.13A). Most integral proteins span the entire width of the phospholipid bilayer, so one part of the protein interacts with the outside of the compartment, another part interacts with the hydrophobic core of the membrane, and a third part interacts with the interior (lumen) of the compartment. Integral membrane proteins are generally dived into five types:

- Type 1 have a single transmembrane helix and a C-terminus on the cytosolic face of membrane.
- Type 2 have a single transmembrane helix with the N-terminus on the cytosolic face.
- Type 3 have multiple transmembrane helices with the N-terminus on the cytosolic face.
- Type 4 comprise multiple distinct polypeptides that assemble to form a functional unit
- Type 5 are integral membrane lipoproteins (proteins with lipids that are covalently linked to amino acid residues).

Proteins that serve as membrane transporters (ion channels, carriers, and pumps; see Chapter 8) are always integral membrane proteins, as are certain receptors that participate in signal transduction pathways (see Chapter 4) and proteins in the endomembrane system that mediate membrane fusion. Some integral membrane proteins recognize and bind tightly to cell wall constituents on the outer surface of the plasma membrane, effectively cross-linking the membrane to the cell wall.

Peripheral membrane proteins are attached to the membrane surface (see Figure 1.13A) by noncovalent bonds and hydrophobic interactions, and can be dissociated from the membrane with high-salt solutions or chaotropic agents, which break ionic and hydrogen bonds, respectively. Peripheral proteins serve a variety of functions in the cell. For example, some are involved in regulating intracellular membrane traffic or mediate interactions between the membranes and the major elements of the cytoskeleton.

Some peripheral membrane proteins are called **anchored proteins** as they are modified with hydrophobic prenyl, acyl, or myristol groups that enhance membrane interactions to varying extents. Such modifications are often reversible, allowing for dynamic interactions of the proteins with the membrane surface. Proteins can also be attached to the plasma membrane surface via a **glycosylphosphatidylinositol anchor** that is covalently attached to the protein in the endoplasmic reticulum (see Figure 1.13C). Because this particular lipid anchor is asymmetrically distributed to the outer leaflets of the plasma membrane, it makes the two sides of the membrane even more distinct.

Specific lateral distribution of membrane components in the same plasma membrane is critical for development, growth, and nutrient transport. Polarized localization of proteins in the plasma membrane results in up to four distinct domains on each cell surface that are broadly designated as outer (peripheral), inner (central), apical (shootward), and basal (rootward). A combination of polar secretion, restricted lateral membrane diffusion, cytoskeleton corralling, and endocytic recycling—all described in this chapter—contributes to polarized distribution of plasma membrane proteins in these domains.

1.5 The Nucleus

The **nucleus** (plural *nuclei*) is the membrane-enclosed organelle that contains the genetic information primarily responsible for regulating the metabolism, growth, and differentiation of the cell. Collectively, these genes and their intervening sequences are referred to as the **nuclear genome**. The size of the nuclear genome in plants is

highly variable, ranging from about 1.2×10^8 base pairs for the mustard relative *Arabidopsis thaliana* to 1×10^{11} base pairs for the lily *Fritillaria assyriaca*. The remainder of the genetic information of the cell is contained in the two semiautonomous organelles—the plastid and the mitochondrion—which we will discuss in Section 1.7.

The nucleus consists of a complex matrix, the **nucleoplasm**, surrounded by a double membrane called the **nuclear envelope** (**Figure 1.14A**), which is a subdomain of the endoplasmic reticulum (ER) (see Section 1.6). **Nuclear pores** form selective channels across both membranes, connecting the nucleoplasm with the cytoplasm (**Figure 1.14B**). There can be very few to many thousands of nuclear pores on an individual nuclear envelope.

The nuclear "pore" is actually an elaborate structure composed of more than 100 different nucleoporin proteins arranged octagonally to form a 105-nm nuclear pore complex. The nucleoporins lining the 40-nm channel of the nuclear pore complex form a meshwork that acts as a supramolecular sieve. A specific amino acid sequence called the nuclear localization signal is required for a protein to gain entry into the nucleus when it exceeds the size of the nuclear pore opening. More details of nuclear pore structure and function can be found in **WEB TOPIC 1.3**.

The nucleus is the site of storage and replication of the **chromosomes**, composed of DNA and its associated proteins (**Figure 1.15**). Collectively, this DNA–protein

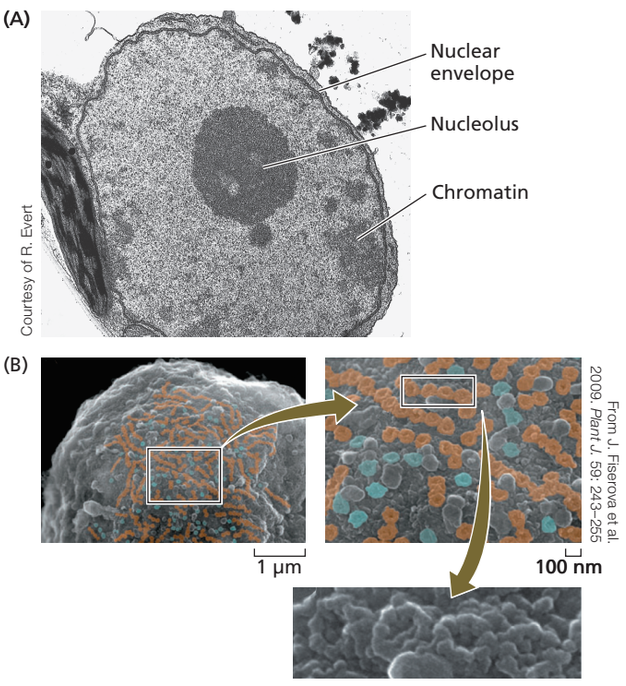


Figure 1.14 **Pore complexes in the nuclear membrane.** (A) Transmission electron micrograph of a plant nucleus, showing the nucleolus and the nuclear envelope. (B) Organization of the nuclear pore complexes (NPCs) on the nuclear surface in tobacco culture cells. The NPCs that touch each other are colored brown; the rest are colored blue. The first inset (top right) shows that most of the NPCs are closely associated, forming rows of 5 to 30 NPCs. The second inset (bottom right) shows the tight associations of the NPCs.

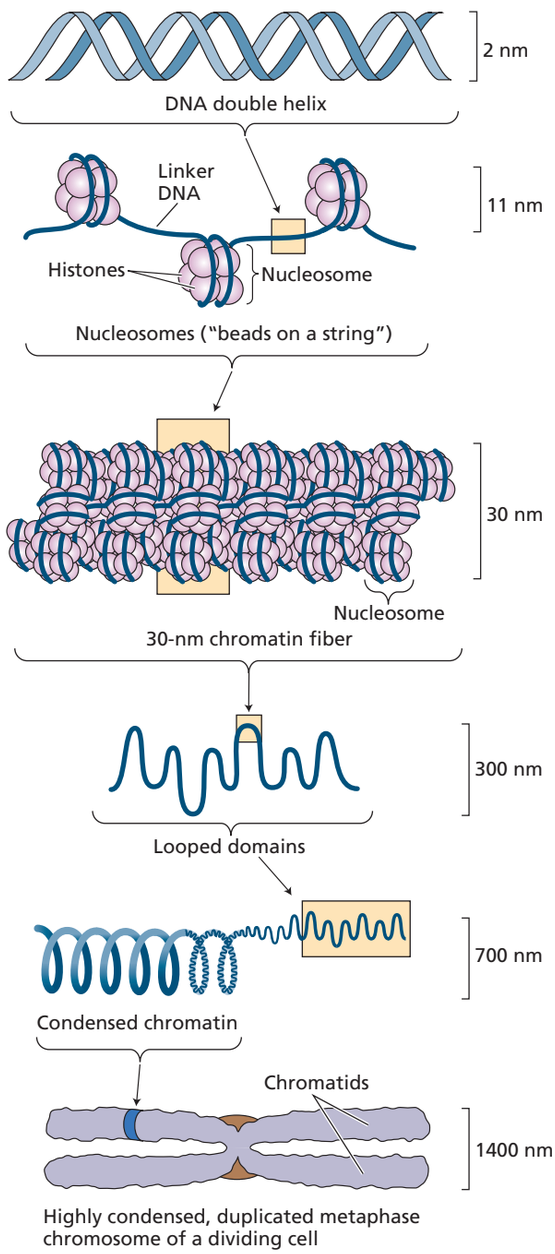


Figure 1.15 **Packaging of DNA in a metaphase chromosome.** The DNA is first aggregated into nucleosomes and then wound to form the 30-nm chromatin fibers. Further coiling leads to the condensed metaphase chromosome. (After B. Alberts et al. 2007. *Molecular Biology of the Cell*, 5th ed. Garland Science, New York.)

complex is known as **chromatin**. The linear length of the entire DNA in any plant genome is usually millions of times greater than the diameter of the nucleus in which it is found. To solve the problem of packaging this chromosomal DNA within the nucleus, segments of the linear double helix of DNA are coiled twice around a solid cylinder of eight **histone** protein molecules, forming a **nucleosome**. Nucleosome assembly is also assisted by large protein complexes called condensins. Nucleosomes are arranged like beads on a string along the length of each chromosome. When the nucleus is not dividing, the chromosomes maintain their spatial independence; they do not "tangle," and instead remain quite discrete, giving rise to the possibility of separate regulation of each chromosome.

During mitosis, the chromatin condenses, first by coiling tightly into a 30-nm chromatin fiber, with six nucleosomes per turn, followed by further folding and packing processes that depend on interactions between proteins and nucleic acids (see Figure 1.15). At interphase (discussed in Section 1.9), two types of chromatin are distinguishable, based on their degree of condensation: heterochromatin and euchromatin. **Heterochromatin** is a highly compact and transcriptionally inactive form of chromatin and accounts for about 10% of the DNA. Most of the heterochromatin is concentrated along the periphery of the nuclear membrane and is associated with regions of the chromosomes that contain few genes, such as telomeres and centromeres. The rest of the DNA consists of **euchromatin**, the dispersed, transcriptionally active form. Only about 10% of the euchromatin is transcriptionally active at any given time. The remainder exists in a state of condensation intermediate between that of the transcriptionally active euchromatin and that of heterochromatin. During the cell cycle, chromatin undergoes dynamic structural changes. In addition to transient local changes that are required for transcription, heterochromatic regions can be converted to euchromatic regions, and vice versa.

Nuclei contain a densely granular region called the **nucleolus** (plural *nucleoli*) (see Figure 1.14A), which is the site of **ribosome** synthesis. Typical cells have one nucleolus per nucleus; some cells have more. The nucleolus includes portions of one or more chromosomes where ribosomal RNA (rRNA) genes are clustered to form a structure called the **nucleolar organizer region**. Even though chromosomes remain largely separate within the nucleus, parts of several may come together to help form the nucleolus. The nucleolus assembles the ribosomal proteins (imported from the cytoplasm) and rRNA of the ribosome into a large and a small subunit, each exiting the nucleus separately through the nuclear pores. The two subunits unite in the cytoplasm to form a complete ribosome (see Figure 1.16A, step 1). Assembled ribosomes are energy-consuming protein-synthesis machines that consume more than 50% of total cellular energy. Those produced by the nucleus for cytoplasmic, "eukaryotic" protein synthesis, the 80S ribosomes (named for their centrifugal sedimentation coefficient), are larger than the ribosomes assembled in and remaining in endosymbiotic mitochondria and plastids for their separate program of "prokaryotic" protein synthesis, the 70S ribosomes.

Gene expression involves transcription, translation, and protein processing

The nucleus is the site of read-out, or **transcription**, of the cell's DNA (**Figure 1.16A**). Some of the DNA is transcribed as messenger RNA (mRNA), which codes for proteins by specific DNA-dependent RNA polymerases. Ribosomes in the cytoplasm then read mRNA exported from the nucleus in one direction, from the 5′ to the 3′ end (**Figure 1.16B**). Other regions of the DNA are transcribed into transfer RNA (tRNA) and rRNA to be used in **translation** (see Figure 1.16A, steps 1–3). The RNA moves through nuclear pores to the cytoplasm, where "free" or cytoskeletally attached polyribosomes (groups of ribosomes translating a single RNA strand) translate the RNA into proteins destined for the cytoplasm and organelles that receive proteins independently of the endomembrane pathway. Stability or degradation of mRNAs is precisely regulated by many interacting proteins and is an important part of gene expression. Most proteins that reside in or are trafficked through the endomembrane system enter the the ER during the process of translation (co-translationally) on polyribosomes situated on the ER membrane. The mechanism of co-translational insertion of proteins into the ER is complex, involving the ribosomes, the mRNA that codes for the secretory protein, and a special protein-translocating pore, the **translocon**, in the ER membrane (see Figure 1.16A, steps 4–7). Proteins that are produced by the endomembrane system are called secretory proteins and can either be secreted from the cell interior to the apoplast, retained in endomembrane organelles as either soluble or membrane-anchored proteins, or trafficked through the endomembrane system to the vacuole.

Most secretory and integral membrane proteins have a **signal peptide**, a hydrophobic leader sequence of 18 to 30 amino acid residues at the amino-terminal end of the chain (see Figure 1.16A). Early in translation, a **signal recognition particle** (**SRP**), made up of protein and RNA, binds both to this hydrophobic leader and to the ribosome, interrupting translation. The ER membrane contains **SRP receptors** that can associate with the translocons, through which the newly synthesized protein is threaded. During co-translational insertion into the ER, the mRNA–ribosome–SRP complex in

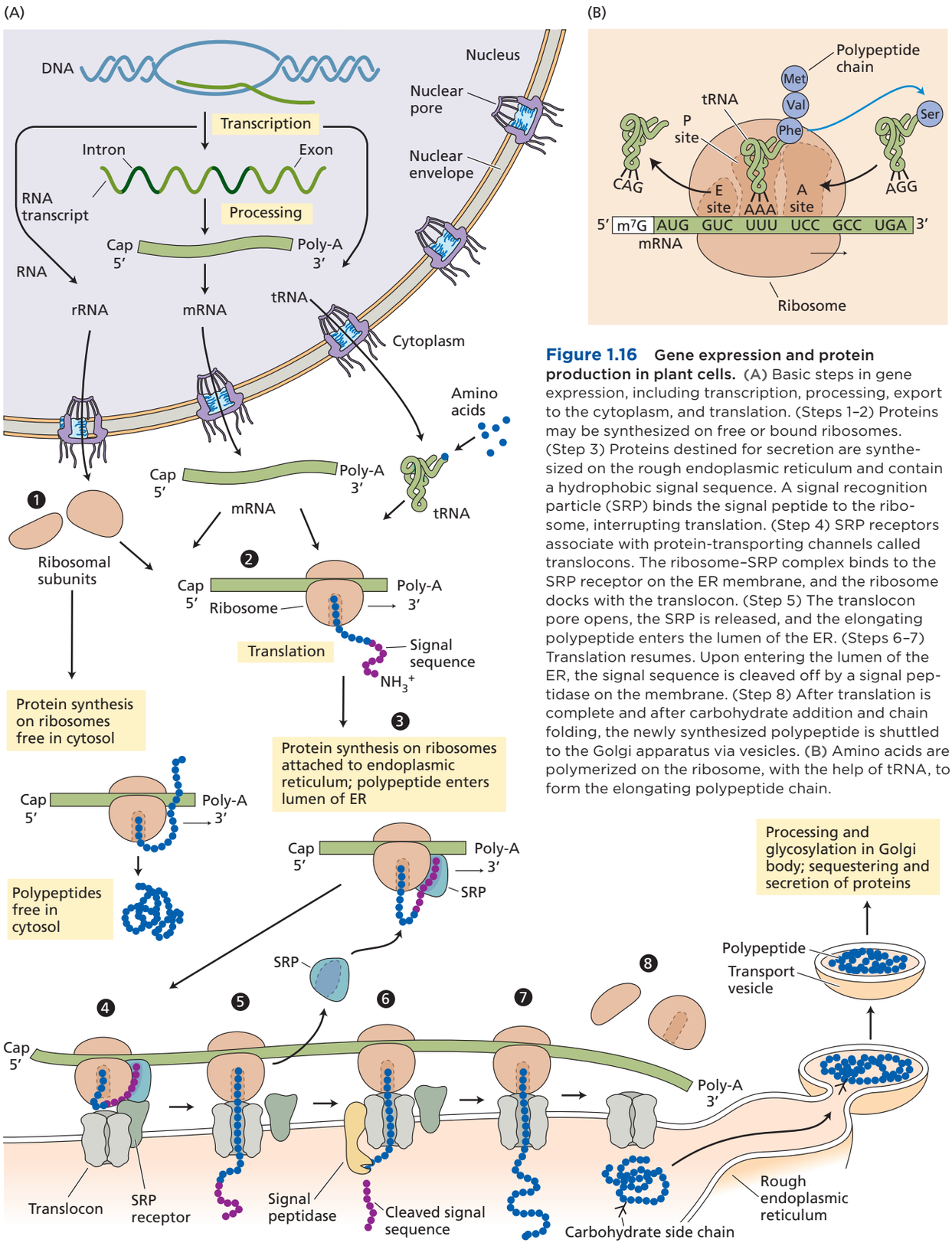


Figure 1.16 **Gene expression and protein production in plant cells.** **(A)** Basic steps in gene expression, including transcription, processing, export to the cytoplasm, and translation. (Steps 1–2) Proteins may be synthesized on free or bound ribosomes. (Step 3) Proteins destined for secretion are synthesized on the rough endoplasmic reticulum and contain a hydrophobic signal sequence. A signal recognition particle (SRP) binds the signal peptide to the ribosome, interrupting translation. (Step 4) SRP receptors associate with protein-transporting channels called translocons. The ribosome–SRP complex binds to the SRP receptor on the ER membrane, and the ribosome docks with the translocon. (Step 5) The translocon pore opens, the SRP is released, and the elongating polypeptide enters the lumen of the ER. (Steps 6–7) Translation resumes. Upon entering the lumen of the ER, the signal sequence is cleaved off by a signal peptidase on the membrane. (Step 8) After translation is complete and after carbohydrate addition and chain folding, the newly synthesized polypeptide is shuttled to the Golgi apparatus via vesicles. **(B)** Amino acids are polymerized on the ribosome, with the help of tRNA, to form the elongating polypeptide chain.

the cytoplasm binds to the SRP receptor on the ER membrane surface, and the ribosome docks with the translocon. Docking opens the translocon pore, the SRP is released, translation resumes, and the elongating polypeptide enters the lumen of the ER. The signal peptide sequence is cleaved off by a signal peptidase associated with the ER membrane (see Figure 1.16A). For integral membrane proteins, some parts of the polypeptide chain are translocated across the membrane while others are not. Completed integral membrane proteins are anchored to the membrane by one or more hydrophobic membrane-spanning domains. Transmembrane proteins that lack a signal peptide integrate into the membrane via internal hydrophobic and protein-protein interaction amino acid sequence motifs.

The proteins synthesized on cytosolic ribosomes that are targeted to membrane organelles (plastids, mitochondria, or peroxisomes) after translation employ posttranslational insertion to cross the organelle membrane. The process of translation on either cytoplasmic or membrane-bound polysomes produces the primary polymer of amino acids, which includes not only the sequence involved in protein function, but also amino acid motifs that interact with "trafficking" proteins to target the "cargo" protein to different destinations in the cell (i.e., molecular addresses) (see **WEB TOPIC 1.4**).

Posttranslational modification of proteins determines their location, activity, and longevity

Protein stability plays an important role in regulating a protein's longevity, and thus gene expression. Once synthesized, a protein has a finite life span in the cell, ranging from a few minutes to hours or days. Thus, steady-state levels of cellular proteins reflect an equilibrium between the synthesis and the degradation of those proteins, a balance referred to as **turnover**. In both plant and animal cells, there are two distinct pathways of protein turnover, one in specialized lytic vacuoles (called lysosomes in animal cells) (see Section 1.6) and the other in the cytoplasm and nucleus.

The pathway of protein turnover that occurs in the cytoplasm and nucleus involves the ATP-dependent formation of a covalent bond between the protein that is to be degraded and a small, 76–amino acid polypeptide called **ubiquitin**. Addition of one or many molecules of ubiquitin to a protein is called *ubiquitination*. Ubiquitination marks a protein for destruction by a large, ATP-dependent proteolytic complex called the **26S proteasome**, which specifically recognizes such "ubiquitin-tagged" molecules (**Figure 1.17**). More than 90% of the short-lived proteins in eukaryotic cells are degraded via the ubiquitin pathway.

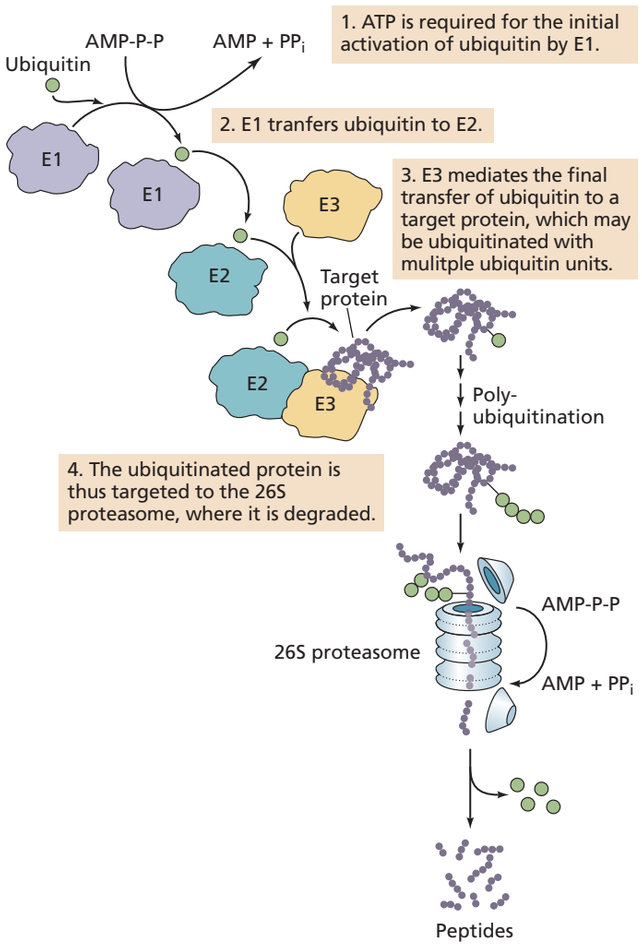


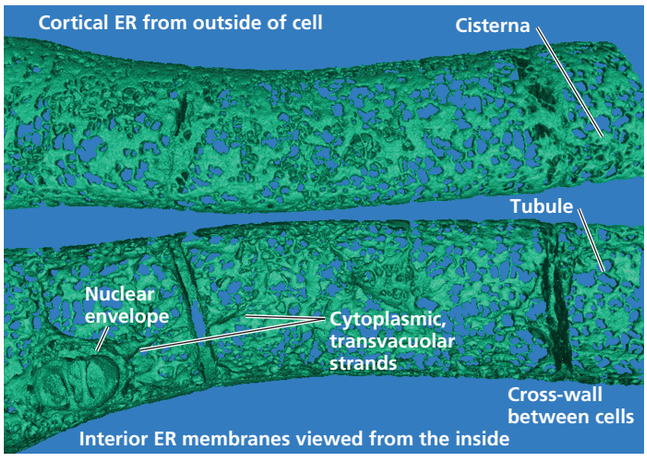
Figure 1.17 Generalized diagram of the cytoplasmic pathway of protein degradation. A similar pathway degrades membrane proteins in the nucleus or after delivery to the vacuole by autophagosomes.

Ubiquitination is initiated when the ubiquitin-activating enzyme (E1) catalyzes the ATP-dependent adenylation of the C terminus of ubiquitin. The adenylated ubiquitin is then transferred to a cysteine residue on a second enzyme, the ubiquitin-conjugating enzyme (E2). Proteins destined for degradation are bound by a third type of protein, a ubiquitin ligase (E3). The E2–ubiquitin complex then transfers its ubiquitin to a lysine residue of the protein bound to E3. This process can occur multiple times to form a polymer of ubiquitin. The ubiquitinated protein is then targeted to the proteasome for degradation.

There are a multitude of protein-specific ubiquitin ligases that regulate the turnover of specific target proteins to regulate development and environmental responses. Chapter 4 will discuss examples of this pathway in more detail in relation to plant hormone action.

1.6 The Endomembrane System

The endomembrane system is a collection of related internal membranes that contributes to the synthesis of roughly one-third of all cellular proteins and allows the cell to communicate with the external environment via vesicular traffic at the plasma membrane. Therefore, although it is not topologically inside the cell, the plasma membrane is also considered part of the endomembrane system. **Exocytosis** is the process that allows forward (anterograde) trafficking of biosynthetic cargo and membranes from the site of synthesis, the endoplasmic reticulum and the **Golgi apparatus**, to distal compartments of the endomembrane system, including the **trans Golgi network** (**TGN**), late endosomes, and ultimately the vacuole, plasma membrane, or cell wall. As exocytosis proceeds through successive endomembrane compartments, increasing luminal acidification contributes to its progression. **Endocytosis** is the opposite (retrograde) process, by which formation of plasma membrane invaginations counterbalances the exocytic flow of membranes to the plasma membrane and allows the cell to incorporate internalized plasma membrane and extracellular material into the cell or recycle those components back to the plasma membrane. Under some conditions, an increase in the specialized form of endomembrane trafficking known as **autophagy** allows cells to consume their own organelles and other cytoplasmic components after transfer to the vacuole. A basal level of autophagy exists in cells to maintain homeostasis; however, in conditions of stress, autophagy is often increased. Autophagy is discussed in more detail in Chapter 23.



Courtesy of L. R. Griffing

Figure 1.18 Three-dimensional reconstruction of ER in tobacco suspension culture cells. When the cells are viewed from the outside looking inward (top), the cortical network of the ER is clearly made up of linked cisternal domains. When the cells are viewed from the inside looking outward (bottom), transvacuolar strands containing ER tubules can be seen, as well as the nuclear envelope, a subdomain of the ER. The nuclei have transnuclear channels and invaginations in the nuclear envelope.

The endoplasmic reticulum is a network of internal membranes

The **endoplasmic reticulum** (**ER**) is composed of an extensive network of tubules that is continuous with the nuclear envelope. The tubules form a network of flattened saccules called **cisternae** (singular *cisterna*) (**Figure 1.18**). The tubules spread throughout the cell, forming close associations with other organelles and the cytoskeleton, mainly actin. The ER network may therefore be a communication network among organelles within a cell, while also serving as a synthesis and delivery system for proteins and lipids. The ER is responsible for initiating the synthesis of secretory proteins; it also produces essential lipids for the cell and cellular organelles. Most of the ER lies just under the plasma membrane, residing in the outer layer of cytoplasm called the cell cortex. This portion of the ER is therefore called the **cortical ER**. The cortical ER is attached to the plasma membrane at membrane subdomains called ER–plasma membrane contact sites. ER contact sites are also formed with other organelles such as mitochondria, plastids, and peroxisomes. Because plant cells generally contain a large central vacuole (see later in this section), the cortical ER on one side of the cell connects with the cortical ER at the other side of the cell via the so-called transvacuolar strands of the ER. The ER is a highly dynamic organelle that remodels tubules into cisternae, and vice versa.

The region of the ER that has many membrane-bound ribosomes associated with co-translational insertion of membrane proteins is called the **rough ER** because the bound ribosomes described previously give the ER a rough appearance in electron micrographs (**Figure 1.19A and B**). Because the ER is the primary site of secretory protein synthesis, a sophisticated protein quality control system is found inside the ER lumen to ensure the production of fully folded proteins. Once secretory proteins enter the ER, they undergo folding processes assisted by specialized resident ER chaperones called reticuloplasmins. High levels of calcium ions and oxidizing conditions contribute to folding and stabilization of the proteins via formation of cystine (cysteine-to-cysteine) linkages. Proteins that do not attain their properly folded conformation are retro-translocated via translocons situated in the ER membrane into the cytosol for degradation. Protein folding in the ER is monitored by conserved sensors that respond to the presence of hydrophobic domains of unfolded or misfolded proteins inside the ER. The activation of these sensors leads to an increased production of proteins that aid the folding and quality control of ER proteins. This process is collectively called the **unfolded protein response** and is depicted in more detail in **WEB TOPIC 1.5**. If the unfolded protein

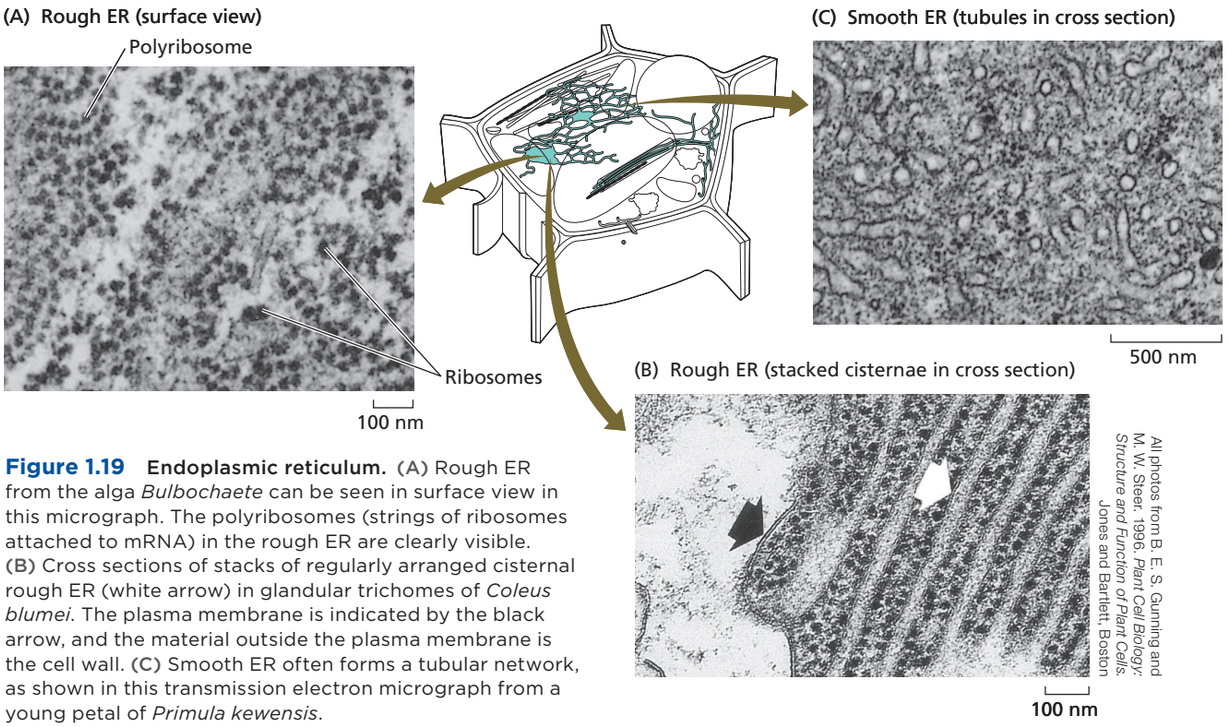


Figure 1.19 **Endoplasmic reticulum.** **(A)** Rough ER from the alga *Bulbochaete* can be seen in surface view in this micrograph. The polyribosomes (strings of ribosomes attached to mRNA) in the rough ER are clearly visible. **(B)** Cross sections of stacks of regularly arranged cisternal rough ER (white arrow) in glandular trichomes of *Coleus blumei*. The plasma membrane is indicated by the black arrow, and the material outside the plasma membrane is the cell wall. **(C)** Smooth ER often forms a tubular network, as shown in this transmission electron micrograph from a young petal of *Primula kewensis*.

response is insufficient, autophagy is activated and cell death is initiated.

The region of the ER without bound ribosomes is called **smooth ER** (**Figure 1.19C**) and is the major source of membrane phospholipids for the other compartments in the endomembrane system. Enzymes that initiate phospholipid and phospholipid head group synthesis on the cytosolic leaflet of the bilayer (i.e., the side of the membrane facing the cytosol) introduce an intrinsic lipid asymmetry in the endomembrane system and plasma membrane formed by exocytosis. Membrane asymmetry can, however, be adjusted by ATP-dependent enzymes called **flippases**, which move phospholipids between membrane leaflets.

The ER is closely associated with the Golgi apparatus. Export of cargo proteins from the ER is facilitated by coatomer type II (COPII) proteins after activation by a secretion associated Ras GTPase. The COPII coat interacts with amino acid motifs in membrane-associated proteins at ER exit sites, which contact the acceptor *cis* cisternae of the Golgi apparatus. This anterograde flow of cargo is counterbalanced by retrograde traffic controlled by the coatomer I (COPI) protein-coated vesicles. This retrograde movement is important for retrieving escaping ER resident proteins (reticuloplasmins) and *cis* to *trans* cisternae–specific enzymes in the Golgi apparatus that participate in the continuous maturation and flow of the Golgi membranes.

Cell wall matrix polysaccharides, secretory proteins and glycoproteins are processed in the Golgi apparatus

The Golgi apparatus is a polarized stack of cisternae, with thicker cisternae occurring on the *cis* side, or forming face, which accepts cargo transported in COPII carriers from the ER (**Figure 1.20**). The opposite, maturing face, or *trans* side, of the Golgi exhibits more flattened, thinner cisternae. Anterograde movement through the

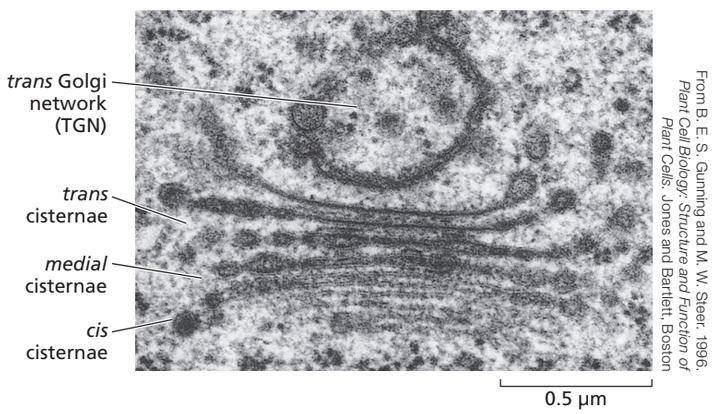
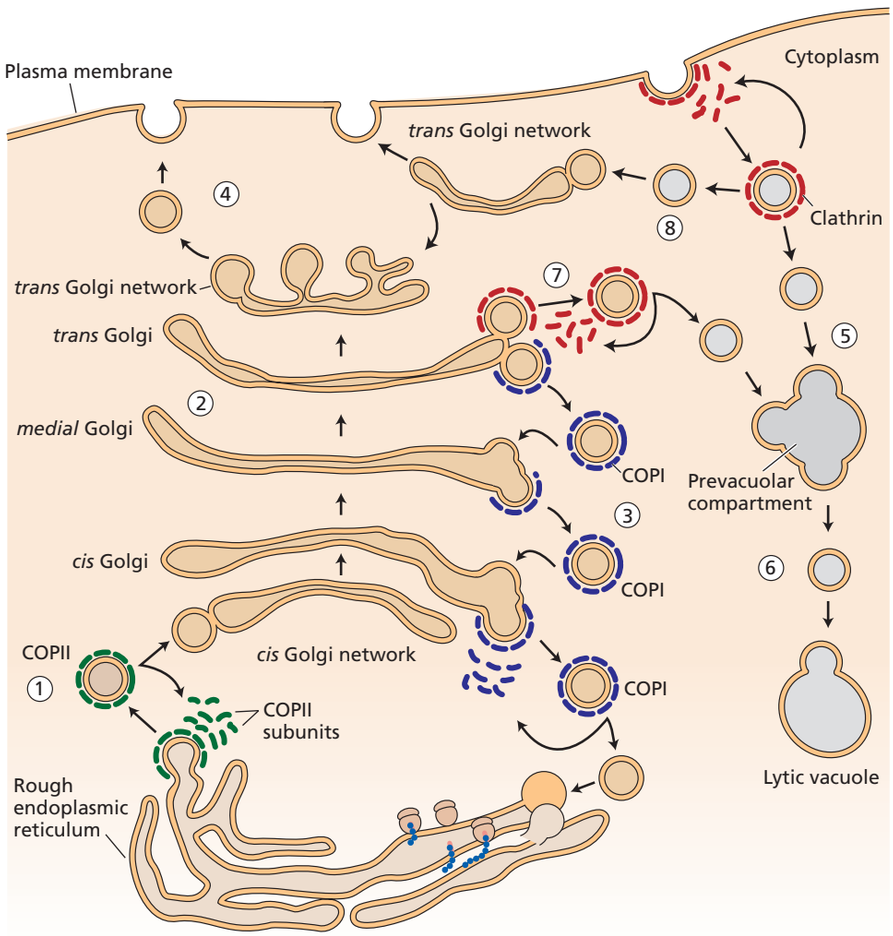


Figure 1.20 **Electron micrograph of a Golgi apparatus in a tobacco (*Nicotiana tabacum*) root cap cell.** The *cis*, *medial*, and *trans* cisternae are indicated. The *trans* Golgi network is associated with the *trans* cisternae and also functions as the early endosome in plant cells.

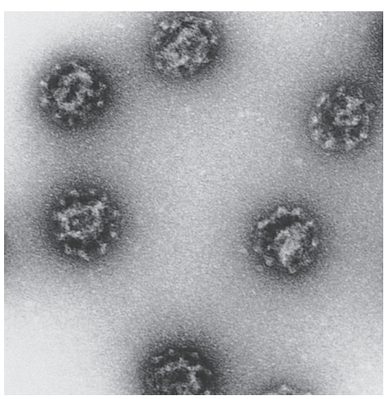
endomembrane system is generally believed to occur via vesicles (**Figure 1.21**). However, anterograde transit through the Golgi body occurs by *cisternal maturation*, whereby *cis* cisternae formed from COPII vesicles mature stepwise into *trans* cisternae. The *trans* cisternae then mature into the *trans* Golgi network (sometimes "falling off" the stack), which then produces secretory vesicles that are mostly uncoated. The *trans* Golgi network also accepts vesicles and their cargo derived from endocytosis at the plasma membrane. In plants,

(A)

1. COPII carriers bud from the ER when in proximity of the *cis* face of the Golgi apparatus.
2. Cisternae progress through the Golgi stack in the anterograde direction, carrying their cargo with them.
3. Retrograde movement of COPI-coated vesicles maintains the correct distribution of enzymes in the *cis*, *medial*, and *trans* cisternae of the stack.
4. Uncoated vesicles bud from the *trans* Golgi membrane and fuse with the plasma membrane.
5. Endocytotic clathrin-coated vesicles fuse with the prevacuolar compartment.
6. Uncoated vesicles bud off from the prevacuolar compartment and carry their cargo to a lytic vacuole.
7. Proteins destined for lytic vacuoles are secreted from the *trans* Golgi to the prevacuolar compartment via clathrin-coated vesicles, and then repackaged for delivery to the lytic vacuole.
8. Endocytic clathrin-coated vesicles can also uncoat and recycle via the *trans* Golgi network. Vesicles produced by the early recycling endosome either directly fuse with the plasma membrane or fuse with the *trans* Golgi.



(B)



Courtesy of D. G. Robinson

Figure 1.21 Vesicular traffic along the secretory and endocytotic pathways. **(A)** Diagram of vesicular traffic mediated by three types of coat proteins. COPII is indicated in green, COPI in blue, and clathrin in red. **(B)** Electron micrograph of clathrin-coated vesicles isolated from a bean leaf.

the *trans* Golgi network functions in the sorting of membrane vesicles containing newly synthesized and recycled proteins and cell wall components secreted to the plasma membrane. Specific membrane domains within the *trans* Golgi network are partially coated with **clathrin**, a protein that works in concert with adaptor proteins to select cargo and shape membranes into vesicles for transport into the vacuole (**Figure 1.22**). Proteins without a vacuolar localization signal are secreted to the cell wall/apoplast in what is often referred to as the *default* pathway.

Many of the proteins found in the lumen of the endomembrane system are **glycoproteins**—proteins with oligomeric sugar chains covalently attached—destined for secretion from the cell or delivery to the other endomembrane compartments. The enzymes that synthesize these sugar chains differ substantially from the enzymes that synthesize polysaccharides for incorporation into the cell wall. In the vast majority of cases, protein glycosylation begins in the ER with the attachment of a branched oligosaccharide chain made up of *N*-acetylglucosamine (GlcNAc), mannose (Man), and glucose (Glc) to one or more specific asparagine residues. This *N-linked glycan* ("N" is the one-letter abbreviation for asparagine) is first assembled on a lipid molecule, **dolichol diphosphate**, which is embedded in the ER membrane. The completed 14-sugar glycan is then transferred to the nascent polypeptide as it enters the ER lumen. These **N-linked glycoproteins** are trimmed in the ER and again during transition from the *cis* to the *trans* Golgi cisternae. Certain sugars, such as mannose, are removed from the oligosaccharide chains, and other sugars are added. In addition to these modifications, glycosylation of the –OH groups of hydroxyproline, serine, threonine, and tyrosine residues (**O-linked oligosaccharides**) occurs in the Golgi apparatus.

Enzymes that function in non-cellulosic cell wall polysaccharide biosynthesis are found in Golgi bodies. These enzymes are mostly Type 2 proteins that contain a single transmembrane helix and a C terminus that extends into the lumen of endomembrane compartments. Enzymes that form cell wall pectins and xyloglucans are also localized in different parts of the Golgi apparatus.

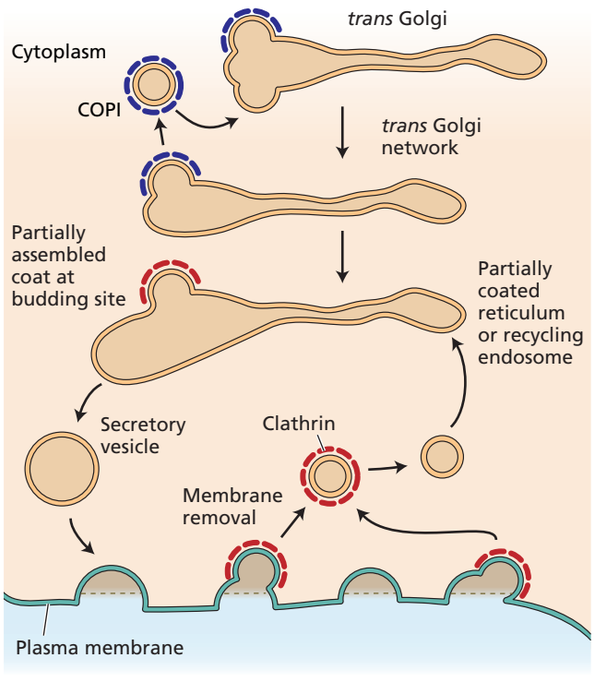


Figure 1.22 Clathrin-coated pits are associated with exocytosis and recycling of membrane components from recent secretion sites on the plasma membrane.

The plasma membrane has specialized regions involved in membrane recycling

Endocytotic membrane internalization at the plasma membrane occurs in small (100 nm) vesicles that are initially coated with clathrin, but clathrin-independent endocytosis has been documented in plant cells. Extracellular materials can be specifically recognized by receptors that are generally proteins spanning the plasma membrane. This process is called receptor-mediated endocytosis. Endocytosis proceeds through clathrin-mediated invagination of the plasma membrane progressing inward, followed by severing of the invagination neck. In plant cells, the difference in osmolarity (or more precisely water potential; see Chapter 5) between the inside and the outside of the cell creates a large internal pressure (in the range of 0.2–1 MPa), called turgor pressure. Turgor pressure pushes the plasma membrane against the cell wall. Therefore, during endocytosis, plasma membrane invagination involves energy and must overcome opposing turgor pressure. After initial endocytosis, vesicles lose their clathrin coat to form endocytic vesicles that are then sorted through the *trans* Golgi network (sometimes called the *early endosome* compartment) for recycling back to the plasma membrane or to *late endosomes*, also called **prevacuolar compartments**, for trafficking to the vacuole (see Figure 1.21A). Prevacuolar compartment endosomes are also called **multivesicular bodies**, as they generally contain smaller intraluminal vesicles.

Endomembrane trafficking pathways are regulated by small GTPase vesicle tethering complexes, and vesicle fusions with target compartments are mediated by a special class of target recognition proteins called **SNAREs** (see **WEB TOPIC 1.6**). An eight-protein tethering complex known as the **exocyst** is regulated by formation of specific SNARE complexes to tether post-Golgi secretory vesicles to the plasma membrane prior to final exocytosis.

Vacuoles have diverse functions in plant cells

The plant vacuole is a compartment enclosed by a membrane called the **tonoplast**. There are two primary types of vacuoles: lytic vacuoles found in vegetative cells and protein storage vacuoles found in developing seeds. The **vacuolar sap**, composed of water and solutes, is actively acidified (pH 5.5 and lower) by tonoplast-localized proton ATPases and pyrophosphatases in both lytic vacuoles and protein storage vacuoles during active growth. In general, vacuoles are small in young meristematic cells and increase in size during cell elongation and maturation, with the membrane being enlarged by fusion with membrane vesicles from the prevacuoloar compartment. Lytic vacuoles (**Figure 1.23A**) can occupy 90 to 95% of plant cell volume, and function in calcium ion signaling, osmotic regulation, lytic digestion, xenobiotic disposal, and defense responses. Expansion of plant cells is driven primarily by increases in lytic vacuolar volume. Inorganic ions, sugars, organic acids, and pigments are some of the solutes that can accumulate in vacuoles in very high concentrations, or even as solid crystals, thanks to the presence of a variety of specific membrane transporters (see Chapter 8). Protein storage vacuoles (**Figure 1.23B**) are specialized compartments that accumulate large amounts of proteins and sugars in developing seeds.

The multivesicular bodies release their cargo of intraluminal vesicles into the lytic vacuole for recycling after fusion with the tonoplast (**Figure 1.24**). Autophagosomes also deliver cargo to the lytic vacuole, either

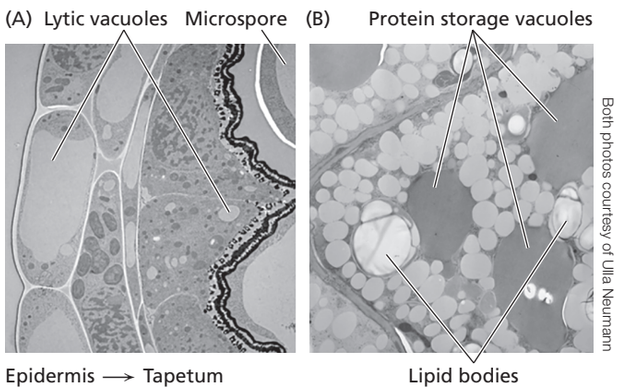


Figure 1.23 Transmission electron micrographs of the two primary types of vacuoles. **(A)** Cross section through a developing barley (*Hordeum vulgare* cv. Bowman) anther showing the four-layered wall (from outside to inside: epidermis, endothecium, middle layer, tapetum) that surrounds the developing microspores (see Chapter 21). The lytic vacuoles can be seen as electron-translucent spaces of various sizes and shapes in the different cell layers. The epidermis is characterized by a single prominent lytic vacuole that makes up most of the cell volume and restricts the cytoplasm to a thin layer pressed against the plasma membrane. By contrast, cells of the tapetum have a much denser cytoplasm and contain numerous small lytic vacuoles. **(B)** Section through castor bean (*Ricinus communis*) endosperm. The endosperm cytoplasm contains protein storage vacuoles of varying diameter that are characterized by an electron-opaque content. The small, globular, electron-translucent structures correspond to lipid bodies. Their contents have been extracted during sample preparation.

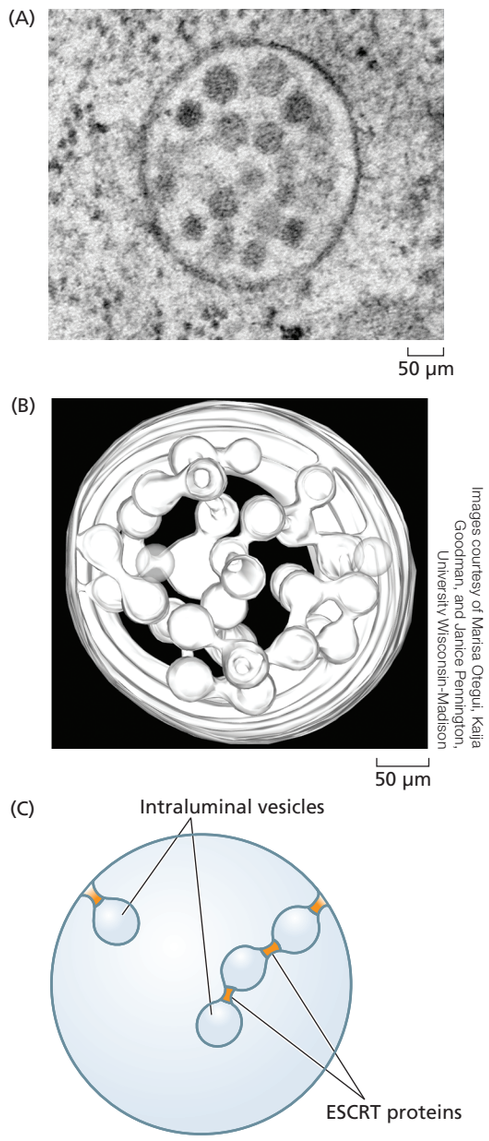
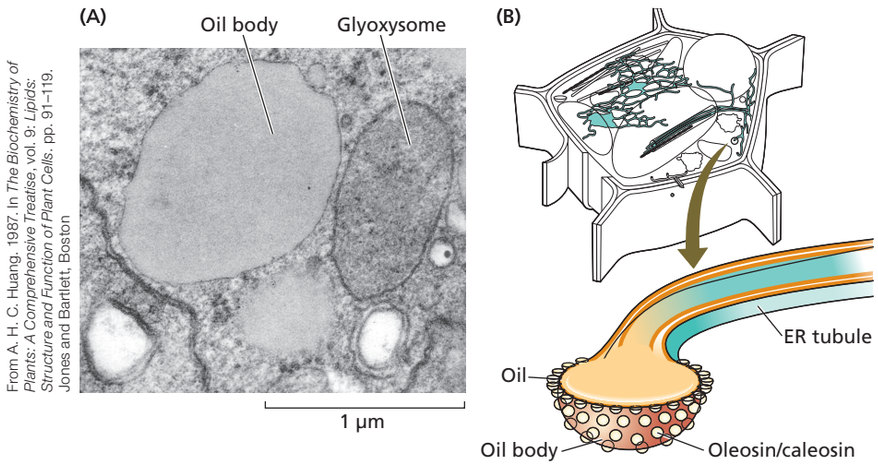


Figure 1.24 Multivesicular bodies. **(A)** A multivesicular body (also called a prevacuolar compartment or late endosome) from a tapetal cell from an anther of Arabidopsis. **(B)** Reconstructed tomographic model of a tapetal multivesicular body. **(C)** Diagram showing the process of vesicular internalization into the multivesicular body. The samples were processed by high-pressure freezing and freeze-substitution (replacement of water with organic molecules and fixatives) followed by embedding in plastic resin.



From A. H. C. Huang. 1987. In *The Biochemistry of Plants: A Comprehensive Treatise*, vol. 9: *Lipids: Structure and Function of Plant Cells*. pp. 91–119. Jones and Bartlett, Boston

Figure 1.25 Oil bodies found in seeds and cotyledons of vascular plants. (A) Electron micrograph of an oil body beside a glyoxisome. (B) Diagram showing the formation of oil bodies by the synthesis and deposition of oil within the phospholipid bilayer of the ER. After budding off from the ER, the oil body is surrounded by a phospholipid monolayer containing specific oil body proteins, such as oleosin. (B after L. A. Staehelin and E. H. Newcomb. 2000. In *Biochemistry and Molecular Biology of Plants*. B. B. Buchanan et al. [eds.]. American Society of Plant Biologists, Rockville, MD.)

directly or after fusion with the late endosome (forming a compartment called an amphisome). By fusing with the vacuole, the membrane of the prevacuolar compartments contributes to the expansion of the tonoplast. During seed formation, embryonic protein storage vacuoles are formed either by regular endomembrane traffic or directly from the ER by local aggregation of storage proteins in the ER lumen.

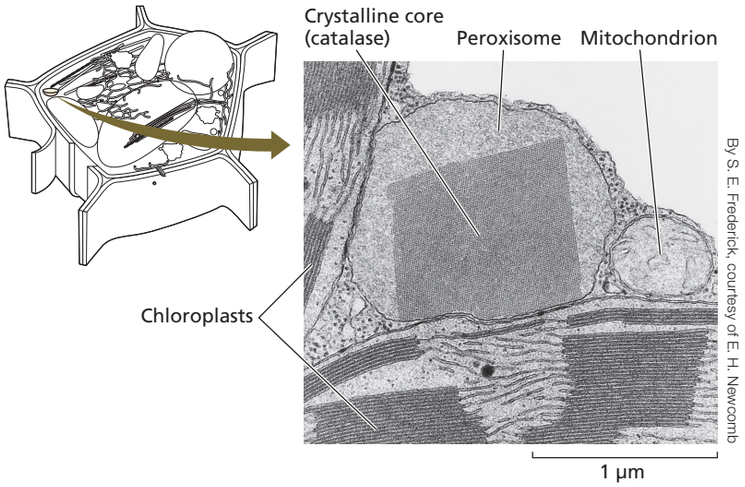
Vacuoles can be inherited during cytokinesis of a mother cell, but also are formed de novo in meristematic cells directly from the ER and from the fusion of endosomal compartments. Therefore, the tonoplast contains proteins and lipids that are originally synthesized in the ER.

Oil bodies are lipid-storing organelles

Many plants synthesize and store large quantities of oil during seed development. These oils accumulate in organelles called **oil bodies** (also known as **oleosomes**) (**Figure 1.25**). Oil bodies are unique among the organelles in that they are surrounded by a "half–unit membrane"—that is, a phospholipid monolayer—derived from the ER (see Figure 1.25B). The phospholipids in the half–unit membrane are oriented with their polar head groups facing the aqueous phase of the cytosol and their hydrophobic fatty acid tails facing the lumen, dissolved in the stored lipid. Oil bodies initially form as regions of differentiation within the ER membrane bilayer. The nature of the storage product, **triacylglycerols** (three fatty acids covalently linked to a glycerol backbone), dictates that this storage organelle will have a hydrophobic lumen. Consequently, as triacylglycerols are stored, they are initially accumulated in the hydrophobic region between the outer and inner leaflets of the ER membrane.

Peroxisomes play specialized metabolic roles in leaves and seeds

Peroxisomes are a class of organelles surrounded by a single membrane bylayer and characterized by the ability to detoxify reactive oxygen species via the enzyme **catalase**, as well as perform other specialized metabolic functions. **Glyoxysomes** are peroxisomes specialized for the β-oxidation of fatty acids (in animals localized to mitochondria) and the metabolism of glyoxylate, a two-carbon acid aldehyde, especially in germinating seeds (see Chapter 13). Glyoxysomes are associated with mitochondria and oil bodies, while leaf peroxisomes function in photorespiration (see Chapter 10) in association with mitochondria and chloroplasts (**Figure 1.26**). While peroxisomes can multiply by division much



By S. E. Frederick, courtesy of E. H. Newcomb

Figure 1.26 Catalase crystal in a peroxisome of a mature leaf of tobacco. Note the close association of the peroxisome with two chloroplasts and a mitochondrion, organelles that exchange metabolites with peroxisomes, especially during photorespiration.

as plastids and mitochondria do, they are more often formed de novo directly from the ER.

1.7 Independently Dividing Semiautonomous Organelles

A typical plant cell has two primary types of semiautonomous organelles: mitochondria and plastids. Both types are separated from the cytoplasm by a double membrane (an outer and an inner membrane) and contain their own DNA and prokaryotic-type ribosomes as descendants of prokaryotic endosymbionts.

Mitochondria (singular *mitochondrion*) are the cellular sites of respiration, a process in which the energy released from sugar metabolism is used for the synthesis of ATP (adenosine triphosphate) from ADP (adenosine diphosphate) and inorganic phosphate (P_i) (see Chapter 13).

Mitochondria are highly dynamic structures that can undergo both fission and fusion. Regardless of shape, all mitochondria have a smooth outer membrane and a highly convoluted inner membrane (**Figure 1.27**). The inner membrane contains an ATP synthase that uses a proton gradient to synthesize ATP for the cell. The proton gradient is generated through the cooperation of electron transporters called the electron transport chain, which is embedded in, and peripheral to, the inner membrane (see Chapter 13). The infoldings of the inner membrane are called **cristae** (singular *crista*). The compartment enclosed by the inner membrane, the mitochondrial **matrix**, contains the enzymes of the pathway of intermediary metabolism called the **tricarboxylic acid** (**TCA**) **cycle** (see Chapter 13).

Plastids are another group of double-membrane–enclosed organelles (derived from an ancestral endosymbiosis event with cyanobacteria). Plastids that function in photosynthesis are called **chloroplasts** (**Figure 1.28A**). In addition to their inner and outer envelope membranes, chloroplasts possess a third system of internal membranes called **thylakoids**. A stack of thylakoids forms a **granum** (plural *grana*) (**Figure 1.28B**). Proteins and pigments (chlorophylls and carotenoids) that function in the photochemical events of photosynthesis are embedded in the thylakoid membrane. Adjacent grana are connected by unstacked membranes called **stroma lamellae** (singular *lamella*). The compartment surrounding the thylakoids, called the **stroma**, is analogous to the matrix of the mitochondrion and contains what may be Earth's most abundant protein, ribulose 1,5-biophosphate carboxylase/oxygenase, called Rubisco for convenience. Rubsico is involved in capturing atmospheric carbon for conversion into organic acids during photosynthesis (see Chapter 10). Although both the large and small subunits of Rubisco are encoded in the plastid genome in algae, in land plants the large subunit of Rubisco is encoded by the chloroplast genome while the small subunit is encoded by the nuclear genome. Coordinated expression of each subunit (and other proteins) by each genome is necessary as chloroplasts grow and divide.

The various components of the photosynthetic apparatus are localized in different areas of the grana and the stroma lamellae. The ATP synthases of the chloroplast are located on the thylakoid membrane (**Figure 1.28C**). During photosynthesis, light-driven electron transfer reactions result in a proton gradient across the thylakoid membrane (**Figure 1.28D**) (see Chapter 9). As in the mitochondria, ATP is synthesized when the proton gradient is dissipated via ATP synthase. In the chloroplast, however, the ATP is not exported to the cytosol, but is used for many stromal reactions, including the fixation of carbon from carbon dioxide in the atmosphere, as described in Chapter 10.

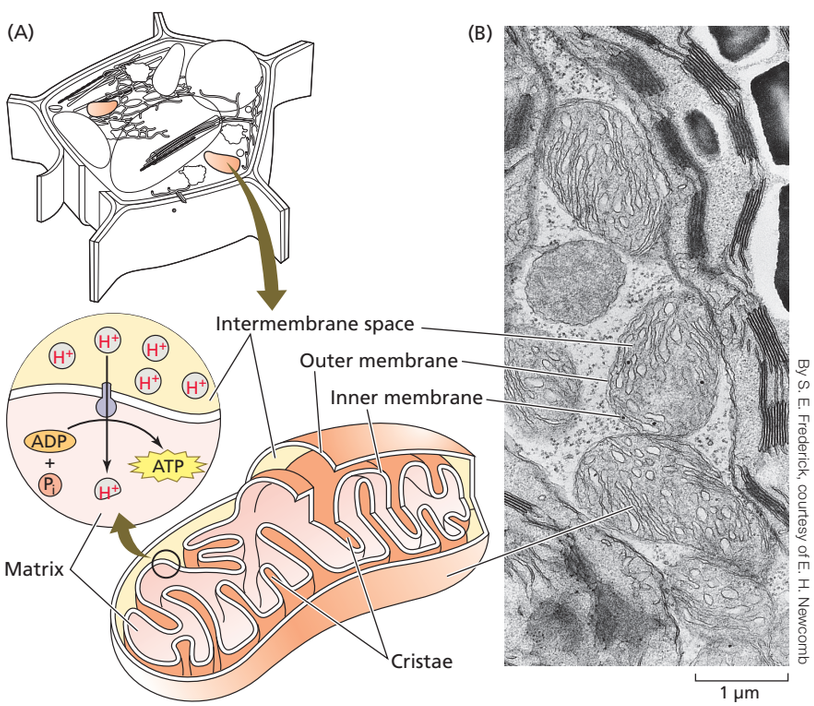


Figure 1.27 **Mitochondria generate ATP via oxidative phosphorylation.** **(A)** Diagrammatic representation of a mitochondrion, including the location of the ATP synthases involved in ATP synthesis on the inner membrane. **(B)** Electron micrograph of mitochondria from a leaf cell of Bermuda grass (*Cynodon dactylon*).

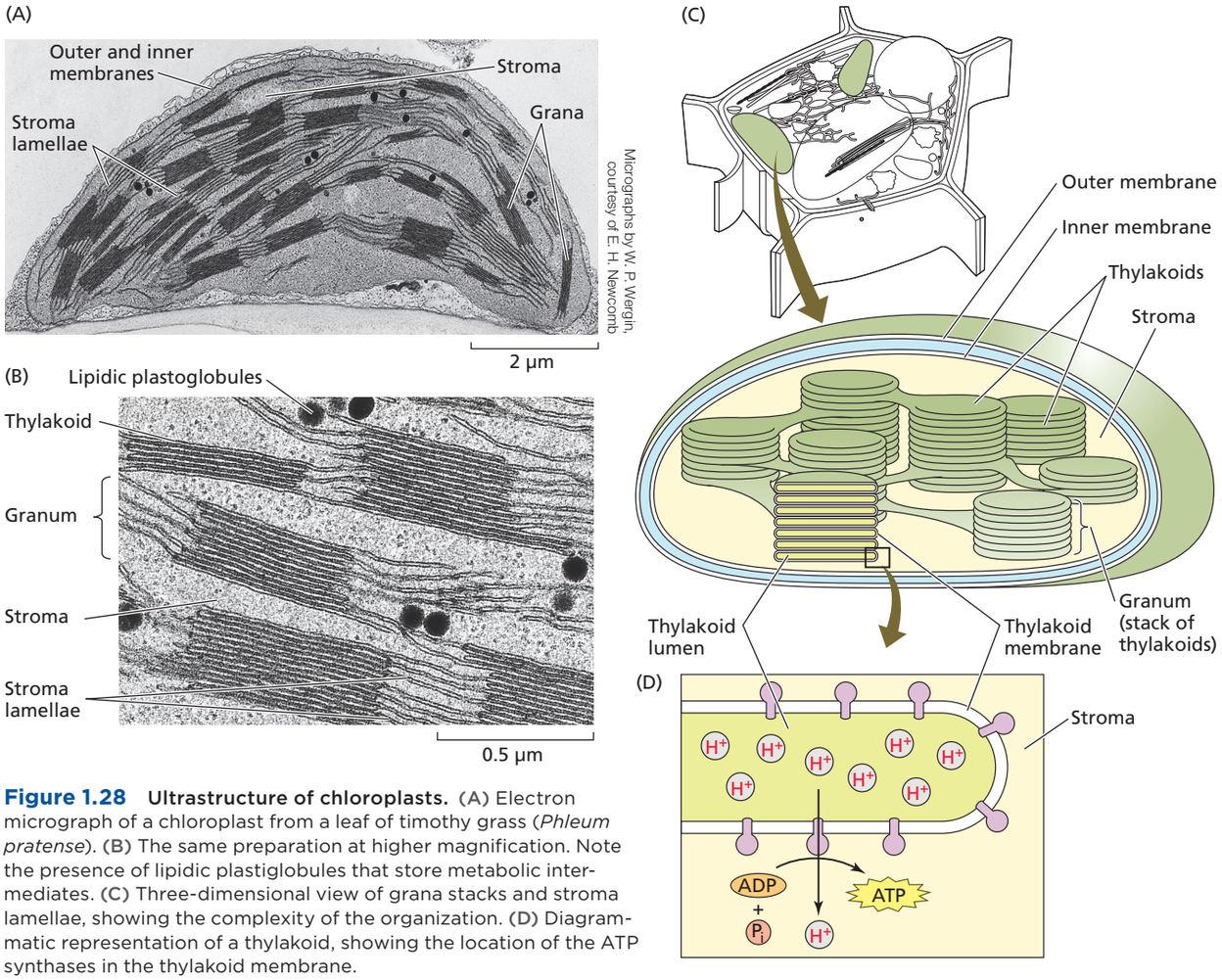


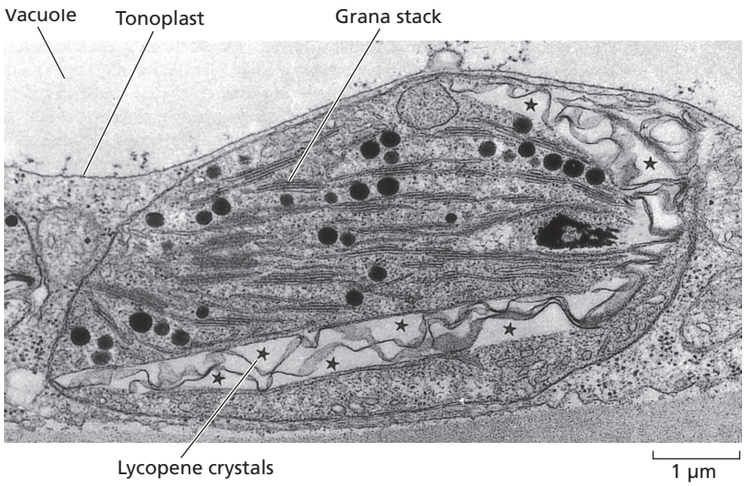
Figure 1.28 **Ultrastructure of chloroplasts.** **(A)** Electron micrograph of a chloroplast from a leaf of timothy grass (*Phleum pratense*). **(B)** The same preparation at higher magnification. Note the presence of lipidic plastiglobules that store metabolic intermediates. **(C)** Three-dimensional view of grana stacks and stroma lamellae, showing the complexity of the organization. **(D)** Diagrammatic representation of a thylakoid, showing the location of the ATP synthases in the thylakoid membrane.

Plastids that contain high concentrations of carotenoid pigments, rather than chlorophyll, are called **chromoplasts**. Chromoplasts are responsible for the yellow, orange, and red colors of many fruits and flowers, as well as of autumn leaves (**Figure 1.29**). Nonpigmented plastids are called **leucoplasts**. Leucoplasts in specialized secretory tissues, such as the nectary, make monoterpenoids, volatile molecules (in essential oils) that often have a strong smell. The most important type of leucoplast is the **amyloplast**, a starch-storing plastid. Amyloplasts are abundant in the storage tissues of shoots and roots, and in seeds. Specialized amyloplasts in the root cap also serve as gravity sensors that enhance directional root growth downward into the soil (see Chapter 17).

Proplastids mature into specialized plastids in different plant tissues

Meristem cells contain **proplastids**, which have few internal membranes, no chlorophyll, and an incomplete complement of the enzymes necessary to carry out photosynthesis (**Figure 1.30A**). While chloroplast development in gymnosperms occurs in both dark and light conditions, angiosperm chloroplast development from proplastids is triggered by light. Upon illumination, regulators of plastidial gene expression are imported into developing plastids to initiate expression of plastidal gene products that interact with nuclear-encoded functional proteins to initiate production of light-absorbing pigments, proliferation of internal membranes, formation of stroma lamellae and grana stacks, and assembly of light-harvesting complexes and other functional structures (**Figure 1.30B**).

Seeds usually germinate in the soil in the dark, and their proplastids mature into chloroplasts only when the young shoot is exposed to light. If germinated seedlings are kept in the dark, the proplastids differentiate into **etioplasts**, which contain semicrystalline tubular arrays of reorganized thylakoid membrane known as **prolamellar**



From B. E. S. Gunning and M. W. Steer. 1996. *Plant Cell Biology: Structure and Function of Plant Cells*. Jones and Bartlett, Boston

Figure 1.29 Electron micrograph of a chromoplast from tomato (*Solanum lycopersicum*) fruit at an early stage in the transition from chloroplast to chromoplast. Small grana stacks are still visible. Stars indicate crystals of lycopene, a type of carotenoid pigment.

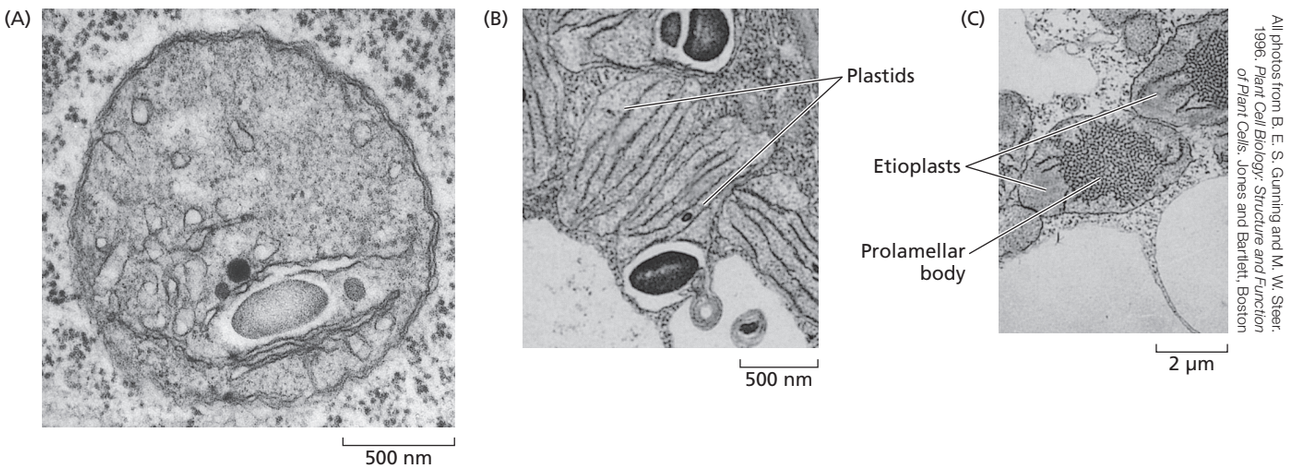
conditions or tissue differentiation, chloroplasts can be converted to chromoplasts, as in autumn leaves and ripening fruit, or to starch-containing amyloplasts in storage organs.

Plastidial and mitochondrial division are independent of nuclear division in land plants

Both mitochondria and plastids divide by the process of fission, consistent with their prokaryotic origins. Fission and organellar DNA replication are regulated independently of nuclear division. For example, the number of chloroplasts per cell volume depends on the cell's developmental history and its local environment. Accordingly, there are many more chloroplasts in the mesophyll cells in the interior of a leaf than in the epidermal cells forming the outer layer of the leaf.

bodies (**Figure 1.30C**). Instead of chlorophyll, etioplasts contain a pale yellow-green precursor pigment, protochlorophyllide. Within minutes after exposure to light, an etioplast differentiates, converting the prolamellar body into thylakoids and stroma lamellae, and the protochlorophyllide into chlorophyll. The maintenance of chloroplast structure depends on the presence of light; mature chloroplasts can revert to etioplasts during extended periods of darkness. Likewise, under different environmental

Although the timing of the fission of chloroplasts and mitochondria is independent of the timing of cell division, these organelles require nuclear-encoded proteins to divide. In both bacteria and the semiautonomous organelles, fission is facilitated by proteins that form co-ordinated rings on the inner and outer membranes at the site of the future division plane. In plant cells, the genes that encode these proteins are located in the nucleus. Mitochondria and chloroplasts can also increase in



All photos from B. E. S. Gunning and M. W. Steer. 1996. *Plant Cell Biology: Structure and Function of Plant Cells*. Jones and Bartlett, Boston

Figure 1.30 Electron micrographs illustrating several stages of plastid development. **(A)** Proplastid from the root apical meristem of broad bean (*Vicia faba*). The internal membrane system is rudimentary, and grana are absent. Large inclusions contain starch. **(B)** Mesophyll cell of a young oat (*Avena sativa*) leaf grown in the light, at an early stage of differentiation. The plastids are developing grana stacks. **(C)** Cell of a young oat leaf from a seedling grown in the dark. The plastids have developed as etioplasts, with elaborate semicrystalline lattices of membrane tubules called prolamellar bodies. When exposed to light, the etioplast can convert to a chloroplast by the disassembly of the prolamellar body and the formation of grana stacks.

size without dividing, in order to meet energy or photosynthetic demand. If, for example, the proteins involved in mitochondrial division are experimentally inactivated, the fewer mitochondria become larger, allowing the cell to meet its energy needs. In plants with compromised chloroplast biogenesis and function (e.g., the *albostrians* mutant in cereals), mitochondrial biogenesis and function are enhanced to compensate for energy deficiencies.

Both plastids and mitochondria can move around plant cells. In some plant cells the chloroplasts are anchored in the outer, cortical cytoplasm of the cell, but in others they are mobile, providing for optimal utilization of light for photosynthesis. Plastids and mitochondria are moved largely by myosins that motor along actin microfilaments (see the discussion of myosins in Section 1.8).

1.8 The Plant Cytoskeleton

The cytoplasm is organized into a dynamic three-dimensional structure by a network of filamentous proteins called the **cytoskeleton**. This network provides the spatial organization for the organelles and serves as scaffolding for the movements of organelles and other cytoskeletal components. It also plays fundamental roles in endomebrane movement, mitosis, meiosis, cytokinesis, wall deposition, the maintenance of cell shape, and cell differentiation.

The plant cytoskeleton consists of microtubules and microfilaments

Two major types of cytoskeletal elements have been demonstrated in plant cells: microtubules and microfilaments. Each type is filamentous, having a fixed diameter and a variable length, up to many micrometers.

Microtubules are polarized hollow cylinders with an outer diameter of 25 nm; they are composed of polymers of the protein **tubulin**. The tubulin monomer is a heterodimer composed of two similar polypeptide chains (α- and β-tubulin) (**Figure 1.31A**). A single microtubule consists of hundreds of thousands of tubulin monomers arranged in columns called **protofilaments**.

Microfilaments are solid, with a diameter of 7 nm. They are composed of the monomeric form of the protein **actin**, called globular actin, or G-actin. Activated by ATP, monomers of G-actin polymerize to form a single polarized chain of actin subunits, also called a protofilament. The actin in the polymerized protofilament is referred to as filamentous actin, or F-actin. A microfilament is helical, a shape resulting from the polarity of association of the G-actin monomers (**Figure 1.31B**).

Actin, tubulin, and their polymers are in constant flux in the living cell

In the cell, actin and tubulin subunits exist as pools of free proteins that are in dynamic equilibrium with their

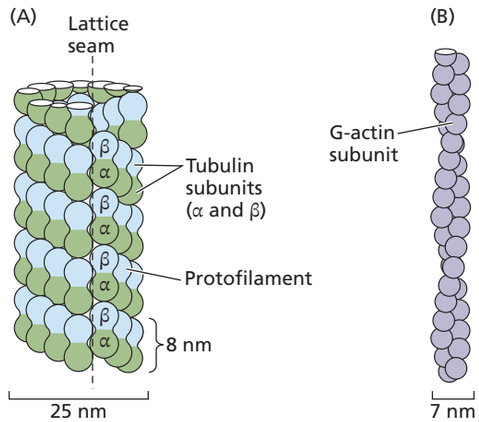


Figure 1.31 **Cytoskeletal microtubules and microfilaments.** **(A)** Drawing of a microtubule in longitudinal view. Each microtubule is typically composed of 13 protofilaments (but varies with species and cell type). The organization of the α and β subunits is shown. **(B)** Diagrammatic representation of a microfilament, showing an F-actin strand (protofilament) with a helical pitch based on the asymmetry of the monomers, the G-actin subunits.

polymerized forms. Compared with animal cells, plants have larger pools of monomeric G-actin and strands made up of F-actin arrays. The cycle of polymerization–depolymerization is essential for cell life. Each of the monomers contains a bound nucleotide: ATP or ADP in the case of actin, GTP or GDP (guanosine tri- or diphosphate) in the case of tubulin. Both microtubules and microfilaments are polarized; that is, the two ends are different. The polarity is displayed by the different rates of growth of the two ends, with the more active end being the plus end and the less active end being the minus end.

In microfilaments, the polarity arises from the polarity of the actin monomer itself; the ATP or ADP nucleotide-binding cleft of the monomer orients toward the slow-growing negative end of the microfilament, while the side opposite the ATP or ADP nucleotide-binding cleft orients toward the fast-growing positive end (**Figure 1.32A**). **Profilin** proteins assist in bringing monomers to the plus end of F-actin, where they are assembled by **formins** (**Figure 1.32B and C**). The proteins **fimbrin** and **villin** function in bundling actin filaments into cables (see Figure 1.32B and C). The **actin related protein 2/3** (**Arp 2/3**) complex creates branched actin filaments (**Figure 1.32D**) that are important for polarized growth of cells. Capping proteins can stabilize filament ends, and depolymerizing proteins enhance turnover. These polarized polymerization and depolymerization events are highly dynamic, and are referred to as **treadmilling** when they occur simultaneously at the minus and plus ends of actin filaments. Treadmilling allows microfilaments to appear to migrate around the cell cortex in the direction of the positive pole. However,

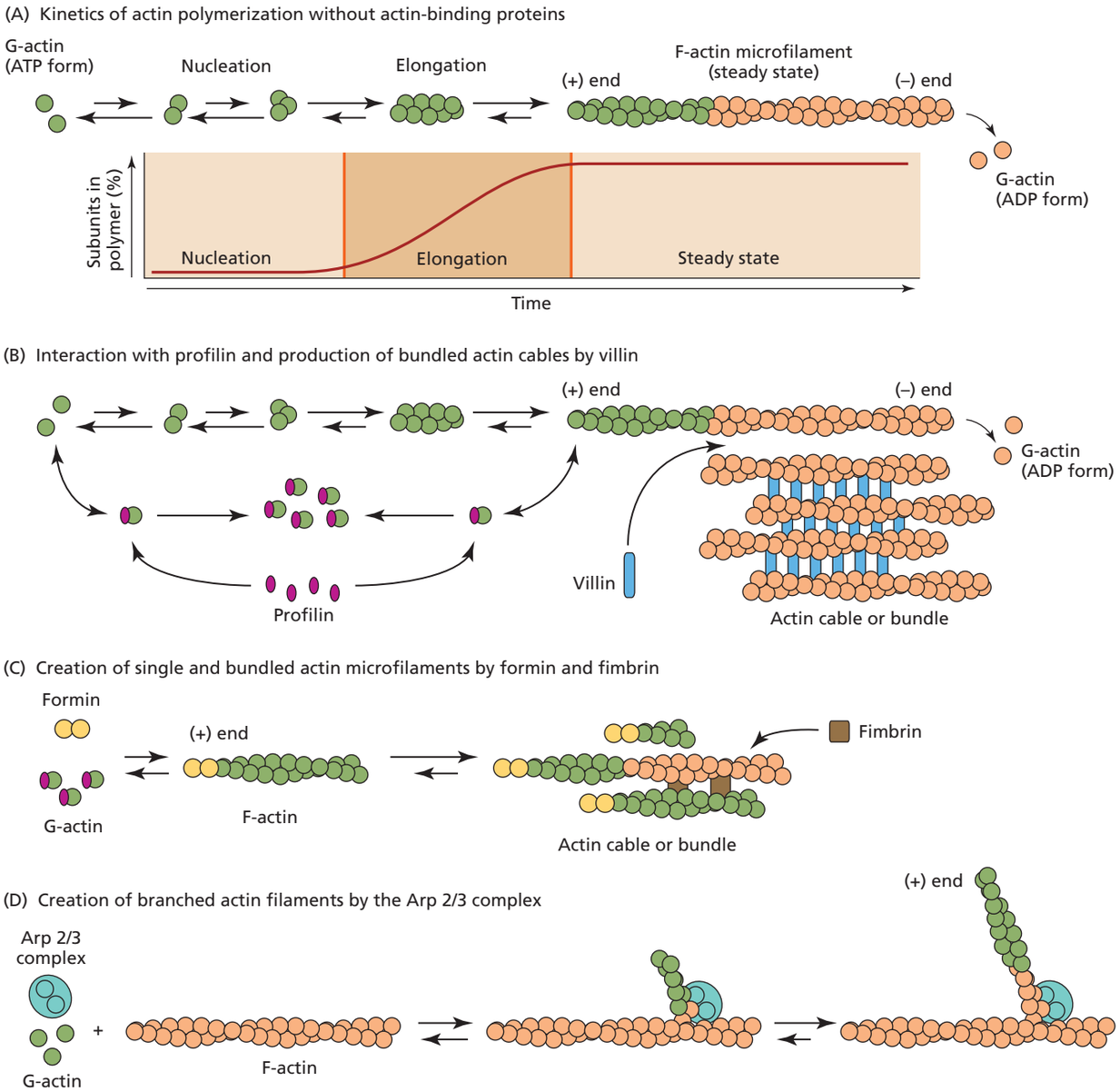


Figure 1.32 Assembly of single, bundled, and branched actin microfilaments. **(A)** Kinetics of polarized microfilament assembly. Green indicates ATP, orange indicates ADP. **(B)** F-actin assembly. Individual G-actin monomers bind ATP and aggregate to form a trimer, which nucleates formation of a new filament. Additional G-actin then polymerizes at the plus and minus ends of the growing F-actin filament. ATP hydrolysis to ADP occurs after the ATP-charged units are polymerized, and the G-actin that comes off has ADP. Formin dimers initiate F-actin assembly. **(C)** Assembly of single and bundled filaments. **(D)** Formation of branched actin by ARP 2/3 complex.

what appears to be microfilament motility is actually caused by growth at the positive ends and degradation at the negative ends.

In microtubules, the polarity arises from the polarity of the α- and β-tubulin heterodimer (see Figure 1.31A). The α-tubulin monomer exists only in the GTP form and is exposed on the minus end, and the β-tubulin can bind either GTP or GDP and is exposed on the plus end (see Figure 1.33A). Microfilaments and microtubules have half-lives, usually counted in minutes, determined by accessory proteins that regulate the dynamics of microfilaments and microtubules.

Microtubules are dynamic cylinders

Microtubule nucleation and initiation of growth occur at *microtubule organizing centers* (*MTOCs*), also called *initiation complexes*, but the precise nature of the initiation complex is still unresolved. One type of initiation complex contains a much less abundant type of tubulin called γ-*tubulin*, which forms ring complexes in the cortical cytoplasm from which microtubules can grow (**Figure 1.33A–C**).

Each tubulin heterodimer contains two GTP molecules, one on the α-tubulin monomer and the other on the β-tubulin monomer. GTP on the α-tubulin monomer is tightly bound and nonhydrolyzable, while the GTP on the β-tubulin site is hydrolyzed to GDP after the heterodimer assembles onto the plus end of a microtubule. The assembly of the tubulin subunits results in the formation of a hollow cylinder. If the rate of GTP hydrolysis "catches up" with the rate of addition of new heterodimers, the GTP-charged cap of tubulin vanishes and the protofilaments come apart from each other, initiating a catastrophic depolymerization (see Figure 1.33C). Such catastrophes can be rescued (depolymerization stopped and polymerization resumed) if the increase in the local free tubulin concentration (with GTP) caused by the catastrophe once again favors polymerization. The slowly growing minus end does not depolymerize if it is capped by γ-tubulin. However, plant microtubules can be released from γ-tubulin ring complexes by an ATPase, katanin (from the Japanese word *katana*, "samurai sword"), which severs the microtubule at the point where the growing microtubule branches off another microtubule (**Figure 1.33D**). Once the microtubules are released by katanin, they move, snakelike, through the cell cortex by treadmilling.

During treadmilling, tubulin heterodimers are added to the growing plus end at about the same rate that they are removed from the shrinking minus end (see Figure 1.33D). The transverse orientation of the cortical microtubules determines the orientation of the newly synthesized cellulose microfibrils in the cell wall by constraining movement of cellulose synthase complexes within the plasma membrane. The presence of transverse cellulose microfibrils in the cell wall reinforces the wall in the transverse direction, promoting growth along the perpendicular longitudinal axis. In this way, microtubules play an important role in the polarity of plant growth.

Cytoskeletal motor proteins mediate cytoplasmic streaming and directed organelle movement

Mitochondria, peroxisomes, endosomesn, and Golgi bodies are extremely mobile in plant cells. These approximately 1-μm particles move at rates of about 1–10 μm s^{-1} in seed plants, depending on cell type and developmental stage. This movement is quite fast; it is equivalent to a 1-m object moving at 10 m s^{-1}, approximately the speed of the world's fastest human. Actin and its motor protein, myosin, act together to generate this movement using energy released by ATP hydrolysis and are therefore frequently referred to as the actomyosin cytoskeleton.

Cytoplasmic streaming refers to the coordinated flow of the cytoplasm with organelles inside the cell. The movement of individual organelles can be part of cytoplasmic streaming but is perhaps better called **directed organelle movement** because organelles can frequently move past each other in opposite directions on neighboring F-actin filaments. If directed organelle movement exerts sufficient viscous drag on the surrounding cytoplasm, then it will drive cytoplasmic streaming. Accordingly, there is almost no cytoplasmic streaming in small meristematic cells. As cells elongate and differentiate, rates of streaming increase. In the giant cells of the green algae *Chara* and *Nitella*, cytoplasmic streaming occurs in a helical path down one side of a cell and up the other side, at speeds of up to 75 μm s^{-1}. Similarly, in rapidly growing pollen tubes, the presence of a forward stream in the center and of return streams at the periphery creates fountainlike cytoplasmic streaming. Both directed organelle movement and stabilization (tethering) involves interactions via attachment sites to other organelles, endomembranes, the cytoskeleton, or the plasma membrane. The endoplasmic reticulum interacts with the plasma membrane and other organelles via F-actin at these attachment sites.

Molecular motors participate in all directed organelle movements. Plants have two types of motors, the myosins and the kinesins. The myosins are actin-binding proteins. The kinesins are associated with microtubules. When myosins and kinesins move along the cytoskeleton, they do so in a particular direction along the polar cytoskeletal polymers. Myosins generally move toward the plus end of the actin filaments, and a plant specific isoform, myosin XI plays an important role in **tip growth** of pollen tubes and root hairs (see Chapter 2). Kinesins can move along microtubules in both directions, and can bind to chromatin or to other microtubules to help organize the spindle apparatus during mitosis (see Section 1.9).

All of the motors we have discussed have separate head, neck, and tail domains (shown with myosin XI in **Figure 1.34**). The globular head domain binds to the cytoskeleton reversibly, depending on the phosphorylation state of the nucleotide in the domain's ATPase active site. The neck region changes angle upon hydrolysis of ATP, flexing the head relative to the tail. The tail domain usually contains regions for dimerization, and the end of the globular tail domain binds to specific organelles or "cargo" and is called the *cargo domain* (see Figure 1.34B). In order for a motor to move an organelle, the motor dimerizes; the two molecules interact and bind to the organelle at the cargo domain. The two

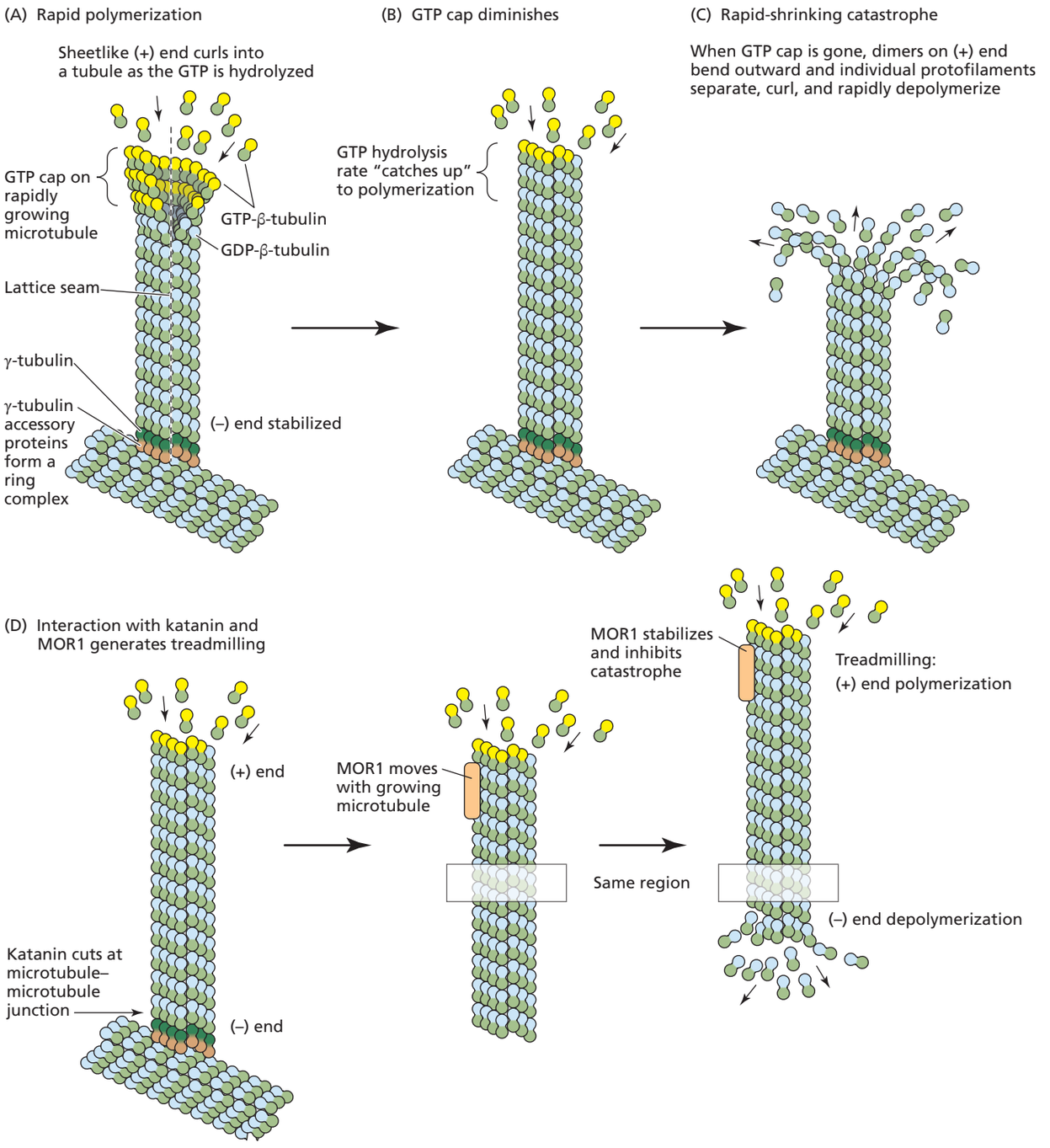


Figure 1.33 Models for microtubule dynamic instability and treadmilling. **(A)** The minus ends of microtubules at new initiation sites can be stabilized by γ-tubulin ring complexes, some of which are found along the sides of previously existing microtubules. Microtubule plus ends grow rapidly, producing a "cap" of tubulin that has GTP bound to the β subunit. The newly added cap has a sheetlike structure that curls into a tubule as the GTP is hydrolyzed. **(B)** As the rate of growth slows or GTP hydrolysis increases, the GTP cap is diminished. **(C)** When the GTP cap is gone, the microtubule protofilaments peel apart because the heterodimer with GDP bound to the β subunit of tubulin is slightly curved. The protofilaments are unstable, and rapid, catastrophic depolymerization ensues. **(D)** If the microtubule is severed at a branch point by the ATPase katanin, the minus end becomes unstable and can depolymerize. If the microtubule is stabilized at the plus end by MOR1 (microtubule organizing 1 protein), a microtubule-associated protein, then the rate of addition on the plus end can match the depolymerization at the minus end and treadmilling ensues.

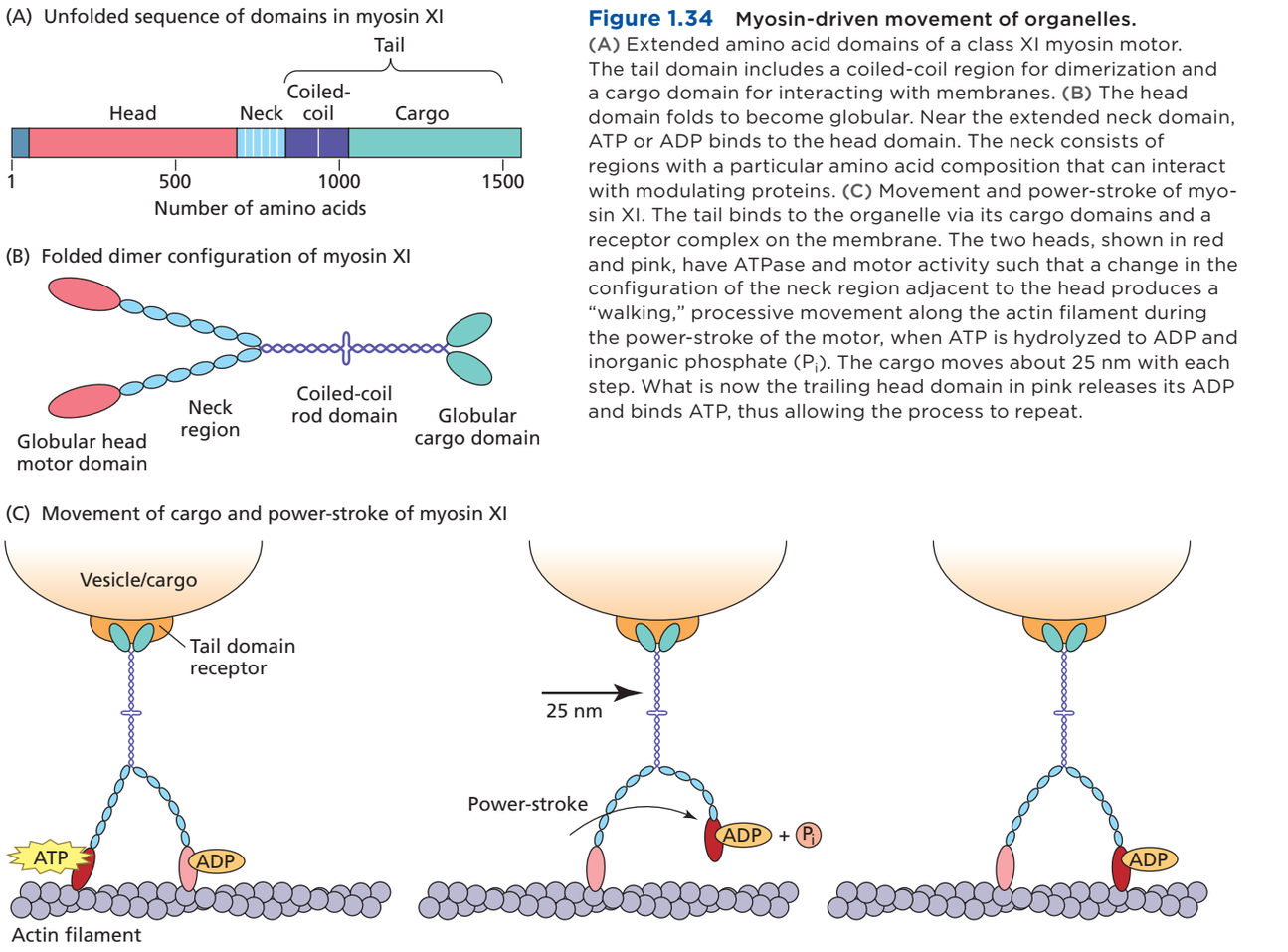


Figure 1.34 **Myosin-driven movement of organelles.** **(A)** Extended amino acid domains of a class XI myosin motor. The tail domain includes a coiled-coil region for dimerization and a cargo domain for interacting with membranes. **(B)** The head domain folds to become globular. Near the extended neck domain, ATP or ADP binds to the head domain. The neck consists of regions with a particular amino acid composition that can interact with modulating proteins. **(C)** Movement and power-stroke of myosin XI. The tail binds to the organelle via its cargo domains and a receptor complex on the membrane. The two heads, shown in red and pink, have ATPase and motor activity such that a change in the configuration of the neck region adjacent to the head produces a "walking," processive movement along the actin filament during the power-stroke of the motor, when ATP is hydrolyzed to ADP and inorganic phosphate (P_i). The cargo moves about 25 nm with each step. What is now the trailing head domain in pink releases its ADP and binds ATP, thus allowing the process to repeat.

heads of the dimer then alternately bind to the cytoskeleton and "walk" forward while the neck flexes as ATP is hydrolyzed (see Figure 1.34C). In this way, the organelle is moved along the cytoskeleton.

The actin cytoskeleton interacts with the membrane of many organelles. Recent studies have identified actin-binding proteins that anchor the ER membrane with the actin cytoskeleton and are necessary for the streaming of this organelle.

1.9 Cell Cycle Regulation

The cell division cycle, or cell cycle, is the process by which cells reproduce themselves and their genetic material, the nuclear DNA (**Figure 1.35**). The cell cycle consists of four phases: **gap 1** (**G_1**), **DNA synthesis phase** (**S**, or **S phase**), **gap 2** (**G_2**), and **mitotic phase** (**M**, or **M phase**). G_1 is the phase of variable duration when a newly formed daughter cell has not yet replicated its DNA. DNA is replicated during S phase. G_2 is the phase when a cell with replicated DNA has not yet proceeded to mitosis, which occurs during M phase. Collectively, G_1, S phase, and G_2 are referred to as **interphase**. M phase includes all the stages of mitosis, from metaphase to telophase (discussed shortly). In vacuolated cells, the vacuole enlarges throughout interphase, and the plane of cell division bisects the vacuole during mitosis (see Figure 1.35). Organelles distribute stochastically into future daughter cells.

Each phase of the cell cycle has a specific set of biochemical and cellular activities

Nuclear DNA is prepared for replication in G_1 by the assembly of a prereplication complex at the origins of replication along the chromatin. DNA is replicated during S phase, and G_2 cells prepare for mitosis.

The whole architecture of the cell is altered as it enters mitosis. If the cell has a large central vacuole, this vacuole must first be divided in two by a coalescence of cytoplasmic transvacuolar strands that contain the nucleus; this becomes the region where nuclear division will occur. Golgi stacks and other organelles partition themselves between the two halves of the cell. As you

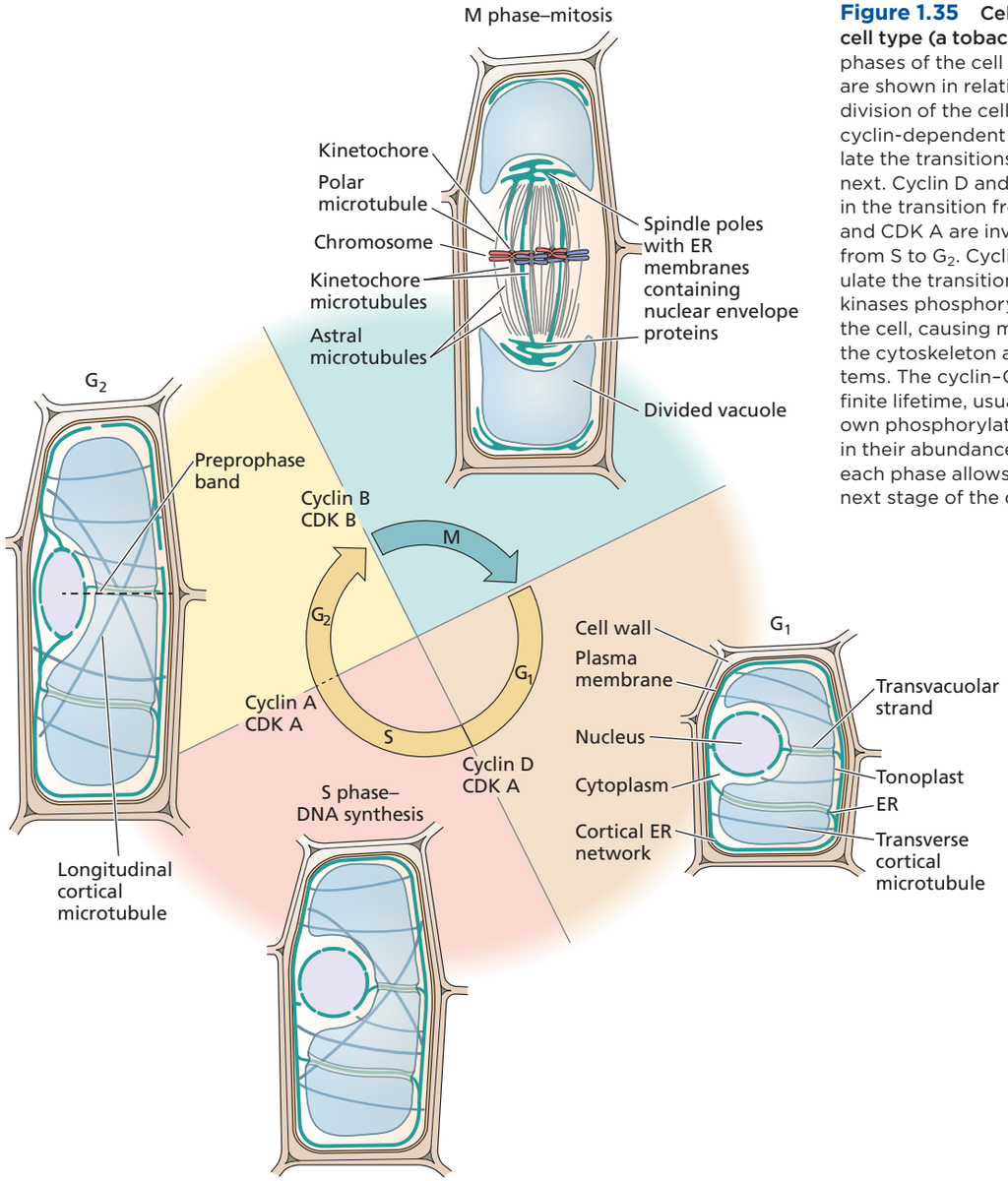
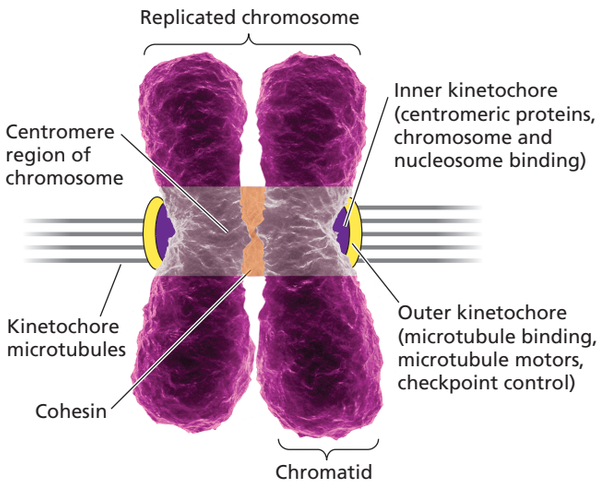


Figure 1.35 Cell cycle in a vacuolated cell type (a tobacco cell). The four phases of the cell cycle, G_1, S, G_2, and M, are shown in relation to elongation and division of the cell. Various cyclins and cyclin-dependent kinases (CDKs) regulate the transitions from one phase to the next. Cyclin D and CDK A are involved in the transition from G_1 to S. Cyclin A and CDK A are involved in the transition from S to G_2. Cyclin B and CDK B regulate the transition from G_2 to M. The kinases phosphorylate other proteins in the cell, causing major reorganization of the cytoskeleton and the membrane systems. The cyclin–CDK complexes have a finite lifetime, usually regulated by their own phosphorylation state; the decrease in their abundance toward the end of each phase allows progression to the next stage of the cell cycle.

will soon see, the endomembrane system and cytoskeleton are extensively rearranged.

As a cell enters mitosis, the chromosomes change from their interphase state of organization within the nucleus and begin to condense to form the metaphase chromosomes (**Figure 1.36**). The metaphase chromosomes are held together by special proteins called *cohesins*, which reside in the centromeric region of each chromosome pair. In order for the chromosomes to separate, these proteins must be cleaved by the enzyme *separase*. This occurs when the kinetochore attaches to spindle microtubules (described later in this section).

At a key regulatory point, or **checkpoint**, late in G_1 of the cell cycle, the cell becomes committed to the initiation of DNA synthesis. In mammalian cells, DNA replication and mitosis are linked—the cell division cycle, once begun, is not interrupted until all phases of mitosis have been completed. In contrast, plant cells can leave the cell division cycle either before or after replicating their DNA (i.e., during G_1 or G_2). Consequently, whereas most animal cells are diploid (having two sets of chromosomes), plant cells are frequently tetraploid (having four sets of chromosomes) or sometimes even polyploid (having many sets of chromosomes) after going through



© Sebastian Kaulitzki/Shutterstock

Figure 1.36 **Structure of a metaphase chromosome.** The centromeric DNA is highlighted, and the region where cohesion molecules bind the two chromosomes together is shown in orange. The kinetochore is a layered structure (the inner layer is shown in purple, the outer layer in yellow) that contains microtubule-associated proteins, including kinesins that help depolymerize the microtubules during shortening of kinetochore microtubules in anaphase.

additional cycles of nuclear DNA replication without mitosis, a process called **endoreduplication**.

The cell cycle is regulated by cyclins and cyclin-dependent kinases

The biochemical reactions governing the cell cycle are evolutionarily highly conserved in eukaryotes, and plants have retained the basic components of this mechanism. Progression through the cycle is regulated mainly at three checkpoints: during late G_1 (as just mentioned), late S phase, and at the G_2–M boundary.

The key enzymes that control the transitions between the different phases of the cell cycle, and the entry of nondividing cells into the cell cycle, are the **cyclin-dependent kinases**, or **CDKs**. Protein kinases are enzymes that phosphorylate proteins using ATP. Most multicellular eukaryotes have several protein kinases that are active in different phases of the cell cycle. All CDKs depend on regulatory subunits called **cyclins** for their activities. Specific cyclins increase in abundance at each cell cycle stage and are degraded before the transition to the next phase. Several classes of cyclins have been identified in plants, animals, and yeast. Three cyclins have been shown to regulate the tobacco cell cycle, as shown in Figure 1.35:

1. G_1/S cyclins, cyclin D, active late in G_1
2. S-type cyclins, cyclin A, active in late S phase
3. M-type cyclins, cyclin B, active just before M phase

The critical checkpoint late in G_1 that commits the cell to another round of DNA replication is regulated primarily by the D-type cyclins and CDKs. D-type cyclin expression is dependent on sugar availability (i.e., enough energy) and the presence of cytokinin (see Chapter 4).

Mitosis and cytokinesis involve both microtubules and the endomembrane system

Mitosis is the process by which previously replicated chromosomes are aligned, separated, and distributed in an orderly fashion to daughter cells (**Figure 1.37**). Microtubule reorganizations are an integral part of mitosis and cytokinesis. The period immediately prior to prophase is called **preprophase**. During preprophase, the G_2 microtubules are completely reorganized into a **preprophase band** of cortical microtubules (with a small number of microfilaments) around the nucleus at the site of the future cell plate—the precursor of the cross-wall. The position of the preprophase band, the underlying *cortical division site*, and the partition of cytoplasm that divides the central vacuoles determine the plane of cell division in plants, and thus play a crucial role in development.

At the start of **prophase**, the microtubules of the preprophase band start to depolymerize, and new microtubules polymerizing on the surface of the nuclear envelope begin to gather at two foci on opposite sides of the nucleus, initiating spindle formation. Although not associated with the centrosomes (which plants, unlike animal cells, lack), these foci serve the same function in organizing microtubules. During prophase, the nuclear envelope remains intact, but it breaks down as the cell enters **metaphase** in a process that involves reorganization and reassimilation of the nuclear envelope into the ER. Throughout the division cycle, cell division kinases (not to be confused with CDKs) interact with microtubules to help reorganize the spindle by phosphorylating microtubule-associated proteins and kinesins. The nucleolus completely disappears during mitosis and gradually reassembles after mitosis, as the chromosomes decondense and reestablish their positions in the daughter nuclei.

In early metaphase, the preprophase band fully disappears and new microtubules polymerize, completing the **mitotic spindle**. The mitotic spindles of plant cells are more boxlike in shape than those in animal cells. The spindle microtubules in a plant cell arise from a diffuse zone consisting of multiple microtubule organizing centers at opposite ends of the cell and extend toward the middle in nearly parallel arrays.

The **centromere**, the region where the two chromatids are attached near the center of the chromosome, contains repetitive DNA, as does the **telomere**, which forms the chromosome ends that protect the chromosome from degradation. Some of the spindle microtubules bind to the chromosome in the special region of the centromere called

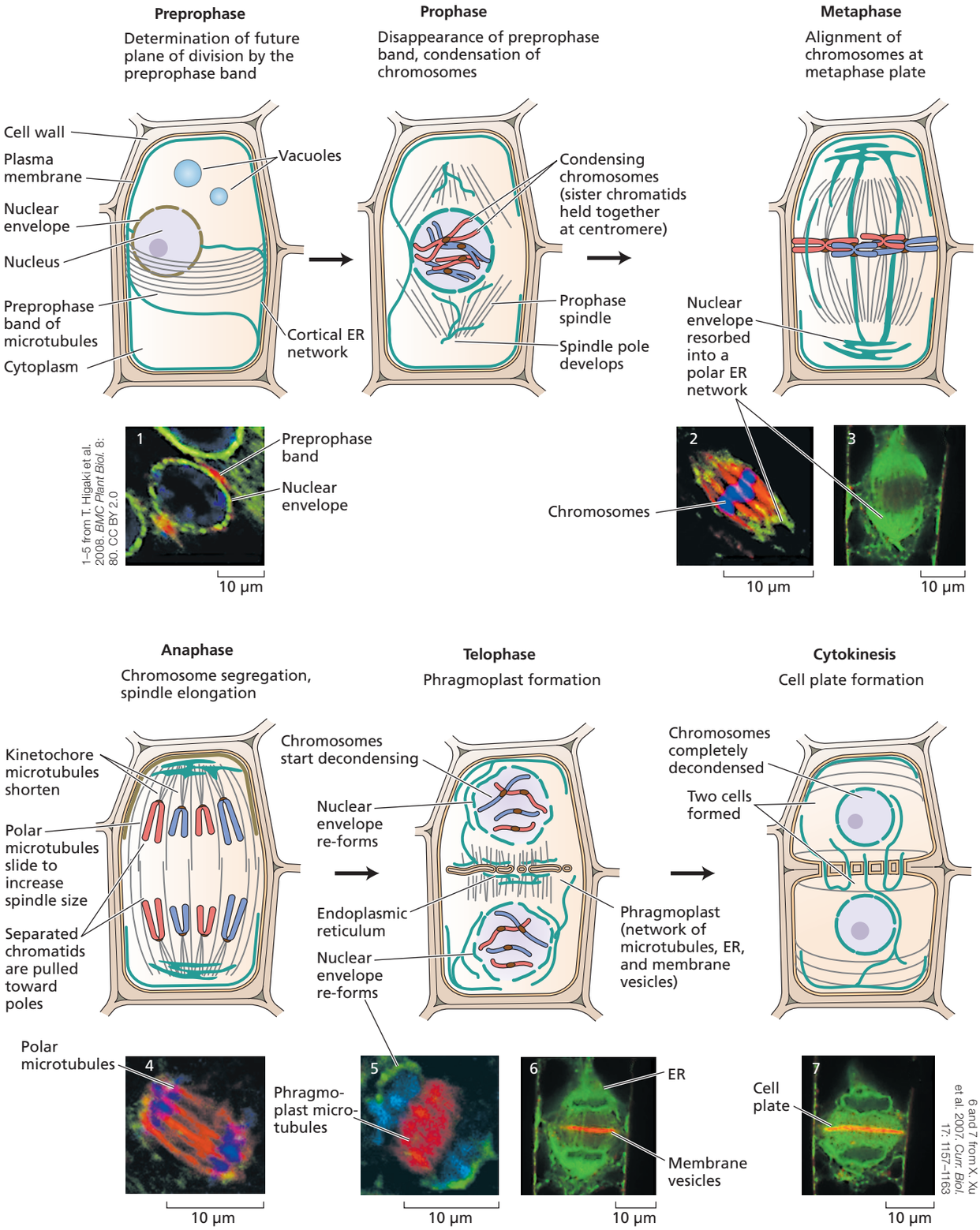


Figure 1.37 Changes in cellular organization that accompany mitosis in a meristematic (nonvacuolated) plant cell.

the **kinetochore**, and the condensed chromosomes align at the metaphase plate (see Figures 1.36 and 1.37). Some of the unattached microtubules overlap with microtubules from the opposite polar region in the spindle midzone.

The mechanism of chromosome separation during **anaphase** has two components. In early anaphase, the sister chromatids separate and begin to move toward their poles by regulated microtubule depolymerization. In late anaphase, the polar microtubules slide relative to each other and elongate, pushing the spindle poles farther apart. At the same time, the sister chromosomes are pushed to their respective poles. In plants, the spindle microtubules are apparently not anchored to the cell cortex at the poles, and so the chromosomes cannot be pulled apart. Instead, they are probably pushed apart by kinesins in the overlapping polar microtubules of the spindle.

At **telophase**, a new network of microtubules, F-actin, and ER called the **phragmoplast** appears. The phragmoplast organizes the region of the cytoplasm where cytokinesis takes place. The microtubules have now lost their spindle shape but retain polarity, with their minus ends still pointed toward the separated, now decondensing, chromosomes, where the nuclear envelope is in the process of re-forming. The plus ends of the microtubules point toward the midzone of the phragmoplast, where small vesicles produced by in the Golgi apparatus and *trans* Golgi network accumulate. Some content of theses vesicles is also recycled from endocytosed parental cell plasma membranes. These vesicles have long tethers formed by the exocyst (see Section 1.6) and may aid in the formation of the cell plate in the next cell cycle stage: cytokinesis.

Cytokinesis is the process that establishes the **cell plate**, a precursor of the cross-wall that will separate the two daughter cells. This cell plate, with its enclosing plasma membrane, is initiated by a large cluster of vesicles that fuse as an island in the center of the cell and then grows by additional vesicle fusion and expansion outward toward the parental wall. The site at which the forming cell plate fuses with the parental plasma membrane is determined by the previous location of the preprophase band (which disappeared earlier). Specific proteins recruited by preprophase band microtubules remain as landmarks within the cortical division zone after disassembly of the preprophase band. As the cell plate assembles, it traps ER tubules in plasmalemma-lined membrane channels spanning the plate, thus connecting the two daughter cells (**Figure 1.38**). These cell plate–spanning ER tubules establish the sites for the primary plasmodesmata (see Figure 1.4). After cytokinesis, microtubules re-form in the cell cortex. The new cortical microtubules have a transverse orientation relative to the future elongation axis of the cell, and this orientation determines the polarity of future cell extension.

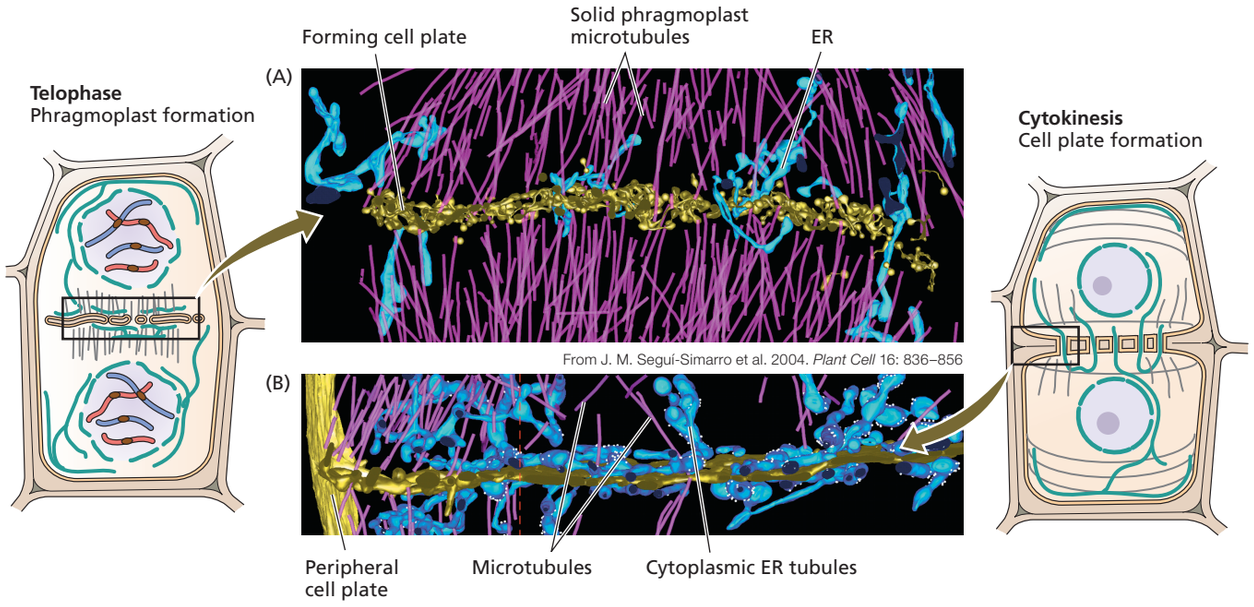


Figure 1.38 Changes in the organization of the phragmoplast and ER during cell plate formation. **(A)** The forming cell plate (yellow, seen from the side) in early telophase has only a few sites where it interacts with the ER (blue). The solid phragmoplast microtubules (purple) also have few ER cisternae among them. **(B)** Side view of the forming peripheral cell plate (yellow), showing that although many cytoplasmic ER tubules (blue) intermingle with microtubules (purple) in the peripheral growth zone, there is little direct contact between ER tubules and cell plate membranes. The small white dots are ER-bound ribosomes. (After J. M. Seguí-Simarro et al. 2004. *Plant Cell* 16: 836–856.)

Summary

- Despite their great diversity in form and size, all plants carry out similar physiological and biochemical processes. These processes depend entirely on structures that interact at every level of scale, from the molecular level to the anatomical level.

1.1 Plant Life Processes: Unifying Principles

- All land plants are sessile organisms and convert solar energy to chemical energy. They use growth instead of motility to obtain resources, and have vascular systems, rigid structures, and mechanisms to avoid desiccation on land. Plants develop from embryos sustained and protected by tissues from the mother plant.
- Plant classification is based on evolutionary relationships (**Figure 1.1**).
- Plant life cycles alternate between diploid and haploid generations (**Figure 1.2**).

1.2 Overview of Plant Structure

- All seed plants have the same basic vegetative body plan, consisting of stem, root, and leaves (**Figure 1.3**).
- Plant cells are surrounded by rigid yet dynamic cell walls that communicate with the cytoplasm (**Figure 1.4**).
- Primary cell walls are synthesized in actively growing cells, whereas secondary cell walls are deposited on the inner surface of the primary walls, after most cell expansion has ended (**Figure 1.4**).
- Because of rigid cell walls, plant development depends solely on patterns of cell division and directional cell enlargement.
- The cytoplasm of neighboring cells is connected by plasmodesmata, forming the symplasm, which allows not only water and small molecules but also proteins and RNAs to move between cells without crossing the plasma membrane (**Figure 1.4**).
- New cells are produced in meristems that produce new organs such as roots, stems, leaves, and after a transition from vegetative growth, flowers (**Figure 1.5**).
- Secondary growth results in the increase in girth of roots and shoots through the action of the specialized meristems, the vascular and cork cambium (**Figure 1.5**).

1.3 Plant Tissue Types

- Dermal tissue, ground tissue, and vascular tissue are the three major tissue systems present in all plant organs (**Figure 1.3**).
- Dermal tissue includes the epidermis, which has multiple cell types, including pavement cells, stomatal guard cells, and trichomes (**Figure 1.6**).
- Parenchyma, collenchyma, and sclerenchyma are types of ground tissue. Parenchyma cells have the capacity to continue division and can differentiate into a variety of other ground tissues and vascular tissues (**Figures 1.8, 1.9**).
- Vascular tissue has thickened secondary cell walls, perforated end walls, and pits that can develop into channels in the walls shared between adjacent cells (**Figures 1.10, 1.11**).

1.4 Plant Cell Compartments

- All plant cells contain cytoplasm, a nucleus, and subcellular organelles, all enclosed by the plasma membrane and cell wall (**Figure 1.12**).
- All plants begin with a similar complement of organelles that arise either semiautonomously or from the endomembrane system.
- The endomembrane system plays a central role in secretory processes, cell signaling, specialized metabolite production, membrane recycling, the cell cycle, and cell expansion (**Figure 1.12**).
- Plastids and mitochondria are semiautonomous, independently dividing organelles of endosymbiotic origin that are not derived from the endomembrane system.
- Biological membranes are composed of lipids and both integral and peripheral membrane proteins. Peripheral membrane proteins with covalently-linked, membrane embedded lipid moieties are called anchored proteins (**Figure 1.13**).
- The composition and fluid-mosaic structure of all plasma membranes permit regulation of transport into and out of the cell and between subcellular compartments (**Figure 1.13**).

1.5 The Nucleus

- The nucleus is the site of storage, replication, and transcription of the DNA in the chromatin, as well as the site for the synthesis of ribosomes and mRNA (**Figures 1.14–1.16**).
- The specialized membranes of the nuclear envelope are derived from and are continuous with the endoplasmic reticulum (ER), a component of the endomembrane system (**Figure 1.14**).
- Translation of mRNA into proteins occurs in the cytoplasm (**Figure 1.16**).
- Posttranslational regulation of gene expression involves mRNA and protein modification as well as turnover (**Figure 1.17**).

1.6 The Endomembrane System

- The ER is a network of membrane-bound tubules and cisternae that form a complex and dynamic structure that is to a large extent aligned with the F-actin cytoskeleton (**Figure 1.18**).

(*Continued*)

Summary (*continued*)

- The rough ER is involved in synthesis of proteins that enter the lumen of the ER; the smooth ER is the site of lipid biosynthesis (**Figure 1.19**).
- Secretion of proteins from cells begins at the rough ER (**Figure 1.19**).
- Glycoproteins destined for secretion are processed first in the ER and then in the Golgi apparatus (**Figures 1.20, 1.21**).
- Matrix polysaccharides are synthesized in the Golgi apparatus and delivered to the cell wall via the exocytosis of vesicles (**Figure 1.22**).
- Vacuoles serve multiple functions in plant cells; in addition to being involved in the uptake of water and solutes, they play a role in cell expansion and in the storage of secondary metabolites that function in plant defense (**Figure 1.23**).
- Oil bodies are derived from the ER and serve as a storage organelle for lipids known as triacylglycerols (**Figure 1.25**).
- Several types of plant peroxisomes are crucial organelles for detoxifying reactive oxygen species, degrading fatty acids, and other metabolic proceses. Glyoxysomes participate in mobilizing lipids during seed germination (**Figure 1.26**).

1.7 Independently Dividing Semiautonomous Organelles

- Mitochondria and plastids each have an inner and an outer membrane (**Figures 1.27, 1.28**).
- Chloroplasts have an internal thylakoid membrane system that contains photosynthetic proteins, chlorophylls and carotenoids, electron transport chains, and ATP synthases (**Figure 1.28**).
- Specialized plastids may contain high concentrations of pigments (chromoplasts) or starch (amyloplasts) (**Figure 1.29**).
- Proplastids in the meristem pass through distinct developmental stages to form specialized plastids (**Figure 1.30**).
- In plastids and mitochondria, fission and organellar DNA replication are regulated independently of nuclear division.

1.8 The Plant Cytoskeleton

- A three-dimensional network of polymerizing and depolymerizing filamentous proteins—tubulin in microtubules, and actin in microfilaments—organizes the cytoplasm and provides a structural framework for endomembrane interactions compartments (**Figures 1.31, 1.32**).
- Microtubules show dynamic instability, but can stabilize and treadmill through the cell with accessory proteins (**Figure 1.33**).
- Molecular motors reversibly bind the cytoskeleton and direct organelle movement (**Figure 1.34**).
- During cytoplasmic streaming, bulk flow of the cytoplasm is driven by the viscous drag in the wake of myosin motor-driven organelles moving along F-actin.

1.9 Cell Cycle Regulation

- The cell cycle, during which cells replicate their DNA and reproduce themselves, consists of four phases (**Figure 1.35**).
- Cyclins and cyclin-dependent kinases (CDKs) regulate the cell cycle, including the separation of paired metaphase chromosomes (**Figures 1.35, 1.36**).
- Successful mitosis (**Figure 1.37**) and cytokinesis (**Figure 1.38**) require the coordinated participation of microtubules and the endomembrane system.

Web Material

- **WEB TOPIC 1.1 Model Organisms** Certain plant species are used extensively in the lab to study their physiology.
- **WEB TOPIC 1.2 Plant Identification, Classification, and Evolutionary Thought** Our organization of how plants are identified started from utilitarian motives but now relies on evolutionary relationships.
- **WEB TOPIC 1.3 The Nuclear Pore and Proteins Involved in Nuclear Import and Export** The nuclear pore is believed to be lined by a meshwork of unstructured nucleoporin proteins and GTP-charged proteins that mediate transfer into and out of the nucleoplasm.
- **WEB TOPIC 1.4 Protein Signals Used to Sort Proteins to Their Destinations** The primary sequence of a protein can include a ticket to its final destination.
- **WEB TOPIC 1.5 Unfolded Protein Response: Quality Control in the ER** Proteins that are misfolded are tagged and sorted for degradation in the lumen of the ER.
- **WEB TOPIC 1.6 SNAREs, Rabs, and Coat Proteins Mediate Vesicle Formation, Fission, and Fusion** Models are presented for the mechanisms of vesicle fission and fusion.

For more study aids, go to oup.com/he/taiz7e.

Suggested Reading

Albersheim, P., Darvill, A., Roberts, K., Sederoff, R., and Staehelin, A. (2011) *Plant Cell Walls: From Chemistry to Biology*. Garland Science, Taylor and Francis Group, New York.

Bell, K., and Oparka, K. (2011) Imaging plasmodesmata. *Protoplasma* 248: 9–25.

Burch-Smith, T. M., Stonebloom, S., Xu, M., and Zambryski, P. C. (2011) Plasmodesmata during development: Re-examination of the importance of primary, secondary, and branched plasmodesmata structure versus function. *Protoplasma* 248: 61–74.

Burgess, J. (1985) *An Introduction to Plant Cell Development*. Cambridge University Press, Cambridge.

Carrie, C., Murcha, M. W., Giraud, E., Ng, S., Zhang, M. F., Narsai, R., and Whelan, J. (2013) How do plants make mitochondria? *Planta* 237: 429–439.

Chapman, K. D., Dyer, J. M., and Mullen, R. T. (2012) Biogenesis and functions of lipid droplets in plants: Thematic Review Series: Lipid droplet synthesis and metabolism: from yeast to man. *J. Lipid Res*. 53: 215–226.

Griffing, L. R. (2010) Networking in the endoplasmic reticulum. *Biochem. Soc. Trans.* 38: 747–753.

Gunning, B. E. S. (2009) *Plant Cell Biology on DVD*. Springer, New York, Heidelberg.

Henty-Ridilla, J. L., Li, J., Blanchoin, L., and Staiger, C. J. (2013) Actin dynamics in the cortical array of plant cells. *Curr. Opinion Plant Biol*. 16: 678–687.

Hu, J., Baker, A., Bartel, B., Linka, N., Mullen, R. T., Reumann, S., and Zolman, B. K. (2012) Plant peroxisomes: biogenesis and function. *Plant Cell* 24: 2279–2303.

Jones, R., Ougham, H., Thomas, H., and Waaland, S. (2013) *The Molecular Life of Plants*. Wiley-Blackwell, Oxford.

Joppa, L. N., Roberts, D. L., and Pimm, S. L. (2011) How many species of flowering plants are there? *Proc. R. Soc. B* 278: 554–559.

Leroux, O. (2012) Collenchyma: a versatile mechanical tissue with dynamic cell walls. *Ann. Bot*. 110: 1083–1098.

McMichael, C. M., and Bednarek, S.Y. (2013) Cytoskeletal and membrane dynamics during higher plant cytokinesis. *New Phytol*. 197: 1039–1057.

Müller, S., Wright, A. J., and Smith, L. G. (2009) Division plane control in plants: new players in the band. *Trends Cell Biol.* 19: 180–188.

Wasteneys, G. O., and Ambrose, J. C. (2009) Spatial organization of plant cortical microtubules: Close encounters of the 2D kind. *Trends Cell Biol*. 19: 62–71.

Williams, M. E. (2013) How to be a plant. Teaching tools in plant biology: Lecture notes. *Plant Cell* 25(7): tpc.113.tt0713.

2 Cell Walls: Structure, Formation, and Expansion



LAURA_VN/Shutterstock

Plant cells, unlike animal cells, are surrounded by a mechanically strong cell wall. This physical structure has arisen in many organisms as a result of independent evolutionary events. As a result of their discrete origins, the cell walls of prokaryotes, fungi, heterokonts (e.g., diatoms and brown algae), algae, and members of the plant kingdom differ from each other in chemical composition and molecular structure. However, they all share three common functions: regulation of cell volume, determination of cell shape, and mechanical protection of the delicate protoplast against biochemical and physical assaults.

Much of the carbon assimilated by photosynthesis in plants (see Chapter 10) is channeled into the polysaccharides that make up the cell wall. The wall, in its simplest conception, comprises a scaffold of cellulose fibrils embedded in a matrix of polysaccharides and proteins produced by the cell. The matrix components and cellulose fibrils assemble into a network linked by a mixture of covalent and noncovalent bonds. The function of the plant cell wall is intimately linked to its composition and structure, which we explore throughout this chapter.

Although our focus here is on the intrinsic organismal functions of the plant cell wall, it is important to note that cell walls also provide the raw material for many products important to humans and our society. Plant cell walls are the material basis of paper, textiles (such as cotton, flax, and linen), wood-based structural products, synthetic fibers, plastics, films, coatings, adhesives, gels, thickeners, and other engineered materials. Globally, aggregated cell walls, described as *cellulosic biomass*, are widely used for energy generation, heat, and fuel. As one of the most abundant reservoirs of organic carbon in nature and a major sink for photosynthetically captured carbon, the plant cell wall also plays an integral role in carbon flow through ecosystems.

We begin this chapter with a description of some general functions of plant cell walls, followed by an overview of their composition, biosynthesis, and assembly. We then turn to the role of the primary cell wall in cell expansion and cell shape, arguably its most essential physiological function. We end by examining how secondary cell walls are produced, via lignification, and their importance for the physiology of water transport and plant structure.

2.1 Overview of Plant Cell Wall Functions and Structures

It is impossible to know what plants would be like had cell walls not evolved in their ancestors; however, we do know that if we remove their cells walls through enzymatic digestion, we are left with vulnerable, spherical, membrane-bound protoplasts that have no organized supracellular structure or function. The cell wall is an essential part of any plant. Indeed, the cell wall is critical for many essential processes in plant growth, development, and physiology:

- Cells walls connecting adjacent cells prevent cell sliding, slippage, and motility. Cell adhesion is thus essential for tissue integrity and defense. The selective release of cell adhesion is equally important for growth, the development of intercellular air spaces for gas exchange, and cell separation during leaf abscission.
- As a mechanically strong layer encapsulating the cell, the wall acts as a cellular "exoskeleton" that controls cell shape and allows high turgor pressures to develop. Without a cell wall to resist the forces generated by turgor pressure, plant water relations would be profoundly different (see Chapter 3). Because of this, cell walls determine the mechanical strength of plant structures that allow plants to grow to great heights.
- Plant morphogenesis ultimately depends on the control of cell wall properties, because the physical enlargement of plant cells is limited principally by when and how the cell wall yields to the force of turgor.
- The cell wall acts as a diffusion barrier that limits the size and kinds of molecules that can reach the plasma membrane, both through sieving effects and through ionic and hydrophobic interactions. Fixed negative charges in the walls profoundly influence the distribution of ions and charged macromolecules.
- Numerous sensory proteins are partly anchored in the cell wall and form a bridge to the plasma membrane, providing a mechanism for sensing cell integrity.
- Cell walls present a major structural and chemical barrier to invasion and spread of pathogens, to entry and proliferation of parasites, and to tissue consumption by herbivores. Moreover, oligosaccharides released from the cell wall by the action of lytic enzymes from invading microbes act as important signaling molecules that elicit defense responses against pathogens.
- Transpirational water flow in the xylem requires a mechanically strong wall that resists collapse in response to the negative pressure in the xylem. Defects in cell wall formation often result in xylem collapse.

The functional diversity and varying roles of the cell wall require diverse cell wall compositions and structures. We begin this section with a brief description of the morphology and basic architecture of plant cell walls. Then we discuss the organization, composition, and synthesis of the wall in some of its diverse forms.

Plant cell walls vary in structure and function

In 1665, Robert Hooke published *Micrographia*, a book detailing early microscopy of biological materials. His observations of sectioned bark from cork oak (*Quercus suber*) led him to coin the term *cell* for the discrete, microscopic units making up that sample. But what Hooke actually described were the cell walls! Cell walls are the most obvious visual objects that can be viewed in stained sections of plant organs and can vary greatly in appearance and composition in different cell types (**Figure 2.1**). For example, the cell walls of parenchyma in the pith and cortex are generally thin (~100 nm) and have few distinguishing features. In contrast, epidermal cells, collenchyma, xylem vessels and tracheids, phloem fibers, and other forms of sclerenchyma cells have thicker walls (~1,000 nm or more, often multilayered). These

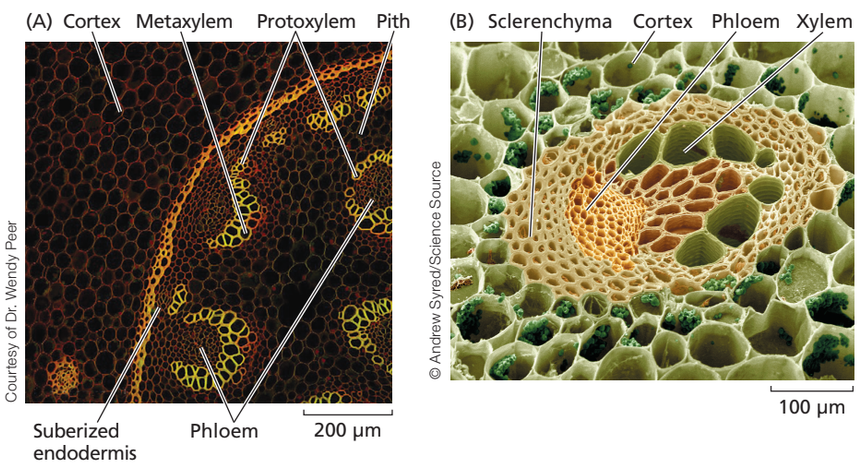


Figure 2.1 Cross-sectional morphology of plant organs showing variation in cell shape, size, and cell wall structure. (A) Cross section of a root of a club moss (*Lycopodium* sp.), showing cells with varying shape and wall morphology in different tissue types. Stained transverse section, light microscopy. (B) Cross section of a vascular bundle in the stem of a buttercup (*Ranunculus repens*), showing cells with varying wall morphology in different tissue types (see labels). Note the highly thickened walls of the sclerenchyma fiber cells and the pitted walls of the xylem vessels. False-colored scanning electron micrograph.

walls may be intricately sculpted and impregnated with substances such as lignin, cutin, suberin, waxes, silicate polymers, or structural proteins, which alter the wall's chemical and physical properties.

The walls on the different sides of a cell may vary in thickness, in the amount and type of impregnating substances, and in the frequency of pitting and plasmodesmata—tiny membrane-lined channels that allow passive transport of small molecules and active transport of proteins and nucleic acids between the cytoplasm of adjacent cells (see Figure 1.4). For example, the outer wall of the epidermis lacks plasmodesmata, is thicker than the other walls of the cell, and is coated externally with cutin and waxes. In some grasses, the epidermal wall may also contain a layer of polymerized silicate. In stomatal guard cells, the wall adjacent to the stomatal pore is much thicker than the walls on the other sides of the cell. Such variations in wall structure and composition within a single cell reflect the cell's polarity and differentiated functions. These variations generally arise from targeted secretion of wall components to the cell surface.

Despite this morphological diversity, cell walls are generally described in terms of three layers: the primary wall, the middle lamella, and secondary wall. As described in Chapter 1, the **cell plate** formed during plant cell division is rich in acidic polysaccharides (pectins). In postmitotic cell walls, this area becomes the pectin-enriched **middle lamella** (**Figure 2.2**). This layer often contains hydroxyproline-rich glycoproteins (HRGPs) and serves as a flexible adhesive layer between cells or as the site of cellular abscission during senescence (see Chapter 22). Shortly after cell plate formation, cellulose and other components are deposited during growth, forming the **primary wall**. Primary cell walls usually are thin and architecturally simple (**Figures 2.3A and 2.4A**), but some primary walls may be thick and multilayered, such as those found in collenchyma or in the epidermis (**Figure 2.3B and C**). **Secondary walls** are formed after cell enlargement stops and thus are usually

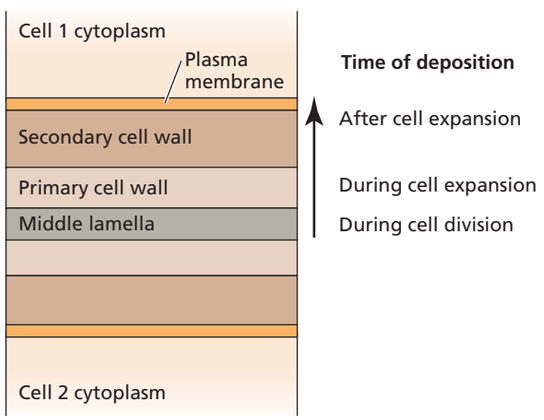


Figure 2.2 The three layers of cell walls, aligned with their time of deposition during the origin, growth, and differentiation of a cell. The middle lamella is pectin-rich and is the first layer deposited during cell plate formation in early cell division. The cell then begins to add cellulose and hemicelluloses, forming the primary cell wall. Once cell expansion has ceased, the secondary cell wall is produced.

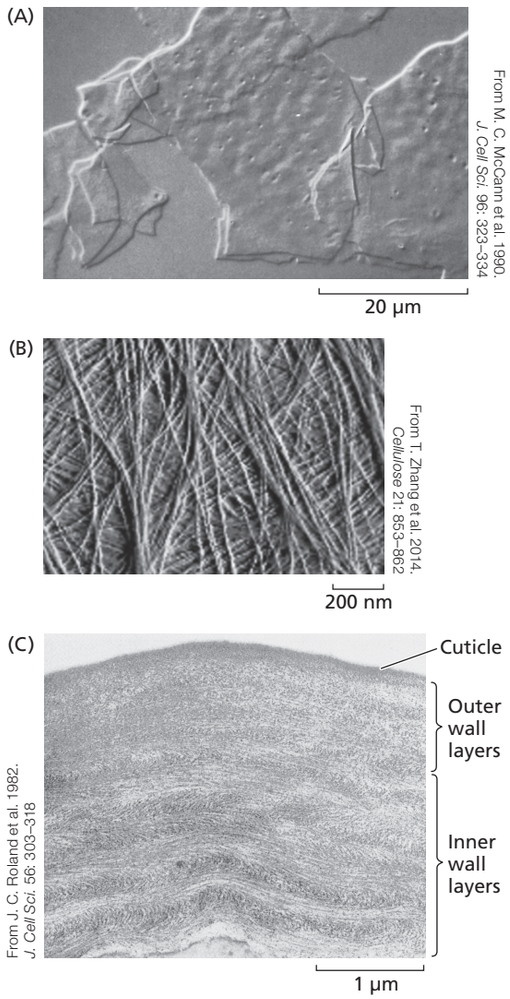


Figure 2.3 Three views of primary cell walls. **(A)** This surface view of cell wall fragments from onion parenchyma was taken with a light microscope using Nomarski optics. Note that at this scale the wall looks like a very thin sheet with small surface depressions; these depressions may be pit fields, places where plasmodesmatal connections between cells are concentrated. **(B)** The inner surface of an unextracted, never-dried wall of onion scale epidermis, imaged underwater by atomic force microscopy. Note the fibrous texture of the wall and the presence of multiple lamellae with fibrils in different orientations. The narrowest fibrils are approximately 3 nm in diameter. They aggregate to form larger bundles. **(C)** Electron micrograph of the outer epidermal cell wall (cross section) from the growing region of a bean hypocotyl. Multiple layers are visible within the wall. The inner layers are thicker and more defined than the outer layers, because the outer layers are the older regions of the wall and have been stretched and thinned by cell expansion.

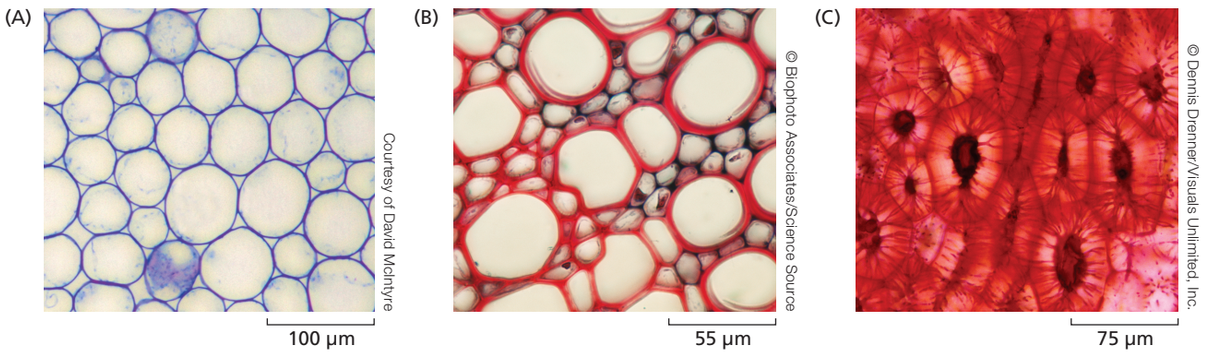


Figure 2.4 Diversity of cell wall structure. The thin walls of buttercup (*Ranunculus occidentalis*) stem parenchyma **(A)** contrast with the thickened secondary cell walls of tracheids in a vascular bundle of a sunflower (*Helianthus* sp.) stem **(B)** and sclereids from a cherry pit (*Prunus* sp.) **(C)**.

the youngest cell wall components. They are deposited between the plasma membrane and the primary cell wall. Secondary walls may be highly specialized in structure and composition, reflecting the differentiated state of the cell (**Figure 2.4B and C**). In the water-conducting tissue (xylem), fiber cells, tracheids, and vessels are notable for possessing thickened, multilayered secondary walls that are strengthened and waterproofed by **lignin** (discussed later in this and other sections). However, not all secondary walls are lignified or thickened. **Pits** and **pit fields** are thin areas of primary cell wall populated with plasmodesmata where there is no secondary wall (see Chapter 6).

Components differ for primary and secondary cell walls

Cell walls contain several types of polysaccharides that are named after the principal sugars they contain (**Figure 2.5** and **WEB TOPIC 2.1**). For example, a **glucan** is a polymer of glucose units linked end to end, a **galactan** is a polymer of galactose, a **xylan** is a polymer of xylose, a **mannan** is a polymer of mannose, and so on. **Glycan** is

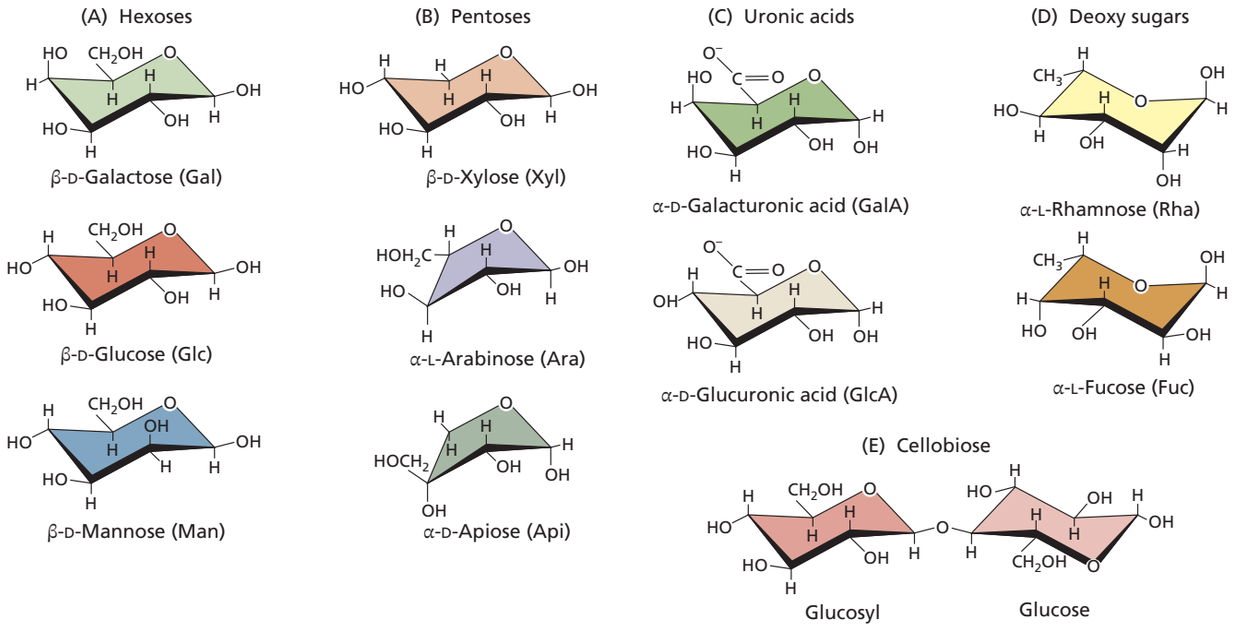


Figure 2.5 Conformational structures of sugars commonly found in plant cell walls. **(A)** Hexoses (six-carbon sugars). **(B)** Pentoses (five-carbon sugars). **(C)** Uronic acids (acidic sugars). **(D)** Deoxy sugars. **(E)** Cellobiose, showing the (1,4)-β-D-linkage between two glucose residues in inverted orientation. All sugars are shown in their pyranose (six-membered ring) forms except arabinose and apiose, which are shown in the furanose (five-membered ring) form.

the general term for a polymer made up of sugars and is synonymous with polysaccharide.

Polysaccharides may be linear unbranched chains of sugar residues (units), or they may contain side branches attached to the backbone. For branched polysaccharides, the backbone of the polysaccharide is usually indicated by the last part of the name. For example, **xyloglucan** has a glucan backbone (a linear chain of glucose residues) with xylose sugars attached as side chains. **Arabinoxylan** has a xylan backbone (a chain of xylose residues) with arabinose side chains. The names can get lengthy. For example, **glucuronoarabinoxylan** (**GAX**) is an arabinoxylan decorated with a low frequency of glucuronic acid units. However, a compound name does not necessarily imply a branched structure. For example, rhamnogalacturonan I is the name given to a polymer containing both rhamnose and galacturonic acid in its backbone (it also has galactan and arabinan side chains that are not included in the name). Thus, the name is based on the major sugars in the polymer but does not indicate its structural details.

Table 2.1 Structural components of plant cell walls

Class	Examples
Cellulose	Microfibrils of (1,4)-β-D-glucan
Pectins	Homogalacturonan
	Rhamnogalacturonan I with arabinan, galactan, and arabinogalactan side chains
	Rhamnogalacturonan II
Hemicelluloses	Xyloglucan
	Glucuronarabinoxylan variants include glucuronoxylan and arabinoxylan
	Glucomannan
	Mixed linkage (1,3;1,4)-β-D-glucan
Nonenzymic proteins	(See Table 2.2)
Lignin	(See Figure 2.22)

The specific linkages between sugar rings, including the specific carbons that are linked together and the configuration of the linkage (see **WEB TOPIC 2.1**), are important for the properties of the polysaccharide. For instance, cellulose is a glucan made of β(1,4)-linked glucose, while callose is made of β(1,3)-linked glucose; both are glucans, but they have very different functions and mechanical properties.

Cell wall polysaccharides are classified into three groups. **Cellulose** is the major fibrillar component of the cell wall and is composed of an array of β(1,4)-linked glucans coalesced to form a microfibril with well-ordered and less-ordered regions. It is insoluble in water and has high tensile strength (see Section 2.2). **Pectin** is the name for a complex and diverse group of hydrophilic, gel-forming polysaccharides rich in acidic sugar residues. The third group of wall polysaccharides are collectively called **hemicelluloses**. Chemically hemicelluloses have been defined as polysaccharides with β(1,4)-linked backbones linked in an equatorial configuration (meaning the link between residues is in line with the plane of the ring). Pectins and hemicelluloses are also called **matrix polysaccharides** because they help form the matrix within which cellulose is embedded.

The composition of the matrix polysaccharides varies by plant species, cell type, and region of the cell wall (**Table 2.1**). Typical primary cell walls of eudicots are rich in pectins, with smaller amounts of cellulose and hemicelluloses, whereas secondary cell walls are high in cellulose and a different form of hemicellulose, with varying amounts of lignin (described in Section 2.4), a polymer of units derived from phenylpropanoid metabolism. As a result of their high pectin content, primary walls have a relatively high water content, which is important for maintaining the ability of the wall to expand during cell enlargement. In contrast, the cellulose–hemicellulose–lignin structure of secondary cell walls is densely packed and contains less water—a structure well designed for strength and compression resistance.

The cell wall matrix also contains proteins. Some of these proteins can catalyze biochemical changes to wall structure. In primary cell walls, 2 to 10% of the dry mass consists of **nonenzymatic proteins** whose exact functions are uncertain. These proteins may be localized in the walls of specific cell types or may be more widespread (**Table 2.2**). They are usually identified by short motifs or repeating sequences of amino acids or a high degree of glycosylation. A variety of functions have been suggested for these proteins, including consolidation of the cell plate following cell division and strengthening of the walls in growing root hairs. Primary cell walls also contain **arabinogalactan proteins** (**AGPs**), which usually amount to less than 1% of the dry mass of the wall. These water-soluble proteins are heavily glycosylated (**Figure 2.6**). More than 90% of the mass of AGPs may be sugar residues—primarily galactose and arabinose (see Figure 2.5). Multiple AGP forms are found in plant tissues, either in the wall or associated with the external face of the plasma membrane (via a glycosylphosphatidylinisitol anchor), and they display tissue- and cell-specific expression patterns. AGPs may function in cell adhesion and in cell signaling during cell differentiation.

By dry mass, primary cell walls typically contain approximately 40% pectin, 25% cellulose, and 20% hemicellulose, with perhaps 5% protein and the remaining percentage composed of diverse other materials. However,

Table 2.2 Nonenzymatic proteins of the cell wall

Class of cell wall protein	Percentage carbohydrate	Notable tissue localization
HRGP (hydroxyproline-rich glycoprotein)	~55	Cambium, vascular parenchyma
PRP (proline-rich protein)	0–20	Xylem, fibers, cortex, root hairs
GRP (glycine-rich protein)	0	Primary xylem and phloem
AGP (arabinogalactan protein)	up to 90	Varied cell-specific expression

large deviations from these typical values may be found across plant organs and species. For example, the walls of grass coleoptiles consist of 60 to 70% hemicellulose, 20 to 25% cellulose, and only about 10% pectin. Cereal endosperm walls may contain as little as 2% cellulose, with hemicellulose making up most of the wall. Parenchyma cell walls of celery and sugar beets contain mostly cellulose and pectin, with as little as 4% hemicellulose. The wall at the tip of pollen tubes appears to be mostly pectin, with small amounts of cellulose to reinforce the tip structure. Wall compositions and polysaccharide structures can also change throughout development as a result of altered patterns of synthesis and the action of enzymes in the wall that can trim side chains or digest pectins and hemicelluloses.

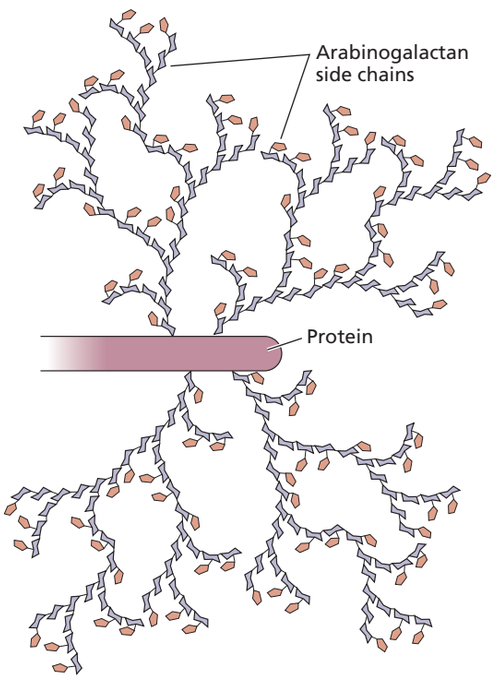


Figure 2.6 **Arabinogalactan protein molecule showing the highly branched arabinogalactan side chains attached to the protein backbone.** AGPs have a wide diversity of structures. (After N. C. Carpita and M. C. McCann. 2000. In *Biochemistry and Molecular Biology of Plants*, B. B. Buchanan et al. [eds.], American Society of Plant Biologists, Rockville, MD.)

Cellulose microfibrils have an ordered structure and are synthesized at the plasma membrane

Cellulose is the most abundant polysaccharide on earth. Its function in plants and utility for humans is based on its packaging into microfibrils. The simplest **cellulose microfibrils** are narrow structures, approximately 3 nm wide, that strengthen the cell wall, sometimes reinforcing more in one direction than in another, depending on how the microfibrils are deposited in the wall (i.e., they give structural bias; see Figure 2.3B). Each microfibril comprises an estimated 18 to 24 (usually 18) parallel chains of (1,4)-linked β-D-glucose tightly packed together to form a highly ordered (crystalline) core with extensive hydrogen bonding within and between glucan chains (**Figure 2.7**). The chains surrounding the core are more flexible, and their positions are influenced by interactions with water and matrix polysaccharides at the surface. Moreover, there is evidence of periodic disorder along the microfibril—that is, short segments where crystalline order is interrupted at intervals of 150 to 300 nm. These areas of disorder are thought to represent sites where pectins or hemicelluloses are woven into the cellulose microfibril.

Native cellulose in plants is found in two variant crystalline forms, called allomorphs Iα and Iβ, which differ slightly in the way the parallel glucan chains are packed. Cellulose Iβ is the dominant allomorph in land plants. The biological significance of these two crystalline forms is unclear at present. Microfibrils have hydrophilic surfaces, populated by polar—OH groups extending from the sides of stacked glucose chains, and hydrophobic surfaces, populated by nonpolar C—H groups populating the plane of the sugar rings (see Figure 2.7E). These surfaces bind water and matrix polymers differently, and as a result the microfibril shape is an important factor for wall construction. It is also important for enzymatic attack by microbial cellulases, which dock onto the hydrophobic surface and remove one glucan chain at a time. A major barrier to enzymatic attack of cellulose is the energetic cost of stripping an individual glucan from this crystalline microfibril.

Cellulose microfibrils in nature vary considerably in width and degree of order, depending on their biological source. For instance, cellulose microfibrils in primary

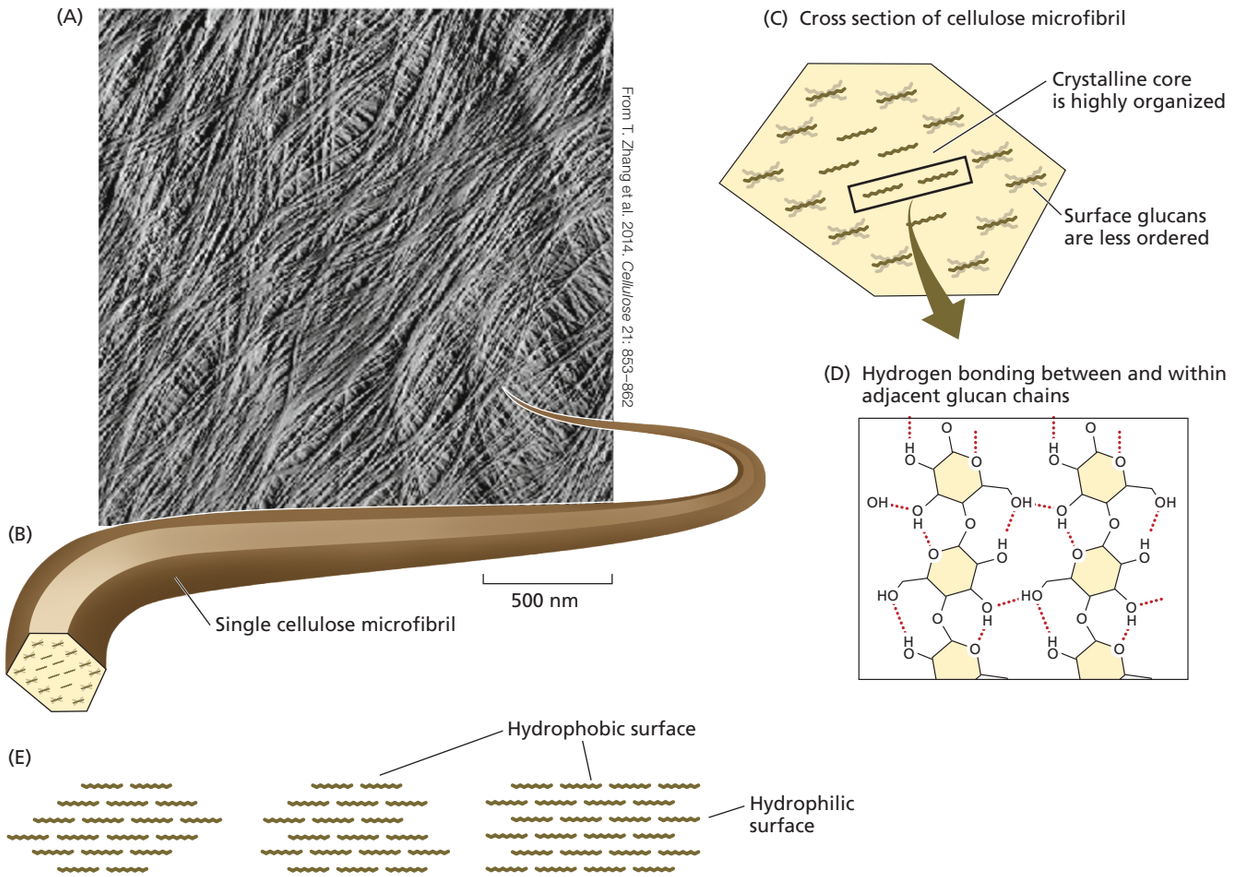


Figure 2.7 **Structure of a cellulose microfibril.** **(A)** Atomic force microscopy image of the primary cell wall from onion epidermis. Note its fibrous texture, which arises from layers of cellulose microfibrils. **(B)** A single cellulose microfibril composed of (1,4)-β-D-glucan chains tightly bonded to each other to form a crystalline microfibril. **(C)** Cross section of a cellulose microfibril, illustrating one model of cellulose structure, with a crystalline core of highly ordered (1,4)-β-D-glucans surrounded by a less organized layer. **(D)** The crystalline regions of cellulose have precise alignment of glucans, with hydrogen bonding within, but not between, layers of (1,4)-β-D-glucans. **(E)** Potential cross-sectional shapes of microfibrils. Note that the hydrophobic surface area varies greatly with shape. (B–E after J. F. Matthews et al. 2006. *Carbohydr. Res.* 341: 138–152.)

cell walls of land plants are approximately 3 nm wide, whereas those formed by some green algae may be up to 20 nm wide and may be more highly ordered (more crystalline) than those found in land plants. This variation corresponds to the number of chains that make up the cross section of a microfibril. Individual microfibrils can also bundle together to form larger **macrofibrils**; this is most common in the cell walls of woody tissues, where cellulose has a higher degree of order (crystallinity) than in primary cell walls. Cellulose chain length (or DP, degree of polymerization) ranges from approximately 2000 to more than 25,000 glucose residues, corresponding to a fully extended length of 1 to 13 μm. The microfibril may be longer than the individual glucans because of overlap and staggering of the glucans in the microfibril. It is very difficult to obtain accurate measures of the length of microfibrils in the cell wall, but our best estimates are in the range of 1 to 13 μm.

Evidence from electron microscopy indicates that cellulose microfibrils are synthesized by large, ordered protein complexes, called cellulose synthase complexes, which are embedded in the plasma membrane (**Figure 2.8**). These rosette-like structures are made up of six subunits, each of which is believed to contain three to six units of **cellulose synthase**, the enzyme that synthesizes the individual glucans that make up the microfibril. The cellulose synthase complexes probably contain additional proteins, but these have not yet been identified.

Cellulose synthases in plants are **sugar–nucleotide polysaccharide glycosyltransferases** encoded by a multigene family named **CESA** (**Cellulose Synthase A**). This family is present in all land plants, but the number of

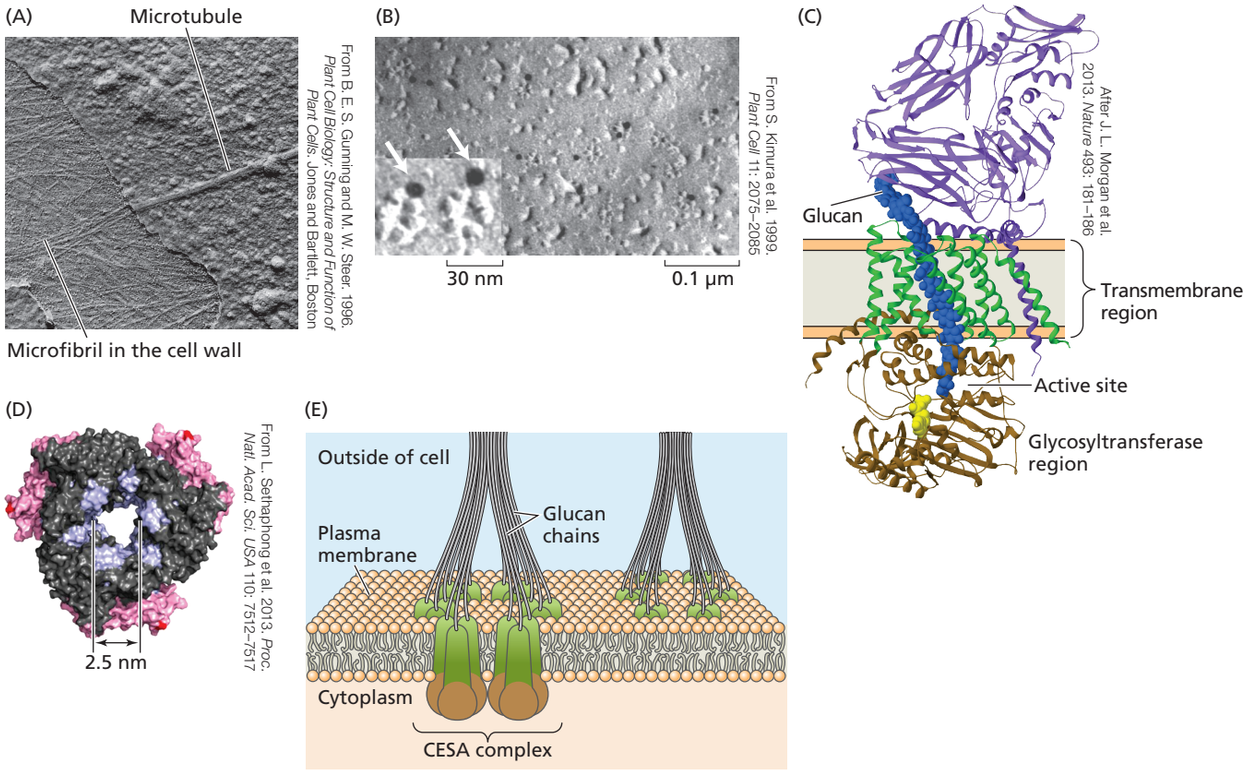


Figure 2.8 **Cellulose microfibrils are synthesized at the cell surface by membrane-bound complexes containing cellulose synthase (CESA) proteins.** **(A)** Electron micrograph showing newly synthesized cellulose microfibrils immediately exterior to the plasma membrane. **(B)** Freeze-fracture replicas showing binding of nanogold antibody against cellulose synthase to rosette structures in the membrane. The inset shows an enlarged view of two selected particle rosettes with immunogold labeling, indicating that the rosette structures contain CESA. The nanogold particles are the dark circles indicated with arrows. **(C)** Structure of a bacterial cellulose synthase. The brown region indicates the catalytic domain of the glycosyltransferase region where the catalytic site is located; this is the business end of the protein that transfers a glucose from uridine diphosphate glucose (UDP-glucose) to the glucan (blue). The green region indicates the transmembrane region, which forms a tunnel for the glucan to cross the membrane. The purple region is a domain not present in plant CESAs. **(D)** One possible oligomeric form of CESA in which three CESAs form a trimeric complex corresponding to one of the particles in the rosette structure seen in (B). **(E)** Computational model of a CESA complex extruding glucan chains that coalesce to form a microfibril.

CESA genes in any given species varies. Genetic evidence in the model eudicot *Arabidopsis thaliana* indicates that three different *CESA* family members are involved in cellulose synthesis in primary cell walls and that a different set of three is used to make cellulose in secondary walls of vascular tissues. Experimentally, specific *CESA* units have been swapped between the cellulose synthase complexes of primary and secondary walls and the complexes have still been able to synthesize cellulose microfibrils.

The catalytic domain of cellulose synthase, which is located on the cytoplasmic side of the plasma membrane, transfers a glucose residue from a sugar–nucleotide donor, uridine diphosphate glucose (UDP-glucose), to the growing glucan chain. Recent studies of the structure of a bacterial cellulose synthase have yielded insights into the details of the formation of glucan and its transport across the membrane through a tunnel in the synthase (see Figure 2.8C). Computational modeling indicates that a similar catalytic mechanism operates in plant CESAs. The modeling also leads to hypotheses of how multiple synthases could be grouped within the cellulose synthesis complex to produce multiple parallel glucan chains that coalesce to form a microfibril immediately after synthesis (see Figure 2.8D and E). There is some evidence that hemicelluloses may get entrapped in the microfibril as it forms; this may create disorder in the crystalline microfibril and also anchor the microfibril to the matrix.

Other proteins are implicated in cellulose microfibril formation, but their detailed functions and whether their roles are direct or indirect are not yet certain. A larger group of related proteins encoded by *CESA-like* (*CSL*) genes appear to function in the synthesis of other specific types of polysaccharides. Another class of

membrane-associated (1,4)-β-D-endoglucanases appear to function in cellulose crystallization, while other groups of proteins function in cellulose crystalline assembly.

Matrix polysaccharides are delivered to the wall via vesicles

In its simplest conception, the wall matrix may be thought of as a hydrogel within which cellulose microfibrils are embedded. Matrix polysaccharides are synthesized by membrane-bound glycosyltransferases in the Golgi apparatus and are delivered to the cell wall via vesicles in the process known as exocytosis (**Figure 2.9** and **WEB TOPIC 2.2**; see also Chapter 1). Some members of the *CSL* gene family encode glycan synthases that contribute to the backbone building of matrix hemiceulluoses. Additional sugar residues may be added as branches to these polysaccharide backbones by other sets of glycosyltransferases, probably acting coordinately in membrane-bound complexes. Pectins are also synthesized in the Golgi apparatus and delivered via exocytosis to the cell wall. The common pectin, homogalacturonan (HG), is synthesized in the Golgi by a glycosyltransferase named GAUT1, which transfers galacturonic acid from a UDP donor to an HG acceptor. GAUT1 is part of a protein complex that is anchored to the inner face of the Golgi apparatus membrane by a related but enzymatically inactive protein, GAUT7. The Golgi apparatus is thought to contain numerous other enzymes that participate in the synthesis of other wall polysaccharides, but these enzymes have not yet been well characterized.

Unlike cellulose, which forms a crystalline microfibril, the matrix polysaccharides are much less ordered and are often described as amorphous. This noncrystalline character is a consequence of the structure of these polysaccharides—their branching and their nonlinear conformation. Nevertheless, studies using various physical techniques, including infrared spectros-

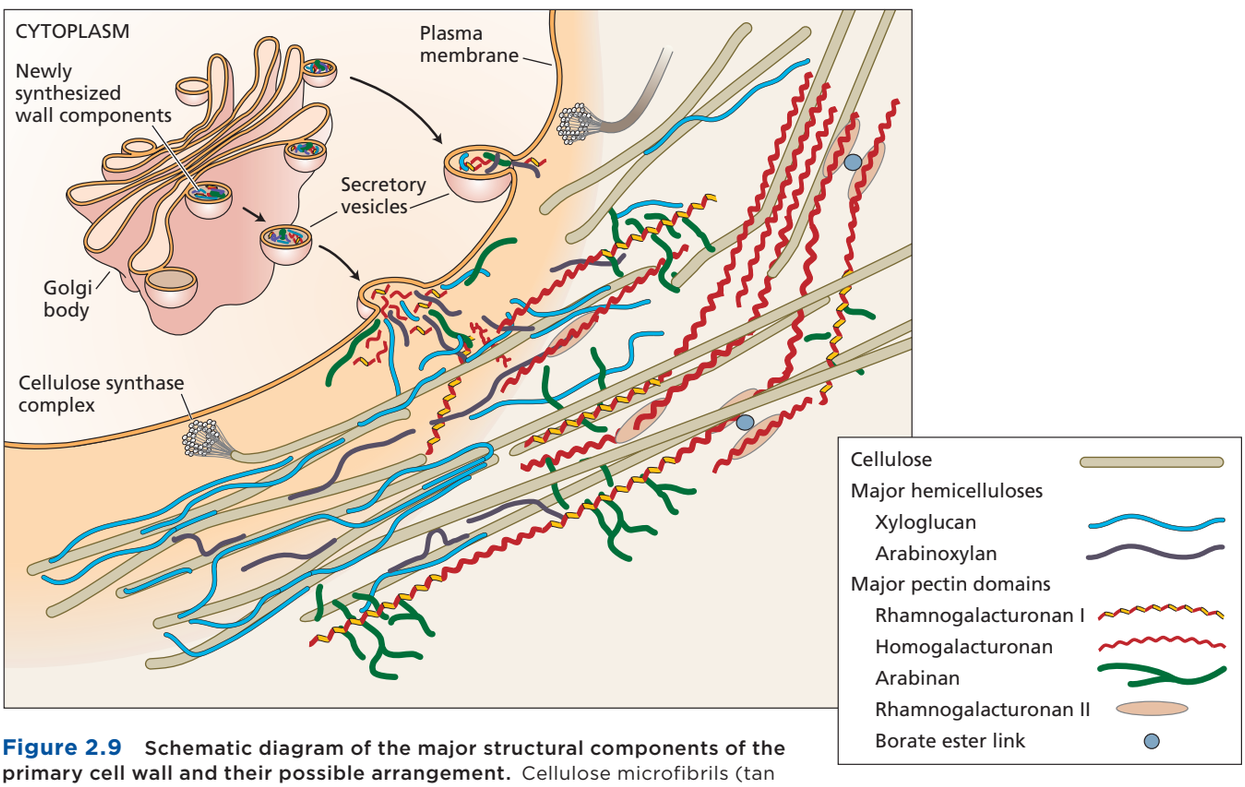


Figure 2.9 Schematic diagram of the major structural components of the primary cell wall and their possible arrangement. Cellulose microfibrils (tan rods) are synthesized at the cell surface and are partially coated with hemicelluloses (blue and brown strands), which may separate microfibrils from one another. Pectins (red, yellow, and green strands) form an interlocking matrix that controls microfibril spacing and wall porosity. Pectins and hemicelluloses are synthesized in the Golgi apparatus and delivered to the wall via vesicles that fuse with the plasma membrane and thus deposit these polymers at the cell surface. For clarity, the hemicellulose–cellulose network is emphasized on the left, and the pectin network is emphasized on the right. (After D. J. Cosgrove. 2005. *Nat. Rev. Mol. Cell Biol.* 6: 580–861.)

copy and nuclear magnetic resonance (NMR), indicate partial order in the orientation of hemicelluloses and pectins in the cell wall, probably as a result of a physical tendency for these polymers to become aligned along the long axis of cellulose fibrils in a manner that alters cellulose crystallinity. Such realignment of pectins after deposition to the cell wall has been visualized by confocal microscopy combined with metabolic labeling with a fucose molecule coupled to a fluorescence dye. In addition, recent work has shown that a deficiency of boron (an ionic cross-linker of pectin) may alter the alignment of cellulose microfibrils within the wall after they are deposited.

Hemicelluloses are matrix polysaccharides that bind to cellulose

Hemicelluloses comprise a heterogeneous group of polysaccharides (**Figure 2.10**) that are usually tightly bound in the wall, as just introduced. Hemicelluloses typically have a pronounced ability to bind to cellulose in vitro and likely play an important role in the assembly of cellulose microfibrils to form a coherent cell wall in vivo (e.g., through altering cellulose crystallinity)

The dominant hemicellulose in primary cell walls of most land plants is xyloglucan, which consists of a (1,4)-β-D-glucan decorated with (1,6)-linked β-D-xylosyl residues (see Figure 2.10A). Xyloglucan structure shows some variability among species. In most eudicots, 30 to 40% of the xylose residues are appended with a galactose residue, which in turn may bear a terminal fucose residue. A concise nomenclature has been developed to refer to the branching pattern of xyloglucan (see Figure 2.10B): For example, G is used for an unsubstituted glucose residue; X means glucose is substituted solely with xylose; L is used for a xylose–galactose side chain; and F denotes a xylose–galactose–fucose side chain.

Xyloglucan has a repeating substructure in which one of every four glucose residues in the backbone is unsubstituted (does not carry a sugar side chain). Endoglucanase digestion of xyloglucan from most eudicot sources yields three major oligosaccharides with four glucose residues in the backbone, designated XXXG, XXFG, and XLFG. Plants in the Solanaceae, such as tomato, use an arabinose residue in place of galactose, which appears to be functionally equivalent for cell wall mechanics. Glycosidases are able to remove the side chain sugars, resulting in xyloglucans with a lower degree of substitution, which bind more tightly to cellulose.

Unlike in most other land plants, the dominant hemicellulose in the primary cell wall of grasses (Poaceae) is arabinoxylan (also called glucuronoarabinoxylan or GAX; see Figure 2.10C). The small amount of xylgoclucans present are mostly made up of XXGG, XXGGG, and XXGGGG repeat units. Pectins are also present in grass cell walls but are greatly reduced in abundance. GAX has a (1,4)-β-D-xylan backbone substituted with (1,3)-α-L-arabinose residues; approximately 1 residue in 50 is substituted with (1,2)-α-D-glucuronic acid. The degree of arabinose substitution varies widely, from more than 80% to less than 10%. Unlike most hemicelluloses, highly substituted GAX is not tightly bound to the cell wall, does not bind cellulose in vitro, and is readily solubilized from the cell wall under mild conditions used to extract pectin. Some of the arabinose residues bear ferulate groups attached by an ester linkage. Oxidative coupling of ferulate groups results in cross-links between GAX; such cross-linking reduces the digestibility of grasses (i.e., for feeding cows and sheep) and may reduce cell wall extensibility. Ferulates also function as nucleation sites for lignin polymerization in grass walls.

In addition to GAX, primary cell walls of grasses also contain mixed-linkage **(1,3;1,4)-β-D-glucan**. The mixed-linkage glucan is thought to bind tightly to the surface of cellulose, reducing cellulose–cellulose interactions, while less-substituted GAX may serve a cross-linking function.

Secondary walls of woody tissues contain little xyloglucan or pectin; instead, the matrix polysaccharides are primarily xylans and glucomannans with a low degree of side chain substitution. These hemicelluloses bind tightly to cellulose and require strong alkali to be solubilized from the wall. The major hemicellulose of secondary walls varies by source: In secondary walls of eudicots the dominant hemicellulose is **glucuronoxylan**, with lesser amounts of glucomannans. Glucuronoxylan is similar to GAX (see Figure 2.10C), but without the arabinose side chains and the glucuronic acid is 4-O-methyl substituted. **Glucomannan** has a backbone consisting of β(1,4)-linked glucose and mannose residues, with infrequent galactose side chains (see Figure 2.10D). In gymnosperm wood the major hemicellulose is glucomannan, with smaller amounts of arabinoxylan substituted with 4-O-methylglucuronyl residues. GAX with low degree of substitution is the major hemicellulose of secondary walls in grasses. The low frequency of side chains in these hemicelluloses enables them to bind more tightly to cellulose and to pack more tightly in the cell wall.

Pectins are hydrophilic gel-forming components of the primary cell wall

Pectins are the most abundant component of most primary cell walls, forming a hydrated gel phase in which cellulose and hemicelluloses are embedded. They act as hydrophilic filler to prevent aggregation and collapse of the cellulose network, and they also determine the porosity of the cell wall to macromolecules. They are often the sole component of the middle lamella (the oldest part of the wall). Release of oligosaccharides from pectins during fungal invasion of plant tissue elicits defense responses that limit pathogen invasion (see Chapter 24).

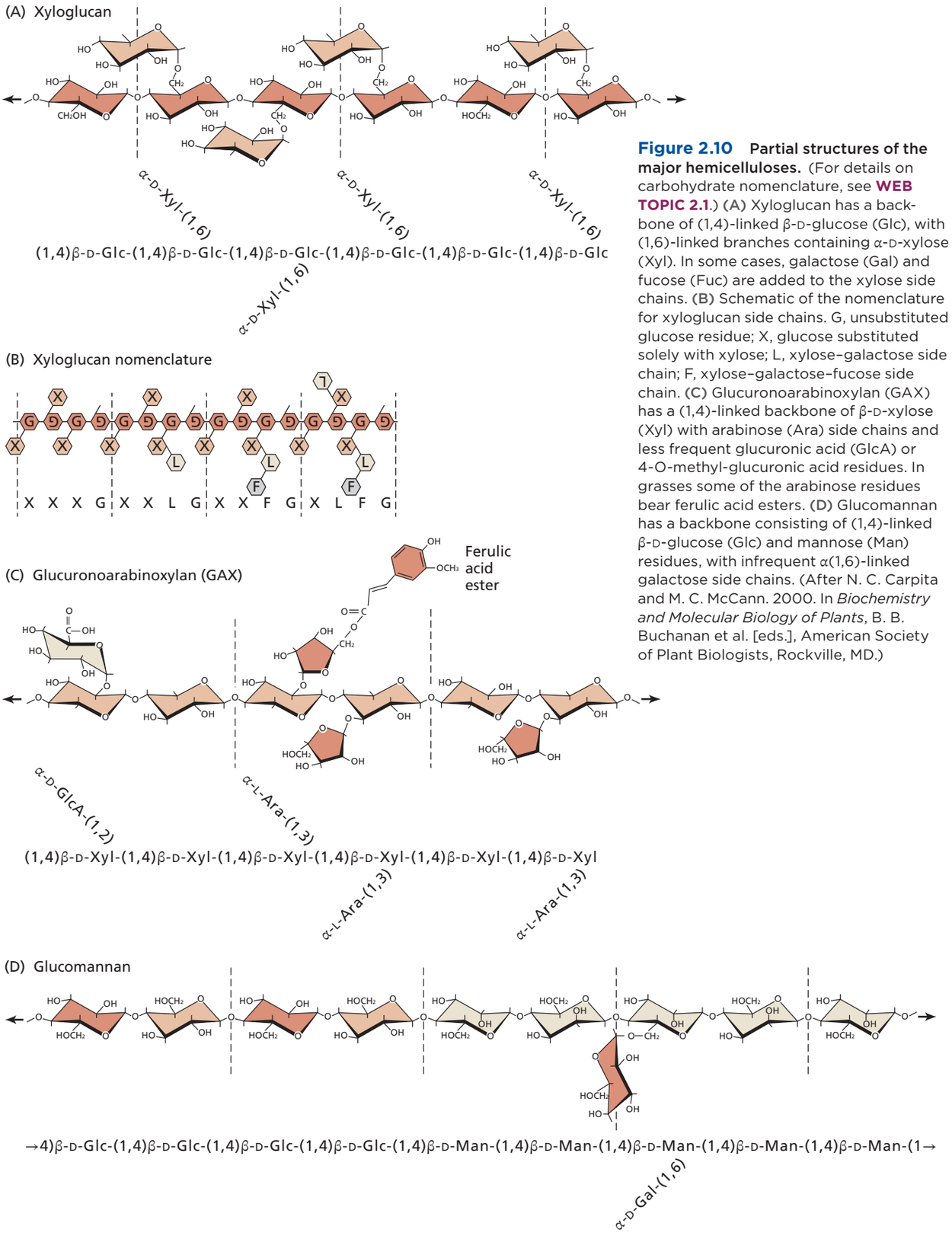


Figure 2.10 **Partial structures of the major hemicelluloses.** (For details on carbohydrate nomenclature, see **WEB TOPIC 2.1**.) **(A)** Xyloglucan has a backbone of (1,4)-linked β-D-glucose (Glc), with (1,6)-linked branches containing α-D-xylose (Xyl). In some cases, galactose (Gal) and fucose (Fuc) are added to the xylose side chains. **(B)** Schematic of the nomenclature for xyloglucan side chains. G, unsubstituted glucose residue; X, glucose substituted solely with xylose; L, xylose–galactose side chain; F, xylose–galactose–fucose side chain. **(C)** Glucuronoarabinoxylan (GAX) has a (1,4)-linked backbone of β-D-xylose (Xyl) with arabinose (Ara) side chains and less frequent glucuronic acid (GlcA) or 4-O-methyl-glucuronic acid residues. In grasses some of the arabinose residues bear ferulic acid esters. **(D)** Glucomannan has a backbone consisting of (1,4)-linked β-D-glucose (Glc) and mannose (Man) residues, with infrequent α(1,6)-linked galactose side chains. (After N. C. Carpita and M. C. McCann. 2000. In *Biochemistry and Molecular Biology of Plants*, B. B. Buchanan et al. [eds.], American Society of Plant Biologists, Rockville, MD.)

Pectins constitute a heterogeneous group of polysaccharides, characteristically containing galacturonic acid and neutral sugars such as rhamnose, galactose, and arabinose. These different polysaccharides are often, but not always, covalently linked to one another, forming large macromolecular structures (~10^6 Da). NMR studies indicate that pectins make contact with cellulose surfaces in the wall, and binding studies have shown that the neutral side chains of pectins can bind to cellulose surfaces, although more weakly than do hemicelluloses. NMR results also indicate that pectins make intimate contact with the hemicellulose xyloglucan. There also is evidence for covalent linkages between pectins and hemicelluloses, and a recent study identified a covalent complex containing an arabinogalactan protein, pectin, and xylan, but the extent and significance of such cross-linking for primary wall function are not yet certain.

The three major pectic polysaccharide groups are **homogalacturonan** (**HG**), **rhamnogalacturonan I** (**RG I**), and **rhamnogalacturonan II** (**RG II**) (**Figure 2.11**). HG is a linear chain of (1,4)-linked β-D-galacturonic acid residues, some of which are methyl esterified. It is the most abundant pectin in primary cell walls. RG I has a long backbone of alternating rhamnose and galacturonic acid residues and carries long side-chains of **arabinans**, galactans, and **type-1 arabinogalactans**, collectively known as neutral pectic polysaccharides. RG II, which is the least abundant of these pectin domains, contains an HG backbone decorated with side chains made of at least ten different sugars in a complicated pattern of

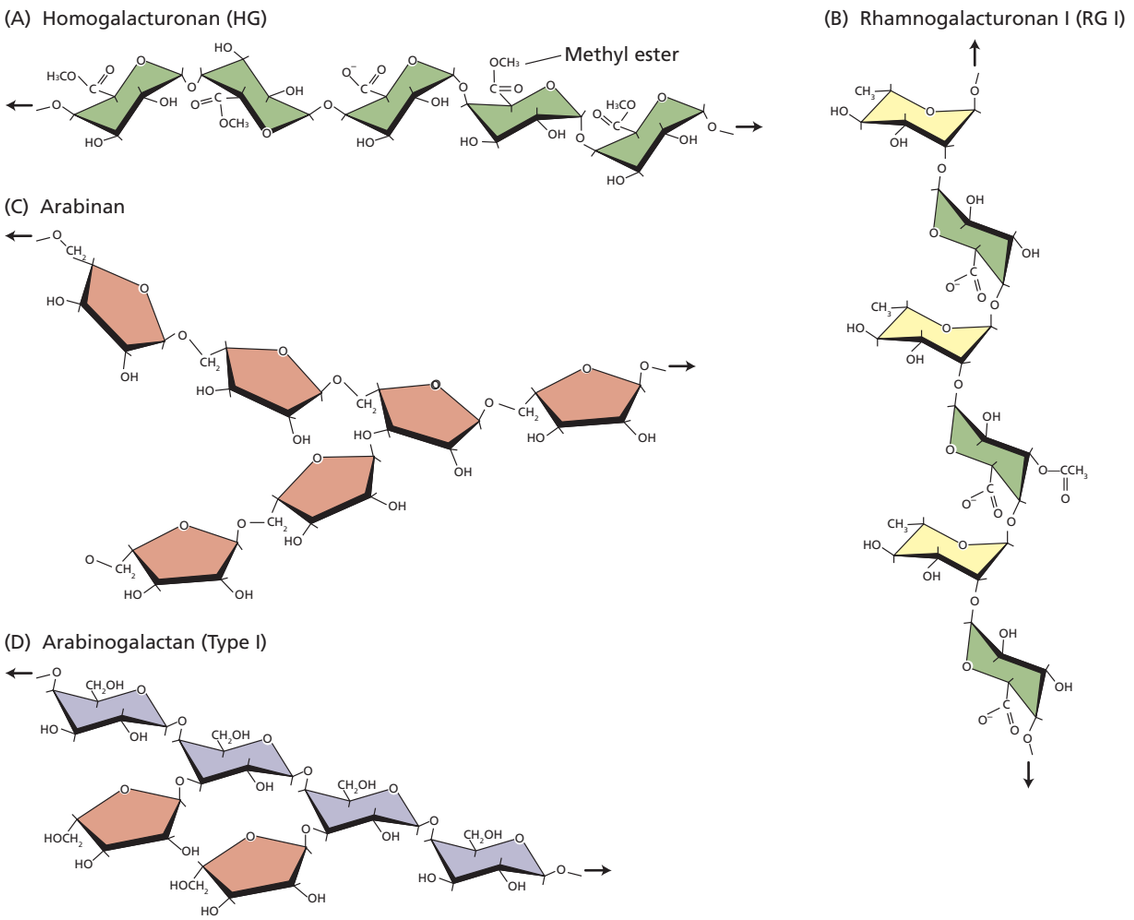


Figure 2.11 **Partial structures of the most common pectins.** **(A)** Homogalacturonan, also known as polygalacturonic acid or pectic acid, is made up of (1,4)-linked α-D-galacturonic acid (GalA). The carboxyl residues are often methyl esterified. **(B)** Rhamnogalacturonan I (RG I) is a very large pectin domain, with a backbone of alternating GalA and (1,2)-α-D-rhamnose (Rha). **(C, D)** Side chains can be attached to rhamnose in RG I and are composed principally of arabinans (C), galactans, and arabinogalactans (D). These side chains may be short or quite long. The galacturonic acid residues are often methyl esterified. (After N. C. Carpita and M. C. McCann. 2000. In *Biochemistry and Molecular Biology of Plants*, B. B. Buchanan et al. [eds.], American Society of Plant Biologists, Rockville, MD.)

linkages. Although RG I and RG II have similar names, they have very different structures.

When HG is initially synthesized, many of the acidic carboxyl groups are methyl esterified, giving a less charged polysaccharide. Subsequent removal of methyl esters in the cell wall by pectin methyl esterase enzymes facilitates ionic cross-linking of HG and gel formation (**Figure 2.12A**). Extensive block-wise de-esterification of HG restores the charged carboxyl group and enables calcium ions to form ionic bridges between adjacent chains, resulting in a relatively stiff gel. The solubilization of pectins by Ca^{2+} chelators is based on the removal of these Ca^{2+} bridges. Ionic gel formation by HG is important for the adhesion of cells by the middle lamella and makes the primary cell wall less extensible. De-esterification of HG also plays a role in initiation of leaf primordia at the shoot apical meristem and in pollen tube growth. By creating free carboxyl groups, de-esterification also increases the electric-charge density in the wall, which in turn may influence the concentration of ions in the wall, the activities of wall enzymes, and possibly the distribution of charged signaling molecules. The possible roles of pectin gelation in cell wall mechanics and cell expansion are discussed in Sections 2.2 and 2.3.

The cross-linking of pectic polysaccharides together to form this hydrogel is based primarily on ionic cross-links formed by cations such as Ca^{2+}, B^{+}, and Na^{+}. The extent of cross-linking is related to the rigidity, porosity, and viscosity of the cell wall material. It has been proposed that pectin domains are also covalently linked end to end in the wall. **Figure 2.12B** illustrates a hypothetical scheme for linkage of HG, RG I, and RG II. Not

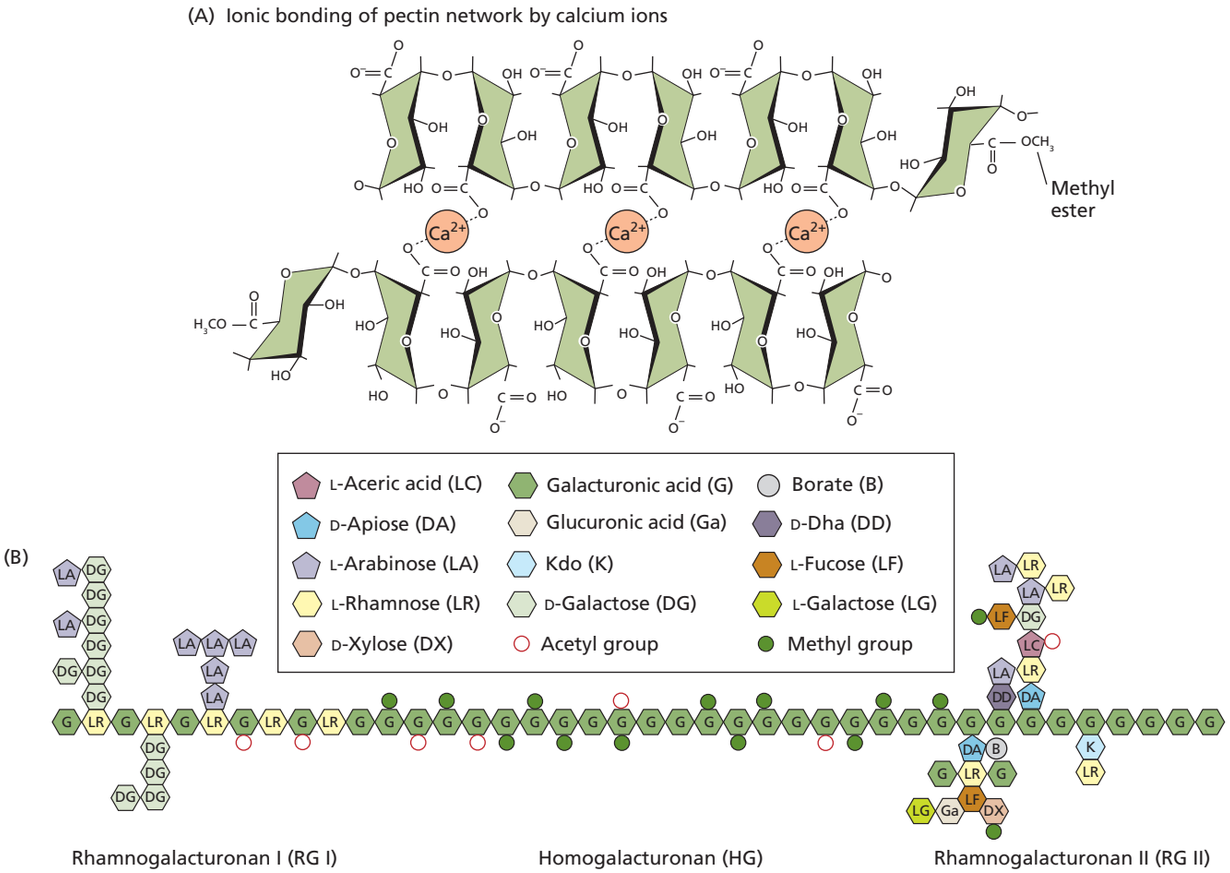


Figure 2.12 Higher-level organization of pectin within the cell wall. **(A)** Formation of a pectin network involves ionic bridging of the nonesterified carboxylate groups (COO^{-}) by calcium ions. When blocked by methyl-esterified groups, the carboxyl groups cannot participate in this type of interchain network formation. Likewise, the presence of side chains on the backbone interferes with network formation. **(B)** Schematic model illustrating the linear arrangement of the various pectin domains to each other, including rhamnogalacturonan I (RG I), homogalacturonan (HG), and rhamnogalacturonan II (RG II). The structure is not quantitatively accurate: HG should be about ten times more abundant and RG I about two times more abundant. Kdo = 3-Deoxy-D-manno-2-octulosonic acid; D-Dha = dihydroxyacetone. (A after After N. C. Carpita and M. C. McCann. 2000. In *Biochemistry and Molecular Biology of Plants*, B. B. Buchanan et al. [eds.], American Society of Plant Biologists, Rockville, MD; B after D. Mohnen. 2008. *Curr. Opin. Plant Biol.* 11: 266–277.)

all the pectic polysaccharides are attached to such large structures, however. For instance, in growing pea stems most arabinans and galactans were not linked to acidic polysaccharides, and in maize (*Zea mays*) HG could be separated from other pectic components by gentle, nonenzymatic methods.

2.2 The Dynamic Primary Cell Wall

Early in the life of a plant cell, its primary cell wall is extensible and able to incorporate new structural material as the cell grows. As discussed in Section 2.1, the primary cell wall is generally simple, comprising thin layers made of long cellulose microfibrils embedded in a hydrated matrix of noncellulosic polysaccharides and small amounts of proteins (see Figure 2.3). This structure imparts an ideal combination of flexibility and strength to the growing cell wall, which must be both extensible and strong at the same time.

Primary cell walls are continually assembled during cell growth

As mentioned in Section 2.1, primary walls originate de novo during the final stages of cell division when the newly formed cell plate separates the two daughter cells and solidifies into a stable wall that is capable of bearing the physical stresses generated by turgor pressure. You may recall that the middle lamella forms in parallel with the cell plate (see Figure 2.2). As each daughter cell grows, new components are continually added to the primary cell wall. As such, the "life" of an individual polymer that is part of the primary wall may be outlined as follows:

Synthesis → deposition → assembly → modification

At any given moment during active wall formation, wall polymers are being deposited, assembled, and modified. As a result, newly formed cell wall comprises a heterogeneous mix of incorporated and unincorporated polymers. Here we consider wall polymer assembly into an existing cohesive network; in Section 2.3 we consider modifications that affect cell enlargement.

After their secretion into the cell wall space, the wall polymers must be assembled into a cohesive structure; that is, the individual polymers must attain the physical arrangement and bonding relationships that are characteristic of the primary (growing) cell wall and that confer on it both tensile strength and extensibility. Although the details of wall assembly are not fully understood, the prime candidates for this integration process are self-assembly and enzyme-mediated assembly.

SELF-ASSEMBLY Self-assembly is an attractive concept because it is mechanistically simple. Many polysaccharides possess a marked tendency to aggregate spontaneously into organized structures. For example, hemicelluloses often aggregate, making their separation into distinct polymers technically difficult. However, in the case of hemicellulose integration into the wall, it is likely that self-assembly alone is an insufficient explanation: When hemicelluloses are bound with cellulose in vitro, their binding is much weaker than is the case in real cell walls, and these artificial composites display different enzyme accessibility. In contrast, evidence suggests that pectin gel assembly and disassembly may be affected by mechanical forces, such as that from turgor; to disrupt ionic cross-linking within pectin gels, these forces need only exceed the strength of such bonds. Models that take this into account indicate that self-assembly may play a role in pectin gel structural dynamics. Thus, it seems likely that self-assembly plays some role in cell wall polymer integration, but it is unlikely to be the only process involved.

ENZYME-MEDIATED ASSEMBLY Enzymes may also guide wall assembly, by facilitating the breaking and forming of covalent bonds. A prime candidate for enzyme-mediated wall assembly is **xyloglucan endotransglucosylase** (**XET**). This enzyme, which belongs to a large family of enzymes named **xyloglucan endotransglucosylase/hydrolases** (**XTHs**), facilitates the severing of the backbone of a xyloglucan and re-joining one end of the cut xyloglucan with the free end of an acceptor xyloglucan (**Figure 2.13**). This transfer reaction integrates newly synthesized xyloglucans into the cell wall, potentially strengthening it. Transglycosylases with other substrate specificities have recently been detected in plant cell walls, but their biological functions have not yet been assessed.

Other wall enzymes that might aid in wall assembly include glycosidases, pectin methyl esterases, pectin acyltransferases, and various oxidases. Some glycosidases remove the side chains of hemicelluloses, increasing the tendency of hemicelluloses to adhere to each other and to the surface of cellulose microfibrils. As we described in Section 2.1, pectin methyl esterase removes methyl esters that block acidic groups of HG, thereby enhancing HG's ability to form a Ca^{2+}-bridged gel network; in this case there is likely to be interplay between enzymatic activity and self-assembly. Oxidases such as peroxidase catalyze cross-linking between phenolic groups (tyrosine, phenylalanine, ferulic acid) in wall proteins, pectins, and other wall polymers. Such oxidative cross-linking is also the basis of lignin formation, which we discuss in Section 2.4.

2.3 Mechanisms of Cell Expansion

During plant cell enlargement, new wall polymers are continually synthesized and secreted at the same time that the preexisting wall is expanding. Wall expansion

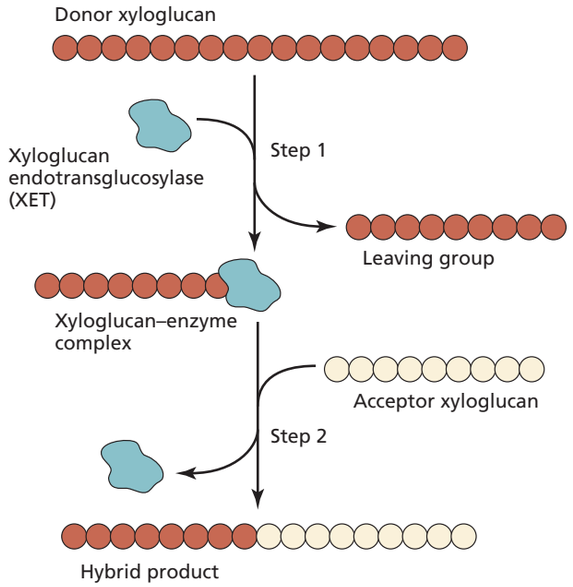


Figure 2.13 Action of xyloglucan endotransglucosylase (XET) to cut and join xyloglucan polymers into new configurations. Step 1: The enzyme cuts a xyloglucan molecule (the donor xyloglucan), forming a long-lived complex where the xyloglucan is covalently attached to the enzyme. Step 2: Subsequently the enzyme transfers the xyloglucan chain to the nonreducing end of a second xyloglucan (the acceptor xyloglucan), resulting in a hybrid product. (After S. C. Fry. 2004. *New Phytol.* 161: 641–675.)

may be highly localized (as in the case of **tip growth**) or more dispersed over the wall surface (**diffuse growth**) (**Figure 2.14**). Tip growth is characteristic of root hairs and pollen tubes; it is closely linked to cytoskeletal processes, especially those of actin microfilaments (see **WEB ESSAY 2.1**). Most of the other cells in the plant body exhibit diffuse growth, which is linked to both microtubules and actin microfilaments. Cells such as fibers, some sclereids, and trichomes grow in a pattern that is intermediate between that of diffuse growth and tip growth.

Even in cells with diffuse growth, however, different parts of the wall may enlarge at different rates or in different directions. For example, in cortical cells of the stem or epidermal cells of the young seedling hypocotyl, the end walls grow much less than the side walls. This difference in growth between cell faces may be due to structural or enzymatic variations in specific walls or to variations in the stresses borne by different walls. As a consequence of such uneven patterns of wall expansion, plant cells may assume irregular forms, often important for their functions.

Microfibril orientation influences growth directionality of cells with diffuse growth

During growth, the loosened cell wall is extended by physical forces generated from cell turgor pressure. Turgor pressure creates an outward-directed force, equal in all directions. While turgor pressure has no directionality, the cell wall may yield more in one direction than another due to its structural characteristics (more detail later in this section). The directionality of growth is determined in large part by the orientation of cellulose microfibrils within the wall.

When cells first form at meristems, they are isodiametric; that is, they have equal diameters in all directions. If the orientation of cellulose microfibrils in the primary cell wall is randomly arranged, the cells grow isotropically (equally in all directions), expanding radially to generate a sphere (**Figure 2.15A**). In most plant cell walls, however, cellulose microfibrils are aligned in a predominant direction. The alignment of cellulose fibers allows the cell wall to hold more stress (generated by turgor) in the direction parallel to the predominant fiber alignment and yield more in the direction perpendicular to the fiber alignment. The result is **anisotropic growth** (as in stems, where cells increase much more in length than in width).

In the lateral walls of elongating cells, such as cortical and vascular cells of some stems and roots, or the giant internode cells of the filamentous green alga *Nitella*, cellulose microfibrils are deposited circumferentially (transversely), at right angles to the long axis of the cell. The circumferential arrangement of cellulose microfibrils restricts growth in girth and promotes growth in length (**Figure 2.15B**). It is important to note that in

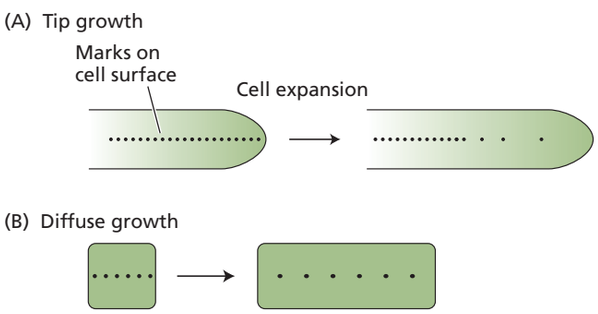


Figure 2.14 The cell surface expands differently during tip growth and diffuse growth. **(A)** Expansion of a tip-growing cell is confined to an apical dome at one end of the cell. If marks are placed on the cell surface and the cell is allowed to continue to grow, only the marks that were initially within the apical dome grow farther apart. Root hairs and pollen tubes are examples of plant cells that exhibit tip growth. **(B)** If marks are placed on the surface of a diffuse-growing cell, the distance between all the marks increases as the cell grows. Most cells in multicellular plants grow by diffuse growth.

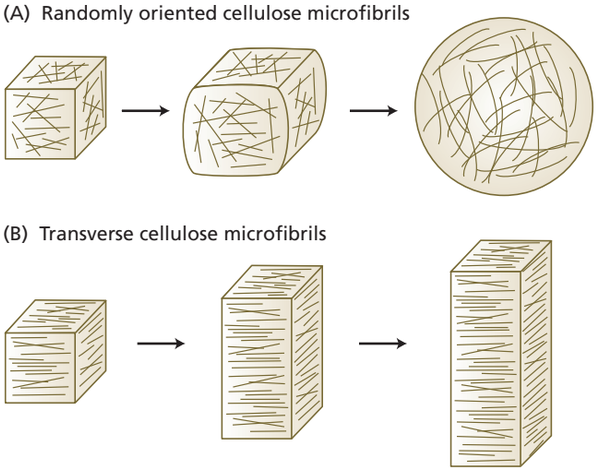


Figure 2.15 The orientation of newly deposited cellulose microfibrils determines the direction of cell expansion. (A) If the cell wall is reinforced by randomly oriented cellulose microfibrils, the cell will expand equally in all directions, forming a sphere. (B) When most of the reinforcing cellulose microfibrils have the same orientation, the cell expands at right angles to the microfibril orientation and is constrained in the direction of the reinforcement. Here the microfibril orientation is transverse, so cell expansion is longitudinal.

multicellular organs, it is not necessary for all cells to display this circumferential alignment in cellulose fibers; as long as enough cells do, they can pull their neighbors with them into anisotropic growth—something that is only possible because of the connection between neighboring cells that the wall provides.

Microfibril orientation in the multilayered cell wall changes over time

As the cell expands and construction of the wall continues, the wall often takes on a layered structure in cross section. According to the **multinet growth hypothesis**, each successive wall layer is stretched and thinned as the cell grows, such that the microfibrils in older cell wall layers would be expected to become passively reoriented in the longitudinal direction as cells elongate. Evidence for passive reorientation has been reported for growing cells in Arabidopsis roots stained with a fluorescent dye to enable imaging of cellulose microfibril bundles by confocal microscopy. However, it is likely that such passive reorientation would be influenced by the properties of the matrix and would require active remodeling of the cell wall structure. Experiments with isolated walls from growing hypocotyls and onion bulb epidermal cells indicate that force alone is unable to reorient fibers without the addition of enzymes that act on the junctions holding microfibrils together. These and other results suggest that wall expansion involves selective loosening of junctions between microfibrils, rather than a generalized loosening of the matrix. We discuss such "hot spots" in more detail later in this section.

Other experiments suggest that the oldest (i.e., outermost) layers of the cell wall may be so fragmented as a result of their history of enlargement that they may contribute little to the control of cell expansion. By this hypothesis, the inner one-fourth of the wall dominates control of cell expansion (see **WEB TOPIC 2.3**). Recent mathematical modelling also supports a progressive lessening of the influence of older wall layers on the direction of cell expansion.

Cortical microtubules influence the orientation of newly deposited microfibrils

Newly deposited cellulose microfibrils usually are coaligned with microtubule arrays in the cytoplasm, close to the plasma membrane (**Figure 2.16**). A striking example occurs in xylem vessel elements, where bands of cortical microtubules mark the sites of secondary wall thickenings and also the sites of CESA localization. Moreover, experimental disruptions of microtubule organization with drugs or by genetic defects often lead to disorganized wall structure and disorganized growth. For example, several drugs bind to tubulin, the subunit protein of microtubules, causing them to depolymerize. When growing roots are treated with a microtubule-depolymerizing drug, such as oryzalin, the region of elongation expands laterally, becoming bulbous and tumorlike (**Figure 2.17A and B**). This disrupted growth is due to the isotropic expansion of the cells; that is, they enlarge like a sphere instead of in a directional manner. The drug-induced destruction of microtubules in the growing cells interferes with the transverse deposition of cellulose. Cellulose microfibrils continue to be synthesized in the absence of microtubules, but they are deposited randomly and have altered crystallinity, and consequently the cells expand equally in all directions.

These and related observations have led to the hypothesis that microtubules serve as tracks that guide or direct the movement of CESA complexes as they synthesize microfibrils (see **WEB ESSAY 2.1**). The movement of CESA in living cells was made visible by expressing a fusion of CESA with a fluorescent protein. Tagged CESA units were observed to move within the plasma membrane along microtubule tracks (**Figure 2.17C**); they were also seen to be inserted into the plasma membrane from the Golgi apparatus at microtubule-tethered compartments. A molecular linker between CESA and microtubules was recently identified as CSI1 (CESA interactive protein 1), providing a link between the cytoskeleton and cellulose orientation. These results, obtained by confocal microscopy and genetics, reveal new details of how the cytoskeleton directs cell wall organization, and lend weight to the hypothesis that microtubules guide cellulose microfibril direction.

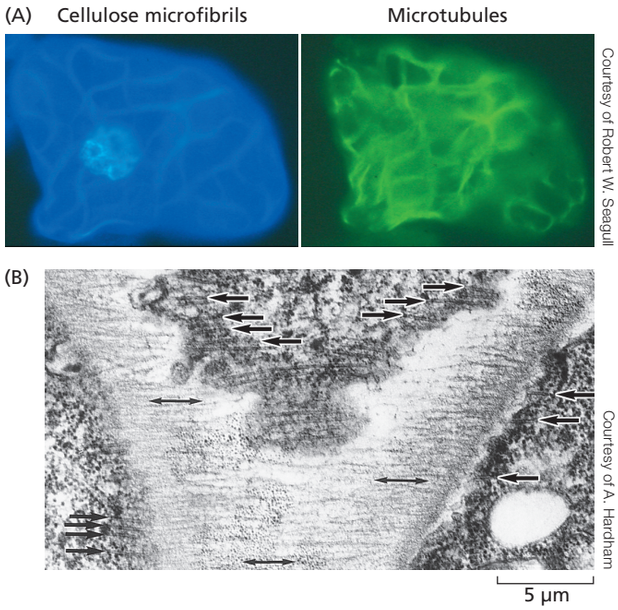


Figure 2.16 The orientation of microtubules in the cortical cytoplasm mirrors the orientation of newly deposited cellulose microfibrils in the walls of cells that are elongating. **(A)** The arrangement of microtubules can be revealed with fluorescently labeled antibodies to the microtubule protein tubulin. In this differentiating tracheary element from a *Zinnia* cell suspension culture, the pattern of microtubules (green) mirrors the orientation of the cellulose microfibrils in the wall, as shown by calcofluor staining (blue). **(B)** The alignment of cellulose microfibrils in the cell wall can sometimes be seen in grazing sections prepared for electron microscopy, as in this micrograph of a developing sieve tube element in a root of *Azolla* (a water fern). The longitudinal axis of the root and the sieve tube element runs vertically. Both the wall microfibrils (double-headed arrows) and the cortical microtubules (single-headed arrows) are aligned transversely.

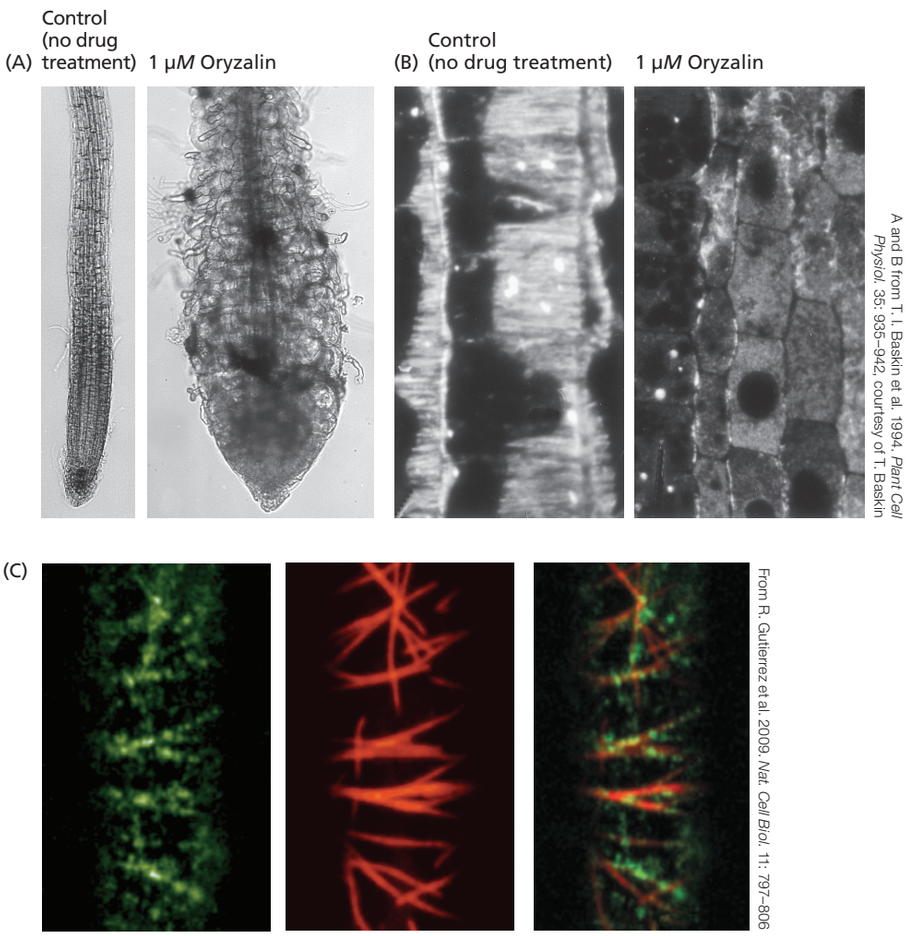


Figure 2.17 Disruption of cortical microtubules results in a dramatic increase in radial cell expansion and a concomitant decrease in elongation. **(A)** Root of Arabidopsis seedling treated with the microtubule-depolymerizing drug oryzalin (1 µ*M*) for 2 days before this photomicrograph was taken. The drug has altered the polarity of growth. **(B)** Microtubules were visualized by means of an indirect immunofluorescence technique and an antitubulin antibody. Whereas cortical microtubules (bright horizontal lines) in the control are oriented at right angles to the direction of cell elongation, very few microtubules remain in roots treated with 1 µ*M* oryzalin. **(C)** Images of fluorescently tagged CESA proteins (left panel) and microtubules (middle panel) indicate that microtubules guide the trajectories of CESA movement in the plasma membrane, thus guiding the orientation of cellulose microfibrils. The right panel shows the superposition of the two images.

Many factors influence the extent and rate of cell growth

Plant cells typically expand 10- to 1000-fold in volume before reaching maturity; this is an important and distinguishing feature of plant growth, whereby the plant body's volume is built by massive increases in cell volume rather than cell number. In extreme cases—for example, xylem vessel elements—cells may enlarge more than 10,000-fold in volume compared with their meristematic initials. The cell wall permits this massive expansion without losing its mechanical integrity as a whole or becoming dramatically thinner. Thus, as we described in Section 2.1, newly synthesized polymers are integrated into the wall without destabilizing it.

This integration process may be particularly critical for cells that display extremely rapid expansion, such as tip-growing root hairs and pollen tubes. In rapidly growing cells with tip growth, the growing wall at the tip doubles its surface area and is displaced to the nonexpanding part of the cell within minutes. This is a much greater rate of wall expansion than is typically found in cells with diffuse growth, where growth rates are approximately 1 to 10% per hour. Because of their fast expansion rates, tip-growing cells are highly susceptible to wall thinning and bursting. Mechanical and cytological models of tip growth in pollen tubes have given hints about how expansion and the addition of wall components need to be coordinated for stable tip growth. Although diffuse growth and tip growth appear to be different growth patterns, both types of wall expansion must have analogous, if not identical, processes of polymer integration, wall stress relaxation, and wall polymer slippage.

There are indications that the cell wall matrix may regulate cell expansion rates. Transgenic alteration of pectin to increase or decrease HG methylation results in concomitant changes in hypocotyl cell elongation rate in Arabidopsis. There are also tissue- and cell-level patterns of HG methylation that are coincident with variations in growth rate. For example, in anisotropically growing hypocotyl epidermal cells, the slower growing end walls have more Ca^{2+}-cross-linked pectin. It is still unclear how changing matrix properties influence cell elongation rate, but it may be through both direct and indirect effects. Directly, changes to the matrix mechanics, perhaps through changes in matrix hydration, could affect the ability of cellulose fibrils to move. Indirectly, changes in pectin methylation would probably alter the porosity of the cell wall and charge distribution, both of which could influence the mobility of factors important for cellulose fibril modification.

Many intrinsic and extrinsic factors influence the rate of cell wall expansion. Cell type and age are important developmental factors. So, too, are hormones such as auxin, gibberellin, and brassinosteroids, which signal when and where cells should grow. Environmental conditions such as light and water availability may likewise modulate cell expansion. These intrinsic and extrinsic factors are most likely to modify cell expansion by altering the way in which the cell wall is loosened, so that it yields (stretches irreversibly) differently. In this context we speak of the **yielding properties of the cell wall**. However, these factors might also alter turgor pressure, which would similarly influence expansion rate. The wall's yielding properties and turgor pressure are probably both regulated during growth, perhaps to different degrees depending on the exact context being considered.

Stress relaxation of the cell wall drives water uptake and cell expansion

Because the cell wall is the major mechanical restraint that limits cell expansion, much attention has been given to its physical properties. As a hydrated polymeric material, the plant cell wall has physical properties that are intermediate between those of a solid and those of a liquid. We call these **viscoelastic**, or **rheological** (flow), **properties**. Walls of cells that are growing are generally less rigid and exhibit less flow than those of mature cells, and under appropriate conditions they exhibit a long-term irreversible stretching, or **yielding**, that is absent or nearly absent in mature walls. This irreversible stretching may also be referred to as *plastic deformation*.

Stress relaxation is a crucial concept for understanding how cell walls enlarge. The term *stress* is used here in the mechanical sense, as force per unit area. As we hinted at earlier, wall stresses arise as an inevitable consequence of cell turgor. The turgor pressure in growing plant cells is typically between 0.3 and 1.0 megapascals (MPa); for contrast, a typical car tire is inflated to about 0.2 MPa. Turgor pressure stretches the cell wall and generates a counterbalancing physical stress or tension in the wall. Because plant cells enclose large pressurized volumes within relatively thin cell walls, the tensile stress generated within the wall is equivalent to 10 to 100 MPa, which is 10- to 100-fold greater than turgor—a very large stress indeed.

This simple fact has important consequences for the mechanics of cell enlargement. To change shape, plant cells must control the direction and rate of wall expansion. The directionality of wall expansion is determined by depositing cellulose in a biased orientation. The rate of expansion is determined by controlled loosening of bonds between microfibrils and between other matrix polysaccharides. This biochemical loosening enables movement or slippage of cellulose microfibrils and their associated matrix polysaccharides, thereby increasing the wall surface area. At the same time, such loosening reduces the physical stress in the wall.

Reduction of cell wall stress by loosening is crucial because it decreases turgor pressure and thus water potential, enabling the water uptake required for expansive

growth. The water ends up mainly in the vacuole, which takes up an ever-larger proportion of the cell volume as the cell enlarges. **WEB ESSAY 2.2** describes how growing cells regulate their water uptake and how this uptake is coordinated with wall yielding.

Leaf epidermal pavement cells provide a model for regulated cell wall expansion

Leaf epidermal pavement cells have an interlocking jigsaw puzzle–like structure that provides a model for studying the interactions of pressure-driven expansion modulated by structural constraints. Pavement cells are initially simple in shape, with straight or curving borders. As they grow, however, they develop interdigitizing lobes and irregular shapes (see Figure 1.6). Studies using atomic force microscopy and imaging of cytoskeletal structures demonstrate that lobing occurs most prominently in regions of the cell where microtubular and microfilament structures (see Chapter 1) are heterogeneous. Microfilament networks regulated by the ROP2 GTPase are particularly enriched in regions of lobing, as are cell wall structures associated with plasticity. Modeling and direct measurements demonstrate that turgor pressure drives differential expansion of cell walls in lobe regions. The dynamics of pavement cell lobing are similar across multiple plant species. In transgenic plants constitutively overexpressing ROP2 GTPase, the actin filament network of pavement cells is dense and relatively homogeneous, and cell extensibility and elasticity are similarly homogeneous. Consequently, lobing is almost completely absent in ROP2 overexpression lines. Modeling of lobing requires consideration of both the forces within each cell and the differential resistance encountered at the margins of adjoining cells.

Acid-induced growth and wall stress relaxation are mediated by expansins

A common characteristic of growing cell walls is that they extend much faster at acidic pH than at neutral pH. This phenomenon is called **acid growth**. In living cells, acid growth is evident when growing cells are treated with acid buffers or with the fungal toxin fusicoccin, which induces acidification of the cell wall space by activating an H^+-ATPase in the plasma membrane. These changes in cell wall acidification can be directly visualized with secreted ratiometric fluorescent protein reporters. These reporters use a red fluorescent protein that is relatively unaffected by pH as a normalizing control and a fusion (pHusion) of a yellow fluorescent protein whose fluorescence is quenched (reduced) by low pH to monitor local changes in pH.

An example of acid-induced growth can be found in the initiation of the root hair, where the local wall pH drops to a value of 4.5 at the time when the epidermal cell begins to bulge outward. Wall acidification also occurs during auxin-induced growth, but is probably not sufficient to account for all the growth induced by this hormone, and other wall-loosening processes may also be involved. Nevertheless, this pH-dependent mechanism of wall extension appears to be an evolutionarily conserved process common to all land plants and is involved in a variety of growth processes.

Acid growth may also be observed in isolated frozen and thawed or heat-treated cell wall segments, which lack normal cellular, metabolic, and synthetic processes. Such an observation entails using an extensometer to place the walls in tension and to measure long-term wall extension, or "creep" (**Figure 2.18**). The term **creep** refers to a time-dependent irreversible extension under a fixed force or load, typically the result of slippage of wall polymers relative to one another. When growing walls are incubated in neutral buffer (pH 7) and clamped in an extensometer with a fixed load (creep test), the walls extend briefly when tension is applied, but extension soon ceases. When transferred to an acidic buffer of pH 5 or less (0 min in Figure 2.18, the wall begins to extend rapidly, in some instances continuing for many hours.

This acid-induced creep is characteristic of walls in growing cells, but it is not observed in mature (nongrowing) walls. When walls are pretreated with heat, proteases, or other agents that denature proteins, they lose their acid growth ability. Such results indicate that acid

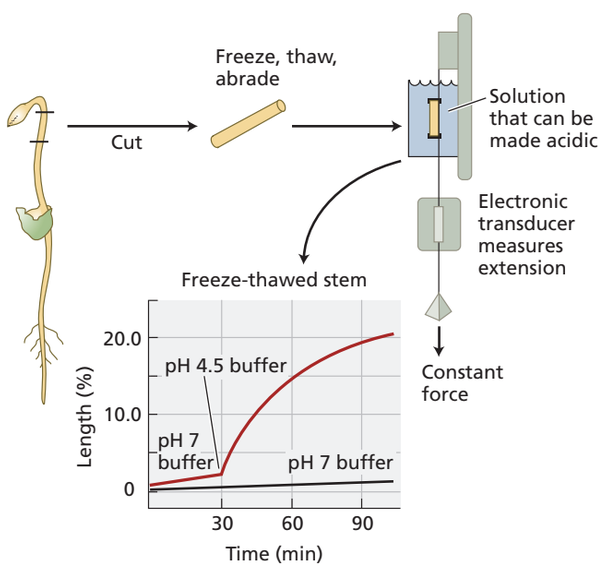


Figure 2.18 Acid-induced extension of isolated cell walls, measured in an extensometer. The wall sample from killed cells is clamped and put under tension in an extensometer that measures the length with an electronic transducer attached to a clamp. When the solution surrounding the wall is replaced with an acidic buffer (e.g., pH 4.5), the wall extends irreversibly in a time-dependent fashion (it creeps). (After D. J. Cosgrove. 1997. *Annu. Rev. Cell Dev. Biol.* 13: 171–201.)

growth is not due simply to the physical chemistry of the wall (e.g., a weakening of the pectin gel), but is catalyzed by wall proteins.

The idea that proteins are required for acid growth was confirmed in reconstitution experiments in which heat-inactivated walls were restored to nearly full acid-growth responsiveness by the addition of proteins extracted from growing walls (**Figure 2.19**). In these experiments, the active components proved to be a group of proteins that were named **expansins**. Expansins catalyze the pH-dependent extension and stress relaxation of cell walls. They are effective in catalytic amounts (about 1 part protein per 5000 parts wall, by dry weight), and they do not exhibit lytic or other enzymatic activities. Expansins exhibit structural similarities with another group of characterized plant endoglucanases, but are classified as wall-modifying proteins, as enzymatic activity cannot be demonstrated.

With the complete sequencing of several plant genomes, we now know that expansins belong to a large superfamily of proteins, divided into two major expansin families, **α-expansins** (**EXPAs**) and **β-expansins** (**EXPBs**), plus two smaller families of unknown function. In extension assays with isolated cell walls, EXPAs are more active on eudicot cell walls, whereas EXPBs are more active on grass cell walls. Current evidence indicates that EXPAs loosen cellulose–cellulose junctions containing xyloglucan, whereas EXPBs loosen wall complexes containing GAX (glucuronoarabinoxylan); this makes sense given the general differences in hemicellulose composition between eudicots and grasses. Expansins have also been discovered in a small set of bacteria and fungi, where they facilitate colonization of plant tissues. Evolutionary analysis indicates that the bacterial expansins probably arose from one or more horizontal gene transfers from a plant to a bacterium, followed by additional horizontal gene transfers among various bacterial species that colonize the vascular system of plants.

The molecular basis for expansin action on wall rheology is still uncertain, but most evidence indicates that expansins cause wall creep by loosening noncovalent adhesion between wall polysaccharides. Structural and binding studies suggest that expansins act at sites in the cell wall where cellulose microfibrils stick to one another. These hypothesized "hot spots" appear to be short, tightly connected junctions that may also be sites of pectin and hemicellulose interactions with cellulose.

Cell wall models are hypotheses about how molecular components fit together to make a functional wall

To understand how plant cells grow, it is essential to understand how the cell wall polymers are connected to produce a structure with enough tensile strength to resist turgor pressure, yet at the same time flexible enough to allow for irreversible expansion of the wall fabric and incorporation of new polymers to strengthen the wall. The complexity of the plant cell wall makes structural elucidation quite difficult. Structural models of cell walls are revised as new structural details are discovered.

The earliest molecular model of primary cell wall architecture envisioned a covalently linked matrix of hemicellulose (xyloglucans), pectins, and structural proteins that were noncovalently bonded to cellulose microfibrils. This model was later replaced by an alternative model in which xyloglucans fully coated the surfaces of cellulose microfibrils and directly tethered them into a load-bearing network, with pectins and glycoproteins forming an independent, interpenetrating matrix (**Figure 2.20A**).

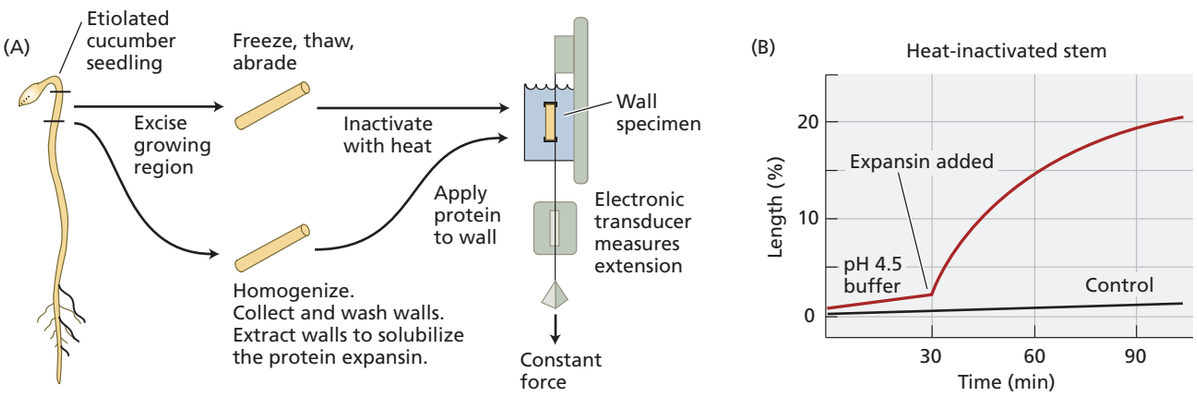


Figure 2.19 Scheme for the reconstitution of extensibility of isolated cell walls. **(A)** Cell walls are prepared as in Figure 2.18 and briefly heated to inactivate the endogenous acid extension response. To restore this response, proteins are extracted from growing walls and added to the solution surrounding the wall. **(B)** Addition of a protein mixture containing expansins restores the acid extension properties of the wall. (After D. J. Cosgrove. 1997. *Annu. Rev. Cell Dev. Biol.* 13: 171–201.)

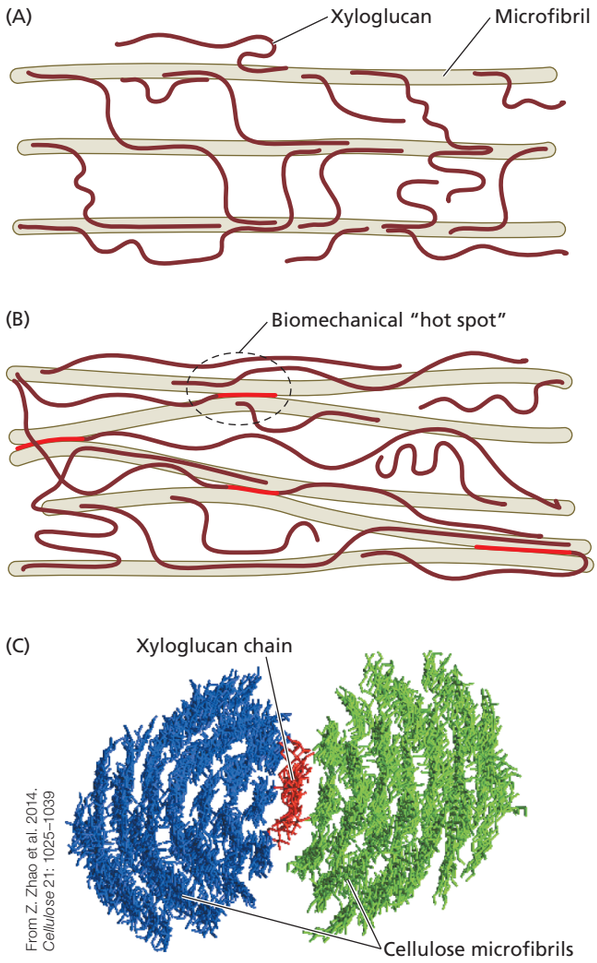


Figure 2.20 Alternative concepts of the structural role of xyloglucan. **(A)** The tethered-network model proposes that xyloglucans bind extensively to cellulose surfaces and form cross-bridges that tether microfibrils together. **(B)** The biomechanical "hot spot" model proposes that most of the xyloglucan is not load-bearing and that wall extension and mechanics are controlled at limited regions where cellulose microfibrils come in close contact, aided by entrapped xyloglucan. **(C)** A computational simulation of two cellulose microfibrils (blue and green, shown in cross section) bonded together by a xyloglucan chain (red). (B after Y. B. Park and D. J. Cosgrove. 2012. *Plant Physiol.* 158: 1933–1943.)

In recent years, the "tethered-network" model has undergone substantial revision as new data have been collected. NMR data indicate that only about 10% of cellulose microfibril surfaces are coated by xyloglucan and that pectins directly contact cellulose surfaces. Biomechanical analyses of cell walls digested with substrate-specific endoglucanases show that the majority of xyloglucan does not contribute to wall mechanics and that cellulose is not directly linked by extensive xyloglucan tethers. Instead, the results suggest that a quantitatively minor pool of xyloglucan intertwines with cellulose to form structurally important junctions that control wall creep and mechanical extensibility. Moreover, expansin has been found to target a site with similar properties, that is, one containing both xyloglucan and cellulose with altered crystalline structure. Last, Arabidopsis mutants have been generated that completely lack xyloglucan, yet exhibit relatively minor growth defects. This surprising result demonstrates that xyloglucan is not essential for plant growth, and also underscores the impressive plasticity and adaptability of plant cell wall composition.

From these studies a new model is emerging about the functional architecture of growing cell walls. The revised view posits a microscale network containing biomechanical "hot spots," which are limited junctions of bundled cellulose microfibrils where wall extensibility and mechanics are controlled (**Figure 2.20B and C**). In support of this idea, computational modeling shows that a monolayer of xyloglucan sandwiched between cellulose microfibrils could provide appreciable mechanical strength to cell walls. This "hot spot" model, like the models before it, must be considered a hypothesis in need of further testing, validation, and with experimental progress, likely revision.

Many structural changes accompany the cessation of wall expansion

The growth cessation that occurs during cell maturation is generally irreversible and is typically accompanied by a reduction in wall extensibility, as measured by various biophysical methods. These physical changes in the wall might come about by (a) a reduction in wall-loosening processes, (b) an increase in wall cross-linking, and/or (c) an alteration in the composition of the wall, making for a more rigid structure or one less susceptible to wall loosening. There is some evidence supporting each of these ideas.

Several modifications of the maturing wall may contribute to wall rigidification:

- Newly secreted matrix polysaccharides may be altered in structure, thereby forming tighter complexes with cellulose or other wall polymers, or they may be resistant to wall-loosening activities.
- Removal of (1,3;1,4)-β-D-glucan in grass cell walls is coincident with growth cessation in these walls and may cause wall rigidification.
- De-esterification of pectins, leading to pectin gels that are more rigid, is similarly associated with growth cessation in both grasses and eudicots.
- Cross-linking of phenolic groups in the wall (such as tyrosine residues in hydroxyproline-rich glycoproteins, ferulic acid residues attached to

matrix polysaccharides, and lignin) generally coincides with wall maturation and is believed to be mediated by peroxidase, a putative wall rigidification enzyme.

- Microtubules and associated cellulose synthase complexes show reorientation of alignment parallel to the growth axis in some anisotropically elongating cells, coincident with growth slowing.

Thus, many structural changes in the wall occur during and after cessation of growth, and it has not yet been possible to identify the significance of individual processes for cessation of wall expansion.

2.4 Secondary Cell Wall Structure and Function

The secondary cell wall (SCW) is a hierarchical structure assembled by some living cells inside the primary cell wall after wall expansion has ceased (**Figure 2.21A and B**). The best-studied SCWs are from cells that are highly lignified and dead at maturity, such as tracheids, xylem

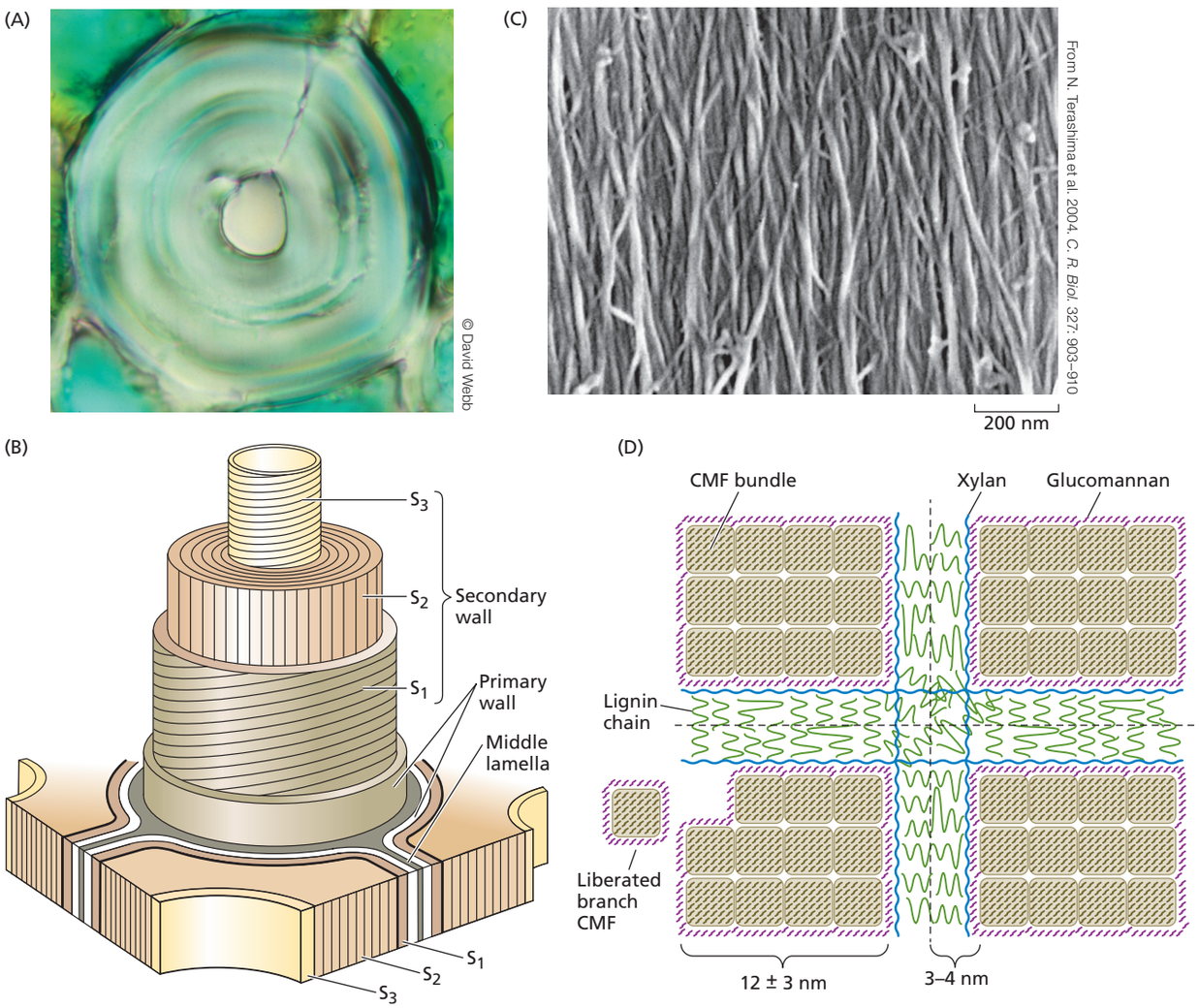


Figure 2.21 **Multi-scale structure of secondary cell walls.** **(A)** Cross section of a *Podocarpus* sclereid, in which multiple layers in the secondary wall are visible. **(B)** Diagram of the cell wall organization often found in tracheids and other cells with thick secondary walls. Three distinct layers (S_1, S_2, and S_3) are formed interior to the primary wall. **(C)** Macrofibrils visible on the inner surface of a *Ginko* tracheid cell wall, as seen by field emission scanning electron microscopy. **(D)** A model of macrofibril structure and packing. Here four macrofibrils are shown in a transverse section as three-by-four arrays of elementary cellulose microfibrils (CMFs) that are tightly packed and coated with glucomannan. Binding the macrofibrils together is a lignin–xylan layer. (D after N. Terashima et al. 2009. *J. Wood Sci.* 55: 409–416.)

vessels, and fibers in woody tissues, but other notable examples include phloem and interfascicular fibers, stone cells, and epidermal cells such as cotton fibers, which are not lignified but do become incredibly thick by amassing strong cellulose-rich walls.

SCWs generally serve a structural, reinforcing role. In contrast to primary cell walls, which can extend dynamically, incorporate new materials, and withstand tensile forces generated by cell turgor, SCWs are structurally designed to resist compressive and tensile forces generated by gravity, external forces causing organ bending, and negative hydrostatic pressures arising during transpiration; they can even deter feeding by herbivores. The mechanical properties of SCWs are stable, enduring even after cell death, and are determined by wall architecture and physical interactions among cell wall polymers.

As mentioned in Section 2.1, SCW cellulose in woody tissues is synthesized by a set of three CESAs different from the three CESAs used to synthesize primary cell wall cellulose. The significance of this fact for cellulose structure is unclear at this time, but possibly it has an impact on how cellulose synthase complexes function, either separately or in clusters to make macrofibrils (assemblages of microfibrils). One striking consequence of defects in SCW cellulose synthesis is xylem vessel collapse. Another important distinction of SCWs is that their hemicelluloses have xylan and (gluco-) mannan backbones with low degrees of substitution (few side chains), whereas the hemicelluloses of primary cell walls are highly substituted. This difference has a major impact on hemicellulose properties, such as conformation, solubility, and binding to cellulose, and probably has a substantial effect on packing of cellulose microfibrils in the cell wall.

Secondary cell walls are rich in cellulose and hemicellulose and often have a hierarchical organization

The temporal history of the SCW, as reflected in its layered structure, is even more obvious than that of the primary wall. The best-studied SCWs consist of sequentially formed concentric layers named, from oldest to youngest, S_1, S_2, S_3, and so on; the number of layers varies with cell type (see Figure 2.21B). SCWs with two or three layers are common in wood and fibers. Cellulose orientation is distinct for each layer, with the first-deposited layer (S_1) oriented in a shallow, nearly transverse helix, whereas cellulose in the thicker S_2 layer is oriented more longitudinally. In fiber cells (see Chapter 1), there is often a special type of SCW deposited in a final step and forming a "gelatinous" layer. This wall section is rich in cellulose and pectins (typically rhamnogalacturonans) that make it strong but also flexible. This structure allows for contraction when needed to balance increasing external forces, as are observed in tension wood. There is some debate about whether this gelatinous layer should be considered a tertiary wall.

MACROFIBRIL FORMATION, STRUCTURE, AND ADHESION SCW lamellae contain highly aligned cellulose microfibrils that are assembled into tightly packed macrofibrils, which in turn coalign with each other and are separated by hemicellulose and lignin (**Figure 2.21C**). The concept of the macrofibril as an aggregate of numerous individual microfibrils is based largely on high-resolution electron microscopy of de-lignified and partially deconstructed cell walls. The appearance of macrofibrils in the wall suggests that their formation is well organized and begins at the earliest stages of cellulose microfibril formation. One possibility is that clusters of cellulose synthesis complexes—one for each elementary microfibril—coordinately produce microfibrils that align and coalesce immediately to form a macrofibril, with hemicellulose interaction occurring afterward. This process may be mediated by auxiliary proteins in the COBRA and KORRIGAN families, as their mutant phenotypes include reduced cell wall organization.

Molecular models of SCWs are much less developed than those developed for primary cell walls. One hypothetical model by Terashima and coworkers (**Figure 2.21D**) illustrates some basic concepts of macrofibril construction at the nanoscale. The model proposes a structured arrangement of matrix polymers, with glucomannans coating the macrofibril surface, xylans positioned in the next layer, and lignin linking xylans and filling the remaining space between macrofibrils. Other models suggest that lignin is intercalated and intertwined among hemicellulose chains. The details of macrofibril structure may also differ among species with different hemicellulose composition.

Physical and computational studies indicate that macrofibrils are prevented from fusing into one massive cellulose crystal by water trapped between the constituent microfibrils. Misalignment and twisting of individual microfibrils may also help prevent such crystallization. Macrofibril diameter also varies with cell type and wall lamella in a manner that correlates with lignin content.

Lignification transforms the SCW into a hydrophobic structure resistant to deconstruction

SCWs are often lignified, a process that starts after SCW formation is well underway. Lignification may even continue after cell death of some cell types, with metabolic contributions from neighboring, living cells. The major building blocks of lignin, called monolignols, are sinapyl and coniferyl alcohols, with minor amounts of *p*-coumaryl alcohol (**Figure 2.22A**). Monolignols are synthesized in the cell from phenylalanine via the phenylpropanoid pathway (see **WEB APPENDIX 4**).

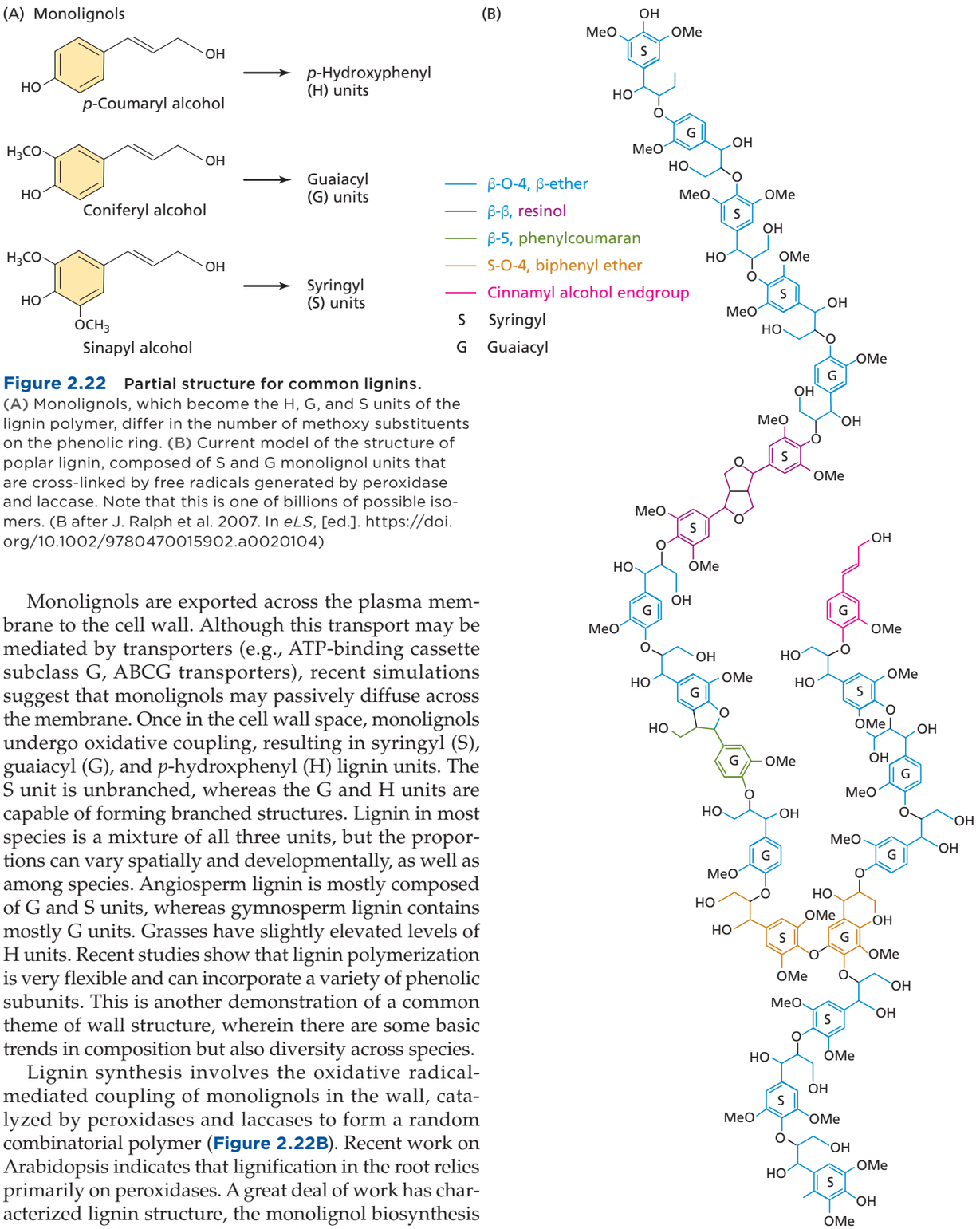


Figure 2.22 **Partial structure for common lignins.** **(A)** Monolignols, which become the H, G, and S units of the lignin polymer, differ in the number of methoxy substituents on the phenolic ring. **(B)** Current model of the structure of poplar lignin, composed of S and G monolignol units that are cross-linked by free radicals generated by peroxidase and laccase. Note that this is one of billions of possible isomers. (B after J. Ralph et al. 2007. In *eLS*, [ed.]. https://doi.org/10.1002/9780470015902.a0020104)

Monolignols are exported across the plasma membrane to the cell wall. Although this transport may be mediated by transporters (e.g., ATP-binding cassette subclass G, ABCG transporters), recent simulations suggest that monolignols may passively diffuse across the membrane. Once in the cell wall space, monolignols undergo oxidative coupling, resulting in syringyl (S), guaiacyl (G), and *p*-hydroxphenyl (H) lignin units. The S unit is unbranched, whereas the G and H units are capable of forming branched structures. Lignin in most species is a mixture of all three units, but the proportions can vary spatially and developmentally, as well as among species. Angiosperm lignin is mostly composed of G and S units, whereas gymnosperm lignin contains mostly G units. Grasses have slightly elevated levels of H units. Recent studies show that lignin polymerization is very flexible and can incorporate a variety of phenolic subunits. This is another demonstration of a common theme of wall structure, wherein there are some basic trends in composition but also diversity across species.

Lignin synthesis involves the oxidative radical-mediated coupling of monolignols in the wall, catalyzed by peroxidases and laccases to form a random combinatorial polymer (**Figure 2.22B**). Recent work on Arabidopsis indicates that lignification in the root relies primarily on peroxidases. A great deal of work has characterized lignin structure, the monolignol biosynthesis pathway, and strategies for modifying this pathway to manipulate lignification. In woody tissues, lignin polymerization usually starts at cell corners in the primary cell

wall and the middle lamella, then spreads progressively to the SCW lamellae. The basis for this pattern of lignification is not well understood, but it is generally speculated that nucleation sites exist in the pectin-rich middle lamella where lignification starts and that physical characteristics of the wall matrix may influence radical-based monolignol polymerization and cross-linking to wall polysaccharides.

A special case of lignification occurs in a narrow region of the root endodermal wall called the Casparian strip (see Chapter 1), which forms a hydrophobic barrier between the stele and the cortex. The Casparian strip contains lignin that is polymerized in a very restricted part of the cell wall. Key factors controlling its synthesis include **CASPARIAN STRIP PROTEIN 1** (**CASP1**), which organizes membrane proteins at the Casparian strip; an NADPH oxidase that generates hydrogen peroxide; and a peroxidase that generates the monolignol radical intermediate (**Figure 2.23**). In addition, the wall protein **ENHANCED SUBERIN 1** (**ESB1**) is essential for proper lignification in this narrow region of the cell wall. ESB1 is a member of the class of proteins known as **dirigent-domain proteins** (from the Latin *dirigere*, "to direct"), which may guide the stereochemistry of a compound synthesized by other enzymes. The exact function of ESB1 is unclear, but it may nucleate lignin formation specifically in the Casparian strip of the endodermal cell wall. A laccase isoform (LACCASE3) appears to function upstream of CASP1 in positioning of the Casparian strip, despite having no evident function in lignin formation.

Although lignification is associated with wall strengthening, the physical basis for this effect is not clear. Lignin was previously thought to form a massive macromolecule that interpenetrated and cross-linked the wall, but more recent results indicate that native lignin (or "protolignin") is smaller than previously believed. Notably, the S-rich lignin of transgenic poplar overexpressing ferulate 5-hydroxylase has a degree of polymerization of only 10, yet the plants appear phenotypically normal. Technical obstacles make it difficult to assess the extent of lignin cross-linking in other cell walls, but extensive cross-linking does not appear to be essential for wood formation in poplar.

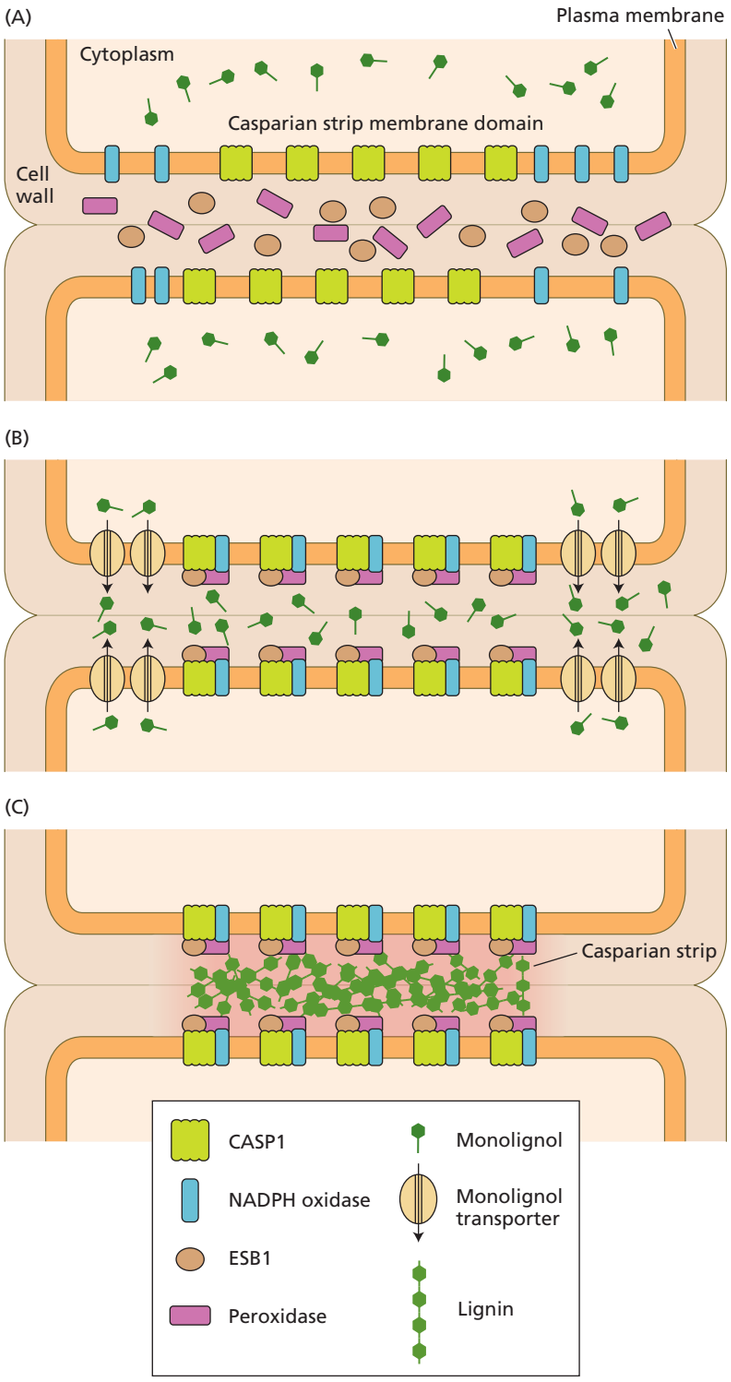


Figure 2.23 **Schematic representation of Casparian strip deposition.** **(A)** CASPs are initially distributed uniformly around the plasma membrane but soon aggregate at a central domain, referred to as the Casparian strip membrane domain (CSD). **(B)** NADPH oxidase and peroxidase are recruited to the CSD, and monolignols are exported in a nontargeted process to the apoplast. **(C)** Lignin polymerization occurs exclusively in the cell wall adjacent to the CSD because the enzymes are localized there. CASP1, CASPARIAN STRIP PROTEIN 1; ESB1, ENHANCED SUBERIN 1. (After D. Roppolo and N. Geldner. 2012. *Curr. Opin. Plant Biol.* 15: 608–617.)

In support of lignin's proposed function in plant cell walls, addition of lignin to composite hydrogel materials made in the lab increases compressive and tensile strength, deformation recoverability, and fracture force. As the SCW becomes lignified, water is removed and is replaced by the hydrophobic lignin molecules. This tends to enhance noncovalant interactions between lignin and polysaccharides, perhaps accounting for some of the wall strengthening. There is also evidence for extensive covalent linking between lignin and wall polysaccharides, but these linkages have been difficult to characterize in detail. In grass cell walls, lignin–carbohydrate linkages are largely via ferulate groups attached to arabinose residues in GAX (see Figure 2.10C).

Summary

The architecture, mechanics, and function of plants depend on the structure of the cell wall. The wall is secreted and assembled as a complex structure that varies in form and composition as the cell differentiates.

2.1 Overview of Plant Cell Wall Functions and Structures

- Cell walls vary greatly in form and composition, depending on cell type and species (**Figures 2.1, 2.3, 2.4**).
- Primary cell walls are synthesized in actively growing cells, whereas secondary cell walls are deposited in certain cells, such as xylem vessel elements and sclerenchyma fibers, after cell expansion ceases (**Figures 2.2–2.4**).
- The middle lamella is a pectin-rich layer between the primary walls of adjoining cells that is formed during cell division (**Figure 2.2**)
- The primary cell wall is a network of cellulose microfibrils embedded in a matrix of hemicelluloses, pectins, and structural proteins (**Figures 2.5, 2.6; Table 2.1**).
- Cellulose microfibrils are highly ordered arrays of glucan chains synthesized at the surface of the cell by protein complexes called cellulose synthase complexes. (**Figures 2.7, 2.8**).
- Matrix polysaccharides are synthesized in the Golgi apparatus and secreted via vesicles (**Figure 2.9**).
- Hemicelluloses bind microfibrils together, and pectins form hydrophilic gels that can become cross-linked by calcium ions (**Figures 2.10–2.12**).
- Secondary walls in woody tissues typically contain xylans and glucomannans instead of xyloglucan and pectin.

2.2 The Dynamic Primary Cell Wall

- Wall assembly occurs partly by spontaneous self-assembly but may also be mediated by enzymes. Xyloglucan endotransglucosylase (XET) has the ability to carry out transglycosylation reactions that integrate newly synthesized xyloglucans into the wall (**Figure 2.13**).

2.3 Mechanisms of Cell Expansion

- Wall expansion may be highly localized (tip growth) or more dispersed over the wall surface (diffuse growth) (**Figure 2.14**).
- In diffuse-growing cells, the orientation of cell growth is determined by the orientation of cellulose microfibrils, which is determined by the orientation of microtubules in the cytoplasm (**Figures 2.15–2.17**).
- The actions of hormones (such as auxin, gibberellin, and brassinosteroids) and environmental conditions (such as light and water availability) modulate cell expansion by altering wall extensibility, or the yield properties of the wall.
- Biochemical loosening of the cell wall leads to wall stress relaxation, which dynamically links water uptake with cell wall expansion in the growing cell.
- Complicated cell growth patterns, like the "jigsaw" pattern seen in leaf epidermal pavement cells, involve localized pressure points generated by cellular expansion and interactions with cytoskeletal elements.
- Acid-induced cell wall extension is characteristic of walls in growing cells and is mediated by proteins called expansins, which loosen the noncovalent adhesions between wall polysaccharides (**Figures 2.18, 2.19**).
- Cessation of cell growth during cell maturation involves multiple mechanisms of cell wall cross-linking and rigidification.

2.4 Secondary Cell Wall Structure and Function

- Secondary cell walls are typically thick layers deposited between the plasma membrane and the primary cell wall. They add strength and compression resistance to stems and other organs.
- The secondary cell walls of woody tissues comprise two or more layers containing cellulose, hemicellulose, and lignin.
- Lignin is formed in the wall by oxidative coupling of monolignols into a random polymer of phenolic subunits. This results in crosslinking of lignin, which locks the secondary cell wall into a hydrophobic material that is resistant to enzymatic deconstruction (**Figures 2.21, 2.22**).

Web Material

- **WEB TOPIC 2.1 Terminology for Polysaccharide Chemistry** A brief review of terms used to describe the structures, bonds, and polymers in polysaccharide chemistry is provided.
- **WEB TOPIC 2.2 Matrix Components of the Cell Wall** The secretion of xyloglucan and glycosylated proteins by the Golgi apparatus can be demonstrated at the ultrastructural level.
- **WEB TOPIC 2.3 The Mechanical Properties of Cell Walls: Studies with Nitella** Experiments have demonstrated that the inner 25% of the cell wall determines the directionality of cell expansion.
- **WEB ESSAY 2.1 Microtubules, Microfibrils, and Growth Anisotropy** The orientations of microtubules and of microfibrils are not always correlated with the directionality of growth.
- **WEB ESSAY 2.2 Biophysical Coordination of Water Uptake and Cell Wall Enlargement** A physical model provides a quantitative framework for relating the physics of water absorption to wall extension and for assessing the limiting physical factors for cell growth.

For more study aids, go to oup.com/he/taiz7e.

Suggested Reading

Albersheim, P., Darvill, A., Roberts, K., Sederoff, R., and Staehelin, A. (2011) *Plant Cell Walls*. Garland Science, New York.

Baskin, T. I. (2005) Anisotropic expansion of the plant cell wall. *Annu. Rev. Cell Dev. Biol.* 21: 203–222.

Boerjan, W., Ralph, J., and Baucher, M. (2003) Lignin biosynthesis. *Annu. Rev. Plant Biol.* 54: 519–546.

Cosgrove, D. J. (2005) Growth of the plant cell wall. *Nat. Rev. Mol. Cell Biol.* 6: 850–861.

Cosgrove, D. J., and Jarvis, M. C. (2012) Comparative structure and biomechanics of plant primary and secondary cell walls. *Front. Plant Sci.* 3: 204.

Lu, F., and Ralph, J. (2010) Lignin. In *Cereal Straw as a Resource for Sustainable Biomaterials and Biofuels*, R. C. Sun (ed.), Elsevier, Amsterdam, pp. 169–207.

Mohnen, D. (2008) Pectin structure and biosynthesis. *Curr. Opin. Plant Biol.* 11: 266–277.

Niklas, K. (2004) The cell walls that bind the tree of life. *Bioscience* 54: 831–841.

Paredez, A. R., Somerville, C. R., and Ehrhardt, D. W. (2006) Visualization of cellulose synthase demonstrates functional association with microtubules. *Science* 312: 291–295.

Plomion, C., Leprovost, G., and Stokes, A. (2001) Wood formation in trees. *Plant Physiol.* 127: 1513–1523.

Sampedro, J., and Cosgrove, D. J. (2005) The expansin superfamily. *Genome Biol.* 6: 242.

Waldron, K. W., and Brett, C. T. (2007) The role of polymer cross-linking in intercellular adhesion. In *Plant Cell Separation and Adhesion,* J. Roberts and Z. Gonzalez-Carranza (eds.), Blackwell, Oxford, pp. 183–204.

Zhong, R., and Ye, Z. H. (2007) Regulation of cell wall biosynthesis. *Curr. Opin. Plant Biol.* 10: 564–572.

3 Genome Structure and Gene Expression



LAURA_VN/Shutterstock

The observable characteristics of a plant (its **phenotype**) are a product of its genotype (all the genes, or alleles, that determine the plant's traits), the pattern of epigenetic chemical modifications of its DNA and associated histones that alter gene expression, and the environment in which it lives. In Chapter 1 we reviewed the fundamental structure and function of DNA, its packaging into chromosomes, and the two major phases of gene expression: transcription and translation. In this chapter we discuss how the composition of the genome beyond its genes influences the physiology and evolution of the organism. First we look at the structure and organization of the nuclear genome and the non-gene elements it contains and contrast that with the cytoplasmic genomes, which are contained inside the mitochondria and plastids. Next we discuss the cellular machinery needed to transcribe and translate the genes into functional proteins, and we see how transcriptional and posttranscriptional processes combine to regulate overall gene expression. We then introduce some of the tools used to study gene function, and we finish up with a discussion of the use of genetic engineering in research and agriculture.

3.1 Nuclear Genome Organization

As discussed in Chapter 1, the nuclear genome contains most of the genes required for the plant's physiological functions. The first plant genome to be fully sequenced was that of a small eudicot angiosperm called thale cress, or Arabidopsis thaliana. The genome of Arabidopsis is made up of only about 157 million base pairs (Mbp), which are distributed over five chromosomes. By contrast, the genome of the monocot Japanese canopy plant (Paris japonica), the plant species with the largest known genome, contains about 150,000 Mbp. Most angiosperms are hermaphroditic, meaning they carry both male and female sex organs on the same plant, and indeed often on the same flower. There are some higher, and many lower, plants that exist in either male or female form. These species with unisexual individuals are called dioecious. These dioecious species also have specific sex chromosomes—sometimes differentiated as X and Y chromosomes—that, just as in humans, carry the information for sex determination. Within its nuclear genome, Arabidopsis holds

27,416 protein-coding genes and another 4827 genes that are either **pseudogenes** (nonfunctional genes) or parts of transposons (mobile DNA elements). The Arabidopsis genome also contains 1359 genes that produce noncoding RNAs (ncRNAs). Some of these ncRNAs include ribosomal and transfer RNAs, whereas others are probably involved in gene regulation. We describe both transposons and ncRNAs in more detail later in this chapter.

The plant genome, however, consists of much more than genes. In this section we examine the organization and chemical makeup of the genome, then see how certain regions of the genome correspond to specific functions.

The nuclear genome is packaged into chromatin

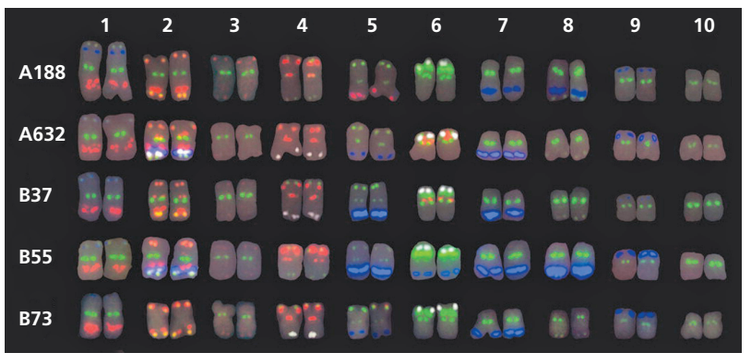
The nuclear genome consists of DNA molecules that are wrapped around histone proteins to form beadlike structures called **nucleosomes** (see Chapter 1). DNA and histones, together with other proteins that bind to the DNA, are referred to as **chromatin** (see Figure 1.15). Two types of chromatin can be distinguished: euchromatin and heterochromatin. Historically, these two types were differentiated based on their appearance in light microscopy when stained with specific dyes. **Heterochromatin** is usually more tightly packaged and thus appears darker than the less condensed **euchromatin**. Most genes that are actively transcribed in a plant are located in the euchromatic regions of a chromosome, while genes located in heterochromatic regions are either inactive or silent, at least in most tissues. Complete silencing of genes will eventually lead to the accumulation of mutations that incur no evolutionary cost (i.e., the mutation does not help or hurt the individual) and render the gene defunct. Such genes are examples of pseudogenes. Compared with euchromatin, heterochromatin is relatively gene-poor. Heterochromatic regions include the centromeres, several so-called knobs, and the regions immediately adjacent to the telomeres, or chromosome ends, known as the **subtelomeric regions**.

Heterochromatic structures often consist of highly repetitive DNA sequences, or **tandem repeats**: blocks of nucleotide motifs of about 150 to 180 bp that are repeated over and over. A second class of repeats is called the **dispersed repeats**. One type of dispersed repeat is known as **simple sequence repeats** (**SSRs**), or **microsatellites**. These repeats consist of sequence motifs that are usually between two and six nucleotides long and that are repeated hundreds or even thousands of times. Another dominant group of dispersed repeats found in heterochromatin is the transposons.

Centromeres, telomeres, and nucleolar organizer regions contain repetitive sequences

The most prominent structural landmarks on chromosomes are centromeres, telomeres, and nucleolar organizer regions. These regions contain repetitive DNA sequences that can be made visible by fluorescent in situ hybridization (FISH), a technique that uses fluorescently labeled molecular probes—usually fragments of DNA—that bind specifically to the sequence to be identified (**Figure 3.1**). **Centromeres** are constrictions of the chromosomes where spindle fibers attach during cell division. The attachment of fibers to the centromere is mediated by the kinetochore, a protein complex surrounding the centromere (see Chapter 1). Usually centromeres consist of highly repetitive DNA regions including tandem repeats and/or inactive transposons. Although these repetitive sequences are often only between 150 and 180 bp long, the total size of plant centromeres can range from hundreds of kilobase pairs to several megabase pairs in length. Because of the length and repetitiveness of centromeres, determining their exact sequence has been difficult for genome scientists, even in the era of routine whole-genome sequencing. **Telomeres** are sequences located at the ends of each chromosome. Telomeres act as caps on the chromosome ends, prevent loss of DNA during DNA replication, and inhibit end-to-end fusion of chromosomes mediated via double-strand break repair mechanisms.

The RNA molecules that make up ribosomes (rRNA) are transcribed from **nucleolar organizer regions** (**NORs**). Because ribosomes are composed mostly of rRNA and proteins, and because many ribosomes are needed for translation, it is not surprising that NORs contain hundreds of repeated copies of each rRNA gene. Depending



From A. Kato et al. 2004. *Proc. Natl. Acad. Sci. USA* 101:13554–13559 © National Academy of Sciences, U.S.A.

Figure 3.1 Chromosomal landmarks, including centromeres, telomeres, and nucleolar organizer regions (NORs), can be used to identify individual chromosomes. Each row shows the ten chromosome pairs of a different inbred line of maize (*Zea mays*; five common lines are shown here, from A188 to B73). DNA sequences (probes) complementary to certain chromosomal landmarks were labeled with fluorescent dyes and hybridized to chromosome preparations. The centromeres can be seen as green dots near the middle of the chromosomes, the NOR as a larger green area on chromosome 6, and the telomeres as faint red dots, most clearly visible at the top of chromosomes 2–4. The larger blue areas are specific heterochromatic regions.

on the plant species, one or several NORs are present within the genome (maize; [*Zea mays*] has one, on chromosome 6; see Figure 3.1). Due to their repetitive nature and high GC content, NORs can be seen through a light microscope (after staining) and thus can serve as chromosome-specific markers. Visible chromosomal markers such as these were used by early geneticists to map phenotypic traits to specific chromosomal regions. Despite its repetitive nature, rDNA (DNA that encodes rRNA) is actively transcribed. The prominent nuclear structure called the nucleolus (see Figure 1.14) consists of the rDNA of the NOR, the proteins that transcribe the rDNA and process the rRNA primary transcripts for assembly into ribosomes, and the immature ribosomes just being assembled.

Transposons are mobile sequences within the genome

One dominant type of repetitive DNA within the heterochromatic regions of the genome is the transposon. **Transposons**, or **transposable elements**, are also known as *jumping genes* because some of them have the ability to insert a copy of themselves into a new location within the genome.

There are two large classes of transposons: the retroelements, or retrotransposons (Class 1), and the DNA transposons (Class 2). These two classes are distinguished by their mode of replication and insertion into a new location (**Figure 3.2**). **Retrotransposons** make an RNA copy of themselves, which is then reverse-transcribed into DNA before it is inserted elsewhere in the genome (see Figure 3.2A). Because they do not normally leave their original location, but rather generate additional copies of themselves, active retrotransposons tend to multiply within the genome. Retrotransposon-derived genome content varies widely among species. In Norway spruce (*Picea abies*), retrotransposons make up an estimated 58% of the genome, while in the carnivorous bladderwort *Utricularia gibba*, retrotransposons occupy no more than about 3.5% of the genome. **DNA transposons**, by contrast, move from one position to another using a cut-and-paste mechanism catalyzed by an enzyme that is encoded within the transposon sequence. This enzyme, **transposase**, splices out the transposon and inserts it elsewhere in the genome, in most cases keeping the total transposon copy number the same (see Figure 3.2B).

Transposition into a gene can result in mutations. If a transposon lands within a coding region, the gene may be inactivated. Insertion of a transposon close to a gene can also alter that gene's expression pattern. For example, the transposon may disrupt the gene's normal regulatory elements, preventing transcription or, since transposons often carry promoters, increasing transcription of the gene. The mutagenic capability of transposons may play an important role in the evolution of the host genome. A low level of mutagenesis can lead to novel

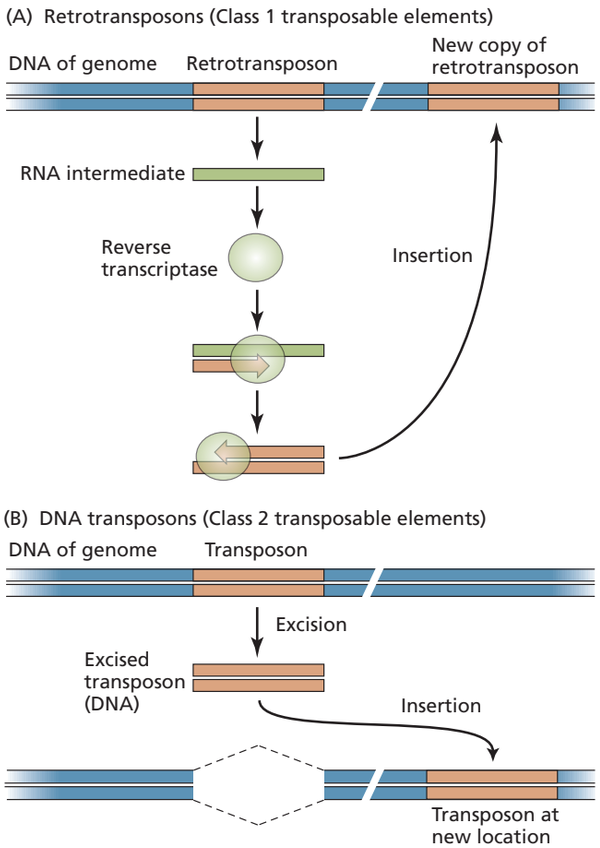


Figure 3.2 The two major classes of transposons differ in their mode of transposition. (A) Retrotransposons move via an RNA intermediate. (B) DNA transposons move using a cut-and-paste mechanism.

variation in an individual that can be passed on to the next generation. However, if the transposition rate is high, resulting in individuals with many mutations, at least some of those mutations are likely to be deleterious and to decrease the overall fitness of the individual.

Plants and other organisms are able to regulate the activity of transposons through the methylation of DNA and histones. As we will see later in this chapter, these same processes are used to repress transcription in heterochromatic regions of the genome. As more genomic DNA sequences have become available, scientists have noticed large numbers of highly methylated transposons in heterochromatic regions. Studies of mutants that are unable to maintain genome methylation have shown that slow loss of methylation over generations can activate dormant transposons and increase the frequency of transpositional mutations (**Figure 3.3**). Such transposon activity may considerably decrease the fitness of offspring. Therefore, methylation and the formation of heterochromatin appear to play important roles in the stability of the genome. Interestingly, in the never-ending evolutionary arms race of two opposing mechanisms, scientists have

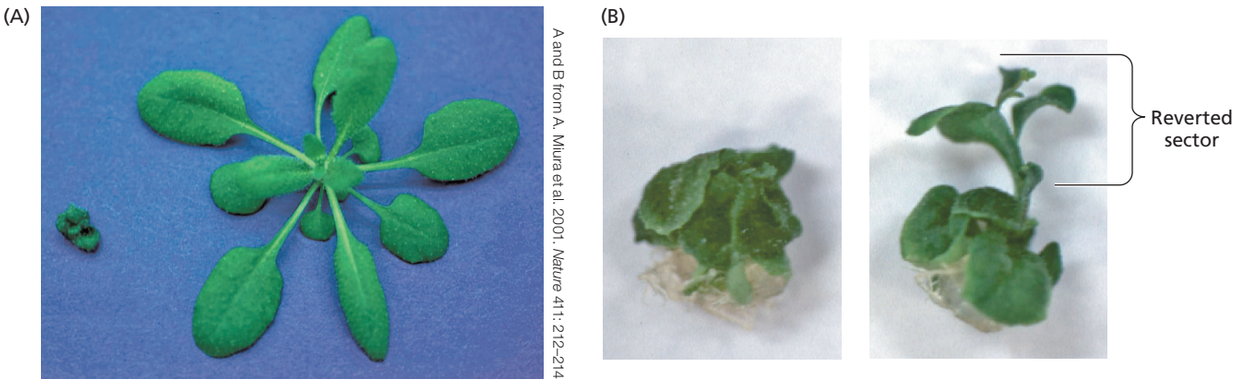


Figure 3.3 Loss of methylation can lead to mutations as unmethylated transposons become active. A mutation called *decrease in dna methylation* (*ddm1*) causes hypomethylation (decreased methylation) of endogenous transposons in Arabidopsis. The *clam* mutation, which arose in a *ddm1* mutant, is the result of insertion of a transposon into the *DWARF4* (*DWF4*) gene, which is required for the biosynthesis of the growth hormone brassinosteroid. **(A)** The transposon-induced *clam* mutant (left) next to wild-type Arabidopsis. **(B)** The *clam* mutant without (left) and with (right) a sector that has reverted to the wild-type phenotype after the transposon jumped back out of the *DWF4* gene.

found transposons whose transposase promoter regions are all but devoid of sequence sites that a methylase could use for methylation, thus evading the plant's silencing mechanisms. Transposons have also been shown to acquire sequence motives that allow them to be regulated by the plant's gene regulatory machinery. One such example is the *ONSEN* transposon, which is activated by heat-sensitive plant transcription factors.

Chromosome organization is not random in the interphase nucleus

During interphase of the cell cycle, the chromosomes decondense. However, interphase chromosomes are not randomly arranged or entangled with each other like a plate of spaghetti; rather, each chromosome occupies a discrete location within the nucleus called the **chromosome territory**. Chromosomes in species with larger genomes orient their chromosomes so that centromeres and telomeres of each chromosome are on opposite poles of the nucleus, a conformation known as the **Rabl configuration**, after the Austrian scientist Carl Rabl, who first proposed such arrangement as early as 1885 (**Figure 3.4A**). However, chromosomes in plants with smaller genomes, such as Arabidopsis, do not adopt a Rabl configuration, and instead seem to cluster their telomeres around the nucleolus in a rosette-like formation (**Figure 3.4B**). Methods that capture chromatin in its native conformation are now being developed. One such technique is called Chromatin Conformation Capture, or 3C. With this technique, parts of the chromosome that are adjacent in the coiled arrangement of the molecule are cross-linked; the DNA is then cut into small pieces, leaving only the cross-linked parts attached to each other. The cross-linked regions are then sequenced, allowing the researcher to identify areas along the chromosome that were adjacent to each other in the cell.

Meiosis halves the number of chromosomes and allows for the recombination of alleles

In Chapter 1 we discussed the events during mitotic cell division. During the production of gametes, cells are divided in a similar fashion as during mitosis but with several important differences. During the first meiotic division, DNA is exchanged between homologous chromosomes before the chromosomes are separated into daughter cells, resulting in the recombination of genetic material (meiotic recombination) (**Figure 3.5**). The second meiotic division segregates the sister chromatids, resulting in four

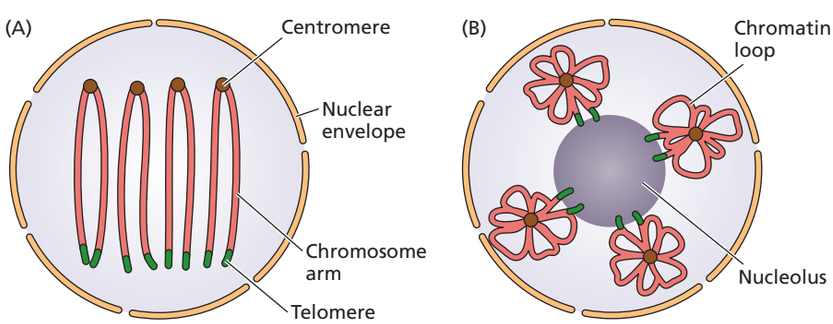


Figure 3.4 Chromosome arrangements in the interphase nucleus. **(A)** Rabl configuration of chromosomes, where centromeres and telomeres of all chromosomes point away from each other. **(B)** Rosette configuration of chromosomes, where the telomeres are oriented toward the nucleolus. (After C. L. Tiang et al. 2013. *Plant Physiol.* 158: 26–34.)

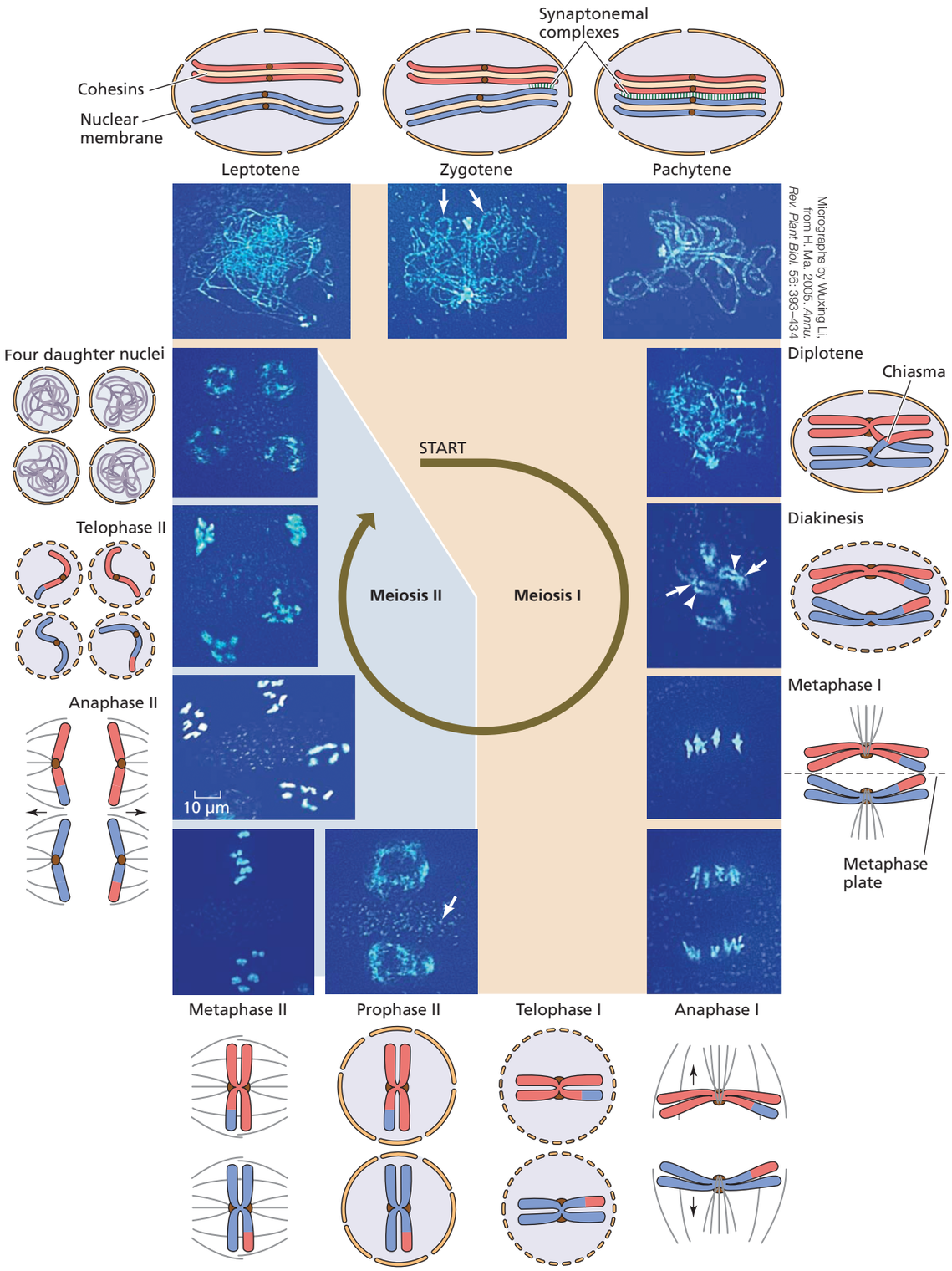
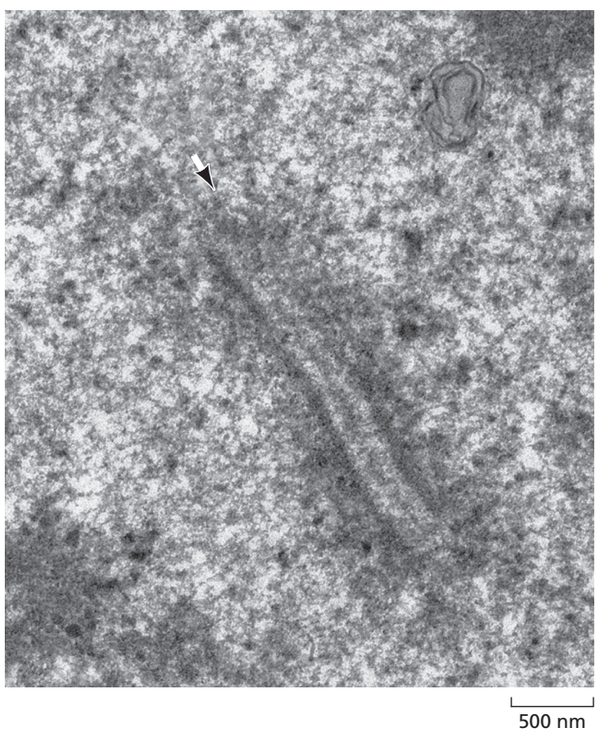


Figure 3.5 **Male meiosis in Arabidopsis.** The illustration shows the chromosomal state at each stage for one chromosome only. Prophase I starts at the leptotene stage and goes through diakinesis. See text for details. Arrows in zygotene of prophase I indicate visible areas of chromosome pairing; in diakinesis of prophase I, arrows indicate chiasmata and arrowheads indicate centromeres. Cohesins are proteins that hold sister chromatids together. Synaptonemal complexes (green lines) are protein complexes that form between homologs. DNA is stained with DAPI. (After L. Grandont et al. 2013. *Cytogenet. Genome Res.* 140: 171–184.)

daughter cells per original cell. Because meiosis involves two cell divisions but only one round of DNA replication, the daughter cells each have half as much genetic material as the original cell: A diploid (2*N*) plant produces haploid (1*N*) gametes. This is called meiotic reduction.

The first major phase in meiosis, prophase, is divided into five stages: leptotene, zygotene, pachytene, diplotene, and diakinesis. During leptotene, homologous regions within pairs of homologous chromosomes begin to associate with each other and meiotic recombination is initiated with the help of several specific proteins. Once homologous regions are identified, homologous chromosomes (homologs) begin to pair during zygotene and form **synaptonemal complexes** (**Figure 3.6**; see also Figure 3.5), which eventually run continuously along the length of each chromosome pair. Paired chromosomes are also referred to as bivalents. Toward the end of pachytene, chromosomes have condensed enough to be seen in the microscope as distinguishable threads (see Figure 3.5). Crossing over (the exchange of DNA between homologs) starts during pachytene, and in diplotene visible junctions, also called chiasmata, can be seen between homologous chromosomes. Chiasmata are resolved (i.e., DNA exchange is completed) toward the end of diplotene and into diakinesis. At this point, chromosomes further condense and the centromeres appear to move away from each other, while the chromosome ends still maintain contact between homologs. The nuclear membrane breaks down at the end of diakinesis. During metaphase I, the still-paired homologs line up along the metaphase plate, where spindle fibers attach to each centromere via the proteinaceous kinetochore. In anaphase I, the homologous pairs are separated with the help of the spindle fibers pulling the homologs to opposite poles. Sister chromatids remain attached to each other during anaphase I. During telophase I, chromosomes may decondense somewhat, as is the case in Arabidopsis, or as in some plants, stay condensed and move quickly through prophase II into metaphase II. During these phases the chromosomes again align at the metaphase plate, and spindle fibers attach at the centromeres. In anaphase II, sister chromatids are separated and pulled toward the poles. Chromosomes begin to decondense during telophase II, and four haploid nuclei form. Cytokinesis then produces four separate cells. In the case of male meiosis in angiosperms, these four cells are the microspores, which stay together in a cluster called a **tetrad**. The tetrad later releases the four microspores, which undergo mitosis to produce mature pollen (the male gametophytes). In the case of female meiosis in angiosperms, only one of the four daughter cells survives, giving rise to the megaspore. The megaspore eventually undergoes mitosis and produces eight haploid nuclei, which form the female gametophyte.



Micrograph by L. Timofejeva, from H. Ma. 2005. *Annu. Rev. Plant Biol.* 56: 393–434

Figure 3.6 **Synaptonemal complex in Arabidopsis.** The arrow points toward a partial synaptonemal complex during pachytene.

Polyploids contain multiple copies of the entire genome

Ploidy level—the number of copies of the entire genome in a cell—is another important aspect of genome structure that may have implications for both physiology and evolution. In many organisms, but especially in plants, the entire diploid (2*N*) genome can undergo one or more additional rounds of replication without undergoing cytokinesis (see Chapter 1) to become **polyploid**. If polyploidy is restricted to vegetative organs, the terminology used to describe this state is **endopolyploidy**. Examples of endopolyploidy are salivary glands in *Drosophila* and liver cells in humans. In plants, endopolyploidy occurs frequently in fully differentiated leaf cells.

If whole-genome duplication is carried into the germ line (gametes), a uniformly polyploid next generation can result. Polyploidy is not a rare event, nor is it normally associated with mutation or disease. In fact, polyploidy is a common phenomenon that has occurred at least once in all angiosperm lineages. Evidence for multiple polyploidization events can be found in many plant genomes, but interestingly, whole-genome duplications appear to be less common in gymnosperms. **Autopolyploid plants** contain multiple complete genomes of a single species, while **allopolyploid plants** contain multiple complete genomes derived from two or more separate species.

Both types of polyploidy can result from incomplete meiosis during gametogenesis. During normal meiosis, the chromosomes of a diploid germ cell undergo DNA replication followed by two rounds of division (meiosis I and meiosis II), producing four haploid cells. If chromosome duplication is not followed by the normal two rounds of cell division during meiosis, diploid **unreduced gametes** may result (**Figure 3.7**). Within a species, or in a self-fertilizing individual, if a diploid egg is fertilized by a diploid sperm, the resulting zygote contains four copies of each chromosome and is said to be *autotetraploid* (see Figure 3.7). Allopolyploids are the result of formation of an interspecies hybrid and also involve genome duplication (see Figure 3.7). Diploid interspecies hybrids occur naturally, but they are frequently sterile.

A classic example from nature where multiple species in the same genus have produced allopolyploid offspring comes from the mustard family, Brassicaceae (**Figure 3.8**). Aside from the natural occurrence of genome duplication, polyploidy can also be induced artificially by treatment with the natural cell toxin colchicine, which is derived from the autumn crocus (*Colchicum autumnale*). Colchicine inhibits spindle fiber formation and prevents cell division, but does not interfere with DNA replication. Treatment with colchicine therefore results in an undivided nucleus containing multiple copies of the genome.

The lack of fertility in diploid interspecies hybrids is in stark contrast to the phenomenon known as **hybrid vigor**, or **heterosis**: the increased vigor often

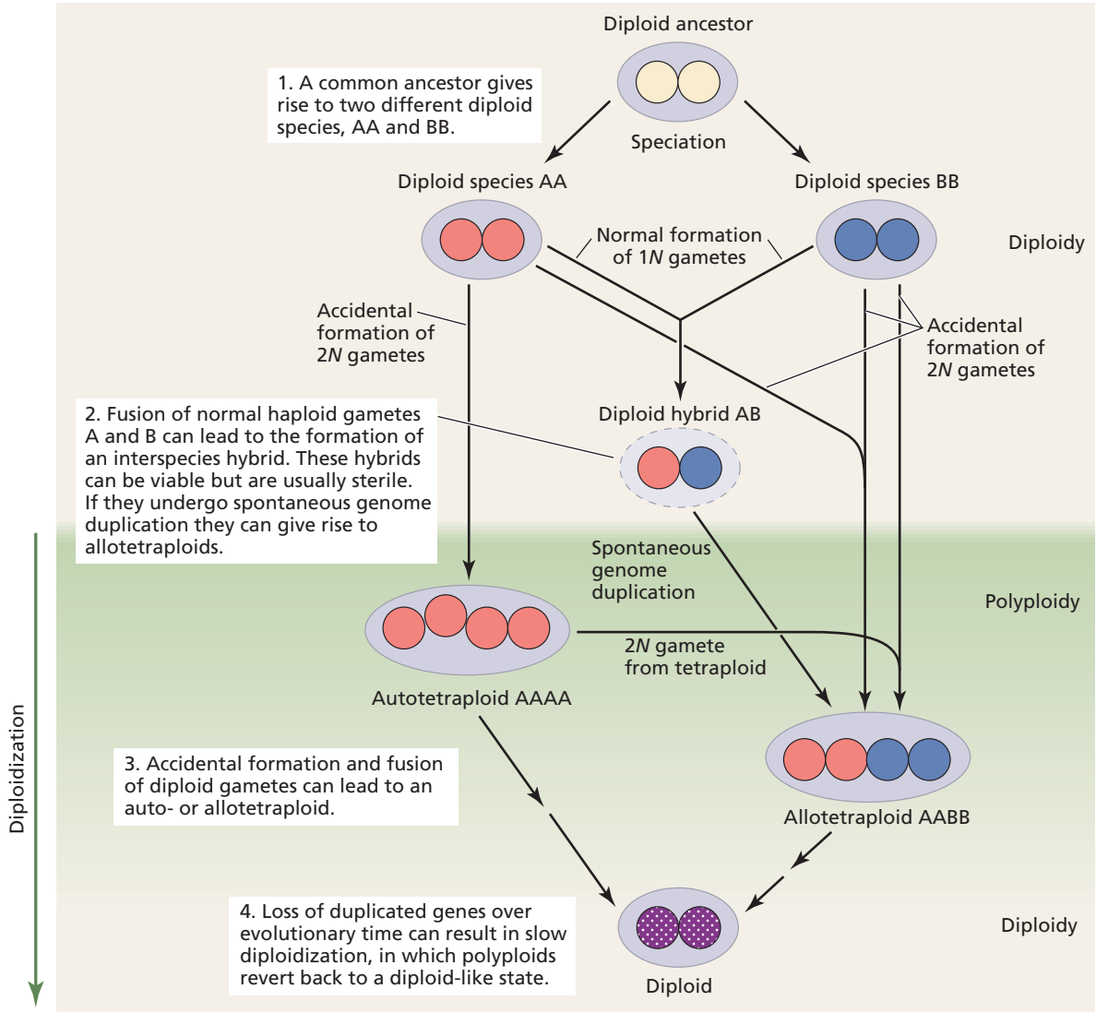


Figure 3.7 Continuum in the evolution of polyploid species. Diploids can give rise to autopolyploids or allopolyploids by the mechanisms outlined in Figure 3.5. Polyploids can revert to a diploid-like state via the gradual loss of DNA, including duplicated genes, over evolutionary time. Light purple underlying ovals represent the nuclei of a species; colored circles inside nuclei represent entire genomes. (After L. Comai. 2005. *Nat. Rev. Genet.* 6: 836–846.)

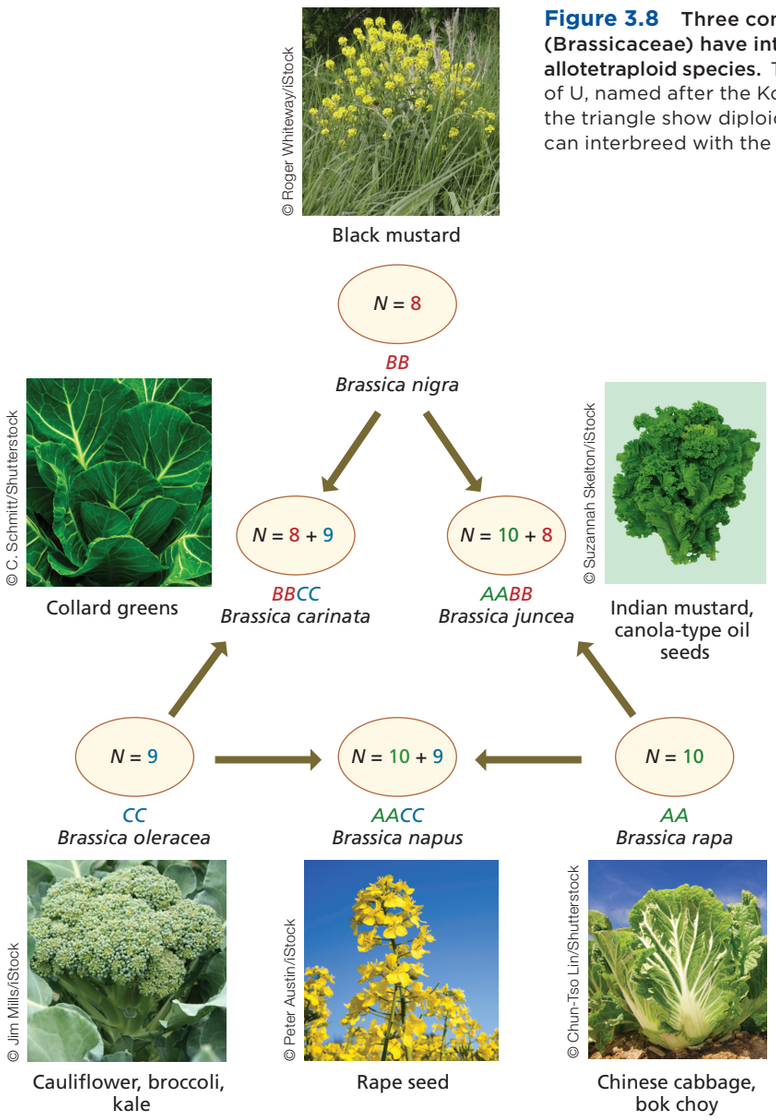


Figure 3.8 **Three common species of plants in the mustard family (Brassicaceae) have interbred with one another in nature to form new allotetraploid species.** Their relationship is depicted in the so-called triangle of U, named after the Korean scientist Nagaharu U. The three corners of the triangle show diploid species of *Brassica*. Each of the three species can interbreed with the two others to form new allopolyploids.

(but not always) observed in the offspring of crosses between two inbred varieties of the same plant species. Heterosis can contribute to larger plants, greater biomass, and higher yields in agricultural crops. The question of exactly which genes are involved in heterosis, and why mechanistically heterozygotes of certain combinations exhibit hybrid vigor over their homozygous (inbred) parents, is still largely unresolved.

As polyploidy leads to multiple, redundant copies of genes in the genome, one copy may be either lost or changed in function over multiple generations. These types of processes are known as **subfunctionalization**. Genome analysis shows that even in many diploid species there is clear evidence of genome duplication in the species' evolutionary history.

3.2 Plant Cytoplasmic Genomes: Mitochondria and Plastids

In addition to the nuclear genome, plant cells contain two cytoplasmic genomes: the mitochondrial genome and the plastid genome. These cytoplasmic genomes are thought to be evolutionary remnants of prokaryotic bacteria and cyanobacteria engulfed in two separate evolutionary events. According to the **endosymbiotic theory**, the original mitochondrion was an oxygen-using (aerobic) bacterium that was absorbed by another prokaryotic organism. Over time, this original endosymbiont evolved into an organelle that was no longer able to live on its own. The host cell, along with its endosymbiont, gave rise to a lineage of cells that were able to use oxygen in aerobic metabolism. Subsequently, a second endosymbiosis event occurred in which a cell engulfed a photosynthetic cyanobacterium that, over time, became a plastid.

Plastid genomes generally range in size from about 120 to 160 kilobase pairs (kbp) and encode genes that are needed for photosynthesis and the expression of plastid genes (see Chapter 9). The mitochondrial genome is much more variable in size than the plastid genome. Plant mitochondrial genomes range between approximately 180 kbp and nearly 11 Mbp—much larger than mitochondrial genomes of animals or fungi, many of which are only 15 to 50 kbp. Much of the difference in size between these genomes is made up by noncoding repeat DNA. Plant mitochondrial DNA contains genes that encode proteins needed in the electron transport chain, or that are involved in providing cofactors for electron transport. Additionally, plant mitochondrial DNA carries genes for proteins required for the organelle's own gene expression, such as ribosomal proteins, tRNAs, and rRNAs (see Chapter 13). In both organelles, most of the genes required for proper plastid or mitochondrial function are no longer encoded in the organellar genome itself, but have been transferred to the nucleus of modern plants over evolutionary time. The proteins

encoded by these genes are synthesized in the cytoplasm and then imported into the organelles. For more on the chromosomal structure of plastid genomes, including a photograph, see **WEB TOPIC 3.1**.

The genetics of organellar genes are governed by two principles that distinguish them from Mendelian genetics. First, both mitochondria and plastids generally show **uniparental inheritance**, which means that sexual offspring (via pollen and eggs) inherit organelles from only one parent. (For a discussion on how uniparental inheritance is achieved during development, see **WEB TOPIC 3.1**.) The second major feature of organellar inheritance is the fact that both plastids and mitochondria can exhibit **vegetative segregation**. This means that a vegetative cell (as opposed to a gamete) can give rise to another vegetative cell via mitosis that is genetically different. For example, consider a vegetative cell that contains a mixture of two genetically distinct types of plastids. During mitosis, the plastids are distributed randomly to the daughter cells. By chance, one daughter cell may receive plastids with one type of genome, while the other daughter cell may receive plastids with different genetic information, perhaps containing one or more mutations. Vegetative segregation, which is also referred to as **sorting-out**, can result in the formation of phenotypically different sectors within a tissue. (For a figure illustrating the sorting-out process, see **WEB TOPIC 3.1**.) The presence of such sectors in leaves may result in what horticulturists often refer to as **variegation**. Leaf variegation can also be caused by mutations in nuclear and mitochondrial genes.

3.3 Transcriptional Regulation of Nuclear Gene Expression

Now that we have looked at the organization of nuclear and cytoplasmic genomes in plants, we turn to the structure of the nuclear genome and how that structure influences the expression of the genes the genome contains. We first review the basic mechanisms of gene transcription, then describe the transcriptional regulation of gene expression.

As we introduced in Chapter 1, the path from gene to protein is a multistep process catalyzed by many enzymes (see Figure 1.16). Each step is subject to regulation by the plant to control the amount of protein that is produced by each gene. Regulation of the first step, transcription, determines when and whether an mRNA is made. This level of regulation, which is referred to as **transcriptional regulation**, includes the control of transcription initiation, maintenance of transcription, and termination. The next level in the regulation of gene expression is known as **posttranscriptional regulation**. This level, which we cover in Section 3.4, includes the control of mRNA stability, translation efficiency, and degradation. Finally, **protein stability** (posttranslational regulation) plays an important role in determining the overall activity of a gene or its product.

RNA polymerase II binds to the promoter region of most protein-coding genes

Gene transcription is facilitated by an enzyme called **RNA polymerase**, which binds to the DNA to be transcribed and makes an mRNA transcript complementary to the DNA sequence. There are several types of RNA polymerase. RNA polymerase II is the polymerase that transcribes most protein-coding genes. An example of a typical eukaryotic gene along with its regulatory sequences is shown in **Figure 3.9**.

Before transcription of a gene can begin, several steps have to occur to allow the RNA polymerase to gain access to the gene's nucleotide sequence. Nuclear DNA is wrapped around histones, forming beadlike nucleosomes. As we will discuss in more detail later in this section, the histones are subject to modifications, and only if those modifications are favorable to transcription will RNA polymerase be able to bind to the DNA. To be functional, eukaryotic RNA polymerases require additional proteins called **general transcription factors** to position the polymerase at the transcription start site. These general transcription factors, together with the RNA polymerase, make up a large, multi-subunit **transcription initiation complex**. Transcription is initiated when the final transcription factor to join the complex phosphorylates the RNA polymerase. The RNA polymerase then separates from the initiation complex and proceeds along the antisense strand (also sometimes referred to as the noncoding, template, negative, or Watson strand) of the DNA in the 3′-to-5′ direction, while adding nucleotides to the new strand of mRNA in the 5′-to-3′ direction of the nascent strand. The mRNA sequence most closely resembles the code of the opposite strand of DNA not used as template by the polymerase, which is therefore referred to as the coding strand (or sense, positive, non-template, or Crick strand).

In addition to requiring RNA polymerase and the general transcription factors, many genes require specific transcription factors (also called gene regulatory proteins) for RNA polymerase to become active. These regulatory proteins bind to the DNA, often at specific sequences, and are a required part of the transcription initiation complex.

The region of the gene that recruits the transcription machinery, including RNA polymerase, is called the **promoter.** The structure of the eukaryotic promoter can be divided into two parts: the **core promoter** or **minimum promoter**, consisting of the minimum sequence required for gene expression, and the **regulatory promoter sequences**, which control the activity of the core

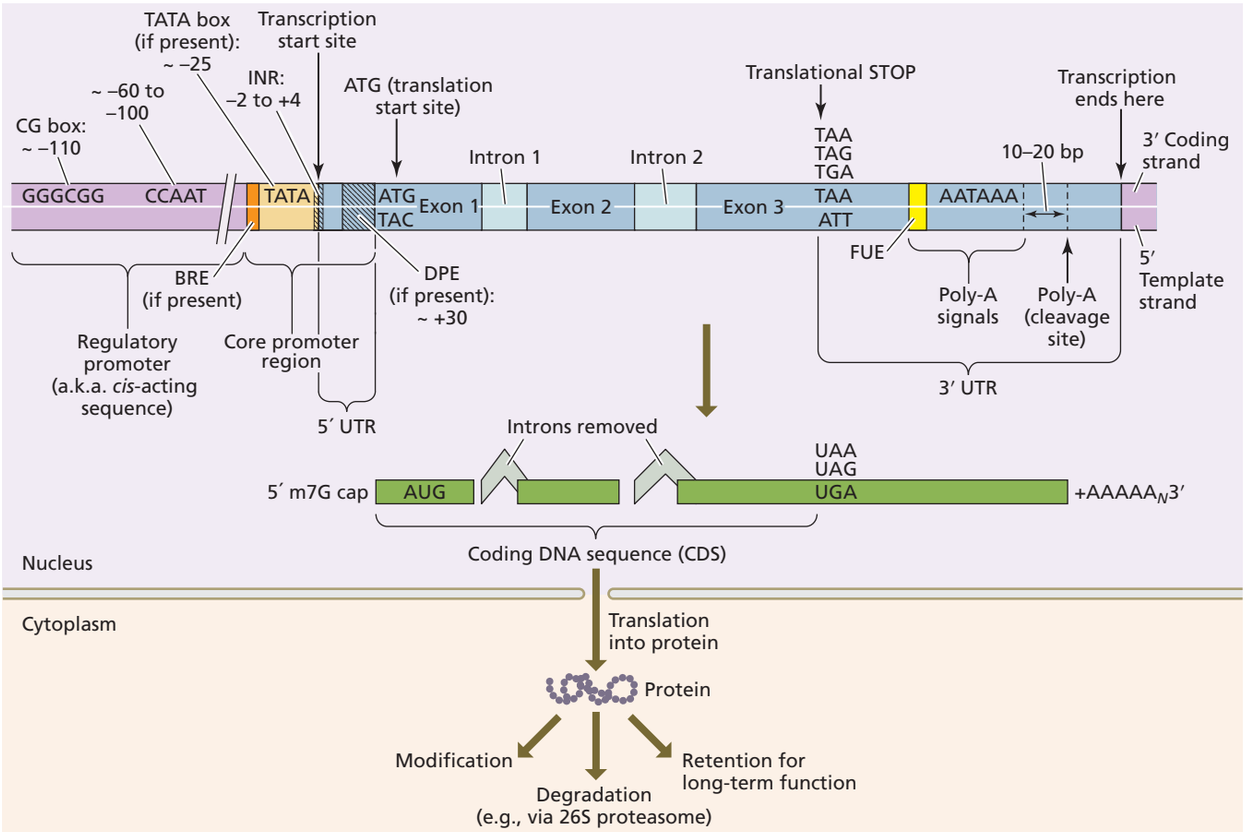


Figure 3.9 **Gene expression in eukaryotes.** RNA polymerase II binds to the promoters of genes that encode proteins. Unlike prokaryotic genes, eukaryotic genes are usually not clustered in operons, and each is divided into introns and exons. Transcription from the template strand proceeds in the 3′-to-5′ direction at the transcription start site, and the growing RNA chain extends one nucleotide at a time in the 5′-to-3′ direction. Translation begins with the first AUG encoding methionine, as in prokaryotes, and ends with a stop codon. The pre-mRNA transcript is first "capped" by the addition of 7-methylguanylate (m7G) to the 5′ end. The 3′ end is shortened slightly by cleavage at a specific site, and a poly-A tail is added. The capped and polyadenylated pre-mRNA is then spliced by a protein complex called the spliceosome, and the introns are removed. The mature mRNA exits the nucleus through the nuclear pores and initiates translation on ribosomes in the cytosol. As each ribosome progresses toward the 3′ end of the mRNA, new ribosomes attach at the 5′ end and begin translating, leading to the formation of polysomes. After translation, some proteins are modified by the addition of chemical groups to the protein chain. The released polypeptides have characteristic half-lives, which are regulated by the ubiquitin pathway and a large proteolytic complex called the 26S proteasome. Eukaryotic genes typically contain binding sites for the RNA polymerase, such as the TATA box within the core promoter region, as well as sites binding general and specific transcription factors in the proximal and distal regulatory promoter. BRE, TFIIB recognition element; DPE, downstream promoter element; FUE, far upstream element; INR, initiator element; UTR, untranslated region.

promoter (**Figure 3.10**). For protein-coding genes, the core promoter generally occupies the approximately 80 bp surrounding the transcription start site.

The core promoter for genes transcribed by RNA polymerase II usually includes several sequence elements referred to as **core promoter elements**. These short nucleotide sequences are responsible for binding the general transcription factors and the RNA polymerase and determine the amount of transcription of a given gene. Many, although by no means all, eukaryotic genes contain a short sequence approximately 25 to 30 bp upstream of the transcription initiation site called the **TATA box** and consisting of the sequence TATA(A/T)AA(G/A), where positions 5 and 8 are more variable than the other positions (see Figure 3.9). Sequence motifs that, like the TATA box, are frequently found in many genes are also referred to as conserved regions. The TATA box plays a crucial role in transcription because it aids in the assembly of the transcription initiation complex just discussed. Genes lacking a TATA box often contain a **downstream promoter element** (**DPE**) with the consensus sequence (A/G)G(A/T)(C/T)(G/A/C), which is located at nucleotides 28 to 32 downstream of the transcription initiation site. A third important part of the core promoter is the

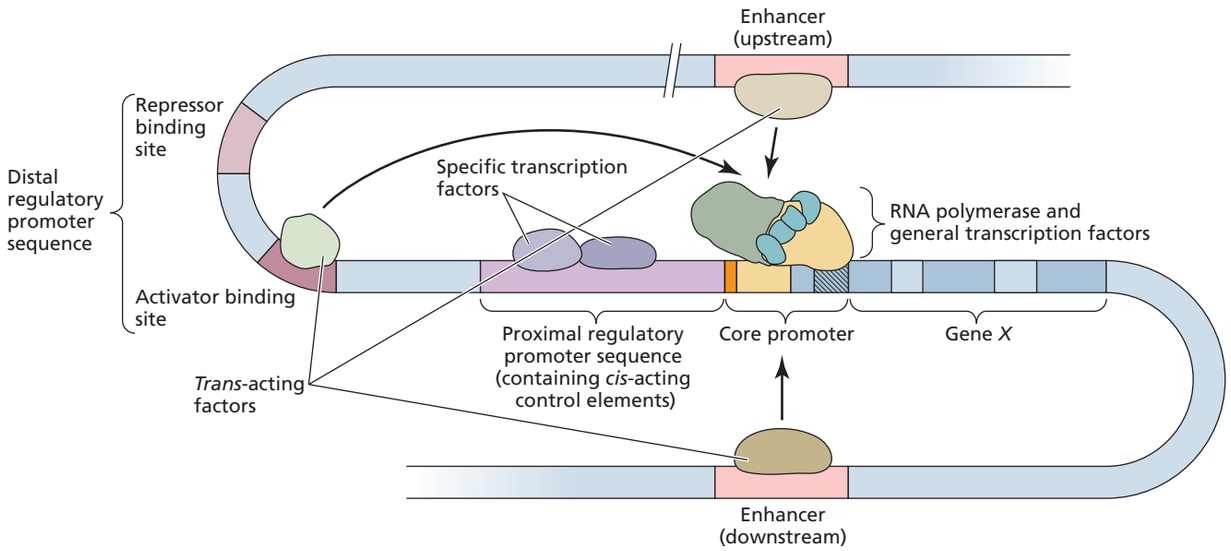


Figure 3.10 Regulation of transcription by distal regulatory promotor sequences, enhancers, and *trans*-acting factors. The *trans*-acting factors can act in concert with the distal regulatory promotor sequences to which they are bound, to activate transcription by making direct physical contact with the transcription initiation complex.

initiator element (**INR**). This nucleotide sequence also binds to general transcription factors and can be found both in TATA box–containing and TATA box–lacking genes around the transcription start site from nucleotide position –2 to +4. The fourth binding element in the core promoter is the so-called **TFIIB recognition element** (**BRE**). This sequence recognizes a different general transcription factor than the other elements. The BRE is located within the six nucleotides immediately adjacent to and upstream of the TATA box (see Figure 3.9).

Farther upstream of the core promoter sequence, many eukaryotic genes also contain two additional conserved sequences: the **CCAAT box** and the **GC box** (see Figure 3.9). The region containing these sequences is called the **regulatory promoter** or the **proximal** (close) **promoter**. This part of the promoter does not bind the RNA polymerase and its associated general transcription factors required for all genes, but instead binds to gene-specific transcription factors. The CCAAT box, if present, is usually located 60 to 100 bp upstream of the transcription start site. It is important to note that not all genes contain all conserved elements. For example, GC boxes are found more frequently in genes that do not contain a TATA box, and one or more GC boxes can be present in a promoter. The various conserved DNA sequences we have described so far are also collectively termed ***cis*-acting control elements**, since they are adjacent (*cis*) to the transcription units they are regulating. The transcription factors that bind to the *cis*-acting control elements are called ***trans*-acting factors**, since the genes that encode them are located elsewhere in the genome.

Numerous *cis*-acting control elements located more distally (farther away) upstream from the proximal promoter sequences can exert either positive or negative control over eukaryotic promoters. These sequences, termed **distal regulatory promoter sequences**, are usually located within 1000 bp of the transcription initiation site (see Figure 3.10). The positively acting transcription factors that bind to these sites are called **activators**, while those that inhibit transcription are called **repressors**. In addition to having regulatory sequences within the promoter itself, eukaryotic genes can be regulated by control elements located tens of thousands of base pairs away from the transcription initiation site. **Enhancers** are one such type of distal regulatory sequence and may be located thousands to hundreds of thousands of base pairs either upstream or downstream from the promoter, or in some cases even reside inside the transcription unit itself. In contrast to the regulation through the core promoter, the proteins binding the proximal and distal promoters jointly determine in which cell types and at what time a given gene is transcribed.

How do all the transcription factors that bind to the *cis*-acting control elements regulate transcription? During the formation of the initiation complex, the DNA between the core promoter and the most distally located regulatory sequences loops out in such a way as to allow all of the transcription factors bound to that segment of DNA to make physical contact with the initiation complex. Through this physical contact, each transcription factor exerts its control, either positive or negative, over transcription.

Conserved nucleotide sequences signal transcriptional termination and polyadenylation

As RNA polymerase II reaches the 3′ region of the gene, it first passes the DNA sequence that codes for the stop codon in the mRNA (see Figure 3.9). The stop codon is part of the mRNA and indicates to the ribosomes where the mRNA region that should be translated into protein ends. The 3′ untranslated region lies 3′ of the sequence (downstream) for the stop codon. Signals for termination of transcription in plants, fungi, and animals have both similarities and differences. Before terminating transcription, plant RNA polymerase II encounters three conserved DNA sequences that aid in the termination of transcription and the addition of the poly-A tail, which helps stabilize the mRNA. The first of these somewhat conserved DNA sequences is the **far upstream element** (**FUE**), which is six nucleotides long and found between 30 and 170 bp before the poly-A addition site. Soon after the FUE many—but by no means all—plant genes contain a conserved AATAAA sequence. This exact sequence seems to be strictly required for polyadenylation in animals, but in plants variations of this sequence with similarity to the AATAAA element are sufficient for proper function. Both the FUE and the AATAA site are also referred to as poly-A signals. The poly-A cleavage site is the DNA sequence that codes for the region on the mRNA where the nascent mRNA strand is cleaved and the poly-A tail added (see Figure 3.9). Together, these three conserved sequences on the DNA strand also promote termination of transcription by RNA polymerase II.

Epigenetic modifications help determine gene activity

As mentioned earlier, transcription can be initiated only if the DNA is accessible to the RNA polymerase and other required binding proteins. In order to make the DNA accessible, its packaging has to be "loosened," a process mediated by covalent modifications of both DNA and histones. Transcription factors generally activate or inactivate gene transcription by recruiting proteins that modify histones to loosen or maintain their interactions with DNA. Because these modifications can change a gene's behavior without changing the DNA sequence of the gene itself, they are referred to as **epigenetic modifications** (from the Greek *epi*, meaning "over" or "on top of").

One common type of DNA modification is the **methylation** of cytosine residues (**Figure 3.11A**). DNA sequences that are frequently methylated in plants are CG, CHG, and CHH (where H can be any base except guanine). In contrast, cytosine methylation in mammals occurs mostly on CG. Cytosine methylation is catalyzed by one of several methyltransferases, whereas DNA demethylation is catalyzed by glycosylases that replace methylcytosine with unmethylated cytosine (see Figure 3.11A).

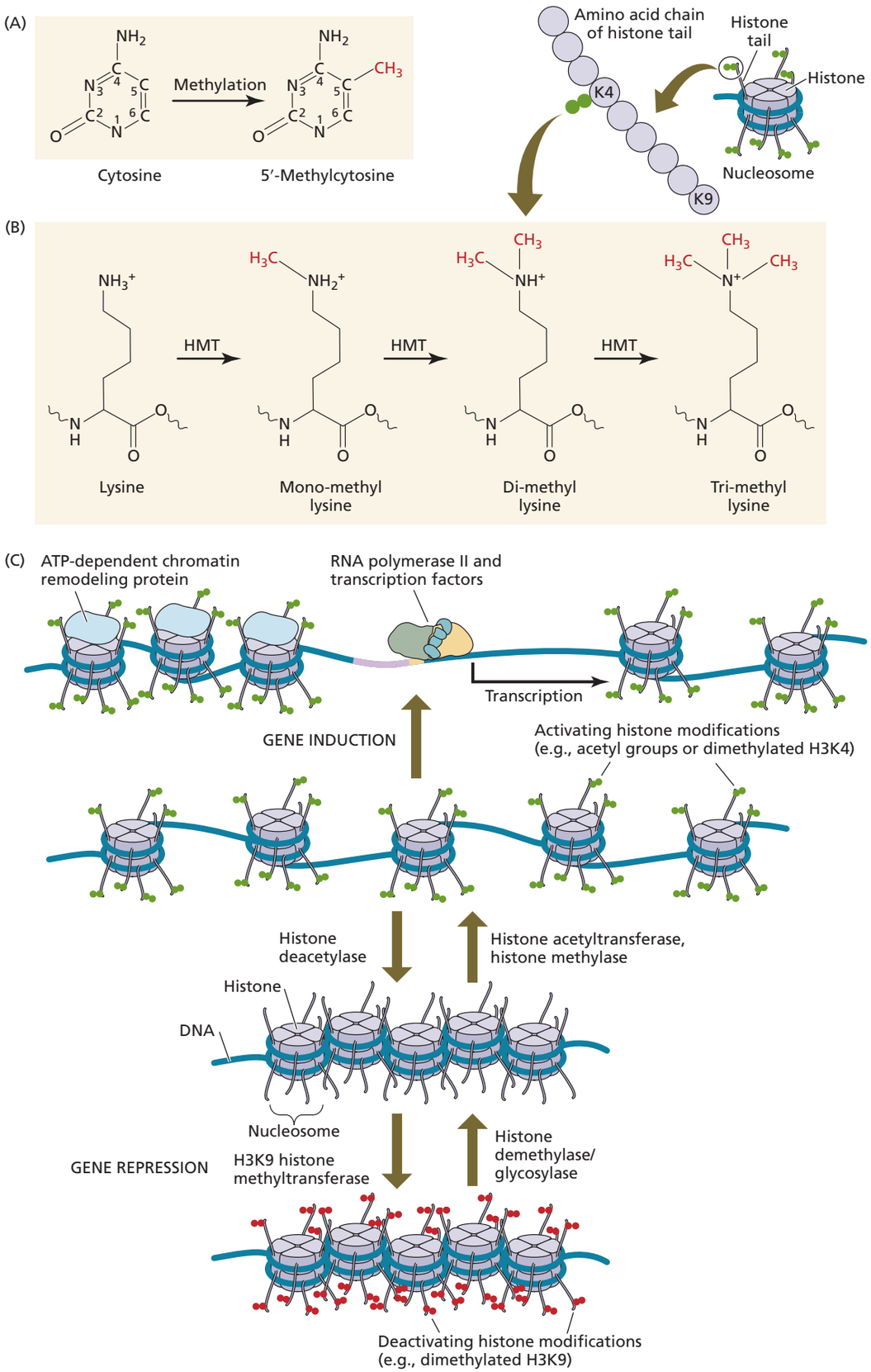
Epigenetic modifications can also occur on histones, which, together with the DNA wrapped around them, make up the nucleosomes. Each histone has a "tail," which is made up of the first part of the histone's amino acid chain and protrudes outward from the nucleosome. Histone modifications occur on these tails, usually within the outermost 40 or so amino acids. These modifications can influence the conformation of the nucleosomes and thereby gene activity in the associated DNA.

One of the histone modifications that influences gene activity is methylation, especially at specific lysine residues (single-letter amino acid abbreviation K) in the tail of histone type H3. These residues are K4, K9, K27, and K36, counting from the outermost amino acid inward to the center of the histone coil. One, two, or three methyl groups can be added to a single lysine (**Figure 3.11B**). Histones dimethylated at position H3K4 are generally associated with active genes, whereas dimethylation at position H3K9 is often associated with inactive genes and elements, such as silent transposons. Methyl groups can be removed by histone demethylases.

Another form of modification that occurs on the histone tail is **acetylation**, which is catalyzed by enzymes called histone acetyltransferases (HATs). In general, acetylated histones are associated with genes that are actively transcribed. Histone deacetylases (HDACs) can reverse this activation by removing acetyl groups.

Both methylation and acetylation change the architecture of the chromatin complex, which may result in condensation or relaxation of the chromatin. These changes occur when multiprotein chromatin remodeling complexes bind to the modified histones. Using the energy released by ATP hydrolysis to drive the reaction, these complexes open up the chromatin by displacing the nucleosomes in the area toward the 5′ or 3′ direction of the remodeling complex. The resulting gap between nucleosomes is now wide enough for RNA polymerase to bind and initiate transcription (**Figure 3.11C**). Alternatively, histone modifications may present novel binding sites for regulatory proteins that affect gene activity. Scientists are only beginning to understand the effects of specific chemical modifications on each of the first 40 or so amino acids of the histone tails. In addition to

Figure 3.11 Gene expression and chromatin remodeling. ▶ **(A)** Addition of a methyl group to the C-5 in cytosine is associated with transcriptional inactivity. **(B)** The amino acid lysine (K), which occurs at several positions in histones, can be mono-, di-, or trimethylated by histone methyltransferase (HMT). **(C)** Histones can be remodeled to activate gene transcription (top) or to repress it (bottom). In many cases, activation is associated with acetylation by histone acetyltransferases (HATs) and methylation by HMT at lysine residue H3K4. These modifications promote ATP-dependent chromatin remodeling and stimulate transcription. Repression of transcription can be achieved by methylation of H3K9 and deacetylation by histone deacetylases.


(A)
Methylation
Cytosine
5′-Methylcytosine
Amino acid chain of histone tail
Histone tail
Histone
K4
K9
Nucleosome
(B)
HMT
HMT
HMT
Lysine
Mono-methyl lysine
Di-methyl lysine
Tri-methyl lysine
(C)
ATP-dependent chromatin remodeling protein
RNA polymerase II and transcription factors
Transcription
GENE INDUCTION
Activating histone modifications (e.g., acetyl groups or dimethylated H3K4)
Histone deacetylase
Histone acetyltransferase, histone methylase
Histone
DNA
Nucleosome
GENE REPRESSION
H3K9 histone methyltransferase
Histone demethylase/ glycosylase
Deactivating histone modifications (e.g., dimethylated H3K9)

methylation and acetylation, other types of histone modifications, including phosphorylation and ubiquitination, can occur both inside the transcription unit of a gene, in the promoter regions, and on enhancers, and can influence the transcriptional activity of a given gene. The entirety of histone modifications on a specific nucleosome is sometimes called the *histone code* to underline the strong link between nucleosome constitution and gene activity.

3.4 Posttranscriptional Regulation of Nuclear Gene Expression

Immediately after transcription, mRNAs are processed: Their introns are removed by splicing, and 5′ caps and 3′ poly-A tails are added. The transcripts are then exported to the cytoplasm for translation. The nucleotide sequence of an mRNA determines its three-dimensional structure as well as interactions with other factors that regulate its stability in response to environmental or developmental cues.

All RNA molecules are subject to decay

Eukaryotic mRNA molecules can be degraded by exonucleases after removal of the poly-A tail (deadenylation) or removal of the 5′ cap (decapping). These processes are guided by environmental cues and other cellular pathways. Some RNA is turned over in small cytoplasmic ribonucleoprotein processing bodies (P-bodies). One mechanism by which mRNA stability is regulated depends on the presence of certain sequences within the mRNA molecule itself, called ***cis*-elements**—an unfortunate choice of terms, since the same term is used for the DNA regions that influence transcriptional activity. These *cis*-elements can be bound by RNA-binding proteins, which may either stabilize the mRNA or promote its degradation by nucleases. Depending on the types of *cis*-elements present, the stability of a given mRNA molecule can vary widely.

Noncoding RNAs regulate mRNA activity via the RNA interference (RNAi) pathway

Another mechanism for regulating mRNA stability is the **RNA interference** (**RNAi**) **pathway**. This pathway involves several types of small RNA molecules that do not code for proteins and are thus called small RNAs (sRNAs) or **noncoding RNAs** (**ncRNAs**). The RNAi pathway has important roles in gene regulation and genomic defense.

The RNAi pathway is a set of cellular reactions to the presence of double-stranded RNA (dsRNA) molecules. Recall that mRNA is usually a single-stranded molecule (ssRNA). In plant cells, dsRNAs usually occur as a result of one of three types of events:

1. The presence of **microRNAs** (**miRNAs**), which are involved in normal developmental processes (see Figure 3.12)
2. The production of **short interfering RNAs** (**siRNAs**), which silence certain genes (see Figure 3.13)
3. The introduction of foreign RNAs, either by viral infection or via transformation by a foreign gene (see Figure 3.14)

Regardless of how the dsRNAs are produced, the cell mounts the RNAi response. The dsRNAs are chopped up, or "diced," into small 21- to 24-nucleotide RNAs, which bind to complementary single-stranded RNAs (e.g., mRNAs) from endogenous genes, viruses, or transgenes and promote their degradation or translational inhibition. In some cases, the RNAi pathway can also lead to gene silencing or **heterochromatization** of endogenous DNA or introduced foreign genes. To explore RNAi in more detail, we first take a look at events leading to dsRNA accumulation in the cell. Then we discuss the molecular components and downstream events of the RNAi process.

microRNAs REGULATE MANY DEVELOPMENTAL GENES POSTTRANSCRIPTIONALLY Plants contain hundreds of genes encoding miRNAs, which act by repressing the translation of mRNAs into protein or by targeting specific mRNAs for degradation. miRNAs are involved in many developmental processes, such as reproduction, cell division, embryogenesis, the formation of new organs (including leaves and flowers), and the transition from the vegetative to the floral phase. miRNAs arise from RNA polymerase II–mediated transcription of a specific locus that codes for the primary miRNA transcripts (pri-miRNAs), which can vary in length from hundreds to thousands of nucleotides (**Figure 3.12**). This primary transcript is capped at the 5′ end, polyadenylated at the 3′ end, and forms a double-stranded stem, whose base-paired arms border a single-stranded loop. Next, pri-miRNAs are processed into pre-miRNAs, which can be up to several hundred nucleotides long. In plants, pri-miRNAs are converted into miRNAs inside the nucleus by the ribonuclease **DICER-LIKE1** (**DCL1**) and the double-stranded RNA-binding domain protein (dsRBP) HYPONASTIC LEAVES 1 (HYL1), both of which are involved in processing the primary transcripts into the mature miRNA duplexes. After processing, the miRNA is transported through the nuclear pores with the help of the nuclear export protein HASTY. Once in the cytoplasm, mature miRNAs are ready to be used in RNAi.

SHORT INTERFERING RNAS ORIGINATE FROM REPETITIVE DNA Mature siRNAs are structurally and functionally similar to miRNAs and also lead to the initiation of RNAi. However, siRNAs differ from miRNAs in the way they are generated. They can arise by transcription from opposing promoters that produce

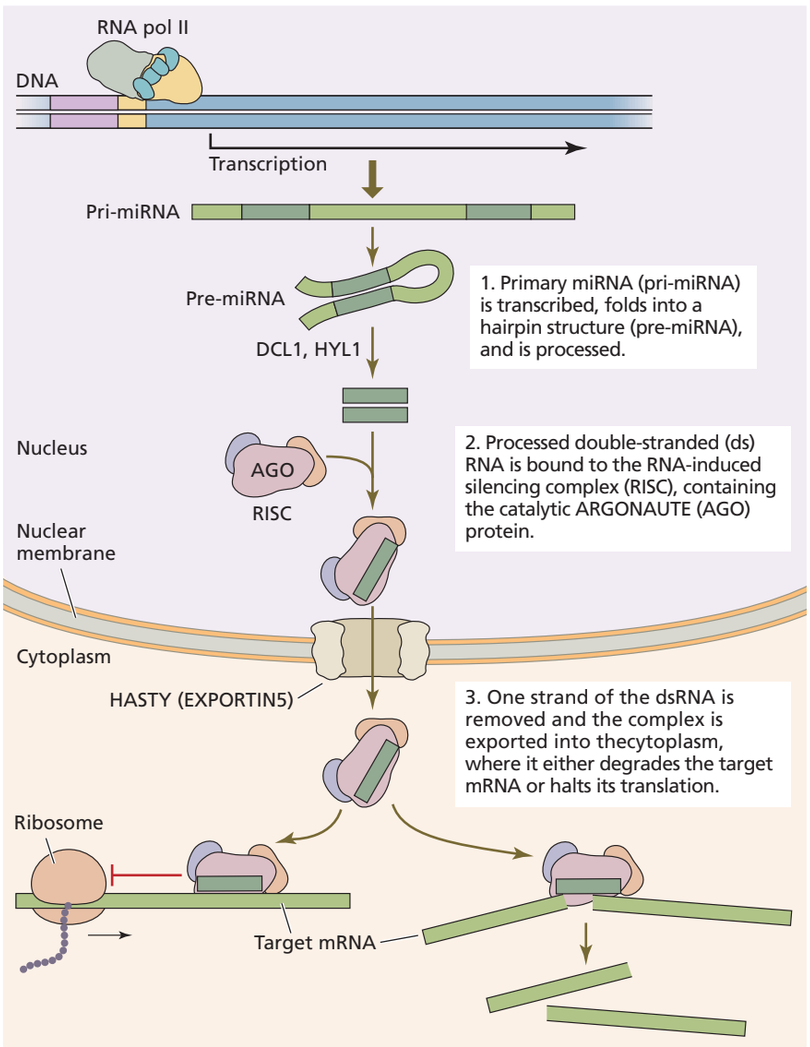


Figure 3.12 **The RNAi pathway in plants: microRNAs.** MicroRNAs (miRNAs) are part of many genetic pathways that are active during plant development. DCL1, DICER-LIKE1, a ribonuclease; HYL1, Hyponastic Leaves 1, an RNA-binding domain protein.

mRNA from opposite strands of a single segment of DNA (**Figure 3.13A**). Simultaneous transcription from such promoters generates two fully or partially complementary single-stranded RNA (ssRNA) molecules that can subsequently form one double-stranded molecule. A different way siRNAs can be formed is by transcription of a duplicated sequence in opposite directions (**Figure 3.13B**). This generates the sense strand of one copy and the antisense strand of the other copy. Short interfering RNA can also be produced from DNA sequences arrayed in such a way that their continuous transcription results in a message that contains at the end of its sequence a mirror image of the beginning of its sequence (a palindrome) and thus can fold back on itself to produce a double-stranded RNA molecule (**Figure 3.13C**). A special class of **RNA-dependent RNA polymerases** (**RdRP**) can generate double-stranded RNA (dsRNA) molecules from single-stranded mRNAs (**Figure 3.13D**). Exactly how RNA-dependent RNA polymerases recognize specific mRNA molecules to convert to dsRNA is still an open question. What is known is that some of the dsRNAs are further processed by the DICER-LIKE4 enzyme (DCL4) into 21–24 nucleotide RNA duplexes that then regulate specific mRNAs in a similar way that miRNAs regulate their mRNA targets. While most protein-coding genes and miRNA-coding sequences are transcribed by RNA polymerase II, transcription of siRNAs initially generated by RNA-dependent RNA polymerases is accomplished by RNA polymerases IV and V.

Not only the biogenesis of the various siRNAs just described differs from that of miRNAs. Unlike miRNAs, endogenous siRNAs are transcribed from chromosomal regions that have in the past often been regarded as transcriptionally inactive: repetitive DNA, transposons, and centromeric regions. Indeed, siRNAs originating from such repeat regions are sometimes referred to as **repeat-associated silencing RNAs** (**ra-siRNAs**) or heterochromatic siRNAs (hc-siRNAs). These siRNAs are produced by DICER-LIKE3 (DCL3). As you will see shortly, the fact that siRNAs are made from repetitive DNA regions may not be coincidental: It appears that the formation of siRNAs and the induction of RNAi actually cause these regions to become heterochromatic and largely transcriptionally silent. Once a dsRNA is produced by direct transcription or by conversion of ssRNA into dsRNA by an RdRP, it is cut into 21- 24-nucleotide RNA duplexes by members of the DICER-LIKE (DCL) protein family (see Figure 3.13). This process takes place in the nucleus in plants, but in some animals, such as *Caenorhabditis elegans*, it occurs in the cytoplasm.

In addition to these siRNAs of endogenous origin, exogenous RNAs can also trigger the formation of siRNAs.

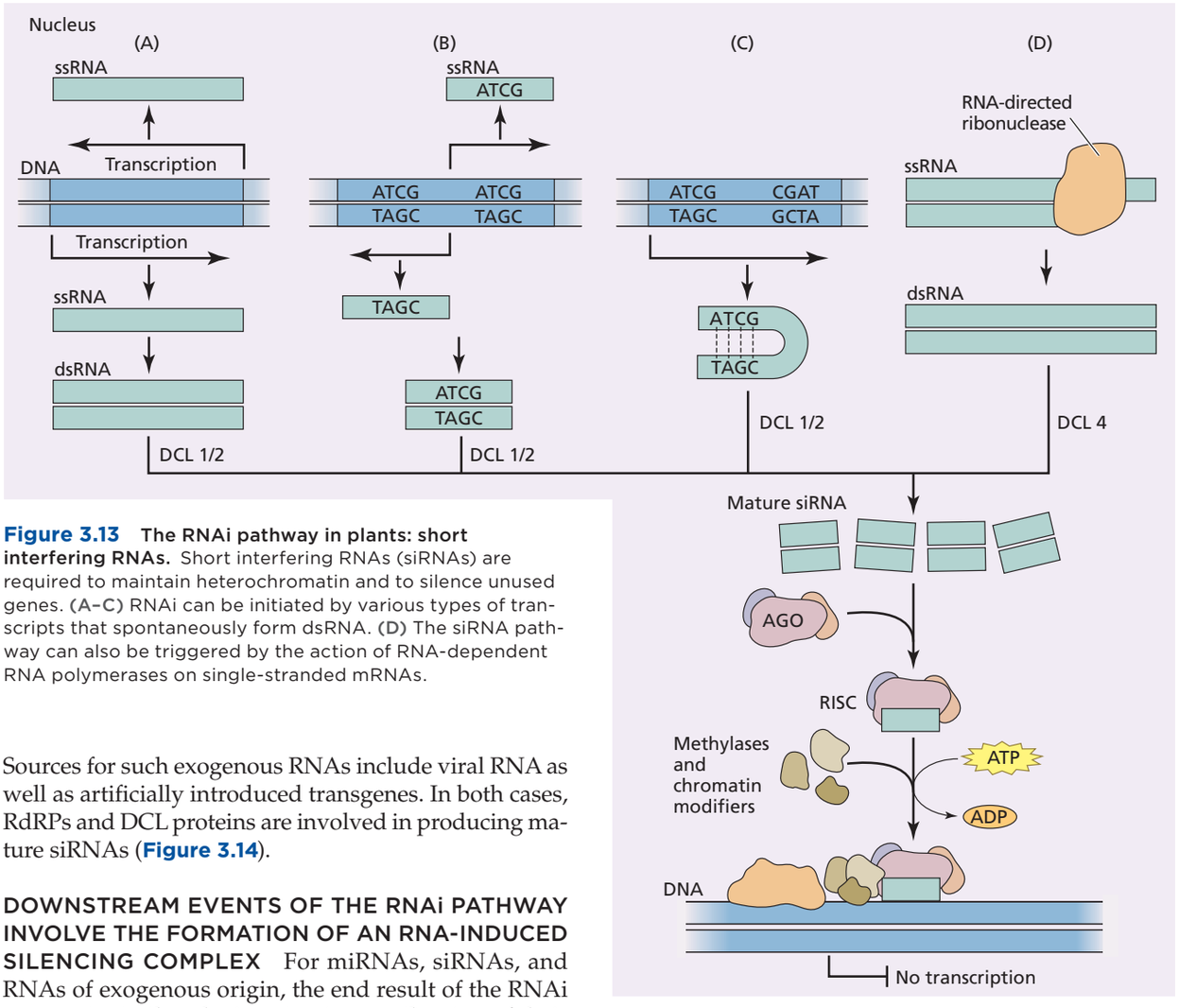


Figure 3.13 **The RNAi pathway in plants: short interfering RNAs.** Short interfering RNAs (siRNAs) are required to maintain heterochromatin and to silence unused genes. (A–C) RNAi can be initiated by various types of transcripts that spontaneously form dsRNA. (D) The siRNA pathway can also be triggered by the action of RNA-dependent RNA polymerases on single-stranded mRNAs.

Sources for such exogenous RNAs include viral RNA as well as artificially introduced transgenes. In both cases, RdRPs and DCL proteins are involved in producing mature siRNAs (**Figure 3.14**).

DOWNSTREAM EVENTS OF THE RNAi PATHWAY INVOLVE THE FORMATION OF AN RNA-INDUCED SILENCING COMPLEX For miRNAs, siRNAs, and RNAs of exogenous origin, the end result of the RNAi process is similar: the inactivation or silencing of their complementary mRNAs or DNA sequences. After 21- to 24-nucleotide miRNAs or siRNAs have been formed by the DICER-LIKE proteins, one strand of the short RNA duplex associates with a ribonuclease complex called the **RNA-induced silencing complex** (**RISC**) (see Figures 3.12 through 3.14). In both animals and plants, RISC contains at least one catalytic **ARGONAUTE** (**AGO**) protein. In some cases, RISC can recruit additional proteins to the complex. In Arabidopsis, ten different members of the AGO gene family are known. After the diced duplex miRNA or siRNA binds to AGO, one of the two RNA strands is removed. Upon this removal, RISC is active. In the case of miRNAs, the small ssRNA strand that binds to AGO now guides RISC to a complementary mRNA. Upon binding of RISC and target mRNA, the target mRNA is cleaved by the "slicer" activity of AGO. The resulting fragments are released into the cytoplasm, where they are further degraded. Instead of slicing the target, the association of RISC with an mRNA molecule may also simply inhibit translation of the mRNA into protein.

While RISC-bound miRNAs primarily target the expression of protein-coding genes, RISC-bound siRNAs also facilitate methylation of DNA and associated histones at sequences complementary to the siRNA. This allows the organism to silence certain genes permanently, and to form heterochromatin, predominantly in the centromeric and subtelomeric regions. Although the mechanism is unclear, RISC with its siRNA somehow guides DNA-modifying enzymes to the genomic sequence to be silenced. The chromatin structure is then "remodeled" in an ATP-requiring reaction and subsequently methylated, resulting in tighter condensation and heterochromatization of the DNA region involved (see Figures 3.11 and 3.13).

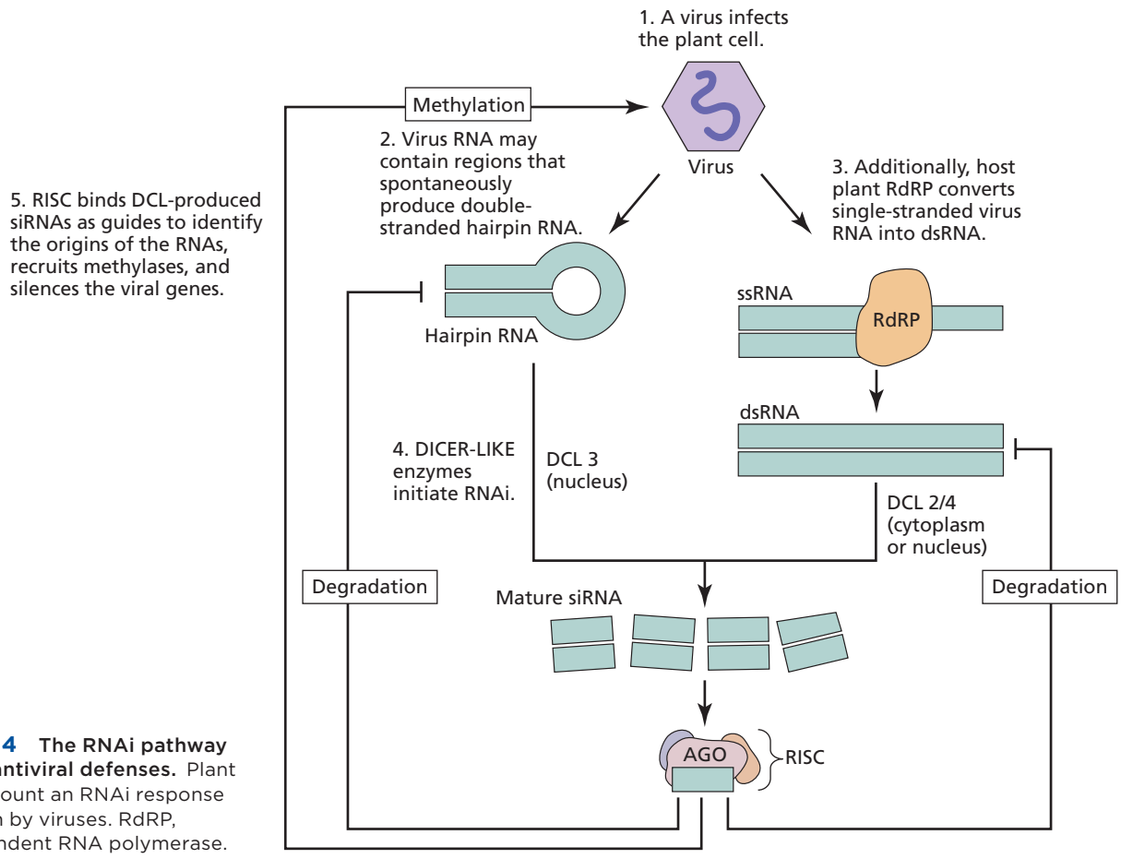


Figure 3.14 **The RNAi pathway in plants: antiviral defenses.** Plant cells can mount an RNAi response to infection by viruses. RdRP, RNA-dependent RNA polymerase.

RNA-INTERFERENCE MAY HELP RESET EPIGENETIC MARKS IN THE GAMETOPHYTE Epigenetic marks such as DNA or histone methylation accumulated by a plant are often silenced over time. Although epigenetic modifications are often necessary for survival, it becomes expensive for a plant to expend the energy to transcribe transposons and other heterochromatic genes just to silence them again via the siRNA pathway. It is not surprising that plants often reset epigenetic marks accumulated by an individual so that they don't accumulate in successive generations. Apparent epigenetic resetting is particularly evident in genes that regulate the onset of flowering (see Chapter 20) and in the gametophyte during fertilization (see Chapter 21).

SMALL RNAS AND RNAi COMBAT VIRAL INFECTION In addition to the processing of miRNAs and endogenous siRNAs, plants have also adopted the RNAi pathway as a type of molecular immune response against infection by viruses. (For other types of plant pathogen defenses, see Chapter 24.) The genomic structures of plant viruses are quite diverse. Some plant viruses inject double-stranded DNA into plant cells, but the majority of plant-infecting viruses use single- or double-stranded RNA. Plants use the siRNA pathway to produce siRNA molecules against the viral genome. Scientists propose three possible ways to generate viral siRNA: (1) via the formation of double-stranded hairpin loops from viral ssRNA, (2) via the generation of complementary sense and antisense viral RNA molecules by host or virus RNA polymerase, and (3) via one of the plant's RdRPs. Regardless of its origin, once dsRNA is recognized by the plant's DCL proteins, siRNAs are produced, loaded onto AGO, and assembled into a RISC (see Figure 3.14). Virus-derived siRNAs can then both degrade viral RNA and methylate the virus genome inside the host cell.

In the process of cutting invasive RNA into 21- to 24-nucleotide siRNAs, the plant generates a pool of "memory" molecules that can travel via plasmodesmata throughout the entire plant body, effectively immunizing the plant before the virus can spread. Not to be outdone by the plant's defenses, viruses have evolved a variety of molecular pathways to circumvent the plant's siRNA mechanism. Some of these counter mechanisms include the inhibition of RISC formation, degradation of AGO, and indirect destabilization of the siRNA molecule itself.

COSUPPRESSION IS A GENE-SILENCING PHENOMENON MEDIATED BY RNA One of the first experiments leading to the discovery of RNAi involved an unexpected plant response to the introduction of transgenes. In the early 1990s, Richard Jorgensen and his colleagues were working with the petunia gene for chalcone synthase, a key enzyme in the pathway that produces purple pigment molecules in petunia flowers. When they inserted a highly active copy of the gene into petunia plants, they expected to see a deepening of the purple color in the flowers of the offspring. To their surprise, the flowers ranged in petal color from dark purple (as expected) to completely white (as if chalcone synthase levels had gone *down* instead of up). This phenomenon—decreased expression of a gene when extra copies are introduced—was termed **cosuppression**. With our present understanding of RNAi, we now know that in some cells, overexpression of chalcone synthase triggered an RNA-dependent RNA polymerase to produce dsRNA molecules, which initiated the RNAi response. This response eventually led to posttranscriptional silencing and to methylation of both the introduced and the endogenous copies of the chalcone synthase gene. Interestingly, posttranscriptional silencing did not occur in all cells. The cells in which gene silencing took place gave rise to white sectors, explaining why some of the transgenic petunia plants had variegated purple and white flowers.

In summary, RNAi is a process in which dsRNA elicits a posttranscriptional response that leads to the silencing of specific transcripts. miRNAs aid in the posttranscriptional regulation of genes in the cytoplasm, while siRNAs act in the nucleus to keep heterochromatin transcriptionally inactive or function as a molecular immune response against viruses.

3.5 Tools for Studying Gene Function

Individuals that contain specific changes in their DNA sequence are called **mutants**. The analysis of mutants is an extremely powerful tool that can help scientists infer the function of a gene or map its location on the chromosomes. In this section we discuss how mutants are generated and how they can be used in genetic analysis. We also discuss some modern biotechnological tools that allow researchers to study or manipulate the expression of genes.

Mutant analysis can help elucidate gene function

Throughout this book we will discuss the genes and genetic pathways involved in physiological functions at length, often referring to certain types of mutants that allowed researchers to understand the genes and pathways under discussion. Why is a mutant gene a more powerful tool for elucidating gene function than the normal, wild-type gene on its own?

The use of mutants for gene identification relies on the ability to distinguish a mutant from a normal individual, so the change in the mutant's nucleotide sequence must result in its observed altered phenotype. If a mutant can be restored to the normal phenotype with a wild-type version of a candidate gene, the researcher knows that a mutation in that gene was responsible for conferring the originally observed mutant phenotype. This method is called **complementation**. For example, assume that a plant with a single-gene mutation shows a delay in producing flowers compared with the wild type. If we can determine the sequence and location of the gene responsible, we will presumably learn something about the mechanisms involved in floral development. Let's now assume that a researcher is able to find a gene in the mutant genome that differs from the wild-type gene in its DNA sequence. If the researcher is able to show that transferring the wild-type gene into the mutant restores the normal phenotype, we can be reasonably certain that the candidate gene plays a role in the initiation of flowering.

In the 1920s, H. J. Muller and L. J. Stadler independently experimented with the effects of X-rays on the stability of chromosomes in flies and in barley, respectively. Both researchers reported heritable changes in the treated organisms. In the following years, other techniques for inducing mutations were developed. These techniques include the use of ultraviolet or fast-neutron radiation and of mutagenic chemicals. For example, treatment with the chemical **ethylmethanesulfonate** (**EMS**) causes the addition of an ethyl group to a nucleotide base, usually guanine. Ethylated guanine pairs with thymine instead of cytosine. The cell's DNA repair machinery then replaces the ethylated guanine with adenine, causing a permanent mutation from G/C to A/T at that site. Mutagenesis with either radiation or chemicals induces nucleotide changes randomly throughout the genome.

There are several ways to map a mutation to its chromosome and ultimately clone the affected gene. **WEB TOPIC 3.2** explains a method called **map-based cloning**, which uses crosses between a mutant and a wild-type plant and genetic analysis of the offspring to narrow down the location of the mutation to a short segment of the chromosome, which is then sequenced.

Another method of mutagenesis is the random insertion of transposons into genes. This technique involves crossing the plant of interest with a plant carrying a single active transposon and screening their offspring for mutant phenotypes caused by random insertion of the transposon into new locations. Because the sequence of the transposon is known, these mutations are "tagged"; thus, the DNA sequences adjacent to the transposon can be readily found and analyzed to identify the mutated gene. This technique is called **transposon tagging** and is explained in detail in **WEB TOPIC 3.3**. Using a technique very similar to transposon tagging, plant genes can also be tagged with known sequences from specific bacteria or viruses. We discuss the example of the soil-borne mutagenic *Agrobacterium* in Section 3.6 in a different context.

This bacterium can transfer a piece of its genome into a host plant's genome, creating a mutation and leaving behind a "tag," similar to that of transposons. DNA markers can be used to associate mutations with phenotypes in marker-assisted breeding.

Although novel mutations can be deliberately introduced into plants to evaluate gene function, mutations can also occur naturally as a result of exposure to utraviolet rays from the sun, mistakes made by the cell during DNA replication, or chemical modification of DNA by toxins. Such mutations are an important source of variation and the basis of evolution. Plant breeders often identify valuable traits in wild relatives of crop plants and *introgress* these traits into elite agricultural varieties (**Box 3.1**).

BOX 3.1 Genetic Traits from Wild Grasses Are Used to Make Grain Crops More Resilient to Climate Change and Global Pathogen Threats

Monoculture of major agricultural crops has reduced their genetic diversity. As a result, food production is increasingly subject to losses from climate volatility, diminished natural resources, and pest pressures. Wild relatives of crop plants are regarded as a treasure trove of useful resistance and resilience **traits**. Unlike modern crop varieties that have been selected for yield under ideal agronomic conditions, wild relatives of crop plants maintain natural survival and dispersal traits that are undesirable for food production and consumption. Historically, the process of crop domestication involved selection of variants that perform reliably due to loss of traits that provide selective advantages in the wild. Examples include loss of free shattering (seed dispersal after ripening) in wheat, barley, rice, and sorghum; apical dominance in maize; and grain quality and threshability in bread wheat (*Triticum aestivum*). These traits are controlled by a small number of genes, and thus were easy to eliminate. Breeding manipulations created a "domestication bottleneck" that reduced the genetic diversity that underpins complex traits such as disease resistance, heat, and water-deficit stress tolerance.

Marker-assisted breeding employs DNA-based markers that are tightly linked to phenotypic traits to assist in the selection process to deliver improved cultivars. Advances in the next-generation sequencing and genotyping technologies have revolutionized the marker-assisted breeding process and have reduced the time and costs required to transfer useful genes and alleles from wild species of crop plants.

(*Continued*)

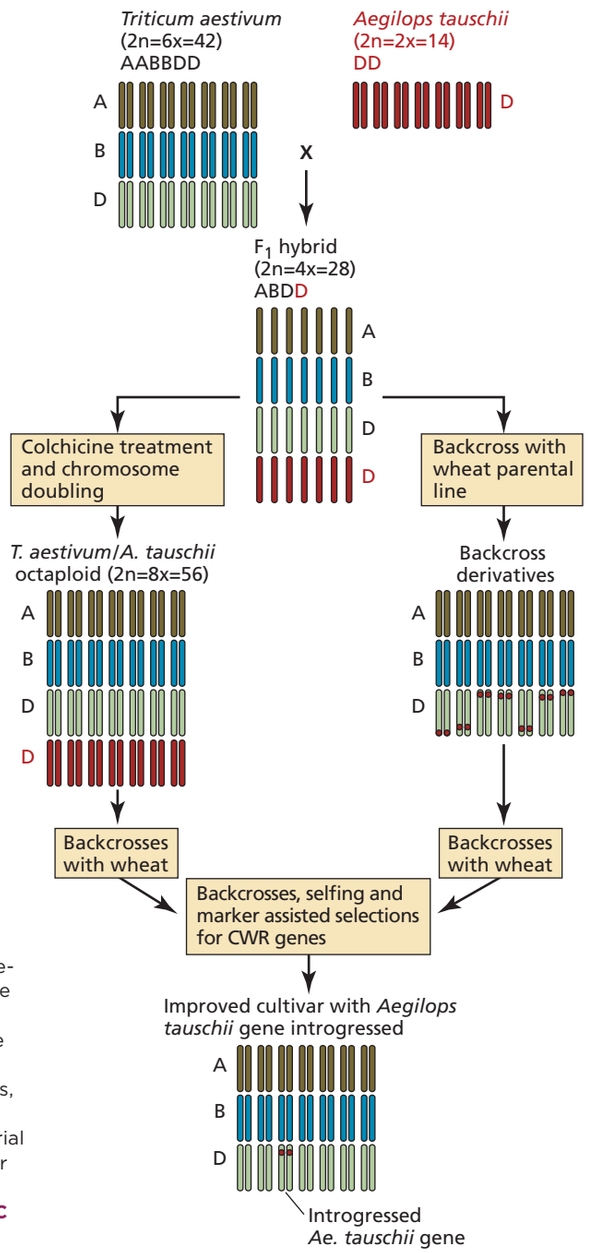


Figure A Commonly used schemes to introgress wild relative genes into wheat varieties. This scheme explains the introgression of genes into wheat from its close wild relative species *Aegilops tauschii*. Bread wheat is hexaploid as a result of the hybridization of three distinct genomes (2n=6x=42; AABBDD), while *Ae. tauschii* is diploid (2n=2x=14; DD) genomes. Colchicine is used by breeders to create viable higher level artificial polyploids for introgressive crosses. Backcrosses of hybrids, mutants, or artificial polyploid lines are made to a recurrent parental line (elite cultivar) to reduce or to eliminate unwanted genetic material and undesirable traits associated with the the CWR. The gene or genes associated with the desired trait are then "mapped" and identified by high-throughput DNA sequencing (see **WEB TOPIC 3.4** for a discussion of map-based gene identification).

BOX 3.1 Genetic Traits from Wild Grasses are Used to Make Grain Crops More Resilient to Climate Change and Global Pathogen Threats *(continued)*

A web-enabled global priority list of 1667 crop wild relatives (CWRs) has been created for collecting, protecting, and using wild plant genetic resources to generate crop plant varieties with resilience to global climate change at the Crop Wild Relatives Project (www.cwrdiversity.org).

Introgression of useful genetic material from CWRs to cultivated varieties has traditionally been performed by direct introduction of wild pollen into the emasculated or female flowers of domesticated crops. Direct crossing schemes have been very effective in transferring genes in crop plants from their close CWRs (**Figure A**). However, successful crossing is often challenging and time-consuming because of the incompatibility of the wild chromosomes, or other systems in the plants to maintain their genomic stability (see Chapter 21). "Bridge" crossing, whereby a CWR gene is first introduced into an intermediate species that is compatible with both the parents, is sometimes used to overcome these barriers and, ultimately, transfer the genes of interest to the desired cultivated background.

In many cases, interspecific hybrids do not form viable seeds or healthy embryos. To overcome this barrier, young embryos (see Chapter 21) are removed from the ovules and cultured in artificial media, a technique known as *embryo rescue*. Technically difficult approaches that artificially insert genetic material from one species into cells from another, such as somatic hybridization or protoplast fusion, are sometimes employed when sexual hybridization is not feasible. Sometimes, breeders increase ploidy (genome) numbers to achieve necessary genetic stability (numbers of genes required for viability) after hybridization. Chromosome doubling using chemicals such as colchicine is employed for this purpose. Synthetic hexaploid wheat lines have been developed using this technique by crossing tetraploid wheat with a diploid progenitor of modern hexaploid wheat, and then doubling the genomes of the triploid interspecific hybrid using colchicine.

γ-Radiation is a physical technique less commonly used to transfer "alien" chromosome segments to wheat. Although useful for introducing shorter (broken) chromosome segments with the gene(s) of interest, the broken chromosome segments may contain chromatin with undesirable genes that also are integrated randomly throughout the genome, making it difficult to retain the segment of interest while eliminating undesirable DNA.

The availability of genomic resources and of high-resolution maps for marker-assisted selections, high-throughput phenotyping capacities, and speed breeding have revolutionized gene discovery and precise transfer of useful genes from CWRs to crop plants and will help address the challenges of twenty-first-century agriculture. ■

Molecular techniques can measure the activity of genes

Once a gene of interest has been identified, scientists are usually interested in where and when the gene is expressed. For example, a gene may be expressed only in reproductive tissues, or only in vegetative ones. Likewise, a gene may encode general cell functions (so-called housekeeping functions) and be expressed continuously, or it may encode special functions and be expressed only in response to a certain stimulus, such as a hormone or an environmental cue. In the past, transcriptional analysis (determination of the amount of mRNA produced from a gene at a given time) has been performed mainly on single genes. Tools developed for this type of analysis include northern blotting and in situ hybridization. However, gene transcription is primarily evaluated by quantitative reverse transcription polymerase chain reaction (qRT-PCR), microarray analysis, and various types of high-throughput **transcriptomics** (RNAseq). Specialized RNAseq methodologies are used to make transcriptional comparisons, determine the extent of epigenetic modification, determine expression in a single cell, and identify chromatin interactions. **Proteomic** techniques are used to identify and quantify the protein products of gene expression as well as protein modifications such as phosphorylation or acylation (see Chapter 4). The application of these transcriptomic technologies is discussed extensively in **WEB TOPIC 3.5**.

Gene fusions can create reporter genes

The identification of a gene containing a mutation provides information about that gene's location in the genome and about the effect of its altered function on the plant's phenotype. From the sequence of a gene alone, scientists can make inferences about the gene's cellular function by comparing the gene's structure with those of other known genes. For example, certain regions within the gene—so-called **domains**—might have similarity to domains found in certain families of genes, such as those encoding kinases, phosphatases, or membrane receptors. However, sequence information alone does not give direct evidence of the gene's cellular function, nor does it indicate where in the plant, or under what conditions, the gene is active.

One way to find out where and when a certain gene is expressed in a plant or cell is to measure the abundance of its mRNA by one of the methods described in the previous subsection. Another way is to make a gene fusion. A **gene fusion** is an artificial construct that combines part of the gene of interest—for example, the promoter—with another gene—referred to as a **reporter gene**—that produces a readily detectable protein. One such reporter gene is the green fluorescent protein (GFP) gene, which produces a fluorescent protein that can be observed in an intact plant or cell by fluorescence microscopy (for an example, see Figure 16.11). Recall that not all genes are transcribed in every cell of the plant at all times. A gene's expression is regulated by transcription factors that fine-tune its activity and allow it to be transcribed only where and when it is needed. If a plant carries a promoter–*GFP* gene fusion in all of its cells, *GFP* will be expressed only in those cells that would normally express the gene whose promoter was fused with *GFP*. In other words, green fluorescence will be visible wherever and whenever the gene under investigation is expressed. Another frequently used reporter of gene activity is a fusion a plant gene promoter sequence to the oportion of a bacterial *β-glucuronidase* (*GUS*). The enzyme encoded by *GUS* hydrolyzes an introduced chemical substrate to produce a blue colored or fluorescent product in the cells where the promoter of interest is active (for an example, see Figure 18.30). This process kills the plant tissue, so is not useful for monitoring of gene activity over time.

3.6 Genetic Modification of Plants

To transform plants with gene fusions, such as reporter genes or those for complementation analysis, scientists have harnessed the power of the microbial plant pathogen *Agrobacterium tumefaciens*. This bacterium causes infected plants to overproduce growth hormones, which induce the formation of a tumor called a **crown gall** (see Figure 4.13). Crown gall disease is a serious problem for certain agricultural crops, such as fruit trees, as it can reduce crop yield and decrease overall plant health.

Agrobacterium is sometimes referred to as a natural genetic engineer because it has the ability to transform plant cells with a small subset of its own genes. The genes transferred to the plant genome are part of a circular extrachromosomal piece of DNA called the tumor-inducing (Ti) plasmid (**Figure 3.15**). The Ti plasmid contains several virulence (*vir*) genes as well as a region called the transfer DNA (T-DNA). The *vir* genes are required for initiating and conducting the transfer of the T-DNA into the plant cell. Once transferred, the T-DNA inserts itself randomly into the plant nuclear genome. It carries genes for two general functions: first, the induction of the crown gall, which will provide housing for the bacterium, and second, the production of nonprotein amino acids called *opines*, which are used by the bacterium as a source of metabolic energy. An overview of the steps involved in the transformation of plant cells by *Agrobacterium* is shown in **Figure 3.16**.

Given that *Agrobacterium* is usually a plant pathogen, how can it be a useful biotechnological tool? We already mentioned in Section 3.5 that *Agrobacterium* can be used to transfer tags to the genome to randomly disrupt genes for mutant analysis. When *Agrobacterium* is used in the laboratory for targeted genome modification, scientists use a strain that has a modified Ti plasmid. The hormone and opine genes are removed from the T-DNA to render the bacterium harmless to plants, and a gene of interest is inserted in their place (see Figure 3.15). If the gene originates from another organism, it is referred to as a *transgene.* Often a gene that confers resistance to an antibiotic is added as a selectable marker gene. The engineered Ti plasmid is then inserted into *Agrobacterium*.

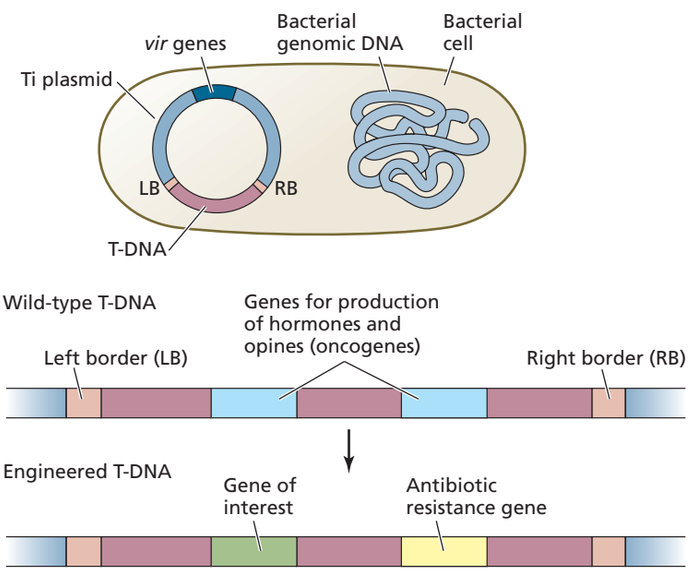


Figure 3.15 ***Agrobacterium*'s tumor-inducing (Ti) plasmid.** The Ti plasmid is a circular extrachromosomal piece of DNA contained inside the bacterial cell. A portion of this plasmid, the transfer DNA (T-DNA), is transferred to the infected plant, where it is inserted into the plant's nuclear genome. The virulence (*vir*) genes, located elsewhere on the Ti plasmid, are essential for initiating the transfer of T-DNA. Wild-type Ti plasmid T-DNA contains genes for production of plant hormones and nonprotein amino acids (opines). When *Agrobacterium* is used for plant transformation, the hormone and opine genes are removed and replaced with the gene of interest, often coupled with a selectable reporter gene such as a gene for antibiotic resistance.

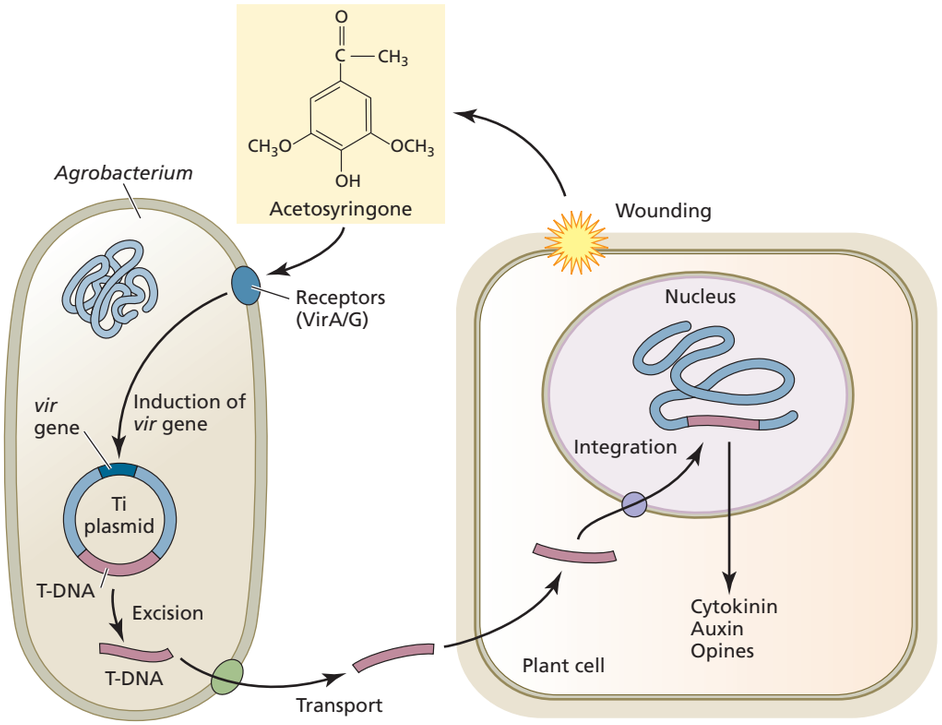


Figure 3.16 Infection of plant cells with *Agrobacterium*.

Any gene now contained within the T-DNA will be transferred into a plant cell infected with the engineered bacterium. The antibiotic resistance gene allows the researcher to easily screen for transformed cells since only transformed cells will survive when grown in the presence of the antibiotic.

Plants can be infected with the engineered bacterium in several ways. Small leaf segments can be cut from a plant and co-cultivated with a solution of the bacterium, before washing the plant cells and culturing them on tissue culture medium. The plant hormones auxin and cytokinin are then used to stimulate the generation of roots and shoots from the tissue, respectively. This technique eventually produces a transformed adult plant. Some plants, including Arabidopsis, are so easily transformed that just dipping the flowers in a suspension of the bacterium is sufficient to result in transformed embryos in the next generation.

Besides *Agrobacterium*-mediated transformation, several other techniques have been developed to incorporate foreign genes into plant genomes. One such technique is the fusion of two plant cells with different genomic information, called **protoplast fusion**. Another is **biolistics**, sometimes referred to as the **gene gun** technique, in which tiny particles of gold coated with the genetic construct of interest are shot into cells growing in culture dishes (**Figure 3.17**). The genetic material is randomly incorporated into the cells' genomes. The cells can then be transferred to solid culture medium and grown into mature transgenic individuals.

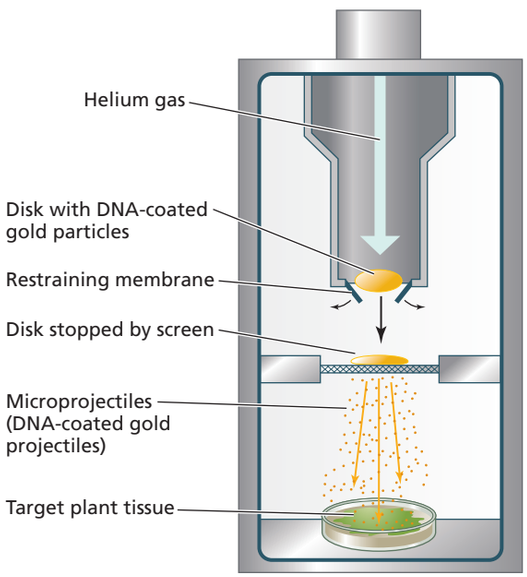


Figure 3.17 Recombinant DNA can be inserted into plant cells using biolistics with a "gene gun."

3.7 Editing Plant Genomes

Genome editing technologies can make targeted modifications in plant genomes. Currently, four major genome editing technologies are used for basic and translational research in plants:

1. Targeted mutagenesis by sequence-specific nucleases
2. Precise gene replacement
3. Base editing
4. Prime editing

This section describes these genome editing technologies, which have begun to revolutionize twenty-first-century plant genetics and crop breeding.

Sequence-specific nucleases induce targeted mutations

To introduce specific mutations into the plant genome, one can engineer sequence-specific nucleases (SSNs), which generate double-strand breaks at the target DNA sequence(s). Early versions of SSNs included engineered meganucleases, zinc finger nucleases (ZFNs), and transcription activator-like effector nucleases (TALENs). The development of TALEN technology was inspired by basic research in plant–pathogen interactions (see Chapter 24). *Xanthomonas* bacterial pathogens secrete transcription activator-like (TAL) effectors into plant cells to disrupt host metabolism and cause disease. TAL effectors bind to the promoters of some host genes and activate their expression, thereby modifying host processes to benefit the bacterial pathogens. How the TAL effectors recognize specific DNA sequences was unknown until 2009, when two research groups decoded the TAL effectors' DNA recognition code. This mechanism was subsequently harnessed to engineer TALENs, a new class of SSN (**Figure 3.18**), providing a great example of how a basic science discovery can be quickly translated into a powerful biotechnology.

The most popular and powerful SSN technologies are based on CRISPR (*C*lustered *R*egularly *I*nterspaced *S*hort *P*alindromic *R*epeats)-Cas (CRISPR-*as*sociated protein)

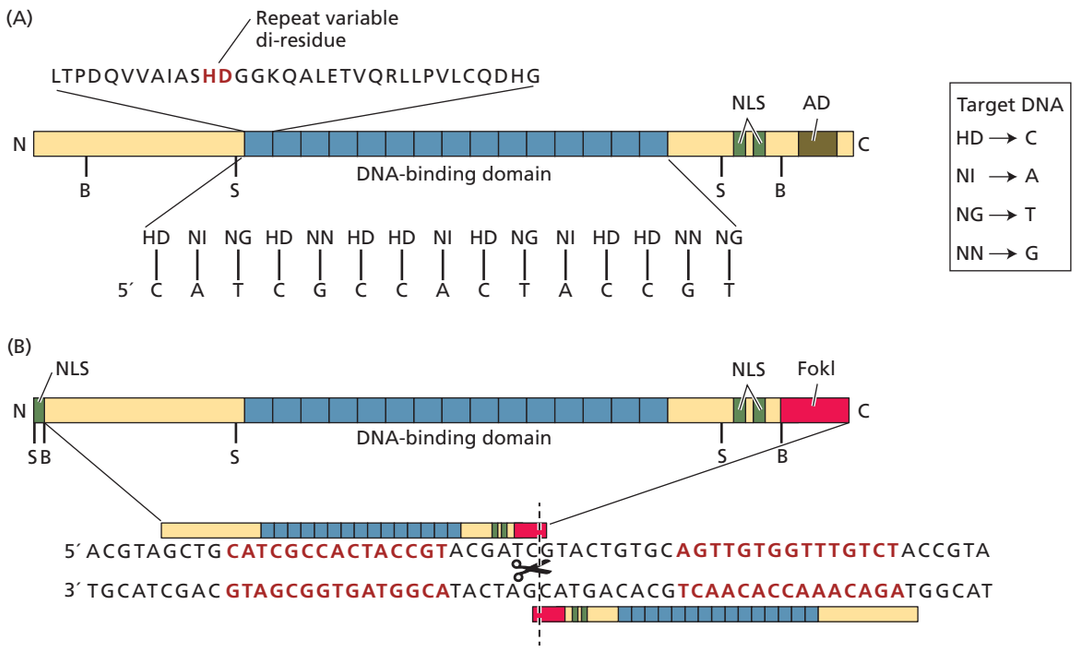


Figure 3.18 **TAL effectors and TALENs.** **(A)** Structure of a naturally occurring TAL effector. The DNA-binding domain is made up of tandemly repeated sequences (blue segments), each of which contains two amino acids that target the protein to a specific DNA base. These amino acids are called repeat variable di-residued (RVDs). One of these consensus repeat sequences is shown above the protein structure with its RVD indicated with bold red font. The box shows the DNA targets that are associated with each RVD. As shown below the protein structure, the RVD sequences vary among the consensus repeat sequences, and the particular set of RVDs in a TAL effector's DNA-binding domain determines its target nucleotide sequence. The four most common RVDs, which are the basis of engineered TALENS, are shown with their most frequently associated nucleotide (e.g., TAL repeat with the RVD of HD recognize Cytosine (C) in DNA) . **(B)** Structure of a TALEN. In TALENs, the transcriptional activation domain (AD) of TAL is replaced with the endonuclease FokI. Two different monomeric TALENs, engineered to bind to sequences flanking the target site (indicated with bold red font), are required to bind the target site and enable FokI to dimerize and cleave the DNA. AD, transcriptional activation domain; B, restriction (cutting) site for BamHI; NLS, nuclear localization signal; S, restriction (cutting) site for SphI. (After T. Cermak et al. 2011. *Nucleic Acids Res.* 39: e82.)

systems. The CRISPR-Cas9 system was originally identified in the immune system of the bacterium *Streptococcus thermophilus*, which is used in the dairy industry to fend off bacteriophages (viruses that attack bacteria) that can spoil the yogurt making process. A functional CRISPR-Cas9 system can snip off a piece of DNA from the genome of an invading phage and insert it between CRISPR repeats in the bacterial genome, creating a "memory" of that phage. This phage-derived memory DNA is called a protospacer and can be transcribed to produce CRISPR RNA (crRNA), which includes both phage and CRISPR sequences. A trans-activating CRISPR RNA (tracrRNA) that can hybridize with the CRISPR sequence in the crRNA is also required by the system. The Cas9 protein is a nonspecific DNA nuclease that is guided by the crRNA-tracrRNA to target and cleave the invading phage DNA at a site adjacent to the protospacer motif (**Figure 3.19A**). In 2012, Jennifer Doudna and Emmanuelle Charpentier demonstrated de novo engineering of a CRISPR-Cas9 system as an RNA-guided SSN. Importantly, a guide RNA (gRNA) was engineered by fusing crRNA and tracrRNA

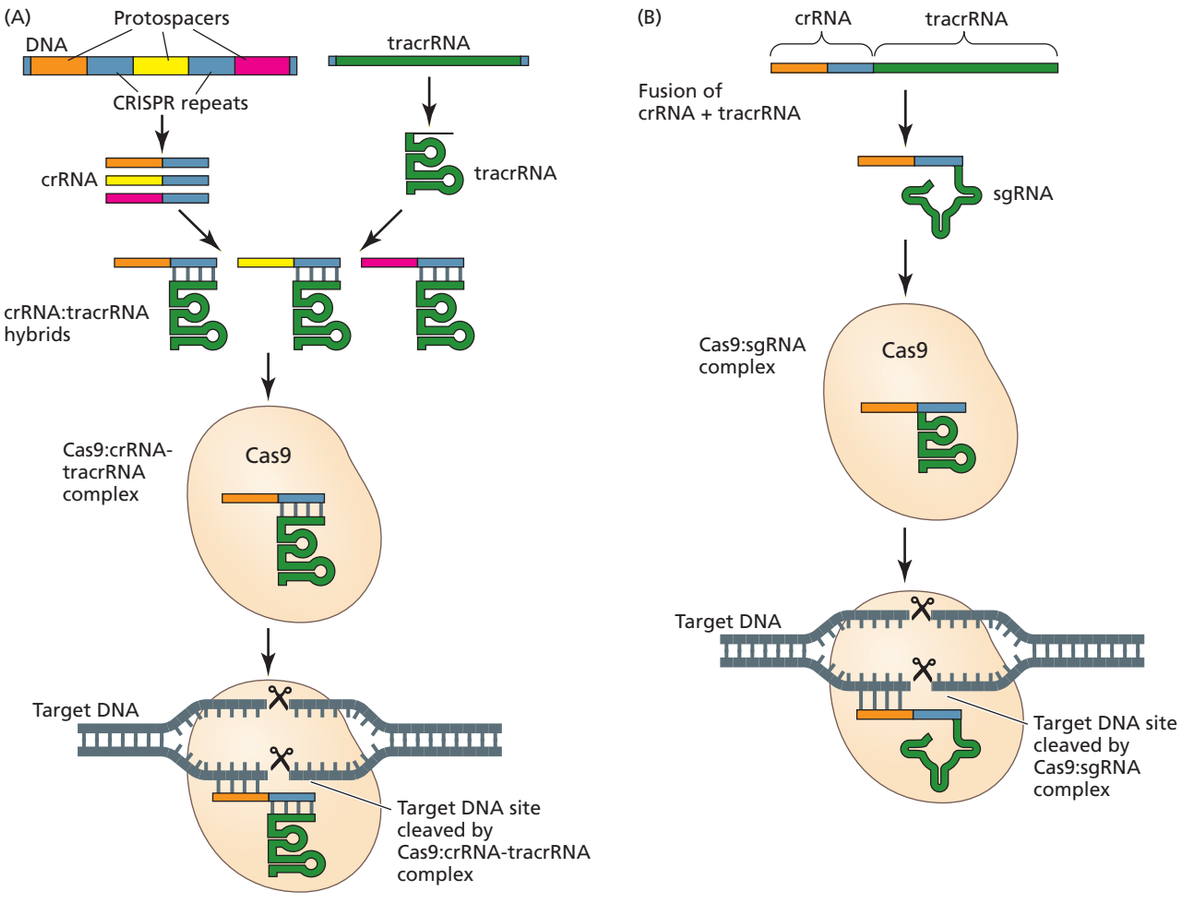


Figure 3.19 **CRISPR-Cas system for gene editing.** **(A)** The CRISPR regions in bacterial genomes contain snippets of DNA (protospacers, depicted as colored segments) that are remnants of invasive DNA from a bacterial or viral attack in the past that did not lead to the host cell's death. Incorporation of these foreign DNA pieces into the bacterial host genome creates a memory bank of DNA sequences to be potentially targeted for destruction in the event of a future attack. Each DNA snippet can be transcribed into RNA, called CRISPR-RNA (or crRNA), each of which is complementary to one specific foreign DNA sequence. The second major component of the host's CRISPR system is the transactivating CRISPR RNA (tracr RNA). crRNA and tracrRNA hybridize and bind to the Cas9 protein, also encoded in the host's genome. This complex can then target complementary invading DNA and cleave it using the nuclease function of the Cas9 protein. Although the cleaved DNA can be repaired, such repairs are imperfect and create mutations in the invading DNA, which often impairs its function. **(B)** CRISPR systems engineered for genome editing use a synthetic piece of RNA, called the guide RNA (gRNA) which is a fusion of the tracrRNA and the target sequence. A synthetic construct made in the lab and encoding the gRNA is transformed into the target host together with a copy of the Cas9 gene. Inside the target cell, the Cas9:gRNA complex can create mutations in a gene of interest by cleavage via Cas9 followed by imperfect repair of the damage by the host cell's DNA repair machinery. (After J. D. Sander and J. K. Joung. 2014. *Nat. Biotechnol.* 32: 347–355.)

together, which reduced the CRISPR-Cas9 system to two components, Cas9 and gRNA (**Figure 3.19B**). Soon after, CRISPR-Cas9 was being used for genome editing in eukaryotes, including plants. Later, additional Cas components such as Cas12a and Cas12b were demonstrated to work in plants. As RNA-guided nucleases, CRISPR-Cas systems are easy to engineer, enabling targeting of nearly any sequence in a genome of interest. For their work on adapting the CRISPR system into a programmable gene editing tool, Doudna and Charpentier were awarded the 2020 Nobel Prize in Chemistry.

In eukaryotic cells, SSN-generated double-strand breaks are repaired through either the **non-homologous end-joining** (**NHEJ**) (**Figure 3.20A**) or **homologous recombination** (**HR**) DNA repair pathway (**Figure 3.20B**). Non-homologous end joining is the preferred pathway and is error-prone, which results in small insertion and deletion mutations. This is the usual mechanism of targeted mutagenesis by SSNs. With a CRISPR-Cas system, a plant biologist can easily introduce mutations into a gene of interest to study its loss-of-function phenotype, which in turn helps deduce the function of the gene. This simple gene knockout technology has greatly boosted basic research in plants. Furthermore, loss-of-function or reduced function for some genes can be of agronomic value. Given that multiple gRNAs can be coexpressed with the Cas nuclease in plant cells, it is feasible to edit genes for multiple traits simultaneously in elite cultivars for rapid crop improvement.

Gene editing can lead to precise gene replacement

Precise gene replacement by homology-directed repair is often considered to be the Holy Grail of plant genome editing (see Figure 3.20B). Two things are required for efficient homology-directed repair: (1) induction of DNA double-strand breaks at the target sequence by SSNs such as CRISPR-Cas, and (2) a double-stranded or single-stranded DNA donor repair template that contains the desired changes and homology to the target sequence. In principle, homology-directed repair can generate base changes or deletions, or even deletion or insertion of whole genes. For example, an herbicide-resistance trait was introduced into rice by CRISPR-Cas9-mediated homology-directed repair that modified specific parts of the acetolactate synthase gene (**Figure 3.21**). However, the efficiency of homology-directed repair editing needs to be drastically improved before this technology can be readily applied in many other plant species. Homology-directed DNA repair occurs primarily in the G_2 and S phases of the cell cycle and is relatively uncommon in the vast majority of plant cell types compared with non-homologous end-joining. It is also a challenge with homology-directed repair to deliver the repair template into plant cells. Given the promise of precise gene

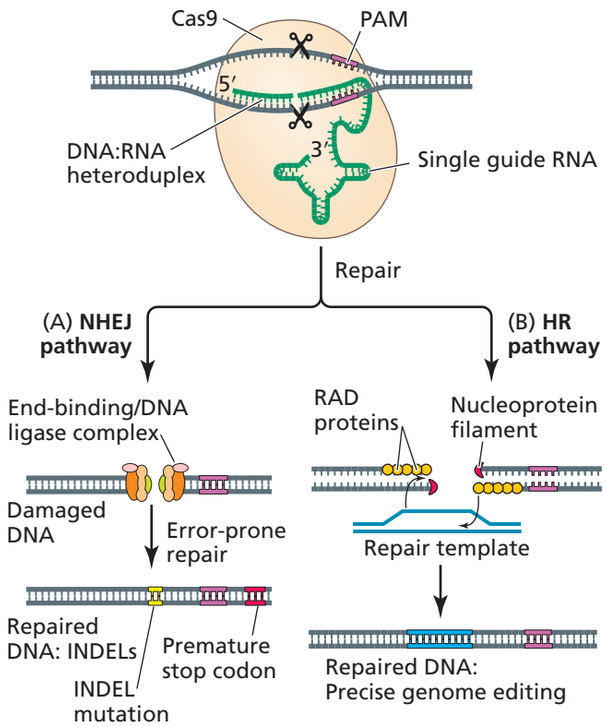


Figure 3.20 CRISPR-Cas9-mediated targeted mutagenesis and precise gene replacement. CRISPR-Cas9 complexes target specific genomic sequences to create double-strand breaks adjacent to the protospacer adjacent motif (PAM) site. **(A)** The error-prone non-homologous end-joining (NHEJ) DNA repair pathway can be harnessed by CRISPR-Cas9 to introduce premature stop codons or other mutations into the coding sequence of a gene. INDELs, small insertions and deletions. **(B)** The homologous recombination (HR) pathway uses a DNA template to guide the repair of double-strand breaks. HR is less efficient, but it is useful for genome editing because it results in precise replacement of genome sequences. (After M. Barresi and S. Gilbert. 2019. *Developmental Biology*, 12th ed. Sinauer Associates/Oxford University Press, Sunderland, MA; J. W. Paul, III and Y. Qi. 2016. *Plant Cell Rep.* 35: 1417–1427.)

replacement for improving crop resilience and yield in suboptimal climatic conditions, innovative solutions to these limitations can be expected.

Base editing can be used as an alternative to homology-directed repair

Base editing is a practical alternative to homology-directed repair if the goal is to introduce base changes into a plant genome. Base editing is achieved by so-called base editors that are derived from CRISPR-Cas9 systems. Cytosine base editors can direct C-to-T substitutions (or G-to-A on the complementary DNA strand). An efficient cytosine base editor system generally comprises a Cas9-based "nickase," which cuts only the targeted DNA strand instead of making a double-strand



From Y. Sun et al. 2016. *Mol. Plant* 9: 628–631

Figure 3.21 Generation of herbicide-resistant rice plants by CRISPR-Cas9-mediated homology-directed repair. The plants are shown 36 days after being sprayed with 100 μM bispyribac sodium at the five-leaf stage. On the left is a rice line with the edited acetolactate synthase (*ALS*) gene involved in the synthesis of branched amino acids and on the right is a wild-type (WT) rice line. The herbicide bispyribac sodium inhibits the WT ALS protein function but fails to inhibit the modified ALS protein. Note that the wild-type plants died whereas the gene-edited plants grew normally.

break; a cytidine deaminase; and one to a few copies of uracil glycosylase inhibitor (**Figure 3.22A**). Adenine base editors catalyze A-to-G (or T-to-C on the complementary DNA strand) base changes. An adenine base editor is composed of a Cas9 nickase and an engineered adenine deaminase.

Base editors can be used to modify plants for different purposes. First, base editors can alter stop codons. A cytosine base editor can convert an amino acid codon to a premature stop codon (TAG, TAA, or TGA) and thus knock out the function of a protein-coding gene. By contrast, an adenine base editor can cause a reversion of a premature stop codon to a codon for Trp (TGG), Glu (CAA, CAG), or Arg (CGA). Second, base editors can target RNA splicing sites to alter splicing. Third, base editors can be used to direct specific amino acid changes for protein engineering, such as editing genes for targeted pathogen resistance. Last, but not least, many agronomic traits are associated with single nucleotide polymorphisms (SNPs) in *cis*-regulatory elements in crop genomes. Base editors are expected to be widely used for directing specific agronomically important SNPs for rapid breeding of elite crop varieties.

Despite their promise, current base editors have some limitations. For example, cytosine and adenine base editors are largely limited to making transition mutations (i.e., purine to purine and pyrimidine to pyrimidine). Also, base editors act on all targetable bases in a targeting window and hence lack sufficient precision for achieving base changes at specific sites. CRISPR-derived base editing systems continue to improve in efficiency and have become standard tools for plant molecular biologists and biotechnologists. Base editing systems based on TAL effectors are increasingly used for editing of plastid and mitochondrial genomes (see Figure 3.18) because guide RNAs used for CRISPR editing cannot effectively enter these organelles. The ability to edit chloroplast and mitochondrial genomes is an important component of efforts to engineer photosynthetic activity and CO_2 utilization under changing climatic conditions.

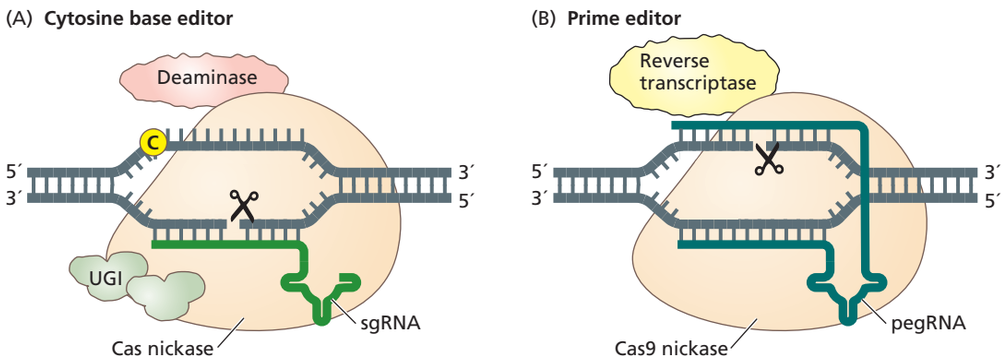
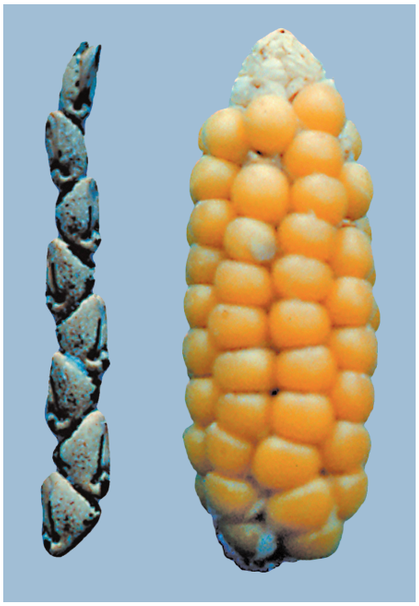


Figure 3.22 Base editors and prime editors derived from CRISPR-Cas9. **(A)** A cytosine base editor bound to its target site, showing the nick in the targeted DNA strand where repair or replacement takes place. UGI, uracil glycosylase inhibitor. **(B)** A prime editor bound to its target site, showing the nick in the nontargeted DNA strand (the complement of the targeted strand). The reverse transcriptase uses the template in the pegRNA to synthesize new DNA to replace the damaged strand. Binding of a second UGI increases the efficiency of base editing. (After A. V. Anzalone et al. 2020. *Nat. Biotechnol.* 38: 824–844.)

Prime editing uses an RNA repair template and reverse transcription

Prime editing is the newest gene editing technology we discuss here and is more versatile and precise than base editing. Prime editors are based on an engineered CRISPR-Cas9 system that contains (1) a Cas9 nickase that cuts the nontargeted strand DNA, (2) a prime editing guide RNA (pegRNA) that carries a 3′ extension with an RNA primer and a reverse transcription template, and (3) a reverse transcriptase that converts RNA to DNA (**Figure 3.22B**). In prime editing, the desired DNA changes are encoded in the reverse transcription template and incorporated into the target site in the plant genome. Prime editors can introduce any of the 12 possible transition and transversion mutations as well as small insertions and deletions (INDELS). Currently, prime editing readily reaches efficiencies of approximately 1% in plant cells, which is roughly on par with the editing efficiency of homology-directed repair. With further improvement, prime editors will likely become major tools for generating precise base changes and defined INDELs in crop genomes.



Courtesy of John Doebley

Figure 3.23 Classic breeding and domestication of the wild grass teosinte (left) have led to the crop plant *Zea mays* (maize, right) over hundreds of years

3.8 Engineering Crop Plants

Humans have modified crop plants through selective breeding for many centuries to produce varieties that have higher yields, are better adapted to specific climates, or are resistant to plant pathogens. For example, modern maize varieties are the domesticated descendants of wild relatives in the genus *Zea*, known as teosinte (**Figure 3.23**). As is apparent from the photo, breeding and domestication have modified this crop plant substantially from its original form. Likewise, selective breeding has produced crop tomatoes that are much larger than the fruit from the original progenitor species. Breeding has even produced entirely new species, such as the common bread wheat *Triticum aestivum*, which is allohexaploid and arose from the cross-pollination of three different progenitor species. While classic breeding techniques rely on random genetic recombination of traits in sexually compatible species, biotechnology allows the transfer of a controlled number of genes between species that cannot be crossed successfully. Here we discuss how breeding using biotechnological tools differs from classic breeding.

In classic breeding, desirable traits are introgressed into elite agricultural lines by cross-pollinating two varieties and selecting for those traits among the offspring. One disadvantage of this approach is that the genetic contributions of both parents are reshuffled in meiosis, so undesirable traits can be introduced into the recipient line along with the desirable ones. The undesirable traits must then be bred out again by repeated, often time-consuming, backcrosses with the elite line while retaining the desirable traits. Biotechnological tools circumvent this problem by introducing transgenes, edited plant genes, or combinations of guide RNAs and Cas proteins into cells using *Agrobacterium*, biolistics, or viruses.

Transgenes can confer resistance to herbicides or plant pests

Any gene artificially transferred into an organism is usually referred to as a **transgene**. Most often transgenes are introduced from one species into another species. However, some researchers prefer to distinguish gene transfer between sexually compatible species that could also exchange genetic material via classic breeding (***cis*genics**) from gene transfer between species that cannot be naturally crossed, for which these researchers reserve the term ***trans*genics**. Two of the types of transgenes most commonly used in commercial crops today are genes that allow plants to resist herbicide applications and genes that allow plants to withstand attack by certain insects. Weed invasion and insect infestation are two of the main causes of crop yield reductions in agriculture.

Plants carrying a transgene for **glyphosate resistance** will survive a field application of glyphosate (the commercial herbicide Roundup), which kills weeds but does not harm resistant crop plants. Glyphosate inhibits the enzyme enolpyruvalshikimate-3-phosphate synthase (EPSPS), which catalyzes a key reaction in the shikimic acid pathway, a plant-specific metabolic pathway necessary for the production of many secondary compounds, including auxin and aromatic amino acids (see **WEB APPENDIX 4**).

Glyphosate-resistant plants carry either a gene encoding a bacterial form of EPSPS that is insensitive to the herbicide, or transgene constructs that fuse high-activity promoters with the wild-type EPSPS gene to achieve herbicide resistance by overproduction of the enzyme.

Another commonly used transgene encodes an insecticidal toxin from the soil bacterium ***Bacillus thuringiensis*** (**Bt**). Bt toxin interferes with a receptor found only in the larval gut of certain insects, eventually killing them. Plants expressing Bt toxin are toxic to susceptible insects but harmless to most other organisms, including nontarget insect species.

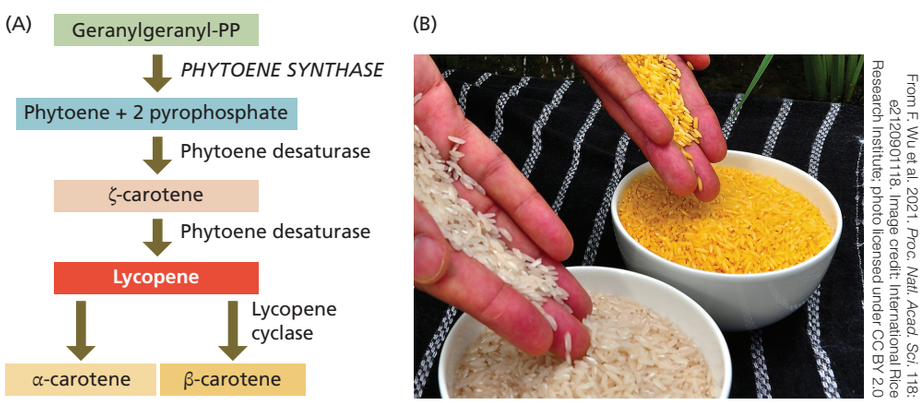
Transgenic plants are also being developed that have enhanced nutritional value. Every year, according to the World Health Organization, dietary vitamin A deficiency causes as many as 500,000 children in developing nations to go blind. Many of these children live in Southeast Asia, where rice is the main part of the diet. Although rice plants synthesize abundant levels of β-carotene (provitamin A) in their leaves, rice endosperm, which makes up the bulk of the grain, does not normally express the genes required for three of the steps in the β-carotene biosynthesis pathway. To overcome this block, Ingo Potrykus, Peter Beyer, and their colleagues developed new strains of rice that carry genes from other species that can complete the β-carotene biosynthesis pathway (**Figure 3.24**). The most efficient strain uses two transgenes: a phytoene synthase gene from maize and a bacterial carotene desaturase gene. Together, these two genes allow the rice plant to accumulate large amounts of β-carotene. Facing many regulatory and intellectual property hurdles, this "golden rice" was field tested for more than ten years and was finally approved for use in the United States in 2018. This was not the first time that the β-carotene content of a crop plant was altered by agriculturalists. Carrots, for example, were either red or yellow before the seventeenth century, when a Dutch horticulturist selected the first orange-colored varieties.

Other researchers are developing transgenic plants that express vaccines in their edible fruit as an alternative, more convenient way to vaccinate people in parts of the world where medical facilities are insufficient for the administration of conventional vaccines.

Genetic engineering of plants remains controversial

The engineering of crop plants has not been greeted with universal enthusiasm and support. In spite of the enormous humanitarian potential of accelerated breeding of sustainable agricultural traits, many individuals, as well as the governments of some countries, look on genetic engineering with suspicion and concern. In particular, opponents to the introduction of genes from other organisms into food plants cite the possibility of inadvertently producing crops that express allergens introduced from another species. They also worry that the overuse of genes encoding Bt toxin might select for insects that develop resistance to the toxin or that windblown pollen from transgenic herbicide-resistant crops could cross-pollinate nearby wild species, thereby producing weeds with herbicide resistance or contaminating organic crops with transgenes. According to the World Health Organization, however, the concern that the ingestion of currently grown and marketed genetically engineered foods poses risks to human health has so far been unsubstantiated.

Crop plants produced by introduction of transgenes or spliced DNA from other organisms are commonly referred to as Genetically Modified Organisms (GMOs). As the sophistication of plant genome editing techniques have become more refined, plant biotechnologists are able to avoid the release of plants containing transgenes into the field. The term Genetically Engineered Organisms (GEOs). Many countries have adopted guidelines that differentiate GMO and GEO crops. For example, a 2016 report from the U.S. National Academies of Science Engineering, and Medicine recommended regulatory differentiation of GMO and GEO approaches, and the United States Department of Agriculture (USDA) has adopted the 2020 Sustainable, Ecological, Consistent, Uniform, Responsible, Efficient (SECURE) rule, which specifies that most genetically engineered crops will not be regulated if they do not contain transgenes.



From F. Wu et al. 2021. *Proc. Natl. Acad. Sci.* 118: e2120901118. Image credit: International Rice Research Institute; photo licensed under CC BY 2.0

Figure 3.24 **Golden rice was produced by inserting a gene encoding a phytoene synthase from maize and another gene encoding a phytoene desaturase enzyme from the soil bacterium *Erwinia uredevora* to catalyze lycopene synthesis in rice grains. A rice lycopene cyclase converts lycopene to a- and β-carotene.** **(A)** The β-carotene biosynthesis pathway in golden rice. **(B)** Normal white rice (left) compared with golden rice (right).

Overall, genetic engineering holds considerable promise for safely modernizing crop breeding to meet the challenges of global climate change. Many of the targeted mutations generated by gene editing technologies already occur in nature or have already arisen during conventional nontargeted mutagenesis or crossbreeding. Given the potential contributions of genome editing to future crop breeding, it is anticipated that these new technologies will be widely used to produce crops that have higher yields, reduced reliance on chemicals to prevent losses to pest and disease, and more resilience to climate-dependent stress.

Research is ongoing to monitor the effects of the new technologies on human health and the environment (see **WEB ESSAY 3.1**). In the end, the controversy may come down to this question: How much risk is acceptable in an attempt to satisfy the needs of an ever-increasing world population for food, clothing, and shelter?

Summary

Genotype, epigenetic modifications of its DNA, and the environment in which it lives determine a plant's phenotype. A thorough understanding of a plant's physiology requires understanding how genotype (nuclear, mitochondrial, and plastid) is translated into phenotype.

3.1 Nuclear Genome Organization

- The most prominent structural landmarks on chromosomes are centromeres, telomeres, and nucleolar organizer regions (NORs) (**Figure 3.1**).
- Heterochromatin (often highly repetitive DNA sequences) is transcriptionally less active than euchromatin.
- Transposons are mobile DNA sequences within the nuclear genome. Some can insert themselves into new places along the chromosomes (**Figure 3.2**).
- Active transposons can significantly damage their host, but most mobile elements are inactivated by epigenetic modifications, such as methylation (**Figure 3.3**).
- Meiosis allows for recombination of genes and the organized reduction of the genome by one half of its chromosomes (**Figure 3.5**).
- All angiosperm lineages have experienced genome duplication at least once in their evolutionary history. Many modern plant species are polyploid, either because of genome multiplication within a species (autopolyploidy) or because of genome duplication in association with hybridization of two or more species (allopolyploidy) (**Figure 3.7**).
- Polyploids have multiple complete genomes; this altered genomic balance can phenotypically distinguish polyploids, especially allopolyploids, from their parents, and may lead to speciation.

3.2 Plant Cytoplasmic Genomes: Mitochondria and Plastids

- Organellar genetics do not obey Mendelian laws, but usually show uniparental inheritance and vegetative segregation.

3.3 Transcriptional Regulation of Nuclear Gene Expression

- Gene expression is regulated at several levels: transcriptional, posttranscriptional, and posttranslational.
- For protein-coding genes, RNA polymerase II binds to the promoter region and requires general transcription factors and other regulatory proteins to initiate gene transcription (**Figures 3.9, 3.10**).
- Epigenetic modifications, such as methylation of DNA and methylation and acetylation of histone proteins, help determine gene activity (**Figure 3.11**).

3.4 Posttranscriptional Regulation of Nuclear Gene Expression

- RNA-binding proteins may either stabilize mRNA or promote its degradation.
- The RNA interference (RNAi) pathway is a post-transcriptional response that leads to the silencing of specific transcripts. MicroRNAs (miRNAs) aid in gene regulation. Short interfering RNAs (siRNAs) help keep heterochromatin transcriptionally inactive, or act as a molecular immune system against viruses (**Figures 3.12–3.14**).

3.5 Tools for Studying Gene Function

- Tools developed for transcriptional analysis of single genes include northern blotting, quantitative reverse transcription polymerase chain reaction (qRT-PCR), and in situ hybridization.
- Transcriptomic technologies use information gained from genome sequencing for high-throughput analysis of gene expression.
- Reporter gene fusions contain part of a gene of interest (e.g., the promoter) fused to a reporter gene that encodes a protein that can be readily detected when expressed. Such constructs can be used to monitor where and when a particular gene is active.

3.6 Genetic Modification of Plants

- *Agrobacterium* can transform plant cells when targeted genes are transferred from the bacterial plasmid called the tumor-inducing (Ti) plasmid (**Figures 3.15, 3.16**).

3.7 Editing Plant Genomes

- CRISPR-Cas-mediated genome editing technologies are also revolutionizing crop breeding. They

(*Continued*)

Summary (*continued*)

allow for introduction of simultaneous changes in many genes at once, thereby greatly accelerating crop breeding.

3.8 Engineering Crop Plants

- In contrast to classic selective breeding, bioengineering allows the transfer of specific genes between species that cannot be crossed successfully, or between crossable species as a means of more precise gene transfer than is possible by traditional breeding.
- Artificially transferred genes can confer resistance to herbicides or plant pests, or provide enhanced nutrition.

Web Material

- **WEB TOPIC 3.1 Inheritance Patterns of Plastid Genomes** Plastid genomes are inherited in a non-Mendelian fashion.
- **WEB TOPIC 3.2 Recombination Mapping and Gene Cloning: Overview** Map-based cloning can be used to identify the gene(s) involved in a phenotype of interest.
- **WEB TOPIC 3.3 Transposon Tagging** Mutagenesis using transposable elements is another approach to gene identification.
- **WEB TOPIC 3.4 The Transcriptome and Data Mining** Advances in high-throughput sequencing of DNA, RNA, and proteins enable genome-scale measurements of gene expression and other genome characteristics.
- **WEB TOPIC 3.5 Transformation by *Agrobacterium*** *Agrobacterium*, a plant pathogen that naturally transforms its host plant, has become the primary biotechnological tool for inserting recombinant DNA into plants.
- **WEB ESSAY 3.1 Agriculture, Population Growth, and the Challenge of Climate Change** The current scientific consensus is that improving crop yields via genetically engineered crops, as well as enhancing soil organic carbon sequestration, are essential components of an overall solution to the problems of population growth and climate change.

For more study aids, go to oup.com/he/taiz7e.

Suggested Reading

Allen, J. F. (2003) The function of genomes in bioenergetic organelles. *Phil. Trans. R. Soc. B.* 358: 19–37.

Bendich, A. (2013) DNA abandonment and the mechanisms of uniparental inheritance of mitochondria and chloroplasts. *Chromosome Res.* 21: 287–296.

Birchler, J. A., Gao, Z., Sharma, A., Presting, G. G., and Han, F. (2011) Epigenetic aspects of centromere function in plants. *Curr. Opin. Plant Biol.* 14: 217–223.

Chen, X. (2012) Small RNAs in development—insights from plants. *Curr. Opin. Genet. Develop.* 22: 361–367.

Chen, Z. J. (2007) Genetic and epigenetic mechanisms for gene expression and phenotypic variation in plant polyploids. *Annu. Rev. Plant Biol. Mol. Biol.* 58: 377–406.

Ghildiyal, M., and Zamore, P. D. (2009) Small silencing RNAs: an expanding universe. *Nat. Rev. Genet.* 10: 94–108.

Gill, N., Hans, C. S., and Jackson, S. (2008) An overview of plant chromosome structure. Cytogenet. *Genome Res.* 120: 194–201.

Grandont, L., Jenczewski, E., and Lloyd, A. (2013) Meiosis and its deviations in polyploid plants. *Cytogenet. Genome Res.* 140:171–84.

Jiao, Y., Wickett, N. J., Ayyampalayam, S., et al. (2011) Ancestral polyploidy in seed plants and angiosperms. *Nature* 473: 97–100.

Leitch, A. R., and Leitch, I. J. (2008) Genomic plasticity and the diversity of polyploid plants. *Science* 320: 481–483.

Liu, C., Lu, F., Cui, X., and Cao, X. (2010) Histone methylation in higher plants. *Annu. Rev. Plant Biol.* 61: 395–420.

Malzahn, A. A., Lowder, L., and Qi, Y. (2017) Plant genome editing with TALEN and CRISPR. *Cell Biosci*. 7: 21.

Madlung, A., and Wendel, J. F. (2013) Genetic and epigenetic aspects of polyploid evolution in plants. *Cytogenet. Genome Res.* 140: 270–285.

Mogensen, L. (1996) The hows and whys of cytoplasmic inheritance in seed plants. *Am. J. Bot.* 83: 383–404.

National Academies of Science, Engineering and Medicine (2016) Genetically Engineered Crops: Experiences and Prospects.

Parisod, C., Alix, K., Just, J., et al. (2010) Impact of transposable elements on the organization and function of allopolyploid genomes. *New Phytol.* 186: 37–45.

Zhang, Y., Malzahn, A. A., Sretenovic, S., and Qi, Y. (2019) The emerging and uncultivated potential of CRISPR technology in plant science. *Nat. Plants* 5: 778–794.

4 Signals and Signal Transduction



LAURA_VN/Shutterstock

As sessile organisms, plants constantly make adjustments in response to their environment, either to take advantage of favorable conditions or to survive unfavorable ones. To facilitate such adjustments, plants have evolved sophisticated sensory systems to optimize water and nutrient usage; to monitor light quantity, quality, and directionality; and to defend themselves from biotic and abiotic threats. Charles and Francis Darwin performed pioneering studies on signal transduction during the bending growth of grass coleoptiles in response to light. They observed that a unidirectional light source was perceived at the coleoptile tip, yet the bending response took place farther back along the shoot tissue. This led the Darwins to conclude that there must be a mobile signal that transferred information from one region of the coleoptile tissue to another and elicited the bending response. The mobile signal was later identified as auxin, indole-3-acetic acid, the first plant hormone to be discovered.

In general, an environmental input that initiates one or more plant responses is referred to as a **signal**, and the physical component that biochemically responds to that signal is designated a receptor. Receptors are either proteins or, in the case of light receptors, proteins associated with light-absorbing pigments. Once receptors sense their specific signal, they must *transduce* the signal (i.e., convert it from one form to another) in order to amplify the signal and trigger the cellular response. Receptors often do this by modifying the activity of other proteins or by employing intracellular signaling molecules called **second messengers**; these molecules then alter cellular processes such as gene transcription. Hence, all signal transduction pathways typically involve the following chain of events:

Signal → receptor → signal transduction → response

In many cases the initial response is the production of **secondary signals**, such as hormones, which are then transported to the site of action and evoke the main physiological response. Many of the specific events and intermediate steps involved in plant signal transduction have now been identified, and these intermediates constitute the **signal transduction pathways**.

We begin this chapter by providing a brief overview of the types of external cues that direct plant growth. Next we discuss how plants employ signal transduction pathways to regulate gene expression and posttranslational responses. A surprising discovery has been that, in the majority of cases, plant signal transduction pathways function by inactivating, degrading, or relocating repressor proteins that modulate transcription. Signal amplification via second messengers is required, as well as mechanisms for signal transmission to coordinate responses throughout the plant. Finally, we examine how individual stimulus-response cascades are often integrated with other signaling pathways, termed *cross-regulation*, to shape plant responses to their environment in time and space.

4.1 Temporal and Spatial Aspects of Signaling

Plant signal transduction mechanisms may be relatively rapid or extremely slow (**Figure 4.1**). When some carnivorous plants, most notably Venus flytrap (*Dionaea muscipula*), catch insects, they use modified leaf traps that close within milliseconds after touch stimulation. Similarly, the sensitive plant (*Mimosa pudica*) folds its leaflets rapidly upon being touched. Young seedlings reorient themselves with respect to gravity minutes after being placed horizontally. Such rapid response mechanisms generally involve release of ions that have been sequestered by energy-dependent processes over time. Environmental responses that occur over a longer

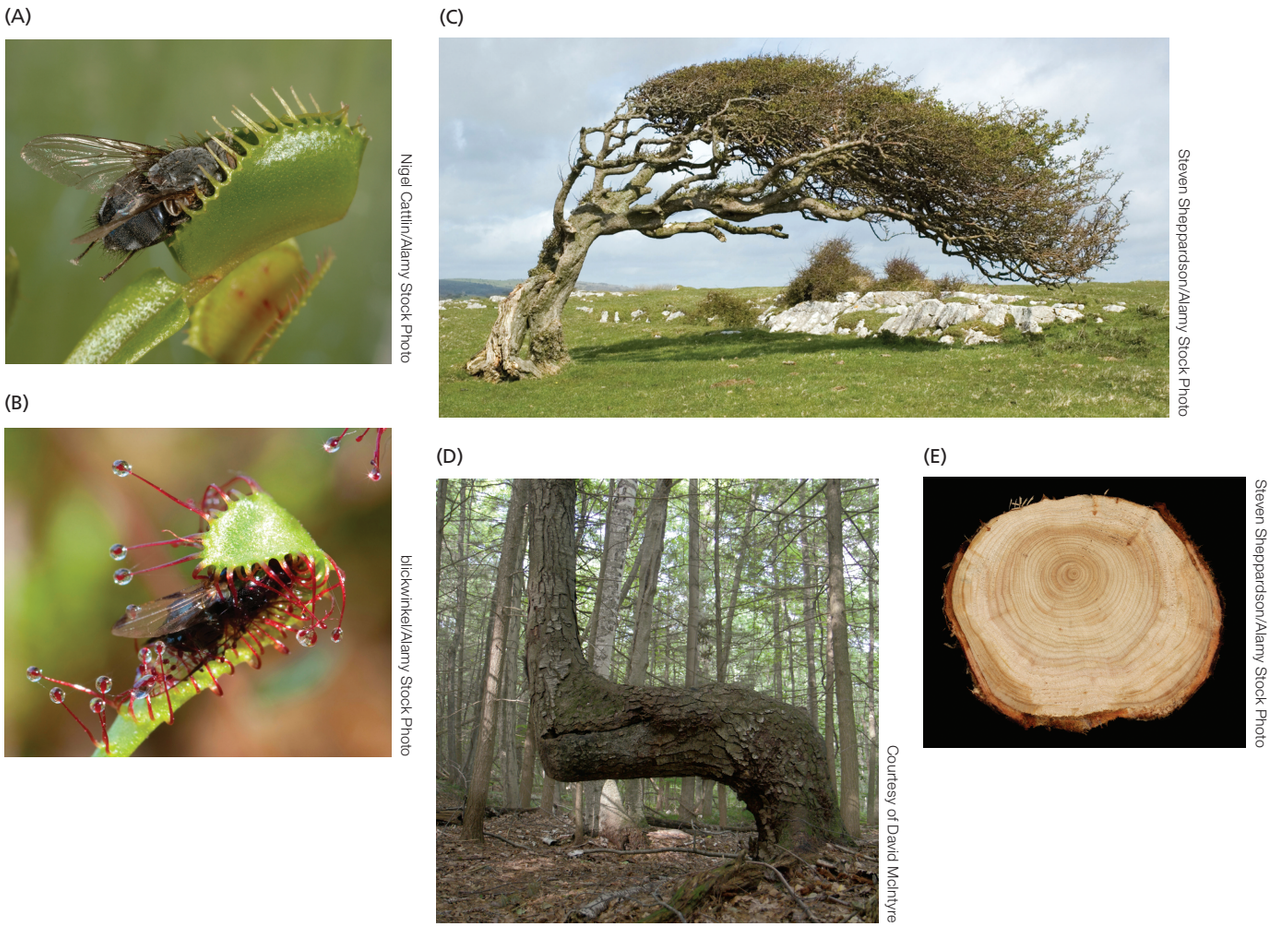


Figure 4.1 Timing of plant responses to the environment ranges from very rapid to extremely slow. **(A)** Insect movements on modified leaves of a Venus flytrap (*Dionaea muscipula*) activate trigger hairs, inducing rapid closure of the leaf lobes. **(B)** The leaves of sundew plants (*Drosera anglica*) capture insects in a sticky fluid produced by stalked glands called tentacles, then roll up to secure the prey and begin digestion. **(C)** A hawthorn tree (*Crataegus* spp.) subjected to prevailing onshore winds responds slowly by growing away from the wind. **(D)** Tree trunks and branches can respond slowly to mechanical stress by producing reaction wood. In this case the tree is an angiosperm, which produces *tension wood* on the adaxial surface. Gymnosperms produce *compression wood* on the abaxial surface. **(E)** Cross section through a gymnosperm tree branch with compression wood, creating an asymmetrical ring structure.

time frame often involve rapid cytoplasmic influx of ionic second messengers, followed by enzyme activation, hormonal responses, and/or gene transcription and protein translation. In contrast, plants attacked by insect herbivores may emit volatiles to attract insect predators within a few hours. Processes occurring on this timescale often involve new transcription and translation activity (see Chapter 3).

Longer-term environmental responses modify developmental programs to shape plant architecture over the entire life of the plant. Examples of long-term responses include modulation of root branching in response to nutrient availability, growth of sun or shade leaves to adjust for light conditions, and activation of lateral bud outgrowth when the shoot apex is damaged by grazing animals. Long-term plant responses can operate over timescales of months or years. For example, a long period of low temperature, termed *vernalization*, is required by many plant species for flowering to occur (see Chapter 20). Chromatin remodeling is often involved in such long-term responses (see Chapter 3).

Plant responses to environmental signals also differ spatially. In a **cell autonomous response** to an environmental signal, both signal reception and response occur in the same cell. In contrast, a **non–cell autonomous response** is one in which signal reception occurs in one cell and the response occurs in distal cells, tissues, or organs. An example of cell autonomous signaling is the opening of guard cells, where blue light activates membrane ion transporters to swell guard cells via the phototropin blue-light photoreceptors (see Chapter 16). An example of non–cell autonomous signaling in the same organs would be the formation of additional stomata when mature leaves are exposed to high light intensity in a process that requires transmission of information from one organ to another (see Chapter 18).

4.2 Signal Perception and Amplification

Although highly varied in nature and makeup, all signal transduction pathways share common features: An initial stimulus is perceived by a receptor and transmitted via intermediate processes to sites where physiological responses are initiated (**Figure 4.2**). The stimulus may derive from developmental programming or from the external environment. When the response mechanism reaches an optimal point, feedback mechanisms attenuate the processes and reset the sensor mechanism.

Receptors are located throughout the cell and are conserved across kingdoms

Receptors can be located at the plasma membrane, cytosol, endomembrane system, or nucleus, as exemplified by hormone and touch receptors (**Figure 4.3**). In some cases, receptors move from one compartment to another. Many plant receptors resemble those found in bacterial systems. For example, homologs of the bacterial mechanosensitive ion channel, **MscS** (**Mechanosensitive channel of Small conductance**), are found both in the plasma membrane and chloroplast envelope (probably the inner membrane) of plant cells. Mechanosensitive channels act as stretch receptors and help cells and plastids adjust to osmotically induced swelling. Plant receptors that perceive the presence of the hormones cytokinin and ethylene, described later in this chapter, are derived from bacterial "two-component" regulatory systems. Several plant photoreceptors diverged from similar proteins in bacteria

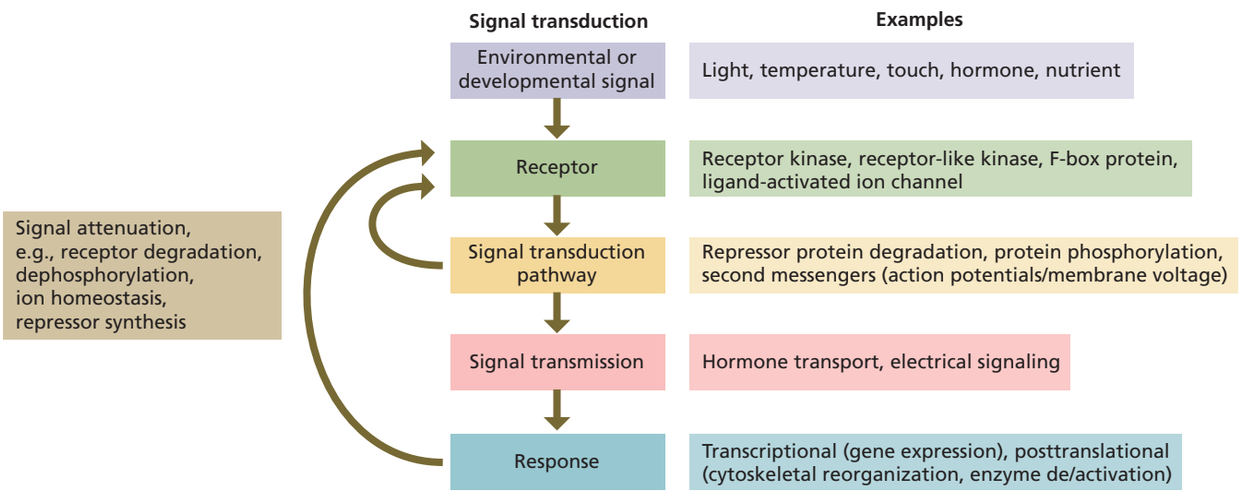


Figure 4.2 **General scheme for signal transduction.** Environmental or developmental signals are perceived by specialized receptors. A signaling cascade is then activated that involves second messengers and leads to a response by the plant cell. When an optimal response has been achieved, feedback mechanisms attenuate the signal.

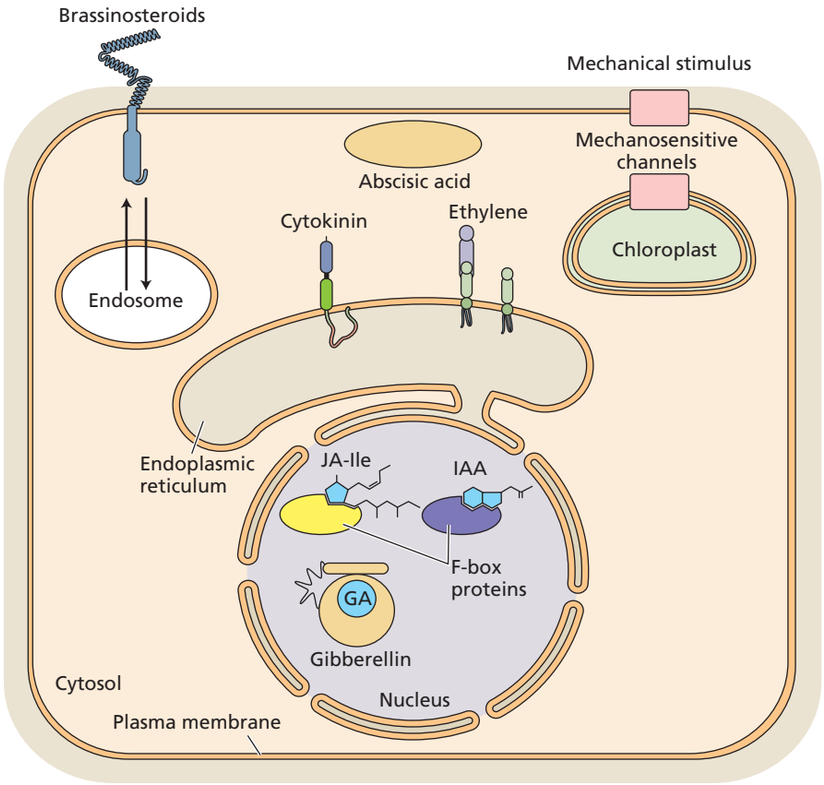


Figure 4.3 Primary locations of plant hormone receptors and mechanosensitive receptors in the cell. The individual receptors are discussed in Section 4.6. GA, gibberellin; IAA, indole-3-acetic acid; JA-Ile, jasmonic acid-isoleucine. (After A. Santer and M. Estelle. 2009. *Nature* 459: 1071–1078.)

and have taken on new functions. For example, bacterial members of the cryptochrome/photolyase superfamily are flavoproteins that repair pyrimidine dimers produced in DNA by UV light. In plants, cryptochromes lack the critical residues required for DNA repair, and instead mediate light control of stem elongation, leaf expansion, photoperiodic flowering, and the circadian clock (see Chapter 16).

Other plant receptors are more similar to those found in animals and fungi, but often have additional or modified components. Examples are found in plant F-box receptor/ubiquitin ligase systems that are integral to several plant hormone receptor complexes (see Figure 4.3). Eukaryotic E3 ubiquitin ligase complexes, which are present in the cytosol and nucleus and are associated with organellar membranes, covalently attach ubiquitin to substrate proteins, tagging them for degradation by the 26S proteasome. In the SCF (*S*kp, *C*ullin, and *F*-box protein) subfamily of E3 ligases, substrate recognition is mediated by **F-box proteins**. SCF-based hormone receptor complexes appear to be a unique adaptation of the ubiquitin ligase machinery in plants.

One of the most conserved mechanisms in all organisms is modification of proteins, lipids, or nucleic acids by **kinase** enzymes that add a phosphate group from ATP to modify the properties of those molecules. Protein kinases function in transducing and amplifying signals by phosphorylating serine, threonine, tyrosine, or histidine residues of target proteins to alter their biological activity or association with other proteins and lipids. When a protein both functions as a receptor and transduces that signal by phosphorylating another molecule, it is called a **receptor kinase**. Although almost all protein kinase families are conserved between animals and plants, they have often diversified differentially. For instance, animals have a large number of plasma membrane G protein–coupled receptors (GPCRs) that detect a diverse array of extracellular signals and transmit them intracellularly via a large family of heterotrimeric G proteins. Plant possess a small number of heterotrimeric G proteins that are of common origin to those in animals, but no analogous GPCR function has been clearly demonstrated to date. Conversely, plants possess hundreds of receptor-like serine/threonine kinases (RLKs) of types that are poorly represented in other kingdoms.

Signals must be amplified intracellularly to regulate their target molecules

If a receptor is considered the gateway through which a signal enters a signaling network, the receptor location to some extent prescribes the length of the subsequent signaling pathway; such pathways can consist either of a few signaling steps or an elaborate cascade of signaling events. The perception of signals at the plasma membrane often activates transduction pathways with many intermediates. In the case of signaling pathways that must

eventually reach the nucleus to regulate gene expression, signal strength along the pathway will dissipate unless it is reinforced by signal amplification events. In the absence of amplification, any activated signaling intermediate that must traverse the cytosol to translocate to the nucleus will become diluted because of its diffusion and deactivation mechanisms (for example, by dephosphorylation, degradation, or sequestration). Furthermore, many chemical signals are present at very low concentrations, and receptors can similarly occur at very low density, such that the initial signal may be quite weak. Signal amplification cascades serve to adjust, maintain, or even enhance signal strength over larger distances. To elevate weak initial signaling events above the threshold of detection or to propagate them across the cytoplasm, cells employ amplification mechanisms such as phosphorylation cascades and second messengers.

Evolutionarily conserved MAP kinases amplify cellular signals

Protein phosphorylation is an important mechanism for regulating protein activity, localization, and abundance in plants. Plants have several protein kinases belonging to prominent protein kinase families. Many of these protein kinase families are also present in animals and yeasts, but their relative abundance and biological role in plants differ significantly from those found in these other systems. Kinases can act at the cell surface or regulate intracellular processes. For example, mitogen-activated protein kinase (MAP kinase) signal amplification cascades function in all eukaryotes and play an important role in multiple plant responses. As shown in **Figure 4.4**, signals perceived by receptors can produce an initial phosphorylation of a MAP kinase kinase kinase (abbreviated as MAP3K), which in turn uses ATP to phosphorylate a MAP kinase kinase (MAP2K). The phosphorylated MAP2K then amplifies the signal by phosphorylating a MAP kinase (MAPK). The MAPK then further amplifies the signal by phosphorylating target proteins to activate or modify a cellular process. Within minutes of signal perception, the MAP3K/MAP2K/MAPK cascade can trigger a suite of downstream responses. The large number of MAP3K, MAP2K, and MAPK family members and the wide range of environmental, developmental, and reproductive cellular responses in which they play important roles suggest that this group of kinases has undergone functional diversification in plants. However, the presence of common MAP kinase modules among multiple responses demonstrates combinatorial interplay with other signaling components.

Evolutionarily conserved kinases regulate programmed and plastic plant development

Histidine-phosphorylating protein kinases may represent the evolutionarily oldest phosphorylation module.

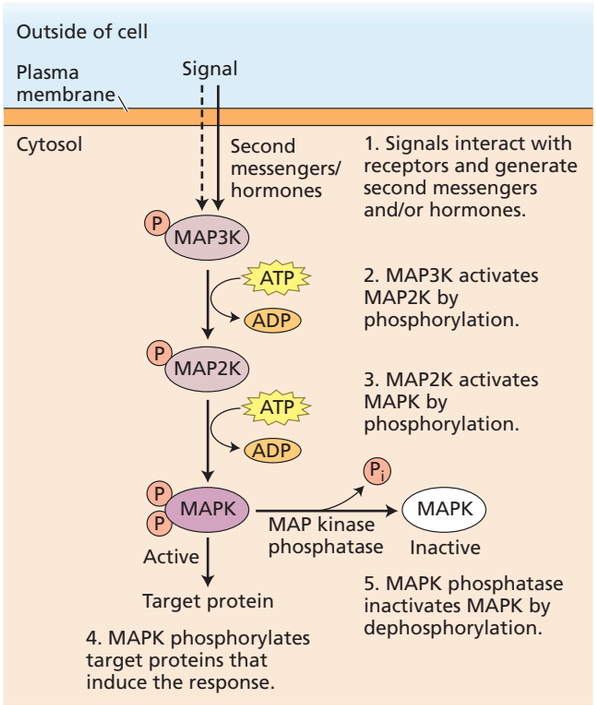


Figure 4.4 Mitogen-activated protein kinase (MAPK) pathways amplify signals to achieve a rapid and massive response to an environmental or developmental stimulus. The solid and dotted arrows leading from the signal indicate direct and indirect activation, respectively.

Bacteria employ two-component receptor systems made up of histidine kinases that phosphorylate proteins with transcriptional activity. The same module can be found in the detection and signal transduction of the plant hormone cytokinin, as described later in this chapter.

The cyclin-dependent protein kinase family is also found in all kingdoms. As their name implies, these kinases require association with cyclins to gain functionality. Cyclins are differentially expressed during the cell cycle, and the association of different cyclins with a particular cyclin-dependent kinase regulate its phosphorylation of discrete regulators at each step of the cell cycle. Programmed interactions between the large number of plant cyclins and cyclin-dependent kinases provide for adaptive control of the fundamental process of cell division.

In plants, a large family of **AGC kinases** that are evolutionarily related to animal cyclic adenosine monophosphate (A-class), cyclic guanosine monophosphate (G-class), and Ca^{2+}-dependent (C-class) protein. Despite an apparent common ancestry with their animal counterparts, the plant AGC kinases are structurally and functionally divergent from them. AGC kinases similar to the phototropin blue-light receptors that function in phototropism, chloroplast movement, and stomatal responses to blue light (see Chapter 16) are present in

algae and vascular plants. In higher plants, the AGC family has expanded and includes the D6 PROTEIN KINASE (D6PK), PROTEIN KINASE ASSOCIATED WITH BREVIX RADIX (PAX), and PINOID kinase, all of which activate directional cellular efflux of the hormone auxin via phosphorylation of the PIN-FORMED (PIN) auxin efflux carrier proteins. The PINOID kinase appears to also regulate the subcellular distribution of PIN proteins to the extent that its name is derived from the similarity of the Arabidopsis *pinoid* and *pin1* loss-of-function mutants. The importance of polar auxin transport is described in Section 4.4. Some plant AGC kinases are linked to lipid signaling processes (described later in this chapter) when they are phosphorylated by PHOSPHOINOSITIDE DEPENDENT KINASE 1 (PDK1).

Ca^{2+}-binding protein kinases represent another group of protein kinase families in plants. These kinases function as a component of Ca^{2+} signaling and are discussed in the context of Ca^{2+} second messengers later in this section.

Extracellular signals are perceived and transmitted by receptor-like kinases

Receptor-like serine/threonine kinases (RLKs) are a prominent family of kinases that phosphorylate serine or, less commonly, threonine protein residues. One large class of RLKs comprises plasma membrane–spanning receptors with extracellular leucine rich repeat (LRR) ligand-binding domains and an intracellular serine/threonine kinase domain for signal transmission. Ligand binding to an RLK receptor results in dimerization with co-receptors to initiate phosphorylation events in the intracellular kinase domains of both RLKs. These, in turn, initiate multiple phosphorylation-dependent signaling processes. One well-studied example of ligand-dependent dimerization and activation of RLKs is binding of the cell surface FLAGELLIN SENSITIVE 2 receptor to the flg22 peptide of pathogenic bacteria that stimulates interactions with the BRI1 ASSOCIATED KINASE (BAK1)/SOMATIC EMBRYOGENESIS RECEPTOR KINASE (SERK) co-receptors to initiate immune responses (**Figure 4.5**). A similar receptor interaction initiates immunity responses to chitin from fungal pathogens. These responses are discussed in detail in Chapter 24.

BAK1/SERK co-receptors also function in intercellular communication that regulates plant growth and development. For instance, binding of EPIDERMAL PATTERNING FACTOR peptide hormones to their RLK results in heteromerization with BAK1/SERK and the TOO MANY MOUTHS co-receptors to regulate epidermal patterning and stomatal development. Similar co-receptors interact with a BAK1/SERK receptor after binding to peptide hormones that control floral abscission. The best-studied RLK hormone receptor is BRASSINOSTEROID INSENSITIVE 1 (BRI1), which heteromerizes with RLKs from the BAK1/SERK family after brassinosteroid binding and regulates multiple aspects of growth and floral identity (see Figures 4.5 and 4.34). In many of the LRR RLK-dependent signaling events, related cytoplasmic kinases play a role in downstream signaling.

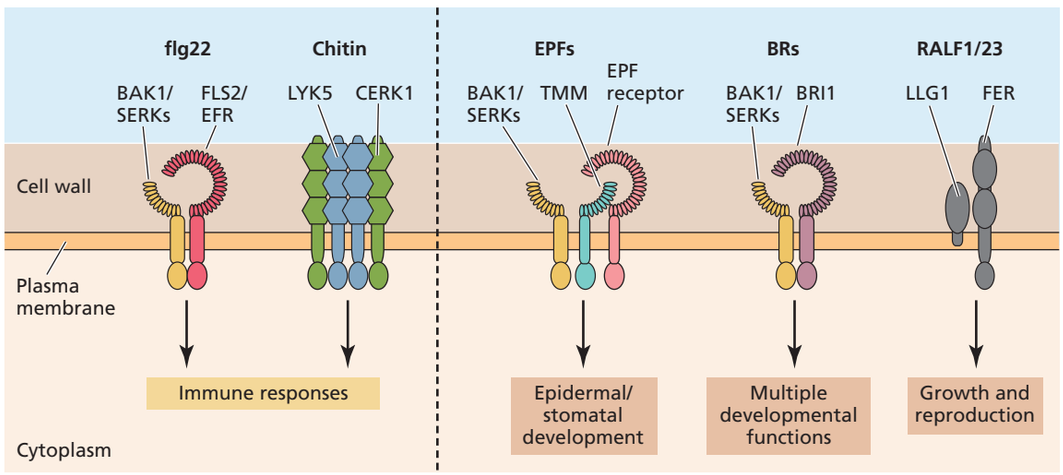


Figure 4.5 Receptor-like serine/threonine kinases (RLKs) bind to extracellular ligands and heteromerize with co-receptors to initiate cellular signal transduction. Ligands can be derived from pathogens such as the flg22 peptide from flagellin, plant signaling peptides (e.g., EPIDERMAL PATTERNING FACTORS [EPFs] and RAPID ALKALINIZATION FACTORS [RALFs]), or hormones (brassinosteroids [BRs]). BAK1/SERKs, BRASSINOSTEROID ACTIVATED KINASE 1/SOMATIC EMBRYOGENESIS RECEPTOR KINASES; BRI1, BRASSINOSTEROID INSENSITIVE 1; CERK1, CHITIN RECEPTOR ELICITOR KINASE 1; EPF, EPIDERMAL PATTERNING FACTOR; FER, FERONIA; flg22, bacterial elicitor fragment; FLS2, Flagellin Sensitive 2; LLG1, LORELEI 1; LYK5, LYSINE MOTIF RECEPTOR KINASE 5; TMM, TOO MANY MOUTHS. (After X. Liang and J.-M. Zhou. 2018. *Ann. Rev. Plant Biol.* 69: 167–299.)

Another group of RLKs plays an important role in monitoring and regulating cell wall integrity and expansion. As described in Chapter 2, the formation of new cell walls after cell division and their maintenance or reorganization during development and growth require fine-tuning. Plant cells need to sense the composition of their cell wall during cellular growth and also during attack from pathogens or herbivores. A group of RLKs similar to a protein first identified in *Catharanthus roseus* (CrRLK1) functions together with the LORELEI family of co-receptors to monitor cell wall integrity. This is achieved through a Glc2-N-glycan–binding malectin domain that is associated with the cell wall–facing outer leaflet of the plasma membrane. The best-studied of these CrRLK1-like RLKs, FERONIA, binds secreted RAPID ALKALINIZATION FACTOR (RALF) peptides and stimulates an increase in apoplastic pH via a transient increase in cytosolic Ca^{2+} and differential phosphorylation of many proteins, including FERONIA itself. A similar mechanism regulates pollen tube integrity during fertilization, while heteromerization of pollen receptor kinase complexes regulates pollen tube growth after binding of LURE pollen guidance peptides.

Phosphatases are the "off switch" of protein phosphorylation

Protein phosphorylation can have a multitude of effects on protein function, localization, and abundance. The effects of phosphorylation can be reversed by **phosphatases** that remove the phosphate addition from substrate proteins. Phosphatases can be grouped by structural similarity, the specific amino acid residues that they dephosphorylate, or by molecular interactions that stimulate their dephosphorylation activity. The cytosolic serine/threonine -specific protein phosphatases of the 2A (PP2A) and 2C (PP2C) subfamilies are the primary protein phosphatases that function in plants. The dephosphorylation of phosphorylated proteins by phosphatases is often part of a negative feedback regulatory circuit, and many of the protein kinase-dependent phosphorylation events mentioned earlier are antagonized by phosphatases.

Other protein modifications can reconfigure cellular processes

Interactions and cellular distribution of proteins can be regulated by modifications other than phosphorylation. As discussed in Chapter 1, *glycosylation* of proteins in the Golgi apparatus and the endoplasmic reticulum (ER) can change their activity and destination within, or even outside, the cell. Other protein modifications modify interactions with other proteins, association with membranes, or even activity of the protein itself. The most common modifications are those that target cytosolic proteins to membrane complexes and surfaces. These include (1) *N-myristoylation*, whereby a 14-carbon myristoyl group is added to the N-terminal glycine residue of a protein; (2) *prenylation*, whereby a farnesyl phosphate or geranylgeranyl molecule derived from terpenoid biosynthesis (see **WEB APPENDIX 4**) is attached to cysteine residues at a signature C-terminal cysteine-containing motif; (3) *S-acylation*, a reversible process that takes place at membrane surfaces whereby a transferase enzyme attaches a C-16 or C-18 fatty acid to a thiol residue to stabilize membrane interactions; and (4) *nitrosylation* of cysteine residues in proteins under conditions where nitric oxide added to cysteine residues prevents formation of cysteine linkages or inhibits enzymatic activity. Protein nitrosylation functions in both programmed development and stress responses (see Chapter 15).

Protein activity can also be modified by the addition of evolutionarily conserved peptides that are similar to ubiquitin (see Chapter 3) but do not tag the protein for degradation. In most cases, addition of modifying peptides activates or stabilizes the target protein. In some cases, peptide modifications alter the nuclear or cytosolic localization of a protein to regulate downstream transcriptional processes.

Ca^{2+} is the most ubiquitous second messenger in plants and other eukaryotes

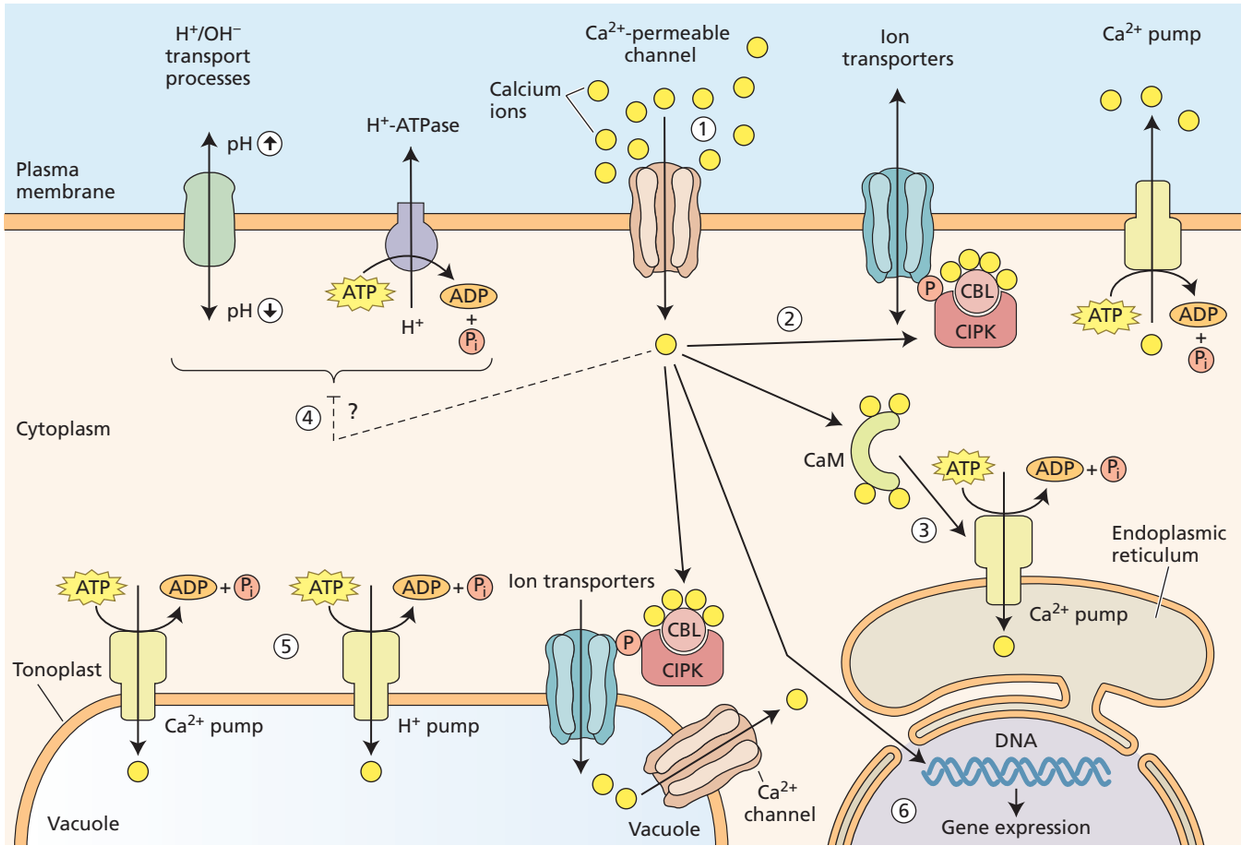
Second messengers represent another strategy to enhance or propagate signals. These small molecules and ions are rapidly produced or mobilized at relatively high levels after signal perception, and can modify the activity of target signaling proteins. Probably the most ubiquitous second messenger in all eukaryotes is the calcium ion, the divalent cation Ca^{2+}, which in plants is involved in a vast number of different signaling pathways, including symbiotic interactions, plant defense responses, and responses to various hormones and abiotic stresses. Cytosolic Ca^{2+} levels increase rapidly when Ca^{2+}-permeable ion channels open to allow passive Ca^{2+} influx from Ca^{2+} stores into the cytosol (**Figure 4.6**). Channel activity must be tightly regulated to maintain precise control over the timing and duration of cytosolic Ca^{2+} elevation. Generally, ion channels are gated, meaning the channel pores are opened or closed by changes in transmembrane electrical potential, membrane tension, posttranslational modification, or binding of a ligand (see Chapter 8). Several families of Ca^{2+}-permeable channels have been identified in plants; these include plasma membrane-localized glutamate-like receptors (GLRs) and cyclic nucleotide-gated channels (CNGCs). Electrophysiological and other evidence supports the presence of Ca^{2+}-permeable channels at the tonoplast and the ER.

Once receptor-mediated signaling activates Ca^{2+}-permeable channels, Ca^{2+} sensor proteins play a pivotal role as signaling intermediaries, linking Ca^{2+} signals to changes in cellular activities. Most plant genomes

contain four major multigene families of Ca^{2+} sensors: the calmodulin (CaM) and calmodulin-like proteins, the Ca^{2+}-dependent protein kinases (CDPKs), the Ca^{2+}/calmodulin-dependent protein kinases (CCaMKs), and the calcineurin-B like proteins (CBLs), which function in concert with CBL-interacting protein kinases (CIPKs). Members of these sensor families modulate the activity of target proteins either by binding to CaM or by phosphorylating the target protein in a Ca^{2+}-dependent manner. Target proteins include transcription factors, various protein kinases, Ca^{2+}-ATPases, enzymes producing reactive oxygen species (ROS), and ion channels. Finally, Ca^{2+} pumps and Ca^{2+} exchangers in organelle and plasma membranes actively remove Ca^{2+} from the cytosol to terminate Ca^{2+} signaling (see Figure 4.6).

Changes in the cytosolic or cell wall pH can serve as second messengers for hormonal and stress responses

Plant cells use the **proton motive force** (i.e., the electrochemical proton gradient) across cellular membranes to drive ATP synthesis (see Chapters 9 and 13) and to



1. Signal-induced activation of Ca^{2+}-permeable ion channels leads to an increase in the concentration of free cytosolic Ca^{2+}.
2. Activated CBL/CIPK Ca^{2+} sensor proteins interact with ion transporters on the plasma membrane and the vacuolar membrane.
3. Activated calmodulin (CaM) stimulates Ca^{2+} pumps on the endoplasmic reticulum.
4. Ca^{2+} may affect membrane transporters, triggering changes in the intracellular and extracellular pH.
5. Pumps on vacuolar membrane create H^+ and Ca^{2+} gradients between cytoplasm and vacuole.
6. Increased Ca^{2+} in nucleus activates Ca^{2+}-dependent transcription.

Figure 4.6 Calcium ions, pH, and reactive oxygen species (ROS) function as second messengers that amplify signals and regulate the activity of target signaling proteins to trigger physiological responses. An increase in the $[Ca^{2+}]_{cyt}$ activates Ca^{2+} sensor proteins (calmodulins [CaMs], Ca^{2+}-dependent protein kinases [CDPKs], and calcineurin-B like proteins/CBL-interacting protein kinases [CBL/CIPKs]), which are located at different subcellular sites. Six types of activation are shown in the figure.

energize secondary active transport (see Chapter 8). In addition to having such "housekeeping" activity, protons also appear to have signaling activity and function as second messengers. In a resting cell, cytosolic pH is typically kept constant at approximately pH 7.5, whereas the cell wall is acidified to pH 5.5 or lower. Extracellular pH can change rapidly in response to a variety of different endogenous and environmental signals, while intracellular pH changes occur more slowly because of cellular buffering capacity. In growing hypocotyls, for example, the plant hormone auxin triggers activation of the plasma membrane H^+-ATPase through phosphorylation of its C terminus. This causes the cell wall to become more acidic, which is thought to promote cell expansion by activating cell wall–loosening enzymes such as expansins (see Chapter 2). In roots, however, where auxin inhibits cell expansion, auxin triggers the rapid alkalization of the cell wall, a process that has been shown to be Ca^{2+}-dependent. Similar Ca^{2+}-dependent pH changes are observed in many environmental stress responses of plants (see Chapter 15).

The transporters that are activated or deactivated by Ca^{2+} to facilitate extra- and intracellular pH changes are currently unknown, as are, for the most part, the downstream targets of these pH changes. Certainly, the pH of the cell wall will affect the protonation status of weakly acidic small molecules such as plant hormones and consequently affect their ability to enter cells by diffusion. Cell wall pH regulation may thus represent a mechanism to fine-tune hormone uptake and signaling. Evidence also exists for pH-dependent gating of potassium ion channels and aquaporins. What has made identification of pH signaling targets difficult is that the presence of acidic and basic amino acids makes all proteins sensitive to pH. Whether this sensitivity is physiologically relevant depends on the pK_a values (dissociation constants) of these amino acids and on how critical their protonation status is to the protein's ability to interact with other proteins, substrates, or ligands.

Reactive oxygen species act as second messengers mediating both environmental and developmental signals

In recent years, **reactive oxygen species** (**ROS**) have emerged not just as cytotoxic by-products of metabolic processes such as respiration and photosynthesis, but also as signaling molecules regulating plant responses to various environmental and endogenous signals. ROS are reactive molecules that are generated through the partial reduction of oxygen (see **WEB ESSAY 13.7**). The majority of ROS are formed in mitochondria, plastids, peroxisomes, and the cell wall. In the context of cell signaling, plasma membrane–localized NADPH oxidases make up the best-understood family of ROS-producing enzymes. NADPH oxidases (or respiratory burst oxidase homologs, RBOHs) transfer electrons from the cytosolic electron donor NADPH across the membrane to reduce extracellular molecular oxygen. The resulting ROS, superoxide, can dismutate to hydrogen peroxide, a more membrane-permeant ROS that also enters cells through specific aquaporin channels.

NADPH oxidase activity is regulated through phosphorylation of its N-terminal amino acids and by direct binding of Ca^{2+} (see Figure 4.6). Some of the kinases responsible for phosphorylating NADPH oxidase N termini have been identified as CDPKs and CBL-dependent CIPKs. NADPH oxidase–mediated oxidative bursts are thus often found downstream of Ca^{2+} signaling pathways, for example in defense signaling, where mutants defective in ROS production exhibit increased susceptibility to pathogens. However, there is also evidence that NADPH oxidase–generated ROS can function upstream of Ca^{2+} signaling.

Targets of ROS signaling include the thiol side chain of cysteine amino acid residues, which can be oxidatively modified to form intramolecular (within the polypeptide/protein) or intermolecular (oxidative cross-linking of different [poly]peptides/proteins) disulfide bonds. Such disulfide bonds usually change the conformation of the affected proteins and thereby their activities (see Chapters 10 and 13). Oxidation of lipids by ROS also functions in stress responses (see Chapter 15), and redox regulation has been shown to alter the DNA-binding activity or cellular localization of several transcription factors and transcriptional activators. Oxidation of secreted polyamines in the apoplast can also contribute to ROS generation as well as adaptation to higher ROS levels in stress responses. In the cell wall, tyrosine residues of structural proteins, feruloyl (ferulic acid) conjugates of polysaccharides, and monolignols are oxidatively cross-linked to modify the strength or the barrier properties of the cell wall (see Chapter 2).

Lipid signaling molecules act as second messengers that regulate a variety of cellular processes

Phosphoglycerolipids and sphingolipids are primary lipid components of plant plasma membranes and are important determinants of their physical properties (e.g., membrane surface charge, fluidity, local membrane curvature). Several phospholipase enzymes hydrolyze specific bonds of phosphoglycerolipids to produce lipid signaling molecules (see Chapter 13). For example, **acyl hydrolases** remove fatty acyl chains, thereby producing a **lysophospholipid**. Lysophospholipids are small bioactive lipids characterized by a single carbon chain and a polar head group (**Figure 4.7A**). They are more hydrophilic than their corresponding phospholipids and have been implicated in the regulation of proton pumping on the

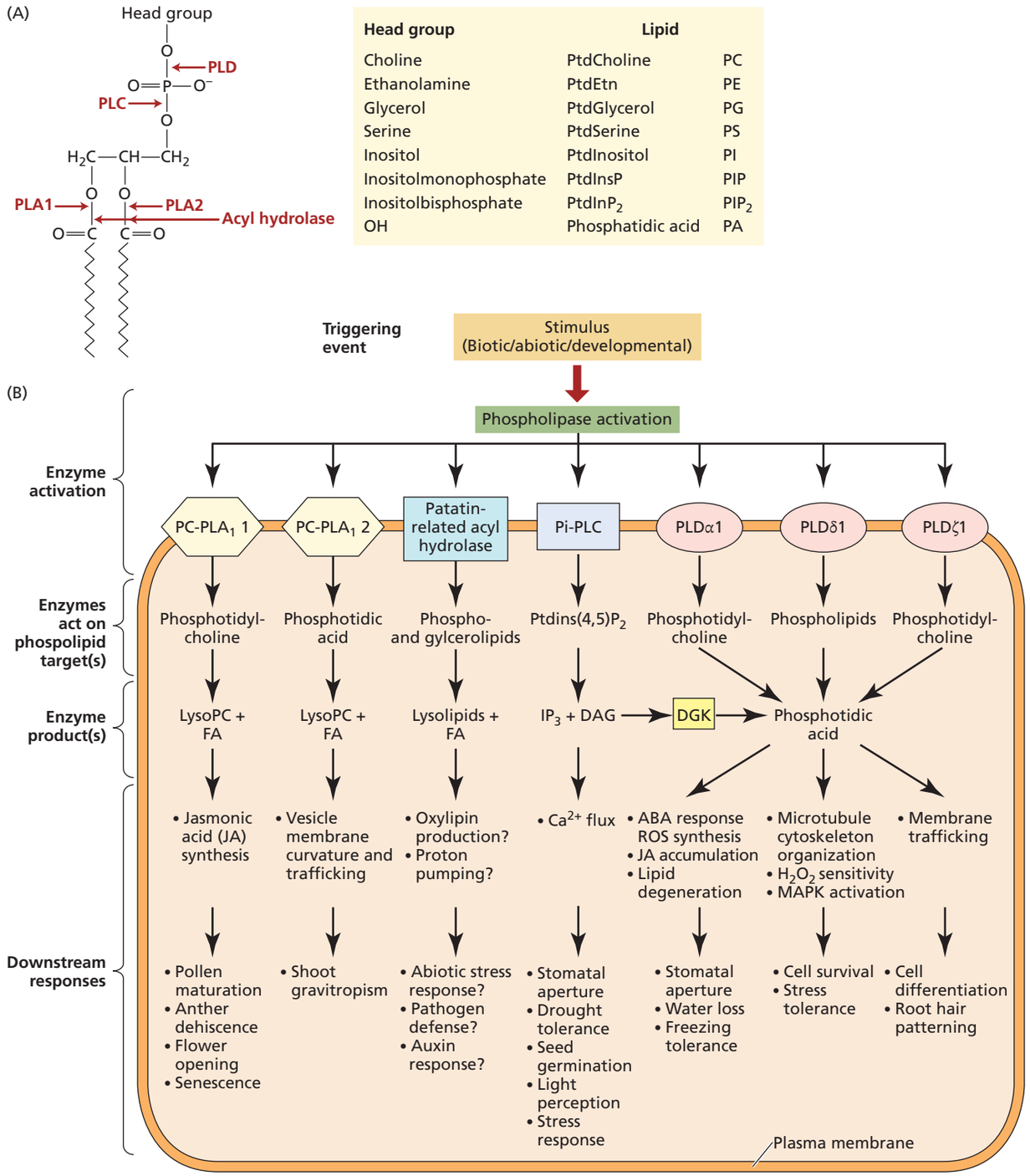


Figure 4.7 **Lipid-modifying enzymes remodel cellular membranes and produce lipid signaling molecules.** **(A)** Structure, hydrolysis, names, and abbreviations of the common phospholipids. (Left) The general structure of a phospholipid is shown, consisting of two fatty acyl chains esterified to a glycerol backbone, a phosphate (creating the "phosphatidyl" moiety [Ptd]), and a variable head group. The positions subject to cleavage by various phospholipases (PLA1, PLA2, PLC, and PLD) are indicated by the red arrows. (Right) A table of possible head groups along with their abbreviations. **(B)** Membrane lipid substrates and messengers produced by different phospholipid- or galactolipid-hydrolyzing enzymes, and their downstream cellular and physiological effects. DAG, diacylglycerol; DGK, diacylglycerol kinase, FA, fatty acid; IP_3, inositol 1,4,5-triphosphate. (After X. Wang. 2004. *Curr. Opin. Plant Biol.* 7: 329–336.)

plasma membrane and other processes. Members of the **phospholipase A** (**PLA**) family cleave either one of the acyl ester bonds, releasing a fatty acid and a lysophospholipid. **Phospholipase C** (**PLC**) hydrolyzes the glycerophosphate bond to produce **diacylglycerol** (**DAG**) and a phosphorylated head group. Many PLCs preferentially cleave phosphatidylinositols, releasing DAG and inositol phosphates such as inositol 1,4,5-triphosphate (IP_3). DAG and IP_3 function as signaling molecules that regulate Ca^{2+} fluxes in a wide variety of developmental and stress response processes (**Figure 4.7B**). DAG functions in cold responses, while IP_3 functions in nitrogen deficiency, temperature, water deficit, and salt stress responses.

DAG is also often rapidly converted by diacylglycerol kinase enzymes to **phosphatidic acid** (**PA**). PA can also be formed when **phospholipase D** (**PLD**) releases the phospholipid head group from **phosphatidylcholine** (**PC**) and other phospholipids to function as a signaling component in drought, salt, cold, and pathogen responses. PA is a cone-shaped lipid that promotes vesicle budding, docking, and fusion, presumably by increasing local negative membrane curvature. PA also enhances some interactions of membrane-associated proteins by facilitating the insertion of hydrophobic amino acids into the lipid bilayer. The negatively charged head group of PA also forms electrostatic interactions with positively charged binding pockets on effector proteins. In guard cells, stomatal closure is promoted when binding of the hormone abscisic acid (ABA) to the PYL/PYR/RCAR receptor (described in Section 4.5) promotes its inhibitory interaction with protein phosphatase 2C isoforms that act on downstream signaling targets (see Chapters 15). ABA-dependent increases in PA have been shown to promote the interaction of PYR/PYL/RCAR with the protein phosphatase 2C ABI1 and to inhibit its activity. PA also appears to modulate the dynamics of both microtubule and actin cytoskeleton. It enhances actin filament formation by binding to, and thereby negatively regulating, the activity of the actin capping protein, a protein that binds in a Ca^{2+}-independent manner to the growing ends of actin filaments, blocking subunit exchange (see Chapter 1).

4.3 Hormones and Plant Development

The form and function of multicellular organisms would not be possible without efficient communication among cells, tissues, and organs. In higher plants, regulation and coordination of metabolism, growth, and morphogenesis often depend on chemical signals from one part of the plant to another. This idea originated in the nineteenth century with the German botanist Julius von Sachs (1832–1897).

Sachs proposed that chemical messengers are responsible for the formation and growth of different plant organs. He also suggested that external factors such as gravity could affect the distribution of these substances within a plant. Indeed, it has since become apparent that a majority of signaling networks that translate environmental cues into growth and developmental responses regulate the metabolism or redistribution of these endogenous chemical messengers. Although Sachs did not know the identity of these messengers, his ideas led to their eventual discovery.

Hormones are chemical messengers that are produced in one cell and modulate cellular processes in another cell by interacting with specific proteins that function as receptors linked to cellular signal transduction pathways. As is the case with animal hormones, most plant hormones are capable of activating responses in target cells at vanishingly low concentrations. Hormonal signaling typically involves the transmission of the hormone from its site of synthesis to its site of action. In general, hormones that are transported to sites of action in tissues distant from their site of synthesis are referred to as *endocrine* hormones, while those that act on cells adjacent to the source of synthesis are referred to as *paracrine* hormones (**Figure 4.8**). Hormones can also function in the same cells in which they are synthesized, in which case they are referred to as *autocrine effectors*. Most plant hormones have paracrine activities, since plants lack the fast-moving circulatory systems found in animals and used by classic endocrine hormones. However, slower, long-distance hormone transport via the vascular system is a common feature in plants, despite the absence of hormone-secreting glands like those in animal endocrine systems.

Although the details of hormonal control of development are quite diverse, all of the basic hormonal pathways share common features (**Figure 4.9**). For example, both signal perception and developmental programming often result in increases or decreases in hormone biosynthesis. The hormone is then transported

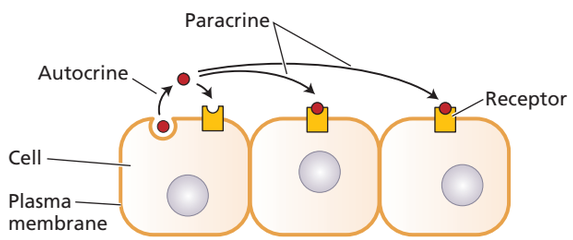


Figure 4.8 **Autocrine versus paracrine signaling.** Autocrine signals bind to receptors on the same cell in which they are synthesized. In contrast, paracrine signals bind to receptors on cells located a short distance away from the site of synthesis. Signaling that involves transport over greater distances is called endocrine signaling.

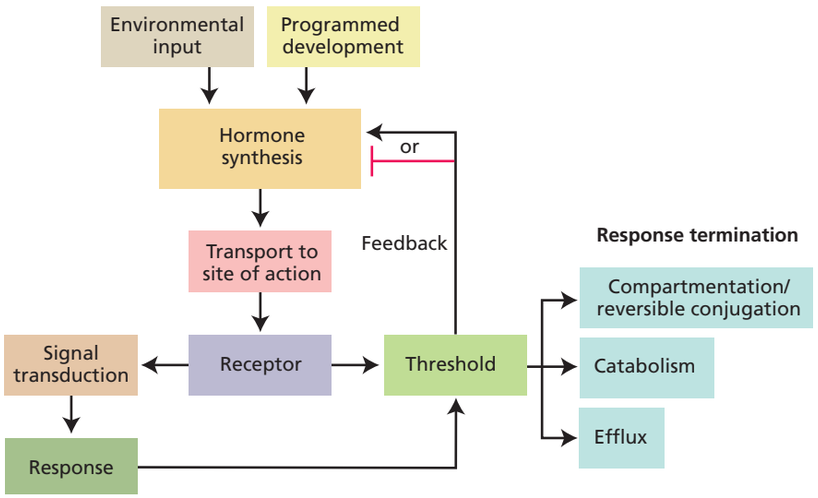


Figure 4.9 Common scheme for hormonal regulation.

to a site of action. Perception of the hormone by a receptor results in transcriptional or posttranscriptional (e.g., phosphorylation, protein turnover, ion extrusion) events that ultimately induce a physiological or developmental response. In addition, the response can be attenuated by negative feedback mechanisms that repress hormone synthesis and by catabolism or sequestration, which combine to cause the return of the active hormone concentration to pre-signal levels. In this way the plant reacquires the ability to respond to the next signal input.

Plant development is regulated by ten major hormones: auxins, gibberellins, cytokinins, ethylene, abscisic acid, brassinosteroids, jasmonates (primarily jasmonic acid-isoleucine), salicylic acid, pipecolates, and strigolactones (**Figure 4.10**). In addition, several peptides trigger responses in adjacent or distal cells to regulate growth. To date the best-studied peptide hormone target in plants is the receptor-like kinase heterodimer CLAVATA1/2. The CLAVATA3 peptide hormone acts over short distances to control embryo development and apical meristem patterning via interactions with CLAVATA1/2 (see Chapters 18 and 22). Other CLAVATA3/Embryo Surrounding Region-Related (CLE) peptides function in conjunction with C-terminally Encoded Peptides (CEPs) in nitrogen assimilation and interactions with rhizobial symbionts (see Chapter 14). Other peptide hormones regulate epidermal cell patterning, tracheary element differentiation in mesophyll cells, and cell wall modification via receptor interactions. Indeed, the list of signaling molecules and growth regulators is likely to continue to expand in the coming years. Here we briefly introduce auxins, gibberellins, cytokinins, ethylene, abscisic acid, brassinosteroids, and strigolactones. The roles of jasmonates, salicylic acid, and pipecolates in biotic interactions will be discussed in Chapter 24.

Auxin was discovered in early studies of coleoptile bending during phototropism

Auxin is essential to plant growth, and auxin signaling functions in virtually every aspect of plant development. Auxin was the first growth hormone to be studied in plants, and was discovered after the prediction of its existence by Charles and Francis Darwin in *The Power of Movement in Plants* (1881). The Darwins studied the bending of seedling sheath leaves (coleoptiles) of canary grass (*Phalaris canariensis*) and seedling hypocotyls of other species in response to unidirectional light, and concluded that a signal produced at the apex travels downward and causes lower cells on the shaded side to grow faster than on the illuminated side. Subsequently, it was shown that the signal was a chemical that could diffuse through gelatin blocks (**Figure 4.11**). Plant physiologists named the chemical signal auxin from the Greek *auxein*, meaning "to increase" or "to grow," and identified indole-3-acetic acid (IAA; see Figure 4.10A) as the primary plant auxin. In some species, 4-chloro-IAA, phenylacetic acid, and indole-3-butyric acid (IBA) function as natural auxins, but IAA is by far the most abundant and physiologically important form. Auxins are also produced by a variety of microbes that live in, on, or near plants (the phytobiome) and are deployed to promote plant growth that benefits the microbes. Because the structure of IAA is relatively simple, researchers were quickly able to synthesize a wide array of molecules with auxin activity. Some of these compounds, such as 1-naphthalene acetic acid (NAA), 2,4-dichlorophenoxyacetic acid (2,4-D), and 2-methoxy-3,6-dichlorobenzoic acid (dicamba), are now used widely as growth regulators and herbicides in horticulture and agriculture.

Gibberellins promote stem growth and were discovered in relation to the "foolish seedling disease" of rice

A second group of plant hormones are the **gibberellins** (abbreviated to GA and numbered in the chronological sequence of their discovery). This group comprises a large number of compounds, all of which are tetracyclic (four-ringed) diterpenoid acids, but only a few of which, primarily GA_1, GA_3, GA_4, and GA_7, have intrinsic biological activity (see Figure 4.10B). One of the most striking effects of biologically active gibberellins, achieved through their role in promoting cell elongation, is the induction of internode elongation in dwarf seedlings. Gibberellins have other diverse roles during the plant life cycle: For

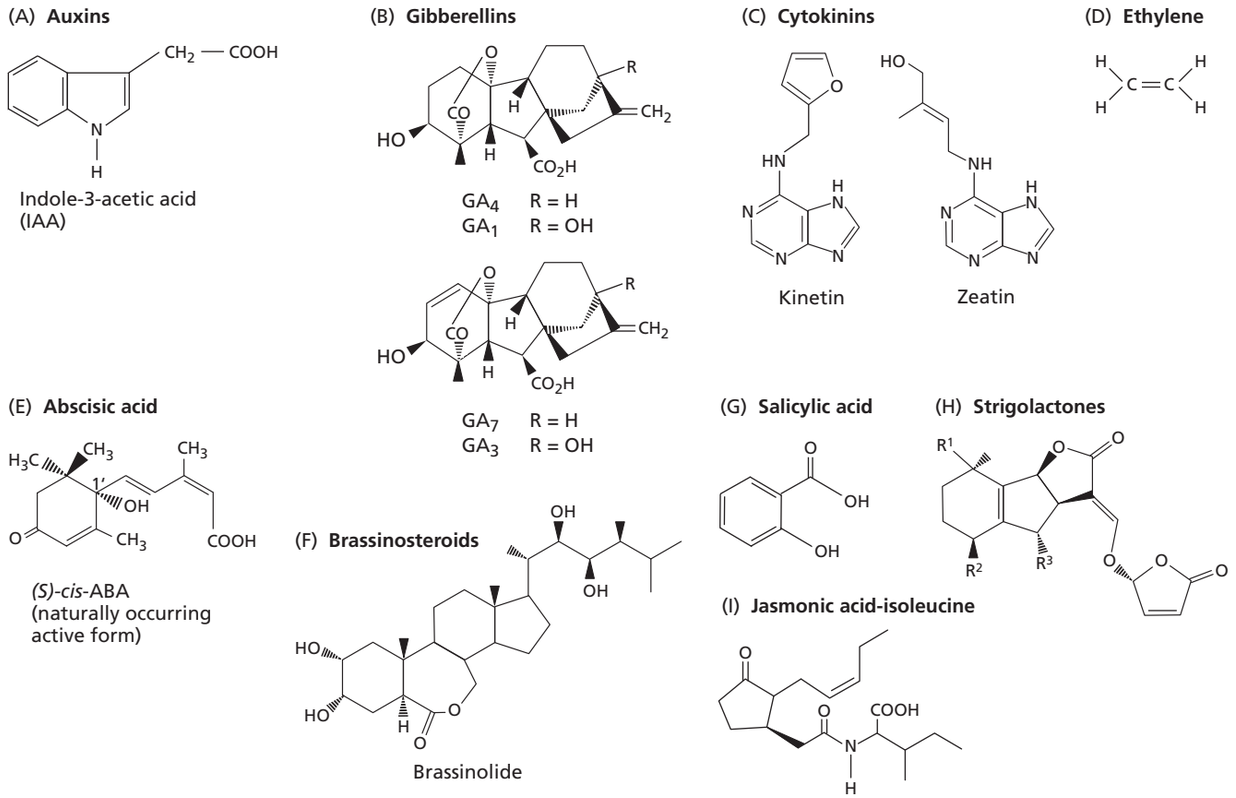
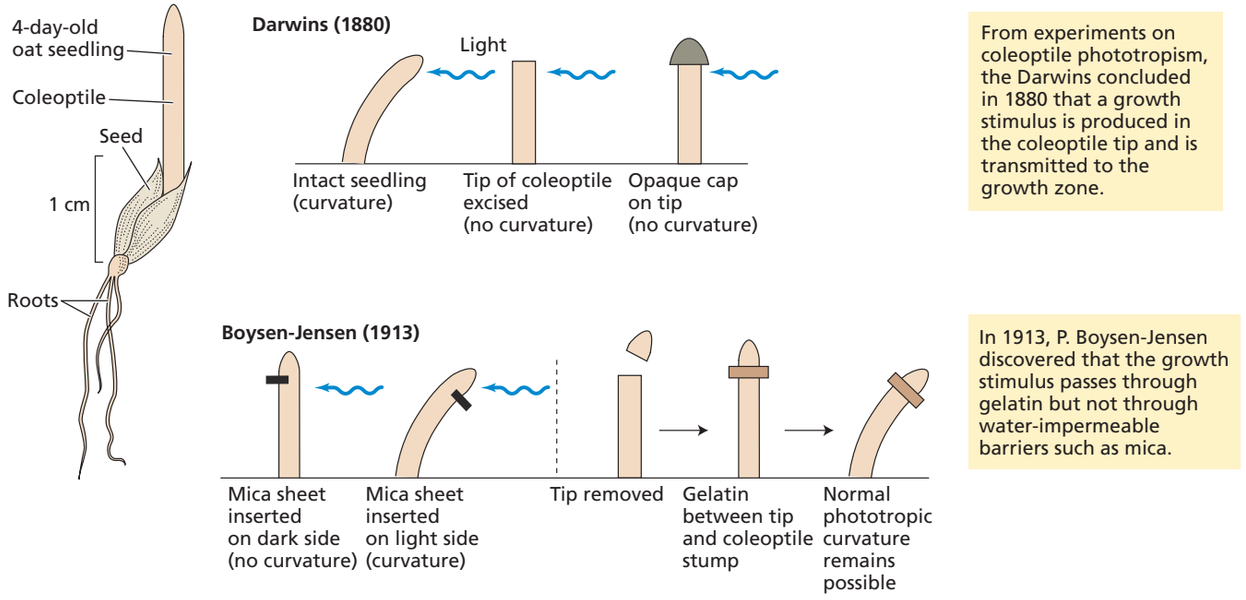


Figure 4.10 Chemical structures of phytohormones.



From experiments on coleoptile phototropism, the Darwins concluded in 1880 that a growth stimulus is produced in the coleoptile tip and is transmitted to the growth zone.

In 1913, P. Boysen-Jensen discovered that the growth stimulus passes through gelatin but not through water-impermeable barriers such as mica.

Figure 4.11 Early experiments on the chemical nature of auxin.

example, they can promote seed germination (see Chapter 17), the transition to flowering (see Chapter 20), pollen development and pollen tube growth (see Chapter 21), and fruit development (see Chapter 21).

Gibberellins were first recognized by Eiichi Kurosawa in 1926 and were isolated by Teijiro Yabuta and Yusuke Sumuki in the 1930s as natural products in the fungus *Gibberella fujikuroi* (now renamed *Fusarium fujikuroi*), from which the hormones derive their unusual name. Rice plants infected with *F. fujikuroi* grow abnormally tall, which leads to lodging (falling over) and reduced yield; hence the name *bakanae*, or "foolish seedling disease." Such overgrowth can be reproduced by applying gibberellins to uninfected rice seedlings. *F. fujikuroi* produces several different gibberellins, the most abundant of which is GA_3, also called gibberellic acid, which can be obtained commercially for horticultural and agronomic use. For example, GA_3 is sprayed onto grape vines to produce the large, seedless grapes we now routinely purchase in the grocery store (**Figure 4.12A**). Spectacular responses were obtained in the stem elongation of dwarf and rosette plants, particularly in genetically dwarf peas (*Pisum sativum*), dwarf maize (corn; *Zea mays*) (**Figure 4.12B**), and many rosette plants (**Figure 4.12C**).

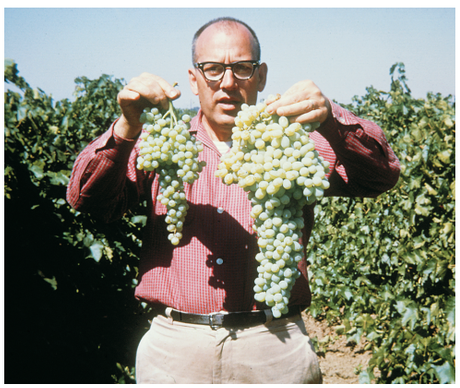
Shortly after the first characterization of gibberellins from *F. fujikuroi*, it was discovered that plants also contain gibberellin-like substances, but in much lower abundance than in the fungus. The first plant gibberellin to be identified was GA_1, which was discovered in extracts of runner bean seeds in 1958. We now know that gibberellins are ubiquitous in plants and are also present in several fungi in addition to *F. fujikuroi*. The majority of plants studied to date contain GA_1 and/or GA_4, so these are the gibberellins to which we assign "hormonal" function. In addition to GA_1 and GA_4, plants contain many inactive gibberellins which represent the precursors or deactivation products of the bioactive gibberellins.

Cytokinins were discovered as cell division–promoting factors in tissue-culture experiments

Cytokinins were discovered in a search for factors that stimulated plant cells to divide (i.e., undergo cytokinesis) in conjunction with the phytohormone auxin. A small molecule was identified that could, in the presence of auxin, stimulate tobacco pith parenchyma tissue to proliferate in culture (**Figure 4.13A**). The cytokinesis-inducing molecule was named *kinetin*. While kinetin is a synthetic cytokinin, its structure is similar to that of naturally occurring cytokinins such as zeatin (see Figure 4.10C).

As we will see in later chapters, cytokinins have been shown to have effects on many physiological and

(A)



© Sylvan Wittwer/Visuals Unlimited

(B)



Courtesy of B. Phinney

(C)



© Sylvan Wittwer/Visuals Unlimited

Figure 4.12 Use of plant hormones as growth regulators. **(A)** Gibberellin induces growth in "Thompson Seedless" grapes. Untreated grapes normally remain small because of natural seed abortion. The bunch on the left is untreated. The bunch on the right was sprayed with GA_3 during fruit development, leading to larger fruits and elongation of the pedicels (fruit stalks). **(B)** The effect of exogenous GA_1 on wild-type (labeled as "normal" in the photograph) and dwarf mutant (*d1*) maize. Gibberellin stimulates dramatic stem elongation in the dwarf mutant but has little or no effect on the tall, wild-type plant. **(C)** Cabbage, a long-day plant, remains a low-growing rosette in short days, but it can be induced to bolt (grow long internodes) and flower by applications of GA_3. In the case illustrated, giant flowering stalks were produced.

developmental processes, including leaf senescence (see Chapter 23), apical dominance (see Chapter 19), formation and activity of apical meristems (see Chapter 18), gametophytic development (see Chapter 21), promotion of sink activity, vascular development, and breaking of bud dormancy (see Chapter 19). In addition, cytokinins play important roles in the interaction of plants with both biotic and abiotic factors, including salinity and drought stresses, macronutrients (including nitrate, phosphate, iron, and sulfate), and symbiotic nitrogen-fixing bacteria and arbuscular mycorrhizal fungi, as well as pathogenic bacteria, fungi, nematodes, and viruses (**Figure 4.13B**) (also see Chapters 15 and 24).

Ethylene is a gaseous hormone that promotes fruit ripening and other developmental processes

Ethylene is a gas with a simple chemical structure (see Figure 4.10D) and was first identified as a plant growth regulator in 1901 by Dimitry Neljubov when he demonstrated its ability to alter the growth of etiolated pea seedlings in the laboratory (**Figure 4.14A**). Subsequently, ethylene was identified as a natural product synthesized by plant tissues.

Ethylene regulates a wide range of processes in plants, including seed germination and seedling growth, cell expansion and differentiation, and leaf and flower senescence and abscission (see Chapters 17 and 22), as well as responses to biotic and abiotic stresses (see Chapters 15 and 24), including epinasty (**Figure 4.14B**). Phytobiome bacteria have been shown to influence plant growth and stress responses by manipulating levels of ethylene and its metabolic precursors.

Abscisic acid regulates seed maturation and stomatal closure in response to water stress

Abscisic acid (ABA) is a ubiquitous hormone in vascular plants and has also been found in mosses, some phytopathogenic fungi, and a wide range of metazoans.

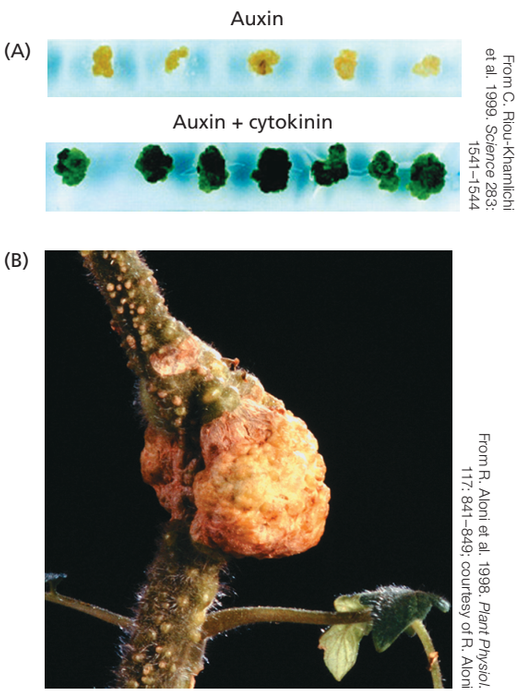


Figure 4.13 **Cytokinin enhances cell division and greening.** **(A)** Wild-type Arabidopsis leaf explants were induced to form callus (undifferentiated cells) by culturing in the presence of auxin alone (top) or auxin plus cytokinin (bottom). Cytokinin was required for callus growth and greening in the presence of light. **(B)** Tumor that formed on a tomato stem expressing increased cytokinin levels after being infected with the crown gall bacterium, *Agrobacterium tumefaciens*. Two months before this photo was taken, the stem was wounded and inoculated with a virulent strain of the crown gall bacterium.

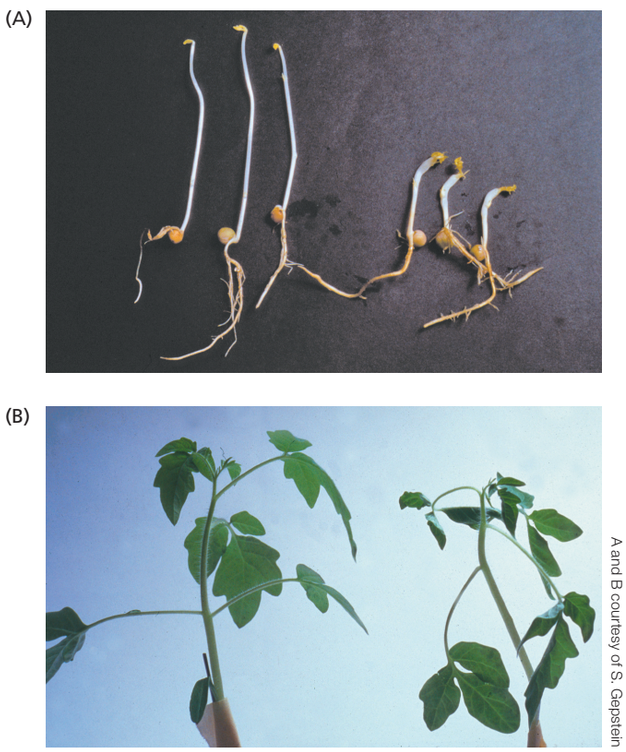


Figure 4.14 **Ethylene responses.** **(A)** Triple response of etiolated pea seedlings. Six-day-old pea seedlings were grown in the dark in the presence of 10 ppm (parts per million) ethylene (right) or left untreated (left). The treated seedlings show radial swelling, inhibition of elongation of the epicotyl, and horizontal growth of the epicotyl (diagravitropism). **(B)** Leaf epinasty in tomato. Epinasty, or downward bending of the tomato leaves (right), is caused by ethylene treatment. An untreated tomato is on the left. Epinasty results when the cells on the adaxial side of the petiole grow faster than those on the abaxial side.

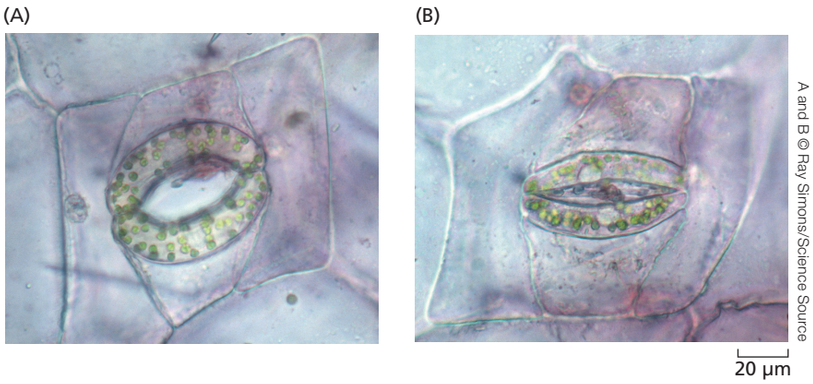


Figure 4.15 **Stomatal closure in response to ABA.** (A) Stomata are open in the light for gas exchange with the environment. (B) ABA treatment closes stomata in the light. This reduces water loss during the day under drought stress conditions.



Figure 4.16 **Loss of the active brassinosteroid in the *nana1* mutant of maize results in dwarfism and altered floral sex determination.** The staminate wild-type tassel is shown on the left, and the feminized *nana1* tassel is shown on the right.

ABA is a four-carbon terpenoid (see Figure 4.10E) that was identified in the 1960s as a growth-inhibiting compound associated with the onset of bud dormancy and promotion of cotton fruit abscission. However, later work showed that ABA promotes senescence, the process preceding abscission, rather than abscission itself. Since then, ABA has also been shown to regulate salinity, dehydration, and temperature stress responses, including stomatal closure (**Figure 4.15**) (see Chapter 15). ABA also promotes seed maturation and dormancy (see Chapter 17) and regulates the growth of roots and shoots, heterophylly (the production of different leaf types on an individual plant), and flowering, as well as some responses to pathogens (see Chapter 24).

Brassinosteroids regulate photomorphogenesis, germination, and other developmental processes

Brassinosteroids, initially named brassins, were first discovered as growth-promoting substances present in the pollen of *Brassica napus* (rape plant). Subsequent X-ray analysis showed that the most bioactive brassin in eudicots, which was named **brassinolide**, is a polyhydroxylated steroid similar to animal steroid hormones (see Figure 4.10F).

Many brassinosteroids have been identified, primarily intermediates of the brassinolide biosynthetic or catabolic pathways. Two brassinosteroids are known to be active, brassinolide and its immediate precursor castasterone, although which form is predominant depends on the plant species and tissue type. Brassinosteroids are ubiquitous plant hormones that, like auxins and gibberellins, appear to predate the evolution of land plants. In the angiosperms, brassinosteroids are found at low levels in various organs (e.g., flowers, leaves, roots) and at higher relative levels in pollen, immature seeds, and fruits.

Brassinosteroids play pivotal roles in a wide range of developmental phenomena in plants, including cell division, cell elongation, cell differentiation, photomorphogenesis, reproductive development, germination, leaf senescence, and stress responses. Mutants deficient in brassinosteroid synthesis show growth and developmental abnormalities, including dwarfism and reduced apical dominance. Brassinosteroid-deficient mutants also exhibit de-etiolated growth in the dark in Arabidopsis, and feminized male flowers and tassels in maize (**Figure 4.16**).

Strigolactones suppress branching and promote rhizosphere interactions

Strigolactones, which occur in about 80% of plant species, are a group of terpenoid lactones (see Figure 4.10H) that were originally discovered as host-derived germination stimulants for root parasitic plants, such as the witchweeds (*Striga* spp.) and broomrapes (*Orobanche* and *Phelipanche* spp.) (**Figure 4.17**). They also promote symbiotic interactions with arbuscular mycorrhizal fungi, facilitating phosphate uptake from the soil. In addition, strigolactones suppress shoot branching and stimulate cambial activity and secondary growth (see Chapter 19). Strigolactones have analogous functions in roots, where they reduce adventitious and lateral root formation and promote root hair growth. In rice, the apocarotenoids zaxinone and β-cyclocitrical, which are derived from the same pathway as strigolactones, have been shown to modify root growth and branching. Karrikins, found in smoke from forest and chaparral fires, are similar to strigolactones and stimulate seed

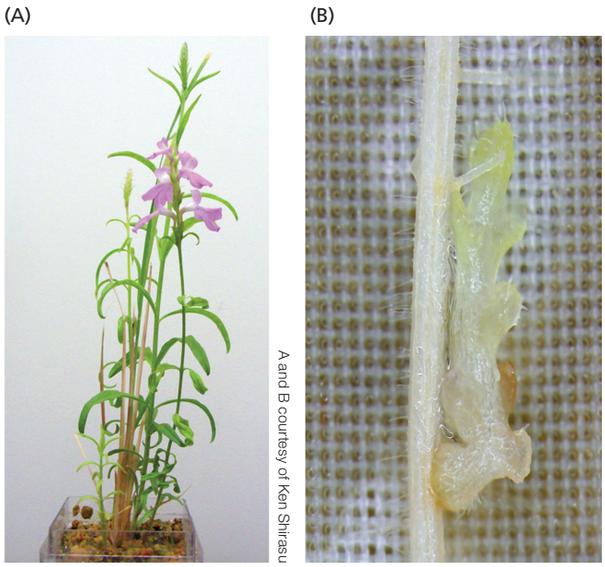


Figure 4.17 **Rice plants colonized by root parasitic plants.** **(A)** Flowering purple witchweed (*Striga hermonthica*) parasitizing a rice plant. **(B)** Etiolated *Striga hermonthica* seedling invading a rice root.

germination (see Chapter 17). Rhizosphere microbial communities also produce carotenoids to modify root growth in multiple plant species.

4.4 Phytohormone Metabolism and Homeostasis

To be effective signals, the concentrations of plant hormones must be tightly regulated in a cell type–specific and tissue-specific manner. In the simplest terms, a hormone's concentration in any given tissue or cell is determined by the balance between the rate of increase in its concentration (e.g., by local synthesis and activation or by import from elsewhere in the plant) and the rate of decrease in its concentration (e.g., by inactivation, degradation, sequestration, or efflux) (**Figure 4.18**). However, the regulation of hormone levels is complicated by many factors. First, primary hormone biosynthetic pathways may be augmented by secondary biosynthetic mechanisms. Second, there may be multiple structural variants of a hormone, which can vary widely in biological activity. Finally, as we will see later, there may be multiple mechanisms for removing active hormone from a system.

In this section we discuss mechanisms for modulating hormone concentrations locally (within a cell or tissue). We cover hormone transport between different parts of a plant in Section 4.5.

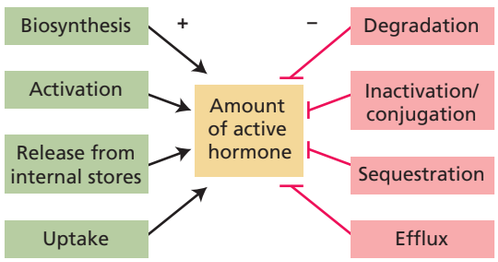


Figure 4.18 **Homeostatic regulatory mechanisms that influence hormone concentration.** Both positive and negative factors work in concert to maintain hormone homeostasis.

Indole-3-pyruvate is the primary intermediate in auxin biosynthesis

IAA is structurally related to the amino acid tryptophan, and is primarily synthesized on the ER surface in a two-step process wherein tryptophan is converted by a tryptophan aminotransferase (TAA) to indole-3-pyruvate (IPyA) as the intermediate (**Figure 4.19**). In the second step of the biosynthetic pathway, members of a flavin monooxygenase family known as YUCCAs (YUCs) rapidly convert IPyA to IAA. The YUCCA enzymes were named for the increased apical dominance, tall inflorescences, and narrow, epinastic leaves that are similar to those of yucca plants and that are found in Arabidopsis when genes encoding YUCCA enzymes are overexpressed (**Figure 4.20**).

IAA biosynthesis is associated with rapidly dividing and growing tissues, especially in shoots. Although virtually all plant tissues appear to be capable of producing low levels of IAA, shoot apical meristems, young leaves, and young fruits are the primary sites of auxin synthesis. In plants that produce indole glucosinolate defense compounds (see Chapter 24), IAA can also be synthesized from tryptophan via a pathway with indole acetonitrile as an intermediate (see **WEB APPENDIX 3**). In maize kernels, IAA also appears to be synthesized by a tryptophan-independent pathway.

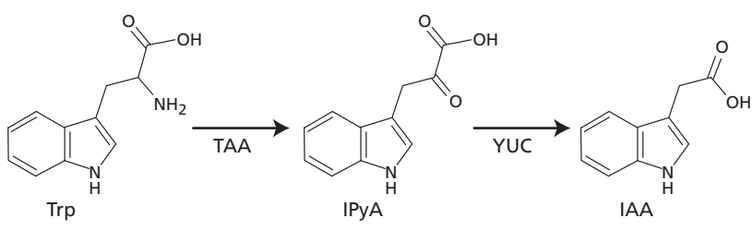


Figure 4.19 **Auxin biosynthesis from tryptophan (Trp).** In the first step, Trp is converted to indole-3-pyruvate (IPyA) by the TAA family of tryptophan aminotransferases. Subsequently, IAA is produced from IPyA by the YUC family of flavin monooxygenases.



Courtesy of Dr. Jeong Im Kim

Wild type *yuc6-1D*

Figure 4.20 Arabidopsis mutant overexpressing the *YUCCA6* (*YUC6*) gene. The dominant *yuc6-1D* activation mutant (right) contains elevated levels of free IAA relative to the wild type (left), because of the overexpression of *YUCCA6*. Note the taller growth and reduced branching of the mutant.

Auxin is toxic at high cellular concentrations, and without homeostatic controls the hormone could easily build up to toxic levels. Auxin can be catabolized by oxidative degradation via dioxygenase of auxin (DAO) in the cytosol and on the cytosolic surface of membranes, ensuring the permanent removal of active hormone when the concentration exceeds the optimal level or when the response to the hormone is complete. The Gretchen Hagen 3 (GH3) family of amido synthetases catalyzes the covalent conjugation of IAA to amino acids in the cytosol, and conjugation to Glu and Asp via this pathway can also result in permanent reduction of signaling activity via subsequent oxidation by DAO. However, most amino acyl conjugates of IAA serve as storage forms from which IAA can be rapidly released by enzymatic processes in the ER. IAA can also be reversibly converted to methyl-IAA via indole-3-acetate O-methyltransferase1 (IAMT1). Indole-3-butyric acid (IBA) is a compound that is routinely used in horticulture to promote rooting of cuttings and is rapidly converted by β-oxidation in the peroxisome to IAA. Both free and conjugated IBA are thought to occur naturally in plants and to serve as auxin sources for specific developmental processes. Auxin has also been shown to be conjugated to peptides, complex glycans (multiple sugar units), or glycoproteins in some plant species, but the precise physiological role of these conjugates is still unknown. A diagram of the storage and catabolic fates of auxin is shown in **Figure 4.21**.

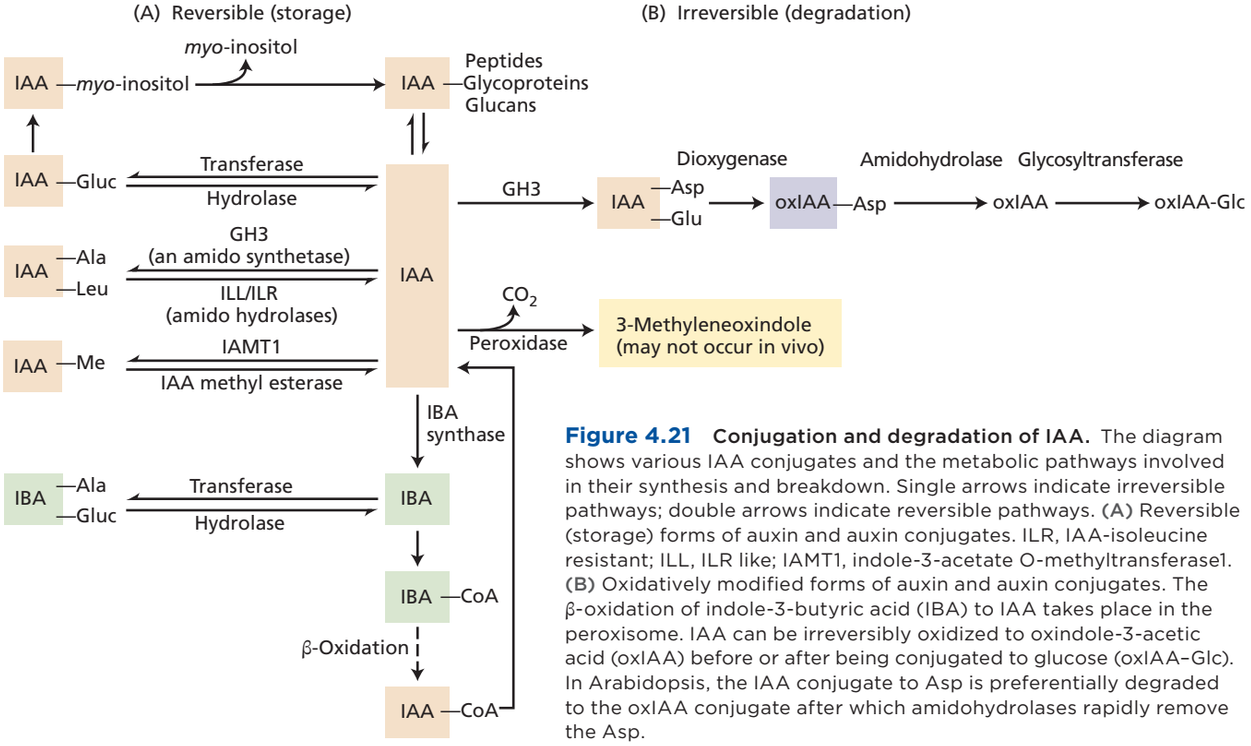


Figure 4.21 Conjugation and degradation of IAA. The diagram shows various IAA conjugates and the metabolic pathways involved in their synthesis and breakdown. Single arrows indicate irreversible pathways; double arrows indicate reversible pathways. **(A)** Reversible (storage) forms of auxin and auxin conjugates. ILR, IAA-isoleucine resistant; ILL, ILR like; IAMT1, indole-3-acetate O-methyltransferase1. **(B)** Oxidatively modified forms of auxin and auxin conjugates. The β-oxidation of indole-3-butyric acid (IBA) to IAA takes place in the peroxisome. IAA can be irreversibly oxidized to oxindole-3-acetic acid (oxIAA) before or after being conjugated to glucose (oxIAA-Glc). In Arabidopsis, the IAA conjugate to Asp is preferentially degraded to the oxIAA conjugate after which amidohydrolases rapidly remove the Asp.

Sequestration of auxin in endomembrane compartments, primarily the ER, also appears to regulate the auxin levels available for signaling. A large store of the AUXIN-BINDING PROTEIN1 (ABP1) is primarily found in the ER lumen, and transporters such as the "short" PIN-FORMED (PIN) proteins (PIN5,6, and 8) as well as PIN-LIKE (PIL) proteins mediate IAA movement across the ER membrane (**Figure 4.22**). Some glutathione S-transferases can bind auxin and may act as chaperones in the cytosol. As described in Chapter 1, the interior of the vacuole is topologically "outside" the cell. Some of the auxin that enters the acidic vacuole would be expected to become protonated (uncharged) and thus readily diffuse back through the tonoplast and into the cytoplasm. However, anionic auxin is exported from the vacuole by the tonoplast membrane transporter WALLS ARE THIN1 (WAT1). Another tonoplast membrane protein, TRANSPORTER OF IBA1 (TOB1), has been shown to mobilize the minor auxin indole butyric acid out of the vacuole.

The well-documented toxicity of exogenously applied auxin, especially on eudicot species, forms the basis for a family of synthetic auxins, such as 2,4-dichlorophenoxyacetic acid (2,4-D), that have long been used as herbicides. Mutations causing auxin overexpression (see Figure 4.20) would tend to be lethal if it were not for homeostatic control of auxin levels. The reason that synthetic auxins are more effective as herbicides than natural auxins is that the synthetic auxins are much less subject to homeostatic control—degradation, conjugation, transport, and sequestration—than natural auxins are.

Synthetic hormones are used as plant growth regulators to optimize crop yield or as herbicides to kill weeds. The efficacy of artificial hormones for plant growth regulation or herbicide use is generally dependent on dosage and timing of application. For example, synthetic auxins are used to thin fruit in apple orchards to ensure that the size of the remaining fruit will yield a high market value. Larger fruit is more desirable to most consumers, so a smaller number of large fruits is usually more profitable than a large number of small fruits. In contrast, synthetic auxins such as 2,4-D and dicamba are often used on row-crop fields several weeks prior to sowing the crop seeds. This "burn down" ensures that weed seeds in the soil die during germination and will not compete with the crop for light, water, and nutrients.

Gibberellins are synthesized by oxidation of the diterpene ent-kaurene

Gibberellins are synthesized in several parts of a plant, including developing seeds, germinating seeds, developing leaves, and elongating internodes. The biosynthetic pathway, which starts in plastids, leads to the production of a linear (straight chain) precursor molecule containing 20 carbon atoms, geranylgeranyl diphosphate or GGPP, which gets converted into *ent*-kaurene. This compound is oxidized sequentially by enzymes associated with the ER, leading to GA_{12}, the first gibberellin formed in all plants studied to date. Dioxygenase enzymes in the cytosol are able to oxidize GA_{12} to all other gibberellins in pathways that may be interconnected in such a way as to form a complex metabolic grid. A summary of gibberellin synthetic pathways is shown in **Figure 4.23**.

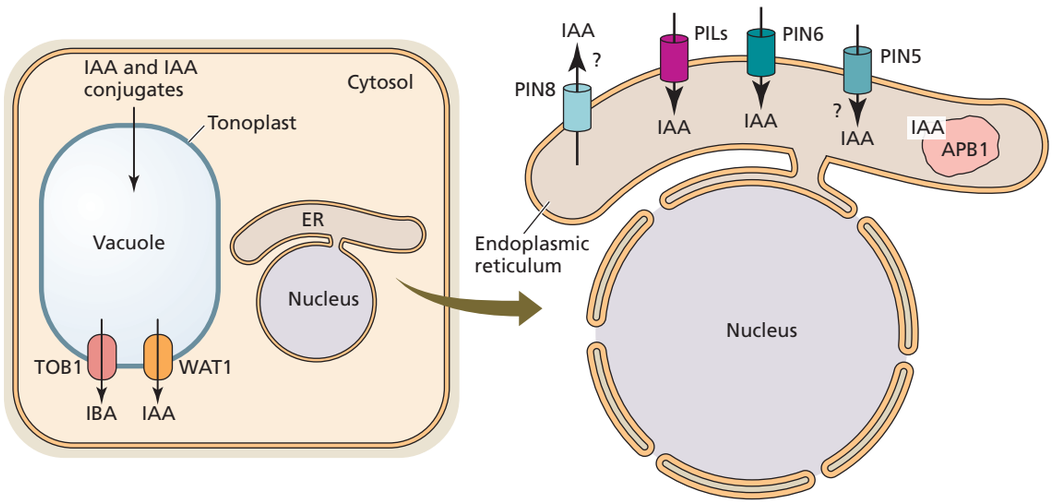


Figure 4.22 Auxin synthesis and metabolism require endomembrane transporters. Auxin is synthesized on the surface of the ER and is found in the ER lumen where the molecular chaperone Auxin-Binding Protein 1 (ABP1) is abundant. The PIN-LIKE proteins (PILs) and "short" PIN proteins mediate movement in and out of the ER. Permeases on the tonoplast mobilize indole acetic acid (IAA) and indole-3-butyric acid (IBA) from the vacuole back to the cytosol. TOB1, Transport of IBA transporter; WAT1, WALLS ARE THIN IAA transporter.

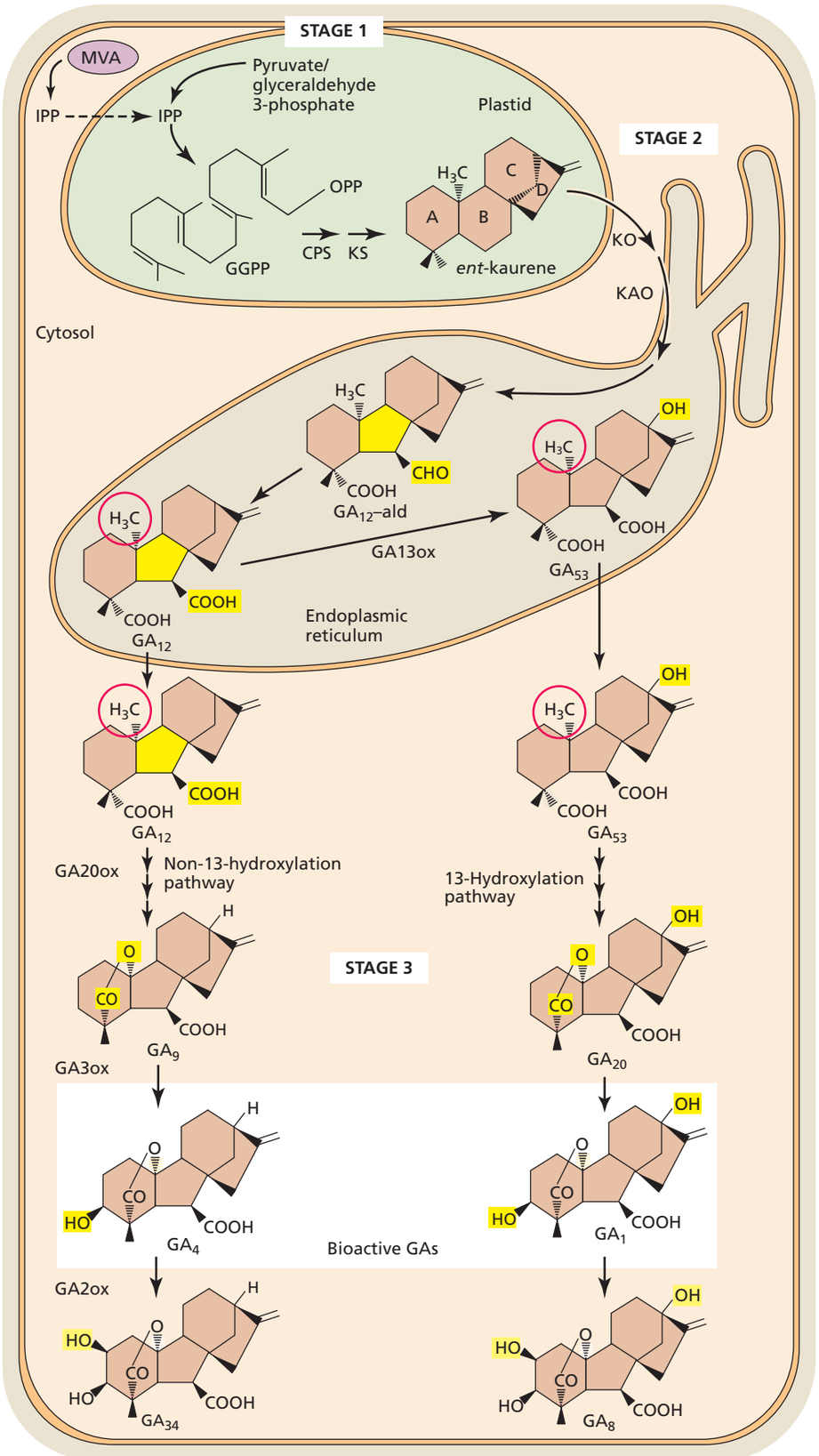


Figure 4.23 **The three stages of gibberellin biosynthesis.** Yellow highlighting indicates the part of the molecule that has been modified in the previous reaction. In stage 1 in the plastid, geranylgeranyl diphosphate (GGPP) is converted to *ent*-kaurene. In stage 2 in the endoplasmic reticulum, *ent*-kaurene is converted to GA_{12}-aldehyde and GA_{12}. GA_{12} is converted to GA_{53} by hydroxylation at C-13. In stage 3 in the cytosol, GA_{12} and GA_{53} are converted, via parallel pathways, to other gibberellins. This conversion proceeds with a series of oxidations at C-20 (red circles), resulting in the eventual loss of C-20 and the formation of the most biologically active gibberellins. 3-β-Hydroxylation then produces GA_4 and GA_1 as the bioactive gibberellins in each pathway. Hydroxylation at C-2 then converts GA_4 and GA_1 to the inactive forms GA_{34} and GA_8, respectively. In most plants the 13-hydroxylation pathway predominates, although in Arabidopsis and some others, the non-13-hydroxylation pathway is the main pathway. MVA, mevalonic acid; IPP, isopentenyl diphosphate; CPS, *ent*-copalyl diphosphate synthase; KS, *ent*-kaurene synthase; KO, *ent*-kaurene oxidase; KAO, *ent*-kaurenoic acid oxidase; GA20ox, GA 20-oxidase; GA3ox, GA 3-oxidase; GA2ox, GA 2-oxidase; GA13ox, GA 13-oxidase.

The pathways involved in gibberellin biosynthesis and catabolism are under tight genetic control. Several mechanisms have been described to date. These include gibberellin inactivation via a family of enzymes termed GA 2-oxidases, methylation via a methyltransferase, and conjugation to sugars. Genetic modulation of these pathways plays an important role in plant development. For example, as we will see in Chapter 18, *KNOXI* gene expression in the shoot apical meristem, which is crucial for proper function of the meristem, reduces gibberellin levels by inhibiting gibberellin biosynthesis and promoting gibberellin inactivation. Gibberellin biosynthesis is also regulated by feedback inhibition when cellular gibberellin exceeds threshold levels. The application of exogenous gibberellin causes down-regulation of the *GA20ox* and *GA3ox* genes, whose products catalyze the two final two steps in the formation of bioactive gibberellins (GA_1 and GA_4).

Gibberellins and gibberellin antagonists are also used as plant growth regulators. For example, application of GA to grapes can increase the size of the individual fruits (see Figure 4.12A). The GA antagonists uniconazole and paclobutrazol can be used to inhibit GA biosynthesis. These plant growth regulators can be used to decrease the stature of the plants, such as maize, to reduce lodging, and in the greenhouse to reduce internode and petiole elongation in horticultural and ornamental crops.

Cytokinins are adenine derivatives with isoprene side chains

Cytokinins are adenine derivatives, and the most common class of cytokinins has isoprenoid side chains, including isopentenyl adenine (iP), dihydrozeatin (DHZ), and the most abundant cytokinin in higher plants, zeatin. Cytokinins are made from ADP/ATP and dimethylallyl diphosphate (DMAPP), primarily in plastids. A simplified schematic of the cytokinin biosynthetic pathway is shown in **Figure 4.24**.

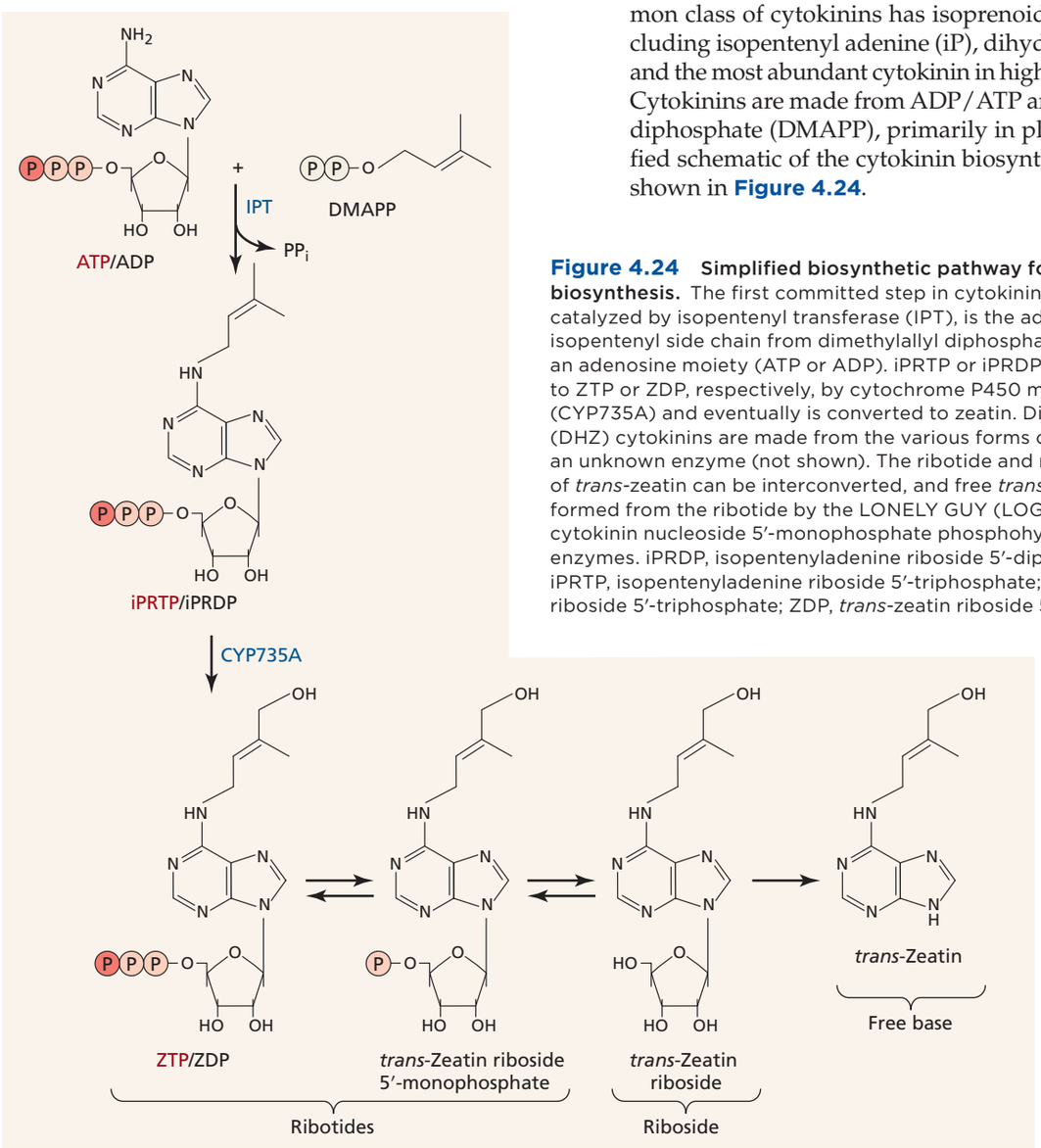


Figure 4.24 Simplified biosynthetic pathway for cytokinin biosynthesis. The first committed step in cytokinin biosynthesis, catalyzed by isopentenyl transferase (IPT), is the addition of the isopentenyl side chain from dimethylallyl diphosphate (DMAPP) to an adenosine moiety (ATP or ADP). iPRTP or iPRDP is converted to ZTP or ZDP, respectively, by cytochrome P450 monooxygenase (CYP735A) and eventually is converted to zeatin. Dihydrozeatin (DHZ) cytokinins are made from the various forms of *trans*-zeatin by an unknown enzyme (not shown). The ribotide and riboside forms of *trans*-zeatin can be interconverted, and free *trans*-zeatin can be formed from the ribotide by the LONELY GUY (LOG) family of cytokinin nucleoside 5′-monophosphate phosphohydrolase enzymes. iPRDP, isopentenyladenine riboside 5′-diphosphate; iPRTP, isopentenyladenine riboside 5′-triphosphate; ZTP, *trans*-zeatin riboside 5′-triphosphate; ZDP, *trans*-zeatin riboside 5′-diphosphate.

In addition to the free bases, which are the only active forms, cytokinins are also present in the plant as ribosides (in which a ribose sugar is attached to the 9 nitrogen of the purine ring), ribotides (in which the ribose sugar moiety contains a phosphate group), or **glycosides** (in which a sugar molecule is attached to the 3, 7, or 9 nitrogen of the purine ring, or to the oxygen of the zeatin or dihydrozeatin side chain). In addition to this glycosylation-mediated inactivation, active cytokinin levels are also decreased catabolically through irreversible cleavage by cytokinin oxidases.

Consistent with its role in promoting cell division, cytokinin is required for proper functioning of the shoot apical meristem and is therefore tightly regulated (see Chapter 18. While inhibiting gibberellin levels, *KNOX* gene expression increases cytokinin levels in the shoot apical meristem by up-regulating the cytokinin biosynthetic gene *ISOPENTENYL TRANSFERASE7* (*IPT7*) (see Figure 4.24).

Ethylene is synthesized from methionine via the intermediate ACC

Ethylene can be produced by almost all parts of higher plants, although the rate of production depends on the type of tissue, the stage of development, and environmental inputs. For example, certain mature fruits undergo a respiratory burst in response to ethylene, and ethylene levels increase in these fruits at the time of ripening (see Chapter 21). Ethylene is derived from the amino acid methionine and the intermediate *S*-adenosylmethionine, which is generated in the Yang cycle (**Figure 4.25**). The first committed and generally rate-limiting step in the biosynthesis is the conversion of *S*-adenosylmethionine to 1-aminocyclopropane-1-carboxylic acid (ACC) by the enzyme ACC synthase. ACC is then converted to ethylene by enzymes called **ACC oxidases**. ACC functions directly as a signaling compound in mosses, and there is some evidence that ACC interacts with glutamate-like receptors (see Chapter 21) in angiosperms. As ethylene is a gaseous hormone, there is no evidence of ethylene catabolism in

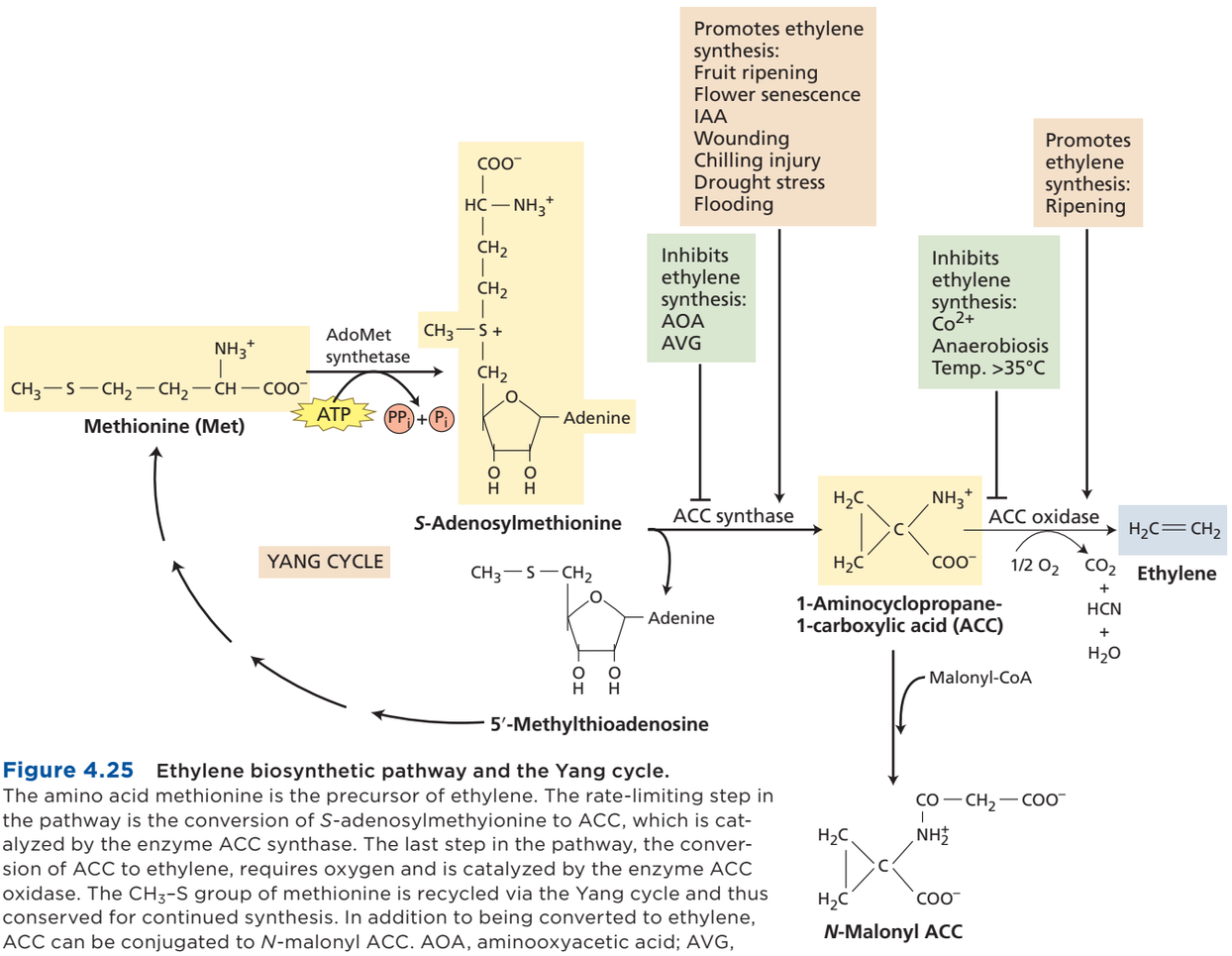


Figure 4.25 **Ethylene biosynthetic pathway and the Yang cycle.** The amino acid methionine is the precursor of ethylene. The rate-limiting step in the pathway is the conversion of *S*-adenosylmethyionine to ACC, which is catalyzed by the enzyme ACC synthase. The last step in the pathway, the conversion of ACC to ethylene, requires oxygen and is catalyzed by the enzyme ACC oxidase. The CH_3–S group of methionine is recycled via the Yang cycle and thus conserved for continued synthesis. In addition to being converted to ethylene, ACC can be conjugated to *N*-malonyl ACC. AOA, aminooxyacetic acid; AVG, aminoethoxy-vinylglycine.

plants, and ethylene rapidly diffuses out of plant tissues when biosynthesis is pharmacologically interrupted.

Abscisic acid is synthesized from a carotenoid intermediate

ABA is synthesized in almost all cells that contain chloroplasts or amyloplasts and has been detected in every major organ and tissue. ABA is a 14-carbon terpenoid, or sesquiterpenoid, which is synthesized in plants by an indirect pathway via 40-carbon carotenoid intermediates (**Figure 4.26**). Early steps of this pathway occur in plastids. Cleavage of the carotenoid by the enzyme NCED (9-*cis*-epoxycarotenoid dioxygenase) is a rate-limiting, highly regulated step in ABA synthesis that produces the 14-carbon precursor molecule xanthoxin, which subsequently moves into the cytosol, where a series of oxidative reactions convert xanthoxin to ABA. Further oxidation by ABA-8′-hydroxylases leads to ABA inactivation. ABA can also be inactivated by conjugation, but this is reversible. Both types of inactivation are also tightly regulated.

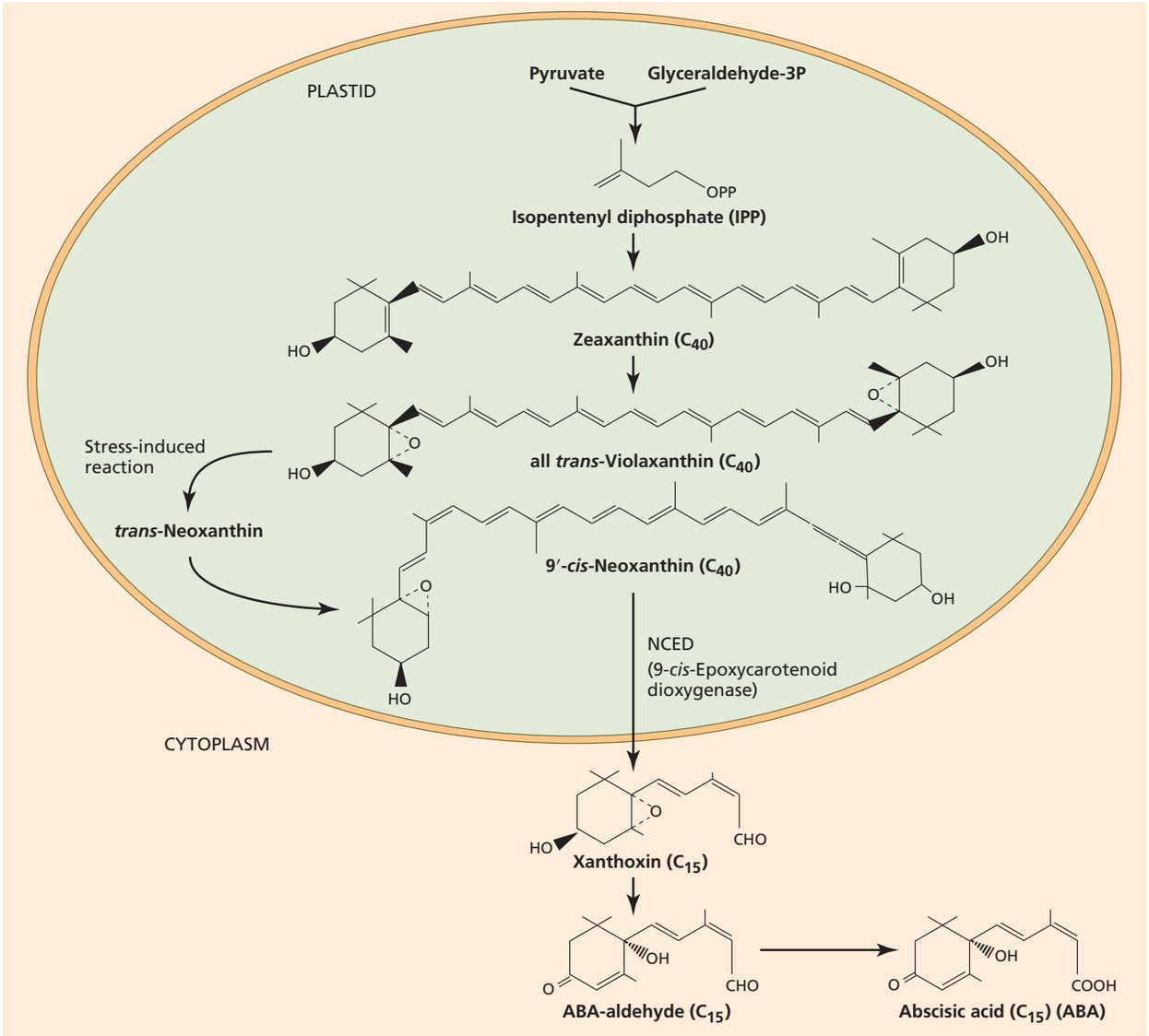


Figure 4.26 Simplified diagram of ABA biosynthesis via the terpenoid pathway. The initial stages occur in plastids, where isopentenyl diphosphate (IPP) is converted to the C_{40} xanthophyll zeaxanthin. Zeaxanthin is further modified to 9-*cis*-neoxanthin, which is cleaved by the enzyme NCED (9-*cis*-epoxycarotenoid dioxygenase) to form the C_4 inhibitor, xanthoxin. Xanthoxin then is converted to ABA in the cytosol. ABA-deficient mutants that have been helpful in elucidating the pathway are shown in **WEB APPENDIX 3**.

ABA concentrations can fluctuate dramatically in specific tissues during development or in response to changing environmental conditions. In developing seeds, for example, ABA levels can increase 100-fold within a few days, reaching average concentrations in the micromolar range, and then decline to very low levels as maturation proceeds (see Chapter 21). Under conditions of water stress (i.e., dehydration stress), ABA in the leaves can increase 50-fold within 4 to 8 h (see Chapter 15).

Brassinosteroids are derived from the sterol campesterol

Brassinosteroids are synthesized from the plant sterol campesterol, which is similar in structure to cholesterol. Members of the **cytochrome P450 monooxygenase** (**CYP**) enzyme family that are associated with the ER catalyze most of the reactions in the brassinosteroid biosynthetic pathway (**Figure 4.27**). Bioactive brassinosteroid levels are also modulated by a variety of inactivation or catabolic reactions, including epimerization, oxidation, hydroxylation, sulfonation, and conjugation to glucose or lipids. However, only few of the enzymes responsible for brassinosteroid catabolism and inactivation have been identified so far.

The levels of active brassinosteroids are also regulated by brassinosteroid-dependent negative feedback mechanisms in which hormone concentrations above a certain threshold cause a decrease in brassinosteroid biosynthesis. This attenuation is brought about by the down-regulation of brassinosteroid biosynthetic genes

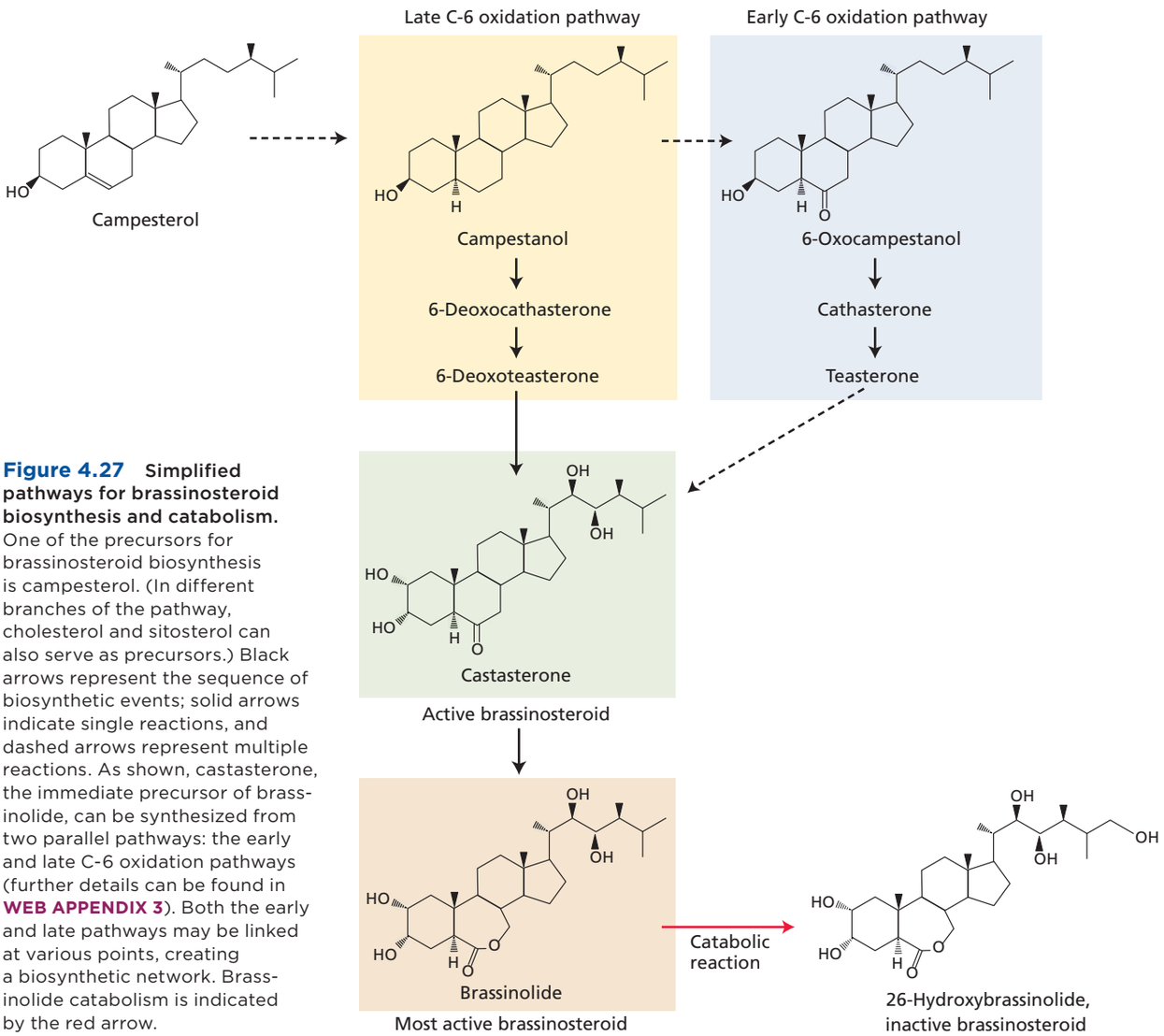


Figure 4.27 Simplified pathways for brassinosteroid biosynthesis and catabolism. One of the precursors for brassinosteroid biosynthesis is campesterol. (In different branches of the pathway, cholesterol and sitosterol can also serve as precursors.) Black arrows represent the sequence of biosynthetic events; solid arrows indicate single reactions, and dashed arrows represent multiple reactions. As shown, castasterone, the immediate precursor of brassinolide, can be synthesized from two parallel pathways: the early and late C-6 oxidation pathways (further details can be found in **WEB APPENDIX 3**). Both the early and late pathways may be linked at various points, creating a biosynthetic network. Brassinolide catabolism is indicated by the red arrow.

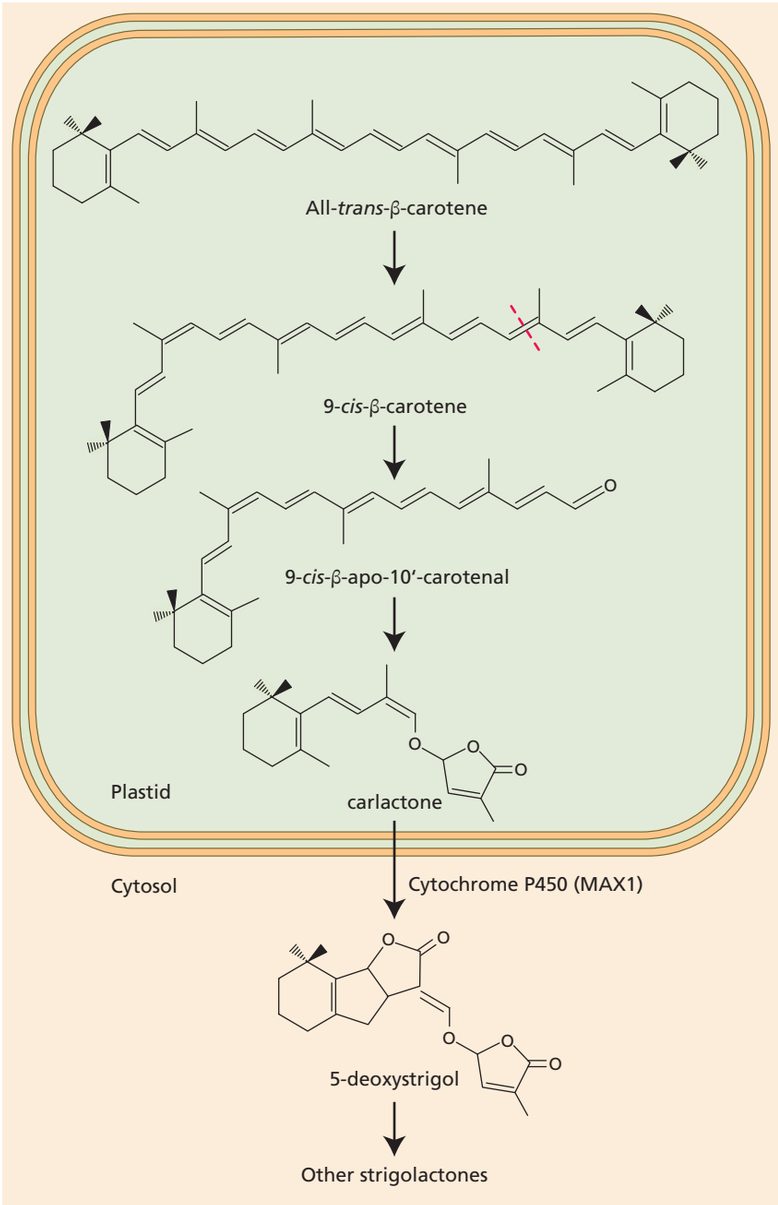


Figure 4.28 Strigolactone biosynthetic pathway and signaling proteins. All-*trans*-β-carotene is isomerized to 9-*cis*-β-carotene by a β-carotene isomerase. 9-*cis*-β-Carotene is cleaved (at the dashed red line) by carotenoid cleavage dioxygenases, to produce carlactone. The final stages of strigolactone synthesis and signaling occur in the cytosol.

and the up-regulation of genes involved in brassinosteroid catabolism. Thus, mutants impaired in their ability to respond to brassinolide accumulate high levels of the active brassinosteroids compared with wild-type plants.

Propiconazole is a commonly used fungicide, because it inhibits the activity of cytochrome P450 enzymes that synthesize the structural sterol ergosterol in fungal pathogens. When used at higher concentrations, this fungicide reduces growth of turf grasses and maize. These observations led to the discovery that the maize *nana1* dwarf and floral sex mutant (see Figure 4.16) is deficient in brassinosteroid biosynthesis.

Strigolactones are synthesized from β-carotene

Like ABA, strigolactones and other apocarotenoid signaling molecules are derived from carotenoid precursors in plastids in a pathway that is conserved up to synthesis of the intermediate carlactone. Synthesis of signaling molecules such as strigolactones begins with cleavage of the carotenoid precursors (**Figure 4.28**). Diverse cytochrome P450 isoforms produce strigolactones and similar signaling molecules that vary among species. Carotenoid cleavage can also occur via non-enzymatic oxidative processes.

The strigolactone signaling pathway will be discussed in Chapter 19.

4.5 Movement of Hormones within the Plant

Hormones that provide positional cues to regulate patterns of cellular differentiation are termed **morphogens**. Through combinations of synthesis, transport, and turnover, morphogen molecules attain a graded distribution within tissues, which in turn evokes a range of concentration-dependent responses. So far we have looked at the mechanisms that control the synthesis, turnover, and intracellular distribution of plant hormones. In this section we focus on the movement of hormones between the cells, tissues, and organs of the plant.

Lipophilic hormones such as ABA and strigolactones can diffuse across membranes, but in some tissues they are also actively transported by ATP-binding cassette subfamily G (ABCG) transporters. For example, an ABCG

protein transports strigolactone from the root apex to differentiating root tissues. ABA and cytokinins can move over long distances in the xylem transpiration stream and have recently been shown to be actively transported into the vascular system in the root. Gibberellins that are synthesized in the root epidermis can also be taken up in those cells via the nitrate/peptide transporter NPF3. Auxins and cytokinins can also move with source–sink fluxes in the phloem. Recent research suggests that an active transport mechanism controls gibberellin levels in root vascular tissues, resulting in accumulation of this growth hormone in expanding endodermal cells that control root elongation. As a gaseous compound, ethylene is more soluble in lipid bilayers than in the aqueous phase and can freely pass through the plasma membrane. In contrast, its precursor, ACC, is water soluble and is thought to be transported via the xylem to shoot tissues. It is currently unknown whether brassinosteroids have endocrine or paracrine activity. Brassinosteroids do not seem to undergo root-to-shoot and shoot-to-root translocation, as experiments in pea and tomato indicate that reciprocal stock/scion grafting of wild-type to brassinosteroid-deficient mutants does not rescue the phenotype of the latter. Instead, components of the brassinosteroid signaling and biosynthetic pathways are expressed throughout the plant, especially in young growing tissues. Despite the existence of diverse hormone transport mechanisms in plants, auxin is the only plant hormone that has been clearly shown to function via highly regulated vectorial streams. These are collectively described as polar auxin transport.

Plant polarity is maintained by polar auxin streams

Polar auxin transport is found in almost all plants, including bryophytes and ferns. Early studies of this phenomenon focused on auxin movement in apical and epidermal tissues during seedling phototropic responses (see Chapter 17). Long-distance polar auxin transport through the vascular parenchyma from sites of synthesis in apical tissues and young leaves to the root tip regulates stem elongation, apical dominance, and lateral branching (see Chapter 19). Auxin flows redirected at the root apex into the root epidermis are necessary for root gravitropic responses (see Chapter 17).

Polar auxin transport has been verified by radiolabeled auxin tracer assays and mass spectroscopic analyses of auxin content in discrete tissues. More recently, the use of auxin reporters to report relative auxin concentrations in individual cells and tissues has become a preferred means of visualizing auxin levels in intact plants. The most commonly used reporters are based on DR5, an artificial auxin-responsive promoter that is fused to a reporter gene (whose activity is easily visualized). DR5 fusions to β-glucuronidase (GUS), which produces a blue color when incubated with chromogenic substrates such as p-nitrophenyl β-D-glucuronide (see Figure 21.10), and green fluorescent protein (GFP) or similar fluorescent proteins, are widely used (for example, see Figures 16.11 and 21.10). However, DR5-based reporters require gene transcription to function, which delays the response to auxin. A more dynamic auxin reporter, DII-Venus, is based on a fusion of a yellow fluorescent protein variant to the "degron" portion of the AUX/IAA auxin co-receptor protein that is rapidly turned over in the presence of auxin (see description later in this section). DII-Venus is rapidly degraded when auxin is present. Auxin reporters have also been developed that contain two fluorescent proteins linked by an auxin-binding protein. For instance, in the AuxSen reporter, binding of auxin to a linker derived from a bacterial Trp repressor results in fluorescence resonance energy transfer (FRET) from one fluorescent protein to another, providing a ratiometric indication of cellular auxin levels.

By convention, auxin transport from the shoot and root apices to the root–shoot transition zone is referred to as a *basipetal* flow, whereas downward auxin flow in the root is referred to as *acropetal* transport. As this terminology can be confusing, a newer terminology assigns the term *rootward* transport to all auxin flows toward the root apex and the term *shootward* transport to any directional flow away from the root apex. Both shootward and rootward polar auxin transport are primary mechanisms for effecting programmed and plastic directional growth.

Polar transport proceeds in a cell-to-cell fashion, rather than via the symplasm; that is, auxin exits a cell through the plasma membrane, diffuses across the cell wall, and enters the next cell through its plasma membrane (**Figure 4.29**). The overall process requires metabolic energy, as evidenced by the sensitivity of polar transport to O_2 deprivation, sucrose depletion, and metabolic inhibitors. The velocity of polar auxin transport can exceed 10 mm h^{-1} in some tissues, which is faster than diffusion but much slower than phloem translocation rates (see Chapter 12). Polar transport is specific for all natural and some synthetic auxins; other weak organic acids, inactive auxin analogs, and IAA conjugates are poorly transported. Although polar auxin concentration gradients in the embryo appear to be initially established by localized auxin synthesis, they are amplified and extended by specific transporter proteins in the plasma membrane. The cellular processes that use the proton gradients generated by plasma membrane ATPases to generate polar auxin streams are described by the **chemiosmotic model** of auxin transport.

AUXIN UPTAKE IAA is a weak acid (pK_a 4.75). In the apoplast, where plasma membrane H^+-ATPases normally maintain a cell wall solution of pH 5 to 5.5, 15 to 25% of the auxin is present in a lipophilic, undissociated

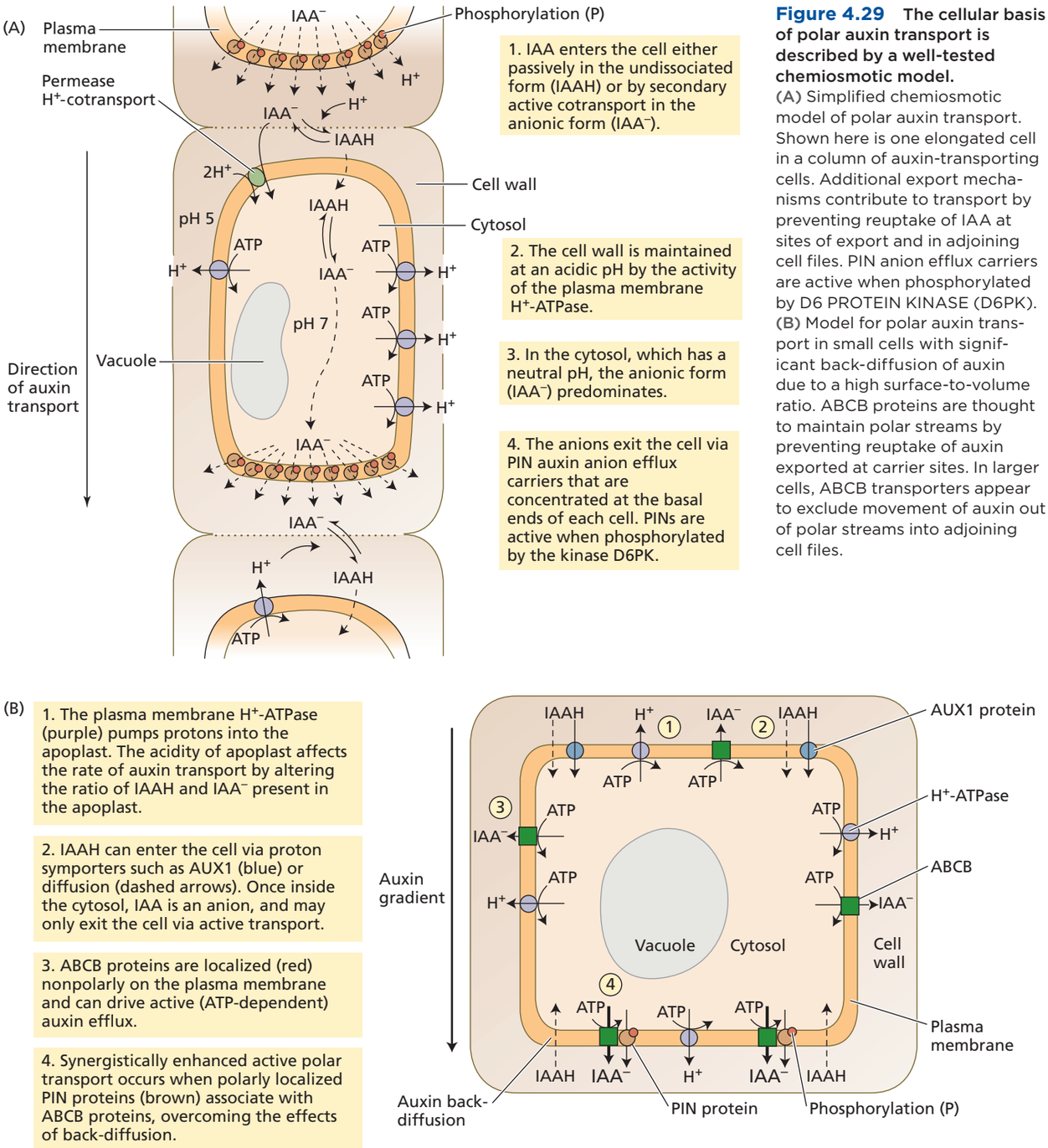


Figure 4.29 **The cellular basis of polar auxin transport is described by a well-tested chemiosmotic model.** **(A)** Simplified chemiosmotic model of polar auxin transport. Shown here is one elongated cell in a column of auxin-transporting cells. Additional export mechanisms contribute to transport by preventing reuptake of IAA at sites of export and in adjoining cell files. PIN anion efflux carriers are active when phosphorylated by D6 PROTEIN KINASE (D6PK). **(B)** Model for polar auxin transport in small cells with significant back-diffusion of auxin due to a high surface-to-volume ratio. ABCB proteins are thought to maintain polar streams by preventing reuptake of auxin exported at carrier sites. In larger cells, ABCB transporters appear to exclude movement of auxin out of polar streams into adjoining cell files.

form (IAAH) that diffuses passively across the plasma membrane down a concentration gradient. Therefore, auxin may enter the cell from any side. Auxin uptake is accelerated by secondary active transport (see Chapter 8) of the amphipathic, anionic IAA^- present in the apoplast via AUXIN1/LIKE AUXIN1 (AUX1/LAX) symporters that cotransport two protons along with the auxin anion. This secondary active transport of auxin allows for greater auxin accumulation than does simple diffusion because anionic auxin is driven across the membrane by the proton motive force (i.e., the high proton concentration in the apoplastic solution). Although

polarized localization of AUX1 on the plasma membrane occurs in some cells, such as the protophloem, the most important contribution of AUX1 is its role in creating cellular sinks that drive polar auxin transport streams. Shootward auxin flows in the *aux1* mutant of Arabidopsis are completely disrupted, resulting in agravitropic root growth; expression of *AUX1* under the control of a promoter associated with the lateral root cap completely restores gravitropic growth in this mutant. The compound 1-naphthoxyacetic acid is often used as an inhibitor of the auxin uptake activity of AUX1/LAX proteins. The NRT1.1 and 1.5 nitrate transporters, which are up-regulated under nitrogen-deficient conditions, also transport auxin, adding to the auxin uptake capacity of root cells.

AUXIN EFFLUX In the neutral pH of the cytosol, the anionic form of auxin, IAA^-, predominates. Transport of IAA^- out of the cell is driven by the negative membrane potential inside the cell. However, because the lipid bilayer of the membrane is impermeable to the anion, auxin export out of the cell must occur via transport proteins in the plasma membrane. Where **PIN auxin efflux carrier proteins** are polarly localized—that is, present on the plasma membrane at only one end of a cell—auxin uptake into the cell and subsequent efflux via PIN give rise to a net polar transport (see Figure 4.29B). The PIN family of proteins is named after the pin-shaped inflorescences formed by the *pin1* mutant of Arabidopsis (**Figure 4.30A**). Different PIN family members mediate auxin efflux in each tissue, and *pin* mutants exhibit phenotypes consistent with this function in these tissues. Of the PIN proteins, PIN1 is the most studied, as it is essential to virtually every aspect of polar development and organogenesis in plant shoots.

A subset of ATP-dependent transporters from the large superfamily of ATP-binding cassette (ABC) integral membrane transporters amplifies efflux and prevents reuptake of exported auxin, especially in small cells where auxin concentrations are high. Defective *ABCB* (ABC "B" class) genes in Arabidopsis, maize, and sorghum result in dwarf phenotypes of varying severity and in altered gravitropism and reduced auxin efflux (**Figure 4.30B**). In general, ABCBs are uniformly, rather than polarly, distributed in the plasma membranes of cells in shoot and root apices. However, when specific ABCB and PIN proteins co-occur in the same location in the cell, the directionality of auxin transport is enhanced; PINs

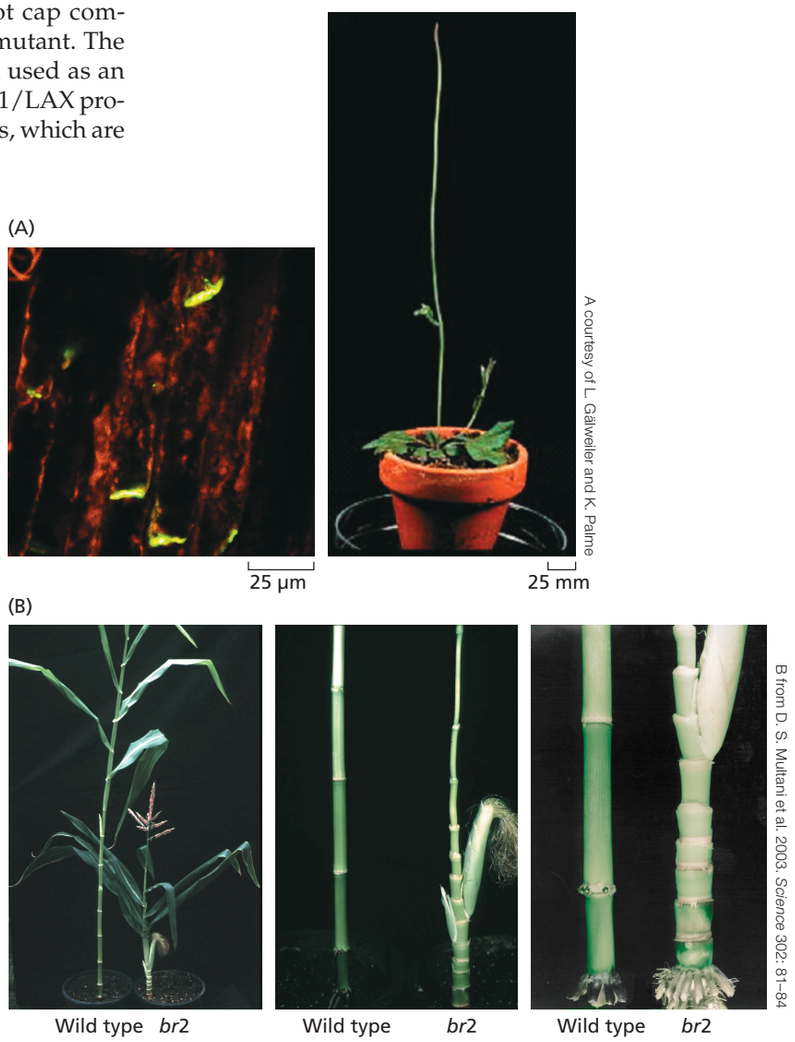


Figure 4.30 Phenotypes associated with the deletion of auxin efflux proteins. **(A)** PIN1 in Arabidopsis. (Left) Localization of the PIN1 protein at the basal ends of conducting cells in Arabidopsis inflorescences as seen by immunofluorescence microscopy. (Right) The *pin1* mutant of Arabidopsis. A normal wild-type Arabidopsis plant can be seen in Figure 17.1B. **(B)** The *BR2* (*Brachytic 2*) gene encodes an ABCB required for normal auxin transport in maize, and *br2* mutants have short internodes. The mutant was created by insertional mutagenesis with the Mutator transposon. Unknown to the investigators, the Mu8 transposon contained a fragment of the *BR2* gene. Expression of the *BR2* gene fragment produced interfering RNA (RNAi), which silenced *BR2* expression (see Chapter 3). The *br2* mutants have compact lower stalks (middle and right) but normal tassels and ear (left and middle).

function synergistically with ABCBs to stimulate polar auxin transport (see Figure 4.29B). The compound *N*-1-naphthylphthalamic acid (NPA) binds to ABCB auxin transport proteins and their regulators and is used as an inhibitor of both ABCB and PIN auxin efflux activity.

Auxin transport is regulated by multiple mechanisms

As would be expected for such an important function, auxin transport is regulated by both transcriptional and posttranscriptional mechanisms. Genes encoding enzymes that function in auxin metabolism (see **WEB APPENDIX 2**), signaling, and transport are regulated by developmental programs and environmental cues. Almost all known plant hormones have an effect on auxin transport or auxin-dependent gene expression. Auxin itself regulates expression of the genes encoding auxin transporters to increase or decrease their abundance and thus to regulate auxin levels.

As is common with many signal transduction pathways, phosphorylation of auxin transporters is a key regulatory mechanism. For instance, the AGC kinase D6PK activates the auxin transport activity of a subset of PIN proteins, and the phototropin 1 photoreceptor kinase inactivates the efflux activity of ABCB19 in phototropic responses (see Chapter 17). Membrane composition and cell wall structure also regulate transporter activity, as both PIN1 and ABCB19 localization in the plasma membrane is dependent on structural sterols or sphingolipids, and PIN1 polar localization is abolished in cellulose synthase–deficient mutants of Arabidopsis. Furthermore, some natural compounds, primarily flavonoids, function as auxin efflux inhibitors. Flavonoids act as reactive oxygen species (ROS) scavengers and are inhibitors of some metalloenzymes, kinases, and phosphatases. Their effects on auxin transport appear to result primarily from these activities.

Regulation of the cellular trafficking of auxin transport proteins to and from the plasma membrane plays a particularly important role in plant development. Specific chaperone proteins are required for successful direction of auxin transporters to the plasma membrane. For instance, the AXR4 protein regulates the trafficking of AUX1, and the immunophilin-like protein TWISTED DWARF 1 (named for the phenotype of the *twd1* mutant in Arabidopsis) regulates the folding and trafficking to the plasma membrane of multiple ABCB auxin transporters. But the most important cellular trafficking processes that regulate polar auxin transport in embryo development are those directing the polar localization of the PIN1 efflux transporter.

Fluorescent protein reporters such as DR-GFP/RFP and DII-Venus have been used to examine how microscopic auxin concentration gradients are reinforced by vectorial localization of PIN1 to form directional auxin transport streams as the embryo develops. In other words, small directional flows of auxin are amplified and stabilized by the establishment of transport proteins and vascular tissue in configurations that maintain directional flows of auxin to growing tissues. The auxin reporters have been extensively validated by comparisons with other auxin measurement methods, as summarized in **Table 4.1**.

Polar localization of the PIN auxin efflux proteins is thought to involve four processes:

- Initial isotropic (nondirectional) trafficking to the plasma membrane. Multiple experimental approaches show that trafficking of PINs to the plasma membrane involves conserved secretory processes (see Chapter 1).

Table 4.1 Methods used to determine auxin levels in plants

Method	Sensitivity	Specificity	Resolution	Comments
Mass spectroscopy	High	High	Tissue or organ level	Can discriminate between different forms of auxin
Immunodetection	Medium	Medium	Cellular	Depends on the accessibility of auxin to antibody binding and specificity of antibody
Reporters	High	High	Cellular	Indicates location of auxin-dependent responses, but reporter activity may in some cases be limited by other factors; these may be artificial promoters (DR5, DII-Venus) or fusions with auxin-responsive gene promoters
PIN localization	Medium	Medium	Cellular	Polarized distribution of PIN-fluorescent protein fusions is used to infer directional auxin flows

- "Transcytosis" and concentration in polarized plasma membrane domains. This process has been observed with PIN2 in mature epidermal cells in the root but is not well characterized and does not appear to be triggered by auxin accumulations. Moreover, PIN2 polar localization is much less dynamic and auxin-sensitive compared with PIN1 and is thought to be determined primarily by developmental programming. Polar alignments of PIN1 and PIN7 with auxin gradients observed during embryogenesis are presumed to result from transcytosis, but to date this has not been verified at the subcellular level. Polar localization and activity of PINs require the activity of the D6PK and PINOID AGC kinases. The name PINOID derives from the phenotypic similarity of the *pinoid* and *pin1* mutants of Arabidopsis.
- Stabilization via interactions with the cell wall. Genetic or pharmacological disruption of cell wall biosynthesis results in a complete loss of PIN1 polarity in Arabidopsis.
- During development, combinatorial phosphorylation of multiple sites on PIN1 by a subset of AGC kinases, which regulates and fine-tunes auxin efflux.

4.6 Hormonal Signaling Pathways

The sites of hormone action are cells that possess specific receptors that can bind the hormone and initiate a signal transduction cascade. Plants employ large numbers of receptor kinases and signal transduction kinases to bring about the physiological responses of hormone target cells. In this section we examine the types of receptors and signal transduction pathways that are associated with each of the main plant hormones.

The cytokinin and ethylene signal transduction pathways are derived from the bacterial two-component regulatory system

In bacteria, **two-component regulatory systems** are important signaling systems that mediate a wide range of responses to environmental stimuli. The two components of this signaling system consist of a membrane-bound histidine kinase **sensor protein** and a soluble **response regulator** protein (**Figure 4.31A**). Sensor proteins receive the input signal, undergo autophosphorylation on a histidine residue, and pass the signal on to response regulators by transferring the phosphoryl group to a conserved aspartate residue on the response regulator. The phosphorylation-activated response regulators, many of which function as transcription factors, then bring about the cellular response. Sensor proteins have two domains, an *input domain*, which receives the environmental signal, and a *transmitter domain*, which transmits the signal to the response regulator. The response regulator proteins also have two domains, a *receiver domain*, which receives the signal from the transmitter domain of the sensor protein, and an *output domain*, which mediates the response.

Modifications of this simple bacterial two-component system are found in the signal transduction pathways activated by the plant hormones cytokinin and ethylene. Cytokinin signaling is mediated by a phosphorylation relay system that consists of a transmembrane cytokinin receptor, a phosphotransfer protein, and a nuclear response regulator (**Figure 4.31B**). The cytokinin receptors, designated CRE1, AHK2, and AHK3 in Arabidopsis, are related in amino acid sequence to the histidine kinases in two-component systems. However, these cytokinin receptors are described as *hybrid sensor histidine kinases* since they contain both the bacterial sensor input and histidine kinase (transmitter) domains as well as the receiver domain of a bacterial response regulator protein.

It was originally assumed that cytokinin receptors are located in the plasma membrane, reflected in the name of the ligand binding domain, CYCLASE HISTIDINE KINASE ASSOCIATED SENSORY EXTRACELLULAR (CHASE). However, the majority of the cytokinin receptors of Arabidopsis and maize are actually in the ER membrane, with the CHASE domain in the ER lumen and the transmitter and receiver domains in the cytosol (**Figure 4.32**). Cytokinin binding to the CHASE domain of its receptor triggers autophosphorylation of a histidine residue on the transmitter domain, followed by transfer of this same phosphate to the aspartate residue on the receiver domain. The phosphate is then transferred to **ARABIDOPSIS HISTIDINE PHOSPHOTRANSFER** (**AHP**) proteins. The newly phosphorylated AHPs function as signaling intermediates that transmit membrane-perceived cytokinin signals to nuclear-localized response regulators (termed **ARABIDOPSIS RESPONSE REGULATOR**, or **ARR**) by transferring the phosphate group to an aspartate on the receiver domain of the ARR (see Figure 4.32). This phosphorylation of the ARRs alters their activity, which brings about the cellular response.

The ARR response regulators are encoded by multigene families. They fall into two basic classes: the **type-A ARR** genes, the products of which are made up solely of a receiver domain, and the **type-B ARR** genes, which also include an output domain containing DNA-binding transcription activation sites (see Figure 4.32). Type-A ARRs negatively regulate cytokinin signaling by interacting with other proteins in a manner dependent on the phosphorylation state of the type-A ARR. Type-B ARRs are activated by phosphorylation, which enables them to regulate the transcription of a set of target genes, including those encoding the type-A ARRs, and thereby bring about the cellular changes involved in the cytokinin response. A family of F-box proteins called KISS

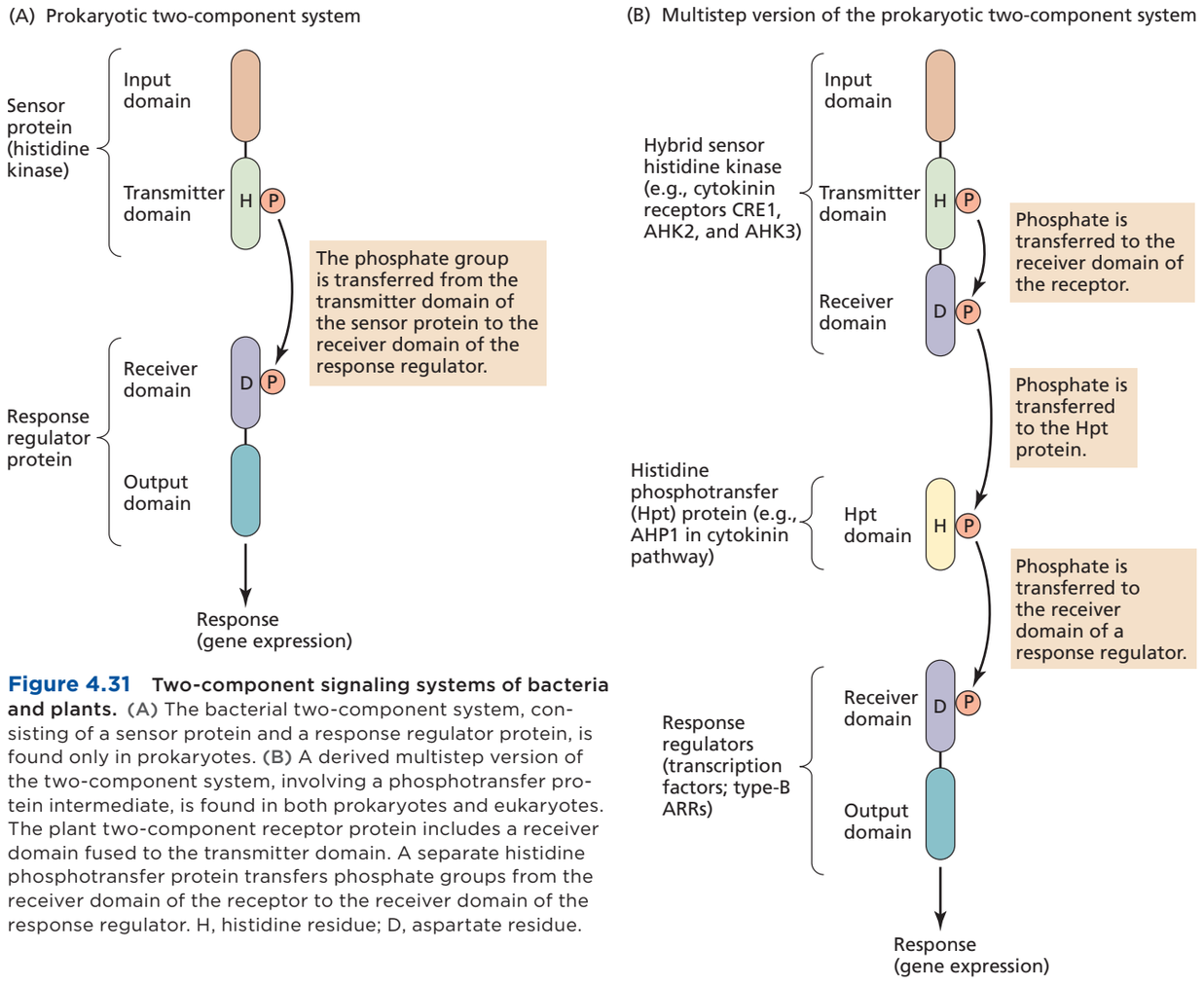


Figure 4.31 Two-component signaling systems of bacteria and plants. (A) The bacterial two-component system, consisting of a sensor protein and a response regulator protein, is found only in prokaryotes. (B) A derived multistep version of the two-component system, involving a phosphotransfer protein intermediate, is found in both prokaryotes and eukaryotes. The plant two-component receptor protein includes a receiver domain fused to the transmitter domain. A separate histidine phosphotransfer protein transfers phosphate groups from the receiver domain of the receptor to the receiver domain of the response regulator. H, histidine residue; D, aspartate residue.

ME DEADLY (KMD) negatively regulates the cytokinin response by targeting type-B ARR proteins for degradation via the E3 ubiquitin ligase complex, SCF^{KMD}.

Ethylene receptors are encoded by a multigene family (in Arabidopsis, ETR1, ETR2, ERS1, ERS2, and EIN4) that is also evolutionarily related to bacterial two-component histidine kinases. However, only two of the ethylene receptors in Arabidopsis (ETR1 and ERS1) have intrinsic histidine kinase activity, and this activity does not appear to play an essential role in signaling. In contrast to cytokinin signaling, the ethylene-signaling pathway thus does not involve a phosphorylation relay system. Ethylene receptors are localized to the ER membrane and interact with two downstream signaling proteins, CONSTITUTIVE TRIPLE RESPONSE 1 (CTR1) and ETHYLENE-INSENSITIVE 2 (EIN2) (**Figure 4.33**). CTR1 is a soluble serine/threonine kinase that is always physically associated with ethylene receptors. EIN2 is an ER transmembrane protein with a cytosolic C-terminal domain that is a target for CTR1 kinase activity. EIN2 is required to stabilize transcription factors of the ETHYLENE-INSENSITIVE 3 (EIN3)/ETHYLENE-INSENSTIVE LIKE (EIL) family, which activate the transcription of ethylene-responsive genes.

Ethylene receptors function as *negative regulators* that actively repress the hormone response in the absence of the hormone. In the absence of ethylene (when receptors are turned on), the ethylene receptors activate the CTR1 kinase, which then directly phosphorylates and thereby inactivates EIN2, which is ubiquitinated and turned over in the proteosome (see Figure 4.33). Active CTR1 is thus also a negative regulator of the ethylene response pathway.

When ethylene binds to the N-terminal transmembrane domain of the ethylene receptors on the lumen side of the ER, the receptors are inactivated and CTR1 is "switched off." This leads to the dephosphorylation of EIN2 by an as-yet-unidentified phosphatase and the

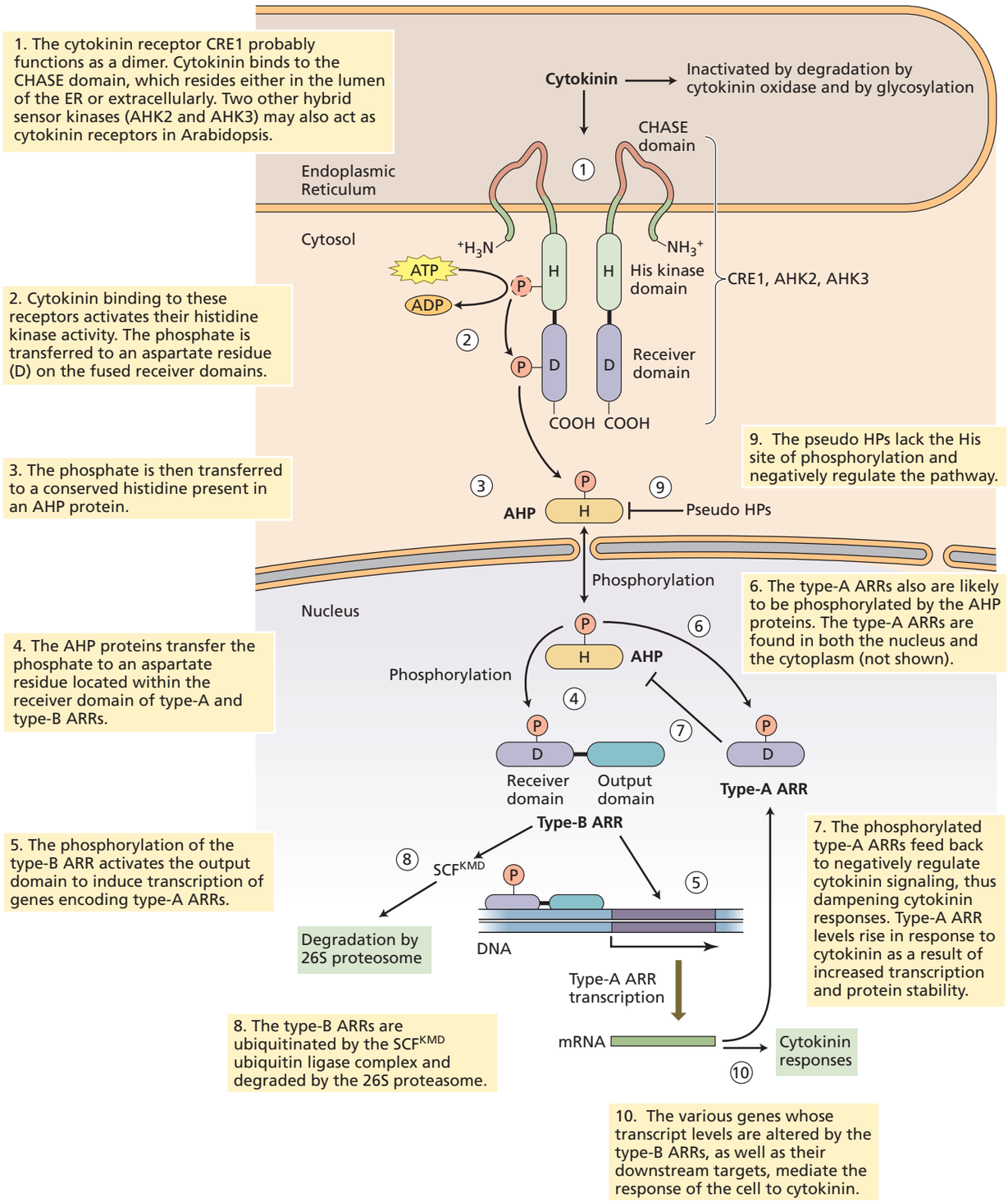


Figure 4.32 Model for the cytokinin signal transduction pathway. Cytokinin binds to the dimerized CRE1 receptor in the endoplasmic reticulum on the lumen side, which initiates a phosphorylation cascade leading to the cytokinin response. Pseudo HP inhibits cytokinin signaling by competing with AHP1-5 for phosphotransfer. AHP, Arabidopsis histidine phosophotransfer protein; ARR, Arabidopsis response regulator; KMDs, KISS ME DEADLY proteins.

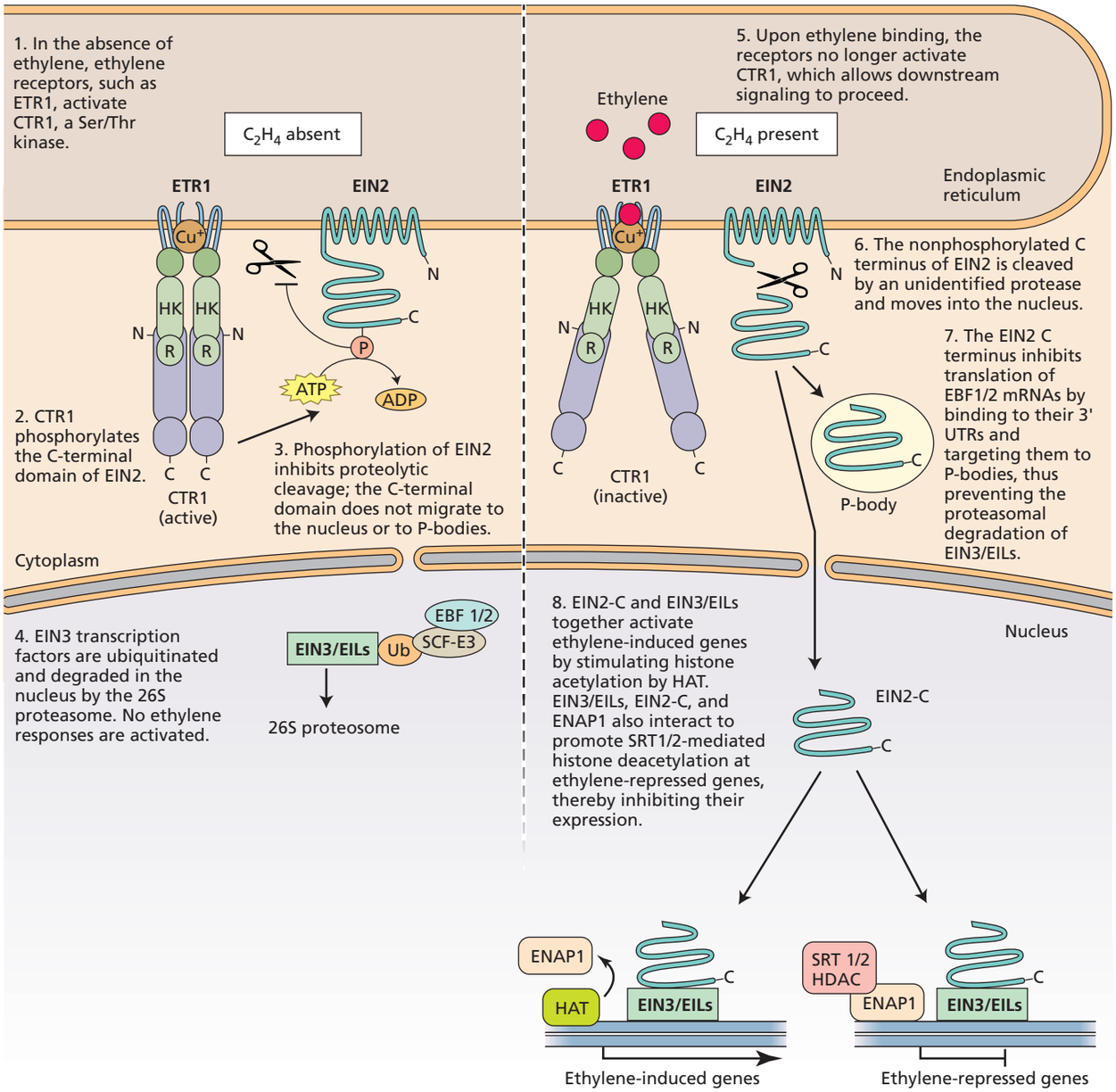


Figure 4.33 **Model of ethylene signaling in Arabidopsis.** Ethylene binds to ETHYLENE RECEPTOR 1 (ETR1), which is an integral membrane protein of the endoplasmic reticulum (ER) membrane. Multiple isoforms of ethylene receptors may be present in a cell; only ETR1 is shown here for simplicity. The receptor is a dimer, held together by disulfide bonds. Ethylene binds on the lumen side within the transmembrane domain, through a copper cofactor, which is assembled into the ethylene receptors. In the absence of ethylene, the kinase CONSITUTIVE TRIPLE RESPONSE 1 (CTR1; see Chapter 17) phosphorylates ETHYLENE-INSENSITIVE 2 (EIN2) to stabilize it and prevent cleavage of the EIN2 C terminus (EIN2-C). Binding of ethylene to the receptor inactivates CTR1, preventing phosphorylation of EIN2 and allowing cleavage of EIN2-C. EIN2-C inhibits degradation of the ETHYLENE-INSENSITIVE 3 (EIN3) and ETHYLENE-INSENSITVE LIKE (EIL) transcription factors, and moves to the nucleus where it interacts with EIN2 ASSOCIATED PROTEIN 1 (ENAP1) to activate ethylene-induced genes and with ENAP1-SRT1/2 to repress ethylene-inactivated genes. EIN2 also binds to the untranslated region of *ETHYLENE BINDING FBOX 1* and *2* (*EBF1/2*) mRNAs and directs them to P-bodies to prevent proteosomal degradation of EIN3/EILs. (After C. Ju and C. Chang. 2012. *AoB PLANTS* 2012: pls031.)

subsequent proteolytic cleavage of its cytosolic C terminus by an unidentified protease. Interaction of CTR1 with EIN2 and similar proteins also regulates the stability of the receptor to ensure that ethylene response mechanisms can rapidly reset. In the presence of ethylene, the cleaved C-terminus of EIN2 binds the 3′ untranslated region of *ETHYLENE BINDING FBOX 1* and *2* (*EBF1/2*) mRNAs to target them to P-bodies (see Chapter 3) for degradation. This prevents EBF1/2 activation of EIN3/EIL degradation via the proteosome. The released EIN2 C-terminal domain migrates into the nucleus where it associates with EIN2 ASSOCIATED PROTEIN 1 (ENAP1) to co-activate EIN3. ENAP1 is associated with chromatin, and its binding to the EIN2 C-terminal domain promotes EIN3 activity at ethylene-responsive genes by increasing access of histone acetyltransferase (HAT) to H3K23 acetylation sites that are associated with transcriptional *activation* (see Chapter 3). In the promoters of ethylene-repressed genes, the interaction between ENAP1, EIN3, and the EIN2 C terminus recruits the SRT1/2 histone deacetylase (HDAC) to deacetylate histone position H3K9 to *repress* transcription. In this way, the EIN2 C terminus acts to stabilize EIN3 as well as activate it. Depending on promoter sequence, transcription of ethylene-regulated genes is induced or repressed by interactions with EIN3/EIL transcription factors. Activation of ETHYLENE RESPONSE FACTOR1 (ERF1) and other transcription factors regulates a second level of ethylene responses to bring about the numerous changes in the function of plant cells in response to ethylene.

Receptor-like kinases mediate brassinosteroid and certain auxin signaling pathways

The largest class of plant receptor kinases consists of the receptor-like serine/threonine kinases (RLKs). Many RLKs localize to the plasma membrane as transmembrane proteins that harbor extracellular ligand-binding domains and cytoplasmic kinase domains, which relay information to the cell interior via phosphorylation of serine or threonine residues of target proteins. Some RLKs have also been shown to phosphorylate tyrosine residues. The ligands for several RLKs have been identified and include chemical signals produced by biotic interactors as well as endogenous plant hormones such as brassinosteroids, auxin, and peptide hormones.

The RLK-mediated brassinosteroid signaling pathway combines signal amplification and repressor inactivation strategies to transduce an extracellular brassinosteroid hormone signal into a transcriptional response. In brief, brassinolide binding to the brassinosteroid receptor kinase BRASSINOSTEROID-INSENSITIVE 1 (BRI1) in the plasma membrane triggers a phosphorylation cascade that causes a repressor protein, BRASSINOSTEROID INSENSITIVE 2 (BIN2), to become inactivated. This results in activation of the transcription factors BRI1-EMS SUPPRESSOR1 (BES1) and BRASSINAZOLE-RESISTANT 1 (BZR1) and subsequent gene expression (**Figure 4.34**).

The BRI1 receptor belongs to the plasma membrane leucine rich repeat (LRR) subfamily of RLKs and contains an N-terminal extracellular domain that binds brassinolide, a single transmembrane domain, and a cytoplasmic kinase domain with specificity toward tyrosine, serine, or threonine residues (see Figure 4.34). Upon binding brassinolide, homodimers of BRI1 are activated and heterooligomerize with the RLK BRI1-ASSOCIATED RECEPTOR KINASE1 (BAK1) (see Figure 4.34); both RLKs undergo auto- and transphosphorylation during activation. In the absence of brassinolide binding, BRI1 interacts with BRI1-KINASE INHIBITOR1 (BKI1), which prevents association with BAK1. Upon BRI1 activation, BKI1 is released from the plasma membrane, BRI1 and BAK1 dimerize, and BRI1 phosphorylates and activates the BR-SIGNALING KINASES (BSKs) and CONSTITUTIVE DIFFERENTIAL GROWTH1 (CDG1). When these plasma membrane–anchored receptor-like cytoplasmic kinases are activated, they phosphorylate and activate the serine/threonine phosphatase BRI1 SUPPRESSOR1 (BSU1). This, in turn, inactivates the repressor protein BIN2.

BIN2 is a serine/threonine protein kinase that, in the absence of brassinolide, negatively regulates the closely related transcription factors BES1 and BZR1 by phosphorylation. Phosphorylation of BES1/BZR1 by active BIN2 has at least two regulatory roles. First, BIN2-mediated phosphorylation of the transcription factors prevents them from shuttling to the nucleus and causes their retention in the cytosol. Second, phosphorylation prevents BES1/BZR1 from binding to target promoters, thus blocking their activity as transcriptional regulators.

In the presence of brassinolide, the activated phosphatase BSU1 dephosphorylates BIN2 and promotes its degradation by the 26S proteasome system, thus blocking its activity (see steps 5 and 6 in Figure 4.34B). BES1 and BZR1 are then dephosphorylated by protein phosphatase 2 A (PP2A), and the active forms of BES1 and BZR1 move into the nucleus where they regulate the expression of brassinolide response genes (see Figure 4.34B).

The core ABA signaling components include phosphatases and kinases

In addition to protein kinases, protein phosphatases (enzymes that remove phosphate groups from proteins) play important roles in signal transduction pathways. A well-described example is the PYR/PYL/RCAR-dependent signal transduction pathway of the hormone ABA. The **PYR/PYL/RCAR** members of the START (*ST*EROIDO-GENIC *A*CUTE *R*EGULATORY PROTEIN-RELATED LIPID-*T*RANSFER) domain protein superfamily, which

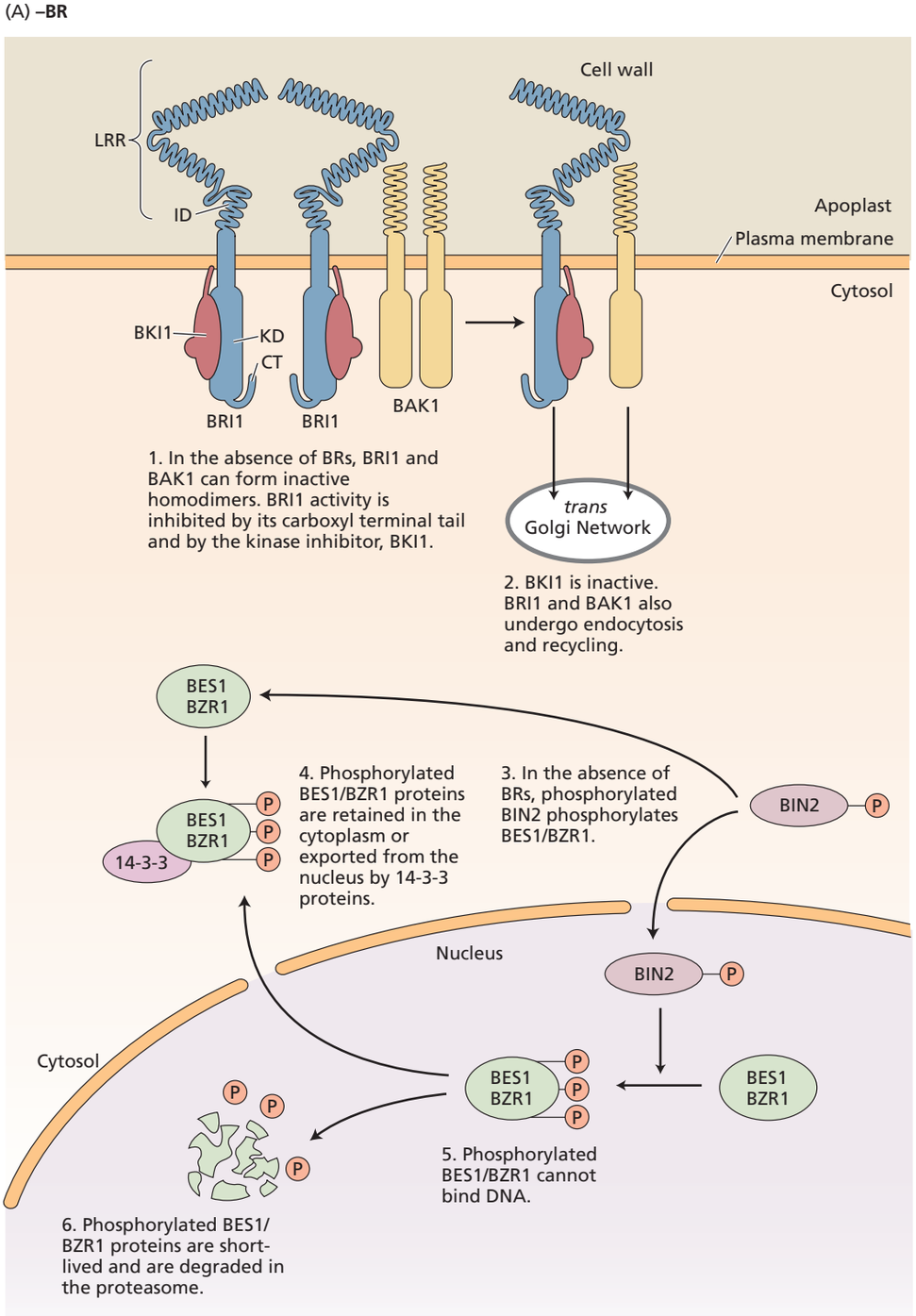


Figure 4.34 Brassinosteroid (BR) signal transduction pathway. The receptor BRI1 is localized in the plasma membrane. The extracellular region consists of a coiled stretch of leucine rich repeat (LRR) sequences containing an island domain (ID) that functions as part of the brassinolide (BL) binding site. The intracellular portion contains a kinase domain (KD) and the C-terminal tail (CT). (A) Without BR, BRI1 and BAK1 form inactive homodimers or are endocytosed and recycled. The BRASSINOSTEROID INSENSITVE 2 (BIN2) kinase is phosphorylated in the absence of BR and phosphorylates both BRI-EMS SUPRESSOR 1 (BES1) and BRASSINOZOLE RESISTANT 1 (BZR1). Phosphorylated BES1 and BZR1are excluded from the nucleus by 14-3-3 proteins and. Thus, prevented from activating target gene transcription.

(*Continued on next page*)

(B) **+BR**

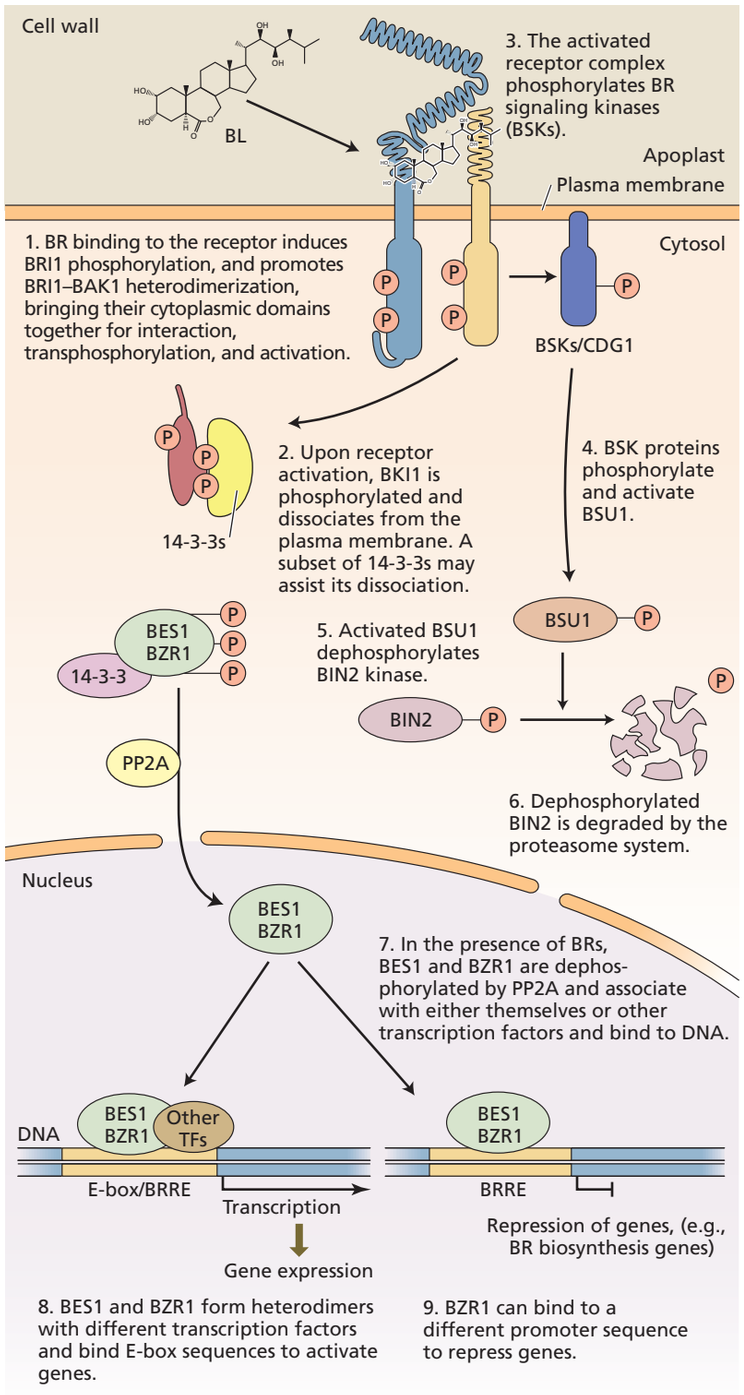


Figure 4.34 (*continued*) **(B)** In the presence of BR, BRI1 can heterodimerize and phosphorylate BR signaling kinases (BSKs) such as CONSTITUTIVE DIFFERENTIAL GROWTH 1. BSK phosphorylation of the phosphatase BRI SUPRESSOR 1 initiates degradation of BIN2, thuis allowing BES1 and BZR1 to activate or repress target gene transcription depending on interactions with other transcription factors that are associated with brassinosteroid response elements (BREEs). (After J. Jiang et al. 2013. *J. Integr. Plant Biol.* 55: 1198–1211.)

contains a predicted hydrophobic ligand-binding pocket, constitute the initial step of the core ABA signal transduction pathway. Fourteen members of this subfamily have been identified in Arabidopsis. Their nomenclature reflects their discoveries: PYRABACTIN RESISTANCE1 (PYR1) for resistance of its mutants to the synthetic sulfonamide compound pyrabactin, which mimics ABA action; PYR1-LIKE (PYL); and REGULATORY COMPONENTS OF ABA RECEPTORS (RCARs).

The PYR/PYL/RCAR protein subfamily is conserved among plants ranging from eudicots to mosses, and the proteins are located in both the cytosol and nucleus. They interact with PP2C phosphatases in an ABA-dependent manner to regulate the downstream activity of serine/threonine protein kinases of the **Sucrose non-Fermenting Related Kinase2** (**SnRK2**) family. In the absence of ABA, these PP2Cs bind to the C termini of SnRK2s and block SnRK2 kinase activity by removing phosphate groups from a region within the kinase domain termed the *activation loop* (**Figure 4.35A**). Because the same domain of the PP2Cs interacts with either the receptor or the kinase, these interactions are mutually exclusive for individual PP2C isoforms. ABA binding changes the conformation of PYR/PYL/RCAR receptors to permit or enhance interaction with PP2C and thereby repress PP2C phosphatase activity. This releases SnRK2 kinases from inhibition. SnRK2 proteins are then free to phosphorylate their many target proteins, including ion channels regulating stomatal aperture and the transcription factors that bind ABA response elements in gene promoters to activate ABA-responsive gene expression (**Figure 4.35B**). ABA signal transduction is therefore based on reversing the balance between PP2C protein phosphatase and SnRK2 kinase activities. As has been described for the auxin receptors, differences in expression of the receptors and PP2Cs, and in their affinities for ABA and each other, permit varied responses to a wide range of ABA concentrations in different cell types.

These same PP2Cs also interact with other proteins implicated in cellular ABA responses, including other protein kinases, Ca^{2+} sensor proteins, transcription factors,

and ion channels, presumably regulating their activity by dephosphorylating specific serine or threonine residues. The PYR/PYL/RCAR-dependent signaling pathway plays a major role in stomatal closing in response to ABA, which will be discussed in Chapter 15.

Plant hormone signaling pathways generally employ negative regulation

The majority of signal transduction pathways ultimately elicit a biological response by inducing changes in the expression of selected target genes. Most animal signal transduction pathways induce a response through the activation of a cascade of positive regulators. In contrast, *the majority of plant transduction pathways induce a response by inactivating repressor proteins*. For example, ethylene binding to ETR1 results in dissociation from the repressor CTR1 and activation of the transcription factor EIN3 (see Figure 4.33). Similarly, brassinosteroid binding to the receptor kinase BRI1 causes the repressor protein BIN2 to become inactivated, resulting in activation of the transcription factors BES1 and BZR1 (see Figure 4.34B).

Why have plant cells evolved signaling pathways based on negative regulation rather than the positive regulation seen in animal cells? Mathematical modeling of signal transduction pathways employing negative regulators suggests that negative regulators result in faster induction of downstream response genes. The speed of a response, particularly to an environmental stress such as drought, may be crucial to the survival of the sessile plant. Hence, the adoption by plants of negative regulatory signaling pathways in the majority of cases is likely to have conferred a selective advantage during evolution.

Several different molecular mechanisms have been described in plant cells to inactivate repressor proteins: These include dephosphorylation to modulate repressor activity, retargeting of the repressor to another cellular compartment, and degradation of the repressor protein. As noted earlier, protein dephosphorylation is employed by the brassinosteroid pathway to inactivate the repressor protein BIN2 (see Figure 4.34).

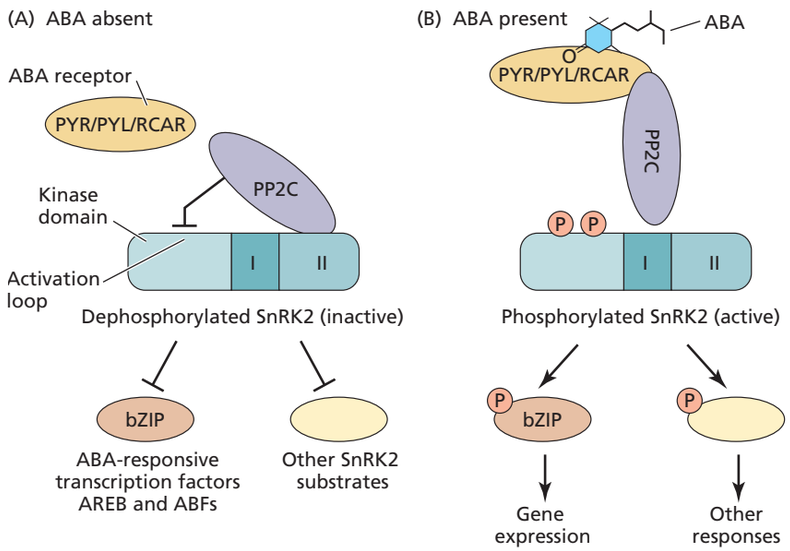
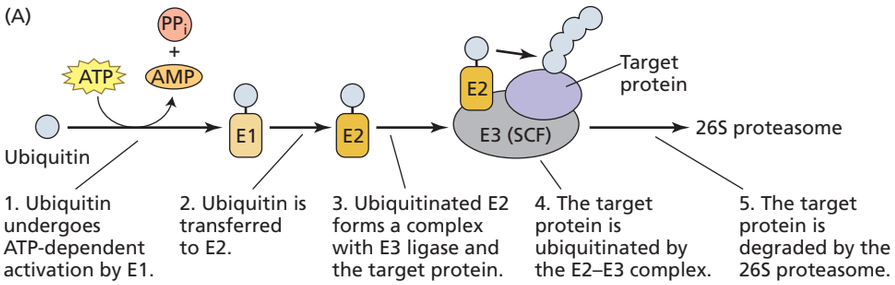
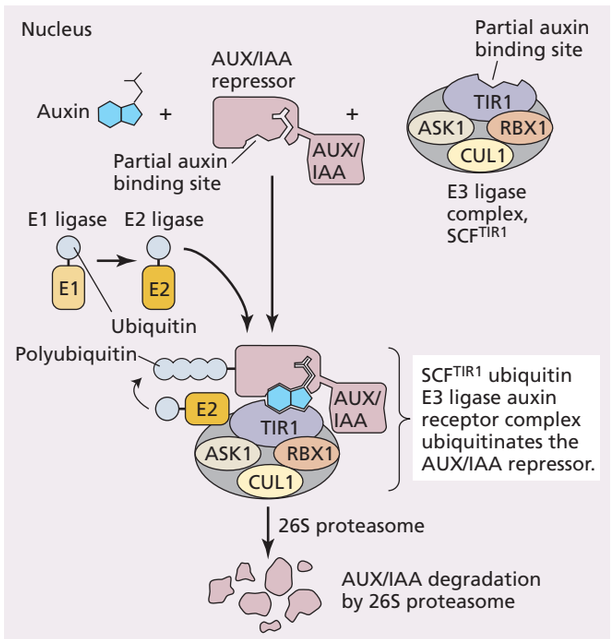


Figure 4.35 Abscisic acid (ABA) signaling involves kinase and phosphatase activities. (A) In the absence of ABA, the protein phosphatase PP2C dephosphorylates and inactivates the SnRK2 kinase. (B) In the presence of ABA, the ABA receptor protein PYR/PYL/RCAR interacts with PP2C, blocking phosphatase action and releasing SnRK2 from negative regulation. The activated SnRK2 phosphorylates ABA-responsive transcription factors (bZIP) and other unknown substrates to induce an ABA response. AREB, ABA response element binding protein; ABF, ABA response element binding factor; PP2C, protein phosphatase 2C; SnRK2,SUCROSE NONFERMENTING RELATED KINASE 2.

Several plant hormone receptors include components of the ubiquitination machinery and mediate signaling via protein degradation

Protein degradation as a mechanism to inactivate repressors of hormone responses was first described as part of the auxin signaling pathway. Since then, the **ubiquitin–proteasome pathway** has been shown to be central to most, if not all, hormone signaling pathways. In brief, a small protein called ubiquitin is first activated by an enzyme termed an *E1 ubiquitin-activating enzyme* in an ATP-dependent manner (**Figure 4.36A**; see also Figure 1.17). The ubiquitin tag is transferred to a second enzyme called an E2 ubiquitin-conjugating enzyme. This enzyme then associates with one of a family of large protein complexes called **S-phase kinase associated protein 1 (Skp1)/Cullin/F-box (SCF) complexes**, which function as E3 ubiquitin ligases. A superscript term is applied to an E3 ligase name (e.g., SCF^{TIR1}) to indicate which F-box protein the complex contains. Within a specific SCF protein complex, the Skp1 and Cullin components are abbreviated in all capitals (*e.g.* Arabidopsis SKP1 and CULLIN) as they are proteins that





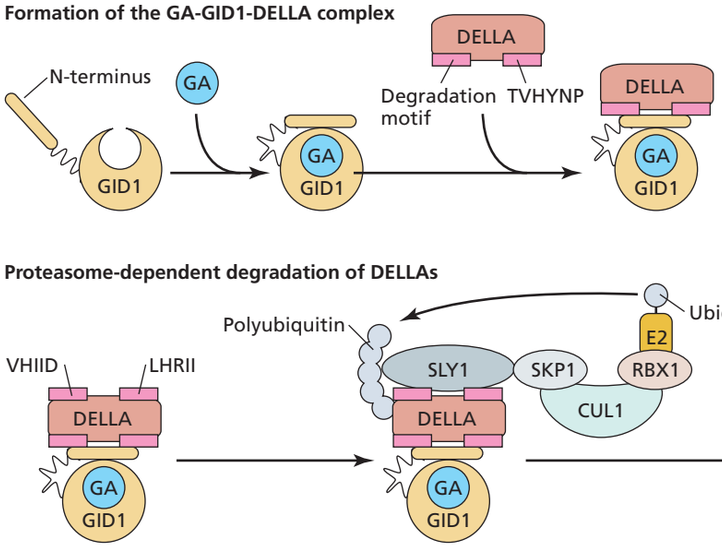


Figure 4.36 Signal transduction pathways in plants often function by inactivating repressor proteins. **(A)** Schematic diagram of the ubiquitin–proteasome degradation pathway, which occurs in both the cytosol and nucleus. **(B)** Binding of auxin to its receptor complex initiates ubiquitin-dependent degradation of the AUX/IAA repressor protein by the 26S proteasome. The auxin receptor is composed of two proteins: the SCF complex component TIR1 and the repressor protein AUX/IAA. Ubiquitin moieties are first activated by E1 ligase and added to target proteins by E2 ligase. TIR1 recruits AUX/IAA proteins to the SCF^{TIR1} complex in an auxin-dependent manner. Once recruited by auxin, AUX/IAA proteins are ubiquitinated by the E3 ligase activity of the SCF^{TIR1} complex, which marks the protein for destruction by the 26S proteasome. **(C)** Binding of gibberellin (GA) to its receptor leads to the degradation of the DELLA transactivating protein by the 26S proteasome. (Top) In the nucleus, gibberellin binds to the GID1 receptor and induces a conformational change in the N-terminal domain of the receptor, allowing the receptor to interact with the Thr-Val-His-Tyr-Asn-Proline (TVHYNP) and DELLA domains of the DELLA protein. (Bottom) Formation of the GID1-repressor complex promotes interactions between the E3 ubiquitin ligase SCF^{SLY} and the Val-His-Asp-Ile-Ile-Asp (VHIID) and Leu Heptad Repeat Protein Interaction (LHRII) motifs within the DELLA protein. This leads to the ubiquitination and degradation of the DELLA protein by the 26S proteasome. With no DELLA present, gene expression is activated where DELLA usually combines to with other trans-acting factors to repress transcription and decreases where DELLA functions as an activator. ASK1, ARABIDOPSIS SKP1-HOMOLOG 1; CUL1, CULLIN1; GID1, GIBBERELLIN INSENSITIVE DWARF 1; LHRII, leucine heptad repeat protein interaction motif; RBX1, RING BOX1; SCF, SKP1-CULLIN-F-Box E3 ligase complex, SLY- SLEEPY1 F-Box protein; TIR1, Transport Inhibitor of Auxin Resistant 1.

are encoded by a specific gene. F-box proteins typically recruit target proteins to the SCF complex so that they can be tagged with multiple copies of ubiquitin by the E3 ligase (see Figure 4.36A). Such polyubiquitination acts as a marker targeting the protein for degradation by the 26S proteasome, a large multiprotein complex that degrades ubiquitin-tagged proteins. In plants, the F-box gene family has been greatly expanded to many hundreds of genes, presumably involved in degrading a similar number of distinct targets. For instance, the KMD proteins described previously function as part of an SCF^{KMD} E3 ubiquitin ligase complex and directly interact with type-B ARR proteins to negatively regulate the cytokinin signaling pathway (see Figure 4.32).

Several of these F-box proteins are components of hormone receptor complexes, and in many hormone signaling pathways, the proteins targeted for degradation are transcriptional repressors (**Figure 4.36B and C**). This occurs in the signaling pathways of auxin, JA-Iles, and gibberellins—all small organic acids—demonstrating the adaption of a common mechanism to specific signals.

In the auxin signaling pathway, genes in the auxin receptor gene family, *TIR1/AFB1-5*, encode F-box components of the SCF complex that functions in the degradation of **AUXIN/INDOLE-3-ACETIC ACID** (**AUX/IAA**) repressors of auxin-responsive gene transcription (**Figure 4.37A**). Auxin-responsive genes typically have **auxin response element** (**AuxRE**) binding sites located in their promoter regions. **Auxin response factors** (**ARFs**) are transcription factors that bind to these AuxRE motifs and repress or activate transcription (see Figure 4.37A). When auxin concentrations are low, AUX/IAA repressor proteins form heterodimers with the ARFs and thus repress transcriptional activation. The AUX/IAA/ARF complexes also recruit chromatin remodeling factors via an interaction with the TOPLESS (TPL) protein. TPL recruits histone deacetylase (HDAC) to maintain the chromatin in a transcriptionally inactive state. In the presence of auxin, AUX/IAA repressors are recruited to the TIR1/AFB receptor complex and are tagged with ubiquitin for degradation by the 26S proteasome (see Figure 4.36B). This allows ARFs to dimerize or even oligomerize and activate gene transcription via recruitment of histone acetyltransferase (HAT). TIR1 and AUX/IAA therefore function as auxin co-receptors, with auxin acting as a "molecular glue" to promote ubiquitination and degradation of the AUX/IAA. Among the many target genes of this pathway are genes encoding auxin-metabolizing enzymes and AUX/IAA repressors, which eventually feedback on the system to reduce active auxin levels and terminate ARF-dependent signaling.

TPL can also directly interact with a specialized ARF (ARF3/ETTIN) that lacks an AUX/IAA interaction domain, but does have an auxin-binding site. When auxin binds to ARF3/ETTIN, TPL dissociates and transcription is de-repressed. This is the only known case where auxin promotes transcription without ubiquitination and degradation of an AUX/IAA repressor protein.

Jasmonates and gibberellins also promote the interaction between an F-box protein of a SCF ubiquitin E3 ligase and its transcriptional repressor target proteins (**Figure 4.37B and C**). The F-box protein CORONATINE-INSENSITIVE1 (COI1) functions as a JA-Ile receptor. Like auxin, JA-Ile promotes the interaction between COI1 and repressors of JA-Ile-induced gene expression called **JA-ILE ZIM-DOMAIN** (**JAZ**) proteins (see Figure 4.37B), thereby targeting JAZ proteins for degradation. Analogous to AUX/IAA proteins, JAZ repressor proteins suppress transcription of jasmonate-responsive genes, but in this case by binding to and repressing basic helix-loop-helix (bHLH) MYC transcription factors via interactions with TPL and a novel interacting protein, NINJA. JA-Ile-induced ubiquitin-dependent degradation of JAZ repressor proteins results in the release and activation of these transcription factors, triggering the induction of jasmonate-responsive gene expression.

Gibberellin signaling also involves components of the SCF complex (see Figure 4.37C). However, the gibberellin receptor **GIBBERELLIN INSENSITIVE DWARF 1** (**GID1**) does not itself function as an F-box protein. Instead, when GID1 binds gibberellin, the receptor undergoes a conformational change that promotes the binding of DELLA repressor proteins (see Figure 4.36C). This in turn induces a conformational change in the DELLA protein and facilitates the interaction of GID1-bound DELLA to SCF^{SLY1}, an E3 ubiquitin ligase in Arabidopsis that contains the F-box protein SLY1 (see Figure 4.36C). In effect, the binding of gibberellin receptor GID1 to DELLA repressor proteins triggers ubiquitination of the latter via the F-box protein SLY1 and subsequent degradation of DELLA proteins by the 26S proteasome. DELLA degradation results in the release and activation of **phytochrome interacting factor** (**PIF**) transcription factors, such as PIF3 and PIF4, as well as other bHLH transcription factors, thus triggering changes in gene expression. In another example, DELLA degradation results in increased expression of a transcriptional activator of α-*AMYLASE* gene expression; α-amylase activity is required for starch degradation during germination (see **WEB TOPIC 17.6**).

As the discussion here indicates, auxin, JA-Ile, and gibberellins signal by *directly* targeting the stability of nuclear-localized repressor proteins and thereby inducing a transcriptional response. Such a short signal transduction pathway provides the means for a very rapid change in nuclear gene expression. However, there is no opportunity for signal amplification as in the case of a signaling pathway involving a kinase cascade or second

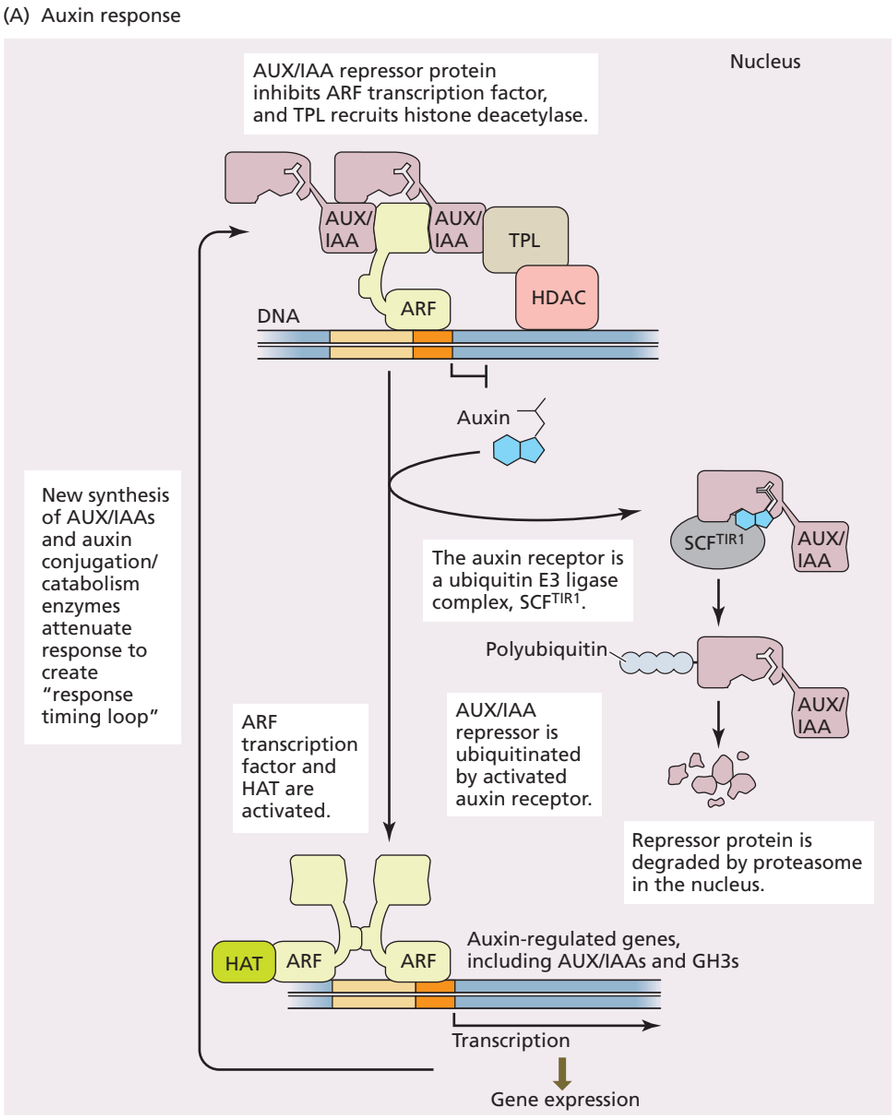
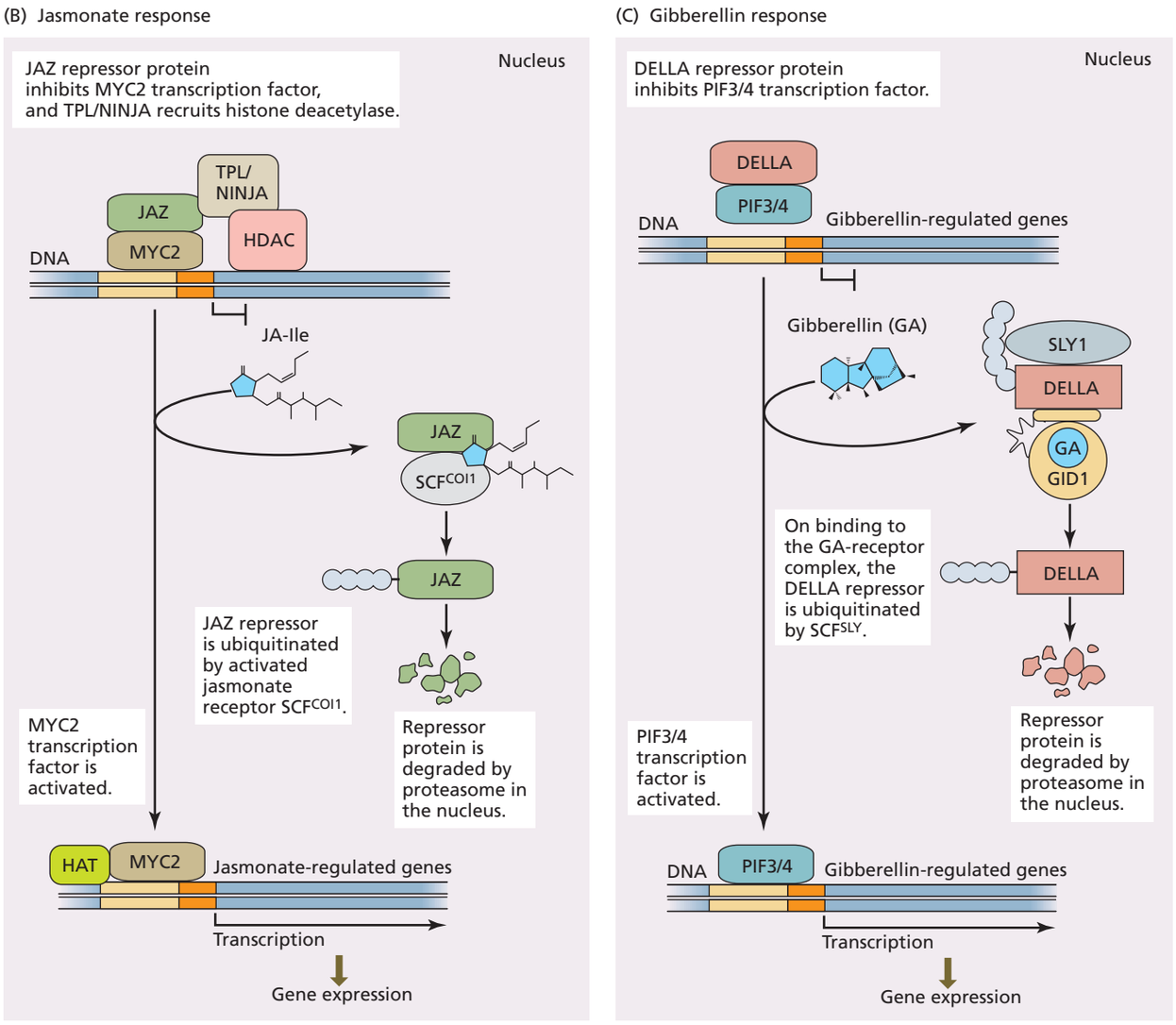


Figure 4.37 Several plant hormone receptors are part of SCF ubiquitination complexes. Auxin, JA-Ile (JA), and gibberellin (GA) signal by promoting interaction between components of the SCF ubiquitination machinery and repressor proteins operating in each hormone's signal transduction pathway. Auxin **(A)** and the jasmonate JA-Ile **(B)** directly promote interaction between the SCF^{TIR1} and SCF^{COI1}complexes and the AUX/IAA and JAZ repressors, respectively. The TOPLESS (TPL) protein functions as a co-repressor with AUX/IAAs and JAZ. In JAZ signaling, TPL functions as a co-repressor after co-recruitment with NINJA. TPL recruits histone deacetylase (HDAC) to the complex to keep the associated chromatin in a repressed state. Release of AUX/IAA and JAZ repression after hormone binding releases TPL and allows activation of the chromatin via histone acetyltransferase (HAT; see Chapter 3). The structural characteristics of the ARF and AUX/IAA proteins that function in auxin signaling have been determined by X-ray crystallography and are reflected in the figure. The structural characteristics of the JAZ repressor protein are only partially known. **(C)** In contrast, gibberellin additionally requires a separate receptor protein, GID1, to form the complex between SCF^{SLY1} and DELLA repressor proteins. In all three cases, addition of multiple ubiquitins (polyubiquitin) marks the repressor proteins for degradation. This triggers the activation of ARF, MYC2, and PIF3/4 transcription factors, resulting in auxin-, JA-Ile-, and gibberellin-induced changes in gene expression.

messengers. Instead, any resulting transcriptional response is directly related to the abundance of the signal molecule, since this determines the number of repressor molecules that are degraded. This important feature in the organization of signal transduction pathways may help explain why comparatively high concentrations of signals such as auxin and gibberellin are required to elicit a biological response.



Plants have evolved mechanisms for switching off or attenuating signaling responses

Arguably, the ability to switch off a response to a signal is just as important as the ability to initiate it. Plants terminate signaling through a variety of mechanisms.

As previously discussed, chemical signals such as plant hormones can be degraded or rendered inactive by oxidation or conjugation to sugars or amino acids. They may also be sequestered into other cellular compartments to spatially separate them from receptors.

Receptors and signaling intermediates that are activated by phosphorylation can be inactivated by phosphatase-mediated dephosphorylation. Activated components of the MAP kinase pathway, for example, are inactivated by MAP kinase phosphatases, ensuring tight cellular control over the duration and intensity of MAP kinase–mediated signaling (see Figure 4.4). Similarly, ion transporters and cellular scavengers can quickly lower elevated concentrations of second messengers to switch off signal amplification. As we have seen, protein degradation provides another mechanism for the plant cell to regulate the abundance of key components of the signal transduction pathway, such as the receptor or a transcription factor.

Feedback regulation represents another key mechanism employed to attenuate a response. For example, the *AUX/IAA* genes, which encode the AUX/IAA auxin repressor proteins, have auxin response element binding sites located in their promoter regions. Thus, AUX/IAA proteins can bind to the promoters of their own genes and repress their own expression. When auxin signaling

triggers the degradation of AUX/IAA repressors, the ensuing transcription of auxin response genes leads to the replacement of AUX/IAA proteins and thus to response attenuation or termination (see Figure 4.37A).

Hormone signaling pathways are often subject to several loops of negative feedback regulation. This is nicely illustrated by the gibberellin pathway (**Figure 4.38**). Bioactive gibberellin (GA_4 in this example) is synthesized through a complex biosynthetic pathway that involves multiple enzyme-catalyzed reactions. The last two enzymes in this pathway are encoded by members of the *GA20ox* and *GA3ox* gene families. As shown in Figure 4.38, in the absence of gibberellin, DELLA transcriptional regulators promote the expression of the genes coding for the GA20ox and GA3ox enzymes, which leads to increased gibberellin biosynthesis. At the same time, DELLA inhibits the expression of genes encoding the gibberellin catabolism enzyme GA2ox, which leads to decreased gibberellin degradation. As of result of these two effects of DELLA, gibberellin concentrations increase. In the presence of gibberellin, DELLA proteins are degraded by the proteasomal pathway. As a result, gibberellin biosynthesis decreases and gibberellin catabolism increases. Thus, gibberellin negatively regulates its own concentration in the cell. These positive and negative feedback loops help ensure that the appropriate gibberellin levels and responses are maintained during plant development.

GA responses are further regulated by light via the nuclear clock protein GIGANTEA (GI). GI is a component of the plant's circadian clock (see Chapter 19) and regulates multiple signaling mechanisms, including the sensing of sugars produced from photosynthesis. GI abundance increases as the day progresses and drops off over the course of the night. Because GI stabilizes the DELLA repressor and GI–DELLA interactions are enhanced at the onset of darkness, expression of GA-responsive genes is highly repressed at the end of the day and during most of the night. This effect decreases as the onset of daylight approaches. This regulation ensures that GA-regulated hypocotyl growth occurs when resources such as photosynthate are available. The timing of GI expression varies across Arabidopsis ecotypes with the latitude at which they were collected. This suggests that GI functions to optimize growth in relation to both day length and growing season.

The cellular response output to a signal is often tissue-specific

Many environmental and endogenous signals can trigger a variety of often highly diverse plant responses. Typically, particular tissue or cell types do not display the entire range of potential responses when exposed to a signal, but instead exhibit distinct response specificity. The plant hormone auxin, for example, promotes cell expansion in growing aerial tissues while inhibiting cell expansion in roots. It elicits lateral root initiation in a subset of cells of the root pericycle, induces leaf primordia at the shoot apical meristem, and controls vascular differentiation in developing plant organs. How can the developmental context of tissues and cells determine such diverse responses to one simple signal? As discussed, auxin signal transduction involves the auxin-dependent interaction of TIR1/AFB receptors and AUX/IAA repressor proteins, leading to AUX/IAA degradation and release of AUX/IAA-mediated repression of ARF transcription factor activity (see Figure 4.37A). All of these signaling components are encoded by multigene families (in Arabidopsis there are 6 *TIR1/AFB* genes, 29 *AUX/IAA*s, and 23 *ARF*s) and have distinct expression patterns, biochemical properties, and biological functions. Where within the plant these components are expressed, how highly they are expressed, the strength of their binding affinity, and the cellular auxin levels they experience all influence the shape of the final auxin response. For example, while it appears that all TIR1/AFBs can potentially interact with many different AUX/IAAs in an auxin-dependent manner, not all of these proteins are expressed in all cell types. Furthermore, the dosage at which auxin promotes these interactions varies significantly with different receptor/repressor combinations, such that some TIR1/AFB–AUX/IAA complexes form at very low auxin concentrations whereas others require substantially higher auxin levels to stably interact. In leaf primordia and floral gynoecia, ARF3 regulates auxin-dependent polar development without AUX/IAA interactions. Differential sensitivity and expression may also be mechanisms to achieve tissue specificity in other hormone signal transduction pathways where receptors or other signaling components are encoded by multigene families.

Hormone responses are modulated by other endogenous molecules

A great deal of what we know about hormone signaling in plants comes from experiments involving pharmacological hormone mimics and inhibitors. In some cases, mimics or inhibitors have been used to identify binding proteins that are potential hormone receptors. In other cases, pharmacological agents have been used to manipulate signaling pathways in ways that facilitate identification of enzymes, transporters, and receptors that are essential to hormone action. In addition to the primary hormones described here, there are many other plant compounds that function as modulators of signaling processes. In some cases, molecules that are structurally similar to primary hormones can act on receptors in specific cell types to produce actions similar to those of the related hormones. This phenomenon is observed with apocarotenoid compounds that are derived from the same biosynthetic pathways that yield abscisic acid and strigolactones. Molecules that

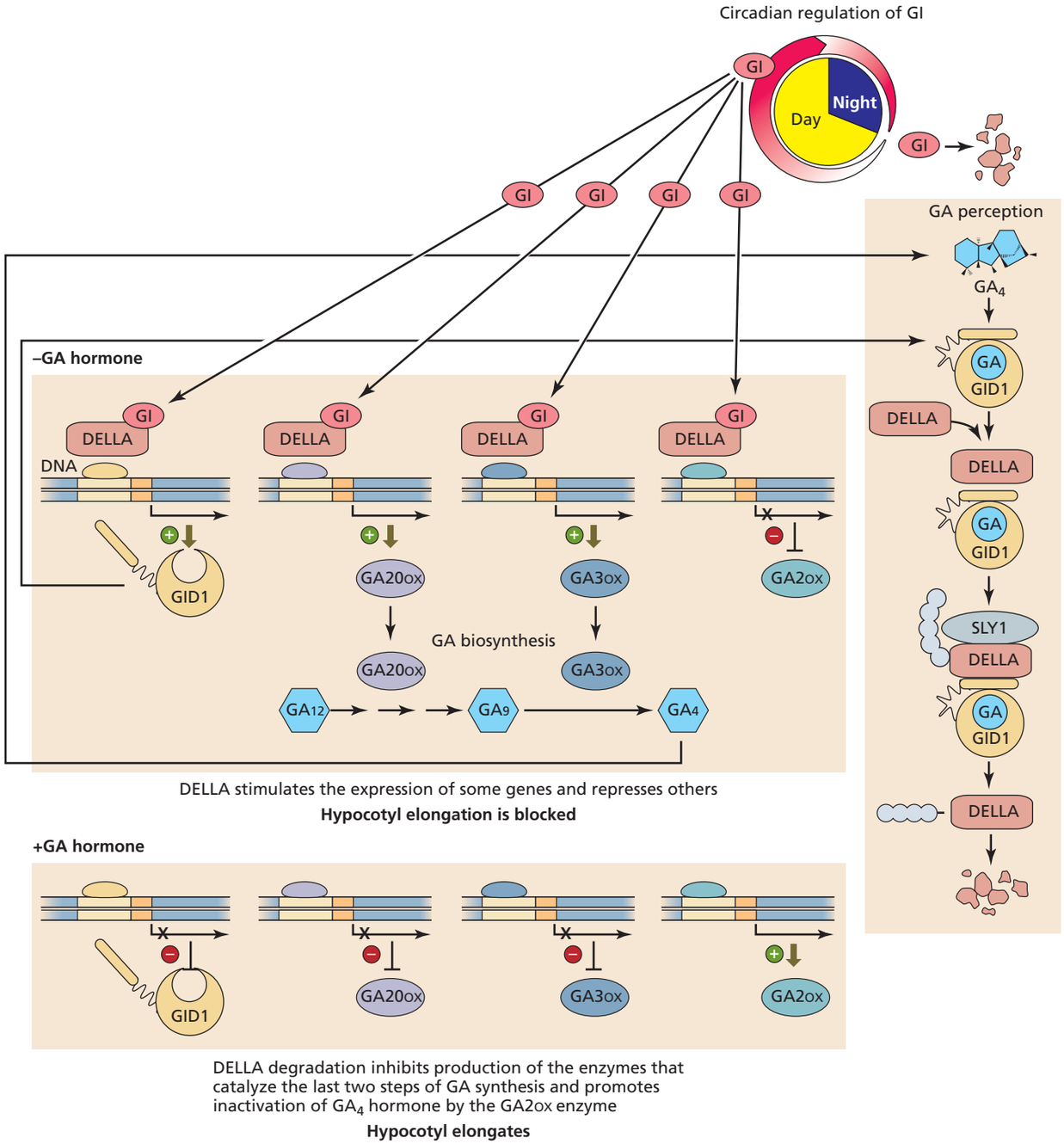


Figure 4.38 **The gibberellin (GA) response is regulated by a series of feedback loops comprising both gibberellin signal transduction and gibberellin biosynthesis.** *GID1* encodes the gibberellin receptor that binds the active hormone GA_4 and recruits DELLA transactivating proteins to the SCF^{SLY1} E3-ubiquitin ligase complex to trigger DELLA degradation. *GA20ox* and *GA3ox* encode enzymes that catalyze the last steps of the gibberellin biosynthetic pathway, while *GA2ox* encodes an enzyme that catabolizes bioactive gibberellin. In the absence of gibberellin, the DELLA proteins positively regulate *GID1*, *GA20ox*, and *GA3ox* (plus signs), and negatively regulate *GA2ox* (minus sign), while the converse occurs in the presence of gibberellin. GA responses are further regulated by the circadian clock whereby the nuclear transcription factor GIGANTEA (GI) stabilizes DELLA. As GI abundance increases over the course of the day, GI interactions with DELLA increase at the end of the day. This enhances DELLA regulation of GA-responsive gene expression. As GI levels fall off during the night, DELLA stability decreases, and DELLA regulation of GA-responsive gene expression feedback loop decreases. So, bioactive gibberellin and the GID1 receptor enhance DELLA degradation during the night, while GA2ox blocks DELLA degradation during the day.

are structurally similar to hormones may also compete for hormone transporters or binding sites. For example, some phenylpropanoid compounds such as *trans*-cinnamic acid appear to moderate auxin transport and response in this manner. Other molecules may protect signaling molecules from oxidation or turnover, as is seen with the decrease in nonenzymatic oxidation of auxin in the presence of endogenous flavonols and flavonol monoglycosides. Finally, some molecules may effect changes in the cellular environment that alter the activity of regulatory components of hormonal pathways. Many of these chemical modulators have more pronounced activity in a subset of plants as a result of selective pressures particular to that lineage.

Plants use electrical signaling for communication between tissues

Although plants lack nervous systems, they do employ long-distance electrical signaling to communicate between distant parts of the plant body. The most common type of electrical signaling in plants is the **action potential**, the transient depolarization of the plasma membrane of a cell generated by voltage-gated ion channels (see Chapter 8). Action potentials have been shown to mediate touch-induced leaflet closure in sensitive plant (*Mimosa pudica*; see Chapter 24), as well as the rapid closure (~0.1 s) of Venus flytrap, which occurs when an insect touches the touch-sensitive trigger hairs on the adaxial sides of the traplike leaf lobes (**Figure 4.39A**). Each touch of a trigger hair is detected by a mechanosensitive receptor that activates an initial Ca^{2+} influx and an action potential (electrical signal) characterized by K^+ efflux. To avoid accidental triggering of flytrap closure, either two hairs must be touched within 20 s of each other, or one hair must be touched twice in rapid succession to reach a threshold Ca^{2+} level (**Figure 4.39B**). A total of five action potentials are required to stimulate jasmonate signaling and the resultant production of digestive enzymes and other components of the "green stomach" that digests the prey.

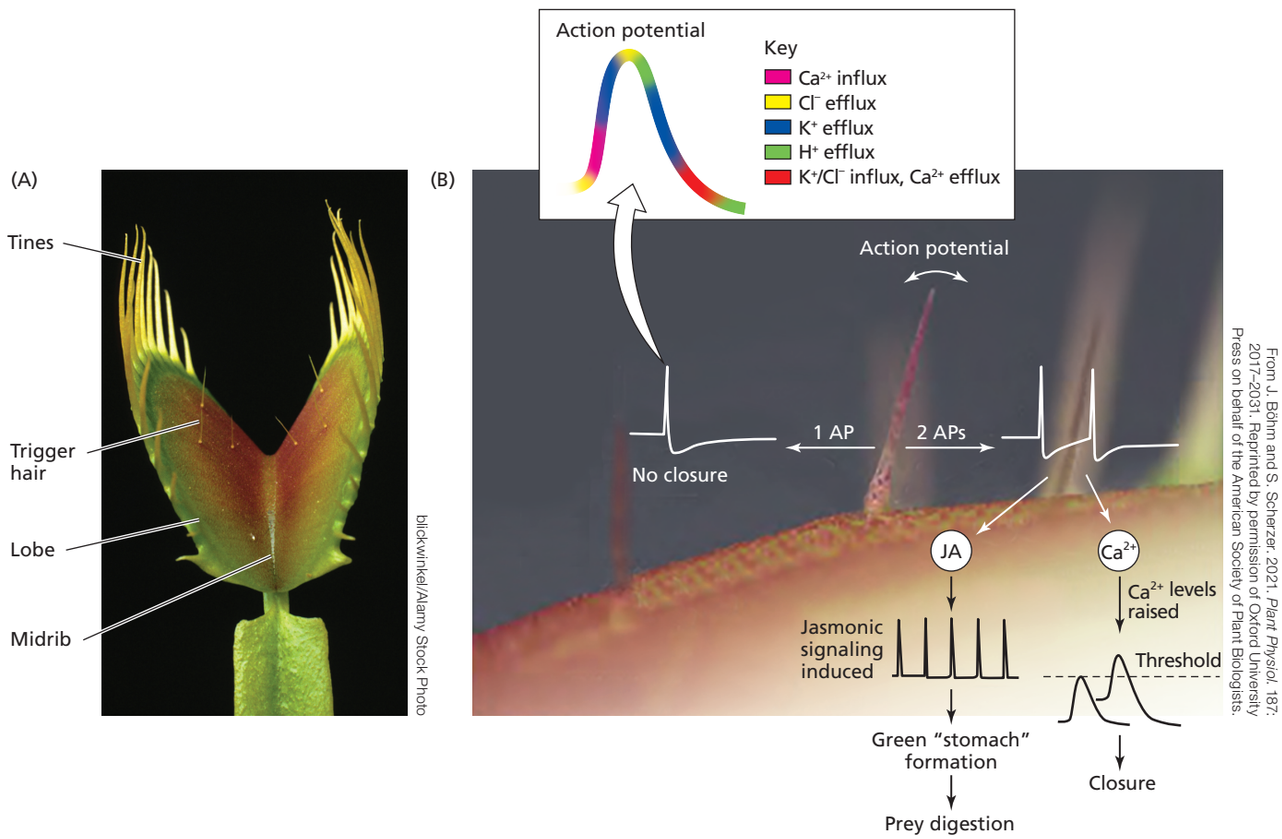


Figure 4.39 Electrical signaling in Venus flytrap (*Dionaea muscipula*). (A) Photograph of the snap-trap leaves with needlelike tines and touch-sensitive trigger hairs. (B) Action potentials (APs) associated with Ca^{2+} influx and K^+ efflux are triggered by movement of mechanosensitive channels in trigger hairs. Mechanical stimulation of the trigger hairs twice by a prey raises Ca^{2+} levels to a threshold that results in flytrap closure. Five triggering events are sufficient to induce jasmonate signaling that stimulates production of digestive enzymes and compounds that create the "green stomach" that digests the prey.

Electrical signaling has been shown to facilitate rapid communication between remote parts of plants in response to various types of stresses, indicating that electrical signaling is a general physiological feature of plants. As we will discuss in Chapter 24, electrical signals can be propagated throughout the plant via the vasculature in response to damage caused by chewing insects. However, unlike in animal nervous systems, plants lack synapses that transmit electrical signals from neuron to neuron via the secretion of neurotransmitters, and the signals travel much more slowly. The mechanism of electrical signal transmission along the vascular system of plants is still poorly understood.

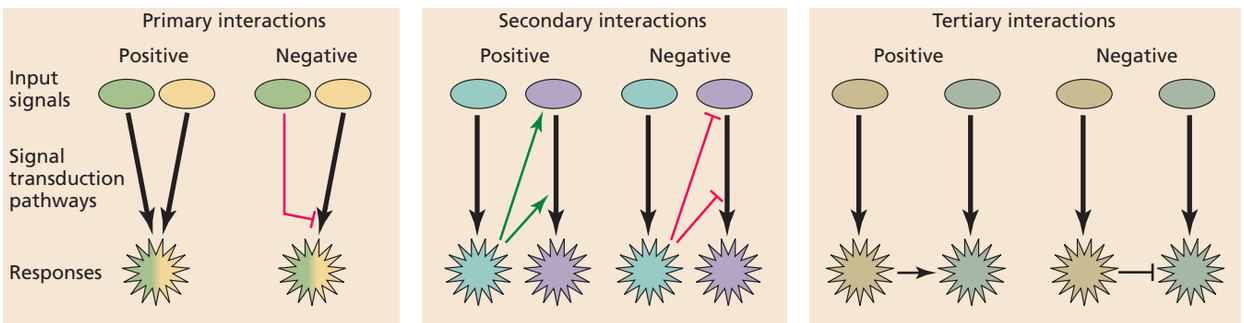
Cross-regulation allows signal transduction pathways to be integrated

Within plant cells, signal transduction pathways never function in isolation, but operate as part of a complex web of signaling interactions. These interactions account for the fact that plant hormones often exhibit *agonistic* (additive or positive) or *antagonistic* (inhibitory or negative) interactions with other signals. Classic examples include the antagonistic interaction between gibberellin and ABA in the control of seed germination (see Chapter 17).

The interaction between signaling pathways has been termed **cross-regulation**, and three categories have been proposed (**Figure 4.40**):

1. **Primary cross-regulation** involves distinct signaling pathways regulating a shared transduction component in a positive or a negative manner.
2. **Secondary cross-regulation** involves the output of one signaling pathway regulating the abundance or perception of a second signal.
3. **Tertiary cross-regulation** involves the outputs of two distinct pathways influencing each other.

Plant signaling is not based on a simple linear sequence of transduction events, but involves cross-regulation among many pathways. Understanding how such complex signaling pathways operate will demand a new scientific approach. This approach is often referred to as **systems biology** and employs mathematical and computational models to simulate these nonlinear biological networks and better predict their outputs.



Two input pathways regulate a single shared protein or multiple shared proteins controlling a response. Both pathways have the same effect on the response.

Two input pathways converge on shared protein(s), but one of the pathways inhibits the effect of the other.

Two input pathways regulate separate responses. In addition, one pathway enhances the input levels or perception of the other pathway.

As in the positive interaction, except that one pathway represses the input levels or perception of the other pathway.

The response of one of the signaling pathways promotes the response of the other pathway.

The response of one of the signaling pathways inhibits the response of the other pathway.

Figure 4.40 Signal transduction pathways operate as part of a complex web of signaling interactions. Three types of cross-regulation have been proposed: primary, secondary, and tertiary. Input signals are shown here as ovals, signal transduction pathways are indicated by heavy arrows, and responses (pathway outputs) are shown as stars. Green (positive) or red (negative) colored lines indicate where one pathway influences the other pathway. The three types of cross-regulation can be either positive or negative.

Summary

Both short- and long-term physiological responses to external and internal signals arise from the transformation (transduction) of signals into mechanistic pathways. In order to activate areas that may be distal from the initial signaling location, signaling intermediates are amplified before dissemination (transmission). Once in play, signaling pathways often overlap into complex signaling networks, a phenomenon termed cross-regulation, to coordinate integrated physiological responses.

4.1 Temporal and Spatial Aspects of Signaling

- Plants use signal transduction to coordinate both rapid and slow responses to stimuli (**Figures 4.1, 4.2**).

4.2 Signal Perception and Amplification

- Receptors are present throughout cells and are conserved among bacteria, plant, animal, and fungal kingdoms (**Figure 4.3**).
- Signaling intermediates must be amplified to prevent dilution of the signaling cascade; the MAPK amplification pathway is conserved among eukaryotes (**Figure 4.4**).
- Diversified families of plant receptor-like serine/threonine kinases (RLKs) function in pathogen responses as well as in growth and development (**Figure 4.5**).
- Signals can also be amplified by second messengers such as Ca^{2+}, H^+, reactive oxygen species (ROS), and modified lipids (lipid signaling molecules), although it can be challenging to parse their signaling targets (**Figure 4.6**).
- Modified lipids regulate growth and stress responses (**Figure 4.7**).

4.3 Hormones and Plant Development

- Hormones can signal cells within, nearby, or far away from their site of synthesis (**Figure 4.8**).
- Hormones are conserved chemical messengers that can, at very low concentrations, transmit signals between cells and initiate physiological responses (**Figure 4.9**).
- Except for ethylene, phytohormones contain ring structures (**Figure 4.10**).
- The first growth hormone to be identified was auxin, during studies of coleoptile bending due to phototropism (**Figure 4.11**).
- The gibberellin group of growth hormones can be used as growth regulators (**Figure 4.12**).
- Tissue-culture experiments revealed the role of cytokinins as cell division–promoting factors (**Figure 4.13**).
- Ethylene is a gaseous hormone that promotes fruit ripening and other developmental processes (**Figure 4.14**).
- Abscisic acid regulates seed maturation and stomatal closure in response to water stress (**Figure 4.15**).
- Brassinosteroids are lipid-soluble hormones that regulate many processes, including photomorphogenesis, germination, and floral sex identity (**Figure 4.16**).
- Strigolactones are derived from enzymatic cleavage of carotinoids and regulate branching from the primary root-shoot axis (**Figure 4.17**)

4.4 Phytohormone Metabolism and Homeostasis

- The concentration of hormones is tightly regulated so that signals produce timely responses without compromising sensitivity to the same signal in the future (**Figure 4.18**).
- Indole-3-acetic acid, the primary auxin, is synthesized from tryptophan with indole-3-pyruvate (IPyA) as an intermediate (**Figure 4.19**).
- Gibberellins (GAs) are all derived from GA_{12}, which is oxidized in the cytosol (**Figure 4.23**).
- Cytokinins are adenine derivatives (**Figure 4.24**). *KNOX* genes promote cytokinin concentrations in the shoot apical meristem while inhibiting gibberellin levels.
- Ethylene is synthesized from methionine (**Figure 4.25**) and diffuses rapidly out of plants as a gas; there is no evidence of ethylene catabolism.
- Abscisic acid is synthesized from 40-carbon carotenoids (**Figure 4.26**); its concentrations can fluctuate dramatically during developmental processes.
- Brassinosteroids are derived from campesterol, which is similar in structure to cholesterol (**Figure 4.27**).
- Strigolactones and other apocarotenoid signaling compounds are derived from carotenoids, similarly to abscisic acid (**Figure 4.28**).

4.5 Movement of Hormones within the Plant

- Auxin gradients and polar transport are central components of programmed and plastic development.
- Polar transport of auxin is driven by chemiosmotic gradients and is primarily regulated by polarized efflux carriers (**Figure 4.29**).
- Polar auxin transport regulates organogenesis and maintains the polarity of plant form (**Figure 4.30**).

4.6 Hormonal Signaling Pathways

- Cytokinin and ethylene pathways use derived two-component regulatory systems, which involve membrane-bound sensor proteins and soluble response regulator proteins (**Figures 4.31–4.33**).
- Brassinosteriod and certain auxin pathways use transmembrane receptor-like serine/threonine

Summary (*continued*)

kinases (RLKs) to phosphorylate serine or threonine regions of target proteins (**Figure 4.34**).

- Abscisic acid pathways modulate phosphatases and kinases via the PYL/PYR/RCAR receptor (**Figure 4.35**).
- Most plant hormone pathways employ negative regulators (inactivating repressors), allowing faster activation of downstream response genes (**Figures 4.36, 4.37**).
- Switching off signaling pathways is accomplished by degradation or sequestration of chemical signals via feedback mechanisms (**Figure 4.38**).
- Multiple receptor isoforms and modulators allow hormones to exhibit tissue- and organ-specific responses.
- Plants can also employ fast-acting, long-distance electrical signaling using action potentials, though the transmission of such signals is poorly understood (**Figure 4.39**).
- Integration of signal transduction pathways is accomplished through cross-regulation (**Figure 4.40**).

Suggested Reading

Davière, J.-M., and Achard, P. (2013) Gibberellin signaling in plants. *Development* 140: 1147–141.

Hwang, I., Sheen, J., and Müller, B. (2012) Cytokinin signaling networks. *Annu. Rev. Plant Biol*. 63: 353–380.

Jiang, J., Zhang, C., and Wang, X. (2013) Ligand perception, activation, and early signaling of plant steroid receptor brassinosteroid insensitive 1. *J. Integr. Plant Biol.* 55: 1198–1211.

Ju, C., and Chang, C. (2012) Advances in ethylene signalling: Protein complexes at the endoplasmic reticulum membrane. *AoB PLANTS* 2012: pls031.

Santner, A., and Estelle, M. (2009) Recent advances and emerging trends in plant hormone signaling. *Nature (Lond.)* 459: 1071–1078.

Suarez-Rodriguez, M. C., Petersen, M., and Mundy, J. (2010) Mitogen-activated protein kinase signaling in plants. *Annu. Rev. Plant Biol.* 61: 621–649.

Wang, X., Devaiah, S. P., Zhang, W., and Welti, R. (200) Signaling functions of phosphatidic acid. *Prog. Lipid Res.* 45: 250–278.

Testerink, C., and Munnik, T. (2011) Molecular, cellular, and physiological responses to phosphatidic acid formation in plants. *J. Exp. Bot.* 62: 2349–2361.



Dancestrokes/
Shutterstock

UNIT II

Transport and Translocation of Water and Solutes

CHAPTER 5 **Water and Plant Cells**

CHAPTER 6 **Water Balance of Plants**

CHAPTER 7 **Mineral Nutrition**

CHAPTER 8 **Solute Transport**



5 Water and Plant Cells



Dancestrokes/ Shutterstock

Water plays a crucial role in the life of the plant. Photosynthesis requires that plants obtain carbon dioxide from the atmosphere, and at the same time exposes them to water loss and the threat of dehydration. To prevent leaf desiccation, water must be absorbed by the roots and transported through the plant body. Imbalances between the uptake and transport of water and the loss of water to the atmosphere result in water deficits that can impair many cellular processes. Thus, balancing the uptake, transport, and loss of water represents an important challenge for land plants.

A major difference between plant and animal cells, which has a large impact on their respective water relations, is that plant cells have cell walls and animal cells do not (see Chapter 2). Cell walls allow plant cells to build up large internal hydrostatic pressures, called **turgor pressure**. In this chapter we consider how water moves into and out of plant cells, emphasizing the molecular properties of water and the physical forces that influence water movement at the cellular level.

5.1 Water in Plant Life

Of all the resources that plants need to grow and function, water is the most abundant and yet often the most limiting. The practice of crop irrigation reflects the fact that water is a key resource limiting agricultural productivity (**Figure 5.1**). Water availability likewise limits the productivity of natural ecosystems (**Figure 5.2**), leading to marked differences in vegetation type along precipitation gradients.

The reason water is frequently a limiting resource for plants, but much less so for animals, is that plants use water in huge amounts. Most (~97%) of the water absorbed by a plant's roots is carried through the plant and evaporates from leaf surfaces. Such water loss is called **transpiration**. In contrast, only a small amount of the water absorbed by roots actually remains in the plant to supply growth (~2%) or to be consumed in the biochemical reactions of photosynthesis and other metabolic processes (~1%).

Water loss to the atmosphere appears to be an inevitable consequence of carrying out photosynthesis on land. The uptake of CO_2 is coupled to the loss of water through a common pathway:

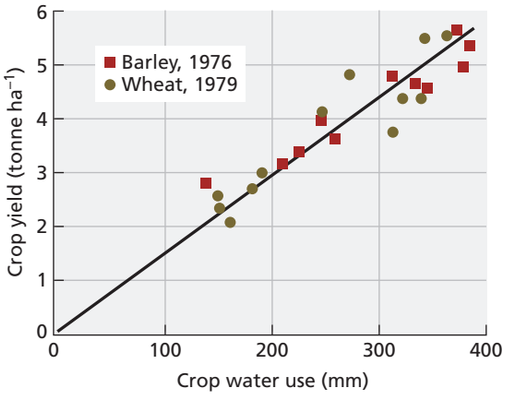


Figure 5.1 Grain yield as a function of water used under a range of irrigation treatments for barley in 1976 and wheat in 1979 in southeastern England. Crop water use is the total amount of water used during the growth of the crop expressed relative to the area over which the crop is grown (i.e., volume of water per area of land). (After H. Jones. 2013. *Plants and Microclimate: A Quantitative Approach to Environmental Plant Physiology* [3rd ed.]. Cambridge, UK: Cambridge University Press. Data from W. Day et al. 1978. *J. Agric. Sci.* 91: 599–623; P. Innes and R. D. Blackwell. 1981. *J. Agric. Sci.* 96: 603–610.)

as CO_2 diffuses into leaves, water vapor diffuses out. Because the driving gradient for water loss from leaves is much larger than that for CO_2 uptake, as many as 400 water molecules are lost for every CO_2 molecule gained. This unfavorable exchange has had a major influence on the evolution of plant form and function and explains why water plays such a key role in the physiology of plants.

We will begin our study of water by considering how its structure gives rise to some of its unique physical properties. We will then examine the physical basis for water movement, the concept of water potential, and the application of this concept to cell water relations.

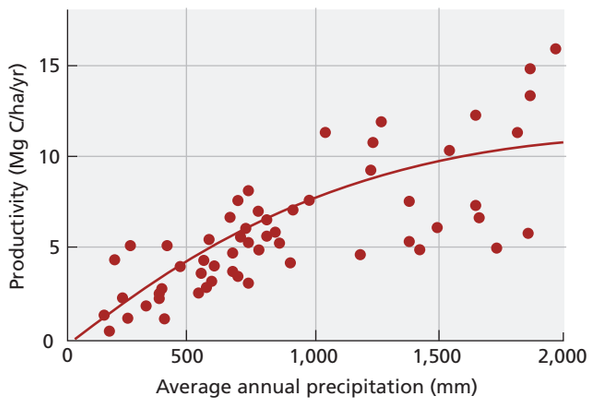


Figure 5.2 Productivity of various ecosystems worldwide as a function of annual pre-cipitation. Above 2,000 to 3,000 mm yearly precipitation productivity actually starts to decrease. (Mg = 10^6 g) (After E. A. Schuur. 2003. *Ecology* 84: 1165–1170.)

5.2 The Structure and Properties of Water

Water has special properties that enable it to act as a wide-ranging solvent and to be readily transported through the body of the plant. These properties derive primarily from the hydrogen bonding ability and polar structure of the water molecule. In this section we examine how the formation of hydrogen bonds contributes to the high specific heat, surface tension, and tensile strength of water.

Water is a polar molecule that forms hydrogen bonds

The water molecule consists of an oxygen atom covalently bonded to two hydrogen atoms (**Figure 5.3A**). Because the oxygen atom is more **electronegative** than hydrogen, it tends to attract the electrons of the covalent bond. This attraction results in a partial negative charge at the oxygen end of the molecule and a partial positive charge at each hydrogen, making water a **polar** molecule. These partial charges are equal, so the water molecule carries no *net* charge.

Water molecules are tetrahedral in shape. At two points of the tetrahedron are the hydrogen atoms, each with a partial positive charge. The other two points of the tetrahedron contain lone pairs of electrons, each with a partial negative charge. Thus, each water molecule has two positive poles and two negative poles. These opposite partial charges create electrostatic attractions between water molecules, known as **hydrogen bonds** (**Figure 5.3B**).

Hydrogen bonds take their name from the fact that effective electrostatic bonds are formed only when highly electronegative atoms such as oxygen are covalently bonded to hydrogen. The small size of the hydrogen atom allows the partial positive charges to be more concentrated, and thus more effective in bonding electrostatically.

Hydrogen bonds are responsible for many of the unusual physical properties of water. Water can form up to four hydrogen bonds with adjacent water molecules, resulting in very strong intermolecular interactions. Hydrogen bonds can also form between water and other molecules that contain electronegative atoms (O or N), especially when these are covalently bonded to H.

Water is an excellent solvent

Water dissolves greater amounts of a wider variety of substances than do other related solvents. Its versatility as a solvent is due in part to the small size of the water molecule. However, it is the hydrogen bonding ability

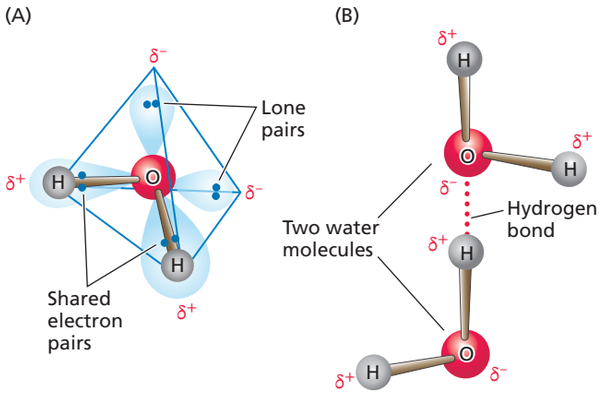


Figure 5.3 **Structure of the water molecule.** (A) Oxygen has six electrons in the outer shell; each hydrogen has one in the inner shell. The strong electronegativity of the oxygen atom means that the two electrons that form the covalent bond with hydrogen are unequally shared, such that each hydrogen atom has a partial positive charge. Each of the two lone pairs of electrons of the oxygen atom produces a partial negative charge. (B) The opposite partial charges (δ^- and δ^+) on the water molecule lead to the formation of intermolecular hydrogen bonds with other water molecules.

of water and its polar structure that make it a particularly good solvent for ionic substances and for molecules such as sugars and proteins that contain polar —OH or —NH_2 groups.

Hydrogen bonding between water molecules and ions, and between water and polar solutes, lowers the free energy of the solute molecules, which helps draw them into solution. Hydrogen bonding also decreases electrostatic interactions between solute molecules and thereby increases their solubility.

Water has distinctive thermal properties relative to its size

The extensive hydrogen bonding between water molecules results in water having both a high specific heat capacity and a high latent heat of vaporization.

Specific heat capacity is the heat energy required to raise the temperature of one unit of mass by one unit of temperature. Temperature is a measure of molecular kinetic energy (energy of motion). When the temperature of water is raised, the molecules vibrate faster and with greater amplitude. Hydrogen bonds act like rubber bands that absorb some of the energy from applied heat, leaving less energy available to increase motion. Thus, compared with other liquids, water requires a relatively large heat input to raise its temperature. This is important for plants because it helps buffer temperature fluctuations.

Latent heat of vaporization is the energy needed to separate molecules from the liquid phase and move them into the gas phase—a process that occurs during transpiration. The term *latent heat* refers to energy released or absorbed during a constant temperature process, in this case a phase change. The latent heat of vaporization decreases as temperature increases, reaching a minimum at the boiling point (100°C). For water at 25°C, the heat of vaporization is 44 kJ mol^{-1}—the highest value known for any liquid. Most of this energy is used to break hydrogen bonds between water molecules.

As anyone who has exited a swimming pool can attest to, evaporation cools the surface from which the liquid has evaporated. The reason for this is that only molecules with enough kinetic energy to overcome the intermolecular forces of the liquid phase are able to escape and enter the gas phase. This reduces the average kinetic energy, and thus the temperature, of the liquid phase. Because water has such a high latent heat of vaporization, it serves to moderate the temperature of transpiring leaves, which would otherwise increase due to the input of radiant energy from the sun.

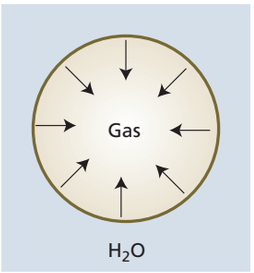
Water has a high surface tension

Water molecules at an air–water interface form fewer hydrogen bonds than water molecules in the bulk liquid. Because hydrogen bonds help balance water's polar charge distribution, water molecules at the surface are in an energetically unfavorable state compared with those surrounded on all sides by other water molecules. As a result, the most stable (i.e., lowest-energy) configuration is one that minimizes the surface area of the air–water interface. To increase the area of an air–water interface, water molecules must move from the bulk liquid to the interface, which requires an input of energy to compensate for the reduction in the number of hydrogen bonds formed by molecules at the surface. The energy required to increase the surface area of a gas–liquid interface is known as **surface tension**.

Surface tension can be expressed in units of energy per area (J m^{-2}) but is generally expressed in the equivalent units of force per length (J m^{-2} = N m^{-1}). A joule (J) is the SI unit of energy, with units of force × distance (N m); a newton (N) is the SI unit of force, with units of mass × acceleration (kg m s^{-2}).

Water has a high surface tension, one of the highest of any liquid. Because hydrogen bonds are attractive forces that pull water molecules together, an air–water interface behaves like a stretched elastic membrane. Surface tension thus describes the tendency of a gas–liquid interface to contract. If the air–water interface is curved, surface tension produces a net force perpendicular to the surface that is directed inward (**Figure 5.4**). An important consequence of this is that an air bubble suspended in water will be squeezed by the surface tension of the water that surrounds it.

The extensive hydrogen bonding in water also gives rise to the property known as **cohesion**, the mutual attraction between molecules. A related property, called



Surface tension of several liquids at 20°C (N/m)	
1% Gelatin	0.0083
Ethanol	0.0228
Phenol	0.0409
Water	0.0728

Figure 5.4 **A gas bubble suspended in a liquid assumes a spherical shape such that its surface area is minimized.** The magnitude of the pressure (force/area) exerted by the gas–liquid interface (arrows) is equal to $2T/r$, where T is the surface tension of the liquid (N/m) and r is the radius of the bubble (m). Water has an extremely high surface tension compared with other liquids at the same temperature.

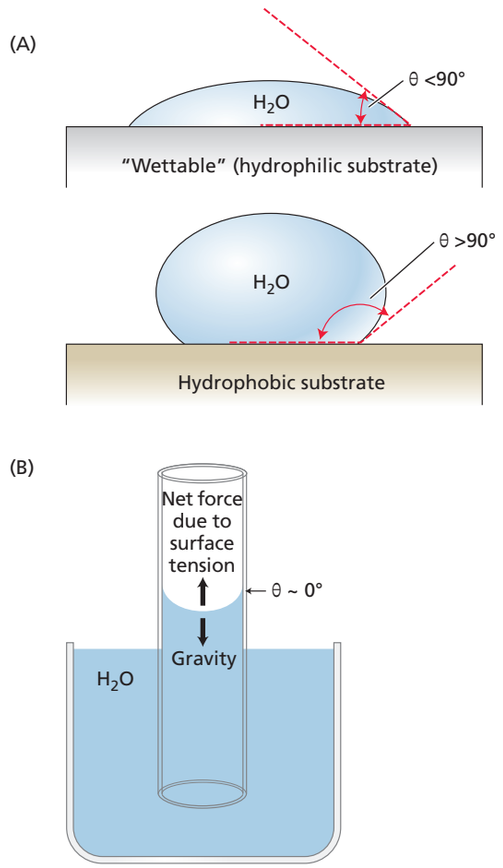


Figure 5.5 **The interaction of water with surfaces.** **(A)** The shape of a droplet placed on a solid surface reflects the relative attraction of the liquid to the solid versus to itself. The contact angle (θ), defined as the angle formed by the intersection of the liquid–vapor and the liquid–solid interface, is used to describe this interaction. "Wettable" surfaces have contact angles of less than 90°; a highly wettable (i.e., hydrophilic) surface (such as water on clean glass or primary cell walls) has a contact angle close to 0°. Water spreads out to form a thin film on highly wettable surfaces. In contrast, nonwettable (i.e., hydrophobic) surfaces have contact angles greater than 90°. Water "beads" up on such surfaces. **(B)** Capillarity can be observed when a liquid is supplied to the bottom of a vertically oriented capillary tube. If the walls are wettable (e.g., water on clean glass), the net force due to surface tension is upward. The water column rises until this upward force is balanced by the weight of the water column.

adhesion, is the attraction of water to a solid phase such as a cell wall or glass surface, which again is due primarily to the formation of hydrogen bonds. The degree to which water is attracted to the solid phase versus to itself can be quantified by measuring the **contact angle** (**Figure 5.5A**). Water tends to spread out (small contact angle) on a "wettable" substrate because the water can form hydrogen bonds with the solid. In contrast, water beads up on a nonwettable or hydrophobic substrate (large contact angle) because the water molecules have a more stable configuration when surrounded by other water molecules than when adjacent to the solid.

Cohesion, adhesion, and surface tension give rise to a phenomenon known as **capillarity** (**Figure 5.5B**). Consider a vertically oriented glass capillary tube with wettable walls (contact angle < 90°). At equilibrium, the water level in the capillary tube will be higher than that of the water supply at its base. Water is drawn into the capillary tube because of (1) the attraction of water to the polar surface of the glass tube (adhesion) and (2) the surface tension of water. Together, adhesion and surface tension pull on the water molecules, causing them to move up the tube until this upward force is balanced by the weight of the water column. The narrower the tube, the higher the equilibrium water level. For calculations related to capillarity, see **WEB TOPIC 5.1**.

Water has a high tensile strength

Hydrogen bonding gives water a high **tensile strength**, defined as the maximum force per unit area that a continuous column of water can withstand before breaking. We do not usually think of liquids as having tensile strength; however, such a property is evident in the rise of a water column in a capillary tube.

We can demonstrate the tensile strength of water by placing it in a clean glass syringe (**Figure 5.6**). When we *push* on the plunger, the water is compressed, and a positive **hydrostatic pressure** builds up. Pressure is measured in units called *pascals* (Pa) or, more conveniently, *megapascals* (MPa). One MPa equals approximately 9.9 atmospheres. Pressure is equivalent to a force per unit area (1 Pa = 1 N m^{-2}) and to an energy per unit volume (1 Pa = 1 J m^{-3}). **Table 5.1** compares units of pressure.

If instead of pushing on the plunger we *pull* on it, a tension, or *negative hydrostatic pressure*, develops as the water molecules resist being pulled apart. Negative

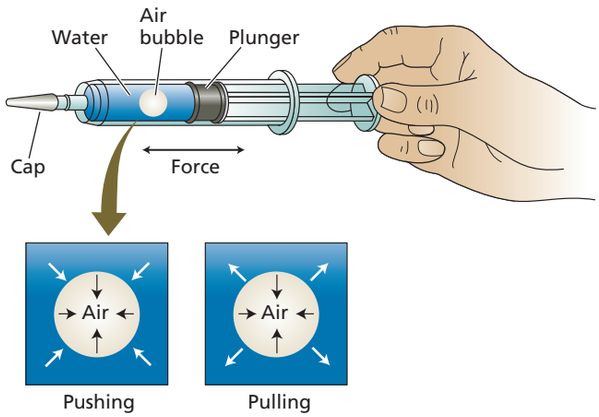


Figure 5.6 **A sealed syringe can be used to create positive and negative pressures in fluids such as water.** Pushing on the plunger causes the fluid to develop a positive, hydrostatic pressure (white arrows) that acts in the same direction as the inward force resulting from the surface tension of the gas–liquid interface (black arrows). Thus, a small air bubble trapped in the syringe will shrink as the pressure increases. Pulling on the plunger causes the fluid to develop a tension, or negative pressure. Air bubbles in the syringe will expand if the outward force on the bubble exerted by the fluid (white arrows) exceeds the inward force resulting from the surface tension of the gas–liquid interface (black arrows).

pressures develop only when molecules are able to pull on one another. Hydrogen bonds between water molecules allow tensions to be transmitted through water, even though it is a liquid. In contrast, gases cannot develop negative pressures because the interactions between gas molecules are limited to elastic collisions.

How hard must we pull on the plunger before the water molecules are torn away from each other and the water column breaks? Careful studies have demonstrated that water can resist tensions greater than 20 MPa. The water column in a syringe (see Figure 5.6), however, cannot sustain such large tensions because of the presence of microscopic gas bubbles in the bulk fluid or attached to the glass wall of the syringe. If the tension in the liquid, which exerts an outward-directed force on the gas–water interface, exceeds the inward-directed force resulting from surface tension, then the bubble will expand. This explains why gas bubbles interfere with the ability of the water in the syringe to resist the pull exerted by the plunger. The expansion of gas bubbles due to tension in the surrounding liquid is known as **cavitation**. As we will see in Chapter 6, cavitation can have a devastating effect on water transport through the xylem.

Table 5.1 **Comparison of units of pressure**

1 atmosphere	= 14.7 pounds per square inch
	= 760 mm Hg (at sea level, 45° latitude)
	= 1.013 bar
	= 0.1013 MPa
	= 1.013×10^5 Pa
A car tire is typically inflated to about 0.2 MPa.	
The water pressure in home plumbing is typically 0.2–0.3 MPa.	
The water pressure under 10 m (~30 feet) of water is 0.1 MPa.	

5.3 Diffusion and Osmosis

Cellular processes depend on the transport of molecules both to the cell and away from it. **Diffusion** is the net movement of substances from regions of higher to lower concentration. At the scale of a cell, diffusion is the dominant mode of transport. **Osmosis** is the net movement of a solvent across a selectively permeable barrier from a region of lower to higher solute concentration. Osmosis is a major factor governing the movement of water across selectively permeable cellular membranes.

Diffusion is the net movement of molecules by random thermal agitation

The molecules in a solution are not static; they are in continuous motion, colliding with one another and exchanging kinetic energy. The trajectory of any particular molecule after a collision is considered to be a random variable. Yet these random movements can result in the net movement of molecules.

Consider an imaginary plane dividing a solution into two equal volumes, A and B. As all the molecules undergo random motion, at each time step there is some probability that any particular solute molecule will cross our imaginary plane. The number we expect to cross from A to B in any particular time step will be proportional to the number at the beginning of the time step on side A, and the number crossing from B to A will be proportional to the number starting on side B.

If the initial concentration on side A is higher than that on side B, more solute molecules will be expected to cross from A to B than from B to A, and we will observe a net movement of solutes from A to B. Thus, diffusion results in the net movement of molecules from regions of high concentration to regions of low concentration, even though each molecule is moving in a random direction. The independent motion of each molecule explains why the system will evolve spontaneously—that is, without an input of energy—toward an equal number of A and B molecules on each side (**Figure 5.7**).

This tendency for a system to evolve toward an even distribution of molecules can be understood as a consequence of the second law of thermodynamics, which tells us that spontaneous processes evolve in the direction of increasing entropy, or disorder. Increasing entropy is synonymous with a decrease in free energy. Thus,

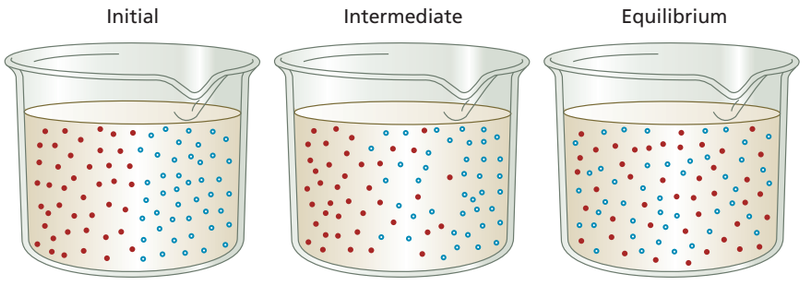


Figure 5.7 Thermal motion of molecules leads to diffusion—the gradual mixing of molecules and eventual dissipation of concentration differences. Initially, two materials containing different molecules are brought into contact. The materials may be gas or liquid. Diffusion is faster in gases and slower in liquids. With time, the mixing and randomization of the molecules diminish net movement. At equilibrium the two types of molecules are randomly (evenly) distributed.

diffusion represents the natural tendency of systems to move toward the lowest possible energy state.

In 1855, Adolf Fick showed that the rate of diffusion is directly proportional to the concentration gradient ($\Delta c_s/\Delta x$)—that is, to the difference in concentration of substance s (Δc_s) between two points separated by a very small distance Δx. In symbols, we write this relation as Fick's first law:

$$J_s = -D_s \frac{\Delta c_s}{\Delta x} \tag{5.1}$$

The rate of transport, expressed as the **flux density** (J_s), is the amount of substance s crossing a unit cross-sectional area per unit time (e.g., J_s may have units of moles per square meter per second [mol m^{-2} s^{-1}]). The **diffusion coefficient** (D_s, units of m^2/s) is a proportionality constant that measures how easily substance s moves through a particular medium. The diffusion coefficient is a characteristic of the substance (larger molecules have smaller diffusion coefficients) and depends on both the medium (diffusion is typically 10,000 times faster in air than in a liquid, for example) and the temperature (substances diffuse faster at higher temperatures). The negative sign in the equation indicates that the flux moves down a concentration gradient.

Fick's first law says that a substance will diffuse faster when the concentration gradient becomes steeper (Δc_s is large) or when the diffusion coefficient is increased. Note that this equation accounts only for movement in response to a concentration gradient, and not for movement in response to other forces (e.g., pressure, electric fields).

Diffusion is most effective over short distances

Consider a mass of solute molecules initially concentrated around a position $x = 0$ (**Figure 5.8**). As the molecules undergo random motion, the average position of the solute molecules remains at $x = 0$ for all time, but the distribution flattens out, as shown for two later time points (see curves 2 and 3 in Figure 5.8). Comparing the distribution of the solutes at the three times, we see that as the substance diffuses away from the starting point, the concentration gradient becomes less steep (Δc_s decreases). As a result, the rate at which solute molecules spread out from $x = 0$ is reduced.

The average time for a particle to diffuse a distance L grows as L^2/D_s. In other words, the average time required for a substance to diffuse a given distance increases as the *square* of that distance. This scaling relationship reflects the "random walk" of diffusion—the fact that each molecule is as likely to move toward some point as away from it.

The diffusion coefficient for glucose in water is about 10^{-9} m^2 s^{-1}. Thus, the average time required for a glucose molecule to diffuse across a cell with a diameter of 50 μm is 2.5 s. However, the average time needed for

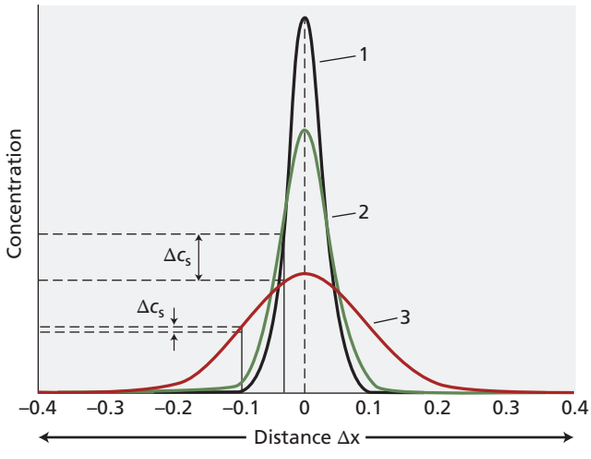


Figure 5.8 Graphical representation of the concentration gradient of a solute that is diffusing according to Fick's first law. The solute molecules were initially located in the plane indicated on the x-axis ("0"). Curve 1 shows the distribution of solute molecules shortly after placement at the plane of origin. Note how sharply the concentration drops off as the distance, *x*, from the origin increases. Curves 2 and 3 shows the solute distribution at two later time points. The average distance of the diffusing molecules from the origin has increased, and the slope of the gradient has flattened out. (After S. Briggs et al. 2014. *J. Rock Mech. Geotech. Eng.* 6: 535–545. © 2014 Institute of Rock and Soil Mechanics, Chinese Academy of Sciences. CC BY-NC-ND 3.0)

the same glucose molecule to diffuse a distance of 1 m in water is approximately 32 years. These values show that diffusion in solutions can be effective within cellular dimensions but is far too slow to be effective over long distances. For additional calculations on diffusion times, see **WEB TOPIC 5.2**.

Osmosis describes the net movement of water across a selectively permeable barrier

Membranes of plant cells are **selectively permeable**; that is, they allow water and other small, uncharged substances to move across them more readily than larger solutes and charged substances. If the concentration of solutes that do not move easily across the membrane is greater in the cell than in the solution surrounding it, water will move spontaneously (i.e., without an input of energy) into the cell. The net movement of water across a selectively permeable barrier toward a region of higher solute concentration is referred to as *osmosis*.

What causes water to move across a membrane into a region with higher solute concentration? As solutes "bounce" off the membrane, they hinder the movement of water molecules toward the membrane. This means that fewer water molecules pass through the membrane from the side with a higher solute concentration. On the side of the membrane without solutes, water molecules move randomly in all directions, including toward the membrane. As a result, the net movement of water across the membrane is toward the side with higher solute concentration.

We can also understand osmosis in relation to the second law of thermodynamics. We saw earlier that the tendency of all systems to evolve toward increasing entropy results in solutes spreading out through the entire available volume. In osmosis, the volume available for solute movement is restricted by the membrane, and thus entropy maximization is realized by the volume of solvent diffusing through the membrane to dilute the solutes. Indeed, in the absence of any countervailing force, *all* the available water will flow to the solute side of the membrane.

Let's imagine what happens when we place a living cell in a beaker of pure water. The presence of a selectively permeable membrane means that water will move into the cell until one of two things happens: (1) The increase in cell volume causes the selectively permeable membrane to rupture, allowing solutes to diffuse freely, or (2) the increase in cell volume is mechanically constrained by the presence of a cell wall such that the driving force for water to enter the cell is balanced by a pressure exerted by the cell wall.

The first scenario describes what would happen to an animal cell, which lacks a cell wall. The second scenario is relevant to plant cells. The plant cell wall is very strong. The resistance of cells walls to deformation creates an inward force that raises the hydrostatic pressure within the cell.

We will soon see how osmosis drives the movement of water into and out of plant cells. First, however, let's discuss the concept of a composite or total driving force, representing the free-energy gradient of water.

5.4 Water Potential

All living things, including plants, require a continuous input of free energy to maintain and repair their highly organized structures, as well as to grow and reproduce. Processes such as biochemical reactions, solute accumulation, and long-distance transport of water and solutes are all driven by an input of free energy. In thermodynamics, free energy represents the potential for performing work, including the work associated with moving water. (For a detailed discussion of the thermodynamic concept of free energy, see **WEB APPENDIX 1**.) In this section we examine how concentration, pressure, and gravity influence the free energy of water and thus affect the movement of water in plants.

The chemical potential of water represents the free-energy status of water

Chemical potential is a quantitative expression of the free energy associated with a substance. The unit of chemical potential is energy per mole of substance ($J\ mol^{-1}$). Note that chemical potential is a relative quantity: It represents the difference between the potential of a substance in a given state and the potential of the same substance in a standard state.

Historically, plant physiologists have most often used a related parameter called **water potential**, defined as the chemical potential of water divided by the partial molal volume of water (the volume of 1 mol of water): 18×10^{-6} $m^3\ mol^{-1}$. Water potential is thus a measure of the free energy of water per unit volume ($J\ m^{-3}$). These units are equivalent to pressure units such as the pascal, which is the common measurement unit for water potential.

Water potential plays a central role in plant physiology because it describes the potential energy that can cause water to move from one part of the plant to another. Water flows spontaneously (i.e., without an input of energy) from regions of higher water potential to regions of lower water potential. Let's look more closely at the important concept of water potential.

Three major factors contribute to water potential

The major factors influencing the water potential in plants are *concentration*, *pressure*, and *gravity*. Water potential is symbolized by Ψ (the Greek letter psi), and the water potential of solutions may be dissected into individual components, usually written as the following sum:

$$\Psi = \Psi_s + \Psi_p + \Psi_g \qquad (5.2)$$

The terms Ψ_s and Ψ_p and Ψ_g denote the effects of solutes, pressure, and gravity, respectively, on the free energy of water. (Alternative conventions for expressing the components of water potential are discussed in **WEB TOPIC 5.3**.) Water potentials are defined in relation to a reference, analogous to how the contour lines on a map specify the distance above sea level. The reference state most often used to define water potential is pure water at ambient temperature and standard atmospheric pressure. The reference height is generally set either at the base of the plant (for whole-plant studies) or at the level of the tissue under examination (for studies of water movement at the cellular level). Let's consider each of the terms on the right-hand side of Equation 5.2.

SOLUTES The term Ψ_s, called the **solute potential** or **osmotic potential**, represents the effect of dissolved solutes on water potential. Solutes reduce the free energy of water by diluting the water. This is primarily an entropy effect; that is, the mixing of solutes and water increases the disorder or entropy of the system and thereby lowers the free energy. This means that *the osmotic potential is independent of the specific nature of the solute*. For dilute solutions of nondissociating substances such as sucrose, the osmotic potential may be approximated by:

$$\Psi_s = -RTc_s \tag{5.3}$$

where R is the gas constant (8.32 J mol^{-1} K^{-1}), T is the absolute temperature (Kelvin, or K), and c_s is the solute concentration of the solution, expressed as **osmolarity** (moles of total dissolved solutes per volume of water [mol L^{-1}]). The minus sign indicates that dissolved solutes reduce the water potential of a solution relative to the reference state of pure water.

Equation 5.3 is valid for "ideal" solutions. Real solutions frequently deviate from the ideal, especially at high concentrations—for example, greater than 0.1 mol L^{-1}. Temperature also affects water potential (see **WEB TOPIC 5.4**). In our treatment of water potential, we will assume that we are dealing with ideal solutions.

PRESSURE The term Ψ_p, called the **pressure potential**, represents the effect of hydrostatic pressure on the free energy of water. Positive pressures raise the water potential (indicating an increase in free energy); negative pressures reduce it. Both positive and negative pressures occur within plants. The positive hydrostatic pressure in cells is referred to as *turgor pressure*. Negative hydrostatic pressures, which frequently develop in xylem conduits, are referred to as **tension**. As we will see, tension is important in moving water long distances through the plant. The question of whether negative pressures can occur in living cells is considered in **WEB TOPIC 5.5**.

Hydrostatic pressure is often measured as the deviation from atmospheric pressure. Remember that water in the reference state is at atmospheric pressure, so by this definition $\Psi_p = 0$ MPa for water in the standard state. Thus, the value of Ψ_p for pure water in an open beaker is 0 MPa, even though its absolute pressure is approximately 0.1 MPa (1 atmosphere).

GRAVITY Gravity causes water to move downward unless the force of gravity is opposed by an equal and opposite force. The **gravitational potential** (Ψ_g) depends on the height (h) of the water above the reference-state water, the density of water (ρ_w), and the acceleration due to gravity (g). In symbols, we write the following:

$$\Psi_g = \rho_w g h \tag{5.4}$$

where $\rho_w g$ has a value of 0.01 MPa m^{-1}. Thus, raising water a distance of 10 m translates into a 0.1 MPa increase in water potential.

The gravitational component (Ψ_g) is generally omitted in considerations of water transport at the cellular level, because differences in this component among neighboring cells are negligible compared with differences in the osmotic potential and the pressure potential. Thus, in these cases Equation 5.2 can be simplified as:

$$\Psi = \Psi_s + \Psi_p \tag{5.5}$$

Water potentials can be measured

Cell growth, photosynthesis, and crop productivity are all strongly influenced by water potential and its components. Plant scientists have thus expended considerable effort in devising accurate and reliable methods for evaluating the water status of plants.

The principal approaches for determining Ψ use either a psychrometer, of which there are two types, or a pressure chamber. Psychrometers take advantage of water's large latent heat of vaporization, which allows accurate measurements of (1) the vapor pressure of water in equilibrium with the sample or (2) the transfer of water vapor between the sample and a solution of known Ψ_s. The pressure chamber measures Y by applying external gas pressure to an excised leaf until water is forced out of the living cells.

In some cells, it is possible to measure Ψ_p directly by inserting a liquid-filled microcapillary that is connected to a pressure sensor into the cell. In other cases, Ψ_p is estimated as the difference between Ψ and Ψ_s. Solute concentrations (Ψ_s) can be determined using a variety of methods, including psychrometers and instruments that measure freezing point depression. A detailed explanation of the instruments that have been used to measure Ψ, Ψ_s, and Ψ_p can be found in **WEB TOPIC 5.6**.

In discussions of water in dry soils and plant tissues with very low water contents, such as seeds, one often finds reference to the **matric potential**, Ψ_m. Under these conditions, water exists as a very thin layer, perhaps one

or two molecules deep, bound to solid surfaces by electrostatic interactions. These interactions are not easily separated into their effects on Ψ_s and Ψ_p, and are thus sometimes combined into a single term, Ψ_m. The matric potential is discussed further in **WEB TOPIC 5.7**.

5.5 Water Potential of Plant Cells

Plant cells typically have water potentials of 0 MPa or less. A negative value indicates that the free energy of water in the cell is less than that of pure water at ambient temperature, atmospheric pressure, and equal height. As the water potential of the solution surrounding the cell changes, water will enter or leave the cell. Because water flows down its gradient in water potential (i.e., from higher to lower water potential), whether water enters or leaves the cell depends on the water potential of the cell and the solution surrounding it. In this section we illustrate the movement of water into and out of plant cells with some numerical examples.

Water enters the cell along a water potential gradient

First imagine an open beaker full of pure water at 20°C (**Figure 5.9A**). Because the water is open to the atmosphere, the pressure potential of the water is the same as atmospheric pressure (Ψ_p = 0 MPa). There are no solutes in the water, so Ψ_s = 0 MPa. Finally, because we focus here on transport processes that take place within the beaker, we define the reference height as equal to the level of the beaker, allowing us to ignore any contribution due to gravity (i.e., Ψ_g = 0 MPa). Therefore, the water potential is 0 MPa ($\Psi = \Psi_s + \Psi_p$).

Now imagine dissolving sucrose in the water to a concentration of 0.1 *M* (**Figure 5.9B**). This addition lowers the osmotic potential (Ψ_s) to –0.244 MPa and decreases the water potential (Ψ) to –0.244 MPa.

Next consider a plant cell that has been allowed to dry until its cell wall is no longer pushing back on the cytoplasm (i.e., a cell with no turgor pressure). We can describe a cell with zero turgor pressure as flaccid because its cell walls do not resist deformation. Let's also assume that the cell has a total internal solute concentration of 0.3 *M* (**Figure 5.9C**). This solute concentration gives an osmotic potential (Ψ_s) of –0.732 MPa. Because the cell is flaccid, the internal pressure is the same as atmospheric pressure, so the pressure potential (Ψ_p) is 0 MPa and the water potential of the cell is –0.732 MPa.

What happens if this cell is placed in the beaker containing 0.1 *M* sucrose (see Figure 5.9C)? Because the water potential of the sucrose solution (Ψ = –0.244 MPa; see Figure 5.9B) is greater (less negative) than the water potential of the cell (Ψ = –0.732 MPa), water will move from the sucrose solution to the cell (from high to low water potential).

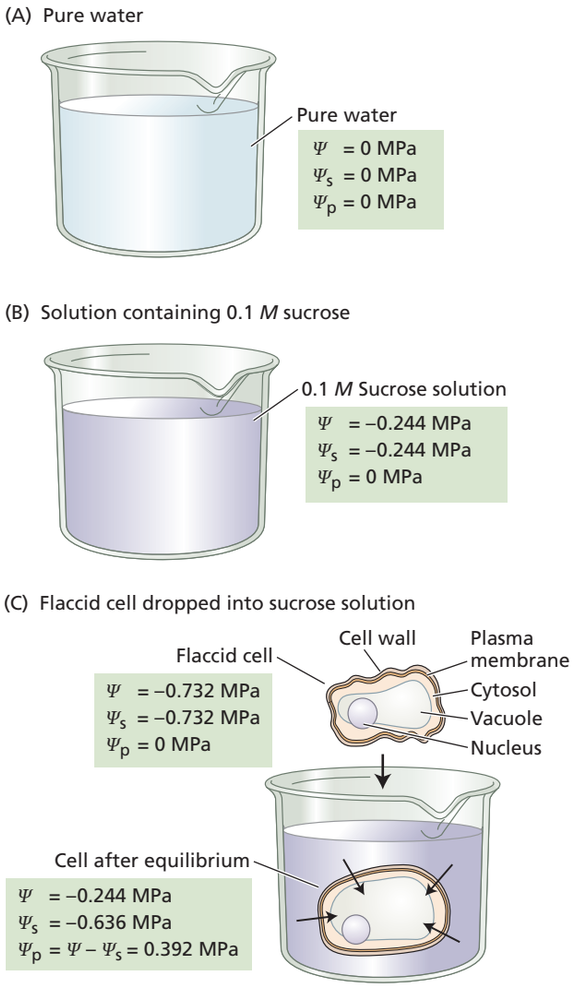


Figure 5.9 Water potential gradients can cause water to enter a cell. **(A)** Pure water. **(B)** A solution containing 0.1 *M* sucrose. **(C)** A flaccid cell (in air) is dropped into a 0.1 *M* sucrose solution. Because the starting water potential of the cell is less than the water potential of the solution, the cell takes up water. After equilibration, the water potential of the cell equals the water potential of the solution, and the result is a cell with a positive turgor pressure.

As water enters the cell, two things happen: The concentration of solutes decreases, and the cell wall is pushed outward. Both of these actions contribute to an increase in the cell's water potential. A lower solute concentration is associated with a lower (less negative) Ψ_s, while as the cell increases in volume, the cell wall stretches a little but also resists deformation. This results in the wall pushing back on the cell contents, which increases the pressure potential (Ψ_p) of the cell.

As the cell's water potential (Ψ) increases, the difference between the inside and outside water potentials ($\Delta\Psi$) is reduced. Eventually the cell Ψ reaches the same value as the Ψ of the sucrose solution. At this point,

the cell is at equilibrium with the surrounding solution —$\Psi_{(cell)} = \Psi_{(solution)}$—and net water transport ceases ($\Delta\Psi = 0$ MPa).

Because the volume of the beaker is much larger than that of the cell, the tiny amount of water taken up by the cell does not significantly affect the solute concentration of the sucrose solution. Hence, Ψ_s, Ψ_p, and Ψ of the sucrose solution are not altered. Therefore, at equilibrium, $\Psi_{(cell)} = \Psi_{(solution)} = -0.244$ MPa.

Calculation of cell Ψ_p and Ψ_s requires knowledge of the change in cell volume. In this example, let's assume that we know that the cell volume increased by 15%, such that the volume of the turgid cell is 1.15 times that of the flaccid cell. If we assume that the number of solutes in the cell remains constant as the cell hydrates, the final concentration of solutes will be diluted by 15%. The new Ψ_s can be calculated by dividing the initial Ψ_s by the relative increase in size of the hydrated cell: $\Psi_s = -0.732/1.15 = -0.636$ MPa. We can then calculate the pressure potential of the cell by rearranging Equation 5.5 as follows: $\Psi_p = \Psi - \Psi_s = (-0.244) - (-0.636) = 0.392$ MPa (see Figure 5.9C).

Water can also leave the cell in response to a water potential gradient

If we now remove our plant cell from the 0.1 *M* sucrose solution (see Figure 5.9C) and place it in a 0.3 *M* sucrose solution (**Figure 5.10A**), $\Psi_{(solution)}$ (–0.732 MPa) is more negative than $\Psi_{(cell)}$ (–0.244 MPa), and water will move from the turgid cell to the solution.

As water leaves the cell, the cell volume decreases. As the cell volume decreases, cell Ψ_p and Ψ decrease until $\Psi_{(cell)} = \Psi_{(solution)} = -0.732$ MPa. As before, we assume that the number of solutes in the cell remains constant as water flows from the cell. We know that Ψ_s in the flaccid cell was –0.732 MPa (see Figure 5.9C) or precisely the same as the new $\Psi_{(solution)}$. This means that the cell volume will decrease back to that of the flaccid cell (from 115 to 100%), where $\Psi_s = -0.732$ MPa. This allows us to calculate that $\Psi_p = 0$ MPa using Equation 5.5.

In this example, the protoplast pulls away from the cell wall (i.e., the cell plasmolyzes), because sucrose molecules are able to diffuse through the water-filled pores of the cell walls. When this occurs, the difference in water potential between the cytoplasm and the solution is entirely across the plasma membrane, and thus the protoplast shrinks independently of the cell wall. In contrast, when a cell desiccates in air (e.g., as in the flaccid cell in Figure 5.9C), plasmolysis does not occur. Instead, the cell (cytoplasm + wall) shrinks as a unit, resulting in the cell wall being mechanically deformed as the cell loses volume (cytorrhysis). **WEB TOPIC 5.8** discusses why cells dehydrated osmotically using solutes that can permeate the cell wall undergo plasmolysis, whereas cells dried in air undergo cytorrhysis.

If, instead of placing the turgid cell in the 0.3 *M* sucrose solution, we leave it in the 0.1 *M* solution and slowly squeeze it by pressing the cell between two plates (**Figure 5.10B**), we effectively raise the cell Ψ_p, consequently raising the cell Ψ and creating a $\Delta\Psi$ such that water now flows *out* of the cell. This is analogous to the industrial process of reverse osmosis in which externally applied pressure is used to separate water from dissolved solutes by forcing it across a semipermeable barrier. If we continue squeezing until half the cell's water is removed and then hold the cell in this condition, the cell will reach a new equilibrium. As in the previous example, at equilibrium $\Delta\Psi = 0$ MPa, and the amount of water added to the external solution is so small that it can be ignored. The cell will thus return to the Ψ value that it had before the squeezing procedure. However, the components of the cell Ψ will be quite different.

Because half of the water was squeezed out of the cell while the solutes remained inside the cell (the plasma membrane is selectively permeable), the cell solution is concentrated twofold, and thus Ψ_s is lower (–0.636 MPa × 2 = –1.272 MPa). Knowing the final values for Ψ and Ψ_s, we can calculate the pressure potential, using Equation 5.5, as $\Psi_p = \Psi - \Psi_s = (-0.244 \text{ MPa}) - (-1.272 \text{ MPa}) = 1.028$ MPa.

In our example we used an external force to change cell volume without a change in water potential. In nature, it is typically the water potential of the cell's environment that changes, and the cell gains or loses water until its Ψ matches that of its surroundings.

One point common to all these examples deserves emphasis: *Water flow across membranes is a passive process. That is, water moves in response to physical forces, toward regions of lower water potential or lower free energy.* There are no known metabolic "pumps" (e.g., reactions driven by ATP hydrolysis) that can be used to drive water across a semipermeable membrane against its free-energy gradient.

The only situation in which water can be said to move across a semipermeable membrane against its water potential gradient is when it is coupled to the movement of solutes. The transport of sugars, amino acids, or other small molecules by various membrane proteins can "drag" up to 260 water molecules across the membrane per molecule of solute transported.

Such transport of water can occur even when the movement is against the usual water potential gradient (i.e., toward a higher water potential), because the loss of free energy by the solute more than compensates for the gain of free energy by the water. The net change in free energy remains negative. The amount of water transported in this way is generally quite small compared with the passive movement of water down its water potential gradient.

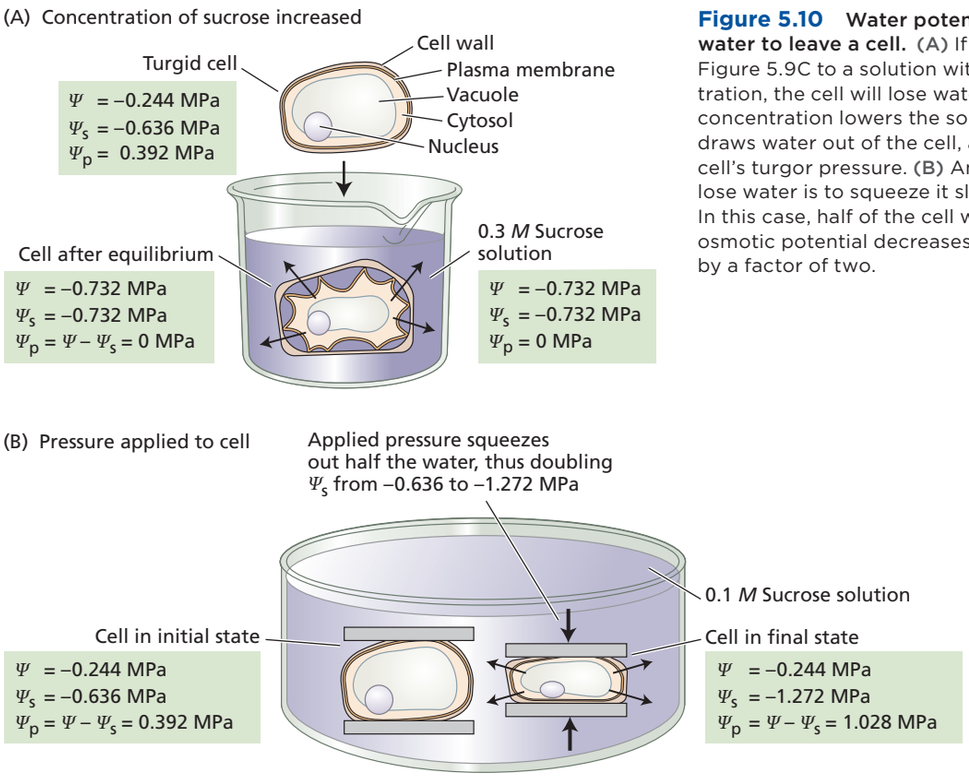


Figure 5.10 Water potential gradients can cause water to leave a cell. (A) If we move the turgid cell in Figure 5.9C to a solution with a higher sucrose concentration, the cell will lose water. The increased sucrose concentration lowers the solution water potential, draws water out of the cell, and thereby reduces the cell's turgor pressure. (B) Another way to make the cell lose water is to squeeze it slowly between two plates. In this case, half of the cell water is removed, so cell osmotic potential decreases (becomes more negative) by a factor of two.

Water potential and its components vary with growth conditions and location within the plant

In leaves of well-watered plants, Ψ ranges from –0.2 to about –1.0 MPa in herbaceous plants and to –2.5 MPa in trees and shrubs. Leaves of plants in arid climates can have much lower Ψ, down to below –10 MPa under the most extreme conditions.

Just as Ψ values depend on the growing conditions and the type of plant, so too, the values of Ψ_s can vary considerably. In cells of well-watered garden plants (examples include lettuce, cucumber seedlings, and bean leaves), Ψ_s may be as high as –0.5 MPa (low cell solute concentration), although values of –0.8 to –1.2 MPa are more typical. In woody plants, Ψ_s tends to be lower (higher cell solute concentration), allowing the more negative midday Ψ typical of these plants to occur without a loss in turgor pressure.

Although Ψ_s *within* cells may be quite negative, the solution surrounding the cells—that is, in the cell walls and in the xylem, collectively referred to as the apoplast—is generally quite dilute. The Ψ_s of the apoplast is typically –0.1 to 0 MPa, although in certain tissues (e.g., developing fruits) and habitats (e.g., high-salinity environments) the concentration of solutes in the apoplast can be large.

Values for Ψ_p in cells of well-watered plants may range from 0.1 to as much as 3 MPa, depending on the value of Ψ_s inside the cell. A plant **wilts** when the turgor pressure inside the cells of its tissues falls toward zero. As more water is lost from the cell, the walls become mechanically deformed, and the cell may be damaged as a result.

5.6 Cell Wall and Membrane Properties

Structural elements make important contributions to the water relations of plant cells. Cell wall elasticity defines the relation between turgor pressure and cell volume, while the permeability of the plasma membrane and the tonoplast (the vacuolar membrane) to water influences the rate at which cells exchange water with their surroundings. In this section we examine how wall and membrane properties influence the water status of plant cells.

Small changes in plant cell volume cause large changes in turgor pressure

Cell walls provide plant cells with a substantial degree of volume homeostasis relative to the large changes in water potential that they experience every day as a consequence of the transpirational water losses associated with photosynthesis (see Chapter 6). Because plant cells have fairly

rigid walls, a change in cell Ψ is generally accompanied by a large change in Ψ_p, with relatively little change in cell (protoplast) volume, as long as Ψ_p is greater than 0.

This phenomenon is illustrated by the *pressure–volume curve* shown in **Figure 5.11**. As Ψ decreases from 0 to –1.2 MPa, the relative or percent water content is reduced by only slightly more than 5%. Most of the decrease in Ψ is due to a reduction in Ψ_p (by about 1.0 MPa); Ψ_s decreases by less than 0.2 MPa as a result of increased concentration of cell solutes.

Measurements of cell water potential and cell volume can be used to quantify how wall properties influence the water status of plant cells. Turgor pressure in most cells approaches zero as the cell volume decreases by 10 to 15%.

The volumetric elastic modulus, symbolized by ε (the Greek letter epsilon), can be determined by examining the relationship between Ψ_p and cell volume: ε is the change in Ψ_p for a given change in relative volume ($\varepsilon = \Delta\Psi_p/\Delta$[relative volume]). Cells with a large ε have stiff cell walls and thus experience larger changes in turgor pressure for the same change in cell volume than cells with a smaller ε and more elastic walls. The mechanical properties of cell walls vary among species and cell types, resulting in significant differences in the extent to which decreases in water potential affect cell volume.

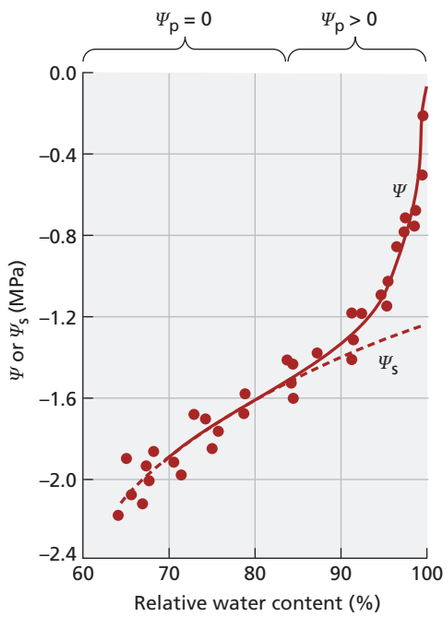
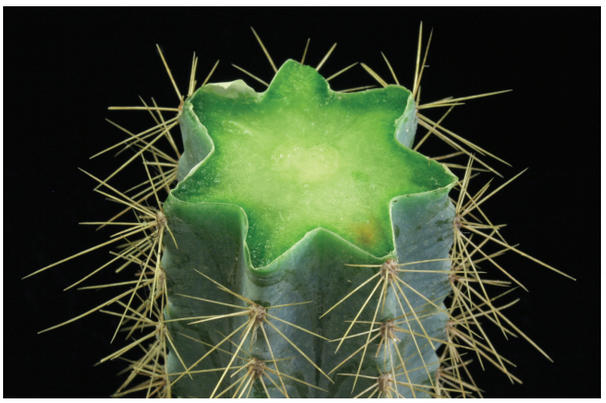


Figure 5.11 The relation between water potential (Ψ), solute potential (Ψ_s), and relative water content ($\Delta V/V$) in cotton (*Gossypium hirsutum*) leaves. Note that Ψ decreases steeply with the initial decrease in relative water content. In comparison, Ψ_s changes little. As cell volume decreases below 90% in this example, the situation reverses: Most of the change in water potential is due to a drop in cell Ψ_s, accompanied by relatively little change in turgor pressure. (After T. C. Hsiao and L. K. Xu. 2000. *J. Exp. Bot.* 51: 1595–1616.)



Courtesy of David McIntyre

Figure 5.12 Cross section of a cactus stem, showing an outer, photosynthetic layer, and an inner, nonphotosynthetic tissue that functions in water storage. During drought, water is lost preferentially from nonphotosynthetic cells, so the water status of the photosynthetic tissue is maintained.

A comparison of the cell water relations within stems of cacti illustrates the important role of cell wall properties. Cacti are stem succulent plants, typically found in arid regions. Their stems consist of an outer, photosynthetic layer that surrounds nonphotosynthetic tissues that serve as a water storage reservoir (**Figure 5.12**). During drought, water is lost preferentially from these inner cells, despite the fact that the water potential of the two cell types remains in equilibrium (or very close to equilibrium). How does this happen?

Detailed studies of *Opuntia ficus-indica* demonstrate that the water storage cells are larger and have thinner walls than the photosynthetic cells, and are thus more flexible (have lower ε). For a given decrease in water potential, a water storage cell will lose a greater fraction of its water content than a photosynthetic cell. In addition, the solute concentration of the water storage cells decreases during drought, in part due to the polymerization of soluble sugars into insoluble starch granules. A more typical plant response to drought is to accumulate solutes, in part to prevent water loss from cells (see Chapter 15). However, in the case of cacti, the combination of more flexible cell walls and a decrease in solute concentration during drought allows water to be withdrawn preferentially from the water storage cells, thus helping maintain the hydration of the photosynthetic tissues.

The rate at which cells gain or lose water is influenced by plasma membrane hydraulic conductivity

So far, we have seen that water moves into and out of cells in response to a water potential gradient. The direction of flow is determined by the direction of the Ψ gradient, and the rate of water movement is proportional to the magnitude of the driving gradient. However, for

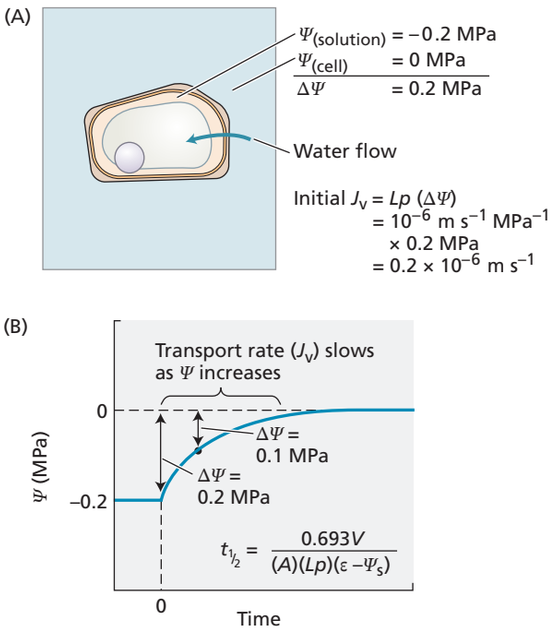


Figure 5.13 **The rate of water transport into a cell depends on the magnitude of the water potential difference ($\Delta\Psi$) and the hydraulic conductivity of the plasma membranes (*Lp*).** **(A)** In this example, the magnitude of the initial water potential difference is 0.2 MPa and *Lp* is 10^{-6} m s^{-1} MPa^{-1}. These values give an initial transport rate (J_v) of 0.2×10^{-6} m s^{-1}. **(B)** As water is taken up by the cell, the water potential difference decreases with time, leading to a slowing in the rate of water uptake. This effect follows an exponentially decaying time course with a half-time ($t_{1/2}$) that depends on the following cell parameters: volume (*V*), surface area (*A*), conductivity (*Lp*), volumetric elastic modulus (ε), and cell osmotic potential (Ψ_s).

a cell that experiences a change in the water potential of its surroundings (e.g., see Figures 5.9 and 5.10), the movement of water across the plasma membrane will decrease with time as the internal and external water potentials converge (**Figure 5.13**). The rate approaches zero in an exponential manner. The time it takes for the rate to decline by half—its half-time, or $t_{1/2}$—is given by the following equation:

$$t_{1/2} = \left(\frac{0.693}{(A)(Lp)}\right)\left(\frac{V}{\varepsilon - \Psi_s}\right) \qquad (5.6)$$

where *V* and *A* are, respectively, the volume and surface of the cell, and *Lp* is the **hydraulic conductivity** of the plasma membrane. Hydraulic conductivity describes how readily water can move across a membrane; it is expressed in terms of volume of water per unit area of membrane per unit time per unit driving force (i.e., m^3 m^{-2} s^{-1} MPa^{-1}). For additional discussion of hydraulic conductivity, see **WEB TOPIC 5.9**.

A short half-time means fast equilibration. Thus, cells with large surface-to-volume ratios, high membrane hydraulic conductivity, and stiff cell walls (large ε) will come rapidly into equilibrium with their surroundings. Cell half-times typically range from 1 to 10 s, although some are much shorter. Because of their short half-times, single cells come to water potential equilibrium with their surroundings in less than 1 min. For multicellular tissues, the half-times may be much longer.

Aquaporins facilitate the movement of water across membranes

For many years, plant physiologists were uncertain about how water moves across plant membranes. Specifically, it was unclear whether water movement into plant cells was limited to the diffusion of water molecules across the plasma membrane's lipid bilayer or if it also involved diffusion through protein-lined pores (**Figure 5.14**). Some studies suggested that diffusion directly across the lipid bilayer was not sufficient to account for observed rates of water movement across membranes, but the evidence in support of microscopic pores was not compelling.

This uncertainty was put to rest in 1991 with the discovery of **aquaporins** (see Figure 5.14). Aquaporins are integral membrane proteins that form water-selective channels across the membrane. Because water diffuses much faster through such channels than through a lipid bilayer, aquaporins facilitate water movement into and out of plant cells.

Although aquaporins may alter the *rate* of water movement across the membrane, they do not change the *direction of transport* or the *driving force* for water

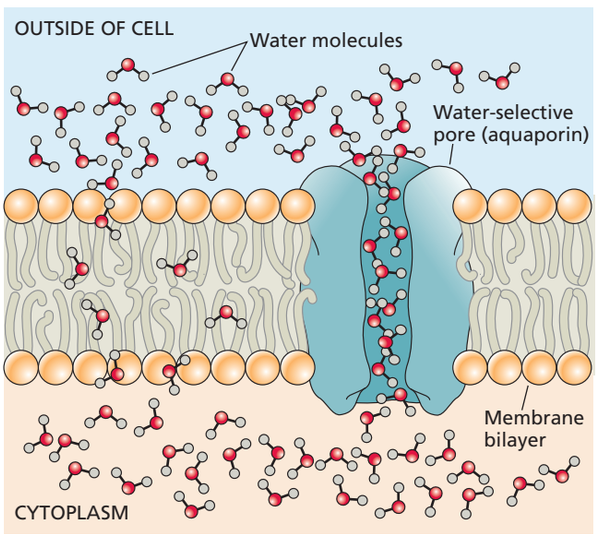


Figure 5.14 **Water can cross biological membranes by diffusion.** Individual water molecules can diffuse through the membrane bilayer, as shown on the left, and by linear diffusion of water molecules through water-selective pores formed by integral membrane proteins such as aquaporins.

movement. However, aquaporins can be reversibly "gated" (i.e., transferred between an open and a closed state) in response to physiological parameters such as intercellular pH and Ca^{2+} concentration. As a result, plants have the ability to regulate the permeability of their membranes to water (see Chapter 8).

5.7 Plant Water Status

The concept of water potential has two principal uses. First, water potential governs transport across plasma membranes, as we have described. Second, water potential is often used as a measure of the *water status* of a plant. In this section we discuss how the concept of water potential helps us evaluate the water status of a plant.

Physiological processes are affected by plant water status

Because of transpirational water loss to the atmosphere, plants are seldom fully hydrated. During periods of drought, they suffer from water deficits that lead to inhibition of plant growth and photosynthesis. **Figure 5.15** lists some of the physiological changes that occur as plants experience increasingly drier conditions.

The sensitivity of any particular physiological process to water deficits is, to a large extent, a reflection of that plant's strategy for dealing with the range of water availability that it experiences in its environment. According to Figure 5.15, the process that is most affected by water deficit is cell expansion. In many plants, reductions in water supply inhibit shoot growth and leaf expansion but *stimulate* root elongation. A relative increase in roots relative to leaves is an appropriate response to reductions in water availability, and thus the sensitivity of shoot growth to decreases in water availability can be seen as an adaptation to drought rather than a physiological constraint.

However, what plants cannot do is to alter the availability of water in the soil. (Figure 5.15 shows representative values for Ψ at various stages of water stress.) Thus, drought does impose some absolute limitations on physiological processes, although the actual water potentials at which such limitations occur vary with species.

Solute accumulation helps cells maintain turgor and volume

The ability to maintain physiological activity as water becomes less available typically incurs some costs. The plant may spend energy to accumulate solutes to maintain turgor pressure, invest in the growth of nonphotosynthetic organs such as roots to increase water uptake capacity, or build xylem conduits capable of transporting water under large tensions (see Chapter 6). Thus, physiological responses to water availability reflect a trade-off between the benefits accrued by being able to carry out physiological processes (e.g., growth) over a wider range of environmental conditions and the carbon investment costs associated with such capability.

Plants that grow in saline environments, called **halophytes**, typically have very low values of Ψ_s. A low Ψ_s lowers cell Ψ enough to allow root cells to extract water from saline water without allowing excessive levels of salts to enter at the same time. Plants may also exhibit quite negative Ψ_s under drought conditions. Water stress typically leads to an accumulation of solutes in the cytoplasm and vacuole of plant cells, thus allowing the cells to maintain turgor pressure despite low water potentials.

Positive turgor pressure ($\Psi_p > 0$) is essential for many physiological processes. For example, the growth of plant cells requires turgor pressure to stretch the cell walls (see Chapter 2). The loss of turgor under water deficits can explain in part why cell growth is so sensitive to water stress, as well as why this sensitivity can be modified by varying the cell's osmotic potential (see Chapter 15). Turgor pressure also contributes to the mechanical rigidity of nonlignified cells and tissues, enables stomata to open (Chapter 6), and powers the movement of sugars through the phloem (Chapter 12).

However, the major benefit of maintaining positive turgor pressure may be in allowing the large fluctuations

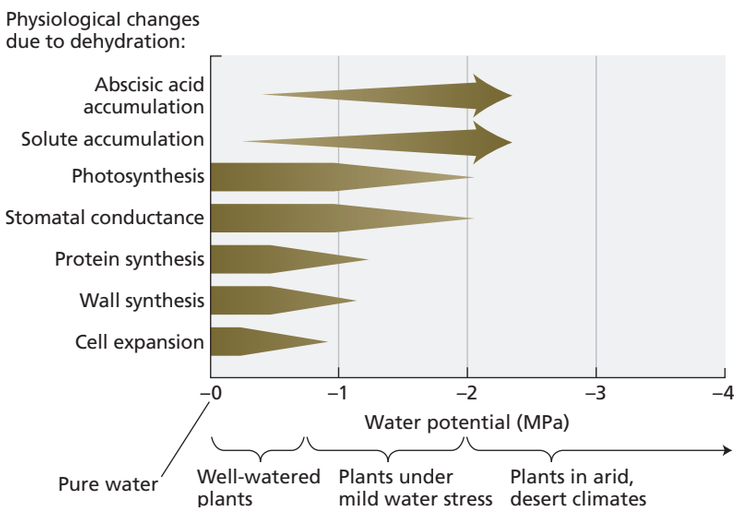


Figure 5.15 Sensitivity of various physiological processes to changes in water potential under various growing conditions. The thickness of the brown bars corresponds to the magnitude of the process. For example, cell expansion decreases as water potential falls (becomes more negative). Arrows indicate processes that are activated by water deficits. Abscisic acid is a hormone that induces stomatal closure during water stress (see Chapters 6 and 15). (After T. C. Hsiao. *Annu. Rev. Plant Physiol.* 24: 519–570.)

in water potential that occur each day to be accommodated primarily through changes in turgor pressure rather than cell volume. Large fluctuations in cell volume can impair metabolic processes through their impact on concentrations of key metabolites. The existence of stretch-activated signaling molecules in the plasma membrane suggests that plant cells may sense changes in their water status via changes in volume, rather than by responding directly to turgor pressure.

Summary

5.1 Water in Plant Life

- Water limits both agricultural and natural ecosystem productivity (**Figures 5.1, 5.2**).
- About 97% of the water absorbed by roots is carried through the plant and is lost by transpiration from the leaf surfaces.
- The uptake of CO_2 is coupled to the loss of water through a common diffusional pathway.

5.2 The Structure and Properties of Water

- The polarity and tetrahedral shape of water molecules permit them to form hydrogen bonds that give water its unusual physical properties: it is an excellent solvent and has a high specific heat capacity, an unusually high latent heat of vaporization, and a high tensile strength (**Figures 5.3, 5.6**).
- Cohesion, adhesion, and surface tension give rise to capillarity (**Figures 5.4, 5.5**).

5.3 Diffusion and Osmosis

- The random thermal motion of molecules results in diffusion (**Figures 5.7, 5.8**).
- Diffusion is important over short distances. The average time for a substance to diffuse a given distance increases as the square of that distance.
- Osmosis is the net movement of water across a selectively permeable barrier toward a region of higher solute concentration.

5.4 Water Potential

- Water's chemical potential is a measure of the free energy of water. It is quantified as the difference between the free energy of water in a given state and the free energy of water in a standard state.
- Concentration, pressure, and gravity contribute to water potential (Ψ) in plants.
- Ψ_s, the solute potential or osmotic potential, represents solutes' dilution of water and the reduction of the free energy of water.
- Ψ_p, the pressure potential, represents the effect of hydrostatic pressure on the free energy of water. Positive pressure (turgor pressure) raises the water potential; negative pressure (tension) reduces it.
- Ψ_g, the gravitational potential, represents the effect of gravity on the free energy of water. Gravity must be taken into account when considering water movement in trees but can be omitted when calculating cell water potential.

5.5 Water Potential of Plant Cells

- Plant cells typically have negative water potentials.
- Water enters or leaves a cell according to the water potential gradient.
- When a flaccid cell is placed in a solution that has a water potential greater (less negative) than the cell's water potential, water will move from the solution into the cell (from high to low water potential) (**Figure 5.9**).
- As water enters, the cell wall resists being stretched, increasing the turgor pressure (Ψ_p) of the cell.
- At equilibrium [$\Psi_{(cell)} = \Psi_{(solution)}$; $\Delta\Psi = 0$], net water movement ceases.
- When a turgid plant cell is placed in a sucrose solution that has a water potential more negative than the water potential of the cell, water will move from the turgid cell to the solution (**Figure 5.10**).
- If a cell is squeezed, its Ψ_p increases, resulting in a $\Delta\Psi$ such that water flows out of the cell (**Figure 5.10**).

5.6 Cell Wall and Membrane Properties

- Cell wall elasticity defines the relation between turgor pressure and cell volume, while the water permeability of the plasma membrane and tonoplast determines how fast cells exchange water with their surroundings.
- Because plant cells have fairly rigid walls, small changes in plant cell volume cause large changes in turgor pressure (**Figure 5.11**).
- For any non-zero initial $\Delta\Psi$, the net movement of water across the membrane will decrease with time as the internal and external water potentials converge (**Figure 5.13**).
- Aquaporins are water-selective membrane channels (**Figure 5.14**).

5.7 Plant Water Status

- During drought, photosynthesis and growth are inhibited, while concentrations of abscisic acid and solutes increase (**Figure 5.15**).
- During drought, plants must use energy to maintain turgor pressure by accumulating solutes, as well as to support root and vascular growth.
- Stretch-activated signaling molecules in the plasma membrane may permit plant cells to sense changes in their water status via changes in volume.

Web Material

- **WEB TOPIC 5.1 Calculating Capillary Rise** Quantification of capillary rise allows us to assess its functional role in water movement in plants.
- **WEB TOPIC 5.2 Calculating Half-Times of Diffusion** The assessment of the time needed for a molecule such as glucose to diffuse across cells, tissues, and organs shows that diffusion has physiological significance only over short distances.
- **WEB TOPIC 5.3 Alternative Conventions for Components of Water Potential** Plant physiologists have developed several conventions to define water potential of plants. A comparison of key definitions in some of these convention systems provides us with a better understanding of the water relations literature.
- **WEB TOPIC 5.4 Temperature and Water Potential** Variation in temperature between 0°C and 30°C has a relatively minor effect on osmotic potential.
- **WEB TOPIC 5.5 Can Negative Turgor Pressures Exist in Living Cells?** It is assumed that Ψ_p is 0 or greater in living cells; is this true for living cells with lignified walls?
- **WEB TOPIC 5.6 Measuring Water Potential** Several methods are available to measure water potential in plant cells and tissues.
- **WEB TOPIC 5.7 The Matric Potential** Matric potential is used to quantify the chemical potential of water in soils, seeds, and cell walls.
- **WEB TOPIC 5.8 Wilting and Plasmolysis** Plasmolysis is a major structural change resulting from major water loss by osmosis.
- **WEB TOPIC 5.9 Understanding Hydraulic Conductivity** Hydraulic conductivity, a measurement of the membrane permeability to water, is one of the factors determining the velocity of water movements in plants.

For more study aids, go to oup.com/he/taiz7e.

Suggested Reading

Bartlett, M. K., Scoffoni, C., and Sack, L. (2012) The determinants of leaf turgor loss point and prediction of drought tolerance of species and biomes: A global meta-analysis. *Ecol. Lett.* 15: 393–405.

Chaumont, F., and Tyerman, S. D. (2014) Aquaporins: Highly regulated channels controlling plant water relations. *Plant Physiol*. 164: 1600–1618.

Goldstein, G., Ortega, J. K. E., Nerd, A., and Nobel, P. S. (1991) Diel patterns of water potential components for the crassulacean acid metabolism plant *Opuntia ficus-indica* when well-watered or droughted. *Plant Physiol.* 95: 274–280.

Kramer, P. J., and Boyer, J. S. (1995) *Water Relations of Plants and Soils*. Academic Press, San Diego.

Maurel, C., Verdoucq, L., Luu, D.-T., and Santoni, V. (2008) Plant aquaporins: Membrane channels with multiple integrated functions. *Annu. Rev. Plant Biol*. 59: 595–624.

Munns, R. (2002) Comparative physiology of salt and water stress. *Plant Cell Environ.* 25: 239–250.

Nobel, P. S. (1999) *Physicochemical and Environmental Plant Physiology*. 2nd ed. Academic Press, San Diego.

Tardieu, F., Parent, B., Caldeira, C. F., and Welcker, C. (2014) Genetic and physiological controls of growth under water deficit. *Plant Physiol.* 164: 1628–1635.

Wheeler, T. D., and Stroock, A. D. (2008) The transpiration of water at negative pressures in a synthetic tree. *Nature* 455: 208–212.

6 Water Balance of Plants



Dancestrokes/ Shutterstock

Life in Earth's atmosphere presents a formidable challenge to land plants. On the one hand, the atmosphere is the source of carbon dioxide, which is needed for photosynthesis. On the other hand, the atmosphere is usually quite dry, leading to a net loss of water due to evaporation. Because plants lack surfaces that can allow the inward diffusion of CO_2 while preventing water loss, CO_2 uptake exposes plants to the risk of dehydration. This problem is compounded because the concentration gradient for CO_2 uptake is much smaller than the concentration gradient that drives water loss. To meet the contradictory demands of maximizing carbon dioxide uptake while limiting water loss, plants have evolved adaptations that control water loss from leaves, and that replace the water lost to the atmosphere with water drawn from the soil.

In this chapter we examine the mechanisms and driving forces operating on water transport within the plant and between the plant and its environment (**Figure 6.1**). We begin our examination of water transport by focusing on water in the soil. We then consider how water moves from the soil into the roots and from the roots up through specialized transport cells to the leaves, from which water is lost to the atmosphere. We end the chapter by considering the ways in which the leaf can control the loss of water, as well as the entry of CO_2, by regulating the opening and closing of stomata, the small openings through which CO_2 uptake and the majority of water loss occur.

6.1 Water in the Soil

The water content and the rate of water movement in soils depend to a large extent on soil type and soil structure. At one extreme is sand, in which the soil particles may be 1 mm or more in diameter. Sandy soils have a relatively low surface area per gram of soil and have large spaces or channels between particles.

At the other extreme is clay, in which particles are smaller than 2 μm in diameter. Clay soils have much greater surface areas and smaller channels between particles. With the aid of organic substances such as humus (decomposing organic matter), clay particles may aggregate into "crumbs," allowing large channels to form that help improve soil aeration and infiltration of water.

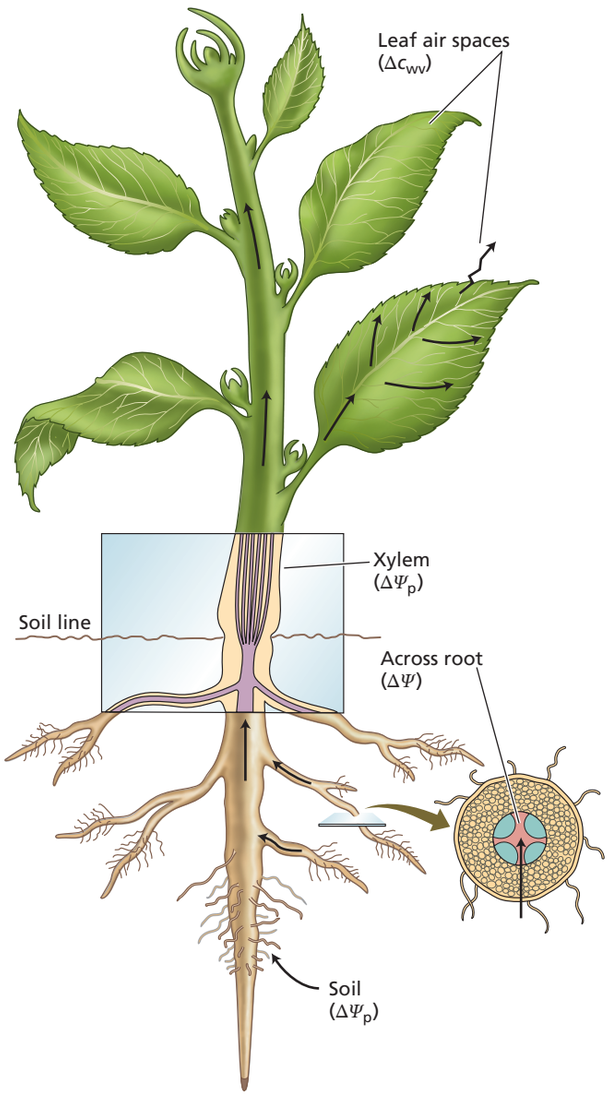


Figure 6.1 Main driving forces for water flow from the soil through the plant to the atmosphere. Differences in water vapor concentration (Δc_{wv}) between leaf and air are responsible for the diffusion of water vapor from the leaf to the air; differences in pressure potential ($\Delta \Psi_p$) drive the bulk flow of water through xylem conduits; and differences in water potential ($\Delta \Psi$) are responsible for the movement of water across the living cells in the root.

When a soil is heavily watered by rain or by irrigation (see **WEB TOPIC 6.1**), the water percolates downward by gravity through the spaces between soil particles, partly displacing, and in some cases trapping, air in these channels. Because water is pulled into the spaces between soil particles by capillarity, the smaller channels become filled first. Depending on the amount of water available, water in the soil may exist as a film adhering to the surface of soil particles, it may fill the smaller but not the larger channels, or it may fill all of the spaces between particles.

In sandy soils, the spaces between particles are so large that water tends to drain from them and remain only on the particle surfaces and in the spaces where particles come into contact. In clay soils, the spaces between particles are so small that much water is retained against the force of gravity. A few days after a soaking rainfall, a clay soil might retain 40% water by volume. In contrast, sandy soils typically retain only about 15% water by volume after thorough wetting.

In this section we examine how the physical structure of the soil influences soil water potential, how water moves in the soil, and how roots absorb the water needed by the plant.

Soil water potential is affected by solutes, surface tension, and gravity

Like the water potential of plant cells, the water potential of soils may be dissected into three components: the osmotic potential, the pressure potential, and the gravitational potential. The **osmotic potential** (Ψ_s) (see Chapter 5) of soil water is generally negligible, because except in saline soils, solute concentrations are low; a typical value might be –0.02 MPa. In soils that contain a substantial concentration of salts, however, Ψ_s can be quite negative, perhaps –0.2 MPa or lower.

The second component of soil water potential is the **pressure potential** (Ψ_p). For wet soils, Ψ_p is very close to zero. As soil dries out, Ψ_p decreases and can become quite negative. Where does the negative pressure potential in soil water come from, and why is Ψ_p related to the water content of the soil?

Recall from our discussion of capillarity in Chapter 5 that water has a high surface tension that tends to minimize air–water interfaces. However, because of adhesive forces, water also tends to cling to the surfaces of soil particles (**Figure 6.2**). As the water content of the soil decreases, the water recedes into the channels between soil particles, forming curved air–water interfaces. In Chapter 5 we learned that surface tension describes the tendency of a gas–liquid interface to contract. If the air–water interface is curved, surface tension produces a net force perpendicular to the surface that acts to reduce the area of the air–water interface. This force causes the Ψ_p of the water in the soil to decrease according to the Young–Laplace equation:

$$\Psi_p = \frac{-2T}{r} \qquad (6.1)$$

where T is the surface tension of water (7.28×10^{-2} N m^{-1} at 20°C, equivalent to 7.28×10^{-8} MPa m), r is the radius of curvature (in meters) of the air–water interface, and the negative sign indicates that surface tension lowers the pressure in the water. Note that this is the same capillarity equation discussed in **WEB TOPIC 5.1** (see also

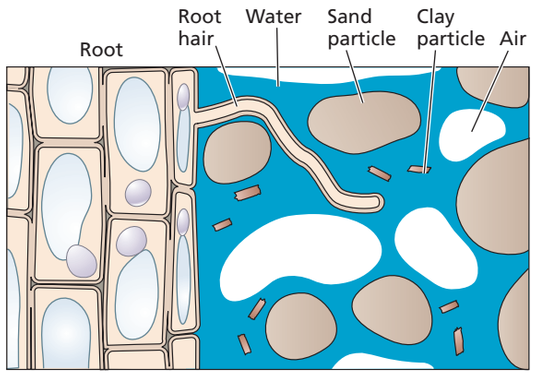


Figure 6.2 Root hairs make intimate contact with soil particles and greatly amplify the surface area used for water absorption by the plant. The soil is a mixture of particles (sand, clay, silt, and organic material), water, dissolved solutes, and air. When the soil is wet, the curvature of air–water interfaces is small. As water is absorbed by the plant, the soil solution recedes into smaller pockets, channels, and crevices between the soil particles. This recession causes the curvature of air–water interfaces in the soil to increase, resulting in a decrease in Ψ_p.

Figure 5.5), where here the soil particles are assumed to be fully wettable (contact angle $\theta = 0$; $\cos \theta = 1$).

As soil dries out, water is first removed from the largest spaces between soil particles and subsequently from successively smaller spaces between and within soil particles. In this process, the value of Ψ_p in soil water can become quite negative because of the increasing curvature of air–water surfaces in pores of successively smaller diameter. For instance, a curvature of $r = 1$ μm (about the size of the largest clay particles) corresponds to a Ψ_p value of –0.15 MPa. The value of Ψ_p may easily reach –1 to –2 MPa as the air–water interface recedes into the smaller spaces between clay particles.

The third component of soil water potential is **gravitational potential** (Ψ_g). Gravity plays an important role in drainage. The downward movement of water is due to the fact that Ψ_g is proportional to elevation: higher at higher elevations, and vice versa. The gradient in Ψ_g is equal to 0.1 MPa over a distance of 10 m.

Water moves through the soil by bulk flow

Bulk or mass flow is the movement of molecules en masse, most often in response to a pressure or gravitational gradient. Common examples of bulk flow are water moving through a garden hose or down a river. The movement of water through soils is predominantly by bulk flow. Both gravity and pressure can drive bulk flow in soils. However, the movement of water toward roots is largely the result of gradients in Ψ_p ($\Delta\Psi_p$) (see Figure 6.1).

Water flows from regions of higher soil water content, where the water-filled spaces are larger and thus Ψ_p is less negative, to regions of lower soil water content, where the smaller size of the water-filled spaces is associated with more curved air–water interfaces and a more negative Ψ_p. Diffusion of water vapor from wetter to drier regions also accounts for some water movement, although its contribution relative to liquid flow is usually negligible except in very dry soils.

As plants absorb water from the soil, they deplete the soil of water near the surface of the roots. This depletion reduces Ψ_p near the root surface and establishes a pressure gradient with respect to neighboring regions of soil that have higher Ψ_p values. Because the water-filled pore spaces in the soil are interconnected, water moves down the pressure gradient to the root surface by bulk flow through these channels.

The rate of water flow in soils depends on two factors: the size of the pressure gradient through the soil, and the hydraulic conductivity of the soil. **Soil hydraulic conductivity** is a measure of the ease with which water moves through the soil, and it varies with the type of soil and its water content. Sandy soils, which have large spaces between particles, have a large hydraulic conductivity when saturated, whereas clay soils, with only minute spaces between their particles, have an appreciably smaller saturated hydraulic conductivity.

As the water content of a soil decreases, the hydraulic conductivity falls dramatically. This decrease in soil hydraulic conductivity is due primarily to the replacement of water in the soil by air. When air moves into a soil channel previously filled with water, water movement through that channel is restricted to the periphery of the channel. As more of the soil spaces become filled with air, water flow is limited to fewer and narrower channels, and the hydraulic conductivity falls. (**WEB TOPIC 6.2** discusses how soil texture influences both the water-holding capacity of soils and their hydraulic conductivity.)

6.2 Water Absorption by Roots

Contact between the surface of the root and the soil is essential for effective water absorption by the root. This contact provides the surface area needed for water uptake and is maximized by the growth of the root and of root hairs into the soil. **Root hairs** are filamentous outgrowths of root epidermal cells that greatly increase the surface area of the root, thus providing greater capacity for absorption of ions and water from the soil. When 3-month-old wheat plants were examined, their root hairs were found to constitute more than 60% of the surface area of the roots (see Figure 7.7).

Water enters the root most readily near the root tip. Mature regions of the root are less permeable to water because they have developed a modified epidermal layer that contains hydrophobic materials in its walls. Although it might at first seem counterintuitive that any portion of

the root system should be impermeable to water, the older regions of the root must be sealed off if there is to be water uptake (and thus bulk flow of nutrients) from the regions of the root system that are actively exploring new areas in the soil (**Figure 6.3**).

The contact between the soil and the root surface is easily broken when the soil is disturbed. It is for this reason that newly transplanted seedlings and plants need to be protected from water loss for the first few days after transplantation. Thereafter, new root growth into the soil reestablishes soil–root contact, and the plant can better withstand water stress.

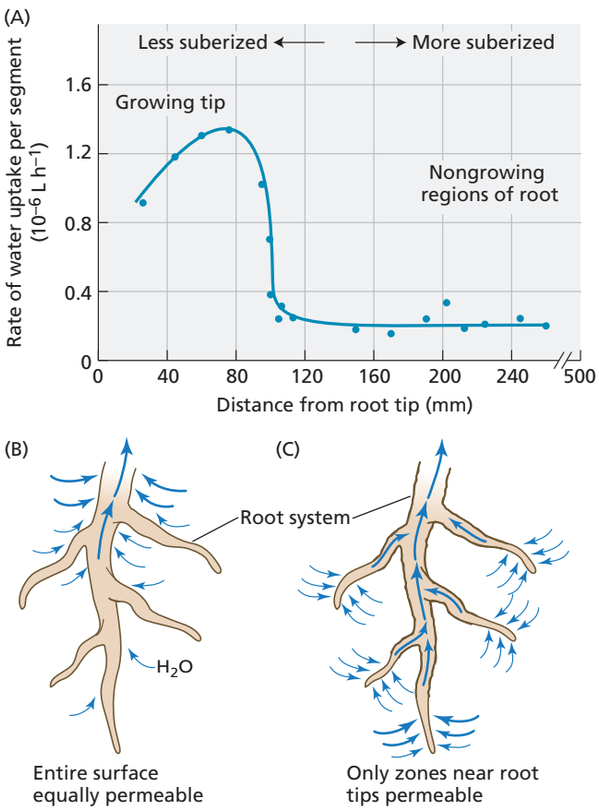


Figure 6.3 **Water uptake by roots.** **(A)** Rate of water uptake by short segments (3–5 mm) at various positions along an intact pumpkin (*Cucurbita pepo*) root. **(B** and **C)** Diagrams of water uptake in which the entire root surface is equally permeable **(B)** or is impermeable in older regions because of the deposition of suberin, a hydrophobic polymer **(C)**. When root surfaces are equally permeable, most of the water enters near the top of the root system, with more distal regions being hydraulically isolated as the suction in the xylem is relieved because of the inflow of water. Decreasing the permeability of older regions of the root allows xylem tensions to extend farther into the root system, allowing water uptake from distal regions of the root system. (A from P. J. Kramer. 1983. Water Relations of Plants, p. 132. Academic Press, San Diego, CA; after *Agricultural Research Council Letcombe Laboratory Annual Report* [1973, p. 10].)

Let's consider how water moves within the root, and the factors that determine the rate of water uptake into the root.

Water moves in the root via the apoplast, symplasm, and transmembrane pathways

In the soil, water flows between soil particles. However, from the epidermis to the endodermis of the root, there are three pathways through which water can flow (**Figure 6.4**): the apoplast, the symplasm, and the transmembrane pathway.

1. The apoplast is the continuous system of cell walls, intercellular air spaces, and the lumens of nonliving cells (e.g., xylem conduits and fibers). In this pathway, water moves through cell walls and extracellular spaces without crossing any membranes as it travels across the root cortex.
2. The symplasm consists of the entire network of cell cytoplasm interconnected by plasmodesmata. In this pathway, water travels across the root cortex via plasmodesmata (see Chapter 1).
3. The transmembrane pathway is the route by which water enters a cell on one side, exits the cell on the other side, enters the next in the series, and so on. In this pathway, water crosses the plasma membrane of each cell in its path twice (once on entering and once on exiting). Transport across the tonoplast may also be involved.

Although the relative importance of the apoplast, symplasm, and transmembrane pathways has not yet been fully established, experiments with the pressure probe technique (see **WEB TOPIC 5.6**) indicate an important role for plasma membranes, and thus the transmembrane pathway, in the movement of water across the root cortex. And though we can define three pathways, it is important to remember that water moves not according to a single chosen path, but rather moves wherever the gradients and resistances direct it. A particular water molecule moving in the symplasm may cross the membrane and move in the apoplast for a moment, and then move back into the symplasm again.

At the endodermis, water movement through the apoplast pathway is obstructed by the Casparian strip (see Figure 6.4). The **Casparian strip** is a band within the radial cell walls of the endodermis that is impregnated with **lignin**, a hydrophobic polymer. The Casparian strip breaks the continuity of the apoplast pathway, forcing water and solutes to pass through the plasma membrane in order to cross the endodermis. The plasma membrane can act selectively in terms of which solutes it allows to enter the cell and which it excludes. The Casparian strip allows the plant to control which solutes enter the xylem, something that would not be possible if water could move continuously through the apoplast from the

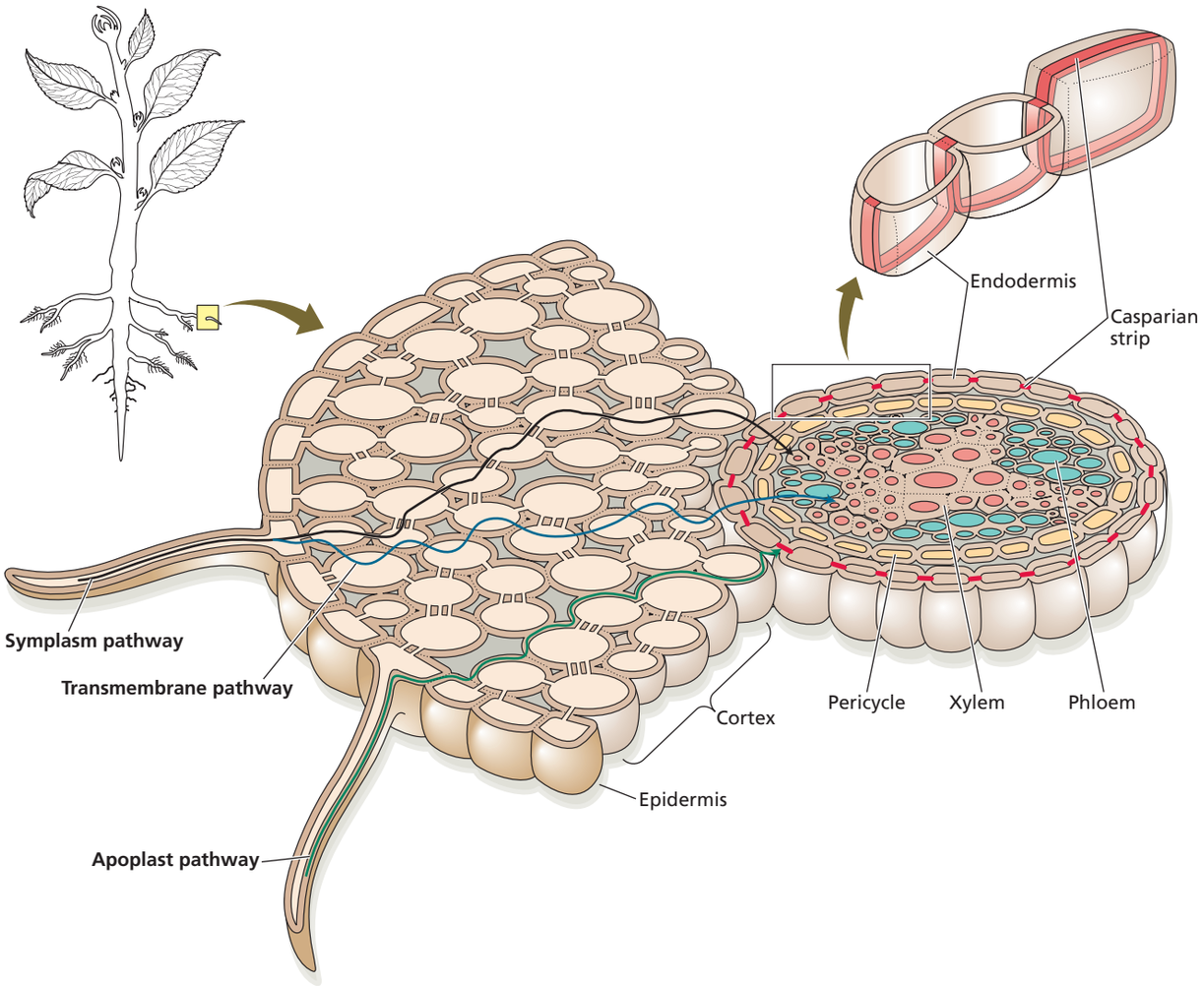


Figure 6.4 **Pathways for water uptake by the root.** Through the cortex, water may travel via the apoplast pathway, the transmembrane pathway, and the symplasm pathway. In the symplasm pathway (black), water flows between cells through the plasmodesmata without crossing the plasma membrane. In the transmembrane pathway (blue), water moves across the plasma membranes, with a short visit to the cell wall space. Note that while these are drawn as three distinct pathways, water molecules will move between the symplasm and apoplast as directed by gradients in water potential and hydraulic resistances. At the endodermis, the apoplast pathway is blocked by the Casparian strip. Many roots also develop a Casparian strip in the outer cell layer of the cortex, forming an exodermis in which flow through the apoplast pathway is blocked.

soil to the xylem. The movement of water across plasma membranes explains why the driving gradient for water uptake by roots is the difference in soil and xylem water potential ($\Delta\Psi$) (see Figure 6.1).

The requirement that water move symplasmically across the endodermis also helps explain why the permeability of roots to water depends strongly on the presence of aquaporins (see Chapters 5 and 8). Down-regulating the expression of aquaporin genes markedly reduces the hydraulic conductivity of roots and can result in plants that wilt easily or that compensate by producing larger root systems.

Water uptake decreases when roots are subjected to low temperature or anaerobic conditions, or when treated with respiratory inhibitors. The reason for this is that the permeability of aquaporins can be regulated in response to intracellular pH. Decreased rates of respiration, in response to low temperature or anaerobic conditions such as occur in flooded soils, lead to an increase in intracellular pH. In turn, the increase in cytosolic pH alters the conductance of aquaporins in root cells, resulting in roots that are markedly less permeable to water. Thus, maintaining membrane permeability to water requires energy expenditure by root cells that is supplied by respiration.

Solute accumulation in the xylem can generate "root pressure"

Plants sometimes exhibit a phenomenon referred to as **root pressure**. For example, if the stem of an actively growing plant is cut off just above the soil, the stump will often exude sap from the cut xylem for many hours. If a manometer is sealed over the stump, positive pressures as high as 0.2 MPa (and sometimes even higher) can be measured.

When transpiration is low or absent, positive hydrostatic pressure builds up in the xylem because roots continue to absorb ions from the soil and transport them into the xylem. The buildup of solutes in the xylem sap leads to a decrease in the xylem osmotic potential (Ψ_s) and thus to a decrease in the xylem water potential (Ψ). This lowering of the xylem Ψ provides a driving force for water absorption, which in turn leads to a positive hydrostatic pressure in the xylem. In effect, the multicellular root tissue behaves as an osmotic membrane does, building up a positive hydrostatic pressure in the xylem in response to the accumulation of solutes.

Root pressure is most likely to occur when soil water potentials are high and transpiration rates are low. As transpiration rates increase, water is transported through the plant and lost to the atmosphere so rapidly that a positive pressure resulting from ion uptake never develops in the xylem.

Plants that develop root pressure frequently produce liquid droplets on the edges of their leaves, a phenomenon known as **guttation** (**Figure 6.5**). Positive xylem pressure causes exudation of xylem sap through specialized pores called *hydathodes* that are associated with vein endings at the leaf margin. The "dewdrops" that can be seen on the tips of grass leaves in the morning are actually guttation droplets exuded from hydathodes. Guttation is most noticeable when transpiration is suppressed and the relative humidity is high, such as at night. It is possible that root pressure reflects an unavoidable consequence of high rates of ion accumulation. However, the existence of positive pressures within the xylem at night can help dissolve gas bubbles, and thus play a role in reversing the deleterious effects of cavitation described in the next section.



Courtesy of David McIntyre

Figure 6.5 Guttation in a leaf from lady's mantle (*Alchemilla vulgaris*). In the early morning, leaves secrete water droplets through the hydathodes, located at the margins of the leaves.

6.3 Water Transport through the Xylem

In most plants, the xylem constitutes the longest part of the pathway of water transport. In a plant 1 m tall, more than 99.5% of the water transport pathway through the plant is within the xylem, and in tall trees the xylem represents an even higher percentage of the pathway. Compared with the movement of water through layers of living cells, the xylem is a pathway of low resistivity. In this section we examine how the structure of the xylem contributes to the movement of water from the roots to the leaves, and how negative pressures generated by transpiration pull water through the xylem.

The xylem consists of two types of transport cells

The conducting cells in the xylem have a specialized anatomy that enables them to transport large quantities of water with great efficiency. There are two main types of water-transporting cells in the xylem: tracheids and vessel elements (**Figure 6.6**). Vessel elements are found in angiosperms, a small group of gymnosperms called the Gnetales, and some ferns. Tracheids are present in both angiosperms and gymnosperms, as well as in ferns and other groups of vascular plants.

The maturation of both tracheids and vessel elements involves the production of secondary cell walls and the subsequent death of the cell—the loss of the cytoplasm and all of its contents. What remain are the thick, lignified cell walls, which form hollow tubes through which water can flow with relatively little resistance. However, because lignin is hydrophobic, it makes the secondary cell wall essentially impermeable to water. For this reason, tracheids and vessel elements develop specialized regions that allow water to flow from one water-transporting cell to another.

Tracheids are elongated, spindle-shaped cells (see Figure 6.6A) that are arranged in overlapping vertical files (**Figure 6.7**). Water flows through the open tracheid lumen and between tracheids by means of the numerous **pits** in the tracheids' lateral walls (see Figure

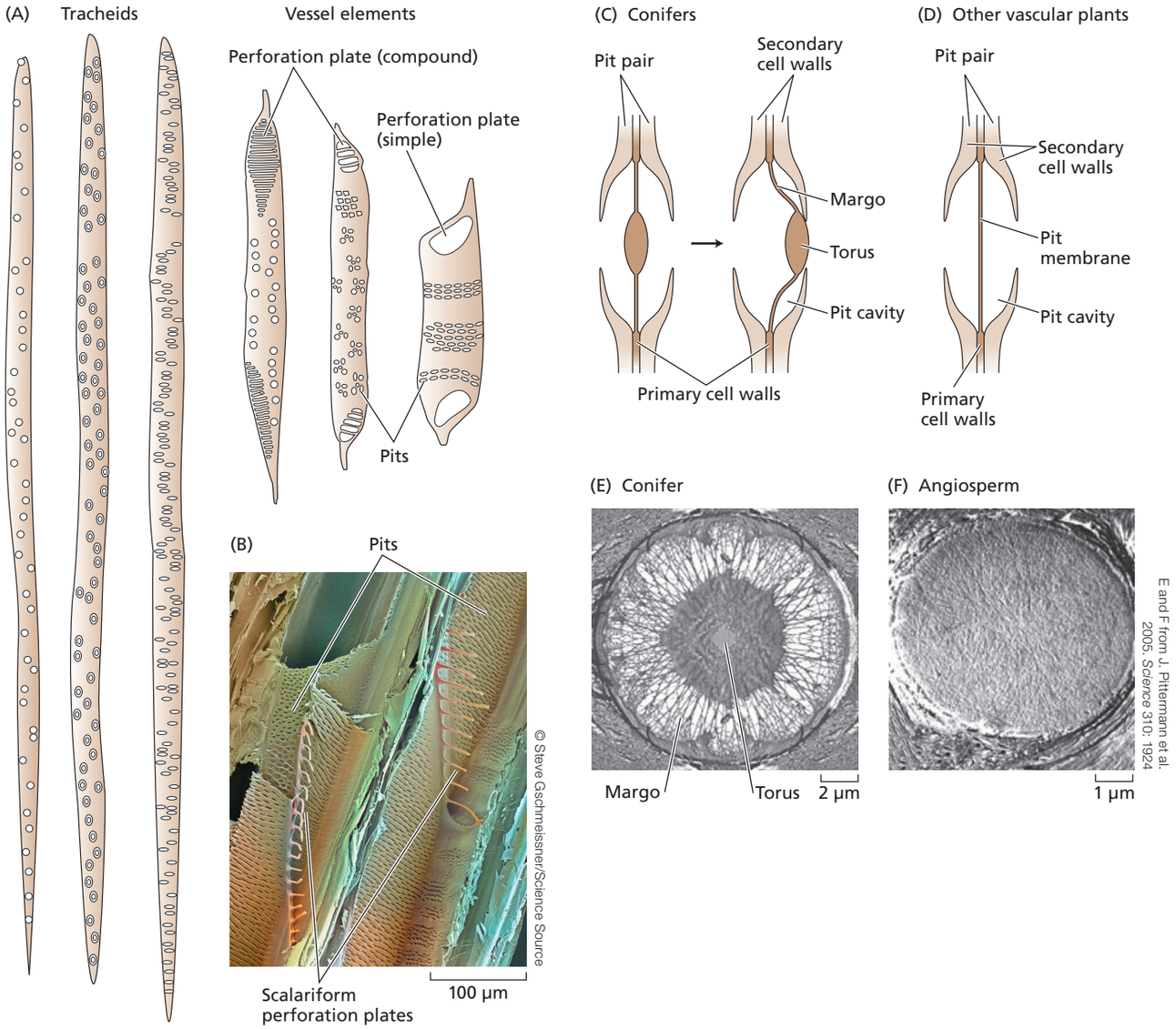


Figure 6.6 **Xylem conduits and their interconnections.** **(A)** Structural comparison of tracheids and vessel elements. Tracheids are elongated, hollow, dead cells with highly lignified walls. The walls contain numerous pits—regions where secondary wall is absent but primary wall remains. The shapes of pits and the patterns of wall pitting vary with species and organ type. Tracheids are present in all vascular plants. Vessels consist of a stack of two or more vessel elements. Like tracheids, vessel elements are dead cells and are connected to one another by perforation plates—regions of the wall where pores or holes have developed. Vessels are connected to other vessels and to tracheids through pits. Vessels are found in most angiosperms and are lacking in most gymnosperms. **(B)** Scanning electron micrograph showing two vessels (running diagonally from lower left to upper right). Pits are visible on the side walls, as are the scalariform (ladderlike) perforation plates between vessel elements. **(C)** Diagram of a coniferous bordered pit pair with the torus centered in the pit cavity (left) or lodged to one side of the cavity (right). When the pressure difference between two tracheids is small, the pit membrane lies close to the center of the bordered pit, allowing water to flow through the porous margo region of the pit membrane; when the pressure difference between two tracheids is large, such as when one has cavitated and the other remains filled with water under tension, the pit membrane is displaced such that the torus becomes lodged against the overarching walls, thereby preventing the embolism from propagating between tracheids. **(D)** In contrast, the pit membranes of angiosperms and other vascular plants are relatively homogeneous in their structure. These pit membranes have very small pores compared with those of conifers, which prevents the spread of embolism but also imparts a significant hydraulic resistance. **(E and F)** Scanning electron microscope images of pit membranes with the overarching secondary wall removed: the torus–margo membrane of a conifer tracheid (E); the homogenous pit membrane of an angiosperm vessel (F). (C after M. H. Zimmerman. 1983. *Xylem Structure and the Ascent of Sap*. Springer, Berlin.)

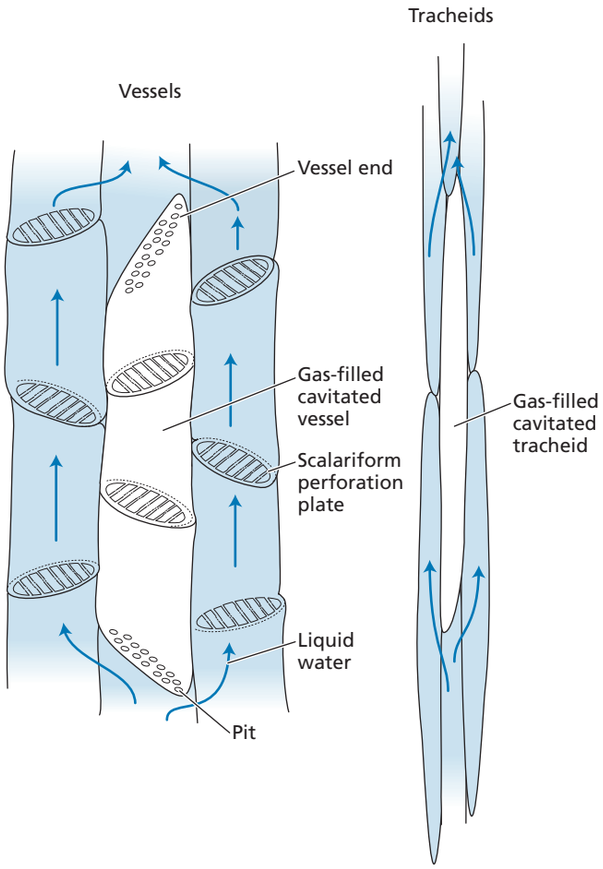


Figure 6.7 **Vessels (left) and tracheids (right) form a series of parallel, interconnected pathways for water movement.** Cavitation blocks water movement because of the formation of gas-filled (embolized) conduits. Because xylem conduits are interconnected through openings ("bordered pits") in their thick secondary walls, water can detour around the blocked vessel by moving through adjacent conduits. Pit membranes help prevent embolisms from spreading between xylem conduits. Thus, in the diagram on the right, the gas is contained within a single cavitated tracheid. In the diagram on the left, gas has filled the entire cavitated vessel, shown here as being made up of three vessel elements, each separated by scalariform perforation plates. In nature, vessels can be very long (up to several meters in length) and thus made up of many vessel elements.

6.6B). Pits are microscopic regions where the lignified secondary wall is absent and only the primary wall is present (see Figure 6.6C). Pits of one tracheid are located opposite pits of an adjoining tracheid, forming **pit pairs**. Pit pairs constitute a low-resistance path for water movement between tracheids. The water-permeable layer between pit pairs, consisting of two primary walls and a middle lamella, is called the **pit membrane**. In **bordered pits**, the secondary wall extends partway over the pit membrane, creating a pit cavity that is connected to the conduit lumen.

Vessel elements have partially or completely open end walls that allow them to be stacked end to end to form a multicellular conduit called a **vessel** (see Figure 6.7). The end walls between adjacent vessel elements form a structure referred to as a **perforation plate**. Each perforation plate contains one or more openings through which water can flow. Simple perforation plates have only a single opening, and often the connection between adjacent vessel elements is completely open. Compound perforation plates have multiple openings, with the plate often consisting of ladderlike bars (scalariform perforation plates).

Vessel elements tend to be shorter and wider than tracheids, but the multicellular vessels formed from vessel elements can be much longer than tracheids. In some species they can be up to a meter or more in length. Like tracheids, vessel elements have pits on their lateral walls (see Figure 6.6B) that allow water to flow from one conduit to another. The vessel elements found at the extreme ends of a vessel have tapered ends and are connected to neighboring vessels via pits.

It is important to emphasize that mature, water-transporting tracheids and vessels do not retain any cell membranes. Thus, the water-filled interiors of xylem conduits form part of the apoplast. Pit membranes, despite their name, do not function like cell membranes. Pit membranes are part of the cell wall, and because they are relatively porous they do not restrict the movement of solutes (i.e., they are not semipermeable and thus cannot cause water to flow by osmosis).

Water moves through the xylem by pressure-driven bulk flow

Pressure-driven bulk flow of water is responsible for long-distance transport of water in the xylem (see Figure 6.1). This pressure gradient must be large enough to overcome the gravitational gradient, which typically opposes the movement of water from the soil to the leaves, as well as the energy dissipated by viscosity. Viscosity describes a fluid's resistance to deformation; in the case of laminar flow through a tube, the relevant deformation arises because water is stationary at the walls of the tube and flows fastest at its center.

If we consider laminar flow through a tube, the rate of flow depends on the radius (r) of the tube, the viscosity (η) of the liquid, and the pressure gradient ($\Delta\Psi_p/\Delta x$) that drives the flow (Δx is a unit of distance along the flow path). Jean Léonard Marie Poiseuille (1797–1869) was a French physician and physiologist, and the relation just described is given by one form of Poiseuille's equation:

$$\text{Volume flow rate} = \left(\frac{\pi r^4}{8\eta}\right)\left(\frac{\Delta\Psi_p}{\Delta x}\right) \qquad (6.2)$$

expressed in cubic meters per second ($m^3\ s^{-1}$). This equation tells us that pressure-driven bulk flow is extremely

sensitive to the radius of the tube. If the radius is doubled, the volume flow rate increases by a factor of 16 (2^4). Vessel elements up to 500 μm in diameter, nearly an order of magnitude greater than that of the largest tracheids, occur in the stems of climbing species. These large-diameter vessels permit vines to transport large amounts of water despite the slenderness of their stems.

Equation 6.2 describes flow through a cylindrical tube and thus does not take into account the fact that xylem conduits are of finite length, such that water must cross many pit membranes as it flows from the soil to the leaves. All else being equal, pit membranes should impede water flow through single-celled (and thus shorter) tracheids to a greater extent than through multicellular (and thus longer) vessels. How then is it possible that conifers are among the tallest trees in the world given that conifer xylem is formed entirely of tracheids?

The answer is that conifers (and the gymnosperm *Ginkgo biloba*) have pit membranes that are much more permeable to water than the pit membranes found in other plants. In conifers, the pit membrane has a central thickening, called a **torus** (plural *tori*), surrounded by a porous and relatively flexible region known as the **margo** (see Figure 6.6C and E). The openings in the margo are large relative to the tiny pores in the pit membranes of other vascular plants. The strong dependence of pressure-driven flow on pore radius (see Equation 6.2) explains why the hydraulic resistance to flow through a conifer pit is much less than in plants that lack margo/torus pit membranes.

As we will see, the major role of pit membranes is to prevent the spread of gas bubbles, called *emboli*, within the xylem. Drought, which results in more negative water potentials (see Chapter 15), can cause xylem conduits to become air-filled, a potentially disastrous situation for a plant because embolized conduits can no longer transport water from the roots to the leaves. The margo/torus structure allows conifer pit membranes to function like valves: When they are centered in the pit cavity, the pits remain open; when they are lodged in the circular or oval wall thickenings bordering the pit, the pits are closed. Such lodging of the torus effectively prevents gas bubbles from spreading into neighboring tracheids (we will discuss this formation of bubbles, a process called cavitation, shortly). Plants that lack margo/torus pit membranes rely on the surface tension of water to prevent gas bubbles from spreading from one xylem conduit to another. For this reason, their pit membranes are constrained to have much smaller pores and thus a much larger hydraulic resistance.

Water movement through the xylem requires a smaller pressure gradient than movement through living cells

The xylem provides a pathway of low resistivity for water movement. Some numerical values will help us appreciate the extraordinary efficiency of the xylem. We will calculate the driving force required to move water through the xylem at a typical velocity and compare it with the driving force that would be needed to move water through a pathway made up of living cells at the same rate.

For the purposes of this comparison, we will use a value of 4 mm s^{-1} for the xylem transport velocity and 40 μm as the vessel radius. This is a high velocity for such a narrow vessel, so it will tend to exaggerate the pressure gradient required to support water flow in the xylem. Using a version of Poiseuille's equation (see Equation 6.2), we can calculate the pressure gradient needed to move water at a velocity of 4 mm s^{-1} through an *ideal* tube with a uniform inner radius of 40 μm. The calculation gives a value of 0.02 MPa m^{-1}. Elaboration of the assumptions, equations, and calculations can be found in **WEB TOPIC 6.3**.

Of course, *real* xylem conduits have irregular inner wall surfaces, and water flow through perforation plates and pits adds resistance to water transport. Such deviations from the ideal increase the viscous drag: Measurements show that the actual resistance is greater by approximately a factor of 2.

Let's now compare this value with the driving force that would be necessary to move water at the same velocity from cell to cell, crossing the plasma membrane each time. As calculated in **WEB TOPIC 6.3**, the driving force needed to move water through a layer of cells at 4 mm s^{-1} is 2×10^8 MPa m^{-1}. This is ten orders of magnitude greater than the driving force needed to move water through our 40-μm-radius xylem vessel. Our calculation clearly shows that water flow through the xylem is vastly more efficient than water flow across living cells. Nevertheless, the xylem can make a significant contribution to the total resistance to water flow through the plant.

What pressure difference is needed to lift water 100 meters to a treetop?

With the foregoing example in mind, let's see what pressure gradient is needed to move water up to the top of a very tall tree. The tallest trees in the world are the coast redwoods (*Sequoia sempervirens*) of North America and the mountain ash (*Eucalyptus regnans*) of Australia. Individuals of both species can exceed 100 m.

If we think of the stem of a tree as a long pipe, we can estimate the pressure difference that is needed to overcome the viscous drag of moving water from the soil to the top of the tree by multiplying the pressure gradient needed to move the water by the height of the tree. The pressure gradients needed to move water through the xylem of very tall trees are on the order of 0.01 MPa m^{-1}, smaller than in our previous example. If we multiply this pressure gradient by the height of the tree (0.01 MPa $m^{-1} \times 100$ m), we find that the total pressure difference

needed to overcome the resistance to water movement through the stem is equal to 1 MPa.

In addition to the hydraulic resistance due to viscosity, we must consider gravity. As described by Equation 5.4, for a height difference of 100 m, the difference in Ψ_g is approximately 1 MPa. That is, Ψ_g is 1 MPa higher at the top of the tree than at the ground level. So the other components of water potential must be 1 MPa more negative at the top of the tree to counter the effects of gravity.

To allow transpiration to occur, the pressure gradient must be large enough to overcome the effects of gravity and the resistance to water movement through the xylem. Thus, we calculate that a pressure difference of roughly 2 MPa, from the base to the top branches, is needed to carry water up the tallest trees.

The cohesion–tension theory explains water transport in the xylem

In theory, the pressure gradient needed to move water through the xylem could result from the generation of positive pressures at the base of the plant. We mentioned previously that some roots can develop positive hydrostatic pressure in their xylem. However, root pressure is typically less than 0.1 MPa and disappears with transpiration or when soils are dry, so it is clearly inadequate to move water up a tall tree. Furthermore, because root pressure is generated by the accumulation of ions in the xylem, relying on this for transporting water would require a mechanism for dealing with these solutes once the water evaporates from the leaves.

Instead, transpiration causes the pressure in the xylem to decrease. It is the lowering of xylem pressures in leaves that creates the pressure gradient that causes water to flow upward from the roots. However, as our earlier calculations show, the $\Delta\Psi_p$ needed to move water through the xylem requires that pressures fall to values far below zero. Negative hydrostatic pressure means that the water molecules pull on one another (and the walls of the xylem conduit). Negative pressures in water are often referred to as tension.

In Chapter 5 we saw how the many hydrogen bonds that form between water molecules make water highly cohesive and give it a high tensile strength. It is these properties of water, coupled with the stiffness of the lignified conduit walls, that allow the xylem to develop and sustain large negative pressures. The idea that transpiration leads to a decrease in xylem pressure and that this tension pulls water through the xylem was first proposed toward the end of the nineteenth century. It is called the *cohesion–tension mechanism of sap ascent* because it requires the cohesive properties of water to sustain large tensions in the xylem water columns.

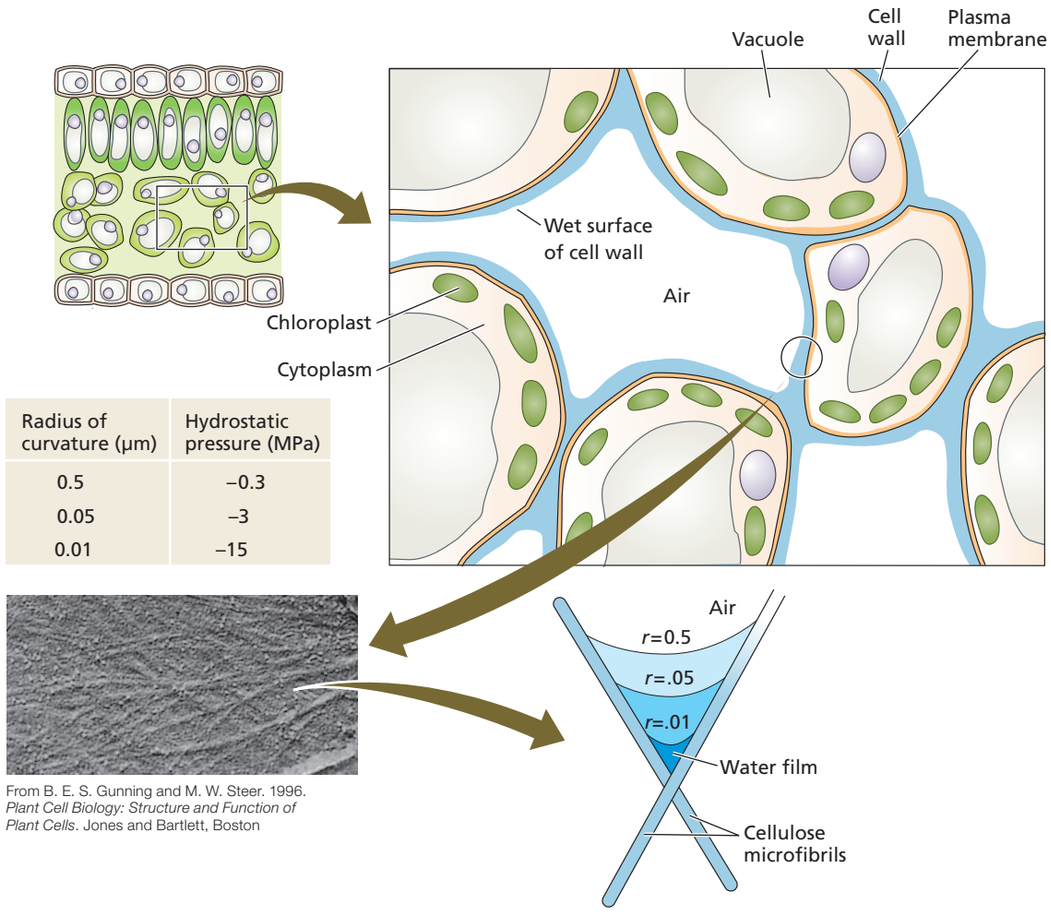
The xylem tensions needed to pull water from the soil develop in leaves as a consequence of transpiration. How does the loss of water vapor through open stomata result in the flow of water from the soil? When leaves open their stomata to obtain CO_2 for photosynthesis, water vapor diffuses out of the leaves. This causes water to evaporate from the surface of cell walls inside the leaves. In turn, the loss of water from the cell walls causes the water potential in the walls to decrease as water is drawn into the interstices of the cell wall where it forms curved air–water interfaces (**Figure 6.8**). Because water adheres to the cellulose microfibrils and other hydrophilic components of the cell wall, the curvature of these interfaces reduces Ψ_p, analogous to what happens in the soil. This creates a gradient in water potential that causes water to flow toward the sites of evaporation. Some of the water that flows toward the sites of evaporation comes from the protoplasts of adjacent cells. However, because leaves are connected to the soil via a low-resistance pathway—the xylem—most of what replaces water lost from the leaves due to transpiration comes from the soil. Water will flow from the soil when the water potential of the leaves is low enough to overcome the Ψ_p of the soil, as well as the resistance associated with moving water through the plant. Note that for water to be pulled from the soil requires that there be a continuous liquid-filled pathway extending from the sites of evaporation, down through the plant, and out into the soil.

The cohesion–tension mechanism explains how the substantial movement of water through plants can occur without the direct expenditure of metabolic energy: The energy that powers the movement of water through plants comes from the sun, which, by increasing the temperature of the leaf, drives the evaporation of water. However, water transport through the xylem is not "free." The plant must build xylem conduits capable of withstanding the large tensions needed to pull water from the soil. In addition, plants must accumulate enough solutes in their living cells that they are able to remain turgid even as water potentials decrease due to transpiration.

The cohesion–tension mechanism has been a controversial subject for more than a century and continues to generate lively debate. The main controversy surrounds the question of whether water columns in the xylem can sustain the large tensions (negative pressures) necessary to pull water up tall trees. Recently, water transport through a microfluidic device designed to function as a synthetic "tree" demonstrated the stable flow of liquid water at pressures lower (more negative) than –7.0 MPa.

Xylem transport of water in trees faces physical challenges

The large tensions that develop in the xylem of trees and other plants present significant physical challenges. First, the water under tension transmits an inward force to the walls of the xylem. If the cell walls were weak or pliant, they would collapse under this



Radius of curvature (μm)	Hydrostatic pressure (MPa)
0.5	–0.3
0.05	–3
0.01	–15

From B. E. S. Gunning and M. W. Steer. 1996. *Plant Cell Biology: Structure and Function of Plant Cells*. Jones and Bartlett, Boston

Figure 6.8 The driving force for water movement through plants originates in leaves. One hypothesis for how this occurs is that as water evaporates from the surfaces of mesophyll cells, water withdraws farther into the interstices of the cell wall. Because cellulose is hydrophilic (contact angle = 0°), the force resulting from surface tension causes a negative pressure in the liquid phase. As the radius of curvature of the air–water interfaces decreases, the hydrostatic pressure becomes more negative, as calculated from Equation 6.1.

tension—analogous to what can happen to a drinking straw if you suck on it too hard. The secondary wall thickenings and lignification of tracheids and vessels are adaptations that offset this tendency to collapse. Plants that experience large xylem tensions tend to have dense wood, reflecting the mechanical stresses imposed on the wood by water under tension.

A second challenge is that water under such tensions is in a *physically metastable state*. Water is stable as a liquid when its hydrostatic pressure exceeds its saturated vapor pressure. When the hydrostatic pressure in liquid water becomes equal to its saturated vapor pressure, the water will undergo a phase change. We are all familiar with the idea of vaporizing water by increasing its temperature (raising its saturated vapor pressure). Less familiar, but still easily observed, is the fact that water can be made to boil at room temperature by placing it in a vacuum chamber (lowering the hydrostatic pressure of the liquid phase by reducing the pressure of the atmosphere).

In our earlier example we estimated that a pressure gradient of 2 MPa would be needed to supply water to leaves at the top of a 100-m-high tree. If we assume that the soil surrounding this tree is fully hydrated and lacks significant concentrations of solutes (i.e., $\Psi = 0$), the cohesion–tension theory predicts that the hydrostatic pressure of water in the xylem at the top of the tree will be –2 MPa. This value is substantially below the saturated vapor pressure (absolute pressure of ~0.002 MPa at 20°C). What maintains the water column in its liquid state?

Water in the xylem is described as being in a metastable state because despite the existence of a thermodynamically lower energy state—the vapor phase—it remains a liquid. This situation occurs because (1) the cohesion and adhesion of water make the free-energy

barrier for the liquid-to-vapor phase change very high, and (2) the structure of the xylem minimizes the presence of *nucleation sites*—sites that lower the energy barrier separating the liquid from the vapor phase.

The most important nucleation sites are gas bubbles. The reason for this is that it takes less energy to expand the gas–liquid interface of an existing bubble than it does to form a bubble (gas void) de novo. Furthermore, the curvature of a bubble, and thus also the inward force resulting from surface tension, is a function of its size. This is why, for the same tension in the xylem, small bubbles remain stable or even contract, losing volume as they push gas back into solution, while large bubbles expand. If the tension in the xylem increases to the point where the inward force on a bubble resulting from surface tension is less than the outward force due to the negative pressure in the liquid phase, the bubble will expand. And once a bubble starts to expand, the force due to surface tension decreases, because the air–water interface of a larger bubble has less curvature. Thus, a bubble that exceeds the critical size for expansion will expand until it fills the entire conduit.

The absence of gas bubbles of sufficient size to destabilize the water column when under tension is due, in part, to the fact that in the roots, water must flow across the endodermis to enter the xylem. The endodermis serves as a filter, preventing gas bubbles from entering the xylem. Pit membranes also function as filters as water flows from one xylem conduit to another. However, when pit membranes are exposed to air on one side—because of injury, leaf abscission, or the existence of a neighboring gas-filled conduit—pit membranes can serve as sites of entry for air. Air enters when the pressure difference across the pit membrane is sufficient either to allow air to penetrate the cellulose matrix of structurally homogeneous pit membranes (see Figure 6.6D), or to dislodge the torus of a coniferous pit membrane (see Figure 6.6C). This phenomenon is called *air seeding*.

A second mode by which bubbles can form in xylem conduits is freezing of the xylem tissues. Because water in the xylem contains dissolved gases and the solubility of gases in ice is very low, freezing of xylem conduits can lead to bubble formation.

In plant physiology, the phenomenon of bubble expansion is referred to as *cavitation*, and the resulting gas-filled void is referred to as an *embolism*. Its effect is similar to that of a vapor lock in the fuel line of an automobile or an embolism in a blood vessel. Cavitation breaks the continuity of the water column and prevents the transport of water under tension.

Vulnerability curves (**Figure 6.9**) provide a way of quantifying a species' susceptibility to cavitation and the impact of cavitation on flow through the xylem. A vulnerability curve plots the measured hydraulic conductivity (usually as a percent of maximum) of a branch, stem, or root segment versus the experimentally imposed level of xylem tension. Due to cavitation, xylem hydraulic conductivity decreases with increasing tensions until flow ceases entirely. However, the decrease in xylem hydraulic conductivity occurs at much lower tensions in species in moist habitats, such as cottonwood than in species from more arid regions, such as sagebrush.

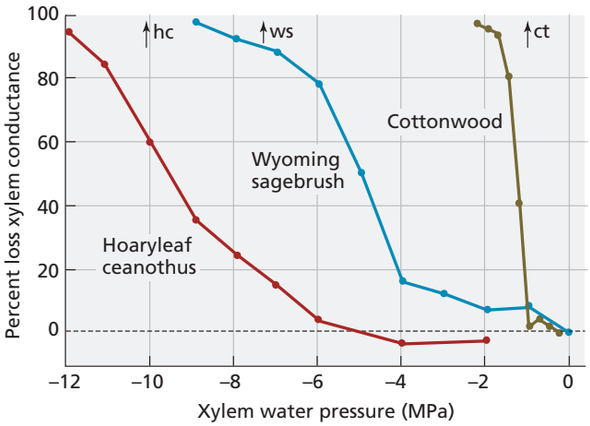


Figure 6.9 Xylem vulnerability curves represent the percentage loss of hydraulic conductance in stem xylem versus xylem water pressure, here in three species of contrasting drought tolerance. Data were obtained from excised branches subjected experimentally to increasing levels of xylem tension using a centrifugal force technique. Arrows on the upper axis indicate the minimum xylem pressure measured in the field for each species. (After J. S. Sperry. 2000. *Agric. For. Meteorol.* 104: 13–23.)

Plants have several mechanisms to overcome losses of xylem conductivity caused by embolism

The impact of xylem cavitation on the plant can be minimized by several means. Pit membranes can prevent an expanding gas bubble from spreading to an adjacent conduit. In this way, pit membranes serve to contain embolism.

Most plants are able to tolerate small amounts of cavitation. Because the capillaries in the xylem are interconnected, water can detour around the embolized conduit by traveling through neighboring, water-filled conduits (see Figure 6.7). Thus, the finite length of the tracheid and vessel conduits of the xylem, while resulting in an increased resistance to water flow, also provides a way to restrict the impact of cavitation. However, any reduction in xylem hydraulic capacity has the potential to affect productivity if it reduces the supply of water to the leaves. Soil drying results in increasingly negative xylem pressures and can lead to substantial amounts of embolism. Plants can mitigate the impact of soil drying by shedding leaves or reducing contact between roots and soil. During prolonged drought, however, xylem

pressures will eventually reach levels that induce cavitation. Recent work shows that embolism is a major factor in drought-induced mortality of trees.

The major way that plants overcome embolism is by producing new xylem conduits or by growing new shoots. This highlights an important benefit of secondary growth (see Chapter 19).

In some species, the development of root pressure allows embolized conduits to be refilled. Recall that root pressure results in the development of positive hydrostatic pressures in the xylem. These positive pressures in the liquid phase are transmitted to any gas bubbles in the xylem. In turn, the increase in pressure forces gas to dissolve and thus allows an embolized conduit to become filled with water.

6.4 Water Movement from the Leaf to the Atmosphere

On its way from the leaf to the atmosphere, water is pulled from the xylem into the cell walls of the mesophyll, where it evaporates into the air spaces of the leaf (**Figure 6.10**). The water vapor then exits the leaf through the stomatal pore. The movement of liquid water through the living tissues of the leaf is controlled by gradients in water potential. However, transport in the vapor phase is by diffusion, so the final part of the transpiration stream is controlled by the *concentration gradient of water vapor*.

The waxy cuticle that covers the leaf surface is an effective barrier to water movement. It has been estimated that only about 5% of the water lost from leaves escapes through the cuticle. Almost all of the water lost from leaves is lost by diffusion of water vapor through the tiny stomatal pores. In most herbaceous species, stomata are present on both the adaxial and abaxial surfaces of the leaf, usually more abundant on the abaxial surface. In many tree species, stomata are located only on the abaxial surface of the leaf.

Leaves have a large hydraulic resistance

Although the distances that water must traverse within leaves are small relative to the entire soil-to-atmosphere pathway, the contribution of the leaf to the total hydraulic resistance is large. On average, leaves constitute 30% of the total liquid-phase resistance, and in some plants their contribution is much larger. This combination of short path length and large hydraulic resistance also occurs in roots, reflecting the fact that in both organs, water transport takes place across highly resistive living tissues as well as through the xylem.

Water enters leaves and is distributed across the leaf lamina in xylem conduits. Water must exit through the xylem walls and pass through multiple layers of living

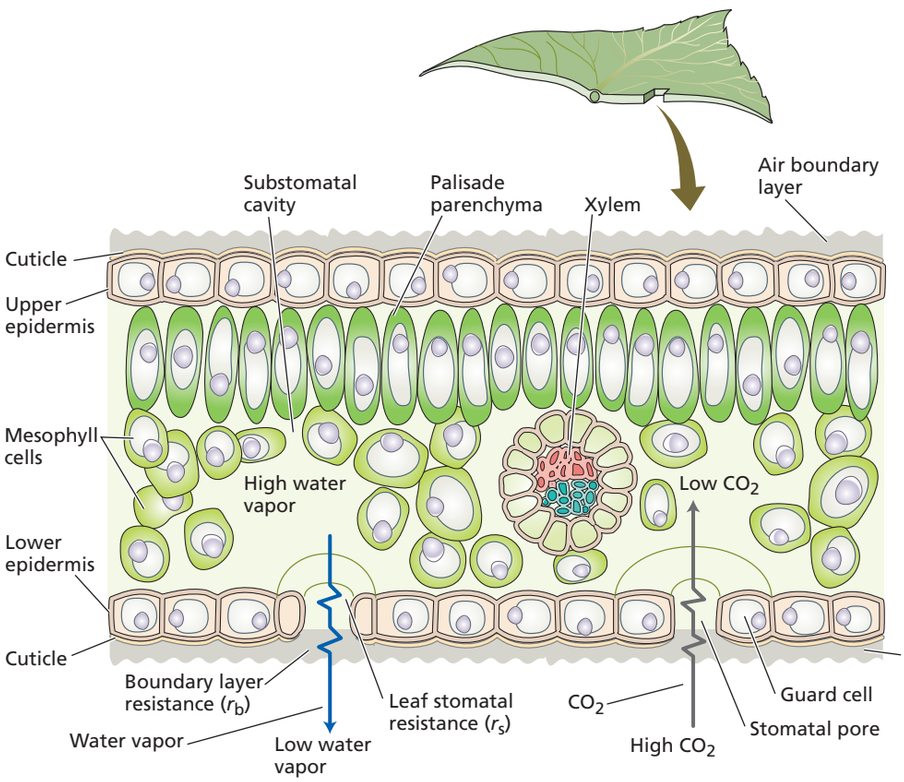


Figure 6.10 Water pathway through the leaf. Water is pulled from the xylem into the cell walls of the mesophyll, where it evaporates into the air spaces within the leaf. Water vapor then diffuses through the leaf air space, through the stomatal pore, and across the boundary layer of still air found next to the leaf surface. CO_2 diffuses in the opposite direction along its concentration gradient (low inside, higher outside).

cells before it evaporates. Leaf hydraulic resistance thus reflects the number, distribution, and size of xylem conduits, as well as the hydraulic properties of leaf mesophyll cells. The hydraulic resistance of leaves of diverse vein architectures varies as much as 40-fold. A large part of this variation appears to be due to the density of veins within the leaf and their distance from the evaporative leaf surface. Leaves with closely spaced veins tend to have lower hydraulic resistance and higher rates of photosynthesis, suggesting that the proximity of leaf veins to sites of evaporation exerts a significant impact on the rates of leaf gas exchange.

The hydraulic resistance of leaves varies in response to growth conditions and exposure to low leaf water potentials. For example, leaves of plants growing in shaded conditions exhibit greater resistance to water flow than do leaves of plants grown in higher light. Leaf hydraulic resistance also typically increases with leaf age. Over shorter time scales, decreases in leaf water potential lead to marked increases in leaf hydraulic resistance. The increase in leaf hydraulic resistance may result from decreases in the membrane permeability of mesophyll cells, cavitation of xylem conduits in leaf veins, or in some cases, the physical collapse of xylem conduits under tension.

Table 6.1 Representative values for relative humidity, absolute water vapor concentration, and water potential for four points in the pathway of water loss from a leaf

Location	Relative humidity	Water vapor	
		Concentration (mol m^{-3}) (c_{wv})	Potential (MPa)[a]
Inner air spaces (25°C)	0.99	1.27	−1.38
Just inside stomatal pore (25°C)	0.97	1.21	−7.04
Just outside stomatal pore (25°C)	0.47	0.60	−103.7
Bulk air (20°C)	0.50	0.50	−93.6

Source: Adapted from P. S. Nobel. 1999. *Physiochemical and Environmental Plant Physiology*, 2nd ed. Academic Press, San Diego, CA.

Note: See Figure 6.10.

[a]Calculated using Equation 6.6.2 in **WEB TOPIC 6.4**, with values for $RT/\overline{V}_w$ of 135 MPa at 20°C and 137.3 MPa at 25°C.

The driving force for transpiration is the difference in water vapor concentration

Transpiration from the leaf depends on two major factors: (1) the **difference in water vapor concentration** between the leaf air spaces and the external bulk air (Δc_{wv}) and (2) the **diffusional resistance** (r) of this pathway. The difference in water vapor concentration is expressed as $c_{wv(leaf)} - c_{wv(air)}$. The water vapor concentration of air ($c_{wv[air]}$) can be readily measured, but that of the leaf ($c_{wv[leaf]}$) is more difficult to assess.

Whereas the volume of air space inside the leaf is small, the wet surface from which water evaporates is large. Air space volume is about 5% of the total leaf volume in pine needles, 10% in maize (corn; *Zea mays*) leaves, 30% in barley, and 40% in tobacco leaves. In contrast to the volume of the air space, the internal surface area from which water evaporates may be from 7 to 30 times the external leaf area. This high surface-to-volume ratio makes for rapid vapor equilibration inside the leaf. Thus, we can assume that the air space in the leaf is close to water potential equilibrium with the cell wall surfaces from which liquid water is evaporating.

Within the range of water potentials experienced by transpiring leaves (generally more positive than –2.0 MPa), the equilibrium water vapor concentration is within 2 percentage points of the saturation water vapor concentration. This allows one to estimate the water vapor concentration within a leaf from its temperature. Because the saturated water vapor content of air increases exponentially with temperature, leaf temperature has a marked impact on transpiration rates. (**WEB TOPIC 6.4** shows how we can calculate the water vapor concentration in the leaf air spaces and discusses other aspects of the water relations within a leaf.)

The concentration of water vapor, c_{wv}, changes at various points along the transpiration pathway. We see from **Table 6.1** that c_{wv} decreases at each step of the pathway from the cell wall surface to the bulk air outside the leaf. The important points to remember are that (1) the driving force for water loss from the leaf is the *absolute* concentration difference (difference in c_{wv}, in mol m^{-3}), and (2) this difference is markedly influenced by leaf temperature.

Water loss is also affected by the pathway resistances

The second important factor governing water loss from the leaf is the diffusional resistance of the transpiration pathway, which consists of two varying components (see Figure 6.10):

1. The resistance associated with diffusion through stomatal pores, the leaf **stomatal resistance** (r_s).
2. The resistance due to the layer of unstirred air next to the leaf surface through which water vapor must diffuse to reach the turbulent air of the atmosphere. This second resistance, r_b, is called the leaf **boundary layer resistance**. We will discuss this type of resistance before considering stomatal resistance.

The thickness of the boundary layer is determined primarily by wind speed and leaf size. When the air

surrounding the leaf is very still, the layer of unstirred air on the surface of the leaf may be so thick that it is the primary deterrent to water vapor loss from the leaf. Increases in stomatal apertures under such conditions have little effect on transpiration rate (**Figure 6.11**), although closing the stomata completely will still reduce transpiration.

When wind velocity is high, the moving air reduces the thickness of the boundary layer at the leaf surface, reducing the resistance of this layer. Under such conditions, stomatal resistance will largely control water loss from the leaf.

Various anatomical and morphological aspects of the leaf can influence the thickness of the boundary layer. Hairs on the surface of leaves can serve as microscopic windbreaks. Some plants have sunken stomata that provide a sheltered region outside the stomatal pore. The size and shape of leaves and their orientation relative to the wind direction also influence the way the wind sweeps across the leaf surface. Most of these factors, however, cannot be altered on an hour-to-hour or even a day-to-day basis. For short-term regulation of transpiration, control of stomatal apertures by the guard cells plays a crucial role in regulating leaf transpiration.

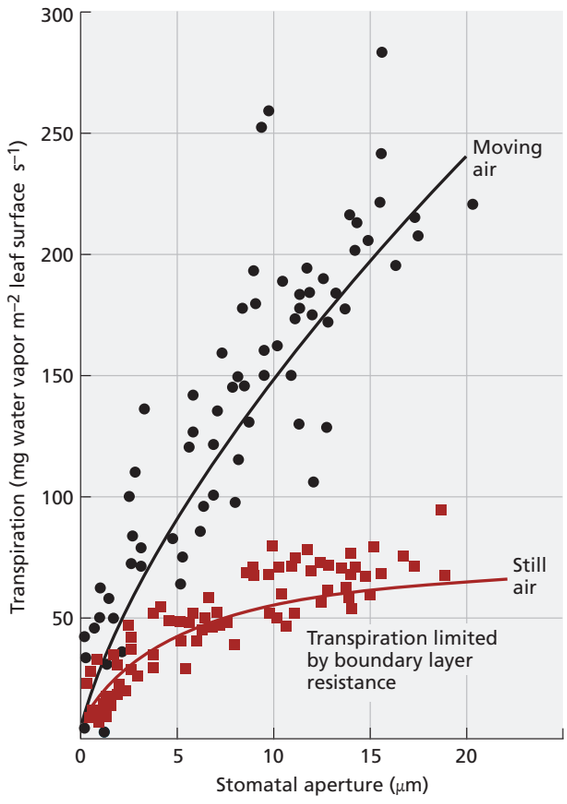


Figure 6.11 Dependence of transpiration on the stomatal aperture of zebra plant (*Zebrina pendula*) in still air and in moving air. The boundary layer is thicker and more rate-limiting in still air than in moving air. As a result, the stomatal aperture has less control over transpiration in still air. (After G. G. J. Bange. 1953. *Acta Bot. Neerl.* 2: 255–296.)

Some species are able to change the orientation of their leaves and thereby influence their transpiration rates. For example, when plants orient their leaves parallel to the sun's rays, leaf temperature is reduced and with it the driving force for transpiration, Δc_{wv}. Many grass leaves roll up as they experience water deficits, in this way reducing light interception. Even wilting can help ameliorate high transpiration rates by reducing the amount of radiation intercepted, resulting in lower leaf temperatures and a decrease in Δc_{wv}.

Stomatal control couples leaf transpiration to leaf photosynthesis

Because the cuticle covering the leaf is nearly impermeable to water, most leaf transpiration results from the diffusion of water vapor through stomata (see Figure 6.10). The microscopic stomatal pores provide a *variable-resistance pathway* for diffusional movement of gases across the epidermis and cuticle. Changes in stomatal resistance are important for regulating water loss by the plant and for controlling the rate of CO_2 uptake necessary for photosynthesis.

On a sunny morning when the supply of water is abundant and the solar radiation incident on the leaf favors high photosynthetic activity, the demand for CO_2 inside the leaf is large and the stomatal pores open wide, decreasing the stomatal resistance to CO_2 diffusion. Water loss by transpiration is substantial under these conditions, but since the water supply from the soil is plentiful, it is advantageous for the plant to accept an increased rate of water loss to obtain more products of photosynthesis, which are essential for growth and reproduction. By contrast, when soil water is less abundant, stomata open less or even remain closed despite abundant sunshine. At night, when there is no photosynthesis and thus no demand for CO_2 inside the leaf, stomata shut, preventing unnecessary loss of water.

The *temporal* regulation of stomatal apertures—open during the day, closed at night—occurs in the majority of plants. Only species that exhibit crassulacean acid metabolism (CAM) photosynthesis, which we will learn about in Chapter 10, exhibit an inverted pattern in which stomata open at night and close during the day. These plants conserve water by capturing and storing CO_2 at night when transpiration rates are low. They then draw on their stored CO_2 during the day, allowing them to photosynthesize despite closed stomata.

The cell walls of guard cells have specialized features

Plants regulate transpiration by opening and closing stomata. This biological control is exerted by a pair of

specialized epidermal cells, the **guard cells**, which surround the stomatal pore (**Figures 6.12** and **6.13**).

Guard cells show considerable morphological diversity, but we can distinguish two main types. The most common type of guard cells have an elliptical contour (often called kidney-shaped) with the pore at their center (see Figure 6.12A). In grasses (see Figure 6.12B), guard cells have a characteristic dumbbell shape, with bulbous ends. The pore is a long slit located between the two "handles" of the dumbbells. These guard cells are always flanked by a pair of differentiated epidermal cells called **subsidiary cells**, which help the guard cells control the stomatal pore. Subsidiary cells are also found in some species with kidney-shaped stomata. The guard cells, subsidiary cells, and pore are collectively called the **stomatal complex**.

A distinctive feature of guard cells is the specialized structure of their walls. Portions of these walls are substantially thickened (see Figure 6.13) and may be up to 5 μm across, in contrast to the 1 to 2 μm typical of epidermal cells. In kidney-shaped guard cells, a differential thickening pattern results in very thick inner and outer walls, a thin wall in contact with surrounding epidermal cells, and a somewhat thickened wall facing the pore. The portions of the outer wall in contact with the atmosphere often extend into well-developed ledges.

The alignment of **cellulose microfibrils**, which reinforce all plant cell walls and are an important determinant of cell shape (see Chapter 2), plays an essential role in the opening and closing of the stomatal pore. In cylindrically shaped cells, cellulose microfibrils are oriented transversely to the long axis of the cell. As a result, the cell expands in the direction of its long axis, because the cellulose reinforcement offers the least resistance at right angles to its orientation.

In guard cells the microfibril organization is different. Kidney-shaped guard cells have cellulose microfibrils fanning out radially from the pore (see Figure 6.12C). As a result, the wall facing the pore is much stronger than the wall in contact with epidermal cells. Thus, as a guard cell increase in volume, the side facing the epidermis expands more than the side facing the pore. This causes the guard cells to bow apart and the pore to open. In grasses, the dumbbell-shaped guard cells function like beams with inflatable ends. The orientation of the cellulose microfibrils is such that as the bulbous ends of the cells increase in volume, the beams move apart from each other and the slit between them widens (see Figure 6.12C).

While the orientation of the cellulose microfibrils is a major determinant of guard cell expansion during stomatal opening, recent computer modeling studies and experiments with cell wall mutants have shown that the matrix polysaccharides (see Chapter 2) play an important role as well. At the early stages of stomatal opening, the microfibril orientation dictates the pattern of opening. As the pressure in the guard cells increases, however, the cell wall pectins undergo strain-induced stiffening, and this property appears to be critical for proper opening of the stomata.

Changes in guard cell turgor pressure cause stomata to open and close

The early aspects of stomatal opening are ion uptake and other metabolic changes in the guard cells, which we will discuss in detail in Chapter 8. Here we will note

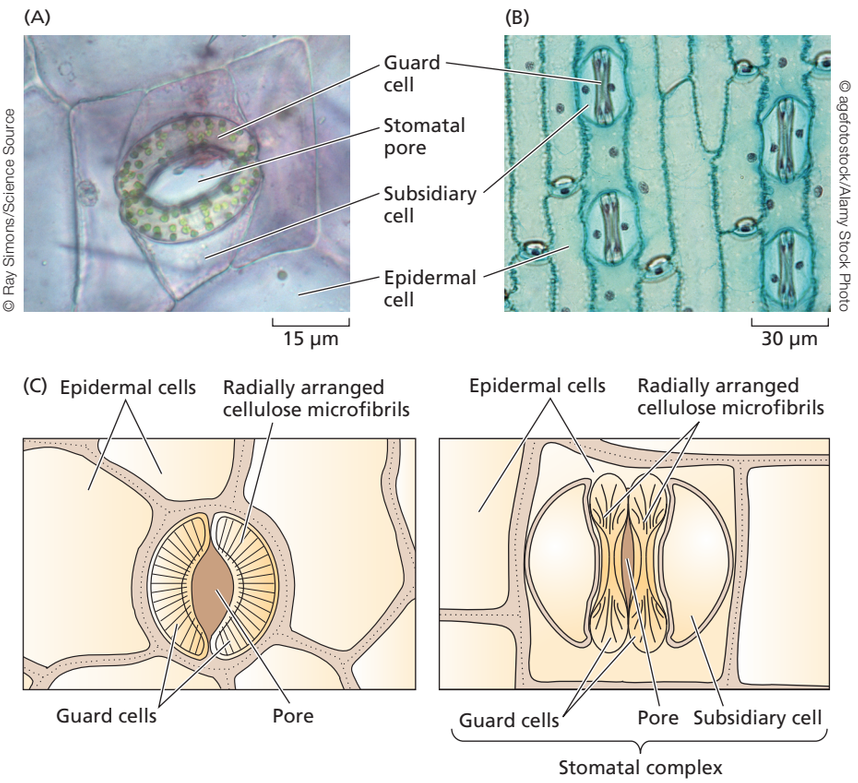


Figure 6.12 **Stomata.** **(A)** Most plants have kidney-shaped guard cells, as seen in this open stoma of *Tradescantia zebrina*. **(B)** Stomata of maize (*Zea mays*), showing the dumbbell-shaped guard cells typical of grasses. **(C)** Radial alignment of the cellulose microfibrils in guard cells and epidermal cells of a kidney-shaped stoma (left) and a grasslike stoma (right). (C after H. Meidner and D. Mansfield. 1968. *Physiology of Stomata*. McGraw-Hill, London.)

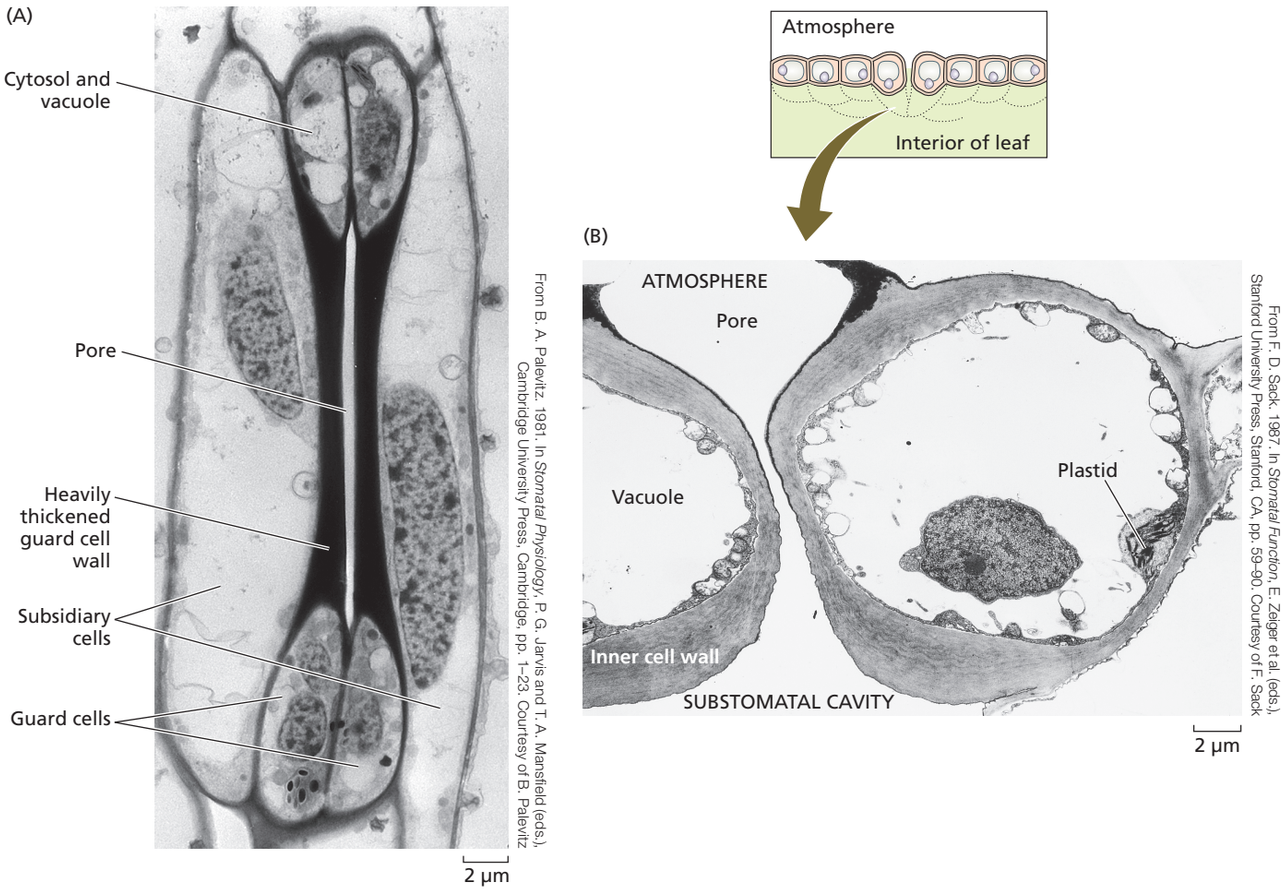


Figure 6.13 **Guard cell wall structure.** **(A)** Electron micrograph of a stoma from a grass (*Phleum pretense*). The bulbous ends of each guard cell show their cytosolic content and are joined by the heavily thickened walls. The stomatal pore separates the two midportions of the guard cells. **(B)** Electron micrograph showing a pair of guard cells from tobacco (*Nicotiana tabacum*). The section was made perpendicular to the main surface of the leaf. In both images, the stomatal pore is very small, indicating that the stomata are essentially closed. Note the uneven thickening pattern of the walls, which determines the asymmetric deformation of the guard cells when their volume increases during stomatal opening.

the effect of decreases in osmotic potential (Ψ_s) resulting from ion uptake and from biosynthesis of organic molecules in the guard cells. The potassium ion concentration in guard cells increases severalfold when stomata open, from 100 m*M* in the closed state to 400 to 800 m*M* in the open state, depending on the species and the experimental conditions. In most species these large concentration changes in K^+ are electrically balanced by varying amounts of the anions Cl^- and malate^{2-}. However, in some species of the genus *Allium*, such as onion (*A. cepa*), K^+ is balanced solely by Cl^-.

Water relations in guard cells follow the same rules as in other cells. A decrease in Ψ_s causes the water potential to decrease, and water consequently moves into the guard cells. As water enters the cell, turgor pressure increases and the stomata open. Stomatal closure results from a decrease in guard cell turgor pressure as a result of solute efflux and polymerization and thus is essentially stomatal opening in reverse.

In grasses, stomatal opening involves the transfer of solutes out of subsidiary cells and into guard cells, resulting in an increase in the turgor pressure of guard cells and a decrease in the turgor pressure of subsidiary cells. As a result, the guard cells are able to move laterally into space previously occupied by subsidiary cells. The reciprocal exchange of solutes between guard cells and subsidiary cells is thought to play an important role in allowing grass stomata to open quickly and to achieve large apertures.

Internal and external signals regulate the osmotic balance of guard cells

Guard cells function as multisensory hydraulic valves. Environmental factors such as light quality and intensity, temperature, leaf water status, and intercellular CO_2

concentrations are sensed by guard cells, and these signals are integrated into well-defined stomatal responses.

Stomatal opening is triggered by both blue and red wavelengths of light. In guard cells, blue light is perceived by the phototropin photoreceptors (see Chapter 16), which trigger responses that drive ion uptake (see Chapter 8) and lower guard cell water potential. The result is water uptake and vacuolar expansion that produces rapid stomatal opening (see Chapter 16 for details). Blue light also stimulates conversion of starches to glucose to provide energy for stomatal opening (see Chapter 10). Because the intensity of blue light needed to promote stomatal opening is extremely low, blue light is thought to be the principal signal for stomata to open at dawn. In most plants, higher intensities of red-enriched photosynthetically active radiation (PAR) (see Chapter 9) induce stomatal opening during the day. The exception are CAM plants, which display the opposite response: Stomata open during the night. In both cases, the regulation of stomatal opening involves ion uptake. Opening responses also correlate with changes in sucrose levels and are integrated with CO_2 sensing (see Chapter 16).

A potent signal for stomatal closure is the hormone abscisic acid, discussed in detail in Chapter 15. Abscisic acid produced by mesophyll cells in response to decreases in mesophyll cell turgor pressure is transported to guard cells, where it triggers the rapid release of solutes and thus a decrease in guard cell turgor pressure that causes stomata to close. Stomatal closure in response to water-deficit stress helps plants avoid developing xylem tensions associated with a high likelihood of cavitation.

The transpiration ratio measures the relationship between water loss and carbon gain

The effectiveness of plants in moderating water loss while allowing sufficient CO_2 uptake for photosynthesis can be assessed by a parameter called the **transpiration ratio**. This value is defined as the amount of water transpired by the plant divided by the amount of carbon dioxide assimilated by photosynthesis.

For plants in which the first stable product of carbon fixation is a three-carbon compound (C_3 plants; see Chapter 10), as many as 400 molecules of water are lost for every molecule of CO_2 fixed by photosynthesis, giving a transpiration ratio of 400. (Sometimes the reciprocal of the transpiration ratio, called the *water-use efficiency*, is cited. Plants with a transpiration ratio of 400 have a water-use efficiency of 1/400, or 0.0025.)

The large ratio of H_2O efflux to CO_2 influx results from three factors:

1. The concentration gradient driving water loss is about 100 times larger than that driving the influx of CO_2. In large part, this difference is due to the low concentration of CO_2 in air (about 0.04%) and the relatively high concentration of water vapor within the leaf.
2. CO_2 diffuses about 1.6 times more slowly through air than water does (the CO_2 molecule is larger than H_2O and has a smaller diffusion coefficient).
3. CO_2 must cross the plasma membrane, the cytoplasm, and the chloroplast envelope before it is assimilated in the chloroplast. These membranes add to the resistance of the CO_2 diffusion pathway.

Some plants use variations in the usual photosynthetic pathway for fixation of carbon dioxide that substantially reduce their transpiration ratio. Plants in which a four-carbon compound is the first stable product of photosynthesis (C_4 plants; see Chapter 10) generally transpire less water per molecule of CO_2 fixed than C_3 plants do; a typical transpiration ratio for C_4 plants is about 150. This is largely because C_4 photosynthesis results in a lower CO_2 concentration in the intercellular air space (see Chapter 10), thus creating a larger driving force for the uptake of CO_2 and allowing these plants to operate with smaller stomatal apertures and thus lower transpiration rates.

Desert-adapted plants with CAM photosynthesis, in which CO_2 is initially fixed into four-carbon organic acids at night (see Chapter 10), have even lower transpiration ratios; values of about 50 are not unusual. This is possible because their stomata have an inverted diurnal rhythm, opening at night and closing during the day. Transpiration is much lower at night, because the cool leaf temperature gives rise to only a very small Δc_{wv}.

6.5 Overview: The Soil–Plant–Atmosphere Continuum

We have seen that movement of water from the soil through the plant to the atmosphere involves different mechanisms of transport:

- In the soil and the xylem, liquid water moves by bulk flow in response to a pressure gradient ($\Delta\Psi_p$).
- When liquid water is transported into and out of cells, the driving force is the water potential difference across the plasma membrane.
- In the vapor phase, water moves primarily by diffusion, at least until it reaches the outside air, where convection (a form of bulk flow) becomes dominant.

However, the key element in the transport of water from the soil to the leaves is the generation of negative pressures within the xylem due to the capillary forces within the cell walls of transpiring leaves. At the other end of the plant, soil water is also held by capillary forces. This results in a "tug-of-war" on a rope of water

by capillary forces at both ends. As a leaf loses water due to transpiration powered by sunlight, water moves through the xylem driven by physical forces.

This simple mechanism makes for tremendous energetic efficiency, which is critical when as many as 400 molecules of water are being transported for every CO_2 molecule being taken up in exchange. Crucial elements that allow this transport system to function are a low-resistivity xylem flow path that is protected from cavitation, a high-surface-area root system for extracting water from the soil, and the ability to limit water loss from leaf surfaces when the soil is dry.

Summary

There is an inherent conflict between a plant's need for CO_2 uptake and its need to conserve water, resulting from water being lost through the same pores that let in CO_2. To manage this conflict, plants have evolved adaptations that control water loss from leaves, and that replace the water that is lost to the atmosphere with water from the soil.

6.1 Water in the Soil

- The water content and rate of movement in soils depend on soil type and structure, which influence the pressure gradient in the soil and its hydraulic conductivity.
- In soil, water may exist as a surface film on soil particles, or it may partially or completely fill the spaces between particles.
- Osmotic potential, pressure potential, and gravitational potential influence the movement of water from the soil through the plant to the atmosphere (**Figure 6.1**).
- The intimate contact between root hairs and soil particles greatly increases the surface area for water absorption (**Figure 6.2**).

6.2 Water Absorption by Roots

- Water uptake is mostly confined to regions near root tips (**Figure 6.3**).
- In the root, water may move via the apoplast, the symplasm, or the transmembrane pathway (**Figure 6.4**).
- Water movement through the apoplast is obstructed by the Casparian strip in the endodermis, which forces water to move symplasmically before it enters the xylem (**Figure 6.4**).
- When transpiration is low or absent, the continued transport of solutes into the xylem fluid leads to a decrease in Ψ_s and a decrease in Ψ, providing the force for water absorption and a positive Ψ_p, which yields a positive hydrostatic pressure in the xylem (**Figure 6.5**).

6.3 Water Transport through the Xylem

- Xylem conduits, which can be either single-celled tracheids or multicellular vessels, provide a low-resistance pathway for the transport of water (**Figure 6.6**).
- Elongated, spindle-shaped tracheids and stacked vessel elements have pits in lateral walls (**Figure 6.6**).
- Pressure-driven bulk flow moves water long distances through the xylem.
- The ascent of water through plants results from the decrease in water potential at the sites of evaporation within leaves (**Figure 6.8**).
- Cavitation breaks the continuity of the water column in the xylem and prevents the transport of water under tension (**Figures 6.7, 6.9**).

6.4 Water Movement from the Leaf to the Atmosphere

- Water is pulled from the xylem into the cell walls of leaf mesophyll before evaporating into the leaf's air spaces (**Figure 6.10**).
- The hydraulic resistance of leaves is large and varies in response to growth conditions and exposure to low leaf water potentials.
- Transpiration depends on the difference in water vapor concentration between the leaf air spaces and the external air and on the diffusional resistance of this pathway, which consists of leaf stomatal resistance and boundary layer resistance (**Figure 6.11, Table 6.1**).
- Opening and closing of the stomatal pore are accomplished and controlled by guard cells (**Figures 6.12, 6.13**).
- Stomatal movements are driven by changes in the solute concentration (Ψ_s) of guard cells. Blue and red wavelengths of light stimulate solute accumulation and thus stomatal opening, while the hormone abscisic acid triggers guard cells to decrease their solute concentration and thus to close.
- The effectiveness of plants in limiting water loss while allowing CO_2 uptake is given by the transpiration ratio.

6.5 Overview: The Soil–Plant–Atmosphere Continuum

- Physical forces, without the involvement of any metabolic pump, drive the movement of water from soil to plant to atmosphere, with the sun being the ultimate source for the energy.

Web Material

- **WEB TOPIC 6.1 Irrigation** Irrigation has a dramatic impact on crop yield and soil salinity.
- **WEB TOPIC 6.2 Physical Properties of Soils** The size distribution of soil particles influences the soil's ability to hold and conduct water.
- **WEB TOPIC 6.3 Calculating Velocities of Water Movement in the Xylem and in Living Cells** Water flows more easily through the xylem than across living cells.
- **WEB TOPIC 6.4 Leaf Transpiration and Water Vapor Gradients** Leaf transpiration and stomatal conductance affect leaf and air water vapor concentrations.

For more study aids, go to oup.com/he/taiz7e.

Suggested Reading

Bramley, H., Turner, N. C., Turner, D. W., and Tyerman, S. D. (2009) Roles of morphology, anatomy and aquaporins in determining contrasting hydraulic behavior of roots. *Plant Physiol*. 150: 348–364.

Brodribb, T. J., McAdam, S. A. M., and Carins Murphy, M. R. (2017) Xylem and stomata, coordinated through space and time. *Plant Cell Environ.* 40: 872–880.

Buckley, T. N. (2019) How do stomata respond to water stress? *New Phytol*. 224: 21–36.

Choat, B., Brodribb, T .J., Brodersen, C. R., Duursma, R. A., López, R., and Medlyn, B. E. (2018) Triggers of tree mortality under drought. *Nature* 558: 531–539.

Hacke, U. G., Sperry, J. S., Pockman, W. T., Davis, S. D., and McCulloh, K. (2001) Trends in wood density and structure are linked to prevention of xylem implosion by negative pressure. *Oecologia* 126: 457–461.

Pickard, W. F. (1981) The ascent of sap in plants. *Prog. Biophys. Mol. Biol*. 37: 181–229.

Pittermann, J., Sperry, J. S., Hacke, U. G., Wheeler, J. K., and Sikkema, E. H. (2005) Torus-margo pits help conifers compete with angiosperms. *Science* 310: 1924.

Roelfsema, M. R. G., and Kollist, H. (2013) Tiny pores with a global impact. *New Phytol*. 197: 11–15.

Sack, L., and Scoffoni, C. (2013) Leaf venation: structure, function, development, evolution, ecology and applications in past, present and future. *New Phytol*. 198: 983–1000.

Stroock, A. D., Pagay, V. V., Zwieniecki, M. A., and Holbrook, N. M. (2014). The physicochemical hydrodynamics of vascular plants. *Annu. Rev. Fluid Mech*. 46: 615–642.

7 Mineral Nutrition



Dancestrokes/
Shutterstock

Mineral nutrients are elements such as nitrogen, phosphorus, and potassium that plants acquire from the soil. Most mineral nutrients originate in the substrate rock and are released as the rock breaks down or is weathered. Although mineral nutrients continually cycle through all organisms, they enter the **biosphere** predominantly through the roots of plants, so in a sense plants act as "miners" of Earth's crust. The large surface area of roots and their ability to absorb nutrients, in elemental or compound form, at low concentrations from the soil solution increase the effectiveness of mineral acquisition by plants. After being absorbed by roots, the mineral elements or compounds that contain them are translocated to the different parts of the plant, where they serve in numerous biological functions. Other organisms, such as mycorrhizal fungi and nitrogen-fixing bacteria, often participate with roots in the acquisition of mineral nutrients.

The study of how plants obtain and use mineral nutrients is called **mineral nutrition**. This area of research is central for improving modern agricultural practices and environmental protection, as well as for understanding plant ecological interactions in natural ecosystems. High agricultural yields often depend on fertilization with mineral nutrients. The application of a **limiting nutrient** will increase plant growth and yield unless another abiotic or biotic stress is also limiting. To meet the demand for food by the increasing world population (**Box 7.1**), annual world use of fertilizer has increased dramatically since 1940. Agricultural production is also increasing, especially grain and livestock production, in part because of fertilizer use but also because of improvements in crop genetics.

More than half of the energy used in agriculture is expended on the production, distribution, and application of nitrogen fertilizers. Moreover, production of phosphorus fertilizers depends on nonrenewable resources that are likely to reach peak production during this century. Crop plants, however, typically use less than half of the fertilizer applied to the soils around them. The remaining minerals may leach into surface waters or groundwater, become associated with soil particles, or contribute to air pollution or climate change after conversion to ammonia or nitrous oxide, for example.

Box 7.1 Nitrogen Fertilizers and Climate Change

Massive use of synthetic nitrogen (N) fertilizers beginning in the twentieth century, and now amounting to more than 120 teragrams (Tg; 1 Tg = 1 million metric tons) of N per year, underpinned the Green Revolution and ensures food security for much of humanity. However, the use of N fertilizers also has unfavorable consequences for the world in that reactive nitrogen species (RNS) adversely affect water and air quality and human and ecosystem health, taking us beyond a safe operating space for humanity. Human intervention in the global N cycle, primarily through the production and use of N fertilizers but also through the production of N oxides (NOx) from burning fossil fuels, has doubled the flux of N through the cycle, with additional impacts on Earth's climate. RNS compounds have many positive and negative influences on greenhouse gas (GHG) balance, although the net climate effect may be cooling, in part because of increased photosynthesis and CO_2 sequestration in the biosphere. Agriculture is the main source of ammonia emissions, which contribute the most to the cooling effect of RNS, mainly through aerosol formation and solar energy reflection and N deposition that stimulates carbon sequestration. Likewise, agriculture is the main source of the potent greenhouse gas N_2O, the primary RNS contributor to global warming. NOx have many interactions, leading to ozone (a GHG) and aerosol production, for example, which together lead to a small net cooling effect. Production and use of synthetic fertilizers have had other direct and indirect effects on climate, including the release of CO_2 from fossil fuels used to produce ammonia, which accounts for about 1% of global energy use. The doubling of the world population has led to a tripling of the consumption of fossil fuels and CO_2 emissions since the 1960s (see **Figure A**).

As a result, there is growing pressure to increase N-use efficiency (NUE) in agriculture, for example through improved management practices that better match supply of fertilizer with crop demand for N, plant breeding to improve uptake and utilization of soil N, and the use of legumes that incorporate atmospheric di-nitrogen into ammonia via symbiotic nitrogen fixation (see Chapter 14). Globally, NUE, defined as nitrogen captured in harvested grain divided by total N inputs, stands at about 40% for the major cereals, wheat, maize, and rice, while it is 80% for the major legume, soybean. Thus, greater use of legumes for food production, or simply as a natural source of fixed N for agricultural systems when used as a cover crop in rotations or intercropped with a non-legume, could increase overall NUE of agriculture and reduce the need for synthetic N fertilizers. This would help ensure food security while reducing the negative environmental impacts of N fertilizers. ■

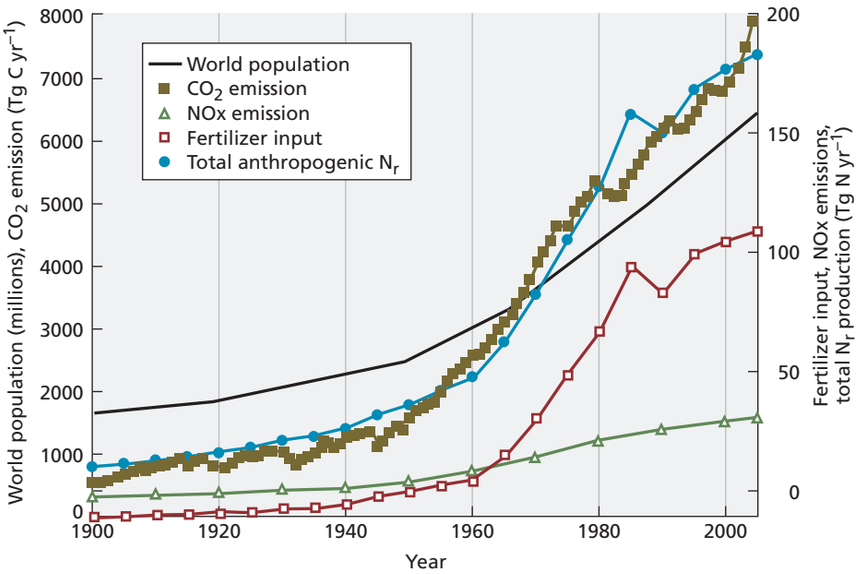


Figure A World trends in human population, N fertilizer consumption, N oxide (NOx) and CO_2 emissions, and human N fixation (total anthropogenic N_r). The rate of human N fixation is now about twice that of biological N fixation in terrestrial ecosystems. N_r, reactive nitrogen. (After J. W. Erisman et al. 2011. *Curr. Opin. Environ. Sustain.* 3: 281–290.)

As a consequence of fertilizer leaching, many water wells in the United States now exceed the federal standard for nitrate (NO_3^-) concentrations in drinking water of 10 mg/L. Infants have the greatest risk from nitrate poisoning (methemoglobinemia). In addition to nitrogen from fertilizer, nitrogen released to the environment by other human activities and deposited in the soil by rainwater, a process known as atmospheric nitrogen deposition, is altering ecosystems throughout the world.

In this chapter we discuss the nutritional needs of plants, the symptoms of specific nutritional deficiencies, and the use of fertilizers to ensure proper plant nutrition. Then we examine how soil structure (the arrangement of solid, liquid, and gas phase components) and root morphology influence the transfer of nutrients from the environment into a plant. Finally, we introduce the topic of symbiotic mycorrhizal associations, which play key roles in nutrient acquisition in the majority of plants. Chapters 8 and 14 address additional aspects of solute transport and nutrient assimilation, respectively.

7.1 Essential Nutrients, Deficiencies, and Plant Disorders

Only certain elements are essential for plants. An **essential element** is defined as one whose absence causes severe abnormalities in plant growth, development, or reproduction and may prevent a plant from completing its life cycle. Essential elements serve myriad functions in plants. They are components of cell walls, membranes, and other structural components, proteins that catalyze metabolism, nucleic acids that store and process genetic information, molecular cascades involved in signal transduction, and are essential for osmotic homeostasis and other functions. If plants are given these essential elements, as well as water and energy from sunlight, they can synthesize all the compounds they need for normal growth. **Table 7.1** lists the elements that are considered to be essential for most, if not all, vascular plants. The first three elements—hydrogen, carbon, and oxygen—are not considered mineral nutrients because they are obtained primarily from water or atmospheric carbon dioxide.

Essential mineral elements are usually classified as *macronutrients* or *micronutrients* according to their relative concentrations in plants. In some cases, the differences in concentration between macronutrients and micronutrients are not as large as those indicated in Table 7.1. For example, some plant tissues, such as the leaf mesophyll, contain almost as much iron or manganese as they do sulfur or magnesium. Often elements are present in concentrations greater than the plant's minimum requirements, with the excess being stored.

The classification of plant nutrients into macronutrients and micronutrients is a traditional approach but is difficult to justify physiologically. Many scientists prefer to classify nutrients according to their biochemical role and physiological function. **Table 7.2** shows such a classification, in which plant nutrients have been divided into four basic groups:

1. Nitrogen, sulfur, and phosphorus constitute the first group of essential elements. These elements form covalent bonds in carbon-containing compounds

TABLE 7.1 Tissue concentrations of essential elements required by most plants

Element	Chemical symbol	Concentration in dry matter (mg g^{-1} or µg g^{-1})[a]	Relative number of atoms with respect to molybdenum
Obtained from water or carbon dioxide			
Hydrogen	H	60	60,000,000
Carbon	C	450	40,000,000
Oxygen	O	450	30,000,000
Obtained from the soil			
Macronutrients			
Nitrogen	N	15	1,000,000
Potassium	K	10	250,000
Calcium	Ca	5	125,000
Magnesium	Mg	2	80,000
Phosphorus	P	2	60,000
Sulfur	S	1	30,000
Silicon	Si	1	30,000
Micronutrients			
Chlorine	Cl	100	3,000
Iron	Fe	100	2,000
Boron	B	20	2,000
Manganese	Mn	50	1,000
Sodium	Na	10	400
Zinc	Zn	20	300
Copper	Cu	6	100
Nickel	Ni	0.1	2
Molybdenum	Mo	0.1	1

Source: After E. Epstein. 1972. *Mineral Nutrition of Plants: Principles and Perspectives*. John Wiley and Sons, New York; E. Epstein. 1999. *Annu. Rev. Plant Physiol. Plant Mol. Biol.* 50: 641—664.

[a]The values for the nonmineral elements (H, C, O) and the macronutrients are in mg g^{-1}, while the values for micronutrients are expressed in µg g^{-1}.

and macromolecules (e.g., nucleic acids, proteins, and lipids). The abundance of such crucial molecules explains why nitrogen, sulfur, and phosphorus are essential macronutrients. Plants assimilate nitrogen and sulfur via biochemical reactions involving oxidation and reduction reactions to form covalent bonds with carbon (see Chapter 14).

2. In the second group, silicon and boron are important for maintaining structural integrity. Silicon is a beneficial nutrient for most plants but is an essential nutrient only in Equisetaceae. Silicon is taken up as silicic acid and accumulates in cell walls as amorphous silica (SiO_2). Boron is an important structural component of pectin in cell walls (see Chapter 2).
3. The third group is present in plants as either free ions dissolved in the plant water or ions electrostatically bound to substances such as the pectic acids present in the plant cell wall. Elements in this group have important roles as enzyme cofactors, in regulating osmotic potentials, and in controlling membrane permeability.
4. The fourth group, including metals such as iron, has important roles in reactions involving electron transfer.

TABLE 7.2 Classification of plant mineral nutrients according to biochemical function

Mineral nutrient	Functions
Group 1	**Nutrients that are part of carbon compounds**
N	Constituent of amino acids, amides, proteins, nucleic acids, nucleotides, coenzymes, hexosamines, etc.
S	Component of amino acids cysteine and methionine. Constituent of lipoic acid, coenzyme A, thiamine pyrophosphate, glutathione, biotin, 5′-adenylylsulfate, and 3′-phosphoadenosine.
P	Component of sugar phosphates, nucleic acids, nucleotides, coenzymes, phospholipids, phytic acid, etc. Has a key role in reactions that involve ATP.
Group 2	**Nutrients that are important for structural integrity**
Si	Deposited as amorphous silica in cell walls. Contributes to cell wall mechanical properties, including rigidity and elasticity.
B	Structural component of pectic polysaccharide RG II (rhamnogalacturonan II). Forms complexes with mannitol, mannan, polymannuronic acid, and other constituents of cell walls. Involved in cell elongation and nucleic acid metabolism.
Group 3	**Nutrients that remain in ionic form**
K	Required as a cofactor for more than 40 enzymes. Principal cation in establishing cell turgor and maintaining cell electroneutrality.
Ca	Constituent of the middle lamella of cell walls. Required as a cofactor by some enzymes involved in the hydrolysis of ATP and phospholipids. Acts as a second messenger in metabolic regulation.
Mg	Required by many enzymes involved in phosphate transfer. Constituent of the chlorophyll molecule.
Cl	Required for the photosynthetic reactions involved in O_2 evolution.
Zn	Constituent of alcohol dehydrogenase, glutamic dehydrogenase, carbonic anhydrase, etc.
Na	Involved with the regeneration of phosphoenolpyruvate in C_4 and CAM plants. Substitutes for potassium in some functions.
Group 4	**Nutrients that are involved in redox reactions**
Fe	Constituent of cytochromes and nonheme iron proteins involved in photosynthesis, N_2 fixation, and respiration.
Mn	Required for activity of some dehydrogenases, decarboxylases, kinases, oxidases, and peroxidases. Involved with other cation-activated enzymes and photosynthetic O_2 evolution.
Cu	Component of ascorbic acid oxidase, tyrosinase, monoamine oxidase, uricase, cytochrome oxidase, phenolase, laccase, and plastocyanin.
Ni	Constituent of urease. In N_2-fixing bacteria, constituent of hydrogenases.
Mo	Constituent of nitrogenase, nitrate reductase, and xanthine dehydrogenase.

Source: After H. J. Evans and G. J. Sorger. 1966. *Annu. Rev. Plant Physiol.* 17: 47–76; K. Mengel and E. A. Kirkby. 2001. *Principles of Plant Nutrition*, 5th ed. Kluwer Academic Publishers, Nordrecht, Netherlands.

Please keep in mind that this classification is somewhat arbitrary because many elements serve several functional roles. For example, manganese is listed in group 4 as a metal involved in several key electron transfer reactions, yet it is a mineral element that remains in ionic form, which would place it in group 3.

Some naturally occurring elements, such as aluminum, selenium, and cobalt, are not essential elements yet can also accumulate in plants. Aluminum, for example, is not considered to be an essential element, although plants commonly contain from 0.1 to 500 μg aluminum per gram dry matter, and the addition of low amounts of aluminum to a nutrient solution may stimulate plant growth. Many species in the genera *Astragalus*, *Xylorhiza*, and *Stanleya* accumulate selenium, although plants have not been shown to have a specific requirement for this element. Cobalt is part of cobalamin (vitamin B_{12} and its derivatives), a component of several enzymes in nitrogen-fixing microorganisms; thus, cobalt deficiency blocks the development and function of nitrogen-fixing nodules, but plants that are not fixing nitrogen do not require cobalt. Crop plants normally contain only relatively small amounts of such nonessential elements.

The following subsections describe the methods used to examine the roles of nutrient elements in plants.

Special techniques are used in nutritional studies

To demonstrate that an element is essential requires that plants be grown under experimental conditions in which only the element under investigation is absent. Such conditions are extremely difficult to achieve with plants grown in a complex medium such as soil. In the nineteenth century, scientists approached this problem by growing plants with their roots immersed in a **nutrient solution** containing only inorganic salts. Their demonstration that plants could grow normally with no soil or organic matter proved unequivocally that plants can fulfill all their needs from only mineral nutrient elements, water, air (CO_2), and sunlight.

The technique of growing plants with their roots immersed in a nutrient solution without soil is called **solution culture** or **hydroponics**. Successful hydroponic culture (**Figure 7.1A**) requires a large volume of nutrient solution or frequent adjustment of the nutrient solution to prevent nutrient uptake by roots from producing large changes in the mineral nutrient concentrations and pH of the solution. A sufficient supply of oxygen to the root system is also critical and may be achieved by vigorous bubbling of air through the solution. Hydroponics is used in the commercial production of many greenhouse and indoor crops, such as tomato (*Solanum lycopersicum*), cucumber (*Cucumis sativus*), and hemp (*Cannabis sativa*). In one form of commercial hydroponic culture, plants are grown in a supporting material such as sand, gravel, vermiculite, rockwool, polyurethane foams, or expanded clay. Nutrient solutions are then flushed through the supporting material, and old solutions are removed by leaching

Another technique, which has sometimes been heralded as the medium of the future for scientific investigations, is to grow the plants in **aeroponics**. In this technique plants are grown with their roots suspended in air while being sprayed continuously with a nutrient solution (**Figure 7.1B**). This approach provides easy manipulation of the gaseous environment around the

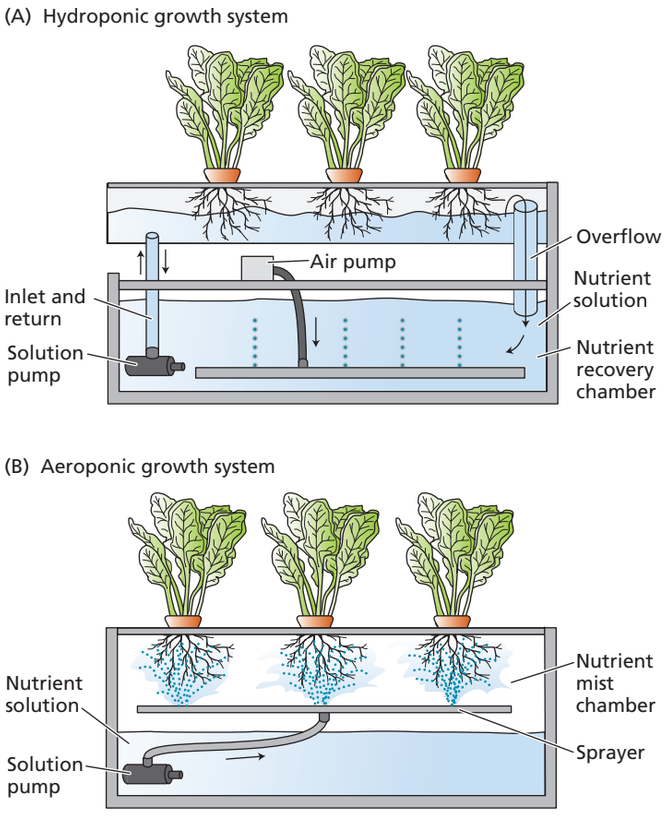


Figure 7.1 Solution culture systems. **(A)** In a hydroponic culture, plants are suspended by the base of the stem over a tank containing a nutrient solution. Air is pumped through a porous solid that generates a stream of small bubbles and keeps the solution fully saturated with oxygen. **(B)** In aeroponics, a high-pressure pump sprays nutrient solution on roots enclosed in a tank. (After E. Epstein and A. J. Bloom. 2005. *Mineral Nutrition of Plants: Principles and Perspectives*, 2nd ed. Oxford University Press/Sinauer, Sunderland, MA.)

roots, but it requires higher concentrations of nutrients than hydroponic culture does to sustain rapid plant growth. Aeroponics is used in commercial food production, especially in indoor vertical agricultural facilities where temperature, humidity, light, and all nutrients are carefully controlled.

Nutrient solutions can sustain rapid plant growth

Over the years, many formulations have been used for nutrient solutions. Early formulations developed by Wilhelm Knop in Germany in the 1860s included only KNO_3, $Ca(NO_3)_2$, KH_2PO_4, $MgSO_4$, and an iron salt. At the time, this nutrient solution was believed to contain all the minerals required by plants, but these experiments were carried out with chemicals that were contaminated with other elements that are now known to be essential (such as boron and molybdenum). **Table 7.3** shows a more modern formulation for a nutrient solution. This formulation is called a modified **Hoagland solution**, named after Dennis R. Hoagland, a scientist who did pioneering work on hydroponics in the 1930s.

A modified Hoagland solution contains all known mineral elements needed for rapid plant growth. The concentrations of these elements are set at the highest possible concentrations without producing toxicity symptoms or salinity stress, and thus may be several orders of magnitude higher than those found in the soil around plant roots. For example, whereas phosphorus is present in the soil solution at concentrations normally less than 0.06 $\mu g\ g^{-1}$ or 2 μM, the modified Hoagland solution calls for 62 $\mu g\ g^{-1}$ or 2 mM. Such high initial concentrations permit plants to be grown in a medium for extended periods without replenishment of the nutrient, but they may injure young plants. Therefore, many researchers dilute their nutrient solutions severalfold and replenish them frequently to minimize fluctuations of nutrient concentration in the medium and in the plants.

TABLE 7.3 Composition of a modified Hoagland nutrient solution for growing plants

Compound	Molecular weight	Concentration of stock solution	Concentration of stock solution	Volume of stock solution per liter of final solution	Element	Final concentration of element	
	$g\ mol^{-1}$	mM	$g\ L^{-1}$	mL		μM	$\mu g\ g^{-1}$
Macronutrients							
KNO_3	101.10	1,000	101.10	6.0	N	16,000	224
$Ca(NO_3)_2 \cdot 4H_2O$	236.16	1,000	236.16	4.0	K	6,000	235
$NH_4H_2PO_4$	115.08	1,000	115.08	2.0	Ca	4,000	160
$MgSO_4 \cdot 7H_2O$	246.48	1,000	246.49	1.0	P	2,000	62
					S	1,000	32
					Mg	1,000	24
Micronutrients							
KCl	74.55	25	1.864		Cl	50	1.77
H_3BO_3	61.83	12.5	0.773		B	25	0.27
$MnSO_4 \cdot H_2O$	169.01	1.0	0.169		Mn	2.0	0.11
$ZnSO_4 \cdot 7H_2O$	287.54	1.0	0.288	2.0	Zn	2.0	0.13
$CuSO_4 \cdot 5H_2O$	249.68	0.25	0.062		Cu	0.5	0.03
H_2MoO_4 (85% MoO_3)	161.97	0.25	0.040		Mo	0.5	0.05
NaFeDTPA	468.20	64	30.0	0.3–1.0	Fe	19.2–64.0	1.1–3.6
Optional[a]							
$NiSO_4 \cdot 6H_2O$	262.86	0.25	0.066	2.0	Ni	0.5	0.03
$Na_2SiO_3 \cdot 9H_2O$	284.20	1,000	284.20	1.0	Si	1,000	28

Source: After E. Epstein and A. J. Bloom. 2005. *Mineral Nutrition of Plants: Principles and Perspectives*, 2nd ed. Oxford University Press/Sinauer, Sunderland, MA.

Note: The macronutrients are added separately from stock solutions to prevent precipitation during preparation of the nutrient solution. A combined stock solution is made up containing all micronutrients except iron. Iron is added as sodium ferric diethylenetriaminepentaacetate; some plants, such as maize, require the higher concentration of iron shown in the table.

[a]Nickel is usually present as a contaminant of the other chemicals, so it may not need to be added explicitly. Silicon, if included, should be added first and the pH adjusted with HCl to prevent precipitation of the other nutrients.

Another important property of this modified Hoagland formulation is that nitrogen is supplied as both ammonium (NH_4^+) and nitrate (NO_3^-). Supplying nitrogen in a balanced mixture of cations (positively charged ions) and anions (negatively charged ions) tends to decrease the rapid rise in the pH of the medium that is commonly observed when the nitrogen is supplied solely as nitrate anion. Even when the pH of the medium is kept neutral, most plants grow better if they have access to both NH_4^+ and NO_3^-, because absorption and assimilation of the two nitrogen forms promote inorganic cation–anion balance in the plant.

A significant problem with nutrient solutions is maintaining the availability of iron. When supplied as an inorganic salt such as $FeSO_4$ or $Fe(NO_3)_2$, iron can precipitate out of solution as iron hydroxide, particularly under alkaline conditions. If phosphate salts are present, insoluble iron phosphate will also form. Precipitation of the iron out of solution makes it physically unavailable to plants, unless iron salts are added at frequent intervals. Earlier researchers solved this problem by adding iron together with citric acid or tartaric acid. Compounds such as these are called **chelators** because they form soluble complexes with cations such as ferric iron (Fe^{3+}) and Ca^{2+} in which the cation is held by ionic forces rather than by covalent bonds. **Figure 7.2** shows the structure of different species of Fe^{3+}-citrate complexes that are biologically relevant. In fact, plants produce and use organic chelators such as citrate to solubilize and transport iron into and around the organism. For example, iron is transported in the xylem (vascular tissue) as Fe^{3+}-citrate complexes.

More modern nutrient solutions use the chelators ethylenediaminetetraacetic acid (EDTA), diethylenetriaminepentaacetic acid (DTPA, or pentetic acid), or ethylenediamine-N,N′-bis(o-hydroxyphenylacetic) acid (o,o-EDDHA) to keep iron in solution where it is available to plants. In fact, plants use different mechanisms for iron uptake (see Chapter 8). Eudicots use a reductase to reduce Fe^{3+} to ferrous iron (Fe^{2+}) at the root surface and then they take up Fe^{2+}. Monocots secrete chelators called phytosiderophores that bind Fe^{3+}, which is then transported into the plant complexed with the phytosiderophore. After uptake into the root, iron is kept soluble by chelation with organic compounds present in plant cells.

Mineral deficiencies disrupt plant metabolism and function

An inadequate supply of an essential element results in a nutritional disorder manifested by characteristic deficiency symptoms. In hydroponic culture, withholding of an essential element can be readily correlated with a given set of symptoms. For example, a particular deficiency might elicit a specific pattern of leaf discoloration.

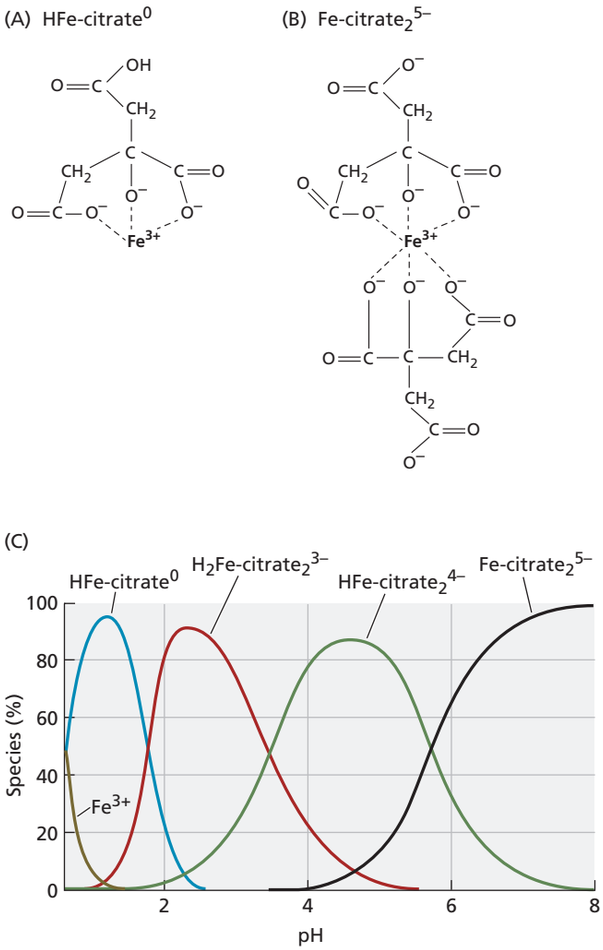


Figure 7.2 Examples of Fe^{3+}-citrate complexes in solution and the effect of pH. (A) HFe-citrate^0. (B) Fe-citrate$_2^{5-}$. (C) The predominance of different Fe^{3+}-citrate complexes in solution depends on pH. For example, Fe-citrate$_2^{5-}$, shown in (B), predominates at neutral pH. (C after P. Vukosav et al. 2012. *Anal. Chim. Acta*. 745: 85–91).

Diagnosis of soil-grown plants can be more complex for the following reasons:

- Deficiencies of several elements may occur simultaneously.
- Deficiencies or excessive amounts of one element may induce deficiency or excessive accumulation of another element.
- Some virus-induced plant diseases may produce symptoms similar to those of nutrient deficiencies.

Nutrient deficiency symptoms in a plant are the expression of metabolic disorders resulting from the insufficient supply of an essential element. These disorders are related to the roles played by essential elements in normal plant metabolism and function (listed in Table 7.2).

Most essential elements have a variety of different physiological functions in plants, but some general statements are possible. The essential elements mainly function in plant structure, metabolism, signal transduction, and cellular osmoregulation. Research continues to reveal specific roles for these elements; for example, calcium ions function structurally in the cell wall and also regulate key enzymes, transporters, and ion channels in the cell.

An important clue in relating an acute deficiency symptom to a particular essential element is the extent to which an element can be recycled from older to younger leaves. Some elements, such as nitrogen, phosphorus, and potassium, can readily move from leaf to leaf, either because they are always primarily in soluble form (e.g., K^+) or because they are easily liberated from macromolecules such as proteins, nucleic acids, and lipids, via the action of proteases, nucleases, and lipases, respectively (e.g., NH_4^+ and HPO_4^{2-}) (see Chapter 23). Other elements, such as boron and calcium, are relatively immobile in most plant species because they are associated with structures such as the cell wall that are more recalcitrant to decomposition (**Table 7.4**). If an essential element can be mobilized quickly, deficiency symptoms tend to appear first in older leaves. Conversely, deficiencies of immobile essential elements become evident first in younger leaves. In the discussion that follows, we describe the particular deficiency symptoms and functional roles of the essential elements as they are grouped in Table 7.2. Please keep in mind that many symptoms are highly dependent on plant species.

GROUP 1: DEFICIENCIES IN MINERAL NUTRIENTS THAT ARE PART OF CARBON COMPOUNDS This first group consists of nitrogen, phosphorus, and sulfur. Nitrogen and phosphorus availability in soils limits plant productivity in most natural and agricultural ecosystems. By contrast, soils generally contain sufficient sulfur, although that is changing as atmospheric sulphate deposition, primarily the result of coal-burning power plants, has been decreasing since 1980. The oxidation–reduction states of nitrogen and sulfur range widely (see Chapter 14); some of the most energy-intensive reactions in life are necessary to convert highly oxidized inorganic forms, such as nitrate and sulfate, that roots absorb from the soil into highly reduced forms found in organic compounds, such as amino acids, within plants. Phosphorus, by contrast, is not reduced after being taken up by plants as phosphate, which forms covalent bonds with carbon via oxygen in compounds such as ATP and other nucleotide phosphates, nucleic acids, phospholipids, phosphoproteins, and phosphorylated intermediates of metabolism.

TABLE 7.4 **Mineral elements classified on the basis of their mobility within a plant and their tendency to retranslocate during deficiencies**

Mobile	Intermediate	Immobile
Nitrogen	Sulfur	Calcium
Potassium	Iron	Boron
Magnesium	Zinc	
Phosphorus	Copper	
Chlorine		
Sodium		
Molybdenum		

Note: Within each group, elements are listed in the order of their abundance in the plant.

NITROGEN Nitrogen is the mineral element that plants require in the greatest amounts (see Table 7.1). It serves as a constituent of many plant cell components, including chlorophyll, proteins, and nucleic acids. Therefore, nitrogen deficiency rapidly limits plant growth. If such a deficiency persists, most species show leaf **chlorosis** (yellowing of the leaves), associated with deconstruction of the photosynthetic apparatus and of macromolecules more generally, especially in the older leaves near the base of the plant (for pictures of nitrogen deficiency and the other mineral deficiencies described in this chapter, see **WEB TOPIC 7.1**). Under severe nitrogen deficiency, these leaves become completely yellow (or tan) while mobilizing and exporting amino acids and nutrients to other organs, and then fall off the plant. Younger leaves may not show these symptoms initially because nitrogen can be mobilized from older leaves. Thus, a nitrogen-deficient plant may have light green upper leaves and yellow or tan lower leaves.

When nitrogen deficiency develops slowly, plants may have markedly slender and often woody stems. This woodiness may be due to a buildup of excess carbohydrates that cannot be used in the synthesis of amino acids or other nitrogen-containing compounds. Carbohydrates not used in nitrogen metabolism may also be used in anthocyanin synthesis, leading to accumulation of that pigment. This condition is revealed as a purple coloration in leaves, petioles, and stems of nitrogen-deficient plants of some species, such as tomato and certain varieties of maize (corn; *Zea mays*).

SULFUR Sulfur is found in certain amino acids (i.e., cysteine and methionine) and is a constituent of several coenzymes and vitamins, such as coenzyme A, *S*-adenosylmethionine, biotin, vitamin B_1, and pantothenic acid, which are essential for metabolism.

Many of the symptoms of sulfur deficiency are similar to those of nitrogen deficiency, including leaf chlorosis,

stunting of growth, and anthocyanin accumulation. This similarity is not surprising, since sulfur and nitrogen are both constituents of proteins. The chlorosis caused by sulfur deficiency, however, generally arises initially in young and mature leaves, rather than in old leaves as in nitrogen deficiency, because sulfur, unlike nitrogen, is not as easily remobilized to the younger leaves in most species. Nonetheless, in some plant species sulfur chlorosis may occur simultaneously in all leaves, or even initially in older leaves.

PHOSPHORUS Phosphorus (as phosphate, PO_4^{3-}) is an integral component of important compounds in plant cells, including the sugar–phosphate intermediates of respiration and photosynthesis as well as the phospholipids that make up most plant membranes (see Chapters 10 and 13). The largest pool of organic phosphorus in cells is in nucleotides used in plant energy metabolism (such as ATP) and in DNA and RNA. Characteristic symptoms of phosphorus deficiency include stunted growth of the entire plant and a dark green coloration of the leaves, which may be malformed and contain small areas of dead tissue called **necrotic spots** (for a picture, see **WEB TOPIC 7.1**).

As in nitrogen deficiency, some species may produce excess anthocyanins under phosphorus deficiency, giving the leaves a slight purple coloration. Unlike in nitrogen deficiency, the purple coloration of phosphorus deficiency is not associated with chlorosis. In fact, the leaves may be a dark greenish purple. Additional symptoms of phosphorus deficiency include the production of slender (but not woody) stems and the death of older leaves. Plant development, including flowering, may also be delayed.

GROUP 2: DEFICIENCIES IN MINERAL NUTRIENTS THAT ARE IMPORTANT FOR STRUCTURAL INTEGRITY This group consists of the macronutrient silicon and the micronutrient boron. These elements are usually present in plants as ester linkages between the element (X) and the carbon atom of an organic compound (i.e., R-C-O-X).

SILICON Only members of the family Equisetaceae—called *scouring rushes* because at one time their ash, rich in gritty silica (SiO_2), was used to scour pots—require silicon to complete their life cycle. Nonetheless, many other species accumulate substantial amounts of silicon and show enhanced growth, fertility, and stress resistance when supplied with adequate amounts of silicon.

Plants deficient in silicon are more susceptible to lodging (the permanent displacement of crop stems from vertical alignment) and fungal infection. Silicon is deposited primarily in the endoplasmic reticulum, cell walls, and intercellular spaces as hydrated, amorphous silica ($SiO_2 \cdot nH_2O$). It also forms complexes with polyphenols and thus serves as a complement to lignin in the reinforcement of cell walls. In addition, silicon can lessen the toxicity of many metals, including aluminum and manganese.

BORON Boron serves as a structural component in the cell wall, where it cross-links RG II (rhamnogalacturonan II, a small pectic polysaccharide) (see Chapter 2). It may also have additional physiological functions in plants; there is evidence for boron functioning in cell elongation, nucleic acid synthesis, hormone responses, membrane function, and cell cycle regulation. Boron-deficient plants may exhibit a wide variety of symptoms, depending on the species and the age of the plant.

A characteristic symptom of boron deficiency is black necrosis of young leaves and terminal buds. The necrosis of the young leaves occurs primarily at the base of the leaf blade. Stems may be unusually stiff and brittle. Apical dominance may also be lost, causing the plant to become highly branched; however, the terminal apices of the branches soon become necrotic because of inhibition of cell differentiation. Structures such as the fruits, fleshy roots, and tubers may exhibit necrosis or abnormalities related to the breakdown of internal tissues.

GROUP 3: DEFICIENCIES IN MINERAL NUTRIENTS THAT REMAIN IN IONIC FORM This group includes some of the most familiar mineral elements: the macronutrients potassium, calcium, and magnesium and the micronutrients chlorine, zinc, and sodium. These elements may be found as ions in solution in the cytosol or vacuoles, or they may be bound electrostatically or as ligands to larger, carbon-containing compounds.

POTASSIUM Potassium, present in plants as the cation K^+, plays an important role in regulation of the osmotic potential of plant cells (see Chapters 5 and 8). It also activates many enzymes involved in photosynthesis and respiration (see Chapters 10 and 13).

The first observable symptom of potassium deficiency is mottled or marginal chlorosis, which then develops into necrosis primarily at the leaf tips, at the margins, and between veins. In monocots, these necrotic lesions may eventually extend toward the leaf base. Because potassium can be mobilized to the younger leaves, these symptoms appear initially on the more mature leaves toward the base of the plant. The leaves may also curl and crinkle. The stems of potassium-deficient plants may be slender and weak, with abnormally short internodal regions. In potassium-deficient maize, the roots may have an increased susceptibility to root-rotting fungi present in the soil, and this susceptibility, together with effects on the stem, results in an increased tendency for the plant to lodge.

CALCIUM Calcium ions (Ca^{2+}) have two distinct roles in plants: (1) a structural/apoplastic role whereby Ca^{2+} binds to acidic groups of membrane lipids (phospho- and sulfolipids) and cross-links pectins, particularly in the middle lamellae that separate newly divided cells (see Chapter 2); and (2) a signaling role whereby Ca^{2+} acts as a second messenger that initiates plant responses to environmental stimuli (see Chapter 4). In its function as a second messenger, Ca^{2+} binds to proteins such as calmodulin (CaM), calmodulin-like proteins (CMLs), or calcineurin B–like proteins (CBLs) in the cytosol of plant cells. These Ca^{2+}-binding proteins regulate many other proteins such as kinases, phosphatases, and cytoskeletal proteins. Some targets of Ca^{2+} signaling bind Ca^{2+} directly through EF-hand motifs, including ion channels, kinases, phospholipases, NADPH oxidases, and others. Ca^{2+} thereby regulates many cellular processes, including cell growth and differentiation and responses to hormones and environmental signals (see Chapter 4). While most essential nutrients are accumulated in plant cells, calcium ions are actively pumped out of the cytosol and into the cell wall space and vacuole (see Chapter 8), facilitating their role as a second messenger in signal transduction.

Characteristic symptoms of calcium deficiency include necrosis of young meristematic regions such as the tips of roots or young leaves, where cell division and cell wall formation are most rapid. Necrosis in slowly growing plants may be preceded by a general chlorosis and downward hooking of young leaves. Young leaves may also appear deformed. The root system of a calcium-deficient plant may appear brownish, short, and highly branched. Severe stunting may result if the meristematic regions of the plant die prematurely.

MAGNESIUM In plant cells, magnesium ions (Mg^{2+}) have a specific role in the activation of enzymes involved in respiration, photosynthesis, and the synthesis of DNA and RNA. Mg^{2+} is also part of the ring structure of the chlorophyll molecule (see Chapter 9). A characteristic symptom of magnesium deficiency is chlorosis between the leaf veins, occurring first in older leaves because of the high mobility of this cation. This pattern of chlorosis occurs because the chlorophyll in the vascular bundles remains unaffected longer than that in the cells between the bundles. If the deficiency is extensive, the leaves may become yellow or white. An additional symptom of magnesium deficiency may be senescence and premature leaf abscission.

CHLORINE The element chlorine is found in plants as the chloride ion (Cl^-). It is required for the water-splitting reaction of photosynthesis through which oxygen is produced (see Chapter 9). In addition, chlorine may be required for cell division in leaves and roots. Plants deficient in chlorine develop wilting of the leaf tips followed by general leaf chlorosis and necrosis. The leaves may also exhibit reduced growth. Eventually the leaves may take on a bronzelike color ("bronzing"). Roots of chlorine-deficient plants may appear stunted and thickened near the root tips.

Chloride ions are highly soluble and are generally available in soils because seawater is swept into the air by wind and delivered to soil when it rains. Therefore, chlorine deficiency is only rarely observed in plants grown in native or agricultural habitats. Most plants absorb chlorine at concentrations much higher than those required for normal growth and development.

ZINC Many enzymes require zinc ions (Zn^{2+}) for their activity, and zinc may be required for chlorophyll biosynthesis in some plants. Zinc deficiency is characterized by a reduction in internodal growth, and as a result plants display a rosette habit of growth in which the leaves form a circular cluster radiating at or close to the ground. The leaves may also be small and distorted, with leaf margins having a puckered appearance. These symptoms may result from loss of the ability to produce sufficient amounts of the auxin indole-3-acetic acid (IAA). Zinc deficiency results in a decrease in chlorophyll synthesis, and in some species (e.g., maize, sorghum, and beans) older leaves may show chlorosis between the leaf veins and then develop white necrotic spots.

SODIUM Species using the C_4 and crassulacean acid metabolism (CAM) pathways of carbon fixation (see Chapter 10) may require sodium ions (Na^+). In these plants, Na^+ appears vital for regenerating phosphoenolpyruvate, the substrate for primary carboxylation in the C_4 and CAM pathways. Under sodium deficiency, these plants exhibit chlorosis and necrosis, or even fail to form flowers. Many C_3 species also benefit from exposure to low concentrations of Na^+. Sodium ions stimulate growth through enhanced cell expansion and can partly substitute for potassium ions as an osmotically active solute.

GROUP 4: DEFICIENCIES IN MINERAL NUTRIENTS THAT ARE INVOLVED IN REDOX REACTIONS

This group of five micronutrients consists of the metals iron, manganese, copper, nickel, and molybdenum. Like the group 3 elements, these elements remain in ionic form. However, all of the group 4 elements can undergo reversible oxidation and reduction (e.g., $Fe^{2+} \leftrightarrow Fe^{3+}$), a property that is essential for their roles in electron transfer and energy transformation. They are usually found in association with larger molecules such as cytochromes, chlorophyll, and proteins (usually enzymes).

IRON Iron has an important role as a component of enzymes involved in the transfer of electrons (redox

reactions), such as cytochromes (see Chapters 9 and 13). In this role it is reversibly oxidized from Fe^{2+} to Fe^{3+} during electron transfer.

As in magnesium deficiency, a characteristic symptom of iron deficiency is interveinal chlorosis. This symptom, however, appears initially on younger leaves because iron, unlike magnesium, is not as readily mobilized from older leaves. Under conditions of extreme or prolonged deficiency, the veins may also become chlorotic, causing the whole leaf to turn white. The leaves become chlorotic because iron is required for the synthesis of some of the chlorophyll–protein complexes in the chloroplast. The low mobility of iron is probably due to its precipitation in the older leaves as insoluble oxides or phosphates. The precipitation of iron diminishes subsequent mobilization of the metal into the phloem for long-distance translocation.

MANGANESE Manganese ions (Mn^{2+}) activate several enzymes in plant cells. In particular, decarboxylases and dehydrogenases involved in the tricarboxylic acid cycle (see Chapter 13) are specifically activated by manganese ions. The best-defined function of Mn^{2+} is in the photosynthetic reaction through which oxygen (O_2) is produced from water (see Chapter 9). The major symptom of manganese deficiency is interveinal chlorosis associated with the development of small necrotic spots. This chlorosis may occur on younger or older leaves, depending on plant species and growth rate.

COPPER Copper is involved in redox reactions in which it is reversibly oxidized from Cu^{+} to Cu^{2+}. An important copper-containing protein is plastocyanin, which functions as an electron carrier during the light reactions of photosynthesis (see Chapter 9). The initial symptom of copper deficiency in many plant species is the production of dark green leaves, which may contain necrotic spots. The necrotic spots appear first at the tips of young leaves and then extend toward the leaf base along the margins. The leaves may also be twisted or malformed. Cereal plants exhibit a white leaf chlorosis and necrosis with rolled tips. Under extreme copper deficiency, leaves may drop prematurely and flowers may be sterile.

NICKEL The only known requirement for nickel in vascular plants is for the nickel-containing (Ni^{2+}) enzyme urease. In addition, nitrogen-fixing microorganisms in legume root nodules require nickel (Ni^{+} through Ni^{4+}) for the enzyme that reprocesses some of the hydrogen gas generated during fixation (hydrogen uptake hydrogenase) (see Chapter 14). Nickel-deficient plants accumulate urea in their leaves and consequently show leaf tip necrosis. Because plants require only minuscule amounts of nickel (see Table 7.1), nickel deficiency in the field has been found in only one crop, pecan trees in the southeastern United States.

MOLYBDENUM Molybdenum ions (Mo^{4+} through Mo^{6+}) are components of several enzymes, including nitrate reductase, nitrogenase, xanthine dehydrogenase, aldehyde oxidase, and sulphite oxidase. Nitrate reductase catalyzes the reduction of nitrate to nitrite during its assimilation by the plant cell; nitrogenase converts nitrogen gas to ammonia in nitrogen-fixing microorganisms (see Chapter 14). Because molybdenum is involved in both nitrate assimilation and nitrogen fixation, a molybdenum deficiency may bring about a nitrogen deficiency if the nitrogen source is primarily nitrate or if the plant depends on symbiotic nitrogen fixation. Consequently, the first indication of a molybdenum deficiency is general chlorosis between veins and necrosis of older leaves. In some plants, such as cauliflower and broccoli, the leaves may not become necrotic but instead may appear twisted and subsequently die (whiptail disease). Flower formation may be prevented, or the flowers may abscise prematurely.

Although plants require only tiny amounts of molybdenum (see Table 7.1), some soils (e.g., acidic soils in Australia) supply inadequate concentrations. Small additions of molybdenum to such soils can greatly enhance crop or forage growth at negligible cost.

Plant tissue analysis reveals mineral deficiencies

Requirements for mineral elements change as a plant grows and develops. In crop plants, nutrient concentrations at certain stages of growth influence the yield of the economically important organs (tuber, grain, etc.). To optimize yields, farmers use analyses of nutrient concentrations in soil and in plants to determine fertilizer schedules.

Soil analysis is the chemical determination of the nutrient content in a soil sample from the root zone. As we discuss in Section 7.3, both the chemistry and the biology of soils are complex, and the results of soil analyses vary with sampling methods, storage conditions for the samples, and nutrient extraction techniques. Perhaps more important is that a particular soil analysis reflects the amount of nutrients *potentially* available to the plant roots from the soil, but soil analysis does not tell us how much of a particular mineral nutrient the plant actually needs or is able to absorb. This additional information is best determined by plant tissue analysis.

The traditional approach to **plant tissue analysis** is to determine the amount of a particular nutrient, usually in leaf samples, and determine if it is in a concentration range that is adequate for that species, the organ sampled, and the stage of growth. If the nutrient concentration is below the adequate range, it is in the **deficiency zone**

and the application of that nutrient as a fertilizer or a soil amendment that would make the nutrient more available to plants, for example by changing soil pH, could improve growth and yield. Plant scientists recognize that this approach is overly simplified and that diagnosis of nutrient deficiency based on plant tissue analysis is complex. Knowing the concentration of some individual nutrients in the shoot is insufficient to identify a deficiency because plants tightly control the cellular concentration of some nutrients. The recent development of ionomics (**Box 7.2**) addresses some of this complexity by considering all nutrients in plant samples at the same time. This approach identifies multi-element patterns that can be used to diagnose plant nutrient deficiencies more accurately.

Because agricultural soils are often limited in the elements nitrogen, phosphorus, and potassium (NPK), many farmers routinely take into account, at a minimum, growth or yield responses for these elements. Fertilizers containing N, P, and K are often applied at planting or early in plant development before deficiency symptoms could occur. These applications are based on soil tests and the farmer's knowledge of the cropping history of the farm. During the growing season, if a nutrient deficiency is suspected, perhaps by agricultural drone monitoring (used in modern precision

Box 7.2 Ionomics: A Powerful Approach to Study Mineral Nutrition

In the same way that the genome is the full complement of genetic material in an organism, the **ionome** is the composition of all inorganic elements, including nutrients, in an organism. Ionomics is the study of the elemental composition of organisms and changes in this composition in response to physiological stimuli, developmental state, and genetic changes. Interactions among nutrients have long been known to affect all aspects of plant nutrition, including nutrient availability in the soil, uptake by roots, and function in the plant. However, it wasn't until the development of ionomics in the early 2000s that patterns of elemental composition were treated as a phenotype. The development of ionomics was made possible by a convergence of new technologies. High-throughput elemental analysis became possible with inductively coupled plasma mass spectrometry (ICP-MS) which can determine concentrations for 18 to 20 elements rapidly and simultaneously. New developments in plant genetics and genomics, as well as statistical methods to analyze large data sets, were also necessary to make ionomics possible.

Many advances have been made using ionomics. Genes that affect the ionome have been identified using these high-throughput methods. For example, ionomic phenotypes were identified in populations of mutants and genes identified using DNA microarrays and next-generation sequencing (NGS). Naturally occurring alleles that affect the ionome have also been identified and their role in environmental adaptation uncovered. Elemental analysis of *Arabidopsis thaliana* accessions, collected from different ecological zones, showed differences in their ionomes. The genes underlying the ionomic phenotypes were identified using a variety of genetic approaches, such as quantitative trait loci (QTL) analysis or genome-wide association mapping. These natural genetic variants were then grown in the landscape where they naturally occur, in order to better understand their role in environmental adaptation. A particularly important finding from ionomic studies is that multiple element patterns provide a better identification of nutrient deficiency than does single elemental analysis. A dramatic example of this involves iron deficiency. The concentration of iron in plants is very stable and provides almost no information to determine whether a plant is iron deficient. Ionomic analysis of iron-deficient Arabidopsis plants identified the pattern shown in **Figure A**. Iron-deficient plants show no change in iron content but have elevated manganese, cobalt, zinc, and cadmium and lower molybdenum, and this pattern is diagnostic for iron deficiency. Another example is phosphate deficiency. Low phosphorus concentration is diagnostic for phosphate deficiency. However, including concentrations of cobalt, zinc, boron, copper, and arsenic greatly improves the ability to diagnose phosphate deficiency.

Ionomic analysis has now been applied to many plant species and also animals. One of the most important challenges is to use ionomics to identify genes that plants have used to adapt to different environmental conditions, including diverse natural soils. This work will identify alleles that can be used in breeding projects to produce crop plants that are adapted to specific environmental conditions. ■

	Fe	P	Mn	Co	Zn	Mo	Cd	B	Cu	As
Iron deficiency	—	—	↑	↑	↑	↓	↑	—	—	—
Phosphate deficiency	—	↓	—	↓	↑	—	—	↑	↓	↑

Figure A **Multi-element patterns can provide a more accurate diagnosis of nutrient deficiencies.** Arabidopsis plants were grown in nutrient-sufficient or nutrient-deficient conditions. Arrows indicate elevated or decreased elemental concentrations that were predictive for nutrient deficiency. Dashes indicate elements that were not significantly different. (After I. R. Baxter et al. 2008. *Proc. Natl. Acad. Sci. USA* 105: 12081–12086. © 2008 National Academy of Sciences)

agriculture), steps are taken to correct the deficiency before it reduces growth or yield.

7.2 Treating Nutritional Deficiencies

Many traditional and subsistence farming practices promote the recycling of mineral elements. Crop plants absorb nutrients from the soil, humans and animals consume locally grown crops, and crop residues and manure from humans and animals return the nutrients to the soil. The main losses of nutrients from such agricultural systems are from leaching that carries dissolved ions, especially nitrate, away with drainage water. In acidic soils (pH < 7), leaching of nutrients other than nitrate may be decreased by the addition of lime—a mix of CaO, $CaCO_3$, and $Ca(OH)_2$—to make the soil more alkaline, because many mineral elements form less soluble compounds when the pH is higher than 7 (**Figure 7.3**).

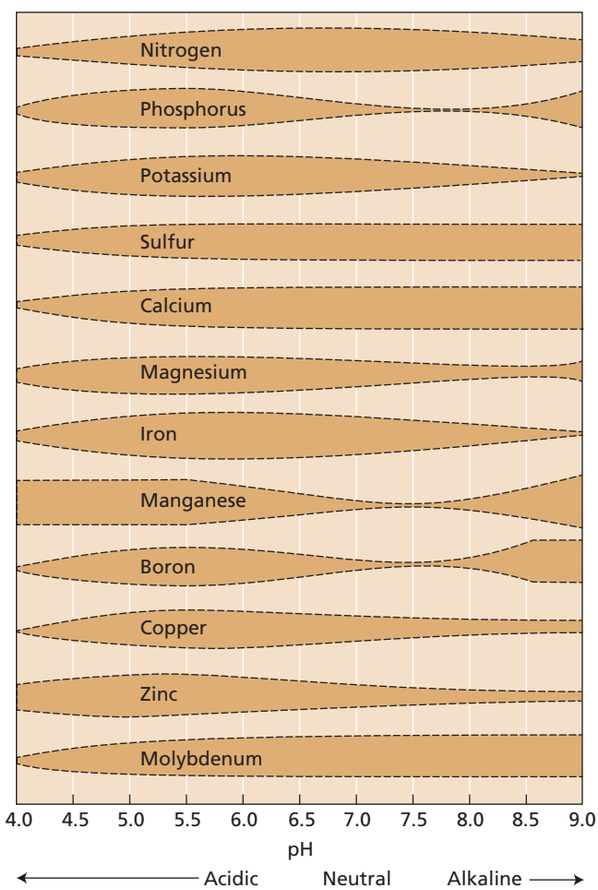


Figure 7.3 Influence of soil pH on the availability of nutrient elements in organic soils. The thickness of the horizontal bars indicates the degree of nutrient availability to plant roots. All of these nutrients are available in the pH range of 5.5 to 6.5. (After R. E. Lucas and J. F. Davis. 1961. *Soil Sci.* 92: 177–182.)

This decrease in leaching, however, may be gained at the expense of decreased availability of some nutrients, especially iron.

In the high-production agricultural systems of industrialized countries, a large proportion of crop biomass leaves the area of cultivation, and returning crop residues to the land where the crop was produced becomes difficult at best. Under most current agricultural practices, this unidirectional removal of nutrients from agricultural soils makes it necessary to restore the lost nutrients to these soils through the addition of fertilizers.

Crop yields can be improved by the addition of fertilizers

Most inorganic fertilizers contain inorganic salts of the macronutrients nitrogen, phosphorus, and potassium (see Table 7.1). Fertilizers that contain only one of these three nutrients are termed *straight fertilizers*. Some examples of straight fertilizers are superphosphate, ammonium nitrate, and muriate of potash (potassium chloride). Fertilizers that contain two or more mineral nutrients are called *compound fertilizers* or *mixed fertilizers*, and the numbers on the package label, such as "10-14-10," refer to the percentages of N, P, and K, respectively, in the fertilizer.

With long-term agricultural production, consumption of micronutrients by crops can reach a point at which they too must be added to the soil as fertilizers. Adding micronutrients to the soil may also be necessary to correct a preexisting deficiency. For example, many acidic, sandy soils in humid regions are deficient in boron, copper, zinc, manganese, molybdenum, or iron and can benefit from nutrient supplementation.

Chemicals may also be applied to the soil to modify soil pH. As Figure 7.3 shows, soil pH affects the availability of all mineral nutrients. Addition of lime, as mentioned previously, can raise the pH of acidic soils; addition of elemental sulfur can lower the pH of alkaline soils (pH > 7). In the latter case, microorganisms absorb the sulfur and subsequently release sulfate and hydrogen ions that acidify the soil.

Fertilizers approved for organic agricultural practices originate from natural rock deposits such as sodium nitrate and rock phosphate (phosphorite) or from the residues of plant or animal life. Natural rock deposits are chemically inorganic but are considered acceptable for use in organic agriculture. Plant and animal residues contain many nutrient elements in the form of organic compounds. Before crop plants can acquire the nutrient elements from these residues, the organic compounds must be broken down to simple organic compounds such as amino acids or inorganic compounds such as ammonium and nitrate, usually by the action of soil microorganisms through a process called **mineralization**. Mineralization depends on many factors,

including temperature, water and oxygen availability, pH, and the type and number of microorganisms present in the soil. As a consequence, rates of mineralization are highly variable, and nutrients from organic residues become available to plants over periods that range from days to months to years. Because mineralization rates from organic residues are often low and limiting to plant growth, at times they may exceed the demand of the crop—for example, before seedling emergence and early in the growing season as soils warm. Asynchrony between mineral nutrient supply and plant demand is a major cause of nutrient loss to the surrounding environment, not only in organic farming systems but also for those that use inorganic fertilizers. Nonetheless, residues from organic fertilizers do improve the physical structure of most soils, enhancing water retention during drought and increasing drainage in wet weather. In some developing countries, organic fertilizers are all that is available or affordable.

Some mineral nutrients can be absorbed by leaves

In addition to absorbing nutrients through their roots, most plants can absorb mineral nutrients applied to their leaves as a spray, a process known as **foliar application**. In some cases this method has agronomic advantages over the application of nutrients to the soil. Foliar application can reduce the lag time between application and uptake by the plant, which could be important during a phase of rapid growth. It can also circumvent the problem of restricted uptake of a nutrient from the soil. For example, foliar application of mineral nutrients such as iron, manganese, and copper may be more efficient than application through the soil, where these ions are bound to soil particles and hence are less available to the root system.

Nutrient uptake by leaves is most effective when the nutrient solution is applied to the leaf as a thin film. Production of a thin film often requires that the nutrient solutions be supplemented with surfactant chemicals, such as the detergent Tween 80® or newly developed organosilicon surfactants, that reduce surface tension. Nutrient movement into the plant seems to involve diffusion through the cuticle and uptake by leaf cells, although uptake through the stomatal pores may also occur.

For foliar nutrient application to be successful, damage to the leaves must be minimized. If foliar sprays are applied on a hot day, when evaporation is high, salts may accumulate on the leaf surface and cause burning or scorching. Spraying on cool days or in the evening helps alleviate this problem. Foliar application has proved economically successful mainly with tree crops and vines such as grapes, but it is also used with cereals. Nutrients applied to the leaves can save an orchard or vineyard when soil-applied nutrients would be too slow to correct a deficiency. In wheat (*Triticum aestivum*), nitrogen applied to the leaves during the later stages of growth enhances the protein content of the seeds.

7.3 Soil, Roots, and Microbes

Soil is complex physically, chemically, and biologically. It is a heterogeneous mixture of substances distributed in solid, liquid, and gas phases (see Chapter 6). All of these phases interact with mineral elements. The inorganic particles of the solid phase provide a reservoir of potassium, phosphorus, calcium, magnesium, and iron. Also associated with this solid phase are organic compounds containing nitrogen, phosphorus, and sulfur, among other elements. The liquid phase of soil constitutes the soil solution that is held in pores between the soil particles. It contains dissolved mineral ions and organic compounds and serves as the medium for solute movement to the root surface. Gases such as oxygen, carbon dioxide, and nitrogen are dissolved in the soil solution, but roots exchange gases with soils predominantly through the air-filled pores between soil particles.

From a biological perspective, soil constitutes a diverse ecosystem in which plant roots and microorganisms interact. Many microorganisms play key roles in releasing (mineralizing) nutrients from organic sources, some of which are then made directly available to plants. Microbes also compete with the plants for mineral nutrients. Some specialized microorganisms, including mycorrhizal fungi and nitrogen-fixing bacteria, can form alliances with plants for their mutual benefit (**symbioses**, singular *symbiosis*). In this section we discuss the importance of soil properties, root structure, and symbiotic mycorrhizal relationships to plant mineral nutrition. Chapter 14 will address the symbiotic relationships of plants with nitrogen-fixing bacteria.

Negatively charged soil particles affect the adsorption of mineral nutrients

Soils are composed of inorganic and organic particles, and both have predominantly negative charges on their surfaces. Many inorganic soil particles are crystal lattices that are tetrahedral arrangements of the cationic forms of aluminum (Al^{3+}) and silicon (Si^{4+}) bound to oxygen atoms, thus forming aluminates and silicates. When cations of lesser charge replace Al^{3+} and Si^{4+} in the crystal lattice, these inorganic soil particles become negatively charged. This process is called isomorphous substitution. The negative charge of inorganic soil particles is called **permanent charge** and is largely pH independent.

Organic soil particles originate from dead plants, animals, and microorganisms that soil microorganisms have decomposed to various degrees. The negative surface charges of organic particles result from the dissociation of hydrogen ions from the carboxylic and

hydroxyl groups present in this component of the soil. The negative charges on organic particles are predominately pH dependent.

Soils are categorized by particle size:

- Gravel consists of particles larger than 2 mm.
- Coarse sand consists of particles between 0.2 and 2 mm.
- Fine sand consists of particles between 0.02 and 0.2 mm.
- Silt consists of particles between 0.002 and 0.02 mm.
- Clay consists of particles smaller than 0.002 mm (2 μm).

The silicate-containing clay materials are further divided into three major groups—kaolinite, illite, and montmorillonite—based on differences in their structure and physical properties (**Table 7.5**). The kaolinite group is generally found in well-weathered soils; the montmorillonite and illite groups are found in less-weathered soils.

Mineral cations such as ammonium (NH_4^+) and potassium (K^+) are adsorbed to the negative surface charges of inorganic and organic soil particles or adsorbed within the lattices formed by soil particles. This cation adsorption is an important factor in soil fertility. Mineral cations adsorbed on the surface of soil particles are not readily leached when the soil is infiltrated by water and thus provide a nutrient reserve available to plant roots. Mineral nutrients adsorbed in this way can be replaced by other cations in a process known as **cation exchange** (**Figure 7.4**). The degree to which a soil can adsorb and exchange ions is termed its *cation exchange capacity* (*CEC*) and is highly dependent on the soil type. A soil with a higher CEC generally has a larger reserve of mineral nutrients. Cation exchange capacity is due primarily to negative charges on clay and organic matter particles. Organic matter has a much higher CEC by weight compared with clay. Therefore, the CEC of a soil depends on its organic matter content. The CEC of inorganic particles, such as clay, is largely pH independent. However, the CEC of organic matter is highly dependent on soil pH: At low pH, organic acid groups are protonated and uncharged, whereas at higher pH they are deprotonated and carry a negative charge. As roots grow, they release protons into the soil, acidifying it. These protons can exchange cationic nutrients from soil particles, making them available for uptake.

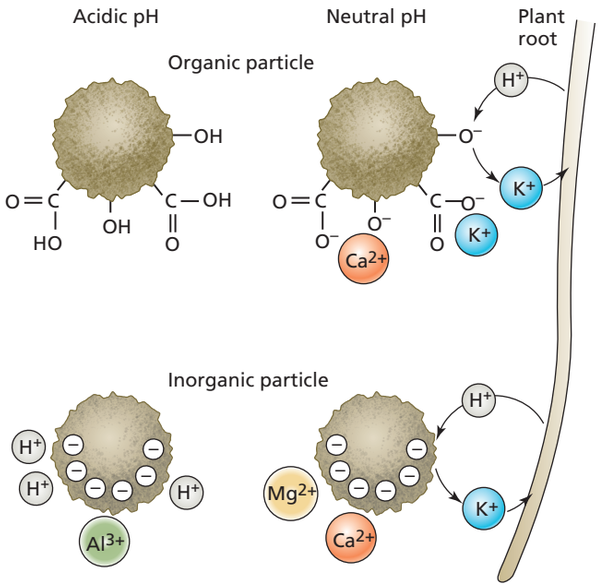


Figure 7.4 Cation exchange on the surface of soil particles. At acidic pH (left side), the cation exchange capacity (CEC) of organic soil particles is lower because organic acid sites (COOH, OH) are protonated. The CEC of inorganic particles is mainly pH independent and at lower pH tends to be occupied by H^+ and Al^{3+}. At neutral pH (right side), the CEC of organic particles is higher. Negatively charged sites on both organic and inorganic particles tend to be occupied by cationic nutrients such as Ca^{2+}, Mg^{2+}, and K^+. As roots grow, they release H^+ that can exchange on soil particles and release cationic nutrients for uptake by the root.

Mineral anions such as nitrate (NO_3^-) and chloride (Cl^-) tend to be repelled by the negative charge on the surface of soil particles and remain dissolved in the soil solution. Thus, the anion exchange capacity of most

TABLE 7.5 Comparison of properties of three major types of silicate clays found in the soil

	Type of clay		
Property	**Montmorillonite**	**Illite**	**Kaolinite**
Size (μm)	0.01–1.0	0.1–2.0	0.1–5.0
Shape	Irregular flakes	Irregular flakes	Hexagonal crystals
Cohesion	High	Medium	Low
Water-swelling capacity	High	Medium	Low
Cation exchange capacity (milliequivalents 100 g^{-1})	80–100	15–40	3–15

Source: After N. C. Brady. 1974. *The Nature and Properties of Soils*, 8th ed. Macmillan, New York.

agricultural soils is small compared with their cation exchange capacity. Nitrate in particular remains mobile in the soil solution, where it is susceptible to leaching by water moving through the soil.

Phosphate solubility in soil is usually controlled by its association with Ca^{2+}, Fe^{3+}, and Al^{3+} to form insoluble inorganic compounds. As a result, phosphate is more soluble in soil solution at slightly acidic pH (see Figure 7.3). However, the availability of phosphate is also controlled by its association with soil particles. Phosphate ions ($H_2PO_4^-$ and HPO_4^{2-}) bind to the edges of soil particles containing aluminum or iron because the positively charged iron and aluminum ions (Fe^{2+}, Fe^{3+}, and Al^{3+}) are associated with hydroxyl ion (OH^-) groups that become protonated and can adsorb phosphate. The lack of phosphate mobility or its low solubility can both limit its availability for uptake by plants. Formation of mycorrhizal symbioses (discussed later in this section) helps overcome this lack of mobility. Additionally, the roots of some plants, such as those of lupine (*Lupinus albus*) and members of the Proteaceae (e.g., *Macadamia*, *Banskia*, *Protea, Hakea*), secrete large amounts of organic acids into the soil that release phosphate from iron, aluminum, and calcium phosphates.

Sulfate (SO_4^{2-}) in the presence of Ca^{2+} forms gypsum ($CaSO_4$). Gypsum is only slightly soluble, but it releases sufficient sulfate to support plant growth. Most nonacidic soils contain substantial amounts of Ca^{2+}; consequently, sulfate mobility in these soils is low, and sulfate is not highly susceptible to leaching.

Soil pH affects nutrient availability, soil microbes, and root growth

Hydrogen ion concentration (pH) is an important property of soils because it affects the growth of plant roots and soil microorganisms. Root growth is generally favored in slightly acidic soils, at pH values between 5.5 and 6.5. Fungi generally predominate in acidic soils ($pH < 7$); bacteria become more prevalent in alkaline soils ($pH > 7$). Soil pH determines the availability of soil nutrients (see Figure 7.3). Acidity promotes the weathering of rocks that releases K^+, Mg^{2+}, Ca^{2+}, and Mn^{2+} and increases the solubility of carbonates, sulfates, and some phosphates. Increasing the solubility of nutrients enhances their availability to roots as concentrations increase in the soil solution.

Major factors that lower the soil pH are the decomposition of organic matter, ammonium assimilation by plants and microbes, and the amount of rainfall. Carbon dioxide is produced as a result of the decomposition of organic matter and equilibrates with soil water in the following reaction:

$$CO_2 + H_2O \leftrightarrow H_2CO_3 \leftrightarrow H^+ + HCO_3^-$$

This releases hydrogen ions (H^+), lowering the pH of the soil. Microbial decomposition of organic matter also produces ammonia/ammonium (NH_3/NH_4^+) and hydrogen sulfide (H_2S) that can be oxidized in the soil to form the strong acids nitric acid (HNO_3) and sulfuric acid (H_2SO_4), respectively. As plant roots absorb ammonium ions from the soil and assimilate them into amino acids, the roots generate hydrogen ions that they excrete into the surrounding soil (see Chapter 13). Hydrogen ions also displace K^+, Mg^{2+}, Ca^{2+}, and Mn^{2+} from the surfaces of soil particles. Leaching may then remove these ions from the upper soil layers, leaving a more acidic soil. By contrast, the weathering of rock in arid regions releases K^+, Mg^{2+}, Ca^{2+}, and Mn^{2+} into the soil, but because of the low rainfall, these ions do not leach from the upper soil layers, and the soil remains alkaline.

Excess mineral ions in the soil limit plant growth

When excess sodium salts are present in soil, the soil is said to be *saline*, and such soils may inhibit plant growth if the mineral ions reach concentrations that limit water availability or exceed the adequate levels for a particular nutrient (see Chapter 14). Sodium chloride and sodium sulfate are the most common salts in saline soils. Excess mineral ions in soils can be a major problem in arid and semiarid regions because rainfall is insufficient to leach them from the soil layers near the surface.

Irrigated agriculture fosters soil salinization if the amount of water applied is insufficient to leach the salt below the root zone. Irrigation water can contain 100 to 1000 g of mineral ions per cubic meter. An average crop requires about 10,000 m^3 of water per hectare. Consequently, 1000 to 10,000 kg of mineral ions per hectare may be added to the soil per crop, and over several growing seasons, high concentrations of mineral ions may accumulate in the soil.

In saline soils, plants encounter **salt stress**. Salt stress involves both water-deficit stress, as plant cells find it harder to extract water from the soil, and ionic stress, as ions (primarily Na^+ and Cl^-) accumulate to toxic levels within cells. Whereas many plants are affected adversely by the presence of relatively low concentrations of salt, other plants can survive (**salt-tolerant plants**) or even thrive (**halophytes**) at high salt concentrations. The mechanisms by which plants tolerate high salinity are complex (see Chapter 15), involving expression of enzymes, biochemical synthesis of hydrophilic osmolytes that promote water uptake into cells, and membrane transport. Plants deal with excess mineral ions in different ways, either excluding them at the plasma membrane, taking them up and excreting them, or sequestering them. To prevent toxic buildup of mineral ions in the cytosol where crucial metabolism occurs,

many plants sequester them in the vacuole. Efforts are underway to bestow salt tolerance on salt-sensitive crop species using both classic plant breeding and biotechnology, as detailed in Chapter 15.

Other mineral ions, including metal ions, can also accumulate to excessive amounts in soil and can cause severe toxicity in plants as well as humans (see **WEB ESSAY 7.1**). These metals include zinc, copper, cobalt, nickel, mercury, lead, cadmium, silver, and chromium.

Some plants develop extensive root systems

The ability of plants to obtain both water and mineral nutrients from the soil is related to their ability to develop an extensive root system and to various other traits such as flexible development in response to nutrient supply and demand, ability to secrete organic anions, and capacity to form mycorrhizal symbioses. In the late 1930s, H. J. Dittmer examined the root system of a single winter rye plant after 16 weeks of growth. He estimated that the plant had 13 million primary and lateral root axes, extending more than 500 km in length and providing 200 m^2 of surface area. This plant also had more than 10^{10} root hairs, providing another 300 m^2 of surface area. The total surface area of roots from a single rye plant equaled that of a professional basketball court. Other plant species may not develop such extensive root systems, which may limit their nutrient absorption capacity and increase their reliance on mycorrhizal symbioses (discussed shortly).

In the desert, the roots of mesquite (genus *Prosopis*) may extend downward more than 50 m to reach groundwater. Annual crop plants have roots that usually grow between 0.1 and 2.0 m in depth and extend laterally to distances of 0.3 to 1.0 m. In orchards, the major root systems of trees planted 1 m apart reach a total length of 12 to 18 km per tree. The annual production of roots in natural ecosystems may easily surpass that of shoots, so in many respects the aboveground portions of a plant represent only "the tip of the iceberg." Nonetheless, making observations on root systems is difficult and usually requires special techniques (see **WEB TOPIC 7.2**).

Plant roots may grow continuously throughout the year if conditions are favorable. Their proliferation, however, depends on the availability of water and minerals in the immediate microenvironment surrounding the root, the so-called **rhizosphere**. If the rhizosphere is poor in nutrients or too dry, root growth is slow. As rhizosphere conditions improve, root growth increases. If fertilization and irrigation provide abundant nutrients and water, plants invest fewer resources into root growth and development and more into shoots, to maximize photosynthesis and growth, which decreases the root to shoot ratio. Under such luxurious conditions, which are rare in nature, a relatively small root system meets the nutrient needs of the whole plant. Fertilization and irrigation cause greater allocation of resources to the shoot and reproductive structures than to roots, and this shift in allocation pattern contributes to higher yield of aboveground parts.

Root systems differ in form but are based on common structures

The *form* of the root system differs greatly among plant species. In monocots, root development starts with the emergence of three to six **primary** (or *seminal*) **root** axes from the germinating seed. With further growth, the plant extends new adventitious roots, called **nodal roots** or *brace roots*. Over time, the primary and nodal root axes grow and branch extensively to form a complex *fibrous root system* (**Figure 7.5**). In fibrous root systems, all the roots generally have similar diameters (except where environmental conditions or pathogenic interactions modify the root structure), so it is impossible to distinguish a main root axis.

In contrast to monocots, eudicots develop root systems with a main single root axis, called a **taproot**, which may thicken as a result of secondary cambial activity. From this main root axis, *lateral roots* develop to form an extensively branched root system. Nutrient availability also influences root development, as we discuss later in this section. Some plants, especially in



Figure 7.5 **Fibrous root systems of wheat (a monocot).** **(A)** The root system of a mature (3-month-old) wheat plant growing in dry soil. **(B)** The root system of a mature wheat plant growing in irrigated soil. It is apparent that the morphology of the root system is affected by the amount of water present in the soil. In a mature fibrous root system, the primary root axes are indistinguishable. (After J. E. Weaver. 1926. *Root Development of Field Crops*. McGraw-Hill, New York.)

the family Proteaceae, produce a proliferation of lateral roots termed *cluster roots* or *proteoid roots* in response to phosphate deficiency. An example of proteoid roots of *Hakea prostrata* is shown in **Figure 7.6**. Proteoid roots secrete organic acids such as citrate or malate that lower the pH of the soil surrounding the root and solubilize calcium, aluminum, and iron phosphate, making phosphate available for uptake by the plant. The development of the root system in both monocots and eudicots depends on the activity of the root apical meristem and the production of lateral root meristems (see Chapters 18 and 19). **Figure 7.7** is a generalized diagram of the apical region of a plant root and identifies three zones of activity: the meristematic, elongation, and maturation zones.

In the **meristematic zone**, cells divide both in the direction of the root base to form cells that will differentiate into the tissues of the functional root and in the direction of the root apex to form the **root cap**. The root cap protects the delicate meristematic cells as the root expands into the soil. It commonly secretes a gelatinous material called *mucigel*, which surrounds the root tip. The precise function of mucigel is uncertain, but it may provide lubrication that eases the root's penetration of the soil, protect the root apex from desiccation, promote the transfer of nutrients to the root, and affect interactions between the root and soil microorganisms. The root cap is central to the perception of gravity, the signal that directs the growth of roots downward. This process is termed the **gravitropic response** (see Chapters 4 and 17).

Cell division in the root apex proper is relatively slow; this region is called the **quiescent center**. After a few generations of slow cell divisions, root cells displaced from the apex by about 0.1 mm begin to divide more rapidly. Cell division again tapers off at about 0.4 mm from the apex, and the cells expand equally in all directions.

The **elongation zone** begins approximately 0.7 to 1.5 mm from the apex (see Figure 7.7). In this zone cells elongate rapidly. A final round of divisions of the innermost layer of cortex produces a central ring of cells called the **endodermis**. The walls of this endodermal cell layer become thickened, and suberin is deposited

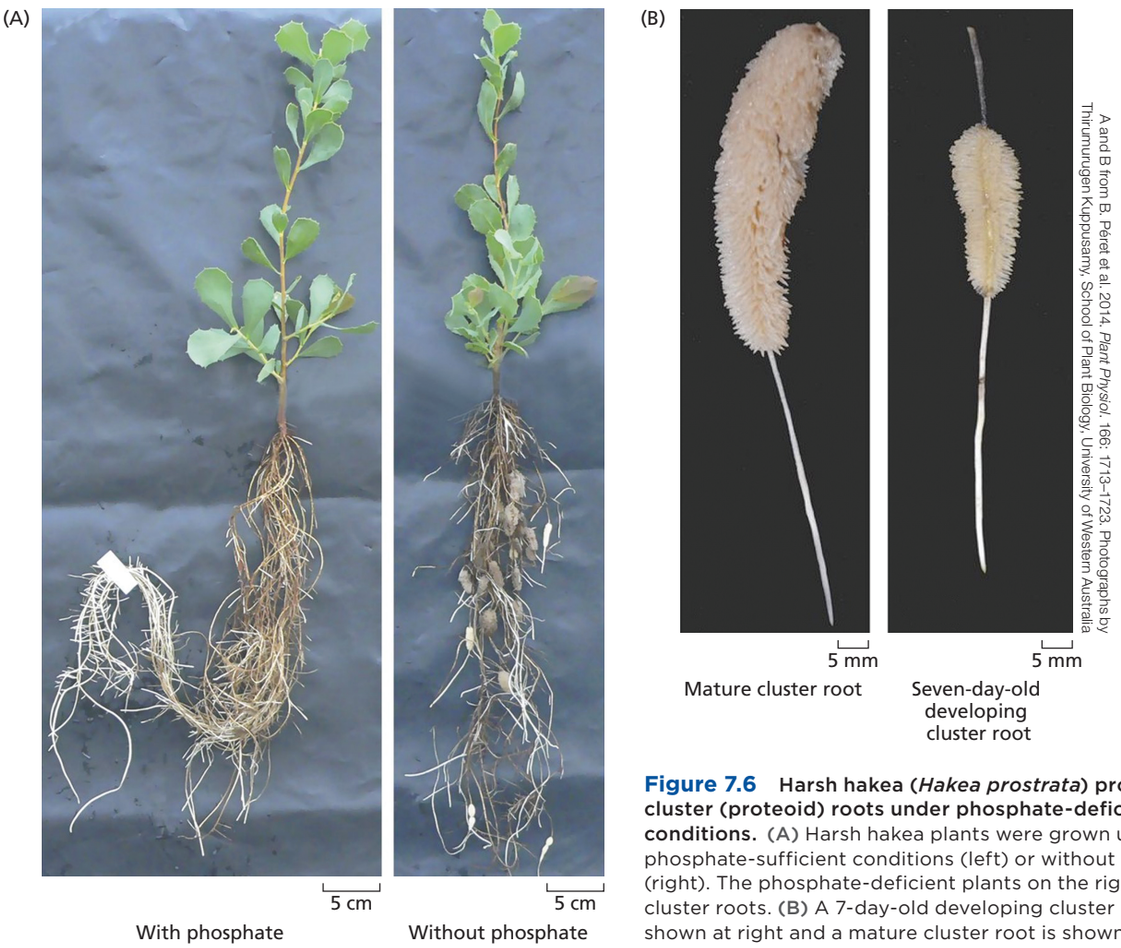


Figure 7.6 **Harsh hakea (*Hakea prostrata*) produces cluster (proteoid) roots under phosphate-deficiency conditions.** **(A)** Harsh hakea plants were grown under phosphate-sufficient conditions (left) or without phosphate (right). The phosphate-deficient plants on the right produced cluster roots. **(B)** A 7-day-old developing cluster root is shown at right and a mature cluster root is shown at left.

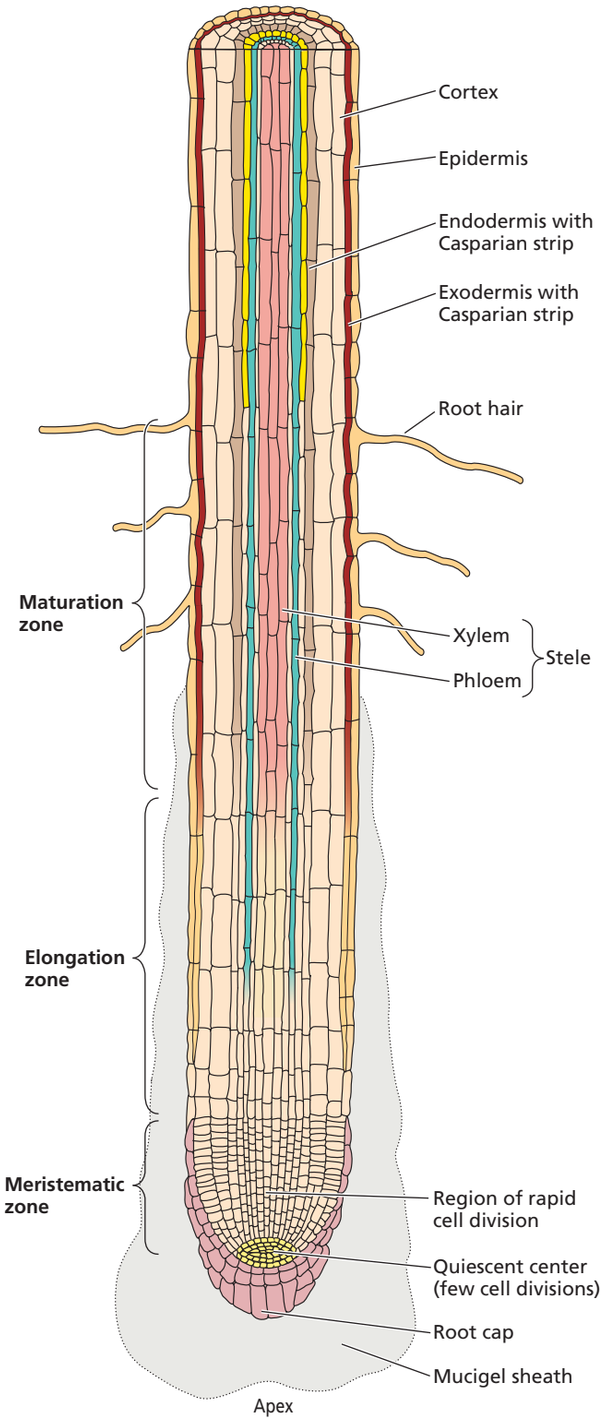


Figure 7.7 Diagrammatic longitudinal section of the apical region of the root. The meristematic cells are located near the tip of the root. These cells generate the root cap and the upper tissues of the root. In the elongation zone, cells differentiate to produce xylem, phloem, and cortex. Root hairs, formed in epidermal cells, first appear in the maturation zone.

on the radial walls and forms the **Casparian strip**, a hydrophobic structure that prevents apoplastic movement of water or solutes across the root (see Figure 6.4). In addition to having an endodermis, 90% of angiosperm species also have an **exodermis**, the outermost layer of the cortex in roots. The exodermis is also suberized and is a barrier to apoplastic movement of water and solutes. The exodermis is absent in gymnosperms.

The area of the root interior to the endodermis is called the **stele**. The stele contains the vascular elements of the root: the **phloem**, which transports metabolites from the shoot to the root and to fruits and seeds, and the **xylem**, which transports water and solutes to the shoot (see Chapter 1). Phloem develops more rapidly than xylem, attesting to the fact that phloem function is critical near the root apex. Large quantities of carbohydrates must flow through the phloem to the growing apical zones in order to support cell division and elongation. Carbohydrates provide rapidly growing cells with an energy source and with the carbon skeletons required to synthesize organic compounds. Six-carbon sugars (hexoses) also function as osmotically active solutes in the root. At the root apex, where the phloem is not yet developed, carbohydrate movement depends on symplasmic transport and is relatively slow.

Root hairs, with their large surface area for absorption of water and solutes and for anchoring the root to the soil, first appear in the **maturation zone** (see Figure 7.7), and here the xylem develops the capacity to translocate substantial quantities of water and solutes to the shoot.

Different areas of the root absorb mineral ions differently

The precise point of entry of minerals into the root system has been a topic of considerable interest. Some researchers have claimed that nutrients are absorbed only at the apical regions of the root axes or branches; others claim that nutrients are absorbed over the entire root surface.

The Casparian strip of the endodermis and exodermis in angiosperms plays a major role in preventing nonselective entry of solutes into the xylem where they would be translocated to the rest of the plant. The mechanism of selective solute uptake that uses both transmembrane transporters and the Casparian strip is discussed in Chapters 6 and 8. But the Casparian strip does not extend to the root apex; the endodermis and exodermis mature and each produces a Casparian strip in the late elongation zone or early maturation zone. This allows for a less-selective solute uptake mechanism at the root tip, and some solutes can be taken up predominantly at the root apex. For example, root absorption of calcium ions in barley (*Hordeum vulgare*) appears to be restricted to the apical region. The extent that particular nutrients (and other solutes) are taken up at the apex compared with the rest of the root depends on many factors, among

them the nutrient's concentration in the soil solution, the demand for the nutrient by the plant, and the expression of uptake transporters in different parts of the root, especially in root hairs. Iron may be taken up either at the apical region, as in barley and other species, or over the entire root surface, as in maize. Potassium ions, nitrate, ammonium, and phosphate can be absorbed by all locations of the root surface, but in maize the elongation zone has the maximum rates of potassium ion accumulation and nitrate absorption. In maize and rice and in wetland species, the root apex absorbs ammonium more rapidly than the elongation zone does. Ammonium and nitrate uptake by conifer roots varies significantly across different regions of the root and may be influenced by rates of root growth and maturation. In several species, the root apex and root hairs are the most active in phosphate absorption. Hyphae of arbuscular mycorrhizal fungi also play a significant role in uptake of phosphate and other nutrients, and the development of this symbiosis can change the regions of the root involved in uptake.

The high rates of nutrient absorption in the apical root zones also result from the strong demand for nutrients in these tissues and the relatively high nutrient availability in the soil surrounding them. For example, cell elongation depends on the accumulation of solutes such as potassium ions, chloride, and nitrate to increase the osmotic pressure within the cell (see Chapter 2). Ammonium is the preferred nitrogen source to support cell division in the meristem because meristematic tissues are often carbohydrate-limited and because assimilation of ammonium into organic nitrogen compounds consumes less energy than assimilation of nitrate (see Chapter 14). The root apex and root hairs grow into fresh soil, where nutrients have not yet been depleted.

Within the soil, nutrients can move to the root surface both by mass flow and by diffusion (see Chapter 6). In mass flow, nutrients are carried by water moving through the soil toward the root. The amounts of nutrients provided to the root by mass flow depend on the nutrient concentrations in the soil solution and the rate of water flow through the soil toward the plant, which itself depends on transpiration rates. When both the rate of water flow and the concentrations of nutrients in the soil solution are high, mass flow can play an important role in nutrient supply. Hence, highly soluble nutrients such as nitrate are largely carried by mass flow, but this process is less important for nutrients with low solubility, such as phosphate and zinc ions.

In diffusion, mineral nutrients move from a region of higher concentration to a region of lower concentration. Nutrient uptake by roots lowers the concentrations of nutrients at the root surface, generating concentration gradients in the soil solution surrounding the root. Diffusion, or more precisely net flux, of nutrients down their concentration gradients, along with mass flow resulting from transpiration, can increase nutrient availability at the root surface.

When the rate of absorption of a nutrient by roots is high and the nutrient concentration in the soil solution is low, mass flow can supply only a small fraction of the total nutrient requirement. Under these conditions, plant nutrient absorption becomes independent of plant transpiration rates, and diffusion rates limit the movement of the nutrient to the root surface. When diffusion is too slow to maintain high nutrient concentrations near the root, a **nutrient depletion zone** forms adjacent to the root surface. This zone may extend from about 0.2 to 2.0 mm from the root surface, depending on the mobility of the nutrient in the soil. The nutrient depletion zone is particularly important for phosphate.

The formation of a depletion zone tells us something important about mineral nutrition. Because roots deplete the mineral supply in the rhizosphere, their effectiveness in mining minerals from the soil is determined not only by the rate at which they can remove nutrients from the soil solution, but also by their continuous growth into undepleted soil. Without continuous growth, roots would rapidly deplete the soil adjacent to their surfaces. Optimal nutrient acquisition therefore depends both on the root system's capacity for nutrient uptake and on its ability to grow into fresh soil. The ability of the plant to form a mycorrhizal symbiosis is also critical in overcoming the effects of depletion zones, because the hyphae of the fungal symbionts grow beyond the depletion zone. These fungal structures take up nutrients far from the root (up to 25 cm in the case of arbuscular mycorrhizas) and translocate them rapidly to the roots, overcoming the slow diffusion in soil.

Nutrient availability influences root growth and development

Plants, which have limited mobility for most of their lives, must deal with changes in their local environment because they cannot move away from unfavorable conditions. Above the ground, light intensity, temperature, and humidity may fluctuate substantially during the day and across the canopy, but CO_2 and O_2 concentrations remain relatively uniform. In contrast, soil buffers the roots from temperature extremes, but the belowground concentrations of CO_2 and O_2, water, and nutrients are extremely heterogeneous, both spatially and temporally. For example, inorganic nitrogen concentrations in soil may range a thousandfold over a distance of centimeters or the course of hours. Given such heterogeneity, plants seek the most favorable conditions within their reach.

Roots sense the belowground environment and respond—through gravitropism, thigmotropism, chemotropism, and hydrotropism—by growing toward soil resources. Roots are able to sense nutrient availability

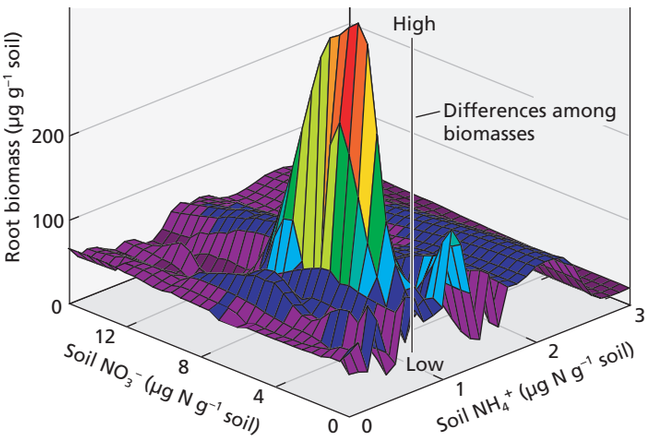


Figure 7.8 Root biomass as a function of extractable soil NH_4^+ and NO_3^-. The root biomass is shown (μg root dry weight g^{-1} soil) plotted against extractable soil NH_4^+ and NO_3^- (μg extractable N g^{-1} soil) for tomato (*Solanum lycopersicum* cv. T-5) growing in an irrigated field that had been fallow the previous 2 years. The colors emphasize the differences among biomasses, ranging from low (purple) to high (red). (After A. J. Bloom et al. 1993. *Plant Cell Environ.* 16: 199–206.)

and grow into areas of the soil with more optimal concentrations (**Figure 7.8**). Roots are also able to alter their metabolism and development to increase nutrient uptake under deficiency conditions.

Phosphate is generally trapped in surface soil horizons (layers), either tightly bound to iron and aluminum oxides or held as biological phosphorus in microorganisms. Phosphorus deficiency can trigger "topsoil foraging" by plant roots. Some bean genotypes, for example, respond to phosphorus deficiency by producing more adventitious lateral roots, decreasing the growth angle of these roots (relative to the shoot) so they are more shallow, increasing the number of lateral roots emerging from the tap root, and increasing root hair density and length (**Figure 7.9**). These changes in root system architecture place more of the roots in the topsoil, where the majority of the phosphate resides. In some plants, these changes are manifest as cluster roots (see Figure 7.6). Under continuous phosphorus deficiency, systemic signals, including miRNAs (see

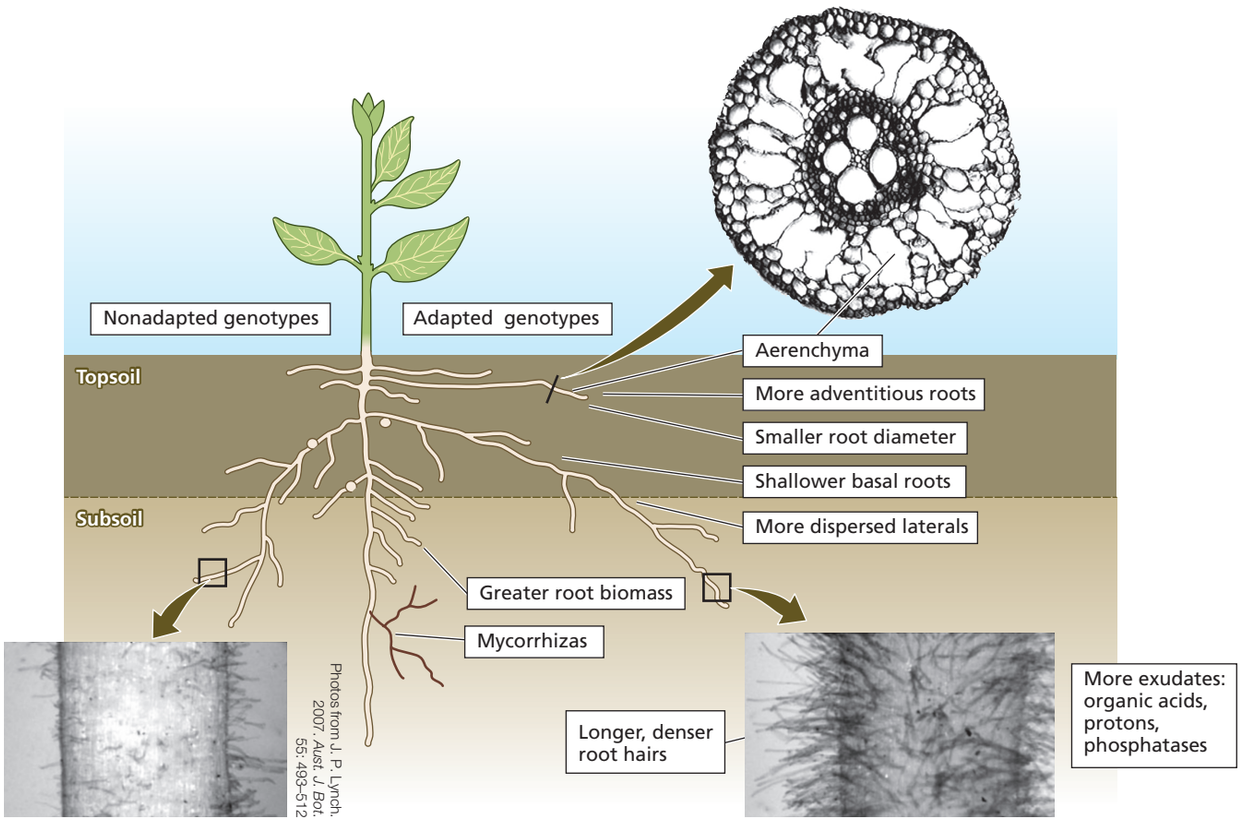


Figure 7.9 Topsoil foraging of phosphorus by phosphorus-efficient bean genotypes. In response to low phosphate availability, some bean varieties, as shown on the right side, display modified root architecture that increases root density in the soil surface layer, increased root hair density, modified metabolism that results in secretion of protons, and organic acids, and the ability to form mycorrhizal interactions. These adaptations all increase phosphate absorption by the root. (After J. P. Lynch. 2007. *Aust. J. Bot.* 55: 493–512.)

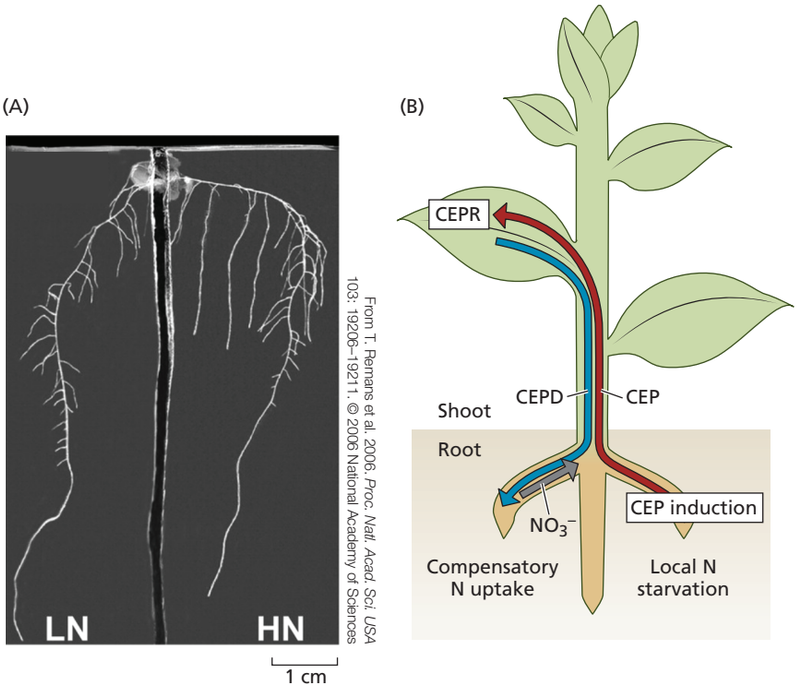
Chapter 4) produced in the shoot, are transduced in the phloem to the roots, where they induce alterations in root architecture via auxin and other hormone signaling mechanisms (see Chapter 19).

Nitrogen deficiency in the roots also results in both local and systemic responses. Under nitrogen deficiency, the NRT1.1 nitrate transporter (see Chapters 8 and 14) directly changes root auxin levels to reduce lateral root growth (see Chapter 19). C-terminally Encoded Peptide 1 (CEP1) is also produced and further represses local lateral root growth. In split-root assays where part of the root system is exposed to nitrate while the rest experiences nitrate limitation, lateral root growth and nitrogen uptake are preferentially increased on the nitrate-sufficient side (**Figure 7.10A**), suggesting that systemic signaling is also involved. CEP is also xylem-mobile and functions together with cytokinins (see Chapter 4) as a systemic nitrogen demand signal that travels to the shoot and is sensed in the phloem by CEP Receptors 1 and 2. Activation of these receptors promotes expression of genes encoding two non-secreted small proteins of the glutaredoxin family that travel in the phloem to the roots and promote nitrogen acquisition in areas of the root system with higher nitrate availability. **Figure 7.10B** shows a model for the regulation of nitrate acquisition via integrated local and systemic nitrogen-demand signaling. Local responses also modify root growth in response to high soil nutrient concentrations, as a few roots—as little as 4% of the root system in spring wheat and 12% in lettuce—are sufficient to supply all the nutrients required. Plants may thus diminish the allocation of their resources to roots while increasing allocations to the shoot and reproductive structures. This resource shifting is one mechanism through which fertilization stimulates crop yields.

Mycorrhizal symbioses facilitate nutrient uptake by roots

Our discussion so far has centered on the direct acquisition of mineral elements and compounds by roots, but this process is usually modified by the association of **mycorrhizal fungi** with the root system to form a **mycorrhiza** (from the Greek words for "fungus" and "root"; plural *mycorrhizas* or *mycorrhizae*). The host plant supplies associated mycorrhizal fungi with carbohydrates and in return receives nutrients from the fungi. There are indications that drought (water-deficit stress) and disease tolerance may also be improved in the host plant.

Mycorrhizal symbioses of two main types—**arbuscular mycorrhizas** and **ectomycorrhizas**—are widespread in nature, occurring in about 90% of terrestrial plant species, including most major crops. The majority, perhaps 80%, are arbuscular mycorrhizas, which are symbioses between a phylum of fungi called the Glomeromycota and a broad range of angiosperms, gymnosperms, ferns, and liverworts. Their importance for herbaceous species and fruit trees makes arbuscular mycorrhizas vital to agricultural production, particularly in nutrient-poor soils.



From T. Remans et al. 2006. *Proc. Natl. Acad. Sci. USA* 103: 19206–19211. © 2006 National Academy of Sciences

Figure 7.10 Root-to-shoot-to-root peptide signaling influences nitrate uptake in the context of uneven nitrogen supply to the root system. **(A)** Split-root experiment with half of an Arabidopsis root system growing on low nitrate (LN) and the other half growing on high nitrate (HN). After 5 days of growth in this setup, the high-nitrate side of the root system has longer lateral roots. **(B)** Model of how C-terminally Encoded Peptide 1 (CEP) signaling from low-nitrate roots stimulates nitrate uptake in high-nitrate roots via integration of nitrogen demand signals in the shoot. CEPD, CEP Downstream; CEPR, CEP Receptor. (B after Y. Matsubayashi. 2018. *Proc. Jpn. Acad. Ser. B. Phys. Biol. Sci.* 94: 59–74.)

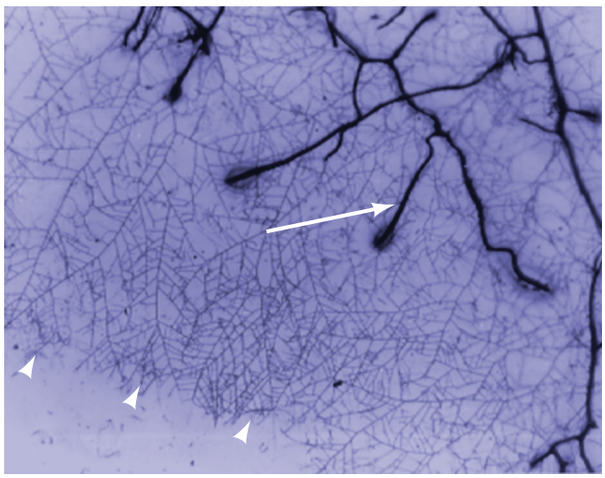
This is the most ancient type of mycorrhiza, occurring in fossils of the earliest land plants. This symbiosis preceded the evolution of true roots and therefore was probably crucial in facilitating plant establishment on land more than 450 million years ago.

By contrast, ectomycorrhizal symbioses evolved more recently. They are formed by far fewer plant species, notably trees in the families Pinaceae (pines, larches, Douglas fir), Fagaceae (beech, oak, chestnut), Salicaceae (poplar, aspen), Betulaceae (birch), and Myrtaceae (*Eucalyptus*). The fungal partners belong to either the Basidomycota or, less frequently, the Ascomycota. These symbioses play major roles in the nutrition of trees and therefore in the productivity of vast areas of boreal forest.

Some plant species, particularly those in the families Salicaceae (*Salix* [willow] and *Populus* [poplar, aspen]) and Myrtaceae (*Eucalyptus*), can form both arbuscular and ectomycorrhizal symbioses. Other plants are unable to form any kind of mycorrhiza. These include members of the families Brassicaceae, such as cabbage (*Brassica oleracea*) and the model plant *Arabidopsis thaliana*; Chenopodiaceae, such as spinach (*Spinacea oleracea*); and Proteaceae, such as macadamia nut (*Macadamia integrifolia*).

Certain agricultural practices may reduce or eliminate mycorrhiza formation in plants that normally form them. These practices include flooding (paddy rice does not form mycorrhizas, whereas upland rice does), extensive soil disturbance caused by plowing, application of high concentrations of fertilizer, and of course soil fumigation and application of some fungicides. Such practices may decrease yields in crops such as maize that are very dependent on mycorrhizas for nutrient uptake. Mycorrhizas also do not form in solution culture or in hydroponic cultivation. Nonetheless, for the majority of plants, mycorrhiza formation is the normal situation and the non-mycorrhizal state is essentially an artifact, brought about by particular agricultural practices.

Mycorrhizas modify the plant root system and influence plant mineral nutrient acquisition, but the way they do so varies between types. Arbuscular mycorrhizal fungi develop a highly branched system (mycelium) of hyphae (fine filamentous structures 2 to 10 μm in diameter) that extend into the soil beyond the root of their host (**Figure 7.11**). Different arbuscular mycorrhizal fungi vary considerably in their distance and intensity of soil exploration, but phosphate transfer from as far as 25 cm away from the root has been measured. The mycelium in soil also helps stabilize aggregates of soil particles, promoting good soil structure. The hyphae extend into soil well beyond the zone of depletion that develops around a root and thus can absorb an immobile nutrient such as phosphate from beyond the depletion zone. Hyphae also penetrate soil pores that are much narrower than those available to roots.



From M. Giovannetti et al. 2006. *Plant Signal Behav.* 1: 1–5

Figure 7.11 Visualization of the intact extraradical mycelium of *Glomus mosseae* spreading from colonized roots of cherry plum (*Prunus cerasifera*). The advancing front of the extraradical mycelium is indicated by arrowheads and the plant roots by an arrow. Note the differences in lengths and diameters of roots and hyphae.

The root of the arbuscular mycorrhizal host plant looks almost the same as a non-mycorrhizal root, and the presence of the fungi can only be detected by staining and microscopy. Hyphae of arbuscular mycorrhizal fungi, growing from spores in the soil or roots of another plant, penetrate the root epidermis and colonize the root cortex. An exodermis is present only in angiosperms as the outermost cell layer of the cortex. Most angiosperms have an exodermis, and mycorrhizal fungi can gain access to the cortex by passing through the exodermis and invading the cortical cells to form either highly branched structures called **arbuscules** (Arum-type colonization; **Figure 7.12A**) or complex **hyphal coils** (Paris-type colonization; **Figure 7.12B**). The fungi are restricted to the cortex and never penetrate the endodermis or colonize the stele of the root. Arbuscules increase the area of contact between the symbionts and remain surrounded by a plant membrane that is involved in transferring nutrients from fungal to plant cells. The penetration process is genetically controlled by a pathway that nearly 400 million years later was partially co-opted for the colonization of legume roots by nitrogen-fixing bacteria (see Chapter 14).

Phosphate is delivered by the fungi directly to the root cortex. After export from the fungal arbuscules or coils, this phosphate is taken up by the plant cells. Some of the suite of plant **phosphate transporters** (see Chapter 8) are specifically or preferentially expressed only in the plant membrane surrounding the arbuscules and coils in the root cortex and are not expressed in non-mycorrhizal roots. These transporters play a key role in the transfer of phosphate from fungus to plant. Plants regulate the level

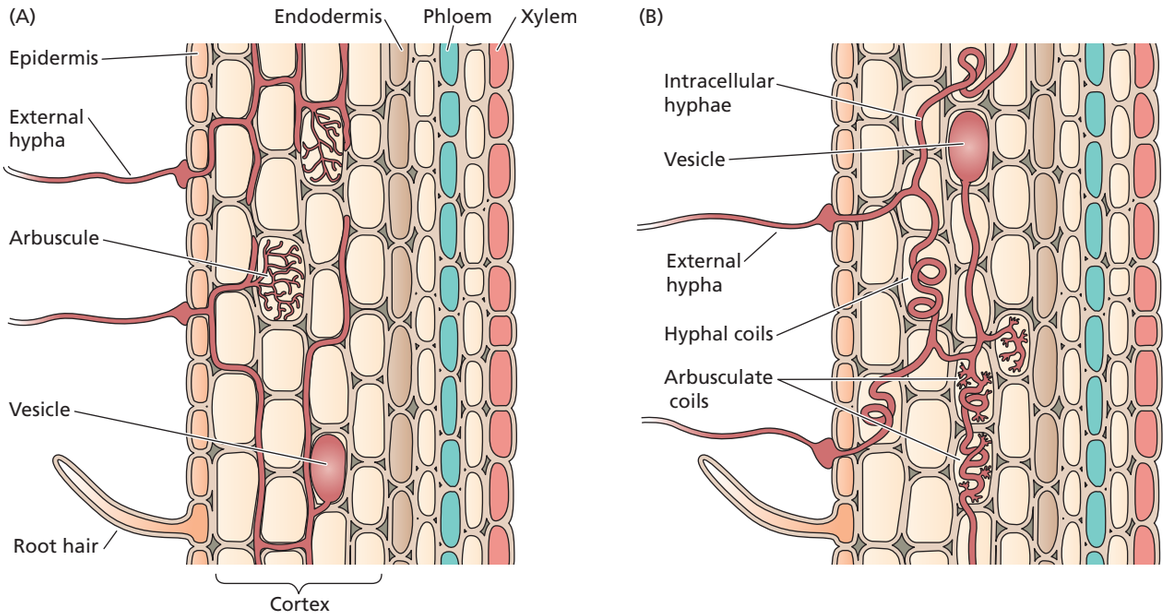


Figure 7.12 Diagrammatic representation of the two major forms of arbuscular mycorrhizal colonization of the root cortex. **(A)** Arum-type colonization is characterized by the formation of intracellular, highly branched arbuscules in root cortical cells. **(B)** Paris-type colonization is characterized by the formation of intracellular hyphal coils in root cortical cells, some of which (called arbusculate coils) bear small arbuscule-like branches.

of fungal colonization in response to their phosphate status, indicating that plants control the amount of fixed carbon delivered to the fungus based on their phosphate requirement. We will need to know more about how the symbiotic partners interact to influence nutrient acquisition in order to harness arbuscular mycorrhizal symbiosis to optimize crop nutrition. In addition to their importance for phosphate uptake, arbuscular mycorrhizal fungi are known to be important in the uptake of nitrogen and zinc.

Roots colonized by ectomycorrhizal fungi can be clearly distinguished from non-mycorrhizal roots; they grow more slowly and often appear thicker and highly branched. The fungi typically form a thick sheath, or *mantle*, of mycelium around roots, and some of the hyphae penetrate between the epidermal and sometimes (in the case of conifers) the cortical cells (**Figure 7.13**). The root cells themselves are not penetrated by the fungal hyphae, but instead are surrounded by a network of hyphae called the **Hartig net**, which provides a large area of contact between the symbionts that is involved in nutrient transfers. The fungal mycelium also extends into the soil, away from the compact sheath, where it is present as individual hyphae, mycelial fans (**Figure 7.14**), or mycelial strands. The fans in particular play important roles in obtaining nutrients from the soil, especially soil organic matter.

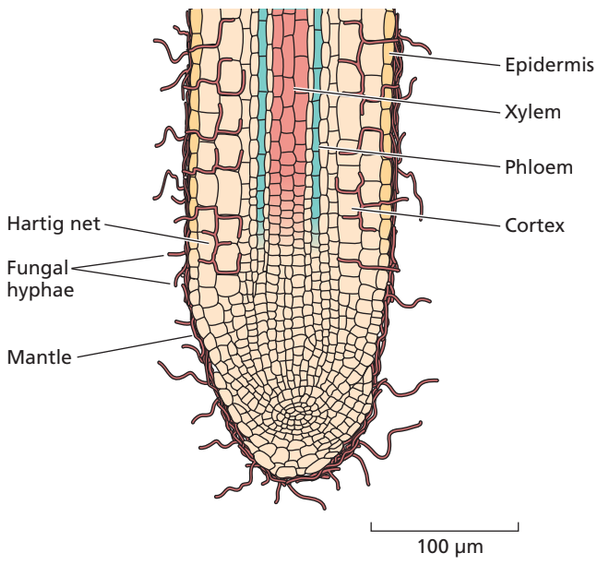


Figure 7.13 Diagrammatic representation of a longitudinal section of an ectomycorrhizal root. Fungal hyphae form a dense fungal mantle over the surface of the root and penetrate between epidermal cells, or epidermal and cortical cells, to form the Hartig net. Hyphae also grow extensively in soil, forming dense mycelium and/or mycelial strands. (After A. D. Rovira et al. 1983. In *Encyclopedia of Plant Physiology, New Series, Vol. 15A: Inorganic Plant Nutrition.* A. Läuchli and R. L. Bieleski [eds.], Springer, Berlin, pp. 61–93.)

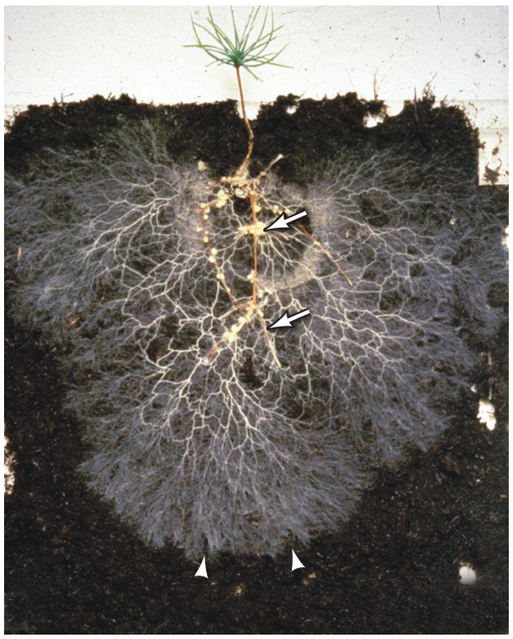


Figure 7.14 **Seedling of pine (*Pinus*) showing mycorrhizal rootlets (upper arrow) colonized by an ectomycorrhizal fungus and grown in an observation chamber in forest soil.** Note the differences between the mycelial front of dense hyphae advancing into the soil (arrowheads) and the aggregated mycelial strands (lower arrow).

Ectomycorrhizal fungi form interconnected networks among trees and produce many of the toadstools, puffballs, and truffles found in forests. Often the amount of fungal mycelium is so extensive that its total mass is much greater than that of the roots themselves. The arrangement and biochemical activities of the fungal structures in relation to the root tissues determine important aspects of nutrient acquisition by ectomycorrhizal roots and the form in which the nutrients pass from fungus to plant. In addition, all nutrients from the soil must pass through the fungal mantle covering the root epidermis before reaching the root cells themselves, giving the fungus a major role in uptake of all nutrients from the soil solution, including phosphate and inorganic forms of nitrogen (nitrate and ammonium). The extent to which fungi compete with the roots when nitrogen is in short supply is a matter of active research. The fungal mycelium that develops in soil proliferates extensively in soil organic matter patches (see Figure 7.14). The hyphae have a marked ability to convert insoluble organic nitrogen and phosphorus to soluble forms and to pass these nutrients to the plants. In this way, ectomycorrhizal fungi enable their host plants to access organic sources of nutrients, avoid competition with free-living mineralizing organisms, and grow in highly organic forest soils that contain very low amounts of inorganic nutrients.

Nutrients move between mycorrhizal fungi and root cells

Movement of nutrients from soil via a mycorrhizal fungus to root cells involves complex integration of structure and function in both fungus and plant symbionts. The interfaces where fungus and plant are juxtaposed are critical zones for transport and are composed of the plasma membranes of both organisms, plus variable amounts of cell wall material. Therefore, nutrient movements from fungus to plant are potentially under the control of these two membrane types and subject to regulatory transport processes as described in Chapter 8. Movement of nutrients from soil to the plant via a mycorrhizal fungus requires (at least) uptake of a nutrient from soil by the fungus, long-distance translocation of the nutrient through fungal hyphae (and mycelial strands when present), transmembrane efflux from the fungus to the apoplastic zone between the two membranes of the interface, and transport across the plant plasma membrane. Important issues to be resolved include the form of nutrient that is transferred and the mechanism and amounts of transfers. Mechanisms promoting efflux from the fungus to the interfacial apoplastic zone are poorly understood, while uptake into the plant has received more attention. In the case of phosphate, the plant uptake step is an active process requiring energy provided by a H^+-ATPase that generates a proton gradient (see Chapter 8) and the presence of proton-coupled phosphate symporters in the plant membrane surrounding the intracellular fungal structures, which are specifically or preferentially expressed when the roots are mycorrhizal.

Transfer of nitrogen is more complex and more controversial. In ectomycorrhizas, for which a major role in plant nitrogen nutrition has long been accepted, organic nitrogen may move from fungus to plant, with the form (glutamine, glutamine and alanine, or glutamate) varying with fungal species and the selectivity of the efflux transporters in the fungus. Some transfer of nitrogen as ammonium or ammonia may also occur.

Mycorrhizal networks can also transfer nutrients between plants. Stable isotope labeling and high-throughput DNA sequencing have been used to demonstrate distribution of nutrients based on plant source–sink relationships via ectomycorrhizal clusters associated with forest trees.

Summary

Plants are autotrophic organisms capable of using the energy from sunlight to synthesize all their components from carbon dioxide, water, and mineral elements. Although mineral nutrients continually cycle through all organisms, they enter the biosphere predominantly through the root systems of plants. After being absorbed by the roots, the mineral elements are translocated to the various parts of the plant, where they serve in numerous biological functions.

7.1 Essential Nutrients, Deficiencies, and Plant Disorders

- Studies of plant nutrition have shown that specific mineral elements are essential for plant life (**Tables 7.1, 7.2**).
- These elements are classified as macronutrients or micronutrients, depending on the relative amounts found in plants (**Table 7.1**).
- Nutritional disorders occur because nutrients have key roles within plants. They serve as components of organic compounds, in energy storage, in plant structures, as enzyme cofactors, and in electron transfer reactions.
- Mineral nutrition can be studied through the use of solution culture, which allows the characterization of specific nutrient requirements (**Figure 7.1; Table 7.3**).
- Certain visual symptoms are diagnostic for deficiencies in specific nutrients in vascular plants.
- Soil and plant tissue analysis can provide information on the nutritional status of the plant–soil system and can suggest corrective actions to avoid deficiencies or toxicities.

7.2 Treating Nutritional Deficiencies

- When crop plants are grown under modern high-production conditions, substantial amounts of nutrients are removed from the soil.
- To prevent the development of deficiencies, nutrients—particularly nitrogen, phosphorus, and potassium—can be added back to the soil in the form of fertilizers.
- Fertilizers that provide nutrients in inorganic forms are called inorganic fertilizers; those that derive from plant or animal residues or from natural rock deposits are considered organic fertilizers. In both cases, plants absorb the nutrients primarily as inorganic ions. Most fertilizers are applied to the soil, but some are sprayed on leaves.

7.3 Soil, Roots, and Microbes

- Soil is a complex substrate—physically, chemically, and biologically.
- Soil pH has a large influence on the availability of mineral elements to plants (**Figure 7.3**).
- The size of soil particles and the cation exchange capacity of the soil determine the extent to which a soil provides a reservoir for water and nutrients (**Table 7.5; Figure 7.4**).
- If mineral elements, especially sodium or metals, are present in excess in the soil, plant growth may be adversely affected. Certain plants are able to tolerate excess mineral elements, and a few species—for example, halophytes in the case of sodium—may thrive under these extreme conditions.
- To obtain nutrients from the soil, plants develop extensive root systems (**Figures 7.5, 7.6**), form symbioses with mycorrhizal fungi, and produce and secrete protons or organic anions into the soil.
- Roots continually deplete the nutrients from the immediate soil around them.
- Nutrient availability influences root growth (**Figures 7.8–7.10**).
- The majority of plants have the ability to form symbioses with mycorrhizal fungi.
- The fine hyphae of mycorrhizal fungi extend the reach of roots into the surrounding soil and facilitate the acquisition of nutrients (**Figures 7.11–7.14**). Arbuscular mycorrhizas increase uptake of mineral nutrients, particularly phosphorus, whereas ectomycorrhizas play a significant role in obtaining nitrogen from organic sources.
- In return, plants provide carbohydrates to the mycorrhizal fungi.

Web Material

- **WEB TOPIC 7.1 Symptoms of Deficiency in Essential Minerals** Deficiency symptoms are characteristic of each essential element and can be diagnostic for the deficiency. The color photographs in this topic illustrate deficiency symptoms for each essential element in tomato.
- **WEB TOPIC 7.2 Observing Roots Belowground** The study of roots growing under natural conditions requires a means to observe roots belowground. State-of-the-art techniques are described in this topic.
- **WEB ESSAY 7.1 From Meals to Metals and Back** Metal accumulation is toxic to plants. Understanding the molecular process involved in toxicity is helping researchers develop better phytoremediation crops.

For more study aids, go to oup.com/he/taiz7e.

Suggested Reading

Armstrong, F. A. (2008) Why did nature choose manganese to make oxygen? *Philos. Trans. R. Soc. Lond., B, Biol. Sci.* 363: 1263–1270.

Baxter, I. R., Vitek, O., Lahner, B., Muthukumar, B., Borghi, M., Morrissey, J., Guerinot, M. L., and Salt, D. E. (2008) The leaf ionome as a multivariable system to detect a plant's physiological status. *Proc. Natl. Acad. Sci. USA* 105: 12081–12086.

Bucher, M. (2007) Functional biology of plant phosphate uptake at root and mycorrhiza interfaces. *New Phytol*. 173: 11–26.

Bücking, H. and Kafle, A. (2015) Role of arbuscular mycorrhizal fungi in the nitrogen uptake of plants: Current knowledge and research gaps. *Agronomy* 5: 587–612.

Burns, I. G. (1991) Short- and long-term effects of a change in the spatial distribution of nitrate in the root zone on N uptake, growth and root development of young lettuce plants. *Plant Cell Environ.* 14: 21–33.

Erisman, J. W., Galloway, J., Seitzinger, S., Bleeker, A., and Butterbach-Bahl, K. (2011) Reactive nitrogen in the environment and its effect on climate change. *Curr. Opin. Environ. Sustain.* 3: 281–290.

Feldman, L. J. (1998) Not so quiet quiescent centers. *Trends Plant Sci.* 3: 80–81.

Godfray, H. C., Beddington, J. R., Crute, I. R., Haddad, L., Lawrence, D., Muir, J. F., Pretty, J., Robinson, S., Thomas, S. M., and Toulmin, C. (2010) Food security: the challenge of feeding 9 billion people. *Science* 327: 812–818.

Hodge, A., and Storer, K.(2015) Arbuscular mycorrhiza and nitrogen: implications for individual plants through to ecosystems. *Plant Soil* 386: 1–19.

Hose, E., Clarkson, D. T., Steudle, E., Schreiber, L., and Hartung, W. (2001) The exodermis: a variable apoplastic barrier. *J. Exp. Bot.* 52: 2245–64.

Huang, X.Y., and Salt, D. E. (2016) Plant ionomics: From elemental profiling to environmental adaptation. *Mol. Plant* 9: 787–797.

Jackson, R. B., Canadell, J., Ehleringer, J. R., Mooney, H. A., Sala, O. A., and Schulze, E.-D. (1996) A global analysis of root distributions for terrestrial biomes. *Oecologia* 108: 389–411.

Jeong, J., and Guerinot, M. L. (2009) Homing in on iron homeostasis in plants. *Trends Plant Sci.* 14: 280–285.

Mengel, K., and Kirkby, E. A. (2001) *Principles of Plant Nutrition*, 5th ed. Kluwer Academic Publishers, Dordrecht, Netherlands.

Péret, B., Desnos, T., Jost, R., Kanno, S., Berkowitz, O., and Nussaume, L. (2014) Root architecture responses: in search of phosphate. *Plant Physiol.* 166: 1713–1723.

Sattelmacher, B. (2001) The apoplast and its significance for plant mineral nutrition. *New Phytol*. 149: 167–192.

Steffen, W., Richardson, K., Rockstrom, J., Cornell, S. E., Fetzer, I., Bennett, E. M., Biggs, R., Carpenter, S. R., de Vries, W., de Wit, C. A., Folke, C., Gerten, D., Heinke, J., Mace, G. M., Persson, L. M., Ramanathan, V., Reyers, B., and Sörlin, S. (2015). Planetary boundaries: Guiding human development on a changing planet. *Science* 347: 1259855.

Vukosav, P., Mlakar, M., and Tomišić, V. (2012) Revision of iron (III)-citrate speciation in aqueous solution. Voltammetric and spectrophotometric studies. *Anal Chim Acta*. 745: 85–91.

Zegada-Lizarazu, W., Matteucci, D., and Monti, A. (2010) Critical review on energy balance of agricultural systems. *Biofuel. Bioprod. Biorefin.* 4: 423–446.

8 Solute Transport



Dancestrokes/ Shutterstock

The interior of a plant cell is separated from the external environment by a plasma membrane that is only two lipid molecules thick. This thin layer separates a relatively constant internal environment from variable external surroundings. In addition to forming a hydrophobic barrier to diffusion, the membrane must facilitate and continuously regulate the inward and outward traffic of selected molecules and ions as the cell takes up nutrients, exports solutes, and regulates its turgor pressure. Similar functions are performed by the internal membranes that separate the various compartments within each cell. The plasma membrane also detects information about the environment, about molecular signals from other cells, and about the presence of invading pathogens. Often these signals are relayed by changes in ion fluxes across the membrane.

The movement of ions and other solutes from one location to another within an organism is known as **transport**. Local transport of solutes into or within cells is regulated mainly by membrane proteins. Larger-scale transport between plant organs, or between plant and environment, is also controlled by membrane transport at the cellular level. For example, the transport of sucrose from leaf to root through the phloem, referred to as **translocation**, is driven and regulated by membrane transport into the phloem cells of the leaf and from the phloem to the storage cells of the root (see Chapter 12).

In this chapter we consider the physical and chemical principles that govern the movement of molecules in solution and show how these principles apply to membranes and biological systems. We discuss the molecular mechanisms of transport in living cells and the great variety of membrane transport proteins that are responsible for the particular transport properties of plant cells. As an example, we discuss the channels, transporters, and pumps of stomatal guard cells and their roles in signal transduction and in the control of osmotic gradients that drive changes in stomatal aperture. Finally, we examine the pathways that ions take when they enter the root as well as the mechanism of xylem loading, the process whereby ions are released into the tracheary elements of the stele. Because transported substances, including carbohydrates, amino acids, and metals such as iron and zinc, are vital for human nutrition, understanding and manipulating solute transport in plants can contribute solutions to sustainable food production.

8.1 Passive and Active Transport

According to Fick's first law (see Equation 5.1), the movement of molecules by diffusion always proceeds spontaneously, down a gradient of free energy or chemical potential, until equilibrium is reached. The spontaneous "downhill" movement of molecules is termed **passive transport**. At equilibrium, no further net movement of solutes can occur without the application of a driving force.

The movement of substances against a gradient of chemical potential, or "uphill," is termed **active transport**. It is not spontaneous, and it requires that work be done on the system by the application of cellular energy. One common way (but not the only way) of accomplishing this task is to couple transport to the hydrolysis of ATP.

Recall from Chapter 5 that we can calculate the driving force for diffusion or, conversely, the energy input necessary to move substances against a gradient by measuring the potential-energy gradient. For uncharged solutes this gradient is often a simple function of the difference in concentration. Biological transport can be driven by four major forces: concentration, hydrostatic pressure, gravity, and electrical fields. (However, recall from Chapter 5 that in small-scale biological systems, gravity seldom contributes substantially to the force that drives transport.)

The **chemical potential** for any solute is defined as the sum of the concentration, electrical, and hydrostatic potentials (and the chemical potential under standard conditions). *The importance of the concept of chemical potential is that it sums all the forces that may act on a molecule to drive net transport.*

$$\underset{\substack{\text{Chemical potential for a given solute, } j}}{\tilde{\mu}_j} = \underset{\substack{\text{Chemical potential of } j \text{ under standard conditions}}}{\mu_j^*} + \underset{\substack{\text{Concentration (activity) component}}}{RT \ln C_j} + \underset{\substack{\text{Electrical-potential component}}}{z_j FE} + \underset{\substack{\text{Hydrostatic-pressure component}}}{\bar{V}_j P} \quad (8.1)$$

Here $\tilde{\mu}_j$ is the chemical potential of the solute species j in joules per mole (J mol^{-1}), μ_j^* is its chemical potential under standard conditions (a correction factor that will cancel out in future equations and so can be ignored), R is the universal gas constant, T is the absolute temperature, and C_j is the concentration (more accurately the activity) of j.

The electrical term, $z_j FE$, applies only to ions; z is the electrostatic charge of the ion (+1 for monovalent cations, –1 for monovalent anions, +2 for divalent cations, and so on), F is Faraday's constant (96,500 Coulombs, equivalent to the electrical charge on 1 mol of H^+), and E is the overall electrical potential of the solution (with respect to ground). The final term, $\bar{V}_j P$, expresses the contribution of the partial molal volume of j ($\bar{V}_j$) and pressure (P) to the chemical potential of j. (The partial molal volume of j is the change in volume per mole of substance j added to the system, for an infinitesimal addition.)

This final term, $\bar{V}_j P$, makes a much smaller contribution to $\tilde{\mu}_j$ than do the concentration and electrical terms, except in the very important case of osmotic water movements. As discussed in Chapter 5, when we consider water movement at the cellular scale, the chemical potential of water (i.e., the water potential) depends on the concentration of dissolved solutes and the hydrostatic pressure on the system.

In general, diffusion (passive transport) always moves molecules energetically downhill from areas of higher chemical potential to areas of lower chemical potential. Movement against a chemical-potential gradient is indicative of active transport (**Figure 8.1**).

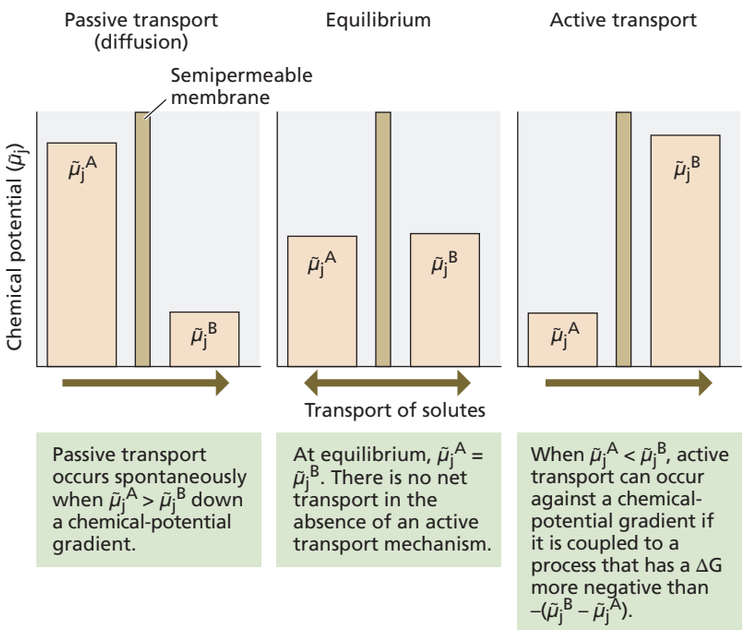


Figure 8.1 Relationship between chemical potential, $\tilde{\mu}$, and the transport of molecules across a semipermeable membrane. The net movement of molecular species j between compartments A and B depends on the relative magnitude of the chemical potential of j in each compartment, represented here by the size of the boxes. Movement down a chemical gradient occurs spontaneously and is called passive transport; movement against, or up, a gradient requires energy and is called active transport.

If we take the diffusion of sucrose across a plasma membrane as an example, we can accurately approximate the chemical potential of sucrose in any compartment by the concentration term alone (unless a solution is concentrated, causing hydrostatic pressure to build up within the plant cell). From Equation 8.1, the chemical potential of sucrose inside a cell can be described as follows (in the next four equations, the subscript *s* stands for sucrose and the superscripts *i* and *o* stand for inside and outside, respectively):

$$\underset{\substack{\text{Chemical potential of sucrose solution inside the cell}}}{\tilde{\mu}_s^i} = \underset{\substack{\text{Chemical potential of sucrose solution under standard conditions}}}{\mu_s^*} + \underset{\substack{\text{Concentration component}}}{RT \ln C_s^i} \tag{8.2}$$

The chemical potential of sucrose outside the cell is calculated in the same way:

$$\tilde{\mu}_s^o = \mu_s^* + RT \ln C_s^o \tag{8.3}$$

We can calculate the difference in the chemical potential of sucrose between the solutions inside and outside the cell, $\Delta\tilde{\mu}_s$, regardless of the mechanism of transport. To get the signs right, remember that for inward transport, sucrose is being removed (–) from outside the cell and added (+) to the inside, so the change in free energy in joules per mole of sucrose transported will be as follows:

$$\Delta\tilde{\mu}_s = \tilde{\mu}_s^i - \tilde{\mu}_s^o \tag{8.4}$$

Substituting the terms from Equations 8.2 and 8.3 into Equation 8.4, we get the following:

$$\begin{aligned} \Delta\tilde{\mu}_s &= \left(\mu_s^* + RT \ln C_s^i\right) - \left(\mu_s^* + RT \ln C_s^o\right) \\ &= \mathrm{RT}\left(\ln \mathrm{C}_s^i - \ln \mathrm{C}_s^o\right) \\ &= \mathrm{RT} \ln \frac{\mathrm{C}_s^i}{\mathrm{C}_s^o} \end{aligned} \tag{8.5}$$

If this difference in chemical potential is negative, sucrose can diffuse inward spontaneously (provided the membrane is permeable to sucrose; see Section 8.2). In other words, the driving force ($\Delta\tilde{\mu}_s$) for solute diffusion is related to the magnitude of the concentration gradient (C_s^i/C_s^o).

If the solute carries an electrical charge (as does, for example, the potassium ion), the electrical component of the chemical potential must also be considered. Suppose the membrane is permeable to K^+ and Cl^- rather than to sucrose. Because the ionic species (K^+ and Cl^-) diffuse independently, each has its own chemical potential. Thus, for inward K^+ diffusion,

$$\Delta\tilde{\mu}_K = \tilde{\mu}_K^i - \tilde{\mu}_K^o \tag{8.6}$$

Substituting the appropriate terms from Equation 8.1 into Equation 8.6, we get

$$\Delta\tilde{\mu}_s = (RT \ln [K^+]^i + zFE^i) - RT \ln [K^+]^o + zFE^o) \tag{8.7}$$

and because the electrostatic charge of K^+ is +1, $z = +1$, and

$$\Delta\tilde{\mu}_K = RT \ln \frac{[K^+]^i}{[K^+]^o} + F(E^i - E^o) \tag{8.8}$$

The magnitude and sign of this expression will indicate the driving force and direction for K^+ diffusion across the membrane. A similar expression can be written for Cl^- (but remember that for Cl^-, $z = -1$).

Equation 8.8 shows that ions, such as K^+, diffuse in response to both their concentration gradients ($[K^+]^i/[K^+]^o$) and any electrical-potential difference between the two compartments ($E^i - E^o$). One important implication of this equation is that ions can be driven passively against their concentration gradients if an appropriate voltage (electrical field) is applied between the two compartments. Because of the importance of electrical fields in the biological transport of any charged molecule, $\tilde{\mu}$ is often called the **electrochemical potential**, and $\Delta\tilde{\mu}$ is the difference in electrochemical potential between two compartments.

8.2 Transport of Ions across Membrane Barriers

If two ionic solutions are separated by a biological membrane, diffusion is complicated by the fact that the ions must move through the membrane as well as across the open solutions. The extent to which a membrane permits the movement of a substance is called **membrane permeability**. As we discuss in Section 8.3, permeability depends on the composition of the membrane as well as on the chemical nature of the solute. In a loose sense, permeability can be expressed in terms of a diffusion coefficient for the solute through the membrane. However, permeability is influenced by several additional factors, such as the ability of a substance to enter the membrane, that are difficult to measure.

Despite its theoretical complexity, we can readily measure permeability by determining the rate at which a solute passes through a membrane under a specific set of conditions. Generally the membrane will hinder diffusion and thus reduce the speed with which equilibrium is reached. For any particular solute, however, the permeability or resistance of the membrane itself cannot alter the final equilibrium conditions. Equilibrium occurs when $\Delta\tilde{\mu}_j = 0$.

In this section we discuss the factors that influence the distribution of ions across a membrane. These parameters can be used to predict the relationship between the electrical gradient and the concentration gradient of an ion.

Different diffusion rates for cations and anions produce diffusion potentials

When salts diffuse across a membrane, an electrical membrane potential (voltage) can develop. Consider the two KCl solutions separated by a membrane in **Figure 8.2**. The K^+ and Cl^- ions will permeate the membrane independently as they diffuse down their respective gradients of electrochemical potential. And unless the membrane is very porous, its permeability to the two ions will differ.

As a consequence of these different permeabilities, K^+ and Cl^- will initially diffuse across the membrane at different rates. The result is a slight separation of charge, which instantly creates an electrical potential across the membrane. In biological systems, membranes are usually more permeable to K^+ than to Cl^-. Therefore, K^+ will diffuse out of the cell (see compartment A in Figure 8.2) faster than Cl^-, causing the cell to develop a negative electrical charge with respect to the extracellular medium. A potential that develops as a result of diffusion is called a **diffusion potential**.

The principle of electrical neutrality must always be kept in mind when the movement of ions across membranes is considered: Bulk solutions always contain equal numbers of anions and cations. The existence of a membrane potential implies that the distribution of charges across the membrane is uneven; however, the actual number of unbalanced ions is negligible in chemical terms. For example, the generation of a membrane potential of –100 millivolts (mV), like that found across the plasma membranes of many plant cells, is due to ions moving across the membrane and results in the presence of only 1 extra anion out of every 100,000 within the cell—a concentration difference of only 0.001%! As Figure 8.2 shows, these extra anions are found immediately adjacent to the surface of the membrane; there is no charge imbalance throughout the bulk of the cell.

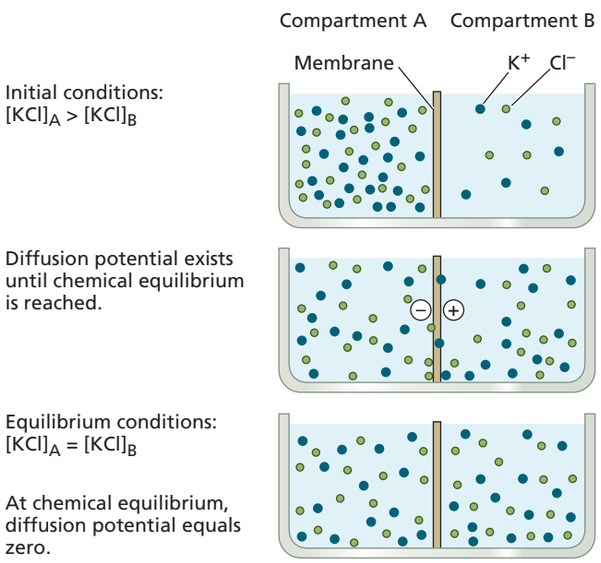


Figure 8.2 Development of a diffusion potential and a charge separation between two compartments separated by a membrane that is preferentially permeable to potassium ions. If the concentration of potassium chloride is higher in compartment A ($[KCl]_A > [KCl]_B$), potassium and chloride ions will diffuse into compartment B. If the membrane is more permeable to potassium ions than to chloride, potassium ions will diffuse faster than chloride ions, and a charge separation (+ and –) will develop, resulting in establishment of a diffusion potential.

In our example of KCl diffusion across a membrane, electrical neutrality is preserved, because as K^+ moves ahead of Cl^- in the membrane, the resulting diffusion potential retards the movement of K^+ and speeds that of Cl^-. Ultimately, both ions diffuse at the same rate, but the diffusion potential persists and can be measured. As the system moves toward equilibrium and the concentration gradient collapses, the diffusion potential also collapses.

How does membrane potential relate to ion distribution?

Because the membrane in the preceding example is permeable to both K^+ and Cl^- ions, equilibrium will not be reached for either ion until the concentration gradients decrease to zero. However, if the membrane were permeable only to K^+, diffusion of K^+ would carry charges across the membrane until the membrane potential balanced the concentration gradient. Because a change in potential requires very few ions, this balance would be reached very quickly. Potassium ions would then be at equilibrium, even though the change in the concentration gradient for K^+ would be negligible.

When the distribution of any solute across a membrane reaches equilibrium, the passive flux, J (i.e., the amount of solute crossing a unit area of membrane per unit time), is the same in the two directions—outside to inside and inside to outside:

$$J_{o\rightarrow i} = J_{i\rightarrow o}$$

Fluxes are related to $\Delta\tilde{\mu}$ (for a discussion on fluxes and $\Delta\tilde{\mu}$, see **WEB APPENDIX 1**); thus, at equilibrium the electrochemical potentials will be the same even if the concentrations are quite different:

$$\tilde{\mu}_j^o = \mu_j^i$$

and for any given ion (the ion is symbolized here by the subscript j),

$$\mu_j^* + RT \ln C_j^o + z_j F E^o = \mu_j^* + RT \ln C_j^i + z_j F E^i \quad (8.9)$$

By rearranging Equation 8.9, we obtain the difference in electrical potential between the two compartments at equilibrium ($E^i - E^o$):

$$E^i - E^o = \frac{RT}{z_j F}\left(\ln \frac{C_j^o}{C_j^i}\right)$$

This electrical-potential difference is known as the **Nernst potential** (ΔE_j) for that ion,

$$\Delta E_j = E^i - E^o$$

And

$$\Delta E_j = \frac{RT}{z_j F}\left(\ln \frac{C_j^o}{C_j^i}\right) \tag{8.10}$$

or

$$\Delta E_j = \frac{2.3RT}{z_j F}\left(\log \frac{C_j^o}{C_j^i}\right)$$

This relationship, known as the *Nernst equation*, states that at equilibrium, the difference in concentration of an ion between two compartments is balanced by the voltage difference between the compartments. The Nernst equation can be further simplified for a univalent cation at 25°C:

$$\Delta E_j = 59 \text{ mV} \log \frac{C_j^o}{C_j^i} \tag{8.11}$$

Note that a tenfold difference in concentration corresponds to a Nernst potential of 59 mV ($C_o/C_i = 10/1$; log 10 = 1). That is, a membrane potential of 59 mV would maintain a tenfold concentration gradient of an ion whose movement across the membrane is driven by passive diffusion. Similarly, if a tenfold concentration gradient of an ion existed across the membrane, passive diffusion of that ion down its concentration gradient (if it were allowed to come to equilibrium) would result in a difference of 59 mV across the membrane.

All living cells exhibit a membrane potential that is due to selective ion movement across the plasma membrane. We can determine these membrane potentials by inserting a microelectrode into the cell and measuring the voltage difference between the inside of the cell and the extracellular medium (**Figure 8.3**).

The Nernst equation can be used at any time to determine whether a given ion is at equilibrium across a membrane. However, a distinction must be made between equilibrium and steady state. *Steady state* is the condition in which influx and efflux of a given solute are equal, and therefore the ion concentrations are constant over time. Steady state is not necessarily the same as equilibrium (see Figure 8.1); in steady state, the existence of active transport across the membrane prevents many diffusive fluxes from ever reaching equilibrium.

The Nernst equation distinguishes between active and passive transport

Table 8.1 shows how experimental measurements of ion concentrations at steady state in pea root cells compare with predicted values calculated from the Nernst equation. In this example, the concentration of each ion in the external solution bathing the tissue and the

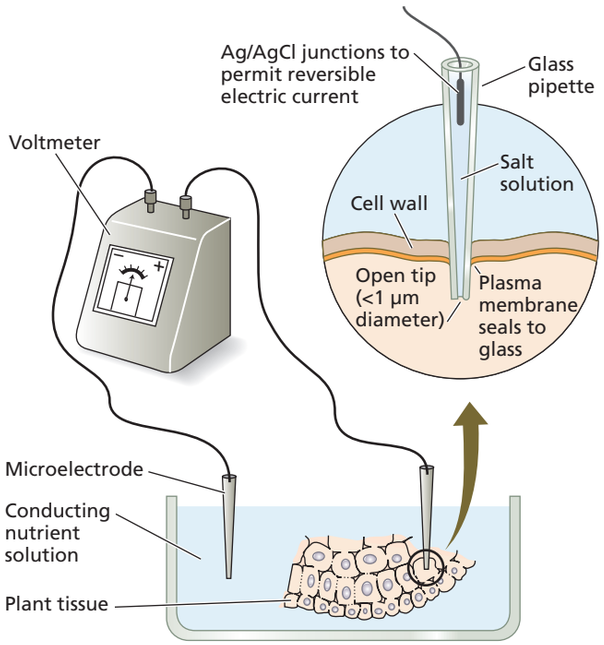


Figure 8.3 Diagram of a pair of microelectrodes used to measure membrane potentials across plasma membranes. One of the glass micropipette electrodes is inserted into the cell compartment under study (usually the vacuole or the cytoplasm), while the other is kept in an electrically conducting solution that serves as a reference. The microelectrodes are connected to a voltmeter, which records the electrical-potential difference between the cell compartment and the solution. Typical membrane potentials across plant plasma membranes range from –100 to –200 mV. The insert shows how electrical contact with the interior of the cell is made through the open tip of the glass micropipette, which contains an electrically conducting salt solution.

Table 8.1 Comparison of observed and predicted ion concentrations in pea root tissue

Ion	Concentration in external medium (mmol L^{-1})	Internal concentration[a] (mmol L^{-1})	
		Predicted	Observed
K^+	1	74	75
Na^+	1	74	8
Mg^{2+}	0.25	1340	3
Ca^{2+}	1	5360	2
NO_3^-	2	0.0272	28
Cl^-	1	0.0136	7
$H_2PO_4^-$	1	0.0136	21
SO_4^{2-}	0.25	0.00005	19

Source: Data from N. Higinbotham et al. 1967. *Plant Physiol.* 42: 37–46.

Note: The membrane potential was measured as –110 mV.

[a]Internal concentration values were derived from ion content of hot water extracts of 1- to 2-cm intact root segments.

measured membrane potential were substituted into the Nernst equation, and the internal concentration of each ion was predicted.

Prediction using the Nernst equation assumes passive ionic distribution, but notice that, of all the ions shown in Table 8.1, only K^+ is at or near equilibrium. The anions NO_3^-, Cl^-, $H_2PO_4^-$, and SO_4^{2-} all have higher internal concentrations than predicted, indicating that their uptake is active. The cations Na^+, Mg^{2+}, and Ca^{2+} have lower internal concentrations than predicted; therefore, these ions are actively exported.

The example shown in Table 8.1 is an oversimplification; plant cells have several internal compartments, each of which can differ in its ionic composition from the others. The cytosol and the vacuole are the most important intracellular compartments in determining the ionic relations of plant cells. In most mature plant cells, the central vacuole occupies 90% or more of the cell volume, and the cytosol is restricted to a thin layer around the periphery of the cell.

Because of its small volume, the cytosol of most angiosperm cells is difficult to assay chemically. For this reason, much of the early work on the ionic relations of plants focused on certain green algae, such as *Chara* and *Nitella*, whose cells are several inches long and may contain an appreciable volume of cytosol. In brief:

- Potassium ions are accumulated passively in the cytosol. When extracellular K^+ concentrations are very low, K^+ may be taken up actively.
- Sodium ions are pumped actively out of the cytosol into the extracellular space and vacuole.
- Protons are also actively extruded from the cytosol. This process helps maintain the cytosolic pH near neutrality, while the vacuole and the extracellular medium are generally more acidic by one or two pH units.
- Anions are taken up actively into the cytosol.
- Calcium ions are actively transported out of the cytosol at both the plasma membrane and the vacuolar membrane, which is called the tonoplast.

Many different ions permeate the membranes of living cells simultaneously, but K^+ has the highest concentrations in plant cells, and it exhibits high permeabilities. A modified version of the Nernst equation, the **Goldman equation**, includes all permeant ions (all ions for which mechanisms of transmembrane movement exist) and therefore gives a more accurate value for the diffusion potential. When permeabilities and ion gradients are known, it is possible to calculate a diffusion potential across a biological membrane from the Goldman equation. The diffusion potential calculated from the Goldman equation is termed the *Goldman diffusion potential* (for a detailed discussion of the Goldman equation, see **WEB TOPIC 8.1**).

Proton transport is a major determinant of the membrane potential

In most eukaryotic cells, K^+ has both the greatest internal concentration and the highest membrane permeability, so the diffusion potential may approach E_K, the Nernst potential for K^+. In some cells of some organisms—particularly in some mammalian cells such as neurons—the normal resting potential of the cell may also be close to E_K. This is not the case with plants and fungi, however, which often show experimentally measured membrane potentials (often –200 to –100 mV) that are much more negative than those calculated from the Goldman equation, which are usually only –80 to –50 mV. Thus, in addition to the diffusion potential, the membrane potential must have a second component. The additional voltage is provided by the plasma membrane H^+-ATPase, an *electrogenic pump* that transports H^+ out of plant cells unaccompanied by a balancing charge.

Energy for active transport by the plasma membrane H^+-ATPase is provided by the hydrolysis of ATP. We can study the dependence of the plasma membrane potential on ATP by observing the effect of cyanide (CN^-) on the membrane potential (**Figure 8.4**). Cyanide rapidly poisons the mitochondria (see Chapter 13), and ATP within cells becomes depleted. As ATP synthesis is inhibited, the membrane potential falls to the level of the Goldman diffusion potential (see **WEB TOPIC 8.1**).

Thus, the membrane potentials of plant cells have two components: a diffusion potential and a component resulting from active, electrogenic ion transport—the net

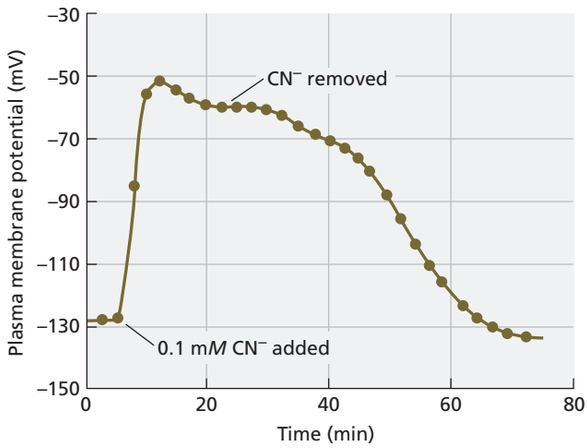


Figure 8.4 The plasma membrane potential of a pea cell collapses when cyanide (CN^-) is added to the bathing solution. Cyanide blocks ATP production in the cell by poisoning the mitochondria. The collapse of the membrane potential upon addition of cyanide indicates that an ATP supply is necessary for maintenance of the potential. Washing the cyanide out of the tissue results in a slow recovery of ATP production and restoration of the membrane potential. (After N. Higinbotham et al. 1970. *J. Membr. Biol.* 3: 210–222.)

transport of a charge across the membrane. When cyanide inhibits electrogenic ion transport, the pH of the external medium increases while the cytosol becomes acidic, consistent with the active transport of protons out of the cell that is electrogenic.

A change in membrane potential caused by an electrogenic pump will change the driving forces for diffusion of all ions that cross the membrane. For example, the outward transport of H^+ can create an electrical driving force for the passive diffusion of K^+ into the cell. Protons are transported electrogenically across the plasma membrane not only in plants but also in bacteria, algae, fungi, and some animal cells, such as those of the kidney epithelia.

ATP synthesis in mitochondria and chloroplasts also depends on a H^+-ATPase. In these organelles, this transport protein is usually called an *ATP synthase* because it forms ATP rather than hydrolyzing it (see Chapters 9 and 13). We discuss the structure and function of membrane proteins involved in active and passive transport in plant cells in detail in Sections 8.3 and 8.4.

8.3 Membrane Transport Processes

Artificial membranes made of pure phospholipids have been used extensively to study membrane permeability. When the permeability of artificial phospholipid bilayers to ions and molecules is compared with that of biological membranes, important similarities and differences become evident (**Figure 8.5**).

Biological and artificial membranes have similar permeabilities to nonpolar molecules and many small polar molecules. However, biological membranes are much more permeable to ions, to some large polar molecules, such as sugars, and to water than artificial bilayers are. This is because biological membranes contain **transport proteins** that facilitate the passage of selected ions and other molecules. The general term *transport proteins* encompasses three main categories of proteins: channels, carriers, and pumps (**Figure 8.6**), each of which we describe in more detail later in this section.

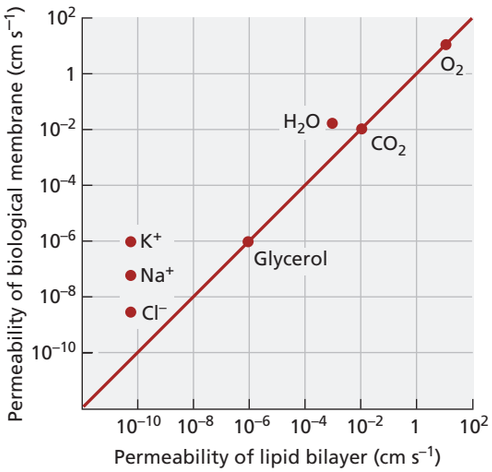


Figure 8.5 Typical values for the permeability of a biological membrane to various substances compared with those for an artificial phospholipid bilayer. For nonpolar molecules such as O_2 and CO_2, and for some small uncharged molecules such as glycerol, permeability values are similar in both systems. For ions and selected polar molecules, including water, the permeability of biological membranes is increased by one or more orders of magnitude because of the presence of transport proteins. Note the logarithmic scale.

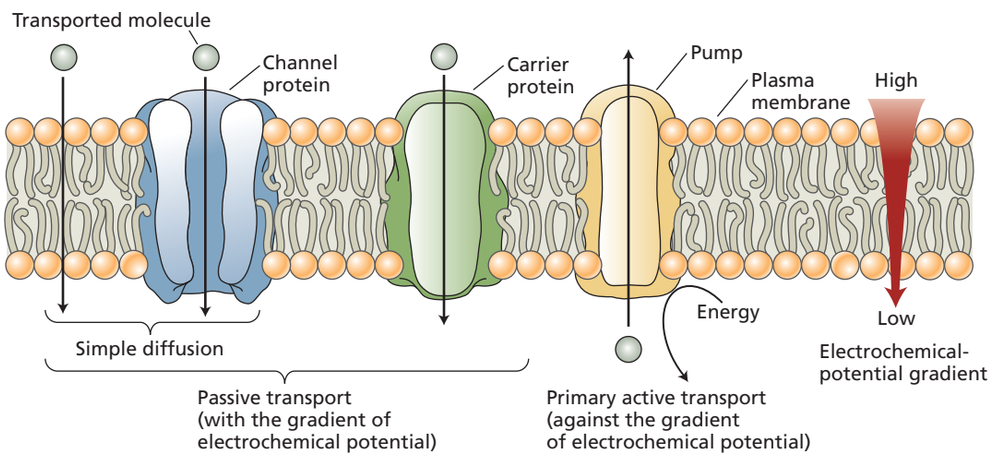


Figure 8.6 Three classes of membrane transport proteins: channels, carriers, and pumps. Channels and carriers can mediate the passive transport of a solute across a membrane down the electrochemical potential gradient of the solute. Channel proteins act as membrane pores, and their specificity is determined primarily by the biophysical properties of the channel. Carrier proteins bind the transported molecule on one side of the membrane and release it on the other side. Primary active transport is carried out by pumps that use energy directly, usually from ATP hydrolysis, to transport solutes against their gradient of electrochemical potential.

Transport proteins exhibit specificity for the solutes they transport, so cells require a great diversity of transport proteins. The simple prokaryote *Haemophilus influenzae*, the first organism for which the complete genome was sequenced, has only 1743 genes, yet more than 200 of those genes (more than 10% of the genome) encode various proteins involved in membrane transport. In Arabidopsis, out of a predicted 33,602 protein-coding genes, as many as 1800 may encode proteins with transport functions.

Transport proteins are usually specific for the kinds of substances they transport, but they may transport other solutes with a similar size and charge. For example, a K^+ transporter in the plasma membrane may transport K^+, Rb^+, and Na^+ with different preferences. In contrast, most K^+ transporters are completely ineffective in transporting anions such as Cl^- or uncharged solutes such as sucrose. Similarly, most sucrose transporters transport a range of uncharged glycosides, but no other substances.

In this section we consider the structures, functions, and physiological roles of the various membrane transporters found in plant cells, especially in the plasma membrane and tonoplast. We begin with a discussion of the role of certain transporters (channels and carriers) in promoting the diffusion of solutes across membranes. We then distinguish between primary and secondary active transport and discuss the roles of the electrogenic H^+-ATPase in driving H^+-coupled secondary active transport.

Channels enhance diffusion across membranes

Channels are transmembrane proteins that function as selective pores through which ions, and in some cases neutral molecules, can diffuse across the membrane. The size of a pore and the density and nature of the surface charges on its interior lining determine the transport specificity of a channel. Transport through channels is always passive, and the specificity of transport depends on the pore size and electrical charge more than on selective binding (**Figure 8.7**).

As long as the channel pore is open, substances that can penetrate the pore diffuse through it extremely rapidly: about 10^8 ions per second through an ion channel. Channel pores are not open all the time, however. Channel proteins contain particular regions called **gates** that open and close the pore in response to signals. Signals that can regulate channel activity include membrane potential changes, ligands, hormones, light, and posttranslational protein modifications such as phosphorylation. For example, voltage-gated channels open or close in response to changes in the membrane potential (see Figure 8.7B). Another intriguing regulatory signal is mechanical force, which changes the conformation and thereby controls the gating of mechanosensitive ion channels in plants and other organisms.

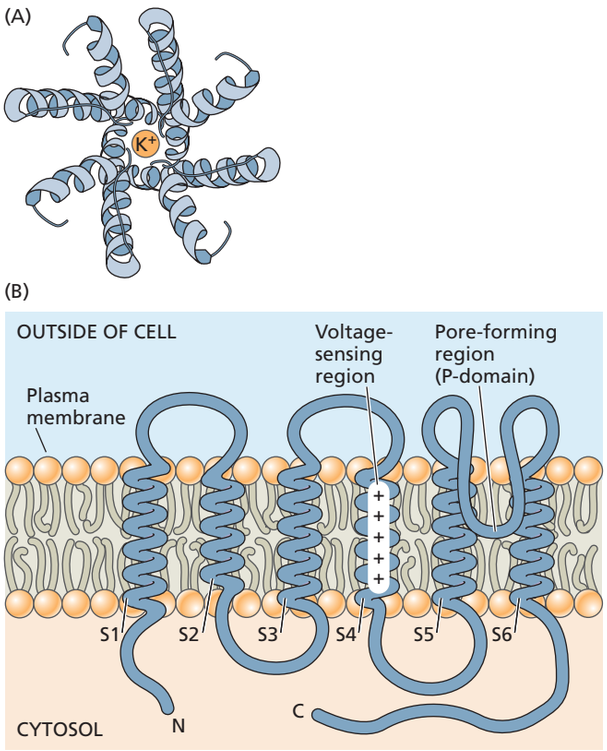


Figure 8.7 **Models of K^+ channels in plants.** **(A)** Top view of a channel, looking through the pore of the protein. Membrane-spanning helices of four subunits come together in an inverted teepee with the pore at the center. The pore-forming regions of the four subunits dip into the membrane, forming a K^+ selectivity finger region at the outer part of the pore. **(B)** Side view of an inwardly rectifying K^+ channel, showing a polypeptide chain of one subunit, with six membrane-spanning helices (S1–S6). The fourth helix contains positively charged amino acids and acts as a voltage sensor. The pore-forming region (P-domain) is a loop between helices 5 and 6. (A after Q. Leng et al. 2002. *Plant Physiol.* 128: 400–410; B after D. Sanders and P. Bethke. 2000. In *Biochemistry and Molecular Biology of Plants*, B. B. Buchanan et al. [eds.], pp. 110–158. American Society of Plant Physiologists, Rockville, MD.)

Individual ion channels can be studied in detail by an electrophysiological technique called patch clamping (see **WEB TOPIC 8.2**), which can detect the electric current carried by ions diffusing through a single open channel or a collection of channels. Patch clamp studies reveal that for a given ion, such as K^+, a membrane has a variety of different channels. These channels may open over different voltage ranges, or in response to different signals, which may include K^+ or Ca^{2+} concentrations, pH, reactive oxygen species, and so on. The ion permeability of a membrane depends on which channels are open and on the substrate specificity of those channels. This allows ion transport to be fine-tuned to the prevailing conditions.

As we saw in the experiment presented in Table 8.1, the distribution of most ions is not close to equilibrium

across the membrane. Therefore, we know that channels for most ions are usually closed. Plant cells generally accumulate more anions than could occur via a strictly passive mechanism. Therefore, when anion channels open, anions flow out of the cell, and active mechanisms are required for anion uptake. Calcium ion channels are tightly regulated and essentially open only during signal transduction. Calcium ion channels function only to allow Ca^{2+} flux into the cytosol, and Ca^{2+} must be expelled from the cytosol by active transport. In contrast, K^+ can diffuse either inward or outward through channels, depending on whether the membrane potential is more negative or more positive than E_K, the potassium ion equilibrium potential.

K^+ channels that open only at potentials more negative than the prevailing Nernst potential for K^+ are specialized for inward diffusion of K^+ and are known as **inwardly rectifying**, or simply *inward*, K^+ channels. Conversely, K^+ channels that open only at potentials more positive than the Nernst potential for K^+ are **outwardly rectifying**, or *outward*, K^+ channels (**Figure 8.8**). Inward K^+ channels function in the accumulation of K^+ from the apoplast, as occurs, for example, during K^+ uptake by guard cells in

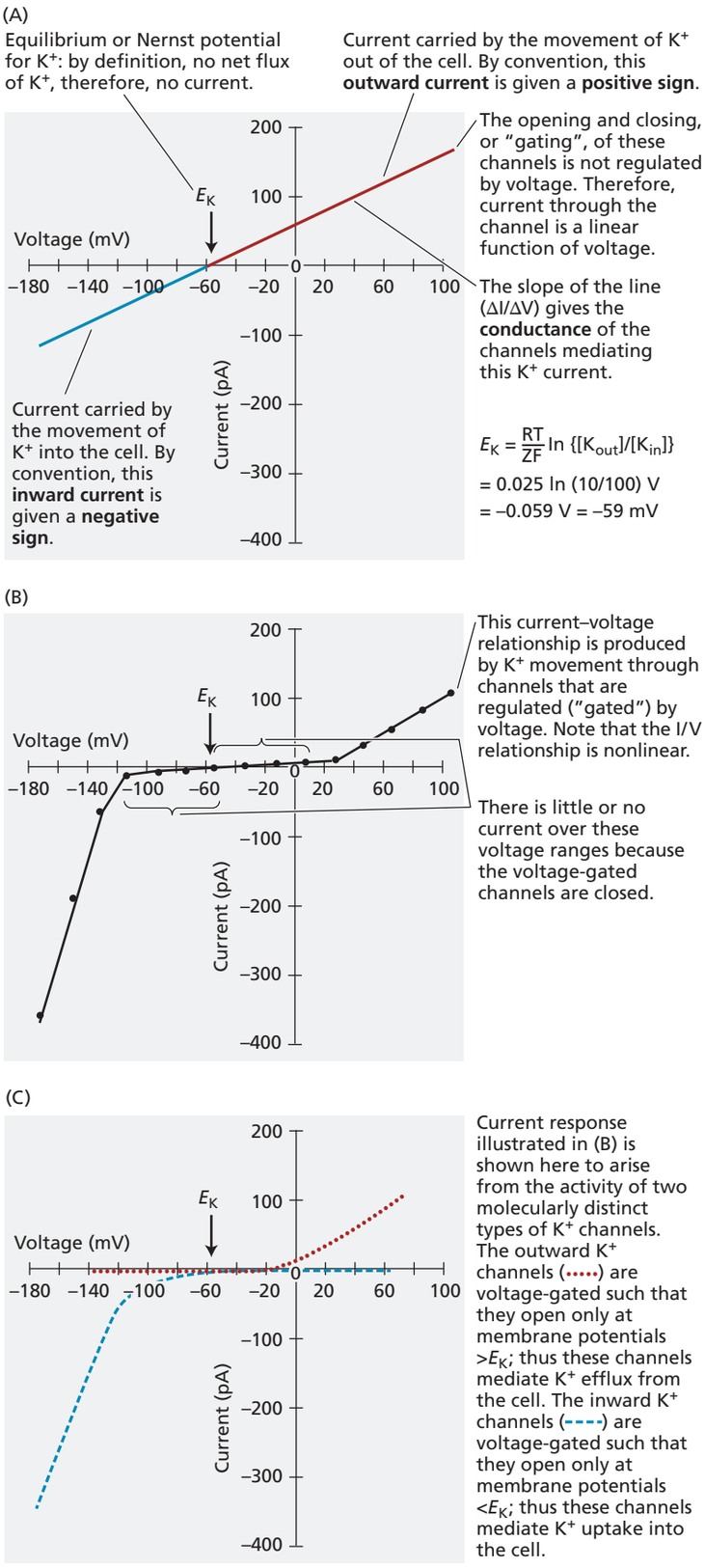


Figure 8.8 **Current–voltage relationships.** **(A)** Diagram showing the current that would result from K^+ flux through a set of hypothetical plasma membrane K^+ channels that were not voltage-regulated, given a K^+ concentration in the cytosol of 100 m*M* and an extracellular K^+ concentration of 10 m*M*. Note that the current would be linear, and that there would be zero current at the equilibrium (Nernst) potential for K^+ (E_K). **(B)** Actual K^+ current data from an Arabidopsis guard cell protoplast, with the same intracellular and extracellular K^+ concentrations as in (A). These currents result from the activities of voltage-regulated K^+ channels. Note that, again, there is zero net current at the equilibrium potential for K^+. However, there is also zero net current over a broader voltage range because the channels are closed over this voltage range in these conditions. When the channels are closed, no K^+ can flow through them, hence zero current is observed over this voltage range. **(C)** The current–voltage relationship in (B) actually results from the activities of two sets of channels—the inwardly rectifying K^+ channels and the outwardly rectifying K^+ channels—which together produce the current–voltage relationship. (After L. Perfus-Barbeoch and S. M. Assmann, unpublished data.)

the process of stomatal opening (see Figure 8.8). Various outward K^+ channels function in stomatal closing and in the release of K^+ into the xylem or apoplast (discussed in Sections 8.5 and 8.6, respectively).

Carriers bind and transport specific substances

Unlike channels, carrier proteins do not have pores that extend completely across the membrane. In transport mediated by a carrier, the substance being transported is initially bound to a specific site on the carrier protein. This requirement for binding allows carriers to be highly selective for a particular substrate to be transported. **Carriers** therefore specialize in the transport of specific inorganic or organic solutes. Binding causes a conformational change in the protein, which exposes the substance to the solution on the other side of the membrane. Transport is complete when the substance dissociates from the transport protein.

Because a conformational change in the protein is required to transport an individual molecule or ion, the rate of transport by a carrier is many orders of magnitude slower than that through a channel. Typically, carriers may transport 100 to 1000 ions or molecules per second, while millions of ions can pass through an open ion channel per second. The binding and release of molecules at a specific site on a carrier protein are similar to the binding and release of molecules by an enzyme in an enzyme-catalyzed reaction. As we discuss later in this section, enzyme kinetics have been used to characterize transport proteins.

While channels function only in passive transport, carriers can function in either passive transport or secondary active transport (the latter is discussed later in this section). Passive transport via a carrier is sometimes called **facilitated diffusion**, although it resembles diffusion only in that it transports substances down their gradient of electrochemical potential, without an additional input of energy. (The term "facilitated diffusion" might seem more appropriately applied to transport through channels, but historically it has not been used in that way.)

Primary active transport requires energy

To carry out active transport, a carrier must couple the energetically uphill transport of a solute with another, energy-releasing event so that the overall free-energy change is negative. **Primary active transport** is coupled directly to a source of energy other than $\Delta\tilde{\mu}_j$, such as ATP hydrolysis, an oxidation–reduction reaction (as in the electron transport chain of mitochondria and chloroplasts; see Chapters 9 and 13), or the absorption of light by the carrier protein (such as bacteriorhodopsin in halobacteria).

Membrane proteins that carry out primary active transport are called **pumps** (see Figure 8.6). Most pumps transport inorganic ions, such as H^+ or Ca^{2+}. However, as we will see in Section 8.4, pumps belonging to the ATP-binding cassette (ABC) family of transporters can carry large organic molecules.

Ion pumps can be further characterized as either electrogenic or electroneutral. In general, **electrogenic transport** refers to ion transport involving the net movement of charge across the membrane. In contrast, **electroneutral transport**, as the name implies, involves no net movement of charge. For example, the Na^+/K^+-ATPase of animal cells pumps three Na^+ out for every two K^+ in, resulting in a net outward movement of one positive charge. The Na^+/K^+-ATPase is therefore an electrogenic ion pump. In contrast, the H^+/K^+-ATPase of the animal gastric mucosa pumps one H^+ out of the cell and one K^+ in for each ATP hydrolyzed, so there is no net movement of charge across the membrane. Therefore, the H^+/K^+-ATPase is an electroneutral pump.

For the plasma membrane of plants, fungi, and bacteria, as well as for plant tonoplast and other plant and animal endomembranes, H^+ is the principal ion that is electrogenically pumped across the membrane. The **plasma membrane H^+-ATPase** generates the gradient of electrochemical potential of H^+ across the plasma membrane, while the **vacuolar H^+-ATPase** (usually called the **V-ATPase**) and the **H^+-pyrophosphatase** (**H^+-PPase**) electrogenically pump protons into the lumen of the vacuole and the Golgi cisternae.

Secondary active transport is driven by ion gradients

Solutes are also actively transported across a membrane against their gradient of electrochemical potential by coupling the uphill transport of one solute to the downhill transport of another. This type of carrier-mediated cotransport is termed **secondary active transport**. In plants and fungi, secondary active transporters mainly use the downhill transport of H^+ to drive the uptake of nutrients such as NO_3^-, SO_4^{2-}, and $H_2PO_4^-$; the uptake of many metabolites such as amino acids, peptides, and sucrose; and the export of Na^+, which at high concentrations is toxic to plant cells. **Figure 8.9** shows how secondary active transport may involve the binding of a substrate (S) and an ion (usually H^+) to a carrier protein and a conformational change in that protein.

Secondary active transport is driven indirectly by pumps. In plant cells, protons are extruded from the cytosol by electrogenic H^+-ATPases operating in the plasma membrane and at the vacuolar membrane. Consequently, a membrane potential and a pH gradient are created at the expense of ATP hydrolysis. This gradient of electrochemical potential for H^+, referred to as $\Delta\tilde{\mu}_{H^+}$, or (when expressed in other units) the **proton motive force** (**PMF**), represents stored free energy in the form of the H^+ gradient (see **WEB TOPIC 8.3**).

There are two types of secondary active transport: symport and antiport. The example shown in Figure 8.9

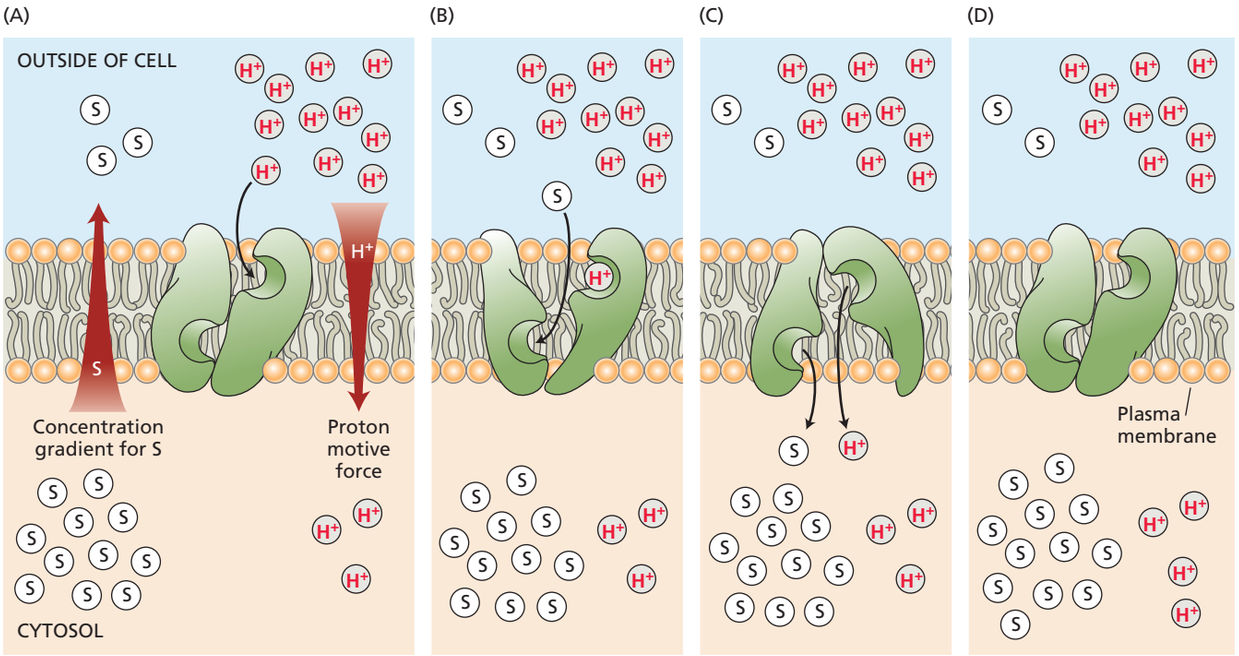


Figure 8.9 **Hypothetical model of secondary active transport.** In secondary active transport, the energetically uphill transport of one solute is driven by the energetically downhill transport of another solute. In the illustrated example, energy that was stored as proton motive force ($\Delta\tilde{\mu}_{H^+}$, symbolized by the red arrow on the right in [A]) is being used to take up a substrate (S) against its concentration gradient (red arrow on the left). **(A)** In the initial conformation, the binding sites on the protein are exposed to the outside environment and can bind a proton. **(B)** This binding results in a conformational change that permits a molecule of S to be bound. **(C)** The binding of S causes another conformational change that exposes the binding sites and their substrates to the inside of the cell. **(D)** Release of a proton and a molecule of S to the interior of the cell restores the original conformation of the carrier and allows a new pumping cycle to begin.

and in **Figure 8.10A** is called **symport** (and the proteins involved are called *symporters*) because the two substances move in the same direction through the membrane. **Antiport** (facilitated by proteins called *antiporters*) refers to coupled transport in which the energetically downhill movement of one solute drives the active (energetically uphill) transport of another solute in the opposite direction (**Figure 8.10B**). Considering the direction of the H^+ gradient, proton-coupled symporters generally function in solute uptake into the cytosol while proton-coupled antiporters function to export solutes out of the cytosol.

In both types of secondary transport, the ion or solute being transported simultaneously with the protons is moving against its gradient of electrochemical potential, so its transport is active. However, the energy driving this transport is provided by the proton motive force rather than directly by ATP hydrolysis.

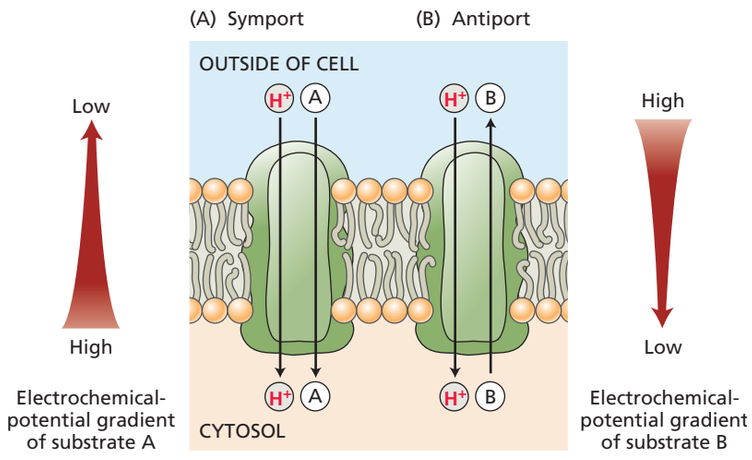


Figure 8.10 **Two examples of secondary active transport coupled to a primary proton gradient.** **(A)** In symport, the energy dissipated by a proton moving back into the cell is coupled to the uptake of one molecule of a solute (e.g., a sugar) into the cell. **(B)** In antiport, the energy dissipated by a proton moving back into the cell is coupled to the active transport of a substrate (e.g., a sodium ion) out of the cell. In both cases, the substrate under consideration is moving against its gradient of electrochemical potential. Both neutral and charged substrates can be transported by such secondary active transport processes.

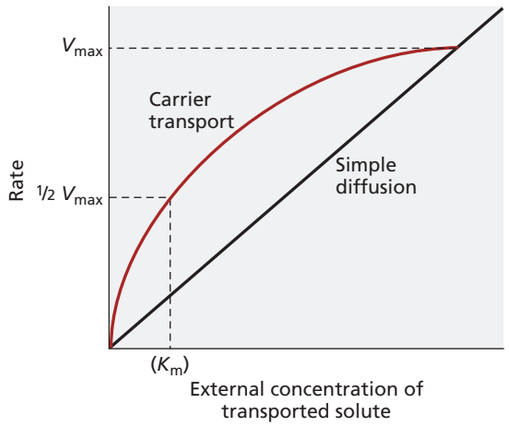


Figure 8.11 **Carrier transport often shows enzyme kinetics, including saturation (V_{max}) (see WEB APPENDIX 1).** In contrast, simple diffusion through open channels is ideally directly proportional to the concentration of the transported solute or, for an ion, to the difference in electrochemical potential across the membrane.

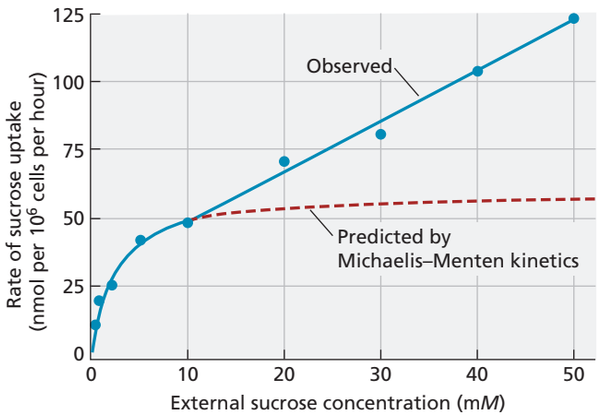


Figure 8.12 **The transport properties of a solute can change with solute concentrations.** For example, at low concentrations (1–10 m*M*), the rate of uptake of sucrose by soybean cells shows saturation kinetics typical of carriers. A curve fitted to these data is predicted to approach a maximum rate (V_{max}) of 57 nmol per 10^6 cells per hour. Instead, at higher sucrose concentrations, the uptake rate continues to increase linearly over a broad range of concentrations, consistent with the existence of additional facilitated transport mechanisms for sucrose uptake. (After W. Lin et al. 1984. *Plant Physiol.* 75: 936–940.)

Kinetic analyses can elucidate transport mechanisms

Thus far we have described transport in terms of its energetics or thermodynamics, which determine the direction of transport. It is equally important to understand the kinetics, or rate, of transport. The same approaches used to study enzyme kinetics are often used to study transport because both involve the binding and dissociation of molecules at binding sites on proteins (see **WEB TOPIC 8.4**). One distinction of the kinetic approach is that it gives new insights into the regulation of transport.

In kinetic experiments, the effects of solute concentrations on transport rates are measured. The kinetic characteristics of the transport rates can then be used to distinguish between different transporters. The maximum rate (V_{max}) of carrier- or channel-mediated transport cannot be exceeded, regardless of the concentration of substrate (**Figure 8.11**). V_{max} is approached when the substrate-binding site on the carrier is always occupied or when flux through the channel is maximal. The concentration of transporter, not the concentration of solute, becomes rate-limiting. Thus, V_{max} is an indicator of the number of molecules of the specific transport protein that are functioning in the membrane.

The constant K_m (which is numerically equal to the solute concentration that yields half the maximum rate of transport) tends to reflect the properties of the particular binding site. Low K_m values indicate high binding affinity of the transport site for the transported substance. Higher values of K_m indicate a lower affinity of the transport site for the solute. The affinity can be so low that in practice V_{max} is never reached.

Cells or tissues often display complex kinetics for the transport of a solute. Complex kinetics usually indicate the presence of more than one type of transport mechanism—for example, both high- and low-affinity transporters. **Figure 8.12** shows the rate of sucrose uptake by soybean cotyledon protoplasts as a function of the external sucrose concentration. Uptake increases sharply with concentration and begins to saturate at about 10 m*M*. At concentrations above 10 m*M*, uptake becomes linear and nonsaturable within the concentration range tested. Inhibition of ATP synthesis with metabolic poisons blocks the saturable component, but not the linear one.

The interpretation of the pattern shown in Figure 8.12 is that sucrose uptake at low concentrations is an energy-dependent, carrier-mediated process (H^+–sucrose symport). At higher concentrations, sucrose enters the cells by transport down its concentration gradient and is therefore insensitive to metabolic poisons. Consistent with these data, both H^+–sucrose symporters and sucrose facilitators (i.e., transport proteins that mediate transmembrane sucrose flux down its free-energy gradient) have been identified at the molecular level.

8.4 Membrane Transport Proteins

Numerous representative transport proteins located in the plasma membrane and the tonoplast are illustrated in **Figure 8.13**. Typically, transport across a biological membrane is energized by one primary active transport system coupled to ATP hydrolysis. In plants and

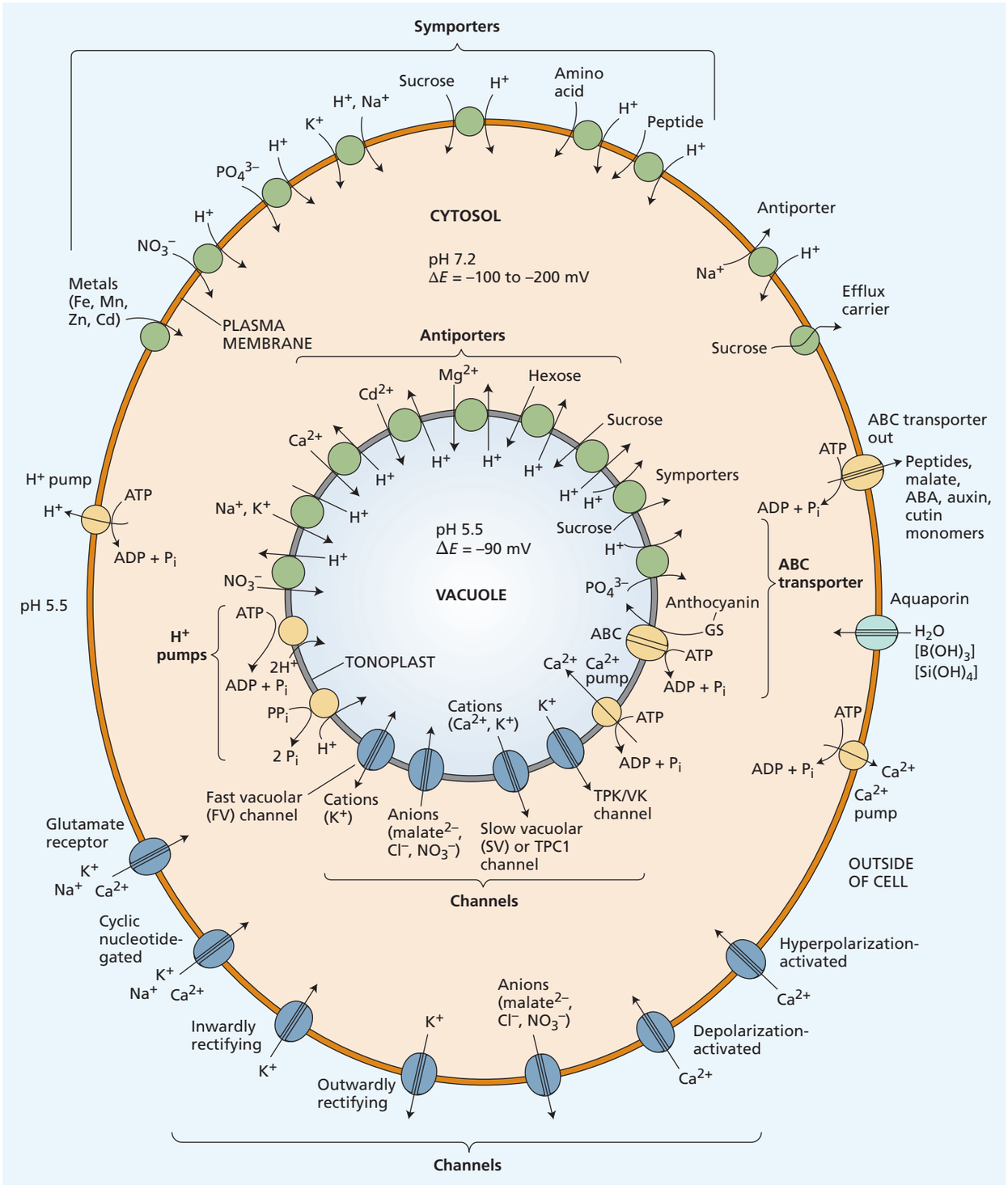


Figure 8.13 Overview of the various transport proteins in the plasma membrane and tonoplast of plant cells.

fungi, the H^+-ATPase is the primary pump that generates the ion gradient and an electrochemical potential. Many other ions or neutral organic solutes can then be transported by a variety of secondary active transport proteins, which energize the transport of their substrates by simultaneously carrying one or two H^+ down their energy gradient. Thus, protons circulate across the membrane, outward through the primary active transport proteins, and back into the cell through the secondary active transport proteins. Most of the ion gradients across membranes of higher plants are generated and maintained by electrochemical-potential gradients of H^+, which are generated by electrogenic proton pumps.

In plants, Na^+ is transported out of cells by a Na^+–H^+ antiporter and Cl^-, NO_3^-, $H_2PO_4^-$, sucrose, amino acids, and other substances enter the cell via specific H^+ symporters. What about potassium ions? Potassium ions are mainly taken up from the apoplast through inwardly rectifying K^+ channels (see Figure 8.8). K^+ uptake through channels is driven by the negative membrane potential. When passive K^+ uptake is not energetically favorable, for example if extracellular K^+ is too low, K^+ can be taken up by symport with H^+. K^+ uptake via a symport mechanism can accumulate more K^+ in cells relative to the extracellular K^+ concentration because transport is driven by both the negative membrane potential and the transmembrane pH gradient, both of which are generated by H^+-ATPases in the plasma membrane. K^+ efflux from cells occurs through outwardly rectifying K^+ channels and is driven by membrane potentials more positive than E_K (see Figure 8.8), which can be achieved by efflux of Cl^- or other anions through anion channels.

Genes encoding many transporters have been identified

Transporter gene identification, genome sequencing, and transport assays using heterologous expression systems have revolutionized the study of transport proteins. Many plant transporter genes were identified using plant complementary DNA (cDNA) libraries to complement (i.e., compensate for) transport deficiencies in yeast. Yeast transporter mutants have been essential to both identify plant transporter genes and as heterologous expression systems to study transporter activity. *Xenopus* oocytes have also been an important heterologous expression system for plant channels and transporters. Because of their large size and generally low background transport activity, *Xenopus* oocytes are convenient for electrophysiological studies. Coexpression in oocytes is relatively easy, which has facilitated studying interactions of channels or transporters with regulatory proteins such as protein kinases. As the number of sequenced genomes has increased, it has become common to identify putative transporter genes by phylogenetic analysis, in which sequence comparison with genes encoding transporters of known function in other organisms allows one to predict function in the organism of interest. Based on such analyses, it has become evident that gene families, rather than individual genes, exist in plant genomes for most transport functions. Within a gene family, variations in transport kinetics, in modes of regulation, in subcellular localization, and in differential tissue expression give plants a remarkable plasticity to respond to a broad range of environmental conditions. In the following subsections we discuss the functions and diversity of transporters for the major categories of solutes found within the plant body (note that sucrose transport was discussed in Sections 8.1 and 8.3 and is also discussed in Chapter 12).

Transporters exist for diverse nitrogen-containing compounds

Nitrogen, one of the macronutrients, can be present in the soil solution as nitrate (NO_3^-), ammonia (NH_3), or ammonium (NH_4^+), and in some soils in organic form such as amino acids. Plants have both electrogenic and electroneutral ammonium transporters, and both types bind NH_4^+, deprotonate it, and transport NH_3. In addition, electrogenic ammonium transporters also transport H^+, and therefore are NH_3–H^+ symporters. The cellular uptake of anions such as NO_3^- requires energy, and NO_3^- is taken up by symport with H^+. Plant NO_3^- transporters are of particular interest because of their complexity. They can function not only in NO_3^- transport but also as receptors for NO_3^-; their expression is regulated by cellular NO_3^- concentrations (see Chapter 14), and their transport activity is regulated at the protein level.

Mutants with defects in NO_3^- transport or NO_3^- reduction can be selected by growth in the presence of chlorate (ClO_3^-). Chlorate is a NO_3^- analog that is taken up and reduced in wild-type plants to the toxic product chlorite. If plants resistant to ClO_3^- are selected, they are likely to show mutations that block NO_3^- transport or reduction. Several such mutations have been identified in Arabidopsis. The first transporter gene identified in this way, named *CHL1/NRT1.1*, encodes an inducible NO_3^-–H^+ symporter that functions as a dual-affinity carrier, with its mode of action (high affinity or low affinity) being switched by its phosphorylation status. Remarkably, this transporter also functions as a NO_3^- sensor that regulates NO_3^--induced gene expression.

Once nitrogen has been incorporated into organic molecules, there are a variety of mechanisms that distribute it throughout the plant. Peptide transporters provide one such mechanism. Peptide transporters are important for mobilizing nitrogen reserves during seed germination and senescence. In the carnivorous pitcher plant *Nepenthes alata*, high levels of expression of a peptide transporter are found in the pitcher, where the transporter presumably mediates uptake of peptides from digested insects into the internal tissues.

Some peptide transporters operate by coupling with the H^+ electrochemical gradient. Other peptide transporters are members of the ABC family of proteins, which directly use energy from ATP hydrolysis for transport; thus, this transport does not depend on a primary electrochemical gradient (see **WEB TOPIC 8.5**). The ABC family is an extremely large protein family, and its members transport diverse substrates, ranging from small inorganic ions to macromolecules. For example, large metabolites such as flavonoids, anthocyanins, and secondary products of metabolism are sequestered in the vacuole via the action of specific ABC transporters, while other ABC transporters mediate the transmembrane transport of the hormone abscisic acid.

Amino acids constitute another important category of nitrogen-containing compounds. The plasma membrane amino acid transporters of eukaryotes have been divided into five superfamilies, three of which rely on the proton gradient for coupled amino acid uptake and are present in plants. In general, amino acid transporters can provide high- or low-affinity transport, and they have overlapping substrate specificities. Many amino acid transporters show distinct tissue-specific expression patterns, suggesting specialized functions in different cell types. Amino acids constitute an important form in which nitrogen is distributed long distances in plants, so it is not surprising that the expression patterns of many amino acid transporter genes include expression in vascular tissues.

Amino acid and peptide transporters have important roles in addition to their function as distributors of nitrogen resources. Because plant hormones are frequently found conjugated with amino acids and peptides, transporters for those molecules may also be involved in the distribution of hormone conjugates throughout the plant. The hormone auxin is derived from tryptophan, and the genes encoding auxin transporters are related to those for some amino acid transporters. In another example, proline is an amino acid that accumulates under salt stress. This accumulation lowers the water potential of the cell, thereby promoting cellular water retention under stress conditions.

Cation transporters are diverse

Cations are transported by pumps, carriers, and channels. The relative contributions of each type of transport mechanism differ depending on the membrane, cell type, and prevailing conditions.

CATION CHANNELS On the order of 50 genes in the Arabidopsis genome encode channels mediating cation uptake across the plasma membrane or intracellular membranes such as the tonoplast. Some of these channels are highly selective for specific ionic species, such as potassium ions. Others allow passage of a variety of cations, sometimes including Na^+, even though this ion is toxic when overaccumulated. As described in **Figure 8.14**,

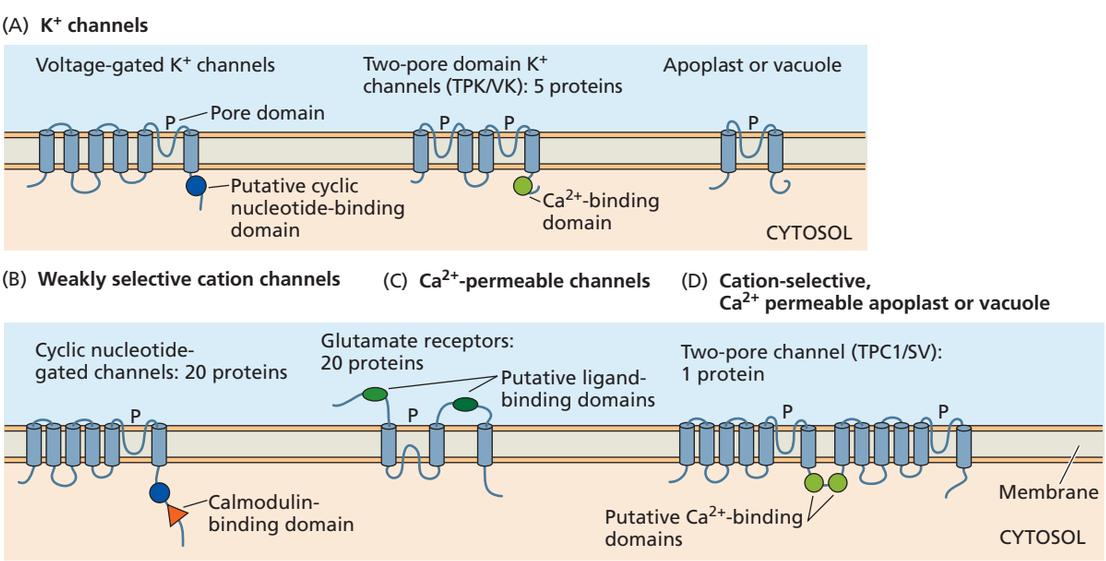


Figure 8.14 Five families of Arabidopsis cation channels. Some channels have been identified from sequence homology with channels of animals, while others have been experimentally verified. **(A)** Two families of K^+-selective channels: voltage-gated K^+ channels and two-pore domain K^+ channels. **(B)** Weakly selective cation channels with activity regulated by binding of cyclic nucleotides. **(C)** Glutamate receptor Ca^{2+} channels; these channels are activated by extracellular glutamate and are Ca^{2+} permeable. **(D)** Two-pore channel: One protein (TPC1/SV) is the sole two-pore channel of this type encoded in the Arabidopsis genome. TPC1/SV is permeable to mono- and divalent cations, including Ca^{2+}. (A after A. Lebaudy et al. 2007. *FEBS Lett.* 581: 2357–2366; B–D after A. A. Very and H. Sentenac. 2002. *Trends Plant Sci.* 7: 168–175.)

cation channels are categorized into five types based on their deduced structures and cation selectivity.

Of the five types of plant cation channels, the voltage-gated K^+ channels have been the most thoroughly characterized. Plant voltage-gated channels are highly K^+-selective and can be either inwardly or outwardly rectifying or weakly rectifying (see Figure 8.8). Some members of this family can:

- Mediate K^+ uptake or efflux across the guard cell plasma membrane.
- Provide a major conduit for K^+ uptake from the soil.
- Participate in K^+ release to xylem vessels from the living stelar cells.
- Play a role in K^+ uptake in pollen, a process that promotes water influx and pollen tube elongation.

Some voltage-gated channels, such as those in roots, can mediate high-affinity K^+ uptake, allowing passive K^+ uptake at micromolar external K^+ concentrations as long as the membrane potential is sufficiently hyperpolarized to drive this uptake.

Not all ion channels are as strongly regulated by membrane potential as the majority of the voltage-gated channels are. For example, channels such as the TPK/VK are not voltage-regulated. Cyclic nucleotide-gated cation channels are an example of a ligand-gated channel, with activity promoted by the binding of cyclic nucleotides such as cGMP. These channels exhibit weak selectivity with permeability to K^+, Na^+, and Ca^{2+}. Cyclic nucleotide-gated cation channels are involved in diverse physiological processes, including disease resistance, senescence, temperature sensing, and pollen tube growth and viability. Another interesting set of ligand-gated channels are the glutamate receptor channels. These channels are homologous to a class of glutamate receptors in the mammalian nervous system that function as glutamate-gated cation channels and are activated in plants by glutamate and some other amino acids. Plant glutamate receptor channels are permeable to Ca^{2+}, K^+, and Na^+ to varying extents, but have been particularly implicated in Ca^{2+} uptake and signaling in nutrient acquisition in roots and in guard cell and pollen tube physiology.

Ion fluxes must also occur in and out of the vacuole, and both cation- and anion-permeable channels have been characterized in the vacuolar membrane. Plant vacuolar cation channels include the Ca^{2+}-activated TPC1/SV cation channel (see Figures 8.13 and 8.14D) and most TPK/VK channels (see Figure 8.13), which are highly selective K^+ channels that are activated by Ca^{2+}. In addition, Ca^{2+} efflux from internal storage sites such as the vacuole plays an important signaling role. For a more detailed description of these signal transduction pathways, see Chapter 4.

CATION CARRIERS A variety of carriers also move cations into plant cells. One family of transporters that specializes in K^+ transport across plant membranes is the HAK/KT/KUP family (which we will refer to here as the HAK family). The HAK family contains both high-affinity and low-affinity transporters, some of which also mediate Na^+ influx at high external Na^+ concentrations. High-affinity HAK transporters are thought to take up K^+ via H^+–K^+ symport, and these transporters are particularly important for K^+ uptake from the soil when soil K^+ concentrations are low. A second family, the cation–H^+ antiporters (CPAs), mediates electroneutral exchange of H^+ and other cations, including K^+. A third family consists of the Trk/HKT transporters (which we will refer to here as the HKT transporters), which can operate as K^+–H^+ or K^+–Na^+ symporters, or as Na^+ channels under high external Na^+ concentrations. The importance of the HKT transporters for K^+ transport remains incompletely elucidated, but as described shortly, HKT transporters are central elements in plant tolerance of saline conditions.

Irrigation increases soil salinity, and salinization of croplands is an increasing problem worldwide. Although halophytic plants, such as those found in salt marshes, are adapted to a high-salt environment, such environments are deleterious to other, glycophytic, plant species, including the majority of crop species. Plants have evolved mechanisms to extrude Na^+ across the plasma membrane, to sequester salt in the vacuole, and to redistribute Na^+ within the plant body.

At the plasma membrane, a Na^+–H^+ antiporter was uncovered in a screen to identify Arabidopsis mutants that showed enhanced sensitivity to salt; hence, this antiporter was named Salt Overly Sensitive, or SOS1. SOS1-type antiporters in the root extrude Na^+ from the plant, thereby lowering internal concentrations of this toxic ion.

In the tonoplast, electroneutral H^+-coupled antiporters for Na^+ or K^+ in the NHX family function to accumulate Na^+ or K^+ in the vacuole. NHX transporters are a subset of CPA proteins, which couple the energetically downhill movement of H^+ into the cytosol with Na^+ or K^+ uptake into the vacuole. When the Arabidopsis *AtNHX1* antiporter gene is overexpressed, it confers greatly increased salt tolerance to both Arabidopsis and crop species such as maize (corn; *Zea mays*), wheat, and tomato.

Whereas SOS1 and NHX antiporters reduce cytosolic Na^+ concentrations, HKT1 transporters transport Na^+ from the apoplast into the cytosol. However, Na^+ uptake by HKT1 transporters in the plasma membrane of root xylem parenchyma cells is important in retrieving Na^+ from the transpiration stream, thereby reducing Na^+ concentrations and attendant toxicity in photosynthetic tissues. Transgenic expression of a HKT1 transporter in a durum (pasta) variety of wheat greatly increases grain yield in wheat grown on saline soils.

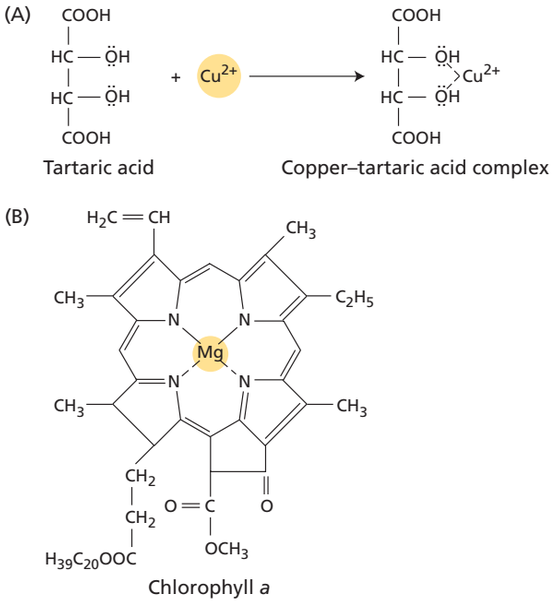


Figure 8.15 **Examples of coordination complexes.** Coordination complexes form when oxygen or nitrogen atoms of a carbon compound donate shared electron pairs (represented by dots) to form a bond with a cation. **(A)** Copper ions share electrons with the hydroxyl oxygens of tartaric acid. **(B)** Magnesium ions share electrons with nitrogen atoms in chlorophyll *a*. Dashed lines represent a coordination bond between electrons from the nitrogen atoms and the magnesium cation.

Calcium ions are actively pumped out of the cytoplasm by Ca^{2+}-ATPases found at the plasma membrane and in some endomembranes such as the tonoplast (see Figure 8.13) and endoplasmic reticulum. Much of the Ca^{2+} inside the cell is stored in the central vacuole, where it is sequestered via Ca^{2+}-ATPases and via Ca^{2+}–H^+ antiporters, which use the electrochemical potential of the proton gradient to energize the vacuolar accumulation of Ca^{2+}. There is a large free-energy gradient for Ca^{2+} that favors its entry into the cytosol from both the apoplast and intracellular stores. This entry is mediated by Ca^{2+}-permeable channels, which we described earlier in this section. Calcium ion concentrations in the apoplast are usually in the millimolar range; in contrast, free cytosolic Ca^{2+} concentrations are kept in the hundreds of nanomolar (10^{-9} *M*) to 1 micromolar (10^{-6} *M*) range.

CATION FUNCTION IN CELLS The noncovalent bonds formed between cations and carbon compounds are of two types: coordination bonds and electrostatic bonds (for a discussion of noncovalent bonds, see **WEB APPENDIX 1**). In the formation of a coordination complex, several oxygen or nitrogen atoms of a carbon compound donate unshared electrons to form a bond with the cation nutrient. As a result, the positive charge on the cation is neutralized or distributed.

Coordination bonds typically form between polyvalent cations and carbon compounds—for example, complexes between copper ions and a chelator such as tartaric acid (**Figure 8.15A**) or between magnesium ions and chlorophyll *a* (**Figure 8.15B**). The nutrients that are assimilated as coordination complexes include copper, zinc, iron, and magnesium ions. Electrostatic bonds form because of the attraction of a positively charged cation for a negatively charged group such as a carboxylate (—COO^-) on a carbon compound. Unlike the situation in coordination bonds, the cation in an electrostatic bond retains its positive charge. Monovalent cations such as potassium ions can form electrostatic bonds with many organic acids (**Figure 8.16A**). Nonetheless, many of the potassium ions that are accumulated by plant cells and function in osmotic regulation and enzyme activation remain in the cytosol and vacuole as free ions. Divalent ions such as the calcium ion form electrostatic bonds with the carboxylic groups of polygalacturonic acid of pectins in the cell wall (**Figure 8.16B**) (see Chapter 2).

Anion transporters have been identified

Nitrate (NO_3^-), chloride (Cl^-), sulfate (SO_4^{2-}), and phosphate ($H_2PO_4^-$) are the main inorganic ions in plant cells,

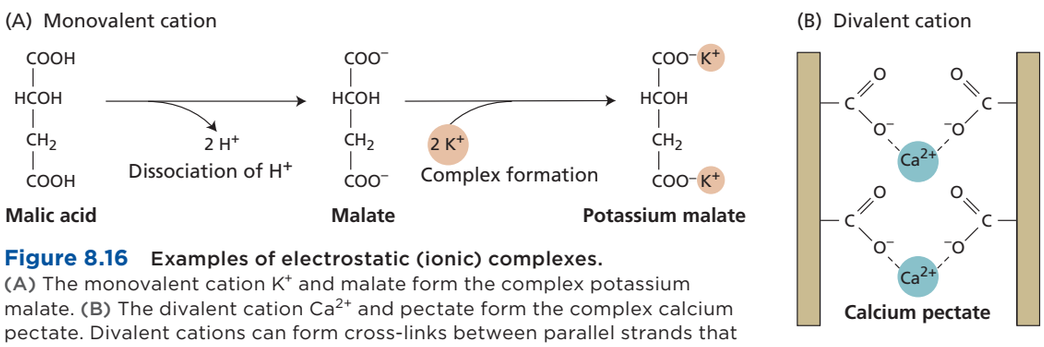


Figure 8.16 **Examples of electrostatic (ionic) complexes.** **(A)** The monovalent cation K^+ and malate form the complex potassium malate. **(B)** The divalent cation Ca^{2+} and pectate form the complex calcium pectate. Divalent cations can form cross-links between parallel strands that contain negatively charged carboxylic acid groups. Calcium ion cross-links play a structural role in the cell walls.

and malate^{2-} is a major organic anion. The free-energy gradient for all of these anions is in the direction of passive efflux, which means that anion efflux occurs if an anion channel opens and that energy is required for anion accumulation in cells. Several types of plant anion channels have been characterized by electrophysiological techniques, and most anion channels appear to be permeable to a variety of anions. In particular, anion channels in the ALMT and SLAC families with differential voltage dependence and anion permeabilities have been shown to be important for anion efflux from guard cells, a topic we discuss in Section 8.5.

Anion–H^+ symporters mediate the energetically uphill transport of anions into plant cells and are specific for particular anions. Plants have specific uptake transporters for nitrate (as discussed earlier in this section), chloride, phosphate, sulfate, and organic anions such as malate and citrate. In Arabidopsis, a family of about nine plasma membrane phosphate transporters, some high affinity and some low affinity, mediates phosphate uptake in symport with protons. These transporters are expressed primarily in the root epidermis and root hairs, and their expression is induced upon phosphate starvation. Other phosphate–H^+ symporters have also been identified in plants and have been localized to membranes of intracellular organelles such as the tonoplast, plastids, and mitochondria. Another group of phosphate transporters, the phosphate translocators, are located in the inner plastid membrane, where they mediate exchange of inorganic phosphate with phosphorylated carbon compounds (see **WEB TOPIC 10.12**).

Transporters for metal and metalloid ions transport essential micronutrients

Several metals are essential nutrients for plants, although they are required in only trace amounts (see Chapter 7). More than 25 ZIP transporters mediate the uptake of iron, manganese, and zinc ions into plants, and other transporter families that mediate the uptake of copper and molybdenum ions have been identified. Metal ions are usually present at low concentrations in the soil solution, so these transporters are typically high-affinity transporters. To absorb sufficient iron from the soil solution, roots have evolved several mechanisms that increase the solubility of iron and therefore its availability for plants (**Figure 8.17**). These mechanisms include:

- Soil acidification, which increases the solubility of ferric iron, followed by the reduction of ferric iron to the more soluble ferrous form (Fe^{2+}). This mechanism is used by eudicots and non-graminaceous monocots.
- Release of compounds that form stable, soluble complexes with iron, the so-called siderophores. This mechanism is used by graminaceous monocots (grasses).

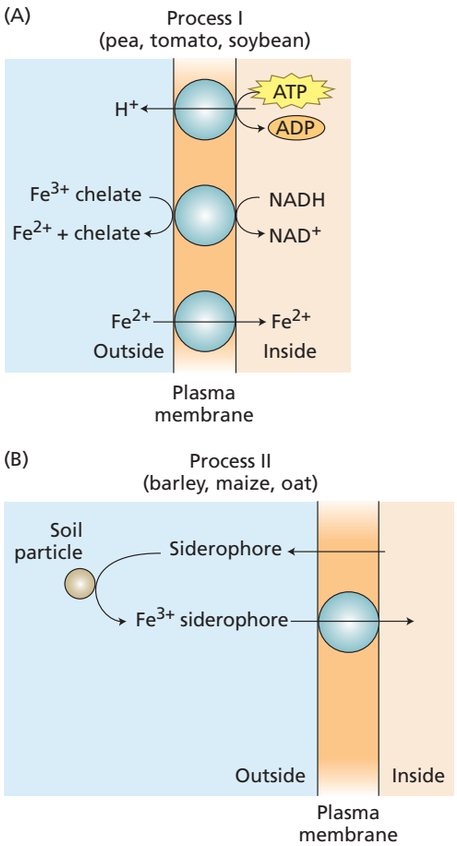


Figure 8.17 **Two mechanisms for iron uptake by plants.** (A) A process used by eudicots such as pea, tomato, and soybean. The chelators include organic compounds such as malic acid, citric acid, phenolics, and piscidic acid. (B) A process used by grasses such as barley, maize, and oat. After the grass excretes a siderophore that removes iron from soil particles, the whole iron-chelate complex is transported into root cells. (After M. L. Guerinot and Y. Yi. 1994. *Plant Physiol.* 104: 815–820.)

In the soil, iron is present primarily as ferric iron (Fe^{3+}), in oxides such as $Fe(OH)^{2+}$, $Fe(OH)_3$, and $Fe(OH)_4^-$. At neutral pH, ferric iron is highly insoluble. Roots generally acidify the soil around them: They pump out protons, respiration in the roots releases CO_2 that forms carbonic acid in the soil, the uptake and assimilation of ammonium cause the release of excess protons, and the roots secrete organic acids that enhance iron and phosphate availability). Iron deficiency stimulates proton export in roots. Plasma membranes in roots contain an enzyme called *iron-chelate reductase*, which reduces ferric iron to ferrous iron, with cytosolic NADH or NADPH serving as the electron donor (see Figure 8.17A). The activity of this enzyme increases under iron deficiency.

Several compounds secreted by roots form stable chelates with iron. Examples include malic acid, citric acid

(see Figure 7.2), phenolics, and piscidic acid. Grasses produce a special class of iron chelators called *siderophores*. Siderophores are composed of amino acids not found in proteins, such as mugineic acid, and form highly stable complexes with Fe^{3+}. Root cell plasma membranes in grasses have Fe^{3+}–siderophore transport systems to take up the chelated iron. Under iron deficiency, grass roots release more siderophore into the soil and increase their capacity for Fe^{3+}–siderophore transport (see Figure 8.17B). Iron deficiency is the most common human nutritional disorder worldwide, so an increased understanding of how plants accumulate iron may also benefit efforts to improve the nutritional value of crops.

Once in the plant, metal ions, usually chelated with other molecules, must be transported into the xylem for distribution throughout the plant body via the transpiration stream, and metals must also be sent to their appropriate subcellular destinations. Ferrous iron absorbed by the roots is oxidized to ferric iron in the cytoplasm. Much of the iron taken up in the roots is transported to leaves in the ferric form as a complex with citrate or nicotianamine. Once in the leaves, an iron cation undergoes an important assimilatory reaction through which it is inserted into the porphyrin precursor of heme groups found in the cytochromes located in the chloroplasts and mitochondria (see Chapter 9). This reaction is catalyzed by the enzyme ferrochelatase (**Figure 8.18**). Most of the iron in plants is found in heme groups. In addition, iron–sulfur proteins of the electron transport chain (see Chapters 9 and 13) contain nonheme iron covalently bound to the sulfur atoms of cysteine residues in the apoprotein. Iron is also found in Fe_2S_2 centers, which contain two irons (each complexed with the sulfur atoms of cysteine residues) and two inorganic sulfides.

Free iron (iron not complexed with carbon compounds) may interact with oxygen to form highly damaging hydroxyl radicals, $HO^{\bullet}$. Plant cells may limit such damage by storing iron in an iron–protein complex called ferritin. Mutants of Arabidopsis show that, although ferritins are essential for protection against oxidative damage, they do not serve as a major pool for either seedling development or proper functioning of the photosynthetic apparatus. Ferritin consists of a protein shell with 24 identical subunits forming a hollow sphere that has a molecular mass of about 480 kDa. Within this sphere is a core of 5400 to 6200 iron atoms present as a ferric oxide–phosphate complex. The mechanism of iron release from ferritin is uncertain but appears to involve breakdown of the protein shell. The concentrationl of free iron in plant cells regulates the de novo biosynthesis of ferritin. Interest in ferritin is high because iron in this protein-bound form may be highly available to humans, and foods rich in ferritin, such as soybean, may address dietary anemia problems.

Metalloids are elements that have properties of both metals and nonmetals. Boron and silicon are two metalloids that are used by plants. Both play important roles in cell wall structure—boron by cross-linking cell wall polysaccharides, and silicon by increasing structural rigidity. Boron (as boric acid [$B(OH)_3$; also written H_3BO_3]) and silicon (as silicic acid [$Si(OH)_4$; also written H_4SiO_4]) both enter cells via aquaporin-type channels (see the next subsection) and are exported via efflux transporters, probably by secondary active transport. Because of similarities in chemical structure, arsenite (a form of arsenic) can also enter plant roots via the silicon channel and be exported to the transpiration stream via the silicon exporter. Rice is particularly efficient at taking up arsenite, and as a result, arsenic poisoning from human consumption of rice is a significant problem in regions of southeast Asia.

Aquaporins have diverse functions

Aquaporins are a class of transporters that are abundant in plant membranes and animal membranes (see Chapters 5 and 6). The Arabidopsis genome encodes approximately 35 aquaporins. As the name implies, many aquaporin proteins function as water channels. In addition, some aquaporin proteins mediate the influx of mineral nutrients (e.g., boric acid and silicic acid). There is also some evidence that aquaporins can act as conduits for carbon dioxide, ammonia (NH_3), and hydrogen peroxide (H_2O_2) movement across the plasma membrane and other plant membranes.

At the protein level, aquaporin activity is regulated by phosphorylation as well as by pH, Ca^{2+} concentration, heteromerization, and reactive oxygen species. Such regulation may account for the ability of plant cells to quickly alter their permeability to water in response to circadian rhythm and to stresses such as salt, chilling, drought (water-deficit stress), and flooding (anoxia). Regulation also occurs at the level of gene expression. Aquaporin genes are highly expressed in epidermal and endodermal

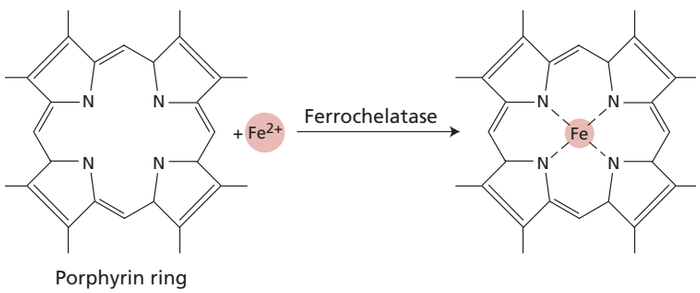


Figure 8.18 **The ferrochelatase reaction.** The enzyme ferrochelatase catalyzes the insertion of iron into the porphyrin ring to form a coordination complex. See Figure 9.33 for illustration of the biosynthesis of the porphyrin ring.

cells and in the xylem parenchyma, which may be critical points for control of water movement.

Plasma membrane H^+-ATPases are highly regulated P-type ATPases

The outward active transport of protons across the plasma membrane creates gradients of pH and electrical potential that drive the transport of many other substances (ions and uncharged solutes) through the various secondary active transporters and channels. H^+-ATPase activity is also important for the regulation of cytosolic pH and for the control of cell turgor, which drives organ (leaf and flower) movement, stomatal opening, and cell growth. **Figure 8.19** illustrates how a membrane H^+-ATPase might work.

Plant and fungal plasma membrane H^+-ATPases and Ca^{2+}-ATPases are members of a class known as P-type ATPases, which are phosphorylated as part of the catalytic cycle that hydrolyzes ATP. Plant plasma membrane H^+-ATPases are encoded by a family of about a dozen genes. The roles of each H^+-ATPase isoform are becoming understood, based on information from gene expression patterns and functional analysis of Arabidopsis plants harboring null mutations in individual H^+-ATPase genes. Some H^+-ATPases exhibit cell-specific patterns of expression. For example, several H^+-ATPases are expressed in guard cells, where they energize the plasma membrane to drive solute uptake during stomatal opening (see Section 8.5 and also Chapter 6).

In general, H^+-ATPase expression is high in cells with key functions in nutrient movement, including root endodermal cells and cells involved in nutrient uptake from the apoplast that surrounds the developing seed. In cells in which multiple H^+-ATPases are coexpressed, they may be differentially regulated or may function redundantly, perhaps providing a "fail-safe" mechanism to this all-important transport function.

Figure 8.20 shows a model of the functional domains of the plasma membrane H^+-ATPase AtAHA2 from *Arabidopsis thaliana*. The protein has ten membrane-spanning domains that cause it to loop back and forth across the membrane. Some of the membrane-spanning domains make up the pathway through which protons are pumped. The N domain binds Mg_2ATP, and the P domain contains the aspartic acid residue that becomes phosphorylated during the catalytic cycle.

Like other enzymes, the plasma membrane H^+-ATPase is regulated by the concentration of substrate (ATP), pH, temperature, and other factors. In addition, H^+-ATPase molecules can be reversibly activated or deactivated by specific signals, such as light, hormones, or pathogen attack. This type of regulation is mediated by a specialized autoinhibitory domain at the C-terminal end of the polypeptide chain, which acts to regulate the activity of the H^+-ATPase. If the autoinhibitory domain is removed by a protease, the enzyme becomes irreversibly activated.

The autoinhibitory effect of the C-terminal domain is also regulated by protein kinases and phosphatases that add phosphate groups to or remove them from serine or threonine residues on this domain. Phosphorylation promotes binding of 14-3-3 proteins which are soluble proteins that participate in many signal transduction pathways and function via protein–protein interaction; 14-3-3 proteins bind to the phosphorylated region of the H^+-ATPase and displace the autoinhibitory domain, leading to H^+-ATPase activation. The fungal toxin **fusicoccin**, which is a strong activator of the H^+-ATPase, activates this pump

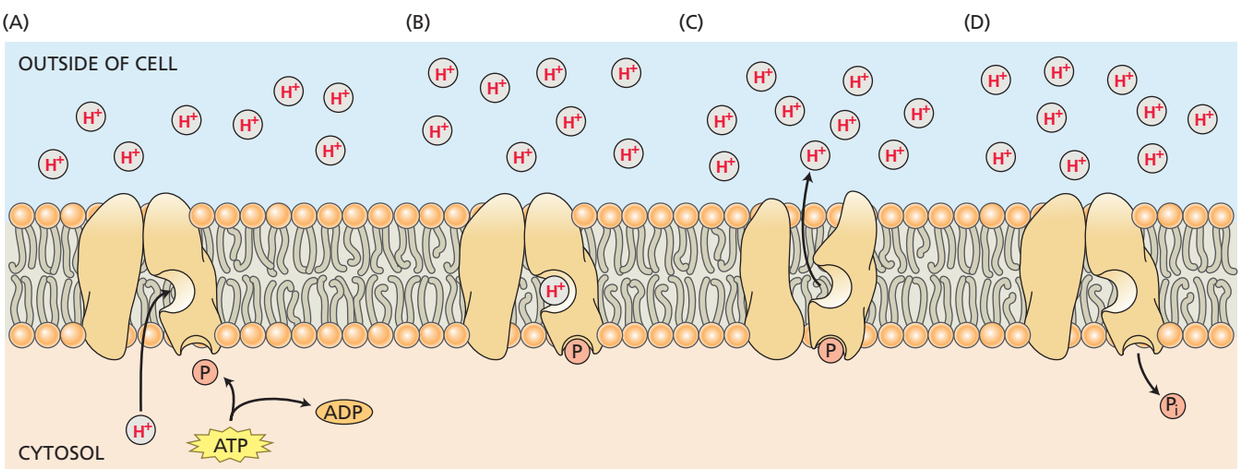


Figure 8.19 Hypothetical steps in the transport of a proton against its chemical gradient by H^+-ATPase. The pump, embedded in the membrane, **(A)** binds the proton on the inside of the cell and **(B)** is phosphorylated by ATP. **(C)** This phosphorylation leads to a conformational change that exposes the proton to the outside of the cell and makes it possible for the proton to diffuse away. **(D)** Release of the phosphate ion (P_i) from the pump into the cytosol restores the initial configuration of the H^+-ATPase and allows a new pumping cycle to begin.

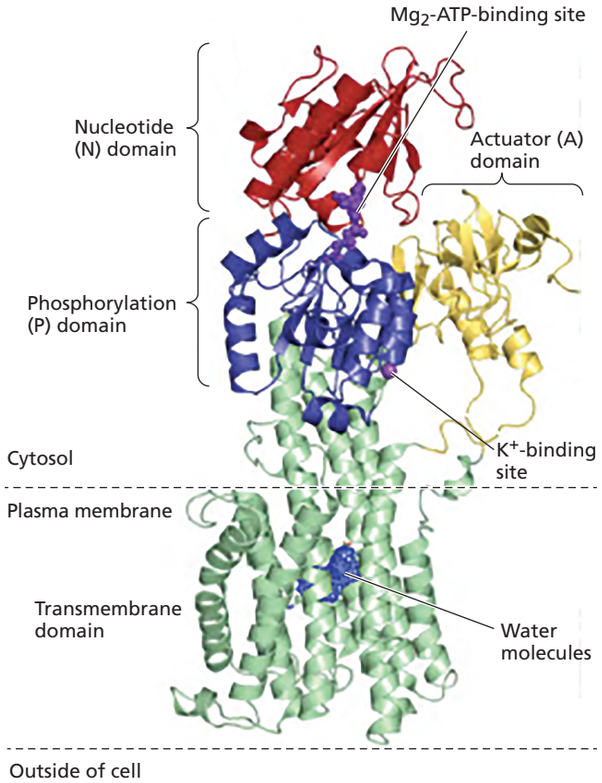


Figure 8.20 **Three-dimensional representation of the plasma membrane H^+-ATPase AtAHA2 from *Arabidopsis thaliana*.** The nucleotide (N) binding domain, phosphorylation (P) domain, actuator (A) domain, and transmembrane domain contain ten transmembrane spans. The solvent cavity within the transmembrane domain contains eight to ten water molecules. Mg_2-ATP- and K^+-binding sites are indicated. Posttranslational modifications lead to displacement of the C-terminal autoinhibitory domain (not shown here), resulting in H^+-ATPase activation. (After D. Focht et al. 2017. *Front. Physiol.* 8: 202. CC BY 4.0.)

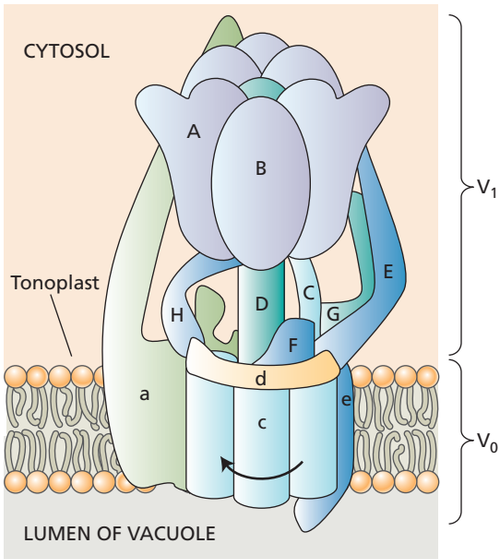


Figure 8.21 **Model of the V-ATPase rotary motor.** Many polypeptide subunits come together to make up this complex enzyme. The V_1 catalytic complex, which is easily dissociated from the membrane, contains the nucleotide-binding and catalytic sites. Components of V_1 are designated by uppercase letters. The integral membrane complex mediating H^+ transport is designated V_0, and its subunits are designated by lowercase letters. It is proposed that ATPase reactions catalyzed by each of the A subunits, acting in sequence, drive the rotation of the shaft (D) and the six c subunits. The rotation of the c subunits relative to the a subunit is thought to drive the transport of H^+ across the membrane. (After C. Kluge et al. 2003. *J. Bioenerg. Biomembr.* 35: 377–388.)

by increasing 14-3-3 binding affinity even in the absence of phosphorylation. The effect of fusicoccin on the guard cell H^+-ATPases is so strong that it can lead to irreversible stomatal opening, wilting, and even plant death.

The tonoplast H^+-ATPase drives solute accumulation in vacuoles

Plant cells increase their size primarily by taking up water into a large central vacuole. Therefore, the water potential of the vacuole must be kept sufficiently low for water to enter from the cytosol. The tonoplast regulates the traffic of ions and metabolites between the cytosol and the vacuole, just as the plasma membrane regulates their uptake into the cell. Tonoplast transport became a vigorous area of research following the development of methods for the isolation of intact vacuoles and tonoplast vesicles (see **WEB TOPIC 8.6**). These studies elucidated a diversity of anion and cation channels in the tonoplast membrane and led to the discovery of a new type of proton-pumping ATPase, the vacuolar H^+-ATPase, which transports protons into the vacuole (see Figure 8.13).

The vacuolar H^+-ATPase differs both structurally and functionally from the plasma membrane H^+-ATPase. The vacuolar ATPase is more closely related to the F-ATPases of mitochondria and chloroplasts (see Chapters 9 and 13), and the vacuolar ATPase, unlike the plasma membrane ATPases discussed earlier, does not form a phosphorylated intermediate during ATP hydrolysis. Vacuolar ATPases belong to a general class of ATPases that are present on the endomembrane systems of all eukaryotes. They are large enzyme complexes, about 750 kDa, composed of multiple subunits. These subunits are organized into a peripheral complex, V_1, that is responsible for ATP hydrolysis, and an integral membrane channel complex, V_0, that is responsible for H^+ translocation across the membrane (**Figure 8.21**). Because of their similarities to F-ATPases, vacuolar ATPases are assumed to operate like tiny rotary motors (see Chapters 9 and 13).

Vacuolar ATPases are electrogenic proton pumps that transport protons from the cytosol to the vacuole

and generate a proton motive force across the tonoplast. Electrogenic proton pumping accounts for the fact that the tonoplast has a membrane potential of –20 to –30 mV (cytosol relative to the vacuole lumen). Electrophysiologists describe membrane potentials relative to the cytoplasm, so the vacuolar lumen is considered equivalent to the extracellular space. Anions such as Cl^- and $malate^{2-}$ are transported from the cytosol into the vacuole through channels in the tonoplast. To generate a membrane potential across the tonoplast requires relatively few protons to be pumped across the membrane. The activity of tonoplast anion channels neutralizes the membrane potential and allows the vacuolar H^+-ATPase to generate a large concentration gradient of protons (pH gradient) across the tonoplast. This gradient accounts for the fact that the pH of the vacuolar sap is typically about 5.5, while the cytosolic pH is typically 7.0 to 7.5. Whereas the electrical component of the proton motive force drives the uptake of anions into the vacuole, the electrochemical-potential gradient for H^+ ($\tilde{\mu}_{H^+}$) is harnessed to drive the uptake of cations and sugars into the vacuole via secondary transport (antiporter) systems (see Figure 8.13).

H^+-pyrophosphatases and P-type H^+-ATPases also pump protons at the tonoplast

Another type of proton pump, a H^+-pyrophosphatase (H^+-PPase), works in parallel with the vacuolar ATPase to create a proton gradient across the tonoplast (see Figure 8.13). This enzyme consists of a single polypeptide that harnesses energy from the hydrolysis of inorganic pyrophosphate (PP_i) to drive H^+ transport.

The free energy released by PP_i hydrolysis is less than that from ATP hydrolysis. However, the H^+-PPase transports only one H^+ ion per PP_i molecule hydrolyzed, whereas the vacuolar ATPase appears to transport two H^+ ions per ATP hydrolyzed. Thus, the energy available per H^+ transported appears to be approximately the same, and the two enzymes seem to be able to generate comparable proton gradients. Interestingly, the plant H^+-PPase is not found in animals or in yeast, although similar enzymes are present in some bacteria and protists.

Both the V-ATPase and the H^+-PPase are found in other compartments of the endomembrane system in addition to the vacuole. Consistent with this distribution, evidence is emerging that V-type ATPases regulate not only H^+ gradients per se, but also vesicle trafficking and secretion. In addition, resistance to salt and drought stress and increased biomass have been observed in many different plants overexpressing H^+-PPase. These phenotypes may have several causes, including increased H^+ transport into vacuoles, localization of H^+-PPase in membranes other than the tonoplast, decreased cytosolic pyrophosphate concentration, and up-regulation of plasma membrane H^+-ATPases.

Although the pH of most plant vacuoles is mildly acidic (~5.5), the pH of the vacuoles of some species is much lower—a phenomenon termed *hyperacidification*. Vacuolar hyperacidification is responsible for the sour taste of certain fruits (lemons) and vegetables (rhubarb) and flower color in petunia. Hyperacidification of the vacuoles of petunia petals and citrus fruit has been shown to require the activity of P-type H^+-ATPases in the tonoplast. Since P-type H^+-ATPases transport one H^+ per ATP hydrolyzed, they are capable of generating a larger pH gradient than either V-type ATPases or H^+-PPases.

8.5 Transport in Stomatal Guard Cells

Stomatal guard cells (**Figure 8.22**), found in the epidermis of leaves and other green tissues, control the aperture of stomatal openings that allow for gas exchange between a plant and the atmosphere—primarily CO_2 uptake into leaves and water vapor efflux into the atmosphere. Guard cells are an important model for studying transport processes for several reasons: Guard cells reversibly change their shape using an osmotic mechanism, they respond to many environmental and internal stimuli, and they are easily accessible and visible in the epidermis. Many ion channels and transporters were initially identified and characterized in guard cells. The osmotic mechanism that guard cells use to change

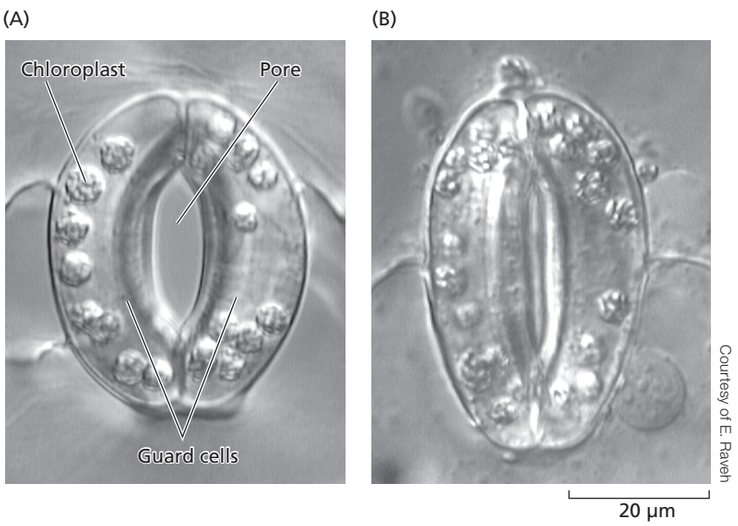


Figure 8.22 Micrograph of a light-stimulated stomatal opening in detached epidermis of *Vicia faba*. An open, light-treated stoma is shown in (A), and a closed, dark-treated stoma is shown in (B). Stomatal aperture is quantified by measuring the width of the stomatal pore.

shape, and thereby regulate stomatal aperture, depends on pumps, transporters, and channels in the plasma membrane and vacuolar membrane of guard cells.

Blue light induces stomatal opening

Opening of the stomatal pore requires guard cells surrounding the pore to increase in volume, which they do by taking in water from the extracellular space. Water movement across membranes is driven by a difference in **water potential** (see Chapter 5), and guard cells generate a more negative water potential by accumulating K^+ salts. An important physiological stimulus that triggers stomatal opening is blue light. As shown in **Figure 8.23A**, blue light is detected by **phototropins** (see Chapter 16), plasma membrane protein kinases that use a flavin cofactor to absorb blue light. Phototropin activation initiates a signaling pathway that leads to phosphorylation and activation of plasma membrane H^+-ATPases. Phototropin does not phosphorylate H^+-ATPases directly—that action is accomplished by

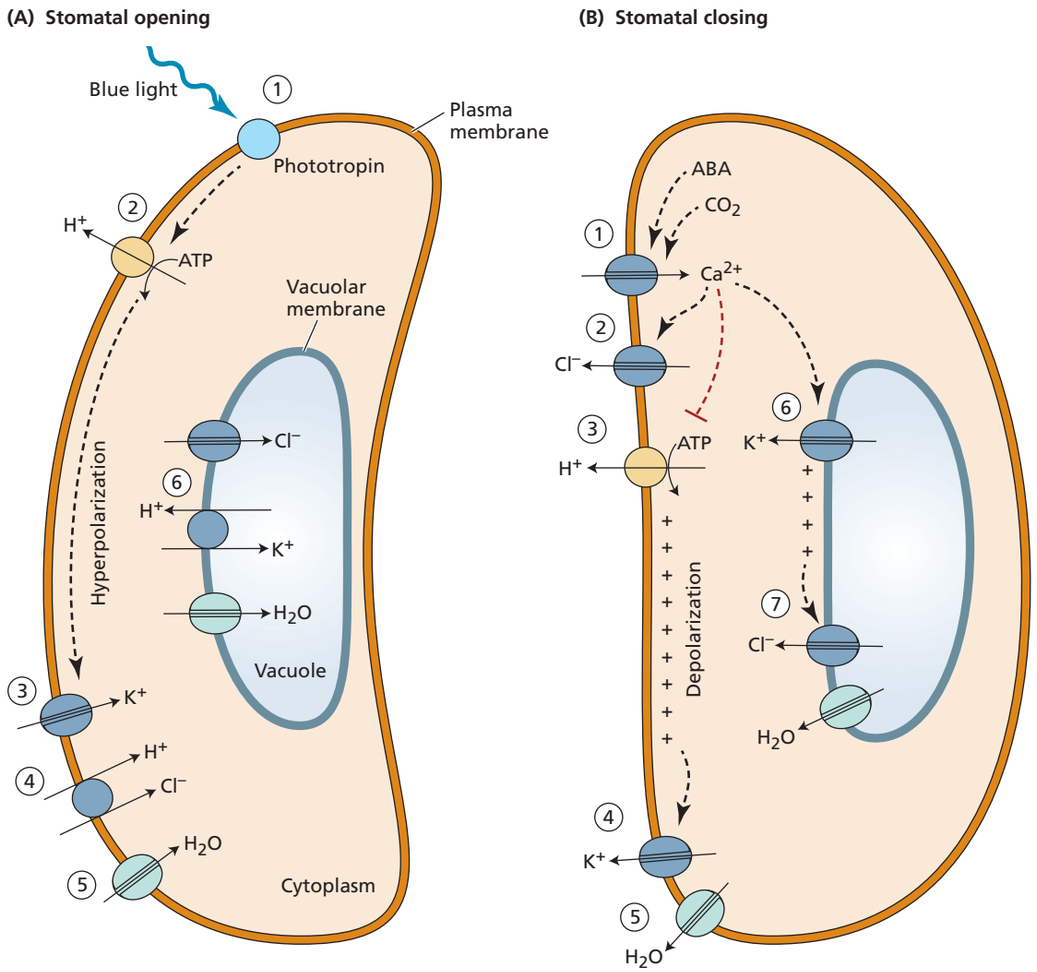


Figure 8.23 Transport activities in guard cells during stomatal opening and closing. **(A)** Stomatal opening. ① Phototropins are blue-light receptors in the plasma membrane. Signaling results in activation of plasma membrane H^+-ATPases ②, which hyperpolarizes the membrane potential and increases the transmembrane pH gradient. Inwardly rectifying K^+ channels ③ are activated by hyperpolarization, and anions such as Cl^- are accumulated via H^+-coupled transporters ④. The resulting accumulation of K^+ salts drives water uptake via aquaporins ⑤. The vacuole also accumulates K^+ salts, but this mechanism involves K^+–H^+ antiporters and anion channels ⑥. **(B)** Stomatal closing. ABA or elevated CO_2 leads to the activation of Ca^{2+} channels ① and elevated cytoplasmic Ca^{2+}, which is a central regulator for stomatal closing. Elevated Ca^{2+} results in activation of anion efflux channels ② and inhibition of plasma membrane H^+-ATPases ③. The resulting plasma membrane depolarization activates outwardly rectifying K^+ channels ④, allowing K^+ efflux. The efflux of K^+ salts drives water efflux from the cells via aquaporins ⑤. Elevated cytoplasmic Ca^{2+} activates TPK/VK K^+ channels in the tonoplast, allowing K^+ efflux from the vacuole ⑥. The resulting tonoplast depolarization drives anion efflux from the vacuole via anion channels ⑦. Dashed lines indicate stimulatory or inhibitory signal transduction steps.

another protein kinase that has not been identified yet. Activation of plasma membrane H^+-ATPases causes hyperpolarization of the membrane potential, a key regulator of transport activities in the cell. Hyperpolarization activates inwardly rectifying K^+ channels, allowing K^+ uptake into the guard cells. Anion uptake is accomplished by H^+-coupled anion transporters that are stimulated by the increased transmembrane pH gradient caused by the activation of plasma membrane H^+-ATPases. The more negative **osmotic potential** due to uptake of K^+ salts drives water uptake into the guard cells via aquaporins, thus increasing guard cell volume and turgor and causing a change in the shape of the cells, which opens the stomatal pore (see Chapter 6).

The volume of the guard cell vacuole also increases during stomatal opening. Proton pumping from the vacuolar H^+-PPase or V-ATPase does not appear to be required. Anion uptake through anion channels and K^+ uptake via K^+–H^+ antiporters (see Figure 8.13A) increases K^+ salt concentration in the vacuole and drives water uptake into the vacuole via aquaporins.

Abscisic acid and high CO_2 induce stomatal closing

The mechanism of stomatal closing is the opposite of stomatal opening in that it is driven by depolarization at the plasma membrane, efflux of K^+ salts from guard cells, loss of water via aquaporins, a decrease in guard cell volume and turgor, and a change in cell shape that results in closing of the stomatal pore. The stress hormone abscisic acid (ABA) (see Chapter 15) and elevated intracellular CO_2 both induce stomatal closing. Elevated cytoplasmic Ca^{2+} in guard cells is an important signaling intermediate in stomatal closing (**Figure 8.23B**). ABA receptor activation triggers the activation of Ca^{2+} channels in the plasma membrane, allowing Ca^{2+} influx. The elevated cytosolic Ca^{2+} in turn leads to activation of plasma membrane anion channels and inhibition of plasma membrane H^+-ATPases, both of which lead to membrane depolarization.

Membrane depolarization, due to anion efflux through plasma membrane anion channels, activates outwardly rectifying K^+ channels in the plasma membrane and drives K^+ efflux. This results in the net efflux of K^+ salts from guard cells, making the osmotic potential of the cells less negative and driving water efflux via aquaporins. The cell volume and turgor decrease, and the shape of the guard cells changes to close the stomatal pore. Note that in both stomatal opening and closing, K^+ movement across the plasma membrane is driven by changes in membrane potential.

The volume of the guard cell vacuole also decreases during stomatal closure. It is expected that K^+ efflux from vacuoles, as well as of anions such as Cl^-, NO_3^-, and malate, is important, but the mechanism is not fully understood. Elevated cytosolic Ca^{2+} activates highly selective TPK/VK channels that may provide a pathway for K^+ efflux from the vacuole. As shown in Figure 8.23B, the resulting vacuolar membrane depolarization may drive anion efflux from the vacuole via anion channels.

8.6 Ion Transport in Roots

Mineral nutrients absorbed by the root are carried to the shoot by the transpiration stream moving through the xylem (see Chapter 6). Both the initial uptake of nutrients and water and the subsequent movement of these substances from the root surface across the cortex and into the xylem are highly specific, well-regulated processes.

Ion transport across the root obeys the same biophysical laws that govern cellular transport. However, as we have seen in the case of water movement (see Chapter 6), the anatomy of roots imposes special constraints on the pathway of ion movement. In this section we discuss the pathways and mechanisms involved in the radial movement of ions from the root surface to the tracheary elements of the xylem.

Solutes move through both apoplast and symplasm

Thus far, our discussion of cellular ion transport has not included the cell wall. In terms of the transport of small molecules, the cell wall is a fluid-filled lattice of polysaccharides through which mineral nutrients diffuse readily. Because all plant cells are separated by cell walls, ions can diffuse across a tissue (or be carried passively by water flow) entirely through the cell wall space without ever entering a living cell. This continuum of cell walls is called the **extracellular space**, or **apoplast** (see Figure 6.4). Typically, 5 to 20% of the plant tissue volume is occupied by cell walls (see Chapter 2).

Just as the cell walls form a continuous phase, so do the cytoplasms of neighboring cells, collectively referred to as the **symplasm**. Plant cells are interconnected by cytoplasmic bridges called plasmodesmata (singular *plasmodesma*) (see Chapter 1), cylindrical pores 20 to 60 nm in diameter (**Figure 8.24**; also see Figure 1.4). Each plasmodesma is lined with plasma membrane and contains a narrow tubule, the *desmotubule*, which is a continuation of the endoplasmic reticulum.

In tissues where significant amounts of intercellular transport occur, neighboring cells contain large numbers of plasmodesmata, up to 15 per square micrometer of cell surface. Specialized secretory cells, such as floral nectaries and leaf salt glands, have high densities of plasmodesmata.

By injecting dyes or by making electrical-resistance measurements on cells containing large numbers of plasmodesmata, investigators have shown that inorganic ions, water, and small organic molecules can move

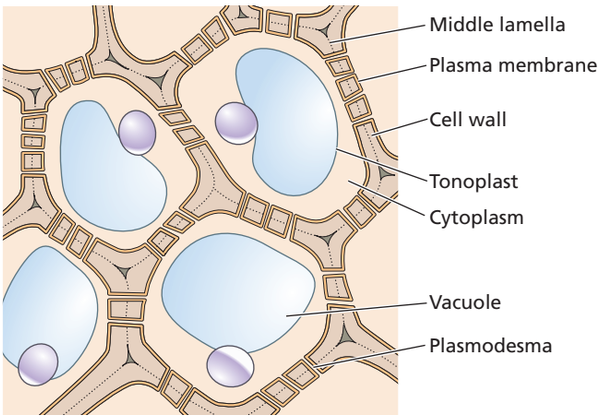
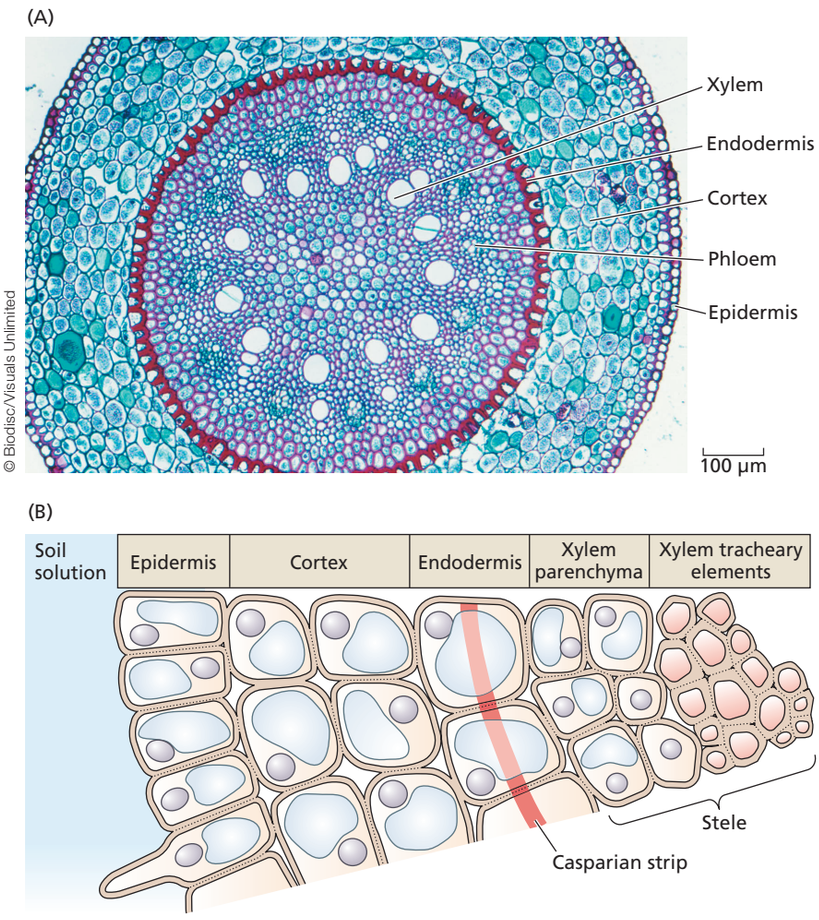


Figure 8.24 **Plasmodesmata connect the cytoplasm of neighboring cells, thereby facilitating cell-to-cell communication.**



© Biodisc/Visuals Unlimited

Figure 8.25 **Tissue organization in roots.** **(A)** Cross section through a root of carrion flower (genus *Smilax*), a monocot, showing the epidermis, cortex parenchyma, endodermis, xylem, and phloem. **(B)** Schematic diagram of a root cross section, illustrating the cell layers through which solutes pass from the soil solution to the xylem tracheary elements.

from cell to cell through these pores. Because each plasmodesma is partly occluded by the desmotubule and its associated proteins (see Chapter 1), the movement of large molecules such as proteins through plasmodesmata requires special mechanisms. Ions, by contrast, appear to move symplasmically through the plant by simple diffusion through plasmodesmata (see Chapter 6).

Ions cross both symplasm and apoplast

Absorption of most ions by the root (see Chapter 6) is more pronounced in the root hair zone than in the meristematic and elongation zones. Cells in the root hair zone have completed their elongation but have not yet begun secondary growth. The root hairs are simply extensions of specific epidermal cells that greatly increase the surface area available for ion absorption.

An ion that enters a root may immediately enter the symplasm by crossing the plasma membrane of an epidermal cell, or it may enter the apoplast and diffuse between the epidermal cells through the cell walls. From the apoplast of the cortex, an ion (or other solute) may either be transported across the plasma membrane of a cortical cell, thus entering the symplasm, or diffuse radially all the way to the endodermis via the apoplast. The apoplast forms a continuous phase from the root surface through the cortex. However, in all cases, ions must enter the symplasm before they can enter the stele, because of the presence of the Casparian strip. As discussed in Chapters 1, 2, and 6, the Casparian strip is a lignified or suberized layer that forms as rings around the specialized cells of the endodermis (**Figure 8.25**) and effectively blocks the entry of water and solutes into the stele via the apoplast.

The stele consists of dead tracheary elements surrounded by living pericycle and xylem parenchyma cells. Once an ion has entered the stele through the symplasmic connections across the endodermis, it continues to diffuse through the living cells. Finally, the ion is exported into the apoplast and diffuses into the conducting cells of the xylem—because these cells are dead, their interiors are continuous with the apoplast. The Casparian strip allows nutrient uptake to be selective; only ions and solutes that enter the symplasm, generally via

transporters, and are exported into the apoplast, also via transporters, will make it into the xylem and be transported to the shoot. The Casparian strip also prevents ions from diffusing back out of the root through the apoplast. Thus, the presence of the Casparian strip allows the plant to maintain a higher ion concentration in the xylem than exists in the soil water surrounding the roots. The roots of most eudicots have an additional cell layer with a Casparian strip called the exodermis (see Figure 7.7). When present, the exodermis is the outermost cell layer of the cortex and serves a function similar to that of the endodermis.

Xylem parenchyma cells participate in xylem loading

The process whereby ions exit the symplasm of a xylem parenchyma cell and enter the conducting cells of the xylem for translocation to the shoot is called **xylem loading**. Xylem loading is a highly regulated process. Xylem parenchyma cells, like other living plant cells, maintain plasma membrane H^+-ATPase activity and a negative membrane potential. Transporters that specifically function in the unloading of solutes to the tracheary elements have been identified by electrophysiological and genetic approaches. The plasma membranes of xylem parenchyma cells contain proton pumps, aquaporins, and a variety of ion channels and carriers specialized for influx or efflux.

In Arabidopsis xylem parenchyma, the stelar outwardly rectifying K^+ channel (SKOR) is expressed in cells of the pericycle and xylem parenchyma, where it functions as an efflux channel, transporting K^+ from the living cells into the tracheary elements. In mutant Arabidopsis plants lacking the SKOR channel protein, or in plants in which SKOR has been pharmacologically inactivated, K^+ transport from the root to the shoot is severely reduced, confirming the function of this channel protein.

Several types of anion-selective channels have also been identified that participate in unloading of Cl^- and NO_3^- from the xylem parenchyma. Drought, abscisic acid (ABA) treatment, or elevation of cytosolic Ca^{2+} concentrations (which often occurs as a response to ABA) all reduce the activity of SKOR and anion channels of the root xylem parenchyma, a response that could help maintain cellular hydration in the root under desiccating conditions.

Other, less-selective ion channels found in the plasma membrane of xylem parenchyma cells are permeable to K^+, Na^+, and anions. Other transport molecules have also been identified that mediate loading of boron (as boric acid [$B(OH)_3$] or borate [$B(OH)_4^-$]), Mg^{2+}, and $H_2PO_4^{2-}$. Thus, the flux of ions from the xylem parenchyma cells into the xylem tracheary elements is under tight metabolic control through the regulation of plasma membrane H^+-ATPases, ion efflux channels, and carriers.

Summary

The movement of ions and other solutes from one location to another within an organism is known as transport. Transport processes are predominantly mediated by membrane proteins. Plants exchange solutes with their local environment, among their tissues and organs, and within their cells. Transport proteins control both cellular transport as well as long-distance transport processes such as metabolite transport in the phloem. Ion transport in plants is vital to their mineral nutrition and stress tolerance, and modulation of plant transport components and properties has potential to improve the nutritive value, stress tolerance, and yield of crops.

8.1 Passive and Active Transport

- Concentration gradients and electrical-potential gradients, the main forces that drive transport across biological membranes, are integrated by a term called the electrochemical potential (**Equation 8.8**).
- Movement of solutes across membranes down their free-energy gradient is facilitated by passive transport mechanisms, whereas movement of solutes against their free-energy gradient is known as active transport and requires energy input (**Figure 8.1**).

8.2 Transport of Ions across Membrane Barriers

- The extent to which a membrane permits the movement of a substance is a property known as membrane permeability (**Figure 8.5**).
- Permeability depends on the membrane proteins that facilitate the transport of specific substances, on the lipid composition of the membrane, and the chemical properties of the solutes.
- For each permeant ion, the distribution of that particular ionic species across a membrane that would occur at equilibrium is described by the Nernst equation (**Equation 8.10**).
- Transport of H^+ across the plant plasma membrane by H^+-ATPases is a major determinant of the membrane potential (**Figure 8.20**).

8.3 Membrane Transport Processes

- Biological membranes contain specialized proteins—channels, carriers, and pumps—that facilitate solute transport (**Figure 8.6**).
- The net result of membrane transport processes is that most ions are maintained in disequilibrum with their surroundings (**Table 8.1**).

Summary (*continued*)

- Channels are regulated protein pores that, when open, greatly enhance fluxes of ions and, in some cases, neutral molecules across membranes (**Figures 8.6, 8.7**).
- Organisms have a great diversity of ion channel types. Depending on the channel type, channels can be nonselective or highly selective for just one ionic species. Channels can be regulated by many parameters, including voltage, intracellular signaling molecules, ligands, hormones, and light (**Figures 8.8, 8.13, 8.14**).
- Carriers bind specific substances and transport them at a rate several orders of magnitude lower than that of channels (**Figures 8.6, 8.11**).
- Pumps require energy for transport. Active transport of H^+ and Ca^{2+} across plant plasma membranes is mediated by pumps (**Figures 8.13, 8.19–8.21**).
- Secondary active transporters in plants harness energy from energetically downhill movement of protons to mediate energetically uphill transport of another solute (**Figure 8.9**).
- In symport, both transported solutes move in the same direction across the membrane, whereas in antiport, the two solutes move in opposite directions (**Figure 8.10**).

8.4 Membrane Transport Proteins

- Many channels, carriers, and pumps of the plant plasma membrane and tonoplast have been identified at the molecular level (**Figure 8.13**) and characterized using electrophysiological (**Figures 8.3, 8.8**) and biochemical techniques.
- Transporters exist for diverse nitrogenous compounds, including ammonium, nitrate, amino acids, and peptides.
- Plants have a great variety of cation channels that can be classified according to their ionic selectivity and regulatory mechanisms (**Figure 8.14**).
- Several different classes of cation carriers mediate K^+ uptake into the cytosol (**Figure 8.13**).
- Na^+–$H^+$and K^+–H^+ antiporters in the tonoplast accumulate Na^+ and K^+ in the vacuole (**Figure 8.13**).
- Ca^{2+} is an important second messenger in signal transduction cascades, and its cytosolic concentration is tightly regulated. Ca^{2+} enters the cytosol passively, via Ca^{2+}-permeable channels, and is actively removed from the cytosol by Ca^+ pumps and Ca^{2+}–H^+ antiporters (**Figure 8.13**).
- Selective carriers that mediate NO_3^-, Cl^-, SO_4^-, and $H_2PO_4^-$ uptake into the cytosol and anion channels that nonselectively mediate anion efflux from the cytosol regulate cellular concentrations of these macronutrients (**Figure 8.13**).
- Both essential and toxic metal ions are transported by high-affinity ZIP transport proteins.
- Aquaporins act as water channels, mediate the influx of mineral nutrients (e.g., boron and silicic acid), and act as conduits for the movement of CO_2, NH_3, and H_2O_2 across the plasma membrane and other plant membranes. Regulation of aquaporins allows plant cells to rapidly change their permeability to water in response to environmental stimuli.
- Plasma membrane H^+-ATPases are encoded by a multigene family, and their activity is reversibly controlled by an autoinhibitory domain (**Figure 8.20**).
- Like the plasma membrane, the tonoplast also contains both cation and anion channels, as well as a diversity of other transporters.
- Three types of proton pumps are found in the vacuolar membrane: vacuolar H^+-ATPases (V-ATPases), H^+-pyrophosphatases (H^+-PPases), and in some cells P-type H^+-ATPases regulate the proton motive force across the tonoplast, which in turn drives the movement of other solutes across this membrane via antiport and symport mechanisms (**Figures 8.13, 8.21**).

8.5 Transport in Stomatal Guard Cells

- Stomatal opening involves activation of P-type H^+-ATPases in the guard cell plasma membrane. The resulting membrane hyperpolarizarion drives the uptake of K^+ salts, a more negative osmotic potential, cellular uptake of water, and stomatal opening (**Figures 8.22, 8.23**).
- Stomatal closing is driven by anion channel activation that depolarizes the guard cell plasma membrane. K^+ efflux follows via outward K^+ channels. The osmotic potential becomes less negative and water efflux results in a decrease in guard cell volume and stomatal closure (**Figures 8.22, 8.23**).

8.6 Ion Transport in Roots

- Solutes such as mineral nutrients move between cells either through the extracellular space (the apoplast) or from cytoplasm to cytoplasm (via the symplasm). The cytoplasm of neighboring cells is connected by plasmodesmata, which facilitate symplasmic transport (**Figure 8.24**).
- When a solute enters the root, it may be taken up into the cytosol of an epidermal cell, or it may diffuse through the apoplast into the root cortex and then enter the symplasm through a cortical or endodermal cell.
- The presence of the Casparian strip prevents apoplastic diffusion of solutes into the stele. Solutes enter the stele via diffusion from endodermal cells to pericyle and xylem parenchyma cells.
- During xylem loading, solutes are released from xylem parenchyma cells to the conducting cells of the xylem, and then move to the shoot in the transpiration stream (**Figure 8.25**).

Web Material

- **WEB TOPIC 8.1 Relating the Membrane Potential to the Distribution of Several Ions across the Membrane: The Goldman Equation** The Goldman equation is used to calculate the membrane permeability to more than one ion.
- **WEB TOPIC 8.2 Patch Clamp Studies in Plant Cells** Patch clamping is applied to plant cells for electrophysiological studies.
- **WEB TOPIC 8.3 Chemiosmosis in Action** The chemiosmotic hypothesis explains how electrical and concentration gradients are used to perform cellular work.
- **WEB TOPIC 8.4 Kinetic Analysis of Multiple Transporter Systems** Application of principles of enzyme kinetics to transport systems provides an effective way to characterize different carriers.
- **WEB TOPIC 8.5 ABC Transporters in Plants** ATP-binding cassette (ABC) transporters are a large family of active transport proteins energized directly by ATP.
- **WEB TOPIC 8.6 Transport Studies with Isolated Vacuoles and Membrane Vesicles** Certain experimental techniques enable the isolation of tonoplast and plasma membrane vesicles for study.

For more study aids, go to oup.com/he/taiz7e.

Suggested Reading

Barbier-Brygoo, H., Vinauger, M., Colcombet, J., Ephritikhine, G., Frachisse, J., and Maurel, C. (2000) Anion channels in higher plants: Functional characterization, molecular structure and physiological role. *Biochim. Biophys. Acta* 1465: 199–218.

Brunkard, J. O., Runkel, A. M., and Zambryski, P. C. (2015) The cytosol must flow: Intercellular transport through plasmodesmata. *Curr. Opin. Cell Biol.* 35: 13–20.

Du, M., Spalding, E. P., and Gray, W. M. (2020) Rapid auxin-mediated cell expansion. *Annu. Rev. Plant Biol.* 71: 379–402.

Eisenach, C., and De Angeli, A. (2017) Ion transport at the vacuole during stomatal movements. *Plant Physiol.* 174: 520–530.

Geldner, N. (2013) The endodermis. *Annu. Rev. Plant. Biol.* 64: 531–558.

Harold, F. M. (1986) *The Vital Force: A Study of Bioenergetics*. W. H. Freeman, New York.

Hamamoto, S., Horie, T., Hauser, F., Deinlein, U., Schroeder, J. I., and Uozumi, N. (2015) HKT transporters mediate salt stress resistance in plants: from structure and function to the field. *Curr. Opin. Biotechnol.* 32: 113–120.

Jammes, F., Hu, H. C., Villiers, F., Bouten, R., and Kwak, J. M. (2011) Calcium-permeable channels in plant cells. *FEBS J.* 278: 4262–4276.

Jeong, J., and Guerinot, M. L. (2009) Homing in on iron homeostasis in plants. *Trends Plant Sci.* 14: 280–285.

Li, G., Santoni, V., and Maurel, C. (2013) Plant aquaporins: Roles in plant physiology. *Biochim. Biophys. Acta* 1840: 1574–1582.

Martinoia, E., Meyer, S., De Angeli, A., and Nagy, R. (2012) Vacuolar transporters in their physiological context. *Annu. Rev. Plant Biol*. 63: 183–213.

Palmgren, M. G., and Nissen, P. (2011) P-type ATPases. *Annu. Rev. Biophys*. 40: 243–266.

Schroeder, J. I., Raschke, K., and Neher, E. (1987) Voltage dependence of K channels in guard-cell protoplasts. *Proc. Natl. Acad. Sci. USA* 84: 4108–4112.

Schroeder, J. I., Delhaize, E., Frommer, W. B., Guerinot, M. L., Harrison, M. J., Herrera-Estrella, L., Horie, T., Kochian, L.V., Munns, R., Nishizawa, N. K., et al. (2013) Using membrane transporters to improve crops for sustainable food production. *Nature* 497: 60–66.

Wang, Y., and Wu, W.-H. (2013) Potassium transport and signaling in higher plants. *Annu. Rev. Plant Biol.* 64: 451–476.

Ward, J. M. (1997) Patch-clamping and other molecular approaches for the study of plasma membrane transporters demystified. *Plant Physiol.* 114: 1151–1159.

Ward, J. M., Mäser, P., and Schroeder, J. I. (2009) Plant ion channels: Gene families, physiology, and functional genomics analyses. *Annu. Rev. Physiol.* 71: 59–82.

Yamaguchi, T., Hamamoto, S., and Uozumi, N. (2013) Sodium transport system in plant cells. *Front. Plant Sci.* 4: 410.

Yazaki, K., Shitan, N., Sugiyama, A., and Takanashi, K. (2009) Cell and molecular biology of ATP-binding cassette proteins in plants. *Int. Rev. Cell Mol. Biol.* 276: 263–299.



Aleksey Sagitov/Shutterstock

UNIT III

Biochemistry and Metabolism

CHAPTER 9 **Photosynthesis: The Light Reactions**

CHAPTER 10 **Photosynthesis: The Carbon Reactions**

CHAPTER 11 **Photosynthesis: Physiological and Ecological Considerations**

CHAPTER 12 **Translocation in the Phloem**

CHAPTER 13 **Respiration and Lipid Metabolism**

CHAPTER 14 **Assimilation of Inorganic Nutrients**

CHAPTER 15 **Abiotic Stress**





9 Photosynthesis: The Light Reactions



Aleksey Sagitov/Shutterstock

Life on Earth ultimately depends on energy derived from the sun. Photosynthesis is the only process of biological importance that can harvest this energy.

A large fraction of the planet's energy resources results from photosynthetic activity in either recent or ancient times (fossil fuels). This chapter introduces the basic physical principles that underlie photosynthetic energy storage and the current understanding of the structure and function of the photosynthetic apparatus.

The term *photosynthesis* means literally "synthesis using light." As we will see in this chapter, oxygenic photosynthetic organisms (those, like plants, that produce O_2 as a by-product) use solar energy to synthesize complex carbon compounds. More specifically, light energy drives the synthesis of carbohydrates and the generation of oxygen from carbon dioxide and water. Energy stored in these carbohydrate molecules can be used later to power cellular processes in the plant and can serve as the energy source for all forms of life.

This chapter deals with the role of light in photosynthesis, the structure of the photosynthetic apparatus, and the processes that begin with the excitation of chlorophyll by light and culminate in the synthesis of ATP and NADPH.

9.1 Photosynthesis in Green Plants

The most active photosynthetic tissue in vascular plants is the mesophyll of leaves. Mesophyll cells have many chloroplasts, which contain the specialized light-absorbing green pigments, the **chlorophylls**. In photosynthesis, the plant uses solar energy to oxidize water, thereby releasing oxygen, and to reduce carbon dioxide, thereby forming large carbon compounds, primarily sugars. The complex series of reactions that culminate in the reduction of CO_2 include the thylakoid reactions and the carbon fixation reactions.

The **thylakoid reactions** of photosynthesis take place in the specialized internal membranes of the chloroplast called thylakoids (see Chapter 1). The end products of these thylakoid reactions are the high-energy compounds ATP and NADPH, which are used for the synthesis of sugars in the **carbon fixation reactions**. These synthetic processes take place in the stroma of the chloroplast, the aqueous region that surrounds the thylakoids. The thylakoid reactions, also called the "light reactions" of

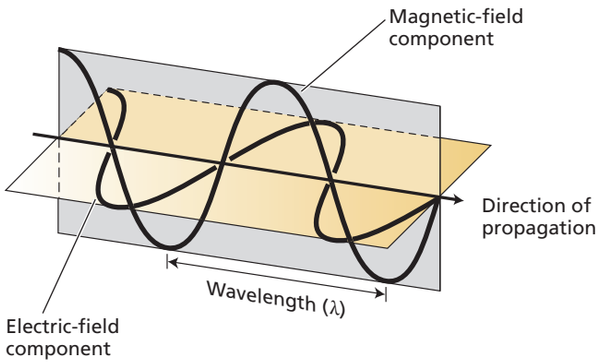


Figure 9.1 Light is a transverse electromagnetic wave, consisting of oscillating electric and magnetic fields that are perpendicular to each other and to the direction of propagation of the light. Light moves at a speed of 3.0×10^8 m s^{-1}. The wavelength (λ) is the distance between successive crests of the wave.

photosynthesis, are the subject of this chapter; the carbon fixation reactions will be discussed in Chapter 10.

In the chloroplast, light energy is converted into chemical energy by two different functional units called *photosystems*. The absorbed light energy is used to power the transfer of electrons through a series of compounds that act as electron donors and electron acceptors. The majority of electrons are extracted from H_2O, which is oxidized to O_2, and ultimately reduce $NADP^+$ to NADPH. Light energy is also used to generate a proton motive force (see Chapter 8) across the thylakoid membrane; this proton motive force is used to synthesize ATP.

9.2 General Concepts

In this section we explore the essential concepts that provide a foundation for understanding photosynthesis. These concepts include the nature of light, the properties of pigments, and the various roles of pigments.

Light consists of photons with characteristic energies

Light has properties of both particles and waves. A wave (**Figure 9.1**) is characterized by a **wavelength**, denoted by the Greek letter lambda (λ), which is the distance between successive wave crests. The **frequency**, represented by the Greek letter nu (ν), is the number of wave crests that pass an observer in a given time. A simple equation relates the wavelength, the frequency, and the speed of any wave:

$$c = \lambda\nu \qquad (9.1)$$

where c is the speed of the wave—in the present case, the speed of light (3.0×10^8 m s^{-1}). The light wave is a transverse (side-to-side) electromagnetic wave, in which both electric and magnetic fields oscillate perpendicularly to the direction of propagation of the wave and at 90° with respect to each other.

Light can also be considered as particles, known as **photons**. Each photon contains an amount of energy that is not continuous but rather is delivered at discrete levels, called **quanta**. The energy (E) of a photon depends on the frequency of the light according to a relation known as Planck's law:

$$E = h\nu \qquad (9.2)$$

where h is Planck's constant (6.626×10^{-34} J s). How photons interact with matter depends strongly on their frequency or energy, and only a narrow range of frequencies, in the visible spectrum, are useful for photosynthesis (**Figure 9.2**). Lower-frequency photons, with energies below that of red light, and higher-frequency photons, with energies above that of violet light, cannot drive photosynthesis.

Absorption of photosynthetically active light changes the electronic states of chlorophylls

For light energy to power photosynthesis, it must be captured and converted into electrical or chemical forms.

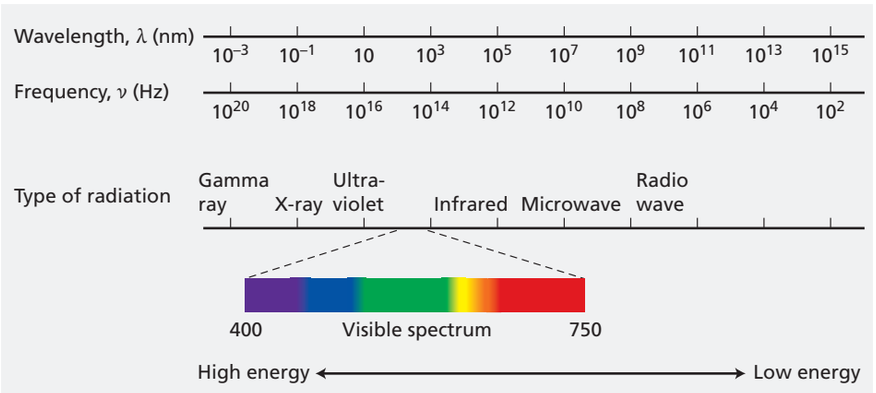


Figure 9.2 Electromagnetic spectrum. Wavelength (λ) and frequency (ν) are inversely related. Our eyes are sensitive to only a narrow range of wavelengths of radiation, the visible region, which extends from about 400 nm (violet) to about 700 nm (red). Short-wavelength (high-frequency) light has a high energy content; long-wavelength (low-frequency) light has a low energy content.

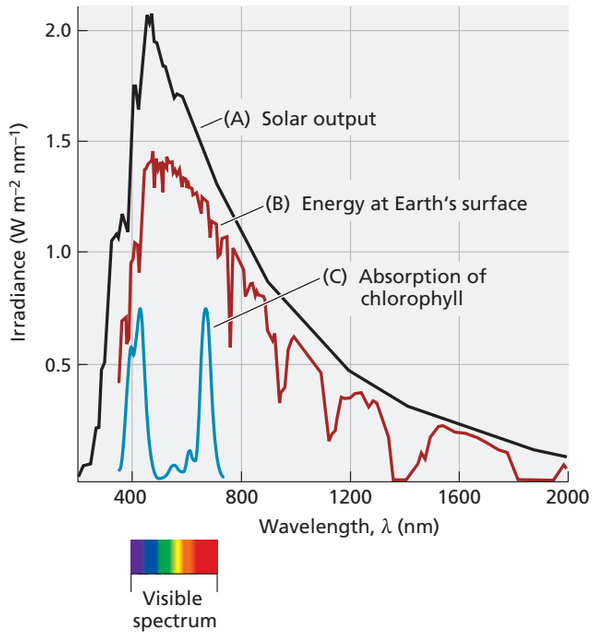


Figure 9.3 **The solar spectrum and its relation to the absorption spectrum of chlorophyll.** Curve A is the energy output of the sun as a function of wavelength. Curve B is the energy that strikes Earth's surface. The sharp valleys in the infrared region beyond 700 nm represent the absorption of solar energy by molecules in the atmosphere, chiefly water vapor. Curve C is the absorption spectrum of chlorophyll, which absorbs strongly in the blue (about 430 nm) and red (about 660 nm) portions of the spectrum. Because the green light in the middle of the visible spectrum is not efficiently absorbed, some of it is reflected into our eyes and gives plants their characteristic green color.

The first step in this process is the absorption of light by pigments associated with the photosynthetic apparatus. Different energies (or frequencies) of light interact with molecules in different ways, inducing different types of transitions. For light to be absorbed, the absorbing pigment must have an energy transition (a process excitable by light) that matches the photon's energy. If the photon's energy does not precisely match such a transition (i.e., it is too low or too high), the light will not be absorbed. Thus, although sunlight that strikes Earth's surface contains photons with a wide range of different energies, as shown in **Figure 9.3**, only a small fraction of this light can be used for photosynthesis. Plant photosynthesis can use light energy between about 400 and 700 nm (ranging from violet to red and far-red wavelengths, nearly matching the visible spectrum; see Figure 9.2).

This range of photon energies can excite electrons in plant pigments, mostly chlorophylls, from low-energy molecular orbitals to higher-energy "excited states" (**Figure 9.4**). Such excited states in chlorophyll molecules are the essential starting points for the light reactions. By contrast, lower-energy infrared radiation tends to excite vibrational motions or rotations of chemical bonds, the energy of which is rapidly dissipated as heat and thus is not useful for driving photosynthesis. Photons with higher energy, including deeper UV light, tend to directly ionize molecules, essentially knocking electrons off the molecules, thereby generating radicals that can damage biological materials.

The **absorption spectrum** (plural *spectra*) of a typical chlorophyll found in chloroplasts is shown by the blue curve in Figure 9.3. An absorption spectrum provides a measure of the amount of **light energy** taken up or absorbed by a molecule or substance as a function of the wavelength of the light. The absorption spectrum for a particular substance can be determined using a spectrophotometer, as illustrated in **Figure 9.5**.

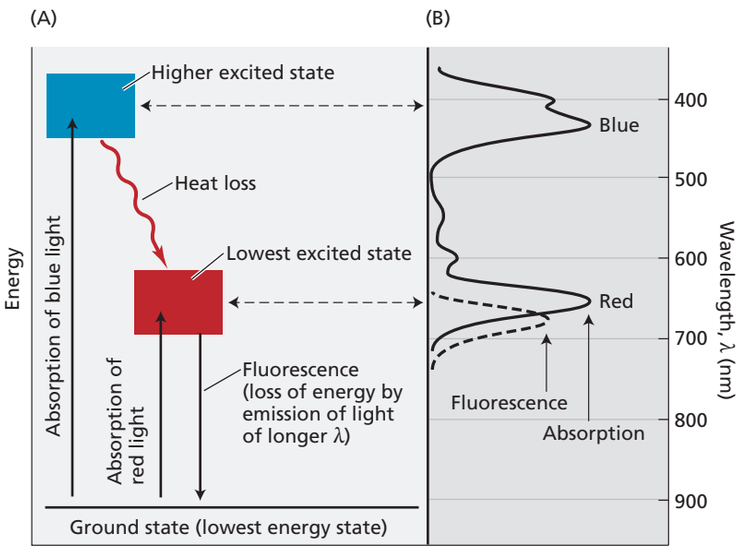


Figure 9.4 **Light absorption and emission by chlorophyll.** (A) Energy level diagram. Absorption or emission of light is indicated by vertical arrows that connect the ground state with excited electron states. The blue and red absorption bands of chlorophyll (which absorb blue and red photons, respectively) correspond to the upward vertical arrows, signifying that energy absorbed from light causes the molecule to change from the ground state to an excited state. The downward-pointing arrow indicates fluorescence, in which the molecule goes from the lowest excited state to the ground state while re-emitting energy as a photon. (B) Spectra of absorption and fluorescence. The long-wavelength (red) absorption band of chlorophyll corresponds to light that has the energy required to cause the transition from the ground state to the first excited state. The short-wavelength (blue) absorption band corresponds to a transition to a higher excited state.

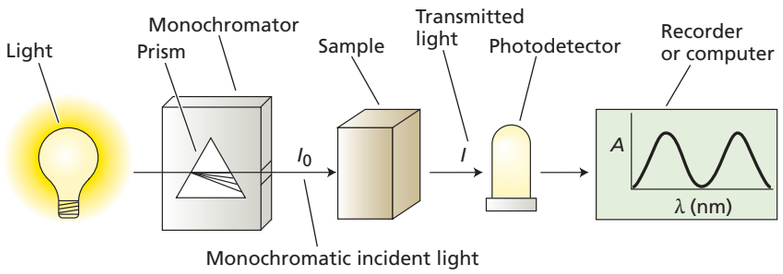


Figure 9.5 Schematic diagram of a spectrophotometer. The instrument consists of a light source, a monochromator that contains a wavelength selection device such as a prism, a sample holder, a photodetector, and a recorder or computer. The output wavelength of the monochromator can be changed by rotation of the prism; the graph of absorbance (*A*) versus wavelength (λ) is called a spectrum.

Spectrophotometry, the technique used to measure the absorption of light by a sample, is discussed more fully in **WEB TOPIC 9.1**. In many cases, absorption spectra are plotted as the absorption of light (on the y-axis) as a function of the wavelength of light (on the x-axis). However, it is also informative to plot absorption as a function of frequency, which, because of the relationship described by Equation 9.2, gives us the dependence of absorption on the energy of the photons.

Chlorophyll appears green to our eyes because it absorbs light mainly in the red and blue parts of the spectrum, so the light that is not absorbed is enriched in green wavelengths (about 550 nm) (see Figures 9.3 and 9.4). The absorption of light is represented by Equation 9.3, in which chlorophyll (Chl) in its lowest energy, or ground, state absorbs a photon (represented by $h\nu$) and makes a transition to a higher energy, or excited, state (Chl*):

$$\text{Chl} + h\nu \rightarrow \text{Chl}^* \qquad (9.3)$$

The distribution of electrons in the excited molecule is different from the distribution in the ground-state molecule. Absorption of red light excites the chlorophyll to a higher-energy "excited state" (the "Lowest excited state" in Figure 9.4) by promoting an electron from a low energy orbital to a higher energy orbital. Blue light can also be absorbed by chlorophyll, initially producing an excited state of even higher energy (the "Higher excited state" in Figure 9.4) than that produced by red light. However, this higher-energy excited state is extremely unstable and rapidly decays to the **lowest excited state**, which is the starting point for reactions that drive photosynthesis. The initial photosynthetic reactions must be extremely rapid to outcompete the decay of the lowest excited state; if the energy in the excited state is not used by these reactions, it will last only several nanoseconds (1 nanosecond = 10^{-9} s) at most.

The lowest excited state of chlorophyll can decay by several alternative pathways:

1. Excited chlorophyll can re-emit a photon and thereby return to its ground state—a process known as **fluorescence**. When it does so, the wavelength of fluorescence is slightly longer (and of lower energy) than the wavelength of absorption, because a portion of the excitation energy is converted into heat before the fluorescent photon is emitted. Chlorophylls fluoresce in the red region of the spectrum (see Figure 9.4).
2. Excited chlorophyll can return to its ground state by directly converting its excitation energy into heat, with no emission of a photon.
3. Excited chlorophyll can participate in **energy transfer**, during which the chlorophyll transfers its energy to another molecule, including other chlorophylls. In this way, hundreds of chlorophyll molecules can transfer energy over long distances of 50 to 100 nm.
4. Excited chlorophyll can form a highly reactive state called triplet chlorophyll, which can react with oxygen to form toxic by-products.
5. Excited chlorophyll can initiate **photochemistry**, in which the energy of the excited state causes chemical reactions to occur, ultimately storing energy in photosynthetic products. The photochemical reactions of photosynthesis are among the fastest known chemical reactions. This speed is necessary for photochemistry to outcompete the non-energy-storing decay pathways.

Photosynthetic pigments absorb the light that powers photosynthesis

The energy of sunlight is first absorbed by the pigments of the plant. All pigments active in photosynthesis are found in the chloroplast. Structures and absorption spectra of several photosynthetic pigments are shown in **Figures 9.6** and **9.7**, respectively. The chlorophylls and **bacteriochlorophylls** (pigments found in certain bacteria) are the typical pigments of photosynthetic organisms.

Chlorophylls *a* and *b* are abundant in green plants, and chlorophylls *c*, *d*, and *f* are found in some protists and cyanobacteria. Several different types of bacteriochlorophylls have been found; type *a* is the most widely distributed. **WEB TOPIC 9.2** shows the distribution of pigments in different types of photosynthetic organisms.

All chlorophylls have a complex ring structure that is chemically related to the heme groups found in hemoglobin and cytochromes (see Figure 9.6A). A long

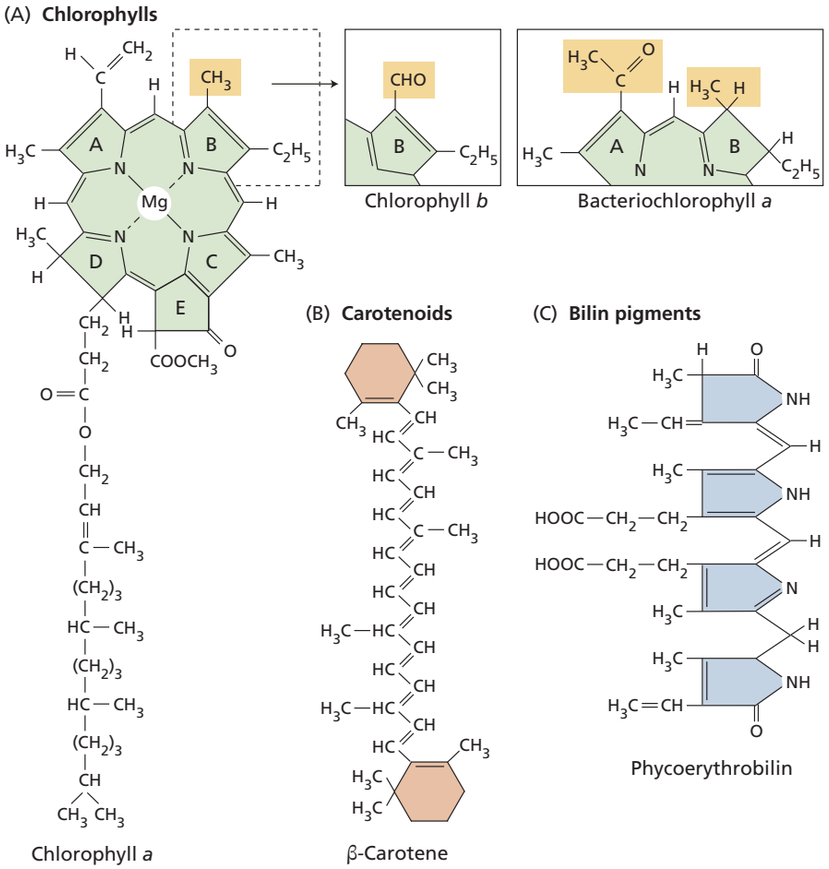


Figure 9.6 **Molecular structure of some photosynthetic pigments.** **(A)** The chlorophylls have a porphyrin-like ring structure (green) with a magnesium ion (Mg) coordinated in the center and a long hydrophobic hydrocarbon tail that anchors them in the photosynthetic membrane. The porphyrin-like ring is the site of the electron rearrangements that occur when the chlorophyll is excited, and of the unpaired electrons when it is either oxidized or reduced. Various chlorophylls differ chiefly in the substituents around the rings and the pattern of double bonds. **(B)** Carotenoids are linear polyenes that serve as both antenna pigments and photoprotective agents. **(C)** Bilin pigments are open-chain tetrapyrroles found in antenna structures known as phycobilisomes that occur in cyanobacteria and red algae.

hydrocarbon tail is almost always attached to the ring structure. The tail anchors the chlorophyll to the hydrophobic portion of its environment. The ring structure contains some loosely bound electrons and is the part of the molecule involved in electronic transitions and redox (reduction–oxidation) reactions.

The different types of **carotenoids** found in photosynthetic organisms are molecules with multiple conjugated double bonds (see Figure 9.6B). Absorption bands in the 400 to 500 nm region give carotenoids their characteristic orange color. The color of carrots, for example, is due to the carotenoid β-carotene, whose structure and absorption spectrum are shown in Figures 9.6 and 9.7, respectively.

Carotenoids are found in all known natural photosynthetic organisms. Carotenoids are integral constituents

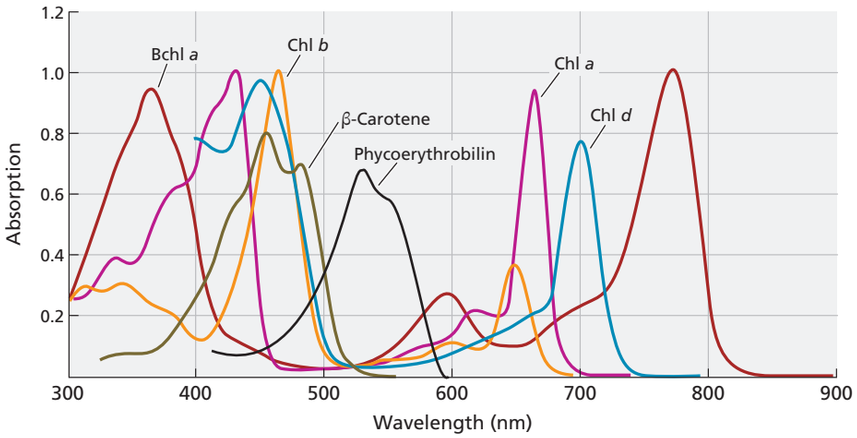


Figure 9.7 **Absorption spectra of some photosynthetic pigments, including β-carotene, chlorophyll *a* (Chl *a*), chlorophyll *b* (Chl *b*), bacteriochlorophyll *a* (Bchl *a*), chlorophyll *d* (Chl *d*), and phycoerythrobilin.** The absorption spectra shown are for pure pigments dissolved in nonpolar solvents, except phycoerythrin, a protein from cyanobacteria that contains a phycoerythrobilin chromophore covalently attached to the peptide chain. In many cases the spectra of photosynthetic pigments in vivo are substantially affected by the environment of the pigments in the photosynthetic membrane.

of the thylakoid membrane and are usually associated intimately with many of the proteins that make up the photosynthetic apparatus. The light energy absorbed by the carotenoids can be transferred to chlorophyll for photosynthesis; because of this role they are called **accessory pigments**. Carotenoids also help protect the organism from damage caused by light, by "quenching" reactive intermediates such as triplet chlorophylls (see Section 9.8 and Chapter 11).

9.3 Key Experiments in Understanding Photosynthesis

Establishing the overall chemical equation of photosynthesis required several hundred years and contributions by many scientists (literature references for historical developments can be found on the website for this book). In 1771, Joseph Priestley observed that a sprig of mint growing in air in which a candle had burned out regenerated something in the air so that another candle could burn. He had discovered oxygen evolution by plants. A Dutch biologist, Jan Ingenhousz, documented the essential role of light in photosynthesis in 1779.

Other scientists established the roles of CO_2 and H_2O and showed that organic matter, specifically carbohydrate, is a product of photosynthesis along with oxygen. By the end of the nineteenth century, the balanced overall chemical reaction for photosynthesis could be written as follows:

$$6\,CO_2 + 6\,H_2O \xrightarrow{\text{Light, plant}} C_6H_{12}O_6 + 6\,O_2 \quad (9.4)$$

where $C_6H_{12}O_6$ represents a simple sugar such as glucose. As we will discuss in Chapter 10, glucose is not the actual product of the carbon fixation reactions, so this part of the equation should not be taken literally. However, the energetics for the actual reaction are approximately the same as represented here.

The chemical reactions of photosynthesis are complex. At least 50 intermediate reaction steps have now been identified, and additional steps undoubtedly will be discovered. An early clue to the chemical nature of the essential chemical process of photosynthesis came in the 1920s from investigations of photosynthetic bacteria that did not produce oxygen as an end product. From his studies on these bacteria, C. B. van Niel concluded that photosynthesis is a redox process. This conclusion has served as a fundamental concept on which all subsequent research on photosynthesis has been based.

We now turn to the relationship between photosynthetic activity and the spectrum of absorbed light. We discuss some of the critical experiments that have contributed to our present understanding of photosynthesis, and we consider equations for the essential chemical reactions of photosynthesis.

Action spectra relate light absorption to photosynthetic activity

The use of action spectra has been central to the development of our current understanding of photosynthesis. An **action spectrum** describes the effectiveness of different wavelengths of light in promoting a biological response. For example, an action spectrum for photosynthesis can be constructed by measuring the rate of oxygen evolution as a function of increasing light intensities (the number of photons per unit of area per second) at different wavelengths (**Figure 9.8**). (Because photosynthesis is saturated at high light, the rate of oxygen evolution should be measured at very low light, or estimated by the half-saturation point.) The efficiency with which a particular wavelength intensity of light induces photosynthesis will be higher when it is more effectively absorbed by photosynthetic pigments. Thus, an action spectrum can identify the *chromophores* (pigments) responsible for a particular light-induced phenomenon.

Some of the first action spectra were measured by T. W. Engelmann in the late 1800s (**Figure 9.9**). Engelmann used a prism to disperse sunlight into a rainbow that was allowed to fall on an aquatic algal filament. A population of O_2-seeking bacteria was introduced into the system. The bacteria congregated in the regions of the filaments that evolved the most O_2. These were the regions illuminated by blue light and red light, which

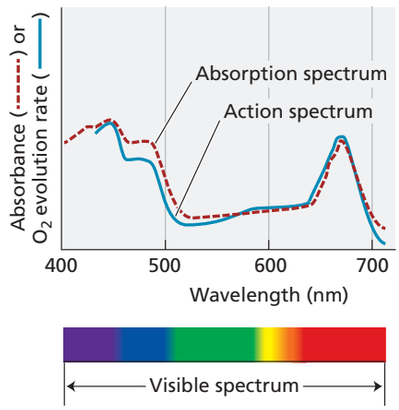


Figure 9.8 Action spectrum compared with an absorption spectrum. The absorption spectrum is measured as shown in Figure 9.5. An action spectrum is measured by plotting a response to light, such as oxygen evolution, as a function of wavelength. If the pigment used to obtain the absorption spectrum is the same as that which causes the response, the absorption and action spectra will match. In the example shown here, the action spectrum for oxygen evolution matches the absorption spectrum of intact chloroplasts quite well, indicating that light absorption by the chlorophylls mediates oxygen evolution. Discrepancies are found in the region of carotenoid absorption, from 450 to 550 nm, indicating that energy transfer from carotenoids to chlorophylls is not as effective as energy transfer between chlorophylls.

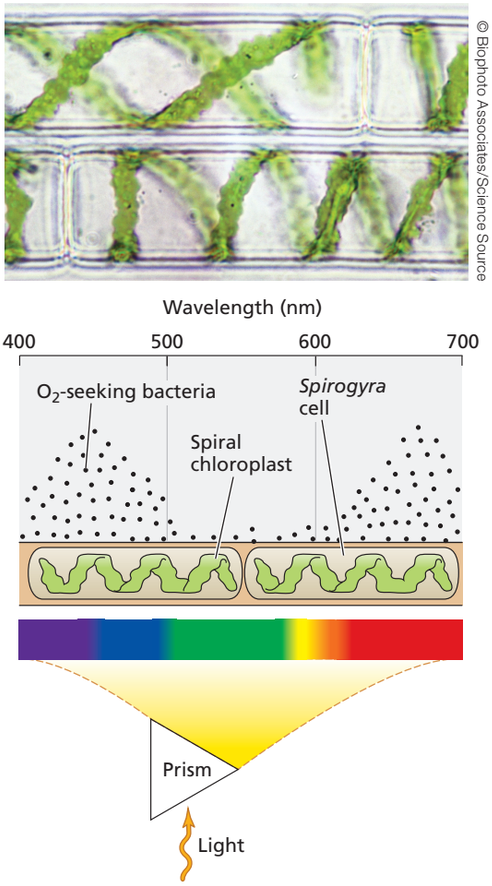


Figure 9.9 Schematic diagram of the action spectrum measurements by T. W. Engelmann. Engelmann projected a spectrum of light onto the spiral chloroplast of the filamentous green alga *Spirogyra* and observed that O_2-seeking bacteria introduced into the system collected in the region of the spectrum where chlorophyll pigments absorb. This action spectrum gave the first indication of the effectiveness of light absorbed by pigments in driving photosynthesis.

are strongly absorbed by chlorophyll. Today, action spectra can be measured in room-sized spectrographs in which a huge monochromator bathes the experimental samples in monochromatic light. The technology is more sophisticated, but the principle is the same as that of Engelmann's experiments.

A special version of the action spectrum measures the effectiveness of the light that is actually absorbed by the plant, rather than the total incident light. In this case, the **quantum yield** of photosynthesis—the fraction of absorbed light that is actually used to drive productive photosynthesis—can be calculated. As we discuss later in this section, the quantum yield of photosynthesis under low light can be close to 1.0, which means nearly every photon that is absorbed is used to drive photosynthesis.

Action spectra were very important for the discovery of two distinct photosystems operating in O_2-evolving photosynthetic organisms. Before we introduce the two photosystems, however, we need to describe the light-gathering antennas and the energy needs of photosynthesis.

Photosynthesis takes place in complexes containing light-harvesting antennas and photochemical reaction centers

A portion of the light energy absorbed by chlorophylls and carotenoids is eventually stored as chemical energy via the formation of chemical bonds. This conversion of energy from one form to another is a complex process that depends on cooperation between many pigment molecules and a group of electron transfer proteins.

The majority of the pigments serve as an **antenna complex**, collecting light and transferring the energy to the **reaction center complex**, where the chemical oxidation and reduction reactions leading to long-term energy storage take place (**Figure 9.10**). Molecular structures of some of the antenna and reaction center complexes are discussed later in the chapter.

How does the plant benefit from this division of labor between antenna and reaction center pigments? Even in bright sunlight, a single chlorophyll molecule absorbs only a few photons each second. If there were a reaction center associated with each chlorophyll molecule, the reaction center enzymes would be idle most of the time, only occasionally being activated by photon absorption. However, if a reaction center receives energy from many

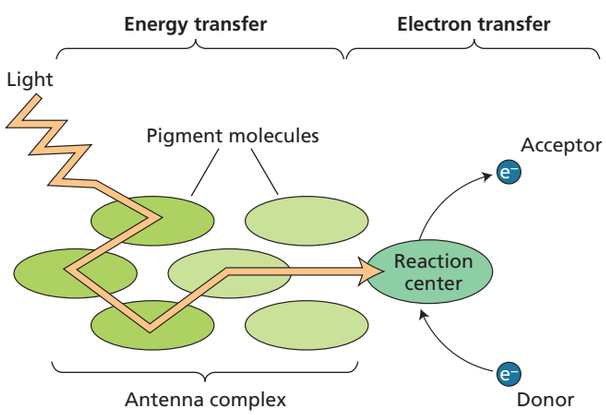


Figure 9.10 Basic concept of energy transfer during photosynthesis. Many pigments together serve as an antenna, collecting light and transferring its energy to the reaction center, where chemical reactions store some of the energy by transferring electrons from a chlorophyll pigment to an electron acceptor molecule. An electron donor then reduces the chlorophyll again. The transfer of energy in the antenna is a purely physical phenomenon and involves no chemical changes.

pigments at once, the system is kept active a large fraction of the time.

In 1932, Robert Emerson and William Arnold performed a key experiment that provided the first evidence for the cooperation of many chlorophyll molecules in energy conversion during photosynthesis. They delivered very brief (10^{-5} s) flashes of light to a suspension of the green alga *Chlorella pyrenoidosa* and measured the amount of oxygen produced. The flashes were spaced about 0.1 s apart, a time that Emerson and Arnold had determined in earlier work was long enough for the enzymatic steps of the process to be completed before the arrival of the next flash. The investigators varied the energy of the flashes and found that at high energies the oxygen production did not increase when a more intense flash was given: The photosynthetic system was saturated with light (**Figure 9.11**).

In their measurement of the relationship of oxygen production to flash energy, Emerson and Arnold were surprised to find that under saturating conditions, only 1 molecule of oxygen was produced for each 2500 chlorophyll molecules in the sample. We know now that several hundred pigments are associated with each reaction center and that each reaction center must operate four times to produce 1 molecule of oxygen—hence the value of 2500 chlorophylls per O_2.

The reaction centers and most of the antenna complexes are integral components of the thylakoid membrane. In eukaryotic photosynthetic organisms, these membranes are found within the chloroplast; in photosynthetic prokaryotes, the site of photosynthesis is the plasma membrane or membranes derived from it.

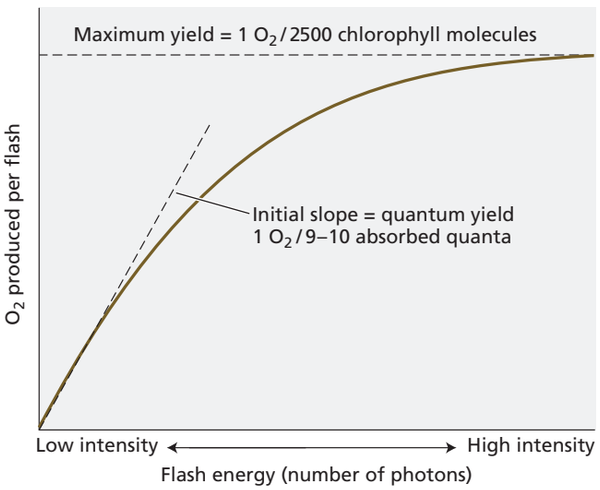


Figure 9.11 Relationship of oxygen production to flash energy, the first evidence for the interaction between the antenna pigments and the reaction center. At saturating energies, the maximum amount of O_2 produced is 1 molecule per 2500 chlorophyll molecules (see text).

The chemical reaction of photosynthesis is driven by light

It is important to realize that the chemical reaction shown in Equation 9.4 is energetically uphill, meaning that it cannot proceed without a large input of energy. The equilibrium constant for Equation 9.4, calculated from tabulated free energies of formation for each of the compounds involved, is about 10^{-500}. This number is so close to zero that one can be quite confident that in the entire history of the universe no molecule of glucose has formed spontaneously from H_2O and CO_2 without external energy being provided. The energy needed to drive the photosynthetic reaction comes from light. Here's a simpler form of Equation 9.4:

$$CO_2 + H_2O \xrightarrow{\text{Light, plant}} (CH_2O) + O_2 \qquad (9.5)$$

where (CH_2O) is one-sixth of a glucose molecule. About ten photons of light are required to drive the reaction of Equation 9.5.

Light drives the reduction of NADP$^+$ and the formation of ATP

The overall process of photosynthesis is a redox chemical reaction, in which electrons are removed from one chemical species, thereby oxidizing it, and added to another species, thereby reducing it. In 1937, Robert Hill found that in the light, isolated chloroplast thylakoids reduce a variety of compounds, such as iron salts. These compounds serve as oxidants in place of CO_2, as the following equation shows:

$$4\ Fe^{3+} + 2\ H_2O \rightarrow 4\ Fe^{2+} + O_2 + 4\ H^+ \qquad (9.6)$$

Many compounds have since been shown to act as artificial electron acceptors in what has come to be known as the Hill reaction. The use of artificial electron acceptors has been invaluable in elucidating the reactions that precede carbon reduction. The demonstration of oxygen evolution linked to the reduction of artificial electron acceptors provided the first evidence that oxygen evolution could occur in the absence of carbon dioxide and led to the now accepted and proven idea that the oxygen in photosynthesis originates from water, not from carbon dioxide.

We now know that during the normal functioning of the photosynthetic system, light reduces NADP$^+$, which in turn serves as the reducing agent for carbon fixation in the Calvin–Benson cycle (see Chapter 10). ATP is also formed during the electron flow from water to NADP$^+$, and it too is used in carbon reduction.

The chemical reactions in which water is oxidized to oxygen, NADP$^+$ is reduced to NADPH, and ATP is formed are known as the *thylakoid reactions* because almost all the reactions up to NADP$^+$ reduction take place in the thylakoids. The carbon fixation

and reduction reactions are called the *stroma reactions* because the carbon reduction reactions take place in the aqueous region of the chloroplast, the stroma. Although this division is somewhat arbitrary, it is conceptually useful.

Oxygen-evolving organisms have two photosystems that operate in series

The light reactions of photosynthesis involve two types of photochemical reaction centers, contained within **photosystems I** and **II** (**PSI** and **PSII**), which operate in series to carry out the early energy storage reactions of photosynthesis. PSI preferentially absorbs far-red light of wavelengths greater than 680 nm; PSII preferentially absorbs red light of 680 nm and is driven very poorly by far-red light. Another difference between the photosystems is that:

- PSI produces a strong reductant, capable of reducing $NADP^+$, and a weak oxidant.
- PSII produces a very strong oxidant, capable of oxidizing water, and a weaker reductant than the one produced by PSI.

The reductant produced by PSII re-reduces the oxidant produced by PSI. These properties of the two photosystems are shown schematically in **Figure 9.12** (see **WEB TOPIC 9.4**).

The scheme of photosynthesis depicted in Figure 9.12, called the *Z scheme* (because it looks like the letter Z), has become the basis for understanding O_2-evolving (oxygenic) photosynthetic organisms. It accounts for the operation of two physically and chemically distinct photosystems (I and II), each with its own pool of antenna pigments and photochemical reaction center. The two photosystems are linked by an electron transport chain.

Almost all the energy for life on our planet comes from photosynthesis, and thus its efficiency controls the maximum overall productivity of our ecosystems. Two distinct parameters determine the efficiency of photosynthesis: the quantum yield and the energy conversion efficiency.

The graph shown in Figure 9.11 permits us to calculate the quantum yield of photochemistry (Φ), defined as follows:

$$\Phi = \frac{\text{Number of photochemical products}}{\text{Total number of quanta absorbed}} \qquad (9.7)$$

At low light intensities, the curve shows its highest, and nearly linear, increase in oxygen evolution with increasing light intensity. Over this range, the quantum yield of photochemistry can be as high as 0.95, meaning that 95% of the photons absorbed by chlorophylls are used in photochemistry. Because the formation of the stable photosynthetic products O_2 and fixed CO_2 (sugars) requires multiple photochemical events, it has a lower quantum yield of formation than the photochemical quantum yield. It takes about ten photons to produce one molecule of O_2, so the quantum yield of O_2 production is about 0.1, even though the quantum yield for each photochemical step in the process is nearly 1.0. A more detailed discussion of quantum yields can be found in **WEB TOPIC 9.3**.

Although the photochemical quantum yield under optimum conditions is nearly 1.0, the fraction of energy that is stored by photosynthesis—that is, the **energy conversion efficiency**—is much less. One major reason for this loss of energy is that a photon's energy is absorbed by generating a series of intermediates in the light

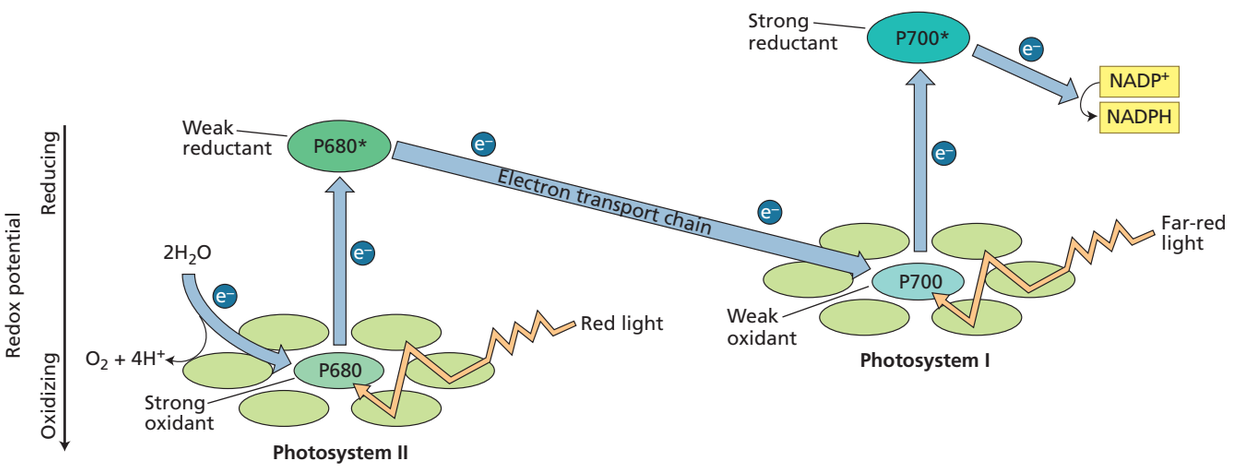


Figure 9.12 Z scheme of photosynthesis. Red light absorbed by photosystem II (PSII) produces a strong oxidant and a weak reductant. Far-red light absorbed by photosystem I (PSI) produces a weak oxidant and a strong reductant. The strong oxidant generated by PSII oxidizes water, while the strong reductant produced by PSI reduces $NADP^+$. This scheme is basic to an understanding of photosynthetic electron transport. P680 and P700 refer to the wavelengths of maximum absorption of the reaction center chlorophylls in PSII and PSI, respectively.

reactions, ultimately forming O_2, NADPH, and ATP. The equilibrium constant for each step in this process has a large drop in free energy, which ensures that the forward reactions are much faster than the reverse reactions. In this way, the energy from the photon is "trapped," preventing it from being lost by reverse reactions, thereby increasing the quantum yield of light capture, but at the cost of a loss in overall energy storage.

When 680-nm red light is absorbed, the total energy input (see Equation 9.2) is 1760 kJ per mole of oxygen formed. This amount of energy is more than enough to drive the reaction in Equation 9.5, which has a standard-state free-energy change of +467 kJ mol^{-1}. The maximum efficiency of conversion of light energy from 680-nm red photons (the optimal wavelength) into chemical energy is therefore about 27%. Blue light is also strongly absorbed by the photosystems, with similar quantum efficiency. Blue photons have about 50% higher energy content than red photons, but once absorbed this extra energy is lost extremely rapidly, resulting in a lower energy conversion efficiency for the formation of stable products. White light from the sun is composed of photons that span the range of photosynthetically active radiation, from about 400 to 700 nm, and the average energy conversion efficiency is intermediate between that of red and blue photons.

At higher light intensities, photosynthesis is limited by downstream processes, such as the fixation of CO_2, leading to lower quantum efficiencies. Figure 9.11 shows that the response of photosynthesis to light saturates at higher light. Note that Figure 9.11 shows the light saturation curve for a short flash of light, but the general shape of the curve under constant light is similar. The higher the light intensity, the smaller the slope of the response of photosynthesis to further increases in light intensity. This flattening of the curve means that that the quantum efficiency of the light reactions decreases at high light intensities—that is, a higher fraction of the energy from photons is lost as heat. The system is "light-limited" when the arrival of photons is slower than the maximum rates at which the system can use them. But when light intensity increases, photons arrive more rapidly than can be used. As we discuss in Section 9.8, having too much light can lead to buildup of reactive intermediates that can lead to photodamage. To prevent these situations, the capture of light is down-regulated by the plant, dissipating more energy as heat.

Most of the energy produced by the light reactions is stored in the form of fixed carbon. A large fraction of this fixed carbon is subsequently used for cellular maintenance processes, with a smaller fraction being used to generate new biomass (see Chapter 11). Thus, the overall energy conversion efficiency for making new plant matter is only a few percent, far below the theoretical maximum, limiting the energy available (and the rate of CO_2 uptake) in our environment. Decreasing these large energy losses is a target of efforts to improve crop productivity, though it is not clear to what extent this can be engineered while still maintaining the robustness of plants in their environments.

9.4 Organization of the Photosynthetic Apparatus

The previous section explained some of the physical principles underlying photosynthesis, some aspects of the functional roles of various pigments, and some of the chemical reactions carried out by photosynthetic organisms. We now turn to the architecture of the photosynthetic apparatus and the structure of its components, and learn how the molecular structure of the system leads to its functional characteristics.

The chloroplast is the site of photosynthesis

In photosynthetic eukaryotes, photosynthesis takes place in the subcellular organelle known as the chloroplast (see Chapter 1). **Figure 9.13** shows a transmission electron micrograph of a thin section from a pea chloroplast. The most striking aspect of the structure of the chloroplast is the extensive system of internal membranes known as **thylakoids**. All the chlorophyll

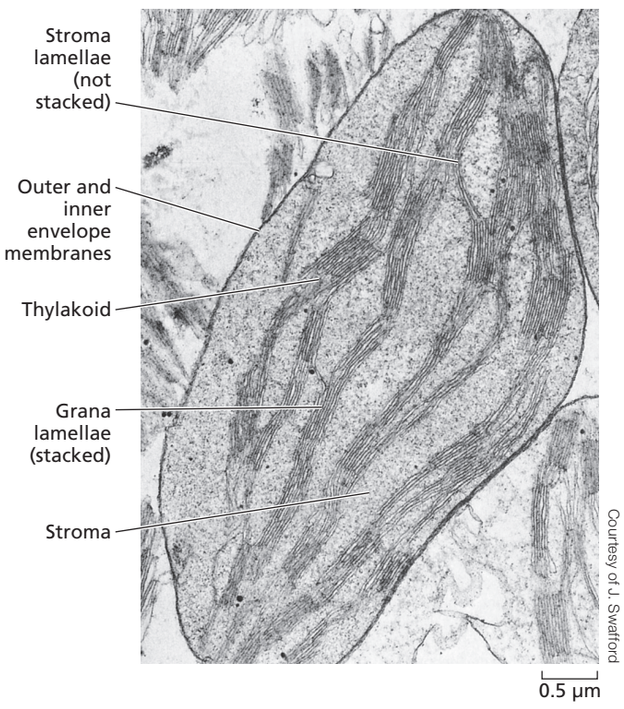


Figure 9.13 Transmission electron micrograph of a chloroplast from pea (*Pisum sativum*) fixed in glutaraldehyde and OsO_4, embedded in plastic resin, and thin-sectioned with an ultramicrotome.

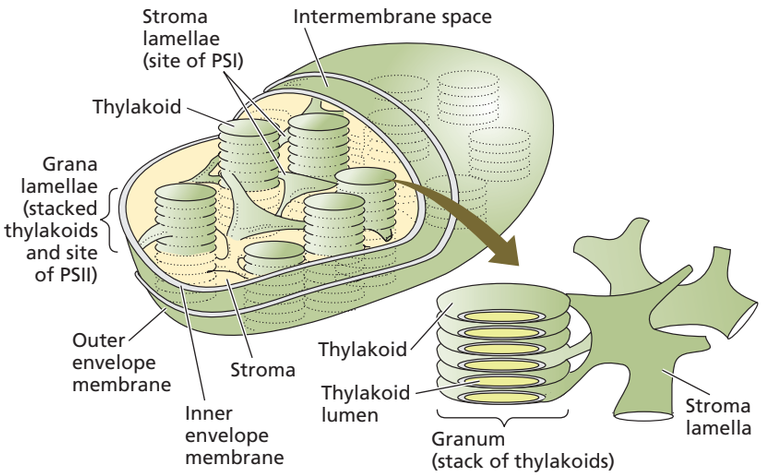


Figure 9.14 Schematic picture of the overall organization of the membranes in the chloroplast. The chloroplast of vascular plants is surrounded by the inner and outer membranes (the envelope). The region of the chloroplast that is inside the inner membrane and surrounds the thylakoid membranes is known as the stroma. It contains the enzymes that catalyze carbon fixation and other biosynthetic pathways. The thylakoid membranes are highly folded and appear in many pictures to be stacked like coins (the granum), although in reality they form one or a few large interconnected membrane systems, with a well-defined interior and exterior with respect to the stroma. (After W. M. Becker. 1986. *The World of the Cell*. Benjamin/Cummings, Menlo Park, CA.)

is contained within this membrane system, which is the site of the light reactions of photosynthesis.

The carbon reduction reactions, which are catalyzed by water-soluble enzymes, take place in the **stroma**, the region of the chloroplast outside the thylakoids. Most of the thylakoids appear to be very closely associated with each other. These stacked membranes are known as **grana lamellae** (singular *lamella*; each stack is called a *granum*), and the exposed membranes in which stacking is absent are known as **stroma lamellae**.

Two separate membranes, each composed of a lipid bilayer and together known as the **envelope**, surround most types of chloroplasts (**Figure 9.14**). This double-membrane system contains a variety of metabolite transport systems. The chloroplast also contains its own DNA, RNA, and ribosomes. Some of the chloroplast proteins are products of transcription and translation within the chloroplast itself, whereas most of the others are encoded by nuclear DNA, synthesized on cytoplasmic ribosomes, and then imported into the chloroplast. This remarkable division of labor, extending in many cases to different subunits of the same enzyme complex, is discussed in more detail later in this chapter. For some dynamic structures of chloroplasts, see **WEB ESSAY 9.1**.

Thylakoids contain integral membrane proteins

A wide variety of proteins essential to photosynthesis are embedded in the thylakoid membranes. In many cases, portions of these proteins extend into the aqueous regions on both sides of the thylakoids. These **integral membrane proteins** contain a large proportion of hydrophobic amino acids and are therefore much more stable in a nonaqueous medium such as the hydrocarbon portion of the membrane (see Figure 1.13).

The reaction centers, the antenna pigment–protein complexes, and most of the electron carrier proteins are all integral membrane proteins. In all known cases, integral membrane proteins of the chloroplast have a unique orientation within the membrane. Thylakoid membrane proteins have one region pointing toward the stromal side of the membrane and the other oriented toward the interior space of the thylakoid, known as the *lumen* (see Figure 9.14).

The chlorophylls and carotenoids in the thylakoid membrane are associated in a noncovalent, but highly specific, way with proteins, thereby forming pigment–protein complexes that are structurally organized to optimize energy transfer to, and subsequent electron transfer by, the reaction centers.

Photosystems I and II are spatially separated in the thylakoid membrane

The PSII reaction center, along with its antenna chlorophylls and associated electron transport proteins, is located predominantly in the grana lamellae (**Figure 9.15A**). The PSI reaction center and its associated antenna pigments and electron transfer proteins, as well as the ATP synthase enzyme that catalyzes the formation of ATP, are found almost exclusively in the stroma lamellae and at the edges of the grana lamellae. The cytochrome b_6f complex of the electron transport chain that connects the two photosystems is distributed between stroma and grana lamellae. The structures of all these complexes are shown in **Figure 9.15B**.

The two photochemical events that take place in O_2-evolving photosynthesis are spatially separated. This separation requires that mobile carriers move electrons between the two photosystems, from the grana region to the stroma region of the thylakoids. These diffusible carriers are the redox cofactor plastoquinone (PQ) and the blue-colored copper protein plastocyanin (PC), which carry electrons from PSII to the cytochrome b_6f complex, and from the cytochrome b_6f complex to PSI,

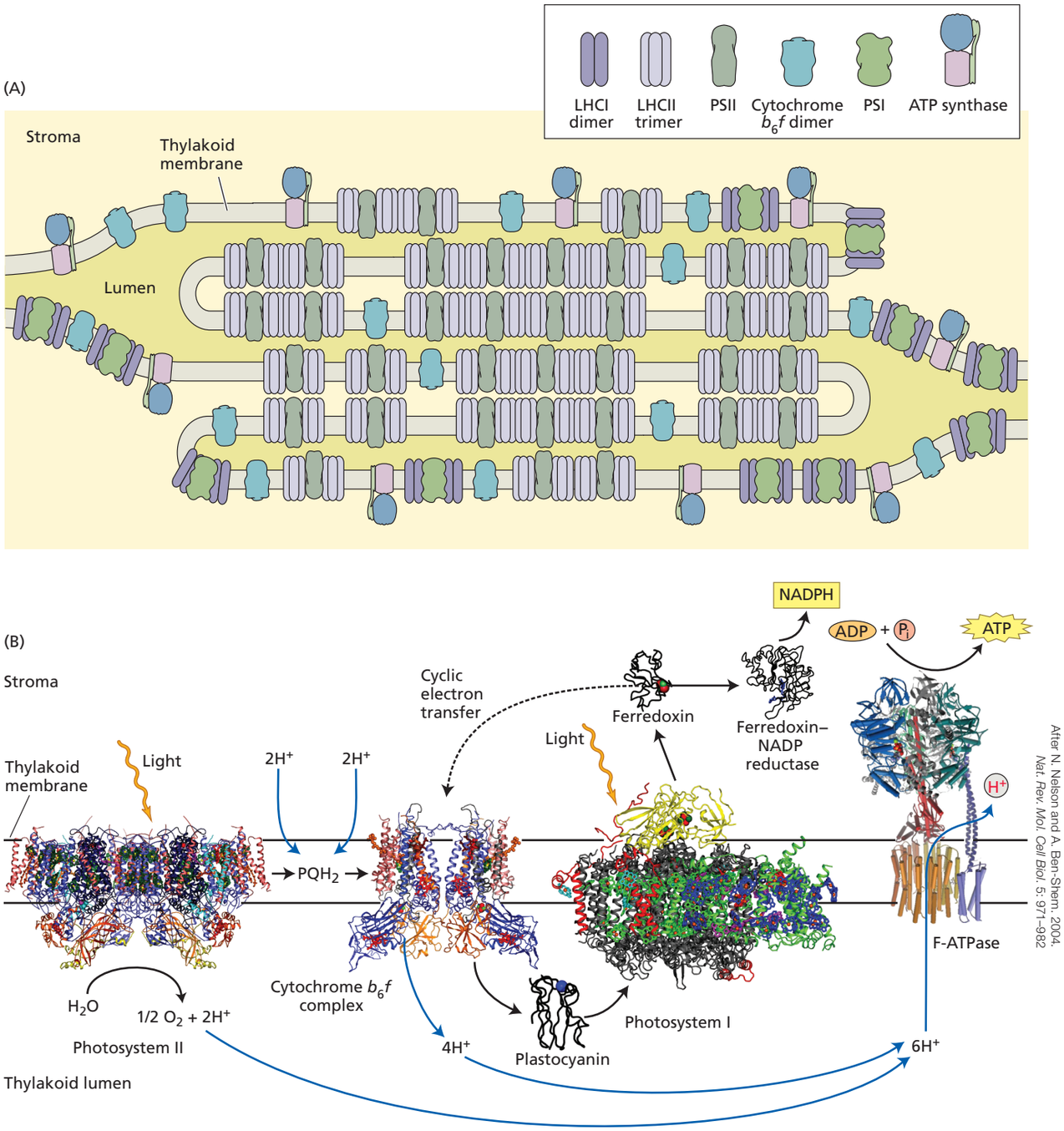


Figure 9.15 Organization and structure of the four major protein complexes of the thylakoid membrane. (A) PSII is located predominantly in the stacked regions of the thylakoid membrane; PSI and ATP synthase are found in the unstacked regions protruding into the stroma. Cytochrome b_6f complexes are evenly distributed. This lateral separation of the two photosystems requires that electrons and protons produced by PSII be transported a considerable distance before they can be acted on by PSI and ATP synthase. (B) Structures of the four main protein complexes of the thylakoid membrane. Shown also are the two diffusible electron carriers—plastocyanin, which is located in the thylakoid lumen, and plastohydroquinone (PQH_2) in the membrane. The lumen has a positive electrical charge with respect to the stroma. The proton pumping stoichiometry shown is for two photons for each reaction center, meaning 6 H^+ per 2e^-. For a description of the mechanism of PQH_2 turnover in electron and proton transfer, see Figure 9.25. (A after J. F. Allen and J. Forsberg. 2001. *Trends Plant Sci.* 6: 317–326.)

respectively, as we discuss in more detail later in Section 9.6. In addition, water oxidation by PSII releases protons into the lumen of the grana (see Section 9.6), which must diffuse to the stroma lamellae to reach the ATP synthase, where they are used to drive the synthesis of ATP. The functional significance of this large separation (many tens of nanometers) between PSI and PSII is not entirely clear but is thought to allow the two photosystems to self-organize and thus improve the efficiency of energy distribution between the two photosystems.

There are more PQ and PC molecules than photocenters in the thylakoids, and these "pools" of electron carriers can interact with multiple PSI or PSII complexes. This allows the photosystems to act cooperatively without requiring a strict one-to-one stoichiometry between the two photosystems or their excitation by light. Instead, PSII reaction centers feed reducing equivalents into a common intermediate pool of lipid-soluble electron carriers (plastoquinone). The PSI reaction centers remove the reducing equivalents from the common pool, rather than from any specific PSII reaction center complex. In some species, including many vascular plants, there is relatively more PSII than PSI in the thylakoids, but in cyanobacteria there is often a higher proportion of PSI. The reasons for these different stoichiometries are not entirely understood, but they are thought to help prevent the buildup of reactive intermediates and balance the relative needs for ATP and NADPH by controlling the relative rates of linear and cyclic electron flow (see Section 9.7).

Anoxygenic photosynthetic bacteria have a single reaction center

Non-O_2-evolving (anoxygenic) organisms contain only a single photosystem similar to either photosystem I or II. These simpler organisms have been very useful for detailed structural and functional studies that have contributed to a better understanding of oxygenic photosynthesis. In most cases these anoxygenic photosystems carry out cyclic electron transfer with no net reduction or oxidation. Part of the energy of the photon is conserved as a proton motive force (see Section 9.7) and is used to make ATP.

Reaction centers from purple photosynthetic bacteria were the first integral membrane proteins to have structures determined to high resolution (see **WEB TOPIC 9.5**). Detailed analysis of these structures, along with the characterization of numerous mutants, has revealed many of the principles involved in the energy storage processes carried out by all reaction centers.

The structure of the purple bacterial reaction center is similar in many ways to that of PSII from oxygen-evolving organisms, especially in the electron acceptor portion of the chain. The proteins that make up the core of the bacterial reaction center are relatively similar in sequence to their PSII counterparts, implying an evolutionary relatedness. A similar situation is found with respect to the reaction centers of the anoxygenic green sulfur bacteria and the heliobacteria, compared with PSI. The evolutionary implications of this pattern are discussed in Section 9.9.

9.5 Organization of Light-Absorbing Antenna Systems

The antenna systems of different classes of photosynthetic organisms are remarkably varied, in contrast to the reaction centers, which appear to be similar even in distantly related organisms. The variety of antenna complexes reflects evolutionary adaptation to the diverse environments in which different organisms live, as well as the need in some organisms to balance energy input to the two photosystems. In this section we learn how energy transfer processes absorb light and deliver energy to the reaction center.

Antenna systems contain chlorophyll and are membrane-associated

Antenna systems function to deliver energy efficiently to the reaction centers with which they are associated. The size of the antenna system varies considerably in different organisms, ranging from a low of 20 to 30 bacteriochlorophylls per reaction center in some photosynthetic bacteria, to generally 200 to 300 chlorophylls per reaction center in vascular plants, to a few thousand pigments per reaction center in some types of algae and bacteria. The molecular structures of antenna pigments are also quite diverse, although all of them are associated in some way with the photosynthetic membrane. In almost all cases, the antenna pigments are associated with proteins to form pigment–protein complexes.

The physical mechanism by which excitation energy is conveyed from the chlorophyll that absorbs the light to the reaction center occurs predominantly through **fluorescence resonance energy transfer**, often abbreviated as FRET. By this mechanism the excitation energy is transferred from one molecule to another by a nonradiative process.

A useful analogy for resonance transfer is the transfer of energy between two tuning forks. If one tuning fork is struck and properly placed near another, the second tuning fork receives some energy from the first and begins to vibrate. The efficiency of energy transfer between the two tuning forks depends on their distance from each other and their relative orientation, as well as on their vibrational frequencies, or pitches. Similar parameters affect the efficiency of energy transfer in antenna complexes, with energy substituted for pitch.

Energy transfer in antenna complexes is usually very efficient: Approximately 95 to 99% of the photons absorbed by the antenna pigments have their energy

transferred to the reaction center, where it can be used for photochemistry. There is an important difference between energy transfer among pigments in the antenna and the electron transfer that occurs in the reaction center: Whereas energy transfer is a purely physical phenomenon, electron transfer involves chemical (redox) reactions.

The antenna funnels energy to the reaction center

The sequence of pigments within the antenna that funnel absorbed energy toward the reaction center has absorption maxima that are progressively shifted toward longer red wavelengths (**Figure 9.16**). This red shift in absorption maximum means that the energy of the excited state is somewhat lower nearer the reaction center than in the more peripheral portions of the antenna system. This loss of energy helps drive flow of the remaining energy toward the reaction centers, where it can initiate the photochemical light reactions.

As a result of this arrangement, when excitation is transferred, for example, from a chlorophyll *b* molecule absorbing maximally at 650 nm to a chlorophyll *a* molecule absorbing maximally at 670 nm, the difference in energy between these two excited chlorophylls is lost to the environment as heat.

For the excitation to be transferred back to the chlorophyll *b*, the energy lost as heat would have to be resupplied. The probability of reverse transfer is therefore smaller simply because thermal energy is not sufficient to make up the deficit between the lower-energy and higher-energy pigments. This effect gives the energy-trapping process a degree of directionality or irreversibility and makes the delivery of excitation to the reaction center more efficient. In essence, the system sacrifices some energy from each quantum so that nearly all of the quanta can be trapped by the reaction center.

Many antenna pigment–protein complexes have a common structural motif

In all eukaryotic photosynthetic organisms that contain both chlorophyll *a* and chlorophyll *b*, the most abundant antenna proteins are members of a large family of structurally related proteins. Some of these proteins are associated primarily with PSII and are called **light-harvesting complex II** (**LHCII**) proteins; others are associated with PSI and are called **light-harvesting complex I** (**LHCI**) proteins. These antenna complexes are also known as **chlorophyll a/b antenna proteins**.

The structure of one of the LHCII proteins has been determined (**Figure 9.17**). The protein contains three α-helical regions and binds 14 chlorophyll *a* and *b* molecules, as well as four carotenoids. The structure of the LHCI proteins is generally similar to that of the LHCII proteins. All of these proteins have significant sequence similarity and are almost certainly descendants of a common ancestral protein.

Light absorbed by carotenoids or chlorophyll *b* in the LHC proteins is rapidly transferred to chlorophyll *a* and then to other chlorophyll-containing antenna pigments

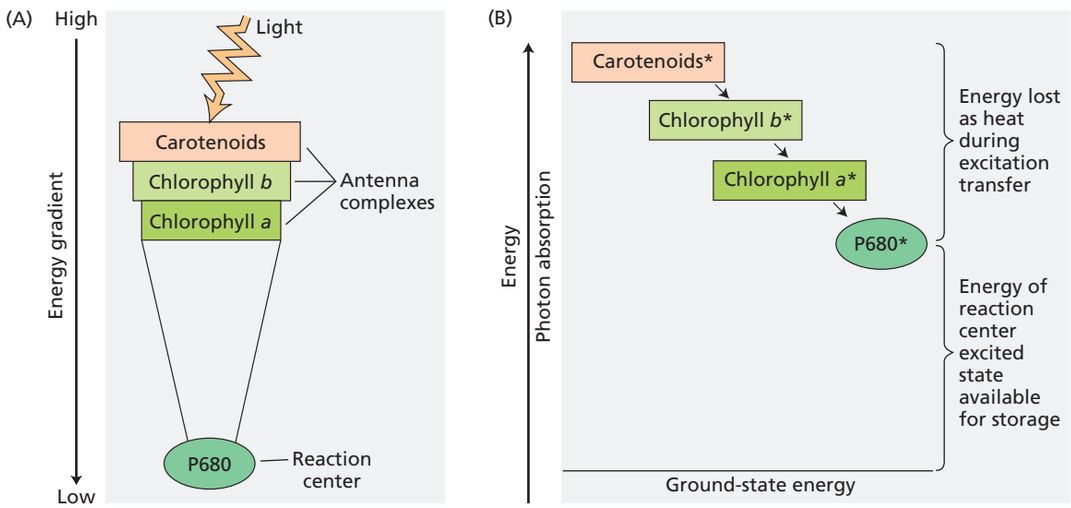


Figure 9.16 Funneling of excitation from the antenna system toward the reaction center. (A) The excited-state energy of pigments increases with distance from the reaction center; that is, pigments closer to the reaction center are lower in energy than those farther from the reaction center. This energy gradient ensures that excitation transfer toward the reaction center is energetically favorable and that excitation transfer back out to the peripheral portions of the antenna is energetically unfavorable. (B) Some energy is lost as heat to the environment by this process, but under optimal conditions almost all the excitation energy absorbed in the antenna complexes can be delivered to the reaction center. The asterisks denote excited states.

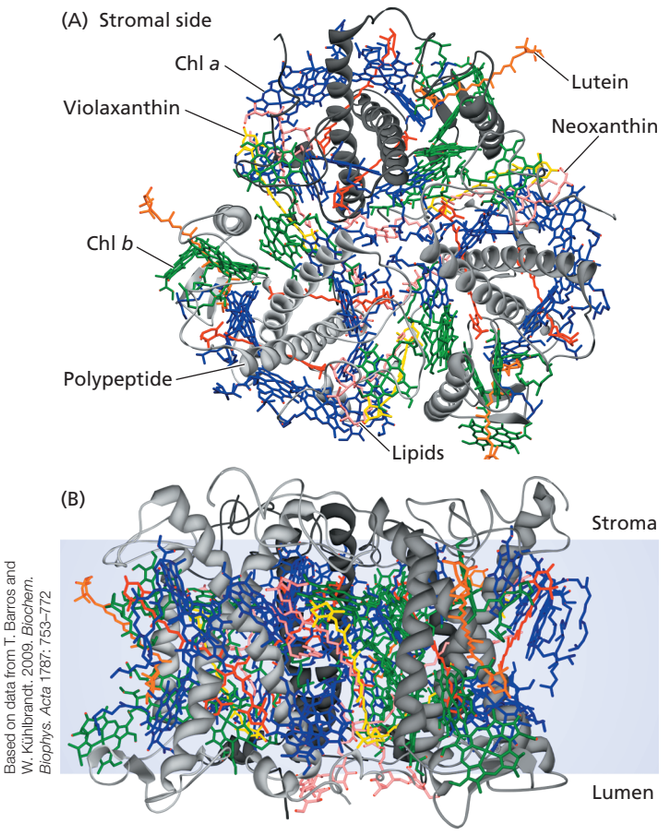


Figure 9.17 Structure of the trimeric LHCII antenna complex from vascular plants. The antenna complex is a transmembrane pigment protein; each monomer contains three helical regions that cross the nonpolar part of the membrane. The trimeric complex is shown from the stromal side (A) and from within the membrane (B). Gray, polypeptide; dark blue, Chl *a*; green, Chl *b*; dark orange, lutein; light orange, neoxanthin; yellow, violaxanthin; pink, lipids.

that are intimately associated with the reaction center. The LHCII complex is also involved in regulatory processes, which we discuss in Section 9.8.

9.6 Mechanisms of Electron Transport

Some of the evidence that led to the idea of two photochemical reactions operating in series was discussed earlier in this chapter. In this section we consider in more detail the chemical reactions involved in electron transfer during photosynthesis. We discuss the excitation of chlorophyll by light and the reduction of the first electron acceptor, the flow of electrons through photosystems II and I, the oxidation of water as the primary source of electrons, and the reduction of the final electron acceptor ($NADP^+$). The chemiosmotic mechanism that mediates ATP synthesis is discussed in detail in Section 9.7.

Electrons from chlorophyll travel through the carriers organized in the Z scheme

Figure 9.18 shows a simplified version of the Z scheme, in which all the electron carriers known to function in electron flow from H_2O to $NADP^+$ are arranged vertically at their midpoint redox potentials, which can be used to estimate the energy stored in those states compared with the unexcited (or ground) state (see **WEB TOPIC 9.6** for further detail). Components known to react with each other are connected by arrows, so the Z scheme is really a synthesis of both kinetic and thermodynamic information. The large vertical arrows represent the input of light energy into the system. Note that this "energy diagram" view of the Z scheme does not represent changes in the positions of the various states or imply that they physically move in these directions. A spatial representation of these reactions is shown in **Figure 9.19**, as well as in a more detailed molecular view in Figure 9.15.

Photons excite the specialized chlorophyll of the reaction centers (P680 for PSII; P700 for PSI), and an electron is ejected. The electron then passes through a series of electron carriers and eventually reduces P700 (for electrons from PSII) or $NADP^+$ (for electrons from PSI). Much of the following discussion describes the movements of these electrons, and how these result in the storage of energy in the final products.

Almost all the chemical processes that make up the light reactions of photosynthesis are carried out by four major protein complexes: PSII, the cytochrome b_6f complex, PSI, and ATP synthase. These four integral membrane complexes are vectorially oriented in the thylakoid membrane to function as follows (see Figures 9.15 and 9.19):

- PSII oxidizes water to O_2 in the thylakoid lumen and in the process releases protons into the lumen. The reduced product of photosystem II is plastohydroquinone (PQH_2). The overall reaction results in transfer of electrons from the lumen to the stromal side of the thylakoid membrane, as well as the release of protons into the stroma (from water oxidation) and uptake of protons from the stroma (by PQ reduction to PQH_2).
- Cytochrome b_6f oxidizes PQH_2 molecules that were reduced by PSII and delivers electrons to PSI via the soluble copper protein plastocyanin. The oxidation is a complex process, called the *Q cycle*, that involves a series of electron and proton transfer reactions that not only provide electrons to PSI but also contribute to the thylakoid proton motive force (see Figure 9.25). The oxidation involves the removal of two protons and two electrons from PQH_2, forming PQ. It occurs at the PQH_2 oxidation site, called Q_o, which faces the thylakoid lumen, so that the two protons are released into the lumen. One of the electrons from PQH_2 is

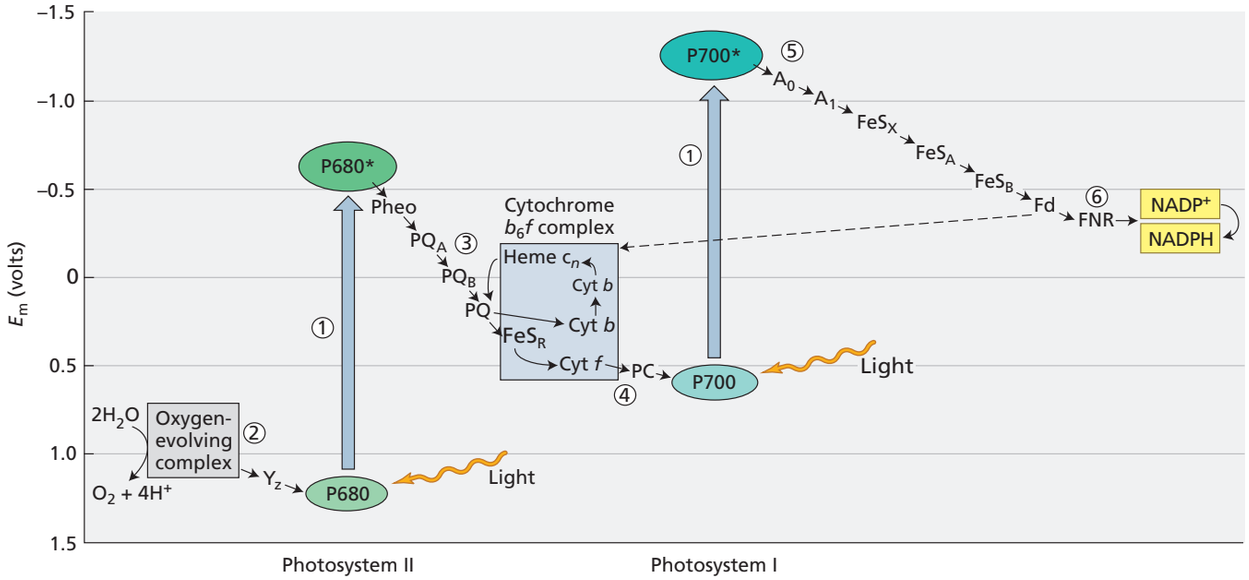


Figure 9.18 Detailed Z scheme for O_2-evolving photosynthetic organisms. The redox carriers are placed at their midpoint redox potentials (at pH 7). ① The vertical arrows represent photon absorption by the reaction center chlorophylls: P680 for photosystem II (PSII) and P700 for photosystem I (PSI). The excited PSII reaction center chlorophyll, P680*, transfers an electron to pheophytin (Pheo). ② On the oxidizing side of PSII (to the left of the arrow joining P680 with P680*), P680 oxidized by light is re-reduced by Y_z (not shown) which has received electrons from oxidation of water. ③ On the reducing side of PSII (to the right of the arrow joining P680 with P680*), pheophytin transfers electrons to the acceptors PQ_A and PQ_B, which are plastoquinones. ④ The cytochrome b_6f complex transfers electrons to plastocyanin (PC), a soluble protein, which in turn reduces $P700^+$ (oxidized P700). ⑤ The acceptor of electrons from P700* (A_0) is thought to be a chlorophyll, and the next acceptor (A_1) is a quinone. A series of membrane-bound iron–sulfur proteins (FeS_X, FeS_A, and FeS_B) transfers electrons to soluble ferredoxin (Fd). ⑥ The soluble flavoprotein ferredoxin–$NADP^+$ reductase (FNR) reduces $NADP^+$ to NADPH, which is used in the Calvin–Benson cycle to reduce CO_2 (see Chapter 10). The dashed line indicates cyclic electron flow around PSI. (After R. E. Blankenship and R. C. Prince. 1985. *Trends Biochem. Sci.* 10: 382–383.)

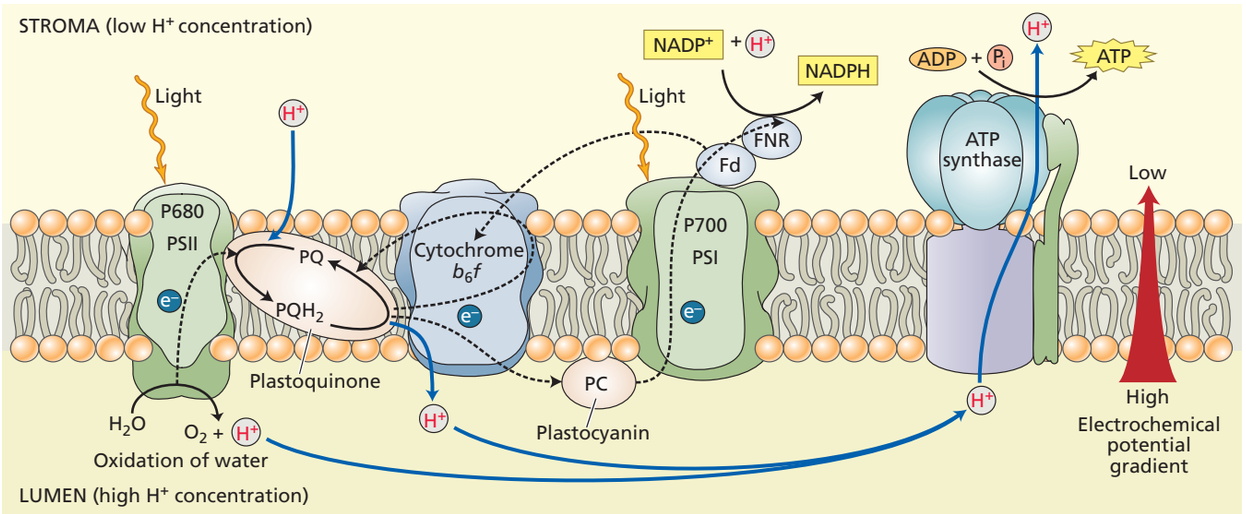


Figure 9.19 Transfer of electrons and protons in the thylakoid membrane is carried out vectorially by four protein complexes (see Figure 9.15B for structures). Water is oxidized and protons are released in the lumen by PSII. PSI reduces $NADP^+$ to NADPH in the stroma, via the action of ferredoxin (Fd) and the flavoprotein ferredoxin–$NADP^+$ reductase (FNR). Protons are also transported into the lumen by the action of the cytochrome b_6f complex and contribute to the electrochemical proton gradient. These protons must then diffuse to the ATP synthase enzyme, where their diffusion down the electrochemical potential gradient is used to synthesize ATP in the stroma. Reduced plastoquinone (PQH_2) and plastocyanin transfer electrons to cytochrome b_6f and to PSI, respectively. The dashed lines represent electron transfer; solid blue lines represent proton movement.

transferred to cytochrome *f*, then to plastocyanin, and finally to PSI. The other electron from PQH_2 is transferred through a chain of hemes, across the thylakoid membrane from the lumen to the stromal side of the thylakoid membrane. This electron transfer results in the reduction of another molecule of PQ taking up protons from the stroma, as well as the generation of an electric field across the thylakoid membrane (lumen side positive).

- PSI reduces $NADP^+$ to NADPH in the stroma by the action of ferredoxin (Fd) and the flavoprotein ferredoxin–$NADP^+$ reductase (FNR). The overall reaction results in the transfer of electrons from the lumen to the stromal side of the thylakoid membrane.
- ATP synthase synthesizes ATP from ADP and inorganic phosphate (P_i) as protons diffuse back through it from the lumen into the stroma. The overall reaction results in the transfer of protons from the lumen to the stromal side of the thylakoid membrane.

Energy is captured when an excited chlorophyll reduces an electron acceptor molecule

As discussed in Section 9.5, the function of light is to excite a specialized chlorophyll in the reaction center, either by direct absorption or, more frequently, via energy transfer from an antenna pigment. This excitation process can be envisioned as the promotion of an electron from the highest-energy filled orbital of the chlorophyll to the lowest-energy unfilled orbital (**Figure 9.20**). The higher orbital has higher free energy, with the electron only loosely bound to the chlorophyll and easily lost if a molecule that can accept the electron is nearby.

This process can occur because of a critical property of the excited-state chlorophyll that allows it to act as a strong electron donor (reductant) and a strong electron acceptor (oxidant). As illustrated in Figure 9.20, the ground-state chlorophyll has a pair of electrons in one of its orbitals (designated by the up and down arrows). The fact that the orbital is occupied by two electrons of different spins makes the state quite stable so that it does not easily lose or gain electrons.

Exciting this chlorophyll promotes one of the two electrons to a higher orbital; in this state, the two orbitals are only partially filled and are therefore unstable. If this excited chlorophyll cannot react with other molecules, it will re-form the ground state and lose the extra energy as either fluorescence (light) or heat. However, if the excited chlorophyll can interact with nearby molecules, it can perform secondary photochemistry because the two partially filled orbitals are reactive. One of these orbitals can readily give up an electron, making it a strong reductant, while the other can readily

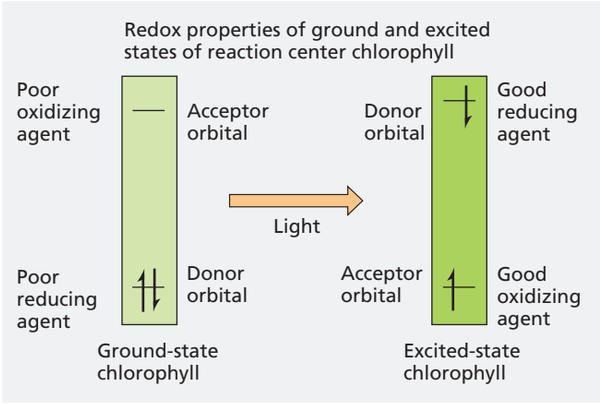


Figure 9.20 Orbital occupation diagram for the ground and excited states of reaction center chlorophyll. In the ground state the molecule is a poor reducing agent (loses electrons from a low-energy orbital) and a poor oxidizing agent (accepts electrons only into a high-energy orbital). In the excited state the situation is markedly different, and an electron can be lost from the high-energy orbital, making the molecule an extremely powerful reducing agent. This is the reason for the extremely negative excited-state redox potential shown by P680* and P700* in Figure 9.18. The excited state can also act as a strong oxidant by accepting an electron into the lower-energy orbital, although this pathway is not significant in reaction centers. (After R. E. Blankenship and R. C. Prince. 1985. *Trends Biochem. Sci.* 10: 382–383.)

accept an electron, making it a strong oxidant, as illustrated in Figure 9.20.

In the reaction centers, the first photochemical reaction involves the transfer of an excited electron on the chlorophyll to an acceptor molecule, forming a **charge-separated state** in which the reduced electron acceptor has a negative charge and the chlorophyll has a positive charge. (Note that the overall charge of the reaction center remains the same; that is, electrons are not "produced" by the light but rather are rearranged or moved from one state or molecule to others.) The PSI and PSII reaction centers have different specific reactions, as we discuss later in this section, but they all involve a similar series of electron transfer processes.

As we mentioned in Section 9.2, the excited state of chlorophyll decays in a few nanoseconds, losing its energy as heat or fluorescence. To compete with this unproductive decay, the initial steps of photosynthesis must be extremely rapid. In other words, the "forward" rates that lead to the products of photosynthesis must be much faster than unproductive decay. Indeed, the formation of the initial charge-separated state in PSI and PSII is about 1000 times faster than the decay of the excited state, and occurs in a few picoseconds (1 picosecond = 10^{-12} s). Such extremely rapid electron transfer reactions require that the donor and acceptor molecules be packed together very closely and have energy levels that are optimized for rapid electron transfer. These requirements

are met by the specific structures of the reaction centers, as discussed shortly.

Going from the excited chlorophyll to the charge-separated state results in some loss of energy, but the first charge-separated state is still highly unstable. The electron can return to the reaction center chlorophyll and re-form the ground state, with the loss of all the stored energy. This wasteful *recombination* process, however, does not appear to occur to any substantial degree in functioning reaction centers. Instead, the acceptor transfers its extra electron to a secondary acceptor and so on down a chain of electron carriers. We refer to this chain as the acceptor-side electron carriers because they accept electrons from the excited reaction center chlorophyll. In parallel, the oxidized chlorophyll can extract an electron from nearby electron donors, which we refer to as donor-side carriers because they ultimately donate electrons to the reaction center chlorophyll cation. The donor-side reactions produce the fully reduced chlorophyll, thus preventing the return of electrons from the acceptor-side carriers.

Each of the electron transfer steps (on both the acceptor and donor sides) progressively stabilizes the charge-separated states of the reaction centers, preventing recombination. However, because energy is conserved, this stabilization results in a loss of energy, so that the more stable the state, the less energy it contains. This trade-off partly explains the differences in quantum yield and energy conversion efficiency discussed in Section 9.3. Because the subsequent charge-separated states are progressively more stable, the following forward reactions can also be slower. This is important because the biochemical reactions that are ultimately powered by the light reactions are much slower than the initial photochemistry, on a scale of milliseconds to seconds.

The reaction center chlorophylls of the two photosystems absorb at different wavelengths

As discussed earlier in the chapter, PSI and PSII have distinct absorption characteristics. For example, the reduced and oxidized states of the reaction center chlorophylls have distinct absorption spectra that can be probed using a spectrophotometer that measures the amount of light of different wavelengths absorbed by a sample (see Figure 9.5). In the oxidized state, chlorophylls lose their characteristic strong light absorbance in the red region of the spectrum; they become **bleached**. It is therefore possible to monitor the redox state of these chlorophylls by time-resolved optical absorbance measurements in which this bleaching is monitored directly (see **WEB TOPIC 9.1**).

Using such techniques, it was found that the reaction center chlorophyll of PSI absorbs maximally at 700 nm in its reduced (ground) state. Accordingly, this chlorophyll is named **P700** (the P stands for *pigment*). The analogous optical transient of PSII is at 680 nm, so its reaction center chlorophyll is known as **P680**. The reaction center bacteriochlorophyll from purple photosynthetic bacteria was similarly identified as **P870**.

The X-ray structure of the bacterial reaction center (see **WEB TOPIC 9.5**) clearly indicates that P870 is a closely coupled pair, or dimer, of bacteriochlorophylls rather than a single molecule. The primary donors of PSI (P700) and PSII (P680) are also composed of chlorophyll *a* molecules, though they may not act as functional dimers. In the oxidized state, reaction center chlorophylls contain an unpaired electron.

The PSII reaction center is a multi-subunit pigment–protein complex

PSII is contained in a multi-subunit protein supercomplex (**Figure 9.21**). In vascular plants, the multi-subunit protein supercomplex has two complete reaction centers and some antenna complexes. The core of the reaction center consists of two membrane proteins known as D1 and D2, as well as other proteins, as shown in **Figure 9.22** and **WEB TOPIC 9.8**.

The primary donor chlorophyll, additional chlorophylls, carotenoids, pheophytins, and plastoquinones (two electron acceptors described later in this section) are bound to the membrane proteins D1 and D2. These proteins have some sequence similarity to the L and M peptides of purple bacteria. Other proteins serve as antenna complexes or are involved in oxygen evolution. Some, such as cytochrome b_{559}, have no known function but may be involved in a protective cycle around PSII.

Water is oxidized to oxygen by PSII

Water is oxidized according to the following chemical reaction:

$$2\,H_2O \rightarrow O_2 + 4\,H^+ + 4\,e^- \qquad (9.8)$$

This equation indicates that four electrons are removed from two water molecules, generating an oxygen molecule and four hydrogen ions (protons). (For more on oxidation–reduction reactions, see **WEB APPENDIX 1** and **WEB TOPIC 9.6**.)

Water is a very stable molecule. Oxidation of water to form molecular oxygen requires the formation of an extremely strong oxidant. The photosynthetic **oxygen-evolving complex** (**OEC**) is the only known biochemical system that carries out this reaction, and it is the source of almost all the oxygen in Earth's atmosphere.

Many studies have provided a substantial amount of information about oxygen evolution (see **WEB TOPIC 9.7**). High-resolution crystal structures and a wide range of biophysical measurements show that the OEC

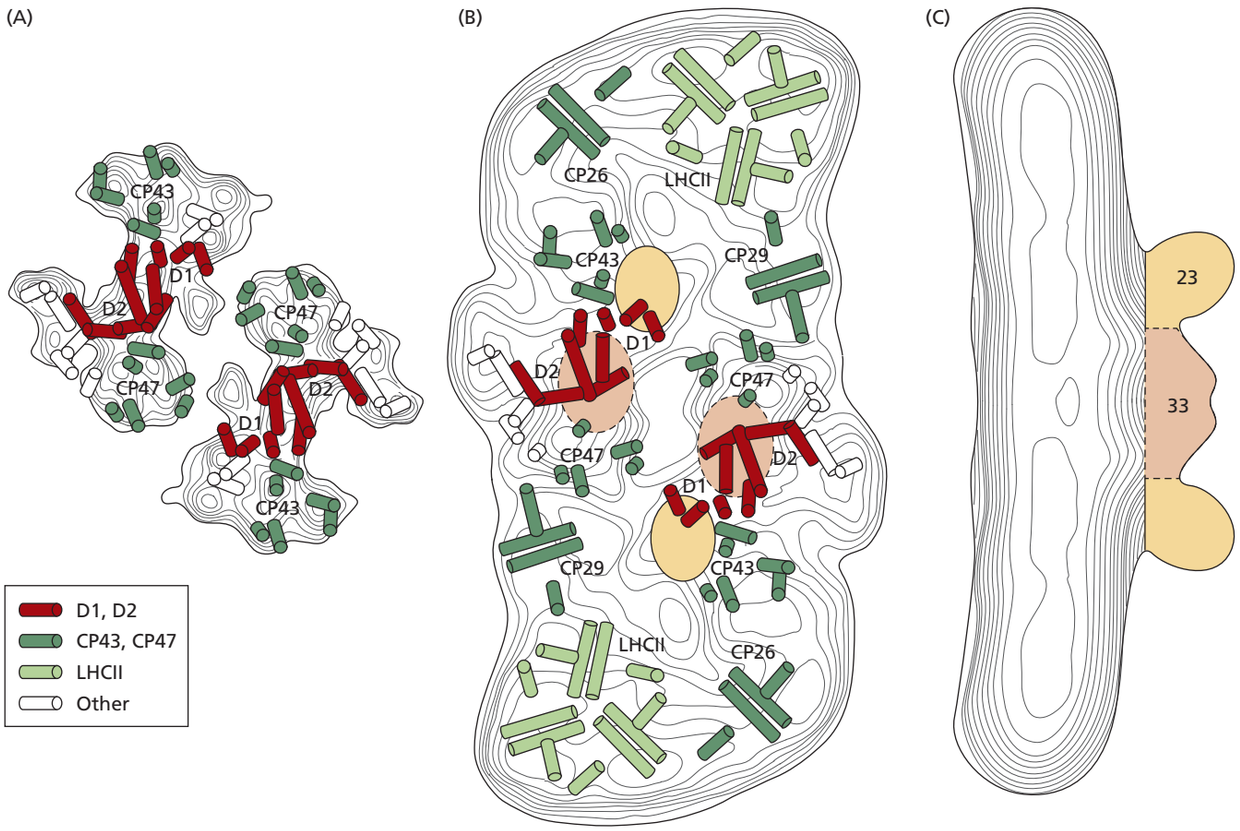


Figure 9.21 Structure of the dimeric multi-subunit protein supercomplex of PSII from vascular plants, as determined by electron microscopy. The figure shows two complete reaction centers, each of which is a dimeric complex. The cylinders represent helical portions of the proteins. **(A)** Arrangement of the D1 and D2 (red) and CP43 and CP47 (green) core subunits. Other helices are shown in white. **(B)** View from the lumenal side of the supercomplex, including additional antenna complexes, LHCII, CP26, and CP29, and an extrinsic oxygen-evolving complex, shown as orange and yellow ovals with solid and dashed outlines. **(C)** Side view of the complex, illustrating the arrangement of the extrinsic proteins of the oxygen-evolving complex. (After J. Barber et al. 1999. *Trends Biochem. Sci.* 24: 43–45.)

contains a catalytic cluster with four manganese (Mn) ions as well as Cl^- and Ca^{2+} ions (see **WEB TOPIC 9.7**). The D1 protein of PSII contains a special tyrosine residue, called Y_z, that acts as the primary electron donor to the excited chlorophyll P680 (see Figure 9.18), forming a free radical oxidized tyrosine residue that, in turn, extracts electrons from the OEC. Each successive excitation of PSII results in an additional oxidation of the OEC, generating a progressive series of oxidation states—known as the *S states* and labeled S_0, S_1, S_2, S_3, and S_4 (see **WEB TOPIC 9.7**).

When four oxidizing equivalents have accumulated in the OEC, it extracts four electrons from two H_2O molecules to generate O_2. The oxidation of water also releases four protons into the lumen of the thylakoid (see Figure 9.19), and these protons are ultimately transferred from the lumen to the stroma by translocation through the ATP synthase (see Section 9.7).

Pheophytin and two quinones accept electrons from PSII

Pheophytin, a chlorophyll in which the central magnesium ion has been replaced by two hydrogen ions, acts as an early acceptor in PSII. The structural change gives pheophytin chemical and spectral properties that are slightly different from those of Mg-containing chlorophylls. Pheophytin passes electrons to a complex of two plastoquinones in close proximity to an iron ion. These processes are very similar to those found in the reaction center of purple bacteria (for details, see Figure 9.5.B in **WEB TOPIC 9.5**).

The two plastoquinones, PQ_A and PQ_B, are bound to the reaction center and receive electrons from pheophytin in a sequential fashion. PQ_A can accept only one electron at a time, so it acts as a relay, transferring electrons from pheophytin to PQ_B. The function of PQ_B is more complex. After one excitation of PSII, PQ_B

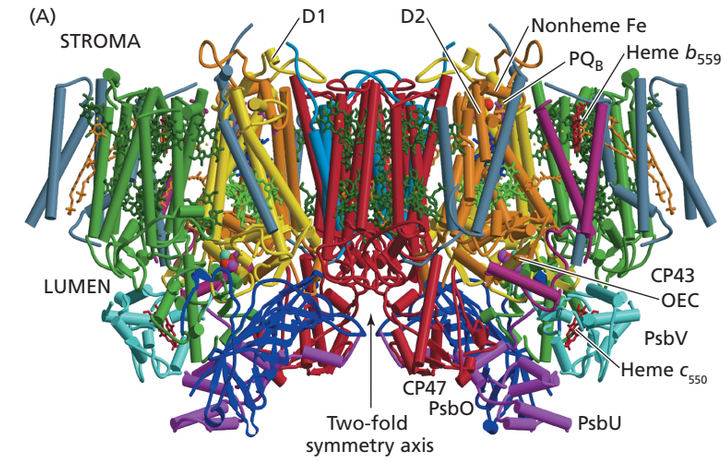
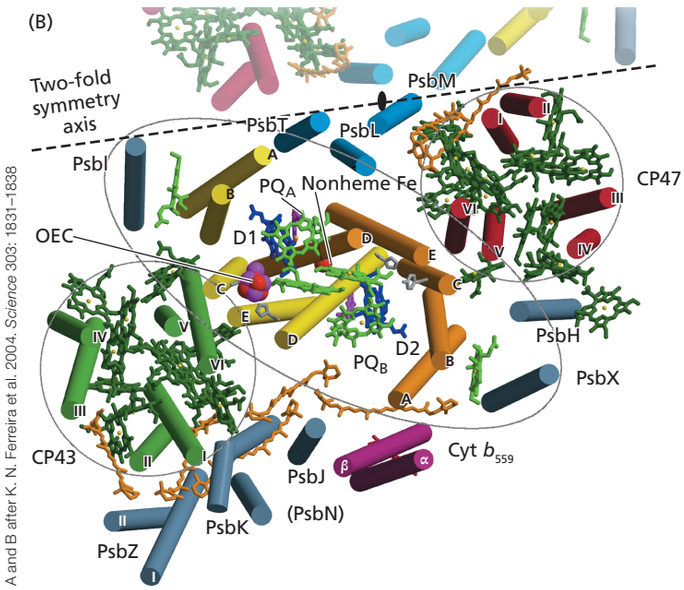
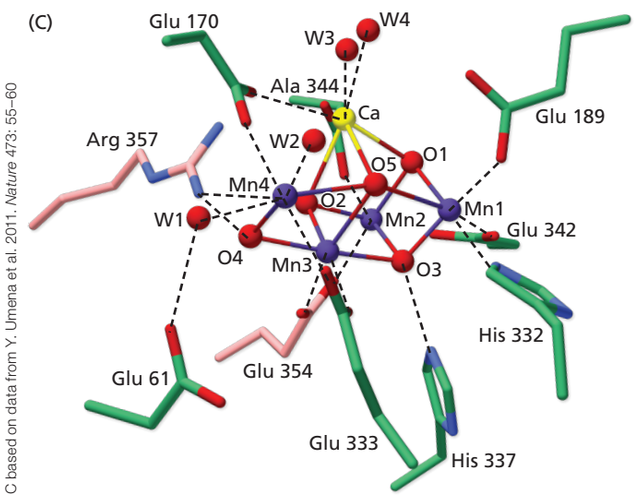


Figure 9.22 Structure of the PSII reaction center from the cyanobacterium *Thermosynechococcus elongatus*, resolved at 3.5 Å (0.35 nm). The structure includes the D1 (yellow) and D2 (orange) core reaction center proteins, the CP43 (green) and CP47 (red) antenna proteins, cytochromes b_{559} and c_{550}, the extrinsic 33-kDa oxygen evolution protein PsbO (dark blue), and the pigments and other cofactors. **(A)** Side view parallel to the membrane plane. **(B)** View from the lumenal surface, perpendicular to the plane of the membrane. CP43, CP47 and D1/D2 are encircled separately. **(C)** Detail of the Mn-containing water-splitting complex. W1 through W4 indicate the positions of bound water molecules. O1 through O5 indicate bridging oxygen atoms in the Mn cluster. Ca indicates the position of a bound Ca^{2+}.



A and B after K. N. Ferreira et al. 2004. *Science* 303: 1831–1838



C based on data from Y. Umena et al. 2011. *Nature* 473: 55–60

can accept one electron, forming a stable, tightly bound free radical intermediate (plastosemiquinone) (**Figure 9.23**). A second PSII excitation results in the uptake of two protons from the stromal side of the thylakoid and the formation of the fully reduced, protonated **plastohydroquinone** (**PQH_2**). The PQH_2 then dissociates from the reaction center complex and enters the hydrophobic portion of the membrane, where it transfers its electrons to the cytochrome b_6f complex. The empty Q_B site on PSII can be repopulated with an oxidized PQ, re-forming PQ_B.

Unlike the large protein complexes of the thylakoid membrane, PQH_2 is a small, nonpolar molecule that diffuses readily in the nonpolar core of the membrane bilayer in both its fully oxidized (PQ) and fully reduced (PQH_2) forms. This allows the PQ/PQH_2 system to act as a transmembrane shuttle for electrons and protons.

Electron flow through the cytochrome b_6f complex also transports protons

The **cytochrome b_6f complex** is a large multisubunit protein with several prosthetic groups (**Figure 9.24**). The complex is a functional dimer and contains two *b*-type hemes and one *c*-type heme (**cytochrome *f***). In *c*-type cytochromes the heme is covalently attached to the protein; in *b*-type cytochromes the chemically similar protoheme group is not covalently attached (see **WEB TOPIC 9.8**). In addition, the complex contains a **Rieske iron–sulfur protein** (named for the scientist who discovered it), in which two iron ions are bridged by two sulfide ions. The functional roles of most of these cofactors are similar to those of the mitochondrial cytochrome bc_1 complex, which functions in oxidative phosphorylation (as described in Chapter 13). However, the cytochrome b_6f complex also

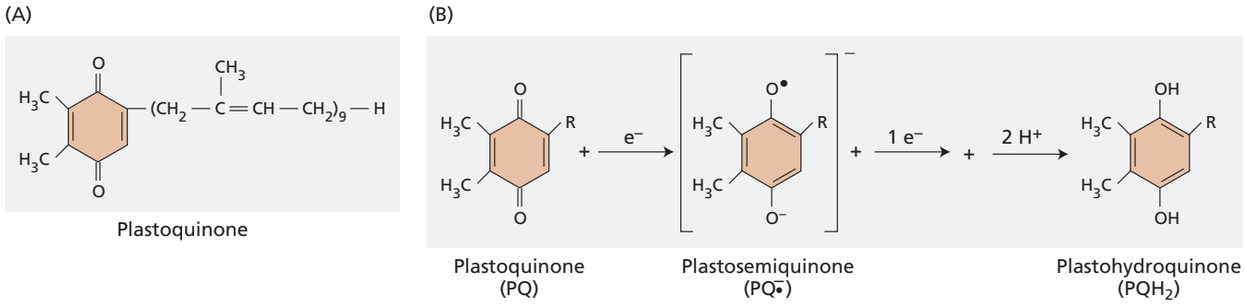


Figure 9.23 Structure and reactions of plastoquinones that operate in PSII. **(A)** The plastoquinone consists of a quinoid head and a long nonpolar tail that anchors it in the membrane. **(B)** Redox reactions of plastoquinone. The fully oxidized plastoquinone (PQ), anionic plastosemiquinone ($PQ^{\bullet}$), and reduced plastohydroquinone (PQH_2) forms are shown; R represents the side chain.

contains additional cofactors, including an additional heme group (called heme c_n), a chlorophyll, and a carotenoid, whose functions are yet to be fully resolved.

The cytochrome b_6f complex and the related cytochrome bc_1 complex in the mitochondrial electron transport chain operate through a mechanism known as the **Q cycle**, which was first proposed by Peter Mitchell in 1975 and later modified by many other researchers (**Figure 9.25**). In this mechanism, PQH_2, formed by light excitation of PSII (see previous subsection) or other processes (see next paragraph), binds to a site called Q_o that faces the lumenal side of the thylakoid. One of the electrons on PQH_2 is transferred to the Rieske iron–sulfur center, then to cytochrome *f*, PC, and finally P700 of PSI. The extraction of one electron from the PQH_2 bound at Q_o results in the formation of plastosemiquinone, which is highly reactive and delivers an electron to the nearby *b*-type heme. This electron is then transferred across the thylakoid, via the *b* and c_n hemes, to a second binding site called Q_i. Note that the reduction of the *b*-type hemes appears in Figure 9.25 to be uphill in terms of free energy, but is driven forward by subsequent reactions. The overall reaction has a negative free energy.

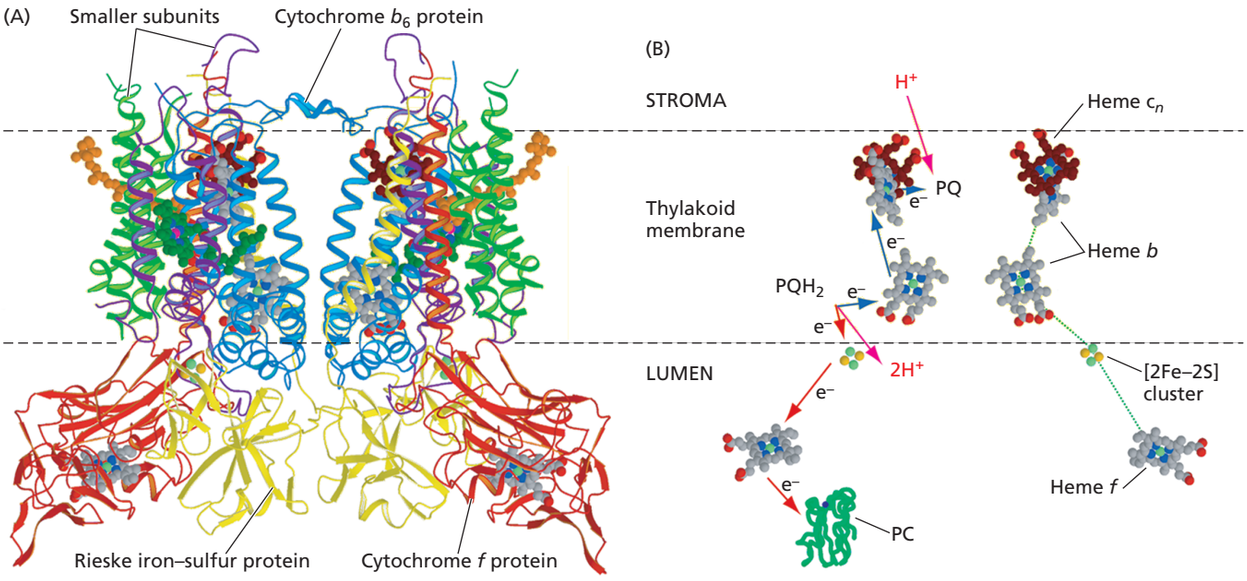


Figure 9.24 Structure of the cytochrome b_6f complex from cyanobacteria. **(A)** Arrangement of the proteins and cofactors in the complex. Cytochrome b_6 protein is shown in blue, cytochrome *f* protein in red, Rieske iron–sulfur protein in yellow, and other, smaller subunits in green and purple. **(B)** Here the proteins are omitted to more clearly show the positions of the cofactors. The movements of electrons and protons associated with the first part of the Q cycle are shown on the left. [2 Fe–2S] cluster, part of the Rieske iron–sulfur protein; PC, plastocyanin; PQ, plastoquinone; PQH_2, plastohydroquinone. (After G. Kurisu et al. 2003. *Science* 302: 1009–1014.)

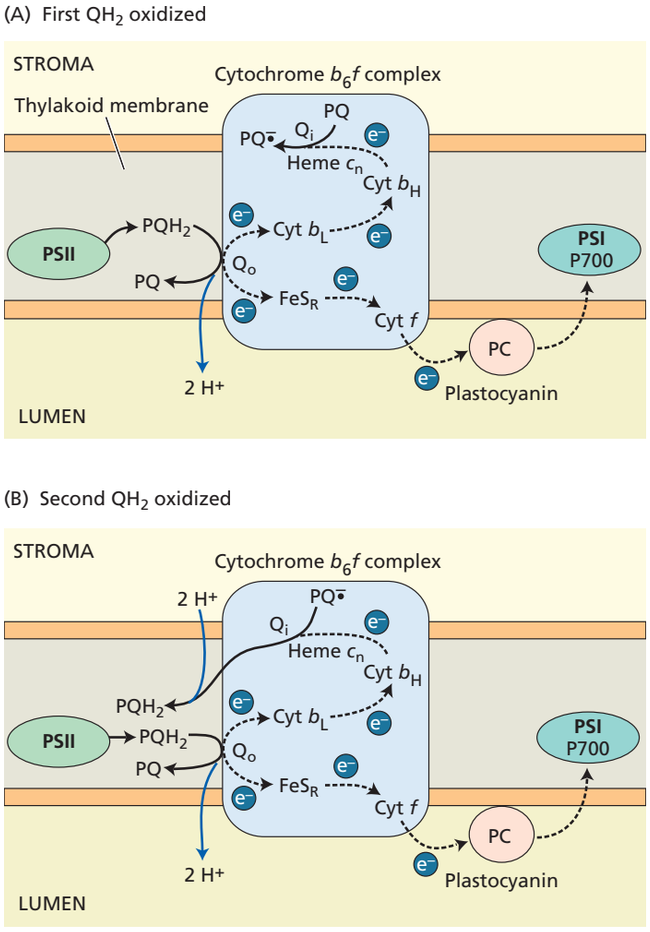


Figure 9.25 Mechanism of electron and proton transfer in the cytochrome b_6f complex. This complex contains two b-type cytochromes (Cyt *b*), a c-type cytochrome (Cyt c, historically called cytochrome *f*), a Rieske Fe–S protein (FeS_R), and two quinone oxidation–reduction sites. **(A)** Oxidation of the first PQH_2: A plastohydroquinone (PQH_2) molecule produced by the action of PSII (see Figure 9.23) binds to a site called Q_o near the lumenal side of the complex, and is oxidized in a special processes in which one of its two electrons is transferred to the FeS_R and the other to heme b_L (a low potential or strongly reducing b heme). Two protons from PQH_2 are released into the lumen during this process. The electron transferred to FeS_R is passed to cytochrome f (Cyt *f*) and then to plastocyanin (PC), which reduces oxidized P700 of PSI. The reduced b_L heme transfers an electron to the higher potential b_H heme. The oxidized PQH_2, called plastoquinone (PQ), is released from the Q_o site into the thylakoid membrane. **(B)** Oxidation of the second PQH_2 results in a cyclic processes: A second PQH_2 is oxidized at the Q_o site, with one electron going from FeS_R to PC and finally to P_{700}. The second electron goes through the two b-type hemes and cyt c_i heme. The two electrons accumulated on the hemes cooperate to reduce PQ to PQH_2, at the Q_i site, which is located near the stromal side of the membrane, taking up two protons from the stroma. The PQH_2 released from Q_i into the thylakoid membrane can be oxidized at the Q_o site. Overall, for each electron that is passed from PQH_2 at the Q_o site to PC, two protons are released into the lumen.

This process results in the transfer of one electron across the thylakoid membrane and the release of two protons into the lumen. A second turnover of the Q_o site introduces a second electron into the cytochrome *b* chain, allowing a PQ bound to the Q_i site to be reduced to PQH_2, with the uptake of protons from the stromal side of the thylakoid membrane. The resulting PQH_2 can then diffuse to Q_o, where it will be oxidized, delivering the protons to the lumen. Overall, the Q cycle results in two protons being deposited into the lumen for each electron that is transferred from PQH_2 to P700, increasing the number of protons available for ATP synthesis.

Plastocyanin carries electrons between the cytochrome b_6f complex and photosystem I

The location of the two photosystems at different sites on the thylakoid membranes (see Figure 9.15) requires that at least one component is capable of moving along or within the membrane in order to deliver electrons produced by PSII to PSI. The cytochrome b_6f complex is distributed equally between the grana and the stroma regions of the membranes, but its large size makes it unlikely that it is a mobile carrier of electrons between the photosystems.

As already described, plastoquinone acts as the mobile carrier of electrons from PSII to the cytochrome b_6f complex. Electrons are then transferred between the cytochrome b_6f complex and P700 by **plastocyanin** (**PC**), a small (10.5 kDa), water-soluble, copper-containing protein. This protein is found in the lumenal space (see Figure 9.25). In certain green algae and cyanobacteria, a *c*-type cytochrome is sometimes found instead of plastocyanin; which of these two proteins is synthesized in these organisms depends on the amount of copper available to the organism.

The PSI reaction center oxidizes PC and reduces ferredoxin, which transfers electrons to $NADP^+$

The PSI reaction center complex is a large multisubunit complex (**Figure 9.26**). In contrast to PSII, in which the antenna chlorophylls are associated with the reaction center but present on separate pigment–proteins, a core antenna consisting of about 100 chlorophylls is an integral part of the PSI reaction center. The core antenna and P700 are bound to two proteins, PsaA and PsaB, with molecular masses in the range of 66 to 70 kDa (see **WEB TOPIC 9.8**). The PSI reaction center complex from pea contains four LHCI complexes in addition to the core structure similar to that found in cyanobacteria (see Figure 9.26). The

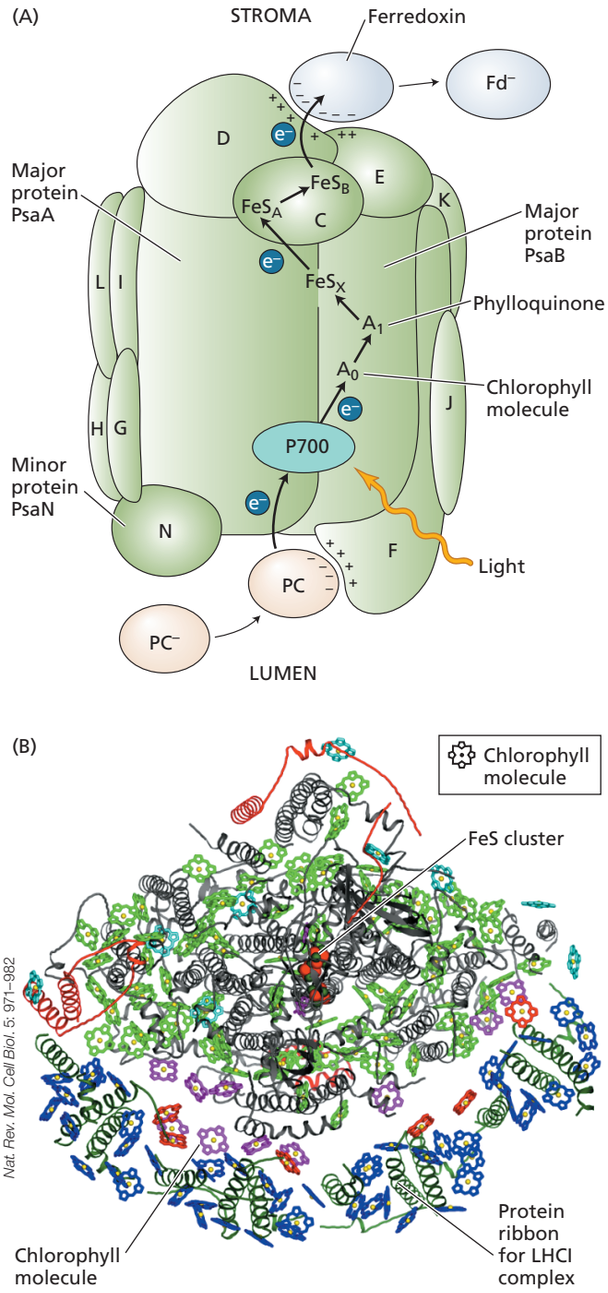


Figure 9.26 **Structure of PSI.** **(A)** Structural model of the PSI reaction center from vascular plants. Components of the PSI reaction center are organized around two major core proteins, PsaA and PsaB. The minor proteins PsaC to PsaN are labeled C to N. Electrons are transferred from plastocyanin (PC) to P700 (see Figures 9.18 and 9.19) and then to a chlorophyll molecule (A_0), to phylloquinone (A_1), to the Fe–S centers FeS_X, FeS_A, and FeS_B, and finally to the soluble iron–sulfur protein ferredoxin (Fd). **(B)** Structure of the PSI reaction center complex from pea at 4.4 Å (0.44 nm) resolution, including the LHCI antenna complexes. This is viewed from the stromal side of the membrane. Chlorophyll molecules associated with different subunit proteins are depicted in different colors. Only portions of the proteins (mainly helices) are shown. (A after R. Malkin and K. Niyogi. 2000. In B. B. Buchanan et al. [eds.]. 2000. *Biochemistry and Molecular Biology of Plants*. American Society of Plant Physiologists, Rockville, MD.)

total number of chlorophyll molecules in this complex is nearly 200. The vast majority of these chlorophylls act as part of an antenna, funneling light energy into the core of the reaction center, where photochemistry takes place.

The core antenna pigments form a bowl surrounding the electron transfer cofactors, which are in the center of the complex. In their reduced form, the electron carriers that function in the acceptor region of PSI are all extremely strong reducing agents. These reduced species are very unstable and thus difficult to identify. One of these early acceptors is a chlorophyll molecule, and another is a quinone species, phylloquinone, also known as vitamin K_1.

Additional electron acceptors include a series of three membrane-associated iron–sulfur proteins, also known as **Fe–S centers**: **FeS_X**, **FeS_A**, and **FeS_B** (see Figure 9.26). FeS_X is part of the P700-binding protein; FeS_A and FeS_B reside on an 8-kDa protein that is part of the PSI reaction center complex. Electrons are transferred through FeS_A and FeS_B to **ferredoxin** (**Fd**), a small, water-soluble iron–sulfur protein (see Figures 9.18 and 9.26). The membrane-associated flavoprotein **ferredoxin–NADP⁺ reductase** (**FNR**) oxidizes the reduced ferredoxin and reduces $NADP^+$ to NADPH, thus completing the sequence of electron flow that begins with the oxidation of water.

In addition to the reduction of $NADP^+$, reduced ferredoxin produced by PSI has several other functions in the chloroplast, such as the supply of reductants to reduce nitrite (see Chapter 14) and the regulation of some of the carbon-fixation enzymes (see Chapter 10).

Some herbicides block photosynthetic electron flow

The use of herbicides to kill unwanted plants is widespread in modern agriculture. Many different classes of herbicides have been developed. Some act by blocking amino acid, carotenoid, or lipid biosynthesis or by disrupting cell division. Other herbicides, such as dichlorophenyldimethylurea (DCMU, also known as diuron) and paraquat, block photosynthetic electron flow (**Figure 9.27**).

DCMU blocks electron flow at the quinone acceptors of PSII, by competing for the binding site of plastoquinone that is normally occupied by PQ_B. Paraquat accepts electrons from the early acceptors of PSI and then reacts with oxygen to form superoxide, $O_2^{\bullet -}$, a species that is very damaging to chloroplast components.

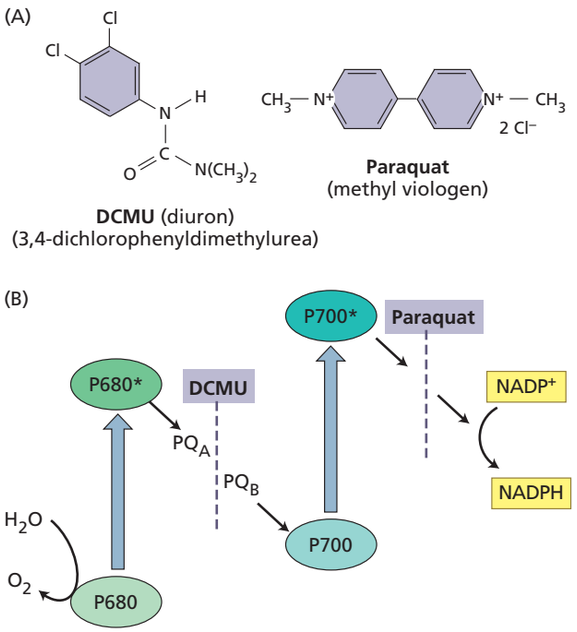


Figure 9.27 Chemical structure and mechanism of action of two important herbicides. (A) Chemical structure of 3,4-dichlorophenyldimethylurea (DCMU, also known as diuron) and methyl viologen (paraquat), two herbicides that block photosynthetic electron flow. (B) Sites of action of the two herbicides. DCMU blocks electron flow at the plastoquinone acceptors of PSII by competing for the binding site of plastoquinone. Paraquat acts by accepting electrons from the early acceptors of PSI.

9.7 Proton Transport and ATP Synthesis in the Chloroplast

In the preceding section we learned how captured light energy is used to reduce $NADP^+$ to NADPH. Several steps in this sequence of electron transfer reactions also store energy in the form of an electrochemical gradient of protons that in turn drives **photophosphorylation**, the light-dependent synthesis of ATP. This process was discovered by Daniel Arnon and his coworkers in the 1950s. Under normal cellular conditions, photophosphorylation requires electron flow, although under some conditions electron flow and photophosphorylation can take place independently of each other. Electron flow without accompanying phosphorylation is said to be **uncoupled**.

It is widely accepted that photophosphorylation works via the chemiosmotic mechanism. This mechanism was first proposed in the 1960s by Peter Mitchell. The same general mechanism drives phosphorylation during aerobic respiration in bacteria and mitochondria (see Chapter 13), as well as the transfer of many ions and metabolites across membranes (see Chapter 8). Chemiosmosis appears to be a unifying aspect of membrane processes in all forms of life.

In Chapter 8 we discussed the role of ATPases in chemiosmosis and ion transport at the cell's plasma membrane. The ATP used by the plasma membrane ATPase is synthesized by photophosphorylation in the chloroplast and oxidative phosphorylation in the mitochondrion. Here we are concerned with chemiosmosis and transmembrane proton concentration differences used to make ATP in the chloroplast.

The basic principle of chemiosmosis is that ion concentration differences and electrical potential differences across membranes are sources of free energy that can be used by the cell. As described by the second law of thermodynamics (see **WEB APPENDIX 1** for a detailed discussion), any nonuniform distribution of matter or energy represents a source of energy. Differences in **chemical potential** of any molecular species whose concentrations are not the same on opposite sides of a membrane provide such a source of energy (see Chapter 8).

The asymmetric nature of the photosynthetic membrane and the electron transfer systems leads to the storage of energy in two forms. First, electrons flow through the photosystems across the thylakoid membrane from the lumen (where water is split) to the stroma (where NADPH is produced). Second, protons flow from one side of the membrane to the other during electron flow, as discussed earlier. The direction of proton translocation is such that the stroma becomes more alkaline (fewer H^+ ions) and the lumen becomes more acidic (more H^+ ions) as a result of electron transport (see Figures 9.19 and 9.25).

Some of the early evidence supporting a chemiosmotic mechanism of photosynthetic ATP formation was provided by an elegant experiment carried out by André Jagendorf and coworkers (**Figure 9.28**). They suspended chloroplast thylakoids in a pH 4 buffer, and the buffer diffused across the membrane, causing the interior, as well as the exterior, of the thylakoid to equilibrate at this acidic pH. They then rapidly transferred the thylakoids to a pH 8 buffer, thereby creating a pH difference of four units across the thylakoid membrane, with the inside acidic relative to the outside. They found that large amounts of ATP were formed from ADP and P_i by this process, with no light input or electron transport. This result supports the predictions of the chemiosmotic mechanism described in the paragraphs that follow.

Mitchell proposed that the total energy available for ATP synthesis, which he called the **proton motive force** (Δp), is the sum of a proton chemical potential and a transmembrane electrical potential. These two components of the proton motive force from the outside of the membrane to the inside are given by the following equation:

$$\Delta p = \Delta E - 59 \text{ mV} \times (\text{pH}_i - \text{pH}_o) \qquad (9.9)$$

where ΔE is the transmembrane electrical potential, and $\text{pH}_i - \text{pH}_o$ (or ΔpH) is the pH difference across the membrane. The constant of proportionality (at 25°C) is

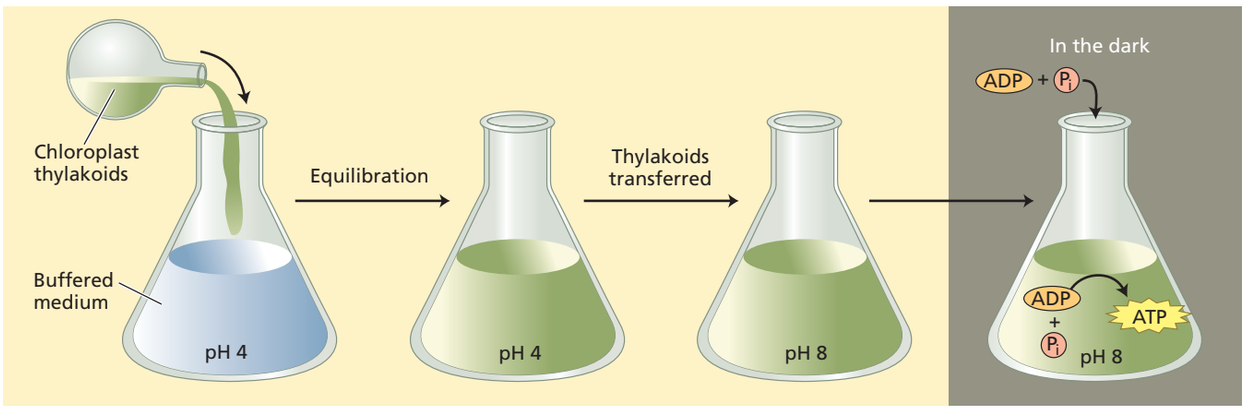
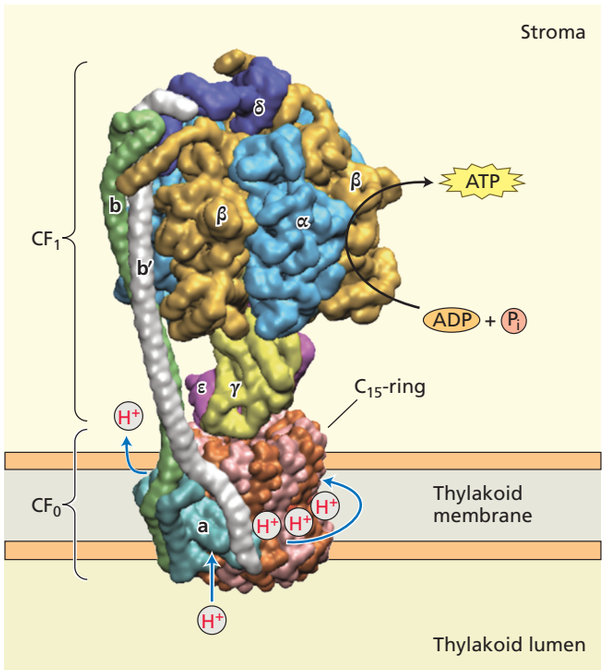


Figure 9.28 **Summary of the experiment carried out by Jagendorf and coworkers.** Isolated chloroplast thylakoids kept previously at pH 8 were equilibrated in an acid medium at pH 4. The thylakoids were then transferred to a buffer at pH 8 that contained ADP and P_i. The proton gradient generated by this manipulation provided a driving force for ATP synthesis in the absence of light. This experiment verified a prediction of the chemiosmotic model stating that a chemical potential across a membrane can provide energy for ATP synthesis. (After A. T. Jagendorf. 1967. *Fed. Proc., Fed. Am. Soc. Exp. Biol.* 26: 1361–1369.)



Courtesy of W. Frasch

Figure 9.29 **Structure of chloroplast F_0F_1-ATP synthase.** This enzyme consists of a large multi-subunit complex, CF_1, attached on the stromal side of the membrane to an integral membrane portion, known as CF_0. CF_1 consists of five different polypeptides, with stoichiometry of $\alpha_3\,\beta_3\,\gamma\,\delta\,\varepsilon$. CF_0 contains probably four different polypeptides, with a stoichiometry of a b b′ c_{14}. Protons from the lumen are transported by the rotating *c* polypeptide and are ejected on the stromal side. The structure closely resembles that of the mitochondrial F_0F_1-ATP synthase (see Chapters 8 and 13) and the vacuolar V-type ATPase (see Chapter 6).

59 mV per pH unit, so a transmembrane pH difference of one pH unit is equivalent to a membrane potential of 59 mV. While it is thought that mitochondria store Δp almost exclusively as electrical potential, the chloroplast also stores some of this energy as a pH gradient, which causes the lumen of the thylakoid to become more acidic with respect to the stroma, which in turn plays key roles in regulating light capture and electron transfer, as we discuss in Section 9.8.

The ATP is synthesized by an enzyme complex (mass ~400 kDa) known by several names: **ATP synthase**, **ATPase** (after the reverse reaction of ATP hydrolysis), and **CF_0–CF_1**. This enzyme consists of two parts: a hydrophobic membrane-bound portion called CF_0 and a portion that sticks out into the stroma called CF_1 (**Figure 9.29**). CF_0 appears to form a channel across the membrane through which protons can pass. CF_1 is made up of several peptides, including three copies of each of the α and β peptides arranged alternately much like the sections of an orange. Whereas the catalytic sites are located largely on the β polypeptide, many of the other peptides are thought to have primarily regulatory functions. CF_1 is the portion of the complex that synthesizes ATP.

The molecular structure of the mitochondrial ATP synthase has been determined by X-ray crystallography and cryo-EM methods. Although there are significant differences between the chloroplast and mitochondrial enzymes, they have the same overall architecture and probably nearly identical catalytic sites. In fact, there are remarkable similarities in the way electron flow is coupled to proton translocation in chloroplasts, mitochondria, and purple bacteria (**Figure 9.30**). Another remarkable aspect of the mechanism of the ATP synthase is that

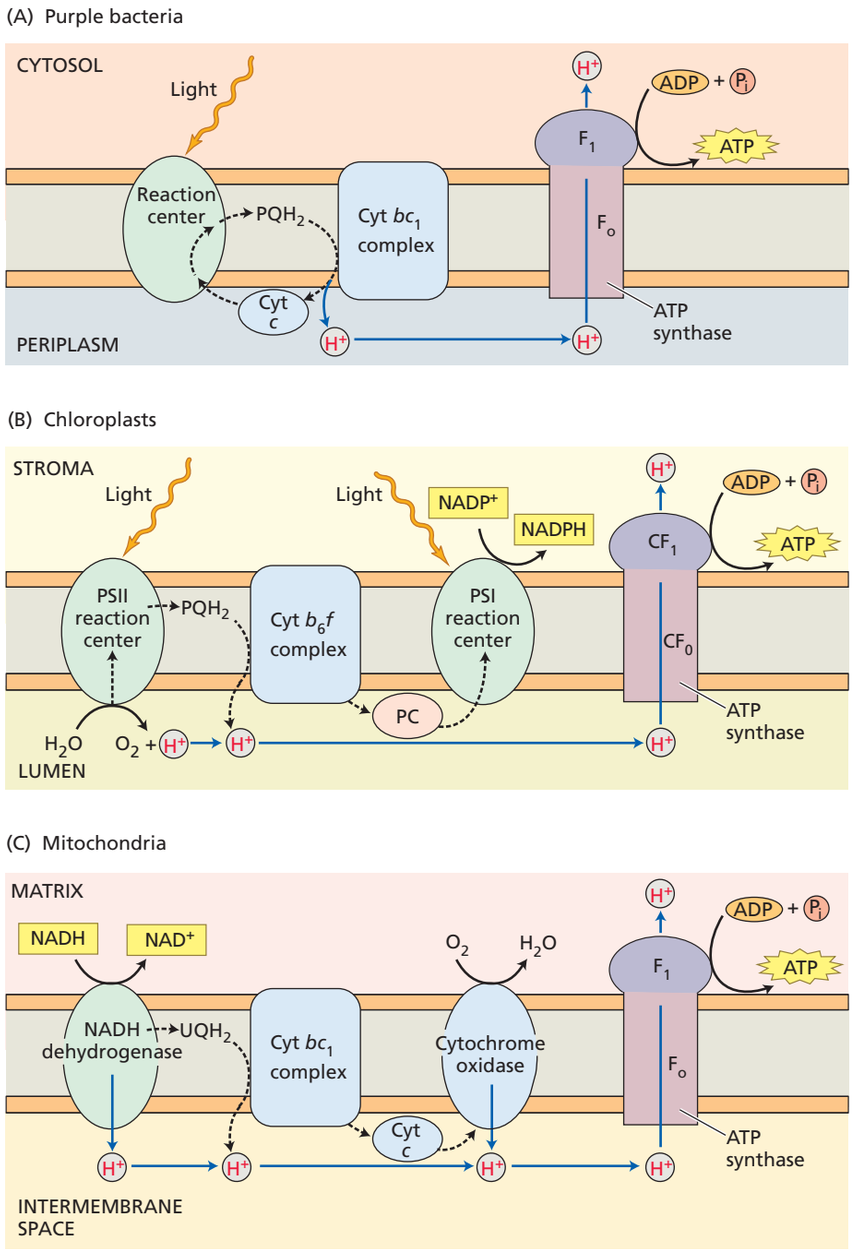


Figure 9.30 **Similarities of photosynthetic and respiratory electron flow in purple bacteria, chloroplasts, and mitochondria.** In all three, electron flow is coupled to proton translocation, creating a transmembrane proton motive force (Δp). The energy in the proton motive force is then used for the synthesis of ATP by ATP synthase. **(A)** A reaction center in purple photosynthetic bacteria carries out cyclic electron flow, generating a proton potential by the action of the cytochrome bc_1 complex. **(B)** Chloroplasts carry out noncyclic electron flow, oxidizing water and reducing $NADP^+$. Protons are produced by the oxidation of water and by the oxidation of PQH_2 by the cytochrome b_6f complex. **(C)** Mitochondria oxidize NADH to NAD^+ and reduce oxygen to water. Protons are pumped by the enzyme NADH dehydrogenase, the cytochrome bc_1 complex, and cytochrome oxidase. The ATP synthases in the three systems are very similar in structure. UQH_2, ubiquinol

the internal stalk and probably much of the CF_0 portion of the enzyme rotate during catalysis. The enzyme is actually a tiny molecular motor (see **WEB TOPICS 9.9** and **13.4**). Three molecules of ATP are synthesized for each rotation of the enzyme.

Direct microscopic imaging of the CF_0 part of the chloroplast ATP synthase indicates that it contains 14 copies (or 15 copies in some cyanobacteria) of the integral membrane subunit c (see Figure 9.29). Each subunit can translocate one proton across the membrane each time the complex rotates. This suggests that the stoichiometry of protons translocated to ATP formed is 14/3, or 4.69. Measured values of this parameter are usually somewhat lower than this value, and the reasons for this discrepancy are not yet understood.

Cyclic electron flow augments the output of ATP to balance the chloroplast energy budget

The linear electron flow pathway described in Section 9.6 produces ATP and NADPH, but at a fixed ratio that is too low to support CO_2 fixation and other processes

that require ATP. Therefore, under certain conditions, the light reactions provide additional sources of ATP. One major source is a process called **cyclic electron flow**, in which electrons flow from the reducing side of PSI back to P700 via plastohydroquinone and the cytochrome b_6f complex. This cyclic electron flow is coupled to proton pumping from the stroma to the lumen and can be used for ATP synthesis without water oxidation or $NADP^+$ reduction (see Figure 9.15B). Cyclic electron flow is especially important as an ATP source in the bundle sheath chloroplasts of some plants that carry out C_4 carbon fixation (see Chapter 10).

9.8 Repair and Regulation of the Photosynthetic Machinery

Photosynthetic systems face a special challenge. To function well at low light, their antenna complexes must be large to absorb sufficient amounts of light energy and process it into chemical energy. However, at the molecular level, the energy in a photon can be damaging, particularly under unfavorable conditions. In excess, light energy can lead to the production of toxic chemical species such as superoxide, singlet oxygen, and hydrogen peroxide, and damage can occur if the light energy is not dissipated safely. Photosynthetic organisms therefore contain complex regulatory and repair mechanisms to protect their photosynthetic apparatus.

Some of these mechanisms regulate energy flow in the antenna system, to avoid excess excitation of the reaction centers and ensure that the two photosystems are equally driven. Although very effective, these processes are not entirely fail-safe, and sometimes reactive intermediates can accumulate, leading to the production of toxic **reactive oxygen species**. **Figure 9.31** provides an overview of the several levels of regulation and repair systems that cope with these problems. The first line of defense is suppression of damage by quenching of excess excitation energy as heat. Second-line defenses include biochemical systems that scavenge or detoxify reactive oxygen species once formed and that repair damage. Superoxide dismutase and ascorbate peroxidase consume superoxide and hydrogen peroxide, while carotenoids and tocopherol (vitamin E) quench $^1O_2$.

Carotenoids serve as photoprotective agents

In addition to their role as accessory pigments, carotenoids play an essential role in **photoprotection**. The photosynthetic membrane can easily be damaged by the large amounts of energy absorbed by the pigments if this energy cannot be stored by photochemistry; this is why a protection mechanism is needed. The photoprotection mechanism can be thought of as a safety valve, venting excess energy before it can damage the organism. When the energy stored in chlorophylls in the excited state is

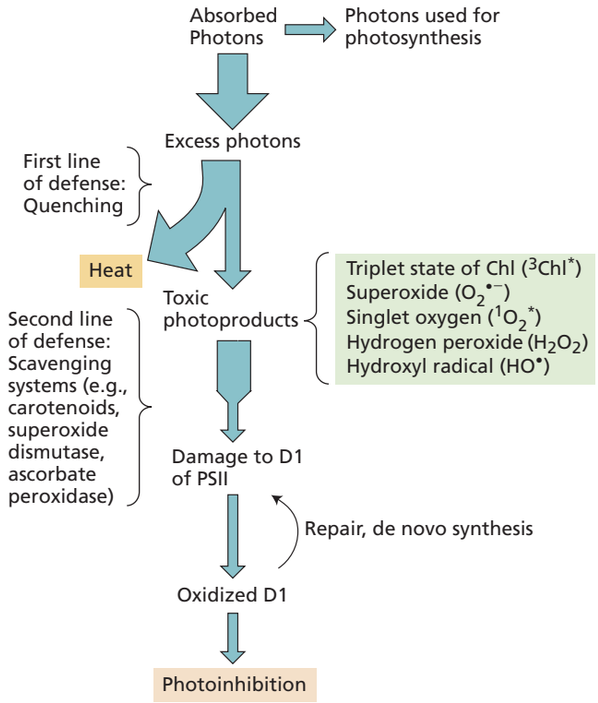


Figure 9.31 Overall picture of the regulation of photon capture and the protection and repair of photodamage. Protection against photodamage is a multilevel process. The first line of defense is suppression of damage by quenching of excess excitation as heat. If this defense is not sufficient and toxic photoproducts form, a variety of scavenging systems eliminate the reactive photoproducts. If this second line of defense also fails, the photoproducts can damage the D1 protein of PSII. This damage leads to photoinhibition. The D1 protein is then excised from the PSII reaction center and degraded. A newly synthesized D1 is reinserted into the PSII reaction center to form a functional unit. (After K. Asada. 1999. *Plant Physiol. Plant Mol. Biol.* 50: 601–639.)

rapidly dissipated by excitation transfer or photochemistry, the excited state is said to be **quenched**.

If the excited state of chlorophyll is not rapidly quenched by excitation transfer or photochemistry, it can react with molecular oxygen to form an excited state of oxygen known as **singlet oxygen** ($^1O_2$). The yield of $^1O_2$* is even higher when excited states of chlorophyll are produced during recombination reactions within the photosystems. This means that the reversal of the light reactions (the return of excited chlorophyll to its ground state) not only dissipates energy, it also can produce harmful by-products. Thus, while recombination occurs for only a small fraction of excited reaction centers, it is extremely important because the singlet oxygen it produces can react with and damage many cellular components, especially lipids.

Another form of reactive oxygen, superoxide ($O_2^{\bullet -}$), can be formed when electrons accumulate on the PSI

reaction center. Superoxide can interact with other redox components to produce hydrogen peroxide (H_2O_2) and the highly reactive hydroxyl radical ($HO^{\bullet}$) which, like singlet oxygen, can damage cellular components.

Carotenoids exert their photoprotective action by rapidly quenching the excited state of chlorophyll. The excited state of carotenoids does not have sufficient energy to form singlet oxygen, so it decays back to its ground state while losing its energy as heat.

Mutant organisms that lack carotenoids cannot live in the presence of both light and molecular oxygen—a rather difficult situation for an O_2-evolving photosynthetic organism. Mutants of non-O_2-evolving photosynthetic bacteria that lack carotenoids can be maintained under laboratory conditions if oxygen is excluded from the growth medium.

Some xanthophylls also participate in energy dissipation

Nonphotochemical quenching, a major process regulating the delivery of excitation energy to the reaction center, can be thought of as a "volume knob" that adjusts the flow of excitations to the PSII reaction center to a manageable level, depending on the light intensity and other conditions. The process appears to be an essential part of the regulation of antenna systems in most algae and plants.

Nonphotochemical quenching is the quenching of excited states of chlorophyll and other antenna pigments (see Figure 9.4) by processes that do not produce stable photochemical products. As a result of nonphotochemical quenching, a large fraction of the excitations in the antenna system caused by intense illumination are dissipated harmlessly as heat, preventing the buildup of reactive intermediates that could otherwise cause photodamage.

There are several distinct nonphotochemical quenching processes with different underlying mechanisms. The most rapidly responding of these is triggered by the acidification of the thylakoid lumen, which activates the interconversion of special carotenoids called **xanthophylls** and directly modulates the antenna complexes to form nonphotochemical quenching states (**Figure 9.32**). In high light, violaxanthin is converted into zeaxanthin, via the intermediate antheraxanthin, by the enzyme violaxanthin de-epoxidase. This enzyme is located in the lumen and is activated at low pH. High concentrations of protons also directly modulate the properties of a protein associated with PSII antenna, called the PsbS protein in vascular plants.

The acidification of the lumen can occur at high light, when the light-driven influx of protons is larger than their efflux through the ATP synthase. It also occurs when downstream metabolic reactions are inhibited, for instance under drought (water-deficit stress), heat, or cold stress. These conditions slow the use of ATP, depleting the chloroplast of ADP or inorganic phosphate (P_i), the substrates for the ATP synthase, and thereby slow the release of protons from the lumen through the ATP synthase. In this way, lumen acidification can act as a central regulatory "signal" to control photosynthesis in response to both energy input by light and its use by metabolism.

The PSII reaction center is easily damaged and rapidly repaired

Another effect that appears to be a major factor in the stability of the photosynthetic apparatus is photoinhibition, which occurs when excess excitation arriving at the PSII reaction center leads to its inactivation and

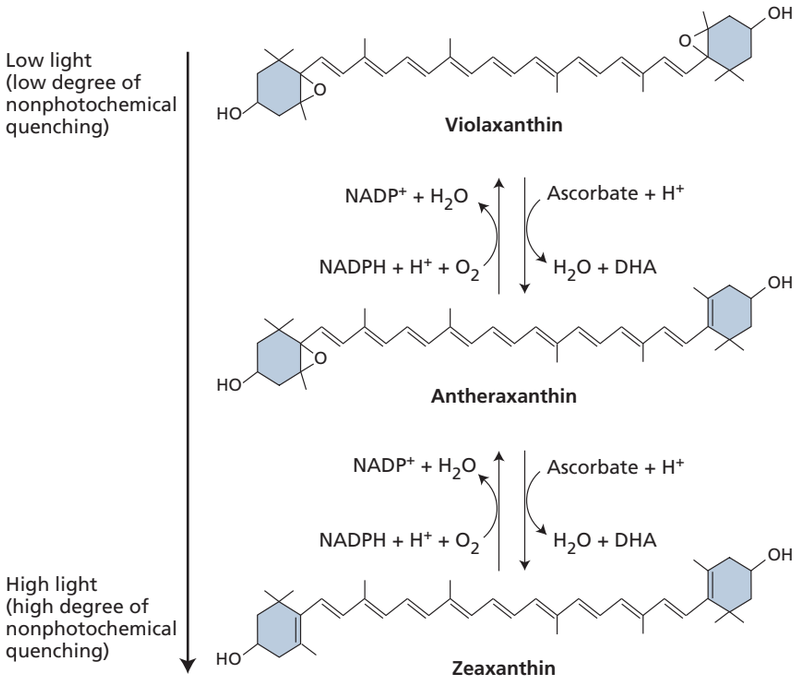


Figure 9.32 Chemical structure of violaxanthin, antheraxanthin, and zeaxanthin. The highly quenched state of PSII is associated with zeaxanthin, the unquenched state with violaxanthin. Enzymes interconvert these two carotenoids, with antheraxanthin as the intermediate, in response to changing conditions, especially changes in light intensity. Zeaxanthin formation uses ascorbate as a cofactor, and violaxanthin formation requires NADPH. DHA, dehydroascorbate.

damage. **Photoinhibition** is a complex set of molecular processes defined as the inhibition of photosynthesis by excess light.

As we will discuss in detail in Chapter 11, photoinhibition is reversible in early stages. Prolonged inhibition, however, results in damage to the system such that the PSII reaction center must be disassembled and repaired. The main target of this damage is the D1 protein that makes up part of the PSII reaction center complex (see Figure 9.21). When D1 is damaged by excess light, it must be removed from the membrane and replaced with a newly synthesized molecule. The other components of the PSII reaction center are not damaged by excess excitation and are thought to be recycled, so the D1 protein is the only component that needs to be synthesized (see Figure 9.31).

PSI is also vulnerable to damage from reactive oxygen species under certain conditions, such as when plants are exposed to high light at low temperatures. The ferredoxin acceptor of PSI is a very strong reductant that can readily reduce molecular oxygen to form superoxide ($O_2^{\bullet -}$). This reduction competes with the normal channeling of electrons to the reduction of $NADP^+$ and other processes. Superoxide is one of a series of reactive oxygen species that can be very damaging to biological membranes, but when formed in this way it can be eliminated by the action of a series of enzymes, including superoxide dismutase and ascorbate peroxidase.

Thylakoid stacking permits energy partitioning between the photosystems

The fact that photosynthesis in vascular plants is driven by two photosystems with different light-absorbing properties poses a special problem. If the rates of delivery of energy to PSI and PSII are not precisely matched and conditions are such that the rate of photosynthesis is limited by the available light (low light intensity), the rate of electron flow will be limited by the photosystem that is receiving less energy. In the most efficient situation, the input of energy would be the same to both photosystems. However, no single arrangement of pigments would satisfy this requirement because at different times of day the light intensity and spectral distribution tend to favor one photosystem or the other. This problem can be solved by a mechanism that shifts energy from one photosystem to the other in response to different conditions. Thylakoid membranes contain a protein kinase that can phosphorylate a specific threonine residue on the surface of LHCII, one of the membrane-bound antenna pigment proteins described earlier in the chapter (see Figure 9.17). The kinase is activated when plastoquinone, one of the electron carriers between PSI and PSII, accumulates in the reduced state. Reduced plastoquinone accumulates when PSII is being activated more frequently than PSI. The phosphorylated LHCII then migrates out of the stacked regions of the membrane into the unstacked regions (see Figure 9.15), probably because of repulsive interactions with negative charges on adjacent membranes. The net result is that when LHCII is not phosphorylated, it delivers more energy to PSII, and when it is phosphorylated, it delivers more energy to PSI.

9.9 Genetics, Assembly, and Evolution of Photosynthetic Systems

Chloroplasts have their own DNA, mRNA, and protein synthesis machinery, but most chloroplast proteins are encoded by nuclear genes and imported into the chloroplast (see Chapter 1). In this section we consider the genetics, assembly, and evolution of the main chloroplast components.

Chloroplast genes exhibit non-Mendelian patterns of inheritance

Chloroplasts and mitochondria reproduce by division rather than by de novo synthesis. This mode of reproduction is not surprising, given that these organelles contain genetic information that is not present in the nucleus. During cell division, chloroplasts are divided between the two daughter cells. In most sexual plants, however, only the maternal plant contributes chloroplasts to the zygote. In these plants the normal Mendelian pattern of inheritance does not apply to chloroplast-encoded genes, because the offspring receive chloroplasts from only one parent. The result is **non-Mendelian**, or **maternal**, **inheritance**. Numerous traits are inherited in this way; one example is the herbicide-resistance trait discussed in **WEB TOPIC 9.10**.

Most chloroplast proteins are imported from the cytoplasm

Chloroplast proteins can be encoded by either chloroplast or nuclear DNA. The chloroplast-encoded proteins are synthesized on chloroplast ribosomes; the nuclear-encoded proteins are synthesized on cytoplasmic ribosomes and then transported into the chloroplast. The genes needed for chloroplast function are distributed between the nuclear and plastid genomes with no evident pattern, but both sets are essential for the viability of the chloroplast. For example, the enzyme Rubisco (see Chapter 10), which functions in carbon fixation, has two types of subunits, a chloroplast-encoded large subunit and a nuclear-encoded small subunit, both of which are required for activity. The small subunits of Rubisco are synthesized in the cytosol and transported into the chloroplast, where the enzyme is assembled. Some chloroplast genes are necessary for other chloroplast

functions, such as heme and lipid synthesis. Control of the expression of the nuclear genes that code for chloroplast proteins is complex and dynamic, involving light-dependent regulation mediated by both phytochrome and blue light (see Chapter 16), as well as other factors.

The transport of chloroplast proteins that are synthesized in the cytosol is a tightly regulated process. Nuclear-encoded chloroplast proteins (such as the small subunit of Rubisco) are synthesized as precursor proteins containing an N-terminal amino acid sequence known as a **transit peptide**. This terminal sequence directs the precursor protein to the chloroplast, facilitates its passage through both the outer and the inner envelope membranes, and is then clipped off. The electron carrier plastocyanin is a water-soluble protein that is encoded in the nucleus, but it functions in the lumen of the chloroplast. It therefore must cross three membranes to reach its destination in the lumen. The transit peptide of plastocyanin is very large and is processed in more than one step as it directs the protein through two sequential translocations across the inner envelope membrane and the thylakoid membrane.

The biosynthesis and breakdown of chlorophyll are complex pathways

Chlorophylls are complex molecules exquisitely suited to the light absorption, energy transfer, and electron transfer functions that they carry out in photosynthesis (see Figure 9.6). Like all other biomolecules, chlorophylls are made by a biosynthetic pathway in which simple molecules are used as building blocks to assemble more complex molecules. Each step in the biosynthetic pathway is enzymatically catalyzed.

The chlorophyll biosynthetic pathway consists of more than a dozen steps (see **WEB TOPIC 9.11**). The process can be divided into several phases (**Figure 9.33**), each of which can be considered separately, but in the cell they are highly coordinated and regulated. This regulation is essential because free chlorophyll and many of the biosynthetic intermediates are damaging to cellular components. The damage results largely because chlorophylls absorb light efficiently, but in the absence of accompanying proteins they lack a pathway for disposing of the energy, with the result that toxic singlet oxygen is formed.

The breakdown pathway of chlorophyll in senescing leaves is quite different from the biosynthetic pathway. The first step is removal of the phytol tail by an enzyme known as chlorophyllase, followed by removal of the magnesium ion by magnesium de-chelatase. Next the porphyrin structure is opened by an oxygen-dependent oxygenase enzyme to form an open-chain tetrapyrrole.

The tetrapyrrole is further modified to form water-soluble, colorless products. These colorless metabolites are then exported from the senescent chloroplast and transported to the vacuole, where they are stored. The chlorophyll-binding proteins are subsequently recycled into new proteins, which is important for the nitrogen economy of the plant.

Complex photosynthetic organisms have evolved from simpler forms

The complicated photosynthetic apparatus found in plants and algae is the end product of a long evolutionary sequence. Much can be learned about this evolutionary process from analysis of simpler prokaryotic photosynthetic organisms, including the anoxygenic photosynthetic bacteria and the cyanobacteria.

The chloroplast is a semiautonomous cell organelle, with its own DNA and a complete protein synthesis apparatus. Many of the proteins that make up the photosynthetic apparatus, as well as all the chlorophylls and lipids, are synthesized in the chloroplast. Other proteins are imported from the cytoplasm and are encoded by nuclear genes. How did this curious division of labor come about? Most experts now agree that the chloroplast is the descendant of a symbiotic relationship between a cyanobacterium and a simple nonphotosynthetic eukaryotic cell. This type of relationship is called **endosymbiosis**.

Originally the cyanobacterium was capable of independent life, but over time much of its genetic information needed for normal cellular functions was lost, and a substantial amount of information needed to synthesize the photosynthetic apparatus was transferred to the nucleus. So the cyanobacterium was no longer capable of life outside its host and eventually became an integral part of the cell, known as the chloroplast.

In some types of algae, chloroplasts have arisen by endosymbiosis of eukaryotic photosynthetic organisms. In these organisms the chloroplast is surrounded by three (and in some cases four) membranes, which are thought to be remnants of the plasma membranes of the earlier organisms. Mitochondria are also thought to have originated by endosymbiosis in a separate event much earlier than chloroplast formation.

The answers to other questions related to the evolution of photosynthesis are less clear. These include the nature of the earliest photosynthetic systems, how the two photosystems became linked, and the evolutionary origin of the oxygen-evolving complex.

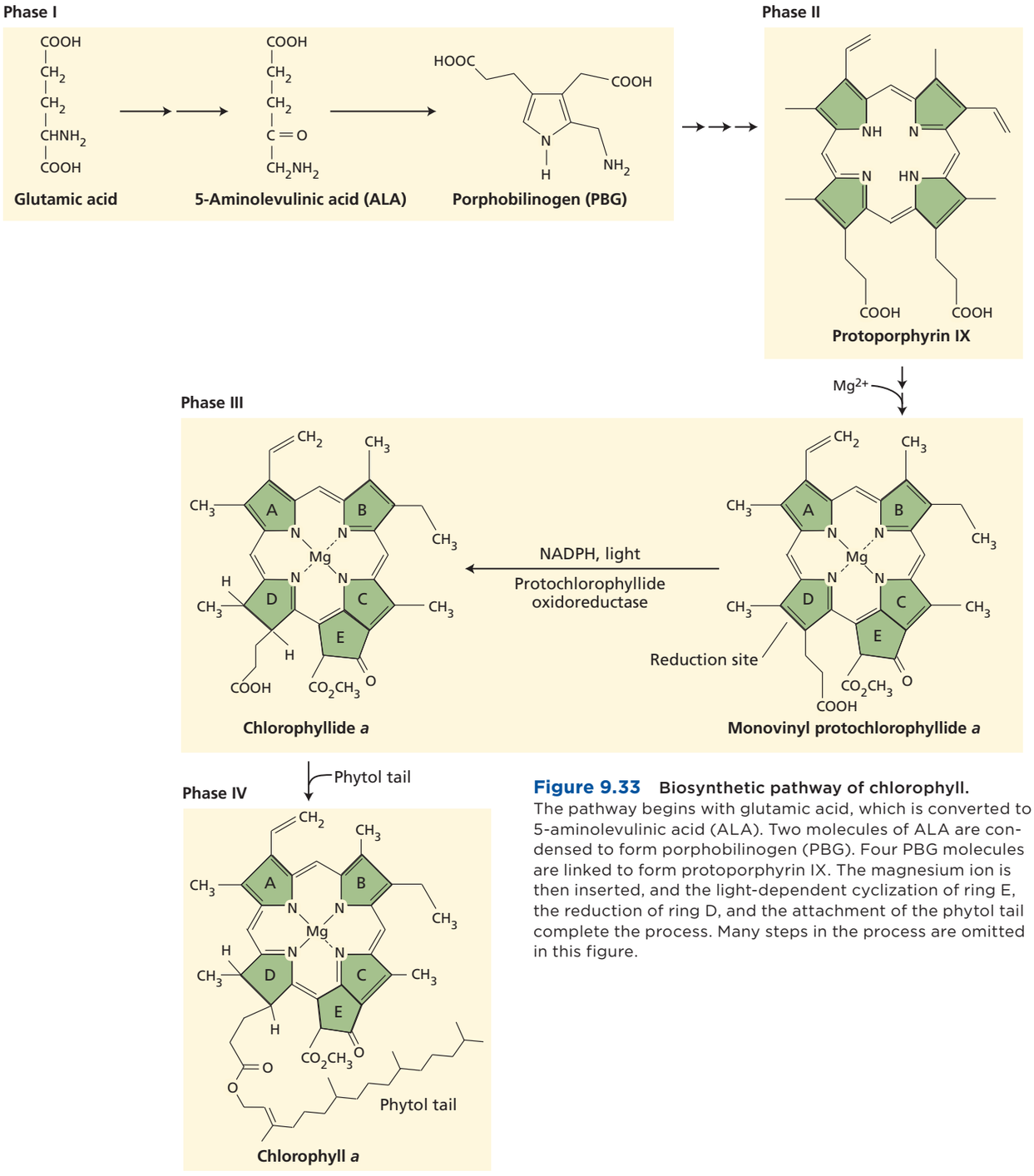


Figure 9.33 **Biosynthetic pathway of chlorophyll.** The pathway begins with glutamic acid, which is converted to 5-aminolevulinic acid (ALA). Two molecules of ALA are condensed to form porphobilinogen (PBG). Four PBG molecules are linked to form protoporphyrin IX. The magnesium ion is then inserted, and the light-dependent cyclization of ring E, the reduction of ring D, and the attachment of the phytol tail complete the process. Many steps in the process are omitted in this figure.

Summary

Photosynthesis in plants captures light energy for the synthesis of carbohydrates and the generation of oxygen from carbon dioxide and water. Energy stored in carbohydrates is used to power cellular processes in the plant and can serve as the energy resource for all forms of life.

9.1 Photosynthesis in Green Plants

- Within chloroplasts, chlorophylls absorb light energy for the oxidation of water, releasing oxygen and generating NADPH and ATP (thylakoid reactions).
- NADPH and ATP are used to reduce carbon dioxide to form sugars (carbon fixation reactions, treated in **Chapter 10**).

9.2 General Concepts

- Light behaves as both a particle and a wave, delivering energy as photons, some of which are absorbed and used by plants (**Figures 9.1–9.3**).
- Light-energized chlorophyll may fluoresce or transfer energy to another molecule to drive chemical reactions (**Figures 9.4, 9.10**).
- All photosynthetic organisms contain a mixture of pigments with distinct structures and light-absorbing properties (**Figures 9.6, 9.7**).

9.3 Key Experiments in Understanding Photosynthesis

- An action spectrum for photosynthesis shows algal oxygen evolution at certain wavelengths (**Figures 9.8, 9.9**).
- Antenna pigment–protein complexes collect light energy and transfer it to the reaction center complexes (**Figures 9.10, 9.16**).
- Light drives the reduction of $NADP^+$ and the formation of ATP. Oxygen-evolving organisms have two photosystems (PSI and PSII) that operate in series (**Figure 9.12**).

9.4 Organization of the Photosynthetic Apparatus

- Within the chloroplast, thylakoid membranes contain the reaction centers, the light-harvesting antenna complexes, and most of the electron carrier proteins. PSI and PSII are spatially separated in thylakoids (**Figure 9.15**).

9.5 Organization of Light-Absorbing Antenna Systems

- The antenna system funnels energy to the reaction center (**Figure 9.16**).
- Light-harvesting proteins of both photosystems are structurally similar (**Figure 9.17**).

9.6 Mechanisms of Electron Transport

- The Z scheme illustrates the flow of electrons from H_2O to $NADP^+$ through carriers in PSII and PSI (**Figures 9.12, 9.18**).
- Three large protein complexes transfer electrons: PSII, the cytochrome b_6f complex, and PSI (**Figures 9.15, 9.19**).
- PSI reaction center chlorophyll absorbs maximally at 700 nm; PSII reaction center chlorophyll absorbs maximally at 680 nm.
- The PSII reaction center is a multi-subunit protein–pigment complex (**Figures 9.21, 9.22**).
- Manganese ions are required to oxidize water.
- Two hydrophobic plastoquinones accept electrons from PSII (**Figures 9.19, 9.23**).
- Protons are transported into the thylakoid lumen when electrons pass through the cytochrome b_6f complex (**Figures 9.19, 9.25**).
- Plastoquinone and plastocyanin carry electrons between PSII and PSI (**Figure 9.25**).
- $NADP^+$ is reduced by the PSI reaction center, using Fe–S centers and ferredoxin as electron carriers (**Figure 9.26**).
- Herbicides may block photosynthetic electron flow (**Figure 9.27**).

9.7 Proton Transport and ATP Synthesis in the Chloroplast

- In vitro transfer of pH 4–equilibrated chloroplast thylakoids to a pH 8 buffer resulted in the formation of ATP from ADP and P_i, supporting the chemiosmotic mechanism (**Figure 9.28**).
- Protons move down an electrochemical gradient (proton motive force), passing through an ATP synthase and forming ATP (**Figure 9.29**).
- During catalysis, the CF_0 portion of the ATP synthase rotates like a miniature motor.
- Proton translocation in chloroplasts, mitochondria, and purple bacteria shows significant similarities (**Figure 9.30**).
- Cyclic electron flow generates ATP, but no NADPH, by proton pumping (**Figure 9.15**).

9.8 Repair and Regulation of the Photosynthetic Machinery

- Protection and repair of photodamage consist of quenching and heat dissipation, neutralizing toxic photoproducts, and synthetic repair of PSII (**Figure 9.31**).
- Xanthophylls (a class of carotenoids) participate in nonphotochemical quenching (**Figure 9.32**).
- Kinase-mediated phosphorylation of LHCII causes its migration to stacked thylakoids and its delivery of energy to PSI. Upon dephosphorylation, LHCII migrates to unstacked thylakoids and delivers more energy to PSII.

Summary (*continued*)

9.9 Genetics, Assembly, and Evolution of Photosynthetic Systems

- Chloroplasts have their own DNA, mRNA, and protein synthesis system. They import most proteins into the chloroplast. These proteins are encoded by nuclear genes and synthesized in the cytosol.
- Chloroplasts show a non-Mendelian, or maternal, pattern of inheritance.
- Chlorophyll biosynthesis can be divided into four phases (**Figure 9.33**).
- The chloroplast is descended from a symbiotic relationship between a cyanobacterium and a simple nonphotosyntheic eukaryotic cell.

Web Material

- **WEB TOPIC 9.1 Principles of Spectrophotometry** Spectrophotometry is a key technique for the study of light reactions.
- **WEB TOPIC 9.2 The Distribution of Chlorophylls and Other Photosynthetic Pigments** The content of chlorophylls and other photosynthetic pigments varies among plant kingdoms.
- **WEB TOPIC 9.3 Quantum Yield** Quantum yields measure how effectively light drives a photobiological process.
- **WEB TOPIC 9.4 Antagonistic Effects of Light on Cytochrome Oxidation** Photosystems I and II were discovered in some ingenious experiments.
- **WEB TOPIC 9.5 Structures of Two Bacterial Reaction Centers** X-ray diffraction studies resolved the atomic structure of the reaction center of PSII.
- **WEB TOPIC 9.6 Midpoint Potentials and Redox Reactions** The measurement of midpoint potentials is useful for analyzing electron flow through PSII.
- **WEB TOPIC 9.7 Oxygen Evolution** The S-state mechanism is a model for water splitting in PSII.
- **WEB TOPIC 9.8 Photosystem I** PSI is a multi-subunit–pigment protein supercomplex.
- **WEB TOPIC 9.9 ATP Synthase** The ATP synthase functions as a molecular motor.
- **WEB TOPIC 9.10 Mode of Action of Some Herbicides** Some herbicides kill plants by blocking photosynthetic electron flow.
- **WEB TOPIC 9.11 Chlorophyll Biosynthesis** Chlorophyll and heme share early steps of their biosynthetic pathways.
- **WEB ESSAY 9.1 A Novel View of Chloroplast Structure** Stromules extend the reach of the chloroplasts.

For more study aids, go to oup.com/he/taiz7e.

Suggested Reading

Armbruster, U., Correa Galvis, V., Kunz, H.-H., and Strand, D. D. (2017) The regulation of the chloroplast proton motive force plays a key role for photosynthesis in fluctuating light. *Curr. Opin. Plant Biol.* 37: 56–62.

Blankenship, R. E. (2002) *Molecular Mechanisms of Photosynthesis*. Blackwell Scientific, Oxford.

Croce, R., and van Amerongen, H. (2020) Light harvesting in oxygenic photosynthesis: Structural biology meets spectroscopy. *Science* 369: eaay2058.

Davis, G. A., Rutherford, A. W., and Kramer, D. M. (2017) Hacking the thylakoid proton motive force for improved photosynthesis: Modulating ion flux rates that control proton motive force partitioning into $\Delta\psi$ and ΔpH. *Philos Trans. R. Soc. Lond. B. Biol. Sci.* 372: 20160381.

Hohmann-Marriott, M. F., and Blankenship, R. E. (2011) Evolution of photosynthesis. *Annu. Rev. Plant Biol.* 62: 515–548.

Kaiser, E., Morales, A., and Harbinson, J. (2018) Fluctuating light takes crop photosynthesis on a rollercoaster ride. *Plant Physiol.* 176: 977–989.

Kanazawa, A., Neofotis, P., Davis, G. A., Fisher, N., and Kramer, D. M. (2020) Diversity in photoprotection and energy balancing in terrestrial and aquatic phototrophs. In A. W. D. Larkum, A. R. Grossman, and J. A. Raven, eds., *Photosynthesis in Algae: Biochemical and Physiological Mechanisms*. Springer International Publishing, Cham, Switzerland, pp. 299–327.

Kramer, D. M., Nitschke, W., and Cooley, J. W. (2009) The cytochrome bc1 and related bc complexes: The Rieske/cytochrome b complex as the functional core of a central electron/proton transfer complex. In C. N. Hunter, F. Daldal, M. C. Thurnauer, and J. T. Beatty, eds., *The Purple Phototrophic Bacteria*. Springer Netherlands, Dordrecht, pp. 451–473.

Kromdijk, J., Głowacka, K., Leonelli, L., Gabilly, S. T., Iwai, M., Niyogi, K. K., and Long, S. P. (2016) Improving photosynthesis and crop productivity by accelerating recovery from photoprotection. *Science* 354: 857–861.

Lubitz, W., Chrysina, M., and Cox, N. (2019) Water oxidation in photosystem II. *Photosynth. Res.* 142: 105–125.

10 Photosynthesis: The Carbon Reactions



Aleksey Sagitov/Shutterstock

We examined the requirements of plants for mineral nutrients and light to grow and complete their life cycle in Chapters 7 and 9, respectively. The amount of matter in our planet remains relatively constant, and a continuous flux of energy is needed to transform, circulate, and order molecules throughout the biosphere. Without this energy input, entropy would increase, the flow of matter would stop, and life would cease to exist. The initial source of energy for nearly all life on our planet comes from solar radiant energy that strikes Earth's surface. Aquatic and terrestrial photosynthetic organisms capture approximately 3×10^{21} Joules per year of sunlight energy and use it to fix approximately 2×10^{11} tonnes of carbon per year.

More than 1 billion years ago, heterotrophic cells acquired the ability to convert sunlight into chemical energy through primary endosymbiosis of an ancient photosynthetic cyanobacterium. Phylogenic analyses of plastids, cyanobacteria, and eukaryotes have determined that the Archaeplastidae, the autotrophic eukaryotic descendants of this ancient monophyletic endosymbiotic event, comprises three major lineages: Chloroplastidae (Viridiplantae: green algae, land plants), Rhodophyceae (red algae), and Glaucophytae (unicellular algae containing cyanobacteria-like plastids called cyanelles). The integration of cyanobacterial genes into the host's genome dramatically reduced the size of the plastid genome (plastome). This transfer of genes required the development of complex transport mechanisms across the outer and inner membrane of the plastid for targeting nucleus-encoded proteins to the endosymbiont, and plastid-encoded proteins to the host. Additionally, the endosymbiotic event required the exchange of numerous compounds between the plastid and the rest of the cell. The ancestral endosymbiont conveyed the ability not only to carry out oxygenic photosynthesis, but also to synthesize novel compounds, such as *starch*, and is now essential for nitrogen and sulfur assimilation, amino acid and fatty acid synthesis, and many other specialized functions.

In Chapter 9 we learned how the thylakoid membranes use energy associated with the photochemical oxidation of water to molecular oxygen to generate ATP, reduced ferredoxin, and NADPH. Subsequently, the products of these light-dependent reactions are used in the surrounding fluid phase (stroma) to drive the enzyme-catalyzed reduction of atmospheric CO_2 to triose

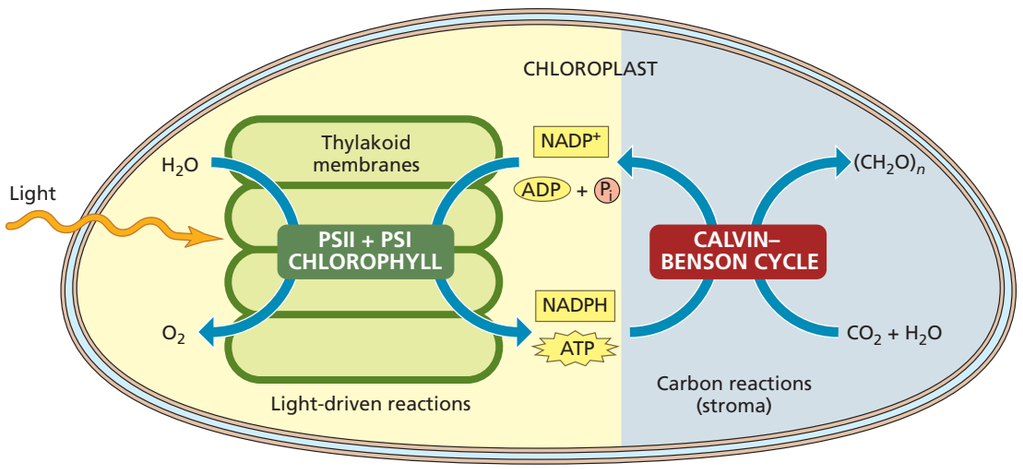


Figure 10.1 Light and carbon reactions of photosynthesis in chloroplasts of land plants. In thylakoid membranes, the excitation of chlorophyll in the photosynthetic electron transport system (photosystem II [PSII] + photosystem I [PSI]) by light elicits the formation of ATP and NADPH (see Chapter 7). In the stroma, both ATP and NADPH are consumed by the Calvin–Benson cycle in a series of enzyme-driven reactions that reduce atmospheric CO_2 to carbohydrates (triose phosphates).

phosphates, ultimately leading to the synthesis of carbohydrates and other cell components (**Figure 10.1**). The reduction of CO_2 within the stroma of chloroplasts was for many years referred to as the *dark reactions* because it is not directly driven by the chemical process of light absorption (photochemistry). However, these stroma-localized reactions are now commonly referred to as the *carbon reactions of photosynthesis* because not only do products of photochemistry (e.g., ATP and NADPH) provide the energy for these reactions, but light is required to activate many of the enzymes required for carbon assimilation.

We begin this chapter by describing the metabolic cycle that incorporates atmospheric CO_2 into organic compounds: the **Calvin–Benson cycle**. Next we consider how the unavoidable reaction of ribulose 1,5-bisphosphate carboxylase/oxygenase (Rubisco) with molecular oxygen decreases the efficiency of photosynthetic CO_2 assimilation, and how photorespiration releases CO_2 while recycling the by-products of this oxygenation reaction that would otherwise be unusable by the cell. We also examine two CO_2-concentrating mechanisms that land plants have evolved for minimizing the oxygenation of Rubisco and the loss of energy and CO_2 during photorespiration (see **WEB TOPIC 10.1**): C_4 photosynthesis and crassulacean acid metabolism (CAM). Finally, we consider the formation of the two major products of the photosynthetic CO_2 fixation: **starch**, the reserve polysaccharide that accumulates transiently in chloroplasts; and **sucrose**, the disaccharide that is generated outside the chloroplast and is exported from leaves (*sources*) to developing tissues and storage organs (*sinks*) of the plant.

10.1 The Calvin–Benson Cycle

A requisite for maintaining life in the biosphere is the fixation of atmospheric CO_2 into organic compounds, which ultimately provide the substrates and energy needed for cellular metabolism. These endergonic (energy-requiring) transformations are driven by the energy coming from the photochemical reactions described in Chapter 9. The predominant pathway of autotrophic CO_2 fixation is termed the Calvin–Benson cycle (see **WEB TOPIC 10.2**), which is found in many prokaryotes and in all photosynthetic eukaryotes, from algae to angiosperms. This pathway decreases the oxidation state of carbon from the highest value, found in CO_2 (+4), to levels found in sugars (e.g., +2 in keto groups [—CO—] and 0 in secondary alcohols [—CHOH—]). In view of its notable capacity for lowering the carbon oxidation state, the Calvin–Benson cycle is also aptly named the *reductive pentose phosphate cycle* and the *photosynthetic carbon reduction cycle*. In this section we examine how CO_2 is fixed via Rubisco and assimilated by the Calvin–Benson cycle using ATP and NADPH generated by the light reactions (see Figure 10.1), and how the cycle is regulated.

The Calvin–Benson cycle has three phases: carboxylation, reduction, and regeneration

In the 1950s, a series of ingenious experiments carried out by M. Calvin, A. Benson, J. A. Bassham, and their colleagues provided convincing evidence for the Calvin–Benson cycle (see **WEB TOPIC 10.2**). The Calvin–Benson cycle can be separated into three phases that are highly coordinated in the chloroplast (**Figure 10.2**):

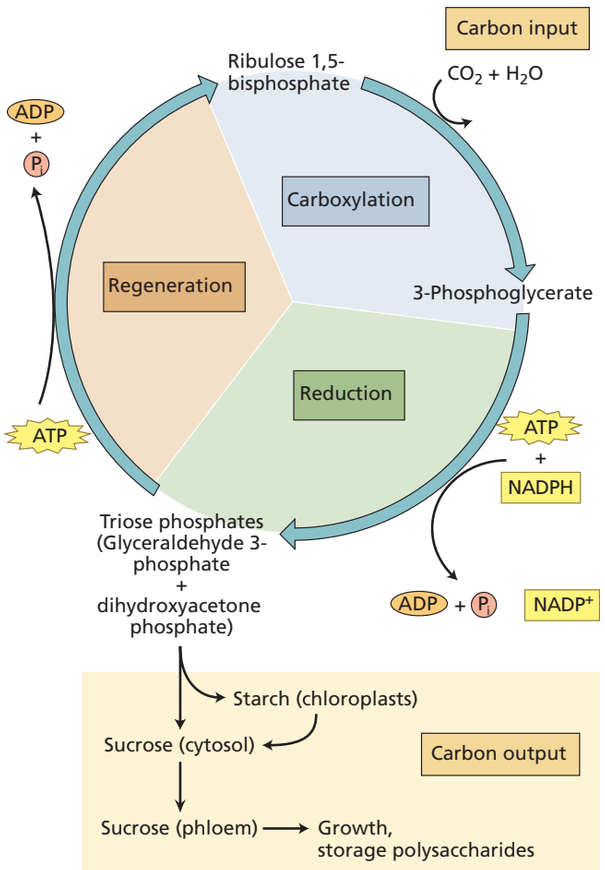


Figure 10.2 **The Calvin–Benson cycle proceeds in three phases:** (1) *carboxylation*, which covalently links atmospheric carbon (CO_2) to a carbon skeleton; (2) *reduction*, which forms a carbohydrate (triose phosphate) at the expense of photochemically generated ATP and reducing equivalents in the form of NADPH; and (3) *regeneration*, which restores the CO_2 acceptor ribulose 1,5-bisphosphate. At steady state, the input of CO_2 equals the output of triose phosphates. The latter either serve as precursors of starch biosynthesis in the chloroplast or flow to the cytosol for sucrose biosynthesis and other metabolic reactions. Sucrose is loaded into the phloem sap and used for growth or polysaccharide biosynthesis in other parts of the plant.

1. *Carboxylation* of the CO2 acceptor molecule. Rubisco catalyzes the reaction of CO2 and water with a five-carbon acceptor molecule (ribulose 1,5-bisphosphate) to generate two molecules of a three-carbon Calvin–Benson cycle intermediate (3-phosphoglycerate).
2. *Reduction* of 3-phosphoglycerate. Two successive enzymatic reactions phosphorylate and reduce 3-phosphoglycerate to the triose phosphate glyceraldehyde 3-phosphate using photochemically generated ATP and NADPH.
3. *Regeneration* of the CO_2 acceptor ribulose 1,5-bisphosphate. The cycle is completed by regeneration of ribulose 1,5-bisphosphate through a series of ten enzyme-catalyzed reactions, consuming additional ATP.

The majority of the triose phosphate generated in the Calvin–Benson cycle is used to regenerate ribulose 1,5-bisphosphate. However, the input of atmospheric CO_2 generates additional triose phosphates that can be used by several other metabolic pathways, including for the generation of high-energy storage compounds such as starch in the chloroplast, or for export to the cytosol for the formation of sucrose or for respiration in cytosol and mitochondria (see Chapter 13).

The fixation of CO_2 via carboxylation of ribulose 1,5-bisphosphate and the reduction of 3-phosphoglycerate yield triose phosphates

In the carboxylation step of the Calvin–Benson cycle, one molecule of CO_2 and one molecule of H_2O react with one molecule of ribulose 1,5-bisphosphate to yield two molecules of 3-phosphoglycerate (**Figure 10.3**, reaction 1). This reaction is catalyzed by the chloroplast enzyme ribulose 1,5-bisphosphate carboxylase/oxygenase, referred to as **Rubisco** (see **WEB TOPIC 10.3**). In the first partial reaction, a H^+ is extracted from the carbon 3 of ribulose 1,5-bisphosphate to generate an enediol intermediate (**Figure 10.4**). The addition of CO_2 to the unstable Rubisco-bound enediol drives the irreversible formation of the six-carbon intermediate 2-carboxy-3-ketoarabinitol 1,5-bisphosphate, which is then split through hydration to yield two molecules of 3-phosphoglycerate.

In the reduction phase of the Calvin–Benson cycle, two successive reactions first phosphorylate and then reduce the 3-phosphoglycerate produced by the carboxylation reaction (see Figure 10.3, reactions 2 and 3):

1. First, ATP, formed by the light reactions, is used to phosphorylate 3-phosphoglycerate at the carboxyl group, yielding 1,3-bisphosphoglycerate in a reaction catalyzed by 3-phosphoglycerate kinase.
2. Next, NADPH, also generated by the light reactions, is used to reduce 1,3-bisphosphoglycerate to glyceraldehyde 3-phosphate, in a reaction catalyzed by the chloroplast enzyme NADP–glyceraldehyde-3-phosphate dehydrogenase.

When three molecules of ribulose 1,5-bisphosphate (3 molecules × 5 carbons/molecule = 15 carbons total) react with three molecules of CO_2 (3 carbons total), six molecules of 3-phosphoglycerate are produced. The carboxylation and reduction of these six molecules of 3-phosphoglycerate produce six molecules of glyceraldehyde 3-phosphate (6 molecules × 3 carbons/molecule

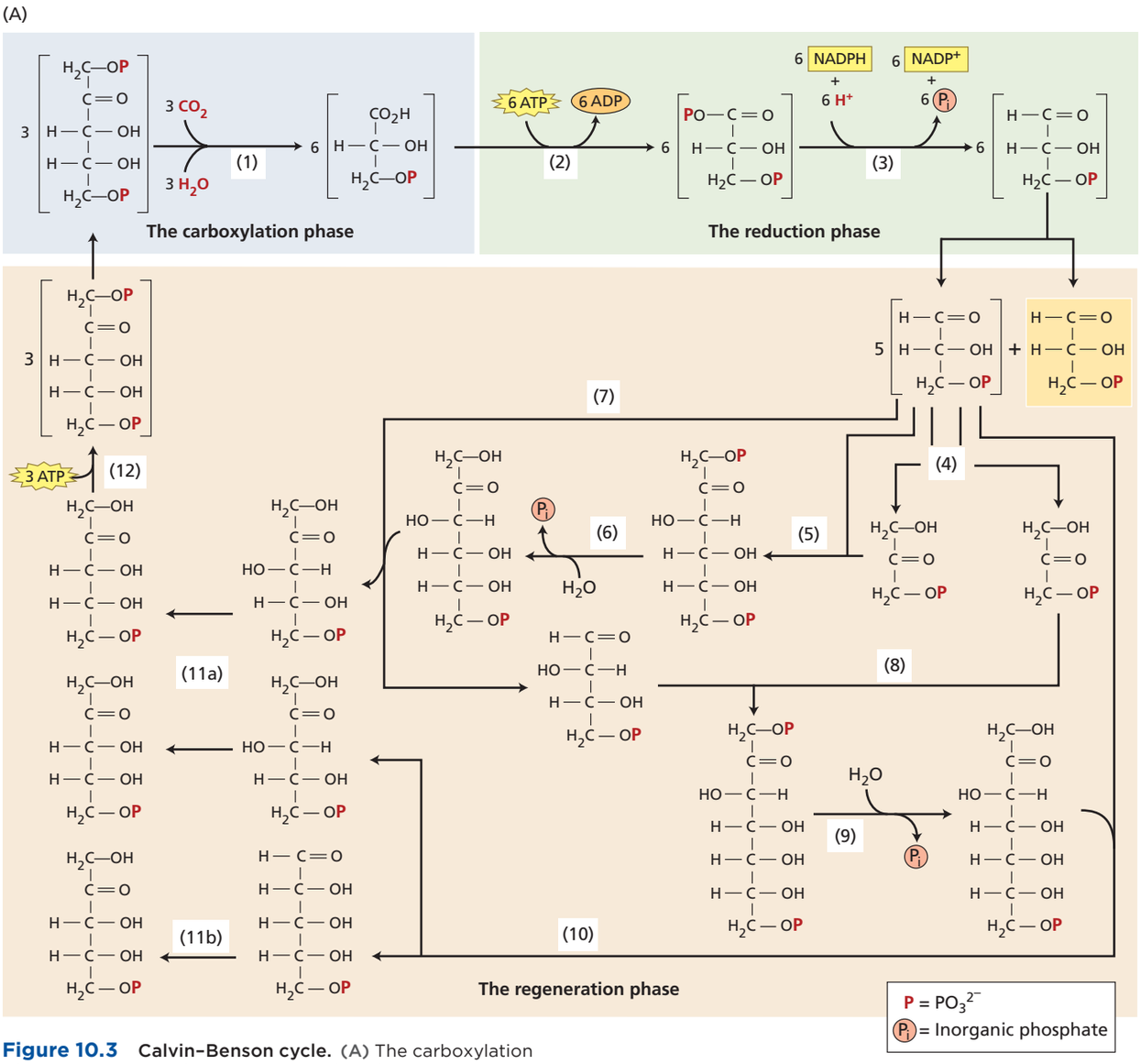


Figure 10.3 **Calvin–Benson cycle.** **(A)** The carboxylation of three molecules of ribulose 1,5-bisphosphate yields six molecules of 3-phosphoglycerate (carboxylation phase). After phosphorylation of the carboxyl group, 1,3-bisphosphoglycerate is reduced to six molecules of glyceraldehyde-3-phosphate with the concurrent release of six molecules of inorganic phosphate (reduction phase). From the total six molecules of glyceraldehyde 3-phosphate, one represents the net assimilation of the three molecules of CO_2 while the other five undergo a series of reactions that finally regenerate the starting three molecules of ribulose 1,5-bisphosphate (regeneration phase). **(B)** A description of the numbered reactions of the Calvin–Benson cycle shown in (A).

= 18 carbons total) (see Figure 10.3). One of the glyceraldehyde 3-phosphate molecules can be removed from the cycle to feed into another metabolic pathway (e.g., starch or sucrose synthesis or respiration), while the other five are used to regenerate three molecules of ribulose 1,5-bisphosphate.

The regeneration of ribulose 1,5-bisphosphate ensures the continuous assimilation of CO_2

In the regeneration phase, the Calvin–Benson cycle facilitates the continuous uptake of atmospheric CO_2 by restoring the CO_2 acceptor ribulose 1,5-bisphosphate. To this end, three molecules of ribulose 1,5-bisphosphate (3 molecules × 5 carbons/molecule = 15 carbons total) are formed by reactions that reshuffle the carbons from five molecules of glyceraldehyde 3-phosphate (5 molecules × 3 carbons/molecule = 15 carbons) (see Figure

(B)

Reactions of the Calvin–Benson cycle	
Reaction number (see Figure 10.3A) and enzyme name	**Reaction**
1. Ribulose 1,5-bisphosphate carboxylase/oxygenase (Rubisco)	Ribulose 1,5-bisphosphate + CO_2 + H_2O → 2 3-phosphoglycerate
2. 3-Phosphoglycerate kinase	3-Phosphoglycerate + ATP → 1,3-bisphosphoglycerate + ADP
3. NADP–glyceraldehyde-3-phosphate dehydrogenase	1,3-Bisphosphoglycerate + NADPH + H^+ → glyceraldehyde 3-phosphate + $NADP^+$ + P_i
4. Triose phosphate isomerase	Glyceraldehyde 3-phosphate → dihydroxyacetone phosphate
5. Aldolase	Glyceraldehyde 3-phosphate + dihydroxyacetone phosphate → fructose 1,6-bisphosphate
6. Fructose 1,6-bisphosphatase	Fructose 1,6-bisphosphate + H_2O → fructose 6-phosphate + P_i
7. Transketolase	Fructose 6-phosphate + glyceraldehyde 3-phosphate → erythrose 4-phosphate + xylulose 5-phosphate
8. Aldolase	Erythrose 4-phosphate + dihydroxyacetone phosphate → sedoheptulose 1,7-bisphosphate
9. Sedoheptulose 1,7-bisphosphatase	Sedoheptulose 1,7-bisphosphate + H_2O → sedoheptulose 7-phosphate + P_i
10. Transketolase	Sedoheptulose 7-phosphate + glyceraldehyde 3-phosphate → ribose 5-phosphate + xylulose 5-phosphate
11a. Ribulose 5-phosphate epimerase	Xylulose 5-phosphate → ribulose 5-phosphate
11b. Ribose 5-phosphate isomerase	Ribose 5-phosphate → ribulose 5-phosphate
12. Phosphoribulokinase (ribulose 5-phosphate kinase)	Ribulose 5-phosphate + ATP → ribulose 1,5-bisphosphate + ADP + H^+

Note: Pi stands for inorganic phosphate.

10.3). The sixth molecule of glyceraldehyde 3-phosphate (1 molecule × 3 carbons/molecule = 3 carbons total) represents the net assimilation of three molecules of CO_2 and becomes available for further carbon metabolism by the plant. The reshuffling of the other five molecules of glyceraldehyde 3-phosphate to yield three molecules of ribulose 1,5-bisphosphate proceeds through reactions 4 to 12 in Figure 10.3.

In summary, triose phosphates are formed in the carboxylation and reduction phases of the Calvin–Benson cycle using energy (ATP) and reducing equivalents (NADPH) generated by the illuminated photosystems of chloroplast thylakoid membranes:

$$3\ CO_2 + 3\ \text{ribulose 1,5-bisphosphate} + 3\ H_2O + 6\ \text{NADPH} + 6\ H^+ + 6\ \text{ATP} \downarrow 6\ \text{Triose phosphates} + 6\ \text{NADP}^+ + 6\ \text{ADP} + 6\ P_i$$

From these six triose phosphates, five are used in the regeneration phase that restores the CO_2 acceptor (ribulose 1,5-bisphosphate) for the continuous functioning of the Calvin–Benson cycle:

$$5\ \text{Triose phosphates} + 3\ \text{ATP} + 2\ H_2O \rightarrow 3\ \text{ribulose 1,5-bisphosphate} + 3\ \text{ADP} + 2\ P_i$$

The sixth triose phosphate represents the net synthesis of an organic compound from CO_2 that is used as a building block for stored carbon or for other metabolic processes. Hence, the fixation of three CO_2 generates one new triose phosphate (glyceraldehyde 3-phosphate) using 6 NADPH and 9 ATP:

$$3\ CO_2 + 5\ H_2O + 6\ \text{NADPH} + 9\ \text{ATP} \downarrow \text{Glyceraldehyde 3-phosphate} + 6\ \text{NADP}^+ + 9\ \text{ADP} + 8\ P_i$$

Stated another way, the Calvin–Benson cycle uses two molecules of NADPH and three molecules of ATP to assimilate each molecule of CO_2. For a detailed analysis of the efficiency of the Calvin–Benson cycle in the use of energy, see **WEB TOPIC 10.4**.

An induction period precedes the steady state of photosynthetic CO_2 assimilation

In the dark, both the activity of photosynthetic enzymes and the concentration of intermediates of the Calvin–Benson cycle are low. Therefore, enzymes of the Calvin–Benson cycle and most of the triose phosphates are committed to restore adequate concentrations of metabolic intermediates when leaves receive light. The rate of

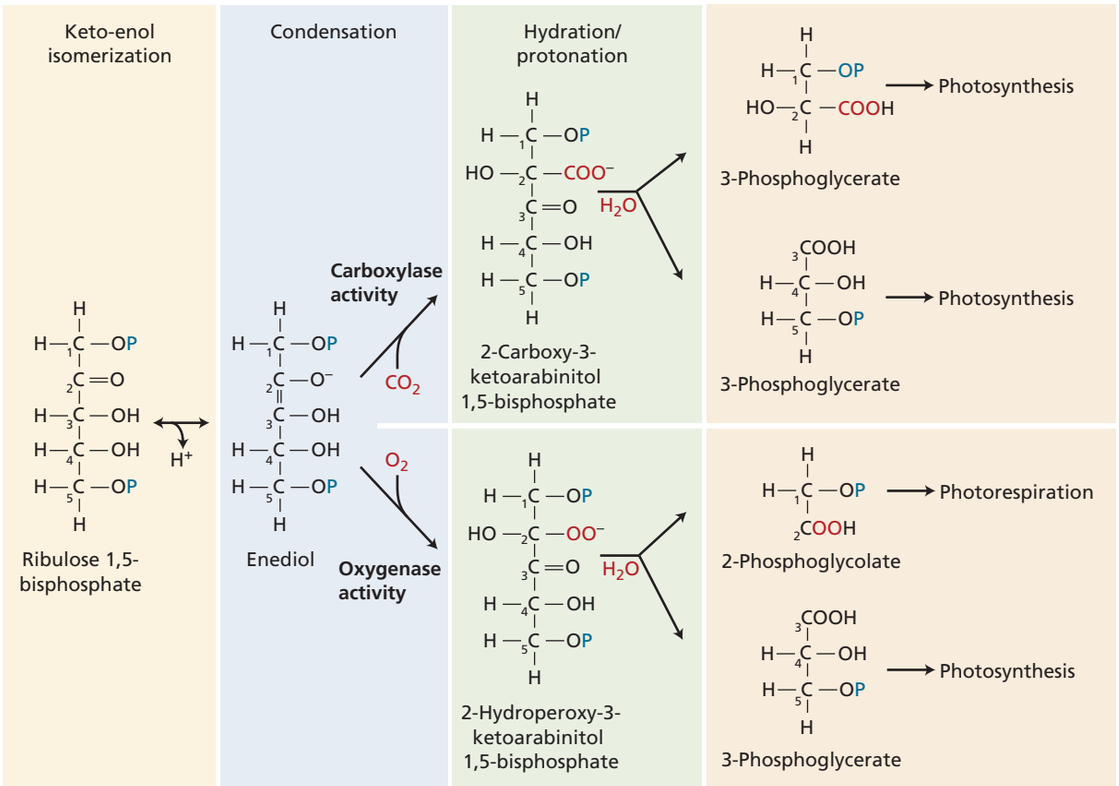


Figure 10.4 Carboxylation and oxygenation of ribulose 1,5-bisphosphate catalyzed by Rubisco. The binding of ribulose 1,5-bisphosphate to Rubisco facilitates the formation of an enzyme-bound enediol intermediate that can be attacked by CO_2 or O_2 at carbon 2. With CO_2, the product is a six-carbon intermediate (2-carboxy-3-ketoarabinitol 1,5-bisphosphate); with O_2, the product is a five-carbon reactive intermediate (2-hydroperoxy-3-ketoarabinitol 1,5-bisphosphate). The hydration of these intermediates at carbon 3 triggers the cleavage of the carbon–carbon bond between carbons 2 and 3, yielding two molecules of 3-phosphoglycerate (carboxylase activity) or one molecule of 2-phosphoglycolate and one molecule of 3-phosphoglyerate (oxygenase activity). The important physiological effects of the oxygenase activity are described in Section 10.2.

CO_2 fixation increases with time in the first few minutes after the onset of illumination—a time lag called the **induction period**. The acceleration of the photosynthetic rate is due to both the activation of enzymes by light (discussed later in this section) and an increase in the concentration of intermediates of the Calvin–Benson cycle. In short, the six triose phosphates formed in the carboxylation and reduction phases of the Calvin–Benson cycle during the induction period are used mainly to build up the intermediates needed to regenerate the CO_2 acceptor ribulose 1,5-bisphosphate.

When photosynthesis reaches a steady state, five of the six triose phosphates formed continue to contribute to the regeneration of the CO_2 acceptor ribulose 1,5-bisphosphate, while the sixth triose phosphate can be used in the chloroplast for starch formation, in the cytosol for sucrose synthesis, and for other metabolic processes (see Figure 10.2), such as respiration (see Chapter 13).

Many mechanisms regulate the Calvin–Benson cycle

The efficient use of energy in the Calvin–Benson cycle requires the existence of specific regulatory mechanisms that ensure not only that all intermediates in the cycle are present at adequate concentrations in the light, but also that the cycle is turned off in the dark. To produce the necessary metabolites in response to environmental stimuli, chloroplasts achieve the appropriate rates of biochemical transformations through the modification

of enzyme levels (μmoles of enzyme/chloroplast) and catalytic activities (moles of substrate converted/[minute × mole of enzyme]).

Gene expression and protein biosynthesis determine the concentrations of enzymes in cell compartments. The amounts of enzymes present in the chloroplast stroma are regulated by the coordinated expression of nuclear and plastid genomes. This coordination is controlled in part by pentatricopeptide repeat (PPR) proteins, which are nucleus-encoded chloroplast RNA-binding proteins that help regulate expression of plastid genes. Nucleus-encoded enzymes are translated on 80S ribosomes in the cytosol and subsequently transported into the plastid. Alternatively, plastid-encoded proteins are translated in the stroma on prokaryotic-like 70S ribosomes.

Light modulates the expression of stromal enzymes encoded by the nuclear genome via specific photoreceptors (e.g., phytochrome and blue-light receptors; see Chapters 16 and 17). However, nuclear gene expression needs to be synchronized with the expression of other components of the photosynthetic apparatus in the organelle. Most of the regulatory signaling between nucleus and plastids is anterograde—that is, the products of nuclear genes control the transcription and translation of plastid genes. Such is the case, for example, in the assembly of stromal Rubisco from eight nucleus-encoded small subunits (S) and eight plastid-encoded large subunits (L). However, in some cases (e.g., the synthesis of proteins associated with chlorophyll), regulation can be retrograde—that is, the regulatory signal flows from the plastid to the nucleus.

In contrast to slow changes in catalytic rates caused by variations in the concentration of enzymes, post-translational modifications rapidly change the specific activity of chloroplast enzymes (moles of substrate converted/[minute × mole of enzyme]). Two general mechanisms accomplish the light-mediated modification of the kinetic properties of stromal enzymes:

1. Change in covalent bonds that result in a chemically modified enzyme, such as the carbamylation of amino groups [$Enz–NH_2 + CO_2 \leftrightarrow Enz–NH–CO_2^- + H^+$], the reduction of disulfide bonds [$Enz–(S)_2 + Prot–(SH)_2 \leftrightarrow Enz–(SH)_2 + Prot–(S)_2$], and (de) phosphorylation by kinases and phosphatases
2. Modification of noncovalent interactions caused by changes in (i) ionic composition of the cellular milieu (e.g., pH, Mg^{2+}), (ii) binding of enzyme effectors, (iii) close association with regulatory proteins in supramolecular complexes, or (iv) interaction with thylakoid membranes

In our further discussion of regulation in this section, we examine light-dependent mechanisms that regulate the specific activity of five pivotal enzymes (see Figure 10.3) within minutes of the dark-to-light transition:

- Rubisco
- Fructose 1,6-bisphosphatase
- Sedoheptulose 1,7-bisphosphatase
- Phosphoribulokinase
- NADP–glyceraldehyde-3-phosphate dehydrogenase

Rubisco activase regulates the catalytic activity of Rubisco

Most life forms in the biosphere depend on photosynthetic organisms that capture inorganic carbon from the environment through the Calvin–Benson cycle. That point notwithstanding, the maximum number of molecules of CO_2 that Rubisco converts to products per catalytic site per second (*turnover rate*) is low (varying from 1–6 CO_2 fixed/s in land plants to 12 CO_2 fixed/s in some cyanobacteria and other bacteria). George Lorimer and colleagues found that Rubisco must even be activated before it can act as a catalyst. Chemical modifications, site-directed mutagenesis, molecular dynamics calculations, and high-resolution crystal structures showed that CO_2 plays a dual role in the activity of Rubisco: CO_2 is required to transform the enzyme from an inactive to an active form (*activation*) and is also the substrate for the carboxylase reaction (*catalysis*) (**Figure 10.5**).

The catalytic activities of Rubisco—carboxylation and oxygenation—require the formation of a lysyl-carbamate (EC) on a conserved lysine residue by a molecule of CO_2 called *activator* CO_2 (see "Rubisco activation" in Figure 10.5). The subsequent binding of Mg^{2+} to the carbamate stabilizes the carbamylated Rubisco (ECM) and converts Rubisco to a catalytically competent enzyme. Another molecule of CO_2—*substrate* CO_2—can then react with the enediol formed from ribulose 1,5-bisphosphate at the active site of Rubisco (see "Catalytic cycle" in Figure 10.5), releasing two molecules of 3-phosphoglycerate (the "Product" in "Catalytic cycle").

Sugar phosphates (such as xylulose 1,5-bisphosphate) and the substrate (ribulose 1,5-bisphosphate) can prevent activation and inhibit catalysis by binding tightly to the uncarbamylated Rubisco. Additionally, 2-carboxy-D-arabinitol 1-phosphate (CA1P) can bind to the activated Rubisco (ECM) and inactivate the enzyme. Plants and green algae overcome this inhibition with the enzyme Rubisco activase, which in an ATP-dependent reaction, modifies the active site and releases the inhibitory sugar phosphates from the inactivated Rubisco, thus reactivating Rubisco (see "Rubisco activase" in Figure 10.5; also see **WEB TOPIC 10.5**).

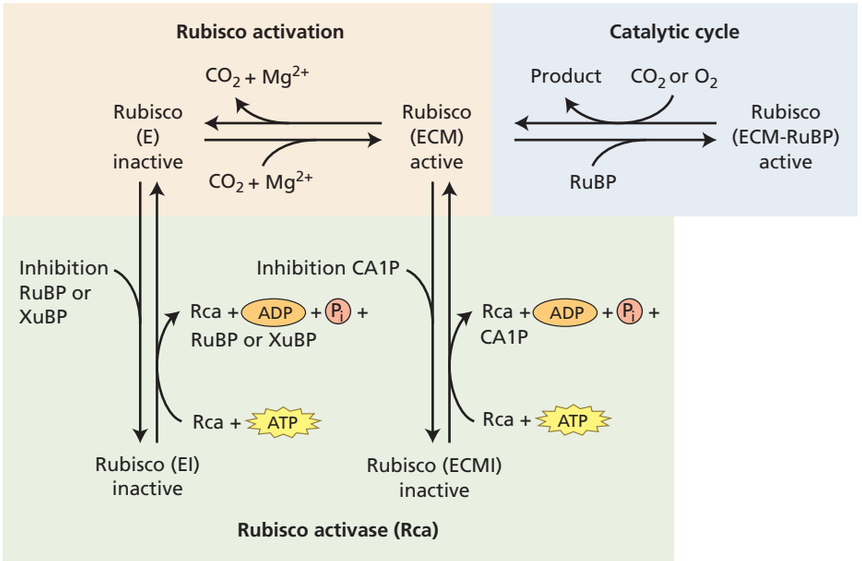


Figure 10.5 **CO_2 functions as both an activator and a substrate in the reaction catalyzed by Rubisco.** *Rubisco activation*: The reaction of activator CO_2 with Rubisco (E) causes formation of the unstable adduct E–carbamate(EC) (not shown), which is stabilized by reaction with Mg^{2+} to yield the E–carbamate-Mg^{2+} adduct (ECM) at the enzyme's active site. In the stroma of illuminated chloroplasts, the increase in both pH (lower H^+ concentration) and concentration of Mg^{2+} facilitates the formation of the ECM complex, which represents the catalytically active form of Rubisco. The tight binding of sugar phosphates, such as xylulose 1,5-bisphosphate (XuBP) or ribulose 1,5-bisphosphate (RuBP) (to give EI), prior to activation either impedes the production of the EC or blocks the binding of substrates to the carbamylated enzyme. Additionally, 2-carboxy-D-arabinitol 1-phosphate (CA1P) can bind to ECM, inactivating Rubisco (ECMI). *Rubisco activase*: In the Rubisco activase–mediated cycle, the hydrolysis of ATP by Rubisco activase (Rca) elicits a conformational change of Rubisco that reduces its binding affinity for sugar phosphates and leads to the formation of the ECM-activated form of Rubisco. *Catalytic cycle:* The ECM can then combine with ribulose 1,5-bisphosphate, forming the enediol that is subsequently attacked by either CO_2 or O_2, initiating the carboxylase or oxygenase activities, respectively (see Figure 10.4).

RUBISCO ACTIVASE In many plant species, the alternative splicing of a unique pre-mRNA yields two identical Rubisco activases that differ only at the carboxyl terminus: the long-form α (46 kDa) and the short-form β (42 kDa). The C-terminal extension of the long-form α carries two cysteines that modulate the sensitivity of ATPase activity to the ATP:ADP ratio by thiol–disulfide exchange. In this way, regulation of Rubisco activase is linked to light via the ferredoxin–thioredoxin system described in the next subsection. However, other, still unknown, components may be involved because light also stimulates the activity of Rubisco in species that naturally produce only the short-form β, which lacks the regulatory cysteines (see **WEB TOPIC 10.5**).

Light regulates the Calvin–Benson cycle via the ferredoxin–thioredoxin system

Light regulates the catalytic activity of four enzymes of the Calvin–Benson cycle directly via the **ferredoxin–thioredoxin system**. This mechanism uses ferredoxin reduced by the photosynthetic electron transport chain together with two chloroplast proteins (ferredoxin–thioredoxin reductase and thioredoxin) to regulate fructose 1,6-bisphosphatase, sedoheptulose 1,7-bisphosphatase, phosphoribulokinase, and NADP–glyceraldehyde-3-phosphate dehydrogenase (**Figure 10.6**).

Light transfers electrons from water to ferredoxin via the photosynthetic electron transport system (see Chapter 9). Reduced ferredoxin converts the disulfide bond of the regulatory protein thioredoxin (—S—S—) to the reduced state (—SH HS—) with the iron–sulfur enzyme ferredoxin–thioredoxin reductase. Subsequently, reduced thioredoxin cleaves a specific disulfide bridge (oxidized cysteines) of the target enzyme, forming free (reduced) cysteines. The cleavage of the enzyme disulfide bonds causes a conformational change that increases catalytic activity (see Figure 10.6). Deactivation of thioredoxin-activated enzymes takes place when darkness relieves the "electron pressure" from photosynthetic electron transport, but the precise details of the deactivation process are unknown.

Proteomic studies have shown that the ferredoxin–thioredoxin system regulates enzymes functional in numerous chloroplast processes other than carbon

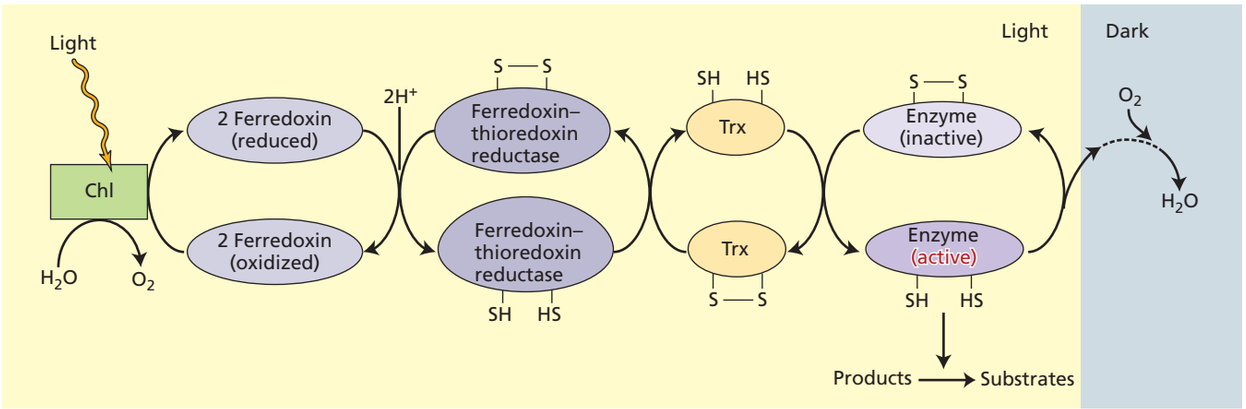


Figure 10.6 **Ferredoxin–thioredoxin system.** The ferredoxin–thioredoxin system links the redox status of the thylakoid membranes to the activity of enzymes in the chloroplast stroma. The activation of enzymes of the Calvin–Benson cycle starts in the light with the reduction of ferredoxin by the photosynthetic electron transport chain (Chl) (see Chapter 9). Reduced ferredoxin, together with two protons, is used to reduce a catalytically active disulfide bond (—S—S—) of the iron-sulfur enzyme ferredoxin–thioredoxin reductase, which in turn reduces the unique disulfide bond (—S—S—) of the regulatory protein thioredoxin (Trx). The reduced form of thioredoxin (—SH HS—) then reduces regulatory disulfide bonds of the target enzyme, triggering its conversion to the catalytically active state that catalyzes the transformation of substrates into products. Darkness halts the electron flow from ferredoxin to the enzyme, and thioredoxin becomes oxidized through an unknown mechanism involving molecular oxygen. Next, the unique disulfide bond (—S—S—) of thioredoxin brings the reduced form (—SH HS—) of the enzyme back to the oxidized form (—S—S—) with the concurrent loss of the catalytic capacity. In contrast to thioredoxin-activated enzymes, a chloroplast enzyme of the oxidative pentose phosphate cycle, glucose 6-phosphate dehydrogenase, does not operate in the light but is functional in the dark because thioredoxin reduces the disulfide critical for the activity of the enzyme.

fixation. Additionally, thioredoxin also protects proteins against damage caused by reactive oxygen species, such as hydrogen peroxide (H_2O_2), the superoxide anion ($O_2^{\bullet -}$), and the hydroxyl radical ($^{\bullet}OH$).

Light-dependent ion movements modulate enzymes of the Calvin–Benson cycle

Upon illumination, the electron transport chain leads to the flow of protons from the stroma into the thylakoid lumen and generates the proton motive force, which leads to the release of Mg^{2+} from the thylakoid lumen to the stroma. These light-actuated ion fluxes decrease the stromal concentration of protons (the pH increases from 7 to 8) and increase Mg^{2+} from 2 to 5 m*M*. The light-mediated increase of pH and the concentration of Mg^{2+} activate enzymes of the Calvin–Benson cycle that require Mg^{2+} for catalysis and are more active at pH 8 than at pH 7: Rubisco, fructose 1,6-bisphosphatase, sedoheptulose 1,7-bisphosphatase, and phosphoribulokinase. Modifications of the ionic composition within the chloroplast stroma are rapidly reversed upon darkening.

Light controls the assembly of chloroplast enzymes into supramolecular complexes

The formation of supramolecular complexes with regulatory proteins also has important effects on the catalytic activity of chloroplast enzymes. For example, glyceraldehyde-3-phosphate dehydrogenase binds noncovalently with phosphoribulokinase and CP12—a protein of approximately 10.5 kDa containing four conserved cysteines able to form two disulfide bridges (**Figure 10.7**). The three proteins form a ternary complex (CP12–phosphoribulokinase–glyceraldehyde 3-phosphate dehydrogenase) wherein glyceraldehyde-3-phosphate dehydrogenase and phosphoribulokinase are catalytically inactive. Light regulates the stability of the ternary complex through the ferredoxin–thioredoxin system. Reduced thioredoxin cleaves the disulfide bonds of both phosphoribulokinase

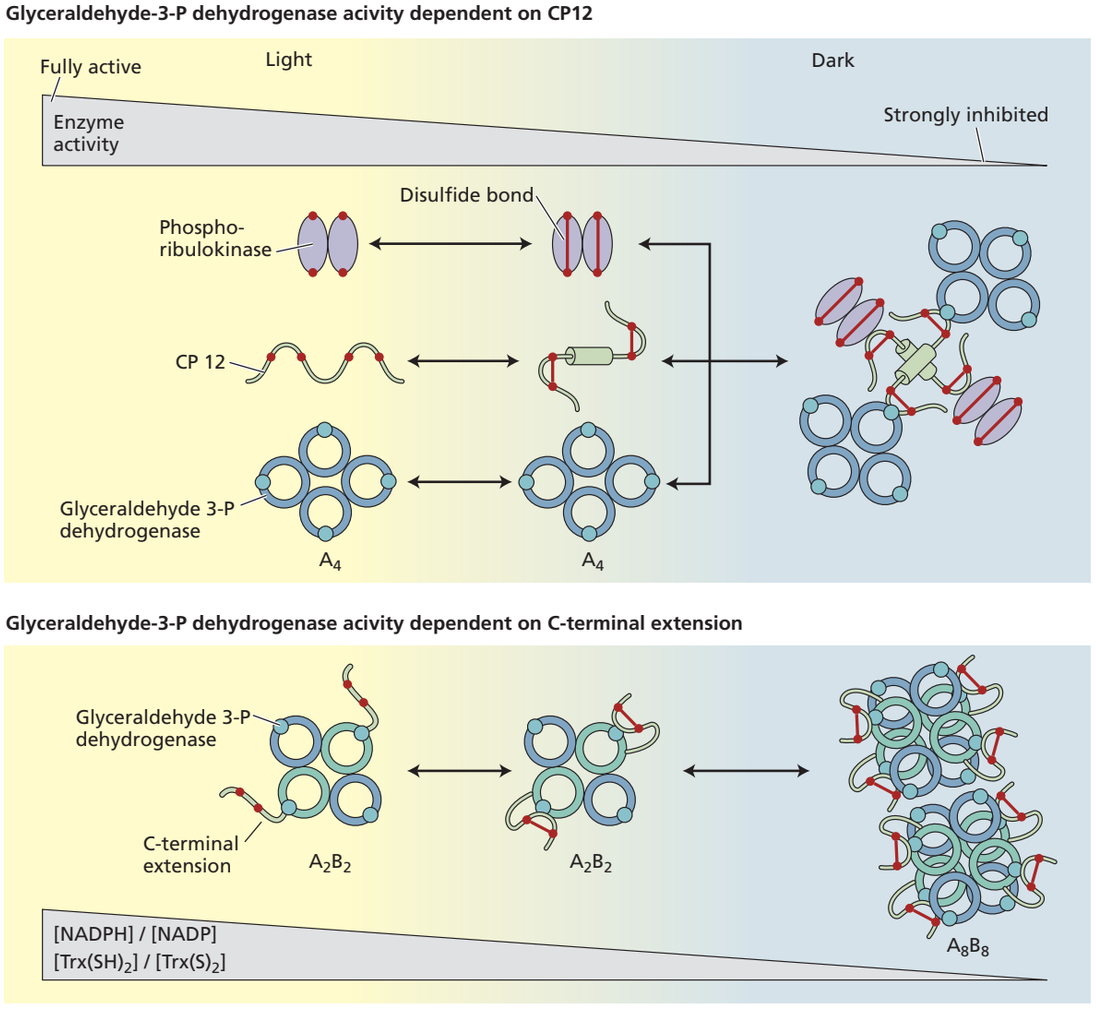


Figure 10.7 **Regulation of chloroplast phosphoribulokinase and glyceraldehyde-3-phosphate dehydrogenase.** Chloroplasts contain two isoforms of glyceraldehyde-3-phosphate dehydrogenases, named A_4 and A_2B_2. The A and B polypeptides of the A_2B_2 isoform are similar except that a C-terminal extension of the subunit B holds two cysteines able to form a disulfide bridge. Under "dark conditions," the interaction of oxidized phosphoribulokinase with the A_4-glyceraldehyde-3-phosphate dehydrogenase and oxidized CP12 stabilizes the complex [(A_4-glyceraldehyde-3-phosphate dehydrogenase)$_2$•(phosphoribulokinase)$_2$•(CP12)$_4$]. Both A_4-glyceraldehyde-3-phosphate dehydrogenase and phosphoribulokinase are catalytically inactive in the ternary complex. The A_2B_2 glyceraldehyde-3-phosphate dehydrogenase also becomes inactive in the dark by forming A_8B_8 oligomers. Under "light conditions," reduced thioredoxin cleaves the disulfide bonds of CP12 and phosphoribulokinase. The reduction of phosphoribulokinase and CP12 separates the components of the ternary complex, releasing the active phosphoribulokinase and the active A_4-glyceraldehyde 3-phosphate dehydrogenase. Reduced thioredoxin (Trx) also cleaves the disulfide bond in subunit B of A_8B_8-glyceraldehyde-3-phosphate dehydrogenase. The reduction converts the inactive oligomer into the active A_2B_2-glyceraldehyde-3-phosphate dehydrogenase.

and CP12, releasing glyceraldehyde-3-phosphate dehydrogenase and phosphoribulokinase in the catalytically active conformations.

10.2 The Oxygenation Reaction of Rubisco and Photorespiration

Rubisco catalyzes both the carboxylation and the oxygenation of ribulose 1,5-bisphosphate (see Figure 10.4). Carboxylation yields two molecules of 3-phosphoglycerate, and oxygenation produces one molecule each of 3-phosphoglycerate and 2-phosphoglycolate. 2-Phosphoglycolate is an inhibitor of two chloroplast enzymes (triose phosphate isomerase and phosphofructokinase) and cannot be directly processed by the Calvin–Benson cycle. To avoid both the drain of carbon out of the Calvin–Benson cycle and enzyme inhibition, 2-phosphoglycolate is metabolized through the oxidative photosynthetic carbon

cycle. This network of coordinated enzymatic reactions, also known as **photorespiration**, occurs in chloroplasts, leaf peroxisomes, and mitochondria (**Figure 10.8**) (see **WEB TOPIC 10.6**).

Recent studies have shown that photorespiration is an essential component of photosynthesis that not only salvages part of the assimilated carbon, but also links to other important pathways (e.g., amino acid biosynthesis, nitrogen assimilation, 1-carbon metabolism) of contemporary land plants. In this section we begin with the relevant features of photorespiration in land plants. Next we describe the integration of photorespiration into plant metabolism and then turn to different approaches to increase the yield of crop biomass through the modification of leaf photorespiration.

The oxygenation of ribulose 1,5-bisphosphate sets in motion photorespiration

In evolutionary terms, Rubisco appears to have evolved from an ancient enolase in the archaeal methionine-salvage pathway. Billions of years ago, oxygenation of ribulose 1,5-bisphosphate was insignificant in non-oxygenic prokaryotes because of the lack of O_2 and high levels of CO_2 in the ancient atmosphere. The high concentrations of O_2 and low levels of CO_2 in the extant atmosphere boost the oxygenase activity of Rubisco, making inevitable the formation of the toxic 2-phosphoglycolate. All Rubiscos catalyze the incorporation of O_2 into ribulose 1,5-bisphosphate. Even homologs from anaerobic autotrophic bacteria exhibit the oxygenase activity, demonstrating that the oxygenase reaction is intrinsically linked to the active site of Rubisco and not an adaptive response to the appearance of O_2 in the biosphere.

The oxygenation of the 2,3-enediol isomer of ribulose 1,5-bisphosphate with one molecule of O_2 yields an unstable intermediate that rapidly splits into one molecule each of 3-phosphoglycerate and 2-phosphoglycolate (see Figure 10.4 and Figure 10.8, reaction 1). In chloroplasts of land plants, 2-phosphoglycolate phosphatase catalyzes the rapid hydrolysis of 2-phosphoglycolate to glycolate (see Figure 10.8, reaction 2). The subsequent transformations of glycolate take place in the peroxisomes and mitochondria (see Chapters 1 and 13). Glycolate leaves the chloroplasts through specific transporters— either the plastidial glycolate/glycerate transporter (PLGG1) or the bile acid sodium symporter BASS6— in the envelope inner membrane and diffuses to the peroxisomes (see Figure 10.8). In peroxisomes, glycolate oxidase catalyzes the oxidation of glycolate by O_2, producing H_2O_2 and glyoxylate (see Figure 10.8, reaction 3). The peroxisomal catalase breaks down the H_2O_2, releasing O_2 and H_2O (see Figure 10.8, reaction 4). The glutamate:glyoxylate aminotransferase catalyzes the transamination of glyoxylate with glutamate, yielding the amino acid glycine (see Figure 10.8, reaction 5).

Glycine exits the peroxisomes and enters the mitochondria, where a multienzyme complex of glycine decarboxylase (GDC) and serine hydroxymethyltransferase (SHMT) catalyzes the conversion of two molecules of glycine and one molecule of NAD^+ into one molecule each of serine, NADH, NH_4^+, and CO_2 (see Figure 10.8, reactions 6 and 7). This sequence of reactions is initiated by GDC, using one molecule of NAD^+ for the oxidative decarboxylation of one molecule of glycine, yielding one molecule each of NADH, NH_4^+, and CO_2 and the activated one-carbon unit methylene tetrahydrofolate (THF) bound to GDC (GDC-THF-CH_2):

$$\text{Glycine} + NAD^+ + \text{GDC-THF} \rightarrow \text{NADH} + NH_4^+ + CO_2 + \text{GDC-THF-}CH_2$$

Next, SHMT catalyzes the addition of the methylene unit to a second molecule of glycine, forming serine and regenerating GDC-THF:

$$\text{Glycine} + \text{GDC-THF-}CH_2 \rightarrow \text{Serine} + \text{GDC-THF}$$

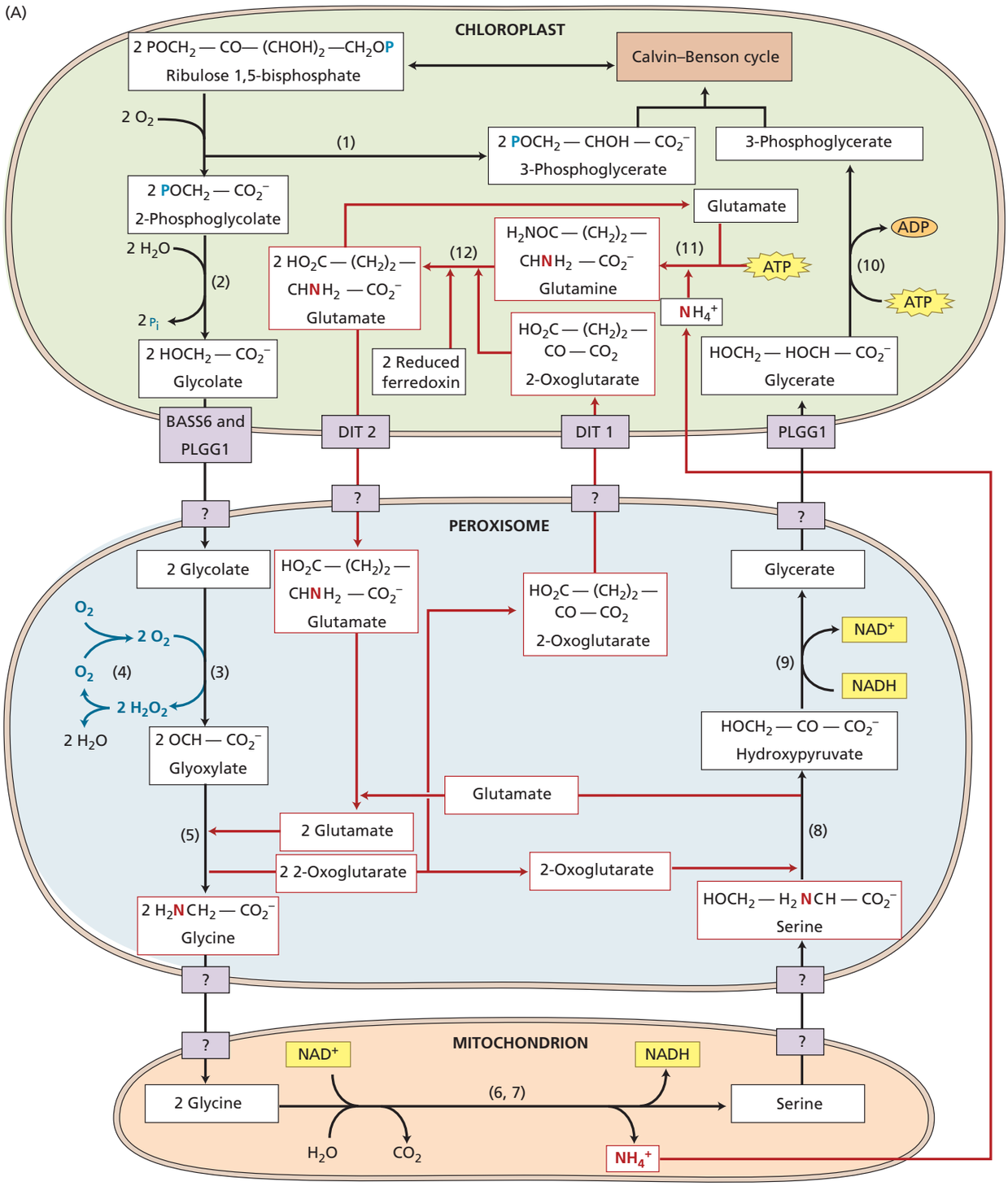
The oxidation of carbon atoms (two molecules of glycine [oxidation states C1: +3; C2: –1] → serine [oxidation states C1: +3; C2: 0; C3: –1] and CO_2 [oxidation state C: +4]) drives the reduction of oxidized pyridine nucleotide:

$$NAD^+ + H^+ + 2\,e^- \rightarrow \text{NADH}$$

The products of the GDC and SHMT reactions are metabolized at different locations in leaf cells. NADH is oxidized to NAD^+ in the mitochondria. NH_4^+ and CO_2 diffuse out of the mitochondria and can be refixed in the chloroplasts, where they are assimilated to form glutamate and 3-phosphoglycerate, respectively.

The newly formed serine diffuses from the mitochondria back to the peroxisomes for donation of its amino group to 2-oxoglutarate via transamination catalyzed by serine:2-oxoglutarate aminotransferase, forming glutamate and hydroxypyruvate (see Figure 10.8, reaction 8). Next, an NADH-dependent reductase catalyzes the transformation of hydroxypyruvate into glycerate (see Figure 10.8, reaction 9). Finally, glycerate reenters the chloroplast, where it is phosphorylated by glycerate kinase using ATP to yield 3-phosphoglycerate and ADP (see Figure 10.8, reaction 10). Hence, the formation of 2-phosphoglycolate (via Rubisco) and the phosphorylation of glycerate (via glycerate kinase) metabolically link the Calvin–Benson cycle to photorespiration.

The NH_4^+ released in the oxidation of glycine diffuses from the matrix of the mitochondria to the chloroplasts (see Figure 10.8). In the chloroplast stroma, glutamine synthetase catalyzes the ATP-dependent incorporation of NH_4^+ into glutamate, yielding glutamine, ADP, and inorganic phosphate (see Figure 10.8, reaction 11). Subsequently, glutamine and 2-oxoglutarate are substrates


(A)
CHLOROPLAST
2 POCH2 — CO— (CHOH)2 —CH2OP
Ribulose 1,5-bisphosphate
Calvin–Benson cycle
2 O2
(1)
2 POCH2 — CHOH — CO2−
3-Phosphoglycerate
3-Phosphoglycerate
2 POCH2 — CO2−
2-Phosphoglycolate
Glutamate
2 H2O
(2)
2 Pi
2 HO2C — (CH2)2 — CHNH2 — CO2−
Glutamate
(12)
H2NOC — (CH2)2 — CHNH2 — CO2−
Glutamine
(11)
ATP
ADP
(10)
ATP
NH4+
2 HOCH2 — CO2−
Glycolate
2 Reduced ferredoxin
HO2C — (CH2)2 — CO — CO2
2-Oxoglutarate
HOCH2 — HOCH — CO2−
Glycerate
BASS6 and PLGG1
DIT 2
DIT 1
PLGG1
?
?
?
?
PEROXISOME
2 Glycolate
HO2C — (CH2)2 — CHNH2 — CO2−
Glutamate
HO2C — (CH2)2 — CO — CO2
2-Oxoglutarate
Glycerate
O2
2 O2
O2
(4)
(3)
2 H2O2
2 H2O
NAD+
NADH
(9)
2 OCH — CO2−
Glyoxylate
HOCH2 — CO — CO2−
Hydroxypyruvate
Glutamate
(5)
2 Glutamate
(8)
2 2-Oxoglutarate
2-Oxoglutarate
HOCH2 — H2NCH — CO2−
Serine
2 H2NCH2 — CO2−
Glycine
?
?
?
?
MITOCHONDRION
NAD+
NADH
2 Glycine
(6, 7)
Serine
H2O
CO2
NH4+

(B)

Reactions of photorespiration

Reaction number (see Figure 10.8A) and enzyme name	Reaction[a]
1. Rubisco	2 Ribulose 1,5-bisphosphate + 2 O_2 → 2 2-phosphoglycolate + 2 3-phosphoglycerate
2. Phosphoglycolate phosphatase	2 2-Phosphoglycolate + 2 H_2O → 2 glycolate + 2 P_i
3. Glycolate oxidase	2 Glycolate + 2 O_2 → 2 glyoxylate + 2 H_2O_2
4. Catalase	2 H_2O_2 → 2 H_2O + O_2
5. Glutamate:glyoxylate aminotransferase	2 Glyoxylate + 2 glutamate → 2 glycine + 2 2-oxoglutarate
6. Glycine decarboxylase complex (GDC)	Glycine + NAD^+ + [GDC] → CO_2 + NH_4^+ + NADH + [GDC-THF-CH_2]
7. Serine hydroxymethyl transferase	[GDC-THF-CH_2] + glycine + H_2O → serine + [GDC]
8. Serine:2-oxoglutarate aminotransferase	Serine + 2-oxoglutarate → hydroxypyruvate + glutamate
9. Hydroxypyruvate reductase	Hydroxypyruvate + NADH + H^+ → glycerate + NAD^+
10. Glycerate kinase	Glycerate + ATP → 3-phosphoglycerate + ADP
11. Glutamine synthetase	Glutamate + NH_4^+ + ATP → glutamine + ADP + Pi
12. Ferredoxin-dependent glutamate synthase (GOGAT)	2-Oxoglutarate + glutamine + 2 Fd_{red} + 2 H^+ → 2 glutamate + 2 Fd_{oxid}

[a]Locations: Chloroplasts; peroxisomes; mitochondria. Fd: ferredoxin.

(C) Net reaction of photorespiration

2 Ribulose 1,5-bisphosphate + 3 O_2 + H_2O + glutamate
↓ **(reactions 1 to 9)**
Glycerate + 2 3-phosphoglycerate + NH_4^+ + CO_2 + 2 P_i + 2-oxoglutarate

Two reactions in the chloroplasts restore the molecule of glutamate:

2-Oxoglutarate + NH_4^+ + [(2 Fd_{red} + 2 H^+), ATP]
↓ **(reactions 11 and 12)**
Glutamate + H_2O + [(2 Fd_{oxid}), ADP + P_i]

and the molecule of 3-phosphoglycerate:

Glycerate + ATP
↓ **(reaction 10)**
3-Phosphoglycerate + ADP

Hence, the consumption of three molecules of atmospheric oxygen in the C_2 oxidative photosynthetic carbon cycle (two in the oxygenase activity of Rubisco and one in peroxisomal oxidations) elicits

- the release of one molecule of CO_2 and
- the consumption of two molecules of ATP and two molecules of reducing equivalents (2 Fd_{red} + 2 H^+)

for

- incorporating a three-carbon skeleton back into the Calvin–Benson Cycle, and
- restoring glutamate from NH_4^+ and 2-oxoglutarate.

Figure 10.8 **Operation of photorespiration.** **(A)** Enzymatic reactions are distributed in three organelles: chloroplasts, peroxisomes, and mitochondria. *In chloroplasts*, the oxygenase activity of Rubisco reacting with two molecules of oxygen yields two molecules of 2-phosphoglycolate, which are converted into two molecules of glycolate. The glycolates are transported from the chloroplast and imported into the peroxisome where they are oxidized by O_2 to glyoxylate. The glyoxylate is converted into glycine, which moves from peroxisomes and into the mitochondria. *In mitochondria*, two molecules of glycine (four carbons) yield a molecule of serine (three carbons) with the concurrent release of CO_2 (one carbon) and NH_4^+. The amino acid serine is then transported back to the peroxisome and transformed to glycerate (three carbons), which return to chloroplasts in a process that recovers part of the carbon (three carbons) and all the nitrogen released by the GDC cycle. For details, see the text. **(B)** A description of the numbered reactions of photorespiration shown in (A). **(C)** Net reaction of the photorespiratory cycle.

of ferredoxin-dependent glutamate synthase (GOGAT) for the production of two molecules of glutamate (see Figure 10.8, reaction 12). The reassimilation of NH_4^+ released from the photorespiratory cycle restores glutamate for the action of the peroxisomal glutamate:glyoxylate aminotransferase in the conversion of glyoxylate to glycine (see Figure 10.8, reaction 5).

Carbon, nitrogen, and oxygen atoms circulate through photorespiration (**Figure 10.9**).

- In the *carbon* cycle, the chloroplasts transfer two molecules of glycolate (four carbon atoms) to peroxisomes and recover one molecule of glycerate (three carbon atoms). The mitochondria release one molecule of CO_2 (one carbon atom).
- In the *nitrogen* cycle, the chloroplasts transfer one molecule of glutamate (one nitrogen atom) and recover one molecule of NH_4^+ (one nitrogen atom).
- In the *oxygen* cycle, Rubisco and glycolate oxidase catalyze the incorporation of two molecules of O_2 each (eight oxygen atoms) when two molecules of ribulose 1,5-bisphosphate enter photorespiration (see Figure 10.8, reactions 1 and 3). However, catalase releases one molecule of O_2 from two molecules of H_2O_2 (two oxygen atoms) (see Figure 10.8, reaction 4). Hence, three molecules of O_2 (six oxygen atoms) are reduced in the photorespiratory cycle.

In vivo, three aspects regulate the distribution of metabolites between the Calvin–Benson cycle and photorespiration: (i) the kinetic properties of Rubisco (inherent to the plant), (ii) the availability of atmospheric CO_2 and O_2, and (iii) the temperature.

The specificity factor ($S_{c/o}$) estimates the preference of Rubisco for CO_2 versus O_2:

$$S_{c/o} = [V_C/K_C]/[V_O/K_O] \qquad (10.1)$$

where V_C and V_O are the maximum velocities for carboxylation and oxygenation, respectively, and K_C and K_O are the Michaelis–Menten constants for CO_2 and O_2, respectively. $S_{c/o}$ determines the ratio of the velocity of carboxylation (v_C) to that of oxygenation (v_O) at given concentrations of CO_2 and O_2:

$$S_{c/o} = v_C/v_O \times [(O_2)/(CO_2)] \qquad (10.2)$$

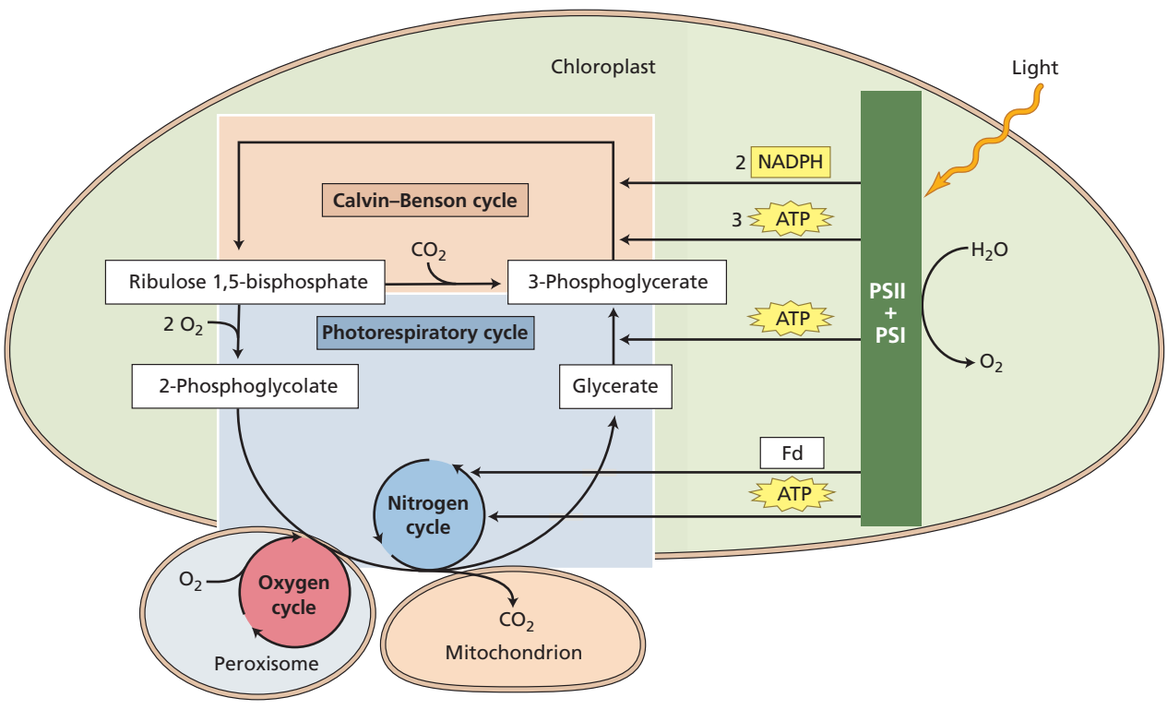


Figure 10.9 Dependence of photorespiration on chloroplast metabolism. The supply of ATP and reducing equivalents from light reactions in thylakoid membranes is needed for the functioning of photorespiration in three compartments: chloroplasts, peroxisomes, and mitochondria. The *carbon cycle* uses (1) NADPH and ATP to maintain the adequate level of ribulose 1,5-bisphosphate in the Calvin–Benson cycle and (2) ATP to convert glycerate to 3-phosphoglycerate in photorespiration. The *nitrogen cycle* employs ATP and reducing equivalents to restore glutamate from NH_4^+ and 2-oxoglutarate coming from the photorespiratory cycle. In the peroxisome, the *oxygen cycle* contributes to the removal of H_2O_2 formed in the oxidation of glycolate by O_2.

When the concentration of CO_2 around the active site is equal to that of O_2 [$(O_2)/(CO_2) = 1$], $S_{c/o}$ estimates the relative capacity of Rubisco for carboxylation and oxygenation (v_C/v_O). $S_{c/o}$ at a given temperature is generally constant but tends to decrease as temperature increases. Additionally, $S_{c/o}$ for Rubisco from different organisms varies: The $S_{c/o}$ of Rubisco from cyanobacteria (~40) is lower than that from C_3 plants (~82–90) and from C_4 species (~70–82) (see the discussion of C_3 and C_4 photosynthesis in Sections 10.3 and 10.4, respectively). There is generally a trade-off in the affinity of Rubisco for CO_2 and the catalytic speed of the carboxylation reaction such that enzymes that evolved under high-CO_2 conditions tend to have a low $S_{c/o}$ and those that evolved under low-CO_2 availability tend to have a high $S_{c/o}$.

The ambient temperature exerts an important influence over $S_{c/o}$ and the concentrations of O_2/CO_2 around the active site of Rubisco. Warmer environments have the effect of:

- Increasing the oxygenase activity of Rubisco more than the carboxylase activity, suggesting that a greater increase of K_C for CO_2 than of K_O for O_2 diminishes $S_{c/o}$.
- Lowering the solubility of CO_2 to a greater extent than O_2. The increase of $[O_2]/[CO_2]$ decreases the v_C/v_O ratio; that is, the oxygenase activity of Rubisco prevails over the carboxylase activity (see **WEB TOPIC 10.8**).
- Reducing the stomatal aperture to conserve water. The stomatal closure lowers the uptake of atmospheric CO_2, thereby decreasing CO_2 at the active site of Rubisco (see Chapter 6).

Overall, warmer environments significantly limit the efficiency of photosynthetic carbon assimilation because the progressive increase in temperature tilts the balance away from carboxylation (photosynthesis) and toward oxygenation (photorespiration) (see Chapter 11).

Photorespiration is linked to the photosynthetic electron transport system

Photosynthetic carbon metabolism in intact leaves reflects the competition for ribulose 1,5-bisphosphate between two mutually opposing cycles, the Calvin–Benson cycle and photorespiration. These cycles are interlocked with the photosynthetic electron transport system for the supply of ATP and reducing equivalents (reduced ferredoxin and NADPH) (see Figure 10.9). For salvaging two molecules of 2-phosphoglycolate by conversion to one molecule of 3-phosphoglycerate, photophosphorylation provides one molecule of ATP necessary for the transformation of glycerate to 3-phosphoglycerate (see Figure 10.8, reaction 10), while the consumption of NADH by hydroxypyruvate reductase (see Figure 10.8, reaction 9) is counterbalanced by its production by glycine decarboxylase (see Figure 10.8, reaction 6).

In photorespiration, nitrogen:

- *Enters* into the peroxisome through the transamination step catalyzed by the glutamate:glyoxylate aminotransferase (two nitrogen atoms) (see Figure 10.8, reaction 5), and
- *Leaves* (1) from the mitochondria as NH_4^+ (one nitrogen atom), in the reaction catalyzed by the glycine decarboxylase–serine hydroxymethyltransferase complex (see Figure 10.8, reactions 6 and 7) (2) from the peroxisomes in the transamination step catalyzed by serine:2-oxoglutarate aminotransferase (one nitrogen atom) (see Figure 10.8, reaction 8).

The photosynthetic electron transport system supplies one molecule of ATP and two molecules of reduced ferredoxin needed for salvaging one molecule of NH_4^+ through its incorporation into glutamate via glutamine synthetase (see Figure 10.8, reaction 11) and ferredoxin-dependent glutamate synthase (GOGAT) (see Figure 10.8, reaction 12).

In summary, each oxygenation reaction produces one molecule each of 3-phosphoglycerate and 2-phosphoglycolate such that the net reaction of two oxygenation reactions is:

$$\begin{gathered}2\ \text{Ribulose 1,5-bisphosphate} + 3\ O_2 + H_2O + ATP + \\ [2\ \text{ferredoxin}_{red} + 2\ H^+ + ATP] \\ \downarrow \\ 3\ \text{3-Phosphoglycerate} + CO_2 + 2\ P_i + ADP + \\ [2\ \text{ferredoxin}_{oxid} + ADP + P_i]\end{gathered}$$

Because of the additional provision of ATP and reducing power for the operation of the photorespiratory cycle, the quantum requirement for CO_2 fixation under photorespiratory conditions (high $[O_2]$ and low $[CO_2]$) is higher than under nonphotorespiratory conditions (low $[O_2]$ and high $[CO_2]$). **Box 10.1** discusses genetically engineered photorespiratory bypasses in land plants. The quantum requirement for CO_2 fixation is further discussed in Chapter 11.

Enzymes of plant photorespiration derive from different ancestors

The complete genomes of different organisms have demonstrated that all photorespiratory enzymes are present in plants and in red and green algae. Moreover, these phylogenetic studies suggest that the distribution of enzymes in plants correlates with the origin of compartments involved in photorespiration. Chloroplast enzymes evolved from a cyanobacterial endosymbiont, while mitochondrial enzymes have a proteobacterial ancestor. For example, chloroplast glycerate kinase is of cyanobacterial origin, and mitochondrial glycine

Box 10.1 Production of Biomass May Be Enhanced by Engineering Photorespiration

Solutions to the current food and energy shortages depend on the degree to which land plants can be altered for higher CO_2 assimilation. When O_2 outcompetes CO_2, the oxygenase activity of Rubisco lowers the amount of carbon that enters the Calvin–Benson cycle. Therefore, to understand how to engineer leaf cells for improving the photosynthetic efficiency, scientists are tackling various aspects of the oxygenation reaction of Rubisco and photorespiration, from modification of the active site of Rubisco to genetically engineering bypasses of the traditional photorespiratory pathways. The engineering of catalytically more efficient Rubiscos in plants has been challenging, but future progress is likely with the rapid development of new genetic tools and a better understanding of Rubisco kinetic constraints. An attractive alternative possibility is to incorporate more efficient mechanisms for retrieving the carbon atoms of the 2-phosphoglycolate that is generated by the reaction of Rubisco with O_2 and the wasteful release of ammonia by the GDC in the mitochondria.

There have been several engineering approaches to lower the flux of photorespiratory metabolites through peroxisomes and mitochondria, releasing photorespired CO_2 in the chloroplast where it can be directly refixed. One of the first approaches was to introduce a bacterial (*E. coli*) glycolate catabolic pathway into chloroplasts of a land plant (Arabidopsis) (see **WEB TOPIC 10.8**). Chloroplasts of these transgenic plants have an entirely functional photorespiratory cycle formed from the bacterial enzymes glycolate dehydrogenase, tartronic semialdehyde synthase, and tartronic semialdehyde reductase. The engineered plants grow faster, have increased biomass, and contain higher levels of soluble sugars under short-day growth conditions.

A second approach used the overexpression of three enzymes in the chloroplast stroma of Arabidopsis—glycolate oxidase, catalase, and malate synthase—to release CO_2 from glycolate. First, the oxidation of glycolate by the novel chloroplast glycolate oxidase yields glyoxylate and H_2O_2, and catalase catalyzes the subsequent decomposition of H_2O_2 [2 glycolate + 2 O_2 → 2 glyoxylate + 2 H_2O_2; 2 H_2O_2 → 2 H_2O + O_2]. Next, the successive action of two enzymes converts two molecules of glyoxylate (two carbon atoms) into pyruvate (three carbon atoms) and CO_2 (one carbon atom):

- Malate synthase catalyzes the condensation of glyoxylate with acetyl-CoA [CoA-S~CO-CH_3], yielding malate [glyoxylate + CoA-S~CO-CH_3 → malate + CoA-SH].
- The chloroplastic NADP–malic enzyme catalyzes the decarboxylation of malate to pyruvate with the concurrent formation of NADPH [malate + $NADP^+$ → pyruvate + CO_2 + NADPH + H^+].

Finally, chloroplastic pyruvate dehydrogenase catalyzes the conversion of pyruvate into acetyl-CoA, yielding NADH and another molecule of CO_2 [pyruvate + CoA-SH + NAD^+ → CoA-S~CO-CH_3 + CO_2 + NADH + H^+]. As a result of this alternative cycle, one molecule of glycolate (two carbon atoms) is converted to two molecules of CO_2 (two carbon atoms). The oxidation of carbon atoms yields reducing power in the form of NADPH and NADH. These Arabidopsis plants also had increased biomass production compared with control plants under short-day growth conditions.

These novel pathways depart from plant photorespiration in sidestepping the mitochondrial and peroxisomal reactions. Therefore, the shift of glycolate from plant photorespiration to the engineered pathways releases CO_2 in the immediate vicinity of Rubisco, allowing rapid refixation of the CO_2, and at the same time avoids the use of energy (ATP and reductant) required to recover NH_4^+.

Recently, similar photorespiratory bypasses have been combined with repression of the chloroplast glycolate exporter (PLGG1) (see Figure 10.8), which leads to further yield increases in field-grown tobacco. There are still questions regarding the mechanisms that confer the yield benefits of these photorespiratory bypasses, but these initial studies are encouraging and there are continued efforts in this area of research (see https://ripe.illinois.edu).

decarboxylase comes from an ancient proteobacterium (see Chapter 1).

Photorespiration interacts with many metabolic pathways

Early research suggested that photorespiration served to salvage carbon diverted by the oxygenase activity of Rubisco and to protect plants from stressful conditions such as high light, drought (water deficit stress), and salt stress. The negative impact of lacking photorespiration on photosynthetic CO_2 assimilation was first demonstrated by plant mutants that do not survive in air (21% O_2; 0.04% CO_2) but resume their normal growth in high-CO_2 environments (2% CO_2). This *photorespiratory phenotype* served to identify previously unknown enzymes and reactions of photorespiration. For example, Arabidopsis mutants lacking glycerate kinase accumulate glycerate and concurrently are incapable of growing in normal air, but are viable in atmospheres with elevated levels of CO_2.

Studies have also revealed a tight connection between photorespiration and other pathways of plant metabolism. For example, key steps of photorespiration interact with:

- *Nitrogen metabolism at multiple levels*: Photorespiration reassimilates NH_4^+ formed in the mitochondria, uses glutamate in peroxisomal transaminations, and produces amino acids (serine, glycine) for other metabolic pathways.
- *Cell redox homeostasis*: H_2O_2 formed by the peroxisomal glycolate oxidase regulates the redox state of leaves. The formation of H_2O_2 induces suicide programs in catalase-deficient barley plants that exhibit the photorespiratory phenotype. Although H_2O_2 damages key cellular molecules such as DNA and lipids, the current view recognizes this reactive oxygen species as a signaling molecule linked to hormone and stress responses.
- *C_1 metabolism*: 5,10-methylene tetrahydrofolate is the cofactor required by glycine decarboxylase–serine hydroxymethyltransferase in the conversion of glycine to serine in the mitochondria. Reactions mediated by folates transfer one-carbon units in the synthesis of precursors for proteins, nucleic acids, lignin, and alkaloids.
- *Expression of transcription factors*: More than 200 transcription factors are differentially expressed when plants are transferred from atmospheres with high levels of CO_2 to normal air. Photorespiratory conditions (high $[O_2]$, low $[CO_2]$) enhance the expression of genes encoding the components of cyclic electron flow pathways, consistent with the additional demand for energy by the photorespiratory pathway. Photorespiratory conditions decrease the expression of genes encoding proteins involved in synthesis of starch and sucrose and in the metabolism of nitrogen and sulfur.

10.3 Inorganic Carbon–Concentrating Mechanisms

Except for some photosynthetic bacteria, all other photoautotrophic organisms in the biosphere use the Calvin–Benson cycle to assimilate atmospheric CO_2. The pronounced reduction in atmospheric CO_2 and rise in O_2 levels that commenced about 350 million years ago triggered a series of adaptations to handle an environment that promoted photorespiration in photosynthetic organisms. These adaptations include various strategies for active uptake of CO_2 and HCO_3^- from the surrounding environment and accumulation of inorganic carbon near Rubisco. The immediate consequence of higher levels of CO_2 around Rubisco is a decrease in the oxygenation reaction. Plasma membrane CO_2 and HCO_3^- pumps have been studied extensively in prokaryotic cyanobacteria, eukaryotic algae, and aquatic plants (see **WEB TOPIC 10.1** and **WEB ESSAY 10.2**) but have not been identified in terrestrial plants.

In land plants, the diffusion of CO_2 from the atmosphere to the chloroplast plays a crucial role in net photosynthesis. During C_3 photosynthesis, once CO_2 is within the leaf it has to cross four barriers (the cell wall, plasma membrane, cytosol, and chloroplast envelope) before reaching Rubisco. Recent evidence has revealed that pore-forming membrane proteins (aquaporins) and leaf anatomy probably both influence the diffusion of CO_2 within the leaf to the initial site of carboxylation. However, the combined effects of relatively low atmospheric CO_2 availability (e.g., low stomatal conductance because of drought) and resistance to CO_2 movement within the leaf can limit rates of C_3 photosynthesis and decrease leaf-level water use efficiency (see Chapter 11).

Land plants evolved two carbon-concentrating mechanisms for increasing the concentration of CO_2 at the site of Rubisco carboxylation:

- C_4 photosynthetic carbon fixation (C_4)
- Crassulacean acid metabolism (CAM)

The uptake of atmospheric CO_2 by these carbon-concentrating mechanisms precedes CO_2 assimilation through the Calvin–Benson cycle.

10.4 Inorganic Carbon–Concentrating Mechanisms: C_4 Photosynthetic Carbon Fixation

C_4 photosynthesis has evolved as one of the major carbon-concentrating mechanisms used by terrestrial plants to compensate for limitations associated with low availability of atmospheric CO_2. This CO_2-concentrating mechanism evolved in more that 60 plant lineages, and some of the most productive crops on the planet (e.g., maize [corn; *Zea mays*], sugarcane, sorghum) use this mechanism to enhance the carboxylation capacity of Rubisco. In this section we examine:

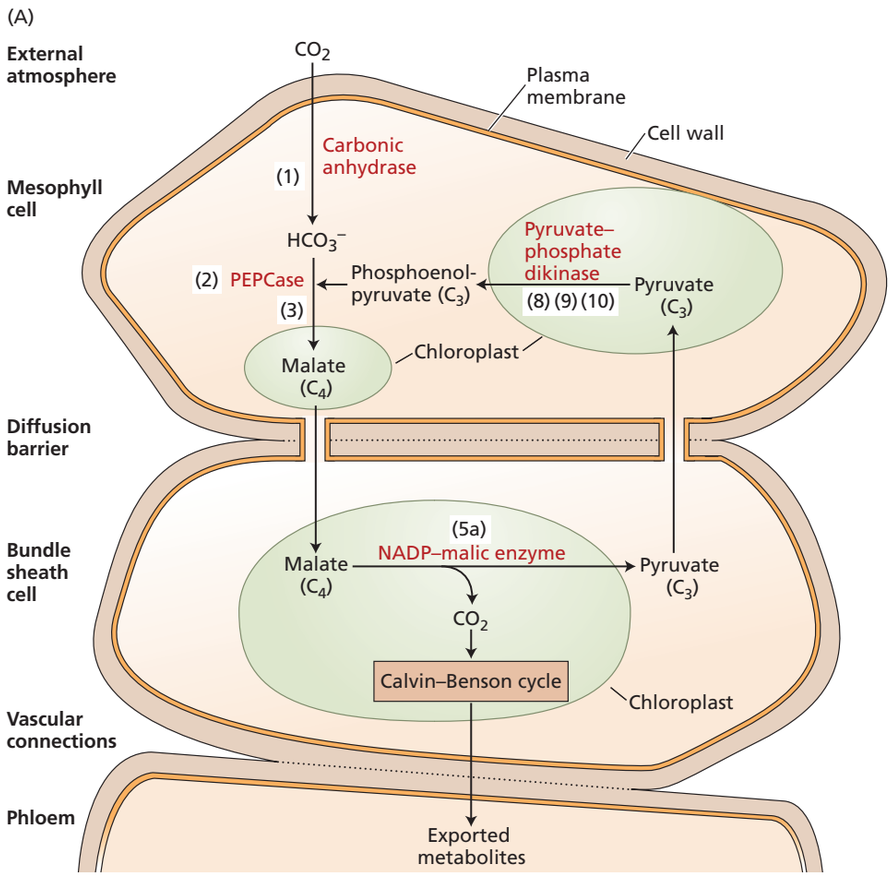
- The biochemical and anatomical attributes of C_4 photosynthesis that minimize the oxygenation reaction of Rubisco oxygenation and the rate of photorespiration
- The requirements of the spatial separation of the C_4 biochemistry and variation in decarboxylation of inorganic carbon
- The light-mediated regulation of enzyme activities, and
- The importance of C_4 photosynthesis for sustaining plant growth in many tropical areas

Malate and aspartate are the primary carboxylation products of the C_4 cycle

In the late 1950s, H. P. Kortschack and Y. Karpilov independently observed that ^{14}C label appeared initially in the four-carbon acids malate and aspartate when $^{14}CO_2$ was provided to leaves of sugarcane and maize in the light. This finding was unexpected because a three-carbon acid, 3-phosphoglycerate, is the first labeled product in the Calvin–Benson cycle. In subsequent experiments, M. D. Hatch and C. R. Slack used "pulse-chase" labeling with $^{14}CO_2$ to demonstrate the transfer of carbon from four-carbon acids to the Calvin–Benson cycle. They found that (1) malate and aspartate are the first stable intermediates of photosynthesis and (2) that the carbon 4 of these four-carbon acids subsequently becomes carbon 1 of 3-phosphoglycerate. These transformations take place in two morphologically distinct cell types—the mesophyll and bundle sheath cells—that are separated by their respective walls and membranes ("Diffusion barrier" in **Figure 10.10**). This pathway is named the *C_4 photosynthetic carbon cycle* (also known as the Hatch–Slack cycle or the C_4 cycle).

During C_4 photosynthesis, the enzyme phosphoenolpyruvate carboxylase (PEPCase), rather than Rubisco, catalyzes the initial carboxylation in mesophyll cytosol close to the external atmosphere (see Figure 10.10, reaction 1) (see **WEB ESSAY 10.1**). The carboxylation by PEPCase uses bicarbonate (HCO_3^-) instead of CO_2, and unlike with Rubisco, this reaction is not inhibited by O_2. The four-carbon acids formed in mesophyll cells flow across the diffusion barrier via the plasmodesmata to the bundle sheath cells, where they are decarboxylated, releasing CO_2 that is refixed by Rubisco via the Calvin–Benson cycle. Although all C_4 plants share primary carboxylation via PEPCase, the other enzymes used to release CO_2 around Rubisco vary among different C_4 biochemical subtypes (see **WEB TOPIC 10.9**).

Since the seminal studies of the 1950s and the 1960s, the C_4 cycle has been associated with a particular leaf structure, called **Kranz anatomy** (*Kranz*, German for "wreath"). Typical Kranz anatomy exhibits an inner ring of bundle sheath cells around vascular tissues and an outer layer of mesophyll cells (**Figure 10.11A and B**). This particular leaf anatomy generates a diffusion barrier that (1) separates the uptake of atmospheric carbon



by PEPCase in mesophyll cells from CO_2 assimilation by Rubisco in bundle sheath cells and (2) limits the leakage of CO_2 from bundle sheath to mesophyll cells. However, there are now clear examples of single-cell C_4 photosynthesis in several green algae, diatoms, and aquatic and land plants (typified in the land plants by *Suaeda aralocaspica* [formerly *Borszczowia aralocaspica*] and three *Bienertia* species) (**Figure 10.11C**) (see **WEB TOPIC 10.10**). In summary, a diffusion gradient is needed to concentrate CO_2 around Rubisco, but this barrier can be *between* or *within* cells as long as the resistance is sufficient to minimize energy-wasteful overcycling and leakage of CO_2 from the compartmentalized area.

Kranz-type C_4 plants assimilate CO_2 by the concerted action of two different types of cells

The key features of the C_4 cycle were initially described in leaves of plants such as maize whose vascular tissues are surrounded by two distinctive photosynthetic cell types. In this anatomical context, the assimilation of CO_2 from the external atmosphere in the bundle sheath cells proceeds through five successive stages (see Figure 10.10):

1. Hydration of CO_2 by carbonic anhydrase, to generate HCO_3^- that is used to carboxylate phosphoenolpyruvate by PEPCase in the mesophyll cell cytosol (see Figure 10.10, reaction 2). The reaction product, oxaloacetate, is subsequently reduced to malate by NADP–malate dehydrogenase in the mesophyll chloroplasts (see Figure 10.10, reaction 3) or converted to aspartate by transamination with glutamate in the cytosol, depending on the C_4 subtype (see Figure 10.10, reaction 4) (see **WEB TOPIC 10.9**).
2. Diffusion of the four-carbon acids (malate or aspartate) through the plasmodesmata into the bundle sheath cells surrounding the vascular bundles.
3. Decarboxylation of the four-carbon acids and generation of CO_2, which is then reduced to triose

(B)

Reactions of C_4 photosynthesis	
Reaction numbers (see Figure 10.10A) and enzyme name	**Reaction**
1. Carbonic anhydrase	$CO_2 + H_2O \rightarrow H_2CO_3 \rightarrow H^+ + HCO_3^-$
2. PEPCase	Phosphoenolpyruvate + $HCO_3^- \rightarrow$ oxaloacetate + P_i
3. NADP–malate dehydrogenase	Oxaloacetate + NADPH + $H^+ \rightarrow$ malate + $NADP^+$
4. Aspartate aminotransferase	Oxaloacetate + glutamate → aspartate + 2-oxoglutarate
Decarboxylating enzymes	
5a. NADP–malic enzyme	Malate + $NADP^+ \rightarrow$ pyruvate + CO_2 + NADPH + H^+
5b. NAD–malic enzyme	Malate + $NAD^+ \rightarrow$ pyruvate + CO_2 + NADH + H^+
6. Phosphoenolpyruvate carboxykinase	Oxaloacetate + ATP → phosphoenolpyruvate + CO_2 + ADP
7. Alanine aminotransferase	Pyruvate + glutamate → alanine + 2-oxoglutarate
8. Pyruvate–phosphate dikinase	Pyruvate + P_i + ATP → phosphoenolpyruvate + AMP + PP_i
9. Adenylate kinase	AMP + ATP → 2 ADP
10. Pyrophosphatase	$PP_i + H_2O \rightarrow 2\ P_i$

Note: P_i and PP_i stand for inorganic phosphate and pyrophosphate, respectively.

Figure 10.10 **(A) The C_4 photosynthetic carbon cycle involves five successive stages in two distinct cell types.** (a) In the mesophyll cells, the enzyme phospho-enolpyruvate carboxylase (PEPCase) catalyzes the reaction of HCO_3^-, provided by the uptake of atmospheric CO_2, with phosphoenolpyruvate, a three-carbon compound (see reaction 2). The reaction product, oxaloacetate, a four-carbon compound, is further transformed to malate by the action of NADP–malate dehydrogenase (see reaction 3). (b) The four-carbon acid moves to the bundle sheath cell, close to vascular connections. (c) The decarboxylating enzyme (here, NADP–malic enzyme in the chloroplast; see reaction 5a) releases the CO_2 from the four-carbon acid, yielding a three-carbon acid (e.g., pyruvate). The released CO_2 in the bundle sheath chloroplast builds up a large excess of CO_2 over O_2 around Rubisco, thereby facilitating the assimilation of CO_2 through the Calvin–Benson cycle. (d) The residual three-carbon acid (pyruvate) flows back to the mesophyll cell. (e) To complete the C_4 cycle, the enzyme pyruvate–phosphate dikinase (reaction 8) catalyzes the regeneration of phosphoenolpyruvate, the acceptor of the HCO_3^-, for another turn of the cycle. The consumption of two molecules of ATP per molecule of fixed CO_2 (see reactions 8–10) drives the C_4 cycle in the direction of the arrows, thus pumping CO_2 from the atmosphere to the Calvin–Benson cycle. The assimilated carbon leaves the chloroplast and, after transformation to sucrose in the cytosol, enters the phloem for translocation to other parts of the plant. **(B)** The reactions of the C4 photosynthetic carbon cycle, some of which are shown in (A).

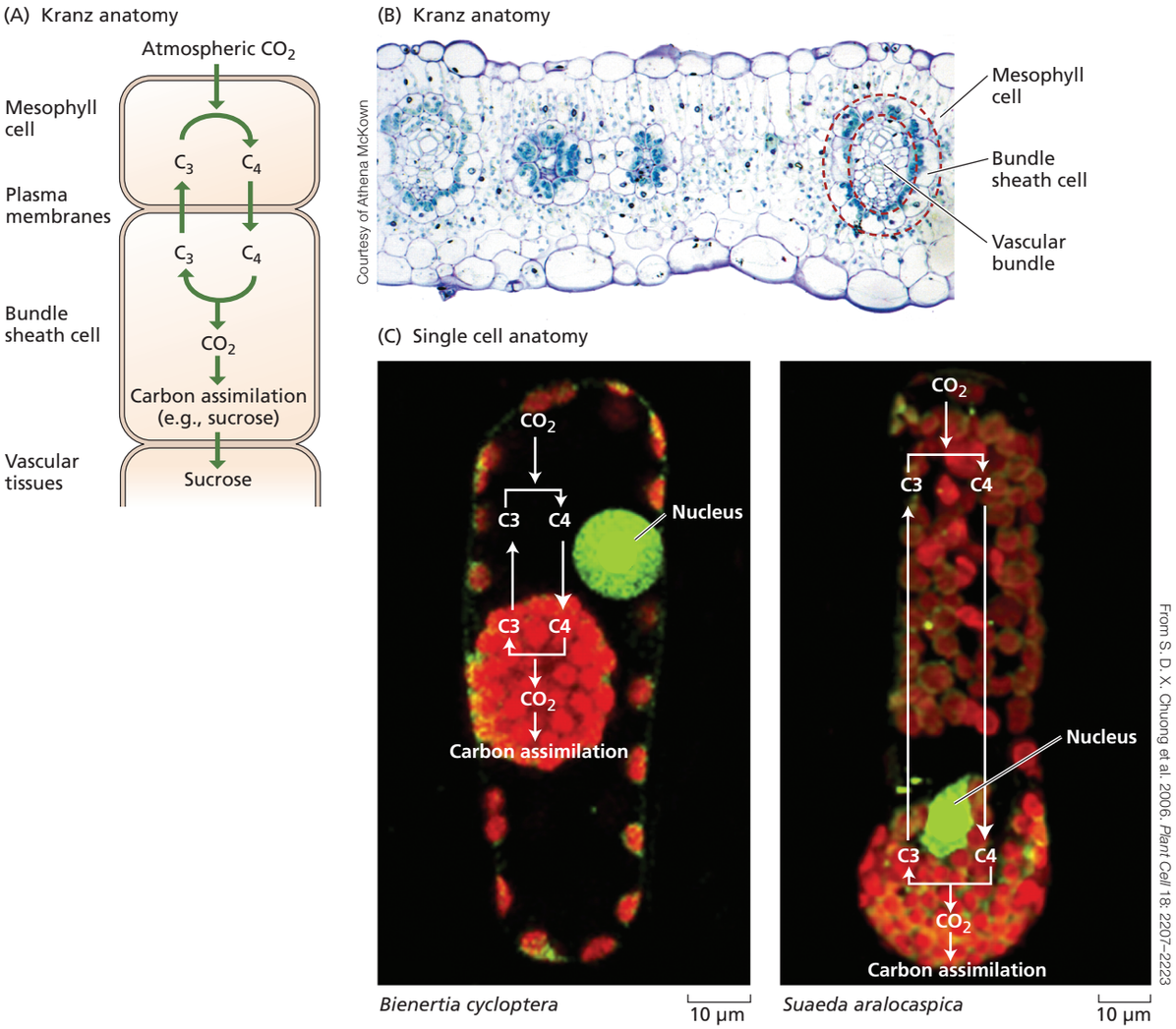


Figure 10.11 **C_4 photosynthetic pathway in leaves of different plants.** **(A and B)** In almost all known C_4 plants, photosynthetic CO_2 assimilation requires the development of Kranz anatomy. This anatomical feature compartmentalizes photosynthetic reactions in two distinct types of cells that are arranged concentrically around the veins: mesophyll and bundle sheath cells. Bundle sheath cells surround the vascular tissue, while an outer ring of mesophyll cells is peripheral to the bundle sheath and adjacent to intercellular spaces. The membrane and cell walls that separate these two cell types reduce the leakage of CO_2 from the bundle sheath cells and are essential for efficient C_4 photosynthesis in land plants. (B) Kranz anatomy. Light micrograph of transverse section of leaf blade of *Flaveria australasica* (NAD–malic enzyme type C_4 photosynthesis). **(C)** Single-cell C_4 photosynthesis occurs in organisms that contain the equivalent of the C_4 compartmentation in a single cell. Studies on the key photosynthetic enzymes of these plants indicate two dimorphic chloroplasts located in different cytoplasmic locations functioning analogously to mesophyll and bundle sheath cells in Kranz-type C_4 plants. Here, diagrams of the C_4 cycle are superimposed on fluorescent staining and immunofluorescence of *Bienertia cycloptera* (left) and *Suaeda aralocaspica* (right).

phosphate via the Calvin–Benson cycle. Prior to this reaction, an aspartate aminotransferase catalyzes the conversion of aspartate back to oxaloacetate in some C_4 plants (see Figure 10.10, reaction 4). Different types of C_4 plants make use of different decarboxylases to release CO_2 for the effective suppression of the oxygenase reaction of Rubisco (see Figure 10.10, reactions 5a, 5b, and 6) (see **WEB TOPIC 10.9**).

4. Diffusion back to the mesophyll cells of the three-carbon backbone (pyruvate or alanine) formed by the decarboxylation step.
5. Regeneration of phosphoenolpyruvate, the HCO_3^- acceptor, which consumes ATP and inorganic

phosphate and releases AMP and pyrophosphate. Two molecules of ATP are consumed in the conversion of pyruvate to phosphoenolpyruvate: one in the reaction catalyzed by pyruvate–phosphate dikinase (see Figure 10.10, reaction 8) and another in the formation of AMP from ADP by adenylate kinase (see Figure 10.10, reaction 9). When alanine is the three-carbon acid returned from the bundle sheath cells, the formation of pyruvate by alanine aminotransferase precedes phosphorylation by pyruvate–phosphate dikinase (see Figure 10.10, reaction 7).

The compartmentation of enzymes ensures that inorganic carbon from the surrounding atmosphere can be taken up initially by mesophyll cells, fixed subsequently by the Calvin–Benson cycle of bundle sheath cells, and finally exported to the phloem (see Figure 10.10 and Chapter 12).

The C_4 subtypes use different mechanisms to decarboxylate four-carbon acids transported to bundle sheath cells

The C_4 biochemical subtypes employ different mechanisms to decarboxylate the four-carbon acids in the bundle sheath cells, and shuttle different three-carbon compounds from bundle sheath cells back to the mesophyll cells (**Table 10.1**). Additionally, the four-carbon acid transported to the bundle sheath cells can be malate or aspartate, produced in the chloroplasts or cytosol of mesophyll cells, respectively.

In the NADP–malic enzyme (NADP–ME) type of C_4 photosynthesis shown in Figure 10.10, malate enters the chloroplast of bundle sheath cells, where it is decarboxylated by NADP–ME (see Figure 10.10, reaction 5a).

In the NAD–malic enzyme (NAD–ME) and PEP carboxykinase (PEPCK) types of C_4 photosynthesis, cytosolic aspartate aminotransferase of the bundle sheath cells catalyzes the conversion of aspartate back to oxaloacetate [aspartate + pyruvate → oxaloacetate + alanine]. In NAD–ME type C_4 plants, the oxaloacetate is reduced to malate in the mitochondria of bundle sheath cells via NAD–malate dehydrogenase and subsequently decarboxylated by NAD–ME (see Figure 10.10, reaction 5b). In PEPCK type C_4 plants, the majority of the oxaloacetate is decarboxylated to phosphoenolpyruvate in the cytosol of bundle sheath cells (see Figure 10.10, reaction 6), but these plants can also use NAD–ME to decarboxylate malate provided by the mesophyll cells. The released CO_2 diffuses from the mitochondria or cytosol to the chloroplasts of bundle sheath cells for fixation by Rubisco and reduction by the Calvin–Benson cycle.

In the chloroplasts of bundle sheath cells, the CO_2 released by the three decarboxylation reactions increases the concentration of CO_2 around the active site of Rubisco, thereby minimizing the inhibition by O_2. Pyruvate (from NADP–ME type C_4 photosynthesis) and alanine (from NAD–ME and PEPCK types) are transported from bundle sheath cells to the mesophyll cells for the regeneration of phosphoenolpyruvate. Although traditionally C_4 plants were classified as one subtype or another, data suggest that in some C_4 plants there is flexibility and overlap between these pathways.

Bundle sheath cells and mesophyll cells exhibit anatomical and biochemical differences

Originally described for tropical grasses and *Atriplex*, the C_4 cycle is now known to occur in at least 62 independent lineages of angiosperms distributed across 21 different families. C_4 plants evolved from C_3 ancestors around 30 million years ago in response to multiple environmental stimuli such as atmospheric changes (decline of CO_2 concentration, increase of O_2), modification of global weather, periods of drought, and intense solar radiation. The transition from C_3 to C_4 plants requires the coordinated modification of genes that affect leaf anatomy, cell ultrastructure, metabolite transport, and regulation of metabolic enzymes. The analyses of (i) specific genes and elements that control their expression; (ii) mRNAs and the deduced amino acid sequences; and (iii) C_3 and C_4 genomes and transcriptomes indicate that convergent evolution underlies the multiple origins of C_4 plants.

Found in all except four terrestrial plants (see next subsection), the distinctive Kranz anatomy increases the

Table 10.1 Mechanisms of C_4 acid decarboxylation in bundle sheath cells

Decarboxylating enzyme (subcellular localization)	C_4 acid transported [mesophyll → bundle sheath] for decarboxylation	C_3 acid moved [bundle sheath → mesophyll] for carboxylation	Plant
NADP–malic enzyme (NADP–ME) (chloroplast)	Malate	Pyruvate	*Sorghum bicolor*, *Zea mays*
NAD–malic enzyme (NAD–ME) (mitochondrion)	Aspartate	Alanine	Cleome, *Atriplex*
PEP carboxykinase (PEPCK) (cytosol)	Aspartate	Alanine, pyruvate, phosphoenolpyruvate	*Megathyrsus maximus*

concentration of CO_2 in bundle sheath cells to almost tenfold higher than that in the external atmosphere (see Figure 10.11A and B). The efficient accumulation of CO_2 in the vicinity of Rubisco reduces the rate of photorespiration to 2 to 3% of photosynthesis. Mesophyll and bundle sheath cells show large biochemical differences. PEPCase and Rubisco are located in mesophyll and bundle sheath cells, respectively, while the decarboxylases are found in different intracellular compartments of bundle sheath cells: NADP–ME in chloroplasts, NAD–ME in mitochondria, and PEPCK in the cytosol. In addition, mesophyll cells contain randomly arranged chloroplasts with stacked thylakoid membranes, while in some C_4 subtypes (primarily NADP–ME) the chloroplasts in bundle sheath cells are concentrically arranged and exhibit unstacked thylakoids. These chloroplast characteristics correlate with the energy requirements of the type of C_4 photosynthesis. For example, C_4 species of the NADP–ME subtype, in which malate is shuttled from mesophyll chloroplasts to bundle sheath cells, exhibit functional photosystems II and I in mesophyll chloroplasts, whereas bundle sheath chloroplasts are deficient in or have low levels of photosystem II and the associated oxygen-evolving complex (i.e., O_2 production from photosystem II is generally low in the bundle sheath cells of NADP–ME plants). In NAD–ME and PEPCK subtypes, by contrast, the bundle sheath chloroplasts and the mesophyll chloroplasts have similar levels of photosystem II.

The C_4 cycle also concentrates CO_2 in single cells

The finding of C_4 photosynthesis in terrestrial plants devoid of Kranz anatomy disclosed a much greater diversity in modes of C_4 carbon fixation than had previously been thought to exist (see **WEB TOPIC 10.10**). Four plants in the Chenopodiaceae that grow in the Middle East and parts of Asia, *Suaeda aralocaspica* (formerly *Borszczowia aralocaspica*) and three *Bienertia* species, perform complete C_4 photosynthesis within single chlorenchyma cells (see Figure 10.11C). The external region, proximal to the external atmosphere, carries out the initial carboxylation and regeneration of phosphoenolpyruvate, whereas the internal region functions in the decarboxylation of four-carbon acids and the refixation of the liberated CO_2 via Rubisco. The chlorenchyma cells of these species have dimorphic chloroplasts with different subsets of enzymes, similar to the two types of chloroplasts found in mesophyll versus bundle sheath cells of Kranz-type C_4 plants. In the single-cell C_4 plants, the large vacuole separating the two types of chloroplasts provides the diffusion resistance that allows the CO_2 concentration to build up around Rubisco.

Aquatic photosynthetic organisms, which account for approximately half of the global primary productivity, also use a single-cell CO_2-concentrating mechanism to suppress the Rubisco oxygenation reaction. As discussed in **WEB ESSAY 10.2**, there are some similarities, but also key differences, between the aquatic and terrestrial CO_2-concentrating mechanisms.

Light regulates the activity of key C_4 enzymes

In addition to supplying ATP and NADPH for the operation of the C_4 cycle, light is essential for the regulation of several participating enzymes. Variations in photon flux density elicit changes in the activities of NADP–malate dehydrogenase, PEPCase, and pyruvate–phosphate dikinase by two different mechanisms: thiol–disulfide exchange [Enz–$(Cys\text{-}S)_2$ ↔ Enz–$(Cys\text{-}SH)_2$] and phosphorylation–dephosphorylation of specific amino acid residues [e.g., serine, Enz–Ser-OH ↔ Enz–Ser-OP].

NADP–malate dehydrogenase is regulated via the ferredoxin–thioredoxin system as in C_3 plants (see Figure 10.6). The enzyme is reduced (activated) by thioredoxin when leaves are illuminated, and is oxidized (deactivated) in the dark. The diurnal phosphorylation of PEPCase by a specific kinase, named PEPCase kinase, is thought to increase the uptake of ambient CO_2, and the nocturnal dephosphorylation by protein phosphatase 2A brings PEPCase back to low activity. A highly unusual enzyme regulates the dark–light activity of pyruvate–phosphate dikinase. Pyruvate–phosphate dikinase is modified by a bifunctional threonine kinase–phosphatase that catalyzes both ADP-dependent phosphorylation and P_i-dependent dephosphorylation of pyruvate–phosphate dikinase. Darkness promotes the phosphorylation of pyruvate–phosphate dikinase (PPDK) by the regulatory kinase–phosphatase [$(PPDK)_{active}$ + ADP → $(PPDK\text{-}P)_{inactive}$ + AMP], causing the loss of enzyme activity. The phosphorolytic cleavage of the phosphoryl group in the light by the same enzyme restores the catalytic capacity of PPDK [$(PPDK\text{-}P)_{inactive} + P_i \rightarrow (PPDK)_{active} + PP_i$].

Photosynthetic assimilation of CO_2 in C_4 plants requires more transport processes than in C_3 plants

The chloroplasts export part of the fixed carbon to the cytosol during active photosynthesis while importing the phosphate released from biosynthetic processes to replenish ATP and other phosphorylated metabolites in the stroma. In C_3 plants, the major factors that modulate the partitioning of assimilated carbon between the chloroplast and cytosol are the relative concentrations of triose phosphates and inorganic phosphate. Triose phosphate isomerases rapidly interconvert dihydroxyacetone phosphate and glyceraldehyde 3-phosphate in the plastid and cytosol (see Figure 10.3B, reaction 4). The triose phosphate translocator—a protein complex in the inner membrane of the chloroplast envelope—exchanges chloroplast triose phosphates for cytosol phosphate. Thus, C_3 plants require one transport process across the chloroplast envelope to export triose

phosphates (three molecules of CO_2 assimilated) from the chloroplasts to the cytosol.

In C_4 plants, the distribution of photosynthetic CO_2 assimilation over two different cells entails a massive flux of metabolites between mesophyll cells and bundle sheath cells. Moreover, three different pathways accomplish the assimilation of inorganic carbon in C_4 photosynthesis. In this context, different metabolites flow from the cytosol of leaf cells to chloroplasts, mitochondria, and conducting tissues. Therefore, the composition and the function of translocators in organelles and plasma membrane of C_4 plants depend on the pathway used for CO_2 assimilation. For example, mesophyll cells of NADP–ME type C_4 photosynthesis use four transport steps across the chloroplast envelope to fix one molecule of atmospheric CO_2: (1) import of cytosolic pyruvate (Na^+-dependent pyruvate transporter); (2) export of stromal phosphoenolpyruvate (phosphoenolpyruvate phosphate translocator); (3) import of cytosolic oxaloacetate (dicarboxylate transporter); and (4) export of stromal malate (dicarboxylate transporter).

In hot, dry climates, the C_4 cycle reduces photorespiration

As noted in Section 10.2, elevated temperatures limit the rate of photosynthetic CO_2 assimilation in C_3 plants by decreasing the solubility of CO_2 and the ratio of the carboxylation to oxygenation reactions of Rubisco. Because of the decrease in the photosynthetic activity of Rubisco, the energy demands associated with photorespiration increase in warmer areas of the world. In C_4 plants, two features help overcome the deleterious effects of high temperature:

- First, atmospheric CO_2 enters the cytoplasm of mesophyll cells where carbonic anhydrase rapidly and reversibly converts CO_2 into bicarbonate [$CO_2 + H_2O \rightarrow HCO_3^- + H^+$] ($K_{eq} = 1.7 \times 10^{-4}$). The equilibrium between CO_2 and HCO_3^- is determined by the pH of the cytoplasm, but carbonic anhydrase speeds up the time to reach equilibration. This reaction by carbonic anhydrase is essential to maintain the high rates of C_4 photosynthesis, particularly in warm climates that tend to decrease the levels of CO_2 within the leaf. PEPCase also has a high affinity for HCO_3^- and thus high activity even when HCO_3^- is low. This enables C_4 plants to reduce their stomatal aperture at high temperatures and thereby conserve water while fixing CO_2 at rates equal to or greater than those of C_3 plants.
- Second, the high concentration of CO_2 in bundle sheath chloroplasts minimizes the oxygenation reaction of Rubisco and the operation of photorespiration.

The response of net CO_2 assimilation to temperature in part influences the distribution of C_3 and C_4 species on Earth. The optimal photosynthetic efficiency of C_3 species generally occurs at temperatures lower than for C_4 species: approximately 20–25°C and 25–35°C, respectively. By enabling more efficient assimilation of CO_2 at higher temperatures, C_4 species become more abundant in the tropics and subtropics and less abundant at latitudes farther from the equator. Although C_4 photosynthesis is commonly dominant in warm environments, a group of perennial grasses (*Miscanthus*, *Spartina*) are chilling-tolerant C_4 species that thrive in areas where the weather is moderately cold (see Chapter 11).

10.5 Inorganic Carbon–Concentrating Mechanisms: Crassulacean Acid Metabolism (CAM)

Another mechanism for concentrating CO_2 around Rubisco is present in approximately 350 genera and 35 terrestrial plant families that inhabit arid environments with seasonal water availability, including commercially important plants such as pineapple (*Ananas comosus*), agave (*Agave* spp.), cacti (Cactaceae), and orchids (Orchidaceae). This photosynthetic carbon fixation is named **crassulacean acid metabolism** (**CAM**), to recognize its initial observation in *Kalanchoe pinnata* a succulent member of the Crassulaceae. Like the C_4 mechanism, CAM appears to have originated during the last 35 million years in habitats where reductions in atmospheric CO_2 coupled with reduced stomatal conductance due to water limitations provided the selective pressure. The leaves of CAM plants have traits that minimize water loss, such as thick cuticles and stomata with small apertures, but which also minimize the access to atmospheric CO_2. The carbon-concentrating mechanism in CAM plants is temporal spacing between night and day reactions (**Figure 10.12**), which differs from that of C_4 plants, in which the carbon-concentrating mechanism is physical separation between the mesophyll and bundle sheath cells.

In all CAM plants, cytosolic PEPCase fixes HCO_3^- from atmospheric and respiratory CO_2 into oxaloacetate using phosphoenolpyruvate formed via the glycolytic breakdown of stored carbohydrates (see Figure 10.12 and Figure 10.10, reaction 2). A cytosolic NADP–malate dehydrogenase converts the oxaloacetate to malate (see Figure 10.10, reaction 3), which is stored in the vacuoles for the remainder of the night. During the day, the stored malate exits the vacuole for decarboxylation by cytosolic NADP–ME, mitochondrial NAD–ME, or cytosolic PEPCK, the same enzymes used in the three C_4 biochemical subtypes (see Table 10.1). The released CO_2 is made available to chloroplasts for fixation via Rubisco, while the three-carbon acid by-product is converted to triose phosphates and subsequently to starch or sucrose via gluconeogenesis (see Figure 10.12).

Changes in the rate of carbon uptake and in enzyme regulation throughout the day create a 24-h CAM cycle.

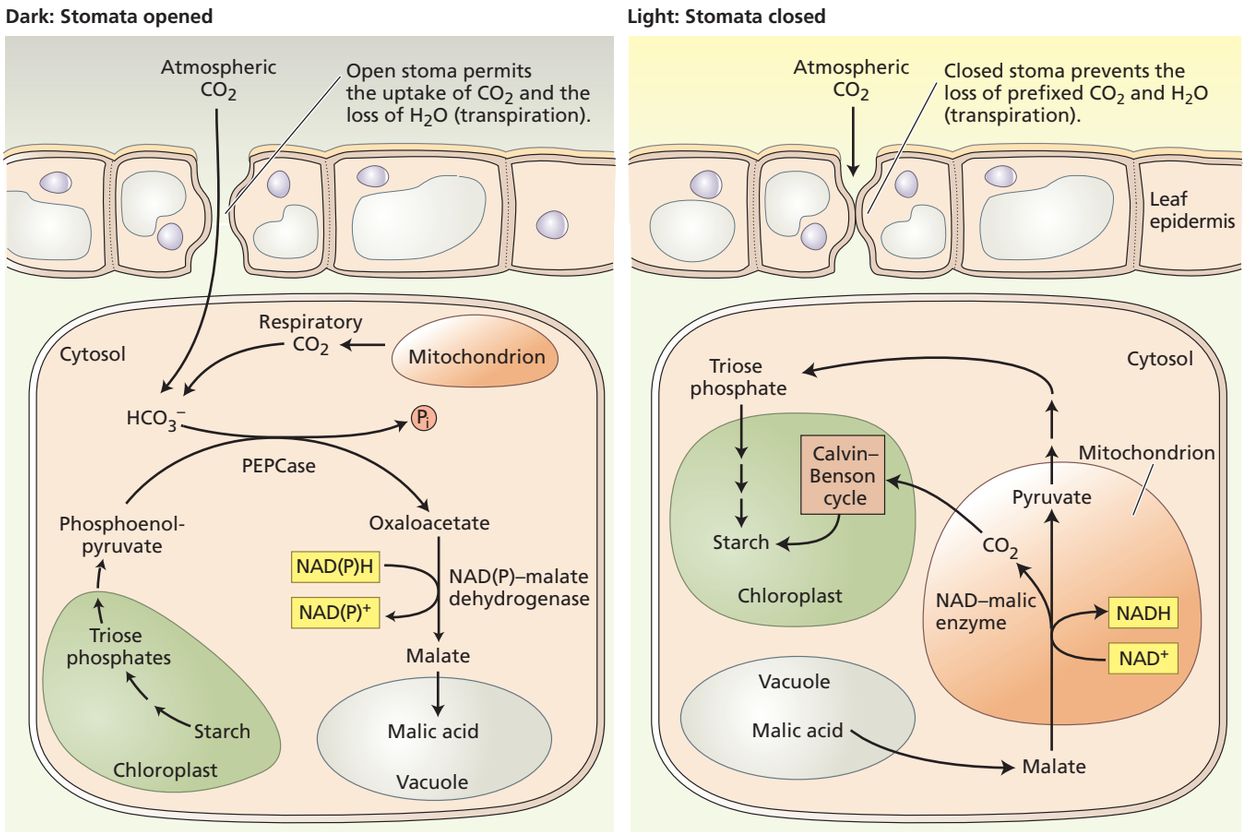


Figure 10.12 **Crassulacean acid metabolism (CAM) in *Kalanchoe*.** In CAM metabolism, CO_2 uptake is separated temporally from refixation via the Calvin–Benson cycle. The uptake of atmospheric CO_2 takes place at night when stomata are open. At this stage, gaseous CO_2 in the cytosol, coming from the external atmosphere and mitochondrial respiration, increases the levels of HCO_3^- ($CO_2 + H_2O \leftrightarrow HCO_3^- + H^+$). Then cytosolic PEPCase catalyzes a reaction between HCO_3^- and phosphoenolpyruvate provided by the nocturnal breakdown of chloroplast starch. The four-carbon acid formed, oxaloacetate, is reduced to malate, which in turn diffuses into the acidic vacuole and becomes protonated to malic acid. During the day, the malic acid stored in the vacuole flows back to the cytosol and dissociates back to malate. Mitochondrial NAD–malic enzyme decarboxylates the malate, releasing CO_2 that is refixed into carbon skeletons by the Calvin–Benson cycle. In essence, the diurnal accumulation of starch in the chloroplast constitutes the net gain of the nocturnal uptake of inorganic carbon. The adaptive advantage of the stomatal closure during the day is that it prevents not only water loss by transpiration, but also the diffusion of internal CO_2 to the external atmosphere. See Figure 10.10B for a description of reactions. Note that different CAM species can have different contributions of NAD-ME, NADP-ME, and PEPCK as the decarboxylating enzyme.

Four distinct phases define the temporal control of C_4 and C_3 carboxylations within the same cellular environment: phase I (night), phase II (early morning), phase III (daytime), and phase IV (late afternoon) (see **WEB TOPIC 10.11**). During the nocturnal phase I, when stomata are open, CO_2 is captured in the form of HCO_3^- by PEPCase and stored as malate in the vacuole. During diurnal phase III, when stomata are closed and the Calvin–Benson cycle is activated by light, the stored malate is decarboxylated and provides high concentrations of CO_2 around the active site of Rubisco, thereby minimizing photorespiration. The transient phases II and IV shift the metabolism in preparation for phases III and I, respectively. In phase II, Rubisco activity increases, but it decreases in phase IV. In contrast, the activity of PEPCase increases in phase IV and declines in phase II. The contribution of each phase to the overall carbon balance varies considerably among different CAM plants and is sensitive to environmental conditions. Constitutive CAM plants use the nocturnal uptake of CO_2 at all times. Facultative CAM plants resort to the CAM pathway only when induced by water deficit stress or salt stress; otherwise, they operate as C_3 plants.

Whether the triose phosphates produced by the Calvin–Benson cycle are stored as starch in chloroplasts or used for the synthesis of sucrose depends on the plant species. However, these carbohydrates ultimately ensure not only plant growth, but also the supply of substrates for the next nocturnal carboxylation phase. To sum up, the temporal separation of nocturnal initial carboxylation from

diurnal decarboxylation increases the concentration of CO_2 near Rubisco and reduces photorespiration, thereby increasing the efficiency of photosynthesis.

Different mechanisms regulate C_4 PEPCase and CAM PEPCase

Comparative analysis of photosynthetic PEPCases provides a remarkable example of the adaptation of enzyme regulation to particular metabolisms. Phosphorylation of plant PEPCases by PEPCase kinase converts the inactive nonphosphorylated form into the active phosphorylated counterpart:

$$\text{PEPCase}_{\text{inactive}} + \text{ATP} \rightarrow \text{PEPCase–P}_{\text{active}} + \text{ADP}$$

Dephosphorylation of PEPCase by protein phosphatase 2A brings the enzyme back to the inactive form. PEPCase in C_4 plants functions during the day and has reduced activity at night, while PEPCase in CAM plants operates at night and has reduced activity in the daytime. The contrasting responses of photosynthetic PEPCases to light are conferred by regulatory elements that control the synthesis and degradation of PEPCase kinases. The synthesis of PEPCase kinase is mediated by light-sensing mechanisms in C_4 leaves and by endogenous circadian rhythms in CAM leaves (see **WEB ESSAY 10.1**).

CAM is a versatile mechanism sensitive to environmental stimuli

The high efficiency of water use in CAM plants probably accounts for their extensive diversification and speciation in water-limited environments. CAM plants that grow in deserts, such as cacti, open their stomata during the cool nights and close them during the hot, dry days. The potential advantage of terrestrial CAM plants in arid environments is well illustrated by the unintentional introduction of the African prickly pear (*Opuntia stricta*) into the Australian ecosystem. From a few plants in 1840, the population of *O. stricta* expanded to occupy 25 million ha in less than a century.

Closing the stomata during the day minimizes the loss of water in CAM plants, but because H_2O and CO_2 share the same diffusion pathway, CO_2 must then be taken up by the open stomata at night (see Figure 10.12). The availability of light mobilizes the reserves of vacuolar malic acid for the action of specific decarboxylating enzymes—NAD–ME, NADP–ME, and PEPCK—and the assimilation of the resulting CO_2 via the Calvin–Benson cycle. CO_2 released by decarboxylation does not escape from the leaf because stomata are closed during the day. As a consequence, the internally generated CO_2 is fixed by Rubisco and converted to carbohydrates by the Calvin–Benson cycle. Thus, stomatal closure during the day not only helps conserve water, but also assists in the buildup of the elevated internal concentration of CO_2 that enhances the photosynthetic carboxylation of ribulose 1,5-bisphosphate.

Genotypic attributes and environmental factors modulate the extent to which the biochemical and physiological capacity of CAM plants is expressed. Although many species in the family Crassulaceae (e.g., *Kalanchoe*) are obligate CAM plants that exhibit circadian rhythmicity, others (e.g., *Clusia*) show C_3 photosynthesis and CAM simultaneously in distinct leaves. The proportion of CO_2 taken up by PEPCase at night or by Rubisco during the day (net CO_2 assimilation) is adjusted by (1) stomatal behavior, (2) fluctuations in organic acid and storage carbohydrate accumulation, (3) the activities of primary (PEPCase) and secondary (Rubisco) carboxylating enzymes, (4) the activities of decarboxylating enzymes, and (5) the rates of synthesis and breakdown of three-carbon skeletons.

Many CAM representatives are able to adjust their pattern of CO_2 uptake in response to longer-term variations of environmental conditions. The ice plant (*Mesembryanthemum crystallinum* L.), agave, and *Clusia* are among the plants that use CAM when water is scarce but undergo a gradual transition to C_3 when water is sufficient. Other environmental conditions, such as salinity, temperature, and light, also contribute to the extent of CAM induction in these species. This form of regulation requires the expression of numerous CAM genes in response to stress signals.

The water-conserving closure of stomata in arid lands may not be the unique basis of CAM evolution, because paradoxically, CAM species are also found among aquatic plants. Perhaps this mechanism also enhances the acquisition of inorganic carbon (as HCO_3^-) in aquatic habitats, where the high resistance to gas diffusion in liquid restricts the availability of CO_2.

10.6 Accumulation and Partitioning of Photosynthates—Starch and Sucrose

Metabolites accumulated in the light—photosynthates—become the ultimate source of energy for plant growth, maintenance, and development. The photosynthetic assimilation of CO_2 by most leaves yields sucrose in the cytosol and starch in the chloroplasts. During the day, sucrose flows from the leaf cytosol to heterotrophic sink tissues, while starch accumulates as dense, insoluble granules in chloroplasts (**Figure 10.13**) (see **WEB TOPIC 10.12**). The onset of darkness not only stops the assimilation of CO_2, but also initiates the degradation of chloroplast starch. The content of starch in the chloroplasts falls through the night because breakdown products flow to the cytosol to sustain the export of sucrose to other organs. The large fluctuation of stromal starch in the light versus the dark is why the polysaccharide stored in chloroplasts is called *transitory starch*. Transitory starch functions as (1) an overflow mechanism that

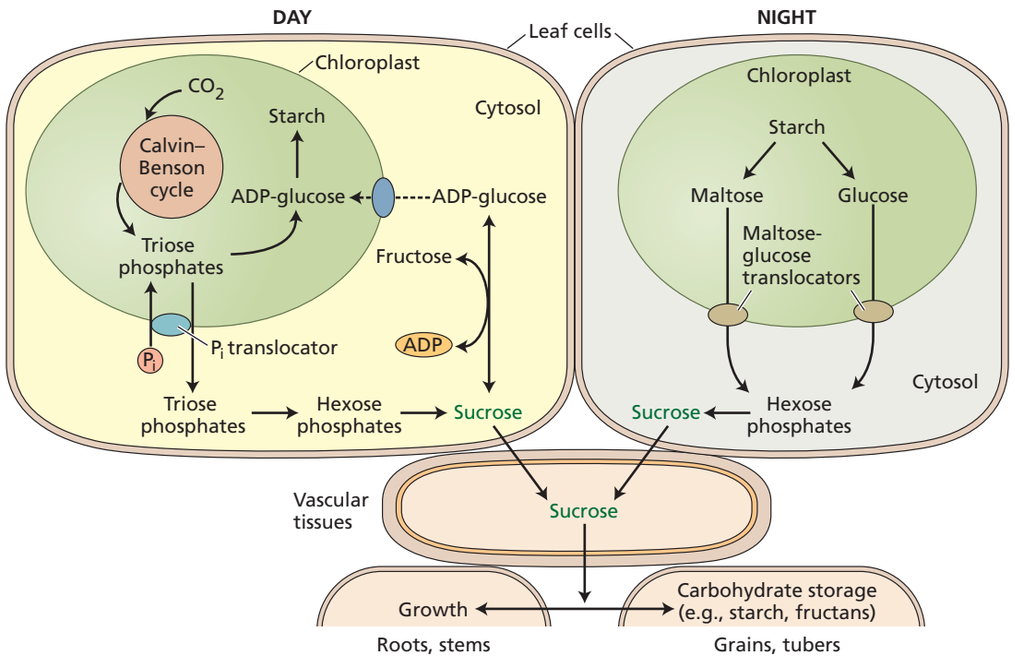


Figure 10.13 **Carbon mobilization in land plants.** During the day, carbon assimilated photosynthetically is used either for the formation of starch in the chloroplast or is exported to the cytosol for the synthesis of sucrose. External and internal stimuli control the partitioning between starch and sucrose. Triose phosphates from the Calvin–Benson cycle may be used for (1) the synthesis of chloroplast ADP-glucose (the glucosyl donor for starch synthesis) or (2) translocation to the cytosol for the synthesis of sucrose. At night, the cleavage of the glycosidic linkages of starch releases both maltose and glucose, which flow across the chloroplast envelope to supplement the hexose phosphate pool and contribute to sucrose synthesis. Transport across the chloroplast envelope, carried out by translocators for phosphate and maltose and glucose, conveys information between the two compartments. As a consequence of the diurnal synthesis and nocturnal breakdown, the levels of chloroplast starch are maximal during the day and minimal at night. This transitory starch serves as the nocturnal energy reserve that provides an adequate supply of carbohydrates to land plants, and also as a diurnal overflow that accepts the carbon excess when photosynthetic CO_2 assimilation proceeds faster than the synthesis of sucrose. Daily, sucrose links the assimilation of inorganic carbon (CO_2) in leaves to the use of organic carbon for growth and storage in nonphotosynthetic parts of the plant.

stores photosynthate when the synthesis and transport of sucrose are limited during the day and (2) an energy reserve to provide an adequate supply of carbohydrate at night when sugars are not formed by photosynthesis. Plants vary widely in the extent to which they accumulate starch and sucrose in leaves (see Figure 10.13). In some species (e.g., soybean, sugar beet, Arabidopsis), the ratio of starch to sucrose in the leaf is almost constant throughout the day. In others (e.g., spinach, French beans), starch accumulates when sucrose exceeds the storage capacity of the leaf or the demand of sink tissues.

The carbon metabolism of leaves also responds to the requirements of sink tissues for energy and growth. Regulatory mechanisms ensure that physiological processes in the chloroplast are synchronized not only with the cytoplasm of the leaf cell but also with other parts of the plant during the day–night cycle. An abundance of sugars in leaves promotes plant growth and carbohydrate storage in reserve organs, while low levels of sugars in sink tissues stimulate the rate of photosynthesis. Sucrose transport links the availability of carbohydrates in source leaves to the use of energy and the formation of reserve polysaccharides in sink tissues (see Chapter 12).

10.7 Formation and Mobilization of Chloroplast Starch

Starch is the main storage carbohydrate in plants, being surpassed only by cellulose as the most abundant polysaccharide. In the light, chloroplasts store part of the assimilated carbon as insoluble starch granules that are degraded at night. The 24-h rhythm of starch turnover adjusts to the ambient situation. For example, Arabidopsis plants grown in short days (6-h day/18-h night) allocate more photosynthate to starch than do plants grown in long days (18-h day/6-h night), but in both cases the transitory starch is consumed by dawn. The co-localization of photosynthesis and starch metabolism in the chloroplast requires efficient coordination between these fundamental metabolic pathways. In this section we consider the chloroplast processes associated with the diurnal accumulation and nocturnal degradation of starch.

Chloroplast stroma accumulates starch as insoluble granules during the day

Starch, like glycogen, is a complex polysaccharide built up from a single monosaccharide—glucose—that consists of two major components, amylopectin and amylose (**Figure 10.14A**). The α-D-glucosyl units associate in long linear chains linked through α-D-1,4 glycosidic linkages wherein α-D-1,6 glycosidic linkages are formed as branch points. The contribution of α-D-1,6 glycosidic linkages to total bonds is lower in amylose (less than 1%) than in amylopectin (~5–6%); thus, the former is essentially linear and the latter branched. The molecular weight of amylose (500–20,000 glucose units) is lower than that of amylopectin (~10^6 glucose units). The structure, size, and proportions of amylose and amylopectin in the starch granule vary among plant species.

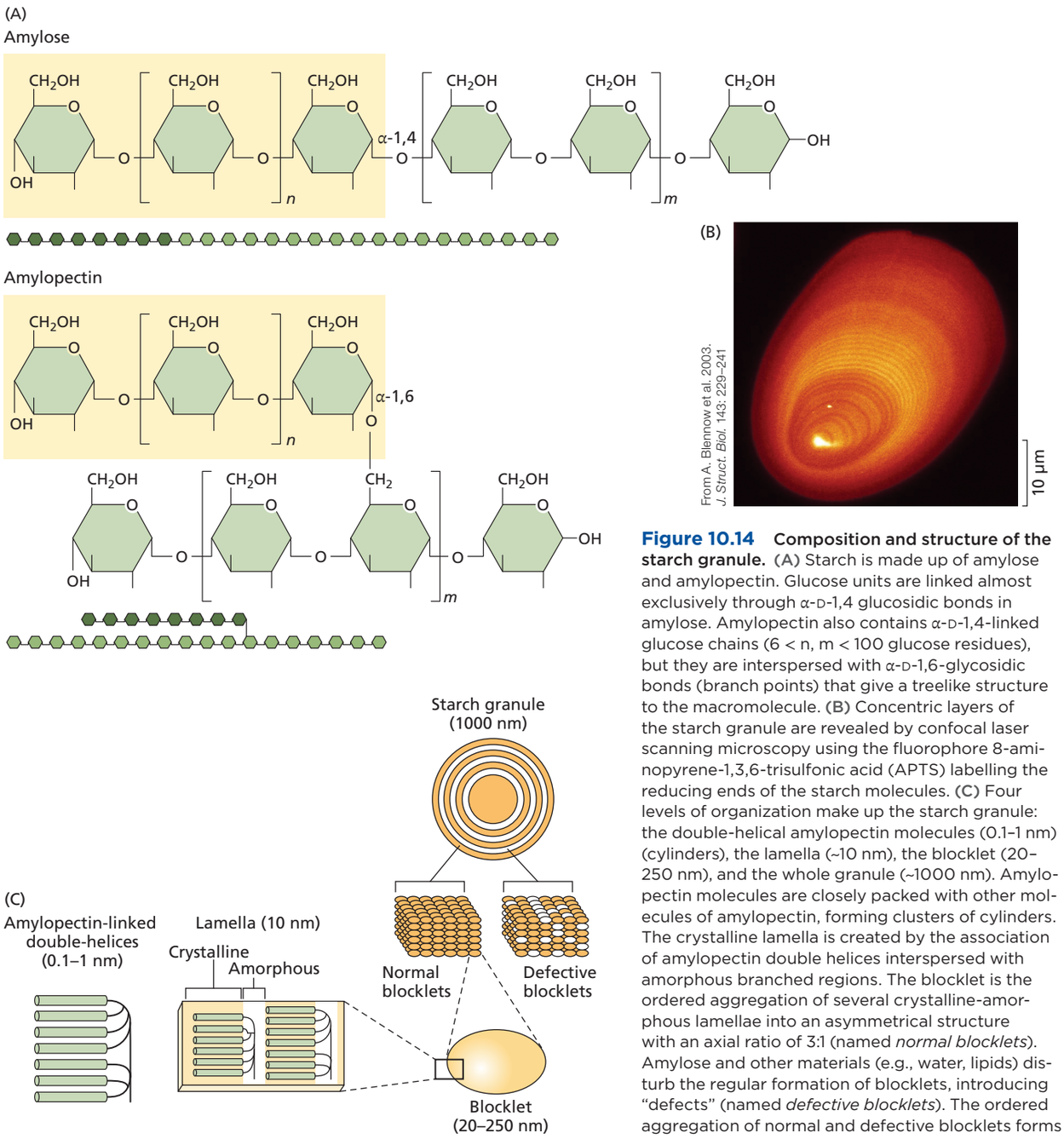
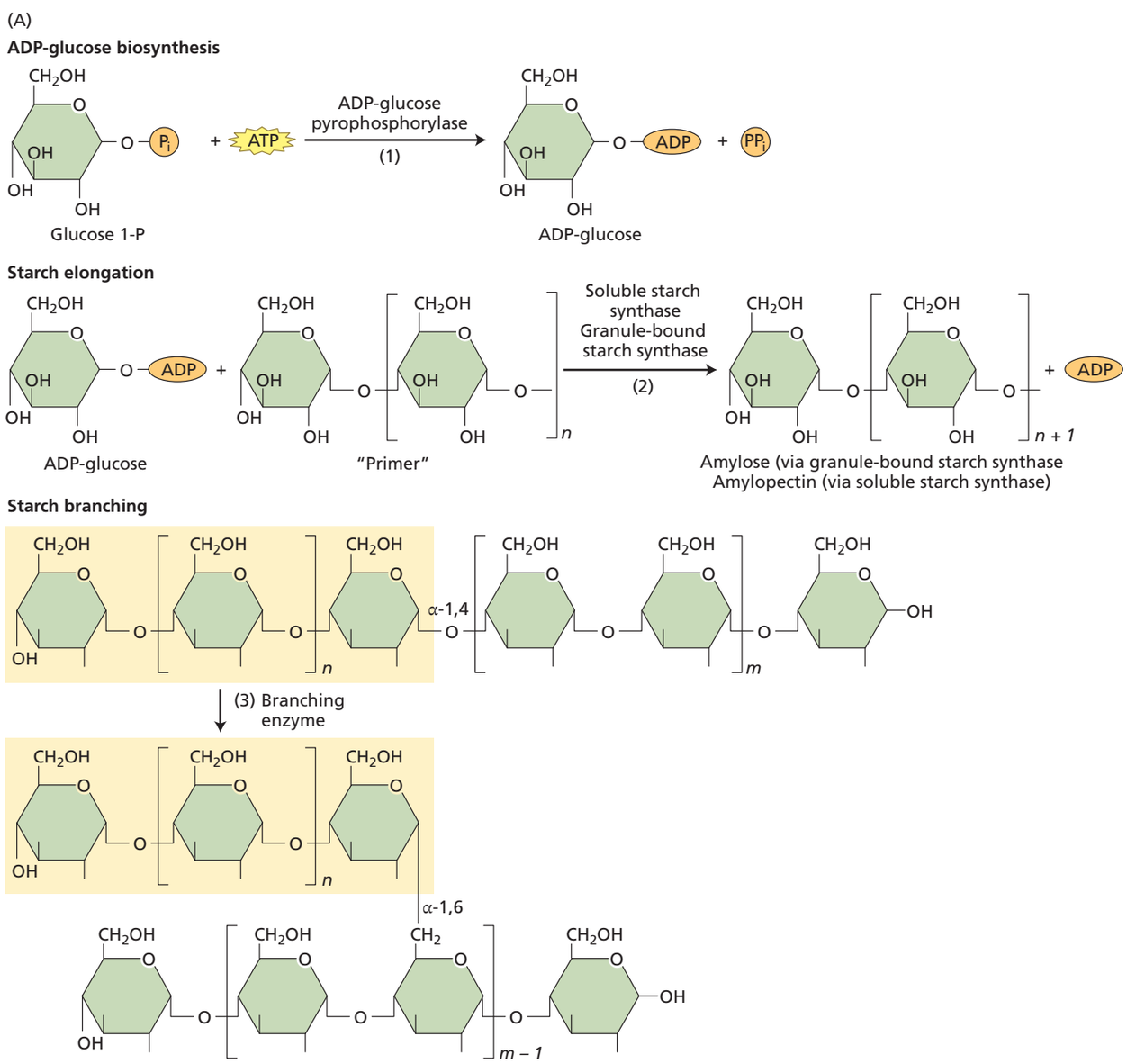


Figure 10.14 Composition and structure of the starch granule. **(A)** Starch is made up of amylose and amylopectin. Glucose units are linked almost exclusively through α-D-1,4 glucosidic bonds in amylose. Amylopectin also contains α-D-1,4-linked glucose chains ($6 < n, m < 100$ glucose residues), but they are interspersed with α-D-1,6-glycosidic bonds (branch points) that give a treelike structure to the macromolecule. **(B)** Concentric layers of the starch granule are revealed by confocal laser scanning microscopy using the fluorophore 8-aminopyrene-1,3,6-trisulfonic acid (APTS) labelling the reducing ends of the starch molecules. **(C)** Four levels of organization make up the starch granule: the double-helical amylopectin molecules (0.1–1 nm) (cylinders), the lamella (~10 nm), the blocklet (20–250 nm), and the whole granule (~1000 nm). Amylopectin molecules are closely packed with other molecules of amylopectin, forming clusters of cylinders. The crystalline lamella is created by the association of amylopectin double helices interspersed with amorphous branched regions. The blocklet is the ordered aggregation of several crystalline-amorphous lamellae into an asymmetrical structure with an axial ratio of 3:1 (named *normal blocklets*). Amylose and other materials (e.g., water, lipids) disturb the regular formation of blocklets, introducing "defects" (named *defective blocklets*). The ordered aggregation of normal and defective blocklets forms the concentric rings of hard (crystalline) and soft (semicrystalline) shells in the starch granule.

Chloroplasts can store large amounts of reduced carbon without changing the osmotic balance of the cell by packing amylose and amylopectin into insoluble starch granules (**Figure 10.14B**) (see **WEB TOPIC 10.12**). The amylose content and the ratio of long to short branch chains in amylopectin regulate the structure and size of the starch granule. Moreover, the association of stromal components (phosphate monoesters, lipids, phospholipids, and proteins) with the granule also controls the molecular architecture (**Figure 10.14C**). As the accumulation of starch granules in the stroma exerts tension on the envelope, ion channels perceive the mechanical stimuli and rapidly adjust the volume and shape of chloroplasts. The fluctuation of transitory starch is accommodated by changes in the size of a fixed number of starch granules.

The biosynthesis of amylose and amylopectin proceeds through successive steps: initiation, elongation, branching, and termination of the polysaccharide chain. Numerous studies have improved our understanding of elongation and branching, but knowledge of initiation and termination remain limited.

The sugar nucleotide ADP-glucose provides the glucosyl moiety for the biosynthesis of the α-D-1,4 glycosidic linkages of the growing glucan chains. Although different sources of the chloroplast ADP-glucose have been proposed, the chloroplast enzyme ADP-glucose pyrophosphorylase (AGPase) is thought to catalyze the synthesis of most of this starch precursor (**Figure 10.15A**, reaction 1). The elongation of the glucan chains proceeds via starch synthases, which catalyze the transfer of the



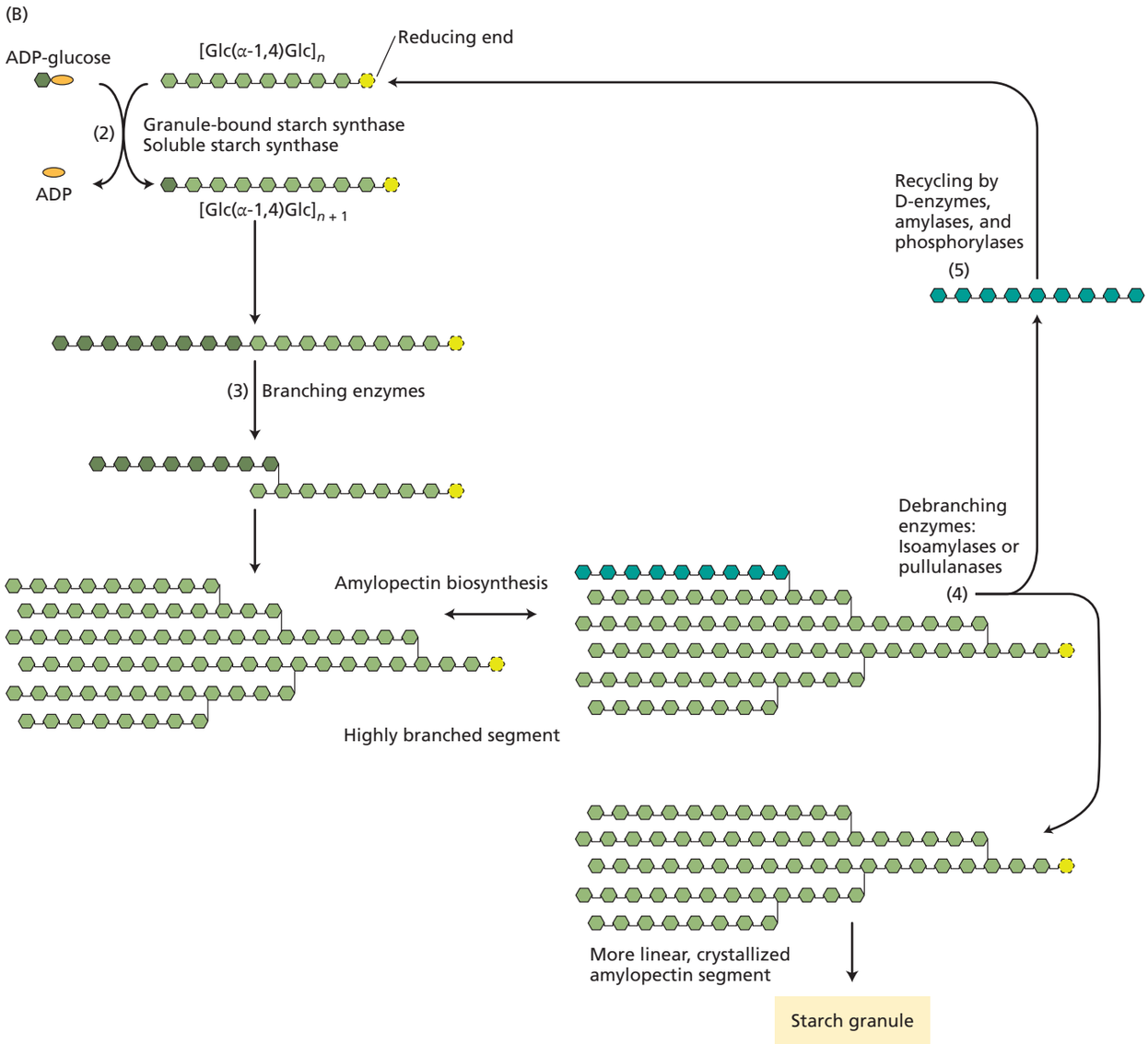


Figure 10.15 **Pathway of starch synthesis.** Starch biosynthesis in plants is a complex process that includes biosynthesis of the sugar nucleotide ADP-glucose, formation of the "primer," elongation of the linear α-D-1,4-linked glucan, and branching of the amylose molecule for the biosynthesis of amylopectin. **(A)** Starch elongation and branching. (1) The first committed step of starch biosynthesis is the formation of ADP-glucose. The enzyme ADP-glucose pyrophosphorylase catalyzes the formation of ADP-glucose from ATP and glucose 1-phosphate with the concurrent release of pyrophosphate. (2) The next step in the formation of starch is the successive addition of glucosyl moieties through α-D-1,4 linkages that elongate the polysaccharide. Starch synthases transfer the glucosyl moiety of ADP-glucose to the nonreducing end of a preexisting α-D-1,4-glucan primer. The biosynthetic pathway for the formation of the primer remains elusive. The multiple isoforms of starch synthases found in plant tissues are the granule-bound starch synthase, located essentially within the granule matrix, and the soluble starch synthases, which are partitioned between granular and stromal fractions according to species, tissues, and developmental stages. (3) Branching enzymes catalyze the formation of branch points within the glucan chains through cleavage of α-D-1,4 linkages and the transfer of the released oligosaccharide to a linear glucan, forming an α-D-1,6 linkage. **(B)** Biosynthesis of amylopectin. Reactions 2 and 3 are as in (A). (4) The yellow unit illustrates the reducing end of the polysaccharide, that is, the glucose moiety whose aldehyde group does form a glycosidic linkage. Debranching enzymes cleave α-D-1,6 linkages off randomly branched water-soluble polysaccharides, yielding small linear α-D-1,4-glucans (malto-oligosaccharides). Depending on their substrate requirements, these enzymes are either isoamylases or pullulanases. The former are active toward distantly spaced branches of amylopectin, while the latter exhibit high activity toward the tightly spaced branches of the glucan polymer. (5) Released soluble malto-oligosaccharides are recycled back into the biosynthetic pathway and transferred to the starch polysaccharides by a complex series of reactions catalyzed by D-enzymes, amylases, and phosphorylases.

glucosyl moiety of ADP-glucose to the nonreducing end of a preexisting α-D-1,4-glucan primer. The glucose added to the glucan chain retains the α-configuration in the new glycosidic bond (see Figure 10.15A, reaction 2). Multiple isoforms of starch synthase are located both soluble in the stroma and in association with the nonsoluble starch granules, and these isoforms differ in their specificity toward glucan chains of different lengths.

During the elongation process, starch-branching enzymes transfer a segment of an α-D-1,4-glucan chain to carbon 6 of a glucosyl moiety in the same glucan, forming a novel α-D-1,6 glycosidic linkage (see Figure 10.15A, reaction 3). Starch-branching enzymes are also present in various isoforms, and similar to the starch synthases, these isoforms differ in the length of the glucan chain transferred and in whether they are located in the stroma or associated with starch granules.

The randomly branched amylopectin produced by starch-branching enzymes generally does not integrate into starch granules. Isoamylases hydrolyze (remove) branches that impede formation of the crystalline regions of amylopectin by long linear α-glucan segments (**Figure 10.15B**, reaction 4). The trimmed polysaccharide is then properly folded at the starch granule surface. The malto-oligosaccharides released by the action of isoamylases are sometimes recycled directly back to the starch granule, possibly by transferases such as the so-called disproportionating enzyme or D-enzyme:

$$(\text{Glucose})_m + (\text{glucose})_n \rightarrow (\text{glucose})_{m+n-x} + (\text{glucose})_x$$

where m and $n \geq 3$ and $x \leq 4$ (see Figure 10.15B, reaction 4). The products of this reaction become substrates for the action of starch synthases and branching enzymes (see Figure 10.15B, reactions 2 and 3). Other enzymes, including amylases and phosphorylases, are also involved here.

Starch degradation at night requires the phosphorylation of amylopectin

Phenotyping of transgenic plants, biochemical analyses, and genome sequence information have provided a new picture of the pathway involved in the nocturnal degradation of transitory starch (**Figure 10.16**). At night, starch is transiently phosphorylated to sterically disrupt the compact glucan structures in the starch granule. This phosphorylation is catalyzed by glucan–water dikinases that phosphoryl groups into the transitory starch. Unlike most kinases, glucan–water dikinases release inorganic phosphate and transfer the β-phosphate of ATP (indicated by the bold P in the reaction below) to carbons 3 and 6 of glucosyl moieties of amylopectin:

$$\text{Adenosine-P-}\mathbf{P}\text{-P (ATP)} + (\text{glucan})\text{–O–H} + H_2O \rightarrow$$
$$\text{adenosine-P (AMP)} + (\text{glucan})\text{–O–}\mathbf{P} + P_i$$

Although phosphoryl groups occur infrequently in leaf starch (1 phosphoryl group per 2000 glucosyl residues in Arabidopsis), transgenic Arabidopsis lines with diminished glucan–water dikinase activity (named *starch excess 1*, or *sex1*) show decreased starch degradation. As a consequence, the content of starch in mature leaves of *sex1* lines is up to seven times that of wild-type leaves. Thioredoxin-dependent processes (see Figure 10.6) regulate (1) the catalytic activity of glucan–water dikinases and (2) the distribution of these enzymes between the stroma and the starch granule. Starch phosphorylation affects both starch biosynthesis and starch hydrolysis during starch mobilization. During mobilization, the starch granule is extensively phosphorylated by glucan–water dikinases to break up the crystalline segments of the granule, followed by dephosphorylation of the starch by glucan phosphatases to permit complete hydrolysis of the α-glucan chains.

The export of maltose prevails in the nocturnal breakdown of transitory starch

Two mechanisms accomplish the cleavage of the α-D-1,4 glycosidic bond of phosphorylated starch (see Figure 10.16).

1. Hydrolysis, catalyzed by amylases:

$$[\text{Glucose}]_n + H_2O \rightarrow [\text{glucose}]_{n-m} + [\text{glucose}]_m$$
$$[\alpha\text{-amylase}]$$

$$[\text{Glucose}]_n + H_2O \rightarrow \text{linear } [\text{glucose}]_{n-2} + \text{maltose}$$
$$[\beta\text{-amylase}]$$

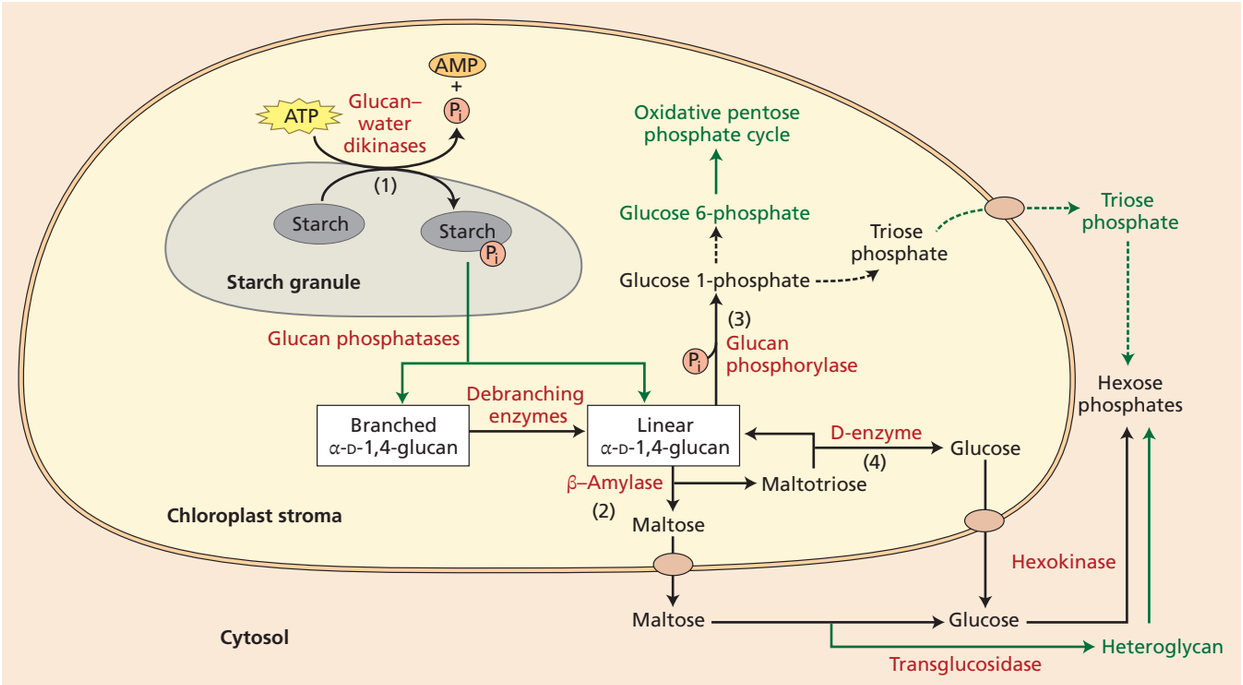
2. Phosphorolysis, catalyzed by α-glucan phosphorylases:

$$[\text{Glucose}]_n + P_i \rightarrow [\text{glucose}]_{n-1} + \text{glucose 1-phosphate}$$

The major product of starch breakdown is maltose, which is exported from the chloroplast to the cytosol at night. This disaccharide is formed by β-amylases acting on the starch granule or on oligosaccharides released from the granule by α-amylases. However, neither α-amylases nor β-amylases hydrolyze the α-D-1,6 glycosidic bond that constitutes 4 to 5% of the glycosidic linkages in amylopectin (see Figure 10.16). Two debranching enzymes, pullulanase (limit dextrinase) and isoamylase, are essential for the complete breakdown of starch granules to linear glucans (see Figure 10.15, reaction 4). The linear glucans produced by these hydrolases are further degraded at night by chloroplast β-amylase.

The production of maltose leads unavoidably to the formation of low amounts of maltotriose, because the exhaustive action of β-amylase cannot further process the trisaccharide (see Figure 10.16). The D-enzyme catalyzes the formation of maltopentaose and glucose (see Figure 10.16, reaction 4). The glucose is exported by a glucose transporter in the inner chloroplast membrane. These reactions prevent the accumulation of the maltotriose as starch is hydrolyzed during the night.

(A)



(B)

1. Adenosine-P-**P**-P (ATP) + [**P**–glucan]–O–H + H_2O → adenosine-P (AMP) + [**P**–glucan]–O–**P** + P_i
2. $[Glucose]_n + H_2O$ → linear $[glucose]_{n-2}$ + maltose
3. $[Glucose]_n + P_i$ → $[glucose]_{n-1}$ + glucose 1-phosphate
4. $2\ [Glucose]_3$ → $[glucose]_5$ + glucose

Figure 10.16 Nocturnal starch degradation in Arabidopsis leaves. **(A)** The release of soluble glucans from the starch granule at night requires prior phosphorylation of the polysaccharide via glucan–water dikinases. At this stage, debranching enzymes transform the branched starch into linear glucans, which in turn can be converted into maltose via β-amylolysis catalyzed by chloroplast β-amylase. The residual maltotriose is degraded into maltose and glucose for export to the cytosol by a cyclic process. First, two maltotrioses are converted into maltopentaose (and a glucose is released) by the D-enzyme (Reaction 4). The maltopentaose is then recycled through the β-amylase to regenerate maltotriose releasing another maltose. Under stress conditions, the phosphorolytic cleavage of α-D-1,4-glucans catalyzed by chloroplast glucan phosphorylase yields glucose 1-phosphate, which can be cleaved to triose phosphate and exchanged for phosphate, or incorporated into the oxidative pentose phosphate cycle. Two transporters in the chloroplast envelope, one for maltose and another for glucose, facilitate the flow of the products of starch degradation to the cytosol. The use of maltose in the leaf cytosol proceeds via a transglucosidase that transfers a glucosyl moiety to a heteroglycan and concurrently releases a molecule of glucose. The cytosolic glucose can be phosphorylated via a hexokinase to glucose 6-phosphate for incorporation into the pool of hexose phosphates. **(B)** The numbered reactions shown in part A.

The fate of maltose in the leaf cytosol was delineated by studies of transgenic plants devoid of a cytosolic transglucosidase. These plants degrade starch poorly and accumulate maltose to levels much higher than in wild-type plants. The transglucosylation reaction catalyzed by this enzyme transfers a glucosyl moiety from maltose to cytosolic heteroglycans constituted of arabinose, galactose, and glucose [(heteroglycans) + maltose → (heteroglycans)-glucose + glucose]. Phosphorylation of the remaining glucose by hexokinase adds glucose 6-phosphate to the hexose phosphate pool for conversion to sucrose.

The synthesis and degradation of the starch granule are regulated by multiple mechanisms

Numerous mechanisms regulate the activity of enzymes involved in starch metabolism.

REDOX CONTROL The importance of reducing and oxidizing conditions in the control of starch breakdown

was uncovered by biochemical experiments (AGPase, glucan–water dikinase, phosphoglucan phosphatase, and β-amylase 1) and by identifying potential targets of thioredoxin (see Figure 10.6) in proteomics screens (β-amylase, α-glucan phosphorylase, ADP-glucose translocator, and starch branching enzyme IIa).

PROTEIN PHOSPHORYLATION Protein phosphorylation is another way to rapidly modulate enzyme activities. In the plastid, specific protein kinases catalyze the transfer of the γ-phosphate from ATP to specific amino acids (generally serine, threonine, and tyrosine) of enzymes related to starch metabolism (phosphoglucoisomerase, phosphoglucomutase, AGPase, glucan–water dikinases, transglucosidase [dpe2], α-amylase 3, β-amylases, limit dextrinase, starch branching enzymes, starch synthases, granule-bound starch synthase, α-glucan phosphorylase, glucose transporter, and maltose transporter). However, the physiological role of these phosphorylations is unknown.

FORMATION OF COMPLEXES WITH PROTEINS Many enzymes involved in the formation of starch granules (soluble and granule-bound starch synthases, α-amylases, and glucan–water dikinases) bind to scaffold proteins that possess starch-binding domains. The formation of these heterocomplexes markedly changes the activity of the enzymes. Moreover, some of the partly soluble enzymes, including branching enzyme, starch synthase, and starch phosphorylase, form complexes in a phosphorylation-dependent manner.

ALLOSTERIC EFFECTORS (LOW MOLECULAR WEIGHT METABOLITES) Small molecules interact with enzyme sites distal to the active site and thereby perturb the catalytic activity over a distance—that is, they have an allosteric effect. Thus, low-molecular-weight metabolites participate actively in starch synthesis. For example, the disaccharide trehalose [α-D-Gluc-(1→1)-α-D-Gluc] does not accumulate to any great extent in the vast majority of plants, but trehalose 6-phosphate significantly increases the reductive activation of ADP-glucose pyrophosphorylase. This enzyme is also allosterically activated by the primary product of photosynthesis, 3-phosphoglycerate, and inhibited by free phosphate.

10.8 Sucrose Biosynthesis and Signaling

The production of sucrose in the leaf cytosol, coupled to loading and translocation in the phloem, ensures a suitable supply of carbohydrates for the optimal development of the plant. Additionally, sucrose communicates the carbon and energy status of tissues sustaining autotrophic assimilation (leaves) to compartments performing heterotrophic consumption (e.g., roots, tubers, and grains). Thus, sucrose not only provides carbon skeletons for growth and polysaccharide biosynthesis, but also is a key signaling molecule that regulates carbon partitioning between source leaves and sink tissues. This section describes the mechanisms that allocate products of photosynthetic CO_2 assimilation to the cytosol for the synthesis of sucrose.

Triose phosphates from the Calvin–Benson cycle build up the cytosolic pool of three important hexose phosphates in the light

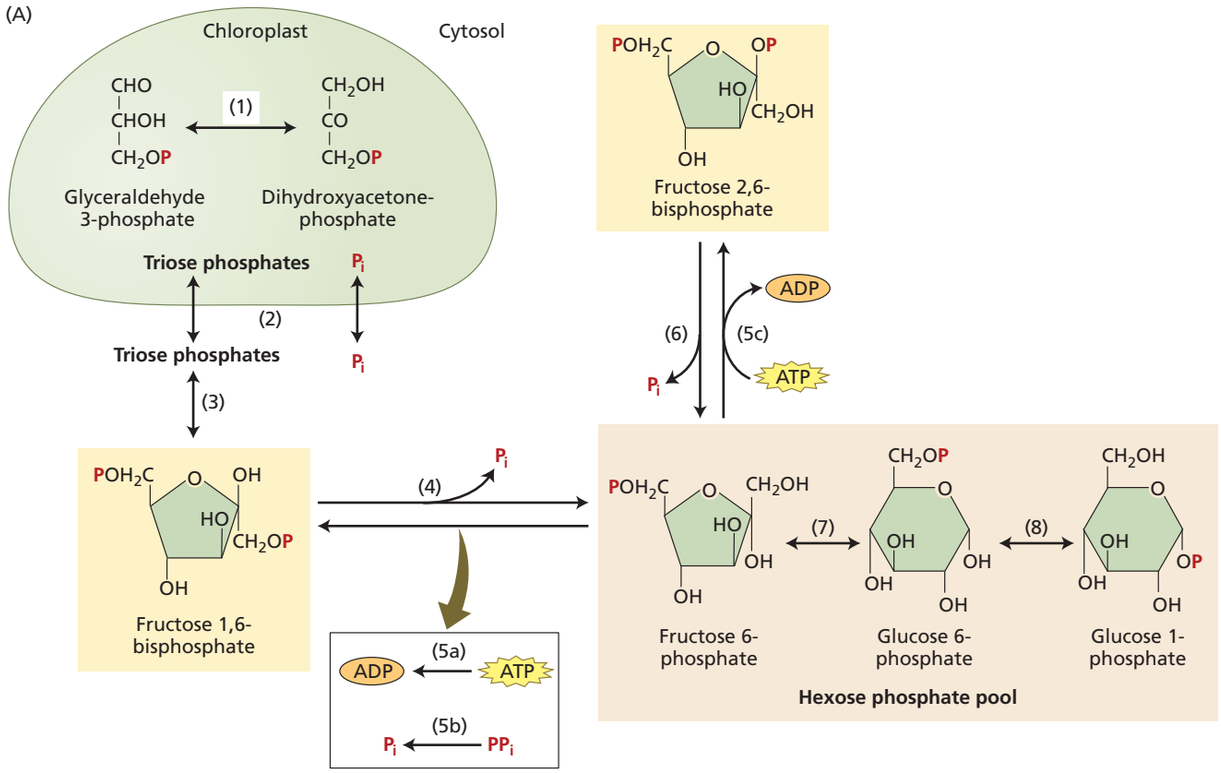
During active photosynthesis, the accumulation of dihydroxyacetone phosphate and glyceraldehyde 3-phosphate in the cytosol increases the formation of fructose 1,6-bisphosphate catalyzed by cytosolic aldolase ($\Delta G^{0\prime} = 24$ kJ/mol) (**Figure 10.17**, reaction 3). Given that the cytosolic aldolase catalyzes the reaction of two triose phosphates, the K_{eq} for this reaction is:

$$K_{eq} = [\text{dihydroxyacetone phosphate}] \times [\text{glyceraldehyde 3-phosphate}] \,/\, [\text{fructose 1,6-bisphosphate}] = [\text{triose phosphates}]^2 \,/\, [\text{fructose 1,6-bisphosphate}],$$

implying that the concentration of fructose 1,6-bisphosphate varies exponentially in response to changes in the concentration of triose phosphates. Hence, a constant input of triose phosphates from photosynthetically active chloroplasts biases the aldolase reaction in the cytosol of leaf cells toward the formation of fructose 1,6-bisphosphate. The reverse reaction—the aldol cleavage of fructose 1,6-bisphosphate to dihydroxyacetone

Figure 10.17 Interconversion of hexose phosphates. ▶ **(A)** Fructose 1,6-bisphosphate, formed from triose phosphates by the action of aldolase, has a phosphate group cleaved from the carbon 1 position by cytosolic fructose 1,6-bisphosphatase, which differs structurally and functionally from the chloroplast counterpart. The generated fructose 6-phosphate constitutes the starting substrate for three transformations. *First*, land plants employ two different phosphorylation reactions of fructose 6-phosphate at the carbon 1 position of the furanose ring: the classic ATP-dependent phosphofructokinase (see glycolysis in Chapter 13), and a pyrophosphate-dependent phosphofructokinase that catalyzes the readily reversible phosphorylation of fructose 6-phosphate using pyrophosphate as substrate. *Second*, fructose 6-phosphate 2-kinase catalyzes the ATP-dependent phosphorylation of fructose 6-phosphate to fructose 2,6-bisphosphate, and in turn, fructose 2,6-bisphosphate phosphatase catalyzes the hydrolysis of fructose 2,6-bisphosphate, releasing the phosphoryl group and again yielding fructose 6-phosphate. *Third*, hexose phosphate isomerase and glucose 6-phosphate isomerase, respectively, favor the isomerization of fructose 6-phosphate to glucose 6-phosphate and of glucose 6-phosphate to glucose 1-phosphate. Collectively, fructose 6-phosphate, glucose 6-phosphate, and glucose 1-phosphate constitute the pool of hexose phosphates. **(B)** A description of the numbered reactions in the interconversion of hexose phosphates shown in (A).

(A)



(B)

Reactions in the conversion of photosynthetically formed triose phosphates to sucrose

1. *Triose phosphate isomerase*
   Dihydroxyacetone phosphate → glyceraldehyde 3-phosphate
2. *Phosphate/triose phosphate translocator*
   Triose phosphate (*chloroplast*) + P_i (*cytosol*) → triose phosphate (*cytosol*) + P_i (*chloroplast*)
3. *Fructose 1,6-bisphosphate aldolase*
   Dihydroxyacetone phosphate + glyceraldehyde 3-phosphate → fructose 1,6-bisphosphate
4. *Fructose 1,6-bisphosphatase*
   Fructose 1,6-bisphosphate + H_2O → fructose 6-phosphate + P_i

5a. *Fructose 6-phosphate 1-kinase (phosphofructokinase)*
   Fructose 6-phosphate + ATP → fructose 1,6-bisphosphate + ADP

5b. *PP_i-dependent phosphofructokinase*
   Fructose 6-phosphate + PP_i → fructose 1,6-bisphosphate + P_i

5c. *Fructose 6-phosphate 2-kinase*
   Fructose 6-phosphate + ATP → fructose 2,6-bisphosphate + ADP

6. *Fructose 2,6-bisphosphatase*
   Fructose 2,6-bisphosphate + H_2O → fructose 6-phosphate + P_i
7. *Hexose phosphate isomerase*
   Fructose 6-phosphate → glucose 6-phosphate
8. *Phosphoglucomutase*
   Glucose 6-phosphate → glucose 1-phosphate

Note: The triose phosphate isomerase (reaction 1) catalyzes the equilibrium between dihydroxyacetone phosphate and glyceraldehyde 3-phosphate in the chloroplast stroma, while the *P_i translocator* (reaction 2) facilitates the exchange between triose phosphates and P_i across the chloroplast inner envelope membrane. All other enzymes catalyze cytosol reactions.

P_i and PP_i stand for inorganic phosphate and pyrophosphate, respectively.

phosphate and glyceraldehyde 3-phosphate—takes place when the proportion of fructose 1,6-bisphosphate is high in relation to triose phosphates, for example in glycolysis.

Cytosolic fructose 1,6-bisphosphatase subsequently catalyzes the hydrolysis of fructose 1,6-bisphosphate at the carbon 1 position, yielding fructose 6-phosphate and phosphate ($\Delta G^{0\prime}$ = 16.7 kJ/mol) (see Figure 10.17, reaction 4).

Cytosolic fructose 6-phosphate can proceed to different destinations through:

1. Phosphorylation of carbon 1, which restores fructose 1,6-bisphosphate, catalyzed by two enzymes, phosphofructokinase and pyrophosphate-dependent phosphofructokinase (see Figure 10.17, reactions 5a and b).
2. Phosphorylation of carbon 2, which yields fructose 2,6-bisphosphate, catalyzed by a unique bifunctional enzyme confined to the cytosol. Fructose 6-phosphate 2-kinase/fructose 2,6-bisphosphatase catalyzes both the incorporation and the hydrolysis of the phosphoryl group (see Figure 10.17, reactions 5c and 6).
3. Isomerization, which produces glucose 6-phosphate, catalyzed by hexose phosphate isomerase (see Figure 10.17, reaction 7).

The cytosolic concentration of fructose 6-phosphate is kept close to equilibrium with glucose 6-phosphate and glucose 1-phosphate by readily reversible reactions catalyzed by hexose phosphate isomerase ($\Delta G^{0\prime}$ = 1.7 kJ/mol) and phosphoglucomutase ($\Delta G^{0\prime}$ = 7.3 kJ/mol) (see Figure 10.17, reactions 7 and 8). These three sugar phosphates are collectively named *hexose phosphates* (see Figure 10.17).

Fructose 2,6-bisphosphate regulates the hexose phosphate pool in the light

The regulatory metabolite cytosolic fructose 2,6-bisphosphate regulates the exchange of triose phosphates and phosphate for the formation of the hexose phosphate pool. A high ratio of triose phosphates to phosphate in the cytosol, typical of photosynthetically active leaves, suppresses the formation of fructose 2,6-bisphosphate, because triose phosphates strongly inhibit the kinase activity of the bifunctional enzyme fructose 6-phosphate 2-kinase/fructose 2,6-bisphosphate phosphatase. By contrast, a low ratio of triose phosphates to phosphate, indicative of limited photosynthesis, promotes the synthesis of fructose 2,6-bisphosphate because phosphate stimulates the fructose 6-phosphate 2-kinase activity and inhibits the fructose 2,6-bisphosphatase activity. Higher concentrations of fructose 2,6-bisphosphate inhibit the activity of cytosolic fructose 1,6-bisphosphatase and, in so doing, deplete the level of hexose phosphates in the cytosol.

In turn, fructose 6-phosphate inhibits the bisphosphatase activity and activates the kinase activity of the bifunctional enzyme fructose 6-phosphate 2-kinase/fructose 2,6-bisphosphatase, and thereby increases the concentration of fructose 2,6-bisphosphate. As fructose 2,6-bisphosphate inhibits fructose 1,6-bisphosphatase, the concentration of fructose 6-phosphate decreases. Thus, fructose 2,6-bisphosphate modulates the pool of hexose phosphates in response not only to photosynthesis, but also to the demands of the cytosolic hexose phosphate pool itself.

Sucrose is continuously synthesized in the cytosol

Photosynthate produced in leaves is transported, primarily as sucrose, to meristems and developing organs such as growing leaves, roots, flowers, fruits, and seeds (see Figure 10.13). The concentration of sucrose in the cytosol of leaves is dependent on two processes:

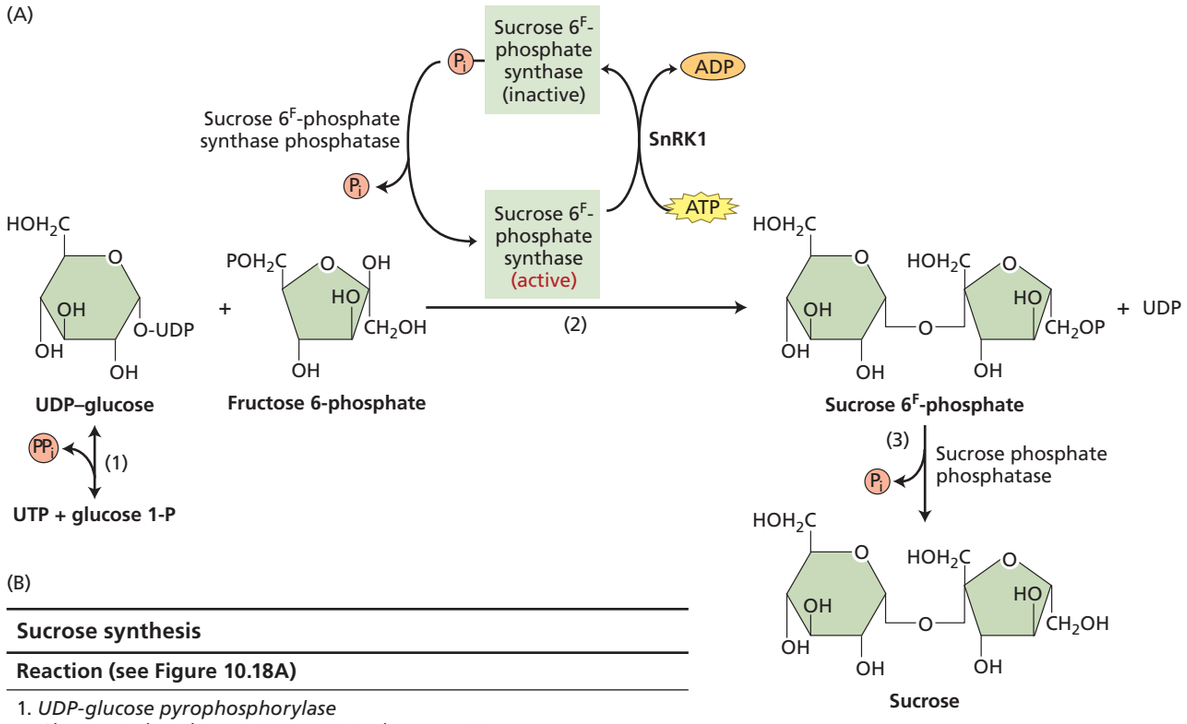
1. Carbon import, which conveys diurnal triose phosphates and nocturnal maltose from chloroplasts to the leaf cytosol for sucrose synthesis
2. Carbon export, which delivers sucrose from the leaf cytosol to other tissues to support energy demands and polysaccharide synthesis

Cell fractionation, the physical separation of organelles for analysis of their intrinsic enzyme activities, has shown that sucrose is synthesized in the cytosol from the hexose phosphate pool as depicted in **Figure 10.18**, reactions 1–3.

The conversion of hexose phosphates to sugar nucleotides precedes the formation of sucrose. In the cytosol, glucose 1-phosphate reacts with UTP to yield UDP-glucose and pyrophosphate in a reaction catalyzed by UDP-glucose pyrophosphorylase (see Figure 10.18, reaction 1). Two consecutive reactions complete the synthesis of sucrose from UDP-glucose. Sucrose 6^F-phosphate synthase (the superscript F indicates that sucrose is phosphorylated at carbon 6 of the fructose moiety) first catalyzes the formation of sucrose 6^F-phosphate from fructose 6-phosphate and UDP-glucose (see Figure 10.18, reaction 2). Subsequently, sucrose 6^F-phosphate phosphatase releases inorganic phosphate from sucrose 6^F-phosphate, yielding sucrose (see Figure 10.18, reaction 3).

The reversible formation of sucrose 6^F-phosphate ($\Delta G^{0\prime}$= –5.7 kJ/mol) followed by its hydrolysis ($\Delta G^{0\prime}$ = –16.5 kJ/mol) renders the synthesis of sucrose essentially irreversible in vivo. Moreover, the association of these enzymes into macromolecular complexes facilitates the direct transfer of sucrose 6^F-phosphate to sucrose 6^F-phosphate phosphatase without mixing with other metabolites.

(A)



(B)

Sucrose synthesis
Reaction (see Figure 10.18A)
1. *UDP-glucose pyrophosphorylase* Glucose 1-phosphate + UTP → UDP-glucose + PP_i
2. *Sucrose 6^F-phosphate synthase* UDP-glucose + fructose 6-phosphate → UDP + sucrose 6^F-phosphate
3. *Sucrose 6^F-phosphate phosphatase* Sucrose 6^F-phosphate + H_2O → sucrose + P_i

Figure 10.18 **Sucrose synthesis.** **(A)** Sucrose 6^F-phosphate synthase catalyzes the transfer of the glucosyl moiety from UDP-glucose to fructose 6-phosphate, yielding sucrose 6^F-phosphate. Desphosphorylation of sucrose 6^F-phosphate by the enzyme sucrose 6^F-phosphate phosphatase releases the disaccharide sucrose. The posttranslational transformation of covalent bonds (via phosphorylation–dephosphorylation) and noncovalent interactions (via allosteric effectors) regulate the activity of sucrose 6^F-phosphate synthase. The phosphorylation of a specific serine residue on the enzyme by the concerted action of ATP and a specific kinase, SnRK1, yields an inactive enzyme. The release of phosphate from phosphorylated sucrose 6^F-phosphate synthase by a specific sucrose 6^F-phosphate synthase–phosphatase restores the basal activity. (The 6^F notation in sucrose 6^F-phosphate indicates that sucrose is phosphorylated at the carbon 6 of the fructose moiety.) **(B)** A description of the numbered reactions in the conversion of hexose phosphates to sucrose shown in (A).

Sucrose 6^F-phosphate synthase is regulated by posttranslational modifications (protein phosphorylation) and metabolites (allosteric control) (see Figure 10.18). In the dark, the phosphorylation of sucrose 6^F-phosphate synthase by a specific kinase lowers its catalytic activity. The kinase, SnRK1 (*S*ucrose *n*on-fermenting-*1*-*R*elated protein *K*inase), is a hub within a network of signaling pathways that phosphorylates and inactivates other enzymes (nitrate reductase, trehalose-phosphate synthase, and fructose 6-phosphate 2-kinase/fructose 2,6-bisphosphatase). In the light, the inactive sucrose 6^F-phosphate synthase is activated by dephosphorylation via a protein phosphatase. The phosphorylation of sucrose 6^F-phosphate synthase is also regulated by cytosolic metabolites: Glucose 6-phosphate inhibits the kinase SnRK1, and phosphate inhibits the phosphatase (**Figure 10.19**). In addition to its regulation by phosphorylation–dephosphorylation, the active form of sucrose 6^F-phosphate synthase is stimulated by glucose 6-phosphate and inhibited by phosphate. Thus, the increased levels of hexose phosphates and decreased levels of phosphate in the cytosol, caused by high rates of photosynthesis, enhance the synthesis of sucrose. Conversely, sucrose 6^F-phosphate synthase is inefficient when increased levels of phosphate in the cytosol, caused by lower rates of photosynthesis, diminish hexose phosphates.

Sucrose synthesized in the cytosol of leaf cells is loaded into the phloem, transported to distant destinations,

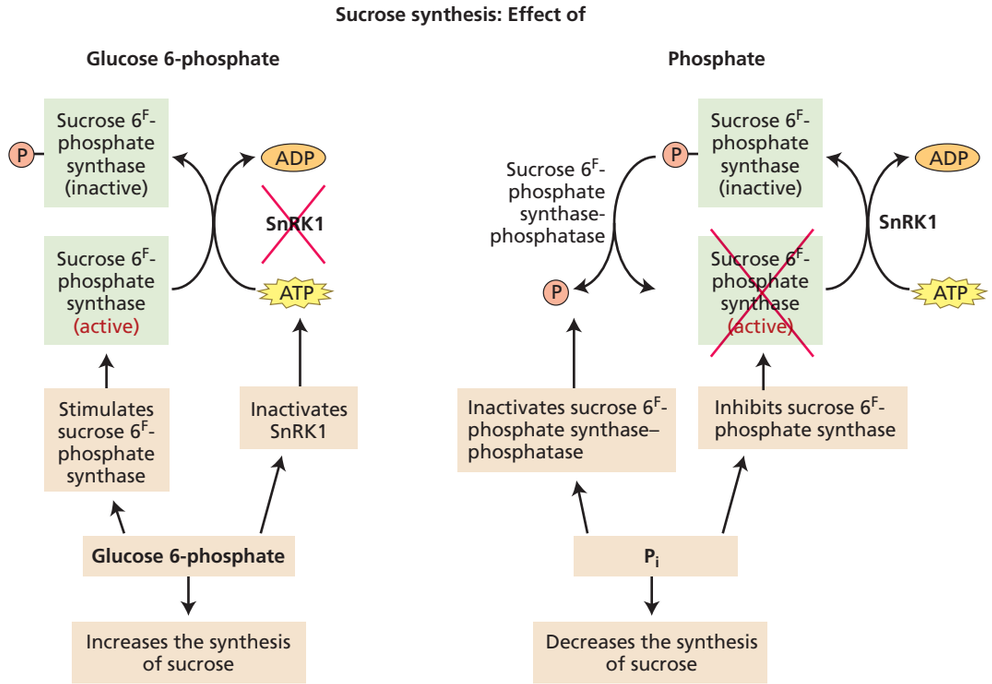


Figure 10.19 Glucose 6-phosphate and phosphate regulate the synthesis of sucrose. Glucose 6-phosphate increases the synthesis of sucrose by modulating the activity of two associated enzymes. Glucose 6-phosphate enhances the activity of sucrose 6^F-phosphate synthase itself, and also impedes formation of the inactive form of sucrose 6^F-phosphate synthase by inhibiting the SnRK1 kinase that phosphorylates and deactivates the enzyme. Phosphate lowers the synthesis of sucrose in a converse manner. Phosphate inhibits the activity of sucrose 6^F-phosphate synthase, and deactivates sucrose 6^F-phosphate synthase–phosphatase, the enzyme that converts sucrose 6^F-phosphate synthase to its active form. The transition of leaves from dark to light increases the concentration of glucose 6-phosphate and concurrently decreases the concentration of phosphate in the cytosol. Thus, the higher level of glucose 6-phosphate and the low level of phosphate jointly enhance sucrose synthesis in the light. The Xs indicate inactive enzymes.

and unloaded in tissues such as developing leaves, apical meristems, and different organs (stems, tubers, grains). Specific membrane proteins, called sucrose transporters, drive the mass flow of sucrose to distant parts of the plant. Sucrose transport acts in concert with other signaling mechanisms—both tissue- and cell-specific—as a long-distance signal that promotes developmental responses through regulation of hormonal responses at the sink level. Thus, the loading and unloading of phloem vessels with sucrose convey bidirectional information on nutrients and energy between the source leaves and the sink tissues (see Chapter 12).

Sucrose plays only a minor role in stomatal regulation

Historically, sucrose has been suggested to play a key osmotic role in regulating stomatal opening and closing. During stomatal opening, sucrose can be broken down by invertase in the vacuole to release the osmolytes fructose and glucose. But recent studies suggest that sucrose does not act primarily as an osmolyte. Sucrose can be used as a carbon supply for glycolysis and the TCA cycle to provide energy to pump counterions into the vacuole and to generate regulatory molecules such as malate to prime tonoplast ion channels or to be used as counterions within the vacuole. Sucrose has also been shown to act as a signaling molecule to help coordinate rates of photosynthesis and stomatal conductance. For example, when the photosynthetic production of sucrose exceeds the export of sucrose via the phloem, sucrose can accumulate in the apoplast, where it can influence stomatal closure. Furthermore, studies have shown that the hexose monomers produced by degradation of sucrose by invertase and sucrose synthase are sensed by hexokinase, triggering abscisic acid (ABA) signaling and stomatal closure. There are still numerous unanswered questions about the role of sucrose in stomatal regulation. For example, what is the main source of sucrose found within the guard cells? What is the molecular mechanism of hexokinase signaling during stomatal closure, and does this signaling pathway also influence stomatal opening? Overall, sucrose accumulation and breakdown appear to influence both stomatal opening and closing, but the role of sucrose may vary over the course of the diurnal period and under different environmental conditions.

Summary

Sunlight ultimately provides energy for the assimilation of inorganic carbon into organic material (autotrophy). The Calvin–Benson cycle is the predominant pathway for this conversion in many prokaryotes and in all plants.

10.1 The Calvin–Benson Cycle

- NADPH and ATP generated by light energy in chloroplast thylakoids drive the endergonic fixation of atmospheric CO_2 through the Calvin–Benson cycle in the chloroplast stroma (**Figure 10.1**).
- The Calvin–Benson cycle has three phases: (1) carboxylation of ribulose 1,5-bisphosphate with CO_2 catalyzed by Rubisco, yielding 3-phosphoglycerate; (2) reduction of the 3-phosphoglycerate to triose phosphates using ATP and NADPH; and (3) regeneration of the CO_2 acceptor molecule ribulose 1,5-bisphosphate (**Figures 10.2, 10.3**).
- CO_2 and O_2 compete in the carboxylation and oxygenation reactions catalyzed by Rubisco (**Figure 10.4**).
- Rubisco activase controls the activity of Rubisco, wherein CO_2 functions as both activator and substrate (**Figure 10.5**).
- Light regulates the activity of Rubisco activase and four enzymes of the Calvin–Benson cycle via the ferredoxin–thioredoxin system and changes in Mg^{2+} concentration and pH (**Figures 10.6, 10.7**).

10.2 The Oxygenation Reaction of Rubisco and Photorespiration

- Photorespiration minimizes the loss of fixed CO_2 by the oxygenase activity of Rubisco (**Figure 10.8**).
- Chloroplasts, peroxisomes, and mitochondria participate in the movement of carbon, nitrogen, and oxygen atoms through photorespiration (**Figures 10.8, 10.9**).
- Kinetic properties of Rubisco, temperature, and the availability of atmospheric CO_2 and O_2 control the balance between the Calvin–Benson cycle and photorespiration.

10.3 Inorganic Carbon–Concentrating Mechanisms

- Terrestrial plants have two carbon-concentrating mechanisms that precede CO_2 assimilation through the Calvin–Benson cycle: C_4 photosynthetic carbon fixation (C_4) and crassulacean acid metabolism (CAM).

10.4 Inorganic Carbon–Concentrating Mechanisms: C_4 Photosynthetic Carbon Fixation

- The C_4 photosynthetic carbon cycle fixes atmospheric CO_2 via PEPCase into carbon skeletons in one compartment. The four-carbon acid products flow to another compartment where CO_2 is released and refixed via Rubisco (**Figure 10.10**).
- The C_4 cycle may be driven by diffusion gradients between mesophyll and bundle sheath cells (Kranz anatomy) as well as by gradients within a single cell (**Figure 10.11; Table 10.1**).
- Light regulates the activity of key C_4 cycle enzymes: NADP–malate dehydrogenase, PEPCase, and pyruvate–phosphate dikinase.
- The CO_2-concentrating mechanism in C_4 plants reduces the oxygenation reaction of Rubisco and water loss in hot, dry climates.

10.5 Inorganic Carbon–Concentrating Mechanisms: Crassulacean Acid Metabolism (CAM)

- CAM photosynthesis captures atmospheric CO_2 at night and scavenges respiratory CO_2 behind closed stomata during the day (**Figure 10.12**).
- CAM is generally associated with anatomical features that minimize water loss and is typically found in plants growing in arid environments.
- Genetics and environmental factors determine CAM expression.

10.6 Accumulation and Partitioning of Photosynthates—Starch and Sucrose

- In most leaves, sucrose in the cytosol and starch in chloroplasts are the end products of photosynthetic CO_2 assimilation (**Figure 10.13**).
- During the day, sucrose flows from the leaf cytosol to sink tissues, while starch accumulates as granules in chloroplasts. At night, the starch content of chloroplasts falls to provide carbon skeletons for sucrose synthesis in the cytosol to nourish heterotrophic tissues.

10.7 Formation and Mobilization of Chloroplast Starch

- Starch biosynthesis during the day proceeds through successive steps: initiation, elongation, branching, and termination of the polysaccharide chain (**Figures 10.14, 10.15**).
- Starch degradation at night requires prior phosphorylation of the polysaccharide. Glucan–water dikinases catalyze transfer of the β-phosphate of ATP to starch. Glucan phosphatases subsequently dephosphorylate the released phospho-malto-oligosaccharides (**Figure 10.16**).
- The hydrolysis of linear glucans by chloroplast β-amylases yields mainly maltose, which is exported to the cytosol for sucrose synthesis.

10.8 Sucrose Biosynthesis and Signaling

- During the day, the ratio of triose phosphates to inorganic phosphate modulates the partitioning of carbon between chloroplasts and cytosol. The accumulation of triose phosphates in the cytosol builds up the pool of hexose phosphates. Hexose

Summary (*continued*)

phosphates are precursors in the cytosolic synthesis of sucrose catalyzed by sucrose 6^F-phosphate synthase and sucrose 6^F-phosphate phosphatase (**Figures 10.17, 10.18**).

- Phosphorylation and noncovalent interactions with metabolites regulate sucrose 6^F-phosphate synthase activity (**Figure 10.19**).
- In addition to providing carbon for growth and polysaccharide biosynthesis, sucrose acts as a signal in regulating genes that encode enzymes, transporters, and storage proteins.
- Sucrose accumulation and breakdown appear to influence both stomatal opening and closing, thereby helping coordinate rates of photosynthesis and transpiration. The role of sucrose regulation of stomata may change throughout the diurnal period and under different environmental conditions.

Web Material

- **WEB TOPIC 10.1 CO_2 Pumps** Cyanobacteria contain protein complexes (CO_2 pumps) and supramolecular complexes for the uptake and fixation of inorganic carbon.
- **WEB TOPIC 10.2 How the Calvin–Benson Cycle Was Elucidated** Experiments carried out in the 1950s led to the discovery of the path of CO_2 fixation.
- **WEB TOPIC 10.3 Rubisco: A Model Enzyme for Studying Structure and Function** As the most abundant enzyme on Earth, Rubisco was early on obtained in quantities sufficient for elucidating its structure and catalytic properties.
- **WEB TOPIC 10.4 Energy Demands for Photosynthesis in Land Plants** This topic evaluates the NADPH and ATP budget during the assimilation of CO_2.
- **WEB TOPIC 10.5 Rubisco Activase** Rubisco is unique among Calvin–Benson cycle enzymes in its regulation by a specific protein, Rubisco activase.
- **WEB TOPIC 10.6 Operation of the Photorespiratory Pathway** The enzymes of photorespiration are localized in three different organelles.
- **WEB TOPIC 10.7 Cyanobacteria and the Oxygenation Reaction of Rubisco** Cyanobacteria use a proteobacterial pathway to bring carbon atoms of 2-phosphoglycolate back to the Calvin–Benson cycle.
- **WEB TOPIC 10.8 Carbon Dioxide: Some Important Physicochemical Properties** Plants have adapted to the properties of CO_2 by altering the reactions catalyzing its fixation.
- **WEB TOPIC 10.9 Three Variations of C_4 Metabolism** Certain reactions of the C_4 photosynthetic pathway differ among plant species.
- **WEB TOPIC 10.10 Single-Cell C_4 Photosynthesis** Some marine organisms and land plants accomplish C_4 photosynthesis in a single cell.
- **WEB TOPIC 10.11 Photorespiration in CAM Plants** During the day, stomatal closing and photosynthesis in CAM leaves lead to very high intracellular concentrations of both oxygen and carbon dioxide. These unusual conditions pose interesting adaptive challenges for CAM leaves.
- **WEB TOPIC 10.12 Starch Granule Architecture** The morphology and composition of the starch granule influence the synthesis and degradation of the polysaccharide.
- **WEB ESSAY 10.1 Modulation of Phosphoenolpyruvate Carboxylase in C_4 and CAM Plants** The CO_2-fixing enzyme phosphoenolpyruvate carboxylase is regulated differently in C_4 and CAM species.
- **WEB ESSAY 10.2 Photosynthesis and CO_2-Concentrating Mechanisms in Marine Plants** This essay discusses the role of marine organisms in global primary productivity.

For more study aids, go to oup.com/he/taiz7e.

Suggested Reading

Abt, M. R., and Zeeman, S. C. (2020) Evolutionary innovations in starch metabolism. *Curr. Opin. Plant Biol.* 55: 109–117.

Barett, J., Girr, P., and Mackinder, L. C. M. (2021) Pyrenoids: CO_2 fixing phase separated liquid organelles. *Biochim. Biophys. Acta.* 1868: 118949.

Bräutigam, A., Schlüter, U., Eisenhut, M., and Gowik., U. (2017) On the evolution of CAM photosynthesis. *Plant Physiol.* 174: 473–477.

Manavski, N., Schmid, L-M., and Meurer, J. (2018) RNA-stabilization factors in chloroplast of vascular plants. *Essays Biochem*. 62: 51–64.

Christin, P. A., Arakaki, M., Osborne, C. P., Bräutigam, A., Sage, R. F., Hibberd, J. M., Kelly, S., Covshoff, S., Wong, G. S., Hancock, L. et al. (2014) Shared origins of a key enzyme during the evolution of C4 and CAM metabolism. *J. Exp. Bot.* 65: 3609–3621.

Damager, I., Engelsen, S. B., Blennow, A., Møller, B. L., and Motawia, S. M. (2010) First principles insight into starch-like α-glucans: their synthesis, conformation and hydration. *Chem. Rev.* 110: 2049–2080.

Balsera, M., Uberegui, E., Schürmann, P., and Buchanan, B. B. (2014) Evolutionary development of redox regulation in chloroplasts. *Antioxid. Redox Signal*. 21: 1327–1355.

Edwards, E. J. (2014) The inevitability of C_4 photosynthesis. *eLife* 3: e03702.

Furbank, R. T. (2011) Evolution of the C_4 photosynthetic mechanism: are there really three C_4 acid decarboxylation types? *J. Exp. Bot.* 62: 3103–3108.

Ermakova, M., Danila, F. R., Furbank, R. T., and von Caemmerer, S. (2020) On the road to C_4 rice: advances and perspectives. *Plant J.* 101: 940–950.

Flamholz, A. I., Prywes, N., Moran, U., Davidi, D., Bar-On, Y. M., Oltroffe, L. M., Alves, R., Savage, D., and Milo R. (2019) Revisiting trade-offs between Rubisco kinetic parameters *Biochemistry* 58: 3365–3376.

Lawson, T., and Matthews, J. (2020) Guard cell metabolism and stomatal function. *Annu. Rev. Plant Biol.* 71: 273–302.

Michelet, L., Zaffagnini, M., Morisse, S., Sparla, F., Pérez-Pérez, M. E., Francia, F., Danon, A., Marchand, C. H., Fermani, S., Trost, P., and Lemaire, S. D. (2013) Redox regulation of the Calvin-Benson cycle: something old, something new. *Front. Plant Sci.* 4: 1–21.

Mueller-Cajar, O. (2017) The Diverse AAA+ machines that repair inhibited rubisco active sites. *Front. Mol. Biol.* 4: 1–31.

Peterhansel, C., and Offermann, S. (2012) Re-engineering of carbon fixation in plants –Challenges for plant biotechnology to improve yields in a high-CO_2 world. *Curr. Opin. Biotechnol.* 23: 204–208.

Sage, R. F., Christin, P. A., and Edwards, E. J. (2011) The C_4 plant lineages of planet Earth. *J. Exp. Bot.* 62: 3155–3169.

Schlüter, U., and Weber, A. P. M. (2020) Regulation and evolution of C_4 photosynthesis. *Annu. Rev. Plant Biol.* 71: 183–215.

Weber, A. P. M., and Bar-Even, A. (2019) Update: Improving the efficiency of photosynthetic carbon reactions. *Plant Physiol.* 179: 803–812.

Zhong, Y., Qu, J. Z., Liu, X., Ding, L., Liu, Y., Bertoft, E., Petersen, B. L. Hamaker, B. R., Hebelstrup, K.H., and Blennow, A. (2022) Different genetic strategies to generate high amylose starch mutants by engineering the starch biosynthetic pathways. *Carbohydr. Polym.* 287: 119327.

11 Photosynthesis: Physiological and Ecological Considerations



Aleksey Sagitov/Shutterstock

The conversion of solar energy to the chemical energy of organic compounds is a complex process that includes electron transport and photosynthetic carbon metabolism (see Chapters 9 and 10). This chapter addresses some of the photosynthetic responses of the intact leaf to its environment. Additional photosynthetic responses to different types of stress will be covered in Chapter 15. When discussing photosynthesis in this chapter, we are referring to the rate of net photosynthesis, the difference between photosynthetic carbon assimilation and the loss of CO_2 via photorespiration and mitochondrial respiration in the light.

The impact of the environment on photosynthesis is of broad interest, especially to physiologists, ecologists, evolutionary biologists, climate change scientists, and agronomists. From a physiological standpoint, we wish to understand the direct responses of photosynthesis to environmental factors such as light, atmospheric CO_2 concentrations, and temperature, as well as the indirect responses (mediated through the effects of stomatal control) to environmental factors such as humidity and soil moisture. The dependence of photosynthetic processes on environmental conditions is also important to agronomists because plant productivity, and hence crop yield, depends strongly on prevailing photosynthetic rates in a dynamic environment. To the ecologist, photosynthetic variation across plant lineages in different environments is of great interest in terms of adaptation and evolution.

In studying the environmental dependence of photosynthesis, a central question arises: How many environmental factors can limit photosynthesis at one time? The British plant physiologist F. F. Blackman hypothesized in 1905 that, under any particular set of conditions, the rate of photosynthesis is limited by the slowest step in the process, the so-called *limiting factor*. The implication of this hypothesis is that at any given time, photosynthesis can be limited either by light or by CO_2 concentration, for instance, but not by both factors. This hypothesis has had a marked influence on the approach used by plant physiologists to study photosynthesis—that is, varying one factor and keeping all other environmental conditions constant. Instrumental to this analysis was the development of a biochemical model of C_3 photosynthesis published in 1980 by Graham Farquhar, Susanne von Caemmerer, and Joe Berry. This model has been expanded over the years to describe the three

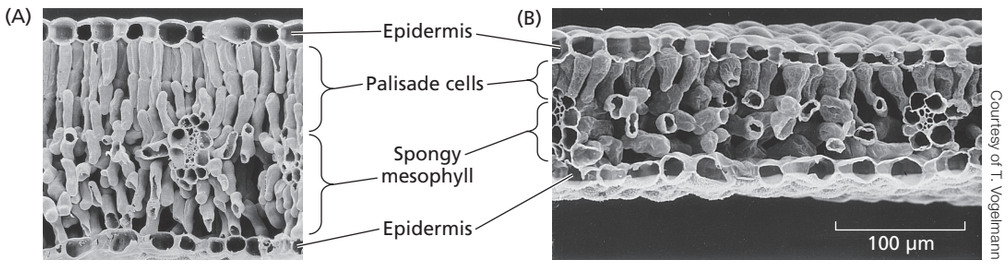


Figure 11.1 Scanning electron micrographs of the leaf anatomy of a legume (*Thermopsis montana*) grown in different light environments. Note that the sun leaf (A) is much thicker than the shade leaf (B), and that the palisade (column-like) cells are much longer in the leaves grown in sunlight. Layers of spongy mesophyll cells can be seen below the palisade cells.

major metabolic processes that have been identified as important for photosynthetic performance:

1. Rubisco capacity
2. Regeneration of ribulose bisphosphate (RuBP)
3. Metabolism of the triose phosphates

Graham Farquhar and Tom Sharkey pointed out that we can think of the controls on the overall net photosynthetic rates of leaves in economic terms, considering "supply" and "demand" functions for carbon dioxide. The major metabolic processes just referred to take place in the palisade cells and spongy mesophyll of the leaf (**Figure 11.1**). These biochemical activities describe the "demand" for CO_2 by photosynthetic metabolism in the cells. However, the rate of CO_2 "supply" to these cells is largely determined by diffusion limitations resulting from boundary layer conductance, stomatal regulation, and subsequent resistance in the mesophyll (see also Chapter 6). The coordinated actions of "demand" by photosynthetic cells and "supply" of atmospheric CO_2 affect leaf photosynthetic rates of net CO_2 uptake.

In the following sections we focus on how naturally occurring variation in light and temperature influences photosynthesis in leaves and how leaves in turn adjust or acclimate to such variation. We also explore how atmospheric CO_2 and temperature influence photosynthesis, an especially important consideration in a world where CO_2 concentrations and temperature are rapidly increasing as humans continue to burn fossil fuels for energy production.

11.1 Photosynthesis Is Influenced by Leaf Properties

Scaling up from the chloroplast (the focus of Chapters 9 and 10) to the leaf adds new levels of complexity to photosynthesis. At the same time, the structural and functional properties of the leaf add additional levels of regulation to CO_2 and H_2O exchange between leaves and the atmosphere.

We will start by examining the capture of light, and how leaf anatomy and leaf orientation maximize light absorption for photosynthesis. Then we will describe how leaves acclimate to their light environment. We will see that the photosynthetic response of leaves grown under different light conditions also reflects the ability of a plant to grow under different light environments. However, there are limits to the extent to which photosynthesis in a species can acclimate to very different light environments. For example, in some situations photosynthesis is limited by an inadequate supply of light. In other situations, absorption of too much light would cause severe problems if special mechanisms did not protect the photosynthetic system from excessive light. While plants have multiple levels of control over photosynthesis that allow them to grow successfully in constantly changing environments, there are ultimately limits to what is possible.

Consider the many ways in which leaves are exposed to different spectra (qualities) and quantities of light. Plants grown outdoors are exposed to sunlight, and the spectrum of that light will depend on whether it is measured in full sunlight or under the shade of a canopy. Plants grown indoors may receive incandescent, fluorescent, or LED lighting, each of which differs in intensity and spectral composition from sunlight. To account for these differences in spectral quality and quantity, we need to define how we measure and express the light availability for photosynthesis.

The light reaching the plant is a flux, and that flux can be measured in either energy or photon flux units. **Irradiance** is the amount of energy that falls on a flat surface of known area per unit time, expressed in watts per square meter (W m^{-2}). Recall that time (seconds) is contained within the term watt: 1 W = 1 joule (J) s^{-1}. Quantum flux, or photon flux density (PFD), is the number of incident **quanta** (singular *quantum*) striking the leaf,

expressed in moles per square meter per second (mol m^{-2} s^{-1}), where *moles* refers to the number of photons (1 mol of light = 6.02×10^{23} photons, Avogadro's number). Quanta and energy units for sunlight can be interconverted relatively easily, provided that the wavelength of the light, λ, is known. The energy of a photon is related to its wavelength as follows:

$$E = \frac{hc}{\lambda} \qquad (11.1)$$

where c is the speed of light (3×10^8 m s^{-1}), h is Planck's constant (6.63×10^{-34} J s), and λ is the wavelength of light, usually expressed in nanometers (1 nm = 10^{-9} m). From Equation 11.1 it can be calculated that a photon at 400 nm has twice the energy of a photon at 800 nm (see **WEB TOPIC 11.1**).

When considering photosynthesis and light, it is appropriate to express light as photosynthetic photon flux density (PPFD)—the flux of light (usually expressed as micromoles per square meter per second [μmol m^{-2} s^{-1}]) within the photosynthetically active range (400–700 nm). How much light is there on a sunny day? Under direct sunlight on a clear day, PPFD is about 2000 μmol m^{-2} s^{-1} at the top of a dense forest canopy, but may be only 10 μmol m^{-2} s^{-1} at the bottom of the canopy because of light absorption by the leaves overhead.

Leaf anatomy and canopy structure optimize light absorption

On average, about 340 W (J s^{-1}) of radiant energy from the sun reach each square meter of Earth's surface. When this sunlight strikes the vegetation, only 5% of the energy is ultimately converted into carbohydrates by photosynthesis (**Figure 11.2**). The reason this percentage is so low is that a major percentage of the light is either too short or too long a wavelength to be absorbed by the photosynthetic pigments (**Figure 11.3**). Furthermore, of the photosynthetically active radiation (PAR) (400–700 nm) that is incident on a leaf, a small percentage is transmitted through the leaf and some is also reflected from its surface. Because chlorophyll absorbs strongly in the blue and red regions of the spectrum (see Figure 9.3), green wavelengths are primarily transmitted and reflected (see Figure 11.3)—hence the green color of vegetation. Lastly, a percentage of the photosynthetically active radiation that is initially absorbed by the leaf is consumed by metabolism and a smaller amount is lost as heat (see Chapter 9).

The anatomy of the leaf is highly specialized for light absorption. The outermost cell layer, the epidermis, is typically transparent to visible light, and the individual cells are often convex. Convex epidermal cells can act as lenses and focus light so that the amount of light reaching some of the chloroplasts can be greater than the amount of incident light. Epidermal focusing is common among herbaceous plants and is especially prominent

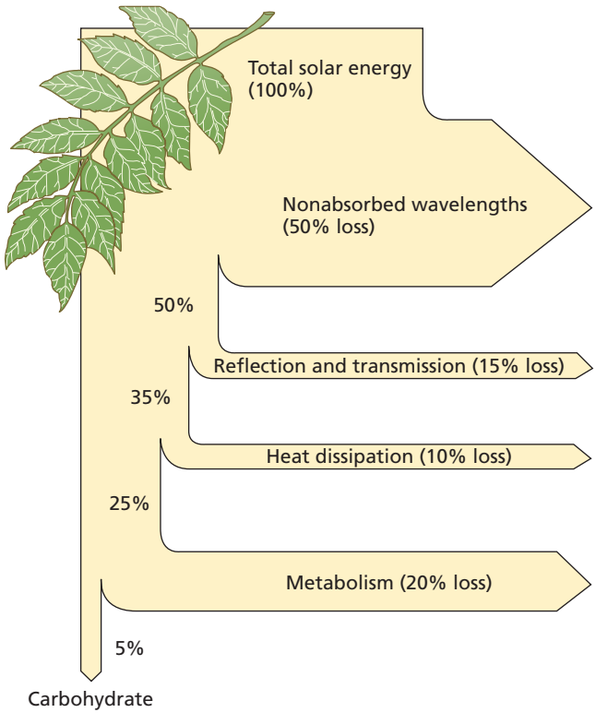


Figure 11.2 Conversion of solar energy into carbohydrates by a leaf. Of the total incident energy, only 5% is converted into carbohydrates.

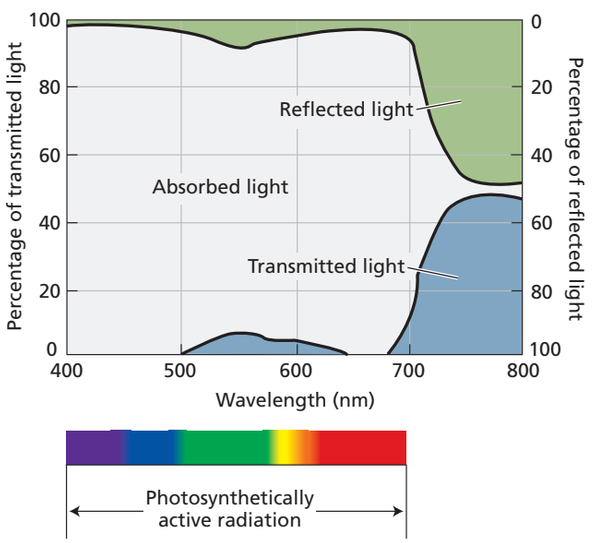


Figure 11.3 Optical properties of a bean leaf. Shown here are the percentages of light absorbed, reflected, and transmitted, as a function of wavelength. The transmitted and reflected green light in the wave band at 500–600 nm gives leaves their green color. Note that most of the light above 700 nm is not absorbed by the leaf. (After H. Smith. 1986. In *Photomorphogenesis in Plants*., 1st ed. R. E. Kendrick and G. H. M. Kronenberg [eds.]. Nijhoff, Dordrecht, Netherlands, pp. 187–217.)

among tropical plants that grow in the forest understory, where the incident light levels are low.

Below the epidermis, the top layers of photosynthetic cells in eudicots are called **palisade cells**; they are shaped like pillars that stand in parallel columns one to three layers deep (see Figure 11.1). Some leaves have several layers of columnar palisade cells, and we may wonder how efficient it is for a plant to invest energy in developing multiple cell layers when the high chlorophyll content of the first layer would appear to allow little transmission of incident light to the leaf interior. In fact, more light than might be expected penetrates the first layer of palisade cells because of the *sieve effect* and *light channeling*.

The **sieve effect** occurs because chlorophyll is not uniformly distributed throughout cells but instead is confined to the chloroplasts. This packaging of chlorophyll results in shading between the chlorophyll molecules and creates gaps between the chloroplasts where light is not absorbed—hence the reference to a sieve. Because of the sieve effect, the total absorption of light by a given amount of chlorophyll in chloroplasts of a palisade cell is less than the light that would be absorbed by the same amount of chlorophyll were it uniformly distributed in solution.

Light channeling occurs when some of the incident light is propagated through the central vacuoles of the palisade cells and through the air spaces between the cells, an arrangement that results in the transmission of light into the leaf interior. In the interior, below the palisade layers, is the **spongy mesophyll**, where the cells are very irregular in shape and are surrounded by large air spaces (see Figure 11.1). The large air spaces generate many interfaces between air and water that reflect and refract the light, thereby randomizing its direction of travel. This phenomenon is called **interface light scattering**.

Light scattering is especially important in leaves because the multiple refractions between cell–air interfaces greatly increase the length of the path over which photons travel, thereby increasing the probability of absorption. In fact, photon path lengths within leaves are commonly four times longer than the thickness of the leaf. Thus, the palisade cell properties that allow light to pass through, and the spongy mesophyll cell properties that are conducive to light scattering, result in more uniform light absorption throughout the leaf.

In some environments, such as deserts, there is so much light that it is potentially harmful to the photosynthetic machinery of leaves. In these environments, leaves often have special anatomic features, such as hairs, salt glands, and epicuticular wax, that increase the reflection of light from the leaf surface, thereby reducing light absorption. Such adaptations can decrease light absorption by as much as 60%, thereby reducing overheating and other problems associated with the absorption of too much solar energy.

At the whole-plant level, leaves at the top of a canopy absorb most of the sunlight, and reduce the amount of radiation that reaches leaves lower down in the canopy. Leaves that are shaded by other leaves experience lower light levels and different light quality than the leaves above them and have much lower photosynthetic rates. However, like the layers of an individual leaf, the structure of most plants, and especially of trees, represents an outstanding adaptation for light interception. The elaborate branching structure of trees vastly increases the interception of sunlight. In addition, leaves at different levels of the canopy have varied morphology and physiology that help improve light capture throughout the canopy. The result is that very little PAR penetrates all the way to the bottom of the forest canopy; almost all of the PAR is absorbed by leaves before reaching the forest floor (**Figure 11.4**).

The deep shade of a forest floor thus makes for a challenging growth environment for plants. However, in many shady habitats **sunflecks** are a common environmental feature that brings high light levels deep into the canopy. These are patches of sunlight that pass through small gaps in the leaf canopy; as the sun moves, the sunflecks move across the normally shaded leaves. In spite of the short, ephemeral nature of sunflecks, the photons in them can comprise nearly 50% of the total light energy available during the day. In a dense forest, sunflecks can change the sunlight impinging on a shade leaf by more than tenfold within seconds. This critical energy is available for only a few seconds to minutes,

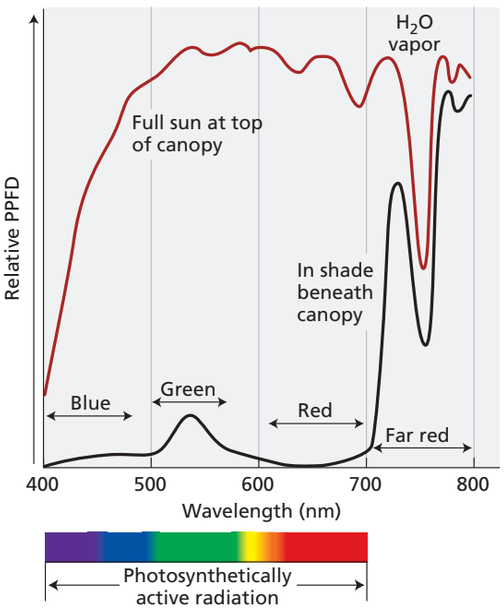


Figure 11.4 Relative spectral distributions of sunlight at the top of a canopy and in the shade under the canopy. Most photosynthetically active radiation is absorbed by leaves in the canopy. (After H. Smith. 1986. In *Photomorphogenesis in Plants*, 2nd ed. R. E. Kendrick and G. H. M. Kronenberg [eds.]. Nijhoff, Dordrecht, Netherlands, pp. 337–416.)

and in a very high dose. Many deep-shade species that experience sunflecks have physiological mechanisms for taking advantage of this burst of light when it occurs. Sunflecks also play an important role in the carbon metabolism of densely planted crops, where the lower leaves are shaded by leaves higher up on the plant.

Leaf angle and leaf movement can control light absorption

The angle of the leaf relative to the sun determines the amount of sunlight incident on it. Incoming sunlight can strike a flat leaf surface at a variety of angles depending on the time of day and the orientation of the leaf. Maximum incident radiation occurs when sunlight strikes a leaf perpendicular to its surface. When the rays of light deviate from perpendicular, however, the incident sunlight on a leaf is proportional to the angle at which the rays hit the surface.

Under natural conditions, leaves exposed to full sunlight at the top of the canopy tend to have steep leaf angles, so less than the maximum amount of sunlight is incident on the leaf blade; this allows more sunlight to penetrate into the canopy. For this reason, it is common to see the angle of leaves within a canopy decrease (become more horizontal) with increasing depth in the canopy.

Some leaves maximize light absorption by **solar tracking**; that is, they continuously adjust the orientation of their laminae (blades) such that they remain perpendicular to the sun's rays (**Figure 11.5**). Many species, including alfalfa, cotton, soybean, bean, and lupine, have leaves capable of solar tracking.

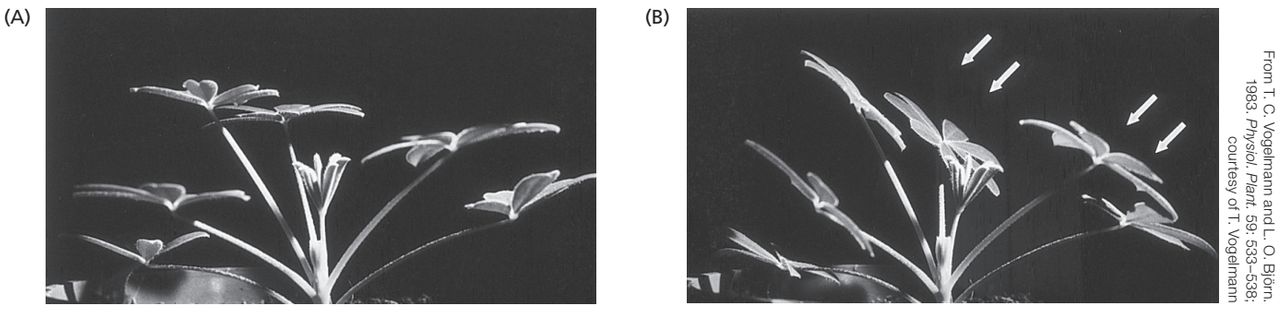
Solar-tracking leaves present a nearly vertical position at sunrise, facing the eastern horizon. Individual leaf blades then begin to track the rising sun, following its movement across the sky with an accuracy of ±15° until sunset, when the laminae are again nearly vertical, facing west. During the night the leaves take a horizontal position and reorient just before dawn so that they face the eastern horizon, ready for another sunrise. Leaves track the sun only on clear days, and they stop moving when a cloud obscures the sun. In the case of intermittent cloud cover, some leaves can reorient as rapidly as 90° per hour and thus can catch up with the new solar position when the sun emerges from behind a cloud.

Solar tracking is a blue-light response (see Chapter 16), and the sensing of blue light in solar-tracking leaves occurs in specialized regions of the leaf or stem. In species of *Lavatera* (Malvaceae), the photosensitive region is located in or near the major leaf veins, but in many species, notably legumes, leaf orientation is controlled by a specialized organ called the **pulvinus** (plural *pulvini*), found at the junction between the blade and the petiole. In lupines (*Lupinus*, Fabaceae), for example, leaves consist of five or more leaflets, and the photosensitive region is in a pulvinus located at the basal part of each leaflet lamina (see Figure 11.5). The pulvinus contains motor cells that change their osmotic potential and generate mechanical forces that determine laminar orientation. In other plants, leaf orientation is controlled by small mechanical changes along the length of the petiole and by movements of the younger parts of the stem.

Heliotropism is another term used to describe leaf orientation by solar tracking. Leaves that maximize light interception by solar tracking are referred to as *diaheliotropic*. Some solar-tracking plants can also move their leaves so that they *avoid* full exposure to sunlight, thus minimizing heating and water loss. These sun-avoiding leaves are called *paraheliotropic*. Some plant species, such as soybean, have leaves that can display diaheliotropic movements when they are well watered and paraheliotropic movements when they experience water stress.

Leaves acclimate to sun and shade environments

Acclimation is a developmental process in which leaves express a set of biochemical and morphological adjustments that are suited to the particular environment in which the leaves are exposed. Acclimation can occur



From T. C. Vogelmann and L. O. Björn. 1983. *Physiol. Plant.* 59: 533–538; courtesy of T. Vogelmann

Figure 11.5 **Leaf movement in a sun-tracking plant.** **(A)** Initial leaf orientation in the lupine *Lupinus succulentus*, with no direct sunlight. **(B)** Leaf orientation 4 h after exposure to oblique light. Arrows indicate the direction of the light beam. Movement is generated by asymmetric swelling of a pulvinus, found at the junction between the lamina and the petiole. In natural conditions, the leaves track the sun's trajectory in the sky.

in both mature leaves and in newly developing leaves. **Plasticity** is the term we use to define how much adjustment can take place. Many plants have developmental plasticity to respond to a range of light regimes, growing as sun plants in sunny areas and as shade plants in shady habitats. The ability to acclimate is important, given that shady habitats can receive less than 20% of the PAR available in an exposed habitat, and deep-shade habitats receive less than 1% of the PAR incident at the top of the canopy.

In some plant species, individual leaves that develop under very sunny or deep shady environments are often unable to persist when transferred to the other type of habitat. In such cases, the mature leaf will abscise (senesce and fall off) and a new leaf will develop that is better suited for the new environment. You may notice this if you take a plant that developed indoors and transfer it outdoors; after some time, if it is the right type of plant, a new set of leaves will develop that are better suited to high sunlight. However, some plant species are not able to acclimate when transferred from a sunny to a shady environment, or vice versa. The lack of acclimation indicates that these plants have lower plasticity and are specialized for either a sunny or a shady environment. When plants adapted to deep-shade conditions are transferred into full sunlight, the leaves experience chronic photoinhibition and leaf bleaching, and they eventually die. We will discuss photoinhibition, introduced in Chapter 9, in Section 11.2.

Sun and shade leaves have contrasting biochemical and morphological characteristics:

- Shade leaves increase light capture by having more total chlorophyll per reaction center, a higher ratio of chlorophyll *b* to chlorophyll *a*, and usually thinner laminae than sun leaves.
- Sun leaves have less total chlorophyll per reaction center, increase CO_2 assimilation by having more Rubisco, and can dissipate excess light energy by having a large pool of xanthophyll-cycle components (see Chapter 9). Morphologically they have thicker leaves and a thicker palisade layer than shade leaves (see Figure 11.1).

These morphological and biochemical modifications are associated with specific acclimation responses to the *amount* of sunlight in a plant's habitat, but light *quality* can also influence such responses. For example, far-red light, which is absorbed primarily by photosystem I (PSI), is proportionally more abundant in shady habitats than in sunny ones (see Chapter 18). To better balance the flow of energy through PSII and PSI, the adaptive response of some shade plants is to produce a higher ratio of PSII to PSI reaction centers, compared with that found in sun plants. Other shade plants, rather than altering the ratio of PSII to PSI reaction centers, add more antenna chlorophyll to PSII to increase absorption by this photosystem. These changes appear to enhance light absorption and optimize energy transfer in shady environments.

11.2 Effects of Light on Photosynthesis in the Intact Leaf

Light is a critical resource that often limits plant growth, but at times leaves can be exposed to too much rather than too little light. In this section we describe typical photosynthetic responses to light as measured by light-response curves. We also consider how features of a light-response curve can help explain contrasting physiological properties between sun and shade plants, and between C_3 and C_4 species (see Chapter 10). The section concludes with descriptions of how leaves respond to excess light.

Photosynthetic light-response curves reveal differences in leaf properties

Measuring net CO_2 fixation in intact leaves across varying PPFD levels generates light-response curves (**Figure 11.6**). In near darkness there is little photosynthetic carbon

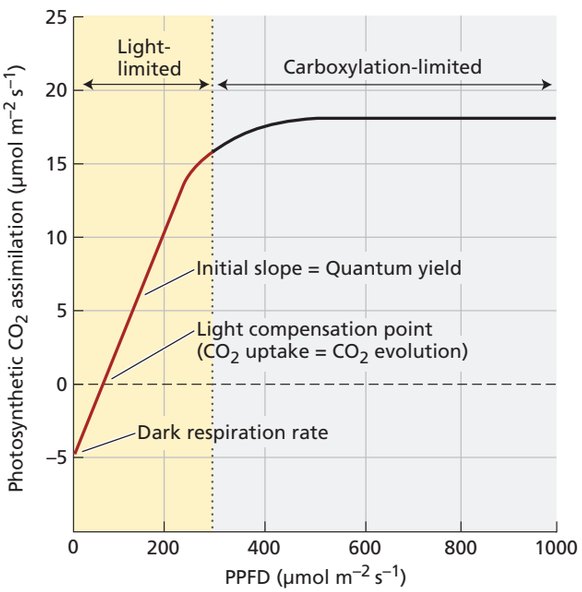


Figure 11.6 Response of photosynthesis to light in a C_3 plant. In darkness, respiration causes a net efflux of CO_2 from the plant. The light compensation point is reached when photosynthetic CO_2 assimilation equals the amount of CO_2 evolved by respiration. Increasing light above the light compensation point proportionally increases photosynthesis, indicating that photosynthesis is limited by the rate of electron transport, which in turn is limited by the amount of available light. This portion of the curve is referred to as light-limited. Further increases in photosynthesis are eventually limited by the carboxylation capacity of Rubisco or the metabolism of triose phosphates. This part of the curve is referred to as carboxylation-limited.

assimilation, but because mitochondrial respiration continues, CO_2 is given off by the leaf (see Chapter 13). The uptake of CO_2 is negative in this part of the light-response curve. At higher PPFD levels, photosynthetic CO_2 assimilation eventually reaches a point where CO_2 uptake exactly balances CO_2 evolution, the **light compensation point**. The PPFD at which different leaves reach the light compensation point can vary among species and developmental conditions. One of the more interesting differences is found between plants that normally grow in full sunlight and those that grow in the shade (**Figure 11.7**). Light compensation points of sun plants range from 10 to 20 μmol m^{-2} s^{-1} PPFD, whereas corresponding values for shade plants are 1 to 5 μmol m^{-2} s^{-1} PPFD.

Why are light compensation points lower for shade plants? For the most part, this is because respiration rates in shade plants are very low; therefore, only low rates of photosynthesis are necessary to bring the net rates of CO_2 exchange to zero. Low respiratory rates are a consequence of slow growth rates of shade plants and allow them to survive in light-limited environments through their ability to achieve positive CO_2 uptake rates at lower PPFD values compared with sun plants.

A linear relationship between PPFD and photosynthetic rate persists at light levels above the light compensation point (see Figure 11.6). Throughout this linear portion of the light-response curve, photosynthesis is light-limited; more light stimulates proportionally more photosynthesis. When corrected for light absorption, the slope of this linear portion of the curve provides the **maximum quantum yield** of photosynthesis for the leaf. Leaves of sun and shade plants show very similar quantum yields despite their different growth habitats. This is because the basic biophysical and biochemical processes that determine quantum yield are the same for these two types of plants. But quantum yield can vary among plants with different photosynthetic pathways (e.g., between C_3 and C_4 plants).

Quantum yield is the ratio of a given light-dependent product to the number of absorbed photons (see Equation 9.7). Photosynthetic quantum yield can be expressed on either a CO_2 or an O_2 basis, and as explained in Chapter 9, the quantum yield of photochemistry is about 0.95. However, the maximum photosynthetic quantum yield of an integrated process such as photosynthesis is lower than the theoretical yield when measured in chloroplasts (organelles) or whole leaves. Based on the biochemistry discussed in Chapter 10, we expect the theoretical maximum quantum yield for photosynthesis to be 0.125 for C_3 plants (one CO_2 molecule fixed per eight photons absorbed). But under today's atmospheric conditions (417 ppm CO_2, 21% O_2), the quantum yields for CO_2 of C_3 and C_4 leaves vary between 0.04 and 0.07 mole of CO_2 per mole of photons.

In C_3 plants the reduction from the theoretical maximum is caused primarily by energy loss through photorespiration. In C_4 plants the reduction is caused by the additional energy requirements of the CO_2-concentrating mechanism and the potential cost of refixing CO_2 that has diffused out from within the bundle sheath cells. If C_3 leaves are exposed to low O_2 concentrations, photorespiration is minimized and the maximum quantum yield increases to about 0.09 mole of CO_2 per mole of photons. In contrast, if C_4 leaves are exposed to low O_2 concentrations, the quantum yields for CO_2 fixation remain constant at about 0.06 to 0.07 mole of CO_2 per mole of photons. This is because the carbon-concentrating mechanism in C_4 photosynthesis eliminates nearly all the oxygenation reaction of Rubisco and consequently the CO_2 evolved via photorespiration.

At higher PPFD along the light-response curve, the photosynthetic response to light starts to level off (see Figures 11.6 and 11.7) and eventually approaches *saturation*. Beyond the light saturation point, net photosynthesis no longer increases, indicating that factors other than incident light, such as electron transport rate, Rubisco activity, or the metabolism of triose phosphates, limit photosynthesis. Light saturation levels for shade plants are substantially lower than those for sun plants (see Figure 11.7). This is also true for leaves of the same plant when grown in sun versus shade (**Figure 11.8**). These levels usually reflect the maximum PPFD to which a leaf was exposed during growth.

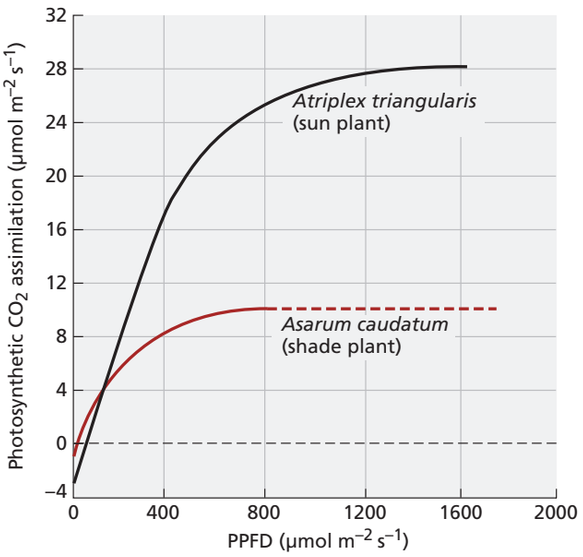


Figure 11.7 Light-response curves of photosynthetic carbon fixation in sun and shade plants. Triangle orache (*Atriplex triangularis*) is a sun plant, and wild ginger (*Asarum caudatum*) is a shade plant. Typically, shade plants have a low light compensation point and have lower maximum photosynthetic rates than sun plants. The dashed red line has been extrapolated from the measured part of the curve. (After G. W. Harvey. 1979. *Carnegie Inst. Wash. Yb.* 79: 161–164. Courtesy, Carnegie Institution for Science.)

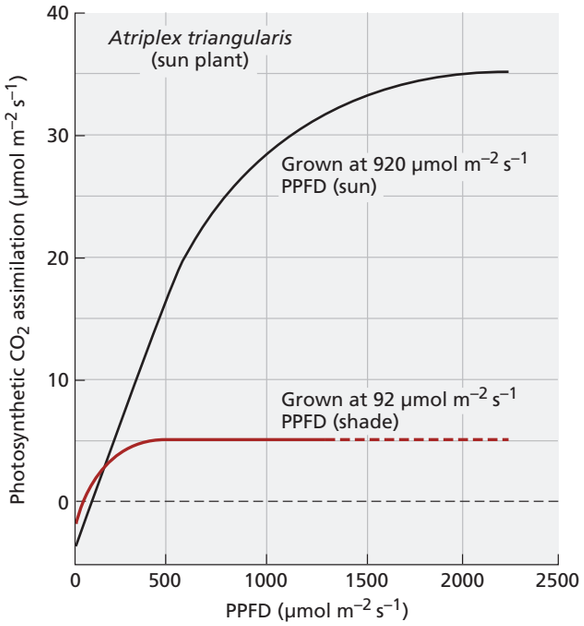


Figure 11.8 **Light-response curve of photosynthesis of a sun plant grown under sun versus shade conditions.** The upper curve represents an *A. triangularis* leaf grown at a PPFD ten times higher than that of the lower curve. In the plant grown at the lower light levels, photosynthesis saturates at a substantially lower PPFD, indicating that the photosynthetic properties of a leaf depend on its growing conditions. The dashed red line has been extrapolated from the measured part of the curve. (After O. Björkman. 1981. In *Encyclopedia of Plant Physiology*, New Series, Vol. 12A. O. L. Lange et al. [eds.], pp. 57–107. Springer, Berlin, Heidelberg.)

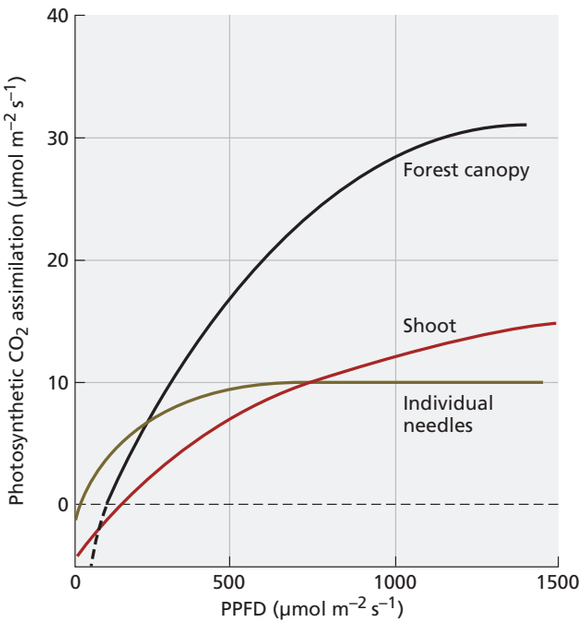


Figure 11.9 **Changes in photosynthesis (expressed on a per-square-meter basis) in individual needles, a complex shoot, and a forest canopy of Sitka spruce (*Picea sitchensis*) as a function of PPFD.** Complex shoots consist of groupings of needles that often shade each other, similar to the situation in a canopy where branches often shade other branches. As a result of shading, much higher PPFD levels are needed to saturate photosynthesis. The dashed portion of the forest canopy trace has been extrapolated from the measured part of the curve. (After P. G. Jarvis and J. W. Leverenz. 1983. In *Encyclopedia of Plant Physiology*, New Series, Vol. 12D. O. L. Lange et al. [eds.], pp. 233–280. Springer, Berlin, Heidelberg.)

The light-response curve of most leaves saturates between 500 and 1000 µmol m^{-2} s^{-1}, well below full sunlight (which is about 2000 µmol m^{-2} s^{-1}). An exception to this is well-fertilized crop leaves, which often saturate above 1000 µmol m^{-2} s^{-1}. Although individual leaves are rarely able to use full sunlight, whole plants usually consist of many leaves that shade each other. Thus, at any given time of the day only a small proportion of the leaves are exposed to full sun, especially in plants with dense canopies. The rest of the leaves receive subsaturating photon fluxes that come from sunflecks that pass through gaps in the leaf canopy, diffuse light, and light transmitted through other leaves.

Because the photosynthetic response of the intact plant is the sum of the photosynthetic activity of all the leaves, only rarely is photosynthesis light-saturated at the level of the whole plant (**Figure 11.9**). It is for this reason that crop productivity is usually related to the total amount of light received during the growing season, rather than to single-leaf photosynthetic capacity. Given enough water and nutrients, the more light a crop receives, the higher the biomass produced.

Leaves must dissipate excess light energy as heat

When exposed to excess light, leaves must dissipate the surplus absorbed light energy to prevent damage to the photosynthetic apparatus (**Figure 11.10**). There are several routes for energy dissipation that involve *nonphotochemical quenching* (see Chapter 9), the quenching of chlorophyll fluorescence by mechanisms other than photochemistry. The most important example involves the transfer of absorbed light energy away from electron transport toward heat production through the xanthophyll cycle.

THE XANTHOPHYLL CYCLE The xanthophyll cycle, which comprises the three carotenoids violaxanthin, antheraxanthin, and zeaxanthin, establishes an ability to dissipate excess light energy in the leaf (see Figure 9.31). Under high light, violaxanthin is converted to antheraxanthin and then to zeaxanthin. Both of the aromatic rings of violaxanthin have a bound oxygen atom. In antheraxanthin only one of the two rings has a bound oxygen, and in zeaxanthin neither does. Zeaxanthin is the most effective of the three xanthophylls in heat dissipation,

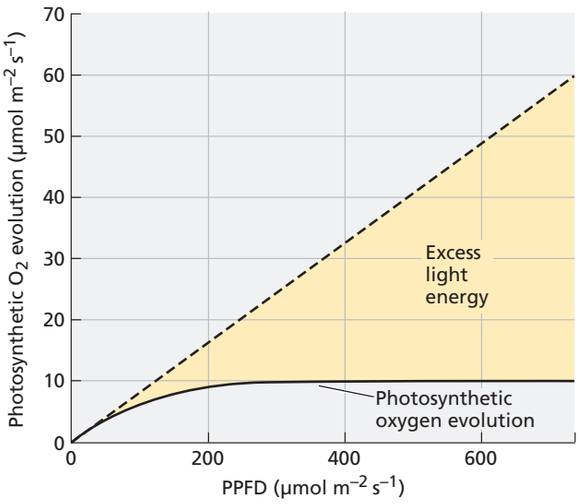


Figure 11.10 Excess light energy in relation to a light-response curve of photosynthetic oxygen evolution in a shade leaf. The dashed line shows theoretical oxygen evolution in the absence of any rate limitation to photosynthesis. At PPFD levels up to 150 μmol m^{-2} s^{-1}, a shade plant is able to use the absorbed light. Above 150 μmol m^{-2} s^{-1}, however, photosynthesis saturates, and an increasingly larger amount of the absorbed light energy must be dissipated. At higher PPFD levels there is a large difference between the fraction of light used by photosynthesis versus that which must be dissipated (excess light energy). The differences are much greater in a shade plant than in a sun plant. (After C. B. Osmond. 1994. In *Photoinhibition of Photosynthesis: From Molecular Mechanisms to the Field*. N. Baker and J. R. Bowyer [eds.]. BIOS Scientific, Oxford, pp. 1–24.)

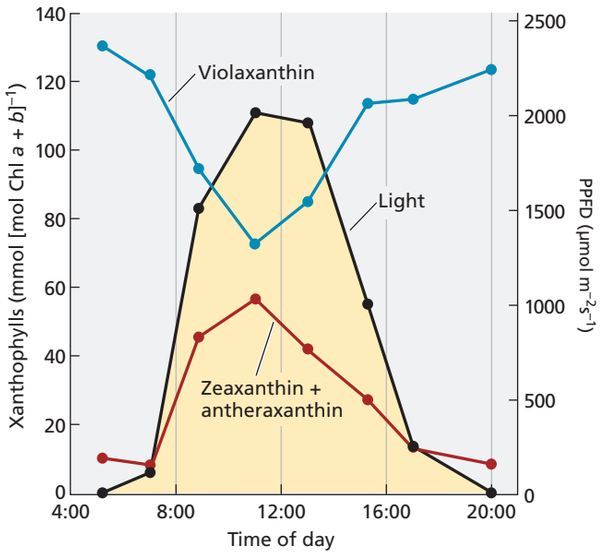


Figure 11.11 Diurnal changes in xanthophyll content as a function of PPFD in sunflower (*Helianthus annuus*). As the amount of light incident to a leaf increases, a greater proportion of violaxanthin is converted to antheraxanthin and zeaxanthin, thereby dissipating excess excitation energy and protecting the photosynthetic apparatus. (After W. W. Adams and B. Demmig-Adams. 1992. *Planta* 186: 390–398.)

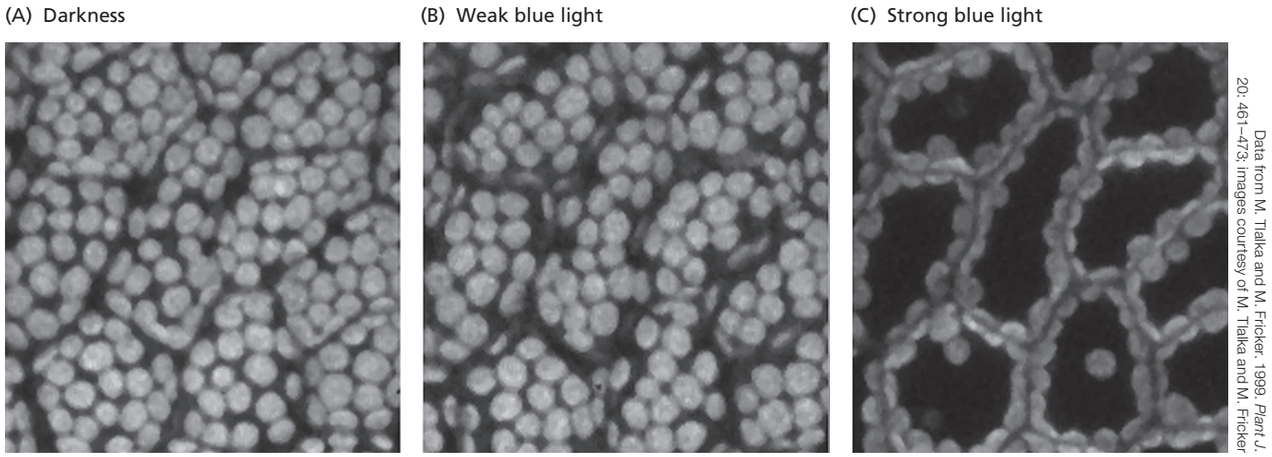
and antheraxanthin is only half as effective. Whereas the antheraxanthin content remains relatively constant throughout the day, the zeaxanthin content increases at high PPFD and decreases at low PPFD.

In leaves growing under full sunlight, zeaxanthin and antheraxanthin can make up 40% of the total xanthophyll-cycle pool at maximum PPFD levels attained at midday (**Figure 11.11**). In these conditions a substantial amount of excess light energy absorbed by the thylakoid membranes can be dissipated as heat, thus preventing damage to the photosynthetic machinery of the chloroplast (see Chapter 9). Leaves that grow in full sunlight contain a substantially larger xanthophyll pool than do shade leaves, so they can dissipate higher amounts of excess light energy. Nevertheless, the xanthophyll cycle also operates in plants that grow in the low light of the forest understory, where they are occasionally exposed to sunflecks. Exposure to just one sunfleck results in the conversion of much of the violaxanthin in the leaf to zeaxanthin.

The xanthophyll cycle is also important in species that remain green during winter, when photosynthetic rates are low yet light absorption remains high. Unlike in the diurnal cycling of the xanthophyll pool observed in the summer, zeaxanthin levels remain high all day during the winter. This mechanism maximizes dissipation of light energy, thereby protecting the leaves against photooxidation when winter cold prevents carbon assimilation.

CHLOROPLAST MOVEMENTS An alternative means of reducing the absorption of excess light energy is to move the chloroplasts within the cell so that they are no longer exposed to high light. Chloroplast movement is widespread among algae, mosses, and leaves of higher plants. If chloroplast orientation and location are controlled, leaves can regulate how much incident light is absorbed. Under low light (**Figure 11.12A and B**), chloroplasts gather at the cell surfaces parallel to the plane of the leaf so that they are aligned perpendicularly to the incident light—a position that maximizes absorption of light.

Under high light (**Figure 11.12C**), the chloroplasts move to the cell surfaces that are parallel to the incident light, thus minimizing absorption of light. Such chloroplast rearrangement can decrease the amount of light absorbed by the leaf by about 15%. Chloroplast movement in leaves is a typical blue-light response (see Chapter 16). Blue light also controls chloroplast orientation in many of the lower plants, but in some algae, chloroplast movement is controlled by phytochrome. In leaves, chloroplasts move along actin



Data from M. Tlalka and M. Fricker. 1999. *Plant J.* 20: 461–473; images courtesy of M. Tlalka and M. Fricker

Figure 11.12 Chloroplast distribution in photosynthesizing cells of the duckweed *Lemna*. These surface views show the same cells under three conditions: **(A)** darkness, **(B)** weak blue light, and **(C)** strong blue light. In (A) and (B), chloroplasts are positioned near the upper surface of the cells, where they can absorb maximum amounts of light. When the cells are irradiated with strong blue light (C), the chloroplasts move to the side walls, where they shade each other, thus minimizing the absorption of excess light.

microfilaments in the cytoplasm, and calcium ions regulate their movement.

LEAF MOVEMENTS Plants have also evolved responses that reduce the excess radiation load on whole leaves during high sunlight periods, especially when transpiration and its cooling effects are reduced because of water stress. These responses often involve changes in the leaf orientation relative to the incoming sunlight. For example, heliotropic leaves of both alfalfa and lupine track the sun, but at the same time can reduce incident light levels by folding leaflets together so that the leaf laminae become nearly parallel to the sun's rays (paraheliotrophic), as discussed earlier. Another common response is mild wilting around solar noon, as seen in many sunflowers, whereby a leaf droops to a vertical orientation, again effectively reducing the incident heat load and reducing transpiration and incident light levels. Many grasses are able to effectively "twist" through loss of turgor in bulliform cells, resulting in reduced incident PPFD.

Absorption of too much light can lead to photoinhibition

When leaves are exposed to more light than they can use (see Figure 11.10), the reaction center of PSII is inactivated and often damaged in a phenomenon called **photoinhibition** (see Chapter 9). The characteristics of photoinhibition in the intact leaf depend on the amount of light to which the plant is exposed. The two types of photoinhibition are dynamic photoinhibition and chronic photoinhibition.

Under moderate excess light, **dynamic photoinhibition** is observed. Quantum yield decreases, but the maximum photosynthetic rate remains unchanged. Dynamic photoinhibition is caused by the diversion of absorbed light energy toward photoprotective heat dissipation—hence the decrease in quantum yield. This decrease is often temporary, and quantum yield can return to its initial higher value when PPFD decreases below saturation levels. **Figure 11.13** shows how photons from sunlight are allocated to photosynthetic reactions versus being thermally dissipated as excess energy over the course of a day under favorable and stressed environmental conditions.

Chronic photoinhibition results from exposure to high levels of excess light that damage the photosynthetic system and decrease both instantaneous quantum yield and maximum photosynthetic rate. This would happen if the stress condition in Figure 11.13B persisted because photoprotection was not possible. In contrast to the effects of dynamic photoinhibition, the effects of chronic photoinhibition are relatively long-lasting, persisting for weeks or months.

Early researchers of photoinhibition interpreted decreases in quantum yield as damage to the photosynthetic apparatus. It is now recognized that short-term decreases in quantum yield reflect protective mechanisms (see Chapter 9), whereas chronic photoinhibition represents actual damage to the chloroplast resulting from excess light and a failure of the protective mechanisms.

How significant is photoinhibition in nature? Dynamic photoinhibition appears to occur daily, when leaves are exposed to maximum amounts of light and there is a corresponding reduction in carbon fixation. Photoinhibition is more pronounced at low temperatures and becomes chronic under more extreme climatic conditions.

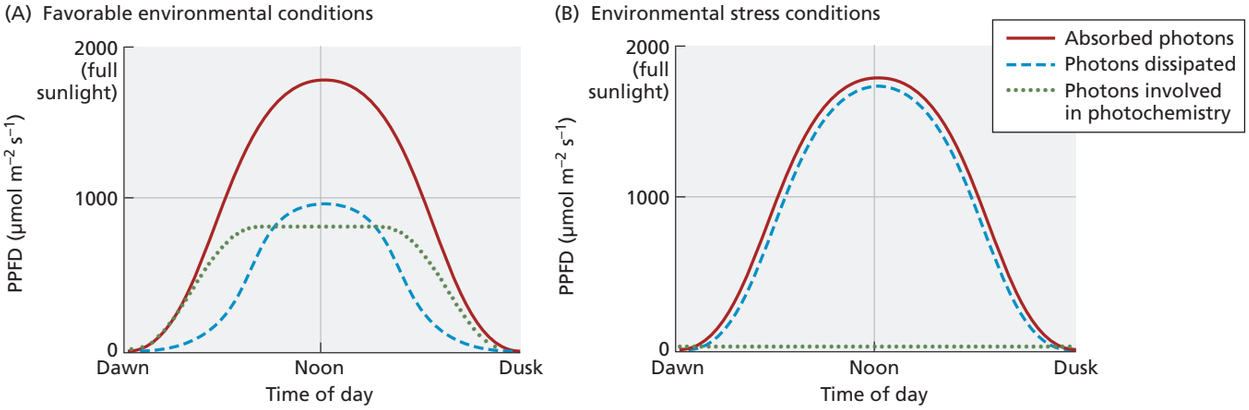


Figure 11.13 Changes over the course of a day in the allocation of photons absorbed by sunlight. Shown here are contrasts in how the photons striking a leaf are either involved in photochemistry or thermally dissipated as excess energy under favorable conditions **(A)** and stress conditions **(B)**. (After B. Demmig-Adams and W. W. Adams. 2000. *Nature* 403: 371–372.)

11.3 Effects of Temperature on Photosynthesis in the Intact Leaf

Photosynthesis (CO_2 uptake) and transpiration (H_2O loss) share a common pathway. That is, CO_2 diffuses into the leaf, and H_2O diffuses out, through the stomatal opening regulated by the guard cells (see Chapter 6). While these are independent processes, vast quantities of water are lost during photosynthetic periods, with the molar ratio of H_2O loss to CO_2 uptake often exceeding 250. The high water-loss rate also removes heat from leaves through evaporative cooling, keeping leaves relatively cool even under full sunlight conditions. Thus, in addition to allowing CO_2 uptake for photosynthesis, transpiration helps prevent leaves from overheating (e.g., high temperature stress), but this water loss comes at a cost, especially in arid and semiarid ecosystems.

Leaves must dissipate vast quantities of heat

The heat load on a leaf exposed to full sunlight is very high. In fact, under normal sunny conditions with moderate air temperatures, a leaf would warm up to a dangerously high temperature if all incident solar energy were absorbed and none of the heat was dissipated. However, this does not occur because leaves absorb only about 50% of the total solar energy (300–3000 nm), with most of the absorption occurring in the visible portion of the spectrum (see Figures 11.2 and 11.3). This amount of energy absorption is still large, and a leaf can typically dissipate this heat load through three processes (**Figure 11.14**):

1. Radiative heat loss: All objects emit long-wave radiation (at about 10,000 nm) in proportion to their temperature to the fourth power (Stephan Boltzman equation). However, the maximum emitted wavelength is inversely proportional to the leaf temperature, and leaf temperatures are low enough that the wavelengths emitted are not visible to the human eye.
2. Sensible heat loss: If the temperature of the leaf is higher than that of the air circulating around the leaf, the heat is convected (transferred) away from the leaf to the air. The size and shape of a leaf influence the amount of sensible heat loss, with

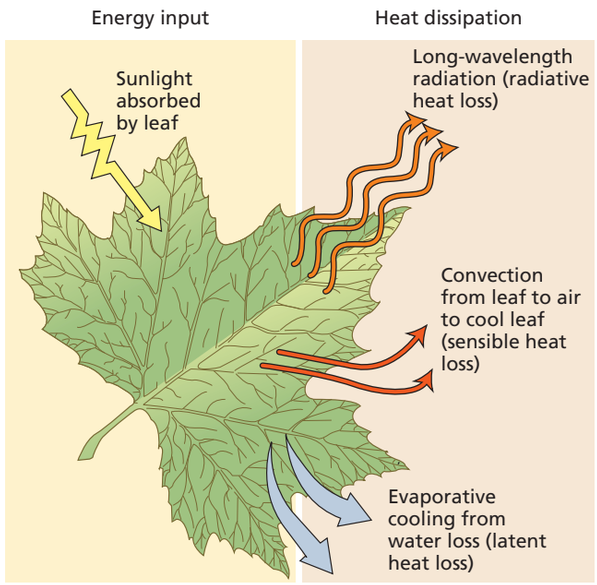


Figure 11.14 Absorption and dissipation of energy from sunlight by the leaf. The imposed heat load must be dissipated in order to avoid damage to the leaf. The heat load is dissipated by emission of long-wavelength radiation, by sensible heat loss to the air surrounding the leaf, and by the evaporative cooling caused by transpiration.

smaller leaves being more efficient in heat loss than larger leaves.

3. Latent heat loss: Because the evaporation of water requires energy, when water evaporates from a leaf (transpiration), it removes large amounts of heat from the leaf and thus cools it. The human body is cooled by the same principle, commonly known as perspiration.

Sensible heat loss and evaporative heat loss are the most important processes in the regulation of leaf temperature, and the ratio of the two fluxes is called the **Bowen ratio**:

$$\text{Bowen ratio} = \frac{\text{Sensible heat loss}}{\text{Evaporative heat loss}} \qquad (11.2)$$

In well-watered crops, transpiration (see Chapter 6), and hence water evaporation from the leaf, is high, so the Bowen ratio is low (see **WEB TOPIC 11.2**). Conversely, when evaporative cooling is limited, the Bowen ratio is high. For example, in a water-stressed crop, partial stomatal closure reduces evaporative cooling and the Bowen ratio is increased. The amount of evaporative heat loss (and thus the Bowen ratio) is influenced by the degree to which stomata remain open.

Plants with very high Bowen ratios conserve water, but consequently may also experience high leaf temperatures. However, the temperature difference between the leaf and the air does increase the amount of sensible heat loss. Reduced growth is usually correlated with high Bowen ratios, because a high Bowen ratio is indicative of at least partial stomatal closure and reduced CO_2 availability for photosynthesis.

There is an optimal temperature for photosynthesis

Maintaining favorable leaf temperatures is crucial to plant growth because maximum photosynthesis occurs within a relatively narrow temperature range. The peak photosynthetic rate across a range of temperatures is the *photosynthetic thermal optimum*. When a plant is either above or below its optimal temperature, photosynthetic rates decrease. The photosynthetic thermal optimum reflects biochemical, genetic (adaptation), and environmental (acclimation) components.

Species adapted to different thermal regimes usually have an optimal temperature range for photosynthesis that reflects the temperatures of the environment in which they evolved. For example, there is an especially clear contrast between the C_3 plant *Atriplex glabriuscula*, which commonly grows in cool coastal environments, and the C_4 plant *Tidestromia oblongifolia*, from a hot desert environment (**Figure 11.15**). The ability to acclimate or biochemically adjust to temperature can also be found within species. When plants of the same species are grown at different temperatures and then tested for their photosynthetic response, they generally show photosynthetic thermal optima that correlate with the temperature at which they were grown. That is, plants of the same species grown at low temperatures have higher photosynthetic rates at low temperatures, whereas those same plants grown at high temperatures have higher photosynthetic rates at high temperatures. Plants with a high thermal plasticity are capable of growing over a wide range of temperatures.

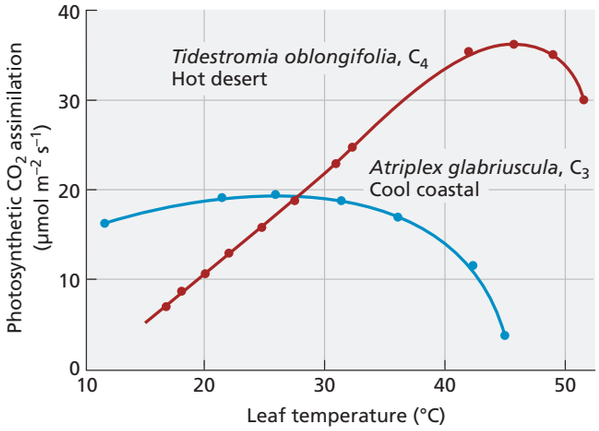


Figure 11.15 Photosynthesis as a function of leaf temperature at normal atmospheric CO_2 concentrations for a C_3 plant grown in its natural cool habitat and a C_4 plant growing in its natural hot habitat. (After O. Björkman et al. 1975. *Carnegie Inst. Wash Yb.* 74: 743–748. Courtesy, Carnegie Institution for Science.)

Changes in photosynthetic rates in response to temperature play an important role in plant adaptations to different environments and contribute to plants being productive even in some of the most extreme thermal habitats. In the lower temperature range, plants growing in alpine areas of Colorado and arctic regions in Alaska are capable of net CO_2 uptake at temperatures close to 0°C. At the other extreme, plants living in Death Valley, California, one of the hottest places on Earth, can achieve positive photosynthetic rates at temperatures approaching 50°C (see Figure 11.15).

Photosynthesis is sensitive to both high and low temperatures

When photosynthetic rates are plotted as a function of temperature, the temperature-response curve has an asymmetric bell-type shape (see Figure 11.15). In spite of some differences in shape, the temperature-response curve of photosynthesis among and within species has many common features. The ascending portion of the curve represents a temperature-dependent stimulation of enzymatic activities; the flat top is the temperature range that is optimal for photosynthesis; and the descending portion of the curve is associated with

temperature-sensitive deleterious effects, some of which are reversible while others are not.

What factors are associated with the decline in photosynthesis above the photosynthetic temperature optimum? Temperature affects all biochemical reactions of photosynthesis as well as membrane integrity in chloroplasts, so it is not surprising that the responses to temperature are complex. Cellular respiration rates also increase as a function of temperature, but they are not the primary reason for the sharp decrease in net photosynthesis at high temperatures. A major impact of high temperature is on membrane-bound electron transport processes, which can become uncoupled or unstable at high temperatures. This cuts off the supply of reducing power and ATP needed to fuel net photosynthesis and leads to a sharp overall decrease in photosynthesis.

Under ambient CO_2 concentrations and with favorable light and soil moisture conditions, the photosynthetic thermal optimum is often limited by the activity of Rubisco. In leaves of C_3 plants, the response to increasing temperature reflects conflicting processes: an increase in carboxylation rate and a decrease in the affinity of Rubisco for CO_2 with a corresponding increase in the oxygenation rate and photorespiration (see Chapter 10). There is also evidence that Rubisco activity decreases because of negative heat effects on Rubisco activase at higher (>35°C) temperatures (see Chapter 10). The reduction in the affinity for CO_2 and the increase in photorespiration attenuate the potential temperature response of photosynthesis under ambient CO_2 concentrations. By contrast, in plants with C_4 photosynthesis, the CO_2 surrounding Rubisco is saturating, or nearly so (as we discussed in Chapter 10), and the negative effect of high temperature on Rubisco's affinity for CO_2 is not realized. This is one reason that leaves of C_4 plants tend to have a higher photosynthetic temperature optimum than do leaves of C_3 plants (see Figure 11.15).

At low temperatures, the oxygenation rate catalyzed by Rubisco is decreased, but C_3 photosynthesis can become limited by factors such as phosphate availability in the chloroplast. When triose phosphates are exported from the chloroplast to the cytosol, an equimolar amount of inorganic phosphate is taken up via translocators in the chloroplast membrane. If the rate of triose phosphate use in the cytosol decreases, phosphate uptake into the chloroplast is inhibited and photosynthesis becomes phosphate-limited. Starch synthesis and sucrose synthesis decrease rapidly with decreasing temperature as the demand by sink tissues diminishes, reducing the consumption of triose phosphates and causing the phosphate limitation observed at low temperatures. C_4 plants are typically warm-adapted species, and their photosynthetic rates decrease sharply at low temperatures. However, some C_4 species, such as *Miscanthus*, appear to be less cold-sensitive than others, such as the warm-adapted maize (corn; *Zea mays*).

Photosynthetic efficiency is temperature-sensitive

Photorespiration (see Chapter 10) and the quantum yield (light-use efficiency) differ between C_3 and C_4 photosynthesis, with changes particularly noticeable as temperatures vary. **Figure 11.16** illustrates quantum yield for photosynthesis as a function of leaf temperature in C_3 and C_4 plants in today's atmosphere of 417 ppm CO_2. In the C_4 plants, the quantum yield remains constant with temperature, reflecting low rates of photorespiration. In the C_3 plants, the quantum yield decreases with temperature, reflecting a stimulation of photorespiration by temperature and an ensuing higher energy cost for net CO_2 fixation.

The reduced quantum yield due to increased photorespiration leads to expected differences in the photosynthetic capacities of C_3 and C_4 plants in habitats with different temperatures. **Figure 11.17** shows the predicted relative rates of primary productivity of C_3 and C_4 grasses along a latitudinal transect in the Great Plains of North America from southern Texas in the United States to Manitoba in Canada. The decline in C_4 relative to C_3 productivity moving northward closely parallels the shift in abundance of

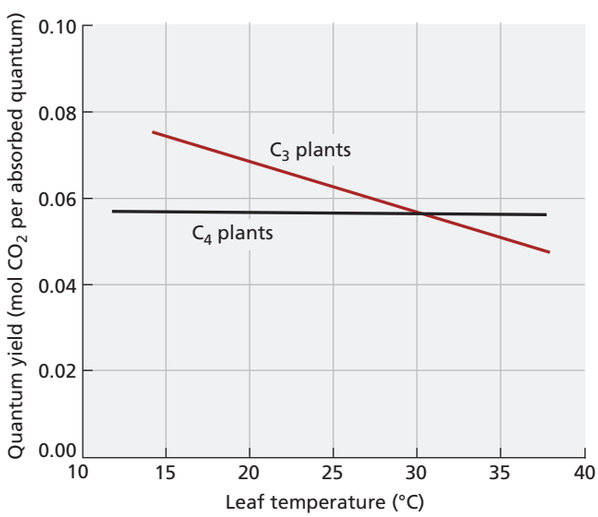


Figure 11.16 Quantum yield of photosynthetic carbon fixation in C_3 and C_4 plants as a function of leaf temperature. Photorespiration increases with temperature in C_3 plants, and the energy cost of net CO_2 fixation increases accordingly. This higher energy cost is reflected in lower quantum yields at higher temperatures. In contrast, photorespiration is very low in C_4 plants and the quantum yield does not show a temperature dependence. Note that at lower temperatures the quantum yield of C_3 plants is higher than that of C_4 plants, indicating that C_3 photosynthesis is more efficient at lower temperatures. (After J. R. Ehleringer et al. 1997. *Oecologia* 112: 285–299.)

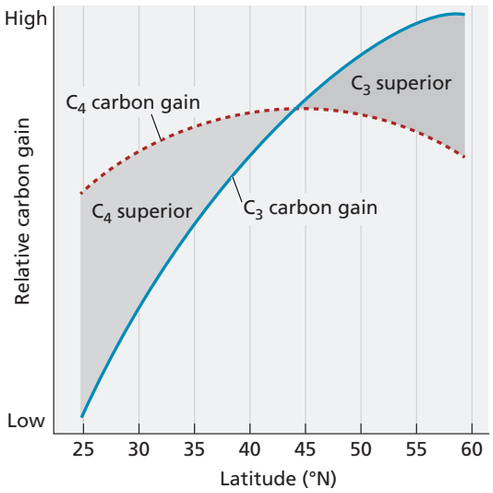


Figure 11.17 **Relative rates of photosynthetic carbon gain predicted for identical C_3 and C_4 grass canopies as a function of latitude across the Great Plains of North America.** (After J. R. Ehleringer. 1978. *Oecologia* 31: 255–267.)

plants with these pathways in the Great Plains: C_4 species are more common below 40°N, and C_3 species dominate above 45°N (see **WEB TOPIC 11.3**).

11.4 Effects of Carbon Dioxide on Photosynthesis in the Intact Leaf

Atmospheric CO_2 diffuses into leaves—first through stomata, then through the intercellular air spaces, and ultimately into cells and chloroplasts. In the presence of adequate amounts of light, higher CO_2 concentrations typically support higher photosynthetic rates. The reverse is also true: Low CO_2 concentrations can limit the amount of photosynthesis, particularly in C_3 plants.

In this section we discuss the concentration of atmospheric CO_2 in recent history, and its availability for carbon-fixing processes. Then we consider the limitations that CO_2 places on photosynthesis and the impact of the CO_2-concentrating mechanisms of C_4 and CAM plants.

Atmospheric CO_2 concentration keeps rising

Carbon dioxide presently accounts for about 0.0417%, or 417 ppm, of atmospheric air. The partial pressure of ambient CO_2 (c_a) varies with atmospheric pressure and is approximately 40 pascals (Pa) at sea level (see **WEB TOPIC 11.4**). Water vapor usually accounts for up to 2% of the atmosphere and O_2 for about 21%. The largest constituent in the atmosphere is diatomic nitrogen, at about 78%.

Today the atmospheric concentration of CO_2 is almost twice the concentration that prevailed over the last 400,000 years, as measured from air bubbles trapped in glacial ice in Antarctica (**Figure 11.18A and B**) (see also **Web Topic 11.5**), and it is higher than any experienced on Earth in the last 2 million years. Most extant plant taxa are therefore thought to have evolved in a low-CO_2 world (~180–280 ppm CO_2). Only when one looks back more than 35 million years does one find much higher CO_2 concentrations (>1000 ppm). Thus, the geologic trend over these many millions of years was one of decreasing atmospheric CO_2 concentrations.

Currently, the CO_2 concentration of the atmosphere is increasing by about 1 to 3 ppm each year, primarily because of the burning of fossil fuels (e.g., coal, oil, and natural gas) and deforestation (**Figure 11.18C**). Since 1958, when C. David Keeling began systematic measurements of CO_2 in the clean air at Mauna Loa, Hawaii, atmospheric CO_2 concentrations have increased by more than 30%. By year 2100 the atmospheric CO_2 concentration could reach 600 to 750 ppm unless fossil fuel emissions and deforestation are diminished (see **WEB TOPIC 11.6**).

CO_2 diffusion to the chloroplast is essential to photosynthesis

For photosynthesis to occur in C_3 plants, CO_2 must diffuse from the atmosphere into the leaf and to the carboxylation site of Rubisco. The diffusion rate depends on the CO_2 concentration gradient in the leaf (see Chapters 6 and 10) and on resistances along the diffusion pathway, which comprises both gas and liquid routes, or phases. The cuticle that covers the leaf is nearly impermeable to CO_2, so the main port of entry of CO_2 into the leaf is the stomatal pore. (The same path is traveled in the reverse direction by H_2O.) CO_2 diffuses through the pore into the substomatal cavity and into the intercellular air spaces between the mesophyll cells. This portion of the diffusion path of CO_2 is in the gas phase. The remainder of the diffusion path to the chloroplast is in the liquid phase, which begins at the water layer that wets the walls of the mesophyll cells and continues through the plasma membrane, the cytosol, and the chloroplast. (For the properties of CO_2 in solution, see **WEB TOPIC 10.9**.)

The sharing of the stomatal entry pathway by CO_2 and H_2O presents the plant with a functional dilemma. In air of high relative humidity, the diffusion gradient that drives water loss is about 50 times larger than the gradient that drives CO_2 uptake. In drier air, this difference can be much larger. Therefore, a decrease in stomatal resistance through the opening of stomata facilitates higher CO_2 uptake, but is unavoidably accompanied by substantial water loss. Not surprisingly, many adaptive features help counteract this water loss in plants in arid and semiarid regions of the world.

Each portion of the CO_2 diffusion pathway imposes a resistance to CO_2 diffusion, so the supply of CO_2 for photosynthesis meets a series of different points of resistance. The gas phase of CO_2 diffusion into the leaf can be divided into three components—the boundary layer, the

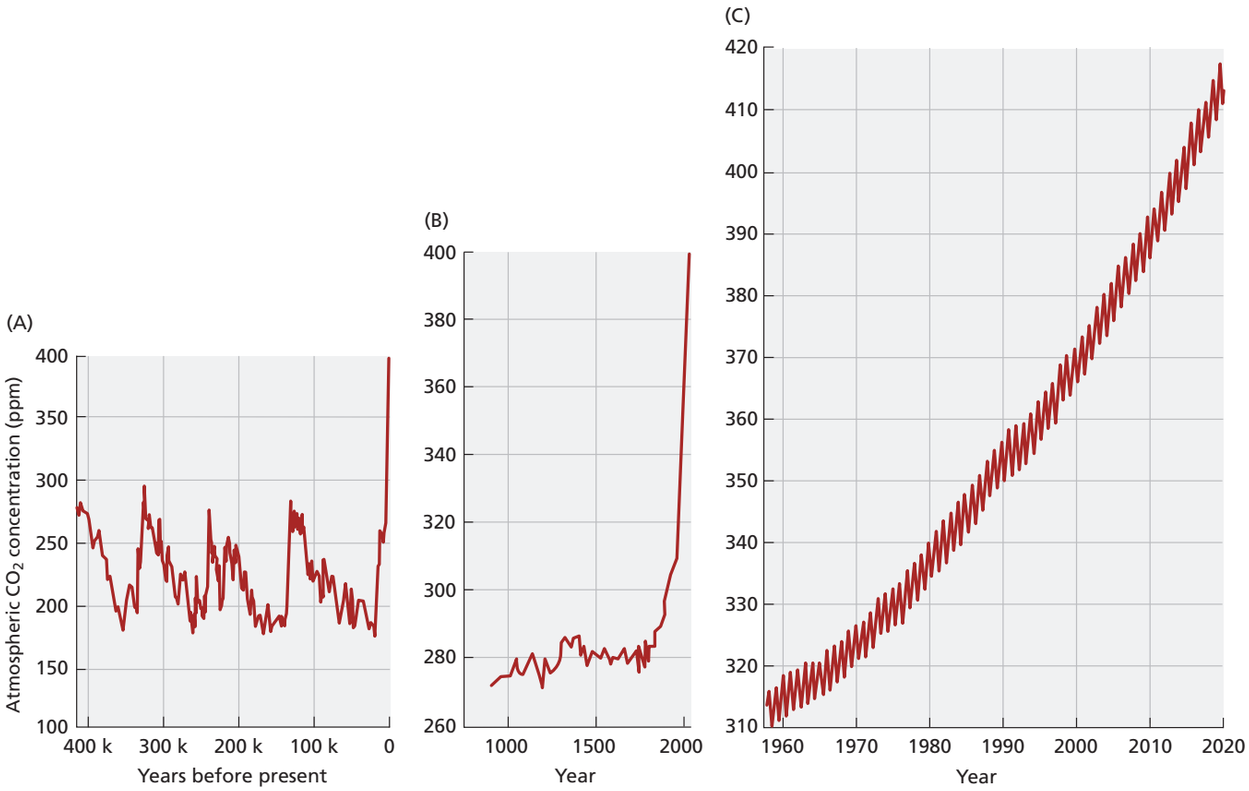


Figure 11.18 Concentration of atmospheric CO_2 from 420,000 years ago to the present. **(A)** Past atmospheric CO_2 concentrations, determined from bubbles trapped in glacial ice in Antarctica, were much lower than current levels. **(B)** In the last 1000 years, the rise in atmospheric CO_2 concentration coincides with the Industrial Revolution and the increased burning of fossil fuels. **(C)** Current atmospheric concentrations of CO_2 measured at Mauna Loa, Hawaii, continue to rise. The wavy nature of the trace is caused by change in atmospheric CO_2 concentrations associated with seasonal changes in relative balance between photosynthesis and respiration rates. Each year the highest CO_2 concentration is observed in May, just before the Northern Hemisphere growing season, and the lowest concentration is observed in October. (A after J. M. Barnola et al. 2003 and B after D. M. Etheridge et al. 1998. In *Trends: A Compendium of Data on Global Change*, Boden et al. [eds.], Oak Ridge, TN: Carbon Dioxide Information Analysis Center, Oak Ridge Natl Lab, USDOE; C after C. D. Keeling and T. P. Whorf. 1994. In *Trends '93: A Compendium of Data on Global Change*; updated using data from www.esrl.noaa.gov/gmd/ccgg/trends/ and https://scrippsco2.ucsd.edu/.)

stomata, and the intercellular spaces of the leaf—each of which can impose a significant resistance to CO_2 diffusion (**Figure 11.19**). An evaluation of the magnitude of each point of resistance is helpful for understanding CO_2 limitations to photosynthesis.

The boundary layer consists of relatively unstirred air near the leaf surface, and its resistance to diffusion is called the **boundary layer resistance**. The boundary layer resistance affects all diffusive processes, including water and CO_2 diffusion as well as sensible heat loss, discussed earlier. The boundary layer resistance decreases with smaller leaf size and greater wind speed. Smaller leaves thus have a lower resistance to CO_2 and water diffusion and tend to have higher sensible heat loss. Leaves of desert plants are usually small, facilitating sensible heat loss. In contrast, large leaves are often found in the humid tropics, especially in the shade. These leaves have large boundary layer resistances, but they can dissipate the radiation heat load by evaporative cooling made possible by the abundant water supply in these habitats.

After diffusing through the boundary layer, CO_2 enters the leaf through the stomatal pores, which impose the next type of resistance in the diffusion pathway, **stomatal resistance**. Under most conditions in nature, in which the air around a leaf is seldom completely still, the boundary layer resistance is much smaller than the stomatal resistance, and the main limitation to CO_2 diffusion into the leaf is imposed by the stomatal resistance.

There are two additional resistances within the leaf. The first is resistance to CO_2 diffusion in the air spaces that separate the substomatal cavity from the walls of the mesophyll cells. This is called the **intercellular air space resistance**. The second is the **mesophyll resistance**, which is resistance to CO_2 diffusion in the liquid phase. In C_3

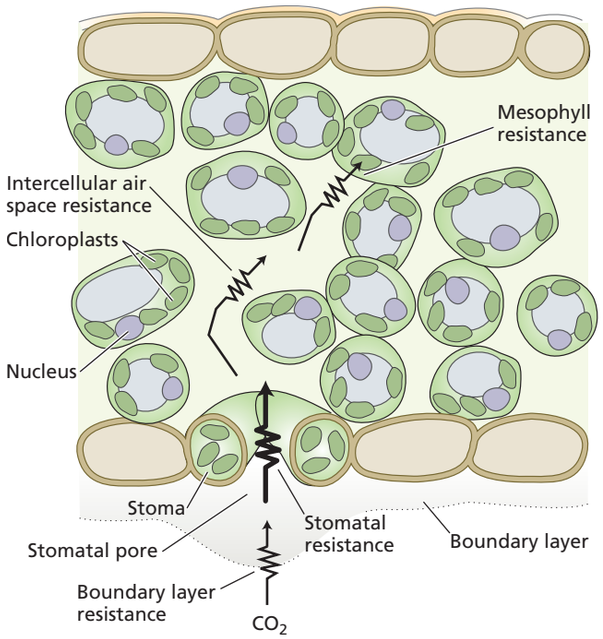


Figure 11.19 Points of resistance to the diffusion and fixation of CO_2 from outside the leaf to the chloroplasts. The stomatal aperture is the major point of resistance to CO_2 diffusion into the leaf. In some cases, the nuclei and chloroplasts are depicted to be in front of the vacuole, not inside it (see Figure 11.12).

plants, localization of chloroplasts near the cell periphery minimizes the distance that CO_2 must diffuse through liquid to reach carboxylation sites within the chloroplast. The mesophyll resistance to CO_2 diffusion can have a similar limitation to photosynthesis as stomatal resistance. Because the stomatal guard cells can impose a variable and potentially large resistance to CO_2 influx and water loss in the diffusion pathway, regulating the stomatal aperture provides the plant with an effective way to control gas exchange between the leaf and the atmosphere (see **WEB TOPIC 11.4**). Alternatively, decreasing mesophyll resistance may increase CO_2 availability for photosynthesis without negatively affecting leaf water loss because mesophyll resistance is not thought to influence the movement of water out of the leaf. Traits such as mesophyll cell wall thickness and the mesophyll cell surface area exposed to the intercellular air space can both influence mesophyll resistance. These traits have potentially important implications for breeding increased photosynthetic water-use efficiency in agronomically important plants, particularly when soil water availability is low.

CO_2 supply imposes limitations on photosynthesis

For C_3 plants growing with adequate light, water, and nutrients, CO_2 enrichment above natural atmospheric concentrations results in increased photosynthesis and enhanced productivity. Expressing photosynthetic rate as a function of the partial pressure of CO_2 in the intercellular air space (c_i) within the leaf (see **WEB TOPIC 11.4**) makes it possible to evaluate limitations to photosynthesis imposed by CO_2 supply. At low c_i concentrations, photosynthesis is strongly limited by the low CO_2. In the absence of photosynthesis, leaves release CO_2 because of mitochondrial respiration (see Chapter 13).

Increasing c_i to the concentration at which photosynthesis and respiration balance each other defines the **CO_2 compensation point**. This is the point at which net assimilation of CO_2 by the leaf is zero (**Figure 11.20**). This concept is analogous to that of the light compensation point discussed earlier in Section 11.2 (see Figure 11.6). The CO_2 compensation point reflects the balance between photosynthesis uptake of CO_2 and the CO_2 released by photorespiration and respiration under constant PPFD, whereas the light compensation point reflects that balance as a function of PPFD under constant CO_2 concentration.

C_3 VERSUS C_4 PLANTS In C_3 plants, increasing c_i above the compensation point increases photosynthesis over a wide concentration range (see Figure 11.20). At low to intermediate CO_2 concentrations, photosynthesis is limited by the carboxylation capacity of Rubisco. At higher c_i concentrations, photosynthesis begins to saturate as the net photosynthetic rate becomes limited by

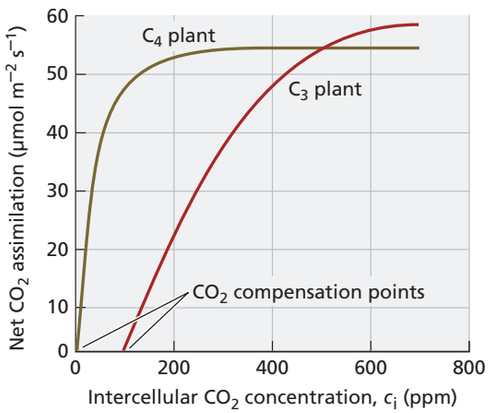


Figure 11.20 Changes in photosynthesis as a function of intercellular CO_2 concentrations in Arizona honeysweet (*Tidestromia oblongifolia*), a C_4 plant, and creosote bush (*Larrea tridentata*), a C_3 plant. Photosynthetic rate is plotted against calculated intercellular CO_2 concentration inside the leaf (see Equation 5 in **WEB TOPIC 11.4**). The intercellular CO_2 concentration at which net CO_2 assimilation is zero defines the CO_2 compensation point. (After J. A. Berry and J. S. Downton. 1982. In *Photosynthesis: Development, Carbon Metabolism and Plant Productivity*, Vol. 2. Govindjee [ed.]. Academic Press, New York.)

another factor (remember Blackman's concept of limiting factors). At these higher c_i concentrations, net photosynthesis becomes limited by the capacity of the light reactions to generate sufficient NADPH and ATP to regenerate the acceptor molecule ribulose 1,5-bisphosphate. Most leaves appear to regulate their c_i values by controlling stomatal opening, so that c_i remains at an intermediate subambient concentration between the limits imposed by carboxylation capacity and the capacity to regenerate ribulose 1,5-bisphosphate. In this way, both the light and dark reactions of photosynthesis are co-limiting. A plot of net CO_2 assimilation as a function of c_i tells us how photosynthesis is regulated by CO_2, independent of the functioning of stomata (see Figure 11.20).

Comparing such a plot for C_3 and C_4 plants reveals interesting differences between the two pathways of carbon metabolism:

- In C_4 plants, photosynthetic rates saturate at CO_2 concentrationsin the intercellular air space (c_i) of about 100–200 ppm, reflecting the effective CO_2-concentrating mechanisms operating in these plants (see Chapter 10).
- In C_3 plants, increasing c_i concentrations continue to stimulate photosynthesis over a much broader CO_2 range than for C_4 plants.
- In C_4 plants, the CO_2 compensation point is nearly zero, reflecting their very low levels of photorespiration (see Chapter 10).
- In C_3 plants, the CO_2 compensation point is about 50–100 ppm at 25°C, reflecting CO_2 produced by photorespiration (see Chapter 10).

These responses reveal that C_3 plants will be more likely than C_4 plants to benefit from today's ongoing increases in atmospheric CO_2 concentrations (see Figure 11.20). Because photosynthesis in C_4 plants is saturated at low CO_2 concentrations, C_4 plants do not benefit as much from increases in atmospheric CO_2 concentrations. However, as we discuss later in this section, the response of photosynthesis in both C_3 and C_4 plants to changes in CO_2 concentrations is strongly influenced by leaf temperature and soil water availability, which are also expected to change as atmospheric CO_2 concentrations rise.

From an evolutionary perspective, the ancestral photosynthetic pathway is C_3 photosynthesis, and C_4 photosynthesis is a derived pathway. During earlier geologic time periods (more than 35 million years ago) when atmospheric CO_2 concentrations were much higher than they are today, CO_2 diffusion through stomata into leaves would have resulted in higher c_i values and therefore high photosynthetic rates and reduced photorespiration in C_3 plants. However, the lower CO_2 concentrations in the atmosphere that have occurred more recently would have led to reduced photosynthetic rates and higher photorespiration. The evolution of C_4 photosynthesis is one biochemical adaptation to a CO_2-limited atmosphere. Our current understanding is that the earliest C_4 plants evolved recently in geologic terms, approximately 25–30 million years ago, when atmospheric CO_2 was relatively low.

C_4 photosynthesis first became a prominent component of terrestrial ecosystems in the warmest growing regions of Earth when global CO_2 concentrations decreased below a critical threshold (**Figure 11.21**), and stomatal conductance was low due to soil aridity and low relative humidity in the atmosphere. The negative impacts of high photorespiration and CO_2 limitation on C_3 photosynthesis would have been greatest under these warm to hot growing conditions, drought, and low atmospheric CO_2. These conditions were likely key factors favoring the evolution and ultimately geographic expansion of C_4 plants.

Because of the CO_2-concentrating mechanisms in C_4 plants, the CO_2 concentration at the site of Rubisco carboxylation within C_4 chloroplasts is typically close to saturating for Rubisco carboxylation activity. As a result, plants with C_4 metabolism require less Rubisco than C_3 plants to achieve a given rate of photosynthesis, and thus use less nitrogen for growth. In addition, the CO_2-concentrating mechanism allows the leaf to maintain high photosynthetic rates at lower c_i values. This permits stomata to remain relatively closed, resulting in less water loss for a given rate of photosynthesis. Thus, the CO_2-concentrating mechanism helps C_4 plants use water and nitrogen more efficiently than C_3 plants. However, the additional energy cost required by the CO_2-concentrating mechanism (see Chapter 10) reduces

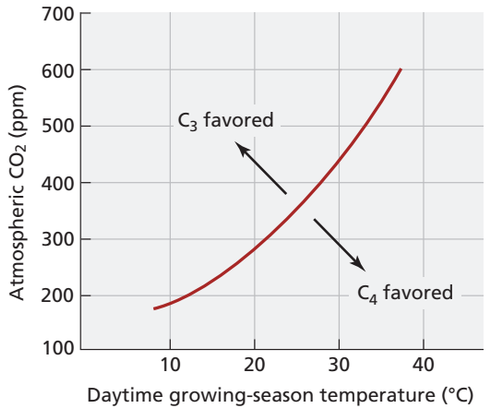


Figure 11.21 Combination of global atmospheric CO_2 concentrations and daytime growing-season temperatures that are predicted to favor C_3 versus C_4 grasses. At any point in time, Earth is at a single atmospheric CO_2 concentration, resulting in the expectation that C_4 plants would be most common in habitats with the warmest growing seasons. (After J. R. Ehleringer et al. 1997. *Oecologia* 112: 285–299.)

the light-use efficiency of C_4 photosynthesis. This is probably one reason that most shade-adapted plants in temperate regions are not C_4 plants and that C_4 plants are typically found in open habitats with high light.

CAM PLANTS Plants with crassulacean acid metabolism (CAM), including many cacti, orchids, bromeliads, and other succulents, have stomatal activity patterns that contrast with those found in C_3 and C_4 plants. CAM plants open their stomata at night and close them during the day, exactly the opposite of the pattern observed in leaves of C_3 and C_4 plants (**Figure 11.22**). At night, atmospheric CO_2 diffuses into CAM plants where it is combined with phosphoenolpyruvate and fixed into oxaloacetate, which is reduced to malate (see Chapter 10). Then during the day CO_2 is released from malate and taken up by Rubisco behind closed stomata. Because stomata are open primarily at night, when lower temperatures and higher humidity reduce transpiration demand, the ratio of water loss to CO_2 uptake is much lower in CAM plants than it is in either C_3 or C_4 plants.

The main photosynthetic constraint on CAM metabolism is that the capacity to store malic acid is limited, and this limitation restricts the total amount of CO_2 uptake. However, the daily cycle of CAM photosynthesis can be very flexible. Some CAM plants are able to enhance total photosynthesis during wet conditions by directly fixing atmospheric CO_2 via the Calvin–Benson cycle at the beginning and end of the day, when temperature gradients are less extreme. Other plants may use CAM as a survival mechanism during severe water limitations. For example, cladodes (flattened stems) of cacti can survive after detachment from the plant for several months without water. Their stomata are closed all the time, and the CO_2 released by respiration is refixed into malate. This process, which has been called *CAM idling*, also allows the intact plant to survive for prolonged drought periods while losing remarkably little water.

How will photosynthesis and respiration change in the future under elevated CO_2 conditions?

The consequences of increasing global atmospheric CO_2 are under intense scrutiny by scientists and government agencies, particularly because of the evidence that the greenhouse effect is altering the world's climate. The **greenhouse effect** refers to the warming of Earth's climate that is caused by the trapping of long-wavelength radiation by the atmosphere.

A greenhouse roof transmits visible light, which is absorbed by plants and other surfaces inside the greenhouse. Some of the absorbed light energy is converted to heat, and some of it is reemitted as long-wavelength radiation. Because glass poorly transmits long-wavelength radiation, this radiation cannot leave the greenhouse through the glass roof, and the greenhouse heats up. Certain gases in the atmosphere, particularly CO_2 and methane, play a role similar to that of the glass roof in a greenhouse. The increased CO_2 concentrations, and elevated temperatures associated with the greenhouse effect, have multiple influences on

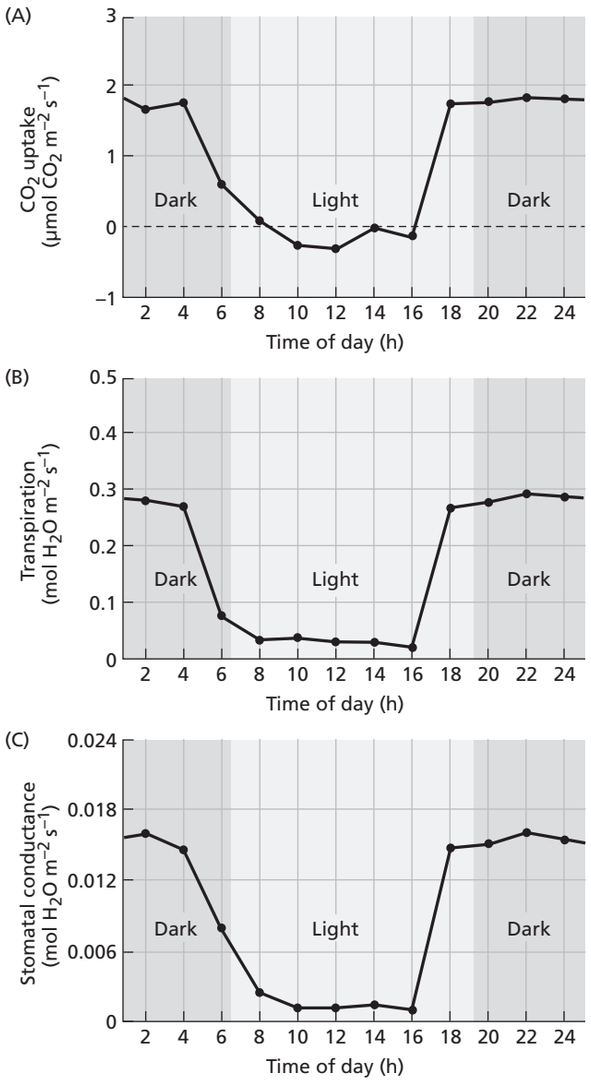


Figure 11.22 Photosynthetic net CO_2 uptake, H_2O transpiration, and stomatal conductance of a CAM plant, the orchid *Doritaenopsis*, during a 24-h period. Whole plants were kept in a gas-exchange chamber in the laboratory. The dark period is indicated by dark areas. Three parameters were measured over the study period: **(A)** photosynthetic rate, **(B)** water loss, and **(C)** stomatal conductance. In contrast to plants with C_3 or C_4 metabolism, CAM plants open their stomata and fix CO_2 at night. (After M.-W. Jeon et al. 2006. *Environ. Exp. Bot.* 55: 183–194.)

photosynthesis and plant growth. At today's atmospheric CO_2 concentrations, photosynthesis in C_3 plants is CO_2-limited, but this situation will change as atmospheric CO_2 concentrations continue to rise. However, as discussed shortly, the response to changes in CO_2 concentrations will also be influenced by concomitant changes in growth temperatures, precipitation patterns, and nutrient availability such that the potential stimulation of photosynthesis by increased CO_2 concentrations could be offset by increased leaf temperatures and decreased stomatal conductance.

A central question in plant physiology today is: How will photosynthesis and respiration differ by the year 2100 when global CO_2 concentrations have reached 600 ppm, 700 ppm, or even higher? This question is particularly relevant as humans continue to add CO_2 derived from fossil fuel combustion to Earth's atmosphere. Under well-watered and highly fertilized laboratory conditions, most C_3 plants grow about 30% faster when the CO_2 concentration reaches 600 to 750 ppm than they do today; above that atmospheric CO_2 concentration, the growth rate becomes more limited by the nutrients available to the plant. To study this question in the field, scientists need to be able to create realistic simulations of future environments. A promising approach to the study of plant physiology and ecology in environments with elevated CO_2 concentrations has been the use of *F*ree *A*ir CO_2 *E*nrichment (FACE) experiments.

For FACE experiments, entire fields of plants or natural ecosystems are encircled by emitters that add CO_2 to the air to create the high-CO_2 environment we might expect to have 20 to 30 years from now. **Figure 11.23** shows FACE experiments in a deciduous forest and a crop canopy.

FACE experiments have provided key new insights into how plants and ecosystems will respond to the CO_2 concentrations expected in the future. One key observation is that plants with the C_3 photosynthetic pathway are much more responsive than C_4 plants under well-watered conditions, with net photosynthetic rates increasing 20% or more in C_3 plants and little to not at all in C_4 plants. Photosynthesis increases in C_3 plants because c_i concentrations increase (see Figure 11.20). At the same time, there is a down-regulation of photosynthetic capacity manifested in reduced activity of the enzymes associated with the enzymatic reactions of photosynthesis. The FACE experiments have also demonstrated that under field conditions, which may have many additional limitations to plant growth, the stimulation of crop yield is generally lower than would be predicted from experiments conducted in greenhouse or growth chambers, which often minimize the influence of these other limiting factors.

Elevated CO_2 concentrations will affect many plant processes. For instance, leaves tend to keep their stomata more closed under elevated CO_2 concentrations. As a direct consequence of reduced transpiration, leaf temperatures are higher (see Figure 11.23C), which may feedback on both photosynthesis, as previously discussed,



Figure 11.23 Free Air CO_2 Enrichment (FACE) experiments are used to study how plants and ecosystems will respond to future CO_2 concentrations. Shown here are FACE experiments in **(A)** a deciduous forest and **(B)** a crop canopy. **(C)** Under elevated CO_2 concentrations, leaf stomata are more closed, resulting in higher leaf temperatures, as shown by the infrared image of a crop canopy.

and mitochondrial respiration. From FACE studies, it has become increasingly clear that acclimation occurs under higher CO_2 concentrations in which photosynthesis and respiration rates are different than they would be under today's atmospheric conditions, but not as high as would have been predicted without the down-regulation of acclimation response.

While CO_2 is indeed important for photosynthesis and respiration, other factors are important for growth under elevated CO_2. For example, a common FACE observation is that plant growth under elevated CO_2 concentrations quickly becomes constrained by nutrient availability (remember Blackman's rule of limiting factors). A second observation is that the presence of pollutant trace gases, such as ozone, can reduce the net photosynthetic response below the maximum values predicted from initial FACE and greenhouse studies of nearly two decades ago.

As a result of increased atmospheric CO_2 concentrations, warmer and drier conditions are also predicted to occur in the near future, which we are already starting to see. The interaction of CO_2, temperature, and water availability has been demonstrated to have important implications for predicting current and future plant productivity, in both managed and natural ecosystems. Of particular importance is that the stimulation of photosynthesis and yield by increases in atmospheric CO_2 concentrations is often partially reduced by increases in temperature and restricted stomatal conductance under drought conditions. Important progress is being made by studying how growth of irrigated and fertilized crops compares with that of plants in natural ecosystems in a world with elevated CO_2. Understanding these responses is crucial as society looks for increased agricultural outputs to support rising human populations and to provide raw materials for biofuels, while minimizing the need for resource inputs.

11.5 Stable Isotopes Record Photosynthetic Properties

We can learn more about the different photosythetic pathways in plants by measuring the relative abundances of stable isotopes in plants. In particular, the stable isotopes of carbon atoms in a leaf contain useful information about photosynthesis.

Recall that isotopes are simply different forms of an element. In the different isotopes of an element, the number of protons remains constant, since that defines the element, but the number of neutrons varies. Radioactive isotopes of an element decay to form different elements over time. In contrast, stable isotopes of an element remain constant and unchanged over time. The two stable isotopes of carbon are ^{12}C and ^{13}C, differing in composition only by an extra neutron in ^{13}C. ^{11}C and ^{14}C are radioactive isotopes of carbon that are frequently used in biological tracer experiments.

How do we measure the stable carbon isotopes of plants?

Atmospheric CO_2 contains the naturally occurring stable carbon isotopes ^{12}C and ^{13}C in the proportions 98.9% and 1.1%, respectively. The chemical properties of $^{13}CO_2$ are identical to those of $^{12}CO_2$, but plants assimilate less $^{13}CO_2$ than $^{12}CO_2$. In other words, leaves discriminate against the heavier isotope of carbon during photosynthesis, and therefore they have smaller $^{13}C/^{12}C$ ratios than are found in atmospheric CO_2.

The $^{13}C/^{12}C$ isotope composition is measured by use of a mass spectrometer, which yields the following ratio:

$$R = \frac{^{13}C}{^{12}C} \tag{11.3}$$

The **carbon isotope ratio** of plants, $\delta^{13}C$, is quantified on a parts per thousand (per mil, ‰) basis:

$$\delta^{13}C‰ = \left(\frac{R_{sample}}{R_{standard}} - 1\right) \times 1000 \tag{11.4}$$

where the standard represents the carbon isotopes contained in a fossil belemnite from the Pee Dee limestone formation of South Carolina. The $\delta^{13}C$ of atmospheric CO_2 has a value of –8‰, meaning that there is less ^{13}C in atmospheric CO_2 than is found in the carbonate of the belemnite standard.

What are some typical values for carbon isotope ratios of plants? Both C_3 and C_4 plants have less ^{13}C than does CO_2 in the atmosphere, which means that leaf tissues discriminate against ^{13}C during the photosynthetic process. Thure Cerling and colleagues provided $\delta^{13}C$ data for a large number of C_3 and C_4 plants from around the world (**Figure 11.24**). What becomes clear from Figure 11.24 is that there is a wide spread of $\delta^{13}C$ values in C_3 and C_4 plants, with averages of –28‰ and –14‰, respectively. These $\delta^{13}C$ variations actually reflect the consequences of small variations in physiology associated with changes in stomatal conductance in different environmental conditions. Thus, $\delta^{13}C$ values can be used both to distinguish between C_3 and C_4 photosynthesis and to further reveal details about stomatal conditions for plants grown in different environments, such as C_3 plants in the tropics versus those in deserts.

Differences in carbon isotope ratio are detectable with mass spectrometers that allow for precise measurements of the abundance of ^{12}C and ^{13}C. Many of our foods grown in temperate climates, such as wheat (*Triticum aestivum*), rice (*Oryza sativa*), potatoes (*Solanum tuberosum*), and beans (*Phaseolus* spp.) are products of C_3 plants. Yet many of our most productive crops, especially those grown under warm summer conditions, are C_4

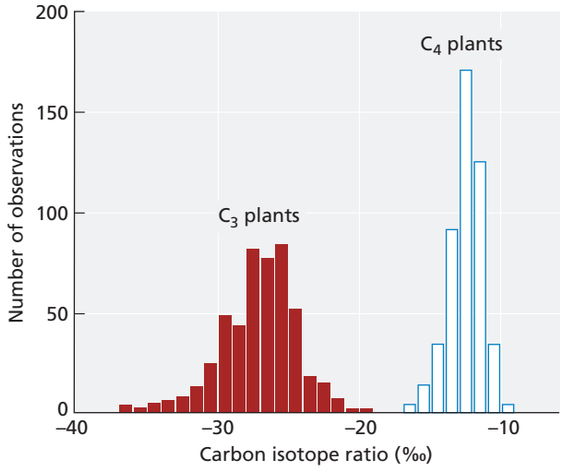


Figure 11.24 **Frequency histograms for observed carbon isotope ratios in C_3 and C_4 plant taxa from around the world.** (After T. E. Cerling et al. 1997. *Nature* 389: 153–158.)

plants such as maize, sugarcane (*Saccharum officinarum*), and sorghum (*Sorghum bicolor*). Starches and sugars extracted from all of these foods may be chemically identical, but these carbohydrates can be related back to their C_3 or C_4 plant source on the basis of their $\delta^{13}C$ values. For example, measuring the $\delta^{13}C$ values of table sugar (sucrose) makes it possible to determine if the sucrose came from sugar beet (*Beta vulgaris*, a C_3 plant) or sugarcane (a C_4 plant) (see **Web Topic 11.7**).

Why does the carbon isotope ratio vary in plants?

What is the physiological basis for ^{13}C depletion in plants relative to CO_2 in the atmosphere? It turns out that both the diffusion of CO_2 into the leaf and the carboxylation selectivity for $^{12}CO_2$ play a role.

We can predict the carbon isotope ratio of a C_3 leaf as

$$\delta^{13}C_{Leaf} = \delta^{13}C_{Air} - a - (b - a)(c_i/c_a) \qquad (11.5)$$

where $\delta^{13}C_{Leaf}$ and $\delta^{13}C_{Air}$ are the carbon isotope ratios of the leaf and atmosphere, respectively; a is the diffusion fraction; b is the net carboxylase fraction in the leaf; and c_i/c_a is the ratio of intercellular to ambient CO_2 concentrations.

CO_2 diffuses from air outside of the leaf to the carboxylation sites within leaves in both C_3 and C_4 plants. We express this diffusion using the term a. Because $^{12}CO_2$ is lighter than $^{13}CO_2$, it diffuses slightly faster toward the carboxylation site, creating an effective diffusion fractionation factor of 4.4‰. Thus, we would expect leaves to have a more negative $\delta^{13}C$ value simply because of this diffusion effect. Yet this factor alone is not sufficient to explain the $\delta^{13}C$ values of C_3 plants as shown in Figure 11.24.

The initial carboxylation event is a determining factor in the carbon isotope ratio of plants. Rubisco represents the only carboxylation reaction in C_3 photosynthesis and has an intrinsic discrimination value against ^{13}C of 30‰, with some variability among species. By contrast, PEP carboxylase, the primary CO_2 fixation enzyme of C_4 plants, has a much different isotope discrimination effect—about 2‰. Thus, the inherent difference between the two carboxylating enzymes contributes to the different isotope ratios observed in C_3 and C_4 plants. We use b to describe the net carboxylation effect. C_4 plants also use Rubisco that has a similar intrinsic discrimination as in C_3 plants, but why is there such a large isotope difference between C_3 and C_4 plants? This is primarily related to the fact that nearly all of the CO_2 supplied by the CO_2-concentrating mechanism is consumed by Rubisco. However, if the leakage of CO_2 from the bundle sheath cells is high, then Rubisco discriminates against the heavier CO_2, causing a more negative $\delta^{13}C$ in C_4 plants. Under most natural growth conditions, the CO_2-concentrating mechanism in C_4 is efficient and there is typically less variation in $\delta^{13}C$ in C_4 than in C_3 plants.

Other physiological characteristics of plants affect their carbon isotope ratio. One primary factor is the partial pressure of CO_2 in the intercellular air spaces of leaves (c_i). In C_3 plants the potential isotope discrimination by Rubisco of –30‰ is not fully realized during photosynthesis because the availability of CO_2 at the carboxylation site becomes a limiting factor restricting the discrimination by Rubisco. Greater discrimination against $^{13}CO_2$ occurs when c_i is high, as when stomata are open. Yet open stomata also facilitate water loss. Thus, lower ratios of photosynthesis to transpiration are correlated with greater discrimination against ^{13}C. When leaves are exposed to water stress, stomata tend to close, reducing c_i values. As a consequence, C_3 plants grown under water-stress conditions tend to have higher carbon isotope ratios (i.e., less discrimination against ^{13}C). Conversely, in C_4 plants the lower c_i due to water stress and closed stomata tends to increase the discrimination against ^{13}C, and C_4 leaves exposed to water stress tend to have a lower carbon isotope ratio.

The application of carbon isotope ratios in plants has become very productive, because Equation 11.5 provides a strong link between the carbon isotope ratio measurement and the intercellular CO_2 value in a leaf. Intercellular CO_2 concentrations are then directly linked with aspects of photosynthesis and stomatal constraints. As stomata close in C_3 plants or as water stress increases, we find that the leaf carbon isotope ratio increases. The carbon isotope ratio measurement then becomes a proxy to estimate several aspects of short-term water stress. These applications include using carbon isotopes to measure plant performance in both agricultural and ecological studies.

One emergent environmental pattern is that, on average, leaf carbon isotope ratios decrease as precipitation increases under natural conditions. **Figure 11.25** illustrates this pattern in a transect across Australia. Here we see that the $\delta^{13}C$ values are highest in the arid regions of Australia and become progressively lower along a precipitation gradient from desert to tropical rainforest ecosystems. Applying Equation 11.5 to interpret these $\delta^{13}C$ data, we conclude that intercellular CO_2 concentrations of leaves of desert plants are lower than what we typically see in leaves of rainforest plants. Because of the sequential nature of tree ring formation (see Chapter 19), $\delta^{13}C$ observations in tree rings can help identify the long-term effects of reduced water availability on plants (e.g., desert versus rainforest habitats) compared with short-term effects that would be recorded in leaves (e.g., seasonal drought cycles).

Carbon isotope ratio analyses are commonly used today to determine the dietary patterns of humans and other animals. The proportion of C_3 to C_4 foods in an animal's diet is recorded in its tissues—teeth, bones, muscles, and hair. Thure Cerling and colleagues described an interesting application of carbon isotope ratio analysis to the eating habits of a family of wild African elephants. They examined sequential $\delta^{13}C$ values in segments of tail hair to reconstruct the daily diets of each animal. They observed predictable seasonal shifts between trees (C_3) and grasses (C_4) as resource availability changed because of rainfall patterns. Carbon isotope ratio analyses can be expanded to include consideration of human diets. One broad-scale observation is that the carbon isotope ratios of North Americans are higher than those observed in Europeans, indicating the prominent role that maize (a C_4 plant) plays in the diets of North Americans. Another application is measuring $\delta^{13}C$ in fossil, carbonate-containing soils and fossil teeth. From such observations it is possible to reconstruct the photosynthetic pathways of the prevailing vegetation from the ancient past. These approaches have been used to determine that C_4 plants became prevalent in grasslands between 6 and 10 million years ago. They have also helped reconstruct the diets of ancient and modern animals (see **WEB TOPIC 11.8**).

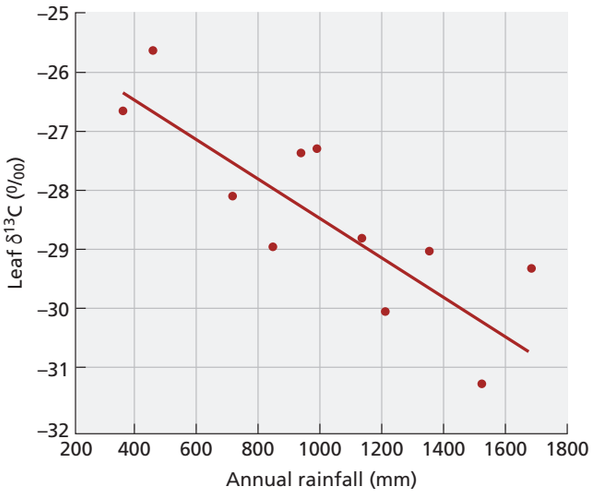


Figure 11.25 Vegetation changes occur along rainfall gradients in southern Queensland, Australia. Here we see that changes in carbon isotope ratios of vegetation appear to be strongly related to precipitation amounts in a region, suggesting that decreased moisture levels influence c_i values and therefore carbon isotope ratios in C_3 species along a geographic gradient in Australian taxa. (After G. R. Stewart et al. 1995. *Aust. J. Plant Physiol.* 22: 51–55.)

CAM plants can have $\delta^{13}C$ values that are very close to those of C_4 plants. In CAM plants that fix CO_2 at night via PEP carboxylase, $\delta^{13}C$ is expected to be similar to that of C_4 plants. However, when some CAM plants are well watered, they can switch to C_3 mode by opening their stomata and fixing CO_2 during the day via Rubisco. Under these conditions the isotope composition shifts toward that of C_3 plants. Thus, the $\delta^{13}C$ values of CAM plants reflect how much carbon is fixed via the C_3 pathway versus the C_4 pathway.

Summary

In considering photosynthetic performance, both the limiting factor hypothesis and an "economic perspective" emphasizing CO_2 "supply" and "demand" have guided research.

11.1 Photosynthesis Is Influenced by Leaf Properties

- Leaf anatomy is highly specialized for light absorption (**Figure 11.1**).
- About 5% of the solar energy reaching Earth is converted into carbohydrates by photosynthesis. Much absorbed light is lost by reflection and transmission, metabolism, and heat (**Figures 11.2, 11.3**).
- In dense forests, almost all photosynthetically active radiation is absorbed by leaves (**Figure 11.4**).

(*Continued*)

Summary (*continued*)

- Leaves of some plants maximize light absorption by solar tracking (**Figure 11.5**).
- Some plants respond to a range of light regimes. However, sun and shade leaves have contrasting morphological and biochemical characteristics.
- To increase light absorption, some shade plants produce a higher ratio of PSII to PSI reaction centers, while others add antenna chlorophyll to PSII.

11.2 Effects of Light on Photosynthesis in the Intact Leaf

- Light-response curves show the PPFD where photosynthesis is limited by light or by carboxylation capacity. The slope of the linear portion of the light-response curve measures the maximum quantum yield (**Figure 11.6**).
- Light compensation points for shade plants are lower than for sun plants because respiration rates in shade plants are low (**Figures 11.7, 11.8**).
- Beyond the saturation point, factors other than incident light, such as electron transport, Rubisco activity, or triose phosphate metabolism, limit photosynthesis. Rarely is an entire plant light-saturated (**Figure 11.9**).
- The xanthophyll cycle dissipates excess absorbed light energy to avoid damaging the photosynthetic apparatus (**Figures 11.10, 11.11**). Chloroplast movements also limit excess light absorption (**Figure 11.12**).
- Dynamic photoinhibition temporarily diverts excess light absorption to heat but maintains maximum photosynthetic rate (**Figure 11.13**). Chronic photoinhibition is irreversible.

11.3 Effects of Temperature on Photosynthesis in the Intact Leaf

- Leaf absorption of light energy generates a heat load that must be dissipated (**Figure 11.14**).
- Plants are remarkably plastic in their adaptations to temperature. Optimal photosynthetic temperatures have strong biochemical, genetic (adaptation), and environmental (acclimation) components.
- Temperature-response curves identify (a) a temperature range where enzymatic events are stimulated, (b) a range for optimal photosynthesis, and (c) a range where deleterious events occur (**Figure 11.15**).
- Below 30°C, the quantum yield of C_3 plants is generally higher than that of C_4 plants; above 30°C, the situation is reversed (**Figure 11.16**). Because of photorespiration, the quantum yield is strongly dependent on temperature in C_3 plants but is nearly independent of temperature in C_4 plants.
- Reduced quantum yield due to photorespiration leads to differences in the photosynthetic capacities of C_3 and C_4 plants and results in a shift of species dominance across different latitudes (**Figure 11.17**).

11.4 Effects of Carbon Dioxide on Photosynthesis in the Intact Leaf

- Atmospheric CO_2 concentrations have been increasing since the Industrial Revolution because of human use of fossil fuels and deforestation (**Figure 11.18**).
- Concentration gradients drive the diffusion of CO_2 from the atmosphere to the carboxylation site in the leaf, using both gas and liquid routes. There are multiple resistances along the CO_2 diffusion pathway, but under most conditions stomatal resistance has the greatest effect on CO_2 diffusion into a leaf (**Figure 11.19**).
- Enrichment of CO_2 above natural atmospheric concentrations results in increased photosynthesis and productivity (**Figure 11.20**), but this can be attenuated by increased leaf temperature and reduced stomatal conductance.
- C_4 photosynthesis may have become prominent due to high rates of photorespiration in Earth's warmest and driest regions when global atmospheric CO_2 concentrations fell below a threshold value (**Figure 11.21**).
- Opening at night and closing during the day, the stomatal activity of CAM plants contrasts with that found in C_3 and C_4 plants (**Figure 11.22**).
- Free Air CO_2 Enrichment (FACE) experiments (**Figure 11.23**) show that C_3 plants are more responsive to elevated CO_2 than are C_4 plants; however, the response of C_3 plants under FACE conditions is often less than that predicted from experiments in greenhouse and growth chambers, as other factors can limit plant growth under field conditions.

11.5 Stable Isotopes Record Photosynthetic Properties

- The carbon isotope ratios of leaves can be used to distinguish photosynthetic pathway differences among different plant species.
- Both C_3 and C_4 plants have less ^{13}C than does CO_2 in the atmosphere, indicating that leaf tissues discriminate against ^{13}C during photosynthesis. However, C_3 plants discriminate against ^{13}C more than C_4 plants do (**Figure 11.24**).
- Conditions that cause stomata to close in C_3 plants, such as water stress, cause the leaf carbon isotope ratio to increase. Thus, the carbon isotope ratio of a leaf can be used as a direct estimate of physiological responses to the environment (e.g., short-term water stress) (**Figure 11.25**).

Web Material

- **WEB TOPIC 11.1 Working with Light** Amount, direction, and spectral quality are important parameters for the measurement of light.
- **WEB TOPIC 11.2 Heat Dissipation from Leaves: The Bowen Ratio** Sensible heat loss and evaporative heat loss are the most important processes in the regulation of leaf temperature.
- **WEB TOPIC 11.3 The Geographic Distributions of C_3 and C_4 Plants** The geographic distributions of C_3 and C_4 plants correspond closely with growing-season temperatures in today's world.
- **WEB TOPIC 11.4 Calculating Important Parameters in Leaf Gas Exchange** Gas exchange methods allow us to measure photosynthesis and stomatal conductance in the intact leaf.
- **WEB TOPIC 11.5 Prehistoric Changes in Atmospheric CO_2** Over the past 800,000 years, atmospheric CO_2 concentration changed between 180 ppm (glacial periods) and 280 ppm (interglacial periods) as Earth moved between ice ages.
- **WEB TOPIC 11.6 Projected Future Increases in Atmospheric CO_2** Atmospheric CO_2 reached 417 ppm in 2021 and is expected to reach 600 to 750 ppm by the end of this century, unless fossil fuel emissions and deforestation are diminished.
- **WEB TOPIC 11.7 Using Carbon Isotopes to Detect Adulteration in Foods** Carbon isotopes are frequently used to detect the substitution of C_4 sugars into C_3 food products, such as the introduction of sugarcane into honey to increase yield.
- **WEB TOPIC 11.8 Reconstruction of the Expansion of C_4 Taxa** The $\delta^{13}C$ of animal teeth faithfully records the carbon isotope ratios of food sources and can be used to reconstruct the abundances of C_3 and C_4 plants eaten by mammalian grazers.

For more study aids, go to oup.com/he/taiz7e.

Suggested Reading

Ainsworth, E. A., and Long, S. P. (2005) What have we learned from 15 years of free-air CO_2 enrichment (FACE)? A meta-analytic review of the responses of photosynthesis, canopy properties and plant production to rising CO_2. *New Phytol.* 165: 351–372.

Blankenship, R. E. (2014) *Molecular Mechanisms of Photosynthesis*, 2nd ed. Blackwell Science Ltd, Oxford.

Demmig-Adams, B. and Adams, W. W. (2006) Photoprotection in an ecological context: the remarkable complexity of thermal energy dissipation. *New Phytol.* 172: 11–21.

Dodd, A. N., Borland A. M., Haslam R. P., et al. (2002) Crassulacean acid metabolism: Plastic, fantastic. *J. Exp. Bot.* 53: 569–580.

Ehleringer, J. R., Cerling, T. E., and Helliker, B. R. (1997) C_4 photosynthesis, atmospheric CO_2, and climate. *Oecologia* 112: 285–299.

Evans, J. R. (2020) Mesophyll conductance: walls, membranes and spatial complexity. *New Phytol.* 229: 1864–1876.

Falkowski, P., and Raven, J. (2007) *Aquatic Photosynthesis*, 2nd ed. Princeton University Press, Princeton.

Farquhar, G. D., Ehleringer, J. R., and Hubick, K. T. (1989) Carbon isotope discrimination and photosynthesis. *Annu. Rev. Plant Physiol. Plant Mol. Biol*. 40: 503–537.

Koller, D. (2000) Plants in search of sunlight. *Adv. Bot. Res*. 33: 35–131.

Laisk, A., and Oja, V. (1998) *Dynamics of leaf photosynthesis*. CSIRO, Melbourne.

Long, S. P., Ainsworth, E. A., Leakey, A. D., et al. (2006) Food for thought: Lower-than-expected crop stimulation with rising CO_2 concentrations. *Science* 312: 1918–1921.

Murchie, E. H., and Niyogi, K. K. (2011) Manipulation of photoprotection to improve plant photosynthesis. *Plant Physiol.* 155: 86–92.

Osborne, C. P., and Sack, L. (2012) Evolution of C_4 plants: A new hypothesis for an interaction of CO_2 and water relations mediated by plant hydraulics. *Philos. Trans. R. Soc. Lond. B. Biol. Sci.* 367: 583–600.

Seibt, U., Rajabi, A., Griffiths, H., and Berry, J. A. (2008) Carbon isotopes and water use efficiency: Sense and sensitivity. *Oecologia* 155: 441–454.

Sharkey, T. D., and Monson, R. K. (2017) Isoprene research – 60 years later, the biology is still enigmatic. *Plant Cell Environ*. 40: 1671–1678.

Terashima, I., Hanba, Y. T., Tholen, D., and Niinemets, Ü. (2011) Leaf functional anatomy in relation to photosynthesis. *Plant Physiol.* 155: 108–116.

Terashima, I., and Hikosaka, K. (1995) Comparative ecophysiology of leaf and canopy photosynthesis. *Plant Cell Environ*. 18: 1111–1128.

Vogelmann, T. C., and Evans, J. R. (2002) Profiles of light absorption and chlorophyll within spinach leaves from chlorophyll fluorescence. *Plant Cell Environ.* 25: 1313–1323.

von Caemmerer, S. (2000) *Biochemical models of leaf photosynthesis*. CSIRO, Melbourne.

Wada, M., Kagawa, T., and Sato, Y. (2003) Chloroplast movement. *Annu. Rev. Plant Biol.* 54: 455–468.

Zhu, X. G., Long, S. P., and Ort, D. R. (2010) Improving photosynthetic efficiency for greater yield. *Annu. Rev. Plant Biol*. 61: 235–261.

12 Translocation in the Phloem



Aleksey Sagitov/Shutterstock

Survival on land poses some serious challenges to terrestrial plants; foremost among these challenges is the need to acquire and retain water. In response to such environmental pressures, plants evolved roots and leaves. Roots anchor the plant and absorb water and nutrients; leaves absorb light and exchange gases. As plants increased in size, the roots and leaves became increasingly separated from each other in space. Thus, systems evolved for long-distance transport that allowed the shoot and the root to efficiently exchange products of absorption and assimilation.

You will recall from Chapters 6 and 8 that the xylem is the tissue that transports water and minerals from the root system to the aerial portions of the plant. The **phloem** is the tissue that transports (*translocates*) the products of photosynthesis—particularly sugars—from mature leaves to areas of growth and storage, including the roots.

Along with the sugars, the phloem also transmits signals in the form of regulatory molecules, and redistributes water and various compounds throughout the plant body. All of these molecules appear to move with the transported sugars. The compounds to be redistributed, some of which initially arrive in the mature leaves via the xylem, can be either transferred out of the leaves without modification or metabolized before redistribution. The fluid that flows through the phloem—the water plus all its solutes—is called *phloem sap*. (*Sap* is a general term used to refer to the fluid contents of plant cells.)

In this chapter we first examine the patterns and pathway of translocation and focus on the loading of sugars in mature leaves. We then follow the sugar movement in the phloem from source to sink and discuss the mechanism of phloem transport, including the rate of movement, magnitude of pressure gradients between sources and sinks, materials translocated in the phloem, and its wound response. The destination of our journey with sugar molecules through the plant is their unloading in sink organs and subsequent consumption and storage. Finally, we explore the role of the phloem in coordinating plant growth by the allocation and partitioning of photosynthetic products and by offering a rapid pathway for signaling.

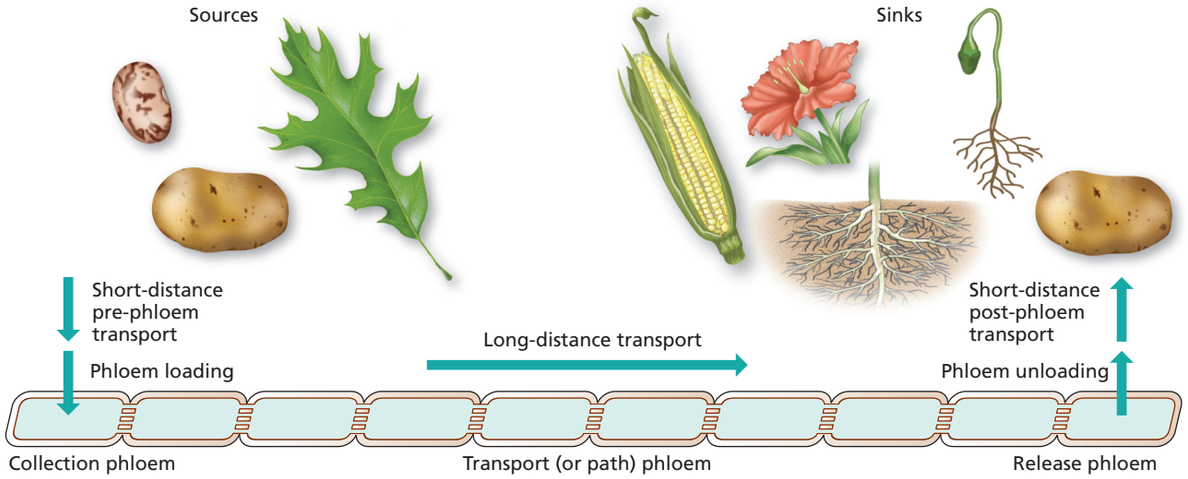


Figure 12.1 Phloem translocates materials from sources to sinks.

12.1 Patterns of Translocation: Source to Sink

The two long-distance transport pathways—the phloem and the xylem—extend throughout the plant body. Unlike the xylem, the phloem does not translocate materials exclusively in either an upward or a downward direction. Rather, sap is translocated from areas of supply, called **sources**, to areas of metabolism or storage, called **sinks** (**Figure 12.1**). The terms **collection phloem**, **transport phloem**, and **release phloem** are often used to characterize the prevalent phloem functions in sources, connecting pathways, and sinks, respectively.

Sources include exporting organs, typically mature leaves that produce photosynthate in excess of their own needs. The term **photosynthate** refers to products of photosynthesis (see Chapter 10). Another type of source is a storage organ during the exporting phase of its development. For example, the storage root of the biennial wild beet (*Beta maritima*) is a sink during the growing season of the first year, when it accumulates sugars received from the source leaves. During the second growing season, the same root becomes a source; the sugars are remobilized and used to produce a new shoot, which ultimately becomes reproductive.

Sinks include all nonphotosynthetic organs of the plant and organs that do not produce enough photosynthetic products to support their own growth or storage needs. Roots, tubers, developing fruits, and immature leaves, which must import carbohydrate for normal development, are all examples of sink tissues. Labeling studies support the source-to-sink pattern of translocation in the phloem (**Figure 12.2A**).

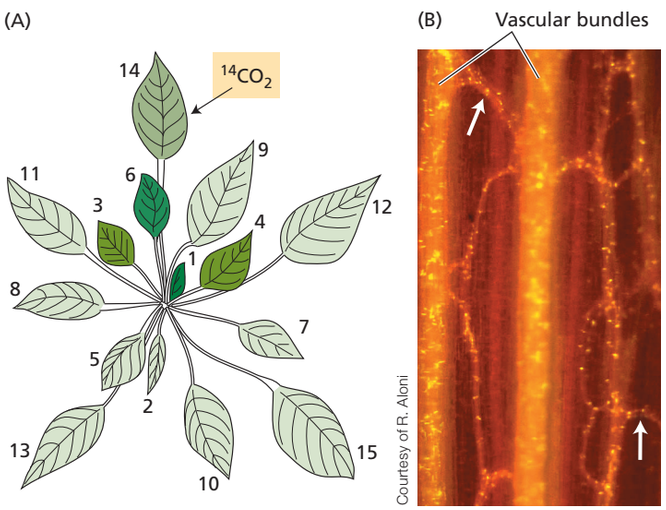


Figure 12.2 Source-to-sink patterns of phloem translocation. **(A)** Distribution of radioactivity from a single labeled source leaf in an intact plant. The distribution of radioactivity in leaves of a sugar beet plant (*Beta vulgaris*) was determined 1 week after $^{14}CO_2$ was supplied for 4 h to a single source leaf (leaf 14, arrow). The degree of radioactive labeling is indicated by the intensity of shading of the leaves. Leaves are numbered according to their age; the youngest, newly emerged leaf is designated 1. The ^{14}C label was translocated mainly to the sink leaves directly above the source leaf (that is, sink leaves with the most direct vascular connections to the source; for example, leaves 1 and 6 are sink leaves directly above source leaf 14). **(B)** Longitudinal view of the typical three-dimensional structure of the phloem in a thick section (from an internode of dahlia [*Dahlia pinnata*]), shown here after clearing, staining with aniline blue (which binds to callose and fluoresces yellow), and viewing under an epifluorescence microscope. The sieve plates of the phloem sieve elements (see Figure 12.7) are seen as numerous small dots because of their callose content. Two large longitudinal vascular bundles are prominent. This staining reveals the delicate sieve tubes forming the phloem network; two phloem anastomoses (vascular interconnections) are marked by arrows. (A after K. W. Joy. 1964. *J. Exp. Bot.* 15: 485–494.)

Although the overall pattern of transport in the phloem can be stated simply as source-to-sink movement, the specific pathways involved are often more complex, depending on proximity, development, vascular interconnections (**Figure 12.2B**), and modification of translocation pathways. Not all sources supply all sinks on a plant; rather, certain sources preferentially supply specific sinks (see Section 12.7).

12.2 Pathways of Translocation

The phloem is generally found on the outer side of both primary and secondary vascular tissues (**Figures 12.3** and **12.4**). In plants with secondary growth, the phloem constitutes the inner bark. Although phloem is commonly located external to the xylem, it is *also* found on the inner side in many eudicot families. In these families, the phloem in the two positions is called external and internal phloem, respectively.

The small veins of leaves, the primary vascular bundles of stems, and the root stele are each separated from the ground parenchyma by a layer of compactly arranged cells, called the bundle sheath (see Figure 12.3), starch sheath, and endodermis, respectively. (Recall the bundle sheath cells involved in C_4 metabolism discussed in Chapter 10.) In the vascular tissue of leaves, the bundle sheath surrounds the small veins all the way to their ends, isolating the veins from the intercellular air spaces of the leaf.

We begin our discussion of translocation pathways with the experimental evidence demonstrating that *sieve elements* are the conducting cells in the phloem. Then we examine their structure and physiology.

Sugar is translocated in phloem sieve elements

Early experiments on phloem transport date back to the nineteenth century, indicating the importance of long-distance transport in plants (see **WEB TOPIC 12.1**). These classic experiments demonstrated that removal of a ring of bark around the trunk of a tree, which removes the secondary phloem (see Figure 12.4), effectively stops sugar transport from the leaves to the roots without altering water transport through the xylem. When radioactively labeled compounds became available, $^{14}CO_2$ was used to show that sugars made in the photosynthetic process are translocated through the phloem sieve elements (see **WEB TOPIC 12.1**).

Mature sieve elements are living cells specialized for translocation

The cells of the phloem that conduct sugars and other organic materials throughout the plant are called **sieve elements**. *Sieve element* is a comprehensive term that includes both the **sieve tube elements** typical of the

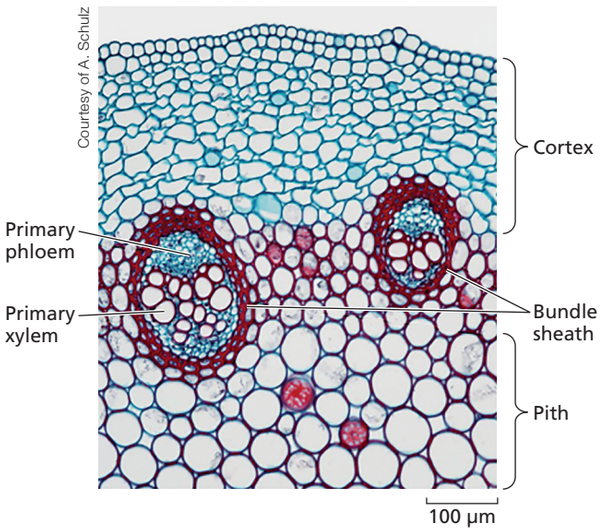


Figure 12.3 Transverse section of a vascular bundle of buttercup (*Ranunculus repens*). The primary phloem is toward the outside of the stem. Both the primary phloem and the primary xylem are surrounded by a bundle sheath of thick-walled sclerenchyma cells, which isolate the vascular tissue from the ground tissue. Fibers and xylem vessels are stained red.

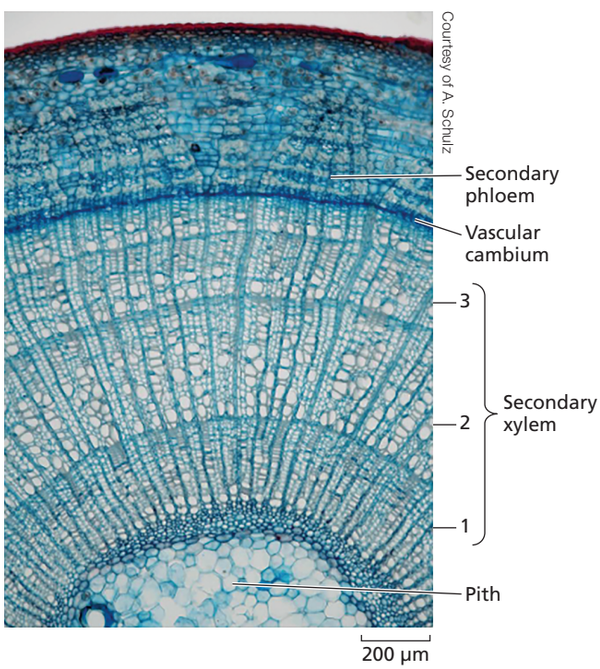


Figure 12.4 Transverse section of a 4-year-old stem of a basswood (*Tilia*) tree. The numbers 1, 2, and 3 indicate growth rings in the secondary xylem. The old (outer) secondary phloem is pushed outward by expansion of the xylem. Only the most recent (innermost) layer of secondary phloem is functional.

angiosperms and the **sieve cells** of gymnosperms. In addition to sieve elements, the phloem tissue contains companion cells (discussed later in this section) and parenchyma cells (which store and release food molecules). In some cases the phloem tissue also includes fibers and sclereids (for protection and strengthening of the tissue) and laticifers (latex-containing cells). However, only the sieve elements are directly involved in translocation.

Mature sieve elements are unique among living plant cells (**Figures 12.5** and **12.6**). They lack many structures normally found in living cells, even in the undifferentiated cells from which they are formed. Although sieve elements retain their plasma membrane, they lose their nuclei and vacuoles during differentiation. Microtubules, Golgi bodies, and ribosomes are also generally absent from the mature cells. Organelles that are retained include somewhat modified mitochondria, plastids, and smooth endoplasmic reticulum. The walls are nonlignified, though they are secondarily thickened in some cases.

Sieve elements of most angiosperms, but not of gymnosperms, are rich in specific structural proteins called P-proteins (see Figure 12.5B and 12.6C). P-protein occurs in several different forms (tubular, fibrillar, granular, and crystalline), depending on the species and maturity of the cell, and is involved in sealing off damaged sieve tubes (see *Damaged sieve elements are sealed off* in Section 12.5).

In conclusion, the cellular structure of sieve elements is different from that of tracheary elements of the xylem, which lack a plasma membrane, have lignified secondary walls, and are dead at maturity (see Chapter 6). As we will see, persistence of the sieve element plasma membrane is critical to the mechanism of translocation in the phloem.

Large pores in cell walls are the prominent feature of sieve elements

Sieve elements (sieve cells and sieve tube elements) have characteristic sieve areas in their cell walls, where pores interconnect the conducting cells (**Figure 12.7**). The sieve area pores range in diameter from less than 1 μm to around 10 μm and develop from plasmodesmata. Unlike sieve areas of gymnosperms, the sieve areas of angiosperms can differentiate into **sieve plates** (see Figure 12.7 and Table 12.1). Sieve plates have larger pores than the other sieve areas in the cell and are generally found on the end walls of sieve tube elements, where the individual cells are joined together to form a longitudinal series called a **sieve tube** (see Figure 12.5).

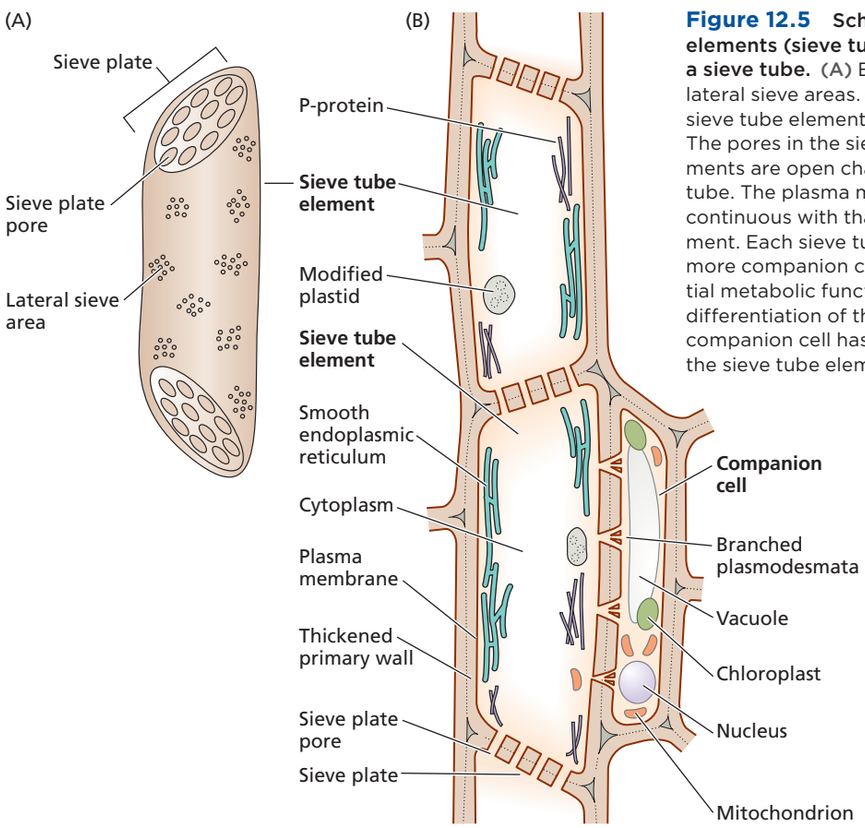


Figure 12.5 **Schematic drawings of mature sieve elements (sieve tube elements) joined together to form a sieve tube.** **(A)** External view, showing sieve plates and lateral sieve areas. **(B)** Longitudinal section, showing two sieve tube elements joined together to form a sieve tube. The pores in the sieve plates between the sieve tube elements are open channels for transport through the sieve tube. The plasma membrane of a sieve tube element is continuous with that of its neighboring sieve tube element. Each sieve tube element is associated with one or more companion cells, which take over some of the essential metabolic functions that are reduced or lost during differentiation of the sieve tube elements. Note that the companion cell has many cytoplasmic organelles, whereas the sieve tube element has relatively few organelles.

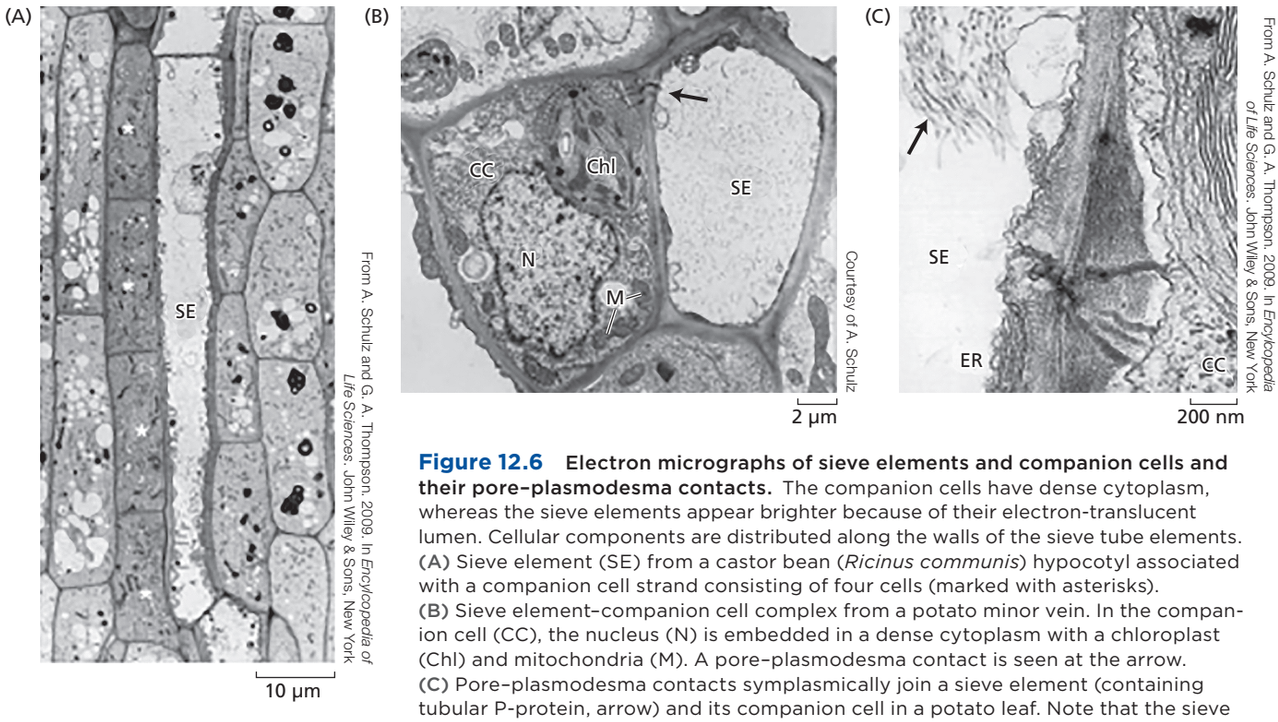


Figure 12.6 Electron micrographs of sieve elements and companion cells and their pore–plasmodesma contacts. The companion cells have dense cytoplasm, whereas the sieve elements appear brighter because of their electron-translucent lumen. Cellular components are distributed along the walls of the sieve tube elements. **(A)** Sieve element (SE) from a castor bean (*Ricinus communis*) hypocotyl associated with a companion cell strand consisting of four cells (marked with asterisks). **(B)** Sieve element–companion cell complex from a potato minor vein. In the companion cell (CC), the nucleus (N) is embedded in a dense cytoplasm with a chloroplast (Chl) and mitochondria (M). A pore–plasmodesma contact is seen at the arrow. **(C)** Pore–plasmodesma contacts symplasmically join a sieve element (containing tubular P-protein, arrow) and its companion cell in a potato leaf. Note that the sieve element plasma membrane is lined with smooth ER cisternae (ER).

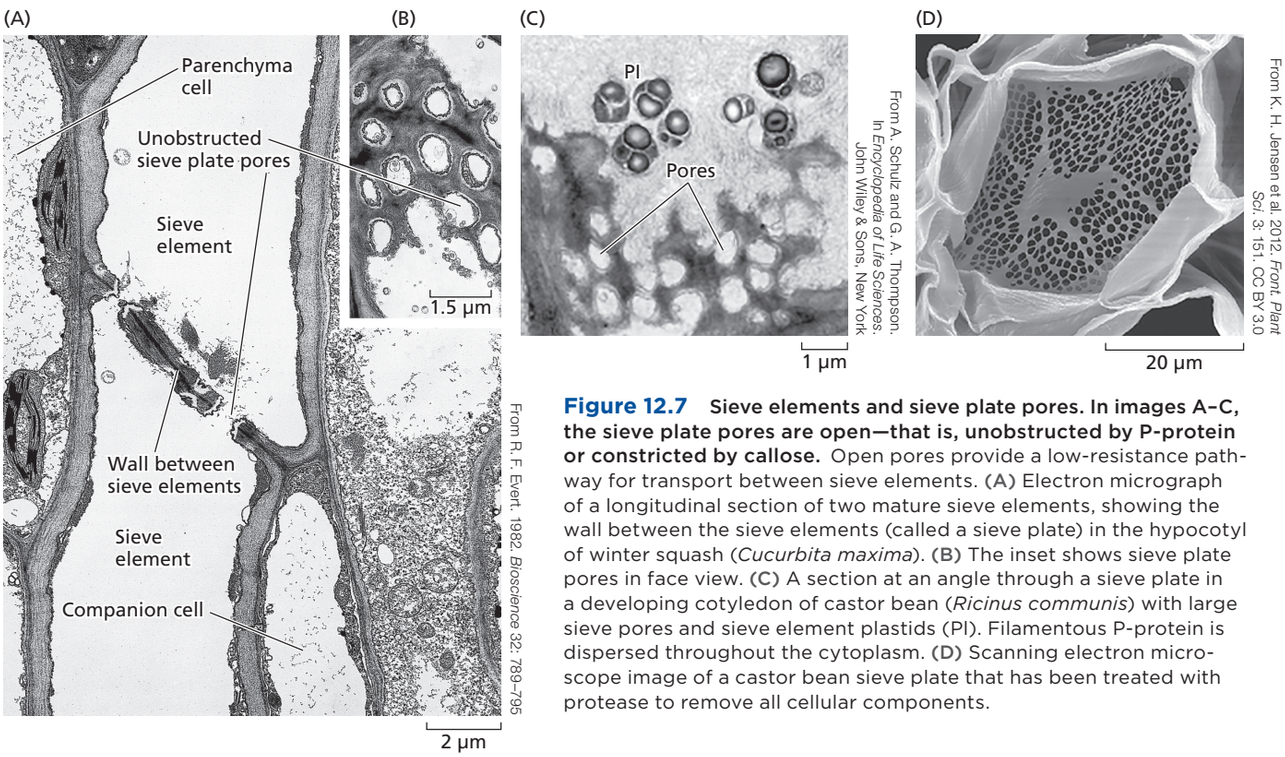
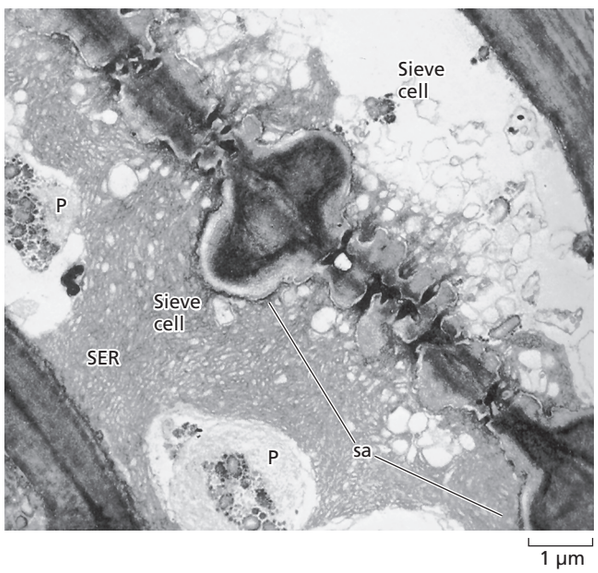


Figure 12.7 Sieve elements and sieve plate pores. In images A–C, the sieve plate pores are open—that is, unobstructed by P-protein or constricted by callose. Open pores provide a low-resistance pathway for transport between sieve elements. **(A)** Electron micrograph of a longitudinal section of two mature sieve elements, showing the wall between the sieve elements (called a sieve plate) in the hypocotyl of winter squash (*Cucurbita maxima*). **(B)** The inset shows sieve plate pores in face view. **(C)** A section at an angle through a sieve plate in a developing cotyledon of castor bean (*Ricinus communis*) with large sieve pores and sieve element plastids (Pl). Filamentous P-protein is dispersed throughout the cytoplasm. **(D)** Scanning electron microscope image of a castor bean sieve plate that has been treated with protease to remove all cellular components.

The distribution of sieve tube contents in functional sieve plate is a critical question when considering the mechanism of phloem transport. Early micrographs showed blocked or occluded pores, thought to be artifacts due to damage as the tissues were prepared for observation. Less invasively prepared phloem depicts the sieve plate pores as open channels that appear to allow unfettered transport (see Figure 12.7A–C; *Functional sieve plate pores appear to be open channels in* Section 12.4) will further consider the distribution of sieve element contents within the cells and within the sieve plate pores.

In contrast to pores in sieve tube elements of angiosperms, sieve areas in gymnosperms do not appear to be open channels. All of the sieve areas in gymnosperms such as conifers are structurally similar, though they can be more numerous on the overlapping end walls of sieve cells. The pores of gymnosperm sieve areas meet in large median cavities in the middle of the wall. Smooth endoplasmic reticulum (SER) covers the sieve areas (**Figure 12.8**) and is continuous through the sieve pores and median cavity, as indicated by ER-specific staining. Observation of living material with confocal laser scanning microscopy confirms that the observed distribution of SER is not an artifact of fixation.

Table 12.1 lists characteristics of sieve tube elements and sieve cells.



From A. Schulz. 1990. In *Sieve Elements: Comparative Structure, Induction, and Development*. H.-D. Behnke and R. D. Sjolund (eds.), Springer-Verlag, Berlin

Figure 12.8 Electron micrograph showing a sieve area (sa) linking two sieve cells in the secondary phloem of a conifer (*Picea abies*). Smooth endoplasmic reticulum (SER) covers the sieve area on both sides and is also found within the pores and the extended median cavity. Such obstructed pores would result in a high resistance to mass flow between sieve cells. P, plastid.

Table 12.1 Characteristics of two types of sieve elements in seed plants

Sieve tube elements found in angiosperms
1. Some sieve areas are differentiated into sieve plates; individual sieve tube elements are joined together into a sieve tube.
2. Sieve plate pores are open channels.
3. P-protein is present in all eudicots and many monocots.
4. Companion cells are sources of ATP and perhaps other compounds. In some species they serve as transfer cells or intermediary cells
Sieve tube elements found in gymnosperms
1. There are no sieve plates; all sieve areas are similar.
2. Pores in sieve areas appear blocked with membranes.
3. There is no P-protein.
4. Strasburger cells have similar functions as companion cells.

Companion cells aid the highly specialized sieve elements

Each sieve tube element is usually associated with one or more **companion cells** (see Figure 12.6). As a rule, the division of a single mother cell forms the sieve tube element and the companion cell in metaphloem and secondary phloem. Numerous specialized plasmodesmatal connections penetrate the walls between sieve tube elements and their companion cells; the plasmodesmata are complex and branched on the companion cell side, while forming a sieve pore on the sieve element side (see Figure 12.6B and C). The presence of these **pore–plasmodesma contacts** suggests a close functional relationship between a sieve element and its companion cell, an association that has been demonstrated by the rapid exchange of fluorescent dyes, and even proteins, between the two cells.

Companion cells differ from sieve elements in having dense, ribosome-rich cytoplasm and many mitochondria. They have taken over some of the critical metabolic functions of sieve elements, such as protein and lipid synthesis, that are reduced or lost during sieve element differentiation. In addition to nursing sieve elements, companion cells are involved in coordinating essential plant functions, such as flowering, tuber development, and emergence of lateral roots (see Section 12.8).

Companion cells play a role in phloem loading, where they are involved in the last step of the transport of photosynthetic products from producing cells in mature leaves to the sieve elements in the minor (small) veins of the leaf. The evolution of different phloem-loading strategies in seed plants is reflected by the existence of at least three different types of companion cells in the minor veins of mature, exporting leaves: “ordinary”

companion cells that are indistinguishable from those in transport phloem, transfer cells, and intermediary cells (discussed in Section 12.3).

Gymnosperm sieve cells are also tightly coupled with pore–plasmodesma contacts to specialized cells with dense cytoplasm and abundant mitochondria. In contrast to companion cells, these *Strasburger cells* are not ontogenetically related (not sister cells) to sieve elements. Like companion cells, they are involved in phloem loading.

The association of sieve elements with specialized cells that have taken over vital functions is an evolutionary advance of seed plants (see **WEB TOPIC 12.2**).

12.3 Phloem Loading

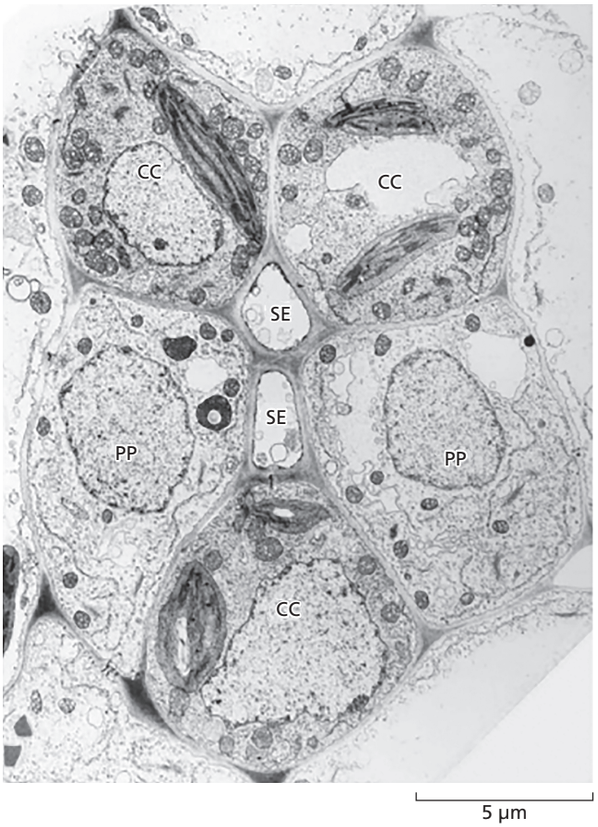
Here we discuss the pathway that photosynthates follow from their origin in mesophyll cells to the minor veins, where they are loaded into the sieve elements. Phloem loading of sugar molecules—often sucrose—provides the driving force for long-distance transport (see Section 12.4).

Several steps are involved in the transport of photosynthate from the mesophyll chloroplasts to the sieve elements of mature leaves:

1. Triose phosphate formed by photosynthesis during the day (see Chapter 10) is transported from the chloroplast to the cytosol, where it is converted to sucrose. During the night, carbon from stored starch exits the chloroplast primarily in the form of maltose and is converted to sucrose.
2. Sucrose moves from producing cells in the mesophyll to cells in the vicinity of the sieve elements in the smallest veins of the leaf (**Figure 12.9**). This **pre-phloem transport** usually covers a distance of only a few cell diameters.
3. In the process called **phloem loading**, sugars are transported into the sieve elements and companion cells. Note that sieve elements and companion cells are often considered a functional unit, called the *sieve element–companion cell complex*. Once inside the sieve elements, sucrose and other solutes are translocated away from the source, a process known as **export**. Translocation through the vascular system to a sink is referred to as **long-distance transport**.

Phloem loading can occur via the apoplast or symplasm

Photosynthates in source leaves must move from the photosynthesizing cells in the mesophyll to the sieve elements. Studies using fluorescent tracers of the molecular size of sucrose suggest that the initial pre-phloem pathway is symplasmic and follows the sugar concentration gradient (**Figure 12.10**). However, sugars might experience an apoplastic step before phloem loading (see Figure 12.10A), or they might move entirely through the symplasm to the sieve elements via the plasmodesmata (see Figure 12.10B). (See Figure 6.4 for a general description of the symplasm and apoplast.) One of the two routes, apoplastic or symplasmic, is predominant in a given plant species; many species, however, show evidence of being able to use more than one loading mechanism. Three distinct mechanisms for phloem loading are now recognized: apoplastic loading, symplasmic loading with oligomer trapping, and passive symplasmic loading. For simplicity's sake, we will initially consider the routes separately, then return to the subject of loading diversity.



From A. Schulz and G. A. Thompson. In *Encyclopedia of Life Sciences*. John Wiley & Sons, New York

Figure 12.9 Electron micrograph showing the relationships among the phloem cell types of the smallest vein in a source leaf of potato. The image shows two sieve elements (SE), three large companion cells (CC), and two phloem parenchyma cells (PP), all surrounded by the bundle sheath. Photosynthates from the mesophyll are loaded from the bundle sheath or the phloem parenchyma into the sieve element–companion cell complexes.

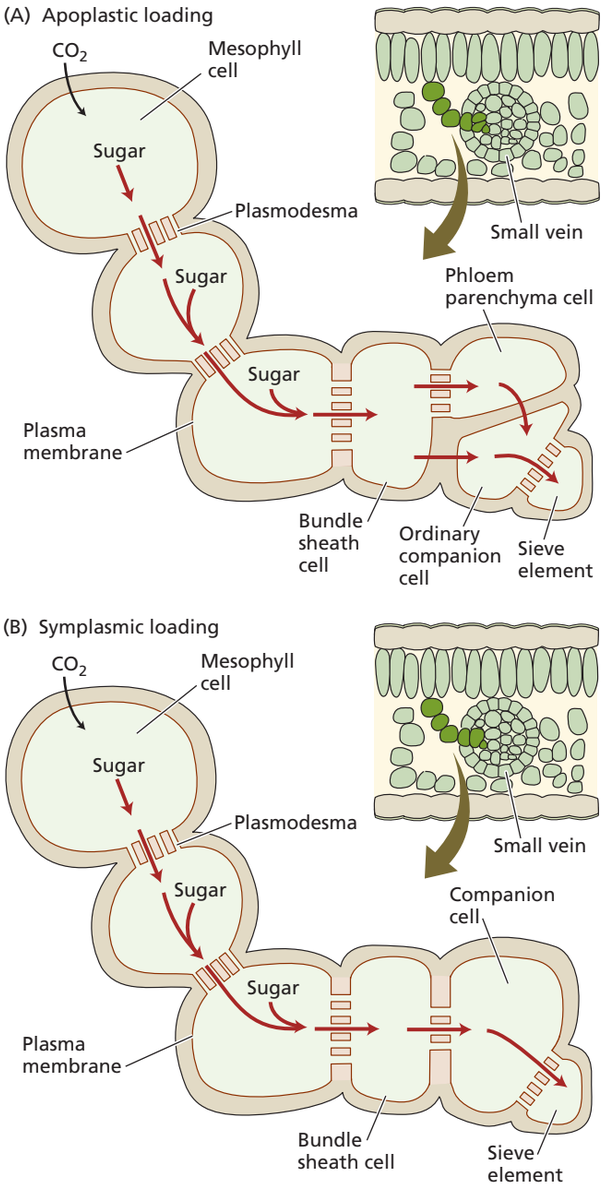


Figure 12.10 Schematic diagram of pathways of phloem loading in source leaves. **(A)** In the partly apoplastic pathway, sugars initially move through the symplasm but enter the apoplast before loading into the companion cells and sieve elements. Sugars loaded into the companion cells are thought to move through plasmodesmata into the sieve elements. **(B)** In the entirely symplasmic pathway, sugars move from one cell to another through plasmodesmata, all the way from the mesophyll to the sieve elements. Note that symplasmically loading plants typically do not contain phloem parenchyma cells.

We will discuss apoplastic loading first and then introduce the two types of symplasmic loading (oligomer trapping and passive), following the order in which their importance was recognized.

Apoplastic loading is characteristic of many herbaceous species

In the case of apoplastic loading, the sugars enter the apoplast surrounding the sieve element–companion cell complex. The sucrose transporters that mediate the efflux of sucrose, most likely from the phloem parenchyma to the apoplast near the sieve element–companion cell complexes, have been identified—first in Arabidopsis and rice—as a subfamily of the SWEET transporters. Sugars are then actively taken up from the apoplast into the sieve element–companion cell complex by a selective transporter located in the plasma membranes of these cells.

The apoplastic phloem-loading model leads to three basic predictions:

1. Transported sugars should be found in the apoplast.
2. In experiments in which sugars are supplied to the apoplast, the exogenously supplied sugars should accumulate in sieve elements and companion cells.
3. Inhibition of sugar efflux from the phloem parenchyma or of uptake from the apoplast should result in inhibition of export from the leaf.

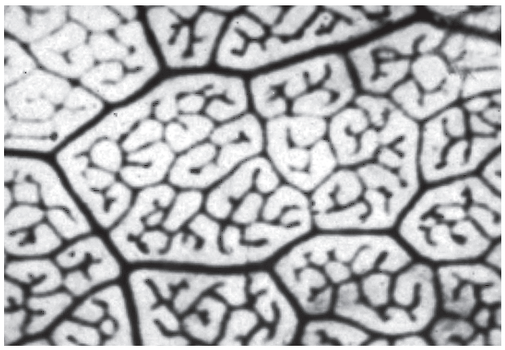
Many studies devoted to testing these predictions have provided solid evidence for apoplastic loading in several species.

Sucrose loading in the apoplastic pathway requires metabolic energy

In many of the species initially studied, sugars become more concentrated in the sieve elements and companion cells than in the mesophyll. This difference in solute concentration can be demonstrated through measurement of the osmotic potential (Ψ_s) of the various cell types in the leaf (see Chapter 6).

In sugar beet, the osmotic potential of the mesophyll is approximately –1.3 MPa, and the osmotic potential of the sieve elements and companion cells is about –3.0 MPa. Most of this difference in osmotic potential is thought to result from accumulated sugar, specifically sucrose, which is the major transport sugar in this species. Experimental studies have also demonstrated that both externally supplied sucrose and sucrose derived from photosynthate accumulate in the phloem of the minor veins of sugar beet source leaves (**Figure 12.11**).

The fact that sucrose is at a higher concentration in the sieve element–companion cell complex than in surrounding cells indicates that sucrose is actively transported against its chemical-potential gradient. The dependence of sucrose accumulation on active transport is supported by the fact that treating source tissue with respiratory inhibitors both decreases the ATP concentration and inhibits loading of exogenous sugar.



From B. R. Fondy, 1975. Sugar selectivity of phloem loading in *Beta vulgaris vulgaris L.* and *Fraxinus americana, americana L.*. Thesis, University of Dayton, Dayton, OH

Figure 12.11 Autoradiograph showing that labeled sugar moves against its concentration gradient from the apoplast into sieve elements and companion cells of a sugar beet source leaf. A solution of ^{14}C-labeled sucrose was applied for 30 min to the adaxial surface of a sugar beet leaf that had previously been kept in darkness for 3 h. The leaf cuticle was removed to allow penetration of the solution to the interior of the leaf. The sieve elements and companion cells of the small veins in the source leaf contain high concentrations of labeled sugar, shown by the black accumulations, indicating that sucrose is actively transported against its concentration gradient.

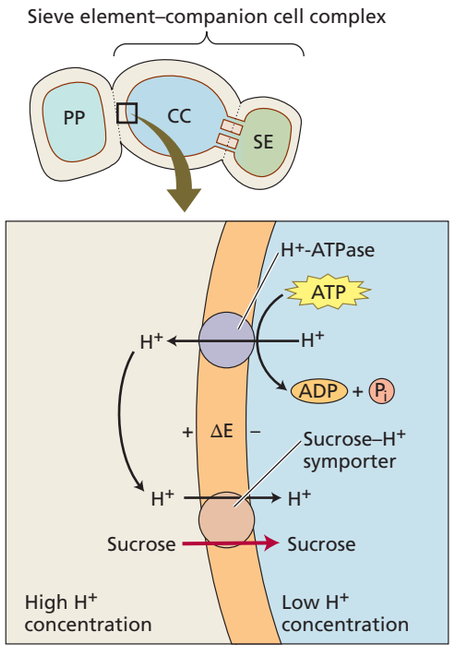


Figure 12.12 ATP-dependent sucrose transport in apoplastic sieve element loading. In the cotransport model of sucrose loading into the symplasm of the sieve element–companion cell complex, the plasma membrane ATPase pumps protons out of the cell into the apoplast, establishing a higher proton concentration in the apoplast and a membrane potential of approximately –120 mV (ΔE). The energy in the electrochemical proton gradient is then used to drive the transport of sucrose into the symplasm of the sieve element–companion cell complex through a sucrose–H^+ symporter. CC, companion cell; PP, phloem parenchyma cell; SE, sieve element.

Plants that load sugars apoplastically into the phloem may also load amino acids and sugar alcohols (sorbitol and mannitol) actively. In contrast, other metabolites, such as organic acids and hormones, may enter sieve elements passively. (See **WEB TOPIC 12.3** for a discussion of these topics.)

Phloem loading in the apoplastic pathway involves a sucrose–H^+ symporter

A sucrose–H^+ symporter is thought to mediate the transport of sucrose from the apoplast into the sieve element–companion cell complex. Recall from Chapter 8 that symport is a secondary transport process that uses the energy generated by the proton pump (see Figures 8.9 and 8.10), in this case a companion cell–specific isoform. The energy dissipated by protons moving back into the cell is coupled to the uptake of a substrate, in this case sucrose (**Figure 12.12**). The symporter selects from the various sugars present in the apoplast the one sugar species that is transported long-distance in the phloem, in this case sucrose.

Many sucrose–H^+ symporters have been cloned and localized in the phloem. SUT1 and SUC2 and their homologs appear to be the major sucrose transporters in phloem loading. They are located in the plasma membrane of either companion cells or sieve elements. (See **WEB TOPIC 12.3**.)

Transfer cells are companion cells that are specialized for membrane transport

Some apoplastically loading plants, such as broad bean (*Vicia faba*), have transfer cells in minor veins. Transfer-type companion cells are similar to intermediary-type companion cells, except for the development of fingerlike wall ingrowths, particularly on the cell walls that face away from source sieve elements (**Figure 12.13**). These wall ingrowths greatly increase the surface area of the plasma membrane, thus increasing the potential for solute transfer across the membrane. Relatively few plasmodesmata connect this type of companion cell to any of the surrounding cells except its own sieve element. Xylem parenchyma cells can also be modified as transfer cells, serving to retrieve and reroute solutes moving in the xylem, which is also part of the apoplast. Transfer cells occur most frequently at nodes in transport phloem, as well as in source phloem and in post–sieve element unloading pathways.

A paucity or virtual absence of plasmodesmata between the sieve element–companion cell complex and neighboring cells (bundle sheath or phloem parenchyma) seems to be correlated with apoplastic loading. The function of the remaining plasmodesmata is not known. The fact that they are present indicates that they must have a function, and an important one, because the cost

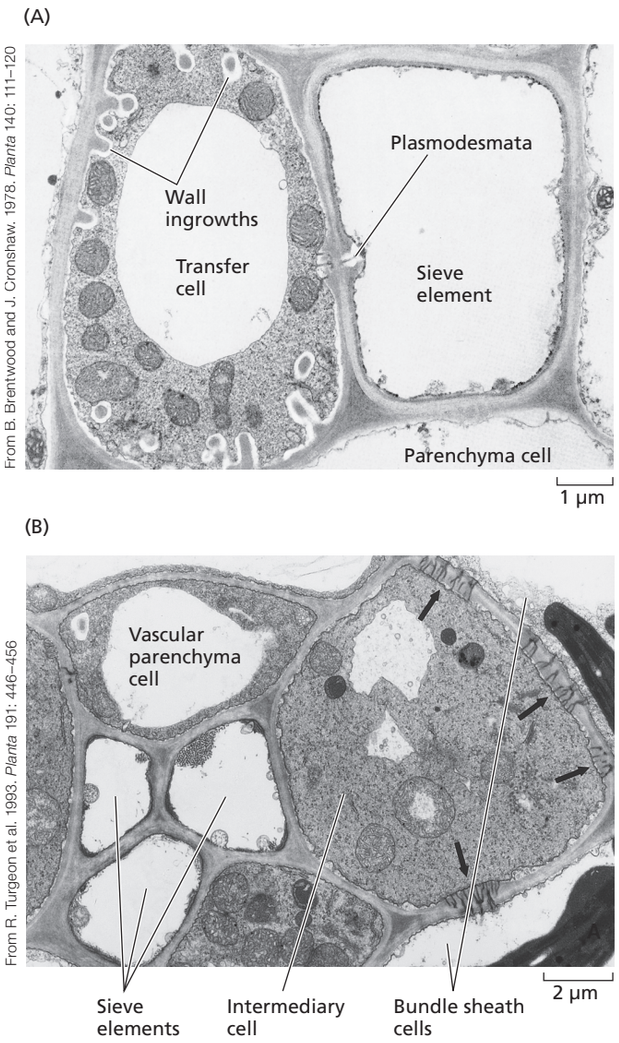


Figure 12.13 **Electron micrographs of specialized companion cells in minor veins of mature leaves.** **(A)** A sieve element adjacent to a transfer-type companion cell with numerous wall ingrowths in pea (*Pisum sativum*). **(B)** A typical intermediary-type companion cell in the minor vein phloem of heartleaf mask flower (*Alonsoa warscewiczii*) with numerous fields of plasmodesmata (arrows) connecting it to neighboring bundle sheath cells. These plasmodesmata are branched on both sides, but the branches are longer and narrower on the intermediary cell side.

of having them is high: They are the avenues by which viruses spread systemically in a plant.

Phloem loading is symplasmic in some species

Apoplastic phloem loading is prevalent in species that transport only sucrose and have few plasmodesmata leading into the minor vein phloem. However, many other species have numerous plasmodesmata at the interface between the sieve element–companion cell complex and the surrounding cells (see Figure 12.13B). The operation of a symplasmic pathway requiring the presence of open plasmodesmata is implied in these species, since phloem isolation seems to be essential for apoplastic loading.

The oligomer-trapping model explains symplasmic loading in plants with intermediary-type companion cells

A symplasmic pathway has become evident in species that transport the tri- and tetrasaccharides raffinose and stachyose, respectively, in addition to the disaccharide sucrose, in the phloem; that have intermediary cells in the minor veins; and that have abundant plasmodesmata leading into the minor veins. Some examples of such species are common coleus (*Coleus blumei*), pumpkin and squash (*Cucurbita pepo*), and melon (*Cucumis melo*). Intermediary cells are companion cells that have numerous plasmodesmata connecting them to bundle sheath cells (see Figure 12.13B). Although the presence of many plasmodesmatal connections to surrounding cells is the most characteristic feature of intermediary cells, they are also distinctive in having numerous small vacuoles, as well as poorly developed thylakoids and a lack of starch grains in the chloroplasts.

Two major questions emerge concerning symplasmic loading:

1. How are raffinose and stachyose selected for transport in the phloem? In apoplastic phloem loading, the involvement of symporters provides a clear mechanism for selectivity because symporters are specific for certain sugar molecules. Symplasmic loading, by contrast, depends on the diffusion of sugars from the mesophyll to the sieve elements via the plasmodesmata. How can diffusion through plasmodesmata during symplasmic loading be selective for certain sugars?
2. Data from several species showing symplasmic loading indicate that sieve elements and companion cells have a higher osmolyte content (more negative osmotic potential) than the mesophyll. How can diffusion-dependent symplasmic loading account for the observed selectivity for transported molecules and the accumulation of sugars against a concentration gradient?

The **oligomer-trapping**[1] **model** (**Figure 12.14**) addresses these questions. This model states that the sucrose synthesized in the mesophyll diffuses from the bundle sheath cells into the intermediary cells through the abundant plasmodesmata that connect the two cell

[1] This textbook uses *oligomer trapping* rather than the originally used term *polymer trapping* because the latter is a misnomer: The involved sugars (up to verbascose) are oligosaccharides, not polysaccharides.

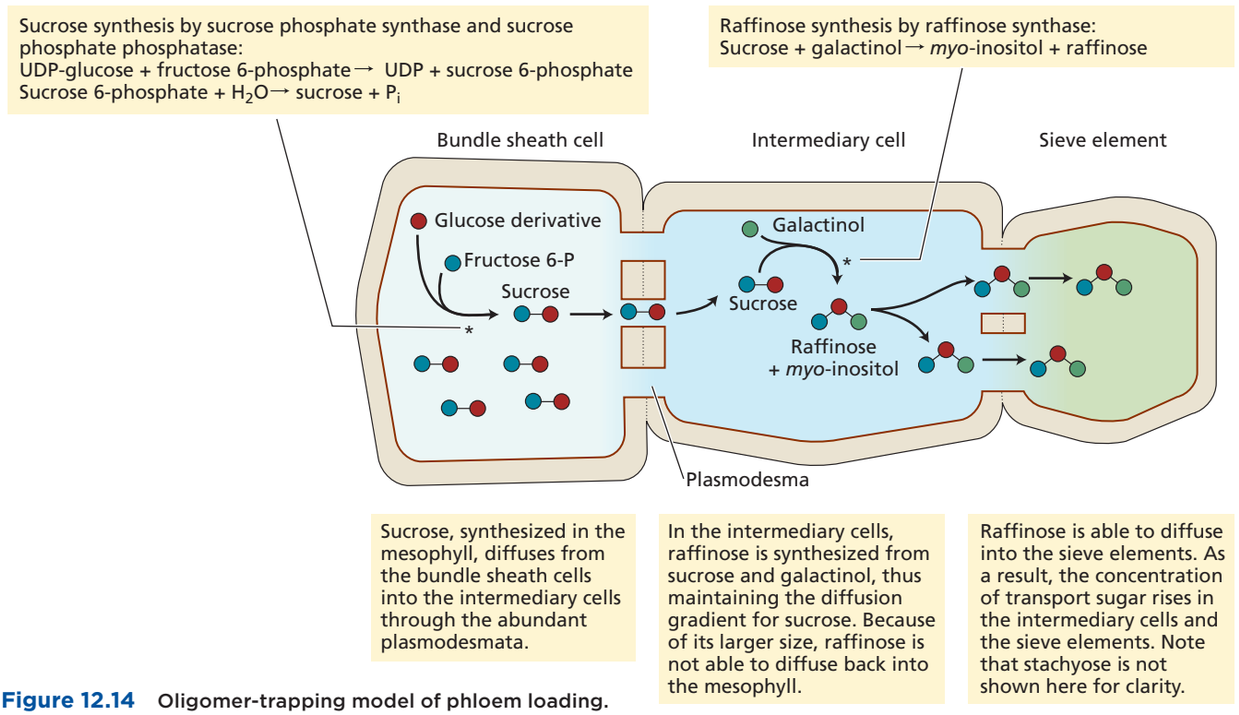


Figure 12.14 **Oligomer-trapping model of phloem loading.** For simplicity, the tetrasaccharide stachyose is omitted. (After A. J. E. van Bel. 1992. *Acta Bot. Neerl.* 41: 121–141.)

types. In the intermediary cells, raffinose and stachyose (oligomers made of three and four hexose sugars, respectively) are synthesized from the transported sucrose and from galactinol (a metabolite of galactose). Because of their relatively large size, raffinose and stachyose cannot diffuse back into the bundle sheath cells, but they can move on into the sieve element. Sugar concentrations in the sieve elements of these plants can reach concentrations equivalent to those in plants that load apoplastically. Sucrose can continue to diffuse into the intermediary cells, because its synthesis in the mesophyll and its use in the intermediary cells maintain the concentration gradient (see Figure 12.14). Like apoplastic loading, oligomer trapping also requires metabolic energy in the companion cells—not for membrane transport, but for the synthesis of tri- and tetrasaccharides.

The oligomer-trapping model makes three predictions:

1. Sucrose should be more concentrated in the mesophyll than in the intermediary cells.
2. The enzymes for raffinose and stachyose synthesis should be preferentially located in the intermediary cells.
3. The plasmodesmata linking the bundle sheath cells and the intermediary cells should exclude molecules larger than sucrose.

Several studies verify the predictions and support the oligomer-trapping model of symplasmic loading in some species. However, recent modeling results suggest that the diffusion of oligosaccharides, such as raffinose and stachyose, back into the mesophyll is prevented not only by the physical size of plasmodesmata, but also by the onset of opposing mass flow from the bundle sheath. (See **WEB TOPIC 12.3** for a discussion of these topics.)

Phloem loading is passive in several tree species

Passive symplasmic phloem loading is widespread among tree species. While the data supporting this mechanism are relatively recent, passive symplasmic loading was actually part of Münch's original conception of pressure flow (see Section 12.4).

It has become apparent that several tree species possess abundant plasmodesmata between the sieve element–companion cell complex and surrounding cells, but do not have intermediary-type companion cells and do not transport raffinose and stachyose. Willow (*Salix babylonica*) and apple (*Malus domestica*) trees are among the species that fall into this category. These plants have no concentrating step in the pathway from the mesophyll into the sieve element–companion cell complex. Since a concentration gradient from the mesophyll into the phloem drives diffusion along the pre-phloem

pathway, the absolute concentrations of sugars in the source leaves of these species must be high to maintain the required high turgor pressures in the sieve elements. Although there is wide variation and considerable overlap among groups of plants with different loading mechanisms, source leaf sugar concentrations are generally higher in the tree species that load passively. Feasibility of this mode of phloem loading was recently demonstrated with a tree-on-a-chip model.

Gymnosperms seem to load photosynthates passively, and have a high frequency of functional plasmodesmata in each interface between mesophyll and sieve elements. Gymnosperm needles have xerophytic adaptations that involve more cells in the pre-phloem pathway. However, water relations in this complex pathway indicate that mass flow starts inside the bundle sheath and drives photosynthates via several parenchyma and Strasburger cells into the sieve elements.

The type of phloem loading is correlated with several significant characteristics

As already discussed, the operation of apoplastic and symplasmic phloem-loading pathways is correlated with several defining characteristics, listed in **Table 12.2**.

- Species that have apoplastic phloem loading as their dominant loading strategy translocate sucrose almost exclusively and have either intermediary-type companion cells or transfer cells in the minor veins. These species usually possess few connections between the sieve element–companion cell complex and the surrounding cells. Active carriers in the sieve element–companion cell complex concentrate sucrose in the phloem cells and generate the driving force for long-distance transport.
- Species that use symplasmic phloem loading with oligomer trapping translocate oligosaccharides such as raffinose in addition to sucrose. They have intermediary-type companion cells in the minor veins, with abundant connections between the sieve element–companion cell complex and the surrounding cells. Oligomer trapping probably concentrates transport sugars in the phloem cells and generates the driving force for long-distance transport.
- Species that have passive symplasmic phloem loading translocate sucrose and sugar alcohols and have ordinary companion cells in the minor veins. These species also possess abundant connections all the way from mesophyll to the sieve element–companion cell complex. Species with passive symplasmic loading are characterized by high overall sugar concentration in the source leaves, which maintains a concentration gradient between the mesophyll and the sieve element–companion cell complex. The high sugar concentrations in the pre-phloem pathway might already—before the sieve-element–companion cell complex—generate the driving force for long-distance transport. Many of the species with passive symplasmic loading are trees.

Table 12.2 Patterns in apoplastic and symplasmic loading

Feature	Apoplastic loading	Symplasmic oligomer trapping	Passive symplasmic loading
Transport sugar	Sucrose	Raffinose and stachyose in addition to sucrose	Sucrose and sugar alcohols
Characteristic companion cells	Ordinary companion cells or transfer cells	Intermediary cells	Ordinary companion cells
Number and conductivity of plasmodesmata connecting the SE–CC complex to surrounding cells	Low	High	High
Dependence on active carriers in SE–CC complex	Transporter driven	Independent of transporters	Independent of transporters
Overall concentration of transport sugars in source leaves	Low	Low	High
Cell type in which driving force for long-distance transport is generated	Sieve element–companion cell complex	Intermediary cells	Mesophyll
Growth habit	Mainly herbaceous	Herbs and woody species	Mainly trees

Sources: Y. V. Gamalei. 1985. *Fiziologiya Rasenii* (Moscow) 32: 886–875; A. J. E. van Bel et al. 1992. *Acta Bot. Neerl.* 41: 121–141; E. A. Rennie and R. Turgeon. 2009. *Proc. Natl. Acad. Sci. USA* 106: 14163–14167

Note: Plants using all three mechanisms of phloem loading may also transport sugar alcohols. In addition, some species may load both apoplastically and symplasmically, since different types of companion cells can be found within the veins of a single species. SE–CC complex, sieve element–companion cell complex.

Our discussion thus far has considered apoplastic loading, symplasmic loading with oligomer trapping, and passive loading separately. However, increasing evidence shows that many, if not all, plants are capable of more than one loading mechanism. For example, both structural and physiological data indicate that some oligomer-trapping plants are also capable of apoplastic loading (see **WEB TOPIC 12.3**).

Plasmodesmatal frequencies suggest that the passive loading strategy is ancestral in the angiosperms, while apoplastic loading and oligomer trapping evolved later. However, the ability to load by multiple mechanisms may have been present even in the earliest angiosperms. Multiple loading mechanisms may allow plants to adapt quickly to abiotic stresses, such as low temperatures. Certainly, the evolution of different loading types and the environmental pressures related to their evolution will continue to be important research areas in the future, as loading pathways are clarified in more species.

12.4 Long-Distance Transport: A Pressure-Driven Mechanism

This section discusses the rates of movement in intact phloem and the mechanism of phloem transport. Once the main transport sugar is loaded into the minor vein sieve elements, it follows the continuous low-resistance pathway of the transport phloem to the organs consuming it (see Figure 12.1). The transport phloem can span long distances: In giant redwoods (*Sequoiadendrum giganteum*) it reaches more than 100 m from the needles at the top of the tree to its finest roots. This long-distance pathway is continuous and comprises first the primary phloem of leaves, petioles, and primary stems; then the secondary phloem in the inner bark of stem and root; and finally the primary phloem of the fine root system. Independent of whether they originated in procambium or cambium, all sieve elements have the same ultrastructure (see Section 12.2), though cell width and sieve pore size are generally larger in the secondary phloem.

An important, but often neglected, aspect of the transport phloem is the unloading and reloading of photosynthates along the pathway. Retrieval of photosynthates might just be to compensate for the leakage of photosynthates caused by the steep sugar gradient between sieve elements and the apoplast. In trees, however, unloading and reloading regularly take place between the transport phloem and the surrounding tissue, such as for storage of proteins and starch in the ray parenchyma. Remobilization of these stored compounds supplies the axial sinks during spring. Companion cells (and Strasburger cells in gymnosperms) in the transport phloem are instrumental for these processes.

Mass transfer is much faster than diffusion

The rate of movement of materials in the sieve elements can be expressed in two ways: as **velocity**, the linear distance traveled per unit time, or as **mass transfer rate**, the quantity of material passing through a given cross section of phloem or sieve elements per unit time. Mass transfer rates based on the cross-sectional area of the sieve elements are preferred because the sieve elements are the conducting cells of the phloem. Values for mass transfer rate range from 1 to 15 g h^{-1} cm^{-2} of sieve elements (in SI units, 2.8–41.7 μg s^{-1} mm^{-2}).

Velocities and mass transfer rates can both be measured with radioactive tracers. (Methods of measuring mass transfer rates are described in **WEB TOPIC 12.4**.) In the simplest type of experiment for measuring velocity, ^{11}C- or ^{14}C-labeled CO_2 is applied for a brief period of time to a source leaf (pulse labeling), and the arrival of label at a sink tissue or at a particular point along the pathway is monitored with an appropriate detector.

In general, velocities measured by a variety of techniques average about 1.0 m h^{-1} (0.28 mm s^{-1}) and range from 0.3 to 1.5 m h^{-1} (in SI units, 0.08–0.42 mm s^{-1}). Transport values exceed the rate of diffusion by many orders of magnitude. Any proposed mechanism of phloem translocation must account for these high velocities.

The pressure-flow model is a passive mechanism for phloem transport

The most widely accepted mechanism of phloem translocation in angiosperms is the pressure-flow model. The pressure-flow model explains phloem translocation as a flow of solution (mass flow or bulk flow) driven by an osmotically generated pressure gradient between source and sink. In the remainder of this section we describe the pressure-flow model, predictions arising from mass flow, and data (both supporting and challenging), and then briefly explore whether the model can possibly be applied to gymnosperms.

The pressure is osmotically generated

Diffusion is far too slow to account for the velocities of solute movement observed in the phloem. Translocation velocities average 1 m h^{-1}; the rate of diffusion would be 1 m per 62 years for sucrose at 25°C! (See Chapter 5 for a discussion of diffusion velocities and the distances over which diffusion is an effective transport mechanism.)

The **pressure-flow model**, first proposed by Ernst Münch in 1930, states that a flow of solution in the sieve elements is driven by an osmotically generated *pressure gradient* between source and sink. Phloem loading at the source and phloem unloading at the sink establish the pressure gradient.

As we discussed earlier (see Section 12.3), three different mechanisms are recognized to generate high

concentrations of sugars in the sieve elements of the source: active membrane transport, oligomer trapping, and passive symplasmic transport. Recall from Chapter 5 (see Equation 5.5) that $\Psi = \Psi_s + \Psi_p$; that is, $\Psi_p = \Psi - \Psi_s$. In source tissues, an accumulation of sugars in the sieve elements generates a low (negative) solute potential (Ψ_s) and causes a steep drop in the water potential (Ψ). In response to the water potential gradient, water enters the sieve elements and causes the turgor pressure (Ψ_p) to increase. Water enters the sieve elements through water channels, called **aquaporins**.

At the receiving end of the translocation pathway, **phloem unloading** leads to a lower sugar concentration in the sieve elements, generating a higher (less negative) solute potential in the sieve elements of sink tissues. As the water potential of the phloem rises above that of the xylem, water tends to leave the phloem in response to the water potential gradient, causing a decrease in turgor pressure in the sieve elements of the sink. **Figure 12.15** illustrates the pressure-flow hypothesis; the figure specifically shows the case of apoplastic phloem loading.

The phloem sap moves by mass flow down the pressure gradient. Mass flow (more precisely *advective* flow) means that solutes move at the same rate as the water molecules and is possible where no membranes are crossed during intercellular transport. Since this is the case between sieve tube elements, mass flow can occur from a source organ with a lower water potential to a sink organ with a higher water potential, or vice versa, depending on the identities of the source and sink organs. In fact, Figure 12.15 illustrates an example in which the flow is against the water potential gradient. Such water movement does not violate the laws of thermodynamics, because mass flow is driven by a pressure gradient, as opposed to osmosis, which is driven by a water potential gradient.

According to the pressure-flow model, movement in the translocation pathway is driven by transport of solutes and water *into* source sieve elements and *out of* sink sieve elements. The passive, pressure-driven, long-distance translocation in the sieve tubes ultimately depends on the mechanisms involved in phloem loading and unloading. These mechanisms are responsible for setting up the pressure gradient.

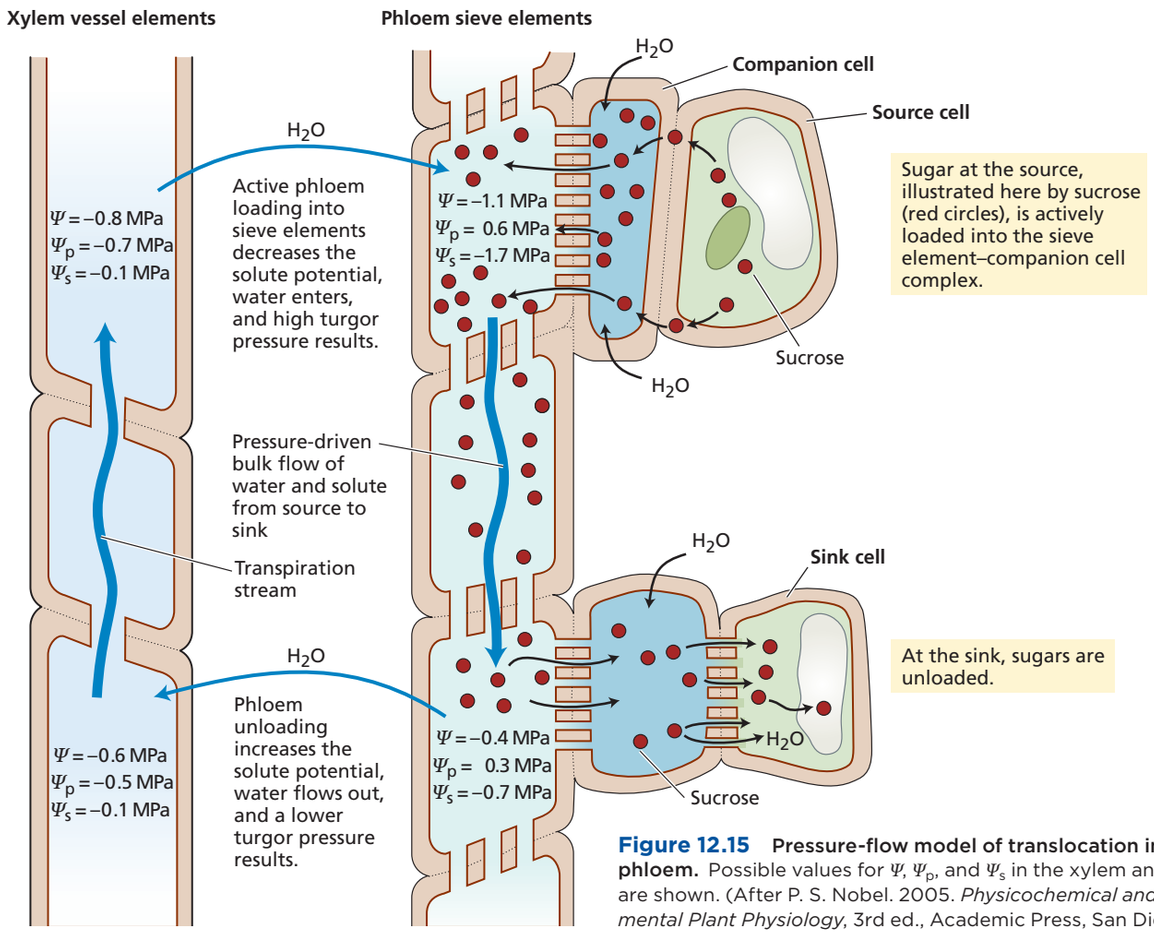


Figure 12.15 Pressure-flow model of translocation in the phloem. Possible values for Ψ, Ψ_p, and Ψ_s in the xylem and phloem are shown. (After P. S. Nobel. 2005. *Physicochemical and Environmental Plant Physiology*, 3rd ed., Academic Press, San Diego, CA.)

Some predictions of pressure flow have been confirmed, while others require further experimentation

Some important predictions emerge from the model of phloem translocation we have just described:

- No true bidirectional transport (i.e., simultaneous transport in both directions) in a single sieve tube can occur. A mass flow of solution precludes such bidirectional movement because a solution can flow in only one direction in a pipe at any one time. Furthermore, water and solutes must move at the same velocity in a flowing solution.
- No great expenditures of energy are required to drive translocation in the tissues along the path. Therefore, treatments that restrict the supply of ATP in the path, such as low temperature, anoxia, and metabolic inhibitors, should not stop translocation. However, the sieve tube lumen and the sieve plate pores must be largely unobstructed. If P-protein or other materials block the pores, the resistance to flow of the sieve element sap might be too great.
- The pressure-flow hypothesis predicts the presence of a positive pressure gradient, with turgor pressure higher in sieve elements of sources than in those of sinks.
- The pressure difference must be large enough to overcome the resistance of the pathway and to maintain flow at the observed velocities. Thus, pressure gradients should be larger in long transport pathways, for example, in trees, than in short transport pathways, as in herbaceous plants.

The available evidence testing the first two predictions is treated in **WEB TOPIC 12.5**. Next we focus on the last two predictions.

Functional sieve plate pores appear to be open channels

Ultrastructural studies of sieve elements are challenging because of the high internal pressure in these cells. When the phloem is excised or killed slowly with chemical fixatives, the turgor pressure in the sieve elements is released. The contents of the cells surge toward the point of pressure release and, in the case of sieve tube elements, accumulate on the sieve plates. This accumulation is probably the reason that many earlier electron micrographs show sieve plates that are obstructed, particularly with P-protein or organelles.

Newer, rapid freezing and fixation techniques provide reliable pictures of undisturbed sieve elements and are confirmed by live microscopy. When young Arabidopsis plants are rapidly frozen by plunging them into slush nitrogen, then freeze-substituted and fixed, sieve plate pores are often unobstructed in the tissue (**Figure 12.16A**). The sieve plate pores of living, translocating

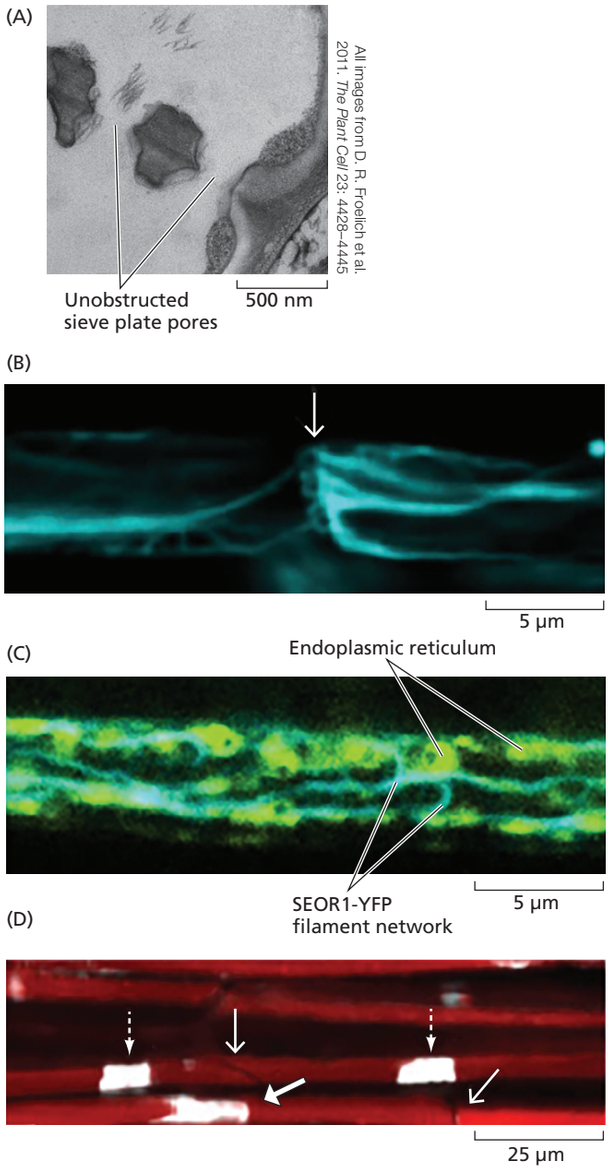


Figure 12.16 Sieve plate pores and sieve tubes in Arabidopsis. **(A)** In plunge-frozen and freeze-substituted tissues, sieve plate pores are often unobstructed and do not contain any detectable callose. **(B)** Living root sieve tubes observed with confocal microscopy show a sieve element occlusion related protein (SEOR1) fused to yellow fluorescent protein (YFP) in cyan. SEOR1–YFP filaments cover or traverse a sieve plate (arrow), outlining the sieve plate pores. **(C)** The endoplasmic reticulum (green) is surrounded by a fine SEOR1–YFP filament meshwork (cyan). **(D)** Masses or agglomerates of SEOR1–YFP protein sometimes fill part of or the entire sieve tube lumen in confocal images (bold arrow and dotted arrows, respectively) but do not necessarily cover sieve plates (thin solid arrows). The sieve tubes in images B–D were living and functional, as seen by the red-colored phloem transport marker carboxy fluorescein diacetate in D. Fluorescence from YFP is false colored as cyan in B and C, and as white in D.

sieve elements of many eudicots have also been observed to be mostly open. Live microscopy, as well as careful preparation for electron microscopy, has observed the sieve element organelles (mitochondria, plastids, and ER) typically at the sieve element periphery. They seem to be anchored to each other or to the sieve element plasma membrane by minute protein "clamps." The open pores and prevention of organelles surging toward sieve plates that are seen in many species (see also Figures 12.6 and 12.7) are consistent with mass flow.

What about the distribution of P-protein in the sieve tube lumen? Electron micrographs of sieve tube members prepared by rapid freezing and fixation have often shown P-protein along the periphery of the sieve elements or as a fine meshwork in the lumen of the cell. Furthermore, the sieve plate pores often contain P-protein in similar positions, lining the pore or in a loose network (see Figures 12.6C and 12.7C).

When a sieve element occlusion related protein (SEOR1 in Arabidopsis) was fused to yellow fluorescent protein (YFP) and observed with confocal microscopy, however, a somewhat different picture emerged. While a meshwork of protein filaments was often shown passing through sieve plates or extending throughout the lumen (**Figure 12.16B and C**), masses or agglomerates of protein were observed to fill large portions of the sieve tube lumen at or close to the sieve plate. The structure of these masses was highly variable, but multiple large masses sometimes filled the entire lumen of the sieve tube (**Figure 12.16D**). These structures were observed in sieve elements of intact, living, translocating sieve elements. The researchers concluded that mass flow is still possible in Arabidopsis; however, knowledge of the porosity of the protein masses, as well as the degree of interaction of the protein with surrounding water molecules, will be needed to fully assess the impact of SEOR1 in Arabidopsis.

Are the pressure gradients in the sieve elements sufficient to drive phloem transport in trees?

Mass flow or bulk flow is the combined movement of all the molecules in a solution, driven by a pressure gradient. What are the pressure values in sieve elements, and how can they be determined? Does a pressure gradient exist between sources and sinks, and if so, is the gradient modest or substantial? Do large plants, such as trees, have proportionally higher pressures in the phloem than small herbaceous species?

Turgor pressure in sieve elements can either be calculated from the water potential and solute potential ($\Psi_p = \Psi - \Psi_s$) or measured directly. A well-established technique uses phloem-sucking aphids. Aphids are small insects that feed by inserting their mouthparts, consisting of four tubular stylets, into a single sieve element of a leaf or stem. Sap can be collected from aphid stylets cut from the body of the insect, usually with a laser, after the aphid has been anesthetized with CO_2. After stylectomy, micromanometers or pressure transducers are sealed over exuding aphid stylets (see **WEB TOPIC 12.6**). The data obtained are accurate because aphids pierce only a single sieve element, and the plasma membrane apparently seals well around the aphid stylet. Pressures measured using the aphid stylet technique range from approximately 0.7 to 1.5 MPa in both herbaceous plants and small trees. These values fit well with direct measurements of the turgor pressures in functional sieve tubes of morning glory (*Ipomoea nil*); in a 7-m stem of this vine, turgor pressure averaged 1.1 MPa.

This study of *Ipomoea* assessed every factor that is necessary to test the feasibility of pressure flow through passive microtubes (= sieve tubes) as described by the Poiseuille equation (see Chapter 6):

$$Velocity = \frac{k \cdot \Delta \Psi p}{\eta \cdot \Delta x} \qquad (12.1)$$

where k is the conductivity of the tube (m^2), $\Delta\Psi_p$ is the pressure differential (Pa), η is the sap viscosity (Pa s), and Δx is the length of the tube (m).

The specific conductivity of sieve tubes was derived from the geometry of sieve elements and dimensions of sieve pores along the transport phloem. The study concluded that a pressure of 0.21 MPa is sufficient to drive transport through 1 m of *Ipomoea* primary phloem. The phloem was able to adjust to increased transport distances: Phloem pressure increased to 2.3 MPa in the petioles of remaining leaves when the basal 10-m stems were defoliated. In these pruned plants, an increase in phloem pressure was accompanied by a fivefold increase in sieve tube conductivity and a doubling of the phloem area, which allowed the plant to compensate for the loss of leaves along the pathway.

This study confirmed earlier studies, deriving turgor pressures from phloem sap concentrations and calculating that the detected pressure gradients are sufficient to drive mass flow. In trees, however, systematic studies of turgor gradients in sieve tubes are lacking. The data are critical to any evaluation of the pressure-flow hypothesis.

One observation is certain, however, and that is that turgor pressures in trees are not proportionally higher than those in herbaceous plants. One study compared calculated turgor pressures (the technique often used in trees) and pressures measured using aphid stylets in small willow saplings. The two techniques yielded comparable values, averaging 0.6 MPa for the calculated pressures and 0.8 MPa for the measured pressures. Calculated pressures were as high as 2.0 MPa in large white ash trees. These values are not substantially different from those measured in herbaceous plants, as previously noted. (Herbaceous plants and trees do often differ in their phloem-loading strategies, in a way that is consistent

with the relatively low pressures in trees; see *Phloem loading is passive in several tree species* in Section 12.3.)

Modified models for translocation by mass flow have been suggested

Even though the pressure-flow model is generally accepted, and its feasibility has been experimentally tested in herbs and vines, doubts have been raised about whether this model is also valid for trees, where the distance between source and sink can reach 50 m or even 100 m. Spread over this distance, the pressure gradient in the phloem system is much smaller than in plants with short transport pathways. Two modifications of the pressure-flow model take this problem into account: the high-pressure manifold model and the relay model.

Key differences in the high-pressure manifold model, compared with the pressure-flow model, include that the pressure in the sieve tube system is high throughout the plant, and that the major resistance to mass flow occurs not in the sieve tubes or sieve plates of the path, but in the plasmodesmata between sieve element–companion cell complexes and sink tissues, particularly vascular parenchyma cells. Since the highest resistance occurs in the plasmodesmata, small pressure gradients would occur between source and sink sieve elements, but the pressure differences between sink sieve elements and phloem parenchyma cells would be large. The resulting system could efficiently and rapidly transmit information on changes in the pressure or concentration of sap over long distances.

The relay model proposes that the phloem consists of functional units joined in series and that solutes are transported actively from one unit to the next, increasing the pressure available to drive transport over long distances such as those that exist in trees. While both models account for some of the observations on sieve tube turgor pressures noted earlier, the relay model also requires energy expenditure along the path, at least in trees. It is not known if the energy requirement along the path is small in trees, as it appears to be in herbaceous plants. Since deciduous trees have axial storage sites that are filled in autumn and remobilized in spring, the transport phloem of trees is not merely a passive translocation pathway, but is active in photosynthate exchange during these periods.

What can we conclude from the experiments and data described here? Some observations are consistent with the operation of mass flow and specifically the pressure-flow mechanism in angiosperm phloem: the movement of solutes and water at the same velocity; the lack of an energy requirement in the pathway of herbaceous plants; the presence of open sieve plate pores; and the failure to detect bidirectional transport. The significance of other observations to pressure flow is more problematic; in particular, the similar pressures in the sieve elements of herbaceous plants and trees are puzzling and show that we don't yet have the whole picture.

Does translocation in gymnosperms involve a different mechanism?

Although mass flow explains translocation in angiosperms, it may not be sufficient for gymnosperms. Very little physiological information on gymnosperm phloem is available (but see *Phloem loading is passive in several tree species* in Section 12.3). On a whole-tree level, the scaling relationship between the structural parameters of phloem transport, leaf length, stem length, and sieve element radius has been derived to be the same in gymnosperms as in angiosperms, supporting the universality of mass flow also in tree species. Recently, the linear—and relatively simple—phloem in needles from different gymnosperm species has been the subject of modeling. Needles can approach 400 mm in length in members of the pine family. Interestingly, phloem export from the tip regions of long needles is incompatible with simple scaling models that assign a uniform function to all sieve elements in the needle. It appears that the models lack data on the distribution of phloem loading and transport along the needle to allow for mass flow.

While the present models can be improved, the phloem ultrastructure raises doubts about mass flow in these species. As discussed previously, the sieve cells of gymnosperms are similar in many respects to sieve tube elements of angiosperms, but do not appear to be connected by open pores (see Figure 12.8). The pores in gymnosperms are filled with numerous membranes of the smooth endoplasmic reticulum. Since live confocal microscopy confirms location of the endoplasmic reticulum, these electron micrographs cannot be rejected as mere artifacts. Such pores seem to be inconsistent with the requirements of a low-resistance pathway. The impact of these membranes to phloem translocation requires further investigation.

12.5 Materials Translocated in the Phloem

Water is the most abundant substance in the phloem. Dissolved in the water are the translocated solutes, including carbohydrates, amino acids, hormones, some inorganic ions, proteins and RNAs, and some specialized metabolites involved in defense and protection. Carbohydrates are the most significant and concentrated solutes in phloem sap (**Table 12.3**), with sucrose being the sugar most commonly transported in sieve elements. There is always some sucrose in sieve element sap, and it can reach concentrations of 0.3 to 0.9 *M*. Sugars, potassium ions, and amino acids and their amides are the principal molecules contributing to the osmotic potential of the phloem.

Table 12.3 The composition of phloem sap, collected as an exudate from cuts in the phloem

Component	mg mL^{-1} [m*M*]	m*M*		
	Ricinus (Hall & Baker, 1972)	*Ricinus* (Peuke, 2010)	*Lupinus* low-saline soil (Pate, 1989)	*Lupinus* high-saline soil (Pate, 1989)
Sugars	80.0–106.0 [234–309]	433	652	600
Amino acids	5.2 [28]	67.5	41	110
Organic acids	2.0–3.2	8.02[a]	60	56
Protein	1.45–2.20	–	–	–
K^+	2.3–4.4 [59–112]	67.1	66.9	52.6
Na^+	–	6.96	8.1	92.6
Cl^-	0.355–0.675 [10–19]	12	7.9	68
SO_4^{2-}	–	1.29	4.3	5.5
PO_4^{3-}	0.350–0.550 [3.7–5.8]	6.56	10	12.6
NO_3^-	–	0.59	–	–
Mg^{2+}	0.109–0.122 [4.5–5.0]	3.71	3.4	2.7
Ca^{2+}	–	1.21	1.5	0.91

Sources: S. M. Hall and D. A. Baker. 1972. *Planta* 106: 131–140; J. S. Pate. 1989. In *Transport of Photoassimilates*, D. A. Baker and J. A. Milburn (eds.). Longman Scientific & Technical, Harlow, UK. pp. 138–166; A. D. Peuke. 2010. *J. Exp. Bot.* 61: 635–655

[a] Malate only.

Complete identification of solutes that are mobile in the phloem and that have a significant function has been difficult; no one method of sampling phloem sap is free of artifacts or provides a complete picture of mobile solutes. The collection of phloem sap is experimentally challenging because of the high turgor pressure in the sieve elements and the wound reactions described later in this section (and in **WEB TOPIC 12.6**). Because of processes that plug sieve plate pores, only a few species exude phloem sap from wounds that sever sieve elements.

A preferable approach for collecting exuded sap is to use an aphid stylet as a "natural syringe," as we described. The high turgor pressure in the sieve element forces the cell contents through the stylet to the cut end, where they can be collected. However, quantities of collected sap are small, and the method is technically difficult. Nonetheless, this method is thought to yield relatively pure sap from the sieve elements and companion cells and to provide a fairly accurate picture of the composition of phloem sap.

Sugars are translocated in a nonreducing form

Results from many analyses of collected sap indicate that the translocated carbohydrates are nonreducing sugars. Reducing sugars, such as the hexoses glucose and fructose, contain an exposed aldehyde or ketone group (**Figure 12.17A**). In a nonreducing sugar, such as sucrose, the ketone or aldehyde group is reduced to an alcohol or combined with a similar group on another sugar. Translocated sugar alcohols include mannitol and sorbitol (**Figure 12.17B**).

Most researchers believe that the nonreducing sugars are the major compounds translocated in the phloem because they are less reactive than their reducing counterparts. In fact, reducing sugars such as hexoses are quite reactive and may be as much of a threat as reactive oxygen and nitrogen species. Animals can tolerate transporting glucose because it is present in fairly low concentrations in the blood, but hexoses cannot be tolerated in the phloem, in which very high sugar concentrations are maintained.

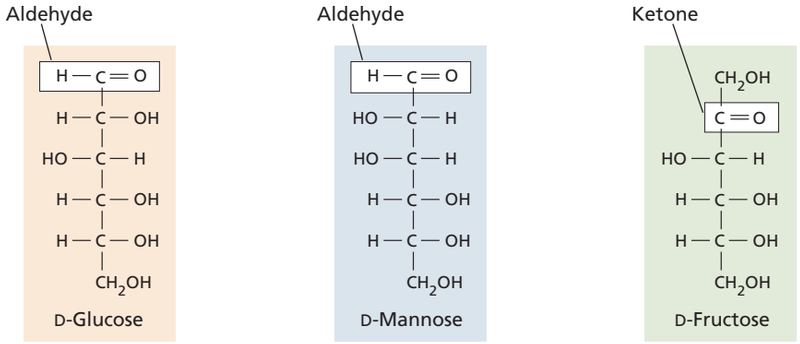
Sucrose is the most commonly translocated sugar; many of the other mobile carbohydrates contain sucrose bound to varying numbers of galactose molecules. Raffinose consists of sucrose and one galactose molecule, stachyose consists of sucrose and two galactose molecules, and verbascose consists of sucrose and three galactose molecules (see Figure 12.17B). Plants translocating raffinose-family sugars typically use oligomer trapping as their loading strategy (see Section 12.3).

Other small organic solutes are translocated in the phloem

Nitrogen is found in the phloem mainly in amino acids—especially glutamate and aspartate—and their respective amides, glutamine and asparagine. Reported concentrations of amino acids and organic acids vary widely, even for the same species, but they are usually low compared with those of carbohydrates (see Table 12.3).

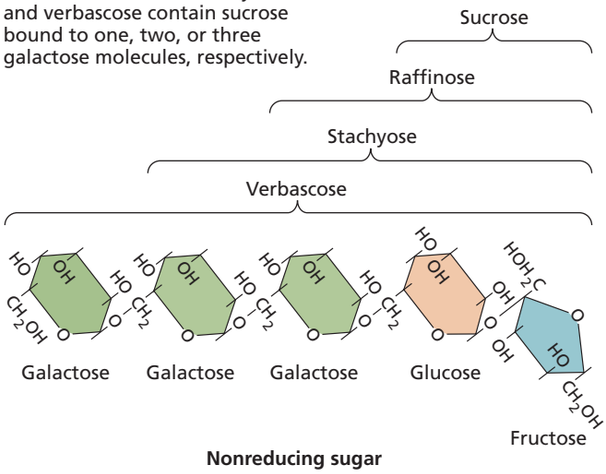
(A) Reducing sugars, which are not generally translocated in the phloem

The reducing groups are aldehyde (glucose and mannose) and ketone (fructose) groups.



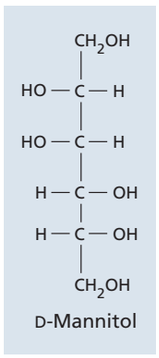
(B) Compounds commonly translocated in the phloem

Sucrose is a disaccharide made up of one glucose and one fructose molecule. Raffinose, stachyose, and verbascose contain sucrose bound to one, two, or three galactose molecules, respectively.



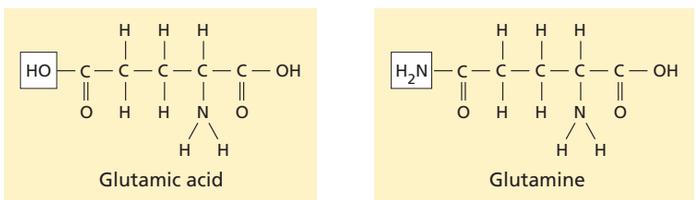
Nonreducing sugar

Mannitol is a sugar alcohol formed by the reduction of the aldehyde grou of mannose.



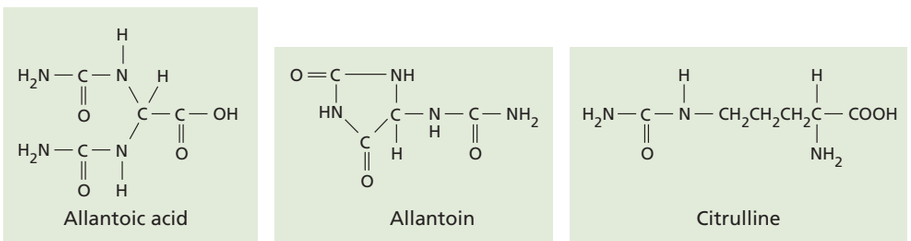
Sugar alcohol

Glutamic acid, an amino acid, and glutamine, its amide, are important nitrogenous compounds in the phloem, in addition to aspartate and asparagine.



Amino acids

Species with nitrogen-fixing nodules also utilize ureides as transport forms of nitrogen.



Ureides

Figure 12.17 **Structures of (A) compounds not normally translocated in the phloem and (B) compounds commonly translocated in the phloem.**

Like sugars, the phloem-mobile amino acids are actively loaded into the phloem, as confirmed by the localization of amino acid transporters in the plasma membrane of companion cells.

Some inorganic ions are also translocated in the phloem, including K^+, NO_3^-, Mg^{2+}, PO_4^{3-}, and Cl^-. By contrast, Ca^{2+} and SO_4^{2-} are relatively immobile in the phloem. Potassium ions appear to serve as a mobile energy source in the phloem by assisting the proton pump in sucrose uptake and retrieval. Posttranscriptional modification of the phloem-localized K^+ channel AKT2 can tap this energy source.

Small cytosolic solutes in companion cells might easily move into the neighboring sieve element, which is well connected by pore–plasmodesma contacts (see Figure 12.6B and C). From here, they are swept along with the phloem sap. It is not settled, however, whether the pore–plasmodesma contacts have a mechanism to retain valuable solutes in the companion cells. Size does not seem to be critical; passage of up to 70-kDa macromolecules was reported using GFP-tagged proteins as tracers. By contrast, the passage of ions and small organic molecules is challenging to test. Simple occurrence in the phloem is not sufficient evidence since collection of phloem sap might lead to displacement of the solute in question. In what may have been a response to sampling, nucleotide phosphates have been found in the phloem sap. It is difficult to imagine that companion cells bleed these energy-rich compounds constitutively.

Hormones do not seem to be retained in the companion cell. Almost all the endogenous plant hormones, including auxin, gibberellins, cytokinins, and abscisic acid, have been found in sieve elements. The long-distance transport of hormones, especially auxin, is thought to occur at least partly in the sieve elements. Hormones might indeed enter the sieve tubes via the pore–plasmodesma contacts, as has been shown for auxin.

Phloem-mobile macromolecules often originate in companion cells

Macromolecules found in the phloem sap include structural P-proteins such as PP1 and PP2 (involved in the sealing of wounded sieve elements in cucurbit species), as well as several water-soluble proteins and RNAs. The function of many of the proteins commonly found in phloem sap is related to stress and defense reactions (see the table in **WEB TOPIC 12.7**). The possible roles of RNAs and proteins as signal molecules will be discussed further in Section 12.8.

The presence of macromolecules in the sap does not necessarily prove that they move with the phloem stream. The gold standard to test phloem mobility is grafting. After grafting, it takes 4 to 7 days for the phloem (and xylem) of the partners to connect in the graft interface. Phloem mobility can only be tested if the macromolecules of the graft partners are sufficiently different to be discriminated from homologous ones in the graft partners.

By this method, evidence has been obtained for the mobility of several companion cell–synthesized macromolecules, including the flower-inducing protein FLOWERING LOCUS T and a large number of different mRNA molecules (see Section 12.8). Recently it was shown that the pore–plasmodesma contacts are indeed able to control the passage of RNAs into sieve elements and thus their appearance in the graft partner. Phloem-mobile messenger RNA sequences seem to have a transfer RNA–like stem-loop structure that mediates transport through pore–plasmodesma contacts. It remains a major challenge to study how these contacts sort organic molecules and hold some in the companion cells and select others for long-distance transport.

Damaged sieve elements are sealed off

As detailed earlier in this section, sieve element sap is rich in sugars and other organic molecules. These molecules represent an energy investment for the plant, and their loss must be prevented when sieve elements are damaged. Short-term sealing mechanisms involve sap proteins (P-proteins), while the principal long-term mechanism for preventing sap loss entails closing sieve plate pores with callose, a glucose polymer.

When a sieve tube is cut or punctured, the release of pressure causes the contents of the sieve elements to surge toward the cut end, from which the plant could lose much sugar-rich phloem sap if there were no sealing mechanism. When surging occurs, however, P-protein is trapped on the sieve plate pores, helping seal the sieve element and prevent further loss of sap (**Figure 12.18A**). Direct support for the sealing function of P-protein has been found in both tobacco and Arabidopsis, in which mutants lacking P-protein lose significantly more transport sugar by sap exudation after wounding than do wild-type plants. No visible phenotypic differences were observed between the mutant and wild-type plants.

Another mechanism for blocking wounded sieve tubes with proteins occurs in plants in the legume family (Fabaceae). These plants contain large crystalloid P-proteins that do not disperse during development. However, following damage or osmotic shock, the P-proteins rapidly disperse and block the sieve tube. The process is reversible and controlled by calcium ions. These P-proteins, known as **forisomes**, occur only in certain legumes and are encoded by members of the sieve element occlusion (SEO) gene family.

Homologous members of the SEO gene family encode conventional P-proteins in other species. These are called SEOR (sieve element occlusion related) genes. The term *P-protein* thus includes similar molecules that are involved in blocking wounded sieve

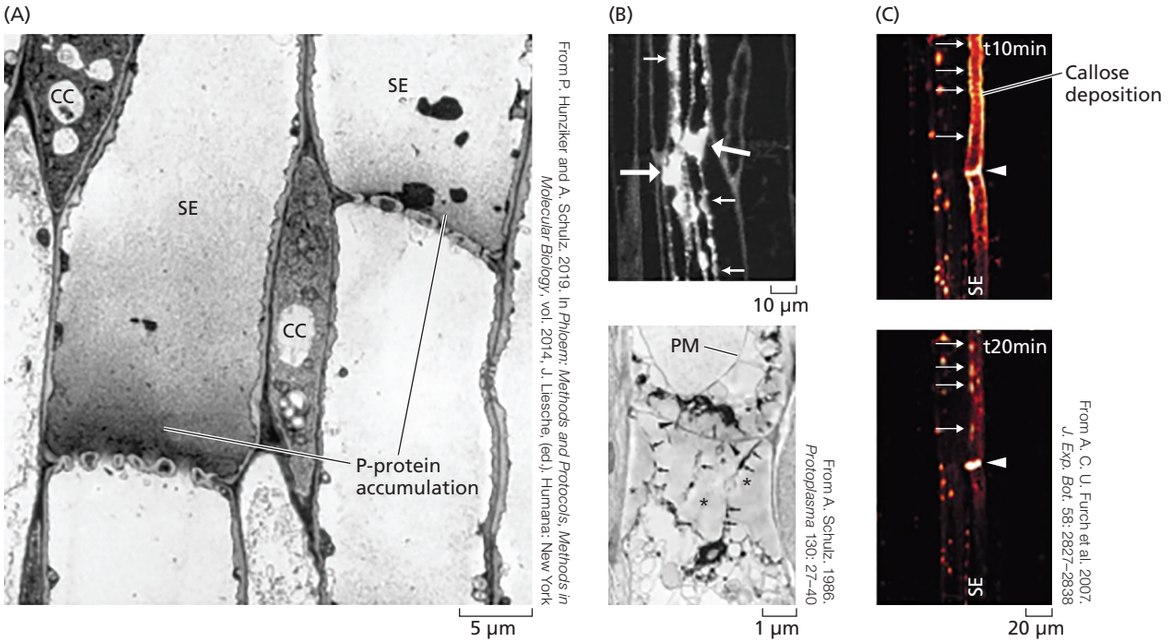


Figure 12.18 Sealing of sieve elements by P-protein and callose. **(A)** P-protein filaments surge toward a phloem cut (about 0.1 mm below this image) and plug the sieve plates of squash (*Cucurbita pepo*). **(B)** Callose covers sieve plates and lateral walls of pea (*Pisum satium*) root phloem 48 h after severing the stele, as seen by bright fluorescence (thick and thin arrows in top image, respectively) and transmission electron microscopy (bottom image). Cytoplasmic compounds (arrows) that initially plug the sieve pores (arrowheads) are subsequently enclosed by callose (asterisks in bottom image). **(C)** Callose deposition (yellow) in leaf phloem is induced by heating the leaf tip 30 mm away at sieve plates (arrowhead) and at lateral sieve pores (arrows). The callose is degraded over time. Top image, 10 min after heating. Bottom image, 20 min after heating. CC, companion cell; PM, plasma membrane; SE, sieve element.

elements in all eudicot angiosperms, as well as special P-proteins, such as forisomes and PP1 and PP2, found in cucurbit species.

A longer-term solution to sieve tube damage is the production of **callose** in the sieve pores (**Figure 12.18B**). Callose, a β-1,3-glucan, is synthesized by an enzyme in the plasma membrane (callose synthase) and is deposited between the plasma membrane and the cell wall. Callose is synthesized in functioning sieve elements in response to damage and other stresses, such as mechanical stimulation and high temperatures, or in preparation for normal developmental events, such as dormancy. The deposition of **wound callose** in the sieve pores efficiently seals off damaged sieve elements from surrounding intact tissue, with complete occlusion occurring about 10 min after injury (**Figure 12.18C**). In all cases, as sieve elements recover from damage or break dormancy, the callose disappears from the sieve pores; its dissolution is mediated by a callose-hydrolyzing enzyme (see Figure 12.18C). While Arabidopsis and tobacco mutants lacking P-protein show no visible phenotypic changes, Arabidopsis mutants lacking a specific callose synthase show lack of wound-induced callose at sieve plates and disturbance of sieve pore development.

Callose deposition is induced and callose synthase genes are up-regulated in rice (*Oryza sativa*) plants attacked by a phloem-feeding insect (brown planthopper); this occurs both in plants resistant to the insect and in susceptible plants. In the susceptible plants, however, feeding by the insects also activates genes for a callose-hydrolyzing enzyme. This unplugs the pores, allows continued feeding, and results in decreased sucrose and starch levels in the leaf sheath being attacked. Sealing off sieve elements that have been penetrated by insect mouthparts can thus play a key role in herbivore resistance.

12.6 Phloem Unloading and Sink-to-Source Transition

Now we have reached the destination of our journey from source to sink. The driving force for phloem translocation is the loading of sugars in source leaves, leading to osmotic pressure in source phloem. The transport phloem forms a continuous pathway to the organs consuming or storing the photosynthates. The plant ensures integrity of this pathway by wound responses that plug the sieve plate pores and seal them with callose. At sink

sites, sugars are released from the phloem, thus reducing its osmotic pressure. Without sugar release, transport would stop since the pressure differential between source and sink would equilibrate (see Figure 12.15). Thus, the rate of phloem transport not only depends on the rate of loading in source leaves, but also on the rate of sugar consumption and removal in the sink organs. Inhibitor studies have shown that import into sink tissue is energy dependent. Accordingly, phloem unloading is coupled to **sink activity**.

Let's take a closer look at **import** into sinks such as developing roots, tubers, and reproductive structures. In many ways the events in sink tissues are simply the reverse of the events in sources. The following steps are involved in the import of sugars into sink cells.

1. *Phloem unloading*. This is the process by which imported sugars leave the sieve elements of sink tissues.
2. *Post-phloem transport*. After unloading, the sugars are transported to cells in the sink by means of a short-distance transport pathway.
3. *Storage and metabolism*. In the final step, sugars are stored or metabolized in sink cells.

In this section we discuss the following questions: Are phloem unloading and short-distance transport symplasmic or apoplastic? Is sucrose hydrolyzed during the process? Do phloem unloading and subsequent steps require energy? Finally, we examine the process by which a young, importing leaf becomes an exporting source leaf.

Phloem unloading and short-distance transport can occur via symplasmic or apoplastic pathways

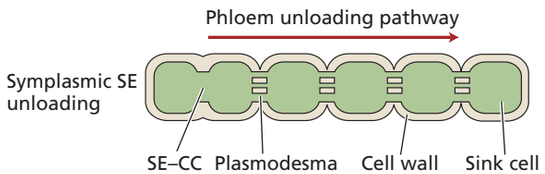
In sink organs, sugars move from the sieve elements to the cells that store or metabolize them. Sinks vary from growing vegetative organs (root tips and young leaves) to storage tissues (roots and stems) to organs of reproduction and dispersal (fruits and seeds). Because sinks vary so greatly in structure and function, there is no single mechanism of phloem unloading and short-distance transport. Differences in import pathways due to differences in sink types are emphasized in this section; however, the pathways often switch during sink development as well.

As in sources, the sugars may move entirely through the symplasm via the plasmodesmata in sinks, or they may enter the apoplast at some point. **Figure 12.19** diagrams the several possible pathways in sinks. Both unloading and the short-distance pathway appear to be completely symplasmic in meristematic and elongating regions of primary root tips and in some young eudicot leaves, such as those of sugar beet and tobacco (see Figure 12.19A). Loading and unloading strategies seem to be independent; plant species that load sugars apoplastically release them at root tips symplasmically.

Symplasmic unloading supplies growing vegetative sinks

Meristematic and elongating regions of plant organs are heterotrophic—that is, they depend on phloem import, as they are not able to meet their energy needs through

(A) Symplasmic phloem unloading and short-distance transport



(B) Apoplastic phloem unloading and short-distance transport

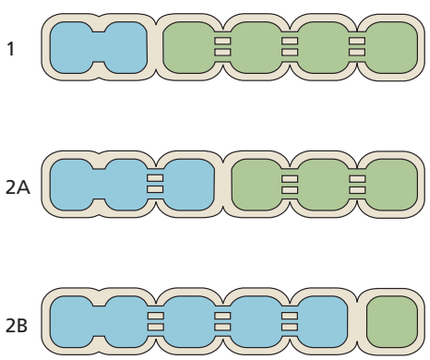


Figure 12.19 Pathways for phloem unloading and short-distance transport. The sieve element–companion cell complex (SE–CC) is considered a single functional unit. The presence of plasmodesmata is assumed to provide functional symplasmic continuity. An absence of plasmodesmata between cells indicates an apoplastic transport step. **(A)** Symplasmic phloem unloading and short-distance transport. All steps are symplasmic. **(B)** Apoplastic phloem unloading and short-distance transport. (After K. J. Oparka and A. J. E. van Bel. 1992. In *Carbon Partitioning within and between Organisms*. C. J. Pollock et al., [eds.]. BIOS Scientific, Oxford.)

Type 1: This short-distance pathway is designated apoplastic because one step, phloem unloading from the sieve element–companion cell complex, occurs in the apoplast. Once the sugars are taken back up into the symplasm of adjoining cells, transport is symplasmic.

Type 2: These pathways also have an apoplastic step. However, phloem unloading from the sieve element–companion cell complex is symplasmic. The apoplastic step occurs later in the pathways. The upper figure (type 2A) shows an apoplastic step close to the sieve element–companion cell complex; the lower figure (type 2B), an apoplastic step that is farther removed.

photosynthesis. This is also the case for young leaves when photosynthesis is not yet meeting their energy needs (discussed later in this section).

Roots grow by cell division and cell elongation at the root tip. Thus, the root tip gets more and more distant from the stem. Development keeps pace with this process by continually extending the phloem system into the root tip, with protophloem sieve elements reaching nearly to the quiescent center. Their maturation involves the disintegration of the nucleus at the same time that they start translocating, as seen with esculin as tracer (**Figure 12.20A and B**). In many eudicots (e.g., garden pea), the protophloem sieve elements are not associated with companion cells. They live only a short time before being replaced by metaphloem sieve elements.

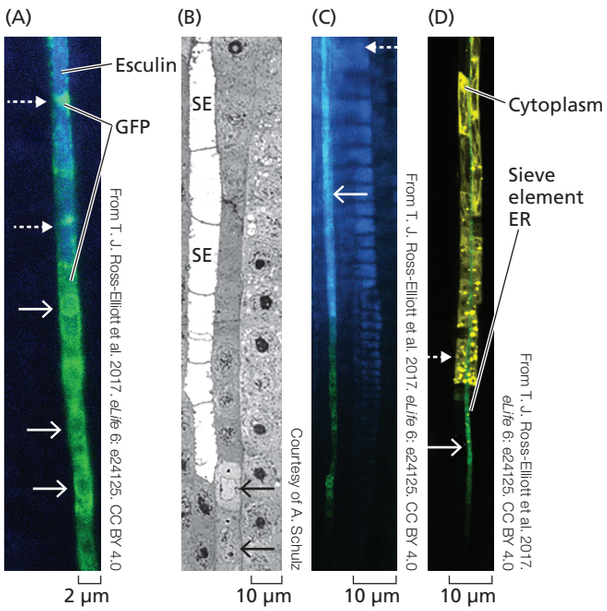


Figure 12.20 Live imaging of translocation in and unloading from root protophloem sieve tubes. **(A)** GFP (green) targeted to the endoplasmic reticulum (ER) of the protophloem sieve tube marks differentiating sieve elements (solid arrows) in Arabidopsis. Esculin (blue) enters from mature sieve elements (dashed arrows) into the differentiating cell file. **(B)** Electron micrograph of the apical end of a protophloem sieve tube from a pea seedling. Six mature sieve elements (SE) and two differentiating ones (arrows) are embedded in dense stele tissue. Mature sieve elements are translucent in electron micrographs. (C and D) Symplasmic unloading from protophloem sieve tubes in roots discriminates small solutes and proteins. **(C)** The small phloem-mobile molecule esculin (blue fluorescence) is unloaded from a protophloem sieve tube (solid arrow) and spreads to neighboring cells (dashed arrow). **(D)** Sieve tube of a transgenic Arabidopsis line expressing SEOR–YFP protein (112 kDa) targeted to the cytoplasm (yellow) and GFP in the sieve element ER (green), both under control of a sieve element–specific promoter. While GFP is restricted to the ER of the protophloem sieve element (solid arrow), cytoplasmic SEOR–YFP escapes into two neighboring cell files consisting of phloem pericycle cells (dashed arrow).

The sieve elements in collection and transport phloem are isolated from all neighbors but their companion cells. However, recent research indicates that protophloem sieve elements in Arabidopsis roots are well connected to phloem pericycle cells. Sugar is unloaded from sieve elements into pericycle cells through specific, funnel-shaped plasmodesmata, and the process involves both diffusion and bulk flow, as suggested by modeling of flow rates per plasmodesma across this interface. Phloem-mobile macromolecules appear to be sorted out at the next post-phloem interface, the pericycle–endodermis interface, through which small solutes and proteins up to 27 kDa, but no larger molecules, pass readily. Differential unloading of small solutes and phloem-mobile macromolecules suggests that the phloem pericycle might have a novel—as yet unknown—function in degrading imported macromolecules that otherwise would pile up in sieve tubes (**Figure 12.20C and D**).

It appears that the phloem–pericycle parenchyma is just as important for selecting which of the phloem-mobile solutes may move on via the endodermis into the root cortex as is the xylem–pericycle parenchyma for xylem loading of selected nutrients (see Chapter 6).

Symplasmic unloading is passive but depends on energy consumption in the sink

In symplasmic unloading, no membranes are crossed during sugar uptake into the sink cells, and transport is passive: Transport sugars move from a high concentration in the sieve elements to a low concentration in the sink cells. Transport sugars are used as substrates for respiration and are metabolized into storage polymers and into compounds needed for growth. Metabolic energy is required in these sink organs mainly for respiration and for biosynthetic reactions. Sucrose metabolism thus results in a low sucrose concentration in the sink cells, extending the source-to-sink sugar gradient in the phloem via the post-phloem pathway right into the sink cells.

Import into seeds, fruits, and storage organs often involves an apoplastic step

While symplasmic unloading predominates in most sink tissues, part of the short-distance pathway is apoplastic in some sink organs at some stages of development—for example, in fruits, seeds, and other storage organs that accumulate high concentrations of sugars. Sugars exit the sieve elements (phloem unloading) via a symplasmic pathway and are transferred from the symplasm to the apoplast at a point removed from the sieve element–companion cell complex (type 2 in Figure 12.19B).

The pathway can switch between symplasmic and apoplastic in these sinks, with an apoplastic step being required when sink sugar concentrations are high. The

apoplastic step can be located at the site of unloading itself (type 1 in Figure 12.19B) or be farther removed from the sieve elements (type 2). The type 2 arrangement, typical of developing seeds, appears to be the most common in apoplastic pathways. Early in ovule development, the phloem end at the chalaza (see Chapter 21) is symplasmically isolated and unloading is apoplastic, but unloading switches to a symplasmic pathway at the time of fertilization (**Figure 12.21**). In developing seeds, an apoplastic step is required farther away from the phloem because there are no symplasmic connections between the maternal tissues and the embryo. This apoplastic step permits membrane control over the substances that enter the embryo, because two membranes must be crossed in the process.

When an apoplastic step occurs in the import pathway, the transport sugar can be partly metabolized in the apoplast, or it can cross the apoplast unchanged (see **WEB TOPIC 12.8**). For example, sucrose can be hydrolyzed into glucose and fructose in the apoplast by invertase, a sucrose-splitting enzyme, and glucose and/or fructose would then enter the sink cells. Sucrose splitting doubles the osmolarity (more negative Ψs) and drags water out of the sucrose-releasing cell. Thus, sucrose-cleaving enzymes play a role in the control of phloem transport by sink tissues.

Apoplastic import is active and requires metabolic energy

In apoplastic import, sugars must cross at least two membranes: the plasma membrane of the cell that is releasing the sugar and the plasma membrane of the sink cell. When sugars are transported into the vacuole of the sink cell, they must also traverse the tonoplast. As discussed earlier, transport across membranes in an apoplastic pathway may be energy dependent. While some evidence indicates that both efflux and uptake of sucrose can be active (see **WEB TOPIC 12.8**), the transporters have yet to be completely characterized.

Since these transporters have been shown to be bidirectional in some studies, some of the same sucrose transporters described earlier for sucrose loading could also be involved in sucrose unloading; the direction of transport would depend on the sucrose gradient, the pH gradient, and the membrane potential. Furthermore, symporters important in phloem loading have been found in some sink tissues—for example, SUT1 in

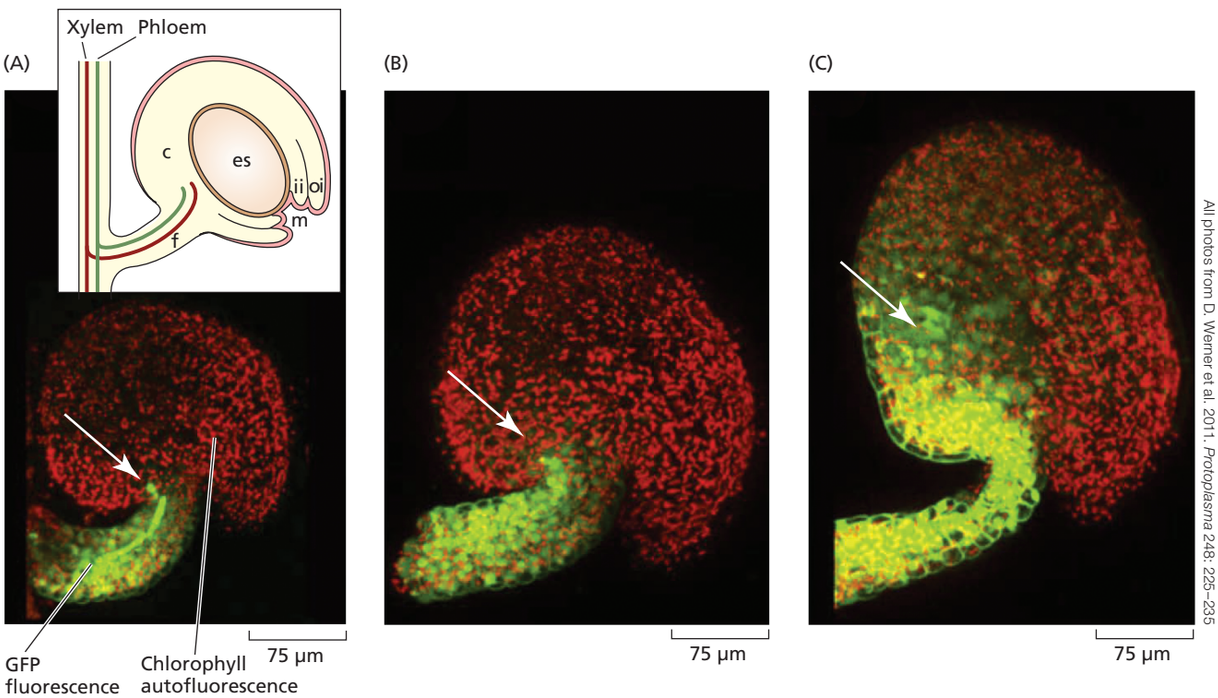
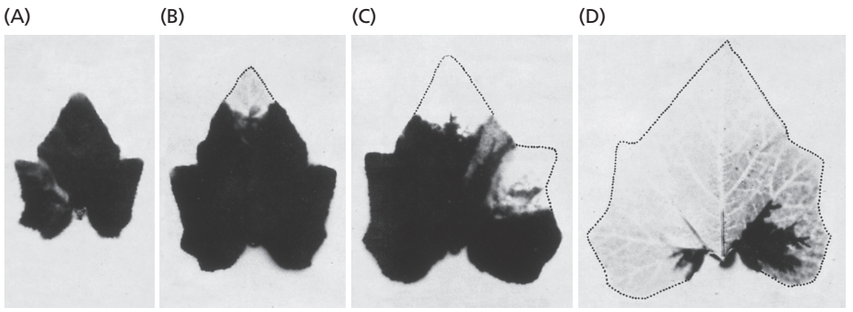


Figure 12.21 The unloading pathway can switch from an apoplastic to a symplasmic pathway. GFP unloading marks the switch from apoplastic to symplasmic unloading into developing seeds. GFP fluorescence is shown in green, chlorophyll autofluorescence in red. **(A)** Developing ovule of a closed flower. The GFP (arrow) is confined to the phloem because there are no functional plasmodesmata connecting the ends of the sieve tubes to surrounding cells (unloading is apoplastic). The inset shows a drawing of an ovule at this stage. Red line = xylem, green line = phloem. c, chalaza; es, embryo sac; f, funiculus; ii, inner integument; m, micropyle; oi, outer integument. **(B)** Mature ovule of a flower that is about to open. GFP is still not being unloaded into the integuments (arrow). **(C)** Ovule of a fertilized flower. The arrow marks GFP that has moved into the integuments via the symplasm. (Inset after D. Werner et al. 2011. *Protoplasma* 248: 225–235.)



All photos from R. Turgeon and J. A. Webb. 1973. *Planta* 113: 179–191

Figure 12.22 Autoradiographs of a leaf of summer squash (*Cucurbita pepo*), showing the transition of the leaf from sink to source status. In each case, the leaf imported ^{14}C from the source leaf on the plant for 2 h. Label is visible as black accumulations. **(A)** The entire leaf is a sink, importing sugar from the source leaf. **(B–D)** The base is still a sink. As the tip of the leaf loses the ability to unload and stops importing sugar (as shown by the loss of black accumulations), it gains the ability to load and to export sugar.

potato tubers. The symporter may function in sucrose retrieval from the apoplast, in import into sink cells, or in both. Monosaccharide transporters must be involved in uptake into sink cells when sucrose is hydrolyzed in the apoplast by cell wall invertases.

The transition of a leaf from sink to source is gradual

Leaves of eudicots such as tomato and bean begin their development as sink organs. A transition from sink to source status occurs later in development, when the leaf is approximately 25% expanded, and is usually complete when the leaf is 40 to 50% expanded. Export from the leaf begins at the tip or apex of the blade and progresses toward the base until the whole leaf becomes a sugar exporter. During the transition period, the tip exports sugar, while the base still imports it from the other source leaves (**Figure 12.22**).

The maturation of leaves is accompanied by functional and anatomic changes, resulting in a reversal of transport direction from importing to exporting. In general, the cessation of import and the initiation of export are independent events. In albino leaves of tobacco, which have no chlorophyll and therefore are incapable of photosynthesis, import stops at the same developmental stage as in green leaves, even though export is not possible. Therefore, a developmental switch besides the initiation of export must occur in developing leaves of tobacco that causes them to cease importing sugars.

Sugars are unloaded and loaded almost entirely via different veins in tobacco (**Figure 12.23**), contributing to the conclusion that import cessation and export initiation are two separate events. The minor veins that are eventually responsible for most of the loading in tobacco and other *Nicotiana* species do not mature until about the time import ceases, as was shown with uptake of

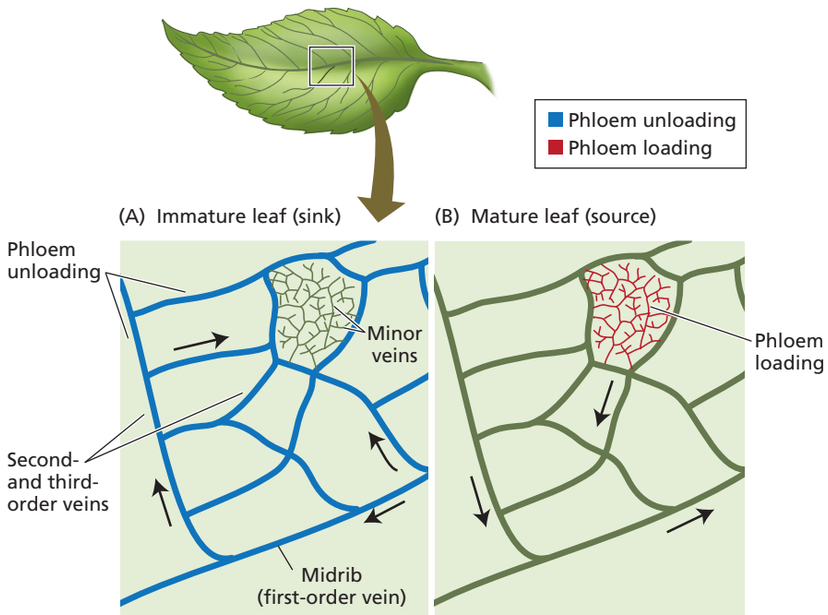
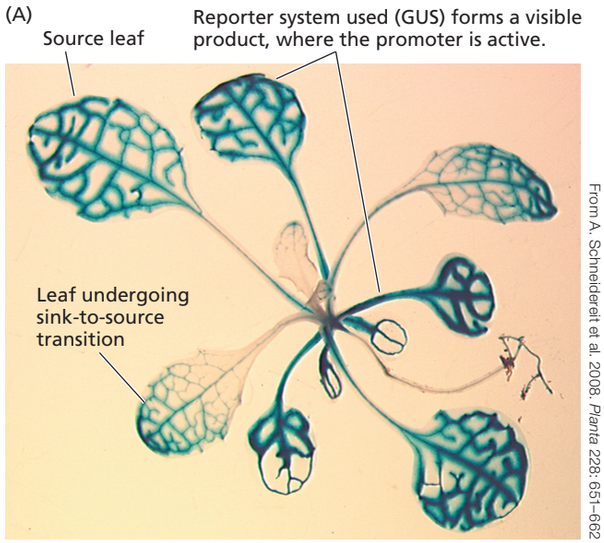


Figure 12.23 Division of labor in the veins of a tobacco leaf. **(A)** When the leaf is immature and still in its sink phase, photosynthate is imported from mature leaves and distributed (arrows) throughout the blade (lamina) via the larger, major veins (thicker lines). The major veins are numbered, with the midrib being the first-order vein. The imported photosynthate unloads from the same major veins into the mesophyll. The smallest, minor veins are found within the areas enclosed by the third-order veins. The minor veins do not function in import and unloading because they are immature. Figure is drawn to scale from an autoradiograph. **(B)** In a mature source leaf, import has ceased and export has begun. Photosynthate loads into the minor veins, while the larger veins serve only in export (arrows); they can no longer unload. Figure is not drawn to scale or in correct proportions, since the lamina grows considerably as the leaf matures. (After R. Turgeon. 2006. *Bioscience* 56: 15–24.)



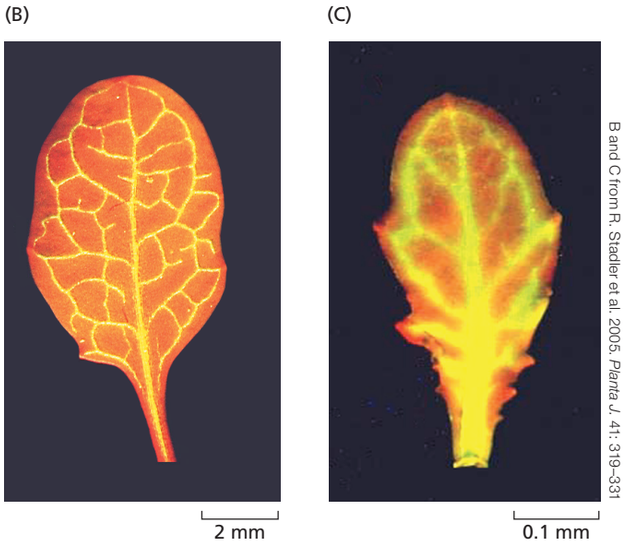


Figure 12.24 Export from source tissue depends on the placement and activity of active sucrose transporters. (A) Arabidopsis rosette transformed with a construct consisting of a reporter gene under control of the *AtSUC2* promoter. SUC2, a sucrose–H^+ symporter, is one of the major sucrose transporters functioning in phloem loading. The reporter system used (GUS) forms a visible product (blue) where the promoter is active. Staining is visible only in the vascular tissue of source leaves and in the tips of leaves undergoing the sink-to-source transition. (B,C) GFP fluorescence in source and sink leaves from transgenic Arabidopsis plants expressing GFP under control of the *SUC2* promoter indicates that GFP moves through plasmodesmata from companion cells into sieve elements of source leaves and from sieve elements into the surrounding mesophyll of sink leaves. (B) GFP is synthesized in companion cells and moves into the sieve elements of the source, as indicated by the bright fluorescence in the veins. (C) Free GFP is imported into sink leaves and moves into the surrounding mesophyll. Because GFP has moved into surrounding tissues, the veins are no longer distinctly delineated, and GFP fluorescence is more diffuse. Note that the scales in (B) and (C) are different; even though the source leaf in (B) appears to be the same size as the sink leaf in (C), the source leaf is actually much larger.

radioactively labeled sucrose. The direction of phloem translocation was also studied by following the expression pattern of the SUC2 sucrose–H^+ symporter (**Figure 12.24**). The ability to accumulate exogenous sucrose in the sieve element–companion cell complex is acquired as the leaves undergo the sink-to-source transition, suggesting that the symporter required for loading has become functional. In developing Arabidopsis leaves, expression of the symporter begins in the tip and proceeds to the base during a sink-to-source transition (see Figure 12.24A). This is the same pattern (basipetal) that is seen in the development of export capacity.

Live microscopy was used to visualize the veins responsible for loading in source leaves, and for unloading in sink leaves. Plants were transformed with the gene for green fluorescent protein (GFP) from jellyfish, under control of the *SUC2* promoter from Arabidopsis. The SUC2 sucrose–H^+ symporter is synthesized within the companion cells, so proteins expressed under the control of its promoter, including GFP, are also synthesized in the companion cells. GFP, which is localized by its fluorescence after excitation with blue light, moves through plasmodesmata from companion cells into sieve elements of source leaves (see Figure 12.24B) and migrates within the phloem to sink tissues. In young leaves, GFP is imported through the large veins, from which it spreads out into the mesophyll (see Figure 12.24C).

The change that stops import during sink-to-source transition must involve blockage of unloading from the large veins at some point in the development of mature leaves. Factors that could account for the cessation of unloading include plasmodesmatal closure and a decrease in plasmodesmatal frequency. Recently it was shown that cessation of phloem unloading from large veins is initiated by activation of the TOR (TARGET OF RAPAMYCIN) regulatory complex. If this metabolic complex is inhibited, GFP spreading into the mesophyll continues beyond the sink-to-source transition.

Export of sugars begins when apoplastic loading is activated and has accumulated sufficient photosynthate in the sieve elements to drive translocation out of the leaf. The following events precede photosynthate export:

- The leaf is synthesizing photosynthate in sufficient quantity that some is available for export. The sucrose-synthesizing genes are being expressed.
- Minor veins responsible for loading have matured. A regulatory element (enhancer) has been identified in the DNA of Arabidopsis that acts as part of a cascade of events leading to minor vein maturation.

The enhancer can activate a reporter gene fused to a companion cell–specific promoter and does so in the same tip-to-base pattern as in the sink-to-source transition.

- The sucrose–H^+ symporter is expressed and in place in the plasma membrane of the sieve element–companion cell complex. Binding sites for transcription factors have been identified in the *SUC2* promoter that mediate this source-specific and companion cell–specific gene expression.

12.7 Photosynthate Distribution: Allocation and Partitioning

The photosynthetic rate determines the total amount of fixed carbon available to the leaf. However, the amount of fixed carbon available for translocation depends on subsequent metabolic events. The regulation of the distribution of fixed carbon into various metabolic pathways is termed **allocation** in this chapter (**Figure 12.25**).

The vascular bundles in a plant form a system of "pipes" that can direct the flow of photosynthates to various sinks: young leaves, stems, roots, fruits, or seeds. However, the vascular system is highly interconnected, forming an open network that allows source leaves to communicate with multiple sinks. Under these conditions, what determines the volume of flow to any given sink? The differential distribution of photosynthates within the plant is termed **partitioning** in this chapter (see Figure 12.25). (The terms *allocation* and *partitioning* are sometimes used interchangeably in current publications.)

After giving an overview of allocation and partitioning, this section examines the coordination of starch and sucrose synthesis. It concludes by discussing how sinks compete, how sink demand might regulate photosynthetic rate in the source leaf, and how sources and sinks communicate with each other.

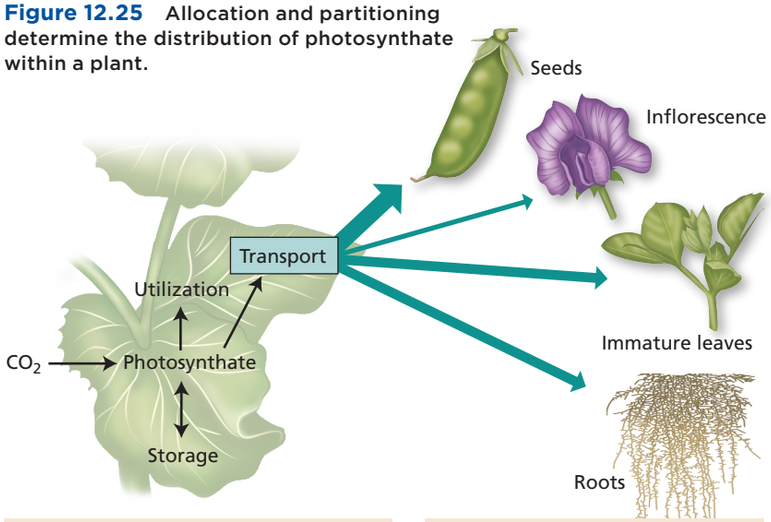
Allocation includes storage, utilization, and transport

The carbon fixed in a source cell can be used for storage, metabolism, and transport:

- *Synthesis of storage compounds*. Starch is synthesized and stored in chloroplasts and, in most species, is the primary storage form that is mobilized for translocation during the night. Plants that store carbon primarily as starch are called *starch storers*.
- *Metabolic utilization*. Fixed carbon can be used within various compartments of the photosynthesizing cell to meet the energy needs of the cell or to provide carbon skeletons for the synthesis of other compounds required by the cell (see Chapter 13).
- *Synthesis of transport compounds*. Fixed carbon can be incorporated into transport sugars for export to various sink tissues. A portion of the transport sugar can also be stored temporarily in the vacuole.

Allocation is also a key process in sink tissues. Once the transport sugars have been unloaded and enter the sink cells, they can remain as such or can be transformed into various other compounds. In storage sinks, fixed carbon can be accumulated as sucrose or hexose in vacuoles or as starch in amyloplasts. In growing sinks, sugars can be used for respiration and for the synthesis of other molecules required for growth.

Figure 12.25 Allocation and partitioning determine the distribution of photosynthate within a plant.



Allocation
The balance among metabolic processes within source cells determines how much photosynthate is available for export to other parts of the plant.

Partitioning
A plant's sinks compete for a share of the available photosynthate. Allocation within sink cells can influence sink strength.

Source leaves regulate allocation

Increases in the rate of photosynthesis in a source leaf generally result in an increase in the rate of translocation from the source. Control points for the allocation of photosynthate include the distribution of triose phosphates to the following processes:

- Regeneration of intermediates in the C_3 photosynthetic carbon reduction cycle (the Calvin–Benson cycle; see Chapter 10)
- Starch synthesis
- Sucrose synthesis, as well as distribution of sucrose between transport and temporary storage pools

Various enzymes operate in the pathways that process the photosynthate. During the day, the rate of starch

synthesis in the chloroplast must be coordinated with sucrose synthesis in the cytosol. Triose phosphates produced in the chloroplast by the Calvin–Benson cycle can be used for either starch or sucrose synthesis or in respiration. Sucrose synthesis in the cytosol diverts triose phosphate away from starch synthesis and storage. The control of these steps is complex and may be different in plants with different loading strategies.

Complexity is exemplified here with species that load sucrose actively from the apoplast. In soybean, when the demand for sucrose by other parts of the plant is high, less carbon is stored as starch in source leaves. The key enzymes involved in the regulation of sucrose synthesis in the cytosol and of starch synthesis in the chloroplast are sucrose phosphate synthase and fructose 1,6-bisphosphatase in the cytosol and ADP-glucose pyrophosphorylase in the chloroplast (see Chapter 10). Further studies will be needed to extend our knowledge to plants using other loading strategies and to the regulation of allocation in those species.

However, there is a limit to the amount of carbon that normally can be diverted from starch synthesis in species that store carbon primarily as starch. Studies of allocation between starch and sucrose under different conditions suggest that a fairly steady rate of translocation throughout the 24-h period is a priority for most plants.

Various sinks partition transport sugars

Sinks compete for the photosynthate being exported by the sources. Such competition determines the partitioning of transport sugars among the various sink tissues of the plant, at least in the short term. The allocation of sugar within a sink (storage or metabolism) affects its ability to compete for available sugars. In this way, the processes of partitioning and allocation interact.

Of course, events in sources and sinks must be synchronized. Partitioning determines the patterns of growth, and growth must be balanced between shoot growth (photosynthetic productivity) and root growth (water and mineral uptake) in such a way that the plant can respond to the challenges of a variable environment. The goal is *not* a constant root-to-shoot ratio but one that secures a supply of carbon and mineral nutrients appropriate to the needs of the plant. So an additional level of control lies in the interaction between areas of supply and demand, as we discuss next.

Sink tissues compete for available translocated photosynthate

Translocation to sink tissues depends on the position of the sink in relation to the source and on the vascular connections between source and sink. Another factor determining the pattern of transport is competition between sinks, for example, between terminal sinks or between terminal sinks and axial sinks along the transport pathway. For example, young leaves might compete with roots for photosynthates in the translocation stream. Competition has been shown by numerous experiments in which removal of a sink tissue from a plant generally results in increased translocation to alternative, and hence competing, sinks. Conversely, increased sink size, for example, increased fruit load, decreases translocation to other sinks, especially the roots. Pruning of grape or fruit trees uses gardeners' traditional knowledge of these processes.

In the reverse type of experiment, the source supply can be altered while the sink tissues are left intact. When the supply of photosynthates from sources to competing sinks is suddenly and drastically reduced by shading of all the source leaves but one, the sink tissues become dependent on a single source. In sugar beet and bean plants, the rates of photosynthesis and export from the single remaining source leaf usually do not change over the short term (approximately 8 h). However, the roots receive less sugar from the single source, while the young leaves receive relatively more. Presumably, the young leaves can deplete the sugar content of the sieve elements more readily and thus increase the pressure gradient and the rate of translocation toward themselves.

Treatments such as making the sink water potential more negative increase the pressure gradient and enhance transport to the sink. Treatment of the root tips of pea (*Pisum sativum*) seedlings with mannitol solutions increased the import of sucrose over the short term by more than 300%, possibly because of a turgor decrease in the sink cells. Longer-term experiments show the same trend. Moderate water stress induced with polyethylene glycol treatment of the roots increased the proportion of photosynthates transported to the roots of apple plants over a period of 15 days, but decreased the proportion transported to the shoot apex. This contrasts with shading treatments just discussed, in which source limitation diverts more sugar to the young leaves.

Sink strength depends on sink size and activity

The ability of a sink to mobilize photosynthate toward itself is often described as **sink strength**. Sink strength depends on two factors—sink size and sink activity—as follows:

$$\text{Sink strength} = \text{sink size} \times \text{sink activity}$$

Sink size is the total biomass of the sink tissue, and **sink activity** is the rate of uptake of photosynthates per unit biomass of sink tissue. Altering either the size or the activity of the sink results in changes in translocation patterns. For example, the ability of a pea pod to import carbon depends on the dry weight of that pod as a proportion of the total number of pods.

Changes in sink activity depend on a balance between processes such as the unloading from the sieve

elements, metabolism in the cell wall, uptake from the apoplast, and photosynthate utilization for either growth or storage.

Experimental treatments to manipulate sink strength, such as cooling the sink tissue, inhibit all activities that require metabolic energy and typically result in a decrease in the velocity of transport toward the sink. More specific are experiments that take advantage of our ability to over- or underexpress enzymes such as those involved in sucrose metabolism. The two major enzymes that split sucrose are invertase and sucrose synthase, both of which can catalyze the first step in sucrose utilization.

The source adjusts over the long term to changes in the source-to-sink ratio

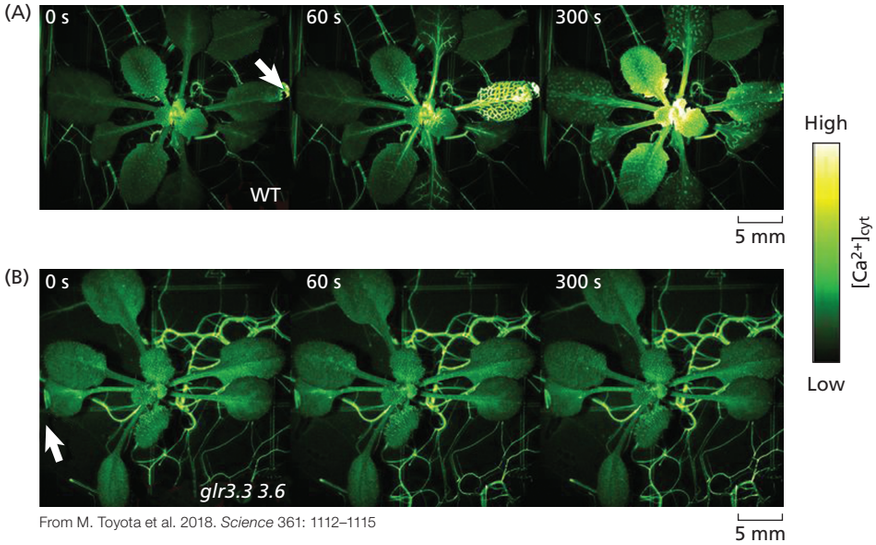
If all but one of the source leaves of a soybean plant are shaded for an extended period (e.g., 8 days), many changes occur in the single remaining source leaf. These changes include a decrease in starch concentration and increases in photosynthetic rate, Rubisco activity, sucrose concentration, transport from the source, and orthophosphate concentration. Thus, the observed short-term changes in the distribution of photosynthate among different sinks are followed, over a longer term, by adjustments in the source leaf's metabolism.

Photosynthetic rate (the net amount of carbon fixed per unit leaf area per unit time) often increases over several days when sink demand increases, and it decreases when sink demand decreases. An accumulation of photosynthate (sucrose or hexoses) in the source leaf can account for the linkage between sink demand and photosynthetic rate in starch-storing plants (see **WEB TOPIC 12.9**). Sugars act as signaling molecules that regulate many metabolic and developmental processes in plants. In general, carbohydrate depletion enhances the expression of genes for photosynthesis, reserve mobilization, and export processes, while abundant carbon resources favor genes for storage and utilization.

Sucrose or hexoses that would accumulate as a result of decreased sink demand are well known to repress photosynthetic genes. Interestingly, the genes for invertase and sucrose synthase, both of which can catalyze the first step in sucrose utilization, and genes for sucrose–H^+ symporters, which play a key role in apoplastic loading, are also among those regulated by carbohydrate supply.

12.8 Transport of Signaling Molecules

Besides its major function in the long-distance transport of photosynthate, the phloem is also a conduit for the transport of signaling molecules from one part of the organism to another. Such long-distance signals coordinate the activities of sources and sinks and regulate plant growth and development (see Chapter 4). As indicated earlier, the signals between sources and sinks might be physical or chemical. Physical signals such as turgor change are transmitted rapidly via the interconnecting system of sieve elements. Sieve tubes can propagate electrical signals like animal neurons do. Depolarization of the negative membrane potential of sieve elements is able to trigger callose deposition and thus plugging of sieve pores (see Section 12.5). Recently it was shown that glutamate receptor–like proteins in the sieve element plasma membrane initiate a calcium ion wave that leads to a systemic wound response, such as after a caterpillar attack (**Figure 12.26**; see Chapter 24). Molecules traditionally considered to be chemical signals, such as proteins and plant hormones,



From M. Toyota et al. 2018. *Science* 361: 1112–1115

Figure 12.26 Glutamate, released from damaged tissue, trigger long-distance Ca^{2+}-based defense signaling in the phloem. (A) Application of a drop of 100 m*M* Glu (arrow) to a wild-type Arabidopsis plant triggers propagation of a Ca^{2+} wave, seen as an increase in Ca^{2+} sensor fluorescence in almost all of the plant's leaves . (B) Glutamate mimics plant response to caterpillars or mechanical wounding anddepends on vascular glutamate receptors, as seen when a drop of 100 m*M* Glu (arrow) is applied to a mutant Arabidopsis plant that does not contain glutamate receptors in the vascular tissue and do not have long-distance signal propagation.

are found in the phloem sap, as are messenger RNAs and noncoding small RNAs. The translocated carbohydrates themselves may also act as signals.

Turgor pressure and chemical signals coordinate source and sink activities

Turgor pressure may play a role in coordinating the activities of sources and sinks. Increase of phloem unloading due to rapid sugar utilization in the sink leads to reduction of turgor pressures in the release phloem to be transmitted to the sources. If sieve element turgor were involved in controlling loading, this signal from the sinks would increase loading. The opposite response would be seen when unloading was slow in the sinks. Loading of sugars from storage along the axial pathway—such as from ray parenchyma in trees—also responds to changes in solute demand. Some data suggest that cell turgor can modify the activity of the proton-pumping ATPase at the plasma membrane and thereby alter sucrose loading rates.

Shoots produce growth regulators such as auxin, which can be rapidly transported to the roots via the phloem, and roots produce cytokinins, which move to the shoots through the xylem. Gibberellins (GA) and abscisic acid (ABA) are also transported throughout the plant in the vascular system. Plant hormones play a role in regulating source–sink relationships. They affect photosynthate partitioning in part by controlling sink growth, leaf senescence, and other developmental processes. Plant defense responses against herbivores and pathogens can also change allocation and partitioning of photosynthates, with plant defense hormones such as jasmonic acid mediating the responses.

Loading of sucrose has been shown to be stimulated by exogenous auxin but inhibited by ABA in some source tissues, whereas exogenous ABA enhances, and auxin inhibits, sucrose uptake by some sink tissues. Hormones might regulate apoplastic loading and unloading by influencing the amount of active transporters in plasma membranes. Other potential sites of hormone regulation of unloading include tonoplast transporters, enzymes for metabolism of incoming sucrose, wall extensibility, and plasmodesmatal permeability in the case of symplasmic unloading, making the target tissue accessible for mobile RNAs and proteins.

As indicated earlier, carbohydrate levels can influence the expression of genes encoding photosynthesis components, as well as genes involved in sucrose hydrolysis. Many genes have been shown to be responsive to sugar depletion and abundance. Thus, not only is sucrose transported in the phloem, but sucrose or its metabolites can also act as signals that modify the activities of sources and sinks. For example, sucrose–H^+ symporter mRNA declines in sugar beet source leaves fed exogenous sucrose through the xylem. The decline in symporter mRNA is accompanied by a loss of symporter activity in plasma membrane vesicles isolated from the leaves. A working model includes the following steps:

1. Decreased sink demand leads to high sucrose levels in the vascular tissue.
2. High sucrose levels lead to down-regulation of the symporter in the source.
3. Decreased loading results in increased sucrose concentrations in the source.

This model is supported by the observation that the down-regulation of the sucrose loading by antisense inhibition of the sucrose–H^+ symporter SUT1 leads to increased sucrose concentrations and starch accumulation, and a lowered photosynthetic rate in source leaves, as compared with the wild type (see **WEB TOPIC 12.9**).

In summary, sugars and other metabolites have been shown to interact with hormonal signals to control and integrate many plant processes. Gene expression in some source–sink systems responds to both sugar and hormonal signals.

Mobile RNAs function as signal molecules in the phloem to regulate growth and development

It has long been known that viruses can move in the phloem, traveling as complexes of proteins and nucleic acids or as intact virus particles. More recently, endogenous RNA molecules and proteins have been found in phloem sap, and at least some of these can function as signal molecules or generate phloem-mobile signals. As viral nucleic acids, the endogenous RNA molecules travel as complexes with specific proteins (ribonucleoproteins [RNPs]) in the phloem sap. Analyses of phloem exudates and of graft transmission suggest that all classes of RNA molecules—siRNA, miRNA, tRNA, rRNA, and mRNA (see Chapter 3)—move with the phloem sap to distant tissues. It appears that most of them are produced in companion cells. After being unloaded in sink tissues, they are able to modify the function of specific cells. For example, it was shown by grafting that silencing spreads in the phloem systemically to young leaves, flowers, and primary roots and follows the same symplasmic unloading pathway as photosynthates do (see Section 12.6). miRNAs are involved in coordinating growth and development such as nutrient starvation response or potato tuberization. rRNA and tRNA fragments in the phloem sap are not part of a functional protein biosynthesis machinery in sieve elements, as previously assumed, but are able to inhibit translation. For example, mRNA for a regulator of gibberellic acid responses (called GAI) was localized to sieve elements and companion cells

of pumpkin (*Cucurbita pepo*) and was found in pumpkin phloem sap. Transgenic tomato plants expressing a mutant version of the regulator gene were dwarf and dark green. The mRNA for the mutant regulator was localized to sieve elements, was able to be transported across graft unions into wild-type scions, and was unloaded into apical tissues. As a result, the mutant phenotype developed new growth on the wild-type scion.

Motifs both in coding sequences and in untranslated regions of the RNA play important roles in the long-distance movement of GAI RNA. Similar results have been obtained for mRNA for the transcription factor BEL5 in potato (*Solanum tuberosum*). *BEL5* transcripts formed in the leaves move in the phloem across graft unions to stolon tips, the site of tuber induction, and the movement is correlated with enhanced tuber production. Preferential accumulation of the mRNA occurs when untranslated regions are present in addition to coding regions.

Mobile proteins also function as signal molecules to regulate growth and development

A classic example of phloem signaling is the FLOWERING LOCUS T (FT) protein, which is a significant component of the floral stimulus that moves from source leaf to apex and that induces flowering at the apex in response to inductive conditions (see Chapter 20). The FT protein has been shown to move from companion cells of source leaves, where it is expressed, into the sieve elements, assisted by an interacting protein that is necessary for passage of the pore–plasmodesma contacts. Long-distance transport of FT protein into the apical tissues is facilitated by yet another protein and takes some 8 h, as has been demonstrated using heat shock–induced FT expression. Unloading from the phloem and transport to the shoot apical meristem, where FT promotes flowering, takes another 4 h. FT mutant analysis indicates that both processes, uploading to and unloading from the phloem, are actively regulated.

During vegetative growth, phloem-mobile transcription factors and peptide hormones were recently shown to integrate plant growth and fine-tune nitrogen acquisition. A light-responsive transcription factor of 18 kDa moves from shoot to root via the phloem to coordinate shoot and root growth with carbon assimilation and nitrogen acquisition. Both nitrogen acquisition and nitrate transport are fine-tuned by three complementary, phloem-mobile peptide hormones, which act downstream of leaf-localized receptor kinases that respond to small xylem-mobile peptides moving from root to shoot.

See **WEB TOPIC 12.7** for further discussion of these topics.

Plasmodesmata function in phloem signaling

Plasmodesmata are involved in nearly every aspect of phloem translocation, from loading to long-distance transport (pores in sieve areas and sieve plates are modified plasmodesmata) to allocation and partitioning. What role might plasmodesmata play in macromolecular signaling in the phloem?

The mechanism of plasmodesmatal transport (called trafficking) can be either passive (nontargeted) or selective and regulated. When a molecule moves passively, its size must be smaller than the **size exclusion limit** (**SEL**) of the plasmodesmata. Phloem plasmodesmata typically have a wider SEL than those in nonvascular tissues. As indicated earlier, GFP (27 kDa) moves passively through plasmodesmata in the phloem. When expressed in the companion cells, it passes the pore–plasmodesma contacts and is swept along with the phloem sap (see Figure 12.24C). By contrast, FT protein (20 kDa) does not enter the phloem stream in the absence of the FT interacting protein. Generally, when a molecule moves in a selective fashion, it must possess a trafficking signal or interact in some other way with the plasmodesmata. The transport of some developmental transcription factors and of viral movement proteins appears to occur by means of a selective mechanism. Viral movement proteins interact directly with plasmodesmata to allow the passage of viral nucleic acids between cells. Once at the plasmodesmata, movement proteins act to increase the SEL of the plasmodesmata to allow the viral genome to move between cells. Endogenous proteins are thought to carry out similar functions for endogenous macromolecules such as FT protein and some P-proteins (see **WEB TOPIC 12.7**). Interaction with components at or within the plasmodesmata, such as chaperones, is also required.

It is fitting to end this chapter with research topics that will continue to engage plant physiologists in the future: regulation of growth and development via the transport of endogenous RNA and protein signals, the nature of the proteins that facilitate the transport of signals through plasmodesmata, and the possibility of targeting signals to specific sinks in contrast to mass flow. Many other potential areas of inquiry have been indicated as well, such as the mechanism of phloem transport in gymnosperms, the nature and role of proteins in the lumen of the sieve elements, and the magnitude of pressure gradients in the sieve elements, especially in trees. As always in science, an answer to one question generates more questions!

From a more applied angle there are many possibilities for applying scientific knowledge about phloem translocation to the improvement of crop yield and resistance to abiotic and biotic stress factors (**Box 12.1**).

Box 12.1 Relevance of Phloem Translocation and Signaling for Climate Change and Biotechnology

Phloem translocation and phloem signaling rapidly respond to abiotic and biotic changes of the environment. These include changes in CO_2 concentration, temperature, and light-induced ROS production, as well as attacks by caterpillars, fungi, and bacteria. The signaling network linking translocation in the phloem with the activity in neighboring tissues is thus of considerable basic agricultural importance. A thorough understanding of the mechanisms regulating photosynthate translocation and phloem signaling should provide the basis for technology aimed at enhancing crop productivity by increasing the accumulation of photosynthate in edible sink tissues, such as cereal grains.

Flower induction is an example of the complexity of phloem signaling. In cells abutting the conducting phloem of mature leaves, the specific flower-inducing protein FLOWERING LOCUS T (FT) is expressed once the day length is appropriate. FT transmission to the apical meristem is regulated by several subsequent checkpoints: It can enter the phloem stream only in the presence of an interacting protein, it can travel only as rapidly as the phloem sap, and its phloem exit has to be accepted by cell contacts in the unloading pathway of the shoot apical meristem. All of these checkpoints are interesting targets for biotechnological and breeding approaches to control flowering, fruit set, and seed filling.

Also, the sugar levels in source and sink organs are involved in coordinating whole-plant physiology: Sucrose or hexoses that would accumulate because of decreased sink demand are well known to repress photosynthetic genes. Among the genes regulated by the carbohydrate supply are those for invertase and sucrose synthase, both of which can catalyze the first step in sucrose utilization, and genes for sucrose–H^+ symporters, which play a key role in apoplastic loading. Regulation of photosynthesis by sink demand suggests that sustained increases in photosynthesis in response to elevated CO_2 in the atmosphere may depend on increasing sink strength. Research should aim at increasing the strength of existing sinks or developing new sinks.

Attaining higher yields of crop plants is one goal of research on photosynthate allocation and partitioning. Whereas grains and fruits are examples of edible yields, total yield includes inedible portions of the shoot. Harvest index, the ratio of economical yield (edible grain) to total aboveground biomass, has increased over the years largely because of the efforts of plant breeders. One goal of modern plant physiology is to further increase yield based on a fundamental understanding of metabolism, development, and in the present context, partitioning.

However, allocation and partitioning in the whole plant must be coordinated such that increased transport to edible tissues does not occur at the expense of other essential processes and structures. Crop yield may also be improved if photosynthates that are normally "lost" by the plant are retained. For example, losses due to nonessential respiration or exudation from roots could be reduced. In the latter case, care must be taken not to disrupt essential processes outside the plant, such as growth of beneficial microbial species in the vicinity of the root that obtain nutrients from the root exudate.

Developmental regulators show feedback mechanisms between the activity of meristems and the arrival of hormones and carbohydrates through the phloem. At the same time, the conducting phloem elements keep pace with organ growth (see **WEB TOPIC 11.9**). If we want to improve crop plants in order to cope with increasing threat levels, such as by drought, flooding, heat, and pests, and to raise productivity, we need to understand and manipulate this regulatory interplay. ■

Summary

Phloem translocation moves the products of photosynthesis from mature leaves to areas of growth and storage. It also transmits chemical signals and redistributes ions and other substances throughout the plant body.

12.1 Patterns of Translocation: Source to Sink

- Phloem does not translocate materials exclusively in either an upward or a downward direction. Sap is translocated from sources to sinks, and the pathways involved are often complex (**Figures 12.1, 12.2**).

12.2 Pathways of Translocation

- Sieve elements of the phloem conduct sugars and other organic materials throughout the plant (**Figures 12.3–12.5**).
- During development, sieve elements retain their plasma membrane but lose many organelles, retaining only modified mitochondria, plastids, and smooth endoplasmic reticulum (**Figures 12.5, 12.6**).
- Sieve elements are interconnected through pores in their cell walls (**Figure 12.7**).

Summary (*continued*)

- Companion cells aid transport of photosynthetic products to the sieve elements. They also supply proteins to the sieve elements (**Figures 12.5, 12.6**).
- In gymnosperms, smooth ER covers the sieve areas and is continuous through the sieve pores and median cavity (**Figure 12.8, Table 12.1**).

12.3 Phloem Loading

- The export of sugars from sources involves allocation of photosynthate to transport sugars, pre-phloem transport, and phloem loading in minor veins (**Figure 12.9**).
- Phloem loading can occur by way of the symplasm or apoplast (**Figure 12.10**).
- Sucrose is actively transported into the sieve element–companion cell complex in the apoplastic pathway (**Figures 12.11, 12.12**).
- The oligomer-trapping model holds that oligomers are synthesized from sucrose in the intermediary cells; the larger oligosaccharides can diffuse only into the sieve elements (**Figures 12.13B, 12.14**).
- Apoplastic and symplasmic phloem-loading pathways have defining characteristics (**Table 12.2**).

12.4 Long-Distance Transport Is Pressure-Driven

- The transport phloem forms a passive, low-resistance pathway but is actively involved in unloading and reloading of sugars to axial sinks.
- Transport velocities in the phloem are high and exceed the rate of diffusion over long distances by many orders of magnitude.
- The pressure-flow model explains phloem translocation as a bulk flow of solution driven by an osmotically generated pressure gradient between source and sink (**Figure 12.15**).
- Phloem loading at the source and phloem unloading at the sink establish the pressure gradient for passive, long-distance bulk flow.
- Pressure gradients in the phloem sieve elements may be modest; pressures in herbaceous plants and trees appear to be similar. Modified models for translocation by mass flow are being developed.

12.5 Materials Translocated in the Phloem

- The composition of sap has been determined; nonreducing sugars are the main transported molecules (**Table 12.3, Figure 12.17**).
- Sap includes proteins, many of which may have functions related to stress and defense reactions.
- P-proteins and callose seal off damaged phloem to limit loss of sap (**Figure 12.18**).

12.6 Phloem Unloading and Sink-to-Source Transition

- The import of sugars into sink cells involves phloem unloading, short-distance transport, and storage or metabolism.
- Phloem unloading and short-distance transport may operate by symplasmic or apoplastic pathways in different sinks (**Figure 12.19**).
- Transport into sink tissues is energy dependent.
- Import cessation and export initiation are separate events, and there is a gradual transition from sink to source (**Figures 12.22, 12.23**).
- The transition from sink to source requires several changes, including the expression and localization of the sucrose–H^+ symporter (**Figure 12.24**).

12.7 Photosynthate Distribution: Allocation and Partitioning

- Allocation in source leaves includes synthesis of storage compounds, metabolic utilization, and synthesis of transport compounds (**Figure 12.25**).
- The regulation of allocation must thus control the distribution of fixed carbon to the Calvin–Benson cycle, starch synthesis, sucrose synthesis, and respiration.
- A variety of chemical and physical signals are involved in partitioning resources among the various sinks.
- In competing for photosynthate, sink strength depends on sink size and sink activity.
- In response to altered conditions, short-term changes alter the distribution of photosynthate among different sinks, while long-term changes take place in source metabolism and alter the amount of photosynthate available for transport.

12.8 Transport of Signaling Molecules

- Plant defense signaling involves glutamate receptor–triggered calcium ion waves, spreading in the phloem (**Figure 12.26**).
- Turgor pressure, cytokinins, gibberellins, and abscisic acid have signaling roles in coordinating source and sink activities.
- Some hormone peptides, transcription factors, and other proteins can move from shoot to root companion cells in the phloem to coordinate carbon and nitrate acquisition with growth.
- Proteins and RNAs transported in the phloem can alter cellular functions.
- Interaction between mobile molecules and pore–plasmodesma contacts may control what passes through plasmodesmata.

Web Material

- **WEB TOPIC 12.1 Sieve Elements as the Transport Cells between Sources and Sinks** Various methods demonstrate that sugar is transported in the sieve elements of the phloem; anatomical and developmental factors affect the basic source-to-sink pattern of transport.
- **WEB TOPIC 12.2 Evolution of the Relationship between Sieve Elements and Neighbor Cells** Comparison of the phloem of vascular plants indicates an increase in intimate contacts and division of functions between sieve elements and their neighboring parenchyma cells.
- **WEB TOPIC 12.3 Experiments on Phloem Loading** Evidence exists for apoplastic loading of sieve elements in some species and for symplasmic loading (oligomer trapping) in others. While active carriers have been identified and characterized for some substances entering the phloem, other substances may enter sieve elements passively.
- **WEB TOPIC 12.4 Monitoring Traffic on the Sugar Freeway: Sugar Transport Rates in the Phloem** A variety of techniques measure mass transfer rate in the phloem, the dry weight moving through a cross-sectional area of sieve elements per unit time.
- **WEB TOPIC 12.5 Evidence for Mass Flow** There is no bidirectional transport in a sieve tube, and no expenditure of energy in the transport pathway.
- **WEB TOPIC 12.6 Sampling Phloem Sap** Exudation from wounds and from severed aphid stylets yields sufficient phloem sap for analysis.
- **WEB TOPIC 12.7 Proteins and RNAs: Signaling Molecules in the Phloem** Some proteins and RNAs are transported between companion cells and sieve elements, travel in sieve elements between sources and sinks, and can modify cellular functions in the sinks. Little evidence exists for movement of proteins outside the companion cells.
- **WEB TOPIC 12.8 Experiments on Phloem Unloading** Apoplastic unloading varies in its energy requirements and in the role of the cell wall invertase.
- **WEB TOPIC 12.9 Possible Mechanisms Linking Sink Demand and Photosynthetic Rate in Starch Storers** Photosynthate accumulation decreases the photosynthetic rate.

For more study aids, go to oup.com/he/taiz7e.

Suggested Reading

Andriunas, F. A., Zhang, H.-M., Xia, X., Patrick, J. W., and Offler, C. E. (2013) Intersection of transfer cells with phloem biology—Broad evolutionary trends, function, and induction. *Front. Plant Sci.* 4: 221.

Comtet, J., Turgeon, R., and Stroock, A. (2017) Phloem loading through plasmodesmata: A biophysical analysis. *Plant Physiol.* 175: 904–915.

Endo, M., Yoshida, M., Sasaki, Y., Negishi, K., Horikawa, K., Daimon, Y., Kurotani, K. I., Notaguchi, M., Abe, M., and Araki, T. (2018) Re-evaluation of florigen transport kinetics with separation of functions by mutations that uncouple flowering initiation and long-distance transport. *Plant Cell Physiol.* 59: 1621–1629.

Jensen, K. H., Berg-Sørensen, K., Bruus, H., Holbrook, N. M., Liesche, J., Schulz, A., Zwieniecki, M. A., and Bohr, T. (2016) Sap flow and sugar transport in plants. *Rev. Mod. Phys.* 88: 1–63.

Kehr, J., and Kragler, F. (2018) Long distance RNA movement. *New Phytol.* 218: 29–40.

Knoblauch, M., Knoblauch, J., Mullendore, D. L., Savage, J. A., Babst, B. A., Beecher, S. D., Dodgen, A. C., Jensen, K. H., and Holbrook, N. M. (2016) Testing the Munch hypothesis of long distance phloem transport in plants. *eLife* 5: e15341.

Liesche, J., and Schulz, A. (2018) Phloem transport in gymnosperms: a question of pressure and resistance. *Curr. Opin. Plant Biol.* 43: 36–42.

Otero, S., and Helariutta, Y. (2017) Companion cells: a diamond in the rough. *J. Exp. Bot.* 68: 71–78.

Patrick, J. W. (2013) Does Don Fisher's high-pressure manifold model account for phloem transport and resource partitioning? *Front. Plant Sci.* 4: 184.

Ross-Elliott, T. J., Jensen, K. H., Haaning, K. S., Wagner, B. M., Knoblauch, J., Howell, A. H., Mullendore, D. L., Monteith, A. G., Paultre, D., Yan, D. W., Otero, S., Bourdon, M., Sager, R., Lee, J. Y., Helariutta, Y., Knoblauch, M., and Oparka, K. J. (2017) Phloem unloading in Arabidopsis roots is convective and regulated by the phloem pole pericycle. *eLife* 6: e15341.

Schulz, A. (2015) Diffusion or bulk flow: how plasmodesmata facilitate pre-phloem transport of assimilates. *J. Plant Res.* 128: 49–61.

Slewinski, T. L., Zhang, C., and Turgeon, R. (2013) Structural and functional heterogeneity in phloem loading and transport. *Front. Plant Sci.* 4: 244.

Thompson, G. A., and van Bel, A. J. E., (eds.). (2013) *Phloem: Molecular Cell Biology, Systemic Communication, Biotic Interactions.* Wiley-Blackwell, Ames, IA.

13 Respiration and Lipid Metabolism



Aleksey Sagitov/Shutterstock

Photosynthesis provides the organic building blocks that plants (and nearly all other organisms) depend on. Respiration, with its associated carbon metabolism, releases the energy stored in carbon compounds for cellular use. At the same time, it generates many carbon precursors for biosynthesis.

We begin this chapter by reviewing respiration in its metabolic context, emphasizing connections between the pathways involved and special features that are peculiar to plants. We also relate this to our understanding of the biochemistry and molecular biology of plant mitochondria and respiratory fluxes in intact plant tissues. Then we describe the pathways of lipid synthesis that lead to the accumulation of fats and oils, which plants use both for energy and carbon storage, and as a principal component of cellular membranes. Finally, we discuss the catabolic pathways involved in the breakdown of lipids and the conversion of their degradation products into sugars that occurs during the germination of fat-storing seeds.

13.1 Overview of Plant Respiration

Aerobic (oxygen-requiring) respiration is common to most eukaryotic organisms, and in its broad outlines the respiratory process in plants is similar to that found in other aerobic eukaryotes. However, some specific aspects of plant respiration distinguish it, especially from its animal counterpart. **Aerobic respiration** is a biological process by which reduced organic compounds are oxidized in a controlled manner. During respiration, energy is released and transiently carried by a compound, **adenosine triphosphate** (**ATP**), which is used by the cell for maintenance and development. Respiration also plays a crucial role in generating organic acids, or their anions, that are used for biosynthesis, nitrogen assimilation, and secretion. The anabolic role of respiration is particularly important in actively growing tissues.

Glucose and fatty acids are usually cited as the substrates for respiration. In plant cells, however, the substrates (reduced carbon) are mainly derived from sources such as the disaccharide sucrose, other sugars, organic acids, triose phosphates from photosynthesis, and to some extent the products from lipid and protein degradation (**Figure 13.1**).

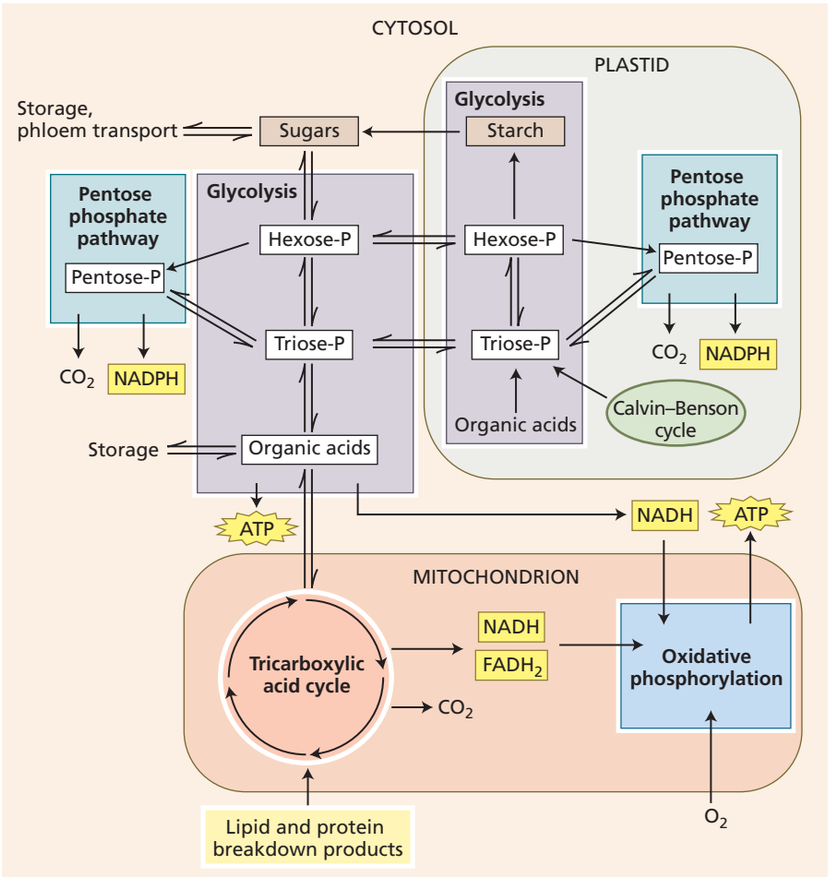


Figure 13.1 **Overview of respiration.** Substrates for respiration are generated by other cellular processes and enter the respiratory pathways. Glycolysis and the oxidative pentose phosphate pathways in the cytosol and plastids convert sugars into organic acids such as pyruvate, via hexose phosphates and triose phosphates, generating NADH or NADPH, and ATP. The organic acids are oxidized in the mitochondrial tricarboxylic acid (TCA) cycle, and the NADH and $FADH_2$ produced provide the energy for ATP synthesis by the electron transport chain and ATP synthase in oxidative phosphorylation. In gluconeogenesis, carbon from lipid breakdown in the glyoxysomes is metabolized in the TCA cycle, and then used to synthesize sugars in the cytosol by reverse glycolysis.

From a chemical standpoint, plant respiration can be expressed as the oxidation of the 12-carbon molecule sucrose and the reduction of 12 molecules of O_2:

$$C_{12}H_{22}O_{11} + 13\ H_2O \rightarrow 12\ CO_2 + 48\ H^+ + 48\ e^- \quad (13.1)$$

$$12\ O_2 + 48\ H^+ + 48\ e^- \rightarrow 24\ H_2O \quad (13.2)$$

giving the following net reaction:

$$C_{12}H_{22}O_{11} + 12\ O_2 \rightarrow 12\ CO_2 + 11\ H_2O \quad (13.3)$$

This reaction is the reversal of the photosynthetic process; it represents a coupled redox reaction in which sucrose is completely oxidized to CO_2 while oxygen serves as the ultimate electron acceptor and is reduced to water in the process. The change in standard **Gibbs free energy** ($\Delta G^{0'}$) for the net reaction is –5760 kJ per mole (342 g) of sucrose oxidized. This large negative value means that the equilibrium point is strongly shifted to the right, and much energy is therefore released by sucrose degradation. The controlled release of this free energy, along with its coupling to the synthesis of ATP, is the primary, although by no means only, role of respiratory metabolism.

To extract energy, the cell oxidizes sucrose in a series of step-by-step reactions, where the steps with the largest energy release are coupled to energy conservation. The reactions can be grouped into four major processes: glycolysis, the oxidative pentose phosphate pathway, the tricarboxylic acid (TCA) cycle, and oxidative phosphorylation. These pathways do not function in isolation, but rather exchange metabolites at several levels. The substrates of respiration enter the respiratory process at different points in the pathways, as summarized in Figure 13.1:

- **Glycolysis** involves a series of reactions catalyzed by enzymes located in the cytosol and the plastids. A sugar—for example, sucrose—is partly oxidized via six-carbon sugar phosphates (hexose phosphates) and three-carbon sugar phosphates (triose phosphates) to produce an organic acid—mainly pyruvate. The process yields a small amount of energy as ATP and reducing power in the form of a reduced nicotinamide nucleotide, NADH.
- In the **oxidative pentose phosphate pathway**, also located in both the cytosol and the plastids, the

six-carbon glucose 6-phosphate is initially oxidized to the five-carbon ribulose 5-phosphate. Carbon is lost as CO_2, and reducing power is conserved in the form of another reduced nicotinamide nucleotide, NADPH. In subsequent near-equilibrium reactions of the pentose phosphate pathway, ribulose 5-phosphate is converted into sugar phosphates containing three to seven carbon atoms. These intermediates can be used in biosynthetic pathways or reenter glycolysis.

- The combined reactions of pyruvate dehydrogenase and the **tricarboxylic acid** (**TCA**) **cycle** completely oxidize pyruvate to 3 CO_2, via stepwise oxidations of organic acids in the innermost compartment of the mitochondrion—the matrix. This process mobilizes the major amount of reducing power (16 NADH + 4 $FADH_2$ per sucrose) and a small amount of energy (ATP) from the breakdown of sucrose.
- In **oxidative phosphorylation**, electrons are transferred along an electron transport chain consisting of a series of protein complexes embedded in the inner of the two mitochondrial membranes. This system transfers electrons from NADH (and related species)—produced by glycolysis, the oxidative pentose phosphate pathway, and the TCA cycle—to oxygen. This electron transfer releases a large amount of free energy, much of which is conserved through the synthesis of ATP from ADP and P_i (inorganic phosphate), catalyzed by the enzyme ATP synthase. Collectively, the redox reactions of the electron transport chain and the synthesis of ATP are called oxidative phosphorylation.

Nicotinamide adenine dinucleotide (NAD^+/NADH) is a soluble organic cofactor (coenzyme) associated with many enzymes that catalyze cellular redox reactions. NAD^+ is the oxidized form that undergoes a reversible two-electron reduction to yield NADH (**Figure 13.2**). The

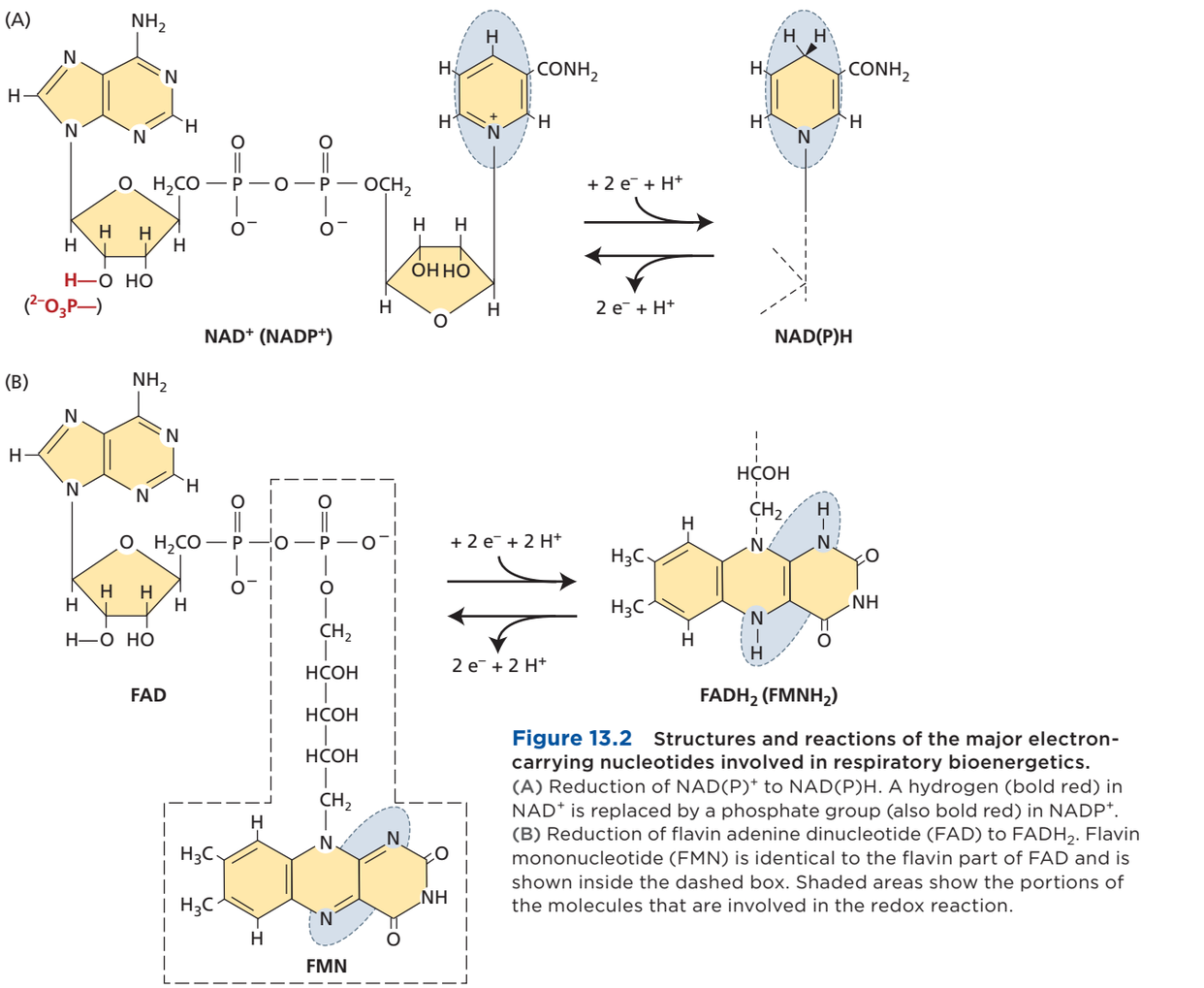


Figure 13.2 **Structures and reactions of the major electron-carrying nucleotides involved in respiratory bioenergetics.** **(A)** Reduction of $NAD(P)^+$ to NAD(P)H. A hydrogen (bold red) in NAD^+ is replaced by a phosphate group (also bold red) in $NADP^+$. **(B)** Reduction of flavin adenine dinucleotide (FAD) to $FADH_2$. Flavin mononucleotide (FMN) is identical to the flavin part of FAD and is shown inside the dashed box. Shaded areas show the portions of the molecules that are involved in the redox reaction.

standard reduction potential for the $NAD^+/NADH$ redox couple is about –320 mV. This tells us that NADH is a relatively strong reductant (i.e., electron donor), which can conserve the free energy carried by the electrons released during the stepwise oxidations of glycolysis and the TCA cycle. A related soluble compound, nicotinamide adenine dinucleotide phosphate ($NADP^+/NADPH$), has a similar function in photosynthesis (see Chapters 9 and 10) and the oxidative pentose phosphate pathway, and also takes part in mitochondrial metabolism. Similarly, the predominantly tightly bound redox couples $FAD/FADH_2$ and $FMN/FMNH_2$ (see Figure 13.2) play important roles in respiration and photosynthesis, as we discuss in Sections 13.4 and 13.5, respectively.

The oxidation of NADH by oxygen via the electron transport chain releases free energy (220 kJ mol^{-1}) that drives the synthesis of approximately 60 ATP per sucrose (as we will see in Section 13.5). We can now formulate a more complete picture of respiration as related to its role in cellular energy metabolism by coupling the following two reactions:

$$C_{12}H_{22}O_{11} + 12\ O_2 \rightarrow 12\ CO_2 + 11\ H_2O \qquad (13.3)$$

$$60\ ADP + 60\ P_i \rightarrow 60\ ATP + 60\ H_2O \qquad (13.4)$$

Recall that not all the carbon that enters the respiratory pathway is fully oxidized to CO_2. Many respiratory carbon intermediates are the starting points for pathways that synthesize amino acids, nucleotides, lipids, and numerous other compounds.

13.2 Glycolysis

In the early steps of glycolysis (from the Greek words *glykos*, "sugar," and *lysis*, "splitting"), carbohydrates are converted into hexose phosphates, each of which is then split into two triose phosphates. In a subsequent energy-conserving phase, each triose phosphate is oxidized and rearranged to yield one molecule of pyruvate, an organic acid. Besides preparing the substrate for oxidation in the TCA cycle, glycolysis yields a small amount of chemical energy in the form of ATP and NADH.

When molecular oxygen is unavailable—for example, in plant roots in flooded soils—glycolysis can be the main source of energy for cells. For this to work, the *fermentative pathways*, which are carried out in the cytosol, must reduce pyruvate to recycle the NADH produced by glycolysis. In this section we describe the basic glycolytic and fermentative pathways, emphasizing features that are specific to plant cells.

Glycolysis metabolizes carbohydrates from several sources

Glycolysis occurs in the cytosol of all organisms (prokaryotes and eukaryotes). The principal reactions associated with the classic glycolytic pathway in plants are almost identical to those in animal cells. However, plant glycolysis has unique regulatory features, alternative enzymatic routes for several cytosolic steps, and a parallel glycolytic pathway in plastids (**Figure 13.3**) (see **WEB ESSAY 13.1**).

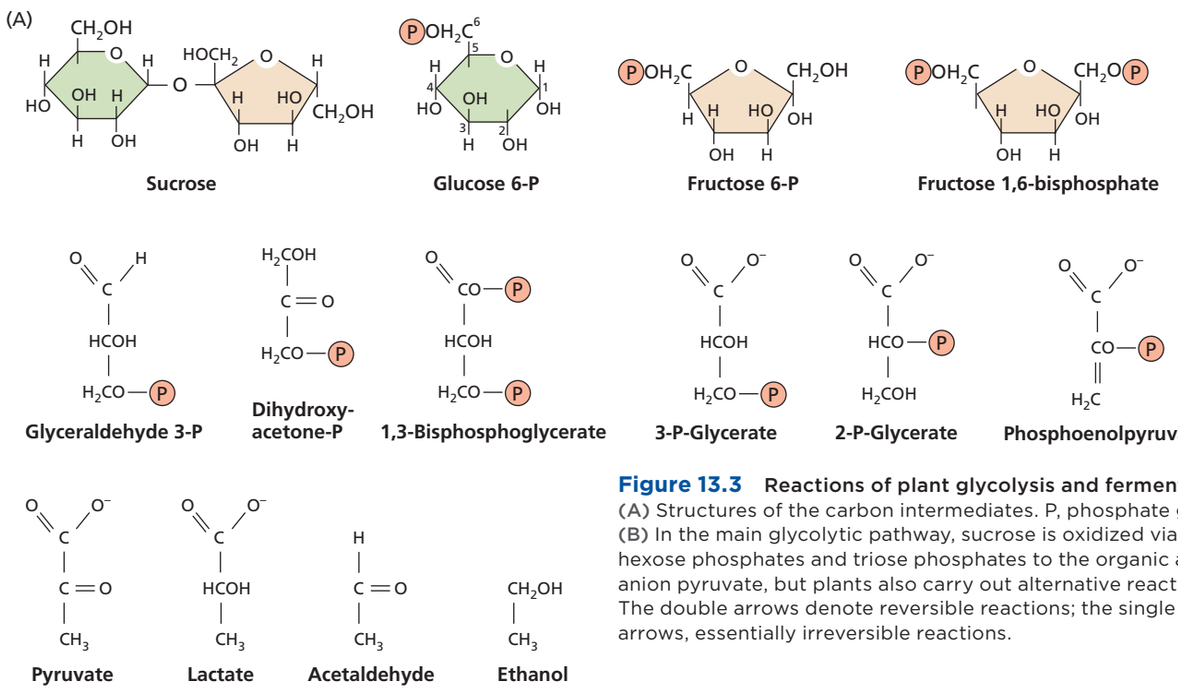
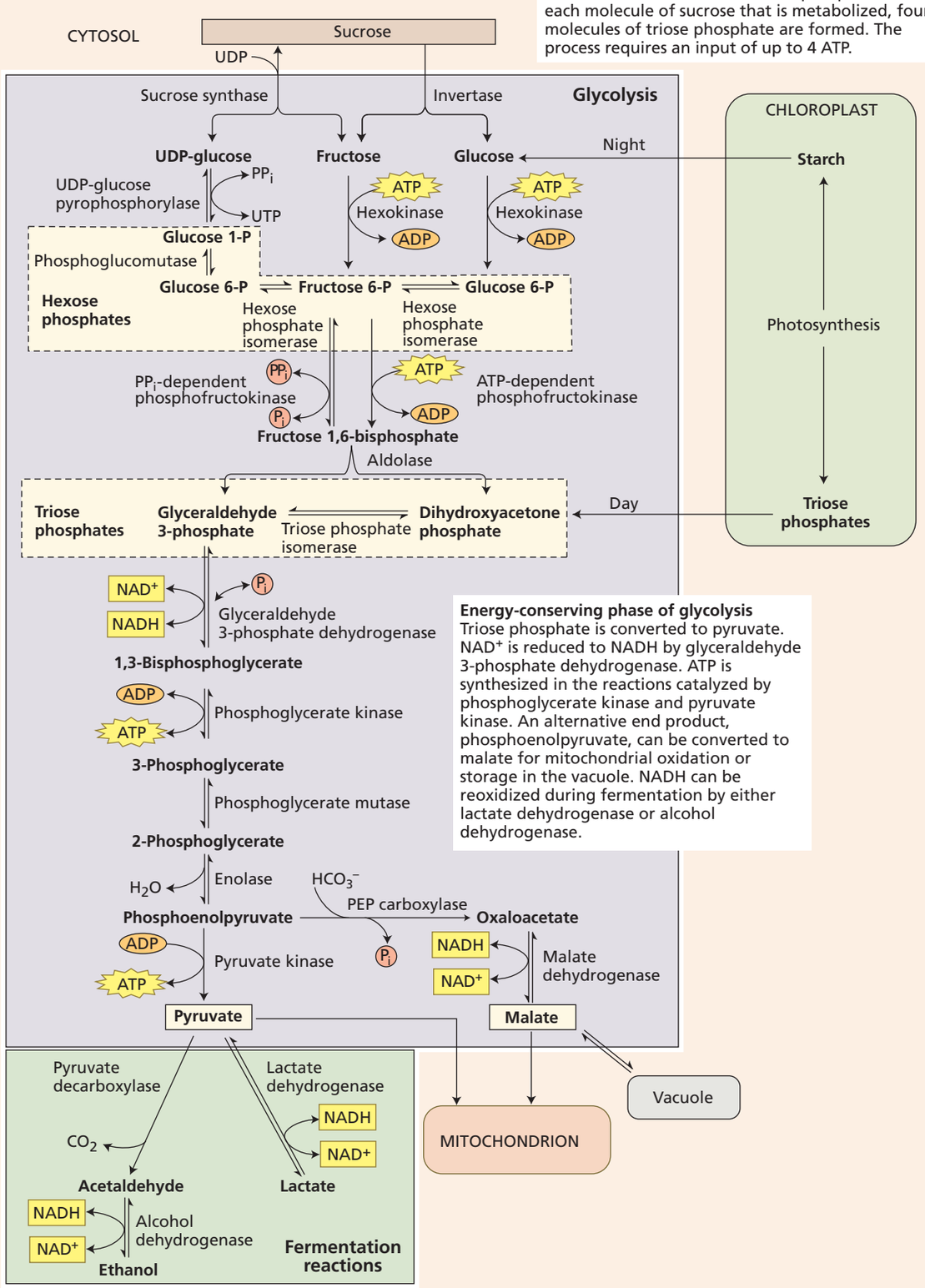


Figure 13.3 **Reactions of plant glycolysis and fermentation.** **(A)** Structures of the carbon intermediates. P, phosphate group. **(B)** In the main glycolytic pathway, sucrose is oxidized via hexose phosphates and triose phosphates to the organic acid anion pyruvate, but plants also carry out alternative reactions. The double arrows denote reversible reactions; the single arrows, essentially irreversible reactions.

(B)

Initial phase of glycolysis Substrates from different sources are channeled into triose phosphate. For each molecule of sucrose that is metabolized, four molecules of triose phosphate are formed. The process requires an input of up to 4 ATP.



Energy-conserving phase of glycolysis Triose phosphate is converted to pyruvate. NAD^+ is reduced to NADH by glyceraldehyde 3-phosphate dehydrogenase. ATP is synthesized in the reactions catalyzed by phosphoglycerate kinase and pyruvate kinase. An alternative end product, phosphoenolpyruvate, can be converted to malate for mitochondrial oxidation or storage in the vacuole. NADH can be reoxidized during fermentation by either lactate dehydrogenase or alcohol dehydrogenase.

In animals, the substrate of glycolysis is glucose, and the end product is pyruvate. Because sucrose is the major translocated sugar in most plants, and is therefore the form of carbon that most nonphotosynthetic tissues import, sucrose (not glucose) can be argued to be the true sugar substrate for plant glycolysis. The end products of plant glycolysis are pyruvate and another organic acid anion, malate.

In the early steps of glycolysis, sucrose is split into its two 6-carbon sugars (hexoses)—glucose and fructose—which can readily enter the glycolytic pathway. Two pathways for the splitting of sucrose are known in plants, both of which take part in the use of sucrose from phloem unloading (see Chapter 12): the invertase pathway and the sucrose synthase pathway.

Invertases in the cell wall, vacuole, and cytosol hydrolyze sucrose into glucose and fructose. The hexoses are then phosphorylated in the cytosol by a hexokinase that uses ATP to form **hexose phosphates**. Alternatively, *sucrose synthase* combines sucrose with UDP to produce fructose and UDP-glucose in the cytosol. UDP-glucose pyrophosphorylase can then convert UDP-glucose and pyrophosphate (PP_i) into UTP and glucose 6-phosphate (see Figure 13.3). While the sucrose synthase reaction is close to equilibrium, the invertase reaction is essentially irreversible, driving the flux in the forward direction.

Through studies of transgenic plants lacking specific invertases or sucrose synthase, each enzyme has been found to be essential for specific life processes, but differences are observed among plant tissues and species. For example, sucrose synthase and cell wall invertase are especially involved in fruit development in several crop species, whereas the cytosolic invertase is important for growth, cell wall integrity, and respiration in *Arabidopsis thaliana*. Both sucrose synthase and invertases can degrade sucrose for glycolysis, and if one of the enzymes is absent, for example in a mutant, the other enzyme(s) can still maintain respiration. The existence of several enzymes or pathways that serve a similar function and can replace each other without a clear loss in function is called **metabolic redundancy**; it is a common feature in plant metabolism. In plastids, there is in many cases a parallel glycolytic pathway that produces metabolites, ATP, and reducing power for plastidial reactions that synthesize, for example, fatty acids, tetrapyrroles, and aromatic amino acids. Starch is synthesized and catabolized only in plastids, and carbon obtained from starch degradation (at night) enters the glycolytic pathway in the cytosol primarily as glucose (see Chapter 10). In the light, photosynthetic products can enter the glycolytic pathway directly as triose phosphate. In overview, glycolysis works like a funnel, with an initial phase collecting carbon from different carbohydrate sources, depending on the physiological situation.

In the initial phase of glycolysis, each hexose unit is phosphorylated twice and then split, producing two molecules of **triose phosphate**. This series of reactions consumes zero to four molecules of ATP per sucrose unit, depending on whether the sucrose is split by sucrose synthase or invertase and whether the ATP- or PPi-dependent phosphofructokinases are active (see **WEB ESSAY 13.1**). The initial phase also includes several essentially irreversible reactions of the glycolytic pathway, which are catalyzed by hexokinase and phosphofructokinase (see Figure 13.3). As we will see later in this section, the phosphofructokinase reaction is one of the control points of glycolysis in both plants and animals.

The energy-conserving phase of glycolysis produces pyruvate, ATP, and NADH

The reactions discussed thus far convert carbon from the various substrate pools to triose phosphates, *glyceraldehyde 3-phosphate*, and its isomer dihydroxyacetone phosphate, which are efficiently interconverted by the triose phosphate isomerase. From this step onward, the glycolytic pathway can extract usable energy in the energy-conserving phase.

Glyceraldehyde 3-phosphate dehydrogenase catalyzes the oxidation of the aldehyde to a carboxylic acid, reducing NAD^+ to NADH. This reaction releases sufficient free energy to allow the phosphorylation (using inorganic phosphate) of glyceraldehyde 3-phosphate to produce 1,3-bisphosphoglycerate. The phosphorylated carboxylate on carbon 1 of 1,3-bisphosphoglycerate (see Figure 13.3A) has a large standard free-energy change ($\Delta G^{0\prime}$) of hydrolysis (–49.3 kJ mol^{-1}). Thus, 1,3-bisphosphoglycerate is a strong donor of P_i groups.

In the next step of glycolysis, catalyzed by *phosphoglycerate kinase*, the phosphate on carbon 1 is transferred to a molecule of ADP, yielding ATP and 3-phosphoglycerate. For each sucrose entering glycolysis, four ATPs are generated by this reaction—one for each molecule of 1,3-bisphosphoglycerate.

This type of ATP synthesis, traditionally referred to as **substrate-level phosphorylation**, involves the direct transfer of a phosphate group from a substrate molecule to ADP to form ATP. ATP synthesis by substrate-level phosphorylation is mechanistically distinct from ATP synthesis by the oxidative phosphorylation in mitochondria (which we describe in Section 13.5) or by photophosphorylation in chloroplasts (see Chapter 9).

In the subsequent two reactions, the phosphate on 3-phosphoglycerate is transferred to carbon 2, and then a molecule of water is removed, yielding the compound *phosphoenolpyruvate* (*PEP*). The phosphate group on PEP has a high $\Delta G^{0\prime}$ of hydrolysis (–61.9 kJ mol^{-1}), which makes PEP an extremely strong substrate for ATP formation. *Pyruvate kinase* catalyzes a second substrate-level phosphorylation by converting ADP and PEP into ATP and pyruvate. This final step, which is the third essentially irreversible step in glycolysis, yields four additional

molecules of ATP for each sucrose molecule that enters the pathway.

Plants have alternative glycolytic reactions

In glycolysis, sugars are degraded to the organic acid pyruvate, but many organisms can also operate a similar pathway in the opposite direction. This process, to synthesize sugars from organic acids, is known as **gluconeogenesis**.

Gluconeogenesis is particularly important in plants (such as the castor oil plant *Ricinus communis* and sunflower) that store carbon in the form of oils (triacylglycerols) in the seeds. Plants cannot transport lipids, so when such a seed germinates, the oil is converted by gluconeogenesis into sucrose, which is transported to the growing cells in the seedling to fuel their energy requirements. In the initial phase of glycolysis, gluconeogenesis overlaps with the pathway for synthesis of sucrose from photosynthetic triose phosphate (described in Chapter 10), which is typical of leaf cells.

Because the glycolytic reaction catalyzed by *ATP-dependent phosphofructokinase* is essentially irreversible (see Figure 13.3), an additional enzyme, *fructose 1,6-bisphosphatase*, converts fructose 1,6-bisphosphate irreversibly into fructose 6-phosphate and P_i during gluconeogenesis. ATP-dependent phosphofructokinase and fructose 1,6-bisphosphate phosphatase represent major control points of carbon flux through the glycolytic and gluconeogenic pathways of both plants and animals as well as in photosynthetic sucrose synthesis in plants (see Chapter 10).

In plants, the interconversion of fructose 6-phosphate and fructose 1,6-bisphosphate is made more complex by the presence of an additional (cytosolic) enzyme, *PP_i-dependent phosphofructokinase* (pyrophosphate:fructose 6-phosphate 1-phosphotransferase), which catalyzes the following reversible reaction (see Figure 13.3):

$$\text{Fructose 6-P} + PP_i \rightarrow \text{fructose 1,6-bisphosphate} + P_i \quad (13.5)$$

where -P represents bound phosphate. PP_i-dependent phosphofructokinase is found in the cytosol of most plant tissues at activities that can be higher than those of ATP-dependent phosphofructokinase. The reaction catalyzed by PP_i-dependent phosphofructokinase is readily reversible, but it is unlikely to operate in sucrose synthesis. Suppression of PP_i-dependent phosphofructokinase in transgenic plants has shown that it contributes to glycolytic flux but that it is not essential for plant survival. The three enzymes that interconvert fructose 6-phosphate and fructose 1,6-bisphosphate are all regulated to match the plant demands for both respiration and synthesis of sucrose and polysaccharides. As a consequence, the operation of the glycolytic pathway in plants has several unique characteristics (see **WEB ESSAY 13.1**).

At the end of the glycolytic process, plants have alternative pathways for metabolizing PEP. In one pathway PEP is carboxylated by the ubiquitous cytosolic enzyme **PEP carboxylase** to form the organic acid anion oxaloacetate. (The same reaction is responsible for the initial CO_2 fixation in CAM plants; see Chapter 10.) The oxaloacetate is then reduced to malate by the action of *malate dehydrogenase*, which uses NADH as a source of electrons (see Figure 13.3). The resulting malate can be exported to the vacuole for storage or to the mitochondrion for degradation in the TCA cycle (discussed in Section 13.4). Thus, the action of pyruvate kinase and PEP carboxylase can produce pyruvate or malate for mitochondrial respiration, although pyruvate dominates in most tissues.

In the absence of oxygen, fermentation regenerates the NAD^+ needed for glycolytic ATP production

Oxidative phosphorylation does not function in the absence of oxygen. Glycolysis then cannot continue because the cell's limited supply of NAD^+ becomes tied up in the reduced state (NADH), and the glyceraldehyde 3-phosphate dehydrogenase comes to a halt. To overcome this limitation, plants and other organisms can further metabolize pyruvate by carrying out one or more forms of **fermentation** (see Figure 13.3).

Alcoholic fermentation (widely known from brewer's yeast) is common in plants. Pyruvate decarboxylase oxidizes pyruvate to CO_2 and acetaldehyde, and alcohol dehydrogenase reduces the latter to ethanol by oxidizing NADH. In lactic acid fermentation (common in mammalian muscle but also in plants), the enzyme lactate dehydrogenase uses NADH to reduce pyruvate to lactate, thus regenerating NAD^+.

Plant tissues may be subjected to low (hypoxic) or zero (anoxic) concentrations of ambient oxygen. Compact and highly active organs such as tubers, seeds, and apical meristems can have highly hypoxic interiors, but the best-studied example involves waterlogged soils in which the diffusion of oxygen is reduced and roots become hypoxic, forcing the tissues to carry out fermentative metabolism. In maize (corn; *Zea mays*), the initial metabolic response to low oxygen concentrations is lactic acid fermentation, but the subsequent response is alcoholic fermentation. Ethanol is thought to be a less toxic end product of fermentation because it can diffuse out of the cell, whereas lactate accumulation promotes deleterious acidification of the cytosol.

It is important to consider the efficiency of fermentation. *Efficiency* is defined here as the energy conserved as ATP relative to the energy potentially available in a molecule of sucrose. The standard free-energy change ($\Delta G^{0\prime}$) for the synthesis of ATP is 32 kJ mol^{-1}. However, under the nonstandard conditions that normally exist in both mammalian and plant cells, the synthesis of ATP

requires an input of free energy of approximately 50 kJ mol^{-1}. The $\Delta G^{0\prime}$ for the complete oxidation of sucrose to CO_2 is –5760 kJ mol^{-1}. Normal glycolysis leads to a net synthesis of four ATP molecules (cost ~200 kJ mol^{-1}) for each sucrose molecule converted into pyruvate. The efficiency of fermentation is therefore only about 4%, because most of the energy available in sucrose remains in the ethanol or lactate. In contrast, the pyruvate produced by glycolysis during aerobic respiration is completely oxidized into CO_2 by mitochondria, resulting in a much more efficient use of the free energy available in sucrose.

Changes in the glycolytic pathway under oxygen deficiency can increase the ATP yield of fermentation. An example of this is when sucrose is degraded via sucrose synthase instead of invertase, avoiding ATP consumption by the hexokinase, or by engaging PP_i-dependent phosphofructokinase. Such modifications emphasize the importance of energetic efficiency for plant survival in the absence of oxygen (see **WEB ESSAY 13.1**).

Because of the low energy recovery of fermentation, an increased rate of glycolytic flux is needed to sustain the ATP production necessary for cell survival. The increase in glycolytic rate in the absence of O_2 is called the *Pasteur effect* after the French microbiologist Louis Pasteur, who first noted it in yeast. Glycolysis is up-regulated by changes in metabolite levels and by the induced synthesis of the glycolytic and fermentation enzymes in response to lower O_2 and energy status, as discussed in Section 13.6.

It was recently discovered that acetate, which is formed by aldehyde dehydrogenases from acetaldehyde, induces epigenetic changes affecting the expression of a battery of genes. This induces drought (water deficit) stress resistance, but the details are not known yet (see Chapter 15). Understanding complex metabolic processes such as glycolysis requires the study of temporal changes in metabolite levels. Rapid extraction, separation, and analysis of many metabolites can be achieved by an approach called *metabolic profiling* (see **WEB ESSAY 13.2**).

13.3 The Oxidative Pentose Phosphate Pathway

The glycolytic pathway is not the only route available for the oxidation of sugars in plant cells. The oxidative pentose phosphate pathway can also accomplish this task (**Figure 13.4**). The reactions are carried out by soluble enzymes present in the cytosol and in plastids. Under most conditions, the pathway in plastids predominates over that in the cytosol.

The first two reactions of this pathway involve the oxidative events that convert the six-carbon molecule glucose 6-phosphate into the five-carbon unit **ribulose 5-phosphate**, with loss of a CO_2 molecule and generation of two molecules of NADPH (not NADH). The remaining reactions of the pathway convert ribulose 5-phosphate into the glycolytic intermediates glyceraldehyde 3-phosphate and fructose 6-phosphate. These products can be further metabolized by glycolysis to yield pyruvate. Alternatively, glucose 6-phosphate can be regenerated from glyceraldehyde 3-phosphate and fructose 6-phosphate by glycolytic enzymes. For six turns of this cycle, we can write the reaction as follows:

$$6\ \text{Glucose 6-P} + 12\ NADP^+ + 7\ H_2O \rightarrow 5\ \text{glucose 6-P} + 6\ CO_2 + P_i + 12\ NADPH + 12\ H^+ \qquad (13.6)$$

The net result is the complete oxidation of one glucose 6-phosphate molecule to CO_2 (five molecules are regenerated) with the concomitant synthesis of 12 NADPH molecules.

Studies of the release of CO_2 from isotopically labeled glucose indicate that the pentose phosphate pathway accounts for 10 to 25% of the glucose breakdown, with the rest occurring mainly via glycolysis. However, the contribution of the pentose phosphate pathway changes during development and with changes in growth conditions as the plant's requirements for specific products vary.

The oxidative pentose phosphate pathway produces NADPH and biosynthetic intermediates

The oxidative pentose phosphate pathway plays several roles in plant metabolism:

- *NADPH supply in the cytosol*. The product of the two oxidative steps is NADPH. This NADPH drives reductive steps associated with biosynthetic and stress defense reactions and is a substrate for reactions that remove reactive oxygen species (ROS). Because plant mitochondria possess an NADPH dehydrogenase located on the external surface of the inner membrane, the reducing power generated by the pentose phosphate pathway can be balanced by mitochondrial NADPH oxidation. The pentose phosphate pathway may therefore also contribute to cellular energy metabolism; that is, electrons from NADPH may end up reducing O_2 and generating ATP through oxidative phosphorylation. For other cytosolic sources of NADPH, see **WEB ESSAY 13.1**.
- *NADPH supply in plastids*. In nongreen plastids, such as amyloplasts in the root, and chloroplasts functioning in the dark, the pentose phosphate pathway is the major supplier of NADPH. The NADPH is used for biosynthetic reactions such as lipid synthesis and nitrogen assimilation. The formation of NADPH by glucose 6-phosphate oxidation in amyloplasts may also signal sugar status to the thioredoxin system for control of starch synthesis.

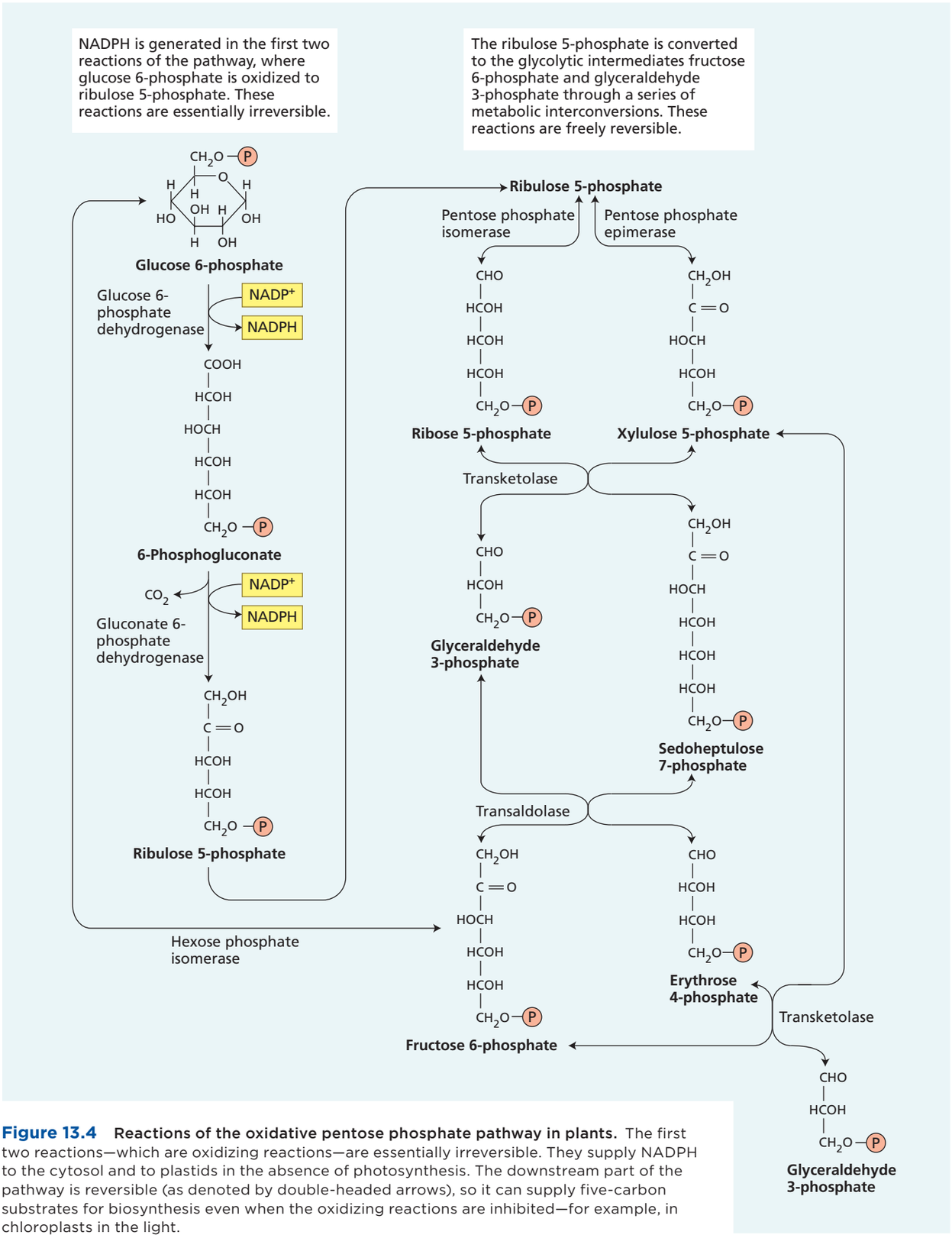


Figure 13.4 **Reactions of the oxidative pentose phosphate pathway in plants.** The first two reactions—which are oxidizing reactions—are essentially irreversible. They supply NADPH to the cytosol and to plastids in the absence of photosynthesis. The downstream part of the pathway is reversible (as denoted by double-headed arrows), so it can supply five-carbon substrates for biosynthesis even when the oxidizing reactions are inhibited—for example, in chloroplasts in the light.

- *Supply of substrates for biosynthetic processes*. In most organisms, the pentose phosphate pathway produces ribose 5-phosphate, which is a precursor of the ribose and deoxyribose needed in the synthesis of nucleic acids. In plants, however, ribose appears to be synthesized by another, as yet unknown, pathway. Another intermediate in the pentose phosphate pathway, the four-carbon erythrose 4-phosphate, combines with PEP in the initial reaction of the shikimic acid pathway that produces plant phenolic compounds, including the aromatic amino acids and the precursors of lignin and flavonoids (see **WEB APPENDIX 4**). This role of the pentose phosphate pathway is supported by the observation that its enzymes are induced by stress conditions such as wounding, under which aromatic compounds are needed for reinforcing and protecting the tissue.

The oxidative pentose phosphate pathway is controlled by cellular redox status

Each enzymatic step in the oxidative pentose phosphate pathway is catalyzed by a group of isoenzymes that vary in their abundance and regulatory properties among plant cell types. The initial reaction of the pathway, catalyzed by **glucose 6-phosphate dehydrogenase**, is inhibited by a high ratio of NADPH to $NADP^+$.

In the light, little operation of the oxidative pentose phosphate pathway occurs in chloroplasts. Plastidic glucose 6-phosphate dehydrogenase is inhibited by a reductive inactivation involving the *ferredoxin–thioredoxin system* (see Chapter 10) and by the NADPH to $NADP^+$ ratio. Moreover, the end products of the pathway, fructose 6-phosphate and glyceraldehyde 3-phosphate, are being synthesized by the Calvin–Benson cycle. Thus, mass action will drive the nonoxidative reactions of the pathway in the reverse direction. In this way, synthesis of erythrose 4-phosphate can be maintained in the light. In nongreen plastids, the glucose 6-phosphate dehydrogenase is less sensitive to inactivation by reduced thioredoxin and NADPH, and can therefore reduce $NADP^+$ to maintain a relatively high reduction level of plastid components in the absence of photosynthesis.

13.4 The Tricarboxylic Acid Cycle

During the nineteenth century, biologists discovered that in the absence of air, glucose-fed yeast cells produce ethanol or lactic acid, whereas in the presence of air, cells consume O_2 and produce CO_2 and H_2O. In 1937 the German-born British biochemist Hans A. Krebs reported the discovery of the citric acid cycle—most commonly known as the *tricarboxylic acid (TCA) cycle*. The elucidation of the TCA cycle explained how pyruvate is broken down into CO_2 and H_2O, and also highlighted the key concept of cycles in metabolic pathways. For his discoveries, Hans Krebs was awarded the Nobel Prize in physiology or medicine in 1953.

Because the TCA cycle occurs in the mitochondrial matrix, we begin with a general description of mitochondrial structure and function, the basic knowledge of which was obtained mainly through experiments on isolated mitochondria (see **WEB TOPIC 13.1**). We then review the steps of the TCA cycle, emphasizing the features that are specific to plants and how they affect respiratory function.

Mitochondria are semiautonomous organelles

The breakdown of sucrose into pyruvate releases less than 25% of the total energy in sucrose; the remaining energy is stored in the four molecules of pyruvate. The next two stages of respiration (the TCA cycle and oxidative phosphorylation) take place within an organelle enclosed by a double membrane, the **mitochondrion** (plural *mitochondria*).

Plant mitochondria are usually spherical or rodlike and range from 0.5 to 1.0 μm in diameter and up to 3 μm in length (**Figure 13.5**), but they can also be branched or reticulated. The number and sizes of mitochondria in a cell can vary dynamically as a result of mitochondrial fission, fusion, and degradation (see Figure 13.5C and **WEB ESSAY 13.3**) while keeping up with cell division. Like chloroplasts, they are semiautonomous organelles, because they contain ribosomes, RNA, and DNA, which encodes a limited number of mitochondrial proteins. Plant mitochondria are thus able to carry out protein synthesis and transmit their genetic information. Metabolically active cells usually contain more mitochondria than less active cells, reflecting the mitochondrial role in energy metabolism. Tapetum cells in the anthers (see Chapter 21), for example, show a marked increase in the number of mitochondria during pollen development.

The ultrastructural features of plant mitochondria are similar to those of mitochondria in other eukaryotes (see Figure 13.5A and B). Plant mitochondria have two membranes: A smooth **outer mitochondrial membrane** completely surrounds a highly invaginated **inner mitochondrial membrane**. The invaginations of the inner membrane are known as **cristae** (singular *crista*). As a consequence of its greatly enlarged surface area, the inner membrane can contain 50% of the total mitochondrial protein. The region between the two mitochondrial membranes is known as the **intermembrane space**. The compartment enclosed by the inner membrane is referred to as the mitochondrial **matrix**. It has a very high content of macromolecules, approximately 50% by weight. Because there is little water in the matrix, mobility is restricted, and it is likely that matrix proteins are organized into multienzyme complexes (so-called metabolons) to facilitate substrate channeling.

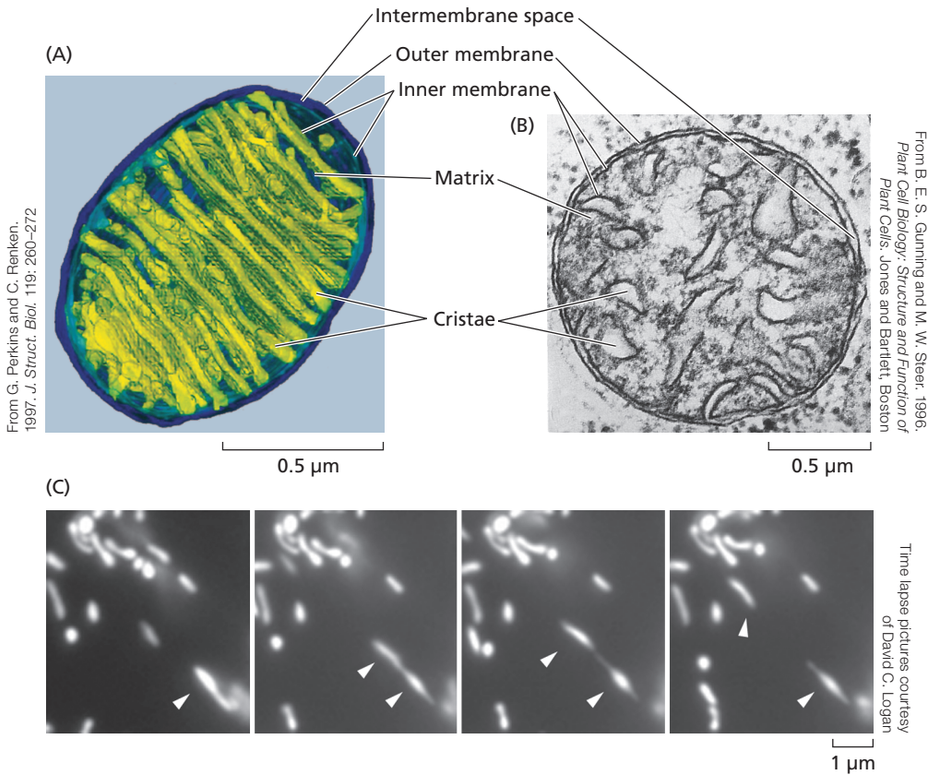


Figure 13.5 Structure of mitochondria from animals and plants. **(A)** Three-dimensional tomography picture of a chicken brain mitochondrion, showing the invaginations of the inner membrane, called cristae, as well as the locations of the matrix and intermembrane space (see also Figure 13.10). **(B)** Electron micrograph of a mitochondrion in a mesophyll cell of broad bean (*Vicia faba*). **(C)** Time-lapse pictures showing a dividing mitochondrion in an Arabidopsis epidermal cell (arrowheads). All the visible organelles are mitochondria labeled with green fluorescent protein. The pictures shown were taken 2 s apart. See **WEB ESSAY 13.3** for the complete video.

Intact mitochondria are osmotically active; that is, they take up water and swell when placed in a hypoosmotic medium. Ions and polar molecules are generally unable to diffuse freely through the inner membrane, which functions as the osmotic barrier. The outer membrane is permeable to solutes that have a molecular mass of less than approximately 6000 Da—that is, most cellular metabolites and ions, but not proteins. The lipid fraction of both membranes is primarily made up of phospholipids, 80% of which are either phosphatidylcholine or phosphatidylethanolamine. About 15% of the inner mitochondrial membrane lipids is diphosphatidylglycerol (also called cardiolipin), which occurs only in that membrane.

Pyruvate enters the mitochondrion and is oxidized via the TCA cycle

The TCA cycle got its name because of the importance of the tricarboxylic acids citric acid (citrate) and isocitric acid (isocitrate) as intermediates (**Figure 13.6**). This cycle constitutes the second stage in respiration and takes place in the mitochondrial matrix. Its operation requires that the pyruvate generated in the cytosol during glycolysis be transported through the inner mitochondrial membrane barrier via a specific transport protein (as we describe in Section 13.5).

Once inside the mitochondrial matrix, pyruvate is decarboxylated in an oxidation reaction catalyzed by **pyruvate dehydrogenase**, a large complex consisting of several enzymes. The products are NADH, CO_2, and acetyl-CoA, in which the acetyl group derived from pyruvate is linked by a thioester bond to a soluble cofactor, coenzyme A (CoA) (see Figure 13.6).

In the next reaction, citrate synthase, formally the first enzyme in the TCA cycle, combines the acetyl group of acetyl-CoA with a four-carbon dicarboxylic acid (*oxaloacetate*) to give a six-carbon tricarboxylic acid (citrate). Citrate is then isomerized to isocitrate by the enzyme aconitase.

The following two reactions are successive oxidative decarboxylations, each of which produces one NADH and releases one molecule of CO_2, yielding a four-carbon product bound to CoA, succinyl-CoA. At this point, all 3 carbons that entered the mitochondrion as pyruvate are oxidized into CO_2.

In the remainder of the TCA cycle, succinyl-CoA is oxidized to oxaloacetate, allowing the continued operation of the cycle. Initially the large amount of free energy available in the thioester bond of succinyl-CoA is conserved through the synthesis of ATP from ADP and P_i via a substrate-level phosphorylation catalyzed by *succinyl-CoA synthetase*. The resulting succinate is oxidized to fumarate by *succinate dehydrogenase*, which is the only membrane-associated enzyme of the TCA cycle and also part of the electron transport chain.

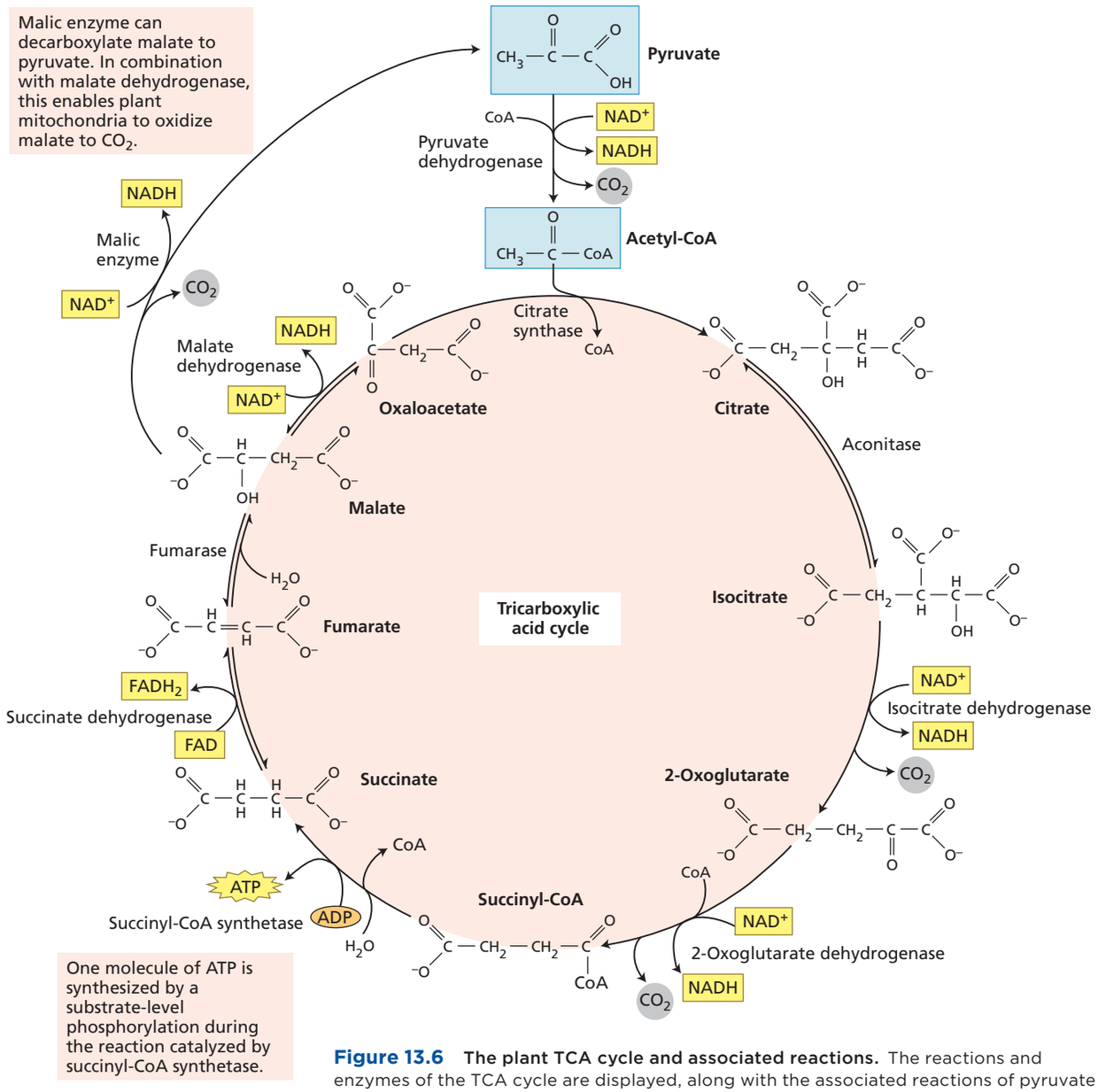


Figure 13.6 **The plant TCA cycle and associated reactions.** The reactions and enzymes of the TCA cycle are displayed, along with the associated reactions of pyruvate dehydrogenase and malic enzyme. Pyruvate is completely oxidized to three molecules of CO_2, and malic enzyme enables plant mitochondria to completely oxidize malate. The electrons released during these oxidations are used to reduce four molecules of NAD^+ to NADH and one molecule of FAD to $FADH_2$.

The electrons and protons removed from succinate end up not on NAD^+, but on another cofactor involved in redox reactions: **flavin adenine dinucleotide** (**FAD**). FAD is covalently bound to the active site of succinate dehydrogenase and undergoes a reversible two-electron reduction to produce $FADH_2$ (see Figure 13.2B).

In the final two reactions of the TCA cycle, fumarate is hydrated to produce malate, which is subsequently oxidized by *malate dehydrogenase* to regenerate oxaloacetate and produce another molecule of NADH. The oxaloacetate produced is now able to react with another acetyl-CoA and continue the cycling.

In total, the stepwise oxidation of one molecule of pyruvate (3C) in the mitochondrion gives rise to three molecules of CO_2, and much of the free energy released during these oxidations is conserved in the form of four

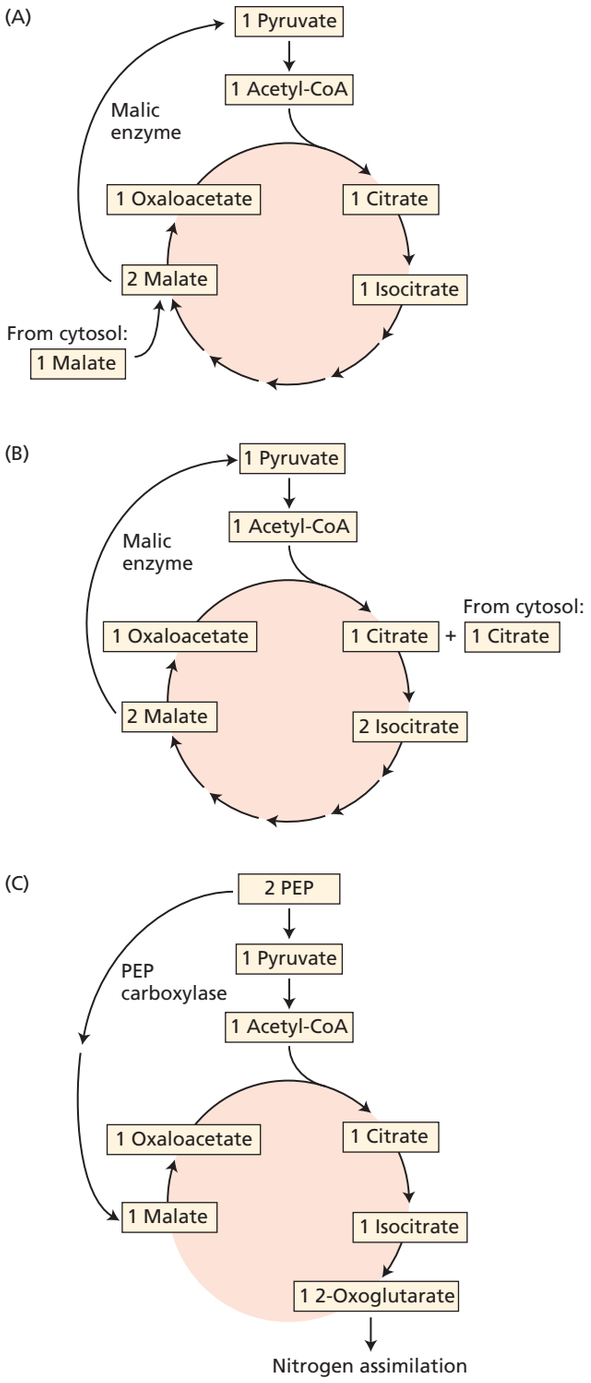


Figure 13.7 Malic enzyme and PEP carboxylase provide plants with metabolic flexibility for the metabolism of PEP and pyruvate. **(A and B)** Malic enzyme converts malate into pyruvate and thus allows plant mitochondria to oxidize both malate (A) and citrate (B) to CO_2 without involving pyruvate delivered by glycolysis. **(C)** With the added action of PEP carboxylase to the standard pathway, glycolytic PEP is converted into 2-oxoglutarate, which is used for nitrogen assimilation.

NADH and one $FADH_2$. In addition, one molecule of ATP is produced by a substrate-level phosphorylation.

The TCA cycle of plants has unique features

The TCA cycle reactions outlined in Figure 13.6 are not all identical to those carried out by animal mitochondria. For example, the step catalyzed by succinyl-CoA synthetase produces GTP or ATP in animals, but exclusively ATP in plants. These nucleotides are energetically equivalent.

A special feature of the plant TCA cycle is the presence of large amounts of **malic enzyme** in the mitochondrial matrix of plants. This enzyme catalyzes the oxidative decarboxylation of malate:

$$\text{Malate} + NAD^+ \rightarrow \text{pyruvate} + CO_2 + \text{NADH} \quad (13.7)$$

The activity of malic enzyme enables plant mitochondria to operate alternative pathways for the metabolism of PEP derived from glycolysis (see **WEB ESSAY 13.1**). As already described, malate can be synthesized from PEP in the cytosol via the enzymes PEP carboxylase and malate dehydrogenase (see Figure 13.3). For degradation, malate is transported into the mitochondrial matrix, where malic enzyme can oxidize it to pyruvate. This reaction makes possible the oxidation of TCA cycle intermediates such as malate (**Figure 13.7A**) or citrate (**Figure 13.7B**) to CO_2. Many plant tissues, not only those that carry out crassulacean acid metabolism (see Chapter 10), store significant amounts of malate or other organic acids in their vacuoles. Degradation of malate via mitochondrial malic enzyme is important for regulating the levels of organic acids in cells—for example, during fruit ripening.

Instead of being degraded, the malate produced via PEP carboxylase can replenish TCA cycle intermediates used in biosynthesis. For example, export of 2-oxoglutarate for nitrogen assimilation in the chloroplast leads to a shortage of oxaloacetate for the citrate synthase reaction. This malate can be replaced through the PEP carboxylase pathway (**Figure 13.7C**). Reactions that replenish intermediates in a metabolic cycle are called *anaplerotic*.

Gamma-aminobutyric acid (GABA) is an amino acid that accumulates under several stress conditions in plants and that may have a role as a signal. GABA is synthesized from 2-oxoglutarate and degraded into succinate by the so-called **GABA shunt**, which bypasses TCA cycle enzymes that may be inhibited under plant stress (see **WEB ESSAY 13.1**).

13.5 Oxidative Phosphorylation

ATP is the energy transmitter used by cells to drive life processes, so chemical energy conserved during the TCA cycle in the form of NADH and $FADH_2$ must be converted into ATP to perform useful work in the cell.

This O_2-dependent process, called oxidative phosphorylation, occurs in the inner mitochondrial membrane.

In this section we describe the process by which the energy level of the electrons from NADH and $FADH_2$ is lowered in a stepwise fashion and conserved in the form of an electrochemical proton gradient across the inner mitochondrial membrane. Oxidative phosphorylation is fundamentally similar in all aerobic cells, yet the mitochondrial electron transport chain of vertebrate and arthropod animals lacks non-energy-conserving NAD(P)H dehydrogenases and alternative oxidase that are present in most eukaryotes, and which are especially rich in variants in plants.

We also examine the enzyme that uses the energy of the electrochemical proton gradient to synthesize ATP: the F_oF_1-ATP synthase. After examining the various stages in the production of ATP, we summarize the energy-conservation steps at each stage, as well as the regulatory mechanisms that coordinate the different pathways.

The electron transport chain catalyzes a flow of electrons from NADH to O_2

For each molecule of sucrose oxidized through glycolysis and the TCA cycle, 4 molecules of NADH are generated in the cytosol, and 16 molecules of NADH plus 4 molecules of $FADH_2$ (associated with succinate dehydrogenase) are generated in the mitochondrial matrix. These reduced compounds must be reoxidized, or the entire respiratory process will rapidly come to a halt.

The electron transport chain catalyzes a transfer of two electrons from NADH (or $FADH_2$) to oxygen, the final electron acceptor of the respiratory process. For the oxidation of NADH, the reaction can be written as

$$NADH + H^+ + \tfrac{1}{2}\,O_2 \rightarrow NAD^+ + H_2O \qquad (13.8)$$

From the reduction potentials for the NADH–NAD^+ pair (–320 mV) and the H_2O–$\frac{1}{2}$ O_2 pair (+810 mV), it can be calculated that the standard free energy released during this overall reaction ($-nF\Delta E^{0\prime}$) is about 220 kJ per mole of NADH. Because the succinate–fumarate reduction potential is higher (+30 mV), only 152 kJ per mole of succinate is released. The role of the electron transport chain is to bring about the oxidation of NADH (and $FADH_2$) and, in the process, use some of the free energy released to generate an electrochemical proton gradient, $\Delta\tilde{\mu}_{H^+}$, across the inner mitochondrial membrane.

The electron transport chain of plants contains the same set of electron carriers found in the mitochondria of other organisms (**Figure 13.8**). The individual electron transport proteins are organized into four transmembrane multiprotein complexes (identified by roman numerals I through IV), all of which are localized in the inner mitochondrial membrane. Three of these complexes (I, III, and IV) are engaged in proton pumping.

COMPLEX I (NADH DEHYDROGENASE) Electrons from NADH generated by the TCA cycle in the mitochondrial matrix are oxidized by complex I (an **NADH dehydrogenase**). The electron carriers in complex I include a tightly bound cofactor (**flavin mononucleotide**, or **FMN**, which is chemically similar to FAD; see Figure 13.2B) and several iron–sulfur centers. Complex I then transfers these electrons to ubiquinone. Four protons are pumped from the matrix into the intermembrane space for every electron pair passing through the complex.

Ubiquinone, a small lipid-soluble electron and proton carrier, is localized within the inner membrane. It is not tightly associated with any protein, and it can diffuse within the hydrophobic core of the membrane bilayer.

COMPLEX II (SUCCINATE DEHYDROGENASE) Oxidation of succinate in the TCA cycle is catalyzed by this complex, and the reducing equivalents are transferred via the cofactors, $FADH_2$ and several iron–sulfur centers, to ubiquinone. Complex II does not pump protons.

COMPLEX III (CYTOCHROME *bc*$_1$ COMPLEX) Complex III oxidizes reduced ubiquinone (ubiquinol) and transfers the electrons via an iron–sulfur center, two *b*-type cytochromes (b_{565} and b_{560}), and a membrane-bound cytochrome c_1 to cytochrome *c*. Four protons per electron pair are pumped out of the matrix by complex III using a mechanism called the **Q cycle** (see **WEB TOPIC 13.2**). Both structurally and functionally, ubiquinone and the cytochrome bc_1 complex are very similar to plastoquinone and the cytochrome b_6f complex, respectively, in the photosynthetic electron transport chain (see Chapter 9).

Cytochrome *c* is a small protein loosely attached to the outer surface of the inner membrane and serves as a mobile carrier to transfer electrons between complexes III and IV, similar to the role of plastocyanin in photosynthetic electron transport (see Chapter 9).

COMPLEX IV (CYTOCHROME *c* OXIDASE) Complex IV contains two copper centers (Cu_A and Cu_B) and cytochromes *a* and a_3. This complex is the terminal oxidase and brings about the four-electron reduction of O_2 to two molecules of H_2O. Two protons are pumped out of the matrix per electron pair (see Figure 13.8).

The electron transport chain may be more complex than the description here implies. Plant respiratory complexes contain several plant-specific subunits whose functions are still unknown. Several of the complexes contain subunits that participate in functions other than electron transport, such as protein import. Finally, the proton-pumping complexes have been observed to form a single supercomplex (called a respirasome), in contrast to being individually mobile in the membrane. However, the functional significance of supercomplexes is still unclear.

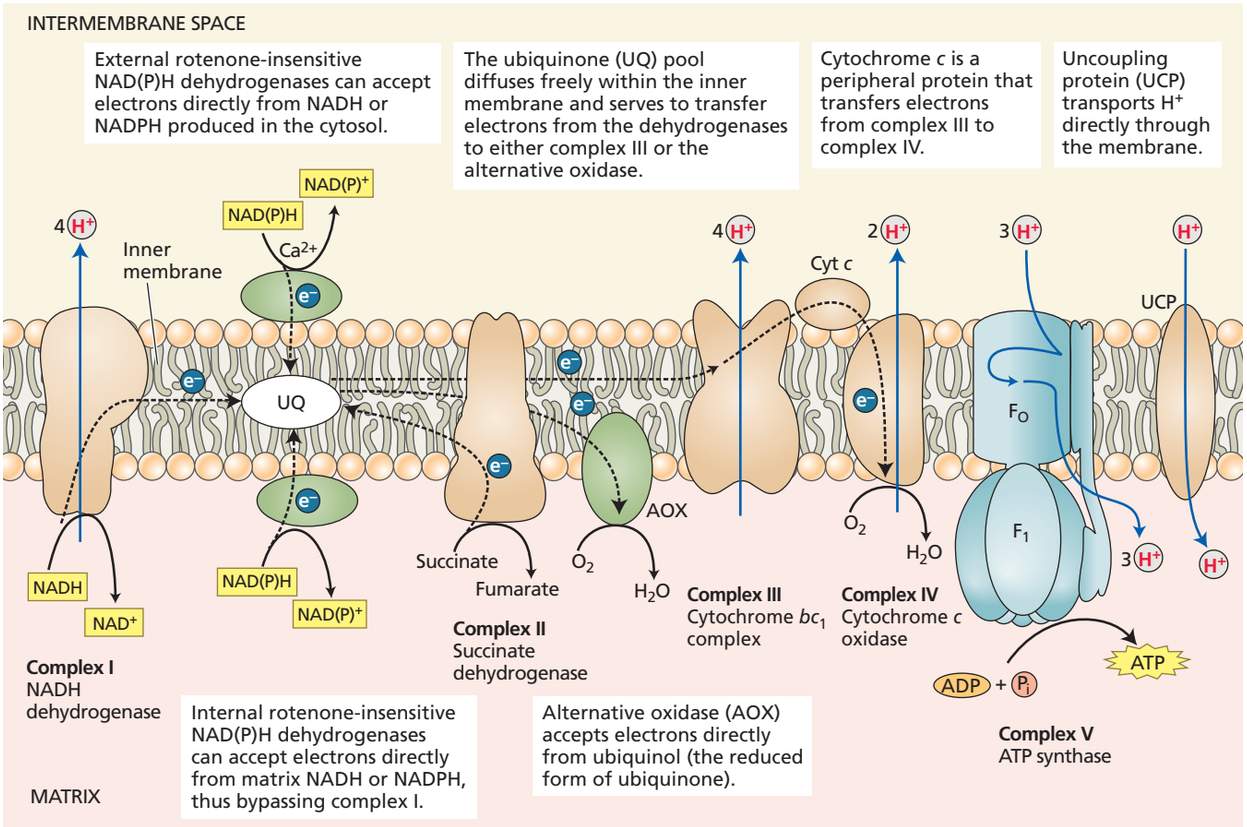


Figure 13.8 Organization of the electron transport chain and ATP synthesis in the inner membrane of the plant mitochondrion. Mitochondria from nearly all eukaryotes contain the four standard protein complexes: I, II, III, and IV. The structures of all complexes have been determined, but they are shown here as simplified shapes. The electron transport chain of the plant mitochondrion contains additional enzymes that do not pump protons, external and internal rotenone-insensitive NAD(P)H dehydrogenases and the alternative oxidase. Additionally, uncoupling proteins directly bypass the ATP synthase by allowing passive proton influx. This multiplicity of bypasses in plants, where vertebrate animals have only the uncoupling protein, gives greater flexibility to plant energy coupling.

The electron transport chain has supplementary branches

In addition to the set of protein complexes just described, the plant electron transport chain contains components not found in mammalian mitochondria (see Figure 13.8 and **WEB TOPIC 13.3**). Especially, additional non-energy-conserving **NAD(P)H dehydrogenases** and a so-called **alternative oxidase** are bound to the inner membrane (**Figure 13.9**). In contrast to the proton-pumping complexes I, III, and IV, these enzymes do not pump protons, so the energy released from oxidation of NADH is not conserved as ATP, but instead is turned into heat.

Plant mitochondria have two pathways for oxidizing matrix NADH. Electron flow through complex I, described in the previous subsection, is sensitive to inhibition by several compounds, including rotenone and piericidin. In addition, plant mitochondria have a rotenone-insensitive dehydrogenase, ND_{in}(NADH), on the matrix surface of the inner mitochondrial membrane. This enzyme oxidizes NADH derived from the TCA cycle, and may also be a bypass engaged when complex I is overloaded, as we will see later in this section. An NADPH dehydrogenase, ND_{in}(NADPH), is also present on the matrix surface, but very little is known about this enzyme.

Rotenone-insensitive NAD(P)H dehydrogenases, mostly Ca^{2+}-dependent, are also attached to the outer surface of the inner membrane facing the intermembrane space. They oxidize either NADH or NADPH from the cytosol. Electrons from these external NAD(P)H dehydrogenases—ND_{ex}(NADH) and ND_{ex}(NADPH)—enter the main electron transport chain at the level of the ubiquinone pool.

Plants have an additional respiratory pathway for the oxidation of ubiquinol and reduction of oxygen. This pathway involves the alternative oxidase,

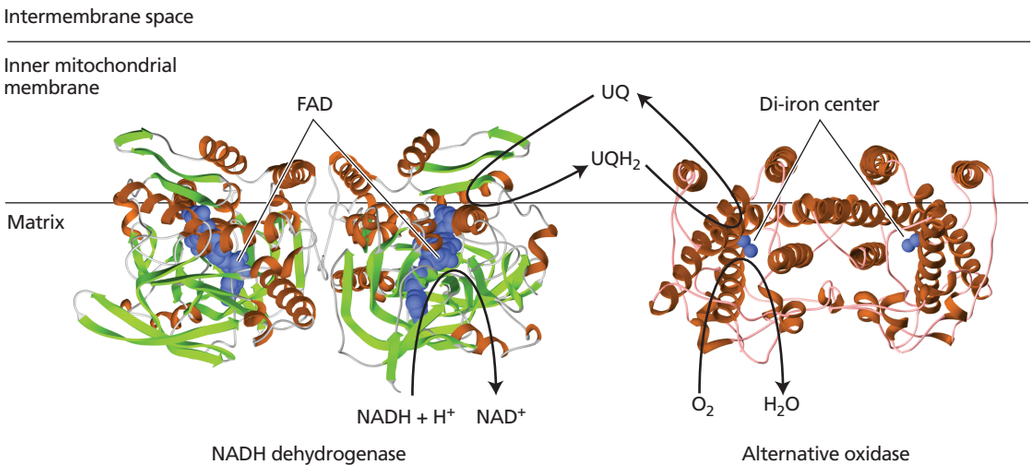


Figure 13.9 Non-energy-conserving electron transport. The internal rotenone-insensitive NADH dehydrogenase and the alternative oxidase are both homodimers, and the reactions are drawn for one monomer each. The enzymes are partly embedded in the inner leaflet of the inner mitochondrial membrane. Therefore, transfer of electrons between the hydrophilic redox couples NADH/NAD^+ and H_2O/O_2, and the hydrophobic ubiquinone (UQH_2/UQ), via single internal redox centers (FAD or di-iron groups), cannot involve proton pumping; the energy released by the reaction is instead given off as heat. Proton pumping across the inner mitochondrial membrane requires large transmembrane protein complexes. (Model of NADH dehydrogenase [from brewer's yeast, *Saccharomyces cerevisiae*] based on data from M. Iwata et al. 2012. *Proc. Natl. Acad. Sci. USA* 109: 15247–15252; model of alternative oxidase [from the sleeping sickness parasite, *Trypanosoma brucei*] based on data from T. Shiba et al. 2013. *Proc. Natl. Acad. Sci. USA* 110: 4580–4585.)

which, unlike cytochrome *c* oxidase, is insensitive to inhibition by cyanide, carbon monoxide, and the signal molecule nitric oxide (see **WEB TOPIC 13.3** and **WEB ESSAY 13.4**).

The physiological significance of these supplementary electron transport enzymes is considered more fully later in this section.

Some additional electron transport chain dehydrogenases present in plant mitochondria directly perform important carbon conversions. A *proline dehydrogenase* oxidizes the amino acid proline. Proline accumulates during drought or salt stress (see Chapter 15), and it is degraded by this mitochondrial pathway when water status returns to normal. An electron transfer flavoprotein:quinone oxidoreductase mediates the degradation of several amino acids that are used by plants as a reserve under carbon starvation conditions induced by light deprivation. A third example is a galactono-gamma-lactone dehydrogenase, specific to plants, that performs the last step in the major pathway for synthesis of the antioxidant *ascorbic acid* (also known as vitamin C). The enzyme uses cytochrome *c* as its electron acceptor, in competition with normal respiration.

ATP synthesis in the mitochondrion is coupled to electron transport

In oxidative phosphorylation, the transfer of electrons to oxygen via complexes I, III, and IV is coupled to the synthesis of ATP from ADP and P_i via the F_oF_1-ATP synthase (complex V). The number of ATPs synthesized depends on the electron donor.

In experiments conducted on isolated mitochondria, electrons donated to complex I (e.g., generated by malate oxidation) give ADP:O ratios (the number of ATPs synthesized per two electrons transferred to oxygen) of 2.4 to 2.7 (**Table 13.1**). Electrons donated to complex II (from succinate) and to the external NADH dehydrogenase give values in the range of 1.6 to 1.8, while electrons donated directly to cytochrome *c* oxidase (complex IV) via artificial electron carriers give values of 0.8 to 0.9. Results such as these have led to the general concept that there are three sites of energy conservation along the electron transport chain, at complexes I, III, and IV.

The experimental ADP:O ratios agree quite well with the values calculated on the basis of the number of H^+ pumped by complexes I, III, and IV and the cost of 4 H^+ for producing 1 ATP (see next subsection and Table 13.1). For instance, electrons from external NADH pass only complexes III and IV, so a total of 6 H^+ are pumped, giving 1.5 ATP (when the alternative oxidase pathway is not used).

The mechanism of mitochondrial ATP synthesis is based on the **chemiosmotic mechanism** described in Chapter 9, which was first proposed in 1961 by Nobel laureate Peter Mitchell as a general mechanism of energy conservation across biological membranes. According to the chemiosmotic mechanism, the orientation of electron

Table 13.1 Theoretical and experimental ADP:O ratios in isolated plant mitochondria

Electrons feeding into	ADP:O ratio	
	Theoretical[a]	Experimental
Complex I	2.5	2.4–2.7
Complex II	1.5	1.6–1.8
External NADH dehydrogenase	1.5	1.6–1.8
Complex IV	1.0[b]	0.8–0.9

[a]It is assumed that complexes I, III, and IV pump 4, 4, and 2 H^+ per 2 electrons, respectively; that the cost of synthesizing 1 ATP and exporting it to the cytosol is 4 H^+; and that the non-energy-conserving pathways are not active.

[b]Cytochrome *c* oxidase (complex IV) pumps only 2 protons. However, 2 electrons move from the outer surface of the inner membrane (where the electrons are donated) across the inner membrane to the inner, matrix side. As a result, 2 H^+ are consumed on the matrix side. This means that the net movement of H^+ and charges is equivalent to the movement of a total of 4 H^+, giving an ADP:O ratio of 1.0.

carriers within the inner mitochondrial membrane allows for the transfer of protons across the inner membrane during electron flow (see Figure 13.8).

Because the inner mitochondrial membrane is highly impermeable to protons, an **electrochemical proton gradient** can build up. The free-energy difference associated with the electrochemical proton gradient, $\Delta\tilde{\mu}_{H^+}$ (expressed in kJ mol^{-1}), is also referred to as the *proton motive force*, Δp, when expressed in units of volts. The transfer of an H^+ from the intermembrane space to the matrix will release energy due to the Δp, which is the sum of an electrical transmembrane potential component (ΔE) and a chemical-potential component (ΔpH), according to the approximate equation:

$$\Delta p = \Delta E - 59 \text{ mV} \times \Delta\text{pH (at 25°C)} \qquad (13.9)$$

where

$$\Delta E = E_{\text{inside}} - E_{\text{outside}} \qquad (13.10)$$

and

$$\Delta\text{pH} = \text{pH}_{\text{inside}} - \text{pH}_{\text{outside}} \qquad (13.11)$$

ΔE results from the asymmetric distribution of charged species (H^+ and other ions) across the membrane, and ΔpH is due to the H^+ concentration difference across the membrane. Because protons are translocated from the mitochondrial matrix to the intermembrane space, the resulting ΔE across the inner mitochondrial membrane has a negative value. Under normal conditions, the ΔpH is approximately 0.5 and the ΔE approximately 200 mV. Because the membrane is only 7 to 8 nm thick, this ΔE corresponds to an electric field of at least 25 million V/m (or ten times the field generating a lightning flash in a thunderstorm), emphasizing the enormous forces involved in electron transport.

As Equation 13.9 shows, both ΔE and ΔpH contribute to the proton motive force in plant mitochondria, although ΔpH constitutes the smaller part, probably because of the large buffering capacity of both cytosol and matrix, which prevents large pH changes. This situation contrasts with that in the chloroplast, where almost all of the proton motive force across the thylakoid membrane is due to ΔpH (see Chapter 9).

The free-energy input required to generate $\Delta\tilde{\mu}_{H^+}$ comes from the free energy released during electron transport. This is done by asymmetric uptake and release of H^+ from reactions (see **WEB TOPIC 13.2**) or via redox-gated H^+ channels. Because of the low permeability (conductance) of the inner membrane to protons, their electrochemical gradient can be consumed to carry out chemical work (ATP synthesis). The $\Delta\tilde{\mu}_{H^+}$ is coupled to the synthesis of ATP by an additional protein complex associated with the inner membrane, the F_oF_1-ATP synthase.

The **F_oF_1-ATP synthase** (also called *complex V*) consists of two major components, F_o and F_1 (see Figure 13.8). **F_o** (subscript "o" for oligomycin-sensitive) is an integral membrane protein complex containing at least three different polypeptides. They form the channel through which protons cross the inner membrane. The other component, **F_1**, is a peripheral membrane protein complex that is composed of at least five different subunits and contains catalytic sites for converting ADP and P_i into ATP. This complex is attached to the matrix side of F_o.

The passage of protons through the channel is coupled to the catalytic cycle of the F_1 component of the ATP synthase, allowing the ongoing synthesis of ATP and the simultaneous use of the $\Delta\tilde{\mu}_{H^+}$. One ATP is synthesized for each 3 H^+ passing through the F_o component from the intermembrane space to the matrix, down the electrochemical proton gradient.

A high-resolution structure for the F_1 component of the mammalian ATP synthase provided evidence for a mechanism in which a part of F_o rotates relative to F_1 to couple H^+ transport to ATP synthesis (see **WEB TOPIC 13.4**). The structure and function of the CF_0CF_1-ATP synthase in chloroplasts are similar to those of the mitochondrial ATP synthase (see Chapter 9).

The operation of a chemiosmotic mechanism of ATP synthesis has several implications. First, the true site of ATP formation on the inner mitochondrial membrane is the ATP synthase, not complex I, III, or IV. These complexes serve as sites of energy conservation whereby electron transport is coupled to the generation of a $\Delta\tilde{\mu}_{H^+}$. The synthesis of ATP decreases the $\Delta\tilde{\mu}_{H^+}$ and, as a consequence, its restriction on the electron transport complexes. Electron transport is therefore stimulated by a large supply of ADP.

The chemiosmotic mechanism also explains the action mechanism of **uncouplers**. These are a wide range

of chemically unrelated, artificial compounds (including 2,4-dinitrophenol and *p*-trifluoromethoxycarbonylcyanide phenylhydrazone [FCCP]) that decrease mitochondrial ATP synthesis but stimulate the rate of electron transport (see **WEB TOPIC 13.5**). All uncouplers make the inner membrane leaky to protons and prevent the buildup of a sufficiently large $\Delta\tilde{\mu}_{H^+}$ to drive ATP synthesis or restrict electron transport. The inner membrane of plant mitochondria, like the mammalian one, has a natural uncoupling protein that can directly lower the $\Delta\tilde{\mu}_{H^+}$ in response to regulatory cues (see Figure 13.8).

Transporters exchange substrates and products

The electrochemical proton gradient also plays a role in the movement of the organic acid anions of the TCA cycle, and of the substrates and products of ATP synthesis, into and out of mitochondria (**Figure 13.10**). Although ATP is synthesized in the mitochondrial matrix, most of it is used outside the mitochondrion, so an efficient mechanism is needed for moving ADP (and P_i) into and ATP out of the organelle.

The ADP/ATP (adenine nucleotide) transporter performs the active exchange of ADP and ATP across the inner membrane. The movement of the more negatively charged ATP^{4-} out of the mitochondrion in exchange for ADP^{3-}—that is, one net negative charge out—is driven by the electrical-potential gradient (ΔE, positive outside) generated by proton pumping.

The uptake of inorganic phosphate (P_i) involves an active phosphate transporter protein that uses the chemical-potential component (ΔpH) of the proton motive force to drive the electroneutral exchange of P_i^- (in) for OH^- (out). As long as a ΔpH is maintained across the inner membrane, the P_i content within the matrix remains high. Similar reasoning applies to the uptake of pyruvate, which is driven by the electroneutral exchange of pyruvate for OH^-, leading to efficient uptake of pyruvate from the cytosol (see Figure 13.10).

The total energetic cost of taking up one P_i and one ADP into the matrix and exporting one ATP is equivalent to the movement of one H^+ from the intermembrane space into the matrix:

- Moving one OH^- out in exchange for P_i^- is equivalent to one H^+ in, so this electroneutral exchange consumes the ΔpH, but not the ΔE.
- Moving one negative charge out (ADP^{3-} entering the matrix in exchange for ATP^{4-} leaving) is the same as moving one positive charge in, so this transport lowers only the ΔE.

This proton, which drives the exchange of ATP for ADP and P_i, should also be included in our calculation of the cost of synthesizing one ATP. Thus, the total cost is 3 H^+ used by the ATP synthase plus 1 H^+ for the exchanges across the membrane, or a total of 4 H^+.

The inner membrane also contains transporters for dicarboxylic acids (malate or succinate) exchanged for P_i^{2-} and for the tricarboxylic acids (citrate, aconitate, or isocitrate) exchanged for dicarboxylic acids (see Figure 13.10 and **WEB TOPIC 13.5**).

Aerobic respiration yields about 60 molecules of ATP per molecule of sucrose

The complete oxidation of a sucrose molecule leads to the net formation of:

- Eight molecules of ATP by substrate-level phosphorylation (four from glycolysis and four from the TCA cycle)
- Four molecules of NADH in the cytosol
- Sixteen molecules of NADH plus four molecules of $FADH_2$ (via succinate dehydrogenase) in the mitochondrial matrix

On the basis of theoretical ADP:O values (see Table 13.1), we can estimate that 52 molecules of ATP will be generated per molecule of sucrose by oxidative phosphorylation. The complete aerobic oxidation of sucrose (including substrate-level phosphorylation) results in a total of about 60 ATPs synthesized per sucrose molecule (**Table 13.2**).

Using 50 kJ mol^{-1} as the actual free energy of formation of ATP in vivo, we find that about 3010 kJ mol^{-1} of free energy is conserved in the form of ATP per mole of sucrose oxidized during aerobic respiration. This amount represents about 52% of the standard free energy available from the complete oxidation of sucrose; the rest is lost as heat. It also represents a vast improvement over fermentative metabolism, in which only 4% of the energy available in sucrose is converted into ATP.

Several subunits of respiratory complexes are encoded by the mitochondrial genome

The genetic system of the plant mitochondrion differs not only from that of the nucleus and the chloroplast, but also from those found in the mitochondria of animals, protists, and fungi. Most notably, mitochondrial processes involving RNA differ between plants and most other organisms (see **WEB TOPIC 13.6**). Major differences are found in plants:

- RNA splicing (for example, special introns are present)
- RNA editing (in which the nucleotide sequence is changed)
- Signals regulating RNA stability
- Translation (plant mitochondria use the universal genetic code, whereas mitochondria in many other eukaryotes have deviant codons)

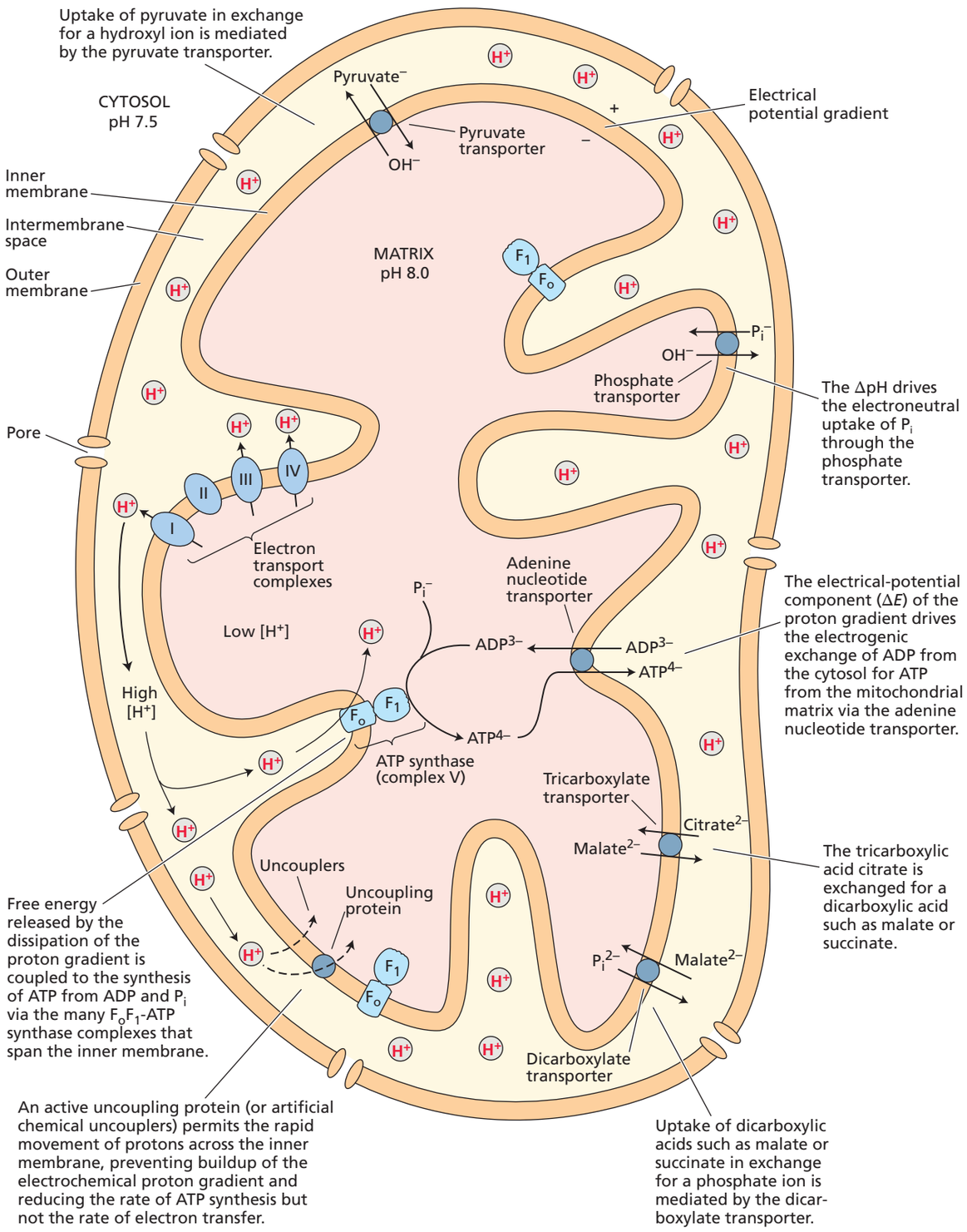


Figure 13.10 Transmembrane transport in plant mitochondria. An electrochemical proton gradient, $\Delta\tilde{\mu}_{H^+}$, consisting of an electrical-potential component (ΔE, –200 mV, negative inside) and a chemical-potential component (ΔpH, alkaline inside), is established across the inner mitochondrial membrane during electron transport. The $\Delta\tilde{\mu}_{H^+}$ is used by specific transporters that move metabolites across the inner membrane.

Table 13.2 The maximum yield of cytosolic ATP from the complete oxidation of sucrose to CO_2 via aerobic glycolysis and the TCA cycle

Part reaction	ATP per sucrose[a]
Glycolysis	
4 substrate-level phosphorylations	4
4 NADH	4 × 1.5 = 6
TCA cycle	
4 substrate-level phosphorylations	4
4 $FADH_2$	4 × 1.5 = 6
16 NADH	16 × 2.5 = 40
Total	**60**

Source: Adapted from M. D. Brand. 1994. *Biochem.* (*Lond.*) 16: 20–24.

Note: Glycolysis is here assumed to use invertase and ATP-phosphofructokinases, but the ATP yield can be higher if other enzymes are active (see **WEB ESSAY 13.1**). Cytosolic NADH is assumed to be oxidized by the external NADH dehydrogenase. The other non-energy-conserving pathways (e.g., the alternative oxidase) are assumed not to be engaged.

[a]Calculated using the theoretical ADP:O values from Table 13.1.

The size of the plant mitochondrial genome varies enormously even among closely related plant species, but at 180 to 11,000 kilobase pairs (kbp), it is always much larger than the compact and uniform 16 kbp genome found in mammalian mitochondria. The size differences are due mainly to the presence of noncoding DNA, including numerous introns, in plant **mitochondrial DNA** (**mtDNA**). Mammalian mtDNA encodes only 13 proteins, in contrast to the 33 proteins encoded by Arabidopsis mtDNA. Both plant and mammalian mitochondria contain genes for rRNAs and tRNAs, but in plants some of the tRNAs are made in the nucleus and imported into the mitochondria. Plant mtDNA encodes several subunits of respiratory complexes I through V, as well as proteins that take part in cytochrome biogenesis. The mitochondrially encoded subunits are essential for the activity of the respiratory complexes.

Except for the proteins encoded by mtDNA, all mitochondrial proteins (probably more than 2000) are encoded by nuclear DNA—including all the proteins of the TCA cycle. These nuclear-encoded mitochondrial proteins are synthesized by cytosolic ribosomes and imported via translocators in the outer and inner mitochondrial membranes. Therefore, oxidative phosphorylation is dependent on expression of genes located in two separate genomes, which must be coordinated to allow synthesis of the respiratory complexes.

Whereas the expression of nuclear genes for mitochondrial proteins is regulated like that of other nuclear genes, less is known about the expression of mitochondrial genes. Genes can be down-regulated by a decreased copy number for the segment of mtDNA that contains the gene. Also, gene promoters in mtDNA are of several kinds and show different transcriptional activities. However, the biogenesis of respiratory complexes appears to be controlled by changes in the expression of the nuclear-encoded subunits; coordination with the mitochondrial genome mainly takes place posttranslationally.

The mitochondrial genome is especially important for pollen development. Naturally occurring rearrangements of genes in the mtDNA lead to so-called cytoplasmic male sterility (CMS). This trait leads to perturbed pollen development by inducing a premature **programmed cell death** (see **WEB ESSAY 13.5**) on otherwise unaffected plants. The CMS traits are used in breeding of several crop plants for making hybrid seed stocks.

Plants have several mechanisms that lower the ATP yield

As we have seen, a complex machinery is required for conserving energy in oxidative phosphorylation. So it is perhaps surprising that plant mitochondria have several functional proteins that reduce this efficiency (see **WEB TOPIC 13.3**). Plants are probably less limited by energy supply (sunlight) than by other factors in the environment (e.g., access to water and nutrients). As a consequence, metabolic flexibility may be more important to them than energetic efficiency.

In the following subsections we discuss the role of three non-energy-conserving pathways and their possible usefulness in the life of the plant: the alternative oxidase, the uncoupling protein, and the rotenone-insensitive NAD(P)H dehydrogenases.

THE ALTERNATIVE OXIDASE Most plants display a capacity for *cyanide-resistant respiration* that is comparable to the capacity of the cyanide-sensitive cytochrome *c* oxidase pathway. The cyanide-resistant oxygen uptake is catalyzed by the alternative oxidase (see Figure 13.9 and **WEB TOPIC 13.3**).

Electrons feed off the main electron transport chain into this alternative pathway at the level of the ubiquinone pool (see Figure 13.8). The alternative oxidase, the only component of the alternative pathway, catalyzes a four-electron reduction of oxygen to water and is specifically inhibited by several compounds, most notably salicylhydroxamic acid. When electrons pass to the alternative pathway from the ubiquinone pool, two sites of proton pumping (at complexes III and IV) are bypassed. Because there is no energy-conservation site in the alternative pathway between ubiquinone and oxygen, the free energy that would normally be conserved as ATP is lost as heat when electrons are shunted through this pathway.

How can a process as seemingly energetically wasteful as the alternative pathway contribute to plant metabolism?

One example of the functional usefulness of the alternative oxidase is in so-called thermogenic flowers of several plant families—for example, the voodoo lily (*Sauromatum guttatum*). In such flowers, a combination of very high respiratory rate and very high alternative oxidase activity leads to massive heat production that is important for pollination (see **WEB ESSAY 13.6**).

In most plants, however, the respiratory rates are too low to generate sufficient heat to raise the temperature significantly. What other role(s) does the alternative pathway play? To answer that question, we need to consider the regulation of the alternative oxidase: Its transcription is often specifically induced, for example, by various types of abiotic and biotic stress. The activity of the alternative oxidase, which functions as a dimer, is regulated by reversible oxidation–reduction of an intermolecular sulfhydryl bridge, by the reduction level of the ubiquinone pool, and by pyruvate. The first two factors ensure that the enzyme is most active under reducing conditions, while the last factor ensures that the enzyme has high activity when there is plenty of substrate for the TCA cycle (see **WEB TOPIC 13.3**).

If the cell consumes relatively little ATP, ADP levels will be low and $\Delta\tilde{\mu}_{H^+}$ will be high. This will restrict the respiration rate, and the reduction level in the mitochondrial electron transport chain will rise and activate the alternative oxidase present. The increased reduction level will also lead to increased formation of reactive oxygen species (ROS), which can cause damage but which also act as a signal for the activation of alternative oxidase expression (see **WEB ESSAY 13.7**). The increased amount of alternative oxidase can prevent overreduction by draining off electrons from the ubiquinone pool (see Figure 13.8), thus limiting the production of ROS and acting as damage control. In this way, the alternative oxidase allows the mitochondrion to adjust the relative rates of ATP production and synthesis of carbon skeletons for use in biosynthetic reactions.

A closely related function of the alternative pathway is in the response of plants to a variety of stresses (e.g., phosphate deficiency, chilling, drought, osmotic stress), many of which can inhibit mitochondrial respiration (see Chapter 15). This inhibition leads to the same induction of the alternative oxidase as that just described. The up-regulation of alternative oxidase expression is an example of *retrograde regulation*, in which nuclear gene expression responds to changes in organellar status by the action of several stress-associated transcription factors (**Figure 13.11**) (see **WEB ESSAY 13.8**).

THE UNCOUPLING PROTEIN A protein found in the inner membrane of mammalian mitochondria, the **uncoupling protein**, can dramatically increase the proton permeability of the membrane and thus act as an uncoupler. As a result, less ATP and more heat are generated. Heat production appears to be one of the uncoupling protein's main functions in mammalian cells.

It had long been thought that the alternative oxidase in plants and the uncoupling protein in mammals were simply two different means of achieving the same end. It was therefore surprising when a protein similar to the uncoupling protein was discovered in plant mitochondria. This protein is induced by stress and stimulated by ROS. In knockout mutants, photosynthetic carbon

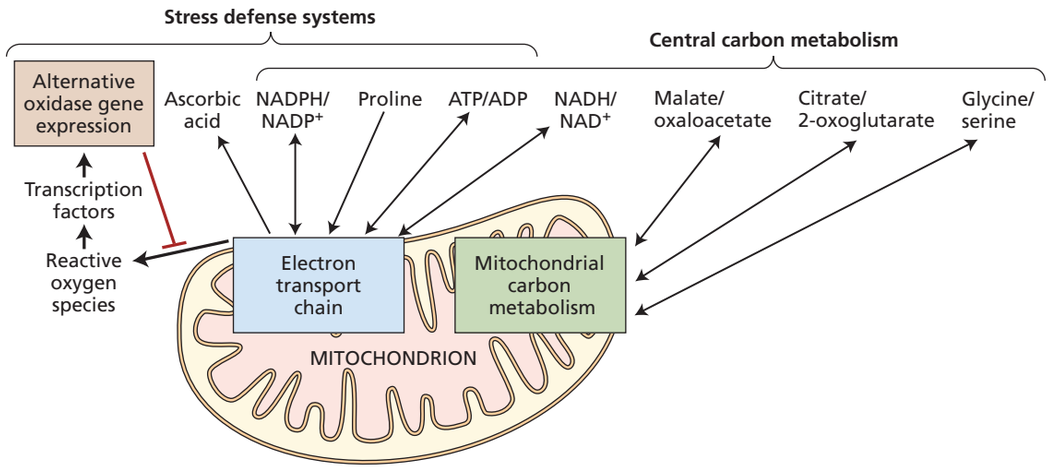


Figure 13.11 Metabolic interactions between mitochondria and cytosol. Mitochondrial activities can influence the cytosolic levels of redox and energy molecules involved in stress defense and in central carbon metabolism (such as growth processes and photosynthesis). An exact distinction between stress defense and carbon metabolism cannot be made because they have components in common. Arrows denote influences caused by changes in mitochondrial synthesis (e.g., reactive oxygen species [ROS], ATP, or ascorbic acid) or degradation (e.g., NAD[P]H, proline, or glycine). The ROS-mediated activation of expression of nuclear genes for the alternative oxidase is an example of retrograde regulation (see **WEB ESSAY 13.8**).

assimilation and growth were decreased consistent with the interpretation that the uncoupling protein, like the alternative oxidase, functions to prevent overreduction of the electron transport chain and formation of ROS (see **WEB TOPIC 13.3** and **WEB ESSAY 13.7**).

ROTENONE-INSENSITIVE NAD(P)H DEHYDROGENASES Multiple rotenone-insensitive dehydrogenases oxidizing NADH or NADPH are found in plant mitochondria (see Figure 13.8 and **WEB TOPIC 13.3**). The internal, rotenone-insensitive NADH dehydrogenase (ND_{in}[NADH]) may work as a non-proton-pumping bypass when complex I is overloaded. Complex I has a higher affinity (ten times lower K_m) for NADH than ND_{in}(NADH). At lower NADH levels in the matrix, typically when ADP is available, complex I dominates, whereas when ADP is rate-limiting, NADH levels increase and ND_{in}(NADH) is more active. ND_{in}(NADH) and the alternative oxidase probably recycle the NADH into NAD^+ to maintain pathway activity. Since reducing power can be shuttled from the matrix to the cytosol by the exchange of different organic acids, external NADH dehydrogenases can have bypass functions similar to those of ND_{in}(NADH). Taken together, these NADH dehydrogenases and the NADPH dehydrogenases are likely to make plant respiration more flexible and allow control of specific redox homeostasis of NADH and NADPH in mitochondria and cytosol (see Figure 13.11).

Respiration is an integral part of a redox and biosynthesis network

In addition to the 2-oxoglutarate provision for nitrogen assimilation mentioned in Section 13.4 (see Figure 13.7C), glycolysis, the oxidative pentose phosphate pathway, and the TCA cycle produce the building blocks for the synthesis of many central plant metabolites, including amino acids, lipids, nucleotides, and hormones and many related compounds (**Figure 13.12**). These are in turn linked to pathways for synthesis of secondary metabolites (see **WEB APPENDIX 4**). Indeed, much of the reduced carbon that is metabolized by glycolysis and the TCA cycle is diverted to biosynthetic purposes and not oxidized to CO_2.

Mitochondria are also a part of the cellular redox network. Variations in consumption or production of redox

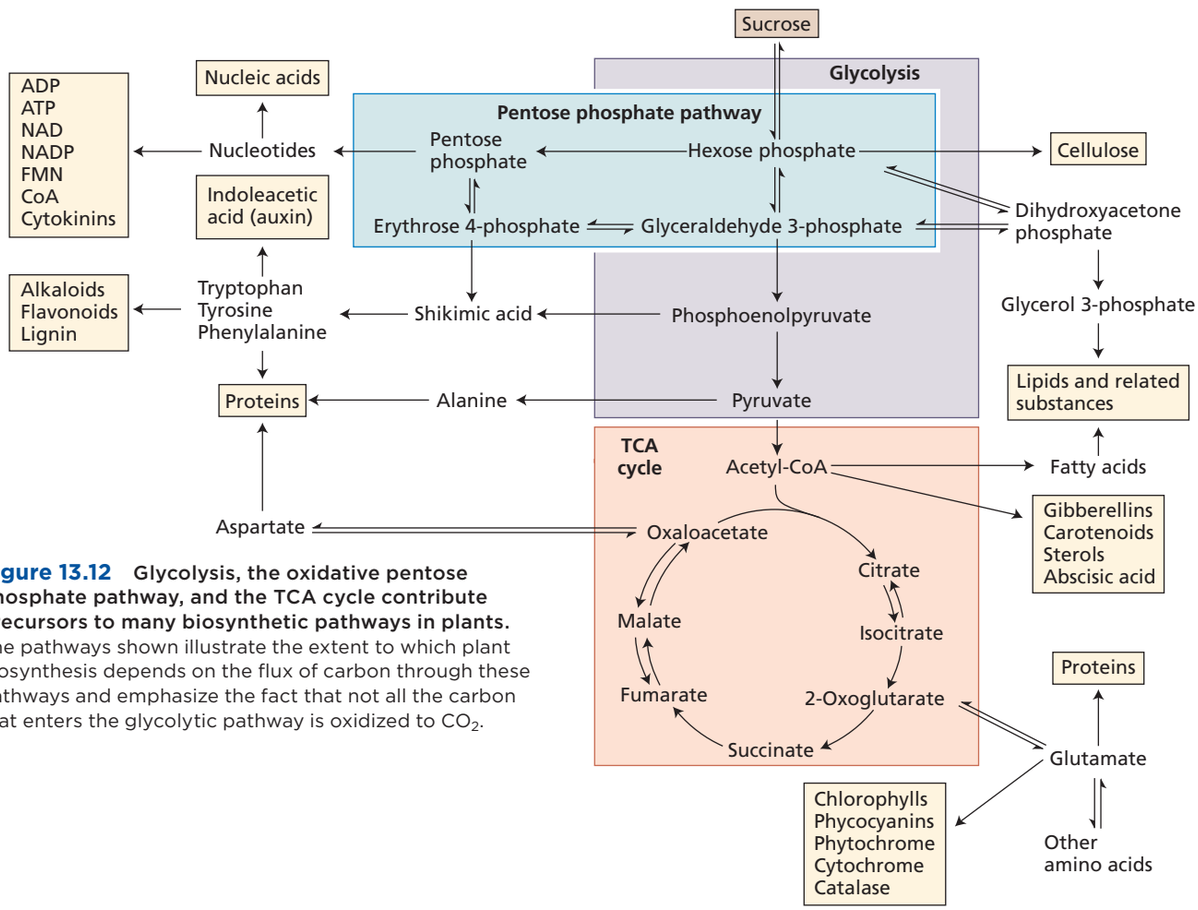


Figure 13.12 Glycolysis, the oxidative pentose phosphate pathway, and the TCA cycle contribute precursors to many biosynthetic pathways in plants. The pathways shown illustrate the extent to which plant biosynthesis depends on the flux of carbon through these pathways and emphasize the fact that not all the carbon that enters the glycolytic pathway is oxidized to CO_2.

and energy-carrying compounds such as NAD(P)H and organic acids affect metabolic pathways in the cytosol and in plastids. Of special importance is the synthesis of ascorbic acid, a central redox and stress defense molecule in plants, by the electron transport chain (see Figure 13.11 and **WEB ESSAY 13.7**). Mitochondria also carry out steps in the biosynthesis of coenzymes necessary for many metabolic enzymes throughout the cell.

Respiration is controlled at multiple levels

Gene expression establishes the protein levels for the respiratory enzymes. The levels change during development, and for some enzymes, such as alternative oxidase and NAD(P)H dehydrogenases, also in response to external factors such as stress, light, and nitrogen supply. However, most respiratory proteins are present in higher abundance than the basic respiration rate requires. Therefore, their activities can be either up- or down-regulated in response to metabolite or redox changes by protein modification or dynamic binding of molecules, and respiration can be rapidly controlled by the demands for its products. Energy-limited shade plants, for example, have been shown to minimize their respiratory rate by minimizing ATP consumption. As a way to achieve this, plant respiratory rate is under "bottom-up" control (**Figure 13.13**). The substrates of ATP synthesis—ADP and P_i—are key short-term regulators of the rates of oxidative phosphorylation, and therefore, via a stepwise series of effects, also of the TCA cycle and glycolysis. Multiple control points exist in all three processes; here we give a brief overview of some major features of the dynamic control of respiration. In contrast to plant cells, animal cells regulate respiration from the "top down," with a primary activation occurring at the phosphofructokinase and secondary activation at the pyruvate kinase.

If a plant cell's demand for ATP in the cytosol decreases relative to the supply, less ADP becomes available for ATP synthesis in the mitochondria, and the electron transport chain will operate at a reduced rate (see Figure 13.13). This slowdown leads to an increase in matrix NADH, which inhibits the activity of pyruvate dehydrogenase and several TCA cycle dehydrogenases, and in matrix NADPH, which is required for thioredoxin function. As in photosynthetic carbon fixation (see Chapter 10), redox levels control TCA cycle enzymes via thioredoxin-mediated removal of cysteine residue dimers. Thus, TCA cycle inhibition results in a buildup of TCA cycle intermediates and their derivatives that directly or indirectly down-regulate the action of upstream steps such as cytosolic pyruvate kinase and PEP carboxylase. This increases the cytosolic PEP concentration, which in turn reduces the rate of conversion of fructose 6-phosphate into fructose 1,6-bisphosphate, thus inhibiting glycolysis (see Figure 13.13). This bottom-up

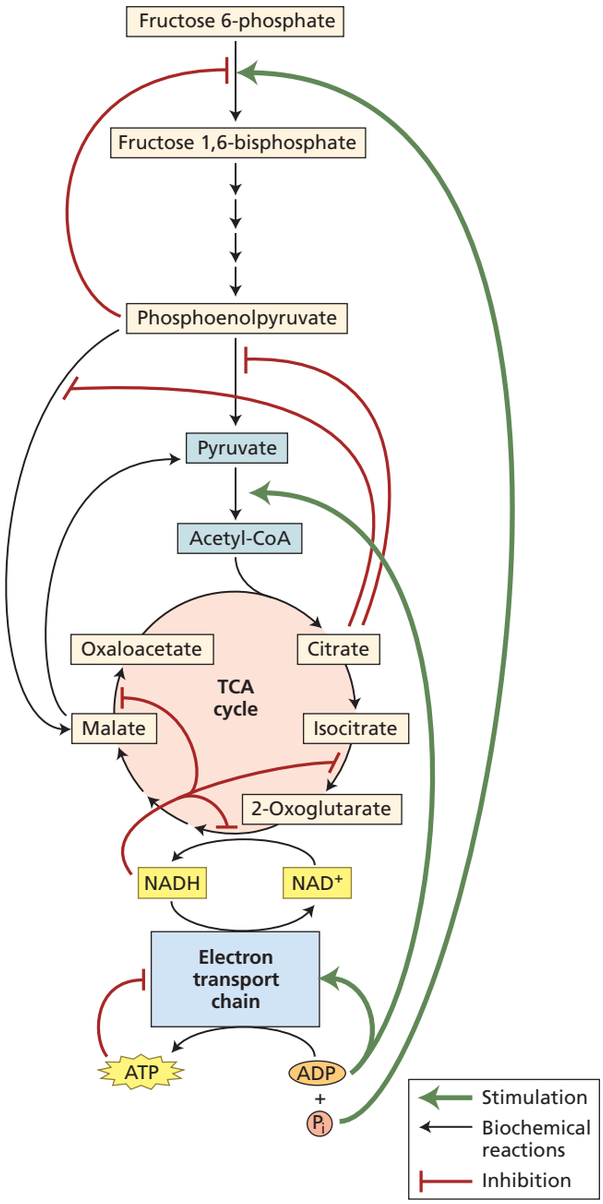
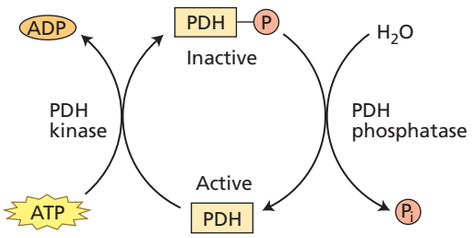


Figure 13.13 Model of bottom-up regulation of plant respiration. Directly or indirectly, several substrates for respiration (e.g., ADP) stimulate while products of respiration (e.g., ATP) inhibit upstream reactions in a stepwise fashion. The image shows a selected set of effects that illustrates the stepwise bottom-up principle. For instance, ATP inhibits the electron transport chain, leading to an accumulation of NADH. NADH inhibits TCA cycle enzymes such as isocitrate dehydrogenase and 2-oxoglutarate dehydrogenase. TCA cycle intermediates such as citrate then inhibit the PEP-metabolizing enzymes in the cytosol. Finally, PEP inhibits the conversion of fructose 6-phosphate into fructose 1,6-bisphosphate and restricts carbon flow into glycolysis. In this way, respiration can be up- or down-regulated in response to changing demands for any of its products: ATP, organic acids, and glycolytic intermediates.



Pyruvate + CoA + NAD^+ ⟶ Acetyl-CoA + CO_2 + NADH + H^+

Effect on PDH activity	Mechanism
Activating	
Pyruvate	Inhibits kinase
ADP	Inhibits kinase
Mg^{2+} (or Mn^{2+})	Stimulates phosphatase
Inactivating	
NADH	Inhibits PDH Stimulates kinase
Acetyl-CoA	Inhibits PDH Stimulates kinase
NH_4^+	Inhibits PDH Stimulates kinase

Figure 13.14 Metabolic regulation of pyruvate dehydrogenase (PDH) activity, directly and by reversible phosphorylation. Upstream and downstream metabolites control PDH activity by direct actions on the enzyme itself or by regulating its protein kinase or protein phosphatase.

inhibitory effect of PEP on ATP-dependent phosphofructokinase activity is strongly decreased by the activator P_i, making the cytosolic ratio of PEP to P_i a critical factor in the control of plant glycolytic activity. Fructose 2,6-bisphosphate (see Chapter 10) also affects the phosphofructokinase reaction, but unlike PEP, it stimulates the reaction in the forward direction by activating *PP_i-dependent phosphofructokinase* and suppresses the reverse direction by inhibiting *fructose 1,6-bisphosphate phosphatase*. In this way, fructose 2,6-bisphosphate affects the partitioning of fixed carbon toward respiration or sugar synthesis.

One benefit of the bottom-up control is that it permits plants to regulate the net glycolytic flux to pyruvate in the cytosol independently of processes such as the photosynthetic sucrose–triose phosphate–starch interconversion. Another benefit is that glycolysis can adjust to the demands for both ATP and biosynthetic precursors from the TCA cycle, such as 2-oxoglutarate needed for nitrogen assimilation (see Chapter 14). The two glycolytic enzymes metabolizing PEP in plant cells—pyruvate kinase and PEP carboxylase—are regulated by similar metabolites, which means that their joint action required for amino acid biosynthesis can be coordinately controlled.

A consequence of bottom-up control of glycolysis is that its rate can influence cellular concentrations of sugars, in combination with sugar-supplying processes such as phloem transport. Glucose and sucrose are potent signaling molecules that help the plant adjust its growth and development to its carbohydrate status. For example, hexokinase not only functions as a glycolytic enzyme, but also as a glucose receptor in the nucleus. This induces sugar-dependent gene expression and works in combination with especially SnRK1- and trehalose 6-phosphate-dependent signaling (see Chapter 10) to adjust plant growth and metabolism to the carbohydrate status.

Pyruvate dehydrogenase is an important control point, especially for reducing TCA cycle activity during photosynthesis. This enzyme is posttranslationally phosphorylated by a *regulatory protein kinase* and dephosphorylated by a *protein phosphatase*. Pyruvate dehydrogenase is inactive in the phosphorylated state, yet the regulatory protein kinase is inhibited by pyruvate, stimulating pyruvate dehydrogenase activity when its substrate is available. In combination with multiple other affectors (**Figure 13.14**), this regulation adjusts the input of substrate to the TCA cycle to the cellular demand.

13.6 Respiration in Intact Plants and Tissues

Many rewarding studies of plant respiration and its regulation have been carried out on organelles and enzymes isolated from plant tissues. But how does this knowledge relate to the function of the whole plant in a natural or agricultural setting?

In this section we examine respiration and mitochondrial function in the context of the whole plant under a variety of conditions. First we explore what happens when green organs are exposed to light: Respiration and photosynthesis operate simultaneously and are functionally integrated in the cell. Next we discuss rates of respiration in different tissues, which may be under developmental control. Finally, we look at the influence of various environmental factors on respiration rates.

Plants respire roughly half of the daily photosynthetic yield

Many factors can affect the respiration rate of an intact plant or of its individual organs. Relevant factors include the species and growth habit of the plant, the type and age of the specific organ, and environmental variables such as light, external O_2 and CO_2 concentrations, temperature, and nutrient and water supply (see Chapter 15). By measuring different oxygen isotopes, it is possible to measure

the in vivo activities of the alternative oxidase and cytochrome *c* oxidase simultaneously. Therefore, we know that a significant part of respiration in most tissues takes place via the "energy-wasting" alternative pathways (see **WEB ESSAY 13.9**).

Whole-plant respiration rates, particularly when considered on a fresh-weight basis, are generally lower than respiration rates reported for animal tissues. This difference is due mainly to the presence in plant cells of a large vacuole and a cell wall, neither of which contains mitochondria. Nonetheless, respiration rates in some plant tissues are as high as those observed in actively respiring animal tissues, so the respiratory process in plants is not inherently slower than in animals (see **WEB ESSAY 13.6**). In fact, isolated plant mitochondria respire as fast as or faster than mammalian mitochondria.

The effect of respiration on the overall carbon economy of the plant can be substantial. Whereas only green tissues photosynthesize, all tissues respire, and they do so 24 h a day. Even in photosynthetically active tissues, respiration, if integrated over the entire day, uses a substantial fraction of the gross photosynthesis. A survey of several herbaceous species indicated that 30 to 60% of the daily gain in photosynthetic carbon is lost to respiration, although these values tend to decrease in older plants. Trees respire a similar fraction of their photosynthetic production, but their respiratory loss increases with age as the ratio of photosynthetic to nonphotosynthetic tissue decreases. In general, unfavorable growth conditions will increase respiration relative to photosynthesis, and thus lower the overall carbon yield available for growth.

Respiratory processes operate during photosynthesis

Mitochondria are involved in the metabolism of photosynthesizing leaves in several ways. Mitochondria are major suppliers of ATP to the cytosol in the light (e.g., for driving biosynthetic pathways), especially under conditions where photosynthetically produced ATP is used in the chloroplasts for carbon fixation. Furthermore, the glycine generated by photorespiration is oxidized to serine in the mitochondrion in a reaction involving mitochondrial oxygen consumption (see Chapter 10). Given that rates of photorespiration often reach 20 to 40% of the gross photosynthetic rate, photorespiration is the largest daytime provider of NADH for the mitochondrial oxidative phosphorylation. By comparison, mitochondria in photosynthesizing tissue do operate some respiration via the TCA cycle, yet far slower than the gross photosynthetic rate, generally by a factor of 6- to 20-fold. The activity of pyruvate dehydrogenase, one of the ports of entry into the TCA cycle, decreases in the light to 25% of its activity in darkness. A basal flux through the respiratory pathways is, however, needed during photosynthesis to supply precursors for biosynthetic reactions, such as the 2-oxoglutarate needed for nitrogen assimilation (see Figures 13.7C and 13.12).

Additional evidence for the involvement of mitochondrial respiration in photosynthesis has been obtained in studies with mitochondrial mutants defective in respiratory complexes. Compared with the wild type, these plants have disturbed leaf development and photosynthesis because changes in levels of redox-active metabolites are communicated between mitochondria and chloroplasts, negatively affecting photosynthetic function.

Different tissues and organs respire at different rates

Respiration is often considered to have two components of comparable magnitude. **Maintenance respiration** is needed to support the function and turnover of the tissues already present. **Growth respiration** provides the energy needed for converting sugars into the building blocks that make up new tissues. A useful rule of thumb is that the greater the overall metabolic activity of a given tissue, the higher its respiration rate. Developing buds usually show very high rates of respiration, and respiration rates of vegetative organs usually decrease from the point of growth (e.g., the leaf tip in eudicots and the leaf base in monocots) to more differentiated regions. A well-studied example is the growing barley leaf.

In mature vegetative organs, stems generally have the lowest respiration rates, whereas leaf and root respiration varies with the plant species and the conditions under which the plants are growing. Low availability of soil nutrients, for example, increases the demand for respiratory ATP production in the root. This increase reflects increased energy costs for active ion uptake and root growth in search of nutrients. **Box 13.1** and **WEB TOPIC 13.7** discuss how crop yield is affected by changes in respiration rates.

When a plant organ reaches maturity, its respiration rate either remains roughly constant or decreases slowly as the tissue ages and ultimately senesces. Exceptions to this pattern include the marked rise in respiration, known as the *climacteric*, that accompanies the onset of ripening in many fruits (e.g., avocado, apple, and banana), and senescence in detached leaves and flowers. During fruit ripening, massive conversion of, for example, starch (banana) or organic acids (tomato and apple) into sugars occurs, accompanied by a rise in the concentration of the hormone ethylene (see Chapter 21) and in the activity of the alternative oxidase pathway.

Different tissues can use different substrates for respiration. Sugars dominate overall, but organic acids contribute in maturing apples and lemons, amino acids in leaves

Box 13.1 Modifying Respiration for Future Needs

To keep up with the growing human population, we need to increase agricultural food production by 70% by year 2060. This must take place without an increase in the cultivated area, with limited water resources in many places, and preferably using fewer agrochemicals. Therefore, we need to develop plants that give a greater net carbon yield by growing more efficiently under future climate conditions.

In plants, a large part (30–60%) of the photosynthetic carbon gain is lost through respiratory processes, and several investigations have shown that respiration can limit the growth rate of plants (see **WEB TOPIC 13.7**). Plant respiration is therefore a relevant target for modification to increase plant productivity.

A simplistic approach would be to remove genes for the non-energy-conserving enzymes NAD(P)H dehydrogenases or alternative oxidase in the mitochondrial electron transport chain. Electrons passing through those enzymes yield 30 to 100% less ATP, so efficiency could potentially be gained by preventing their activity. Unfortunately, suppression of dehydrogenases oxidizing internal NADH or external NADPH in Arabidopsis or suppression of the alternative oxidase in soybean have all given reduced growth under standard greenhouse conditions. This shows that these enzymes have important and nonredundant functions in normal plant growth.

J. S. Amthor and colleagues identified several strategies for specifically decreasing respiratory carbon loss by decreasing the cellular demand for ATP. Here are some examples:

- In plant cells, several ATP-consuming metabolic cycles, so-called futile cycles, take place, such as the simultaneous synthesis and degradation of sucrose and fructose 1,6-bisphosphate in glycolysis. In both cases there is a synthesis enzyme using ATP and another enzyme that performs the reverse reaction, but without ATP recovery (see Figure 13.3). These reactions take place simultaneously, simply consuming ATP without apparent function. If the enzymes could be modified, without creating side effects, to prevent the cycling, ATP could be saved and less respiration would be needed.
- Reschedule the expression of the alternative oxidase so that it is active only during the day, where its activity is required to balance the dissipation of excess reducing power generated by photosynthesis.
- Relocate nitrate assimilation from root to shoot so that the nitrate assimilation in the cytosol and chloroplasts can use the excess reducing power generated by photosynthesis in a more productive way instead of "burning it off' through the alternative oxidase.

To estimate the improvement in net carbon yield that can be achieved, Amthor and colleagues calculated that if all futile cycles could be eliminated (which is quite unrealistic), this could give a reduction in maintenance respiration of 15%, which would give a biomass gain of about 5%. This may not seem like much, but the effects of the various strategies should be additive.

An important issue is to breed plants that are adapted for optimal function at future higher atmospheric CO_2 concentrations and associated higher temperatures and drought. CO_2 release by plant respiration is approximately six times that of anthropogenic release. However, it has been difficult to predict the impact of atmospheric changes on respiration, because it strongly interacts with photosynthesis, photorespiration, and nitrogen assimilation. Therefore, respiratory components of prediction models for future plant growth and the plants' impact on the future atmosphere are less certain.

Another respiratory factor important for global warming is the aerenchyma in flooded plants (see Section 13.6 and Chapter 15). This structure forms the dominant pathway for emission of methane, the second most important greenhouse gas, from flooded soils, especially from rice paddies. ■

during light deprivation, and reductant (NADH) generated from photorespiration in illuminated leaves and lipid degradation, in germinating lipid-containing seeds (see Section 13.7 and Chapter 10). These compounds have different ratios of carbon to oxygen atoms, so the ratio of CO_2 release to O_2 consumption, called the **respiratory quotient** or **RQ**, varies with the substrate oxidized. Since RQ can be determined in the field, it is an important parameter in analyses of carbon metabolism on a larger scale. Alcoholic fermentation releases CO_2 without consuming O_2, so a high RQ is also a marker for fermentation.

Environmental factors alter respiration rates

Many environmental factors can alter the operation of metabolic pathways and change respiratory rates. Disadvantageous growth conditions will generally increase respiration to supply energy for protective reactions. However, environmental oxygen (O_2), temperature, and carbon dioxide (CO_2) can either stimulate or suppress respiration.

OXYGEN Plant respiration can be limited by the supply of oxygen, the terminal substrate in the overall respiratory process. Respiration rates typically decrease if the atmospheric O_2 concentration is below 5% for whole organs or below 2 to 3% for tissue slices. Many plant species, such as tomato and the dogwood tree *Cornus florida*, can survive only in well-drained, aerated soils, because of the need for constant supply of oxygen to their roots from the soil. Oxygen diffuses slowly in aqueous

solutions, both inside and outside the cells. Compact organs such as seeds and potato tubers have a significant O_2 concentration gradient, decreasing from the surface to the center, which can restrict respiration and therefore also the ATP:ADP ratio. The diffusion limitation is most significant in seeds with a thick seed coat and in plant organs submerged in water. The problem of oxygen supply is particularly important in plants growing in very wet or recurrently flooded soils, where limitation in oxygen supply to the root can be severe (see also Chapter 15). Such roots must survive on anaerobic (fermentative) metabolism (see Figure 13.3) or develop structures that can supply oxygen to the roots.

Intercellular air spaces (called **aerenchyma**) form continuous gaseous passageways from the leaves to the roots to provide them with oxygen, avoiding the restriction of respiration and potential death of the plant. Aerenchyma can be permanent, as in rice and water lilies, or be induced by hypoxia, as in maize, which can survive temporary flooding. Extreme examples of permanent oxygen-supplying structures are outgrowths of roots, called *pneumatophores*, that protrude out of the water and provide a gaseous pathway for oxygen diffusion to the root cells. Pneumatophores are found in *Avicennia* and *Rhizophora*, trees that grow in mangrove swamps under continuously flooded conditions.

TEMPERATURE Respiration operates over a wide temperature range (see **WEB ESSAYS 13.4**, **13.6**, and **13.9**). Over short time, it typically increases with temperatures between 0 and 30°C and reaches a plateau at 40 to 50°C. At higher temperatures, it again decreases because of inactivation of the respiratory machinery. The increase in respiration rate for every 10°C increase in temperature is called the **temperature coefficient**, Q_{10}. This ratio varies with plant development and external factors. On a longer timescale, plants acclimate to low temperatures by increasing their respiratory capacity so that ATP production can be maintained.

Low temperatures are used to retard postharvest respiration during the storage of fruits and vegetables, but those temperatures must be adjusted with care. For instance, when potato tubers are stored at temperatures above 10°C, respiration and ancillary metabolic activities are sufficient to allow sprouting. However, below 5°C, stored starch is converted into sucrose (which protects against frost damage), imparting an unwanted sweetness to the tubers. Therefore, potatoes are best stored at 7 to 9°C, which prevents the breakdown of starch while minimizing respiration and germination (see also **WEB ESSAY 13.4** for other temperature effects on respiration).

CARBON DIOXIDE It is common in commercial practice to store fruits at low temperatures under 2 to 3% O_2. The reduced temperature lowers the respiration rate, as does the reduced O_2 level. Low levels of oxygen, instead of anoxic conditions, are used in order to avoid fermentative metabolism. Additionally, an artificially elevated CO_2 concentration (3–5%) is used because it has a direct inhibitory effect on respiration.

The atmospheric CO_2 concentration is currently (2020) about 415 ppm, but because of human activities it is projected to reach about 700 ppm before year 2100 (see Chapter 11). Plant CO_2 uptake by photosynthesis and release by plant respiration are both much larger processes than the release of CO_2 caused by burning of fossil fuels. Therefore, small effects of elevated CO_2 concentrations on plant respiration will affect future global atmospheric changes.

Within the range relevant for atmospheric changes, there is no direct effect of CO_2 concentration on plant respiration. Over longer time, changes in carbon substrate availability, allocation and partitioning (see Chapter 12), and in gene expression will affect plant respiration, yet this is highly variable among plant species, making global predictions difficult. The CO_2-induced increase in temperature (global warming) is expected to generate an increase in respiration that is, however, smaller than the increase in photosynthesis. There is no present concensus that elevations in atmospheric CO_2 would be attenuated by a feedback inhibition of respiration.

13.7 Lipid Metabolism

Lipids are essential for life because of their roles in membrane structure and function as well as for energy and carbon storage. All plant cell membranes have distinct lipid compositions, such as the inner membrane of mitochondria in which cardiolipin contributes to cristae architecture and interacts with electron transfer chain components. Fats and oils are important storage forms of reduced carbon in many seeds, including those of agriculturally important species such as soybean, sunflower, canola, peanut, and cotton. Some fruits, such as olives and avocados, also store fats and oils.

In this final part of the chapter we describe the biosynthesis of two types of glycerolipids: the *triacylglycerols* (the fats and oils stored in seeds) and the *polar glycerolipids* (which form the lipid bilayers of cellular membranes) (**Figure 13.15**). We will see that the biosynthesis of triacylglycerols and polar glycerolipids requires the cooperation of two organelles: the plastid and the endoplasmic reticulum. We also examine the complex process by which germinating seeds obtain carbon skeletons and metabolic energy from the oxidation of fats and oils.

Fats and oils store large amounts of energy

Fats and oils belong to the general class termed *lipids*, a structurally diverse group of hydrophobic compounds

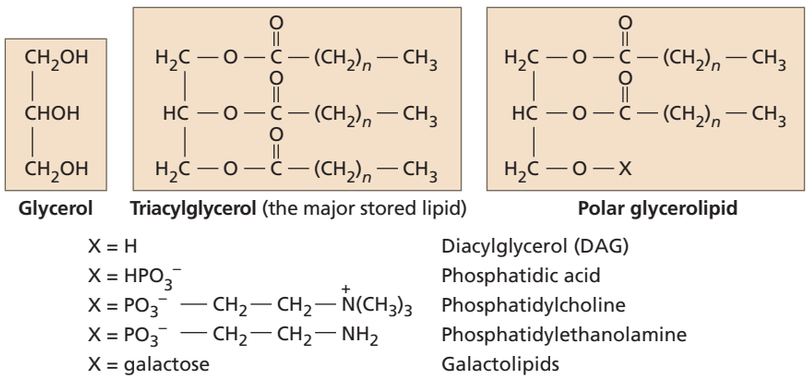


Figure 13.15 Structural features of triacylglycerols and polar glycerolipids in higher plants. The carbon chain lengths of the fatty acids, which always have an even number of carbons, range from 8 to 30 but are typically 16 or 18. Thus, the value of *n* is usually 14 or 16.

that are soluble in organic solvents and highly insoluble in water. Lipids represent a more reduced form of carbon than carbohydrates, so the complete oxidation of 1 g of fat or oil (which contains about 40 kJ of energy) can produce considerably more ATP than the oxidation of 1 g of starch (about 15.9 kJ). Conversely, the biosynthesis of lipids requires a correspondingly large investment of metabolic energy.

Other lipids are important for plant structure and function but are not used for energy storage. These lipids include the phospholipids and galactolipids that are components of plant membranes, as well as sphingolipids, which are also important membrane components; cutin and waxes, which make up the protective cuticle that reduces water loss from exposed plant tissues; and terpenoids (also known as isoprenoids), which include carotenoids involved in photosynthesis and sterols present in many plant membranes.

Triacylglycerols are stored in oil bodies

Fats and oils exist mainly in the form of **triacylglycerols** (*acyl* refers to the fatty acid portion), in which fatty acid molecules are linked by ester bonds to the three hydroxyl groups of glycerol (see Figure 13.15).

The fatty acids in plants are usually straight-chain carboxylic acids having an even number of carbon atoms. The carbon chains can be as short as 8 units and as long as 30 or more, but most commonly are 16 or 18 carbons long. Fatty acids are often indicated by a numerical abbreviation that contains their number of carbons and number of double bonds, separated by a colon (e.g., 16:0, 18:1). *Oils* are liquid at room temperature, primarily because of the presence of carbon–carbon double bonds (unsaturation) in their component fatty acids; *fats*, which have a higher proportion of saturated fatty acids, are solid at room temperature. The major fatty acids in plant lipids are shown in **Table 13.3**. However, several plant species synthesize unusual, industrially useful fatty acids in their seed oils (see **WEB ESSAY 13.10**). **Box 13.2** discusses why plant lipids are a focus of biotechnology.

The proportions of fatty acids in plant oils vary with the plant species. For example, peanut oil is about 9% palmitic acid, 59% oleic acid, and 21% linoleic acid, and soybean oil is 13% palmitic acid, 7% oleic acid, 51% linoleic acid, and 23% linolenic acid. We discuss the biosynthesis of these fatty acids later in this section.

In most seeds, triacylglycerols are stored in the cytoplasm of either cotyledon or endosperm cells in

Table 13.3 Common fatty acids in higher plant tissues

Name[a]	Structure
Saturated fatty acids	
Lauric acid (12:0)	$CH_3(CH_2)_{10}CO_2H$
Myristic acid (14:0)	$CH_3(CH_2)_{12}CO_2H$
Palmitic acid (16:0)	$CH_3(CH_2)_{14}CO_2H$
Stearic acid (18:0)	$CH_3(CH_2)_{16}CO_2H$
Unsaturated fatty acids	
Oleic acid (18:1)	$CH_3(CH_2)_7CH{=}CH(CH_2)_7CO_2H$
Linoleic acid (18:2)	$CH_3(CH_2)_4CH{=}CH{-}CH_2{-}CH{=}CH(CH_2)_7CO_2H$
Linolenic acid (18:3)	$CH_3CH_2CH{=}CH{-}CH_2{-}CH{=}CH{-}CH_2{-}CH{=}CH{-}(CH_2)_7CO_2H$

[a]Each fatty acid has a numerical abbreviation. The number before the colon represents the total number of carbons; the number after the colon is the number of double bonds.

Box 13.2 Biotechnology of Lipids in a Changing World

The glycerolipids in cellular membranes are integral to temperature responses of plants. As the climate transition takes hold, our knowledge of how the biochemistry and membrane physiology of lipids affect the temperature responses of photosynthesis, respiration, and other processes will be used to strengthen the adaptability of crops and other plants to the altered environments in which they will be grown.

Plant lipids, especially vegetable oils produced by soybean, canola, oil palm, and other crops, have been a focus of biotechnology for several decades. The most successful use of biotechnology has been the production of high-oleic soybean (Qualisoy) and canola varieties that have allowed for the elimination of unhealthy trans fats from food. Researchers are also exploring possibilities for producing oil in leaves of crop plants to provide for energy-dense biofuels. Finally, transferring the pathways for synthesis of unusual fatty acids found in some wild plant species to crop plants will provide chemical feedstocks for the synthesis of plastics, resins, and other products for society. ■

organelles known as **oil bodies** (also called *lipid droplets*) (see Chapter 1). The oil-body membrane is a single layer of phospholipids (i.e., a half-bilayer) with the hydrophilic ends of the phospholipids exposed to the cytosol and the hydrophobic acyl hydrocarbon chains facing the triacylglycerol interior (see Chapter 1). The oil body is stabilized by the presence of specific proteins, called oleosins, that coat its outer surface and prevent the phospholipids of adjacent oil bodies from coming in contact and fusing.

The unique membrane structure of oil bodies results from the pattern of triacylglycerol biosynthesis. Triacylglycerol synthesis is completed by enzymes located in the membranes of the endoplasmic reticulum (ER), and the resulting fats accumulate between the two monolayers of the ER membrane bilayer. The bilayer swells apart as more fats are added to the growing structure, while the oleosins are synthesized by ribosomes attached on the ER, and ultimately a mature oil body coated with oleosins buds off from the ER.

Polar glycerolipids are the main structural lipids in membranes

As outlined in Chapter 1, each membrane in the cell is a bilayer of *amphipathic* (i.e., having both hydrophilic and hydrophobic regions) lipid molecules in which a polar head group interacts with the aqueous environment while hydrophobic fatty acid chains form the core of the membrane. This hydrophobic core prevents unregulated diffusion of solutes between cell compartments and thereby allows the metabolism of the cell to be organized.

The main structural lipids in membranes are the **polar glycerolipids** (see Figure 13.15), in which the hydrophobic portion consists of two 16-carbon or 18-carbon fatty acid chains esterified to positions 1 and 2 of a glycerol backbone. The polar head group is attached to position 3 of the glycerol. There are two categories of polar glycerolipids:

1. **Glyceroglycolipids**, in which sugars form the head group (**Figure 13.16A**)
2. **Glycerophospholipids**, in which the head group contains phosphate (**Figure 13.16B**)

Plant membranes have additional structural lipids, including sphingolipids and sterols, which are structural and functional components of the plasma membrane (see Chapters 1 and 4). Other lipids perform specific roles in photosynthesis and other processes. Included among these lipids are chlorophylls, plastoquinone, ubiquinone, carotenoids, and tocopherols, which together account for about one-third of the lipids in plant leaves.

Figure 13.16 shows the nine major polar glycerolipid classes in plants, each of which can be associated with many different fatty acid combinations. The structures shown in Figure 13.16 illustrate some of the more common molecular species.

Chloroplast membranes, which account for 70% of the membrane lipids in photosynthetic tissues, are dominated by glyceroglycolipids; other membranes of the cell contain glycerophospholipids (**Table 13.4**). In nonphotosynthetic tissues, glycerophospholipids are the major membrane glycerolipids. Interestingly, under phosphate starvation, many plant species partially replace glycerophospholipids with glyceroglycolipids, to allow some recovery of phosphate for the synthesis of RNA and other phosphorus-rich compounds.

Fatty acid biosynthesis consists of cycles of two-carbon addition

Fatty acid biosynthesis involves the cyclic condensation of two-carbon units derived from acetyl-CoA. In plants, fatty acids are synthesized primarily in the plastids, while in animals they are synthesized primarily in the cytosol.

The enzymes of the biosynthesis pathway are thought to be held together in a complex that is collectively referred to as *fatty acid synthase*. The complex probably allows the series of reactions to occur more efficiently than it would if the enzymes were physically separated from one another. In addition, the growing acyl chains are covalently bound to a low molecular weight acidic protein called the **acyl carrier protein** (**ACP**). When conjugated to the acyl carrier protein, an acyl chain is referred to as **acyl-ACP**.

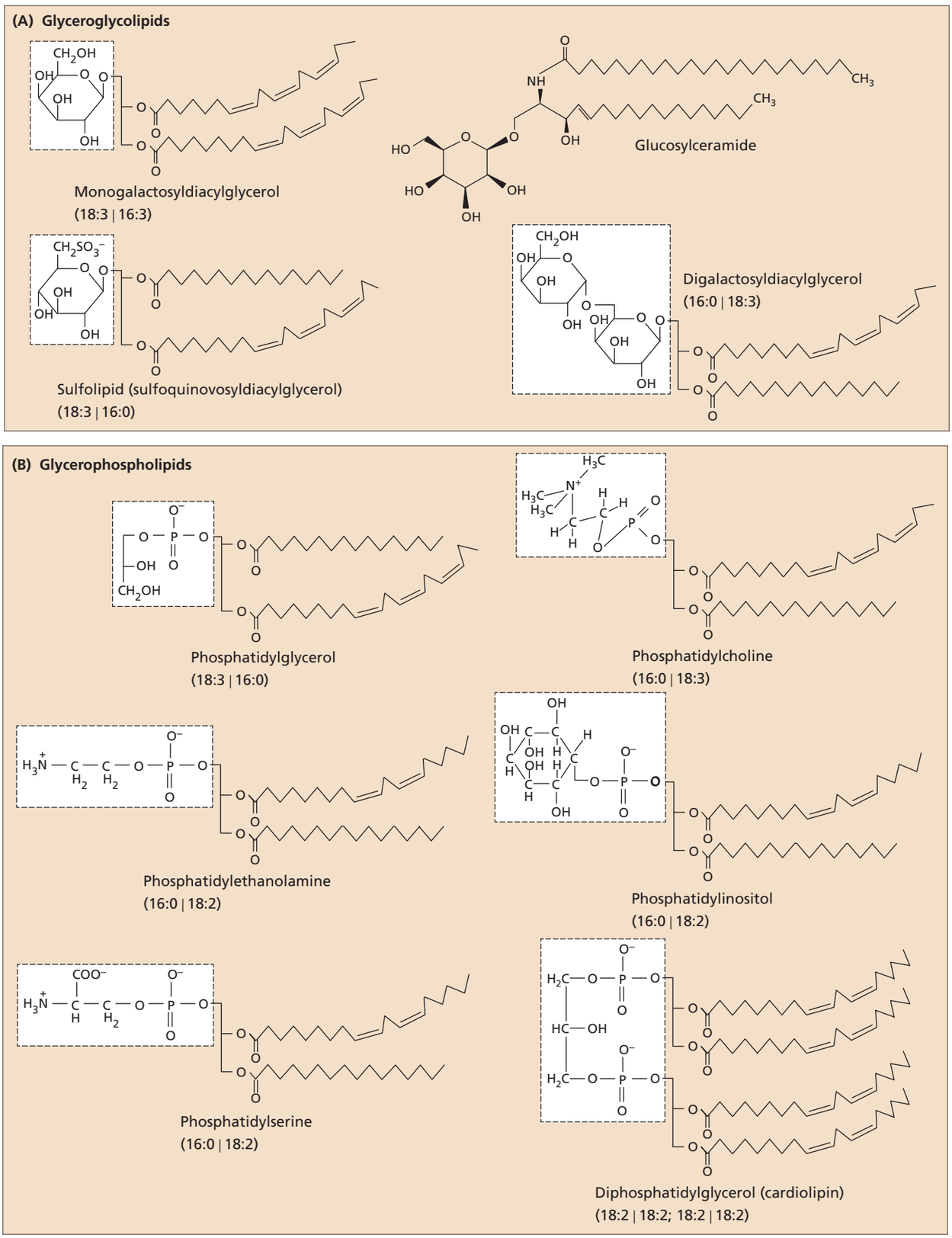

(A) Glyceroglycolipids
Monogalactosyldiacylglycerol
(18:3 | 16:3)
Glucosylceramide
Sulfolipid (sulfoquinovosyldiacylglycerol)
(18:3 | 16:0)
Digalactosyldiacylglycerol
(16:0 | 18:3)
(B) Glycerophospholipids
Phosphatidylglycerol
(18:3 | 16:0)
Phosphatidylcholine
(16:0 | 18:3)
Phosphatidylethanolamine
(16:0 | 18:2)
Phosphatidylinositol
(16:0 | 18:2)
Phosphatidylserine
(16:0 | 18:2)
Diphosphatidylglycerol (cardiolipin)
(18:2 | 18:2; 18:2 | 18:2)

Figure 13.16 **Major polar glycerolipid classes found in plant membranes:** (A) Glyceroglycolipids and a sphingolipid and (B) glycerophospholipids. Two of at least six different fatty acids may be attached to the glycerol backbone. One of the more common molecular species is shown for each glycerolipid class. The numbers given below each name refer to the number of carbons (number before the colon) and the number of double bonds (number after the colon).

The first committed step in the pathway (i.e., the first step unique to the synthesis of fatty acids) is the synthesis of malonyl-CoA from acetyl-CoA and CO_2 by the enzyme *acetyl-CoA carboxylase* (**Figure 13.17**). The tight regulation of acetyl-CoA carboxylase appears to control the overall rate of fatty acid synthesis. The malonyl-CoA reacts with ACP to yield malonyl-ACP, then fatty acid synthesis proceeds through repeated cycles of the following four steps:

1. In the first cycle of fatty acid synthesis, the acetate group from acetyl-CoA is transferred to a specific cysteine of condensing enzyme (3-ketoacyl-ACP synthase) and then combined with malonyl-ACP to form acetoacetyl-ACP, with loss of CO_2.
2. Next the keto group at carbon 3 is removed (reduced, using 2 NADPH) by the action of three enzymes to form a new acyl chain (butyryl-ACP), which is now four carbons long (see Figure 13.17).
3. The four-carbon fatty acid and another molecule of malonyl-ACP then become the new substrates for condensing enzyme, resulting in the addition of another two-carbon unit to the growing chain. The cycle continues until 16 or 18 carbons have been added.
4. Some 16:0-ACP is released from the fatty acid synthase machinery, but most molecules that are

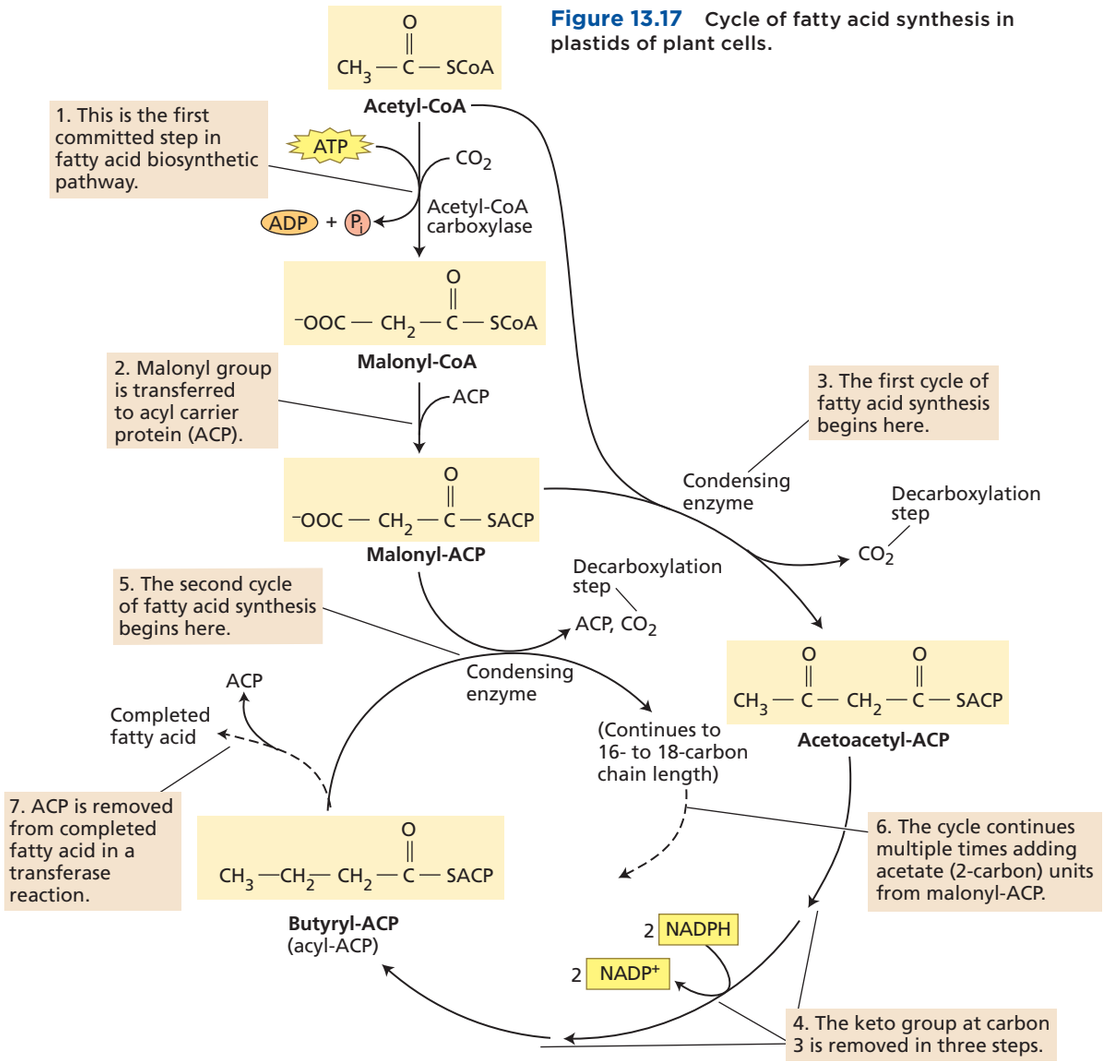


Figure 13.17 **Cycle of fatty acid synthesis in plastids of plant cells.**

Table 13.4 Glycerolipid components of cellular membranes

	Lipid composition (mole percentages of total)		
Lipid	Chloroplast	Endoplasmic reticulum	Mitochondrion
Phosphatidylcholine	4	47	43
Phosphatidylethanolamine	—	34	35
Phosphatidylinositol	1	17	6
Phosphatidylglycerol	7	2	3
Diphosphatidylglycerol (cardiolipin)	—	—	13
Monogalactosyldiacylglycerol	55	—	—
Digalactosyldiacylglycerol	24	—	—
Sulfolipid	8	—	—

elongated to 18:0-ACP are efficiently converted into 18:1-ACP by a desaturase enzyme. Thus, 16:0-ACP and 18:1-ACP are the major products of fatty acid synthesis in plastids (**Figure 13.18**).

Fatty acids may undergo further modification after they are linked with glycerol to form glycerolipids. Additional double bonds are placed in the 16:0 and 18:1 fatty acids by a series of desaturase isozymes. *Desaturase isozymes* are integral membrane proteins found in the chloroplast and the ER. Each desaturase inserts a double bond at a specific position in the fatty acid chain, and the enzymes act sequentially to produce the final 18:3 and 16:3 products.

Glycerolipids are synthesized in the plastids and the ER

The fatty acids synthesized in the chloroplast are next used to make the glycerolipids of membranes and oil bodies. The first steps of glycerolipid synthesis are two acylation reactions that transfer fatty acids from acyl-ACP or acyl-CoA to glycerol-3-phosphate to form **phosphatidic acid**.

The action of a specific phosphatase produces **diacylglycerol** (**DAG**) from phosphatidic acid. Phosphatidic acid can also be converted directly into phosphatidylinositol or phosphatidylglycerol; DAG can give rise to phosphatidylethanolamine or phosphatidylcholine (see Figure 13.18).

The localization of the enzymes of glycerolipid synthesis reveals a complex and highly regulated interaction between the chloroplast, where fatty acids are synthesized, and other membrane systems of the cell. In simple terms, the biochemistry involves two pathways referred to as the prokaryotic (or chloroplast) pathway and the eukaryotic (or ER) pathway:

1. In chloroplasts, the **prokaryotic pathway** uses the 16:0-ACP and 18:1-ACP products of chloroplast fatty acid synthesis to synthesize phosphatidic acid and its derivatives. Alternatively, the fatty acids may be exported to the cytoplasm as CoA esters.
2. In the cytoplasm, the **eukaryotic pathway** uses a separate set of acyltransferases in the ER to incorporate the fatty acids into phosphatidic acid

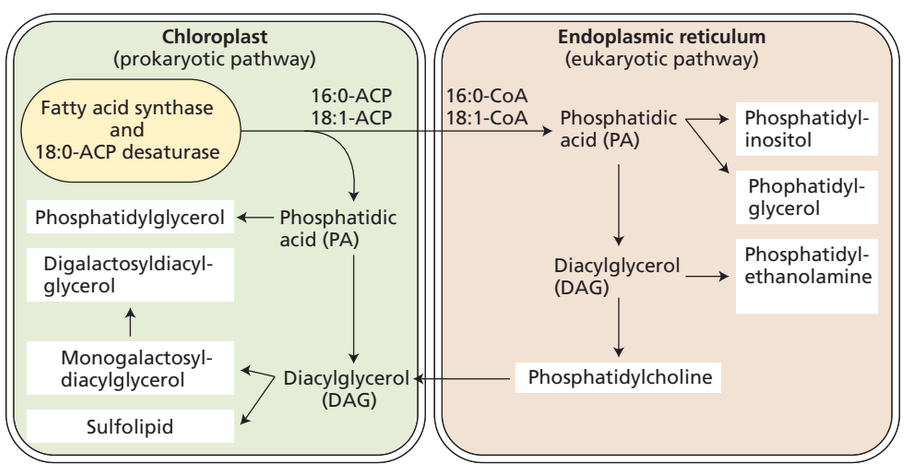


Figure 13.18 **The two pathways for glycerolipid synthesis in the chloroplast and endoplasmic reticulum of Arabidopsis leaf cells.** The major membrane components are shown in boxes. Desaturases in the chloroplast and the ER convert 16:0 and 18:1 fatty acids into the more highly unsaturated fatty acids shown in Figure 13.16.

and its derivatives. Fatty acids are also incorporated directly into phosphatidylcholine (PC) by an exchange reaction. A large proportion of the PC synthesized is turned over to return lipid molecules to the chloroplast.

A simplified version of this two-pathway model is depicted in Figure 13.18.

In some higher plants, including Arabidopsis and spinach, the two pathways contribute almost equally to chloroplast lipid synthesis. In many other angiosperms, however, phosphatidylglycerol is the only product of the prokaryotic pathway, and the remaining chloroplast lipids are synthesized entirely by the eukaryotic pathway.

The biochemistry of triacylglycerol synthesis in oilseeds is generally the same as described for the glycerolipids: 16:0-ACP and 18:1-ACP are synthesized in the plastids of the cell and exported as CoA thioesters for incorporation into DAG and PC in the ER (see Figure 13.18).

The key enzymes in oilseed metabolism (not shown in Figure 13.18) are *PC:DAG cholinephosphotransferase*, which interconverts phosphatidylcholine and diacylglycerol, and *acyl-CoA:DAG acyltransferase* and *PC:DAG acyltransferase*, which catalyze triacylglycerol synthesis. As noted earlier, triacylglycerol molecules accumulate in specialized subcellular structures—the oil bodies—from which they can be mobilized during germination and converted into sugars.

Lipid composition influences membrane function

A central question in membrane biology is the functional reason behind lipid diversity. Each membrane system of the cell has a characteristic and distinct complement of lipid types, and within a single membrane, each class of lipids has a distinct fatty acid composition (see Table 13.4). Why is lipid diversity needed?

One aspect of membrane biology that might offer answers to this central question is the relationship between lipid composition and the ability of organisms to adjust to temperature changes. For example, chill-sensitive plants experience sharp reductions in growth rate and development at temperatures between 0 and 12°C (see Chapter 15). Many economically important crops, such as cotton, soybean, maize, rice, and many tropical and subtropical fruits, are classified as chill-sensitive. In contrast, most plants that originate from temperate regions are able to grow and develop at chilling temperatures and are classified as chill-resistant plants.

It has been suggested that, because of the decrease in lipid fluidity at lower temperatures, the primary event of chilling injury is *a transition from a liquid-crystalline phase to a gel phase* in cellular membranes. According to this hypothesis, such a transition results in alterations in the metabolism of chilled cells and would lead to injury and death of the chill-sensitive plants. Several lines of evidence indicate that high levels of saturated fatty acids in phosphatidylglycerol are specifically associated with chilling sensitivity.

Other research, however, suggests that the relationship between membrane unsaturation and plant responses to temperature is more subtle and complex (see **WEB TOPIC 13.8**). The responses of Arabidopsis mutants with increased saturation of fatty acids to low temperatures are not what is predicted by the chill-sensitivity hypothesis, suggesting that normal chilling injury may not be strictly related to the level of unsaturation of membrane lipids.

These findings make it clear that either the extent of membrane unsaturation or the presence of particular lipids, such as desaturated phosphatidylglycerol, can affect the responses of plants to low temperatures. As discussed in **WEB TOPIC 13.8**, more work is required to fully understand the relationship between lipid composition and membrane function.

Membrane lipids are precursors of important signaling compounds

Plants, animals, and microbes all use membrane lipids as precursors for compounds that are used for intracellular or long-range signaling. For example, jasmonate hormone—derived from linolenic acid (18:3)—activates plant defenses against insects and many fungal pathogens (see Chapters 4 and 24). In addition, jasmonate regulates other aspects of plant growth, including flower and seed development.

Phosphatidylinositol 4,5-bisphosphate (**PIP_2**) is the most important of several phosphorylated derivatives of phosphatidylinositol known as *phosphoinositides*. In animals, receptor-mediated activation of phospholipase C leads to the hydrolysis of PIP_2 into inositol trisphosphate ($InsP_3$) and diacylglycerol, both of which act as intracellular secondary messengers.

The action of $InsP_3$ in releasing Ca^{2+} into the cytoplasm (through Ca^{2+}-sensitive channels in the tonoplast and other membranes), and thereby regulating cellular processes, has been demonstrated in several plant systems, including the stomatal guard cells. Information about other types of lipid signaling in plants is becoming available through biochemical and molecular genetic studies of phospholipases and other enzymes involved in the generation of these signals.

Storage lipids are converted into carbohydrates in germinating seeds

After germinating, oil-containing seeds metabolize stored triacylglycerols by converting them into sucrose. Plants are not able to transport fats from the cotyledons to other tissues of the germinating seedling, so they must convert stored lipids into a more mobile form of carbon, generally

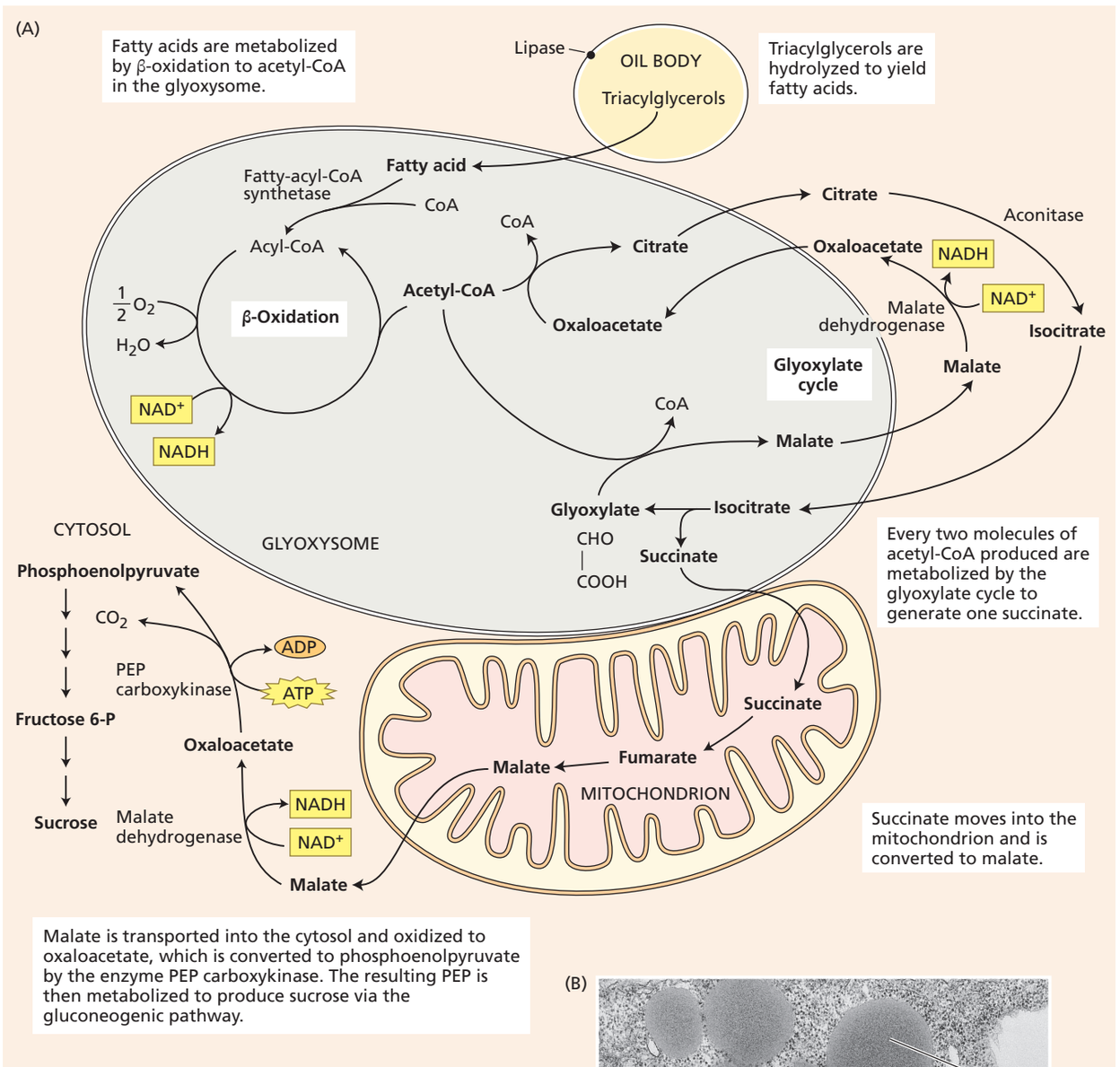


Figure 13.19 **Conversion of fats into sugars during germination in oil-storing seeds.** (A) Carbon flow during fatty acid breakdown and gluconeogenesis (see Figures 13.2, 13.3, and 13.6 for chemical structures). (B) Electron micrograph of a cell from the oil-storing cotyledon of a cucumber seedling, showing glyoxysomes, mitochondria, and oil bodies.

sucrose. This process involves several steps that are located in different cellular compartments: oil bodies, glyoxysomes, mitochondria, and the cytosol.

OVERVIEW: LIPIDS TO SUCROSE In oilseeds, the conversion of lipids into sucrose is triggered by germination. It begins with the hydrolysis of triacylglycerols stored in oil bodies into free fatty acids, followed by oxidation of those fatty acids in glyoxysomes to produce acetyl-CoA (**Figure 13.19**). In most oilseeds, approximately 30% of the acetyl-CoA is used for energy production via respiration, and the rest is converted into sucrose through the glyoxylate cycle and gluconeogenesis.

LIPASE-MEDIATED HYDROLYSIS The initial step in the conversion of lipids into carbohydrates is the breakdown of triacylglycerols stored in oil bodies by a lipase, which hydrolyzes triacylglycerols into three fatty acid molecules and one molecule of glycerol. During the breakdown of lipids, oil bodies and glyoxysomes are generally in close physical association (see Figure 13.19B).

β–OXIDATION OF FATTY ACIDS The fatty acid molecules enter the glyoxysome, where they are activated by conversion into fatty-acyl-CoA by *fatty-acyl-CoA synthetase*. Fatty-acyl-CoA is the initial substrate for the **β-oxidation** series of reactions, in which C_n fatty acids (fatty acids composed of n carbons) are sequentially broken down into $n/2$ molecules of acetyl-CoA (see Figure 13.19A). This reaction sequence involves the reduction of ½ O_2 to H_2O and the formation of one NADH for each β-oxidation cycle.

In mammalian tissues, the four enzymes associated with β-oxidation are present in the mitochondrion. In plant seed storage tissues, they are located exclusively in the glyoxysome or the equivalent organelle in vegetative tissues, the peroxisome (see Chapter 1).

THE GLYOXYLATE CYCLE The function of the **glyoxylate cycle** is to convert two molecules of acetyl-CoA into succinate. The acetyl-CoA produced by β-oxidation is metabolized in the glyoxysome through a series of reactions that make up the glyoxylate cycle (see Figure 13.19A). Initially, the acetyl-CoA reacts with oxaloacetate to give citrate, which is then transferred to the cytoplasm for isomerization to isocitrate by aconitase. Isocitrate is reimported into the glyoxysome and converted into malate by two reactions that are unique to the glyoxylate cycle:

1. First, isocitrate (C_6) is cleaved by the enzyme isocitrate lyase to give succinate (C_4) and glyoxylate (C_2). The succinate is exported to the mitochondria.
2. Next, malate synthase combines a second molecule of acetyl-CoA with glyoxylate to produce malate (C_4).

Malate is then transferred to the cytoplasm and converted into oxaloacetate by the cytoplasmic isozyme of malate dehydrogenase. Oxaloacetate is reimported into the glyoxysome and combines with another acetyl-CoA to continue the cycle (see Figure 13.19A). The glyoxylate produced keeps the cycle operating, but the succinate is exported to the mitochondria for further processing.

THE MITOCHONDRIAL ROLE Moving from the glyoxysomes to the mitochondria, the succinate is converted into malate by the two corresponding TCA cycle reactions. The resulting malate can be exported from the mitochondria in exchange for succinate via the dicarboxylate transporter located in the inner mitochondrial membrane. Malate is then oxidized to oxaloacetate by malate dehydrogenase in the cytosol, and the resulting oxaloacetate is converted into carbohydrates by the reversal of glycolysis (gluconeogenesis). This conversion requires circumventing the irreversibility of the PEP carboxylase reaction (see Figure 13.3) and is facilitated by PEP carboxykinase, which uses ATP as a phosphate group donor to convert oxaloacetate into PEP and CO_2 (see Figure 13.19A).

From PEP, gluconeogenesis can proceed to the production of glucose, as described in Section 13.2. Sucrose is the final product of this process, and is the primary form of reduced carbon translocated from the endosperm or cotyledons to the growing seedling tissues. Not all seeds quantitatively convert fat into sugar.

Summary

Using the building blocks provided by photosynthesis, respiration releases the energy stored in carbon compounds in a controlled manner for cellular use. At the same time, it generates many carbon precursors for biosynthesis.

13.1 Overview of Plant Respiration

- In plant respiration, reduced cellular carbon generated by photosynthesis is oxidized to CO_2 and water, and this oxidation is coupled to the synthesis of ATP.
- Respiration takes place via four main processes: glycolysis, the oxidative pentose phosphate pathway, the TCA cycle, and oxidative phosphorylation (the electron transport chain and ATP synthesis) (**Figure 13.1**).

13.2 Glycolysis

- In glycolysis, carbohydrates are converted into pyruvate in the cytosol, and a small amount of ATP is synthesized via substrate-level phosphorylation. NADH is also produced (**Figure 13.3**).
- Plant glycolysis has alternative enzymes for several steps. These allow differences in substrates used, products made, and the direction of the pathway.
- When insufficient O_2 is available, fermentation regenerates NAD^+ for glycolysis. Only a minor fraction of the energy available in sugars is conserved by fermentation (**Figure 13.3**).
- Plant glycolysis is regulated from the "bottom-up" by its products (**Figure 13.13**).

13.3 The Oxidative Pentose Phosphate Pathway

- Carbohydrates can be oxidized via the oxidative pentose phosphate pathway, which provides building blocks for biosynthesis and reducing power in the form of NADPH (**Figure 13.4**).

13.4 The Tricarboxylic Acid Cycle

- In the mitochondrial matrix, pyruvate is oxidized into CO_2 via the TCA cycle, generating a large number of reducing equivalents in the form of NADH and $FADH_2$ (**Figures 13.5, 13.6**).
- In plants, the TCA cycle is involved in alternative pathways that allow oxidation of malate or citrate and export of intermediates for biosynthesis (**Figures 13.6, 13.7**).

13.5 Oxidative Phosphorylation

- Electron transport from NADH and $FADH_2$ to oxygen is coupled by enzyme complexes to proton transport across the inner mitochondrial membrane. This generates an electrochemical proton gradient used for powering synthesis and export of ATP (**Figures 13.8–13.10**).
- During aerobic respiration, up to 60 molecules of ATP are produced per molecule of sucrose (**Table 13.2**).
- Typical for plant respiration is the presence of several proteins (alternative oxidase, NAD[P]H dehydrogenases, and uncoupling protein) that lower the energy recovery, but also give increased metabolic flexibility (**Figures 13.8, 13.9**).
- The main products of the respiratory process are ATP and metabolic intermediates used in biosynthesis. The cellular demand for these compounds regulates respiration via control points in the electron transport chain, the TCA cycle, and glycolysis (**Figures 13.11–13.14**).

13.6 Respiration in Intact Plants and Tissues

- More than 50% of the daily photosynthetically fixed carbon may be respired by a plant.
- Many factors can affect the respiration rate observed at the whole-plant level. These factors include the nature and age of the plant tissue and environmental factors such as light, temperature, nutrient and water supply, and O_2 and CO_2 concentrations.

13.7 Lipid Metabolism

- Triacylglycerols (fats and oils) are an efficient form for storage of reduced carbon, particularly in seeds. Polar glycerolipids are the primary structural components of membranes (**Figures 13.15, 13.16; Tables 13.3, 13.4**).
- Triacylglycerols are synthesized in the ER and accumulate within the phospholipid bilayer, forming oil bodies.
- Fatty acids are synthesized in plastids using acetyl-CoA, in cycles of two-carbon addition. Fatty acids from the plastids can be transported to the ER, where they are further modified (**Figures 13.17, 13.18**).
- The function of a membrane may be influenced by its lipid composition. The degree of unsaturation of the fatty acids influences the sensitivity of plants to cold, but does not seem to be involved in typical chilling injury.
- Some lipid derivatives, such as jasmonate, are important plant hormones.
- During germination in oil-storing seeds, the stored lipids are metabolized to carbohydrates in a series of reactions that include the glyoxylate cycle. The glyoxylate cycle takes place in glyoxysomes, and subsequent steps occur in the mitochondria (**Figure 13.19**).
- Acetyl-CoA generated during lipid breakdown in the glyoxysomes is used for respiration or converted into carbohydrates in the cytosol by gluconeogenesis (**Figure 13.19**).

Web Material

- **WEB TOPIC 13.1 Isolation of Mitochondria** Intact, functional mitochondria can be purified for analysis in vitro.
- **WEB TOPIC 13.2 The Q Cycle Explains How Complex III Pumps Protons across the Inner Mitochondrial Membrane** A cyclic process allows for a higher proton-to-electron stoichiometry.
- **WEB TOPIC 13.3 Multiple Energy-Conservation Bypasses in Oxidative Phosphorylation of Plant Mitochondria** The enigmatic non-energy-conserving pathways of respiration are important for metabolic flexibility.
- **WEB TOPIC 13.4 F_oF_1-ATP Synthases: The World's Smallest Rotary Motors** Rotation of the γ subunit brings about the conformational changes that couple proton flux to ATP synthesis.
- **WEB TOPIC 13.5 Transport into and out of Plant Mitochondria** Plant mitochondria transport metabolites, coenzymes, and macromolecules.
- **WEB TOPIC 13.6 The Genetic System in Plant Mitochondria Has Several Special Features** The mitochondrial genome encodes about 40 mitochondrial proteins.
- **WEB TOPIC 13.7 Does Respiration Reduce Crop Yields?** Crop yield is correlated with low respiration rates in a way that is not fully understood.
- **WEB TOPIC 13.8 The Lipid Composition of Membranes Affects the Cell Biology and Physiology of Plants** Lipid mutants are expanding our understanding of the ability of organisms to adapt to temperature changes.
- **WEB ESSAY 13.1 Metabolic Flexibility Helps Plants to Survive Stress** The ability of plants to carry out a metabolic step in different ways increases plant survival under stress.
- **WEB ESSAY 13.2 Metabolic Profiling of Plant Cells** Metabolic profiling complements genomics and proteomics.
- **WEB ESSAY 13.3 Mitochondrial Dynamics: When Form Meets Function** Fluorescence microscopy has shown that mitochondria dynamically change shape, size, number, and distribution in vivo.
- **WEB ESSAY 13.4 Seed Mitochondria and Stress Tolerance** Seeds experience a wide range of stresses and are dependent on respiration for germination.
- **WEB ESSAY 13.5 Balancing Life and Death: The Role of the Mitochondrion in Programmed Cell Death** Programmed cell death is an integral part of the life cycle of plants, often directly involving mitochondria.
- **WEB ESSAY 13.6 Respiration by Thermogenic Flowers** The temperature of thermogenic flowers, such as the *Arum* lilies, can increase up to 35°C above their surroundings.
- **WEB ESSAY 13.7 Reactive Oxygen Species (ROS) and Plant Respiration** The production of reactive oxygen species is an unavoidable consequence of aerobic respiration.
- **WEB ESSAY 13.8 Transcriptional Regulation of Respiration/Retrograde Regulation** Retrograde regulation allows the nuclear genes to respond to changes in mitochondrial function.
- **WEB ESSAY 13.9 In Vivo Measurement of Plant Respiration** The activities of the alternative oxidase and cytochrome *c* oxidase can be measured simultaneously.
- **WEB ESSAY 13.10 Extreme Diversity of Triacylglycerol and Fatty Acid Structures in Plant Oils Used for Food, Biofuels, and Chemicals** Specialty plant oils have industrial applications.

For more study aids, go to oup.com/he/taiz7e.

Suggested Reading

Amthor, J. S., Bar-Even, A., Hanson, A. D., Millar, A. H., Stitt, M., Sweetlove, L. J., and Tyerman, S. D. (2019) Engineering strategies to boost crop productivity by cutting respiratory carbon loss. *Plant Cell* 31: 297–314.

Atkin, O. K., Meir, P., and Turnbull, M. H. (2014) Improving representation of leaf respiration in large-scale predictive climate-vegetation models. *New Phytol.* 202: 743–748.

Bates, P. D., Stymne, S., and Ohlrogge, J. (2013) Biochemical pathways in seed oil synthesis. *Curr. Opin. Plant Biol.* 16: 358–364.

Dusenge, M. E., Duarte, A. G., and Way, D. A. (2019) Plant carbon metabolism and climate change: elevated CO_2 and temperature impacts on photosynthesis, photorespiration and respiration. *New Phytol.* 221: 32–49.

Holzl, G., and Doermann, P. (2019) Chloroplast lipids and their biosynthesis. *Annu. Rev. Plant Biol.* 70: 51–81.

Markham, J. E., Lynch, D.V., Napier, J. A., Dunn, T. M., and Cahoon, E. B. (2013) Plant sphingolipids: function follows form. *Curr. Opin. Plant Biol.* 16: 350–357.

Millar, A. H., Whelan, J., Soole, K. L. and Day, D. A. (2011) Organization and regulation of mitochondrial respiration in plants. *Annu. Rev. Plant Biol.* 62: 79–104.

Millar, A. H., Siedow, J. N., and Day, D. A. (2015) Respiration and photorespiration. In: Buchanan, B. B., Gruissem, W., and Jones,

R. L. (eds.), *Biochemistry and Molecular Biology of Plants*, 2nd ed., pp. 610–655. Somerset, NJ: Wiley.

Møller, I. M., Jensen, P. E., and Hansson, A. (2007) Oxidative modifications to cellular components in plants. *Annu. Rev. Plant Biol.* 58: 459–481.

Møller, I. M., Igamberdiev, A. U., Bykova, N.V., Finkemeier, I., Rasmusson, A. G., and Schwarzländer, M. (2020) Matrix redox physiology governs the regulation of plant mitochondrial metabolism through post-translational protein modifications. *Plant Cell* 32: 573–594.

Møller, I. M., Rasmusson, A. G., and Van Aken, O. (2021) Plant mitochondria: Past, present and future. *Plant J.* 108: 912–959.

Mower, J. P. (2020) Variation in protein gene and intron content among land plant mitogenomes. *Mitochondrion* 53: 203–213.

Nakamura, Y. (2017) Plant phospholipid diversity: Emerging functions in metabolism and protein–lipid interactions. *Trends Plant Sci.* 22: 1027–1040.

Nicholls, D. G., and Ferguson, S. J. (2013) *Bioenergetics*, 4th ed. Academic Press, San Diego, CA.

O'Leary, B. M., and Plaxton, W. C. (2016) Plant Respiration. In ELS, John Wiley & Sons, Ltd (Ed.). doi.org/10.1002/9780470015902.a0001301.pub3.

Rasmusson, A. G., Geisler, D. A., and Møller, I. M. (2008) The multiplicity of dehydrogenases in the electron transport chain of plant mitochondria. *Mitochondrion* 8: 47–60.

Sweetlove, L. J., Beard, K. F. M., Nunes-Nesi, A., Fernie, A. R., and Ratcliffe, R. G. (2010) Not just a circle: Flux modes in the plant TCA cycle. *Trends Plant Sci.* 15: 462–470.

van Dongen, J. T., and Licausi, F. (2015) Oxygen sensing and signaling. *Annu. Rev. Plant Biol.* 66: 345–367.

Vanlerberghe, G. C. (2013) Alternative oxidase: A mitochondrial respiratory pathway to maintain metabolic and signaling homeostasis during abiotic and biotic stress in plants. *Int. J. Mol. Sci.* 14: 6805–6847.

Wallis, J. G., and Browse, J. (2010) Lipid biochemists salute the genome. *Plant J.* 61: 1092–1106.

14 Assimilation of Inorganic Nutrients



Aleksey Sagitov/Shutterstock

Higher plants are autotrophic organisms that can synthesize all of their organic molecular components out of inorganic nutrients obtained from their surroundings. For many inorganic nutrients, this process involves absorption from the soil by the roots (see Chapter 8) and incorporation into the organic compounds that are essential for growth and development. This incorporation of inorganic nutrients into organic substances such as pigments, enzyme cofactors, lipids, nucleic acids, and amino acids is termed **nutrient assimilation**.

Assimilation of some nutrients—particularly nitrogen and sulfur—involves a complex series of biochemical reactions that are among the most energy-consuming reactions in living organisms:

- In nitrate (NO_3^-) assimilation, the nitrogen in NO_3^- is converted to a higher-energy (more reduced) form in nitrite (NO_2^-), then to a yet-higher-energy (even more reduced) form in ammonium (NH_4^+), and finally into the amide nitrogen of the amino acid glutamine. This process consumes the equivalent of 12 ATPs per amide nitrogen.
- Plants such as legumes form symbiotic relationships with nitrogen-fixing bacteria to convert molecular nitrogen (N_2) into ammonia (NH_3). Ammonia is the first stable product of natural fixation; at physiological pH, however, ammonia is protonated to form the ammonium ion (NH_4^+). The process of biological nitrogen fixation, together with the subsequent assimilation of NH_3 into an amino acid, consumes the equivalent of about 16 ATPs per amide nitrogen.
- The assimilation of sulfate (SO_4^{2-}) into the amino acid cysteine via the two pathways found in plants consumes about 14 ATPs.
- For some perspective on the enormous energies involved, consider that if these reactions run rapidly in reverse—say, from NH_4NO_3 (ammonium nitrate) to N_2—they become explosive, liberating vast amounts of energy as motion, heat, and light. Nearly all explosives, including nitroglycerin, TNT (trinitrotoluene), and gunpowder, are based on the rapid oxidation of nitrogen or sulfur compounds.

Assimilation of other nutrients, especially the macronutrient and micronutrient cations (see Chapter 7), involves the formation of complexes with organic compounds. For example, Mg^{2+} associates with chlorophyll pigments, Ca^{2+} associates with pectates

within the cell wall, and Mo^{6+} associates with enzymes such as nitrate reductase and nitrogenase. These complexes are highly stable, and removal of the nutrient from the complex may result in total loss of function.

This chapter outlines the primary reactions through which the major nutrients (nitrogen, sulfur, and phosphate) are assimilated and discusses the organic products of these reactions. We emphasize the physiological implications of the required energy expenditures and introduce the topic of symbiotic nitrogen fixation. Plants serve as the major conduit through which nutrients pass from slower geophysical domains into faster biological ones; this chapter thus highlights the vital role of plant nutrient assimilation in the human diet.

14.1 Nitrogen in the Environment

Many prominent biochemical compounds in plant cells contain nitrogen (see Chapter 7). For example, nitrogen is found in the nucleotides and amino acids that form the building blocks of nucleic acids and proteins, respectively. Only the elements oxygen, carbon, and hydrogen are more abundant in plants than nitrogen. Most natural and agricultural ecosystems show dramatic gains in productivity after fertilization with inorganic nitrogen, attesting to the importance of this element and to the fact that it is present in suboptimal amounts.

In this section we discuss the biogeochemical cycle of nitrogen, the crucial role of nitrogen fixation in the conversion of molecular nitrogen into ammonium and nitrate, and the fate of ammonium and nitrate in plant tissues.

Nitrogen passes through several forms in a biogeochemical cycle

Nitrogen is present in many forms in the biosphere. The atmosphere contains vast quantities (about 78% by volume) of molecular nitrogen (N_2) (see Chapter 7). For the most part, this large reservoir of nitrogen is not directly available to living organisms. Acquisition of nitrogen from the atmosphere requires the breaking of an exceptionally stable triple covalent bond between two nitrogen atoms ($N{\equiv}N$) to produce ammonia (NH_3) or nitrate (NO_3^-). These reactions, known as **nitrogen fixation**, occur through both industrial and natural processes.

Industrial processes use elevated temperature (about 200°C), high pressure (about 200 atmospheres, or 20 MPa), and a metal catalyst (usually iron) to combine N_2 with hydrogen and form ammonia. These extreme conditions are required to overcome the high activation energy of the reaction. This nitrogen fixation reaction, called the *Haber–Bosch process*, is a starting point for the manufacture of nitrogen fertilizers, which globally exceeds 110 million metric tons per year (110 Mt y^{-1}, or 110×10^{12} g y^{-1}). It has been estimated that half of the nitrogen in the human body comes from this process.

The following natural processes fix about 260 Mt y^{-1} ($\pm$ 100 Mt y^{-1}) of nitrogen (**Table 14.1**):

TABLE 14.1 The major processes of the biogeochemical nitrogen cycle

Process	Definition	Rate (Mt y^{-1}, 10^{12}g y^{-1})[a]
Industrial fixation	Industrial conversion of molecular nitrogen to ammonia	110–120
Atmospheric fixation	Lightning and photochemical conversion of molecular nitrogen to nitrate	2–10
Biological fixation	Prokaryotic conversion of molecular nitrogen to ammonia	150–380
Plant acquisition	Plant absorption and assimilation of ammonium or nitrate	1000–1200
Immobilization	Microbial absorption and assimilation of ammonium or nitrate	N/C
Ammonification	Bacterial and fungal catabolism of soil organic matter to ammonium	N/C
Anammox	Anaerobic ammonium oxidation: bacterial conversion of ammonium and nitrite to molecular nitrogen	N/C
Nitrification	Bacterial (*Nitrosomonas* spp.) oxidation of ammonium to nitrite and subsequent bacterial (*Nitrobacter* spp.) oxidation of nitrite to nitrate	N/C
Mineralization	Bacterial and fungal catabolism of soil organic matter to mineral nitrogen through ammonification or nitrification	N/C
Volatilization	Physical loss of gaseous ammonia to the atmosphere	60–80
Ammonium fixation	Physical embedding of ammonium into soil particles	10
Denitrification	Bacterial conversion of nitrate to nitrous oxide and molecular nitrogen	100–280
Nitrate leaching	Physical flow of nitrate dissolved in groundwater out of the topsoil and eventually into the oceans	40–70

[a]N/C, not calculated.
Source: W. H. Schlesinger. 1997. *Biogeochemistry: An Analysis of Global Change*, 2nd ed., Academic Press, San Diego, CA.

- *Lightning.* Lightning is responsible for about 2% of the nitrogen fixed by natural processes. Lightning converts water vapor and oxygen into highly reactive hydroxyl free radicals, free hydrogen atoms, and free oxygen atoms that attack molecular nitrogen (N_2) to form nitric acid (HNO_3). This nitric acid subsequently falls to Earth with rain.
- *Biological nitrogen fixation.* The remaining 98% results from biological nitrogen fixation, in which bacteria or cyanobacteria (blue-green algae) fix N_2 into ammonia (NH_3). This ammonia dissolves in water to form ammonium (NH_4^+):

$$NH_3 + H_2O \rightarrow NH_4^+ + OH^- \qquad (14.1)$$

The high cost of fertilizers, especially for poor farmers, combined with negative impact of fertilizers on the environment, has resulted in intense efforts to better understand and implement biological nitrogen fixation, as well as to improve the nitrogen use efficiency of crops.

Once fixed into ammonia or nitrate, nitrogen enters a biogeochemical cycle and passes through several organic or inorganic forms before it eventually returns to molecular nitrogen (**Figure 14.1**; see also Table 14.1). The ammonium (NH_4^+) and nitrate (NO_3^-) ions in the soil solution that are generated through fixation or released through decomposition of soil organic matter become the object of intense competition among plants and microorganisms. To be competitive, plants have evolved mechanisms for scavenging these ions rapidly from the soil solution (see Chapter 8). Under the elevated soil concentrations that occur after fertilization, the absorption of ammonium and nitrate by the roots may exceed the capacity of a plant to assimilate these ions, leading to their accumulation within the plant's tissues.

Unassimilated ammonium or nitrate may be dangerous

If it accumulates to high concentrations in living tissues, ammonium is toxic to both plants and animals. Ammonium dissipates the transmembrane proton gradients (**Figure 14.2**) that are required for photosynthetic and respiratory electron transport (see Chapters 9 and 13), for sequestering metabolites in the vacuole (see Chapter 8), and for transporting nutrients across biological membranes (see Chapter 8). Since high concentrations of ammonium are dangerous, animals have developed a strong aversion to its smell. The active ingredient in smelling salts, a medicinal vapor released under the nose to revive a person who has fainted, is ammonium carbonate. To avoid the toxic effects of ammonium, plants suppress ammonium uptake by a phosphorylation-dependent allosteric feedback mechanism involving the ammonium transporter AMT1;1, they assimilate ammonium near the site of absorption or generation, and rapidly store any excess in their vacuoles.

Unlike the case with ammonium, plants can store high concentrations of nitrate, and they can translocate

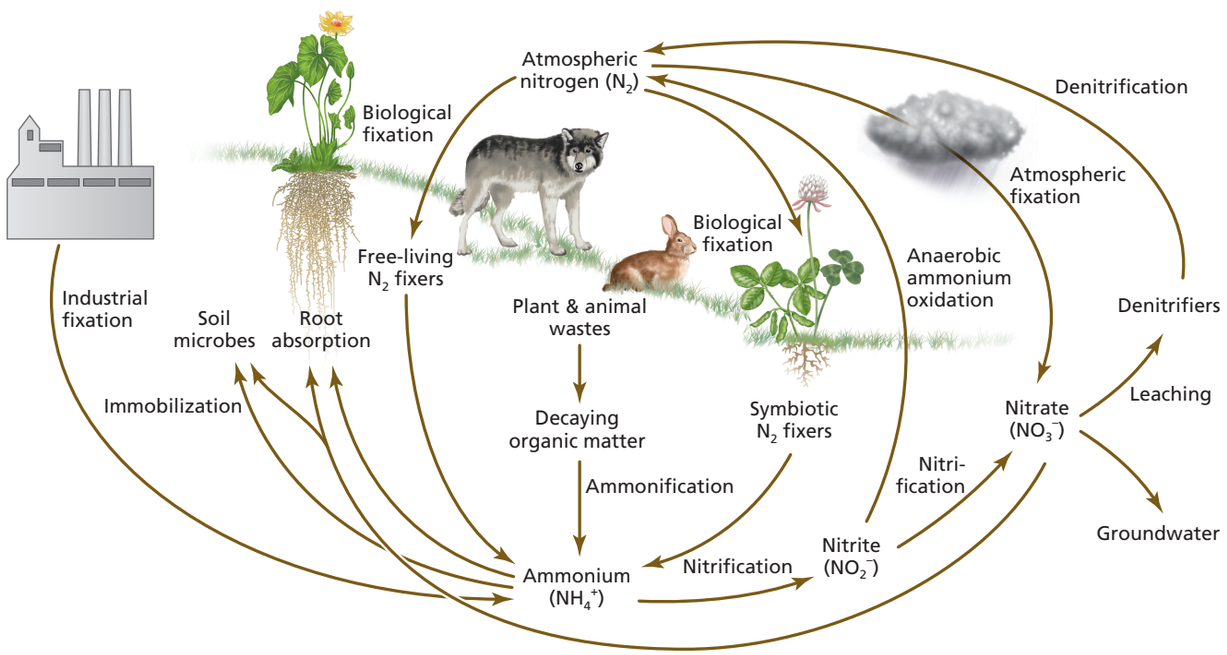


Figure 14.1 Nitrogen cycles through the atmosphere, changing from a gas to soluble ions before it is incorporated into organic compounds in living organisms. Some of the steps involved in the nitrogen cycle are shown.

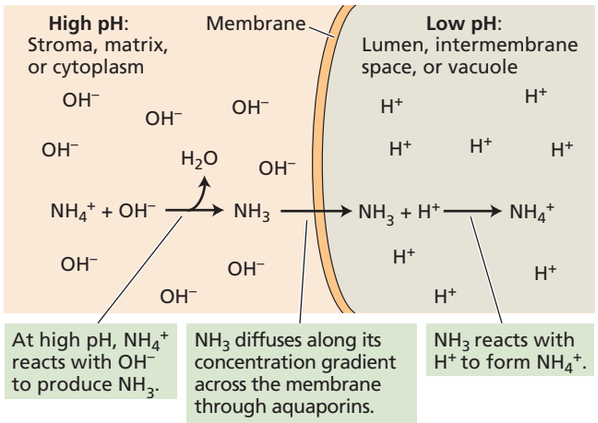


Figure 14.2 **NH_4^+ toxicity derives from dissipation of pH gradients.** The left side represents the stroma, matrix, or cytoplasm, where the pH is high; the right side represents the lumen, intermembrane space, or vacuole, where the pH is lower; and the membrane represents the thylakoid, inner mitochondrial, or tonoplast membrane for a chloroplast, mitochondrion, or root cell, respectively. The net result of the reaction shown is that both the OH^- concentration on the left side and the H^+ concentration on the right side have been diminished; that is, the pH gradient has been dissipated. The movement of ammonia across membranes can occur through aquaporins (see Chapter 8). $\Delta\psi$, membrane potential. (After A. J. Bloom. 1997. In *Ecology in Agriculture*, L. E. Jackson [ed.], pp. 145–172, Academic Press, San Diego, CA.)

it from tissue to tissue without deleterious effect. Yet if livestock or humans consume plant material that is high in nitrate, they may suffer methemoglobinemia, a disease in which the liver reduces nitrate to nitrite, which combines with hemoglobin and renders hemoglobin unable to bind oxygen. Humans and other animals may also convert nitrate into nitrosamines, which are potent carcinogens, or into nitric oxide, a potent signaling molecule involved in many physiological processes such as widening of blood vessels. Some countries limit the nitrate content in plant materials sold for human consumption.

In the next three sections we discuss the process by which plants assimilate nitrate into organic compounds via the enzymatic reduction of nitrate first into nitrite, next into ammonium, and then into amino acids.

14.2 Nitrate Assimilation

Plant roots actively absorb nitrate from the soil solution via several low- and high-affinity nitrate–proton cotransporters in the NRT1 and NRT2 family (see Chapter 8). Plants eventually assimilate most of this nitrate into organic nitrogen compounds. The first step in this process is the conversion of nitrate to nitrite in the cytosol, a reduction reaction (for redox properties, see Chapter 13) that involves the transfer of two electrons (**Figure 14.3**).

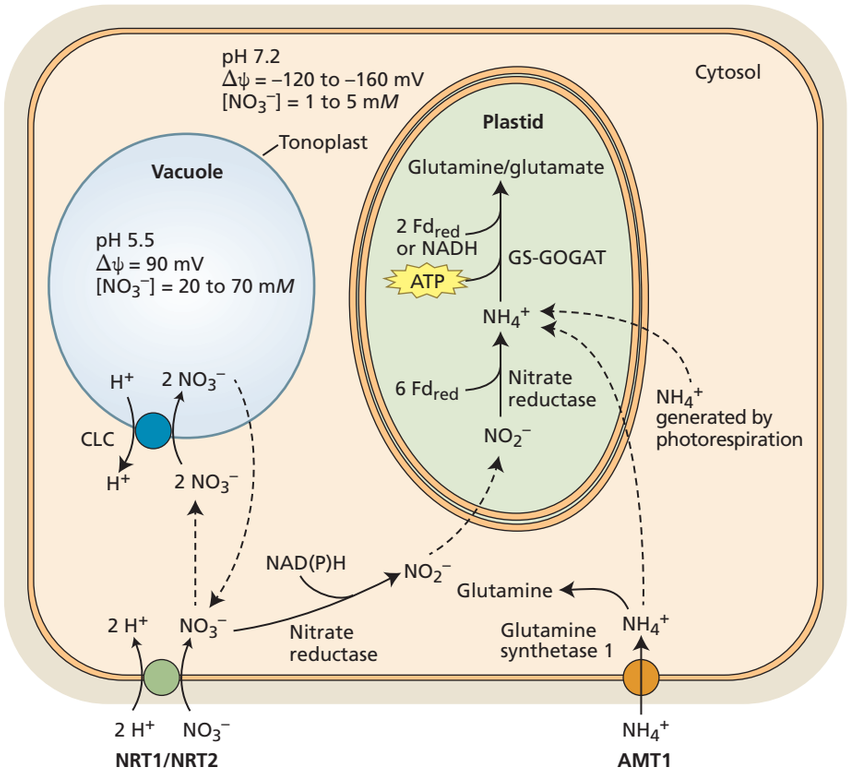


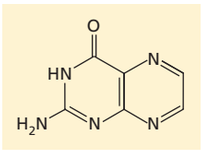
Figure 14.3 **Overview of nitrogen assimilation in plant cells.** Nitrate is taken up across the plasma membrane by proton-coupled symporters NRT1 or NRT2, using the proton gradient as the driving force. Nitrate is then converted to ammonium in a two-step process by nitrate reductase in the cytosol and nitrite reductase in the plastids. Nitrate can be transported across the tonoplast by the proton-nitrate antiporter CLC and stored in the vacuole up to a concentration of 70 m*M*. Ammonium, taken up by AMT1 transporters or produced intracellularly by nitrate assimilation or photorespiration, can be assimilated into glutamine and glutamate by glutamine synthetase (GS) and glutamate synthase, which has the systematic name glutamine:2-oxoglutarate aminotransferase (GOGAT). $\Delta\psi$, membrane potential.

The enzyme **nitrate reductase** (**Figure 14.4**) catalyzes this reaction:

$$NO_3^- + NAD(P)H + H^+ \rightarrow NO_2^- + NAD(P)^+ + H_2O \quad (14.2)$$

where NAD(P)H indicates either NADH or NADPH. The most common form of nitrate reductase uses only NADH as an electron donor; another form of the enzyme that is found predominantly in nongreen tissues such as roots can use either NADH or NADPH.

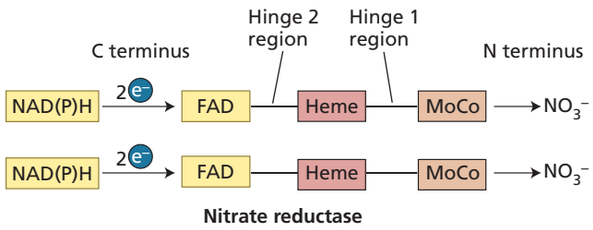
The nitrate reductases of higher plants are composed of two identical subunits, each containing three prosthetic groups: flavin adenine dinucleotide (FAD), heme, and a molybdenum ion complexed to an organic molecule called a *pterin*.



A pterin (fully oxidized)

Nitrate reductase is the main molybdenum-containing protein in vegetative tissues; one symptom of molybdenum deficiency is the accumulation of nitrate that results from diminished nitrate reductase activity.

X-ray crystallography and comparison of the amino acid sequences for nitrate reductase from several species with the sequences of other well-characterized proteins that bind FAD, heme, or molybdenum ions have led to a multiple-domain model for nitrate reductase; a simplified three-domain model is shown in Figure 14.4. The FAD-binding domain accepts two electrons from NADH or NADPH. The electrons then pass through the heme domain to the molybdenum complex, where they are transferred to nitrate.



Nitrate reductase

Figure 14.4 Model of the nitrate reductase dimer, illustrating the three binding domains whose polypeptide sequences are similar in eukaryotes: FAD, heme, and molybdenum complex (MoCo). The NAD(P)H binds at the FAD-binding region of each subunit and initiates a two-electron transfer from the carboxyl (C) terminus, through each of the electron transfer components, to the amino (N) terminus. Nitrate is reduced at the molybdenum complex near the amino terminus. The polypeptide sequences of the hinge regions are highly variable among species.

Many factors regulate nitrate reductase

Nitrate, light, and carbohydrates influence the abundance and activity of nitrate reductase at the transcriptional, translational, and posttranslational levels. Nitrate reductase mRNA in roots is induced very quickly after addition of nitrate, and maximum levels can be reached within 30 min. In contrast to the rapid accumulation of mRNA, there is a gradual linear increase in nitrate reductase activity upon addition of nitrate, reflecting that the synthesis of the nitrate reductase protein requires the presence of the nitrate reductase mRNA.

The posttranslational modification of the protein (involving a reversible phosphorylation) is analogous to the regulation of sucrose phosphate synthase (see Chapters 10 and 13). Carbohydrate concentrations, light, and other environmental factors stimulate a protein phosphatase that dephosphorylates a key serine residue in the hinge 1 region of nitrate reductase (between the molybdenum complex and heme-binding domains; see Figure 14.4) and thereby activates the enzyme. Operating in the reverse direction, darkness and Mg^{2+} stimulate a protein kinase that phosphorylates the same serine residues, which then interact with a 14-3-3 inhibitor protein, and thereby inactivate nitrate reductase. *Regulation of nitrate reductase activity through phosphorylation and dephosphorylation provides more rapid control than can be achieved through synthesis or degradation of the enzyme (minutes versus hours).*

Nitrite reductase converts nitrite to ammonium

Nitrite (NO_2^-) is a highly reactive, and potentially toxic, ion. Plant cells immediately transport the nitrite generated by nitrate reduction (see Reaction 14.2) from the cytosol into the plastid, where nitrite is rapidly converted into ammonium by the enzyme nitrite reductase. Nitrite reduction involves the transfer of six electrons, according to the following overall reaction:

$$NO_2^- + 6\ Fd_{red} + 8\ H^+ \rightarrow NH_4^+ + 6\ Fd_{ox} + 2\ H_2O \quad (14.3)$$

where Fd is ferredoxin and the subscripts *red* and *ox* stand for *reduced* and *oxidized*, respectively. Reduced ferredoxin is derived from photosynthetic electron transport in the chloroplasts (see Chapter 9) and from NADPH generated by the oxidative pentose phosphate pathway in the plastids of nongreen tissues (see Chapter 13).

In some species, chloroplasts and root plastids contain different forms of nitrite reductase, but both forms consist of a single polypeptide containing two prosthetic groups: an iron–sulfur cluster (Fe_4S_4) and a specialized heme. These groups act together to bind nitrite and reduce it to ammonium. Although no nitrogen compounds of intermediate redox states accumulate, a small percentage (0.02–0.2%) of the nitrite reduced is released

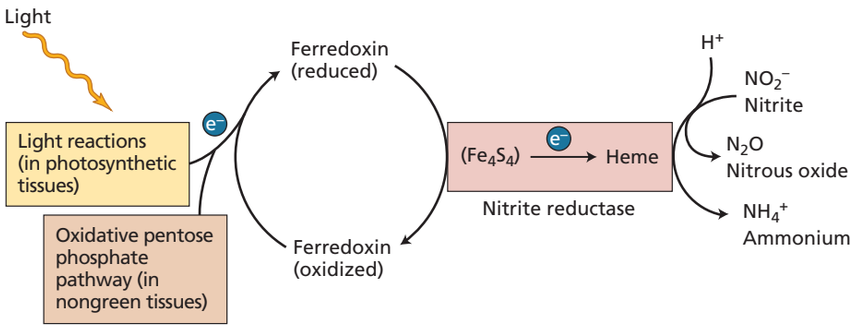


Figure 14.5 Model for coupling of photosynthetic electron flow, via ferredoxin, to the reduction of nitrite by nitrite reductase. The enzyme contains two prosthetic groups, an iron–sulfur cluster (Fe_4S_4) and heme, which participate in the reduction of nitrite to ammonium.

as nitrous oxide (N_2O), a greenhouse gas. The electron flow through ferredoxin, Fe_4S_4, and heme can be represented as in **Figure 14.5**.

Nitrite reductase is encoded in the nucleus and synthesized in the cytoplasm with an N-terminal transit peptide that targets it to the plastids. Elevated concentrations of NO_3^- or exposure to light induce the transcription of nitrite reductase mRNA. Accumulation of the end products in the process—asparagine and glutamine—represses this induction.

Both roots and shoots assimilate nitrate

In many plants, when the roots receive small amounts of nitrate, nitrate is reduced primarily in the roots. As the supply of nitrate increases, a greater proportion of the absorbed nitrate is translocated via the xylem to the shoot and assimilated there. Even under similar conditions of nitrate supply, the balance between root and shoot nitrate metabolism—as indicated by the proportion of nitrate reductase activity in each of the two organs or by the relative concentrations of nitrate and reduced nitrogen in the xylem sap—varies among species.

In plants such as cocklebur (*Xanthium strumarium*), nitrate metabolism is restricted to the shoot, whereas in other plants, such as white lupine (*Lupinus albus*), most nitrate is metabolized in the roots (**Figure 14.6**). Generally, species native to temperate regions rely more heavily on nitrate assimilation by the roots than do species in tropical or subtropical regions. Apart from species-based differences, partitioning of nitrate assimilation between the root and the shoot is also affected by environmental conditions such as salt stress and elevated CO_2, among others.

Nitrate can be transported in both xylem and phloem

Proper partitioning of nitrate assimilation among various tissues is important to maximize nitrogen use efficiency and to optimize plant growth. Root-to-shoot nitrate transport, a key factor in determining the partitioning of nitrate assimilation between root and shoot, occurs via the xylem, using transpiration as the driving force.

Root-to-shoot nitrate transport is controlled mainly at the step of xylem loading. In Arabidopsis, Nitrate Transporter 1.5 (NRT1.5), expressed in the xylem pole pericycle, is responsible for loading nitrate into the xylem. In addition to xylem transport, phloem nitrate transport, driven by osmotic gradients and from source to sink tissues, is responsible for redistributing nitrate to nitrogen-demanding tissues. Nitrate can be stored in large quantities in the vacuole, up to a concentration of 70 m*M* (see Figure 14.3), from which it can be retrieved

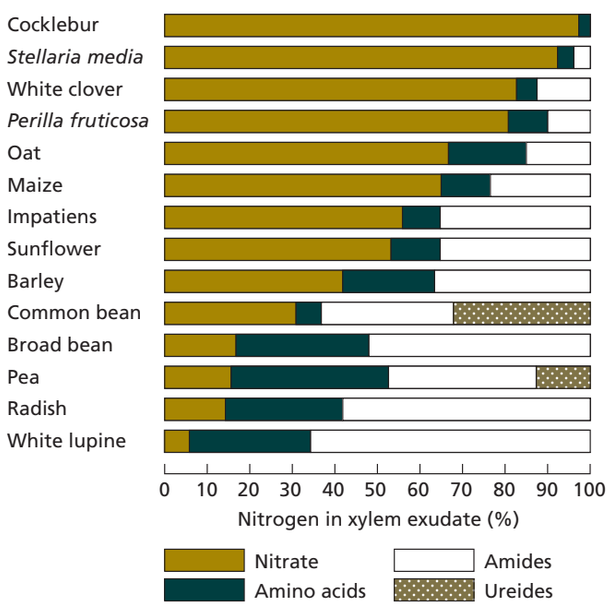


Figure 14.6 Relative amounts of nitrate and other nitrogen compounds in the xylem sap of various plant species. The plants were grown with their roots exposed to nitrate solutions, and xylem sap was collected by severing the stem. Note the presence of ureides in common bean and pea; only legumes of tropical origin export nitrogen in such compounds. (After J. S. Pate. 1973. *Soil Biol. Biochem.* 5: 109–119.)

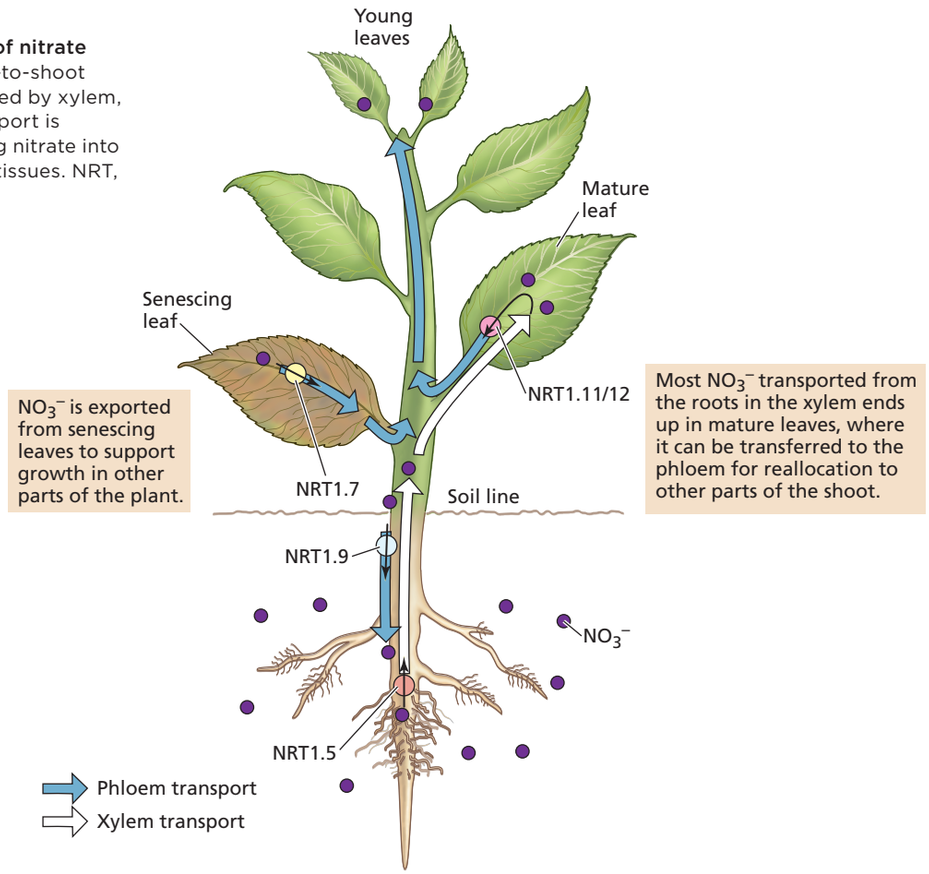


Figure 14.7 Overview of nitrate transport in plants. Root-to-shoot nitrate transport is mediated by xylem, while phloem nitrate transport is responsible for distributing nitrate into nitrogen-demanding sink tissues. NRT, nitrate transporter.

when needed. Nitrate storage capacity and retrieval efficiency are well correlated with yield in grain crops. When the external nitrate supply is low, nitrate stored in old leaves is retrieved and loaded into phloem by the nitrate transporter NRT1.7 to feed growing tissues such as young leaves and seeds (**Figure 14.7**). This phloem-mediated remobilization can help plants sustain growth under nitrogen deficiency. In contrast, when soil nitrate supply is high, nitrate from the roots is directed via the xylem stream to mature leaves where transpiration is greatest. In this case, xylem-borne nitrate can be transferred into the phloem by the nitrate transporters NRT1.11 and NRT1.12 in the major vein of mature leaves to satisfy the high nitrogen demand of young leaves. Plants rely on phloem nitrate transport to reallocate xylem-borne and stored nitrate under nitrogen-sufficient and nitrogen-deficient conditions, respectively, to feed growing tissues. Similar to NRT1.11 and NRT1.12, root-expressed NRT1.9 also mediates xylem-to-phloem transfer of nitrate, serving as a negative regulatory module for root-to-shoot nitrate transport. Depending on external and internal nitrogen status, xylem and phloem nitrate transport work together to ensure that nitrate is properly distributed and assimilated in various tissues.

Transceptor contributes to nitrate signaling

CHL1/NRT1.1 is a dual-affinity nitrate transporter involved in nitrate uptake (see Chapter 8), and it also functions as a nitrate transceptor (transporter with receptor function). Nitrate rapidly induces the expression of approximately 500 nitrate-related genes—including those encoding nitrate reductase, nitrite reductase, and nitrate transporters—in a coordinate manner. This rapid transcriptional response is termed the primary nitrate response, and it prepares plants to acquire and assimilate nitrate when external nitrate is available. Expression levels of nitrate-related genes are stringently regulated according to the external nitrate concentration and display a biphasic saturation pattern (**Figure 14.8A**). As part of the primary nitrate response, plants use dual-affinity binding and altered phosphorylation of the transceptor CHL1/NRT1.1 to sense wide-ranging variations of the external nitrate levels, and then use the transcription factor NLP7 to bind to the promoters of the nitrate reductase and nitrite reductase genes (**Figure 14.8B**). To ensure that nitrate acquisition is well coordinated with C assimilation and internal N status, nitrate transporter gene NRT2.1 is also fine-tuned by CEP1-mediated systemic nitrogen-demand signaling (see Chapter 7) and light-responsive 18 kDa transcription factor HY5 (see Chapter 12).

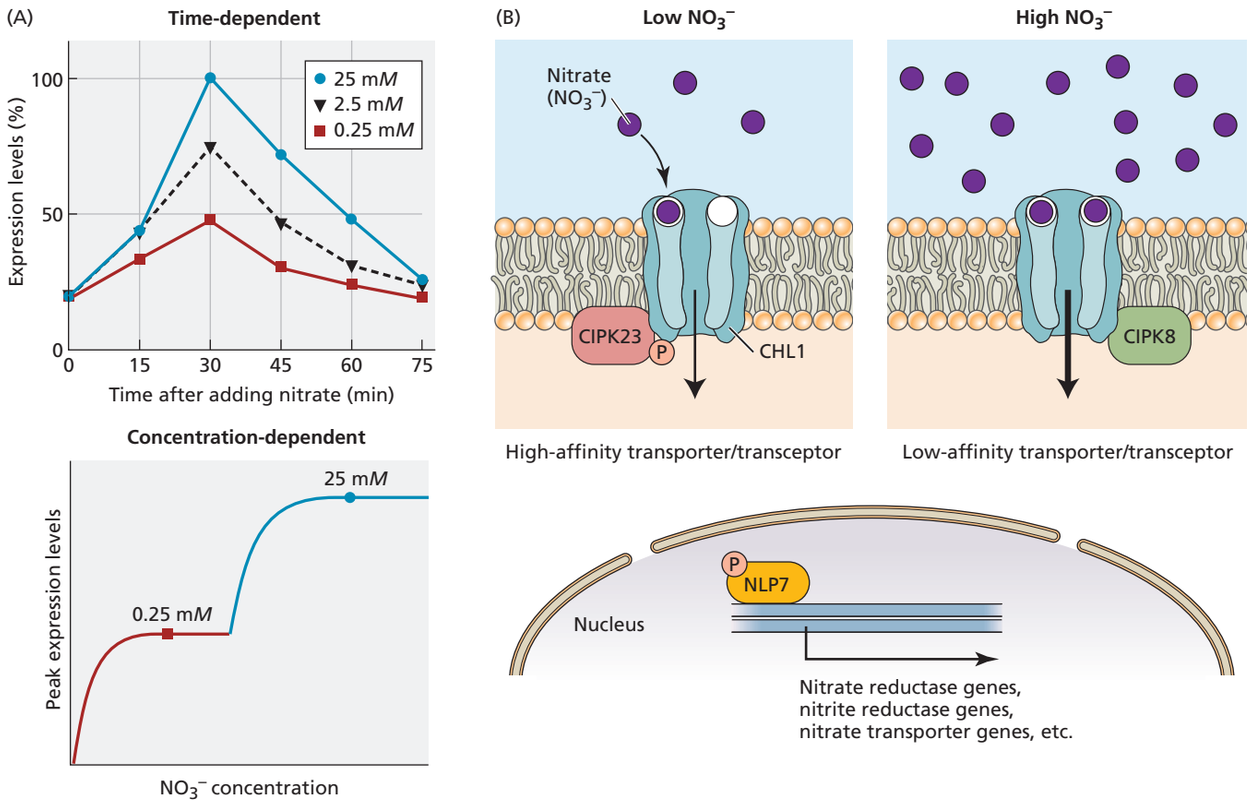


Figure 14.8 **The primary nitrate response.** **(A)** Time-dependent (top) and concentration-dependent (bottom) expression patterns of the nitrate-related genes including nitrate reductase. **(B)** The transceptor CHL1 uses dual-affinity binding to sense a wide range of changes in soil nitrate concentration with the help of two protein kinases, CIPK23 and CIPK8 (see Chapter 4), which operate in the high- and low-affinity phases, respectively. Transcription factor NLP7 can then bind the promoters of nitrate-related genes to elicit their expression.

14.3 Ammonium Assimilation

Plant cells avoid ammonium toxicity by rapidly converting the ammonium generated from nitrate assimilation or photorespiration (see Chapter 10) into amino acids. The primary pathway for this conversion involves the sequential actions of glutamine synthetase (GS) and glutamate synthase, which has the systematic name glutamine:2-oxoglutarate aminotransferase (GOGAT). In this section we discuss the enzymatic processes that mediate the assimilation of ammonium into essential amino acids, and the role of amides in the regulation of nitrogen and carbon metabolism.

Converting ammonium to amino acids requires two enzymes

Glutamine synthetase (**GS**) combines ammonium with glutamate to form glutamine (**Figure 14.9A**):

$$\text{Glutamate} + NH_4^+ + \text{ATP} \rightarrow \text{glutamine} + \text{ADP} + P_i \quad (14.4)$$

This reaction requires the hydrolysis of one ATP and involves a divalent cation such as Mg^{2+}, Mn^{2+}, or Co^{2+} as cofactor. Plants have two classes of GS, GS1 in the cytosol and GS2 in chloroplasts/plastids.

Cytosolic GS1 isozymes, expressed specifically in phloem and predominantly in the vascular bundles of roots, function in primary ammonia assimilation and produce glutamine for long-distance nitrogen transport. The GS2 in root plastids generates amide nitrogen for local consumption, whereas the GS2 in the chloroplasts of mesophyll cells is involved in both primary ammonium assimilation and the reassimilation of photorespiratory NH_4^+. Loss-of-function *gs2* mutants die under photorespiratory conditions because of the accumulation of toxic concentrations of NH_4^+, but *gs1* mutants do not display this phenotype. Light and carbohydrate concentrations alter the expression of the plastid forms of the enzyme GS2, but they have little effect on the cytosolic forms GS1.

Elevated plastid levels of glutamine stimulate the activity of **glutamate synthase** (also known as *glutamine:*

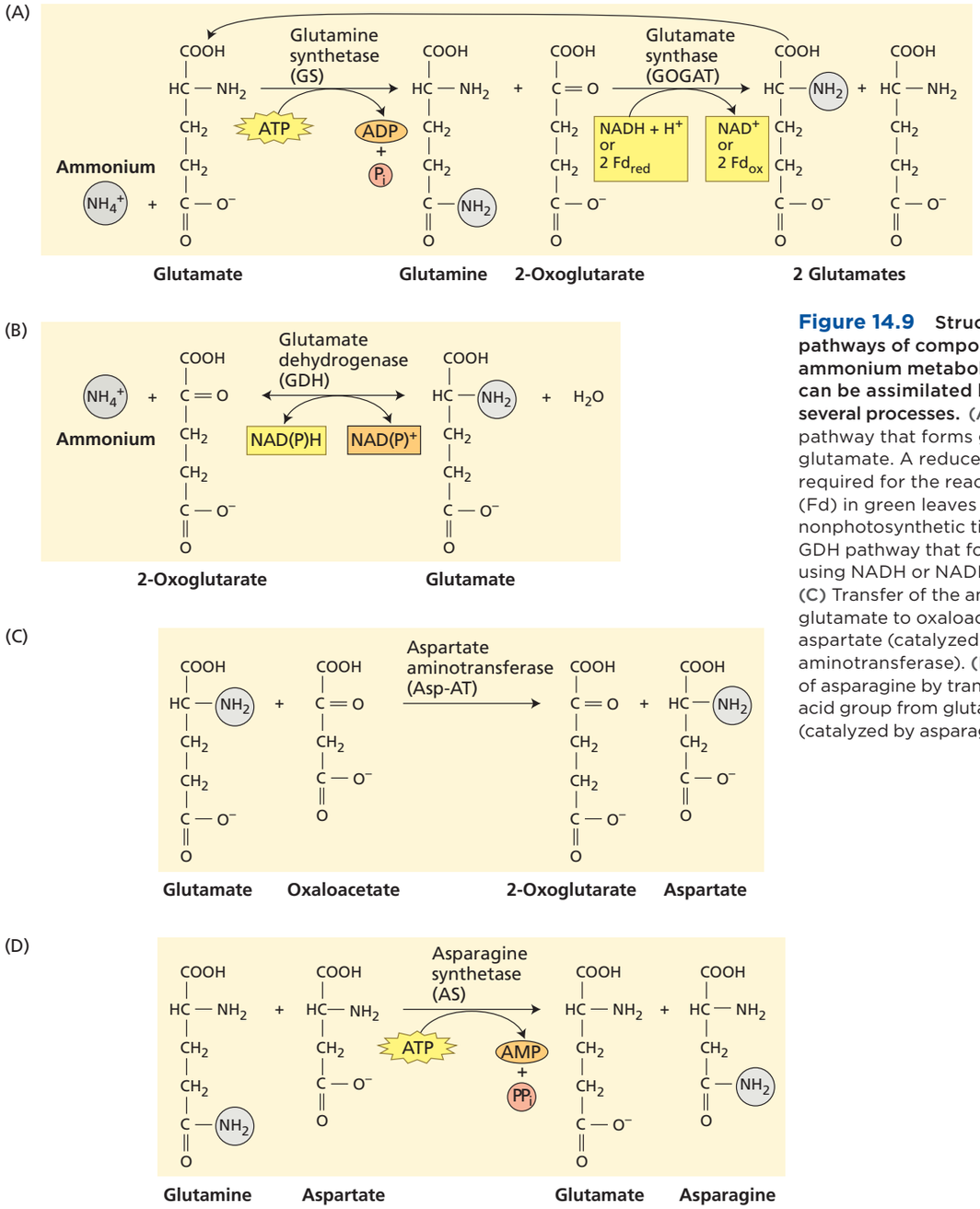


Figure 14.9 **Structure and pathways of compounds involved in ammonium metabolism. Ammonium can be assimilated by one of several processes.** **(A)** The GS–GOGAT pathway that forms glutamine and glutamate. A reduced cofactor is required for the reaction: ferredoxin (Fd) in green leaves and NADH in nonphotosynthetic tissue. **(B)** The GDH pathway that forms glutamate using NADH or NADPH as a reductant. **(C)** Transfer of the amino group from glutamate to oxaloacetate to form aspartate (catalyzed by aspartate aminotransferase). **(D)** Synthesis of asparagine by transfer of an amino acid group from glutamine to aspartate (catalyzed by asparagine synthetase).

2-oxoglutarate aminotransferase, or **GOGAT**). This enzyme transfers the amide group of glutamine to 2-oxoglutarate, yielding two molecules of glutamate (see Figure 14.9A). Plants contain two types of GOGAT; one accepts electrons from NADH, and the other accepts electrons from ferredoxin (Fd):

$$\text{Glutamine} + \text{2-oxoglutarate} + \text{NADH} + \text{H}^+ \rightarrow 2\ \text{glutamate} + \text{NAD}^+ \qquad (14.5)$$

$$\text{Glutamine} + \text{2-oxoglutarate} + 2\ \text{Fd}_{red} \rightarrow 2\ \text{glutamate} + 2\ \text{Fd}_{ox} \qquad (14.6)$$

The NADH type of the enzyme (NADH-GOGAT) is located in plastids of nonphotosynthetic tissues such as roots or the vascular bundles of developing leaves. In roots, NADH-GOGAT is involved in the assimilation of NH_4^+ absorbed from the rhizosphere (the soil near the surface of the roots); in vascular bundles of developing

leaves, NADH-GOGAT assimilates glutamine translocated from roots or senescing leaves.

The ferredoxin-dependent type of glutamate synthase (Fd-GOGAT) is found in chloroplasts and participates in both primary ammonium assimilation and photorespiratory nitrogen metabolism. Both the amount of protein and its activity increase with light levels. Roots, particularly those under nitrate nutrition, have Fd-GOGAT in their plastids. Fd-GOGAT in the roots presumably functions to incorporate the glutamine generated during nitrate assimilation. Electrons to reduce Fd in roots are generated by the oxidative pentose phosphate pathway (see Chapter 13).

Ammonium can be assimilated via an alternative pathway

Glutamate dehydrogenase (**GDH**) catalyzes a reversible reaction that synthesizes or deaminates glutamate (**Figure 14.9B**):

$$\text{2-Oxoglutarate} + NH_4^+ + \text{NAD(P)H} \rightarrow \text{glutamate} + H_2O + \text{NAD(P)}^+ \quad (14.7)$$

An NADH-dependent form of GDH is found in mitochondria, and an NADPH-dependent form is localized in the chloroplasts of photosynthetic organs. Although both forms are relatively abundant, they cannot substitute for the GS–GOGAT pathway to assimilate ammonium. GDH has a very low affinity for ammonium (K_m of 10–80 m*M*), which is much higher than the ammonium concentration typically found in plant tissue (0.2–1.0 m*M*). Therefore, the primary function of GDH is to deaminate glutamate and thereby provide five-carbon skeletons (2-oxoglutarate) to plants in darkness or to germinating seeds (see Figure 14.9B).

Transamination reactions transfer nitrogen

Once assimilated into glutamine and glutamate, nitrogen can be further incorporated into other amino acids via transamination reactions. The enzymes that catalyze these reactions are known as aminotransferases. An example is **aspartate aminotransferase** (**Asp-AT**), which catalyzes the following reaction (**Figure 14.9C**):

$$\text{Glutamate} + \text{oxaloacetate} \rightarrow \text{2-oxoglutarate} + \text{aspartate} \quad (14.8)$$

in which the amino group of glutamate is transferred to the carboxyl group of oxaloacetate to produce aspartate. Aspartate is a metabolically reactive amino acid that serves as a nitrogen donor in numerous aminotransferase reactions to produce lysine, threonine, and methionine. Aspartate also participates in the malate–aspartate shuttle to transfer reducing equivalents from the mitochondrion and chloroplast into the cytosol in C_3 plants and in the transport of carbon from the mesophyll to the bundle sheath for C_4 carbon fixation in some C_4 plants (see Chapter 10). All transamination reactions require pyridoxal phosphate (vitamin B_6) as a cofactor.

Aminotransferases are found in the cytosol, chloroplasts, mitochondria, and peroxisomes. The aminotransferases in chloroplasts may have a significant role in amino acid biosynthesis, because plant leaves or isolated chloroplasts exposed to radioactively labeled carbon dioxide rapidly incorporate the label into glutamate, aspartate, alanine, serine, and glycine.

Asparagine and glutamine link carbon and nitrogen metabolism

Asparagine, isolated from asparagus as early as 1806, was the first amide to be identified. It serves not only as a component of proteins, but also as a key compound for nitrogen transport and storage because of its stability and high nitrogen-to-carbon ratio (2 N to 4 C for asparagine compared with 2 N to 5 C for glutamine and 1 N to 5 C for glutamate).

The major pathway for asparagine synthesis involves the transfer of the amide nitrogen from glutamine to aspartate (**Figure 14.9D**):

$$\text{Glutamine} + \text{aspartate} + \text{ATP} \rightarrow \text{glutamate} + \text{asparagine} + \text{AMP} + PP_i \quad (14.9)$$

Asparagine synthetase (**AS**), the enzyme that catalyzes this reaction, is found in the cytosol of leaves and roots and in nitrogen-fixing nodules (see Section 14.5). In maize (corn; *Zea mays*) roots, particularly those under potentially toxic levels concentrations of ammonia, ammonium may replace glutamine as the source of the amide group.

High levels of light and carbohydrate, conditions that stimulate plastid GS2 (see Reaction 14.4) and Fd-GOGAT (see Reaction 14.5 and 14.6), inhibit the expression of genes coding for AS and the activity of the enzyme. Thus, they favor nitrogen assimilation into glutamine and glutamate, compounds that are rich in carbon and participate in the synthesis of new plant materials.

In contrast, energy-limited conditions inhibit GS2 and GOGAT, stimulate AS, and thus favor nitrogen assimilation into asparagine, a compound that is rich in nitrogen and sufficiently stable for long-distance transport or long-term storage.

14.4 Amino Acid Biosynthesis

Humans and most animals are heterotrophic for nitrogen, relying on organic nitrogen in the foods they eat. Furthermore, they cannot synthesize certain amino acids—histidine, isoleucine, leucine, lysine, methionine, phenylalanine, threonine, tryptophan, valine, and in the case of young humans, arginine (adult humans can synthesize arginine)—and thus must obtain these so-called essential amino acids from their diet. In contrast, plants acquire inorganic nitrogen from the soil and can synthesize all

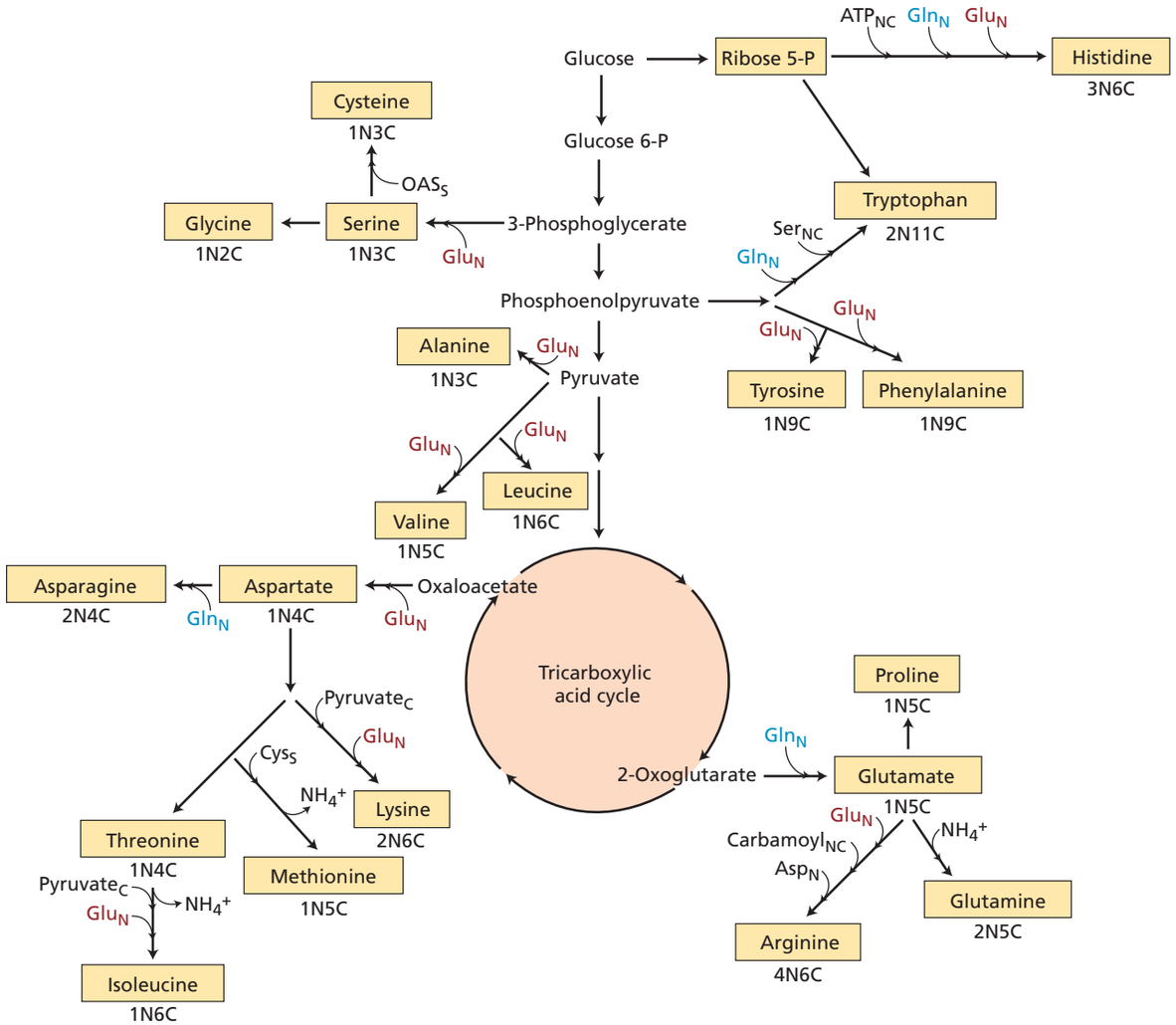


Figure 14.10 Biosynthetic pathways for the carbon skeletons of the 20 standard amino acids. N sources, S sources, and additional C sources in the biosynthetic pathways are also indicated. Asp_N, aspartate (N source); ATP_{NC}, ATP (N and C source); $carbamoyl_{NC}$, carbamoyl (N and C source); Cys_S, cysteine (S-source); Gln_N (blue), glutamine (N source); Glu_N (red), glutamate (N source); OAS_S, O-acetyl-serine (S-source); Pyr_C, pyruvate (C source); Ser_{NC}, serine (N and C source).

of the 20 amino acids that are common in proteins. The nitrogen-containing amino group, as discussed in Section 14.3, is derived from transamination reactions with glutamine or glutamate. The carbon skeletons for amino acids derive from 3-phosphoglycerate, phosphoenolpyruvate, or pyruvate generated during glycolysis, or from 2-oxoglutarate or oxaloacetate generated in the tricarboxylic acid cycle (**Figure 14.10**). Parts of these pathways required for synthesis of the essential amino acids are appropriate targets for herbicides (such as Roundup®; see Chapter 3), because they are missing from animals, so substances that block these pathways are lethal to plants, but in low concentrations do not injure animals.

14.5 Biological Nitrogen Fixation

Biological nitrogen fixation accounts for most of the conversion of atmospheric N_2 into ammonium, and thus serves as the key entry point of molecular nitrogen into the biogeochemical cycle of nitrogen (see Figure 14.1). In this section we describe the symbiotic and associative relationships between nitrogen-fixing organisms and higher plants; nodules, the specialized plant-produced structures infected by nitrogen-fixing bacteria; the genetic and signaling interactions that regulate nitrogen fixation by symbiotic prokaryotes and their hosts; and the properties of the nitrogenase enzymes that fix nitrogen.

Free-living and symbiotic bacteria fix nitrogen

Some bacteria, as stated earlier, can convert atmospheric nitrogen into ammonia (**Table 14.2**). Most of these nitrogen-fixing prokaryotes, also known as diazotrophs, live in the soil, generally independent of other organisms. Several form symbiotic associations with higher plants in which the prokaryote directly provides the host plant with fixed nitrogen in exchange for other nutrients and carbohydrates (see Table 14.2, top). Such symbioses occur in nodules that form on the roots or sometimes stems of the plant and contain the nitrogen-fixing bacteria.

The most common type of symbiosis occurs between members of the plant family Fabaceae (Leguminosae) and soil bacteria of the genera *Azorhizobium*, *Bradyrhizobium*, *Mesorhizobium*, *Rhizobium*, and *Sinorhizobium* (collectively called **rhizobia**; **Figure 14.11** and **Table 14.3**; also see Table 14.2). Another common type of symbiosis occurs between several woody plant species, such as alder trees, and soil bacteria of the genus *Frankia*; these plants are known as **actinorhizal** plants. Still other types of nitrogen-fixing symbioses involve the South American herb *Gunnera* and the tiny water fern *Azolla*, which form associations with the cyanobacteria *Nostoc* and *Anabaena*, respectively (**Figure 14.12**; also see Table 14.2). Finally, several types of nitrogen-fixing bacteria are associated with grasses or cereals.

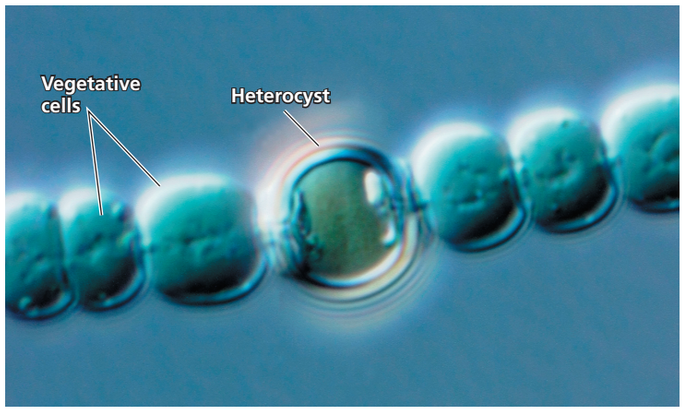


David McIntyre

Figure 14.11 Root nodules on a common bean (*Phaseolus vulgaris*). The nodules, the spherical structures, are a result of infection by *Rhizobium* sp.

TABLE 14.2 Examples of organisms that can carry out nitrogen fixation

SYMBIOTIC NITROGEN FIXATION Host plant	N-fixing symbionts
Leguminous: legumes, *Parasponia* (nonlegume)	*Azorhizobium*, *Bradyrhizobium*, *Mesorhizobium*, *Rhizobium*, *Sinorhizobium*
Actinorhizal: alder (tree), *Ceanothus* (shrub), *Casuarina* (tree), *Datisca* (shrub)	*Frankia*
Gunnera	*Nostoc*
Azolla (water fern)	*Anabaena*
Sugarcane	*Acetobacter*
Miscanthus	*Azospirillum*
FREE-LIVING NITROGEN FIXATION **Type**	**N-fixing genera**
Cyanobacteria (blue-green algae)	*Anabaena*, *Calothrix*, *Nostoc*
Other bacteria	
Aerobic	*Azospirillum*, *Azotobacter*, *Beijerinckia*, *Derxia*, *Gloeothece*
Facultative	*Bacillus*, *Klebsiella*
Anaerobic	
Nonphotosynthetic	*Clostridium*, *Methanococcus* (archaebacterium)
Photosynthetic	*Chromatium*, *Rhodospirillum*



© Dr. Peter Siver

Figure 14.12 **A heterocyst in a filament of the nitrogen-fixing cyanobacterium *Anabaena*, which forms associations with the water fern *Azolla*.** The thick-walled heterocysts, interspersed among vegetative cells, have an anaerobic inner environment that allows cyanobacteria to fix nitrogen in aerobic conditions.

Nitrogen fixation requires microanaerobic or anaerobic conditions

Because nitrogen fixation involves the expenditure of large amounts of energy, the nitrogenase enzymes that catalyze these reactions have sites that facilitate the high-energy exchange of electrons. Oxygen, being a strong electron acceptor, can damage these sites and irreversibly inactivate nitrogenase, so nitrogen must be fixed under anaerobic conditions. Each of the nitrogen-fixing organisms listed in Table 14.2 either functions under natural anaerobic conditions or creates an internal, local anaerobic (microanaerobic) environment separated from the oxygen in the atmosphere that surrounds it.

In filamentous cyanobacteria, nitrogen fixation occurs in specialized cells called *heterocysts* (see Figure 14.12). The low oxygen concentration in heterocysts is achieved by the elimination of oxygen-producing photosystem II activity (see Chapter 9), an increased respiration rate, and synthesis of a heterocyst-specific peptidoglycan layer that thickens the cell wall. Heterocysts differentiate from vegetative cells when cyanobacteria are deprived of NH_4^+. As a result of nitrogen starvation, 2-oxoglutarate accumulates in vegetative cells, inducing the synthesis of the transcription factors nitrogen control gene (NtcA) and heterocyst differentiation master regulator (HetR), which act as a global nitrogen regulator and a specific master regulator, respectively, and leading to heterocyst differentiation. HetR interacts with heterocyst commitment protein (HetP), a protein containing no domain of known function, to commit the cell to irreversibly differentiate into a heterocyst. The number of heterocysts in filaments depends on the environmental conditions. Usually one heterocyst cell is present for every ten vegetative cells, enabling an efficient use of energy resources for carbon and nitrogen metabolism in the two types of cells.

Cyanobacteria can fix nitrogen under anaerobic conditions such as those that occur in flooded fields. In Asian countries, nitrogen-fixing cyanobacteria of both the heterocyst and nonheterocyst types are a major means for maintaining an adequate nitrogen supply in the soil of rice fields. Cyanobacteria fix nitrogen when the fields are flooded and die as the fields dry, releasing the fixed nitrogen to the soil. Another important source of available nitrogen in flooded rice fields is the *Azolla–Anabaena* association, which can fix as much as 0.5 kg of atmospheric nitrogen per hectare per day, a rate of fertilization that is sufficient to attain moderate rice yields. **Box 14.1** discusses how plants can obtain fixed nitrogen in future agriculture.

TABLE 14.3 **Associations between host plants and rhizobia**

Plant host	Rhizobial symbiont
Parasponia (a nonlegume)	Bradyrhizobium spp.
Soybean (*Glycine max*)	*Bradyrhizobium japonicum* (slow-growing type); *Sinorhizobium fredii* (fast-growing type)
Alfalfa (*Medicago sativa*)	*Sinorhizobium meliloti*
Sesbania (aquatic)	*Azorhizobium* (forms both root and stem nodules; the stems have adventitious roots)
Bean (*Phaseolus*)	*Rhizobium leguminosarum* bv. *phaseoli*; *R. tropicii*; *R. etli*
Clover (*Trifolium*)	*Rhizobium leguminosarum* bv. *trifolii*
Pea (*Pisum sativum*)	*Rhizobium leguminosarum* bv. *viciae*
Aeschynomene (aquatic)	Photosynthetic *Bradyrhizobium* clade (photosynthetically active rhizobia that form stem nodules, probably associated with adventitious roots)

Box 14.1 Challenges and Solutions for Solving Nitrogen Deficiency in Future Agriculture

Nutrient acquisition, especially of phosphorus and nitrogen, is crucial for balancing plant growth and reproduction. The agricultural revolution has led to developing technologies and practices that were required for supporting an increasing human population. In the coming decades the challenge will be to meet future food demands while facing the necessity to reduce the environmental impact of intensive agriculture, which is currently based on a high input of industrial fertilizers. Acquisition of nutrients through beneficial plant–microbe associations is recognized as a sustainable solution to this challenge. Identifying microbes that can efficiently provide these nutrients to plant hosts in return for carbon resources, without inducing a pathogenic effect, is now a prime target for research.

In the legume–*Rhizobium* symbiosis, the nitrogen-fixing bacteria have the capacity to provide most of the nitrogen required by the plant host. Consequently, the areas cultivated with legumes are increasing in order to meet societal demands for protein production in a sustainable manner. Elite nitrogen-fixing rhizobial strains are used as inoculum, but to take full advantage of their symbiotic capacities there is a need to understand how to increase bacterial persistence across diverse soils, and to ensure their effective selection by the legume hosts. Cereals lack this endosymbiotic capacity and are therefore dependent on nitrogen fertilizers, but current research aims at changing this high dependence using different strategies. Identification of root-associative diazotrophs is one of them. This could become efficient if we understand how to manipulate and adapt diazotrophs to agricultural settings. Plant genotype, the isolate, and the environment all have a major effect on the establishment of root–diazotroph associations, as well as on the amount of fixed nitrogen received by the host. Parallel efforts based on biotechnological approaches target genetic engineering of cereals by expression of the nitrogenase complex in the chloroplasts and mitochondria of cereal cells, or by transferring the ability to recognize and accommodate the nitrogen-fixing bacteria through symbiotic association. Once successful, these biotechnological approaches will have the potential to create a new agricultural revolution. ■

Free-living bacteria that are capable of fixing nitrogen are aerobic, facultative, or anaerobic (see Table 14.2, bottom):

- *Aerobic* nitrogen-fixing bacteria such as *Azotobacter* are thought to maintain a low oxygen concentration (microaerobic conditions) through their high levels of respiration. Others, such as *Gloeothece*, evolve O_2 photosynthetically during the day and fix nitrogen during the night when respiration lowers oxygen concentrations.
- *Facultative* organisms, which are able to grow under both aerobic and anaerobic conditions, generally fix nitrogen only under anaerobic conditions.
- Obligate *anaerobic* nitrogen-fixing bacteria that grow in environments devoid of oxygen can be either photosynthetic (e.g., *Rhodospirillum*) or non-photosynthetic (e.g., *Clostridium*).

Cereals can develop associative relationships with nitrogen-fixing bacteria, but in these interactions root nodules are not produced. Instead, the nitrogen-fixing bacteria attach to the root surfaces, mainly around the elongation zone and the root hairs, or live as endophytes, colonizing the apoplastic space of plant tissues without causing disease. For example, *Acetobacter diazotrophicus* and *Herbaspirillum* species live in the apoplast of stem tissues in sugarcane and may provide their host with about 30% of its nitrogen. Recent studies of indigenous maize native cultivars grown in nitrogen-poor, high-humidity environments of Mexico's highlands showed that their aerial roots secrete carbohydrate-rich mucilage and associate with nitrogen-fixing bacteria. Under these conditions, the fixation of atmospheric nitrogen contributed 29 to 82% of the nitrogen nutrition of these maize genotypes. The potential for associative and endophytic nitrogen-fixing bacteria to supplement the nitrogen nutrition of cereals has been explored, but the large diversity of bacterial species, and the variety of plant responses to these bacteria, have impeded progress.

Symbiotic nitrogen fixation occurs in specialized structures

Some symbiotic nitrogen-fixing prokaryotes dwell within **nodules**, the special organs of the plant host that enclose the nitrogen-fixing bacteria (see Figure 14.11). In the case of *Gunnera*, these organs are preexisting stem glands that develop independently of the symbiont. In the case of legumes and actinorhizal plants, bacteria induce the plant to form the nodules.

Legumes and actinorhizal plants regulate gas permeability in their nodules, maintaining oxygen concentrations of 20 to 40 nanomolar (n*M*) within the nodule (about 10,000 times lower than equilibrium concentrations in water). These concentrations can support

respiration but are sufficiently low to avoid inactivation of the nitrogenase. Gas permeability increases in the light and decreases under drought (water-deficit stress) or upon exposure to nitrate. The mechanism for regulating gas permeability is not yet known, but it may involve potassium ion fluxes into and out of infected cells.

Nodules contain oxygen-binding heme proteins called **leghemoglobins** that have a high affinity for oxygen (a K_m of about 10 n*M*), about ten times higher than that of the β chain of human hemoglobin. Leghemoglobins are the most abundant proteins in nodules, giving them a heme-pink color, and are crucial for symbiotic nitrogen fixation.

Leghemoglobins increase the rate of oxygen transport to the respiring symbiotic bacteria, decreasing substantially the steady-state concentration of oxygen in infected cells. To continue aerobic respiration under such conditions, the bacteroid uses a specialized electron transport chain (see Chapters 9 and 13) in which the terminal oxidase has an affinity for oxygen even higher than that of leghemoglobins, a K_m of about 7 n*M*.

Establishing symbiosis requires an exchange of signals

The symbiosis between legumes and rhizobia is not obligatory. Legume seedlings germinate without any association with rhizobia, and they may remain unassociated throughout their life cycle. Rhizobia also occur as free-living organisms in the soil. Under nitrogen-limited conditions, however, the symbionts seek each other out through an elaborate exchange of signals. This signaling, the subsequent infection process, and the development of nitrogen-fixing nodules involve specific genes in both the host and the symbionts.

Plant genes up-regulated during root nodule symbiosis have been generically called **nodulin genes**. A set of rhizobial genes called **nodulation** (**nod**) **genes** is responsible for the biosynthesis and secretion of specific signaling molecules, the Nod factors. The *nod* genes are classified as common *nod* genes or host-specific *nod* genes. The common *nod* genes—*nodA*, *nodB*, and *nodC*—are found in all rhizobial strains; the host-specific *nod* genes—such as *nodP*, *nodQ*, and *nodH*; or *nodF*, *nodE*, and *nodL*—may be present or not in different rhizobial species and determine the host range (the plants that can be infected). Only one of the *nod* genes, the regulatory *nodD*, is constitutively expressed, and as we will explain in detail, its protein product (NodD) regulates the transcription of the other *nod* genes.

The first stage in the formation of the symbiotic relationship between the nitrogen-fixing bacteria and their host is migration of the bacteria toward the roots of the host plant. This migration is a chemotactic response mediated by chemical attractants, especially (iso)flavonoids and betaines, secreted by the roots. These attractants activate the rhizobial NodD protein, which then induces transcription of the other *nod* genes. The promoter region of all *nod* operons, except that of *nodD*, contains a highly conserved sequence called the *nod* box. Binding of the activated NodD to the *nod* box induces transcription of the other *nod* genes.

Nod factors produced by bacteria act as signals for symbiosis

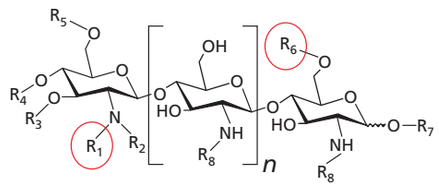
Nod factors are lipochitin oligosaccharide signal molecules, all of which have a chitin β-1,4-linked *N*-acetyl-D-glucosamine backbone (varying in length from three to six sugar units) and a fatty acid chain on the C-2 position of the nonreducing sugar (**Figure 14.13**).

Three of the *nod* genes (*nodA*, *nodB*, and *nodC*) encode enzymes (NodA, NodB, and NodC, respectively) that are required for synthesizing the basic lipochitinous structure:

1. NodA is an *N*-acyltransferase that catalyzes the addition of a fatty acyl chain.
2. NodB is a chitin-oligosaccharide deacetylase that removes the acetyl group from the terminal nonreducing sugar.
3. NodC is a chitin-oligosaccharide synthase that links *N*-acetyl-D-glucosamine monomers.

The NOD proteins, whose presence varies among rhizobial species, are primarily involved in the modification of the fatty acyl chain or the addition of groups important in determining host specificity:

- NodE and NodF determine the length and degree of saturation of the fatty acyl chain; those of *Rhizobium leguminosarum* bv. *viciae* and *R. meliloti* result



R1: fatty acid: C18:0; C18:1, C16:0; C16:1
R2: methyl, hydrogen
R3: hydrogen, carbomyl
R4: hydrogen, carbomyl
R5: hydrogen, carbomyl, acetyl
R6: hydrogen, fucose, sulphate, acetyl, 4-*O*-acetyl fucose, 2-*O*-methyl fucose
R7: hydrogen, glycerol, mannosyl
R8: acetyl
n=1, 2, 3

Figure 14.13 **Nod factors are lipochitin oligosaccharides.** The fatty acid chain typically has 16 to 18 carbons. The number of repeated middle sections (*n*) is usually two or three. (After T. J. Stokkermans et al. 1995. *Plant Physiol.* 108: 1587–1595.)

in the synthesis of an 18:4 and a 16:2 fatty acyl group, respectively. (Recall from Chapter 13 that the number before the colon gives the total number of carbons in the fatty acyl chain, and the number after the colon gives the number of double bonds.)

- Other enzymes, such as NodS, NodH, and NodZ, contribute to host specificity of Nod factors through the addition of specific substituents at the reducing or nonreducing sugar moieties.

Legume hosts use Nod factor receptors (NFRs) to recognize and respond to specific Nod factors (**Figure 14.14**). These receptors have extracellular regions with three sugar-binding LysM domains (for lysin motif, a widespread protein module originally identified in enzymes that degrade bacterial cell walls, but also present in many other proteins), a single-pass transmembrane domain, and an intracellular protein kinase domain. Binding of Nod factors to the NFR extracellular domains activates the intracellular protein kinase domain, which then initiates a signaling cascade. Some components of this signaling cascade, such as symbiosis receptor-like kinase (SYMRK), nucleoporins, cation channels, and cyclic nucleotide–gated channels, are also crucial for plant symbiosis with arbuscular mycorrhizal fungi (see Chapters 7, 19, and 24), and are required for activation of oscillations in the Ca^{2+} concentration in the nuclei of root epidermal cells (see Figure 14.14). Nuclear Ca^{2+} oscillations are interpreted by a Ca^{2+}/calmodulin-dependent protein kinase (CCaMK) that associates with CYCLOPS, a transcriptional activator. CYCLOPS, together with specific transcription factors, activates the expression of early nodulin genes, leading to root nodule formation and bacterial infection. Among these early nodulin genes, NIN has emerged as a central hub controlling both nodulation and infection.

Nodule formation involves phytohormones

Infection and nodule organogenesis occur simultaneously during root nodule symbiosis. Nod factor–producing rhizobia attach to developing root hairs, which then reorient their tip growth and curl around the bacteria (**Figure 14.15A and B**). The rhizobia enclosed in the curl multiply and form a microcolony. The cell wall of the curling root hair undergoes major remodeling in response to Nod factors, and an apoplastic infection chamber is formed. The next step is formation of the **infection thread** (**Figure 14.15C**), an internal tubular extension of the plasma membrane that is produced by the fusion of Golgi-derived membrane vesicles at the site of infection. The thread grows at its tip by the fusion of secretory vesicles to the end of the tube. In parallel with infection thread formation in the root hairs, cells deeper within the root cortex dedifferentiate and start dividing, forming a distinct area called a *nodule primordium*, from which the nodule will develop. The nodule primordia form opposite the protoxylem poles of the root vascular bundle (see **WEB TOPIC 14.1**).

Different signaling compounds, acting either positively or negatively, control the development of nodule primordia. Nod factors activate localized cytokinin signaling in the root cortex and pericycle, leading to the

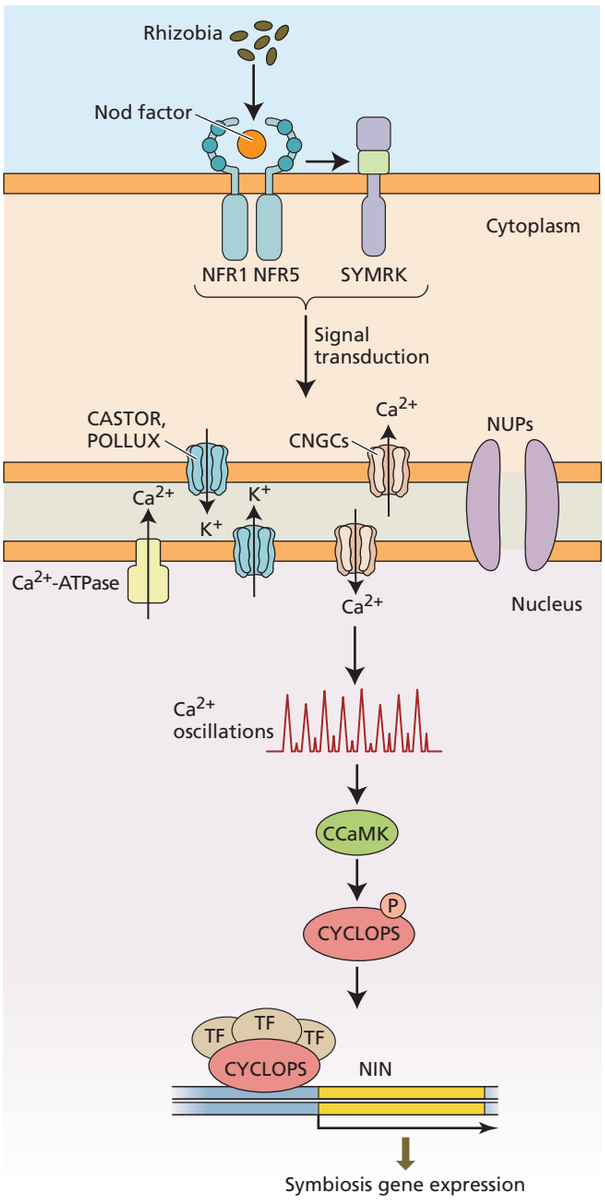


Figure 14.14 Simplified intracellular signaling cascade initiated by Nod factor receptors (NFR1 and NFR5) after binding compatible Nod factors. CASTOR/POLLUX, cation channels; CNGCs, cyclic nucleotide–gated channels; NIN, Nodule inception protein; NUPs, nucleoporins; SYMRK, symbiotic receptor kinase; TF, transcription factor.

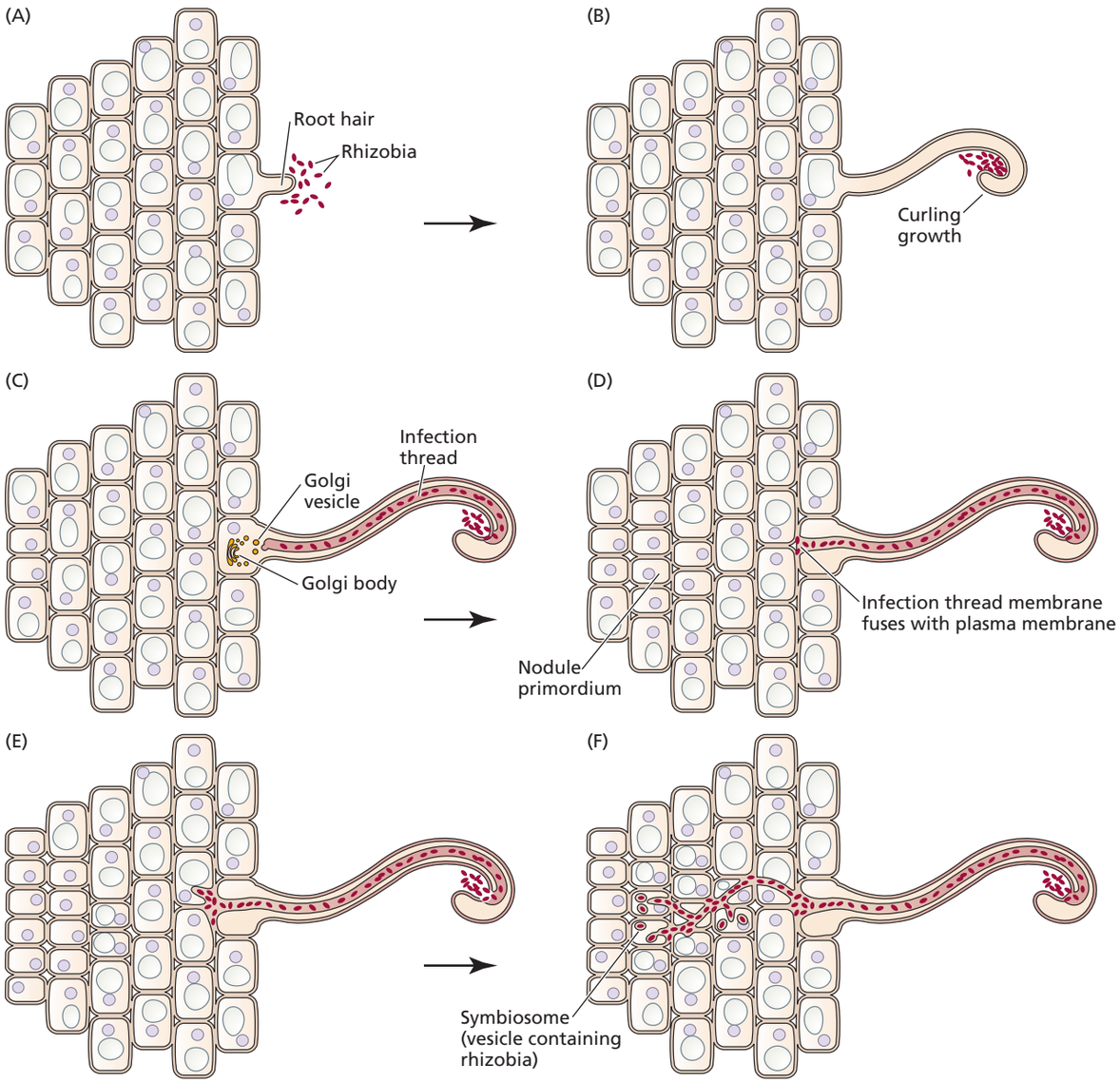


Figure 14.15 The infection process during nodule organogenesis. **(A)** Rhizobia bind to an emerging root hair in response to chemical attractants sent by the plant. **(B)** In response to factors produced by the bacteria, the root hair exhibits abnormal curling growth, and rhizobia cells proliferate within the coils. **(C)** Localized degradation of the root hair wall leads to infection and formation of the infection thread from Golgi secretory vesicles of root cells. **(D)** The infection thread reaches the end of the cell, and its membrane fuses with the plasma membrane of the root hair cell. **(E)** Rhizobia are released into the apoplast and penetrate the compound middle lamella to the subepidermal cell plasma membrane, leading to the initiation of a new infection thread, which forms an open channel with the first. **(F)** The infection thread extends and branches until it reaches target cells, where vesicles (symbiosomes) composed of plant membrane that enclose bacterial cells are released into the cytosol.

localized suppression of polar auxin transport, inducing localized cell division. Ethylene is synthesized in the region of the pericycle, diffuses into the cortex, and blocks cell division opposite the phloem poles of the root.

The infection thread filled with proliferating rhizobia elongates through the root hair and cortical cell layers, in the direction of the nodule primordium, where it branches leading to increased access to multiple plant cells. When the infection thread reaches the cells of the nodule primordium, its tip fuses with the plasma membrane of a host cell (**Figure 14.15D**) and bacterial cells surrounded by host-derived membrane are released into the cytoplasm, forming the *symbiosomes* (**Figure 14.15E and F**).

At first the bacteria within symbiosomes continue to divide, and the surrounding symbiosome membrane (also called the *peribacteroid membrane*) increases in surface area to accommodate this growth by fusing with smaller vesicles. Soon thereafter, upon an undetermined signal from the plant, the bacteria stop dividing and begin to differentiate into nitrogen-fixing **bacteroids**.

The mature nodule develops a vascular system (which facilitates the exchange of fixed nitrogen produced by the bacteroids for nutrients contributed by the plant) and a layer of cells to limit diffusion of O_2 into the root nodule interior. In some temperate legumes (e.g., pea), the nodules are elongated and cylindrical because of the presence of a *nodule meristem* at the tip. The nodules of tropical legumes, such as soybean and peanut, lack a persistent meristem and are spherical.

The nitrogenase enzyme complex fixes N_2

Biological nitrogen fixation, like industrial nitrogen fixation, produces ammonia from molecular nitrogen. The overall reaction is

$$N_2 + 8\ e^- + 8\ H^+ + 16\ ATP \rightarrow 2\ NH_3 + H_2 + 16\ ADP + 16\ P_i \qquad (14.10)$$

Note that the reduction of N_2 to two NH_3, a six-electron transfer, is coupled to the reduction of two protons to evolve H_2. The **nitrogenase enzyme complex** catalyzes this reaction.

The nitrogenase enzyme complex has two components—the Fe protein and the MoFe protein—neither of which has catalytic activity by itself (**Figure 14.16**). For one dinitrogen molecule to be reduced to two ammonia molecules, the Fe protein and the MoFe protein have to interact eight times:

- The Fe protein, known as the reductase, participates in the redox reactions that convert N_2 to NH_3. It is a homodimeric protein with two iron–sulfur clusters (four Fe^{2+}/Fe^{3+} and four S^{2-}) and two ATP-binding sites. The Fe protein is irreversibly inactivated by O_2 with a typical half-decay time of 30 to 45 s.
- The MoFe protein has four subunits, each with two Mo–Fe–S clusters. The MoFe protein is also inactivated by O_2, with a half-decay time in air of 10 min.

In the overall nitrogen reduction reaction (see Figure 14.16), ferredoxin serves as an electron donor to the Fe protein, which in turn hydrolyzes ATP and reduces the MoFe protein. The MoFe protein can then reduce numerous substrates (**Table 14.4**), although under natural conditions it reacts only with N_2 and H^+. One of the reactions catalyzed by nitrogenase, the reduction of acetylene to ethylene, is used in estimating nitrogenase activity (see **WEB TOPIC 14.2**).

The energetics of nitrogen fixation are complex. Production of NH_3 from N_2 and H_2 is an exergonic reaction (see **WEB APPENDIX 1** for a discussion of exergonic reactions), with a $\Delta G^{0'}$ (change in free energy) of –27 kJ mol^{-1}, but industrial production of NH_3 from N_2 and H_2 is *endergonic*, requiring a very large energy input because of the activation energy needed to break the triple bond in N_2. For the same reason, the enzymatic reduction of N_2 by nitrogenase also requires a large investment of energy (see Reaction 14.10), although the exact changes in free energy are not yet known. Calculations based on the carbohydrate metabolism of legumes show that a plant respires 7 to 12 moles of CO_2 per mole of N_2 fixed. On the basis of Reaction 14.10, the $\Delta G^{0'}$ for the overall reaction of biological nitrogen fixation is about –200 kJ mol^{-1}. To compensate for the exergonic reaction, ammonium production is limited by the slow operation (number of N_2 molecules reduced per unit time is about 5 s^{-1}) of the nitrogenase complex. To compensate for this slow turnover rate, the bacteroid synthesizes large amounts of nitrogenase (up to 20% of the total protein in the cell).

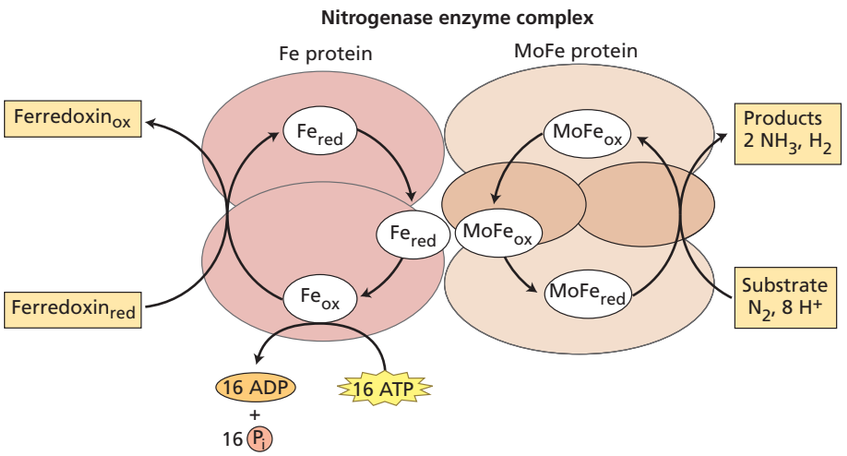


Figure 14.16 The reaction catalyzed by nitrogenase. Ferredoxin reduces the Fe protein. Binding and hydrolysis of ATP to the Fe protein are thought to cause a conformational change of the Fe protein that facilitates the redox reactions. The Fe protein reduces the MoFe protein, and the MoFe protein reduces the N_2. (After R. O. D. Dixon and C. T. Wheeler. 1986. *Nitrogen Fixation in Plants*. Chapman and Hall, New York; B. Buchanan et al. 2000. *Biochemistry and Molecular Biology of Plants*. American Society of Plant Physiologists, Rockville, MD.)

TABLE 14.4 Reactions catalyzed by nitrogenase

$N_2 \rightarrow NH_3$	Molecular nitrogen fixation
$N_2O \rightarrow N_2 + H_2O$	Nitrous oxide reduction
$N_3^- \rightarrow N_2 + NH_3$	Azide reduction
$C_2H_2 \rightarrow C_2H_4$	Acetylene reduction
$2\ H^+ \rightarrow H_2$	H_2 production
$ATP \rightarrow ADP + P_i$	ATP hydrolytic activity

Source: R. H. Burris. 1976. Nitrogen fixation. In *Plant Biochemistry*, 3rd ed., J. Bonner and J. Varner, eds., Academic Press, NY, pp. 887–908.

Under natural conditions, substantial amounts of H^+ are reduced to H_2 gas, and this process can compete with N_2 reduction for electrons from nitrogenase. In rhizobia, 30 to 60% of the energy supplied to nitrogenase may be lost as H_2, diminishing the efficiency of nitrogen fixation. Some rhizobia, however, contain hydrogenase, an enzyme that can split the H_2 formed and generate electrons for N_2 reduction, thus improving the efficiency of nitrogen fixation.

Amides and ureides are the transported forms of nitrogen

The symbiotic nitrogen-fixing prokaryotes release ammonia that, to avoid toxicity, must be rapidly converted into organic forms in the root nodules before being transported to the shoot via the xylem. Nitrogen-fixing legumes can be classified as amide exporters or ureide exporters, depending on the composition of the xylem sap. Amides (principally the amino acids asparagine or glutamine) are exported by temperate-region legumes, such as pea (*Pisum*), clover (*Trifolium*), broad bean (*Vicia*), and lentil (*Lens*) (see Figure 14.6).

Ureides are exported by legumes of tropical origin, such as soybean (*Glycine*), common bean (*Phaseolus*), peanut (*Arachis*), and southern pea (*Vigna*) (see Figure 14.6). The three major ureides are allantoin, allantoic acid, and citrulline (**Figure 14.17**). Allantoin is synthesized in peroxisomes from uric acid, and allantoic acid is synthesized from allantoin in the endoplasmic reticulum. The site of citrulline synthesis from the amino acid ornithine has not yet been determined. All three compounds are ultimately released into the xylem and transported to the shoot, where they are rapidly catabolized to ammonium. This ammonium enters the assimilation pathway described earlier.

14.6 Sulfur Assimilation

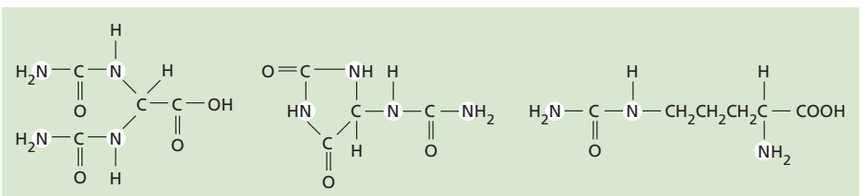
Sulfur is among the most versatile elements in living organisms. Disulfide bridges in proteins play structural and regulatory roles (see Chapter 10). Sulfur participates in electron transport through iron–sulfur clusters (see Chapters 9 and 13). The catalytic sites for several enzymes and coenzymes, such as urease and coenzyme A, contain sulfur. Secondary metabolites (compounds that are not involved in primary pathways of growth and development) that contain sulfur range from the rhizobial Nod factors discussed in Section 14.5 to the antiseptic alliin in garlic and the anticarcinogen sulforaphane in broccoli.

The versatility of sulfur derives in part from the property that it shares with nitrogen: *multiple stable oxidation states*. In this section we discuss the enzymatic steps that mediate sulfur assimilation, and the biochemical reactions that catalyze the reduction of sulfate into the two sulfur-containing amino acids, cysteine and methionine.

Sulfate is the form of sulfur transported into plants

Most of the sulfur in higher-plant cells derives from sulfate (SO_4^{2-}) transported via an H^+–SO_4^{2-} symporter (see Chapter 8) from the soil solution. Sulfate in the soil comes predominantly from the weathering of parent rock material. Industrialization, however, adds an additional source of sulfate: atmospheric pollution. The burning of fossil fuels releases several gaseous forms of sulfur, including sulfur dioxide (SO_2) and hydrogen sulfide (H_2S), which find their way to the soil in rain.

In the gas phase, sulfur dioxide reacts with a hydroxyl radical and oxygen to form sulfur trioxide (SO_3). SO_3 dissolves in water to become sulfuric acid (H_2SO_4), a strong acid, which is the major cause of acid rain. Plants can metabolize sulfur dioxide taken up in the gaseous form through their stomata. Nonetheless, prolonged exposure (more than 8 h) to high atmospheric concentrations (greater than 0.3 ppm) of SO_2 causes extensive tissue damage because of the formation of sulfuric acid inside the plant leaf.



Allantoic acid Allantoin Citrulline

Figure 14.17 The major ureide compounds used to transport nitrogen from sites of fixation to sites where their deamination will provide nitrogen for amino acid and nucleoside synthesis.

Sulfate assimilation requires the reduction of sulfate to cysteine

Synthesis of sulfur-containing organic compounds from inorganic sulfate takes place in plastids, mitochondria and cytosol.

SULFATE ACTIVATION The first step in the synthesis of sulfur-containing organic compounds is activation of inorganic sulfate (**Figure 14.18**). Sulfate is very stable and thus needs to be activated before any subsequent reactions may proceed. Activation begins with a reaction between sulfate and ATP to form adenosine-5′-phosphosulfate (APS) and pyrophosphate (PP_i) (see Figure 14.18):

$$SO_4^{2-} + ATP \rightarrow APS + PP_i \qquad (14.11)$$

There are two forms of the enzyme, ATP sulfurylase, that catalyzes this reaction. The major form is found in plastids and accounts for 90 to 95% of total ATP sulfurylase activity, and a minor form is found in the cytosol (**Figure 14.19**). Some plant species, including Arabidopsis, have no cytosolic ATP sulfurylase. Expression of the ATP sulfurylase–encoding gene *ATPS* and respective protein activity can be up-regulated by sulfur starvation or repressed by an end product of the pathway, such as cysteine or glutathione.

The sulfate activation reaction is energetically unfavorable. To drive this reaction forward, the products APS and PP_i must be converted immediately to other compounds. PP_i, the phosphate donor and energy source, is hydrolyzed to inorganic phosphate (P_i) by inorganic pyrophosphatase according to the following reaction:

$$PP_i + H_2O \rightarrow 2\ P_i \qquad (14.12)$$

Plants contain two types of pyrophosphatase: One is soluble pyrophosphatase and the other is vacuolar H^+-pyrophosphatase. The other product of the Reaction 14.11, APS, is rapidly reduced or phosphorylated, with reduction being the dominant pathway.

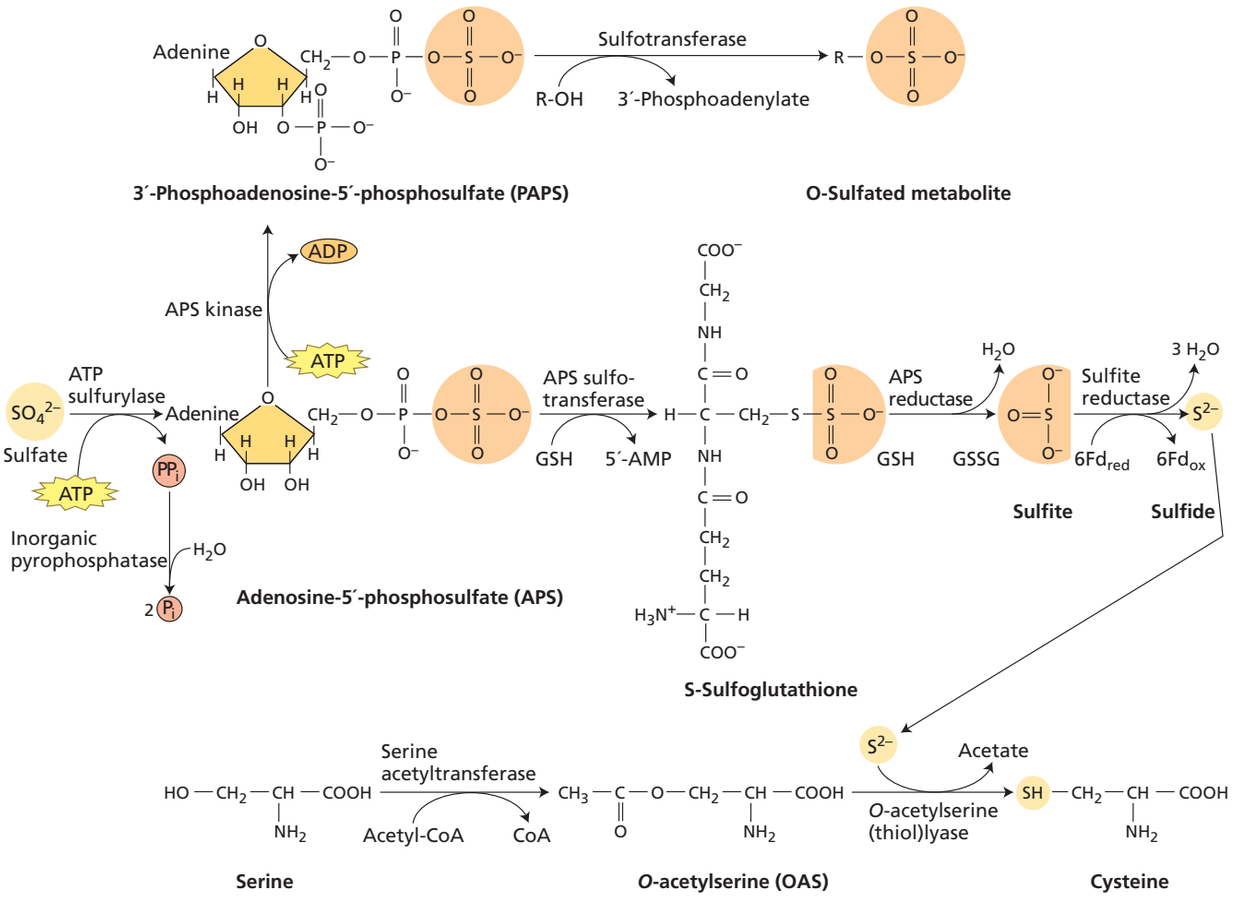


Figure 14.18 Structure and pathways of compounds involved in sulfur assimilation. The enzyme ATP sulfurylase cleaves pyrophosphate from ATP and replaces it with sulfate. Sulfide is produced from APS through reactions involving reduction by glutathione and ferredoxin. The sulfide reacts with *O*-acetylserine to form cysteine. Fd, ferredoxin; GSH, glutathione, reduced; GSSG, glutathione, oxidized.

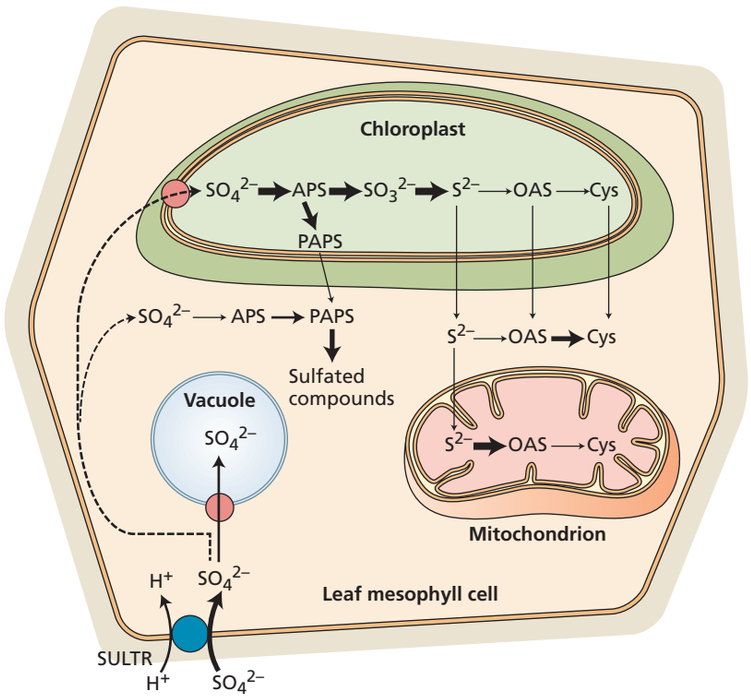
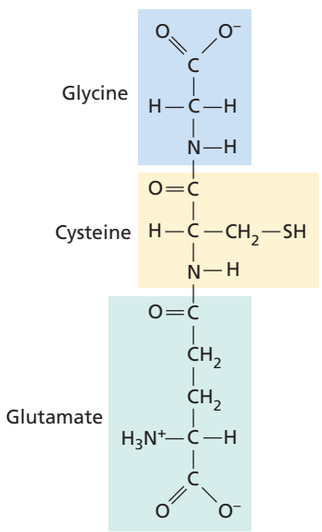


Figure 14.19 Overview of sulfur assimilation in plant cells. Sulfate is taken up across the plasma membrane by the proton-coupled symporters SULTRs. Sulfate can be stored in vacuoles or processed further in other parts of the cell. Reduction of sulfate to sulfide takes place in the chloroplasts/plastids. Incorporation of sulfide into cysteine takes place in the cytosol, chloroplasts/plastids, and mitochondria. Synthesis of sulfated compounds takes place in the cytosol. The thickness of the arrows shows the relative importance of the reactions.

The reduction of APS is a multistep process that occurs exclusively in plastids (see Figures 14.18 and 14.19). First, APS reductase transfers two electrons, apparently from reduced glutathione (GSH), to produce sulfite (SO_3^{2-}):

$$APS + 2\,GSH \rightarrow SO_3^{2-} + 2\,H^+ + GSSG + AMP + H_2O \quad (14.13)$$

where GSSG stands for oxidized glutathione. (The *SH* in GSH and the *SS* in GSSG represent S—H and S—S bonds, respectively.)



Reduced glutathione

The N terminus of the APS reductase protein is a reductase domain containing an iron–sulfur cluster (Fe–S), whereas its C terminus is a glutaredoxin-like (Grx) domain. APS reductase forms a dimer, and during the reaction, disulfide bridges can alternatively be formed between the two enzyme subunits or between the N-terminal Fe–S and C-terminal Grx domains. As is similar with ATP sulfurylase, the activity of APS reductase and expression of the encoding gene *APR* are also up-regulated by sulfur starvation and repressed by the reduced forms of sulfur.

Second, sulfite reductase transfers six electrons from ferredoxin (Fd_{red}) to produce sulfide (S^{2-}):

$$SO_3^{2-} + 6\,Fd_{red} \rightarrow S^{2-} + 6\,Fd_{ox} + 3\,H_2O \quad (14.14)$$

The reduction of sulfate into sulfide is an energy-intensive process that consumes more energy than either nitrate or CO_2 assimilation. Since sulfite is a toxic anion, sulfite reductase activity is maintained in excess, and unlike with ATP sulfurylase and APS reductase, neither its expression nor its activity is regulated by sulfur nutrition.

INCORPORATION OF SULFIDE INTO CYSTEINE

The resultant sulfide then reacts with *O*-acetylserine (OAS) to form cysteine and acetate. The *O*-acetylserine that reacts with S^{2-} is formed via a reaction catalyzed by serine acetyltransferase:

$$Serine + acetyl\text{-}CoA \rightarrow OAS + CoA \quad (14.15)$$

OAS and sulfide then react to form cysteine through a reaction catalyzed by OAS (thiol)-lyase:

$$\text{OAS} + S^{2-} \rightarrow \text{cysteine} + \text{acetate} \qquad (14.16)$$

Serine acetyltransferase and OAS (thiol)-lyase are encoded by small multiple gene families called *SERAT* and *BSAS* , respectively. Expression levels of *SERAT* and *BSAS* are not regulated by sulfate starvation. Serine acetyltransferase and OAS (thiol)-lyase can be found in the cytosol, plastids, and mitochondria. Mutant analysis has indicated that the major site of OAS synthesis is the mitochondria, whereas the major site of cysteine synthesis is the cytosol. These two enzymes can operate separately or form a multienzyme complex. Assembly of the complex is negatively regulated by OAS, but positively regulated by sulfide. Complex formation serves to fine-tune regulation of sulfate assimilation, as the protein–protein interactions in the complex enhance serine acetyltransferase activity but repress that of OAS (thiol)-lyase.

PHOSPHORYLATION OF APS APS phosphorylation operates at the interface between primary and secondary sulfur metabolism (see Figures 14.18 and 14.19). To be incorporated into sulfated compounds, APS is phosphorylated by APS kinase in plastids and cytosol to form 3′-phosphoadenosine-5′-phosphosulfate (PAPS):

$$\text{APS} + \text{ATP} \rightarrow \text{PAPS} + \text{ADP} \qquad (14.17)$$

Sulfotransferases in the cytosol may then transfer the sulfate group from PAPS to various compounds (R-OH in Figure 14.18), including choline, brassinosteroids, flavonol, gallic acid glucoside, glucosinolates, peptides, and polysaccharides.

Sulfate assimilation occurs mostly in leaves

The reduction of sulfate to cysteine changes the oxidation number of sulfur from +6 to –2, thus involving the transfer of eight electrons. Glutathione, ferredoxin, NAD(P)H, or *O*-acetylserine may serve as electron donors at various steps of the pathway (see Figure 14.18). In Arabidopsis, all the enzymes involved in sulfate assimilation—with the exception of sulfite reductase and the enzymes catalyzing the synthesis of reduced glutathione—are encoded by small multigene families.

Leaves are generally much more active than roots in sulfur assimilation, presumably because photosynthesis provides reduced ferredoxin, and photorespiration generates serine (see Chapter 10), which may stimulate the production of *O*-acetylserine. The sulfur assimilated in leaves is exported via the phloem to sink organs (shoot and root apices, and fruits). Uptake of sulfate in roots, transport of sulfate from roots to shoots, and several steps of sulfate assimilation are regulated by the demands for sulfur assimilation via a feedback mechanism.

Methionine is synthesized from cysteine

Methionine, the other sulfur-containing amino acid found in proteins, is synthesized in plastids from cysteine (see **WEB TOPIC 14.3** for further detail). After cysteine and methionine are synthesized, sulfur can be incorporated into proteins and a variety of other compounds, such as acetyl-CoA and *S*-adenosylmethionine. The latter compound is important in the synthesis of ethylene (see Chapters 4, 15 and 21) and in reactions involving the transfer of methyl groups, as in histone modification (see Chapter 3).

14.7 Phosphate Assimilation

Phosphate (HPO_4^{2-}) in the soil solution is readily transported into plant roots via an H^+–HPO_4^{2-} symporter (see Chapter 8) and incorporated into a variety of organic compounds, including sugar phosphates, phospholipids, and nucleotides. The main entry point of phosphate into assimilatory pathways occurs during the formation of ATP, the energy "currency" of the cell. In the overall reaction for this process, inorganic phosphate is added to the second phosphate group in adenosine diphosphate to form a phosphate ester bond.

In mitochondria, the energy for ATP synthesis derives from the oxidation of NADH or succinate by oxidative phosphorylation (see Chapter 13). ATP synthesis is also driven by light-dependent photophosphorylation in the chloroplasts (see Chapter 9). In addition to these reactions in mitochondria and chloroplasts, reactions in the cytosol such as glycolysis also assimilate phosphate.

Glycolysis incorporates inorganic phosphate into 1,3-bisphosphoglyceric acid, forming a high-energy acyl phosphate group. This phosphate can be donated to ADP to form ATP in a substrate-level phosphorylation reaction (see Chapter 13). Once incorporated into ATP, the phosphate group may be transferred via many different reactions to form the various phosphorylated compounds found in higher-plant cells.

miRNAs contribute to phosphate and sulfate signaling

Mediated by the transcription factor PHR1, phosphate deficiency quickly induces the expression of miR399 in shoots, and later in roots. Shoot-derived miR399 is transported via phloem transport into roots (see Chapter 12), where it facilitates cleavage of *PHOSPHATE 2* (*PHO2*) mRNA that encodes a ubiquitin-conjugating E2 enzyme. This action relieves the degradation of PHO1 and PHOSPHATE TRANSPORTER 1 (PHT1) to enhance root-to-shoot phosphate translocation and phosphate uptake, respectively, under conditions of phosphate deficiency.

In a similar process, mediated by the transcription factor SULFUR LIMITATION 1 (SLIM1), sulfate deficiency induces an accumulation of miR395 in phloem, thereby limiting the expression of its target *SULFATE*

TRANSPORTER 2;1 (*SULTR2;1*) in xylem parenchyma to enhance root-to-shoot sulfate transport. Additional targets of miR395 include three ATP sulfurylase isoforms (*ATPS1*, *ATPS3*, and *ATPS4*), with this regulatory circuit modulating not only sulfate assimilation flux but also sulfate translocation.

14.8 Oxygen Assimilation

Respiration accounts for the bulk (about 90%) of the O_2 assimilated by plant cells (see Chapter 13). Another major pathway for the assimilation of O_2 into organic compounds involves the incorporation of O_2 from water (e.g., see reaction 1 in Figure 10.3). A small proportion of oxygen can be directly assimilated into organic compounds in the process of *oxygen fixation* via enzymes known as *oxygenases*. The most prominent oxygenase in plants is ribulose 1,5-bisphosphate carboxylase/oxygenase (Rubisco), which during photorespiration incorporates oxygen into an organic compound and releases energy (see Chapter 10).

14.9 The Energetics of Nutrient Assimilation

Nutrient assimilation generally requires large amounts of energy to convert stable, low-energy, highly oxidized inorganic compounds into high-energy, highly reduced organic compounds. For example, the reduction of nitrate to nitrite and then to ammonium requires the transfer of about eight electrons and accounts for about 25% of the total energy expenditures in both roots and shoots. Consequently, a plant may use one-fourth of its energy to assimilate nitrogen, a constituent that accounts for less than 2% of the total dry weight of the plant.

Many of these assimilatory reactions occur in the stroma of the chloroplast, where they have ready access to powerful reducing agents, such as NADPH, thioredoxin, and ferredoxin, generated during photosynthetic electron transport. This process—coupling nutrient assimilation to photosynthetic electron transport—is called **photoassimilation** (**Figure 14.20**).

Photoassimilation and the C_3 carbon fixation cycle occur in the same compartment. However, only when photosynthetic electron transport generates reductant in excess of the needs of the C_3 carbon fixation cycle—for example, under conditions of high light and low CO_2—does photoassimilation proceed. High concentrations of CO_2 inhibit nitrate assimilation in the shoots of C_3 plants (**Figure 14.21A**).

One physiological mechanism responsible for this phenomenon involves photorespiration (see Chapter 10). Photorespiration has been erroneously portrayed as a wasteful process. In fact, photorespiration plays a positive role in plant carbon–nitrogen relations. It stimulates the export of malate from chloroplasts, and this malate in the cytoplasm generates NADH that powers the first step of NO_3^- assimilation, the reduction of NO_3^- to NO_2^-. Carbon dioxide enrichment decreases photorespiration, decreasing the amount of NADH available for NO_3^- reduction.

Unlike in C_3 carbon fixation, the first carboxylation reaction in the C_4 carbon fixation pathway generates

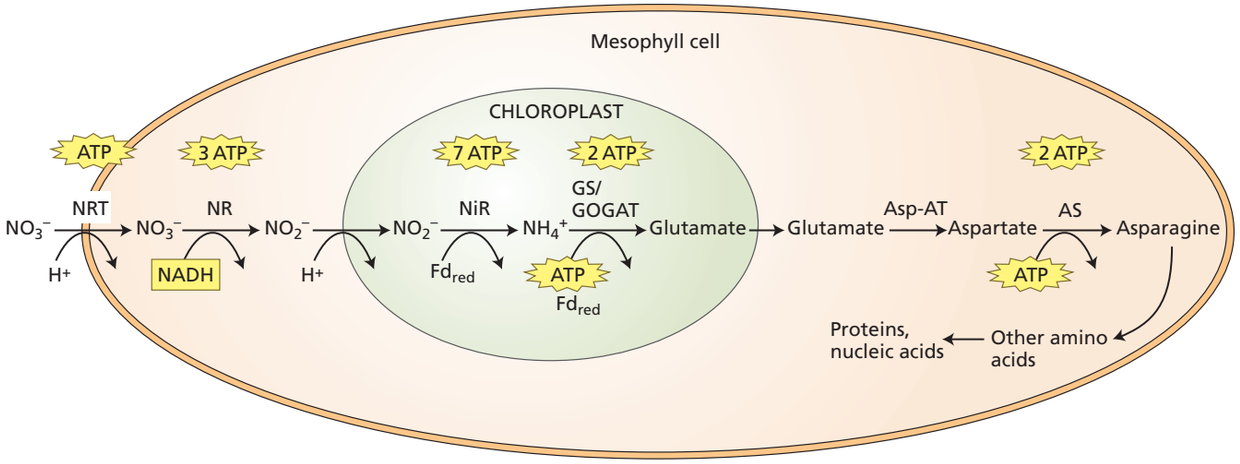


Figure 14.20 Summary of processes involved in the assimilation of mineral nitrogen in the leaf. Nitrate translocated from the roots through the xylem is absorbed by a mesophyll cell via one of the nitrate ransporters (NRT) into the cytoplasm. There it is reduced to nitrite via nitrate reductase (NR). Nitrite is translocated into the stroma of the chloroplast along with a proton. In the stroma, nitrite is reduced to ammonium via nitrite reductase (NiR), and this ammonium is converted into glutamate via the sequential action of glutamine synthetase (GS) and glutamate synthase (GOGAT). Once again in the cytoplasm, the glutamate is transaminated to aspartate via aspartate aminotransferase (Asp-AT). Finally, asparagine synthetase (AS) converts aspartate into asparagine. The approximate amounts of ATP equivalents are given above each reaction.

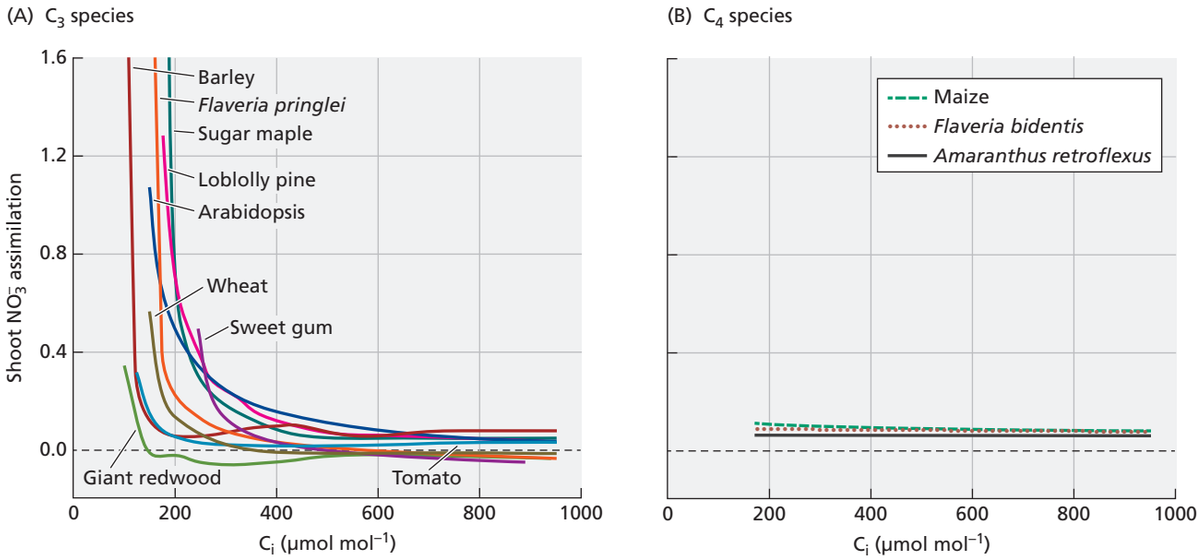


Figure 14.21 Shoot NO_3^- assimilation as a function of shoot internal CO_2 concentration (C_i) for nine C_3 species (A) and three C_4 species (B). Shoot NO_3^- assimilation is assessed by ΔAQ (decrease in the ratio of shoot CO_2 consumption to O_2 evolution with a shift from NH_4^+ to NO_3^- nutrition). (Modified from A. J. Bloom et al. 2012. *Ecology* 93: 355–367 with data from P. S. Searles and A. J. Bloom. 2003. *Plant Cell Environ*. 26: 1247–1255.)

ample amounts of malate and NADH in the cytoplasm of mesophyll cells. This explains the CO_2-independence of shoot NO_3^- assimilation in C_4 plants (**Figure 14.21B**). Also, the rapid malate catabolism and high CO_2 concentrations in bundle sheath cells explain why C_4 plants assimilate NO_3^- exclusively in mesophyll cells.

If, as expected, atmospheric levels of CO_2 increase to about 700 ppm during this century (see Chapter 11), CO_2 inhibition of shoot nitrate assimilation will increasingly affect plant–nutrient relations. Food quality of C_3 crops such as wheat has already suffered losses and will decline even more during the coming decades. Breeding crops for enhanced root nitrate and ammonium assimilation has the potential to mitigate such losses in food quality, but this approach is yet untapped.

Summary

Nutrient assimilation is the often energy-requiring process by which plants incorporate inorganic nutrients into the carbon constituents necessary for growth and development.

14.1 Nitrogen in the Environment

- When nitrogen is fixed into ammonia (NH_3) or nitrate (NO_3^-), it passes through several organic or inorganic forms before it eventually returns to molecular nitrogen (N_2) (**Table 14.1, Figure 14.1**).
- At high concentrations, ammonium (NH_4^+) is toxic to living tissues, but nitrate can be safely stored and translocated in plant tissues (**Figures 14.2, 14.3**).

14.2 Nitrate Assimilation

- Plant roots actively absorb nitrate, then reduce it to nitrite (NO_2^-) in the cytosol by nitrate reductase, and further reduce it to ammonium in the plastids by nitrite reductase (**Figure 14.3**).
- Nitrate reductase contain three domains that bind FAD, heme, and molybdenum ions, respectively (**Figure 14.4**).
- Nitrate, light, and carbohydrate levels affect the transcription and translation of nitrate reductase.
- Darkness and Mg^{2+} can inactivate nitrate reductase. Such inactivation is faster than regulation by decreased synthesis or degradation of the enzyme.
- In chloroplasts and root plastids, the enzyme nitrite reductase reduces nitrite to ammonium (**Figure 14.5**).
- Both roots and shoots assimilate nitrate (**Figures 14.6, 14.7**).
- Nitrate can be transported in both the xylem and phloem (**Figure 14.7**).

Summary (*continued*)

- Nitrate transceptor (transporter with receptor function) CHL1 not only helps the plant acquire nitrate from soil, but also senses nitrate concentration differences in the soil and elicits different levels of gene expression (**Figure 14.8**).

14.3 Ammonium Assimilation

- Plant cells avoid ammonium toxicity by rapidly converting ammonium into amino acids (**Figure 14.9**).
- Nitrogen is incorporated into other amino acids via transamination reactions involving glutamine and glutamate.
- The amino acid asparagine is a key compound for nitrogen transport and storage.

14.4 Amino Acid Biosynthesis

- The carbon skeletons for amino acids derive from intermediates of glycolysis and the tricarboxylic acid cycle (**Figure 14.10**).

14.5 Biological Nitrogen Fixation

- Biological nitrogen fixation accounts for most of the ammonia formed from atmospheric N_2 (**Figure 14.1; Table 14.1**).
- Several types of nitrogen-fixing bacteria form symbiotic associations with higher plants (**Figures 14.11, 14.12; Tables 14.2, 14.3**).
- Nitrogen fixation requires anaerobic or microaerobic conditions.
- Symbiotic nitrogen-fixing prokaryotes function within nodules, specialized structures formed by the plant host (**Figure 14.11**).
- The symbiotic relationship is initiated by the migration of the nitrogen-fixing bacteria toward the roots of the host plant, which is mediated by chemical attractants secreted by the roots.
- Attractants activate the rhizobial NodD protein, which then induces the biosynthesis of Nod factors that act as signals for symbiosis (**Figures 14.13, 14.14**).
- Nod factors induce root hair curling, sequestration of rhizobia, cell wall degradation, and bacterial access to the root hair plasma membrane, from which an infection thread forms (**Figure 14.15**).
- Filled with proliferating rhizobia, the infection thread elongates through root tissue in the direction of the developing nodule, which arises from cortical cells (**Figure 14.15**).
- In response to a signal from the plant, the bacteria in the nodule stop dividing and differentiate into nitrogen-fixing bacteroids.
- The reduction of N_2 to NH_3 is catalyzed by the nitrogenase enzyme complex (**Figure 14.16**).
- Fixed nitrogen is transported as amides or ureides (**Figures 14.6, 14.17**).

14.6 Sulfur Assimilation

- Most assimilated sulfur derives from sulfate (SO_4^{2-}) absorbed from the soil solution, but plants can also metabolize gaseous sulfur dioxide (SO_2) entering via stomata.
- Synthesis of sulfur-containing organic compounds begins with the reduction of sulfate to the amino acid cysteine (**Figure 14.18**).
- Sulfate is mainly assimilated in leaves, involving three subcellular compartments of cytosol, chloroplast, and mitochondria (**Figure 14.19**).

14.7 Phosphate Assimilation

- Roots absorb phosphate (HPO_4^{2-}) from the soil solution, and its assimilation occurs with the formation of ATP.
- From ATP, the phosphate group can be transferred to many different carbon compounds in plant cells.

14.8 Oxygen Assimilation

- Respiration and the oxygenase activity of Rubisco account for most of the O_2 assimilated by plant cells, but direct oxygen fixation is also catalyzed by other oxygenases.

14.9 The Energetics of Nutrient Assimilation

- Energy-requiring nutrient assimilation is coupled to photosynthetic electron transport, which generates powerful reducing agents (**Figure 14.20**).
- Photoassimilation operates only when photosynthetic electron transport generates reductant in excess of the needs of the C_3 carbon fixation cycle.
- Rising levels of atmospheric CO_2 inhibit nitrate assimilation in the shoots of C_3 plants (**Figure 14.21**).

Web Material

- **WEB TOPIC 14.1 Development of a Root Nodule** Nodule primordia form opposite the protoxylem poles of the root vascular bundles.
- **WEB TOPIC 14.2 Measurement of Nitrogen Fixation** Acetylene reduction is used as an indirect measurement of nitrogen reduction.
- **WEB TOPIC 14.3 The Synthesis of Methionine** Methionine is synthesized in plastids from cysteine.

For more study aids, go to oup.com/he/taiz7e.

Suggested Reading

Chiou, T.-J., and Lin, S.-I. (2011) Signaling network in sensing phosphate availability in plants. *Annu. Rev. Plant Physiol.* 62: 185–206.

Crawford, N. M., and Forde, B. J. (2002) Molecular and developmental biology of inorganic nitrogen nutrition. In: *The Arabidopsis Book*, C. Somerville and E. Meyerowitz (eds.), American Society of Plant Physiologists, Rockville, MD.

Fowler, D., Coyle, M., Skiba, U., Sutton, M. A., Cape, J. N., Reis, S., Sheppard, L. J., Jenkins, A., Grizzetti, B., Galloway, J. N., Vitousek, P., Leach, A., Bouwman, A. F., Butterbach-Bahl, K., Dentener, F., Stevenson, D., Amann, M., and Voss, M. (2013) The global nitrogen cycle in the twenty-first century. *Philos. Trans. R Soc. Lond B Biol. Sci*. 368: 20130164.

Geurts, R., Lillo, A., and Bisseling, T. (2012) Exploiting an ancient signalling machinery to enjoy a nitrogen fixing symbiosis. *Curr. Opin. Plant Biol.* 15: 438–443.

Herridge, D. F., Peoples, M. B., and Boddey, R. M. (2008) Global inputs of biological nitrogen fixation in agricultural systems. *Plant Soil* 311: 1–18.

Ho, C.-H., Lin, S.-H., Hu, H.-C., and Tsay, Y.-F. (2009) CHL1 functions as a nitrate sensor in plants. *Cell* 138: 1184–1194.

Maillet, F., Poinsot, V., Andre, O., Puech-Pages, V., Haouy, A., Gueunier, M., Cromer, L., Giraudet, D., Formey, D., Niebel, A., et al. (2011) Fungal lipochitooligosaccharide symbiotic signals in arbuscular mycorrhiza. *Nature* 469: 58–63.

Marschner, H., and Marschner, P. (2012) *Marschner's Mineral Nutrition of Higher Plant*s, 3rd ed. Elsevier/Academic Press, London; Waltham, MA.

Oldroyd, G. E., Murray, J. D., Poole, P. S., and Downie, J. A. (2011) The rules of engagement in the legume-rhizobial symbiosis. *Annu. Rev. Gen.* 45: 119–144.

Santi, C., Bogusz, D., and Franche, C. (2013) Biological nitrogen fixation in non-legume plants. *Ann. Bot.* 111: 743–767.

Schroeder, J. I., Delhaize, E., Frommer, W. B., Guerinot, M. L., Harrison, M. J., Herrera-Estrella, L., Horie, T., Kochian, L.V., Munns, R., Nishizawa, N. K., Tsay, Y. F., and Sanders, D. (2013) Using membrane transporters to improve crops for sustainable food production. *Nature* 497: 60–66.

Takahashi, H., Kopriva, S., Giordano, M., Saito, K., and Hell, R. (2011) Sulfur Assimilation in Photosynthetic Organisms: Molecular Functions and Regulations of Transporters and Assimilatory Enzymes. *Annu. Rev. Plant Biol.* 62: 157–184.

Wang, Y.-Y., Cheng, Y.-H., Chen, K.-E., and Tsay, Y. F. (2018) Nitrate transport, signaling, and use efficiency. *Annu. Rev. Plant Biol.* 69: 85–122.

15 Abiotic Stress



Aleksey Sagitov/Shutterstock

Plants grow and reproduce in environments containing a multitude of abiotic (nonliving), chemical, and physical factors, which vary both with time and geographic location. The primary abiotic environmental parameters that affect plant growth are light (intensity, quality, and duration), water (soil availability and humidity), carbon dioxide, oxygen, soil nutrient content and availability, temperature, and toxins (i.e., heavy metals and salinity). Fluctuations of these abiotic factors outside their normal ranges usually have negative biochemical and physiological consequences for plants. Being sessile, plants are unable to avoid abiotic stress simply by moving to a more favorable environment. Instead, plants have evolved the ability to compensate for stressful conditions by altering physiological and developmental processes to maintain growth and reproduction.

In the past several decades, the introduction of greenhouse gases into our atmosphere has resulted in a cumulative warming of air, land, and ocean (global warming). This warming has become a major contributor to changes in our climate, causing an increase in the frequency and intensity of weather events that subject plants to abiotic stress conditions, such as prolonged droughts, heat waves, flooding, and salinity (**WEB TOPIC 15.1**). As we describe in this chapter, these conditions can have a negative impact on plant growth and yield, threatening our food supply and highlighting the importance of studying abiotic stress responses in different crops, herbaceous plants, and trees.

In this chapter we provide an integrated view of how plants adapt and respond to abiotic stresses in the environment. Like all living organisms, plants are complex biological systems containing thousands of different genes, proteins, regulatory molecules, signaling agents, and chemical compounds that form hundreds of interlinked pathways and networks. Under normal growing conditions, the different biochemical pathways and signaling networks act in a coordinated manner to balance environmental inputs with the plant's genetic imperative to grow and reproduce. When exposed to unfavorable environmental conditions, this complex interactive system adjusts homeostatically to minimize the negative impacts of stress and maintain metabolic equilibrium (**Figure 15.1**).

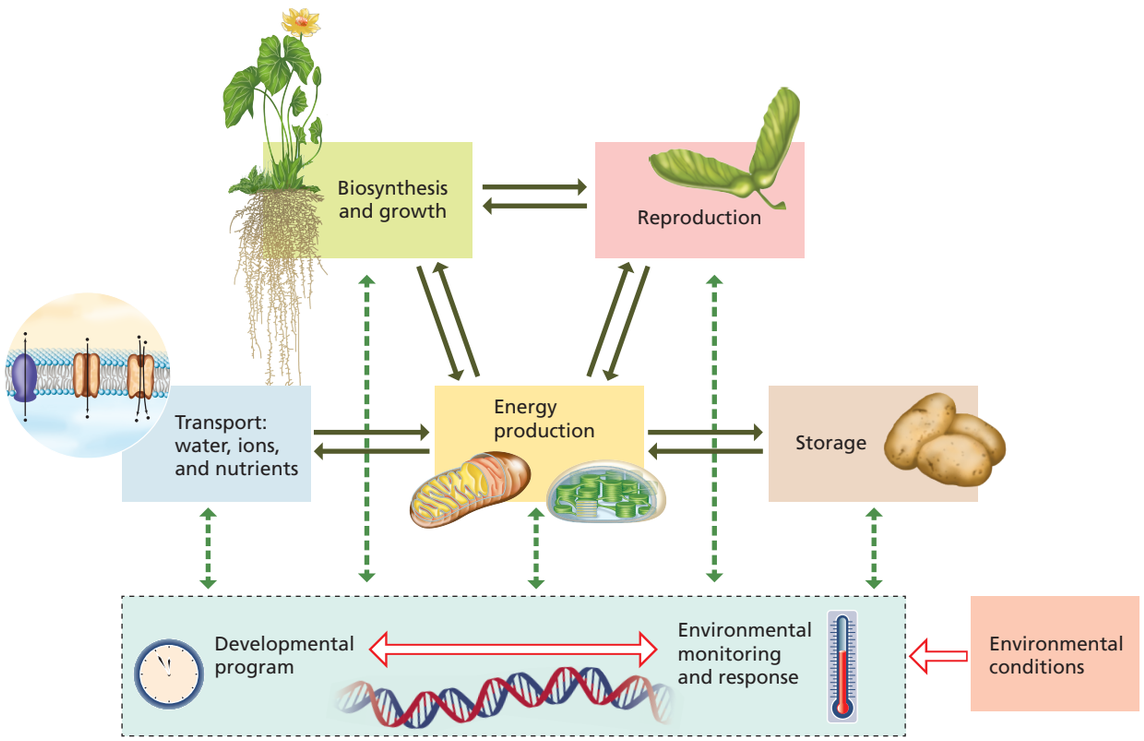


Figure 15.1 Interactions between environmental conditions and plant development, growth, energy production, and ion and nutrient balance and storage. The balance between these processes is controlled by the plant genome (bottom box), which encodes sensors and signal transduction pathways that monitor and adjust for environmental and internal inputs (open and dashed arrows). Based on the different environmental stress signals, the plant genome can thus direct the flow of energy between the different processes (solid arrows) to establish a new homeostatic state matched to the specific stress conditions.

We begin by distinguishing between adaptation and acclimation in relation to abiotic stress. Next we describe the various abiotic factors in the environment that can negatively affect plant growth and development. In the remainder of the chapter we discuss plant stress-sensing mechanisms and the processes that transform sensory signals into physiological responses, as well as describe the specific metabolic, physiological, and anatomical changes that result from these signaling pathways and enable plants to adapt or acclimate to abiotic stress. Finally, we describe how efforts to enhance the abiotic stress tolerance of plants can improve agricultural yield, and how the different physiological processes affected in plants during abiotic stress can be used for plant monitoring and treatment in the field using precision agriculture practices (**WEB TOPIC 15.2**).

15.1 Defining Plant Stress

The ideal growth conditions for a given plant can be defined as the conditions that allow the plant to achieve its maximum growth and reproductive potential as measured by plant weight, height, and seed number, which together make up the *total biomass* of the plant. **Stress** can be defined as any environmental condition that prevents the plant from achieving its full genetic potential. For example, a decrease in light intensity would cause a reduction in photosynthetic activity with a concomitant decrease in the energy supply to the plant. Under these conditions, the plant could compensate either by slowing down biosynthesis, thus reducing its growth rate or yield, or by drawing on its stored food reserves in the form of starch or oil (see Figure 15.1).

Similarly, a decrease in water availability would also have a deleterious effect on growth. One way that plants compensate for a decrease in water potential is by closing their stomata, which reduces water loss by transpiration. However, stomatal closure also decreases CO_2 uptake by the leaf, thereby reducing photosynthesis and suppressing growth. In addition to suppressing growth, abiotic stresses can reduce seed production, due to limited photosynthetic resources and other deleterious effects of stress on reproductive processes. For example, water-deficit treatments inhibit the growth of rice plants, and salinity decreases ear size and kernel size in maize (corn; *Zea mays*) (**Figure 15.2**).

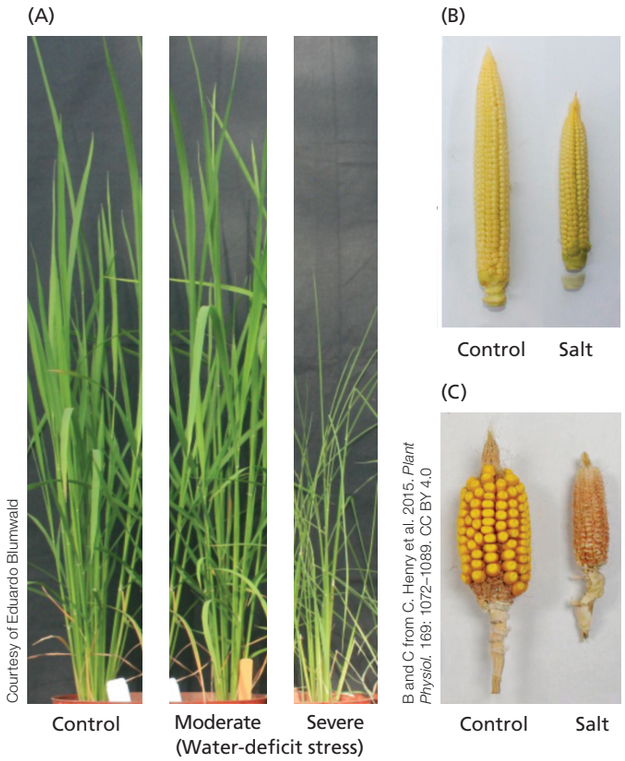


Figure 15.2 Impact of abiotic stress on plant growth and reproduction. **(A)** Whereas moderate water-deficit stress does not have a significant effect on the growth of rice plants, severe water-deficit stress reduces growth. **(B)** Effect of salt stress on maize ear size. **(C)** Effect of salt stress on maize kernel size.

Physiological adjustment to abiotic stress involves trade-offs between vegetative and reproductive development

How do changes in environmental conditions affect seed production? Under optimal growing conditions, the competition for resources among the different plant organs or developmental phases is minimal. The transition to reproductive growth occurs only after the vegetative adult phase completes its genetically determined developmental program (see Chapter 20). Under abiotic stress conditions, however, the vegetative growth program may terminate prematurely, and the plant may go immediately to the reproductive phase. In this case the plant undergoes a transition to flowering, fertilization, and seed set before the plant has reached its full size, resulting in a smaller plant (see Figure 15.2A). With fewer leaves to provide photosynthates, plants growing under suboptimal conditions may also produce fewer and smaller viable seeds (see Figure 15.2B and C).

The particular developmental pathway that a plant uses to maximize its reproductive potential under abiotic stress depends to a large extent on the plant's life cycle. For example, *annual plants* complete their life cycle in a single season. It is thus advantageous for annual plants to adjust their metabolism and developmental programs so as to produce the maximum number of viable seeds under whatever environmental conditions are encountered during the season. By contrast, *perennial plants*, which have multiple seasons in which to produce seeds, tend to adjust their metabolism and developmental programs to ensure the optimal storage of food resources that will enable the plants to survive to the next season, even at the expense of seed production. Perennial plants faced with a severe abiotic stress period could therefore abort flowering altogether and enter dormancy until conditions improve.

15.2 Acclimation and Adaptation

Individual plants respond to changes in the environment by directly altering their physiology or morphology in ways that enhance their survival and reproduction. Such responses require no new genetic modifications. If the response of the individual plant improves with repeated exposure to the environmental stress, then the response is termed **acclimation**. Acclimation represents a nonpermanent change in the physiology or morphology of the individual that can be reversed if the prevailing environmental conditions change. Epigenetic mechanisms that alter the expression of genes without changing the genetic code of an organism can extend the duration of acclimation responses and make them heritable. When genetic changes in an entire plant population have been fixed over many generations by selective environmental pressure, those changes are referred to as **adaptation**.

Adaptation to stress involves genetic modification over many generations

A remarkable example of adaptation to an extreme abiotic environment is the growth of plants in serpentine soils. Serpentine soils are characterized by low moisture, low concentrations of macronutrients, and elevated levels of heavy metals. These conditions would result in severe stress conditions for most plants. However, it is not unusual to find populations of plants that have become genetically adapted to serpentine soils growing not far from closely related nonadapted plants growing on "normal" soils. Simple transplant experiments have shown that only the adapted populations can grow and reproduce on the serpentine soil, and genetic crosses reveal the stable genetic basis of this adaptation.

The evolution of adaptive mechanisms in plants to a particular set of environmental conditions generally involves processes that allow *avoidance* of the potentially damaging effects of these conditions. For example,

populations of the weed Yorkshire fog grass (*Holcus lanatus*) that are adapted to growth on arsenic-contaminated mine sites in southwestern England contain a specific genetic modification that reduces the uptake of arsenate, allowing the plants to avoid arsenic toxicity and thrive on contaminated mine sites. In contrast, populations growing on uncontaminated soils are less likely to contain this genetic modification.

Acclimation allows plants to respond to environmental fluctuations

In addition to genetic changes in entire populations, individual plants may acclimate to periodic changes in the environment by directly altering their morphology or physiology. The physiological changes associated with acclimation require no genetic modifications, and many are reversible. One example of acclimation from gardening is a process known as *hardening off*. To speed up the growth of plants, gardeners often start by growing them indoors in pots under optimal growth conditions. The gardeners then move the plants outdoors for part of the day over a period long enough to acclimate, or "harden," the plants to outdoor weather before moving them outdoors permanently.

Both genetic adaptation and acclimation can contribute to the plants' overall tolerance of extremes in their abiotic environment. In the example just discussed, genetic adaptation in the arsenic-tolerant Yorkshire fog grass population only *reduces* arsenate uptake—it does not stop it. To mitigate the toxic effects of the arsenate that does accumulate, the adapted plants use the same biochemical mechanism that nonadapted plants use to respond to the toxic effects of arsenate accumulation in tissues. This mechanism involves the biosynthesis of low-molecular-weight, metal-binding molecules called *phytochelatins* (discussed in more detail in Section 15.6), which reduce arsenic toxicity. Thus, the ability of Yorkshire fog grass to thrive on arsenic-contaminated mine waste depends on both a genetic adaptation specific to the tolerant population (arsenate exclusion; see *Exclusion and internal tolerance mechanisms allow plants to cope with toxic ions* in Section 15.6) and on acclimation, which is common to all plants that respond to arsenic by producing phytochelatins.

Another example of acclimation is the response of salt-sensitive, or *glycophytic*, plants to salinity. Although glycophytic plants are not genetically adapted to growth in saline environments, when exposed to elevated salinity they can activate several stress responses that allow the plants to cope with the physiological perturbations imposed by elevated salinity in their environment. For example, the SOS pathway (a signaling pathway discovered in *salt overly sensitive* mutants) leads to enhanced efflux of Na^+ from cells and a reduction in salinity-induced toxicity.

15.3 Environmental Factors and Their Biological Impacts on Plants

In this section we briefly describe the ways in which various environmental stresses can disrupt plant metabolism. As with every biological system, plant survival and growth depend on complex networks of coupled anabolic and catabolic pathways that direct the flow of energy and resources within and among cells. Disruption of these networks by environmental factors can result in uncoupling of the pathways. For example, metabolic enzymes can, and often do, have different temperature optima. An increase or decrease in ambient temperature can inhibit a subset of enzymes without affecting other enzymes in the same or connected pathways. Such functional uncoupling of metabolic pathways could result in the accumulation of intermediate compounds that could be converted to toxic by-products.

In recent years, scientists have begun to use advanced tools such as transcriptomics, proteomics, and metabolomics to simultaneously study thousands of transcripts, proteins, and chemical compounds altered in plants in response to abiotic stress. These large-scale genomic analyses have enabled researchers to identify important stress-response pathways and networks involved in plant acclimation.

One of the most common groups of toxic intermediates produced by stress are **reactive oxygen species** (**ROS**), that are highly reactive forms of oxygen possessing at least one unpaired electron in their orbitals. ROS are capable of rapidly reacting with, and oxidizing, a wide variety of cellular constituents, including proteins, DNA, RNA, and lipids (see **WEB ESSAY 13.7**). The most common forms of ROS in plant cells are superoxide ($O_2^{\bullet -}$), singlet oxygen ($^1O_2$), hydrogen peroxide (H_2O_2), and hydroxyl radicals ($OH^{\bullet}$) (**Figure 15.3**). ROS can also trigger an autocatalytic process of membrane oxidation that can result in the degradation of organelles and the plasma membrane, and cell death. Despite

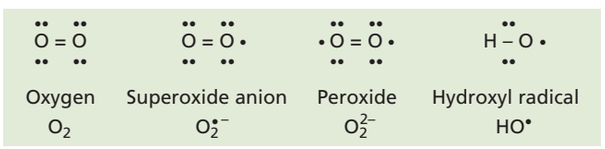


Figure 15.3 **Chemistry of reactive oxygen species (ROS).** Molecular oxygen does not have any available unpaired electrons in its orbitals, but different forms of ROS have at least one unpaired electron. Various cellular metabolites can therefore transfer an electron to ROS and be oxidized in the process.

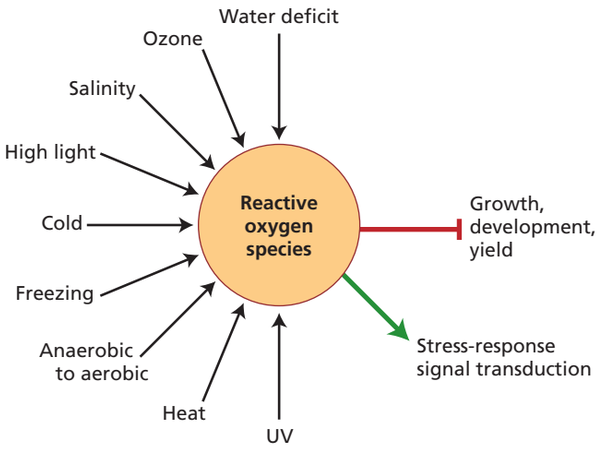


Figure 15.4 Dual role of reactive oxygen species (ROS) during abiotic stress. A variety of abiotic stresses result in the accumulation of ROS in cells. On the one hand, ROS have a negative effect on plant growth, development, and yield. On the other hand, ROS accumulation has a positive effect on cells by activating signal transduction pathways that induce acclimation mechanisms. These, in turn, counteract the negative effects of stress (including ROS accumulation).

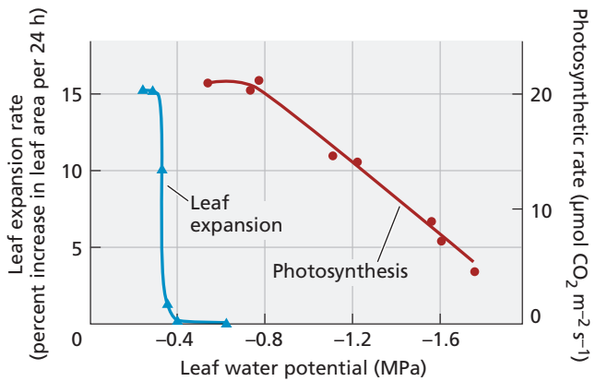


Figure 15.5 Effects of water stress on photosynthesis and leaf expansion of sunflower (*Helianthus annuus*). In this species, leaf expansion is completely inhibited under mild stress levels that barely affect photosynthetic rates. (After J. S. Boyer. 1970. *Plant Physiol.* 46: 233–235.)

their mechanistic differences, most abiotic stresses result in the production of ROS (**Figure 15.4**), and ROS are used by plants as signal transduction molecules for stress sensing (discussed in more detail in Section 15.5).

Environmental stresses can also disrupt the compartmentation of metabolic processes that isolates them from other cellular components. The same temperature extremes that can inhibit enzyme activity can also affect membrane fluidity: High temperature causes increased fluidity, and low temperature causes decreased fluidity. Changes in membrane fluidity can disrupt the coupling between different protein complexes in chloroplast or mitochondrial membranes, resulting in the uncontrolled transfer of electrons to oxygen and the formation of ROS.

Water deficit decreases turgor pressure, increases ion toxicity, and inhibits photosynthesis

As in most other organisms, water makes up the largest proportion of the cellular volume in plants and is the most limiting resource. About 97% of water taken up by plants is lost to the atmosphere (mostly by transpiration). About 2% is used for volume increase or cell expansion, and 1% for metabolic processes, predominantly photosynthesis (see Chapters 5 and 6). Water deficit (insufficient water availability) occurs in most natural and agricultural habitats and is caused mainly by intermittent to continuous periods without precipitation. *Drought* is the meteorological term for a period of insufficient precipitation that ultimately results in plant water deficit. In this chapter we use the term *water-deficit stress* since the amount of stress a plant experiences under drought conditions depends on the soil's water-holding capacity and the depth of the water table.

Water deficit can affect plants differently during vegetative versus reproductive growth. When plant cells experience water deficit, cell dehydration occurs. Cell dehydration adversely affects many basic physiological processes (**Table 15.1**). For example, during water deficit the water potential (Ψ) of the apoplast becomes more negative than that of the symplasm, causing reductions in pressure potential (turgor) (Ψ_p) and volume (see Chapter 5). A secondary effect of cell dehydration is that ions become more concentrated and may become cytotoxic. Water deficit also induces the accumulation of abscisic acid (ABA), which promotes stomatal closure, reducing gas exchange and inhibiting photosynthesis (**Figure 15.5**). As a result of dehydration-induced uncoupling of the photosystems, free electrons produced by the reaction centers are not transferred to $NADP^+$, leading to the generation of ROS that could cause cellular damage if not removed.

Temperature stress affects a broad spectrum of physiological processes

Temperature stress disrupts plant metabolism because of its differential effect on protein stability and enzymatic reactions, causing the uncoupling of different reactions and the accumulation of toxic intermediates and ROS. As mentioned earlier, heat stress increases membrane fluidity, whereas cold stress decreases membrane fluidity, causing the uncoupling of different multiprotein complexes, disruption of electron flow and energetic reactions, and disruption of ion homeostasis and regulation. Heat stress can also destabilize (melt) RNA and DNA secondary structures, and cold stress can overstabilize (harden) them, disrupting transcription,

TABLE 15.1 Physiological and biochemical perturbations in plants caused by fluctuations in the abiotic environment

Environmental factor	Primary effects	Secondary effects
Water deficit	Water potential (ψ) reduction (see Chapter 5)	Reduced cell/leaf expansion
	Cell dehydration	Reduced cellular and metabolic activities
	Hydraulic resistance	Stomatal closure
		Photosynthetic inhibition
		Leaf abscission
		Altered carbon partitioning
		Cell wall damage
		Cavitation
		Membrane and protein destabilization
		ROS production
		Ion cytotoxicity
		Cell death
Salinity	Water potential (ψ) reduction (see Chapter 5)	Same as for water deficit (see above)
	Cell dehydration	
	Ion cytotoxicity	
Flooding and soil compaction	Hypoxia (see Chapter 13)	Reduced respiration
	Anoxia	Fermentative metabolism
		Inadequate ATP production
		Production of toxins by anaerobic microbes
		ROS production
		Stomatal closure
High temperature	Membrane and protein destabilization	Photosynthetic and respiratory inhibition
		ROS production
		Cell death
Chilling	Membrane destabilization	Membrane dysfunction
Freezing	Water potential (ψ) reduction	Same as for water deficit (see above)
	Cell dehydration	Physical destruction
	Symplasmic ice crystal formation	
Trace element toxicity	Disturbed cofactor binding to proteins and DNA	Disruption of metabolism
	ROS production	
High light intensity	Photoinhibition (see Chapters 9 and 11)	Inhibition of PSII repair
	ROS production	Reduced CO_2 fixation

translation, and RNA processing and turnover. In addition, temperature stress can affect protein structure and block protein degradation, causing the buildup of protein aggregates. Such protein clumps can disrupt normal cellular functions by interfering with the function of the cytoskeleton and associated organelles. Heat stress is also known to negatively affect plant reproduction by causing decreased pollen viability, fertilization, and seed filling, as well as increased flower and fruit abortion. Because of the effects of heat stress on plant reproductive processes, global warming (see **WEB TOPIC 15.1**) is expected to cause an overall decrease in the yield of major grain crops such as wheat, maize, and rice.

Flooding results in anaerobic stress to the root

When a field is flooded, the O_2 levels at the root surface decrease dramatically because most of the air in the soil is displaced by water, and the O_2 concentration of water is significantly lower than that of air: The atmosphere

contains about 20% O_2 or 200,000 ppm, compared with less than 10 ppm dissolved O_2 in flooded soil. Under these conditions, respiration in roots is suppressed and fermentation is enhanced. This metabolic shift can cause energy depletion, acidification of the cytosol, and toxicity from ethanol accumulation. As a consequence of energy depletion, many processes such as protein synthesis are suppressed. Anaerobic stress can cause cell death within hours or days, depending on the degree of genetic adaptation of the species. Even if the O_2-deprived plant is returned to normal O_2 levels, the recovery process itself can pose a hazard. While the roots are under anaerobic stress, the absence of O_2 prevents the formation of ROS. But if the O_2 level in the soil is rapidly increased, much of it is used to form ROS, causing oxidative damage to the root cells.

Salinity stress has both osmotic and cytotoxic effects

Excess soil salinity brought about by a combination of over-irrigation and poor soil drainage affects large regions of the world's land mass and has a severe impact on agriculture. About 20% of all cultivatable land, feeding about 2.4 billion people, is currently under irrigation, and roughly 20% of all irrigated land is affected by salinity stress. It is likely that the percentage of irrigated land will increase significantly in areas most affected by global warming.

Salinity stress has two components: nonspecific **osmotic stress** that causes water deficits, and specific ion effects resulting from the accumulation of toxic ions, which interfere with nutrient uptake and cause cytotoxicity. Salt-tolerant plants genetically adapted to salinity are termed **halophytes** (from the Greek *halo*, "salty"), while less salt-tolerant plants that are not adapted to salinity are termed **glycophytes** (from the Greek *glyco*, "sweet"). Under nonsaline conditions, the cytosol of higher plant cells contains about 100 m*M* K^+ and less than 10 m*M* Na^+, an ionic environment in which enzymes are optimally functional. In saline environments, cytosolic Na^+ and Cl^- increase to more than 100 m*M*, and these ions become cytotoxic. One reason that Na^+ is toxic at high concentrations is that it is chemically similar to K^+ and can competitively inhibit K^+-dependent cellular processes. Several enzymes, including pyruvate kinase, nitrate reductase, Rubisco, starch synthase, sucrose phosphate synthase, β-amylase, invertase, and phosphofructokinase (see Chapters 10, 13, and 14), require K^+ for their function and can be inhibited in the presence of high cytosolic Na^+ levels. At high concentrations, apoplastic Na^+ can also compete for sites on transport proteins that are necessary for high-affinity uptake of K^+ (see Chapter 8), an essential macronutrient (see Chapter 7).

The effects of high salinity in plants occur through a two-phase process: a fast response to the high osmotic pressure at the root–soil interface and a slower response caused by the accumulation of Na^+ (and Cl^-) in the leaves. In the osmotic phase there is a reduction in shoot growth, with reduced leaf expansion and inhibition of lateral bud formation. The second phase starts with the accumulation of toxic amounts of Na^+ in the leaves, leading to the inhibition of photosynthesis and other biosynthetic processes. Although in most species Na^+ reaches toxic concentrations before Cl^-, some plant species, such as citrus, grapevine, and soybean, are highly sensitive to excess Cl^-.

During freezing stress, extracellular ice crystal formation causes cell dehydration

Plants subjected to freezing temperatures must contend with the formation of ice crystals, either extracellularly or intracellularly. Intracellular ice crystal formation nearly always proves lethal to the cell. However, the water in the apoplast is relatively dilute and therefore has a higher freezing point than that of the more concentrated symplasm. As a result, ice crystals tend to form in the apoplast and in the xylem tracheids and vessels, along which the ice can quickly propagate. The formation of ice crystals lowers the apoplastic water potential (Ψ), which becomes more negative than that of the symplasm. Unfrozen water within the cell moves down this gradient out of the cell towards the ice crystals in the intercellular spaces. As water leaves the cell, the plasma membrane contracts and pulls away from the cell wall. During this process the plasma membrane, rigidified by the low temperature, may become damaged. The lower the temperatures, the more water travels down the gradient toward the frozen water. For example, at –10°C the symplasm loses about 90% of its osmotically active water to the apoplast. In this respect, freezing stress has much in common with water-deficit stress. As with water-deficit stress, cells that are already dehydrated, like those in seeds and pollen, are less likely to undergo further dehydration by extracellular ice crystal formation and therefore less likely to be damaged.

Heavy metals can both mimic essential mineral nutrients and generate ROS

The uptake of heavy metal ions such as Cd^{2+} by plant cells can lead to the accumulation of ROS, inhibition of photosynthesis, disruption of membrane structure and ion homeostasis, inhibition of enzymatic reactions, and activation of programmed cell death (PCD) (see Chapter 23). One of the reasons that heavy metals are so toxic is that they can mimic other essential metals (e.g., Cd^{2+} can mimic Zn^{2+}), take their place in essential reactions, and disrupt these reactions. The mimicking of essential elements can also explain the uptake of Cd^{2+} and other heavy metal ions into cells via channels that evolved to transport essential elements. Cd^{2+} can also inhibit the uptake of Zn^{2+}, Fe^{2+}, and Mn^{2+} by competing with these ions

for the same transport systems. (Note that Fe^{+3} is transported by a different mechanism, as discussed in Chapter 8). In addition to having these toxic effects, heavy metals can directly interact with oxygen to form ROS.

Ozone and ultraviolet light generate ROS that cause lesions and induce PCD

Ozone enters the plant through open stomata and is converted to different forms of ROS. These ROS cause lipid peroxidation and the oxidation of proteins, RNA, and DNA. These toxic effects induce the formation of lesions in leaves that are characteristic of the activation of PCD. In general, the type of lesions (leaf chlorosis and tissue necrosis) and the severity of the injuries are dependent on the extent of exposure to ozone and can vary among different plant species. The thinning of the ozone layer in Earth's upper atmosphere reduces the filtering of ultraviolet (UV) radiation, resulting in an increase in UV radiation reaching Earth's surface. In addition to its effects on photosynthesis, UV radiation also induces the formation of ROS that can cause mutations during DNA replication. The UV-induced accumulation of ROS induces PCD and the formation of lesions. Both ozone and UV stress cause suppression of plant growth and reduction of agronomic yields.

Combinations of abiotic stresses can induce unique signaling and metabolic pathways

In the field, plants are often subjected to a combination of different abiotic stresses simultaneously. Water-deficit stress and heat stress are examples of two different abiotic stresses that almost always occur together in the environment, with devastating results. Between 1980 and 2012 in the United States, the cost of crop damage due to droughts combined with heat waves was four times greater than that due to droughts alone (**Figure 15.6A**), and these extreme weather events are forecast to increase in frequency and intensity because of global climatic changes driven by global warming (see **WEB TOPIC 15.1**).

Plants respond differently to different abiotic stresses, but the physiological responses to the different stresses are not additive when they occur in combination. **Figure 15.6B** shows the effects of heat and water deficit, applied separately, on four different physiological parameters of Arabidopsis: photosynthesis, respiration, stomatal conductance, and leaf temperature. The physiological profiles under the two stresses applied individually are quite different. For example, during heat stress alone, plants *increase* their stomatal conductance, which cools their leaves by transpiration. However, if heat stress is combined with water-deficit stress, the stomata close to

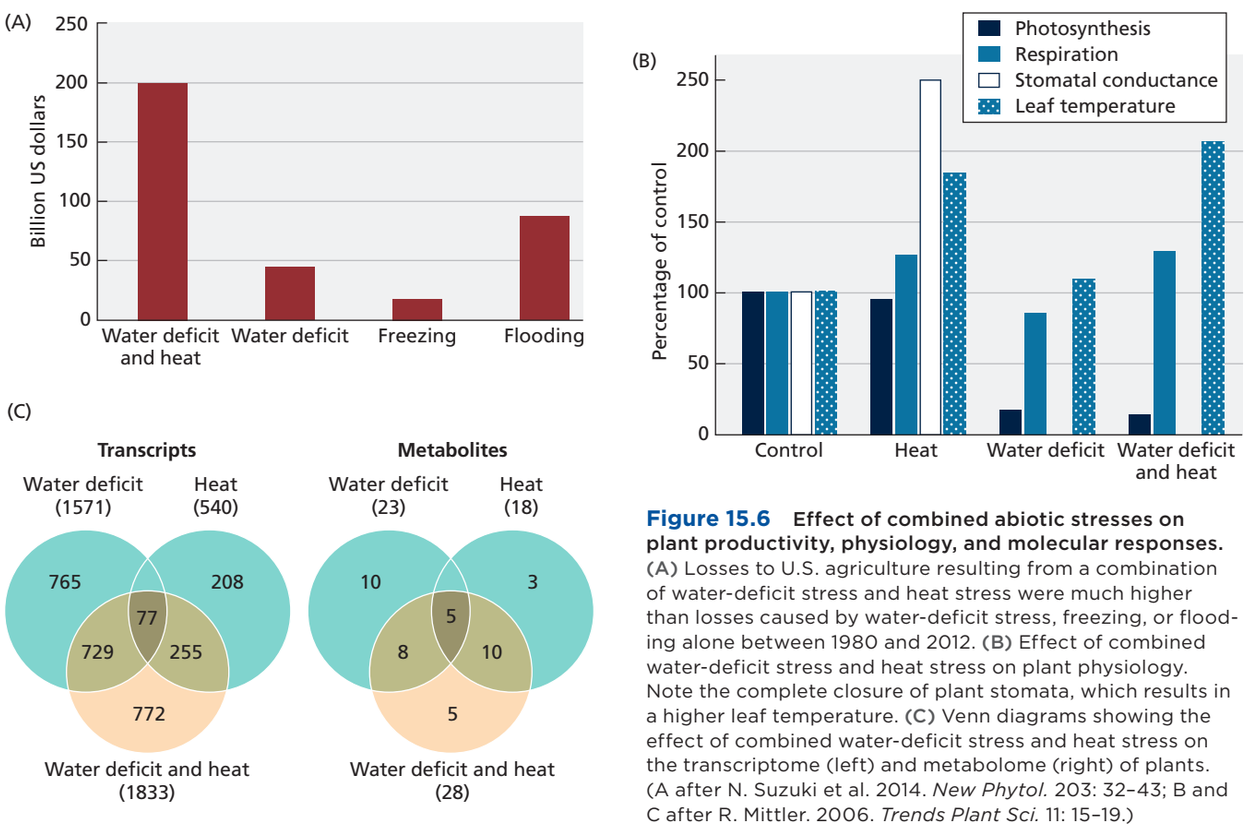


Figure 15.6 Effect of combined abiotic stresses on plant productivity, physiology, and molecular responses. **(A)** Losses to U.S. agriculture resulting from a combination of water-deficit stress and heat stress were much higher than losses caused by water-deficit stress, freezing, or flooding alone between 1980 and 2012. **(B)** Effect of combined water-deficit stress and heat stress on plant physiology. Note the complete closure of plant stomata, which results in a higher leaf temperature. **(C)** Venn diagrams showing the effect of combined water-deficit stress and heat stress on the transcriptome (left) and metabolome (right) of plants. (A after N. Suzuki et al. 2014. *New Phytol.* 203: 32–43; B and C after R. Mittler. 2006. *Trends Plant Sci.* 11: 15–19.)

conserve water, causing the leaf temperature to rise by 2 to 5°C. In other words, water-deficit stress exacerbates the effects of heat stress on leaf temperature, and the combination can be lethal.

The combination of heat stress plus water-deficit stress also induces different patterns of gene expression and metabolite turnover than either stress alone. As shown in **Figure 15.6C**, water deficit plus heat caused the accumulation of 772 unique transcripts and 5 unique metabolites, demonstrating that the acclimation of plants to the combination of water-deficit stress and heat stress is different in many aspects from the acclimation of plants to water-deficit or heat stress applied individually. Differences in physiological parameters, transcript accumulation, and metabolites could be a result of conflicting physiological responses to the two stresses. Because global warming is likely to be accompanied by more frequent droughts in many regions of the world, both agriculture and natural ecosystems are likely to be negatively affected (see **WEB TOPIC 15.1**).

A similar problem can arise when heat stress occurs in combination with salinity or heavy metal stress, because enhanced transpiration can lead to greater uptake of salt or heavy metals. In contrast, some stress combinations could have beneficial effects on plants compared with the individual stresses applied separately. For example, water-deficit stress, which causes stomatal closure, could potentially enhance tolerance to ozone. The stress matrix shown in **Figure 15.7** summarizes different combinations of environmental conditions that could have a significant impact on agricultural production. Among the several stress interactions that could have a deleterious effect on crop productivity are water deficit and heat, salinity and heat, nutrient deficiency stress and water deficit, and nutrient deficiency and salinity. Interactions that could have a beneficial impact include water deficit and ozone, ozone and UV, and high CO_2 combined with water deficit, ozone, or high light.

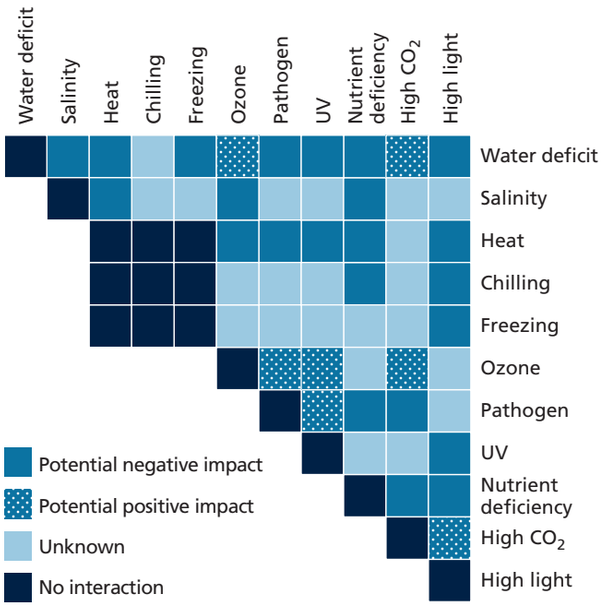


Figure 15.7 Stress matrix. Different combinations of potential environmental stresses can have different effects on field crops. The matrix is color-coded to indicate stress combinations that were studied with different crops and their overall effect on plant growth and yield. (After R. Mittler and E. Blumwald. 2010. *Annu. Rev. Plant Biol.* 61: 443–462.)

Interactions occur between abiotic and biotic stresses

Some of the most studied stress interactions are those of different abiotic stresses with biotic stresses, such as pests or pathogens. Typically, prolonged exposure to abiotic stresses, such as heat or water deficit, results in weakening of plant defenses and enhanced susceptibility to pests or pathogens. Plant interactions with different pathogens (covered in Chapter 24) rely in many cases on innate immune receptors expressed in plant cells. These receptors recognize pathogen-generated invasion signals and activate different plant defenses, including PRR-triggered immunity (PTI) and/or effector-triggered immunity (ETI). In recent years, several links were identified between innate immunity genes and abiotic stresses. These findings are starting to untangle the molecular mechanisms that balance responses to biotic versus abiotic stresses.

Sequential exposure to different abiotic stresses sometimes confers cross-protection

Several studies have reported that the application of a particular abiotic stress condition can enhance the tolerance of plants to a subsequent exposure to a different type of abiotic stress. This phenomenon is called **cross-protection**. It occurs because many stresses result in the accumulation of the same general stress-response proteins and metabolites, for example ROS-scavenging enzymes, molecular chaperones, and osmoprotectants, and these persist in plants for some time even after the stress conditions have subsided. The application of a second stress to the same plants that experienced the initial stress may therefore have a decreased effect because the plants are already primed and ready to deal with several different aspects of the new stress condition. We discuss the example of heat shock proteins in Section 15.6.

Beneficial microbes can improve plant tolerance to abiotic stress

In nature, plants are exposed to diverse root and leaf microbiota that they interact with in complex ways (see Chapters 7, 14, and 24). These interactions can result in several beneficial outcomes, including improved

acquisition of nutrients, accelerated growth, pathogen resistance, and improved tolerance to different abiotic stress conditions such as heat, water deficit, and salinity. These beneficial effects depend on the types and abundances of bacteria and fungi in the soil, the plant, and on the interactions these microbes establish with the plant. The plant microbiome can include many different beneficial microorganisms that modulate and improve plant resilience and growth via different molecular and hormonal interactions. In turn, the different microbes benefit from these interactions by absorbing nutrients, sugars, and other metabolites secreted by the plant. Although studies of the plant microbiome and its effects on abiotic stress tolerance are in their infancy, the potential to improve crop tolerance to abiotic stress by controlling their microbiome is significant and promising.

15.4 Stress-Sensing Mechanisms in Plants

Plants use a variety of mechanisms to sense abiotic stress. As discussed earlier, environmental stress disrupts or alters many physiological processes in the plant by affecting protein and RNA stability, ion transport, the coupling of reactions, or other cellular functions. Any of these primary disruptions can signal to the plant that a change in environmental conditions has occurred and that it's time to respond by altering existing pathways or by activating stress-response pathways. At least five different types of stress-sensing mechanisms can be distinguished:

1. *Physical sensing* refers to the mechanical effects of stress on the plant or cell structure—for example, the contraction of the plasma membrane from the cell wall during water-deficit stress.
2. *Biophysical sensing* might involve changes in protein structure or enzymatic activity, such as the inhibition of different enzymes during heat stress.
3. *Metabolic sensing* usually results from the detection of by-products that accumulate in cells due to the uncoupling of enzymatic or electron transfer reactions, such as the accumulation of ROS during stress caused by too much light.
4. *Biochemical sensing* often involves the presence of specialized proteins that were selected during evolution for their ability to sense a particular stress—for example, Ca^{2+} channels that can sense changes in osmotic stress and alter Ca^{2+} homeostasis.
5. *Epigenetic sensing* refers to modifications of DNA or RNA structure that do not alter genetic sequences, such as the changes in chromatin structure that occur during temperature stress.

Each of these stress-sensing mechanisms can act individually or in combination to activate downstream signal transduction pathways.

Early-acting stress sensors provide the initial signal for the stress response

Transcriptional regulators, or transcription factors, are proteins that bind specific DNA sequences and activate or suppress the expression of different genes. A particular transcription factor can bind to the promoters of hundreds of different genes and affect their expression simultaneously. A transcription factor can also bind to the promoter of a gene encoding another transcription factor, thereby activating or suppressing its expression. In this way a cascade of transcriptional regulation of gene expression can occur. A diagram of the possible early events in the sensing of abiotic stress and the signal transduction and acclimation pathways activated by these events is presented in **Figure 15.8**. Thus far, several stress-sensing mechanisms that act early in the pathway have been identified, including the following representative examples:

- A kinase (SNF1-related kinase 1) that senses energy depletion during stress (through cellular energy-dependent posttranslational modifications) and activates hundreds of stress-response transcripts.

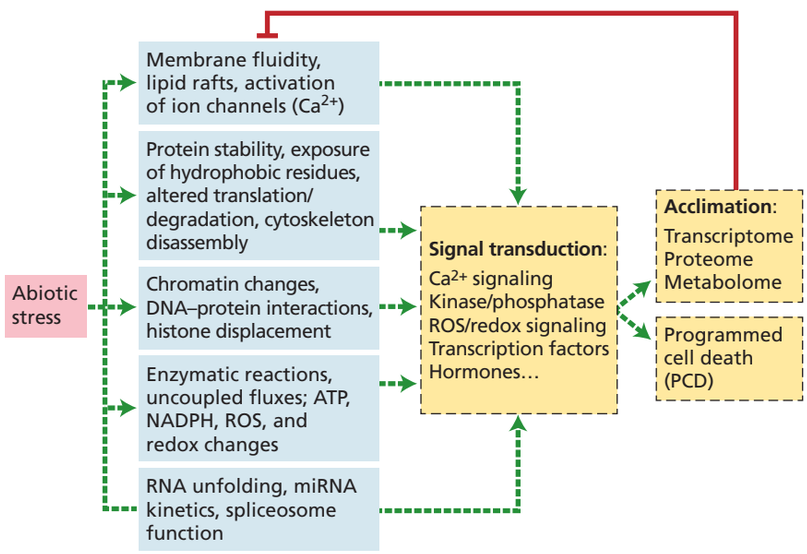


Figure 15.8 **Early events in the sensing of abiotic stress by plants (blue boxes) and the signal transduction and acclimation pathways activated by these events (boxes with dashed borders).** (After R. Mittler et al. 2012. *Trends Biochem. Sci.* 37: 118–125.)

- Ca^{2+}-permeable channels such as the hyperosmolality-gated Ca^{2+}-permeable channel and mechanosensitive channel-like 10 that, together with Histidine kinase 1 and small GTPase proteins, detect the effects of osmotic stress on membranes and activate ABA-dependent and -independent responses.
- Heat shock transcription factors that are released from their association with heat shock proteins (which instead bind heat stress–induced denatured proteins) and turn on heat-response gene transcription.
- Ethylene-response factor group VII transcription factors that lose the oxidation status of their N terminus during low oxygen conditions and regulate the expression of hypoxia-induced transcripts.
- Ca^{2+}-permeable channels such as annexins and cyclic nucleotide-gated channels that detect the effects of heat stress on membranes and trigger heat stress–response mechanisms.
- Open Stomata 1 (OST1), a kinase that undergoes cold-induced myristoylation and phosphorylates the transcription factor Inducer of C-Repeat Binding Factor 1, which activates cold responses.

In the next section we discuss some of the major signaling pathways used by plants to transduce stress-specific signals and acclimate to newly arising stress conditions.

15.5 Signaling Pathways Activated in Response to Abiotic Stress

The initial stress-sensing mechanisms described in Section 15.4 trigger a downstream response that comprises multiple signal transduction pathways. These pathways involve Ca^{2+}, protein kinases, protein phosphatases, ROS signaling, activation of transcriptional regulators, accumulation of plant hormones, and so on. The stress-specific signals that emerge from these pathways, in turn, activate or suppress various networks that trigger different acclimation mechanisms to enable the plant to survive the stress. Acclimated plants may continue to grow and reproduce under the stress conditions or may suppress these processes until more favorable conditions return. In this section we consider stress signaling pathways and their interactions in greater detail.

The signaling intermediates of many stress-response pathways can interact

Stress-induced oscillations in the concentrations of cytosolic Ca^{2+} and ROS are important early signaling events in many acclimation pathways. Cellular Ca^{2+} levels are controlled by Ca^{2+} channels, Ca^{2+}–H^+ antiporters, and Ca^{2+}-ATPases, which mediate the transport of Ca^{2+} from storage compartments such as the vacuole, the endoplasmic reticulum, and the cell wall (see Chapter 8). Ca^{2+} regulates transcription factors by a variety of

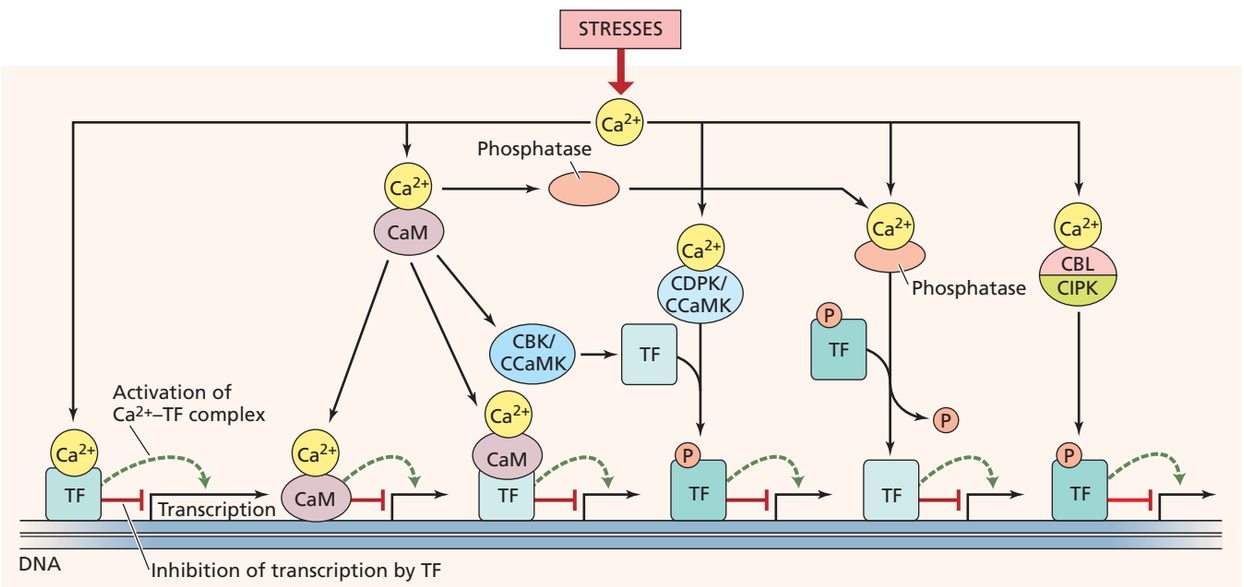


Figure 15.9 Stress-induced elevation of cellular Ca^{2+} can regulate transcription by various mechanisms. Elevated Ca^{2+} levels can result in Ca^{2+} binding to different proteins, including transcription factors (TF), various calmodulins (CaM), kinases (e.g., Ca^{2+}-dependent protein kinases [CDPKs]) or kinase-binding proteins (e.g., calcineurin B-like proteins [CBLs] that bind CBL-interacting protein kinases [CIPKs]), and phosphatases that directly or indirectly activate or suppress transcription, causing the activation of acclimation pathways. CBK, calmodulin-binding protein kinase; CCaMK, Ca^{2+}/calmodulin-dependent protein kinase. (After A. S. Reddy et al. 2011. *Plant Cell* 23: 2010–2032. CC BY)

mechanisms. As shown in **Figure 15.9**, Ca^{2+} can activate gene expression by binding directly to certain transcription factors. Alternatively, Ca^{2+} forms Ca^{2+}–CaM complexes, which can activate transcription either directly or indirectly, by binding to a transcription factor. Ca^{2+} also activates various protein kinases and phosphatases that regulate gene expression, either by phosphorylating (activating) or dephosphorylating (inhibiting) transcription factors. The vast cellular networks of protein kinases and phosphatases therefore play an essential role in integrating different stress-response pathways.

The steady-state level of ROS in the cell is governed by the balance between ROS-generating reactions and ROS-scavenging reactions (**Figure 15.10**). ROS generation occurs in several cellular compartments and as a result of the activities of specialized oxidases, such as NADPH oxidases, amine oxidases, and cell wall–bound peroxidases (**Table 15.2**). ROS scavenging is carried out by antioxidant molecules such as ascorbate, glutathione, vitamin E, and carotenoids, and by antioxidant enzymes such as superoxide dismutase, ascorbate peroxidase, and catalase. Many types of biotic and abiotic stresses trigger the production of ROS (see Figure 15.4). Because ROS can trigger the opening of Ca^{2+} channels, and increases in cytosolic Ca^{2+} concentrations can activate Ca^{2+}-dependent protein kinases (CDPKs) that activate NADPH oxidase, the Ca^{2+} and ROS pathways interact in a positive feedback cycle (**Figure 15.11**). The elevation of Ca^{2+} and ROS levels during the early stages of the stress response activates protein kinases and phosphatases that phosphorylate or dephosphorylate different transcription factors (see Figure 15.9). Activation or inhibition of transcription factors during abiotic stress can also result from changes in the redox status of the cell that are directly sensed by certain transcriptional regulators.

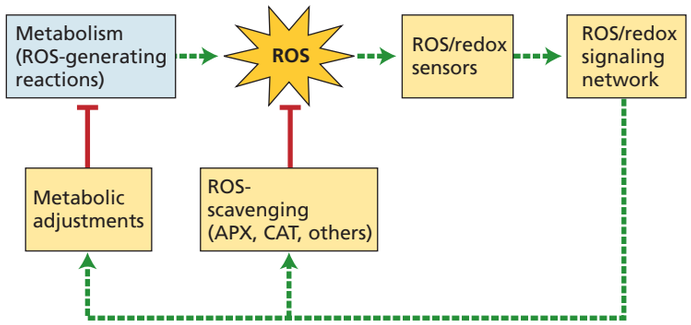


Figure 15.10 Basic ROS cycle. Normal metabolic reactions in cells, such as photosynthesis, respiration, photorespiration, and lipid oxidation, generate ROS. Various sensors monitor ROS levels in cells; an increase in ROS activates a signal transduction network that in turn activates ROS-scavenging mechanisms such as ascorbate peroxidase (APX), catalase (CAT), and superoxide dismutase (SOD). The signaling network also modulates various metabolic reactions and suppresses, when needed, some of the ROS-producing pathways. The overall result of the cycle is controlled maintenance of ROS levels in cells.

When plants are subjected to multiple stresses, cross talk can occur among the hormones, secondary messengers, and protein kinases or phosphatases involved in each of the stress pathways (see Chapter 4). For example, mitogen-activated protein kinases (MAPKs) exist in all eukaryotic cells and are involved in virtually all

TABLE 15.2 Reactive oxygen species

Molecule	Abbreviation(s)	Sources
Molecular oxygen (triplet ground state)	O_2; $^3\Sigma$	Most common form of dioxygen gas
Singlet oxygen (first excited singlet state)	$^1O_2$; $^1\Delta$	UV irradiation, photoinhibition, PSII electron transfer reactions
Superoxide anion	$O_2^{\bullet-}$	Mitochondrial electron transfer reactions, Mehler reaction (reduction of O_2 by iron–sulfur center of PSI), photorespiration in glyoxysomes, peroxisome reactions, plasma membrane, paraquat oxidation, nitrogen fixation, pathogen defense, reaction of O_3 and OH^- in apoplast, respiratory burst homolog (NADPH oxidase)
Hydrogen peroxide	H_2O_2	Photorespiration, β-oxidation, proton-induced decomposition of $O_2^{\bullet-}$, pathogen defense
Hydroxyl radical	$HO^{\bullet-}$	Decomposition of O_3 in apoplast, pathogen defense, Fenton reaction
Perhydroxyl radical	$HO_2^{\bullet-}$	Reaction of O_3 and OH^- in apoplast
Ozone	O_3	Electrical discharge or UV irradiation in stratosphere, UV irradiation of combustion products in troposphere
Nitric oxide	NO	Nitrate reductase, nitrite reduction by the mitochondrial electron transport chain

Source: After R. Jones et al. 2013. *The Molecular Life of Plants.* Wiley-Blackwell, Chichester, West Sussex, UK, p. 567.

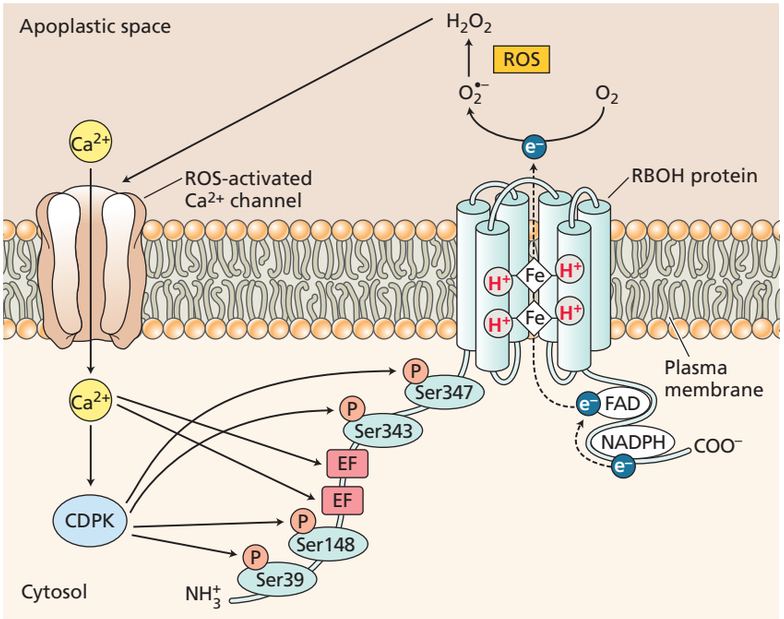


Figure 15.11 **Interaction between ROS and Ca^{2+} signaling mediated by respiratory burst oxidase homolog (RBOH) proteins (NADPH oxidases), Ca^{2+}-dependent protein kinases (CDPKs), and ROS-activated Ca^{2+} channels.** ROS are shown to activate Ca^{2+} channels on the plasma membrane (left). The elevated Ca^{2+} levels in the cytosol then activate CDPKs (bottom) that phosphorylate and activate RBOH proteins (right), which generate more ROS. RBOH proteins have six transmembrane domains. The amino-terminal cytoplasmic domain of RBOH proteins contains many serines (Ser) that can be phosphorylated by CDPKs and two Ca^{2+}-binding EF hands that can bind Ca^{2+} directly. Similar ROS-activated Ca^{2+} channels are found in the vacuole membrane (not shown).

important aspects of plant life. MAPKs participate in MAP3K/MAP2K/MAPK signal transduction cascades, collectively known as **MAPK modules**, that affect a variety of downstream targets. As shown in **Figure 15.12**, MAPK modules may target metabolic enzymes, other kinases, or transcription factors. In this way, the same basic MAPK modules can regulate responses to temperature, oxidative, salinity, osmotic, and water-deficit stresses. These different stress responses also share upstream signaling intermediates, such as Ca^{2+}, phosphatidic acid, and ROS. Therefore, changes in the level of signaling intermediates caused by any one of these stress responses can affect the other stress-response pathways.

Acclimation to stress involves transcriptional regulatory networks called regulons

Combinations of different transcription factors can regulate a gene network responding to a particular abiotic stimulus, with some genes being activated and some suppressed. Such transcriptional regulatory networks responding to abiotic stress have been termed **stress-response regulons**. An example of a stress-response regulon is shown in **Figure 15.13**. The advantage of using regulons to control the response of plants to a particular abiotic stress is that they simultaneously activate specific stress-response pathways while suppressing other pathways that are not needed or could even damage the plant during stress. For example, in response to high light conditions, certain genes that encode the photosynthetic antenna proteins might need to be suppressed, while other genes that code for ROS scavenging might need to be activated.

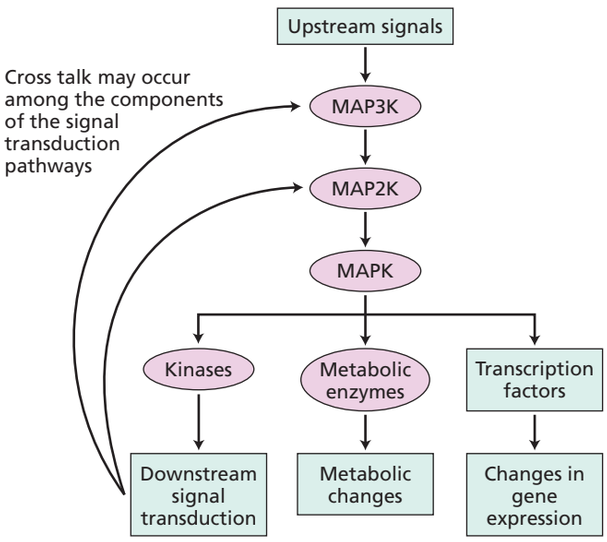


Figure 15.12 **Schematic diagram of mitogen-activated protein kinase (MAPK) cascades involved in plant signal transduction during abiotic stress responses.** Upstream signals activate a MAPK kinase kinase (MAP3K), which phosphorylates and activates a MAPK kinase (MAP2K). The MAP2K then phosphorylates and activates a MAPK, which can phosphorylate a wide variety of downstream targets, including other kinases, metabolic enzymes, or transcription factors. Note that cross talk may also occur among the components of the signal transduction pathways of different stress responses, allowing integration of the responses to various types of stress. (After B. Buchanan et al. 2015. *Biochemistry and Molecular Biology of Plants*, 2nd ed. Wiley-Blackwell, New York.)

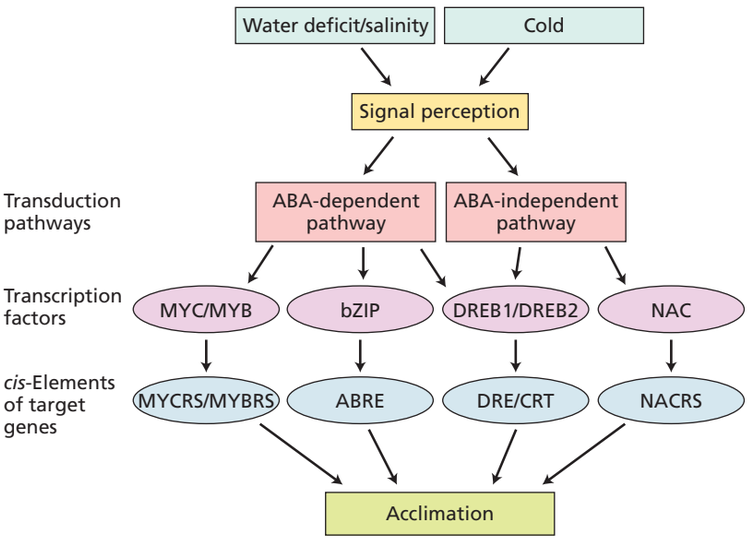


Figure 15.13 Example of two abiotic stress-activated signal transduction pathways that use four different types of regulons (transcription factor networks) to activate acclimation mechanisms. The regulons shown belong to the MYC/MYB, bZIP, DREB, and NAC families. For each regulon, the name of the DNA *cis*-element bound by the transcription factors is shown. (After C. Lata and M. Prasad. 2011. *J. Exp. Bot.* 62: 4731–4748.)

Chloroplasts and mitochondria respond to abiotic stress by sending stress signals to the nucleus

We usually think of the nucleus as the master organelle of the cell, controlling the activities of the other organelles by regulating nuclear gene expression. However, it has been shown that retrograde, or reverse, signaling from the chloroplast or the mitochondria to the nucleus can also play a key role in abiotic stress perception. Many abiotic stress conditions affect chloroplasts and mitochondria, either directly or indirectly, and can potentially generate signals that can influence nuclear gene expression and acclimation responses. Light stress, for example, can cause over-reduction of the electron transport chain, enhanced accumulation of ROS, and altered redox potential.

During the acclimation to light stress, the levels of light-harvesting complex II (LHCII) decline because of the down-regulation of the *LHCB* gene, which encodes the apoprotein of the LHCII complex (see Chapter 9). Because *LHCB* is a nuclear gene, the chloroplast sends a stress signal to the nucleus that down-regulates *LHCB* gene expression. The nuclear gene *ABI4* encodes a transcription factor that suppresses the expression of *LHCB* genes. In Arabidopsis there is evidence that the chloroplast gene *GUN1* acts upstream of *ABI4* during the acclimation to light stress. In other words, the GUN1 protein perceives the original stress signal in the chloroplast and either generates or transmits a second signal to the nucleus, which causes ABI4 to bind to the promoter of the *LHCB* gene and block transcription.

Plant-wide waves of Ca^{2+} and ROS mediate systemic acquired acclimation

As in systemic acquired resistance (SAR) during biotic stress (see Chapter 24), abiotic stress applied to one part of the plant can generate signals that are transported to the rest of the plant, initiating acclimation even in parts of the plant that have not been subjected to the stress. This process is called **systemic acquired acclimation** (**SAA**). Rapid SAA responses to different abiotic stress conditions, including heat, cold, salinity, and high light intensity, have been demonstrated to be mediated by systemic plant-wide waves of ROS production and Ca^{2+} signaling, which travel at rates of 1 to 4 cm min^{-1} and are dependent on the presence of specific NADPH oxidases, such as **respiratory burst oxidase homolog D**, and various Ca^{2+} channels, such as glutamate-like receptors (**Figure 15.14**). The rapid movement of abiotic stress–triggered ROS and Ca^{2+} signals through the plant suggests that many abiotic stress responses may occur much more quickly than previously thought. In fact, transcriptomics and metabolomics studies have recently demonstrated that changes in thousands of transcripts and tens to hundreds of metabolites can occur within minutes of abiotic stress application.

Epigenetic mechanisms, retrotransposons, and small RNAs provide additional protection against stress

Thus far we have discussed responses to abiotic stress in terms of signaling cascades and altered gene expression—acclimation processes that can be reversed when more favorable conditions arise. Recently, attention has focused on epigenetic changes, which can potentially provide long-term adaptations to abiotic stress. Because some chromatin modifications are mitotically and meiotically heritable, stress-induced epigenetic changes might even have evolutionary implications. Chromatin immunoprecipitation of DNA cross-linked to modified histones, coupled with modern sequencing technologies, has opened the door to genome-wide analyses of changes in the **epigenome**. Stable or heritable DNA methylation and histone modifications have now been linked with specific abiotic stresses (**Figure 15.15**).

The role of epigenetic regulation of flowering time has been studied in Arabidopsis in relation to genes known to be involved in abiotic stress. Mutations in some of

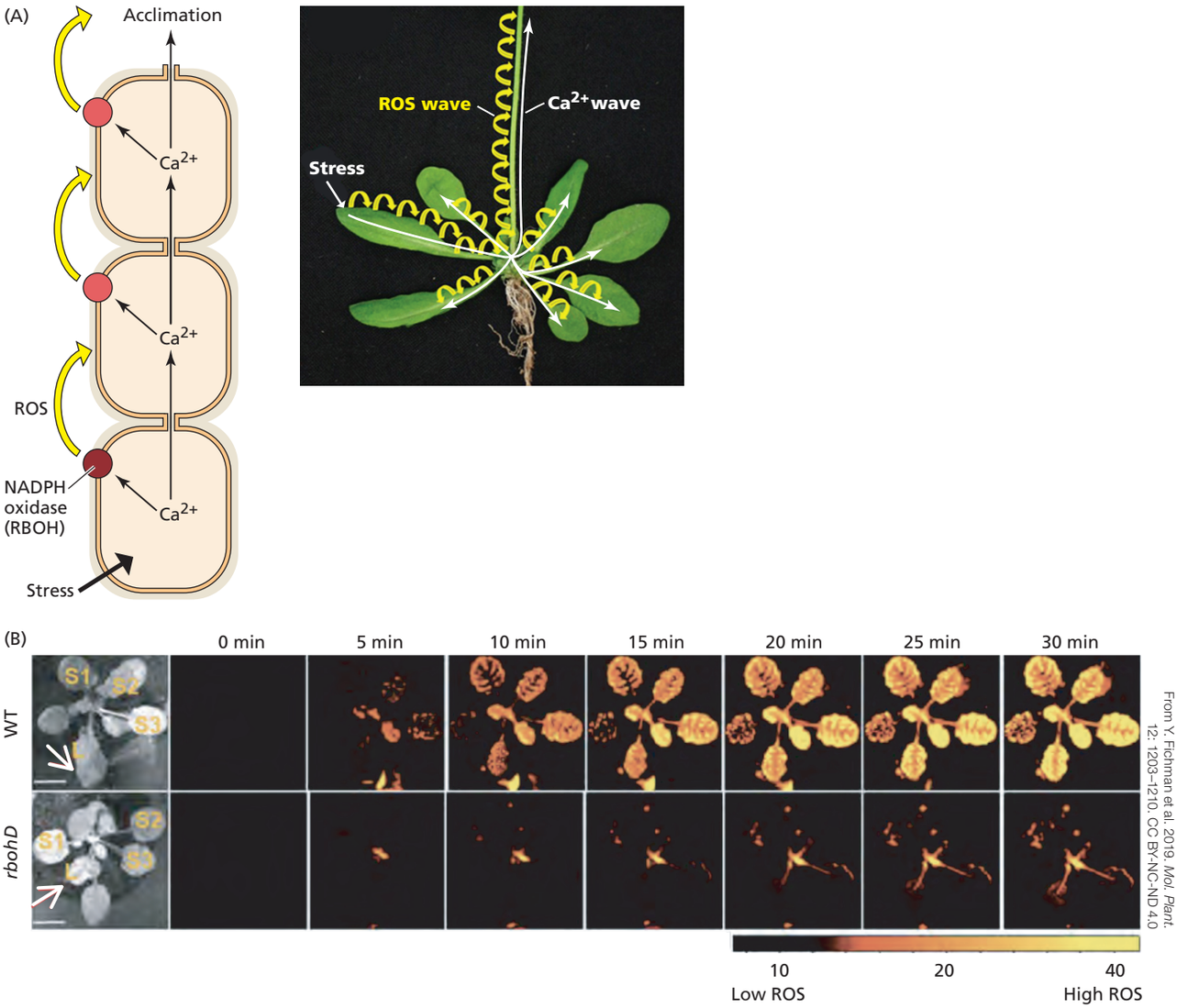


Figure 15.14 **Rapid systemic signaling in response to local sensing of abiotic stress.** **(A)** Schematic model of the ROS and Ca^{2+} waves that are required to mediate rapid systemic signaling in response to abiotic stress. The ROS wave is generated by an active, self-propagating wave of ROS production that starts at the initial tissue subjected to stress and spreads to the entire plant. As shown in the left panel, each cell along the path of the signal activates its RBOH proteins (NADPH oxidase) and generates ROS. The ROS wave is accompanied by a Ca^{2+} wave that requires various Ca^{2+} channels (e.g., glutamate-like receptors), as well as Ca^{2+}-dependent kinases (e.g., CDPKs), and the two waves are coordinated. As the ROS and Ca^{2+} waves spread systemically through the plant, they activate acclimation mechanisms in distal tissues (right panel). **(B)** Time-lapse images of live whole-plant ROS detection in Arabidopsis plants subjected to a localized excess light stress treatment on a single leaf (arrows). Prior to stress treatment, plants were fumigated with a permeant fluorescent dye that detects ROS. Subsequently visible light and fluorescence images were captured every 30 s for 30 min. The localized light treatment is shown to trigger the ROS wave in wild type (WT) plants but not in a mutant deficient in the NADPH oxidase RBOHD (*rbohD*). L, treated leaf; S1, S2, and S3, non-treated systemic leaves. (A after S. I. Zandalinas and R. Mittler. 2018. *Free Radic. Biol. Med.* 122: 21–27.)

these genes result in changes in flowering times. For example, late flowering of the freezing-sensitive mutant *hos15* has been shown to result from deacetylation of the flowering genes *SOC* and *FT* (see Chapter 20). Normally, the flowering repressor FLC (a MADS box protein) is epigenetically repressed during vernalization, allowing acquisition of the competence to flower after exposure to prolonged low temperatures. This process has been shown to involve several different proteins that could alter chromatin remodeling.

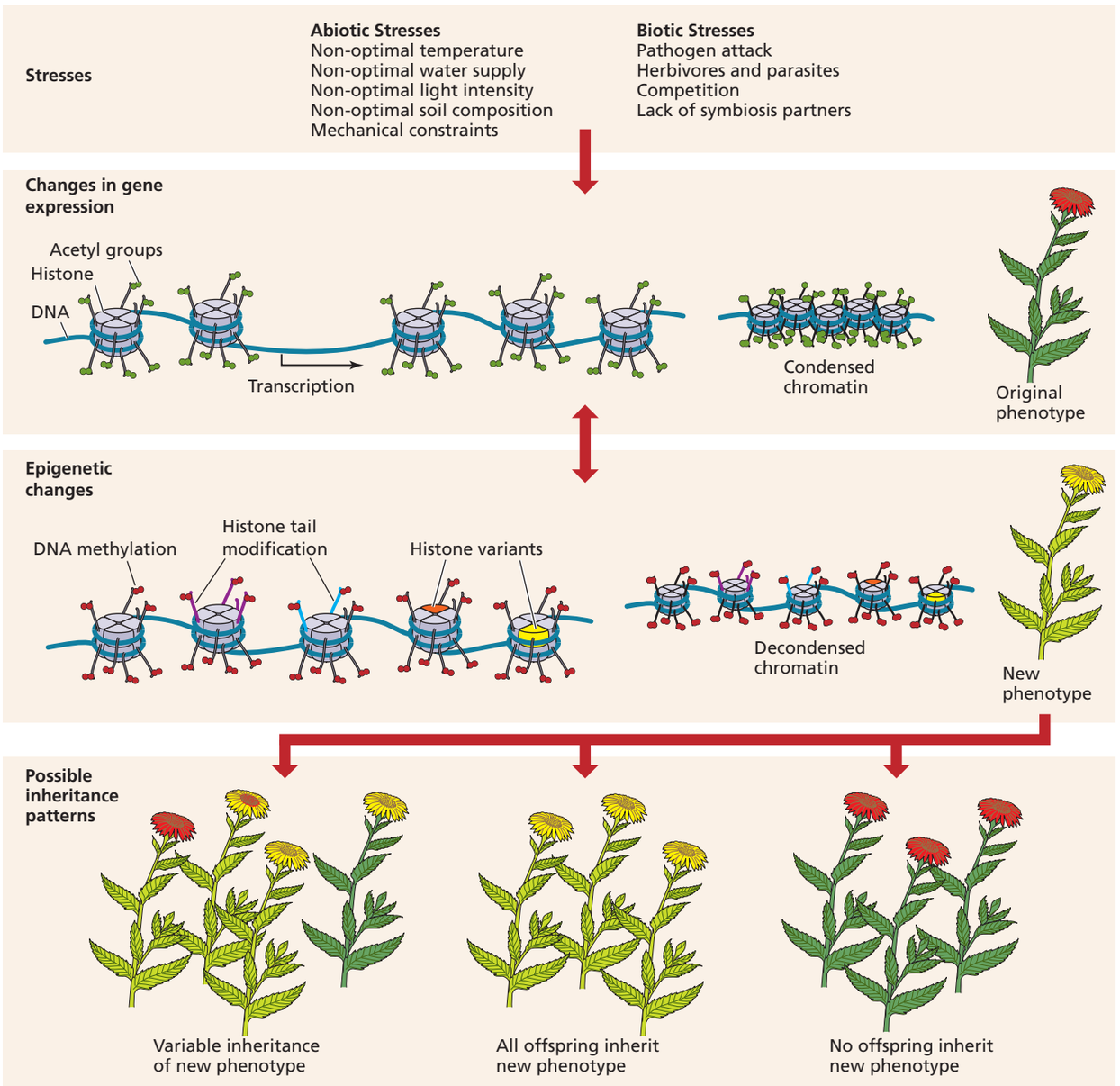


Figure 15.15 **Stress-induced changes in gene expression can be mediated by protein, lipid, or nucleic acid modification, second messengers, or hormones (e.g., abscisic acid, salicylic acid, jasmonic acid, and ethylene).** Transcription changes or stress factors can affect chromatin via DNA methylation, histone tail modifications, histone variant replacements, or nucleosome loss and chromatin de-condensation. These changes are reversible and can modify plant metabolism or morphology under stress conditions. Usually, the new phenotypes are not transmitted to progeny; however, chromatin-associated changes have the potential to be heritable, which could result in maintenance of the new features and epigenetic diversity in the next generation. (After R. Gutzat and O. Mittelsten-Scheid. 2012. *Curr. Opin. Plant Biol.* 15: 568–573.)

Increased attention has also been given in recent years to the involvement of small RNAs in abiotic stress responses. Small RNAs belong to at least two different groups: microRNAs (miRNAs) and endogenous small interfering RNAs (siRNAs). Both miRNAs and siRNAs can cause posttranscriptional gene silencing via RISC (RNA-induced silencing complex)-mediated degradation of mRNA in the cytosol (see Chapter 2). Furthermore, siRNAs can suppress gene expression by altering chromatin properties in the nuclei via **RNA-induced transcriptional silencing** (**RITS**). It has also been proposed that small RNAs may be involved

in suppressing protein translation during stress. Both miRNAs and siRNAs have been shown to control gene expression during various abiotic stresses, including cold, heat, nutrient deficiency, dehydration, salinity, and oxidative stresses.

Another interesting epigenetic mechanism discovered in recent years is that of transposon activation in response to stress. For example, heat stress triggers the retrotransposon *ONSEN* (Japanese for "hot spring") to jump into the promoters of nearby genes, making these promoters (and the genes they control) heat-responsive.

Hormonal interactions regulate abiotic stress responses

Plant hormones mediate a wide range of adaptive responses and are essential for the ability of plants to adapt to abiotic stresses. ABA biosynthesis is among the most rapid responses of plants to abiotic stress. ABA concentrations in leaves can increase up to 50-fold under water-deficit conditions—the most dramatic change in concentration reported for any hormone in response to an environmental signal. ABA accumulation in stressed leaves, via redistribution or biosynthesis, is very effective in causing stomatal closure and plays an important role in reducing water loss by transpiration under water-stress conditions (see Section 15.6). Increases in humidity reduce ABA levels by increasing ABA breakdown, thereby permitting stomata to reopen. ABA biosynthesis or response mutants are unable to close their stomata under water-deficit conditions and are called *wilty* mutants. Many genes associated with ABA biosynthesis and genes encoding ABA receptors and downstream signaling components have been identified (see Chapter 4 and **WEB APPENDIX 3**). ABA also plays important roles in the adaptation of plants to cold temperatures and salinity stress. Cold stress induces the synthesis of ABA, and the exogenous application of ABA improves the cold tolerance of plants.

Another plant hormone that plays a key role in acclimation to various abiotic stresses is cytokinin. Cytokinin and ABA have antagonistic effects on stomatal opening, transpiration, and photosynthesis. Water deficit results in decreased cytokinin levels and increased ABA levels. Although ABA is normally required for stomatal closure, preventing excessive water loss, water-deficit stress conditions can also inhibit photosynthesis and cause premature leaf senescence. Cytokinins appear to be able to ameliorate the effects of water deficit. As shown in **Figure 15.16**, transgenic plants expressing *IPT* (the gene encoding isopentenyl transferase, the enzyme that catalyzes the rate-limiting step in cytokinin synthesis) under the control of a water-deficit-specific promoter exhibit enhanced tolerance for water deficit compared with wild-type plants. Thus, cytokinins are able to protect biochemical processes associated with photosynthesis and delay senescence during water-deficit stress.

In addition to ABA and cytokinin, other hormones play important roles in the response of plants to abiotic stress, including gibberellic acid, auxin, salicylic acid, ethylene, jasmonic acid, strigolactones, brassinosteroids, and several newly identified plant peptide hormones. The extensive overlap among the different sets of genes controlled by these hormones implies the existence of complex regulatory networks with

(A) Wild type

(B) P_{SARK}::*IPT*



A and B courtesy of E. Blumwald

Figure 15.16 **Effects of water deficit on wild-type and transgenic tobacco plants expressing isopentenyl transferase (a key enzyme in the production of cytokinin) under the control of P_{SARK} (*P*romoter region of *S*enescence-*A*ssociated *R*eceptor *K*inase), a maturation and stress-induced promoter.** Shown are wild-type (A) and transgenic (B) plants after 15 days of water deficit followed by 7 days of rewatering.

significant cross talk between the different hormone signaling pathways. Hormones can act synergistically or antagonistically during stress, and the coordinated regulation of hormone biosynthetic pathways is of great importance for the ability of plants to acclimate to abiotic stress conditions.

Auxin provides an example of how complex the cross talk between hormones can be. Interactions between auxin and other hormones can play crucial roles in the acclimation of plants to water-deficit conditions. The expression of *TLD1*[1], which encodes an indole-3-acetic acid (IAA)–amido synthetase, has been shown to induce the expression of genes encoding LEA (*L*ate *E*mbryogenesis *A*bundant) proteins, which accumulate during seed maturation in an ABA-dependent manner and are also correlated with enhanced water-deficit tolerance in rice. Ethylene regulates the expression of several genes linked with auxin synthesis, auxin transporters (*PIN1, PIN2, PIN4, AUX1*), and auxin-responsive transcription factors (*ARF2, ARF19*). Conversely, cellular auxin levels greatly influence ethylene biosynthesis. Several genes encoding ACC (1-aminocyclopropane-1-carboxylic acid) synthase, the rate-limiting step in ethylene biosynthesis, are regulated by auxin.

15.6 Physiological and Developmental Mechanisms That Protect Plants against Abiotic Stress

Thus far in the chapter we have discussed the various types of abiotic stress, the mechanisms by which plants sense abiotic stress, the signal transduction pathways that convert stress signals into altered gene expression, and the role of hormonal interactions in regulating networks of genetic pathways. Now we discuss the fruits of the labors of all these genetic networks—the metabolic, physiological, and anatomical changes that are triggered to counter the effects of abiotic stress. Terrestrial plants first emerged onto land more than 500 million years ago. Thus, they have had ample time to evolve mechanisms to cope with various types of abiotic stresses. These mechanisms include the abilities to accumulate protective metabolites and proteins and to regulate growth, morphogenesis, photosynthesis, membrane transport, stomatal aperture, and resource allocation. The effects of these and other changes are to attain cellular homeostasis so that the plant's life cycle can be completed under the new environmental regime. In this section we discuss some of the major physiological mechanisms of acclimation. In **WEB TOPIC 15.1** we describe ongoing efforts to develop crops with enhanced abiotic stress tolerance.

[1] The rice gene *TLD1* gets its name from the increased number of *t*illers, enlarged *l*eaf angles, and *d*warfism in the *tld1* mutant.

Plants adjust osmotically to drying soils by accumulating solutes

Water can only move through the soil–plant–atmosphere continuum if water potential decreases along that path (see Chapters 5 and 6). Recall from Chapter 5 that $\Psi = \Psi_s + \Psi_p$, where Ψ = water potential, Ψ_s = osmotic potential, and Ψ_p = pressure potential (turgor). When the water potential of the rhizosphere (the microenvironment surrounding the root) decreases because of water deficit or salinity, plants can continue to absorb water only as long as Ψ is lower (more negative) in the plant than it is in the soil water. **Osmotic adjustment** is the capacity of plant cells to accumulate solutes and use them to lower Ψ during periods of osmotic stress. This adjustment involves a net increase in solute content per cell that is independent of the volume changes that result from loss of water. The decrease in Ψ_s is typically limited to about 0.2 to 0.8 MPa, except in plants adapted to extremely dry conditions.

There are two main ways by which osmotic adjustment can take place, one involving the vacuole and the other the cytosol. A plant may take up ions from the soil, or transport ions from other plant organs to the root, so that the solute concentration of the root cells increases. For example, increased uptake and accumulation of K^+ will lead to decreases in Ψ_s, because of the effect of the K^+ on the osmotic pressure within the cell. This response is common in plants growing in saline soils, where ions such as K^+ and Ca^{2+} are readily available to the plant. The uptake of K^+ and other cations must be electrically balanced either by the uptake of inorganic anions, such as Cl^-, or by the production and vacuolar accumulation of organic acids such as malate or citrate.

There is a potential problem, however, when ions are used to decrease Ψ_s. Some ions, such as Na^+ or Cl^-, are essential to plant growth in low concentrations but in higher concentrations can have a detrimental effect on cellular metabolism. Other ions, such as K^+, are required in larger quantities, but at high concentrations can still have a detrimental effect on the plant, mostly through disruption of plasma membranes or proteins. The accumulation of ions during osmotic adjustment is predominantly restricted to the vacuoles, where the ions are kept out of contact with cytosolic enzymes or organelles. For example, many halophytes (plants adapted to salinity) use vacuolar compartmentation of Na^+ and Cl^- to facilitate osmotic adjustment that sustains or enhances growth in saline environments.

When the ion concentration in the vacuole increases, other solutes must accumulate in the cytosol to maintain water potential equilibrium between the two compartments. These solutes are called compatible solutes (or compatible osmolytes). **Compatible solutes** are organic compounds that are osmotically active in the cell but do not destabilize the membrane or interfere with enzyme

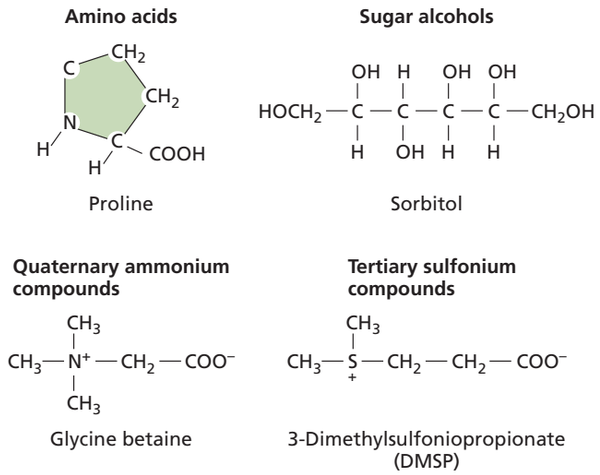


Figure 15.17 **Four groups of molecules frequently serve as compatible solutes: amino acids, sugar alcohols, quaternary ammonium compounds, and tertiary sulfonium compounds.** Note that these compounds are small and have no net charge.

function at high concentrations, as ions do. Plant cells can tolerate high concentrations of these compounds without detrimental effects on metabolism. Common compatible solutes include amino acids such as **proline**, sugar alcohols such as **sorbitol**, and quaternary ammonium compounds such as **glycine betaine** (**Figure 15.17**). Some of these solutes, such as proline, also seem to have an osmoprotectant function, whereby they protect plants from toxic by-products produced during periods of water shortage, and provide a source of carbon and nitrogen to the cell when conditions return to normal. Each plant family tends to use one or two compatible solutes in preference to others. Because the synthesis of compatible solutes is an active metabolic process, energy is required. The amount of carbon used for the synthesis of these organic solutes can be rather large, and for this reason the synthesis of these compounds tends to reduce crop yield.

Submerged organs develop aerenchyma tissue in response to hypoxia

We now turn to the mechanisms used by plants to cope with too much water. In most wetland plants, such as rice, and in many plants that acclimate well to wet conditions, the stem and roots develop longitudinally interconnected, gas-filled channels that provide a low-resistance pathway for the movement of O_2 and other gases. The gases (air) enter through stomata, or through lenticels (porous regions of the periderm that allow gas exchange) on woody stems and roots, and travel by molecular diffusion or by convection driven by small pressure gradients. In many plants adapted to wetland growth, root cells are separated by prominent, gas-filled spaces that form a tissue called aerenchyma. These cells develop in the roots of wetland plants independently of environmental stimuli. In some nonwetland monocots and eudicots, however, O_2 deficiency induces the formation of aerenchyma in the stem base and newly developing roots.

An example of induced aerenchyma occurs in maize (**Figure 15.18**). Hypoxia stimulates the activity of ACC synthase and ACC oxidase in the root tips of maize and causes ACC and ethylene to be produced faster. Ethylene triggers programmed cell death and disintegration of cells in the root cortex. The spaces formerly occupied by these cells provide gas-filled voids that facilitate movement of O_2. Ethylene-triggered cell death is highly selective; only some cells have the potential to initiate the developmental program that creates the aerenchyma.

When aerenchyma formation is induced, a rise in cytosolic Ca^{2+} concentration is thought to be part of the

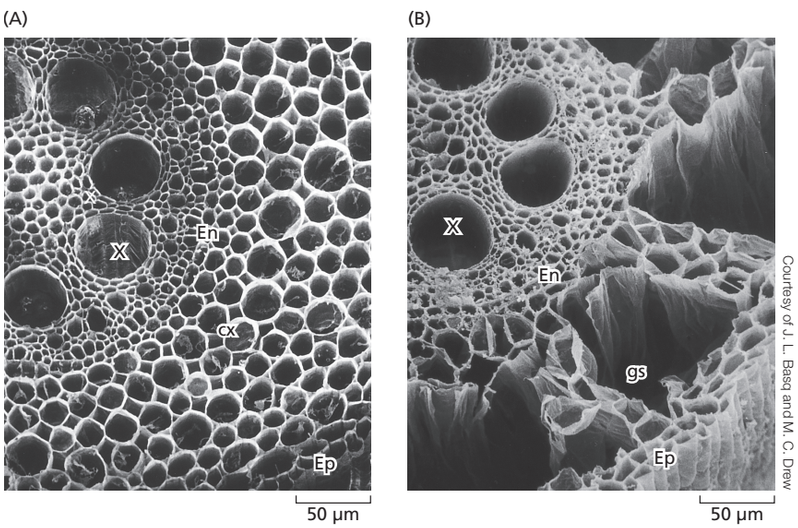


Figure 15.18 **Scanning electron micrographs of transverse sections through roots of maize, showing changes in structure with O_2 supply.** (A) Control root, supplied with air, with intact cortical cells. (B) O_2-deficient root growing in a nonaerated nutrient solution. Note the prominent gas-filled spaces (gs) in the cortex (cx), formed by degeneration of cells. The stele (all cells interior to the endodermis, En) and the epidermis (Ep) remain intact. X, xylem.

ethylene signal transduction pathway leading to cell death. Signals that elevate cytosolic Ca^{2+} concentration can promote cell death in the absence of hypoxia. Conversely, signals that lower cytosolic Ca^{2+} concentration block cell death in hypoxic roots that would normally form aerenchyma.

In roots of rice and other typical wetland plants, structural barriers composed of suberized and lignified cell walls prevent O_2 diffusion outward to the soil. The O_2 thus retained supplies the apical meristem and allows growth to extend 50 cm or more into anaerobic soil. In contrast, roots of nonwetland species, such as maize, leak O_2. Internal O_2 becomes insufficient for aerobic respiration in the root apex of these nonwetland plants, and this lack of O_2 severely limits the depth to which such roots can extend into anaerobic soil.

Antioxidants and ROS-scavenging pathways protect cells from oxidative stress

Reactive oxygen species accumulate in cells during many different types of environmental stresses and are detoxified by specialized enzymes and antioxidants, a process referred to as **ROS scavenging**. Biological antioxidants are small organic compounds or small peptides that can accept electrons from ROS, such as superoxide or H_2O_2, and neutralize them. Common antioxidants in plants include the water-soluble ascorbate (vitamin C), the reduced tripeptide glutathione (GSH in reduced form, GSSG in oxidized form), the lipid-soluble α-tocopherol (vitamin E), and β-carotene (vitamin A). To maintain an adequate supply of these compounds in the reduced state, cells rely on various reductases, such as glutathione reductase, dehydroascorbate reductase, and monodehydroascorbate reductase, which use the reducing power of NADPH or NADH produced by respiration or photosynthesis.

Some ROS may react spontaneously with cellular antioxidants, and some are unstable and decay before they cause cellular damage. However, plants have evolved several different **antioxidative enzymes** that dramatically increase the efficiency of these processes (see **WEB ESSAY 13.7**). For example, **superoxide dismutase** is an enzyme that simultaneously oxidizes and reduces the superoxide anion to produce hydrogen peroxide and oxygen according to the reaction: $2\ O_2^- + 2\ H^+ \rightarrow O_2 + H_2O_2$. Variants of superoxide dismutase are found in chloroplasts, peroxisomes, mitochondria, the cytosol, and the apoplast. Different forms of **ascorbate peroxidase** are present in the same cellular compartments as superoxide dismutase. Ascorbate peroxidase catalyzes the destruction of hydrogen peroxide using ascorbic acid as a reducing agent in the following reaction: 2 L-ascorbate + H_2O_2 + $2\ H^+ \rightarrow$ 2 monodehydroascorbate + $2\ H_2O$. **Catalase** catalyzes the detoxification of hydrogen peroxide in peroxisomes by converting it to water and oxygen according to the reaction: $2\ H_2O_2 \rightarrow 2\ H_2O + O_2$. Reduced forms of **peroxiredoxins** (**Prx**) reduce hydrogen peroxide, and are themselves re-reduced by thioredoxin (Trx), according to the coupled reactions: Prx(reduced) + H_2O_2 → Prx(oxidized) + $2\ H_2O$, and Prx(oxidized) + Trx(reduced) → Prx(reduced) + Trx(oxidized). Finally, **glutathione peroxidase** catalyzes the detoxification of hydrogen peroxide using reduced glutathione (GSH) as a reducing agent: $H_2O_2 + 2$ GSH → GSSG + $2\ H_2O$.

ROS detoxification enzymes and antioxidants function in cells as a network supported by various antioxidant recycling systems that replenish the level of reduced antioxidants (**Figure 15.19**) (see also **WEB ESSAY 13.7**). This ROS-scavenging network maintains ROS at safe, low levels in cells, while allowing cells to use ROS for signal transduction reactions.

Molecular chaperones and molecular shields protect proteins and membranes during abiotic stress

Protein structure is sensitive to disruption by changes in temperature, pH, or ionic strength associated with different types of abiotic stresses. Plants have several mechanisms to limit or avoid such problems, including osmotic adjustment for maintenance of hydration, proton pumps to maintain pH homeostasis, and **molecular chaperone proteins** that physically interact with other proteins to facilitate protein folding, reduce misfolding, stabilize tertiary structure, and prevent aggregation or disaggregation. A unique set of chaperones, called **heat shock proteins** (**HSPs**), are synthesized in response to a variety of environmental stresses. Cells that synthesize HSPs in response to heat stress show improved thermal tolerance and can tolerate subsequent exposures to higher temperatures that would otherwise be lethal. HSPs are induced by widely different environmental conditions, including water deficit, wounding, low temperature, and salinity. In this way, cells that have previously experienced one stress may gain cross-protection against another stress.

HSPs were discovered in the fruit fly (*Drosophila melanogaster*) and appear to be ubiquitous in plants, animals, fungi, and microorganisms. The heat shock response appears to be mediated by one or more signal transduction pathways, one of which involves a specific set of transcription factors, called **heat shock factors**, that regulate the transcription of HSP mRNAs. There are several different classes of HSPs, including HSP70s that bind and release misfolded proteins, HSP60s that produce huge barrel-like complexes that are used as chambers for protein folding, HSP101s that mediate the disaggregation of protein aggregates, and sHSPs and other HSPs that bind and stabilize different complexes and membranes. These different classes of HSPs function together as a molecular network to alleviate the impact of heat stress (**Figure 15.20**).

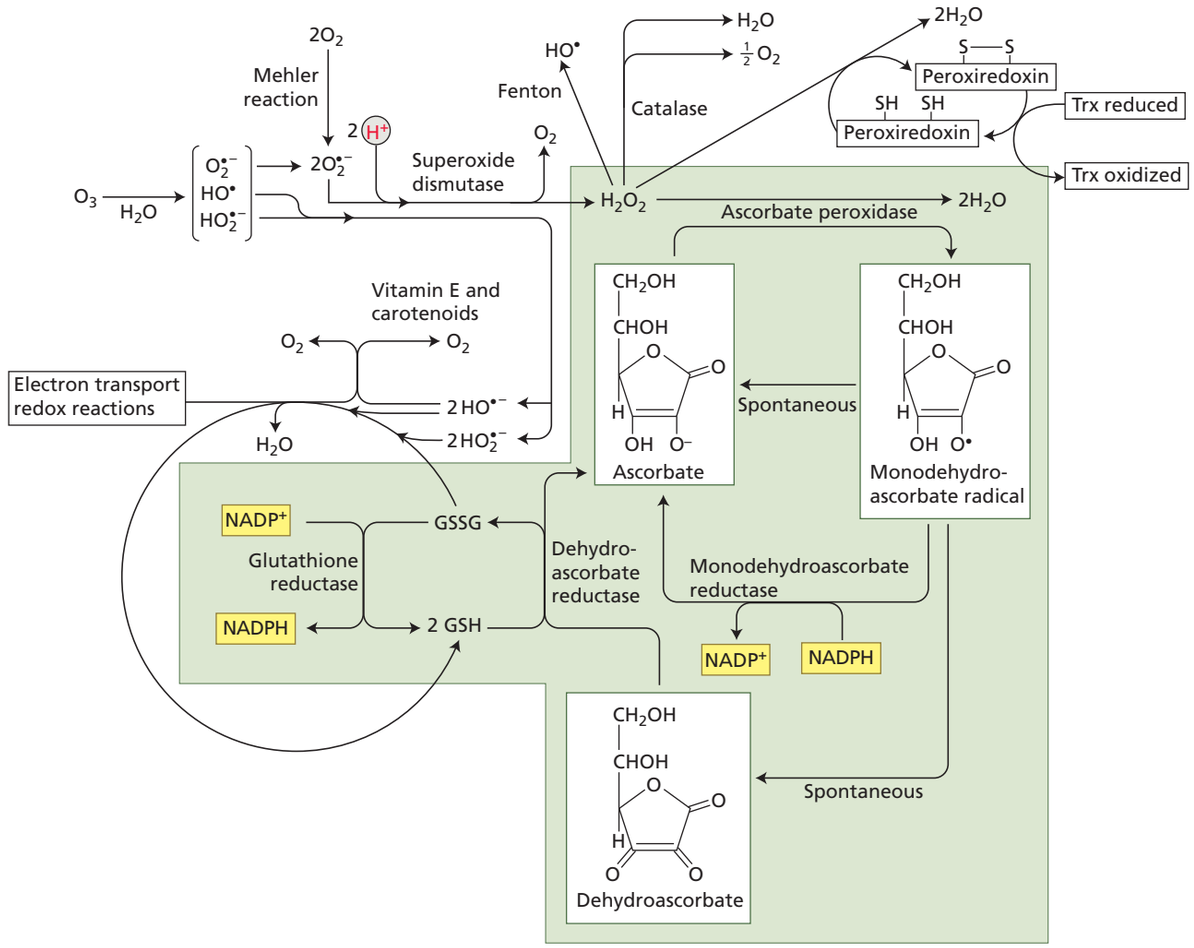


Figure 15.19 **Antioxidant biosynthetic pathways that regulate the levels of reactive oxygen species (ROS) in the cell.** Superoxide dismustase converts superoxide radicals to hydrogen peroxide (H_2O_2), which is broken down to H_2O and O_2 by catalase. H_2O_2 can also be reduced to water by ascorbate peroxidase, and hydroxyl ion and singlet oxygen can be consumed by the glutathione pathway, indicated by the colored background. Trx, thioredoxin. (After R. Jones et al. 2013. *The Molecular Life of Plants.* Wiley-Blackwell, Chichester, West Sussex, UK, p. 568.)

Numerous other proteins have been identified that act in a similar fashion to stabilize proteins and membranes during dehydration, temperature extremes, and ion imbalance. These include the **LEA/DHN/RAB protein family**. LEA (Late Embryogenesis Abundant) proteins accumulate in response to dehydration during the latter stages of seed maturation (see Chapter 21). Most LEA proteins belong to a more widespread group of proteins called **hydrophilins**. Hydrophilins have a strong attraction for water, fold into α helices upon drying, and have the ability to reduce aggregation of dehydration-sensitive proteins, a property termed **molecular shielding**. DHNs (dehydrins) accumulate in plant tissues in response to a variety of abiotic stresses, including salinity, dehydration, cold, and freezing stress. Dehydrins, like LEA proteins, are highly hydrophilic and are intrinsically disordered proteins. Their ability to serve as molecular shields and as cryoprotectants has been attributed to their flexibility and minimal secondary structure. Since both LEAs and DHNs are often induced by ABA, they are sometimes referred to as RABs (responsive to ABA).

Plants can alter their membrane lipids in response to temperature and other abiotic stresses

As temperatures drop, membranes may go through a phase transition from a flexible liquid-crystalline structure to a solid gel structure. The phase transition temperature varies depending on the lipid composition of the membranes. In general, saturated fatty acids that have no double bonds solidify at lower temperatures

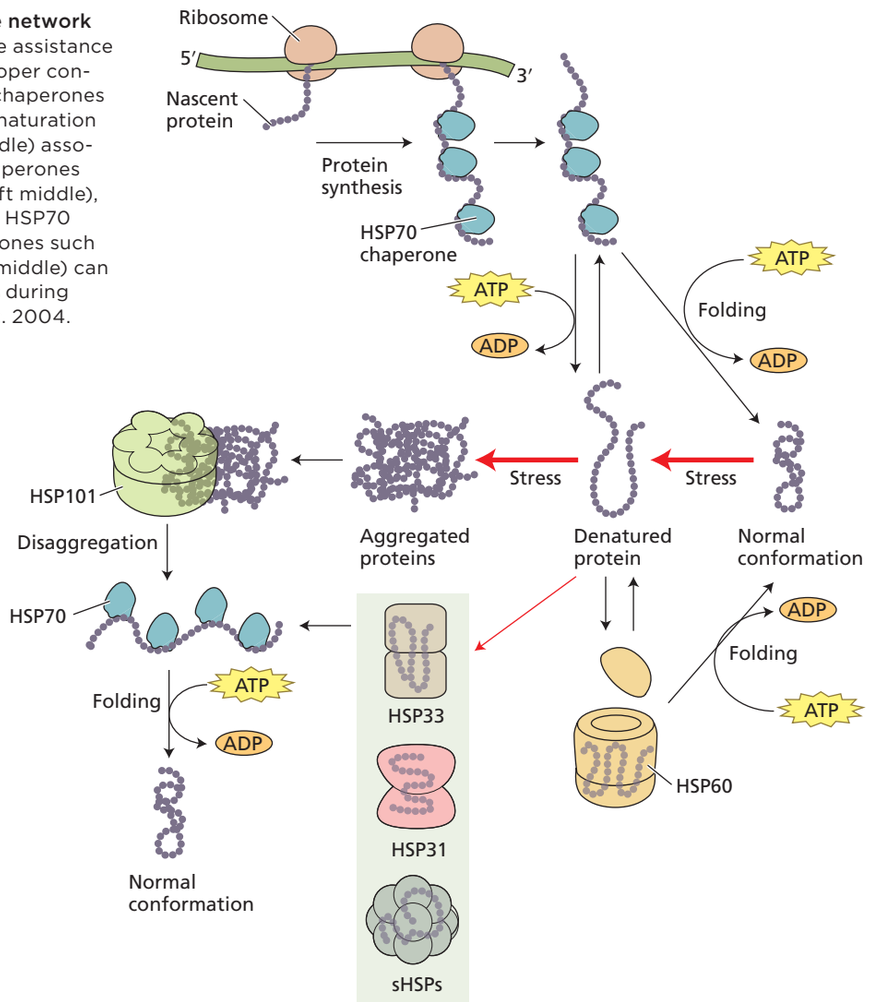


Figure 15.20 Molecular chaperone network in cells. Nascent proteins requiring the assistance of molecular chaperones to reach a proper conformation are associated with HSP70 chaperones (top). Native proteins that undergo denaturation during stress (denatured proteins; middle) associate with HSP70 (top) and HSP60 chaperones (bottom). If aggregates are formed (left middle), they are disaggregated by HSP101 and HSP70 (left). Additional stress-related chaperones such as HSP31, HSP33, and sHSPs (bottom middle) can also associate with denatured proteins during stress. (After F. Baneyx and M. Mujacic. 2004. *Nat. Biotechnol.* 22: 1399–1408.)

than do lipids that contain polyunsaturated fatty acids, because the latter have kinks in their hydrocarbon chains and do not pack as closely as saturated fatty acids. Chilling-resistant plants tend to have membranes with more unsaturated fatty acids that increase their fluidity, whereas chilling-sensitive plants have a high percentage of saturated fatty acid chains that tend to solidify at low temperatures (**Table 15.3**; also see Chapter 1).

Prolonged exposure to extreme temperatures may result in an altered composition of membrane lipids, a form of acclimation. Certain transmembrane enzymes can alter lipid saturation, by introducing one or more double bonds into fatty acids. For example, during acclimation to cold temperatures, the activities of **desaturase enzymes** increase and the proportion of unsaturated lipids rises. This modification lowers the temperature at which the membrane lipids begin a gradual phase change from fluid to semicrystalline form and allows membranes to remain fluid at lower temperatures, thus protecting the plant against damage from chilling. Conversely, a greater degree of saturation of the fatty acids in membrane lipids makes the membranes less fluid. Certain Arabidopsis mutants have reduced activity of omega-3 fatty acid desaturases. These mutants show an increased tolerance of photosynthesis at high temperatures, presumably because the degree of saturation of chloroplast lipids is increased.

Exclusion and internal tolerance mechanisms allow plants to cope with toxic ions

Two basic mechanisms are employed by plants to tolerate the presence of high concentrations of toxic ions in the environment, including Na^+, AsO_4^{3-}, Cd^{2+}, Cu^{2+}, Ni^{2+}, Zn^{2+}, and selenium (Se^{2-}, SeO_3^{2-}, or SeO_4^{2-}): exclusion and internal tolerance. **Exclusion** refers to the ability to block the uptake of toxic ions into the cell or to actively secrete them, thereby preventing the concentrations of these ions from reaching a toxic threshold level. **Internal tolerance**

TABLE 15.3 Fatty acid composition of mitochondria isolated from chilling-resistant and chilling-sensitive species

	Percent weight of total fatty acid content					
	Chilling-resistant species			Chilling-sensitive species		
Major fatty acids[a]	Cauliflower bud	Turnip root	Pea shoot	Bean shoot	Sweet potato	Maize shoot
Palmitic (16:0)	21.3	19.0	17.8	24.0	24.9	28.3
Stearic (18:0)	1.9	1.1	2.9	2.2	2.6	1.6
Oleic (18:1)	7.0	12.2	3.1	3.8	0.6	4.6
Linoleic (18:2)	16.1	20.6	61.9	43.6	50.8	54.6
Linolenic (18:3)	49.4	44.9	13.2	24.3	10.6	6.8
Ratio of unsaturated to saturated fatty acids	3.2	3.9	3.8	2.8	1.7	2.1

Source: After J. M. Lyons et al. 1964. *Plant Physiol.* 39: 262–268.
[a]Shown in parentheses are the number of carbon atoms in the fatty acid chain and the number of double bonds.

typically involves biochemical adaptations that enable the plant to tolerate, compartmentalize, or chelate elevated concentrations of potentially toxic ions.

Glycophytes (salt-sensitive plants) generally rely on exclusion mechanisms to protect themselves from moderate levels of salinity in the soil. Glycophytes are able to tolerate moderate levels of salinity because of root mechanisms that either reduce the uptake of potentially harmful ions or actively pump these ions back into the soil. Ca^{2+} plays a key role in minimizing the uptake of Na^+ from the external medium. As a charged ion, Na^+ has a very low permeability through the lipid bilayer, but it can be transported across the plasma membrane by both low- and high-affinity transport systems, many of which normally transport K^+ into root cells. External Ca^{2+} at millimolar concentrations (the normal physiological concentration of Ca^{2+} in the apoplast) increases the selectivity of the K^+ transporters and minimizes Na^+ uptake. Different Na^+–H^+ antiporters in the plasma membrane and tonoplast can also lower the cytosolic level of Na^+ by actively pumping it back into the apoplast or into the vacuole. The energy used to drive these processes is supplied by different H^+-pumping ATPases in these membranes (see Chapter 8).

In contrast to glycophytes, halophytes can tolerate high levels of Na^+ in the shoot because they have a greater capacity for vacuolar sequestration of ions in their leaf cells. Furthermore, halophytes seem to have a greater ability to restrict net Na^+ uptake into leaf cells. As a result of this increased vacuolar compartmentation and reduced cellular uptake of Na^+ in the shoots, halophytes have an enhanced capacity to sustain an increased flux of Na^+ from roots in the transpirational stream.

An extreme example of internal tolerance to toxic ions is the **hyperaccumulation** of certain trace elements, which occurs in a limited number of species. Hyperaccumulating plants can tolerate foliar concentrations of various trace elements, such as arsenic, cadmium, nickel, zinc, and selenium, of up to 1% of their shoot dry weight (10 mg per gram dry weight). Hyperaccumulation is a relatively rare plant adaptation to potentially toxic ions that requires heritable genetic changes that enhance the expression of the ion transporters involved in the uptake and vacuolar compartmentation of these ions.

Phytochelatins and other chelators contribute to internal tolerance of toxic metal ions

Chelation is the binding of an ion with at least two ligating atoms within a chelating molecule. Chelating molecules can have different atoms available for ligation, such as sulfur (S), nitrogen (N), or oxygen (O), and these different atoms have different affinities for the ions they chelate (see Chapters 7 and 8). By wrapping itself around the ion it binds to form a complex, the chelating molecule renders the ion less chemically active, thereby reducing its potential toxicity. The complex is then usually translocated to other parts of the plant or stored away from the cytoplasm (typically in the vacuole). Long-distance transport of chelated ions from roots to shoots is also a critical process for hyperaccumulation of metals in shoot tissues. Both the iron chelator nicotianamine and the free amino acid histidine have been implicated in chelation of metals during this transport process. In addition, plants also synthesize other ligands for ion chelation, such as phytochelatins.

Phytochelatins are low-molecular-weight thiols consisting of the amino acids glutamate, cysteine, and glycine, with the general form of $(\gamma\text{-Glu-Cys})_n\text{Gly}$. Phytochelatins are synthesized by the enzyme phytochelatin synthase. The thiol groups of cysteine act as ligands for ions of trace elements such as cadmium and arsenic

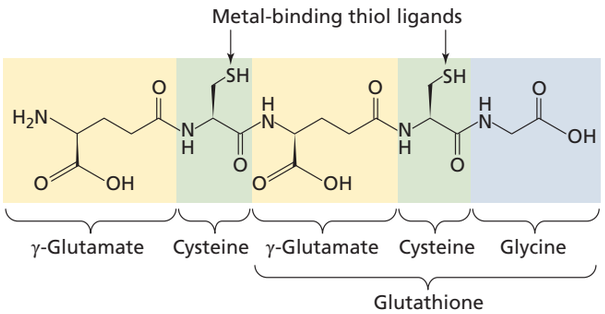


Figure 15.21 **Molecular structure of the metal chelate phytochelatin.** Phytochelatin uses the sulfhydryl groups in cysteine to bind metals such as cadmium, zinc, and arsenic.

(**Figure 15.21**). Once formed, the phytochelatin–metal complex is transported into the vacuole for storage. Synthesis of phytochelatins has been shown to be necessary for resistance to Cd^{2+}. In addition to chelation, active transport of metal ions into the vacuole and out of the cell also contributes to internal metal tolerance.

Plants use cryoprotectant molecules and antifreeze proteins to prevent ice crystal formation

During freezing, the protoplast, including the vacuole, may **supercool**—that is, the cellular water may remain liquid even at temperatures several degrees below its theoretical freezing point. Supercooling is common in many species of the hardwood forests of southeastern Canada and the eastern United States. Cells can supercool only to about –40°C, the temperature at which ice forms spontaneously. Spontaneous ice formation sets the *low-temperature limit* at which many alpine and subarctic species that undergo deep supercooling can survive. It may also explain why the altitude of the timberline in mountain ranges is at or near the –40°C minimum isotherm.

Several specialized plant proteins, termed **antifreeze proteins**, limit the growth of ice crystals through a mechanism independent of lowering of the freezing point of water. Synthesis of these antifreeze proteins is induced by cold temperatures. The proteins bind to the surfaces of ice crystals to prevent or slow further crystal growth. Sugars, polysaccharides, osmoprotectant solutes, dehydrins, and other cold-induced proteins can also have cryoprotective effects.

ABA signaling during water stress causes the massive efflux of K^+ and anions from guard cells

Hormones play an important signaling role in a variety of plant stress responses. During water stress, ABA increases dramatically in leaves, which leads to stomatal closure (**Figure 15.22**). Physiologically, stomatal closure

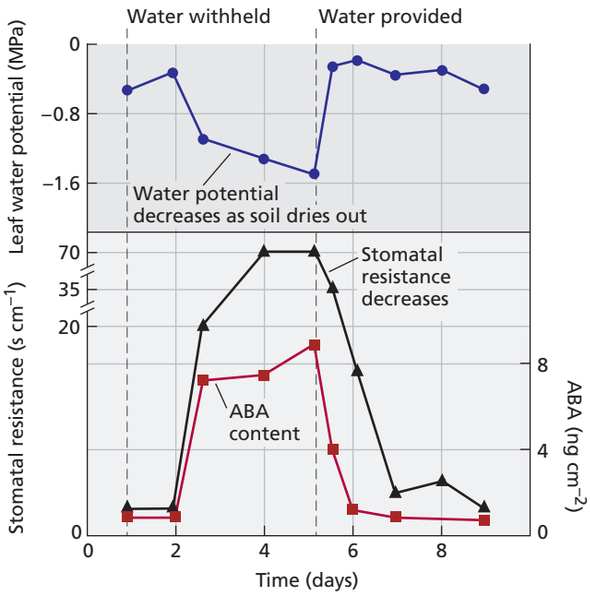


Figure 15.22 **Changes in leaf water potential, stomatal resistance (the inverse of stomatal conductance), and ABA content in maize in response to water stress.** As the soil dries out, the water potential of the leaf decreases, and the ABA content and stomatal resistance increase. Re-watering reverses the process. (After M. F. Beardsell and D. Cohen. 1975. *Plant Physiol.* 56: 207–212.)

is brought about by a reduction in turgor pressure that follows the massive efflux of K^+ and anions from guard cells. Activation of specialized ion efflux channels on the plasma membrane is required for such a large-scale loss of K^+ and anions from guard cells to occur. How does ABA bring this about?

Plasma membrane K^+ efflux channels are *voltage-gated* (see Chapter 8)—that is, they open only if the plasma membrane becomes **depolarized**. ABA causes depolarization by elevating cytosolic Ca^{2+} in two ways: (1) by triggering a transient influx of Ca^{2+} ions and (2) by promoting the release of Ca^{2+} from internal stores, such as the endoplasmic reticulum and the vacuole. As a result, the cytosolic Ca^{2+} concentration rises from 50 to 350 n*M* to as high as 1100 n*M* (1.1 μ*M*) (**Figure 15.23**). This increase in cytosolic Ca^{2+} then opens Ca^{2+}-activated anion channels on the plasma membrane.

The prolonged opening of anion channels permits large quantities of Cl^- and $malate^{2-}$ ions to escape from the cell, moving down their electrochemical gradients. The outward flow of negatively charged Cl^- and $malate^{2-}$ ions depolarizes the membrane, triggering the opening of the voltage-gated K^+ efflux channels. The elevated levels of cytosolic Ca^{2+} also cause K^+ influx channels to close, reinforcing the depolarization effect.

In addition to increasing cytosolic Ca^{2+}, ABA causes alkalinization of the cytosol from about pH 7.7 to

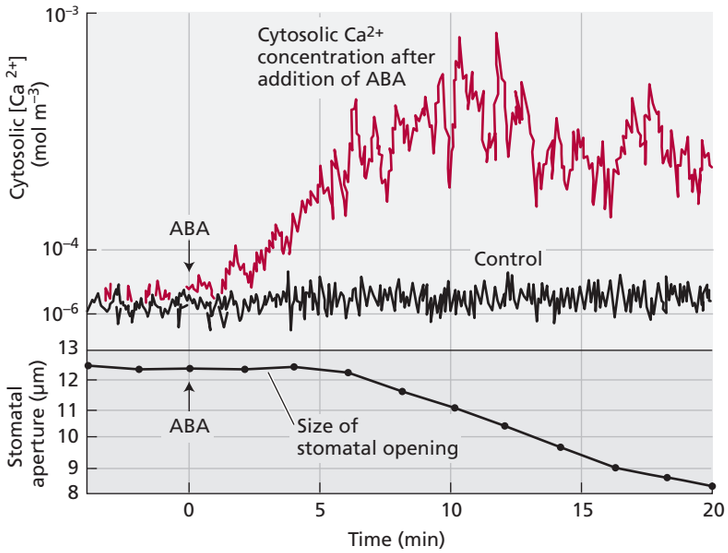


Figure 15.23 Time course of the ABA-induced increase in guard cell cytosolic Ca^{2+} concentration (upper panel) and ABA-induced stomatal aperture (lower panel). The rise in Ca^{2+} begins within approximately 3 min of the addition of ABA, followed by a steady decrease in the size of the stomatal aperture within an additional 5 min. (After M. R. McAinsh et al. 1990. *Nature* 343: 186–188.)

pH 7.9. The increase in cytosolic pH has been shown to further stimulate the opening of the K^+ efflux channels. ABA also inhibits the activity of the plasma membrane H^+-ATPase, resulting in additional membrane depolarization. ABA inhibition of the plasma membrane proton pump is apparently caused by the combination of elevated cytosolic Ca^{2+} concentration and alkalinization of the cytosol.

During stomatal closure, the surface area of the guard cell plasma membrane may contract by as much as 50%. Where does the extra membrane go? The answer seems to be that it is taken up as small vesicles by endocytosis—a process that also involves ABA-induced reorganization of the actin cytoskeleton mediated by a family of plant Rho GTPases, or ROPs (*Rho* GTPases in *P*lants) (see Chapter 1).

Signal transduction in guard cells, with their multiple sensory inputs, involves protein kinases and phosphatases. For example, the activities of the H^+-ATPases that drive the guard plasma membrane potential are reduced by several protein kinases. Protein phosphatases have also been implicated in modifying specific H^+-ATPase activities, leading to changes in the anion channel activities. In view of these results, it appears that protein phosphorylation and dephosphorylation play important roles in the ABA signal transduction pathway in guard cells. A simplified general model for ABA action in stomatal guard cells is shown in **Figure 15.24**. For a more detailed discussion, see **WEB TOPIC 15.3**.

Plants can alter their morphology in response to abiotic stress

In response to abiotic stress, plants can activate developmental programs that alter their phenotype, a phenomenon known as **phenotypic plasticity**. Phenotypic plasticity can result in adaptive anatomical changes that enable plants to avoid some of the harmful effects of abiotic stress.

An important example of phenotypic plasticity is the ability to alter leaf shape. As biological solar panels, leaves must be exposed to sunlight and air, which makes them vulnerable to environmental extremes. Plants have thus evolved the ability to modify leaf morphology in ways that enable them to avoid or mitigate the effects of abiotic extremes. Such mechanisms include changes in leaf area, leaf orientation, leaf rolling, trichomes, and waxy cuticles, as we outline here.

LEAF AREA Large, flat leaves provide optimal surfaces for the production of photosynthates, but they can be detrimental to crop growth and survival under stressful conditions because they provide a large surface area for evaporation of water, which can lead to quick depletion of soil water or excessive, damaging absorption of solar energy. Plants can reduce their overall leaf area by reducing leaf cell division and expansion, by altering leaf shapes (**Figure 15.25A**), and by initiating the senescence and abscission of leaves (**Figure 15.25B**). This phenomenon can lead to certain types of heterophylly, as in aquatic plants (**WEB ESSAY 15.1**).

LEAF ORIENTATION For protection against overheating during water deficit, the leaves of some plants may orient themselves away from the sun; such leaves are said to be **paraheliotropic**. Leaves that gain energy by orienting themselves perpendicular to the sunlight are referred to as **diaheliotropic**. Another morphological factor that can alter the interception of radiation is leaf rolling, which minimizes the profile of tissue exposed to the sun (**Figure 15.25C**) (see Chapter 11). Leaf wilting, while not an example of phenotypic plasticity, can alter leaf angle and thereby reduce the amount of sunlight absorbed.

TRICHOMES Many leaves and stems have hairlike epidermal cells known as trichomes or hairs. Densely packed trichomes on a leaf surface keep leaves cooler by reflecting radiation, and can also mechanically impede insect infestation (see Chapter 23). Both the structure and chemical constituents of trichomes can change in response to light, herbivory, water stress, salinity, or the presence of heavy metals. For example, the leaves

1. Abscisic acid (ABA) binds cytosolic ABA receptors (RCAR/PYR/PYL) (see Chapter 4).

2. The ABA-bound receptors form a complex with type 2C protein phosphatases (PP2Cs), inhibiting their activity. PP2Cs represent a major negative regulator within this signaling network.

3. Inhibition of PP2C activity releases the positive regulator kinase OST1 from inhibition, resulting in both phosphorylation and activation of NADPH oxidases (RBOHs). RBOHs catalyze the formation of apoplastic reactive oxygen species (ROS) such as H_2O_2 and $O_2^{\bullet-}$, which triggers opening of plasma membrane Ca^{2+}-permeable ion channels. Ca^{2+} enters the cell.

4. The resulting elevation of cytosolic Ca^{2+}, augmented by Ca^{2+}-promoted release of Ca^{2+} stored in organelles, including the vacuole, leads to activation of calcium-dependent protein kinases (CPKs). CPKs can also activate RBOH proteins, further promoting Ca^{2+} influx into the cytosol.

5. Both OST1 and CPKs phosphorylate and thereby activate plasma membrane anion channels, leading to efflux of anions (A^-). This process can be inhibited directly by PP2Cs in the absence of ABA. Two types of anion channels are activated: slow (S-type) and rapid (R-type).

6. Anion efflux leads to depolarization of the plasma membrane, which drives K^+ efflux via outward-rectifying potassium (K^+_{out}) channels (GORK). The majority of A^- and K^+ in a plant cell are stored in the vacuole and are released into the cytosol via Ca^{2+}-activated K^+ channels and anion release transporters present in the tonoplast. The efflux of ions (A^- and K^+) reduces the turgor pressure of guard cells, resulting in stomatal closure.

7. Inhibition of PP2C by ABA and RCAR/PYR/PYL also leads to inhibition of channels and pumps that mediate accumulation of ions during stomatal opening, such as H^+-ATPases and inward rectifying K^+ (K^+_{in}) channels. These channels would otherwise counteract the closure-promoting effects of ion efflux.

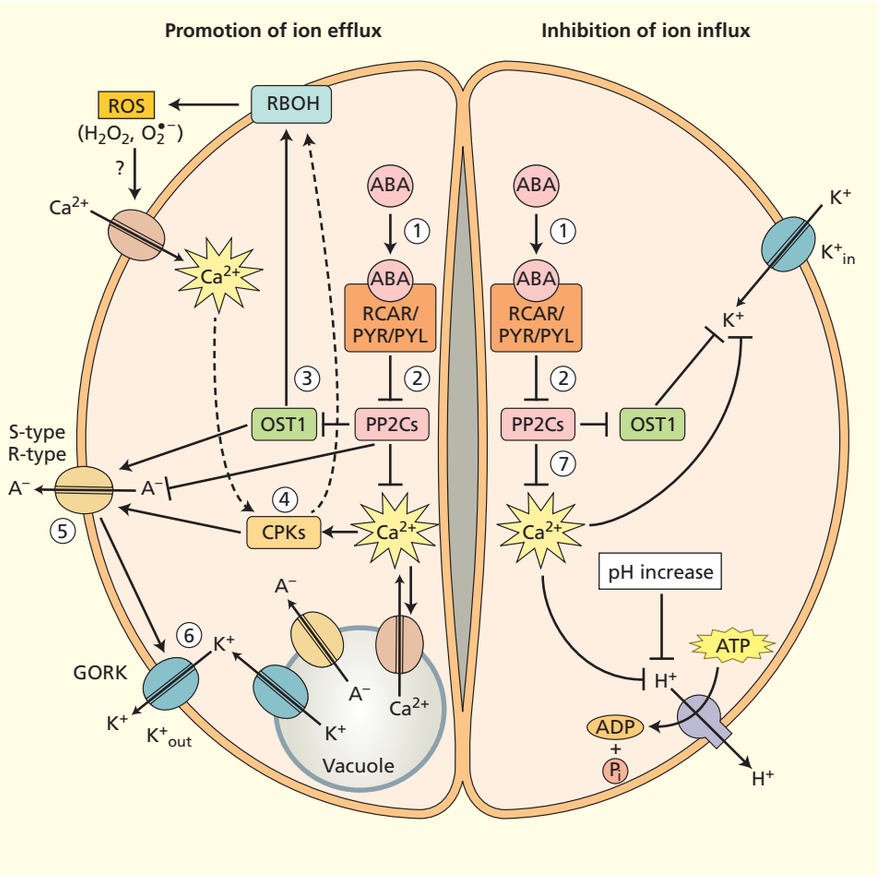


Figure 15.24 Simplified model for ABA signaling in stomatal guard cells. The net effect is the loss of potassium (K^+) and its anion (Cl^- or malate^{2-}) from the cell. CPK, Ca^{2+}-dependent protein kinase; GORK, K^+-outward-rectifying channel; OST1, OPEN STOMATA 1 protein kinase; PP2C, protein phosphatase 2C; RBOH, respiratory burst oxidase homolog, an NADPH oxidase; ROS, reactive oxygen species. (After B. Brandt and J. Schroeder, unpublished.)

of the yellow monkey flower (*Mimulus guttatus*) often produce glandular trichomes that may serve as a chemical deterrent to herbivory. When the early leaves of *Mimulus* are experimentally damaged to simulate herbivory, it causes an increase in the production of glandular trichomes in the later leaves, a plastic response that is probably adaptive.

CUTICLE The cuticle is a multilayered structure of waxes and related hydrocarbons deposited on the outer cell walls of the leaf epidermis. The cuticle, like trichomes, can reflect light, thereby reducing heat load. The cuticle appears to also restrict the diffusion of water and gases, as well as the entrance of pathogens. A developmental response to water deficit in some plants is the production of a thicker cuticle, which decreases transpiration.

ROOT-TO-SHOOT RATIO The **root-to-shoot ratio** is another important example of phenotypic plasticity. The root:shoot ratio appears to be governed by a functional balance between water uptake by the root and photosynthesis by the shoot. Within the limits set by the plant's

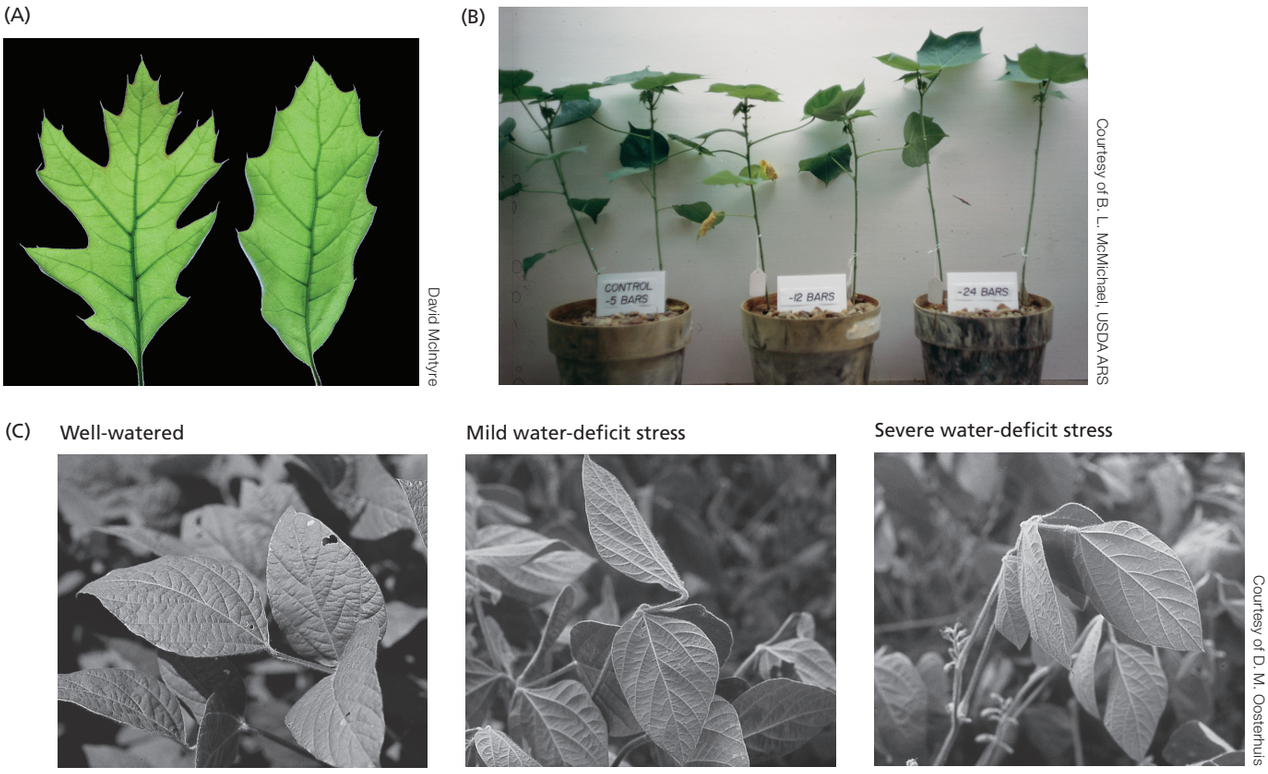


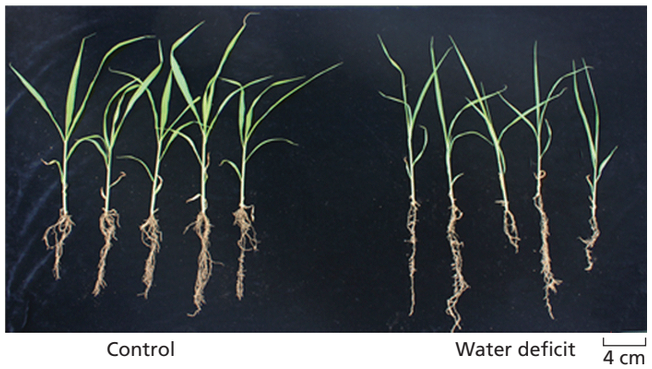
Figure 15.25 Morphological changes in response to abiotic stress. **(A)** Altered leaf shape can occur in response to environmental changes. The oak (*Quercus* sp.) leaf on the left is from the outside of a tree canopy, where temperatures are higher than they are inside the canopy. The leaf on the right is from the inside of the canopy. The deeper sinuses of the leaf on the left result in a thinner boundary layer, which allows for better evaporative cooling. **(B)** The leaves of young cotton (*Gossypium hirsutum*) plants abscise in response to water-deficit stress. The plants at left (control) were watered throughout the experiment; those in the middle and at right were subjected to moderate water-deficit stress and severe water-deficit stress, respectively, before being watered again. Only a tuft of leaves at the top of the stem is left on the severely stressed plants. The –5, –12, and –24 bars = –0.5, –1.2, and –2.4 MPa, respectively. **(C)** Leaf movements in soybean in response to osmotic stress. Leaflet orientation of field-grown soybean (*Glycine max*) plants in the well-watered, unstressed position; during mild water-deficit stress; and during severe water-deficit stress. The large leaf movements induced by mild stress are quite different from wilting, which occurs during severe stress. Note that during mild stress the terminal leaflet has been raised, whereas the two lateral leaflets have been lowered; each is almost vertical.

genetic potential, a shoot tends to grow until water uptake by the roots becomes limiting to further growth; conversely, roots tend to grow until their demand for photosynthates from the shoot exceeds the supply. This functional balance is shifted if the water supply decreases. When water to the shoot becomes limiting, leaf expansion is reduced before photosynthetic activity is affected (see Figure 15.5). Inhibition of leaf expansion reduces the consumption of carbon and energy, and a greater proportion of the plant's assimilates can be allocated to the root system, where they can support further root growth. However, root growth is also sensitive to the water status of the soil microenvironment; root apices lose turgor in dry soil, while roots in moist soils continue to grow (**Figure 15.26**).

ABA plays an important role in regulating the root:shoot ratio during water-deficit stress. As shown in **Figure 15.27**, under water-deficit stress conditions the root-to-shoot biomass ratio increases, allowing the roots to grow at the expense of the leaves. However, ABA-deficient mutants are unable to change their root:shoot ratio in response to water-deficit stress. Thus, ABA is required for the change in the root:shoot ratio to occur.

The process of recovery from stress can be dangerous to the plant and requires a coordinated adjustment of plant metabolism and physiology

Once a plant acclimates to a specific set of environmental stress conditions, it achieves a state of metabolic homeostasis that enables it to grow optimally under these conditions. However, when the stress is removed, for example by re-watering in the case of a water-deficit-stressed plant, the plant must shift its metabolism back to its



From J. Pan et al. 2018. *BMC Plant Biol.* 18: 315. CC BY 4.0

Figure 15.26 **Effect of water-deficit conditions on root and shoot growth of fox millet (*Panicum italicum* L.) seedlings.** The soil moisture was maintained at 80 to 90% of field capacity in well-watered (control) conditions and at 50% in water-deficit conditions. Pots were weighed daily to record the mass of water loss by evapotranspiration, and the amount of water needed to bring each pot to appropriate field capacity was added to each pot. Both root and shoot growth were inhibited.

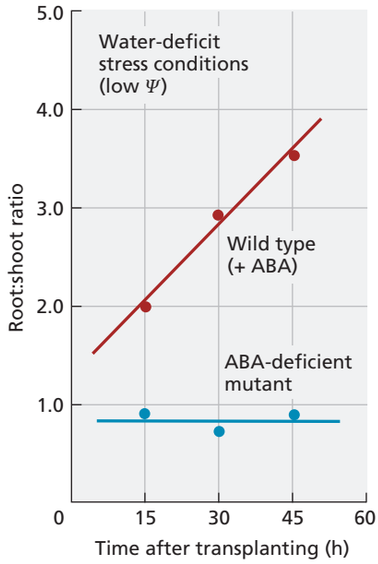


Figure 15.27 **Under water-deficit stress conditions (low Ψ, defined slightly differently for shoot and root), the ratio of root growth to shoot growth is much higher when ABA is present (i.e., in the wild type) than when it is absent (in the ABA-deficient mutant).** (After I. N. Saab et al. 1990. *Plant. Physiol.* 93: 1329–1336.)

previous state in order to acclimate to the new set of nonstressed conditions. In some instances, for example when the plant needs to shift from a highly reduced anaerobic environment to oxidized aerobic conditions during a relief from flooding stress, the metabolic shift may be highly dangerous to the plant because high levels of ROS can damage cells.

The recovery process from stress is therefore as much a synchronized process as is the acclimation to stress. The plant must remove and recycle all the unneeded mRNAs, proteins, and protective chemicals and compounds that accumulated in cells during the acclimation process and throughout the stress period. In addition, the plant must shift its metabolic energy flow to prepare for, and adjust to, the new conditions. Reactivation of certain processes such as photosynthesis, respiration, and lipid biosynthesis may require a delicate and synchronized process, because these pathways can produce high levels of ROS, and the ROS-scavenging pathways that protect the plant should be in place before the pathways become fully functional. Although from an energy standpoint it is best for the plant to remove and recycle all stress-response mechanisms when the stress subsides, some plants maintain a readiness to counter the reoccurrence of stress by keeping certain stress-response regulatory mechanisms, hormones, or epigenetic modifications active even after the stress subsides. This process is often referred to metaphorically as *memory* because the plant seems to "remember" the stress even long after it is over and will respond much faster to its reoccurrence compared with the first time it encountered it.

Summary

Plants sense changes in their environment and respond to them by means of dedicated stress-response pathways. These pathways involve gene networks, regulatory proteins, and signaling intermediates, as well as proteins, enzymes, and molecules that act to protect cells from the detrimental effects of abiotic stress. Together these anti-stress mechanisms enable plants to acclimate or adapt to stresses such as water deficit, heat, cold, and salinity, as well as their possible combinations. A major research goal is to use some of these acclimation or adaptation mechanisms to protect crops from the adverse climatic conditions that are expected to result from global warming (**WEB TOPIC 15.1**).

15.1 Defining Plant Stress

- Stress can be defined generally as any environmental condition that prevents the plant from achieving its full genetic potential measured under ideal growth conditions (**Figures 15.1, 15.2**).
- Plant responses to abiotic stress involve trade-offs between vegetative and reproductive growth, which may differ depending on whether the plant is an annual or a perennial.

15.2 Acclimation and Adaptation

- Adaptation is characterized by genetic changes in an entire population that have been fixed by natural selection over many generations.
- Acclimation is the process whereby individual plants respond to periodic changes in the environment by directly altering their morphology or physiology. The physiological changes associated with acclimation require no genetic modifications, and many are reversible.

15.3 Environmental Factors and Their Biological Impacts on Plants

- Environmental stresses can disrupt plant metabolism through a variety of mechanisms, most of which result in the accumulation of reactive oxygen species (ROS) (**Figures 15.3, 15.4**).
- Cell dehydration leads to decreased turgor pressure, increased ion toxicity, and inhibition of photosynthesis (**Figure 15.5, Table 15.1**).
- Temperature stress affects protein stability, enzymatic reactions, membrane fluidity, and the secondary structures of RNA and DNA (**Table 15.1**).
- Flooded soil is depleted of oxygen, leading to anaerobic stress to the root (**Table 15.1**).
- Salinity stress causes cell dehydration coupled with inhibition of enzymatic activity due to ion toxicity, thereby reducing aboveground plant growth and inhibiting photosynthesis (**Table 15.1**).
- Freezing stress, like water-deficit stress, causes cell dehydration, but can also disrupt cellular integrity due to membrane damage (**Table 15.1**).
- Heavy metals can replace other essential metals and disrupt key reactions (**Table 15.1**).
- Ozone and ultraviolet light induce the formation of ROS, which in turn induce the formation of leaf lesions and programmed cell death.
- Combinations of abiotic stresses can have effects on plant physiology and productivity that are different than those of individual stresses (**Figures 15.6, 15.7**).
- Plants can gain cross-protection when they are sequentially exposed to different abiotic stresses.

15.4 Stress-Sensing Mechanisms in Plants

- Plants use physical, biophysical, metabolic, biochemical, and epigenetic mechanisms to detect stresses and activate response pathways (**Figure 15.8**).

15.5 Signaling Pathways Activated in Response to Abiotic Stress

- Many stress-response pathways share signaling intermediates, allowing these pathways to be integrated (**Figures 15.9–15.12**).
- Regulons simultaneously activate specific stress-response pathways and suppress other pathways that are not needed or could even damage the plant during stress (**Figure 15.13**).
- Chloroplasts and mitochondria can send distress signals to the nucleus.
- A systemic plant-wide wave of ROS production and Ca^{2+} signaling alerts as-yet unstressed parts of the plant of the need for a response (**Figure 15.14**).
- Epigenetic stress-response mechanisms may lead to heritable protection (**Figure 15.15**).
- Hormones act separately and together to regulate abiotic stress responses.

15.6 Physiological and Developmental Mechanisms That Protect Plants against Abiotic Stress

- Global warming and climate change are expected to have complex and potentially severe impacts on the growth and yield of many crops in many different areas on our planet (**Web Topic 15.1**).
- Agricultural researchers study how plants sense and acclimate to stressful conditions, and then try to develop crops with enhanced tolerance (**Web Topic 15.1**).
- Precision agriculture is a modern approach to farm management that uses advanced imaging, artificial intelligence, and robotics to ensure that the crops and soils of any given agricultural land receive exactly what they need for optimum growth, health, and productivity (**Web Topic 15.2**).

(*Continued*)

Summary (*continued*)

- Plants lower root Ψ to continue to absorb water in drying soil.
- Aerenchyma tissue allows O_2 to diffuse down to submerged organs (**Figure 15.18**).
- ROS can be detoxified through scavenging pathways that reduce oxidative stress (**Figure 15.19**).
- Molecular chaperone proteins protect sensitive proteins and membranes during abiotic stress (**Figure 15.20**).
- Prolonged exposure to extreme temperatures can alter the composition of membrane lipids, thereby allowing plants to maintain membrane fluidity (**Table 15.3**).
- Plants cope with toxic ions through exclusion and internal tolerance mechanisms (**Figure 15.21**).
- Plants generate antifreeze proteins to prevent ice crystal formation.
- Stomatal closure is prompted by ABA-induced efflux of K^+ and anions from guard cells (**Figures 15.22–15.24**).
- Plants can alter their leaf morphology and their root-to-shoot biomass ratio to avoid or mitigate abiotic stress (**Figures 15.25–15.27**).
- Reversal of stress-response pathways must occur in a synchronized manner to avoid production of ROS.

Web Material

- **WEB TOPIC 15.1 Climate Change, Global Warming, and Abiotic Stress** Global warming has become a major contributor to changes in our climate, causing an increase in the frequency and intensity of weather events that subject plants to abiotic stress conditions such as prolonged droughts, heat waves, flooding, and salinity.
- **WEB TOPIC 15.2 Abiotic Stress and Precision Agriculture** Different physiological processes in plants are affected during abiotic stress, which can be efficiently monitored and treated in the field using precision agriculture practices.
- **WEB TOPIC 15.3 A Closer Look at ABA Signaling in Guard Cells** Recent studies have helped elucidate the complex interactions during ABA-induced stomatal closure.
- **WEB ESSAY 15.1 Heterophylly in Aquatic Plants** Abscisic acid induces aerial-type leaf morphology in many aquatic plants.

For more study aids, go to oup.com/he/taiz7e.

Suggested Reading

Bailey-Serres, J., Parker, J. E., Ainsworth, E. A., Oldroyd, G. E. D., and Schroeder, J. I. (2019) Genetic strategies for improving crop yields. *Nature* 575: 109–115.

Cheung, A.Y., Qu, L. J., Russinova, E., Zhao,Y., and Zipfel, C. (2020) Update on receptors and signaling. *Plant Physiol.* 182: 1527–1530.

Kollist, H., Zandalinas, S. I., Sengupta, S., Nuhkat, M., Kangasjärvi, J., and Mittler, R. (2019) Rapid responses to abiotic stress: Priming the landscape for the signal transduction network. *Trends Plant Sci.* 24: 25–37.

Lamers, J., van der Meer, T., and Testerink, C. (2020) How plants sense and respond to stressful environments. *Plant Physiol.* 182: 1624–1635.

Lobell, D. B., Schlenker, W., and Costa-Roberts, J. (2011) Climate trends and global crop production since 1980. *Science* 333: 616–620.

Mhamdi, A., and Van Breusegem, F. (2018) Reactive oxygen species in plant development. *Development* 145: dev164376.

Mittler, R. (2017) ROS are good. *Trends Plant Sci.* 22: 11–19.

Ohama, N., Sato, H., Shinozaki, K., and Yamaguchi-Shinozaki, K. (2017) Transcriptional regulatory network of plant heat stress response. *Trends Plant Sci.* 22: 53–65.

Rodriguez, P. A., Rothballer, M., Chowdhury, S. P., Nussbaumer, T., Gutjahr, C., and Falter-Braun, P. (2019) Systems biology of plant-microbiome interactions. *Mol. Plant.* 12: 804–821.

Saijo,Y., and Loo, E. P. (2020) Plant immunity in signal integration between biotic and abiotic stress responses. *New Phytol.* 225: 87–104.

Yeung, E., Bailey-Serres, J., and Sasidharan, R. (2019) After the deluge: Plant revival post-flooding. *Trends Plant Sci.* 24: 443–454.

Zandalinas, S. I., Fichman,Y., Devireddy, A. R., Sengupta, S., Azad, R. K., and Mittler, R. (2020) Systemic signaling during abiotic stress combination in plants. *Proc. Natl. Acad. Sci. USA* 117: 13810–13820.

Zandalinas, S. I, Fritschi, F. B., Mittler, R. (2021) Global warming, Climate change, and environmental pollution: Recipe for a multifactorial stress combination disaster. *Trends Plant Sci.* 26: 588–599.

Zhu, J. K. (2016) Abiotic stress signaling and responses in plants. *Cell* 167: 313–324.



schankz/Shutterstock

UNIT IV

Growth and Development

CHAPTER 16 **Signals from Sunlight**

CHAPTER 17 **Seed Dormancy, Germination, and Seedling Establishment**

CHAPTER 18 **Vegetative Growth and Organogenesis: Primary Growth of the Plant Axis**

CHAPTER 19 **Vegetative Growth and Organogenesis: Branching and Secondary Growth**

CHAPTER 20 **The Control of Flowering and Floral Development**

CHAPTER 21 **Sexual Reproduction: From Gametes to Fruits**

CHAPTER 22 **Embryogenesis: The Origin of Plant Architecture**

CHAPTER 23 **Plant Senescence and Developmental Cell Death**

CHAPTER 24 **Biotic Interactions**



16 Signals from Sunlight



schankz/Shutterstock

Sunlight serves not only as an energy source for photosynthesis, but also as a signal that regulates various developmental processes, from seed germination to fruit development and senescence (**Figure 16.1**). Sunlight also provides directional cues for plant growth as well as nondirectional cues for plant movements. We have already touched on several light-sensing mechanisms in the preceding chapters. In Chapter 11 we saw that chloroplasts move within leaf palisade cells to orient either their face or edge toward the sun (see Figure 11.12). The leaves of many species are able to bend toward the sun during its progress across the sky, a phenomenon known as **solar tracking** (see Figure 11.5). The range of light intensity and quality under a variety of conditions is shown in **Table 16.1**.

In subsequent chapters we will encounter examples of light-regulated plant development. For example, many seeds require light to germinate, a process called **photoblasty**. Sunlight inhibits stem growth and stimulates leaf expansion in growing seedlings, two of several light-induced phenotypic changes collectively referred to as **photomorphogenesis** (**Figure 16.2**; also see Chapter 17). Most of us are familiar with the observation that the branches of houseplants placed near a window grow toward the incoming light. This phenomenon, called **phototropism**, is an example of how plants alter their growth patterns in response to the direction of incident radiation (**Figure 16.3**; also see Chapter 17). In some species the leaves fold up at night (**nyctinasty**) and open at dawn (**photonasty**). Photonastic movements are plant movements in response to nondirectional light. As we will discuss in Chapter 20, many plants flower at specific times of the year in response to changing day length, a phenomenon called **photoperiodism**.

In addition to visible light (**Figure 16.4**), sunlight also contains ultraviolet (UV) radiation, which can damage membranes, DNA, and proteins (see Chapter 15). Many plants can sense the presence of UV radiation and protect themselves against cellular damage by synthesizing simple phenolics and flavonoids that act as sunscreens and remove damaging oxidants and free radicals that are induced by the high-energy UV photons.



SHOSEI/Aflo/Getty Images

Figure 16.1 Sunlight exerts multiple influences on plants. Plants expose their leaves to sunlight to transform solar energy into chemical energy, and they also use sunlight for a wide range of developmental signals that optimize photosynthesis and detect seasonal changes.

In this chapter we discuss the primary signaling mechanisms involved in light-regulated growth and development, focusing primarily on the red-light (600–700 nm), far-red light (700–750 nm), blue light (400–500 nm), and UV-B radiation (290–320 nm) receptors.

16.1 Plant Photoreceptors

Pigments, such as chlorophyll and the accessory pigments of photosynthesis, are molecules that absorb visible light at specific wavelengths, and reflect or transmit the nonabsorbed wavelengths, which are perceived as colors. Unlike the photosynthetic pigments, photoreceptors absorb a photon of a given wavelength and use this energy as a signal that initiates a photoresponse. With the exception of UVR8 (discussed at the end of this chapter), all the known photoreceptors consist of a protein plus a light-absorbing prosthetic group (a nonprotein molecule attached to the photoreceptor protein) called a **chromophore**. As we will see later, the protein structures of the different photoreceptors vary. Other common aspects of photoreceptors include sensitivity to light quantity (number of photons), light quality (wavelength dependency), light intensity, and duration

All of the photoresponses noted thus far, including the responses to UV radiation, involve receptors that detect specific wavelengths of light and induce developmental or physiological changes. As we saw in Chapter 4, hormone signal transduction involves a chain of reactions beginning with a hormone receptor and ending with a physiological response. The receptor molecules that plants use to detect sunlight are termed **photoreceptors**. Like hormone receptors, photoreceptors respond to a signal, in this case light, by initiating signaling reactions that typically involve second messengers and phosphorylation cascades (see Figure 4.4).

TABLE 16.1 Ecologically important light parameters

	Fluence rate (μmol m^{-2} s^{-1})	R:FR[a]
Daylight	1900	1.19
Sunset	26.5	0.96
Moonlight	0.005	0.94
Ivy canopy	17.7	0.13
Soil, at a depth of 5 mm	8.6	0.88

Source: H. Smith. 1982. *Annu. Rev. Plant Physiol.* 33: 481–518

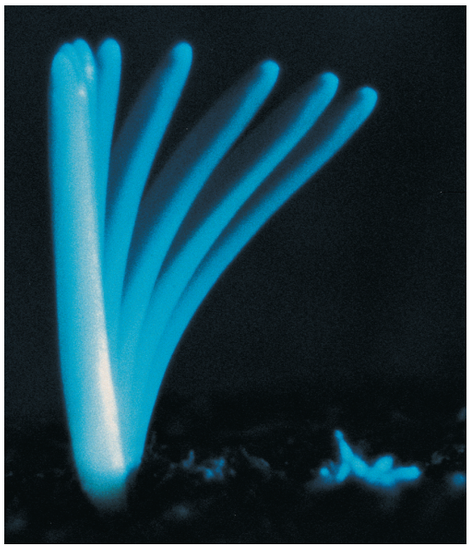
Note: The light intensity factor (400–800 nm) is given as the photon flux density, and phytochrome-active light is given as the R:FR ratio.

[a]Absolute values taken from spectroradiometer scans; the values should be taken to indicate the relationships between the various natural conditions and not as actual environmental means.



© Nigel Cattlin/Alamy Stock Photo

Figure 16.2 Comparison of seedlings grown in the light versus the dark. (Left) Cress seedlings grown in the light. (Right) Cress seedlings grown in the dark. The dark-grown seedlings exhibit etiolation, characterized by elongated hypocotyls and a lack of chlorophyll.



Courtesy of M. A. Quiñones

Figure 16.3 **Time-lapse photograph of a maize (corn; *Zea mays*) coleoptile growing toward unilateral blue light given from the right.** The coleoptile is about 3 cm long. The consecutive exposures were made 30 min apart. Note the increasing angle of curvature as the coleoptile bends.

of the exposure to light. In each case, perception of light by specific photoreceptors initiates cellular signals that ultimately regulate specific photoresponses.

Among the photoreceptors that can promote photomorphogenesis in plants, the most important are those that absorb red and blue light. **Phytochromes** are photoreceptors that absorb red and far-red light most strongly (600–750 nm), but they also absorb blue light (400–500 nm) and UV-A radiation (320–400 nm). Phytochromes mediate many aspects of vegetative and reproductive development, as we will describe in subsequent chapters. Three main classes of photoreceptors mediate the effects of UV-A/blue light: the cryptochromes, the phototropins, and the **ZEITLUPE** (**ZTL**, German for "slow motion") family. Cryptochromes, like the phytochromes, play a major role in plant photomorphogenesis, while **phototropins** primarily regulate phototropism, chloroplast movements, and stomatal opening. The ZTL family of photoreceptors plays roles in day length perception and circadian rhythms. As in the case of hormone signaling, light signaling typically involves interactions between multiple photoreceptors and their signaling intermediates.

By convention, plant photoreceptors are designated in lowercase (e.g., phy, cry, phot) when the holoprotein (protein plus chromophore) is described, and in uppercase (PHY, CRY, PHOT) when the apoprotein (protein minus chromophore) is described. To be consistent with genetic conventions, we will use uppercase italics (*PHY*, *CRY*, *PHOT*) for the genes encoding the photoreceptor apoproteins.

A unique photoreceptor system has also been isolated from Arabidopsis that is specific for the perception of ultraviolet radiation (**UV RESISTANCE LOCUS 8**, or **UVR8**) and is responsible for several UV-B-induced photomorphogenic responses. UVR8 is discussed at the end of the chapter.

Photoresponses are driven by light quality or spectral properties of the energy absorbed

As in the case of hormone receptors (see Chapter 4), the different photoreceptor systems in plants can interact with each other, and it can be difficult to separate specific responses within the full solar spectrum since many photoreceptors may be absorbing energy at the same time. For example, the process of **de-etiolation**, characterized by the production of chlorophyll in dark-grown (etiolated; from the French *étiolier*, "to make pale") seedlings when exposed to light, results from the coaction of phytochrome and protochlorophyllide (see Chapter 9) absorbing red light and cryptochrome absorbing blue

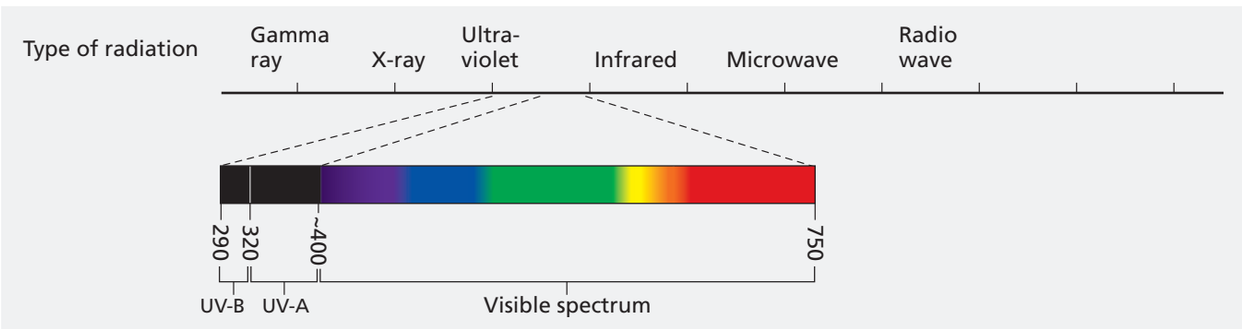


Figure 16.4 **Plants can use visible light, UV-A, and UV-B radiation as developmental signals (all wavelengths in nm).**

light from sunlight. How, then, can we functionally distinguish intrinsic responses to individual photoreceptors? In many cases, a contribution from photosynthesis cannot be excluded since photosynthetic pigments also absorb red light and blue light.

To determine which wavelengths of light are necessary to bring about a particular plant response, photobiologists typically produce what is known as an action spectrum. Action spectra describe the wavelength specificity of a biological response to sunlight. Each photoreceptor differs in its atomic composition and arrangement and thus exhibits different absorption characteristics. As we saw in Chapter 9, a photosynthetic action spectrum is a graph that plots the magnitude of a light response (photosynthesis) as a function of wavelength (see **WEB TOPIC 8.1** for a detailed discussion of spectroscopy and action spectra). The action spectrum of the response can then be compared with the absorption spectra of candidate photoreceptors.

Similar approaches have been used to identify photoreceptors involved in signaling pathways. For example, red light stimulates lettuce seed germination, and far-red light inhibits it (**Figure 16.5**). The action spectra for these two antagonistic effects of light on Arabidopsis seed germination are shown in **Figure 16.6A**. Stimulation shows a peak in the red region (660 nm), while inhibition has a peak in the far-red region (720 nm). When the absorption spectra of each of the two forms of phytochrome (Pr and Pfr) are measured separately in a spectrophotometer designed to study photoreversible molecules, they correspond closely to the action spectra for the stimulation and inhibition of seed germination, respectively (**Figure 16.6B**). As we discuss in Section 16.2, the close correspondence between the action and absorption spectra of phytochrome not only confirmed its identity as the photoreceptor involved in regulating seed germination, it also established that the red/far-red reversibility of seed germination was due to the photoreversibility of phytochrome itself.

Similarly, action spectra for blue light–stimulated phototropism, stomatal movements, and other key blue-light responses all exhibit a peak in the UV-A region (at 370 nm) and a peak in the blue region (~410–500 nm) that has a characteristic "three-finger" fine structure (**Figure 16.7A**), suggesting a common photoreceptor. The absorption spectrum for the LIGHT-OXYGEN-VOLTAGE 2 (LOV2) domain of phototropin, which contains the chromophore flavin mononucleotide (FMN), is identical to the action spectrum for phototropism (**Figure 16.7B**), consistent with phototropin acting as the photoreceptor for these responses. The mechanism of phototropin action is discussed later in the chapter.

Plants responses to light can be distinguished by the amount of light required

Light responses can also be distinguished by the amount of light required to induce them. The amount of light is referred to as the **fluence**, which is defined as the total number of photons impinging on a unit of surface area. Total fluence = fluence rate × the length of time (duration) of irradiation. Note that this formula involves two components: the number of incident photons at any given moment and the duration of exposure. The standard units for fluence are micromoles of quanta (photons) per square meter (μmol m^{-2}). Some responses are sensitive not only to the total fluence but also to the **irradiance**, or fluence rate, of light. The units of irradiance are micromoles of quanta per square meter per second (μmol m^{-2} s^{-1}). (For definitions of these and other terms used in light measurement, see Chapter 9 and **WEB TOPIC 9.1**).

Because photochemical responses are stimulated only when a photon is absorbed by its photoreceptor, there can be a difference between incident irradiation and absorption. For example, in photosynthesis the apparent quantum efficiency is assessed as the electron transport rate or total carbon assimilation as a function

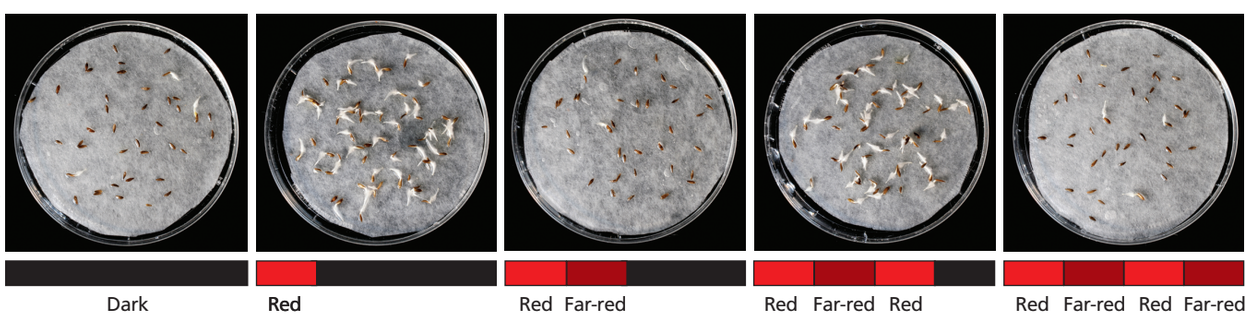


Figure 16.5 Lettuce seed germination is a typical photoreversible response controlled by phytochrome. Red light promotes lettuce seed germination, but this effect is reversed by far-red light. Imbibed (hydrated) seeds were given alternating treatments of red followed by far-red light. The effect of the light treatment depended on the last treatment given. Very few seeds germinated following the last far-red treatment.

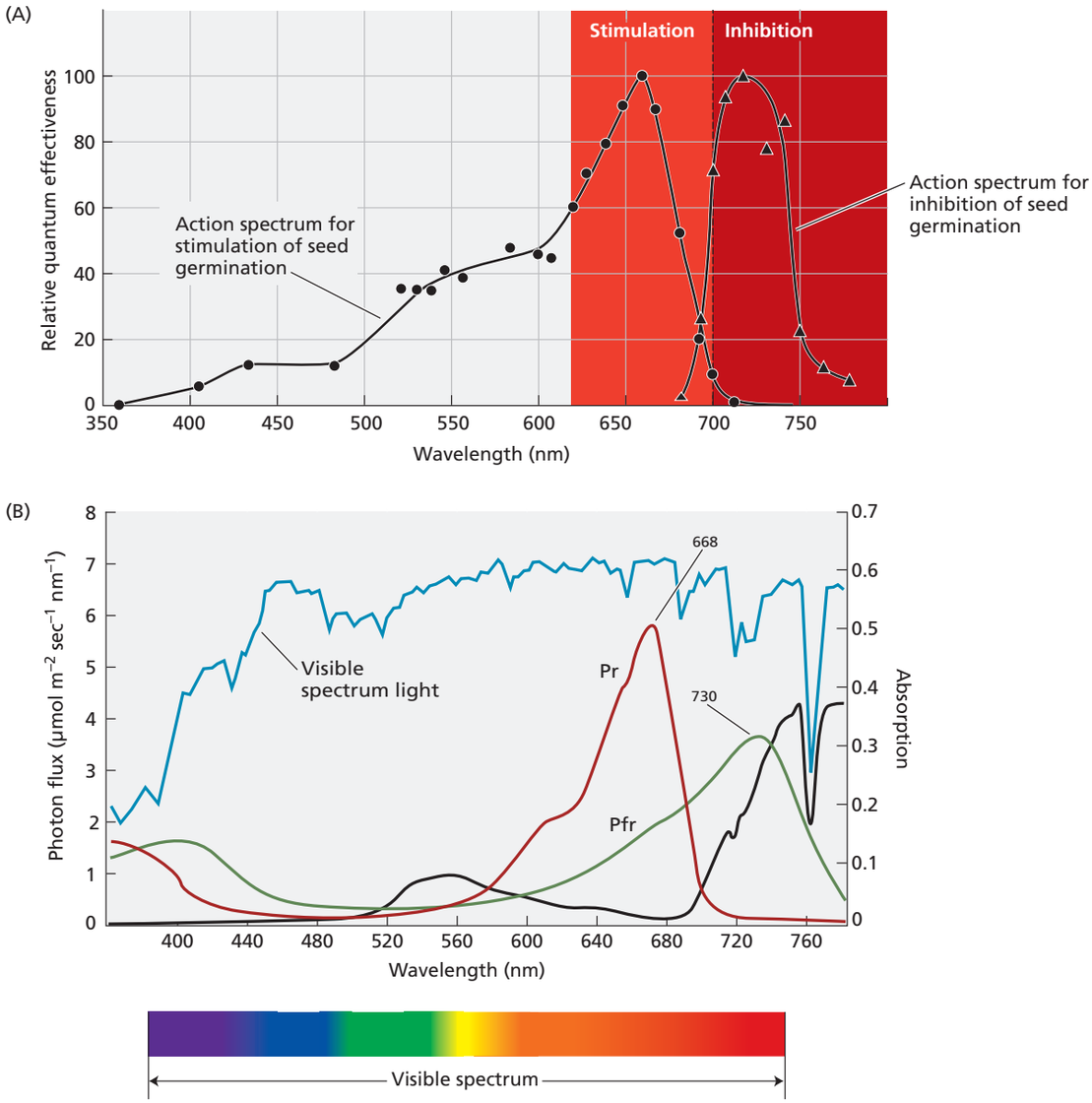


Figure 16.6 **The action spectrum of phytochrome function matches its absorption spectrum.** **(A)** Action spectra for the photoreversible stimulation and inhibition of seed germination in Arabidopsis. **(B)** Absorption spectra of purified oat phytochrome in the Pr (red line) and Pfr (green line) forms overlap. At the top of the canopy, there is a relatively uniform distribution of visible-spectrum light (blue line), but under a dense canopy much of the red light is absorbed by plant pigments, resulting in transmittance of mostly far-red light. The black line shows the spectral properties of light that is filtered through a leaf. Thus, the relative proportions of Pr and Pfr are determined by the degree of vegetative shading in the canopy. (A after W. Shropshire et al. 1961. *Plant Cell Physiol.* 2: 63–69; B after J. M. Kelly and J. C. Lagarias. 1985. *Biochemistry* 24: 6003–3010, courtesy of Patrice Dubois.)

of the incident photosynthetic photon flux density (PPFD). However, this measure underestimates the *actual* quantum efficiency because not all the incident photons are absorbed. This caveat is also important in assessing the dose response of the photomorphogenic responses of green plants to red or blue light, because much of the light is absorbed by chlorophyll. The same principle applies to the responses to UV radiation, since the epidermis may absorb just under 100% of the incident UV radiation. Thus, the amount of radiation required to induce a photoresponse may be quite high based on the amount of incident irradiation required and quite low based on actual photon absorption by the photoreceptor.

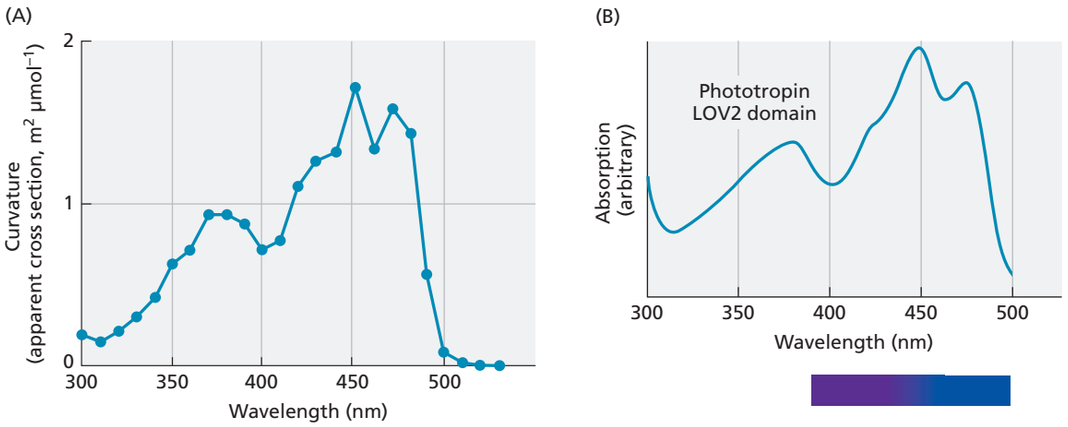


Figure 16.7 The action spectrum of phototropism matches the absorption spectrum of the light-sensing domain of phototropin. (A) Action spectrum for blue light–stimulated phototropism in alfalfa hypocotyls. The "three-finger" pattern in the 400- to 500-nm region is characteristic of many blue-light responses. (B) The absorption spectrum of the light-sensing domain of phototropin. (A after T. I. Baskin and M. Iino. 1987. *Photochem. Photobiol.* 46: 127–136; B after W. R. Briggs and J. M. Christie. 2002. *Trends Plant Sci.* 7: 204–210.)

16.2 Phytochromes

Phytochromes were first identified in flowering plants as the photoreceptors responsible for photomorphogenesis in response to red and far-red light. However, they are members of a gene family present in all land plants, and have also been found in streptophyte algae, cyanobacteria, other bacteria, fungi, and diatoms. For example, **bacteriophytochromes** (**BphPs**) regulate the biosynthesis of the photosynthetic apparatus in *Rhodopseudomonas palustris*, and of pigments in *Deinococcus radiodurans* and *Rhodospirillum centenum*. The phytochrome from the filamentous fungus *Aspergillus nidulans* appears to play a role in sexual development. These functions of bacterial and fungal phytochromes are thus conceptually analogous to photomorphogenesis in flowering plants.

Because neither red nor far-red light penetrate water to depths greater than a few meters, phytochrome would appear to be less useful as a photoreceptor for aquatic organisms. However, recent studies have shown that different algal phytochromes can sense orange, green, or even blue light, suggesting that phytochromes have the potential to be spectrally tuned during natural selection to absorb different wavelengths.

Phytochrome is the primary photoreceptor for red and far-red light

Phytochrome is a cyan-blue (midway between green and blue) or cyan-green protein with a subunit molecular mass of about 125 kilodaltons (kDa). Many of the biological properties of phytochrome were established in the 1930s through studies of red light–induced morphogenic responses, especially seed germination. A key breakthrough in the history of phytochrome was the discovery that the effects of red light (620–700 nm) could be reversed by a subsequent irradiation with far-red light (700–750 nm). This phenomenon was first demonstrated in germinating lettuce seeds (see Figure 16.5) but was also observed in stem and leaf growth, as well as in floral induction and other developmental phenomena (**Table 16.2**). The reversibility of the red and far-red responses ultimately led to the discovery that a single photoreversible photoreceptor, phytochrome, was responsible for both activities. It was subsequently demonstrated that the two forms of phytochrome could be distinguished spectroscopically (see Figure 16.6B).

Phytochrome can interconvert between Pr and Pfr forms

In dark-grown, or etiolated, seedlings, phytochrome is present in a red light–absorbing form, referred to as **Pr**. This cyan-blue-colored inactive form is converted by red light to a far-red light–absorbing form called **Pfr**, which is pale cyan-green in color and is considered to be the active form of phytochrome. Pfr can revert back to inactive Pr in darkness, but this is a relatively slow process. However, Pfr can be rapidly converted to Pr by irradiation with far-red light. This conversion–reconversion property, termed **photoreversibility** (also referred to as *photochromism*), is the most distinctive feature of phytochrome and can be measured in vivo or in vitro with almost identical results. It is often diagrammed as follows:

$$\mathrm{Pr} \underset{\text{Far-red light}}{\overset{\text{Red light}}{\rightleftharpoons}} \mathrm{Pfr} \qquad \text{Equation 1}$$

Photoreversibility is thus a defining feature of phytochromes. Even algal phytochromes with peak absorbances

Table 16.2 Typical photoreversible responses induced by phytochrome in a variety of higher and lower plants

Group	Genus	Stage of development	Effect of red light
Angiosperms	*Lactuca* (lettuce)	Seed	Promotes germination
	Avena (oat)	Seedling (etiolated)	Promotes de-etiolation (e.g., leaf unrolling)
	Sinapis (mustard)	Seedling	Promotes formation of leaf primordia, development of primary leaves, and production of anthocyanins
	Pisum (pea)	Adult	Inhibits internode elongation
	Xanthium (cocklebur)	Adult	Inhibits flowering (photoperiodic response)
Gymnosperms	*Pinus* (pine)	Seedling	Enhances rate of chlorophyll accumulation
Pteridophytes	*Onoclea* (sensitive fern)	Young gametophyte	Promotes growth
Bryophytes	*Polytrichum* (moss)	Germling	Promotes replication of plastids
Chlorophytes	*Mougeotia* (alga)	Mature gametophyte	Promotes orientation of chloroplasts to directional dim light

in the orange, green, or blue regions of the spectrum exhibit photoreversibility at a different wavelength.

It is important to note that the phytochrome pool is never fully converted to the Pfr or Pr forms following red or far-red irradiation, because the absorption spectra of the Pfr and Pr forms overlap. Thus, when Pr molecules are exposed to red light, most of them absorb the photons and are converted to Pfr, but some of the Pfr made also absorbs the red light and is converted back to Pr (see Figure 16.6B). The proportion of phytochrome in the Pfr form after saturating irradiation by red light is only about 88%. Similarly, the very small amount of far-red light absorbed by Pr makes it impossible to convert Pfr entirely to Pr by broad-spectrum far-red light. Instead, an equilibrium of 98% Pr and 2% Pfr is achieved. This equilibrium is termed the **photostationary state**. Pfr will also revert back to Pr in the absence of red light. This process, known as *thermal reversion*, contributes to the photostationary state and is sensitive to changes in temperature, which can affect phytochrome performance, leading to the proposal that phytochrome can also function as a temperature sensor.

Pfr is the physiologically active form of phytochrome

Because phytochrome responses are induced by red light, they could, in theory, result from either the appearance of Pfr or the disappearance of Pr. In most cases studied, a quantitative relationship holds between the magnitude of the physiological response and the amount of Pfr generated by light, but no such relationship holds between the physiological response and the loss of Pr. Evidence such as this has led to the conclusion that Pfr is the physiologically active form of phytochrome.

The use of narrow waveband red (R) and far-red (FR) light was central to the discovery and eventual isolation of phytochrome. However, unlike the plants used in laboratory-based photobiological experiments, a plant growing outdoors is never exposed to pure "red" or "far-red" light. In natural settings plants are exposed to a much broader spectrum of light, and it is under these conditions that phytochrome must work to regulate developmental responses to changes in the light environment. Indeed, as shown in Figure 16.6B, the plant canopy itself can have a dramatic effect on both the quantity and quality of incident light reaching individual plants. Of particular importance is the red:far red (R:FR) ratio, which is strongly affected by the presence of a canopy because chlorophyll absorbs red but not far-red light (see Table 16.1). Thus, as we will discuss in Chapter 18, plants growing beneath a canopy use phytochrome to sense the R:FR ratio in regulating such processes as shade avoidance, competitive interactions, and seed germination.

The phytochrome chromophore and protein both undergo conformational changes in response to red light

Phytochrome in the functionally active dimeric form is a soluble protein with a molecular mass of about 250 kDa. The evolutionary origin of phytochrome is ancient, predating the appearance of eukaryotes. Bacterial phytochromes are light-dependent histidine kinases that function as **sensor proteins** that phosphorylate corresponding **response regulator** proteins (see Chapter 4). However, as discussed shortly, phytochromes retain a histidine kinase–related domain, which is characteristic of bacterial two-component systems.

In higher plants the phytochrome chromophore is a linear tetrapyrrole called **phytochromobilin** (**Figure 16.8**). Phytochromobilin is synthesized inside plastids and is derived from heme via a pathway that branches

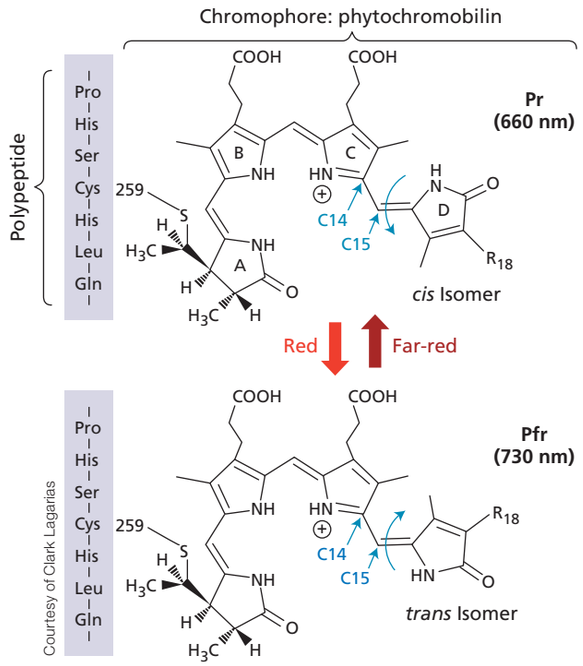


Figure 16.8 **Structure of the Pr and Pfr forms of the tetrapyrrole (A–D) chromophore (phytochromobilin) and the peptide region bound to the chromophore through a thioether linkage.** The chromophore undergoes a *cis–trans* isomerization at carbon 15 in response to red and far-red light. (After F. Andel et al. 1996. *Biochemistry* 35 (50): 15997–16008, courtesy of Clark Lagarias)

from the chlorophyll biosynthetic pathway. Phytochromobilin is exported from the plastid to the cytosol where it autocatalytically attaches to the PHY apoprotein through a thioether linkage to a cysteine residue. (Thioether linkages are ethers in which the oxygen is replaced by a sulfur: R^1—S—R^2.) There are three phytochrome isoforms in most angiosperms (phyA–C), although many broadleaf plant species contain up to five (phyA–E). Each phy isoform is encoded by a separate gene, and each plays a unique role in development.

Figure 16.9A illustrates several of the structural domains in phytochrome. The N-terminal half of phytochrome contains **PAS** and **GAF** domains that covalently bind the chromophore and confer bilin-lyase activity. The N-terminus also includes the **PHY** domain, which stabilizes phytochrome in the Pfr form. The **PAS-GAF-PHY** domains comprise the chromophore-binding, photosensory region of phytochrome. A "hinge" region separates the N-terminal and C-terminal halves of the molecule. The crystal structure of the light-sensing N-terminal half of Arabidopsis phyB is shown in **Figure 16.9B**.

Downstream of the hinge region are two **PAS-related domain** (**PRD**) repeats that mediate phytochrome dimerization. The PRD has been implicated in targeting the Pfr form of phyB to the nucleus, although it lacks a canonical nuclear localization signal (NLS). The C-terminal region of plant phytochromes contains an ATP-binding histidine kinase–related domain (HKRD) that does not target histidine residues for phosphorylation.

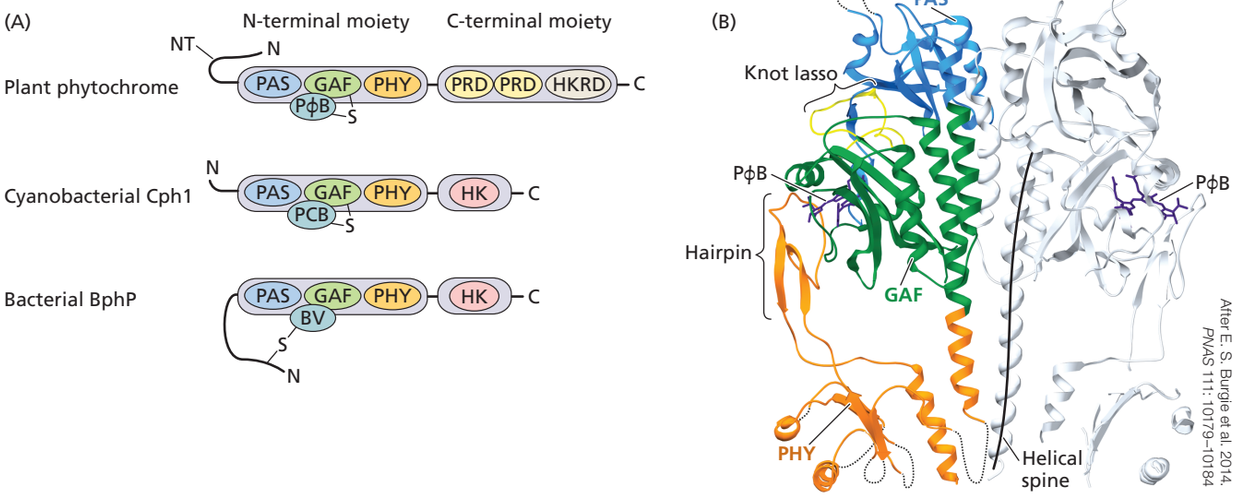


Figure 16.9 **Phytochrome domains and their functions.** **(A)** Schematic representation of plant phytochrome (PHY), prokaryotic Cph1 (cyanobacterial phytochrome 1), and BphP (bacterial phytochrome-like protein). The chromophore is attached to cysteine residues in the proteins via a thioether link (–S–). Note that the cysteine residue that forms the linkage is located in the GAF domain in canonical phytochromes such as PHY and Cph1, whereas it is located in the N-terminal extension in BphP-type bacterial phytochromes. BV, biliverdin; HK, histidine kinase domain; HKRD, histidine kinase–related domain; NT, N-terminal extension; PφB, phytochromobilin; PRD (PAS-related domain). **(B)** Ribbon structure of the N-terminal, light-sensing half of the Pr form of the Arabidopsis PhyB dimer. The three domains are colored as follows: PAS, blue; GAF, green; PHY, orange. The chromophore phytochromobilin (PφB) is indicated in purple.

A comparison of the domain structures of plant phytochrome with the prokaryotic phytochromes Cph1 (*c*yanobacterial *ph*ytochrome *1*) and BphPs highlights several differences between plant and prokaryotic phytochromes, including the absence of the two PRD domains in prokaryotes and the substitution of the prokaryotic histidine kinase domain with the HKRD in plants (see Figure 16.9A). Although all phytochromes contain tetrapyrrole chromophores, phytochromobilin differs from the chromophores found in prokaryotic phytochromes.

Exposure of the Pr form of phytochrome to red light causes atomic-scale structural changes in the chromophore phytochromobilin: The Pr chromophore undergoes a *cis–trans* isomerization between carbons 15 and 16 and rotation of the C14—C15 single bond (see Figure 16.8). The change in the chromophore leads to the rearrangement of crucial secondary-structure elements in the protein.

Pfr is partitioned between the cytosol and the nucleus

The primary step in phytochrome signaling is when the photoreceptor migrates from the cytoplasm to the nucleus, which appears to be a conserved feature found in all phytochromes from algae to plants. In the cytosol, phytochrome holoproteins dimerize in the inactive Pr state (**Figure 16.10**). The conversion of Pr to Pfr by red light is associated with a conformational change in the dimer that is still unresolved. Both phyA and phyB move from the cytosol into the nucleus in a light-dependent fashion (**Figure 16.11**), but they do so by different mechanisms. Neither phyA nor phyB contains a canonical nuclear localization signal (NLS). The PRD domain of phyB can potentially serve as an NLS, but it is apparently masked in the Pr form. Conversion of Pr to Pfr by red light may expose the functional NLS of the PRD domain of phyB, facilitating phyB's import into the nucleus. In contrast, the PRD domain of phyA cannot act as an NLS, and it is therefore dependent on other proteins, such as **FAR-RED ELONGATED HYPOCOTYL1** (**FHY1**) and its homolog FHY1-LIKE (FHL), to transport it into the nucleus (see Figure 16.10).

Once in the nucleus, phytochromes interact with transcriptional regulators to mediate changes in gene transcription. Thus, one important function of phytochrome is

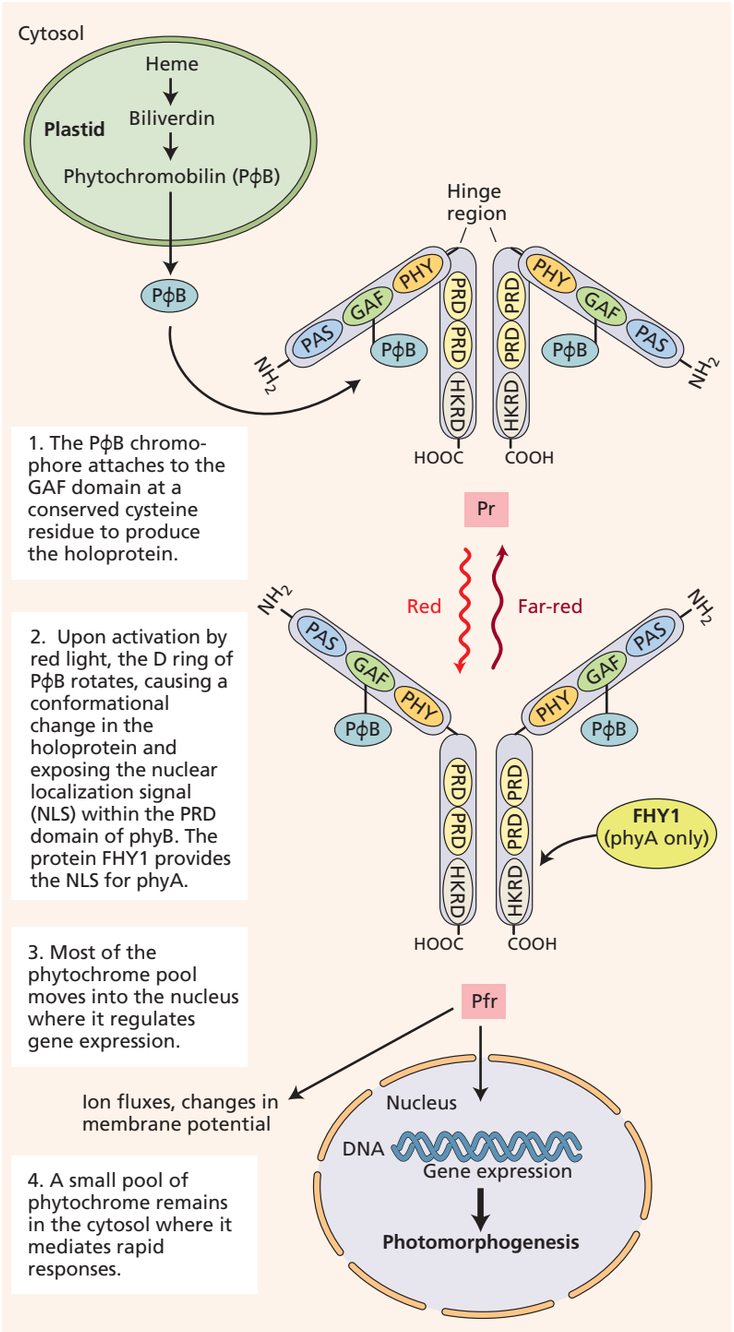
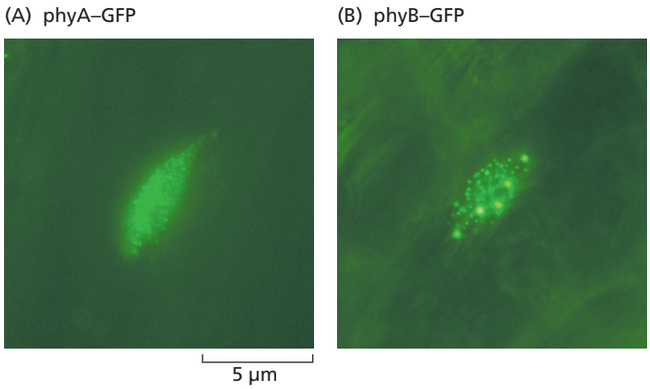


Figure 16.10 Steps in phytochrome activation and signal transduction in photomorphogenesis. After synthesis of phytochromobilin in the plastid and assembly with the apoprotein (1), phytochrome is activated by red light (2) and moves into the nucleus (3) to modulate gene expression. A small pool of phytochrome remains in the cytosol, where it may regulate rapid biochemical changes (4). Whereas phyB has its own nuclear localization signal, phyA requires the protein FHY1 to enter the nucleus. Several conserved domains of phytochrome are shown: PAS, GAF (contains bilin-lyase domain), PHY, PRD (PAS-related domain), and HKRD (histidine kinase–related domain). PΦB, phytochromobilin.



A and B from R. Yamaguchi et al. 1999. *J. Cell Biol.* 145: 437–445, courtesy of A. Nagatani

Figure 16.11 Nuclear localization of phy–GFP fusion proteins in epidermal cells of Arabidopsis hypocotyls. Transgenic Arabidopsis plants expressing phyA–GFP (A) or phyB–GFP (B) were exposed to either continuous far-red light (A) or continuous white or red light (B) and observed under a fluorescence microscope. Only nuclei are visible, demonstrating that the light treatments induced nuclear accumulation of the phy–GFP fusion proteins. In darkness, phy is absent from the nucleus. These results indicate a role for nuclear–cytoplasmic partitioning in controlling phytochrome signaling. The smaller bright green dots inside the nucleus in (B) are called "speckles." The number and size of these speckles have been correlated with light responsiveness.

to serve as a light-activated switch to bring about global changes in gene expression. However, as discussed in the next section, several phytochrome responses, such as the inhibition of stem elongation, occur extremely rapidly, within minutes or even seconds following exposure to red or far-red light. Thus, phytochromes can also play important roles in the cytosol, regulating membrane potentials and ion fluxes in response to red and far-red light.

16.3 Phytochrome Responses

The variety of different phytochrome responses in intact plants is extensive, in terms of both the kinds of responses (see Table 16.2) and the quantity of light needed to induce the responses. A survey of this variety will show how diversely the effects of a single photoevent—the absorption of light by Pr—are manifested throughout the plant. For ease of discussion, phytochrome-induced responses may be logically grouped into two types:

- Rapid biochemical events
- Slower morphological changes, including movements and growth

Some of the early biochemical reactions affect later developmental responses. The nature of these early biochemical events, which comprise signal transduction pathways, is treated in detail later in the chapter. Here we focus on the effects of phytochrome on whole-plant responses. As we will see, such responses can be classified into various types depending on the amount and duration of light required and on their action spectra.

Phytochrome responses vary in lag time and escape time

Morphological responses to the photoactivation of phytochrome are often observed visually after a *lag time*—the time between stimulation and the observed response. The lag time may be as brief as a few minutes or as long as several weeks. These differences in response times result from the multiple signal transduction pathways that function downstream of phytochrome signaling as well as interactions with other developmental mechanisms. The more rapid of these responses are usually reversible movements of organelles (see **WEB TOPIC 16.1**) or reversible volume changes (swelling, shrinking) in cells, but even some growth responses are remarkably fast. For instance, red-light inhibition of the stem elongation rate of light-grown pigweed (*Chenopodium album*) and Arabidopsis is observed within minutes after the proportion of Pfr to Pr in the stem is increased. However, lag times of several weeks are observed for the induction of flowering in Arabidopsis and other species.

Variety in phytochrome responses can also be seen in the phenomenon called **escape from photoreversibility**. Red light–induced events are reversible by far-red light for only a limited period of time, after which the response is said to have "escaped" from reversal control by light. This escape phenomenon can be explained by a model based on the assumption that phytochrome-controlled morphological responses are the end result of a multistep sequence of linked biochemical reactions in the responding cells. Early stages in the sequence may be fully reversible by removing Pfr, but at some point in the sequence a point of no return is reached, beyond which the reactions proceed irreversibly toward the response. The escape time therefore represents the amount of time it takes before the overall sequence of reactions becomes irreversible—essentially, the time it takes for Pfr to complete its primary action. The escape time for different phytochrome responses ranges remarkably, from less than a minute to hours.

Phytochrome responses fall into three main categories based on the amount of light required

As **Figure 16.12** shows, phytochrome responses fall into three major categories based on the amount of light they require: very low fluence responses (VLFRs), low-fluence responses (LFRs), and high-irradiance responses (HIRs).

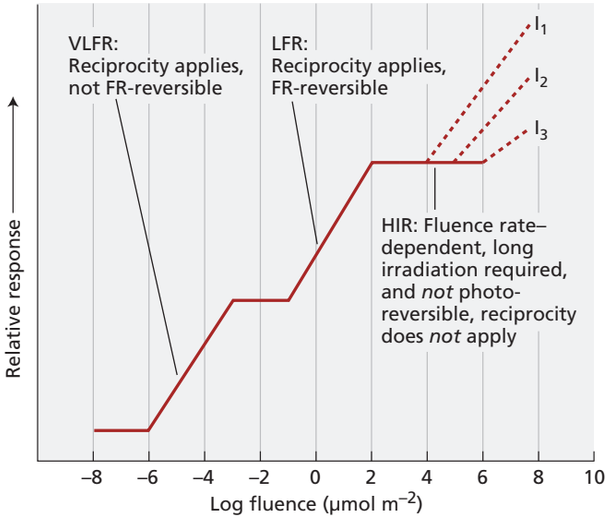


Figure 16.12 Three types of phytochrome responses, based on their sensitivities to fluence. The relative magnitudes of representative responses are plotted against increasing fluences of red light. Short light pulses activate very low fluence responses (VLFRs) and low-fluence responses (LFRs).The fluence at which LFRs are intiated vary with species. Because high-irradiance responses (HIRs) are proportional to irradiance as well as to fluence, the effects of three different irradiances given continuously are illustrated by dashed lines ($I_1 > I_2 > I_3$). (After W. R. Briggs et al. 1984. In *Sensory Perception and Transduction in Aneural Organisms*, G. Columbetti et al. [eds.], Plenum, New York, pp. 265–280.)

VLFRs and LFRs have a characteristic range of light fluences within which the magnitude of the response is proportional to the fluence. HIRs, however, are proportional to the irradiance.

VERY LOW FLUENCE RESPONSES (VLFRS) Some phytochrome responses can be initiated by fluences as low as 0.0001 μmol m^{-2} (a few seconds of starlight, or one-tenth of the amount of light emitted by a firefly in a single flash), and they become saturated (i.e., reach a maximum) at about 0.05 μmol m^{-2}. For example, Arabidopsis seeds can be induced to germinate with red light in the range of 0.001 to 0.1 μmol m^{-2}. In dark-grown oat (*Avena* spp.) seedlings, red light can stimulate the growth of the coleoptile and inhibit the growth of the mesocotyl (the elongated axis between the coleoptile and the root) at similarly low fluences.

VLFRs are non-photoreversible. The minute amount of light needed to induce VLFRs converts less than 0.02% of the total phytochrome to Pfr. Because the far-red light that would normally reverse a red-light effect converts only 98% of the Pfr to Pr (as discussed earlier), about 2% of the phytochrome remains as Pfr—significantly more than the 0.02% needed to induce VLFRs. In other words, far-red light cannot lower the Pfr concentration below 0.02%, so it is unable to inhibit VLFRs. Although VLFRs are non-photoreversible, the action spectrum for VLFR responses (e.g., seed germination) is similar to those for LFR responses (discussed next), supporting the view that phytochrome is the photoreceptor involved in VLFRs. This hypothesis was confirmed using phytochrome-deficient mutants, as described later in the chapter.

LOW-FLUENCE RESPONSES (LFRS) Another set of phytochrome responses cannot be initiated until the fluence reaches 1.0 μmol m^{-2}, and they are saturated at about 1000 μmol m^{-2}. These low-fluence responses (LFRs) include processes such as the promotion of lettuce seed germination, inhibition of hypocotyl elongation, and regulation of leaf movements (see Table 16.2). As we saw in Figure 16.6, the LFR action spectrum for Arabidopsis seed germination includes a main peak for stimulation in the red region (660 nm) and a major peak for inhibition in the far-red region (720 nm).

Both VLFRs and LFRs can be induced by brief pulses of light, provided that the total amount of light energy adds up to the required fluence. The total fluence is a function of two factors: the fluence rate (μmol m^{-2} s^{-1}) and the time of irradiation. Thus, a brief pulse of red light will induce a response, provided that the light is sufficiently bright, and conversely, very dim light will work if the irradiation time is long enough. This reciprocal relationship between fluence rate and time is known as the **law of reciprocity**. VLFRs and LFRs both obey the law of reciprocity; that is, the magnitude of the response (e.g., percent germination or degree of inhibition of hypocotyl elongation) is dependent on the product of the fluence rate and the time of irradiation.

However, reciprocity holds true only when photon absorption by the photoreceptor studied is the rate-limiting step in the response being studied. Reciprocity is confounded when any step between photoreceptor activation and the response measured (e.g., hypocotyl elongation) becomes limiting. Thus, the concept of reciprocity is difficult to demonstrate for many responses.

HIGH-IRRADIANCE RESPONSES (HIRS) Phytochrome responses of the third type are termed high-irradiance responses (HIRs), several of which are listed in **Table 16.3**. HIRs require prolonged or continuous exposure to light of relatively high irradiance. The response is proportional to the irradiance until the response saturates and additional light has no further effect (see **WEB TOPIC 16.2**). The reason these responses are called high-irradiance responses rather than high-fluence responses is that they are proportional to fluence rate—the number of photons striking the plant tissue per second—rather than to fluence—the total number of photons striking the plant in a given period

Table 16.3 Some plant photomorphogenic responses induced by high irradiances

Synthesis of flavonoids, including anthocyanins, in various eudicot seedlings and in apple skin segments
Inhibition of hypocotyl elongation in mustard, lettuce, and petunia seedlings
Induction of flowering in henbane (*Hyoscyamus*)
Plumular hook opening in lettuce
Enlargement of cotyledons in mustard
Production of ethylene in sorghum

of illumination. HIRs saturate at much higher fluences than LFRs—at least 100 times higher. Because neither continuous exposure to dim light nor transient exposure to bright light can induce HIRs, these responses do not obey the law of reciprocity.

Many of the LFRs listed in Table 16.2, particularly those involved in de-etiolation, also qualify as HIRs. For example, at low fluences the action spectrum for anthocyanin production in seedlings of white mustard (*Sinapis alba*) is indicative of phytochrome and shows a single peak in the red region of the spectrum. The effect is reversible with far-red light (a photochemical property unique to phytochrome), and the response obeys the law of reciprocity. However, if the dark-grown seedlings are instead exposed to high-irradiance light for several hours, the action spectrum contains peaks in the far-red and blue regions, the effect is no longer photoreversible, and the response becomes proportional to the irradiance. Thus, the same effect can be either a LFR or a HIR, depending on the history of a seedling's exposure to light. As we will discuss in the remainder of this section, different phytochrome molecules are responsible for these various types of responses.

Phytochrome A mediates responses to continuous far-red light

Arabidopsis contains five genes encoding phytochromes, *PHYA–PHYE*. Four of the five phytochromes, phyB–phyE, appear to be mostly light-stable in the plant and function primarily in the regulation of LFRs such as shade avoidance involving changes in the R:FR ratio. In contrast, phyA is rapidly degraded as Pfr and controls plant VLFRs and far-red HIRs. Recent studies suggest that phyB also is degraded in the nucleus along with its phytochrome interacting factor (PIF) targets during signaling. Thus, Pfr turnover appears to be a conserved property of plant phytochromes.

In early mutant screens of Arabidopsis, mutations in phyB were identified in mutants with altered hypocotyl elongation under continuous white light, collectively termed *hy* mutants. Continuous white light is detected by the light-stable phytochromes, phyB–phyE. Since far-red HIRs were known to require light-labile phytochrome, it was suspected that phyA must be the photoreceptor involved in the perception of continuous far-red light. Screens of mutants that fail to respond to continuous far-red light and instead grow tall and spindly led to the identification of phyA mutants as well as additional mutants that were defective in chromophore formation, indicating that phyA mediates the response to continuous far-red light.

Mutants lacking phyA also failed to germinate in response to millisecond pulses of light, but showed a normal response to red light in the low-fluence range (mediated by phyB). This result demonstrates that phyA also functions as the primary photoreceptor for this VLFR. When *phyA/phyB* double mutants are grown under high-fluence red light (>100 μmol m^{-2} s^{-1}), they are even more elongated than the *phyB* single mutant. PhyA has also been shown to play a role in the photoperiod control of flowering in Arabidopsis and rice.

Phytochrome B mediates responses to continuous red or white light

The characterization of the *hy3* mutant revealed an important role for phyB in de-etiolation, since mutant seedlings grown in continuous white light had long hypocotyls. The *phyB* mutant is deficient in chlorophyll and in some mRNAs that encode chloroplast proteins, and it is impaired in its ability to respond to plant hormones.

In addition to regulating white and red light–mediated HIRs, phyB also appears to regulate LFRs, such as photoreversible seed germination, the phenomenon that originally led to the discovery of phytochrome. Wild-type Arabidopsis seeds require light for germination, and the response shows red/far-red reversibility in the low-fluence range (see Figure 16.6A). Mutants that lack phyA respond normally to red light, whereas mutants deficient in phyB are unable to respond to low-fluence red light. This experimental evidence strongly suggests that phyB mediates photoreversible seed germination.

PhyB also plays an important role in regulating plant responses to shade treatments. Plants that are deficient in phyB often look like wild-type plants that are grown under dense vegetative canopies. In fact, mediating responses to vegetative shade such as accelerated flowering and increased elongation growth may be one the most ecologically important roles of phytochromes (see Chapter 18).

Roles for phytochromes C, D, and E are emerging

Although phyA and phyB are the predominant forms of phytochrome in Arabidopsis, phyC, phyD, and phyE play unique roles in regulating responses to red and

far-red light. The creation of double and triple mutants has made it possible to assess the relative role of each phytochrome in a given response. phyD and phyE are structurally similar to phyB but are not functionally redundant. Responses mediated by phyD and phyE include petiole and internode elongation (see Chapter 18) and the control of flowering time (see Chapter 20). The characterization of *phyC* mutants in Arabidopsis suggests a complex interplay between phyC, phyA, and phyB response pathways. This specialization in phytochrome gene function is likely to be important in fine-tuning phytochrome responses to daily and seasonal changes in light regimes. Light-stable phytochromes are known to heterodimerize. Thus, their relative expression will determine light responsiveness. Indeed, their relative expression can vary among plant species, accounting for differences in light responsiveness.

16.4 Phytochrome Signaling Pathways

All phytochrome-regulated changes in plants begin with absorption of light by the photoreceptor. After light absorption, the molecular properties of phytochrome are altered, affecting the interaction of the phytochrome protein with other cellular components that ultimately bring about changes in the growth, development, or position of an organ (see Tables 16.2 and 16.3).

Molecular and biochemical techniques are helping unravel the early steps in phytochrome action and the signal transduction pathways that lead to physiological or developmental responses. These responses fall into two general categories:

- Ion fluxes, which cause relatively rapid turgor responses
- Altered gene expression, which typically results in slower, longer-term responses

In this section we examine the effects of phytochrome on both membrane permeability and gene expression, as well as the possible chain of events constituting the signal transduction pathways that bring about these effects.

Phytochrome regulates membrane potentials and ion fluxes

Phytochrome can rapidly alter phosphoinositol composition in isolated pulvinus cells that exhibit rapid turgor changes within seconds of a light pulse. Such rapid membrane modulation has been inferred from the effects of red and far-red light on the surface potential of roots and oat coleoptiles, in which the lag time between the production of Pfr and the onset of measurable hyperpolarization (membrane potential changes) is brief. Changes in the electrical potential of these cells imply changes in the flux of ions across the plasma membrane and suggest that some of the cytosolic responses of phytochrome are initiated at or near the plasma membrane.

One long-standing conundrum has been how the filamentous green alga *Mougeotia* uses red light to stimulate rapid chloroplast movement (see **WEB TOPIC 16.1**). In many species, including Arabidopsis, chloroplast movements are mediated by blue light through the action of phototropin photoreceptor proteins. In *Mougeotia*, the photoreceptor that regulates chloroplast movements consists of a fusion between phytochrome and a phototropin known as **neochrome**, which shows typical bilin binding as well as red/far-red reversibility. Thus, *Mougeotia* appears to have evolved the ability to exploit red light as a signal to induce a response (chloroplast movement) that is typically mediated by blue light.

Phytochrome regulates gene expression

As the term *photomorphogenesis* implies, plant development is profoundly influenced by light. Elongated stems, folded cotyledons, and the absence of chlorophyll characterize the development of dark-grown, etiolated seedlings. Complete reversal of these symptoms by light involves major long-term alterations in metabolism that can only be brought about by changes in gene expression. Light-regulated plant promoters are similar to those of other eukaryotic genes: a collection of modular elements, the number, position, flanking sequences, and binding activities of which can lead to a wide range of transcriptional patterns. No single DNA sequence or binding protein is common to all phytochrome-regulated genes.

At first, it may appear paradoxical that light-regulated genes have such a range of regulatory elements, any combination of which can confer light-regulated expression. However, as discussed in Chapter 3, such complex promoter elements allow for the differential light- and tissue-specific regulation of many genes through the action of multiple photoreceptors.

The stimulation and repression of transcription by light can be very rapid, with lag times as short as 5 min. Using DNA microarray analysis, global patterns of gene expression in response to changes in light can be monitored. (For a discussion of methods for transcriptional analysis, see **WEB TOPIC 3.4**.) These studies have indicated that nuclear import triggers a transcriptional cascade involving thousands of genes that are involved in photomorphogenic development. By monitoring gene expression profiles over time following a shift of plants from darkness to light, both early and late targets of *PHY* gene action have been identified.

The nuclear import of phyA and phyB is highly correlated with the light quality that stimulates their activities. That is, nuclear import of phyA is activated by either red or far-red light, or low-fluence broad-spectrum light, whereas phyB import is driven by red-light exposure and is reversible by far-red light. Nuclear import

of the phytochrome proteins represents a major control point in phytochrome signaling.

Some of the early gene products that are rapidly up-regulated following a shift from darkness to light are themselves transcription factors that activate the expression of other genes. The genes encoding these rapidly up-regulated proteins are called **primary response genes**. Expression of the primary response genes depends on signal transduction pathways (discussed next) and is independent of protein synthesis. In contrast, the expression of the late genes, or **secondary response genes**, requires the synthesis of new proteins.

Phytochrome interacting factors (PIFs) act early in signaling

Phytochrome interacting factors (**PIFs**) are a family of basic helix-loop-helix (bHLH) transcription factors that regulate various aspects of phytochrome-mediated activity, including photomorphogenesis, seed germination, chlorophyll biosynthesis, shade avoidance, and hypocotyl elongation. PIFs promote etiolated development in the dark (**skotomorphogenesis**) primarily by serving as transcriptional activators of dark-induced genes (**Figure 16.13A**), and also by repressing some light-induced genes (**Figure 16.13B**). PIFs that interact with *either* phyA or phyB define branch points in the phy signaling networks, whereas proteins that interact with *both* phyA and phyB are likely to represent points of convergence. One of the most extensively characterized of these factors is **PIF3**, which interacts with *both* phyA and phyB. PIF3 and several related PIF or **PIF-like proteins** (**PILs**) are particularly notable because at least five members of this gene family selectively interact with phytochromes in their active Pfr conformations. The fact that these proteins are localized to the nucleus and can bind to DNA suggests an intimate association between phytochrome and gene transcription.

Under high R:FR ratios, Pfr formation initiates the degradation of PIF proteins through phosphorylation, followed by degradation via the proteasome complex (see Chapters 1 and 4). The rapid degradation of PIFs may provide a mechanism for modulating light responses that is tightly coupled to the activities of phy proteins. For instance, under low R:FR ratios that induce shade avoidance (see Chapter 18), PIF7 is dephosphorylated and binds to DNA in the promoters of target genes. PIF7 interactions with a subunit of a conserved chromatin remodeling complex known as INO80 results in eviction of the of a specialized Histone 2A subunit (see Chapter 3) known as H2A.Z that normally strongly binds DNA to prevent transcription. Eviction of H2A.Z results in increased transcription. Phosphorylation of PIF7 under white light or high R:FR ratios, as in emergence from shade, resets the system and represses transcription.

Phytochrome signaling involves protein phosphorylation and dephosphorylation

Reversible phosphorylation plays an important role in regulating phytochrome signaling. Phytochromes themselves are phosphorylated, and this posttranslational modification can modulate their rate of thermal reversion and affect their photosensitivity in Arabidopsis. Knowledge of the kinases and phosphatases responsible for controlling phytochrome phosphorylation is limited.

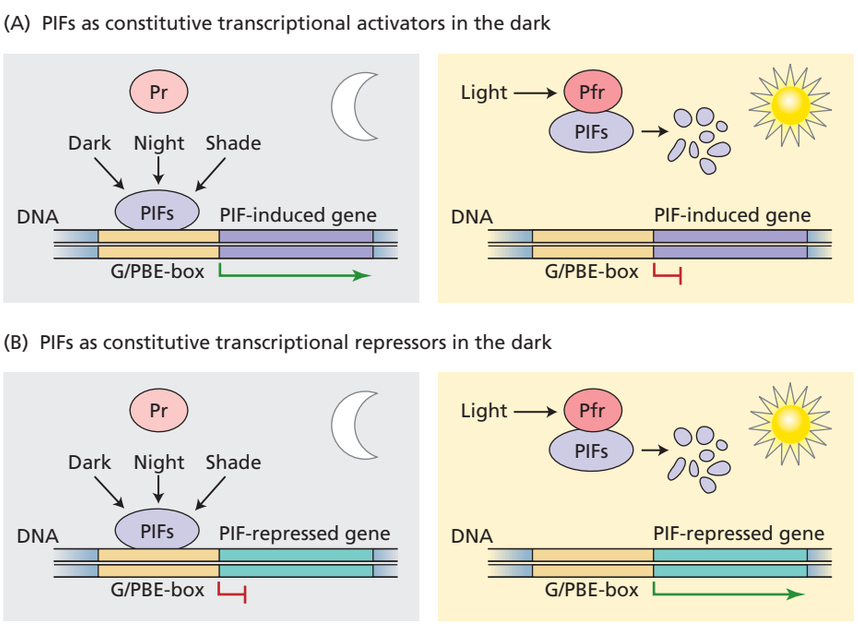


Figure 16.13 **Phytochrome interacting factors (PIFs) act as negative regulators of photomorphogenesis.** (A) Most PIFs are constitutive activators of genes that are expressed in the dark or in response to shade. In the light, Pfr promotes degradation of the PIFs, blocking the transcription of skotomorphogenesis genes. (B) During de-etiolation, PIFs also can act as constitutive repressors of some light-induced genes by binding to either G-Box motifs or (CACGTG) or PIF Binding Elements (CACATG) that are collectively referred to as G/PBE boxes. Pfr causes the turnover of these PIFs, allowing the expression of photomorphogenesis genes. (After P. Leivar and E. Monte. 2014. *Plant Cell* 26: 56–78.)

Although recent evidence adds to an ongoing debate as to whether phytochrome itself possesses phosphotransfer activity, phytochrome is known to control the phosphorylation status of signaling partners such as PIF3 through the action of photoregulatory kinases. A group of membrane-associated **phytochrome kinase substrate** (**PKS**) proteins appears to modify phytochrome activity via phosphorylation either directly or via interactions with other kinases. PKS1 interacts with phyA and phyB in both the active Pfr and inactive Pr forms. Molecular and genetic analyses suggest that these proteins act selectively to promote phyA-mediated VLFR. Several phosphatases have also been shown to interact with phy and regulate its phosphorylation state.

Phytochrome-induced photomorphogenesis involves protein degradation

As discussed in Chapter 4, plant signal transduction pathways can involve the inactivation, degradation, or removal of repressor proteins. The phytochrome signaling pathway can also follow this general principle. For example, phyA is rapidly degraded following its activation by light. Thus, protein degradation, in addition to phosphorylation, is emerging as a ubiquitous mechanism regulating many cellular processes, including light and hormone signaling, circadian rhythms, and flowering time (for examples, see Chapter 4).

Genetic screens for Arabidopsis mutants that exhibit partial photomorphogenesis in the dark led to the discovery of the repressor proteins that regulate the light-dependent stability of phytochrome and transcription factors that activate gene expression associated with photomorphogenesis. In the dark, the E3-ligase component **CONSTITUTIVE PHOTOMORPHOGENESIS 1** (**COP1**) is recruited in the cytoplasm by a protein complex known as the COP 9 SIGNALOSOME (CSN) and moved into the nucleus. COP1 interacts with the protein kinase SUPPRESSOR OF PHYTOCHROME A1 (**SPA1**) to phosphorylate, ubiquitinate, and target for degradation photomorphogenic transcription factors, including PIF1 (**Figure 16.14**). The result is that photomorphogenic genes are not expressed in darkness.

In the light, COP1 activity is repressed by the action of photoreceptors, although the complete mechanism underlying COP1 inactivation in the light is unknown. Light-dependent export of COP1 to the cytoplasm is a

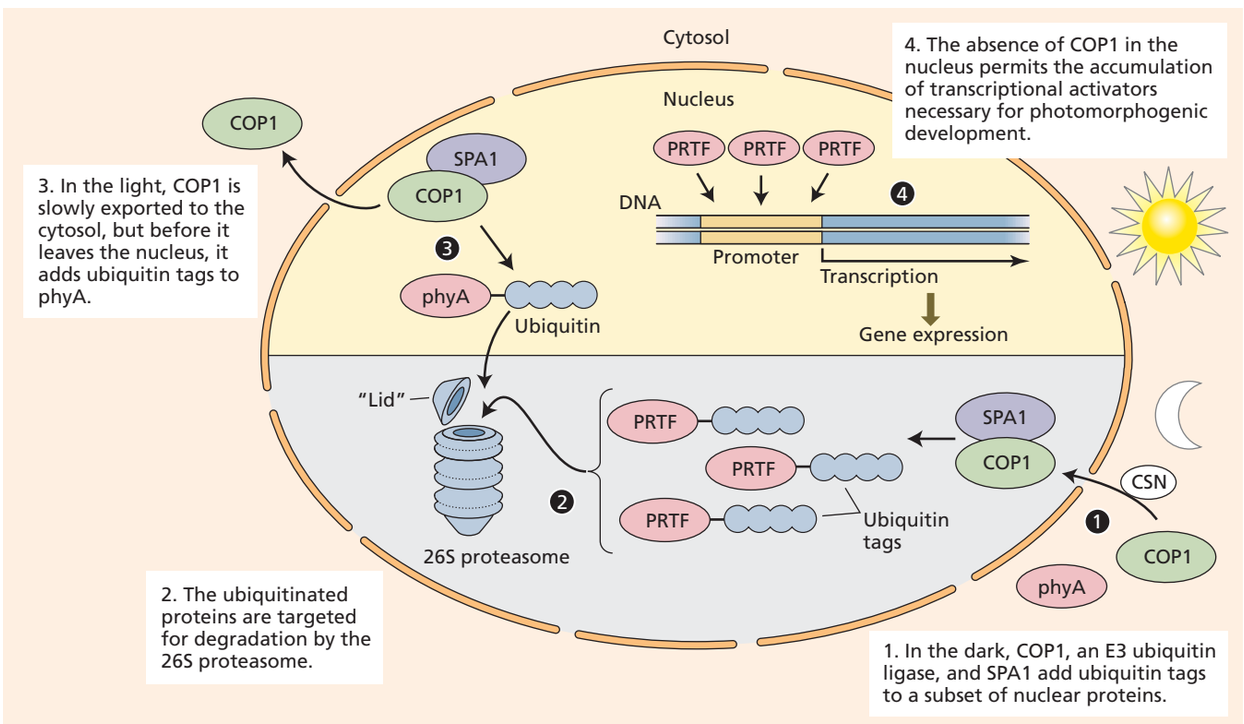


Figure 16.14 COP proteins regulate the turnover of proteins required for photomorphogenic development. During the night, COP1 enters the nucleus with the help of the COP9 signalosome complex (CSN). COP1 forms a complex with SUPPRESSOR OF PHYTOCHROME A1 (SPA1), and the COP1–SPA1 complex adds ubiquitin to a subset of phytochrome-responsive transcription factors (here abbreviated PRTF) that promote photomorphogenesis. The transcription factors are then degraded by the proteasome complex. During the day, COP1 exits the nucleus, allowing the transcriptional activators to accumulate.

slow process (see Figure 16.14), requires long exposure to light (more than 24 h), and is probably a mechanism to suppress COP1 activation under extended light conditions. Together, the repression of COP1 activity and export to the cytoplasm allow transcription factors to bind to promoter elements in genes that mediate photomorphogenic development.

As we will discuss in Chapter 20, COP1 is also required for degradation of the flowering regulators CONSTANS (CO) and GIGANTEA (GI).

16.5 Blue-Light Responses and Photoreceptors

Blue-light responses have been reported in higher plants, algae, ferns, fungi, and prokaryotes. In addition to phototropism, these responses include anion uptake in algae, inhibition of seedling hypocotyl (stem) elongation, stimulation of chlorophyll and carotenoid synthesis, activation of gene expression, and enhancement of respiration. Among motile unicellular organisms such as certain algae and bacteria, blue light mediates *phototaxis*, the movement of motile unicellular organisms toward or away from light. Blue light also stimulates the infection process in bacteria, such as the animal pathogen *Brucella abortus*. Some blue-light responses were introduced in relation to photosynthesis in Chapter 11, including chloroplast movements, solar tracking, and stomatal opening. In Chapter 17 several key blue-light responses —photoblasty, phototropism, and photomorphogenesis —will be discussed in the context of seed germination and seedling establishment.

Blue-light responses have characteristic kinetics and lag times

The inhibition of stem elongation and the stimulation of stomatal opening by blue light illustrate two important temporal properties of blue-light responses:

1. A significant lag time separating the light signal and the maximum response rate
2. Persistence of the response after the light signal has been switched off

Blue-light responses can be relatively rapid compared with most photomorphogenic changes. However, in contrast to typical photosynthetic responses, which are fully activated almost instantaneously after a "light on" signal, and which cease as soon as the light goes off, blue-light responses exhibit a lag time of variable duration and proceed at maximum rates for several minutes after application of a light pulse.

For example, blue light induces a decrease in growth rate and a transient membrane depolarization in etiolated cucumber seedlings only after a lag time of about 25 s (**Figure 16.15**). The persistence of blue-light responses in the absence of blue light has been studied using blue-light pulses. For example, blue light–induced activation of the H^+-ATPase in guard cells decays following a pulse of blue light, but only after several minutes have elapsed. This persistence of the blue-light response after the pulse can be explained by a photochemical cycle in which the physiologically active form of the photoreceptor, which has been converted from the inactive form by blue light, slowly reverts to the inactive form after the blue light is switched off. As we will discuss in Section 16.8, in the case of phototropins this cycle appears to involve four main processes: receptor dephosphorylation by a protein phosphatase, breaking the covalent carbon–sulfur bond with the cysteine side-chain in the apoprotein (see Figure 16.9), dissociation of the receptor from its target molecules, and the dark reversion of light-driven conformational changes. The rate of decay of the response to a blue-light pulse would thus depend on the time course of the reversion of the active form of the photoreceptor back to the inactive form.

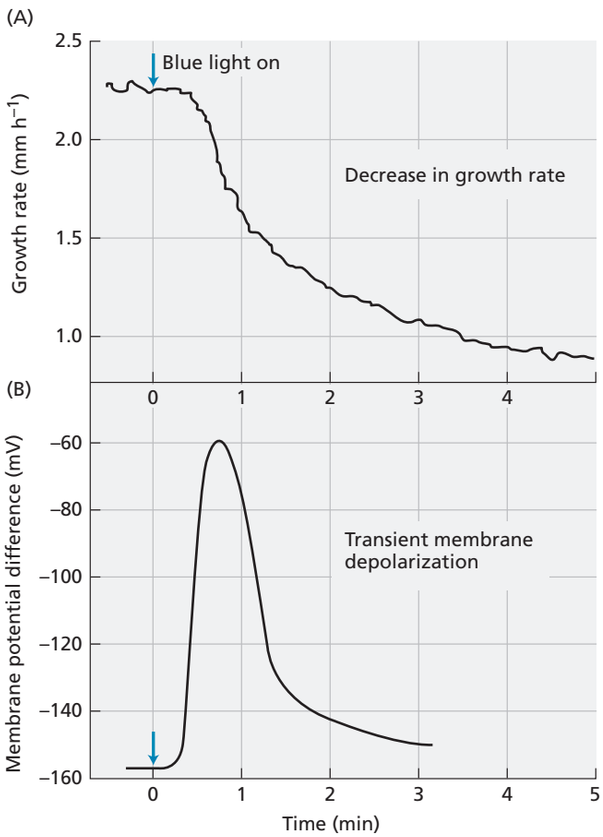


Figure 16.15 Blue light reduces hypocotyl elongation after rapid membrane depolarization. (A) Blue light–induced changes in elongation rates of etiolated cucumber hypocotyls. (B) Blue light–induced transient membrane depolarization of hypocotyl cells. (After E. P. Spalding and D. J. Cosgrove. 1989. *Planta* 178: 407–410.)

16.6 Cryptochromes

Cryptochromes are blue-light photoreceptors that mediate several blue-light responses, including suppression of hypocotyl elongation, promotion of cotyledon expansion, membrane depolarization, inhibition of petiole elongation, anthocyanin production, and circadian clock entrainment. ***CRYPTOCHROME 1*** (***CRY1***) was originally identified in screens wherein Arabidopsis mutant hypocotyls were elongated when grown in white light but were still inhibited by red, thus indicating a defect in a light-signaling pathway distinct from that of phytochrome. As discussed later in the chapter, cryptochromes are responsible for the long-term blue light–induced inhibition of hypocotyl elongation, while phototropins mediate the rapid inhibitory response.

The three cryptochrome isoforms in Arabidopsis (cry1, 2, and 3) are proteins with significant sequence homology to microbial **photolyase**, a blue light–activated enzyme that repairs pyrimidine dimers in DNA caused by exposure to ultraviolet radiation. However, cryptochromes show no photolyase activity. Cryptochrome proteins were later discovered in many organisms, including cyanobacteria, ferns, algae, fruit flies, mice, and humans.

The activated FAD chromophore of cryptochrome causes a conformational change in the protein

The domain structure of Arabidopsis cryptochromes is shown in **Figure 16.16A**. Similar to a major class of photolyases, cryptochromes bind a **flavin adenine dinucleotide** (**FAD**) and the pterin 5,10-methylenetetrahydrofolate

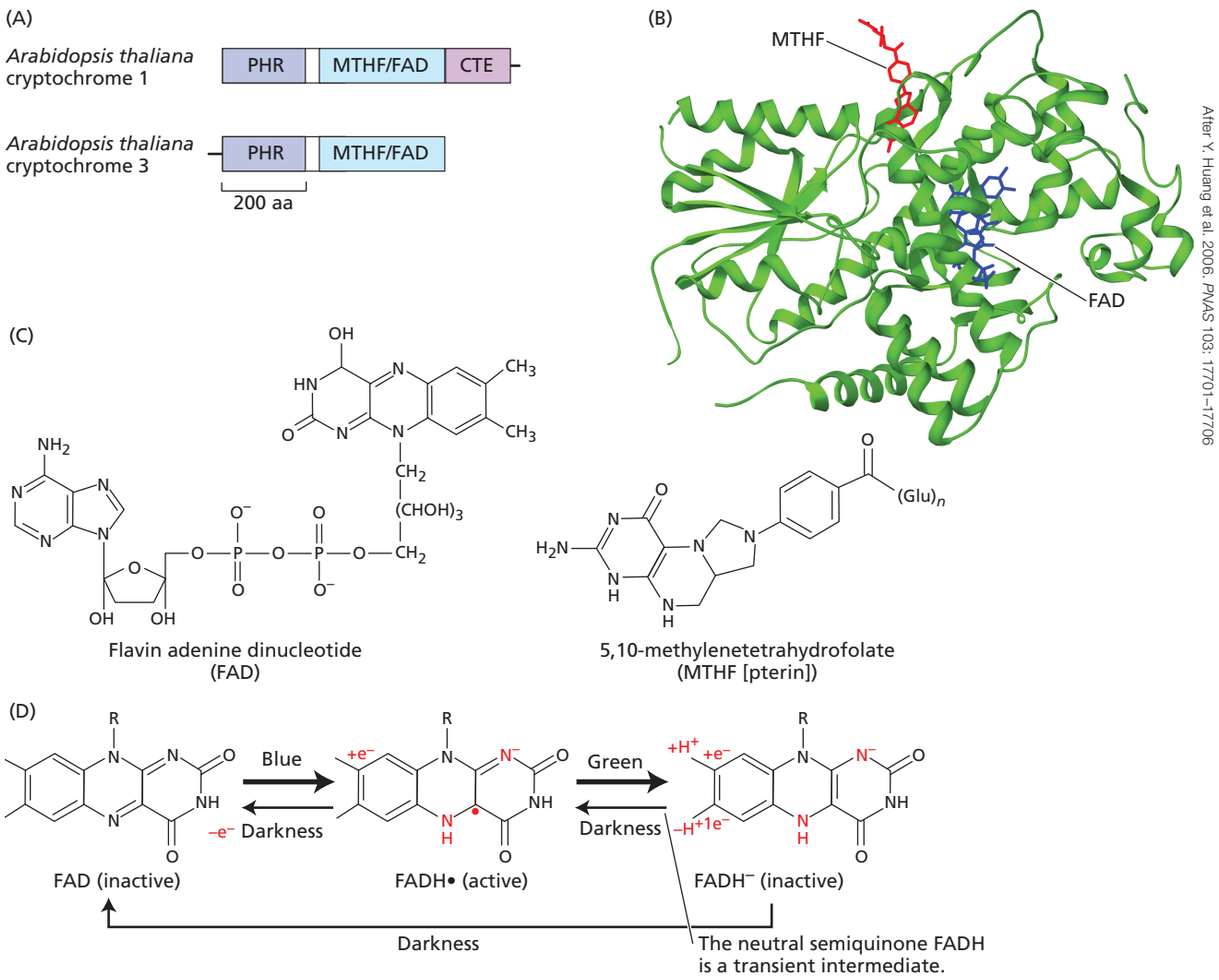


Figure 16.16 Cryptochrome domain and chromophore structure. **(A)** Alignment of two cryptochromes from Arabidopsis showing the photolyase-homology region (PHR) with the FAD-binding domain and the cryptochrome C-terminal (CCT). **(B)** Cryptochrome is a dimer, but the monomer is shown in this ribbon diagram. The light-harvesting cofactor 5,10-methylenetetrahydrofolate (MTHF) and the catalytic cofactor flavin adenine dinucleotide (FAD) are noncovalently bound to the protein, as indicated. **(C)** The structures of FAD and MTHF. **(D)** The FAD photocycle of cryptochrome.

(MTHF) as chromophores (**Figure 16.16B and C**). Pterins are light-absorbing pteridine derivatives often found in pigmented cells of insects, fishes, and birds. In photolyases, blue light is absorbed by the pterin, and the excitation energy is then transferred to FAD. A similar mechanism may operate in cryptochrome, but definitive evidence is lacking. However, it is clear that FAD is the primary chromophore regulating cryptochrome activity.

Blue-light absorption alters the redox status of the bound FAD chromophore, and it is this primary event that triggers photoreceptor activation (**Figure 16.16D**). Cryptochromes bind fully oxidized FAD in the inactive or resting state. Blue light results in the formation of a semi-reduced (semiquinone) neutral FAD radical (FADH•). FADH• is generated by photoreduction and subsequent protonation of the FAD chromophore. Light-driven generation of FADH• occurs within microseconds (and is considered to represent the signaling state that triggers photoreceptor activation). In the absence of blue light, FADH• reverts back to FAD. Inhibitory effects of green light have been observed on cryptochrome function, presumably by antagonizing FADH• formation, which absorbs in this spectral region. As occurs in phytochromes and phototropins, the activation mechanism of blue-light absorption promotes protein conformational changes. In the case of cryptochromes, light absorption by the N-terminal photolyase-homology region (PHR) is thought to alter the conformation of a C-terminal extension (CTE), which is necessary for signaling. This C-terminal extension is absent from photolyase enzymes but is clearly essential for cryptochrome signaling. We can therefore view plant cryptochrome as a molecular light switch wherein absorption of blue photons at the PHR results in conformational changes of the protein at the C terminus to initiate binding to specific partner proteins to initiate gene transcription via trans acting factors such ELONGATED HYPOCOCTYL 5 (HY5). As in phytochromes, dimerization of cryptochromes, mediated by the PHR, may be important for their signaling. Indeed, cryptochrome homodimerization contributes to controlling cryptochrome's photosensitivity by regulating an appropriate balance of active/inactive receptor molecules. This is facilitated by the binding of BLUE-LIGHT INHIBITORS OF CRYPTOCHROMES (BICs), which can suppress cryptochrome photoactivation by inhibiting its homodimerization.

cry1 and cry2 have different developmental effects

Overexpression of the CRY1 apoprotein in transgenic tobacco or Arabidopsis plants results in a stronger blue light–induced inhibition of hypocotyl elongation, as well as increased production of anthocyanin (**Figure 16.17**). A second cryptochrome, named cry2, was later isolated

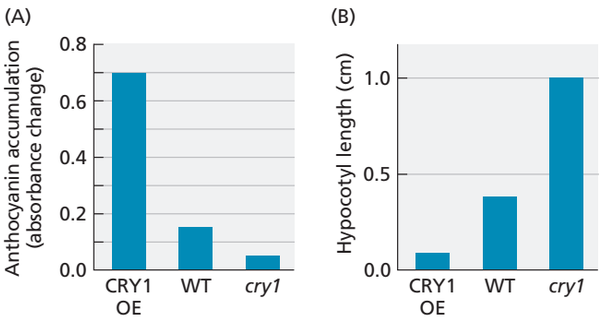


Figure 16.17 Blue light stimulates the accumulation of anthocyanins (A) and the inhibition of stem elongation (B) in transgenic and mutant seedlings of Arabidopsis. These bar graphs show the phenotypes of a transgenic plant overexpressing the gene that encodes CRY1 (CRY1 OE), the wild type (WT), and *cry1* loss-of-function mutants. The enhanced blue-light response of the CRY1 overexpressor demonstrates the important role of this gene product in stimulating anthocyanin biosynthesis and inhibiting stem elongation. (After M. Ahmad et al. 1998. *Nature* 392: 720–723.)

from Arabidopsis. Both cry1 and cry2 appear to be ubiquitous throughout the plant kingdom. A major difference between them is that the cry2 protein is preferentially degraded under blue light, whereas cry1 is much more stable. Transgenic plants overexpressing the *CRY2* gene show only a small enhancement of the inhibition of hypocotyl elongation found in the wild type, indicating that unlike cry1, cry2 does not play a primary role in inhibiting stem elongation. However, transgenic plants overexpressing *CRY2* show a large increase in blue light–stimulated cotyledon expansion. In addition, cry1, and to a lesser extent cry2, is involved in setting the circadian clock in Arabidopsis, whereas cry2 plays a major role in the induction of flowering (see Chapter 20). Cryptochrome homologs have also been shown to function in regulating the circadian clock in flies, mice, and humans.

It is also worth noting that in Arabidopsis the nuclear and cytoplasmic pools of cry1 have been shown to have distinct biological functions. Contrary to expectations, nuclear, rather than cytoplasmic, cry1 molecules were found to mediate blue light–mediated changes in membrane depolarization. This response, showing a time course of several seconds, is one of the fastest cry1-mediated responses to blue light. The mechanism involved in this blue light–dependent, anion-channel activation is not yet known.

While cry1 and cry2 are generally found in the nucleus, cry3 is localized to chloroplasts and mitochondria. The function of cry3 is not yet known, although it has been shown to have photolyase activity specific to single-stranded DNA lesions. Furthermore, the mechanism of cry3 signaling is obviously different from that of cry1 and cry2 since it lacks a prominent C-terminal extension.

Nuclear cryptochromes inhibit COP1-induced protein degradation

Both cry1 and cry2 are present in the nucleus and the cytoplasm, and there is no evidence that cryptochrome moves into the nucleus in response to light. **Figure 16.18** shows that in darkness, COP1, in concert with SPA1 and other factors, acts to degrade transcription factors that induce the expression of genes required for photomorphogenesis (see also Figure 16.14). Upon activation by blue light, cry1 in the nucleus forms a complex with SPA1 and COP1 that prevents them from acting, thereby preventing the degradation of transcription factors that promote photomorphogenesis. As in the case of phytochrome signaling, the increased transcription factor abundance promotes photomorphogenic development.

It is the C terminus of cryptochrome that binds to SPA1 and prevents SPA1/COP1 action. Arabidopsis plants overexpressing only the cryptochrome C-terminal extension (CTE) show phenotypes similar to those of *cop* mutants, which resemble light-grown seedlings when grown in darkness. The model shown in Figure 16.18 can explain the phenotype of CTE-overexpressing plants. Without the PHR, the CTE can adopt an active conformation that sequesters the activity of COP1 and SPA1 even in the absence of light, thereby promoting an increase in transcription of key photomorphogenic genes.

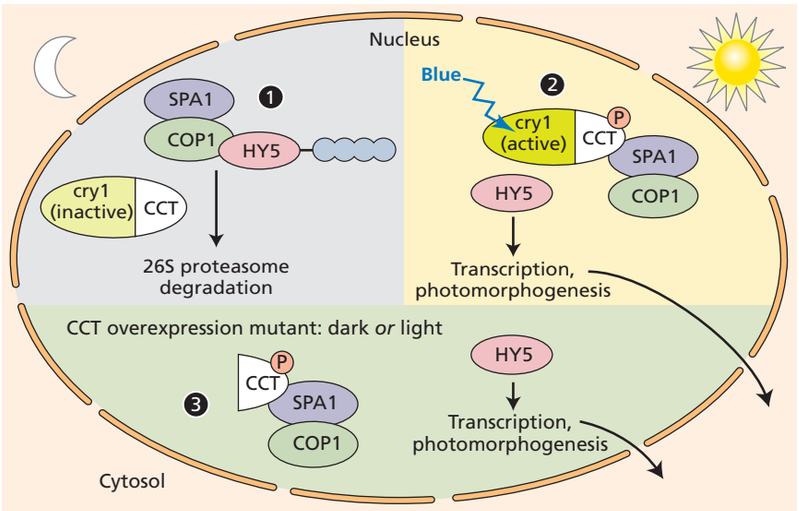


Figure 16.18 **Model of cry1 interactions with COP1 and SPA1 in the regulation of photomorphogenesis.** ❶ In the dark, COP1/SPA1 acts to degrade the phytochrome-responsive transcription factor HY5, which is required for photomorphogenesis. ❷ In the light, cry1 is activated directly by blue light and indirectly by blue light–induced phosphorylation. Activated cry1 forms a complex with COP1 and SPA1 via the C-terminal domain, preventing them from degrading protein targets such as HY5. ❸ In the absence of the photosensory N terminus as in the truncation mutant diagrammed on the bottom, the CTE region can adopt an active conformation that sequesters COP1/SPA1 in the absence of light, thereby promoting an increase in HY5 protein levels and transcription of key morphogenic genes.

Blue light–induced phosphorylation of cryptochrome also appears to be important in modulating its activity and, in the case of cry2, promoting its degradation. Photoregulatory kinases are involved in phosphorylating cryptochromes, and this process appears to be important for maintaining their C terminus in an active conformation (see Figure 16.18).

Cryptochrome can also bind to transcriptional regulators directly

In addition to controlling the levels of transcription factors, cryptochrome can also directly bind to and regulate the activity of specific DNA-binding proteins. In the case of flowering, cry2 has been shown to bind directly to bHLH transcription factors such as Cry-Interacting bHLH1 (CIB1). CIB1 regulates floral initiation by binding to the promoter of *FLOWERING LOCUS T* (*FT*). FT is the mobile transcriptional regulator that migrates from leaves to the apical meristem and activates transcription of floral meristem identity genes (see Chapter 20). Plants overexpressing CIB1 flower earlier than wild-type plants. Similarly, cry1 has been shown to regulate light-dependent production of other mobile factors in soybean shoots. Those mobile factors move through the vascular system to the roots where they stimulate nodulation (see Chapter 14).

16.7 Interactions of Cryptochrome with Other Photoreceptors

Interaction between cryptochrome and phytochrome was long suspected because several developmental processes, such as photomorphogenesis and flowering, were known to be under phytochrome control, yet mutations in the *CRY2* gene led to alterations in these responses. We now understand that interactions exist between several of the plant photoreceptors. Many of the developmental processes affected by these interactions can be grouped into three general categories: stem or hypocotyl elongation, flowering, and regulation of circadian rhythms.

Stem elongation is inhibited by both red and blue photoreceptors

As noted earlier, the stems of seedlings growing in the dark elongate very rapidly, and the inhibition of stem

elongation by light is a key photomorphogenic response of the seedling emerging from the soil surface (see Chapter 18). Although phytochrome is involved in this response, the action spectrum for the decrease in elongation rate also shows strong activity in the blue region, which cannot be explained by the absorption properties of phytochrome. In fact, the 400- to 500-nm blue region of the action spectrum for the inhibition of stem elongation closely resembles that of phototropism.

A specific blue light–mediated hypocotyl response can be distinguished from one mediated by phytochrome by their contrasting time courses. Whereas phytochrome-mediated changes in elongation rates can be detected within approximately 10 to 90 min, depending on the species, blue-light responses show lag times of less than 1 min. High-resolution analysis of the changes in growth rate mediating the inhibition of hypocotyl elongation by blue light has provided valuable information about the interactions among phototropin, cry1, cry2, and phyA. After a lag of 30 s, blue light–treated, wild-type Arabidopsis seedlings show a rapid decrease in elongation rates during the first 30 min, and then they grow very slowly for several days.

Another rapid response elicited by blue light is a depolarization of the membrane of hypocotyl cells that precedes the inhibition of growth rate (see Figure 16.15B). This membrane depolarization is caused by the activation of anion channels (see Chapter 8), which facilitates the efflux of anions such as chloride. Application of an anion channel blocker, NPPB (5-nitro-2,3 -phenylpropylaminobenzoic acid), prevents the blue light–dependent membrane depolarization and decreases the inhibitory effect of blue light on hypocotyl elongation.

Analysis of the same response in *cry1*, *cry2*, *phyA*, and *phot1* mutants has shown that suppression of stem elongation by blue light during seedling de-etiolation is initiated by phot1, with cry1, and to a limited extent cry2, modulating the response after 30 min (**Figure 16.19**). The slow rate of stem growth in blue light–treated seedlings is primarily a result of the persistent action of cry1, and this is the reason that *cry1* mutants of Arabidopsis show a long hypocotyl, compared with the short hypocotyl of the wild type. PhyA appears to play a role in at least the early stages of blue light–regulated growth, because growth inhibition does not progress normally in *phyA* mutants.

Phytochrome interacts with cryptochrome to regulate flowering

In Arabidopsis, continuous blue or far-red light promotes flowering, and red light inhibits flowering. Far-red light acts through phyA, and the antagonistic effect of red light is produced by phyB. One might expect the *cry2* mutant to be delayed in flowering, since blue light promotes flowering. However, *cry2* mutants flower at the same time as the wild type under either continuous blue or continuous red light. A delay is observed only if both

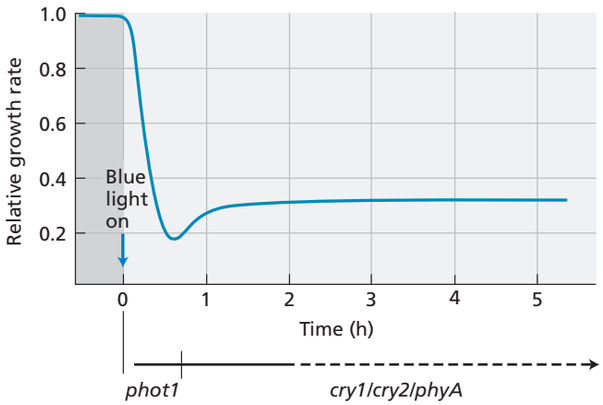


Figure 16.19 Sensory transduction process of blue light–stimulated inhibition of stem elongation in wild-type Arabidopsis. Elongation rates in the dark (0.25 mm h^{-1}) were normalized to 1. Within 30 s of the onset of blue-light irradiation, growth rates decreased; they approached zero within 30 min, then continued at very reduced rates for several days. If blue light was applied to a *phot1* mutant, dark-growth rates remained unchanged for the first 30 min, indicating that the inhibition of elongation in the first 30 min is under phototropin control. Similar experiments with *cry1*, *cry2*, and *phyA* mutants indicated that the respective gene products control elongation rates at later times consistent with regulation of gene expression (represented by dotted line on *x*-axis). (After B. M. Parks et al. 2001. *Curr. Opin. Plant Biol.* 4: 436–440.)

blue light and red light are given together. Therefore, cry2 probably promotes flowering in blue light by repressing phyB function. Cry2 apparently inhibits phyB function by suppressing the activity of EARLY FLOWERING 3 (elf3), which interacts with phytochrome, indicating that these signaling pathways converge.

The circadian clock is regulated by multiple aspects of light

As noted previously in this chapter, several plant processes show oscillations of activity that roughly correspond to a 24-h, or circadian, cycle. This endogenous rhythm uses an oscillator that must be **entrained** (synchronized) to the daily light–dark cycles of the external environment. In experiments designed to characterize the role of photoreceptors in this process, phytochrome-deficient mutants were crossed with lines carrying the luciferase reporter gene that is regulated by the circadian clock. The pace of the oscillator was slowed (i.e., the period length increased) when *phyA* mutants were grown under dim red light but not under high-irradiance red light. However, *phyB* mutants showed timing defects only under high-irradiance red light. The cryptochromes cry1 and cry2 were required for blue light–mediated entrainment of the circadian clock. These studies indicate that both phytochromes and cryptochromes entrain the circadian clock in Arabidopsis. This light input appears to be modulated by the genes *EARLY FLOWERING 3* (*elf3*) and *TIME FOR COFFEE*

(*TIC*). Mutations in *elf3* stop the oscillations of the clock at dusk, whereas mutations in *TIC* stop the clock at dawn. The *elf3/tic* double mutant is completely arrhythmic, suggesting that *TIC* and *ELF* interact with different components of the clock at different phases in the rhythm.

16.8 Phototropins

Early attempts to identify blue-light photoreceptor mutants of Arabidopsis with defective phototropic responses were later extended by Winslow Briggs and colleagues and resulted in the isolation of several nonphototropic hypocotyl (*nph*) mutants, which showed impaired phototropic responses to low intensities of blue light. Subsequent cloning of the *NPH1* locus resulted in the identification of the photoreceptor for phototropism. The encoded protein was named phototropin after its role in mediating phototropic responses, but these receptors also control several blue-light responses that collectively function to optimize photosynthetic efficiency and promote plant growth, particularly under low light conditions.

Angiosperms contain two phototropin genes, *PHOT1* and *PHOT2*. *PHOT1* is the primary phototropic receptor in Arabidopsis and mediates phototropism in response to low and high fluence rates of blue light. phot2 mediates phototropism in response to high light intensities. Similar overlaps in the functions of the phot1 and phot2 photoreceptors are observed for other blue-light responses in Arabidopsis, including chloroplast movements, stomatal opening, leaf movements, and leaf expansion. Together with phototropism, these processes integrate efficient light capture and CO_2 uptake for photosynthesis. Consequently, growth of phototropin-deficient mutants is severely compromised, particularly under low light intensities.

Blue light induces changes in FMN absorption maxima associated with conformation changes

In contrast to cryptochromes, which are predominantly localized in the nucleus, phototropin receptors are associated with the plasma membrane, where they function as light-activated serine/threonine kinases. **Figure**

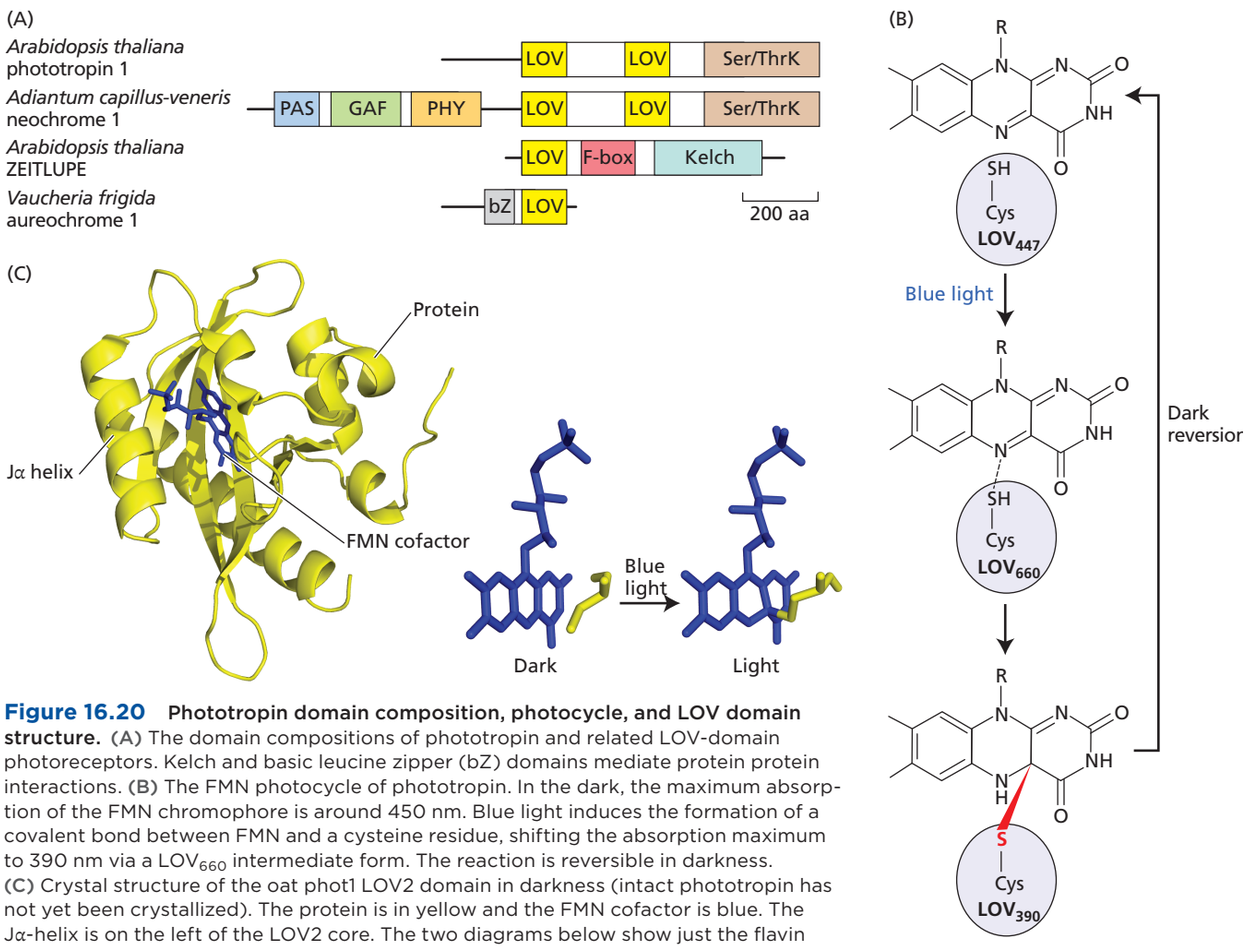


Figure 16.20 Phototropin domain composition, photocycle, and LOV domain structure. **(A)** The domain compositions of phototropin and related LOV-domain photoreceptors. Kelch and basic leucine zipper (bZ) domains mediate protein protein interactions. **(B)** The FMN photocycle of phototropin. In the dark, the maximum absorption of the FMN chromophore is around 450 nm. Blue light induces the formation of a covalent bond between FMN and a cysteine residue, shifting the absorption maximum to 390 nm via a LOV_{660} intermediate form. The reaction is reversible in darkness. **(C)** Crystal structure of the oat phot1 LOV2 domain in darkness (intact phototropin has not yet been crystallized). The protein is in yellow and the FMN cofactor is blue. The Jα-helix is on the left of the LOV2 core. The two diagrams below show just the flavin and the formation of the cysteine adduct after irradiation with blue light. (After J. M. Christie. 2007. *Annu. Rev. Plant Biol.* 58: 21–45.)

16.20A illustrates the domain structure of Arabidopsis phototropin 1 and of three related blue-light photoreceptors found in plants or algae: neochrome, ZEITLUPE, and aureochrome. Phototropin contains two light-sensing **LIGHT-OXYGEN-VOLTAGE** (**LOV**) domains, LOV1 and LOV2, each binding a chromophore flavin mononucleotide (FMN). Spectroscopic studies have shown that in the dark, one FMN molecule is noncovalently bound to each LOV domain. Upon blue-light illumination, the FMN molecule becomes covalently bound to a cysteine residue in the phototropin molecule, forming a cysteine–flavin covalent adduct (Figure 16.20B). As we discuss shortly, this reaction induces a major protein conformational change, which can be reversed by a dark treatment. The three-dimensional structure of the LOV2 domain resembles a closed molecular hand holding the FMN tightly by noncovalent interactions inside its core (Figure 16.20C). Figure 16.20 also shows the formation of the covalent bond between the flavin cofactor and a cysteine residue in response to blue light.

The LOV2 domain is primarily responsible for kinase activation in response to blue light

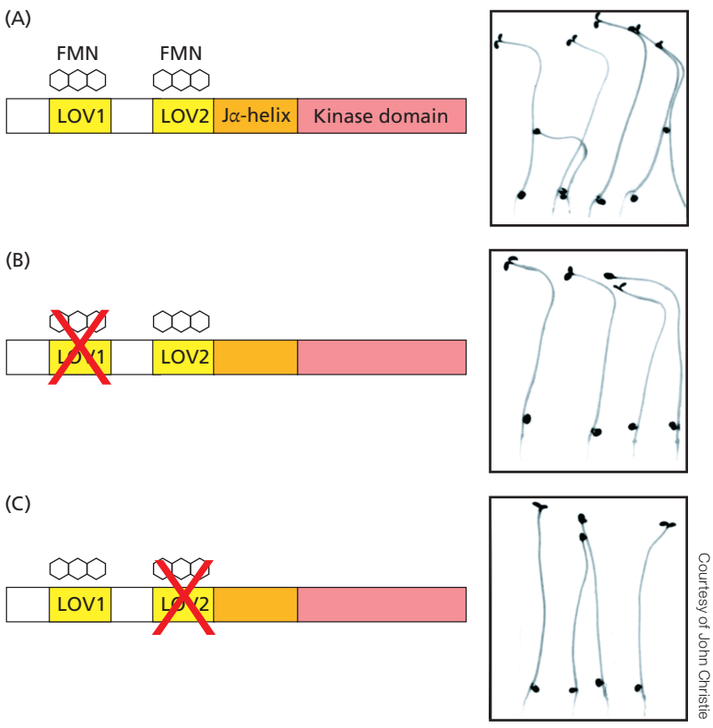
As demonstrated in mutagenesis experiments, the LOV2 domain, in particular, is essential for blue light–induced kinase activation and autophosphorylation of the phototropin photoreceptor. Mutating the conserved cysteine in the LOV1 domain of phot1 does not affect phototropic responsiveness (Figure 16.21A and B), whereas the equivalent mutation in LOV2 abolishes the response (Figure 16.21C). These and other studies have demonstrated the importance of LOV2 in controlling phototropin function. This is due in part to the position of LOV2 within the phototropin molecule, where it is coupled to a protein region known as the Jα-helix that is important for propagating light-driven changes within LOV2 to the kinase domain. The function of LOV1 is still poorly understood, but the domain is thought to play a role in receptor dimerization.

Blue light induces a conformational change that "uncages" the kinase domain of phototropin and leads to autophosphorylation

Although a three-dimensional structure for the entire phototropin molecule is still lacking, many genetic, biochemical, and biophysical studies have provided a good understanding of how the phototropin light switch works. As with cryptochrome and phytochrome, the N-terminal photosensory region of the phototropins controls the activity of the C-terminal half of the protein, which contains a serine/threonine kinase domain (see Figure 16.21A). In the dark, the N-terminal region, including the LOV domains, "cages" and inhibits the activity of the kinase domain (Figure 16.22). Absorption of blue photons by the LOV domains results in primary photochemical changes that lead to the uncaging of the kinase domain and its activation by the unfolding of the Jα-helix. The activation of the C-terminal kinase domain then leads to receptor autophosphorylation on multiple serine residues. Autophosphorylation of the kinase domain is required for all phototropin-mediated responses in Arabidopsis. A type 2A protein phosphatase mediates dephosphorylation and inactivation of phototropin in the dark (see Figure 16.22).

Phototropins trigger plant movements that enhance light use

Activation of phototropin kinases triggers signal transduction events that change the orientation of organs or organelles to improve photosynthetic light use. One of these responses is phototropism, or bending toward light, described in Chapter 17. The intracellular distribution of chloroplasts in leaves can also change in response



Courtesy of John Christie

Figure 16.21 Phototropism in Arabidopsis seedlings can be used as the bioassay for phototropin activity. **(A)** Wild type, with both LOV1 and LOV2 domains. **(B)** Mutating the cysteine in the LOV1 domain of phot1 does not affect phototropic responsiveness (the seedlings bend toward blue light). **(C)** The equivalent mutation in the LOV2 domain abolishes the response, demonstrating that only the LOV2 domain is required for phototropism.

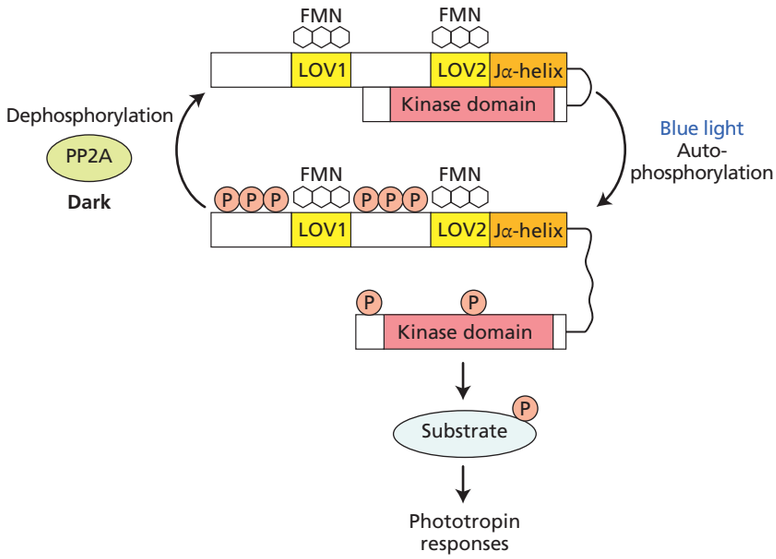


Figure 16.22 Model for blue light–induced autophosphorylation of phototropin. Phototropin has two LOV domains (yellow) and a kinase domain (red), separated by an α-helical region (Jα). In the absence of light, the N-terminal region, including the LOV domains, "cages" and represses the activity of the kinase domain. Absorption of blue photons by the LOV domains results in primary photochemical changes that lead to the uncaging of the kinase domain and its activation. Although not shown in the diagram, the Jα-helix completely loses its helical structure. Photoexcitation of the LOV domains results in activation of the C-terminal kinase domain, which leads to receptor autophosphorylation on multiple serine residues. Autophosphorylation within the kinase domain is essential for initiating all phototropin-mediated responses in Arabidopsis. Dephosphorylation resulting in inactivation occurs in the dark. PP2A, protein phosphatase 2a. (After S.-I. Inoue et al. 2010. *Curr. Opin. Plant Biol.* 13: 587–593.)

to light conditions. As discussed in Chapter 11, this feature is adaptive, as the redistribution of chloroplasts within the cells modulates light absorption and prevents photodamage (see Figure 11.12). Under weak illumination, chloroplasts accumulate near the upper and lower walls of the leaf palisade cells to maximize light absorption (**Figure 16.23**). Under strong illumination, the chloroplasts move to the lateral walls that are parallel to the incident light to avoid excess light absorption and photodamage. In the dark, the chloroplasts move to the bottom of the cell, although the physiological function of this position is unclear. The action spectrum for the redistribution response shows the typical three-finger fine structure typical of specific blue-light responses (see Figure 16.7).

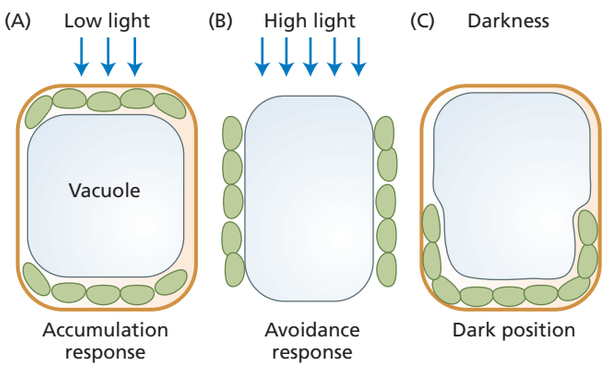


Figure 16.23 Schematic diagram of chloroplast distribution patterns in Arabidopsis palisade cells in response to different light intensities. **(A)** Under low light conditions, chloroplasts optimize light absorption by accumulating at the adaxial and abaxial sides of palisade cells. **(B)** Under high light conditions, chloroplasts avoid sunlight by migrating to the side walls of palisade cells. **(C)** Chloroplasts move to the bottom of the cell in darkness. (After M. Wada. 2013. *Plant Sci.* 210: 177–182.)

Arabidopsis *phot1* mutants have a normal avoidance response and a poor accumulation response. In contrast, *phot2* mutants lack the avoidance response but retain a fairly normal accumulation response. Cells from the *phot1/phot2* double mutant lack both the avoidance and accumulation responses. These results indicate that phot2 plays a key role in the avoidance response, and that both phot1 and phot2 contribute to the accumulation response. Studies have shown that phot2 mutants in fact do not survive in the field under conditions of full sunlight because of photooxidative damage.

The isolation of Arabidopsis mutants impaired in the chloroplast avoidance response led to the identification of a novel F-actin-binding protein, CHLOROPLAST UNUSUAL POSITIONING1 (CHUP1), consistent with earlier work showing that chloroplast movements occur through changes in the cytoskeleton. CHUP1 localizes to the chloroplast envelope and functions in chloroplast positioning and movement. A model of chloroplast movement in Arabidopsis is shown in **Figure 16.24**. Both phot1 and phot2 mediate the accumulation response and are localized at the plasma membrane. phot2, which mediates the avoidance response, is also localized on the chloroplast envelope. In the presence of full sunlight, CHUP1, which appears to anchor to the plasma membrane via protein interactions, binds to the chloroplast envelope. CHUP1 recruits G-actin and actin-polymerizing proteins to extend an existing F-actin filament (see Figure 1.32). CHUP1 and the chloroplast

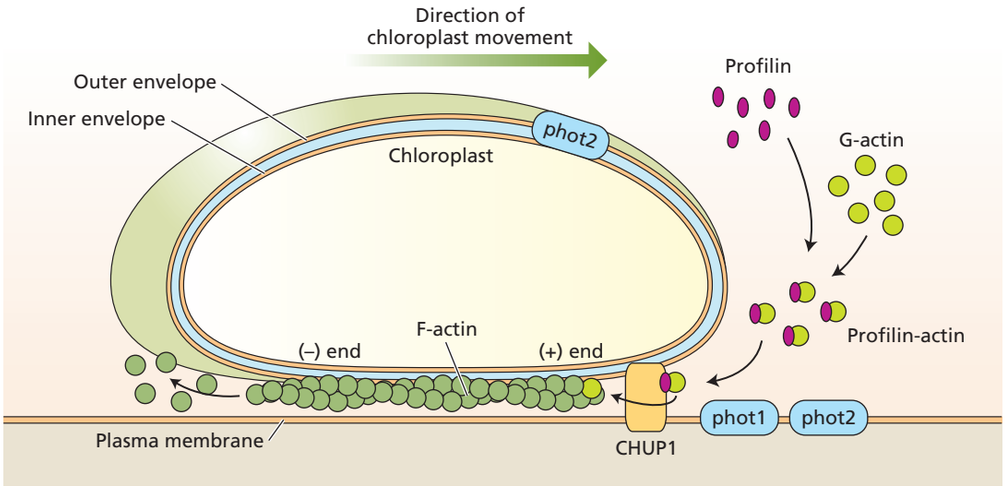


Figure 16.24 Model for phototropin-mediated chloroplast movement in *Arabidopsis thaliana*. Both phot1 and phot2 mediate the accumulation response and are localized at the plasma membrane. phot2 is also localized on the chloroplast envelope and probably mediates the avoidance response. CHUP1 binds to the chloroplast envelope via its N terminus and may also be anchored to the plasma membrane. CHUP1 initiates profilin-mediated actin polymerization (see Chapter 1) to extend an existing F-actin filament that is associated with the chloroplast. As a result, the actin filament lengthens and CHUP1 and the chloroplast are pushed in the direction of filament elongation The actin filaments are depolymerized at their minus ends. The green arrow shows the direction of chloroplast movement. (After M. Wada. 2013. *Plant Sci.* 210: 177–182.)

are then pushed by the inserted G-actin, generating the motive force for chloroplast movement.

Blue light initiates stomatal opening via activation of the plasma membrane H^+-ATPase

Stomatal photophysiology and sensory transduction in relation to water and photosynthesis were introduced in Chapters 6 and 8, and were discussed again in stress responses described in Chapter 15. Studies with *phot1/phot2* double mutants have shown that phototropins are the primary blue-light photoreceptors for stomatal opening. Several key steps in the sensory transduction process of phototropin-stimulated stomatal opening have been identified. In particular, the guard cell proton-pumping H^+-ATPase plays a central role in the regulation of stomatal movements (**Figure 16.25**). The activated H^+-ATPase transports H^+ across the membrane and increases the inside-negative electrical potential, driving the K^+ uptake through the voltage-gated inward-rectifying K^+ channels. The accumulation of K^+ facilitates the influx of water into the guard cells, leading to an increase in turgor pressure and stomatal opening. The C terminus of the H^+-ATPase has an autoinhibitory domain that regulates the activity of the enzyme. If this autoinhibitory domain is experimentally removed by a protease, the H^+-ATPase becomes irreversibly activated. The autoinhibitory domain of the C terminus is thought to lower the activity of the enzyme by blocking its catalytic site. Conversely, the fungal toxin fusicoccin appears to activate the enzyme by displacing the autoinhibitory domain away from the catalytic site.

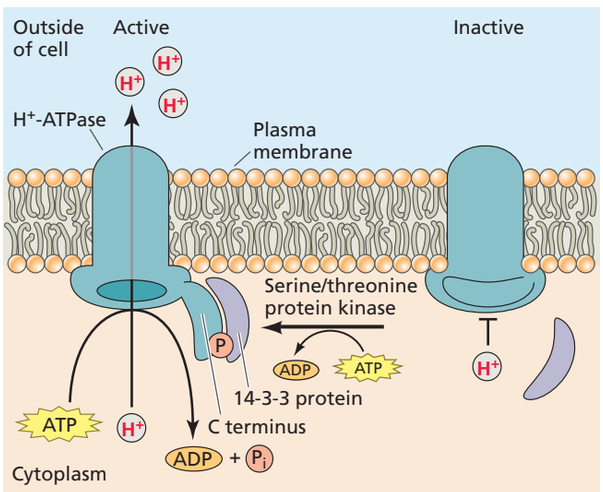


Figure 16.25 Role of the proton-pumping ATPase in the regulation of stomatal movement. Blue light activates the H^+-ATPase. Activation of the enzyme involves the phosphorylation of serine and threonine residues of its C-terminal domain. A regulatory protein termed 14-3-3 protein binds to the phosphorylated C terminus of the guard cell H^+-ATPase, but not to the nonphosphorylated one. Pumping protons out of the cell increases the entry of K^+ to balance the charge.

Upon blue-light irradiation, the H^+-ATPase shows a lower K_m for ATP and a higher V_{max}, indicating that blue light activates the H^+-ATPase. Activation of the enzyme involves the phosphorylation of serine and threonine residues in the C-terminal region of the H^+-ATPase. Inhibitors of protein kinases, which might block phosphorylation of the H^+-ATPase, prevent blue light–stimulated proton pumping and stomatal opening. As with fusicoccin, phosphorylation of the C-terminus appears also to displace the autoinhibitory domain from the catalytic site of the enzyme.

A regulatory 14-3-3 protein (see Chapter 8) binds to the phosphorylated C terminus of the guard cell H^+-ATPase, but not to the nonphosphorylated one (see Figure 16.25). The same 14-3-3 isoform binds to the guard cell H^+-ATPase in response to both fusicoccin and blue-light treatments. The 14-3-3 protein dissociates from the H^+-ATPase upon dephosphorylation of the C-terminal domain.

However, phototropins do not phosphorylate the H^+-ATPase directly. The kinase involved in phosphorylating the H^+-ATPase has not yet been identified. However, early signal transduction events following phototropin excitation at the guard cell plasma membrane have been identified and are illustrated in **Figure 16.26**. The membrane-associated, guard cell–specific protein kinase called BLUE LIGHT SIGNALING 1 (BLUS1) is phosphorylated by phot1 and phot2 redundantly. Arabidopsis mutants lacking BLUS1 show no blue light–induced stomatal opening but are not impaired in other phototropin responses, including phototropism and chloroplast

1. Blue light activates phototropin photoreceptor kinases that then activate CONVERGENCE OF BLUE LIGHT AND CO_2 (CBC) kinases. Activated CBCs inhibit transport of Cl^- out of the cell, which increases Cl^- import into the vacuole.

2. Phosphorylation of a BLUE LIGHT SIGNALING 1 (BLUS1) / kinase complex activates sequential protein phosphorylation steps that activate plasma membrane H^+-ATPases by releasing inhibitory 14-3-3 proteins.

3. Activation of H^+-ATPases hyperpolarizes the plasma membrane, which increases K^+ movement into the guard cell. Vacuolar K^+ uptake is coordinated with that of Cl^- and malate^{2-}. These ion movements lower the water potential of the vacuole and drive water uptake, vacuolar expansion, and turgor-driven stomatal opening.

4. Photosynthetically active radiation increases production of ATP by chloroplasts, increasing cytosolic ATP levels and leading to increased rates of cytosolic ATPase activity. Photosynthetically active radiation also increases production of carotenoids, which protect membranes from photooxidative damage and are precursors for synthesis of the stomatal closure hormone abscisic acid.

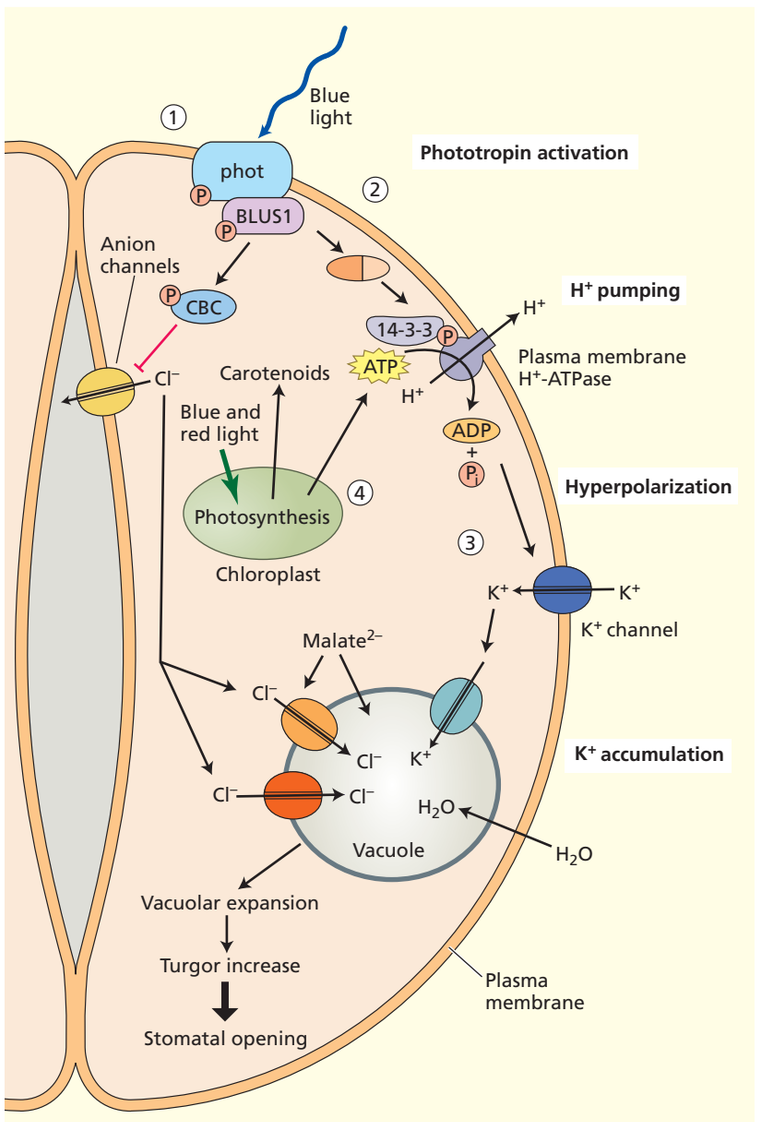


Figure 16.26 **Phototropin signal transduction leading to stomatal opening.** (After S. Inoue and T. Kinoshita. 2017. *Plant Physiol.* 174: 531–538. CC BY 4.0)

relocation. This phosphorylation event is essential in initiating the early transduction events that ultimately lead to phosphorylation and activation of the H^+-ATPase.

The signals from BLUS1 converge on the PROTEIN PHOSPHATASE 1 (PP1) complex that regulates the activation of the H^+-ATPase. PP1 is a serine/threonine protein phosphatase composed of a catalytic protein phosphatase 1c subunit and a regulatory subunit, PRSL1 (PP1 REGULATORY SUBUNIT2-LIKE PROTEIN1), which modulates catalytic activity, subcellular localization, and substrate specificity. PP1 positively regulates stomatal opening through blue-light signaling between phototropins and the plasma membrane H^+-ATPase.

The protein kinase CONVERGENCE OF BLUE LIGHT AND CO_2 1 (CBC1) is also activated by phot-mediated phosphorylation. Phosphorylation of CBC1 and its paralog CBC2 in response to blue light promotes stomatal opening through the inhibition of S-type anion channels. As CBCs also promote stomatal opening when they are phosphorylated under low CO_2 concentrations, they are regarded as integrators of the light and CO_2 responses in guard cells.

16.9 Responses to Ultraviolet Radiation

In addition to its cytotoxic effects, UV-B radiation can elicit a wide range of photomorphogenic responses, some of which are listed in **Table 16.4**. Moderate increases in UV-B levels can enhance differential growth of "sun-loving" plants and have been shown to enhance bud set in poplar trees. The photoreceptor responsible for UV-B-induced developmental responses, UVR8, is a seven-bladed β-propeller protein, which forms functionally inactive homodimers in the absence of UV-B (**Figure 16.27**). Unlike phytochrome, cryptochrome, and phototropin, UVR8 lacks a prosthetic chromophore. The two identical subunits of UVR8 are linked in the dimer by a network of salt bridges formed between tryptophan residues, which serve as the primary UV-B sensors, and nearby arginine residues.

Upon absorbing UV-B photons, the tryptophans undergo structural changes that break the salt bridges, leading to the dissociation of the two functionally active monomers. The monomers then interact with COP1–SPA complexes to activate gene expression, as illustrated in **Figure 16.28**. Thus, although COP1–SPA acts as a negative regulator that targets transcription factors for degradation during phytochrome and cryptochrome responses (see Figures 16.14 and 16.18, COP1–SPA acts as a positive regulator during UV-B signaling by interacting with the C-terminal region of UVR8 in the nucleus. The UVR8–COP1–SPA complex then activates the transcription of photomorphogenic transcription factors, to control the expression of many of the genes induced by UV-B. These include REPRESSOR OF UVR8 proteins that mediate reassociation of inactive UVR8 dimers to reset the system.

Table 16.4 Photomorphogenic responses to UV-B

Gene regulation
UV-B tolerance
Flavonoid biosynthesis
Hypocotyl growth suppression
Leaf/epidermal cell expansion
Endoreduplication in epidermal cells
Stomatal density
Entrainment of circadian clock
Increased photosynthetic efficiency

Source: G. I. Jenkins. 2014. *Plant Cell* 26: 21–37.

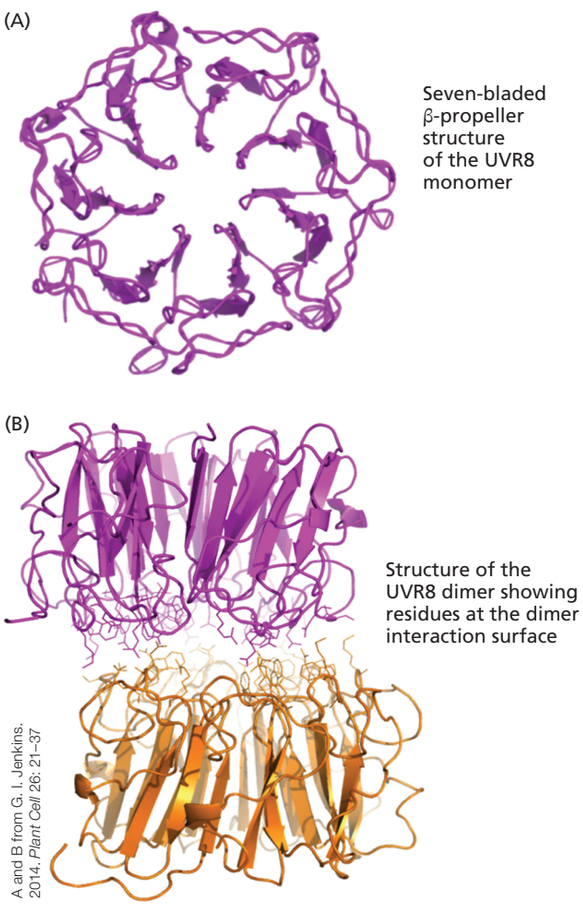


Figure 16.27 UVR8 structure and dimerization. **(A)** End-on view showing the seven blades of the β-propeller. **(B)** Side view of the UVR8 dimer, showing the amino acid residues at the interaction surface.

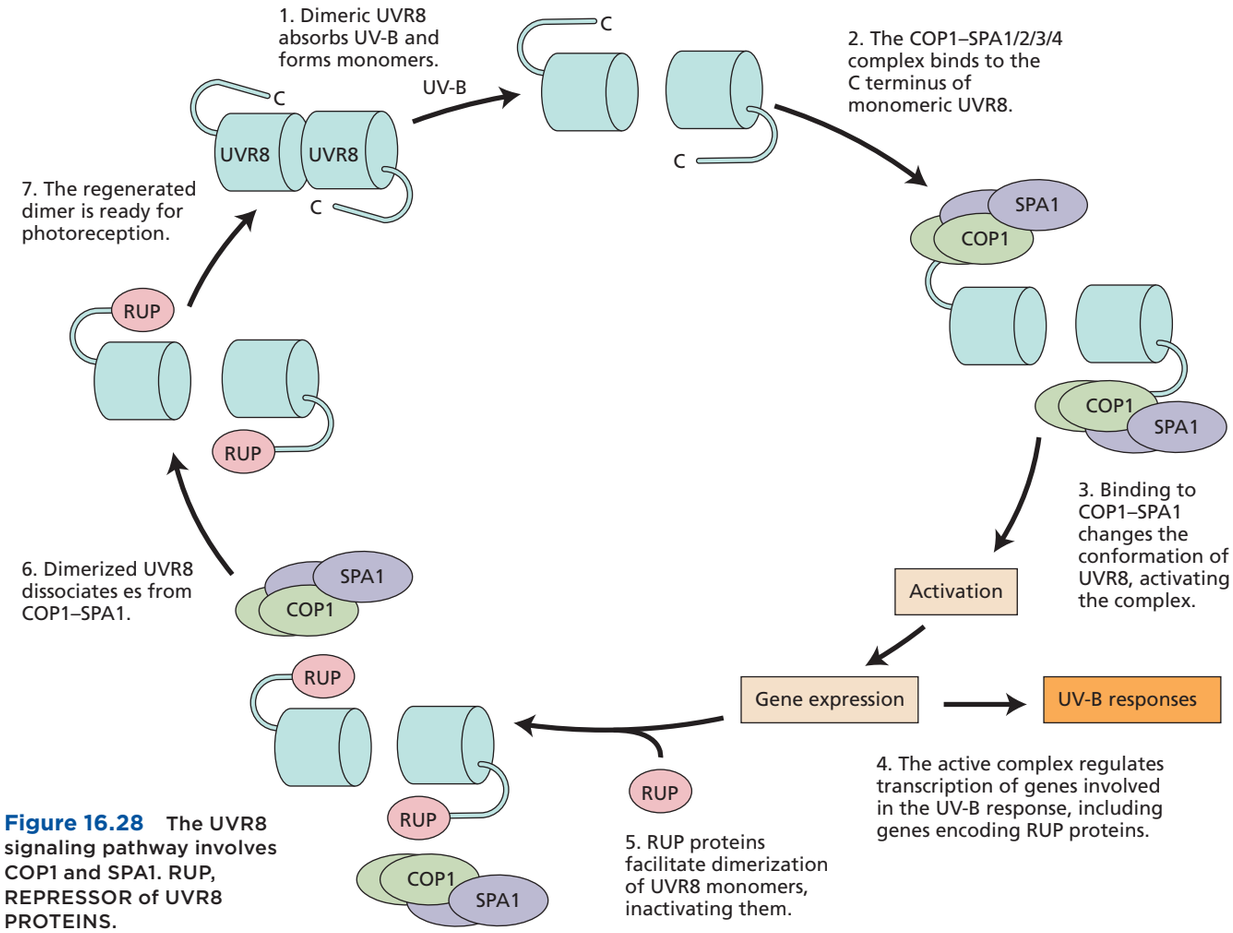


Figure 16.28 The UVR8 signaling pathway involves COP1 and SPA1. RUP, REPRESSOR of UVR8 PROTEINS.

Summary

Photoreceptors, including phytochromes, cryptochromes, and phototropins, help plants regulate developmental processes over their lifetimes by sensitizing plants to incident light. Photoreceptors also initiate protective processes in response to harmful radiation.

16.1 Plant Photoreceptors

- Sunlight regulates developmental processes over the life of the plant and provides directional and nondirectional cues for growth and movement. Sunlight also contains UV radiation that can harm plant tissues (**Figures 16.1–16.4**).
- Phytochromes (which absorb red and far-red light) and phototropins and cryptochromes (which absorb blue light and UV-A) are photoreceptors that are sensitive to light quantity, quality, and duration.
- Action spectra and absorption spectra help researchers determine which wavelengths of light lead to specific photoresponses (**Figures 16.6, 16.7**).
- Light fluence and irradiance also govern whether a photoresponse occurs.

16.2 Phytochromes

- Phytochrome is generally sensitive to red and far-red light, and it exhibits the ability to interconvert between Pr and Pfr forms.
- The physiologically active form of phytochrome is Pfr.
- Red light triggers conformational changes in both the phytochrome chromophore and protein (**Figures 16.8–16.10**).
- Pfr movement from the cytosol to the nucleus enables phytochrome-regulated transcription in the nucleus (**Figures 16.10, 16.11**).

16.3 Phytochrome Responses

- Photoresponses exhibit various lag times (between exposure to light and the subsequent response)

(*Continued*)

Summary (*continued*)

and escape times (wherein the response is only reversible for a certain amount of time).

- Phytochrome-initiated responses fall into one of three main categories: very low fluence responses (VLFRs), low-fluence responses (LFRs), or high-irradiance responses (HIRs) (**Figure 16.12**).
- Phytochrome A mediates responses to continuous far-red light.
- Phytochrome B mediates responses to continuous red or white light.

16.4 Phytochrome Signaling Pathways

- Phytochrome can be associated with changes in lipid composition and membrane potentials.
- Phytochrome regulates gene expression through a wide range of modular elements.
- Phytochrome itself can be phosphorylated and dephosphorylated.
- Phytochrome-induced photomorphogenesis involves protein degradation (**Figures 16.13, 16.14**).

16.5 Blue-Light Responses and Photoreceptors

- In contrast to red- and far-red-light responses, blue-light responses generally exhibit longer lag times and are more persistent after the disappearance of the light signal (**Figures 16.15, 16.19**).

16.6 Cryptochromes

- Activation of the flavin adenine dinucleotide (FAD) chromophore causes a conformational change in cryptochrome, enabling cryptochrome to bind to other protein partners (**Figure 16.16**).
- Light-dependent anthocyanin accumulation is regulated by cry1 in Arabidopsis (**Figure 16.17**).
- Cryptochrome homologs 1, 2, and 3 have different developmental effects, and are localized differently than phytochromes.
- Activation of both phytochromes and cryptochromes can inactivate COP1 to inhibit protein degradation and promote the accumulation of factors leading to photomorphogenesis (compare **Figures 16.14** and **16.18**).

16.7 Interactions of Cryptochromes with Other Photoreceptors

- Both phytochrome and cryptochrome inhibit stem elongation (**Figure 16.19**).
- Phytochrome interacts with cryptochrome to regulate flowering, and both types of photoreceptors are necessary to maintain circadian cycles.

16.8 Phototropins

- Similar to cryptochromes, phototropins mediate photoresponses to blue light; phototropin 1 and 2 are sensitive to different and overlapping intensities of blue light.
- Phototropins are located in the plasma membrane, and each has two flavin mononucleotide (FMN) chromophores that can induce conformational changes (**Figures 16.20, 16.21**).
- When phototropins are activated by blue light, their kinase domain is "uncaged," causing autophosphorylation (**Figure 16.22**).
- Phototropins mediate chloroplast accumulation and avoidance responses to weak and strong light via F-actin filament assembly (**Figures 16.23, 16.24**).
- Blue light, sensed by phototropins, causes activation of plasma membrane H^+-ATPases and ultimately regulates stomatal opening. However, the kinase that activates H^+-ATPases has not been identified (**Figures 16.25, 16.26**).

16.9 Responses to Ultraviolet Radiation

- The photoreceptor involved in responses to UV-B irradiation is UVR8 (**Figure 16.27**).
- Unlike other phytochromes, cryptochromes, and phototropins, UVR8 lacks a prosthetic chromophore and is activated by UV absorption of discrete tryptophan residues.
- UVR8 interacts with the COP1–SPA1 complex to activate the transcription of UV-B-induced genes (**Figure 16.28**).

Web Material

- **WEB TOPIC 16.1** ***Mougeotia*: A Chloroplast with a Twist** Microbeam irradiation experiments have been used to localize phytochrome in this filamentous green alga.
- **WEB TOPIC 16.2 Phytochrome and High-Irradiance Responses** Dual-wavelength experiments helped demonstrate the role of phytochrome in HIRs.

For more study aids, go to oup.com/he/taiz7e.

Suggested Reading

Burgie, E. S., Bussell, A. N., Walker, J. M., Dubiel, K., and Vierstra, R. D. (2014) Crystal structure of the photosensing module from a red/far-red light-absorbing plant phytochrome. *Proc. Natl. Acad. Sci. USA* 111: 10179–10184.

Christie, J. M., and Murphy, A. S. (2013) Shoot phototropism in higher plants: New light through old concepts. *Am. J. Bot.* 100: 35–46.

Christie, J. M., Kaiserli, E., and Sullivan, S. (2011) Light sensing at the plasma membrane. In *Plant Cell Monographs*, Vol. 19: *The Plant Plasma Membrane*, A. S. Murphy, W. Peer, and B. Schulz, eds., Springer-Verlag, Berlin, Heidelberg, pp. 423–443.

Hiyama, A., Takemiya, A., Munemasa S., Okuma, E., Sugiyama, N., Tada, Y., Murata, Y., and Shimazaki, K.-I. (2017) Blue light and CO2 signals converge to regulate light-induced stomatal opening. *Nat. Comm.* 8: 1284.

Inoue, S.-I., Takemiya, A., and Shimazaki, K.-I. (2010) Phototropin signaling and stomatal opening as a model case. *Curr. Opin. Plant Biol.* 13: 587–593.

Leivar, P., and Monte, E. (2014) PIFs: Systems integrators in plant development. *Plant Cell* 26: 56–78.

Liscum, E., Askinosie, S. K., Leuchtman, D. L., Morrow, J., Willenburg, K. T., and Coats, D. R. (2014) Phototropism: Growing towards an understanding of plant movement. *Plant Cell* 26: 38–55.

Rizzini, L., Favory, J.-J., Cloix, C., Faggionato, D., O'Hara, A., Kaiserli, E., Baumeister, R., Schäfer, E., Nagy, F., Jenkins, G. I., et al. (2011) Perception of UV-B by the *Arabidopsis* UVR8 protein. *Science* 332: 103–106.

Rockwell, R. C., Duanmu, D., Martin, S. S., Bachy, C., Price, D. C., Bhattachary, D., Worden, A. Z., and Lagarias, J. C. (2014) Eukaryotic algal phytochromes span the visible spectrum. *Proc. Natl. Acad. Sci. USA* 111: 3871–3876.

Swartz, T. E., Corchnoy, S. B., Christie, J. M., Lewis, J. W., Szundi, I., Briggs, W. R. and Bogomolni, R. A. (2001) The photocycle of a flavin-binding domain of the blue light photoreceptor phototropin. *J. Biol. Chem.* 276: 36493–36500.

Takala, H., Bjorling, A., Berntsson, O., Lehtivuori1, H., Niebling, S., Hoernke, M., Kosheleva, I., Henning, R., Menzel, A., Janne, A., et al. (2014) Signal amplification and transduction in phytochrome photosensors. *Nature* 509: 245–249.

Takemiya, A., Sugiyama, N., Fujimoto, H., Tsutsumi, T., Yamauchi, S., Hiyama, A., Tadao, Y., Christie, J. M., and Shimazaki, K.-I. (2013) Phosphorylation of BLUS1 kinase by phototropins is a primary step in stomatal opening. *Nat. Commun.* 4: 2094. doi: 10.1038/ncomms3094

Takemiya, A., Yamauchi, S., Yano, T., Ariyoshi, C., and Shimazaki, K.-I. (2013) Identification of a regulatory subunit of protein phosphatase 1, which mediates blue light signaling for stomatal opening. *Plant Cell Physiol.* 54: 24–35.

Wada, M. (2013) Chloroplast movement. *Plant Sci*. 210: 177–182.

Wang, Q., Zuo, Z. C., Wang, X., Gu, L. F., Yoshizumi, T., Yang, Z. H., Yang, L., Liu, Q., Liu, W., Han, Y. J., et al. (2016) Photoactivation and inactivation of Arabidopsis cryptochrome 2. *Science* 354: 343–347.

17 Seed Dormancy, Germination, and Seedling Establishment



schankz/Shutterstock

Seeds are specialized plant structures adapted for the dispersal of the next sporophyte generation. Seeds are unique to the Spermatophyta (seed plants), which includes both the angiosperms and gymnosperms. Seeds develop from ovules, which before fertilization contain the female gametophytes and where, after fertilization, embryogenesis occurs (see Chapters 21 and 22). The seed tissues surrounding the embryo provide stored foods to the embryo throughout embryogenesis and early seedling development. The seed also protects the embryo from the environment after the seed is released from the parent plant. The packaging of the embryo into a self-contained seed was one of many evolutionary adaptations that freed plant reproduction from a dependence on water. The evolution of seed plants thus represents an important milestone in the adaptation of plants to dry land.

We begin this chapter by describing the structure and composition of various types of seeds. Next we describe the processes of seed germination and seedling establishment—by which we mean the production of the first photosynthetic leaves and a minimal root system. Between embryogenesis and germination there is typically a period of *seed maturation* that culminates in *quiescence*, a non-germinating state characterized by a reduced metabolic rate, after which the seed is released from the parent plant. Quiescence ensures that germination is delayed until the seed reaches the soil, where it can receive the water and oxygen required for seedling growth. Although some seeds have the capacity to germinate as soon as they are mature, others remain in a state known as a *dormancy* and require an additional treatment or tigger, such as light, chilling, or physical abrasion, before they can germinate. For many agricultural crops this is not a problem, because human selection for rapidly germinating seeds has resulted in the gradual loss of dormancy-inducing genes.

Once a seed begins to germinate, its food reserves are mobilized to support the growth of the emerging seedling. A wide variety of enzymes are produced that degrade the stored proteins, lipids, and starch stored in the seed. Hormones play an important role in coordinating the processes of germination and food mobilization.

Later in the chapter we consider the processes involved in the ongoing growth of the plant. These include photomorphogenesis (light-induced development), the development of a functioning vascular system, and the mechanisms regulating growth rate. Finally, we discuss the differential growth responses that allow the plant to navigate its environment, including gravitropism and phototropism, the processes by which plants orient themselves to gravity and light.

17.1 Seed Structure

Although this chapter focuses on the seeds of angiosperms because of their extraordinary diversity and importance to agriculture, it is important to appreciate the differences between the seeds of angiosperms and gymnosperms, which are discussed in **WEB TOPIC 17.1**. All seeds contain three basic structural features: an embryo, food storage tissue, and a protective outer layer of dead cells called the **seed coat** (or **testa**). The angiosperm embryo consists of the embryonic axis, which is composed of the **radicle**, or embryonic root; the **hypocotyl**, to which one or two **cotyledons** are attached; and the **shoot apex** bearing the **plumule**, or first true leaf primordium. In angiosperms, the food storage tissue that nourishes the growing embryo is the triploid endosperm that results from double fertilization (see Chapter 21). In some angiosperm species, the seed coat is fused to the fruit wall, or **pericarp**, which is derived from the ovary wall. In cereals, the seed coat pericarps are fused, technically making these "seeds" fruits, and will be referred to as seeds throughout the book. **Figure 17.1** shows a variety of familiar true seeds as well as fruits with a seedlike appearance.

Seed anatomy varies widely among different plant groups

Despite their common features, seeds range widely in size, from the dust-sized particles of orchids, weighing



Figure 17.1 Seeds and seedlike fruits. **(A–D)** True seeds. (A) Rapeseed (*Brassica napus*). (B) Brazil nut (*Bertholletia excelsa*). (C) Coffee bean (*Coffea* sp.). (D) Coconut (*Cocos nucifera*). **(E–I)** Simple dried indehiscent fruits. (E) Samara, a winged achene, from maple (*Acer* sp.). (F) Achene from strawberry (*Fragaria* sp.). (G) Caryopses, from wheat and other cereals (e.g., *Triticum* spp.). (H) Nut from oak (*Quercus* sp.). (I) Cypselae, an achene with 2 carpals, from sunflower and other composites (e.g., *Helianthus* spp.). Monocot caryopses and Asteraceae cypselae are routinely referred to as seeds.

1 μg, to the massive seeds of the coco de mer (*Lodoicea maldivica*), which can reach 30 cm in length and weigh 20 kg. Despite the relative simplicity of the embryo, and the limited number of tissues surrounding it, seed anatomy exhibits considerable diversity among the different plant groups.

Seeds can be categorized broadly as endospermic or non-endospermic, depending on the presence or absence of a well-formed triploid endosperm at maturity. **Figure 17.2** shows representative examples from both categories. For example, beet seeds are non-endospermic because the triploid endosperm is largely used up during embryo development. Instead, the perisperm and storage cotyledons serve as the main sources of nutrients during germination. The **perisperm** is derived from the nucellus, the maternal tissue that gives rise to the ovule (see Chapter 21). Garden bean seeds (*Phaseolus vulgaris*) and legume seeds in general are also non-endospermic, relying on their large storage cotyledons, which make up most of the bulk of the seed, for their food reserves. In

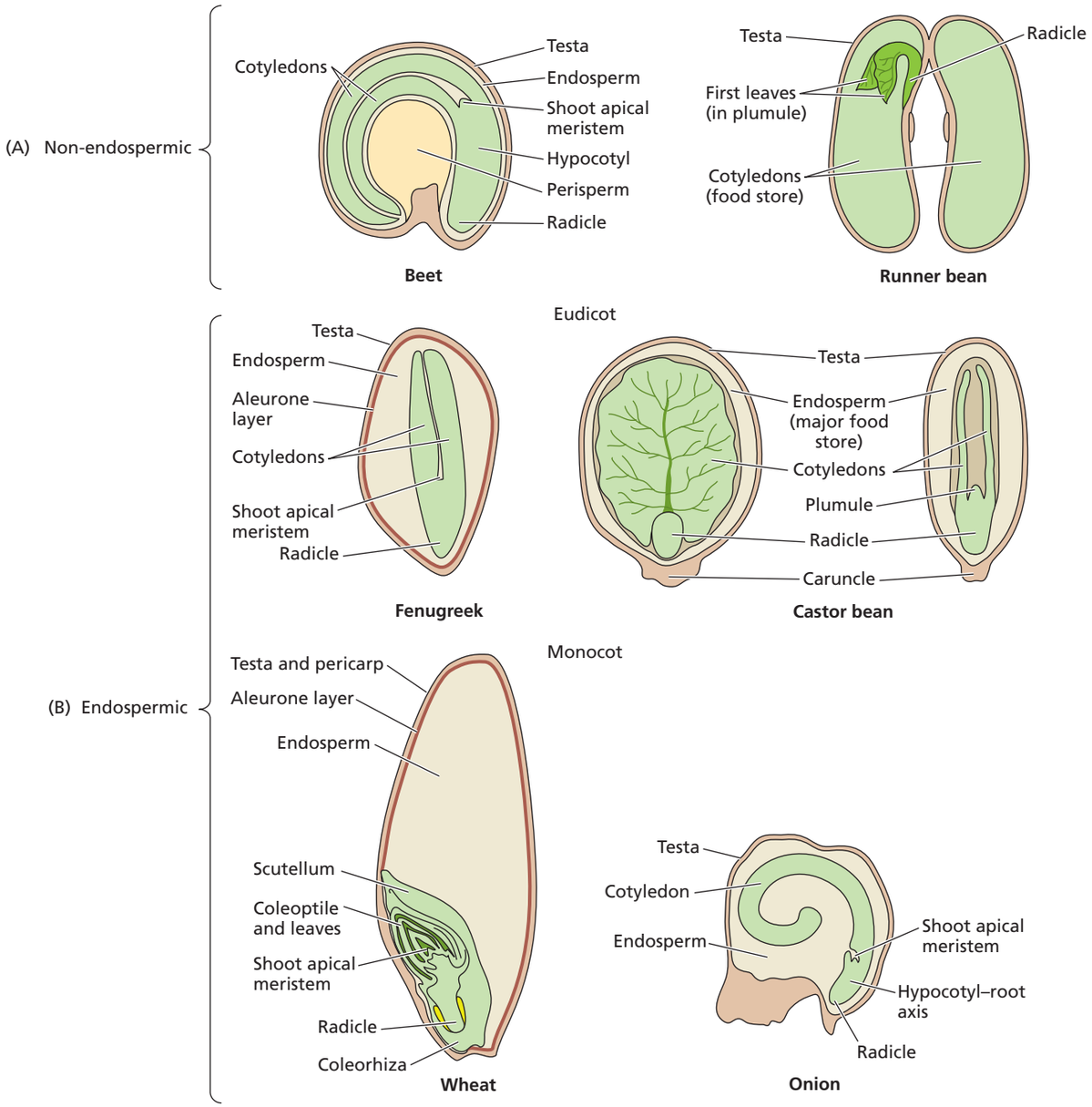


Figure 17.2 Seed structures. Structure of non-endospermic seeds (A) and endospermic seeds (B).

contrast, castor bean (*Ricinus communis*), onion (*Allium cepa*), bread wheat (*Triticum* spp.), and maize (corn; *Zea mays*) seeds are all endospermic.

In keeping with its role as a food storage tissue, the endosperm is typically rich in starch, lipids, and proteins. Some endosperm tissue has thick cell walls that break down during germination, releasing a variety of sugars. The outermost layer of the endosperm in some species differentiates into a specialized secretory tissue with thickened primary walls called the *aleurone layer*, so named because it is composed of cells filled with **protein storage vacuoles** (**PSVs**), originally called *aleurone grains* (see Figure 1.23). As you will see in Section 17.5, the aleurone layer plays an important role in regulating dormancy in certain eudicot seeds. In seeds of wheat and other members of the Poaceae (grass family), secretory aleurone layers are also responsible for the mobilization of stored food reserves during germination.

The embryos of cereal grains are highly specialized and merit closer examination both because of their agricultural importance and because they have been widely used as model systems to study the hormonal regulation of food mobilization during germination. Specialized embryonic structures are found in seeds from the grass family and are discussed in Chapter 22. These include the following structures (see Figure 17.2B):

- The single cotyledon has been modified by evolution to form an absorptive organ, the **scutellum**, which forms the interface between the embryo and the starchy endosperm tissue. During germination, mobilized sugars from the endosperm are absorbed by the scutellum and transported to the embryo proper.
- The basal sheath of the scutellum has been elongated to form a **coleoptile** that covers and protects the first leaves while the shoot is growing up through the soil.
- The base of the hypocotyl has been elongated to form a protective sheath around the radicle called the **coleorhiza**.
- In some members of the grass family, such as maize, the upper hypocotyl has been modified to form a **mesocotyl** (not shown in Figure 17.2B). During seedling development, the growth of the mesocotyl helps raise the shoot to the soil surface, especially in the case of deeply planted seeds (see **WEB TOPIC 17.2**).

17.2 Seed Dormancy

During seed maturation, the embryo dehydrates and enters a quiescent phase. Seed germination requires rehydration and can be defined as the resumption of growth of the embryo in the mature seed. The process of germination encompasses all the events that take place between the start of *imbibition* (moistening) of the dry seed (discussed in Section 17.4 in the context of seed germination) and the *emergence* of the embryo, usually starting with the radicle, from the structures that surround it. Successful completion of germination depends on the same environmental conditions as vegetative growth (see Chapter 18): Water and oxygen must be available, and the temperature must be in the *physiological range* (that is, the range that does not inhibit physiological processes). However, a viable (living) seed may not germinate even if the appropriate environmental requirements are satisfied, a phenomenon known as **seed dormancy**. Seed dormancy is an intrinsic temporal block to the initiation of germination that provides additional time for seed dispersal over greater distances. It also maximizes seedling survival by preventing germination under unfavorable conditions. *Seed banks* are repositories where seeds are stored under conditions that maintain both dormancy and viability. A seed bank may comprise a naturally occurring repository (such as the soil) or an artificial repository built by humans.

Most mature seeds typically have less than 0.1 g water g^{-1} dry weight at the time of shedding. As a consequence of dehydration, metabolism comes nearly to a halt and the seed enters a quiescent, or "resting," state. In some cases the seed becomes dormant as well. Unlike **seed quiescence**, defined as the failure to germinate because of a lack of water, O_2, or proper temperature for growth, seed dormancy requires additional treatments or signals for germination to occur.

Different types of seed dormancy can be distinguished on the basis of the developmental timing of dormancy onset. Newly dispersed, mature seeds that fail to germinate under favorable conditions exhibit **primary dormancy**. Once primary dormancy has been lost, non-dormant seeds may acquire **secondary dormancy** if exposed to unfavorable conditions that inhibit germination over an extended period of time (see **WEB TOPIC 17.3**).

There are two basic types of seed dormancy mechanisms: exogenous and endogenous

Seed dormancy may have both physical and physiological mechanisms. According to one classification scheme, primary seed dormancy can be divided into two main types, *exogenous dormancy* and *endogenous dormancy*.

Exogenous dormancy, or **coat-imposed dormancy**, refers to the physical inhibitory effects of the seed coat or other enclosing tissues, such as the endosperm, pericarp, or extrafloral organs, on the growth of the embryo during germination. The embryos of such seeds germinate readily in the presence of water and oxygen once the seed coat and other surrounding tissues have either been removed or damaged. There are several ways that seed coats can impose dormancy on the embryo:

- *Water impermeability.* This type of dormancy, also called hard-seededness, is common in plants found in arid and semiarid regions, especially among legumes, such as clover (*Trifolium* spp.) and alfalfa (*Medicago* spp.). The classic example is Indian lotus (*Nelumbo nucifera*) seeds, which can survive up to 1200 years because of their impermeable coats. Waxy cuticles, suberized layers, and the cell walls of palisade layers consisting of lignified sclereids all combine to restrict the penetration of water into the seed. This type of dormancy can be broken by mechanical or chemical scarification. In the wild, passage through the digestive tracts of animals can cause chemical scarification.
- *Interference with gas exchange*. Dormancy in some seeds can be overcome by oxygen-enriched atmospheres, suggesting that the seed coat and other surrounding tissues limit the supply of oxygen to the embryo. In wild mustard (*Sinapis arvensis*), the permeability of the seed coat to oxygen is less than that to water by a factor of 10^4. In other seeds, oxidative reactions involving phenolic compounds in the seed coat may consume large amounts of oxygen, reducing oxygen availability to the embryo.
- *Mechanical constraint*. The first visible sign of germination is typically the radicle (embryonic root) breaking through its surrounding structures, such as the endosperm, if present, and seed coat. In some cases, however, the thick-walled endosperm may be too rigid for the radicle to penetrate, as in Arabidopsis, tomato, coffee, and tobacco. For such seeds to complete germination, the endosperm cell walls must be weakened by the production of cell wall–degrading enzymes, typically where the radicle emerges.
- *Retention of inhibitors*. Dormant seeds often contain secondary metabolites, including phenolic acids, tannins, and coumarins, and repeated rinsing of such seeds with water often promotes germination. The seed coat may impose dormancy by preventing the escape of inhibitors from the seed, or the seed coat may produce inhibitors that diffuse into the embryo.

Endogenous dormancy, also known as **embryo dormancy**, refers to seed dormancy that is intrinsic to the seed and is not due to any physical or chemical influence of the seed coat or other surrounding tissues. Endogenous dormancy is regulated by the ratio of the hormones abscisic acid (ABA) and gibberellin (GA) (discussed at the end of this section), and may be due to arrested embryogenesis, resulting in small, immature embryos (see **WEB TOPIC 17.4**), or to a lack of sucrose availability in the embryonic axis, as in apple (*Malus domestica*). Endogenous dormancy is typically induced by ABA at the end of embryogenesis. Fully mature seeds require endogenous ABA for the regulation and maintenance of primary dormancy following imbibition of the dry seed. For example, in Arabidopsis, lettuce, barley, and tobacco seeds, the degree of seed dormancy correlates with endogenous ABA concentration in imbibed, rather than in dry, seeds. After dormancy is broken, the seed is able to germinate over the range of conditions permissible for the particular genotype.

Non-dormant seeds can exhibit vivipary and precocious germination

In some species the mature seeds not only lack dormancy, but also germinate while still on the mother plant, a phenomenon known as **vivipary**. True vivipary is extremely rare in angiosperms and is largely restricted to mangroves and other plants growing in estuarine or riparian ecosystems in the tropics and subtropics. A well-known example of a viviparous species is red mangrove (*Rhizophora mangle*) (**Figure 17.3**). Seeds of this species germinate while still inside the attached fruit and produce an elongated, dartlike propagule that can drop from the tree and root itself in the surrounding soft mud.

The germination of physiologically mature seeds on the mother plant is known as **preharvest sprouting** and is characteristic of some grain crops when they mature in



© Larry Larsen/Alamy Stock Photo

Figure 17.3 Vivipary in a wetland plant. Viviparous seeds of red mangrove (*Rhizophora mangle*).

(A)



Jaswinder Singh/McGill University

(B)



Photo by Jenny Rees



© Branex/Dreamstime.com

Figure 17.4 **Xivipary in crop plants.** Preharvest sprouting in wheat (*Triticum aestivum*) **(A)** and maize (*Zea mays*) **(B)**. For both species, non-sprouting heads and ears, respectively, are shown to the right for comparison.

wet weather (**Figure 17.4A**). Preharvest sprouting in cereals (e.g., wheat, barley, rice, and sorghum) reduces grain quality and causes serious economic losses. In maize, *viviparous* (*vp*) mutants have been selected in which the embryos germinate directly on the cob while still attached to the parent plant (**Figure 17.4B**). Several of these mutants are ABA deficient and one is ABA insensitive, preventing the normal ABA-mediated dormancy. Vivipary in the ABA-deficient mutants can be partially prevented by treatment with exogenous ABA. Vivipary in maize also requires GA biosynthesis early in embryogenesis as a positive signal to induce germination; double mutants deficient in GA and ABA do not exhibit vivipary. This shows that germination is regulated by the ABA:GA ratio, not the actual amount of ABA.

The ABA:GA ratio is the primary determinant of embryonic seed dormancy

It has long been known that ABA exerts an inhibitory effect on seed germination, whereas GA exerts a positive effect. According to the **hormone balance theory**, the ratio of these two hormones serves as the primary determinant of seed dormancy and germination. The relative hormonal activities of ABA and GA in the seed depend on two main factors: the amounts of each hormone present in the target tissues, and the ability of the target tissues to detect and respond to each of the hormones. Hormonal sensitivity, in turn, is determined by the hormonal signaling pathways in the target tissues (**Figure 17.5**).

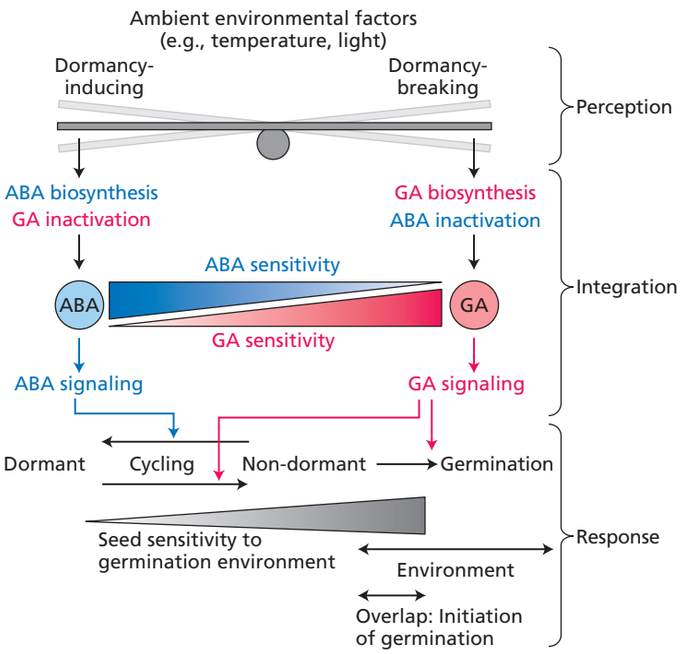


Figure 17.5 **Model for ABA and gibberellin (GA) regulation of dormancy and germination in response to environmental factors.** Environmental factors such as temperature affect the ABA:GA ratios and the responsiveness of the embryo to ABA and GA. In dormancy, GA is inactivated and ABA biosynthesis and signaling predominate. In the transition to germination, ABA is inactivated and GA biosynthesis and signaling predominate. The complex interplay between ABA and GA metabolism and sensitivity in response to environmental conditions can result in cycling between dormant and non-dormant states (dormancy cycling). Germination can proceed to completion when favorable environmental conditions and non-dormancy coincide. (After W. E. Finch-Savage and G. Leubner-Metzger. 2006. *New Phytol.* 171: 501–523.)

The amounts of ABA and GA are determined by their relative rates of biosynthesis versus inactivation (see Chapter 4 and **WEB APPENDIX 3**). The balance between the biosynthesis and inactivation pathways is regulated by the action of transcription factors. As discussed in Section 17.3, certain environmental factors can alter the ABA:GA balance in seeds and thereby stimulate germination. Certain treatments, such as *after-ripening*, can promote germination by reducing ABA concentrations, while other treatments, such as chilling (or *stratification*) can promote germination by increasing GA biosynthesis (see Figure 17.5). We discuss both after-ripening and chilling in greater detail later in Section 17.3.

Another factor that appears to regulate seed dormancy is the relative sensitivities of the embryo to ABA and GA. According to a recent model, the hormonal sensitivity of the embryo is under both developmental and environmental control (see Figure 17.5). During the early stages of seed development, ABA sensitivity is high and GA sensitivity is low, which favors dormancy over germination. Later in seed development, ABA sensitivity declines and GA sensitivity increases, favoring germination. At the same time, the seed becomes progressively more sensitive to environmental cues, such as temperature and light, that can either stimulate or inhibit germination.

ABA and GA are not the only hormones regulating seed dormancy. For example, both ethylene and brassinosteroids reduce the ability of ABA to inhibit germination, apparently by negatively regulating the ABA signal transduction pathway. ABA also inhibits ethylene biosynthesis, while brassinosteroids enhance it. Thus, hormonal networks are probably involved in regulating seed dormancy, as they are in regulating most other developmental phenomena.

17.3 Release from Dormancy

Breaking dormancy involves a change in the metabolic state of the seed that enables the embryo to reinitiate growth. Because germination is an irreversible process that commits the seed to grow into a seedling, many species have developed sophisticated mechanisms for sensing the optimal environmental conditions for this to occur. Often there are seasonal components to the ultimate "decision" of a seed to germinate, as in the examples of secondary dormancy noted in **WEB TOPIC 17.3**. In this section we discuss some of the environmental cues that bring about the release from dormancy. Although each external signal is discussed separately, seeds in nature must integrate responses to multiple environmental factors, perceived either simultaneously or in succession.

Because the ABA:GA ratio plays such a decisive role in maintaining seed dormancy, environmental conditions that break dormancy ultimately are thought to activate gene networks that affect the balance between the responses to ABA and GA. This hypothesis is consistent with the fact that treatment of seeds with GA often can substitute for a positive environmental signal in breaking dormancy.

Light is an important signal that breaks dormancy in small seeds

Many seeds have a light requirement for germination (termed *photoblasty*), which may involve only a brief exposure, as in the case of the 'Grand Rapids' cultivar of lettuce (*Lactuca sativa*); an intermittent treatment (e.g., succulents of the genus *Kalanchoe*); or even a specific photoperiod involving short or long days. For example, birch (*Betula* spp.) seeds require long days (16 h light) to germinate, while seeds of the conifer eastern hemlock (*Tsuga canadensis*) require short days. Phytochrome, which senses red (R) and far-red (FR) wavelengths of light (see Chapter 16), is the primary sensor for light-regulated seed germination. All light-requiring seeds exhibit coat-imposed dormancy, and removal of the seed coat and endosperm allows the radicle (embryonic root) to elongate in the absence of light. The effect that light has on the embryo is thus to enable the radicle to penetrate the endosperm, a process facilitated in some species by enzymatic weakening of the cell walls in the micropylar region, adjacent to the radicle.

Light is required for germination of the small seeds of numerous herbaceous and grassland species, many of which remain dormant if they are buried below the depth to which light penetrates the soil. Even when such seeds are on or near the soil surface, the amount of shading by the vegetation canopy (i.e., the R:FR light ratio the seeds receive) is likely to affect their germination. We will return to the effects of the R:FR ratio in Chapter 19 in relation to the phenomenon of shade avoidance.

Some seeds require either chilling or after-ripening to break dormancy

Many seeds require a period of low temperature (1–10°C) to germinate. For species adapted to temperate climates, this requirement has obvious survival value, since such seeds will not germinate in the fall, but rather in the following spring. Chilling seeds to break their dormancy is called **stratification**, named for the agricultural practice of overwintering dormant seeds in layered mounds of soil or moist sand. Today seeds are simply stored moist in a refrigerator. Stratification has the added benefit that it synchronizes germination, which ensures that plants will mature at the same time. **Figure 17.6A** shows the effects of chilling on apple seed germination. Intact seeds require 80 days of chilling for maximum germination, whereas isolated embryos exhibit maximum germination after approximately 50 days. Thus, the presence of the surrounding tissues (seed coat and endosperm) increases the chilling requirement of the embryo by about 30 days.

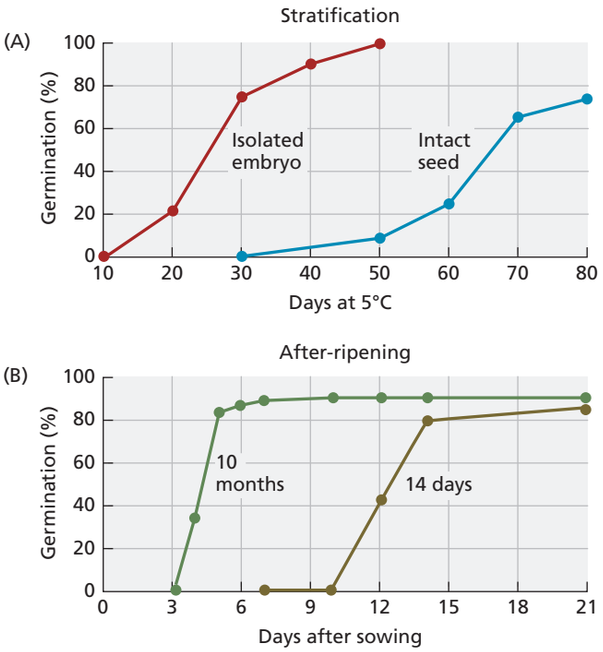


Figure 17.6 Seed dormancy can be overcome by stratification and after-ripening. **(A)** Release of apple seeds from dormancy by stratification, or moist chilling. Imbibed seeds were stored at 5°C and periodically removed to test the seeds or isolated embryos for germination. The germination of intact seeds (defined as emergence of the radicle) was significantly delayed compared with that of isolated embryos (defined as elongation of the radicle). **(B)** Effect of after-ripening on the germination of *Nicotiana plumbaginifolia seeds*. After-ripening for 10 months or longer greatly accelerated germination compared with after-ripening for only 14 days. (A after J. D. Bewley et al. 2013. In *Seeds: Physiology of Development, Germination, and Dormancy*, 3rd edition. Springer, New York.; B after P. Grappin et al. 2000. *Planta* 2010: 279–285.)

Some seeds may require a period of **after-ripening**, meaning dry storage at room temperature, before they can germinate. The duration of the after-ripening requirement may be as short as a few weeks (e.g., barley, *Hordeum vulgare*) or as long as 5 years (e.g., curly dock, *Rumex crispus*). In the field, after-ripening may occur in winter annuals in which dormancy is broken by high summer temperatures, allowing the seeds to germinate in the fall. In contrast, moist chilling during the cold winter months is effective in many summer annuals. After-ripening of horticultural and agricultural crop seeds is usually performed in special drying cupboards that maintain the appropriate temperature, aeration, and low moisture conditions.

The effect of the duration of after-ripening on the germination of seeds of *Nicotiana plumbaginifolia* is shown in **Figure 17.6B**. Seeds after-ripened for only 14 days began to germinate after about 10 days of subsequent wetting, while seeds after-ripened for 10 months began germinating after only 3 days. Seeds are considered "dry" when their water content drops below 20%. However, if the seeds become too dry (5% water content or less), the effectiveness of after-ripening is diminished. In several species, ABA concentrations decrease during after-ripening, and even a small decline may be sufficient to break dormancy. For example, in *N. plumbaginifolia* seeds, the ABA concentration decreases by about 40% during after-ripening. In general, after-ripening promotes a decrease in ABA concentration and sensitivity, and a rise in GA concentration and sensitivity.

Seed dormancy can be broken by various chemical compounds

Numerous chemicals, such as respiratory inhibitors, sulfhydryl compounds, oxidants, and nitrogenous compounds, have been shown to break seed dormancy in specific species. However, only a few of these chemicals occur naturally in the environment. Of these, nitrate, often in combination with light, is probably the most important. Some plants, such as hedge mustard (*Sisymbrium officinale*), have an absolute requirement for nitrate and light for seed germination. Another chemical agent that can break dormancy is nitric oxide (NO), a signaling molecule that also functions in multiple stress responses (see Chapter 15). Mutants unable to synthesize NO exhibit reduced germination, and the effect can be reversed by treating the seeds with exogenous NO. Another strong chemical stimulant of seed germination in many species under natural conditions is smoke, which is produced during forest fires. Smoke is likely to contain multiple germination stimulants; one of the most active of these is **karrikinolide**, a member of the karrikin class of molecules, which structurally resemble strigolactone plant hormones (see Chapter 4).

In all three of these examples, the chemical stimulants appear to break dormancy by the same basic mechanism: by down-regulating ABA biosynthesis or signaling, and up-regulating GA biosynthesis or signaling, thus altering the ABA:GA ratio.

17.4 Seed Germination

Germination is the process that begins with water uptake by the dry seed and ends with the emergence of part of the embryo, usually the radicle, from its surrounding tissues. Strictly speaking, germination concludes with radicle emergence and does not include subsequent seedling growth. The rapid mobilization of stored food reserves that fuels the initial growth of the seedling is initiated during germination.

Germination requires permissive ranges of water, temperature, and oxygen, and often light and nitrate as well. Of these, water is the most essential factor. The

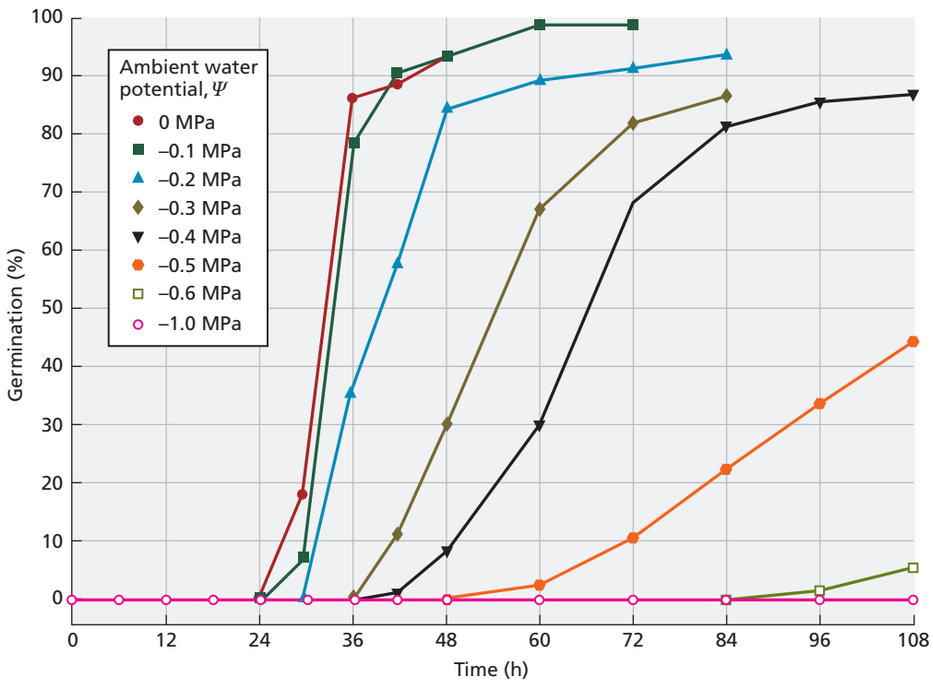


Figure 17.7 Time course of tomato seed germination at different ambient water potentials. (After G. Leubner [seedbiology.de] and A. Liptay and P. Schopfer. 1983. *Plant Physiol.* 73: 935–938.)

water content of mature, air-dried seeds is in the range of 5 to 15%, well below the threshold required for fully active metabolism. In addition, water uptake is needed to generate the turgor pressure that powers cell expansion, the basis of vegetative growth and development. As we discussed in Chapter 6, water uptake is driven by the gradient in water potential (Ψ) from the soil to the seed. For example, incubating tomato seeds at high ambient water potential (Ψ = 0 MPa) allows 100% germination, whereas incubation at low water potential (Ψ = –1.0 MPa), which nullifies the gradient in water potential, completely suppresses germination (**Figure 17.7**).

Germination and postgermination can be divided into three phases corresponding to the phases of water uptake

Under normal conditions, water uptake by the seed is triphasic (**Figure 17.8**):

- *Phase I*. The dry seed takes up water rapidly by the process of imbibition.
- *Phase II*. Water uptake by imbibition declines and metabolic processes, including transcription and translation, are reinitiated. The embryo expands, and the radicle emerges from the seed coat.
- *Phase III*. Water uptake resumes because of a decrease in Ψ as the seedling grows, and the stored food reserves of the seed are fully mobilized.

The initial rapid uptake of water by the dry seed during Phase I is referred to as **imbibition**, to distinguish it from water uptake during Phase III. Although the water potential gradient drives water uptake in both cases, the causes of the gradients are different. In the dry seed, the **matric potential** (Ψ_m) component of the water potential equation lowers Ψ and creates the gradient. The matric potential arises from the binding of water to solid surfaces, such as the microcapillaries of cell walls and the surfaces of proteins and other macromolecules (see Chapter 5). The rehydration of cellular macromolecules activates basal metabolic processes, including respiration, transcription, and translation.

Imbibition ceases when all the potential binding sites for water become saturated, and Ψ_m becomes less negative. During Phase II the rate of water uptake slows down until the water potential gradient is reestablished. Phase II can thus be thought of as the lag phase preceding growth, during which the solute potential (Ψ_s) of the embryo gradually becomes more negative because of the breakdown of stored food reserves and the liberation of osmotically active solutes. The seed volume may increase as a result, rupturing the seed coat. At the same time, additional metabolic functions come online, such as the re-formation of the cytoskeleton and the activation of DNA repair mechanisms.

The emergence of the radicle through the seed coat in Phase II marks the end of the process of germination. The cell walls of the radicle are loosened and extend in response to the increase in turgor pressure that accompanies the uptake of water, which causes cell elongation. However, in many seeds the radicle must first break

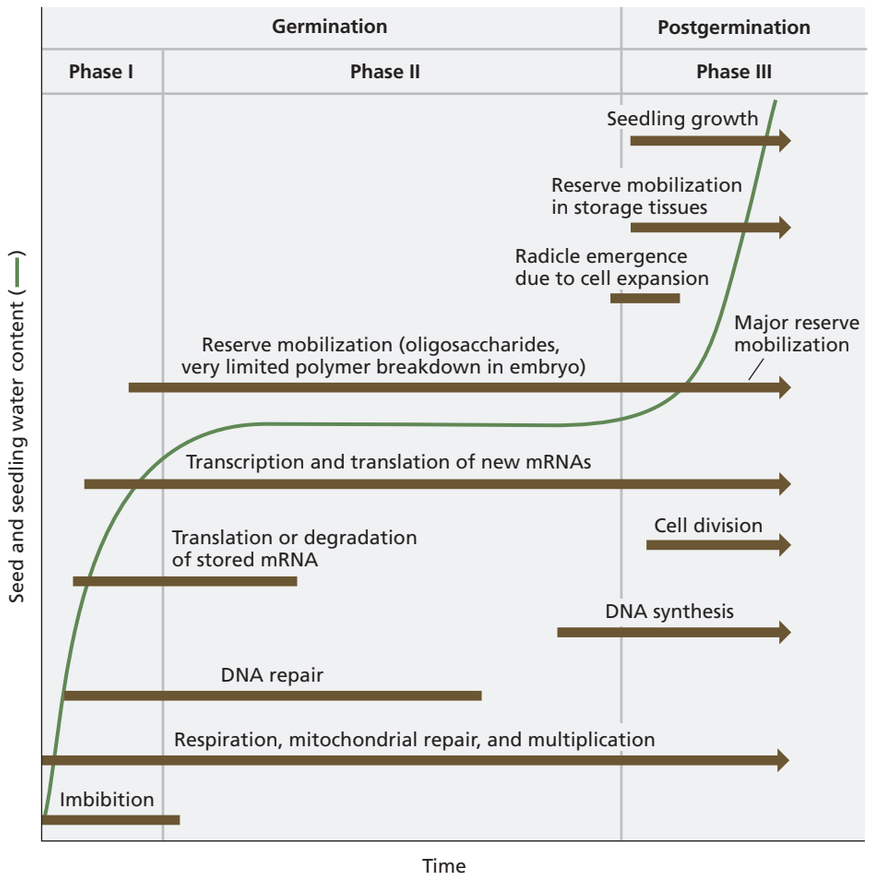


Figure 17.8 Phases of water uptake in seeds. In Phase I, dry seeds imbibe (take up) water rapidly. Since water flows from the higher to the lower water potential, the water uptake by the seed stops when the difference in water potential between the seed and the environment becomes zero. During Phase II the cells expand and the radicle emerges from the seed, completing germination. Metabolic activity increases and cell wall loosening occurs. In Phase III, water uptake resumes as the seedling becomes established. (After J. D. Bewley. 1997. *Plant Cell* 9: 1055–1066; H. Nonogaki et al. 2007. In *Annual Plant Reviews, Vol. 27: Seed Development, Dormancy, and Germination*; H. Nonogaki et al. 2010. *Plant Sci.* 179: 574–581.)

through the barrier imposed by the surrounding endosperm, seed coat, or pericarp before it can emerge from the seed. Radicle emergence can be a one- or two-step process. In the one-step process, either the surrounding tissues become physically weakened during imbibition, allowing the radicle to emerge unimpeded, or the radicle expands sufficiently during imbibition to rupture the surrounding tissues. In the two-step process, the surrounding tissues must first undergo metabolic weakening before the radicle can emerge from the seed (see **WEB TOPIC 17.5**).

During Phase III the rate of water uptake increases rapidly because of the onset of cell wall loosening and cell expansion, as seedling growth begins. Thus, the water potential gradient in Phase III embryos is maintained by both cell wall relaxation and solute accumulation.

17.5 Mobilization of Stored Reserves

The major food reserves of angiosperm seeds are typically stored in the cotyledons or in the endosperm. Proteins, lipids, and carbohydrates (starch) are stored in specialized structures within these tissues. Starch is stored in **amyloplasts**, which are specialized plastids (see Chapter 1); proteins are stored in protein storage vacuoles (PSVs); and lipids are stored in **oil bodies**, or lipid droplets. All plants have these three types of specialized food storage structures, although in many plants one type predominates. After germination there is a massive mobilization of reserves to provide nutrients, carbon, nitrogen, minerals, and so on to the growing seedling until it becomes autotrophic.

Starch is an important form of stored carbon and is the major food reserve in cereals. The endosperm is the major tissue that stores starch in cereals, though it can also accumulate in the embryo. Starch degradation is initiated by the enzymes α-amylase and β-amylase. α-Amylase hydrolyzes starch chains internally to produce oligosaccharides consisting of α(1,4)-linked glucose residues. β-Amylase degrades these oligosaccharides from the ends to produce the disaccharide maltose, which is then converted to glucose by maltase. Mobilization of stored food reserves is important industrially for producing malted grains for bread, beverages, and other products.

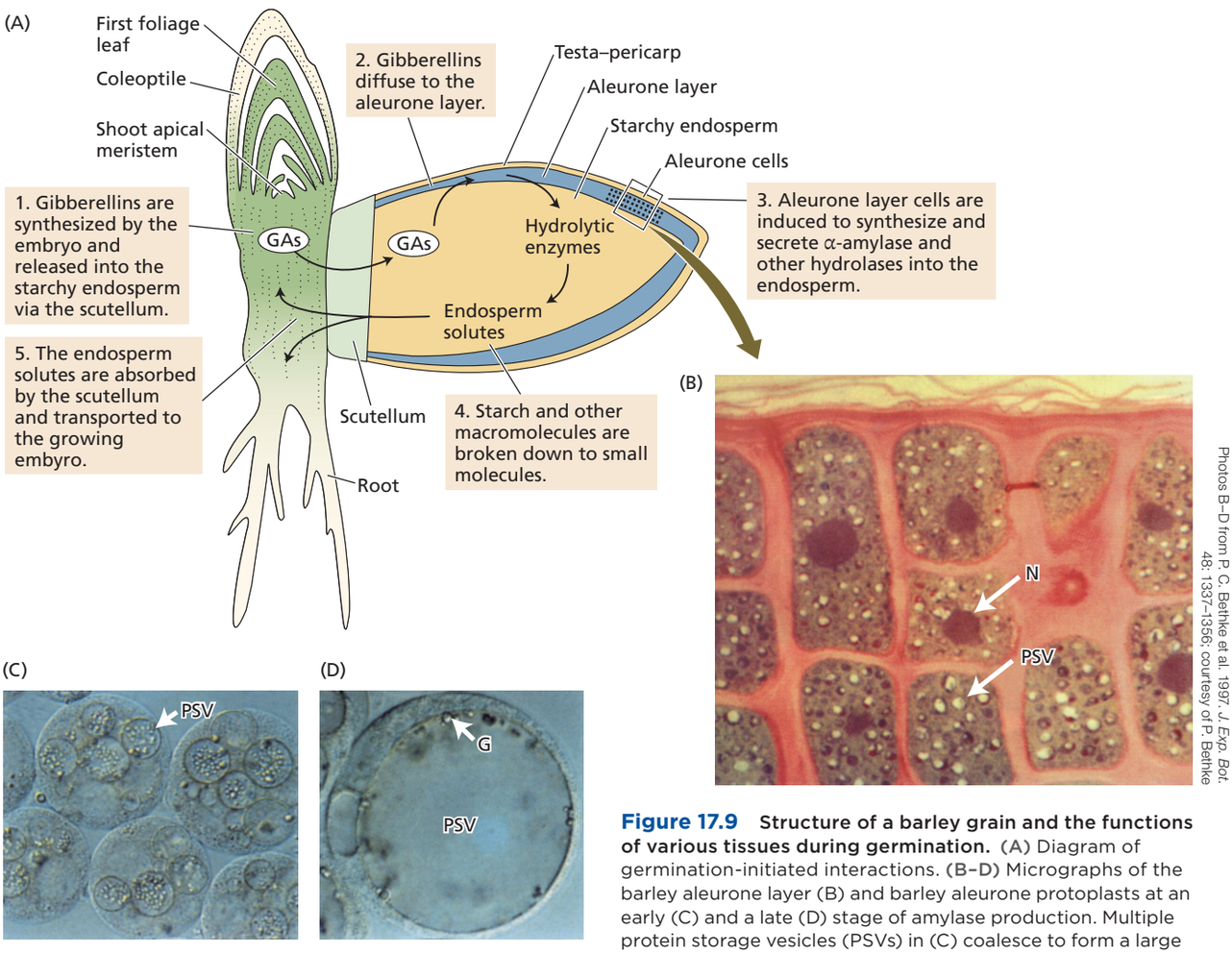
Protein storage vacuoles are the primary source of nitrogen and amino acids for new protein synthesis in the seedling. (See Figure 1.23 for a micrograph of PSVs.) The stored proteins are hydrolyzed by proteases. Protein

storage vacuoles also contain phytin, the K^+, Mg^{2+}, or Ca^{2+} salt of phytic acid (*myo*-inositol hexaphosphate, a sugar alcohol), the major storage form of phosphate in seeds. During food mobilization, the enzyme phytase hydrolyzes phytin to release phosphate and the other ions for use by the growing seedling. Legumes are an example of plants that store a large amount of protein in their seeds.

Oil bodies contain lipids, which are high-energy carbon sources and are converted to sucrose during germination. (See Figure 1.25 and Figure 13.19 for electron micrographs of oil bodies.) In addition to storing triacylglycerides and phospholipids, oil bodies also store proteins, such as oleosins, caleosins, and steroleosins, with oleosins being predominant. Oil bodies are prevalent in oilseed plants such as rapeseed, mustard, cottonseed, flax, maize, peanut, sesame, copra, palm kernel, soybean, and sunflower seed. In oilseed plants, the oil bodies are synthesized in the embryo. As discussed in Chapter 13, lipids are catabolized during seed germination via the activity of lipases, β-oxidation, and the glyoxylate cycle.

Cereal seeds are a model for understanding starch mobilization

Cereals have a specialized starch mobilization mechanism that has been extensively studied as a model for how ABA and GA function during germination and seedling establishment. Cereal seeds consist of three parts: the embryo, the endosperm, and the fused seed coat pericarp (**Figure 17.9**). The embryo, which will grow into the new seedling, has a specialized absorptive organ, the scutellum. The triploid endosperm is composed of two tissues: the centrally located **starchy endosperm** and, surrounding it, a peripheral **aleurone layer**. The aleurone layer is a specialized digestive tissue; the starchy endosperm consists of thin-walled cells with amyloplasts filled with starch grains. Living cells of



Photos B–D from P. C. Bethke et al. 1997. *J. Exp. Bot.* 48: 1337–1356; courtesy of P. Bethke

Figure 17.9 Structure of a barley grain and the functions of various tissues during germination. **(A)** Diagram of germination-initiated interactions. **(B–D)** Micrographs of the barley aleurone layer (B) and barley aleurone protoplasts at an early (C) and a late (D) stage of amylase production. Multiple protein storage vesicles (PSVs) in (C) coalesce to form a large vesicle in (D), which will provide amino acids for α-amylase synthesis. G, phytin globoid that sequesters minerals; N, nucleus.

the aleurone layer synthesize and release α-amylase and other hydrolytic enzymes into the starchy endosperm during germination. As a consequence, the stored food reserves of the endosperm are broken down, and the solubilized sugars, amino acids, and other products are transported to the growing embryo via the scutellum.

As shown in Figure 17.9, GA is released from the embryo during germination stimulate the production and release of α-amylase by the aleurone layer of cereal seeds. Once inside the aleurone cells, GA binds to its receptor and initiates a signal transduction pathway, as described in Chapter 4. (See **WEB TOPIC 17.6** for a discussion of GA signaling during germination.) GA signaling results in increased expression of a transcriptional activator, *GA-MYB*, which in turn induces expression of the α-amylase gene in the aleurone layer (**Figure 17.10**), leading to the production and secretion of α-amylase into the endosperm. GA also promotes programmed cell death of the aleurone layer after germination. During seed dormancy, this process is inhibited by ABA, ensuring that the aleurone layer will not undergo programmed cell death prior to germination. Experiments carried out in the 1960s confirmed earlier observations that the secretion of starch-degrading enzymes by barley aleurone layers depends on the presence of the embryo. It was soon discovered that GA_3 could substitute for the embryo in stimulating starch degradation. The significance of the GA effect became clear when it was shown that the embryo synthesizes and releases GAs into the endosperm during germination. Genetic studies demonstrated that while GA_1 is the only bioactive GA produced by cereals, the aleurone layers can respond to any bioactive GA, such as GA_3.

ABA inhibits the GA-induced synthesis of hydrolytic enzymes that are essential for the breakdown of storage reserves during seedling growth. In the case of α-amylase, ABA acts by inhibiting GA-dependent transcription of α-*amylase* mRNA.

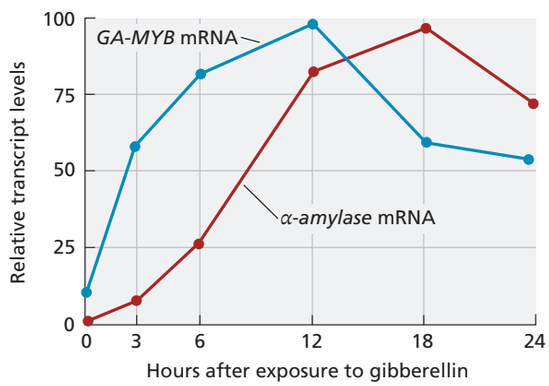


Figure 17.10 Time course for the induction of GA-responsive transcription factor (*GA-MYB*) and α-amylase mRNAs by GA_3. *GA-MYB* expression precedes that of α-amylase by about 3 h. In the absence of gibberellin, the concentrations of both the *GA-MYB* and α-amylase mRNAs are negligible. (After F. Gubler et al. 1995. *Plant Cell* 7: 1879–1891.)

Legume seeds are a model for understanding protein mobilization

In addition to being food reserves for the developing seedling, stored proteins may also increase tolerance to desiccation and reactive oxygen species and help stabilize membranes. Seed storage proteins can accumulate in the embryo and endosperm, as well as in the aleurone layer in cereals, and different proteins may be stored in different tissue types. Examples of seed storage proteins are presented in **Table 17.1**. These include water-insoluble globulins (e.g., legumins and vicilins in legumes), alcohol-soluble prolamins and alkali-soluble glutelins (in cereals), and water-soluble albumins (in many plants). Some storage proteins are similar to amylases but lack hydrolytic activity, indicating that these proteins have been repurposed specifically for storage. Compared with other proteins, seed storage proteins usually contain a greater percentage of nitrogen-rich amino acids, such as lysine, arginine, glutamine, and asparagine, as well as the sulphur-containing amino acid cysteine. Storage proteins are also a reservoir of reduced carbon, as well as minerals such as K^+, Mg^{2+}, or Ca^{2+}complexed with phytin or globulins. While seeds are dormant, their storage proteins are stabilized in various ways. For example, globulins can aggregate electrostatically via Mg^{2+} and Ca^{2+} ions to prevent proteolysis. Storage proteins also fold into compact sheets via disulphide bonds between cysteines such that only a few proteolytic sites are exposed.

During germination, proteases degrade storage proteins to mobilize the amino acids and nitrogen they contain. Proteases that are present in dormant seeds are usually stored separately from storage proteins within the cell, and rarely within PSVs. Proteases are inactive until the seed imbibes, and seeds often contain protease inhibitors that must be degraded before the proteases can hydrolyze the stored proteins. After imbibition and activation, proteases are moved to the PSVs, via trafficking of the proteases or by fusion of the compartments. Once the pH and redox balance become suitable for enzymatic activity, the storage proteins are cleaved by serine proteases, aspartic proteases, metalloproteases, and endo- and exopeptidases to provide the raw materials to synthesize new amino acids and proteins as the embryo germinates and the seedling becomes established. In cereals, GA increases expression of cysteine proteases in the aleurone layer needed for the mobilization of seed storage proteins. Similar proteases also function in the seasonal remobilization of storage proteins in the bark and roots of woody perennials and the roots of perennial grasses. **WEB TOPIC 17.7** discusses protein mobilization during Phases I and II of germination.

Table 17.1 Major families of seed storage proteins

Seed storage protein	Protein types and representative plants containing them
11S globulin (legumins)	Glycinin (*Glycine max*)
	Cruciferins (*Brassica canola*)
	Glutelins (*Oryza sativa*), e.g., glutenin (*Triticum* spp.)
7S globulin (vicilins)	Vicilin-type subunits: Phaseolin (*Phaseolus vulgaris*)
	Convicilin-type subunits: Convicilin (*Pisum sativum*)
	Beta-conglutin (*Lupinus albus*)
2S albumins	Single-chain type: SFA-8 (*Helianthus* spp.)
	Two-chain type: Napin (*Brassica napus*); Conglutin δ_2 (*L. albus*)
Sulfur-rich prolamins	α/β-gliadin (*Triticum* spp.)
	γ-gliadin (*Triticum* spp.)
	B-hordein (*Hordeum vulgare*)
Sulfur-poor prolamins	ω-gliadin (*Triticum* spp.)
	C-hordein (*H. vulgare*)
High-molecular-weight prolamins	D-hordein (*H. vulgare*)

Source: Adapted from A. L. Tan-Wilson and K. A. Wilson. 2012. *Physiol. Plant.* 145: 140–153.

Oilseeds are a model for understanding lipid remobilization

Oil bodies are mainly composed of triacylglycerides, that are synthesized by the embryo. Aggregates of triacylglycerides are enclosed by a phospholipid monolayer and oleosins, structural proteins embedded in the lipid monolayer (see **WEB TOPIC 17.8**). Oleosins stabilize the oil bodies during dormancy, regulate oil body size, emulsify the oil bodies during germination to allow for lipid catabolism, and regulate lipid metabolism. Oleosins also provide tolerance to freezing stress. The oil body phospholipid membrane also contains the proteins caleosins and steroleosins, which have peroxygenase and β-hydroxysteroid dehydrogenase activities, respectively. The Ca^{2+}-binding caleosins are also found in single-cell algae and fungi. Oleosins are found only in land plants and are thought to be derived from caleosins. The breakdown of oil bodies by proteases and lipases and the β-oxidation of the released fatty acids provide energy and raw materials for germination and seedling establishment. For oilseeds such as *Brassica napus* ssp. *napus* (canola), catabolism of lipids in the embryo oil bodies is essential for germination. If lipolysis is blocked genetically or chemically, these oilseeds cannot germinate.

17.6 Seedling Growth and Establishment

Broadly defined, seedling establishment is the stage when the seedling becomes competent to photosynthesize, assimilate water and nutrients from the soil, undergo normal cellular and tissue differentiation and maturation, and respond appropriately to environmental stimuli. The transition between germination and growth independent of the seed is crucial, since seedlings are highly susceptible to unfavorable biotic and abiotic factors during this stage. For example, in the field, about 10 to 55% of maize seedlings and 48 to 70% of soybean seedlings fail at this stage. Seed size is an important factor in surviving this stage because larger seeds have larger food reserves, allowing more time for seedling establishment. However, this advantage must be balanced against the larger cost to the parent plant of providing these extra reserves.

The development of emerging seedlings is strongly influenced by light

While germination is strictly defined as the emergence of the radicle from the seed, the rest of the embryo also needs to emerge from the seed, marking the beginning of seedling establishment. In monocots, the coleoptile protects the shoot apical meristem as it emerges from the seed and grows through the soil to the light. In eudicots, the shoot apical meristem is protected by the apical hook formed by the upper hypocotyl and the two closed cotyledons. The formation, maintenance, and opening of the apical hook are regulated by interactions between light and hormones.

A key event in seedling establishment is the emergence of the shoot from the soil into the light, which triggers profound changes in shoot development. The shoots of dark-grown seedlings are **etiolated**—that is, they have long, spindly hypocotyls, an apical hook (in the case of eudicots), closed cotyledons, and nonphotosynthetic proplastids, which causes the unexpanded leaves to have a pale yellow color. In contrast, seedlings grown in nondirectional light have shorter, thicker hypocotyls, no apical hook, open cotyledons, and expanded leaves with photosynthetically active chloroplasts (**Figure 17.11**). Development in the dark is termed **skotomorphogenesis**, while development in the presence of light is called **photomorphogenesis**. When dark-grown seedlings are transferred to the light, photomorphogenesis takes over and the seedlings are said to be de-etiolated.

The switch between dark- and light-grown development involves genome-wide transcriptional and translational changes triggered by the perception of light by several classes of photoreceptors (see Chapter 16).

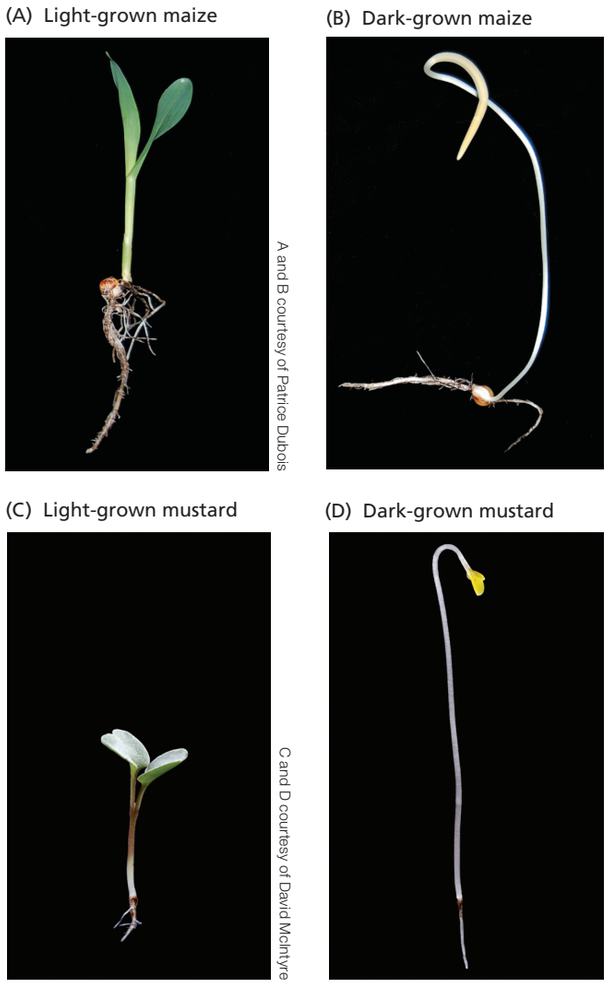


Figure 17.11 Light- and dark-grown monocot and eudicot seedlings. **(A and B)** Maize (corn; *Zea mays*) and **(C and D)** mustard (*Eruca* sp.) seedlings grown either in the light (A and C) or the dark (B and D). Symptoms of etiolation in maize, a monocot, include the absence of greening, reduction in leaf width, failure of leaves to unroll, and elongation of the coleoptile and mesocotyl. In mustard, a eudicot, etiolation symptoms include absence of greening, reduced leaf size, hypocotyl elongation, and maintenance of the apical hook.

Despite the complexity of the process, the transition from skotomorphogenesis to photomorphogenesis is surprisingly rapid. Within minutes of applying a single flash of light to a dark-grown bean seedling, several developmental changes occur:

- A decrease in the rate of stem elongation
- The beginning of apical hook opening
- Initiation of the synthesis of photosynthetic pigments

Light thus acts as a signal that induces a change in the shape of the seedling, from one that facilitates growth beneath the soil to one that will enable the plant to efficiently harvest light energy and convert it into the essential sugars, proteins, and lipids necessary for growth.

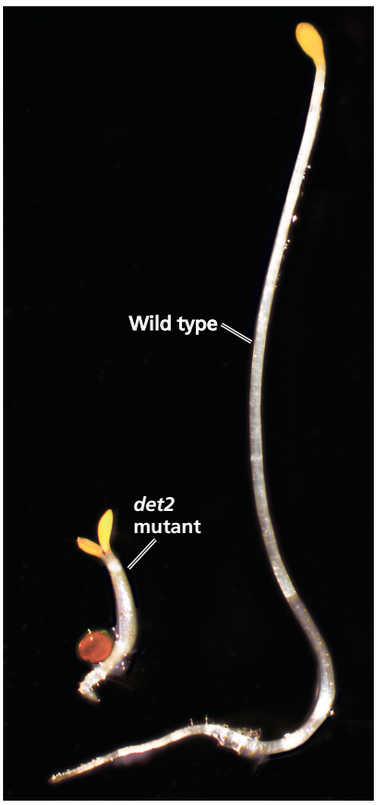
Among the different **photoreceptors** that can promote photomorphogenic responses in plants, the most important are those that absorb red and blue light. **Phytochrome** is a protein–pigment photoreceptor that absorbs red and far-red light most strongly, but it also absorbs blue light (see Chapter 16). **Cryptochromes** are flavoproteins that mediate many blue-light responses involved in photomorphogenesis, including the inhibition of hypocotyl elongation, cotyledon expansion, and petiole elongation.

Gibberellins and brassinosteroids both suppress photomorphogenesis in darkness

As we saw in Chapter 16, photomorphogenesis is negatively regulated. In the dark, many of the transcription factors that promote photomorphogenesis are degraded in the nucleus via CONSTITUTIVE PHOTOMORPHOGENESIS 1 (COP1)–mediated ubiquitination and the 26S proteasome, while in the light this degradation process is prevented, allowing photomorphogenesis to proceed. Plant hormones act to coordinate these changes throughout the plant.

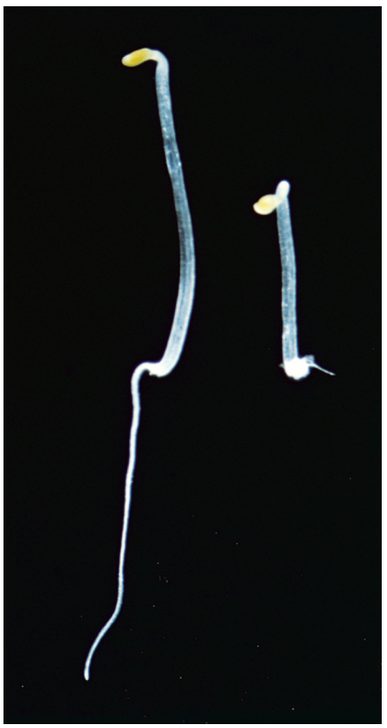
In the dark, the concentration of phytochrome in the Pfr (far-red light–absorbing) form is low. Since Pfr reduces hypocotyl *sensitivity* to GA, endogenous GAs promote hypocotyl cell elongation to a greater extent in the dark than in the light, causing the spindly appearance of dark-grown seedlings. In the light, Pr (the red light–absorbing form of phytochrome) is converted to Pfr, which causes the hypocotyl to become less sensitive to GAs. As a result, hypocotyl elongation is greatly reduced and the seedling appears to undergo partial photomorphogenesis. For this reason, GA-deficient mutant peas grown in the dark look somewhat like light-grown seedlings, although they lack chlorophyll. Taken together, these results indicate that GAs suppress some aspects of photomorphogenesis in the dark, and the suppression is reversed by red light.

Brassinosteroids play a parallel role in suppressing photomorphogenesis in the dark. Genetic screens for mutants that appeared de-etiolated when grown in the dark led to the identification of brassinosteroid biosynthetic genes. When grown in the dark, brassinosteroid-deficient Arabidopsis mutants are short and lack the apical hooks observed in normal etiolated seedlings (**Figure 17.12**). GA also suppresses photomorphogenesis in the dark, and mutants in GA biosynthesis also exhibit characteristics of light-grown seedlings. The signal transduction pathways of GA and brassinosteroids interact with the phytochrome pathway through their regulation of phytochrome interacting factors (see Chapter 16).



Courtesy of S. Savaldi-Goldstein

Figure 17.12 The dark-grown brassinosteroid-deficient mutant (*det2*) seedling of Arabidopsis on the left has a short, thick hypocotyl and open cotyledons. A dark-grown wild type is on the right.



Courtesy of Joe Kieber

Figure 17.13 Effects of ethylene on growth in Arabidopsis seedlings. Three-day-old etiolated seedlings grown in the presence (right) or absence (left) of 10 ppm ethylene. Note the shortened hypocotyl, reduced root elongation, and exaggeration of the curvature of the apical hook that result from the presence of ethylene are collectively known as the triple response.

Hook opening is regulated by phytochrome, auxin, and ethylene

During embryogenesis, a single cell undergoes cell division, cell expansion, and differentiation to form all of the different cell types and organs of the embryo, including the root and shoot apical meristems (see Chapter 22). After the embryo germinates, the cells of the seedling undergo cell division, cell expansion, and further differentiation. The influence of light and hormones on this growth can be observed as the apical hook opens, the vascular system and root hairs are formed, and finally lateral roots and true leaves develop (see Chapter 18).

As mentioned earlier, etiolated eudicot seedlings usually form an apical hook located just behind the shoot apex and which protects the shoot apical meristem. Hook formation and maintenance in darkness result from ethylene-induced asymmetric growth (**Figure 17.13**). In compacted soils, the gaseous hormone ethylene cannot diffuse in the soil and accumulates around the germinated seedling. This results in the triple response, in which the apical hook is tighter, the hypocotyl is shorter and thicker, and the root is very short. This change in morphology aids seedlings as they push through compacted soils and around small obstacles such as stones to reach the soil surface. Auxin-insensitive mutants do not develop an apical hook, and treatment of wild-type Arabidopsis seedlings with NPA (*N*-1-naphthylphthalamic acid), an inhibitor of polar auxin transport, also blocks apical hook formation. The closed shape of the hook is a consequence of the more rapid elongation of the outer side of the hypocotyl compared with the inner side, and auxin inhibition of cell elongation on the inner side. Therefore, auxin and ethylene function synergistically in apical hook formation. The more rapid growth of the outer tissues relative to the inner tissues could reflect an ethylene-dependent lateral redistribution of auxin analogous to what is seen during phototropic bending, which we discuss in Section 17.8.

After exposure to light, the elongation rate of the inner side of the apical hook increases, equalizing the growth rates on both sides and causing the hook to open (see **WEB APPENDIX 2**). Red light induces hook opening, and this effect is reversed by far-red light, indicating that phytochrome is the photoreceptor involved in this

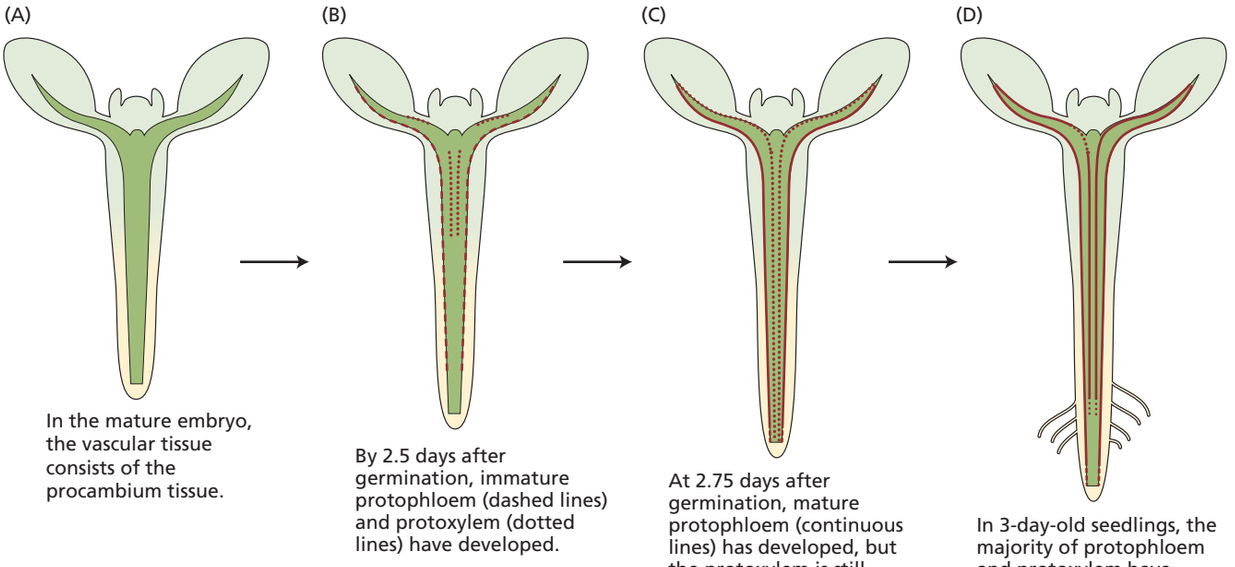


Figure 17.14 **Vascular patterning and differentiation in Arabidopsis embryos and seedlings.** (After J. S. Busse and R. F. Evert. 1999. *Int. J. Plant Sci.* 160: 1–13.)

process. A close interaction between phytochrome and ethylene controls hook opening. As long as ethylene is produced by the hook tissue in the dark, elongation of the cells on the inner side is inhibited. Red light inhibits ethylene formation, promoting growth on the inner side, thereby causing the hook to open.

Vascular differentiation begins during seedling emergence

During embryogenesis within the seed, symplasmic and apoplastic transport are sufficient to distribute water, nutrients, and signals throughout the embryo by the process of diffusion. Following germination, however, the emerging seedling requires a continuous vascular system to distribute materials quickly and efficiently throughout the plant. The vascular system of the embryo consists only of procambial strands—immature vascular tissue.

During seedling emergence, first protoxylem and protophloem cells appear, followed by the larger metaxylem and metaphloem cells (**Figure 17.14**). As the protophloem and protoxylem differentiate and mature, the vascular tissue becomes continuous between the root and the hypocotyl, which is rootlike in the organization of its vascular tissue. The pattern of differentiation and maturation is different in a germinating seedling compared with a mature plant (see Chapter 19). The protophloem matures earlier than the protoxylem in the emerging radicle and during primary growth: Phloem sieve tube development occurs nearly simultaneously in the hypocotyl and root, while xylem differentiation occurs acropetally in roots.

The root tip has specialized cells

The **root cap** occupies the most distal part of the root and is composed of columella cells and cells that form the lateral cap (**Figure 17.15**). It represents a unique set of cells that are situated below the meristematic zone and cover the apical meristem (see Chapter 18) and protect it

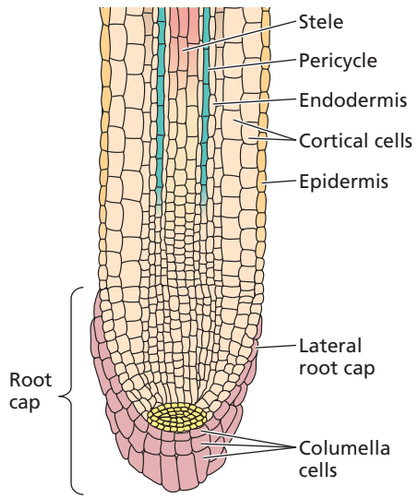


Figure 17.15 **Root cell types.** The root cap comprises columella cells and cells that form the lateral cap. Epidermal cells are exposed to the rhizosphere above the lateral root cap. Moving toward the center of the root, the tissue layers are the cortex, endodermis, pericycle, and stele. The stele is composed of the xylem, phloem, and their companion and supporting parenchyma cells.

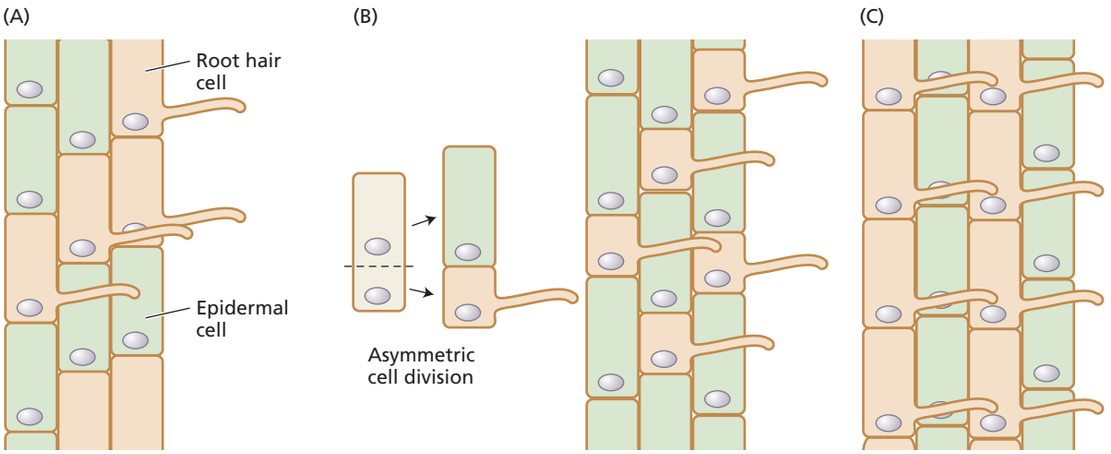


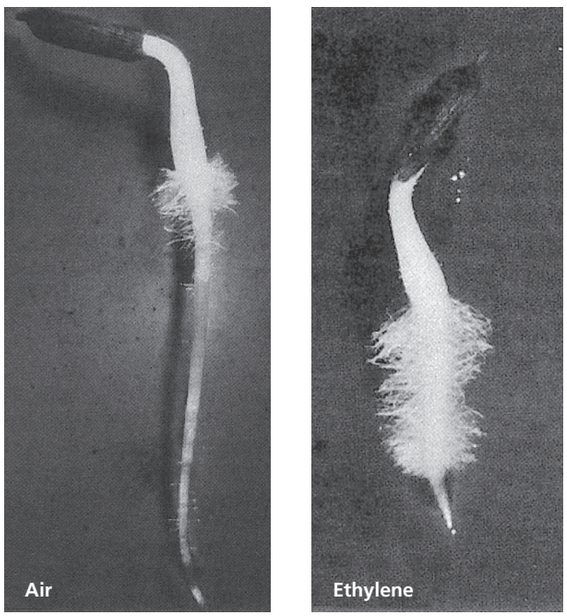
Figure 17.16 Three patterns of trichoblast differentiation. **(A)** In some plants, all root epidermal cells have the potential to become trichoblasts and the pattern is specified by developmental cues. **(B)** In basal vascular plants and some monocots, the trichoblast results from an asymmetric cell division. **(C)** In the Brassicaceae, trichoblasts and atrichoblasts occur in alternating cell files. (After T. Bibikova and S. Gilroy. 2003. *J. Plant Growth Regul.* 21: 383–415.)

from mechanical injury as the root tip is pushed through the soil. The first layer of root cap cells of emerging radicles has modified cell walls with a cuticle that protects the emerging root tip from abiotic stress. Other functions of the root cap include the perception of gravity by the columella cells during gravitropism and the secretion of compounds, such as mucilage, that help the root penetrate the soil and mobilize mineral nutrients. The root cap cells are constantly renewed by the meristematic cells and undergo developmentally programmed cell death that influences future root architecture. Epidermal cells lie beneath the root cap and become exposed to the rhizosphere above the lateral root cap.

Ethylene and other hormones regulate root hair development

Root hairs are extensions of root epidermal cells that increase the surface area of the root for water and mineral uptake and also serve a mechanical role to help anchor plants in the soil. Root tips are also an example of tip growth. While all epidermal cells have the potential to differentiate into a root hair (trichoblast) or not (atrichoblast), developmental cues specify the pattern of trichoblasts and atrichoblasts (**Figure 17.16A**). Species-specific signals and cell-to-cell communication determine the basic pattern of root hair position. In early vascular plants such as *Lycopodium*, *Selaginella*, and *Equisetum*, the basal angiosperm family Nymphaeaceae (water lilies), and some monocots, root hairs arise from the smaller cell produced by an asymmetric cell division in the root meristem (**Figure 17.16B**). In the Brassicaceae the root epidermis consists of alternating files of cells that are either atrichoblasts or trichoblasts (**Figure 17.16C**). Trichoblast differentiation is regulated by gene expression (see **WEB TOPIC 17.9**).

Ethylene is a positive regulator of root hair development, and ethylene-treated roots produce extra root hairs in abnormal locations (**Figure 17.17**). Conversely, fewer root hairs form in ethylene-insensitive mutants or in wild types treated with ethylene biosynthesis inhibitors. These observations suggest that ethylene acts as a positive regulator in the differentiation of root hairs.



Both photos from F. B. Abeles et al. 1992. *Ethylene in Plant Biology*. 2nd ed. Academic Press, San Diego, CA; courtesy of F. Abeles

Figure 17.17 Promotion of root hair formation by ethylene in lettuce seedlings. Two-day-old seedlings were treated with air (left) or 10 ppm ethylene (right) for 24 h before the photo was taken. Note the profusion of root hairs on the ethylene-treated seedling.

Root hairs elongate by tip growth (see Chapters 2 and 21) that responds to nutritional and water status via a combination of auxin, methyl jasmonate, brassinosteroids, and Ca^{2+} signaling. Intracellular auxin concentrations regulate root hair elongation. In Arabidopsis, auxin is delivered from the apex in shootward streams maintained by the coordinated activity of the auxin transporters AUXIN RESISTANT 1 (AUX1), PIN-FORMED 2 (PIN2), and ATP-BINDING CASSETTE TRANSPORTER SUBFAMILY B 4 (ABCB4). Atrichoblasts have higher auxin concentrations as a result of AUX1 uptake. AUX1 is lacking in trichoblasts, where ABCB4 activity maintains optimal auxin concentrations for root hair elongation. Methyl jasmonate has also been shown to enhance root hair growth, while brassinosteroids inhibit root hair growth.

17.7 Differential Growth Enables Successful Seedling Establishment

To survive, seedlings require a functional root–soil interface, adequate gas exchange, and functional photosynthetic carbon fixation. Seedlings employ programmed and environmental responses involving preferential cell elongation to achieve establishment. As described in Chapter 4, the experiments of Charles and Francis Darwin detailed in the *Power of Movement in Plants* (1881) recorded organ bending and rotation during growth in various species. This movement is called **nutation**. **Circumnutation** is the circular or elliptical movement of the tips of growing organs, such as roots, hypocotyls, and stems, caused by oscillating changes in growth rate around the circumference of the organ (**Figure 17.18**). As the organ elongates, the circular movements of its tip trace a spiral pattern through space. Nutation and circumnutation are nastic movements, meaning they are autonomous and independent of external stimuli, although external factors such as light, temperature, and gravity can modify the oscillations observed in spiral growth. For example, experiments conducted under altered gravity, such as in low gravity Earth orbit or on a clinostat, have shown that circumnutation still occurs near zero gravity but that its period and amplitude are affected. Genetic evidence also suggests that gravity influences circumnutation in shoots.

The mechanics of these nastic movements can be modeled to include observed changes in turgor and cell volume. When seedling hypocotyls or epicotyls elongate, the epidermal cells often elongate more on one side of the organ than the other, and more than the cortical cells adjacent to them. Then the epidermal cells on the other side "catch up" and overshoot, thus maintaining the differential growth. This results in torsion in the stem or roots that can produce nutation. Furthermore, differential growth can result in a curve that oscillates, which will also produce torsion resulting in circumnutation (see Figure 17.18B). The degree of curvature affects the amplitude of

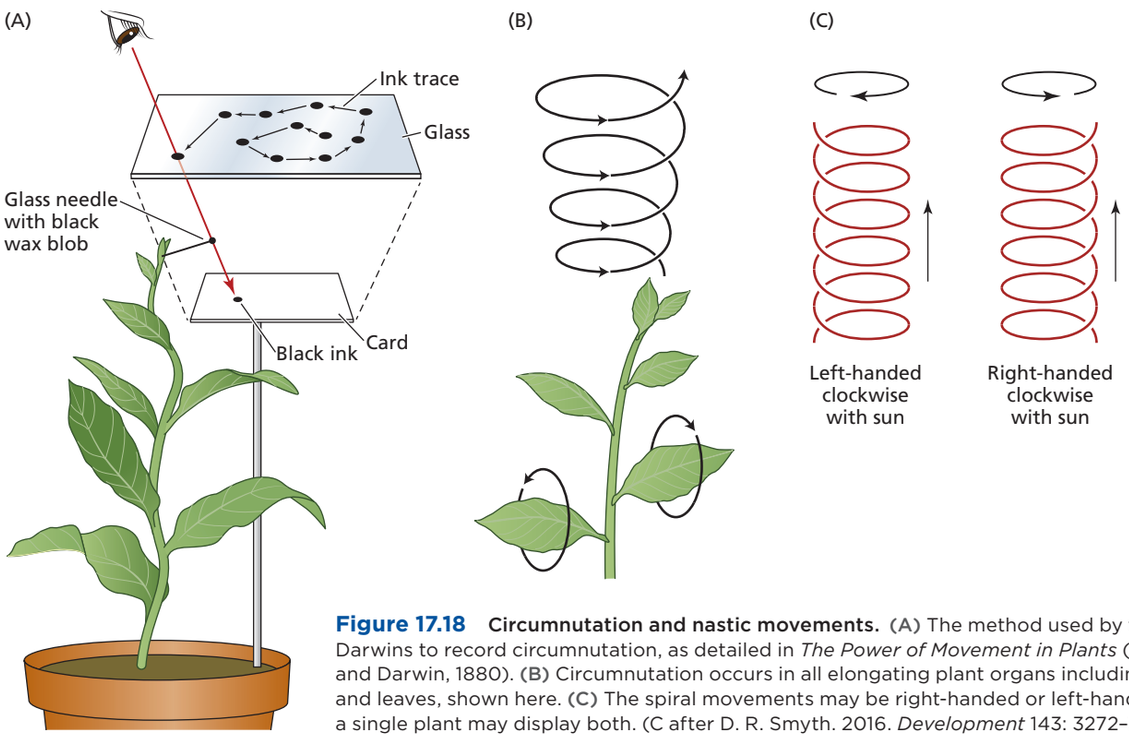


Figure 17.18 **Circumnutation and nastic movements.** **(A)** The method used by the Darwins to record circumnutation, as detailed in *The Power of Movement in Plants* (Darwin and Darwin, 1880). **(B)** Circumnutation occurs in all elongating plant organs including stems and leaves, shown here. **(C)** The spiral movements may be right-handed or left-handed, and a single plant may display both. (C after D. R. Smyth. 2016. *Development* 143: 3272–3282.)

the circumnutation. The spiral is predominantly counterclockwise across species but is clockwise in some, such as hops. The handedness appears to be related to microtubule orientation in the growing cells, an observation that also points to the intrinsic nature of nutation.

Cell-to-cell communication via plasmodesmata or transported hormones is likely to be involved in the local elongation of cells. As the cells expand, plasmodesmatal connections are interrupted with the cellular remodeling, and this may affect growth locally. Therefore, local communication, as well as cell elongation, is temporarily disrupted until the plasmodesmata are repaired, which can take 10 min to several hours depending on the species. Several methods have detected transient accumulations of auxin and GA on the lower side of circumnutating hypocotyls, but as we will see later in Section 17.8, this may reflect transient gravity responses. Furthermore, auxin appears to maintain, but not initiate, nutation. In the twisted dwarf mutant of Arabidopsis, in which auxin efflux in the hypocotyl and roots is disrupted by a loss of ABCB auxin transporters in the plasma membrane, both roots and hypocotyls exhibit exaggerated hypernutation. Oscillating acid growth in different cells could play a role in circumnutation, but the measured pH oscillations are faster than the observed oscillations in growth.

Nutational growth in seedling roots is also based on differential elongation of cortical and epidermal cells and is important for penetration of soil layers. Root nutation is regulated by ethylene and is highly dependent on auxin reuptake into shootward flows mediated by the AUX1 auxin-uptake transporter.

Ethylene affects microtubule orientation and induces lateral cell expansion

At concentrations above 0.1 $\mu L\ L^{-1}$, ethylene can reduce the rate of elongation and increase lateral expansion, leading to swelling of the hypocotyl or the epicotyl. The directionality of plant cell expansion is determined by the orientation of the cellulose microfibrils in the cell wall. Transverse microfibrils reinforce the cell wall in the lateral direction, so that turgor pressure is channeled into cell elongation. The orientation of the microfibrils is in turn determined by the orientation of the cortical array of microtubules in the cortical (peripheral) cytoplasm. In typical elongating plant cells, the cortical microtubules are arranged transversely, giving rise to transversely arranged cellulose microfibrils.

When etiolated seedlings are treated with ethylene (see Figure 17.13), the microtubule alignment in the cells of the hypocotyl switches from a transverse to a diagonal or longitudinal orientation (**Figure 17.19**). This approximately 90-degree shift in microtubule orientation leads to a parallel shift in cellulose microfibril deposition. The newly deposited wall is reinforced in the longitudinal direction rather than the transverse direction, which promotes lateral expansion instead of elongation. Exogenous ethylene inhibits elongation and promotes lateral expansion within 10 min of application (**Figure 17.20A**). When ethylene is removed (replaced with air), then cell elongation resumes (see Figure 17.20A). If ethylene is not removed, then growth in elongation remains inhibited (**Figure 17.20B**). This experiment can be repeated by examining the effects in the absence of different components regulating the ethylene response. In the absence of one of the ethylene signal transduction components that interacts with the ethylene receptor (e.g., *ein2*; see Chapter 4), no response to ethylene can be measured (see Figure 17.20B). In contrast, if the downstream transcriptional activation

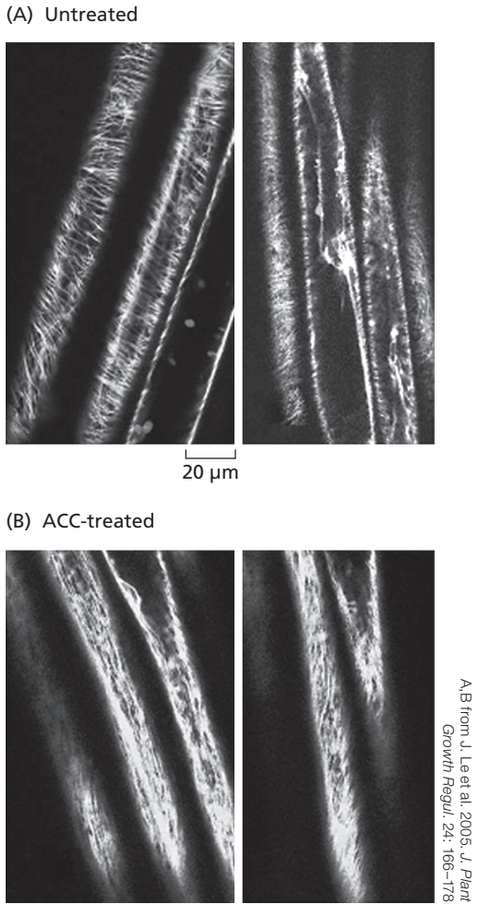


Figure 17.19 **Ethylene affects microtubule orientation.** **(A)** Microtubule orientation is transverse in hypocotyls of control dark-grown transgenic Arabidopsis seedlings expressing a tubulin gene tagged with green fluorescent protein. **(B)** Microtubule orientation is longitudinal and diagonal in hypocotyl cells from seedlings treated with the ethylene precursor 1-aminocyclopropane-1-carboxylic acid (ACC), which increases ethylene production.

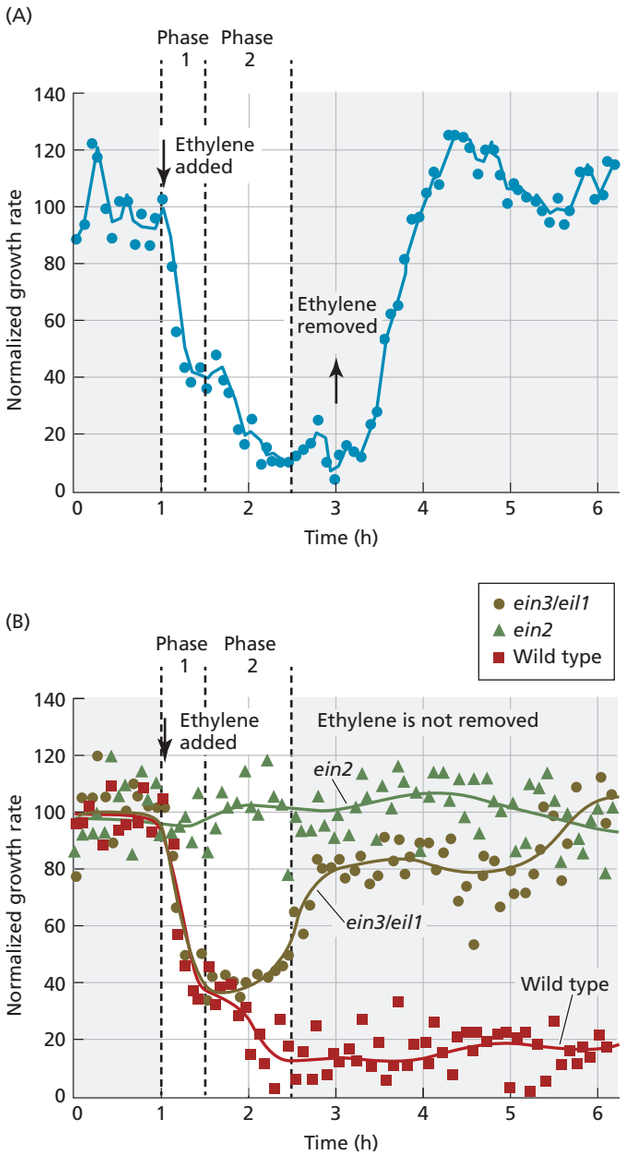


Figure 17.20 **Kinetics of the effects of ethylene on hypocotyl elongation in dark-grown Arabidopsis seedlings.** **(A)** Growth rate of etiolated wild-type Arabidopsis after exposure to ethylene and subsequent removal of ethylene at the times indicated by the arrows. Note that the reduction in the growth rate following exposure to ethylene occurs in two distinct phases. Growth inhibition is transient in phase 1 and sustained in phase 2. **(B)** Growth rate of etiolated wild-type seedlings and *ETHYLENE INSENSITIVE 2* and *3* and *ETHYLENE INSENSITIVE 3-LIKE 1* (*ein2* and *ein3/eil1*) mutant seedlings following exposure to ethylene at the time indicated by the arrow. The phase 1 response of the *ein3/eil1* mutant seedlings with a defective ethylene signaling pathway (see Chapter 4) is identical to that of the wild type, but the phase 2 response is absent, whereas the growth rate of *ein2* is insensitive to ethylene. (After B. M. Binder et al. 2004a. *Plant Physiol.* 136: 2913–2920; B. M. Binder et al. 2004b. *Plant Physiol.* 136: 2921–2927.)

is absent (e.g., *ein3/eil1*), then the rapid decrease in growth corresponding to microtubule reorganization is observed; however, growth rate resumes in the presence of ethylene (see Figure 17.20B), as if ethylene were removed (as in Figure 17.20A).

Auxin promotes growth in stems and coleoptiles, while inhibiting growth in roots

The observations of Charles and Francis Darwin ultimately led to the identification of auxin as the transported hormone that primarily regulates differential organ bending in seedlings. Auxin synthesized in the shoot apex is transported toward the tissues below. The steady supply of auxin arriving at the subapical region of a stem or coleoptile is required for the continued elongation of these cells. Because the concentration of endogenous auxin in the elongation region of a normal healthy plant is nearly optimal for growth, spraying the plant with exogenous auxin causes only a modest and short-lived stimulation in growth. Such spraying may even be inhibitory in the case of dark-grown seedlings, which are more sensitive to supraoptimal auxin concentrations than light-grown plants are.

However, when the endogenous source of auxin is removed by excision of stem or coleoptile sections containing the elongation zone, the growth rate rapidly decreases to a low basal rate. Such excised sections often respond to exogenous auxin by rapidly increasing their growth rate back to the concentration in the intact plant (**Figure 17.21A and B**). Most of the elongation takes place in outer tissues, and is not just a matter of tissue penetration of the auxin. When the sections are split longitudinally, they curve inward as they elongate, thus demonstrating greater auxin-responsive elongation by the outer layers of cells.

Auxin control of root elongation has been more difficult to demonstrate, perhaps because auxin induces the production of ethylene, which inhibits root growth. Elongation of root cells also requires the GA biosynthesis in epidermal cells. These three hormones interact differentially in root tissue to control growth. GA appears to be required for basal growth. However, even when ethylene biosynthesis is specifically blocked, low concentrations (10^{-10} to 10^{-9} M) of auxin promote the growth of intact roots, whereas higher concentrations (10^{-6} M) inhibit growth. Thus, while roots may require a minimum concentration of auxin to grow, root growth is strongly inhibited by auxin concentrations that promote elongation in stems and coleoptiles. When roots grow in well-drained or sandy soil, ethylene produced by the roots can freely diffuse in the soil, and root elongation is observed. However, in compacted soils, ethylene cannot diffuse away from the root, and the root stops elongating and increases

in girth. These roots resemble the root phenotype of the ethylene-treated etiolated seedlings (see Figure 17.13).

The minimum lag time for auxin-induced elongation is 10 minutes

When a stem or coleoptile section is excised and inserted into a sensitive growth-measuring device, the lag time for the auxin response can be monitored with great precision. For example, addition of auxin markedly stimulates the growth rates of oat (*Avena sativa*) coleoptile and soybean (*Glycine max*) hypocotyl sections after a lag period of only 10 to 12 min. The maximum growth rate, which represents a five- to tenfold increase over the basal rate, is reached after 30 to 60 min of auxin treatment. As is shown in **Figure 17.21C**, auxin-induced elongation is dose-dependent—that is, a threshold concentration of auxin must be reached to initiate this response. Beyond the optimal concentration, auxin becomes inhibitory. The stimulation of growth by auxin requires energy, and metabolic inhibitors inhibit the response within minutes. Auxin-induced growth is also sensitive to inhibitors of protein synthesis such as cycloheximide, suggesting that

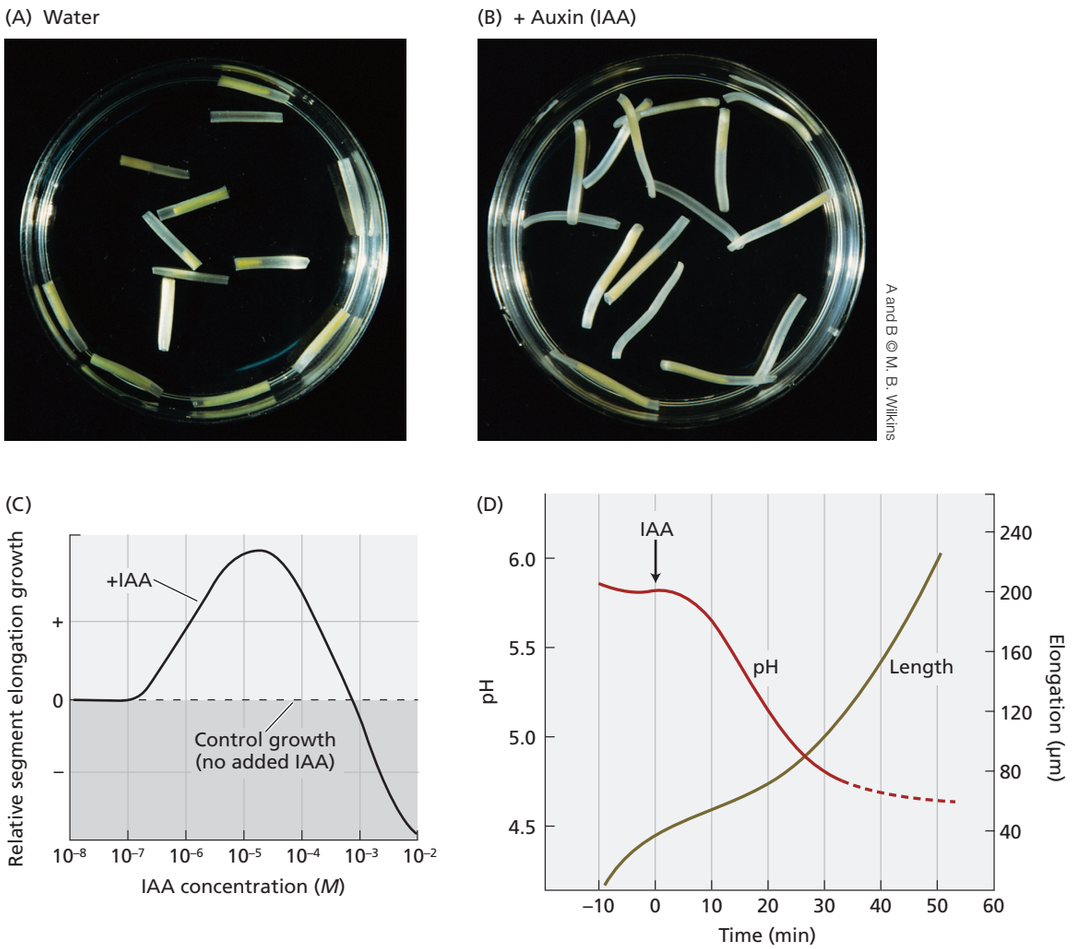


Figure 17.21 **Auxin stimulates elongation.** Oat coleoptile sections depleted of endogenous auxin were incubated for 18 h in either water **(A)** or auxin (IAA) **(B)**. The yellow material inside the translucent coleoptile is the primary leaf tissue. **(C)** Typical dose-response curve for IAA-induced growth in pea stem or oat coleoptile sections. Elongation growth of excised sections of coleoptiles or young stems is plotted versus increasing concentrations of exogenous IAA. At concentrations above 10^{-5} *M*, IAA becomes less and less effective. Above about 10^{-4} *M* it becomes inhibitory, as shown by the fact that the stimulation decreases and the curve eventually falls below the dashed line, which represents growth in the absence of added IAA. **(D)** Kinetics of auxin-induced elongation and cell wall acidification in maize coleoptiles. The pH of the cell wall was measured with a pH microelectrode. Note the similar lag times (10–15 min) for both cell wall acidification and the increase in the rate of elongation, although the pH change is slightly slower since it is mediated by auxin-dependent transcriptional activation. (D after M. Jacobs and P. M. Ray. 1976. *Plant Physiol.* 58: 203–209.)

protein synthesis is required for the response. Inhibitors of RNA synthesis also inhibit auxin-induced growth after a slightly longer delay.

Auxin-induced proton extrusion loosens the cell wall

Auxin induces acidification of the apoplast by increasing the activity of plasma membrane H^+-ATPases. Cell wall acidification occurs 10 to 15 min after auxin exposure, consistent with the growth kinetics, as shown in **Figure 17.21D**. As discussed in Chapter 2, cell wall proteins called expansins mediate wall loosening at acid pH. Once the cell wall is sufficiently loosened by expansin activity, turgor pressure initiates cell expansion.

In Arabidopsis, auxin is perceived at the surface of hypocotyl cells and results in phosphorylation of the plasma membrane H^+-ATPases by TRANSMEMBRANE KINASE 1 (TMK1). This activates localized apoplastic acidification and results in cellular elongation. Auxin binding to TMK1 or an associated protein at the cell surface also stabilizes nuclear AUX/IAA proteins in the apical hook (see Chapter 4), which represses auxin signaling. In roots, perception of inhibitory concentrations of auxin is mediated by TMK1 and involves nuclear auxin responses that, in turn, regulate ABA signaling via the ABA INSENSITIVE 1 and 2 transcription factors (see Chapter 4).

Other biochemical processes, such as new cell wall biosynthesis, are required to sustain cell expansion over the long term. Auxin increases transcription of *Small Auxin Up RNAs* (*SAURs*), a group of early auxin response genes. The *SAUR* gene family is large (79 genes in Arabidopsis), with several members in each clade (10 clades in Arabidopsis). Because of the SAUR proteins' large number and functional redundancy, their functions have been difficult to fully characterize. However, we know that SAUR19 inhibits the activity of Protein Phosphatase 2C, D clade (PP2C.D1), which dephosphorylates and inactivates the plasma membrane H^+-ATPase. Thus, inhibition of PP2C.D1 results in increased H^+-ATPase activity and affects acid growth (see Chapter 2).

17.8 Tropisms: Growth in Response to Directional Stimuli

As sessile organisms, plants must rely on growth responses to compete for sunlight and to forage for water and minerals in the soil. Plants respond to external stimuli by altering their growth and developmental patterns. During seedling establishment, abiotic factors such as gravity, touch, and light influence the initial growth habit of the young plant. **Tropisms** are directional growth responses in relation to environmental stimuli caused by the asymmetric growth of the plant axis (stem or root) and anisotropic cell growth. Tropisms may be positive (growth toward the stimulus) or negative (growth away from the stimulus).

One of the first forces that emerging seedlings encounter is gravity. **Gravitropism**, growth in response to gravity, enables shoots to grow upward toward sunlight for photosynthesis, and roots to grow downward into the soil for water and nutrients. As soon as the shoot tip penetrates the soil surface, it encounters sunlight. **Phototropism** enables leafy shoots to grow toward sunlight, thus maximizing photosynthesis, while some roots grow away from sunlight. **Thigmotropism** is differential growth in response to touch and mechanosensing and helps roots grow around obstacles and Venus flytrap leaves to close on prey. **Hydrotropism** is directional growth in response to a water or a water vapor gradient and enables roots to grow toward a source of water.

Gravitropism involves the lateral redistribution of auxin

When dark-grown *Avena* seedlings are oriented horizontally, the coleoptiles bend upward in response to gravity. According to a model independently put forward by Went and Cholodny in the early twentieth century, auxin in a horizontally oriented coleoptile tip is transported laterally to the lower side, causing the lower side of the coleoptile to grow faster than the upper side (see the next subsection). This general **Cholodny–Went model** has subsequently been shown to apply to phototropism. Two key features that contribute to the Cholodny–Went model are the polarity and gravity independence of long-distance auxin transport. The primary *rootward* and *shootward* polar auxin streams maintained by polar export of auxin are shown in **Figure 17.22A**. The velocity of polar auxin transport can exceed 3 mm h^{-1} in some tissues, which is faster than diffusion but slower than phloem translocation rates (see Chapter 11). **Figure 17.22B** illustrates an experiment using radiolabeled auxin to demonstrate rootward polar auxin transport in a seedling hypocotyl section.

A demonstration that polar auxin transport is gravity-independent is shown in **Figure 17.23**. Grape cuttings were placed in a moist chamber, which led to the formation of adventitious roots at the basal ends of the cuttings and bud outgrowth at the apical ends. When the cuttings were inverted, the polarity of root and shoot formation was preserved. Roots formed at the basal end (now pointing upward) because root differentiation was stimulated by the auxin that accumulated there due to basipetal (rootward) polar transport. Shoots tended to form at the apical end where the auxin concentration was lowest, no matter which way the cutting was oriented with respect to gravity.

The gravitropic stimulus perturbs the symmetric movements of auxin

In a young seedling, most of the auxin in the root is derived from the shoot. IAA is delivered to the root apex by

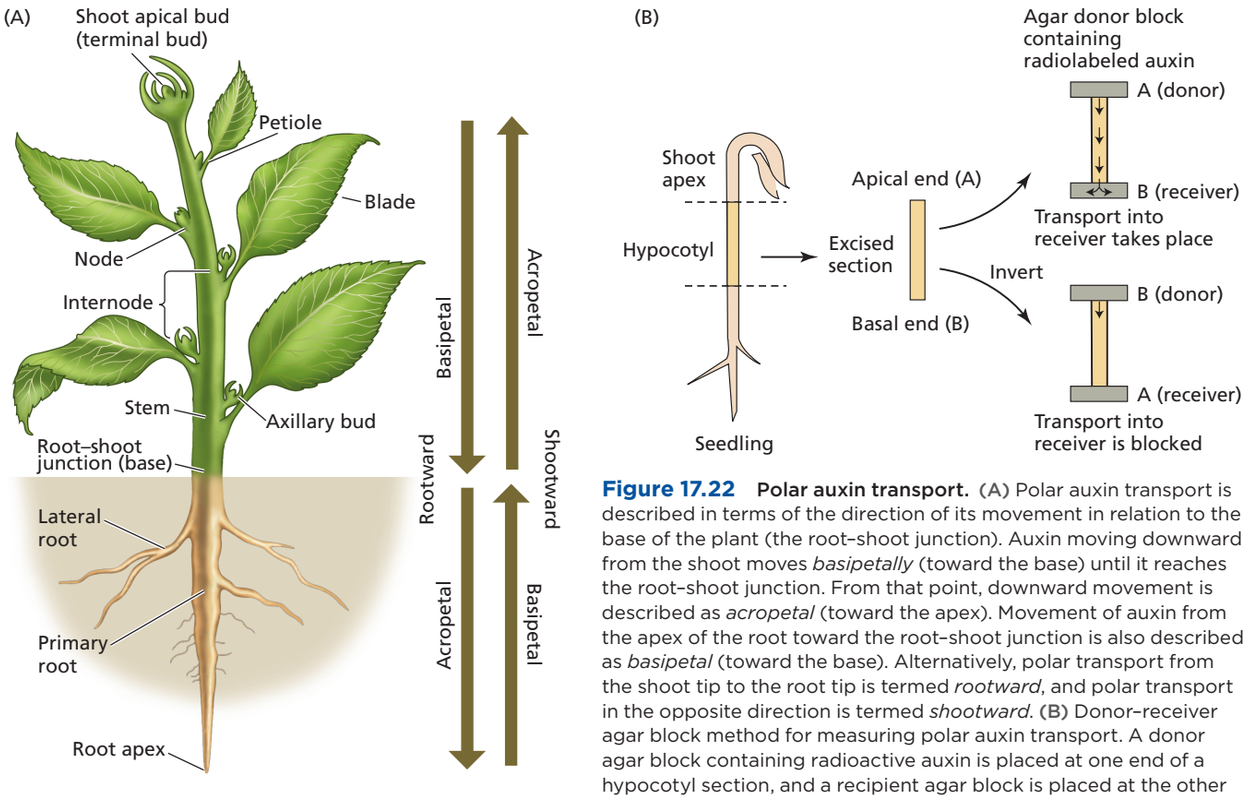


Figure 17.22 **Polar auxin transport.** (A) Polar auxin transport is described in terms of the direction of its movement in relation to the base of the plant (the root–shoot junction). Auxin moving downward from the shoot moves *basipetally* (toward the base) until it reaches the root–shoot junction. From that point, downward movement is described as *acropetal* (toward the apex). Movement of auxin from the apex of the root toward the root–shoot junction is also described as *basipetal* (toward the base). Alternatively, polar transport from the shoot tip to the root tip is termed *rootward*, and polar transport in the opposite direction is termed *shootward*. (B) Donor–receiver agar block method for measuring polar auxin transport. A donor agar block containing radioactive auxin is placed at one end of a hypocotyl section, and a recipient agar block is placed at the other end. The amount of radioactive auxin that accumulates in the recipient block is a measure of how much auxin is transported through the hypocotyl section. When the hypocotyl is inverted, no radiolabeled auxin is transported from the donor to the receiver block.

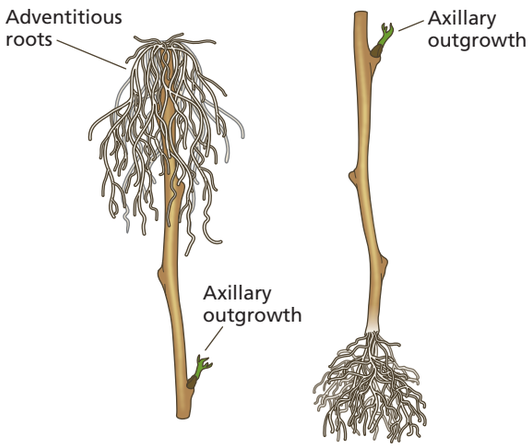


Figure 17.23 **Adventitious root growth is polar.** Adventitious roots grow from the basal ends of grape hardwood cuttings and axillary outgrowth occurs at the apical end, whether the cuttings are maintained in the inverted orientation (the cutting on the left) or the upright orientation (the cutting on the right). Auxin accumulates at the basal end and is depleted at the apical end because of polar transport that is independent of gravity. (After H. T. Hartmann and D. E. Kester. 1983. *Plant Propagation: Principles and Practices*, 4th ed. Prentice-Hall, Inc., NJ.)

a rootward directional stream directed by the efflux carrier PIN1 and maintained by the ATP-dependent activity of a group of ABCB transporters best represented by Arabidopsis ABCB19 (see Chapter 4). As shown in **Figure 17.24**, PIN proteins in the shoot apical meristem are responsible for directing auxin movement, first toward the tip of the apex, and then down the stem and into the root. In the root, PIN proteins in the cells of the vascular cylinder transport auxin to the columella (central) region of the root cap. In older plants, IAA is also synthesized in the root meristem. PIN3 efflux carriers move auxin out of the columella and provide the directional vector of auxin movement out of the columella in tropic responses in the root. Auxin is taken up into the adjacent lateral root cap cells via the AUX1 permease and then moves into a shootward epidermal stream driven by combined PIN and ABCB efflux activity. That shootward epidermal stream is primarily determined by PIN2 and maintained by ABCB4 (see Figure 17.24). PIN2 is localized on the upper side of root epidermal cells, conducting auxin away from the lateral root cap toward the elongation zone, where auxin acts to stimulate cell elongation. Upon

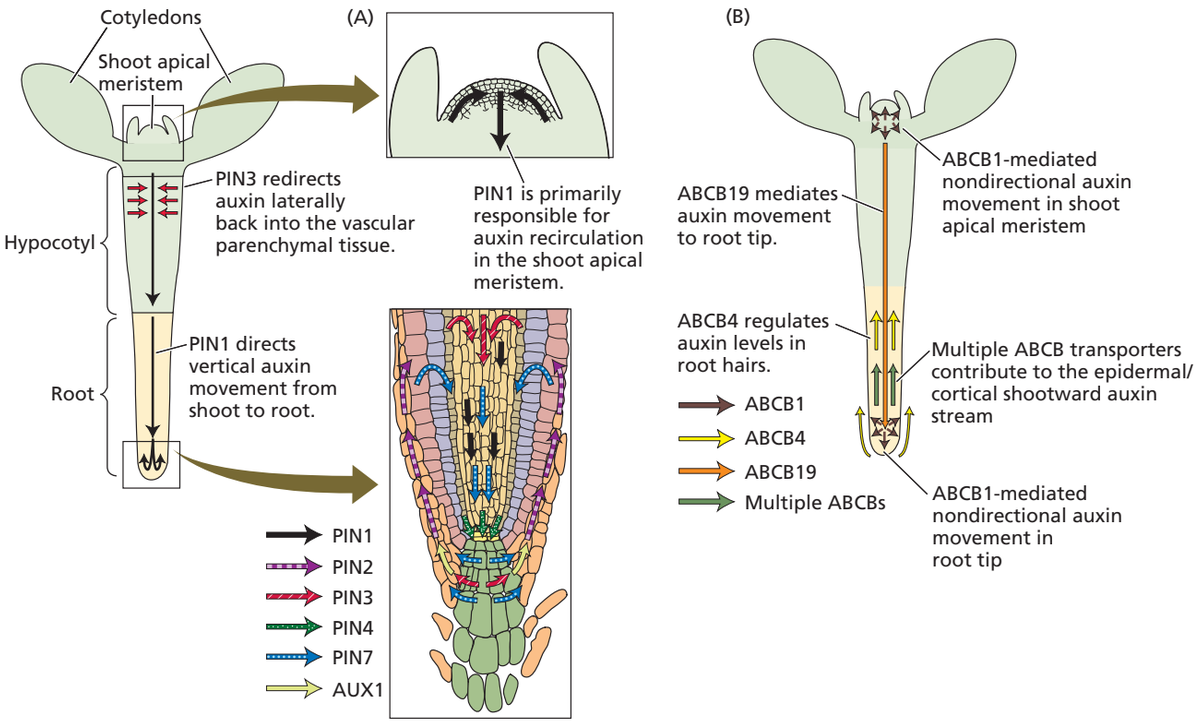


Figure 17.24 Polar auxin transport in Arabidopsis seedlings. **(A)** PIN transport proteins in the vascular tissue direct auxin to the root (see text for discussion). PIN proteins in the root vascular cylinder then transport auxin to the columella of the root cap. Auxin then moves into the lateral root cap cells and is redirected by the combined uptake via AUX1 in the lateral root cap and export by PIN proteins in the epidermis. PIN proteins are also involved in redirecting auxin toward the elongation zone, after which some auxin moves back into the vascular cylinder. The term *fountain model* was suggested by the fact that the stream of auxin coming from the shoot reverses direction after reaching the root cap. The two inserts show PIN1-mediated auxin movement in the shoot apical meristem (top inset) and PIN-regulated auxin circulation in the root tip (bottom inset). **(B)** Auxin flow associated with ATP-dependent ABCB transport proteins. The multidirectional arrows at the shoot and root apices indicate nondirectional auxin transport. However, when combined with polarly localized PIN proteins, directional transport occurs. Multiple ABCBs function in the mobilization of auxin in cortical and epidermal tissues to the elongation and differentiation zones. ABCB4 regulates auxin concentrations in elongating root hairs. (After I. Blilou et al. 2005. *Nature* 433: 39–44.)

reaching the elongation zone, auxin is transported laterally back into the vascular cylinder, apparently via PIN2 localized on the inner lateral side of cortical cells. This recirculation of auxin from the root cap to the elongation zone and back again is referred to as the *fountain model*.

Early experimental studies established that the tips of coleoptiles are the site of perception for blue light–induced phototropic bending, and that the lateral movement of auxin to the shaded side is involved in the response (see Chapters 4 and 16). The tips of coleoptiles are also able to sense gravity and redistribute auxin to the lower side. For example, if the excised tip of a coleoptile is placed on agar blocks and oriented horizontally, a greater amount of auxin diffuses into the agar block from the lower half of the tip than from the upper half, as demonstrated by a bioassay (**Figure 17.25**).

Gravitropism in roots also depends on auxin redistribution. The site of perception of gravity in roots

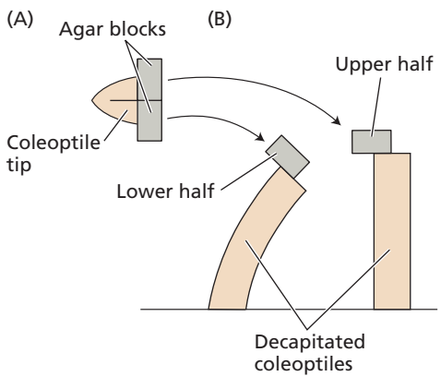


Figure 17.25 Auxin is transported to the lower side of a horizontally oriented oat coleoptile tip. **(A)** Auxin from the upper and lower halves of a horizontal tip is allowed to diffuse into two agar blocks. **(B)** The agar block from the lower half (left) induces greater curvature in a decapitated coleoptile than the agar block from the upper half (right) does.

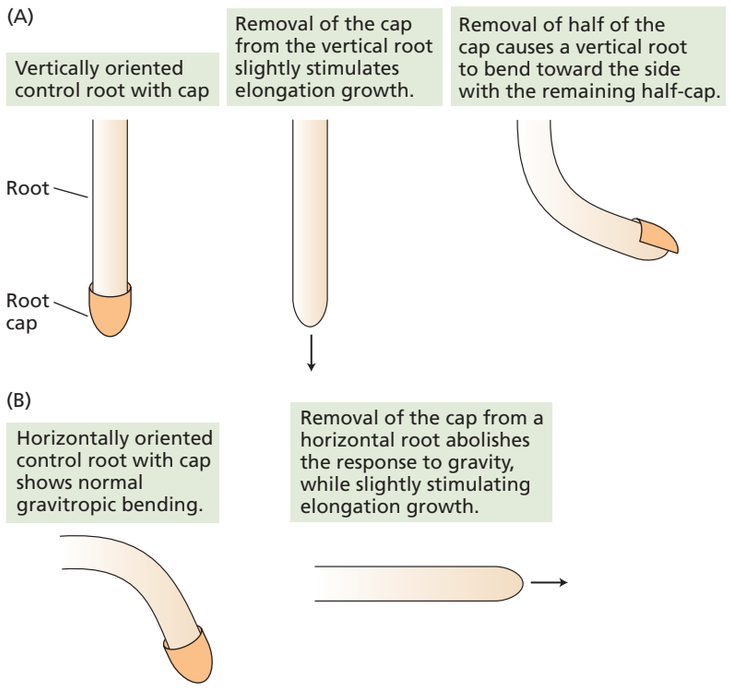


Figure 17.26 Effects of microsurgery on the direction of root growth. Microsurgery experiments demonstrate that the root cap is required for redirection of auxin and subsequent differential inhibition of elongation in root gravitropic bending. **(A)** Vertically growing root. **(B)** Horizontally growing root. (After S. Shaw and M. B. Wilkins. 1973. *Planta* 109: 11–26.)

is the root cap. When the root cap is removed from a growing root, the root no longer bends downward in response to gravity (**Figure 17.26**). In fact, the growth rate of the root actually increases slightly, suggesting that the root cap supplies an inhibitor that modulates growth in the elongation zone. Microsurgery experiments in which half of the cap was removed confirmed that the cap transports a root growth inhibitor, later identified as auxin, to the lower side of the root during gravitropic bending. Experiments with auxin transport inhibitors and auxin transporter mutants have shown that the shootward transport of auxin from the root cap to the elongation zone is required for gravitropic growth.

According to the current model for root gravitropism, shootward auxin transport in a vertically oriented root is equal on all sides. When the root is oriented horizontally, however, the signals from the cap redirect most of the auxin to the lower side, thus inhibiting the growth of that lower side (**Figure 17.27**). Consistent with this model, IAA rapidly accumulates on the lower side of a horizontally oriented root and concentrates in the epidermal cells of the elongation zone. The movement of auxin across a horizontally oriented root cap has been confirmed using the reporter gene construct DR5:*GFP*, consisting of green fluorescent protein (GFP) expressed from the auxin-sensitive DR5 promoter. In addition, SAURs are observed on the upper side of gravitropically stimulated roots (see later in this section).

Gravity perception is triggered by the sedimentation of amyloplasts

The primary mechanism by which gravity can be detected by cells is via the motion of a falling or sedimenting intracellular body. Root cap columella cells contain large, dense amyloplasts (starch-containing plastids) called **statoliths**. These statoliths readily sediment to the bottom of the cell to align with the gravity vector within 60 s (see Figure 17.27). As we have seen, removal of the root cap from otherwise intact roots prevents root gravitropism without inhibiting growth, suggesting that the root cap columella cells function as gravity-sensing cells, or **statocytes**. Perception of the stimulus (statolith displacement by gravity) is thought to occur via membrane receptors and/or cytoskeletal interactions. Since starchless mutants show a reduced response to gravity, additional signals must be involved in gravity perception.

In a vertically oriented root, PIN3 is uniformly distributed around the columella cells, but when the root is placed on its side, PIN3 is preferentially targeted to the lower side of these cells within 6 min (see Figure 17.27). This redistribution of PIN3 occurs after sedimentation of the statoliths and before the root begins to bend, and is thought to accelerate auxin transport to the lower side of the root. As a result, auxin is transported out of the columella to the lower side of the root cap. From there it is transported back to the elongation zone via the epidermal cells. However, as *pin3* mutants are not completely agravitropic, other asymmetric events might act along with PIN3 localization to alter auxin flows. The most likely event would be an asymmetric change in apoplastic acidification, which would impose an asymmetric chemiosmotic potential to redirect auxin flow. This would cause PIN3 redistribution, which would amplify the flow of auxin in the new direction (canalization; see Chapter 18). The activities of AUX1 and PIN2 in their respective expression domains are also necessary for gravitropic responses, as their loss-of-function mutants are agravitropic.

In eudicot stems and stemlike organs, the statoliths involved in gravity perception are located in the **starch sheath**, the innermost layer of cortical cells that

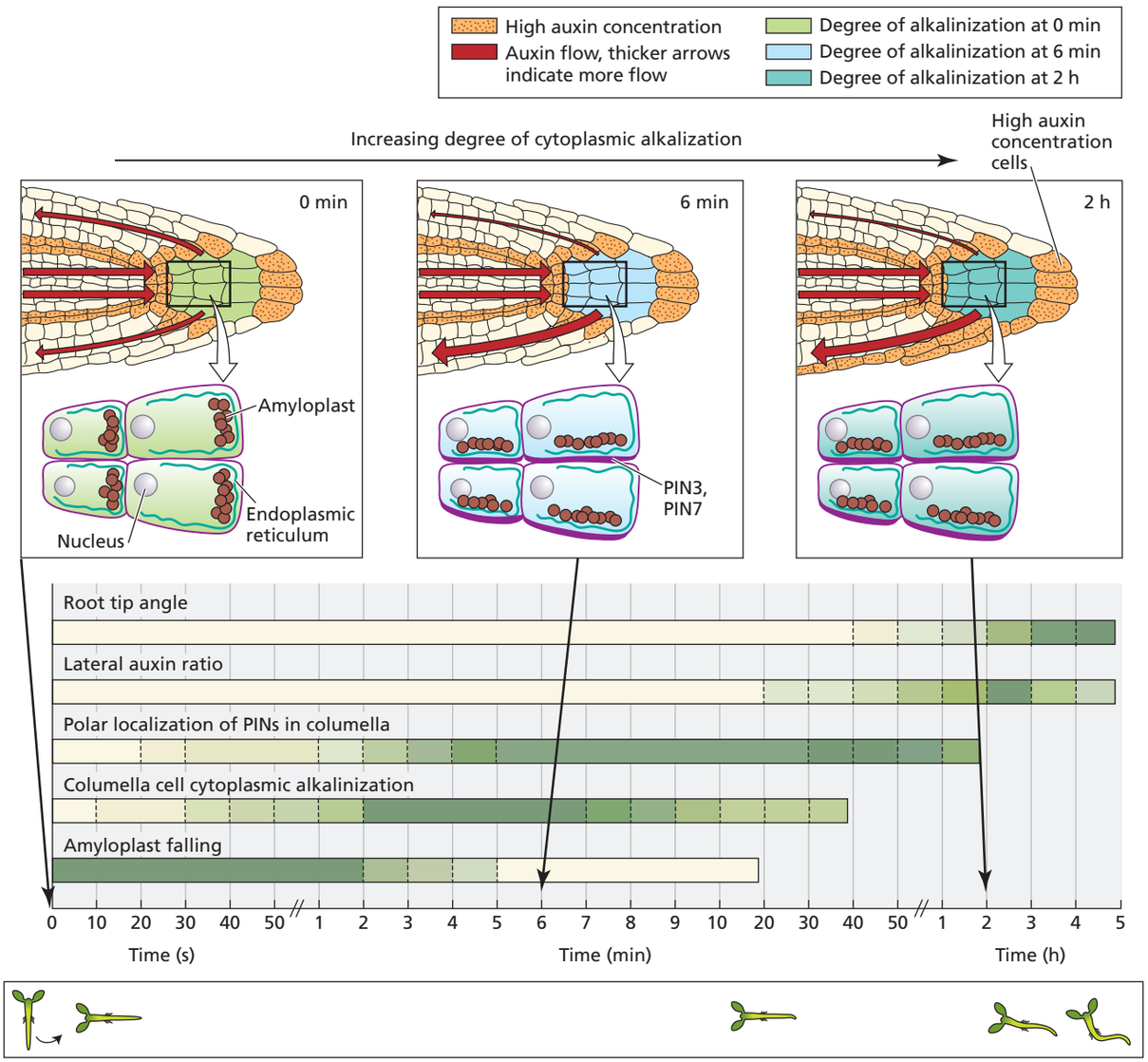


Figure 17.27 Sequence of events following gravistimulation of an Arabidopsis root. The timescale on the bottom is nonlinear. The differential growth of the shoot and roots of the seedling at different stages of the response is illustrated below the timescale. Three stages of statolith sedimentation are shown on the top. The left panel shows time zero, when the seedling is first rotated 90 degrees. The second and third stages shown are at about 6 min and 2 h after rotation. The red arrows indicate auxin flow, with thicker arrows indicating more flow. Cells with relatively high auxin concentrations are shown in orange. Columella cells of the root tip are shown in green at time zero; the color changes to blue and then to blue-green at 2 hours to indicate the degree of alkalinization of the cytoplasm (see Figure 15.33). The distribution of PIN proteins is diagrammed as a purple outline on the plasma membrane of the columella cells. (After K. I. Baldwin et al. 2013. *Am. J. Bot.* 100: 126–142.)

surrounds the ring of vascular bundles of the shoot (**Figure 17.28**). The starch sheath is continuous with the endodermis of the root, and the amyloplasts are redistributed when the gravity vector is changed. The starch sheath cells contain ABCB19 and PIN3, which function coordinately to restrict auxin streams to the vascular system (**Figure 17.29**). Selective regulation of the downward auxin transport stream conducted by PIN1 inside the vascular cylinder and selective restriction of lateral auxin movement into the starch sheath cells by ABCB19 and PIN3 appear to play a fundamental role in tropic bending. In response to a change in the gravity vector, such as occurs when a plant is lodged by heavy rain, the amyloplasts reorient to the bottom of the starch sheath cells and the hypocotyl will bend upward in less than 1 h. The exact sequence of subsequent events remains unresolved, but PIN3 signals are absent on the lower side of the bend in the hypocotyl starch sheath cells 4 h after gravitropic

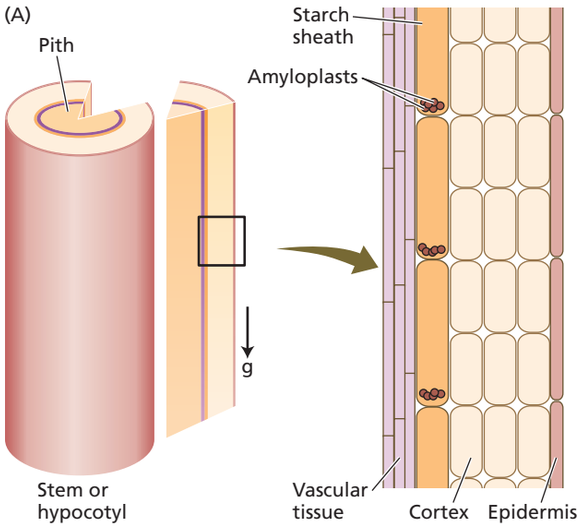


Figure 17.28 **Gravity sensing in the starch sheath of shoots.** **(A)** Diagram of the starch sheath located outside the ring of vascular tissue in a hypocotyl. The cutaway view shows the amyloplasts at the bottom of the cells. **(B)** Amyloplasts in the starch sheath cells relocalize after a gravitropic stimulus. (After M. Palmieri and J. Z. Kiss. 2007. In R. R. Wise and J. K. Hoober [Eds.], *The Structure and Function of Plastids. Advances in Photosynthesis and Respiration*, vol. 23. Springer, Dordrecht, pp. 507–525.)

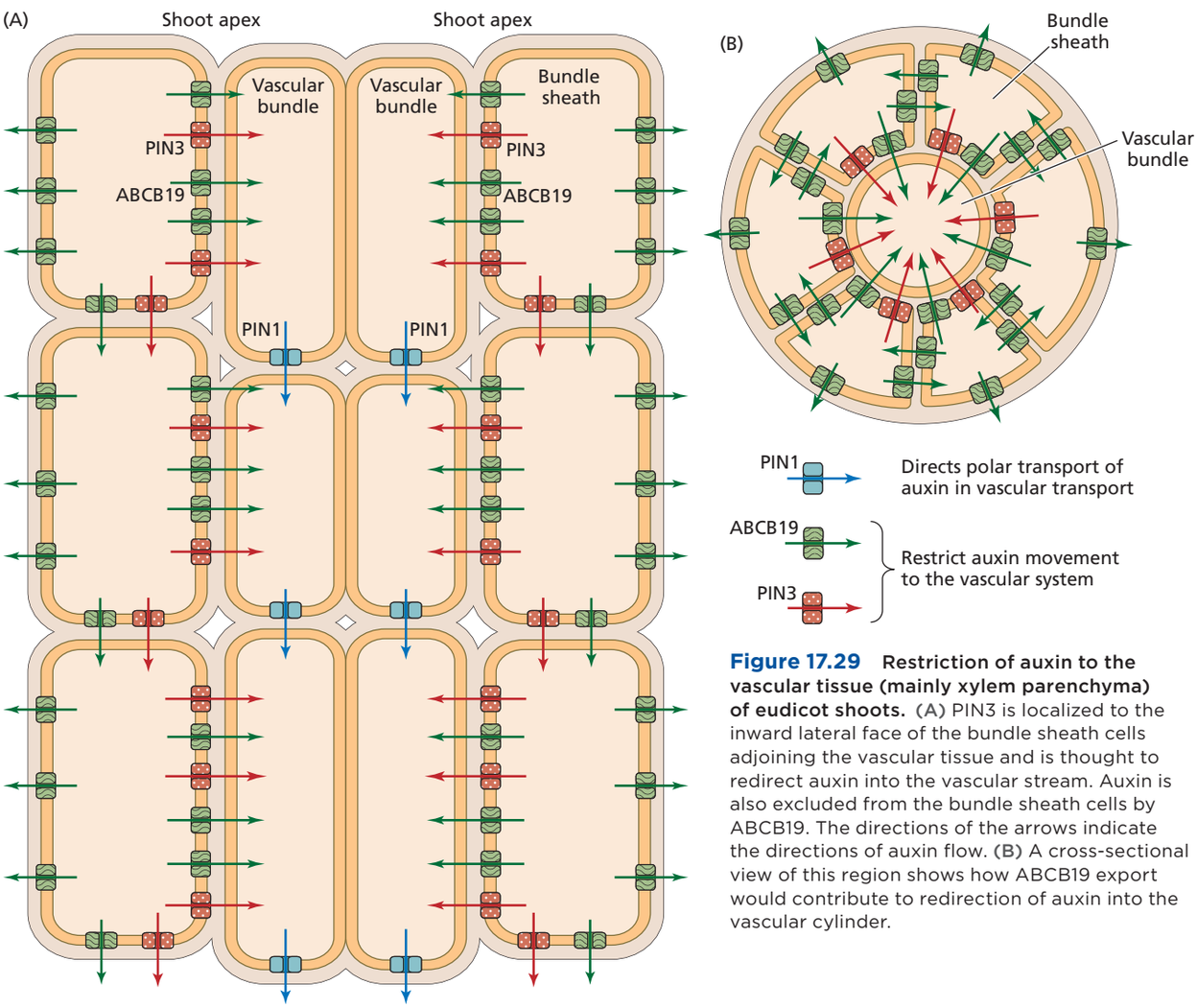


Figure 17.29 **Restriction of auxin to the vascular tissue (mainly xylem parenchyma) of eudicot shoots.** **(A)** PIN3 is localized to the inward lateral face of the bundle sheath cells adjoining the vascular tissue and is thought to redirect auxin into the vascular stream. Auxin is also excluded from the bundle sheath cells by ABCB19. The directions of the arrows indicate the directions of auxin flow. **(B)** A cross-sectional view of this region shows how ABCB19 export would contribute to redirection of auxin into the vascular cylinder.

stimulation. Genetic studies have confirmed the role of the starch sheath in shoot gravitropism, and Arabidopsis and tomato mutants lacking amyloplasts in the starch sheath display reduced gravitropic shoot growth.

Gravity sensing may involve pH and calcium ions (Ca^{2+}) as second messengers

A variety of experiments suggest that localized changes in pH and Ca^{2+} gradients are part of the signaling that occurs during gravitropism. When pH-sensitive dyes were used to monitor both intracellular and extracellular pH in Arabidopsis roots, rapid changes were observed soon after roots were rotated to a horizontal position (**Figure 17.30**). Within 2 min of gravistimulation, the cytoplasmic pH of the columella cells of the root cap increased from 7.2 to 7.5, while the apoplastic pH declined from 5.5 to 4.5. These changes preceded any detectable tropic curvature by about 10 min. Changes in extracellular pH may also be an important signaling element that could modulate auxin responses by altering the chemiosmotic proton gradient.

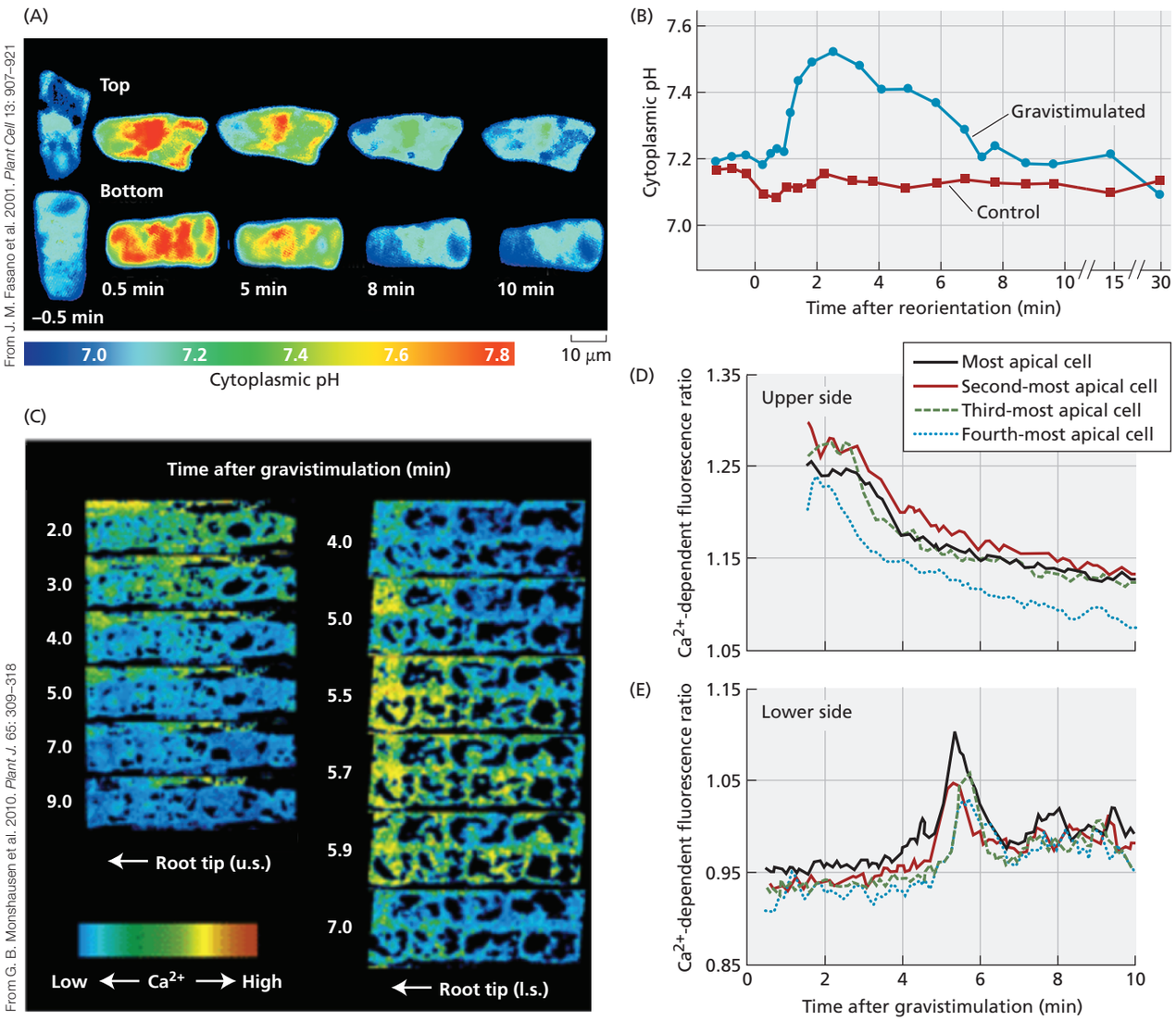


Figure 17.30 Gravitropic pH changes are regulated by a Ca^{2+}-dependent pathway. **(A)** Imaging of pH-sensitive dyes in the response of the columella cells to gravitropic stimulus. The color scale was used to generate the pH data in (B). **(B)** The cytoplasmic pH increases in less than 2 min after gravistimulation. **(C)** Visualization of cytosolic Ca^{2+} concentrations in epidermal cells of the apical elongation zone on the upper side (u.s., left) and lower side (l.s., right) of the gravistimulated root using a Ca^{2+} sensor. **(D and E)** Quantification of cytosolic Ca^{2+} concentrations in cells on the upper side (D) and lower side (E) of the gravistimulated root. Plots show the most apical cell (i.e., closest to root tip), second-most apical cell, third-most apical cell, and fourth-most apical cell in the epidermal cell file. (B after J. M. Fasano et al. 2001. *Plant Cell* 13: 907–921; D,E after G. B. Monshausen et al. 2010. *Plant J.* 65: 309–318.)

The alkalinization of the cytosol combined with the acidification of the apoplast suggests that activation of the plasma membrane H^+-ATPase is one of the initial events that mediates root gravity perception or signal transduction. The chemiosmotic model of polar auxin transport (described in Chapter 4) predicts that differential acidification of the apoplast and alkalinization of the cytosol would result in increased directional uptake and efflux of IAA from the affected cells.

Early physiological studies suggested that Ca^{2+} release from storage compartments might also be involved in root gravitropic signal transduction. For example, treatment of maize roots with EGTA (ethylene glycol-bis[b-aminoethyl ether]-N,N,N′,N′-tetraacetic acid), a compound that can chelate (form a complex with) Ca^{2+}, prevents Ca^{2+} uptake by cells and inhibits root gravitropism. As in the case of [^{3}H]IAA, $^{45}Ca^{2+}$ is polarly transported to the lower half of a root cap that is stimulated by gravity. Ca^{2+} and pH signaling thus appears to regulate root gravitropic bending through the propagation of a Ca^{2+}-dependent signaling pathway.

Thigmotropism involves signaling by Ca^{2+}, pH, and reactive oxygen species

When the radicle emerges from the seed coat, gravity is not the only force it encounters; the radicle also immediately encounters forces imposed by the soil. Depending on where the seed ended up, the soil might be predominantly sand, clay, loam, or some other composition. The plant responds to obstacles in the soil, such as rocks, by redirecting growth around them (thigmotropism) until it can resume growth in alignment with the gravity vector. In nature, roots integrate gravitropic and thigmotropic stimuli to control their growth response.

Auxin mediates differential cell elongation growth during thigmotropism. In roots, the columella cells are the site of perception of the touch stimulus, and the signal is transduced within the columella cells (**Figure 17.31**). The mechanical stimulus induces changes in the concentrations of the secondary messengers Ca^{2+}, pH, and reactive oxygen species. After the touch response, the concentration of cytosolic Ca^{2+} increases in the epidermal cells on the side of the root distal to the touch stimulus (**Figure 17.32A**). This triggers an increase in reactive oxygen species in the apoplast as well as acidification of the cytosol, and alkalization of the apoplast on the untouched side of the root (**Figure 17.32B and C**). The asymmetric growth of the root is mediated by the redistribution of auxin which accumulates on the lower side of the root, as observed in the gravitropic response. Obstacle avoidance has two stages. Roots first bend away from the obstacle (thigmotropism) and continue to grow parallel to the obstacle.

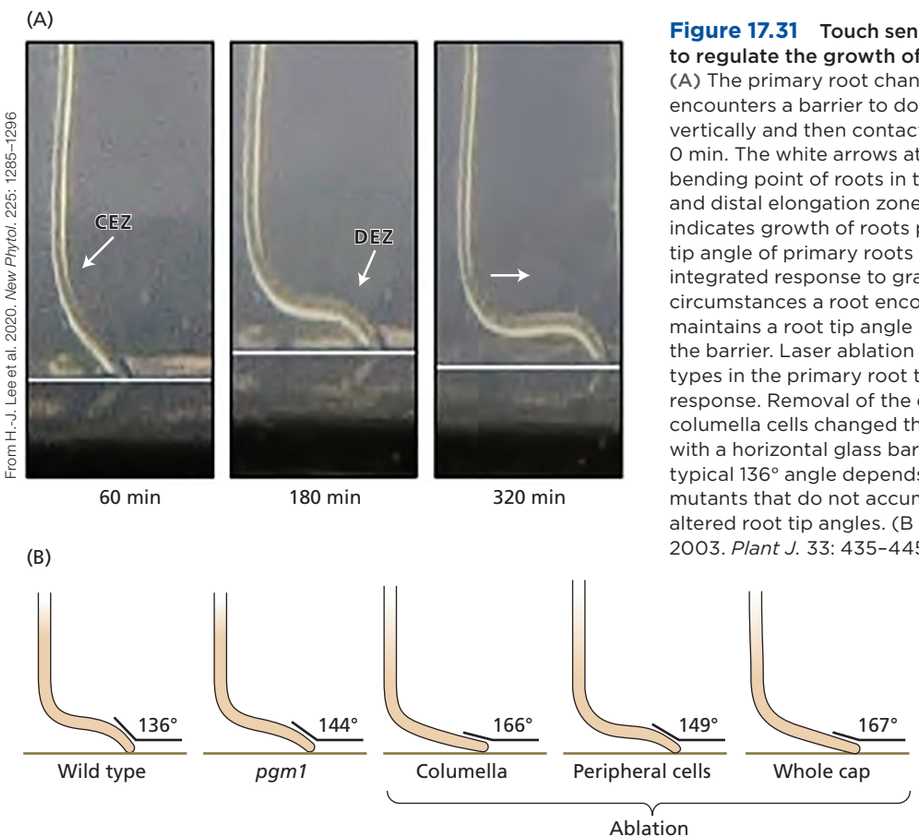


Figure 17.31 **Touch sensing interacts with gravity sensing to regulate the growth of primary roots of Arabidopsis.** **(A)** The primary root changes its growth direction when it encounters a barrier to downward growth. Roots were grown vertically and then contacted a horizontal glass barrier at 0 min. The white arrows at 60 min and 180 min indicate the bending point of roots in the central elongation zone (CEZ) and distal elongation zone (DEZ). The white arrow at 320 min indicates growth of roots parallel to the barrier. **(B)** The root tip angle of primary roots growing around a barrier is an integrated response to gravity and touch. Under normal circumstances a root encountering a horizontal barrier maintains a root tip angle of 136° until it reaches the edge of the barrier. Laser ablation was used to remove different cell types in the primary root tip, to interfere with the gravitropic response. Removal of the entire root cap or peripheral or columella cells changed the root tip angle of roots interacting with a horizontal glass barrier, indicating that maintaining the typical 136° angle depends on gravitropism. Similarly, *pgm1* mutants that do not accumulate starch in columella cells have altered root tip angles. (B after G. D. Massa and S. Gilroy. 2003. *Plant J.* 33: 435–445.)

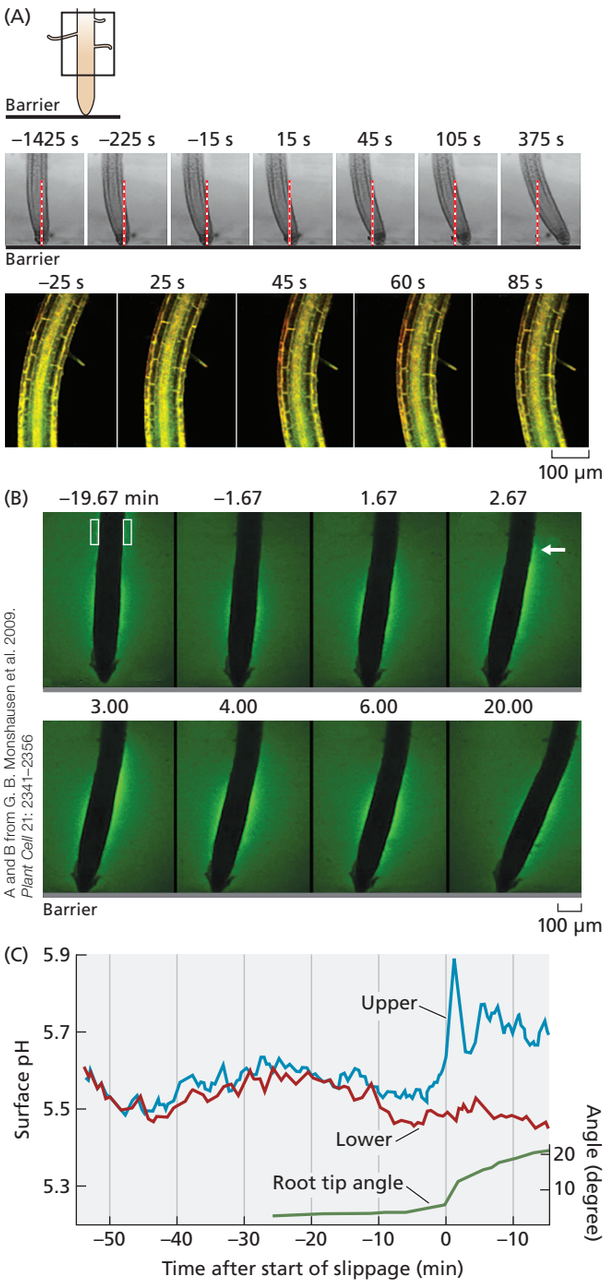


Figure 17.32 **Ca^{2+} and pH changes occur during thigmotropism.** **(A)** Cytosolic Ca^{2+} increases transiently when a vertically growing root tip touches a horizontal glass barrier (see cartoon at top). Top panels: As the root encounters the barrier (at the position marked by the red line), it first presses against the obstacle and finally slides to the side, stretching cells on the upper side of the developing bend. Numbers indicate the time after the start of slippage, here 25 min after first contact was made with the barrier. Bottom panels: Cytosolic Ca^{2+} fluorescence images of a root after it has encountered a barrier. The root region corresponds to the boxed area in the cartoon, and numbers indicate the time after the start of slippage. Note that the Ca^{2+} concentration (red signal) increases in the epidermis and cortex of the upper side of the bend. **(B)** Images of a primary root growing through agarose containing a fluorescent pH indicator dye (green fluorescence), before and after encountering a horizontal barrier. Numbers indicate the time after the start of slippage. When the root is growing vertically, the apoplastic pH is fairly symmetrical on either side of the root. When the root encounters a barrier and subsequently slides to the side, the apoplastic pH rapidly increases on the upper side of the root where the bend forms. Boxes indicate the regions of interest for the pH measurement. The arrow indicates the position where the root bends. **(C)** pH changes were measured along the upper (blue) and lower (red) sides of the root in (B). The green line indicates the root tip angle. Bar = 100 µm. (After G. B. Monshausen et al. 2009. *Plant Cell* 21: 2341–2356).

When the obstacle is no longer perceived via touch sensing, the roots bend again to align root growth with gravity (gravitropism). Therefore, touch sensing modulates gravity sensing until the touch signal is no longer perceived.

Touch responses are also triggered when a growing root encounters denser soil, resulting in root skewing or waving. This response involves the integration of gravitropism, thigmotropism, and circumnutation. For a discussion of how root gravitropism interacts with circumnutation and thigmotropism, see **WEB TOPIC 17.10**.

Hydrotropism involves ABA signaling and asymmetric cytokinin responses

Hydrotropsim is root growth in response to asymmetric water potential of the soil (**Figure 17.33**). The adaptive response of water-foraging root growth toward areas of high water potential is essential for plant survival in soils where water is limiting. In Arabidopsis, pea, rice, and cucumber, hydrotropism still occurs when the root cap is removed using laser ablation, indicating that the root cap is not the site of perception. Instead, water gradients seem to be sensed by the cortical cells in the root elongation zone, where ABA signaling is triggered in response to a water gradient. The hydrotropism responses are dependent on ABA signaling, as the response is not observed in mutants that are insensitive to ABA, and ABA hyper-responsive mutants show rapid hydrotropism. ABA induces expression and accumulation of MIZU-KUSSEI 1 (MIZ1), named for two Japanese words meaning "water" and "tropism." MIZ1 negatively regulates the activity of the endoplasmic reticulum (ER) Ca^{2+}-ATPase 1 (ECA1). As a result, an asymmetric Ca^{2+} gradient is formed in the phloem, and Ca^{2+} diffuses down this gradient to the cortical cells in the root elongation zone on the low water potential side.

Cytokinin signaling is also involved in hydrotropism, as the behavior is reduced in cytokinin biosynthesis or response mutants. Asymmetric cytokinin biosynthesis and accumulation in the meristematic zone are also dependent on MIZ1 activity. The type-A cytokinin

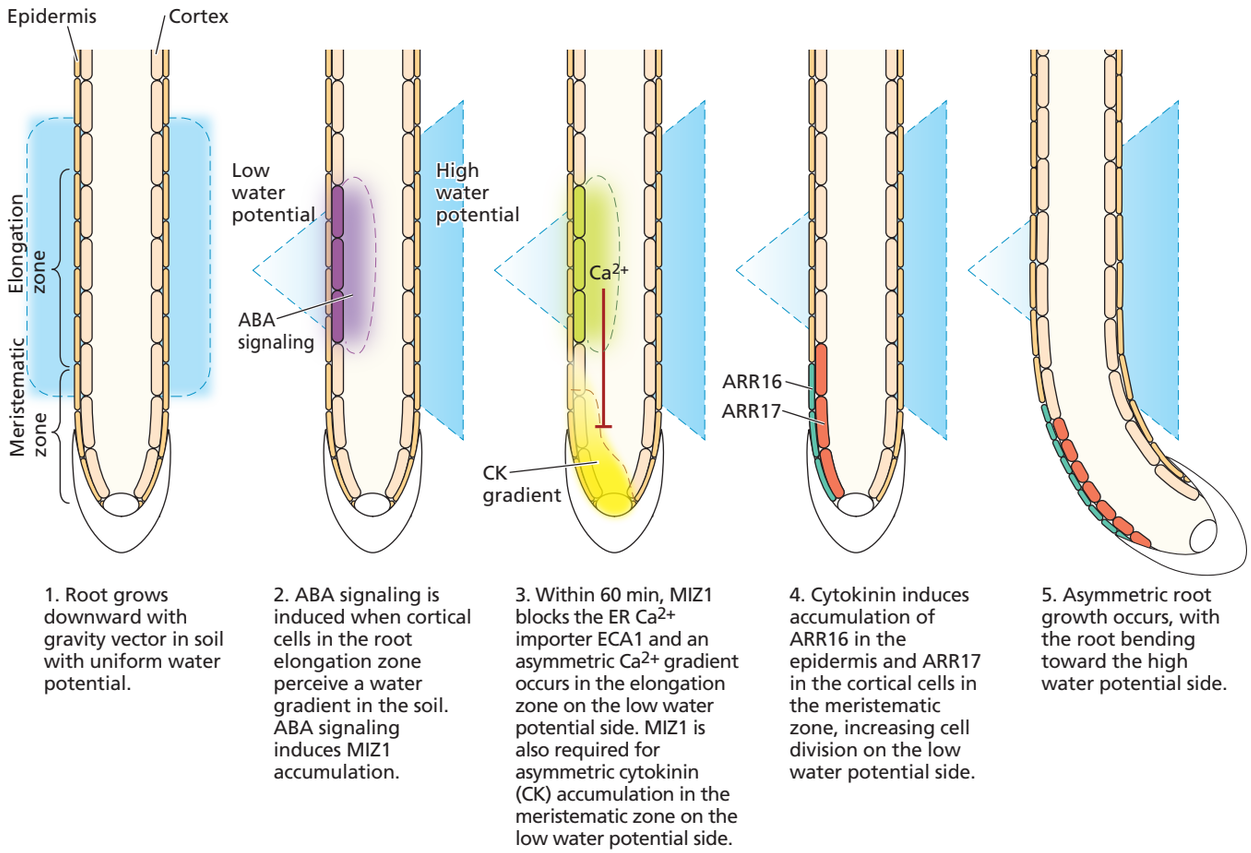


Figure 17.33 Hydrotropic growth of roots toward high water potential. Roots respond to water gradients by a pathway involving Ca^{2+} and ABA signaling events. ABA stimulates expression of MIZ1, which negatively regulates the ER Ca^{2+}-ATPase ECA1, resulting in higher Ca^{2+} concentrations on the side of the root in contact with low water potential soil. Cytokinin induces cell division on the side with low water potential via ARR16 and 17 resulting in asymmetric growth and root bending towards the high water potential side.

response regulators ARR16 and ARR17, in the epidermal and cortical cells, respectively, are up-regulated, resulting in more cells available for elongation on the low water potential side. While cell elongation must occur for the root to bend toward higher moisture, the role of auxin in hydrotropic responses is species-specific. Auxin signaling or polar auxin transport resulting in the lateral redistribution of auxin is required for hydrotropism in rice and pea, but not in Arabidopsis or lotus.

Phototropins are the light receptors involved in phototropism

An emerging seedling is able to bend in any direction toward sunlight to optimize light absorption. This phenomenon is known as phototropism. As we saw in Chapter 16, blue light is particularly effective in inducing phototropism, and two flavoproteins, **phototropin 1** and **phototropin 2**, are the photoreceptors for phototropic bending. Phototropism results from rapid signaling events that are initiated by light-activated phototropins on the lit side of plant organs and that result in differential elongation growth. As in the case of gravitropism, the bending response to directional blue light can be explained by the Cholodny–Went model of lateral auxin redistribution.

Phototropism is mediated by the lateral redistribution of auxin

Charles and Francis Darwin provided the first clue concerning the mechanism of phototropism by demonstrating that while light is perceived at the tip of coleoptiles, bending occurs in the region below the tip. The Darwins proposed that some "influence" was transported from the tip to the growing region, thus causing the observed asymmetric growth response. This influence was later shown to be auxin.

When a shoot is growing vertically, auxin is transported polarly from the growing tip to the elongation zone. However, auxin can also be transported laterally, and this lateral diversion of auxin lies at the heart of

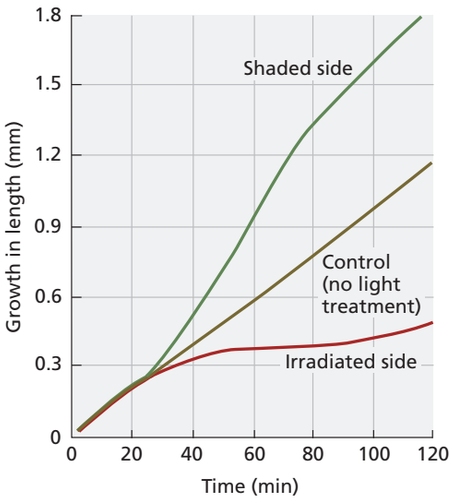


Figure 17.34 Time course of growth on the irradiated and shaded sides of a coleoptile responding to a 30-s pulse of unidirectional blue light at zero minutes. Control coleoptiles were not given a light treatment. (After M. Iino and W. R. Briggs. 1984. *Plant Cell Environ.* 7: 97–104.)

the Cholodny–Went model for tropisms. In phototropic bending, auxin from the shoot tip is redirected laterally to the shaded side of the stem and stimulates cell elongation. The resulting differential growth causes the shoot to bend toward the light (**Figures 17.34** and **17.35**).

Although phototropic mechanisms appear to be highly conserved across plant species, the precise sites of auxin production, light perception, and lateral transport have been difficult to define. In maize coleoptiles, auxin accumulates in the upper 1 to 2 mm of the tip. The zones of photosensing and lateral transport extend farther down, to 5 mm from the tip. The response is also strongly dependent on the light fluence (the number of photons per unit of area). Similar zones of auxin biosynthesis and accumulation, light perception, and lateral transport are seen in the true shoots of all monocots and eudicots examined to date.

For a description of negative phototropism in roots, see **WEB TOPIC 17.11**.

Shoot phototropism occurs in a series of steps

As we mentioned earlier, the events in phototropic bending occur rapidly. Phototropism can be divided into a series of four steps: perception and early signal amplification events, rapid phototropic bending, attenuation, and elongation at the new angle (**Figure 17.36**). Perception and early events in phototropism, such as phosphorylation and dephosphorylation, occur within 1 s to 30 min after blue-light irradiation. Rapid hototropic bending occurs from about 30 min to 150 min after perception of a blue-light signal. The signal is then attenuated from about 150 min to 220 min, and finally,

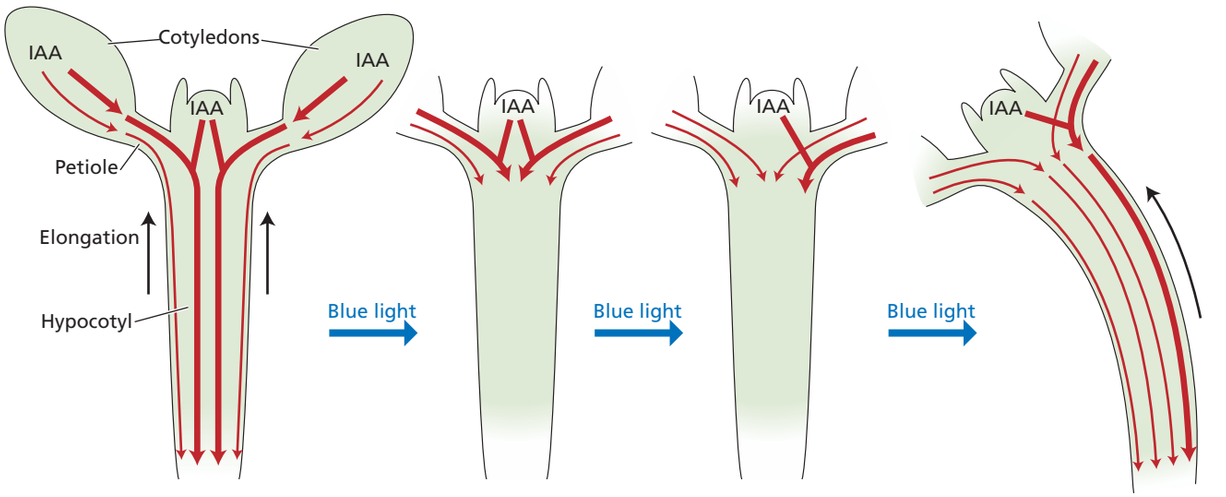


Figure 17.35 Model of rootward auxin movement (red arrows within the seedlings) associated with phototropin 1–dependent phototropism in dark-acclimated seedlings of Arabidopsis. (After J. M. Christie et al. 2011. *PLOS Biol.* 9: e1001076; CC BY.)

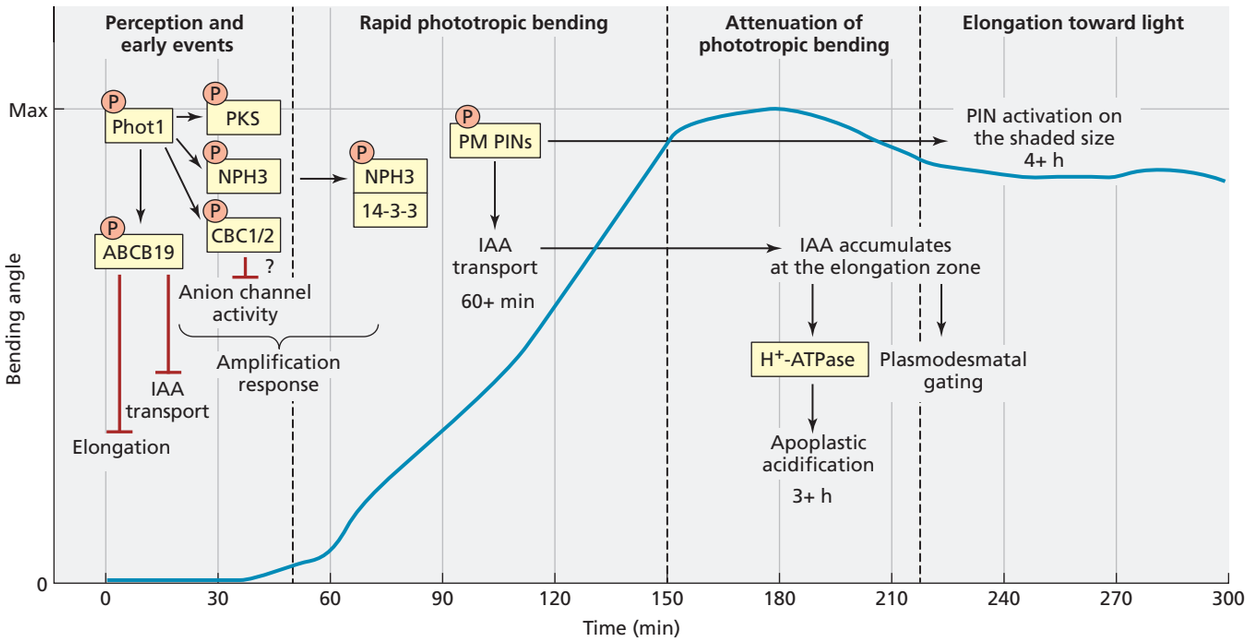


Figure 17.36 Summary of events during successive stages of phototropism. During perception and the early events of phototropism (1 s–50 min), phot1 perceives the signal and autophosphorylates, thereby becoming activated. Active phot1 directly phosphorylates the auxin transporter ABCB19 to block auxin transport, and hypocotyl elongation stops. Active phot1 also phosphorylates other proteins—NPH3, PKS, CBC1, and CBC2—to amplify the phototropic signal. CBCs are present in the hypocotyl, but it is not known if they mediate anion channel activity during phototropsim. The exact order of these steps is not known. During rapid phototropic bending (50–150 min), plasma membrane (PM)–localized PIN auxin efflux proteins are activated via phosphorylation on the shaded side to promote elongation toward the light source. During the attenuation phase (150–220 min), auxin accumulates on the newly shaded side of the hypocotyl elongation zone. Cell wall acidification in the attenuation phase is essential for cell elongation and prepares the hypocotyl for the post-phototropic elongation phase. In the elongation phase on the phototropic axis, plasmodesmatal gating occurs and asymmetric PIN localization is observed 4 h after blue-light perception. (Courtesy of Candace Pritchard and Wendy Peer.)

elongation commences about 220 min after perception of the initial blue-light signal.

Although phototropins are hydrophilic proteins, they are primarily associated with the plasma membrane. Low-fluence blue light is perceived by the cells on the irradiated side of the hypocotyl and a series of signal transduction events is initiated. During the first minute after irradiation, the plasma membrane is transiently depolarized, and the cytoskeleton is reoriented; existing microtubules are degraded and new, longitudinally oriented microtubules are formed (see **WEB TOPIC 17.12**).

After approximately 3 min of unilateral blue-light irradiation, phototropin 1 (phot1) undergoes autophosphorylation. Next, the activated phot1 phosphorylates the auxin transporter ABCB19. As a result of ABCB19 inhibition, auxin accumulates above the cotyledonary node and less auxin is delivered to the elongation zone, causing a rapid stop in hypocotyl elongation and circumnutation. After this pause in elongation, the pooled auxin is laterally diverted to the shaded side of the hypocotyl via a poorly understood process. Auxin accumulation on the shaded side of the upper hypocotyl can be detected after approximately 15 min of exposure to unilateral blue light. Diverted auxin is then transported to the hypocotyl elongation zone in the vascular tissues and epidermis.

As perception of blue light continues, phototropic signal amplification occurs via activated phot1 acting on additional substrates. Another primary substrate for activated phot1 is NONPHOTOTROPIC HYPOCOTYL 3 (NPH3), originally identified from the *nph3* mutant that did not exhibit hypocotyl bending in response to low-fluence blue light. Along with ROOT PHOTOTROPISM 2 (RPT2), NPH3 is a member of a group of NPH3/RPT2 LIKE (NRL) proteins that contain a conserved C-terminal phosphorylation site. NPH3 phosphorylation allows it to bind the 14-3-3 phospho-binding proteins that regulate multiple cellular functions, including proton pumping by plasma membrane H^+-ATPses (see Chapter 8), membrane channel activities, and receptor function. Phosphorylation of NPH3 by phot1 establishes a gradient of 14-3-3 proteins from the lit to the shaded side of the seedling to modulate auxin transport functions that initiate differential bending. The plasma membrane–localized PHYTOCHROME KINASE SUBSTRATE (PKS) proteins are also directly phosphorylated by activated

phot1. PKS4 also interacts with NPH3, and may function in a negative feedback loop that regulates phototropism.

Autophosphorylated phot1 is then internalized by clathrin-mediated endocytosis. The function of internalization is unclear, but it may play a role in either phototropin signaling or receptor desensitization. In guard cells, phot1 phosphorylates the cytosolic kinases CONVERGENCE OF BLUE LIGHT 1 and 2 (CBC1/2) (see Chapter 16). Cytosolic phot1 may phosphorylate CBCs in the hypocotyl as well, as loss of CBCs results in a partial delay in phototropic bending. BLUE LIGHT SIGNALING 1 (BLUS1) is also a known substrate for phot1, but a role for BLUS1 in phototropism has not been demonstrated.

Rapid auxin-dependent activation of plasma membrane H^+-ATPase activity occurs on the shaded side of the hypocotyl. As observed during gravitropism, *SAURs* are differentially expressed during phototropism, with greater expression on the side with the greater auxin concentrations within 1 h of blue-light treatment, and thus mediate the activation of cell wall acidification by the plasma membrane H^+-ATPase. The TRANSMEMBRANE KINASE 1 and 4 (TMK1 and 4) also positively regulate the plasma membrane H^+-ATPase in an auxin-dependent manner. Acidification of the apoplast appears to play a role in phototropic growth: The apoplastic pH is more acidic on the shaded side of phototropically bending stems or coleoptiles than on the irradiated side. Decreased pH would be expected to enhance cellular elongation and amplify auxin movement from cell to cell. Both processes would be expected to contribute to bending toward light. SAURs also accumulate on the shaded side of the hypocotyl after phototropic stimulus, supporting the differential cell wall acidification.

Bending toward the blue-light source can be detected after approximately 30 min. After the intial blue-light perception and early events, blue light perception continues and rapid phototropic bending involves activation of PIN proteins by the AGCVIII protein kinases D6PK and PAX on the shaded side of the hypocotyl, thus functioning with ABCB19 in rapid phototropic bending. During attenuation, the phototropic signal is diminished by degradation of phot1 and bending is completed. After bending is completed, elongation toward the light source occurs. Circumnutation resumes as phototropic and gravitropic signals are integrated during elongation. While no differential pH changes are noted during early phototropic events, the activity of the plasma membrane H^+-ATPase is essential for cell wall acidification to enable hypocotyl elongation after phototropic bending. Plasmodesmatal gating (see Chapter 1) also has a role in the attenuation and elongation phases of phototropism, as callose depositions are observed 4 h after the initial phototropic stimulus. Asymmetric PIN localization is also observed 4 h after blue-light perception.

Although phototropins are the primary photoreceptors for phototropism, phytochromes and cryptochromes can also contribute to the response (see **WEB TOPIC 17.13**).

Summary

Seeds require rehydration, and sometimes additional treatments, to germinate. During germination and establishment, food reserves maintain the seedling until it is autotrophic. Following emergence, the shoot responds to nondirectional cues from sunlight to undergo photomorphogenesis. At the same time, shoots are also responding to directional signals to orient themselves with respect to sunlight (phototropism), gravity (gravitropism), and a source of water (hydrotropism). The root extends downward into the soil, adjusting its growth to avoid obstacles (thigmotropism). Vascular tissue differentiates to facilitate the movement of water, minerals, and sugars from seed reserves and the environment to all parts of the seedling. Hormones play central roles as signaling agents in all of the developmental pathways associated with seedling establishment.

17.1 Seed Structure

- Seeds are surrounded by a seed coat (testa), whereas fruits are enclosed by the pericarp (**Figure 17.1**).
- Seed anatomy varies widely in the types and distributions of stored food resources and the nature of the seed coat (**Figure 17.2**).

17.2 Seed Dormancy

- Seed dormancy may be either exogenous (imposed by surrounding tissues) or endogenous (arising from the embryo itself).
- Endogenous dormancy can be due to high ABA:GA concentrations, or to arrested embryogenesis.
- Seeds that do not become dormant may exhibit vivipary and precocious germination (**Figures 17.3, 17.4**).
- The primary hormones regulating seed dormancy are abscisic acid (ABA) and gibberellins (GAs) (**Figure 17.5**).

17.3 Release from Dormancy

- Light, especially red light, breaks dormancy in many small seeds, a phenomenon mediated by phytochrome.
- Some seeds require chilling or after-ripening to break dormancy (**Figure 17.6**).
- ABA and GA are not the only chemicals regulating seed dormancy. In some seeds, nitrate, nitric oxide (NO), and chemicals in smoke can break dormancy.

Summary (*continued*)

17.4 Seed Germination

- Germination and postgermination take place in three phases relating to water uptake (**Figures 17.7, 17.8**).

17.5 Mobilization of Stored Reserves

- The cereal aleurone layer responds to gibberellins by secreting hydrolytic enzymes (including α-amylase) into the surrounding endosperm, making starch breakdown products available to the embryo (**Figure 17.9**).
- Gibberellins are secreted by the embryo and promote α-amylase transcription and production (**Figure 17.10**).
- ABA inhibits α-amylase transcription.
- Protein storage vacuoles (PSVs) contain phytin, the K^+, Mg^{2+}, and Ca^{2+} salt of phytic acid (*myo*-inositol hexaphosphate, a sugar alcohol), a major storage form of phosphate in seeds. Phytase releases the phosphate and other cations during germination.
- Stored proteins protect the seed against desiccation and reactive oxygen species.
- Proteases are stored in a separate compartment in the cell and are rarely packaged in the seed protein storage vacuole.
- Oil bodies store triacyglycerides and phospholipids.
- Oil bodies also store oleosins, caleosins, and steroleosins, proteins embedded in the lipid monolayer that stabilize the oil body during dormancy, regulate oil body size, and emulsify the oil bodies during germination.
- Oil bodies are broken down by proteases, lipases, and β-oxidation of the released fatty acids during germination and seedling establishment The breakdown of oil bodies by proteases and lipases and the β-oxidation of the released fatty acids provide energy and raw materials for germination and seedling establishment (see Chapter 13).

17.6 Seedling Growth and Establishment

- Seedlings transition from skotomorphogenesis (development in the dark, i.e., underground) to photomorphogenesis (development in the presence of light) at the first instance of light (**Figure 17.11**).
- In etiolated shoots, gibberellins and brassinosteroids suppress photomorphogenesis (**Figure 17.12**).
- Phytochrome, auxin, and ethylene regulate hook opening (**Figure 17.13**).
- Vascular differentiation begins during seedling emergence (**Figure 17.14**).
- The root cap covers the root apical meristem and protects it as the root pushes through the soil (**Figure 17.15**).
- Root hairs are specialized epidermal cells that increase the surface area of the root for water and mineral uptake and help anchor the plant in the soil.
- Root hair formation is regulated by ethylene (**Figure 17.17**).

17.7 Differential Growth Enables Successful Seedling Establishment

- Nutation is organ rotation during growth. Circumnutation is the spiral growth observed in the tips of organs, such as roots, hypocotyls, and stems, in circular or elliptical oscillating patterns (**Figure 17.18**).
- Nutation and circumnutation are nastic movements, meaning they are autonomous and independent of external stimuli.
- Ethylene causes reorientation of microtubules and induces lateral cell expansion (**Figures 17.19, 17.20**).
- At optimal concentrations, auxin promotes stem and coleoptile growth and inhibits root growth. However, higher concentrations of auxin can inhibit stem and coleoptile growth (**Figure 17.21**).

17.8 Tropisms: Growth in Response to Directional Stimuli

- Polarized seedling growth is directed by polar auxin streams (**Figures 17.22, 17.23**).
- Most of the auxin that is redirected shootward in the apex of young seedling roots is derived from the shoot (**Figure 17.24**).
- Lateral redistribution of auxin in coleoptile tips facilitates gravitropism in coleoptiles (**Figure 17.25**).
- A horizontally oriented root redirects auxin to the lower side, inhibiting growth at the elongation zone, an activity that is mediated by the root cap (**Figures 17.26, 17.27**).
- Statoliths in the columella cells of the root cap serve as gravity sensors (**Figure 17.27**).
- The statoliths that regulate gravitropism in eudicot stems and hypocotyls are located in the starch sheath (**Figure 17.28)**.
- Auxin is restricted to the vascular tissue in eudicot stems (**Figure 17.29**).
- pH and Ca^{2+} act as second messengers in the signaling that occurs during gravitropism (**Figure 17.30**).
- pH, Ca^{2+}, and reactive oxygen species act as second messengers in the signaling that occurs during thigmotropism (**Figures 17.31, 17.32**).
- Auxin redistribution occurs during thigomotropism.
- The cortical cells in the root elongation zone are the site of perception of soil water potential (**Figure 17.33**).
- The shaded side of the hypocotyl elongates during phototropic bending (**Figure 17.34**).

(*Continued*)

Summary (*continued*)

- Like gravitropism and thigmotropism, phototropism involves lateral redistribution of auxin (**Figure 17.35**).
- Phototropism in hypocotyls begins within seconds of irradiation and within minutes phototropin 1 autophosphorylates and then temporarily blocks auxin transport and initiates signal amplification (**Figure 17.36**).
- Bending can be observed at 30 min and rapid bending commences at 50 min and continues until the signal is attenuated.
- After phototropic bending is complete, the phototropic signal is attenuated.
- The final step in phototropism is elongation of the hypocotyl toward the light.

Web Material

- **WEB TOPIC 17.1 The Evolution of Seeds** When and how did seeds evolve?
- **WEB TOPIC 17.2 Seedling Growth Can Be Divided into Two Types: Epigeal and Hypogeal** Some cotyledons rise above the soil surface and others remain under the soil.
- **WEB TOPIC 17.3 Seeds Exhibit Both Primary and Secondary Dormancy** Secondary dormancy can be hard to break.
- **WEB TOPIC 17.4 A Special Case of Endogenous Dormancy** Arrested embryogenesis in carrot is an example of endogenous dormancy.
- **WEB TOPIC 17.5 Phase II of Germination Can Be Either a One-Step or a Two-Step Process** The presence or absence of an endosperm at germination determines the Phase II process.
- **WEB TOPIC 17.6 A Classic Experiment—Split Cereal Seeds** One half has only endosperm, the other half has endosperm and the embryo. Which half can degrade starch?
- **WEB TOPIC 17.7 Mobilization of Seed Storage Proteins during Germination** Seed storage proteins are hydrolyzed into small peptides and amino acids that can be transported and synthesized into new proteins and peptides.
- **WEB TOPIC 17.8 Oil Body Organization and Function during Germination** Proteins on the oil body surface prevent oil body fusion and control oil body size.
- **WEB TOPIC 17.9 Trichoblast Identity in Arabidopsis** Mobile transcription factors control root hair formation.
- **WEB TOPIC 17.10 Thigmotropism, Gravitropism, and Circumnutation Are Integrated Signals** Plants perceive multiple signals simultaneously and need to integrate them.
- **WEB TOPIC 17.11 Roots Are Phototropic** Roots exhibit negative phototropism.
- **WEB TOPIC 17.12 Microtubule Orientation and Blue Light** Blue light causes cortical microtubules to reorient in the longitudinal direction.
- **WEB TOPIC 17.13 Chromophores and Phototropism** Phytochromes and cryptochromes contribute to phototropism.

For more study aids, go to oup.com/he/taiz7e.

Suggested Reading

Bewley, J. D., Bradford, K. J., Hilhorst, H. W. M., and Nonogaki, H. (2013) *Seeds: Physiology of Development, Germination and Dormancy*, 3rd ed. Springer, New York.

Chang, J., Li, X., Fu, W., Wang, J., Yong, Y., Shi, H., Ding, Z., Kui, H., Gou, X., He, K., and Li, J. (2019) Asymmetric distribution of cytokinins determines root hydrotropism in *Arabidopsis thaliana*. *Cell Res.* 29: 984–993.

Christie, J. M., and H. Yang et al. (2011) phot1 inhibition of ABCB19 primes lateral auxin fluxes in the shoot apex required for phototropism. *PLOS Biol.* 9: e1001076.

Dietrich, D., Pang, L., Kobayashi, A., Fozard, J. A., Boudolf, V., Bhosale, R., Antoni, R., et al. (2017) Root hydrotropism is controlled via a cortex-specific growth mechanism. *Nat. Plants* 3: 17057.

Migliaccio, F., Tassone, P., and Fortunati, A. (2013) Circumnutation as an autonomous root movement in plants. *Am. J. Bot.* 100: 4–13.

Shkolnik, D., Nuriel, R., Bonza, M. C., Costa, A., and Fromm, H. (2018) MIZ1 regulates ECA1 to generate a slow, long-distance phloem-transmitted Ca^{2+} signal essential for root water tracking in Arabidopsis. *Proc. Natl. Acad. Sci. USA* 115: 8031–8036.

Shao, Q., Liu, X., Su, T., Ma, C., and Wang, P. New insights into the role of seed oil body proteins in metabolism and plant development. *Front. Plant Sci.* 10: 1568.

Wang, X., Yu, R., Wang, J., Lin, Z., Han, X., Deng, Z., Fan, L., He, H., Deng, X. W., and Chen, H. (2020) The asymmetric expression of SAUR genes mediated by ARF7/19 promotes the gravitropism and phototropism of plant hypocotyls. *Cell Rep.* 31: 107529.

18 Vegetative Growth and Organogenesis: Primary Growth of the Plant Axis



schankz/Shutterstock

As we discussed in Chapter 17, developmental programming in the seedling ensures functional establishment of a photosynthesizing plant capable of taking up nutrients and water from the soil. In the next phase of growth, undifferentiated cells in juvenile plants adopt new fates to generate specialized cell types or organs that enhance competition for resources under variable environmental conditions. The pattern of differentiation and growth results in a huge diversity of organ shapes and functions.

In this chapter we discuss the developmental processes by which plants transition from the seedling state, expand on their primary axis, and begin production of determinate lateral organs such as leaves. We begin by considering the basic features of cell division and initiation of processes that lead to differentiation in the root and shoot apical meristems, and then discuss leaf development. We examine blade formation in simple leaves, which involves the marginal expansion of leaf tissues, differentiation into adaxial and abaxial domains, and morphogenesis along the proximal–distal axis. We also discuss how compound leaves are produced by variations of these developmental pathways. Finally, we discuss the gene networks and hormonal signals that control development of the specialized cells of the epidermis and vascular tissue.

The regulated formation and outgrowth of indeterminate branch systems, as well as secondary growth in perennial plants, will be discussed in Chapter 19.

18.1 Meristematic Tissues: Foundations for Indeterminate Growth

Plant development exhibits a remarkable degree of plasticity, which can be largely attributed to specialized tissues called **meristems**. A meristem can be broadly defined as a region that contains cells that divide to both replicate themselves and produce founder cells for the differentiated plant body. Several types of meristems contribute to the vegetative development of plants.

The **root apical meristem** (**RAM**) and **shoot apical meristem** (**SAM**) are found at the tips of the root and shoot, respectively. **Intercalary meristems**, such as the **vascular cambium** and the stem tissues from which grass leaves emerge, represent proliferative tissues that are flanked by differentiated tissues. Small, superficial clusters of cells known as **meristemoids** give rise to structures such as trichomes or stomata (see **WEB ESSAY 18.1** for a historical overview of plant meristems).

The root and shoot apical meristems use similar strategies to enable indeterminate growth

Although it might seem difficult to imagine two parts of a plant more different than a shoot and a root, the RAM and SAM function in similar ways. Both contain a spatially defined cluster of cells, termed **initials**, that are distinguished by their slow rate of division and undetermined fate. As polarized patterns of cell division displace some initials to the meristem edge, they take on various differentiated fates that contribute to the radial and longitudinal organization of the root or shoot and to the development of lateral organs.

Both the RAM and the SAM must balance the production of new cells with the ongoing recruitment of cells into differentiated tissues to maintain a constant size. Is it possible that common aspects of RAM and SAM behavior can be traced to similar underlying mechanisms? How are these mechanisms regulated to maintain the characteristic organizations of the shoot and root and to enable adaptive growth responses to a range of different environments? Do the distinct patterns of growth and organogenesis in root and shoot impose special requirements on RAM and SAM function? To address these questions, Sections 18.2 and 18.3 discuss basic features of the RAM and the SAM as well as examples of genetically defined signaling pathways that contribute to their establishment and maintenance.

18.2 The Root Apical Meristem

Many aspects of root growth reflect adaptations to a demanding environment. Roots, which anchor the plant and absorb water and mineral nutrients from the soil, display complex patterns of growth and tropisms that allow them to explore and exploit a heterogeneous environment laden with obstacles. Although cells produced by the RAM divide, differentiate, and elongate as they are displaced away from the tip, lateral outgrowths such as root hairs (see Chapter 17) and lateral branches (see Chapter 19) emerge farther away from the root tip in regions where cell elongation is complete. This spatial separation, which helps prevent damage to lateral organs from shearing forces, affords a useful opportunity to focus on just those processes at the root tip that serve to maintain a set of initials and regulate their division activity. In this section we consider the generation of root organization at the apex in more detail, discussing regional differences in cellular behavior that contribute to the growth and functionality of the root. We then review experimental evidence suggesting that the coordinated growth of the root depends on a combination of auxin-dependent and cytokinin-dependent programs of gene activity that are coordinated by specific classes of transcription factors and response regulators.

The root tip has four developmental zones

The basic features of root development can best be described by first distinguishing zones within the root with distinct cellular behaviors. Although it is impossible to define their boundaries with absolute precision, the division of the root into the following zones provides a useful spatial framework that is relevant to our discussion of the underlying mechanisms (**Figure 18.1**).

- The **root cap** occupies the most distal part of the root. It represents a unique set of initial derivatives that are displaced distally away from the meristematic zone. The differentiated products of these divisions cover the apical meristem and protect it from mechanical injury as the root tip is pushed through the soil. Other functions of the root cap include perception of gravity, to enable gravitropism (see Chapter 17), and the secretion of compounds that help the root penetrate the soil and mobilize mineral nutrients.
- The **meristematic zone** lies just under the root cap. It contains a cluster of cells that act as initials, dividing with characteristic polarities to produce cells that divide further and differentiate into the various mature tissues that make up the root. Cells surrounding these initials have small vacuoles and expand and divide rapidly.
- The **elongation zone** is the site of rapid and extensive cell elongation. Although some cells continue to divide while they elongate within this zone, the rate of division decreases progressively to zero with increasing distance from the meristem.
- The **maturation zone** is the region in which cells acquire their differentiated characteristics. Cells enter the maturation zone after division and elongation have ceased, and in this region cell outgrowths called root hairs and lateral organs such as lateral roots may begin to form. Differentiation may begin much earlier, but cells do not achieve their mature state until they reach this zone. Lateral root development is described in detail in Chapter 19.

Depending on the species, these four developmental zones can occupy little more than the first millimeter of the root or extend over a longer portion of the distal regions of the root.

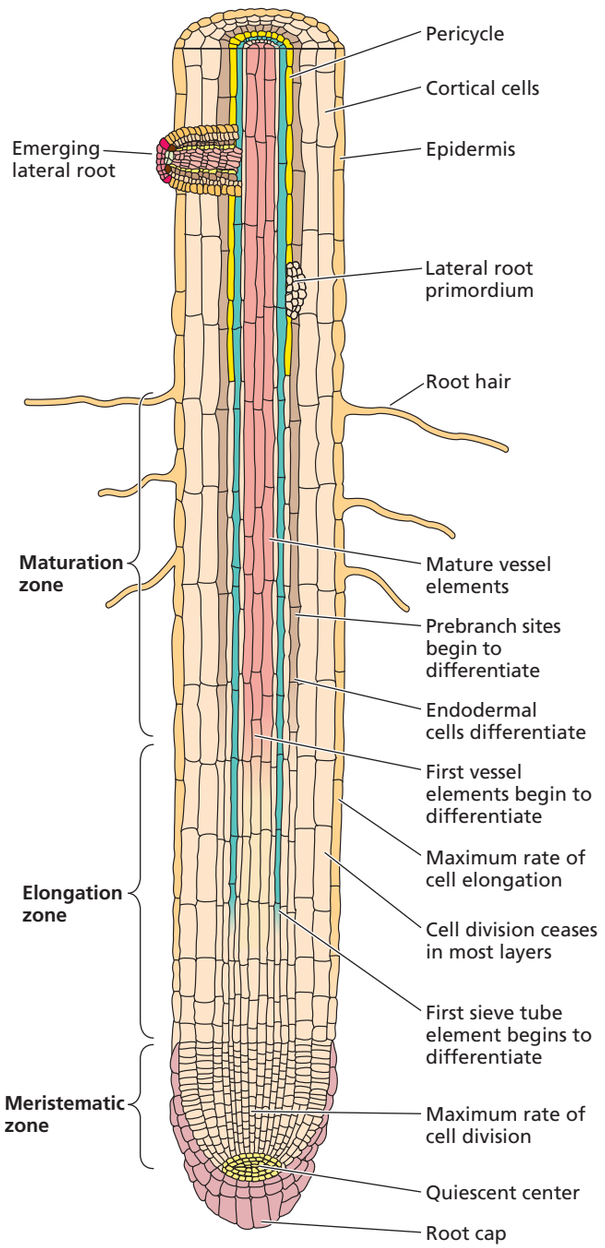


Figure 18.1 Simplified diagram of a primary root showing the root cap, meristematic zone, elongation zone, and maturation zone.

The origin of different root tissues can be traced to specific initial cells

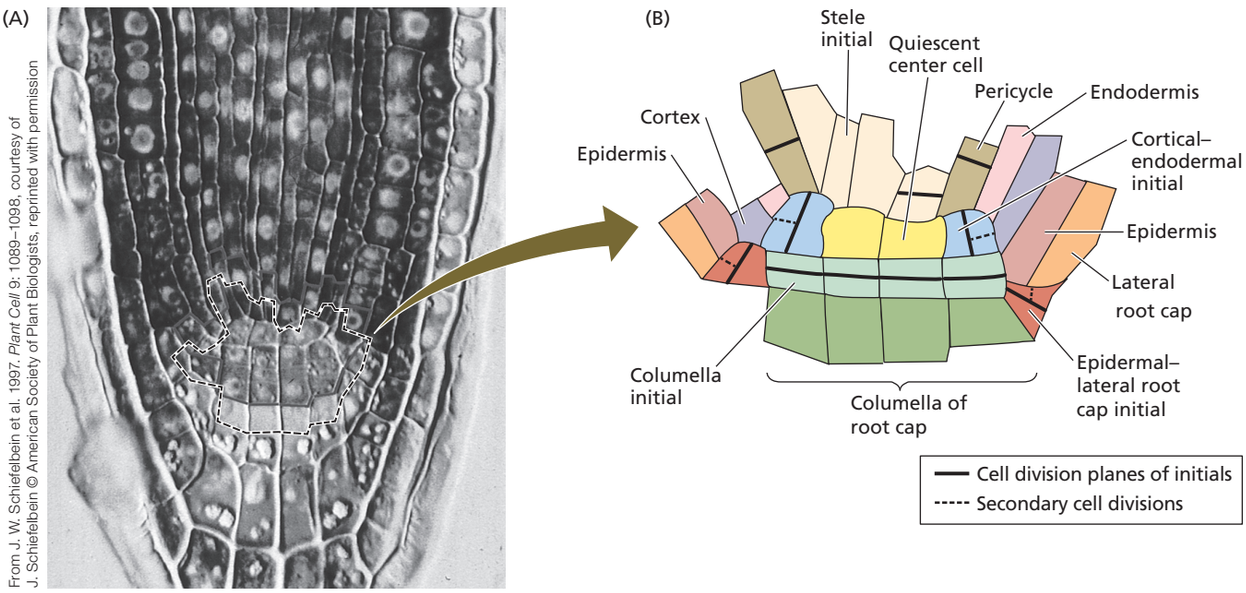
Given the progressive and linear development of the tissues that make up the root, it is relatively simple to trace their origin back to specific initial cells in the subapical region. In most plant roots, a medial longitudinal cross section (**Figure 18.2A**) reveals long cell files that converge near the apex at the **quiescent center** (**QC**), named for its relatively low rate of cell division compared with those of surrounding tissues. The QC can consist of as few as one or as many as hundreds of cells and is often difficult to distinguish from adjacent initial cells. In the water fern *Azolla*, a single, centrally positioned apical cell appears to fulfill the roles of both QC and initials by retaining low, but consistent, mitotic activity throughout vegetative development (see **WEB TOPIC 18.1**). For our discussion here, we will use the well-defined and relatively simple Arabidopsis root as a model.

The QC of Arabidopsis consists of only four cells, and because division of these cells during postembryonic development is rare, mechanical or genetic ablation of the QC or surrounding initials produces visible changes in growth. In Arabidopsis, four distinct sets of initials, all of which are adjacent to the QC, can be defined in terms of their position and the tissues they produce (**Figure 18.2B**):

- *Columella initials.* Located directly below (distal to) the QC, these initials give rise to the central portion (columella) of the root cap.
- *Epidermal–lateral root cap initials.* Located to the side of the QC, these initials first divide anticlinally to produce daughter cells, which then divide periclinally to form two files of cells that mature into the lateral root cap and epidermis.
- *Cortical–endodermal initials.* Located interior and adjacent to the epidermal–lateral root cap initials, the cortical–endodermal initials divide anticlinally to set off daughter cells, which then divide periclinally to form the cortical and endodermal cell layers.
- *Stele initials.* Located directly above (proximal to) the QC, these initials give rise to the vascular system, including the pericycle.

Auxin and cytokinin contribute to the maintenance and function of the RAM

Auxin and cytokinin play important roles in RAM maintenance. Auxin is initially supplied to the primary root apex by rootward transport from the shoot, but is replaced by auxin produced in or around the QC as the primary root elongates and branches. A discrete set of AUXIN RESPONSE FACTORS (ARFs) and cytokinin-responsive ARABIDOPSIS RESPONSE REGULATORS (ARRs) (see Chapter 4) are required for root growth. Auxin accumulation and synthesis in the QC and surrounding cells maintain the expression of genes encoding a group of transcription factors that function in RAM organization (**Figure 18.3**). Two transcription factors known as PLETHORA 1 and 2, as well as members of the WOX (for *W*USCHEL homeo*box*) family of transcription factors, are abundant in these cells and are required for normal RAM function. In particular, WOX5 is expressed in a small group of



From J. W. Schiefelbein et al. 1997. *Plant Cell* 9: 1089–1098, courtesy of J. Schiefelbein © American Society of Plant Biologists, reprinted with permission

Figure 18.2 **All the tissues in the Arabidopsis root are derived from a small number of initial cells in the root apical meristem.** **(A)** Longitudinal section through the center of a root. The meristem containing the initials that give rise to all the tissues of the root is outlined with a dashed line. **(B)** Diagram of the region outlined in (A). Only two of the four quiescent center cells are depicted in this section. The heavier black lines indicate the cell division planes that occur in the initials. The dashed black lines indicate the secondary cell divisions that occur in the cortical–endodermal and epidermal–lateral root cap initials.

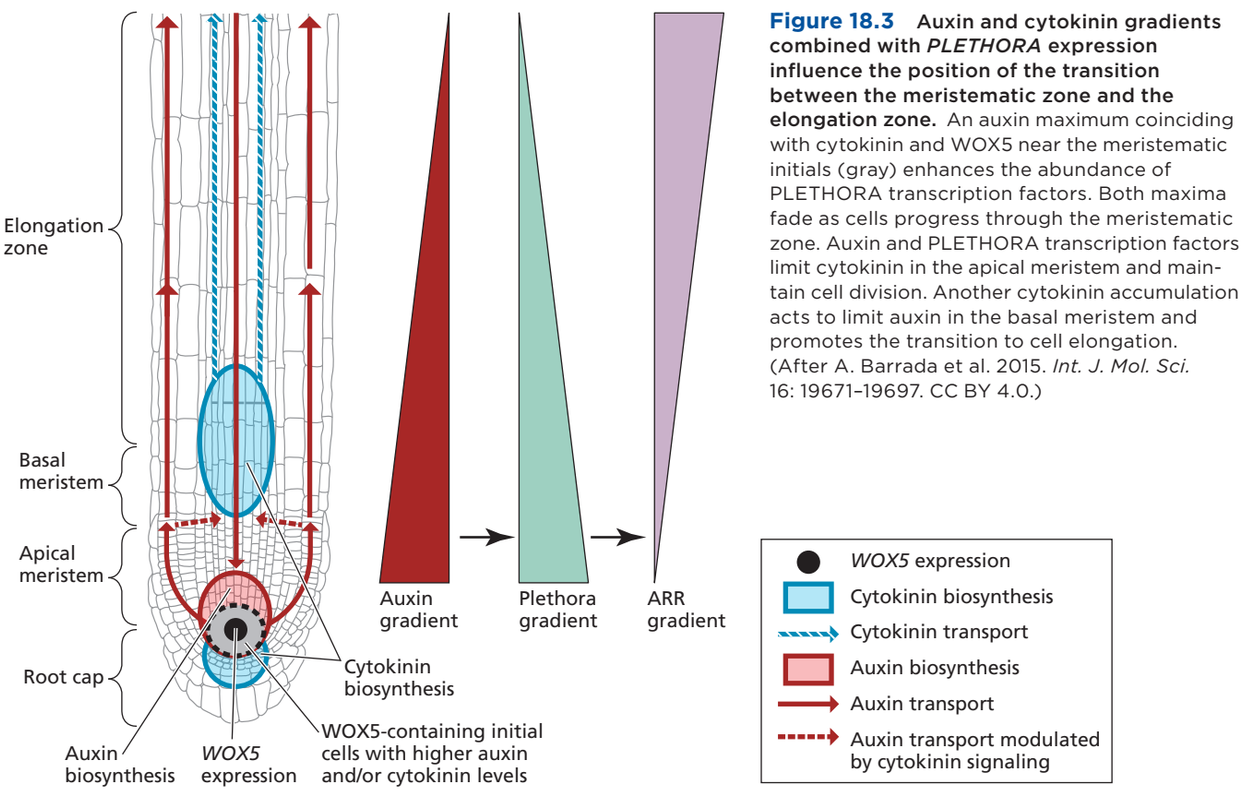


Figure 18.3 **Auxin and cytokinin gradients combined with *PLETHORA* expression influence the position of the transition between the meristematic zone and the elongation zone.** An auxin maximum coinciding with cytokinin and WOX5 near the meristematic initials (gray) enhances the abundance of PLETHORA transcription factors. Both maxima fade as cells progress through the meristematic zone. Auxin and PLETHORA transcription factors limit cytokinin in the apical meristem and maintain cell division. Another cytokinin accumulation acts to limit auxin in the basal meristem and promotes the transition to cell elongation. (After A. Barrada et al. 2015. *Int. J. Mol. Sci.* 16: 19671–19697. CC BY 4.0.)

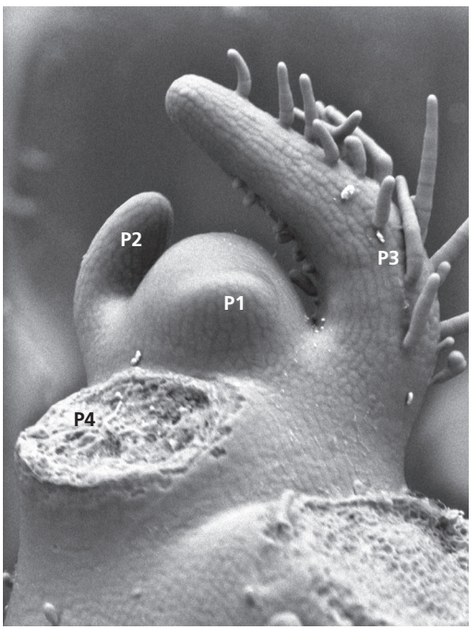
cells in the root tip that includes the QC and the surrounding initials and is important in maintaining their undifferentiated state.

Auxin-dependent meristem maintenance in the root also involves cytokinin. When maturing cells move further away from the QC in the meristematic zone, also known as the division zone, of the root, high auxin and PLETHORA expression in the absence of WOX5 promotes cell division and represses ARR genes that activate cytokinin responses. As progressive cell divisions gradually diminish PLETHORA levels via dilution, increased ARR gene expression and cytokinin signaling lower auxin concentrations, inhibit cell division, and promote the transition to cell elongation (see Figure 18.3). This antagonism between auxin and cytokinin responses is similar to that observed in undifferentiated callus cultures, where alterations in auxin:cytokinin ratios can be used to selectively initiate development of shoots or roots. Excision of the root apex, application of auxin and cytokinin, and overexpression of *PLETHORA* and *WOX* genes can all be used to alter meristem size and position in the root.

18.3 The Shoot Apical Meristem

Like the root apical meristem, the shoot apical meristem (SAM) first forms during embryogenesis and maintains a group of undetermined cells. However, there are significant differences between the two meristem types in how the descendants of those cells become incorporated into organs. Whereas lateral root initiation occurs well back of the root tip (see Chapter 19), leaves and associated axillary branches form close to apical initials in the shoot. In place of the root cap that protects the apical initials of the root, young leaf primordia overlap and enclose the shoot tip (**Figure 18.4**).

The term *shoot apical meristem* refers specifically to the initial cells and their undifferentiated derivatives, but excludes adjacent regions that contain cells fully committed to particular developmental fates.[1] The moreinclusive term **shoot apex** (plural *apices*) refers to the apical meristem plus the most recently formed leaf primordia. The size, shape, and organization of the SAMvary according to plant species, developmental stage, and growth conditions. Cycads have the largest SAM among vascular plants, measuring over 3 mm in diameter; at the other extreme, the SAM of Arabidopsis is less than 50 μm in diameter and contains only a few dozen cells. Within a given species, significant variations in SAM size can also occur over time, and SAM shapes may range from flat to mounded. Some of these variations are related to nutrient availability or seasonal differences in growth rate, including the onset of dormancy or flowering.



Courtesy of D. Reinhardt

Figure 18.4 Shoot apex of a tomato plant. This SEM micrograph shows the basic features of the shoot apex, including a central dome-shaped region, which maintains uncommitted initials, and a series of leaf primordia (P1, P2, P3), which have successively emerged at lateral positions on the flanks of the shoot apex. P4 indicates the base of an older leaf primordium that was removed to expose the younger primordia.

In this section we first consider the basic organization of the SAM, discussing the regional differences in cellular behavior that contribute to its function. We then discuss evidence suggesting that, like the RAM, the SAM relies on localized differences in mobile hormone, peptide, and transcription factor activities for its formation and maintenance.

The shoot apical meristem has distinct zones and layers

At the center of an active SAM lies the **central zone** (**CZ**), containing a cluster of infrequently dividing initial cells that can be compared to similar cells in the QC of roots (**Figure 18.5A**). The **peripheral zone** (**PZ**) flanks the CZ and consists of cytoplasmically dense cells that divide more frequently to produce cells that later become incorporated into lateral organs such as leaves. The **rib zone** (**RZ**) is proximal to the CZ and contains dividing cells that produce the internal tissues of the stem.

Superimposed on these regional differences in the frequency of division are distinct patterns in the planes of cell division. In most angiosperm meristems, the two outermost cell layers divide anticlinally and maintain

[1] The terms *initial cells* and *stem cells* are often used interchangeably by developmental biologists. To avoid confusion with the term applied to the primary plant axis, we use the terms *undifferentiated cells*, *initial cells*, or *initials* throughout this textbook.

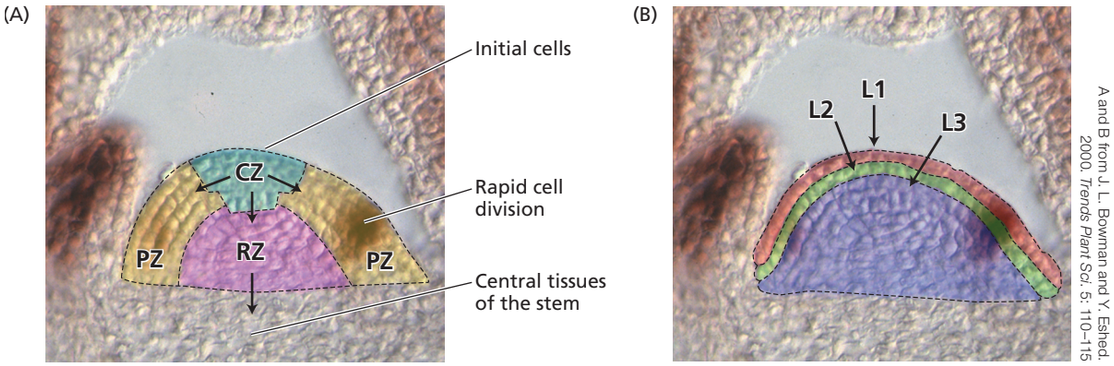


Figure 18.5 **The Arabidopsis shoot apical meristem can be analyzed in terms of cytological zones or cell layers.** **(A)** The shoot apical meristem has cytological zones that represent regions with different identities and functions. The central zone (CZ) contains meristematic cells that divide slowly but are the ultimate source of the tissues that make up the plant body. The peripheral zone (PZ), in which cells divide rapidly, surrounds the central zone and produces the leaf primordia. A rib zone (RZ) lies interior to the central zone and generates the central tissues of the stem. **(B)** The shoot apical meristem also has cell layers that contribute to specific tissues of the shoot. Most cell divisions are anticlinal in the L1 and L2, layers; the planes of cell division are more randomly oriented in the L3 layer. The outermost (L1) layer generates the shoot epidermis; the L2 and L3 layers generate internal tissues.

the **L1** (epidermal) and **L2** layers (**Figure 18.5B**), each a single cell thick. L1 and L2 are sometimes referred to collectively as the tunica. The cells lying interior to the tunica, known as **L3** or the corpus, display more variable division planes, which increases cell number in three dimensions and increases tissue volume. These differences in division planes were discovered by elegant experiments tracking patterns of cell division in the SAM (see **WEB TOPIC 18.2**).

A combination of positive and negative interactions determines apical meristem size

Throughout development, the SAM maintains its size by balancing the loss of cells to differentiation in the peripheral zone with the production of more cells by division of initials in the central zone. The logic of the core size control mechanism is simple: Positive regulators are produced proximal to the initials in the central zone and increase the number of meristematic cells, and negative regulators are produced in the initials and suppress the positive regulator. Larger meristems have more initial cells and produce a higher dose of negative regulator, naturally limiting meristem size; and smaller meristems produce less negative regulator, allowing more positive regulator to increase meristem size. Eventually these two interacting factors reach an equilibrium and maintain constant meristem size.

The key positive regulator of meristem size is the WUSCHEL (WUS) homeodomain transcription factor. *WUSCHEL* was the first characterized *WOX* gene and was named for the irregular "mop-top" appearance of the shoot apex in the Arabidopsis *wuschel* mutant (see Chapter 22 for a description of homeobox genes). WUS, like WOX5 in the root, is essential to maintaining the identity of apical initials. Opposing the activity of WUS are key negative regulators of meristem size that are encoded by the *CLAVATA* (*CLV*) genes (from the Latin for "club-shaped," to describe the enlarged SAM of Arabidopsis *clv* mutants). Molecular and biochemical analyses have shown that the CLV proteins physically interact with each other to function as a peptide-receptor-protein kinase signaling relay whose outputs act to limit meristem size. CLV1 is a leucine rich repeat (LRR) receptor-like kinase (RLK), with an extracellular ligand binding domain, and an

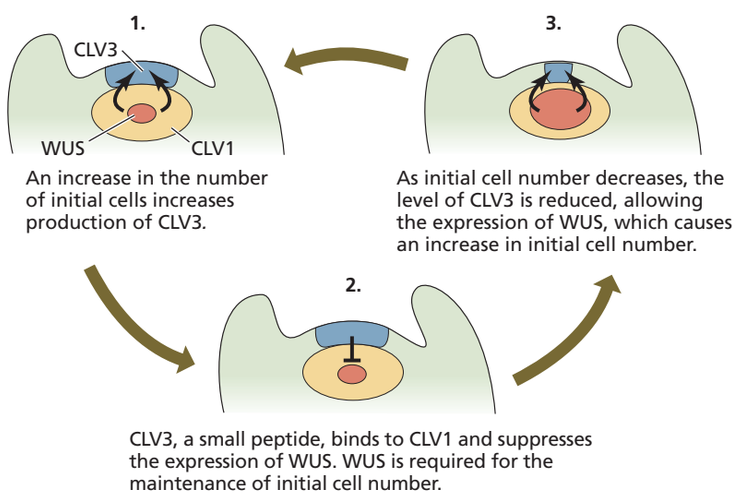


Figure 18.6 **Model of the feedback loop that maintains initial cells in the SAM.**

intracellular kinase signaling domain (see Chapter 4). CLV2 resembles CLV1 but lacks the intracellular kinase domain, and thus appears to depend on interaction with other intracellular proteins for its signaling outputs. CLV3 is a small 13–amino acid member of the CLAVATA3/Embryo Surrounding Region-Related (CLE) signaling peptide family that is expressed in undifferentiated cells (**Figure 18.6**) and binds CLV1 and CLV2 to initiate signaling processes that repress WUS expression. WUS is required to maintain initial cell indeterminancy and numbers. This, in turn, results in decreased production of CLV3 and consequent de-repression of WUS-dependent production of undifferentiated cells. This feedback loop provides a stable pool of initial cells in the SAM during growth.

KNOX class homeodomain transcription factors help maintain proliferation in the SAM through regulation of cytokinin and GA concentrations

We have discussed maintenance mechanisms in the SAM that are similar to those in the RAM, but some unique mechanisms are present in the SAM. For example, the production of lateral organs close to the more pluripotent cells of the meristem appears to require an additional level of regulation, which is mediated by members of the KNOX (*KN*OTTED 1 homeob*ox*) family of transcription factors. The name KNOTTED is derived from the knotlike protuberances observed in maize (corn; *Zea mays*) with mutations in the genes encoding these transcription factors. Subsequently, studies of the Arabidopsis *shoot meristemless* (*stm*) mutant showed that the mutation resulted from loss of a KNOX transcription factor required for SAM formation and maintenance. STM is present throughout almost the entire body of the meristem, but not in the groups of cells in flanking positions that are committed to become leaf primordia (labeled P0 in Figure 18.7).

KNOX proteins function in part by modulating the concentrations of the plant hormones cytokinin and gibberellin (GA) (**Figure 18.7**). Applying cytokinin to the meristem rescues meristem collapse in *stm* mutants, and *STM* expression in the SAM activates the transcription of genes encoding isopentenyl transferases that are involved in the biosynthesis of cytokinin. These observations support the idea that STM up-regulates cytokinin-mediated stabilization of meristems.

As well as up-regulating cytokinin synthesis, *KNOX* genes also stabilize the meristem by suppressing the accumulation of GA in the SAM. Genetic experiments have shown that artificial activation of GA signaling in the SAM destabilizes the meristem. In a variety of species, *KNOX* gene expression directly represses transcription of *GA 20-OXIDASE1*, an enzyme that catalyzes the rate-limiting step in biosynthesis of the active form of GA (see Chapter 4).

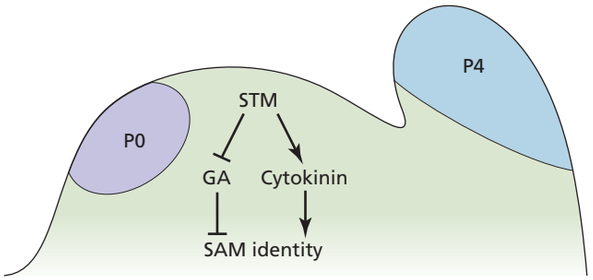


Figure 18.7 Model for how expression of the KNOX transcription factor STM elevates cytokinin concentrations while repressing GA in the SAM. P4 is a developing leaf, and P0 is the site where the next leaf primordium will form. (After A. Hudson. 2005. *Curr. Biol.* 15: R803–805.)

Localized auxin accumulation promotes leaf initiation

The arrangement of leaves on the shoot, or **phyllotaxy**, is usually characteristic of a species and can be classified in three basic patterns: alternate, decussate (opposite), and spiral (**Figure 18.8**). Phyllotactic patterns are directly linked to the pattern of initiation of leaf primordia on the shoot apical meristem (**Figure 18.9A**) but can be altered by environmental conditions, by mutations that affect meristem size, or by ablation of discrete sets of apical cells.

Disruption of microscale polar auxin transport in the shoot apex by use of the auxin efflux inhibitor *N*-1-naphthylphthalamic acid (NPA) or by mutation of the PIN-FORMED 1 (PIN1) auxin efflux transporter (see Chapter 4) results in altered positioning or complete elimination of leaf primordia (**Figure 18.9B**). In tomato and Arabidopsis, leaf initiation also slows or stops in the dark as auxin concentrations decrease. Placement of a microdroplet of auxin on the shoot apex of an Arabidopsis *pin1* mutant results in ectopic leaf initiation (**Figure 18.9C**). Auxin fluxes and accumulations in the shoot apex can also be inferred by microscopic observation of fluorescent auxin reporters and PIN1-GFP

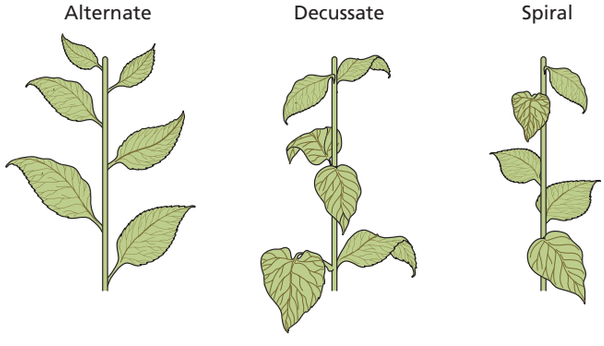


Figure 18.8 Three types of leaf arrangements (phyllotactic patterns) along the shoot axis. The same terms are also used for inflorescences and flowers.

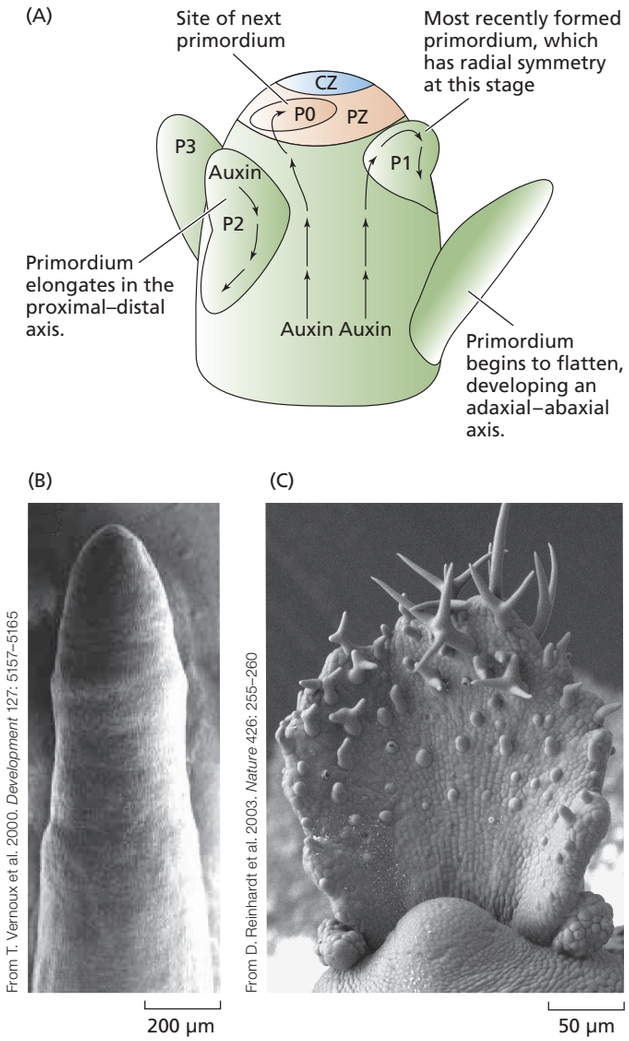


Figure 18.9 **Local auxin maxima determine the position of leaf primordia.** **(A)** Sites of leaf formation are related to patterns of polar auxin transport. Patterns of auxin movement (arrows) can be inferred from asymmetric localization of PIN proteins. P0, P1, P2, and P3 refer to the ages of leaf primordia; P0 corresponds to the stage at which the leaf begins its overt development, and P1, P2, and P3 represent increasingly older leaves. Leaf primordia are initiated where auxin accumulates. Acropetal (toward tip) movement of auxin is blocked at the boundary separating the central and peripheral zones (CZ and PZ, respectively), leading to increased auxin concentrations at this position and the initiation of a leaf (P0). The newly formed leaf primordium (P1) acts as an auxin sink, thus preventing initiation of new leaves directly above it. The displacement of a more mature leaf (P2) away from the PZ allows acropetal auxin movements to become reestablished, thus enabling the initiation of another leaf. **(B)** Scanning electron micrograph of a *pin1* inflorescence meristem that fails to produce leaf primordia. See Figure 4.30 for a photo of a *pin1* mutant plant. **(C)** Leaf primordium induced on the inflorescence meristem of a *pin1* mutant by placing a microdrop of IAA in lanolin paste on the side of the meristem. (A after D. Reinhardt et al. 2003. Nature 426: 255–260.)

(see Chapter 4). Coordination of PIN asymmetry across several cells amplifies directional flow of auxin derived from basal cell layers across the shoot apex. These results demonstrate a role for auxin in leaf initiation, although an additional role of cytokinin is also likely.

Mechanical stress and physical interactions of expanding cells can also regulate meristem development. Some of these interactions and the methods used to study them are described in **WEB TOPIC 18.3**.

Axillary meristems form in the axils of leaf primordia

Axillary meristems are located where the adaxial (upper) leaf surface meets the stem. They form at the same time as leaf primordia and remain dormant until they grow out later in development to form branches. Initial suppression of axillary meristems not only allows plants to pattern branches in response to the environment, but also reduces the accumulation of mutations that are due to DNA replication. This may allow large perennial plants such as trees to live for many years without accumulating deleterious mutations.

Axillary meristem initiation involves three main steps: correct positioning of initial cells, delineation of the meristem boundaries, and establishment of the meristem proper. Many of the same genes that control leaf initiation and lamina outgrowth also regulate axillary meristem initiation. Auxin biosynthesis, transport, and signaling are all required for the initiation of axillary meristems, and mutants defective in these pathways fail to form new axillary meristems.

Other regulators are unique to axillary branches: Mutations of the gene encoding the LATERAL SUPPRESSOR transcription factor from tomato (**Figure 18.10**), rice, and Arabidopsis do not affect leaf development but cause a

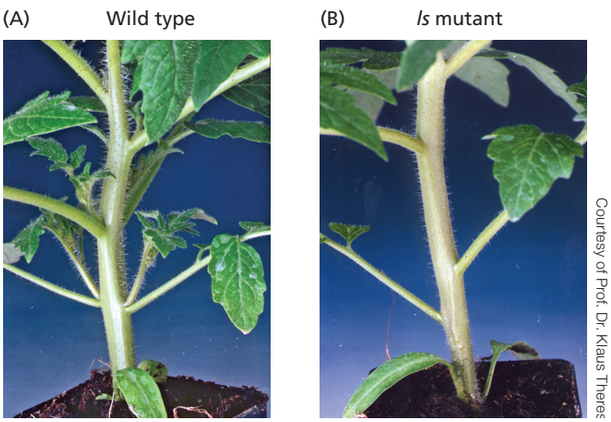
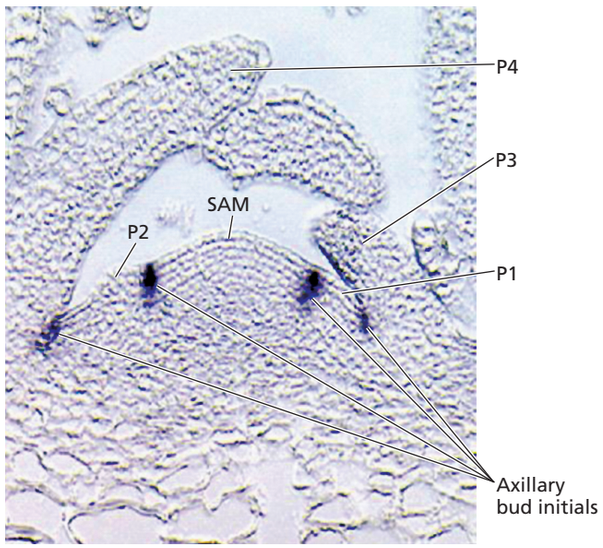


Figure 18.10 **The tomato mutant *lateral suppressor* (*ls*) shows defects in axillary bud formation.** **(A)** Wild-type tomato. **(B)** The *ls* mutant, in which axillary buds fail to form in most of the leaf axils.



From T. Greb et al. 2003. *Genes Dev.* 17: 1175–1187

Figure 18.11 **Accumulation of *LATERAL SUPPRESSOR* mRNA as indicated by in situ hybridization in the axillary bud regions of an Arabidopsis shoot tip.** P1–P4 are leaf primordia.

complete block in axillary bud formation during the vegetative phase of development. *LATERAL SUPRESSOR* mRNA accumulates in the axils of leaf primordia, where new axillary meristems develop (**Figure 18.11**).

18.4 Leaf Development

Morphologically, the leaf is the most variable of all the plant organs. The collective term for any type of leaf on a plant, including structures that evolved from leaves, is **phyllome**. Phyllomes include the photosynthetic **foliage leaves** (what we usually mean by "leaves"), protective **bud scales**, **bracts** (leaves associated with inflorescences, or flowers), and **floral organs**. In angiosperms the main part of the foliage leaf is expanded into a flattened structure known as the **blade** or **lamina** (**Figure 18.12**). The appearance of a flat lamina in seed plants in the middle to late Devonian was a key event in leaf evolution, as it maximizes light capture. Lamina formation also creates two distinct leaf domains: **adaxial** (upper surface) and **abaxial** (lower surface). Several types of leaves have evolved based on their adaxial–abaxial leaf structure (see **WEB TOPIC 18.4**).

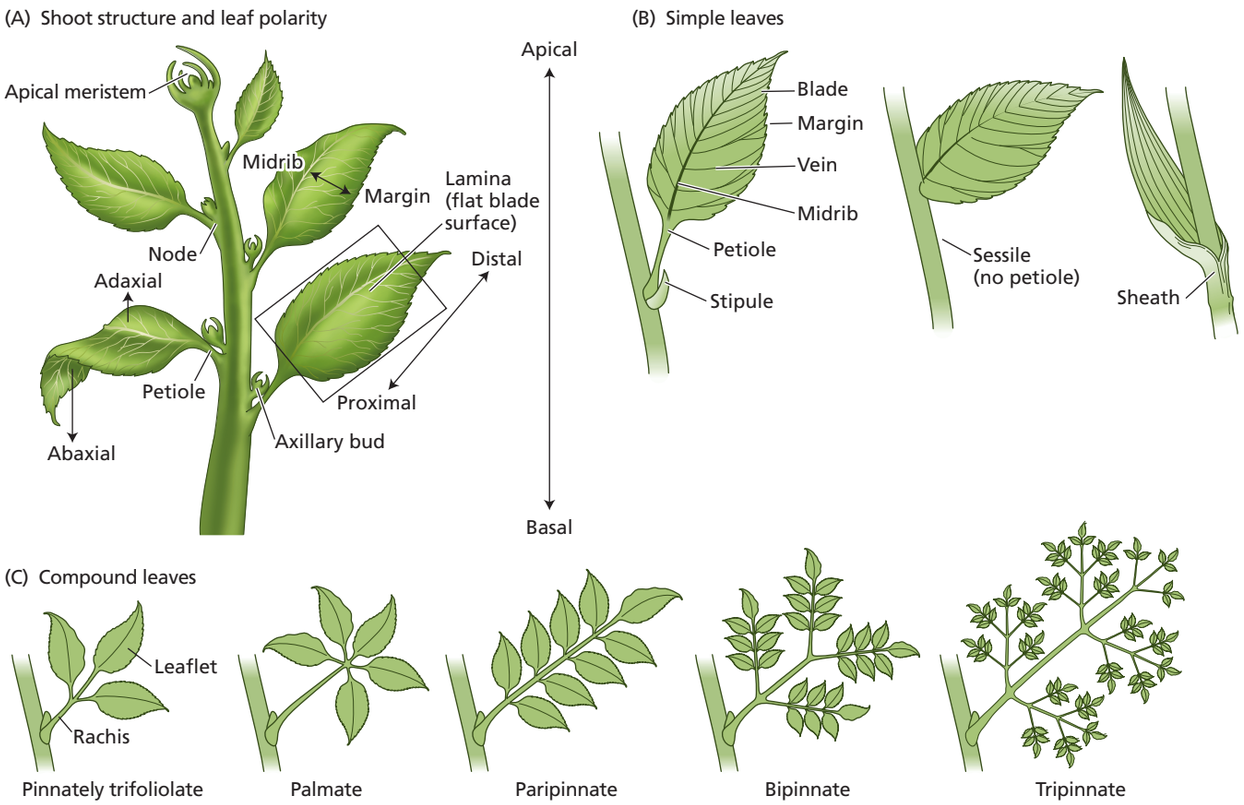


Figure 18.12 **Overview of leaf structure.** **(A)** Shoot structure, showing three types of leaf polarity: adaxial–abaxial, distal–proximal, and midrib–margin. **(B)** Examples of simple leaves. Variations in lower leaf structure include the presence or absence of stipules and petioles, and leaf sheaths. **(C)** Examples of compound leaves.

In the majority of plants the leaf blade is attached to the stem by a stalk called the **petiole**. However, some plants have **sessile leaves**, with the leaf blade attached directly to the stem (see Figure 18.12B). In most monocots and certain eudicots the base of the leaf is expanded into a sheath around the stem. Many eudicots have **stipules**, small outgrowths of the leaf primordia, located on the abaxial side of the leaf base. Stipules protect the young developing foliage leaves and are sites of auxin synthesis during early leaf development.

Leaves may be **simple** or **compound** (see Figure 18.12B and C). A simple leaf has one blade, whereas a compound leaf has two or more blades, the **leaflets**, attached to a common axis, or **rachis**. Some leaves, like the adult leaves

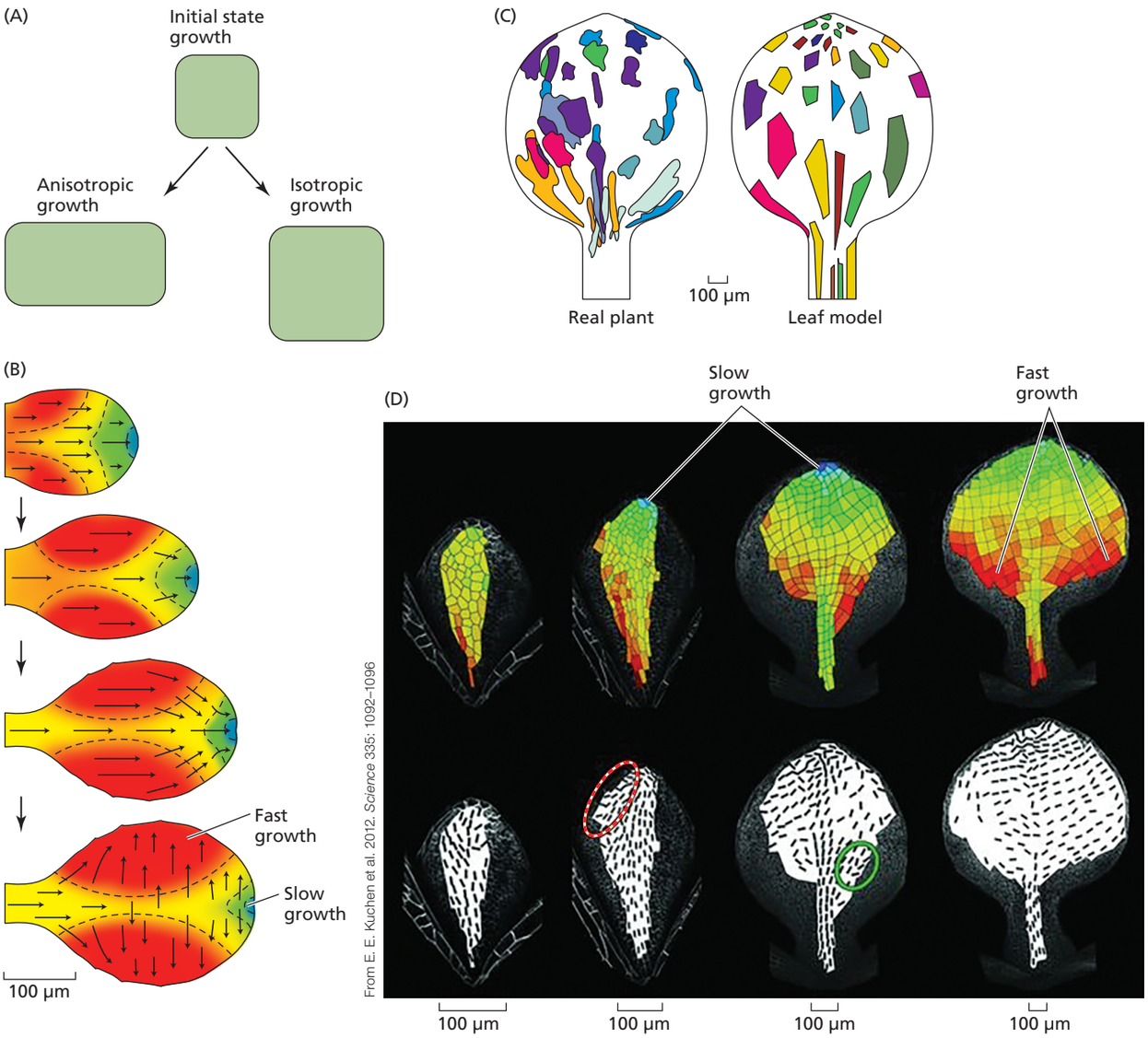


Figure 18.13 Growth patterns determine organ shape. **(A)** Isotropic growth increases size with no change in shape, whereas anisotropic growth increases one axis preferentially. Here, both final shapes have doubled in area. **(B)** Computational model of Arabidopsis leaf development, color-coded to represent growth rate (red fast, green slow) and with arrows on the leaves representing principal orientations of growth. **(C)** Comparison of predicted sectors from a leaf model (right) with sectors from a real plant (left). **(D)** Live tracking of Arabidopsis leaf growth, color-coded to represent growth rate (top row; red fast, blue slow) and with lines representing principal orientations of growth (bottom row). The solid circle highlights a slow growing tip region, and the dashed circle highlights a faster growing lateral region. DAI, days after leaf initiation (B, C and D after E. E. Kuchen et al. 2012. *Science* 335: 1092–1096.)

of some *Acacia* species, lack a blade and instead have a flattened petiole simulating the blade, the **phyllode**. In some plants the stems themselves are flattened like blades and are called **cladodes**, as in the cactus *Opuntia*.

Growth determines leaf shape

Despite the many different shapes, all leaves begin as dome-shaped primordia on the flanks of the SAM (see Figure 18.9A). In Chapter 17 we discussed the anisotropic (directional) growth of seedling hypocotyls and roots in nutational growth and in their responses to environmental stimuli. Nutational growth results from differing rates of anisotropic expansion between cell files constrained by cell wall interactions, as described in Chapter 2. Hypocotyl tropisms are also based on anisotropic cellular elongation. Tropic responses in the root involve anisotropic growth of the organ, but also involve inhibition of anisotropic growth to achieve organ bending. More complex combinations of regulated isotropic and anisotropic growth determine the shape of leaves (**Figure 18.13**).

The patterns of differential growth in leaves are determined by regions of gene expression associated with a particular identity—for example, the adaxial and abaxial side of leaves or different zones of the meristem. Local cell wall alterations within these regions can then alter growth rates or directions and create new shapes through development. The complexity of mechanical constraints on programmed cellular expansion in the leaf can be further elaborated by functional differentiation of cells for metabolic or reproductive specialization and environmental interactions.

Dynamic imaging of leaves during development provides the basis for detailed models of the contributions of cells in specific domains to leaf shape and growth (see Figure 18.13B). Sectors of leaves that are associated with expression of particular genes or clusters of genes can then be measured to determine their contributions to leaf shape and rates of growth during a particular interval (see Figure 18.13C and D). Comparisons of actual measurements to computational models are used to refine growth models. These are then compared to observations of growth in mutants lacking key regulatory genes, as well as to imaging of gene expression patterns using reporters (see Chapter 3), to understand gene function at high resolution. This approach has become the standard for studying growth of all plant organs.

18.5 The Establishment of Leaf Polarity

Leaves are patterned along three axes: from base to tip (proximal–distal), from midline to margin (medial–lateral), and from top to bottom (adaxial–abaxial) (see Figure 18.12). The amount of growth along each of these axes determines the final shape of the leaf. For example, flat leaves grow preferentially along the medial–lateral and proximal–distal axes. Cell types form patterns along these axes: The relatively simple leaves in Arabidopsis contain an adaxial epidermis and a single layer of adaxial palisade mesophyll cells, and three abaxial layers of spongy mesophyll and an abaxial epidermis. But how are these patterns set up and maintained during development? As we will see, the patterning of these axes is interlinked and involves shared molecular regulators.

A signal from the SAM initiates adaxial–abaxial polarity

Because leaf primordia develop from a group of cells on the flanks of the SAM, leaves possess inherent positional relationships with the SAM: The adaxial side of a leaf primordium is derived from cells adjacent to the SAM, while the abaxial side is derived from cells farther away. Microsurgical studies in the 1950s demonstrated that communication between the SAM and the leaf primordium is required to establish leaf adaxial–abaxial polarity. For example, a transverse incision dividing the SAM from the primordium initial (I) caused the initial to develop radially without forming any adaxial tissue (**Figure 18.14A**). The resulting "leaf" was cylindrical and contained only abaxial tissues (it was *abaxialized*). However, two marginal incisions that allowed unimpeded communication between the SAM and the primordium did not disrupt adaxial–abaxial symmetry (**Figure 18.14B**).

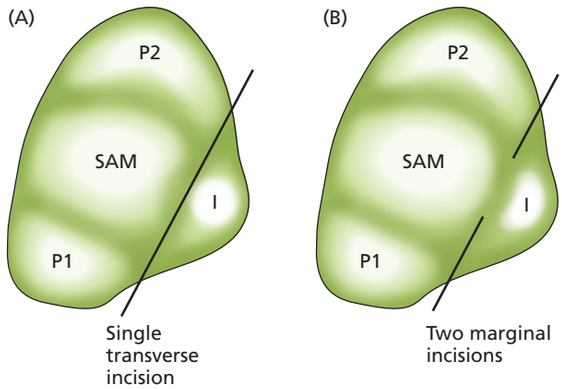


Figure 18.14 Diagram of microsurgical technique used in early experiments in potato (*Solanum tuberosum*) to determine the influence of the SAM on leaf primordium (P) development. **(A)** A primordium initial (I) isolated from the SAM by a transverse incision subsequently grows radially and contains only abaxial tissues. **(B)** A primordium initial (I) that is only partially isolated from the SAM subsequently shows normal adaxial–abaxial symmetry. (After I. M. Sussex. 1951. *Nature* 167: 651–652.)

Refinements of these surgical experiments using laser ablation and microdissection produced similar results, suggesting that a signal between the SAM and leaf is required for specification or maintenance of adaxial identity. Traditionally this signal has been interpreted as being a signal from the meristem to the leaf, but recent work has raised the possibility that the signal may travel from the leaf to the meristem, and experiments suggest that auxin removal from the adaxial side of leaves may be necessary for adaxial specification. However, it is not clear whether auxin removal from the leaf is the signal itself or a downstream consequence of it, and the nature of the adaxializing signal remains a mystery. These results also highlight another key feature of leaf development, which is that adaxial–abaxial patterning is required for growth along the medial–lateral axis. We examine this in more detail later in this section.

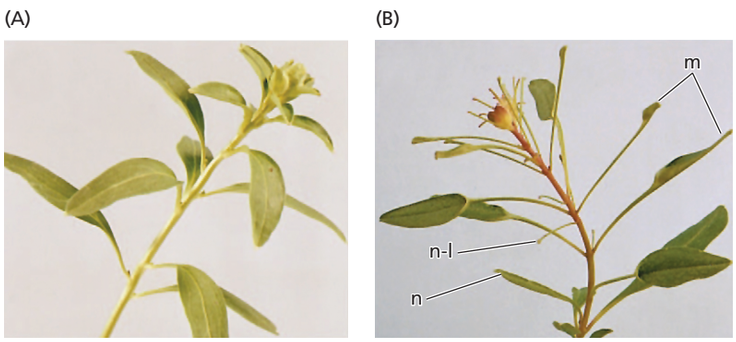
Antagonism between sets of transcription factors determines adaxial–abaxial leaf polarity

The first insights into the molecular basis of adaxial and abaxial identity came from analysis of the loss-of-function mutant *phantastica* (*phan*) in snapdragon (*Antirrhinum majus*) (**Figure 18.15A**). *phan* mutants produce leaves with altered adaxial–abaxial symmetry, ranging from abaxialized needlelike leaves that fail to produce lamina, to leaves with blades with a mosaic of adaxial and abaxial characters (**Figure 18.15B**). Molecular genetic experiments in Arabidopsis and other species using mutants such as *phan* have elucidated the mechanisms that regulate adaxial–abaxial polarity.

A complex gene expression network specifies adaxial and abaxial fate and keeps these two identities spatially separate (**Figure 18.16**). Our current understanding is that genes specifying adaxial fate repress genes specifying abaxial fate and vice versa, producing mutually exclusive domains on each side of the leaf. *KNOX1* expression in leaf primordia is initially induced by auxin and prevents precocious leaf differentiation, but is then repressed in both adaxial and abaxial zones in most plant species. Detailed gene expression studies suggest that alongside a signal between leaf and SAM, adaxial and abaxial patterning of the leaf is inherited from the SAM, where *Class III Homeodomain-Leucine Zipper* (*HD-ZIP III*) genes are expressed in the center and genes encoding KANADI (Malayalam for "mirror") transcription factors are expressed at the perimeter. Leaf primordia form at the boundary between the two and inherit the pattern.

MYB transcription factors, HD-ZIP III proteins, and *KNOX1* repression promote adaxial identity

The *PHAN* gene in snapdragon encodes a MYB (**Myelobastosis**) transcription factor, and the *ASYMMETRIC LEAVES 1* and *2* (*AS1* and *AS2*) genes in Arabidopsis encode similar proteins. Arabidopsis AS1 and AS2 repress *KNOX1* genes on the adaxial side of the leaf indirectly by activating genes that encode HD-ZIP III transcription factors to, in turn, activate WOX3 repression of *KNOX1* (see Figure 18.16A). The HD-ZIP III transcription factors derive their name from a characteristic structure: a DNA-binding homeodomain, a sterol-binding domain, and a leucine zipper protein dimerization domain. Expression of the HD-ZIP III adaxial identity genes is normally limited to the adaxial domains of the leaf primordia (see Figure 18.16A). When these genes are mutated or inactivated, adaxial characters are lost. When HD-ZIP III genes are ectopically expressed throughout the leaf, abaxial tissues take on adaxial characteristics such as production of axillary buds. The importance of HD-ZIP III to adaxial identity is demonstrated by an additional level of regulation by microRNA interference (see Chapter 3). Expression of miR166 in the abaxial region targets multiple *HD-ZIP III* mRNAs (see Figure 18.16B).



From R. Waites and A. Hudson. 1995. *Development* 121: 5143–2154

Figure 18.15 **Effects of *phan* mutations on leaf morphology in *Antirrhinum majus*.** (A) The vegetative shoot of a wild-type plant with normal leaves. (B) The vegetative shoot of a *phan* mutant shows altered adaxial–abaxial symmetry, with narrow (n), needlelike (n-l), and mosaic (m) leaves.

Abaxial identity is determined by auxin, KANADI, and YABBY

Auxin plays an important role in abaxial leaf development. ARF3 and ARF4 are unique auxin response factors that are activated directly by auxin binding (see Chapter 4) and enhance abaxial *YABBY* expression and abaxial identity (see Figure 18.16). Abaxial identity is also dependent on the presence of KANADI transcription factors that suppress *AS1/2* gene expression and activate transcription of *YABBY* genes in abaxial tissues. YABBYs are zinc finger helix-loop-helix transcription factors that are named for the similarity of the leaves of some *yabby* family mutants to the claws of Australian crayfish (yabbies). Almost complete loss of abaxial

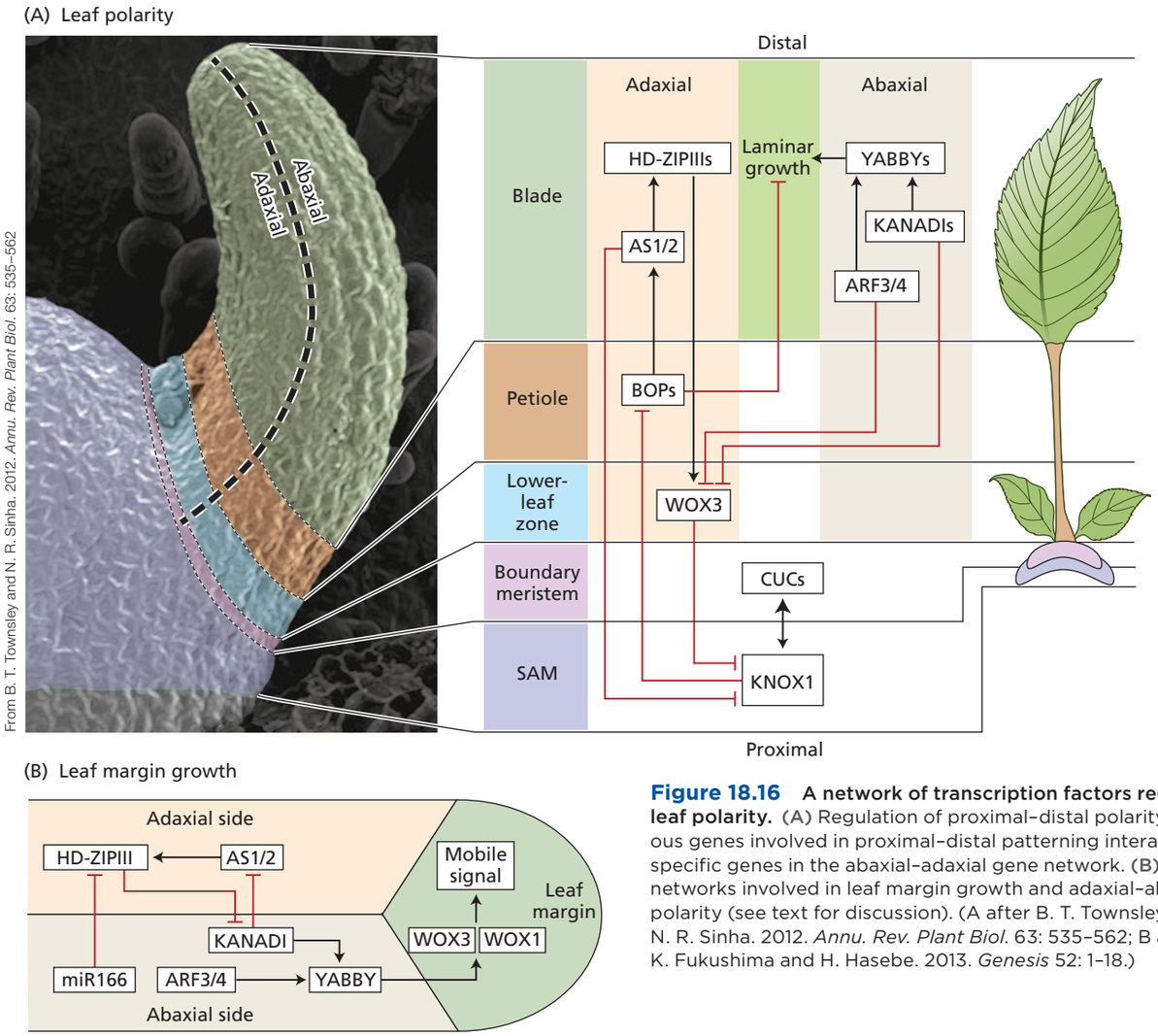


Figure 18.16 **A network of transcription factors regulates leaf polarity.** (A) Regulation of proximal–distal polarity. Various genes involved in proximal–distal patterning interact with specific genes in the abaxial–adaxial gene network. (B) Gene networks involved in leaf margin growth and adaxial–abaxial polarity (see text for discussion). (A after B. T. Townsley and N. R. Sinha. 2012. *Annu. Rev. Plant Biol.* 63: 535–562; B after K. Fukushima and H. Hasebe. 2013. *Genesis* 52: 1–18.)

identity is observed when *yabby* and *kanadi* mutations are combined. Conversely, ectopic formation of abaxial tissues is observed when KANADI genes are overexpressed. It is still unclear how KANADI transcription factors promote abaxial identity.

Blade outgrowth is auxin dependent and regulated by the YABBY and WOX genes

As well as contributing to adaxial–abaxial polarity, *YABBY* genes also promote lamina outgrowth. In the absence of all *YABBY* gene activity, leaf primordia retain a small amount of adaxial–abaxial polarity but fail to initiate lamina outgrowth. During blade outgrowth, YABBYs positively regulate expression of *WOX1* and *WOX3* in the adaxial–abaxial domain interface, where they are required for blade and margin outgrowth (see Figure 18.16B). As shown in Figure 18.16B, WOX1 and WOX3 activate expression of the gene encoding a cytochrome p450 monooxygenase that produces an unknown mobile signal that promotes cell division activity in aerial organs, including leaves. Auxin appears to be another signal acting in blade formation, as higher-order mutants with reduced auxin biosynthesis or distribution have smaller and narrower leaves.

Leaf proximal–distal polarity also depends on specific gene expression

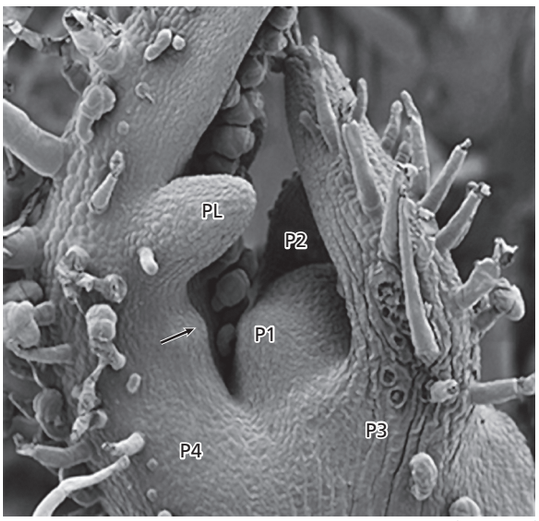
Leaf development also exhibits polarity along its length, called **proximal–distal polarity**. Developing leaf primordia can be divided lengthwise into four main zones extending from the meristem: boundary meristem, lower-leaf zone, petiole, and blade (see Figure 18.16A).

Proximal–distal polarity becomes evident as the primordium begins to grow out and away from the SAM. The boundary between the SAM and primordia forms a zone of low cell division and expansion that

separates these two cell groups and allows the leaf to grow out physically separate from the meristem. The CUP-SHAPED COTYLEDON (CUC) 1 and 2 transcription factors are key regulators of this process, and as their name implies, *cuc1/cuc2* double mutants display cotyledon and leaf organ fusions as well as growth arrest.

The lower-leaf zone plays an important role in leaves that develop stipules or form leaf sheaths (see Figure 18.12). In these cases, the founder cells (which give rise to the leaf primordium) recruit additional cells into the primordium through a mechanism that is dependent on *WOX* gene expression. Cells that are recruited to become stipules or sheath originate in the flanks of the primordium.

The region of the leaf primordium destined to become the petiole is characterized by the expression of *Blade on Petiole* (*BOP*) genes, which encode dimeric zinc finger transcriptional activators that are required to establish petiole identity in the proximal portion of the Arabidopsis leaf (see Figure 18.16A). The *bop1/bop2* double mutant lacks the proper distinction between leaf blade and petiole, and both single mutants form leaf blades on what would normally be the petiole. *BOP1* and *BOP2* are both expressed in the adaxial domain, where they act redundantly to suppress laminar outgrowth in the petiole region.



From J. Kang and N. R. Sinha. 2010. *Botany* 88: 710–724

Figure 18.17 Scanning electron micrograph of tomato shoot tip showing developing compound leaf. Primordia 1 through 4 (P1–P4) are shown. The first primary leaflet pair (PL) and the second leaflet pair (arrow) are visible on P4.

In compound leaves, de-repression of the *KNOX1* gene promotes leaflet formation

Compound leaves have evolved independently many times from simple leaf forms. Despite wide variations in the form and complexity of compound leaves, the developmental mechanisms that lead to their formation are remarkably similar. By delaying differentiation, individual leaf primordia can redeploy gene regulatory networks used by the SAM during leaf initiation to form leaflet primordia and produce compound leaves (**Figure 18.17**). Similar to what happens during the initiation of leaf primordia on the SAM, PIN1 proteins focus auxin flow, forming local auxin maxima spaced along the flanks of the primordia (**Figure 18.18**). These regions then grow out to form leaflets.

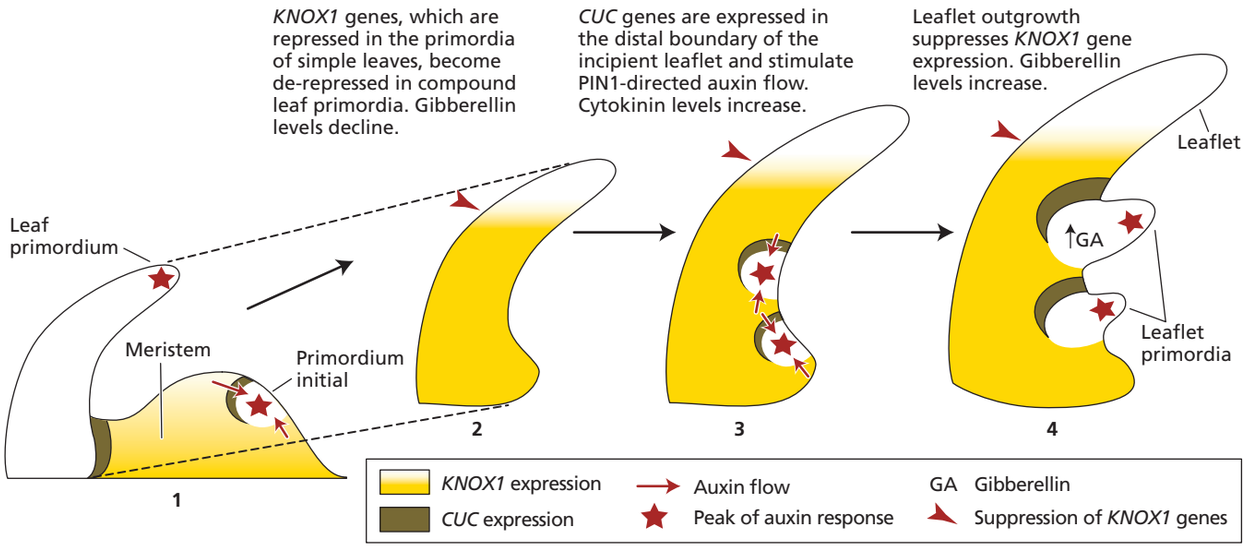


Figure 18.18 Development of compound leaves. The initial stages of simple and compound leaf development are similar. *KNOX1* genes are repressed in the primordium initial (1) and are subsequently reactivated (2), thereby maintaining the primordium in an undifferentiated state. Leaflet primordia are then initiated in a process resembling the initiation of leaf primordia involving PIN1-mediated auxin flow (3 and 4). (After A. Hasson et al. 2010. *C. R. Biol.* 333: 350–360.)

KNOX1 is also an important component of the regulatory network involved in compound leaf development as it inhibits differentiation of the leaf and allows leaflets to form (see Figure 18.18). Cytokinins act downstream of KNOX proteins in promoting leaflet development. For example, overexpression of a key cytokinin biosynthesis gene in tomato leaf primordia causes an increase in the number of leaflets. Conversely, overexpression of a cytokinin degradation gene results in a decrease in the number of leaflets. Shared pathways control the formation of leaf serrations and leaflets in different species, as discussed in **WEB TOPIC 18.5**.

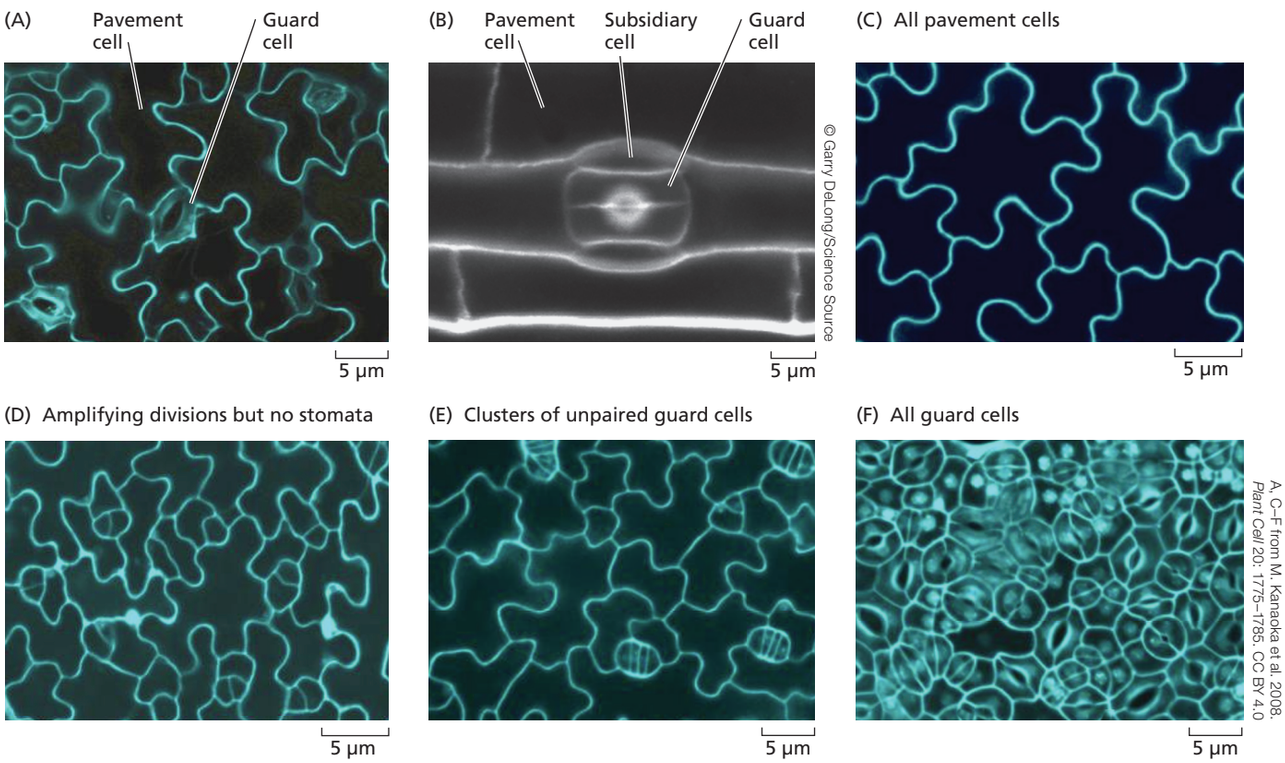
18.6 Differentiation of Epidermal Cell Types

The epidermis is the outermost layer of cells on the primary plant body, including both vegetative and reproductive structures. The epidermis usually consists of a single layer of cells derived from the L1 layer, or **protoderm**. In some plants, such as certain species of the Moraceae, Begoniaceae, and Piperaceae, the epidermis has two or more cell layers derived from periclinal divisions of the protoderm.

There are three main types of epidermal cells found in all angiosperms: pavement cells, trichomes, and guard cells. **Pavement cells** are relatively unspecialized epidermal cells that can be regarded as the default developmental fate of the protoderm (see Chapter 22). **Trichomes** are unicellular or multicellular extensions of the shoot epidermis that have diverse forms, structures, and functions, including protection against insect and pathogen attack, reduction of water loss, and increased tolerance of abiotic stress conditions. Trichome development and function are discussed in **WEB TOPIC 18.6**. **Guard cells** are pairs of cells that surround the **stomata**, or pores, that are present in the photosynthetic parts of the shoot. Guard cells regulate gas exchange between the leaf and the atmosphere by undergoing tightly regulated turgor changes in response to light and other factors (see Chapters 6, 8, and 16). Here we describe the development of stomata as a model system for pattern formation and cytodifferentiation.

Guard cell identity is determined by a specialized epidermal lineage

Stomata are found in nearly all land plants. Stomatal development depends on the cells sequentially adopting a series of different identities. Our understanding of stomatal development is derived from tracing of cell lineages, but really began to advance after the identification of Arabidopsis mutants with more, fewer, or distorted stomata (**Figure 18.19**). The names of many of these mutants allude to the mouthlike shape of stomata.



© Garry DeLong/Science Source

A, C–F from M. Kanaoka et al. 2008. *Plant Cell* 20: 1775–1785. CC BY 4.0

Figure 18.19 **Stomatal development mutants.** **(A)** Wild-type Arabidopsis. **(B)** Wild-type grass leaf. **(C)** *spch* mutant in which no cells enter the stomatal lineage. **(D)** *mute* mutant in which amplifying cell divisions occur but no mature stomata form. **(E)** *fama* mutant in which clusters of unpaired guard cells are visible. **(F)** *scrm* mutant in which all the cells become guard cells.

In eudicots, such as Arabidopsis, a population of **meristemoid mother cells** (**MMCs**) is established in the developing protoderm (which will give rise to the leaf epidermis). Each MMC divides asymmetrically to give rise to two morphologically distinct daughter cells—a larger **stomatal lineage ground cell** (**SLGC**) and a smaller meristemoid (**Figure 18.20**). The meristemoid can undergo a variable number of asymmetric amplifying divisions giving rise to as many as three SLGCs, with the meristemoid ultimately differentiating into a **guard mother cell** (**GMC**), which is recognizable because of its rounded morphology. The GMC then undergoes one symmetric division, forming a pair of guard cells surrounding a pore—the stomate (from the Greek word meaning "mouth"). Following amplifying divisions of the meristemoid, the resulting SLGCs can differentiate into pavement cells, which are the most abundant cell type in the epidermis of a mature leaf, or they can divide asymmetrically (**spacing divisions**) to give rise to a secondary meristemoid. Although this lineage is called the *stomatal lineage*, the ability of meristemoids and SLGCs to undergo repeated divisions means that this lineage is actually responsible for generating the majority of the epidermal cells in the leaves.

Two groups of bHLH transcription factors govern stomatal cell identity transitions

In Arabidopsis stomatal lineage, the transition from one cell identity to another is associated with, and requires the specific expression of, one of three basic helix-loop-helix (bHLH) transcription factors: SPEECHLESS (SPCH), MUTE, and FAMA (named after the Roman goddess of rumor) (see Figures 18.20 and 18.21. Transcriptional activity regulated by SPCH drives MMC formation and leads to the entry into asymmetric division of these cells. SPCH also regulates subsequent asymmetric amplifying and spacing divisions. MUTE promotes the differentiation of meristemoids into GMCs and promotes the terminal cell division of the GMC. In parallel, MUTE induces FAMA, which promotes differentiation of stomatal guard cells and halts further divisions. Arabidopsis *mute* mutants have amplifying divisions but no stomata, while *fama* mutants form clusters of thin unpaired guard cells. In addition, two related bHLH leucine zipper (bHLH-LZ) proteins, SCREAM (SCRM) and SCRM2, have been identified as the partners of SPCH, MUTE, and FAMA. In *scrm* mutants, the entire epidermis becomes stomata.

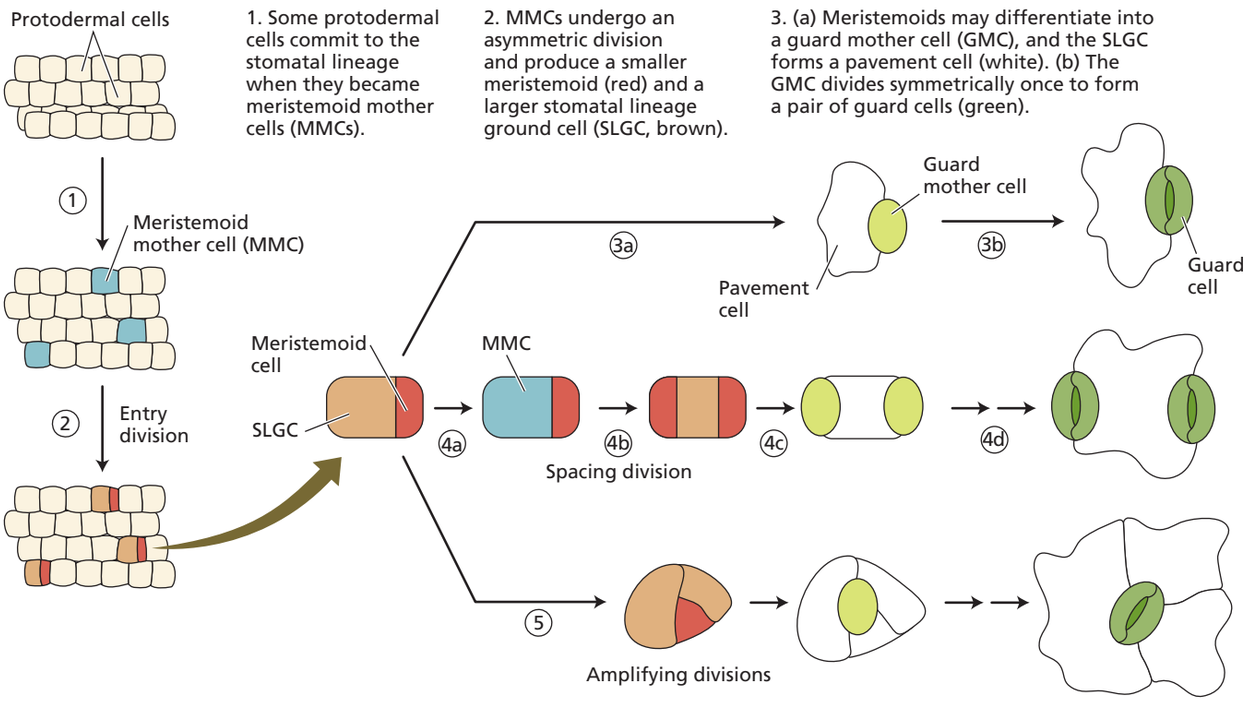


Figure 18.20 **Stomatal development in Arabidopsis.** The spacing pathway is shown in Figure 18.21. (After S. Lau and D. C. Bergmann. 2012. *Development* 139: 3683–3692.)

Cell-to-cell peptide signals regulate stomatal patterning

Stomata are spaced apart by at least one cell length to maximize gas exchange between the leaf and the atmosphere. The spacing is regulated by cell-to-cell communication and intrinsic factors that orient the cell divisions (**Figure 18.21A**). The secreted peptides from the EPIDERMAL PATTERNING FACTOR (EPF) family are expressed by stomatal lineage cells. EPF2 is expressed by MMCs and early meristemoids, while EPF1 is expressed by late meristemoids, GMCs and young guard cells. Binding of EPF peptides to the receptor-like kinase (RLK) heterodimer formed by ERECTA (or an ERECTA-like protein) and TOO MANY MOUTHS results in recruitment of a BAK1/SERKs component to activate kinase activity (see Chapter 4). EPF2 is detected by receptors in protodermal cells, while EPF1 is detected in SLGCs and in GMCs. EPF1 prevents stomata from forming in clusters or pairs by providing positional information. EPF2 inhibits adjacent cells from entering the stomatal lineage and promotes the formation of pavement cells. Mutations in these pathways result in changes in stomatal density or clustering of stomata. The mesophyll also contributes to stomatal patterning. One of the EPF-like peptides, EPFL9, a positive regulator of stomatal density, is produced by the underlying mesophyll and released to the epidermis where it binds to an RLK complex. Experiments have shown that the depletion of EPFL9 results in a decrease in stomatal numbers, indicating that its function is important for normal stomatal development.

Intrinsic polarity in the stomatal lineage aids stomatal spacing

The orientation of some key divisions during stomatal development helps maintain the "one-cell-spacing rule." The division of the MMC and meristemoids is said to be asymmetric because the two daughter cells have different fates; in this case the daughters are also physically different in that the SLGC is larger than the meristemoid. Shortly after division both daughters express the SPCH protein, but it is then down-regulated in the larger of the

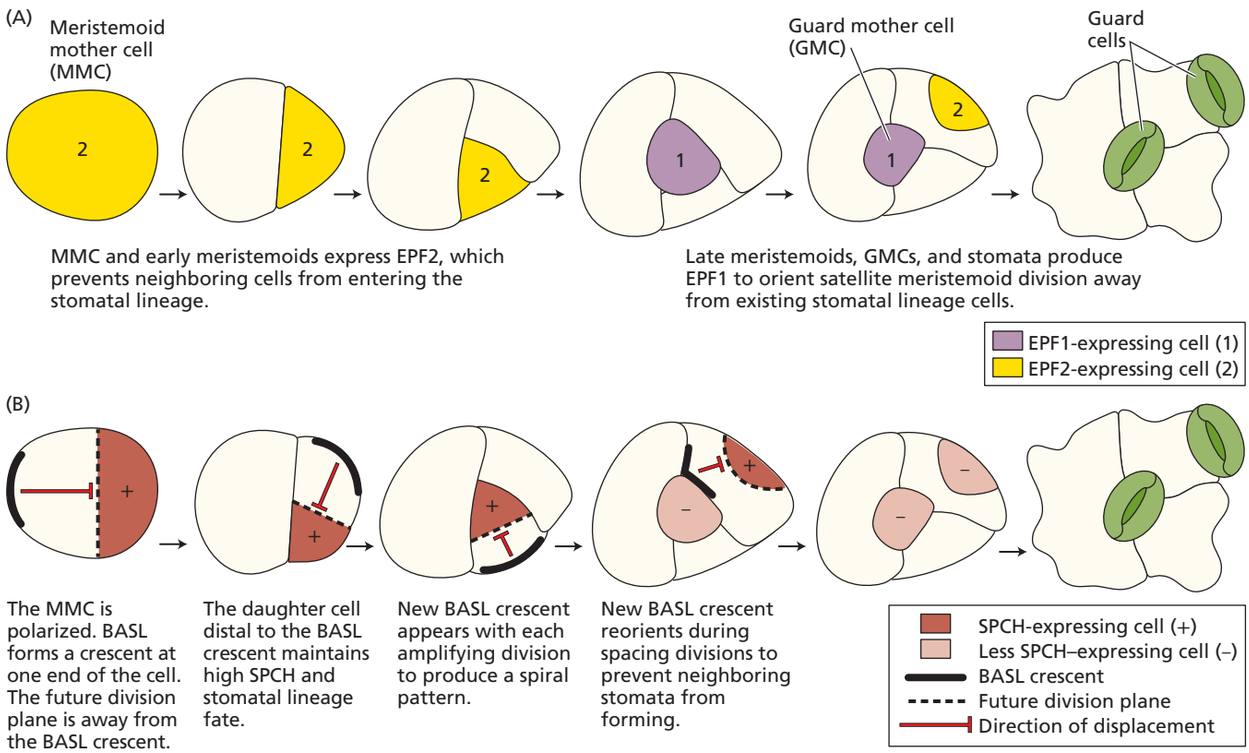


Figure 18.21 Polarized cell division and peptide signaling regulate stomatal spacing. Three related transcription factors—SPCH, MUTE, and FAMA—form heterodimers with SCRM and are required for the production of meristemoids, GMCs, and guard cells. **(A)** EPF2 and EPF1 peptides negatively regulate stomatal density and patterning. EPF2 is synthesized and secreted by meristemoid mother cells (MMCs) and early meristemoids. The presence of extracellular EPF2 is detected by an RLK complex that activates intracellular signaling that represses the production of new meristemoids. EPF1 is synthesized in late meristemoids, GMCs, and stomata. It prevents neighboring stomata from forming. **(B)** BASL polarizes the stomatal lineage cells to orient the successive asymmetric division and to orient spacing divisions.

two cells. Polarity plays an important role in orienting the asymmetric divisions. The polarity is controlled by polarity proteins that mark one end of the MMC. The division is then orientated such that the polarity proteins are in only one of the daughter cells (**Figure 18.21B**). One such protein identified in Arabidopsis is BREAKING OF ASYMMETRY IN THE STOMATAL LINEAGE (BASL). BASL regulates multiple aspects of asymmetric epidermal cell divisions and is independent of stomatal lineage, but it is present as a crescent on the membrane of epidermal cells, including the MMC and meristemoid cells prior to division, and remains in the SLGC after division (see Figure 18.21B).

Environmental factors also regulate stomatal density

Stomatal density and aperture are sensitive to the environment. Factors such as water deficit, light, and CO_2 concentration cause a change in stomatal density in order to balance CO_2 uptake with limiting water loss. For example, water deficit induces abscisic acid (ABA), and this has been found to activate the MAP kinase signaling cascade that down-regulates SPCH. Elevated temperature decreases stomatal density via phyB and the bHLH transcription factor PHYTOCHROME INTERACTING FACTOR 4 (PIF4) that coordinates light and temperature responses with growth (see Chapters 4 and 16). Elevated temperatures repress phyB activity, and both phyB and PIF4 then accumulate in stomatal lineage precursors and suppress SPCH expression. In contrast, high light activation of phyB represses PIF4 levels and increases SPCH expression, with the result that stomatal density increases. Stomatal formation is repressed in the dark via repression of EPFL9 and CONSTITUTIVE PHOTOMORPHOGENIC 1 (COP1) targeting SCRM for degradation (see Chapter 16 for discussion of COP1 function in light responses). At high CO_2 concentrations, stomatal density is reduced. This occurs via an activation of extracellular EPF2 by the tripeptidyl peptidase CO_2 RESPONSE SECRETED PROTEASE and induced expression of EPF2 in response to high CO_2.

Stomata development in monocots involves some genes that are orthologous to those in Arabidopsis

The guard cells in grasses are dumbbell-shaped rather than kidney-shaped as in eudicots and some other monocots (see Figure 6.12). Monocot guard cells are flanked by a subsidiary cell that contributes to their function. In grasses, stomata form in discrete cell files (**Figure 18.22**). In these files, an undifferentiated cell divides asymmetrically to produce a smaller and a

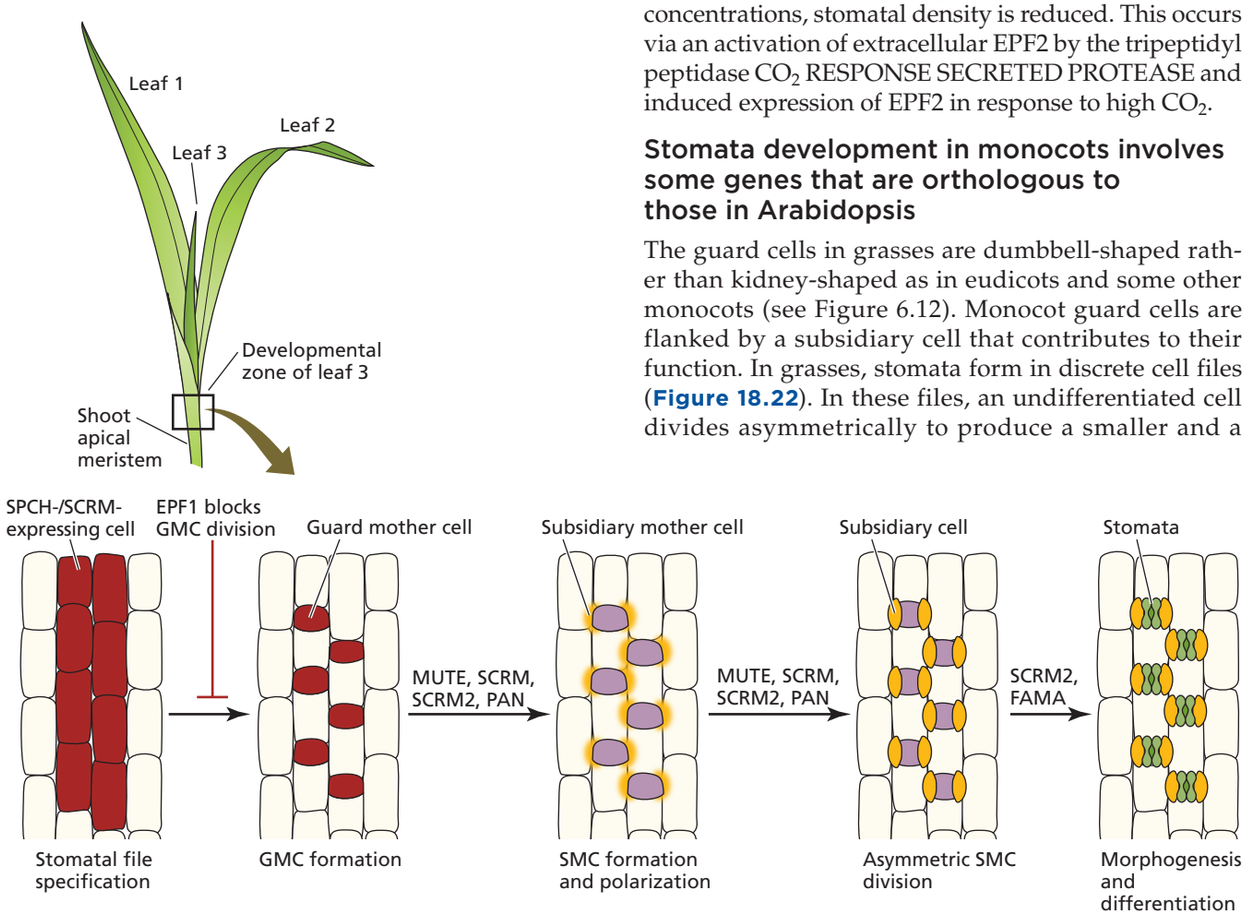


Figure 18.22 Stomatal development in grasses involves orthologs of many of the genes involved in stomatal development in eudicots. However, the roles are different. SCRM and SPCH specify the early asymmetric division. The cells then progress to become guard mother cells and finally stomata without amplifying divisions. Instead, a polarized asymmetric division creates subsidiary cells that surround the stomata. SMC, subsidiary mother cell. (After T. D. G. Nunes et al. 2019. *Plant J.* 101: 780–799. CC BY 4.0)

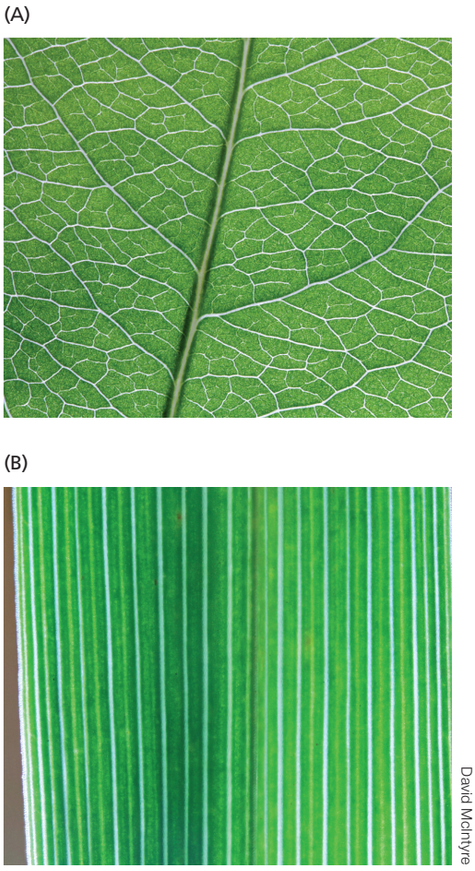


Figure 18.23 **Two basic patterns of leaf venation in angiosperms.** **(A)** Reticulate venation in *Prunus serotina*, a eudicot. **(B)** Parallel venation in *Iris sibirica*, a monocot.

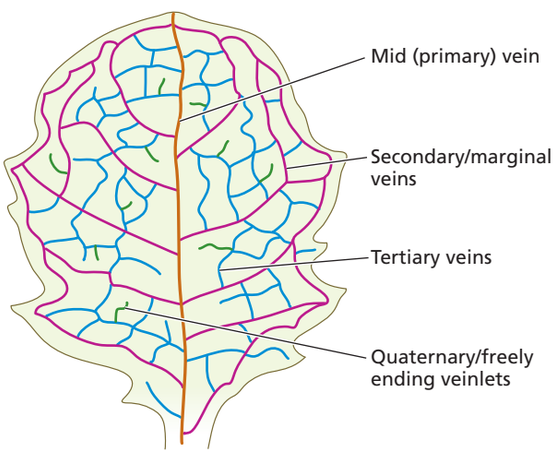


Figure 18.24 **Hierarchy of venation in the mature Arabidopsis leaf based on the diameter of the veins at the site of attachment to the parent vein.** (After W. J. Lucas et al. 2013. *J. Integr. Plant Biol.* 55: 294–388.)

larger cell. The smaller cell becomes a guard mother cell, which will divide symmetrically to make the two guard cells that surround the central pore. The cells next to the GMC divide asymmetrically to make two subsidiary cells, one on each side of the guard cells, which increases their opening efficiency. Orthologs of the major bHLHs are found in grasses but have slightly different roles than in Arabidopsis. In the model grass *Brachypodium*, SPCH has been duplicated and is partially redundant, and SCRM1 controls early asymmetric divisions while SCRM2 acts later in differentiation of the GMC. The MUTE ortholog moves from the GMC to specify subsidiary cell identity. Orthologs of TOO MANY MOUTHS, EPF1, and ERECTA are also found in grasses and mosses, suggesting conservation of their function. However, orthologs of BASL have not been identified in grasses, suggesting that other proteins perform BASL-like functions instead. For instance, the oriented asymmetric division that forms the subsidiary cell in maize is performed cooperatively by *PANGLOSS1* (PAN1) and PAN2. The PANs are leucine rich repeat receptor-like kinases that localize in the subsidiary mother cell at the sites of contact with the GMC to induce polarized cell division. They are likely up-regulated by the maize MUTE ortholog.

18.7 Venation Patterns in Leaves

The leaf vascular system is a complex network of interconnecting veins consisting of two main conducting tissue types, xylem and phloem, as well as nonconducting cells, such as parenchyma, sclerenchyma, and fibers. The spatial organization of the leaf vascular system—its **venation pattern**—is both species- and organ-specific. Venation patterns fall into two broad categories: *reticulate venation*, found in most eudicots, and *parallel venation*, typical of many monocots (**Figure 18.23**).

Despite the diversity of leaf venation patterns, they all share a hierarchical organization. Veins are organized into distinct size classes—primary, secondary, tertiary, and so on—based on their width at the point of attachment to the parent vein (**Figure 18.24**). The smallest veinlets end blindly in the mesophyll. The hierarchical structure of the leaf vascular system reflects the hierarchical functions of different-sized veins, with larger-diameter veins functioning in the **bulk transport** of water, minerals, sugars, and other metabolites, and smaller-diameter veins functioning in **phloem loading** (see Chapter 11).

The question of how leaf venation patterns develop has long intrigued plant biologists. For the leaf vascular system to carry out its long-distance transport functions effectively, veins must be efficiently distributed throughout photosynthetic tissues and a vein's many cell types must be arranged properly within the radial

and longitudinal dimensions of the vascular bundle. It is not surprising, then, that the differentiation of vascular tissues is under strict developmental control. In this section we first describe the development of a leaf's vascular connection to the rest of the plant. Then we discuss how the higher-order venation pattern of a leaf is established.

The primary leaf vein is initiated discontinuously from the preexisting vascular system

In the mid-nineteenth century, the Swiss plant anatomist Carl Wilhelm von Nägeli made a surprising discovery while tracing the source of vascular bundles in the primary shoot. In the mature part of the stem of seed plants, the longitudinal vascular bundles form a continuous conducting system that begins at the root–shoot juncture and ends near the growing tips. Nägeli had assumed that the vascular system must grow upward (acropetally) from the preexisting vascular system to the growing tips of the shoot. Instead, he discovered that the leaf vascular bundles, arising from vascular precursor cells called the **procambium**, were initiated discontinuously in association with the emerging leaf primordia in the SAM (**Figure 18.25**). From there the vascular bundles differentiated downward (basipetally) toward the node directly below the leaf and formed a connection to the older vascular bundle. The portion of the vascular bundle that enters the leaf was later called the **leaf trace** (see Figure 18.25).

What Nägeli had discovered was that the continuous longitudinal vascular bundles in the stem are actually composed of individual leaf traces. Species may differ in the exact course of leaf trace development, but the basic interpretation of the seed plant shoot primary vascular system as a sympodium of leaf traces appears to be universal.

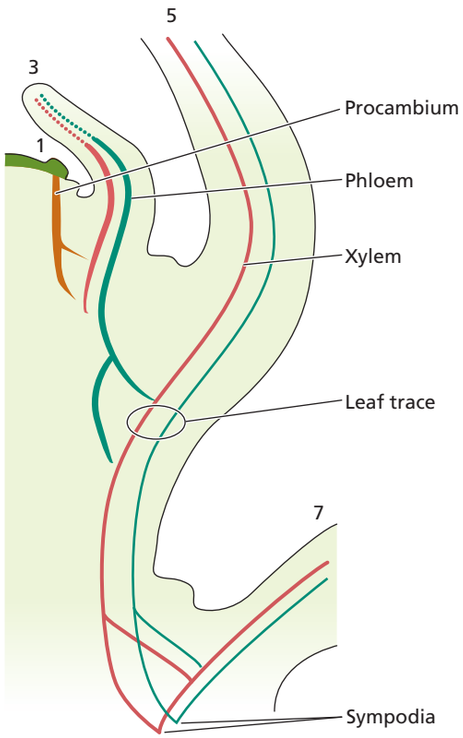


Figure 18.25 Early vascular development in a shoot with decussate phyllotaxy. The SAM and a young leaf primordium are indicated in green with procambial strands of a leaf trace extending from this primordium in orange. Leaf traces develop basipetally toward the mature vascular system and join to form a sympodium. Numbers correspond to the leaf order, starting with the primordia (not all leaves are shown). (After K. Esau. 1953. *Plant Anatomy*. Wiley, New York.)

Auxin canalization initiates development of the leaf trace

Several lines of evidence indicate that auxin stimulates formation of vascular tissues. An example is the role of auxin in regeneration of vascular tissue after wounding (**Figure 18.26A**). Vascular regeneration is prevented by removal of the leaf and shoot above the wound but can be restored by the application of auxin to the cut petiole above the wound, suggesting that auxin from the leaf is required for vascular regeneration. As shown in **Figure 18.26B**, the files of regenerating xylem elements originate at the source of auxin at the upper cut end of the vascular bundle, and progress basipetally until they reconnect with the cut end of the vascular bundle below, matching the presumed direction of the flow of auxin. The upper end of the cut vascular bundle thus acts as the **auxin source** and the lower cut end as the **auxin sink**.

These and similar observations in other systems, such as bud grafting, have led to the hypothesis that as auxin flows through tissues it stimulates and polarizes its own transport, which gradually becomes channeled—or canalized—into files of cells leading away from auxin sources; these cell files can then differentiate to form vascular tissue.

Consistent with this idea, local auxin application (as in the wounding experiments just described) induces vascular differentiation in narrow strands leading away from the application site, rather than in broad fields of cells. New vasculature usually develops toward, and unites with, preexisting vascular strands, resulting in a connected vascular network. We would therefore predict that a developing leaf trace acts as an auxin source and the existing stem vasculature as an auxin sink. Recent studies on leaf venation have supported this source–sink model, or **canalization model**, for auxin flow at the molecular level. In this model, auxin synthesized in one or more cells is exported and a directional flow is created by uptake into adjacent cells. This gradient is then amplified by directional export mechanisms to *canalize* the transport vector.

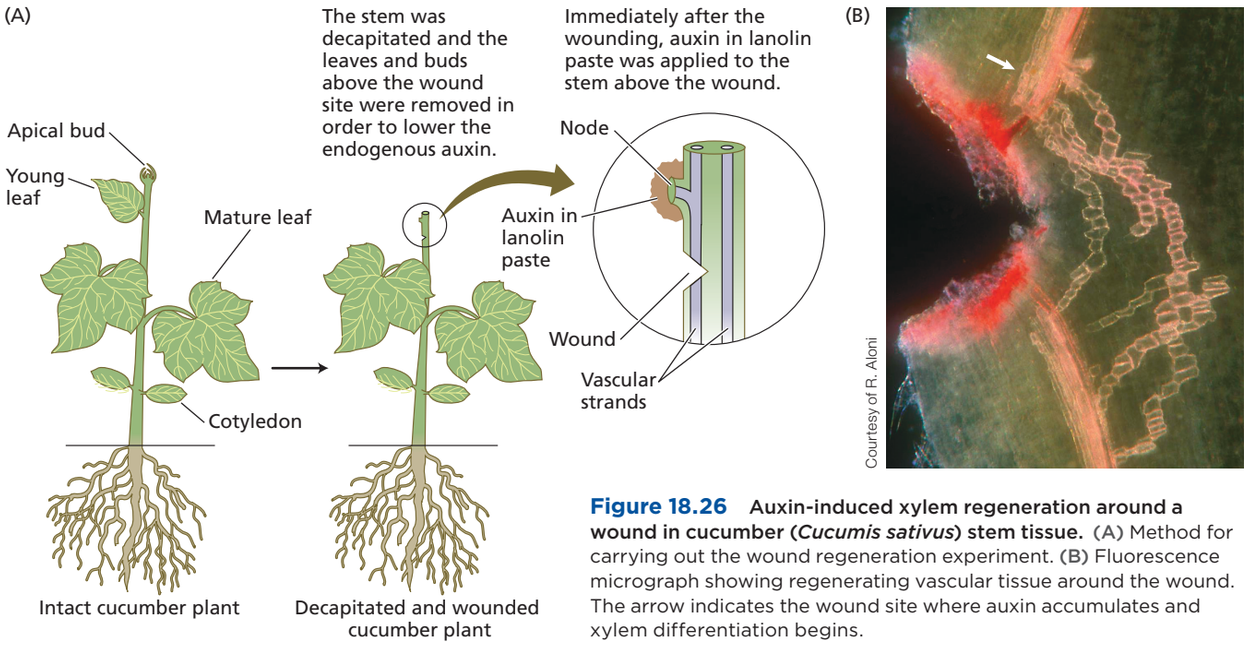
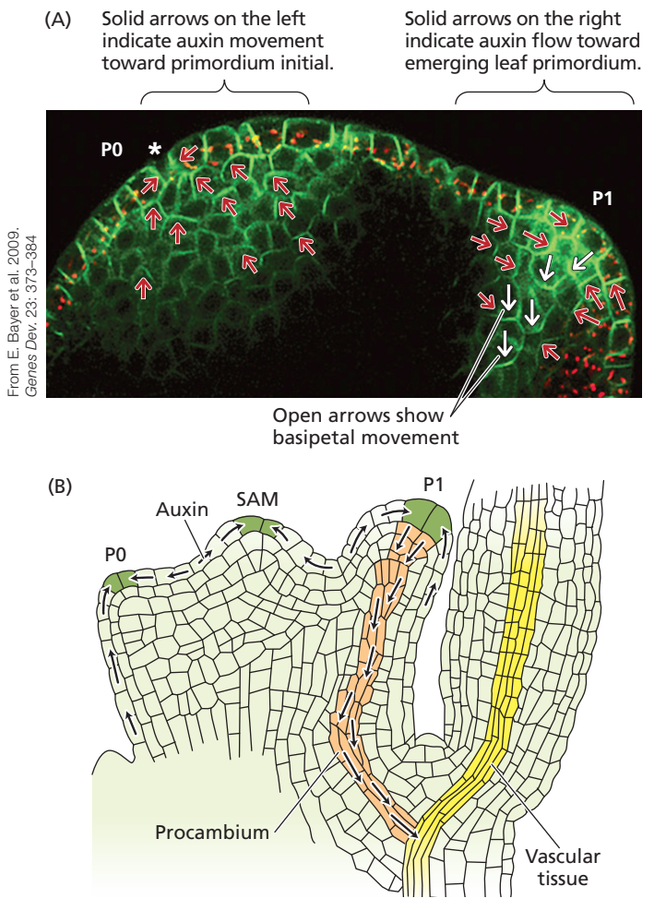


Figure 18.26 **Auxin-induced xylem regeneration around a wound in cucumber (*Cucumis sativus*) stem tissue.** **(A)** Method for carrying out the wound regeneration experiment. **(B)** Fluorescence micrograph showing regenerating vascular tissue around the wound. The arrow indicates the wound site where auxin accumulates and xylem differentiation begins.



Basipetal auxin transport from the L1 layer of the leaf primordium initiates development of the leaf trace procambium

Auxin canalization is accompanied by redistribution of PIN1 auxin efflux carriers to the extent that distribution of PIN1 can be used to predict the direction of auxin flow within a tissue. **Figure 18.27A** shows the SAM of a tomato plant expressing the Arabidopsis PIN1 protein fused to green fluorescent protein (GFP). Based on the cellular localization of the PIN1 proteins, auxin is directed to a convergence point in the L1 layer of the leaf primordium initial (P0). In contrast, auxin is directed basipetally in the initiating midvein (leaf trace) of the emerging leaf primordium (P1).

A model for midvein formation in Arabidopsis is shown in **Figure 18.27B**. The canalization of auxin toward the tip of the leaf primordium (P1) in the L1 layer via PIN1 transporters leads to an accumulation of auxin at the tip. Auxin efflux from this region of

Figure 18.27 **PIN1-mediated auxin flow during midvein formation.** **(A)** Longitudinal section through a tomato vegetative meristem expressing AtPIN1:GFP (green). The red arrows on the left indicate the direction of auxin movement toward the site of the leaf primordium initial (P0, white asterisk). The red arrows on the right indicate auxin flow toward the emerging leaf primordium (P1). The white arrows show basipetal auxin movement, which initiates the differentiation of the midvein. **(B)** Schematic diagram of auxin flow through the L1, L2, and L3 tissue layers and midvein differentiation during the formation of leaf primordia. Primordium initial (P0), primordium (P1).

high auxin concentration becomes canalized via PIN1 proteins in the basipetal direction toward the older leaf trace directly below it.

The existing vasculature guides the growth of the leaf trace

Microsurgical experiments have shown that the existing vascular bundle in the stem is required for the directional development of the leaf trace procambium. **Figure 18.28A** shows PIN1 distribution in the apex of a tomato plant expressing Arabidopsis PIN1 fused to GFP. The leaf trace emerging from the leaf primordium initial (P0) has connected to the existing leaf trace of the leaf primordium below it (P3), as shown diagrammatically in **Figure 18.28B**. However, if P3 is surgically removed, the leaf trace from P0 connects instead to the vascular bundle of the leaf primordium on the other side of the stem (P2) (**Figure 18.28C and D**). These results suggest that either the existing vascular bundle is serving as an auxin sink and thus facilitating auxin canalization, or that it is producing a different signal that guides the development of the leaf trace.

Vascular development proceeds from procambium differentiation

During vein formation, ground meristem cells differentiate into pre-procambium cells—a stable intermediate state between ground cells and procambium cells. Pre-procambium cells are isodiametric in shape (approximately cube-shaped) and are anatomically indistinguishable from ground meristem cells. Cell divisions of the pre-procambium are parallel to the direction of growth of the vascular strand, resulting in the elongated cells characteristic of the procambium (**Figure 18.29A**). This differentiation of the procambium proceeds in the basipetal direction.

Protophloem is the first vascular tissue to form from procambium cells, and its differentiation begins at the vascular bundle below and proceeds acropetally into the leaf primordium. In contrast, primary xylem differentiation lags behind primary phloem, is discontinuous, and proceeds both acropetally into the leaf primordium and basipetally toward the vascular bundle below.

Higher-order leaf veins differentiate in a predictable hierarchical order

The hierarchical order of leaf vascularization has been best studied in Arabidopsis. In general, vein development and patterning progress in the basipetal direction (**Figure 18.29B**). In other words, venation is generally at a more advanced stage of development at the tip of a developing leaf than it is at the base.

The pattern of vein formation follows a stereotypical course in Arabidopsis. The first procambium that forms in the leaf primordium—the leaf trace—represents the future **primary vein**, or **midvein**. As the leaf grows, secondary pre-procambium of the first pair of secondary veins (orange arrows in Figure 18.29B) develops out from the midvein and then loops acropetally toward the midvein at the leaf tip. The pre-procambium of tertiary

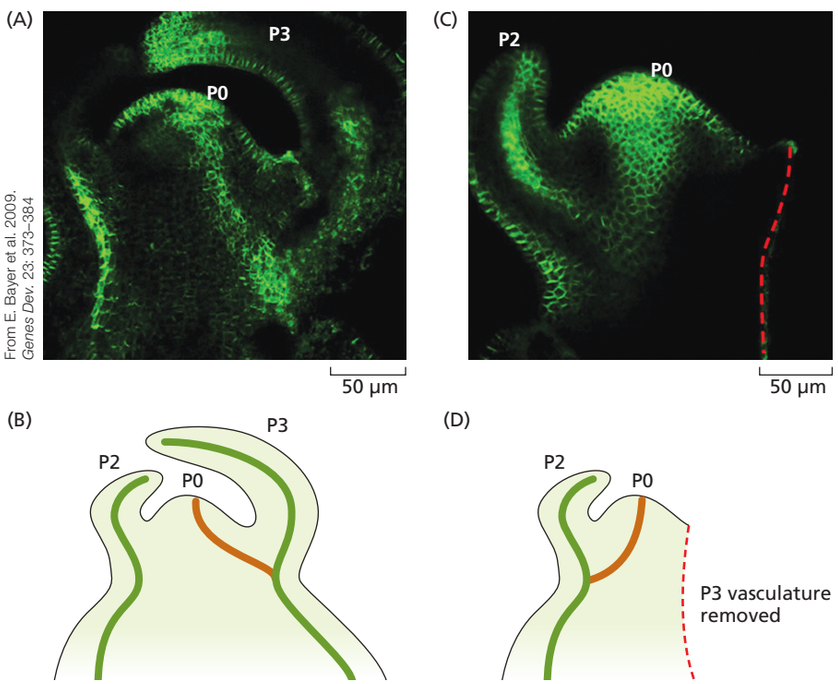


Figure 18.28 Preexisting vascular bundle guides basipetal development of the leaf trace. **(A and B)** In the control Arabidopsis meristem expressing AtPIN1:GFP (green), the newly initiated P0 leaf trace grows toward, and connects to, the P3 leaf trace directly below it. **(C and D)** When the P3 vasculature is surgically removed (dashed red line), the P0 leaf trace connects instead to the P2 leaf trace on the other side of the stem. (B and D after E. Bayer et al. 2009. *Genes Dev.* 23: 373–384.)

veins progresses out from the secondary veins and either reconnects with other extending strands or ends in the mesophyll (orange arrows in Figure 18.29B). The procambium differentiates from the pre-procambium simultaneously along the procambial strand (green lines in Figure 18.29B). Xylem differentiation occurs approximately 4 days later and can develop either continuously, or as discontinuous islands, along the vascular strand (magenta arrows in Figure 18.29B).

Proper differentiation of the vascular tissues within the veins depends on normal adaxial–abaxial polarity of the leaf. The four circles shown in **Figure 18.29C** represent vascular differentiation in the presence and absence of adaxial–abaxial polarity. The green circle on the left represents the undifferentiated procambial strand. Under conditions of normal adaxial–abaxial polarity, xylem develops on the adaxial side and phloem on the abaxial side. However, if the leaf has become adaxialized, as is *phan* mutants, the xylem cells surround the phloem, whereas in abaxialized mutants, such as those of the KANADI gene family, phloem cells surround the xylem cells.

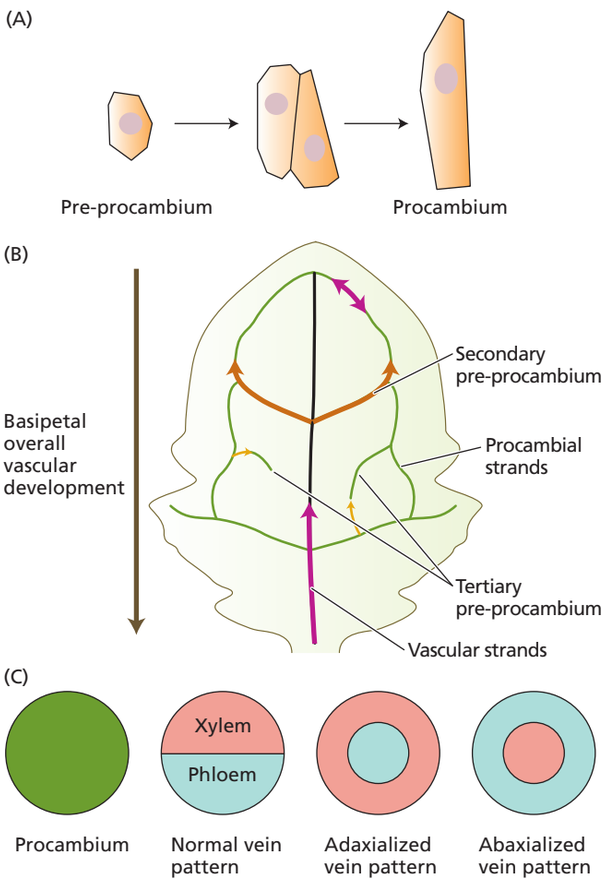


Figure 18.29 **Patterning of leaf vein formation.** **(A)** Formation of procambium cells from a pre-procambium cell. When a pre-procambium cell divides, either both daughter cells can become procambium cells or one cell can retain pre-procambium identity (not shown). **(B)** Development of vein pattern in young leaves. **(C)** Radial vein pattern in leaves. Left to right: procambial strand; normal vein pattern; vein pattern in adaxialized mutants; vein pattern in abaxialized mutants. (After W. J. Lucas et al. 2013. *J. Integr. Plant Biol.* 55: 294–388.)

Auxin regulates higher-order vein formation and patterning

As it is for leaf trace development, the distribution of auxin is critical for directing the development of higher-order leaf veins. At leaf margins, the adaxial–abaxial interface triggers the expression of auxin biosynthetic genes. The resulting auxin accumulation at the leaf margins is thought to stimulate the expansion of the lamina, and this accumulation is strongest in the regions where serrations are formed (**Figure 18.30**). The auxin maxima along the leaf margins also correspond to

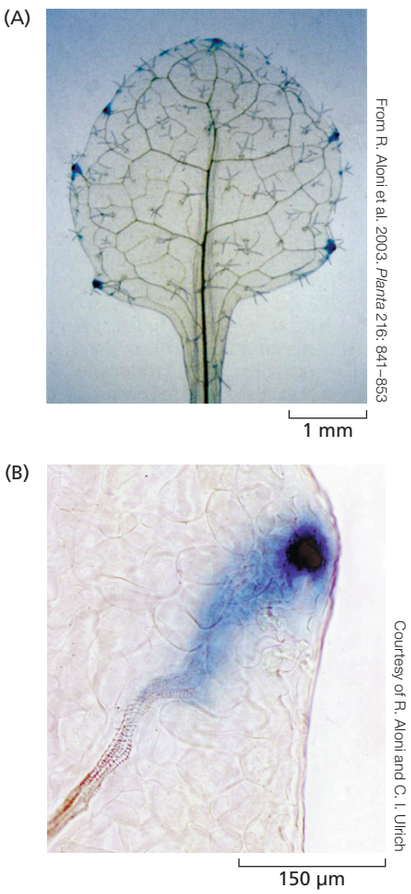
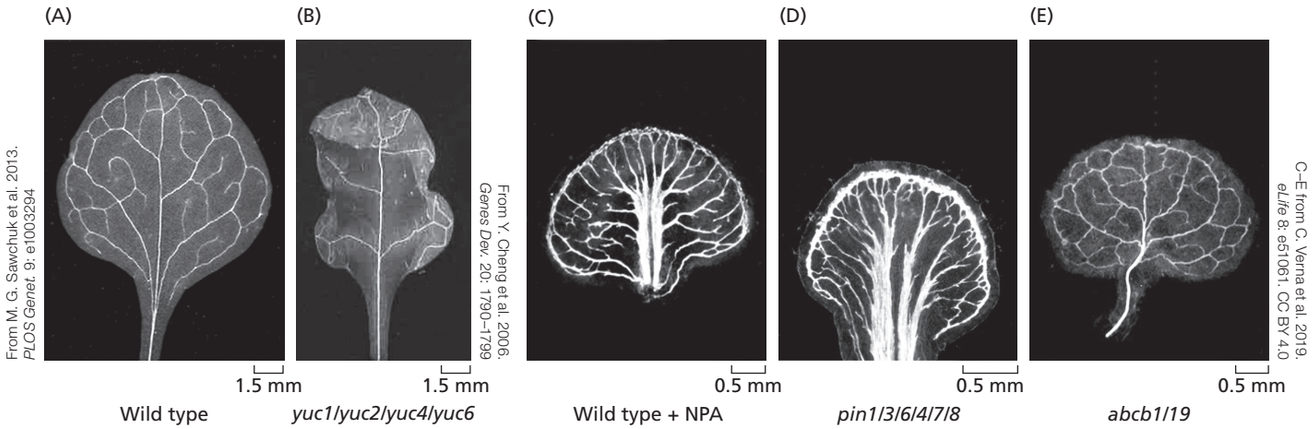


Figure 18.30 **Auxin biosynthesis at the hydathodes of Arabidopsis leaves, as indicated by the expression of the *GUS* reporter gene driven by the auxin-responsive DR5 promoter.** **(A)** An Arabidopsis leaf that has been cleared to reveal the blue stain. **(B)** Auxin flow and canalization from the hydathode toward a developing leaf vein.



From M. G. Sawchuk et al. 2013. *PLOS Genet.* 9: e1003294

From Y. Cheng et al. 2006. *Genes Dev.* 20: 1790–1799

C–E from C. Verna et al. 2019. *eLife* 8: e51061. CC BY 4.0

Figure 18.31 Mutations that affect auxin transport or auxin biosynthesis alter leaf venation patterns in young Arabidopsis rosette leaves. **(A)** Wild-type leaf. **(B)** *yuc1/yuc2/yuc4/yuc6* quadruple mutant. In the absence of significant auxin biosynthesis, the venation pattern is highly reduced. **(C)** Wild-type leaf treated with the auxin efflux inhibitor NPA, which inhibits both PIN and ABCB efflux activity. Venation and expansion are reduced. **(D)** Leaf of a mutant lacking six *PIN* genes showing reduced venation and intermediate size. **(E)** An *abcb1/19* mutant exhibits reduced expansion, similar to what is seen with NPA treatment. All leaves are imaged by darkfield microscopy.

specialized pores associated with vein endings at the leaf margin called hydathodes (see Chapter 6). Auxin moves away from these auxin maxima toward the primary vein and initiates differentiation of pre-procambium to eventually form a secondary leaf vein. Figure 18.30B illustrates the canalization of auxin from its site of synthesis in the hydathode region to a developing vein forming from the midvein in the center of the leaf.

The importance of auxin synthesis and transport for leaf venation is dramatically demonstrated by the phenotypes of Arabidopsis mutants deficient in auxin synthesis or polar transport (**Figure 18.31**). The normal venation pattern is almost entirely eliminated in *yuc1/yuc2/yuc4/yuc6* quadruple mutants (see Figure 18.31B), in which auxin biosynthesis is substantially reduced. Pharmacological blockage of cellular auxin efflux by *N*-1-naphthylphthalamic acid (NPA) reduces venation branching and overall leaf expansion (see Figure 18.31C). Loss of PIN activity in a sextuple mutant largely recapitulates the effect of NPA on branching but has less effect on overall leaf size (see Figure 18.31D). However, the ATP-BINDING CASSETTE B (ABCB) auxin efflux transporters also bind and are inhibited by NPA, and a double *abcb* mutant retains PIN activity but exhibits the reduction in leaf expansion seen with NPA treatment (see Figure 18.31E).

Summary

This chapter has illustrated that the great variety of plant cell types and organ shapes are controlled by common themes. Mobile signals such as auxin and peptide hormones integrate environmental and spatial cues to pattern growth and differentiation. Interlocking signaling pathways involving transcription factors, signaling peptides, and hormones balance environmental inputs to maintain characters such as meristem size and epidermal cell spacing. As we will see in the next chapter, this integration of long distance signaling with conserved local signaling pathways allows plants to make decentralized decisions that conserve basic plant architecture while enhancing prospects for survival and reproduction.

18.1 Meristematic Tissues: Foundations for Indeterminate Growth

- The root and shoot apical meristems use similar strategies to enable indeterminate growth.

18.2 The Root Apical Meristem

- The origin of different root tissues can be traced to distinct types of initial cells surrounding the quiescent center (**Figures 18.1, 18.2**).
- Auxin, cytokinin, and transcription factor gradients influence developmental transitions in the root apex (**Figure 18.3**).

Summary (*continued*)

18.3 The Shoot Apical Meristem

- The shoot apical meristem has a structure distinct from that of the root apical meristem (**Figure 18.4**).
- Shoot tissues are derived from several discrete sets of apical initials (**Figure 18.5**).
- The CLV–WUS feedback loop maintains meristem size (**Figure 18.6**).
- Expression of KNOX transcription factors promotes cytokinin production in the SAM while suppressing the accumulation of GA (**Figure 18.7**).
- Phyllotactic patterns are directly linked to the pattern of leaf development (**Figure 18.8**).
- Leaf initiation occurs at sites of localized auxin accumulation (**Figure 18.9**).
- Axillary bud formation begins in the shoot apex (**Figures 18.10, 18.11**).

18.4 Leaf Development

- Flat leaves have diversified into a huge range of leaf shapes (**Figure 18.12**).
- Differential growth controls leaf shape (**Figure 18.13**).

18.5 The Establishment of Leaf Polarity

- Adaxial–abaxial polarity in a leaf primordium is established by a signal from the SAM (**Figure 18.14**).
- Adaxial and abaxial identity are specified by hormonal interactions and a network of genes (**Figures 18.15, 18.16**).
- Leaf primordia also differentiate proximally–distally, into a boundary meristem, lower-leaf zone, petiole, and blade (**Figure 18.16**).

18.6 Differentiation of Epidermal Cell Types

- The epidermis is derived from the protoderm (L1) and has three main cell types—pavement cells, trichomes, and stomatal guard cells—as well as other cell types.
- Mechanistic studies of guard cell development began with mutant studies in Arabidopsis (**Figure 18.19**).
- Not only guard cells, but the majority of leaf epidermal cells, arise from specialized meristemoid mother cells (MMCs), stomatal lineage ground cells (SLGCs), meristemoids, and guard mother cells (GMCs) (**Figure 18.20**).
- Stomatal spacing is regulated by mobile peptides and polarity factors (**Figure 18.21**).
- Monocot stomatal development is regulated by conserved transcription factors functioning in a modified spatial context (**Figure 18.22**).

18.7 Venation Patterns in Leaves

- Leaf venation patterns indicate the spatial organization of the vasculature (**Figures 18.23, 18.24**).
- Triggered by auxin that is transported downward, leaf veins are initiated separately from established vasculature and grow *down* to rejoin it, directed by the vascular bundle in the stem (**Figures 18.25–18.27**).
- Similarly to initial development of veins, development of higher-order veins proceeds from tip to base and is regulated by auxin canalization (**Figures 18.28, 18.29**).
- Localized auxin biosynthesis allows for development of higher-order veins, and auxin transporters contribute to the appropriate specification of vein spacing and patterning (**Figures 18.30, 18.31**).

Web Material

- **WEB TOPIC 18.1** ***Azolla*** **Root Development** Anatomical studies of the root of the aquatic fern *Azolla* have provided insights into cell fate during root development.
- **WEB TOPIC 18.2 Shoot Tissues Are Derived from Several Discrete Sets of Apical Initials** Clonal analysis using treatment with colchicine to produce larger polyploid cells was used to determine cell lineages in the meristem.
- **WEB TOPIC 18.3 Mechanical Signaling in the Meristem** Cell divisions in the meristem exert mechanical pressures that contribute to cell and organ shapes.
- **WEB TOPIC 18.4 Bifacial, Unifacial, and Equifacial Leaves** Bifacial, unifacial, and equifacial leaves can be distinguished based on their anatomical and morphological differences.
- **WEB TOPIC 18.5 Development of Serrated and Compound Leaves** While marginal serrations are modified by many genes, the key components are auxin and the CUP-SHAPED COTYLEDON genes.
- **WEB TOPIC 18.6 Trichomes Are Specialized Cells in the Leaf Epidermis** In Arabidopsis, trichomes develop from single protodermal cells.
- **WEB ESSAY 18.1 Plant Meristems: A Historical Overview** Scientists have used many approaches to unravel the secrets of plant meristems.

For more study aids, go to oup.com/he/taiz7e.

Suggested Reading

Caño-Delgado, A., Lee, J.Y., and Demura, T. (2010) Regulatory mechanisms for specification and patterning of plant vascular tissues. *Annu. Rev. Cell Dev. Biol*. 26: 605–637.

Heisler, M. G., Hamant, O., Krupinski, P., Uyttewaal, M., Ohno, C., Jönsson, H., Traas, J., and Meyerowitz, E. M. (2010) Alignment between PIN1 polarity and microtubule orientation in the shoot apical meristem reveals a tight coupling between morphogenesis and auxin transport. *PLOS Biol.* 8: e1000516.

Kuchen, E. E., Fox, S., Barbier de Reuille, P., Kennaway, R., Bensmihen, S., Avondo, J., Calder, G. M., Southam, P., Robinson, S., Bangham, A., and Coen, E. (2012) Generation of leaf shape through early patterns of growth and tissue polarity. *Science* 335: 1092–1096.

Kierzkowski, D., Runions, A., Vuolo, F., Strauss, S., Lymbouridou, R., Routier-Kierzkowska, A.-L., Wilson-Sánchez, D., Jenke, H., Galinha, C., Mosca, G., Zhang, Z., Canales, C., Dello Ioio, R., Huijser, P., Smith, R. S., and Tsiantis, M. (2019) A growth-based framework for leaf shape development and diversity. *Cell* 177: 1405–1418.

Mazur, E., Kulik, I., Hajný, J., and Friml, J. (2020) Auxin canalization and vascular tissue formation by TIR1/AFB-mediated auxin signaling in Arabidopsis. *New Phytol.* 226: 1375–1383.

Nunes, T. D. G., Zhang, D., and Raissig, M. T. (2020) Form, development and function of grass stomata. *Plant J.* 101: 780–799.

Robinson, S., Barbier de Reuille, P., Chan, J., Bergmann, D., Prusinkiewicz, P., and Coen, E. (2011) Generation of spatial patterns through cell polarity switching. *Science* 333: 1436–40.

Steeves, T. A., and Sussex, I. M. (1989) *Patterns in Plant Development*. Cambridge University Press, Cambridge, UK.

Verna, C., Ravichandran, S. J., Sawchuk, M. G., Linh, N. M., and Scarpella, E. (2019) Coordination of tissue cell polarity by auxin transport and signaling. *eLife* 8: e51061.

19 Vegetative Growth and Organogenesis: Branching and Secondary Growth



schankz/Shutterstock

Seedlings and juvenile plants tend to allocate more photosynthate to vertical growth than to lateral growth because it helps them compete more effectively for sunlight aboveground, and for water belowground. As the plant increases its biomass, indeterminate growth is sustained by the emergence of additional shoot and root axes, a process called *branching*. In shoots, branches arise superficially from buds located in the axils of the leaves (*axillary buds*), while in roots branches are initiated internally in a layer of cells called the *pericycle*, located on the interior side of the endodermis (see Chapter 1).

Variations in the spatial arrangements, angles, and morphologies of branches generate the *architecture* of the shoot and root systems. Shoot architecture is a complex adaptive feature that depends on the regulated production of determinate lateral organs, such as leaves, as well as the regulated formation and outgrowth of indeterminate branch systems. The "Green Revolution" of the mid-20th century, a period of dramatic yield increases in global agriculture due to the introduction of high-yielding varieties, was brought about in part by intentional modifications in the shoot architecture of key cereal crops (see **WEB TOPIC 19.1**). Root architecture has comparable levels of complexity that arise from the regulated formation and outgrowth of indeterminate lateral roots. These include lateral roots that branch from primary roots as well as lateral roots that branch from previously formed lateral roots. Some root systems also include *adventitious roots*, which form in structures other than roots—for example, from the lower underground stem nodes in both monocots and eudicots, and from aboveground stems or branches in the case of epiphytes.

A defining feature of primary growth is the near absence of lignified cell walls in primary tissues other than the xylem conducting elements. The relative lack of lignin in herbaceous plants limits their abilities to grow very tall or to support large branches. For herbaceous annuals, biennials, and even some perennial plants that are either small in stature or climbers that rely on other plants for support, the vegetative growth phase of development consists entirely of primary growth. In perennial plants (trees and shrubs), however, primary growth is quickly

followed by *secondary growth*—growth in girth. Secondary growth arises from the activities of two cambial layers: the *vascular cambium*, which produces secondary xylem and phloem, and the *cork cambium*, which produces the *periderm*, a corky layer that replaces the epidermis as the outer protective layer on the stems and roots (see Chapter 1). Another type of secondary growth is found in arborescent monocots, such as palm trees. Instead of a ring of secondary xylem (i.e., wood) and phloem produced by a vascular cambium, palm trees have specialized initial cells in the cortex that give rise to secondary vascular bundles. These additional vascular bundles, which contain lignified xylem, provide sufficient structural reinforcement to allow palm trees to grow to great heights.

In this chapter we continue our survey of vegetative growth begun in Chapter 18 by examining the mechanisms of branching and secondary growth. Although the branches of shoots and roots originate from very different structures (axillary buds versus the pericycle, respectively), the two developmental pathways converge on a common endpoint: the production of new apical meristems, which greatly enhance the rate of increase in plant biomass. As we will see, the two pathways also share key similarities in their hormonal responses and genetic control mechanisms.

We conclude our discussion of vegetative growth with a description of some of the regulatory pathways that underly the production of secondary xylem and phloem. Secondary growth allows further increases in plant biomass by greatly extending the limits on height. Even after the height limit of a species has been attained, tree biomass continues to increase in the lateral direction because of the activity of the vascular cambium, which persists until the tree dies (see Chapter 23).

19.1 Shoot Branching and Architecture

The shoot and inflorescence architecture of flowering plants is determined to a large extent by the branching patterns established during postembryonic development. The most primitive type of branching is **dichotomous branching**, which is typically present only in nonvascular and non-seed plants, but also occurs in several seed plant taxa, such as cacti. During dichotomous branching the shoot apical meristem (SAM) enlarges and divides in half, producing two equal shoots (see **WEB TOPIC 19.2**).

In contrast, shoot architecture in seed plants is characterized by iterations of a basic module called a **phytomer**,[1] consisting of an internode, a node, a leaf, and an axillary bud (**Figure 19.1**). Modifications of the position, size, and shape of the individual phytomer, plus variations in the pattern of axillary bud outgrowth, explain the remarkable diversity of shoot architecture among seed plants. Vegetative and inflorescence branches, as well as the floral primordia produced by inflorescences, are derived from axillary meristems initiated in the axils of leaves. During vegetative development, axillary meristems, like the apical meristem, initiate the formation of leaf primordia, resulting in axillary buds (see Chapter 18). These buds either become dormant or develop into lateral shoots, depending on their position along the shoot axis, the developmental stage of the plant, and environmental factors. During reproductive development, axillary meristems initiate formation of inflorescence branches and flowers. Hence, shoot architecture depends not only on the patterns of axillary meristem formation, but also on meristem identity and subsequent growth characteristics. One important growth characteristic of shoots (and roots, as discussed in Section 19.2) is the **gravitropic setpoint angle**, the angle at which gravitropic organs are maintained with respect to gravity. Variation in the gravitropic setpoint angle of branches can lead to a wide variety of shoot architectures (**Figure 19.2**). As we discuss in Section 19.2, the angle of branch growth is determined by both genetic and environmental factors.

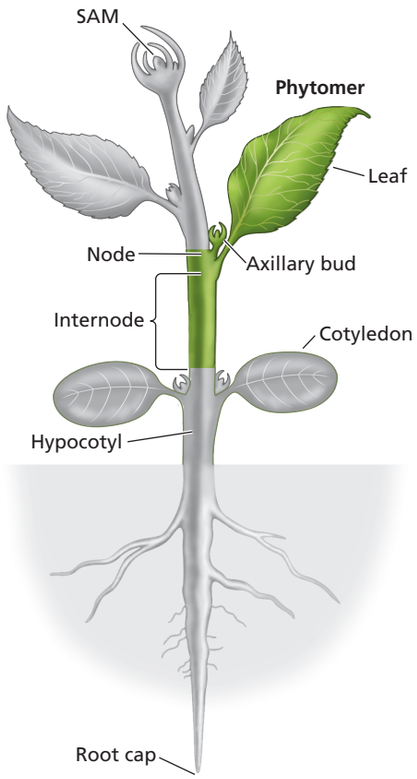


Figure 19.1 Schematic drawing of a phytomer, the basic module of shoot organization in seed plants.

[1] Some authors use the alternative term *metamer*.



Figure 19.2 The gravitropic setpoint angle of tree branches creates different patterns of tree architecture.

Auxin, cytokinins, and strigolactones regulate axillary bud outgrowth

Once the axillary meristems are formed, they may enter a phase of highly restricted growth (dormancy), or they may be released to grow into axillary branches. The "go or no go" decision is determined by developmental programming and environmental responses mediated by plant hormones that act as local and long-distance signals. Interactions of hormonal signaling pathways coordinate the relative growth rates of different branches and the shoot tip, ultimately determining shoot architecture. The main hormones involved are auxin, cytokinins, and strigolactones (see Chapter 15). All three types of hormones are produced in varying quantities in the root and shoot, but their translocation allows them to exert effects far from their site of synthesis (**Figure 19.3**).

Auxin is synthesized predominantly in young leaves and the shoot apex, and is transported downward (i.e., basipetally in the stem and acropetally in the root) in a specialized polar auxin transport stream via ATP-BINDING CASSETTE subfamily B (ABCB) and PIN-formed (PIN) proteins in the vascular cylinder and starch sheath or endodermis (see Chapters 4, 17, and 18). Auxin can also be transported in the phloem, where it moves by mass flow from source to sink (see Chapter 11).

Strigolactones are transported out of sites of synthesis via plasma membrane ABC transporters and have been shown to move upward in the xylem from root to shoot. Cytokinins, too, are transported from sites of synthesis to the xylem by an ABC transporter, and they can also move in the phloem. Consequently, there is considerable scope for long-distance communication via these hormones.

Auxin from the shoot tip maintains apical dominance

The role of auxin in regulating axillary bud growth is most easily demonstrated in experiments on apical dominance. **Apical dominance** is the control exerted by the shoot tip over axillary buds and branches below. Plants with strong apical dominance are typically weakly branched and show a strong branching response to

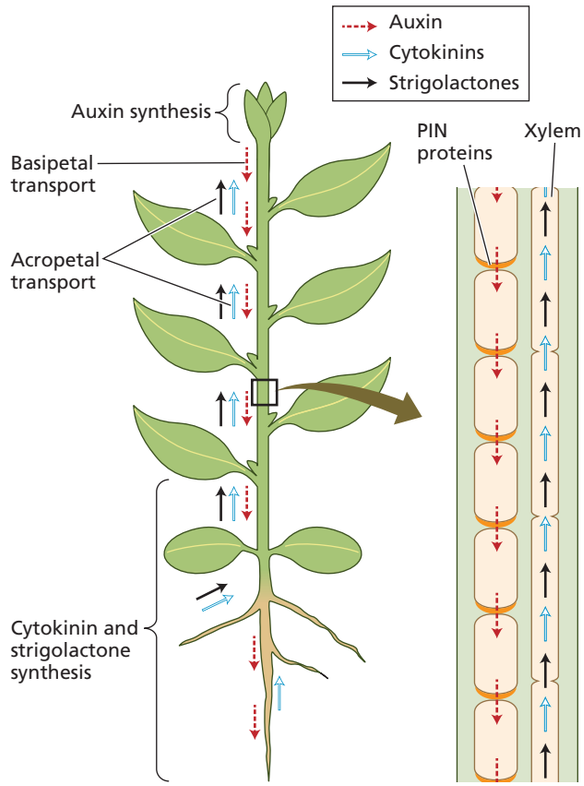


Figure 19.3 **Long-distance transport of three types of hormones that regulate shoot branching: auxin, cytokinins, and strigolactones.** Auxin is produced primarily in young expanding leaves and is transported basipetally by PIN1-mediated polar auxin transport. Strigolactones and cytokinins are synthesized mainly in the root and can be translocated acropetally to the shoot in the xylem. These two hormones can also be synthesized in shoot tissues adjacent to axillary buds. (After M. A. Domagalska and O. Leyser. 2011. *Nat. Rev. Mol. Cell Biol.* 12: 211–221.)

decapitation (removal of the growing or expanding leaves and the shoot tip). Plants with weak apical dominance are typically highly branched and show little, if any, response to decapitation.

More than a century of experimental evidence suggests that in plants with strong apical dominance, auxin produced in the shoot tip inhibits axillary bud outgrowth. In such plants, mutants with decreased rootward auxin transport exhibit increased branching, and treatment of the shoot apex with auxin transport inhibitors results in increased branching. Addition of auxin to the shoot at the point of apical excision inhibits outgrowth, while application of auxin transport inhibitors to the stem releases the axillary buds below from apical dominance (**Figure 19.4A**). Gardeners take advantage of this phenomenon when they "pinch back" chrysanthemums with strong apical dominance to create dense, dome-shaped bushes of blossoms.


(A)
Stump
Auxin
Auxin transport inhibitor
Intact plant
De-tipped
De-tipped plus IAA
PAT inhibitor
(B)
Wild type
max2 mutant
max1;3;4 mutant
max1;3;4 shoot, wild-type root
max2 shoot, wild-type root
Wild-type shoot, max2 root
max1;3;4 shoot, max2 root
Wild-type shoot, max1;3;4 root

Figure 19.4 Axillary bud outgrowth is inhibited by auxin and strigolactones. **(A)** Classic physiological experiments demonstrating the role of auxin in apical dominance. In de-tipped shoots the axillary buds are released from apical dominance. Replacing the missing shoot tip with auxin (indole-3-acetic acid, or IAA) prevents axillary bud outgrowth. Applying an inhibitor of polar auxin transport (PAT) to the stem causes bud outgrowth below the application site. **(B)** Grafting experiments carried out with mutants defective in strigolactone biosynthesis or signaling that have increased branching. Grafting the shoots of the strigolactone biosynthesis mutants (*max1*, *max3*, or *max4*) to wild-type roots restored shoot branching of the mutants to wild-type levels. Grafting the roots of the strigolactone signaling mutant *max2* onto the shoots of the wild type and synthesis mutants *max1*, *max3*, or *max4* also prevented bud outgrowth, demonstrating that *max2* can produce the signal in the roots, even though it cannot respond to it. The branch-inhibiting hormone can also be produced in the shoot, as grafting of the wild-type shoot to the strigolactone-deficient roots (*max1*, *max3*, or *max4*) did not increase the number of branches. (After M. A. Domagalska and O. Leyser. 2011. *Nat. Rev. Mol. Cell Biol.* 12: 211–221.)

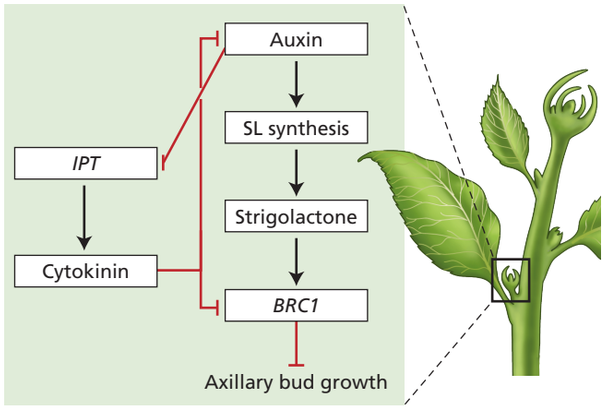


Figure 19.5 Hormonal network regulating apical dominance. Auxin from the shoot apex promotes strigolactone synthesis in the nodal area via the *max4* gene. In eudicots, auxin up-regulate the *BRANCHED 1* (*BRC1*) gene and down-regulate *IPT* genes. BRC1 inhibits axillary bud growth. Strigolactones also inhibit cytokinin biosynthesis, which otherwise would prevent BRC1 production. (After S. El-Showk et al. 2013. *Development* 140: 1373–1383.)

A key requirement in the activation of a lateral branch is its connection to the existing vasculature. Branch outgrowth requires auxin export from the developing leaves in the bud. The growing bud therefore acts as an auxin source, exporting auxin into the auxin transport stream of the main stem, itself an auxin sink because of its ability to transport auxin. A theoretical model has been proposed to describe the role of auxin in regulating bud outgrowth (see **WEB TOPIC 19.3**). There is also evidence for a role of sucrose in this process.

Strigolactones act locally to repress axillary bud growth

Strigolactones are thought to act in conjunction with auxin during apical dominance. Arabidopsis mutants defective either in strigolactone biosynthesis (*max1* [*more axillary growth 1*], *max3*, or *max4*) or signaling (*max2*) show increased branching without decapitation (**Figure 19.4B**). Grafting a shoot from a biosynthesis mutant onto a wild-type root restores apical dominance, indicating that strigolactones can move from the root to the shoot. However, root-derived strigolactones are not required for bud repression, since wild-type shoots grafted onto strigolactone-deficient roots have normal apical dominance.

Cytokinins antagonize the effects of strigolactones

Direct application of cytokinin to axillary buds stimulates their growth, suggesting that cytokinins are involved in breaking apical dominance. Consistent with this hypothesis, the expression of two cytokinin biosynthesis genes (*ISOPENTENYL TRANSFERASE 1* and *2* [*IPT1* and *IPT2*]) increases in the second nodal stem of peas following decapitation, suggesting that auxin from the shoot apex normally represses these genes. This was confirmed by incubating excised stem segments with and without auxin; *IPT1* and *IPT2* expression persisted only in segments incubated without auxin. In addition, application of the auxin transport inhibitor 2,3,5-triiodobenzoic acid (TIBA) around the internode led to increased *IPT1* and *IPT2* expression below the site of application, demonstrating that these genes are normally repressed by auxin transported down from the shoot apex. Thus, it appears that the cytokinins involved in breaking apical dominance are synthesized locally at the node.

A simplified scheme for the antagonistic interactions between cytokinins and strigolactones is shown in **Figure 19.5**. Auxin maintains apical dominance by stimulating strigolactone synthesis. In eudicots, strigolactones then activate the gene for BRANCHED 1 (BRC1), a transcription factor that suppresses axillary bud growth. Besides activating *BRC1*, strigolactones also inhibit cytokinin biosynthesis by negatively regulating the *IPT* genes. In contrast, cytokinins inhibit BRC1 action, and prevent auxin-induced strigolactone biosynthesis. The *BRC1* homolog in rice, *FINE CULM 1* (*FC1*), and in maize (corn; *Zea mays*), *TEOSINTE BRANCHED 1* (*TB1*), are the primary genes regulating branching in these crops. *TB1* is also responsible for a major trait involved in the domestication of maize, transforming the highly branched maize progenitor teosinte into the more desirable reduced-branching phenotype of modern maize (**Figure 19.6**).



Figure 19.6 **Comparison of teosinte (*Zea mays* ssp. *parviglumis*) and modern maize (*Zea mays* ssp. *mays*).**

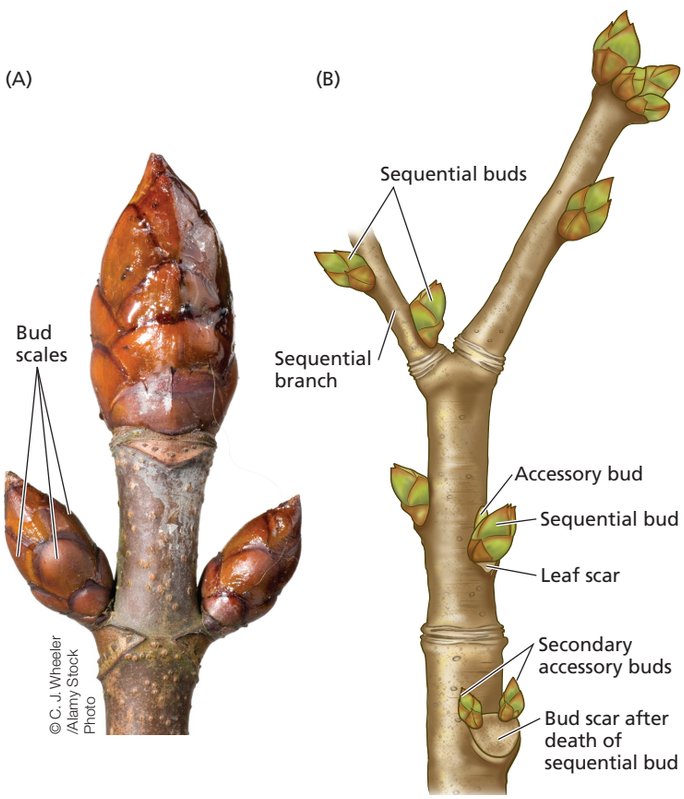


Figure 19.7 **Types of dormant buds.** **(A)** Dormant axillary buds of horse chestnut (*Aesculus hippocastanum*) surrounded by bud scales. **(B)** Diagram of sequential axillary buds, accessory buds, and secondary accessory buds.

Integration of environmental and hormonal branching signals is required for plant fitness

In some cases, a plant can adjust its default shoot branching pattern in response to environmental conditions. Two classic examples are the shade avoidance response and the nutrient deficiency response. Both of these responses involve the regulatory pathways described earlier.

Plants avoid shade through enhanced shoot elongation and suppressed branching. Shade avoidance involves phytochrome B signaling in response to the decreased R:FR light ratio that results when sunlight is filtered through green leaves containing chlorophyll. Genetic studies in Arabidopsis have shown that phytochrome B requires both auxin and strigolactone signaling pathways, as well as the bud-specific *BRC1* and *BRC2* genes to inhibit axillary bud outgrowth under shading conditions.

The response to nutrient deficiency is mediated by strigolactones. Well-nourished plants are bushy, whereas plants growing under nutrient-poor conditions tend to be weakly branched. The involvement of strigolactones in this branching response presumably relates, evolutionarily, to the role of these hormones in enhancing nutrient acquisition. Mycorrhizal plant species secrete strigolactones into the rhizosphere to promote the mycorrhizal symbiosis and thereby enhance nutrient uptake. The details vary among different species, but even in non-mycorrhizal plant species, strigolactone concentration in the shoot is elevated under low nutrient conditions. The increase in strigolactone concentration suppresses axillary bud outgrowth. Reduced branching in response to nutrient deficiency is adaptive because the plant is able to focus its resources on development of the main shoot and existing branches, rather than on promoting the growth of additional branches that cannot be supported by the nutrient supply. In high nitrogen conditions, which promote branching, cytokinin synthesis in the root is up-regulated. Plants in which multiple cytokinin biosynthesis genes are mutated are unable to increase branching in response to high nitrogen, suggesting a functional connection.

Axillary bud dormancy is affected by season, position, and age factors

Many woody perennial plants in temperate regions stop growing during the winter and produce dormant terminal and axillary buds that are protected by thick, leathery bud scales (**Figure 19.7A**).

Often these buds remain dormant throughout the winter. Major environmental factors that influence bud dormancy include temperature, light, photoperiod, water, and nutrients. Bud position and plant age are also important factors. Circadian clock genes and flowering genes (see Chapter 20), together with phytochrome A, are involved in controlling dormancy in deciduous trees in relation to photoperiod and temperature. In aspen trees, for example, this system regulates the cell cycle in buds. Even in herbaceous plants, pathways that regulate flowering in response to photoperiod interact with pathways regulating axillary bud outgrowth. For example, strigolactone-related branching mutants of garden pea (*Pisum sativum*) show dramatic shifts in the position and number of axillary branches when grown under different photoperiods, and flowering genes affect branching at cauline nodes in Arabidopsis.

Besides the terminal buds and the axillary buds (also called *sequential buds*) formed by the shoot apical meristem, many trees produce **accessory buds**, defined as buds that form near and in addition to the normal (i.e., *sequential*) axillary buds (**Figure 19.7B**). Accessory buds may form on the scars of sequential axillary buds or in the axils of the bud scales. Both axillary and accessory dormant buds can become buried under bark after the onset of secondary growth. As we discuss in Section 19.3, such buried dormant buds can become activated in response to fire and other stimuli.

19.2 Root Branching and Architecture

Most living vascular plants have root systems that anchor them to the soil and absorb water and nutrients required for growth. Through natural selection, plant root systems have evolved the ability to adapt to variations in soil composition, competition with other root systems, abiotic stress, and biotic interactions in the rhizosphere. Diversity and phenotypic plasticity are therefore key features of root architecture and are essential to the plant's survival. Recent research on the structure of root systems has been driven by advances in root system phenotyping (see **WEB TOPIC 19.4**). These and other studies have shown that plants have evolved complex control mechanisms that regulate root system architecture. **Root system architecture** is the spatial configuration of the entire root system in the soil. More specifically, root system architecture refers to the geometric arrangement of individual roots within the plant's root system in the three-dimensional soil space. Root systems are composed of different root types, and different plant species are able to control the types of roots they produce as well as their growth rates, degree of branching, and growth angles.

Postembryonic roots arising from existing roots are termed **lateral** or **branch roots**, while roots arising from non-root tissues are termed **adventitious roots**. In general, monocots such as the grasses have fibrous root systems consisting mainly of adventitious roots which in turn produce abundant lateral roots. By contrast, eudicots such as Arabidopsis typically produce a single dominant primary root, or taproot, which gives rise to all of the lateral roots and their branches.

In shoots, leaf and axillary bud primordia are periodically initiated on the flanks of apical meristems in spiral arrangements or other precise patterns—a phenomenon referred to as *phyllotaxis* (see Chapter 18). Lateral root primoridia are initiated in the zone of differentiation of the growing root (see Chapter 18). The arrangement of lateral roots along the surface of a root is termed **rhizotaxis**, and is determined by a combination of endogenous and environmental factors.

During root growth, the developmental zones (meristematic [cell division], elongation, and maturation [differentiation]) move acropetally by the addition of new cells at the growing tip (see Figure 19.9A). As a result, the developing lateral roots are shifted in the shootward direction through the maturation zone toward the fully mature region of the root. (Note that the developing lateral roots do not change their position relative to the root base.) This process generates a developmental gradient between the youngest lateral root primordia near the growing tip and the oldest lateral roots near the root base.

Lateral root primordia arise from the xylem pole pericycle cells

In most plants, including Arabidopsis, lateral roots are initiated exclusively in the pericycle, the tissue located just inside the endodermis (see Chapter 1). The arrangement of vascular tissue in the root is characterized as diarch (as in Arabidopsis), triarch, tetrarch, and so on, depending on the number of xylem arms, which corresponds to the number of protoxylem strands (**Figure 19.8**). The **phloem pole pericycle** cells are the pericycle cells located adjacent to the phloem strands, while the **xylem pole pericycle** cells are adjacent to the tips of the xylem arms. In Arabidopsis and most other eudicots and nongrass monocots, lateral root initiation occurs exclusively in the xylem pole pericycle cells, while in the grasses (e.g., maize and barley) lateral root initiation is restricted to the phloem pole pericycle cells. This difference raises the important question of how the pericycle cells of the xylem pole (in the case of most angiosperms) or the phloem pole (in the case of some monocots) become specified from the other pericycle cells. Because most of the research in this area has been conducted on Arabidopsis, we will focus on the development of lateral roots from xylem pole pericycle cells.

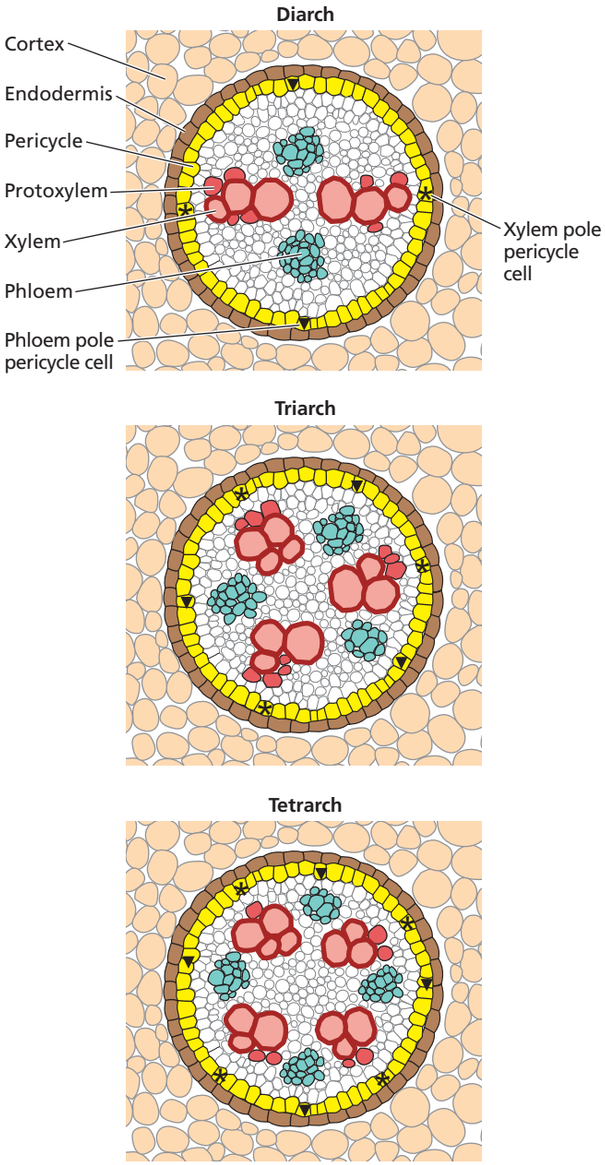


Figure 19.8 **Examples of different protoxylem and protophloem arrangements in eudicot roots.** (After M. Megías et al. 2019. *Atlas of Plant and Animal Histology*. Dept. Func. Biol. Hlth. Sci., University of Vigo, Spain. https://mmegias.webs.uvigo.es/02-english/2-organos-v/guiada_o_v_rprimario.php.)

Lateral root formation can be divided into four distinct stages

Lateral root primordia arise in the pericycle from **lateral root founder cells**, a subset of the xylem pole pericycle cells. Prior to specification of the founder cells, lateral root development involves largely invisible cellular changes that prepare the pericycle adjacent to the xylem pole to become founder cells. These invisible changes may occur in stages as the cells pass from the meristematic zone to the elongation zone. For example, there is evidence that the gene expression patterns of both xylem pole pericycle cells and phloem pole pericycle cells begin to resemble those of their respective vascular tissues while still in the meristematic zone at the root tip. However, whatever changes occur in the meristematic zone, xylem pole pericycle cells do not achieve full competence to differentiate into lateral root founder cells until they reach the elongation zone.

The location in the root where xylem pole pericycle cells become fully competent to become founder cells is called a **prebranch site**, which roughly corresponds to the start of the maturation zone (**Figure 19.9A**). It is here that some xylem pole pericycle cells (**Figure 19.9B**) undergo **priming**, which conditions them to become lateral root founder cells (**Figure 19.9C**). While the new lateral root primordium is undergoing initiation at the prebranch site, it is being displaced in the shootward direction. Periodically, new lateral root founder cells differentiate to form a new prebranch site, and the process repeats itself as long as primary root growth continues.

Lateral root formation can be divided into four distinct stages:

I. *Differentiation of the lateral root founder cells*, which specify the locations of the prebranch sites along the root

II. *Lateral root initiation*, which involves nuclear migration and asymmetric and anticlinal cell divisions in the lateral root founder cells

III. *Lateral root primordium formation*, which produces a new root apical meristem perpendicular to the parental root

IV. *Lateral root emergence*, which involves interactions between the lateral root primordium and surrounding tissues, thereby allowing passage through the overlying cell layers and emergence of a new lateral root

Given their importance for root system architecture, the mechanisms involved in creating prebranch sites have received considerable attention. For example, there is now abundant evidence suggesting that specification of prebranch sites requires auxin and occurs predominantly in the oscillation zone. An **auxin clock model** has been proposed to account for the spacing of prebranch sites. Briefly, the model proposes that the spacing of prebranch sites is regulated by periodic oscillations of either auxin activity or auxin concentrations in the oscillation zone, which extends roughly from midway in the meristematic zone to the beginning of

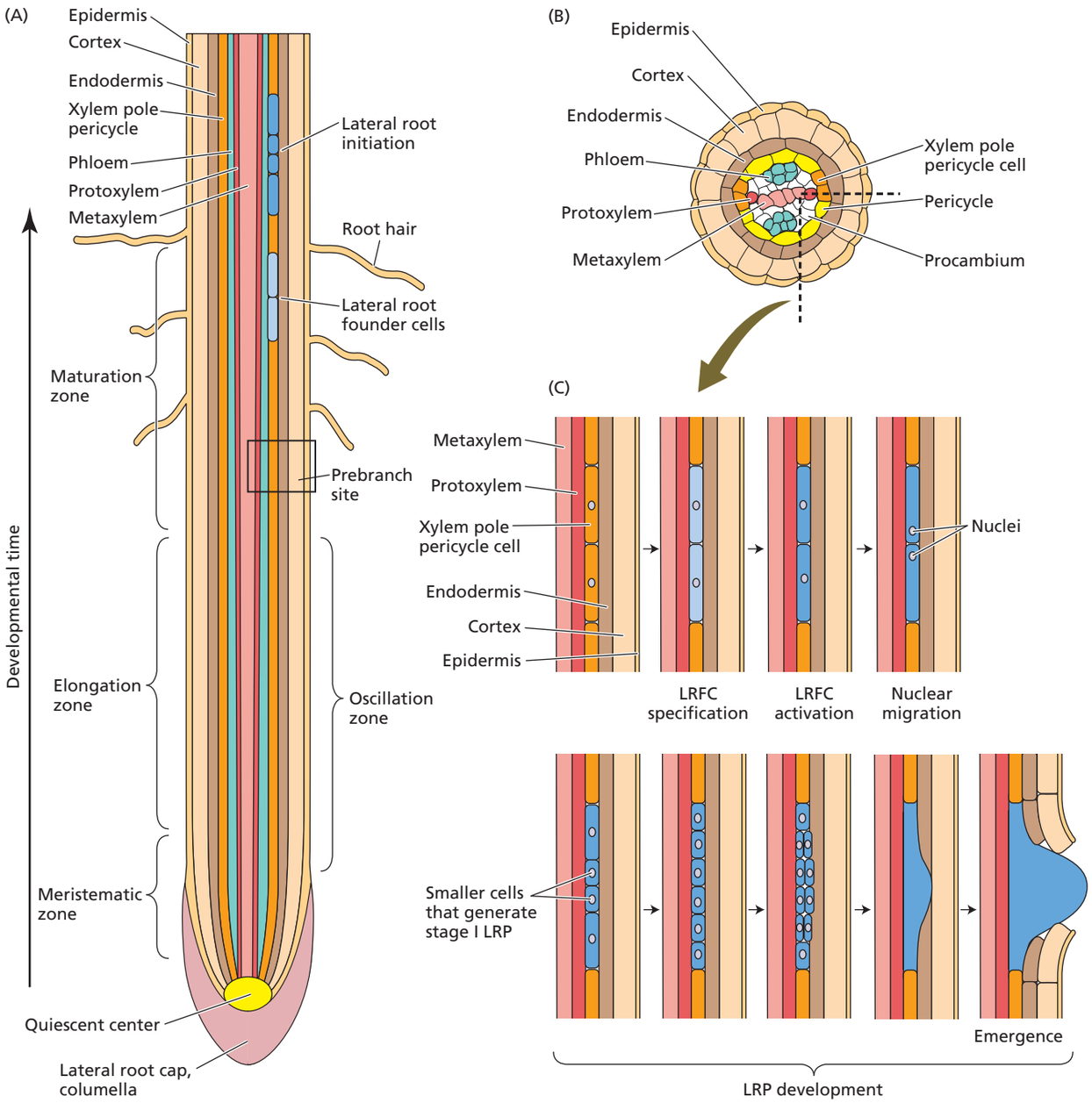


Figure 19.9 **Lateral root development in Arabidopsis.** **(A)** Longitudinal section of the primary root showing its developmental zones. The prebranch site, where a branch root will form if given the appropriate signals, forms after an oscillatory phase of auxin responsive gene expression within the oscillation zone. The oscillation zone confers competence on the xylem pole pericycle cells to differentiate into lateral root founder cells (light blue). **(B)** Cross section of primary root. Oscillating auxin responses occur in the protoxylem (red); however, because lateral root initiation occurs in the adjacent xylem pole pericycle cells (orange), signaling between these two cell types might be required for the specification of lateral root founder cells. **(C)** Longitudinal sections of a small portion of the root, showing initiation and development of a lateral root. Specific xylem pole pericycle cells (orange) are specified as lateral root founder cells (LRFC; light blue) and then are activated to undergo cell division (dark blue). Activation causes migration of the nuclei of a pair of vertically stacked LRFCs toward the cell wall they share. These cells then undergo asymmetric anticlinal divisions, giving rise to several smaller cells (dark blue). Continued anticlinal and periclinal divsions generate a lateral root primordium (LRP). The LRP grows through the outer cell layers of the primary root until it emerges from the epidermis. (Drawing not to scale.) (After J. M. Van Norman et al. 2013. *Development* 140: 4301–4310.)

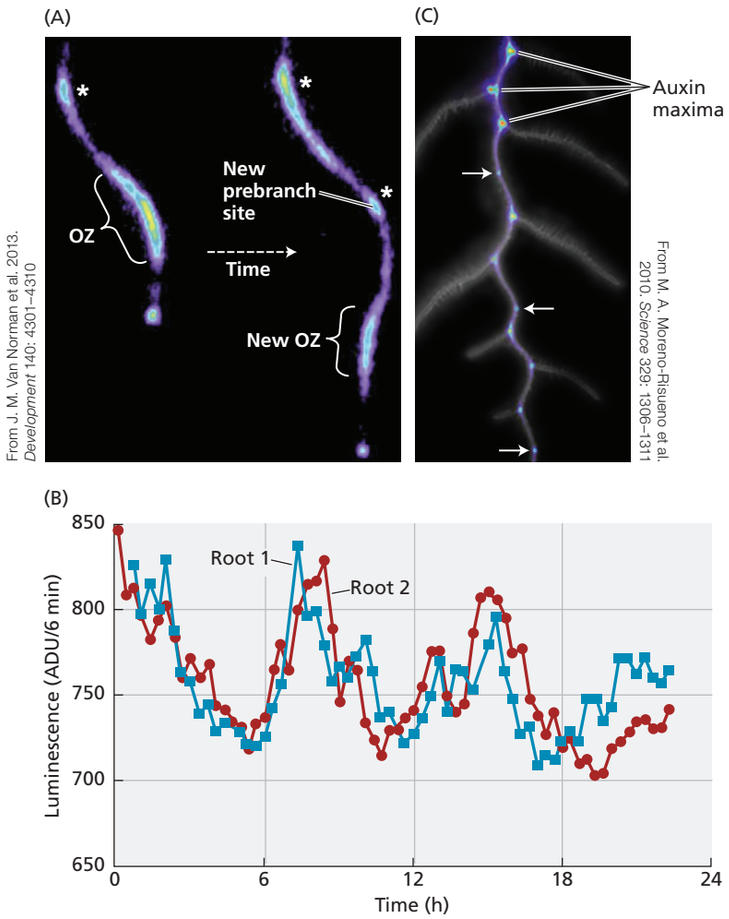


Figure 19.10 **Prebranch sites form in the oscillation zone, immediately below the maturation zone.** **(A)** Expression of the luciferase gene driven by the auxin-sensitive DR5 promoter in an Arabidopsis root. Auxin signaling levels, as indicated by luminescence caused by luciferase activity, fluctuate over time in the oscillation zone (OZ). Asterisks indicate prebranch sites, which correspond to the auxin activity maxima. **(B)** Auxin signaling levels measured by luminescence in two Arabidopsis roots oscillate with a period of about 6 h in the oscillation zone. ADU, analog digital units. **(C)** Auxin maxima along the root (light blue areas) correspond to sites of bending, lateral root formation, and lateral root emergence. Sites of lateral root formation are indicated by arrows. (B after M. A. Moreno-Risueno et al. 2010. *Science* 329: 1306–1311.)

the maturation zone (**Figure 19.10**). According to the model, only those cells exposed to an auxin maximum (activity or concentration) are competent to form a prebranch site (see **WEB TOPIC 19.5**).

Lateral root founder cells undergo asymmetric cell divisions to initiate formation of lateral root primordia

In Arabidopsis, several vertical files of founder cells participate in the initiation stage of lateral root growth. The first visible sign of the activation of the lateral root founder cells is nuclear migration toward the cell wall between two abutting lateral root founder cells in a file, followed by *formative* cell divisions in both cells (see Figure 19.9C). A formative division is an asymmetric cell division in which the two daughter cells acquire different cell fates. Lateral root initiation is defined as being completed when the first formative divisions are finished and the daughter cell fates have been established. This stage of lateral root development is termed stage II. Stage II also includes the activation of specific transcription factor genes required for the coordination of various stages in primordium formation. For example, members of the PLETHORA (PLT) family of transcription factors are essential for the regulation of all post-initiation steps of lateral root formation (see Chapter 18).

The formation of the lateral root primordium marks the onset of outgrowth of the lateral root. A combination of cell growth and several rounds of proliferative (anticlinal, periclinal, and tangential) cell divisions generates a dome-shaped primordium that emerges as a lateral root at the final stage of lateral root outgrowth. Cell wall softening enzymes are produced in the cortical and epidermal tissues that overlie the emerging primordium, easing its progression toward the root surface and into the soil. Once the new meristem is fully formed, it acquires the ability to synthesize its own auxin. Emerged lateral roots thus possess a functional root apical meristem (RAM), including a quiescent center and the surrounding initial cells that give rise to all the tissues of the growing lateral root.

Monocots and eudicots differ in their predominant root types

Both monocot and eudicot root systems are roughly similar in structure, consisting of an embryonically derived primary root (the radicle), lateral roots, and adventitious roots derived from shoot nodes. However, there are also significant differences in their root systems. Monocot root systems, especially those of the cereals, are generally more complex than the root systems of eudicots. For example, the maize seedling root system consists of a **primary root** that develops from the radicle, **seminal roots** that branch from the scutellar node, and postembryonically derived **crown roots** that branch from the lowermost nodes of the stem and are also referred to as adventitious roots (**Figure 19.11**). The primary and seminal roots form fibrous root systems, highly branched systems with many fine lateral roots. Crown roots are relatively unimportant in seedlings, but in contrast to

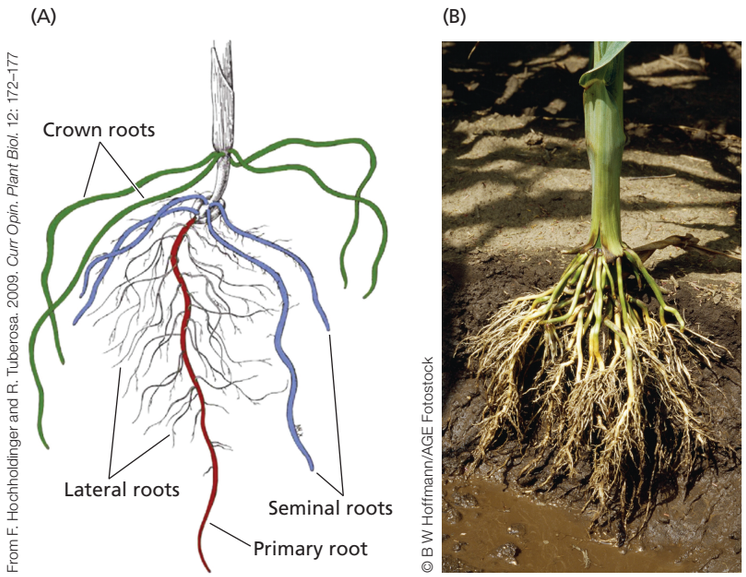


Figure 19.11 **Monocot root systems.** **(A)** Root system of a 14-day-old maize seedling composed of primary root derived from the embryonic radicle, seminal roots derived from the scutellar node, postembryonically formed crown roots that arise at nodes above the mesocotyl, and lateral roots. **(B)** Mature maize root system.

the primary and seminal roots, they continue to form, develop, and branch throughout vegetative growth. Later in development, a specialized type of crown root, the brace root, emerges from nodes above the soil surface. Brace roots have a distinct morphology and are thought to provide structural support for larger plants.

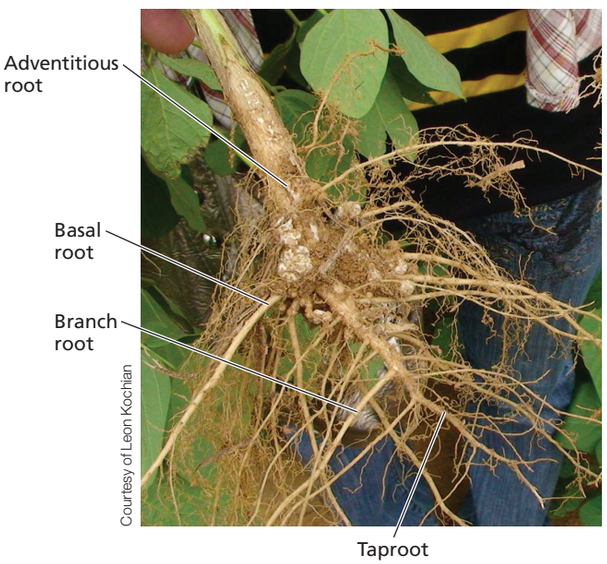


Figure 19.12 **Soybean root system showing primary root (taproot), branch roots, basal roots, and adventitious roots.**

The crown root system makes up the vast majority of the root system in adult maize plants (see Figure 19.11B).

The root system of a young eudicot consists of the primary root (or taproot) and its branch roots. As the root system matures, basal roots arise from the oldest part of the taproot, near the junction with the shoot. In addition, adventitious roots can arise from subterranean stems or from the hypocotyl; these roots are loosely analogous to the adventitious crown roots in the cereals. The root system of a soybean plant as a representative eudicot is depicted in **Figure 19.12**, where the tap, branch, basal, and adventitious roots can be seen.

Transcription factors regulate the gravitropic setpoint angles of lateral roots and shoots

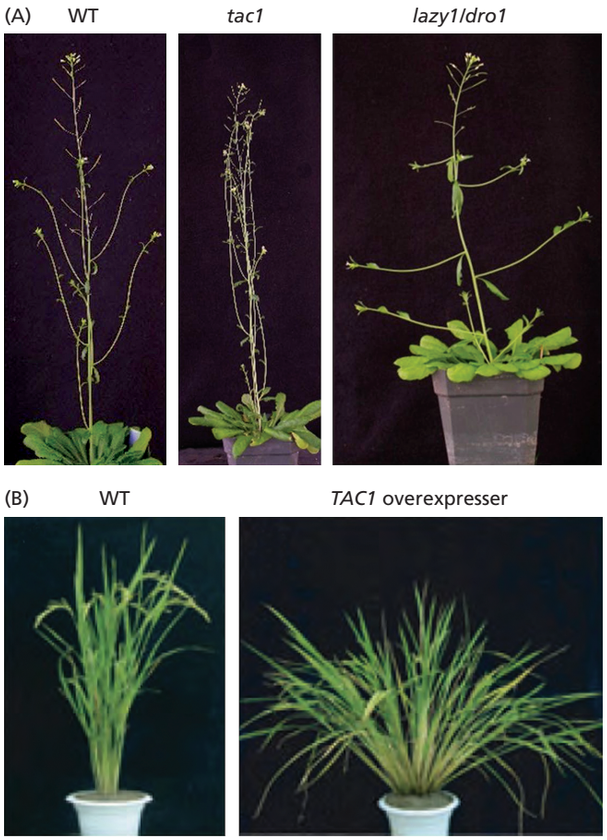
As mentioned in Section 19.1, the various components of shoot systems and root systems tend to grow at characteristic gravitropic setpoint angles. By convention, a primary root growing vertically downward has a gravitropic setpoint angle of 0°, while that of a primary shoot growing vertically upward is 180°. Lateral shoots and roots tend to have setpoint angles that deviate from the vertical.

Immediately following emergence, the lateral roots have not yet developed an elongation zone, which means they are incapable of gravitropic bending. As a result, newly emerged lateral roots initially grow away from the primary axis at an angle perpendicular to gravity. This horizontal growth helps expand the root system in the radial direction, increasing access to nutrients and stabilizing the plant. Once lateral roots have formed elongation zones, they bend at their predetermined gravitropic setpoint angles, and continue growing at this same angle for a variable period of time called the *plateau phase*. In general, early lateral roots have longer plateau phases than later lateral roots. Eventually, another gravitropic response kicks in, which causes a second bending with more pronounced downward growth, resulting in an angle between 0° and 30°.

In general, if a graviresponsive branch (root or shoot) is mechanically displaced, upward or downward, from its gravitropic setpoint angle, it will undergo tropic growth to shift it back toward that gravitropic setpoint angle. This means that lateral roots with nonvertical gravitropic setpoint angles can be negatively gravitropic—that is, grow against the gravity vector. Conversely, nonvertical shoot branches can be positively gravitropic and grow downward. This observation provides a simple demonstration that the mechanistic basis for the maintenance of graviresponsive nonvertical growth cannot lie solely in

differences in gravitropic competence between primary and lateral organs. There must be another, unidentified mechanism that can drive upward growth in lateral roots and downward growth in lateral shoots.

Several regulatory factors have been identified that influence the gravitropic setpoint angle of lateral organs in both shoots and roots and across diverse plant phyla. These proteins belong to the IGT family, named for a highly conserved IGT amino acid motif. This family has three distinct clades, LAZY, DEEPER ROOT-ING (DRO), and TILLER ANGLE CONTROL (TAC), which variously increase or decrease growth angles of root and shoot lateral organs (**Figure 19.13**). Deciphering the functions of these transcription factors should help reveal the mechanisms controlling gravitropic setpoint angle. Manipulation of these mechanisms could prove valuable for increasing crop yield and resilience. For example, in rice, genetic variations in several IGT transcription factor loci have been linked to important agronomic traits: *DRO1* to deeper rooting, which improves drought tolerance; *DRO1-LIKE 1* to enhanced soil surface rooting, which improves tolerance to saline and waterlogged soils; and *TAC1* to optimal shoot branch angle, which promotes efficient photosynthesis in densely planted fields.



From C. A. Hollender et al. 2020. *Sci. Rep.* 10: 6051. CC BY 4.0

From B. Yu et al. 2007. *Plant J.* 52: 891–898

Figure 19.13 Regulation of shoot gravitropic setpoint angles by IGT transcription factors. **(A)** The branch angles of an Arabidopsis *tac1* mutant are more upright than those of the wild type (WT), while a *lazy1/dro1* double mutant has more horizontal stem angles. **(B)** In rice, shoot and root growth angles are more horizontal in *TAC1* overexpressors.

Plants can modify their root system architecture to optimize water and nutrient uptake

Root system architecture is highly plastic within species, as plants can modulate root development to optimize water and nutrient uptake (see Chapter 7). For example, water heterogeneity in soils can be caused by air pockets or variations in soil water potential, as occurs during partial drying or in response to salinity gradients. This heterogeneity can stimulate directional root growth toward areas of higher humidity or water availability, a behavior called *hydrotropism* (see Chapter 17). As discussed in Chapter 7, plant roots typically form mycorrhizal associations that can enhance nutrient uptake, particularly in the case of phosphate ions. Such associations frequently involve anatomical and morphological changes that facilitate nutrient exchange between the root and its fungal symbiont. Plant roots can also form symbiotic associations with nitrogen-fixing bacteria, as described in Chapter 14.

19.3 Secondary Growth

All gymnosperms and most eudicots—including woody shrubs and trees, as well as large herbaceous species—develop lateral meristems that cause radial growth (growth in width) in stems and roots. Growth in girth that results from lateral meristems is called **secondary growth** (**Figure 19.14**), and it contributes to the continual enlargement of woody plants, allowing them to become thicker and more robust. It has been estimated that wood makes up more than half the world's biomass, and forest biomes provide homes for about 80% of the world's biodiversity.

The development of a vascular cambium responsible for secondary growth has occurred repeatedly during the evolution of vascular plants (see **WEB TOPIC 19.6**). Wood is composed of secondary xylem tissues with thickened secondary cell walls, and its formation is dynamic and continuous. Physiologically, wood serves transport, storage, and mechanical functions, and the response of wood to various environmental factors reflects changes that facilitate these functions. (For a discussion of adaptive secondary growth responses to environmental stresses, see **WEB TOPIC 19.7**.)

Two types of lateral meristems are involved in secondary growth

Secondary growth is generated by the activities of two types of lateral meristems: the **vascular cambium**,

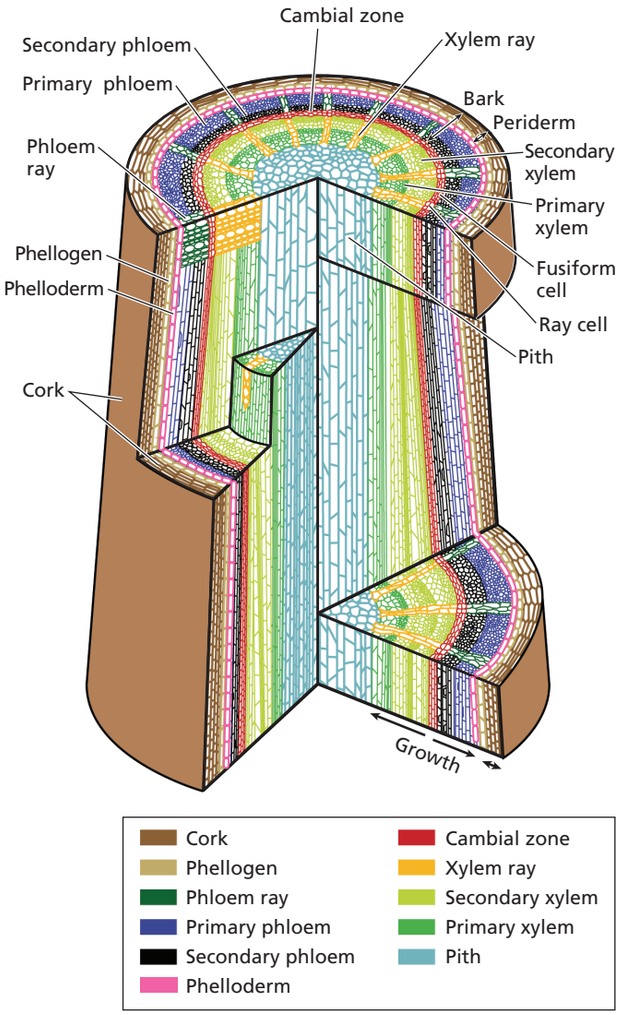


Figure 19.14 **Internal anatomy of a woody stem.** The vascular cambium (red region) consists of a single layer of cambial initial cells and its immediate derivatives on either side, and is surrounded by an outer layer of secondary phloem cells (black) and an inner layer of secondary xylem cells (light green). The primary phloem (dark blue), primary xylem (dark green), and pith (light blue) are also shown. The periderm includes the phellogen (tan cell layer), phelloderm (pink), and phellem (cork cells, in brown). The bark layer includes all tissues external to the vascular cambium, including the primary and secondary phloem. Most angiosperm and gymnosperm tree species also contain radial files of ray cells that play a role in nutrient transport and storage. (After J. P. M. Risopatron et al. 2010. *Protoplasma* 247: 145–161.)

which produces secondary vascular tissues, and the **cork cambium**, or **phellogen**, which produces the outer protective layers of the secondary plant body called the **periderm** (**Figure 19.15A**). The vascular cambium and the cork cambium are typically organized in concentric cylinders. However, other forms of secondary woody growth have evolved that produce various other shapes that are probably adaptive in nature, as occurs in lianas (see **WEB TOPIC 19.8**).

The secondary xylem and phloem produced from the vascular cambium allow the plant to modulate long-distance transport capacities and adapt to different ecological niches and to environmental changes. The periderm produced from the cork cambium is more superficial and protects the plant from biotic and abiotic stresses and prevents water loss. Both tissues increase mechanical support and are considered a key anatomical innovation for the evolution of tall, robust plants. Such plants can live longer and have the option to reproduce less frequently, doing so only when the conditions are optimal.

The transition from primary to secondary growth in gymnosperms and eudicots is readily visible along the shoot axis. In poplar (*Populus* spp.), for example, primary growth occurs in the top eight internodes, up to approximately 15 cm from the shoot apical meristem (SAM). Primary growth then gives way to secondary (woody) growth that produces secondary xylem and secondary phloem (see Figure 19.15A). The primary and secondary growth zones are separated both spatially and temporally, are easily discernible, and develop rapidly (within 1–2 months) in fast-growing species such as poplar.

The vascular cambium produces secondary xylem and phloem

In contrast to the terminally positioned SAM and RAM, the vascular cambium presents a very distinct meristem organization that extends along nearly the entire length of the apical–basal axis of the plant, and which functions to produce vascular tissues along the radial axis. The vascular cambium consists of initial cells (cambial initials) organized in radial files that form a continuous cylinder around the stem. Cambial initials divide to produce mother cells for xylem, phloem, and rays (discussed shortly), which in turn undergo several rounds of division to form the cambium zone, a zone of relatively undifferentiated cells with variable numbers of cells per radial cell file. These cells then differentiate into several different cell types as they progress away from the cambium zone.

The vascular cambium displays two main division patterns—anticlinal (perpendicular to the stem surface) and periclinal (parallel to the stem surface) (see Figure 19.15B). Anticlinal divisions add more cells to the cambium to accommodate the increasing girth of the stem and are thought to indicate the position of the cambium initials, which are otherwise morphologically indistinguishable from the other cells in the cambium zone. The peak of anticlinal division is typically within the first or second cell file proximal to the phloem and is usually used to pinpoint the approximate position of the vascular

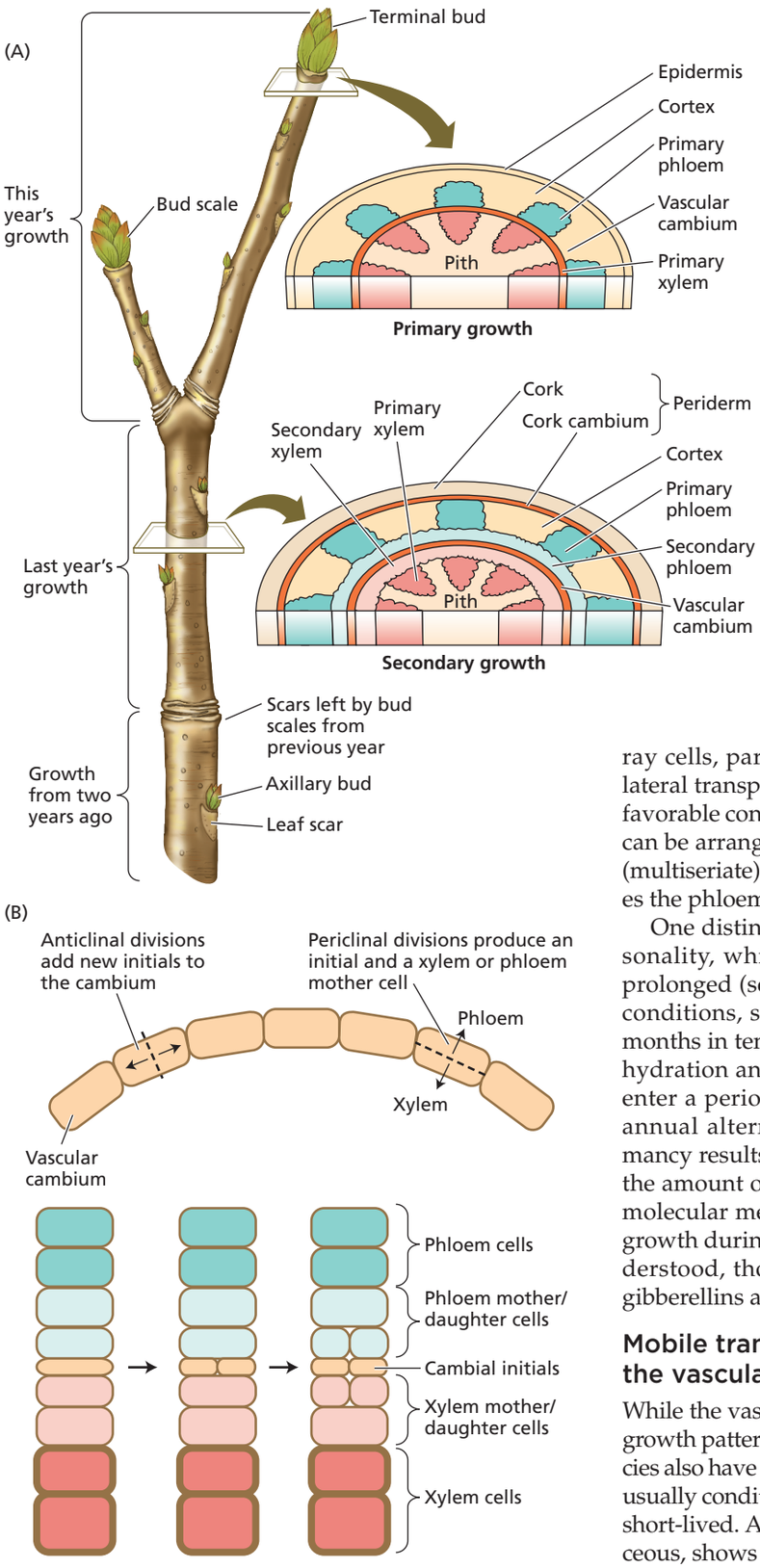


Figure 19.15 Development of secondary vascular tissue. **(A)** Primary growth in woody stems occurs in the spring, followed by secondary growth. **(B)** Orientations of the cell division planes in the cambial zone maintain the proper balance between growth in diameter versus circumference. Cambial cells initially divide anticlinally to produce new initials and increase the circumference of the cambium. The same initials also divide periclinally to produce xylem and phloem mother cells, always leaving behind another initial. (B after R. Spicer and A. Groover. 2010. *New Phytol.* 186: 577–592.)

cambium. While other meristems produce cells only on one side, both of the lateral meristems involved in secondary growth are bifacial, forming new cells on both sides. The vascular cambium produces xylem inward and phloem outward (see Figure 1.5), while, as we discuss later in this section, the cork cambium produces phellem outward and phelloderm inward.

In addition to phloem and xylem cells, the vascular cambium produces ray cells, parenchyma cells that serve as conduits for lateral transport in the stem and for storage during unfavorable conditions such as winter dormancy. Ray cells can be arranged in one file (uniseriate) or multiple files (multiseriate) to form a tissue known as *rays* that traverses the phloem, cambium, and xylem (see Figure 19.14).

One distinct challenge that trees face is climate seasonality, which poses risks to their survival during prolonged (seasonal) unfavorable or potentially lethal conditions, such as those encountered during winter months in temperate and boreal regions. To endure dehydration and freezing stress during the winter, trees enter a period of dormancy. The vascular cambium's annual alternation between active growth and dormancy results in the formation of tree rings that record the amount of lateral growth of the tree each year. The molecular mechanisms that control vascular cambium growth during growth–dormancy cycles are poorly understood, though phytohormones such as auxin and gibberellins are thought to play major roles.

Mobile transcription factors pre-pattern the vascular cambium

While the vascular cambium is responsible for perennial growth patterns in woody species, many herbaceous species also have a vascular cambium, though its formation is usually conditional (e.g., in response to stress) or it is very short-lived. Arabidopsis, despite being small and herbaceous, shows notable secondary development in several

organs and has proved very useful for studying the molecular basis for cambial development and wood formation.

Well before secondary development begins, young Arabidopsis roots have cambial precursor cells (the *procambium*) that are situated between the protophloem and protoxylem (**Figure 19.16A**). The divisions that generate procambial cells are directed by mobile PHLOEM EARLY DOF (PEAR) proteins—transcription factors that are expressed in the *protophloem sieve element precursor* cells upon cytokinin induction (**Figure 19.16C**). PEAR proteins then move to cells surrounding the sieve element precursor, activating their division potential and thereby generating procambial cells in the inner vascular cylinder. Auxin and class III homeodomain-leucine

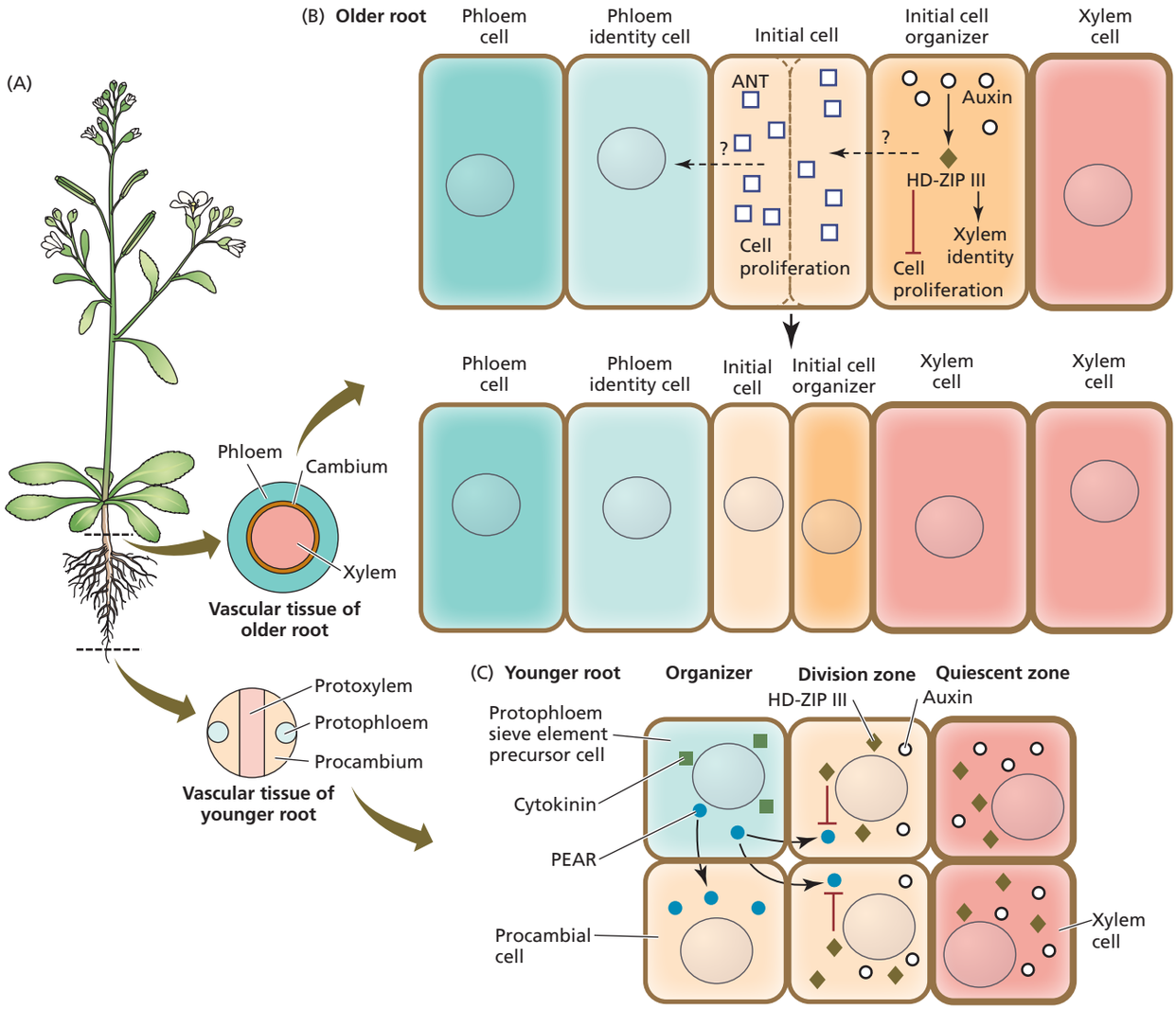


Figure 19.16 Development of cambial tissue in roots. **(A)** In young roots, procambial cells separate protophloem and protoxylem, forming the vascular cylinder. In older roots, the vascular cambium is switched on to produce new phloem and xylem. **(B)** In older root, xylem cells with high concentrations of auxin act as organizers of the vascular cambium, with HD-ZIP III proteins keeping them quiescent. Unknown signals travel from the initial cell organizer to adjacent cells to specify them as initial cells, which express ANT and divide to produce xylem on the inner side and phloem on the outer side. Only the events that lead to xylem production are pictured in the model: the mechanism for phloem production from the bifacial stem cell is unknown, and therefore not shown in the scheme. **(C)** In younger root, PEAR transcription factors travel from the protophloem sieve element precursor cell, which has high concentrations of cytokinin, to neighboring cells, where PEAR promotes cell divisions that will form procambial cells and result in radial growth. The high concentration of auxin in more central cells of the developing vascular cylinder and the presence of PEAR proteins activate the transcription of HD-ZIP III transcription factors, which block PEAR movement into adjacent cells, restricting the division zone. (A and C after S. Wolf and J. U. Lohmann. 2019. *Nature* 565: 433–435; B after O. Smetana et al. 2019. *Nature* 565: 485–489.)

zipper transcription factors (HD-ZIPs) in the procambial cells prevent further movement of PEARs, creating a quiescent zone with fewer cell divisions that corresponds to the protoxylem. The protophloem sieve element precursor cells in the root tip thus serve as the *organizers* of the lateral meristem that generates procambial cells through periclinal cell divisions, pre-patterning radial growth before secondary growth is activated.

Secondary growth occurs in more mature parts of the root, near the root–hypocotyl junction (see Figure 19.16A). Lineage tracing experiments have determined that the initial cell organizers of the mature root vascular cambium are protoxylem cells (**Figure 19.16B**), not protophloem cells as in the young root. As in the root tip, the organizer cells are quiescent and are defined by an auxin response maximum. HD-ZIP III transcription factors are involved in specifying xylem identity and are also responsible for the quiescence of the organizer, but the presence of these transcription factors is not sufficient to establish cambium on its own. In contrast, a local peak in auxin signaling within vascular tissues is sufficient to respecify a new cambium organizer (see Figure 19.16B). This is an important characteristic, as—contrary to organizers in other meristems—the cambium organizer is dynamic. When the xylem cells undergo programmed cell death to differentiate into xylem vessels, the previous organizer is replaced by initial cells that acquire organizer identity, ensuring the maintenance of the vascular cambium (see **WEB TOPIC 19.9**). The role of organizers in phloem cell formation is still poorly understood.

The xylem cells acting as the organizer send mobile signals (see Figure 19.16B, dashed arrow) to adjacent cells, giving them stem cell capabilities. All the cells in physical contact with the xylem (both xylem procambial cells and xylem pole pericycle cells) can become initial cells and generate vascular cambium. The requirement for direct contact with the xylem indicates that the ability to function as an initial cell is determined by cell position and the signals received from the organizer during secondary development. Lineage tracing experiments have confirmed that a single bifacial initial cell in each radial cell file, marked by the expression of transcription factor *AINTEGUMENTA* (*ANT*), is able to divide, alternately producing both phloem and xylem precursors.

The gene networks that control secondary meristems share similarities and differences with those that control the apical meristems

The patterns of growth and development during secondary growth are governed by processes and genes that are similar to those that regulate development of the SAM and RAM (see Chapter 18). This similarity has aided the molecular dissection of the mechanisms controlling secondary growth.

As we saw in Chapter 18, the activities of initials in both the SAM and the RAM depend on the activity of WOXs: *WUSCHEL* (*WUS*) promotes the activity of initials in the SAM (**Figure 19.17A**), while WOX5 contributes to the function of initials in the RAM (**Figure 19.17B**). The vascular cambium appears to rely on a similar mechanism, whereby maintenance of the cambium depends on the activity of *WOX4* (**Figure 19.17C**). *WOX4* activation promotes procambial and cambial cell divisions and is required for cambial meristematic activity (**Figure 19.18A**). In plants with extensive secondary growth, such as poplar trees, plants with deficient *WOX4* expression have narrower cambium and decreased stem girth. Like *WUS* and *WOX5*, *WOX4* is regulated via the interaction of small peptides with a receptor kinase. In this case the receptor kinase is PHLOEM INTERCALATED WITH XYLEM/TDIF RECEPTOR (PXY/TDR) (see Figure 19.18A), which is preferentially expressed in the procambium and vascular cambium, while the CLAVATA3/Embryo Surrounding Region-Related (CLE) peptides are expressed in the phloem. However, unlike in the apical meristems, the expression of CLE peptides promotes *WOX4* activity instead of inhibiting it.

Initial cell maintenance, proliferation, and differentiation also require spatial separation, which is achieved through transcription factors that define the developmental boundaries. In the SAM, one such class of transcription factors with this function is the LATERAL ORGAN BOUNDARIES (LBD) family. LBD genes help establish a boundary between the undifferentiated cells in the SAM and the differentiating tissues of the leaf primordium. Members of the LBD family play a similar role in secondary growth by separating the cambium zone from the differentiating secondary phloem and xylem. One phenotype of *pxy* mutants is that phloem and xylem layers are intercalated (i.e., a layer of phloem can become inserted between two layers of xylem, and vice versa). One of the genes regulated by PXY is *LBD4*, which is also controlled by WOX14 and TARGET OF MONOPTEROS 6 (TMO6) and promotes the formation of phloem (see Figure 19.18A). Expressed at the phloem–procambium boundary, LBD4 is likely to be involved in defining this boundary. Similarly, LBD1, which is expressed primarily in phloem and cambium, has been found to promote the formation of secondary phloem in *Populus*.

Several transcription factors, including WOX4, SHORT VEGETATIVE PHASE (SVP), and PETAL LOSS (PTL), have dual functions in regulating cambial cell proliferation and xylem differentiation. When overexpression of the cambial activator WOX4 was combined with removal of the PTL cambial inhibitor, the resulting double mutant showed enhanced radial growth (**Figure 19.18B**).

Despite the broad similarities between apical and cambial meristems, significant differences also exist.

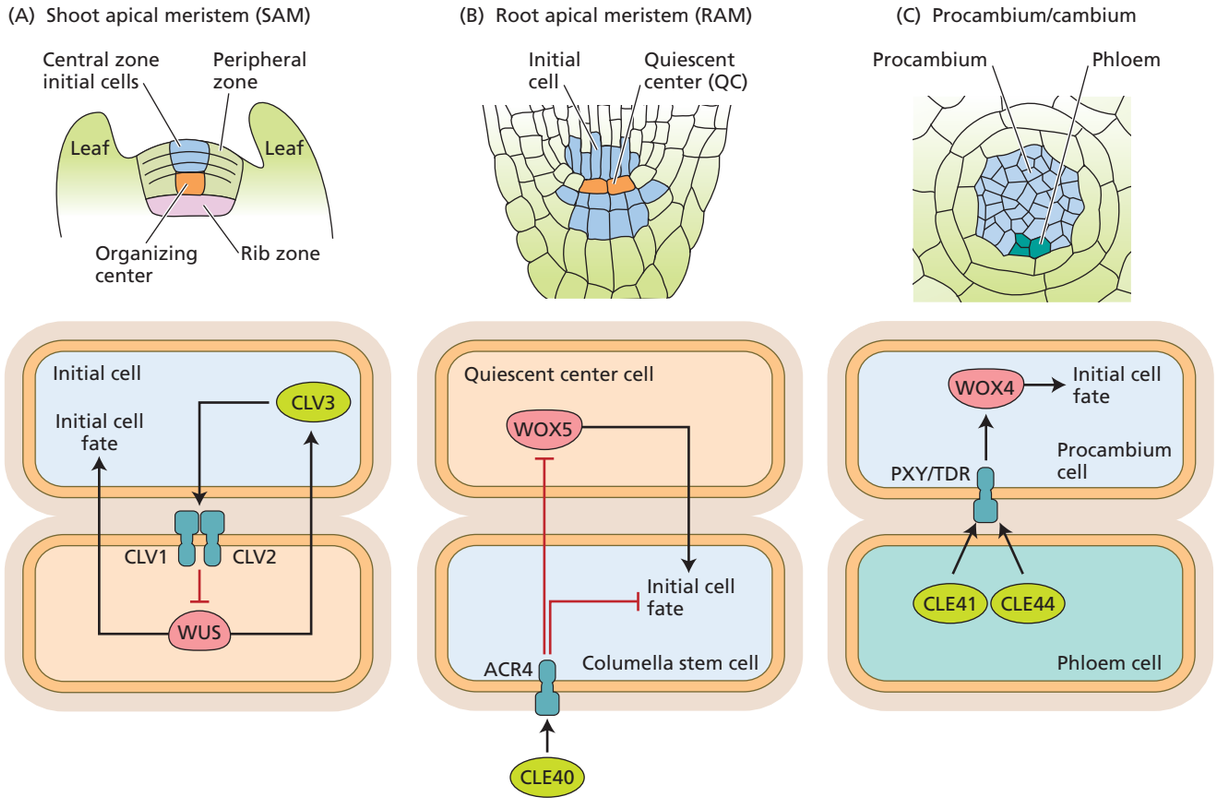
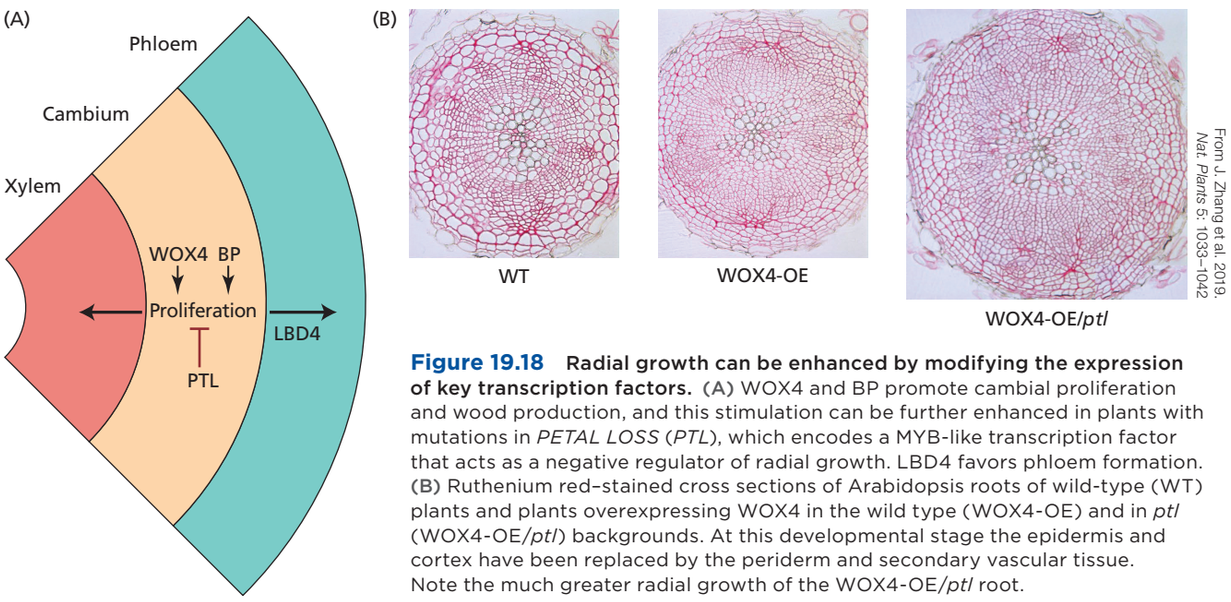


Figure 19.17 **Comparison of three distinct patterning processes that exploit regulatory interactions between small peptides and WOX class transcription factors.** **(A)** WUS promotion of apical initials in the SAM. **(B)** WOX5 promotion of initials in the RAM. **(C)** WOX4 promotion of initials in the vascular cambium. (After S. Miyashima et al. 2013. *EMBO J.* 32: 178–193.)



From J. Zhang et al. 2019. *Nat. Plants* 5: 1033–1042.

Figure 19.18 **Radial growth can be enhanced by modifying the expression of key transcription factors.** **(A)** WOX4 and BP promote cambial proliferation and wood production, and this stimulation can be further enhanced in plants with mutations in *PETAL LOSS* (*PTL*), which encodes a MYB-like transcription factor that acts as a negative regulator of radial growth. LBD4 favors phloem formation. **(B)** Ruthenium red–stained cross sections of Arabidopsis roots of wild-type (WT) plants and plants overexpressing WOX4 in the wild type (WOX4-OE) and in *ptl* (WOX4-OE/*ptl*) backgrounds. At this developmental stage the epidermis and cortex have been replaced by the periderm and secondary vascular tissue. Note the much greater radial growth of the WOX4-OE/*ptl* root.

For example, the two kinase receptor families PXY and ERECTA genetically interact to guide secondary vascular development. However, the interactions between these two gene families are wired differently in stems and hypocotyls, leading to distinct phenotypes in each organ.

Several phytohormones regulate vascular cambium activity and differentiation of secondary xylem and phloem

As with many other processes in plants, hormones play important roles in the regulation of secondary growth. Several hormones provide positional cues and signals for growth and differentiation of different cell types and tissues (**Figure 19.19**). Here we focus on four hormones, because a significant amount of experimental evidence supports their role in the regulation of secondary growth.

Although auxin movements in trees have not been extensively studied, it is assumed that auxin is produced in leaves and apical meristems and transported via polar auxin transport to the stem and vascular cambium. Auxin concentrations have been measured in the vascular cambium and differentiating xylem and phloem in both angiosperm and gymnosperm trees. Similar to the recently identified auxin response maximum that specifies the cambium organizer in Arabidopsis, the peak auxin concentration in trees occurs at the xylem face of the cambium and decreases toward the differentiating xylem and phloem. The decrease is steeper toward the phloem and much more gradual toward the xylem. This auxin concentration gradient across the cambial zone has led to the speculation that the role of auxin in xylem and phloem differentiation is based on a radial morphogen gradient.

The critical role of auxin is also supported by exogenous treatments showing that auxin application in decapitated trees, in which the vascular cambium has become inactive, induces the reactivation of the cambium. More recently, direct manipulation of the auxin response in transgenic poplar trees has shown that auxin sensitivity is critical for both periclinal and anticlinal divisions in the cambium and affects the growth and differentiation of xylem cells.

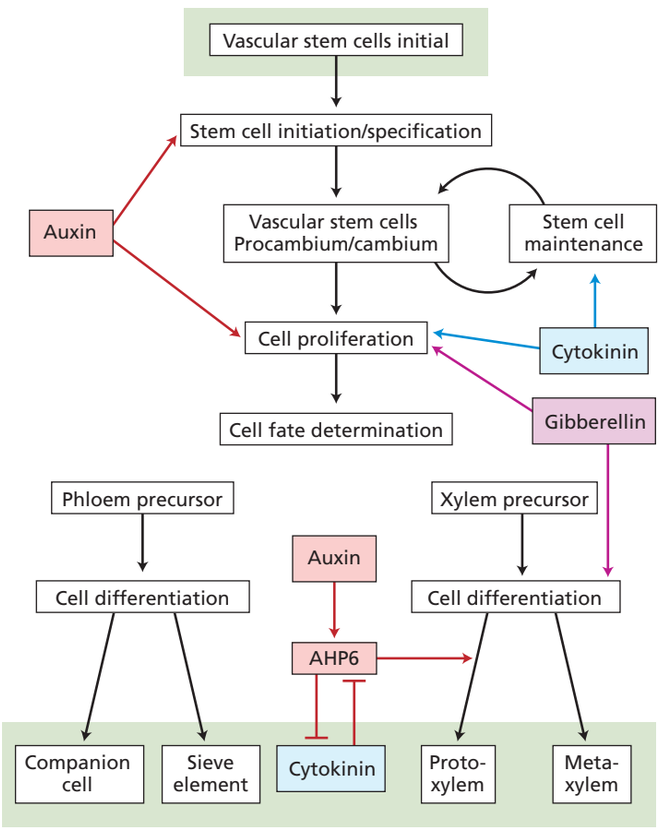


Figure 19.19 Hormones are involved in regulating key stages of secondary vascular tissue development. The protein ARABIDOPSIS HISTIDINE PHOSPHOTRANSFER PROTEIN 6 (AHP6) acts as a cytokinin signaling inhibitor that restricts the domain of cytokinin activity, thus allowing protoxylem differentiation in a spatially specific manner.

Gibberellins also play a major and distinct role in secondary growth. Like auxin, bioactive gibberellins exhibit a concentration gradient across the wood-forming zone, but unlike in auxin, the peak is shifted toward the developing xylem. Exogenous treatment of decapitated seedlings lacking auxin with gibberellins resulted in the activation of cambium cell divisions. However, the dividing cells lost their typical shape and failed to differentiate into xylem. Simultaneous application of auxin and gibberellins prevented the abnormalities observed in the gibberellin treatment alone, and stimulated cambium division to an extent not seen in the gibberellin or auxin treatment alone, suggesting that the two hormones act synergistically (see Figure 19.19).

Metabolic profiling and expression of several genes from the gibberellin biosynthesis pathway indicate that gibberellin metabolism in the wood-forming tissues also involves transport of gibberellin precursors from the phloem laterally through the rays into the differentiating xylem, where they are then converted to bioactive forms. Both exogenous treatments and transgenic manipulations indicate that gibberellins have a positive effect on elongation of fiber cells, which have a structural function in the plant, with thick cell walls and a high length-to-diameter ratio (see Chapter 1). This suggests a role for gibberellins in xylem cell differentiation and growth.

Cytokinins have also been implicated in regulation of secondary growth (see Figure 19.19). A specific decrease in the cytokinin concentration in the cambium zone of transgenic poplar trees led

to significant impairment of radial growth and cell division in the cambium. This result was correlated with cytokinin concentrations peaking on the phloem-side of cambium and the expression in the cambium zone of a gene encoding the cytokinin receptor and the primary response regulator involved in cytokinin signaling. This suggests that cytokinin is an important regulator of cell proliferation in the cambium.

Ethylene is yet another hormone that has been strongly implicated as a regulator of secondary growth. The concentration of the ethylene precursor, 1-aminocyclopropane-1-carboxylic acid (ACC), was found to be high at the cambium zone, but unlike with auxin and gibberellin, no gradient was detected. Ethylene treatment and ACC feeding experiments demonstrated that ethylene is a positive regulator of cambial activity, radial growth, and secondary xylem formation. These results are also consistent with the results of transgenic manipulation of ethylene biosynthesis and action in poplar. Ethylene plays an important role in the formation of **tension wood**, a specialized type of reaction wood in angiosperms formed in tissues experiencing tension caused by stem bending or tilting (see **WEB TOPIC 19.7**). Expression of both ethylene biosynthesis and signaling genes is elevated in the tension wood–forming zone, and ethylene-insensitive transgenic poplars fail to produce tension wood.

The cork cambium gives rise to the outer corky layer called the periderm

Most woody eudicots and gymnosperms develop a secondary cambium known as phellogen that gives rise to the periderm. The periderm replaces the protective functions of the epidermis during secondary growth. Collectively the periderm consists of phellogen, phellem, and phelloderm (**Figure 19.20A**). **Phellem**, or **cork**,

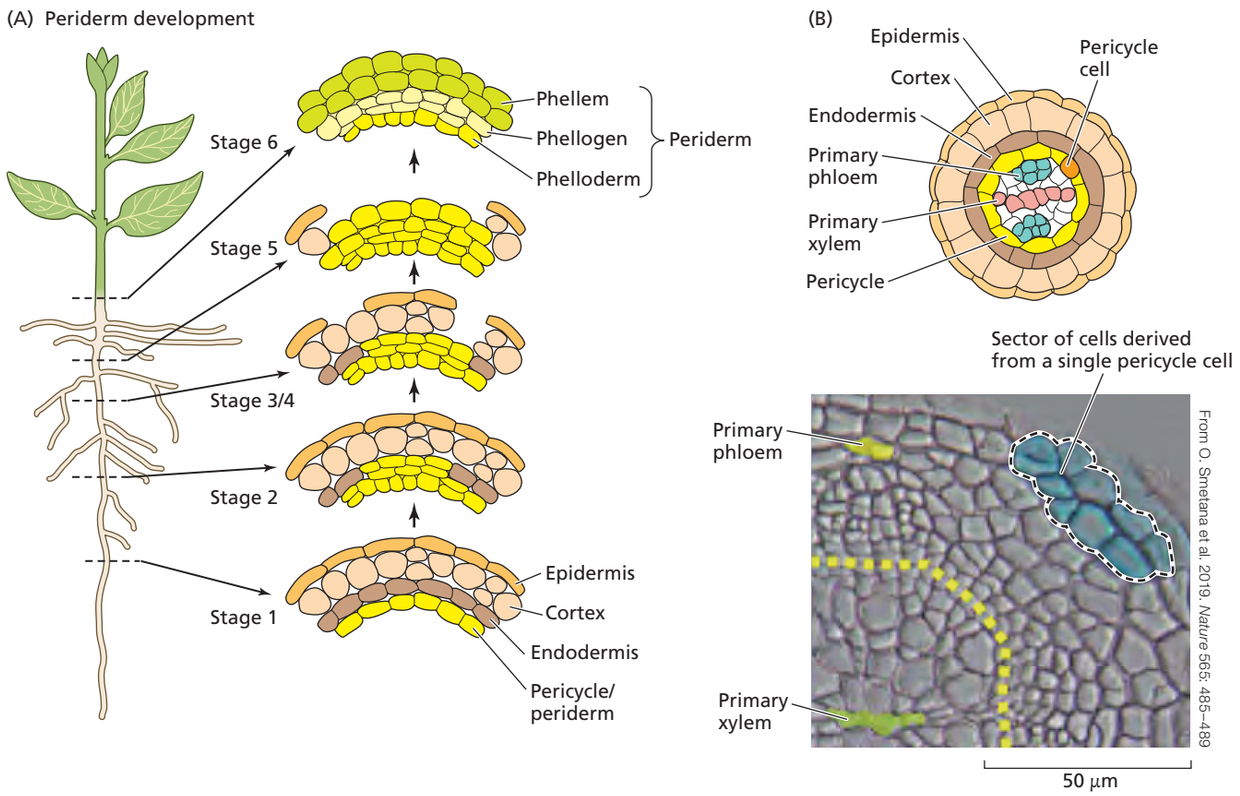


Figure 19.20 **Periderm formation in Arabidopsis roots.** **(A)** Phellogen is a bifacial meristem that produces phellem on the outside and phelloderm on the inside. The periderm is formed from the pericycle, the outer layer of the vascular cylinder (stele). In stage 2, the endodermis undergoes programmed cell death, and in stage 4 it disappears. The cortex and epidermis slough off at stage 3/4 while the tissues are still alive. Stage 5 is defined by a full ring of suberized cells, and in stage 6 the periderm is fully formed and devoid of any epidermal or cortical cells. **(B)** A schematic of a root cross section highlights the initial pericycle cell followed by lineage tracing in the micrography below. Lineage tracing experimentsshow that any pericycle cell can form phellogen. In this case the phellem contains a sector of cells (blue) derived from a single pericycle cell (orange in the upper diagram). The yellow dashed line marks cambium while primary phloem and primary xylem are colored in yellow and green respectively. (After A. Campilho et al. 2020. *Curr. Opin. Plant Biol.* 53: 10–14.)

is the multilayered protective tissue of dead cells with suberized walls, which is formed outward by the phellogen. The **phelloderm** is living parenchyma tissue that is formed inward.

The amount of phellem produced by the phellogen varies among tree species, with cork oak (*Quercus suber*) representing an extreme example that contains a permanent phellogen layer producing cork or phellem indefinitely. The resulting thick, corky layer probably protects the main trunk of cork oak from dehydration in the hot, dry Mediterranean climate. It is also an excellent insulator, with low density and permeability, and is used in construction, clothing, and wine preservation. Cork wine stoppers prevent wine contamination and allow the penetration of a small amount of oxygen, just enough to keep the wine developing while avoiding oxidation. The periderm also protects against pathogen penetration, either by simply thickening the surface barrier with additional layers or by increasing suberization (as in the case of the Casparian strip; see Chapter 4) or the content of other active metabolites.

Although the periderm originates directly under the epidermis in shoots, in roots it has a deeper origin, arising from the pericycle, which is surrounded by three concentric tissue layers (endodermis, cortex, and epidermis). Through lineage tracing experiments, it was possible to confirm that all pericycle cells contribute to the phellogen lineage (**Figure 19.20B**), meaning that xylem pole pericycle cells act as initial cells for both vascular cambium and phellogen. The plasticity of xylem pole pericycle cells is remarkable, since in addition to contributing to both secondary meristems, they also give rise to regenerated calli in plant tissue culture and initiate lateral roots in some species (although lateral roots can sometimes derive from other pericycle cells).

When the xylem pole pericycle cells in the root divide periclinally, increasing the number of layers radially, the endodermal cells start to flatten (see Figure 19.20A, stage 1). On the phloem pole pericycle side, the endodermal cells initiate programmed cell death in stage 2 and then die gradually as the new meristem progresses. In areas where the endodermis has already disappeared and there is suberized (differentiated) phellem, cortical and epidermal cells start to slough off, probably through abscission, since these cells are still alive (stages 3 and 4), resulting in a gradual elimination of the former protective layers. Stage 5 culminates in a full ring of differentiated cork and a complete absence of epidermis, while any leftover cortex and endodermis are eliminated in stage 6. Interestingly, the emergence of lateral roots also involves a combination of programmed cell death and abscission (see Chapter 18). The regulatory networks underlying periderm formation are now being uncovered, which will show if the molecular mechanisms are also conserved.

Bark has diverse protective and storage functions

The outer protective layer of trees is commonly referred to as **bark**. This term, often applied incorrectly to the periderm alone, actually consists of all the tissues outside the vascular cambium, including the functional secondary phloem, crushed nonfunctional secondary phloem, crushed primary phloem, and periderm. Therefore, bark originates from two different meristems, the phellogen and the vascular cambium. Bark tends to peel easily from a tree because the vascular cambium, with its dividing cell layers, is much more fragile than the secondary tissues on either side. Despite the importance of this array of tissues to safeguard phloem and protect woody plants from biotic and abiotic threats, the composition of bark and the genetic pathways controlling its formation are not well understood, mainly because it is highly diverse among different species. For instance, in some trees, such as oaks, the bark is thick and cracked, while in others, such as cherry trees and birch, it is smooth. Bark can also have different colors, even among closely related tree species.

Bark also varies in the types and amounts of secondary metabolites it contains. While many of these are produced by the plant as a defense mechanism, humans have also found them to be useful. Classic examples of bark-derived drugs are the antiseptic and anti-inflammatory salicylic acid (from willow), the antimalarial quinine (from cinchona), and the chemotherapy medication paclitaxel (from Pacific yew). A recent study analyzed gene expression and metabolites in the barks of different species of the Betulaceae family and found that betulin, the triterpene responsible for the white color of silver birch, was much less abundant in other species of the family, such as black alder. The study also highlighted the importance of phellem for producing secondary metabolites for plant defense, since many of the relevant metabolic pathways function in the formation of this tissue.

Bark can also function as a storage organ. Growth seasonality imposes a significant challenge for perennial plants with respect to nutrient use, storage, and recycling. Although all plant species have mechanisms to recycle, store, and remobilize nutrients during the growing season, the seasonal cycling of nitrogen, the most abundant macronutrient, is a hallmark of the perennial life habit. For example, nitrogen from the senescing leaves is stored in the form of **bark storage proteins** (**BSPs**) in small vacuoles of the phloem parenchyma (inner bark). These proteins are synthesized early in the autumn but are rapidly mobilized during the spring as growth is reinitiated.

Epicormic buds covered by bark can sprout after forest fires

In Section 19.2 we made the distinction between branch roots, which arise internally in the pericycle, and branch shoots, which arise from external buds in the axils of

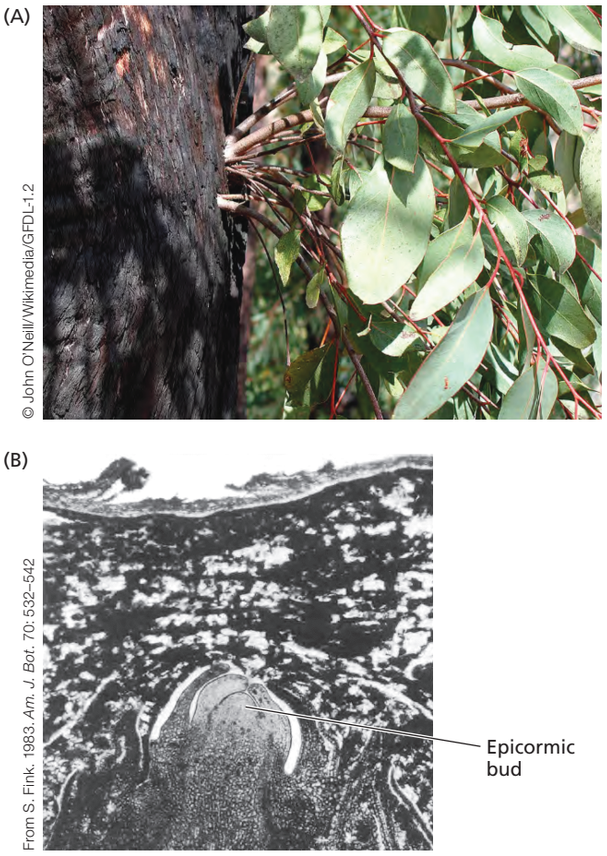


Figure 19.21 **Epicormic branches and bud.** **(A)** Eucalyptus tree 2 years after the 2003 Eastern Victoria alpine bushfires in Australia. **(B)** Epicormic bud of *Tilia platyphyllos*, covered by bark.

leaves. However, there are some types of branch shoots that can arise internally from **epicormic buds** located beneath the bark of tree trunks. These are called *epicormic* branches, from the Greek words for "on the trunk." The sprouting of epicormic branches and "stool shoots," lateral shoots produced in the absence of a terminal bud, on the trunks and stumps of old trees is widespread among angiosperms and conifers, and plays an important role in shaping tree architecture. This is especially true for trees adapted to fire-prone ecosystems, such as eucalyptus trees growing in the grasslands and forests of Australia. Eucalyptus trees have the capacity to produce numerous epicormic buds that sprout in the aftermath of a severe burn (**Figure 19.21A**). Unlike axillary buds, epicormic buds often survive such fires because they are insulated from the intense heat by the tree's thick layer of bark (**Figure 19.21B**).

Epicormic branches can arise from two types of epicormic buds: **preventitious buds**, which are axillary buds that have remained dormant during secondary growth and have become covered by bark, and **adventitious buds**, which differentiate de novo from mature stem tissue or from callus tissue at wound sites. An example of the latter are redwood burls that form on aerial parts of the trunk in response to injury. In contrast, the redwood burls that form at the base of the tree arise from large clusters of axillary buds that begin forming in the cotyledonary axils and then spread to the axils of the leaves above. This induces swelling and secondary growth, resulting in a basal burl. These basal burls are filled with clusters of preventitious epicormic buds, which can regenerate new trees following a fire or after the main trunk has been harvested.

Summary

Much of the diversity of plant form comes from their ability to initiate and pattern new organs such as branches or lateral roots throughout their lifetime. The organs are initiated from meristems that are established and maintained in similar ways as those associated with primary development seen in Chapter 18. The trigger to produce a new organ requires the integration of environmental and internal signals through the action of mobile signals in a way that is comparable to the mechanisms that pattern the cell types, tissues, and organ shapes during primary development. Specific signaling pathways have also been repurposed repeatedly throughout evolution to control different aspects of development. For example, meristematic tissues in the root, shoot, and vascular cambium all use similar receptor kinase–WOX feedback loops to regulate initial cell number and position, and the hormone auxin patterns vasculature, positions lateral organs, and regulates branch outgrowth, among many other functions. Overall, this integration of mobile signaling molecules with conserved local signaling pathways allows plants to make decentralized developmental decisions and to adjust their development rapidly to a changing environment while also maintaining robust organ shapes and tissue patterns.

19.1 Shoot Branching and Architecture

- In seed plants, shoot architecture is based on repeating units called phytomers, consisting of an internode, a node, a leaf, and an axillary bud (**Figure 19.1**).
- There is strong experimental evidence that auxin from the shoot tip and strigolactones from the root maintain apical dominance (**Figures 19.3–19.5**).
- Cytokinins break apical dominance and promote axillary dominance (**Figure 19.5**).
- Environmental signals can override default hormonal signals to shape vegetative architecture. For example, the nitrogen status of the plant alters branching.

(*Continued*)

Summary (*continued*)

19.2 Root Branching and Architecture

- There are two types of postembryonic roots: lateral, or branch, roots arising from existing roots, and adventitious roots arising from non-root tissues.
- Lateral root primordia arise from the xylem pole pericycle cells (**Figures 19.8, 19.9**).
- An auxin clock in the oscillation zone primes the xylem pole pericycle cells to become lateral root founder cells (**Figure 19.10**).
- Shoot and root systems exhibit different architectures based on branching patterns and gravitropic setpoint angles, which vary with species and the environment.
- Monocot roots systems are composed largely of seminal and crown roots, while eudicot root systems are derived largely from the primary root (taproot) (**Figures 19.11, 19.12**).
- Gravitropic setpoint angles are fundamental to plant architecture and are controlled by IGT transcription factors (**Figure 19.13**).
- Root system architecture is highly sensitive to heterogeneity in the aqueous environment.
- Mycorrhizal relationships among root systems are ubiquitous and involve nutrient transport along source–sink gradients.

19.3 Secondary Growth

- Growth in width is accomplished by the vascular cambium and cork cambium, which are secondary bifacial meristems that give rise to secondary vascular tissue and the periderm, respectively (**Figures 19.14, 19.15**).
- Mobile transcription factors establish the pre-pattern of the vascular cambium (**Figure 19.16**).
- The protophloem sieve element precursor cells are the organizers of a lateral meristem within the root tip that generates procambial cells through periclinal cell divisions, thus pre-patterning secondary growth (**Figure 19.16**).
- In more mature roots, the cambial initial cell organizer has xylem identity and is characterized by quiescence and an auxin maximum (**Figure 19.16**).
- Any cell type in close proximity to the xylem can become a cambial initial cell, whereas the periderm originates in the pericycle (**Figure 19.16, 19.20**).
- WOX transcription factors and small peptide signaling modules are used in several contexts to promote initial cell identity in the SAM and RAM, as well as maintenance of the vascular cambium (**Figure 19.17**).
- Radial growth and wood formation can be manipulated by altering the expression of several key transcription factors (**Figure 19.18**).
- Auxin, gibberellins, cytokinins, and ethylene regulate vascular cambium activity and differentiation of secondary vascular tissues (**Figure 19.19**).
- Periderm arises from pericycle. In the process, endodermis undergoes PCD and cortex and epidermis break (**Figure 19.20**).
- Tree architecture can be regenerated after forest fires by the activation of long-dormant epicormic buds (**Figure 19.21**).
- Vascular cambium activity is sensitive to stimuli (e.g., gravity, weight) that ultimately influence wood properties.

Web Material

- **WEB TOPIC 19.1 Plant Architecture, Crop Yields, and Environmental Sustainability** A major genetic basis of the Green Revolution was semidwarf mutations in cereal food crops that altered shoot architecture, either as the result of reduced gibberellin hormone concentrations or signaling.
- **WEB TOPIC 19.2 Dichotomous Branching** The earliest type of branching in vascular plants was dichotomous branching, characteristic of early vascular plants and some modern angiosperms.
- **WEB TOPIC 19.3 Model of Auxin-Regulated Branching.** A model that describes the relationships among auxin flux, the concentration of PIN proteins, and the activation of lateral buds can explain experimental observations.
- **WEB TOPIC 19.4 Advances in Root System Phenotyping** Modern root system image capture methods include two-dimensional (2D) and three-dimensional (3D) imaging techniques.
- **WEB TOPIC 19.5 An Auxin Clock Model for the Spacing of Prebranch Sites** According to the auxin clock model, cells migrating through the root oscillation zone are exposed to fluctuating levels either of auxin activity or auxin concentration.
- **WEB TOPIC 19.6 Evolution of Secondary Growth** Judging from the fossil record, secondary growth arose independently several times in many lineages, predating modern seed plants.
- **WEB TOPIC 19.7 Reaction Wood** Trees can form a specialized type of wood called "reaction wood" in response to gravitational or water stress.
- **WEB TOPIC 19.8 Secondary Growth in Lianas** Variant secondary growth patterns have arisen in lianas as adaptations for climbing tall trees.
- **WEB TOPIC 19.9 Organizers of Root Vascular Cambium** Organizer cells near the root tip promote cell divisions in nearby cells. In this case the organizers are xylem cells that induce neighboring initial cells to generate xylem daughter cells toward the root interior and periphery.

For more study aids, go to oup.com/he/taiz7e.

Suggested Reading

Aloni, R. (2021) *Vascular Differentiation and Plant Hormones.* Springer Nature, Switzerland.

Alonso-Serra, J., Shi, X., Peaucelle, A., Rastas, P., Bourdon, M., Immanen, J., Takahashi, J., Koivula, H., Eswaran, G., Muranen, S., Help, H., Smolander, O.-P., Su, C., Safronov, O., Gerber, L., Salojärvi, J., Hagqvist, R., Mähönen, A. P., Helariutta, Y., and Nieminen, K. (2020) ELIMÄKI Locus is required for vertical proprioceptive response in birch trees. *Curr. Biol.* 30: 589–599.

Bao, Y., Aggarwal, P., Robbins, N. E., Sturrock, C. J., Thompson, M. C., Tan, H. Q., Tham, C., Duan, L., Rodriguez, P. L., Vernoux, T., Mooney, S. J., Bennett, M. J., and Dinneny, J. R. (2014) Plant roots use a patterning mechanism to position lateral root branches toward available water. *Proc. Natl. Acad. Sci. USA* 111: 9319–9324.

Barlow, P. W. (1994) Evolution of structural initial cells in apical meristems of plants. *J. Theor. Biol.* 169: 163–177.

Campilho, A., Nieminen, K., and Ragni, L. (2020) The development of the periderm: the final frontier between a plant and its environment. *Curr. Opin. Plant Biol. Growth Dev.* 53: 10–14.

Chery, J. G., Pace, M. R., Acevedo-Rodríguez, P., Specht, C. D., and Rothfels, C. J. (2020) Modifications during early plant development promote the evolution of nature's most complex woods. *Curr. Biol.* 30: 237–244.

Di Mambro, R., De Ruvo, M., Pacifici, E., Salvi, E., Sozzani, R., Benfey, P. N., Busch, W., Novak, O., Ljung, K., Di Paola, L., Marée, A. F. M., Costantino, P., Grieneisen, V. A., and Sabatini, S. (2017) Auxin minimum triggers the developmental switch from cell division to cell differentiation in the Arabidopsis root. *Proc. Natl. Acad. Sci. USA* 114: E7641–E7649.

Hirakawa, Y., Kondo, Y., and Fukuda, H. (2010) TDIF Peptide signaling regulates vascular initial cell proliferation via the WOX4 Homeobox gene in Arabidopsis. *Plant Cell* 22: 2618–2629.

Miyashima, S., Roszak, P., Sevilem, I., Toyokura, K., Blob, B., Heo, J., Mellor, N., Help-Rinta-Rahko, H., Otero, S., Smet, W., Boekschoten, M., Hooiveld, G., Hashimoto, K., Smetana, O., Siligato, R., Wallner, E.-S., Mähönen, A. P., Kondo, Y., Melnyk, C. W., Greb, T., Nakajima, K., Sozzani, R., Bishopp, A., De Rybel, B., and Helariutta, Y. (2019) Mobile PEAR transcription factors integrate positional cues to prime cambial growth. *Nature* 565: 490–494.

Prusinkiewicz, P., Crawford, S., Smith, R. S., Ljung, K., Bennett, T., Ongaro, V., and Leyser, O. (2009) Control of bud activation by an auxin transport switch. *Proc. Natl. Acad. Sci. USA* 106: 17431–17436.

Risopatron, J. P. M., Sun, Y., and Jones, B. J. (2012) The vascular cambium: Molecular control of cellular structure. *Protoplasma* 247: 145–161.

Smetana, O., Mäkilä, R., Lyu, M., Amiryousefi, A., Sánchez Rodríguez, F., Wu, M.-F., Solé-Gil, A., Leal Gavarrón, M., Siligato, R., Miyashima, S., Roszak, P., Blomster, T., Reed, J. W., Broholm, S., and Mähönen, A. P. (2019) High levels of auxin signaling define the stem-cell organizer of the vascular cambium. *Nature* 565: 485–489.

Uga, Y., Sugimoto, K., Ogawa, S., Rane, J., Ishitani, M., Hara, N., Kitomi, Y., Inukai, Y., Ono, K., Kanno, N., Inoue, H., Takehisa, H., Motoyama, R., Nagamura, Y., Wu, J., Matsumoto, T., Takai, T., Okuno, K., and Yano, M. (2013) Control of root system architecture by DEEPER ROOTING 1 increases rice yield under drought conditions. *Nat. Genet.* 45: 1097–102.

Verna, C., Ravichandran, S. J., Sawchuk, M. G., Linh, N. M., and Scarpella, E. (2019) Coordination of tissue cell polarity by auxin transport and signaling. *eLife* 8: 51061.

Wu, K., Wang, S., Song, W., Zhang, J., Wang, Y., Liu, Q., Yu, J., Ye, Y., Li, S., Chen, J., Zhao, Y., Wang, J., Wu, X., Wang, M., Zhang, Y., Liu, B., Wu, Y., Harberd, N. P., and Fu, X. (2020) Enhanced sustainable green revolution yield via nitrogen-responsive chromatin modulation in rice. *Science* 367: eaaz2046.

Zhang, J., Eswaran, G., Alonso-Serra, J., Kucukoglu, M., Xiang, J., Yang, W., Elo, A., Nieminen, K., Damén, T., Joung, J.-G., Yun, J.-Y., Lee, J.-H., Ragni, L., Barbier de Reuille, P., Ahnert, S. E., Lee, J.-Y., Mähönen, A. P., and Helariutta, Y. (2019) Transcriptional regulatory framework for vascular cambium development in Arabidopsis roots. *Nat. Plants* 5: 1033–1042.

20 The Control of Flowering and Floral Development



schankz/Shutterstock

Most people look forward to the spring season and the profusion of flowers it brings. Many vacationers carefully time their travels to coincide with specific blooming seasons: *Citrus* along Blossom Trail in southern California, tulips in Holland. In Washington, DC, and throughout Japan, the cherry blossoms are received with spirited ceremonies. As spring progresses into summer, summer into fall, and fall into winter, wildflowers bloom at their appointed times. Flowering at the correct time of year is crucial for the reproductive fitness of the plant; plants that are cross-pollinated must flower in synchrony with other individuals of their species as well as with their pollinators at the time of year that is optimal for seed set.

Although the strong correlation between flowering and seasons is common knowledge, the phenomenon poses fundamental questions that we address in this chapter:

- How do plants keep track of the seasons of the year and the time of day?
- Which environmental signals influence flowering, and how are those signals perceived?
- How are environmental signals transduced to bring about the developmental changes associated with flowering?

In Chapter 19 we discussed the role of the root and shoot apical meristems in vegetative growth and development. The transition to flowering involves major changes in the pattern of morphogenesis and cell differentiation at the shoot apical meristem. Ultimately, as we will see, this process leads to the production of the floral organs—sepals, petals, stamens, and carpels.

20.1 Floral Evocation: Integrating Environmental Cues

A particularly important developmental decision during the plant life cycle is when to flower. The process by which the shoot apical meristem becomes committed to forming flowers is termed **floral evocation**. Delaying this commitment to flower will increase the carbohydrate reserves that will be available for mobilization, allowing more and better-provisioned seeds to mature. Delaying flowering, however, also potentially increases the danger that the plant will be eaten, killed by abiotic stress, or outcompeted

by other plants before it reproduces. Reflecting this, plants have evolved an extraordinary range of reproductive adaptations—for example, annual versus perennial life cycles.

Annual plants such as groundsel (*Senecio vulgaris*) may flower within a few weeks after germinating. But trees may grow for 20 or more years before they begin to produce flowers. Across the plant kingdom, different species flower at a wide range of ages, indicating that the age, or perhaps the size, of the plant is an internal factor controlling the switch to reproductive development.

The case in which flowering occurs strictly in response to internal developmental factors, independently of any particular environmental condition, is referred to as *autonomous regulation*. In species that exhibit an absolute requirement for a specific set of environmental cues in order to flower, flowering is considered to be an *obligate* or *qualitative* response. If flowering is promoted by certain environmental cues, but will eventually occur in the absence of such cues, the flowering response is *facultative* or *quantitative*. A species with a facultative flowering response, such as Arabidopsis, relies on both environmental and autonomous signals to promote reproductive growth.

Photoperiodism and vernalization are two of the most important mechanisms underlying seasonal responses. Photoperiodism (see Chapter 16) is a response to the length of day or night; vernalization is the promotion of flowering by prolonged cold temperature. Other signals, such as light quality, ambient temperature, and abiotic stress, are also important external cues for plant development.

The evolution of both internal (autonomous) and external (environment-sensing) control systems enables plants to precisely regulate flowering so that it occurs at the optimal time for reproductive success. For example, in many populations of a particular species, flowering is synchronized, which favors cross-pollination. Flowering in response to environmental cues also helps ensure that seeds are produced under favorable conditions, particularly with respect to water and temperature. However, this makes plants especially vulnerable to rapid climate change, such as global warming, which can alter the regulatory networks that govern floral timing (see **WEB TOPIC 20.1**).

20.2 The Shoot Apex and Phase Changes

All multicellular organisms pass through a series of more or less defined developmental stages, each with its characteristic features. In humans, infancy, childhood, adolescence, and adulthood represent four general stages of development, with puberty as the dividing line between the nonreproductive and the reproductive phases. Similarly, plants pass through distinct developmental phases. However, unlike animals, plants continually produce new organs from the shoot apical meristem. This ability enables plants to synchronize their development with a changing environment by controlling the timing of phase transitions. In addition, the plant must integrate information from the environment as well as autonomous signals to maximize its reproductive fitness. This section describes the major pathways that control these decisions.

Plants progress through three developmental phases

Postembryonic development in plants can be divided into three phases:

1. The juvenile phase
2. The adult vegetative phase
3. The adult reproductive phase

The transition from one phase to another is called **phase change**.

The primary distinction between the juvenile and the adult vegetative phases is that the latter has the ability to form reproductive structures: flowers in angiosperms, cones in gymnosperms. However, flowering, which represents the expression of the reproductive competence of the adult phase, often depends on specific environmental and developmental signals. Thus, the absence of flowering itself is not a reliable indicator of juvenility.

The transition from juvenile to adult is frequently accompanied by changes in vegetative characteristics, such as leaf morphology, phyllotaxy (the arrangement of leaves on the stem), thorniness, rooting capacity, and leaf retention in deciduous plants such as English ivy (*Hedera helix*) (**Figure 20.1**; see also **WEB TOPIC 20.2**). Such changes are most evident in woody perennials, but they are apparent in many herbaceous species as well. Unlike the abrupt transition from the adult vegetative phase to the reproductive phase, the transition from juvenile to adult vegetative is usually gradual, involving intermediate forms.

Juvenile tissues are produced first and are located at the base of the shoot

The time sequence of the three developmental phases results in a spatial gradient of juvenility along the shoot axis. Because growth in height is restricted to the apical meristem, the juvenile tissues and organs, which form first, are located at the base of the shoot. In rapidly flowering herbaceous species, the juvenile phase may last only a few days, and few juvenile structures are produced. In contrast, woody species have a more prolonged juvenile phase, in some cases lasting 30 to 40 years (**Table 20.1**). In these cases the juvenile structures can account for a significant portion of the mature plant.

Once the meristem has switched to the adult phase, only adult vegetative structures are produced, culminating in flowering. The adult and reproductive phases



Figure 20.1 **Juvenile and adult forms of English ivy (*Hedera helix*).** The juvenile form has lobed palmate leaves arranged alternately, a climbing growth habit, and no flowers. The adult form has entire ovate leaves arranged in spirals, an upright growth habit, and flowers that develop into fruits.

are therefore located in the upper and peripheral regions of the shoot.

Attainment of a sufficiently large size appears to be more important than the plant's chronological age in determining the transition to the adult phase. Conditions that retard growth, such as mineral deficiencies, low light, water stress, defoliation, and low temperature, tend to prolong the juvenile phase or even cause reversion to juvenility of adult shoots. In contrast, conditions that promote vigorous growth accelerate the transition to the adult phase. When growth is accelerated, exposure to the correct flower-inducing treatment can result in flowering.

Although plant size seems to be the most important factor, it is not always clear which specific component associated with size is critical. In some *Nicotiana* species, it appears that plants must produce a certain number of leaves to transmit a sufficient amount of the floral stimulus to the apex.

Once the adult phase has been attained, it is relatively stable and is maintained during vegetative propagation or grafting. For example, cuttings taken from the basal region of mature plants of English ivy develop into juvenile plants, while those taken from the tip develop into adult plants. When scions were taken from the base of a flowering silver birch (*Betula verrucosa*) and grafted onto seedling rootstocks, there were no flowers on the grafts for the first 2 years. In contrast, grafts taken from the top of the mature tree flowered freely.

The term *juvenility* has different meanings for herbaceous and woody species. Whereas juvenile herbaceous meristems flower readily when grafted onto flowering adult plants (see **WEB TOPIC 20.3**), juvenile woody meristems generally do not. Juvenile woody meristems are thus said to lack the competence to flower (see **WEB TOPIC 20.4**).

TABLE 20.1 **Length of juvenile period in some woody plants**

Species	Length of juvenile period
Rose (*Rosa* [hybrid tea])	20–30 days
Grape (*Vitis* spp.)	1 year
Apple (*Malus* spp.)	4–8 years
Citrus spp.	5–8 years
English ivy (*Hedera helix*)	5–10 years
Redwood (*Sequoia sempervirens*)	5–15 years
Sycamore maple (*Acer pseudoplatanus*)	15–20 years
English oak (*Quercus robur*)	25–30 years
European beech (*Fagus sylvatica*)	30–40 years

Source: After J. R. Clark. 1983. *J. Arboriculture* 9: 201–205

Phase changes can be influenced by nutrients, gibberellins, and other signals

The transition at the shoot apex from the juvenile to the adult phase can be affected by transmissible factors from the rest of the plant. In many plants, exposure to low-light conditions prolongs juvenility or causes reversion to juvenility. A major consequence of a low-light regime is a reduction in the supply of carbohydrates to the apex; thus, carbohydrate supply, especially sucrose, may play a role in the transition between juvenility and maturity. Carbohydrate supply as a source of energy and raw material can affect the size of the apex. For example, in the florist's chrysanthemum (*Chrysanthemum morifolium*), flower primordia are not initiated until a minimum apex size has been reached. In Arabidopsis, carbohydrate status in the plant is transmitted by the small signaling molecule trehalose 6-phosphate, a disaccharide. Plants lacking trehalose 6-phosphate exhibit very delayed flowering, even under inductive conditions, and trehalose 6-phosphate activates flowering pathways in both the leaves and shoot apex.

The apex receives a variety of hormonal and other factors from the rest of the plant in addition to carbohydrates and other nutrients. Experimental evidence shows that the application of gibberellins causes reproductive

structures (cones) to form in young, juvenile plants of several conifer families. The involvement of endogenous gibberellins in the control of reproduction is also indicated by the fact that other treatments that accelerate cone production in pines (e.g., root removal, water stress, and nitrogen starvation) often also result in a buildup of gibberellins in the plant.

A major class of conserved molecules that control phase transitions in plants is the microRNAs. MicroRNAs are small noncoding RNA molecules that target the mRNA transcripts of other genes through short regions of sequence homology, thus interfering with their function (see Chapter 3). In Arabidopsis and many other plants, including trees, the microRNA156 (miR156) is key for controlling the juvenile-to-adult transition (**Figure 20.2**). Some of the target genes of miR156 promote the transition to flowering. The level of miR156 decreases over time, and once it falls below a threshold the targeted genes are expressed and phase change becomes possible. Overexpressing the microRNA is sufficient to greatly delay phase changes in Arabidopsis and poplar trees.

In addition to miR156, the microRNA172 (miR172) has been implicated in phase transitions in Arabidopsis (see Figure 20.2). miR172 levels increase during development as miR156 levels decline. In contrast to miR156, the abundance of which is controlled by plant age, miR172 appears to be under photoperiodic control (discussed in Section 20.4). The targets of miR172 include several transcripts that encode transcription factors involved in the repression of flowering. Thus, miR172 promotes the phase change from adult vegetative growth to reproductive growth.

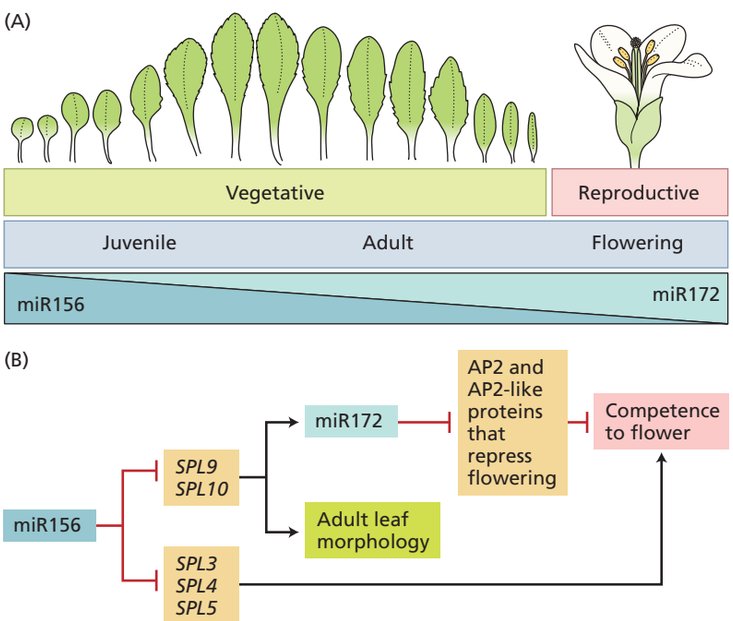


Figure 20.2 **Regulation of phase change in Arabidopsis by microRNAs.** **(A)** During the earliest stages of development, the level of miR156 is very high and the level of miR172 is very low, promoting the juvenile vegetative growth phase. Juvenile leaves are small and round, and exhibit trichomes only on their adaxial side. Over time, the level of miR156 declines, and the level of miR172 increases, promoting the transition to the adult vegetative phase. Adult vegetative leaves are larger and more elongated, with abaxial trichomes. **(B)** The decline in the level of miR156 allows the expression of the *SQUAMOSA PROMOTER BINDING PROTEIN-LIKE 9* (*SPL9*) and *SPL10* genes, which up-regulate miR172. miR172 down-regulates six AP2-like transcription factors that repress flowering. Release from repression, combined with up-regulation of the flower-promoting genes *SPL3–5*, makes the plant competent to flower, allowing the transition to flowering. The decline in adult leaf size reflects a gradual shift in the allocation of sugars from the leaves to the developing reproductive structures.

20.3 Circadian Rhythms: The Clock Within

Organisms are normally subjected to daily cycles of light and darkness, and both plants and animals often exhibit rhythmic behavior in association with these changes. A 24-h rhythm consisting of a light period followed by a dark period is called a **diel rhythm**. Examples of diel rhythms include leaf and petal movements (day and night positions), stomatal opening and closing, growth and sporulation patterns in fungi (e.g., *Pilobolus* and *Neurospora*), time of day of pupal emergence (the fruit fly *Drosophila*), and activity cycles in rodents, as well as daily changes in the rates of metabolic processes such as photosynthesis and respiration.

When organisms are transferred from daily light–dark cycles to continuous darkness or continuous light, many of these rhythms continue to be expressed, at least for several days. Under such uniform conditions the period of the rhythm is close to 24 h, and consequently the term *circadian rhythm* (from the Latin *circa*, "about," and *diem*, "day") is applied (see Chapter 4). Because they continue in a constant light or dark environment, these circadian rhythms cannot be direct responses to the presence or absence of light but must be based on an internal pacemaker, often called an endogenous oscillator.

A single oscillator mechanism can be tied to multiple downstream processes at different times. Endogenous oscillators are thought to be regulated by the interactions of four sets of genes expressed in the dawn, morning, afternoon, and evening hours. Light may augment the amplitude of the oscillation by activating the morning and evening genes (**Figure 20.3**).

(A)

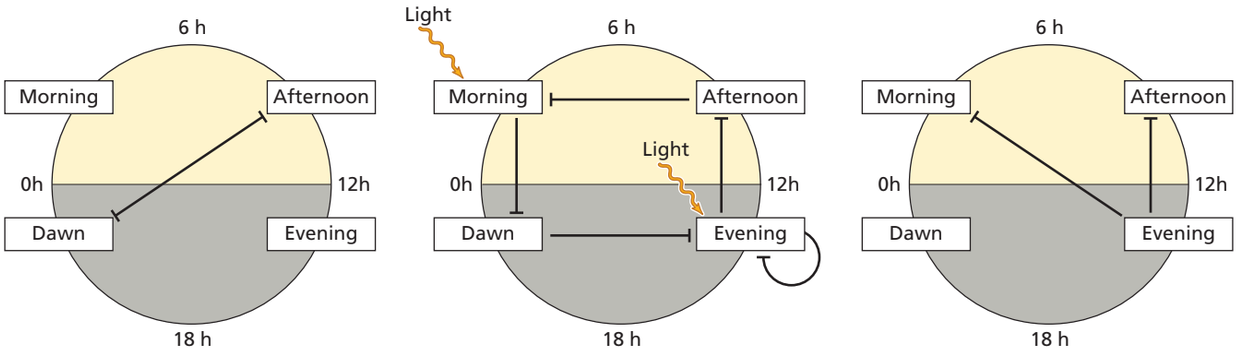
Mutual inhibition of Dawn and Afternoon genes. This motif is known as a "toggle switch." When one of the pair is high, the other is low. This motif alone does not oscillate.

(B)

The switch is located within a four-member ring, in which each set of genes turns off the set expressed before. In steady state, the ring alone does not oscillate either: Diagonally opposite pairs are on or off. This outcome is prevented by (A).

(C)

The Evening genes turn off all genes except Dawn genes in the early night, "clearing the decks" before Dawn gene expression starts again in the mid- to late night.

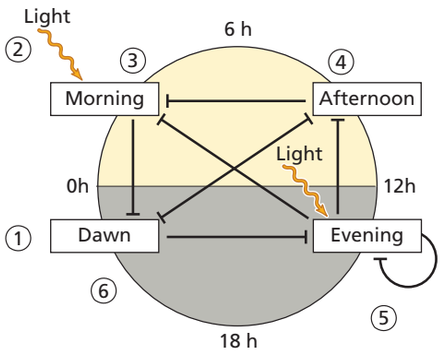


(D) The daily cycle, step by step

1. Dawn gene expression starts in the mid- to late night, continuing repression of Afternoon genes (A).

2. Light activates Morning and Evening gene expression. Evening genes are repressed by Dawn genes (B), so only Morning genes are expressed.

3. Morning genes turn off Dawn genes (B), allowing expression of Afternoon genes (A) and Evening genes (B). Ongoing light activation of Evening genes also helps.



4. Afternoon genes turn off Morning genes (B) and also keep Dawn genes off (A).

5. Evening genes turn off all genes except Dawn genes (C).

6. Dawn genes are expressed again in the late night.

Figure 20.3 **Model for the endogenous circadian oscillator.** The circles represent a 24-h cycle, marked at 6-h intervals (0 h, 6 h, 12 h, and 18 h); daylight is from 0 h to 12 h. (Based on O. Purcell et al. 2010. *J. R. Soc. Interface* 7: 1503–1524; and Andrew Millar, personal communication.)

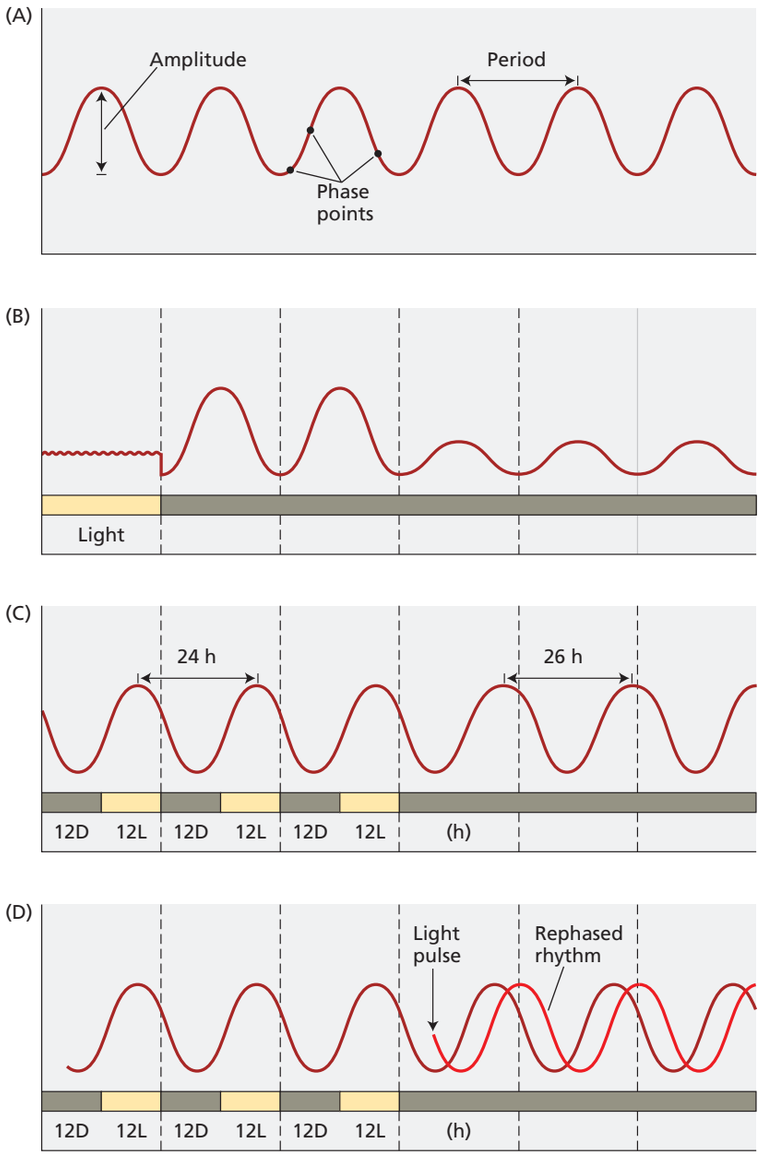
The endogenous oscillator is coupled to a variety of physiological processes, such as leaf movement or photosynthesis, and it maintains the rhythm. For this reason, the endogenous oscillator can be considered the clock mechanism, and the physiological functions that are being regulated, such as leaf movements or photosynthesis, are sometimes referred to as the hands of the clock.

Circadian rhythms exhibit characteristic features

Circadian rhythms arise from cyclic phenomena that are defined by three parameters:

1. **Period** is the time between comparable points in the repeating cycle. Typically the period is measured as the time between consecutive maxima (peaks) or minima (troughs) (**Figure 20.4A**).
2. **Phase** is any point in the cycle that is recognizable by its relationship to the rest of the cycle. The most obvious phase points are the peak and trough positions.
3. **Amplitude** is usually considered to be the distance between peak and trough. The amplitude of a biological rhythm can often vary while the period remains unchanged (as, for example, in **Figure 20.4B**).

In constant light or darkness, rhythms depart from an exact 24-h period. The rhythms then drift in relation to solar time, either gaining or losing time depending on whether the period is shorter or longer than 24 h. Under natural conditions, the endogenous oscillator is **entrained** (synchronized) to a true 24-h period by environmental signals, the most important of which are



A typical circadian rhythm. The period is the time between comparable points in the repeating cycle; the phase is any point in the repeating cycle recognizable by its relationship with the rest of the cycle; the amplitude is the distance between peak and trough.

Suspension of a circadian rhythm in continuous bright light and the release or restarting of the rhythm following transfer to darkness.

A circadian rhythm entrained to a 24-h light–dark (L–D) cycle and its reversion to the free-running period (26 h in this example) following transfer to continuous darkness.

Typical phase-shifting response to a light pulse given shortly after transfer to darkness. The rhythm is rephased (delayed) without its period being changed.

Figure 20.4 Some characteristics of circadian rhythms.

the light-to-dark transition at dusk and the dark-to-light transition at dawn (**Figure 20.4C**).

Such environmental signals are termed **zeitgebers** (German for "time givers"). When such signals are removed—for example, by transfer to continuous darkness—the rhythm is said to be **free-running**, and it reverts to the circadian period that is characteristic of the particular organism (see Figure 20.4C).

Although the rhythms are generated internally, they normally require an environmental signal to initiate their expression. In addition, many rhythms damp out (i.e., the amplitude decreases) when the organism is subjected to a constant environment for several cycles. When this occurs, an environmental zeitgeber, such as a transfer from light to dark or a change in temperature, is required to restart the rhythm (see Figure 20.4B).

The circadian clock would be of no value to the organism if it could not keep accurate time under the fluctuating temperatures experienced in natural conditions. Indeed, temperature has little or no effect on the period of the free-running rhythm. The feature that enables the clock to keep time at different temperatures is called **temperature compensation**.

Phase shifting adjusts circadian rhythms to different day–night cycles

In circadian rhythms, physiological responses are coupled to a specific time point of the endogenous oscillator so that the response occurs at a particular time of day. A single oscillator can be coupled to multiple circadian rhythms, which may even be out of phase with each other.

How do such responses remain on time when the daily durations of light and darkness change with the seasons? Investigators typically test the response of the endogenous oscillator by placing the organism in continuous darkness and examining the response to a short pulse of light (usually less than 1 h) given at different phase points in the free-running rhythm. When an organism is entrained to a cycle of 12 h light and 12 h dark and then allowed to free-run in constant light or darkness, the phase of the rhythm that coincides with the light period of the previous entraining cycle is called the **subjective day**, and the phase that coincides with the dark period is called the **subjective night**.

If a light pulse is given during the first few hours of the subjective night, the rhythm is delayed; the organism interprets the light pulse as the end of the previous day (**Figure 20.4D**). In contrast, a light pulse given toward the end of the subjective night advances the phase of the rhythm. In other words, the organism interprets the light pulse as the beginning of the following day.

This is precisely the response that would be expected if the light pulse allowed the rhythm to stay on local time even when the seasons change. These phase-shifting responses enable the rhythm to be entrained to approximately 24-h cycles with different durations of light and darkness, and they demonstrate that the rhythm can adjust to seasonal variations in day length.

Phytochromes and cryptochromes entrain the clock

The molecular mechanism whereby a light signal causes phase shifting is not yet known, but studies in Arabidopsis have identified some of the key elements of the circadian oscillator and its inputs and outputs (see Chapter 16). The low levels and specific wavelengths of light that can induce phase shifting indicate that the light response must be mediated by specific photoreceptors rather than by photosynthetic rate. For example, the red-light entrainment of rhythmic day–night leaf movements in *Samanea*, a semitropical leguminous tree, is a low-fluence response mediated by phytochrome (see Chapter 16).

Each type of phytochrome acts as a specific photoreceptor for red, far-red, or blue light. Plants also sense light through cryptochromes (CRYs), and the CRY1 and CRY2 proteins participate in blue-light entrainment of the clock in plants, as they do in insects (see Chapter 16). In contrast, CRYs in mammals do not seem to function as circadian photoreceptors. Surprisingly, CRY proteins also appear to be required for normal entrainment by red light. Since these proteins do not absorb red light, this requirement suggests that CRY1 and CRY2 may act as intermediates in phytochrome signaling during entrainment of the clock.

In *Drosophila*, CRY proteins interact physically with clock components and thus constitute part of the oscillator mechanism. However, this does not appear to be the case in Arabidopsis, in which *cry1/cry2* double mutants are impaired in entrainment but otherwise have normal circadian rhythms. In plants, photoactivated CRY2 activates flowering in response to blue light by directly up-regulating expression of a key flowering gene, *FLOWERING LOCUS T* (*FT*) (discussed in detail in Section 20.6).

20.4 Photoperiodism: Monitoring Day Length

As we have seen, the circadian clock enables organisms to repeat particular molecular or biochemical events at specific times of day or night. **Photoperiodism**, or the ability of an organism to detect day length, makes it possible for an event to occur at a particular time of year, thus allowing for a seasonal response. Circadian rhythms and photoperiodism have the common property of responding to cycles of light and darkness.

Precisely at the equator, day length and night length are equal and constant throughout the year. As one moves away from the equator toward the poles, the days become longer in summer and shorter in winter (**Figure 20.5**). Plant species have evolved the ability to detect these seasonal changes in day length, and their specific photoperiodic responses are strongly influenced by the latitude in which they originated.

Photoperiodic phenomena are found in both animals and plants. In the animal kingdom, day length controls such seasonal activities as hibernation, development of summer and winter coats, and reproductive activity. Plant responses controlled by day length are numerous; they include the initiation of flowering, asexual reproduction, the formation of storage organs, and the onset of dormancy.

Plants can be classified according to their photoperiodic responses

Numerous plant species flower during the long days of summer, and for many years plant physiologists believed that the correlation between long days and flowering was a consequence of the accumulation of photosynthetic products synthesized during long days.

This hypothesis was shown to be incorrect by the work of Wightman Garner and Henry Allard, conducted in the 1920s at the U.S. Department of Agriculture laboratories in Beltsville, Maryland. Garner and Allard

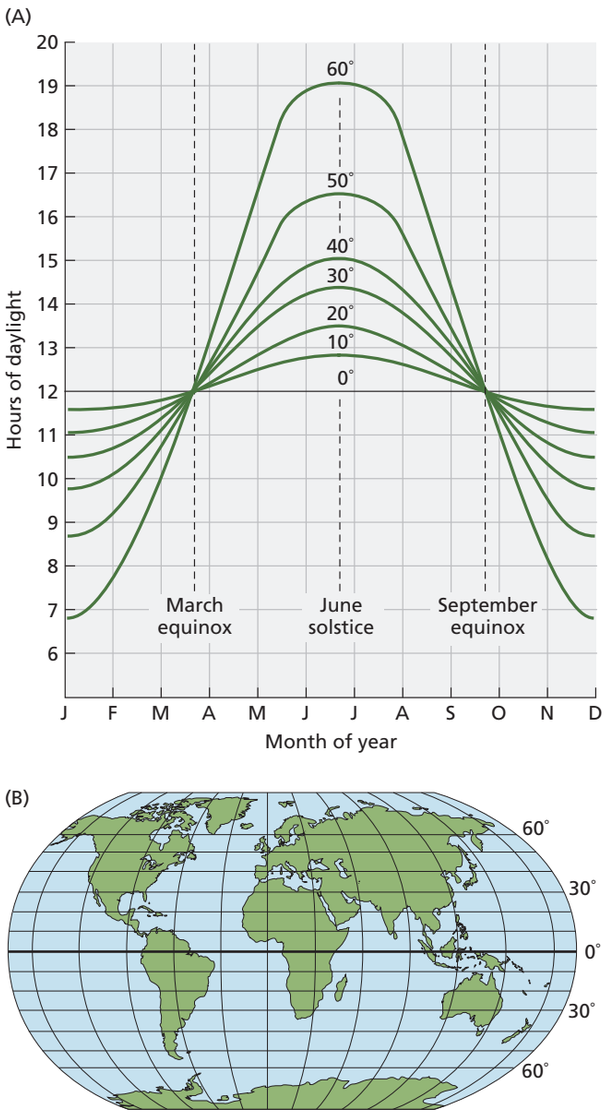


Figure 20.5 **Correlation between seasons and day length according to latitude.** (A) Effect of latitude on day length at different times of the year in the northern hemisphere. Day length was measured on day 20 of each month. (B) Global map showing longitudes and latitudes.

found that a mutant variety of tobacco, 'Maryland Mammoth', grew profusely to about 5 m in height but failed to flower in the prevailing conditions of summer (**Figure 20.6**). However, the plants flowered in the greenhouse during the winter under natural light conditions.

These results ultimately led Garner and Allard to test the effect of artificially shortened days by covering plants grown during the long days of summer with a light-tight tent from late in the afternoon until the following morning. These artificial short days also caused the plants to flower. Garner and Allard concluded that day length,



Figure 20.6 **'Maryland Mammoth' mutant of tobacco (right) compared with wild-type tobacco (left).** Both plants were grown during summer in the greenhouse. (University of Wisconsin graduate students used for scale.)

rather than the accumulation of photosynthate, was the determining factor in flowering. They were able to confirm their hypothesis in many different species and conditions. This work laid the foundations for the extensive subsequent research on photoperiodic responses.

Although many other aspects of plants' development may also be affected by day length, flowering is the response that has been studied the most. Flowering species tend to fall into one of two main photoperiodic response categories: short-day plants and long-day plants.

- **Short-day plants** (**SDPs**) flower only in short days (*qualitative* SDPs), or their flowering is accelerated by short days (*quantitative* SDPs).
- **Long-day plants** (**LDPs**) flower only in long days (*qualitative* LDPs), or their flowering is accelerated by long days (*quantitative* LDPs).

The essential distinction between long-day and short-day plants is that flowering in LDPs is promoted only when the day length *exceeds* a certain duration, called the **critical day length**, in every 24-h cycle, whereas promotion of flowering in SDPs requires a day length that is *less than* the critical day length. The absolute value of the critical day length varies widely among species, and only when flowering is examined for a range of day lengths can the correct photoperiodic classification be established (**Figure 20.7**).

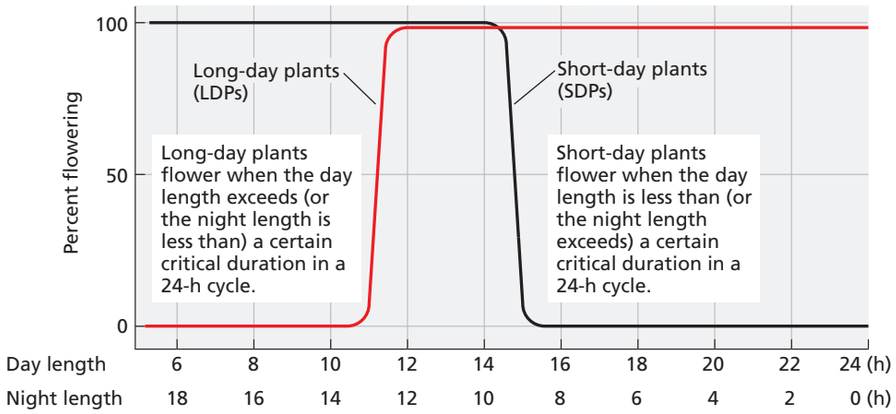


Figure 20.7 Photoperiodic response in long- and short-day plants. The critical duration varies among species. In this example, both the SDPs and the LDPs would flower in photoperiods between 12 and 14 h long.

LDPs can effectively measure the lengthening days of spring or early summer and delay flowering until the critical day length is reached. Many varieties of wheat (*Triticum aestivum*) behave in this way. SDPs often flower in the fall when the days shorten below the critical day length, as in many varieties of *Chrysanthemum morifolium*. However, day length alone is an ambiguous signal, because it cannot distinguish between spring and fall.

Plants exhibit several adaptations for avoiding the ambiguity of the day-length signal. One is the presence of a juvenile phase that prevents the plant from responding to day length during the spring. Another mechanism for avoiding the ambiguity of day length is the coupling of a temperature requirement to a photoperiodic response. Certain plant species, such as winter wheat, do not respond to photoperiod until after a cold period (vernalization or overwintering) has occurred. (We discuss vernalization in Section 20.7.)

Other plants avoid seasonal ambiguity by distinguishing between *shortening* and *lengthening* days. Such "dual–day length plants" fall into two categories:

- **Long–short-day plants** (**LSDPs**) flower only after a sequence of long days followed by short days. LSDPs, such as *Bryophyllum*, *Kalanchoe*, and night-blooming jasmine (*Cestrum nocturnum*), flower in the late summer and fall, when the days are shortening.
- **Short–long-day plants** (**SLDPs**) flower only after a sequence of short days followed by long days. SLDPs, such as white clover (*Trifolium repens*), Canterbury bells (*Campanula medium*), and echeveria (*Echeveria harmsii*), flower in the early spring in response to lengthening days.

Finally, species that flower under any photoperiodic condition are referred to as day-neutral plants. **Day-neutral plants** (**DNPs**) are insensitive to day length. Flowering in DNPs is typically under autonomous regulation—that is, internal developmental control. Some day-neutral species, such as kidney bean (*Phaseolus vulgaris*), evolved near the equator where the day length is constant throughout the year. Many desert annuals, such as desert paintbrush (*Castilleja chromosa*) and desert sand verbena (*Abronia villosa*), evolved to germinate, grow, and flower quickly whenever sufficient water is available. These are also DNPs.

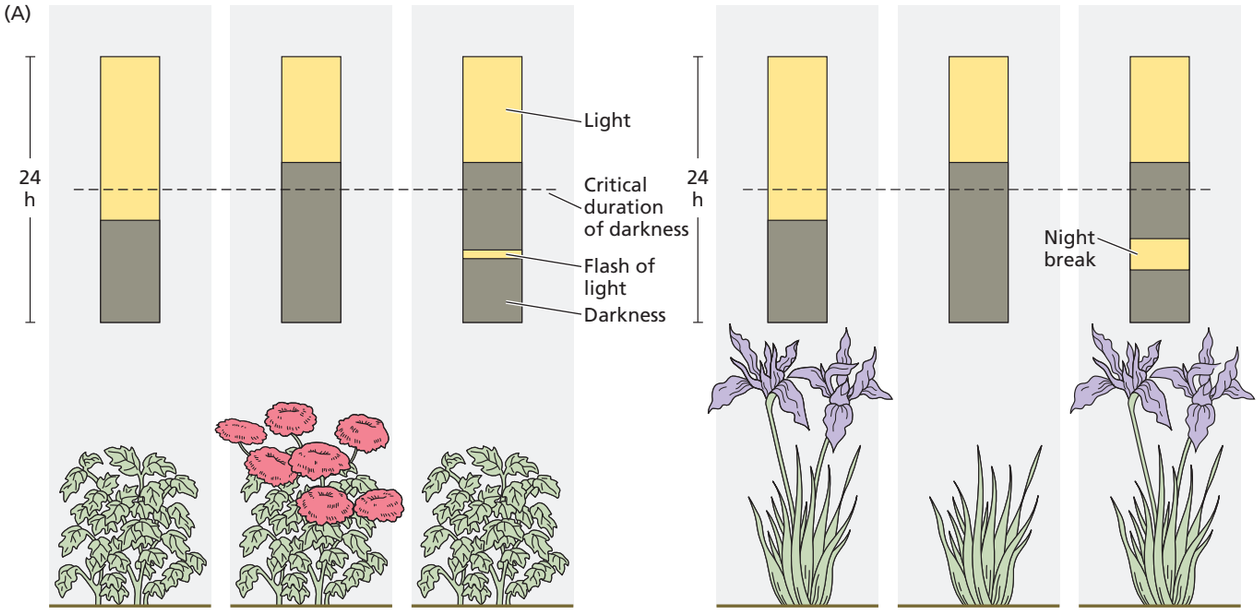
The leaf is the site of perception of the photoperiodic signal

The photoperiodic stimulus in both LDPs and SDPs is perceived by the leaves. For example, treatment of a single leaf of the SDP *Xanthium* with short photoperiods is sufficient to cause the formation of flowers, even when the rest of the plant is exposed to long days. Thus, in response to photoperiod the leaf transmits a signal that regulates the transition to flowering at the shoot apex. The photoperiod-regulated processes that occur in the leaves resulting in the transmission of a floral stimulus to the shoot apex are referred to collectively as **photoperiodic induction**.

Photoperiodic induction can take place in a leaf that has been separated from the plant. For example, in the SDP *Perilla crispa* (a member of the mint family), an excised leaf exposed to short days can cause flowering when subsequently grafted to a noninduced plant maintained in long days. This result indicates that photoperiodic induction depends on events that take place exclusively in the leaf.

The length of the night is important for floral induction

Under natural conditions, day and night lengths configure a 24-h cycle of light and darkness. In principle, a plant could perceive a critical day length by measuring the duration of either light or darkness. Much experimental work in the early studies of photoperiodism was devoted to establishing which part of the light–dark cycle is the controlling factor in flowering. Results



Short-day (long-night) plants flower when night length exceeds a critical dark period. Interruption of the dark period by a brief light treatment (a night break) prevents flowering.

Long-day (short-night) plants flower if the night length is shorter than a critical period. In some long-day plants, shortening the night with a night break induces flowering.

Figure 20.8 **Photoperiodic regulation of flowering.** **(A)** Effects on SDPs and LDPs. **(B)** Effects of the duration of the dark period on flowering. Treating SDPs and LDPs with different photoperiods clearly shows that the critical variable is the length of the dark period.

showed that flowering of SDPs is determined primarily by the duration of darkness (**Figure 20.8A**). It was possible to induce flowering in SDPs with light periods longer than the critical value, provided that these were followed by sufficiently long nights (**Figure 20.8B**). Similarly, SDPs did not flower when short days were followed by short nights.

More detailed experiments demonstrated that photoperiodic timekeeping in SDPs is a matter of measuring the duration of darkness. For example, flowering occurred only when the dark period exceeded 8.5 h in cocklebur (*Xanthium strumarium*) or 10 h in soybean (*Glycine max*). The duration of darkness was also shown to be important in LDPs (see Figure 20.8). These plants were found to flower in short days, provided that the accompanying night length was also short; however, a regime of long days followed by long nights was ineffective.

Night breaks can cancel the effect of the dark period

A feature that underscores the importance of the dark period is that it can be made ineffective by interruption with a short exposure to light, called a **night break** (see Figure 20.8A). In contrast, interrupting a long day with a brief dark period does not cancel the effect of the long day (see Figure 20.8B). Night-break treatments of only a few minutes are effective in *preventing* flowering in many SDPs, including *Xanthium* and *Pharbitis*, but much longer exposures are often required to *promote* flowering in LDPs.

In addition, the effect of a night break varies greatly according to the time when it is given. For both LDPs and SDPs, a night break was found to be most effective when given near the middle of a dark period of 16 h (**Figure 20.9**). The discovery of the night-break effect

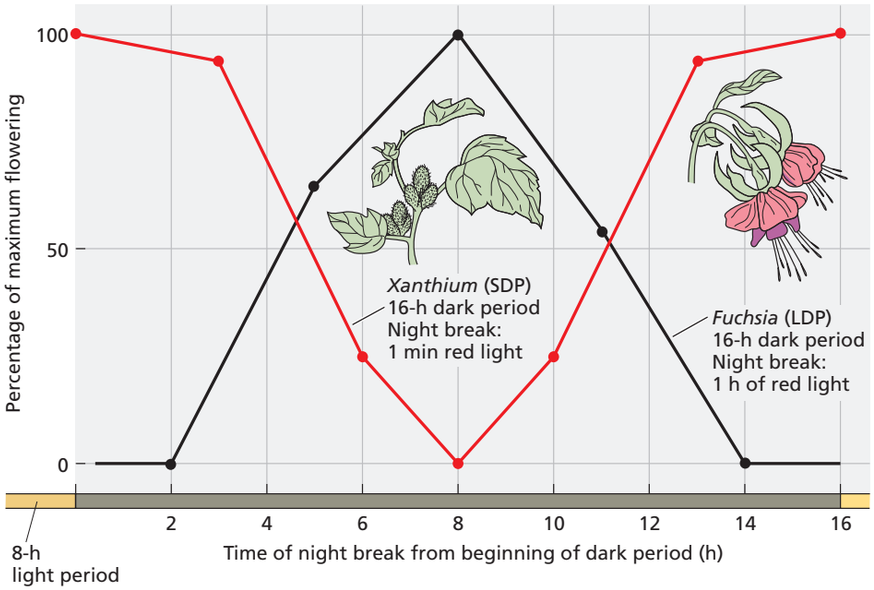


Figure 20.9 **The time at which a night break is given determines the flowering response.** When given during a long dark period, a night break promotes flowering in LDPs and inhibits flowering in SDPs. In both cases, the greatest effect on flowering occurs when the night break is given near the middle of the 16-h dark period. The LDP *Fuchsia* was given a 1-h exposure to red light in a 16-h dark period. *Xanthium* was exposed to red light for 1 min in a 16-h dark period. (Data for *Fuchsia* from D. Vince-Prue. 1975. *Photoperiodism in Plants*. London: McGraw-Hill; data for *Xanthium* from F. B. Salisbury. 1963. *Planta* 49: 518–524; H. D. Papenfuss and F. B. Salisbury. 1967. *Plant Physiol.* 42: 1562–1568.)

has led to the development of commercial methods for regulating the time of flowering of horticultural species, such as *Kalanchoe*, chrysanthemum, and poinsettia (*Euphorbia pulcherrima*).

Photoperiodic timekeeping during the night depends on a circadian clock

The decisive effect of night length on flowering indicates that measuring the passage of time in darkness is important for photoperiodic timekeeping. Most of the available evidence favors a mechanism based on a circadian rhythm. According to the **clock hypothesis**, photoperiodic timekeeping depends on an endogenous circadian oscillator of the type discussed in Section 20.3 (see Figure 20.3; see also Chapter 16). The central oscillator is coupled to various physiological processes that involve gene expression, including flowering in photoperiodic species.

Measurements of the effect of a night break on flowering can be used to investigate the role of circadian rhythms in photoperiodic timekeeping. For example, when soybean plants, which are SDPs, are transferred from an 8-h light period to an extended 64-h dark period, the flowering response to night breaks shows a circadian rhythm (**Figure 20.10**).

This type of experiment provides strong support for the clock hypothesis. If this SDP were simply measuring the length of night by the accumulation of a particular intermediate in the dark, any dark period greater than the critical night length should cause flowering. Yet long dark periods are not inductive for flowering if the light break is given at a time that does not properly coincide with a certain phase of the endogenous circadian

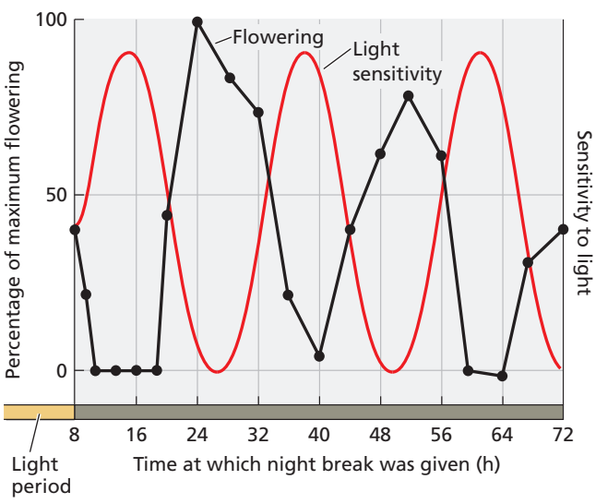


Figure 20.10 **Rhythmic flowering in response to night breaks.** In this experiment, the SDP soybean (*Glycine max*) received cycles of an 8-h light period followed by a 64-h dark period. A 4-h night break was given at various times during the long inductive dark period. The flowering response, plotted as the percentage of the maximum, was then plotted for each night break given. Note that a night break given at 26 h induced maximum flowering, while no flowering was observed when the night break was given at 40 h. Moreover, this experiment demonstrates that the sensitivity to the effect of the night break shows a circadian rhythm. These data support a model in which flowering in SDPs is induced only when dawn (or a night break) occurs after the completion of the light-sensitive phase. In LDPs the light break must coincide with the light-sensitive phase for flowering to occur. (Data from M. W. Coulter and K. C. Hamner. 1964. *Plant Physiol.* 39: 848–856.)

oscillator. This finding demonstrates that flowering in SDPs requires both a dark period of sufficient duration and a dawn signal at an appropriate time in the circadian cycle (see Figure 20.3).

Further evidence for the role of a circadian oscillator in photoperiod measurement is the observation that the photoperiodic response can be phase-shifted by light treatments (see **WEB TOPIC 20.5**).

The external coincidence model is based on oscillating light sensitivity

How does an oscillation with a 24-h period measure a critical duration of darkness of, say, 8 to 9 h, as in the SDP *Xanthium*? In 1936 Erwin Bünning proposed that the control of flowering by photoperiodism is achieved by an oscillation of phases with different sensitivities to light. This proposal has evolved into the **external coincidence model**, in which the circadian oscillator controls the timing of light-sensitive and light-insensitive phases.

The ability of light either to promote or to inhibit flowering depends on the phase in which the light is given. When a light signal is administered during the light-sensitive phase of the rhythm, the effect is either to *promote* flowering in LDPs or to *prevent* flowering in SDPs. As shown in Figure 20.10, the phases of sensitivity and insensitivity to light continue to oscillate in darkness. Flowering in SDPs is induced only when exposure to light from a night break or from dawn occurs after completion of the light-sensitive phase of the rhythm.

If a similar experiment is performed with an LDP, flowering is induced only when the night break occurs *during* the light-sensitive phase of the rhythm. In other words, *flowering in both SDPs and LDPs is induced when the light exposure is coincident with the appropriate phase of the rhythm*. This continued oscillation of sensitive and insensitive phases in the absence of dawn and dusk light signals is characteristic of a variety of processes controlled by the circadian oscillator (see Figure 20.3).

The coincidence of CONSTANS expression and light promotes flowering in LDPs

The duration of daylight by itself serves as a strong external stimulus that helps plants sense when the seasons are changing and when it is the right time to flower. According to the external coincidence model, plant flowering responses are sensitive to light only at certain times of the day–night cycle. A key component of a regulatory pathway that promotes flowering of Arabidopsis in long days is a gene called ***CONSTANS*** (***CO***), which encodes a zinc finger transcription factor. *CO* was first identified in an Arabidopsis mutant, *co*, that was incapable of a photoperiodic flowering response. The expression of *CO* is controlled by the circadian clock, as shown by the daily oscillations in its mRNA abundance (**Figure 20.11A and B**, top curve). However, genetic and molecular studies have shown that in the LDP Arabidopsis, CO protein accumulates only in response to long days (see Figure 20.11A and B, middle curve), and this is what accelerates flowering.

A critical feature of the external coincidence mechanism is that flowering in LDPs is promoted when a light-sensitive phase of the *CO* diel rhythm, which is generated in the leaf (the site of perception of the photoperiodic stimulus), coincides with the presence of light (an external signal). The increase in *CO* mRNA that occurs during short days does not lead to an increase in CO protein, because *CO* expression occurs entirely in the dark. In contrast, during long days, *CO* gene expression is accompanied by sharp increases in CO protein level, because at least some of the period of *CO* expression overlaps with the light period (see Figure 20.11B).

Long days are inductive for Arabidopsis flowering because CO protein levels increase under these conditions, and an important feature of the external coincidence model is that light can permit active CO protein to accumulate to a level that promotes flowering. The circadian oscillation of *CO* mRNA provides an explanation for the link between photoperiod perception and the circadian clock, allowing plants to measure day-length changes. But how does light bring about the accumulation of CO protein?

A clue to the function of light was provided by evidence that the abundance of CO protein fluctuates throughout the day–night cycle under long-day conditions, with two peak inductions during the light period. One peak occurs just before daybreak and the other at the end of the day (see Figure 20.11B). The diel CO protein profile is based in part on differences in the rates of CO degradation in the light versus the dark. In the dark, CO is tagged with ubiquitin and rapidly degraded by the 26S proteasome (see Chapter 4). Light appears to enhance the stability of the CO protein, allowing it to accumulate during the day. This explains why *CO* promotes flowering only when its mRNA accumulates during the light period.

However, the situation is more complicated than a simple light–dark switch regulating CO protein turnover. The effect of light on CO stability depends on the functions of several different photoreceptors. In the morning, when CO is at its predawn peak, phytochrome B (phyB) and ZEITLUPE (ZTL), the latter a light, oxygen, or voltate (LOV) domain blue-light photoreceptor (see Chapter 16), appear to promote light-induced CO degradation, sharply reducing its levels by unknown mechanisms. In the early evening, by contrast, cryptochromes, phyA, and FLAVIN-BINDING KELCH REPEAT, F-BOX 1 (FKF1), a ZTL homologous blue-light photoreceptor, antagonize this degradation and allow the CO protein to build up (see Figure 20.11B; see also **WEB TOPIC 20.6**). The regulation of

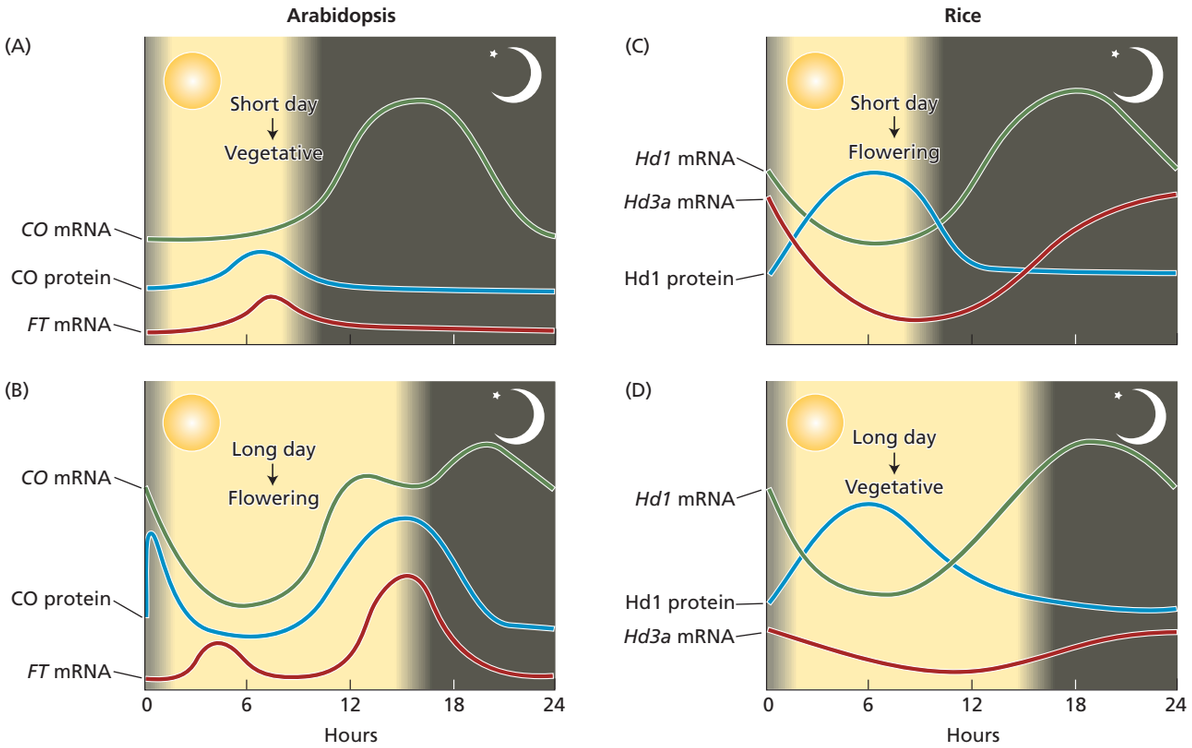


Figure 20.11 Molecular basis of the external coincidence model in Arabidopsis (A and B) and rice (C and D). **(A)** In Arabidopsis under short days, there is little overlap between *CO* mRNA expression and daylight. CO protein does not accumulate to sufficient levels in the phloem to promote the expression of the transmissible floral stimulus, FT protein, and the plant remains vegetative. **(B)** Under long days, the peak of *CO* mRNA abundance overlaps with daylight (early in the day and late in the afternoon), allowing CO protein to accumulate. (The sharp rise in CO protein in the early morning is caused by a transient increase in protein upon exposure to light at dawn.) CO activates *FT mRNA* expression in the phloem, which causes flowering when the FT protein is translocated to the apical meristem. **(C)** In rice under short days, the lack of coincidence between *Hd1 mRNA* expression and daylight stimulates the expression of the gene encoding the rice transmissible floral stimulus and FT relative, Hd3a. In this condition, Hd1 acts as an activator of *Hd3a*, allowing the accumulation of Hd3a protein (not shown), which is translocated to the apical meristem where it causes flowering. (Note that there is a lag time before the activation of *Hd3a* expression by Hd1.) **(D)** Under long days, the coincidence of *Hd1 mRNA* expression with daylight inhibits *Hd3a* expression. In response to long days, the function of Hd1 is converted to a repressor of *Hd3a* expression. As a result, *Hd3a mRNA* does not accumulate, and the plant remains vegetative. (A and B after Y. H. Song. et al. 2015. *Ann. Rev. Plant Biol.* 66: 441–464 and Y. H. Song et al. 2018. *Nat. Plants* 4: 824–835; C and D after H. Wei et al. 2020. *aBIOTECH* 1: 219–232.)

day length–dependent *CO* expression and CO accumulation is the core mechanism that enables Arabidopsis to measure changes in day length.

SDPs use a coincidence mechanism to inhibit flowering in long days

Studies of flowering in the SDP rice have shown that the basic external coincidence mechanism for photoperiod-sensing is conserved in rice and Arabidopsis. The rice genes ***Heading-date1*** (***Hd1***) and ***Heading-date3a*** (***Hd3a***) encode proteins homologous to Arabidopsis *CO* and *FT* (*FLOWERING LOCUS T*), respectively. In transgenic plants, overexpression of *FT* in Arabidopsis, and of *Hd3a* in rice, results in rapid flowering regardless of photoperiod, demonstrating that both *FT* and *Hd3a* are strong promoters of flowering. Moreover, expression of the native *FT* and *Hd3a* genes is substantially elevated during inductive photoperiods (long days in Arabidopsis and short days in rice) (**Figure 20.11C**). In addition, rice *Hd1* and Arabidopsis *CO* exhibit similar diel patterns of mRNA accumulation. The difference between rice and Arabidopsis is that in the SDP rice, Hd1 acts as a *repressor* of *Hd3a* expression in long days (**Figure 20.11D**), and as an *activator* of its expression in short days (see Figure 20.11C).

In contrast to what happens in Arabidopsis, in rice the coincidence of *Hd1* expression and light under long days suppresses flowering by inhibiting the expression of *Hd3a*. Flowering in the SDP rice thus occurs only under short-day conditions, when *Hd1* is expressed mainly in the dark. In addition, the effect of Hd1 on *Hd3a* expression (inhibition versus induction) seems to

be differently regulated according to day length. Hd1 accumulates during the light period regardless of photoperiod but is in a biochemically active state that initiates *Hd3a* transcription only in short days. Remarkably, the different responses to photoperiod of SDPs versus LDPs are due in part to the opposite effects of day length on the activity of CO/Hd1 in the photoperiodic sensing system.

However, it is important to note that photoperiodism is even more complex, and other regulatory mechanisms that fine-tune the responses of SDPs and LDPs to changing day length are certain to be present (**Box 20.1**).

Box 20.1 Refining Molecular Mechanisms of Photoperiodic Flowering Happening in Natural Environments

As seen in this chapter, flowering is controlled by the combinations of environmental factors such as light quality, photoperiod, temperature, and so on. Like laboratory animals, plants used in physiological research are usually grown under controlled environmental conditions, such as a light–dark cycle with fixed temperature. Indeed, most biology research laboratories employ simplified environmental conditions to minimize environmental variations and obtain reliable and reproducible data. The application of this approach with model plants has been extremely successful in elucidating a wide range of fundamental physiological processes.

However, as in the case with animals, plants often exhibit different responses in laboratory versus natural environments at the physiological and molecular levels. For example, recent research revealed that the LDP Arabidopsis flowered earlier in natural long days than in long days under controlled conditions. In addition, surprisingly, the abundance of *FT* transcripts peaked in the morning and at dusk in the outdoors (**Figure A**). The high accumulation of *FT mRNA* early in the day is not normally observed in laboratory conditions (see Figure 20.11 in the main text). The discrepancies in flowering time and the *FT* expression profile between laboratory and outdoor conditions were caused by a combination of changes in the red:far red (R:FR) ratio and of daily temperature. The R:FR ratio in sunlight is almost 1.0, but it is more than 2.0 in light sources typically used in laboratories, indicating that the laboratory growth conditions used in the studies are red light–enriched. This can in part explain the delayed flowering of Arabidopsis in laboratory conditions compared with the outdoors, because red light inhibits flowering by destabilizing CO protein. Additionally, the degradation rate of CO protein in the morning under natural environments was decreased, suggesting a correlation between increased CO stability and *FT* induction in this condition (see Figure A). Furthermore, the temperature fluctuation throughout the day strongly affected the *FT* expression pattern. By adjusting the settings for the R:FR ratio and daily temperature cycle closer to natural conditions, it is possible to reproduce the flowering response observed outdoors under controlled laboratory conditions.

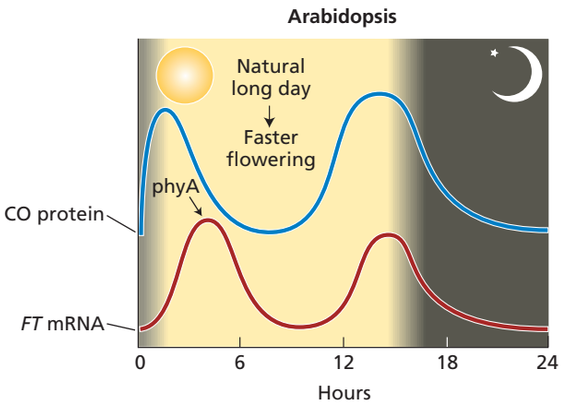


Figure A **Expression profile of *FT* in natural long days.** *FT mRNA* abundance peaks in the morning and at dusk in the outdoors. Compared with the *FT* expression pattern in conventional laboratory long-day conditions, the additional morning peak of *FT* in the outdoors accelerates flowering in Arabidopsis. Under natural long days, the degradation rate of CO protein in the morning is decreased, suggesting that the induction of *FT* peak in this condition is due to the increase in CO stability. In addition, phyA, the main photoreceptor that absorbs far-red light, seems to contribute to the generation of *FT* morning peak in response to the R:FR ratio to 1.0 and daily temperature cycle in the outdoors. (After Y. H. Song et al. 2018. *Nat. Plants* 4: 824–835.)

PhyA is the main photoreceptor responsible for absorbing far-red light and probably is also involved in temperature sensing. In Arabidopsis, the loss-of-function alleles in the *PHYA* gene exhibit slightly delayed flowering under long days in a growth chamber. In contrast, the delay in flowering of the *phyA* mutant in the field is more marked. In addition, the levels of *FT* transcripts in the morning under natural conditions are greatly reduced by the *phyA* mutation, suggesting the crucial role of phyA in flowering regulation, which has been underestimated in laboratories conditions.

Clearly, studying plants under natural conditions is essential for improving our understanding of plant biology and physiology, and will help us prepare future scenarios for food security in the face of climate change. ■

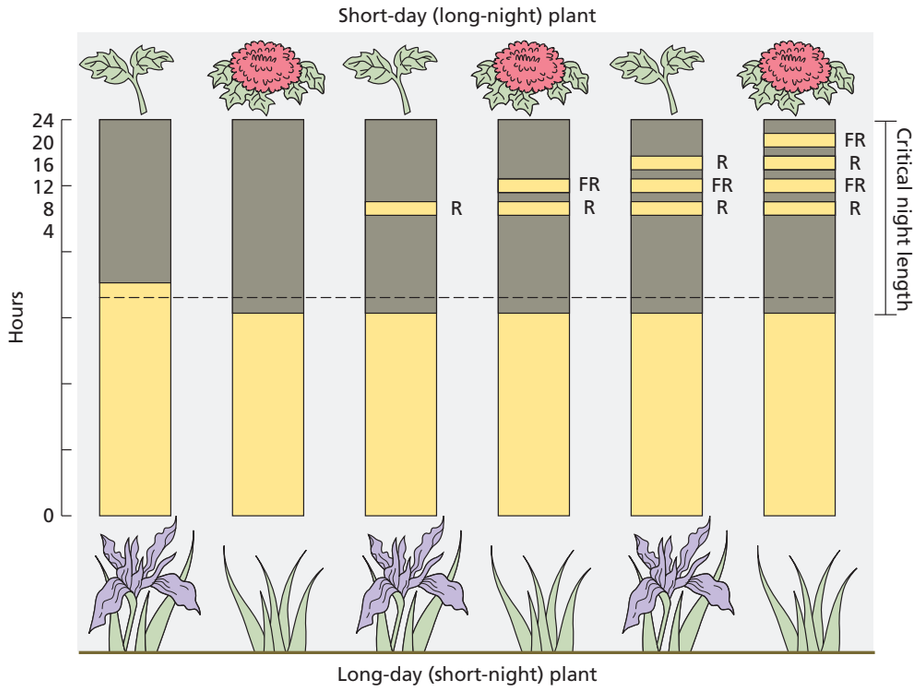


Figure 20.12 Phytochrome control of flowering by red (R) and far-red (FR) light. A flash of red light during the dark period induces flowering in an LDP, and the effect is reversed by a flash of far-red light. This response indicates the involvement of phytochrome. In SDPs, a flash of red light prevents flowering, and the effect is reversed by a flash of far-red light.

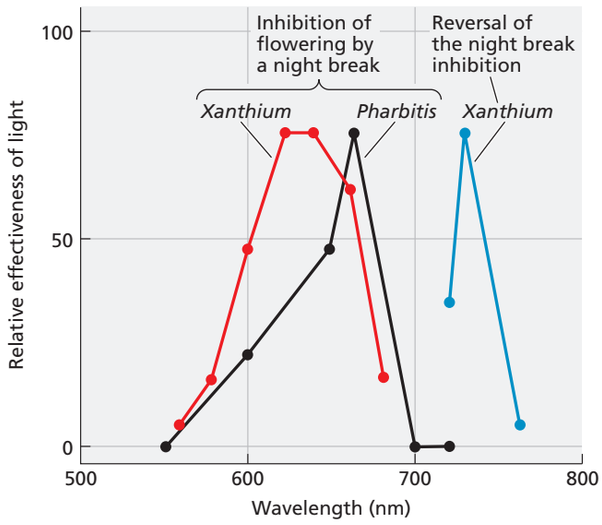


Figure 20.13 Action spectra for the control of flowering by night breaks implicate phytochrome. Flowering in SDPs is inhibited by a short light treatment (night break) given in an otherwise inductive period. In the SDP *Xanthium strumarium*, red-light night breaks of 620 to 640 nm are the most effective. Reversal of the red-light effect is maximal at 725 nm. In the dark-grown SDP *Pharbitis nil*, which is devoid of chlorophyll and its interference with light absorption, night breaks of 660 nm are the most effective. This 660-nm maximum coincides with the absorption maximum of phytochrome. (Data for *Xanthium* from S. B. Hendricks and H. W. Siegelman. 1967. *Comp. Biochem.* 27: 211–235; data for *Pharbitis* from H. Saji et al. 1983. *Plant Cell Physiol.* 24: 1183–1189.)

Phytochrome is the primary photoreceptor in photoperiodism

Night-break experiments are well suited for studying the nature of the photoreceptors (see Chapter 16) involved in the reception of light signals during the photoperiodic response. The inhibition of flowering in SDPs by night breaks was one of the first physiological processes shown to be under the control of phytochrome (**Figure 20.12**).

In many SDPs, a night break becomes effective only when the supplied dose of light is sufficient to saturate the photoconversion of **Pr** (phytochrome that absorbs red light) to **Pfr** (phytochrome that absorbs far-red light) (see Chapter 16). A subsequent exposure to far-red light, which photoconverts the pigment back to the physiologically inactive Pr form, restores the flowering response.

Action spectra for the inhibition and restoration of the flowering response in SDPs are shown in **Figure 20.13**. A peak at 660 nm, the absorption maximum of Pr, is obtained when dark-grown *Pharbitis* seedlings are used to avoid interference from chlorophyll. In contrast, the spectra for *Xanthium* provide an example of the response in green plants, in which the presence of chlorophyll can cause some discrepancy between the action spectrum and the absorption spectrum of Pr. These action spectra plus the red/far-red reversibility of the night break responses confirm the role of phytochrome as the photoreceptor that is involved in photoperiod measurement in SDPs. Night break experiments with LDPs have also implicated phytochrome. Thus, in some LDPs a night

break of red light promotes flowering, and a subsequent exposure to far-red light prevents this response.

A circadian rhythm in the promotion of flowering by far-red light has been observed in the LDPs barley (*Hordeum vulgare*), darnel ryegrass (*Lolium temulentum*), and Arabidopsis (**Figure 20.14**). The response is proportional to the irradiance and duration of far-red light and is therefore a high-irradiance response (HIR; see Chapter 16). As in other HIRs, phyA is the phytochrome that mediates the response to far-red light. Consistent with a role of phyA in promoting the flowering of LDPs, mutations in the *PHYA* gene delay flowering in Arabidopsis. In contrast, when phyB absorbs red light, it acts to delay flowering, and consistent with the antagonistic effects of red and far-red light, *phyB* mutations promote flowering in Arabidopsis. However, in some LDPs the role of phytochrome is more complex than in SDPs, because a blue-light photoreceptor also participates in the response.

A blue-light photoreceptor regulates flowering in some LDPs

In some LDPs, such as Arabidopsis, blue light can promote flowering, suggesting the possible participation of a blue-light photoreceptor in the control of flowering. As we discussed in Chapter 16, the cryptochromes, encoded by the *CRY1* and *CRY2* genes, are blue-light photoreceptors that control seedling growth in Arabidopsis. As noted in Section 20.3, the CRY protein has also been implicated in the entrainment of the circadian oscillator. The role of blue light in flowering and its relationship to circadian rhythms have been investigated by use of the luciferase reporter gene construct mentioned in **WEB TOPIC 20.7**.

Blue-light regulation of both circadian rhythmicity and flowering is also supported by studies with an Arabidopsis flowering-time mutant, *ztl* (see **WEB TOPICS 20.7** and **20.8**). Several blue-light photoreceptors are involved in sensing inductive photoperiods in Arabidopsis. Mutations in one of the cryptochrome genes, *CRY2* (see Chapter 18), caused delayed flowering in long days. In addition, the *cry1*/*cry2* double mutants flowered slightly later than *cry2* in long days, indicating some functional redundancy of CRY1 and CRY2 in promoting flowering time in Arabidopsis.

Another type of blue-light photoreceptor plays a crucial role in photoperiodic flowering in Arabidopsis. FKF1 functions to align the induction of *CO* expression with the light period in long days, but not in short days, enabling Arabidopsis to differentiate seasons. In long days, loss-of-function *fkf1* mutants have very delayed flowering and an inability to perceive inductive photoperiods. In contrast, the overproduction of FKF1 protein promotes flowering in long days. In addition, ZTL, a FKF1 homolog, appears to antagonize FKF1 in the regulation of flowering. Like the *fkf1* mutants, plants carrying elevated ZTL protein levels flower much later than the wild type in long days. Conversely, loss-of-function alleles of the *ZTL* gene cause early flowering.

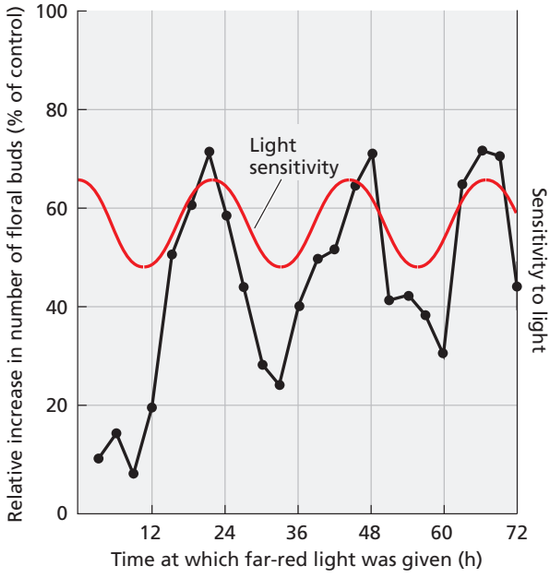


Figure 20.14 Effect of far-red light on floral induction in Arabidopsis. At the indicated times during a continuous 72-h daylight period, 4 h of far-red light were added. Data points in the graph are plotted at the centers of the 4-h treatments. The data show a circadian rhythm of sensitivity to the far-red promotion of flowering (red line). This supports a model in which flowering in LDPs is promoted when the light treatment (in this case far-red light) coincides with the peak of light sensitivity. (After G. Deitzer. 1984. In *Light and the Flowering Process*, D. Vince-Prue et al. [eds.], Academic Press, New York, pp. 51–63.)

It is likely that the cryptochromes, FKF1, and ZTL regulate flowering by modulating CO protein stability, allowing it to accumulate under long day conditions. As noted earlier, the CO protein acts as a promoter of flowering in LDPs.

20.5 Long-Distance Signaling Involved in Flowering

Although floral evocation occurs at the apical meristems of shoots, in photoperiodic plants inductive photoperiods are sensed by the leaves. This suggests that a long-range signal must be transmitted from the leaves to the apex, which has been shown experimentally through extensive grafting experiments in many different plant species. The biochemical nature of this signal had long baffled physiologists. The problem was finally solved using molecular genetic approaches, and the floral stimulus was identified as a protein. In this section we review the background for the discovery of the floral stimulus, referred to as **florigen**, which serves as the long-distance signal during flowering.

Grafting studies provided the first evidence for a transmissible floral stimulus

The production in photoperiodically induced leaves of a biochemical signal that is transported to a distant target tissue (the shoot apex) where it stimulates a response (flowering) satisfies an important criterion for a hormonal effect. In the 1930s, Mikhail Chailakhyan postulated the existence of a universal flowering hormone, which he named florigen.

The evidence in support of florigen comes mainly from experiments in which noninduced receptor plants were stimulated to flower by having a leaf or shoot from a photoperiodically induced donor plant grafted to them. For example, in the SDP *Perilla crispa*, grafting a leaf from a plant grown under inductive short days onto a plant grown under noninductive long days causes the latter to flower (**Figure 20.15A**). Moreover, the floral stimulus seems to be the same in plants with different photoperiodic requirements. Thus, grafting an induced shoot from the LDP *Nicotiana sylvestris*, grown under long days, onto the SDP 'Maryland Mammoth' tobacco caused the latter to flower under noninductive (long-day) conditions.

The leaves of DNPs have also been shown to produce a graft-transmissible floral stimulus (**Table 20.2**). For example, grafting a single leaf of a flowering day-neutral variety of soybean, 'Agate', onto the short-day variety, 'Biloxi', caused flowering in 'Biloxi' even when the latter was maintained in noninductive long days. Similarly, a shoot from a flowering day-neutral variety of tobacco (*Nicotiana tabacum*, cv. Trapezond) grafted onto the LDP *Nicotiana sylvestris* induced the latter to flower under noninductive short days.

Grafting studies also showed that in some species, such as *Xanthium* (SDP), *Bryophyllum* (SLDP), and *Silene* (LDP), not only can flowering be induced by grafting, but the induced state itself appears to be self-propagating (see **WEB TOPIC 20.9**). In a few cases, flowering has even been induced by grafts between different genera. The SDP *Xanthium strumarium* flowered under long-day conditions when shoots of flowering *Calendula officinalis* were grafted onto a vegetative *Xanthium* stock. Similarly, grafting a shoot from the LDP *Petunia hybrida* onto a stock of the cold-requiring biennial henbane (*Hyoscyamus niger*) caused the latter to flower under long days, even though it was nonvernalized (**Figure 20.15B**).



Figure 20.15 Two grafting experiments demonstrating the translocation of a leaf-generated floral stimulus. **(A)** At left, grafting an induced leaf from a plant grown under short days onto a noninduced shoot causes the axillary shoots to produce flowers. The donor leaf has been trimmed to facilitate grafting, and the upper leaves have been removed from the stock to promote phloem translocation from the scion to the receptor shoots. At right, grafting a noninduced leaf from a plant grown under long days results in the formation of vegetative branches only. **(B)** This grafting experiment demonstrates the transfer of the floral stimulus between different genera. The stock (left branch) is nonvernalized henbane (*Hyoscyamus niger*), which requires cold treatment to flower. The scion (right branch) is the LDP *Petunia hybrida*. Maintaining the graft combination under long days at room temperature resulted in the movement of the floral stimulus from the scion to the stock.

TABLE 20.2 Transmission of the flowering signal occurs through a graft junction

Donor plants maintained under flower-inducing conditions	Photoperiod type[a,b]	Vegetative receptor plant induced to flower	Photoperiod type[a,b]
Helianthus annuus	DNP in LD	*H. tuberosus*	SDP in LD
Nicotiana tabacum 'Delcrest'	DNP in SD	*N. sylvestris*	LDP in SD
Nicotiana sylvestris	LDP in LD	*N. tabacum* 'Maryland Mammoth'	SDP in LD
Nicotiana tabacum 'Maryland Mammoth'	SDP in SD	*N. sylvestris*	LDP in SD

Note: The successful transfer of a flowering induction signal by grafting between plants of different photoperiodic response groups shows the existence of a transmissible floral hormone that is effective.

[a]LDPs = long-day plants; SDPs = short-day plants; DNPs = day-neutral plants.

[b]LD, long days; SD, short days.

In *Perilla crispa* (see Figure 20.15A), the movement of the floral stimulus from a donor leaf to the stock across the graft union correlated closely with the translocation of ^{14}C-labeled assimilates from the donor, and this movement was dependent on the establishment of vascular continuity across the graft union. These results confirmed earlier girdling studies showing that the floral stimulus is translocated along with photoassimilates in the phloem.

Florigen is translocated in the phloem

The leaf-derived photoperiodic floral stimulus is translocated via the phloem to the shoot apical meristem, where it promotes floral evocation. Treatments that block phloem translocation, such as girdling or localized heat-killing, block flowering by preventing the movement of the floral stimulus out of the leaf.

It is possible to measure rates of movement of florigen by removing a leaf at different times after induction, and comparing the time it takes for the signal to reach two buds located at different distances from the induced leaf. The rationale for this type of measurement is that a threshold amount of the signaling compound has reached the bud when flowering takes place, despite the removal of the leaf. In this way, the time for a sufficient amount of signal to exit the leaf can be determined. Furthermore, comparing the times of induction for two differently positioned buds provides a measure of the rate of movement of the signal along the stem.

Studies using this method have shown that the rate of movement of the flowering signal is comparable to, or somewhat slower than, the rate of translocation of sugars in the phloem (see Chapter 11). For example, export of the floral stimulus from adult leaves of the SDP *Chenopodium* is complete within 22.5 h from the beginning of the long night period. In the LDP *Sinapis*, movement of the floral stimulus out of the leaf is complete as early as 16 h after the start of the long-day treatment.

Because the floral stimulus is translocated along with sugars in the phloem, it is subject to source–sink relations. An induced leaf positioned close to the shoot apex is more likely to cause flowering than an induced leaf at the base of a stem, which normally feeds the roots. Similarly, noninduced leaves positioned between the induced leaf and the apical bud will tend to inhibit flowering by serving as the preferred source leaves for the bud, thus preventing the floral stimulus from the more distal induced leaf from reaching its target.

20.6 The Identification of Florigen

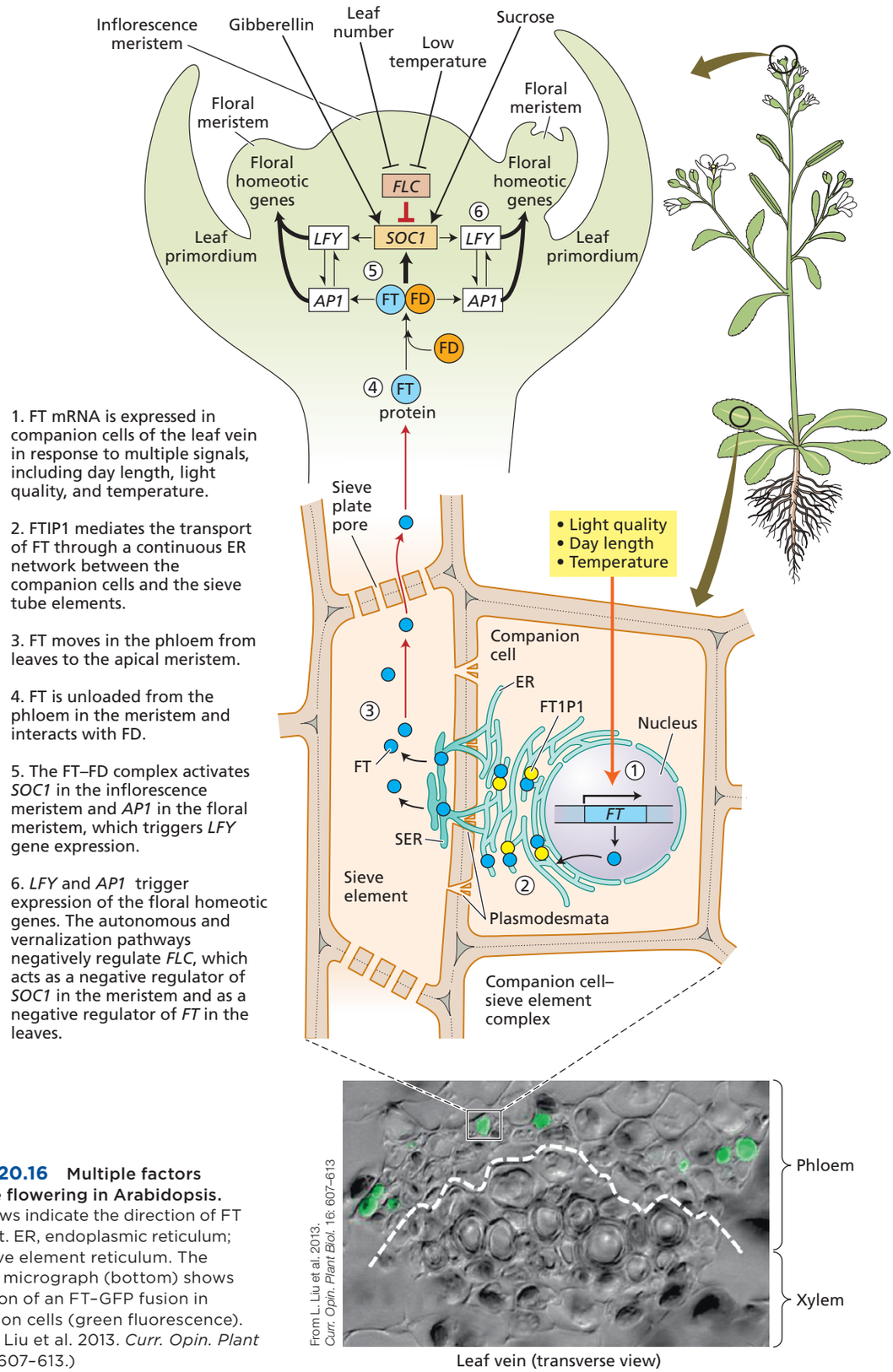
Pioneering grafting experiments of the kind described in Section 20.5 established the importance of a long-range signal from the leaf to the apical meristem to stimulate flowering. Since the 1930s, there have been many unsuccessful attempts to isolate and characterize florigen. A major breakthrough was the identification of *FLOWERING LOCUS T* (*FT*) in Arabidopsis through genetic screens.

The Arabidopsis protein FLOWERING LOCUS T (FT) is florigen

According to the external coincidence model, flowering in LDPs such as Arabidopsis occurs when the *CONSTANS* gene is expressed during the light period. *CO* gene expression appears to be highest in the companion cells of the phloem of leaves and stems. One set of experiments showed that the photoperiod-insensitive flowering of *co* mutants could be rescued by expressing *CO* specifically in the phloem of the minor veins of mature leaves. In contrast, expressing *CO* in the apical meristems of *co* mutants did not restore the flowering phenotype, supporting the notion that *CO* acts specifically in the phloem of leaves to stimulate flowering in response to long days. Other work showed that when transgenic shoots expressing *CO* in their leaf phloem were grafted onto the *co* mutant, flowering was induced in all the shoots, not just those expressing *CO*. This observation suggests that *CO* expression gives rise to a graft-transmissible floral stimulus that can cause flowering at the apical meristem.

The signaling output of CO activity is directly mediated by the expression of *FT*, which is also exclusively observed in the companion cells. In Arabidopsis, *CO* expression during long days results in an increase in *FT mRNA* (see Figure 20.11). However, unlike *CO*, *FT* stimulates flowering when expressed in either the companion cells or the apical meristem. Expression of the *FT* gene (or its relatives, such as *Hd3a* in rice, discussed earlier) is induced in a range of species during their floral-inductive photoperiods. When the *FT* gene is introduced into a range of plant species whose flowering is not influenced by photoperiod, it accelerates flowering. In addition, FT protein can move from the leaves to the apical meristem and thus exhibits all the properties that would be expected of florigen.

According to the current model, FT protein moves via the phloem from the leaves to the meristem under inductive photoperiods. There are two critical steps in this process: the export of FT from companion cells to the sieve tube elements, and the activation of FT target genes at the shoot apex, which triggers flower development. The endoplasmic reticulum (ER) is one of the major routes for the transport of proteins from the companion cells to the sieve tube elements. The ER-localized protein, FT INTERACTING PROTEIN1 (FTIP1), is required for FT movement into the phloem translocation stream, which takes it to the meristem (**Figure 20.16**). Once in the floral meristem, the FT protein enters the nucleus and forms a complex with **FLOWERING D** (**FD**), a basic leucine zipper (bZIP) transcription factor that is expressed in the meristem. The complex formed by FT and FD then activates floral identity genes such as *APETALA1* (*AP1*).



1. FT mRNA is expressed in companion cells of the leaf vein in response to multiple signals, including day length, light quality, and temperature.

2. FTIP1 mediates the transport of FT through a continuous ER network between the companion cells and the sieve tube elements.

3. FT moves in the phloem from leaves to the apical meristem.

4. FT is unloaded from the phloem in the meristem and interacts with FD.

5. The FT–FD complex activates *SOC1* in the inflorescence meristem and *AP1* in the floral meristem, which triggers *LFY* gene expression.

6. *LFY* and *AP1* trigger expression of the floral homeotic genes. The autonomous and vernalization pathways negatively regulate *FLC*, which acts as a negative regulator of *SOC1* in the meristem and as a negative regulator of *FT* in the leaves.

From L. Liu et al. 2013. *Curr. Opin. Plant Biol.* 16: 607–613

Figure 20.16 Multiple factors regulate flowering in Arabidopsis. Red arrows indicate the direction of FT transport. ER, endoplasmic reticulum; SER, sieve element reticulum. The leaf vein micrograph (bottom) shows expression of an FT-GFP fusion in companion cells (green fluorescence). (After L. Liu et al. 2013. *Curr. Opin. Plant Biol.* 16: 607–613.)

In Arabidopsis, these events set in motion positive feedback loops that keep the meristem in a flowering state. After being activated by the FT protein, FD triggers the expression of *SUPPRESSOR OF OVEREXPRESSION OF CONSTANS1* (*SOC1*) and *AP1*. Both of these targets activate *LEAFY* (*LFY*; a floral identity gene we discuss later in this chapter), and *LFY* directly activates the expression of *AP1* and *FD*, forming two positive feedback loops (see Figure 20.16). Because of the action of these positive feedback loops, floral initiation in Arabidopsis is irreversible. However, the meristems of some species lack such positive feedback loops and, as a consequence, revert to producing leaves in the absence of a continuous inductive photoperiod.

In addition, it is likely that the FT protein synthesized in a host plant is able to travel into stems of parasitic plants attached to it. Once there, the host FT protein triggers the activation of flowering-related genes by physically interacting with FD protein produced by the parasite. By using an interplant mobile signal—the FT protein—parasitic plants can synchronize their flowering with that of their host plant and optimize their reproductive fitness.

20.7 Vernalization: Promoting Flowering with Cold

Vernalization is the process whereby repression of flowering is alleviated by a prolonged cold treatment given to a hydrated seed (i.e., a seed that has imbibed water) or to a growing plant (dry seeds do not respond to the cold treatment because vernalization is an active metabolic process). Without the cold treatment, plants that require vernalization show delayed flowering or remain vegetative, and they are not competent to respond to floral signals such as inductive photoperiods. In many cases these plants grow as rosettes with no elongation of the stem (**Figure 20.17**).

In this section we examine some of the characteristics of the cold requirement for flowering, including the range and duration of the inductive temperatures, the sites of perception, the relationship to photoperiodism, and a possible molecular mechanism.

Vernalization results in competence to flower at the shoot apical meristem

Plants differ considerably in the age at which they become sensitive to vernalization. Winter annuals, such as the winter forms of cereals (which are sown in the fall and flower in the following summer), respond to low temperature very early in their life cycle. In fact, many winter annuals can be vernalized before germination (i.e., radicle emergence from the seed) if the seeds have imbibed water and become metabolically active. Other plants, including most biennials (which grow as rosettes during the first season after sowing and flower in the following summer), must reach a minimal size before they become sensitive to low temperature for vernalization.

The effective temperature range for vernalization is from just below freezing to about 10°C, with a broad optimum usually at 1 to 7°C. The effect of cold increases with the duration of the cold treatment until the response is saturated. The response usually requires several weeks of exposure to low temperature, but the precise duration varies widely with species and variety.

Vernalization can be lost as a result of exposure to devernalizing conditions, such as high temperature (**Figure 20.18**), but the longer the exposure to low temperature, the more permanent the vernalization effect.

Vernalization appears to take place primarily in the shoot apical meristem. Localized cooling causes flowering when only the stem apex is chilled, and this effect appears to be largely independent of the temperature experienced by the rest of the plant. Excised shoot tips have been successfully vernalized, and where seed vernalization is possible, fragments of embryos consisting essentially of the shoot tip are sensitive to low temperature.

In developmental terms, vernalization results in the acquisition of competence of the meristem to undergo the floral transition. Yet, as discussed earlier in the chapter, competence to flower does not guarantee that flowering will occur. A vernalization requirement is often linked to a requirement for a particular photoperiod. The most common combination is a requirement



Courtesy of Colleen Bizzell

Winter-annual Arabidopsis without vernalization

Winter-annual Arabidopsis with vernalization

Figure 20.17 Vernalization induces flowering in the winter-annual types of *Arabidopsis thaliana*. The plant on the left is a winter-annual type that has not been exposed to cold. The plant on the right is a genetically identical winter-annual type that was exposed to 40 days of temperatures slightly above freezing (4°C) as a seedling. It flowered 3 weeks after the end of the cold treatment with about nine leaves on the primary stem.

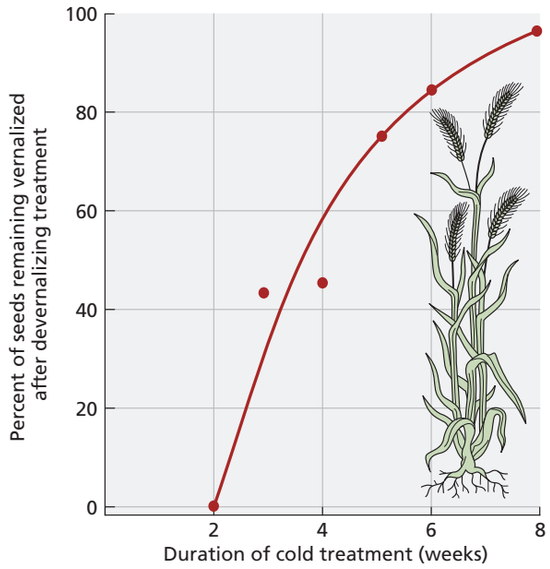


Figure 20.18 **Duration of exposure to low temperature increases the stability of the vernalization effect.** The longer that winter rye (*Secale cereale*) is exposed to a cold treatment, the greater the number of plants that remain vernalized when the cold treatment is followed by a devernalizing treatment. In this experiment, seeds of rye that had imbibed water were exposed to 5°C for different lengths of time, then immediately given a devernalizing treatment of 3 days at 35°C. (Data from O. N. Purvis and F. G. Gregory. 1952. *Ann. Bot.* 1: 569–592.)

for cold treatment *followed* by a requirement for long days—a combination that leads to flowering in early summer at high latitudes (see **WEB TOPIC 20.10**). In some varieties of wheat and barley, short days can substitute for cold-mediated vernalization, a process called SD vernalization in cereals.

Vernalization can involve epigenetic changes in gene expression

For vernalization to occur, active metabolism is required during the cold treatment. Sources of energy (sugars) and oxygen are required, and temperatures below freezing at which metabolic activity is suppressed are not effective for vernalization. Furthermore, cell division and DNA replication also appear to be required. In some plant species, vernalization causes a stable change in the competence of the meristem to form an inflorescence.

One explanation for how vernalization stably affects competence is that there are changes in the pattern of gene expression in the meristem after cold treatment that persist into the spring and throughout the remainder of the life cycle. Stable changes in gene expression that do not involve alterations in the DNA sequence and which can be passed on to descendant cells through mitosis or meiosis are known as epigenetic changes. As such, epigenetic changes in gene expression are stable even after the signal (in this case cold) that induced the change is no longer present. Epigenetic changes of gene expression occur in many organisms, from yeast to mammals, and often require cell division and DNA replication, as is the case for vernalization.

The involvement of epigenetic regulation of a specific target gene in the vernalization process has been confirmed in the LDP Arabidopsis. In winter-annual types of Arabidopsis that require both vernalization and long days for flowering to be accelerated, a gene that acts as a repressor of flowering has been identified: *FLOWERING LOCUS C* (*FLC*). *FLC* is highly expressed in nonvernalized shoot apical regions. After vernalization, this gene is epigenetically switched off for the remainder of the plant's life cycle, permitting flowering in response to long days to occur (**Figure 20.19**). In the next generation,

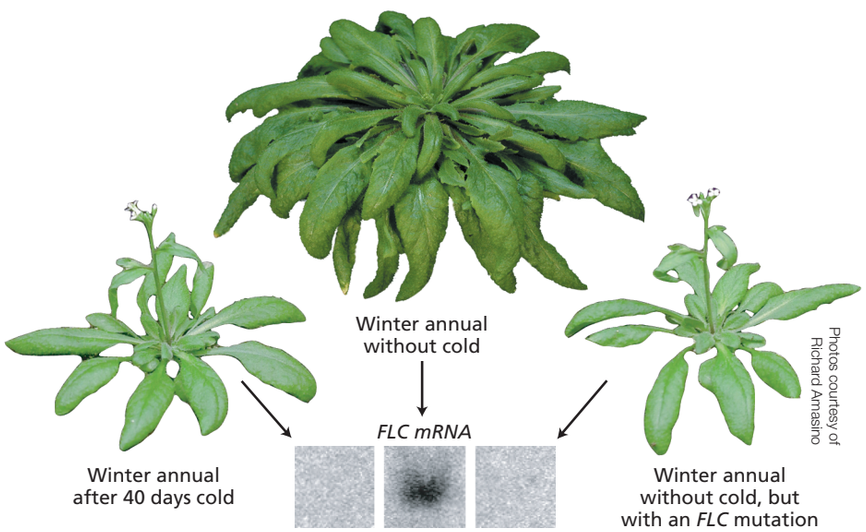


Figure 20.19 **Plants with a vernalization requirement are either quite delayed in flowering or do not flower unless they experience a period of prolonged cold.** (Left) Vernalization blocks the expression of the gene *FLOWERING LOCUS C* (*FLC*) in cold-requiring winter-annual ecotypes of Arabidopsis. (Right) A winter annual with an inhibitory mutation in the *FLC* gene exhibits rapid flowering without cold treatment.

however, the gene is switched on again, restoring the requirement for cold. Thus, in Arabidopsis the state of expression of the *FLC* gene represents a major determinant of meristem competence. In Arabidopsis it has been shown that FLC works by directly repressing the expression of the key floral signal *FT* in the leaves as well as the transcription factor genes *SOC1* and *FD* at the shoot apical meristem (see Figure 20.16).

The epigenetic regulation of *FLC* involves stable changes in chromatin structure resulting from **chromatin remodeling** (see Chapter 3). Vernalization causes the chromatin of the *FLC* gene to lose histone modifications characteristic of euchromatin (transcriptionally active DNA) and to acquire modifications, such as the methylation of specific lysine residues, characteristic of heterochromatin (transcriptionally inactive DNA). The cold-induced conversion of *FLC* from euchromatin to heterochromatin effectively silences the gene.

A range of vernalization pathways may have evolved

Many vernalization-requiring plants germinate in the fall, taking advantage of the cool and moist conditions optimal for their growth. The vernalization requirement of such plants ensures that flowering does not occur until spring, allowing the plants to survive winter vegetatively (flowers are especially sensitive to frost). A vernalizing plant must not only sense cold exposure, but also have a mechanism to measure the duration of cold exposure. For example, if a plant is exposed to a short period of cold early in the fall followed by a return of warm temperatures later that fall, it is important for the plant not to perceive the brief exposure to cold as winter and the following warm weather as spring. Accordingly, vernalization occurs only after exposure to a duration of cold sufficient to indicate that a complete winter season has passed.

A similar system of measuring the duration of cold before buds can be released from dormancy operates in many perennials that grow in temperate climates. The mechanism that plants have evolved to measure the duration of cold is not known, but in Arabidopsis there are genes that are induced only after exposure to a long period of cold, and these genes are critical to the vernalization process.

There does not appear to be a particular vernalization pathway that is conserved among all flowering plants. As discussed earlier, *FLC* is the flowering repressor that is responsible for the vernalization requirement in Arabidopsis. *FLC* encodes a MADS box protein that is related to regulatory proteins that we discuss later in this chapter, such as DEFICIENS and AGAMOUS, that are involved in floral development. In cereals, a gene encoding a different type of protein, a zinc finger–containing protein called VRN2 (*vern*alization 2), acts as the flowering repressor that creates a vernalization requirement.

It appears that the major groups of flowering plants evolved in warm climates and therefore did not evolve a mechanism to measure the duration of winter. Over geologic time, regions of Earth gradually developed a temperate climate because of continental drift and other factors. Members of many groups of plants adapted to these new temperate niches with the development of responses such as vernalization and bud dormancy, and thus these responses are likely to have evolved independently in different groups of plants.

20.8 Multiple Pathways Involved in Flowering

It is clear that the transition to flowering involves a complex system of interacting factors. Leaf-generated transmissible signals, including plant hormones, are required for determination of the shoot apex in both autonomously regulated and photoperiodic species.

Gibberellins and ethylene can induce flowering

Among the naturally occurring growth hormones, gibberellins (see Chapter 15) can have a strong influence on flowering (see **WEB TOPIC 20.11**). Exogenous gibberellin can evoke flowering when applied either to rosette LDPs such as Arabidopsis, or to dual–day length plants such as *Bryophyllum*, when grown under short days.

Gibberellin appears to promote flowering of Arabidopsis weakly in long days and strongly in short days. The central repressors of gibberellin signaling, DELLA proteins, down-regulate expression of the *FT*, *LFY*, and *SOC1* genes. DELLA proteins also interact with transcriptional regulators of *FT*, such as CO, FLC, and PHYTOCHROME INTERACTING FACTOR4 (PIF4) (see Chapter 4). Gibberellin stimulates the proteasomal degradation of DELLA, resulting in the up-regulation of *FT*, *LFY*, and *SOC1*, which promotes flowering (see Figure 20.16).

Exogenously applied gibberellins can also evoke flowering in a few SDPs under noninductive conditions and in cold-requiring plants that have not been vernalized. As noted in the discussion of phase change in Section 20.2, cone formation can also be promoted in juvenile plants of several gymnosperm families by the addition of gibberellins. Thus, in some plants exogenous gibberellins can bypass the endogenous trigger of age in autonomous flowering, as well as the primary environmental signals of day length and temperature. As discussed in Chapter 4, plants contain many gibberellin-like compounds. Most of these compounds are either precursors to, or inactive metabolites of, the active forms of gibberellin.

Gibberellin metabolism in the plant is strongly affected by day length. For example, in the LDP spinach (*Spinacia oleracea*), the levels of gibberellins are relatively low in short days, and the plants maintain a rosette form. After the plants are transferred to long days, the levels of all the gibberellins of the 13-hydroxylated pathway ($GA_{53} \rightarrow GA_{44} \rightarrow GA_{19} \rightarrow GA_{20} \rightarrow GA_1$; see **WEB APPENDIX 3**) increase. However, the fivefold increase in the physiologically active gibberellin, GA_1, is what causes the marked stem elongation that accompanies flowering.

In addition to gibberellins, other growth hormones can either inhibit or promote flowering. One commercially important example is the striking promotion of flowering in pineapple (*Ananas comosus*) by ethylene and ethylene-releasing compounds—a response that appears to be restricted to members of the pineapple family (Bromeliaceae).

The transition to flowering involves multiple factors and pathways

Genetic studies have established that there are four distinct developmental pathways that control flowering in the LDP Arabidopsis (see Figure 20.16):

- The *photoperiodic pathway* begins in the leaf and involves several photoreceptors. In LDPs under long-day conditions, the complex relationships among these photoreceptors result in the accumulation of CO protein in the phloem companion cells of the leaf. CO activates the expression of its downstream target gene, *FT*, in the phloem. FT protein ("florigen") moves into the sieve tube elements and is translocated to the apical meristem, where it stimulates flowering. As shown in the enlargement of the meristem in Figure 20.16, FT protein forms a complex with the transcription factor FD. The FD–FT complex then activates downstream target genes such as *SOC1*, *AP1*, and *LFY*, which turn on floral homeotic genes on the flanks of the inflorescence meristem.
- In the *autonomous* and *vernalization pathways*, flowering occurs either in response to internal signals—the production of a fixed number of leaves—or to prolonged low temperatures. In the autonomous pathway of Arabidopsis, all of the genes associated with the pathway are expressed in the meristem. The autonomous pathway acts by reducing the expression of the flowering repressor gene *FLOWERING LOCUS C* (*FLC*), an inhibitor of *SOC1* expression. Vernalization also represses *FLC*, but by a different mechanism (an epigenetic switch). Because the *FLC* gene is a common target, the autonomous and vernalization pathways are grouped together.
- The *gibberellin pathway* is required for flowering mainly under noninductive short days and marginally in long days. Exogenous gibberellins can promote flowering under these noninductive conditions by promoting the expression of *FT*, *SOC1*, and *LFY*.

All four pathways primarily converge on the expression of the key floral regulator, *FT,* in the vasculature. FT protein then conveys inductive signals for the expression of *SOC1*, *LFY*, and *AP1* in the meristem (see Figure 20.16), which in turn activate downstream genes required for floral organ development such as *AP3*, *PISTILLATA* (*PI*), and *AGAMOUS* (*AG*), as we will see in the next section.

20.9 Floral Meristems and Floral Organ Development

Once flowering has been evoked, the business of building flowers begins. The shapes of flowers are extremely diverse, reflecting adaptations to protect developing gametophytes, attract pollinators, promote self-pollination or cross-pollination as appropriate, and produce and disperse fruits and seeds. Despite this diversity, genetic and molecular studies have now identified a network of genes that control floral morphogenesis in flowers as different as those of Arabidopsis and snapdragon (*Antirrhinum majus*). Variations on this regulatory network now seem to account for floral morphogenesis in other species as well.

In this section we focus on floral development in Arabidopsis, which has been studied extensively. First we outline the basic morphological changes that occur during the transition from the vegetative to the reproductive phase. Then we consider the arrangement of the floral organs in four whorls on the meristem, and the types of genes that govern the normal pattern of floral development.

The shoot apical meristem in Arabidopsis changes with development

Floral meristems can usually be distinguished from vegetative meristems by their larger size. In the vegetative meristem, the cells of the central zone complete their division cycles slowly. The transition from vegetative to reproductive development is marked by an increase in the frequency of cell divisions within the central zone of the shoot apical meristem (see Chapter 18). The increase in the size of the meristem is largely a result of the increased division rate of these central cells.

During the vegetative phase of growth, the Arabidopsis apical meristem produces leaves with very short internodes, resulting in a basal rosette of leaves (**Figure 20.20**). When reproductive development is initiated, the vegetative meristem is transformed into the primary

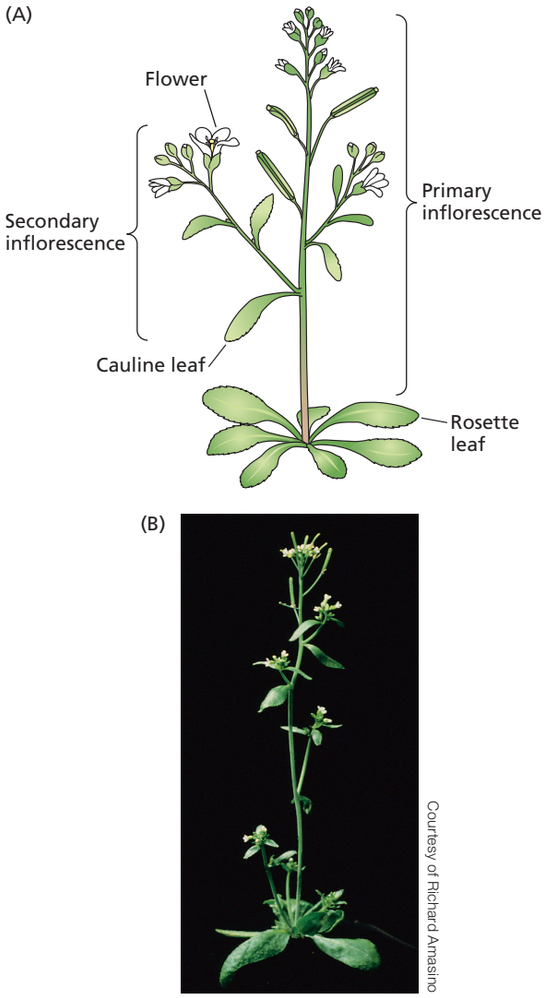


Figure 20.20 **Inflorescence architecture in Arabidopsis.** **(A)** The shoot apical meristem in *Arabidopsis thaliana* generates different organs at different stages of development. Early in development the shoot apical meristem forms a rosette of basal leaves. When the plant makes the transition to flowering, the shoot apical meristem is transformed into a primary inflorescence meristem that ultimately produces an elongated stem bearing flowers. Leaf primordia initiated prior to the floral transition develop on the stem (cauline leaves), and secondary inflorescences develop in the axils of these stem-borne leaves. **(B)** Photograph of a flowering Arabidopsis plant.

inflorescence meristem. The **primary inflorescence meristem** produces an elongated inflorescence axis bearing two types of lateral organs: stem-borne (or inflorescence) leaves and flowers. The axillary buds of the stem-borne leaves develop into **secondary inflorescence meristems**, and their activity repeats the pattern of development of the primary inflorescence meristem. The Arabidopsis inflorescence meristem has the potential to grow indefinitely and thus exhibits *indeterminate* growth.

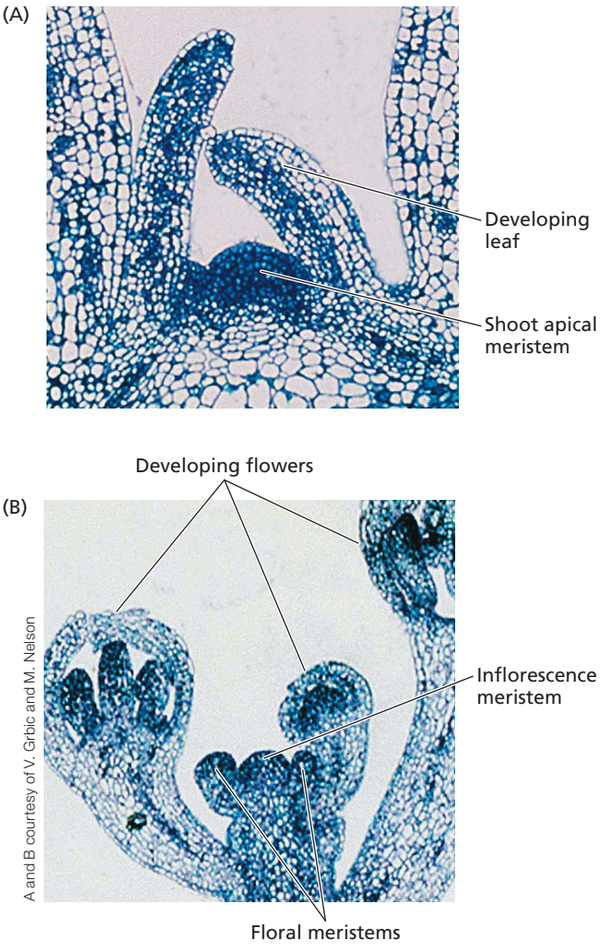


Figure 20.21 **Longitudinal sections through a vegetative (A) and a reproductive (B) shoot apical region of Arabidopsis.**

Flowers arise from **floral meristems** that form on the flanks of the inflorescence meristem (**Figure 20.21**). In contrast to the inflorescence meristem, the floral meristem is determinate.

The four different types of floral organs are initiated as separate whorls

Floral meristems initiate four different types of floral organs: sepals, petals, stamens, and carpels. These sets of organs are initiated in concentric rings, called **whorls**, around the flanks of the meristem (**Figure 20.22**). The initiation of the innermost organs, the carpels, consumes all of the meristematic cells in the apical dome, and only the floral organ primordia (localized regions of cell division) are present as the floral bud develops. In Arabidopsis, the whorls are arranged as follows:

- The first (outermost) whorl consists of four sepals, which are green at maturity.

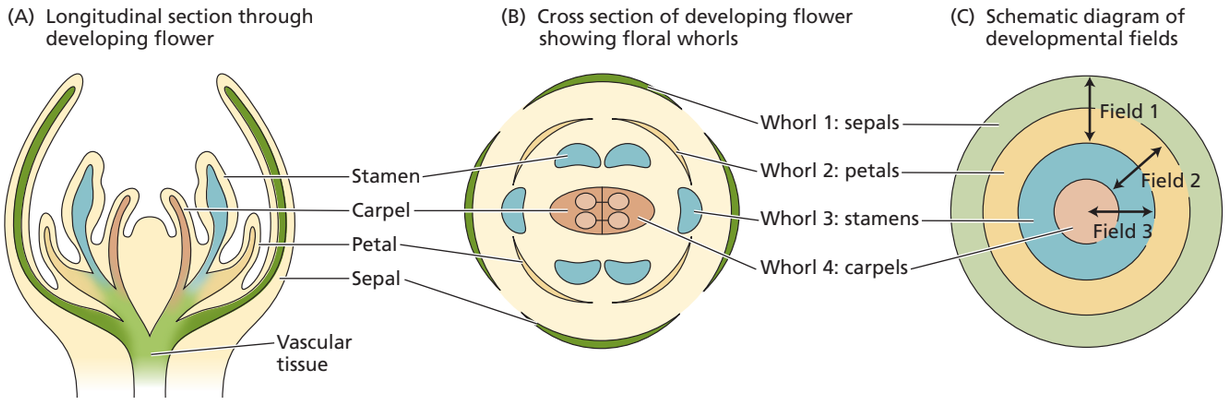


Figure 20.22 Floral organs are initiated sequentially by the floral meristem of Arabidopsis. (A and B) The floral organs are produced as successive whorls (concentric circles), starting with the sepals and progressing inward. (C) According to the combinatorial model, the functions of each whorl are determined by three overlapping developmental fields. These fields correspond to the expression patterns of specific floral organ identity genes. (After J. D. Bewley et al. 2000. In *Biochemistry and Molecular Biology of Plants*, B. B. Buchanan et al. [eds.], Rockville, MD: American Society of Plant Biologists.)

- The second whorl is composed of four petals, which are white at maturity.
- The third whorl contains six stamens (the male reproductive structures), two of which are shorter than the other four.
- The fourth (innermost) whorl is a single complex organ, the gynoecium or pistil (the female reproductive structure), which is composed of an ovary with two fused carpels, each containing numerous ovules, and a short style capped with a stigma.

Two major categories of genes regulate floral development

Studies of mutations have enabled identification of two key categories of genes that regulate floral development: floral meristem identity genes and floral organ identity genes.

1. Floral meristem identity genes encode transcription factors that are necessary for the initial induction of floral organ identity genes. They are the positive regulators of floral organ identity in the developing floral meristem.
2. **Floral organ identity genes** directly control floral organ identity. The proteins encoded by these genes are transcription factors that interact with other protein cofactors to control the expression of downstream genes whose products are involved in the formation or function of floral organs.

While certain genes fit neatly within these two general categories, it is important to keep in mind that floral development involves complex, nonlinear gene networks. In these networks, individual genes often play multiple roles. For example, evolution has recruited the same transcription factor, APETALA2, to first regulate floral meristem identity and then floral organ identity (**Table 20.3**).

Floral meristem identity genes regulate meristem function

Floral meristem identity genes must be active for the immature primordia formed at the flanks of the shoot apical meristem or inflorescence meristem to become floral meristems. (Recall that an apical meristem that is forming floral meristems on its flanks is known as an inflorescence meristem; see Figure 20.21.) For example, mutants of snapdragon (*Antirrhinum*) that have a defect in the floral meristem identity gene *FLORICAULA* (*FLO*) develop an inflorescence that does not produce flowers. Instead of developing floral meristems in the axils of the bracts, *flo* mutants develop additional inflorescence meristems in the bract axils. Thus, the wild-type *FLO* gene controls the determination step that establishes floral meristem identity.

In Arabidopsis, *LEAFY* (*LFY*), *FLOWERING D* (*FD*), *SUPPRESSOR OF OVEREXPRESSION OF CONSTANS1* (*SOC1*), and *APETALA1* (*AP1*) are among the critical genes in the genetic pathway that must be activated to establish floral meristem identity (see Table 20.3). *LFY* is the Arabidopsis version of the snapdragon *FLO* gene. As we saw in Figure 20.16, *LFY*, *FD*, and *SOC1* play central roles in floral evocation by integrating signals from several different pathways involving both environmental and internal cues. *lfy* and *fd* double mutants fail to form flowers, highlighting the roles of *LFY* and *FD* as floral meristem identity genes that serve as master regulators for the initiation of floral development.

TABLE 20.3 Genes that regulate flowering

Gene	Transcription Factor Family	Functions	Expression Domain	Orthologs
CONSTANS (*CO*)	Zinc finger	Activates flowering in response to long photoperiods	In leaves under long photoperiods	*AtCO* (potato); *Hd1* (rice)
FLOWERING D (*FD*)	bZIP	Receptor for florigen, activates flowering via AP1	In shoot apex	*OsFD1* (rice)
SUPPRESSOR OF OVEREXPRESSION OF CONSTANS1 (*SOC1*)	MADS	Activates flowering downstream of florigen	Leaves and apex	-
PHYTOCHROME INTERACTING FACTOR4 (*PIF4*)	bHLH	Activates florigen in response to high temperature	Leaves and apex	-
FLOWERING LOCUS C	MADS	Floral repressor	Leaves and apex	-
SHORT VEGETATIVE PHASE (*SVP*)	MADS	Represses flowering at low temperature	Leaves and apex	-
FLOWERING LOCUS M (*FLM*)	MADS	Represses flowering	Leaves and apex	-
LEAFY (*LFY*)	LFY	Floral meristem identity gene	Shoot apex	*RLF* (rice); *FLORICAULA* (*Antirrhinum*)
APETALA1 (*AP1*)	MADS	Class A homeotic gene, meristem identity	Floral meristems, whorl 1	*SQUAMOSA* (*Antirrhinum*); *ZAP1*, *GLOSSY15* (maize [corn, *Zea mays*])
APETALA2 (*AP2*)	AP2/EREBP	Class A homeotic gene, floral meristem identity	Floral meristems, whorl 1	*BRANCHED FLORETLESS1* (maize)
PISTILLATA (*PI*)	MADS	Class B homeotic gene	Whorls 2 and 3	*GLOBOSA* (*Antirrhinum*)
AGAMOUS (*AG*)	MADS	Class C homeotic gene	Whorls 3 and 4	*PLENA* and *FARINELLI* (*Antirrhinum*); *ZAG1* and *ZMM2* (maize)
SEPALLATA (*SEP*) *1*, *2*, *3*, *4*	MADS	Class E homeotic genes	Whorls 1–4	*DEFH49*, *DEFH200*, *DEFH72*, *AmSEP3B* (*Antirrhinum*); *ZMM3*, *8*, *14* (maize)
CAULIFLOWER (*CAL*)	MADS	Meristem identity	Floral meristem	-
FRUITFULL (*FUL*)	MADS	Floral meristem identity	Floral meristem and cauline leaves	-

Homeotic mutations led to the identification of floral organ identity genes

The genes that determine floral organ identity were discovered as floral homeotic mutants. Mutations in the fruit fly (*Drosophila*) led to the identification of a set of homeotic genes encoding transcription factors that determine the locations at which specific structures develop. Homeotic genes act as major developmental switches that activate the entire genetic program for a particular structure. The expression of homeotic genes thus gives organs their identity.

The floral organ identity genes were first identified as single-gene homeotic mutations that altered floral organ identity, causing some of the floral organs to appear in the wrong places. Five key genes initially were identified in Arabidopsis that specify floral organ identity: *APETALA1* (*AP1*), *APETALA2* (*AP2*), *APETALA3* (*AP3*), *PISTILLATA* (*PI*), and *AGAMOUS* (*AG*). Mutations in these genes dramatically altered the structure, and thus the identity, of the floral organs produced in two adjacent whorls (**Figure 20.23**). For example, plants with the *ap2* mutation lacked sepals and petals (see Figure 20.23B). Plants bearing *ap3* or *pi* mutations produced sepals instead of petals in the second whorl, and carpels instead of stamens in the third whorl (see Figure 20.23C). Plants homozygous for the *ag* mutation lacked

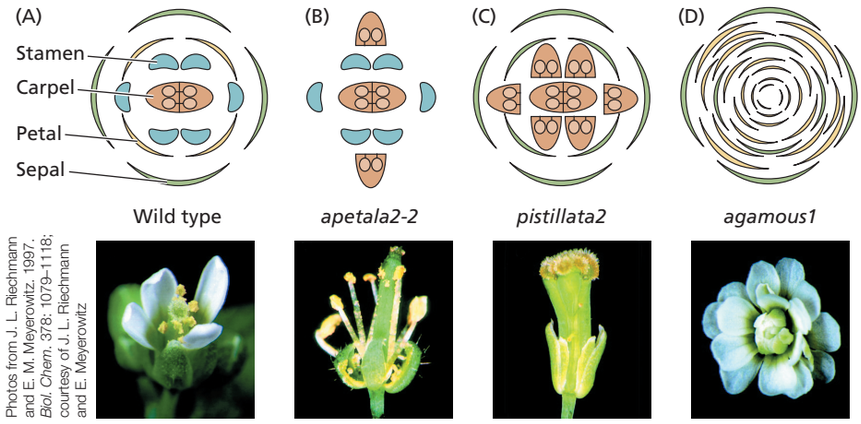


Figure 20.23 **Mutations in the floral organ identity genes dramatically alter the structure of the flower.** **(A)** Wild-type Arabidopsis shows normal structure in all four floral components. **(B)** *apetala2-2* mutants lack sepals and petals. **(C)** *pistillata2* mutants lack petals and stamens. **(D)** *agamous1* mutants lack both stamens and carpels. (After J. D. Bewley et al. 2000. In: *Biochemistry and Molecular Biology of Plants*, B.B. Buchanan et al. [eds.], Rockville, MD: American Society of Plant Biologists.)

both stamens and carpels (see Figure 20.23D). Because mutations in these genes change floral organ identity without affecting the initiation of flowers, they are, by definition, homeotic genes.

The role of organ identity genes in floral development is dramatically illustrated by experiments in which two or three activities are eliminated by loss-of-function mutations. In quadruple-mutant Arabidopsis plants (*ap1, ap2, ap3/pi*, and *ag*), floral meristems no longer produce floral organs, but rather produce green leaflike structures; these leaflike organs are produced with a whorled phyllotaxy typical of normal flowers (**Figure 20.24**). This experimental result shows that leaves are the "ground state" of organs produced by shoot meristems, and that the activity of additional genes such as *AP1* and *AP2* are required to convert the leaflike, "ground-state" organs into petals, sepals, stamens, and pistils. This result supports the idea of the eighteenth-century German poet and natural scientist Johann Wolfgang von Goethe (1749–1832), who speculated that floral organs are highly modified leaves.



Figure 20.24 **A quadruple mutant of Arabidopsis (*ap1, ap2, ap3/pi, ag*) produces leaflike structures in place of floral organs.**

The ABC model partially explains the determination of floral organ identity

The five floral organ identity genes we have just described fall into three classes—A, B, and C—defining three different kinds of activities encoded by three distinct types of genes (**Figure 20.25**):

- Class A activity, encoded by *AP1* and *AP2*, controls organ identity in the first and second whorls. Loss of Class A activity results in the formation of carpels instead of sepals in the first whorl, and of stamens instead of petals in the second whorl.
- Class B activity, encoded by *AP3* and *PI*, controls organ determination in the second and third whorls. Loss of Class B activity results in the formation of sepals instead of petals in the second whorl, and of carpels instead of stamens in the third whorl.
- Class C activity, encoded by *AG*, controls events in the third and fourth whorls. Loss of Class C activity results in the formation of petals instead of stamens in the third whorl. Moreover, in the absence of Class C activity, the fourth whorl (normally a carpel) is replaced by a *new flower*. As a result, the fourth whorl of an *ag* mutant flower is occupied by sepals. The floral meristem is no longer determinate. Flowers continue to form *within* flowers, and the pattern of organs (from outside to inside) is: sepal, petal, petal; sepal, petal, petal; and so on.

The **ABC model** accounts for many observations in two distantly related eudicot species (snapdragon and Arabidopsis), and provides a way of understanding how relatively few key regulators can combinatorially provide a complex outcome. The ABC model postulates that organ identity in each whorl is determined by a unique combination of the three organ identity gene activities (see Figure 20.25):

- Class A activity alone specifies sepals.
- Class A and B activities are required for the formation of petals.

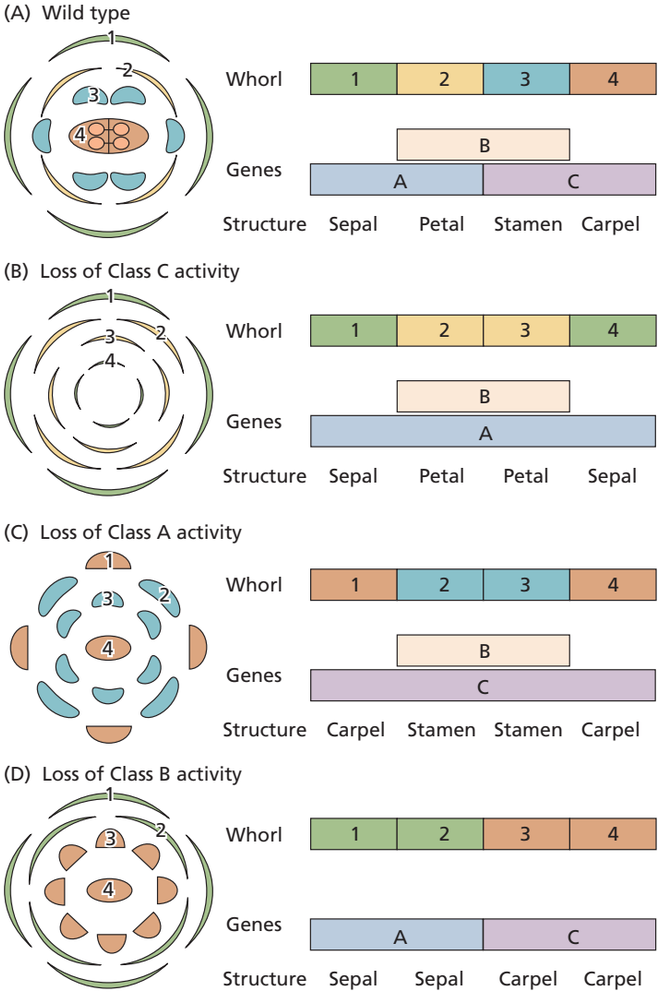


Figure 20.25 **Interpretation of the phenotypes of floral homeotic mutants based on the ABC model.** **(A)** All three activity classes are functional in the wild type. **(B)** Loss of Class C activity results in expansion of Class A activity throughout the floral meristem. **(C)** Loss of Class A activity results in the spread of Class C activity throughout the meristem. **(D)** Loss of Class B activity results in the expression of only Class A and C activities. (After J. D. Bewley et al. 2000. In: *Biochemistry and Molecular Biology of Plants*, B.B. Buchanan et al. [eds.], Rockville, MD: American Society of Plant Biologists.)

- Class B and C activities form stamens.
- Class C activity alone specifies carpels.

The model further proposes that Class A and C activities mutually repress each other; that is, both A- and C-class genes exclude each other from their expression domains, in addition to their function in determining organ identity.

Although the patterns of organ formation in wild-type flowers and most of the mutants are predicted and explained by this model, not all observations can be accounted for by the ABC genes alone. For example, expression of the ABC genes throughout the plant does not transform vegetative leaves into floral organs. Thus, the ABC genes, while necessary, are not sufficient to impose floral organ identity onto a leaf developmental program. As we discuss next, transcription factors encoded by floral meristem identity genes are also required for the formation of petals, stamens, and carpels.

Arabidopsis Class E genes are required for the activities of the A, B, and C genes

Since the A, B, and C genes were identified, another class of floral homeotic genes, the Class E genes, has been discovered. Mutations in three of the other genes identified in mutant screens for floral homeotic mutants, *AGAMOUS-LIKE1-3* (*AGL1-3*), produced only subtle phenotypes when mutated individually. However, the flowers of the *agl1/agl2/agl3* triple mutants consisted of sepal-like structures only, suggesting that the subtle phenotypes previously observed in the three individually mutated *AGL* genes were due to functional redundancy. Because of the sepal-rich phenotype of the triple mutant, the three *AGL* genes were renamed *SEPALLATA1-3* (*SEP1-3*) and were added to the ABC model as Class E genes (**Figure 20.26**). (Class D genes are required for ovule formation and are described later in this section.)

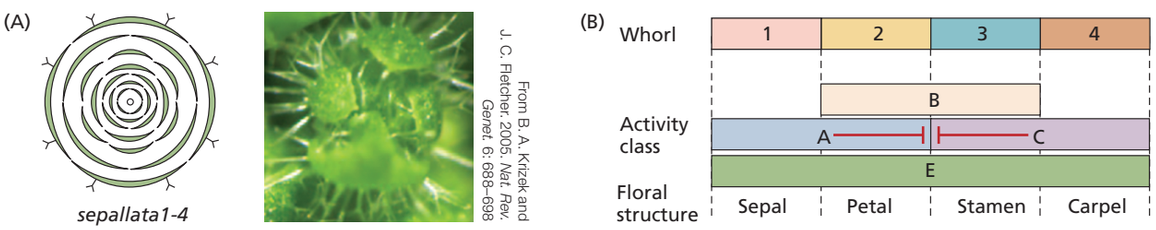


Figure 20.26 **ABCE model for floral development.** **(A)** In *sepallata1–4* mutants, all of the floral organs resemble vegetative leaves, suggesting that *SEP* genes are required for floral meristem identity. **(B)** ABCE model for floral organ determination in which *SEP*s act as Class E genes required for floral organ identity. (From B. A. Krizek and J. C. Fletcher. 2005. *Nat. Rev. Genet.* 6: 688–698.)

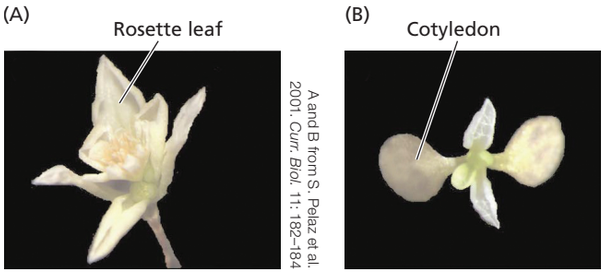


Figure 20.27 **Conversion of cotyledons and vegetative leaves into petals by ectopic expression of Class E genes in combination with Class A and B genes.** Arabidopsis plants overexpressing *SEP3/AP1/AP3/PI* **(A)** or *AP1/AP3/PI/SEP2/SEP3* **(B)** transgenes.

Another *SEPALLATA* gene, *SEP4*, is required redundantly with the other three *SEP* genes to confer sepal identity, and contributes to the development of the other three organ types. *sep* quadruple mutants show a conversion of all four floral organ types into leaflike structures, similar to the *ap1, ap2, ap3/pi,* and *ag* quadruple mutant (see Figures 20.24 and 20.26). Remarkably, by expressing Class E genes in combination with Class A and B genes, it is possible to convert both cotyledons and vegetative leaves into petals (**Figure 20.27**).

The ABCE model was formulated based on genetic experiments in Arabidopsis and *Antirrhinum*. Flowers from different species have evolved diverse structures by modifying the regulatory networks described by the ABCE model (see **WEB TOPIC 20.12**).

According to the Quartet Model, floral organ identity is regulated by tetrameric complexes of the ABCE proteins

All homeotic genes that have been identified so far, in both plants and animals, encode transcription factors. However, unlike animal homeotic genes, which contain homeobox sequences, most plant homeotic genes belong to a class of related sequences known as **MADS box genes**. The acronym MADS is based on the four founding members (*MINICHROMOSOME MAINTENANCE1* [*MCM1*], *AGAMOUS*, *DEFICIENS*, and *SERUM RESPONSE FACTOR* [*SRF*]) of a large gene family.

Many of the genes that determine floral organ identity are MADS box genes, including the *DEFICIENS* gene of snapdragon and the *AGAMOUS* (*AG*), *PISTILLATA* (*PI*), and *APETALA3* (*AP3*) genes of Arabidopsis (see Table 20.3). The MADS box genes share a characteristic, conserved nucleotide sequence known as a MADS box, which encodes a protein structure known as the MADS domain (**Figure 20.28A**). Adjacent to the MADS domain is an intervening region followed by the K domain, which is a coiled-coil region primarily involved in protein–protein interactions. The MADS

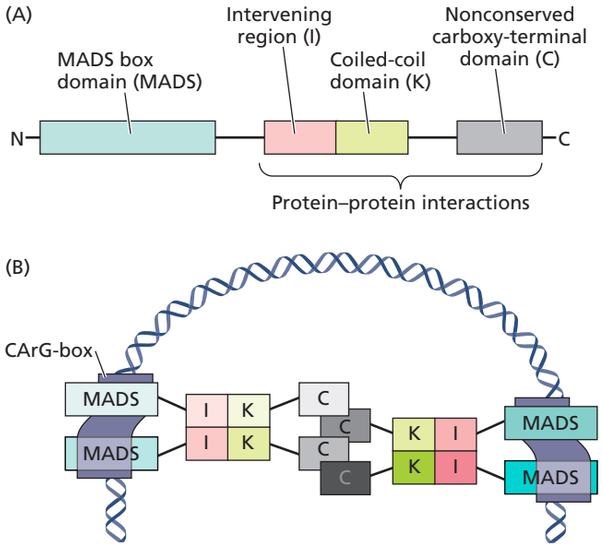


Figure 20.28 **Model of MADS box domain interaction with target genes.** **(A)** Domain structure of MADS box transcription factors. **(B)** Tetramers of MADS box transcription factors bind to a pair of CArG-box motifs in the regulatory regions of their target genes, which causes DNA bending. DNA bending may either activate or repress the target genes.

box gene transcription factors form tetramers that bind to $CC(A/T)_6GG$ sequences, the so-called CArG-box, in the regulatory regions of their target genes. When the tetramers bind two different CArG-boxes on the same target gene, the boxes are brought into close proximity, causing DNA bending (**Figure 20.28B**).

Not all homeotic genes are MADS box genes, and not all genes containing the MADS box domain are homeotic genes. For example, the homeotic gene *AP2* is a member of the AP2/ERF (ethylene-responsive element-binding factor) family of transcription factors, and the floral meristem identity gene *SOC1* is a MADS box gene.

To gain a more mechanistic understanding of the ABCE model, a biochemical interaction model, called the **Quartet Model**, has been proposed (**Figure 20.29**). In the Quartet Model, tetramers of combinations of the ABCE genes directly bind DNA and specify floral organs. The model is based on the observation that MADS box genes dimerize, and two dimers can come together, forming a tetramer. These tetramers are hypothesized to bind CArG-boxes on target genes and modify their expression (see Figure 20.28B). Although all MADS box proteins can form higher-order complexes, not all of these are able to bind DNA. For example, Class B factors (AP3 and PI) bind DNA only as heterodimers, whereas both homodimers and heterodimers of Classes A, C, and E can bind DNA. According to the model, tetramers composed of different homodimers and heterodimers of MADS domain proteins can exert combinatorial control

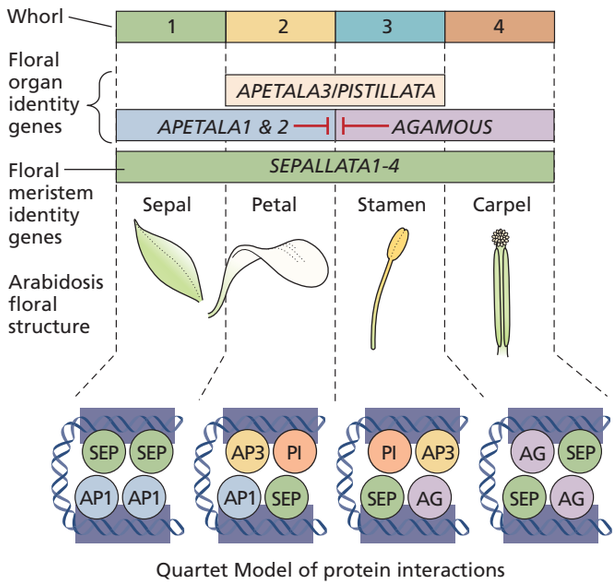


Figure 20.29 Quartet Model of floral organ specification in Arabidopsis. In whorl 1, expression of Class A (*AP1* and *AP2*) and E (*SEP*) genes results in the formation of sepals. In whorl 2, expression of Class A (*AP1*, *AP2*), B (*AP3*, *PI*), and E (*SEP*) genes results in the formation of petals. In whorl 3, the expression of Class B (*AP3*, *PI*), C (*AG*), and E (*SEP*) genes causes the formation of stamens. In whorl 4, Class C (*AG*) and E (*SEP*) genes specify carpels. In addition, Class A activity (*AP1* and *AP2*) represses Class C activity (*AG*) in whorls 1 and 2, while Class C activity represses Class A activity in whorls 3 and 4. According to the Quartet Model, the identity of each of the floral organs is determined by four combinations of the floral homeotic proteins known as the MADS box proteins. Two dimers of each tetramer recognize two different DNA sites (termed CArG-boxes, shown here in purple) on the same strand of DNA, which are brought into close proximity by DNA bending. Note that SEPALLATA proteins are present in all four complexes, serving to recruit the other proteins to the complex. The exact structures of the multimeric complexes are hypothetical.

over floral organ identity. For example, the AP3–PI heterodimer interacts *directly* with AP1 and SEP3 to promote petal formation, and *indirectly* with AG with the help of SEP3 acting as a scaffold. In general, the SEP proteins seem to act as cofactors that provide flower-specific activity to the ABC genes by making complexes with their products and seem to be required for activating the expression of ABC genes.

Class D genes are required for ovule formation

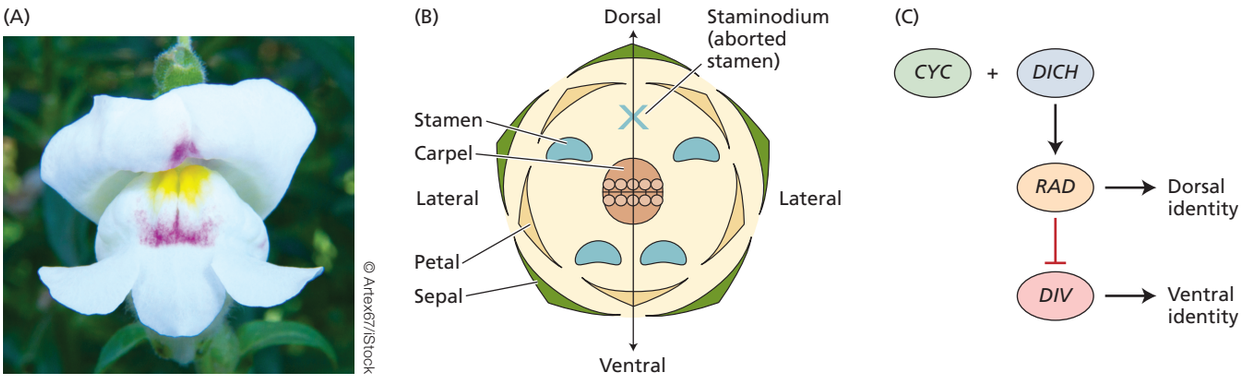
According to the ABCE model, carpel formation requires the activities of the Class C and E genes. However, it appears that a third group of MADS box genes closely related to the Class C genes is required for ovule formation. These ovule-specific genes have been called Class D genes. Since the ovule is a structure within the carpel, Class D genes are not, strictly speaking, "organ identity genes," although they function in much the same way in specifying ovules. Class D activities were first discovered in petunia. Silencing two MADS box genes known to be involved in floral development in petunia, *FLORAL-BINDING PROTEIN7/11* (*FBP7/11*), resulted in the growth of styles and stigmas in the locations normally occupied by ovules. When the *FBP11* was overexpressed in petunia, ovule primordia formed on the sepals and petals.

In Arabidopsis, the ectopic expression of either *SHATTERPROOF1* or *SHATTERPROOF2* (*SHP1*, *SHP2*) or *SEEDSTICK* (*STK*) is sufficient to induce the transformation of sepals into carpeloid organs bearing ovules. Moreover, *stk/shp1/shp2* triple mutants lack normal ovules. Thus, in addition to the Class C and E genes, Class D genes are required for normal ovule development.

Floral asymmetry in flowers is regulated by gene expression

While many flowers, such as those of Arabidopsis, are radially symmetrical, many plants have evolved flowers with bilateral symmetry, which allowed them to form specialized structures to attract pollinators. For example, *Antirrhinum* flowers show distinct differences in the shapes of the adaxial (dorsal) petals compared with the abaxial (ventral) petals (**Figure 20.30**). How has this occurred? Again, as with the ABCE model, genetics has provided the answer. Mutations that disrupt the development of zygomorphic flowers have been known since the eighteenth century. Carl Linnaeus was the first to describe a naturally occurring mutant of toadflax (*Linaria vulgaris*) that converted the bilaterally symmetrical flower to a radially symmetrical form (**Figure 20.31**). Flowers of the genus *Linaria* normally have corollas with four stamens and a single nectar spur. The bizarre specimen described by Linnaeus had five stamens and five nectar spurs. This abnormal, radially symmetrical state was dubbed *peloria* by Linnaeus, from the Greek word for "monster."

More recently, analogous ("peloric") mutants in *Antirrhinum majus* have allowed a genetic dissection of the molecular mechanisms of floral symmetry specification. The cloning of the mutated gene *RADIALIS* (*RAD*) revealed a regulatory mechanism by which *RAD* controls floral asymmetry (see Figure 20.30). *RAD* encodes a transcription factor of the MYB family that represses another key gene called *DIVARICATA* (*DIV*). When *DIV* is mutated, it causes all the petals of the flower to look like the adaxial petals. *DIV* therefore specifies abaxial petal identity in the flower. Analysis of other mutants



© Artex67/iStock

Figure 20.30 **Floral asymmetry in Antirrhinum.** **(A and B)** Antirrhinum flowers exhibit bilateral symmetry. **(C)** The *DIVARICATA* (*DIV*) gene encodes a MYB transcription factor that promotes abaxial identity throughout the flower. *CYCLOIDEA* (*CYC*) and *DICHOTOMA* (*DICH*) encode related transcription factors that activate the *RADIALIS* (*RAD*) gene. The RAD protein antagonizes DIV in the adaxial part of the flower and limits its activity to the lateral and abaxial domains. (B and C after B. A. Krizek and J. C. Fletcher. 2005. *Nat. Rev. Genet.* 6: 688–698.)

indicated that *RAD* determines adaxial petal identity. The RAD transcription factor is activated by two other genes, *CYCLOIDEA* and *DICHOTOMA*, that are expressed in the adaxial petals. The expression of *RAD* thus allows *DIV* to be repressed in the adaxial part of the flower. Where *RAD* is not expressed in the bottom of the flower, *DIV* is expressed and specifies abaxial fate.

Thus far, our understanding of floral development has been based primarily on three model species, Arabidopsis, *Antirrhinum,* and rice. One of the challenges of the future will be to explore the variations in the gene networks that regulate floral development across a wider spectrum of flowering plants. A second challenge will be to try to understand how floral developmental pathways evolved from nonflowering ancestors. Such studies may one day lead to the solution of Darwin's "abominable mystery"—the evolution of angiosperms.



From A. Busch and S. Zachgo. 2009. *BioEssays* 31: 1181–1190.

Figure 20.31 **The *peloria* mutant of toadflax (*Linaria vulgaris*).** The normal flower of *Linaria* with bilateral symmetry is shown on the left, and the radially symmetrical *peloria* mutant is shown on the right. The peloric toadflax flower is now known to be caused by inactivation of the *Linaria CYCLOIDEA* gene through DNA methylation.

Summary

Formation of the floral organs (sepals, petals, stamens, and carpels) occurs at the shoot apical meristem and is linked to both internal (autonomous) and external (environmental) signals. A network of genes that control floral morphogenesis has been identified in several species.

20.1 Floral Evocation: Integrating Environmental Cues

- Internal (autonomous) and external (environment-sensing) control systems enable plants to precisely regulate and time flowering for reproductive success.
- Two of the most important seasonal responses that affect floral development are photoperiodism (response to changes in day length) and vernalization (response to prolonged cold).
- Synchronized flowering favors cross-pollination and helps ensure seed production under favorable conditions.

20.2 The Shoot Apex and Phase Changes

- In plants, the transition from juvenile to adult is usually accompanied by changes in vegetative characteristics (**Figure 20.1**).

(*Continued*)

Summary (*continued*)

20.3 Circadian Rhythms: The Clock Within

- Circadian rhythms are based on an endogenous oscillator consisting of interacting transcription factors, not the presence or absence of light (**Figure 20.3**).
- Circadian rhythms are defined by three parameters: period, phase, and amplitude (**Figure 20.4A**).
- Temperature compensation prevents temperature changes from affecting the period of the circadian clock.
- Phytochromes and cryptochromes entrain the circadian clock.

20.4 Photoperiodism: Monitoring Day Length

- Plants can detect seasonal changes in day length at latitudes away from the equator (**Figure 20.5**).
- Flowering in LDPs requires that the day length exceed a certain duration, called the critical day length. Flowering in SDPs requires a day length that is less than the critical day length (**Figure 20.7**).
- Leaves perceive the photoperiodic stimulus in both LDPs and SDPs.
- Measurement of the length of night is important for monitoring changes in day length; flowering in both SDPs and LDPs can be determined by the duration of darkness (**Figure 20.8**).
- For both LDPs and SDPs, the dark period can be made ineffective by interruption with a short exposure to light (a night break) (**Figure 20.9**).
- The flowering response to night breaks shows a circadian rhythm, supporting the clock hypothesis (**Figure 20.10**).
- In the external coincidence model, flowering is induced in both SDPs and LDPs when light exposure is coincident with the appropriate phase of the oscillator.
- CO (in Arabidopsis) and Hd1 (in rice) regulate flowering by controlling the transcription of floral stimulus genes (**Figure 20.11**).
- CO protein is degraded at different rates in the light versus the dark. Light enhances the stability of CO, allowing it to accumulate during the day; in the dark it is rapidly degraded.
- The effects of red and far-red night breaks implicate phytochrome in the control of flowering in SDPs and LDPs (**Figures 20.12, 20.13**).
- Flowering in LDPs is promoted when the inductive light treatment coincides with a peak in light sensitivity, which follows a circadian rhythm (**Figure 20.14**).

20.5 Long-Distance Signaling Involved in Flowering

- In photoperiodic plants, a long-range signal is transmitted in the phloem from the leaves to the apex, permitting floral evocation (**Figure 20.15**).

20.6 The Identification of Florigen

- FT protein moves via the phloem from the leaves to the shoot apical meristem under inductive photoperiods. In the meristem, FT forms a complex with the transcription factor FD to activate floral identity genes (**Figure 20.16**).

20.7 Vernalization: Promoting Flowering with Cold

- In sensitive plants, a cold treatment is required for plants to respond to floral signals such as inductive photoperiods (**Figures 20.17**, **20.18**).
- For vernalization to occur, active metabolism is required during the cold treatment.
- After vernalization, the *FLC* gene is epigenetically switched off for the remainder of the plant's life cycle, permitting flowering in response to long days to occur in Arabidopsis (**Figure 20.19**).
- The epigenetic regulation of *FLC* involves stable changes in chromatin structure.
- A variety of vernalization pathways have evolved in flowering plants.

20.8 Multiple Pathways Involved in Flowering

- The four distinct pathways that control flowering converge to increase the expression of key floral regulators: *FT* in the vasculature and *SOC1*, *LFY*, and *AP1* in the meristem (**Figure 20.16**).

20.9 Floral Meristems and Floral Organ Development

- The four different types of floral organs are initiated sequentially in separate, concentric whorls (**Figure 20.22**).
- Mutations in homeotic floral identity genes alter the types of organs produced in each of the whorls (**Figures 20.23, 20.24**).
- The ABC model suggests that organ identity in each whorl is determined by the combined activity of three organ identity genes (**Figure 20.25**).
- Expression of Class E floral meristem identity genes (e.g., *SEPALLATA*) is required for expression of Class A, B, and C genes (**Figure 20.26**).
- Many floral organ identity genes encode MADS domain–containing transcription factors that function as heterotetramers (**Figure 20.28, Table 20.3**). The Quartet Model describes how these

Summary (*continued*)

transcription factors might act together to specify floral organs (**Figure 20.29**).

- Variations on the ABCE model can explain the diversity of angiosperm flower structures (**Figures 20.30, 20.31**).

Web Material

- **WEB TOPIC 20.1 Climate Change Has Caused Measurable Changes in Flowering Time of Wild Plants** Plants are able to sense as little as a 1ºC difference in temperature, and increasing ambient temperature accelerates flowering in many species.
- **WEB TOPIC 20.2 Contrasting the Characteristics of Juvenile and Adult Phases of English Ivy (*Hedera helix*) and Maize (*Zea mays*)** A table of juvenile versus adult morphological characteristics is presented.
- **WEB TOPIC 20.3 Flowering of Juvenile Meristems Grafted to Adult Plants** The competence of juvenile meristems to flower can be tested in grafting experiments.
- **WEB TOPIC 20.4 Competence and Determination Are Two Stages in Floral Evocation** Experiments have been carried out to define competence and determination during floral evocation.
- **WEB TOPIC 20.5 Characteristics of the Phase-Shifting Response in Circadian Rhythms** Petal movements in Kalanchoe have been used to study circadian rhythms.
- **WEB TOPIC 20.6 The Contrasting Effects of Phytochromes A and B on Flowering** PhyA and phyB affect flowering in Arabidopsis and other species.
- **WEB TOPIC 20.7 Support for the Role of Blue-Light Regulation of Circadian Rhythms** ELF3 plays a role in mediating the effects of blue light on flowering time.
- **WEB TOPIC 20.8 Genes That Control Flowering Time** A discussion of genes that control different aspects of flowering time is presented.
- **WEB TOPIC 20.9 The Self-Propagating Nature of the Floral Stimulus** In certain species, the induced state can be transferred by grafting almost indefinitely.
- **WEB TOPIC 20.10 Regulation of Flowering in Canterbury Bells by Both Photoperiod and Vernalization** Short days acting on the leaf can substitute for vernalization at the shoot apex in Canterbury bells.
- **WEB TOPIC 20.11 Examples of Floral Induction by Gibberellins in Plants with Different Environmental Requirements for Flowering** A table of the effects of gibberellins on plants with different photoperiodic requirements is presented.
- **WEB TOPIC 20.12 Floral Organ Identity Genes in Monocot Plants** Variations in the ABCE model are associated with contrasting floral morphology in different monocots and eudicots.

For more study aids, go to oup.com/he/taiz7e.

Suggested Reading

Ali, Z., Raza, Q., Atif, R. M., Aslam, U., Ajmal, M., and Chung, G. (2019) Genetic and molecular control of floral organ identity in cereals. *Int. J. Mol. Sci*. 20: 2743.

Amasino, R. (2010) Seasonal and developmental timing of flowering. *Plant J*. 61: 1001–1013.

Andrés, F., and Coupland, G. (2012) The genetic basis of flowering responses to seasonal cues. *Nat. Rev. Genet.* 13: 627–639.

Busch, A., and Zachgo, S. (2009) Flower symmetry evolution: Towards understanding the abominable mystery of angiosperm radiation. *BioEssays* 31: 1181–1190.

Causiera, B., Schwarz-Sommerb, Z., and Davies, B. (2010) Floral organ identity: 20 years of ABCs. *Semin. Cell Dev. Biol.* 21: 73–79.

Huijser, P., and Schmid, M. (2011) The control of developmental phase transitions in plants. *Development* 138: 4117–4129.

Jaeger, E., Pullen, N., Lamzin, S., Morris, R. J., and Wigge, P. A. (2013) Interlocking feedback loops govern the dynamic behavior of the floral transition in Arabidopsis. *Plant Cell* 25: 820–833.

Krizek, B. A., and Fletcher, J. C. (2005) Molecular mechanisms of flower development: An armchair guide. *Nat. Rev. Genet.* 6: 688–698.

Lee, J., and Lee, I. (2010) Regulation and function of SOC1, a flowering pathway integrator. *J. Exp. Bot.* 61: 2247–2254.

Liu, L., Liu, C., Hou, X., Xi, W., Shen, L., Tao, Z., Wang, Y., and Yu, H. (2012) FTIP1 is an essential regulator required for florigen transport. *PLOS Biol*. 10(4): e1001313.

Liu, L., Zhu, Y., Shen, L., and Yu, H. (2013) Emerging insights into florigen transport. *Curr. Opin. Plant Biol.* 16: 607–613.

Rijpkemaa, A. S., Vandenbusscheb, M., Koesc, R., Heijmansd, K., and Gerats, T. (2010) Variations on a theme: Changes in the floral ABCs in angiosperms. *Semin. Cell Dev. Biol.* 21: 100–107.

Song, Y. H., Shim, J. S., Kinmonth-Schultz, H. A., and Imaizumi, T. (2015) Photoperiodic flowering: time measurement mechanisms in leaves. *Annu. Rev. Plant Biol*. 66: 441–464.

Song, Y. H., Kubota, A., Kwon, M. S., Covington, M. F., Lee, N., Taagen, E. R., Cintrón, D. L., Hwang, D. W., Akiyama, R., Hodge, S. K., Huang, H., Nguyen, N. H., Nusinow, D. A., Millar, A. J., Shimizu, K. K., and Imaizumi, T. (2018) Molecular basis of flowering under natural long-day conditions in Arabidopsis. *Nat. Plants* 4: 824–835.

Taoka, K.-I., Ohki, I., Tsuji, H., Kojima, C., and Shimamoto, K. (2013) Structure and function of florigen and the receptor complex. *Trends Plant Sci.* 18: 287–294.

21 Sexual Reproduction: From Gametes to Fruits



schankz/Shutterstock

Prior to the discovery of sexual reproduction in plants in the late seventeenth century, seeds were thought to be produced by an asexual, vegetative process similar to bud formation. In the mid-eighteenth century the role of pollen in fertilization was experimentally demonstrated, and by the late nineteenth century the major features of the plant life cycle had been established. The most profound difference between sexual reproduction in plants and animals is the presence in the plant life cycle of two entirely separate haploid individuals called the male and female gametophytes. Strictly speaking, the stamens and carpels of flowers are spore-producing structures rather than sexual structures. The spores produced in flowers develop into the male and female gametophytes, the true sexual phases of the plant life cycle (see Chapter 1).

We begin our discussion with the development of the male and female gametophytes, which produce the gametes. As sessile organisms, plants depend on gravity and vectors such as wind or insects to bring about pollination and fertilization. As we will see, plants are not entirely passive in this process: They have evolved complex mechanisms, both anatomical and biochemical, that ensure outcrossing. As in the case of animals, Darwinian evolution involves both natural selection and sexual selection. Sexual selection in plants occurs not by visual displays by males as in animals, but by competition between male gametophytes to reach the female gametophyte and fertilize the egg within the ovule. The final step in the process is the development of the seed and fruit—the structures that protect and nourish the embryo, and deliver it to a suitable substrate on which to germinate and establish itself as a new seedling.

21.1 Development of the Male and Female Gametophyte Generations

The plant life cycle differs fundamentally from that of animals in that it encompasses two separate multicellular generations, a diploid (2*N*) *sporophyte generation* and a haploid (1*N*) *gametophyte generation* (see Chapter 1; for a discussion of the evolution of diploidy in plants, see **WEB TOPIC 21.1**). The presence of two genetically distinct multicellular stages in the plant life cycle is called *alternation of generations*. Alternation of generations takes

place in the two reproductive "houses" of the flower—the stamens (*androecium* or "male house") and the carpels (*gynoecium* or "female house").

Because of alternation of generations, there is a crucial difference between plant and animal life cycles in the outcome of meiosis. In animals, the haploid cells produced by meiosis differentiate directly into the gametes—sperm or egg. In contrast, the haploid cells produced by meiosis in plants differentiate into spores—microspores (male) or megaspores (female) (**Figure 21.1**) (see Chapter 3 for a review of meiosis). Spores are cells formed by meiosis that develop into a separate multicellular generation called the gametophyte generation, rather than differentiating directly into gametes as in animals. Specifically, the microspores and megaspores undergo mitotic divisions to produce haploid individuals called *male* (or *micro-*) *gametophytes*, and *female* (or *mega-*) *gametophytes*, respectively. The male gametophytes form in the anther of the stamen, while the female gametophyte develops inside the ovule, or immature seed, which is contained within the hollow base of the *carpel*, called the *ovary* (see Figure 21.1). The presence of the haploid multicellular gametophyte generation in the plant life cycle means that gametes in plants are produced by mitosis rather than by meiosis. That is, specialized cells within the mature male and female gametophytes divide mitotically to produce the 1*N* gametes—the sperm and egg cells. The male and female gametes eventually participate in *syngamy*, in which one sperm cell fuses with one egg cell. Upon being fertilized by the sperm cell, the egg cell is transformed into the 2*N* *zygote*, the first cell of the future embryo (see Figure 21.1 and Chapter 22).

In addition to syngamy between the male and female gametes, a unique type of gametophytic cell fusion occurs within the embryo sacs of angiosperms: A second sperm cell fuses with the diploid *central cell* of the female gametophyte (itself the result of the fusion of two haploid polar nuclei) to produce the triploid *primary endosperm cell*, which goes on to form the nutritive endosperm tissue of the seed. The participation of two sperm cells during fertilization, unique to flowering plants, is called *double fertilization*. These two processes of cell fusion are only possible because the cells involved (sperm, egg, and central cell), unlike all other cells in the plant body, lack true cell walls, which would prevent membrane fusion.

Besides contributing to the evolutionary success of the angiosperms, double fertilization in certain crop plants, especially the big-seeded cereals developed in the Fertile Crescent of the Middle East, played a pivotal role in the early rise of human civilization. The seeds of early wheat varieties were prized by hunter–gatherers because of their abundance of carbohydrate-rich

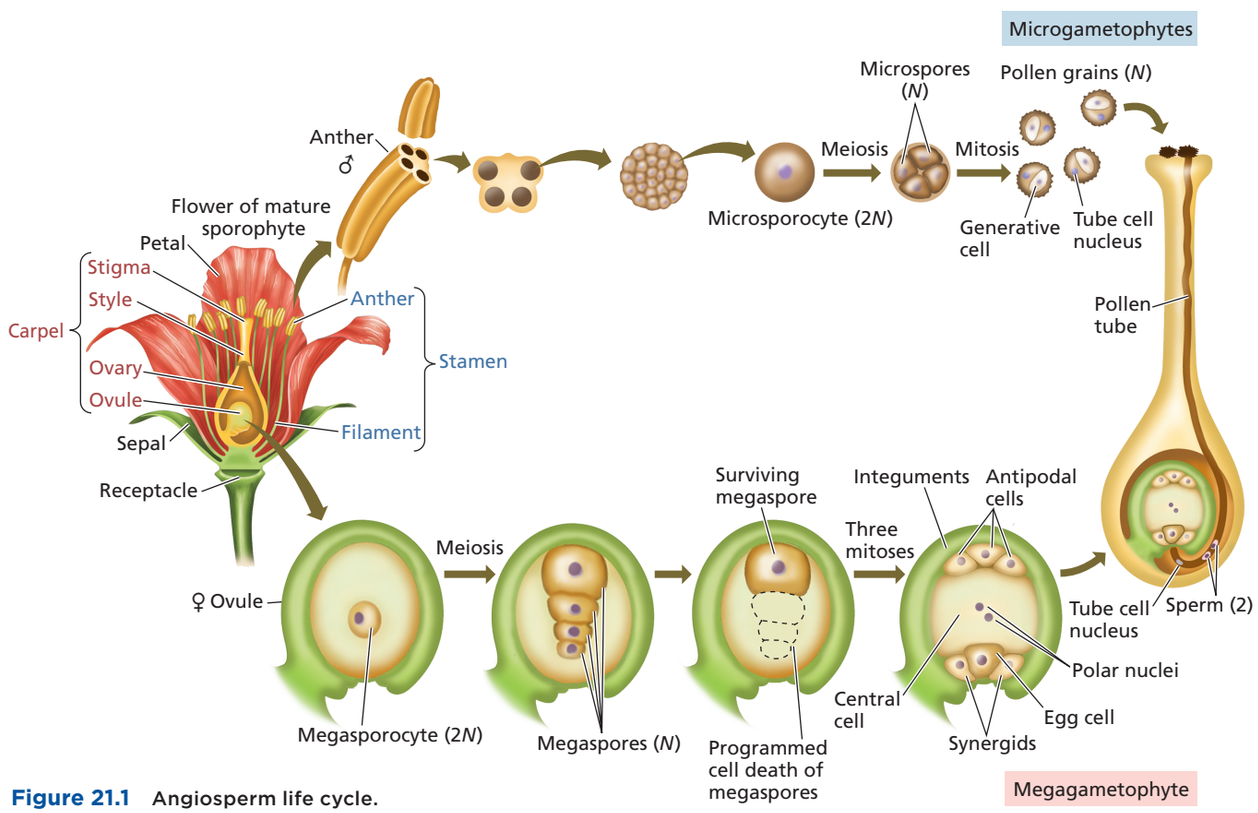


Figure 21.1 Angiosperm life cycle.

endosperm tissue. The planting of wheat seeds in the Middle East eventually led to the momentous shift from hunting and gathering to agriculture.

21.2 Formation of Male Gametophytes in the Stamen

The male gametophyte is formed in the stamen of the flower. Typically, the stamen is made up of a delicate filament attached to an anther composed of four microsporangia (or *pollen sacs*) arranged in opposite pairs (**Figure 21.2A**). Each pair of microsporangia is separated from the other by a central region of sterile tissue surrounding a vascular bundle.

The precise sequence of microsporangium development varies from species to species. In Arabidopsis, the mature anther contains **pollen mother cells**, the cells that undergo meiosis, surrounded by four somatic layers: the epidermis, endothecium, middle layer, and tapetum, a nutrient-transfer tissue that supports the development of the sporogenic tissue. These layers are originally derived from the three layers of the floral meristem (L1, L2, and L3) (see Chapter 20). The L1 layer becomes the epidermis, and the L2 layer gives rise to the archesporial cells as well as the inner surrounding layers, as shown in **Figure 21.2B**. The central region containing the archesporial cells is called the **locule**.

Pollen grain formation occurs in two successive stages

The pollen grain is the male gametophyte of flowering plants. Its development is temporally divided into two sequential phases: microsporogenesis and microgametogenesis. During **microsporogenesis**, sporogenous cells within the anther locules differentiate into pollen mother cells (also referred to as **microsporocytes**), which are the diploid cells that undergo meiosis to produce the microspores (**Figure 21.3A**). The end result of the meiotic process is a tetrad of haploid **microspores** joined together at their cell walls, which are composed largely of callose, a (1,3)-β-glucan polysaccharide (see Chapter 2). The **tapetum**, a layer of secretory cells surrounding the

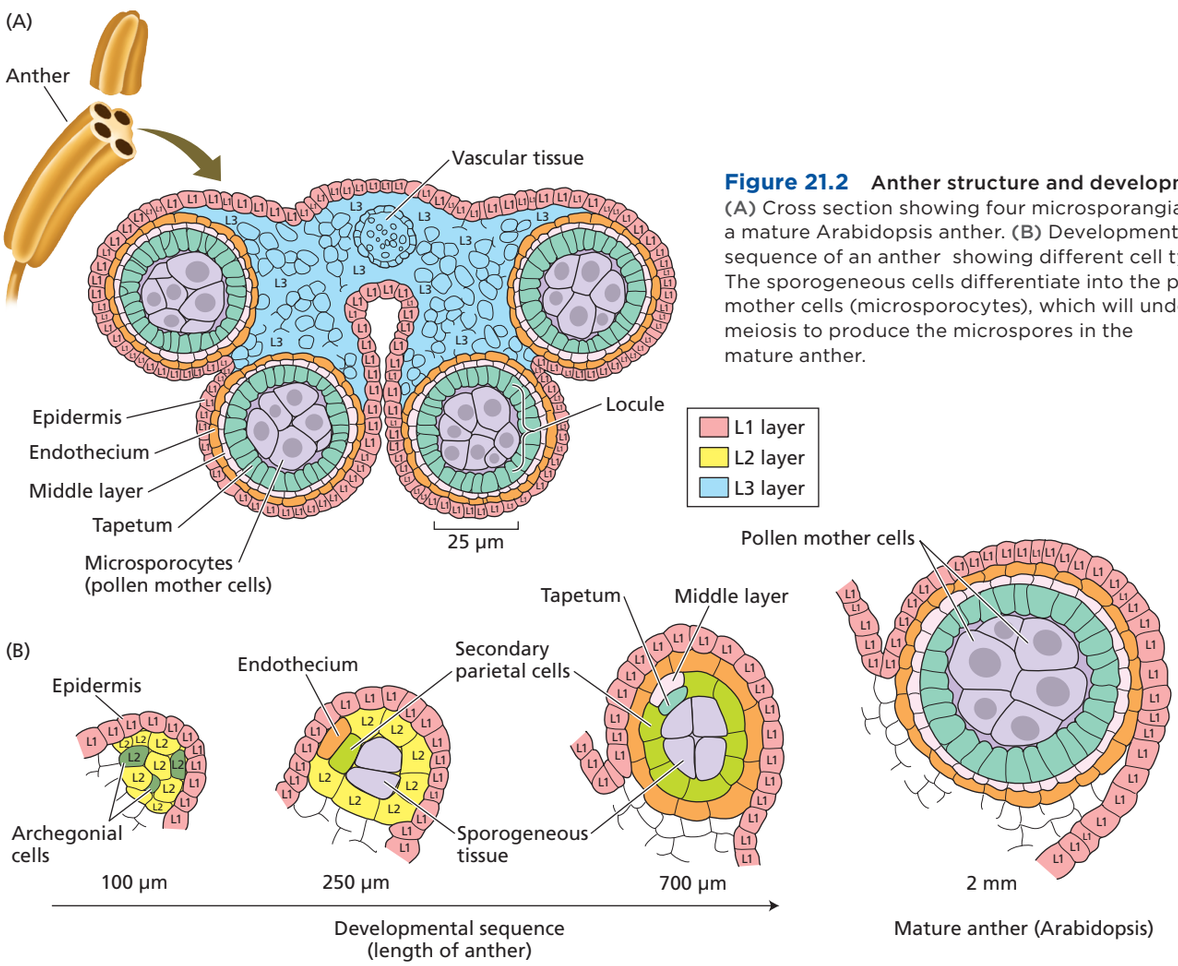


Figure 21.2 Anther structure and development. **(A)** Cross section showing four microsporangia of a mature Arabidopsis anther. **(B)** Developmental sequence of an anther showing different cell types. The sporogeneous cells differentiate into the pollen mother cells (microsporocytes), which will undergo meiosis to produce the microspores in the mature anther.

locule, secretes the hydrolytic enzyme *callase* and other cell wall–degrading enzymes into the locule, which partially digests the cell walls and separates the tetrad into individual microspores (see Figure 21.3A). In some insect-pollinated species, pollen is normally shed either as **tetrads**, as in the common heather (*Calluna vulgaris*), larger assemblages termed **polyads**, or even larger **massulae** and **pollinia**, which aggregate all the pollen in an anther, as in many species of orchids (see **WEB TOPIC 21.2**). Once the microspores have formed inside the anther locules, the microsporogenesis phase of microgametophyte development is completed.

The second stage is **microgametogenesis**, the formation of male gametes. During microgametogenesis, the haploid microspore develops mitotically into the mature male gametophyte, composed of the **vegetative** (or **tube**) **cell** and two **sperm cells** (**Figure 21.3B**). Prior to the first mitotic division, the microspore expands substantially, a process associated with the formation of a large vacuole. In parallel, the microspore nucleus migrates away from the vacuole to the other side of the cell, resulting in a *polarized microspore*. The polarized microspore then undergoes a highly asymmetric cell division (pollen mitosis I), giving rise to a large vegetative cell and a small **generative cell** (or male germ cell). In many species, this asymmetric mitosis leads to a dramatic division of the cytoplasm, excluding all plastids from the generative cell. Consequently the plastid genome is usually inherited through the maternal lineage.

Note that the generative cell plasma membrane on the side facing the cell wall is shared with the outer membrane of the microgametophyte. As a result, the generative cell initially remains attached to the microspore cell wall and is enclosed by a hemispherical wall of callose that separates the generative cell from the vegetative cell. Eventually, however, the callose layer breaks down and the generative cell pinches off from the outer microgametophyte plasma membrane. The generative cell then migrates to the center of the pollen grain, resulting in a unique anatomical structure: a cell within a cell (bicellular stage).

During maturation, pollen grains accumulate carbohydrate and/or lipid reserves to support the active metabolism required for rapid germination and pollen tube growth. At this stage, pollen development can take one of two routes. Many angiosperm families (e.g.,

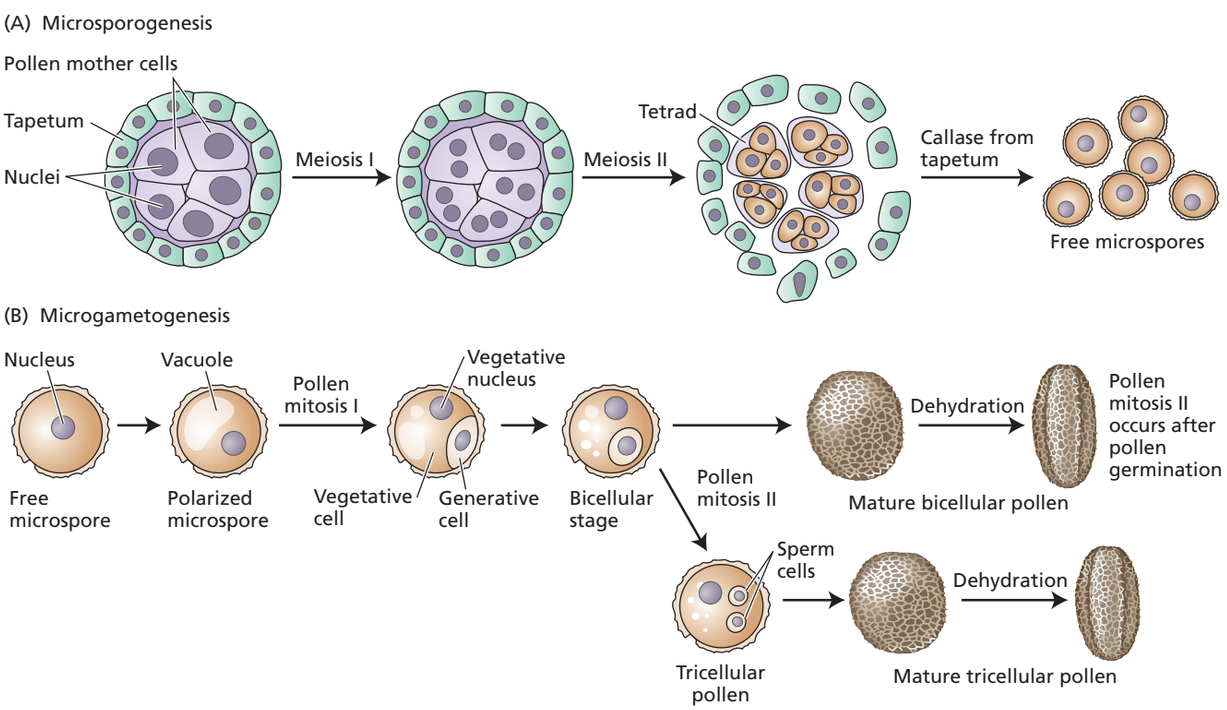


Figure 21.3 Male gametophyte development. (A) Microsporogenesis. Pollen mother cells undergo meiosis to produce a tetrad of microspores. (B) Microgametogenesis. The haploid nucleus divides mitotically to produce the vegetative (tube) cell and the generative cell (bicellular stage). After the generative cell is engulfed by the vegetative cell, pollen grains can follow two types of development: Either they move into desiccation and are shed to the atmosphere (species with bicellular pollen, top), or they divide mitotically to produce two sperm cells, desiccate, and are shed to the atmosphere (species with tricellular pollen, bottom). In species with bicellular pollen, the second mitotic division occurs after germination of the pollen grain. As the pollen grain matures, it forms a specialized cell wall.

Solanaceae, Orchidaceae, Rosaceae) release bicellular pollen: The pollen dehydrates at the bicellular stage and is released from the anther by dehiscence (opening) of the anther wall. Upon pollination and germination of the pollen grain, the generative cell then divides to produce the two sperm cells (pollen mitosis II) inside the growing pollen tube. In other families (e.g., Brassicaceae, Poaceae), the generative cell undergoes pollen mitosis II while still inside the anther, and tricellular pollen is released. In both cases, the production of the two sperm cells marks the end of microgametogenesis. Like the generative cell, the two sperm cells are enclosed within the vegetative, or pollen tube, cell and lack a proper cell wall, enabling them to fuse with either the egg or the central cell during double fertilization.

Depending on the species, tapetal cells may either remain at the periphery of the locule (as they do in Arabidopsis) or become amoeboid and migrate into the locule, intermingling with the developing microspores. In both cases tapetal cells perform a secretory function and eventually undergo programmed cell death (see Chapter 23), releasing their contents into the locule. Because of the essential role of tapetal cells in supplying enzymes, nutrients, and cell wall constituents to the developing pollen grains, defects in the tapetum usually cause abnormal pollen development and decreased fertility. Although male sterility is usually a harmful trait in nature, the ability to generate male-sterile plants by expressing cytotoxic proteins in the tapetum is extremely useful in agriculture for the production of hybrid seeds, such as for canola.

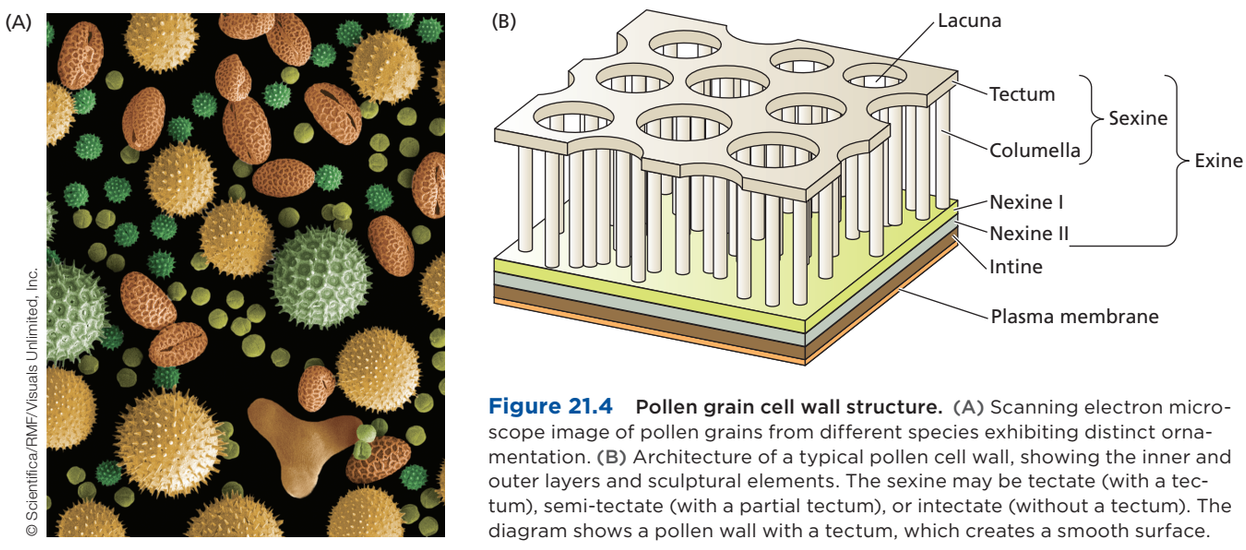
The multilayered pollen cell wall is surprisingly complex

The outer surfaces of pollen grain cell walls exhibit a remarkable variety of sculptural features that play important ecological roles in the transfer of pollen from flower to flower (**Figure 21.4A**). Equally complex, however, are the multiple subsurface wall layers that provide a labyrinth of internal spaces where lipids and proteins may be deposited (**Figure 21.4B**).

Initiation of pollen cell wall formation begins in the microspores immediately following meiosis. An ephemeral callose wall is the first of several layers to be deposited by the microspore onto the cell surface. This is followed by the *primexine* (a precursor of the *sexine*), the *nexine*, and finally the *intine*. (Note that because the microspore is the source of these layers, the innermost layer is the last to be deposited.)

The primexine, composed largely of polysaccharide, acts as a template that guides the accumulation of *sporopollenin*, the main structural component of the *exine*, or outer layer, which includes both the nexine and sexine. While the microspores are still in a tetrad, the early exine is assembled from sporopollenin precursors synthesized and secreted by the microspores themselves. However, once the outermost, callose walls are dissolved and the microspores are released from the tetrad, most of the sporopollenin precursors are supplied by the tapetum. The intine, or inner layer, consists primarily of cellulose and pectins.

Recent studies in Arabidopsis suggest that the sporopollenin polymer consists of phenolic and fatty acid–derived constituents that are covalently coupled, similar to lignin and suberin. In addition, most pollen grain walls include zones where the exine is either thin or missing (**Figure 21.5A and B**). These gaps in the exine where the pollen wall is weakened, called *apertures* or *pores*, enable the pollen tube to emerge from the pollen grain when it germinates on a compatible stigma. Instead of exine, these apertures are filled with pectins in the form of a hydrogel,



© Scientifica/RMF/Visuals Unlimited, Inc.

Figure 21.4 Pollen grain cell wall structure. (A) Scanning electron microscope image of pollen grains from different species exhibiting distinct ornamentation. (B) Architecture of a typical pollen cell wall, showing the inner and outer layers and sculptural elements. The sexine may be tectate (with a tectum), semi-tectate (with a partial tectum), or intectate (without a tectum). The diagram shows a pollen wall with a tectum, which creates a smooth surface.

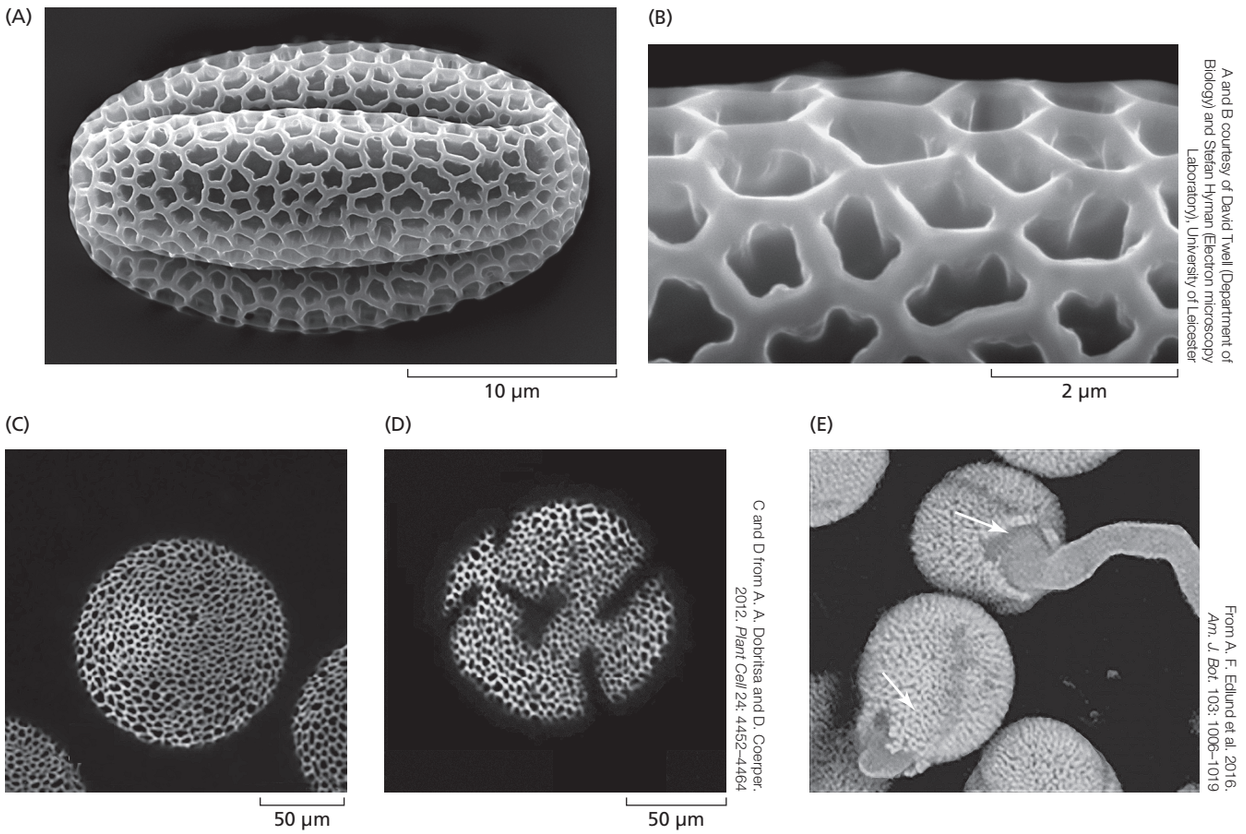


Figure 21.5 **Arabidopsis pollen grain.** **(A)** Scanning electron microscope image of Arabidopsis pollen showing two of its three apertures, which are elongated furrows where the wall is weaker and thinner. **(B)** Higher magnification SEM image of the tectate exine of an Arabidopsis pollen grain. **(C and D)** The *INAPERTURATE POLLEN1* gene controls the number and size of Arabidopsis pollen apertures, which are missing when the gene is mutated (C) or supernumerary when the gene is overexpressed (D). **(E)** Pollen tube emergence by rupture (arrows) of the pollen cell wall, outside the aperture in Arabidopsis.

which appears to facilitate the emergence of the pollen tube. The number and distribution of these apertures vary among different species and are under genetic control. In Arabidopsis, for example, the mutation or overexpression of the gene *INAPERTURATE POLLEN1* can cause either the complete absence of apertures or supernumerary apertures, respectively (**Figure 21.5C and D**). Although pollen wall apertures were once thought to be essential for the emergence of pollen tubes, in Arabidopsis, at least, pollen tubes can occasionally break through the exine in the absence of an aperture (**Figure 21.5E**).

The number of apertures and pattern of exine sculpturing are characteristic for an angiosperm family, genus, and often species. Smooth pollen is associated with wind pollination, as in oaks (*Quercus*) and grasses (maize [corn; *Zea mays*]), while plants pollinated by insects, birds, and mammals tend to have highly sculptured patterns consisting of spines, hooks, or sticky threadlike projections, which enable the pollen to adhere to foraging pollinators. Because sporopollenin is resistant to decay, pollen is well represented in the fossil record, and the distinctive surface patterns of the exine are useful for identifying which species were present, as well as suggesting the conditions of early climates. In species with dry stigmas (discussed in Section 21.4), such as Arabidopsis, the tapetum also coats the pollen grains with **tryphine**, a sticky, adhesive layer that covers the exine layer. Tryphine is rich in proteins, fatty acids, waxes, and other hydrocarbons.

21.3 Female Gametophyte Development in the Ovule

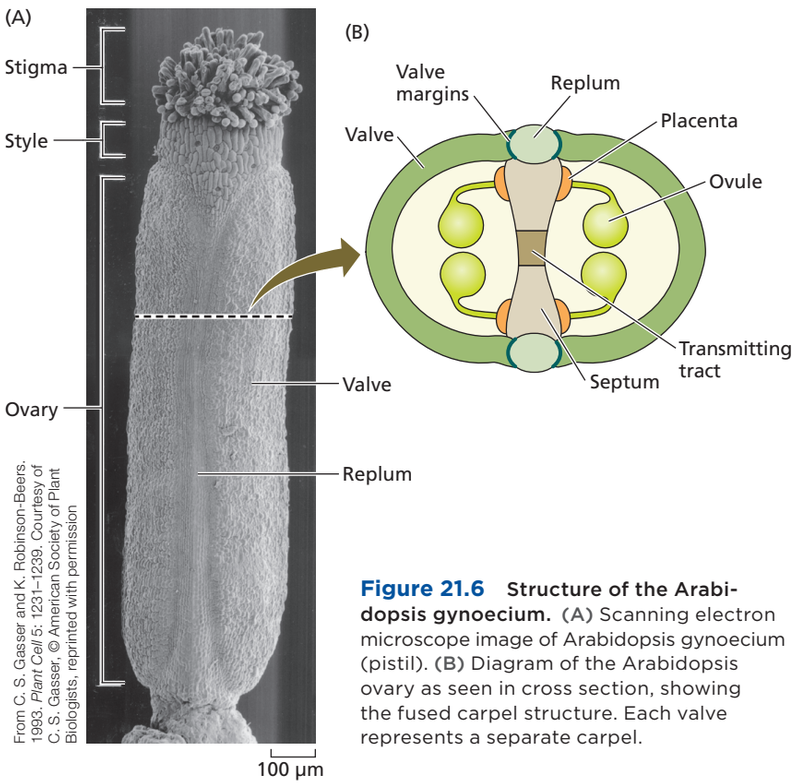
In angiosperms, *ovules* are located within the *ovary* of the *gynoecium*, the collective term for the carpels. Ovules are the sites of both megasporogenesis and megagametogenesis. Upon fertilization of the female gamete (egg cell) by a sperm cell, embryogenesis is initiated

and the ovule develops into a seed. Simultaneously, the ovary enlarges and becomes a fruit. We discuss fertilization and fruit development later in the chapter.

Ovule primordia arise in a specialized ovary tissue called the *placenta*. The locations of placental tissue vary among different plant groups, and include the marginal, parietal, axile, basal, and free-central types of placentation (see **WEB TOPIC 21.3**). The type of placentation in the ovary determines the positions and arrangement of the seeds within the fruit.

The Arabidopsis gynoecium is an important model system for studying ovule development

The gynoecium of Arabidopsis, as in many members of the Brassicaceae (mustard family), consists of two fused carpels, referred to as *valves*, separated by a medial partition called the *septum* (**Figure 21.6**). The edges of valves and the septum are joined at a strip of tissue called the *replum*, which plays an important role in the dehiscence (splitting) of the dry fruit, allowing seeds to disperse. In each carpel there are two strips of placental tissue on either side of the septum.



From C. S. Gasser and K. Robinson-Beers. 1993. *Plant Cell* 5: 1231–1239. Courtesy of C. S. Gasser, © American Society of Plant Biologists, reprinted with permission

Figure 21.6 Structure of the Arabidopsis gynoecium. **(A)** Scanning electron microscope image of Arabidopsis gynoecium (pistil). **(B)** Diagram of the Arabidopsis ovary as seen in cross section, showing the fused carpel structure. Each valve represents a separate carpel.

Ovule primordia first appear along the placenta as conical projections with rounded tips (**Figure 21.7**). Three zones can already be distinguished internally at an early stage of primordium development: the proximal region at the base, which gives rise to the stalklike *funiculus* (blue in Figure 21.7); the distal or *micropylar* region at the tip, which produces the *nucellus*, where meiosis takes place (pink in Figure 21.7); and the central region, called the *chalaza*, which gives rise to the *integuments*, the outer layers of the ovule (yellow in Figure 21.7). The cell that will differentiate into the *megaspore mother cell* is clearly visible in the primordial nucellus because of its large size, large nucleus, and dense cytoplasm.

Typically there are two integument layers: inner and outer. The inner integument forms a ridge some distance

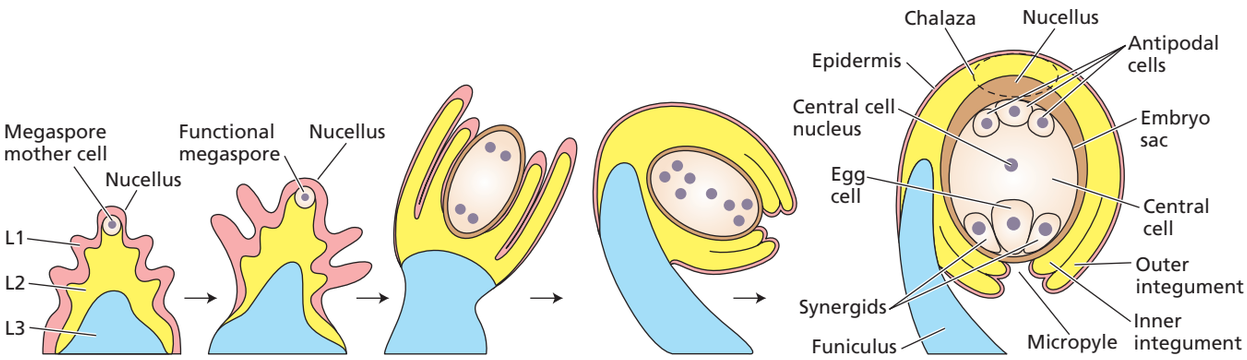


Figure 21.7 Ovule morphogenesis in Arabidopsis showing several stages of development and tissue types. The L1 layer (pink) gives rise to the epidermis, the L2 layer (yellow) gives rise to the bulk of the integuments and chalaza, and the L3 layer (blue) gives rise to the funiculus. The central cell nucleus is formed by fusion of the two polar nuclei (see Figure 21.8) and is the only diploid (2*N*) nucleus in the embryo sac.

behind the apex of the nucellus, followed by the outer integument layer (see Figure 21.7). The two integument layers continue to grow over the nucellus, eventually forming a pore around the micropyle. At the same time, the funiculus curves slightly, causing the ovule to bend inward toward the septum. In this way the micropyle is brought closer to the *transmitting tract*, a specialized tissue within the septum, through which the pollen tube grows during pollination. We discuss the function of the transmitting tract in more detail in Section 21.4.

The vast majority of angiosperms exhibit Polygonum-type embryo sac development

The development of the female gametophyte, or *embryo sac*, is more complex and more diverse than that of the male gametophyte. According to one classification scheme, there are more than 15 different patterns of embryo sac development in angiosperms, with mature embryo sacs that have from 4 to more than 12 cells. The most common pattern was first described in the genus *Polygonum* ("knotweed") and is therefore called the *Polygonum* type of embryo sac. *Polygonum*-type embryo sacs have 8 cells at maturity (sometimes referred as 3+2+3). We discuss this type of embryo sac development next; deviations from *Polygonum*-type development are described in **WEB TOPIC 21.4**.

Functional megaspores undergo a series of free nuclear mitotic divisions followed by cellularization

The nucellus gives rise to the **megaspore mother cell**, the cell that undergoes meiosis to produce the megaspores. In the *Polygonum* type of embryo sac, meiosis of the diploid megaspore mother cell produces four haploid megaspores (**Figure 21.8**). Three of the megaspores, usually those at the micropylar end of the nucellus, subsequently undergo programmed cell death, leaving only one functional megaspore. Functional megaspores then undergo three rounds of free nuclear mitotic divisions (i.e., mitoses without cytokinesis) to produce a *syncytium*—a multinucleate cell formed by nuclear divisions. The result is an eight-nucleate, immature embryo sac. Four of the nuclei then migrate to the chalazal pole, and the other four migrate to the micropylar pole. Three of the nuclei at each pole undergo cellularization without the formation of a cell wall. The three cells at the chalazal pole are termed the **antipodal cells**, while the three cells at the micropylar end of the embryo sac are called the **egg apparatus**, composed of an **egg cell** (the female gamete that combines with a sperm cell to form the zygote) in the middle, flanked by two **synergid cells**. The remaining two nuclei, called **polar nuclei**, migrate toward the central region of the embryo sac, which also contains a large vacuole. The cytoplasm and the two polar nuclei generate a plasma membrane around them, giving rise to a large binucleate **central cell**. Note that the two polar nuclei may either remain separate until the discharge of the male gametes into the embryo sac, or they may fuse before fertilization to form a dipolid (2*N*) **secondary nucleus**. The fully cellularized embryo sac, consisting of seven cells and either seven or eight nuclei, represents the mature female gametophyte or embryo sac.

There are many variations on the *Polygonum*-type embryo sac. For example, antipodal cells are absent in the order Nymphaeales, which includes the water lilies, as well as in members of the evening primrose family (Onagraceae). As a result, these two plant groups have only four-nucleate embryo sacs at maturity. In many other species, including Arabidopsis, the antipodal cells degenerate before fertilization, whereas in members of the grass family (Poaceae) the antipodal cells can proliferate. Given the variable presence of antipodal cells in mature embryo sacs, their function(s) during embryo sac development remain undetermined.

The egg apparatus includes a structure called a **filiform apparatus** at the micropylar end of each synergid (**Figure 21.9**). The filiform apparatus consists of a convoluted, thickened cell wall that increases the surface area

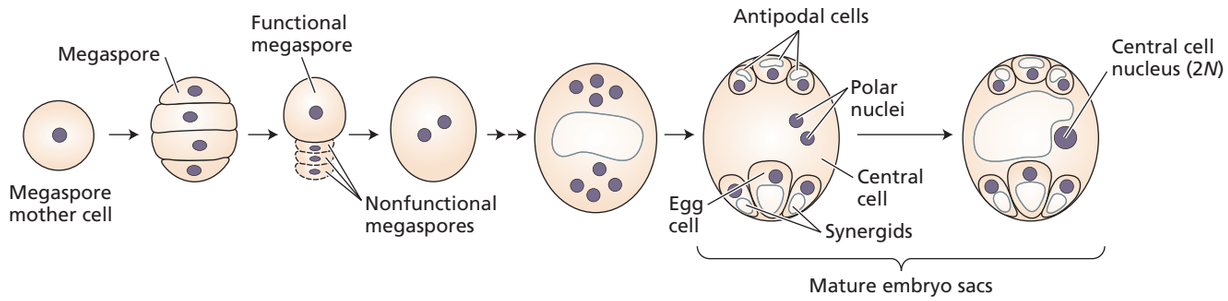


Figure 21.8 Developmental stages in the *Polygonum* type of embryo sac of Arabidopsis. The stages are as described in the text. The beige areas represent cytoplasm, the white areas represent vacuoles, and the brown circles represent nuclei. The chalazal pole is depicted up and the micropylar pole down. As in many other species, the antipodal cells degenerate before fertilization. The central cell nucleus is formed by fusion of the polar nuclei and becomes diploid (2*N*).

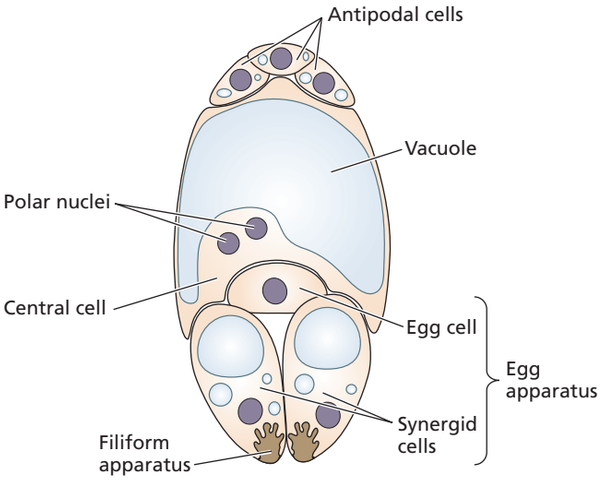


Figure 21.9 Diagram of the egg apparatus and filiform apparatus of the *Polygonum*-type embryo sac of Arabidopsis.

of the plasma membrane. As discussed in Section 21.4, synergid cells are involved in the final stages of pollen tube attraction, the discharge of pollen tube contents into the embryo sac, and gamete fusion. Embryo sacs from the genera *Plumbago* and *Plumbagella* are exceptions to this principle, as they lack synergid cells at maturity.

During double fertilization, the egg cell fuses with one of the sperm cells discharged by the pollen tube, while the central cell fuses with the other sperm cell. Although the term *double fertilization* implies that both the egg cell and the central cell function as female gametes, only the fertilized egg goes on to develop into an embryo. For this reason, the central cell is not considered to be a true gamete. In Arabidopsis, the two polar nuclei of the central cell fuse to form a single diploid nucleus prior to fusion with the sperm cell (see Figure 21.8). Depending on the type of embryo sac, the number of polar nuclei may range from one in *Oenothera* to eight or more in *Peperomia*. During double fertilization in the *Polygonum*-type embryo sac, one sperm cell fuses with the egg to produce the diploid 2*N* zygote, and the other fuses with the central cell to produce the triplod (3*N*) primary endosperm cell, which divides mitotically to give rise to the nutritive endosperm of the seed. Because different types of embryo sacs contain different numbers of polar nuclei, the ploidy level of the endosperm ranges from 2*N* in *Oenothera* to 15*N* in *Peperomia*.

21.4 Pollination and Fertilization in Flowering Plants

Pollination in angiosperms is the process of transferring pollen grains from the anther of the stamen (the microspore-producing structure of the flower) to the stigma of the carpel (the megaspore-producing structure of the flower) (see Figure 21.1). In some species, such as *Arabidopsis thaliana* and rice, reproduction typically occurs via self-pollination, or selfing—that is, the pollen and the stigma arise from the same individual. In other species, **cross-pollination**, or **outcrossing**, is the norm—the male parent and the female parent are separate sporophytes. Many species can reproduce by either self- or cross-pollination; other species (discussed later) have various mechanisms for promoting cross-pollination, and may even be incapable of reproducing by self-pollination.

During cross-pollination, pollen may travel great distances before landing on a suitable stigma. Typically produced in great excess, pollen grains are dispersed by wind, insects, birds, and mammals. The evolution of pollen grains as vehicles for transporting sperm cells made the reproduction of seed plants (gymnosperms and angiosperms) independent of a water medium. Because pollination benefits both plants and their pollinators, many animals coevolved with plants to facilitate the process.

Successful pollination depends on several factors, including ambient temperature, timing, and the receptivity of the stigma of a compatible flower. Many pollen grains can tolerate desiccation and high temperatures during their journey to the stigma. However, some pollen grains, such as those of tomato, are damaged by heat. Understanding how some pollen grains tolerate periods of high temperature will help ensure our food supply as the global climate changes.

The progamic phase includes everything from pollen landing and tube growth to the fusion of sperm and egg

The female gametes are well protected from the environment by ovary tissues. Consequently, to reach an unfertilized egg, sperm cells must be delivered by a pollen tube that grows from the stigma through the style and into the ovule. The developmental stage from pollen deposition on the stigma to the delivery of the sperm cells to the embryo sac is called the **progamic phase** of reproduction. In the Arabidopsis pistil (or gynoecium), which is similar to those of other angiosperms, this process can be divided into six steps (**Figure 21.10**).

Note that in Arabidopsis, as in many angiosperms, the style is solid and the pollen tubes grow intrusively through the apoplast of the transmitting tissue. Flowers with hollow styles (e.g., *Lilium longiflorum*, *Medicago sativa*, orchids) have what are termed *stylar canals*. In these species the transmitting tissue lines the inner surface of the stylar canal and the pollen tubes grow along the canal surface to the ovary.

After the sperm cells are discharged from the pollen tube, double fertilization occurs: One sperm unites with the egg cell to produce the zygote, and the second sperm fuses with the central cell to form the triploid

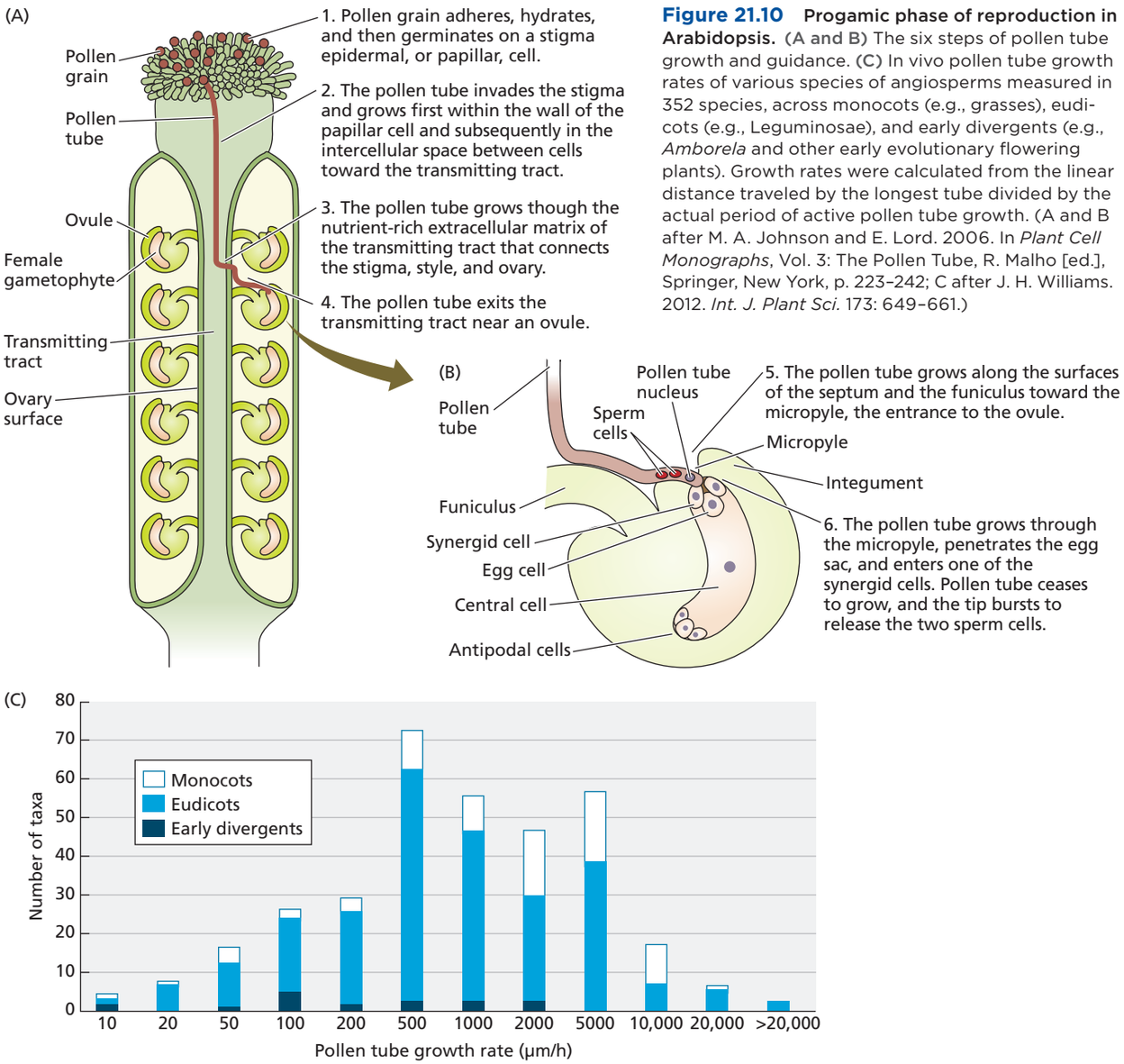


Figure 21.10 Progamic phase of reproduction in Arabidopsis. (A and B) The six steps of pollen tube growth and guidance. (C) In vivo pollen tube growth rates of various species of angiosperms measured in 352 species, across monocots (e.g., grasses), eudicots (e.g., Leguminosae), and early divergents (e.g., *Amborela* and other early evolutionary flowering plants). Growth rates were calculated from the linear distance traveled by the longest tube divided by the actual period of active pollen tube growth. (A and B after M. A. Johnson and E. Lord. 2006. In *Plant Cell Monographs*, Vol. 3: The Pollen Tube, R. Malho [ed.], Springer, New York, p. 223–242; C after J. H. Williams. 2012. *Int. J. Plant Sci.* 173: 649–661.)

primary endosperm cell. As we discuss next, successful delivery of the two sperm cells to the two female gametes (egg and central cell) throughout the six steps of the progamic phase depends on extensive interactions and communication between the pollen tube, the pistil, and the female gametophyte. As shown in Figure 21.10C, the pollen tube growth rate of angiosperms ranges from approximately 10 μm per hour to more than 20,000 μm (20 mm) per hour—on average about 100 times faster than the growth rate of gymnosperm pollen tubes. The pollen grains from an individual plant can have variable pollen tube growth rates, a phenomenon that is thought to constitute male competition (e.g., in *Hibiscus* and *Quercus* species and in Arabidopsis) and should therefore be considered as the plant equivalent of Darwinian sexual selection.

Adhesion and hydration of a pollen grain on a compatible flower depend on recognition between pollen and stigma surfaces

Angiosperm reproduction is highly selective. The surfaces of stigmas can discriminate among diverse pollen grains, accepting those from the appropriate species and rejecting others from unrelated species. When pollen lands on a compatible stigma, the grains physically adhere to the stigma cells, named papillae (plural), due to biophysical and chemical interactions between pollen proteins and lipids and stigma surface proteins. In

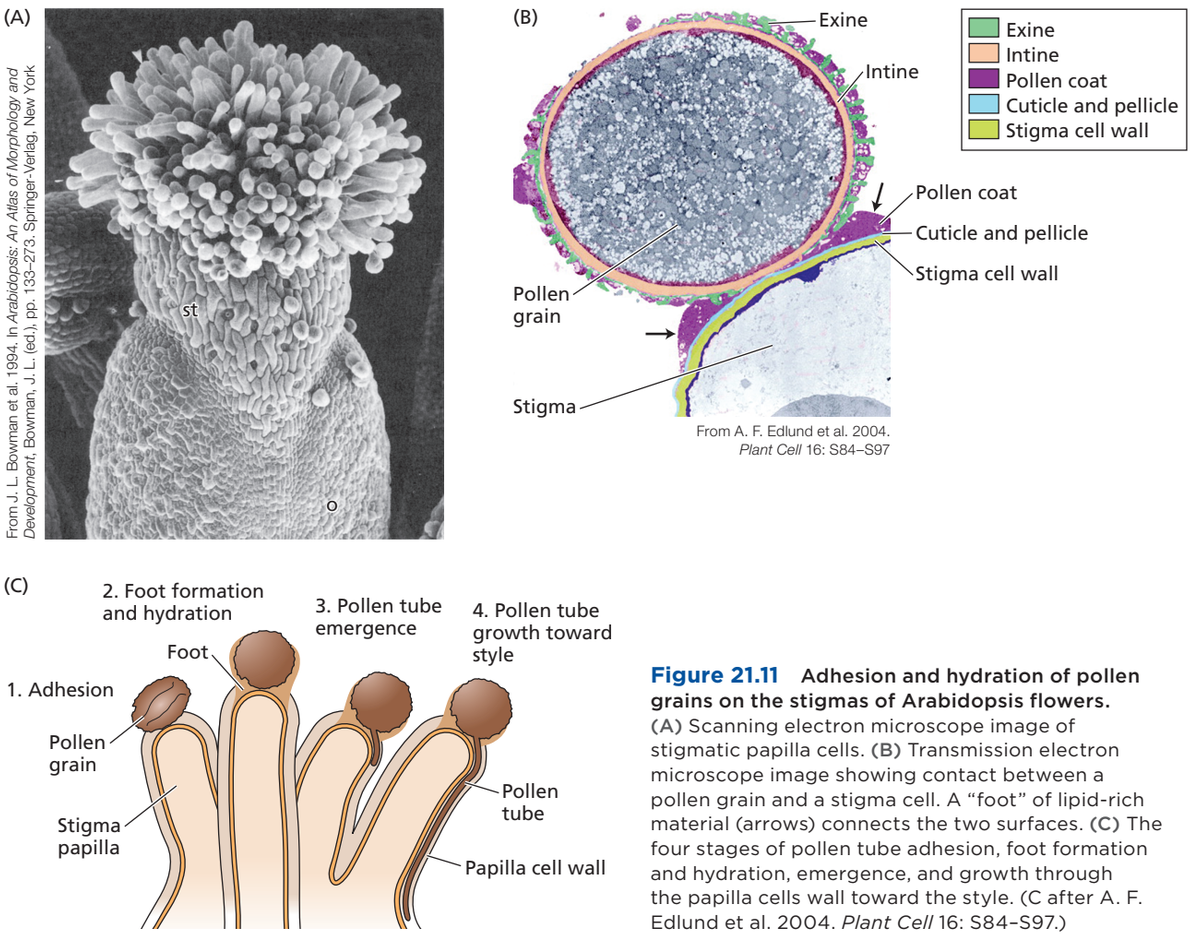


Figure 21.11 **Adhesion and hydration of pollen grains on the stigmas of Arabidopsis flowers.** **(A)** Scanning electron microscope image of stigmatic papilla cells. **(B)** Transmission electron microscope image showing contact between a pollen grain and a stigma cell. A "foot" of lipid-rich material (arrows) connects the two surfaces. **(C)** The four stages of pollen tube adhesion, foot formation and hydration, emergence, and growth through the papilla cells wall toward the style. (C after A. F. Edlund et al. 2004. *Plant Cell* 16: S84–S97.)

general, pollen grains adhere less effectively to stigmas of plants from other families.

Flowers have either wet or dry stigmas. The surface cells of wet stigmas release a viscous mixture of water, proteins, lipids, and polysaccharides; the surface cells of dry stigmas, such as those found in the Brassicaceae, are covered by a cell wall, cuticle, and protein pellicle (**Figure 21.11**). Pollen grains become hydrated by default on wet stigmas by the uptake of the secreted water (e.g., in tobacco and orchids). By contrast, the hydration process on dry stigmas is highly regulated. After landing on a dry stigma, lipids and proteins from the pollen coat flow out onto the stigmatic surface and mingle with materials from the papillae cell to form the "foot," a structure that attaches the pollen grain firmly to the tip of the papilla cells (see Figure 21.11B and C). During this process, the lipids in the foot are thought to reorganize, creating a capillary system through which water and ions can flow from the stigma to the pollen grain. This mechanism apparently allows the pollen grain to perform the paradoxical feat of becoming hydrated on a dry stigma. Remarkably, the pistils of tobacco plants whose stigmas had been genetically ablated could still support pollen germination and fertilization, provided that exogenous lipids (including olive oil) were supplied. Such experiments indicate that lipid interfaces are crucial for the early steps of in vivo pollen germination.

In further support of the role of lipids in pollen hydration, Arabidopsis mutants with defects in long-chain lipid metabolism produce pollen without a pollen coat, and these pollen grains fail to hydrate on the stigma. This defect can be rescued by either high humidity or the application of lipids to the stigma, both of which allow the pollen grain to hydrate and form a pollen tube.

Ca^{2+}-triggered polarization of the pollen grain precedes tube formation

During hydration, the pollen grain becomes physiologically activated. Ca^{2+} influx into the vegetative cell triggers reorganization of the cytoskeleton and causes the cell to become physiologically and structurally polarized. Live imaging of free Ca^{2+} in Arabidopsis pollen grains has shown that the cytosolic Ca^{2+} concentration increases at the future germination site soon after hydration and

remains elevated until tube emergence. Both actin microfilaments and secretory vesicles accumulate below the germination pore or aperture, while the vegetative nucleus and the sperm cells migrate into the germinating pollen tube. In addition to water and Ca^{2+}, boric acid is also necessary for germination of pollen in vitro. As discussed in Chapter 7, boric acid is an essential micronutrient in plants. One of its primary functions is to cross-link the small pectic polysaccharide rhamnogalacturonan II in the cell wall (see Chapter 2). Consistent with its role in wall assembly, boron is required both by the tapetum, which secretes polysaccharides and other materials for the proper assembly of microspore cell walls, and by the pollen grain for germination. The stigma is also known to supply a variety of factors that promote pollen germination, but these appear to be species-specific.

Pollen tubes grow by tip growth

Following germination on the stigma, Arabidopsis pollen tubes penetrate through gaps in the waxy cuticle of the papillae cell and enter the papillae cell wall (see Figure 21.11C). Throughout their transit to the ovules, pollen tubes of all species grow by tip growth facilitated by the exocytosis of cell wall precursors exclusively at the tip (see Chapter 1). As noted earlier (see Figure 21.10C), the growth rate of pollen tubes in some flowering plants (e.g., *Tradescantia*, daylily, maize) is extremely rapid, reaching rates of about 6 μm per second in vivo. (For comparison, tip growth in root hairs is only about 10 to 40 nm per second.) These rates make pollen tubes among the fastest growing cells in nature. Remarkably, an individual tube can reach up to 40 cm in length, as occurs when a maize pollen tube grows through a strand of silk, which is the style of maize carpels. Such rapid rates of pollen tube growth are all the more impressive considering that many angiosperms have solid styles, and that pollen tube growth proceeds by the invasive disruption of the cell wall inside the transmitting tract (see Figure 21.6).

Growing pollen tubes restrict the cytoplasm, the two sperm nuclei, and the vegetative nucleus to the region located a few hundred micrometers behind the growing apical region by forming large vacuoles and callose plugs that seal off the rear portion of the tube, which eventually dies (**Figure 21.12**). At the apical end of the pollen tube is an area known as the *clear zone*, from which most large organelles, such as amyloplasts, nuclei, and most endoplasmic reticulum and mitochondria, are excluded (**Figure 21.13A**). In the region closest to the tip, this size exclusion phenomenon is even more strict, and only small secretory vesicles that carry the cell wall precursors are present. These vesicles accumulate just beneath the tip, where exo- and endocytosis occur, and are frequently organized in an inverted cone shape, or a triangle when seen in section (**Figure 21.13B**).

The molecular basis for the formation of the clear zone is unknown, but it has been associated with the disruption or reorganization of the actin cables at the tip. Actin microfilament dynamics (see Chapter 1) drive cytoplasmic streaming following a "reverse fountain" flow (**Figure 21.13C**). Organelles move along actin fibers that run along the pollen tube shank, but these fibers break up into small, short-lived filaments in the clear zone. Consequently, streaming is disrupted in the clear zone, and the movements of secretory vesicles and small organelles in this region resemble disorganized, Brownian-like motion.

How pollen tubes and other tip-growing cells establish and maintain their polarity remains a fundamental question in plant development. The vast majority of evidence suggests that ion gradients at the growing tip are involved. For example, the tip of a growing pollen tube is polarized due to tip-focused Ca^{2+} and pH gradients, as well as an inverted gradient of chloride (Cl^-) (**Figure 21.14**). These cytosolic gradients can reach nearly

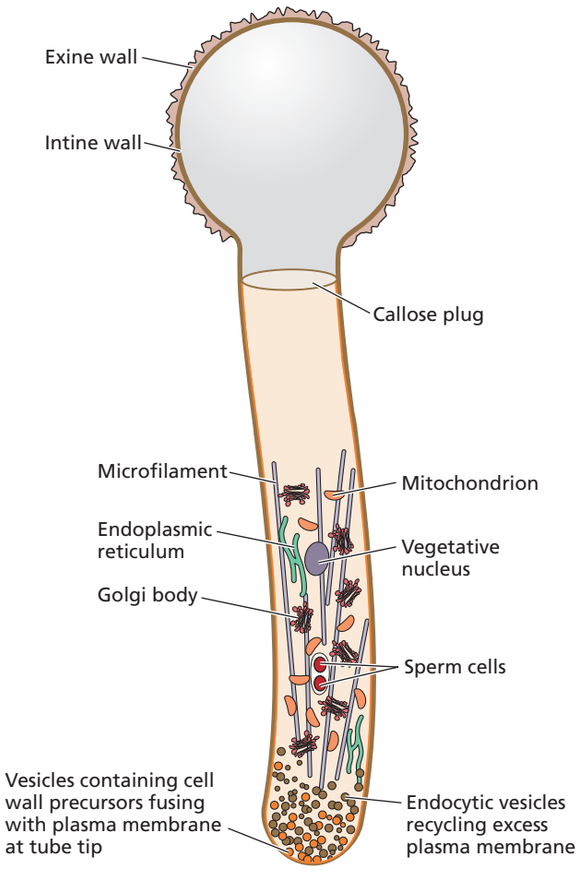


Figure 21.12 **Pollen tube elongating by tip growth.** The cytoplasm is concentrated in the growing region of the tube by large vacuoles and callose partitions. (After R. L. Jones et al. 2013. *The Molecular Life of Plants*. New York: Wiley-Blackwell.)

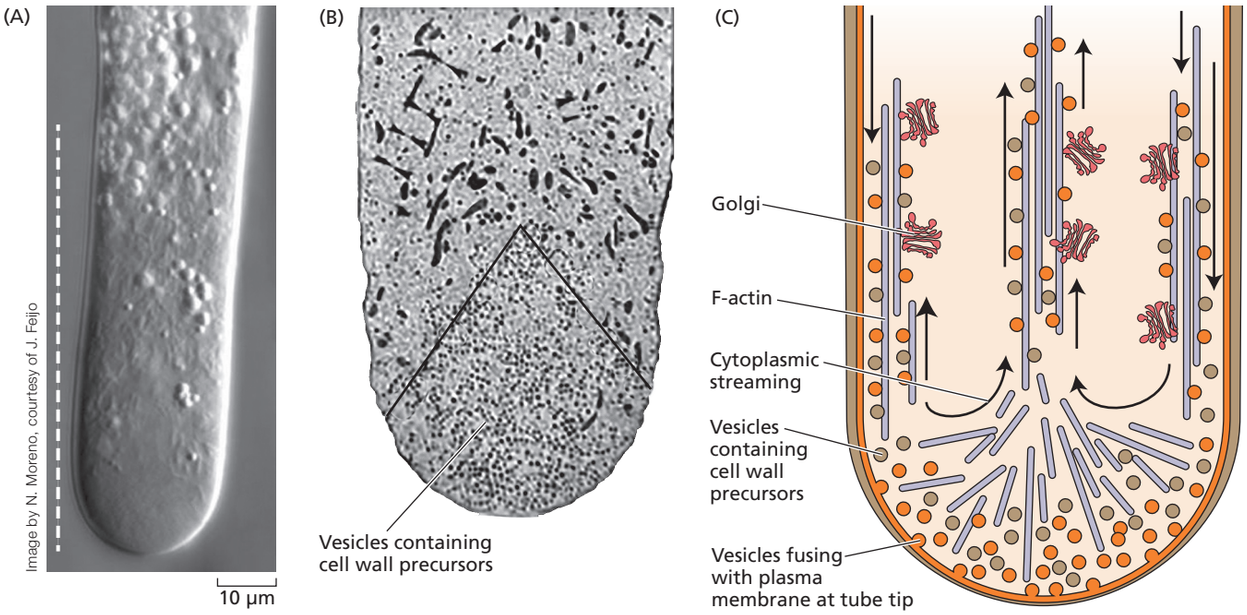
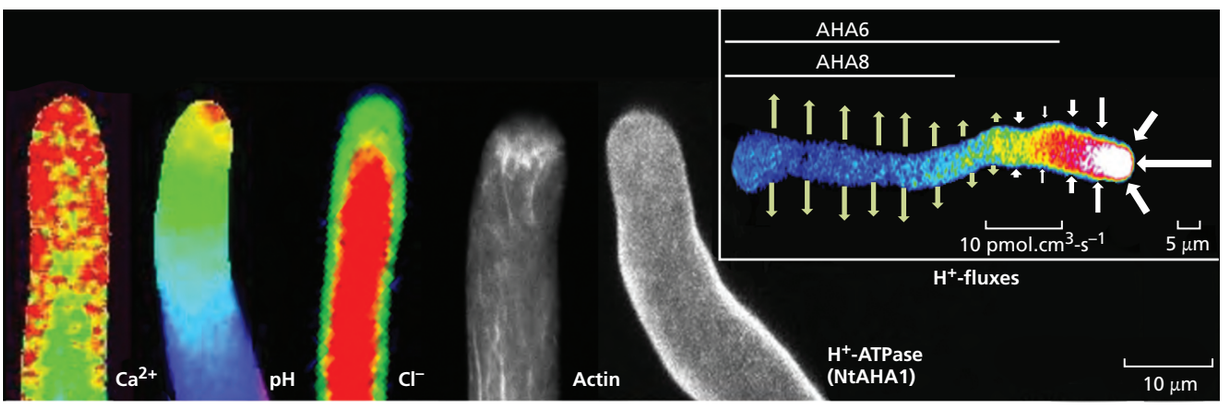


Figure 21.13 **Clear zone of a growing pollen tube.** **(A)** Light micrograph of the clear zone (white dashed line) of elongating lily pollen. **(B)** Electron micrograph of the clear zone of lily pollen, showing the cone of numerous small vesicles (within the two lines) at the extreme end of the tip. **(C)** Diagram of ultrastructural components of the clear zone. As indicated in the illustration, the "clear zone" is not really clear, but contains Golgi bodies, F-actin filaments, and numerous small vesicles. Arrows indicate the circularity of cytoplasmic streaming on either side of the central axis. (B after S. A. Lancelle et al. 1997. *Protoplasma* 196: 21–33; C after A. Y. Cheung et al. 2010. *Proc. Natl. Acad. Sci. USA* 107: 16390–16395.)



Inset from D. Hoffmann et al. 2020. *Nat. Comm.* 11: 2395. CC BY 4.0

Figure 21.14 **Tobacco pollen tubes showing cytosolic concentration gradients for Ca^{2+}, pH/H^+, Cl^-, short actin filaments imaged with a fluorescent probe, and the plasma membrane H^+-ATPase NtAHA1.** Concentration gradients are color-coded, from red (high) to blue (low). The acidic tip corresponds to the region of secretory vesicles, and the clear zone corresponds to the Ca^{2+} and the acidic gradients. Long actin filaments that support organelle streaming begin at the basal edges of these ion gradients. The pattern of extracellular H^+ fluxes at the tip is correlated with the absence of the plasma membrane H^+-ATPase NtAHA1. The inset shows a similar pH/H^+ pattern in an Arabidopsis pollen tube. The image shows the cytosolic gradient of pH, extracellular fluxes of H^+, and localization of the more expressed proton pumps (AHA6 and AHA8) in Arabidopsis pollen tubes. Not only the localization of these pumps correlates with the extracellular fluxes (presence = effluxes, absence = influxes) and consequent pH inside the pollen tune (effluxes = higher pH, influxes = lower pH), but in the double mutant *aha6/aha8* the pollen tube is impaired and seed set is highly reduced. (After E. Michard et al. 2017. *Plant Physiol.* 173: 91–111, partially based on T. Gutermuth et al. 2013. *Plant Cell* 25: 4525–4543 and E. Michard et al. 2008. *Sex. Plant Reprod.* 21: 169–181.)

an order of magnitude in concentration over a distance of only 10 to 20 μm (e.g., Ca^{2+} goes from > 3 μ*M* at the tip to ~0.25 μ*M* just below the tip). The Ca^{2+} gradient correlates closely with the distribution of the actin microfilaments and organelle sorting in the tip (see Figure 21.13C). The molecular mechanism of the formation of the pH gradient (typically 0.5 to 1.0 pH unit within the tip) is thought to involve the exclusion from the tip of H^+-pumping plasma membrane ATPases (see Chapter 8) (see Figure 21.14). The absence of the plasma membrane H^+-ATPase from this zone allows an influx of protons to acidify the cytosol immediately below the tip (see Figure 21.14). Presumably the other ion gradients are also formed by differential positioning or exclusion of ion channels at the tip of the pollen tube.

In laboratory experiments, the concentrations of all these ions in the pollen tube tips of many species have been shown to oscillate. While it is not clear if these oscillations also occur in the wild, the fact that the periodicity of ion oscillations correlates with oscillations in pollen tube growth rate is reminiscent of the correlations observed between ion oscillations at the tips of root hairs and root hair growth. Ca^{2+} oscillations have also been associated with the interaction between pollen tubes and synergid cells that precedes fertilization. Electrical as well as chemical changes associated with changes in ion concentrations, particularly of Ca^{2+}, H^+, and Cl^-, are known to play roles in cell signaling, cytoskeletal dynamics, membrane trafficking, and exocytosis, all of which are involved in maintaining pollen tube polarity and growth.

Receptor-like kinases are thought to regulate the ROP1 GTPase switch, a master regulator of tip growth

To regulate tip growth in a variety of cells, plants use a highly conserved mechanism based on the polar localization of small GTPases (enzymes that hydrolyze GTP to GDP). These regulatory GTPases are molecular switches that can cycle between an active, GTP-binding form and an inactive, GDP-binding form (**Figure 21.15**). When a regulatory GTPase is in its active form, it triggers downstream signal transduction pathways (see Chapter 4). Conversion from the active form back to the inactive form is catalyzed by the GTPase itself, which hydrolyzes the bound GTP to GDP. The GTPase switch is operated by other proteins that affect the rate of either GDP-GTP exchange or GTP hydrolysis. **Guanine nucleotide exchange factors** (**GEFs**) activate inactive GTPases by replacing GDP with GTP, while **GTPase-activating proteins** (**GAPs**) inactivate GTPases by promoting GTP hydrolysis.

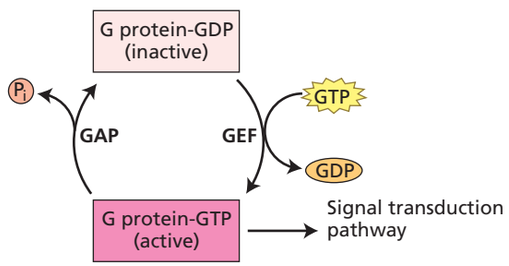


Figure 21.15 Diagram of GEF activation of a GTPase. Guanine nucleotide exchange factors (GEFs) and GTPase-activating proteins (GAPs) regulate the activities of small GTPases (ROPS), which act as molecular switches in pollen tubes.

The GTPases that regulate tip growth and polar cell expansion in plants belong to a unique family of small GTPases called ROPs (for Rho-like GTPase). Arabidopsis has 11 different *ROP* genes, 7 of which are expressed in pollen. One of them produces the protein ROP1-GTPase, that resides exclusively in the plasma membrane at the tips of growing pollen tubes and is a regulator of tip growth. ROP1 activity can be switched on and off by GEFs and GAPs, respectively, but the mechanisms by which ROP1 helps restrict pollen tube growth to the tip are incompletely understood. Ca^{2+} signaling and actin cytoskeleton reorganization are regulated by ROP1, but other proteins specifically interacting with ROP1 may play important roles. Such is the case for a group of proteins called **RICs** (**ROP-interactive CRIB motif–containing proteins**). When overexpressed in Arabidopsis, RIC3 and RIC4 alter pollen tube polarity and exocytosis. Further studies have shown that RIC4 promotes actin filament formation and induces the accumulation of exocytic vesicles at the tip. There is also evidence from studies of root hair development that GEFs are themselves activated by a signaling mechanism involving **receptor-like kinases** (**RLKs**), which are encoded by a large gene family in the Arabidopsis genome. One RLK subfamily comprises the CrRLK1s (C*atharanthus* r*oseus* R*eceptor-L*ike *K*inase 1), also known as FERONIA-like RLKs. (FERONIA was the first member cloned in Arabidopsis and is expressed in the embryo sac.) Two such kinases, ANXUR 1 and 2, are expressed in pollen, and when they are mutated, pollen tubes burst spontaneously (**WEB TOPIC 21.5**) and fail to reach the ovules. These RLKs are regulated by a large family of peptides called RALFs (RAPID ALKALINIZATION FACTORs). Specific RALFs bind specific RLKs, triggering downstream mechanisms (including interactions with the ROP1 signaling pathway) in ways that are believed to regulate tip growth.

Pollen tube tip growth in the pistil is guided by both physical and chemical cues

For successful fertilization to occur, the pollen tube must find its way to the micropyle of an ovule. In fact, there is often competition among pollen tubes to arrive at the micropyle first and thus be the one to fertilize the egg. In many species the number of pollen tubes that reach

the ovary outnumbers the available ovules, reinforcing the idea that faster pollen tube growth rates should increase male reproductive fitness and thus be subject to a form of sexual selection as defined by Darwin. Genetic analysis of this male competition in various species has provided evidence that sexual selection does occur.

In some species, such as oaks, the ovary of the pistil contains multiple ovules but only one of them becomes fertilized to produce a seed. This occurs because only one pollen tube succeeds in reaching the ovary. In other species, such as Arabidopsis, the narrow diameter of the transmitting tract (discussed below) provides a physical constraint that restricts the total number of pollen tubes that can access the ovary.

Two major models have been proposed to explain how pollen tubes grow toward an ovule: the mechanical hypothesis and the chemotropic hypothesis. In the **mechanical hypothesis**, pistil architecture dictates the path of the tube, which follows a narrow **transmitting tract** leading to the ovule (see Figure 21.10A). The transmitting tract of the stigma and style spatially constrains pollen tube growth to the correct path, and in the case of Arabidopsis, limits the number of pollen tubes that can take that path.

Spatial constraints of this kind could also be mediated by secreted molecules. For example, during growth toward the ovule, pollen tubes are in intimate contact with the components of the extracellular matrix of the transmitting tract (or in the case of species with hollow styles, such as lily and orchids, with secretions emanating from the transmitting tissue cells). The extracellular matrix supplies not only nutrients that could support the tube's metabolic activity, but also other molecules that are thought to have adhesive properties that help define the spatial constraints for pollen tube growth. In lily, for example, a small, secreted protein—**stigma/style cysteine-rich adhesin** (**SCA**), a lipid transfer protein—is secreted by the transmitting tract epidermis that lines the hollow style and is involved in growth and adhesion of the tube along the tract. Although experimental evidence favors the mechanical hypothesis as the explanation for pollen tube movements through most of the style, it doesn't explain the sharp turns pollen tubes must make to approach and enter the micropyle.

According to the **chemotropic hypothesis**, pollen tubes are guided toward the ovule by following a gradient of molecular cues called *chemoattractants*. In all species of animals and in early land plants (e.g., mosses), sperm cells swim toward the egg cell by a process named **chemotaxis**: The sperm are able to decode a concentration gradient of a chemoattractant and follow it to its most concentrated source. For example, the sperm cells of ferns are thought to be attracted to the egg-containing archegonia by a concentration gradient of malate. A similar mechanism is known to guide pollen tube growth, but since pollen tubes *grow instead of swim*, the process is referred to as **chemotropism**, a phenomenon also observed in fungal hyphae and neuronal growth. Several types of molecules have been identified that function in pollen tube guidance, mostly from *in vitro* and semi–*in vivo* assays (see the next subsection).

It is important to note that the mechanical and chemotropic mechanisms are not mutually exclusive and can work either by complementarity, in which chemotropism is involved only in regions along the path where the mechanical mechanism is absent, or by redundancy, in which the two mechanisms work in tandem to ensure successful fertilization. In addition, while the early stages of pollen tube growth are regulated by sporophytic cells in the transmitting tract, genetic analyses of Arabidopsis and in vitro guidance experiments in *Torenia fournieri* (discussed in the next subsection) support the idea that chemical signals from the female gametophyte also play critical roles during the final stages of pollen tube growth toward the micropyle.

Style tissue may condition pollen tubes to grow toward the embryo sac

To travel from the stigma to the ovary, a pollen tube must grow through the style. Various experimental approaches have been developed to determine the mechanisms that guide pollen tubes toward the ovule. For example, early research showed that dissected unfertilized ovules of *Gasteria verrucosa* are capable of attracting pollen tubes in vitro. More recently, the unique anatomical features of *Torenia fournieri* (a member of the order Lamiales, which includes lavender and lilac) have made it the preferred model system to study the response of pollen tubes to attractants produced by the female gametophyte (**Figure 21.16A**).

In seed plants, the ovule is enclosed within one or more layers of sporophytic tissue called the integuments, which represent the future seed coat. Gymnosperm seeds are typically enclosed within a single-layered integument, whereas angiosperm ovules are most commonly surrounded by a double-layered integument. The integuments of most angiosperms cannot easily be removed to gain access to the embryo sac, but in *T. fournieri* and some other species the embryo sac naturally protrudes from the micropyle, causing the egg cell, the two synergid cells, and approximately half of the central cell to be located outside the ovule, where they can be observed under a light microscope (**Figure 21.16B and C**).

When ovules of *T. fournieri* are excised from the placenta, the naked embryo sacs are directly exposed to the medium. Experiments have demonstrated that when excised *T. fournieri* ovules are co-cultivated with pollen tubes that have been germinated on a nutrient medium, the pollen tubes are only weakly attracted to the ovule. However, if the *T. fournieri* pollen grains are

first germinated on a living stigma and then allowed to emerge from the cut end of the style into the nutrient medium, the tendency of the pollen tubes to grow toward the micropylar end of the embryo sac is greatly increased (**Figure 21.16D–F**). This system for studying pollen tube attraction has also been adapted for use in Arabidopsis. Experiments in both *Torenia* and Arabidopsis have led to the hypothesis that the interaction between the pollen tube and the style conditions the pollen tube (i.e., makes it competent) to respond to the cues from the embryo sac and grow toward the micropyle.

This principle does not seem to apply to all plants, however. In some species (e.g., *Lilium*, *Gasteria*), the ability of pollen tubes to be attracted to the ovule may develop autonomously rather than through interaction with the stigma. Pollen tubes undergo major changes in gene expression while germinating or during passage from the stigma to the ovary. In *Lilium* and *Gasteria* such developmental changes may play a role in the establishment of the sensing and transducing mechanisms required to sense the pistil guidance mechanisms.

Synergid cells release chemoattractants that guide pollen tube growth to the micropyle

The cellular source of the first pollen tube attractant detected in *T. fournieri* was identified by laser ablation of specific cells of the embryo sac. Pollen tubes failed to grow toward the ovule only if the two synergid cells—but not the egg or central cell—had been killed. These pollen tube chemoattractants have now been identified as cysteine-rich polypeptides, appropriately called **LUREs**, and they can attract pollen tubes growing in vitro. LUREs are related to the **defensins**, a group of antimicrobial proteins found in animals and

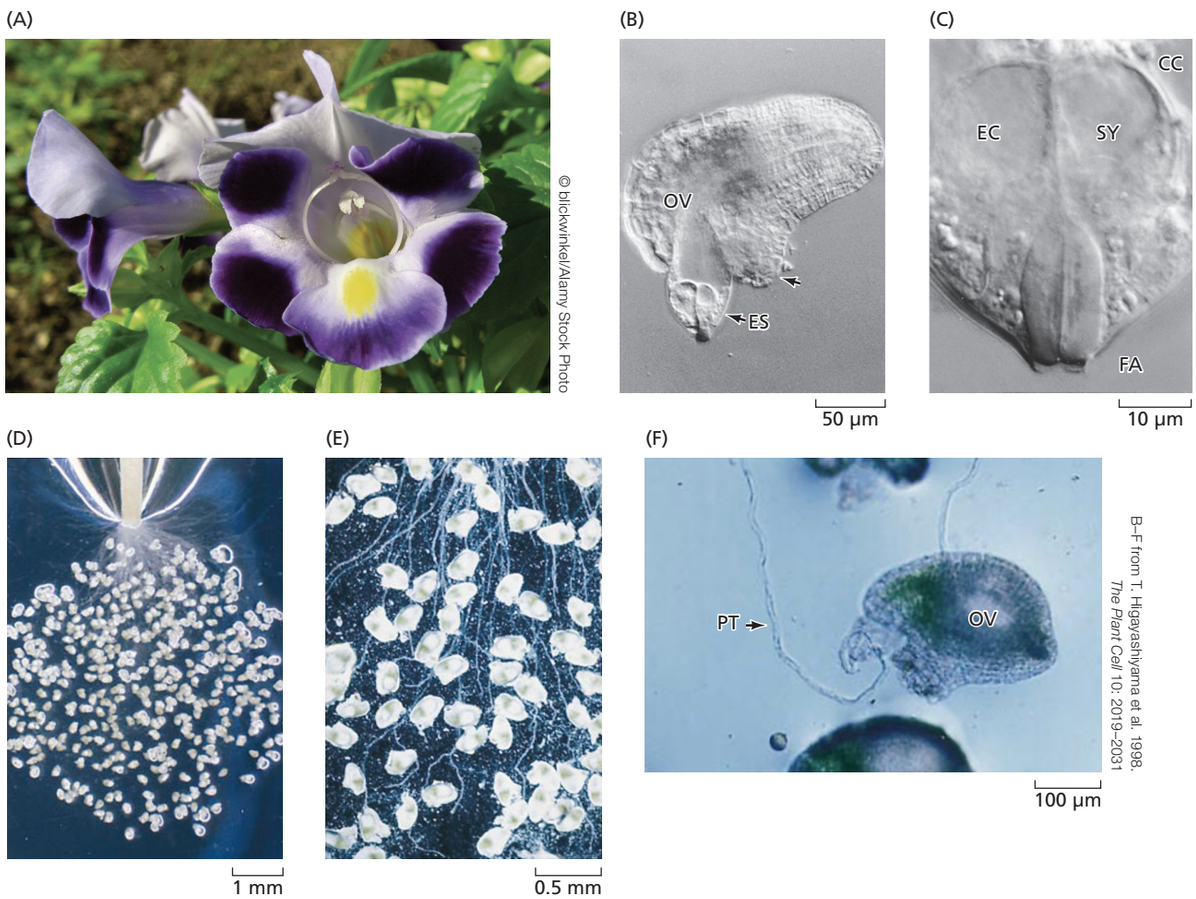


Figure 21.16 Use of excised *Torenia fournieri* ovules to study the influence of the style on the directed growth of the pollen tube. **(A)** Flower of *T. fournieri*. **(B)** *T. fournieri* embryo sac (ES) extending from the micropylar region of the excised ovule (OV). **(C)** Magnified view of the naked embryo sac showing the central cell (CC), the egg cell (EC), and one of the two synergids (SY) with its filiform apparatus (FA). **(D)** Ovules placed near a pollinated style. **(E)** Dark-field image showing pollen tubes growing toward ovules. **(F)** Micrograph of a pollen tube (PT) that has reached the micropylar end of a naked embryo sac in an ovule (OV).

plants. The various LUREs of *Torenia* apparently act in a species-specific manner. LURE-like proteins have also been identified in Arabidopsis, and *T. fournieri* ovules expressing an Arabidopsis LURE attract Arabidopsis pollen tubes preferentially, and vice versa.

LUREs have been shown to bind to two specific receptors, the receptor kinase PRK6 and the receptor-like kinases MDIS1-MIK1 and MDIS1-MIK2. However, mutating all seven of the LURE genes in Arabidopsis had no impact on fertility, and mutating their two known receptors had only a marginal effect. Thus, LUREs do not appear to be strictly required for pollen chemotropism in vivo, suggesting there are other, redundant mechanisms. This finding led to the discovery of a second class of cysteine-rich polypeptides, named **XIUQIU** (pronounced "shiy-chou") after a traditional Chinese embroidered silk ball used as a token of love during dancing festivities. XIUQIU polypeptides attract pollen tubes in vitro almost as strongly as LUREs, but as in the case of LUREs, XIUQIU null mutants retain their fertility. Given the critical role of fertilization in the plant life cycle, it is not surprising that a great deal of redundancy seems to have been built into the system. However, the functions of LUREs and XIUQUIs do not appear to be the same. Detailed analysis of pollen tube competition experiments, in which plants were pollinated with a mixture of pollen from *Arabidopsis thaliana* and a close relative, *A. lyrate*, showed that XIUQIUs are unspecific with respect to species, whereas LUREs can promote species-specific pollination. This phenomenon, called **incongruity**, was characterized in detail by Charles Darwin and enforces species isolation, even when pollen tubes of a closely related species can germinate and grow toward the ovule.

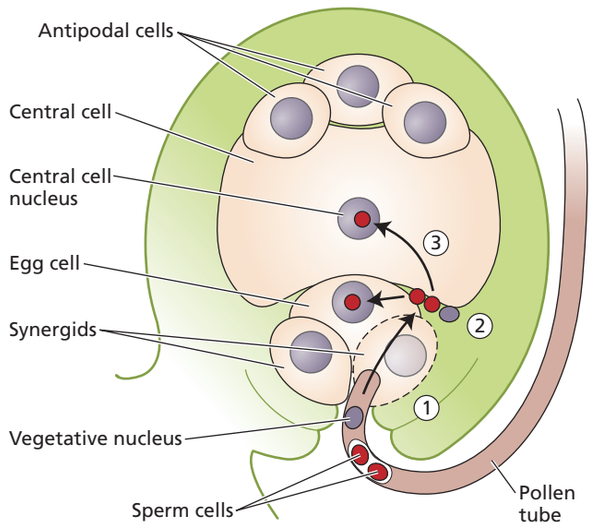
For a brief overview of other potential signaling agents guiding pollen tube growth, see **WEB TOPIC 21.6**.

Double fertilization occurs in three distinct stages

When the pollen tube senses chemical attractants secreted by the synergids, it grows through the micropyle, penetrates the embryo sac, and enters one of the synergid cells. In Arabidopsis, the micropylar end of the egg sac is blocked by the thickened walls of the filiform apparatus, which forms a barrier to pollen tube penetration. Arabidopsis pollen tubes therefore do not enter the synergid at the micropyle, but grow slowly for an hour in close proximity to the synergid cells until a suitable penetration site is located. Once inside the synergid cell, the pollen tube stops growing, the tip bursts to release the two sperm cells, and the synergid cell degenerates.

Studies of pollen tubes and synergid cells labeled with reporters for cytosolic Ca^{2+} concentration have shown that as the pollen tube nears the receptive synergid cell, both undergo a series of Ca^{2+} pulses. This suggests that Ca^{2+} oscillations are part of the signaling mechanism between the pollen tube and the synergid that leads to penetration of the receptive synergid and bursting of the pollen tube. The receptor-like kinase FERONIA is probably involved in this process, given that in *feronia* mutant plants the embryo sacs show altered Ca^{2+} oscillation patterns, and that following the pollen tube's entry into the synergid of a *feronia* mutant embryo sac, the pollen tube tip not only fails to burst but continues to grow inside the embryo sac, coiling and occasionally exiting the ovule.

Based on live imaging of fluorescently tagged sperm cells, sperm cell behavior in Arabidopsis can be divided into three stages (**Figure 21.17**). First, the pollen tube bursts within a few seconds of entering the synergid, triggering the degeneration of the receptive synergid cell. Second, the two sperm cells remain stationary at a boundary region between the egg cell and the central cell for approximately 7 min. Third, the two sperm cells begin moving along the embryo sac; one sperm fuses with the egg and the other fuses with the central cell, completing double fertilization. Experiments using different-colored cellular markers have shown that the two isomorphic (morphologically identical) sperm cells of Arabidopsis randomly fertilize either the egg cell or



1. The pollen tube bursts and discharges. Sperm cells are delivered rapidly from the pollen tube into the female gametophyte. The receptive synergid cell is likely to break down just after the start of pollen tube discharge.

2. Two sperm cells remain at the boundary region between the egg cell and the central cell for several minutes.

3. One sperm cell fuses with the egg cell and the other fuses with the central cell, and their nuclei move toward the target gamete nuclei.

Figure 21.17 **Sperm cell behavior during double fertilization in Arabidopsis can be divided into three stages.**

the central cell. Although the sperm cells of angiosperms are typically isomorphic, some species are dimorphic, having sperm cells with two different morphologies that determine which female gametophyte cell the sperm cell will fuse with. For example, in *Plumbago zeylanica* the larger sperm cell, containing numerus mitochondria, preferentially fuses with the central cell, while the smaller sperm cell, which is enriched with plastids, fuses with the egg cell. Various fail-safe mechanisms have evolved during the final steps of fertilization to ensure that proper gamete fusion takes place (see **WEB TOPIC 21.7**).

There is evidence that the discharged sperm cells exchange additional signals with the egg and central cells that prepare them for fusion. Gamete fusion itself appears to be mediated primarily by the specific fusion protein HAPLESS2 (HAP2), an ancient protein that was originally discovered in plants but was subsequently shown to be essential for gamete fusion in most organisms, with the exception of fungi and vertebrates. HAP2 has also been co-opted by many pathogens—among them *Plasmodium* (malaria), *Toxoplasma*, and viruses (e.g., rubella, dengue)—to promote fusion with target cells. In Arabidopsis, HAP2 is expressed in the sperm cells and is necessary for fusion with the egg cell, in a process that also involves the cysteine-rich protein EC1. When a sperm cell arrives at the egg cell, the egg cell releases EC1. The sperm cell then responds to EC1 by secreting HAP2 onto its surface, allowing fusion to proceed. Consistent with this mechanism, mutant sperm cells lacking HAP2 are unable to fuse with either the egg or the central cell.

21.5 Selfing versus Outcrossing

Most angiosperms—more than 85%—are hermaphroditic, and of these about half are capable of self-fertilization, or **selfing**. According to one hypothesis, species capable of selfing are more likely to become established (i.e., "naturalized") after long-distance dispersal. Consistent with this rule, a positive correlation was found between selfing ability and the extent of global naturalization. However, selfing is also associated with inbreeding depression, which is the likely explanation why so many flowering plants have evolved mechanisms that promote outcrossing. Outcrossing increases genetic diversity and thereby the ability to adapt to different environmental conditions. The most common mechanism used by angiosperms to prevent selfing is *pollen self-incompatibility*, which we discuss later in the section. Certain features of floral morphology or developmental timing also promote outcrossing, as when the stamens and pistils of a bisexual flower or monoecious plant mature at different times. Finally, the production of male-sterile (functionally female) individuals prevents selfing and promotes outcrossing in plants.

Hermaphroditic and monoecious species have evolved floral features to ensure outcrossing

Once sex in plants was discovered, botanists initially assumed that hermaphroditic flowers must all be self-pollinating. It thus came as a surprise when at the end of the eighteenth century it was demonstrated that, in the majority of cases, floral morphology was optimized for attracting insect pollinators, and that these pollinators facilitated outcrossing rather than self-pollination. Temporal and spatial features of flower morphology were identified that prevented self-pollination in both hermaphroditic and monoecious species. In **dichogamy**, the stamens and pistils mature at different times. There are two types of dichogamy: *protandry* and *protogyny*. In protandrous flowers the stamens mature before the pistils, while in protogynous flowers the pistils mature before the stamens (**Figure 21.18A**). A protandrous flower thus functions as a "male flower" early in its development and as a "female flower" later in development; in a protogynous flower the pattern is reversed. Since individuals in a wild population are at different developmental stages at any given time, there will always be pollen available for every pistil, and vice versa.

Another flower feature that promotes outcrossing is **heterostyly**. In heterostylous species, two or three morphological types of flowers, termed *morphs*, exist in the same population. The flower morphs differ in the lengths of their pistils and stamens. In one morph the stamens are short and the pistils are long, while in the second morph it is the reverse (**Figure 21.18B**). The lengths of the stamens and pistils in the two morphs are adapted for pollination by different pollinators or by different body parts of the same pollinator, thus promoting outcrossing. The morph phenotype is also genetically linked to a unique type of self-incompatibility, such that pollen from one morph cannot fertilize another flower on the same morph.

Cytoplasmic male sterility (CMS) occurs in the wild and is of great utility in agriculture

Male sterility—the inability to produce functional pollen—is widespread among plants and effectively prevents self-pollination. Male sterility is often maternally inherited, caused by gain-of-function mutations in the mitochondrial genome, and is therefore called *cytoplasmic male sterility* (*CMS*). CMS has been studied extensively in a wide variety of crops, where it has been exploited in breeding programs.

Most types of CMS mutations are caused by mitochondrial chromosomal rearrangements that produce chimeric genes with new functions. Plant mitochondrial genomes are large, variable in size, and tend to undergo recombination in specific regions (see Chapters 3 and 13). Mitochondrial genome rearrangements can result in fusions between two distinct mitochondrial sequences, sometimes

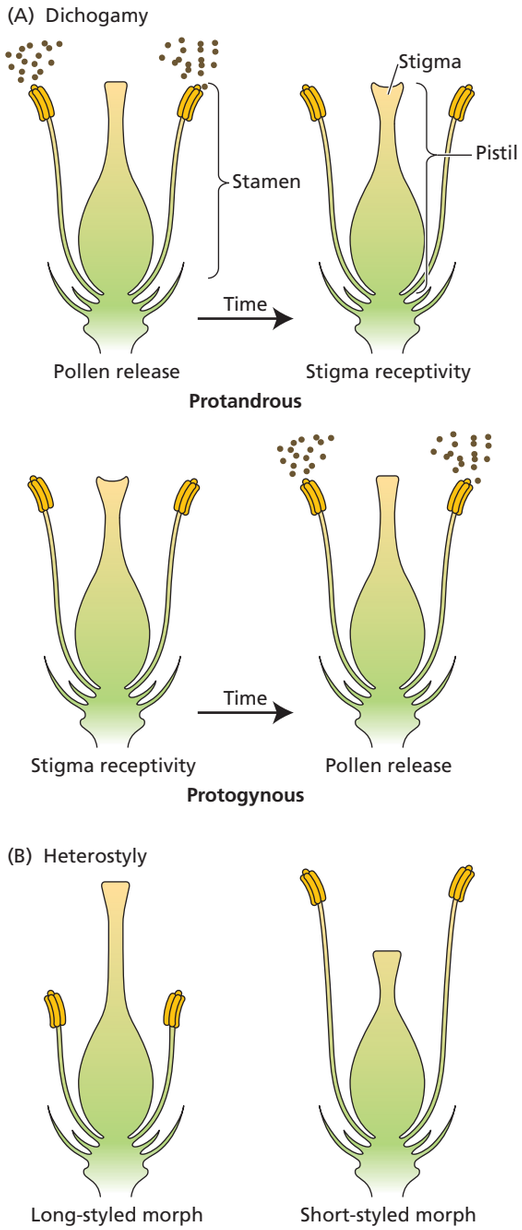


Figure 21.18 **Morphological adaptations in flowers that promote outcrossing.** (A) Dichogamy. In protandrous flowers, pollen release from the anthers occurs prior to stigma receptivity (indicated by the open stigma). In protogynous flowers, stigma receptivity precedes pollen release. (B) Heterostyly. Two anatomically different types of flowers are produced: long-styled morphs and short-styled morphs. Due to incompatibility reactions, the two types can pollinate each other but not themselves.

producing a novel, functional gene. Although no two CMS mutations isolated so far have been the same, all seem to inhibit mitochondrial function when expressed in the anther, resulting in the production of reactive oxygen species (ROS) and ROS-mediated programmed cell death. For a discussion of the molecular mechanism of CMS in rice, and its reversal, see **WEB TOPIC 21.8**.

Male sterility is one of the most sought-after traits in crop plants in which hybrid vigor, or **heterosis**, is of paramount importance for yield (e.g., maize and canola) (see Chapter 3). Hybrid seed displaying heterosis must be produced anew every season from a cross between two genetically distinct inbred lines. The main practical problem in producing hybrid seed is preventing self-pollination, which would result in nonhybrid seeds. Without male sterility, the pollen recipient has to be manually emasculated to prevent self-pollination, a laborious procedure. Cell ablation has been widely used to generate male-sterile varieties of various crops (e.g., canola). In this technique, gene promoters specific for anthers or tissues that pollen depends on to develop (e.g., tapetum) are used to drive the expression of cytotoxic proteins, such as RNAses. These cytotoxic proteins specifically kill the targeted cells or tissues, rendering the adult plants male-sterile. Sown in lines alternating with pollen producing plants, these varieties generate hybrid seeds with the desired phenotype.

Self-incompatibility (SI) is the primary mechanism that enforces outcrossing in angiosperms

Floral morphology and cytoplasmic male sterility promote outcrossing in some species. However, in most hermaphroditic species in which selfing never occurs, outcrossing is strictly enforced by a self/nonself recognition mechanism termed **self-incompatibility** (**SI**). SI systems have evolved independently several times in flowering plants, leading to a diverse array of mechanisms. SI creates a biochemical barrier that prevents self-pollination, usually by killing pollen grains or tubes generated by the same individual, while allowing pollination by another individual of the same species.

The ability to discriminate between self and nonself is a ubiquitous and essential function of both multicellular and microbial species. In vertebrates, for example, recognition of nonself is a major function of immune systems, which depend on a group of genes called the major histocompatibility complex (MHC), in which allelic variability, or polymorphisms, at the MHC loci facilitates self/nonself discrimination. In plants, self/nonself recognition during sexual reproduction is mediated by the self-incompatibility locus, *S* (for *S*elf-incompatibility), which directs the recognition and rejection of self-pollen. This functional analogy between the MHC and the *S* locus in determining the discrimination of self from nonself has long inspired proposals regarding evolutionary homologies between animals and plants. Yet the discovery of the first molecular mechanisms of self-incompatibility in plants showed them to be completely different in every

way from those of animals. The *S* locus is a complex of genes that are expressed either in the anther and pollen grain (male) or in the pistil (female). The pollen and pistil determinant genes are inherited as a single segregating unit and have many alleles. The allelic variants of this gene complex are called **S haplotypes**. A haplotype is any combination of alleles at adjacent loci on a chromosome that are inherited together.

Two distinct genetic mechanisms govern self-incompatibility

During pollination of the stigma, and pollen tube growth within the style and ovary, the proteins expressed by the alleles of the SI genes determine whether the pollen or pollen tube will be perceived as self or nonself by the cells of the pistil. If the cells of the pollen grain (or tube) carry the *same* alleles as the *S* haplotype of the pistil, the pollen is perceived as self and an incompatible reaction occurs that aborts tube development. If, however, the pollen grain (or tube) expresses *S* haplotype alleles that are *different* from those of the pistil, the pollen is perceived as nonself, allowing pollination, tube growth, and fertilization to proceed.

Microscopy of SI processes across many species led to an early grouping of SI mechanisms into two main types based on the stage at which fertilization is arrested. In one set of families (e.g., Brassicaceae, Poaceae), pollen grains are blocked at a very early stage, sometimes even before hydration, and fail to germinate. In the second set of families (e.g., Solanaceae, Rosaceae), pollen grains germinate normally on the stigma, but the pollen tubes die on their way to the ovule. These two types of SI reflect two very different genetic mechanisms (**Figure 21.19**).

In **sporophytic self-incompatibility** (**SSI**), the pollen grain's incompatibility phenotype is determined by the diploid genome of the pollen parent, or more precisely, the sporophytic tissue that supports pollen formation—the tapetum of the anther. The diploid tapetum deposits proteins produced by both copies of its *S* haplotypes onto the surface of the pollen of SSI species. Consequently, even though each haploid pollen grain carries only one *S* haplotype in its genome, its incompatibility phenotype reflects both *S* haplotypes carried by its parent. The stigma is also sporophytic and therefore diploid, and also contains proteins from two different *S* haplotypes. If either of the *S* haplotypes of the pollen parent matches either of the *S* haplotypes on the stigma of the recipient plant, then *rejection* will occur. Since the SSI proteins react immediately after contact on the stigma, the SSI reactions typically block pollen grains prior to hydration or germination. However, if the ungerminated SSI pollen is removed from the incompatible stigma and placed on a compatible stigma, it will recover.

In **gametophytic self-incompatibility** (**GSI**), the incompatibility phenotype of the pollen is determined by the pollen's own (haploid) genotype. In this case, rejection occurs if the single *S* haplotype of the pollen grain matches either of the *S* haplotypes in the pistil. GSI reactions typically arrest pollen tube development after the tube has grown partway through the style. This is because the protein that triggers the incompatibility reaction in the pistil is not already present in the pollen cell wall as it is in SSI. Instead, the protein must first be synthesized by the haploid genome of the pollen grain and then must accumulate in sufficient quantities to elicit GSI within the style. In contrast to SSI, which typically arrests pollen germination, GSI acts later, resulting in pollen tube death.

The type of self-incompatibility reaction present in a given species has been shown to correlate with other aspects of reproductive development. For example, SSI is often associated with a dry stigma, while GSI is more common in species with wet stigmas. Thus, SSI pollen must obtain water from the stigma before the pollen tube can emerge, whereas GSI pollen becomes hydrated and metabolically active as soon as it lands on the stigma.

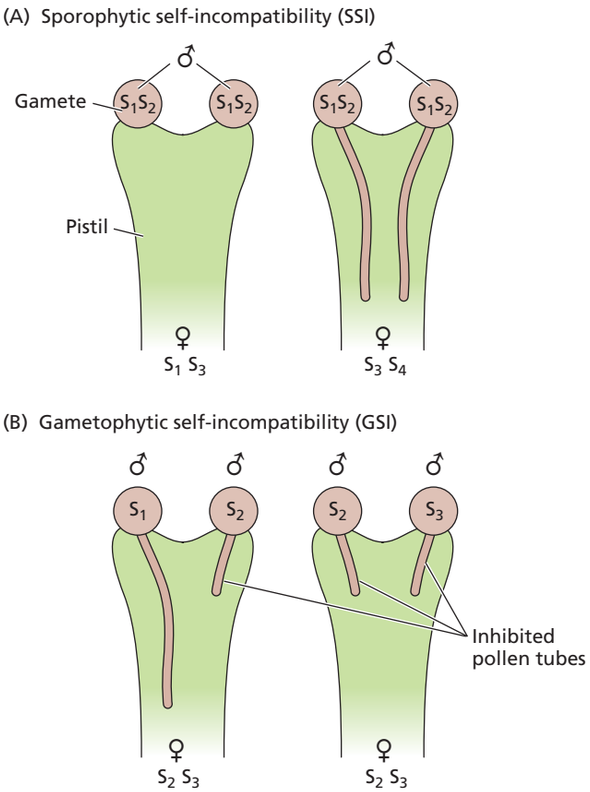


Figure 21.19 Comparison of gametophytic and sporophytic self-incompatibility. (A) Sporophytic self-incompatibility (SSI). Pollen tube growth proceeds only if the parent diploid genotype does not match the female parent. (B) Gametophytic self-incompatibility (GSI). Pollen tube growth proceeds only if the haploid genotype does not match the female *S* locus.

Despite these differences, germination of compatible pollen is equally rapid in both types of SI. Nevertheless, the correlation between these anatomical features and SI type may indicate that the two main types of SI diverged early during angiosperm evolution.

The Brassicaceae sporophytic SI system is mediated by S locus–encoded receptors and ligands

The only SSI system that has been characterized at the molecular level thus far is that of the Brassicaceae. In the Brassicaceae, two highly polymorphic genes (i.e., genes with many different alleles) of the *S* locus are involved in the SI response (**Figure 21.20**). The male *S*-determinants are cysteine-rich proteins located in the pollen coat and are called **S-locus Cysteine-Rich proteins** (**SCRs**). Although SCRs are expressed in both the diploid tapetum and the haploid pollen grain, only the SCRs produced by the tapetum are required for the self-incompatibility reaction. Because the tapetum is a sporophytic tissue, the SI system in Brassicaceae is regarded as sporophytic. The pistil *S*-determinant is a serine/threonine receptor kinase, called the **S-locus receptor kinase** (**SRK**), which is located in the plasma membrane of stigma cells. SRKs are highly variable among different *S* haplotypes, as expected for proteins involved in self-recognition.

During microgametogenesis, the diploid tapetum secretes various proteins, including two types of SCRs—one from each *S* haplotype of the diploid genome—which are incorporated into the exine, the outer layer of the pollen grain cell wall. After pollination, the SCRs diffuse onto the stigma surface and penetrate the papillae cell wall until they reach the plasma membrane. Because the stigma is diploid, the papillae cell plasma membrane also contains two types of SRKs, one for each *S* haplotype in the stigma. Each SRK recognizes and binds only to its cognate SCR encoded by the same *S*-locus haplotype. When this occurs, binding of SCR to SRK causes autophosphorylation of the receptor. Phosphorylation of the SRK receptor then initiates a signaling cascade that rapidly inhibits functions that would normally facilitate pollen hydration and germination. For example, pollen activation compounds or proteins needed for secretion may be targeted for degradation. The SSI reaction occurs even if only one of the two *S* haplotypes represented in the pollen coat (as SCRs) is present in the genome of the stigma.

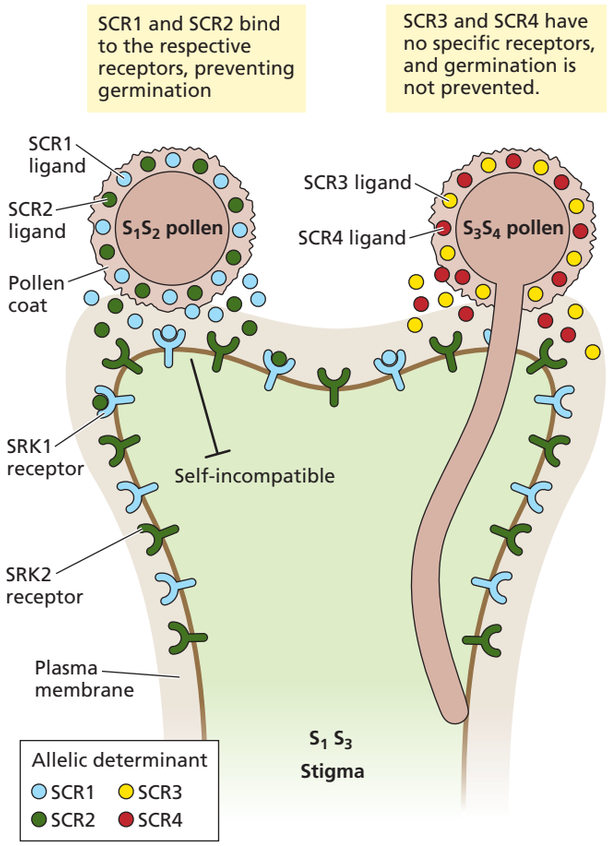


Figure 21.20 Brassicaceae sporophytic SI system involving receptor–ligand interactions and recognition of "self" pollen at the stigma epidermal surface. In the sporophytic SI system, the SI phenotype of the pollen is determined by the SI phenotype of the anther in which it was formed. The pollen and pistil therefore express the gene products of two different SI alleles (dots in the pollen wall). The diagram shows two pollen grains with different haplotypes (S_1S_2 and S_3S_4) on the stigma papillae cell of a self-incompatible S_1S_3 heterozygote. The *S*-locus Cysteine-Rich protein (SCR) ligands of each pollen grain are located in the pollen exine or pollen coat and are delivered to the epidermal surface when the grain lands on the stigma. The stigma papillae cells in the diagram are expressing the SRK1 and SRK2 receptors. Both the S_1 and S_2 ligands from the pollen grain bind and activate their respective receptors on the surface of the S_1S_2 stigma cell, triggering a signaling cascade that leads to inhibition of hydration, germination, and tube growth. In contrast, the S_3 and S_4 ligands of a pollen grain derived from a plant expressing neither the S_3 or S_4 haplotype fail to bind and activate SRK receptors, allowing pollen tube growth to proceed.

Cytotoxic S-RNases and F-box proteins determine gametophytic self-incompatibility (GSI)

Gametophytic self-incompatibility (GSI) is the more prevalent form of self-incompatibility among flowering plants and is thought to have evolved before SSI. Like SSI, GSI is controlled by a single multiallelic locus (*S* locus) containing two tightly linked genes that encode the pollen-expressed male determinant and the pistil-expressed female determinant. In the Solanaceae, Scrophulariaceae, and Rosaceae families, the pollen determinant is specified by a gene encoding an F-box protein, SLF/SFB (SLF and SFB denote the same protein

identified in different species), which is involved in targeting proteins for degradation via the ubiquitination pathway (see Chapter 4). The pistil determinant is specified by a cytotoxic S-ribonuclease (S-RNase) gene, which is specifically expressed in the transmitting tract of the style and secreted into the extracellular spaces where pollen tubes grow (**Figure 21.21A**). Pollen tube rejection occurs whenever there is a match between the *S*-determinant of the haploid pollen and one of the two *S*-determinants expressed in the diploid style.

A key advance in our understanding of the mechanism of GSI was the discovery that the S-RNases produced in

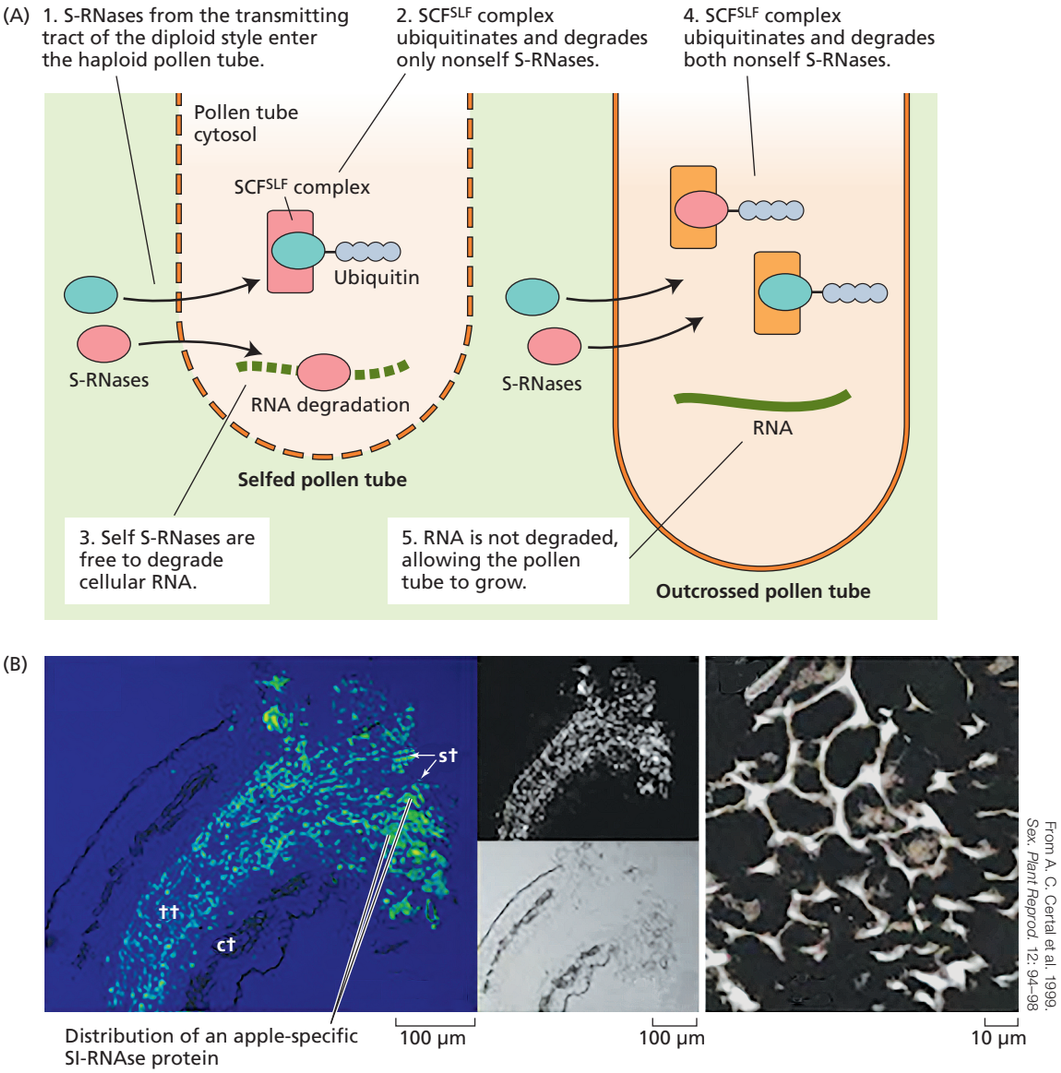


Figure 21.21 RNase degradation model for gametophytic self-incompatibility (GSI). **(A)** (Left) Selfed pollen tube. Because the pollen is haploid, its SCF^{SLF} complex recognizes and degrades only the nonself S-RNAse produced by the diploid transmitting tract. As a result, the remaining self S-RNase is free to degrade cellular RNA. (Right) Outcrossed pollen tube. During cross-pollination, the pollen tube SCF^{SLF} complex recognizes and degrades both of the nonself S-RNases, which eliminates toxicity and allows pollen tube growth to proceed. **(B)** Immunolabeling of SI-RNAses in the style of *Malus domestica* (apple), a member of the Rosaceae family. Left panel shows a microscopic section of an apple pistil. The false-color image was produced by merging a fluorescence image (top center), obtained using fluorescent-labelled antibodies, and a widefield microscopy image (bottom center). Green indicates the distribution of an apple-specific SI-RNAase protein The SI proteins accumulate where pollen and pollen tubes will grow, from the external stigma cells (st), through the transmitting tissue (tt), while none is seen the cortical tissue (ct) and epidermis.. Right panel shows the accumulation of SI proteins in the cell walls and intercellular spaces. Pollen tubes take up these proteins inside while growing through the intercellular spaces.

the transmitting tract can be taken up into the cytosol of the pollen tube, whether or not the pollen determinant matches either of the pistil determinants. In other words, the recognition between the S-RNase from the pistil and the *S*-determinant of the pollen occurs *inside* the pollen tube and results in only self S-RNases being cytotoxic. This observation is consistent with the pollen determinant SLF/SFB being an intracellular protein. As an F-box protein, SLF/SFB is a component of the E3 ligase complex SCF, which is involved in protein degradation through the ubiquitin–26S proteasome-dependent pathway. The function of SLF/SFB suggests a model in which recognition of a nonself S-RNase by the pollen tube SCF^{SLF} proteins leads to the ubiquitination and degradation of the nonself S-RNases in the pollen tube (**Figure 21.21B**). Degradation of nonself S-RNases by SCF^{SLF} would prevent RNase cytotoxicity and allow the pollen tube to continue growing. In the case of self-pollen, however, the SCF^{SLF} protein complex fails to bind to the S-RNase taken up from the transmitting tract. As a result, the S-RNase is not degraded and digests the RNA of the pollen tube vegetative cell, leading to cell death. This model accounts for some aspects of GSI, but not all. For example, sequestration of S-RNase in the tube cell vacuole appears to play an important role in protecting against cytotoxicity. During incompatible reactions, the breakdown of the vacuolar membrane may trigger programmed cell death of the tube cell.

A simpler molecular mechanism of GSI was described in poppy (*Papaver rhoeas*) (see **WEB TOPIC 21.9**).

21.6 Apomixis: Asexual Reproduction by Seed

In some species the embryo is not produced as a result of meiosis and fertilization, but from a somatic diploid cell in the ovule that differentiates directly into a zygote and is therefore genetically identical to the female parent. This type of asexual or clonal reproduction by seed is known as *apomixis*, and the plants produced in this way are known as *apomicts*. Apomixis is known to occur in approximately 0.1% of angiosperms, including both monocots and eudicots in more than 40 angiosperm families. Common examples include citrus species, mango, dandelion, blackberry, crabapple, and the fodder grass *Panicum*. The various types of apomixis are described in **WEB TOPIC 21.10**.

Apomixis is not an evolutionary dead end

Because of its clonal nature, apomixis was once regarded as an evolutionary blind alley, genetically distinct from sexual reproduction. This hypothesis was based on the assumption that apomixis represented an irreversible phylogenetic branch point that would inevitably lead to the extinction of the lineage. This view has now been superseded by phylogenetic analyses that have shown that apomixis is not only widely distributed in both early- and late-branching lineages, but that it is reversible as well. That is, lineages that were once apomictic sometimes revert to obligate sexual reproduction. In a few cases, environmental stress has been shown to induce a switch from sexual reproduction to apomixis.

The genetic control of apomixis is based on the altered expression of the same genes that control the normal development of the nucellus and megagametophyte. Because the vast majority of apomictic genotypes are polyploid, it has been suggested that the evolution of apomixis may have contributed to the fitness of at least some polyploid species.

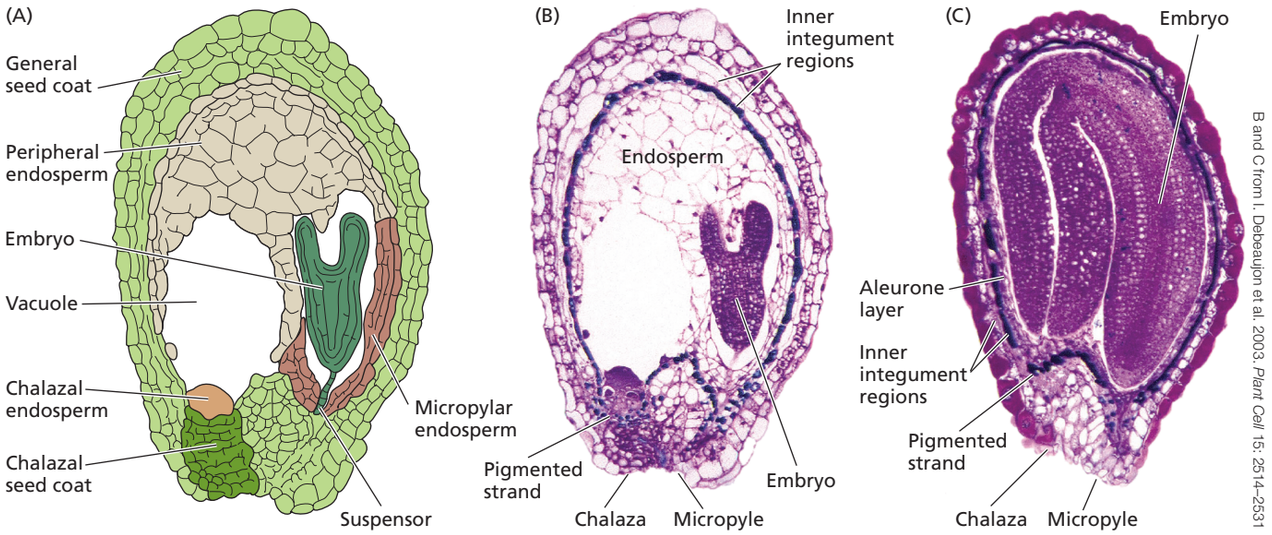
Elucidating the mechanism of apomixis could potentially provide plant breeders with an important new tool for improving crops. Many of our most productive crops, such as maize, are hybrids that have been developed to take advantage of the phenomenon of heterosis. As noted earlier, hybrid plants do not breed true and cannot be propagated by seed. Therefore, hybrid seeds must be generated each season by repeating the original cross. But if apomixis were to be introduced into the F_1 hybrid, the hybrid plant could produce seeds clonally, thus avoiding the problem of the loss of heterosis in the F_2 generation. The development of methods to induce apomixis in F_1 hybrids by transforming them with the appropriate genes offers the exciting possibility of greatly accelerating progress in crop improvement in the future.

21.7 Endosperm Development

From both an ecological and agricultural perspective, the plant life cycle begins and ends with a seed. We now pick up the story of the angiosperm ovule immediately after double fertilization, and follow its transformation into a mature seed.

The endosperm develops from mitotic divisions of the primary endosperm nucleus resulting from double fertilization. There are three types of endosperm development in angiosperms: *nuclear*, *cellular*, and *helobial*. Of these, the nuclear type is the most common and has been extensively studied in seeds of cereals and Arabidopsis, as we discuss in this section. (For a description of the other endosperm types, see **WEB TOPIC 21.11**.)

During seed morphogenesis, the endosperm provides nutrition to the developing embryo. In some species there is sufficient endosperm remaining to provide nutrition to the germinated seedling as well. In Arabidopsis and many other species, the endosperm is almost entirely reabsorbed (solubilized and absorbed) during embryogenesis, and the reserves that will support early seedling growth are stored in the embryo's cotyledons (**Figure 21.22**). The fleshy cotyledons of legumes are highly specialized for food storage (see Chapter 17). In



B and C from I. Debeaujon et al. 2003. *Plant Cell* 15: 2514–2531

Figure 21.22 **Arabidopsis seed structure.** **(A)** Diagram of an Arabidopsis seed with the embryo at the torpedo stage of development. **(B)** Light micrograph of a stained section of an Arabidopsis seed at the same stage as in (A). The embryo is embedded in mature endosperm tissue. The seed is covered by a seed coat derived from the inner and outer integument tissues of the ovule. **(C)** Mature seed. The endosperm has mostly been reabsorbed, and the embryo fills the seed. The cotyledons contain stored reserves that will support early seedling growth following germination. (A after I. Debeaujon et al. 2003. *Plant Cell* 15: 2514–2531.)

cereals and other grasses, the endosperm persists during seed development and becomes the major site for the storage of starch and protein (**Figure 21.23**). Mobilization of these reserves for transport to the embryo is the final function of the endosperm before it undergoes programmed cell death as the seedling becomes established.

In seeds with a nuclear-type endosperm, development proceeds in two phases: a *coenocytic phase* and a *cellular phase*. Just after double fertilization, the endosperm nucleus undergoes several rounds of mitosis without cytokinesis, forming a multinucleate coenocyte. At a specific time that varies with species, the coenocyte deposits cell walls around each nucleus as it gradually undergoes cellularization.

Cellularization of coenocytic endosperm in Arabidopsis progresses from the micropylar to the chalazal region

Several stages in the development of the endosperm coenocyte of Arabidopsis are shown in **Figure 21.24**. The primary endosperm nucleus that results from the fusion of the central cell with one of the sperm cells undergoes a series of eight mitotic divisions without cytokinesis, leading to the production of about 200 nuclei, mostly located at the periphery of the large central cell. By the globular embryo stage, the endosperm coenocyte of Arabidopsis has three regions that become distinct as the seed grows: the **micropylar endosperm** that surrounds the embryo, the peripheral endosperm in the central chamber, and the chalazal endosperm.

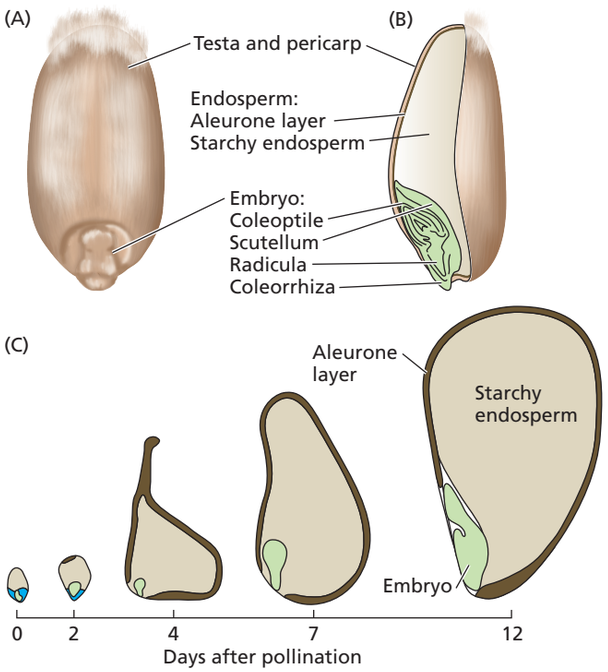


Figure 21.23 **Cereal seed structure, as illustrated by wheat (*Triticum aestivum*).** **(A)** Surface view of the seed, showing the location of the embryo in relation to the endosperm. **(B)** Longitudinal section through a seed. **(C)** Development of the embryo. (A and B after W. Troll. 1937. *Vergleichende Morphologie der hoheren Pflanzen*, Gebruder Borntrager, Berlin; C after M. Cosségal et al. 2007. In *Endosperm: Plant Cell Monographs*, vol 8. Olsen, O.-A. [ed.], pp. 57–71. Springer: Berlin, Heidelberg.)

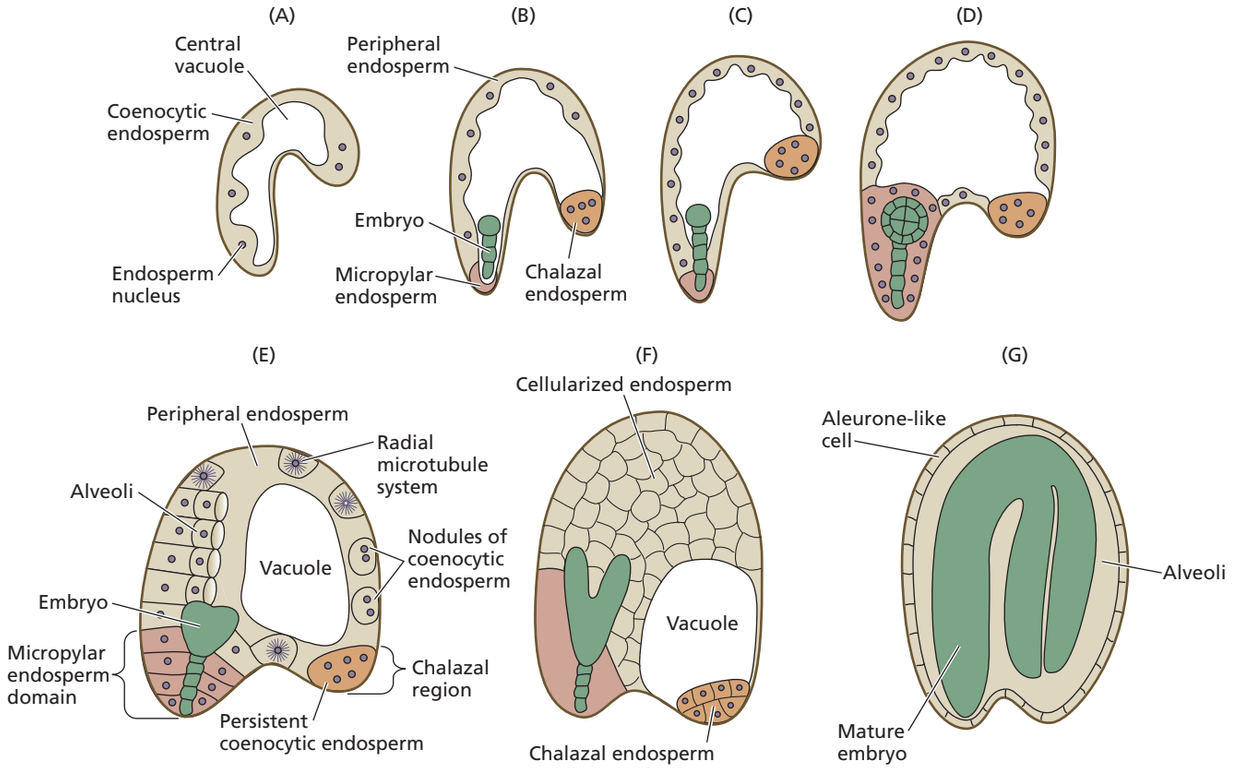


Figure 21.24 Development of the endosperm coenocyte of Arabidopsis. **(A–D)** The primary endosperm nucleus undergoes free nuclear divisions, and the resulting nuclei migrate to the periphery of the coenocytic central cell. **(E–G)** Cellularization of the endosperm coenocyte begins at the micropylar endosperm region and progresses to the chalazal region. All but a thin layer of endosperm at the periphery (the aleurone layer) is reabsorbed by the growing embryo during development. (After O.-A. Olsen. 2004. *Plant Cell* 16: S214–S227.)

Cellularization of the coenocytic endosperm in Arabidopsis begins in the micropylar endosperm region and progresses to the chalazal region (see Figure 21.24E and F). The process is initiated during the globular stage of embryogenesis, when the coenocyte is organized into evenly spaced nuclei kept in position by radial arrays of microtubules (**Figure 21.25A and B**). Mini-phragmoplasts (see Chapter 1) assemble equidistant from adjacent nuclei and later give rise to a cell plate by the fusion of tubular membranes into porous sheets (**Figure 21.25C**). The last stage is the fusion of one side of the cell plate with the parental plasma membrane (**Figure 21.25D**). Walls form between neighboring nuclear cytoplasmic domains but not between the domains and the central cavity of the embryo sac, resulting in open-ended cells referred to as **alveolar cells** because of their tubelike nature. Subsequent divisions of the alveolar cells inward lead to cross-wall formation in the peripheral cell layers, displacing the inner layer of alveoli, along with an overlying layer of residual coenocytic cytoplasm, inward toward the central cavity, until eventually the central vacuole disappears and the entire endosperm is cellularized (see Figure 21.24E and F).

Unlike in cereals, in which most of the endosperm remains in the mature seed,[1] in Arabidopsis the cellular endosperm is largely consumed as the embryo grows. At maturity, the embryo fills the entire seed and only a single layer of endosperm persists in the mature seed (see Figures 21.22C and 21.24G). As discussed in Chapter 17, the persistent endosperm layer, sometimes referred to as the *aleurone layer* by analogy to cereal grains, contributes to coat-imposed dormancy in Arabidopsis and other small-seeded species, and breakdown of its cell wall is required for the completion of germination.

Cellularization of the coenocytic endosperm of cereals progresses centripetally

In cereals, the endosperm is not consumed during embryogenesis, and as a result it takes up a much larger volume of the mature seed (see Figure 21.23).

During cereal endosperm development, the triploid primary endosperm nucleus undergoes a series of

[1] Cereal grains are technically fruits instead of seeds because they are enclosed by a fused *testa–pericarp*, which includes the seed coat and fruit wall (see Chapter 17).

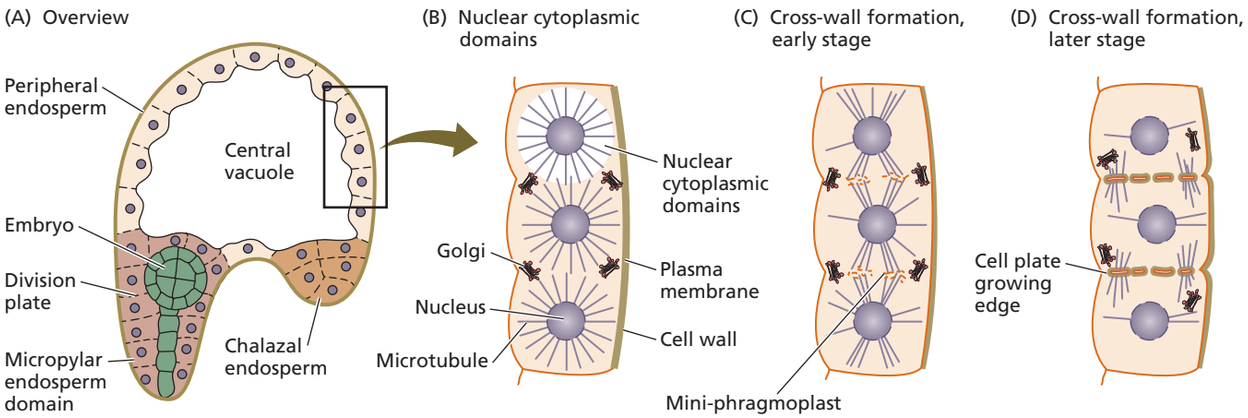


Figure 21.25 Cross-wall formation in the peripheral endosperm of Arabidopsis. **(A)** Cellularization begins during the globular stage of embryogenesis. **(B)** The coenocyte is organized into nuclear cytoplasmic domains by radial microtubules. **(C)** Mini-phragmoplasts form at the boundaries between adjacent domains. **(D)** Vesicles fuse to form cross-walls. (After M. S. Otegui. 2007. *In Endosperm: Plant Cell Monographs*, vol 8. Olsen, O.-A. [ed.], pp. 159–178. Springer: Berlin, Heidelberg.)

mitotic divisions without cytokinesis, and the nuclei migrate to the periphery of the central cell, which also contains a large central vacuole (**Figure 21.26A–D**). As in the Arabidopsis coenocyte, each nucleus is surrounded by radially arranged microtubules (**Figure 21.26E**). Anticlinal walls form initially between adjacent nuclei, resulting in the tubelike alveolar cells, with the open end pointing toward the central vacuole (**Figure 21.26F**). The alveolar nuclei then undergo one or more periclinal mitotic divisions followed by cytokinesis, producing daughter cells. The innermost layer of daughter cells remains alveolar in structure and continues to divide periclinally until cellularization is complete (**Figure 21.26G and H**).

The most important precursors of starchy endosperm tissue are the interior cells of the files that are present at the completion of endosperm cellularization (see Figure 21.26H). Soon after this stage the cells undergo further divisions, with the division planes now oriented randomly so that the cell file pattern is soon lost. The second source of starchy endosperm cells is the inner daughter cells produced by periclinal divisions of the aleurone layer. These cells redifferentiate to become the outer layers of the starchy endosperm.

Endosperm development and embryogenesis can occur autonomously

Although embryogenesis and endosperm formation occur concurrently and in close proximity in seeds, these two processes are not obligately coupled. For example, embryogenesis can take place in vegetative tissue without endosperm development during **somatic embryogenesis** in *Bryophyllum* and *Kalanchoe*, which can reproduce

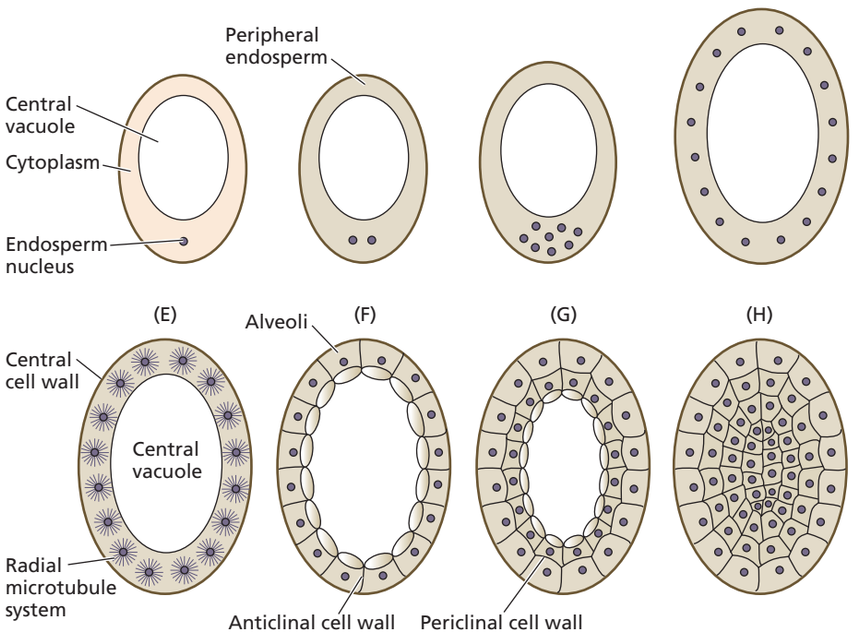


Figure 21.26 Development of the endosperm coenocyte of cereals. **(A–D)** The triploid endosperm nucleus is located in the basal cytoplasm of the central cell. After a series of free nuclear divisions, the nuclei migrate to the periphery of the large coenocytic cell. **(E–H)** Cellularization of the coenocytic endosperm of cereals. (After O.-A. Olsen. 2004. *Plant Cell* 16: S214–S227.)

asexually by producing plantlets on their leaf margins (**Figure 21.27A**). Somatic embryos can also be generated experimentally via tissue culture, a routine procedure in many biotechnology laboratories (**Figure 21.27B**). Once initiated, somatic embryos produced via tissue culture pass through the same developmental stages as normal embryos do (see Chapter 22) and can grow into otherwise normal plants, demonstrating that a nutrient medium can substitute for the nutritive endosperm during in vitro embryogenesis. Despite this apparent morphological recapitulation of zygotic embryogenesis, somatic embryos are formed through different processes. For example, rather than developing from a single-celled zygote, they develop from small groups of cells, and the somatic embryos are typically larger than zygotic embryos.

(A)



Patrice78500/Wikimedia/CC BY-SA 3.0

(B)



From P. P. Kumar and C. S. Loh. 2012. In *Plant Biotechnology and Agriculture*. A. Altman and P. M. Hasegawa, (eds.), pp. 131–138. Academic Press: Amsterdam. Photo by Wendy Shu

Figure 21.27 **Examples of asexual embryogenesis.** **(A)** In *Kalanchoe*, small embryos, sometimes referred as propagules, differentiate from the border of the leaves. They eventually fall off the leaf and start growing as a germinated seed in the floor. **(B)** Somatic embryos can be generated in tissue culture from many species, using young tissue or anthers. These explants are first subjected to a strong osmotic, hormonal, or temperature shock, and afterward grown in a recovery media as calli or cells in suspension. Some clusters of cells then assume an "egglike" fate and start recapitulating all the morphogenetic steps of zygotic embryogenesis. Here, a heart-stage embryo is seen emanating from a callus of undifferentiated cells.

The endosperm can also develop independently of the embryo. Autonomous development of endosperm in the seed appears to be under partial genetic control. In Arabidopsis, mutations in any one of three *FERTILIZATION-INDEPENDENT SEED* (*FIS*) genes (*FIS1*, *FIS2*, and *FIS3*) trigger autonomous endosperm development in the absence of double fertilization and embryo formation.[2] However, the mutant endosperm never cellularizes, whether due to being diploid rather than triploid or other causes. Given that the seed coat (testa) and fruit (silique) also are formed in the *fis* mutants, the development of the endosperm, testa, and ovary wall appears to be coordinated.

Many of the genes that control endosperm development are differentially expressed maternal or paternal genes

Animal breeders have known about parent-of-origin effects for thousands of years. For example, crossing donkeys with horses produces hinnies when the horse is the male parent and mules when the horse is the female parent. **Parent-of-origin effects** are defined as phenotypes that depend on the sex of the parent from which the trait is inherited.

A subset of parent-of-origin effects is caused by **imprinted gene expression**. Such genetic imprinting may have evolved in response to selective pressure in both plants and animals (see **WEB TOPIC 21.12**). Among the first demonstrations of the imprinting of individual genes was a study of the inheritance of maize kernel coloration. It was shown that whether or not a maize kernel was a solid color or exhibited purple mottling depended on whether the *R* alleles controlling mottling came from the maternal or paternal parent. These and subsequent studies demonstrated that the two sets of chromosomes from the female and male parents, while containing the same genes, differed in their developmental effects. Genetic imprinting is thus the process by which alleles on the maternal and paternal chromosomes become differentially "marked" to ensure parent-of-origin-specific expression after fertilization.

We now know that genomic imprinting involves the transmission from gametes to offspring of epigenetic information ("marks") in the form of chemical modification

[2] The *FIS1* gene was originally discovered as a maternal effect in a mutant Arabidopsis plant, and called *medea*. *FIS1* codes for a protein identical to the *MEDEA* gene. The proteins FIS1, FIS2, and FIS3 are Polycomb group proteins that function in histone methylation (see Section 21.7). The gene *FIS3* is also known as *FERTILIZATION-INDEPENDENT ENDOSPERM 1* (*FIE1*).

of DNA or its associated proteins (e.g., histones) by methylation or acetylation (see Chapter 3). As a result, a small subset of genes, termed imprinted genes, are expressed from only one of the two chromosomes in diploid cells. In contrast, most genes of the genome are nonimprinted, meaning that alleles from both parents are expressed equally.

Genes that are maternally expressed and paternally silent due to imprinting are referred to as **maternally expressed genes** (**MEGs**), and those that are paternally expressed and maternally silent are referred to as **paternally expressed genes** (**PEGs**). Studies in Arabidopsis and other species (including monocots) have shown that in flowering plants sexually imprinted gene expression is almost entirely confined to endosperm tissue. The majority of the differentially expressed genes are maternally expressed genes (one study found 100–165 MEGs vs. 10–43 PEGs). The evolutionary significance of the role of MEGs in the endosperm is that the female parent controls the nutrition of the developing plant embryo. While imprinting primarily affects endosperm development, the embryo also expresses a few imprinted genes as well. Our understanding of parental imprinting in plants relies on the study of a limited number of gene mutations, namely the maternally expressed *FIS1*, *FIS2*, and *FLOWERING WAGENIGEN* (*FWA*) loci, and the paternally expressed *PHERES1* (*PHE1*) gene. A possible scheme for the genetic regulation of endosperm development and cell proliferation is presented in **WEB TOPIC 21.13**.

Cells of the starchy endosperm and aleurone layer follow divergent developmental pathways

Whereas seeds of many species store reserves as proteins and oils, the endosperm of cereals stores large quantities of starch. The **starchy endosperm** is a unique tissue, accounting for the bulk of the endosperm in cereal grains (see Figure 21.23). The starchy endosperm of cereals also contains storage proteins, which are deposited in protein storage vacuoles.

Endoreduplication—that is, chromosomal replication without mitosis, resulting in high DNA content and polyploidy (see Chapter 1)—appears to play an important role in starchy endosperm development. In maize, for example, up to five rounds of endoreduplication may lead to a DNA content per nucleus of 96C—that is, 96 times the amount (*c*ontent) present in the haploid nucleus. Endoreduplication begins during reserve deposition, and the accumulation of DNA prevents further nuclear or cell division. The typical size of cells seems to be limited by the amount of DNA in the nucleus. Therefore, endoreduplication enables certain cells of plants and other organisms to expand to larger than normal volumes, maximizing their capacity to store food reserves (e.g., endosperm, up to 96C) or secretory compounds (e.g., leaf trichomes, up to 16C).

The starchy endosperm of cereals is dead at maturity due to programmed cell death, an event linked to the ethylene signaling pathway. In the maize mutant *shrunken2*, which overproduces ethylene, endosperm cell death is accelerated.

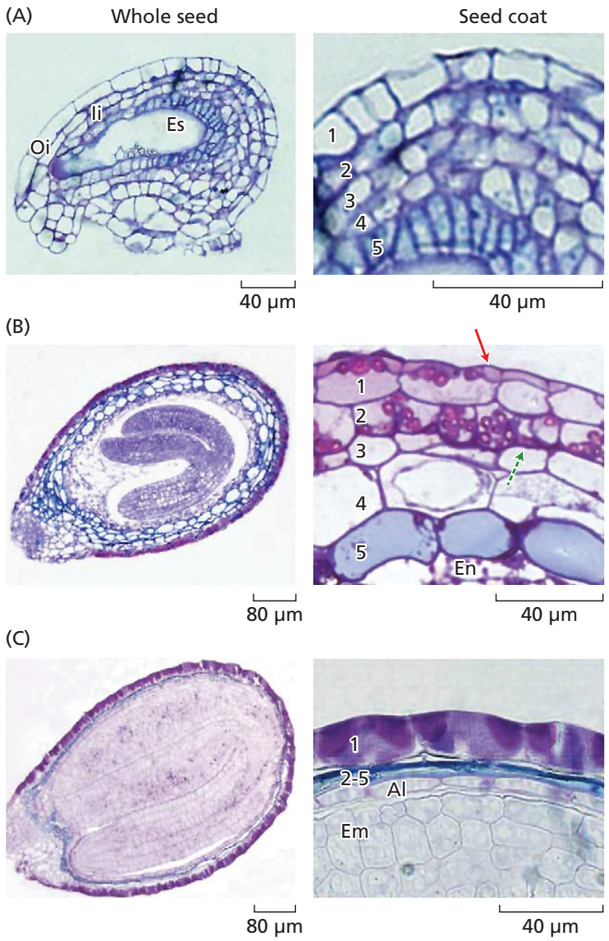
As discussed in Chapter 17, the aleurone layer (the outermost layer[s] of the endosperm) functions during early seedling growth by mobilizing starch and storage protein reserves in the starchy endosperm through the production of an α-amylase, protease, and other hydrolases in response to gibberellins produced by the embryo. Maize and wheat have one layer of aleurone cells, rice has one to several layers, and barley has three layers. In cereal grains, the aleurone layer is the only part of the endosperm that may become pigmented. Genetic studies have identified two genes that play a central role in regulating aleurone layer differentiation (see **WEB TOPIC 21.14**).

21.8 Seed Coat Development

By serving as the outer protective layer of the seed, the seed coat is the first line of defense for the embryonic plant against adverse environmental factors, both abiotic and biotic. However, as discussed in Chapter 17, seed coats can also regulate dormancy, ensuring that external conditions are favorable for growth before germination starts. Following fertilization, the seed coat differentiates from the cells of the maternally derived ovule integuments over a 2- to 3-week period (**Figure 21.28**). Cells in both layers of the outer integument and all three layers of the inner integument undergo a dramatic period of growth in the first few days after fertilization through both cell division and expansion. The resulting five cell layers undergo one of four distinct fates. Cells of the innermost layer, derived from the ovule **endothelium**, synthesize **proanthocyanidin** flavonoid compounds, also known as **condensed tannins** (see **WEB APPENDIX 4**), which accumulate in the central vacuole of the endothelial cells during the first week after fertilization and later become oxidized, imparting a brown color to the differentiated cells (known as the pigmented cell layer) and the whole seed coat. By contrast, cells of the other two inner integument layers do not appear to differentiate further, undergo early programmed cell death, and are crushed as the seed develops (see Figure 21.28C).

Seed coat development appears to be regulated by the endosperm

The seed coat is derived from the integuments of the ovule and is thus maternal, sporophytic tissue. Seed coat growth and differentiation are initiated by fertilization



All photos from G. Haughn and A. Chaudhury. 2005. *Trends Plant Sci.* 10: 472–477

Figure 21.28 **Development of the ovule integuments into the seed coat of Arabidopsis following fertilization.** Several stages of seed development for the whole seed (left) and a detail of the developing seed coat (right) are shown. **(A)** Prior to fertilization. **(B)** Ten days after fertilization. Cells of individual layers have almost completed differentiation into specialized cell types, including endothelium (5), palisade (2), and epidermis (1). The solid arrow indicates mucilage in the apoplast. The dashed arrow indicates the secondary cell wall of the palisade. **(C)** Fifteen days (seed maturity). The cells of all five layers are dead and have been crushed together, except for the epidermis, the shape of which is maintained by the thick cellulose-rich, secondary cell wall, named the columella. Al, endosperm aleurone layer; Em, embryo; En, endosperm; Es, embryo sac; Ii, inner integument; Oi, outer integument. 1 and 2 indicate the two cell layers of the outer integument; 3–5 are the three cell layers of the inner integument.

and normally proceed coordinately with the development of the growing embryo and endosperm of the seed, which represents the next sporophytic generation. Because the seed coat surrounds the seed, its growth in surface area must be coordinated with the growth of the embryo and endosperm for the seed to reach its mature size. If the seed coat fails to expand, seed size is reduced.

Seed coat development seems to depend directly on the endosperm. In crosses between wild-type Arabidopsis and mutants producing only one sperm cell (and which were thus able to fuse with only one of the female gametes), seeds in which only the central cell was fertilized produced normal seed coats, whereas seeds in which only the egg cell was fertilized did not, suggesting that seed coat development depends on endosperm development, and not on embryo development. The reason that the endosperm is required for seed coat development is that, following fertilization, the endosperm, which synthesizes several hormones, supplies auxin to the outer tissues of the ovule, which serves as a trigger for seed coat development. Prior to fertilization, seed coat development genes appear to be epigenetically repressed by POLYCOMB REPRESSIVE COMPLEX 2–(PRC2-) mediated histone trimethylation (see Footnote 2 in Section 2.7), and auxin produced by the endosperm removes this inhibition.

The *TRANSPARENT TESTA GLABRA2* (*TTG2*) gene provides an example of how the seed coat can regulate seed size. *TTG2* positively regulates both the biosynthesis of proanthocyanidin, a plant defense compound produced in the seed coat, and seed coat expansion. As a result, loss-of-function *ttg2* mutants have smaller seeds, presumably because the embryo and endosperm are mechanically constrained by the seed coat during development.

In contrast, mutations in the *HAIKU* gene result in limited growth of the coenocytic endosperm. This defect in endosperm growth also affects the growth of the developing seed coat, such that cell elongation in the expanding seed coat is restricted. This suggests that the growing endosperm regulates the extent to which the ovule integument cells elongate following the initiation of seed coat development.

21.9 Seed Maturation and Desiccation Tolerance

The final phase of seed development, termed **maturation**, is accompanied by the evaporative loss of water to produce a dry seed, a prerequisite for the quiescent state that precedes germination in many species of plants. For many species, maturation also includes the acquisition of **desiccation tolerance**. Desiccation tolerance is often correlated with **seed longevity**, the ability of the seed to remain viable in the dry state over long periods of time.

The term **orthodox seed** has been used to denote those seeds that can tolerate desiccation down to a moisture content as low as 5%, and are storable in a dry state for variable periods of time depending on the species. Examples of familiar orthodox seeds include cereals, legumes, and Arabidopsis. The longest-lived orthodox seed is the 2000-year-old Judaean date palm (*Phoenix*

dactylifera) seed that was successfully germinated in 2005. In contrast, **recalcitrant seeds** are those that are released from the plant with a relatively high water content and active metabolism. Unlike orthodox seeds, recalcitrant seeds deteriorate upon further dehydration and do not survive storage. Mango and avocado are examples of plants with recalcitrant seeds.

Seed filling and desiccation tolerance phases overlap in most species

The timing of the development of desiccation tolerance and seed longevity, in relation to the attainment of mature size and seed dispersal, varies across species. For most species, the acquisition of desiccation tolerance occurs during seed filling. Subsequently, during late maturation, seeds progressively acquire longevity, the ability to remain alive in the dry state for prolonged periods.

For example, four stages of seed growth and development (embryogenesis, seed filling, late maturation, and pod abscission) for seeds of barrel clover (*Medicago truncatula*) are shown in **Figure 21.29A**. Embryogenesis proceeds during the first 10 days after pollination, after which seed filling begins, as indicated by the increase in seed dry weight. Simultaneously, the water content of the seed declines (**Figure 21.29B**). The acquisition of desiccation tolerance begins approximately 24 days after pollination, and overlaps with the seed-filling stage and dehydration phases. From 28 days after pollination onward, seeds gradually acquire longevity (**Figure 21.29C**). Freshly harvested seeds acquire the ability to germinate at approximately 16 days after pollination, and the ability to complete germination increases to 50% from 22 to 32 days after pollination, after which it declines to 10% due to the onset of dormancy (**Figure 21.29D**) (seed dormancy is discussed in Chapter 17). However, this dormancy can be overcome by dry storage for 6 months (after-ripening), after which the fully mature seeds germinate within 24 h.

The acquisition of desiccation tolerance involves many metabolic pathways

For orthodox seeds, seed desiccation involves more than just the physical drying of the seed. It is associated with distinct patterns of gene expression and metabolism that affect multiple physiological processes, including

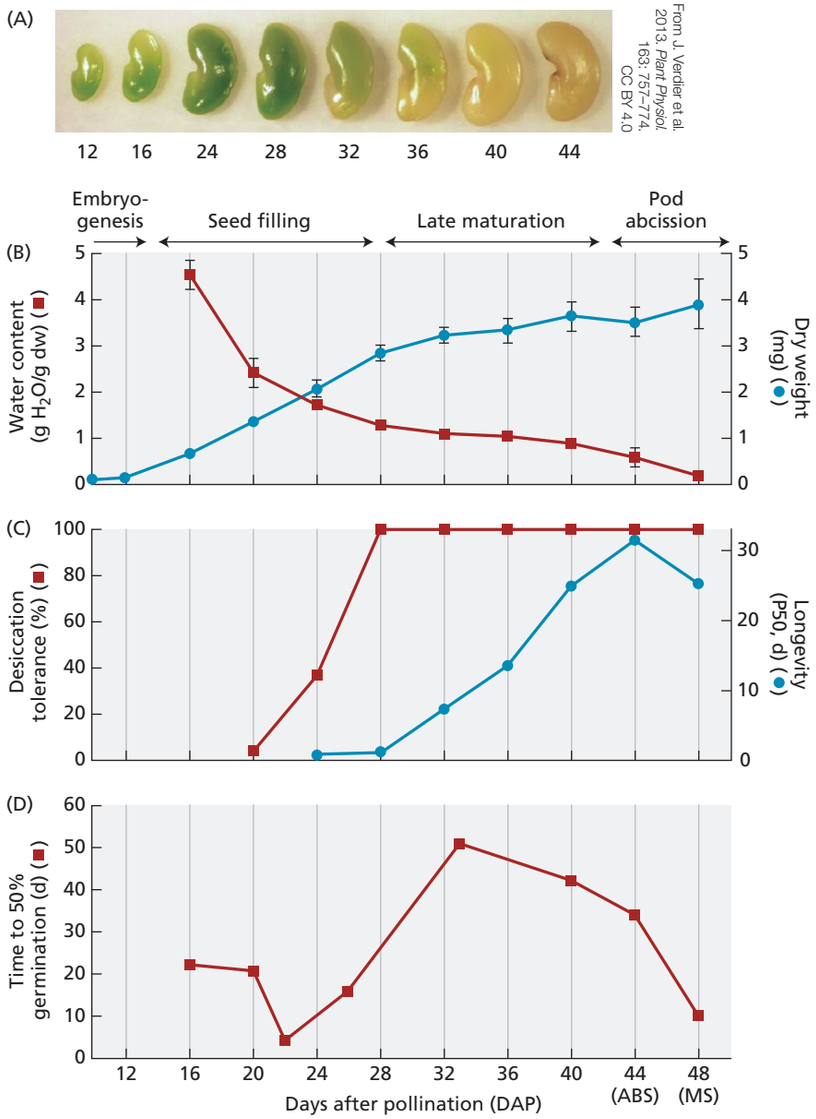


Figure 21.29 Metabolic and physiological changes during seed maturation of *Medicago truncatula*. Seed development is divided into four major phases: embryogenesis, seed filling, late maturation, and pod abscission. **(A)** Time course of seed development. **(B)** Water content and dry weight (dw) changes. Error bars represent ± standard error of the mean. **(C)** Acquisition of desiccation tolerance, measured as the percentage germination after rapid drying to 43% relative humidity, and longevity, determined as the time to reduce viability to 50% under storage at 75% relative humidity and 35°C. **(D)** Changes in germination speed or dormancy, determined as the time required for 50% of seeds to complete germination at 20°C. ABS, abscission; MS, mature seed. (After J. Verdier et al. 2013. *Plant Physiol.* 163: 757–774. CC BY 4.0)

dormancy, after-ripening, and germination. During mid- to late embryogenesis of orthodox seeds, when seed abscisic acid (ABA) content is highest (see Chapter 18), multiple metabolic processes are activated that contribute to the acquisition of desiccation tolerance. In Arabidopsis, the expression patterns of more than 6900 genes, approximately one-third of the genome, change during this period. These changes include metabolic processes (e.g., accumulation of disaccharides and oligosaccharides, synthesis of storage proteins and late-embryogenesis-abundant [LEA] proteins), activation of stress defense mechanisms (e.g., synthesis of small heat shock proteins [smHSPs], activation of antioxidative defenses), and alterations in physical structure and density of cells.

During the acquisition of desiccation tolerance, the cells of the embryo acquire a glassy state

Desiccation can severely damage membranes and other cellular constituents (see Chapter 24). Mature seeds have as little as 0.1 g water g^{-1} dry weight, with water potentials between –350 and –50 MPa. As seeds begin to dehydrate, embryos accumulate sugars and a specific set of proteins. These groups of molecules are thought to interact to produce a *glassy state*. In general, a glass is defined as an amorphous, metastable state that resembles a solid, brittle material but retains the disorder and physical properties of the liquid state. Biological glasses are highly viscous liquids with very low molecular diffusion rates, and therefore can participate only in limited chemical reactions. Because nonreducing sugars such as sucrose, raffinose, and stachyose accumulate during the late stages of seed maturation, it was initially assumed that they were primarily responsible for cellular glass formation. However, the physical properties of sugar glasses are significantly different from those of desiccated embryos, which led to the hypothesis that proteins, specifically LEA proteins, are required for glass formation in seeds.

LEA proteins and nonreducing sugars have been implicated in seed desiccation tolerance

Late-embryogenesis-abundant (LEA) proteins are small, hydrophilic, largely disordered, and thermostable proteins that are synthesized in orthodox seeds during mid- to late maturation and in vegetative tissues in response to osmotic stress. They are thought to have a range of protective functions against desiccation with different efficiencies, including ion binding, antioxidant activity, hydration buffering, and membrane and protein stabilization. Since LEA proteins were first described in the early 1980s in cotton seeds, related proteins have been identified in seeds and pollen grains of other plant species, as well as in bacteria, cyanobacteria, and some invertebrates, and LEA proteins have been shown to increase osmotolerance in transgenic yeast. The ability of "resurrection plants" (e.g., *Craterostigma plantagineum*) to survive extreme desiccation has been linked to the accumulation of LEA proteins in the vegetative organs. In addition, LEA proteins may play a role in the response to freezing and salinity stress, both of which involve cellular dehydration (see Chapter 15).

Most LEA proteins show a biased amino acid composition, resulting in high hydrophilicity, and they are related to a group of proteins called the **dehydrins**. A key feature of LEA proteins is their ability to form hydrogen bonds with sucrose. Since sugars accumulate during seed maturation, it is thought that LEA proteins interact with sucrose and other disaccharides and oligosaccharides to form the glassy state required for desiccation tolerance (see **WEB TOPIC 21.15**).

Abscisic acid plays a key role in seed maturation

Seeds of ABA-insensitive mutants of *M. truncatula* fail to develop desiccation tolerance and are therefore recalcitrant. The synthesis of LEA proteins, storage proteins, and lipids is promoted by ABA, as shown by physiological and genetic studies of cultured embryos of many species. ABA-deficient mutants fail to accumulate these proteins. Furthermore, synthesis of some LEA proteins, or of related family members, can be induced in vegetative tissues by ABA treatment. These results suggest that the synthesis of many LEA proteins is under ABA control during seed maturation.

As we discussed in Chapter 4, ABA induces changes in cellular metabolism by activating, either directly or indirectly, a network of transcription factors. In particular, ABSCISIC ACID INSENSITIVE3 (ABI3) induces the synthesis of storage proteins and LEA proteins through interactions with bZIP transcription factors such as ABI5. An analysis of the gene regulatory network in *M. truncatula* seeds has shown that *ABI5* genes occupy a central position in the regulatory network and are highly connected to *LEA* and desiccation tolerance genes. Thus, *ABI3* and *ABI5*, along with several other genes, are the core components of the seed-specific ABA signaling pathway that regulates survival in the dry state.

Coat-imposed dormancy is correlated with long-term seed viability

The seeds of many herbs and garden vegetables, such as onion, okra, and soybean, can remain viable under storage for only 1 to 2 years. Others, such as those of cucumber and celery, remain viable for up to 5 years. In 1879, W. J. Beal initiated the longest-running experiment on seed longevity by burying the seeds of 20 different species in unstoppered bottles in a sandy hilltop near the Michigan Agricultural College in East Lansing. After 120 years (in the year 2000), only one

species, moth mullein (*Verbascum blattaria*), remained viable, with half of the 50 seeds in the bottle germinating. In 2021 another bottle was dug up and the seeds tested for viability; as of this writing in 2021, only 11 seeds have germinated. However, 142 years is by no means the maximum longevity for seeds. For example, seeds of canna lily (*Canna compacta*) apparently can live for at least 600 years, while the oldest authenticated surviving seeds are those of sacred, Indian, or Asian lotus (*Nelumbo nucifera*), at nearly 1300 years, and a single date palm (*Phoenix dactylifera*) seed, which was found buried at Masada in Israel, at a remarkable 2000 years. These two species have highly impermeable seed coats, suggesting that coat-imposed dormancy is associated with long-term viability. However, many orthodox seeds of lesser longevity can be stored for a long time under seed-bank conditions at low temperature.

21.10 Fruit Development and Ripening

True fruits are found only in the flowering plants. In fact, fruits are a defining feature of the angiosperms, since *angio* means "vessel" or "container" in Greek and *sperm* means "seed." Diverse fruit types are represented in early Cretaceous fossils, including nuts and fleshy drupes and berries. Fruits are typically derived from a seed containing mature ovary; ovary-derived fruit is often referred to as *botanical fruit*. Examples of botanical fruits are peaches, tomatoes, and Arabidopsis siliques. However, fruits can also develop from a variety of non-ovary tissues, and in these cases they are referred to as *accessory fruit* (or *false fruit*). Strawberry is an example of accessory fruit. The fleshy part of the strawberry is actually the receptacle subtending the ovaries, while the true fruits are the dry achenes embedded in this tissue.

Fruits are seed-dispersal units, and they can be grouped according to several features (see **WEB TOPIC 21.16**). Based on their composition and moisture content, they can be either dry or fleshy. Some dry fruits, such as soybean pods, split to release the seeds and hence are **dehiscent**. Other dry fruits, such as the winged seeds (samaras) of maple and cypselae of dandelion, do not undergo this process and are **indehiscent**. The fleshy fruits we are most familiar with are indehiscent and occur in a variety of forms. Tomatoes, bananas, and grapes are defined botanically as **berries**, in which the seeds are embedded in a fleshy mass, while peaches, plums, and apricots are classified as **drupes**, in which the seed is enclosed in a stony endocarp. Apples and pears are **pome** fruits, in which the edible tissue is derived from an accessory structure called a *hypanthium*, the fused bases of the sepals, petals, and sometimes stamens. Fruits can also be defined as *simple*, with a mature single or compound ovary, as in hazelnut, Arabidopsis, and tomato. Alternatively, they may be *aggregate*, where flowers have multiple carpels that are not joined together, as in raspberry. Finally, they may be *multiple*, where the fruit is formed from a cluster of flowers and each flower produces a fruit, as in pineapple. Some examples of fleshy and dry fruit types are illustrated in **Figure 21.30**. It is interesting to note that even within a single plant family, a wide variety of fruit types can be found, including fleshy fruits such as berries, pomes, and drupes and dry fruits such as achenes, capsules, and follicles. This developmental plasticity in fruit type probably reflects rapid evolutionary adaptation in modes of seed protection and dispersal.

The phytohormones auxin and gibberellic acid (GA) regulate fruit set and parthenocarpy

In most angiosperms, the floral organs senesce and die if unfertilized. The developmental switch that turns a floral tissue into a growing fruit depends on pollination of the stigma or fertilization of the ovules. This developmental switch is also called **fruit set**. The mechanisms underlying this induction of fruit set are evolutionarily conserved, and they have been studied in Arabidopsis,

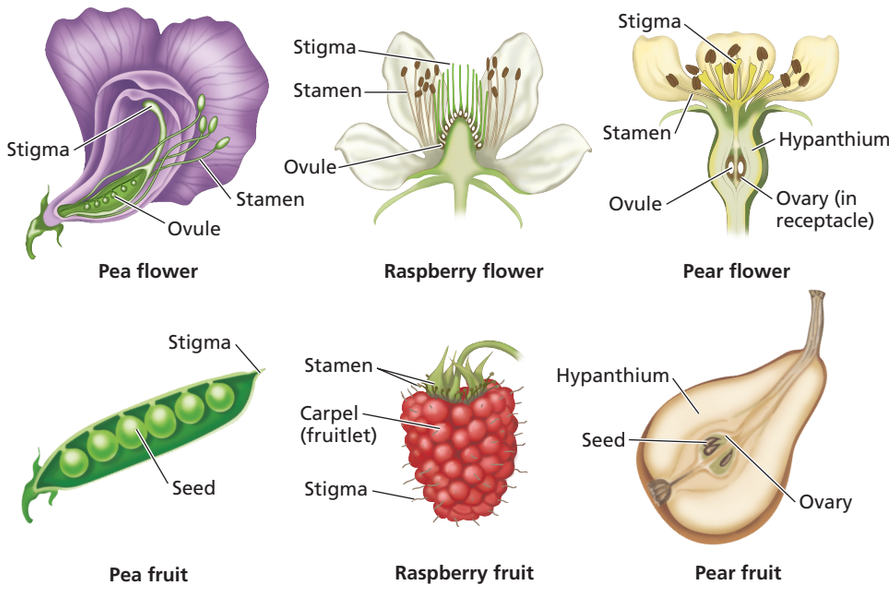
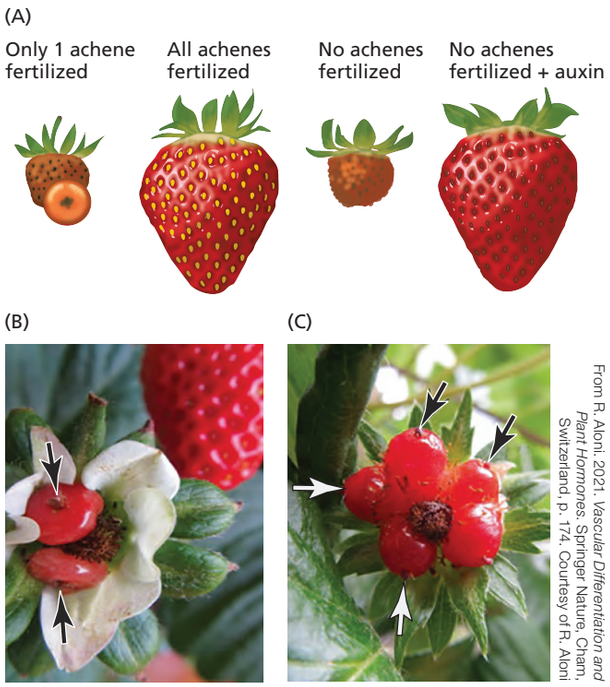


Figure 21.30 Three types of fruit and their flowers: pea, raspberry, and pear.

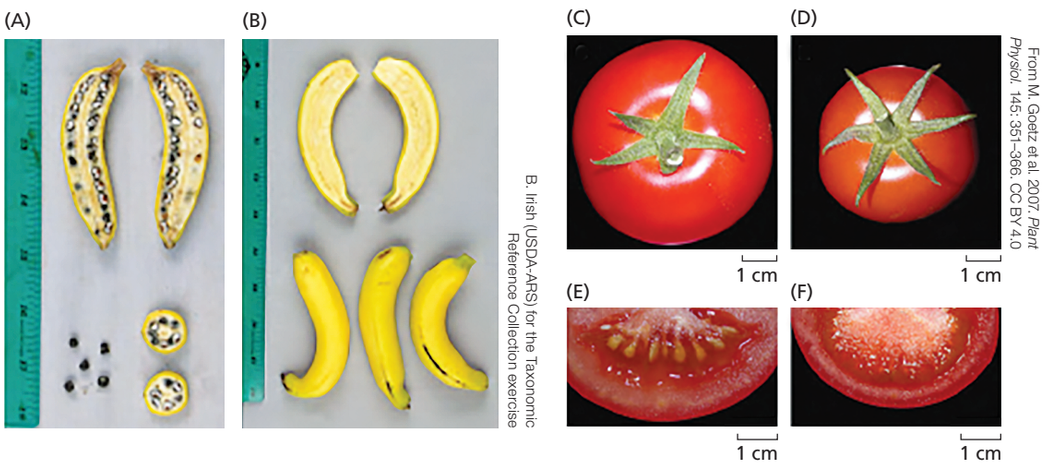


From R. Aloni: 2021. *Vascular Differentiation and Plant Hormones*. Springer Nature, Cham, Switzerland, p. 174. Courtesy of R. Aloni

Figure 21.31 Nitsch's 1950 experiment on strawberry fruit development. **(A)** From left to right: a small fruit flesh induced by the removal of all but a single achene; a fully fertilized and enlarged fruit; a fruit that failed to develop any fruit flesh due to the removal of all achenes; and a fruit with no achenes that still enlarged to form fruit flesh due to the exogenous application of auxin. **(B)** Selective removal of most of the fertilized ovaries in a strawberry flower resulted in the development of two separate miniature "fleshy red fruits" induced by the two remaining achenes (black arrowheads). **(C)** Aggregation of five separate "tiny red fruits" that developed below an inducing achene (white and black arrowheads).

tomato, strawberry, and other angiosperms. Historically, strawberry has been a model for the study of fruit set. A strawberry fruit consists of a receptacle dotted with about 200 seed-containing ovaries (achenes) on its surface, which makes the achenes (the true fruits) easily accessible for experimental manipulation. In 1950, Nitsch showed that removal of the achenes prevented development of the receptacle into a fruit. However, application of auxin to the receptacle could substitute for the achenes and stimulate receptacle enlargement (**Figure 21.31**). This simple experiment suggested that achenes were the source of auxin that stimulated the development of the receptacle. This and later experiments showed that the phytohormones auxin and GA are produced by the seed upon successful fertilization and that the production or exogenous application of these phytohormones is required to promote fruit set and subsequent fruit enlargement.

The molecular mechanisms regulating fruit set have been investigated mainly in Arabidopsis and tomato, which possess abundant molecular genetic tools. In tomato and eggplant, overexpression of the auxin biosynthesis gene *iaaM* or the auxin receptor gene *Transport Inhibitor of Auxin Resistant 1* (*TIR1*) in transgenic plants was sufficient to induce the development of seedless fruits. Such fertilization-independent fruits are termed *parthenocarpic fruits* (**Figure 21.32**). Mutations in genes coding for repressors of auxin responses—for example, auxin response factors (ARFs)—also lead to parthenocarpy. For example, Arabidopsis *arf8* mutants can develop elongated siliques without fertilization. In tomato, transgenic knockdowns of *ARF7*, *ARF8*, or *IAA9* cause parthenocarpy (see Figure 21.32), indicating that these three genes may normally repress fruit set when auxin is not produced.



B. Irish (USDA-ARS) for the Taxonomic Reference Collection exercise

From M. Goetz et al. 2007. *Plant Physiol.* 145: 351–366. CC BY 4.0

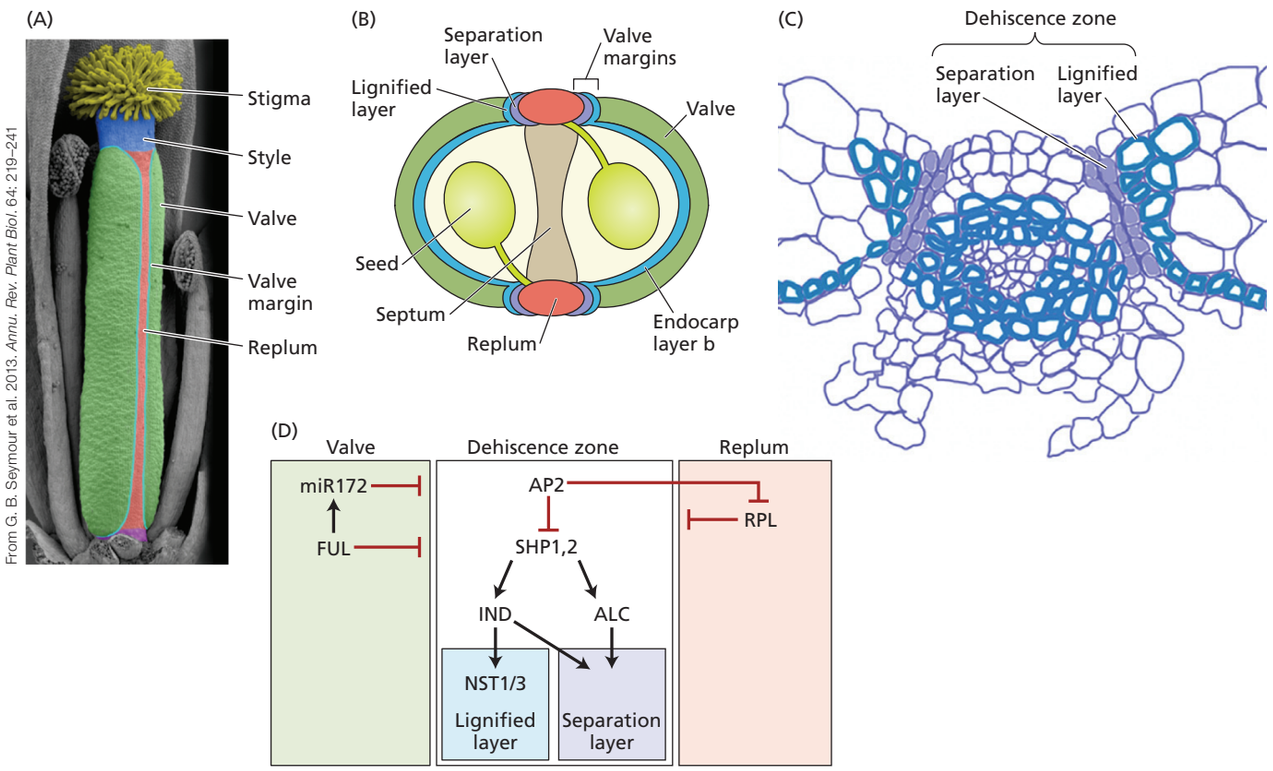
Figure 21.32 Parthenocarpic fruits compared with fertilized fruits. **(A)** Fruits of wild, seeded banana (*Musa acuminata banksia*). **(B)** Domesticated parthenocarpic banana fruits. **(C)** Fertilization-induced wild-type tomato fruit of the 'Monalbo' variety. **(D)** Parthenocarpic 'Monalbo' fruit containing the abnormal *arf8* mutant transgene. **(E)** The 'Monalbo' wild-type fruit cut in half; the locule is filled with pulp and seeds. **(F)** The parthenocarpic 'Monalbo' fruit cut in half to show the seedless endocarp.

Similarly, DELLA proteins repress GA responses. When GA is produced, the GA–GID1 (GIBBERELLIN INSENSITIVE DWARF 1) receptor complex targets DELLA proteins for proteasome-mediated degradation to activate downstream processes, including fruit set. In Arabidopsis, the quintuple *della* mutant shows strong parthenocarpy. The tomato *procera* mutant, which carries a *DELLA* point mutation, and transgenic tomato plants with silenced *DELLA* also develop parthenocarpic fruit.

Efficient fertilization or pollination is usually critical for fruit development. Induction of parthenocarpy has the potential to enhance fruit yield, especially when pollination and fertilization are negatively affected by adverse environmental conditions or lack of pollinators. Parthenocarpy could also improve fruit quality by producing seedless fruits for human consumption. Research on the molecular genetic mechanisms of parthenocarpy is revealing candidate target genes for gene editing and engineering to produce parthenocarpic fruits without application of hormones.

Specific transcription factors regulate the development of the dehiscence zone

Upon maturation, dehiscent fruits open spontaneously to release their seeds. The dry, dehiscent fruits of Arabidopsis serve as a model for the study of fruit dehiscence. In Arabidopsis the gynoecium arises from the fusion of two carpels, referred to collectively as the pistil, at the center of the flower. The Arabidopsis gynoecium consists of two ovary walls or pericarps (also known as valves), a central replum, a septum, and valve margins (**Figure 21.33A**). After fertilization, the valve margins differentiate into a



From G. B. Seymour et al. 2013. *Annu. Rev. Plant Biol.* 64: 219–241

Figure 21.33 The structure and regulation of the dehiscence zone. **(A)** False-color scanning electron micrograph of the Arabidopsis gynoecium showing the stigma, style, valves, replum, and valve margins. **(B)** Diagram of a transverse cross section of the ovary region of the gynoecium, showing the septum and seeds and the two layers of the dehiscence zone. The endocarp layer b, which is interior to the epidermal layer on the inside surface, is lignified and contributes to the tension mechanism of pod shatter. **(C)** Drawing of a cross section through the dehiscence zone (DZ) in Arabidopsis. The separation and lignified layers are indicated by different colors. **(D)** Summary of the network of transcription factors regulating dehiscence zone formation. Four main transcription factors are expressed at the valve margin and direct dehiscence zone formation. SHATTERPROOF1 and SHATTERPROOF2 (SHP1,2) redundantly upregulate INDEHISCENT (IND) and ALCATRAZ (ALC). The fruits of *shp* and *ind* mutants lack lignified and separation layers and are fully indehiscent, while *alc* mutants show only defects in the separation layer. Two additional transcription factors, FRUITFULL (FUL) and REPLUMLESS (RPL), act in the valves and the replum, respectively, to confine the expression of the dehiscence zone genes to the valve margin. Furthermore, FUL (in the valves) activates miR172, a repressor of APETALA2 (AP2), which inhibits SHP in the dehiscence zone. (B after J. R. Dinneny and M. F. Yanofsky. 2004. *BioEssays* 27: 42–49; C and D after P. Ballester and C. Ferrándiz. 2017. *Curr. Opin. Plant Biol.* 35: 68–75.)

dehiscence zone that consists of a lignified layer and a separation layer (**Figure 21.33B and C**). The separation layer contains small cells held together weakly by extracellular matrix; at maturity the springlike tension in the lignified layer and adjoining tissues splits open the fruit along the separation layer, causing the valve to detach from the replum during pod shattering.

In Arabidopsis, the morphogenesis and differentiation of the dehiscence zone are regulated by four transcription factors expressed at the valve margins (**Figure 21.33D**). Two MADS box genes, *SHATTERPROOF1* (*SHP1*) and *SHP2*, act redundantly to activate two basic helix-loop-helix (bHLH) transcription factor genes, *INDEHISCENT* (*IND*) and *ALCATRAZ* (*ALC*). *IND* and *ALC* promote the formation of the lignified layer and the separation layer, respectively. The expression of these four genes is restricted to the dehiscence zone due to the activities of *FRUITFULL* (*FUL*) and *REPLUMLESS* (*RPL*) in the valves and replum, respectively (see Figure 21.33D). The floral homeotic gene *APETALA2* (*AP2*) also plays a role by repressing the dehiscence zone transcription factors SHP and IND and the replum factor RPL to restrict expansion of the dehiscence zone and replum. At the same time, FUL prevents *AP2* expression in the valves by activating miR172, which negatively regulates *AP2* posttranscriptionally. NAC SECONDARY WALL THICKENING PROMOTING FACTOR1 (NST1) and NST3, both NAC transcription factors, act downstream of *IND* to regulate lignin and cellulose synthesis genes.

In seed crops such as legumes (e.g., soybean) and canola (rapeseed), loss of fruit dehiscence (pod shattering resistance) is a key agronomical trait selected for to prevent significant yield loss. Quantitative genetic methods and morphological characterization of shattering resistance have been conducted in soybean and rapeseed varieties. In soybean, a NAC transcription factor, SHATTERING1-5 (SHAT1-5), enhances shattering resistance by promoting excessive lignification of fiber cap cells located at the valve margins near the suture, which prevents the pod from splitting.

Tomato is an important model system for studying fleshy fruit development

The pericarp of fleshy fruits is typically divided into three layers: exocarp (skin), mesocarp (intermediate layer), and endocarp (innermost layer) (**Figure 21.34**). The soft edible part of the fruit is often the mesocarp. In peach, pistachio, and other drupe fruits, the hardened endocarp is referred to as the **stone** or **pit**. The stone provides a physical barrier around the seed to protect seeds from pathogens and herbivores. Analyses of gene expression during stone development have revealed that similar regulatory genes are induced during lignification of the stone in peach and the pericarp in Arabidopsis.

Much of what we know about the development of fleshy fruits has come from work on tomato (*Solanum lycopersicum*), a member of the nightshade family (Solanaceae) (**Figure 21.35A**). In tomato, as in Arabidopsis, the fruit is derived from the fusion of carpels, and the seeds are attached to the placenta. However, unlike Arabidopsis fruits, tomato fruits are indehiscent and the carpels remain completely fused. In fleshy fruits, cell division is usually followed by massive cell expansion (**Figure 21.35B**). In some varieties of tomato, pericarp cell diameters may reach 0.5 mm. About 30 quantitative trait loci (QTLs) have been shown to control fruit size in tomato, and several of the genes for these QTLs have been cloned. A specific locus (*Fw2*) encodes a plant-specific and fruit-specific protein that regulates cell division in the fruit and therefore affects fruit size. Two other loci, *FASCIATED* and *LOCULE NUMBER*, tomato homologs of *CLV3* and *WUS* respectively, control locule number and fruit size.

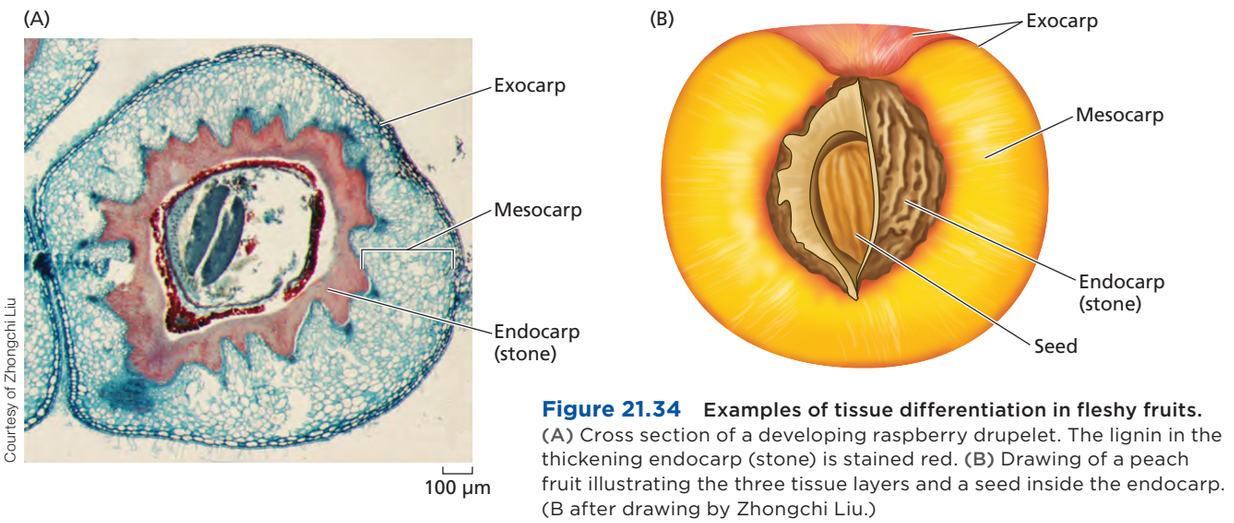


Figure 21.34 **Examples of tissue differentiation in fleshy fruits.** **(A)** Cross section of a developing raspberry drupelet. The lignin in the thickening endocarp (stone) is stained red. **(B)** Drawing of a peach fruit illustrating the three tissue layers and a seed inside the endocarp. (B after drawing by Zhongchi Liu.)

Domestication of the modern tomato involved dramatic changes in fruit weight, shape, and color, as well as in plant architecture. The identification of genes controlling these traits, combined with the advent of the CRISPR-Cas9 technology, has made it possible to engineer "domestication" of tomato directly from its wild relative *Solanum pimpinellifolium*. Four to six loci in *S. pimpinellifolium*, including *SELF-PRUNING, FASCIATED, Fw2.2,* and *OVATE,* were simultaneously edited to improve flowering time, enhance fruit size and shape, optimize shoot architecture, and increase fruit lycopene accumulation, while at the same time preserving the wild species' polygenic disease resistance and salt tolerance traits. Such rapid, CRISPR-Cas9-based trait improvement from wild relatives foreshadows the designer fruits that may soon appear in our fruit baskets.

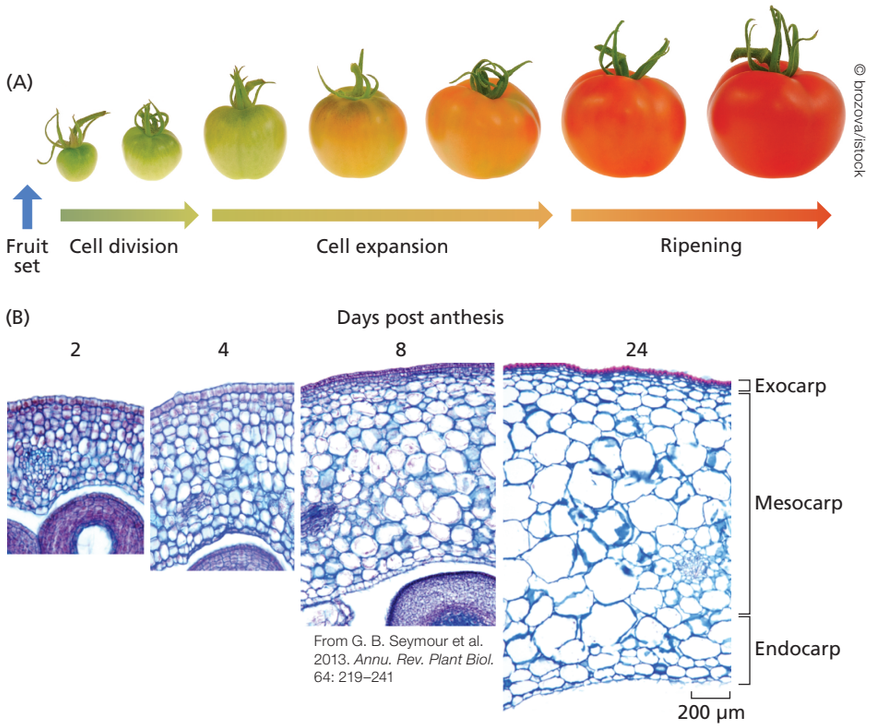


Figure 21.35 **Tomato fruit growth.** (A) Photographs of developmental stages in a miniature tomato. (B) Light microscope images of a cross section of tomato pericarp at 2, 4, 8, and 24 days after flower opening (anthesis).

Fleshy fruits undergo ripening

Ripening in fleshy fruits refers to the changes that make them attractive (to humans and other animals) and ready to eat. Such changes typically include color development, softening, starch hydrolysis, sugar accumulation, production of aroma compounds, and the disappearance of organic acids and phenolic compounds, including tannins. Dry fruits do not undergo a true ripening process, many of the same families of genes that control dehiscence in dry fruits seem to have been recruited to new functions in ripening in fleshy fruits. Because of the importance of fruits in agriculture and their health benefits, the vast majority of studies on fruit ripening have focused on edible fruits. Tomato is the established model for studying fruit ripening, as it has proved highly amenable to biochemical, molecular, and genetic studies on the mechanism of ripening.

Ripening involves changes in the color of fruit

Fruits ripen from green to a range of colors, including red, orange, yellow, purple, and blue. The pigments involved affect not only the visual appeal of the fruit but also its taste and aroma, and are known to have health benefits for humans. Fruits typically contain a mixture of pigments, including the green chlorophylls; yellow, orange, and red carotenoids; red, blue, and violet anthocyanins; and yellow flavonoids. The loss of the green pigment at the onset of ripening is caused by the degradation of chlorophyll and the conversion of chloroplasts to chromoplasts, which act as the site for the accumulation of carotenoids (see Chapter 1).

Carotenoids are responsible for the red color of tomato fruits. During ripening in tomato, the concentration of carotenoids increases between 10- and 14-fold, mainly due to the accumulation of the deep red pigment lycopene. Fruit ripening involves the active biosynthesis of carotenoids, the chemical precursors for which are synthesized in the plastids. The first committed step is the formation of the colorless molecule phytoene by the enzyme phytoene synthase. In tomato, phytoene is then converted to the red pigment lycopene through a series of further reactions. Experiments with transgenic tomatoes have demonstrated that silencing the gene for phytoene synthase prevents the formation of lycopene (**Figure 21.36**).

Anthocyanins are the pigments responsible for the blue and purple color in some berries and red in strawberry (**Figure 21.37**). Anthocyanins are made through the phenylpropanoid pathway; that is, they are derived from the amino acid phenylalanine. Phenylpropanoids constitute some of the most important sets of secondary metabolites in plants. They contribute not only to the characteristic color and flavor of fruits but also to unfavorable traits, such as browning of fruit tissues via enzymatic oxidation of phenolic compounds by polyphenol oxidases.



From R. G. Fray and D. Grierson. 1993. *Plant Mol. Biol.* 22: 589–602

Figure 21.36 Phytoene synthase plays a role in lycopene production in tomato pericarp. The tomato on the left is a wild-type, red ripe fruit. The tomato on the right has reduced levels of phytoene synthase gene expression and therefore fails to accumulate the red pigment lycopene.

Fruit softening involves the coordinated action of many cell wall–degrading enzymes

Softening of fruit involves changes in the fruit's cell walls. In most fleshy fruits, the cell walls consist of a semirigid composite of cellulose microfibrils—thought to be tethered by a xyloglucan network—which is embedded in a gel-like pectin matrix. In tomato, more than 50 genes related to cell wall structure show changes in expression during ripening, indicating a highly complex set of events connected with cell wall remodeling during the ripening process.

Experiments in transgenic plants have demonstrated that no single cell wall–degrading enzyme can account for all aspects of softening in tomato or other fruits. It appears that texture changes result from the synergistic action of a range of cell wall–degrading enzymes and that suites of texture-related genes give different fruits their unique melting, crisp, or mealy textures. However, even in tomato, the precise contribution of each type of enzyme to fruit texture is still poorly understood. Changes in the cuticle of the fruit that affect water loss also affect texture and shelf life.

Taste and flavor reflect changes in acids, sugars, aroma, and other compounds

Most fleshy fruits that are consumed by humans undergo changes that make them especially palatable to eat when they are ripe. These chemical changes include alterations in sugars and acids, the release of aroma compounds, and the reduction of unpalatable metabolites.

One example of human selection for more palatable fruits is the selection against bitterness in cucumber. Wild cucumbers produce cucurbitacins, triterpenoids that confer a bitter taste that repels herbivores. Two bHLH transcription factors, BL (BITTER LEAF) and BT (BITTER FRUIT), promote cucurbitacin C (CuC) biosynthesis in leaves and fruits, respectively; they regulate the expression of *Bitter* (*Bi*), which codes for cucurbitadienol synthase, the first committed step of CuC biosynthesis. Cultivated nonbitter varieties of cucumber are found to possess mutations in *Bi* or *Bt*. Loss of *Bi* leads to nonbitterness of the entire plant, while DNA variants reducing the expression of *Bt* remove bitterness in fruits only. The DNA variants found in *Bi* and *Bt* in nonbitter cucumbers reveal human selections imposed on these genes during domestication.

In many fruits, starch is converted at the onset of ripening to glucose and fructose, and citric and malic acids are also abundant. However, although sugars and acids are vital for taste, volatiles are what really determine the unique flavors of fruits. Flavor volatiles arise from a wide range of compounds. Some of the most detailed studies have been undertaken in tomato. They show that of the 400 or so volatiles produced by tomato, only a small number have a positive effect on flavor. The most important flavor volatiles in tomato are derived from the catabolism of fatty acids such as linoleic acid (hexanal) and linolenic acid (*cis*-3-hexenal, *cis*-3-hexenol, *trans*-2-hexenal) via lipoxygenase activity. Other important volatiles, including 2- and 3-methylbutanal, 3-methylbutanol, phenylacetaldehyde, 2-phenyl-ethanol, and methyl salicylate, are derived from the essential amino acids leucine, isoleucine, and phenylalanine. A third class of volatiles are the apocarotenoids, which are derived via the oxidative cleavage of carotenoids. Apocarotenoids such as β-damascenone are important in tomato, apple, and grape.

Volatile production is intimately connected with the ripening process, but the regulation of these events is not well understood. It is probably controlled by some

(A) (B)



David McIntyre

Courtesy of Zhongchi Liu

Figure 21.37 Examples of pigment formation during fruit ripening. **(A)** Blueberries accumulate more than a dozen different anthocyanins during ripening, including malvidin-, delphinidin-, petunidin-, cyanidin-, and peonidin-glycosides, which give them a deep purple color. **(B)** A pelargonidin-based anthocyanin contributes to the red color of strawberry fruit.

of the diverse transcription factors that show altered expression during ripening.

The causal link between ethylene and ripening was demonstrated in transgenic and mutant tomatoes

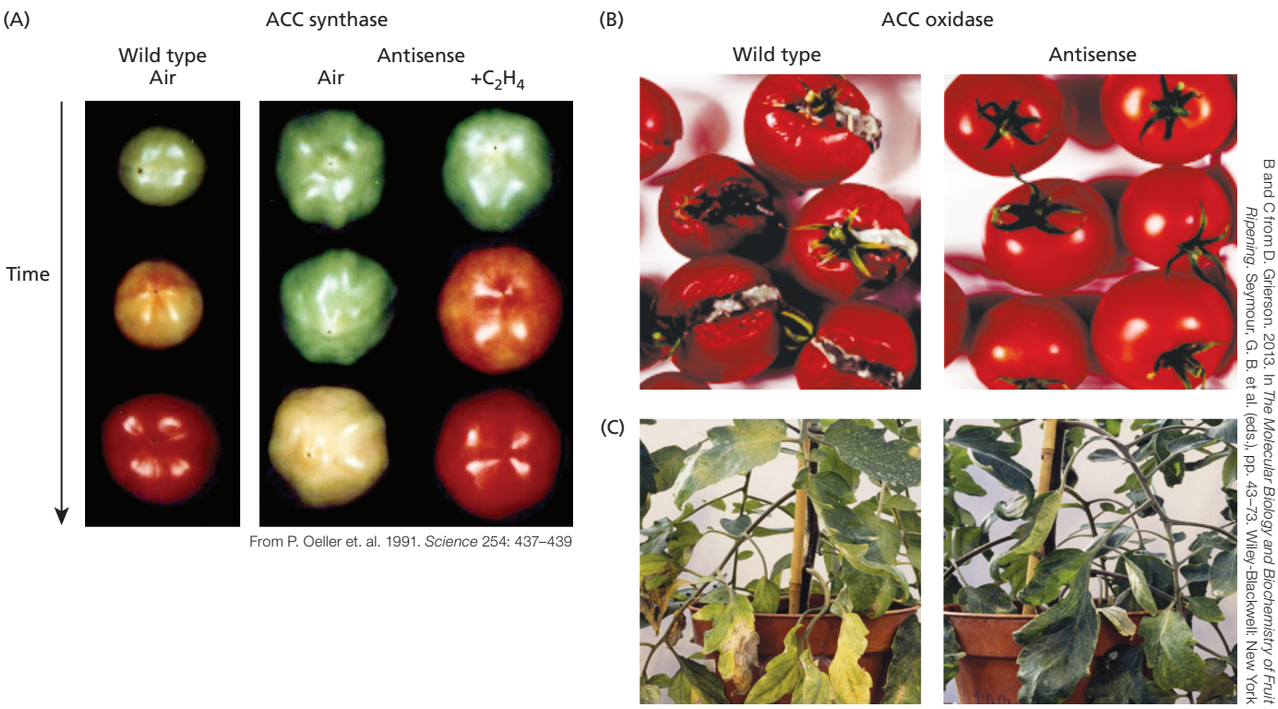
Ethylene has long been recognized as the hormone that can accelerate the ripening of many edible fruits. However, the definitive demonstration that ethylene is required for fruit ripening was provided by experiments in which ethylene biosynthesis was blocked by inhibiting expression of either ACC synthase (ACS) or ACC oxidase (ACO). ACS and ACO are the enzymes involved in the second-to-last and last steps in ethylene synthesis, respectively (see Chapter 4). These two steps in the pathway are normally tightly regulated. Silencing the genes encoding either of these enzymes using antisense RNA constructs inhibits ripening in transgenic tomatoes (**Figure 21.38**). Exogenous ethylene restores normal ripening in the transgenic tomato fruits.

Further demonstration of the requirement for ethylene in fruit ripening came from analysis of the *Never-ripe* mutation in tomato. As the name implies, this mutation completely blocks the ripening of tomato fruit. Molecular analysis has revealed that the *Never-ripe* phenotype is caused by a mutation in an ethylene receptor that renders the receptor unable to bind ethylene. These results, together with the demonstration that inhibiting ethylene biosynthesis blocks ripening, provided unequivocal proof of the role of ethylene in fruit ripening.

The role of plant hormones other than ethylene in controlling ripening is much less well understood, although auxin, ABA, and gibberellins are known to have an effect on this important developmental process.

Climacteric and non-climacteric fruit differ in their ethylene responses

Fleshy fruits have traditionally been placed in two groups as defined by the presence or absence of a characteristic respiratory rise called a **climacteric** at the onset of ripening. Climacteric fruits show this respiratory increase, and also a spike of ethylene production immediately before, or coincident with, the respiratory rise (**Figure 21.39**). Apple, banana, avocado, and tomato are examples of climacteric fruits. In contrast, fruits such as citrus fruits, strawberry, and grape do not exhibit such large changes in respiration and ethylene production and are termed **non-climacteric** fruits.



From P. Oeller et. al. 1991. *Science* 254: 437–439

B and C from D. Grierson. 2013. In *The Molecular Biology and Biochemistry of Fruit Ripening*. Seymour, G. B. et al. (eds.). pp. 43–73. Wiley-Blackwell: New York

Figure 21.38 Antisense silencing of ACC synthase (A) and ACC oxidase (B) inhibits ripening and senescence (C). (A) Fruit expressing an *ACS2* (*ACC SYNTHASE2*) antisense gene, together with controls (wild type). Note that in air the antisense fruit did not ripen, but did senesce after 70 days (yellow); ripening could be restored by adding external ethylene (C_2H_4). (B) The *ACO1* (*ACC OXIDASE*) antisense gene only inhibited ethylene synthesis by approximately 95%: Fruit ripened, but overripening and deterioration were greatly reduced. (C) In addition, leaf senescence was delayed in the *ACO1* antisense plant (right) when compared with the non-transgenic plant (left).

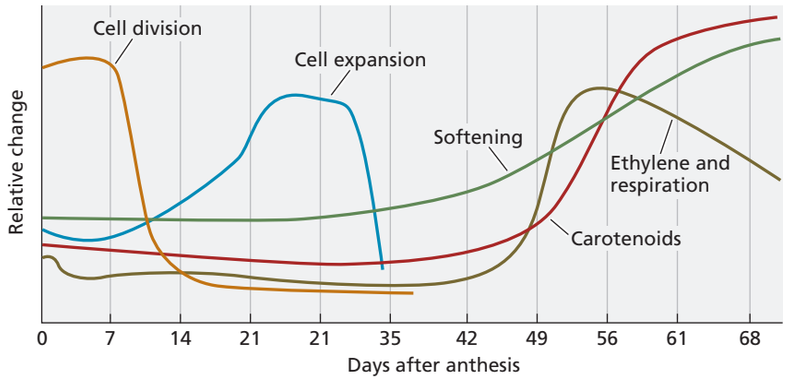


Figure 21.39 **Growth and development of tomato fruits in relation to the effects of ethylene and ripening.** Climacteric fruits show a characteristic increase in respiration and ethylene production, which signals the onset of ripening. (After J. J. Giovannoni. 2004. *Plant Cell* 16: S170–S180.)

In plants with climacteric fruits, two systems of ethylene production operate, depending on the stage of development:

- In System 1, which acts in immature climacteric fruit, ethylene inhibits its own biosynthesis by negative feedback.
- In System 2, which occurs in mature climacteric fruit and in senescing petals in some species, ethylene stimulates its own biosynthesis.

The positive feedback loop for ethylene biosynthesis in System 2 ensures that the entire fruit ripens evenly once ripening has commenced.

When mature climacteric fruits are treated with ethylene, the onset of the climacteric rise and the changes associated with ripening are hastened. In contrast, when immature climacteric fruits are treated with ethylene, the respiration rate increases gradually as a function of the ethylene concentration, but the treatment does not trigger production of endogenous ethylene or induce ripening. Ethylene treatment of non-climacteric fruits, such as citrus, strawberry, and grape, does not cause an increase in respiration and is not required for ripening. However, it can alter ripening characteristics in some species, such as the enhancement of color in citrus.

Although the distinction between climacteric and non-climacteric fruits is a useful generalization, some non-climacteric fruits may also respond to ethylene; for example, citrus fruits de-green in response to exogenous ethylene. Indeed, the distinction between climacteric and non-climacteric fruits may be less dramatic than previously thought, with some species showing contrasting behavior depending on the cultivar. For example, melon (*Cucumis melo*) can be climacteric or non-climacteric depending on the variety.

Considerably less is known about the molecular control of the ripening process in non-climacteric fruits. Strawberry has long been used as a model system for studying non-climacteric fruit ripening. Accumulating evidence suggests that the phytohormone abscisic acid and sucrose act cooperatively to promote fruit ripening in strawberry. Auxin, in contrast, inhibits strawberry fruit ripening, despite the fact that auxin, as we saw earlier, is initially required for fruit set and fruit enlargement.

The ripening process is transcriptionally regulated

Several rare, spontaneous, monogenic mutants in tomato show abnormal ripening or the complete abolition of this process. They include *ripening inhibitor* (*rin*), *non-ripening* (*nor*) (not shown), and *Colorless non-ripening* (*Cnr*) (**Figure 21.40**). The *rin* locus encodes a SEPALLATA class MADS box transcription factor termed MADS-RIN, which is induced at the onset of ripening. The *nor* locus codes for a NAC transcription factor, NAC-NOR, and the *Cnr* locus codes for a SQUAMOSA promoter binding protein-like (SPL) family of transcription factor, SPL-CNR. The lack of ripening in these three mutants suggests the important roles these genes play in controlling tomato ripening.

MADS-RIN interacts with the promoters of ACC synthase genes, suggesting that MADS-RIN regulates ethylene biosynthesis (see Chapter 20). MADS-RIN also binds to the regulatory regions of numerous ripening-related genes to directly control their expression (**Figure 21.41**). These include genes involved in cell wall metabolism, carotenoid formation, and aroma compound biosynthesis.

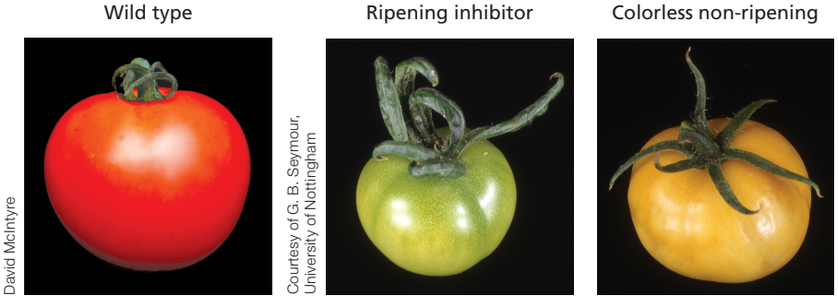
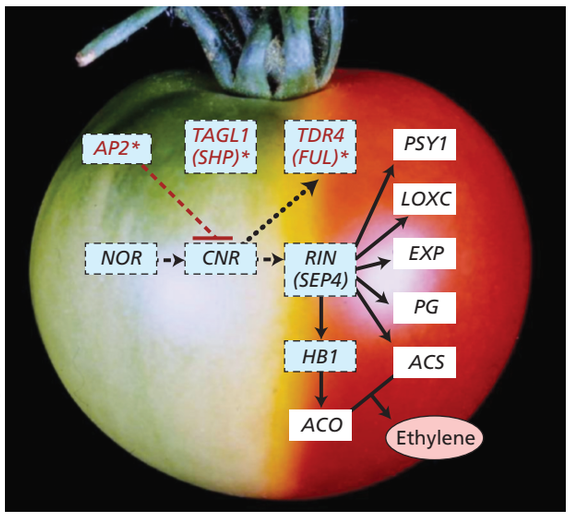


Figure 21.40 **In the tomato mutants ripening inhibitor (rin) and Colorless non-ripening (Cnr), the mutation prevents normal ripening.**



After G. B. Seymour et al. 2013. *Annu. Rev. Plant Biol.* 64: 219–241; image by Don Grierson and Kevin Davies

Figure 21.41 **Major known regulators of ripening in tomato.** The blue rectangles with dashed outlines are transcription factors; the red labels are genes where orthologs are also found in dry dehiscent fruits. Downstream effectors are shown in white boxes. Solid lines between *RIN* and other genes indicate activation, while dashed lines indicate possible activation. The red dashed line between *AP2* and *CNR* indicates repression. (After G. B. Seymour et al. 2003. *Annu. Rev. Plant Biol.* 64: 219–241.)

The *rin* mutation, discovered a half-century ago, is caused by a deletion between *MADS-RIN* and its neighboring gene *MACROCALYX* (*MC*), also a MADS box gene. The resulting fusion protein was recently shown to be a gain-of-function repressor protein rather than a defective activator protein as previously thought. CRISPR-CAS9 was employed to generate true knockouts of *RIN*. Remarkably, the resulting *RIN-KO* mutant still exhibits, albeit at a reduced level, ripening-associated processes, from ethylene production to lycopene accumulation. This result indicates that the role of *RIN* in tomato ripening may need to be reevaluated.

Since the cloning of the genes underlying the *rin*, *nor*, and *Cnr* mutations, a large number of other genes encoding transcription factors required for ripening have been described. These genes are involved in a regulatory network with downstream effectors to promote ethylene biosynthesis and the biochemical changes associated with ripening (see Figure 21.41).

Studying the molecular mechanism of ripening can have commercial applications

Elucidation of the role of ethylene in the ripening of climacteric fruits has resulted in many practical applications aimed at either uniform ripening or the delay of ripening. For example, banana bunches are picked when they are still green and hard, which helps them survive the journey from the fields of Central and South America to their final destinations around the world. The clusters of unripe fruits are cut from the bunch, treated with fungicide, packed in cartons, and shipped overseas. On arrival at their destination, the bananas are placed in temperature-controlled rooms and treated with small amounts of ethylene gas to initiate ripening. This mirrors the natural ripening process but ensures that fruits at different stages of maturity will initiate ripening at the same time, making them easier to market.

In the case of fruits such as apples, ripening can be delayed using controlled atmosphere (i.e., ~2.5% oxygen and 2.5% carbon dioxide) storage and refrigeration, thus extending the marketable period for the crop. In elite varieties of tomato, the *rin* mutation is widely used in the heterozygous form to slow the rate of ripening and extend shelf life. A major disadvantage of using *rin* mutant is that it delays all aspects of ripening so that the fruits often have suboptimal levels of flavor, aroma, and other quality-associated compounds. A more effective approach would be to target individual ripening processes, for instance slowing softening to extend shelf life, without detrimental effects on color and flavor. This goal is becoming a reality as access to the tomato genome sequence is making it easier to identify the genes underlying the complex traits controlling individual aspects of fruit quality.

It is also possible to manipulate the nutritional quality of fruit. For example, anthocyanins, like carotenoids, are thought to protect against heart disease and certain cancers, as they are strong antioxidants that can scavenge excessive damaging ROS. Anthocyanin levels in fruits can be manipulated by transgenic approaches, even to the extent of introducing high levels of these compounds in tomato flesh, where they do not normally occur (**Figure 21.42**). A greater understanding of the molecular determinants of other aspects of fruit development, such as the production of volatiles, will presumably offer other opportunities to improve fruit quality.



Courtesy of Andy Davis, John Innes Centre

Figure 21.42 **Anthocyanin production can be induced in tomato by overexpressing transcription factors that control the biosynthesis of these compounds in snapdragon (*Antirrhinum*).**

Summary

Plants exhibit alternation of generations, where diploids tend to be dominant but haploids produce the gametes. Genetic diversity is encouraged through outcrossing, which is enabled by vectors such as wind or insects, while inbreeding is minimized by active preventive mechanisms in the plant. The new diploid generation develops in the seed or fruit, which ripens and becomes attractive to vectors that disperse seeds.

21.1 Development of the Male and Female Gametophyte Generations

- Plants undergo both a diploid and a haploid generation in order to make gametes and reproduce (**Figure 21.1**).
- Diploidy allows individuals to mask deleterious recessive alleles and allows populations to exhibit greater genetic diversity.

21.2 Formation of Male Gametophytes in the Stamen

- Pollen forms in two stages: first microsporogenesis, then microgametogenesis (**Figure 21.3**).
- In the locule, diploid pollen mother cells divide meiotically to produce the microspores, surrounded by a nutritive tapetum (**Figures 21.2, 21.3**).
- Pollen cell walls are complex, with multiple layers for nutrient storage and for pollen dispersal (**Figures 21.4, 21.5**).

21.3 Female Gametophyte Development in the Ovule

- Eggs are formed in the female gametophyte (embryo sac) first by megasporogenesis and then by megagametogenesis (**Figures 21.7, 21.8**).
- Most angiosperms exhibit *Polygonum*-type megagametophyte development, wherein meiosis of a diploid mother cell produces four immature haploid megagametophytes, only one of which undergoes megagametogenesis.
- Megagametogenesis begins with three mitotic divisions without cytokinesis, followed by cellularization (**Figure 21.9**).

21.4 Pollination and Fertilization in Flowering Plants

- Once pollen has been delivered to the stigma, sperm cells travel to the female gametophyte through a newly grown pollen tube (**Figures 20.10, 21.11**).
- A pollen tube will not form unless there is recognition between pollen and stigma (**Figure 21.11**).
- Pollen tubes grow by tip growth (**Figures 21.12–21.14**).
- Tip-focused ion concentration gradients and a GTPase switch are essential for controlling the polarity of cell expansion of the pollen tube (**Figure 21.15**).
- The path of pollen tube growth is determined by physical and chemical cues from the pistil and the megagametophyte.
- Once the pollen tube has reached the ovule, two sperm are released to fertilize the egg and the central cell (**Figure 21.17**).

21.5 Selfing versus Outcrossing

- Outcrossing is ensured in hermaphroditic and monoecious species by dichogamy and heterostyly (**Figure 21.18**).
- Self-pollination is reduced by cytoplasmic male sterility.
- Self-incompatibility (SI) biochemically prevents self-pollination in angiosperms (**Figure 21.19**).
- Sporophytic SI reactions require expression of two highly variable *S*-locus genes, while gametophytic SI is mediated by cytotoxic S-RNases and F-box proteins (**Figures 21.20, 21.21**).

21.6 Apomixis: Asexual Reproduction by Seed

- Apomixis, or clonal reproduction by a diploid cell, may contribute to the fitness of polyploid species.
- Being able to induce apomixis would reduce loss of hybrid vigor in agricultural crops.

21.7 Endosperm Development

- After fertilization, the diploid endosperm, which will provide nutrition to the embryo, becomes multinucleate, making it a coenocyte (**Figures 21.24, 21.25**).
- Cellularization of the coenocytic endosperm in Arabidopsis proceeds from the micropylar to the chalazal region, while cellularization of cereal endosperms proceeds centripetally (**Figures 21.25, 21.26**).
- Endosperm development is controlled primarily by maternally expressed genes (MEGs), not by the embryo.

21.8 Seed Coat Development

- The seed coat arises from maternal integuments, but its development is regulated by the endosperm (**Figure 21.28**).

21.9 Seed Maturation and Desiccation Tolerance

- Seed filling and the acquisition of dessication tolerance overlap in most species (**Figure 21.29**).
- The acquisition of dessication tolerance is aided by LEA proteins, which form hydrogen bonds with nonreducing sugars, allowing embryo cells to acquire a glassy state that makes them more stable than cells that are simply dehydrated.

(*Continued*)

Summary (*continued*)

- Synthesis of LEA proteins is controlled by abscisic acid.
- Impermeable seed coats and low temperatures can increase seed longevity, which otherwise is highly variable across species.

21.10 Fruit Development and Ripening

- Fruits are seed-dispersal units that either arise from the pistil and contain the seed(s) or are derived from accessory floral tissues (**Figure 21.30**).
- Fruit initiation is triggered by fertilization of the ovules and pollination of the stigma. This developmental switch, also called *fruit set*, can be induced by auxin and GA (**Figure 21.31**).
- Induction of parthenocarpy—the development of fruit without fertilization—can improve fruit quality and yield (**Figure 21.32**).
- Dehiscent fruits release their seeds through pod shattering. Proper morphogenesis and differentiation of the dehiscence zone rely on a network of transcription factors and miRNAs (**Figure 21.33**).
- Fleshy fruits undergo ripening, which involves color changes, highly coordinated fruit softening, and other changes (**Figures 21.34–21.37**).
- Acids, sugars, and volatiles determine the flavor of ripe and unripe fleshy fruits.
- Ethylene accelerates ripening, particularly in climacteric fruits (**Figures 21.38, 21.39**).
- A mechanistic understanding of the ripening process has commercial applications (**Figure 21.42**).

Web Material

- **WEB TOPIC 21.1 Evolution Has Favored Diploidy in Plant Life Cycles** The possible selective advantages of diploidy over haploidy are discussed.
- **WEB TOPIC 21.2 Orchids, Champions of Pollination Deception** The flowers of several orchid species have evolved to mimic female wasps, stimulating pseudocopulation by male wasps.
- **WEB TOPIC 21.3 Types of Placentation in Fruits** A diagram of the various types of placentation in fruits is presented.
- **WEB TOPIC 21.4 Variations in Gametophyte Development** Deviations from *Polygonum*-type placental development. The characteristics of monosporic, bisporic, and tetrasporic embryo sacs are described.
- **WEB TOPIC 21.5 ANXUR 1 and 2 Are FERONIA-like RLKs Required for Tip Growth** Pollen grains with defective Anxur 1 and 2 genes burst immediately after germination.
- **WEB TOPIC 21.6 Other Signaling Molecules Involved in Pollen Tube Guidance** The ovules of Arabidopsis mutants defective in synthesizing ACC are incapable of attracting pollen tubes.
- **WEB TOPIC 21.7 Fail-Safe Mechanisms Ensure That Proper Fertilization Occurs** Various mechanisms have evolved to ensure the robustness of angiosperm fertilization.
- **WEB TOPIC 21.8 The Molecular Mechanism of Cytoplasmic Sterility in Rice** The molecular mechanism of cytoplasmic male sterility (CMS) has been elucidated in the "wild abortive" or CMS-WA rice system.
- **WEB TOPIC 21.9 The Molecular Mechanism of GSI in Poppy (*Papaver rhoeas*)** Although simpler than the GSI mechanism in the Solanaceae, Scrophulariaceae, and Rosaceae, when transferred into Arabidopsis the poppy GSI mechanism conferred self-incompatibility in Arabidopsis.
- **WEB TOPIC 21.10 Various Types of Apomixis** The mechanisms of sporophytic versus gametophytic apomixes are described.
- **WEB TOPIC 21.11 Three Types of Endosperm Development** Endosperm development falls into three basic categories: nuclear, cellular, and helobial.
- **WEB TOPIC 21.12 Evolution of Epigenetic Imprinting** Epigenetic imprinting may have evolved in response to similar selective pressures in plants and animals.
- **WEB TOPIC 21.13 The FIS Proteins and Endosperm Development** Endosperm development is repressed until after fertilization by FIS proteins, which methylate and demethylate DNA and histones in the endosperm.
- **WEB TOPIC 21.14 The Genes Regulating Aleurone Layer Differentiation** Two genes, *DEK1* and *CR4*, have been implicated in cereal aleurone layer differentiation.
- **WEB TOPIC 21.15 The Role of LEA Proteins in Desiccation Tolerance** A subset of LEA proteins has been correlated with desiccation tolerance in *Medicago*.
- **WEB TOPIC 21.16 Fruit Types and Examples** A table of the commonly encountered fruit types and examples is presented.

For more study aids, go to oup.com/he/taiz7e.

Suggested Reading

Angelovici, R., Galili, G., Fernie, A. R., and Fait, A. (2010) Seed desiccation: a bridge between maturation and germination. *Trends Plant Sci*. 15: 201–208.

Batista, R., and Köhler, C. (2020) Genomic imprinting in plants-revisiting existing models. *Genes Dev.* 34: 24–36.

Dinneny, J. R., and Yanofsky, M. F. (2005) Drawing lines and borders: How the dehiscent fruit of Arabidopsis is patterned. *BioEssays* 27: 42–49.

Doucet, J., Lee, H. K., and Goring, D. R. (2016) Pollen Acceptance or Rejection: A tale of two pathways. *Trends Plant Sci.* 20: 1058–1067.

Gehring, M. (2013) Genomic imprinting: Insights from plants. *Annu. Rev. Genet.* 47: 187–208.

Hater, F., Nakel, T., and Groß-Hardt, R. (2020) Reproductive Multitasking: The female gametophyte. *Annu. Rev. Plant Biol.* 71: 517–546.

Higashiyama, T., and Takeuchi, H. (2015) The mechanism and key molecules involved in pollen tube guidance. *Annu. Rev. Plant Biol.* 66: 393–413.

Johnson, M. A., Harper, J. F., and Palanivelu, R. (2019) A fruitful journey: pollen tube navigation from germination to fertilization. *Annu. Rev. Plant Biol.* 70: 809–837.

Klee, H. J., and Giovannoni, J. J. (2011) Genetics and control of tomato fruit ripening and quality attributes. *Annu. Rev Genet.* 45: 41–59.

Knapp, S. (2002) Tobacco to tomatoes: A phylogenetic perspective on fruit diversity in the Solanaceae. *J. Exp. Bot.* 53: 2001–2022.

Knapp, S., and Litt, A. (2013) Fruit—An angiosperm innovation. In *The Molecular Biology and Biochemistry of Fruit Ripening*, G. B. Seymour, G. A. Tucker, M. Poole, and J. J. Giovannoni, eds., Wiley-Blackwell, Oxford, UK, p. 206.

Li, J., and Berger, F. (2012) Endosperm: Food for humankind and fodder for scientific discoveries. *New Phytol.* 195: 290–305.

Li, J., Cocker, J. M., Wright, J., Webster, M. A., McMullan, M., Dyer, S., Swarbreck, D., Caccamo, M., van Oosterhout, C., and Gilmartin, P. M. (2016) Genetic architecture and evolution of the *S* locus supergene in *Primula vulgaris*. *Nat. Plants* 2: 16188.

Li, N., Xu, R., and Li, Y. (2019) Molecular networks of seed size control in plants. *Annu. Rev. Plant Biol*. 70: 435–463.

Manning, K., Tor, M., Poole, M., Hong, Y., Thompson, A. J., King, G. J., Giovannoni, J. J., and Seymour, G. B. (2006) A naturally occurring epigenetic mutation in a gene encoding an SBP-box transcription factor inhibits tomato fruit ripening. *Nat. Genet.* 38: 948–952.

McCann, M., and Rose, J. (2010) Blueprints for building plant cell walls. *Plant Physiol.* 153: 365.

Michard, E., Simon, A. A., Tavares, B., Wudick, M. M., and Feijó, J.A. (2016) Signaling with ions: the keystone for apical cell growth and morphogenesis in pollen tubes. *Plant Physiol*. 173: 91–111.

Nasrallah, J. B. (2011) Self-incompatibility in the Brassicaceae. In *Plant Genetics and Genomics: Crops and Models*, Vol. 9: *Genetics and Genomics of the Brassicaceae*, R. Schmidt, and I. Bancroft, eds., Springer, Berlin, pp. 389–412.

Rodrigues, J. C. M., Luo, M., Berger, F., and Koltunow, A. M. G. (2010) Polycomb group gene function in sexual and asexual seed development in angiosperms. *Sex. Plant Reprod.* 23: 123–133.

Rudall, P. J. (2021) Evolution and patterning of the ovule in seed plants. *Biol. Rev.* 96: 943-960.

Seymour, G. B., Østergaard, L., Chapman, N. H., Knapp, S., and Martin, C. (2013) Fruit development and ripening. *Annu. Rev. Plant Biol.* 64: 209–241.

Tomato Genome Consortium. (2012) The tomato genome sequence provides insights into fleshy fruit evolution. *Nature* 485: 635–641.

Tonnabel, J., David, P., Janicke, T., Lehner, A., Mollet, J.-C., Pannell, J. R., and Dufay, M. (2021) The scope for post-mating sexual selection in plants. *Trends Ecol.Evol.* 36: 556–567.

Twell, D. (2010) Male gametophyte development. In: *Plant Developmental Biology—Biotechnological Perspectives*, Vol. 1, E. C. Pua and M. R. Davey, eds., Springer-Verlag, Berlin, pp. 225–244.

Vrebalov, J., Ruezinsky, D., Padmanabhan, V., White, R., Medrano, D., Drake, R., Schuch, W., and Giovannoni, J. (2002) A MADS-box gene necessary for fruit ripening at the tomato ripening-inhibitor (rin) locus. *Science* 296: 343–346.

Wilkinson, J. Q., Lanahan, M. B., Yen, H.-C., Giovannoni, J. J., and Klee, H. J. (1995) An ethylene-inducible component of signal transduction encoded by Never-ripe. *Science* 270: 1807–1809.

Yang, W.-C., Shi, D.-Q., and Chen, Y.-H. (2010) Female gametophyte development in flowering plants *Annu. Rev. Plant Biol.* 61: 89–108.

Zhong, S., Fei, Z., Chen, Y.-R., Zheng, Y., Huang, M., Vrebalov, J., McQuinn, R., Gapper, N., Liu, B., Xiang, J., et al. (2013) Single-base resolution methylomes of tomato fruit development reveal epigenome modifications associated with ripening. *Nat. Biotechnol.* 31: 154–159.

Zhong, S., Liu, M., Wang, Z., Huang, Q., Hou, S., Xu, Y., Ge, Z., Song, Z., Huang, J., Qiu, X., Shi, Y., Xiao, J., Liu, P., Guo, Y. L., Dong, J., Dresselhaus, T., Gu, H., and Qu, L. J. (2019) Cysteine-rich peptides promote interspecific genetic isolation in Arabidopsis. *Science* 364: eaau9564.

22 Embryogenesis: The Origin of Plant Architecture



schankz/Shutterstock

Land plants comprise a monophyletic group called the embryophytes—plants that make embryos. What sets them apart from their aquatic, algal sisters is the ability to develop a multicellular sporophyte following fertilization of the egg cell by the sperm cell. The fate of the zygote (the fertilized egg cell) differs greatly among plant groups. For example, in nonvascular land plants (bryophytes) such as mosses, the zygote undergoes mitotic divisions to produce a multicellular, diploid sporophyte that is dependent on the gametophyte (to which it is attached) for most of its nourishment (see Chapter 1 for overview). The cells of the moss sporophyte undergo minimal differentiation and development, producing a relatively simple stalk and capsule that lack true vascular tissue. In vascular plants (tracheophytes), by contrast, the zygote divides to produce a diploid sporophyte that lives independently of the gametophytes that produced it. Furthermore, cells of vascular plant sporophytes differentiate into the three main tissue types—dermal, ground, and vascular tissues—that become further specialized into a wide variety of cell and tissue types comprising the major organ systems of the vegetative and reproductive structures. In seed plants (spermatophytes, which include gymnosperms and angiosperms), embryogenesis terminates with the formation of a dormant (or quiescent) seed. The analogous resting stage of bryophytes and non-seed plants is the haploid spore, which represents the start of the gametophyte phase of the life cycle. Given the primary research focus on flowering plants, and the tremendous importance of seed plants to food production, we know much more about embryogenesis in seed plants than in non-seed plants. Accordingly, this chapter focuses on the embryogenesis of seed plants, with an emphasis on the angiosperms. However, it should be kept in mind that seed plant embryogenesis, which evolved about 320 million years ago, is derived from a much older process that has defined land plants since their origin about 450 million years ago.

In seed plants, embryogenesis transforms the single-celled zygote into a complex, multicellular individual contained within a mature seed. As such, embryogenesis provides many examples of developmental processes by which the basic architecture of the plant is established, including the elaboration of forms (**morphogenesis**), the associated formation of functionally

organized structures (**organogenesis**), and the **differentiation** of cells to produce anatomically and functionally distinct tissues (**histogenesis**). An essential feature of the plant's basic architecture is the presence of apical meristems at the tips of the shoot and root axes, which are key to sustaining indeterminate patterns of vegetative growth (see Chapter 18). The development of the embryo also features complex changes in physiology that enable the embryo to withstand prolonged periods of reduced metabolic activity (**dormancy**) and to recognize and respond to environmental cues that signal the plant to resume growth (**germination**) (see Chapter 17). Our primary focus is on embryogenesis in the angiosperms, the most important group of seed plants in terms of agriculture and ecological dominance.

22.1 Embryogenesis in Monocots and Eudicots

We begin by comparing embryogenesis in the two main groups of angiosperms, the monocots and eudicots, represented by maize (corn; *Zea mays*) and Arabidopsis, respectively. Next we consider the signals that guide complex patterns of growth and differentiation in the embryo, including the importance of position-dependent cues. We conclude our survey of plant embryogenesis with a discussion of the molecular and genetic mechanisms that translate position-dependent cues into organized patterns of growth. An overview of the history of plant embryogenesis can be found in **WEB ESSAY 18.1**.

Embryogenesis differs between monocots and eudicots, but also shares common features

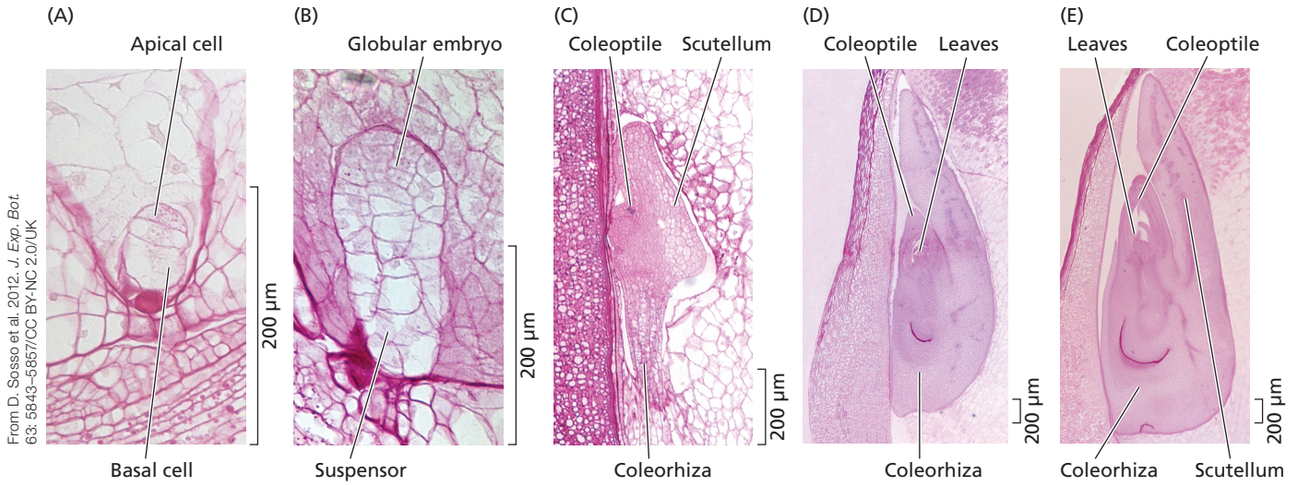
Anatomical comparisons have revealed differences in the patterns of embryogenesis among different seed plant groups, such as those between monocots and eudicots and those between non-flowering gymnosperms and flowering angiosperms. Angiosperm embryogenesis tends to be more predictable in eudicot species, with two cotyledons (embryonic leaves), than in monocot species, with one cotyledon. Embryogenesis in gymnosperms is more unpredictable than in either eudicots or monocots, with embryos from the same gymnosperm species capable of exhibiting a range of cotyledon numbers. Importantly, though, the central elements of embryogenesis are common among nearly all seed plant species, probably reflecting shared developmental processes.

Among flowering plants, Arabidopsis (a eudicot) and maize (a monocot) provide two examples of embryogenesis that differ in detail but share certain fundamental features relating to the establishment of major growth axes. In both species, developmental and physiological events follow the same sequence. In both, tissues and organs are established in similar arrangements. However, there are also major differences between monocot and eudicot embryogenesis. For example, the shoot apical meristem is inactive during embryogenesis in Arabidopsis, whereas several small leaves are formed during embryogenesis in maize. Furthermore, while Arabidopsis is representative of a group of plants in which embryonic cell divisions appear to be strictly controlled and are nearly invariable among individuals, maize displays a superficially less ordered pattern of cell divisions. Maize and Arabidopsis therefore represent opposite ends of a spectrum in embryological development, from the relatively complex and less predictable to the relatively simple and more predictable.

Here we describe maize embryogenesis in brief and Arabidopsis embryogenesis, about which more is known, in detail.

MAIZE EMBRYOGENESIS The large and nearly ubiquitous grass family (Poaceae or Gramineae), of which maize is a member, represents a specialized group of monocots in which, according to one interpretation, the single cotyledon appears to have become functionally divided into two structures, the **scutellum** and the **coleoptile**. The scutellum serves as an absorptive organ that takes up sugars from the endosperm during germination, while the coleoptile forms a tubular sheath that protects the emerging primary leaves from mechanical damage from the soil. The cell division patterns that give rise to these specialized monocot structures are necessarily more complex, yet predictable, than those required to form the two cotyledons of most eudicots. Nevertheless, despite a lack of obvious regularity in cell division patterns, it is possible to describe embryogenesis in maize in terms of six morphologically defined developmental stages (**Figure 22.1**):

1. **Zygotic stage**. This stage begins with the fusion of the haploid egg and sperm to form the zygote (not shown in Figure 22.1) (see Chapter 21). The zygote undergoes polarized growth followed by asymmetric transverse divisions, giving rise to a small apical cell and an elongated basal cell (see Figure 22.1A).
2. **Globular stage**. Following the creation of the apical and basal cells, a series of variable cell divisions creates a multilayered globular embryo consisting of the embryo proper and the larger multicellular suspensor (see Figure 22.1B).
3. **Transition stage**. During the early transition stage, the scutellum appears on the inner side of the embryo (relative to the future seed coat). By the late transition stage, the future shoot apical meristem is evident on the outer side of the embryo, relative to the future seed coat. (The transition stage is not shown in Figure 22.1.)



From D. Sosso et al. 2012. *J. Exp. Bot.* 63: 5843–5857/CC BY-NC 2.0/UK

Figure 22.1 Stages of maize embryogenesis. (A) Zygotic stage. (B) Globular stage. (C) Coleoptile stage. (D) Leaf primordia stage. (E) Maturation stage. (The transition stage, between the globular and coleoptile stages, is not shown.) Longitudinal sections of maize embryos are stained with periodic acid-Schiff's reagent.

4. **Coleoptile stage**. This stage is marked by the formation of a distinct coleoptile, scutellum, shoot apical meristem, root apical meristem, **radicle** (embryonic root), and **coleorhiza**, a protective sheath that covers the embryonic root tip (see Figure 22.1C).
5. **Leaf primordia stage**. The shoot apical meristem initiates several leaves inside the coleoptile (see Figure 22.1D).
6. **Maturation stage**. During the final stage of embryogenesis (see Figure 22.1E), expression of maturation-related genes precedes the onset of dormancy.

ARABIDOPSIS EMBRYOGENESIS The Arabidopsis embryo is relatively small and consists of a minimal number of cells, a common feature among the Brassicaceae (cabbage family), to which Arabidopsis belongs. Perhaps as a consequence of this "minimalist" style of embryogenesis, there is very little variation among individuals in the pattern and timing of cell divisions. This ordered pattern of cell divisions has allowed detailed investigation of the events occurring during embryogenesis and their regulation. Embryogenesis in Arabidopsis occurs in five main stages, each of which is linked to the shape of the embryo:

1. Zygotic stage. The first stage of the diploid life cycle commences with the fusion of the haploid egg and sperm to form the single-celled zygote. As in maize, polarized growth of this cell, followed by an asymmetric transverse division, gives rise to a small apical cell and an elongated basal cell (**Figure 22.2A**).
2. Globular stage. The apical cell undergoes a series of divisions (**Figure 22.2B–D**) to generate a spherical, eight-cell (**octant**) globular embryo exhibiting radial symmetry (see Figure 22.2C). Additional cell divisions increase the number of cells in the globular embryo (see Figure 22.2D) and create the outer layer, the *protoderm*, which later becomes the epidermis. In a next cell division cycle, the inner cells divide once more to generate the inner vascular and outer ground tissue precursors, which completes the establishment of the radial pattern of cell layers. As the globular embryo grows, the shoot and root meristems are initiated at either end.
3. **Heart stage**. While the embryo grows, focused cell division in two regions occurs on either side of the future shoot apical meristem to form the two cotyledons, giving the embryo bilateral symmetry (**Figure 22.2E and F**).
4. **Torpedo stage**. Cell elongation and cellular differentiation processes occur throughout the embryonic axis. Visible distinctions between the adaxial and abaxial tissues of the cotyledons become apparent (**Figure 22.2G**). At the end of this stage, the embryo bends to fill the seed cavity.
5. **Mature stage**. Toward the end of embryogenesis, the embryo and seed lose water and become metabolically inactive as they enter dormancy (discussed in Chapter 17). Storage compounds accumulate in the cells at the mature stage (**Figure 22.2H**).

A comparison of embryogenesis in Arabidopsis and maize illustrates differences in embryo size, shape, cell number, and division patterns. Despite these differences,

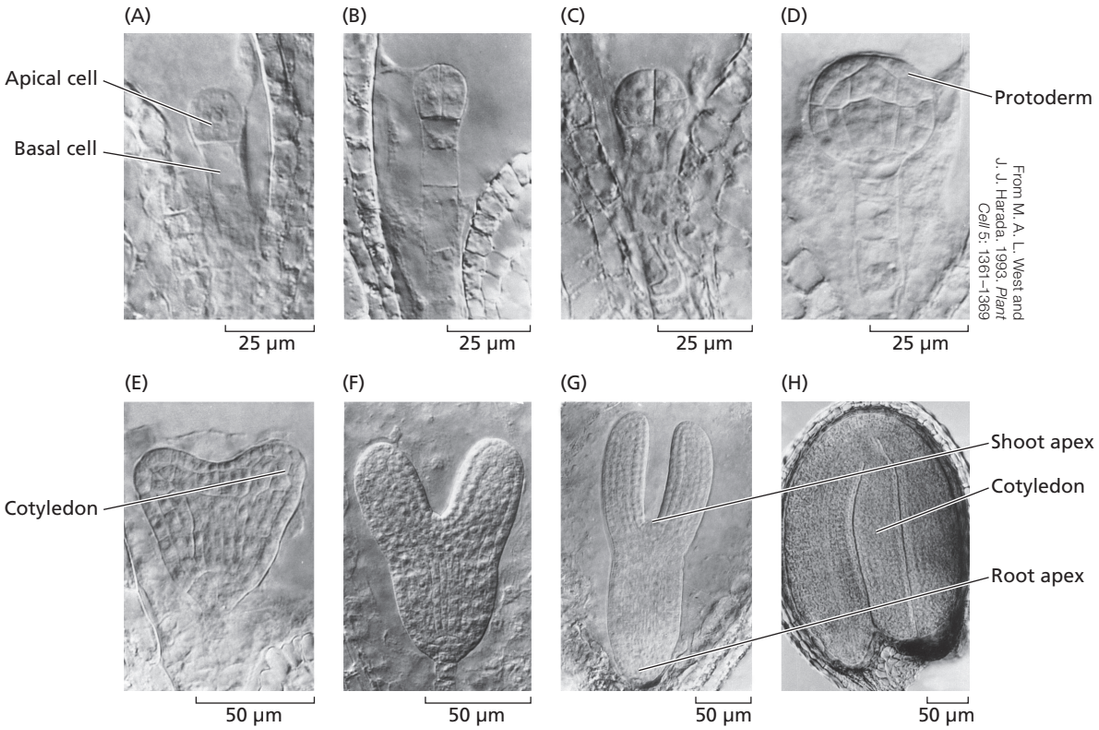


Figure 22.2 The stages of Arabidopsis embryogenesis are characterized by precise patterns of cell division. **(A)** One-cell embryo after the first division of the zygote, which forms the apical and basal cells. **(B)** Two-cell embryo. **(C)** Eight-cell embryo. **(D)** Mid-globular stage embryo, which has developed a distinct protoderm (surface layer). **(E)** Early heart stage embryo. **(F)** Late heart stage embryo. **(G)** Torpedo stage embryo. **(H)** Mature embryo.

several common themes emerge that can be generalized to all seed plants. Perhaps the most fundamental of these relates to **polarity**. Beginning with the single-celled zygote, embryos become progressively more polarized along two axes: the **apical–basal axis**, which runs between the tips of the embryonic shoot and root, and a **radial axis**, perpendicular to the apical–basal axis, which extends from the center of the plant outward (**Figure 22.3**). In the following sections we consider how these axes are established and discuss how specific molecular processes guide their development.

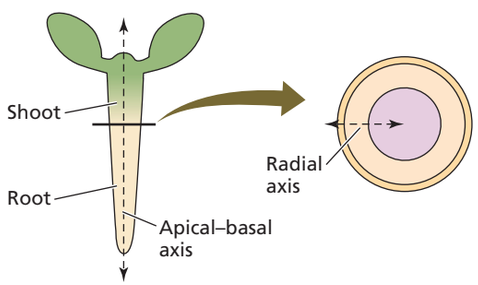


Figure 22.3 The seedling is organized along two axes. In a longitudinal cross section (left), the apical–basal axis extends between the tips of the embryonic root and shoot. In a transverse cross section (right), the radial axis extends from the center to the surface across vascular, ground, and epidermal tissues.

22.2 Establishment of Apical–Basal Polarity

Much of our discussion of apical–basal polarity focuses on Arabidopsis, which is not only a powerful model for molecular and genetic studies, but also displays simple and highly stereotyped cell divisions during the early stages of its embryonic development. By observing changes in this simple pattern, we can more easily recognize both physiological and genetic factors that influence embryonic development. A graphic diagrammatic depiction of the earliest cell divisions in Arabidopsis, provided in **Figure 22.4**, offers a convenient guide for the discussion that follows. (For a discussion of the establishment of polarity in a simpler, algal zygote, see **WEB TOPIC 22.1**.)

Apical–basal polarity is established early in embryogenesis

A characteristic feature of seed plants is a polarity in which tissues and organs are arrayed in a highly

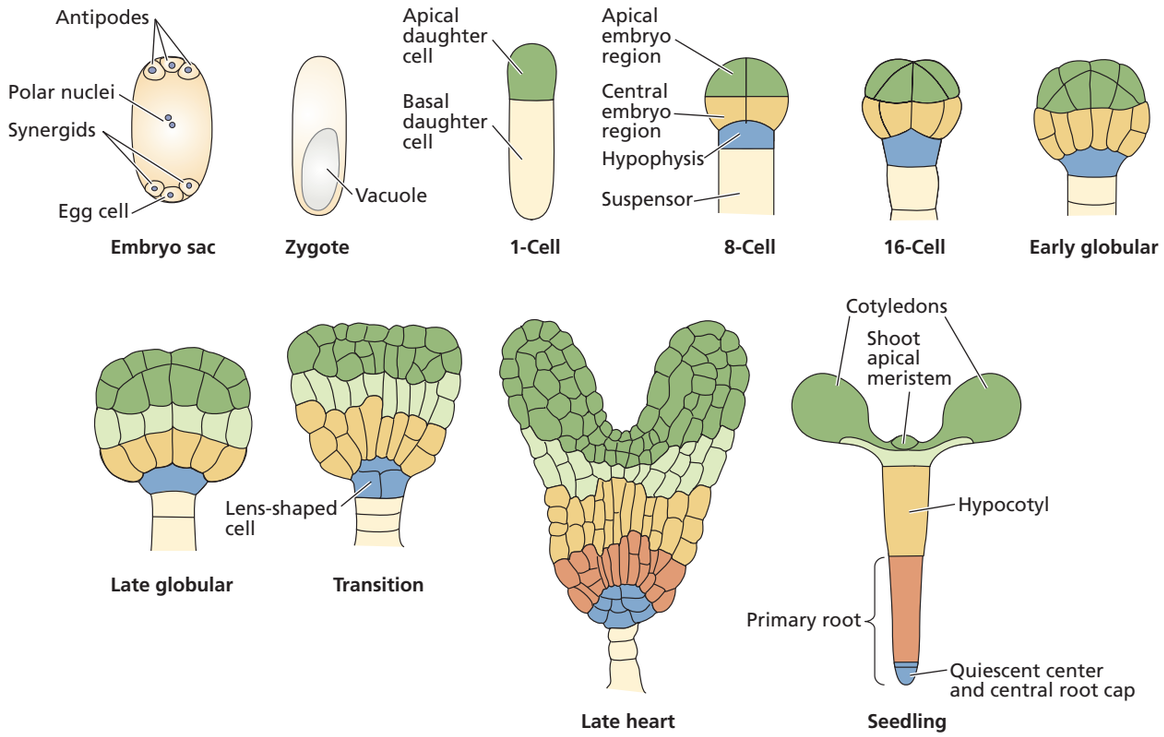


Figure 22.4 Pattern formation during Arabidopsis embryogenesis. A series of successive stages are shown to illustrate how specific cells in the young embryo contribute to specific anatomically defined features of the seedling. Clonally related groups of cells (cells that can be traced back to a common progenitor) are indicated by distinct colors. Following the asymmetric division of the zygote, the smaller, apical daughter cell divides to form an eight-cell embryo consisting of two tiers of four cells each. The upper tier gives rise to the shoot apical meristem and most of the flanking cotyledon primordia. The lower tier produces the hypocotyl and some of the cotyledons, the embryonic root, and the upper cells of the root apical meristem. The basal daughter cell produces a single file of cells that make up the suspensor. The uppermost cell of the suspensor becomes the hypophysis, which is part of the embryo. The hypophysis divides to form the quiescent center and the initial cells that form the root cap. (After T. Laux et al. 2004. *Plant Cell* 16: S190–S202.)

conserved order along an axis that extends from the shoot apical meristem to the root apical meristem. An early manifestation of this apical–basal axis is seen in the zygote itself, which elongates approximately threefold and becomes polarized with respect to its intracellular composition. The apical end of the zygote is densely cytoplasmic, in contrast to the basal end, which contains a large central vacuole. These differences in cytoplasmic density are captured when the zygote divides asymmetrically to give a short, cytoplasmically dense **apical cell** and a longer, vacuolated **basal cell** (see Figures 22.1A, 22.2A, and 22.4).

This first cell division is a critical step in embryogenesis because it defines the polar axis of the plant. A similar asymmetric division is observed in many (but not all) flowering plants. In Arabidopsis the polarity of the zygote, with its apical nucleus and basal vacuole, mirrors the polarity of the egg cell prior to fertilization. Intuitively, one might conclude from this that the polarity of the embryo is inherited directly from the unfertilized egg cell, but this is not what happens. Instead, egg cell polarity breaks down after fertilization by the sperm cell and is subsequently reestablished.

Zygote polarization can be studied using live imaging

The process of zygote polarization has been investigated by live imaging of transgenic Arabidopsis lines in which certain cellular structures were fluorescently labeled (**Figure 22.5**). Polarization can be seen soon after fertilization, is tightly coupled to zygote elongation, and involves distinct partitioning of the cytoskeleton, the nucleus, and the vacuoles to either end of the cell.

The two cells produced by the division of the zygote differ not only in size but also in their subsequent developmental fates. Nearly the entire embryo, and ultimately the mature plant, is derived from the smaller apical cell, which first undergoes two longitudinal divisions, then a set of transverse divisions (producing new cell walls at right angles to the apical–basal axis) to generate the

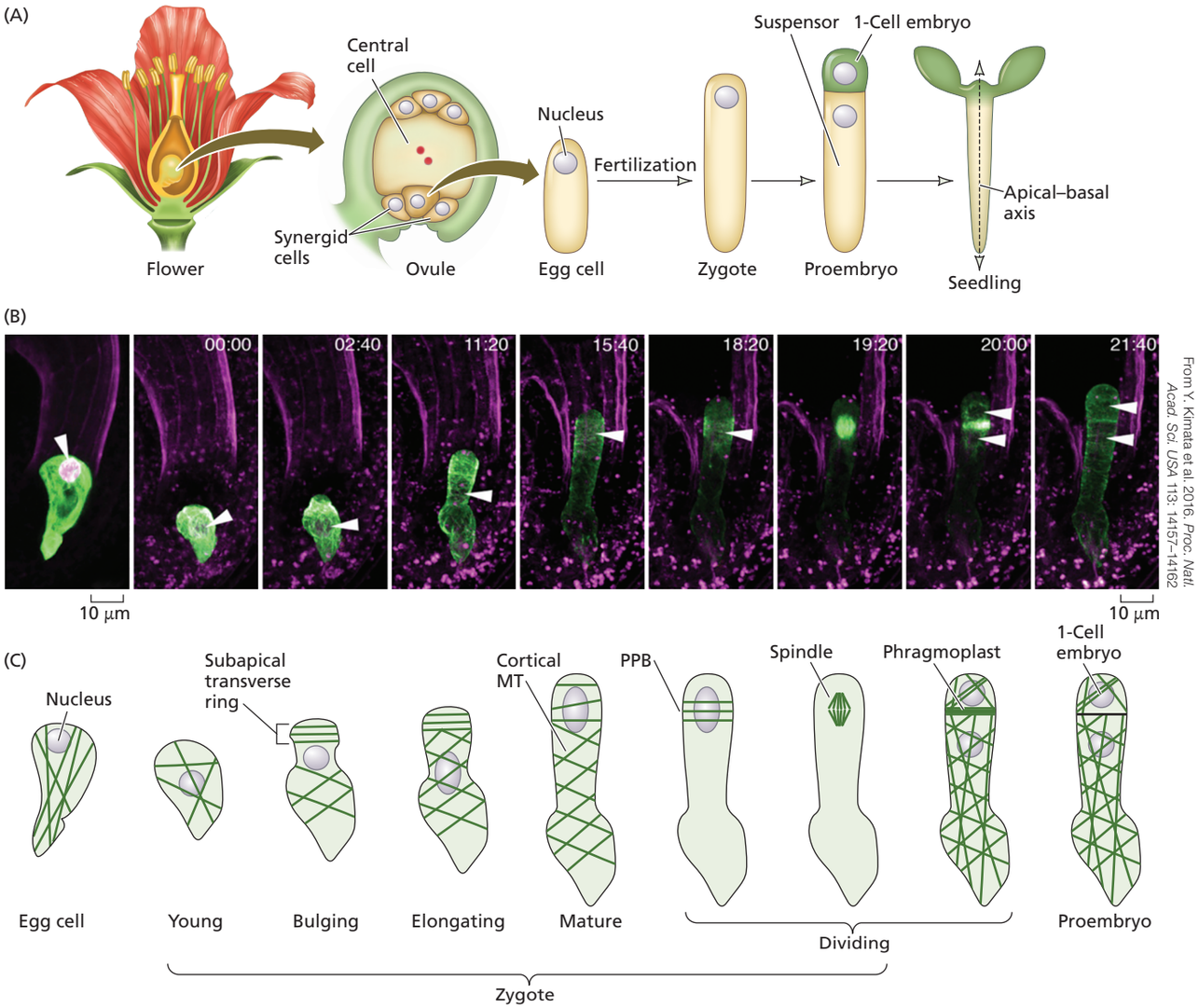


Figure 22.5 Live-cell imaging of cytoskeletal dynamics during early Arabidopsis embryo development. **(A)** Schematic diagram of Arabidopsis zygote development in the ovary of the flower. **(B)** Time-lapse series of fluorescence microscopy images of an egg cell (left-most image), a zygote just after fertilization (time 00:00), and successive stages of zygote development up to the first division. Microtubules are marked by green fluorescence, and the surrounding ovule cells are marked by magenta autofluorescence. Numbers indicate time (hours:minutes) from the first frame. Following fertilization, the zygote shrinks and the cortical microtubules become isotropically (i.e., randomly) oriented. The zygote then bulges at its apical end, where a ring of transversely oriented microtubules forms. This bulge then grows until the zygote reaches its full size. A preprophase band (PPB) of microtubules (see Chapter 1) forms at the position of the nucleus (white arrowheads), and mitosis occurs. **(C)** Illustrations summarize the respective stages in (B). MT, microtubule; PPB, preprophase band. (After Y. Kimata et al. 2016. *Proc. Natl. Acad. Sci. USA* 113: 14157–14162.)

eight-cell (octant) globular embryo (see Figures 22.1B, 22.2C, and 22.4).

The basal cell has a more limited developmental potential. A series of transverse divisions produces the filamentous **suspensor**, which attaches the embryo to the vascular system of the parent plant. Only the uppermost of the division products, known as the **hypophysis**, becomes incorporated into the mature embryo. Through further cell division, the hypophysis contributes to essential parts of the root apical meristem, including the columella and associated root cap tissues, and the quiescent center (see Figure 22.4), which we discussed in detail in Chapter 18.

In the cells that make up the octant globular embryo, there is little, apart from position, to distinguish the appearance of the upper and lower tiers of cells. All eight

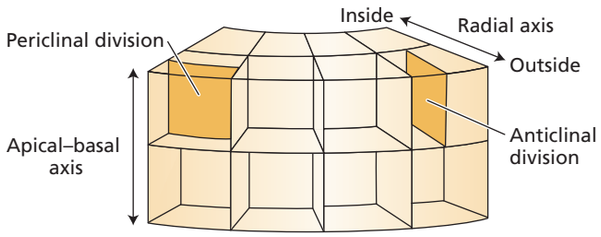


Figure 22.6 Periclinal and anticlinal cell division. Periclinal divisions produce new cell walls parallel to the tissue surface, and thus contribute to the establishment of a new layer. Anticlinal divisions produce new cell walls perpendicular to the tissue surface, and thus increase the number of cells within a layer.

cells then divide periclinally (new cell walls form parallel to the tissue surface) (**Figure 22.6**) to form a new cell layer called the **protoderm**, which ultimately forms the epidermis. As the embryo increases in volume, cells of the protoderm divide anticlinally (new cell walls form perpendicular to the tissue surface) to increase the area of this one-cell-thick tissue. By the early globular stage, broad distinctions between the fates of cells from the upper and lower tiers begin to emerge (see Figure 22.4):

- The apical region, derived from the apical quartet of cells, gives rise to the cotyledons and the shoot apical meristem.
- The middle region, derived from the basal quartet of cells, gives rise to the hypocotyl (embryonic stem), the root, and the apical regions of the root meristem.
- The hypophysis, derived from the uppermost cell of the suspensor, gives rise to the rest of the root meristem.

The ordered sequence of events that brings about the progression from a single, apical cell to a young globular embryo with multiple tissue layers requires several oriented cell divisions. What are the "rules" that govern these planes of cell division, and what are the cellular mechanisms that underpin them?

Analyses of the shapes and division planes in early Arabidopsis embryos led to the hypothesis that cells divide in the plane that minimizes the surface area of the new cross-wall separating the two daughter cells. This hypothesis was tested using three-dimensional microscopic imaging and computational analysis, which demonstrated that the minimum surface area rule does indeed seem to apply during the first three rounds of division (1 → 2, 2 → 4, and 4 → 8 cells) (**Figure 22.7**). At the fourth round of division (8 → 16 cells), however, the pattern abruptly changes. The top image in Figure 22.7 shows four cells of an eight-cell Arabidopsis embryo. If the cells divided according to the minimum surface area rule, they would lay down new cross-walls in the

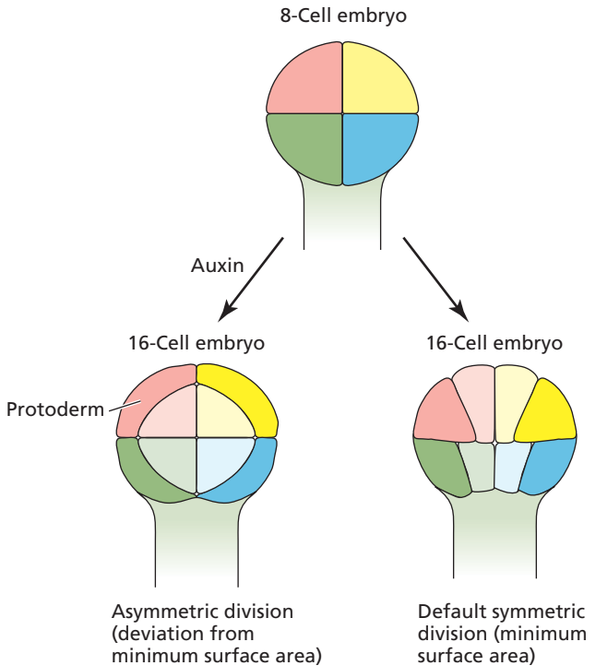


Figure 22.7 Orientation of cell divisions in the Arabidopsis embryo. Shown at the top are four cells of an eight-cell embryo. Each cell can divide symmetrically through the center of the cell (anticlinally), following the minimum surface area rule and generating two cells with equal volume (bottom right). Alternatively, under the influence of regulation, such as by auxin, each cell can divide asymmetrically (periclinally), deviating from the minimum surface area rule and generating outer and inner cell layers (bottom left). (After S. Yoshida et al. 2014. *Dev. Cell* 29: 75–87.)

anticlinal plane at the center of each cell, thereby generating two daughter cells of equal volume. The resulting hypothetical globular embryo (lower right side in Figure 22.7) would consist of only one layer of radially arranged embryonic cells of roughly equal volume. However, this is not what a normal 16-cell Arabidopsis embryo looks like.

Instead, the cells of the eight-cell embryo form cross-walls *asymmetrically* (i.e., off-center) in the periclinal orientation, thereby generating a 16-cell embryo consisting of two distinct cell layers. Note that in this case the volumes of the two daughter cells differ, and the minimum surface area rule for the cross-wall is violated. The daughter cells produced by asymmetric divisions typically have different developmental fates in the mature plant. In this case the outer cell layer, or protoderm, develops into the epidermis, while the inner cells give rise to the ground and vascular tissues.

The symmetric pattern of the first three rounds of embryonic cell division, which obey the minimum surface area rule, can be thought of as the default pathway. This raises the question of why the embryo deviates from this

pathway in the fourth round of divisions. Presumably some genetically determined mechanism intervenes to alter the pattern. As we will see later in the chapter, the hormone auxin functions as a signaling molecule during the shift to asymmetric cell divisions in early embryogenesis. (For a discussion of the establishment of polarity in a simpler, algal zygote, see **WEB TOPIC 22.1**.)

22.3 Mechanisms Guiding Embryogenesis

The reproducible patterns of cell division during early embryogenesis in Arabidopsis might suggest that a fixed sequence of cell division is essential to this phase of development. Absolute consistency in the patterns of cell division would imply that the fates of individual cells within the embryo became fixed, or determined, very early in development; once their fates were established, these cells would be committed to fixed programs of development. Such a *lineage-dependent* mechanism can be likened to assembling a structure from a standard set of parts according to self-contained instructions.

Although many examples of lineage-dependent mechanisms have been documented in animal development, this type of model alone does not readily explain several general features of plant embryogenesis. First, assuming that similar mechanisms operate in controlling embryo development across plant species, lineage-dependent mechanisms are difficult to reconcile with the more variable patterns of cell division typically seen during embryogenesis in many other plant species, including rice and even close relatives of Arabidopsis. Second, even for Arabidopsis, some limited variation in cell division behavior during normal embryogenesis, particularly during later stages, can be seen by following the fates of individual cells with sensitive fate-mapping techniques (**Figure 22.8**). Finally, one can consider the extreme examples provided by certain Arabidopsis mutants that have markedly different patterns of cell division but still retain the ability to form basic embryonic structures (**Figure 22.9**). There seems to be a certain amount of robustness in the plant developmental program with regard to variations in cell division patterns. From this perspective, the more or less predictable

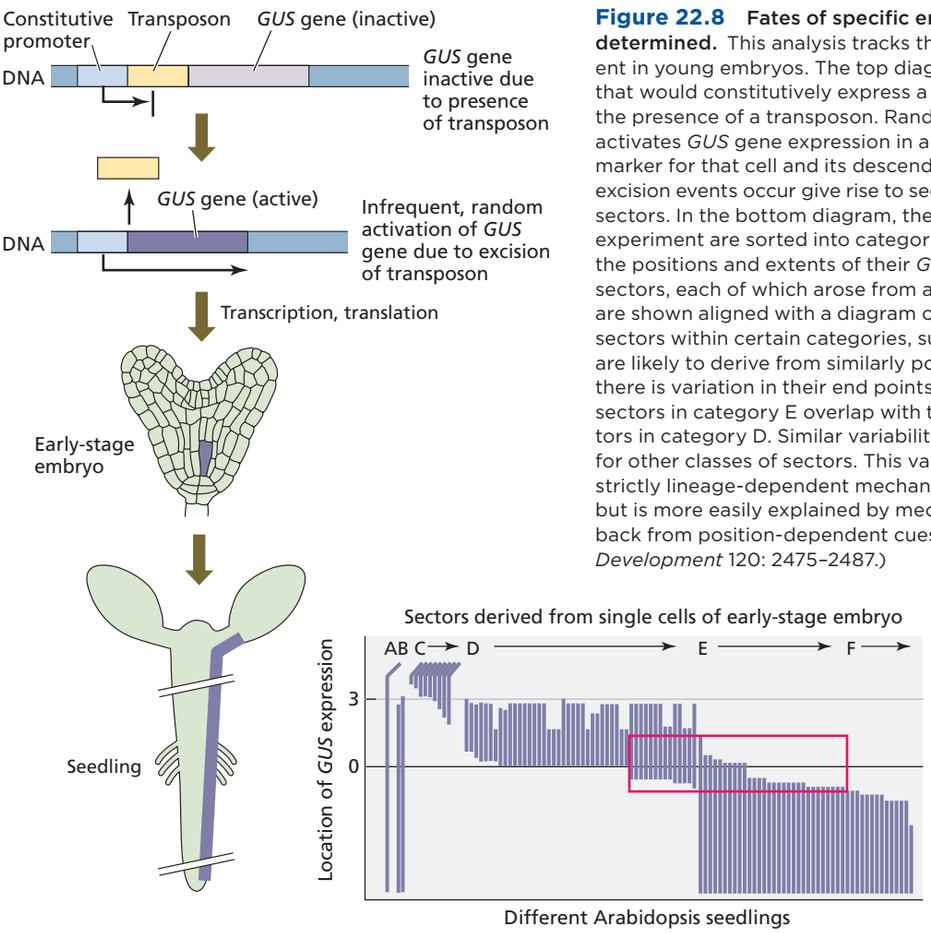
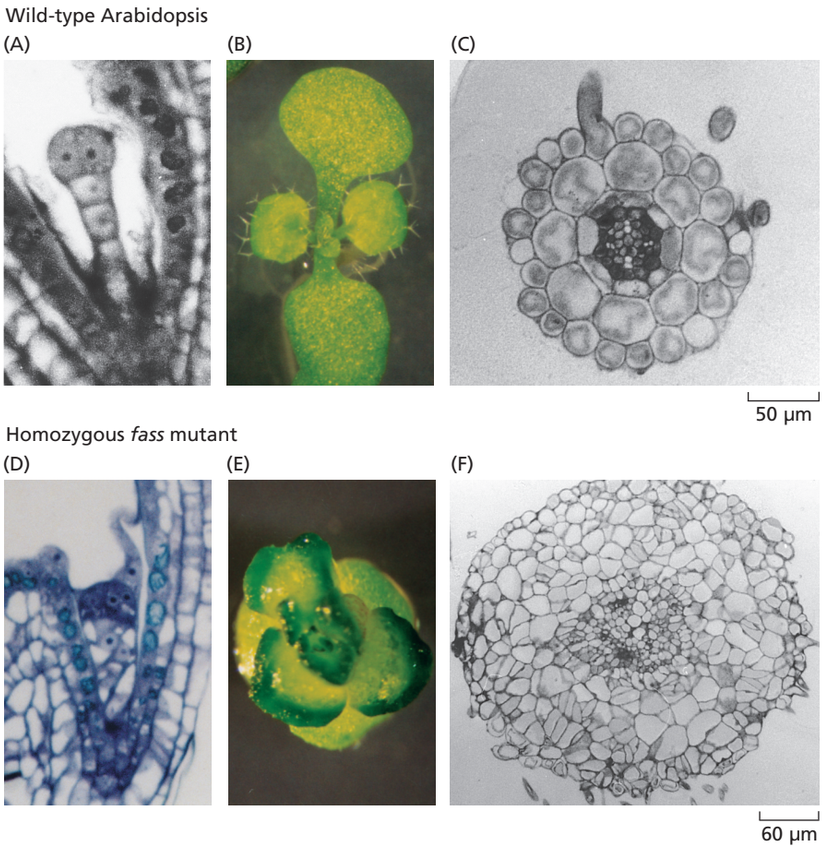


Figure 22.8 Fates of specific embryonic cells are not rigidly determined. This analysis tracks the fates of individual cells present in young embryos. The top diagram shows an artificial gene that would constitutively express a GUS reporter but is blocked by the presence of a transposon. Random excision of the transposon activates *GUS* gene expression in a single cell, providing a heritable marker for that cell and its descendants. Embryos in which these excision events occur give rise to seedlings with *GUS*-expressing sectors. In the bottom diagram, the seedlings from one such experiment are sorted into categories (labeled A–F) according to the positions and extents of their *GUS*-expressing sectors. These sectors, each of which arose from a single cell in the young embryo, are shown aligned with a diagram of a seedling to the left. Although sectors within certain categories, such as E and F, are similar and are likely to derive from similarly positioned cells in the embryo, there is variation in their end points. For example, the top ends of sectors in category E overlap with the bottom ends of some sectors in category D. Similar variability can be seen in the end points for other classes of sectors. This variability is inconsistent with a strictly lineage-dependent mechanism for cell fate determination, but is more easily explained by mechanisms that respond to feedback from position-dependent cues. (After B. Scheres et al. 1994. *Development* 120: 2475–2487.)



All photos from J. Traas et al. 1995. *Nature* 375: 676–677

Figure 22.9 Extra cell divisions do not block the establishment of basic radial pattern elements. Arabidopsis plants with mutations in the *FASS* gene are unable to form a preprophase band of microtubules in cells at any stage of division. Plants carrying this mutation are highly irregular in their cell division and expansion planes, and as a result are severely deformed. However, they continue to produce recognizable tissues and organs in their correct positions. Although the organs and tissues produced by these mutant plants are highly abnormal, a radially oriented tissue pattern is still evident. (Top) Wild-type Arabidopsis: **(A)** early globular stage embryo; **(B)** seedling seen from the top; **(C)** cross section of a root. (Bottom) Comparable stages of Arabidopsis homozygous for the *fass* mutation: **(D)** early embryogenesis; **(E)** mutant seedling seen from the top; **(F)** cross section of a mutant root, showing the random orientation of the cells but a nearly wild-type tissue order: An outer epidermal layer covers a multicellular cortex, which in turn surrounds the vascular cylinder.

pattern of cell division seen in Arabidopsis may simply reflect the small size of its embryo, which places physical limits on the polarity and probable positions of early cell divisions. Therefore, plant embryogenesis would seem to involve a variety of mechanisms, including those that do not rely solely on a fixed sequence of cell divisions.

Intercellular signaling processes play key roles in guiding position-dependent development

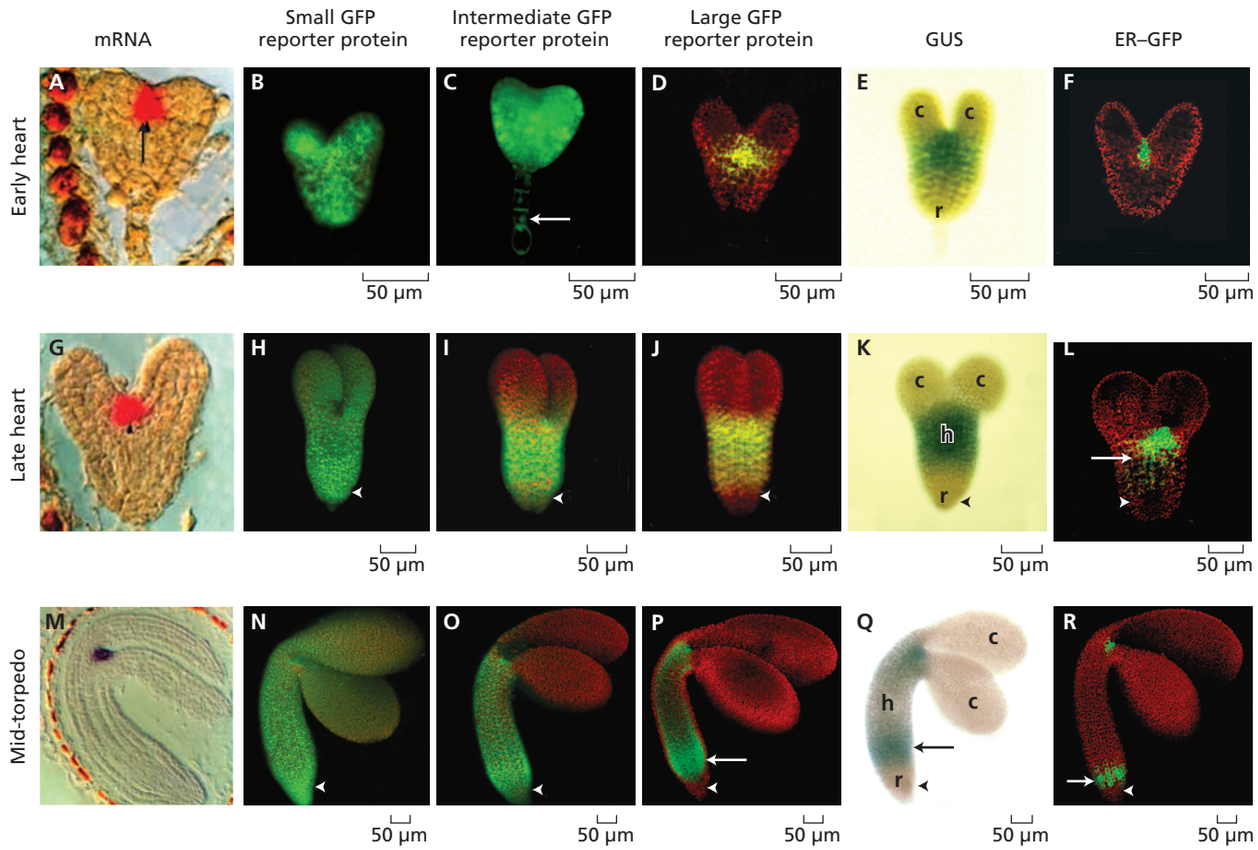
Given that the morphogenesis of the embryo can accommodate variable patterns of cell division, developmental processes that rely on **position-dependent** mechanisms that determine cell fate seem likely to play significant roles. Such mechanisms would operate by modulating the behavior of cells in a manner that reflects their position in the developing embryo, rather than their lineage (ancestry). This type of mechanism would explain how equivalent forms can arise through different patterns of cell division. Such position-dependent determination processes could be expected to feature three general kinds of functional elements:

1. There must be cues that signify unique positions within the developing structure.
2. Individual cells must have the means to assess their location in relation to the positional cues.
3. Cells must have the ability to respond in an appropriate way to the positional cues.

These basic requirements focus attention on the cellular context in which signaling processes operate. How is the propagation of signals across space and time affected by the physical makeup of the cell and its relationship to surrounding tissue? Do physical features such as membranes and cell walls merely represent obstacles to intercellular communication, or are they integral to mechanisms that enable signaling outputs to be regulated in response to additional inputs? In the following subsection we consider several examples that illustrate how genetically defined signaling processes contribute to embryo development.

Cell-cell communication during early embryo development may be regulated by plasmodesmata

Perhaps in a manner analogous to individuals within a social group, individual cells within the developing embryo display a range of facilities that may serve to enable, limit, and transform information during



From I. Kim et al. 2005. *Proc. Natl Acad. Sci. USA* 102: 11945–11950. © 2005 National Academy of Sciences. A, G, and M from J. A. Long and M. K. Barton. 1998. *Development* 125: 3027–3035

Figure 22.10 The potential for intercellular protein movement changes during development. Images show the distribution of small (B, H, N), intermediate (C, I, O), and large (D, J, P) GFP reporter proteins in embryos of different ages (early heart, A–F; late heart, G–L; mid-torpedo, M–R). All constructs are transcribed from an *STM* promoter, which produces transcripts in relatively small regions of the embryos, as shown by in situ hybridization (A, G, M) or by fusion to the nondiffusible GUS (E, K, Q) or ER–GFP reporters (F, L, R). Small proteins appear to move readily at all stages of embryogenesis (B, H, N), but the mobility of larger proteins is lower and becomes more restricted in older embryos (C and D, I and J, O and P). Arrows indicate the nucleus in suspensor cells (C) and ectopic expression of the *STM* promoter in hypocotyls (L, P–R). Arrowheads indicate the root. Abbreviations: c, cotyledons; h, hypocotyl; r, root.

communication. One remarkable aspect of early-stage embryos is the relatively small effect that cell walls have on the intercellular movement of certain classes of large molecules. Studies in intact plants show that large artificial dyes and fluorescently tagged protein molecules can move from cell to cell throughout the embryo (**Figure 22.10**), probably via cytoplasmic bridges provided by plasmodesmata. As development progresses, movement of these molecules becomes more size-restricted and spatially limited, suggesting that plasmodesmata-regulated flow of information becomes more important for later stages of development, perhaps to enable regionalized patterns of histogenesis. Paradoxically, during these same early stages of development, the movement of certain classes of relatively small molecules, including the wide-ranging plant hormone auxin, appears more restricted. As we will see, this regulated intercellular movement of molecules plays an essential role in a variety of developmental processes, including the establishment of the axial architecture of the embryo.

Mutant analyses have identified genes for signaling processes that are essential for embryo organization

Various types of mutants have been analyzed to gain insight into the processes that help establish the basic polarity of the embryo. Many of these processes affect proteins that are likely to contribute to some aspect of signal transduction. Genetic analyses of Arabidopsis mutants have identified genes that are required for the development of a viable embryo. All of the embryos shown in **Figure 22.11** have been arrested and will abort at the stage shown in the figure, well before the heart

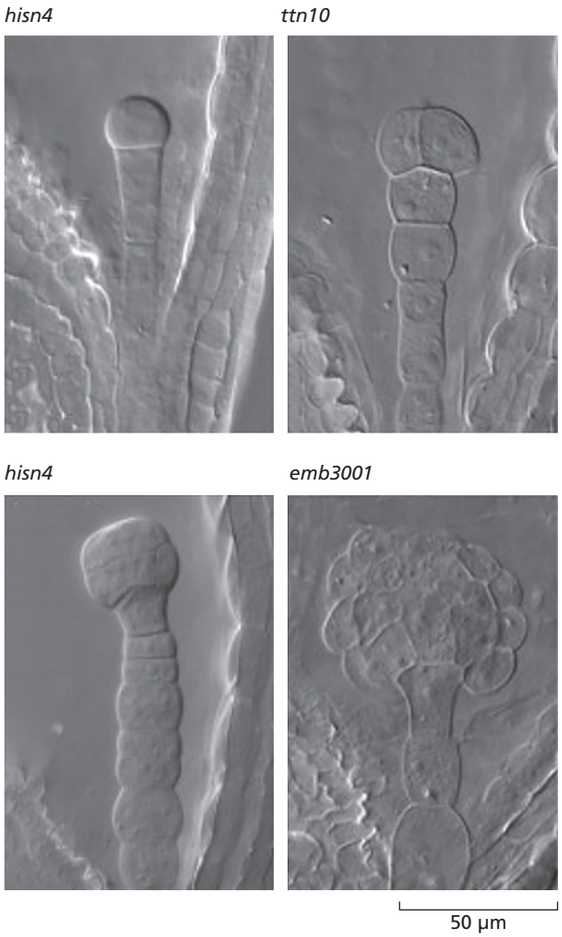


Figure 22.11 **Representative embryo lethal Arabidopsis mutants.** Each panel shows the arrested stage of the embryo lethal mutant indicated at top left. HSN4 is involved in histidine biosynthesis. TTN10 is involved in mitotic DNA replication initiation. EMB3001 contributes to a pathway for proteolysis.

stage. While the defects observed in such *embryo lethal* mutants indicate that the mutated gene is required for the viability or progression of embryogenesis, it cannot be concluded that the gene is directly involved in regulating the developmental process. Indeed, many mutations that affect development do so indirectly, either by altering cellular structure or by modifying the expression of genes required for basic metabolic functions.

Several genes that function in embryonic patterning have been isolated by screening for defective seedlings. Unlike embryo lethal mutants, *seedling defective* mutants are capable of developing into mature seeds that germinate, indicating that basic metabolic activity is relatively intact. However, this class of mutants displays abnormal organization when germinated and examined at the seedling stage. Among such mutants are those in which the normal apical–basal patterning is disrupted so that the shoot apical meristem, the root apical meristem, or both are missing. The nature of the defects seen in these loss-of-function mutants suggests that the corresponding genes are required for establishing normal apical–basal polarity (**Figure 22.12**). The cloning of several of these genes has led to insights into their molecular functions, which are summarized below. As our discussion here is focused on the morphologies of the mutants, we identify each gene using the name of its eponymous mutant (see the discussion of gene names and nomenclature systems in Chapter 3).

- ***GURKE*** (***GK***) (see Figure 22.12C), named for the cucumber-like shape of the mutant, in which the cotyledons and shoot apical meristem are reduced or missing, encodes an acetyl-CoA carboxylase. Since acetyl-CoA carboxylase is required for the proper synthesis of very-long-chain fatty acids (VLCFAs) and sphingolipids, these molecules or their derivatives appear to be crucial for proper patterning of the apical portion of the embryo.
- ***MONOPTEROS*** (***MP***) (see Figure 22.12B and C), necessary for the normal formation of basal elements such as the root and hypocotyl, as well as vascular tissue, encodes an auxin response factor (ARF). ARFs regulate gene expression in response to auxin, and the mutant's defects can be considered to arise from a failure to properly respond to auxin.
- ***FACKEL*** (***FK***) (see Figure 22.12C) was originally interpreted to be required for hypocotyl formation. Mutants exhibit complex pattern formation defects that include malformed cotyledons, short hypocotyl and root, and often multiple shoot and root meristems. *FK* encodes a sterol C-14 reductase, suggesting that sterols are critical for pattern formation during embryogenesis.
- ***GNOM*** (***GN***) (see Figure 22.12C) encodes a guanine nucleotide exchange factor (GEF) that acts in endomembrane trafficking. This GEF is required for the directional transport of auxin because it contributes to polar distribution of PIN auxin efflux proteins in membranes. The mutation's effects on embryo development are therefore due in part to a failure in properly distributing auxin.

This small collection of mutants highlights the potential significance of specific signaling processes to embryogenesis. Though it is not well understood how *GK* and *FK* mutations lead to characteristic embryonic pattern defects, the predicted biochemical activities of the proteins encoded by both genes are consistent with disruption of some form of lipid-mediated signaling. Similarly, both *GN* and *MP* can be linked to signaling processes, both of which feature auxin. Given the

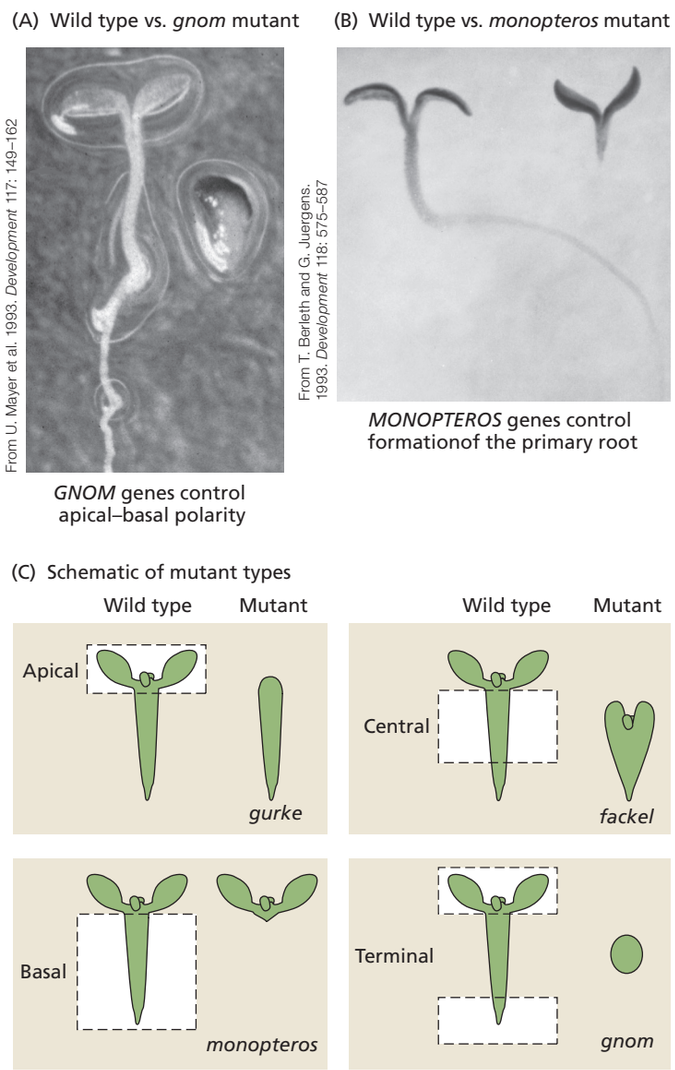


Figure 22.12 Genes essential for Arabidopsis embryogenesis have been identified from their seedling defective mutant phenotypes. The development of mutant seedlings is contrasted here with that of wild-type seedlings at the same stage of development. **(A)** The *GNOM* gene helps establish apical–basal polarity. A plant homozygous for the *gnom* mutation is shown on the right. **(B)** The *MONOPTEROS* gene is necessary for basal patterning and formation of the primary root. A plant homozygous for the *monopteros* mutation (on the right) has a hypocotyl, a normal shoot apical meristem, and cotyledons but lacks the primary root. **(C)** Schematic of four deletion mutant types. In each pair, the boxed regions of the wild-type plant on the left are missing from the mutant on the right. (C after U. Mayer et al. 1991. *Nature* 353: 402–407.)

wealth of background information on auxin-dependent responses, we next consider the importance of auxin and the specific roles of *GN* and *MP* in more detail, including how they contribute to an auxin-dependent establishment of the apical–basal axis of the developing embryo.

22.4 Auxin Signaling During Embryogenesis

As described in Chapters 4 and 18, the hormone auxin orchestrates many growth and developmental processes in plants and has profound effects during embryogenesis. The distribution of auxin and auxin signaling activity have both been mapped using fluorescent reporter constructs that can report either the presence of active auxin (DII domain–based reporters, e.g., DII-VENUS) or transcriptional activation in response to auxin (DR5 promotor-based reporters). Using these tools, it is clear that throughout embryogenesis, cells display dynamic auxin accumulation and response patterns (**Figure 22.13**). At the two-cell stage, the apical cell shows a more active auxin response than the basal cell, while at the globular stage the hypophysis and cells in the lower domain of the embryo proper exhibit higher levels of auxin activity. Indeed, many stages of embryogenesis, such as the formation of the radicle (embryonic root), the initiation of cotyledons, and the differentiation of vascular tissue, are closely linked to an increase in local auxin activity.

Spatial patterns of auxin accumulation regulate key developmental events

Genetic studies have confirmed that increases in local auxin accumulation are causally related to the developmental events with which they are associated. Gene mutations that inhibit auxin biosynthesis (due to defective biosynthesis genes) or the auxin response (due to defective receptors, non-degradable Aux/IAA repressors, or defective ARFs) specifically block those stages in embryonic development that are associated with increases in local auxin activity. The phenotypes of these mutants include the failure to initiate roots or cotyledons and the failure to properly specify vascular and ground tissue. If the spatial pattern of auxin accumulation provides the template for patterning in the embryo, what processes determine where auxin accumulates?

The spatial pattern of auxin accumulation arises from a combination of local biosynthesis and transport. The genes responsible for auxin biosynthesis are expressed in specific cells, which become auxin sources. These cells, however, are not the only ones that show auxin signaling activity, and this discrepancy can be explained by polar auxin transport within the embryo. For example, *pin1* mutants of Arabidopsis, which are defective in polar transport of auxin, often exhibit abnormalities in embryo development such as fused cotyledons (**Figure 22.14**), consistent with a role for auxin transport during embryo development. The PIN proteins, which function as auxin efflux

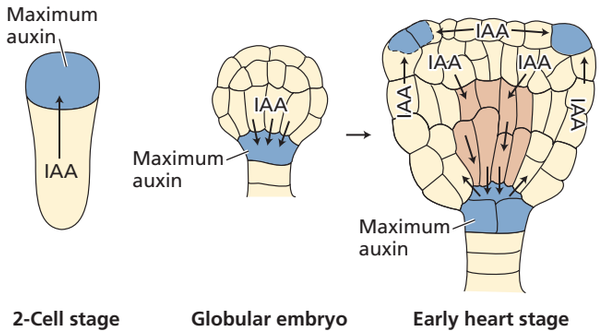
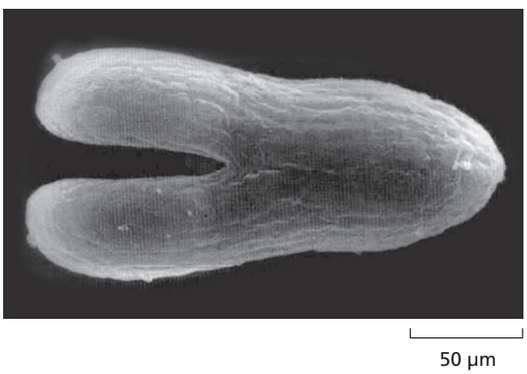


Figure 22.13 **PIN1-dependent movement of auxin (IAA) during early stages of embryogenesis.** Auxin movement, as inferred from the asymmetric distribution of the PIN1 protein and the activity of a DR5 auxin-responsive reporter, is depicted by arrows. Blue areas denote cells with maximum auxin concentrations; brown shading indicates the vascular cylinder. Auxin maxima resulting from synthesis of the hormone create gradients that are then reinforced by the polar orientation of PIN1.

(A) Wild-type Arabidopsis



(B) Mutant *pin1-1* Arabidopsis



A and B from C. Liu et al. 1993. *Plant Cell* 5: 621–630

Figure 22.14 **Evidence for a role for auxin in embryonic development.** **(A)** Wild-type Arabidopsis embryo. **(B)** A *pin1-1* mutant Arabidopsis embryo. Note the failure in cotyledon separation caused by chemical inhibition of auxin transport in vitro and by disruption of auxin transport by mutations in the *PIN* gene.

carriers (see Chapter 4), are prominently expressed in the Arabidopsis embryo. Their localization in the plasma membranes at the basal ends of the transporting cells (consistent with the chemiosmotic model of auxin transport) suggests a well-defined path of auxin transport, from the sites of biosynthesis to sites of action. Thus, auxin acts as a mobile cell-to-cell signal that controls morphogenesis in the embryo. Note that the auxin responses of the targeted cells differ markedly depending on the cells' position within the embryo. Thus, cells in the apical domain of the embryo respond to auxin by initiating the cotyledons, while cells in the basal domain respond by forming the radicle.

The GNOM protein establishes a polar distribution of PIN auxin efflux proteins

PIN proteins are rate-limiting auxin transport proteins, and their asymmetric targeting to polarized membrane domains defines the path of auxin transport. Central to the dynamic nature of PIN protein localization is their trafficking via vesicles through an endomembrane compartment characterized by the presence of the GNOM protein. The GNOM protein establishes a polar distribution of auxin efflux proteins, and not surprisingly, *gnom* mutants have severe developmental defects (see Figure 22.12A and C). Many aspects of the *gnom* mutant phenotype can be mimicked, or **phenocopied**, by the application of auxin transport inhibitors, consistent with the idea that GNOM is required for normal auxin transport.

When the *GNOM* gene was sequenced, its predicted protein was found to be similar to guanine nucleotide exchange factors (GEFs). GEFs promote the intracellular movement of vesicles that deliver specific proteins to targeted sites within the cell. An explanation for how GNOM facilitates polar auxin transport emerged through experiments demonstrating that the GEF activity of GNOM is required for the polarized localization of PIN proteins. Mutation of *GNOM* disrupts the normal polarized distribution of PIN proteins. Disruption of PIN localization is observed in cells treated with brefeldin A, an inhibitor of GEF activity, but not in cells that contain an altered form of GNOM to which brefeldin A is unable to bind. The notion that the altered pattern of embryonic development in *gnom* mutants reflects a disruption of PIN activity is supported by the similar developmental defects that result from directly disrupting genes that encode PIN proteins.

MONOPTEROS encodes a transcription factor that is activated by auxin

The cloning of the *MONOPTEROS* gene (see Figure 22.12B and C) revealed that it encodes a member of a family of proteins called **auxin response factors** (**ARFs**), implicating it in auxin-dependent processes. In the presence of auxin, ARFs regulate the transcription of specific

genes involved in auxin responses. In the absence of auxin, the activity of these proteins is inhibited through their physical association with specific repressors, termed Aux/IAA proteins. Auxin-dependent responses occur when auxin triggers the targeted degradation of these repressors, allowing ARFs to control their target genes (see Chapter 4).

Several lines of evidence support the view that *MONOPTEROS* mediates at least a subset of auxin responses. *monopteros* mutant embryos not only lack hypocotyls and radicles (see Figure 22.12B and C) but also have defects in vascular patterning similar to those observed when auxin levels or movements are artificially disturbed, suggesting that MONOPTEROS is likely to regulate genes that guide auxin-dependent vascular development. Separate genetic studies have confirmed that MONOPTEROS activity is regulated by auxin. These studies focused on the *bodenlos* (*bdl*) mutant, which, like *monopteros* mutants, lacks the basal region of the embryo. This similarity suggested that the two genes might be functionally related. Molecular cloning of *BDL* showed that it encodes one of the many Aux/IAA repressor proteins. The normal form of BDL associates with MONOPTEROS to repress MONOPTEROS activity, but this repression can be relieved by auxin-induced degradation of BDL. Biochemical studies demonstrated that the mutant form of BDL is resistant to auxin-induced degradation and would thus remain bound to MONOPTEROS, repressing its activity and producing a phenotype similar to that of *monopteros*.

Taken together, GNOM and MONOPTEROS can be seen to form part of a more complex mechanism by which the movement of auxin and the responses it elicits help guide the establishment of the apical–basal axis. The overall output of this mechanism is the activation of a set of genes that trigger the establishment of the various pattern elements or cell types. Molecular genetic studies using mutants, combined with whole-genome transcriptional analyses, have identified several such target genes. Given the position dependence of auxin action, it is to be expected that the genes that are activated by this pathway will vary depending on the context of the cell. These genes encompass a variety of functions, including a transcription factor, TARGET OF MONOPTEROS 7 (TMO7), that can move from cell to cell and contributes to root formation, as well as a regulator of vascular tissue formation, TMO5, which we discuss later in the chapter.

22.5 Radial Patterning During Embryogenesis

In addition to the distinctions among cells and tissues positioned along the apical–basal axis of the developing embryo, differences can also be seen along a radial axis that runs perpendicular to the apical–basal axis, extending from the interior to the surface. In Arabidopsis, differentiation of tissues along the radial axis is first observed in the globular embryo (**Figure 22.15**), where periclinal divisions separate the embryo into

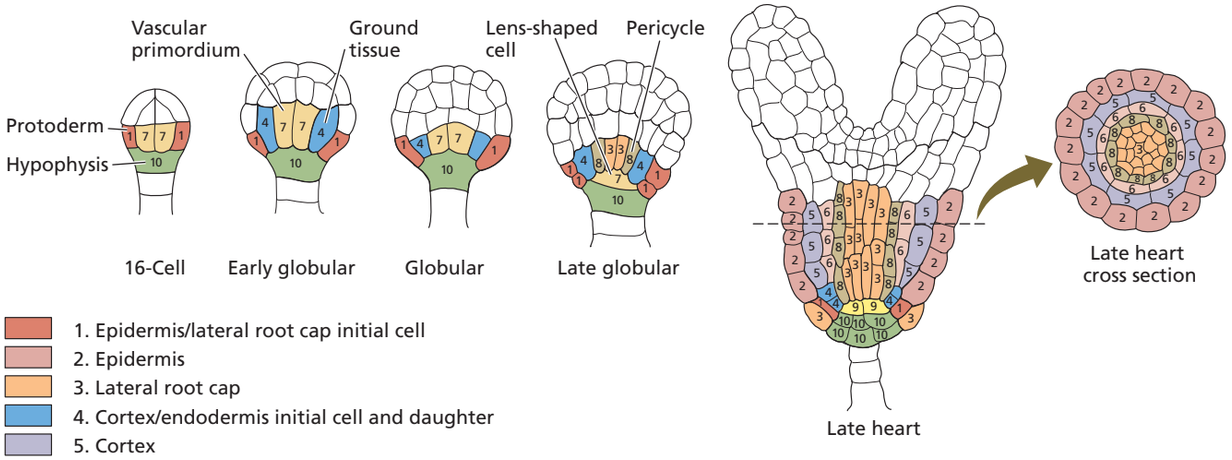


Figure 22.15 Summary of the sequence of radial patterning events during Arabidopsis embryogenesis. The five successive embryonic stages shown in longitudinal section illustrate the origin of distinct tissues, beginning with the delineation of the protoderm (left) and ending with the formation of the vascular tissues (right). Note how the number of tissues increases through the action of initial cells. A cross-sectional view of the basal portion of the late heart stage embryo is shown at the far right (the level of the cross section is shown by the line in the longitudinal section to its left). (After T. Laux et al. 2004. *Plant Cell* 16: S190–S202.)

three radially defined regions. The outermost cells form a one-cell-thick surface layer known as the protoderm, which eventually differentiates into the epidermis. Below this layer lie cells that will later become the **ground tissue**, which in turn differentiates into cortex (the ground tissue between the vascular system and the epidermis) and, in the root and hypocotyl, the endodermis (the layer of suberized cells that restricts water and ion movements into and out of the stele via the apoplast; see Chapter 6). In the most central domain lies the **procambium**, which generates the vascular tissues, including the pericycle of the root.

As we saw for apical–basal patterning of the embryo, a precisely defined sequence of cell divisions does not appear to be essential for basic radial patterning. Significant variability in the patterns of cell divisions associated with the formation of radial patterns can be seen among related species, and basic pattern elements can still be established in mutants with disturbed patterns of cell division, suggesting a prominent role for position-dependent mechanisms. In the following subsections we discuss experiments that address the nature of these mechanisms, providing further examples of the utility of molecular genetic analyses. Further discussion of the physical aspects of cell division can be found in **WEB ESSAY 18.1**. The epidermis provides an interface and boundary at the edge of the radial pattern

One obvious and singular aspect of the radial axis of the embryo is provided by the protoderm, a tissue that can be uniquely defined by its superficial position and which eventually produces the epidermis, a critical tissue that mediates communication between the plant and the outside world. Originating early in embryogenesis, protodermal cells have a set of exposed walls that could, in theory, facilitate the exchange of signals with the external environment or, alternatively, act as a boundary as signals move from cell to cell within the embryo. In either case, the protoderm would exhibit unique properties distinguishing it from the internal cell layers, and thus provide potential cues for radial patterning. For example, studies in *Citrus* have shown the presence of a cuticle layer on the surface of the embryo from the earliest zygotic stages through maturity, suggesting that the walls of protodermal cells form a communication boundary. Some studies also suggest that the epidermis can act as a physical constraint to the growth of more internal layers.

Genetic studies have helped us understand the processes that contribute to the unique character of the epidermis. For example, two genes, *ARABIDOPSIS THALIANA MERISTEM LAYER 1* (*ATML1*) and *PROTODERMAL FACTOR 2* (*PDF2*), have been identified as having essential roles in promoting the epidermal identity of superficially positioned cells. Both genes encode homeodomain transcription factors and are expressed from early stages of embryogenesis in the outer cells of the embryo. This expression appears necessary for the establishment of normal epidermal identity, since loss-of-function mutant plants have an abnormal epidermis in which cells display characteristics normally associated with mesophyll cells (**Figure 22.16**). Conversely, **ectopic** (in the wrong location) expression of *ATML1* in internal tissues has been shown to induce abnormal epidermal characteristics. Together, these results suggest that *ATML1* and the related *PDF2* are likely to function by promoting the activity of downstream genes that mediate the development of epidermal characters.

Procambial precursors for the vascular stele lie at the center of the radial axis

It is easy to imagine that the unique geometric properties at the center of the developing embryo would afford further potential positional cues for patterning tissues along the radial axis, with vascular tissues of the stele eventually occupying the most central positions. Genetic and developmental analyses suggest that this process is progressive, with periclinal divisions first producing additional layers of cells along the radial axis that then become patterned to particular fates by the activity of specific gene networks. For example, Arabidopsis

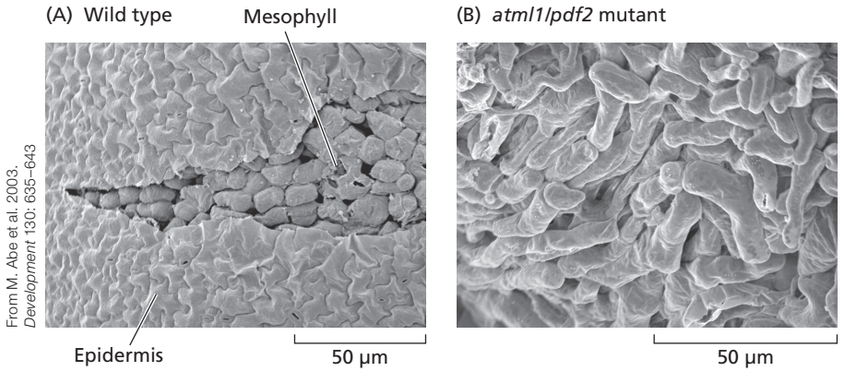


Figure 22.16 ***ATML1* and *PDF2* are required for the establishment of a normal epidermis.** Comparison of a wild-type plant (A) and a double *atml1/pdf2* mutant (B) shows the similarity of the superficial layers of the mutant to the mesophyll of the wild-type plant (partially exposed in A).

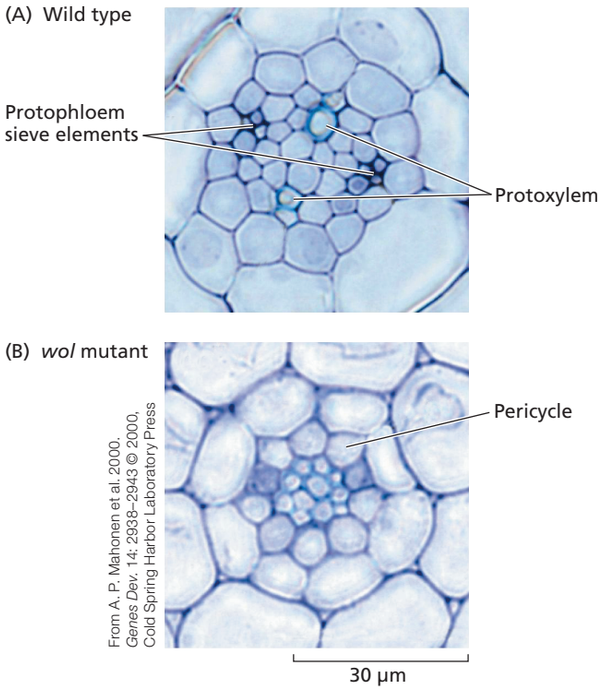


Figure 22.17 The cytokinin receptor encoded by the Arabidopsis *WOODEN LEG* (*WOL*) gene is required for normal phloem development. Comparison of wild-type (A) and *wol* (B) mutant roots shows an absence of phloem elements in *wol* that is accompanied by an apparent decrease in the number of cell layers.

mutants that are deficient for the *WOODEN LEG* (*WOL*) gene fail to undergo a critical round of cell division that normally produces precursors for xylem and phloem (**Figure 22.17**). This defect leads to the development of a vascular system that contains xylem but not phloem. *WOL* (also known as *CYTOKININ RESPONSE 1* [*CRE1*]) encodes one of several related receptors for cytokinin, implicating this hormone in the establishment of radial pattern elements (see Chapter 4). However, these defects can be **rescued** (reversing a phenotype by altering a second factor) by *fass* (i.e., by making a *wol/fass* double mutant), which causes extra rounds of cell division. Thus, it appears that the absence of phloem in *wol* may simply reflect the absence of an appropriately positioned precursor cell layer rather than the inability to specify phloem cell identity.

An understanding of the critical roles of cell division and an adequate number of cells for patterning the vascular tissues also comes from studies of the *TARGET OF MONOPTEROS 5* (*TMO5*) gene. This gene is activated by MONOPTEROS, the auxin-dependent transcription factor discussed earlier, and thus represents a local auxin output. *TMO5* is expressed only in the vascular precursor cells in the center of the globular embryo and encodes a transcription factor. TMO5 forms a heterodimer with a second transcription factor, LONESOME HIGHWAY (LHW). Overexpression of these two transcription factors together induces additional periclinal divisions, and mutation of either factor results in fewer periclinal divisions, indicating that these factors are key regulators of cell division in the vascular tissue (**Figure 22.18**). By titrating the levels of TMO5 and LHW, researchers can control the number of cell layers in the vascular tissue, which led to the discovery that the number of vascular elements (xylem and phloem) scales with the total number of cells in the tissue. For example, mutants with only half the normal number of cell files (produced both anticlinally and periclinally) make only one phloem pole instead of two. When a mutant has excess cell files, multiple (more than two) phloem poles are produced. Once TMO5 and LHW are activated by auxin, they act by locally promoting the synthesis of a second plant hormone, cytokinin. Thus, the interaction between these two plant hormones sets the size of the vascular tissue, and thereby its composition and structure.

The differentiation of cortical and endodermal cells involves the intercellular movement of a transcription factor

The development of endodermal and cortical tissues provides a classic example of how the radial patterning process can be regulated by gene activity communicated between adjacent layers. Two Arabidopsis genes, *SCARECROW* (*SCR*) and *SHORT ROOT* (*SHR*), are both essential for the normal formation of cortical and endodermal cell layers. The similar protein sequences encoded by these two genes place them in the *GRAS* family of transcription factors, whose name derives from the first known members, *GIBBERELLIN-INSENSITIVE* (*GAI*), *REPRESSOR OF GA1–3* (*RGA*), and *SCR*.

Mutants in which either *SCR* or *SHR* activity is reduced fail to undergo a round of cell division that produces the two layers that later differentiate as separate cortex and endodermis. Mutations in either gene block the round of cell division that creates these separate layers (**Figure 22.19**). In *scr* mutants, the single layer that remains exhibits characteristics of both endodermis and cortex, suggesting that the mutant is still able to express these characteristics but is unable to separate them into discrete layers. This interpretation is supported by the ability of *fass* to restore more normal growth patterns. Much as it rescues *wol*, *fass* appears to compensate for the division defect of *scr*, and thus provides separate layers in which distinct endodermal and cortical traits can be expressed.

The mutant *shr* not only exhibits a cell division defect similar to that of *scr*, but is also unable to elaborate cellular characteristics typical of the endodermis. The single undivided layer in *shr* lacks endodermal traits, such as

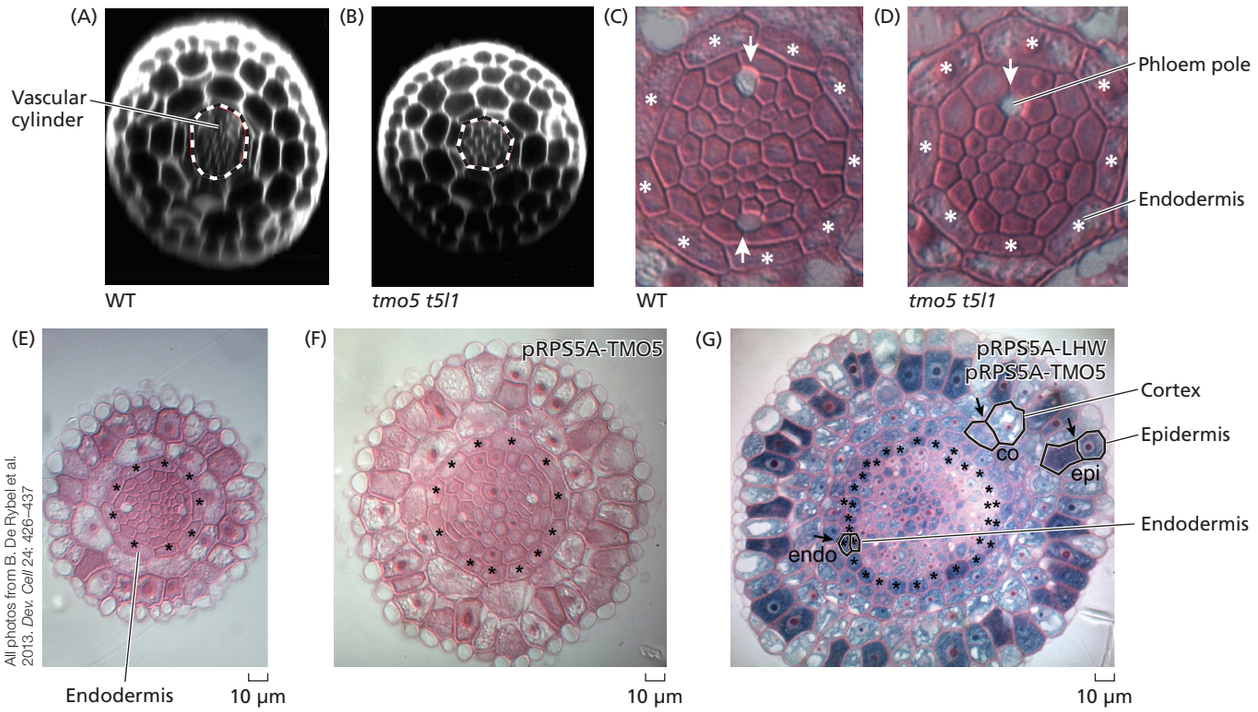


Figure 22.18 ***TMO5* and *LHW* control the number of xylem and phloem cell files in all dimensions in the Arabidopsis root.** **(A and B)** Cross sections of mature embryos of wild type (A) and the *tmo5 tmo5-like1 (t5l1)* double mutant (B). The area inside the dashed line is the vascular tissue, which is smaller in the mutant. **(C and D)** Cross sections of postembryonic root meristems in wild type (C) and the *tmo5/t5l1* mutant (D) show that the latter has fewer vascular cells (cells in the surrounding endodermis are marked with asterisks) and phloem poles (arrows). **(E–G)** Cross sections of root meristems of wild type (E), pRPS5A-TMO5, a line overexpressing TMO5 (F), and pRPS5A-LHW, pRPS5A-TMO5, a line overexpressing both LHW and TMO5 (G). Compared with the wild type, the double overexpression line has more cell files and periclinal divisions. Examples of cell pairs produced by a periclinal division are indicated with outlines and arrows. Endodermal cells are marked with asterisks.

the Casparian strip, and instead displays gene activities that are normally limited to the cortex. This apparent requirement for *SHR* gene activity to specify endodermal traits is puzzling, since the expression of *SHR* mRNA is normally restricted to more internal, provascular tissues.

More detailed analyses involving the use of fluorescently tagged proteins have addressed this paradox, showing that although *SHR* mRNA is confined to the vascular cylinder, its translation product is not. The SHR protein is able to move into the adjacent, more

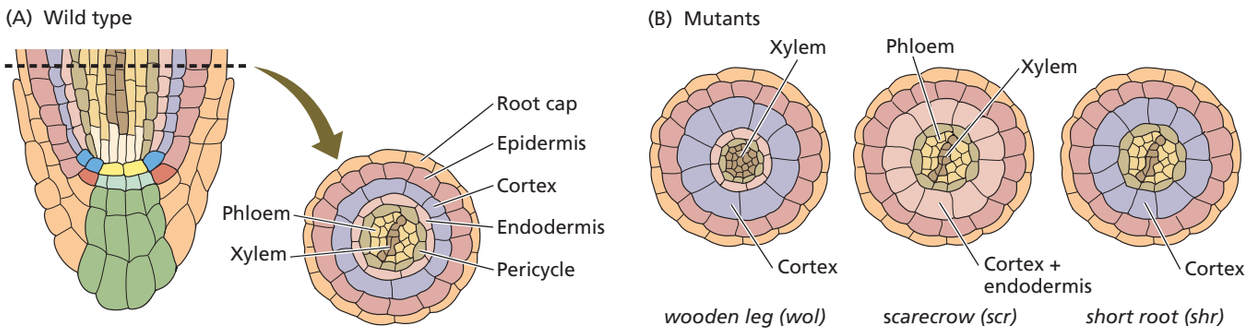


Figure 22.19 **Comparison of normal and mutant radial root patterns shows the spatially defined functions of specific genes.** **(A)** Wild-type root. **(B)** Defective radial root patterns of three Arabidopsis mutants: *wooden leg* (*wol*), *scarecrow* (*scr*), and *short root* (*shr*). (After K. Nakajima and P. N. Benfey. 2002. *Plant Cell* 14: S265–S276.)

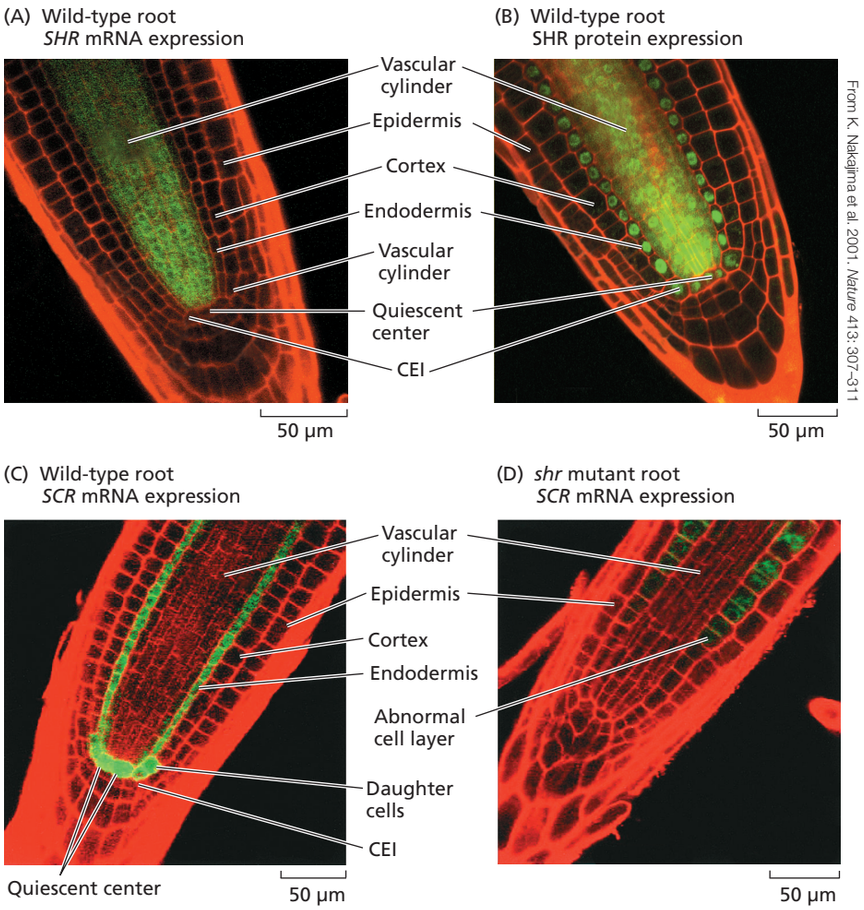


Figure 22.20 The *SHORT ROOT* (*SHR*) and *SCARECROW* (*SCR*) genes in Arabidopsis control tissue patterning during root development. Here, the mRNAs or proteins for *SHR* and *SCR* have been localized by confocal laser scanning microscopy. **(A and B)** *SHR* expression. (A) During early root development, *SHR* promoter activity is restricted to the stele (as visualized using an *SHR* promoter–green fluorescent protein [GFP] fusion). (B) The SHR protein shows a distinct pattern of localization, which includes the central stele and also the nuclei of adjacent endodermis (as visualized using an *SHR* promoter + coding region + GFP fusion). **(C and D)** *SCR* expression (monitored using an *SCR* promoter–GFP fusion). (C) In wild-type roots, the *SCR* is transcribed in the quiescent center, endodermis, and cortical–endodermal initial cell (CEI). It is not present in the cortex, vascular cylinder, or epidermis. (D) The expression of *SCR* is markedly reduced in the *shr* mutant root and appears only in an abnormal cell layer that has characteristics of both endodermis and cortex.

external layer via plasmodesmata, where it has several activities, including promoting enhanced transcription of *SCR*. Following the translation of the *SCR* mRNA, SHR forms a heterodimer with the SCR protein to enhance the transcription of genes associated with endodermal programs of development (**Figure 22.20**). The contribution of the SHR protein to the differentiation of cortical and endodermal cells provides a clear example of how the functions of specific transcription factors may depend on their movement between cell layers.

22.6 Formation of the Root and Shoot Apical Meristems

The most important outcome of embryogenesis is arguably the formation of apical meristems at either end of the mature embryo. These shoot and root apical meristems are home to the initial cells that sustain the vegetative growth of the shoot and root systems. Failure to initiate either of the two apical meristems leads to the arrest of seedling growth, indicative of the critical importance of this step in plant development.

Root formation involves *MONOPTEROS* and other auxin-regulated transcription factors

As we saw earlier in the chapter, mutants lacking an embryonic root (e.g., *monopteros* [*mp*] and *bodenlos* [*bdl*]) have helped elucidate the root-specifying role played by auxin. Analyses of the genes regulated by MONOPTEROS led to the discovery of the mobile transcription factor TMO7 and the vascular tissue regulator TMO5 (discussed earlier in the chapter), but neither of these alone is sufficient to specify a root. Indeed, genetic analyses have identified two additional transcription factors that are activated by auxin and which appear to be responsible for embryonic root formation.

These two transcription factors, belonging to the AP2/Ethylene Responsive Factor class, are encoded by the *PLETHORA 1* (*PLT1*) and *PLETHORA 2* (*PLT2*) genes. Both are activated in the embryo in the lower half of the globular embryo (**Figure 22.21**). Mutants in which

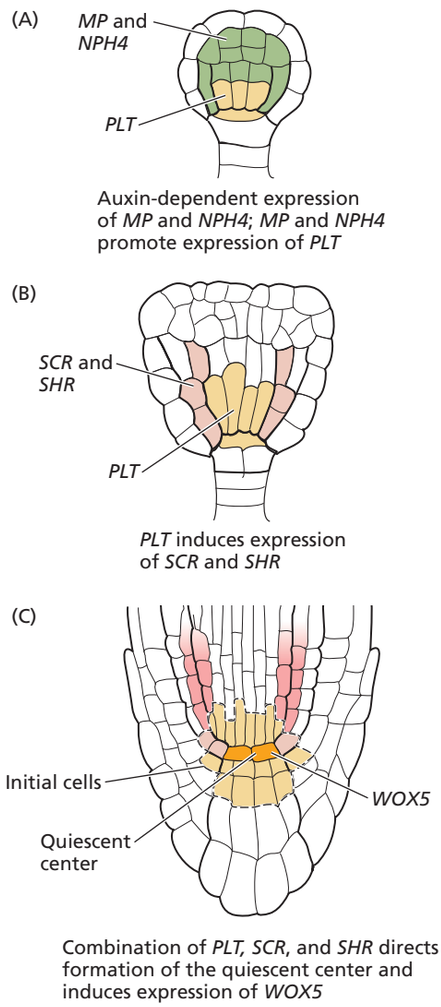


Figure 22.21 Model for the specification of cell identity in the root. **(A)** Early auxin-dependent expression of the *MONOPTEROS* (*MP*) and *NONPHOTOTROPIC HYPOCOTYL 4* (*NPH4*) genes. *MONOPTEROS* and *NPH4* promote *PLETHORA* (*PLT*) expression in a basal domain. **(B)** *PLT* promotes the expression of *SCARECROW* (*SCR*) and *SHORT ROOT* (*SHR*). **(C)** The combination of *PLT*, *SCR*, and *SHR* gene expression directs centrally positioned cells to become the quiescent center, and also induces the expression of *WOX5*, which contributes to the maintenance of surrounding initial cells. The area denoted by a dashed line contains initial cells. (After M. Aida et al. 2004. *Cell* 119: 109–120.)

PLT genes have been disrupted are unable to form an embryonic root. Conversely, the ectopic expression of *PLT* in the upper half of the globular embryo (or in other, postembryonic tissues) is sufficient to form a new root in these locations. Together, these experiments support a model in which auxin activates a set of genes in the lower half of the embryo (including *PLT* genes) that instruct these cells to adopt a root identity.

Shoot formation requires HD-ZIP III, *SHOOT MERISTEMLESS*, and *WUSCHEL* genes

Another set of transcription factors is activated in the upper half of the globular embryo, and it appears to mediate either the establishment of the entire shoot domain or the shoot apical meristem. For example, members of a small family of related transcription factors belonging to the HD-ZIP III class are specifically expressed in the upper half of the globular embryo. Expression of these HD-ZIP III genes in the upper half of the embryo is required for shoot apical meristem formation in the embryo, as well as for the adaxial–abaxial polarity of leaves during vegetative growth (see Chapter 18). When ectopically expressed in the lower half of the embryo, one of these factors, PHABULOSA (PHB), is able to trigger the formation of a second shoot domain (**Figure 22.22C**). This is the opposite of what happens when the PLT protein is artificially expressed in the upper half of the embryo (**Figure 22.22B**), suggesting that HD-ZIP III and PLT transcription factors act antagonistically. Indeed, further experiments have shown that HD-ZIP III factors inhibit the expression of *PLT* genes (**Figure 22.22A**).

Mutations in the *SHOOT MERISTEMLESS* (*STM*) or *WUSCHEL* (*WUS*) genes, which encode transcription factors, cause a loss of the embryonic shoot apical meristem. Although neither of these two transcription factors on its own can trigger the formation of new shoot apical meristems when ectopically expressed in other tissues, in combination they can. *STM* and *WUS* are both expressed in the apical domain of young embryos, and it would seem that both are necessary for meristem formation. Because of this interaction, the position of the embryonic shoot apical meristem can be precisely defined by the domain where the expression of the two genes overlaps.

Plants can initiate embryogenesis in multiple types of cells

In this chapter we have discussed embryogenesis with an emphasis on the familiar context of seed development. However, as indicated in the introduction, the process of embryogenesis is evolutionarily older than seed development, as it also occurs in the non-seed vascular plants, such as the ferns and horsetails. Even in seed plants a variety of other cells besides zygotes are capable of undergoing embryogenesis (**Figure 22.23**). These processes include natural forms of asexual embryogenesis, such as apomixis (asexual embryogenesis from cells within an ovule—i.e., an immature seed) as well as somatic embryogenesis from the leaf margin (e.g., in *Kalanchoe*) (see Chapter 21). In both cases, cells other than the zygote are genetically programmed to undergo embryogenesis and can form an embryo that is

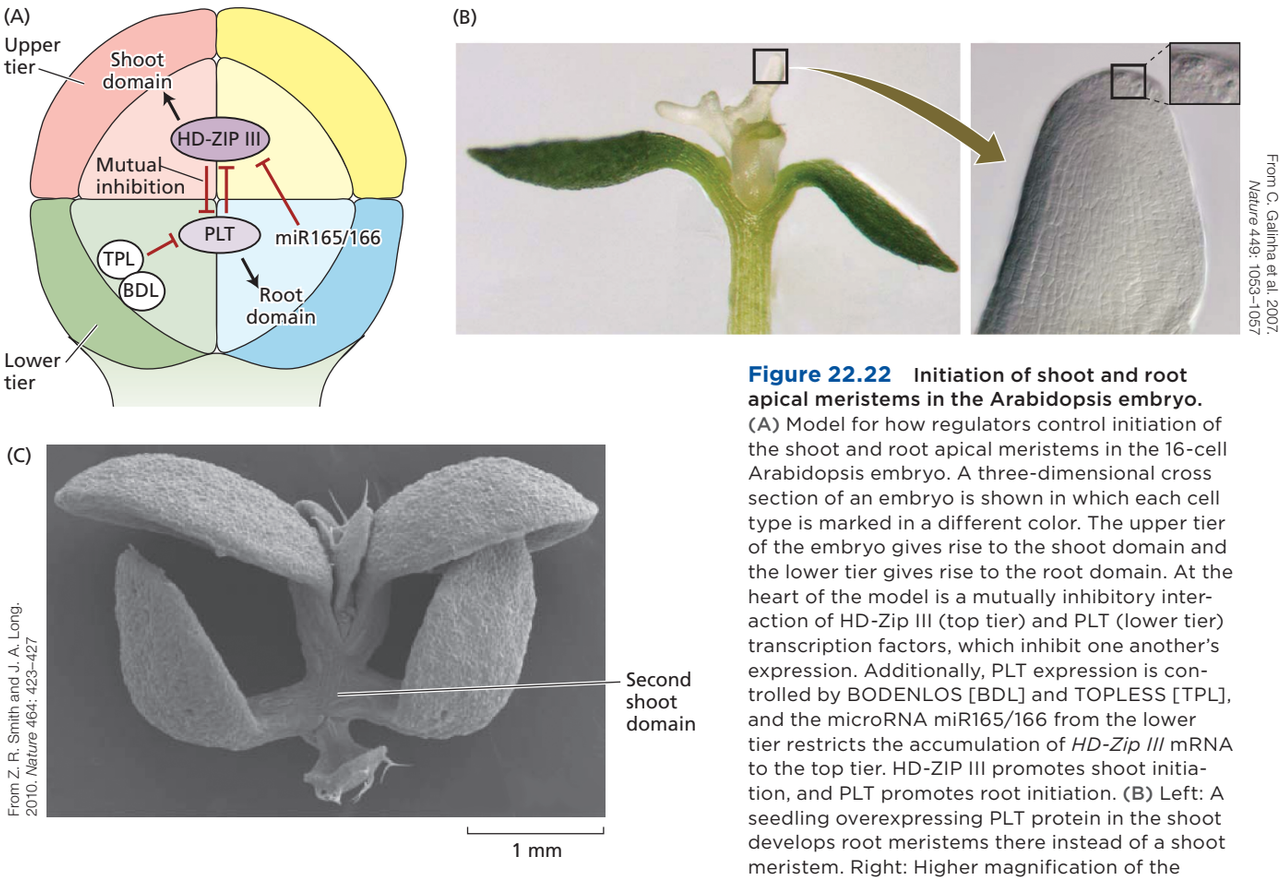


Figure 22.22 **Initiation of shoot and root apical meristems in the Arabidopsis embryo.** **(A)** Model for how regulators control initiation of the shoot and root apical meristems in the 16-cell Arabidopsis embryo. A three-dimensional cross section of an embryo is shown in which each cell type is marked in a different color. The upper tier of the embryo gives rise to the shoot domain and the lower tier gives rise to the root domain. At the heart of the model is a mutually inhibitory interaction of HD-Zip III (top tier) and PLT (lower tier) transcription factors, which inhibit one another's expression. Additionally, PLT expression is controlled by BODENLOS [BDL] and TOPLESS [TPL], and the microRNA miR165/166 from the lower tier restricts the accumulation of *HD-Zip III* mRNA to the top tier. HD-ZIP III promotes shoot initiation, and PLT promotes root initiation. **(B)** Left: A seedling overexpressing PLT protein in the shoot develops root meristems there instead of a shoot meristem. Right: Higher magnification of the boxed area in the left panel shows the presence of statoliths, a typical root characteristic. **(C)** A seedling overexpressing HD-Zip III in the lower tier of the embryo develops a second shoot domain. (A after J. Palovaara et al. 2016. *Annu. Rev. Cell Dev. Biol.* 32: 47–75.)

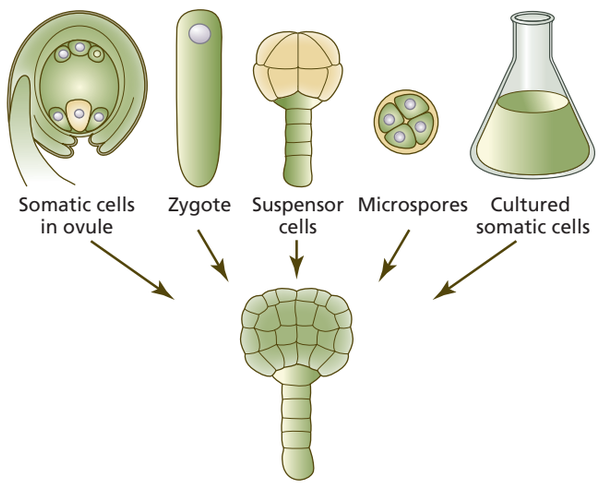


Figure 22.23 **Diverse sources of plant embryos.** In addition to the zygote, many different cells can give rise to plant embryos. The examples shown here are somatic cells in the ovule, suspensor cells, microspores, and cultured somatic cells. (After T. Radoeva and D. Weijers. 2014. *Trends Plant Sci.* 19: 709–716.)

often morphologically (nearly) indistinguishable from sexual, zygote-derived embryos. Embryogenesis can also be artificially induced. For example, artificial somatic embryogenesis, whereby embryos are induced to form from callus tissue following hormone treatments, is often used for plant propagation. Likewise, exposure of microspores to a stress, such as heat, can cause certain plant species to form embryos. Finally, alternative embryogenesis can occur within seeds. Suspensor cells, descendants of the basal cell produced by the first cell division of the zygote, normally become quiescent after a few rounds of cell division. If the embryo is damaged, however, suspensor cells can resume division and form a second embryo. Thus, given the right triggers, plant cells of many types can form embryos, attesting to the tremendous developmental potential of plant cells.

Summary

The sporophyte generation of plants begins with the fertilization events that initiate embryogenesis. Regulated cell divisions produce the polar axis and bilateral symmetry of the embryo. Both mobile and positional signals function as morphogenic regulators. An extended set of these regulatory mechanisms functions in the further elaboration of plant organs during postembryonic growth. Postembryonic plants retain meristems (initial cell niches) that are sites of undifferentiated cell division to provide for plastic or adaptive growth.

22.1 Embryogenesis in Monocots and Eudicots

- Embryogenesis differs between monocots and eudicots but also shares common features.
- Maize (a monocot) and Arabidopsis (a eudicot) represent opposite ends of a spectrum in embryological development, from the relatively complex and less predictable to the relatively simple and more predictable.

22.2 Establishment of Apical–Basal Polarity

- Among seed plants, the apical–basal polarity is established early in embryogenesis (**Figures 22.1–22.5**).

22.3 Mechanisms Guiding Embryogenesis

- Position-dependent mechanisms for determining cell fate guide embryogenesis (**Figure 22.8**).
- Arabidopsis mutants demonstrate that some process other than a fixed sequence of cell divisions must guide radial pattern formation (**Figure 22.9**).
- The potential for intercellular protein movement changes during development (**Figure 22.10**).
- Screens for embryo lethal and seedling defective mutants reveal genes that are essential for normal Arabidopsis embryogenesis (**Figures 22.11, 22.12**).

22.4 Auxin Signaling During Embryogenesis

- Auxin may function as a mobile chemical signal during embryogenesis (**Figures 22.13, 22.14**).

22.5 Radial Patterning During Embryogenesis

- Radial patterning guides formation of tissue layers (**Figure 22.15**).
- Two Arabidopsis genes establish normal epidermal identity (**Figure 22.16**).
- Different genes establish internal tissues, including the vasculature and cortex (**Figures 22.17–22.20**).

22.6 Formation of the Root and Shoot Apical Meristems

- During embryogenesis, initiation of shoot and root apical meristems is controlled by a mutually inhibitory interaction of HD-Zip III and PLT transcription factors (**Figures 22.21, 22.22**).
- Plant embryos can be derived from various types of cells (**Figure 22.23**).

Web Material

- **WEB TOPIC 22.1 Polarity of *Fucus* Zygotes**
  A wide variety of external gradients can polarize the growth of cells that are initially apolar.

For more study aids, go to oup.com/he/taiz7e.

Suggested Reading

Aichinger, E., Kornet, N., Friedrich, T. and Laux, T. (2012) Plant stem cell niches. *Annu. Rev. Plant Biol.* 63: 615–636.

Barlow, P. W. (1994) Evolution of structural initial cells in apical meristems of plants. *J. Theor. Biol.* 169: 163–217.

Dresselhaus, T., and Jürgens G. (2021) Comparative embryogenesis in angiosperms: Activation and patterning of embryonic cell lineages. *Annu. Rev. Plant Biol.* 72: 641–676.

Esau, K. (1965) *Plant Anatomy*, 2nd ed. Wiley, New York.

Hudson, A. (2005) Plant meristems: Mobile mediators of cell fate. *Curr. Biol.* 15: R803–R805.

Jenik, P. D., and Barton, M. K. (2005) Surge and destroy: The role of auxin in plant embryogenesis. *Development* 132: 3577–3585.

Laux, T., Wurschum, T., and Breuninger, H. (2004) Genetic regulation of embryonic pattern formation. *Plant Cell* 16 (Suppl): S190–S202.

Maule, A. J., Benitez-Alfonso, Y., and Faulkner, C. (2011) Plasmodesmata - Membrane tunnels with attitude. *Curr. Opin. Plant Biol.* 14: 683–690.

Miyashima, S., Sebastian, J., Lee, J.-Y. and Helariutta, Y. (2013) Stem cell function during plant vascular development. *EMBO J.* 32: 218–193.

Palovaara, J., de Zeeuw, T., and Weijers, D. (2016) Tissue and organ initiation in the plant embryo: A first time for everything. *Annu. Rev. Cell Dev. Biol.* 32: 47–75.

Poethig, R. S. (1997) Leaf morphogenesis in flowering plants. *Plant Cell* 9: 1077–1087.

Radoeva, T., Vaddepalli, P., Zhang, Z., and Weijers, D. (2019) Evolution, initiation and diversity in early plant embryogenesis. *Dev. Cell* 50: 533–543.

Raghavan, V. (1986) *Embryogenesis in Angiosperms*. Cambridge University Press, Cambridge, UK.

Sachs, T. (1991) Cell polarity and tissue patterning in plants. *Development* 113 (Supplement 1): 83–93.

Scheres, B., Wolkenfelt, H., Willemsen, V., Terlouw, M., Lawson, E., Dean, C., and Weisbeek, P. (1994) Embryonic origin of the Arabidopsis primary root and root meristem initials. *Development* 120: 2475–2487.

Scheres, B. (2013) Rooting plant development. *Development* 140: 939–941.

Silk, W. K. (1984) Quantitative descriptions of development. *Annu. Rev. Plant Physiol*. 35: 479–518.

Sparks, E., Wachsman, G., and Benfey, P. N. (2013) Spatiotemporal signalling in plant development. *Nat. Rev. Genet.* 14: 631–644.

Steeves, T. A., and Sussex, I. M. (1989) *Patterns in Plant Development*. Cambridge University Press, Cambridge, UK.

23 Plant Senescence and Developmental Cell Death



schankz/Shutterstock

Every autumn, people living in temperate climates enjoy the spectacular color changes that can precede the falling of leaves from deciduous trees. Autumn leaves turn yellow, orange, or red and fall from their branches in response to shorter day lengths and cooler temperatures, which trigger two related developmental processes: senescence and abscission (**Figure 23.1**). Senescence is the last developmental stage, ultimately leading to the death of targeted tissues, and it can be distinguished from the related term *necrosis* in several ways. **Senescence** is the age-dependent disassembly and degeneration process of cells, organs, or organisms that is controlled by the interaction of environmental factors with genetically regulated developmental programs. **Necrosis**, despite having some overlap with senescence, is usually defined as non-programmed cell death that is directly caused by physical damage, poisons (such as herbicides or toxins released by pathogens), or nonphysiological conditions, such as temperature or anoxia. **Abscission** refers to the separation of cell layers that occurs at the bases of leaves, floral parts, and fruits, which allows them to be shed easily without damaging the plant.

In plants, senescence at the cellular level involves genetically encoded and actively controlled cellular suicide, otherwise known as **programmed cell death** (**PCD**). PCD is induced as an intrinsic part of regular development in specific cell types or tissues, and can also be triggered by abiotic and biotic stresses (**Figure 23.2**). Different forms of PCD play crucial roles in development, immunity, and response to the environment.

Organ senescence (the senescence of whole leaves, branches, flowers, or fruits) occurs at various stages of vegetative and reproductive development and typically includes abscission of the senescing organ. The importance of organ senescence to plant fitness is easily seen in leaf senescence. In annual plants, leaf senescence serves as a means to disassemble and release the nutrients accumulated during the growth phase and to relocate them to developing seeds for the next generation. In trees, the nutrients disassembled during leaf senescence are relocated and stored in stems or roots in preparation for the next season. Senescence in other organs (e.g., petals) is described in **WEB TOPIC 23.1**.



Chuck Savage/Getty Images

Figure 23.1 Fall colors along Blue Ridge Parkway in Virginia. The combination of several deciduous tree species (e.g., dogwood, red maple, sugar maple, and sorrel trees) produces a wide range of hues.

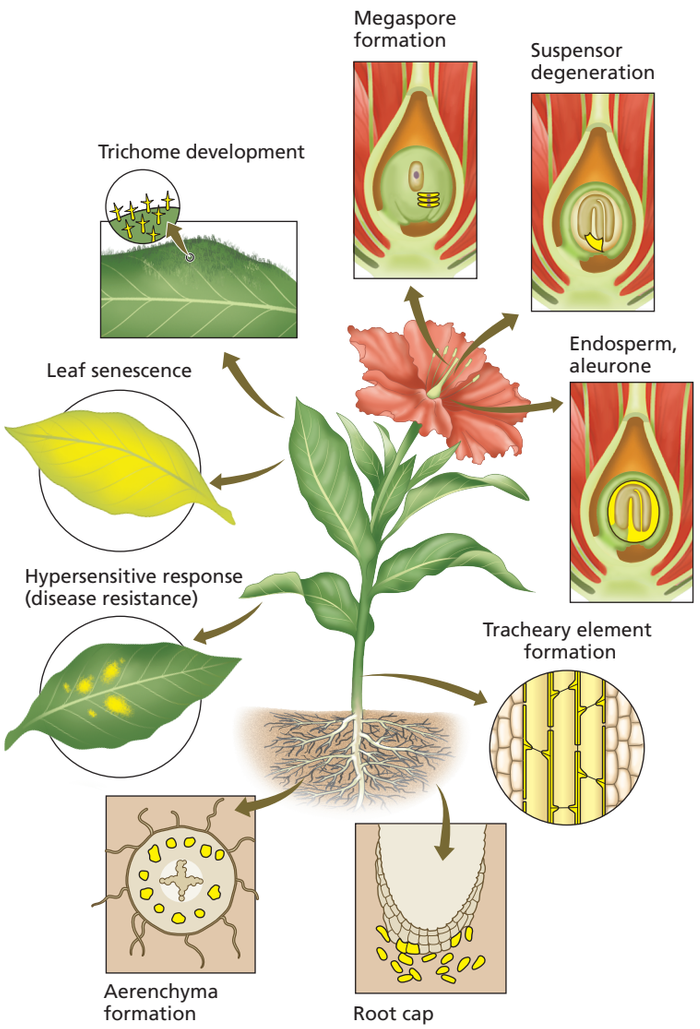


Figure 23.2 Programmed cell death (PCD) is a normal part of the plant life cycle that occurs in a wide range of developmental processes and responses to environmental signals and pathogens. Cells and tissues that undergo PCD are highlighted in yellow here.

Whole-plant senescence, when the entire plant senesces and dies, differs from aging in animals and is much more variable. For example, individual plant life spans may range from a few weeks for some desert annuals to as long as 4600 years for bristlecone pine. Clonal perennial plants can live even longer. Because of the presence of continuously dividing apical meristems, plants could potentially live forever, yet all apical meristems eventually fail and the plant dies.

We begin this chapter with a brief overview of the features of and mechanisms responsible for cell death in plants. We then introduce the various forms of PCD, including senescence-associated cell death, and discuss how a key process, autophagy, is involved in plant cell death. Next we turn to senescence at the organ level, focusing on leaf senescence and abscission and describing the mechanism of orderly degeneration during leaf senescence and its regulation by developmental and environmental signals. Finally, we discuss the factors that govern the two different types of whole-plant senescence: monocarpic and polycarpic senescence.

23.1 Programmed Cell Death

All eukaryotic organisms have evolved mechanisms of programmed cell death. In multicellular plants and animals, the organized destruction of cells is required for normal growth and development and for the removal of unwanted, damaged, or infected cells. PCD can be initiated by specific developmental signals or by potentially lethal events, such as pathogen attacks or errors in DNA replication during cell division. It involves the expression of a characteristic set of genes that orchestrates the dismantling of cellular components and ultimately causes cell death.

PCD, sometimes referred to as **apoptosis** (Greek for "falling off") or **autolysis**, involves the controlled activities of endonucleases, ribonucleases, bifunctional nucleases, and proteases in the cell undergoing the process. Endonucleases digest the chromosomes, producing fragments that form a "ladder" when the DNA is size-separated by gel electrophoresis. A wide variety of proteases, including caspase-like cysteine

endopeptidases, serine proteases, phytepsin aspartyl proteases, metalloproteases, and the ubiquitin–proteasome complex, degrade cellular proteins and accelerate their turnover rates.

Distinct types of PCD occur in plants

Various forms of PCD have been shown to be an intrinsic part of normal plant development, as well as responses to biotic and abiotic stresses. Developmental PCD functions to eliminate senescing or no-longer-required cells, or to generate tissues composed of modified cell "corpses" that retain structural or storage functions when dead. This process occurs during gametophyte maturation, degeneration of embryo suspensor cells, formation of xylem tracheary elements, root development, and senescence (see Figure 23.2). Although **senescence-associated cell death** is a form of developmental PCD, it has many distinct features. During senescence, PCD occurs over broad areas of plant organs and at a relatively slow rate, whereas other types of developmental PCD involve rapid and localized cell death. The slow progression of PCD in senescing leaf cells appears to be required to allow sufficient time for remobilization of nutrients and their translocation to other parts of the plant. Optimal reallocation of nutrients accumulated during the growing season is critical for plant fitness and requires precise control of senescence-associated cell death.

The hypersensitive response and other forms of pathogen-triggered PCD play prominent roles in plant biotic defense responses and are distinct from developmental PCD. The types of PCD involved in responses to abiotic and biotic stresses are discussed in detail in Chapters 15 and 24, respectively.

Developmental PCD and pathogen-triggered PCD involve distinct processes

The two broad types of PCD in plants differ not only in function but in the associated molecular and cytological processes. Plant cells are fundamentally different from animal cells in that they are surrounded by rigid cell walls. Because of the presence of the cell wall, and thus the absence of phagocytes (i.e., animal cells specialized for engulfing and digesting cells targeted for destruction), the cytological changes that occur during apoptosis in animals seldom, if ever, occur in plants. Instead, ultrastructural studies have led to the identification of two plant-specific cytological pathways of PCD: the vacuolar type associated with developmental PCD and the hypersensitive response-type associated with pathogen-triggered PCD (**Figure 23.3**).

Vacuolar-type PCD occurs during normal development and reflects the fact that the large central vacuole is the main repository of proteases, nucleases, and other lytic enzymes. The cytological changes associated with tracheary element differentiation, during which cells undergo vacuolar-type PCD, are illustrated in Figure 23.3A. Before PCD commences, however, hormones such as methyl jasmonate (MeJA), ethylene, auxin, and strigolactones help prime the cells for PCD. Hormone signaling directs transcriptional reprogramming, leading to the activation of developmental PCD genes (e.g., genes encoding proteases and nucleases). For example, in Arabidopsis a member of the NAC transcription factor family (TF), a regulator of leaf senescence, induces the enzyme BIFUNCTIONAL NUCLEASE 1 (BFN1), which degrades DNA and RNA. During developmental PCD, the vacuolar membrane, or tonoplast, ruptures and releases the vacuolar contents, including several proteases. For example, the Arabidopsis cysteine proteases XYLEM CYSTEINE PEPTIDASE 1 (XCP1), XCP2, and METACASPASE 9 (MC9) have been shown to promote cytoplasmic clearance in differentiating tracheary elements.

After hormones have primed cells for developmental PCD, the process may be initiated by various second messengers, including a rise in the Ca^{2+} concentration, the accumulation of reactive oxygen species (ROS), or a drop in intracellular pH. During vacuolar-type PCD, the vacuole swells and either permeabilizes or ruptures, releasing hydrolases into the cytosol and causing large-scale degradation. The cytosol and all its organelles, as well as the plasma membrane, are completely broken down, and in many cases the cell wall is either partially or completely digested as well, as in endosperm tissue. Cell wall degradation does not occur in cells that have acquired lignified secondary cell walls during the process, such as tracheary elements and fibers. (Senescence-associated cell death involving vacuolar-type PCD is described in **WEB TOPIC 23.2**.)

Hypersensitive response-type PCD is induced by a range of abiotic stresses or by detection of a pathogen during the hypersensitive response (see Chapter 24). Cytological hallmarks that distinguish hypersensitive response-type PCD from vacuolar-type PCD include vacuolar water loss and cell shrinkage (see Figure 23.3B). Because the contents of the vacuoles are not released into the cytoplasm during this type of PCD, the corpses of necrotic cells remain largely unprocessed. Hypersensitive response-type PCD will be discussed in greater detail in Chapter 24.

The autophagy pathway captures and degrades cellular constituents within lytic compartments

Cells, like complex machines, experience wear and tear over time, and parts need to be replaced on an ongoing basis to extend the cells' life spans. **Autophagy** (from the Greek words meaning "self-eating") was first characterized in animal cells as the catabolic mechanism that delivers cellular components to lysosomes, where they are

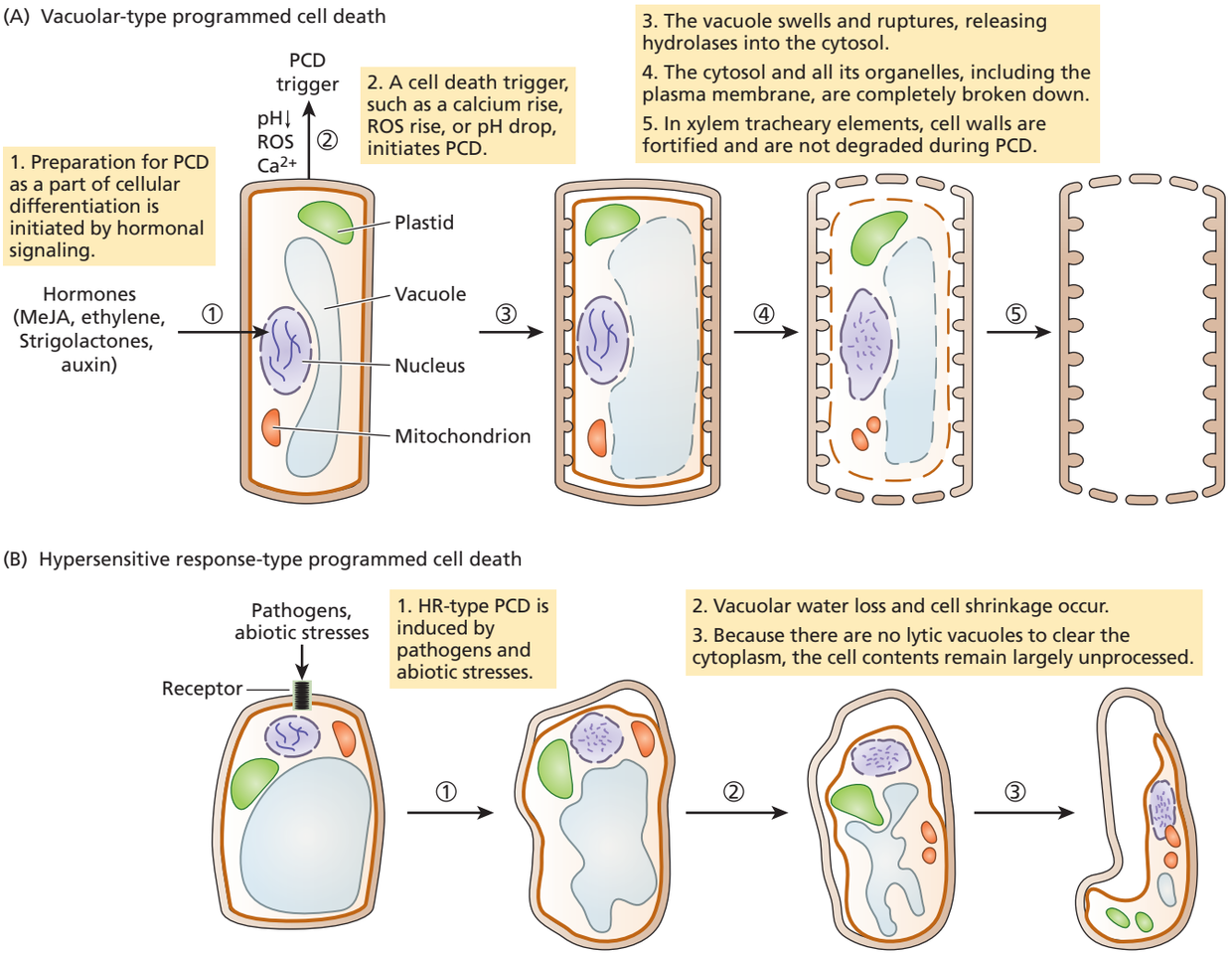


Figure 23.3 **Two types of programmed cell death in plants.** **(A)** Vacuolar-type PCD, also referred to as developmental PCD, is exemplified here by xylem tracheary element differentiation. Preparation for PCD as a part of cellular differentiation is mediated by hormonal signaling. However, PCD is executed only in response to a cell death trigger, such as an increase in the Ca^{2+} or reactive oxygen species (ROS) concentration or a decrease in pH. In xylem tracheary elements, the early stages of PCD involve simultaneous deposition of secondary cell wall and swelling of the vacuole. As PCD progresses, the tonoplast breaks down, releasing hydrolases that digest the cellular contents. **(B)** Hypersensitive response-type PCD occurs in leaves in response to microbial attack or abiotic stresses. The vacuole loses water, resulting in marked cell shrinkage, contraction from the cell wall, and nuclear DNA degradation. Continued water loss from the cytosol leads to the breakdown of the plasma membrane and the release of residual cellular contents into the apoplast. MeJA, methyl jasmonate.

degraded. Autophagy protects the cell from the harmful or lethal effects of damaged or unnecessary proteins and organelles. During starvation, the autophagic breakdown and recycling of cellular components also ensure cellular survival by maintaining cellular energy levels.

In autophagy, the endoplasmic reticulum (ER) first gives rise to a cup-shaped, membranous cisterna called the **phagophore** (**Figure 23.4**). In animals, the phagophore has been shown to form at a specialized site on the ER. The early phagophore then acquires additional membrane lipids, expands, and pinches off from the ER. The expansion and fusion of the phagophore enable it to engulf cytoplasmic components targeted for destruction, which includes misfolded proteins, ribosomes, ER, and mitochondria. The phagophore becomes spherical, and the inner and outer phospholipid bilayers fuse to form the completed **autophagosome**, which is surrounded by a double membrane. In plants, the outer membrane of the autophagosome fuses with the tonoplast. In the process, a single-membrane vesicle called the **autophagic body** enters the vacuole and is degraded (see Figure 23.4). The monomers (amino acids, sugars, nucleosides, etc.) generated by hydrolytic breakdown of the autophagic body are returned to the cytosol for reuse, either as an energy source or as building blocks for new cellular structures.

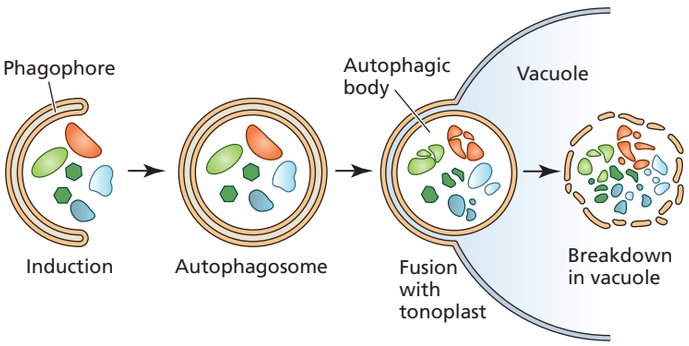


Figure 23.4 Autophagosome formation in plants. Autophagosome biogenesis begins with the formation of a cup-shaped double-membrane structure called a phagophore. The edges of the phagophore grow and engulf cargo (macromolecules and organelles). The edges then fuse, forming a double-membrane vesicle called the autophagosome. Some digestion occurs within the autophagosome during its transit toward the vacuole. Upon reaching the vacuole, the outer membrane of the autophagosome fuses with the tonoplast, and the remaining cargo enters the vacuole within a single-membrane vesicle (autophagic body), which can then be degraded by lytic enzymes.

Autophagy plays a dual role in the regulation of plant PCD

Although they have long been studied as separate processes, autophagy and PCD both play central roles in plant immunity and development. Genetic and biochemical studies have indicated that autophagy is a crucial regulator of PCD.

Autophagy was initially thought to be a mechanism for cell survival during plant immune responses (see Chapter 24). A typical hypersensitive response produces a small region of dead tissue at the site of pathogen infection (**Figure 23.5**). However, mutations of autophagy-related (ATG) genes caused the symptoms of cell death to spread far beyond the site of infection following a 14-day incubation with an avirulent strain of the bacterial pathogen *Pseudomonas syringae*. This phenotype suggests that autophagy helps suppress the spreading of hypersensitive response-type PCD.

Counterintuitively, another aspect of the *atg* mutant phenotype supports a pro-death function for autophagy. Despite there being more extensive necrosis in *atg* mutants, they had smaller areas of hypersensitive response-type PCD at the primary infection sites (see Figure 23.5). Additional evidence for the pro-death function of autophagy comes from the analysis of transgenic Arabidopsis lines displaying enhanced autophagic activity because of overexpression of the small GTP-binding protein RabG3b, a component functioning in autophagosome formation. When RabG3b-overexpressing plants were inoculated with the avirulent bacteria, PCD was significantly accelerated at the primary infection sites compared with the wild type and expanded rapidly into surrounding non-infected tissue within 2 days (unrestricted

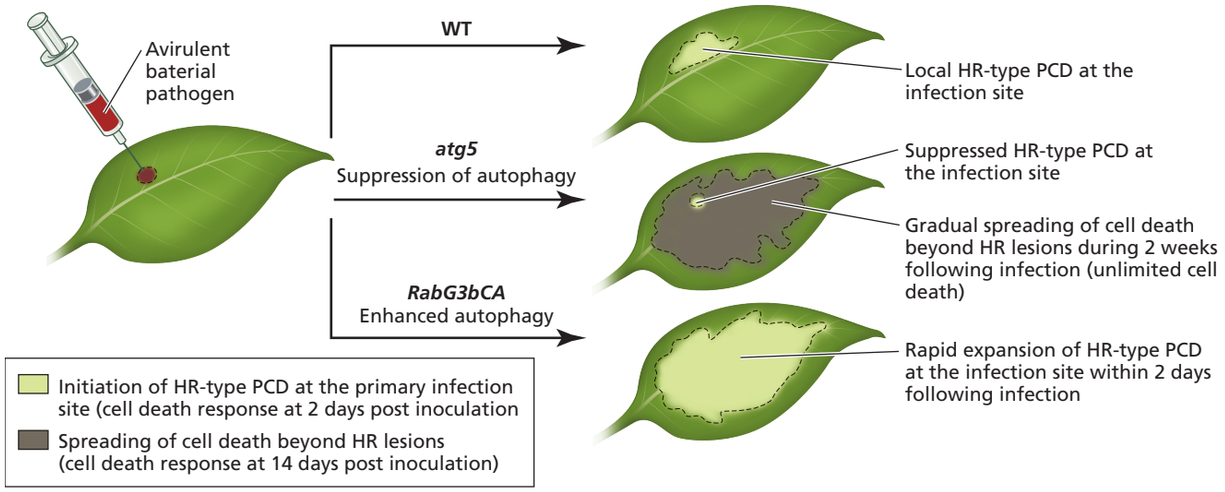
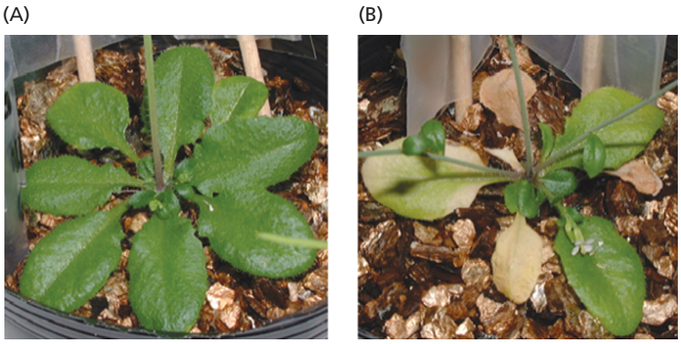


Figure 23.5 Autophagy plays dual roles in the regulation of plant PCD. In wild-type (WT) plants, inoculation with an avirulent pathogen (*Pseudomonas syringae* DC3000, *AvrRpm1*) induced hypersensitive response-type (HR-type) PCD at the infected leaf site. Compared with the WT, the autophagy-deficient *atg5* mutant showed suppressed HR-type PCD, and RabG3b-overexpressing (RabG3bCA) plants, which have enhanced autophagy, had greatly expanded HR lesions that developed within 2 days of inoculation. These phenotypes support a pro-death role for autophagy in pathogen-induced PCD. However, over 2 weeks following inoculation, the *atg5* mutant gradually developed chlorotic cell death at uninfected sites, suggesting a distinct pro-survival role for autophagy. (After S. I. Kwon et al. 2013. *Plant Physiol.* 161: 1722–1736.)

hypersensitive response-type PCD). The rapid spreading of PCD in the RabG3b overexpression lines was quite different from the slowly progressing cell death observed in leaves of *atg* mutants (see Figure 23.5). Taken together, the evidence makes it clear that autophagy plays a dual role in pathogen-triggered PCD: It acts as a pro-death mechanism by initiating the hypersensitive response at the primary infection site, and plays a pro-survival role by suppressing the spread of cell death beyond the localized hypersensitive response lesions.

During embryogenesis, autophagy may be required for the normal differentiation of some types of cells. The role of autophagy in developmental PCD has been studied in somatic embryos of Norway spruce. Suppression of ATG5 or ATG6 did not inhibit cell death, but it impaired the formation of a morphologically normal suspensor. The impaired suspensor phenotype is caused by an alteration in the way the cells die, causing a switch from vacuolar cell death, which is associated with gradual but complete cell clearance, to rapid cell death with typical signs of necrosis. The changes in the mode of cell death in *atg* mutants imply that autophagy plays an ongoing role in developmental PCD, rather than simply acting as an initiator. Cell disassembly during vacuolar PCD is highly ordered and regulated, which requires the maintenance of cellular activity to prevent necrosis. Autophagy is likely to be involved by allowing growth of the vacuole as well as by providing terminally differentiated cells with substrates for energy metabolism during developmental PCD. This would account for the fact that suppression of autophagy during somatic embryo development leads to necrosis.



From D. C. Bassham et al. 2006. *Autophagy* 2: 2–11

Figure 23.6 **Phenotype of wild-type Arabidopsis and the autophagy-defective mutant *atg4a4b-1*.** (A) Wild-type rosette leaves. (B) Autophagy-defective mutant rosette leaves exhibiting accelerated senescence.

Autophagy is required for nutrient recycling during plant senescence

In non-senescing cells, autophagy serves as a homeostatic mechanism that maintains the metabolic and structural integrity of the cell. The inhibitory role of autophagy on plant senescence was demonstrated by means of genetic analysis. As shown in **Figure 23.6**, Arabidopsis mutants with defective autophagy exhibit accelerated leaf senescence. Further molecular and biochemical studies revealed that during leaf senescence, enhancement of autophagy facilitates the degradation and clearance of toxic and damaged cellular components. The recycled cell material is then used to remobilize nutrients throughout the plant. Therefore, as in other types of PCD, autophagy appears to play both pro-death and pro-survival roles during plant senescence. These antagonistic roles sustain the life of senescing cells by maintaining cellular energy levels and promoting the controlled degradation of cell constituents. The tight balance between these two effects enables the efficient recycling and remobilization of nutrients as long as possible before cell death.

23.2 The Leaf Senescence Syndrome

All leaves, including those of evergreens, undergo senescence—whether in response to age-dependent factors, environmental cues, biotic stress, or abiotic stress. In nature, the leaf senescence syndrome is typically observed in the autumn leaves turning from green to yellow, orange, or red in trees and other perennial plants. Annual plants such as grain crops also undergo leaf senescence as part of whole-plant-level senescence at the grain-filling stage.

Senescence in animal cells primarily refers to mitotic (or replicative) senescence—that is, loss of the capacity for further cell division upon aging. In contrast, leaf senescence is postmitotic senescence, in which a degenerative process occurs after cellular maturation or differentiation and leads to cell death. Leaf senescence is a specialized form of PCD that allows the efficient remobilization of nutrients from the source leaf to growing vegetative or reproductive sinks via the phloem. As is the case for the other examples of PCD shown in Figure 23.2, leaf senescence is an evolutionarily selected process that contributes to the overall fitness of the plant.

Leaf senescence occurs even under optimal growth conditions as part of the plant's normal developmental program. However, it can be induced prematurely by environmentally adverse conditions such as abiotic and biotic stresses (see Chapters 15 and 24), which can shorten the lifetime of the entire plant or its individual organs. During unfavorable conditions, leaf senescence can serve as a survival mechanism as well. For example, a diseased leaf may senesce, die, and fall off the plant, thus helping prevent the spread of disease. Similarly, nitrogen deficiency, light limitation, and water-deficit



Courtesy of Andreas M. Fischer

Figure 23.7 Sequential leaf senescence of wheat stems showing a gradient of senescence from the older leaves at the base to the younger leaves near the tip.

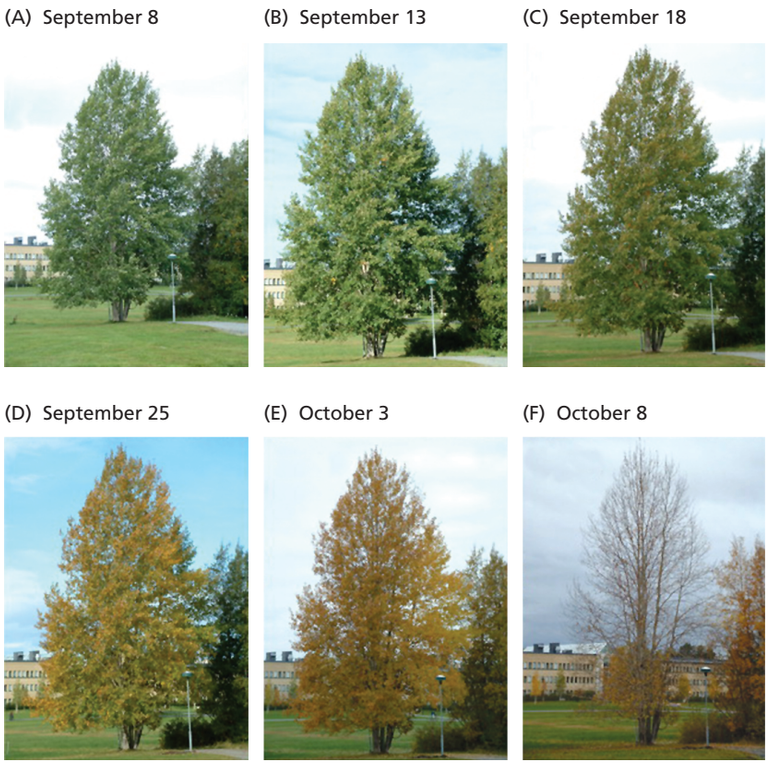
stress can induce the onset of senescence, which may result in early seed development and a shortened plant life span. Therefore, it is obvious that multiple pathways responding to environmental factors exist and are interconnected with endogenous developmental programs. In eudicots, senescence is usually followed by abscission, which is the process that enables plants to shed senescent leaves from the plants. Together, the coupled programs of leaf senescence and abscission help optimize the photosynthetic and nutrient-use efficiency of the plant.

Leaf senescence may be sequential, seasonal, or stress-induced

Leaf senescence under normal growth conditions is governed by the developmental age of the leaf and is a function of hormones and other regulatory factors. Under these circumstances there is usually a senescence gradient from the youngest leaves near the growing tip to the oldest leaves near the base of the shoot—a pattern known as **sequential leaf senescence** (**Figure 23.7**). In eudicots, such age gradients can be seen within individual leaves as well. Cells in the leaf tip emerge earlier from the leaf primordium and are therefore older compared with cells at the leaf base. In many monocots, particularly grasses, the intercalary meristem continues to produce new fully differentiated leaf tissue at the base of the leaf until the leaf reaches its full size.

In contrast to sequential leaf senescence, the leaves of deciduous trees in temperate climates senesce all at once in response to the shorter days and cooler temperatures of autumn—a pattern known as **seasonal leaf senescence** (**Figure 23.8**). Both sequential and seasonal leaf senescence are variations of developmental senescence because they occur under normal growing conditions.

The morphological changes associated with stress-induced leaf senescence differ from those of developmental leaf senescence. As noted earlier, in developmentally senescing leaves, senescence is coordinated at the whole-leaf level, starting at the leaf tips or margins and spreading toward the leaf base (see Figure 23.7). Environmental stress, by contrast, may occur at specific sites on a leaf. When such localized stress occurs, the stressed tissue senesces earlier than the unstressed tissue. Mineral nutrient stress can also alter sequential leaf senescence (see Chapter 7).



From J. Keskitalo et al. 2005. *Plant Physiol.* 139: 1635–1648

Figure 23.8 Seasonal leaf senescence in an aspen tree (*Populus tremula*). All of the leaves begin to senesce in late September and undergo abscission in early October.

Leaves undergo massive structural and biochemical changes during leaf senescence

During senescence, leaf cells are subject to a dramatic transition in cellular metabolism and an orderly degradation of cellular structures. Chloroplasts are the first organelles to be targeted for breakdown (**Figure 23.9**). Chloroplast degeneration begins with chlorophyll breakdown, the first visible symptom of senescence. Protein and RNA degradation parallels the loss of photosynthetic activity, releasing nutrients, such as nitrogen, phosphorus, metal ions, and minerals, that are transferred out of the leaf.

In senescing leaves, anabolic activities such as protein synthesis generally decline, which can be observed as a decline in the number of polysomes and ribosomes during the early stages of leaf senescence. Consistent with the decrease in protein synthesis, the synthesis of rRNAs and tRNAs also decreases during leaf senescence. Concurrently, catabolic activities increase, including the hydrolysis of macromolecules, such as proteins, lipids, nucleic acids, and pigments. Chloroplasts contain about 70% of the total leaf protein, most of which consists of Rubisco localized in the stroma, and light-harvesting chlorophyll-binding protein II (LHCP II) associated with the thylakoid membranes (see Chapters 9 and 10). Senescence-associated stromal and vacuolar proteases play key roles in chloroplast protein degradation. Catabolism and remobilization of chloroplast proteins are thus the primary source of amino acids and nitrogen for sink organs. A variety of lipid-degrading enzymes, including phospholipase D, phosphatidic acid phosphatase, and lipoxygenase, are involved in hydrolysis and metabolism of membrane lipids. The increased activity of RNases during leaf senescence combined with the decline in RNA biosynthesis results in a massive decrease in total RNA levels.

Like the chloroplasts, other organelles, such as the peroxisome, also undergo biochemical changes as senescence proceeds. In contrast, the nucleus and mitochondria remain intact until the later stages of senescence. This reflects the need for leaf cells to maintain gene expression and energy production to properly complete the senescence program. However, chromatin condensation and DNA laddering, typical symptoms of PCD, are eventually observed in senescing leaves. The leaf cells finally undergo disintegration of the plasma and vacuolar membranes, leading to disruption of cellular homeostasis and death.

The autolysis of chloroplast proteins occurs in multiple compartments

The degradation of chloroplast proteins during senescence involves both plastid-localized enzymes, including proteases, as well as other proteolytic systems outside the chloroplasts. For example, the breakdown of Rubisco and other stromal proteins occurs mainly outside the chloroplast via two kinds of autophagic structures: the **Rubisco-containing bodies** (**RCBs**) and **senescence-associated vacuoles** (**SAVs**) (**Figure 23.10**). A major difference between these two structures is that RCBs use the autophagy machinery, whereas SAVs do not. RCBs are surrounded by a double membrane and are thought to be formed when vesicles bud off from the senescing chloroplast, thus shrinking its size. Newly formed RCBs, which contain only Rubisco and other stromal enzymes, are enclosed by autophagosomes that deliver their contents to the vacuole for subsequent degradation. In contrast, SAVs are small, protease-rich, acidic vacuoles that increase in number during senescence in leaf mesophyll and guard cells, but not in the nongreen epidermal

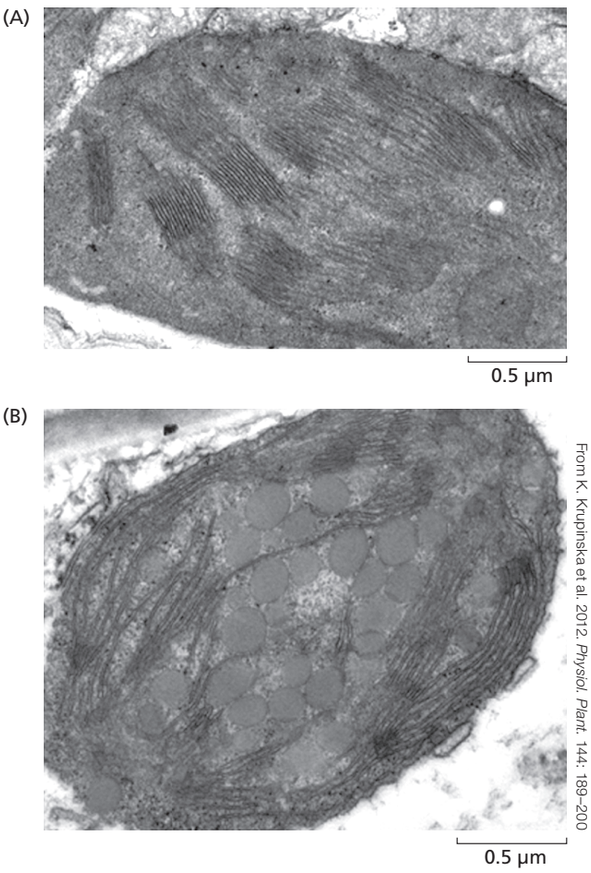


Figure 23.9 Ultrastructure of chloroplasts and gerontoplasts in mesophyll cells of barley leaf. Chloroplasts before senescence (A) and gerontoplasts from leaves in which about 50% of the chlorophyll has been lost (B). During leaf senescence, chloroplasts are transformed into gerontoplasts, showing the progressive unstacking of grana and the loss of thylakoid membranes. The structural dismantling of the grana in gerontoplasts is accompanied by a decline in the primary photochemical reactions and in the efficiency of the Calvin–Benson cycle enzymes.

cells. Like RCBs, SAVs contain Rubisco and other stromal enzymes, and can degrade them directly, although they may also fuse with the central vacuole. RCBs and SAVs reduce the size of the senescing chloroplast and degrade stromal proteins, but they are not involved in the breakdown of the chloroplast membranes. Residual chloroplasts are transported into the central vacuole via an ATG4-dependent process.

It is likely that the early stages of chloroplast protein breakdown occur inside the chloroplast. Chloroplasts contain several ATP-dependent proteases of the *Clp* (*Caseinolytic protease*) and *FtsH* (*Filamentation temperature-sensitive H*) gene families, which are required for chloroplast development. Some of these proteases are specifically up-regulated during leaf senescence, although their precise roles in senescence remain unknown. In addition, isolated chloroplasts can partially degrade Rubisco in vitro, suggesting that chloroplast proteases participate in the early stages of the leaf senescence.

The STAY-GREEN (SGR) protein is required for both LHCP II protein recycling and chlorophyll catabolism

As discussed in Chapter 9, chlorophyll is tightly bound in complexes with proteins. During senescence these

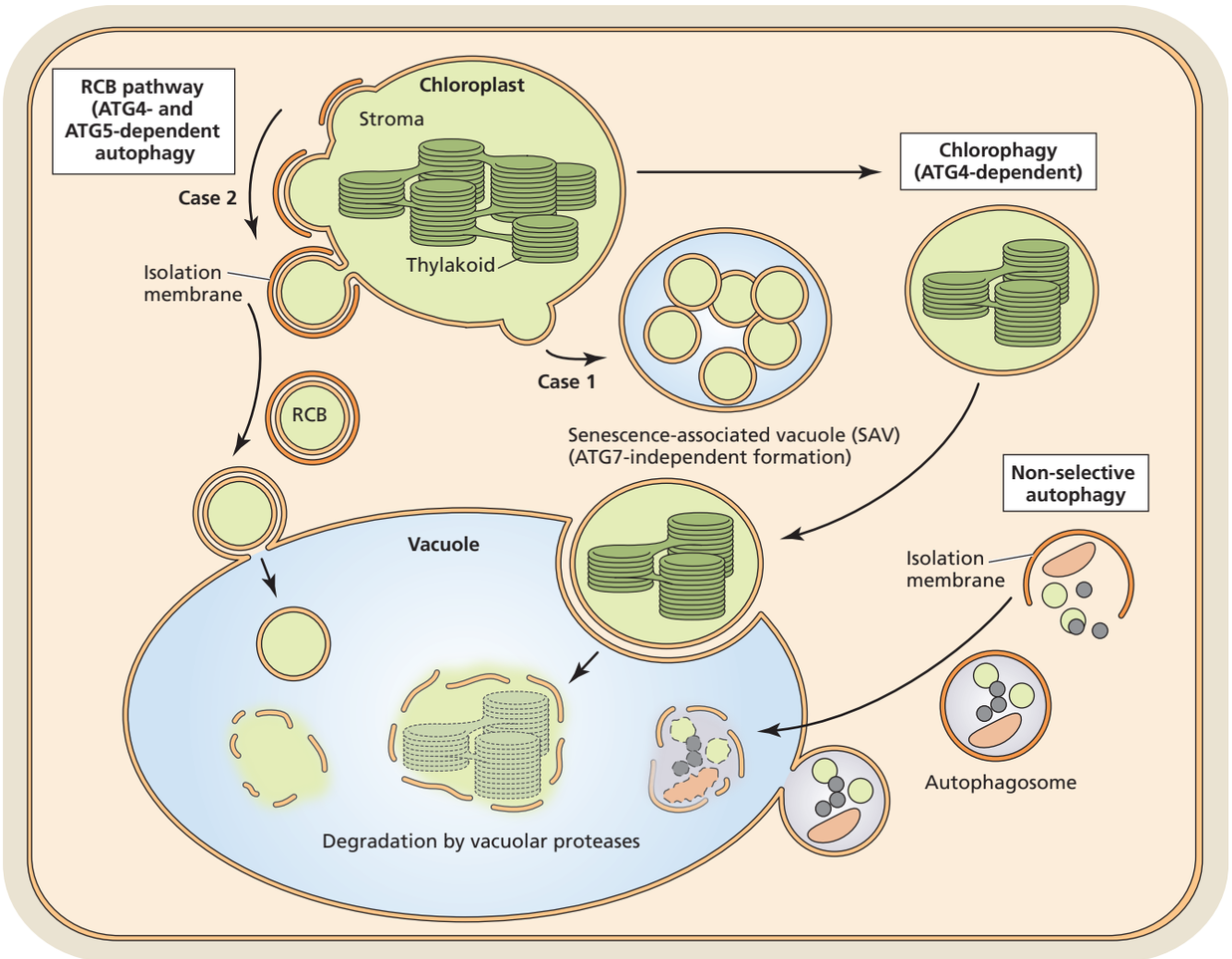


Figure 23.10 Pathways for vacuolar degradation of chloroplasts and their proteins. Chloroplasts can be selectively degraded via several different pathways. In the Rubisco-containing body (RCB) pathway, a chloroplast protrusion is sequestered by an isolation membrane to form an autophagosome specifically containing stromal proteins enclosed by a chloroplast envelope. The resulting RCB is transported into the central vacuole by ATG4- and ATG5-dependent autophagy and degraded by vacuolar proteases. Alternatively, stromal proteins may be transported via vesicles to a senescence-associated vacuole (SAV) (Case 1) or enter a SAV by sequestration of a part of the chloroplast (Case 2). The remaining chloroplast, shrunken by the production of RCBs and SAVs, is then transported into the central vacuole via an ATG4-dependent pathway (chlorophagy). (After H. Ishida et al. 2014. *Biochim. Biophys. Acta. Bioenerg.* 1837: 512–521.)

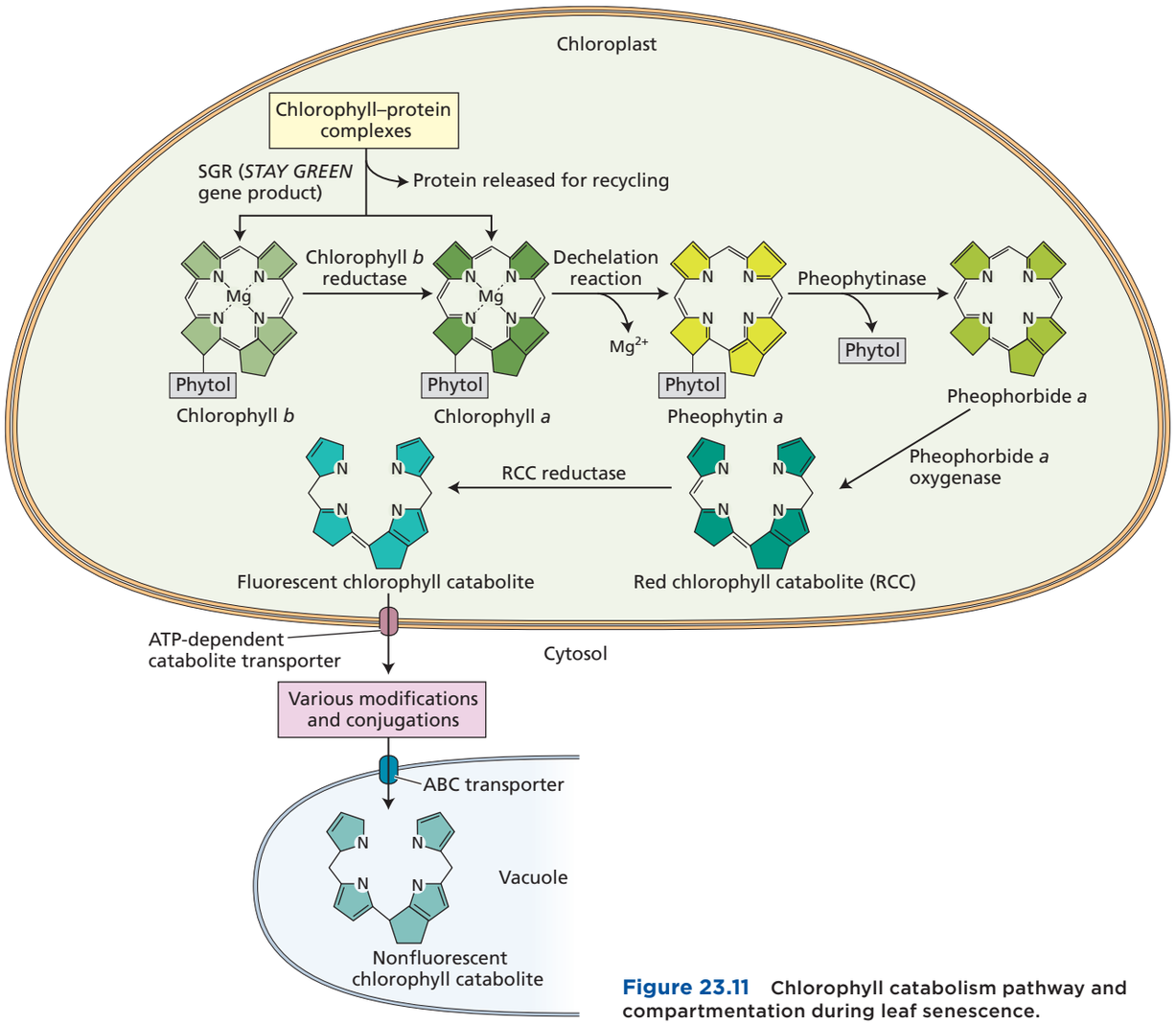


Figure 23.11 Chlorophyll catabolism pathway and compartmentation during leaf senescence.

chlorophyll–protein complexes must be dismantled to allow chlorophyll and the apoproteins to be recycled. STAY-GREEN (SGR) is a chloroplast protein that appears to act by destabilizing chlorophyll–protein complexes and is thought to be required for the proteolysis of LHCP II within the chloroplast. Mutants deficient in SGR stay green during senescence because chlorophyll cannot be catabolized when it is complexed to protein. The *green cotyledon* phenotype in Gregor Mendel's classic crossing experiments with peas (*Pisum sativum*) was caused by a mutation in the *SGR* gene. Despite their ability to retain their chlorophyll, *sgr* mutants exhibit the same decline in photosynthetic efficiency during senescence as wild-type plants do, because the turnover of the soluble proteins of the stroma is unaffected by the mutation. Destabilization of chlorophyll–protein complexes by SGR, perhaps aided by partial proteolytic cleavage, releases LHCP II proteins for autolysis. The liberated chlorophyll molecules are then partially catabolized in the plastid and exported to the cytosol for further modification, before being permanently stored in the vacuole (**Figure 23.11**). Chlorophyll is broken down in a multistep biochemical pathway comprising a set of chlorophyll catabolic genes (CCGs) (see **WEB TOPIC 23.3**).

23.3 Regulation of Leaf Senescence: A Multi-Layered Network

The transition from a mature, photosynthetically active leaf to a senescing leaf is a major phase change that requires the massive reprogramming of gene expression. A global analysis of gene expression in Arabidopsis has identified thousands of genes whose transcript levels are increased during leaf senescence. Up-regulated genes

are termed **senescence-associated genes** (**SAGs**), and among the earliest of these to be up-regulated are those encoding TFs required for the expression of other SAGs. Genes whose expression is suppressed by senescence are called **senescence down-regulated genes** (**SDGs**). A comparison of metabolic pathways that are either stimulated (by SAGs) or repressed (by SDGs) during sequential leaf senescence in Arabidopsis is shown in **Figure 23.12**. SAGs include many genes associated with abiotic and biotic stresses, such as autophagy, the response to reactive oxygen species (ROS), metal ion binding, pectinesterase (cell wall breakdown), lipid breakdown, and genes involved in abscisic acid (ABA), MeJA, and ethylene hormonal signaling (see Chapter 4).

Since senescence can have both internal and external causes, the question arises whether stress-related leaf senescence involves the same metabolic pathways and genetic programs as developmental leaf senescence. Comparisons have been made between the gene expression patterns of Arabidopsis leaves treated with a variety of abiotic stresses and those of naturally senescing leaves. At the earliest stages of treatment, the gene expression patterns of the stressed leaves were distinct from those of naturally senescing leaves. However, by the time the leaves had begun to yellow, the two sets of data converged. These findings suggest that abiotic stress initially involves specific stress-related signal transduction pathways, but that the stress-induced pathways overlap with the developmental senescence pathway once PCD begins.

Leaf senescence depends on the comprehensive regulation of pathways that respond to endogenous and environmental factors

Extensive molecular genetic studies have identified many key regulatory molecules and signaling pathways that play important roles in leaf senescence, including transcription regulators, receptors and signaling components for hormones and stress responses, and regulators of metabolism. An overview of the signaling pathways and regulatory networks involved in regulating leaf senescence is shown in **Figure 23.13**. More recently, numbers of omics and systems analyses of leaf senescence have significantly expanded our knowledge of the highly complex regulatory mechanisms underlying leaf senescence and how they are fine-tuned at the chromatin, transcriptional, posttranscriptional, translational, and posttranslational regulatory levels.

TRANSCRIPTIONAL REGULATION Leaf senescence is accompanied by an extensive, genome-wide reprogramming of gene expression, and the dynamic activation and/or deactivation of TFs is critical to this process. Accordingly, the expression of approximately 20% of TF genes in Arabidopsis is altered during leaf senescence. Some of these TFs have been identified as master regulators of the leaf senescence program. Further efforts to identify regulatory networks involving those TFs have provided a deeper understanding of the complex process of leaf senescence, such as how the

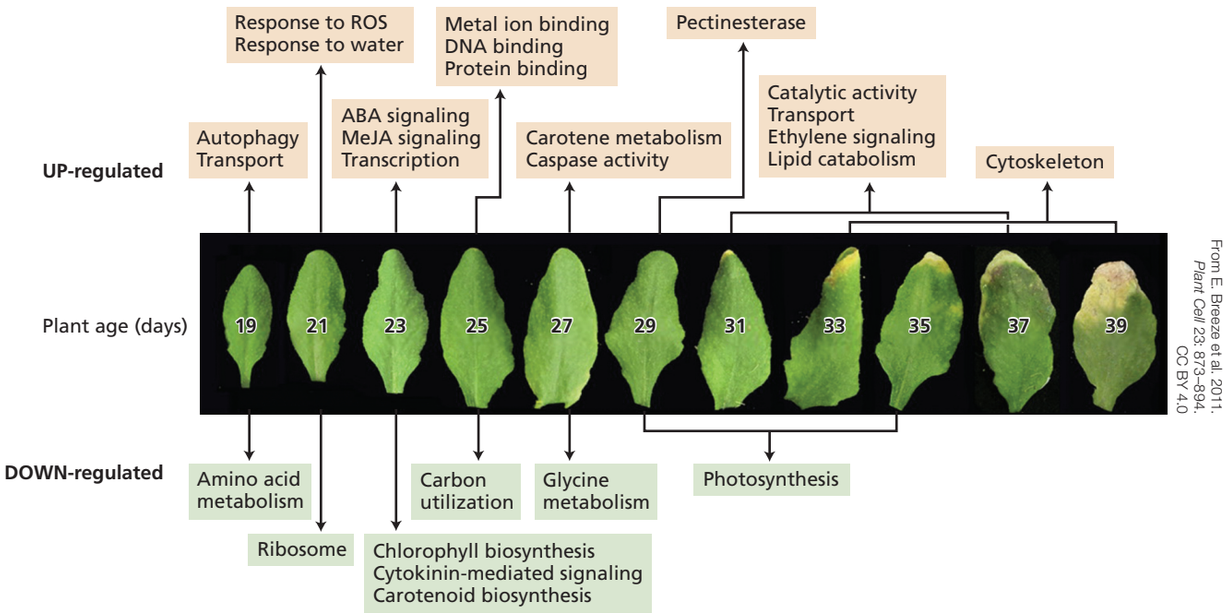


Figure 23.12 Metabolic pathways that are either up-regulated or down-regulated during senescence in Arabidopsis. ABA, abscisic acid; JA, jasmonic acid; MeJA, methyl jasmonate.

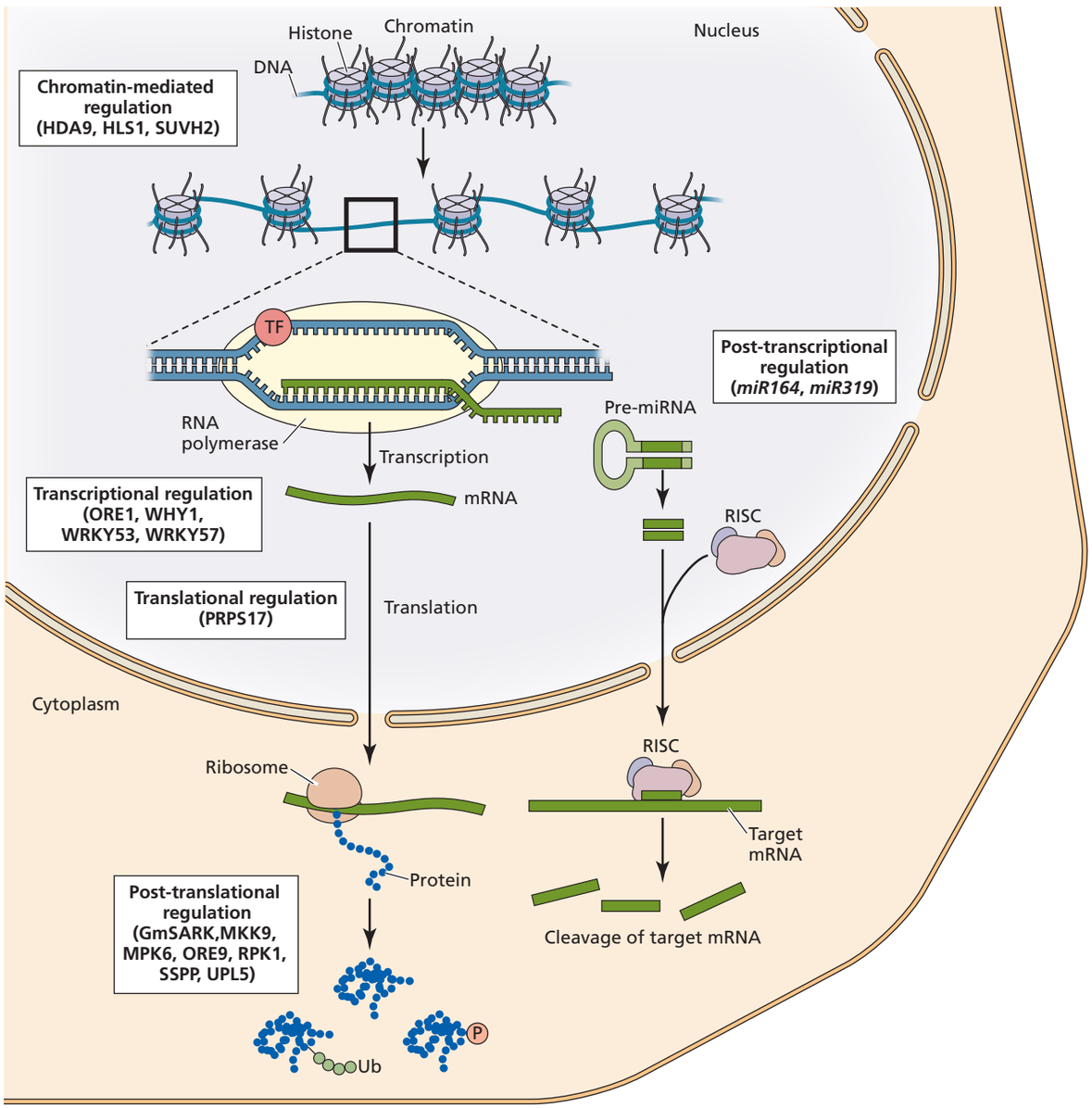


Figure 23.13 Overview of the signaling pathways and regulatory networks involved in leaf senescence. Leaf senescence is finely regulated at the level of chromatin, transcription, posttranscription, translation, and posttranslation. Control of the chromatin structure through histone modifiers such as HDA9, HLS1, and SUVH2 is a key mechanism of leaf senescence. Dynamic regulation of transcription factors (TFs) such as ORE1 and WRKY53 is important for modulating leaf senescence. In addition, miRNAs, including *miR164*, play a role in controlling leaf senescence. Posttranslational modifications such as phosphorylation and ubiquitination provide an additional layer of regulation. Pre-miRNA, premature microRNA; RISC, RNA-induced silencing complex; Ub, ubiquitin. (After H. R. Woo et al. 2013. *J. Cell Sci.* 126: 4823–4833.)

developmental program is integrated with environmental signals during senescence.

The involvement of NAC family TFs in leaf senescence has been intensively characterized in diverse plant species. One of these TFs, ORESARA 1 (ORE1), positively regulates leaf senescence in Arabidopsis. *ORE1* expression is positively regulated by ETHYLENE-INSENSITIVE 2 (EIN2), but in young leaves this is counteracted by negative regulation by *miRNA164* (*miR164*). *miR164* expression gradually decreases with leaf age through negative regulation by EIN2, leading to up-regulation of *ORE1* expression (**Figure 23.14**). These and other results have

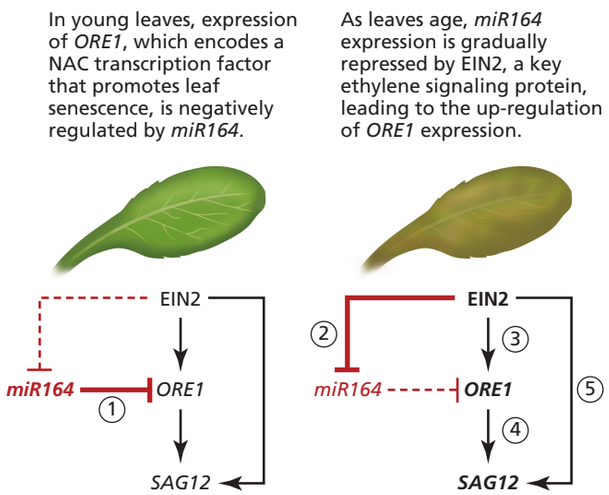


Figure 23.14 Regulation of leaf senescence in Arabidopsis by a trifurcate feed-forward pathway involving EIN2, *miR164*, and *ORE1*. *ORE1* promotes leaf senescence, and its expression is induced in an age-dependent manner by EIN2. *ORE1* is negatively regulated at the posttranscriptional level by *miR164* at earlier stages of leaf life; this repression is alleviated at later stages because of the age-dependent down-regulation of *miR164* expression by EIN2. (After H. R. Woo et al. 2013. *J. Cell Sci.* 126: 4823–4833, based on J. H. Kim et al. *Science* 323: 1053–1057.)

led to a trifurcate pathway model for the regulation of senescence-associated cell death as leaves age. EIN2 also functions in other pathways, including ethylene signaling and stress responses, and ORE1 is also induced by salt stress. Therefore, the age-dependent trifurcate pathway involving ORE1 is probably interlinked with other developmental and environmental signals to fine-tune leaf senescence and cell death processes. Another regulatory network involving ORE1 links light signaling with the leaf senescence program (discussed later) and with ethylene-mediated chlorophyll degradation during leaf senescence.

Plant WRKY (pronounced "worky") TFs are important regulators of senescence as well as plant–pathogen interactions. Like NAC proteins, WRKY TFs promote leaf senescence. WRKY53 positively regulates leaf senescence by modulating the expression of various pathogen- and stress-related SAGs and is therefore thought to be a convergence node between senescence and biotic and abiotic stress-response pathways. The WRKY53 regulatory network that controls leaf senescence involves multiple levels and mechanisms of regulation (**Figure 23.15**). During leaf senescence, *WRKY53* transcription is directly suppressed by the WHIRLY 1 (WHY1) TF (see Figure 23.15, #4) and further regulated by SUPPRESSOR OF VARIEGATION 3-9 HOMOLOG 2 (SUVH2)–mediated histone modification (see Figure 23.15, #1). Posttranslational modification of WRKY53 by ubiquitination and phosphorylation alters its stability and target-binding affinity, respectively (see Figure 23.15, #5 and #6). WRKY53 activity is further modulated by interacting with EPITHIOSPECIFYING SENESCENCE REGULATOR (ESR), which inhibits WRKY53 activity directly, or with the HISTONE DEACETYLASE 9 (HDA9)–POWERDRESS (PWR) complex (see Figure 23.15, #2 and #3), which leads to repression of target genes of WRKY53 (e.g., *WRKY57*). This multi-layered regulation of WRKY53 illustrates how important it is for cells to fine-tune the activity of this TF and to precisely control gene expression during leaf senescence.

CHROMATIN-MEDIATED REGULATION The alteration of chromatin conformation through histone modification and chromatin-remodeling enzymes (see Chapter 3) is a key mechanism for regulating leaf senescence. Genome-wide analysis of histone modifications during Arabidopsis leaf senescence uncovered a strong correlation between histone H3 lysine 4 trimethylation (H3K4me3) and transcription of a subset of genes whose expression is altered during leaf senescence. Histone acetylation is also important for modulating global gene expression during leaf senescence. For example, HDA9 is a positive regulator of leaf senescence that binds to the promoters of genes encoding key negative regulators of senescence and suppressing their expression. Conversely, an Arabidopsis histone acetyltransferase gene, *HOOKLESS 1* (*HLS1*), plays a negative role in leaf senescence. Further evidence of the involvement of dynamic chromatin modifications in controlling leaf senescence comes from mutants with defects in genes coding for SWIch 2/Sucrose Non-Fermentable 2 (SWI2/SNF2)-like chromatin-remodeling proteins.

POSTTRANSCRIPTIONAL REGULATION Leaf senescence is regulated posttranscriptionally by microRNAs. Hundreds of miRNAs are differentially expressed during leaf senescence and form miRNA-mediated regulatory networks involved in a variety of biological processes associated with senescence, including transcriptional regulation, hormone responses, nutrient

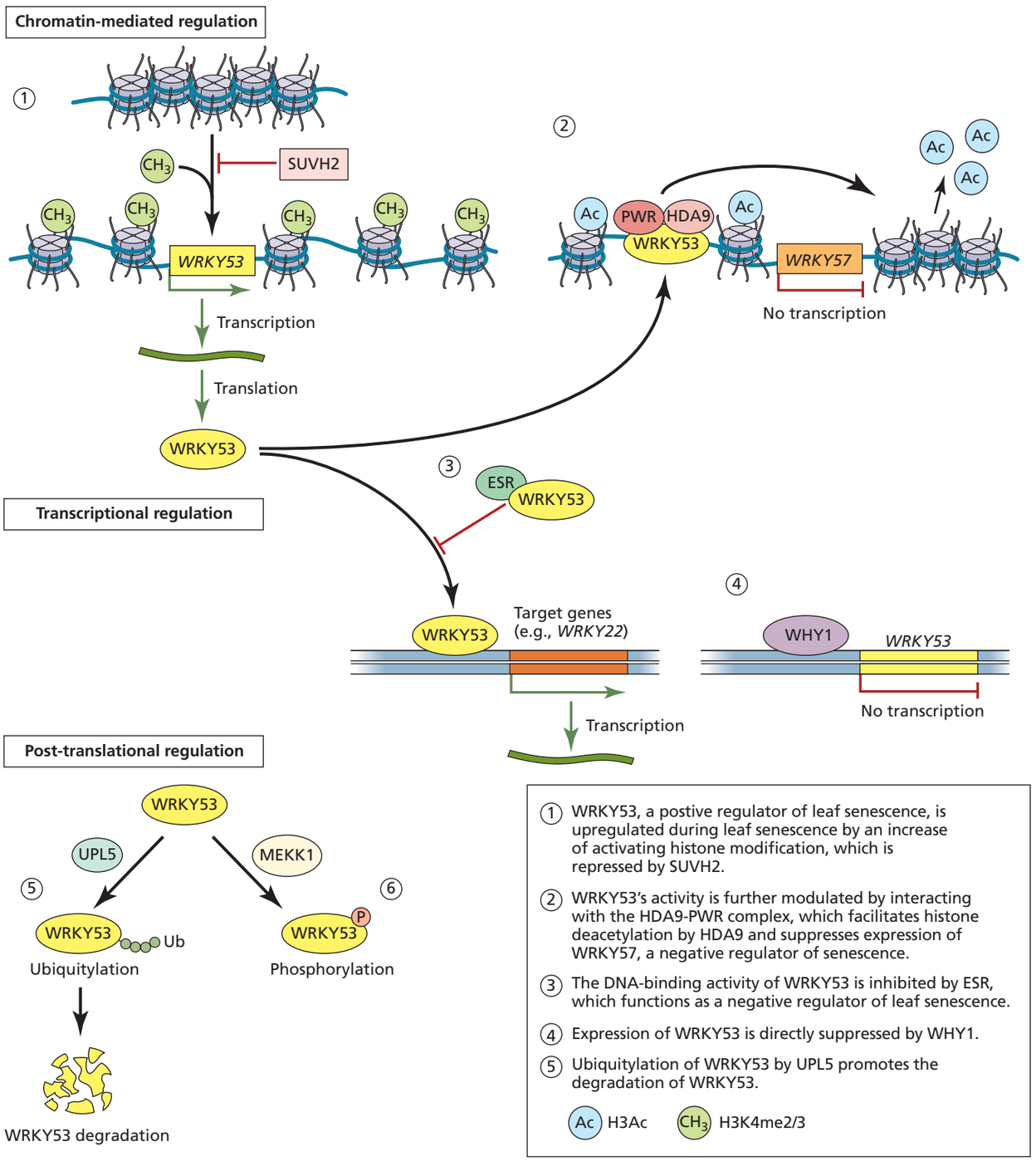


Figure 23.15 Multi-layered regulation of leaf senescence by WRKY53. Up-regulation of *WRKY53* expression during leaf senescence is partially regulated by SUVH2-mediated histone methylation. WRKY53 recruits HDA9 and PWR to its target sites, which facilitates histone deacetylation by HDA9 and suppresses the expression of the associated genes, including *WRKY57*. The expression of *WRKY53* is directly suppressed by WHY1. Binding activity of WRKY53 to its target genes can be inhibited by interaction with ESR. UBIQUITIN PROTEIN LIGASE 5 (UPL5) ubiquitinates WRKY53, causing its degradation, and MITOGEN-ACTIVATED PROTEIN KINASE KINASE KINASE 1 (MEKK1) phosphorylates WRKY53, which increases its binding to its target genes. (After H. R. Woo et al. 2019. *Annu. Rev. Plant Biol.* 70: 15.1–15.30.)

mobilization, and cell structural integrity. In addition to *miR164*, which as discussed earlier targets ORE1 (see Figure 23.14), *miR319* controls leaf senescence by targeting TEOSINTE BRANCHED/CYCLOIDEA/PCF (TCP).

TRANSLATIONAL REGULATION During leaf senescence, synthesis of the large and small subunits of Rubisco is controlled at the translational level. The large and small subunits are encoded in the plastid and nuclear genomes, respectively. The subunits are assembled stoichiometrically to form the Rubisco holoenzyme, and thus their expression needs to be tightly coordinated. However, mRNA levels for the small subunit decline faster during leaf senescence than do those for the large subunit, creating an imbalance. Remarkably, this difference in mRNA levels is compensated for by alterations in their rates of translation. A knockdown mutation of the Arabidopsis *PLASTID RIBOSOMAL SMALL SUBUNIT PROTEIN 17* (*PRPS17*) gene leads to reduced amounts of PRPS17 protein and delayed leaf senescence phenotypes, consistent with a regulatory role for the translational regulation of plastid genes in leaf senescence.

POSTTRANSLATIONAL REGULATION Posttranslational modifications, such as phosphorylation, ubiquitination, methylation, and acetylation, comprise another important layer of regulation underlying leaf senescence (see Figure 23.15). The expression of numerous protein kinases and phosphatases is altered during leaf senescence. Mitogen-activated protein kinase (MAPK) signaling cascades play an important role in modulating leaf senescence triggered by diverse plant hormones (see Chapter 4). For example, the MAPK signaling cascade involving MKK9–MAPK6 (MPK6) has been implicated in salicylic acid (SA)–induced leaf senescence. MPK6 indirectly increases the expression of NONEXPRESSER OF PR GENES 1 (NPR1) by positively regulating SA-triggered *WRKY6* expression and also facilitates nuclear localization of NPR1.

Receptor-like kinases are also involved in regulating leaf senescence. Mutations of *RECEPTOR PROTEIN KINASE 1* (*RPK1*) in Arabidopsis and of *SENESCENCE-ASSOCIATED RECEPTOR-LIKE KINASE* (*GmSARK*) in soybean cause altered senescence phenotypes, which demonstrates the regulatory roles of these kinases in leaf senescence. The role of reversible protein phosphorylation in leaf senescence is demonstrated by the Arabidopsis *SENESCENCE-SUPPRESSED PROTEIN PHOSPHATASE* (*SSPP*) gene. SSPP dephosphorylates and deactivates SARK, a positive regulator of leaf senescence, thereby inhibiting leaf senescence.

The importance of ubiquitin-dependent protein degradation in leaf senescence was first demonstrated by the identification of ORE9, an F-box protein, and UPL5, a HECT domain E3 ubiquitin–protein ligase, as positive regulators of leaf senescence. (For a discussion of the molecular components of the ubiquitination pathway see Chapter 4.) Plant U-box (PUB) E3 and RING-type ubiquitin ligases are also involved in regulating leaf senescence.

LIGHT SIGNALING Light deprivation can induce premature leaf senescence in plants. In Arabidopsis, a high red:far red light ratio (high R:FR) inhibits leaf senescence, while a low R:FR promotes it, suggesting that light regulation of leaf senescence is mediated by one of the phytochromes (see Chapter 16). Phytochrome B (phyB) has been proposed to be the main photoreceptor responsible for the high R:FR-mediated retardation of senescence. Phytochromes that have absorbed red light inactivate phytochrome-interacting a basic helix–loop–helix (bHLH) TFs (PIFs), which inhibit light responses in the dark. PIF4 and PIF5 are the main PIFs involved in promoting leaf senescence. Mutations in PIF4 and PIF5 delay leaf senescence in prolonged darkness as well as under natural low R:FR conditions such as in shade cast by other plants. Under high R:FR conditions, phyB causes degradation of PIF4/5, thereby inhibiting senescence (**Figure 23.16**). Under low R:FR conditions, PIF4 and PIF5 interact with the signaling pathways of two senescence-promoting hormones, ethylene and ABA, by directly activating expression of the TFs EIN3, ABSCISIC ACID INSENSITIVE 5 (ABI5), and ENHANCED EM LEVEL (EEL). These TFs (PIF4, PIF5, EIN3, ABI5, and EEL) in turn activate the expression of the major senescence-promoting NAC TF ORE1, which regulates hundreds of SAGs. Thus, ORE1 probably functions to integrate phyB-mediated light signaling to promote leaf senescence under low light conditions. Moreover, PIF4 directly represses expression of GOLDEN2-LIKE (*GLK*) TFs that are important for maintaining chloroplast activity. Together, this evidence shows that the PIF proteins are core components of a pathway that conveys photoreceptor-mediated light information to key regulators of leaf senescence.

CIRCADIAN RHYTHMS Making developmental transitions in the correct sequence and at the right times is critical for a plant's fitness. Recently there is growing evidence that the circadian clock interacts with the leaf senescence developmental program (for a discussion of the circadian clock mechanism, see Chapter 20). The first clue was provided by the finding that the circadian rhythm varies with leaf age. The circadian period of clock-regulated genes and the core clock genes shortens from 24 h in young leaves to 22 to 23 h in older leaves. This change appears to be regulated by the circadian clock oscillator TIMING OF CAB EXPRESSION 1 (TOC1)

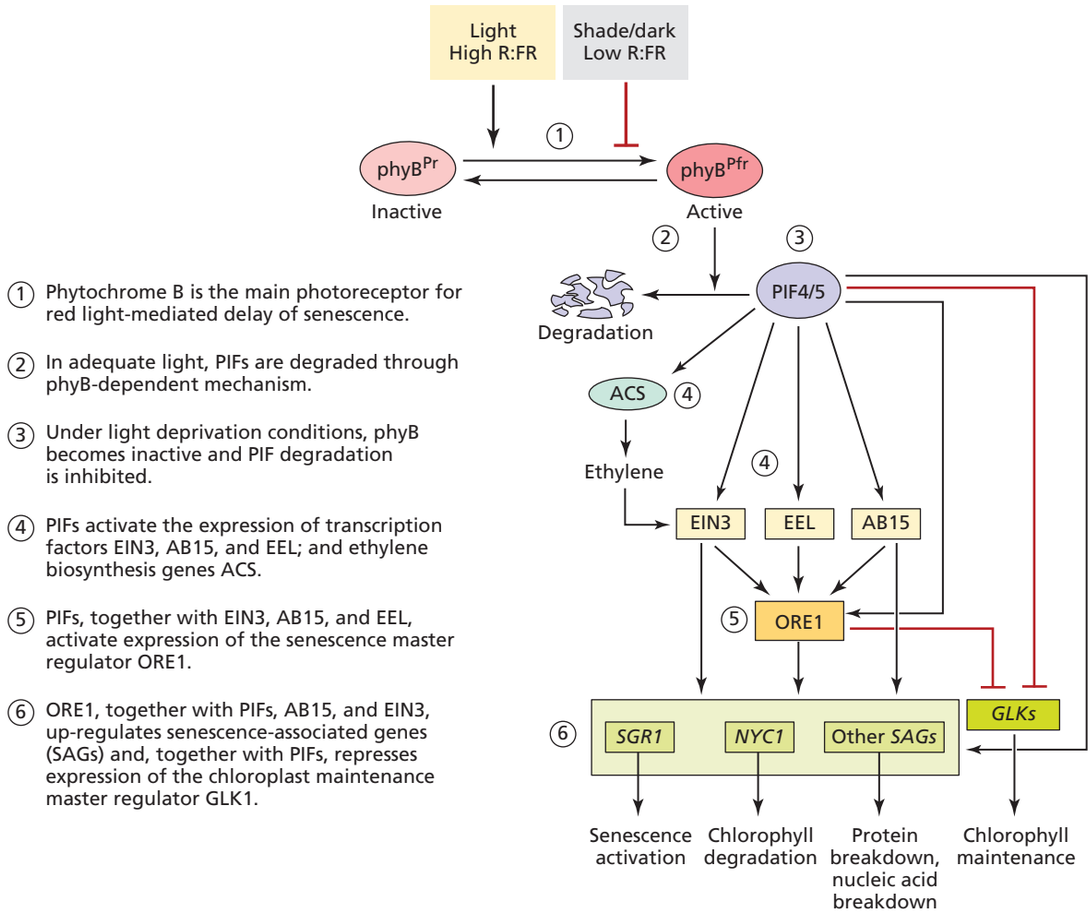


Figure 23.16 The regulatory network that induces leaf senescence in response to extended darkness. In sufficient light (high R:FR), PIFs are degraded through a phytochrome B (phyB)–dependent mechanism, thus suppressing PIF–dependent activation of senescence. In deep shade and darkness (low R:FR), phyB–mediated PIF degradation is inhibited. PIFs can activate the expression of the TFs *EIN3, ABI5,* and *EEL*. In addition, PIFs activate ethylene biosynthesis (by up-regulating *ACC synthase* [*ACS*]), and the accumulating ethylene stabilizes EIN3. PIFs, together with EIN3, ABI5, and EEL, activate the expression of *ORE1*. Finally, ORE1, together with PIFs, ABI5, and EIN3, up-regulates the genes required for chlorophyll degradation and, together with PIFs, down-regulates the chloroplast maintenance master regulator *GLKs*. ORE1 also activates other *SAGs* required for downstream senescence processes. NYC1, NON-YELLOW COLORING 1; SGR1, STAY-GREEN 1. (After D. Liebsch and O. Keech. 2016. *New Phytol.* 212: 563–570.)

(**Figure 23.17A**). As in animal aging systems, disruption of the circadian clock leads to altered life span in plants. For example, mutation of CIRCADIAN CLOCK–ASSOCIATED 1 (CCA1), one of the core components of the clock, accelerates leaf senescence. At the juvenile stage, CCA1 represses the positive senescence regulator ORE1 and activates the chloroplast maintenance gene *GLK2* by directly binding to the promoters of both genes. However, the amount of CCA1 declines with age, attenuating the inhibition of leaf senescence (**Figure 23.17B**). Notably, ORE1 is under circadian regulation. Thus, it is likely that ORE1 is an integrator of age-dependent senescence and the circadian clock.

Plant hormones and other signaling agents can act as positive or negative regulators of leaf senescence

Leaf senescence of higher plants involves genetically and environmentally regulated processes. Thus, both the timing and progression of senescence are flexible, and hormones are key developmental signals that accelerate or delay the timing of leaf senescence. Global gene expression analysis and characterization of genetic mutants have revealed that some hormones act as positive regulators of senescence, while others act as negative regulators. However, the same hormone can act as either a positive or negative regulator of the senescence

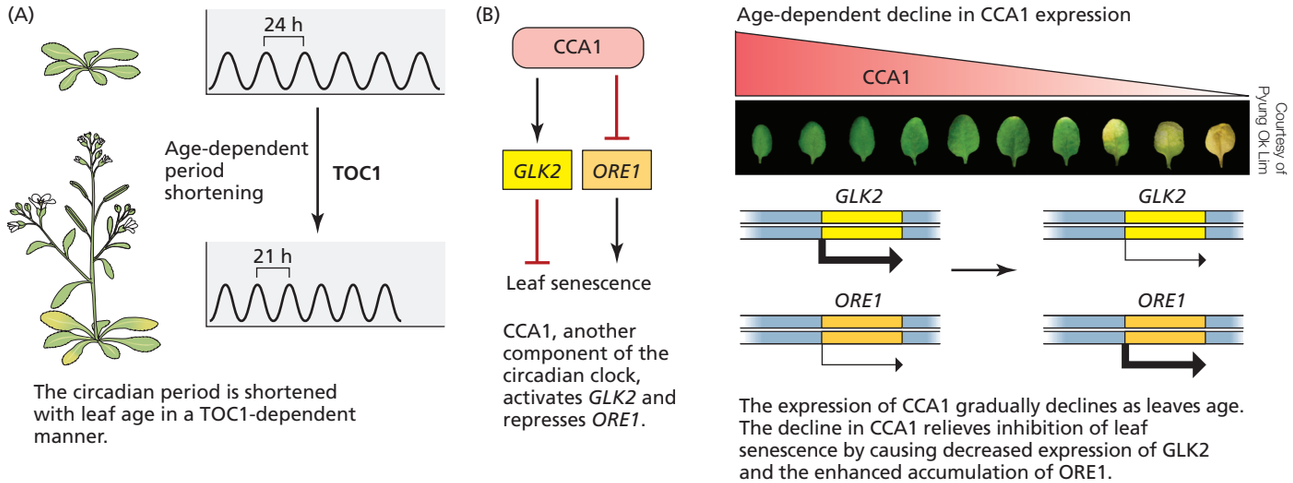


Figure 23.17 Interaction between the circadian clock and aging in Arabidopsis. **(A)** The senescence signal is integrated with the circadian clock through TOC1, one of the core oscillators, resulting in shortening of the circadian period with leaf age. **(B)** The expression of CCA1, another component of the circadian clock, gradually declines with aging. The decrease in CCA1 abundance causes decreased expression of *GLK2* and increased expression of *ORE1*, promoting the transition from growth to senescence.

process depending on the age of the leaf. Hormones also mediate responses to environmental cues, enabling the plant to maximize remobilization under varying environmental conditions. Recently, several TFs, protein kinases, and other regulatory molecules associated with hormone signaling have been identified as key regulators of leaf senescence. In the following subsections we discuss hormones individually, but it is important to keep in mind that hormonal pathways overlap and interact both cooperatively and antagonistically in the regulation of leaf senescence, consistent with a network-type control mechanism.

Positive senescence regulators

ETHYLENE Ethylene is a widely acknowledged senescence-promoting hormone because exogenous ethylene treatment accelerates leaf and flower senescence. Ethylene biosynthetic genes are up-regulated in senescing leaves, and ethylene levels increase during leaf senescence. The significance of ethylene signaling during senescence was initially inferred from the delayed senescence phenotype of ethylene-insensitive mutants in Arabidopsis, such as *ethylene-resistant 1* (*etr1-1*). The stability of key proteins in ethylene-signaling pathways is known to fine-tune the leaf senescence program. For example, accumulation of 1-AMINO-CYCLOPROPANE-1-CARBOXYLATE SYNTHASE 7 (ACS7), an ethylene biosynthetic enzyme, causes precocious leaf senescence. Degradation of ACS7 is inhibited by leaf senescence signaling, a mechanism that fine-tunes ethylene levels as appropriate for leaf development.

ABSCISIC ACID (ABA) ABA levels increase in senescing leaves, and exogenous application of ABA rapidly induces expression of several SAGs and promotes leaf senescence. During leaf senescence, genes associated with ABA synthesis and signaling are up-regulated. ABA levels are also significantly elevated under environmental stress conditions, which often induce leaf senescence (see Chapter 15). Three essential core components of the ABA-signaling pathway—PYRABACTIN RESISTANT 1 (PYR1)/PYR1-LIKE (PYL)/REGULATORY COMPONENTS OF ABA RECEPTOR (RCAR), PROTEIN PHOSPHATASE 2Cs (PP2Cs), and SNF1-RELATED PROTEIN KINASE 2s (SnRK2s) (see Chapter 4)—are known to mediate ABA-promoted leaf senescence. NAC TFs, such as Arabidopsis thaliana NAC-LIKE, ACTIVATED BY AP3/PI (AtNAP) and Oryza sativa NAC2 (OsNAC2), positively regulate ABA levels and induce the expression of chlorophyll degradation genes. Thus, there is a close interaction between ABA-induced stress signaling and leaf senescence signaling pathways.

METHYL JASMONATE (MeJA) Exogenous application of MeJA stimulates leaf senescence and influences the expression of several senescence-related genes. Jasmonate content also increases in leaves as they senesce developmentally; 10-week-old Arabidopsis leaves have been shown to have 50-fold more MeJA than 6-week-old leaves. Consistent with the increase in endogenous MeJA during leaf senescence, the transcript abundance of MeJA biosynthesis genes such as *LIPOXYGENASE 1*

(*LOX1*), *ALLENE OXIDE SYNTHASE* (*AOS*), and *ALLENE OXIDE CYCLASE 1* (*AOC1*), is increased in senescing leaves. MeJA-induced leaf senescence is impaired in an Arabidopsis mutant of the MeJA receptor coronatine-insensitive 1 (COI1), demonstrating the importance of the MeJA signaling pathway. Furthermore, key repressors in the MeJA signaling pathway, such as JAZ4 and JAZ8, were found to negatively regulate MeJA-induced leaf senescence through physical interaction with WRKY57.

SALICYLIC ACID (SA) Salicylic acid regulates many aspects of plant growth and development and responses to various biotic and abiotic stresses. SA also positively regulates developmental leaf senescence. For example, Arabidopsis mutants defective in either SA biosynthesis or SA signaling exhibit delayed senescence when compared with wild-type plants. Furthermore, the SA content gradually increases as a leaf ages, which induces the expression of several SAGs. Transcriptome analysis has confirmed that many of the genes involved in SA biosynthesis are up-regulated in senescing leaves, and that about 20% of SAGs are up-regulated by the SA signaling pathway. SA treatment induces the expression of many SAGs, including *WRKY53*, which (as discussed earlier) acts as a master switch that regulates other *WRKY* genes associated with leaf senescence (see Figure 23.15). Furthermore, the WRKY46 and WKRY75 TFs were found to directly promote *SALICYLIC ACID INDUCTION–DEFICIENT 2* (*SID2*) transcription and thus induce SA production. It is notable that cross talk between SA and ROS responses is important for keeping the levels of antioxidants sufficiently low to protect the senescing leaf cells from premature death, which ensures the slow, controlled degeneration of cells during leaf senescence.

REACTIVE OXYGEN SPECIES There is growing evidence that reactive oxygen species (ROS), especially H_2O_2, play important roles as signals during leaf senescence. ROS are toxic chemicals that cause oxidative damage to DNA, proteins, and membrane lipids (see **WEB TOPIC 13.7** and Chapter 15). They are produced primarily as by-products of normal metabolic processes, such as respiration and photosynthesis, in chloroplasts, mitochondria, and peroxisomes. They can also be produced on the plasma membrane. However, ROS do not trigger senescence by causing physicochemical damage to the cell, but rather act as signals that activate genetically programmed pathways of gene expression that lead to regulated cell death events.

In Arabidopsis, *WRKY53* gene expression increases in leaves at the time of bolting (rapid stem elongation associated with flowering and leaf senescence). Leaf H_2O_2 levels increase at the time of bolting as well. Treating leaves with H_2O_2 has been shown to induce the expression of *WRKY53*. Thus, there is good circumstantial evidence that H_2O_2 acts as a signal that triggers leaf senescence in Arabidopsis. ROS signaling during leaf senescence is coupled to the activity of the MAPK signal transduction pathway.

SUGARS Besides serving as an energy source and as building blocks for macromolecules, sugars may also act as signaling molecules, regulating metabolic pathways as well as developmental events. For example, trehalose 6-phosphate, which stimulates starch biosynthesis (see Chapter 10), may serve as a signal that couples starch biosynthesis to the carbon status of the cytosol in leaves. Studies have shown that high concentrations of sugars lower photosynthetic activity and may even trigger leaf senescence when the sugar concentration exceeds a certain threshold. Sugar-induced senescence is especially important under conditions of low nitrogen availability. It has recently been shown that both trehalose 6-phosphate and sugars accumulate in senescing Arabidopsis leaves. This suggests that trehalose 6-phosphate may play a role in the onset of leaf senescence under conditions of high carbon availability.

Negative senescence regulators

CYTOKININ The senescence-repressing role of cytokinins appears to be universal in plants and has been demonstrated in many studies. Exogenous application of active cytokinins and an increase in the content of endogenous cytokinins can delay senescence. To test the role of cytokinin in regulating the onset of leaf senescence, tobacco plants were transformed with a chimeric gene in which a SAG-specific promoter was used to drive the expression of the *Agrobacterium tumefaciens* gene *isopentenyl transferase* (*ipt*), which encodes a key enzyme in cytokinin biosynthesis (see **WEB APPENDIX 3**). The transgenic plants had wild-type levels of cytokinins and developed normally until the onset of leaf senescence. As the leaves aged, however, the senescence-specific promoter was activated and thus triggered the expression of the *ipt* gene within leaf cells just as senescence would have been initiated (**Figure 23.18A**). The resulting elevated cytokinin levels not only blocked senescence but also limited further expression of the *ipt* gene, preventing cytokinin overproduction (**Figure 23.18B**).

The molecular mechanism of cytokinin action in delaying leaf senescence depends on the canonical two-component cytokinin signaling system (see Chapter 4). The ARABIDOPSIS HISTIDINE KINASE 3 (AHK3) receptor appears to be the primary cytokinin receptor regulating leaf senescence in Arabidopsis. Elevated AHK3 activity results in a significant delay in leaf senescence. Conversely, disruption of *AHK3*, but not of other cytokinin receptor genes, results in premature leaf senescence. CYTOKININ RESPONSE FACTORs (CRFs), which are



Figure 23.18 Cytokinin is a negative regulator of leaf senescence in transgenic tobacco. (A) To generate the construct used in this experiment, a senescence-induced promoter was fused to a cytokinin biosynthesis gene, *ipt*, from *Agrobacterium tumefaciens*. At the onset of senescence of transgenic plants carrying this construct, the promoter directs the expression of *IPT*, increasing the level of cytokinin, which in turn inhibits senescence. The inhibition of senescence attenuates expression from the senescence-induced promoter, preventing cytokinin overproduction. (B) Leaf senescence is delayed in a transgenic tobacco plant containing the senescence-induced *ipt* construct. (After S. Gan and R. M. Amasino. 1995. *Science* 270: 1986–1988.)

part of a side branch of the canonical two-component pathway, are also known to play a negative role in regulating dark-induced senescence.

AUXIN Elucidating the role of auxin in the regulation of leaf senescence has been complicated because auxin has been shown to play a central role in so many aspects of plant growth and development. Adding to the complexity, high auxin concentrations stimulate ethylene production, which promotes senescence in mature leaves. However, much of the evidence obtained thus far points to a role for auxin as a negative regulator of leaf senescence. Application of exogenous auxin in Arabidopsis leads to a decrease in the expression of many SAGs and to overexpression of YUCCA6, the flavin-containing monooxygenase that catalyzes the rate-limiting step in auxin biosynthesis, delays leaf senescence, and decreases SAG expression. In addition, the delayed-senescence Arabidopsis mutant *arf2* has a mutation in the gene *AUXIN RESPONSE FACTOR 2* (*ARF2*), which is a repressor of auxin-response genes. By inactivating the *ARF2* repressor, the *arf2* mutation causes a constitutive auxin response, which delays leaf senescence.

23.4 Abscission

The shedding of leaves, fruits, flowers, and unhealthy structures is termed abscission (see **WEB TOPICS 23.4** and **23.5**). Abscission takes place within specific layers of cells in the **abscission zone**. In leaves, the abscission zone is located near the base of the petiole (**Figure 23.19A–C**). Prior to abscission, a separation layer forms within the abscission zone. In flowers, the abscission zone is positioned where petals and sepals are attached to the receptacle. The abscission zone can often be morphologically identified as one or more layers of isodiametrically flattened cells and becomes differentiated during organ development, many months before organ separation actually takes place. The abscission zone consists of two neighboring cell types: **residuum cells** in the receptacle and **secession cells** in the abscising organs, both of which have distinct cellular activities and structures (**Figure 23.19D and E**).

Organ abscission involves cell separation, which plays a crucial role in many developmental processes in plants, including seed germination, the formation of stomata, pollen tube growth, and fruit dehiscence. Some of these processes are particularly important for agriculture. For example, crop domestication that led to the development of cultivated rice and maize (corn; *Zea mays*) involves a reduction in seed shattering—an important agricultural trait. Because plant cells are embedded within cell walls, cell separation during developmental processes requires the controlled breakdown of the surrounding cell walls. During abscission, the middle lamella binding the cell walls of the two neighboring cell types in the abscission zone is degraded. The dissolution of the walls between the cells of the separation layer subsequently results in the organ being shed from the plant. Uncontrolled cell wall processing by cell wall–hydrolyzing enzymes during organ abscission results in cell separation at ectopic sites, interfering with precise abscission of the organs (see subsequent sections for more information).

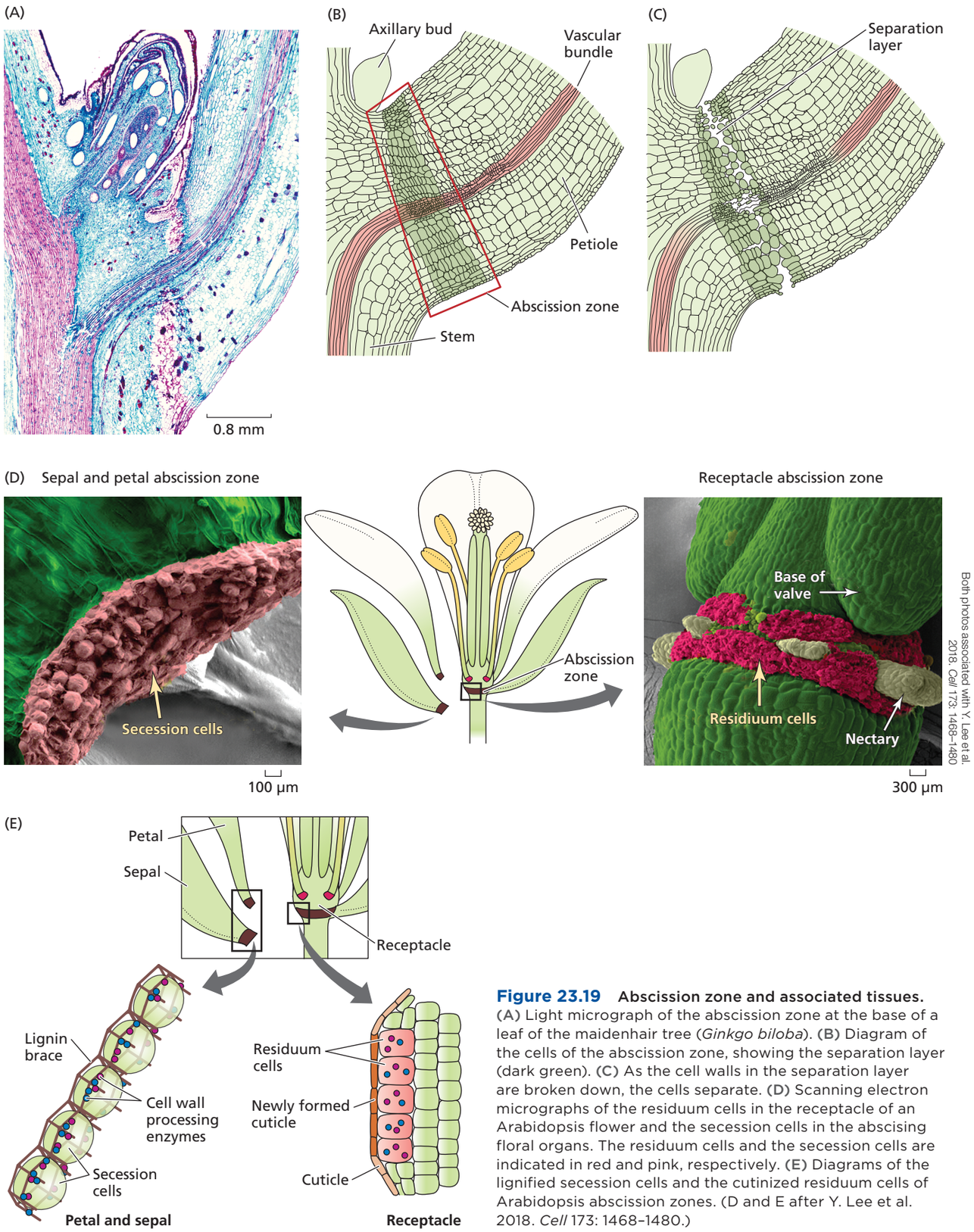


Figure 23.19 **Abscission zone and associated tissues.** **(A)** Light micrograph of the abscission zone at the base of a leaf of the maidenhair tree (*Ginkgo biloba*). **(B)** Diagram of the cells of the abscission zone, showing the separation layer (dark green). **(C)** As the cell walls in the separation layer are broken down, the cells separate. **(D)** Scanning electron micrographs of the residuum cells in the receptacle of an Arabidopsis flower and the secession cells in the abscising floral organs. The residuum cells and the secession cells are indicated in red and pink, respectively. **(E)** Diagrams of the lignified secession cells and the cutinized residuum cells of Arabidopsis abscission zones. (D and E after Y. Lee et al. 2018. *Cell* 173: 1468–1480.)

Two mutants of tomato, *jointless* and *lateral suppressor*, fail to develop an abscission zone on the flower pedicel, and the mutated genes responsible for these phenotypes have been identified. The wild-type *JOINTLESS* gene encodes a MADS box protein, one of a group of TFs that control many aspects of development, including floral organ identity (see Chapter 20). JOINTLESS is known to interact with another MADS box transcription factor, MACOCALYX, to regulate abscission. The *LATERAL SUPPRESSOR* gene also regulates axillary bud development (see Chapter 18).

Organ abscission is regulated by developmental and environmental cues

Ethylene plays a key role in the activation of the events leading to cell separation within the abscission zone. The ability of ethylene gas to cause defoliation in birch trees is shown in **Figure 23.20**. The wild-type tree on the left has lost most of its leaves and only the younger leaves at the top fail to abscise. The tree on the right has been transformed with a copy of the gene for the Arabidopsis ethylene receptor, *ETR1*, carrying the dominant *etr1* mutation (discussed earlier). This tree is unable to respond to ethylene and therefore does not shed any of its leaves after ethylene treatment.



From J. Vahala et al. 2003. *Plant Physiol.* 132: 185–195

Figure 23.20 Effect of ethylene on abscission in the birch *Betula pendula*. The tree on the left is the wild type; the tree on the right was transformed with a mutated version of the Arabidopsis ethylene receptor gene, *ETR1*. The expression of this gene was under the transcriptional control of its own promoter. One of the characteristics of these mutant trees is that they do not drop their leaves when fumigated for 3 days with 50 ppm ethylene.

Molecular genetic studies of Arabidopsis and tomato have added to our current understanding of organ abscission. The process of organ abscission can be divided into four distinct developmental phases, during which the cells of the abscission zone become competent to respond to developmental and environmental cues, including ethylene and auxin (**Figure 23.21**).

1. *Abscission zone formation and abscission suppression phase*. Prior to the perception of any signal (internal or external) that initiates the abscission process, an abscission zone forms at the base of the separating organs. Abscission can be induced only after the abscission zone is formed and differentiated. Early in the abscission zone formation and abscission suppression phase of leaves, auxin from the leaf blade prevents abscission by maintaining the cells of the abscission zone in an ethylene-insensitive state. It has long been known that removal of the leaf blade (the site of auxin production) promotes petiole abscission. Application of exogenous auxin to petioles from which the leaf blade has been removed delays the abscission process. It remains unclear how and when abscission zone cell identity is specified.
2. *Abscission induction phase*. A reduction or reversal in the auxin gradient from the leaf blade, normally associated with leaf senescence, causes the abscission zone to become sensitive to ethylene. As abscission approaches, the amount of auxin from the leaf blade decreases and the ethylene level rises. Treatments that accelerate leaf senescence may promote abscission by interfering with auxin synthesis or transport in the leaf. Ethylene appears to decrease the activity of auxin by reducing its synthesis and transport and increasing its catabolism. The reduction in the concentration of free auxin increases the response of specific target cells in the abscission zone to ethylene.
3. *Cell separation and abscission phase*. The cell separation and abscission phase is characterized by the induction of abscission-related genes encoding specific hydrolytic and remodeling enzymes that loosen the cell walls in the abscission layer. Once sensitized, cells of the abscission zone respond to low concentrations of endogenous ethylene by synthesizing and secreting cell wall–degrading enzymes and cell wall–remodeling proteins, including β-1,4-glucanase (cellulase),

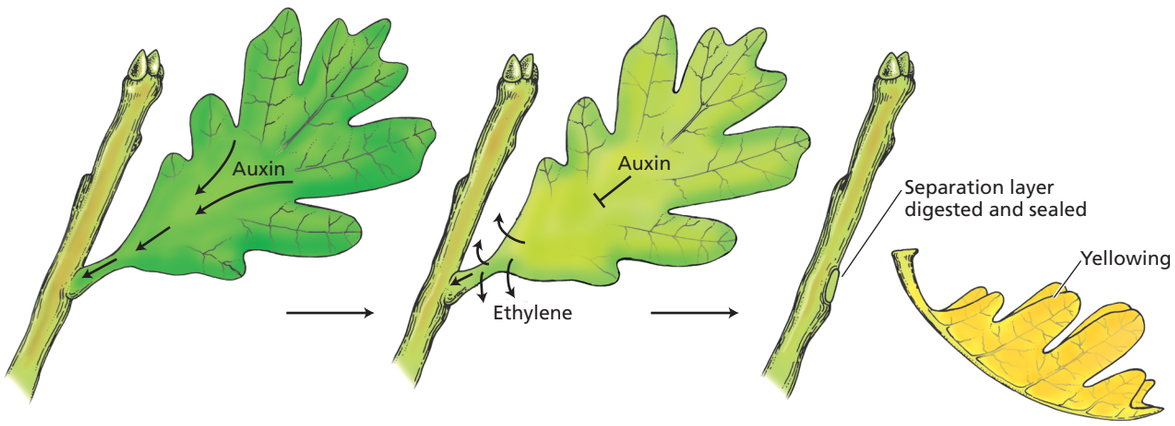


Figure 23.21 Schematic view of the roles of auxin and ethylene during leaf abscission. In the abscission induction phase, the level of auxin decreases, and the level of ethylene increases. These changes in the hormonal balance increase the sensitivity of the target cells to ethylene. (After P. W. Morgan. 1984. In *Ethylene: Biochemical, Physiological and Applied Aspects.* Y. Fuchs and E. Chalutz [Eds.], Martinus Nijhoff, The Hague, Netherlands, pp. 231–240.)

polygalacturonase, xyloglucan endotransglucosylase/hydrolase, and expansin, resulting in degradation of the middle lamella. In this phase, cell separation is precisely controlled by localizing cell wall–processing enzymes to a restricted area. Clean abscission is aided by a honeycomb structure of lignin that is formed by the secession cells in the abscising organ and that acts as a brace that isolates abscising cells and restricts diffusion of the wall-degrading enzymes and expansin proteins they secrete (see Figure 23.19D and E).

4. *Post-abscission phase*. After the completion of floral organ abscission, the residuum cells in the receptacle *transdifferentiate* (i.e., convert directly from one cell type to another) into epidermal cells that form a cuticle, a defining feature of epidermis. The newly formed cuticle protects the exposed surface from infection or other harm. Epidermal cell identity is typically determined during early embryogenesis, so the formation of cuticle on the newly formed surface indicates de novo specification of epidermal cells, which appears to be prearranged in the developmental program.

Although leaf abscission is arguably the most ubiquitous type of abscission in nature, the absence of a suitable genetic model to study it (Arabidopsis leaves do not abscise) has been a barrier to elucidating the developmental genetics of leaf abscission. Fortunately, the abscission of Arabidopsis flowers has allowed a dissection of some of the genes regulating flower abscission. For example, delayed flower abscission mutants in Arabidopsis have led to the identification of several genes that regulate abscission initiation and the subsequent signal transduction. The proteins encoded by these genes include the small, secreted peptide INFLORESCENCE DEFICIENT IN ABSCISSION (IDA) and its receptors on the plasma membrane surface, the leucine-rich repeat receptor-like kinases HAESA (HAE) and HAESA-LIKE2 (HSL2) (**Figure 23.22A**). When IDA binds to HAE/HSL2, the latter forms a receptor complex with BRI1-ASSOCIATED KINASE (BAK1) and SOMATIC EMBRYOGENESIS RECEPTOR KINASES 1 and 2 (SERK1/2) that triggers activation of a MAPK cascade consisting of MKK4/5 and MPK3/6. The MAPK cascade in turn negatively regulates the activity of the TF KNOTTED-LIKE FROM ARABIDOPSIS THALIANA 1 (KNAT1, also known as BREVIPEDICELLUS, or KNAT1/BP), which leads to the transcription of *KNAT2/6*, thereby promoting floral organ abscission (**Figure 23.22B**). The transcription factors KNAT2/6 help transcribe genes encoding cell wall–hydrolyzing enzymes, leading to cell expansion and separation. Loss-of-function mutations in *IDA*, *HAE/HSL2*, or *KNAT2/6* result in retention of the floral organs on the receptacle.

Abscission is remarkable in that two neighboring cell types (the residuum cells and the secession cells) undergo distinct changes in cellular architecture and activity that accomplish organ abscission in a precise manner.

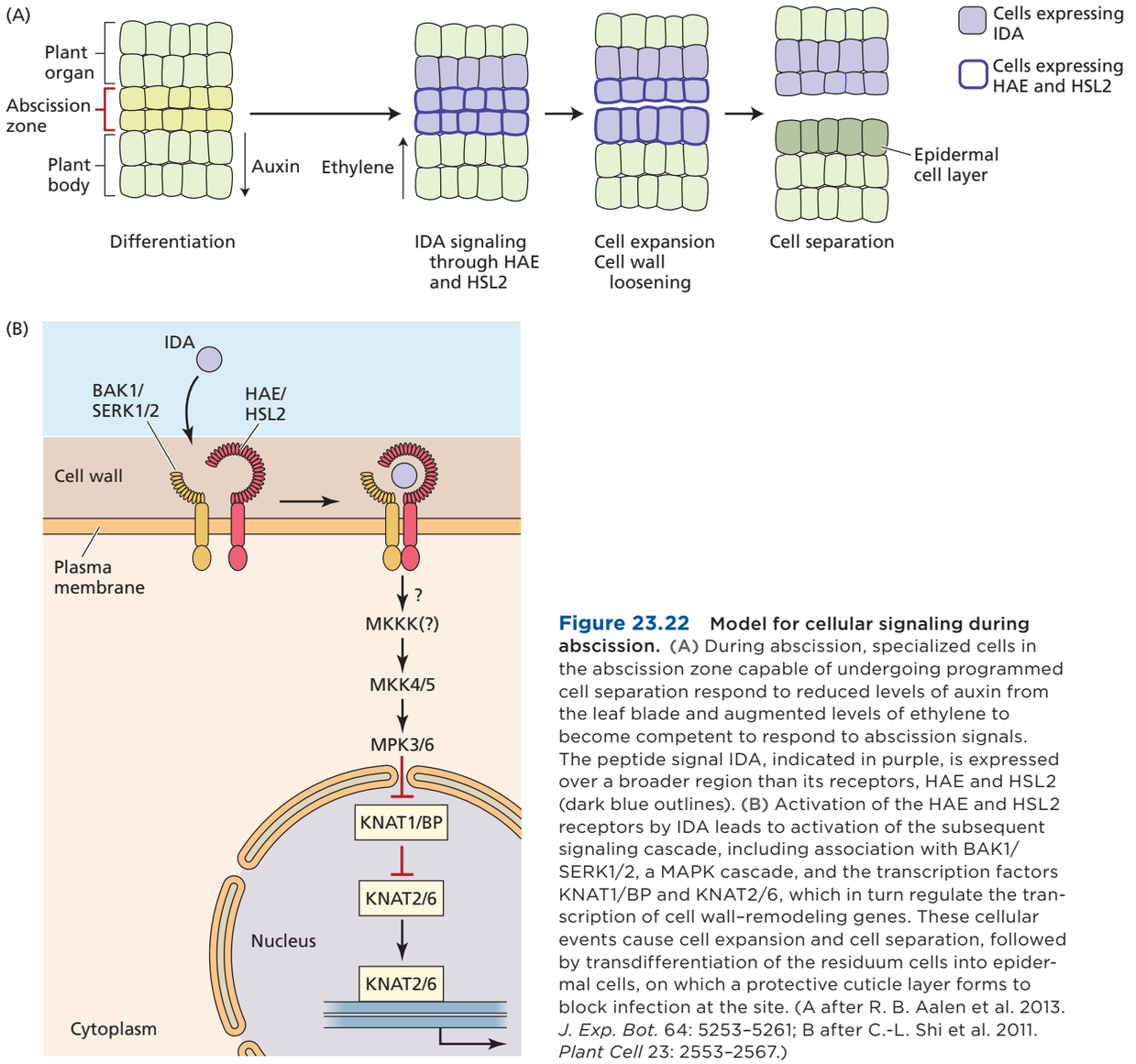


Figure 23.22 Model for cellular signaling during abscission. **(A)** During abscission, specialized cells in the abscission zone capable of undergoing programmed cell separation respond to reduced levels of auxin from the leaf blade and augmented levels of ethylene to become competent to respond to abscission signals. The peptide signal IDA, indicated in purple, is expressed over a broader region than its receptors, HAE and HSL2 (dark blue outlines). **(B)** Activation of the HAE and HSL2 receptors by IDA leads to activation of the subsequent signaling cascade, including association with BAK1/SERK1/2, a MAPK cascade, and the transcription factors KNAT1/BP and KNAT2/6, which in turn regulate the transcription of cell wall–remodeling genes. These cellular events cause cell expansion and cell separation, followed by transdifferentiation of the residuum cells into epidermal cells, on which a protective cuticle layer forms to block infection at the site. (A after R. B. Aalen et al. 2013. *J. Exp. Bot.* 64: 5253–5261; B after C.-L. Shi et al. 2011. *Plant Cell* 23: 2553–2567.)

How these two cellular neighbors communicate with one another to accomplish precise organ abscission awaits further investigation.

23.5 Whole-Plant Senescence

The programmed deaths of individual plant cells and organs are adaptations that benefit the plant by increasing its evolutionary fitness. The death of the whole plant, however, cannot easily be rationalized in evolutionary terms despite the life spans of individual plants being, to a large extent, genetically determined and varying widely across species. In this final section of the chapter we address some of the major questions that have been studied regarding whole-plant senescence: Is whole-plant senescence similar to aging in animals? What is the relationship, if any, between the life span of an individual plant and the longevity of its component cells, tissues, and organs? What is the role of reproduction in whole-plant senescence? Why do meristems stop dividing, and does meristem failure lead to whole-plant senescence? How does the senescence of single plants differ from that of clonal plants? As we will see, the regulation of source–sink relations figures prominently in all models for whole-plant senescence that have been advanced thus far.

Angiosperm life cycles may be annual, biennial, or perennial

Individual plant life spans vary from a few weeks in the case of desert ephemerals, which grow and reproduce rapidly in response to brief episodes of rain, to about 4600 years in the case of bristlecone pine. **Annual plants** generally grow, reproduce, senesce, and die in a single season. **Biennial plants** devote their first year to vegetative growth and food storage and their second year to reproduction, senescence, and death. Annual and biennial plants undergo whole-plant senescence following fruit and seed production, and both are thus termed **monocarpic** because they reproduce only once (**Figure 23.23**).

Perennial plants live for 3 years or longer and may be herbaceous or woody. The range of maximum life spans for perennial plants is given in **Table 23.1**. Perennial plants are usually **polycarpic**, producing fruits and seeds over multiple seasons. However, there are also examples of monocarpic perennials, such as the century plant (*Agave americana*) (**Figure 23.24**) and Japanese timber bamboo (*Phyllostachys bambusoides*). The century plant grows vegetatively for 10 to 30 years before flowering, fruiting, and senescing, while Japanese timber bamboo can grow vegetatively for 60 to 120 years before reproduction and death.



Courtesy of L. Nooden

Figure 23.23 Monocarpic senescence in soybean (*Glycine max*). The entire plant on the left underwent senescence after flowering and producing fruit (pods). The plant on the right remained green and vegetative because its flowers were continually removed.

Remarkably, all clones from the same bamboo stock flower and senesce simultaneously, regardless of geographic location or climatic condition, which suggests the presence of a long-term biological clock of some kind.

Many perennial plants that form clones by asexual reproduction can proliferate into community-sized interconnected "individuals" that achieve astounding ages, such as King's lomatia (*Lomatia tasmanica*), a Tasmanian shrub in the Proteaceae family that may be more than 43,000 years old. Each individual lomatia plant lives only about 300 years, but because it does not transfer any senescence signal to its clones, the clonal community apparently grows and proliferates indefinitely.

Whole-plant senescence differs from aging in animals

Aging in animals is generally associated with gradual deterioration—the cumulative effect of normal wear

Table 23.1 Longevity of various individual and perennial clonal plants

Species	Age (yr)
Individual plants	
Bristlecone pine (*Pinus longaeva*)	4600
Giant sequoia (*Sequoiadendron giganteum*)	3200
Stone pine (*Pinus cembra*)	1200
European beech (*Fagus sylvatica*)	930
Blackgum (*Nyssa sylvatica*)	679
Scots pine (*Pinus silvestris*)	500
Chestnut oak (*Quercus montana*)	427
Red oak (*Quercus rubra*)	326
European ash (*Fraxinus excelsior*)	250
English ivy (*Hedera helix*)	200
Flowering dogwood (*Cornus florida*)	125
Bigtooth aspen (*Populus grandidentata*)	113
Scots heather (*Calluna vulgaris*)	42
Spring heath (*Erica carnea*)	21
Scandinavian thyme (*Thymus chamaedrys*)	14
Clonal plants	
King's lomatia (*Lomatia tasmanica*)	43,000+
Creosote (*Larrea tridentata*)	11,000+
Bracken (*Pteridium aquilinum*)	1400
Sheep fescue (*Festuca ovina*)	1000+
Ground pine (*Lycopodium complanatum*)	850
Reed grass (*Calamagrostis epigeios*)	400+
Wood sage (*Teucrium scorodonia*)	10

Source: H. Thomas. 2013. *New Phytol.* 197: 696–711.



© WildPictures/Alamy Stock Photo

Figure 23.24 Century plant (*Agave americana*) flowers after 10–30 years of vegetative growth, after which it undergoes monocarpic senescence.

and tear on the organism. In contrast, senescing organs, tissues, and cells in plants are *programmed* either to fail quickly or to be deficient in the mechanisms that would otherwise protect against physiological decline. According to this model of whole-plant senescence, the ability of long-lived perennials to maintain the integrity of their meristems for thousands of years derives from developmental programs that successfully ward off the deteriorative effects of time.

One type of time-based cellular damage that has been investigated in plants is **mutational load**. Even the highest-fidelity cell replication mechanisms would be expected to propagate a significant number of errors over thousands of years. The mutation rate might even increase over time due to the buildup of reactive oxygen species (ROS). However, in bristlecone pine trees, no statistically significant relationship was found between the age of the individual and the frequency of mutations in pollen, seed, and seedlings. By contrast, a significant decline in the average number of viable pollen grains per catkin per ramet was found in *Populus tremuloides* with increasing clone age. However, while decreasing pollen viability is consistent with mutational load, it would play no direct role in determining the longevity of clonal communities.

Age-dependent increases in somatic mutations leading to the production of chimeras and sports (plant parts that differ phenotypically from the parent plant) have also been observed in many perennial species. However, the evidence that such mutations contribute to whole-plant senescence is very weak. Indeed, plants seem to have a high tolerance for **genetic mosaicism**, and they possess robust mechanisms for purging deleterious mutant cells.

Another type of time-based damage to cells that potentially could contribute to whole-plant senescence is **telomere shortening**. Telomeres are regions of repetitive DNA that form the chromosome ends and protect them from degradation (see Chapter 3). Normal chromosome replication results in telomere shortening, and without some mechanism for telomere repair, telomeres would eventually disappear after successive rounds of cell division. **Telomerase**—a ribonucleoprotein enzyme complex—extends the ends of telomeres after replication through the activity of telomerase reverse transcriptase. Although animals with dysfunctional telomerase age prematurely, Arabidopsis mutants lacking telomerase activity grow and reproduce for up to ten generations. In addition, observations on bristlecone pine and *Ginkgo biloba* plants failed to demonstrate progressive shortening of telomeres with increasing age. The cause of the differences between plant and animal telomeres with respect to aging is as yet unclear.

The determinacy of shoot apical meristems is developmentally regulated

Plants are often described as having indeterminate growth due to the activities of the apical meristems, but the determinacy of the apical meristems is also under strict developmental control. For example, shoot apical meristems may be continuously meristematic (indeterminate), or may cease activity (be determinate), either by differentiating into a terminal organ such as a flower, or by undergoing growth arrest or senescence. Indeed, the growth habits, life cycles, and senescence profiles of different plant species are intimately connected to their patterns of apical meristem determinacy.

In monocarpic species, all indeterminate vegetative shoot apices become determinate floral apices, and the entire plant senesces and dies after seed dispersal. In contrast, polycarpic perennials retain a population of indeterminate shoot apices as well as apices that become reproductive and determinate.

Monocarpic senescence typically involves three coordinated events: (1) senescence of somatic organs and tissues such as leaves; (2) growth arrest and senescence of shoot apical meristems; and (3) suppression of axillary buds. In peas, shoot apical meristem senescence has

been shown to be regulated by both photoperiod and gibberellins (GAs). As discussed in Chapter 19, auxin from actively growing terminal buds suppresses the growth of axillary buds, a phenomenon known as apical dominance. Strigolactone and cytokinin play antagonistic roles during apical dominance, with strigolactone repressing axillary bud growth and cytokinin promoting it (see Chapter 19). Removal or death of the terminal bud reduces auxin transport and favors cytokinin signaling in the lateral buds, promoting branch formation. However, shoot apical meristem arrest during monocarpic senescence does not lead to activation of the axillary buds.

The molecular mechanism of axillary bud suppression during monocarpic senescence has been investigated in Arabidopsis. Expression of the gene for the TF AtMYB2 in the basal internode is associated with the suppression of both cytokinin biosynthesis and branch formation during monocarpic senescence. T-DNA insertion mutants lacking a functional AtMYB2 protein are bushy because of increased cytokinin production. Senescence is delayed in the bushy mutant, which indicates that cytokinin acts as a negative regulator of whole-plant senescence.

Nutrient redistribution may trigger senescence in monocarpic plants

A diagnostic feature of monocarpic senescence is the ability to delay senescence well beyond the plant's normal life span by the removal of the reproductive structures. For example, repeated depodding enables soybean plants to remain vegetative for many years under favorable growing conditions, leading to a treelike appearance. What is the relationship between fruit development (reproduction) and whole-plant senescence? One of the earliest explanations for monocarpic senescence was based on the redistribution of vital nutrients via the phloem from vegetative sources to reproductive sinks.

Plant hormones are considered to play important roles in regulating source–sink relationships. Many studies have shown that alterations in the source–sink relations of vegetative and reproductive tissues can affect the course of senescence. As discussed earlier in relation to leaf senescence, cytokinins increase sink strength in leaves and delay leaf senescence. During monocarpic senescence in peas, high endogenous GA levels in the vegetative buds are correlated with high sink strength, vigorous vegetative growth, and delayed whole-plant senescence. In contrast, high auxin levels in floral buds are correlated with high sink strength of the reproductive structures and rapid reproductive development followed by whole-plant senescence.

If developing seeds and fruits are such strong sinks that they can trigger the senescence of the rest of the plant, why do male plants of dioecious species such as spinach (*Spinacea oleracea*), which produce neither seeds nor fruits, senesce at the same age as female plants, which produce copious seeds and fruits? Experiments carried out in the late 1950s showed that removing the tiny pollen-producing flowers from the male plants delayed senescence to the same extent that removing the female flowers did. This result seemed to contradict the resource redistribution model, since it was assumed that the use of carbohydrate resources by staminate spinach flowers would be negligible compared with the carbohydrate use of pistillate flowers. However, more recent studies have shown that the nutritional demand of the staminate flowers actually *exceeds* the nutritional demand of the pistillate flowers, especially during early flower development. This could be a determining factor in triggering monocarpic senescence, even in male plants.

Although resource redistribution may well trigger monocarpic senescence, the critical compound is not carbohydrate, because many studies have now shown that the carbohydrate content of leaves increases during senescence. This observation is consistent with the ability of exogenous sugars to trigger leaf senescence. Rather than carbohydrate loss, alterations in source–sink relations caused by floral development may induce a global shift in the hormonal or nutrient balance of the vegetative organs. For example, a loss of nitrogen coupled with a simultaneous accumulation of carbohydrate would cause an increase in the C:N ratio, which has been associated with vacuolar-type PCD in senescing leaves.

The productivity of tall trees continues to increase right up to the onset of senescence

All individual trees die eventually, and it has long been assumed that the growth rate of trees declines with increasing tree size and mass. In fact, it is well established that as trees grow taller, their rate of growth in height decreases (**Figure 23.25**). To explain this decline in the rate of elongation growth over time, it has been reasoned that at some point the height of a tree will begin to approach the limits of the vascular system to deliver adequate supplies of water, minerals, and sugars to the growing tips of the extensive shoot and root systems. As water and other resources become limiting, declines in photosynthetic productivity should occur. The decline in leaf photosynthetic efficiency with increasing age of the tree is well documented. Age-related declines in tree growth have also been viewed as an inevitable consequence of increasing resource allocation to reproduction.

Although the results of a few single-species studies have been consistent with decreases in growth rates as trees increase in height, most of the evidence cited in support of declining tree growth has not been based on measurements of individual tree mass, but on age-related declines in either the *net primary productivity*

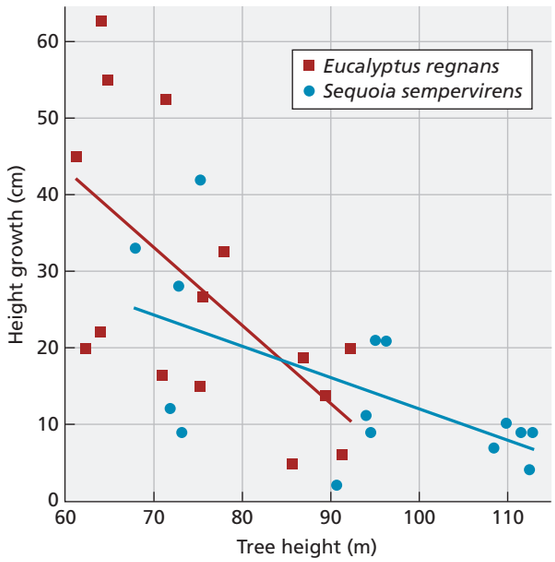


Figure 23.25 **Annual growth in height of eucalyptus and sequoia trees as a function of the beginning height of the tree in the year 2006.** In both cases, the growth in height declined with tree height. (After S. C. Sillett et al. 2010. *For. Ecol. Manage.* 259: 976–994.)

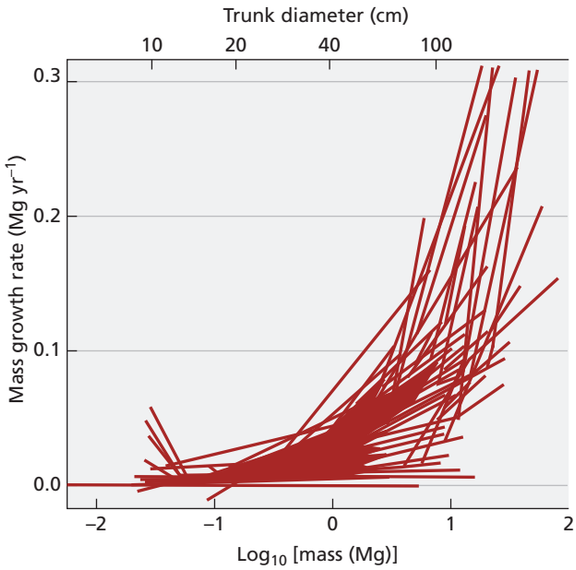


Figure 23.26 **Aboveground mass growth rates for 110,153 trees belonging to 89 species in North America (USA).** Trunk diameters (cm) are shown on the upper horizontal axis; the aboveground tree mass, expressed as $\log_{10}$ (mass in Mg [megagrams]), is shown on the lower horizontal axis; the mass growth rate (Mg yr^{-1}) is shown on the vertical axis. The mass growth rate increases with the aboveground tree mass. Similar results were obtained for 562,893 trees belonging to 314 species growing in five other continents. (After N. L. Stephenson et al. 2014. *Nature* 507: 90–93.)

of forest stands in which the trees are all of a similar age, or in the *rate of mass gain per unit leaf area*, with the implicit assumption that productivity declines at the individual leaf level can be extrapolated to the entire tree.

Recently, however, an analysis was undertaken of the mass growth rates of 673,046 trees belonging to 403 tropical, subtropical, and temperate tree species on every forested continent. In every continent, the aboveground tree mass growth rates for most species increased continuously with the $\log_{10}$ of the tree mass. The results for North America are shown in **Figure 23.26**. In the case of the largest trees, 97% of the species exhibited this trend. In absolute terms, different species of trees with 100-cm trunk diameters typically added from 10 to 200 kg of aboveground dry mass each year, averaging 103 kg per year. This is nearly three times the rate for trees of the same species with 50-cm trunk diameters. In the case of the most massive tree species, such as *Eucalyptus regnans* and *Sequoia sempervirens*, individual trees can add as much as 600 kg to the aboveground mass every year.

The findings just discussed demonstrate that although **growth efficiency** (tree mass growth per unit leaf area or leaf mass) often declines with increasing tree size, total tree leaf mass increases as the square of trunk diameter. A typical tree that experiences a 10-fold increase in diameter will therefore undergo a roughly 100-fold increase in total leaf mass and a 50- to 100-fold increase in total leaf area. Increases in the total leaf area are therefore sufficient to overcome the decline in growth efficiency and cause the whole-tree carbon accumulation rate to increase as the tree increases in size. However, at some point a limit is reached, and senescence occurs while the vascular cambium is still producing new, functional xylem and phloem tissue and the mass growth rate is still increasing. These findings suggest that tall tree senescence involves as yet unidentified factors leading to system collapse rather than simple wear and tear associated with aging. The extent to which the senescence of tall trees is brought about by internal versus external factors, such as fire, nutrient depletion, water stress, or pathogen attack, is still poorly understood.

Summary

Plant cells, organs, and organisms experience wear both from the effects of aging and from external stress. To break down old or damaged tissues, or to further some developmental pathways, plants undergo senescence, or genetically programmed cell death (Figure 23.2). Senescence involves coordinated actions at the cellular, organ, and organismal levels and is intricately regulated through multiple layers and pathways. When and how plants die is critical for plants' fitness.

23.1 Programmed Cell Death

- In plants, various types of PCD are an inherent part of development, as well as a response to biotic and abiotic stresses. Two distinctive types of PCD are developmental PCD and pathogen-triggered PCD (**Figure 23.3**).
- PCD during normal development occurs via vacuolar swelling and cell rupturing and is called vacuolar-type PCD, whereas PCD during the hypersensitive response occurs via vacuolar water loss and cell shrinkage and is called hypersensitive response-type PCD (**Figure 23.3**).
- Autophagosomes capture damaged cellular constituents and release their contents into the central vacuole to be degraded into reusable monomers (**Figure 23.4**).
- Autophagy is a homeostatic mechanism that maintains the metabolic and structural integrity of the cell. It also plays an important role in nutrient recycling during plant senescence. This ensures cellular survival by maintaining cellular energy levels and promoting the ordered degradation of cell constituents (**Figures 23.5, 23.6**).

23.2 The Leaf Senescence Syndrome

- Leaf senescence under normal growth conditions is governed by the developmental age of the leaf and may exhibit a sequential or seasonal pattern (**Figures 23.7, 23.8**). It can also occur prematurely under stressful environmental conditions.
- The earliest cellular changes during leaf senescence occur in the chloroplast (**Figure 23.9**).
- Autolysis of chloroplast proteins occurs in multiple compartments via different pathways (**Figure 23.10**).
- Chlorophyll degradation is governed by the pheophorbide *a* oxygenase (PAO)/phyllobilin pathway (**Figure 23.11**).

23.3 Regulation of Leaf Senescence: A Multi-Layered Network

- Leaf senescence is preceded by a massive reprogramming of gene expression (**Figure 23.12**).
- Leaf senescence is intricately regulated through multiple layers and pathways. A network of overlapping signaling pathways integrates internal and external inputs to regulate senescence through gene expression (**Figure 23.13**).
- The NAC family is one of the most intensively characterized TF families involved in leaf senescence. A trifurcate feed-forward pathway involving EIN2, *miR164*, and ORE1 plays an important role in regulating leaf senescence (**Figure 23.14**).
- The highly complex regulatory mechanisms underlying leaf senescence are fine-tuned at the chromatin, transcriptional, posttranscriptional, translational, and posttranslational levels (**Figure 23.15**).
- The PIF proteins are core components that convey photoreceptor-mediated light information to key leaf senescence regulators (**Figure 23.16**).
- The circadian clock, a part of the endogenous time measurement system, is linked to leaf senescence (**Figure 23.17**).
- Plant hormones such as ethylene, abscisic acid, methyl jasmonate, and salicylic acid act as positive regulators of senescence, while cytokinins and auxins act as negative regulators (**Figure 23.18**).
- There is growing evidence that reactive oxygen species (ROS), especially H_2O_2, can serve as internal signals to promote senescence.
- High concentrations of sugars may also serve to signal leaf senescence, especially under conditions of low nitrogen availability.

23.4 Abscission

- Abscission is the shedding of leaves, fruits, flowers, or other plant organs, and takes place within specific layers of cells called the abscission zone (**Figure 23.19**).
- In addition to the plant hormones auxin and ethylene, the developmental program precisely controls organ abscission. A honeycomb structure of lignin in the secession cells acts as a molecular brace that spatially restricts cell wall breakdown, and the residuum cells transdifferentiate into epidermal cells after the completion of abscission (**Figures 23.19–23.22**).

23.5 Whole-Plant Senescence

- In general, annuals and biennials reproduce only once before senescing, while most perennials can reproduce multiple times before senescing (**Figures 23.23, 23.24**).
- Nutrient redistribution from vegetative structures to reproductive sinks may trigger whole-plant senescence in monocarpic plants.
- While growth efficiency in trees declines with increasing tree size, leaf mass increases as the square of trunk diameter and can overcome this loss in efficiency, until internal or external factors initiate whole-tree senescence (**Figures 23.25, 23.26**).

Web Material

- **WEB TOPIC 23.1 Petal Senescence** Petal senescence is distinct from leaf senescence but shares common physiological and biochemical processes with it.
- **WEB TOPIC 23.2 Senescence-Associated Cell Death** The slower process of vacuolar-type PCD, which is required for sink-to-source transition at the cellular level, occurs during leaf cell senescence.
- **WEB TOPIC 23.3 Biochemical Pathways of Chlorophyll Breakdown** Chlorophyll breakdown is governed by the pheophorbide *a* oxygenase (PAO)/phyllobilin pathway.
- **WEB TOPIC 23.4 Abscission and the Dawn of Agriculture** A short essay discusses the domestication of modern cereals based on artificial selection for nonshattering rachises.
- **WEB TOPIC 23.5 Abscission, Plant Biotechnology, and Food Security** Investigation of organ abscission and cell separation can provide strategies to improving desirable traits in crops, thereby helping address the challenges of food security caused by the increasing global population.

For more study aids, go to oup.com/he/taiz7e.

Suggested Reading

Avila-Ospina, L., Moison, M., Yoshimoto, K., and Masclaux-Daubresse, C. (2014) Autophagy, plant senescence, and nutrient recycling. *J. Exp. Bot.* 65: 3799–3811.

Brusslan, J. A., Bonora, G., Rus-Canterbury, A. M., Tariq, F., Jaroszewicz, A., and Pellegrini, M. (2015) A genome-wide chronological study of gene expression and two histone modifications, H3K4me3 and H3K9ac, during developmental leaf senescence. *Plant Physiol.* 168: 1246–1261.

Gao, S., Gao, J., Zhu, X., Song, Y., Li, Z., Ren, G., Zhou, X., and Kuai, B. (2016) ABF2, ABF3, and ABF4 promote ABA-mediated chlorophyll degradation and leaf senescence by transcriptional activation of chlorophyll catabolic genes and senescence-associated genes in *Arabidopsis*. *Mol. Plant* 9: 1272–1285.

Guo, P., Li, Z., Huang, P., Li, B., Fang, S., Chu, J., and Guo, H. (2017) A tripartite amplification loop involving the transcription factor WRKY75, salicylic acid, and reactive oxygen species accelerates leaf senescence. *Plant Cell* 29: 2854–2870.

Humbeck, K. (2013) Epigenetic and small RNA regulation of senescence. *Plant Mol. Biol.* 82: 529–537.

Huysmans, M., Lema A. S., Coll, N. S., and Nowack, M. K. (2017) Dying two deaths - programmed cell death regulation in development and disease. *Curr. Opin. in Plant Biol.* 35: 37–44.

Ishida, H., Izumi, M., Wada, S., and Makino, A. (2014) Roles of autophagy in chloroplast recycling. *Biochim. Biophys. Acta Bioenerg.* 1837: 512–521.

Kim, J. H., Woo, H. R., Kim, J., Lim, P. O., Lee, I. C., Choi, S. H., Hwang, D., and Nam, H. G. (2009) Trifurcate feed-forward regulation of age-dependent cell death involving miR164 in Arabidopsis. *Science* 323: 1053–1057.

Kwon, S. I., Cho, H. J., Kim, S. R., Park, O. K. (2013) The Rab GTPase RabG3b positively regulates autophagy and immunity-associated hypersensitive cell death in Arabidopsis. *Plant Physiol.* 161: 1722–1736.

Lee, Y., Yoon, T. H., Lee, J., Jeon, S.Y., Lee, J. H., Lee, M. K., Chen, H., Yun, J., Oh, S.Y., Wen, X., et al. (2018) A lignin molecular brace controls precision processing of cell wall critical for surface integrity in Arabidopsis. *Cell* 173: 1468–1480.

Liebsch, D. and Keech, O. (2016) Dark-induced leaf senescence: new insights into a complex light-dependent regulatory pathway. *New Phytol.* 212: 563–570.

Liljegren, S. J., Roeder, A. H. K., Kempi, S. A., Gremski, K., Østergaard, L., Guimil, S., Reyes, D. K., and Yanofsky, M. F. (2004) Control of fruit patterning in Arabidopsis by INDEHESCENT. *Cell* 116: 843–853.

Luo, P. G., Deng, K. J., Hu, X.Y., Li, L. Q., Li, X., Chen, J. B., Zhang, H.Y., Tang, Z. X., Zhang, Y., Sun, Q. X., et al. (2013) Chloroplast ultrastructure regeneration with protection of photosystem II is responsible for the functional 'stay-green' trait in wheat. *Plant Cell Environ*. 36: 683–696.

Minina, E. A., Bozhkov, P. V., and Hofius, D. (2014) Autophagy as initiator or executioner of cell death. *Trends Plant Sci*. 19: 692–697.

Ono, Y. (2013) Evidence for contribution of autophagy to rubisco degradation during leaf senescence in *Arabidopsis thaliana*. *Plant Cell Environ*. 36: 1147–1159.

Sakuraba, Y., Jeong, J., Kang, M-Y., Kim, J., Paek, N-C., and Choi, G. (2014) Phytochrome-interacting transcription factors PIF4 and PIF5 induce leaf senescence in Arabidopsis. *Nat. Commun*. 5: 4636.

Thomas, H. (2013) Senescence, ageing and death of the whole plant. *New Phytol.* 197: 696–711.

Woo, H. R., Kim, H. J., Lim, P. O., and Nam, H. G. (2019) Leaf Senescence: Systems and Dynamics Aspects. *Annu. Rev. Plant Biol.* 70: 347–376.

Woo, H. R., Koo, H. J., Kim, J., Jeong, H., Yang, J. O., Lee, I. H. Jun, J. H., Choi, S. H., Park, S. J., Kang, B., et al. (2016) Programming of plant leaf senescence with temporal and inter-organellar coordination of transcriptome in Arabidopsis. *Plant Physiol.* 171: 452–467.

Zhu, X., Chen, J., Xie, Z., Gao, J., Ren, G., Gao, S., Zhou, X., and Kuai, B. (2015) Jasmonic acid promotes degreening via MYC2/3/4- and ANAC019/055/072-mediated regulation of major chlorophyll catabolic genes. *Plant J.* 84: 597–610.

24 Biotic Interactions



schankz/Shutterstock

In natural habitats, plants live in complex, diverse environments in which they interact with a wide variety of organisms (**Figure 24.1**). Some of these interactions are clearly beneficial, if not essential, to both the plant and the other organism. Such a mutually beneficial biotic interaction is termed a **mutualism**. Examples of mutualism include plant–pollinator interactions, the symbiotic relationship between nitrogen-fixing bacteria (rhizobia) (see Chapter 14) and leguminous plants, and the mycorrhizal associations observed between most plants and fungi (see Chapter 7). Other types of biotic interactions, including **herbivory**, infection by **microbial pathogens** or **parasites** (organisms living in or on the plant and gaining their nutrition at the expense of their hosts), and **allelopathy** (chemical warfare between plants), are detrimental. Plants have evolved intricate defense mechanisms to protect themselves against harmful organisms, and these harmful organisms have in turn evolved counter mechanisms to defeat the plants' defenses. Such tit-for-tat evolutionary processes are examples of **coevolution**, which accounts for the complex interactions between plants and other organisms.

However, it would be an oversimplification to characterize all organisms that interact with plants as either beneficial or harmful. For example, the grazing of flowers by mammals decreases fitness in some plant species, but in others it can lead to an increase in the number of flowering stalks, thus increasing fitness. There are also organisms that benefit from their interaction with the plant without causing any harmful effects. Such neutral interactions (from the plant's perspective) are termed **commensalism**. Commensal organisms can become beneficial if they protect the plant from a second, harmful organism. For example, nonpathogenic soil bacteria and fungi, which cause no harm to the plant, may nevertheless stimulate the plant's innate immune system (discussed in Section 24.4) and thus protect the plant from other, pathogenic microorganisms.

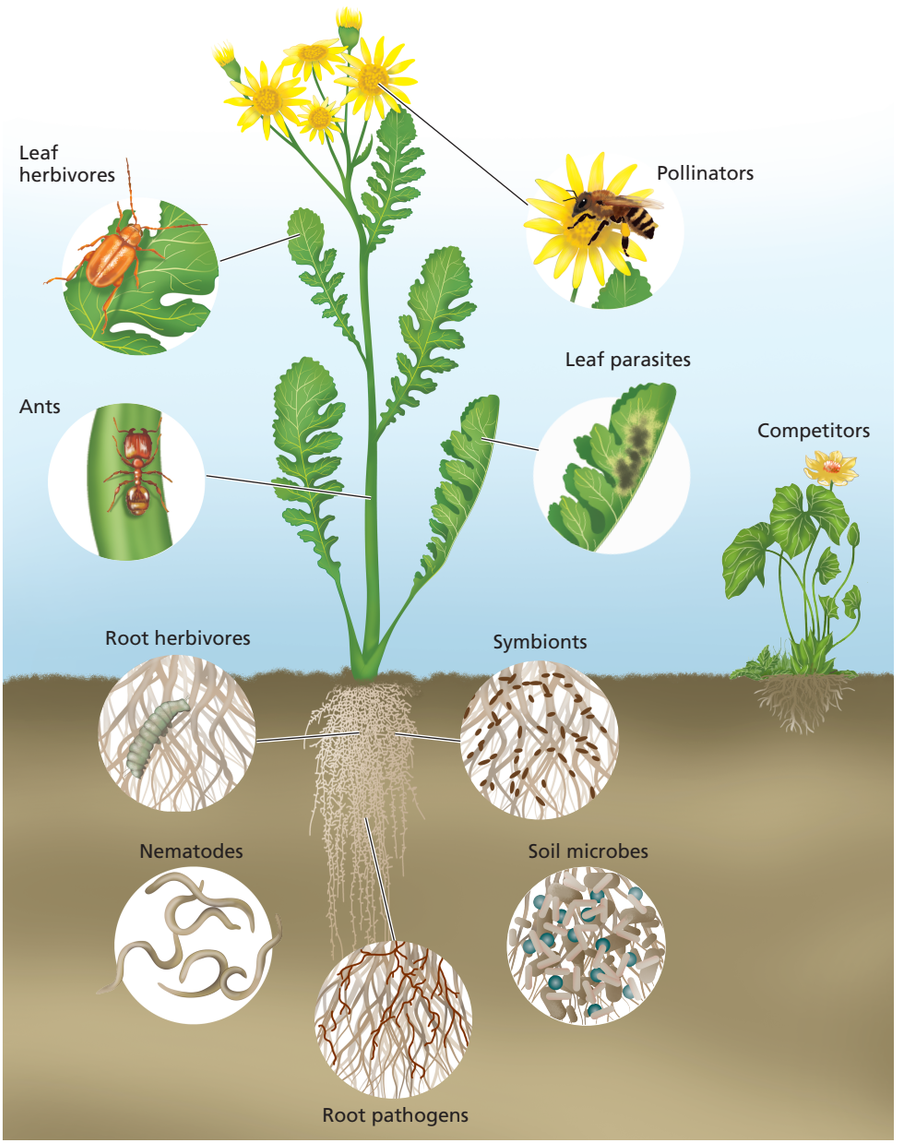


Figure 24.1 **Virtually every part of the plant is adapted to coexist with the organisms in its immediate environment.** (After N. M. van Dam. 2009. *Plant Biol.* 11: 1–5.)

The first line of defense against potentially harmful organisms is the plant's preexisting **constitutive defenses**. Structures such as spines, thorns, and hairs filled with toxins can deter animals from eating the plant. The cuticle (a waxy outer layer), the periderm, and other mechanical barriers also help block bacterial, fungal, and insect entry (see **WEB TOPIC 24.1**). Plants also accumulate toxic specialized metabolites to deter herbivores or defend against pathogen invasion. The second line of defense typically involves **inducible defenses** such as the production of a toxic chemical in response to attack. Inducible defenses require the plant to deploy specific detection systems and signal transduction pathways that can sense the presence of an herbivore or pathogen and alter defense-related gene expression and metabolism accordingly.

We begin our discussion of these biotic interactions with examples of beneficial associations between plants and microorganisms. Next we consider various types of harmful interactions between plants, herbivores, and pathogens. We then survey the wide range of inducible defenses that plants have evolved to fend off insect herbivores, and the signaling molecules and signal transduction pathways that regulate them. We follow with a discussion of plant responses to microbial pathogens, for which some of the same themes of constitutive and inducible defenses are employed. Although plants lack vertebrate-type adaptive immunity, several plant-specific responses to biotic stress can confer both local and **systemic** (plant-wide) resistance to pathogens. Finally, we discuss the mechanisms of two other types of plant

biotic interactions, nematodes and parasitic plants, and the ecological role that toxic root exudates play during plant–plant competition.

24.1 Plant Interactions with Beneficial Microorganisms

The first land plants appear in the fossil record about 450–500 million years ago (mya), with the first fossil plants that also show fungal associations with roots (i.e., mycorrhizal associations) dated at approximately 400 mya. Thus, a mutualistic symbiosis between plant and fungus appears to have occurred very early in the land plant lineage and was probably an important factor in helping plants invade the terrestrial environment. Indeed, land plants are colonized by a wide variety of beneficial microorganisms: endophytic and mycorrhizal fungi, bacteria in the form of biofilms on the surfaces of roots and leaves, endophytic bacteria within the plant, and nitrogen-fixing bacteria contained in specialized root or stem nodules.

In this section we focus on the signaling mechanisms involved in beneficial interactions of plants with three types of microorganisms: nitrogen-fixing bacteria, mycorrhizal fungi, and rhizobacteria. In Chapters 7 and 14 we discussed these biotic interactions from an anatomical and physiological perspective. Here we examine the molecular signaling mechanisms that control the formation of the associations.

The fungal partner in arbuscular mycorrhizal associations belongs to the ancient phylum Glomeromycota. The interaction of Glomeromycota with plant roots is so finely tuned that these fungi have lost the ability to complete their life cycles outside the plant. In part, the fungal dependence on plant partners results from a need to incorporate plant membrane lipids in periarbuscular membrane structures formed by mycorrhizal fungi within plant root cells. Because arbuscular mycorrhizas can be grown only in the presence of their host, progress on dissecting the signaling between the mycorrhizas and their host initially proceeded slowly. However, the rhizobium–legume association proved to be much easier to approach because the bacterial partner in this symbiosis could be cultured independently, allowing the chemicals it produced to be more easily defined, isolated, and then tested to determine their effects on the plant. Once the molecular details of this plant–bacterium interaction were characterized, researchers could ask whether similar processes also occurred during plant–mycorrhizal associations. The similarities that these comparisons revealed have led to the proposal that the rhizobium–legume signaling pathway actually evolved from the more ancient arbuscular mycorrhizal–plant interaction pathway. This idea fits well with the timing of the evolution of the rhizobium–legume symbiosis, which is thought to have formed relatively recently, approximately 60 mya.

Nod factors are recognized by the Nod factor receptor (NFR) in legumes

As described in Chapter 14, symbiotic nitrogen-fixing rhizobia release chemical **nodulation** (**Nod**) **factors** as signaling agents as they near the surface of a legume root. The interaction of specific Nod factors with corresponding Nod factor receptor-like kinases (RLKs) in the plant is the basis for host–symbiont specificity (**Figure 24.2**). Upon binding of Nod factors, the receptors initiate a series of signaling processes within the plant. These signaling pathways facilitate the entry of the symbiotic bacterium into the tissues of the root via the root hairs at the root surface, as well as the activation of a set of genes that regulate the formation of the root nodules deeper in the root's cortical tissues. These nodules are the plant-derived structures that will eventually house the bacteria and provide conditions for them to perform nitrogen fixation. A second type of receptor, called the **symbiosis receptor-like kinase** (**SYMRK**), also participates in these processes. Upon binding of Nod factors, this complex of NFR and SYMRK is thought to activate a cascade of subsequent steps, including fluctuations in the plant's cellular Ca^{2+} concentration, called Ca^{2+} spiking, inside and around the nucleus of the infected epidermal cell (**Figure 24.3**). These events eventually cause the activation of the **core symbiotic genes** (see Figure 24.2) and a series of steps such as signaling via the plant hormone cytokinin (see Chapter 4) that lead to nodulation.

Arbuscular mycorrhizal associations and nitrogen-fixing symbioses involve related signaling pathways

In legumes, *SYMRK* and several other core symbiotic genes have been shown to be required both for legume nodulation and for arbuscular mycorrhizal association. Similarly, the chemical structures of the Nod factors that trigger this system in nodulation resemble those of the Myc factor signaling molecules that elicit similar events in response to mycorrhizal fungi. Taken together, these parallels have led to the idea that the interaction between legumes and nitrogen-fixing rhizobia probably evolved from the more ancient interaction between plants and mycorrhizal fungi, with shared signaling elements forming a **common symbiotic pathway**. Non-nodulating or non-mycorrhizal plants such as Arabidopsis appear to have lost some elements of this core symbiotic pathway, but they do have close relatives of some components such as the Myc factor receptors. However, in these plants the receptors are used to trigger defenses against fungi (discussed in Section 24.4). This observation suggests that a defense response

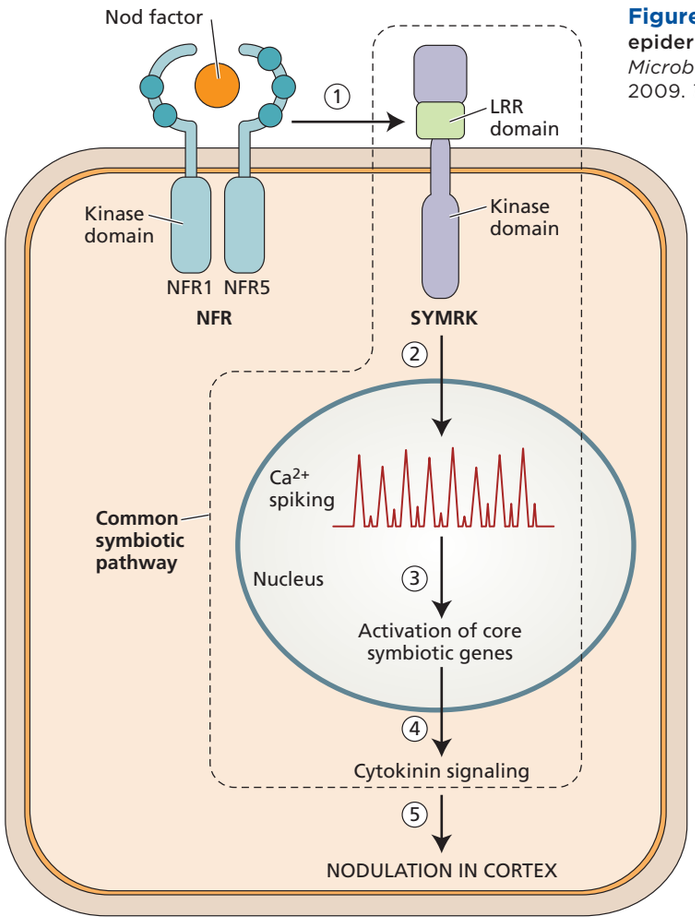


Figure 24.2 Model for Nod factor signaling in the root epidermis. (After C. Gough and J. Cullimore. 2011. *Mol. Plant Microbe. Interact.* 24: 867–878; K. Markmann and M. Parniske. 2009. *Trends Plant Sci.* 14: 77–86.)

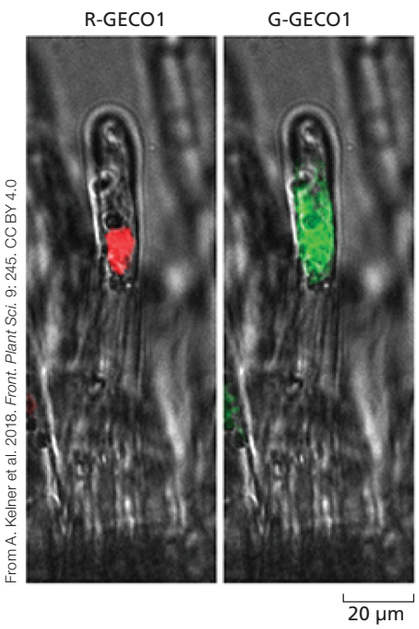
1. The binding of Nod factors to the Nod factor receptors (NFRs) initiates an interaction with the conserved symbiosis receptor-like kinases (SYMRK) containing a leucine rich repeat (LRR) domain. Binding of a Myc factor to a similar receptor in response to mycorrhizal fungal interaction also stimulates SYMRK signaling.

2. The interaction between NFR and SYMRK initiates Ca^{2+} spiking in the nucleus, presumably via a second messenger molecule.

3. Core symbiotic genes are activated.

4. Cytokinin signaling is initiated.

5. Cytokinin signaling brings about the morphological changes associated with nodulation.



From A. Kelner et al. 2018. *Front. Plant Sci.* 9: 245. CC BY 4.0

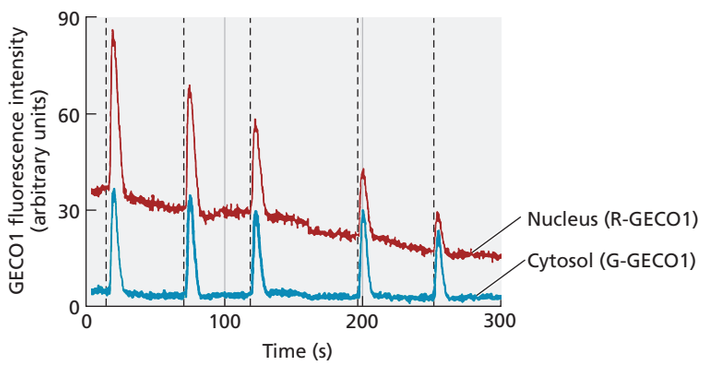


Figure 24.3 Oscillations in the Ca^{2+} concentration in an emerging root hair of *Medicago truncatula* responding to the addition of Nod factor. The plant has been engineered with two Ca^{2+}-sensitive fluorescent proteins (genetically encoded Ca^{2+} indicators for optical imaging, or GECOs), one targeted to the nucleus and one to the cytoplasm. Prominent Ca^{2+} spiking occurs around the nucleus, followed by increases in the cytoplasm near the nucleus and then throughout the root hair cytoplasm. (After A. Kelner et al. 2018. *Front. Plant Sci.* 9: 245. CC BY 4.0)

system was recruited first for initiation of mycorrhizal associations and subsequently for legume–rhizobium signaling. Some plant lineages then lost the symbiotic associations for this pathway, which has been repurposed for the detection of pathogenic fungi.

Rhizobacteria can increase nutrient availability, stimulate root branching, and protect against pathogens

Plant roots provide a nutrient-rich habitat for the proliferation of soil bacteria that thrive on root exudates and lysates, which can represent as much as 40% of the total carbon fixed during photosynthesis. Population densities of bacteria in the rhizosphere can be up to 100-fold higher than in bulk soil, and up to 15% of the root surface may be covered by microcolonies of a variety of bacteria. While these bacteria use the nutrients that are released from the host plant, they also secrete metabolites into the rhizosphere.

A loosely defined group of **plant growth-promoting rhizobacteria** (**PGPR**) provides several beneficial services to growing host plants (**Figure 24.4**). For example, volatile chemicals (i.e., molecules that easily vaporize into the air) produced by the bacterium *Bacillus subtilis* alter root architecture by changing root length and lateral root density. In addition to having these developmental effects, the same volatiles have been shown to enhance proton release by Arabidopsis roots in iron-deficient growth media. These protons acidify the soil, thereby facilitating increased iron uptake and leading to plants with higher chlorophyll content, higher photosynthetic efficiency, and increased size.

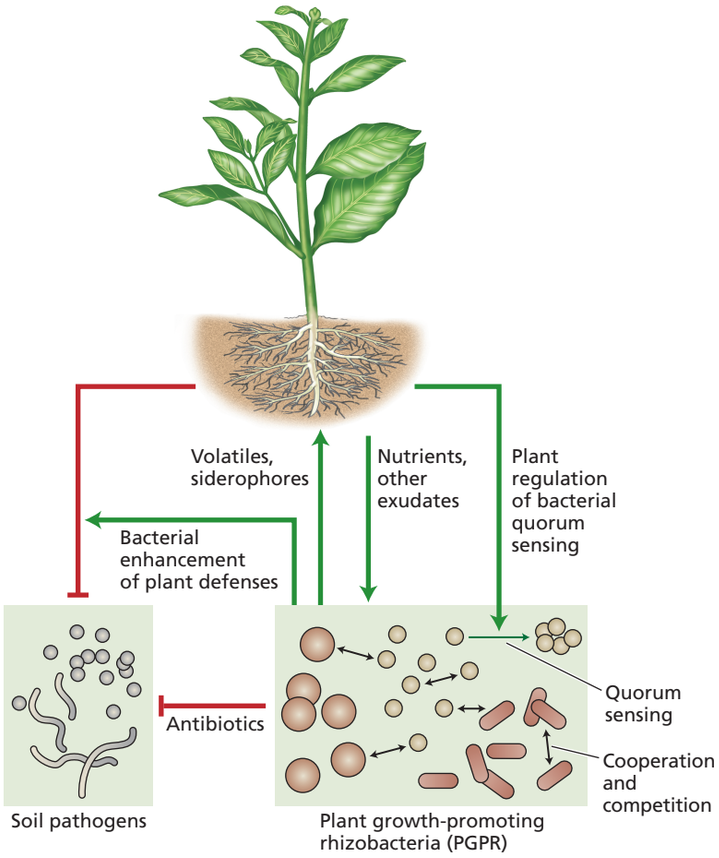


Figure 24.4 **Diagram of the interactions between plants and plant growth-promoting rhizobacteria,** such as *Pseudomonas aeruginosa*, which is thought to release antibiotics or siderophores into the soil that alleviate plant abiotic or biotic stress. The plant exerts control over the bacterial population by regulating bacterial quorum sensing signaling pathways through the release of exudates by the roots. (After C.-H. Goh et al. 2013. *J. Chem. Ecol.* 39: 826–839.)

PGPR can also control the buildup of harmful soil organisms. For example, root-associated *Pseudomonas* species synthesize the antifungal compound 2,4-diacetylphloroglucinol, suppressing the growth of the pathogenic fungus *Gaeumannomyces graminis*. In addition, several studies have suggested that *Pseudomonas aeruginosa* can alleviate the symptoms of biotic and abiotic stress by the release of antibiotics or iron-scavenging **siderophores** (see Chapter 8). The amounts of the compounds released by *P. aeruginosa* are controlled by the bacterium's own **quorum sensing** signaling pathways, which are activated when the bacterium population density reaches a certain level. Plants influence the amount of antibiotics or siderophores released by rhizobacteria through the production of root exudates that regulate these bacterial quorum sensing pathways. In addition to producing chemicals that act to alter the microbial populations or characteristics of the soil around the root, PGPR microbes can also provide protection against pathogenic organisms by activating the *systemic acquired resistance* (*SAR*) pathway within the plant, a defense network we discuss more fully in Section 24.4.

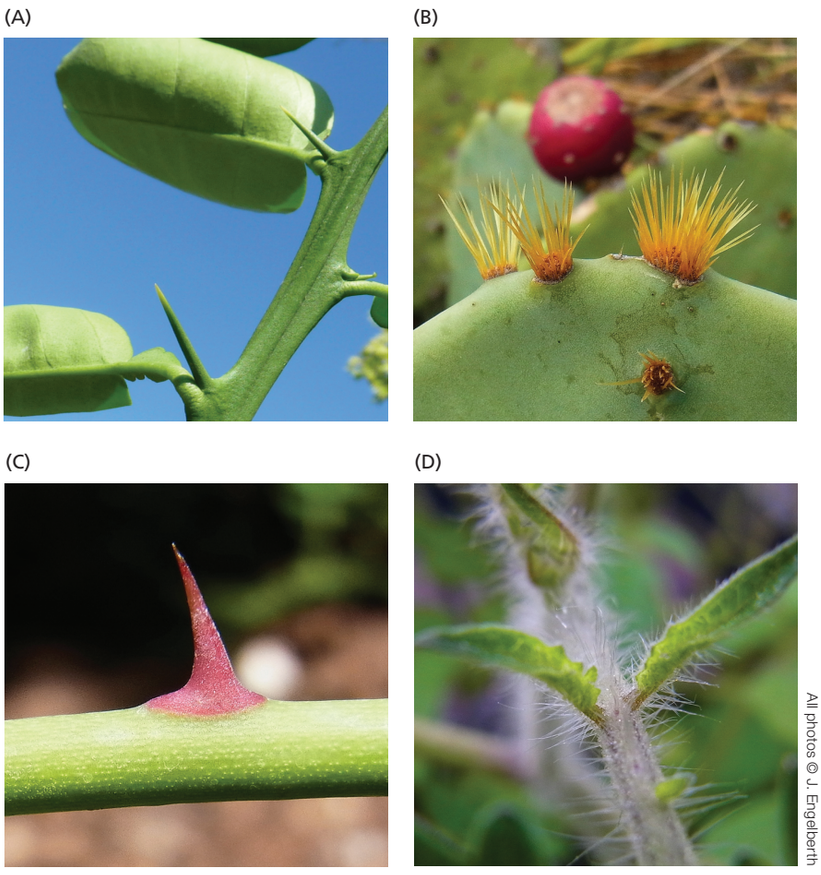
24.2 Herbivore Interactions That Harm Plants

Along with microbial pathogens, vertebrate and invertebrate herbivores represent a major cause of biotic plant damage. Numerous mammals, reptiles, and mollusks feed on plants, as do about half of the more than 1 million insect species, with 20 to 40% of global crop productivity being lost annually to these pests. In more than 350 million years of plant–herbivore coevolution, herbivores have developed diverse feeding styles and behaviors, while plants have evolved mechanisms to

defend themselves against herbivory. Plants employ an array of strategies to resist being eaten, including mechanical barriers, constitutive chemical defenses, and both direct and indirect inducible defenses. These defense mechanisms are in general quite effective, since most plant species are resistant to a wide range of herbivores. For example, about 90% of insect herbivores are restricted to consuming a single family of plants or just a few closely related plant species, while only 10% are generalists, able to eat a wide range of plants. This observation suggests that the vast majority of plant–herbivore interactions have involved coevolution, whereby the insect has had to develop specific strategies tailored to circumventing the defenses of its particular family of plant targets, but then cannot cope with the different defenses employed by other plants.

Mechanical barriers provide a first line of defense against insect pests and pathogens

Mechanical barriers, including surface structures, mineral crystals, and thigmonastic (touch-induced) leaf movements, often provide a first line of defense against pests and pathogens for many plant species. The most common surface structures are thorns, spines, prickles, and trichomes (**Figure 24.5**). **Thorns** are modified branches, as in citrus and acacia; **spines** are modified leaves, as in cacti; and **prickles** are derived mainly from the epidermis, as in roses. All of these structures possess sharp, pointed tips that physically protect plants from larger herbivores, such as mammals. However, they are less effective against smaller, insect herbivores, which can easily avoid such defenses and reach the edible parts of the shoot. **Trichomes**, or hairs, provide another layer of defense that can be effective against insect pests. These structures occur in a variety of forms, either as simple hairs that can mechanically interfere with insect locomotion, or as glandular trichomes that can wage chemical warfare against a potential herbivore. Glandular trichomes store species-specific noxious specialized metabolites (discussed in the next subsection) such as terpenoids and phenolics in a pocket formed between the cell wall and the cuticle. These pockets burst and release their contents upon herbivore contact, and the strong smell and bitter taste of these compounds often repel insect pests; in some cases, the sticky exudate from the trichome can actually immobilize the attacker. In addition to serving as barriers to insect herbivory, trichomes—when bent or damaged—may also act as



All photos © J. Engelberth

Figure 24.5 Examples of mechanical barriers developed by plants. **(A)** Thorns on a lemon tree (*Citrus* sp.) are modified branches, as can be seen by their position in the axil of a leaf. **(B)** Spines, which are characteristic of cacti (*Opuntia* spp.) in the New World, are modified leaves. **(C)** Prickles can be found on the stem and petioles of roses (*Rosa* spp.) and are formed by the epidermis. **(D)** Trichomes on shoot and leaves of tomato (*Solanum lycopersicum*) are also derived from epidermal cells.

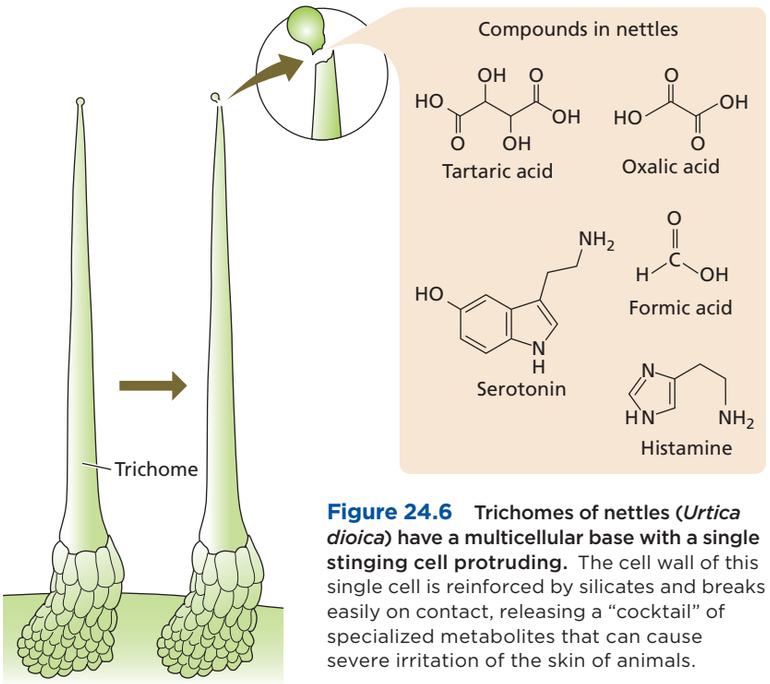


Figure 24.6 **Trichomes of nettles (*Urtica dioica*) have a multicellular base with a single stinging cell protruding.** The cell wall of this single cell is reinforced by silicates and breaks easily on contact, releasing a "cocktail" of specialized metabolites that can cause severe irritation of the skin of animals.

herbivore sensors, sending electrical or chemical signals to surrounding cells. Such signals can trigger the formation of inducible defense compounds, a topic we discuss in more detail in Section 24.3.

The leaves of the stinging nettle (*Urtica dioica*) possess highly specialized "stinging hairs" that form an effective physical and chemical barrier against larger herbivores. The cell walls of these hollow, needlelike trichomes are reinforced with silicates (glass) and filled with a nasty "cocktail" of acids such as oxalic acid, tartaric acid, formic acid, the neurotransmitter serotonin, and the inflammatory agent histamine (**Figure 24.6**). Prior to contact, the tip of the stinging hair is covered by a tiny glass bulb that readily snaps off when touched by an herbivore (or an unlucky human who happens to brush against it), leaving an extremely sharp point to puncture the animal's skin. The pressure of contact also pushes the needlelike trichome shaft down onto the spongy plant tissue at its base, which acts like the plunger of a syringe, injecting the cocktail and causing severe irritation and inflammation.

A different type of mechanical obstacle to herbivory is provided by mineral crystals that are present in many plant species. For example, silica crystals, called **phytoliths**, form in the epidermal cell walls, and sometimes in the vacuoles, of many grass species. Phytoliths add toughness to the cell walls and make the leaves of grasses difficult for herbivores to chew. The cell walls of the horsetail *Equisetum hyemale* contain so much abrasive silica that the indigenous peoples of North America and Mexico used the stems of these plants to clean their cooking pots.



Courtesy of Agong1/Wikipedia

Figure 24.7 **Calcium oxalate crystals (raphides) from the leaf of an agave (*Agave weberi*).** These raphides are tightly packed in specialized cells called idioblasts and are released upon damage. Note the size and pointed ends of these structures.

Calcium oxalate crystals provide another, widespread mechanical deterrent to eating certain plants. These crystals are present in the vacuoles of more than 200 families of plants, including species in the genera *Vitis* (grapes), *Agave*, and *Medicago* (medick, or burclover). Much as with phytoliths, these crystals act as physical deterrents, for example, having abrasive effects on the mouthparts of insect herbivores, especially the mandibles. They therefore serve as a mechanical deterrent for attack by insects, mollusks, and other herbivores. These crystals may be distributed evenly throughout the leaf or restricted to specialized cells called **idioblasts**, with some also forming bunches of needlelike structures called **raphides** (**Figure 24.7**). Raphides have extremely sharp tips that can penetrate the soft tissue in the throat and esophagus of an herbivore. The raphide-rich *Dieffenbachia*, a popular tropical houseplant, is called "dumb cane" because chewing the leaves reputedly renders the victim speechless due to the inflammation caused by consuming the oxalate crystals. Besides inflicting mechanical damage, raphides may also allow other toxic compounds produced by the plant to penetrate through the wounds they produce.

A very different means of avoiding herbivory is employed by sensitive plant (*Mimosa* spp.). *Mimosa* species possess composite leaves consisting of many individual leaflets that are connected to the midrib by a jointlike structure called the pulvinus. This pulvinus acts as a turgor-driven hinge, swelling or deflating and so causing each pair of attached leaflets to move. The pulvinus is responsive to various stimuli, including heat, diurnal cycles (in what is called *nyctinasty*, or sleep movements), solar tracking, water deficiency, and most important in the context of escaping being eaten, touch and damage. If an insect herbivore attempts to chew on a *Mimosa* leaflet, the pulvinus at the base of the damaged leaflet almost immediately deflates, causing the attached leaflets to fold together. Over the course of just a few seconds, this response then spreads to the other undamaged parts of the leaf, causing a wave of leaflet movements. If the stress signal is strong enough, the entire leaf collapses downward due to the action of another pulvinus located at the base of the petiole. Such rapid movements of leaflets and leaves may deter feeding insects and grazing herbivores by startling them (**Figure 24.8**).



Figure 24.8 Leaves of the sensitive plant (here *Mimosa pudica*) respond rapidly to touch by folding in their individual leaflets within seconds. This rapid movement may deter potential insect herbivores. **(A)** Untouched (control) leaves. **(B)** Leaves 5 s after touch.

Plant specialized metabolites can deter insect herbivores

Plants are amazing biochemical factories, so it should not be surprising that chemical defense mechanisms compose a further line of defense against plant pests and pathogens. Plants produce a wide array of chemicals that can be categorized into primary metabolites and specialized metabolites. **Primary metabolites** are those compounds that all plants produce and that are directly involved in growth and development. They include sugars, amino acids, fatty acids and lipids, and nucleotides, as well as the larger compounds that are made of these building blocks, such as proteins, polysaccharides, DNA, and RNA. In contrast, **specialized metabolites** (also called *secondary metabolites*) are often species-specific and usually belong to one of three major classes of chemicals: terpenoids, phenolics, or alkaloids (**Figure 24.9**).

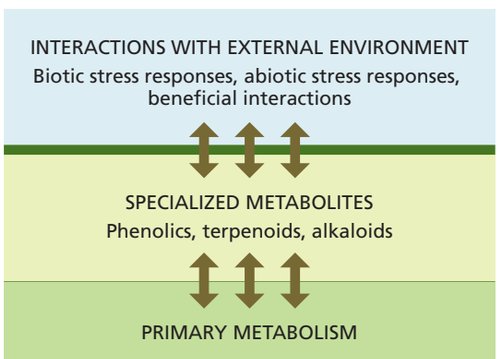


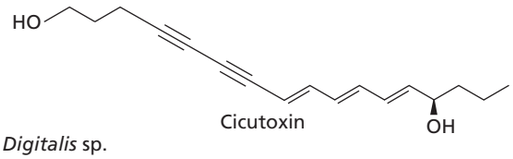
Figure 24.9 Specialized metabolites are located at the interface between primary metabolism and the interaction of organisms with their environment. As such, they play important roles in the plant defense response against pests and pathogens; the regulation of beneficial interactions, including the attraction of pollinators; and as modulators in response to abiotic stresses.

Plants store constitutive toxic compounds in specialized structures

Plants can synthesize a broad range of specialized metabolites that have negative effects on the growth and development of other organisms. Classic examples of plants that are toxic to humans because of their specialized metabolites are hemlock (*Cicuta* spp.) and foxglove (*Digitalis* spp.), which produce the highly toxic cicutoxin (a neurotoxin) and digitoxin (a cardiac toxin), respectively (**Figure 24.10**). In some cases these compounds have proven useful for medicinal purposes. For example, digitoxin is a **cardiac glycoside** that acts by inhibiting the Na^+/K^+-ATPase pump in the plasma membranes of

(A) *Cicuta* sp.





(B) *Digitalis* sp.



Both photos © J. Engelberth

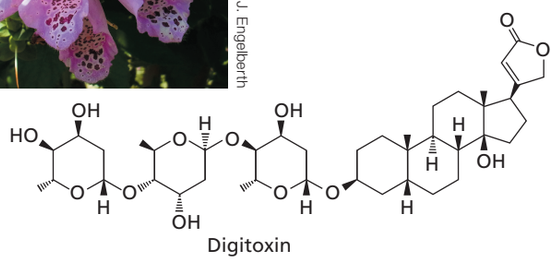


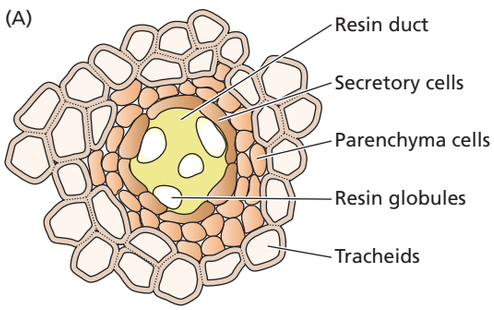
Figure 24.10 Constitutive chemical defenses are effective against many different herbivores, including insects and mammals. Hemlock (*Cicuta* sp.) produces cicutoxin, a diacetylene that prolongs the repolarization of neuronal action potentials. The active principle in foxglove (*Digitalis* sp.) is digitoxin, a cardiac glycoside that inhibits ATPase activity and can increase myocardial contraction.

heart cells. This inhibition leads to increased myocardial contraction, and although fatal at high levels, in therapeutic doses digitoxin has been used to treat congestive heart failure and cardiac arrhythmia. Indeed, plants continue to be a rich source for the discovery of such bio-medicinal compounds. However, it is important to remember that the reason these compounds exist is largely because plants use them to prevent themselves from being eaten, by conducting chemical warfare on their herbivores.

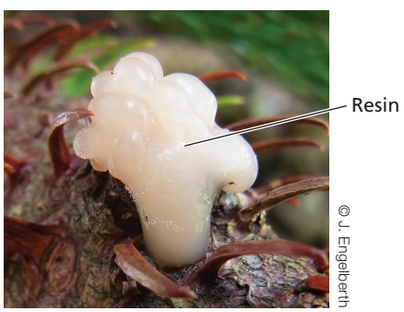
Some of these constitutively produced defensive specialized metabolites can also have deleterious effects on the plant itself. To avoid such autotoxicity, these compounds must be safely stored within the cell, and they must also be relatively isolated from susceptible tissues in the event of release due to cellular damage. Plants therefore tend to accumulate toxic specialized metabolites in storage organelles such as vacuoles, or in specialized anatomical structures such as *resin ducts*, *laticifers* (latex-producing cells), or glandular trichomes. Following an attack by herbivores or pathogens, the toxins are released and become active at the site of damage, without adversely affecting vital growing areas. **Conifer resin ducts**, which are found in the cortex and phloem, contain a mixture of diverse terpenoids (**Figure 24.11**), as well as resin acids. This cocktail is released immediately upon damage to the plant, acting either to poison the attacking herbivore or, because the resin is sticky, to glue the herbivore's mouthparts together. In extreme cases the resin may even engulf the whole insect or pathogen, effectively killing it. However, some herbivores have evolved strategies to avoid these effects. For example, bark beetles circumvent this defense by attacking water-stressed or weakened trees where the flow of resin is much reduced.

Most of the resin ducts in coniferous plants are considered constitutive defenses, but they can also be induced upon herbivore damage. The formation of these adventitious resin ducts, sometimes referred to as

(A)



(B)



© J. Engelberth

(C)

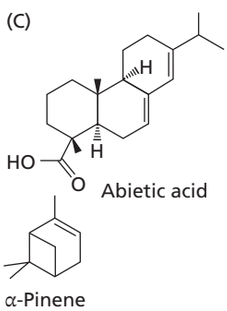


Figure 24.11 Resin stored in its resin ducts is released when herbivores damage the plant. **(A)** Resin duct in the wood of a conifer (*Araucaria* sp.). Note that the resin duct is surrounded by secretory cells that release resin components into the duct system. **(B)** Upon wounding, resin is released at the damage site. There it seals off the damage and serves as a repellent against further herbivory. **(C)** Two terppenoids that are common components of resin.

traumatic resin ducts, as well as the biosynthesis of their resin contents, are regulated by the hormone methyl jasmonate, a volatile derivative of jasmonic acid (JA, discussed in Section 24.3).

Laticifers are composed of cells that produce **latex**, a milky fluid of emulsified components that coagulate upon exposure to air. Compared with resins, latex is usually chemically much more complex and may also contain proteins and sugars besides toxic or repelling specialized metabolites. Laticifers may consist of a series of fused cells (articulated laticifers) or one long syncytial cell (non-articulated laticifers) (**Figure 24.12**). Most notable among the latex-producing plants is the rubber plant (*Hevea brasiliensis*), which has been grown commercially as a source of natural rubber. Upon wounding, this plant releases huge amounts of latex, which is collected by humans and later converted into rubber. Under natural conditions, the rubber released by wounded trees defends the plant against herbivores and pathogens, either by repelling or engulfing them.

Effective though such specialized metabolites can be at deterring herbivores, some animals have evolved adaptations to avoid them (e.g., the bark beetles described earlier) or actually capitalize on their production for their own defense. For example, milkweed (*Asclepias curassavica*) and related genera, such as oleander (*Nerium oleander*), produce latex that contains significant amounts of poisonous steroids called cardenolides. Generalist insect herbivores respond to these compounds either by being repelled or by suffering spasms that lead to death. In contrast, the specialist caterpillars of the monarch butterfly (*Danaus plexippus*) are insensitive to the toxins. They feed on milkweed leaves and retain the cardenolides in their bodies for their own defense, a trick also adopted by the large milkweed bug (*Oncopeltus fasciatus*) and the milkweed aphid (*Aphis nerii*) (**Figure 24.13**). As a result, most insectivorous birds quickly learn to avoid eating these insects. Indeed, the bright and distinctive coloration of the monarch caterpillars and butterflies serves to advertise their toxic nature.

In a further embellishment to the milkweed saga, the parasitic fly *Zenillia adamsoni* can obtain its cardenolide secondhand from the monarch caterpillar. When the female fly is ready to lay eggs, she seeks out a monarch caterpillar and deposits her eggs on its surface. Upon hatching, the fly larvae bore into the caterpillar and consume it from within. Besides using the caterpillar for nourishment, the fly larvae are able to store the caterpillar's toxic cardenolide and retain it as a defense throughout their adult stage.

Plants often store defense chemicals as nontoxic water-soluble sugar conjugates in the vacuole

In addition to accumulation within specialized structures, another common mechanism used by plants to safely store potentially dangerous specialized metabolites is to conjugate the toxic compound with a sugar such as glucose to produce a glycoside. This chemical modification produces a nontoxic precursor as well as making the specialized metabolite more water soluble. To become active, the glycosidic linkages often need to be enzymatically

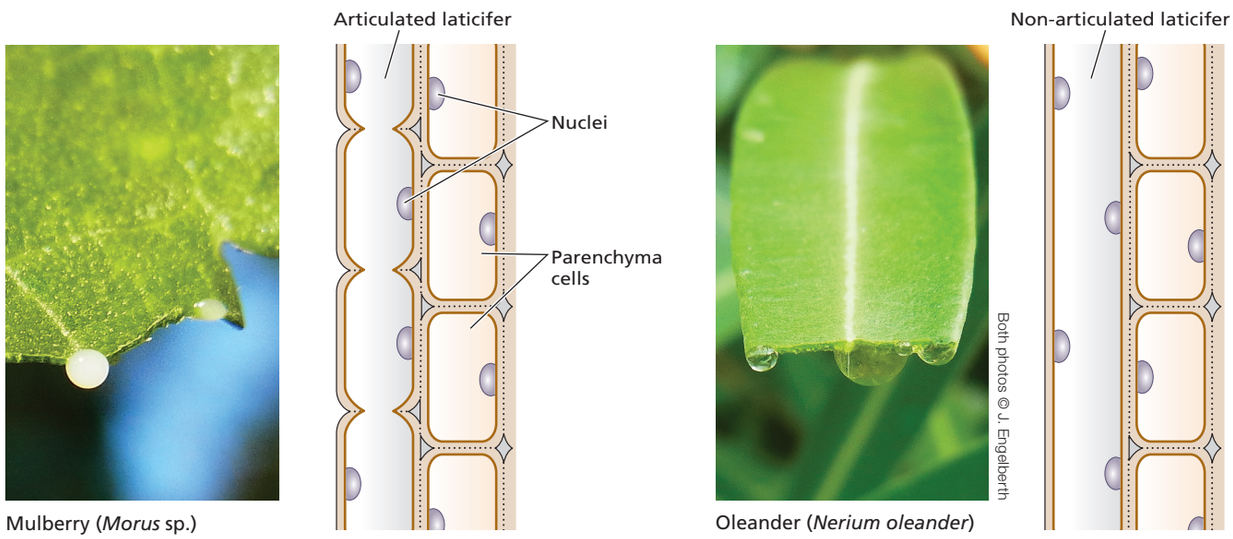


Figure 24.12 Laticifers are made of individual cells and can occur either as articulated systems (single cells connected by a small tube) or non-articulated systems (one large syncytial cell). Latex in the laticifers is released upon damage and often contains cardiac glycosides which fend off herbivores. While mulberry (*Morus* sp.) produces a milky latex in its articulated laticifers, oleander (*Nerium oleander*) releases a clear latex from non-articulated laticifers.

(A) Monarch butterfly (*Danaus plexippus*)



(B) Milkweed bug (*Oncopeltus fasciatus*)



(C) Milkweed aphid (*Aphis nerii*)



All photos © J. Engelberth

Figure 24.13 While most herbivores are very susceptible to the toxic metabolites in the latex of milkweed and oleander plants, some insect herbivores incorporate these compounds into their bodies and show this to potential predators by presenting bright colors. Shown here are three specialist insect herbivores that feed on these latex-producing plants: the caterpillar of the monarch butterfly (A), the milkweed bug (B), and the milkweed aphid (C). Of these, the milkweed bug and the milkweed aphid will use oleander as a food source if milkweed plants are not available.

hydrolyzed. Uncontrolled activation is prevented by the spatial separation of the activating hydrolases and their respective toxic substrates, which come together only when an herbivore starts chewing on the plant.

Vacuolar storage of glycosylated chemical defenses is used to deter both insects and pathogens. In some members of the Poaceae (grass) family, benzoxazinoids (toxic alkaloids) are constitutively produced defensive specialized metabolites. These compounds are usually stored in the vacuole as glycosides coupled to D-glucose (Glc) (**Figure 24.14**). When a cell is damaged by herbivory or pathogen invasion, the inactive glycosides are hydrolyzed, generating products that are toxic not only to insect herbivores but also against pathogens. Furthermore, benzoxazinoids released into the soil can also be toxic to microbes, insects, or competing plants, making these metabolites a powerful general chemical defense against the biotic challenges these plants are going to endure as they grow.

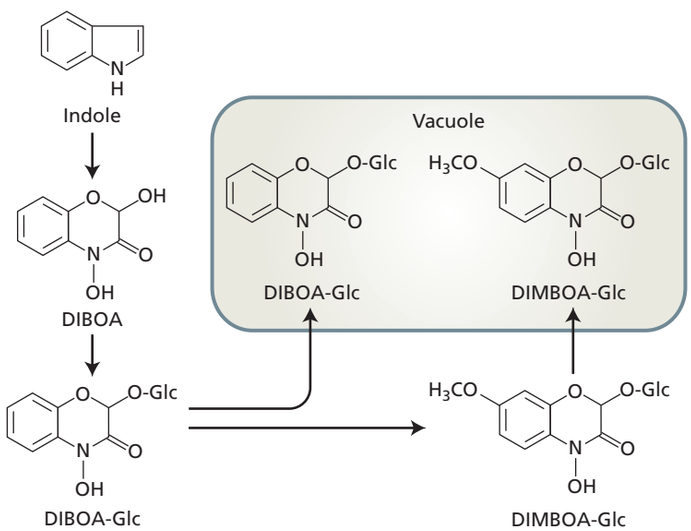
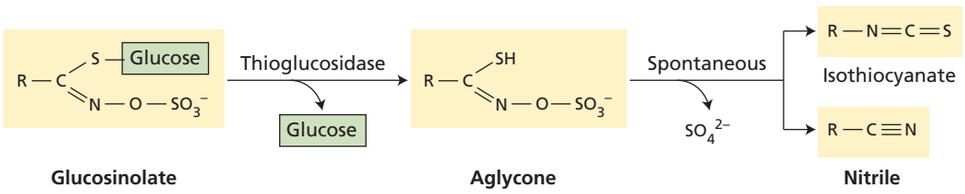


Figure 24.14 In members of the Poaceae family, benzoxazinoids, alkaloids derived from the tryptophan pathway, are major defensive specialized metabolites. The compound 2,4-dihydroxy-1,4-benzoxazin-3-one (DIBOA) and its derivative 2,4-dihydroxy-7-methoxy-1,4-benzoxazin-3-one (DIMBOA) are stored in the vacuole as glycosides (coupled to D-glucose, Glc). After damage, the glycosides are hydrolyzed and release their toxic products.

In the order Brassicales (cabbages and their relatives), many species produce glucosinolates —sulfur-containing organic compounds derived from glucose and an amino acid—as their major defensive specialized metabolites (see **WEB APPENDIX 4**). The hydrolyzing enzyme, myrosinase, is stored in different cells than its substrates. Thus, while myrosinase-containing cells are mostly glucosinolate-free, the so-called sulfur-rich cells contain high concentrations of glucosinolates. When the tissue is damaged, the released myrosinase and glucosinolates mix, resulting in the production of a variety of biologically active compounds that deter most generalist insect herbivores (**Figure 24.15**). The flavors of mustard, wasabi, radish, brussels sprout, and other related vegetables are due to these isothiocyanates. Indeed, humans



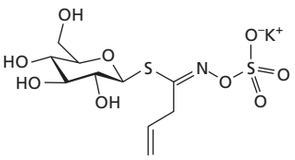


Figure 24.15 Hydrolysis of glucosinolates into mustardy volatiles. The isothiocyanates and nitriles are noxious products of these reactions. First the sugar is cleaved by the enzymatic action of a thiohydrolase to yield an aglycone product that spontaneously decomposes into the volatile toxic products. R represents various alkyl or aryl substituents. For example, if R is CH_2=CH—CH_2–, the compound is sinigrin, a major glucosinolate of black mustard seeds and horseradish roots.

often prize plants, or parts of them, for the culinary flavors imparted by these compounds. However, the high content of the specialized metabolites in these plants is primarily there not for our use in cooking, but to provide the noxious chemical defenses for protection from damage by pests and pathogens.

Cyanogenic glycosides represent a particularly toxic class of specialized metabolites. Upon tissue damage, these glycosides break down and release hydrogen cyanide (HCN). Cyanide inhibits mitochondrial function, so ultimately the herbivore's cells run out of energy and die. Several plant species of economic and nutritional importance, including sorghum (*Sorghum bicolor*) and cassava (*Manihot esculenta*), produce different types of cyanogenic glycosides (**Figure 24.16**). Cassava roots are a major source of dietary calories for people in tropical regions, but they must be carefully prepared by extensive washing and thorough cooking to remove the glycosides and so avoid cyanide toxicity when they are eaten.

24.3 Inducible Defense Responses to Insect Herbivores

While constitutive chemical defenses provide plants with protection against many pests and pathogens, and are common among plants in nature, there are disadvantages to this type of defense strategy. First, constitutive defenses are costly to the plant. The production of specialized metabolites requires a significant energy investment derived from primary metabolism, which is then unavailable for use in growth and reproduction. This trade-off is most obvious in agricultural crops, in

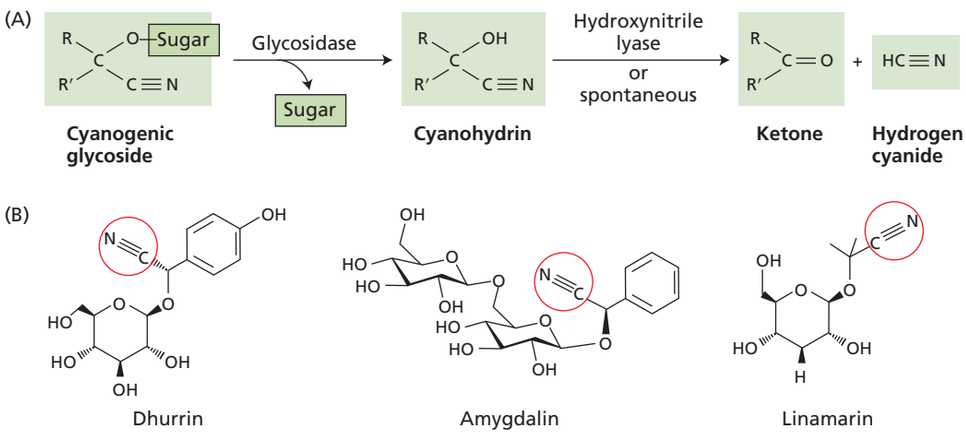


Figure 24.16 Cyanogenic glycosides break down to produce hydrogen cyanide providing a constitutive chemical defense against herbivores. **(A)** Enzyme-catalyzed hydrolysis of cyanogenic glycosides to release hydrogen cyanide. The cyanohydrin produced by glycosidase action on the stored cyanogenic glycoside decomposes either spontaneously or catalyzed by a hydroxynitrile lyase to form hydrogen cyanide. R and R′ represent various alkyl or aryl substituents. For example, if R is phenyl, R′ is hydrogen, and the sugar is the disaccharide β-gentiobiose, then the compound is amygdalin (the common cyanogenic glycoside found in the seeds of almonds, apricots, cherries, and peaches). **(B)** Other compounds that release toxic cyanide are dhurrin from sorghum and linamarin from cassava. The cyanide group is marked by a circle.

which yield is increased, in part, by reducing the capacity of the plant to defend itself. Second, pests and pathogens can adapt to the plant's constitutive chemical defenses, as we saw in the case of the monarch caterpillar and milkweed, even using these compounds to defend themselves against their own predators or parasites. Accordingly, most plants have evolved inducible defense systems in addition to whatever constitutive defenses they may have. Inducible defense systems enable plants to respond more flexibly to the full panoply of threats presented by pests and pathogens.

Inducible defenses require systems to monitor for signs of damage or of an attack and then trigger a response. Plants have many such systems, and in this section we discuss some of the mechanisms by which plants recognize insect herbivores and how they then mount their inducible defenses. Then, in Section 24.4 we investigate similar processes triggered by pathogen attack. For herbivory, these plant responses include not only the de novo synthesis of toxic specialized metabolites and proteins, but also the recruitment of natural enemies of the attacker along with the sending of signals to nearby plants to prepare them against impending herbivory.

Based on their feeding behaviors, three major types of insect herbivores can be distinguished:

1. *Phloem feeders*, such as aphids and whiteflies, cause little direct tissue damage. Phloem feeders insert their narrow *stylet*, which is an elongated mouthpart, between the cells of the epidermis and mesophyll and into the phloem sieve tubes of leaves and stems. The plant defense response to phloem feeders more closely resembles the response to pathogens (discussed in Section 24.4) than to other herbivores. Although the amount of direct tissue injury to the plant from insertion of the stylet is low, these insects can serve as vectors for plant viruses that can then cause great damage.
2. *Cell-content feeders*, such as mites and thrips, are piercing-and-sucking insects that cause an intermediate amount of physical damage to plant cells.
3. *Chewing insects*, such as caterpillars (the larvae of moths and butterflies), grasshoppers, and beetles, cause significant damage to plants. In the discussion that follows, our definition of "insect herbivory" mostly relates to this type of insect damage.

Plants can recognize specific components of insect saliva

To mount an effective inducible defense against pests or pathogens, the host plant must be able to sense that damage has occurred and determine that the source is a biotic attack. Mechanical damage, be it from an insect chewing on a leaf or from hailstones damaging the leaf surface, releases plant compounds that are not normally present in the apoplast. These include contents of the cytoplasm of the damaged cells, such as ATP or peptides, as well as fragments of cell wall such as oligogalacturonides. These compounds can then trigger responses to mechanical damage. However, most plant responses to insect herbivory involve both this general mechanical wound response and the recognition of certain compounds abundant in the insect's saliva or regurgitant that trigger further levels of defense. These insect compounds belong to a broad group of chemicals called **elicitors**, which trigger defense responses in plants to a wide variety of herbivores and pathogens. Although repeated mechanical wounding can induce responses similar to those caused by insect herbivory in some plants, certain molecules in insect saliva can serve as enhancers of this stimulus. In addition, wounding and insect-derived elicitors can trigger signaling pathways *systemically*—that is, throughout the plant—thereby initiating defense responses that can minimize further damage in regions of the plant that are not yet being directly attacked.

The first elicitor identified in insect saliva was a fatty acid–glutamine amide conjugate in the oral secretions of larvae of the beet armyworm (*Spodoptera exigua*) that was given the name volicitin (**Figure 24.17A**). Volicitin is produced only when the insect feeds on a plant, as the fatty acid component is derived from the ingested plant tissue and enzymatically conjugated in the gut to an insect-derived amino acid, typically glutamine.

Since the discovery of volicitin in *Spodoptera*, a variety of fatty acid amides have been identified in lepidopteran species as well as in crickets and fruit flies. Most of them were found to function as elicitors when applied to a broad range of plants. The fatty acid amides are now known to be just one of a variety of insect-produced

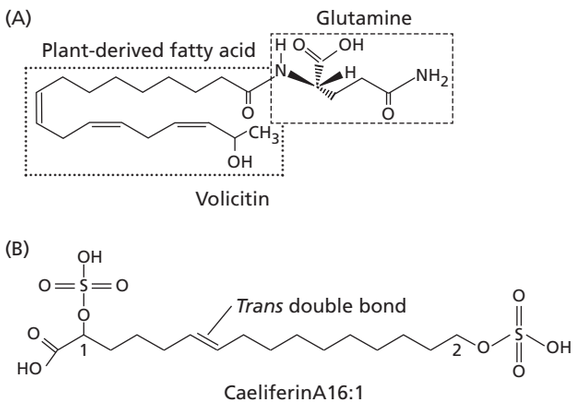


Figure 24.17 **Structures of major insect-derived elicitors.** **(A)** Linolenic acid–amino acid conjugates such as volicitin have been found to induce the release of volatile specialized metabolites in maize seedlings. **(B)** Two classes of caeliferins have been isolated and identified from regurgitant of the grasshopper *Schistocerca americana*. Shown is CaeliferinA16:1 in which two hydroxyls in the α (1) and ω (2) position are sulfated.

elicitors. For example, when *Spodoptera* feeds on cow pea, it breaks down an enzyme found in the plant's chloroplasts and thereby produces a protein fragment named inceptin. Inceptin appears in the oral secretions from the caterpillar and acts as an elicitor of plant defense, once again linking the triggering of the defense pathways to chemical evidence that the insect has been eating a plant.

Some insect-derived compounds elicit responses in a narrower range of species. For example, a class of elicitors named **caeliferins** (**Figure 24.17B**) is found in the oral secretions of a grasshopper (*Schistocerca americana*). Although this elicitor is active in maize (corn; *Zea mays*), neither legumes nor solanaceous plants respond to it with increased defense signaling. Unlike the fatty acid amides, the caeliferins appear to originate entirely within the grasshoppers, as they contain irregular fatty acid chain lengths and a *trans* double bond not found in plants.

We should note here that not all components of insect oral secretions trigger plant defense. For example, the enzyme glucose oxidase found in corn earworm (*Helicoverpa zea*) secretions actually suppresses maize defenses, demonstrating the complex chemical warfare being employed by both sides in the battles between herbivores and hosts.

Ca^{2+} signaling and activation of the MAP kinase pathway are early events associated with insect herbivory

When plants recognize they have been damaged and when they detect elicitors from insect saliva, a complex signal transduction network is activated in which an increase in the cytosolic free Ca^{2+} concentration ($[Ca^{2+}]_{cyt}$) is an early event. Ca^{2+} is a ubiquitous second messenger in multiple cellular responses of all eukaryotic systems (see Chapter 3). Under normal conditions, $[Ca^{2+}]_{cyt}$ is very low (~100 n*M*). Following stimulation by mechanical damage or by an elicitor, Ca^{2+} ions are rapidly released into the cytosol by a combination of influx across the plasma membrane and release from storage compartments such as mitochondria, endoplasmic reticulum, and the vacuole. These fluxes lead to an approximately tenfold increase in $[Ca^{2+}]_{cyt}$ that then activates an array of target Ca^{2+}-binding proteins, which in turn activate downstream targets of the signaling pathway. These downstream targets typically include networks of biochemical events controlled by protein phosphorylation and the reprogramming of gene expression (see Chapter 4). For example, in Arabidopsis a protein called IQD1 was identified as an important mediator of defense responses against insect herbivory, which it accomplishes by activating genes involved in glucosinolate biosynthesis. Accordingly, overexpression of IQD1 in Arabidopsis reduces its susceptibility to herbivory. The action of IQD1 was found to be regulated by Ca^{2+}. Thus, IQD1 is activated by binding calmodulin, a major Ca^{2+}-binding protein, making glucosinolate production responsive to the herbivory-triggered $[Ca^{2+}]$ signal.

It is important to remember that these defenses are costly to the plant; when there are such "on" switches, there are likely to be equally important "off" switches carefully controlling the degree to which defenses are induced. Thus, in addition to its defense-activating role, Ca^{2+} can also be involved in the down-regulation of defense signaling. When the production of two Ca^{2+}-dependent protein kinases (CDPKs) was suppressed by gene silencing in a wild tobacco (*Nicotiana attenuata*), the accumulation of wound signals (such as the plant defense hormone JA, discussed shortly) after herbivory continued over a much longer period than it did in wild-type plants. Consequently, gene-silenced plants produced more defense metabolites and significantly slowed the growth of a specialist herbivore, the tobacco hornworm (*Manduca sexta*). These observations suggest that these two CDPKs are part of the system needed to switch off these induced defenses. Thus, Ca^{2+}-regulated processes are likely to be involved in balancing the induction of defenses with the need to limit their overall costs to the plant.

Insect herbivore–induced defense signaling also involves several types of mitogen-activated protein kinases (MAPKs). In tobacco, silencing the genes for **wound-induced protein kinase** (**WIPK**) and **stress-induced protein kinase** (**SIPK**), both members of the MAPK family, revealed that both are involved in regulating antiherbivore defenses. Both genes are significantly induced after insect herbivory and treatment with fatty acid amide elicitors. SIPK and WIPK also appear to be essential for different aspects of the JA pathway and wound-related synthesis of another plant hormone, ethylene. Similar effects are seen upon manipulating MAPK activity in plants as diverse as tomato and Arabidopsis, demonstrating the likely widespread importance of MAPKs in regulating plant defenses against insect herbivores.

Jasmonate activates defense responses against insect herbivores

A major signaling pathway involved in most plant defenses against insect herbivores is triggered by the hormone jasmonate (primarily in the form of the amino acid conjugate jasmonic acid-isoleucine, JA-Ile). Jasmonate levels rise steeply in response to damage and trigger the production of many proteins involved in plant defenses. Direct demonstration of the role of jasmonate in insect resistance has come from research with JA-deficient mutant lines of Arabidopsis, tomato, and maize. Such mutants are easily killed by insect pests that normally cannot damage wild-type plants. Application of exogenous jasmonic acid restores resistance nearly to the levels of the wild-type plant.

In plants, JAis synthesized from the fatty acid linolenic acid (see Chapter 13), which is released from membrane lipids and then converted to JA-Ile, as outlined in **Figure 24.18**. Two organelles participate in JA biosynthesis, chloroplasts and peroxisomes. Jasmonate triggers a wide range of defense processes, including inducing the transcription of multiple genes for enzymes in all major pathways for specialized metabolite biosynthesis. Jasmonate also shuts down growth, allowing the plant to reallocate its resources toward metabolic pathways involved in defense.

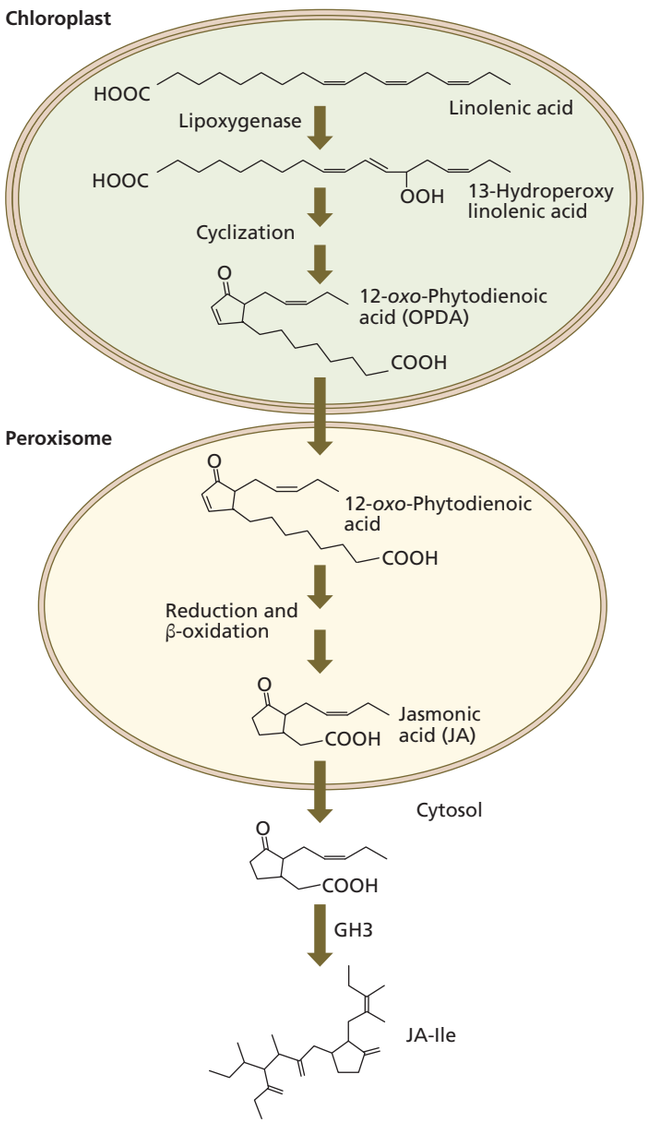


Figure 24.18 Steps in the pathway for conversion of linolenic acid into JA. The first enzymatic steps occur in the chloroplast, resulting in the cyclized product 12-*oxo*-phytodienoic acid (OPDA). This intermediate is transported to the peroxisome, where it is first reduced and then converted into JA by β-oxidation. The amino acid leucine is conjugated to JA by the enzyme JAR1.

Jasmonate acts through a conserved ubiquitin ligase signaling mechanism

As introduced in Chapter 4, JA-Ile acts through a conserved ubiquitin ligase–based signaling mechanism that bears close resemblance to those described for auxin and gibberellin (**Figure 24.19**). Although adding unconjugated jasmonic acid to plants can trigger some defenses, most responses involve JA-Ile as a hormonal signal. This conjugation is performed by enzymes referred to as **jasmonate resistance** (**JAR**) **proteins**, one of which, JAR1, appears to be of particular importance for jasmonate-dependent defense signaling.

When levels of bioactive jasmonate are low, induced defenses are similarly low because the expression of jasmonate-responsive genes is being actively inhibited by members of the **JA-ILE ZIM-DOMAIN** (**JAZ**) **protein family**. These JAZ repressors act by binding to the **MYC2 transcription factor** and inactivating it. MYC2 is a major activator of jasmonate-dependent genes. JAZ proteins also maintain the chromatin in a "closed" state that prevents jasmonate-responsive transcription factors from binding to their targets (see Figure 24.19). Jasmonate triggers the degradation of JAZ proteins by binding to both JAZ proteins and CORONATINE-INSENSITIVE1 (COI1) that function together as jasmonate co-receptors. As described in Chapter 4, COI1 is part of the SKP1-CULLIN-F-Box (SCF) protein complex that attaches the small molecule ubiquitin to proteins to tag them for degradation via the 26S proteasome (see Figure 24.19). Destruction of JAZ liberates the MYC2 transcription factor, which then brings about the expression of jasmonate-responsive genes to trigger induced defense responses.

Hormonal interactions contribute to plant–insect herbivore interactions

In addition to jasmonate, several other signaling agents—including ethylene, salicylic acid, and methyl salicylate—are often induced by insect herbivory. In particular, ethylene appears to play an important role in this context. When applied alone to plants, ethylene has little effect on defense-related gene activation. However, when applied together with JA it seems to enhance jasmonate-related responses. Similarly, when plants are treated with elicitors such as fatty acid amides (which by themselves do not induce the production of significant amounts of ethylene) in combination with ethylene, defense responses are significantly increased. Results such as these demonstrate that a concerted action of these signaling compounds is required for

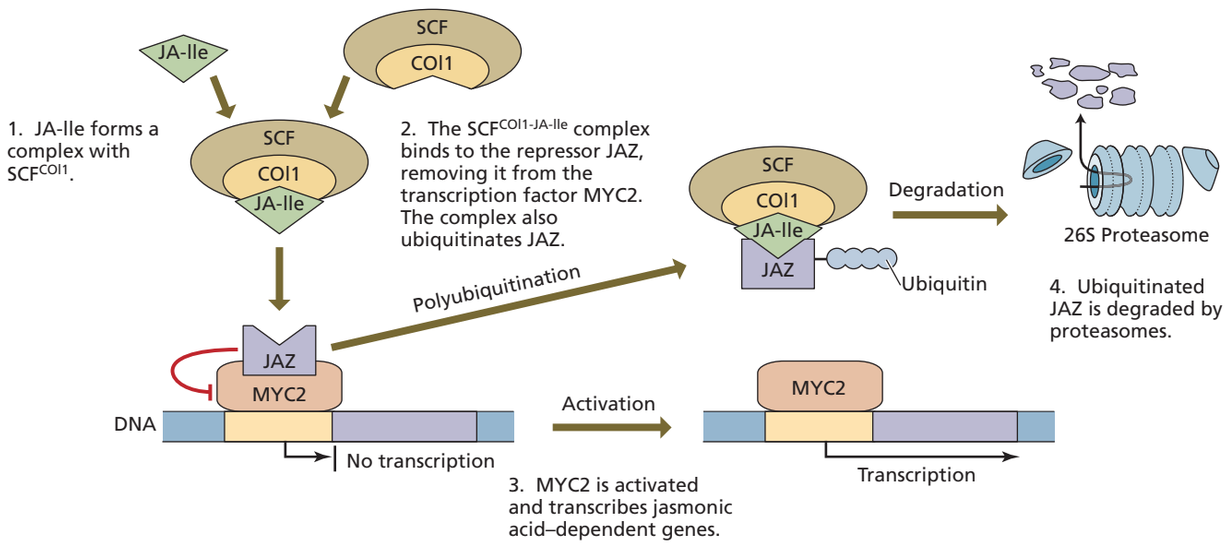


Figure 24.19 **Jasmonic acid signaling.** Jasmonic acid needs to be conjugated first to an amino acid (primarily isoleucine) to bind to COI1 as part of a SCF^{COI1} receptor protein complex. This complex targets JAZ, a repressor of transcription, leading to the degradation of this protein in a proteasome. Transcription factors such as MYC2 then initiate transcription of JA-dependent genes, including those for defense.

the full activation of induced defense responses. Such control through multiple factors allows plants to integrate numerous environmental signals in modulating the defense response.

JA initiates the production of defense proteins that inhibit herbivore digestion

Besides activating pathways for the production of toxic or repelling specialized metabolites, JA also initiates the biosynthesis of defense proteins. Most of these proteins interfere with the herbivore digestive system. For example, some legumes synthesize **α-amylase inhibitors**, which block the action of the starch-digesting enzyme α-amylase in the insect gut. Other plant species produce **lectins**, defense proteins that bind to carbohydrates or carbohydrate-containing proteins. After ingestion by an herbivore, lectins bind to the epithelial cells lining the digestive tract and interfere with nutrient absorption.

A more direct attack on the insect herbivore's digestive system is performed by some plants through the production of a specific cysteine protease that disrupts the membrane that protects the gut epithelium of many insects. Plants also produce **proteinase inhibitors**. Found in legumes, tomato, and other plants, these substances block the action of herbivore proteolytic enzymes. After entering the herbivore's digestive tract, they hinder protein digestion by binding tightly and specifically to the active site of protein-hydrolyzing enzymes such as trypsin and chymotrypsin. Insects that feed on plants containing proteinase inhibitors suffer reduced rates of growth and development. Experiments have shown that this effect can be offset by adding supplemental amino acids to their diet, directly linking their impaired growth to disruption of their ability to digest proteins in their diet.

On the plant side, the defensive role of proteinase inhibitors has also been confirmed by experiments with transgenic tobacco. Plants that had been transformed to accumulate increased levels of proteinase inhibitors suffered less damage from insect herbivores than did untransformed control plants. However, coevolution is a powerful force in plant–insect interactions, and just as has occurred with glucosinolates, some insect herbivores have evolved to avoid this defense, becoming adapted to feed on plants producing plant proteinase inhibitors by production of digestive proteinases resistant to inhibition.

Herbivore damage induces systemic defenses

In tomato, insect feeding leads to the rapid accumulation of proteinase inhibitors throughout the plant, even in undamaged areas far from the initial feeding site. Similarly, in Arabidopsis the wounding of one leaf leads within minutes to the production of JA and JA-Ile in unwounded leaves. These observations indicate that plants possess a system capable of rapid signaling throughout the plant body to trigger preemptive defenses even in undamaged parts. In tomato plants under attack from herbivores, this communication is accomplished in part by damaged cells releasing a signaling peptide called systemin, which triggers JA production. The JA, systemin mRNA, and possibly even systemin itself are then

thought to move systemically in the phloem (see **WEB TOPIC 24.2**). Although peptide signals such as systemin were originally thought to be restricted to solanaceous plants, it has become clear in recent years that peptide signaling in plants is widespread, and that other plants produce peptides as signaling molecules in response to a wide range of stimuli in addition to insect herbivory.

Glutamate receptor-like (GLR) genes are required for long-distance electrical signaling during herbivory

Several lines of evidence suggest a role for electrical signaling in systemic defense responses. For example, the feeding of Egyptian cotton leafworm (*Spodoptera littoralis*) on bean leaves induces a wave of plasma membrane depolarizations that spreads to undamaged areas of the leaf. Similarly, measurements of Arabidopsis responses have now confirmed the role of electrical signaling in the spread of the JA-induced defenses to undamaged leaves in response to both purely mechanical damage and insect herbivory. During feeding of *S. littoralis* larvae, electrical signals induced near the site of attack subsequently spread to neighboring leaves at a maximum speed of 9 cm per min (**Figure 24.20**). These changes are also accompanied by propagating waves of Ca^{2+} and reactive oxygen species (ROS, another ubiquitous cellular signaling molecule). These signals propagate rapidly through the vasculature and then spread throughout the undamaged leaves, probably moving from cell to cell through plasmodesmata to initiate JA-Ile-mediated defense responses. A family of glutamate receptor-like (GLR) genes has been identified as playing an important

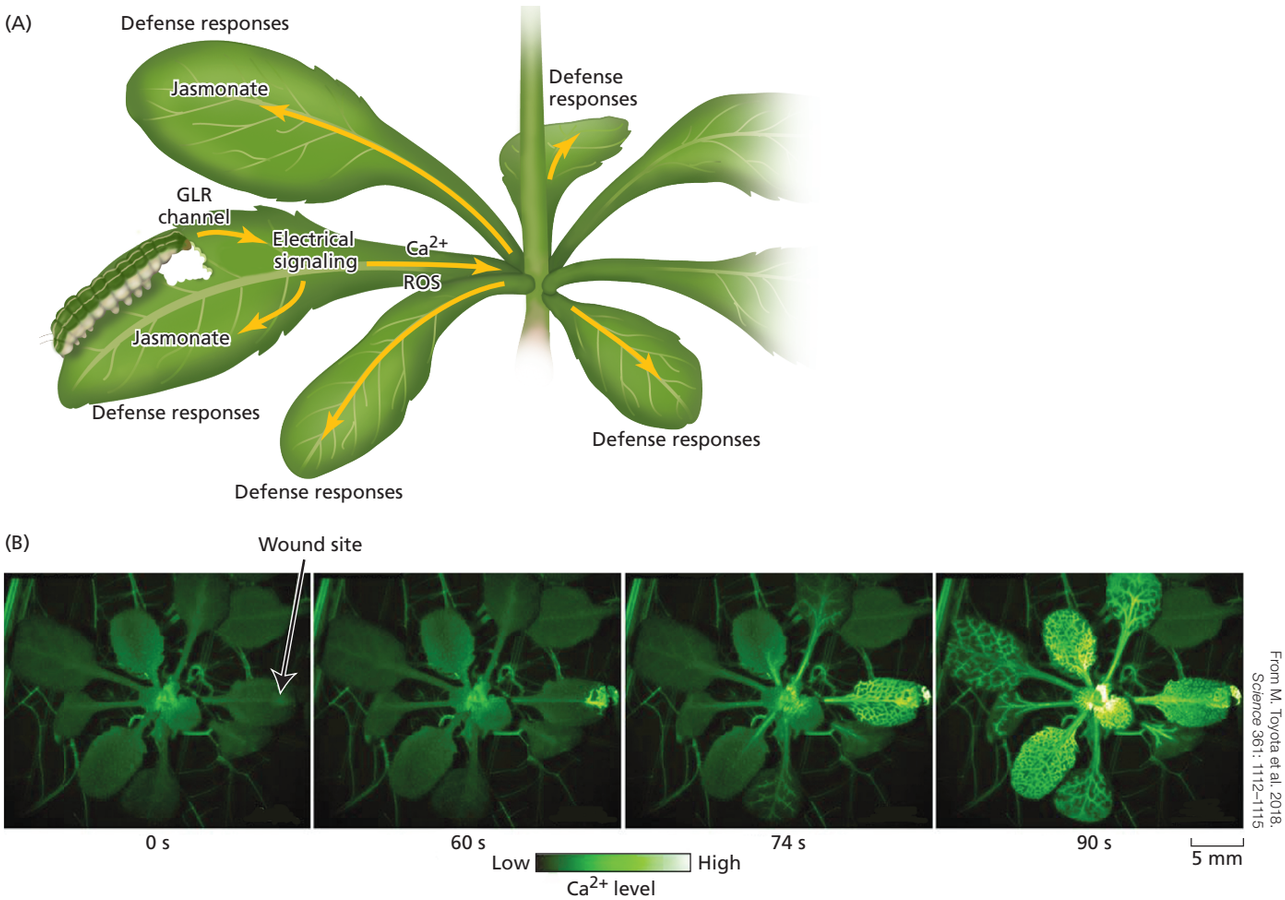


Figure 24.20 Systemic response of Arabidopsis to herbivore attack. **(A)** Injury to the leaf caused by herbivory activates glutamate receptor-like (GLR) ion channels. The GLRs trigger electrical signals that are thought to travel through the vascular system alongside waves of chemical signaling such as changes in the concentration of Ca^{2+} and ROS, thereby stimulating JA production both locally and in other leaves. Jasmonic acid-Ile then initiates defense responses that discourage further herbivory. **(B)** Spread of Ca^{2+} signal through a plant in response to local application of a wound elicitor. The plant is expressing a Ca^{2+}-sensitive fluorescent reporter protein. (A after A. Christmann and E. Grill. *Nature* 500: 404–405.)

role in this process. These GLRs encode Ca^{2+}-permeable ion channels, and both the electrical and Ca^{2+} waves no longer propagate after wounding when these genes are mutated. Similarly, JA-Ile response gene expression and herbivore defense in the unwounded leaves are reduced. The GLRs have also previously been implicated in microbe-related defense responses, suggesting a potentially widespread role in the pathways leading to inducible defenses in the plant.

Herbivore-induced volatiles can repel herbivores and attract natural enemies

Volatile organic compounds (VOCs), or volatiles, are plant-derived organic molecules that are induced or released upon damage. The response of insects to these volatiles provides an excellent example of how coevolution can shape plant–insect interactions. The combination of emitted molecules is often specific for each insect herbivore species and typically includes representatives from the three major pathways of secondary metabolism: the terpenoids, alkaloids, and phenolics. In addition, all plants also emit lipid-derived products, such as **green-leaf volatiles** (a mixture of six-carbon aldehydes, alcohols, and esters) in response to mechanical damage. The ecological functions of these volatiles are manifold (**Figure 24.21**). Many of these compounds, although volatile, remain attached to the surface of the leaf and serve as feeding deterrents because of their taste. In other cases they can act almost like a cry for help from the plant, attracting natural enemies of the attacking insect herbivores—predators or parasites—which use the volatile cues to find their prey or a host for their

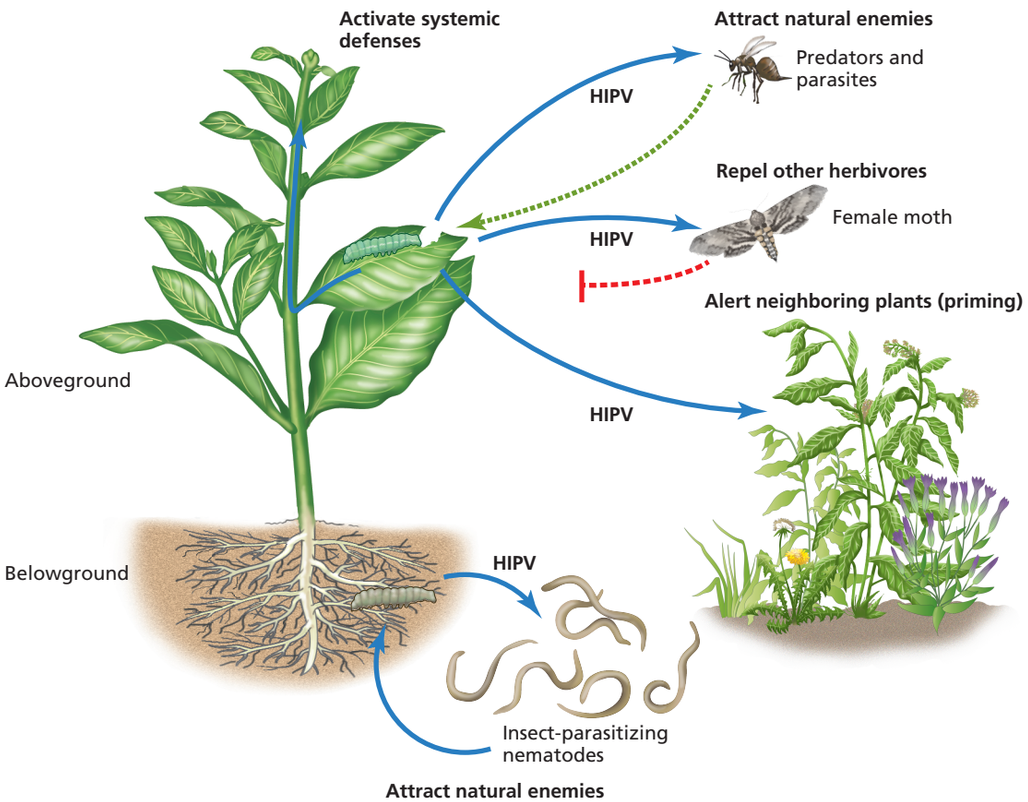


Figure 24.21 Ecological functions of herbivore–induced plant volatiles (HIPV). Many plants release a specific bouquet of volatile organic compounds when attacked by insect herbivores. These volatiles can consist of compounds from all major pathways for specialized metabolite biosynthesis, including terpenoids (mono- and sesquiterpenes), alkaloids (indole), and phenylpropanes (methyl salicylate), as well as green-leaf volatiles. These volatiles can act as cues for natural enemies of the insect herbivore, for example parasitic wasps. Belowground parts of plants can also release volatiles when attacked by herbivores. It has been shown that these volatiles attract insect-parasitizing nematodes, which then attack the herbivore. Volatiles may also serve as a repellant for female moths, thereby reducing further egg deposition. Most recently, volatiles have been found to act as a systemic defense signal in highly sectorial plants with interrupted vascular connections, and also between plants over short distances. There, these volatile signals prepare the receiving plant against impending herbivory by priming (preparing) defense responses, resulting in a stronger and faster response when the receiving plant is actually attacked.

offspring. For example, in maize the elicitor present in the saliva of beet armyworm larvae can induce the synthesis of volatiles that attract parasitoids. Maize seedlings that are treated with very low concentrations of the armyworm elicitor release relatively large amounts of terpenoids, which attract the tiny parasitoid wasp *Microplitis croceipes* that then lays its eggs on the invading armyworms. In contrast, some herbivores actually capitalize on these volatile emissions. For example, volatiles released by leaves during moth oviposition (egg laying) can act as repellents to other female moths, thereby preventing further egg deposition and reducing subsequent competition among the larvae that emerge. Similarly, benzyl cyanide produced by rice leaves during herbivory is taken up by female brown plant hoppers and acts as a pheromone for the males of the species.

Plants have the ability to distinguish among various insect herbivore species and to respond differentially. For example, following herbivory, *Nicotiana attenuata*, a wild tobacco that grows in the deserts of the Great Basin in the western United States, typically produces higher levels of nicotine, which poisons the insect central nervous system. However, when wild tobacco plants are attacked by nicotine-tolerant caterpillars, the plants show no increase in nicotine. Instead, they release volatile terpenes that attract insect predators of the caterpillars. Clearly, wild tobacco and other plants must have ways of determining what type of insect herbivore is damaging their foliage, perhaps by the type of damage they inflict or the distinctive chemical compounds they release in their oral secretions.

Herbivore-induced volatiles can serve as long-distance signals between plants

The role of herbivore-induced plant volatiles is not limited to the interactions between plants and insects. Certain volatiles emitted by infested plants can also serve as signals for neighboring plants to initiate preemptive antiherbivore defenses (see Figure 24.21). In addition to several terpenoids, green-leaf volatiles act as potent signals in this process. Green-leaf volatiles are the major components of the familiar scent of freshly cut grasses. When maize plants were exposed to green-leaf volatiles, JA and JA-related gene expression was rapidly induced, and in addition, these plants were found to respond more strongly to subsequent direct attacks by insect herbivores. Green-leaf volatiles have been shown to prime or sensitize the defense mechanisms of a variety of other plant species, including lima bean (*Phaseolus lunatus*), sagebrush (*Artemisia tridentata*), mouse ear cress (*Arabidopsis thaliana*), poplar (*Populus tremula*), and blueberry (*Vaccinium* spp.). Furthermore, they activate the production of phytoalexins and other antimicrobial compounds (discussed in Section 24.4) and appear to play an important role in the overall defense strategies of plants.

Herbivore-induced volatiles can also act as systemic signals within a plant

Besides providing a signal for neighboring plants, infested plants may well send a volatile signal to other parts of themselves (see Figure 24.21). From an evolutionary point of view, this may have been the original function of those volatiles. Volatiles have been shown to act as inducers of herbivore resistance between different branches of sagebrush. It was found that airflow was essential for the induction of the induced resistance, indicating that the chemical messages were indeed moving in the air outside the plant. Sagebrush, like other desert plants, is highly *sectorial*, meaning that the vascular system of the plant is not well integrated by interconnections, possibly as a safeguard against water deficit. Although many plants are capable of responding systemically to herbivores by means of chemical signals that move internally through vascular interconnections, sagebrush and many other desert plants with more internal sectoring are less able to do so. Instead, volatiles are used to overcome these constraints and provide systemic signaling. In lima bean, volatiles aid recruitment of defensive insect partners. Lima bean uses the nectar from extrafloral nectaries located at the base of leaf blades to attract predacious and parasitoid arthropods, which in turn protect the bean against various types of herbivores (**Figure 24.22**). When leaf beetles attack lima bean, volatiles are released immediately from the damage site and signal other parts of the same plant to activate their defenses and produce **extrafloral nectar** to draw in their protective insect partners.

Defense responses to herbivores and pathogens are regulated by circadian rhythms

Many aspects of plant metabolism and development are regulated by circadian rhythms (see Chapter 20). It has been estimated that about one-third of all plant genes exhibit circadian regulation in their expression. The list



David McIntyre

Figure 24.22 Extrafloral nectaries of lima bean (*Phaseolus lunatus*).

of genes with diurnally regulated transcription includes not only the predictable genes involved in photosynthesis, carbon metabolism, and water uptake, but numerous genes involved in plant defense. This observation has led to the proposal that resistance to insect herbivory may be under circadian control to tailor maximum plant defense to times of maximum herbivore activity.

This hypothesis was supported by a study of the interactions between Arabidopsis and cabbage looper (*Trichoplusia ni*), a generalist lepidopteran herbivore (**Figure 24.23A**). Both cabbage looper herbivory and JA-mediated plant defenses follow circadian rhythms that peak during the day. This observation suggests that the timing of the JA-mediated defense response may be an adaptation that maximizes protection against herbivory. To test whether the plant circadian clock enhances defense against insect pests, herbivory was compared in Arabidopsis plants whose JA-mediated defense responses were either in phase (**Figure 24.23B**) or out of phase (**Figure 24.23C**) with the circadian rhythm of cabbage looper feeding activity. This was accomplished by growing some of the plants on a reversed day–night cycle for several days such that their "day" was the loopers' "night" and vice versa. The rhythm in JA-linked plant defenses was remembered for several days even when the light cycles were shifted back to being synchronized with that of the loopers. After cabbage loopers had been allowed to feed freely on the plants for 72 h, plants whose defense responses were in phase with the loopers had visibly less tissue damage than plants whose circadian rhythm was out of phase with that of the insects (**Figure 24.23D**). As a result, cabbage loopers that fed on the phase-shifted Arabidopsis plants gained three times as much weight over the same period as the synchronized control plants did (**Figure 24.23E**).

Salicylic acid (SA) mediates defense responses to pathogens and is produced from nonenzymatic breakdown of isochorismate-9-glutamate in the cytosol. Isochorismate is synthesized by isochorismate synthase from pools of chorismate in the chloroplast and then exported to the cytoplasm where conjugation to glutamate occurs. CIRCADIAN CLOCK–ASSOCIATED 1 (CCA1) regulation (see Chapter 20) of isochorismate synthesis results in increased levels overnight. Pathogen infection increases isochorismate export to the cytoplasm, where it is conjugated to glutamate that rapidly degrades to

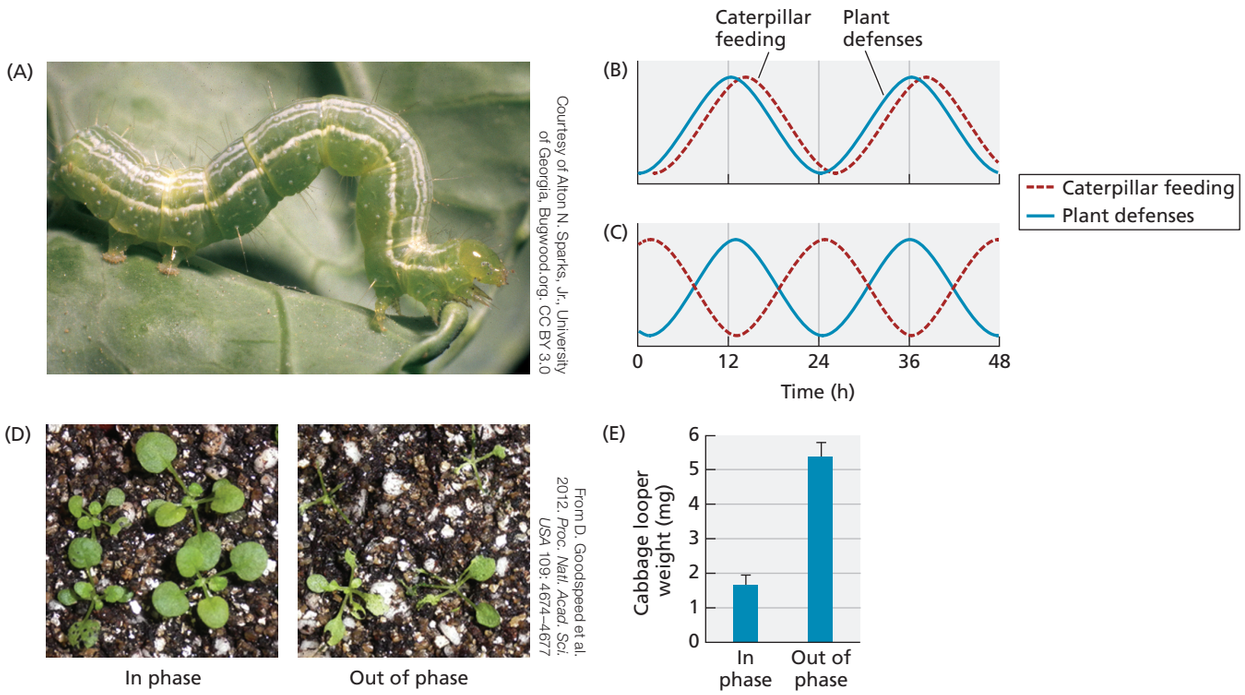


Figure 24.23 Example of circadian rhythms influencing plant defense against herbivory. **(A)** *Trichoplusia ni* (cabbage looper) caterpillar feeding on Arabidopsis. **(B)** Normally the circadian clocks of the caterpillars and the plants are synchronized, and both caterpillar feeding activity and jasmonate-mediated plant defenses peak during the day. This optimizes plant defenses and reduces caterpillar growth rate. **(C)** If the circadian rhythm of Arabidopsis is shifted by 12 h, the plant's defense response is at a minimum when the caterpillar's feeding activity is at a maximum, and the caterpillar grows more rapidly. **(D)** Out-of-phase Arabidopsis plants (right) suffered more damage than in-phase plants (left). **(E)** Comparison of weights of cabbage loopers growing on in-phase or out-of-phase Arabidopsis plants. Error bars represent mean ± standard error; n = 15. (B–E After D. Goodspeed et al. 2012. *Proc. Natl. Acad. Sci. USA* 109: 4674–4677.)

form SA (see **WEB APPENDIX 3**). Diurnal accumulation of isochorismate is thought to contribute to the enhanced resistance of Arabidopsis to pathogenic bacteria where infection tends to occur in the early morning as opposed to the evening.

Insects have evolved mechanisms to defeat plant defenses

This section has demonstrated how plants have evolved an array of physical and chemical mechanisms to protect themselves. These defenses are generally highly effective, but as we have seen, some herbivorous insects have evolved mechanisms for circumventing or overcoming these plant defenses by the process of *reciprocal evolutionary change between plant and insect*, a type of coevolution. These insect adaptations, like plant defense responses, can be either constitutive or induced. Constitutive adaptations are more widely distributed among specialist herbivorous insects, which can feed on only a few plant species, whereas induced adaptations are more likely to be found among insects that are dietary generalists. Although it is not always obvious, in most natural environments plant–insect interactions have led to a standoff where there are effective defenses and countermeasures to elude these defenses and in which plant and insect can each develop and survive, albeit under suboptimal conditions.

24.4 Plant Defenses against Pathogens

Plant pathology is the study of plant diseases. Pathogens that cause infectious diseases in plants include viruses, bacteria, fungi, oomycetes, and nematodes. Oomycetes are filamentous organisms that are evolutionarily closer to brown algae than to fungi and include some of the most destructive plant pathogens in history. Oomycetes include the genus *Phytophthora*, cause of the disastrous potato late blight of the Great Irish Famine (1845–1849). Collectively, these pathogens lead to an estimated reduction in global crop production of 15% annually, despite massive use of pesticides that are costly to both farmers and the environment. A major goal of plant pathology is to understand the molecular and cellular basis of the plant immune system so that this knowledge can be applied to developing crop plants with more robust immune systems, which would then enable a reduction in pesticide use.

In this section we examine the diverse array of mechanisms that plants have evolved to resist infection locally, including **pattern recognition receptor** (**PRR**)**–triggered immunity** (**PTI**), **effector-triggered immunity** (**ETI**), the production of antimicrobial agents, and a type of programmed cell death called the **hypersensitive response**. We also discuss a form of systemic plant immunity referred to as **systemic acquired resistance** (**SAR**).

Microbial pathogens have evolved various strategies to invade host plants

Throughout their lives, plants are continuously exposed to a diverse array of pathogens. Successful pathogens have evolved various mechanisms to invade their host plant and cause disease (**Figure 24.24**). Some penetrate the cuticle and cell wall directly by secreting lytic enzymes, which digest these mechanical barriers. Others enter the plant through natural openings such as stomata, hydathodes, and lenticels. A third category invades the plant through wound sites, for example those caused by insect herbivores. Additionally, many viruses, as well as other types of pathogens, are transferred by insect herbivores, which serve as vectors, and invade the plant from the insect feeding site. Phloem feeders such as whiteflies and aphids deposit these pathogens directly into the vascular system, from which they can easily spread throughout the plant.

Once inside the plant, pathogens generally employ one of three main attack strategies to subdue the host plant and obtain nutrients for their own proliferation. **Necrotrophic pathogens** attack their host by secreting cell wall–degrading enzymes or toxins, which eventually kill the affected plant cells, leading to extensive tissue maceration (softening of the tissues after death by autolysis). This dead tissue is then colonized by the pathogens and serves as a food source. A different strategy is used by **biotrophic pathogens**; after infection, most of the plant tissue remains alive and only minimal cell damage can be observed, as the pathogens feed on substrates that are stolen from their host. **Hemibiotrophic pathogens** are characterized by an initial biotrophic stage, in which the host cells are kept alive as described for biotrophic pathogens. This phase is followed by a necrotrophic stage, in which the pathogens can cause extensive tissue damage.

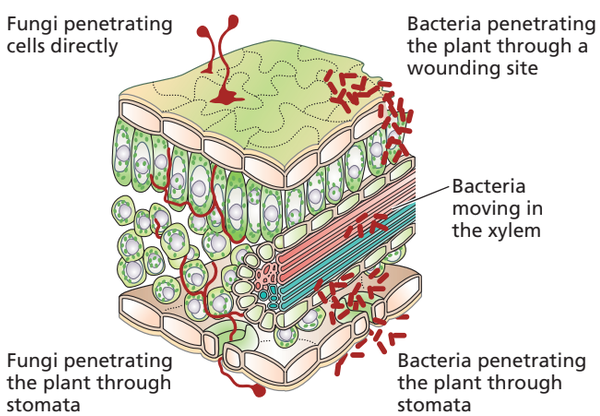


Figure 24.24 Plant pathogens such as bacteria and fungi have developed various methods for invading plants. Some fungi have mechanisms that allow them to directly penetrate the cuticle and cell wall of the plant. Other fungi, and also pathogenic bacteria, enter through natural openings such as stomata or through existing wounds caused by herbivores.

Although these invasion and infection strategies are individually successful, plant disease epidemics are rare in natural ecosystems. This is because plants have evolved effective defense strategies against this diverse array of pathogens.

Pathogens produce effector molecules that aid in the colonization of their plant host cells

Plant pathogens can produce a wide array of effectors that support their ability to successfully colonize their host and gain nutritional benefits. **Effectors** are secreted molecules that can suppress the host immune system, and/or alter the plant's structure, metabolism, or hormonal regulation to the advantage of the pathogen. Because invasion of a suitable host is often the most difficult step for a pathogen, many pathogens produce enzymes that can degrade the plant cuticle and cell wall. Among those enzymes are cutinases, cellulases, xylanases, pectinases, and polygalacturonases. These enzymes have the ability to compromise the integrity of the cuticle as well as the primary and secondary cell walls (see Chapter 2).

Degradation of cutin and host cell walls by pathogen enzymes leads to release of molecules that signal to the plant that it is under attack. These **damage-associated molecular patterns** (**DAMPs**) are sensed by cell surface **pattern recognition receptors** (**PRRs**) that then induce a strong immune response—PRR-triggered immunity, or PTI—which we describe in more detail shortly. To be successful, pathogens must suppress this PTI response (**Figure 24.25**). This is most often accomplished by

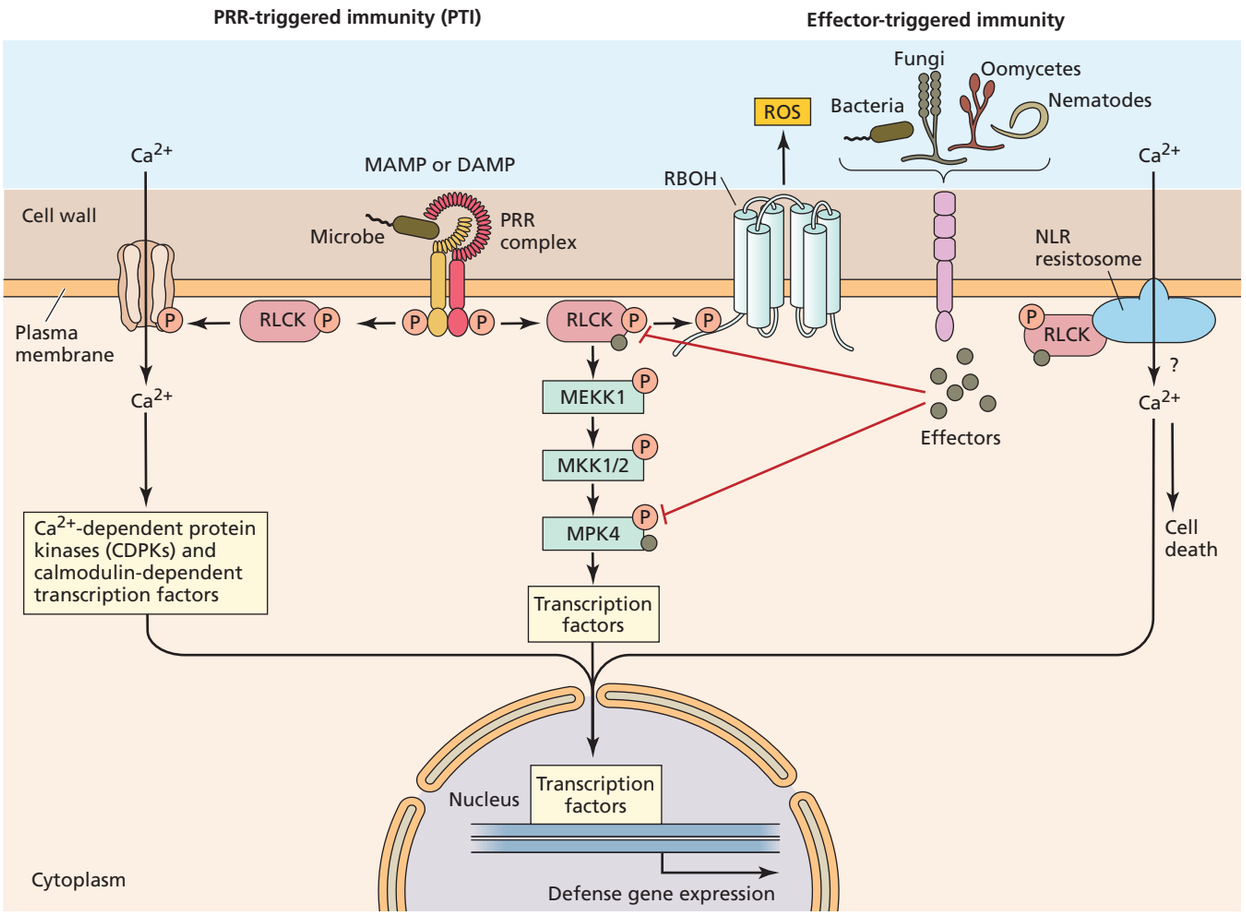


Figure 24.25 **Plants have evolved defense responses to a variety of danger signals of biotic origin.** These danger signals include microbe-associated molecular patterns (MAMPs), damage-associated molecular patterns (DAMPs), and effectors. Extracellular MAMPs produced by microbes, and DAMPs released by microbial enzymes, bind to pattern recognition receptors (PRRs) on the cell surface. As plants coevolved with pathogens, the pathogens acquired effectors as virulence factors that mainly function to suppress PRR signaling. When MAMPs, DAMPs, and effectors bind to their PRRs and resistance (R) proteins, two types of defense responses are induced: PRR-triggered immunity and effector-triggered immunity. Receptor-like cytoplasmic kinases (RLCKs) are phosphorylated by receptor-like kinases, which are part of the PRR complex. NLR, nucleotide-binding site–leucine rich repeat protein; RBOH, respiratory burst oxidase homolog. (After S. Lolle et al. 2020. *Curr. Opin. Immunol.* 62: 99–105.)

translocation of protein effectors from the pathogen into host cells, where the proteins bind to and inactivate key components of the PTI signaling pathway. A single bacterial pathogen strain such as *Pseudomonas syringae* pathovar *tomato* is known to secrete more than 30 different protein effectors that target several different steps in the PTI pathway. Even more striking, oomycete pathogens such as *P. infestans* are believed to translocate several hundred different protein effectors. Such effectors are proving to be very useful tools for identifying proteins in the host that contribute to immune signaling.

In addition to suppressing PTI, some effectors promote host cell susceptibility by inducing cellular responses that promote pathogen growth, such as the release of sugars from cells. A particularly interesting example of this comes from bacterial pathogens in the genus *Xanthomonas*, which secrete so-called transcription activator-like (TAL) effectors that bind to the host plant DNA and activate the expression of genes encoding sugar transporters.

In addition to secreting protein-based effectors, many pathogens secrete toxins that target specific proteins in the plant (**Figure 24.26**). For example, the **HC-toxin** from the fungus *Cochliobolus carbonum*, which causes northern leaf blight disease, inhibits specific histone deacetylases in maize. In general, decreased deacetylation of histones, which are essential in the organization of the chromatin, tends to increase the expression of associated genes (see Chapter 3). However, it is not yet known whether this is how HC-toxin causes disease in maize.

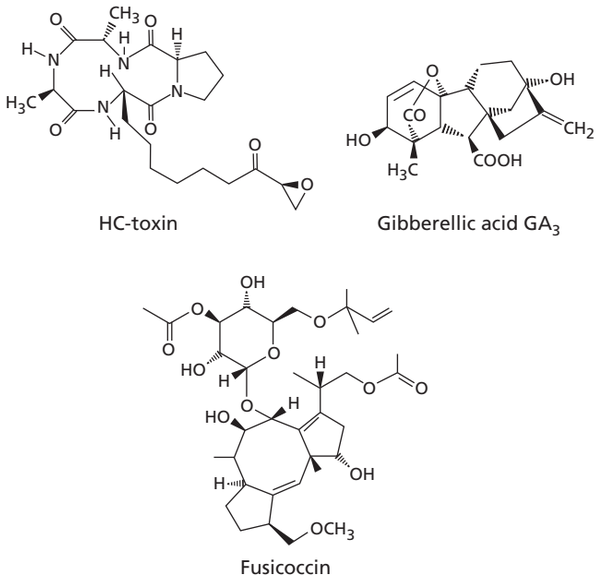


Figure 24.26 Toxins and hormones produced by pathogens help pathogens infect plants. Some pathogens produce specific toxins that significantly alter the physiology of the plant. The HC-toxin, a cyclic peptide, inhibits the enzyme histone deacetylase in the nucleus, and may have a compromising effect on the expression of genes involved in defense. Fusicoccin binds to plant plasma membrane H^+-ATPases, in particular those in stomata, and activates them irreversibly. Gibberellins, produced by the fungus *Gibberella fujikuroi*, accelerate growth, resulting in taller plants, which may promote dispersal of fungal spores. The gibberellins produced by the fungi are identical to those produced endogenously by the plant.

Fusicoccin (see Figure 24.26) is a nonspecific toxin from the fungus *Fusicoccum amygdali*. **Fusicoccin** constitutively activates the plant plasma membrane H^+-ATPase by first binding to a specific protein of the 14-3-3 group of regulators. This complex then binds to the C-terminal region of the H^+-ATPase and activates it irreversibly, leading to cell wall overacidification and plasma membrane hyperpolarization. These effects of fusicoccin are of particular importance for stomatal guard cells (see Chapters 8 and 16). Fusicoccin-induced plasma membrane hyperpolarization in guard cells causes massive K^+ uptake and permanent stomatal opening, which leads to wilting and ultimately the death of the plant. It is not yet clear if and how the pathogen benefits from the excessive wilting of its host.

Some pathogens produce effector molecules that significantly interfere with the hormonal balance of the plant host. The fungus *Gibberella fujikuroi*, which causes infected rice shoots to grow much faster relative to uninfected plants, produces gibberellic acid (GA_3) and other gibberellins. Gibberellins are responsible for the "foolish seedling disease" of rice. It is thought that fungal spores released from the taller, infected plants are more likely to spread to surrounding plants because of their height advantage. It was subsequently demonstrated that gibberellins are naturally occurring plant hormones (see Chapter 4).

Plants can detect pathogens through perception of pathogen-derived "danger signals"

As mentioned earlier, immune signaling in plants is initiated by cell surface receptors called PRRs. Based on transcriptome sequences, we know that plants express hundreds of different PRRs. In addition to sensing host cell–derived DAMPS, these PRRs detect **microbe-associated molecular patterns** (**MAMPs**), which are conserved among a specific class of microorganisms (e.g., chitin fragments for fungi, flagellin for bacteria) but are absent in the host. Receptor-like kinases (RLKs, which we introduced in Chapter 4 and mentioned in Section 24.1 in connection with beneficial plant–microbe interactions) are key PRRs for microbe- and plant-derived molecular signals associated with pathogen infection (see Figure 24.25). RLKs typically contain an extracellular domain such as a leucine rich repeat (LRR) or lysin motif (LysM) domain, a transmembrane domain, and an intracellular kinase domain. In addition to RLKs, some PRRs include receptor-like proteins that contain an extracellular domain and a transmembrane domain,

but lack an intracellular kinase domain. These typically associate with RLKs to form heterodimers, with the kinase domain of the RLK providing the intracellular signaling function.

Systemin, introduced in Section 24.3, is an example of a plant-derived DAMP found in tomato that is produced in response to wounding associated with herbivore activity. Among the well-studied microorganism-derived MAMPs are Pep-13, a 13–amino acid peptide from a cell wall–localized transglutaminase of the oomycete *Phytophthora*, the cause of the infamous potato blight in Ireland; flg22, a 22–amino acid peptide derived from the bacterial flagellin protein; and elf18, an 18–amino acid fragment of the bacterial elongation factor Tu. Because these molecules are common to many, if not all, species within groups of microorganisms, their detection allows the plant to recognize entire classes of potentially pathogenic organisms, such as fungi versus bacteria.

Perception of MAMPs or DAMPs by cell surface PRRs initiates PTI, which inhibits the growth and activity of nonadapted pathogens or pests. The signaling pathways from cell surface PRRs to activation of diverse defense responses is complex, and invariably includes activation of receptor-like cytoplasmic kinases (RLCKs; see Figure 24.25), which are phylogenetically related to the kinase domains of PRRs but lack a transmembrane domain. Once activated by PRRs, RLCKs phosphorylate and activate multiple target proteins, including plasma membrane–localized NADPH/respiratory burst oxidase homologs (RBOHs), anion channels, mitogen-associated protein kinase kinase kinases (MAPKKKs), and plasma membrane–localized Ca^{2+} channels. Opening of the last leads to an influx of Ca^{2+} ions that then activate Ca^{2+}-dependent protein kinases (CDPKs). CDPKs constitute a plant-specific family of protein kinases with 34 members in *Arabidopsis thaliana*. These various signaling pathways ultimately lead to dramatic changes in gene expression, with approximately 30% of the transcriptome responding to a single pathogen molecule such as flg22, which consequently induces a major shift in cellular resources away from growth and toward defense. Included among the up-regulated genes are those encoding hydrolytic enzymes that attack the cell walls of pathogens, such as glucanases, chitinases, and other hydrolases. The resulting breakdown of pathogen cell walls, in turn, releases additional MAMPs thus producing a self-amplifying loop that produces a robust defense response.

The activation of RBOH enzymes is especially significant, as this leads to dramatic increases in extracellular ROS such as the superoxide anion (O_2^-), hydrogen peroxide (H_2O_2), and the hydroxyl radical (•OH) as is seen in some abiotic stress responses (see Chapter 15). The hydroxyl radical is the strongest oxidant of these ROS and can initiate radical chain reactions with a range of organic molecules, leading to lipid peroxidation and enzyme inactivation, which are directly toxic to many microbes.

The ROS burst also contributes to strengthening of the plant cell wall, as certain proline-rich proteins of the wall become oxidatively cross-linked after pathogen attack in an H_2O_2-mediated reaction. Cell wall strengthening is further enhanced by deposition of lignin and callose at the infection site. These polymers are thought to serve as barriers, walling off the pathogen from the rest of the plant and physically blocking its spread.

R genes provide resistance to individual pathogens by recognizing strain-specific effectors

The evolution of effector proteins by pathogens that can suppress PTI placed plants under tremendous evolutionary pressure to evolve additional resistance mechanisms. Plants have responded by evolving specialized **resistance** (**R**) **proteins** that recognize these intracellular effectors and then trigger the opening of Ca^{2+} channels by an independent pathway, which then activates many of the same defense systems as PTI. This second pathway is called effector-triggered immunity (ETI) (see Figure 24.25).

Most R proteins contain a **nucleotide-binding domain** (**NBD**) and **leucine rich repeats** (**LRRs**) and hence are commonly referred to as **nucleotide-binding site–leucine rich repeat proteins** (**NLRs**). There are two major classes of NLRs, with one class characterized by an N-terminal coiled-coil (CC) domain, and the other class defined by an N-terminal domain shared with many mammalian immune signaling proteins, including Toll-like receptors and Interleukin receptors (TIRs). Recent structural analyses have revealed that these two classes form distinct oligomeric structures upon activation by effectors, with the TIR-NLR class (not to be confused with the TIR1 auxin co-receptor) forming a tetrameric clover leaf–shaped structure and the CC-NLR class forming a pentameric propeller-shaped structure (**Figure 24.27**). These oligomeric structures are referred to as **resistosomes**.

Most TIR-NLRs appear to detect pathogen effectors directly via a physical association between the effector and the LRR domain plus a C-terminal jelly roll/immunoglobulin-like domain found on many TIR-NLRs. Binding of the effector to the NLR protein induces a conformational change that enables oligomerization, bringing four TIR domains into close association (see Figure 24.27). This, in turn, forms a binding pocket between adjacent TIRs for nicotinamide adenine dinucleotide (NAD), which is broken down, releasing a cyclic nucleotide that functions as a second messenger. This second messenger appears to then activate a subfamily of CC-NLR proteins through a mechanism that is actively being investigated but is not yet understood.

In contrast to TIR-NLR proteins, most CC-NLRs appear to recognize pathogen effectors indirectly by binding

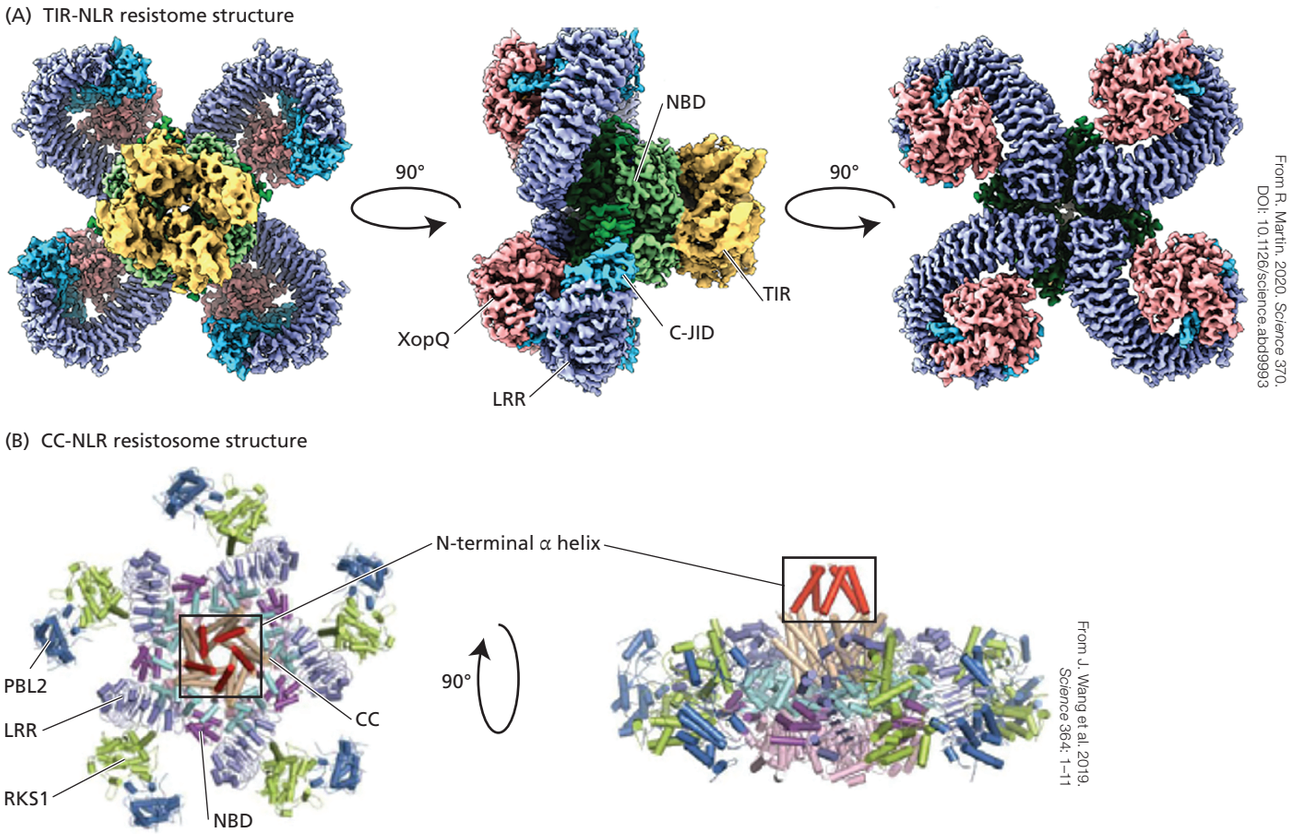


Figure 24.27 **Three-dimensional structures of plant resistosomes.** **(A)** A TIR-NLR resistosome. The pink color indicates a pathogen effector protein (XopQ) bound to the C-terminus of a TIR-NLR protein (Roq1). Light blue indicates the C-terminal jelly roll/immunoglobulin-like domain (C-JID); dark blue, the LRR domain; green, the nucleotide-binding domain (NBD); and yellow, the TIR domain. **(B)** A CC-NLR resistosome (ZAR1). Dark blue on the perimeter of the structure represents the effector target (PBL2), and green represents a bridging protein kinase (RKS1). The remaining colors represent different subdomains of the CC-NLR protein: Lavender indicates the LRR domain; purple, the NBD; light brown, the CC domain; and red, the N-terminal α helix that comes together to form a potential pore structure (inside box).

to plant proteins that are the targets of pathogen effectors. In the absence of pathogen effectors, CC-NLRs are distributed in the cytoplasm and associate with effector targets in a monomeric inactive state. However, when the effector interacts with its target, either altering its conformation or chemically modifying it, the CC-NLR protein undergoes a conformational change that enables oligomerization to form a pentameric structure (see Figure 24.27).

The hypersensitive response is a common defense against pathogens

Although there is considerable overlap between ETI- and PTI-induced defense responses, ETI differs from PTI in that it commonly leads to a localized form of cell death called the **hypersensitive response** (**HR**), in which the attacked cell and cells immediately surrounding the infection site die rapidly. In the case of biotrophic pathogens, especially viruses, this cell death is highly effective at walling off the pathogen and preventing its spread. After a successful hypersensitive response, a small region of dead tissue is left at the site of the attempted invasion, but the rest of the plant is unaffected.

Exactly how ETI leads to cell death is not well understood, but it appears to require the influx of Ca^{2+} from the extracellular space, as the addition of a Ca^{2+} chelator such as ethylene glycol-bis(β-aminoethyl ether)-N,N,N′,N′-tetraacetic acid (EGTA) to this space blocks ETI-induced death. This Ca^{2+} influx must differ qualitatively from that induced by PTI, however, since PTI does not typically induce cell death. Upon oligomerization, the N-terminal α helix of CC-NLR proteins forms a funnel-shaped structure that is inserted into the plasma membrane, forming a pentameric channel in the plasma membrane (see Figure 24.27) that allows Ca^{2+} influx, which in turn activates a defense response. Regardless of the precise mechanism, a hallmark of ETI-induced cell

death is disruption of the plasma membrane and leakage of electrolytes into the apoplastic space.

A single encounter with a pathogen may increase resistance to future attacks

In addition to triggering defense responses locally, microbial pathogens also induce the production of signals such as salicylic acid, methyl salicylate, and other compounds that lead to systemic expression of the antimicrobial **pathogenesis-related** (**PR**) **genes**. *PR* genes encode low molecular weight proteins (6–43 kDa) composed of a diverse group of hydrolytic enzymes, wall-modifying enzymes, antifungal agents, and components of signaling pathways. PR proteins are localized either in vacuoles or in the apoplast and are most abundant in leaves, where they are presumed to confer protection against secondary infections. This phenomenon of local pathogen challenge enhancing resistance to secondary infection is called **systemic acquired resistance** (**SAR**) and normally develops over a period of several days.

Although the phenomenon of SAR has been known for decades, the identity of the molecule responsible for systemic signaling was not uncovered until 2018, when N-hydroxy-pipecolic acid (NHP) was shown to move systemically in plants and to induce defense genes. NHP is an amino acid derived from L-lysine, and its biosynthesis is dramatically up-regulated locally in response to pathogen attack (**Figure 24.28**). Exogenously applied NHP is rapidly converted to N-OGlc-pipecolic acid, which is conjugated to a sugar and then rapidly accumulates in distal leaves. Importantly, this distal accumulation occurs after NHP application even in plants that lack FLAVIN-DEPENDENT MONOOXYGENASE1 (FMO1), which is required for the synthesis of NHP. This observation demonstrates that the exogenously added NHP is transported and that NHP produced by the plant after attack probably moves in a similar manner. Significantly, NHP application causes rapid global changes in defense gene expression and metabolic pathways that lead to enhanced resistance to pathogens, including induction of SA production and downstream induction of defense-related genes.

The main components of the salicylic acid signaling pathway have been identified

Genetic screens of Arabidopsis mutants that are insensitive to salicylic acid identified *NPR1* (*NONEXPRESSOR of PR GENES 1*) as an SA receptor. NPR1 is a copper-containing protein that is found predominantly in inactive multimeric cytoplasmic aggregates under normal conditions. Binding of SA to NPR1 causes a confirmational change in NPR1 that enables it to interact with transcription factors in the nucleus to activate transcription of SA-inducible genes (see Figure 24.28). NPR3 and NPR4 are proteins with

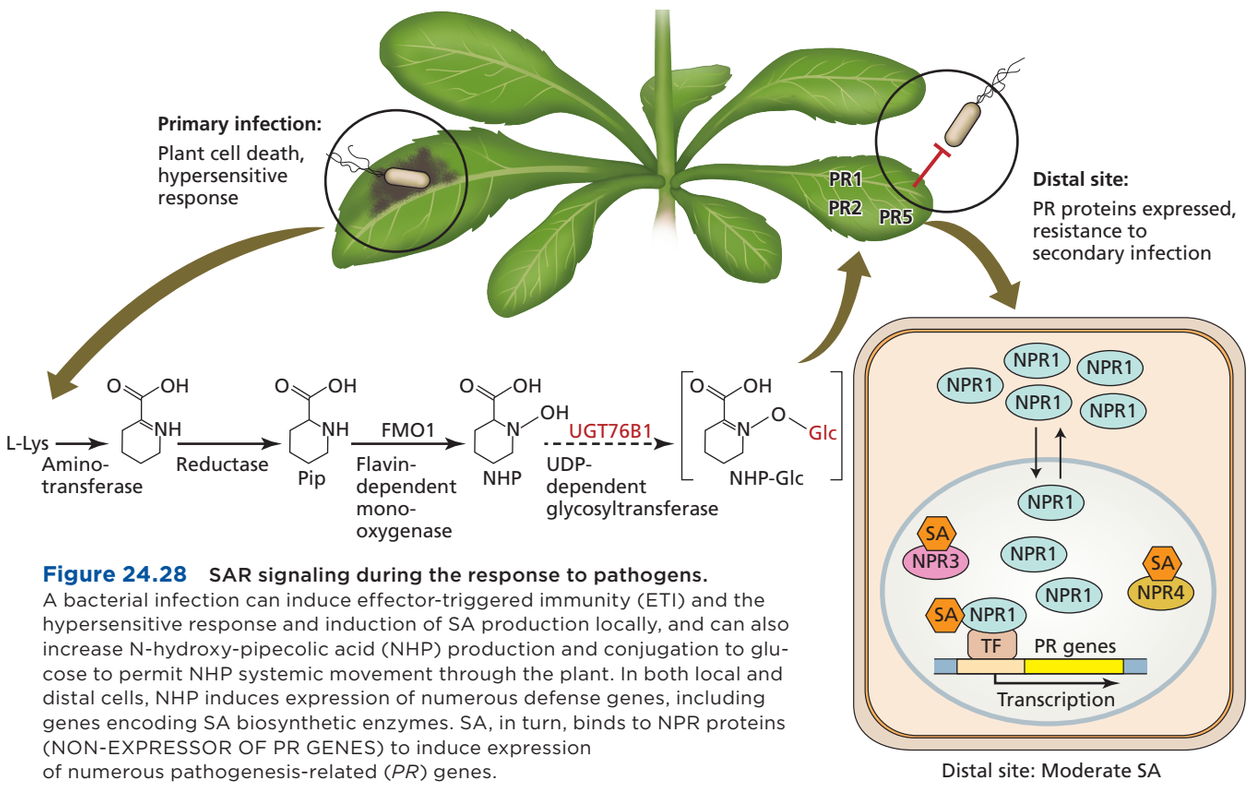


Figure 24.28 **SAR signaling during the response to pathogens.** A bacterial infection can induce effector-triggered immunity (ETI) and the hypersensitive response and induction of SA production locally, and can also increase N-hydroxy-pipecolic acid (NHP) production and conjugation to glucose to permit NHP systemic movement through the plant. In both local and distal cells, NHP induces expression of numerous defense genes, including genes encoding SA biosynthetic enzymes. SA, in turn, binds to NPR proteins (NON-EXPRESSOR OF PR GENES) to induce expression of numerous pathogenesis-related (*PR*) genes.

N-terminal SA-binding domains that are highly similar to NPR1. When not bound to SA, NPR3 and NPR4 function as co-repressors of gene expression by binding to the same transcription factors as NPR1, but in this case, their C-terminal domains function as transcriptional repressors. Upon binding SA, this repressor domain is neutralized, allowing transcription to commence. SA signaling via NPR receptors occurs both at the site of initial infection and at distal sites after NHP priming (see Figure 24.28).

Phytoalexins with antimicrobial activity accumulate after pathogen attack

Phytoalexins are a chemically diverse group of specialized metabolites with strong antimicrobial activities that accumulate around the infection site. Phytoalexin production appears to be a common mechanism of resistance to pathogenic microbes in a wide range of plants. However, different plant families employ different types of specialized products as phytoalexins. For example, in leguminous plants, such as alfalfa and soybean, isoflavonoids are common phytoalexins, whereas in solanaceous plants, such as potato, tobacco, and tomato, various sesquiterpenes are produced as phytoalexins (**Figure 24.29**). (For discussions of the biosynthesis of these compounds, see **WEB APPENDIX 4**.)

Phytoalexins are generally undetectable in the plant prior to infection, but they are synthesized rapidly after microbial attack. The point of control is usually the expression of genes encoding enzymes for phytoalexin biosynthesis. Plants do not appear to store any of the enzymatic machinery required for phytoalexin synthesis. Instead, soon after microbial invasion they begin transcribing the appropriate genes into mRNA and translating the mRNAs into enzymes that synthesize phytoalexins de novo.

Although phytoalexins accumulate in concentrations that have been shown to be toxic to pathogens in bioassays, the defensive significance of these compounds in the intact plant is not fully understood. Experiments on genetically modified plants and pathogens have provided the first direct proof of phytoalexin function in vivo. For example, tobacco plants transformed with a gene for an enzyme catalyzing the biosynthesis of the phenylpropanoid phytoalexin resveratrol become much more resistant to a fungal pathogen than nontransformed control plants. Similarly, resistance of Arabidopsis to a fungal pathogen depends on the tryptophan-derived phytoalexin camalexin, as mutants deficient in camalexin production are more susceptible to the pathogen than is wild-type Arabidopsis. In other experiments, pathogens transformed with genes encoding phytoalexin-degrading enzymes were able to infect plants normally resistant to them.

RNA interference plays a central role in antiviral immune responses in plants

The mechanisms of RNA-mediated gene silencing described in Chapter 3 are important components of plant antiviral immune responses. A key breakthrough in our understanding of the molecular mechanisms underlying RNA interference (RNAi) came when it was discovered that infection of plants with a positive-strand RNA virus (potato virus X) induces accumulation of small RNAs homologous to the infecting virus, which are now known as small-interfering RNAs (siRNAs). This discovery indicated that RNAi might be associated with an RNA-based immune response that occurs even in nontransgenic plants. This was based on the observation that plants frequently recover from a virus infection, with newly emerging leaves on a virus-infected plant displaying greatly enhanced resistance to reinfection by the same virus—as well as to infection by viruses with closely related sequences, but not to more distantly related viruses. This finding indicates that some sort of sequence-specific immune response must be occurring. In support of this idea, it was found that inserting an endogenous plant gene's antisense cDNA sequence into an RNA virus can induce silencing of that gene upon viral infection. Such virus-induced gene silencing (VIGS) has become a useful tool in plant biotechnology, as it provides a rapid method for systemic silencing of genes in plants.

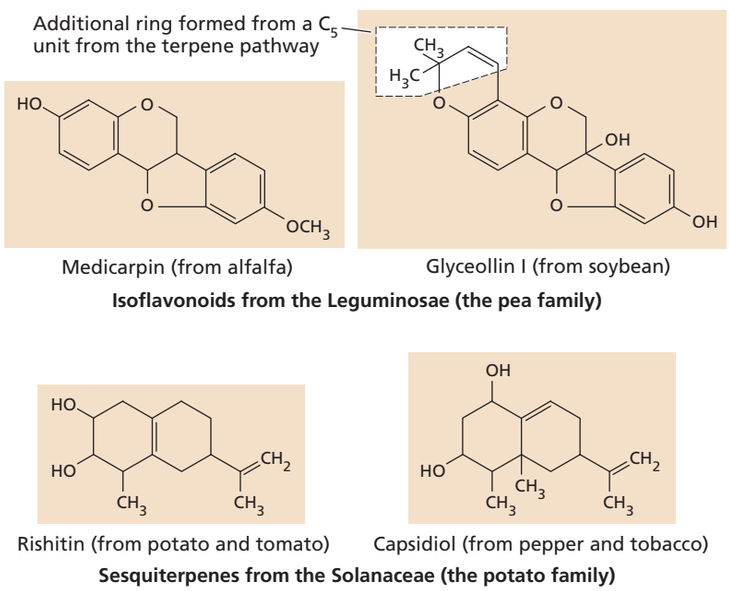


Figure 24.29 Structures of some phytoalexins found in two different plant families.

Some plant parasitic nematodes form specific associations through the formation of distinct feeding structures

Nematodes, or roundworms, are water and soil inhabitants that often outnumber all other animals in their respective environments. Many nematodes exist as parasites relying on other living organisms, including plants, to complete their life cycle. Nematodes can cause severe losses of agricultural crops and ornamental plants. Plant parasitic nematodes can infect all parts of a plant, from roots to leaves, and may even live in the bark of forest trees. Nematodes feed through a hollow stylet that can easily penetrate plant cell walls. In the soil, nematodes can move from plant to plant, thereby causing extensive damage. Arguably the best studied among the plant parasitic nematodes are the **cyst nematodes** and those causing gall formation on infected roots, the so-called **root knot nematodes**. Both are endoparasites that depend on a living plant as host to complete their life cycles and are therefore categorized as biotrophs. The life cycle of parasitic nematodes begins when dormant eggs recognize specific compounds secreted by the plant root (**Figure 24.30**). Once hatched, the juvenile nematodes swim to the root and penetrate it. There they migrate to the vascular tissue, where they begin feeding on the cells of the vascular system.

At the permanent feeding site, usually in the root cortex, a cyst nematode larva pierces a cell with its stylet and injects saliva. The saliva contains numerous effector proteins produced by the salivary glands of the nematode. Based on gene silencing experiments, these effector proteins are required for formation of a **syncytium** (see Figure 24.30A). The syncytium is a large, metabolically active feeding site that becomes multinucleate as neighboring plant cells are incorporated into it by cell wall dissolution and cell fusion. The syncytium continues to spread centripetally toward the vascular tissue, incorporating pericycle cells and xylem parenchyma. The outer walls of the syncytium adjacent to the conducting elements form protuberances resembling those of transfer cells (see Chapter 12), indicating that the syncytium now functions as a nutrient sink.

The cyst nematode, after establishing itself in such a feeding structure, grows and undergoes three molting stages while becoming a vermiform (wormlike) adult. At maturity, the female produces eggs internally, swells, and protrudes from the root surface. The mature male nematodes are released from the root into the soil and are attracted by pheromones to protruding females on the root surface.

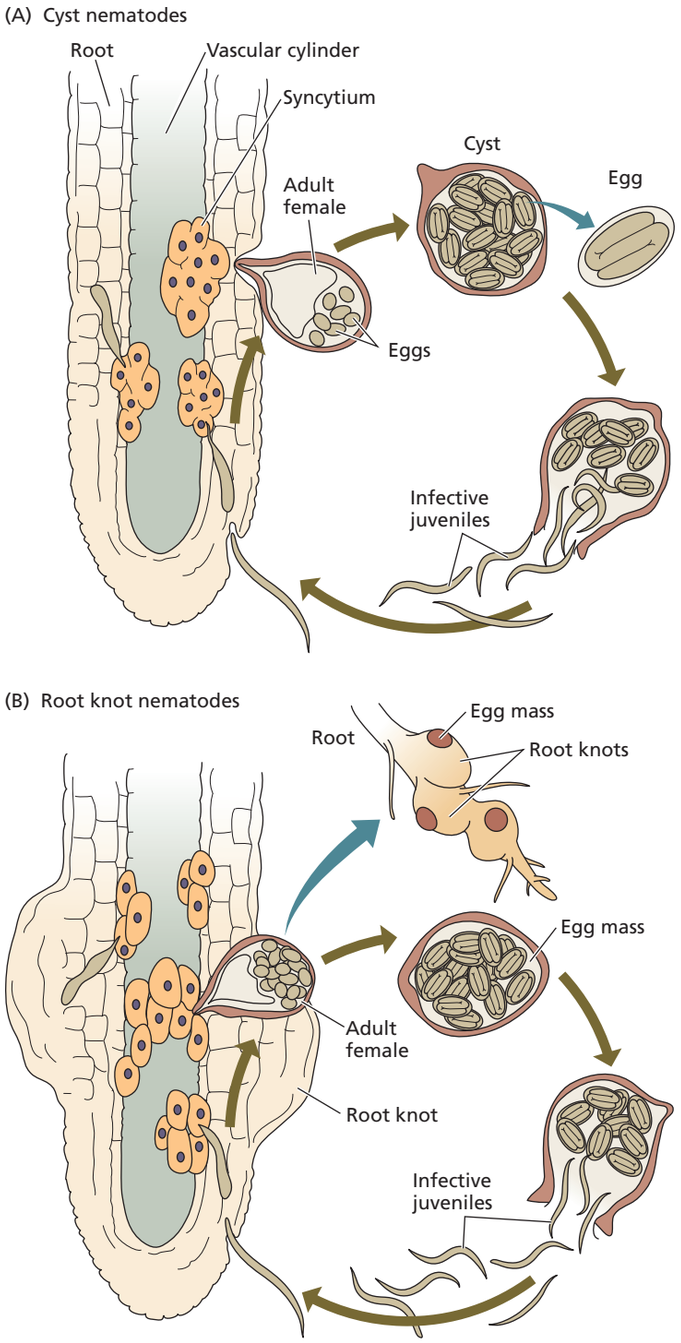


Figure 24.30 Free-living juvenile nematodes are attracted to secretions by the roots. After penetration, the nematode starts feeding on cells in the vasculature. **(A)** Cyst nematodes cause the formation of a specific feeding structure (syncytium) in the vasculature but do not cause other morphological changes. After fertilization, the female cyst nematode dies, thereby forming a cyst containing the fertilized eggs, from which a new generation of infective juveniles hatches. **(B)** Infection by root knot nematodes causes the formation of giant cells, resulting in the typical root knots. Upon maturation, the female nematode releases an egg mass from which new infective juveniles hatch and cause further infestations of plants.

After fertilization, the female dies, forming a cyst containing the fertilized eggs.

Roots infected by root knot nematodes form large cells, resulting in the establishment of the characteristic knot or gall, which also remains in close contact with the vasculature and provides the nematode with nutrients (see Figure 24.30B).

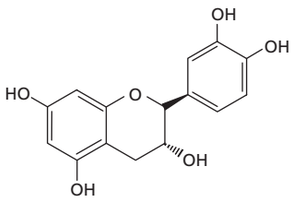
As already mentioned, plant parasitic nematodes secrete a large number of effector proteins that affect the morphology and physiology of the plant. Among those effector proteins are some that are specifically recognized by plants and activate defense responses through recognition by NLR proteins, as described earlier for plant–pathogen interactions. For example, the potato NLR protein H1 binds specifically to a nematode-derived effector, and thus activates defense responses. Several of these plant NLR proteins have been identified to date, and interestingly, all have been shown to participate in plant resistance to microbial pathogens as well, suggesting that nematode effectors and microbial effectors may target some of the same host proteins.

Plants compete with other plants by secreting allelopathic specialized metabolites into the soil

Plants release compounds (**root exudates**) into their environment that change soil chemistry, thus increasing nutrient uptake or protecting against metal toxicity. Plants also secrete chemical signals that are essential for mediating interactions between plant roots and nonpathogenic soil bacteria, including nitrogen-fixing bacterial symbionts. However, microbes are not the only organisms that are influenced by specialized metabolites released by plant roots. Some of these chemicals are also involved in direct communication between plants. Plants release specialized metabolites to the soil to inhibit the roots of other plants, a phenomenon known as allelopathy.

Interest in allelopathy has increased in recent years because of the problem of invasive species that outcompete native species and take over natural habitats. A devastating example is spotted knapweed (*Centaurea maculosa*), an invasive exotic weed introduced to North America that releases phytotoxic specialized metabolites into the soil. Spotted knapweed, a member of the aster family (Asteraceae), is native to Europe, where it is not a dominant or problematic species. However, in the northwestern United States it has become one of the worst invasive weeds, infesting more than 1.8 million ha (~4.4 million acres) in Montana alone. Spotted knapweed often colonizes disturbed areas in North America, but it also invades rangelands, pastures, and prairies, where it displaces native species and establishes dense monocultures.

The phytotoxic specialized metabolites that spotted knapweed roots release into the soil have been identified as a racemic mixture of (±)-catechin (hereafter catechin)



(–)-Catechin

Figure 24.31 **Phytotoxic allelopathic compound produced by spotted knapweed (*Centaurea maculosa*).**

(**Figure 24.31**). The mechanism by which catechin acts as a phytotoxin has been elucidated. In susceptible species such as Arabidopsis, catechin triggers a wave of ROS initiated at the root meristem, which leads to a Ca^{2+} signaling cascade that triggers genome-wide changes in gene expression. In Arabidopsis, catechin doubled the expression of about 1000 genes within 1 h of treatment. By 12 h, many of these same genes were repressed, which may reflect the onset of cell death. Laboratory experiments examining the effects of catechin on plant germination and growth showed that native North American grassland species vary considerably in their sensitivity to catechin. Resistant species may produce root exudates that detoxify this allelochemical.

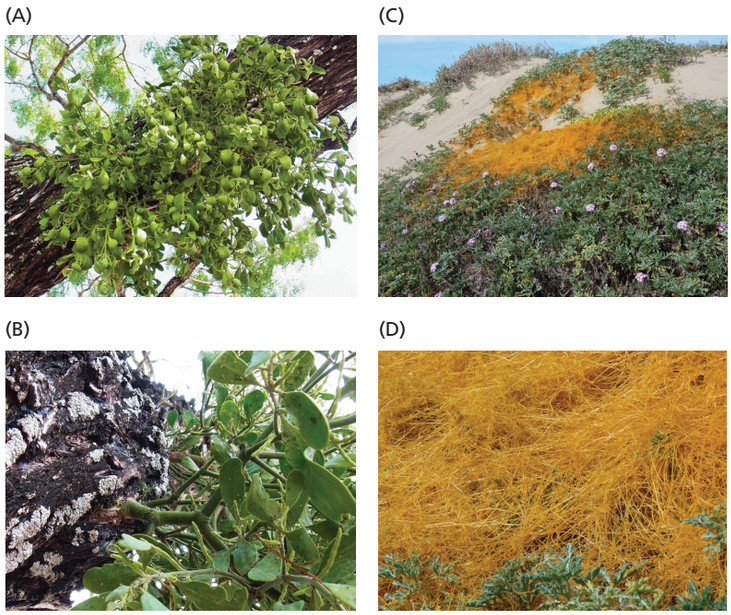
Some plants are parasites of other plants

While most plants are autotrophic, some plants have evolved into parasites that rely on other plants to provide essential nutrients for their own growth and development. Parasitic plants can be divided into two main groups depending on the degree of parasitism. **Hemiparasitic plants** retain the ability to perform at least some photosynthesis, while **holoparasitic plants** are completely parasitic on their host plants and have lost the ability to carry out photosynthesis. For example, mistletoe (genus *Viscum*), which has green leaves and is able to perform photosynthesis, is a hemiparasite (**Figure 24.32A and B**). In contrast, dodder (genus *Cuscuta*), which has lost the ability to photosynthesize and depends entirely on the host for sugars, is a holoparasite (**Figure 24.32C and D**).

Parasitic plants have developed a specialized structure, the **haustorium**, which is a modified root (**Figure 24.33A**). After establishing contact with its host plant, the haustorium penetrates the epidermis or bark and then the parenchyma to grow into the vascular tissue and absorb nutrients from the host (**Figure 24.33B–D**). To reach the host plant, seeds of parasitic plants are either directly deposited by birds or are more randomly distributed by wind or other means. After germination, the seedlings must rely for a time on their seeds for their food supply, until they can find a suitable host. Recent research has shown that low amounts of species-specific plant volatiles may serve as cues for dodder seedlings and direct their growth toward

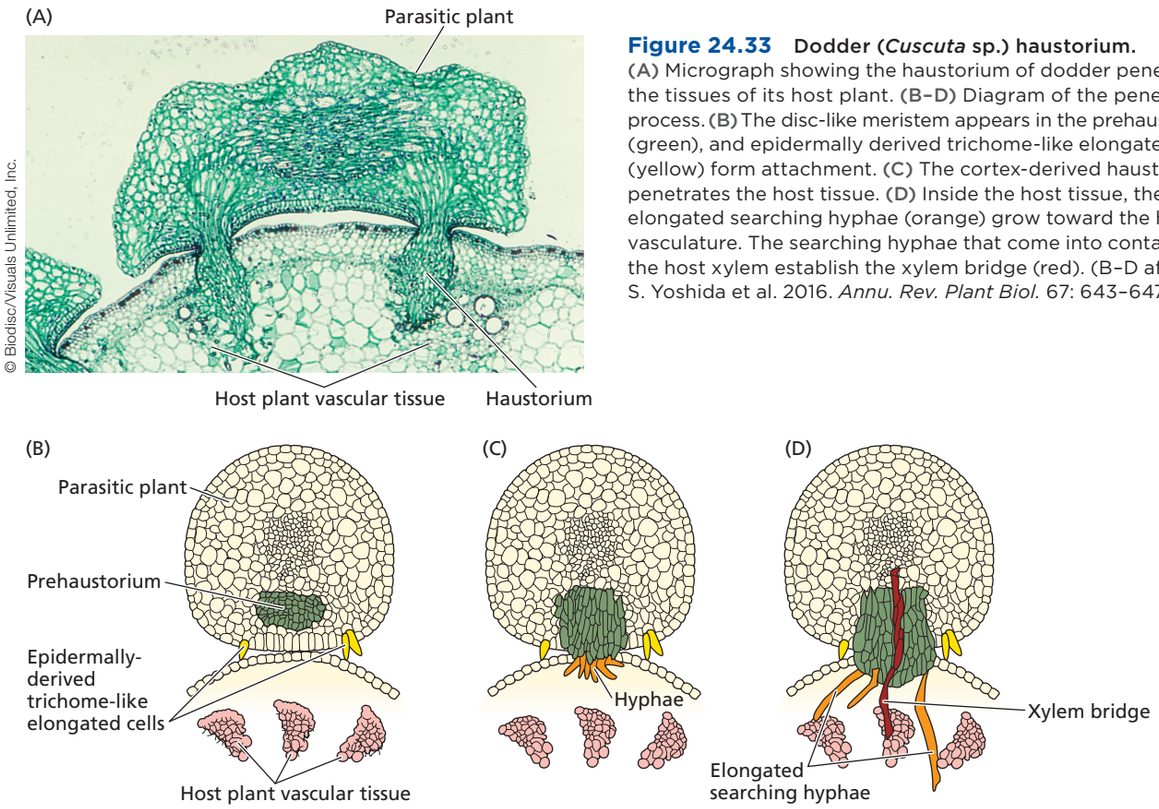
the host. Alternatively, in the case of root parasites, such as *Striga*, compounds secreted by the host root guide the growth of the seedling roots toward the host. Upon contacting the host root, the *Striga* seedling root develops into a haustorium. The haustorium then penetrates the host root and grows directly into the vascular system through the pits of xylem vessels, where it absorbs the necessary nutrients through tubelike protoplasmic structures not covered by a cell wall.

The mechanisms of these interactions between parasitic plants and their hosts have been studied mostly at the morphological level, and little is known about the signaling mechanisms involved. Emerging data, however, indicate that RNA molecules, especially microRNAs, move from the parasitic plant into the host plant, where they affect gene expression in the host. There is also little known about the defense mechanisms of the host plant. It is likely that common defense signaling pathways, including JA, salicylic acid, and ethylene, may play an important role in the defense against parasitic plants, but much more research is needed.



All photos © J. Engelberth

Figure 24.32 **Parasitic plants.** **(A)** Mistletoe (*Viscum* sp.) on a mesquite tree (genus *Prosopis*). **(B)** Clearly visible is the green stem of the mistletoe growing through the bark of the host plant. **(C)** Dodder (*Cuscuta* sp.) growing on a patch of sand verbenas (*Abronia umbellata*) on dunes at the Pacific coast in California. **(D)** Close-up showing the high density of infestation of dodder on its host plant.



© Biodisc/Visuals Unlimited, Inc.

Figure 24.33 **Dodder (*Cuscuta* sp.) haustorium.** **(A)** Micrograph showing the haustorium of dodder penetrating the tissues of its host plant. **(B–D)** Diagram of the penetration process. **(B)** The disc-like meristem appears in the prehaustorium (green), and epidermally derived trichome-like elongated cells (yellow) form attachment. **(C)** The cortex-derived haustorium penetrates the host tissue. **(D)** Inside the host tissue, the elongated searching hyphae (orange) grow toward the host vasculature. The searching hyphae that come into contact with the host xylem establish the xylem bridge (red). (B–D after S. Yoshida et al. 2016. *Annu. Rev. Plant Biol.* 67: 643–647.)

Summary

Plants have evolved many strategies to cope with the threats posed by pests and pathogens. These strategies include sophisticated detection mechanisms and the production of toxic and repelling specialized metabolites. While some of these strategies are constitutive, others are inducible. Overall, these defenses have led to a stand-off in the coevolutionary arms race between plants and their enemies.

24.1 Plant Interactions with Beneficial Microorganisms

- Symbiotic nitrogen-fixing bacteria release Nod factors, which set off a series of reactions leading to infection and the formation of nodules (**Figures 24.2, 24.3**).
- Rhizobacteria can release metabolites that assist plant growth by increasing nutrient availability and pathogen protection (**Figure 24.4**).

24.2 Herbivore Interactions That Harm Plants

- Mechanical barriers that provide a first line of defense against pests and pathogens include thorns, spines, prickles, trichomes and raphides (**Figures 24.5–24.8**).
- Specialized metabolites that serve defense functions are stored in specialized structures that release their contents only upon damage (**Figures 24.10–24.12**).
- Some specialized metabolites are stored in the vacuole as water-soluble sugar conjugates that are spatially separated from their activating enzymes (**Figures 24.14–24.16**).

24.3 Inducible Defense Responses to Insect Herbivores

- Rather than producing defensive specialized metabolites continuously, plants can save energy by producing defense compounds only when induced by mechanical damage or specific components of insect saliva (elicitors) (**Figure 24.17**).
- The jasmonate concentration increases rapidly in response to insect damage and induces transcription of genes involved in plant defense (**Figures 24.18, 24.19**).
- Herbivore damage can induce systemic defenses by causing the synthesis of polypeptide signals or by rapidly propagating electrical and chemical signals to initiate defense responses in as-yet undamaged tissues (**Figure 24.20**).
- Plants may release volatile compounds to attract natural enemies of herbivores, or to signal neighboring plants to initiate defense mechanisms (**Figure 24.21**).

24.4 Plant Defenses against Pathogens

- Pathogens can invade plants through cell walls by secreting lytic enzymes, through natural openings such as stomata and lenticels, and through wounds. Insect herbivores may also be pathogen vectors (**Figure 24.24**).
- Pathogens generally use one of three attack strategies: necrotrophism, biotrophism, or hemibiotrophism.
- Pathogens often produce effector proteins that aid in initial infection (**Figure 24.25**).
- All plants have pattern recognition receptors (PRRs) that set off defense responses when activated by evolutionarily conserved microbe-associated molecular patterns (MAMPs; e.g., flagellin, chitin) or host-derived damage-associated molecular patterns (DAMPS; e.g., cell wall fragments, extracellular ATP, specific peptides) (**Figure 24.25**).
- Plant resistance (*R*) genes encode cytosolic receptors (NLR proteins) that recognize pathogen-derived protein effectors in the cytosol. NLR proteins can recognize pathogen effectors by direct binding, or indirectly by sensing conformational changes in effector targets (**Figures 24.25, 24.27**).
- Upon activation, NLR proteins induce a hypersensitive response, in which cells surrounding the infected site die rapidly, thereby limiting the spread of infection.
- A plant that survives local pathogen infection often develops increased resistance to subsequent attack, a phenomenon called systemic acquired resistance (SAR) (**Figure 24.28**).
- In response to infection, many plants produce phytoalexins, specialized metabolites with strong antimicrobial activity (**Figure 24.29**).
- RNA interference probably evolved as an antiviral defense response (see Chapter 3).
- Nematodes (roundworms) are parasites that can move between hosts and that induce formation of feeding structures and galls from vascular plant tissues. In response, plants use defense signaling pathways similar to those used for pathogen infection (**Figure 24.30**).
- Some plants produce allelopathic specialized metabolites that enable them to outcompete nearby plant species.
- Some plants are parasitic on other plants. Parasitic plants can be divided into two main groups (hemiparasites and holoparasites) depending on their ability to perform some photosynthesis (**Figure 24.32**).
- Parasitic plants use a specialized structure, the haustorium, to penetrate their host, grow into the vasculature, and absorb nutrients (**Figure 24.33**).
- Some parasitic plants detect their host by the specific volatile profile that is constitutively released.

Web Material

- **WEB TOPIC 24.1 Cutin, Waxes, and Suberin** Plant surfaces are covered with layers of lipid material protecting them against water losses and blocking the entry of pathogenic microorganisms.
- **WEB TOPIC 24.2 Systemin Is a Peptide Defense Signal in Tomato** Systemin functions in the rapid induction of protease inhibitor biosynthesis in a wounded tomato plant.

For more study aids, go to oup.com/he/taiz7e.

Suggested Reading

Guo, Q., Major, I. T., and Howe, G.A. (2018) Resolution of growth defense conflict: mechanistic insights from jasmonate signaling. *Curr. Opin. Plant Biol.* 44: 72–81.

Farmer, E. E., Gao, Y.-Q., Lenzoni, G., Wolfender, J.-L., and Wu, Q. (2020) Wound- and mechanostimulated electrical signals control hormone responses. *New Phytol*. 227: 1037–1050.

Lolle, S., Stevens, D., and Coaker, G. (2020) Plant NLR-triggered immunity: from receptor activation to downstream signaling. *Curr. Opin. Immunol.* 62: 99–105.

Martin, R., Qi, T., Zhang, H., Liu, F., King, M., Toth, C., Nogales, E., and Staskawicz, B. J. (2020) Structure of the activated ROQ1 resistosome directly recognizing the pathogen effector xopQ. *Science* 370: eabd9993.

Rosa, C., Kuo, Y. W., Wuriyanghan, H., and Falk, B. W. (2018) RNA interference mechanisms and applications in plant pathology. *Annu. Rev. Phytopathol.* 56: 581–610.

Sharifi, R., Lee, S.-M., and Ryu, C.-M. (2018) Microbe-induced plant volatiles. *New Phytol.* 220: 684–691.

Chen, C.Y., Liu, Y. Q., Song, W. M., Chen, D.Y., Chen, F.Y., Chen, X.Y., Chen, Z. W., Ge, S. X., Wang, C. Z., Zhan, S., Chen, X.Y., and Mao, Y. B. (2019) An effector from cotton bollworm oral secretion impairs host plant defense signaling. *Proc. Natl. Acad. Sci. USA* 116: 14331–14338.

Wang, J., Hu, M., Wang, J., Qi, J., Han, Z., Wang, G., Qi, Y., Wang, H. W., Zhou, J. M., and Chai, J. (2019) Reconstitution and structure of a plant NLR resistosome conferring immunity. *Science* 364: eaav5870.

Zhou, J. M., and Zhang, Y. (2020) Plant immunity: Danger perception and signaling. *Cell* 181: 978–989.

Glossary

(1,3;1,4)-β-D-glucan Mixed-linkage glucan found in cell walls of grasses. It may bind tightly to cellulose surface, producing a less sticky network.

1N (haploid) Having a single unpaired set of chromosomes; the gametophyte generation is characteristically haploid.

26S proteasome A large proteolytic complex that degrades intracellular proteins marked for destruction by the attachment of one or more copies of the small protein ubiquitin.

2N (diploid) Having a paired set of chromosomes; the sporophyte generation is characterized by a diploid set of chromosomes.

A

abaxial Refers to the lower surface of the leaf.

ABC model Proposal for the way in which floral homeotic genes control organ formation in flowers. According to the model, organ identity in each whorl is determined by a unique combination of the three organ identity gene activities.

abscission zone A region that contains the abscission layer and is located near the base of floral organs and the petiole of leaves.

abscission The shedding of leaves, flowers, and fruits from a living plant. The process whereby specific cells in the leaf petiole (stalk) differentiate to form an abscission layer, allowing a dying/dead organ to separate from the plant.

absorption spectrum A graphic representation of the amount of light energy absorbed by a substance plotted against the wavelength of the light.

ACC oxidases Catalyzes the conversion of ACC to ethylene, the last step in ethylene biosynthesis.

accessory bud A bud that is situated either above or on the side of an axillary bud.

accessory pigments Light-absorbing molecules in photosynthetic organisms that work with chlorophyll a in the absorption of light used for photosynthesis. They include carotenoids, other chlorophylls, and phycobiliproteins.

acclimation The increase in plant stress tolerance due to exposure to prior stress. May involve gene expression. Contrast with adaptation.

acetylation The catalyzed chemical addition of an acetate group to another molecule.

acid growth A characteristic of growing cell walls in which they extend more rapidly at acidic pH than at neutral pH.

actin related protein 2/3 (Arp 2/3) Actin related proteins 2 and 3 which bind to the side of a pre-existing actin filament and form a complex with actin to initiate growth of an actin filament branch.

actin A major ATP-binding cytoskeletal protein. The monomer, globular actin (or G-actin), can bind either ADP or ATP. ATP-charged G-actin can self-associate to form long polar filaments of F-actin. In the F-actin form, the ATP is slowly hydrolyzed. The filaments grow by adding new monomers to the plus end (also called the barbed end) and shrink by releasing ADP-bound actin monomers from the minus end (also called the pointed end).

actinorhizal Pertaining to several woody plant species, such as alder trees, in which symbiosis occurs with soil bacteria of the nitrogen-fixing genus *Frankia*.

action potential A transient event in which the membrane potential difference rapidly rises (hyperpolarizes) and abruptly falls (depolarizes). Action potentials, which are triggered by the opening of ion channels, can be self-propagating along linear files of cells, especially in the vascular systems of plants.

action spectrum A graphic representation of the magnitude of a biological response to light as a function of wavelength.

activators In the control of transcription, positively acting transcription factors that bind to distal regulatory sequences usually located within 1000 bp of the transcription initiation site.

active transport The use of energy to move a solute across a membrane against a concentration gradient, a potential gradient, or both (electrochemical potential). Uphill transport.

acyl carrier protein (ACP) A low-molecular-weight, acidic protein to which growing acyl chains are covalently bonded on fatty acid synthetase.

acyl hydrolases Enzymes that remove acyl groups (consisting of a carbonyl group and an alkyl group) from other functional groups.

acyl-ACP A fatty acid chain bonded to the acyl carrier protein.

adaptation An inherited level of stress resistance acquired by a process of selection over many generations. Contrast with acclimation.

adaxial Refers to the upper surface of a leaf.

adenosine triphosphate (ATP) The major carrier of chemical energy in the cell, which by hydrolysis is converted to adenosine diphosphate (ADP) or adenosine monophosphate (AMP).

adhesion The attraction of water to a solid phase such as a cell wall or glass surface, due primarily to the formation of hydrogen bonds.

adventitious bud The bud occurring elsewhere on the plant (such as on trunks, roots, or leaves) except from the leaf axils, stem tips, and plant apices.

adventitious root A root that arises from an organ other than the root—typically a stem.

aerenchyma Anatomical feature of roots found in hypoxic conditions, showing large, gas-filled intercellular spaces in the root cortex.

aerobic respiration The complete oxidation of carbon compounds to CO_2 and H_2O, using oxygen as the final electron acceptor. Energy is released and conserved as ATP.

aeroponics The technique by which plants are grown without soil with their roots suspended in air while being sprayed continuously with a nutrient solution.

after-ripening Technique for breaking seed dormancy by storage at room temperature under dry conditions, usually for several months.

albuminous cells Sieve element-associated cells in the phloem of gymnosperms. Although similar to companion cells in angiosperms, they have a different developmental origin. Also called Strasburger cells.

aleurone layer Layer of aleurone cells surrounding and distinct from starchy endosperm of cereal grains.

allelopathy Release by plants of substances into the environment that have harmful effects on neighboring plants.

allocation The regulated diversion of photosynthate into storage, utilization, and/or transport.

25_Taiz7e-Glossary.indd 1 5/2/22 11:26 AM

α-amylase inhibitors Substances synthesized by some legumes that interfere with herbivore digestion by blocking the action of the starch-digesting enzyme α-amylase.

α-expansins (EXPAs) One of two major families of expansin proteins that catalyze the pH-dependent extension and stress relaxation of cell walls.

allopolyploid plants Polyploids with multiple complete genomes derived from two separate species.

alternation of generations The presence of two genetically distinct multicellular stages, one haploid and one diploid, in the plant life cycle. The haploid gametophyte generate begins with meiosis, while the diploid sporophyte generation begins with the fusion of sperm and egg.

alternative oxidase An enzyme in the mitochondrial electron transport chain that reduces oxygen and oxidizes ubiquinol.

alveolar cells A layer of cells surrounded by tube-like cell walls, formed during the cellularization of coenocytic endosperm.

amplitude In a biological rhythm, the distance between peak and trough; it can often vary while the period remains unchanged.

amyloplast A starch-storing plastid found abundantly in storage tissues of shoots and roots, and in seeds. Specialized amyloplasts in the root cap also serve as gravity sensors.

anaphase The stage of mitosis during which the two chromatids of each replicated chromosome are separated and move toward opposite poles.

angiosperms The flowering plants. With their innovative reproductive organ, the flower, they are a more advanced type of seed plant and dominate the landscape. Distinguished from gymnosperms by the presence of a carpel that encloses the seeds.

anisotropic growth Enlargement that is greater in one direction over another; for example, elongating cells in the stem or root axis grow more in length than in width.

annual plants Plants that complete their life cycle from seed to seed, senesces, and die within one year.

antenna complex A group of pigment molecules that cooperate to absorb light energy and transfer it to a reaction center complex.

antifreeze proteins Proteins that confer to aqueous solutions the property of thermal hysteresis. When induced by cold temperatures, these plant proteins bind to the surfaces of ice crystals to prevent or slow further crystal growth, thereby limiting or preventing freeze damage. Some antifreeze proteins may be identical to pathogenesis-related proteins.

antioxidative enzymes Proteins that detoxify reactive oxygen species.

antipodal cells Cells located at the challazal end of the embryo sac in a mature female gametophyte.

antiport A type of secondary active transport in which the movement of two solutes in opposite directions across the membrane is coupled.

apical cell In ferns and other primitive vascular plants, the single initial or stem cell of roots and shoots that gives rise to all the other cells of the organ. In angiosperm embryogenesis, the smaller, cytoplasm-rich cell formed by the first division of the zygote.

apical dominance In most higher plants, the growing apical bud's inhibition of the growth of lateral buds (axillary buds).

apical meristems Localized regions made up of undifferentiated cells undergoing cell division without differentiation at the tips of shoots and roots.

apical–basal axis An axis that extends from the shoot apical meristem to the root apical meristem.

apoplast The mostly continuous system of cell walls, intercellular air spaces, and xylem vessels in a plant.

apoplastic transport Movement of molecules through the cell wall continuum that is called the apoplast. Molecules may move through the linked cell walls of adjacent cells, and in that way move throughout the plant without crossing the plasma membrane.

apoptosis A type of programmed cell death found in animals showing characteristic morphological and biochemical changes, including fragmentation of nuclear DNA between the nucleosomes. Apoptosis-like changes also occur in some senescing plant tissues, differentiating xylem tracheary elements, and in the hypersensitive response against pathogens.

aquaporin An integral membrane protein that forms water-selective channels across the membrane. Such channels facilitate the movement of water and other small neutral molecules across the membrane.

ARABIDOPSIS HISTIDINE PHOSPHOTRANSFER (AHP) Gene involved in cytokinin signal propagation from the plasma membrane receptor to the nucleus.

ARABIDOPSIS RESPONSE REGULATOR (ARR) Arabidopsis genes that are similar to bacterial two-component signaling proteins called response regulators. There are two classes: Type-A ARRs, whose transcription is up-regulated by cytokinin; type-B ARRs, whose expression is not affected by cytokinin.

arabinans Neutral polysaccharides with a backbone of 1,5-linked arabinose residues decorated with single or short side chains made of arabinose. Arabinans may be separate polymers or may be domains attached to the backbone of rhamnogalacturonan I.

arabinogalactan proteins (AGPs) A family of extensively glycosylated (mostly galactose and arabinose), water-soluble cell wall proteins that usually amount to less than 1% of the wall dry mass. Some may associate with the plasma membrane via a glycosylphosphatidylinositol anchor. They often display tissue- and cell-specific expression.

arabinoxylan A branched cell wall polysaccharide consisting of a backbone of xylose residues with arabinose side chains.

arbuscular mycorrhiza A symbiosis between a fungus belonging to the Glomeromycota, and the roots of a broad range of angiosperms, gymnosperms, ferns, and liverworts. Facilitates the uptake of mineral nutrients by roots.

arbuscule Branched structure of mycorrhizal fungus that forms within penetrated plant cells; the site of nutrient transfer between the fungus and the host plant.

ARGONAUTE (AGO) A catalytic protein that is part of the RNA-induced silencing complex.

ascorbate peroxidase An enzyme that converts peroxide and ascorbate to dehydroascorbate and water.

asparagine synthetase (AS) Enzyme that transfers nitrogen as an amino group from glutamine to aspartate, forming asparagine.

aspartate aminotransferase (Asp-AT) An aminotransferase that transfers the amino group from glutamate to the carboxyl atom of oxaloacetate to form aspartate.

ATP synthase The multi-subunit protein complex that synthesizes ATP from ADP and phosphate (P). The F_oF_1 type, where the subscript o indicates that it is sensitive to the inhibitor oligomycin, is present in bacteria and the inner membrane of mitochondria. Also called Complex V in mitochondria. The CF_0-CF_1 type, where the subscript 0 indicates that it is *not* oligomycin-sensitive, is present in the thylakoid membranes of chloroplasts.

ATPase A transmembrane enzyme that can split ATP into ADP and P_i and use the released energy for driving transmembrane solute transport. *See also* ATP synthase, which has ATPase activity.

autolysis The destruction of a cell through the action of its own enzymes, such as endonucleases, ribonucleases, bifunctional nucleases, and proteases.

autophagic body The single membrane-bound organelle, derived from the autophagosome, that enters the vacuole and releases its contents for degradation.

autophagosome A double membrane-bound organelle that delivers cellular components to the vacuole for degradation.

autophagy A catabolic mechanism that conveys cellular macromolecules and organelles via autophagosomes to lytic vacuoles where they are degraded and recycled.

autopolyploid plants Polyploids containing multiple complete genomes of a single species.

auxin clock model A model for the spacing of prebranch sites in roots based on the periodic fluctuation of auxin activity or concentration in the oscillation zone.

auxin response element (AuxRE) A DNA promoter sequence that modulates gene expression when bound by auxin-responsive transcription factors.

auxin response factors (ARFs) A family of proteins that regulate the transcription of specific genes involved in auxin responses; they are inhibited by association with specific Aux/IAA repressor proteins, which are degraded in the presence of auxin.

auxin sink A cell or tissue that takes up auxin from a nearby auxin source. Participates in auxin canalization during vascular differentiation.

auxin source A cell or tissue that exports auxin to other cells or tissues by polar transport.

AUXIN/INDOLE-3-ACETIC ACID (AUX/IAA) A family of short-lived small proteins that combine with the TIR1/AFB proteins to form the primary auxin receptor. This family of short-lived small proteins in Arabidopsis regulates auxin-induced gene expression by binding to ARF protein that is bound to DNA. If the specific ARF is a transcriptional activator, the Aux/IAA binding represses transcription.

axillary buds Secondary meristems that are formed in the axils of leaves. If they are also vegetative meristems, they will have a structure and developmental potential similar to that of the vegetative apical meristem. Axillary buds can also form flowers, as in inflorescences.

B

***Bacillus thuringiensis* (Bt)** A soil bacterium that is the source for a commonly used transgene encoding an insecticidal toxin.

bacteriochlorophylls Light-absorbing pigments active in photosynthesis in anoxygenic photosynthetic organisms.

bacteriophytochromes (BphPs) Members of a widespread family of photosensors that include plant phytochromes (Phy family), cyanobacteria (Cph1 and Cph2), and purple and other nonphotosynthetic bacteria (BphP), and even fungi (Fph).

bacteroid A nitrogen-fixing organelle that develops from an endosymbiotic bacterium upon invagination into a plant host cell.

bark storage proteins (BSPs) Storage proteins that accumulate in the phloem parenchyma (inner bark) of woody species at the end of the growing season in temperate climates. These proteins are mobilized to support growth in the spring.

bark Collective term for all the tissues outside the cambium of a woody stem or root, and composed of phloem and periderm.

basal cell In embryogenesis, the larger, vacuolated cell formed by the first division of the zygote. Gives rise to the suspensor.

berry A simple, fleshy fruit produced from a single ovary and consisting of a an outer pigmented exocarp, a fleshy, juicy mesocarp, and a membranous inner endocarp.

β-expansins (EXPBs) One of two major families of expansins; the number of EXPB genes is particularly numerous in grasses, where a subset are abundantly expressed in pollen and facilitate pollen tube penetration of the stigma.

β-oxidation Oxidation of fatty acids into fatty acyl-CoA, and the sequential breakdown of the fatty acids into acetyl-CoA units. NADH is also produced.

biennial plants Plants that require two growing seasons to flower and produce seed.

biolistics A procedure, also called the "gene gun" technique, in which tiny gold particles coated with the genes of interest are mechanically shot into cultured cells. Some of the DNA is randomly incorporated into the genome of the targeted cells.

biosphere Parts of the surface and atmosphere of the Earth that support life as well as the organisms living there.

biotrophic pathogens Pathogens that leave infected tissue alive and only minimally damaged while the pathogen continues to feed on host resources.

blade (lamina) The blade of a leaf.

bleached The loss of chlorophyll's characteristic absorbance due to its conversion into another structural state, often by oxidation.

bordered pit A pit pair in which the pit chamber is over-arched by the cell wall, creating a larger pit chamber and smaller pit aperture.

boundary layer resistance The resistance to the diffusion of water vapor due to the layer of unstirred air next to the leaf surface. A component of diffusional resistance.

Bowen ratio The ratio of sensible heat loss to evaporative heat loss, the two most important processes in the regulation of leaf temperature.

bracts Small leaf-like structure with underdeveloped blade.

brassinolide A plant steroidal hormone with growth-promoting activity, first isolated from *Brassica napus* pollen. One of a group of plant steroidal hormones with similar activities called brassinosteroids.

brassinosteroids A group of plant steroid hormones that play important roles in many developmental processes, including cell division and cell elongation in stems and roots, photomorphogenesis, reproductive development, leaf senescence, and stress responses.

bud scales Small, scale-like leaves that form a protective sheath around a dormant bud.

bulk transport Translocation of water and solutes by mass flow down a pressure gradient, as in the xylem or phloem.

C

C_4 photosynthesis The photosynthetic carbon metabolism of certain plants in which the initial fixation of CO_2 and its subsequent reduction take place in different cells, the mesophyll and bundle sheath cells, respectively. The initial carboxylation is catalyzed by phosphoenylpyruvate carboxylase (not by Rubisco as in C_3 plants), producing a four-carbon compound (oxaloacetate), which is immediately converted to malate or aspartate.

caeliferins A family of sulfated α-hydroxy fatty acids that elicit plant volatile production and immune responses.

calcium oxalate crystals Crystals of calcium oxalate that form in the vacuoles of some plant species to deter herbivory by insects and mammals.

callose A β-1,3-glucan synthesized in the plasma membrane and deposited between the plasma membrane and the cell wall at plasmodesmata and sieve pores. Synthesized by sieve elements in response to damage, stress, or as part of a normal developmental process.

Calvin–Benson cycle The biochemical pathway for the reduction of CO_2 to carbohydrate. The cycle involves three phases: the carboxylation of ribulose 1,5-bisphosphate with atmospheric CO_2, catalyzed by Rubisco, the reduction of the formed 3-phosphoglycerate to trioses phosphate by 3-phosphoglycerate kinase and NADP-glyceraldehyde-3-phosphate dehydrogenase, and the regeneration of ribulose 1,5-bisphospate through the concerted action of ten enzymatic reactions.

cambium Layer of meristematic cells between the xylem and phloem that produces cells of these tissues and results in the lateral (secondary) growth of the stem or root.

canalization model The hypothesis that as auxin flows through tissues it stimulates and polarizes its own transport, which gradually becomes channeled—or canalized—into files of cells leading away from auxin sources; these cell files can then differentiate to form vascular tissue.

capillarity The movement of water over small distances up a glass capillary tube or within the cell wall, due to water's cohesion, adhesion, and surface tension.

carbon fixation reactions The synthetic reactions occurring in the stroma of the chloroplast that use the high-energy compounds ATP and NADPH for the incorporation of CO_2 into carbon compounds.

carbon isotope ratio The ratio $^{13}C/^{12}C$ isotope composition of carbon compounds as measured by use of a mass spectrometer.

cardiac glycoside Glycosylated organic plant defense compound similar to oleandrin from Oleander bushes that is poisonous to animals and inhibits sodium/potassium channels to cause contractions in cardiac muscles.

carotenoids Linear polyenes arranged as a planar zigzag chain, with conjugated double bonds. These orange pigments serve both as antenna pigments and photoprotective agents.

carrier A membrane transport protein that binds to a solute, undergo conformational change, and release the solute on the other side of the membrane.

CASPARIAN STRIP PROTEIN 1 (CASP1) A protein that regulates membrane-cell wall junctions and cell wall deposition required for formation modification of the endodermis to form the Casparian strip that functions as an apoplastic barrier surrounding the root vascular cylinder.

Casparian strip A band in the cell walls of the endodermis that is impregnated with the waxlike, hydrophobic substance suberin. Prevents water and solutes from entering the xylem by moving between the endodermal cells.

catalase An enzyme that breaks hydrogen peroxide down into water and oxygen. When it is abundant in peroxisomes it may form crystalline arrays.

cation exchange The replacement of mineral cations adsorbed to the surface of soil particles by other cations.

cavitation The collapse of tension in a column of water resulting from the indefinite expansion of a tiny gas bubble.

CCAAT box A sequence of nucleotides involved in the initiation of transcription in eukaryotes.

cell autonomous response A response to an environmental stimulus or genetic mutation that is localized to a particular cell.

cell plate Wall-like structure that separates newly divided cells. Formed by the phragmoplast and later becomes the cell wall.

cell wall The rigid cell surface structure external to the plasma membrane that supports, binds, and protects the cell. Composed of cellulose and other polysaccharides and proteins. *See also* primary cell walls and secondary cell walls.

cellulose microfibril Thin, ribbon-like structure of indeterminate length and variable width composed of 1→4-linked β-D-glucan chains tightly packed in crystalline arrays alternating with less organized amorphous regions. Provides structural integrity to the cell walls of plants and determines the directionality of cell expansion.

cellulose synthase Enzyme that catalyzes the synthesis of individual 1→4-linked β-D-glucans that make up cellulose microfibrils.

cellulose A linear chain of 1→4-linked β-D-glucose. The repeating unit is cellobiose.

central cell The cell in the embryo sac that fuses with the second sperm cell, giving rise to the primary endosperm cell.

central zone (CZ) A central cluster of relatively large, highly vacuolate, slow-dividing cells in shoot apical meristems, comparable to the quiescent center of root meristems.

centromere The constricted region on the mitotic chromosome where the kinetochore forms and to which spindle fibers attach.

***CESA* (Cellulose Synthase A)** A multigene family of cellulose synthases found in all land plants.

CF_0–CF_1 ATP synthase *See* ATP synthase.

channel A transmembrane protein that functions as a selective pore for passive transport of ions or uncharged molecules like water across the membrane.

charge-separated state State produced in photosynthetic reaction centers after excitation by light in which an electron is moved from the lumen side to the stromal side. This movement of electrons forms an electric field across the thylakoid.

checkpoint A key regulatory point early in G_1 of the cell cycle that determines if the cell is committed to the initiation of DNA synthesis.

chelator An organic compound that can form a noncovalent complex with certain cations facilitating their uptake (e.g., malic acid, citric acid).

chemical potential The free energy, which is available to perform work, associated with a substance.

chemiosmotic model The mechanism whereby the electrochemical gradient of protons established across a membrane by an electron transport process is used to either drive energy-requiring ATP synthesis (mitochondria and chloroplasts) or carrier-mediated anion efflux at the plasma membrane (as in polar auxin transport).

chemotaxis The process by which some cells (e.g., bacteria, protozoa, motile sperm) are able to decode a concentration gradient of a molecule (chemoattractant) and swim by independent motility (flagella, cilia) towards its most concentrated source. In all species of animals and early land plants (e.g., mosses, ferns), sperm cells swim toward the egg cell, or the egg cell producing organs, by chemotaxis.

chemotropic hypothesis The hypothesis that a hierarchy of molecular cues directs the pollen tube to its destination by stimulating the tip to grow toward the ovule.

chemotropism The directed growth of an organ (e.g., roots) or tip-growing cell (e.g., pollen tubes and fungal hyphae) toward an external chemical stimulus. In all flowering plants (gymno- and angiosperms), non-motile sperm cells are borne inside a pollen tube, which grows chemotropically toward the egg cell.

chlorophyll *a/b* antenna protein Chlorophyll-containing protein associated with one or the other of the two photosystems in eukaryotic organisms. Also known as light-harvesting complex protein (LHC protein).

chlorophyll Light-absorbing green pigment active in photosynthesis.

chloroplast The organelle that is the site of photosynthesis in eukaryotic photosynthetic organisms.

chlorosis The yellowing of plant leaves such as occurs as a result of mineral deficiency. The leaves affected and the chlorosis localization on the leaf can be diagnostic for the type of deficiency.

Cholodny–Went model Early mechanism proposed for tropisms involving stimulation of the bending of the plant axis by lateral transport of auxin in response to a stimulus, such as light, gravity, or touch. The original model has been supported and expanded by recent experimental evidence.

chromatin The DNA–protein complex found in the interphase nucleus. Condensation of chromatin forms the mitotic and meiotic chromosomes.

chromophore A light-absorbing pigment molecule that is usually bound to a protein (an apoprotein).

chromoplasts Plastids that contain high concentrations of carotenoid pigments, rather than chlorophyll. Chromoplasts are responsible for the yellow, orange, or red colors of many fruits, flowers, and autumn leaves.

chromosome territory The specific region inside a nucleus that a chromosome occupies.

chromosomes The condensed form of chromatin that forms early in mitosis and meiosis.

chronic photoinhibition Photoinhibition of photosynthetic activity in which both quantum efficiency and the maximum rate of photosynthesis are decreased. Occurs under high levels of excess light.

circumnutation The tendency of a shoot or root tip to oscillate in a spiral pattern during growth.

***cis*-acting control elements** DNA sequences that bind transcription factors and are adjacent (*cis*) to the transcription units they regulate. Not to be confused with *cis*-elements.

***cis*-elements** Certain nucleotide sequences within the mRNA molecule by which mRNA stability is regulated. Not to be confused with *cis*-acting sequences in DNA that influence transcriptional activity.

cisgenics Genetic engineering techniques, in which genes are transferred between plants that could also otherwise be crossed sexually.

cisternae (singular *cisterna*) A network of flattened saccules and tubules that compose the endoplasmic reticulum, the ER.

cladodes Flattened, photosynthetic stems that perform the functions of leaves, as in the pads of prickly pear cacti (*Opuntia*).

clathrin Proteins that have a unique *triskelion* structure that spontaneously assemble into 100-nm cages that coat vesicles associated with endocytosis at the plasma membrane and other cellular trafficking events.

climacteric Marked rise in respiration at the onset of ripening that occurs in all fruits that ripen in response to ethylene, and in the senescence process of detached leaves and flowers.

clock hypothesis Currently accepted hypothesis of how plants measure night length. Proposes that photoperiodic timekeeping depends on the endogenous oscillator of circadian rhythms.

CO_2 compensation point The CO_2 concentration at which the rate of respiration balances the photosynthetic rate.

coat-imposed dormancy Dormancy imposed on the embryo by the seed coat and other enclosing tissues, such as endosperm, pericarp, or extrafloral organs. *See also* exogenous dormancy.

coevolution Linked genetic adaptations of two or more organisms.

cohesion The mutual attraction between water molecules due to extensive hydrogen bonding.

coleoptile stage The stage of embryogenesis in monocotyledonous plants in which the coleoptile becomes distinguishable.

coleoptile A modified ensheathing leaf that covers and protects the young primary leaves of a grass seedling as it grows through the soil. Unilateral light perception, especially blue light, by the tip results in asymmetric growth and bending due to unequal auxin distribution in the lighted and shaded sides.

coleorhiza A protective sheath surrounding the embryonic radicle in members of the grass family.

collection phloem Sieve elements of the minor veins in sources.

collenchyma A specialized parenchyma with irregularly thickened, pectin-rich, primary cell walls that function in support in growing parts of a stem or leaf.

commensalism A relationship between two organisms where one organism benefits without negatively affecting the other.

common symbiotic pathway A sequence of common cellular events in plant roots that occurs in both mycorrhizal formation and root nodulation.

companion cell In angiosperms, a metabolically active cell that is connected to its sieve element by abundant pore-plasmodesma contacts and takes over many of the metabolic activities of the sieve element. It is ontogenetically related to its sieve element, i.e., a sister cell. In source leaves, it functions in the transport of photosynthate into the sieve elements.

compatible solutes Organic compounds that are accumulated in the cytosol during osmotic adjustment. Compatible solutes do not inhibit cytosolic enzymes unlike high concentrations of ions. Examples of compatible solutes include proline, sorbitol, mannitol, and glycine betaine.

complementation Genetic procedure by which two recessive mutations are introduced into the same cell to discover whether they effect the same genetic function and are therefore alleles. If the *trans* configuration ($m +/+ m_1$) exhibits a mutant phenotype, the mutations are allelic, but if they show a wild-type phenotype, they are nonallelic.

compound A leaf subdivided into leaflets.

condensed tannins Tannins that are polymers of flavonoid units. Require use of strong acid for hydrolysis.

conifer resin ducts Ducts or channels in conifer leaves and woody tissue that conduct terpenoid defense compounds. They may be constitutive or their formation may be induced by wounding/defense responses.

conifers Cone-bearing trees.

***CONSTANS* (*CO*)** Gene for a key component of a regulatory pathway that promotes flowering of Arabidopsis in long days; it encodes a protein that regulates the transcription of other genes.

constitutive defenses Plant defenses that are always immediately available or operational; that is, defenses that are not induced.

CONSTITUTIVE PHOTOMORPHOGENESIS1 (COP1) A constitutive repressor of photomorphogenesis that interacts with photomorphogenesis-promoting factors such as HY5 to promote their degradation via the ubiquitin–proteasome pathway.

contact angle A quantitative measure of the degree to which a water molecule is attracted to a solid phase versus to itself.

core promoter element The minimal portion of a promoter that is required to correctly initiate transcription.

core promoter (minimum promoter) One part of the two-part eukaryotic promoter consisting of the minimum upstream sequence required for gene expression.

core symbiotic genes Genes encoding components of the common symbiotic pathway.

cork cambium (phellogen) A layer of lateral meristem that develops within mature cells of the cortex and the secondary phloem. Produces the secondary protective layer, the periderm.

cork cambium A layer of lateral meristem that develops within mature cells of the cortex and the secondary phloem. Produces the secondary protective layer, the periderm. *Also called* phellogen.

cork *See* phellem.

cortex The outer layer of the root delimited on the outside by the epidermis and on the inside by the endodermis.

cortical ER The network of ER that lies just under the plasma membrane and is associated with the plasma at specific contact points. Distinct from internal ER which is found deeper in the cytoplasm and in trans-vacuolar strands.

cosuppression Decreased expression of a gene when extra copies are introduced.

cotyledons Also called "seed leaves," they are the main sources of nutrients during germination and post-germination photosynthesis before the first true leaves develop.

crassulacean acid metabolism (CAM) A biochemical process for concentrating CO_2 at the carboxylation site of Rubisco. Found in the family Crassulaceae (*Crassula*, *Kalanchoë*, *Sedum*) and numerous other families of angiosperms. In CAM, CO_2 uptake and fixation take place at night, and decarboxylation and reduction of the internally released CO_2 occur during the day.

creep pH-dependent cell wall extension. Contributes to cell wall expansion along with polymer integration and wall stress relaxation.

cristae Folds in the inner mitochondrial membrane that project into the mitochondrial matrix.

critical day length The minimum length of the day required for flowering of a long-day plant; the maximum length of day that will allow short-day plants to flower. However, studies have shown that it is the length of the night, not the length of the day, that is important.

cross-pollination (outcrossing) Pollination of a flower by pollen from the flower of a different plant.

cross-protection A plant response to one environmental stress that confers resistance to another stress.

cross-regulation The interaction of two or more signaling pathways.

crown gall A tumor-forming plant disease resulting from wound infection of the stem or trunk by the soil-dwelling bacterium *Agrobacterium tumefaciens*. A tumor resulting from the disease.

crown roots Adventitious roots that emerge from the lowermost nodes of a stem.

CRYPTOCHROME1 (CRY1) A flavoprotein implicated in many blue light responses that has homology with photolyase. Formerly HY4.

cryptochromes A family of flavoprotein photoreceptors that absorb primarily blue-light and regulate plant growth and development.

cyanogenic glycosides Nonalkaloid, nitrogenous protective compounds that break down to give off the poisonous gas hydrogen cyanide when the plant is crushed.

cyclic electron flow In photosystem I, flow of electrons from the electron acceptors through the cytochrome b_6f complex and back to P700, coupled to proton pumping into the lumen. This electron flow energizes ATP synthesis, but does not oxidize water or reduce $NADP^+$.

cyclin-dependent kinases (CDKs) Protein kinases that regulate the transitions from G_1 to S, and from G_2 to mitosis, during the cell cycle.

cyclins Regulatory proteins associated with cyclin-dependent kinases that play a crucial role in regulating the cell cycle.

cyst nematodes Parasitic nematodes that invade roots and transform into a non-motile cyst. The soybean cyst nematode *Heterodera glycines* is a major threat to soybean production.

cytochrome b_6f complex A large multi-subunit protein complex containing two *b*-type hemes, one *c*-type heme (cytochrome *f*), and a Rieske iron–sulfur protein. An immobile protein distributed equally between the grana and the stroma regions of the membranes.

cytochrome *c* A peripheral, mobile component of the mitochondrial electron transport chain that oxidizes complex III and reduces complex IV.

cytochrome *f* A subunit in the cytochrome b_6f complex that plays a role in electron transport between Photosystem I and II.

cytochrome P450 monooxygenase (CYP) A generic term for a large number of related, but distinct, mixed-function oxidative enzymes localized on the endoplasmic reticulum. CYPs participate in a variety of oxidative processes, including steps in the biosynthesis of gibberellins and brassinosteroids.

cytokinesis In plant cells, following nuclear division, the separation of daughter nuclei by the formation of new cell wall.

cytoplasm The cellular matter enclosed by the plasma membrane exclusive of the nucleus, that contains the cytosol, ribosomes, and the cytoskeleton which, in eukaryotes, surrounds intracellular and membrane-limited organelles (chloroplasts, mitochondria, endoplasmic reticulum, etc.).

cytoplasmic streaming The coordinated movement of particles and organelles through the cytosol.

cytoskeleton Composed of polarized microfilaments of actin or microtubules of tubulin, the cytoskeleton helps control the organization and polarity of organelles and cells during growth.

D

day-neutral plants (DNPs) A plant whose flowering is not regulated by day length.

de-etiolation Rapid developmental changes associated with loss of the etiolated form due to the action of light. *See* photomorphogenesis.

defensins A group of small, cysteine-rich antimicrobial proteins found in animals and plants.

deficiency zone Concentrations of a mineral nutrient in plant tissue below the critical concentration that reduces plant growth.

dehiscent The spontaneous opening of a mature anther or fruit, releasing its contents.

dehydrins Hydrophilic plant proteins that accumulate in response to drought stress and cold temperatures.

depolarized Refers to a decrease in the usually negative membrane potential difference across the plasma membrane of plant cells. May be caused by the activation of anion channels and loss of anions, such as chloride, from the cell interior, which is negative with respect to the outside.

dermal tissue The system that covers the outside of the plant body; the epidermis or periderm.

desaturase enzymes Enzymes that remove hydrogens in a carbon chain to create a double bond between carbons or to add an ethyl group to elongate a carbon chain.

desiccation tolerance A plant's ability to function while dehydrated.

diacylglycerol (DAG) A molecule consisting of the three-carbon glycerol molecule to which two fatty acids are covalently attached by ester linkages.

diaheliotropic Refers to leaf movements that maximize light interception by solar tracking and minimize overexposure to light.

DICER-LIKE1 (DCL1) One of the plant nuclear proteins that convert pri-miRNAs into miRNAs.

dichogamy The production of stamens and pistils at different times in hermaphroditic flowers—an adaptation that promotes cross-pollination.

dichotomous branching Branching that occurs by the division of the shoot apical meristem to produce two equal shoots.

diel rhythm A biological rhythm in which physiological or gene expression patterns are regular and repetitive with a daily cycle.

difference in water vapor concentration Referring to the difference between the water vapor concentration of the air spaces inside the leaf and that of the air outside the leaf. One of the two major factors that drive transpiration from the leaf.

differentiation Process by which a cell acquires metabolic, structural, and functional properties that are distinct from those of its progenitor cell. In plants, differentiation is frequently reversible, when excised differentiated cells are placed in tissue culture.

diffuse growth A type of cell growth in plants in which expansion occurs more or less uniformly over the entire surface. Contrast with tip growth.

diffusion coefficient The proportionality constant that measures how easily a specific substance *s* moves through a particular medium. The diffusion coefficient is a characteristic of the substance and depends on the medium.

diffusion potential The potential (voltage) difference that develops across a semipermeable membrane as a result of the differential permeability of solutes with opposite charges (for example K^+ and Cl^-).

diffusion The movement of substances due to random thermal agitation from regions of high free energy to regions of low free energy (e.g., from high to low concentration).

diffusional resistance Restriction posed by the boundary layer and the stomata to the free diffusion of gases from and into the leaf.

dioecious Refers to plants in which male and female flowers are found on different individuals, such as spinach (*Spinacia*) and hemp (*Cannabis sativa*). Contrast with monoecious.

directed organelle movement Movement of an organelle in a particular direction, which can be driven by the interaction with molecular motors associated with the cytoskeleton.

dirigent-domain proteins Homologs of a protein that positions two coniferyl alcohol substrates for oxidative radical dimerization in a specific stereospecific conformation for the formation of (+)-pinoresinol. Dirigent proteins have also been invoked in a disputed hypothesis about ordered lignin formation.

dispersed repeat A type of repeated sequence that is not restricted to a single location in the genome. May occur as microsatellites or transposons.

distal regulatory promoter sequences Located upstream of the proximal promoter sequences, these *cis*-acting sequences can exert either positive or negative control over eukaryotic promoters.

DNA synthesis phase (S, or S phase) In the cell cycle, the stage during which DNA is replicated; it follows G_1 and precedes G_2.

DNA transposons Dominant group of dispersed repeats found in heterochromatin that can move or be copied from one location to another within the genome of the same cell.

dolichol diphosphate Embedded in the ER membrane, this lipid is the assembly site for a branched oligosaccharide (*N*-acetylglucosamine, mannose, and glucose) that will be transferred to the free amino group of one or more asparagine residues of a protein in the ER that is destined for secretion.

domains (1) Regions (nucleotide sequences) within the gene that are similar to regions found in other genes. (2) Regions of a protein (amino acid sequence) with a particular

structure or function. (3) The three major taxonomic groups of living organisms.

dormancy A living condition in which growth does not occur under conditions that are normally favorable to growth.

downstream promoter element (DPE) A distinct type of core promoter element located approximately 30 nucleotides downstream from the transcription start site.

drupe A fruit similar to a berry, but with a hardened, shell-like endocarp (pit or stone) that contains a seed.

dynamic photoinhibition Photo-inhibition of photosynthesis in which quantum efficiency decreases but the maximum photosynthetic rate remains unchanged. Occurs under moderate, not high, excess light.

E

ectomycorrhiza A symbiosis where the fungus typically forms a thick sheath, or mantle, of mycelium around roots. The root cells themselves are not penetrated by the fungal hyphae, but instead are surrounded by a network of hyphae called the Hartig net, which provides a large area of contact between the symbionts that is involved in nutrient transfers.

ectopic Outside of the normal context. Used in gene expression, i.e., expression of a gene product in a domain where it is not normally expressed.

effectors Molecules (including proteins) secreted by pathogens that bind to specific plant proteins to change their activity. Some act on proteins inside plant cells.

effector-triggered immunity (ETI) Immune responses activated by intracellular nucleotide-binding–leucine rich repeat (NLRs) proteins that are encoded by *R* genes.

egg apparatus The three cells at the micropylar end of the embryo sac consisting of the egg cell and two synergid cells.

egg cell The female gamete.

electrochemical potential The chemical potential of an electrically charged solute.

electrochemical proton gradient The sum of the electrical charge gradient and the pH gradient across the membrane, resulting from proton pumping across a membrane.

electrogenic transport Active ion transport involving the net movement of charge across a membrane.

electronegative Having the capacity to attract electrons and thus producing a slightly negative electric charge.

electroneutral transport Active ion transport that involves no net movement of charge across a membrane.

elicitors Specific pathogen molecules or cell wall fragments that bind to plant proteins and thereby signal for plant defense against a pathogen. *See* avirulence genes.

elongation zone The region of rapid and extensive root cell elongation showing few, if any, cell divisions.

embryo dormancy Seed dormancy that is caused directly by the embryo and is not due to any influence of the seed coat or other surrounding tissues. *See also* endogenous dormancy.

endocytosis The formation of small vesicles from the plasma membrane, which detach and move into the cytosol, where they fuse with elements of the endomembrane system.

endodermis A specialized layer of cells with a Casparian strip surrounding the vascular tissue in roots and some stems.

endogenous dormancy Seed dormancy that is intrinsic to the seed and is not due to any physical or chemical influence of the seed coat or other surrounding tissues. Endogenous dormancy is regulated by the ratio of the hormones abscisic acid (ABA) and gibberellin (GA).

endoplasmic reticulum (ER) An organelle comprising a network of membranes that function in protein secretion and biosynthesis of small molecules. The ER is continuous with the nuclear membrane. The *rough* ER region is associated with protein folding and has ribosomes that synthesize ER proteins on the surface. The *smooth* ER region is associated with lipid modification and other biosynthetic activities.

endopolyploidy Polyploidy caused by replication of chromosomes without division of the nucleus.

endoreduplication Cycles of nuclear DNA replication without mitosis resulting in polyploidization.

endosymbiosis A theory that explains the evolutionary origin of the chloroplast and mitochondrion through formation of a symbiotic relationship between a prokaryotic cell and a simple nonphotosynthetic eukaryotic cell, followed by extensive gene transfer to the nucleus.

endosymbiotic theory *See* endosymbiosis.

endothelium A cell layer derived from the innermost layer of the integument that surrounds the embryo sac and supplies it with nutrients, similar to the tapetal layer in anthers.

energy conversion efficiency The fraction of energy from photons that is stored in photochemical reactions. Energy is lost in making reactions go forward, which prevents back reactions. This is distinct from the quantum yield, which describes the fraction of light that induces stable photochemistry.

energy transfer In the light reactions of photosynthesis, the direct transfer of energy from an excited molecule, such as carotene, to another molecule, such as chlorophyll. Energy transfer can also take place between chemically identical molecules, such as chlorophyll-to-chlorophyll transfer.

ENHANCED SUBERIN 1 (ESB1) A protein involved in the restricted formation of lignin in the narrow strip of cell wall that forms the Casparian strip in the root endodermis. Mutants in the *ESB1* gene are characterized by a spread of lignification beyond the Casparian strip as well as elevated levels of suberin in the root.

enhancers Positive regulatory sequences located tens of thousands of base pairs away from a gene's start site. Enhancers may be located either upstream or downstream from the promoter.

entrained The synchronization of the period of biological rhythms by external controlling factors, such as light and darkness.

envelope The double-membrane system surrounding the chloroplast or the nucleus. The outer membrane of the nuclear envelope is continuous with the endoplasmic reticulum.

epicormic bud A dormant bud that becomes covered by bark. Epicormic buds can act as reserve buds that can grow in the presence of increased light or after a forest fire; may be preventitious or adventitious.

epidermis The outermost layer of plant cells, typically one cell thick.

epigenetic modifications Chemical modifications to DNA and histones that cause heritable changes in gene activity without altering the underlying DNA sequence.

epigenome Heritable chemical modifications to DNA and chromatin including DNA methylation, histone methylation and acylation, and DNA sequences that generate noncoding RNA sequences that interfere with gene expression.

escape from photoreversibility The loss of photoreversibility by far-red light of phytochrome-mediated red light–induced events after a short period of time.

essential element An element whose absence causes severe abnormalities in plant growth, development, or reproduction and may prevent a plant from completing its life cycle.

ethylmethanesulfonate (EMS) A chemical mutagen that causes the addition of an ethyl group to a nucleotide, and results in a permanent mutation from G/C to A/T at that site.

etiolated Effects of seedling growth in the dark, in which the hypocotyl and stem are more elongated, cotyledons and leaves do not expand, and chloroplasts do not mature.

etioplast Photosynthetically inactive form of chloroplast found in etiolated seedlings. Does not synthesize chlorophyll or most of the enzymes and structural proteins required for the formation of thylakoids and operation of photosynthesis. Contains an elaborate system of interconnected membrane tubules called the prolamellar body.

euchromatin The dispersed, transcriptionally active form of chromatin. *See also* heterochromatin.

eudicots Abbreviated name for the eudicotyledons, one of two major classes of the angiosperms, and refers to the fact that plants in this class have two seed leaves (cotyledons).

eukaryotic pathway In the cytoplasm, the series of reactions for the synthesis of glycerolipids. *See also* prokaryotic pathway.

exclusion The ability to block the uptake of toxic ions into the cell or to actively secrete them.

exocyst In plants, a multifunctional, multimeric protein complex that functions in tethering of secretory vesicles to the plasma membrane prior to membrane fusion.

exocytosis The process by which vesicle contents are distributed to the plasma membrane or apoplast.

exodermis A specialized layer of cells in most angiosperms, but not gymnosperms, containing a Casparian strip, in the outer layer of the cortex of the root.

exogenous dormancy Physical inhibitory effects of the seed coat or other enclosing tissues, such as the endosperm, pericarp, or extrafloral organs, on the growth of the embryo during germination.

expansins Class of wall-loosening proteins that accelerate wall stress relaxation and cell expansion, typically with an optimum at acidic pH. Appear to mediate acid growth.

export The movement of photosynthate in sieve elements away from the source tissue.

external coincidence model A concept that explains how plants respond appropriately to seasonal changes. When the light-sensitive phase of an internal rhythm coincides with an external light signal, photoperiodic responses including flowering can be induced in long day plants.

extracellular space, or apoplast In plants, the space continuum outside the plasma membrane made up of interconnecting cell walls through which water and mineral nutrients readily diffuse. *See* apoplast.

extrafloral nectar Nectar produced outside of the flower and not involved in pollination events.

F

F_1 The ATP-binding matrix-facing part of the F_oF_1-ATP synthase.

facilitated diffusion Passive transport across a membrane using a carrier or channel.

***FACKEL* (*FK*)** An Arabidopsis gene that encodes a sterol C-14 reductase necessary for structural sterols that define ordered membrane nanodomains. Mutants exhibit pattern formation defects: malformed cotyledons, short hypocotyl and root, and often multiple shoot and root meristems.

far upstream element (FUE) A conserved genetic sequence located upstream of the polyA site in eukaryotic genes.

FAR-RED ELONGATED HYPOCOTYL1 (FHY1) A protein that facilitates the entry of phyA into the nucleus in response to light.

F-box proteins Components of ubiquitin E3 ligase complexes.

fermentation The metabolism of pyruvate in the absence of oxygen, leading to the oxidation of the NADH generated in glycolysis to NAD^+. Allows glycolytic ATP production to function in the absence of oxygen.

ferredoxin (Fd) A small, water-soluble iron-sulfur protein involved in electron transport in photosystem I.

ferredoxin–$NADP^+$ reductase (FNR) Membrane-associated flavoprotein that receives electrons from Photosystem I and reduces $NADP^+$ to NADPH.

ferredoxin–thioredoxin system Three chloroplast proteins (ferredoxin, ferredoxin-thioredoxin reductase, thioredoxin). The concerted action of the three proteins uses reducing power from the photosynthetic electron transport system to reduce protein disulfide bonds by a cascade of thiol/disulfide exchanges. As a result, light controls the activity of several enzymes of the Calvin–Benson cycle.

fertilization The formation of a diploid (2*N*) zygote from the cellular and nuclear fusion of two haploid (1*N*) gametes, the egg and the sperm.

Fe–S center Prosthetic group consisting of inorganic iron and sulfur that are abundant in proteins in respiratory and photosynthetic electron transport.

FeSA Membrane-bound iron–sulfur protein that transfers electrons between Photosystem I and ferredoxin.

FeSB Membrane-bound iron–sulfur protein that transfers electrons between Photosystem I and ferredoxin.

FeSX Membrane-bound iron–sulfur protein that transfers electrons between Photosystem I and ferredoxin.

fiber An elongated, tapered sclerenchyma cell that provides support in vascular plants.

filiform apparatus A convoluted, thickened cell wall that increases the surface area of the plasma membrane at the extreme micropylar end of a synergid cell.

fimbrin An actin-binding protein that bundles F-actin filaments together into larger filamentous bundles.

flavin adenine dinucleotide (FAD) A riboflavin-containing cofactor that undergoes a reversible two-electron reduction to produce $FADH_2$.

flavin mononucleotide (FMN) A riboflavin-containing cofactor that undergoes a reversible one- or two-electron reduction to produce FMNH or $FMNH_2$.

flippases Enzymes that "flip" newly synthesized phospholipids across the bilayer from the outer (cytoplasmic) face of the membrane to the inner leaflet, thereby assuring symmetrical lipid composition of the membrane.

floral evocation The events occurring in the shoot apex that specifically commit the apical meristem to produce flowers.

floral meristems Form floral (reproductive) organs: sepals, petals, stamens, and carpels. May form directly from vegetative meristems or indirectly via an inflorescence meristem.

floral organ identity genes Three types of genes that control the specific locations of floral organs in the flower.

floral organs Angiosperm organs involved directly or indirectly in sexual reproduction; sepals, petals, stamens, and carpels.

florigen The hypothetical, universal flowering hormone synthesized by leaves and translocated to the shoot apical meristem via the phloem. So far, it has not been isolated or characterized.

FLOWERING D (FD) The protein that forms a complex with FT and activates a transcriptional cascade of floral identity genes at the shoot apical meristem, where it stimulates flowering.

flowering plants *See* angiosperms.

fluence The number of photons absorbed per unit surface area.

fluid mosaic The common molecular lipid–protein structure for all biological membranes. A double layer (bilayer) of polar lipids (phospholipids or, in chloroplasts, glycosylglycerides) has a hydrophobic, fluid-like interior. When structural sterols and sphingolipids are present in the bilayer, the fluidity of the interior is decreased. Membrane proteins are embedded in the bilayer and may move laterally.

fluorescence resonance energy transfer The physical mechanism by which excitation energy is conveyed from the pigment that absorbs the light to the reaction center.

fluorescence Following light absorption, the emission of light at a slightly longer wavelength (lower energy) than the wavelength of the absorbed light.

flux density The rate of transport of a substance *s* across a unit area per unit time. J_s may have units of moles per square meter per second (mol m^{-2} s^{-1}).

F_O The integral membrane part of the F_oF_1-ATP synthase in mitochondria. *See also* ATP synthase.

F_OF_1-ATP synthase *See* ATP synthase.

foliage leaves The principal lateral appendages of stems that carry out photosynthesis.

foliar application The application, and subsequent absorption, of some mineral nutrients to leaves as sprays.

forisome A protein body that rapidly disperses and blocks a sieve tube. Occurs only in certain legumes.

formins Proteins that bind actin and actin-profilin complexes to initiate polymerization of the actin filament.

free-running Designation of the biological rhythm that is characteristic for a particular organism when environmental signals are removed, as in total darkness. *See* zeitgeber.

frequency A unit of measurement that characterizes waves, in particular light energy. The number of wave crests that pass an observer in a given time.

fruit set The commitment to initiate fruit development. It is a key developmental switch that normally occurs following successful fertilization and/or pollination.

fruits In angiosperms, one or more mature ovaries containing seeds and sometimes adjacent attached parts.

fusicoccin A fungal toxin that induces acidification of plant cell walls by activating an H^+-ATPase in the plasma membrane. Fusicoccin stimulates rapid acid growth in stem and coleoptile sections. It also stimulates stomatal opening by stimulating proton pumping at the guard cell plasma membrane.

G

GABA shunt A pathway supplementing the citric acid cycle with the ability to form and degrade γ-aminobuteric acid (GABA).

GAF The chromophore-binding domain of phytochrome.

galactan A cell wall polysaccharide composed of galactose residues.

gamete A haploid (1*N*) reproductive cell.

gametophyte generation The stage, or generation, in the life cycle of plants that produces gametes. It alternates with the sporophyte generation, in a process called alternation of generations.

gametophyte The haploid (1*N*) multicellular structure that produces haploid gametes by mitosis and differentiation.

gametophytic self-incompatibility (GSI) The type of self-incompatibility in which the incompatibility phenotype of the pollen is determined by the pollen's own (haploid) genotype.

gap 1 (G_1) The phase of the cell cycle preceding the synthesis of DNA.

gap 2 (G_2) The phase of the cell cycle following the synthesis of DNA.

gate A structural domain of the channel protein that opens or closes the channel in response to external signals such as voltage changes, hormone binding, or light.

GC box A sequence of nucleotides involved in the initiation of transcription in eukaryotes.

gene fusion An artificial construct that links a promoter for one gene with the coding sequence of another gene. Often includes a reporter gene, such as green fluorescent protein gene, *GFP*, that produces a readily detected protein.

general transcription factors Proteins that are required by RNA polymerases of eukaryotes for proper positioning at the transcription start site.

generative cell A cell formed by pollen mitosis I of meiosis from the microspores. Generative cells define the male germ line of hereditary transmission in plants, and divide by pollen mitosis II to give rise to two sperm cells that will proceed to double fertilization of the egg and central cells.

genetic mosaicism The presence of two or more populations of cells with different genotypes caused by somatic mutations in a plant that has developed from a single fertilized egg.

genome Refers to all the genes in a haploid complement of eukaryotic chromosomes, in an organelle, a microbe, or the DNA or RNA content of a virus.

germination The events that take place between the start of imbibition of the dry seed and the emergence of the embryo, usually the radicle, from the structures that surround it. May also be applied to other quiescent structures, such as pollen grains or spores.

GIBBERELLIN INSENSITIVE DWARF 1 (GID1) Gibberellin receptor protein in rice.

gibberellins A large group of chemically related plant hormones synthesized by a branch of the terpenoid pathway and associated with the promotion of stem growth (especially in dwarf and rosette plants), seed germination, and many other functions.

Gibbs free energy The energy that is available to do work; in biological systems the work of synthesis, transport, and movement.

globular stage The first stage of embryogenesis. A radially symmetrical, but not developmentally uniform, sphere of cells produced by initially synchronous cell divisions of the zygote. *See* heart stage, torpedo stage.

glucan A polysaccharide made from glucose units.

glucomannan A polysaccharide made from both glucose and mannose units.

gluconeogenesis The synthesis of carbohydrates through the reversal of glycolysis.

glucose 6-phosphate dehydrogenase A cytosolic and plastidic enzyme that catalyzes the initial reaction of the oxidative pentose phosphate pathway.

glucuronoarabinoxylan (GAX) A hemicellulose with a (1,4)-linked backbone of β-D-xylose (Xyl) and side chains containing arabinose (Ara) and 4-O-methyl-glucuronic acid (4-O-Me-α-D-GlcA).

glucuronoxylan A major hemicellulose in some secondary cell walls, consisting of a backbone of 1→4-linked β-D-xylose residues with occasional glucuronic acid side chains.

glutamate dehydrogenase (GDH) Catalyzes a reversible reaction that synthesizes or deaminates glutamate as part of the nitrogen assimilation process.

glutamate synthase (GOGAT) Enzyme that transfers the amide group of glutamine to 2-oxoglutarate, yielding two molecules of glutamate. Also known as glutamine:2-oxoglutarate aminotransferase (GOGAT).

glutamine synthetase (GS) Catalyzes the condensation of ammonium and glutamate to form glutamine. The reaction is critical for the assimilation of ammonium into essential amino acids. Two forms of GS exist—one in the cytosol and one in chloroplasts/plastids.

glutathione peroxidase A family of enzymes that reduce peroxide to water and lipid hydroperoxides to alcohols.

glycan A general term for a polymer made up of sugar units; it is synonymous with polysaccharide.

glyceroglycolipids Glycerolipids in which sugars form the polar head group. Glyceroglycolipids are the most abundant glycerolipids in chloroplast membranes.

glycerophospholipids Polar glycerolipids in which the hydrophobic portion consists of two 16-carbon or 18-carbon fatty acid chains esterified to positions 1 and 2 of a glycerol backbone. The phosphate-containing polar head group is attached to position 3 of the glycerol.

glycine betaine *N*,*N*,*N*-trimethyl-glycine, which functions in drought stress protection, and was originally identified in sugar beet (*Beta vulgaris*).

glycolysis A series of reactions in which a sugar is oxidized to produce two molecules of pyruvate. A small amount of ATP and NADH is produced.

glycophytes Plants that are not able to resist salts to the same degree as halophytes. Show growth inhibition, leaf discoloration, and loss of dry weight at soil salt concentrations above a threshold. Contrast with halophytes.

glycoproteins Proteins that have covalently attached sugar oligomers or polymers.

glycosides Compounds containing an attached sugar or sugars.

glycosylphosphatidylinositol anchor In plants, a phosphoglyceride protein modification that anchors proteins to ordered plasma membrane domains

glyoxylate cycle The sequence of reactions that convert two molecules of acetyl-CoA to succinate in the glyoxysome.

glyoxysome An organelle found in the oil-rich storage tissues of seeds in which fatty acids are oxidized. A type of microbody.

glyphosate resistance Genetic capacity to survive a field application of the commercial herbicide Roundup, which kills weeds but does not harm resistant crop plants.

***GNOM* (*GN*)** An Arabidopsis gene encoding a regulator of vesicular trafficking in plant cells that is required for normal growth. Homozygous *gnom* mutants lack both roots and cotyledons.

Goldman equation An equation that predicts the diffusion potential across a membrane, as a function of the concentrations and permeabilities of all ions (e.g., K^+, Na^+ and Cl^-) that permeate the membrane.

Golgi apparatus Endomembrane organelle that modifies and packages secreted proteins and some cell wall components. A site of key steps in protein glycosylation. Named for its discoverer Camillo Golgi.

grana lamellae Stacked thylakoid membranes within the chloroplast. Each stack is called a granum, while the exposed membranes in which stacking is absent are known as stroma lamellae.

granum (plural *grana*) In the chloroplast, a stack of thylakoids.

gravitational potential The part of the chemical potential caused by gravity. It is only of a significant size when considering water transport into trees.

gravitropic response The growth initiated by the root cap's perception of gravity and the signal that directs the roots to grow downward.

gravitropic setpoint angle The angle at which gravitropic organs are maintained with respect to gravity.

gravitropism Plant growth in response to gravity, enabling roots to grow downward into the soil and shoots to grow upward.

greenhouse effect The warming of Earth's climate, caused by the trapping of long-wavelength radiation by CO_2 and other gases in the atmosphere. Term derived from the heating of a greenhouse resulting from the penetration of long-wavelength radiation through the glass roof, the conversion of the long-wave radiation to heat, and the blocking of the heat escape by the glass roof.

green-leaf volatiles A mixture of lipid-derived six-carbon aldehydes, alcohols, and esters released by plants in response to mechanical damage.

ground tissue The internal tissues of the plant, other than the vascular, transport tissues.

growth efficiency The growth in mass of a tree per unit leaf area or leaf mass.

growth respiration The respiration that provides the energy needed for converting sugars into the building blocks that make up new tissue. Contrast with maintenance respiration.

GTPase-activating proteins (GAPs) Proteins that inactivate GTPases by promoting GTP hydrolysis.

guanine nucleotide exchange factors (GEFs) Proteins that activate inactive GTPases by replacing GDP with GTP.

guard cells A pair of specialized epidermal cells that surround the stomatal pore and regulate its opening and closing.

guard mother cell (GMC) The cell that gives rise to a pair of guard cells to form a stoma.

***GURKE* (*GK*)** An Arabidopsis gene that encodes an acetyl-CoA carboxylase that functions in synthesis of very-long-chain fatty acids and sphingolipids that characterize ordered mebrane nanodomains that support proteins involved in the proper patterning of the apical portion of the embryo.

guttation An exudation of liquid from the leaves due to root pressure, most commonly occuring in grasses and other herbaceous plants.

gymnosperms An early group of seed plants. Distinguished from angiosperms by having seeds borne unprotected (naked) in cones.

H

H^+-pyrophosphatase (H^+-PPase) An electrogenic pump that moves H^+ (protons) into the vacuole, energized by the hydrolysis of pyrophosphate.

halophytes Plants that are native to saline soils and complete their life cycle in that environment. Contrast with glycophytes.

Hartig net A fungal network of hyphae that surrounds, but does not penetrate, the cortical cells of roots.

haustorium The hyphal tip of a fungus or root tip of a parasitic plant that penetrates host plant tissue.

HC-toxin A cell permeant cyclic tetrapeptide produced by the maize pathogen *Cochliobolus carbonum* that inhibits histone deacetylases.

***Heading-date1* (*Hd1*)** A gene for a *CO* homolog that acts as an inhibitor of flowering in rice.

***Heading-date3a* (*Hd3a*)** The gene for the FT-like protein in rice that is translocated via the sieve tubes to the apical meristem.

heart stage The second stage of embryogenesis. A bilaterally symmetrical structure produced by rapid cell divisions in two regions on either side of the future shoot apex. *See* globular stage, torpedo stage.

heat shock factors Transcription factors that regulate expression of heat shock proteins.

heat shock proteins (HSPs) A specific set of proteins that are induced by a rapid rise in temperature, and by other factors that lead to protein denaturation. Most act as molecular chaperones.

heliotropism Movements of leaves toward or away from the sun.

hemibiotrophic pathogens Plant pathogens that show an initial biotrophic stage, which is followed by a necrotrophic stage, in which the pathogen causes extensive tissue damage.

hemicelluloses Heterogeneous group of polysaccharides that bind to the surface of cellulose, linking cellulose microfibrils together into a network. Typically solubilized by strong alkali solutions.

hemiparasitic plants Photosynthetic plants that are also parasites.

herbivory Consumption of plants or parts of plants as a food source.

heterochromatin Chromatin that is densely packed, darkly staining, and transcriptionally inactive; it accounts for about 10% of the nuclear DNA.

heterochromatization The condensation of euchromatin into heterochromatin, resulting in gene silencing.

heterostyly The condition of having two or three different flower "morphs" in which the stamens and pistils are different lengths. In longistylous flowers the stamens are shorter than the pistils. In brevistylous flowers the stamens are longer than the pistils.

hexose phosphate A six-carbon sugar with a phosphate groups attached.

histogenesis The differentiation of cells to produce various tissues.

histones A family of proteins that interact with DNA and around which DNA is wound to form a nucleosome.

Hoagland solution A nutrient solution for plant growth, originally formulated by Dennis R. Hoagland.

holoparasitic plants Non-photosynthetic plants that are obligate parasites.

homogalacturonan (HG) This pectin polysaccharide is a (1,4)-linked polymer of β-D-galacturonic acid residues; also called polygalacturonic acid.

homologous recombination (HR) A process by which genetic information is exchanged between two double-stranded or single-stranded nucleic acid molecules that share identical or similar base sequences.

hormone balance theory The hypothesis that seed dormancy and germination are regulated by the balance of ABA and gibberellin.

hybrid vigor (heterosis) The increased vigor often observed in the offspring of crosses between two inbred varieties of the same plant species.

hydraulic conductivity Describes how readily water can move across a membrane; it is expressed in terms of volume of water per unit area of membrane per unit time per unit driving force (i.e., $m^3\ m^{-2}\ s^{-1}\ MPa^{-1}$).

hydrogen bond Weak chemical bond formed between a hydrogen atom and an oxygen or nitrogen atom.

hydrophilins Small proteins that function in seed dehydration/dormancy and drought stress responses.

hydroponics A technique for growing plants with their roots immersed in nutrient solution without soil.

hydrostatic pressure Pressure generated by compression of water into a confined space. Measured in units called pascals (Pa) or, more conveniently, megapascals (MPa).

hydrotropism Plant growth in response to root perception of water potential gradients in the soil, enabling root growth toward areas of greater water potential.

hyperaccumulation Accumulation of metals in a healthy plant to levels much higher than those found in the soil and that are generally toxic to non-accumulators.

hypersensitive response-type PCD A common plant defense following microbial infection, in which cells immediately surrounding the infection site die rapidly, depriving the pathogen of nutrients and preventing its spread.

hyphal coil Branched structure of mycorrhizal fungus that form within penetrated plant cells; the site of nutrient transfer between the fungus and the host plant. Also called arbuscules.

hypocotyl The region of the seedling stem below the cotyledons and above the root.

hypophysis In seed plant embryogenesis, the apical-most progeny of the basal cell which contributes to the embryo and will form part of the root apical meristem.

I

idioblast A "special" cell that differs markedly in form, content, or size from the other cells in the same tissue.

imbibition The initial phase of water uptake in dry seeds which is driven by the matric potential component of the water potential, that is, by the binding of water to surfaces, such as the cell wall and cellular macromolecules.

import The movement of photosynthate in sieve elements into sink organs.

imprinted gene expression Imprinted genes are expressed predominantly from either the maternal or the paternal allele, in contrast to nonimprinted genes in which alleles from both parents are expressed equally.

incongruity A reproductive feature brought about by mechanisms that favor fertilization between members of the same species, as opposed to individuals of closely related species. For example, female selection during pollen tube competition in the carpel may favor fertilization by pollen tubes of the same species.

indehiscent Lacking spontaneous opening of a mature anther or fruit.

inducible defenses Defense responses that exist at low levels until a biotic or abiotic stress is encountered.

induction period The period of time (time lag) elapsed between the perception of a signal and the activation of the response. In the Calvin–Benson cycle, the time elapsed between the onset of illumination and the full activation of the cycle.

infection thread An internal tubular extension of the plasma membrane of root hairs through which rhizobia enter root cells.

initials In the root and shoot meristems, a cluster of slowly dividing and undetermined cells. Their descendants are displaced away by polarized patterns of cell division and take on various differentiated fates, contributing to the radial and longitudinal organization of the root or shoot and to the development of lateral organs.

initiator element (INR) A conserved DNA sequence found in the core promoter region of eukaryotic genes.

inner mitochondrial membrane The inner of the two mitochondrial membranes containing the electron transport chain, the F_oF_1-ATP synthase, and numerous transporters.

inorganic fertilizer A fertilizer that provides nutrients in inorganic forms.

integral membrane protein Protein that is embedded in the lipid bilayer. Most span the entire width of the bilayer (so-called transmembrane proteins), so one part of the protein interacts with one side of the membrane, another part interacts with the hydrophobic core of the membrane, and a third part interacts with the other side of the membrane.

intercalary meristem Meristem located near the base, rather than the tip, of a stem or leaf, as in grasses.

intercellular air space resistance The resistance or hindrance that slows down the diffusion of CO_2 inside a leaf, from the substomatal cavity to the walls of the mesophyll cells.

interface light scattering The randomization of the direction of photon movement within plant tissues due to the reflecting and refracting of light from the many air–water interfaces. Greatly increases the probability of photon absorption within a leaf.

intermembrane space The fluid-filled space between the two mitochondrial membranes or between the two chloroplast envelope membranes.

internal tolerance Tolerance mechanisms that function in the symplast (as opposed to exclusion mechanisms).

internode Portion of a stem between nodes.

interphase Collectively the G_1, S, and G_2 phases of the cell cycle.

inwardly rectifying Refers to ion channels that open only at potentials more negative than the prevailing Nernst potential for a cation, or more positive than the prevailing Nernst potential for an anion, and thus mediate inward current.

irradiance The amount of energy that falls on a flat sensor of known area per unit time. Expressed as watts per square meter (W m^{-2}). Note, time (seconds) is contained within the term watt: 1 W = 1 joule (J) s^{-1}, or as moles of quanta per square meter per second (mol m^{-2} s^{-1}), also referred to as fluence rate.

J

JA-ILE ZIM-DOMAIN (JAZ) A transcriptional repressor that serves as a switch for jasmonate signaling. In the presence of JA, JAZ is degraded, allowing positive transcriptional regulators to activate JA-induced genes.

jasmonate resistance (JAR) proteins Defense proteins that are induced by jasmonic acid.

JAZ (jasmonate ZIM-domain) protein family Transcriptional repressor proteins that are proteolytically degraded after jasmonate-induced tagging by an E3 ubiquitin ligase complex.

K

karrikinolide Component of smoke that stimulates seed germination; similar in structure to strigolactones.

kinases Enzymes that have the capacity to transfer phosphate groups from ATP to other molecules.

kinetochore The site of spindle fiber attachment to the chromosome in anaphase. A layered structure associated with the centromere that contains microtubule-binding proteins and kinesins that help depolymerize and shorten the kinetochore microtubules.

Kranz anatomy (G: *kranz*: wreath or halo.) The wreathlike arrangement of mesophyll cells around a layer of large bundle-sheath cells. The two concentric layers of photosynthetic tissue surround the vascular bundle. This anatomical feature is typical of leaves of many C_4 plants.

L

L1 A clonally distinct epidermal layer derived from one set of initials in the shoot apical meristem.

L2 A subepidermal layer of cells derived from an internal set of initials in the shoot apical meristem.

L3 A centrally positioned layer of cells derived from an internal set of initials in the shoot apical meristem.

land plants, or embryophytes All the families of plants inclusive of the non-seed, nonvascular plants.

late-embryogenesis-abundant (LEA) proteins Proteins involved in desiccation tolerance. They interact to form a highly viscous liquid with very slow diffusion and therefore limited chemical reactions. Encoded by a group of genes that are regulated by osmotic stress, first characterized in desiccating embryos during seed maturation.

latent heat of vaporization The energy needed to separate molecules from the liquid phase and move them into the gas phase at constant temperature.

lateral or branch roots Arise from the pericycle in mature regions of the root through establishment of secondary

meristems that grow out through the cortex and epidermis, establishing a new growth axis.

lateral root founder cells Cells in the pericycle that give rise to lateral root primordia.

lateral roots Arise from the pericycle in mature regions of the root through establishment of secondary meristems that grow out through the cortex and epidermis, establishing a new growth axis.

latex A complex, often milky solution exuded from cut surfaces of some plants that represents the cytoplasm of laticifers and may contain defensive substances.

laticifer In many plants, an elongated, often interconnected network of separately differentiated cells that contain latex (hence the term laticifer), rubber, and other specialized metabolites.

law of reciprocity The reciprocal relationship between fluence rate (mol m^{-2} s^{-1}) and duration of light exposure characteristic of many photochemical reactions as well as some developmental responses of plants to light. Total fluence depends on two factors: the fluence rate and the irradiation time. A brief light exposure can be effective with bright light; conversely, dim light requires a long exposure time. Also referred to as Bunsen–Roscoe Law.

LEA/DHN/RAB protein family A family of proteins that shield and protect other proteins and membranes from extreme biophysical effects.

leaf blade The broad, expanded area of the leaf; also called the lamina.

leaf primordia stage The stage of embryogenesis in monocotyledonous plants in which the first leaf primordium emerges.

leaf stomatal resistance Resistance to CO_2 diffusion imposed by the stomatal pores.

leaf trace The portion of the shoot primary vascular system that diverges into a leaf.

leaflet A subdivision of a compound leaf.

leaves The main lateral appendages radiating out from stems and branches. Green leaves are usually the major photosynthetic organs of the plant.

lectins Defensive plant proteins that bind to carbohydrates; or carbohydrate-containing proteins inhibiting their digestion by an herbivore.

leghemoglobin An oxygen-binding heme protein found in the cytoplasm of infected nodule cells that facilitates the diffusion of oxygen to the respiring symbiotic bacteria.

leucoplasts Nonpigmented plastids, the most important of which is the amyloplast.

LHCI Light-harvesting complexes associated with photosystem I.

light channeling In photosynthetic cells, the propagation of some of the incident light through the central vacuole of the palisade cells and through the air spaces between the cells.

light energy The energy associated with photons.

light-harvesting complex II (LHCII) The most abundant antenna protein complex, associated primarily with photosystem II.

LIGHT-OXYGEN-VOLTAGE (LOV) Domains that are sites of binding of the FMN chromophore to phototropins and are thus the part of the protein that senses light.

lignin Highly branched phenolic polymer with a complex structure made up of phenylpropanoid alcohols that may be associated with celluloses and proteins. Deposited in secondary walls, it adds strength allowing upward growth and permitting conduction through the xylem under negative pressure. Lignin has significant defensive functions.

limiting nutrient A nutrient that is not sufficiently available to support plant growth. Its application will normally increase growth as long as other factors (abiotic or biotic) are not also limiting.

locules The pollen-containing cavities inside anthers. The term is also applied to the chambers within the ovary in which seeds develop.

long-day plants (LDPs) Plants that flower only in long days (qualitative LDP) or whose flowering is accelerated by long days (quantitative LDP).

long-distance transport Translocation through the phloem to the sink.

long–short-day plants (LSDPs) Plants that flowersin response to a shift from long days to short days.

lowest excited state Excited state with the lowest energy attained when a chlorophyll molecule in a higher energy state gives up some of its energy to the surroundings as heat.

LUREs The pollen chemoattractants of *Torenia fournieri*, consisting of cysteine-rich polypeptides.

lysophospholipid A phospholipid from which one or both fatty acid groups have been removed.

M

macrofibrils Structures found in secondary cell walls of tracheids and fibers, consisting of ~10–20 aggregated cellulose microfibrils.

MADS box genes Genes encoding a family of transcription factors containing a conserved sequence called the MADS box. It is the family that includes most floral homeotic genes and some of the genes involved in regulating flowering time.

maintenance respiration The respiration needed to support the function and turnover of existing tissue. Contrast with growth respiration.

malic enzyme An enzyme that catalyzes the oxidation of malate to pyruvate, permitting plant mitochondria to oxidize malate or citrate to CO_2 without involving pyruvate generated by glycolysis.

mannan A hemicellulose with a backbone made of 1→4-linked β-D-mannose.

map-based cloning A technique that uses genetic analysis of the offspring of crosses between a mutant and a wild-type plant to narrow the location of the mutation to a short segment of the chromosome, which can then be sequenced.

MAPK modules A cascade of different MAPKs that propagates signals within cells.

margo A porous and relatively flexible region of the pit membranes in tracheids of conifer xylem surrounding a central thickening, the torus.

mass transfer rate The quantity of material passing through a given cross section of phloem or sieve elements per unit time.

massulae Masses of pollen that form in species where individual microspores do not separate after meiosis, and tetrads remain aggregated by cell wall bridges. Massulae can carry tens of thousands pollen grains, and are usually associated with insect pollinated species, increasing the probability that one single insect visit may result in high pollen load, that will be spread in many other flowers.

maternally expressed genes (MEGs) Genes for which only the maternal alleles are expressed.

matric potential (Ψm) The sum of osmotic potential (Ψ_s) + hydrostatic pressure (Ψ_p). Useful in situations (dry soils, seeds, and cell walls) where the separate measurement of Ψ_s and Ψ_p is difficult or impossible.

matrix polysaccharides Polysaccharides comprising the matrix of plant cell walls. In primary cell walls they consist of pectins, hemicelluloses, and proteins.

matrix The colloidal-aqueous phase contained within the inner membrane of a mitochondrion.

maturation stage The stage of embryogenesis at which the embryo matures.

maturation zone The region of the root that has completed its differentiation and shows root hairs for the absorption of water and solutes; and competent vascular tissue.

mechanical hypothesis A type of pollen tube growth that is dictated by pistil architecture.

megaspore mother cell The cell inside the ovule that gives rise to the megaspores by meiosis.

megaspore The haploid (1*N*) spore that develops into the female gametophyte.

megastrobili The strobili or cones that contain the female gametophytic tissue.

meiosis The "reduction division" whereby two successive cell divisions produce four haploid (1*N*) cells from one diploid (2*N*) cell. In plants with alternation of generations, spores are produced by meiosis. In animals, which don't have alternation of generations, gametes are produced by meiosis.

membrane permeability The extent to which a membrane permits or restricts the movement of a substance.

meristematic zone A region at the tip of the root containing the meristem that generates the body of the root. Located just above the root cap.

meristemoid mother cells (MMCs) (singular *stoma*) A microscopic pore in the leaf epidermis surrounded by a pair of guard cells and in some species, also including subsidiary cells. Stomata regulate the gas exchange (water and CO_2) of leaves by controlling the dimension of a stomatal pore.

meristemoids Small, superficial clusters of dividing cells that give rise to structures such as trichomes or stomata.

meristems Localized regions of ongoing cell division that enable growth during post-embryonic development.

mesocotyl In members of the grass family, the part of the elongating axis between the scutellum and the coleoptile.

mesophyll resistance The resistance to CO_2 diffusion imposed by the liquid phase inside leaves. The liquid phase includes diffusion from the intercellular leaf spaces to the carboxylation sites in the chloroplast.

mesophyll Leaf tissue found between the upper and lower epidermal layers, consisting of palisade parenchyma and spongy mesophyll.

metabolic redundancy A common feature of plant metabolism in which different pathways serve a similar function. They can therefore replace each other without apparent loss in function.

metaphase A stage of mitosis during which the nuclear envelope breaks down and the condensed chromosomes align in the middle of the cell.

methylation The chemical addition of methyl groups to alter structure or function. A common modification of cytosine residues in DNA.

microbe-associated molecular patterns (MAMPs) Molecules that are conserved across a large group of microbes (e.g., bacteria or fungi) that trigger defense responses (e.g., flagellin from bacteria or chitin from fungi).

microbial pathogens Bacterial or fungal organisms that cause disease in a host plant.

microfilament A component of the cell cytoskeleton made of actin; it is involved in organelle motility within cells.

microgametogenesis The process in the pollen grain that gives rise to the male gametes, the sperm cells.

microgametogenesis The process in the pollen grain that gives rise to the male gametes, the sperm cells.

micropyle A small opening in the integument of the ovule through which the tip of the pollen tube penetrates during fertilization. The egg cell is located at the micropylar end of the embryo sac.

microRNAs (miRNAs) Short (21–24 nt) RNAs that have double-stranded stem-loop structures and mediate RNA interference.

microspores The haploid (1*N*) cell that develops into the pollen tube or male gametophyte.

microspores The haploid (1*N*) cell that develops into the pollen tube or male gametophyte.

microsporogenesis The process in which microspores are formed by the microsporocyte.

microstrobili The strobili or cones that contain the male gametophytic tissue.

microtubule Component of the cell cytoskeleton made of tubulin, a component of the mitotic spindle, and a player in the orientation of cellulose microfibrils in the cell wall.

middle lamella A thin layer of pectin-rich material at the junction where the primary walls of neighboring cells come into contact. Originates as the cell plate during cell division.

mineral nutrition The study of how plants obtain and use mineral nutrients.

mineralization Process of breaking down organic compounds by soil microorganisms that releases mineral nutrients in forms that can be assimilated by plants.

mitochondrial DNA (mtDNA) The DNA found in mitochondria. Plant mtDNA deviates in many ways from mtDNA in animals or fungi. Mitochondrial genes encode a variety of proteins necessary for cellular respiration.

mitochondrion (plural *mitochondria*) The organelle that is the site for most reactions in the respiratory process in eukaryotes.

mitosis The ordered cellular process by which replicated chromosomes are distributed to daughter cells formed by cytokinesis.

mitotic phase (M, or M phase) The cell cycle phase the nucleus of a cell is divided into two nuclei with an equal amount of genetic material.

mitotic spindle The mitotic structure involved in chromosome movement. Polymerized from α- and β-tubulin monomers formed by the disassembly of the preprophase band in early metaphase.

model organisms Organisms that are particularly accessible and convenient for research and which provide information for hypothesis testing in other organisms.

molecular chaperone proteins Proteins that maintain and/or restore the active three-dimensional structures of other macromolecules.

molecular shielding The protection of one molecule from extreme biophysical factors by another molecule.

monocarpic Refers to plants, typically annuals, that produce fruits only once and then die.

monocots One of the two classes of flowering plants, characterized by a single seed leaf (cotyledon) in the embryo.

monoecious Refers to plants in which male and female flowers are found on the same individuals, such as cucumber (*Cucumis sativus*) and maize (corn; *Zea mays*). Contrast with dioecious.

MONOPTEROS (MP) Gene involved in embryonic patterning. Encodes an auxin response factor that is necessary for the normal formation of basal elements such as the root and hypocotyls.

morphogenesis The developmental processes that give rise to biological form.

morphogens In animals, substances that play key roles in providing positional cues in certain types of position-dependent development.

MscS (Mechanosensitive channel of Small conductance) A mechanically gated ion channel that senses osmotically driven changes in cell volume or physical contact with an object, herbivore, or pathogen.

multinet growth hypothesis Concerns cell wall deposition during cell expansion. Holds that each successive wall layer is stretched and thinned during cell expansion, so the microfibrils would be expected to be passively reoriented in the direction of growth.

multivesicular bodies Part of the prevacuolar sorting compartment that functions in the degradation of endocytosed membrane proteins and endomembrane components destined for the vacuole.

mutant An individual that contains specific changes in its DNA sequence and may show an altered phenotype.

mutational load The total number of deleterious genes that have accumulated in the genome of an individual or a population, which may cause disease.

mutualism A symbiotic relationship in which both organisms benefit.

MYC2 transcription factor A basic helix-loop-helix leucine zipper motif protein that binds an extended G-box promoter. Its transcription is induced by dehydration stress and ABA. MYC2 regulates JA-dependent functions and some light responses.

mycorrhiza (plural *mycorrhizas* or *mycorrhizae*) The symbiotic (mututalistic) association of certain fungi and plant roots. Facilitates the uptake of mineral nutrients by roots.

mycorrhizal fungus A fungus that can form mycorrhizal symbiosis with plants.

N

NAD(P)H dehydrogenases A collective term for membrane-bound enzymes that oxidize NADH or NADPH, or both, and reduce quinone. Several are present in the electron transport chain of mitochondria; for example, the proton-pumping complex I, but also simpler non-proton-pumping enzymes.

NADH dehydrogenase (complex I) A rotenone-sensitive multi-subunit protein complex in the mitochondrial electron transport chain that catalyzes oxidation of NADH and reduction of ubiquinone linked to the pumping of protons from the matrix to the intermembrane space.

necrosis Death that is directly caused by physical damage, toxins, or other external agents.

necrotic spots Small spots of dead leaf tissue. For example, a characteristic of phosphorus deficiency.

necrotrophic pathogens Refers to cell and tissue killing pathogens that attack their host plant first by secreting cell wall-degrading enzymes and/or toxins, which will lead to massive tissue laceration and plant death.

neochrome A photoreceptor in the alga *Mougeotia* that consists of a fusion between phytochrome and a phototropin.

Nernst potential The electrical potential at equilibrium with a transmembrane gradient of ions as described by the Nernst equation.

night break An interruption of the dark period with a short exposure to light that makes the entire dark period ineffective.

nitrate reductase Enzyme located in the cytosol that reduces nitrate (NO_3^-) to nitrite (NO_2^-). Catalyzes the first step by which nitrate absorbed by roots is assimilated into organic form.

nitrogen fixation The natural or industrial processes by which atmospheric nitrogen N_2 is converted to ammonia (NH_3) or nitrate (NO_3^-).

nitrogenase enzyme complex The two-component protein complex that conducts biological nitrogen fixation in which ammonia is produced from molecular nitrogen.

N-linked glycoproteins Glycan linked via a nitrogen atom to a protein. Formed by transfer of a 14-sugar glycan from the ER membrane-embedded dolichol diphosphate to the nascent polypeptide as it enters the lumen of the ER.

nodal roots Adventitious roots that form after the emergence of primary roots.

node Position on the stem where leaves are attached.

nodulation (Nod) factors Lipochitin oligosaccharide signal molecules active in regulating gene expression during nitrogen-fixing nodule formation. All Nod factors have a chitin β-1→4-linked *N*-acetyl-D-glucosamine backbone (varying in length from three to six sugar units) and a fatty acid chain on the C-2 position of the nonreducing sugar.

nodulation (*nod*) gene Rhizobial gene, the products of which participates in nodule formation.

nodule Specialized organ of a plant host containing symbiotic nitrogen-fixing bacteria.

nodulin gene A plant gene specific to nodules.

non–cell autonomous response A cellular response to an environmental stimulus or genetic mutation that is induced by other cells.

non-climacteric Refers to a type of fruit that does not undergo a climacteric, or respiratory burst, during ripening.

noncoding RNAs (ncRNAs) RNAs that do not encode proteins, but may instead be involved in gene regulation or active in the RNA interference (RNAi) pathway.

nonenzymatic proteins Proteins without enzymatic activity, including arabinogalactan proteins, hydroproline-rich glycoproteins, various structural and signaling proteins. Expansins are included in this category.

non-homologous end-joining (NHEJ) A pathway that repairs double-strand breaks in DNA by directly ligating break ends without the need for a homologous template, usually in the presence of a "guide" template.

non-Mendelian, or maternal, inheritance A non-Mendelian pattern of inheritance in which offspring receive genes from only the female parent.

nonphotochemical quenching The quenching of chlorophyll fluorescence by processes other than photochemistry—the converting of excess excitation into heat.

non-seed plants Plant families that do not produce a seed.

nonvascular plants, or bryophytes Plants that do not have vascular tissues, such as xylem and phloem.

nuclear envelope The double membrane surrounding the nucleus.

nuclear genome The entire complement of DNA found in the nucleus.

nuclear pores Sites where the two membranes of the nuclear envelope join, forming a partial opening between the interior of nucleus and the cytosol. Contains an elaborate structure of more than a hundred different nucleoporin proteins that form a nuclear pore complex (NPC).

nucleolar organizer region (NOR) Associated with the nucleolus in the interphase nucleus. Site where portions of one or more chromosomes containing genes, repeated in tandem, coding for ribosomal RNA are clustered and are transcribed.

nucleolar organizer region Associated with the nucleolus in the interphase nucleus. Site where portions of one or more chromosomes containing genes, repeated in tandem, coding for ribosomal RNA are clustered and are transcribed.

nucleolus (plural *nucleoli*) A densely granular region in the nucleus that is the site of ribosome synthesis.

nucleoplasm The cellular contents contained within the nuclear envelope.

nucleosome A structure consisting of eight histone proteins around which DNA is coiled.

nucleotide-binding domain (NBD) Protein domain that binds nucleotides such as ATP. Found in NLR proteins.

nucleotide-binding site–leucine rich repeat (NLR) Class of R proteins that contain an NBD and leucine-rich repeat.

nucleus The membrane-bound structure that contains a cell's hereditary information (chromosomes) and where non-organeller gene transcription occurs.

nutation The bending and rotation of plants organs (e.g., roots, stems, leaves) during growth.

nutrient assimilation The incorporation of inorganic mineral nutrients into organic carbon compounds such as pigments, enzyme cofactors, lipids, nucleic acids, or amino acids.

nutrient depletion zone The region surrounding the root surface showing diminished nutrient concentrations due to uptake into the roots and slow replacement by diffusion.

nutrient solution A solution containing only inorganic salts that supports the growth of plants in sunlight without soil or organic matter.

nyctinasty Sleep movements of leaves. Leaves extend horizontally to face the light during the day and fold together vertically at night.

O

octant The spherical, eight-cell, globular embryo exhibiting radial symmetry.

oil bodies Also known as oleosomes or spherosomes, these organelles accumulate and store triacylglycerols. They are bounded by a single phospholipid leaflet ("half–unit membrane" or "phospholipid monolayer") derived from the ER.

oligomer-trapping model A model that explains the active accumulation of tri-, tetra- and pentasaccharides in sieve element-companion cell complexes of symplasmically loading species.

O-linked oligosaccharides Small polysaccharides that are covalently linked to the side chain hydroxyl of serine or threonine residues in a subgroup of plant glycoproteins. O-linked glycosylation occurs in the Golgi apparatus.

organ senescence The senescence of whole leaves, branches, flowers, or fruits. It occurs at various stages of vegetative and reproductive development and typically includes abscission of the senescing organ.

orthodox seed A seed that can tolerate desiccation and remain viable after storage in a dry state.

osmolarity A unit of concentration expressed as moles of total dissolved solutes per liter of solution (mol L^{-1}). In biology, the solvent is usually water.

osmosis The movement of water across a selectively permeable membrane toward the region of more negative water potential, Ψ (lower concentration of water).

osmotic adjustment The ability of the cell to accumulate compatible solutes and lower water potential during periods of osmotic stress.

osmotic potential The effect of dissolved solutes on water potential. Also called solute potential.

osmotic stress Stress imposed on cells or whole plants when the osmotic potential of external solutions is more negative than that of the solution inside the plant.

outer mitochondrial membrane The outer of the two mitochondrial membranes, which appears to be freely permeable to all small molecules.

outwardly rectifying Refers to ion channels that open only at potentials more positive than the prevailing Nernst potential for a cation, or more negative than the prevailing Nernst potential for an anion, and thus mediate outward current.

oxidative pentose phosphate pathway A cytosolic and plastidic pathway that oxidizes glucose and produces NADPH and a number of sugar phosphates.

oxidative phosphorylation Transfer of electrons to oxygen in the mitochondrial electron transport chain that is coupled to ATP synthesis from ADP and phosphate by the ATP synthase.

oxygen-evolving complex (OEC) The complex associated with photosystem II that oxidizes water and produces molecular oxygen (O_2).

P

P680 The chlorophyll of the photosystem II reaction center that absorbs maximally at 680 nm in its neutral state. The P stands for pigment.

P700 The chlorophyll of the photosystem I reaction center that absorbs maximally at 700 nm in its neutral state. The P stands for pigment.

P870 The reaction center bacteriochlorophyll from purple photosynthetic bacteria that absorbs maximally at 870 nm in its neutral state. The P stands for pigment.

palisade cell Below the leaf upper epidermis, the top one to three layers of pillar-shaped photosynthetic cells are palisade cells.

paraheliotropic Refers to movement of leaves away from incident sunlight.

parasites An organism that lives on or in an organism of another species, known as the host, from the body of which it obtains nutriment.

parenchyma (plural *nuclei*) The organelle that contains the genetic information primarily responsible for regulating cellular metabolism, growth, and differentiation.

parent-of-origin effects A phenotypic difference in the progeny that depends on whether it was transmitted by the maternal or paternal parent.

partitioning The differential distribution of photosynthate to multiple sinks within the plant.

PAS A domain of phytochrome, which is necessary for chromophore attachment to the protein.

PAS-GAF-PHY The N-terminal half of phytochrome containing the photosensory domain.

PAS-related domain (PRD) On the phytochrome protein, two domains that mediate phytochrome dimerization.

passive transport Diffusion across a membrane. The spontaneous movement of a solute across a membrane in the direction of a gradient of (electro)chemical potential (from higher to lower potential). Downhill transport.

paternally expressed genes (PEGs) Genes for which only the paternal alleles are expressed.

pathogenesis-related (PR) genes Genes that encode small proteins that function either as antimicrobials or in initiating systemic defense responses.

pattern-recognition receptor (PRR) Cell surface receptor that is activated by MAMPs or DAMPs

pavement cells The predominant type of leaf epidermal cells, which secrete a waxy cuticle and serve to protect the plant from dehydration and damage from ultraviolet radiation.

pectins A heterogeneous group of complex cell wall polysaccharides that form a gel in which the cellulose–hemicellulose network is embedded. Typically contain acidic sugars such as galacturonic acid and neutral sugars such as rhamnose, galactose, and arabinose. Often include calcium as a structural component, allowing extractions from the wall with chelators or dilute acids.

PEP carboxylase A cytosolic enzyme that forms oxaloacetate by the carboxylation of phosphoenolpyruvate.

perennial plants Plants that live for more than two years.

perforation plate The perforated end wall of a vessel element in the xylem.

pericarp The fruit wall surrounding a fruit, derived from the ovary wall.

pericycle Meristematic cells forming the outermost layer of the vascular cylinder in the stem or root, interior to the endodermis. An internal meristematic tissue from which lateral roots arise.

periderm Tissue produced by the cork cambium that contributes to the outer bark of stems and roots during secondary growth of woody plants, replacing the epidermis. Also forms over wounds and abscission layers after the shedding of plant parts.

period In cyclic (rhythmic) phenomena, the time between comparable points in the repeating cycle, such as peaks or troughs.

peripheral membrane proteins Proteins that are bound to the membrane surface by noncovalent bonds, such as ionic bonds or hydrogen bonds.

peripheral zone (PZ) A doughnut-shaped region surrounding the central zone in shoot apical meristems consisting of small, actively dividing cells with inconspicuous vacuoles. Leaf primordia are formed in the peripheral zone.

perisperm Storage tissue derived from the nucellus, often consumed during embryogenesis.

permanent charge Ionic charge of soil minerals caused by substitution of ions (for example Al^{3+} for Si^{4+}) in the crystal structure during mineral formation.

peroxiredoxins (Prx) A family of antioxidant enzymes that inactivate peroxides.

peroxisome Organelle in which organic substrates are oxidized by O_2. These reactions generate H_2O_2 that is broken down to water by the peroxisomal enzyme catalase.

petiole The leaf stalk that joins the leaf blade to the stem.

Pfr The far-red light–absorbing form of phytochrome converted from Pr by the action of red light. The blue-green colored Pfr is converted back to Pr by far-red light. Pfr is the physiologically active form of phytochrome.

phagophore A double membrane that encloses and isolates cytoplasmic components during macroautophagy.

phase change The phenomenon in which the fates of the meristematic cells become altered in ways that cause them to produce new types of structures.

phase In cyclic (rhythmic) phenomena, any point in the cycle recognizable by its relationship to the rest of the cycle, for example, the maximum and minimum positions.

phellem A part of the secondary dermal system, or periderm, of woody plants, consisting of dead cells with secondary cell walls rich in suberin and lignin. Also called cork.

phelloderm In some plants, one or more layers of parenchyma-like tissue derived from the phellogen.

phellogen *See* cork cambium.

phenocopied A condition that resembles the phenotype of another condition (mutant, treatment).

phenotype A set of observable characteristics of an individual that results from expression of its genome under specific environmental conditions.

phenotypic plasticity Physiological or developmental responses of a plant to its environment that do not involve genetic changes.

pheophytin A chlorophyll in which the central magnesium atom has been replaced by two hydrogen atoms.

phloem fibers Elongated, tapering sclerenchyma cells associated with the other cells in the phloem.

phloem loading The movement of photosynthates from the mesophyll chloroplasts to the sieve elements of mature leaves. Includes short-distance transport steps (*see* pre-phloem transport) and final uptake in the sieve-element-companion cell complex. *See also* phloem unloading.

phloem pole pericycle Pericycle cells adjacent to protophloem.

phloem unloading The movement of photosynthate from the sieve elements to the sink cells that store or metabolize them. Includes sieve-element unloading and short-distance transport. *See also* phloem loading.

phloem The tissue that transports the products of photosynthesis from mature leaves to areas of growth and storage, including the roots.

phosphatases Enzymes that remove a phosphate group from a protein.

phosphate transporter Protein in the plasma membrane specific for the uptake of phosphate by the cell.

phosphatidic acid (PA) A diacylglycerol that has a phosphate on the third carbon of the glycerol backbone.

phosphatidylcholine (PC) Phospholipid having a choline head group and varying fatty acid chain lengths and saturation. Major component of plant membranes.

phosphatidylinositol 4,5-bisphosphate (PIP_2) A group of phosphorylated derivatives of phosphatidylinositol.

phospholipase A (PLA) An enzyme that removes one of the fatty acid chains from a phospholipid.

phospholipase C (PLC) An enzyme whose action on phosphoinositides releases inositol triphosphate ($InsP_3$), along with diacylglycerol (DAG).

phospholipase D (PLD) An enzyme active in ABA signaling; it releases phosphatidic acid from phosphatidylcholine.

photoassimilation The coupling of nutrient assimilation to photosynthetic electron transport.

photoblasty Light-induced seed germination.

photochemistry Very rapid chemical reactions in which light energy absorbed by a molecule causes a chemical reaction to occur.

photoinhibition The inhibition of photosynthesis by excess light.

photolyase A blue light–activated enzyme that repairs pyrimidine dimers in DNA that have been damaged by ultraviolet radiation. Contains an FAD and a pterin.

photomorphogenesis The influence and specific roles of light on plant development. In the seedling, light-induced changes in gene expression to support aboveground growth in the light rather than belowground growth in the dark.

photon A discrete physical unit of radiant energy.

photonasty Plant movements in response to non-directional light.

photoperiodic induction The photoperiod-regulated processes that occur in leaves resulting in the transmission of a floral stimulus to the shoot apex.

photoperiodism A biological response to the length and timing of day and night, making it possible for an event to occur at a particular time of year.

photophosphorylation The formation of ATP from ADP and inorganic phosphate (P_i), catalyzed by the CF_0F_1-ATP synthase and using light energy stored in the proton gradient across the thylakoid membrane.

photoprotection A carotenoid-based system for dissipating excess energy absorbed by chlorophyll in order to avoid forming singlet oxygen and damaging pigments. Involves quenching.

photoreceptors Proteins that sense the presence of light and initiate a response via a signaling pathway.

photorespiration Uptake of atmospheric O_2 with a concomitant release of CO_2 by illuminated leaves. Molecular oxygen serves as substrate for Rubisco and the formed 2-phosphoglycolate enters the photorespiratory carbon oxidation cycle. The activity of the cycle recovers some of the carbon found in 2-phosphoglycolate, but some is lost to the atmosphere.

photoreversibility The intercon-version of the Pr and Pfr forms of phytochrome.

photostationary state Relating to phytochrome under natural light conditions, the equilibrium of 97% Pr and 3% Pfr.

photosynthate The carbon-containing products of photosynthesis.

photosystems I and II (PSI and PSII) Photosystem I (PSI) is a system of photoreactions that absorbs maximally far-red light (700 nm), oxidizes plastocyanin, and reduces ferredoxin. Photosystem II (PSII) is a system of photoreactions that absorbs maximally red light (680 nm), oxidizes water, and reduces plastoquinone. Operates very poorly under far-red light.

phototropin 1 and phototropin 2 Two flavoproteins that are the photoreceptors for the blue-light signaling pathway that induces phototropic bending in eudicots and monocots. They also mediate chloroplast movements and participate in stomatal opening in response to blue light. Phototropins are autophosphorylating protein kinases whose activity is stimulated by blue light.

phototropism The alteration of plant growth patterns in response to the direction of incident radiation, especially blue light.

phragmoplast An assembly of microtubules, membranes, and vesicles that forms during late anaphase or early telophase and precedes fusion of vesicles to form cell plate.

PHY The designation for the phytochrome apoprotein (without the chromophore).

phyllode An expanded petiole resembling and having the function of a leaf, but without a true blade.

phyllome The collective term for all the leaves of a plant including structures that evolved from leaves, such as floral organs.

phyllotaxis The arrangement of leaves on the stem.

phytoalexins Chemically diverse group of specialized metabolites with strong antimicrobial activity that are synthesized following infection and accumulate at the site of infection.

phytochelatins Low-molecular-weight peptides synthesized from glutathione by the enzyme phytochelatin synthase. These peptides can bind a variety of metal(oids) and play an important role in tolerance of plants to As, Cd, and Zn.

phytochrome interacting factors (PIF) Families of phytochrome-interacting proteins that may activate and repress gene transcription; some are targets for phytochrome-mediated degradation.

phytochrome kinase substrate (PKS) Proteins that participate in the regulation of phytochrome via direct phosphorylation or via phosphorylation by other kinases.

phytochromes Plant growth-regulating photoreceptor proteins that absorb primarily red light and far-red light, but also absorb blue light. Phytochromes contain the chromophore phytochromobilin.

phytochromobilin The linear tetrapyrrole chromophore of phytochrome.

phytoliths Discrete cells that accumulate silica in leaves or roots.

phytomer A developmental unit consisting of one or more leaves, the node to which the leaves are attached, the internode below the node, and one or more axillary buds.

PIF3 A basic helix-loop-helix transcription factor that interacts with both phyA and phyB.

PIF-like proteins (PILs) Nuclear, DNA-binding proteins that selectively interact with phytochromes in their active Pfr conformations.

PIN auxin efflux carrier proteins Plasma membrane transport proteins that amplify localized, directional auxin streams associated with embryonic development, organogenesis, and tropic growth.

pit fields Depressions in the primary cell walls where numerous plasmodesmata make connections with adjacent cells. When present, secondary walls are not deposited in the locations of pit fields, giving rise to pits.

pit membrane The porous layer in the xylem between pit pairs, consisting of two thinned primary walls and a middle lamella.

pit pair The adjacent pits of adjoined tracheid cells in the xylem. A low-resistance path for water movement between tracheids.

pit A microscopic region where the secondary wall of a tracheary element is absent and the primary wall is thin and porous, facilitating sap movement between one tracheid and the adjacent one.

pith The ground tissue in the center of the stem or root.

plant growth promoting rhizobacteria (PGPR) Soil bacteria associated with root surfaces that promote plant growth by producing plant growth regulators and/or fixing nitrogen.

plant tissue analysis In the context of mineral nutrition, the analysis of the concentrations of mineral nutrients in a plant sample.

plasma membrane (plasmalemma) A fluid mosaic structure composed of a bilayer of polar lipids (phospholipids or glycosylglycerides) and embedded proteins that together confer selective permeability on the structure. Also called plasmalemma.

plasma membrane H^+-ATPase An ATPase that pumps H^+ (protons) across the plasma membrane energized by ATP hydrolysis.

plasmodesmata (singular *plasmodesma*) Microscopic membrane-lined channel connecting adjacent cells through the cell wall and filled with cytoplasm and a central rod derived from the ER called the desmotubule. Allows the movement of molecules from cell to cell through the symplast. The pore size can apparently be regulated by globular proteins lining the channel inner surface and the desmotubule to allow particles as large as viruses to pass through.

plasticity The ability to adjust morphologically, physiologically, and biochemically in response to changes in the environment.

plastids Cellular organelles found in eukaryotes, bounded by a double membrane, and sometimes containing extensive membrane systems. They perform many different functions: photosynthesis, starch storage, pigment storage, and energy transformations.

plastocyanin (PC) A small (10.5 kDa), water-soluble, copper-containing protein that transfers electrons between the cytochrome b_6f complex and P700. This protein is found in the lumenal space.

plastohydroquinone (PQH2) The fully reduced form of plastoquinone.

plumule First true leaf of a growing seedling.

polar auxin transport Directional auxin streaming that functions in programmed development and plastic growth responses. Long-distance polar auxin transport maintains the overall polarity of the plant axis and supplies auxin for direction into localized streams.

polar glycerolipids The main structural lipids in membranes, in which the hydrophobic portion consists of two 16-carbon or 18-carbon fatty acid chains esterified to positions 1 and 2 of a glycerol.

polar nuclei The two haploid nuclei at the center of the embryo sac that normally fuse to form the diploid nucleus of the central cell.

polar A small difference in charge between two atoms in a molecule. An example is the water molecule where the oxygen atom has a partial negative charge relative to the two hydrogen atoms.

polarity Refers to the distinct ends and intermediate regions along an axis. Beginning with the single-celled zygote, the progressive development of distinctions along two axes: an apical–basal axis and a radial axis.

pollen mother cells (microsporocytes) The microsporocyte that divides meiotically to produce the microspores in the anther.

pollinia An aggregation of pollen composed of hundreds of massulae produced in the anthers of certain flowers. Pollinia can carry millions of pollen grains, and are found in insect pollinated orchids.

polyads Large assemblages of pollen that facilitate bulk transfer of multiple grains during insect-mediated pollination.

polycarpic Refers to perennial plants that produce fruit many times.

polyploid A condition wherein an organism has more than two complete sets of chromosomes.

pome An accessory fruit, such as an apple, composed of one or more carpels surrounded by accessory tissue derived from the hypanthium.

pore–plasmodesma contacts Specific symplasmic contacts between a sieve element and its companion cell, consisting of sieve pores and branched plasmodesmata on the sieve element and companion cell side, respectively.

position-dependent Refers to mechanisms that operate by modulating the behavior of cells in a manner that depends on the position of the cells within the developing embryo.

post-phloem transport The movement of photosynthates from the phloem parenchyma to the sink tissue, after release from the phloem.

posttranscriptional regulation Following transcription, the control of gene expression by altering mRNA stability or translation efficiency.

P-protein A structural protein in angiosperm sieve elements forming filaments, tubules or crystalline structures (*see as specialized form* forisome).

Pr Red light–absorbing phytochrome form. This is the form in which phytochrome is assembled. The blue-colored Pr is converted by red light to the far-red light–absorbing form, Pfr.

prebranch site The location in the root where xylem pole pericycle cells become fully competent to become lateral root founder cells, roughly corresponding to the start of the maturation zone.

precocious germination Germination of viviparous mutant seeds while still attached to the mother plant.

preharvest sprouting Germination of physiologically mature wild-type seeds on the mother plant caused by wet weather.

pre-phloem transport The movement of photosynthates from to mesophyll to bundle sheath and phloem parenchyma, prior to their uptake by sieve element-companion cell complexes

preprophase band A circular array of microtubules and microfilaments formed in the cortical cytoplasm just prior to cell division that encircles the nucleus and predicts the plane of cytokinesis following mitosis.

preprophase In mitosis, the stage just before prophase during which the G_2 microtubules are completely reorganized into a preprophase band.

pressure potential (Ψp) The hydrostatic pressure of a solution in excess of ambient atmospheric pressure.

pressure-flow model A widely accepted model of phloem translocation in angiosperms. It states that transport in the sieve elements is driven by a pressure gradient between source and sink. The pressure gradient is osmotically generated and results from the loading at the source and unloading at the sink.

prevacuolar compartment A membrane compartment equivalent to the late endosome in animal cells where sorting occurs before cargo is delivered to the lytic vacuole.

preventitious buds Dormant axillary buds that have remained dormant during secondary growth and have become covered by bark.

prickles Pointed plant structures that physically deter herbivory and are derived from epidermal cells.

primary active transport The direct coupling of a metabolic energy source such as ATP hydrolysis, oxidation-reduction reaction, or light absorption to active transport by a carrier protein.

primary cell walls The thin (less than 1 μm), unspecialized cell walls that are characteristic of young, growing cells. About 85% polysaccharide and 10% protein by dry weight.

primary cross-regulation Involves distinct signaling pathways regulating a shared transduction component in a positive or a negative manner.

primary dormancy The failure of newly dispersed, mature seeds to germinate under normal conditions, typically induced by abscisic acid (ABA) during seed maturation.

primary growth The phase of plant development that gives rise to new organs and to the basic plant form. It results from cell proliferation in apical meristems, followed by cell elongation and differentiation.

primary inflorescence meristem The meristem that produces stem-bearing flowers; it is formed from the shoot apical meristem.

primary metabolites Metabolites associated with basic cellular functions (e.g., sugars, amino acids, lipids, etc.).

primary plant axis The longitudinal axis of the plant defined by the positions of the shoot and root apical meristems.

primary plant body The part of the plant directly derived from the shoot and root apical meristems and primary meristems. It is composed of tissues resulting from primary, as opposed to secondary, growth.

primary response genes Genes whose expression is necessary for plant morphogenesis and that are expressed rapidly following exposure to a light signal. Often regulated by phytochrome-linked activation of transcription factors. Genes whose expression does not require protein synthesis. *See* secondary response genes.

primary root Root generated directly by growth of the embryonic root or radicle.

primary vein, or midvein Also known as primary vein, the first formed vascular bundle that runs down the middle of the leaf blade in dicot leaves.

priming During lateral root formation, the metabolic process that conditions some xylem pole parenchyma to become lateral root founder cells.

proanthocyanidin A group of condensed tannins that are present in many plants that serve as defensive chemicals against plant pathogens and herbivores.

procambium Primary meristematic tissue that differentiates into xylem, phloem, and cambium.

profilins Actin binding proteins that keep the depolymerized globular G-actin monomers charged with ATP, so that they can be rapidly re-integrated into F-actin. They also bind formins and thereby accelerate the formation of F-actin from formins.

progamic phase During angiosperm reproduction, the set of events from pollen deposition on the stigma surface to fertilization of the egg cell by the sperm.

programmed cell death (PCD) Process whereby individual cells activate an intrinsic senescence program accompanied by a distinct set of morphological and biochemical changes similar to mammalian apoptosis.

prokaryotic pathway In the chloroplast, the series of reactions for the synthesis of glycerolipids. *See also* eukaryotic pathway.

prolamellar bodies Elaborate semicrystalline lattices of membrane tubules that develop in plastids that have not been exposed to light (etioplasts).

promoter The region of the gene that binds RNA polymerase.

prophase The first stage of mitosis (and meiosis) prior to disassembly of the nuclear envelope, during which the chromatin condenses to form distinct chromosomes.

proplastid Type of immature, undeveloped plastid found in meristematic tissue that can convert to various specialized plastid types, such as chloroplasts, amyloplasts, and chromoplasts, during development.

PROTEIN PHOSPHATASE1 (PP1) A signaling intermediate of the phototropin pathway during blue light-induced stomatal opening.

protein stability The rate of protein destruction or inactivation; can contribute to posttranslational regulation and also plays an important role in the overall activity of a gene or its product.

protein storage vacuoles (PSVs) Specialized small vacuoles that accumulate storage proteins, typically in seeds.

proteinase inhibitors Compounds that inhibit the enzymatic activity of proteases.

proteomics The study of proteomes, including the relative abundance and modifications of proteins.

protoderm In the plant embryo, the surface layer one cell thick that covers both halves of the embryo and will generate the epidermis.

protofilaments Polymerized α- and β-tubulin heterodimers.

proton motive force (PMF) The energetic effect of the electrochemical H^+ gradient across a membrane, expressed in units of electrical potential.

proton motive force The energetic effect of the electrochemical H^+ gradient across a membrane, expressed in units of electrical potential.

protoplast fusion A technique for incorporating foreign genes into plant genomes by fusion of two genetically different cells from which the cell walls have been removed.

proximal–distal polarity Polarity that develops along the length of a leaf.

PRR-triggered immunity (PTI) Immune response activated by PRRs.

pseudogenes Stable but nonfunctional genes; apparently derived from active genes by mutation.

pulvinus (plural *pulvini*) A turgor-driven organ found at the junction between the blade and the petiole of the leaf that provides a mechanical force for leaf movements.

pump A membrane protein that carries out primary active transport across a biological membrane. Most pumps transport ions, such as H^+ or Ca^{2+}.

PYR/PYL/RCAR A family of soluble ABA receptors identified as proteins that interact with the PP2C protein phosphatases.

pyruvate dehydrogenase An enzyme in the mitochondrial matrix that decarboxylates pyruvate, producing NADH (from NAD^+), CO_2, and acetic acid in the form of acetyl-CoA (acetic acid bound to coenzyme A).

Q

Q cycle A mechanism for oxidation of plastohydroquinone in chloroplasts and ubiquinol in mitochondria.

quanta (singular *quantum*) Discrete packets of energy contained in a photon.

quantum efficiency The fraction of light hitting a plant that is used for productive photochemistry. Also called the quantum yield.

quantum yield The ratio of the yield of a particular product of a photochemical process to the total number of quanta absorbed.

Quartet Model A molecular model that accounts for the interactions of the A-, B-, C-, and E-class genes in specifying floral organ identity during flowering. According to the model, MADS box genes dimerize, and two dimers can form a tetramer. These tetramers are hypothesized to bind CArG-boxes on target genes and modify their expression.

quenching Or excitation quenching. The process by which energy captured in excited states of chlorophylls is rapidly dissipated, either by photochemistry or by dissipation as heat.

quiescent center (QC) Central region of root meristem where cells divide more slowly than surrounding cells, or do not divide at all.

quorum sensing A system of coordinated signals and responses by which populations regulate growth and environmental responses. This is a common mechanisms in microbial organisms.

R

Rabl configuration Proposed positioning of chromosomes inside a nucleus in which all centromeres and all telomeres point in opposite direction.

rachis The main axis of a compound leaf to which leaflets are attached; the main axis of an inflorescence to which flowers are attached.

radial axis The pattern of concentric tissues extending from the outside of a root or stem into its center.

radicle The embryonic root. Usually the first organ to emerge on germination.

raphides Needles of calcium oxalate or carbonate that function in plant defense.

rays Tissues of various height and width that radiate through the secondary xylem and phloem, and are formed from ray initials in the vascular cambium.

reaction center complex A group of electron transfer proteins that receive energy from the antenna complex and convert it into chemical energy using oxidation-reduction reactions.

reactive oxygen species (ROS) These include the superoxide anion ($O_2^{\bullet -}$), hydrogen peroxide (H_2O_2), and the hydroxyl radical ($HO^{\bullet}$) and singlet oxygen. They are generated in several cell compartments and can act as signals or cause damage to cellular components.

recalcitrant seeds Seeds that are released from the plant with a relatively high water content and active metabolism and, as a consequence, deteriorate upon dehydration and do not survive storage.

receptor kinase A protein in a signaling pathway that detects the presence of a ligand, such as a hormone, by phosphorylating itself or another protein.

receptor-like kinases (RLKs) Transmembrane proteins with putative amino-terminal extracellular domains and carboxyl-terminal intracellular kinase domains, which resemble animal receptor tyrosine kinases. Many plant RLKs specifically phosphorylate serine or threonine residues.

regulatory promoter sequences Sequence elements that are part of the core promoter.

regulatory promoter (proximal promoter) Sequence within or adjacent to a gene that regulates the activity of the gene via its core promoter.

release phloem Sieve elements of sinks.

repeat-associated silencing RNAs (ra-siRNAs) Repeat regions from which short interfering RNAs originate.

reporter gene A gene whose expression conspicuously reveals the activity of another gene. Gene engineered to share the same promoter as another gene.

repressor A protein that either alone or in concert with other proteins represses expression of a gene.

rescued When used in genetics, restoration of wild type growth and development.

residuum cells Abscission zone cells located in the receptacle.

resistance (R) proteins Intracellular receptors that detect pathogen effectors and then activate immune responses, thereby conferring resistance to infection.

resistosomes A multi-subunit complex made of 4 or 5 NLR proteins plus effector targets and sometimes pathogen effectors.

respiratory burst oxidase homolog D An enzyme that generates superoxide using NADPH as an electron donor.

respiratory quotient (RQ) The ratio of CO_2 evolution rate to O_2 consumption rate.

response regulator One component of the two-component regulatory systems that are composed of a histidine kinase sensor protein and a response regulator protein.

retrotransposons In contrast to DNA transposons, these make an RNA copy of themselves, which is then reverse transcribed into DNA before it is inserted elsewhere in the genome.

rhamnogalacturonan I (RG I) An abundant pectic polysaccharide that has a long backbone of alternating rhamnose and galacturonic acid residues.

rhamnogalacturonan II (RG II) A pectic polysaccharide with a complex structure including apiose residues that may be cross linked by borate esters.

rhizobia Collective term for the genera of soil bacteria that form symbiotic (mutualistic) relationships with members of the plant family Leguminosae.

rhizosphere The immediate soil microenvironment surrounding the root.

rhizotaxis The arrangement of lateral roots along the surface of a root.

rib zone (RZ) Meristematic cells beneath the central zone in shoot apical meristems that give rise to the internal tissues of the stem.

ribosome The site of cellular protein synthesis and consisting of RNA and protein.

ribulose 5-phosphate In the pentose phosphate pathway, the initial five-carbon product of the oxidation of glucose 6-phosphate; in subsequent reactions, it is converted into sugar phosphates containing three to seven carbon atoms.

RICs (ROP-interactive CRIB motif–containing proteins) Proteins that interact with ROP1 to regulate pollen tube growth and polarity.

Rieske iron–sulfur protein A protein subunit in the cytochrome b_6f complex, in which two iron atoms are bridged by two sulfur atoms, with two histidine and two cysteine ligands.

ripening The process that causes fruits to become more palatable, including softening, increasing sweetness, loss of acidity, and changes in coloration.

RNA interference (RNAi) pathway An RNA-dependent gene silencing process that is controlled by the RNA-induced silencing complex (RISC) and is initiated by short double-stranded RNA molecules in a cell's cytoplasm.

RNA polymerases A class of enzymes that bind to a gene and transcribe it into an RNA complementary to the DNA sequence.

RNA-dependent RNA polymerases A special class of RNA polymerases that convert single-stranded RNA into double-stranded RNA.

RNA-induced silencing complex (RISC) A multiprotein complex that incorporates one strand of a small interfering RNA (siRNA) or microRNA (miRNA). RISC complexes bind to and cleave mRNA, thereby preventing translation.

RNA-induced transcriptional silencing (RITS) Targeted inactivation of messenger RNA when a short interfering RNA sequence hybridizes to form a double-stranded hybrid.

root apical meristem (RAM) A group of cells at the tip of the root that retain the capacity to proliferate and whose ultimate fate remains undetermined.

root cap Cells at the root apex that cover and protect the meristematic cells from mechanical injury as the root moves through the soil. Site for the perception of gravity and signaling for the gravitropic response.

root exudates Sugars and other compounds secreted into the soil by roots.

root hairs Microscopic extensions of root epidermal cells that greatly increase the surface area of the root, thus providing greater capacity for absorption of soil ions and, to a lesser extent, soil water.

root knot nematodes Plant parasites from the genus *Meloidogyne* found in tropical and subtropical soils. Root-knot nematode larvae infect plant roots to form root-knot galls and are a major cause of crop losses.

root pressure A positive hydrostatic pressure in the xylem of roots.

root system architecture The overall geometric arrangement of roots comprising the plant's root system.

root The tissues descending, usually below ground, from the root–shoot junction and which anchor the plant and absorb and conduct water and minerals into the plant.

root-to-shoot ratio The ration between root and shoot length.

ROS scavenging Detoxification of reactive oxygen species via interactions with proteins and electron acceptor molecules.

rough ER The endoplasmic reticulum to which ribosomes are attached.

Rubisco The acronym for the chloroplast enzyme *rib**u**lose **bis**phosphate **c**arboxylase/**o**xygenase. In a carboxylase reaction, Rubisco uses atmospheric CO_2 and ribulose 1,5-bisphosphate to form two molecules of 3-phosphoglycerate. It also functions as an oxygenase that incorporates O_2 to ribulose 1,5-bisphosphate to yield one molecule of 3-phosphoglycerate and another one molecule of 2-phosphoglycolate. The competition between CO_2 and O_2 for ribulose 1,5-bisphosphate limits net CO_2 fixation.

Rubisco-containing bodies (RCBs) Rubisco-containing vesicles that are thought to bud off from senescing chloroplasts, and are subsequently engulfed by autophagosomes and delivered to the vacuole for degradation.

S

S haplotypes Multiple genes, inherited as a single segregating unit, that make up the S locus.

salt stress The adverse effects of excess minerals on plants.

salt-tolerant plant A plant that can survive or even thrive in high-salt soils. *See also* halophyte.

sclerenchyma Plant tissue composed of cells, often dead at maturity, with thick, lignified secondary cell walls. It functions in support of nongrowing regions of the plant.

scutellum The single cotyledon of the grass embryo, specialized for nutrient absorption from the endosperm.

seasonal leaf senescence The pattern of leaf senescence in which the leaves of deciduous trees in temperate climates senesce all at once in response to the shorter days and cooler temperatures of autumn.

secession cells Abscission zone cells located in separated floral organs (sepals, petals, and stamens).

second messenger Intracellular molecule (e.g., calcium, ROS, IP_3, or diacylglycerol) whose production or release from compartmental storage has been elicited by the stimulation of a receptor. Diffuses intracellularly to the target enzymes or intracellular receptor to produce and amplify the response.

secondary active transport Active transport that uses energy stored in the proton motive force or other ion gradient, and operates by symport or antiport.

secondary cell wall Cell wall synthesized by nongrowing cells. Often multilayered and containing lignin, it differs in composition and structure from the primary wall. Forms during cell differentiation after cell expansion ceases.

secondary cross-regulation Regulation by the output of one signal pathway of the abundance or perception of a second signal.

secondary dormancy Seeds that have lost their primary dormancy may become dormant again if exposed to unfavorable conditions that inhibit germination over a period of time.

secondary growth The tissue growth that occurs after elongation is complete. It involves the vascular cambium (producing the secondary xylem and phloem) and the cork cambium (producing the periderm).

secondary inflorescence meristems The inflorescence meristems that develop from the axillary buds of stem-borne leaves.

secondary nucleus Diploid (2*N*) nucleus formed in the embryo sac's central cell by fusion of the two haploid (*N*) polar nuclei.

secondary phloem Phloem produced by the vascular cambium.

secondary response genes Genes whose expression requires protein synthesis and follows that of primary response genes.

secondary signal A signaling component that is produced or released by activation of a primary signaling pathway. Often a hormone that acts on sites distal to the site of activation.

secondary wall Cell wall synthesized by nongrowing cells. Often multilayered and containing lignin, it differs in composition and structure from the primary wall. Forms during cell differentiation after cell expansion ceases.

secondary walls of woody tissues Thickened walls produced inside the primary cell wall; they are often lignified and play a structural role in supporting the weight of the stem.

secondary xylem Xylem produced by the vascular cambium.

seed coat *See* testa.

seed dormancy The state in which a living seed will not germinate even if all the necessary environmental conditions for growth are met. Seed dormancy introduces a temporal delay in the germination process, providing additional time for seed dispersal.

seed longevity The length of time a seed can remain dormant without losing viability.

seed maturation The final stage of seed development in which the seed loses water by evaporation; mature seeds may also acquire desiccation tolerance and become dormant.

seed plants Plants in which the embryo is protected and nourished within a seed. The gymnosperms and angiosperms.

seed quiescence A non-germinating state characterized by a reduced metabolic rate, after which the seed is released from the parent plant.

selectively permeable Membrane property that allows diffusion of some molecules across the membrane to a different extent than other molecules.

self-incompatibility (SI) A general term for various genetic mechanisms in angiosperms for preventing self-fertilization and thus promoting outcrossing (not to be confused with temporal or anatomical mechanisms, such as heterostyly, that also reduce self-pollination).

selfing Selfing or self-fertilization is the union of male and female gametes generated by the same individual, usually within the same flower, or between flowers from the same individual plant. It is the most extreme form of "inbreeding," a term also applied to the mating of closely related individuals.

seminal roots Lateral roots that develop from the embryonic root, or radicle.

senescence down-regulated genes (SDGs) Genes whose expression levels decline during leaf senescence.

senescence An active, genetically controlled, developmental process in which cellular structures and macromolecules are broken down and translocated away from the senescing organ (typically leaves) to actively growing regions that serve as nutrient sinks. Initiated by environmental cues, regulated by hormones.

senescence-associated cell death One type of developmental PCDs. During senescence, PCD occurs over broad areas of plant organs and at a relatively slow rate.

senescence-associated genes (SAGs) Genes whose expression levels rise during leaf senescence.

senescence-associated vacuoles (SAVs) Small, protease-rich, acidic vacuoles that increase in number during senescence in the leaf mesophyll and guard cells, but not in the nongreen epidermal cells. Although they are distinct from Rubisco-containing bodies, senescence-associated vacuoles contain Rubisco and other stromal enzymes, which they are capable of degrading directly, independent of the autophagic machinery.

sensor proteins Specialized plant cellular receptor proteins that perceive external or internal signals. They consist of two domains, an *input domain*, which receives the environmental signal, and a *transmitter domain*, which transmits the signal to the response regulator.

sequential leaf senescence The pattern of leaf senescence in which there is a gradient of senescence from the growing tip of the shoot to the oldest leaves at the base.

sessile leaves A leaf without a petiole, attached directly to the node via the blade.

shoot apex Consists of the shoot apical meristem plus the most recently formed leaf primordia (organs derived from the apical meristem).

shoot apical meristem (SAM) Meristem at the tip of a shoot. Consists of the terminal central zone (CZ), which contains slowly dividing, undetermined initials, and the flanking peripheral zone (PZ) and rib zone (RZ), in which derivatives of the CZ divide more rapidly and then differentiate.

shoots The aboveground tissues above the root–shoot junction and usually including the stem and leaves.

short interfering RNAs (siRNAs) RNAs that are structurally and functionally quite similar to miRNAs and also lead to the initiation of the RNA interference pathway.

short-day plants (SDPs) A plant that flowers only in short days (qualitative SDP) or whose flowering is accelerated by short days (quantitative SDP).

short–long-day plants (SLDPs) Plants that flower only after a sequence of short days followed by long days.

siderophores Small molecules secreted by non-grass plants and some microbes to chelate iron, which is then taken up into cells at the root surface.

sieve cells The relatively unspecialized sieve elements of gymnosperms. Contrast with angiosperm sieve tube elements.

sieve effect The penetration of photosynthetically active light through several layers of cells due to the gaps between chloroplasts permitting the passage of light.

sieve element Phloem cell that conducts sugars and other organic materials throughout the plant. Refers to both sieve tube elements (angiosperms) and sieve cells (gymnosperms).

sieve plate End wall connecting angiosperm sieve tube elements through many sieve pores; this sieve area has larger pores (sieve pores) than lateral sieve areas.

sieve tube element The sieve element typical of the angiosperms and generally associated with a companion cell. Contrast with sieve cell.

sieve tube Tube formed by the joining together of individual sieve tube elements at their end walls.

signal peptide A hydrophobic sequence of 18 to 30 amino acid residues at the amino-terminal end of a chain; it is found on all secretory proteins and most integral membrane proteins and permits their transit across the membrane of the rough ER.

signal recognition particle (SRP) A ribonucleoprotein (protein-RNA complex) that recognizes and targets specific proteins to the endoplasmic reticulum in eukaryotes.

signal transduction pathway A sequence of processes by which an extracellular signal (typically light, a hormone, or a neurotransmitter) interacts with a receptor at the cell surface, causing a change in the level of a second messenger and ultimately a change in cell functioning.

simple sequence repeats (SSRs) (microsatellites) One group of heterochromatic dispersed repeats that consist of sequences as short as two nucleotides repeated hundreds or even thousands of times. Also known as microsatellites.

simple A leaf with one blade.

singlet oxygen An extremely reactive and damaging form of oxygen formed by reaction of excited chlorophyll with molecular oxygen. Causes damage to cellular components, especially lipids.

sink activity The rate of uptake of photosynthate per unit weight of sink tissue.

sink size The total weight of the sink.

sink strength The ability of a sink organ to mobilize assimilates toward itself. Depends on two factors: sink size and sink activity.

sink Any organ that imports photosynthate, including non-photosynthetic organs and organs that do not produce enough photosynthetic products to support their own growth or storage needs, such as roots, tubers, developing fruits, and immature leaves. Contrast with source.

size exclusion limit (SEL) The restriction on the size of molecules that can be transported via the symplast. It is imposed by the width of the cytoplasmic sleeve that surrounds the desmotubule in the center of the plasmodesma

size exclusion limit The restriction on the size of molecules that can be transported via the symplast. It is imposed by the width of the cytoplasmic sleeve that surrounds the desmotubule in the center of the plasmodesma.

skotomorphogenesis The developmental program plants follow when seeds are germinated and grown in the dark.

S-locus Cysteine-Rich proteins (SCRs) A cysteine-rich protein located in the pollen coat that represents the male *S* determinant in the Brassicaceae.

S-locus receptor kinase (SRK) A serine/threonine receptor kinase located in the plasma membrane of stigma cells that represents the female *S*-determinant in the Brassicaceae.

smooth ER The endoplasmic reticulum lacking attached ribosomes and usually consisting of tubules.

SNAREs A class of targeting recognition proteins for the selective fusion and fission of vesicles and tubules within the endomembrane system.

soil analysis The chemical determination of the nutrient content in a soil sample typically from the root zone.

soil hydraulic conductivity A measure of the ease with which water moves through the soil.

solar tracking The movement of leaf blades throughout the day so that the planar surface of the blade remains perpendicular to the sun's rays.

solute potential *See* osmotic potential

solution culture The technique of growing plants without soil whereby their roots are immersed in a nutrient solution. *See also* hydroponics.

somatic embryogenesis The process by which somatic cells (i.e., non-germline cells) de-differentiate and undergo an autonomous embryogenesis process that re-capitulates all the zygotic embryogenesis steps and results in viable embryos.

sorbitol A sugar alcohol formed by reduction of aldehyde glucose.

sorting-out *See* vegetative segregation.

source Any exporting organ that is capable of producing photosynthetic products in excess of its own needs, such as a mature leaf or a storage organ. Contrast with sink.

spacing divisions Asymmetric divisions of the stomatal lineage ground cells that can give rise to secondary meristemoids during stomatal patterning.

specialized metabolites Plant compounds that have no direct role in plant growth and development, but function as defenses against herbivores and microbial infection by microbial pathogens, attractants for pollinators and seed-dispersing animals, and as agents of plant–plant competition.

specific heat capacity Ratio of the heat capacity of a substance to the heat capacity of a reference substance, usually water. Heat capacity is the amount of heat needed to change the temperature of a unit mass by 1°C. The heat capacity of water is 1 calorie (4.184 Joule) per gram per degree Celsius.

sperm cells Male gametes. Some plant sperm cells are nonflagellated and non-motile (angiosperms, conifers, and Gnetales), while others (bryophytes, ferns, ginkgo, and cycads) are flagellated and motile. The former are delivered to the female gametophyte by the pollen tube, while the latter must swim at least part of the distance to reach the egg.

S-PHASE KINASE-ASSOCIATED PROTEIN1 (Skp1)/Cullin/F-box (SCF) complexes Large protein complexes that function as E3 ubiquitin ligases in the signaling pathways of several plant hormones.

spines Sharp, stiff plant structures that physically deter herbivores and may assist in water conservation and are derived from leaves.

spongy mesophyll Mesophyll cells of very irregular shape located below the palisade cells and surrounded by large air spaces.

spores Reproductive cells formed in plants by meiosis in the sporophyte generation. They give rise, without fusion with another cell, to the gametophyte generation.

sporophyte generation The stage, or generation, in the life cycle of plants that produces spores. It alternates with the gametophyte generation, in a process called alternation of generations.

sporophyte The diploid (2*N*) multicellular structure that produces haploid spores by meiosis.

sporophytic self-incompatibility (SSI) A type of self-incompatibility in which the pollen grain's incompatibility phenotype is determined by the diploid genome of the pollen parent—specifically, the tapetum of the anther.

SRP receptors A receptor protein on the ER membrane that binds to the ribosome-SRP complex, permitting the ribosome to dock with the translocon pore through which the elongating polypeptide will enter the lumen of the ER.

starch sheath A layer of cells that surrounds the vascular tissues of the shoot and coleoptile and is continuous with the root endodermis. Required for gravitropism in Arabidopsis shoots.

starch A polyglucan consisting of long chains of 1,4-linked glucose molecules and branch-points where 1,6-linkages are used. Starch is the carbohydrate storage form in most plants.

starchy endosperm A starch-storing triploid endosperm tissue that comprises the bulk of the seeds of cereals and other members of the grass family.

statocytes Specialized gravity-sensing plant cells that contain statoliths.

statoliths Cellular inclusions such as amyloplasts that act as gravity sensors by having a high density relative to the cytosol and sedimenting to the bottom of the cell.

stele In the root, the tissues located interior to the endodermis. The stele contains the vascular elements of the root: the phloem and the xylem.

stem The primary axis of the plant that is generally above ground, but anatomically similar belowground modified stems, such as rhizomes and corms, are common.

stigma/style cysteine-rich adhesin (SCA) A protein secreted by the transmitting tract of lily styles that is involved in the growth and adhesion of pollen tubes.

stipules Small, leaf-like appendages at the bases of leaves in many dicot species.

stomata (singular *stoma*) A microscopic pore in the leaf epidermis surrounded by a pair of guard cells and in some species, also including subsidiary cells. Stomata regulate the gas exchange (water and CO_2) of leaves by controlling the dimension of a stomatal pore.

stomatal complex The guard cells, subsidiary cells, and stomatal pore, which together regulate leaf transpiration and CO_2 uptake.

stomatal lineage ground cell (SLGC) One of the two daughter cells of the dividing meristemoid mother cell during guard cell differentiation.

stomatal resistance A measurement of the limitation to the free diffusion of gases from and into the leaf posed by the stomatal pores. The inverse of stomatal conductance.

stone (pit) A hardened endocarp (the inner layer of the ovary) in drupe fruits such as peach.

Strasburger cell In gymnosperms, a metabolically active cell that is connected to sieve cells by abundant pore-plasmodesma contacts and takes over many of the metabolic activities of the sieve cell. It contrasts with companion cells by not being ontogenetically related. In source leaves, it functions in the transport of photosynthate into the sieve elements

stratification A process to break dormancy by chilling seeds.

stress relaxation Selective loosening of bonds between primary cell wall polymers, allowing the polymers to slip by each other, simultaneously increasing the wall surface area and reducing the physical stress in the wall.

stress Disadvantageous influences exerted on a plant by external abiotic or biotic factor(s), such as infection, or heat, water, and anoxia. Measured in relation to plant survival, crop yield, biomass accumulation, or CO_2 uptake.

stress–induced protein kinase (SIPK) A mitogen-activated protein kinase similar to WIPK that is activated by diverse environmental signals associated with stress.

stress-response regulons DNA regulatory sequences that function coordinately in stress responses.

strigolactones Carotenoid-derived plant hormones that inhibit shoot branching. They also play roles in the soil by stimulating the growth of arbuscular mycorrhizas and the germination of parasitic plant seeds, such as those of *Striga*, the source of their name.

stroma lamellae Unstacked thylakoid membranes within the chloroplast.

stroma The fluid component surrounding the thylakoid membranes of a chloroplast.

subfunctionalization The process by which evolution acts on duplicate genes, causing one copy to be either lost or changed in function, while the other retains its original function.

subjective day When an organism is placed in total darkness, the phase of the rhythm that coincides with the light period of a preceding light/dark cycle. *See* subjective night.

subjective night When an organism is placed in total darkness, the phase of the rhythm that coincides with the dark period of a preceding light/dark cycle. *See* subjective day.

subsidiary cells Specialized epidermal cells that flank the guard cells and work with the guard cells in the control of stomatal apertures.

substrate-level phosphorylation A process that involves the direct transfer of a phosphate group from a substrate molecule to ADP to form ATP.

subtelomeric regions Regions of a chromosome just proximal to the telomeres.

Sucrose non-Fermenting Related Kinase2 (SnRK2) A family of kinases that includes ABA-activated protein kinases or stress-activated protein kinases.

sucrose A disaccharide consisting of a glucose and a fructose molecule linked via an ether bond between C-1 on the glucosyl subunit and C-2 on the fructosyl unit. The full chemical name is α-D-glucopyranosyl-(1→2)-β-D-fructofuranoside. Sucrose is the carbohydrate transport form, (e.g., in the phloem between source and sink).

sugar–nucleotide polysaccharide glycosyltransferases A group of enzymes that synthesize the backbones of cell wall polysaccharides.

sunfleck A patch of sunlight that passes through an opening in a forest canopy to the forest floor. Major source of incident radiation for plants growing under the forest canopy.

supercool The condition in which cellular water remains liquid because of its solute content, even at temperatures several degrees below its theoretical freezing point.

superoxide dismutase An enzyme that converts superoxide radicals to hydrogen peroxide.

surface tension A force exerted by water molecules at the air–water interface, resulting from the cohesion and adhesion properties of water molecules. This force minimizes the surface area of the air–water interface.

suspensor In seed plant embryogenesis, the structure that develops from the basal cell following the first division of the zygote. Supports, but is not part of, the embryo that develops from the apical cell and hypophysis.

symbiosis receptor-like kinase (SYMRK) A protein kinase involved in perception of chemical signals from symbiotic microbes.

symbiosis The close association of two organisms in a relationship that may or may not be mutually beneficial. Often applied to beneficial (mutualistic) relationships. *See* mutualism.

symplasm The continuum of cellular cytoplasm connected by plasmodesmata.

symplasmic transport The intercellular transport of water and solutes through plasmodesmata.

symport A type of secondary active transport in which the movement of two solutes in the same direction across a membrane is coupled.

synaptonemal complexes Protein structures that form between homologous chromosomes during prophase I of meiosis.

syncytium A multinucleate cell that can result from multiple cell fusions of uninuclear cells, usually in response to viral infection.

synergid cells Two cells adjacent to the egg cell of the embryo sac, one of which is penetrated by the pollen tube upon entry into the ovule.

systemic acquired acclimation (SAA) A photoprotective system wherein leaves exposed to higher light levels transmit a signal to preacclimate shaded leaves.

systemic acquired resistance (SAR) The increased resistance throughout a plant to a range of pathogens following infection by a pathogen at one site.

systemic Movement of a signal or molecule from one location in a plant to distal locations in the plant.

systems biology An approach to examining complex living processes that employs mathematical and computational models to simulate nonlinear biological networks and to better predict their operation.

T

tandem repeats Heterochromatic structures that consist of highly repetitive DNA sequences.

tapetum A layer of secretory cells surrounding the locule of the anther that contribute to the formation of the pollen cell wall.

taproot The main single root axis from which lateral roots develop.

TATA box Located about 25 to 35 bp upstream of the transcriptional start site, this short sequence TATAAA(A) serves as the assembly site for the transcription initiation complex.

telomerase An enzyme that repairs the ends of chromosomes after cell division and prevents them from shortening.

telomere shortening The process by which the telomere (a region of DNA at the end of a chromosome that protects the start of the genetic coding sequence against degradation) undergoes shortening.

telomeres Region of repetitive DNA that form the chromosome ends and protect them from degradation.

telophase Prior to cytokinesis, the final stage of mitosis (or meiosis) during which the chromatin decondenses, the nuclear envelope re-forms, and the cell plate extends.

temperature coefficient (Q_{10}) The increase in the rate of a process (e.g., respiration) for every 10°C increase in temperature.

temperature compensation A characteristic of circadian rhythms, which can maintain their circadian periodicity over a broad range of temperatures within the physiological range.

tensile strength The ability to resist a pulling force. Water has a high tensile strength.

tension wood A type of reaction wood found in arborescent dicots that forms on the upper side of leaning or horizontal stems or branches.

tension Negative hydrostatic pressure.

tertiary cross-regulation Regulation that involves the outputs of two distinct signaling pathways exerting influences on one another.

testa The outer layer of the seed, derived from the integument of the ovule.

tetrad A pair of replicated homologous chromosomes that are synapsed. Consists of four chromatids.

tetrads A pair of replicated homologous chromosomes that are synapsed. Consists of four chromatids.

TFIIB recognition element (BRE) A conserved DNA binding sequence within the core promoter that helps in the regulation of the transcriptional activity of a given gene.

thigmotropism Plant growth in response to touch, enabling roots to grow around rocks and shoots of climbing plants to wrap around structures for support.

thorns Sharp plant structures that physically deter herbivores and are derived from branches.

thylakoid reactions The chemical reactions of photosynthesis that occur in the specialized internal membranes of the chloroplast (called thylakoids). Include photosynthetic electron transport and ATP synthesis.

thylakoids The specialized, internal, chlorophyll containing membranes of the chloroplast where light absorption and the chemical reactions of photosynthesis take place.

tip growth Localized growth at the tip of a plant cell caused by localized secretion of new wall polymers. Occurs in pollen tubes, root hairs, some sclerenchyma fibers, and cotton fibers, as well as moss protonema and fungal hyphae.

tonoplast The vacuolar membrane.

torpedo stage The third stage of embryogenesis. The structure produced by elongation of the axis of the heart stage embryo and further development of the cotyledons. *See also* globular stage, heart stage.

torus A central thickening found in the pit membranes of tracheids in the xylem of most gymnosperms.

tracheary elements Water-transporting cells of the xylem.

tracheids Spindle-shaped, water-conducting cells with tapered ends and pitted walls without perforations found in the xylem of both angiosperms and gymnosperms.

trait A specific character of an organism that is determined by genetic factors (genotype) and environment.

trans Golgi network (TGN) The tubulo-vesicular network that derives from the sloughing *trans* (secretory) cisternae of the Golgi. It is separate from the early recycling endosome, which is also called the partially coated reticulum in plants.

***trans*-acting factors** The transcription factors that bind to the *cis*-acting sequences.

transcription initiation complex A multiprotein complex of transcription factors required for binding RNA polymerase and initiating transcription.

transcription The process by which the base sequence information in DNA is copied into an RNA molecule.

transcriptional regulation The level of regulation that determines if and when RNA is transcribed from DNA

transcriptomics The study of transcriptomes.

transgene A foreign or altered gene that has been inserted into a cell or organism.

transgenic A plant expressing a foreign gene introduced by genetic engineering techniques.

transit peptide An N-terminal amino acid sequence that facilitates the passage of a precursor protein through both the outer and the inner membranes of an organelle such as the chloroplast. The transit peptide is then clipped off.

transition stage The stage of embryogenesis in which the globular embryo transitions toward a bilaterally symmetric stage.

translation The process whereby a specific protein is synthesized according to the sequence information encoded by the mRNA.

translocation (1) In protein synthesis, the movement of protein from its site of synthesis (cytoplasm) into the membrane or lumen of an organelle. (2) The movement of photosynthate from sources to sinks in the phloem.

translocon Protein-lined channel in the rough endoplasmic reticulum that forms associations with SRP receptors and enables proteins synthesized on ribosomes to enter the ER lumen.

transmitting tract The path of pollen tube growth from the stigma to the micropyle of the ovary.

transpiration ratio The ratio of water loss to photosynthetic carbon gain. Measures the effectiveness of plants in moderating water loss while allowing sufficient CO_2 uptake for photosynthesis.

transpiration The evaporation of water from the surface of leaves and stems.

transport phloem Sieve elements of the pathway connecting source and sinks such as the phloem of midribs and stem internodes.

transport protein A transmembrane protein that is involved in the movement of molecules or ions from one side of a membrane to the other side.

transport Movement of molecules or ions from one location to another; may involve crossing a diffusion barrier such as one or more membranes.

transposase An enzyme that catalyzes the movement of a DNA sequence from one site to a different site in the DNA molecule.

transposon tagging The technique of inserting a transposon into a gene and thereby marking that gene with a known DNA sequence.

transposons (transposable elements) DNA elements that can move or be copied from one site in the genome to another site.

treadmilling During interphase, a process by which microtubules in the cortical cytoplasm appear to migrate around the cell periphery due to addition of tubulin heterodimers to the plus end at the same rate as their removal from the minus end.

triacylglycerols Three fatty acyl groups in ester linkage to the three hydroxyl groups of glycerol. Fats and oils.

tricarboxylic acid (TCA) cycle A cycle of reactions localized in the mitochondrial matrix that catalyzes the oxidation of acetyl-CoA (from pyruvate) to CO_2. ATP and NADH are generated in the process.

trichomes Unicellular or multicellular hairlike structures that differentiate from the epidermal cells of shoots and roots. Trichomes may be structural or glandular and function in biotic or abiotic plant responses.

triose phosphate A three-carbon sugar with a phosphate group attached.

tropisms Oriented plant growth in response to a perceived directional stimulus such as light, gravity, touch, or water potential.

tryphine A sticky, adhesive substance rich in proteins, fatty acids, waxes, and other hydrocarbons that coats the exine layer of pollen cell walls.

tubulin A family of cytoskeletal GTP-binding proteins with three members, α-, β-, and γ-tubulin. α-tubulin forms heterodimers with β-tubulin which polymerize to form microtubules. β-tubulin is exposed at the growing plus end and undergoes GTP hydrolysis, while GTP is not hydrolyzed in α-tubulin. The initiation of microtubules is mediated by γ-tubulin, which forms a ring-shaped "primer" for the construction of the microtubule at the minus end of the microtubule.

turgor pressure Force per unit area in a liquid. In a plant cell, the turgor pressure pushes the plasma membrane against the rigid cell wall and provides a force for cell expansion.

turnover The balance between the rate of synthesis and the rate of degradation, usually applied to protein or RNA. An increase in turnover typically refers to an increase in degradation.

two-component regulatory systems Signaling pathways common in prokaryotes. They typically involve a membrane-bound histidine kinase sensor protein that senses environmental signals and a response regulator protein that mediates the response. Although rare in eukaryotes, two-component systems are involved in both ethylene and cytokinin signaling.

type-1 arabinogalactans A pectic polysaccharide with a (1,4)-β-D-galactan backbone decorated with single arabinose residues.

type-A ARR In Arabidopsis, genes that encode response regulators that are made up solely of a receiver domain.

type-B ARR In Arabidopsis, genes that encode response regulators that have an output domain in addition to a receiver domain.

U

ubiquinone A mobile electron carrier of the mitochondrial electron transport chain. Chemically and functionally similar to plastoquinone in the photosynthetic electron transport chain.

ubiquitin A small polypeptide that is covalently attached to proteins by the enzyme ubiquitin ligase using energy from ATP, and that serves as a recognition site for a large proteolytic complex, the proteasome.

ubiquitin–proteasome pathway Mechanism for the specific degradation of cellular proteins involving two discrete steps: the polyubiquitination of proteins via the E3 ubiqutin ligase and the degradation of the tagged protein by the 26S proteasome.

uncoupler A chemical compound that increases the proton permeability of membranes and thus uncouples the formation of the proton gradient from ATP synthesis.

uncoupling protein A protein that increases the proton permeability of the inner mitochondrial membrane and thereby decreases energy conservation.

uncoupling A process by which protons translocated into the lumen by the light reactions can escape to the stroma without the synthesis of ATP, bypassing the ATP synthase. Similarly, uncoupling occurs in the mitochondria when protons translocated out of the matrix as a result of electron transport activity through complexes I, III and IV return to the matrix bypassing the F_oF_1-ATP synthase.

unfolded protein response A cellular response that eliminates misfolded proteins in the lumen of the endoplasmic reticulum.

uniparental inheritance Form of inheritance shown by both mitochondria and plastids, meaning that offspring of sexual reproduction (via pollen and eggs) inherit organelles from only one parent.

unreduced gametes Gametes that have the same number of chromosome sets as the parent cell.

UV RESISTANCE LOCUS 8 (UVR8) The protein receptor that mediates various plant responses to UV-B irradiation.

V

vacuolar H^+-ATPase (V-ATPase) A large, multi-subunit enzyme complex, related to F_oF_1-ATPases, present in endomembranes (tonoplast, Golgi). It acidifies the organelle lumen and provide the proton motive force for the secondary transport of a variety of solutes into the lumen. V-ATPases also function in the regulation of intracellular protein trafficking.

vacuolar sap The fluid contents of a vacuole, which may include water, inorganic ions, sugars, organic acids, and pigments.

vacuolar-type PCD The type of programmed cell death associated with developmental senescence in plant cells in which the vacuole breaks down, releasing various hydrolases into the cytoplasm.

vacuole A membrane-bound cellular organelle containing water and dissolved substances such as salts, sugars, enzymes, and amino acids. Vacuoles function in maintaining water balance and cellular turgor. Lytic vacuoles are characterized by a more acidic pH and can often occupy a majority of the space within a cell. Specialized protein storage vacuoles are found primarily in seeds and very young seedlings.

variegation A condition in which leaves show patterns of white and green. Produced by vegetative segregation and may be due to mutations in nuclear, mitochondrial, or chloroplast genes.

vascular cambium A lateral meristem consisting of fusiform and ray stem cells, giving rise to secondary xylem and phloem elements, as well as ray parenchyma.

vascular plants (tracheophytes) Plants that have xylem and phloem.

vascular tissue Plant tissues specialized for the transport of water (xylem) and photosynthetic products (phloem).

vegetative (tube) cell One of two cells produced by the division of the microspore nucleus during microgametogenesis in angiosperm pollen grains. After engulfing the generative cell, the vegetative cell gives rise to the pollen tube following pollination.

vegetative segregation A major consequence of organellar inheritance (choroplasts and mitochondria) is that a vegetative cell (as opposed to a gamete) can give rise to another vegetative cell via mitosis that is genetically different because one daughter cell may receive organelles with one type of genome, while the other receives organelles with different genetic information.

venation pattern The pattern of veins of a leaf.

vernalization In some species, the cold temperature requirement for flowering. The term is derived from the word for "spring."

vessel elements Nonliving water-conducting cells with perforated end walls found only in angiosperms and a small group of gymnosperms.

vessel A stack of two or more vessel elements in the xylem.

villin An actin binding protein that bundles F-actin filaments.

viscoelastic, or rheological (flow), properties Properties that are intermediate between those of a solid and those of a liquid and combine viscous and elastic behavior.

vivipary The precocious germination of seeds in the fruit while still attached to the plant.

W

water potential A measure of the free energy associated with water per unit volume ($J\ m^{-3}$). These units are equivalent to pressure units such as pascals. Ψ is a function of the solute potential, the pressure potential, and the gravitational potential: $\Psi = \Psi_s + \Psi_p + \Psi_g$. The term Ψ_g is often ignored because it is negligible for heights under five meters.

wavelength A unit of measurement for charactering light energy. The distance between successive wave crests. In the visible spectrum, it corresponds to a color.

whole-plant senescence The death of the entire plant, as opposed to the death of individual cells, tissues, or organs.

whorls Pertaining to the concentric pattern of a set of organs that are initiated around the flanks of the meristem.

wilting Loss of rigidity, leading to a flaccid state, due to turgor pressure falling to zero.

wound callose Callose deposited in the sieve pores of damaged sieve elements that seals them off from surrounding intact tissue. As sieve elements recover, the callose disappears from pores.

wound-induced protein kinase (WIPK) A mitogen-activated protein kinase that is activated by wounding and other environmental signals.

X

xanthophyll Carotenoid involved in nonphotochemical quenching. The xanthophyll zeaxanthin is associated with the quenched state of photosystem II, and violaxanthin is associated with the unquenched state.

XIUQIU A group of small cysteine-rich defensin-like peptides that are involved in the chemo-attraction of pollen tubes to ovules. They are related to the similar family called LUREs, but are less species specific, and are thus considered to be more generic attractants.

xylan A polymer of the five-carbon sugar xylose.

xylem loading The process whereby ions exit the symplasm and enter the conducting cells of the xylem.

xylem pole pericycle Pericycle cells adjacent to protoxylem.

xylem The vascular tissue that transports water and ions from the root to the other parts of the plant.

xyloglucan endotransglucosylase (XET) *See* xyloglucan endotransglucosylase/hydrolases.

xyloglucan endotransglucosylase/hydrolases (XTHs) A large family of enzymes, including xyloglucan endotransglucosylase (XET), that have the ability to cut the backbone of a xyloglucan in the cell wall and join one end of the cut chain with the free end of an acceptor xyloglucan.

xyloglucan A hemicellulose with a backbone of 1→4-linked β-D-glucose residues and short side chains that contain xylose, galactose, and sometimes fucose. It is the most abundant hemicellulose in the primary walls of most plants (in grasses it is present, but less abundant).

Y

yielding properties of the cell wall The capacity of the cell wall to loosen and irreversibly stretch in different ways in response to different internal and external factors.

yielding Long-term irreversible stretching that is characteristic of growing (expanding) cell walls. Nearly lacking in nonexpanding walls.

Z

zeitgebers Environmental signals such as light-to-dark or dark-to-light transitions that synchronize the endogenous oscillator to a 24-hour periodicity.

ZEITLUPE (ZTL) A blue light photoreceptor that regulates day length perception (photoperiodism) and circadian rhythms.

zygotic stage The single-celled product of the union of an egg and a sperm.

25_Taiz7e-Glossary.indd 26 5/2/22 11:26 AM

Illustration Credits

Chapter 1

Alberts, B., et al. (2007) *Molecular Biology of the Cell*. 5th ed. Garland Science, New York.

Fiserova, J., et al. (2009) Nuclear envelope and nuclear pore complex structure and organization in tobacco BY-2 cells. *Plant J.* 59(2): 243–255.

Fitzgibbon, J., et al. (2013) A developmental framework for complex plasmodesmata formation revealed by large-scale imaging of the Arabidopsis leaf epidermis. *Plant Cell* 25: 57–70.

Froelich, D. R., et al. (2011) Phloem ultrastructure and pressure flow. *Plant Cell* 23: 4428–4445.

Gunning, B. E. S. (2009) *Plant Cell Biology on DVD: Information for students and a resource for teachers*. Springer: New York.

Gunning, B. E. S., and Steer, M. W. (1996) *Plant Cell Biology: Structure and Function of Plant Cells*. Jones and Bartlett, Boston.

Higaki, T., et al. (2008) Quantitative analysis of changes in actin microfilament contribution to cell plate development in plant cytokinesis. *BMC Plant Biol.* 8: 80.

Huang, A. H. C. (1987) Lipases. In *The Biochemistry of Plants: A Comprehensive Treatise*. Vol. 9, Lipids: Structure and Function of Plant Cells, pp. 91–119. Jones and Bartlett, Boston.

Leroux, O. (2012) Collenchyma: a versatile mechanical tissue with dynamic cell walls. *Ann. Bot.* 110: 1083–1098.

Rudall, P. J. (1987) Laticifers in *Euphorbiaceae*. *Bot. J. Linn. Soc.* 94: 143–163.

Seguí-Simarro, J. M., et al. (2004) Electron tomographic analysis of somatic cell plate formation in meristematic cells of arabidopsis preserved by high-pressure freezing. *Plant Cell* 16: 836–856.

Staehelin, L. A., and Newcomb, E. H. (2000) In *Biochemistry and Molecular Biology of Plants*. B. B. Buchanan et al. (eds.). American Society of Plant Biologists, Rockville, MD.

Ueki, S., and V. Citovsky. (2011) To gate, or not to gate. *Mol. Plant* 4(5): 782–793.

Xu, X., et al. (2007) Anchorage of plant RanGAP to the nuclear envelope involves novel nuclear-pore-associated proteins. *Curr. Biol*. 17: 1157–1163.

Zhang, W., et al. (2011) The protective shell: sclereids and their mechanical function in corollas of some species of *Camellia* (*Theaceae*). *Plant Biol.* 13: 688–692.

Chapter 2

Baskin, T. I., et al. (1994) Morphology and microtubule organization in Arabidopsis roots exposed to oryzalin or taxol. *Plant Cell Physiol.* 35: 935–942.

Carpita, N. C., and McCann, M. C. (2000) In *Biochemistry and Molecular Biology of Plants*. B. B. Buchanan et al. (eds.). American Society of Plant Biologists, Rockville, MD.

Cosgrove, D. J. (1997) Assembly and enlargement of the primary cell wall in plants. *Annu. Rev. Cell Dev. Biol*. 13: 171–201.

Cosgrove, D. J. (2005) Growth of the plant cell wall. *Nat. Rev. Mol. Cell Biol.* 6: 850–861.

Fry, S. (2004) Primary cell wall metabolism: tracking the careers of wall polymers in living plant cells. *New Phytol.* 161(3): 641–675.

Gunning, B. E. S., and Steer, M. W. (1996) *Plant Cell Biology: Structure and Function of Plant Cells*. Jones and Bartlett, Boston.

Kimura, S., et al. (1999) Immunogold labeling of rosette terminal cellulose-synthesizing complexes in the vascular plant Vigna angularis. *Plant Cell* 11: 2075–2085.

Matthews, J. F., Skopec, C. E., Mason, P. E., Zuccato, P., Torget, R. W., Sugiyama, J., Himmel, M. E., and Brady, J. W. (2006) Computer simulation studies of microcrystalline cellulose Ib. *Carbohydr. Res.* 341: 138–152.

McCann, M. C., et al. (1990) Direct visualization of cross-links in the primary plant cell wall. *J. Cell Sci.* 96: 323–334.

Mohnen, D. (2008) Pectin structure and biosynthesis. *Curr. Opin. Plant Biol.* 11(3): 266–277

Morgan, J. L. W., et al. (2013) Crystallographic snapshot of cellulose synthesis and membrane translocation. *Nature* 493: 181–186. https://doi.org/10.1038/nature11744

Park, Y. B., and Cosgrove, D. J. (2012) A revised architecture of primary cell walls based on biomechanical changes induced by substrate-specific endoglucanases. *Plant Physiol.* 158(4): 1933–1943. https://doi.org/10.1104/pp.111.192880

Ralph, J., et al. (2007) Lignins. In *eLS*, (Ed.). https://doi.org/10.1002/9780470015902.a0020104

Roppolo, D., and Geldner, N. (2012) Membrane and walls: who is master, who is servant? *Curr. Opin. Plant Biol.* 15(6): 608–617. https://doi.org/10.1016/j.pbi.2012.09.009

Sethaphong, L. et al. (2013) Tertiary model of a plant cellulose synthase. *PNAS* 110: 7512–7517. http://www.pnas.org/content/110/18/7512.full

Terashima, N., et al. (2004) Formation of macromolecular lignin in ginkgo xylem cell walls as observed by field emission scanning electron microscopy. *Comptes Rendus Biologies* 327: 903–910. doi:10.1016/j.crvi.2004.08.001 http://www.sciencedirect.com/science/article/pii/S1631069104001738

Zha, Z., et al. (2014) Molecular dynamics simulation study of xyloglucan adsorption on cellulose surfaces: effects of surface hydrophobicity and side-chain variation. *Cellulose* 21: 1025–1039. http://link.springer.com/article/10.1007%2Fs10570-013-0041-1

Zhang, T., et al. (2014) Visualization of the nanoscale pattern of recently-deposited cellulose microfibrils and matrix materials in never-dried primary walls of the onion epidermis. *Cellulose* 21: 853–862. https://doi.org/10.1007/s10570-013-9996-1

Chapter 3

Anzalone, A. V., et al. (2020) Genome editing with CRISPR–Cas nucleases, base editors, transposases and prime editors. *Nat. Biotechnol.* 38: 824–844. https://doi.org/10.1038/s41587-020-0561-9

Barresi, M., and Gilbert, S. (2019) *Developmental Biology*, 12th ed. Oxford University Press/Sinauer, Sunderland, MA.

Cermak, T., et al. (2011) Efficient design and assembly of custom TALEN and other TAL effector-based constructs for DNA targeting. *Nucleic Acids Res.* 39(12): e82. https://doi.org/10.1093/nar/gkr218

Comai, L. (2005) The advantages and disadvantages of being polyploid. *Nat. Rev. Genet.* 6: 836–846. https://doi.org/10.1038/nrg1711

Grandont, L., et al. (2013) Meiosis and its deviations in polyploid plants. *Cytogenet. Genome Res.* 140: 171–184.

Kato, A., et al. (2004) Chromosome painting using repetitive DNA sequences as probes for somatic chromosome identification in maize. *Proc. Natl. Acad. Sci. USA* 101: 13554-13559. © 2004 National Academy of Sciences, U.S.A.

Ma, H. (2005) Molecular genetic analyses of microsporogenesis and microgametogenesis in flowering plants. *Annu. Rev. Plant Biol.* 56: 393–434. http://www.annualreviews.org/doi/pdf/10.1146/annurev.arplant.55.031903.141717

Miura, A., et al. (2001) Mobilization of transposons by a mutation abolishing full DNA methylation in Arabidopsis. *Nature* 411: 212–214.

26_Taiz7e-Illustration Credits.indd 1 4/29/22 3:49 PM

Paul III, J. W., and Qi., Y. (2016) CRISPR/Cas9 for plant genome editing: accomplishments, problems and prospects. *Plant Cell Rep*. 35: 1417–1427.

Sander, J., and Joung, J. (2014) CRISPR-Cas systems for editing, regulating and targeting genomes. *Nat. Biotechmol.* 32: 347–355. https://doi.org/10.1038/nbt.2842

Sun, Y., et al. (2016) Engineering herbicide-resistant rice plants through CRISPR/Cas9-mediated homologous recombination of acetolactate synthase. *Mol. Plant* 9(4): 628–631.

Tiang, C.-L., et al. (2012) Chromosome organization and dynamics during interphase, mitosis, and meiosis in plants. *Plant Physiol.* 158(1): 26–34.

Wu, F., et al. (2021) Opinion: Allow golden rice to save lives. *Proc. Natl. Acad. Sci. USA* 118 (51): e2120901118.

Chapter 4

Aloni, R., et al. (1998) The Never ripe mutant provides evidence that tumor-induced ethylene controls the morphogenesis of Agrobacterium tumefaciens-induced crown galls in tomato stems. *Plant Physiol.* 117: 841–849.

Böhm, J., and Scherzer, S. (2021) Signaling and transport processes related to the carnivorous lifestyle of plants living on nutrient-poor soil. *Plant Physiol.* 187(4): 2017–2031.

Hartwig, T., et al. (2011) Brassinosteroid control of sex determination in maize. *PNAS* 108: 19814–19819.

Jiang, J., et al. (2013) Ligand perception, activation, and early signaling of plant steroid receptor brassinosteroid insensitive 1. *J. Integr. Plant Biol.* 55 (12): 1198–1211.

Ju, C., and Chang, C. (2012) Advances in ethylene signalling: protein complexes at the endoplasmic reticulum membrane. *AoB PLANTS* 2012: pls031. https://doi.org/10.1093/aobpla/pls031.

Liang, X., and Zhou, J.-M. (2018) Receptor-like cytoplasmic kinases: Central players in plant receptor kinase–mediated signaling. *Annu. Rev. Plant Physiol*. 69(1): 267–299.

Multani, D. S., et al. (2003) Loss of an MDR Transporter in Compact Stalks of Maize br2 and Sorghum dw3 Mutants. *Science* 302(5642): 81–84.

Riou-Khamlichi, C., et al. (1999) Cytokinin activation of Arabidposis cell division through a D-type cyclin. *Science* 283: 1541–1544.

Santner, A., Estelle, M. (2009) Recent advances and emerging trends in plant hormone signalling. *Nature* 459: 1071–1078. https://doi.org/10.1038/nature08122.

Wang, X. (2004) Lipid signaling. *Curr. Opin. Plant Biol.* 7(3): 329–336. https://doi.org/10.1016/j.pbi.2004.03.012.

Chapter 5

Briggs, S., et al. (2014) Numerical modelling of flow and transport in rough fractures. *JRMGE* 6(6): 535–545. https://doi.org/10.1016/j.jrmge.2014.10.004.

Day, W., et al. (1978) A drought experiment using mobile shelters: The effect of drought on barley yield, water use and nutrient uptake. *J. Agric. Sci.* 91: 599–623.

Hsiao, T. C. (1973) Plant responses to water stress. *Ann Rev. Plant Physiol*. 24: 519–570.

Hsiao, T. C., and Xu, L. K. (2000) Sensitivity of growth of roots versus leaves to water stress: Biophysical analysis and relation to water transport. *J. Exp. Bot.* 51: 1595–1616.

Innes, P., and Blackwell, R. D. (1981) The effect of drought on the water use and yield of two spring wheat genotypes. *J. Agric. Sci.* 96: 603–610.

Jones, H. (2013). *Plants and Microclimate: A Quantitative Approach to Environmental Plant Physiology* (3rd ed.). Cambridge: Cambridge University Press. doi:10.1017/CBO9780511845727.

Schuur, E. A. (2003) Productivity and global climate revisited: The sensitivity of tropical forest growth to precipitation. *Ecology* 84: 1165–1170.

Chapter 6

Bange, G. G. J. (1953) On the quantitative explanation of stomatal transpiration. *Acta Bot. Neerl*. 2: 255–296.

Gunning, B. E. S. and Steer, M. W. (1996) *Plant Cell Biology: Structure and Function of Plant Cells*. Jones and Bartlett, Boston.

Kramer, P. J. (1983) *Water Relations of Plants*, p. 132. Academic Press: San Diego, CA; after Agricultural Research Council Letcombe Laboratory Annual Report (1973, p. 10).

Meidner, H., and Mansfield, D. (1968) *Physiology of Stomata*. McGraw-Hill, London.

Nobel, P. S. (1999) *Physiochemical and Environmental Plant Physiology*, 2nd ed. Academic Press, San Diego, CA.

Palevitz, B. A. (1981) The structure and development of guard cells. In *Stomatal Physiology*, P. G. Jarvis and T. A. Mansfield, eds., Cambridge University Press, Cambridge, pp. 1–23.

Pittermann, J., et al. (2005) Torus-margo pits help conifers compete with angiosperms. *Science* 310(5756): 1924.

Sack, F. D. (1987) The development and structure of stomata. In *Stomatal Function*, E. Zeiger, G. Farquhar, and I. Cowan, Eds., Stanford University Press, Stanford, CA, pp. 59–90.

Sperry, J. S. (2000) Hydraulic constraints on plant gas exchange. *Agric. For. Meteorol*. 104(1): 13–23.

Zimmerman, H. 1983. *Xylem Structure and the Ascent of Sap*. Springer, Berlin.

Chapter 7

Baxter, I. R., et al. (2008) The leaf ionome as a multivariable system to detect a plant's physiological status. *Proc. Natl. Acad. Sci. USA* 105(33): 12081–12086.

Bloom, A. J., et al. (1993) Root growth as a function of ammonium and nitrate in the root zone. *Plant Cell Environ.* 16: 199–206.

Brady, N. C. (1974) *The Nature and Properties of Soils*, 8th ed. Macmillan, New York.

Epstein, E. (1972) *Mineral Nutrition of Plants: Principles and Perspectives*. John Wiley and Sons, New York.

Epstein, E. (1999) Silicon. *Annu. Rev. Plant Physiol. Mol. Biol*. 50: 641–664.

Epstein, E., and Bloom, A. J. (2005) *Mineral Nutrition of Plants: Principles and Perspectives*, 2nd ed. Oxford University Press/Sinauer, Sunderland, MA.

Erisman, J. W., et al. (2011) Reactive nitrogen in the environment and its effect on climate change. *Curr. Opin. Environ. Sustain.* 3(5): 281–290. https://doi.org/10.1016/j.cosust.2011.08.012.

Evans, H. J., and Sorger, G. J. (1966) Role of mineral elements with emphasis on the univalent cations. *Annu. Rev. Plant Physiol.* 17: 47–76.

Giovannetti, M., et al. (2006) At the root of the wood wide web. *Plant Signal. Behav.* 1(1): 1–5.

Lucas, R. E., and Davis, J. F. (1961) Relationships between pH values of organic soils and availabilities of 12 plant nutrients. *Soil Sci.* 92: 177–182.

Lynch, J. P. (2007) Roots of the second Green Revolution. *Aust. J. Bot*. 55: 493–512. http://dx.doi.org/10.1071/BT06118

Matsubayashi, Y. (2018) Exploring peptide hormones in plants: identification of four peptide hormone-receptor pairs and two post-translational modification enzymes. *Proc. Jpn. Acad. Ser. B. Phys. Biol. Sci.* 94(2): 59–74.

Mengel, K., and Kirkby, E. A. (2001*) Principles of Plant Nutrition*, 5th ed. Kluwer Academic Publishers, Dordrecht, Netherlands.

Péret, B., et al. (2014) Root architecture responses: In search of phosphate. *Plant Physiol.* 166(4): 1713–1723. https://doi.org/10.1104/pp.114.244541.

Remans, T., et al. (2006) The Arabidopsis NRT1.1 transporter participates in the signaling pathway triggering root colonization of nitrate-rich patches. *Proc. Natl. Acad. Sci. USA* 103 (50): 19206–19211.

Rovira, A. D., et al. 1983. The significance of rhizosphere microflora and mycorrhizas in plant nutrition. In *Encyclopedia of Plant Physiology*, New Series, Vol. 15A: Inorganic Plant Nutrition, A. Läuchli and R. L. Bieleski, eds., Springer, Berlin, pp. 61–93.

Vukosav, P., et al. (2012) Revision of iron(III)–citrate speciation in aqueous solution. Voltammetric and spectrophotometric studies. *Analytica Chimica Acta* 745: 85–91. https://doi.org/10.1016/j.aca.2012.07.036.

Weaver, J. E. (1926) *Root Development of Field Crops*. McGraw-Hill, New York.

Chapter 8

Focht, D., et al. (2017) Improved model of proton pump crystal structure obtained by interactive molecular dynamics flexible fitting expands the mechanistic model for proton translocation in P-Type ATPases. *Front. Physiol.* 8: 202.

Guerinot, M. L., and Yi, Y. (1994) Iron: Nutritious, noxious, and not readily available. *Plant Physiol.* 104: 815–820.

Higinbotham, N., et al. (1967) Mineral ion contents and cell transmembrane electropotentials of pea and oat seedling tissue. *Plant Physiol.* 42(1): 37–46.

Higinbotham, N., et al. (1970) Evidence for an electrogenic ion transport pump in cells of higher plants. *J. Membr. Biol.* 3: 210–222.

Kluge, C., et al. (2003) New insight into the structure and regulation of the plant vacuolar H+-ATPase. *J. Bioenerg. Biomembr.* 35: 377–388.

Lebaudy, A., et al. (2007) K+ channel activity in plants: Genes, regulations and functions. *FEBS Lett.* 581: 2357–2366.

Leng, Q., et al. (2002) Electrophysiological analysis of cloned cyclic nucleotide-gated ion channels. *Plant Phys.* 128(2): 400–410. https://doi.org/10.1104/pp.010832.

Lin, W., et al. (1984) Sugar transport into protoplasts isolated from developing soybean cotyledons : I. Protoplast isolation and general characteristics of sugar transport. *Plant Phys*. 75(4): 936–940. https://doi.org/10.1104/pp.75.4.936

Sanders, D., and Bethke, P. (2000) Membrane Transport. In *Biochemistry and Molecular Biology of Plants*, B. B. Buchanan et al. [eds.], pp. 110-158. American Society of Plant Physiologists: Rockville, MD.

Very, A. A., and Sentenac, H. (2002) Cation channels in the Arabidopsis plasma membrane. *Trends Plant Sci.* 7: 168–175.

Chapter 9

Allen, J. F., and Forsberg, J. (2001) Molecular recognition in thylakoid structure and function. *Trends Plant Sci.* 6(7): 317–326.

Asada, K. (1999) The water-water cycle in chloroplasts: Scavenging of active oxygens and dissipation of excess photons. *Annu. Rev. Plant Physiol. Plant Mol. Biol.* 50(1): 601–639.

Barber, J., et al. (1999) Subunit positioning in photosystem II revisited. *Trends Biochem. Sci.* 24(2): 43–45.

Barros, T., and Kühlbrandt, W. (2009) Crystallisation, structure and function of plant light-harvesting Complex II. *Biochim. Biophys. Acta.* 1787(6): 753–772. https://doi.org/10.1016/j.bbabio.2009.03.012.

Becker, W. M. (1986) *The World of the Cell*. Benjamin/Cummings, Menlo Park, CA.

Blankenship, R. E., and Prince, R. C. (1985) Excited-state redox potentials and the Z scheme of photosynthesis. *Trends Biochem. Sci.* 10(10): 382–383. https://doi.org/10.1016/0968-0004(85)90059-3.

Ferreira, K. N., et al. (2004) Architecture of the photosynthetic oxygen-evolving center. *Science* 303(5665): 1831–1838.

Jagendorf, A. T. (1967) Acid-base transitions and phosphorylation by chloroplasts. *FASEB* 26: 1361–1369.

Kurisu, G., et al. (2003) Structure of cytochrome b6f complex of oxygenic photosynthesis: tuning the cavity. *Science* 302(5647): 1009–1014.

Malkin, R., and Niyogi, K. (2000) Photosynthesis. In *Biochemistry and Molecular Biology of Plants*, B. B. Buchanan et al. (eds.), pp. 568–628. American Society of Plant Physiologists: Rockville, MD.

Nelson, N., and Ben-Shem, A. (2004) The complex architecture of oxygenic photosynthesis. *Nat. Rev. Mol. Cell Biol.* 5: 971–982.

Umena, Y., et al. (2011) Crystal structure of oxygen-evolving photosystem II at a resolution of 1.9 Å. *Nature* 473: 55–60.

Chapter 10

Blennow, A., et al. (2003) The molecular deposition of transgenically modified starch as imaged by high-resolution microscopy. *J. Struct. Biol.* 143(3): 229–241.

Chuong, S. D. X., et al. (2006) The cytoskeleton maintains organelle partitioning required for single-cell C_4 photosynthesis in Chenopodiaceae species. *Plant Cell* 18(9): 2207–2223. https://doi.org/10.1105/tpc.105.036186.

Chapter 11

Adams, W. W., and Demmig-Adams, B. (1992) Operation of the xanthophyll cycle in higher plants in response to diurnal changes in incident sunlight. *Planta* 186: 390–398.

Barnola, J. M., et al. (2003) Historical CO_2 record from the Vostok ice core. In *Trends: A Compendium of Data on Global Change*, T. A. Boden, D. P. Kaiser, R. J. Sepanski, and F. W. Stoss, eds., Carbon Dioxide Information Analysis Center, Oak Ridge National Laboratory, U.S. Dept. of Energy, Oak Ridge, TN, pp. 7–10.

Berry, J. A., and Downton, J. S. (1982) Environmental regulation of photosynthesis. In *Photosynthesis: Development, Carbon Metabolism and Plant Productivity*, Vol. 2, Govindjee, ed., Academic Press, New York, pp. 263–343.

Björkman, O. (1981) Responses to Different Quantum Flux Densities. In *Physiological Plant Ecology I. Encyclopedia of Plant Physiology* (New Series), vol 12A, Lange, O. L. et al. (eds), pp. 57–107. Springer: Berlin, Heidelberg.

Björkman, O., et al. (1975) Photosynthetic responses of plants from habitats with contrasting thermal environments: comparison of photosynthetic characteristics of intact plants. *Carnegie Inst. Wash. Yb*. 74: 743-48.

Cerling, T., et al. (1997) Global vegetation change through the Miocene/Pliocene boundary. *Nature* 389: 153–158.

Demmig-Adams, B., and Adams, W. (2000) Harvesting sunlight safely. *Nature* 403: 371–373. https://doi.org/10.1038/35000315.

Ehleringer, J. R. (1978) Implications of quantum yield differences on the distributions of C_3 and C_4 grasses. *Oecologia* 31: 255–267.

Ehleringer, J. R., et al. (1997) C_4 photosynthesis, atmospheric CO_2, and climate. *Oecologia* 112: 285–299.

Etheridge, D. M., et al. (1998) Historical CO_2 records from the Law Dome DE08, DE08-2, and DSS ice cores. In *Trends: A Compendium of Data on Global Change*. Carbon Dioxide Information Analysis Center, Oak Ridge National Laboratory, U.S. Department of Energy, Oak Ridge, Tenn., U.S.A.

Harvey, G. W. (1979) Photosynthetic performance of isolated leaf cells from sun and shade plants. *Carnegie Inst. Wash. Yb*. 79: 161–164.

Jarvis, P. G., and Leverenz, J. W. (1983) Productivity of Temperate, Deciduous and Evergreen Forests. In *Physiological Plant Ecology IV. Encyclopedia of Plant Physiology* (New Series), vol 12D, Lange O. L. et al. (eds.), pp. 233–280. Springer: Berlin, Heidelberg.

Jeon, M.-W., et al. (2006) Photosynthetic pigments, morphology and leaf gas exchange during ex vitro acclimatization of micropropagated CAM Doritaenopsis plantlets under relative humidity and air temperature. *Env. Exp. Bot.* 55(Issues 1–2): 183–194. https://doi.org/10.1016/j.envexpbot.2004.10.014.

Keeling, C. D., and Whorf, T. P. (1994) Atmospheric CO_2 records from sites in the SIO air sampling network. In *Trends '93: A Compendium of Data on Global Change*, T. A. Boden, D. P. Kaiser, R. J. Sepanski, and F. W. Stoss, eds., Carbon Dioxide Information Center, Oak Ridge National Laboratory, Oak Ridge, TN, pp. 16–26; updated using data from Dr. Pieter Tans, NOAA/ESRL (www.esrl.noaa.gov/gmd/ccgg/trends/) and Dr. Ralph Keeling, Scripps Institution of Oceanography (scrippsco2.ucsd.edu/).

Long, S. P., et al. (2006) Foord for thought: Lower-than-expected crop stimulation with rising CO_2 concentrations. *Science* 312: 1918-1921.

Osmond, C. B. (1994) What Is Photoinhibition? Some insights from comparisons of shade and sun plants. In *Photoinhibition of Photosynthesis: From Molecular Mechanisms to the Field*, N. Baker and J. R. Bowyer, eds., BIOS Scientific, Oxford, pp. 1–24.

Smith, H. (1986) The Light Environment. In *Photomorphogenesis in Plants*, 1st ed, R. E. Kendrick and G. H. M. Kronenberg, eds., Nijhoff, Dordrecht, Netherlands, pp. 187–217.

Smith, H. (1994) Sensing the light environment: The functions of the phytochrome family. In *Photomorphogenesis in Plants*, 2nd ed., R. E. Kendrick and G. H. M. Kronenberg, eds., Nijhoff, Dordrecht, Netherlands, pp. 377–416.

Stewart G. R., et al. (1995) 13C natural abundance in plant communities along a rainfall gradient: a biological integrator of water availability. *Funct. Plant Biol.* 22(1): 51–55.

Tlalka, M., and Fricker, M. (1999) The role of calcium in blue-light-dependent chloroplast movement in *Lemna trisulca* L. *Plant J.* 20: 461–473.

Vogelmann, T. C., and Björn, L. O. (1983) Response to directional light by leaves of a suntracking lupine (*Lupinus succulentus*). *Physiol. Plant.* 59(4): 533–538.

Chapter 12

Bentwood, B. J., Cronshaw, J. (1978) Cytochemical localization of adenosine triphosphatase in the phloem of *Pisum sativum* and its relation to the function of transfer cells. *Planta* 140: 111–120.

Evert, R. F. (1982) Sieve-tube structure in relation to function. *Bioscience* 32: 789–795.

Froelich, D. R., et al. (2011) Phloem ultrastructure and pressure flow: Sieve-element-occlusion-related agglomerations do not affect translocation. *Plant Cell* 23(12): 4428–4445.

Fondy, B. R. (1975) Sugar selectivity of phloem loading in *Beta vulgaris*, *vulgaris L.* and *Fraxinus americanus, americana L.* Thesis, University of Dayton, Dayton, OH.

Furch, A. C. U., et al. (2007) Ca^{2+}-mediated remote control of reversible sieve tube occlusion in *Vicia faba*. *J. Exp. Bot.* 58(11): 2827–2838.

Gamalei, Y. V. (1985) Features of phloem loading in woody and herbaceous plants. *Fiziologiya Rastenii* (Moscow) 32: 866–875.

Hall, S. M., and Baker, D. A. (1972) The chemical composition of Ricinus phloem exudate. *Planta* 106: 131–140.

Hunziker, P., and Schulz, A. (2019) Transmission electron microscopy of the phloem with minimal artefacts. In *Phloem: Methods and Protocols, Methods in Molecular Biology*, vol. 2014, J Liesche, (ed.), pp. 17–27. Humana: New York.

Jensen, K. H., et al. (2012) Modeling the hydrodynamics of phloem sieve plates. *Front. Plant Sci.* 3(151): 1-11.

Joy, K. W. (1964) Translocation in sugar beet. I. Assimilation of $14CO_2$ and distribution of materials from leaves. *J. Exp. Bot*. 15: 485–494.

Nobel, P. S. (2005) *Physicochemical and Environmental Plant Physiology*, 3rd ed., Academic Press, San Diego, CA.

Oparka, K. J., and van Bel, A. J. E. (1992) Pathways of phloem loading and unloading: a plea for a uniform terminology. In *Carbon Partitioning within and between Organisms*, Pollock, C. J. et al., (eds.), pp. 249–254. BIOS Scientific: Oxford.

Pate, J. S. (1989) Origin, destination and fate of phloem solutes in relation to organ and whole plant functioning. In: *Transport of Photoassimilates*, Baker, D. A. and Milburn, J. A. (eds). Longman Scientific and Technical, Harlow, Essex, pp. 138–166.

Peuke, A. D. (2010) Correlations in concentrations, xylem and phloem flows, and partitioning of elements and ions in intact plants. A summary and statistical re-evaluation of modelling experiments in *Ricinus communis*. *J. Exp. Bot*. 61(3): 635–655.

Rennie, E. A., and Turgeon, R. (2009) A comprehensive picture of phloem loading strategies. *Proc. Natl. Acad. Sci. USA* 106: 14163–14167.

Ross-Elliott, T. J., et al. (2017) *eLife* 6: e24125. doi: 10.7554/eLife.24125.

Schneidereit, et al. (2008) Conserved cis-regulatory elements for DNA-binding-with-one-finger and homeo-domain-leucine-zipper transcription factors regulate companion cell-specific expression of the Arabidopsis thaliana SUCROSE TRANSPORTER 2 gene. *Planta* 228(4): 651–662.

Schulz, A., and Thompson, G. A. (2009) Phloem Structure and Function (Version 2). In *Encyclopedia of Life Sciences* (eLS). John Wiley & Sons, Ltd.

Schulz, A. (1990) Conifers. In *Sieve Elements: Comparative Structure, Induction, and Development*, H.-D. Behnke and R. D. Sjolund, (eds.), pp. 63–88. Springer-Verlag: Berlin.

Schulz, A. (1986) Wound phloem in transition to bundle phloem in primary roots of *pisum sativum* ii. II: The plasmatic contact between wound sieve tubes and regular phloem. *Protoplasma* 130(1): 27–40.

Stadler, R., et al. (2005) Expression of GFP-fusions in Arabidopsis companion cells reveals non-specific protiein trafficking into sieve elements and identifies a novel post-phloem domain in roots. *Plant J.* 41: 319–331.

Toyota, M., et al. (2018) Glutamate triggers long-distance, calcium-based plant defense signaling. *Science* 361(6407): 1112–1115.

Turgeon, R. (2006) Phloem loading: How leaves gain their independence. *Bioscience* 56(1): 15–24.

Turgeon, R., et al. (1993) The intermediary cell: Minor-vein anatomy and raffinose oligosaccharide synthesis in the Scrophulariaceae. *Planta* 191: 446–456.

Turgeon, R., and Webb, J. A. (1973) Leaf development and phloem transport in *Cucurbita pepo*: Transition from import to export. *Planta* 113: 179–191.

van Bel, A. J. E. (1992) Different phloem-loading machineries correlated with the climate. *Acta Bot. Neerl.* 41: 121–141.

Werner, D., et al. (2011) A dual switch in phloem unloading during ovule development in Arabidopsis. *Protoplasma* 248: 225–235. https://doi.org/10.1007/s00709-010-0223-8.

Chapter 13

Brand, M. D. (1994) The stoichiometry of proton pumping and ATP synthesis in mitochondria. *Biochem. (Lond.)* 16: 20–24. © 1994. The Biochemical Society.

Gunning, B. E. S., and Steer, M. W. (1996) *Plant Cell Biology: Structure and Function of Plant Cells*. Jones and Bartlett, Boston.

Iwata, M., et al. (2012) The structure of the yeast NADH dehydrogenase (Ndi1) reveals overlapping binding sites for water- and lipid-soluble substrates. *Proc. Natl. Acad. Sci. USA* 109: 15247–15252.

Perkins, G., and Renken, C. (1997) Electron tomography of neuronal mitochondria: Three-dimensional structure and organization of cristae and membrane contacts. *J. Struct. Biol.* 119: 260–272.

Shiba, T., et al. (2013) Structure of the trypanosome cyanide-insensitive alternative oxidase. *Proc. Natl. Acad. Sci. USA* 110: 4580–4585.

Chapter 14

Bloom, A. J. (1997) Nitrogen as a Limiting Factor: Crop Acquisition of Ammonium and Nitrate. In *Ecology in Agriculture*, L. E. Jackson (ed.), pp. 145–172, Academic Press, San Diego, CA.

Bloom, A. J., et al. (2012) CO_2 enrichment inhibits shoot nitrate assimilation in C_3 but not C_4 plants and slows growth under nitrate in C_3 plants. *Ecology* 93: 355–367.

Buchanan, B., et al. (2000) *Biochemistry and Molecular Biology of Plants*. American Society of Plant Physiologists, Rockville, MD.

Burris, R. H. (1976) Nitrogen fixation. In *Plant Biochemistry*, 3rd ed., J. Bonner and J. Varner, (eds.), Academic Press, NY. pp. 887–908.

Dixon, R. O. D., and Wheeler, C. T. (1986) *Nitrogen Fixation in Plants*. Chapman and Hall, New York.

Pate, J. S. (1973) Uptake, assimilation and transport of nitrogen compounds by plants. *Soil Biol. Biochem.* 5(1): 109–119.

Schlesinger, W. H. (1997) *Biogeochemistry: An Analysis of Global Change*, 2nd ed., Academic Press, San Diego, CA.

Schroeder, J. I., et al. (2013) Using membrane transporters to improve crops for sustainable food production. *Nature* 497: 60–66.

Searles, P. S., and Bloom, A. J. (2003) Nitrate photo-assimilation in tomato leaves under short-term exposure to elevated carbon dioxide and low oxygen. *Plant Cell Environ.* 26(8): 1247–1255.

Stokkermans, T. J., et al. (1995) Structural requirements of synthetic and natural product lipo-chitin oligosaccharides for induction of nodule primordia on Glycine soja. *Plant Physiol.* 108(4): 1587–1595.

Chapter 15

Baneyx, F., and Mujacic, M. (2004) Recombinant protein folding and misfolding in *Escherichia coli*. *Nat. Biotechnol.* 22: 1399–1408.

Beardsell, M. F., and Cohen, M. (1975.) Relationships between leaf water status, abscisic acid levels, and stomatal resistance in maize and sorghum. *Plant Physiol.* 56(2): 207–212.

Boyer, J. S. (1970) Leaf enlargement and metabolic rates in corn, soybean, and sunflower at various leaf water potentials. *Plant Physiol.* 46: 233–235.

Buchanan, B., et al. (2015) *Biochemistry and Molecular Biology of Plants*, 2nd ed. Wiley Blackwell, New York.

Fichman, Y., et al. (2019) Whole-plant live imaging of reactive oxygen species. *Mol. Plant* 12: 1203–1210. CC BY-NC-ND 4.0.

Gutzat, R., and Mittelsten-Scheid, O. (2012) Epigenetic responses to stress: Triple defense? *Curr. Opin. Plant. Biol.* 15: 568–573.

Henry, C., et al. (2015) Differential role for trehalose metabolism in salt-stressed maize. *Plant Physiol*. 169(2): 1072–1089. https://doi.org/10.1104/pp.15.00729. (https://creativecommons.org/licenses/by/4.0/)

Jones, R., et al. 2013. *The Molecular Life of Plants*. Wiley-Blackwell, Chichester, West Sussex, UK, p. 568.

Lata, C., and Prasad, M. (2011) Role of DREBs in regulation of abiotic stress responses in plants. *J. Exp. Bot.* 62: 4731–4748.

Lyons, J. M., et al. (1964) Relationship between the physical nature of mitochondrial membranes and chilling sensitivity in plants. *Plant Physiol.* 39(2): 262–268.

McAinsh, M. R., et al. (1990) Abscisic acid-induced elevation of guard cell cytosolic Ca^{2+} precedes stomatal closure. *Nature* 343: 186–188.

Mittler, R. (2006) Abiotic stress, the field environment and stress combination. *Trends Plant Sci.* 11: 15–19.

Mittler, R., and Blumwald, E. (2010) Genetic engineering for modern agriculture: Challenges and perspectives. *Annu. Rev. Plant Biol.* 61: 443–462.

Mittler, R., et al. (2012) How do plants feel the heat? *Trends Biochem. Sci.* 37: 118–125.

Pan, J., et al. (2018) Comparative proteomic investigation of drought responses in foxtail millet. *BMC Plant Biol.* 18: 315. CC BY 4.0.

Reddy, A. S. N., et al. (2011) Coping with stresses: Roles of calcium- and calcium/calmodulin-regulated gene expression. *Plant Cell* 23(6): 2010–2032. https://doi.org/10.1105/tpc.111.084988.

Saab, I. N., et al. (1990) Increased endogenous abscisic acid maintains primary root growth and inhibits shoot growth of maize seedlings at low water potentials. *Plant Physiol.* 93(4): 1329–1336.

Suzuki, N., et al. (2014) Abiotic and biotic stress combinations. *New Phytol.* 203: 32–43.

Zandalinas, S. I., and Mittler, R. (2018) ROS-induced ROS release in plant and animal cells. *Free Radic. Biol. Med.* 122: 21–27.

Chapter 16

Ahmad, M., et al. (1998) Cryptochrome blue-light photoreceptors of Arabidopsis implicated in phototropism. *Nature* 392: 720–723.

Andel, F., et al. (1996) Resonance raman analysis of chromophore structure in the lumi-R photoproduct of phytochrome. *Biochemistry* 35(50): 15997–16008. DOI: 10.1021/bi962175k

Baskin, T. I., and Iino, M. (1987) An action spectrum in the blue and ultraviolet for phototropism in Alfalfa. *Photochem. Photobiol.* 46: 127–136.

Briggs, W. R., and Christie, J. M. (2002) Phototropins 1 and 2: versatile plant blue-light receptors. *Trends Plant Sci.* 7: 204–210.

Briggs, W. R., et al. 1984. In *Sensory Perception and Transduction in Aneural Organisms*, G. Columbetti et al. (eds.), Plenum, New York, pp. 265–280.

Burgie, E. S., et al. (2014) Crystal structure of the photosensing module from a red/far-red light-absorbing plant phytochrome. *PNAS* 111(28): 10179–10184.

Christie, J. M. (2007) Phototropin blue-light receptors. *Annu. Rev. Plant Biol.* 58(1): 21-45.

Huang, Y., et al. (2006) Crystal structure of cryptochrome 3 from Arabidopsis thaliana and its implications for photolyase activity. *PNAS* 103(47): 17701–17706.

Inoue, S.-I., and Kinoshita, T. (2017) Blue light regulation of stomatal opening and the plasma membrane H^+-ATPase. *Plant Physiol.* 174(2): 531–538.

Inoue, S.-I., et al. (2010) Phototropin signaling and stomatal opening as a model case. *Curr. Opin. Plant Biol.* 13(5): 587–593.

Jenkins, G. I. (2014) The UV-B photoreceptor UVR8: From structure to physiology. *Plant Cell* 26(1): 21–37. https://doi.org/10.1105/tpc.113.119446.

Kelly, J. M., and Lagarias, J. C. (1985) Photochemistry of 124-kilodalton Avena phytochrome under constant illumination in vitro. *Biochemistry* 24(21): 6003–3010, courtesy of Patrice Dubois

Leivar, P., and Monte, E. (2014) PIFs: Systems integrators in plant development. *Plant Cell* 26: 56–78.

Parks, B. M., et al. (2001) Photocontrol of stem growth. *Curr. Opin. Plant Biol.* 4(5): 436-440. https://doi.org/10.1016/S1369-5266(00)00197-7.

Shropshire Jr., W., et al. (1961) Action spectra of photomorphogenic induction and photoinactivation of germination in *Arabidopsis Thaliana*. *Plant Cell Physiol.* 2(1): 63–69.

Smith, H. (1982) Light quality, photoperception, and plant strategy. *Annu. Rev. Plant Physiol.* 33(1): 481–518.

Spalding, E. P., and Cosgrove, D. J. (1989) Large plasma-membrane depolarization precedes rapid blue-light-induced growth inhibition in cucumber. *Planta* 178: 407–410.

Wada, M. (2013) Chloroplast movement. *Plant Sci.* 210: 177–182.

Yamaguchi, R., et al. (1999) Light-dependent translocation of a phytochrome B-GFP fusion protein to the nucelus in transgenic Arabidopsis. *J. Cell Biol.* 145: 437-445.

Chapter 17

Abeles, F. B., et al. (1992) *Ethylene in Plant Biology*, 2nd ed. Academic Press, San Diego, CA.

Baldwin, K. I., et al. (2013) Gravity sensing and signal transduction in vascular plant primary roots. *Am. J. Bot.* 100: 126–142.

Bethke, P. C., et al. (1997) Hormonal signalling in cereal aleurone. *J. Exp. Bot.* 48: 1337–3365.

Bewley, J. D. (1997) Seed germination and dormancy. *Plant Cell* 9(7): 1055–1066.

Bewley, J. D., et al. (2013) In *Seeds: Physiology of Development, Germination, and Dormancy*, 3rd edition. Springer, New York.

Bibikova, T., and Gilroy, S. (2003) Root hair development. *J. Plant Growth Regul.* 21: 383–415.

Binder, B. M., et al. (2004a) Arabidopsis seedling growth response and recovery to ethylene: A kinetic analysis. *Plant Physiol.* 136(2): 2913–2920.

Binder, B. M., et al. (2004b) Short-term growth responses to ethylene in Arabidopsis seedlings are EIN3/EIL1 independent. *Plant Physiol.* 136(2): 2921–2927.

Blilou, I., et al. (2005) The PIN auxin efflux facilitator network controls growth and patterning in Arabidopsis roots. *Nature* 433: 39–44.

Busse, J. S., and Evert, R. F. (1999) Vascular differentiation and transition in the seedling of *Arabidopsis thaliana* (Brassicaceae). *Int. J. Plant Sci.* 160(2): 241–251.

Christie, J. M., et al. (2011) phot1 Inhibition of ABCB19 primes lateral auxin fluxes in the shoot apex required for phototropism. *PLOS Biol.* 9(6): e1001076. https://doi.org/10.1371/journal.pbio.1001076.

Fasano, J. M., et al. (2001) Changes in root cap pH are required for the gravity response of the Arabidopsis root. *Plant Cell* 13: 907–921.

Finch-Savage, W. E., and Leubner-Metzger, G. (2006) Seed dormancy and the control of germination. *New Phytol.* 171: 501–523.

Grappin, P., et al. (2000) Control of seed dormancy in *Nicotiana plumbaginifolia*: post-imbibition abscisic acid synthesis imposes dormancy maintenance. *Planta* 2010: 279–285.

Gubler, F., et al. (1995) Gibberellin-regulated expression of a myb gene in barley aleurone cells: evidence for Myb transactivation of a high-pI alpha-amylase gene promoter. *Plant Cell* 7: 1879–1891.

Hartmann, H. T., and Kester, D. E. (1983) *Plant Propagation: Principles and Practices*, 4th ed. Prentice-Hall, Inc., NJ.

Iino, M., and Briggs, W. R. (1984) Growth distribution during first positive phototropic curvature of maize coleoptiles. *Plant Cell Environ.* 7: 97–104.

Jacobs, M., and Ray, P. M. (1976) Rapid auxin-induced decrease in free space pH and its relationship to auxin-induced growth in maize and pea. *Plant Physiol.* 58: 203–209.

Le, J., Vandenbussche, et al. (2005) Cell elongation and microtubule behavior in the Arabidopsis hypocotyl: Responses to ethylene and auxin. *J. Plant Growth Regul.* 24: 166–178.

Lee, H.-J., et al. (2020) PIN-mediated polar auxin transport facilitates root-obstacle avoidance. *New Phytol.* 225: 1285–1296.

Leubner, G. [seedbiology.de]

Liptay, A., and Schopfer, P. (1983.) Effect of water stress, seed coat restraint, and abscisic acid upon different germination capabilities of two tomato lines at low temperature. *Plant Physiol.* 73: 935–93.

Massa, G. D., and Gilroy, S. (2003) Touch modulates gravity sensing to regulate the growth of primary roots of *Arabidopsis thaliana*. *Plant J.* 33: 435-445. https://doi.org/10.1046/j.1365-313X.2003.01637.x

Monshausen, et al. (2009) Ca^{2+} regulates reactive oxygen species production and pH during mechanosensing in Arabidopsis roots. *Plant Cell* 21: 2341–2356.

Monshausen, G. B., et al. (2010) Dynamics of auxin-dependent Ca^{2+} and pH signaling in root growth revealed by integrating high-resolution imaging with au-

tomated computer vision-based analysis. *Plant J.* 65: 309–318.

Nonogaki, H., et al. (2007) Mechanisms and Genes Involved in Germination Sensu Stricto. In *Annual Plant Reviews* Volume 27: Seed Development, Dormancy and Germination, K. J. Bradford and H. Nonogaki, eds. doi:10.1002/9780470988848.ch11.

Nonogaki, H., et al. (2010) Germination—Still a mystery. *Plant Sci.* 179: 574–581.

Palmieri, M., and Kiss, J. Z. (2007) The Role of Plastids in Gravitropism. In *The Structure and Function of Plastids. Advances in Photosynthesis and Respiration*, vol. 23, R. R. Wise and J. K. Hoober (eds.), pp. 507–525. Springer, Dordrecht.

Shaw, S., and Wilkins, M. B. (1973) The source and lateral transport of growth inhibitors in geotropically stimulated roots of *Zea mays* and *Pisum sativum*. *Planta* 109: 11–26.

Smyth, D. R. (2016) Helical growth in plant organs: mechanisms and significance. *Development* 143: 3272–3282.

Tan-Wilson, A. L., and Wilson, K. A. (2012) Mobilization of seed protein reserves. *Physiol. Plant.* 145: 140–153.

Chapter 18

Aloni, R., et al. (2003) Gradual shifts in sites of free-auxin production during leaf-primordium development and their role in vascular differentiation and leaf morphogenesis in Arabidopsis. *Planta* 216: 841–853.

Barrada, A., et al. (2015) Spatial regulation of root growth: Placing the plant TOR pathway in a developmental perspective. *Int. J. Mol. Sci.* 16(8): 19671–19697. https://doi.org/10.3390/ijms160819671

Bayer, E., et al. (2009) Integration of transport-based models for phyllotaxis and midvein formation. *Genes Dev*. 23: 373–384.

Bowman, J. L., and Eshed, Y. (2000) Formation and maintenance of the shoot apical meristem. *Trends Plant Sci.* 5: 110–115.

Cheng, Y., et al. (2006) Auxin biosynthesis by the YUCCA flavin monooxygenases controls the formation of floral organs and vascular tissues in Arabidopsis. Genes & Development. 20: 1790–1799

Esau, K. (1953) *Plant Anatomy*. NY: Wiley.

Fukushima, K., and Hasebe, M. (2013) Adaxial–abaxial polarity: The developmental basis of leaf shape diversity. *Genesis* 52: 1–18.

Greb, T., et al. (2003) Molecular analysis of the LATERAL SUPPRESSOR gene in Arabidopsis reveals a conserved control mechanism for axillary meristem formation. *Genes Dev*. 17: 1175–1187.

Hasson, A., et al. (2010) Leaving the meristem behind: The genetic and molecular control of leaf patterning and morphogenesis. *C. R. Biol.* 333: 350–360.

Kanaoka, M. M., et al. (2008) SCREAM/ICE1 and SCREAM2 specify three cell-state transitional steps leading to Arabidopsis stomatal differentiation. *Plant Cell* 20(7): 1775–1785.

Kang, J., and Sinha, N. R. (2010) Leaflet initiation is temporally and spatially separated in simple and complex tomato (*Solanum lycopersicum*) leaf mutants: A developmental analysis. *Botany* 88: 710–724.

Kuchen, E. E., et al. (2012) Generation of leaf shape through early patterns of growth and tissue polarity. *Science* 335: 1092–1096.

Lau, S., and Bergmann, D. C. (2012) Stomatal development: A plant's perspective on cell polarity, cell fate transitions and intercellular communication. *Development* 139: 3683–3692.

Lucas, W. J., et al. (2013) The plant vascular system: Evolution, development and functions. *J. Int. Plant Biol.* 55: 294–388.

Nunes, T. D. G., et al. (2020) Form, development and function of grass stomata. *Plant J.* 101: 780–799.

Reinhardt, D., et al. (2003) Regulation of phyllotaxis by polar auxin transport. *Nature* 426: 255–260. https://doi.org/10.1038/nature02081.

Sawchuk, M. G., et al. (2013) Patterning of leaf vein networks by convergent auxin transport pathways. *PLOS Genet*. 9: e1003294. CC BY 4.0

Schiefelbein, J. W., et al. (1997) Building a root: The control of patterning and morphogenesis during root development. *Plant Cell* 9: 1089–1098, courtesy of J. Schiefelbein, © American Society of Plant Biologists, reprinted with permission.

Sussex, I. M. (1951) Experiments on the cause of dorsiventrality in leaves. *Nature* 167: 651–652.

Townsley, B. T., and Sinha, N. R. (2012) A new development: Evolving concepts in leaf ontogeny. *Annu. Rev. Plant Biol.* 63: 535–562.

Verna, C., et al. (2019) Coordination of tissue cell polarity by auxin transport and signaling. *eLife* 8: e51061. CC BY 4.0

Vernoux, T., et al. (2000) PIN-FORMED 1 regulates cell fate at the periphery of the shoot apical meristem. *Development* 127: 5157–5165.

Waites, R., and Hudson, A. (1995) Phantastica: A gene required for dorsoventrality of leaves in *Antirrhinum majus*. *Development* 121: 2143–2154.

Chapter 19

Campilho, A., et al. (2020) The development of the periderm: the final frontier between a plant and its environment. *Curr. Opin. Plant Biol*. 53: 10–14.

Domagalska, M. A., and Leyser, O. (2011) Signal integration in the control of shoot branching. *Nat. Rev. Mol. Cell Biol.* 12: 211–221.

El-Showk, S., et al. (2013) Crossing paths: cytokinin signalling and crosstalk. *Development* 140(7): 1373–1383. doi: https://doi.org/10.1242/dev.086371.

Fink, S. (1983) The occurrence of adventitious and preventitious buds within the bark of some temperate and tropical trees. *Am. J. Bot*. 70(4): 532–542.

Hochholdinger, F., and Tuberosa, R. (2009) Genetic and genomic dissection of maize root development and architecture. *Curr. Opin. Plant Biol*. 12: 172–177.

Hollender, C. A., et al. (2020) Opposing influences of TAC1 and LAZY1 on lateral shoot orientation in Arabidopsis. *Sci. Rep*. 10: 6051. CC BY 4.0

Megías, M., et al. (2019) Plant Organs: Root. Primary Growth. *Atlas of Plant and Animal Histology*. Dept. of Functional Biology and Health Sciences, University of Vigo, Spain. Updated: 2020-01-19. https://mmegias.webs.uvigo.es/02-english/2-organos-v/guiada_o_v_rprimario.php.

Miyashima, S., et al. (2013) Stem cell function during plant vascular development. *EMBO J*. 32(2): 178–193.

Moreno-Risueno, M. A., et al. (2010) Oscillating gene expression determines competence for periodic Arabidopsis root branching. *Science* 329(5997): 1306–1311.

Risopatron, J. P. M., et al. (2010) The vascular cambium: molecular control of cellular structure. *Protoplasma* 247: 145–161.

Smetana, O., et al. (2019) High levels of auxin signalling define the stem-cell organizer of the vascular cambium. *Nature* 565: 485–489.

Spicer, R., and Groover, A. (2010) Evolution of development of vascular cambia and secondary growth. *New Phytol.* 186(3): 577-592.

Van Norman, J. M., et al. (2013) To branch or not to branch: the role of pre-patterning in lateral root formation. *Development* 140: 4301–4310.

Wolf, S., and Lohmann, J. U. (2019) Plant-thickening mechanisms revealed. *Nature* 565: 433–435.

Yu, B., et al. 2007. TAC1, a major quantitative trait locus controlling tiller angle in rice. *Plant J.* 52: 891–898.

Zhang, J., et al. (2019) Transcriptional regulatory framework for vascular cambium development in Arabidopsis roots. *Nat. Plants* 5: 1033–1042.

Chapter 20

Bewley, J. D., et al. (2000) Reproductive Development. In: *Biochemistry and Molecular Biology of Plants*, B.B. Buchanan et al. (eds.), Rockville, MD: American Society of Plant Biologists.

Busch, A., and Zachgo, S. (2009) Flower symmetry evolution: towards understanding the abominable mystery of angiosperm radiation. *Bioessays* 31(11): 1181–1190.

Clark, J. R. (1983) Age-related changes in trees. *J. Arboric*. 9(8): 201–205.

Coulter, M. W., and Hamner, K. C. (1964) Photoperiodic flowering response of Biloxi soybean in 72 hour cycles. *Plant Physiol.* 39(5): 848–856.

Deitzer, G. (1984) Photoperiodic induction in long-day plants. In *Light and the Flowering Process*, D. Vince-Prue et al. (eds.), Academic Press, New York, pp. 51–63.

Hendricks, S. B., and Siegelman, H. W. (1967) Phytochrome and

photoperiodism in plants. *Comp. Biochem.* 27: 211–235.

Krizek, B. A., and Fletcher, J. C. (2005) Molecular mechanisms of flower development: an armchair guide. *Nat. Rev. Genet*. 6: 688–698.

Liu, L., et al. (2013) Emerging insights into florigen transport. *Curr. Opin. Plant Biol*. 16: 607–613.

Papenfuss, H. D., and Salisbury, F. B. (1967) Aspects of clock resetting in flowering of Xanthium. *Plant Physiol.* 42: 1562–1568.

Pelaz, S., et al. (2001) Conversion of leaves into petals in Arabidopsis. *Curr. Biol.* 11(3): 182–184.

Purcell, O., et al. (2010) A comparative analysis of synthetic genetic oscillators. *J. R. Soc. Interface* 7(52): 1503–1524.

Purvis, O. N., and Gregory, F. G. (1952) Studies in vernalization of cereals. XII. The reversibility by high temperature of the vernalized condition in Petkus winter rye. *Ann. Bot*. 1: 569–592.

Riechmann, J. L., and Meyerowitz, E. M. (1997) Mad domain proteins in plant development. *Biol. Chem.* 378(10): 1079–1118.

Saji, H., et al. (1983) Studies on the photoreceptors for the promotion and inhibition of flowering in dark-grown seedlings of *Pharbitis nil choisy*. *Plant Cell Physiol*. 24(7): 1183–1189.

Salisbury, F. B. (1963) Biological timing and hormone synthesis in flowering of Xanthium. *Planta* 49: 518–524.

Song, Y. H., et al. (2018) Molecular basis of flowering under natural long-day conditions in Arabidopsis. *Nat. Plants* 4: 824–835.

Song, Y. H., et al. 2015. Photoperiodic flowering: Time measurement mechanisms in leaves. *Annu. Rev. Plant Biol.* 66(1): 441–464.

Vince-Prue, D. (1975) *Photoperiodism in Plants*. McGraw-Hill, London.

Wei, H., et al. (2020) Molecular basis of heading date control in rice. *aBIOTECH* 1: 219–232.

Chapter 21

Aloni, R. (2021) Flower Biology and Vascular Differentiation. In *Vascular Differentiation and Plant Hormones*, p. 174. Springer Nature: Cham, Switzerland.

Ballester, P., and Ferrándiz, C. (2017) Shattering fruits: Variations on a dehiscent theme. *Curr. Opin. Plant Biol.* 35: 68–75.

Bowman, J. L., et al. (1994) Flowers. In *Arabidopsis: An Atlas of Morphology and Development*, Bowman, J. L. (ed.), p. 133–273. Springer-Verlag, New York.

Certal, A. C., et al. (1999) S-RNases in apple are expressed in the pistil along the pollen tube growth path. *Sex. Plant Reprod*. 12: 94–98.

Cheung, A. Y., et al. (2010) A transmembrane formin nucleates subapical actin assembly and controls tip-focused growth in pollen tubes. *Proc. Natl. Acad. Sci. USA* 107: 16390–16395.

Cosségal, M., et al. (2007) The Embryo Surrounding Region. In *Endosperm: Plant Cell Monographs*, vol. 8. Olsen, O. A. (ed.), pp. 57–71. Springer: Berlin, Heidelberg.

Debeaujon, I., et al. (2003) Proanthocyanidin-accumulating cells in Arabidopsis testa: Regulation of differentiation and role in seed development. *Plant Cell* 15: 2514–2531.

Dinneny, J. R., and Yanofsky, M. F. (2004) Drawing lines and borders: how the dehiscent fruit of Arabidopsis is patterned. *BioEssays* 27(1): 42–49.

Dobritsa, A. A., and Coerper, D. (2012) The novel plant protein INAPERTURATE POLLEN1 marks distinct cellular domains and controls formation of apertures in the Arabidopsis pollen exine. *Plant Cell* 24(11): 4452–4464. https://doi.org/10.1105/tpc.112.101220.

Edlund, A. F., et al. (2004) Pollen and stigma structure and function: The role of diversity in pollination. *Plant Cell* 16(Suppl. 1): S84–S97.

Edlund, A. F., et al. (2016) Pollen from *Arabidopsis thaliana* and other Brassicaceae are functionally omniaperturate. *Am. J. Bot.* 103: 1006–1019. https://doi.org/10.3732/ajb.1600031.

Fray, R. G., and Grierson, D. (1993) Identification and genetic analysis of normal and mutant phytoene synthase genes of tomato by sequencing, complementation and co-suppression. *Plant Mol. Biol.* 22: 589–602.

Gasser, C. S., and Robinson-Beers, K. (1993) Pistil development. *Plant Cell* 5: 1231–1239.
© American Society of Plant Biologists, reprinted with permission.
Giovannoni, J. J. (2004) Genetic regulation of fruit development and ripening. *Plant Cell* 16 (Suppl 1): S170–S180.

Goetz, M., et al. (2007) Expression of aberrant forms of AUXIN RESPONSE FACTOR8 stimulates parthenocarpy in Arabidopsis and tomato. *Plant Physiol*. 145: 351–366.

Grierson, D. (2013) Ethylene and the control of fruit ripening. In *The Molecular Biology and Biochemistry of Fruit Ripening*. Seymour, G. B. et al. (eds.), pp. 43–73. Wiley-Blackwell: New York.

Gutermuth, T., et al. (2013) Pollen tube growth regulation by free anions depends on the interaction between the anion channel SLAH3 and calcium-dependent protein kinases CPK2 and CPK20. *Plant Cell* 25: 4525–4543.

Haughn, G., and Chaudhury, A. (2005) Genetic analysis of seed coat development in Arabidopsis. *Trends Plant Sci.* 10: 472–477.

Higashiyama, T., et al. (1998) Guidance in vitro of the pollen tube to the naked embryo sac of *Torenia fournieri*. *Plant Cell* 10(12): 2019–2031.

Hoffmann, D., et al. (2020) Plasma membrane H^+-ATPases sustain pollen tube growth and fertilization. *Nat. Comm.* 11: 2395.

Johnson, M. A., and Lord, E. (2006) Extracellular Guidance Cues and Intracellular Signaling Pathways that Direct Pollen Tube Growth. In *Plant Cell Monographs*, Vol. 3: The Pollen Tube, R. Malho (ed.), Springer, New York, p. 223–242.

Jones, R. L., et al. (2013) *The Molecular Life of Plants*. NY: Wiley-Blackwell.

Kumar, P. P., and Loh, C. S. (2012) Plant tissue culture for biotechnology. In *Plant Biotechnology and Agriculture*. A. Altman and P.M. Hasegawa, (eds.), pp. 131–138. Academic Press: Amsterdam. Photo by Wendy Shu.

Lancelle, S. A., et al. (1997) Growth inhibition and recovery in freeze-substitutedLilium longiflorum pollen tubes: structural effects of caffeine. *Protoplasma* 196: 21–33.

Michard, E., et al. (2008) Tobacco pollen tubes as cellular models for ion dynamics: improved spatial and temporal resolution of extracellular flux and free cytosolic concentration of calcium and protons using pHluorin and YC3.1 CaMeleon. *Sex. Plant Reprod*. 21: 169–181.

Michard, E., et al. (2017) Signaling with ions: The keystone for apical cell growth and morphogenesis in pollen tubes. *Plant Physiol*. 173: 91–111.

Oeller, P., et. al. (1991) Reversible inhibition of tomato fruit senescence by antisense RNA. *Science* 254: 437–439.

Olsen, O. A. (2004) Nuclear endosperm development in cereals and *Arabidopsis thaliana*. *Plant Cell* 16(Suppl. 1): S214–S227, https://doi.org/10.1105/tpc.017111.

Otegui, M. S. (2007) Endosperm Cell Walls: Formation, Composition, and Functions. In *Endosperm: Plant Cell Monographs*, vol 8. Olsen, O. A. (ed.), pp.159–178. Springer: Berlin, Heidelberg.

Seymour, G. B., et al. (2013) Fruit development and ripening. *Annu. Rev. Plant Biol.* 64: 219–241.

Troll, W. (1937) Vergleichende Morphologie der hoheren Pflanzen, Gebruder Borntrager, Berlin.

Verdier, J., et al. (2013) A regulatory network-based approach dissects late maturation processes related to the acquisition of desiccation tolerance and longevity of *Medicago truncatula* Seeds. *Plant Physiol*. 163(2): 757–774.

Williams, J. H. (2012) Pollen tube growth rates and the diversification of flowering plant reproductive cycles. *Int. J. Plant Sci.* 173(6): 649–661.

Chapter 22

Abe, M., et al. (2003) Regulation of shoot epidermal cell differentiation by a pair of homeodomain proteins in Arabidopsis. *Development* 130(4): 635–643.

Aida, M., et al. (2004) The PLETHORA genes mediate patterning of the Arabidopsis root stem cell niche. *Cell* 119(1): 109–120. https://doi.org/10.1016/j.cell.2004.09.018.

Berleth, T., and Juergens, G. (1993) The role of the monopteros gene in organising the basal body region of the Arabidopsis embryo. *Development* 118(2): 575–587.

De Rybel, B., et al. (2013) A bHLH complex controls embryonic vascular tissue establishment and indeterminate growth in Arabidopsis. *Dev. Cell* 24(4): 426–437.

Galinha, C., et al. (2007) PLETHORA proteins as dose-dependent

master regulators of Arabidopsis root development. *Nature* 449: 1053–1057.

Helariutta, Y., et al. (2000) The SHORT-ROOT gene controls radial patterning of the Arabidopsis root through radial signaling. *Cell* 101(5): 555–567.

Kim, I., et al. (2005) Subdomains for transport via plasmodesmata corresponding to the apical-basal axis are established during Arabidopsis embryogenesis. *Proc. Natl Acad. Sci. USA* 102(33): 11945–11950. © 2005 National Academy of Sciences.

Kimata, Y., et al. (2016) Cytoskeleton dynamics control the first asymmetric cell division in Arabidopsis zygote. *Proc. Natl. Acad. Sci. USA* 113: 14157–14162.

Laux, T., et al. (2004) Genetic regulation of embryonic pattern formation. *Plant Cell* 16(Suppl 1): S190–S202.

Liu, C., et al. (1993) Auxin polar transport 1s essential for the establishment of bilateral symmetry during early plant embryogenesis. *Plant Cell* 5(6): 621–630.

Long, J. A., and Barton, M. K. (1998) The development of apical embryonic pattern in Arabidopsis. *Development* 125(16): 3027–3035.

Mahonen, A. P., et al. (2000) A novel two-component hybrid molecule regulates vascular morphogenesis of the Arabidopsis root. *Genes Dev*. 14: 2938–2943 © 2000, Cold Spring Harbor Laboratory Press.

Mayer, U., et al. (1991) Mutations affecting body organization in the Arabidopsis embryo. *Nature* 353: 402–407.

Mayer, U., et al. (1993) Apical-basal pattern formation in the Arabidopsisembryo: Studies on the role of the gnom gene. *Development* 117(1): 149–162.

Meinke, D., et al. (2008) Identifying essential genes in *Arabidopsis thaliana*. *Trends Plant Sci*. 13(9): 483–491.

Nakajima, K., and Benfey, P. N. (2002) Signaling in and out: Control of cell division and differentiation in the shoot and root. *Plant Cell* 14: S265–S276.

Nakajima, K., et al. (2001) Intercellular movement of the putative transcription factor SHR in root patterning. *Nature* 413: 307–311.

Palovaara, J., et al. (2016) Tissue and organ initiation in the plant embryo: A first time for everything. *Annu. Rev. Cell Dev. Biol.* 32: 47–75.

Radoeva, T., and Weijers, D. (2014) A roadmap to embryo identity in plants. *Trends Plant Sci*. 19: 709–716.

Scheres, B., et al. (1994) Embryonic origin of the Arabidopsis primary root and root meristem initials. *Development* 120(9): 2475–2487.

Smith, Z. R., and Long, J. A. (2010) Control of Arabidopsis apical–basal embryo polarity by antagonistic transcription factors. *Nature* 464: 423–427.

Sosso, D., et al. (2012) PPR8522 encodes a chloroplast-targeted pentatricopeptide repeat protein necessary for maize embryogenesis and vegetative development. *J. Exp. Bot*. 63(16): 5843–5857.

Traas, J., et al. (1995) Normal differentiation patterns in plants lacking microtubular preprophase bands. *Nature* 375: 676–677.

West, M. A. L., and Harada, J. J. (1993) Embryogenesis in higher plants: An overview. *Plant Cell* 5(10): 1361–1369.

Yoshida, S., et al. 2014. Genetic control of plant development by overriding a geometric division rule. *Dev. Cell* 29(1): 75–87.

Chapter 23

Aalen, R. B., et al. (2013) IDA: a peptide ligand regulating cell separation processes in Arabidopsis. *J. Exp. Bot.* 64(17): 5253–5261.

Bassham, D.C., et al. (2006) Autophagy in development and stress responses of plants. *Autophagy* 2(1): 2–11.

Breeze, E., et al. (2011) High-resolution temporal profiling of transcripts during Arabidopsis leaf senescence reveals a distinct chronology of processes and regulation. *Plant Cell* 23(3): 873–894.

Gan, S., and Amasino, R. M. (1995) Inhibition of leaf senescence by autoregulated production of cytokinin. *Science* 270: 1986–1988.

Ishida, H., et al. (2014) Roles of autophagy in chloroplast recycling. *Biochim. Biophys. Acta Bioenerg*. 1837(4): 512–521.

Keskitalo, J., et al. (2005) A cellular timetable of autumn senescence. *Plant Physiol*. 139: 1635–1648.

Kim, J. H., et al. (2009) Trifurcate feed-forward regulation of age-dependent cell death involving miR164 in Arabidopsis. *Science* 323(5917): 1053–1057.

Krupinska, K., et al. (2012) An alternative strategy of dismantling of the chloroplasts during leaf senescence observed in a high-yield variety of barley. *Physiol. Plant*. 144: 189–200.

Kwon, S. I., et al. (2013) The Rab GTPase RabG3b positively regulates autophagy and immunity-associated hypersensitive cell death in Arabidopsis. *Plant Physiol*. 161(4): 1722–1736.

Lee, Y., et al. (2018) A lignin molecular brace controls precision processing of cell walls critical for surface integrity in Arabidopsis. *Cell* 173: 1468–1480.

Liebsch, D., and Keech, O. (2016) Dark-induced leaf senescence: new insights into a complex light-dependent regulatory pathway. *New Phytol.* 212: 563–570.

Morgan, P. W., et al. (1984) Ethylene: The Natural Regulator of Abscission? In *Ethylene: Biochemical, Physiological and Applied Aspects*. Y. Fuchs and E. Chalutz (eds.), Martinus Nijhoff, The Hague, Netherlands, pp. 231–240.

Shi, C.-L., et al. (2011) Arabidopsis class I KNOTTED-like homeobox proteins act downstream in the IDA-HAE/HSL2 floral abscission signaling pathway. *Plant Cell* 23(7): 2553–2567.

Sillett, S. C., et al. (2010) Increasing wood production through old age in tall trees. *For. Ecol. Manage*. 259(5): 976–994.

Stephenson, N. L., et al. (2014) Rate of tree carbon accumulation increases continuously with tree size. *Nature* 507: 90–93.

Thomas, H. (2013) Senescence, ageing and death of the whole plant. *New Phytol*. 197: 696–711.

Vahala, J., et al. (2003) Ethylene insensitivity modulates ozone-induced cell death in birch (*Betula pendula*). *Plant Phys.* 132(1): 185–195.

Woo, H. R., et al. (2013) Plant leaf senescence and death – regulation by multiple layers of control and implications for aging in general. *J. Cell Sci*. 126(21): 4823–4833.

Woo, H. R., et al. (2019) Leaf senescence: Systems and dynamics aspects. *Annu. Rev. Plant Biol.* 70: 15.1–15.30.

Chapter 24

Christmann, A., and Grill, E. (2013) Plant biology: Electric defence. *Nature* 500: 404–405.

Goh, C.-H., et al. (2013) The impact of beneficial plant-associated microbes on plant phenotypic plasticity. *J. Chem. Ecol.* 39: 826–839.

Goodspeed, D., et al. (2012) Arabidopsis synchronizes jasmonate-mediated defense with insect circadian behavior. *Proc. Natl. Acad. Sci. USA* 109: 4674–4677.

Gough, C., and Cullimore, J. (2011) Lipo-chitooligosaccharide signaling in endosymbiotic plant-microbe interactions. *Mol. Plant Microbe. Interact*. 24: 867–878.

Kelner, A., et al. (2018) Dual color sensors for simultaneous analysis of calcium signal dynamics in the nuclear and cytoplasmic compartments of plant cells. *Front. in Plant Sci*. 9: 245.

Lolle, S., et al. (2020) Plant NLR-triggered immunity: from receptor activation to downstream signaling. *Curr. Opin. Immunol*. 62: 99–105.

Markmann, K., and Parniske, M. (2009) Evolution of root endosymbiosis with bacteria: how novel are nodules? *Trends Plant Sci*. 14: 77–86.

Martin, R. (2020) Structure of the activated ROQ1 resistosome directly recognizing the pathogen effector XopQ. *Science* 370(6521). DOI: 10.1126/science.abd9993.

Toyota, M., et al. (2018) Glutamate triggers long-distance, calcium-based plant defense signaling. *Science* 361(6407): 1112–1115.

van Dam, N. M. (2009) How plants cope with biotic interactions. *Plant Biol*. 11: 1–5.

Wang, J., et al. (2019) Reconstitution and structure of a plant NLR resistosome conferring immunity. *Science* 364(6435): 1–11.

Yoshida, S., et al. (2016) The haustorium, a specialized invasive organ in parasitic plants. *Annu. Rev. Plant Biol.* 67: 643–647.

Index

Page numbers in *italic* type indicate that the information will be found in an illustration or table.

A

AATAAA sequence, *82,* 84
AB14 gene, 456
ABA. *See* Abscisic acid
ABA INSENSITIVE 1 and 2, 526
ABA-8′-hydroxylases, 126
Abaxial, 7, *8,* 549
Abaxial–adaxial leaf polarity, 551–553, 563
ABC model of floral organ identity, 617–618
ABC proteins. *See* ATP-binding cassette membrane transporters
ABCB proteins (auxin transporters)
  auxin efflux and, 130
  auxin regulation of axillary bud outgrowth and, 569
  gravitropism and, 530, *531*
  mechanisms regulating, 131
  plant nastic movements and, 523
  polar auxin transport in seedlings, 527, *528*
  root hair development and, 522
  shoot phototropism and, 537, 538
ABCE model of floral organ identity, 618–620
ABCG transporters, 127–128
ABI proteins, 655, 705, *706*
Abietic acid, *729*
Abiotic stress
  acclimation and adaptation, 445–446
  beneficial effects of plant microbiota and, 451–452
  cross-protection, 451
  definition of stress, 444
  effects of combined stresses, 450–451
  hypersensitive response-type programmed cell death, 693, *694*
  interactions with biotic stress, 451
  overview and significance of, 443–444
  overview of major environmental stresses, 447–450
  plant adjustments in the recovery from, 469–470
  protective physiological and developmental mechanisms, 460–470
  reactive oxygen species and, 446–447
  responses to (*see* Abiotic stress response)
  stress matrix, 451
  trade-offs between reproductive and vegetative growth, 445
Abiotic stress response
  epigenetic mechanisms, 456–459
  hormonal interactions and the regulation of, 459–460
  plant adjustments in the recovery from, 469–470
  protective physiological and developmental mechanisms, 460–470
  signal transduction pathways activated, 453–460
  stress-sensing mechanisms, 452–453
  trade-offs between reproductive and vegetative growth, 445
ABP1. *See* AUXIN-BINDING PROTEIN1
Abronia
  A. umbellata, 750
  A. villosa, 599
Abscisic acid (ABA)
  abiotic stress responses, 459
  auxin-regulated ABA signaling in roots, 526
  breaking of seed dormancy, 511, 512
  chemical structure, *115*
  fruit ripening in strawberry, 663
  functions, 117–118
  LEA/DHN/RAB protein family and, 463
  leaf senescence and, 707
  mobilization of starch endosperm, 515, 516
  movement within the plant, 127–128
  plant development and, 114
  primary locations of receptors, *106*
  regulation of root-to-shoot ratio, 469, *470*
  root hydrotropism, 534, *535*
  seed dormancy, 509, 510–511
  seed maturation, 655
  signal transduction pathway, 138–139
  stomatal closure, 113, *118,* 186, *239,* 240, 466–467, *468*
  synthesis and homeostatic regulation, 125–126
  water deficit-induced accumulation of, 447
  water deficit-mediated stomata development, 558
ABSCISIC ACID INSENSITIVE (ABI) proteins, 655, 705, *706*
Abscission, 691, 709–713
Abscission zone, 709, *710,* 711–713
Absorption spectra
  of chlorophyll, 249–250, *251*
  compared to action spectra, *252*
  defined, 249–250
  of other photosynthetic pigments, *251*
  photoreceptors, 478, *479, 480*
Acacia, 551
ACC. *See* 1-Aminocyclopropane-1-carboxylic acid
ACC oxidase (ACO), 124, 461, 662
ACC synthase (ACS), 124, 460, 461, 662, 663, *706*
Accessory buds, *572,* 573
Accessory fruit, 656
Accessory pigments, 251–252
Acclimation
  abiotic stress and signaling pathways altering gene expression, 453–459
  adjustments in the recovery from stress, 469–470
  aerenchyma, 461–462
  antioxidants and ROS scavenging, 462, *463*
  chelation and phytochelatins, 465–466
  cryoprotectants and antifreeze proteins, 466
  defined, 325–326
  definition and description of, 445, 446
  hormonal interactions and, 459–460
  of leaves to sun and shade environments, 325–326
  membrane lipid alterations, 463–464, *465*
  molecular chaperones and molecular shields, 462–463, *464*
  osmotic adjustment, 460–461
  phenotypic plasticity, 467–469, *470*
  stress response pathways and, *452*
  stress-response regulons and, 455, *456*
  to toxic ions, 464–465
  water stress and ABA-induced stomatal closure, 466–467, *468*
Acer, 506
  A. pseudoplatanus, 593
Acetaldehyde, *382, 383,* 385
Acetate, 386, 437
Acetoacetyl-ACP, 409
Acetobacter, 428
  A. diazotrophicus, 430
Acetolactate synthase gene, 97, *98*
Acetosyringone, *94*
Acetylation, of histones, 84, *85,* 86
Acetyl-CoA
  bioengineered photorespiratory bypass pathways, 296
  conversion of storage lipids into carbohydrates, *412,* 413
  fatty acid biosynthesis, 407, 409
  malic enzyme reaction, *391*
  metabolic regulation of pyruvate dehydrogenase, *402*
  sulfur assimilation, *436*
  tricarboxylic acid cycle, 389, 390
Acetyl-CoA carboxylase, 409, 679
N-Acetylglucosamine, 26
O-Acetylserine (OAS), *436,* 437–438
O-Acetylserine (thiol)lyase, *436,* 438
Achenes, *506,* 656, 657
Acid growth, 63–64
Acid rain, 435
Acids, in ripening fruit, 661
ACO. *See* ACC oxidase
Aconitase, *412,* 413
Aconitate, 396, *397*
ACP. *See* Acyl carrier protein
Acropetal transport, 128
ACS. *See* ACC synthase
ACS7 protein, 707
Actin
  defined, 32
  dynamic equilibrium in the cell, 32–33
  myosins and cytoplasmic streaming, 34, 36
  See also Actin microfilaments; Filamentous actin
Actin capping protein, 113
Actin microfilaments
  ABA-induced stomatal closure in response to water stress, 467
  chloroplast movements in response to light, 329–330
  cytoplasmic streaming, 34, 36

defined, 32
modulation by phosphatidic acid, 113
plant cell structure, *16*
polarity and treadmilling, 32–33
pollen tube tip growth, 636, *637,* 638
Actin related protein 2/3 (Arp 2/3), 32, *33*
Actinorhizal plants, 428, 430–431
Action potentials, 146–147
Action spectra
compared to absorption spectra, *252*
defined, 252
photoreceptors, 477–478, *479, 480*
for photosynthesis, 252–253
Activation loop, 138
Activators, 83
Active transport
chemical potential and, 218
defined, 218
primary active transport, 226
proton transport and membrane potential, 222–223
secondary active transport, 226–227
Acyl carrier protein (ACP), 407, 409–410, 411
Acyl hydrolases, 111, *112*
Acyl-ACP, 407, 409, 410
Acyl-CoA, 410
Acyl-CoA:DAG acyltransferase, 411
N-Acyltransferase, 431
Adaptation, 445–446
Adaxial, 7, *8,* 549
Adaxial–abaxial leaf polarity, 551–553, 563
Adenine base editors, 98
Adenine deaminase, 98
Adenine nucleotide transporter, 396, *397*
Adenosine diphosphate (ADP)
actin microfilaments and, 32
C_4 photosynthesis, *299,* 301
carbon mobilization in land plants, *306*
cytokinin synthesis, 123
dynamic regulation of respiration, 401
metabolic regulation of pyruvate dehydrogenase, *402*
mitochondrial ATP synthesis, 395
mitochondrial transmembrane transport, 396, *397*
phosphate assimilation, 438
photorespiration, 291, *292–293*
Adenosine monophosphate (AMP)
C_4 photosynthesis, *299,* 301
starch degradation, 310, *311*
Adenosine triphosphate (ATP)
actin microfilaments, 32
ammonium assimilation, 424
biological nitrogen fixation, 434
C_4 photosynthesis, *299,* 300–301
Calvin–Benson cycle, 282, 283, *284–285,* 285
cytokinin synthesis, 123
dynamic regulation of respiration, 401
energy costs of nutrient assimilation, 417
glycolysis, *383,* 384
H^+-ATPase and, 222–223
membrane transport proteins, 228–230
mitochondrial respiration in photosynthesis, 403
modifying plant respiration and, 404
motor proteins and cytoplasmic streaming, 34, 36
photorespiration, 291, *292–293, 294,* 295
protein kinases, 107
role in respiration, 379
starch degradation, 310, *311,* 312
sucrose biosynthesis, *313,* 314, *315, 316*
sulfate assimilation, 436
synthesis (*see* ATP synthesis)
Adenosine-5′-phosphosulfate (APS), 436–437, 438
S-Adenosylmethionine, 124, 438
Adenylate kinase, *299,* 301
Adhesion, 155–156
ADP/ATP transporter, 396, *397*
ADP-glucose, *306,* 308, *309,* 310
ADP-glucose pyrophosphorylase (AGPase), 308, *309,* 312, 372
ADP-glucose transporter, 312
ADP:O ratio, 394, *395,* 396
Advective flow, 358
Adventitious buds, 587
Adventitious resin ducts, 729–730
Adventitious roots
defined, 573
description of, 567
eudicot root systems, 577
gravity-independent auxin transport, 526, *527*
Aegilops tauschii, 91
Aerenchyma, 404, 405, 461–462
Aerobic respiration
definition and overview, 379–382
glycolysis, 382–385
overall equation for, 380, 382
oxidative pentose phosphate pathway, 386–388
oxidative phosphorylation, 391–402 (*see also* Oxidative phosphorylation)
oxygen assimilation, 439
in plant biosynthetic and redox networks, 400–401
regulation at multiple levels, 401–402
total ATP yield, 396, *398*
tricarboxylic acid cycle, 388–391
Aeroponics, 193–194
Aerosols, 190
Aeschynomene, 429
Aesculus hippocastanum (horse chestnut), *572*
African elephants, 342
African prickly pear (*Opuntia stricta*), 305
After-ripening treatment, 511, 512
AGAMOUS (*AG*) gene
ABC model of floral organ identity, 617
ABCE model of floral organ identity, 619, 620
a floral organ identity gene, 616–617
a MADS box gene, 619
AGAMOUS-LIKE1-3 (*AGL1-3*) gene, 617
Agave, 303, 305, 727
A. americana, 714, *715*
A. weberi, 727
AGC kinases, 107–108, 131, 132
AGCVIII protein kinases, 538
Aggregate fruits, 657
AGL1-3 gene, 617
Aglycone, *732*
AGO. *See* ARGONAUTE protein
Agonistic interactions, 147
AGPase. *See* ADP-glucose pyrophosphorylase
AGPs. *See* Arabinogalactan proteins
Agriculture
apomixis and future crop improvement, 647
commercial manipulation of fruit ripening, 664
cytoplasmic male sterility, 642–643
fertilizers, 189, 190, 191, 200–201
foliar application of nutrients, 202
hydroponics and aeroponics, 193–194
impact on mycorrhizas, 211
nitrogen-use efficiency, 190
water and agricultural productivity, 153, *154*
wheat seeds, 626–627
See also Cereals; Crop plants
Agrobacterium, 90–91
A. tumefaciens, 93–94, 708, *709*
AHK. *See* ARABIDOPSIS HISTIDINE KINASE proteins
AHP. *See* ARABIDOPSIS HISTIDINE PHOSPHOTRANSFER proteins
AINTEGUMENTA (*ANT*) gene, 582
Air seeding, 180
Air space volume, of leaves, 182
Alanine, *299,* 300, 301, *427*
Alanine aminotransferase, *299,* 301
Albuminous cells, 15
Albumins, 516, *517*
ALCATRAZ (*ALC*) gene, 659
Alchemilla vulgaris (lady's mantle), *174*
Alcohol dehydrogenase, *383,* 385
Alcoholic fermentation, *383,* 385, 404
Aldehyde, 362, *363*
Alders, 428
Aldolase, *284–285,* 312, *313, 383*
Aleurone grains. *See* Protein storage vacuoles
Aleurone layer
Arabidopsis seed structure, *648,* 649
cereal seed structure, *648*
defined, 508
description and functions of, 652
development of starchy endosperm, 650
mobilization of starch endosperm, 515–516
programmed cell death, 516
structure of, *515*
Alfalfa (*Medicago sativa*)
action spectrum of phototropism, *480*
exogenous seed dormancy, 509
leaf movements and light energy absorption, 330
phytoalexins, *747*
rhizobial symbiont, *429*
Algae
chloroplast movements in response to light, 329
endosymbiosis and chloroplasts, 276
See also Green algae
Alkaloids, 738
Allantoic acid, *363,* 435
Allantoin, *363,* 435
Allard, Henry, 597–598
Allelopathy, 721, 749
ALLENE OXIDE CYCLASE 1 (*AOC1*) gene, 708
ALLENE OXIDE SYNTHASE (*AOS*) gene, 708
Allium, 185
A. cepa, 185
Allocation, 371–372, 376
Allopolyploidy, 78–79
Allotetraploidy, *79, 80*
Alonsoa warscewiczii (mask flower), *354*
Alternate phyllotaxis, 547
Alternation of generations, 5–7, 625–626
Alternative oxidase, 393–394, 398–399, 404
Aluminates, 202
Aluminum, 193, 202, 204
Alveolar cells, 649, 650
Amaranthus retroflexus, 440
Amide exporters, 435
Amino acid transporters, 231
Amino acids
ammonium assimilation, 424, *425,* 426
biosynthesis, 426–427
as compatible solutes, 461
phloem loading, 353
in phloem sap, 361, 362, *363,* 364
Amino group, amino acid biosynthesis, 427
1-AMINO-CYCLOPROPANE-1-CARBOXYLATE SYNTHASE 7 (ACS7), 707
1-Aminocyclopropane-1-carboxylic acid (ACC), 124, 128, 585
5-Aminolevulinic acid, *277*
Aminotransferases, *425,* 426

Ammonia
  biological nitrogen fixation, 417, 419, 434, 435
  conversion to organic forms, 435
  NH_3–H^+ symporters, 230
  nitrogen biochemical cycle, 419
  nitrogen fertilizers and climate change, 190
  nitrogen fixation, 418
  soil pH, 204
Ammonia transporters, 230
Ammonification, *418, 419*
Ammonium
  adsorption by soil particles, 203
  assimilation of, 424–426
  biological nitrogen fixation, 417, 419
  metabolic regulation of pyruvate dehydrogenase and, *402*
  modified Hoagland solution, 195
  nitrate assimilation, 417, 420, 421–422
  nitrogen biogeochemical cycle, *418*
  photorespiration, 291, *292–293,* 294, 295
  root absorption, 208
  soil pH, 204
  toxicity, 419, *420,* 424
Ammonium nitrate, 201, 417
Ammonium transporters, 230
Amorphous silica, 192, 197
Amphisome, 28
Amplitude, of circadian rhythms, 595, *596*
AmSEP3B gene, *616*
AMT1 transporters, *420*
Amthor, J. S., 404
Amygdalin, *732*
α-Amylase inhibitors, 736
Amylases
  gibberellin-mediated production, 141
  mobilization of endosperm starch, 514, 516
  regulation of starch metabolism, 312
  starch breakdown, 310, *311*
  starch synthesis, *309,* 310
  α-amylase, 141, 514, 516
  β-amylase, 514
Amylopectin
  degradation of, 310
  starch degradation at night, 310, *311*
  structure and synthesis, 307–310
Amyloplasts
  conversion of chloroplasts into, 31
  definition and functions of, 30
  gravitropism, 529–532
  mobilization of starch in, 515–516
  oxidative pentose phosphate pathway, 386
  in starchy endosperm, 515
  storage of starch, 514
Amylose, 307–310
Anabaena, 428, 429
Anaerobic stress, 448–449
Anammox, *418*
Ananas comosus (pineapple), 303, 613
Anaphase
  meiosis, *77,* 78
  mitosis, *39,* 40
Anaplerotic reactions, 391
Anchored proteins, *17,* 18
Androecium, 626
Angiosperms
  annuals, biennials, and perennials, 714, *715*
  companion cells, *14,* 15
  composition of lignin, 68
  defined, 4
  embryogenesis (*see* Embryogenesis)
  fruit development and ripening, 656–664
  life cycle, *6,* 7, *626*
  photoreversible responses induced by phytochrome, *481*
  phototropin genes, 495
  pit membranes, *175*
  in plant evolution, 4, *5*
  pressure-flow model of phloem translocation, 357–361
  root exodermis, 207
  seed structure, 506–508
  shoot branching and architecture, 568–573
  sieve elements and phloem characteristics, 347–348, *350*
  sieve tube elements and sieve tubes, 14
  tension wood, *104,* 585
  xylem cell types, 174, *175,* 176
Animal diets, carbon isotope ratio and, 342
Anion channels
  ABA-induced stomatal closure in response to water stress, 466, *468*
  overview, 225
  xylem loading, 242
Anion exchange capacity, 203–204
Anion transporters, 233–234
Anions
  diffusion potential, 220
  observed and predicted concentrations in pea root tissue, *221,* 222
  transport into the vacuole, 238
Anisotropic growth, 59–60, *550,* 551
Annexins, 453
Annual plants, 445, 714
Anoxygenic photosynthesis, 259
ANT gene, 582
Antagonistic interactions, 147
Antenna complexes
  energy transfer in photosynthesis, 253–254
  photosystem I, 268
  plant acclimation to shade, 326
  structure and function, 259–261
  thylakoid integral membrane proteins, 257
Antheraxanthin, 274, 328, 329
Anthers
  male gametophytes, 626, 627–630
  S locus and mechanisms of self-incompatibility, 644–647
  structure and development, *627*
Anthocyanins
  fruit ripening, 660, *661*
  mineral deficiencies, 196, 197
  nutritional quality of fruit, 664
Antibiotic resistance genes, 93, 94
Anticlinal divisions, 579–580
Antifreeze proteins, 466
Antioxidative enzymes (antioxidants), 462, *463*
Antipodal cells, *626, 631,* 632, *633, 634*
Antiport, 226, 227
Antiporters, 227, *229,* 230, 232, 233
Antirrhinum, 619, 620, *621*
  A. majus, 552, 620
Antisense strand, gene expression, 81, *82*
ANXUR 1 and 2 kinases, 638
AOC1 gene, 708
AOS gene, 708
AP1 gene. *See* APETALA1 gene
AP2 gene. *See* APETALA2 gene
AP2/Ethylene Responsive Factors, 686–687
AP3 gene. *See* APETALA3 gene
Apertures, in pollen cell walls, 629–630
APETALA1 (*AP1*) gene
  ABC model of floral organ identity, 617
  ABCE model of floral organ identity, 620
  activation in flowering, 608, *609,* 610, 613
  characteristics and functions of, *616*
  a floral meristem identity gene, 615, 616, 617
APETALA2 (*AP2*) gene, 615, 616, 617, 659
APETALA3 (*AP3*) gene, 616, 617, 619, 620
Aphids
  collecting phloem sap with, 362
  measuring phloem turgor pressure with, 360
  as phloem feeders, 733
  transfer of pathogens to plants, 741
Aphis nerii (milkweed aphid), 730, *731*
Apical cell, 670, 671, *672,* 673–674
Apical dominance, 569–571, *572*
Apical hook
  opening of, 519–520
  in seedling emergence, 517
  seedling photomorphogenesis and, 517, 518
Apical meristems, 10
  See also Root apical meristem; Shoot apical meristem
Apical–basal axis/polarity, 672–676
Apiose, *48*
Apocarotenoids, 118, 146, 661
Apomixis, 647, 687–688
Apoplast
  acidification in shoot phototropism, 538
  defined, 10, 240
  freezing stress and, 449
  impact of water deficit on, 447, *448*
  solute potential, 163
Apoplastic transport
  defined, 10
  of ions in roots and, 240, 241
  phloem loading, 351–354, 356, 357
  phloem unloading, 366, 368–369
  water movement in roots, 172, *173*
  water movement in xylem, 176
Apoptosis, 692–693
  See also Programmed cell death
Apple (*Malus domestica*)
  commercial manipulation of ripening, 664
  endogenous seed dormancy, 509
  gametophytic self-incompatibility, *646*
  length of juvenile period, *593*
  passive symplasmic phloem loading, 355–356
  seed stratification, 511, *512*
APS. *See* Adenosine-5′-phosphosulfate
APS kinase, *436,* 438
APS reductase, *436,* 437
APS sulfotransferase, *436*
Aquaporins
  defined, 165
  functions of, 235
  pressure-flow model of phloem translocation, 358
  regulation of, 235–236
  stomatal movements and, *239,* 240
  water movement across membranes, 165–166
  water movement in roots, 173
Aquatic grasses, 4n1
Arabidopsis
  apical hook formation, 519
  aquaporins, 235
  ARGONAUTE protein family, 88
  AtNHX1 antiporter gene, 232
  autophagy, 695–696
  auxin-induced cell wall acidification, 526
  auxin-mediated leaf initiation and, 547
  axillary bud suppression during monocarpic senescence, 716
  axillary meristem formation, 548–549
  bioengineered photorespiratory bypass pathways, 296

callose, 365
cation channels, 231–232
chloroplast movement and phototropin, 497, *498*
chloroplasts and light stress perception, 456
circadian clock and aging in, *707*
circadian oscillator, 597
circadian rhythms influencing inducible defenses in, 740, 741
combined effects of heat and water-deficit stress, 450
cryptochromes, 491, 492, 493
cytokinin and tissue culture, *117*
cytokinin receptors, 132
development of stomata, 556, 558
development of vascular cambium, 580–582
effects of catechin on gene expression in, 749
effects of ethylene on seedling growth, *519, 523, 524*
embryogenesis (*see* Arabidopsis embryogenesis)
establishment of adaxial leaf identity, 552
ethylene receptors, 133
ferritins, 235
flowering (*see* Arabidopsis reproduction)
forms of phytochrome in, 486–487
fruit (*see* Arabidopsis reproduction)
glycerolipid biosynthesis, 411
inducible plant defenses, 734
interactions of root thigmotropism and gravitropism, *533,* 534
leaf senescence regulation, 700–701
leaf transition from sink to source, 370–371
leaf venation and vein development, *559,* 561–563, 564
lignification, 68
male meiosis, *77*
membrane lipids and chill sensitivity, 411
mitochondria, *389*
multivesicular bodies, *27*
mutation and unmethylated transposons, *76*
omega-3 fatty acid desaturase mutants, 463
origin and development of lateral roots, 573–576
periderm formation in roots, *585*
phloem import in growing roots, 367
photorespiratory phenotype, 296
phototropins, 495–496, 497, *498,* 499–500
phytochrome and seed germination, 478, *479,* 485
phytochrome structure, 482
phytochrome-mediated morphogenesis, 489
phytohormones regulating leaf senescence, 707, 708, 709
polar auxin transport, 130, *528*
pollen (*see* Arabidopsis reproduction)
P-protein, 364
red and blue light inhibitors of stem elongation, 494
regulation of juvenile-to-adult phase changes, 593, 594
regulation of shoot gravitropic setpoint angles, *578*
repression of axillary bud outgrowth by strigolactones, 571
root hair development, 522
root initials, 543, *544*
root response to gravistimulation, *530*
root system architecture, 573
seedling growth of brassinosteroid mutants, 518, *519*
seeds (*see* Arabidopsis reproduction)
shoot CO_2 levels and nitrate assimilation, *440*
shoot meristemless mutant, 547
sieve plate pores, sieve tubes, and mass flow, *359,* 360
starch degradation, 310, *311*
starch production, 306
stomata development mutants, 555
sulfur assimilation, 438
synaptonemal complex, *78*
systemic defenses, 736, 737
transformation, 94
transport proteins, 224
transporter genes, 230
trichomes, 11, *12*
twisted dwarf mutant, 523
UV RESISTANCE LOCUS 8 photoreceptor, 477
vernalization, *610,* 611–612
whole plant responses to nitrogen deficiency, *210*
wuschel mutant, 546
xylem parenchyma, 242
xylem transport of nitrate, 422
YUCCA enzymes, 119, *120*
See also Arabidopsis thaliana
Arabidopsis embryogenesis
auxin signaling during, 680–682
establishment of apical–basal polarity, 672, 673–676
formation of the root and shoot apical meristems, *688*
mechanisms guiding, 676–677, 678–680
overview and stages in, 670, 671–672
Polygonum-type embryo sac, *633*
radial patterning during, 682–686
ARABIDOPSIS HISTIDINE KINASE (AHK) proteins, 132, *133, 134,* 708
ARABIDOPSIS HISTIDINE PHOSPHOTRANSFER (AHP) proteins, 132, *134, 584*
Arabidopsis lyrae, 641
Arabidopsis reproduction
ABCE model of floral organ identity, 618–619
autonomous endosperm development, 651
autonomous flowering pathway, 613
blue light and floral induction, 606
cellularization of the coenocytic endosperm, 648–649, *650*
CONSTANS protein and flowering in, 602, *603*
development of the fruit dehiscence zone, 658–659
double fertilization, 633, 641–642
epigenetic regulation of flowering time, 456–457
far-red light and floral induction, *606*
floral meristem identity genes, 615
floral meristems, 613–614
floral organ identity genes, 616–617
flower abscission, *710,* 711, 712–713
fruit set and parthenocarpy, 657, 658
induction of flowering by gibberellin, 612
initiation of floral organs in whorls, 614, 615
molecular mechanisms of flowering in natural environments, 604
nuclear-type endosperm development, 647, 648–649
ovule development, 620, 631–632
pollen cell walls, 629, 630
pollen grain activation, 635–636
pollen hydration, 635
pollen mother cells, 627
pollen tube growth, 636, 638, 639, 640, 641
Polygonum-type embryo sac, *633*
programic phase of reproduction, 633–634
regulation of flowering by florigen, 608–610
seed coat development, *653*
seed desiccation tolerance, 655
seed structure, *648*
tapetal cells, 630
ARABIDOPSIS RESPONSE REGULATOR (ARRs) proteins
cytokinin maintenance of the root apical meristem, 543, *544,* 545
cytokinin signaling transduction, 132–133, *134*
hydrotropism, 534–535
Arabidopsis thaliana
absence of mycorrhizas, 211
AtAHA2 H^+-ATPase, 236, *237*
Ca^{2+}-dependent protein kinases, 744
Cellulose Synthase A, 52
cytosolic invertase, 384
green-leaf volatiles, 739
ionomics, 200
nuclear genome, 19, 73–74
self-pollination, 633
XIUQUIs, 641
xyloglucan mutant, 65
ARABIDOPSIS THALIANA MERISTEM LAYER 1 (*ATML1*) gene, 683
Arabidopsis thaliana NAC-LIKE, ACTIVATED BY AP3/PI (AtNAP), 707
Arabinan, *53, 56,* 57, 58
Arabinogalactan proteins (AGPs), 49, *50, 56,* 57
Arabinose
arabinogalactan proteins, 49
in cell wall polysaccharides, *48*
glucoronoarabinoxylan, 54, *55*
pectins, 56
Arabinoxylan, 49, *53,* 54
Arachis (peanut), 435
Araucaria, 729
Arbuscular mycorrhizal associations, 208, 210–212, 723, 725
Arbuscules, 211, *212*
Archaeplastidae, 281
Archesporial cells, 627
ARFs. *See* Auxin response factors
Arginine, *427*
ARGONAUTE (AGO) protein, *87,* 88, 89
Arizona honeysweet, *336*
Arnold, William, 254
Arnon, Daniel, 270
ARRs. *See* ARABIDOPSIS RESPONSE REGULATOR proteins
Arsenic, 446, 465–466
Arsenic poisoning, 235
Arsenite, 235
Artemisia tridentata (sagebrush), 739
Articulated laticifers, 730
Artificial membranes, 223
Artificial somatic embryogenesis, 688
AS. *See* Asparagine synthetase
Asarum caudatum, 327
Asclepia curassavica (milkweed), 730, *731*
Ascomycota, 211
Ascorbate peroxidase, 273, 462, *463*
Ascorbic acid (ascorbate; vitamin C), 394, 401, 462, *463*
Asexual embryogenesis, 687–688
Asexual reproduction, 647
Asian lotus (*Nelumbo nucifera*), 509, 656
Asparagine, 422, *425,* 426, *427*
Asparagine synthetase (AS), *425,* 426
Asparagus, 426
Aspartate
ammonium assimilation, *425,* 426
asparagine biosynthesis, 426
biosynthetic pathway, *427*
C_4 photosynthesis, 298, 299, 300, 301

Aspartate aminotransferase (Asp-AT), *299,* 301, *425,* 426
Aspartic proteases, 516
Asp-AT. *See* Aspartate aminotransferase
Aspens, 573, *697*
Aspergillus nidulans, 480
Astragalus, 193
ASYMMETRIC LEAVES genes, 552
Asymmetry, in floral development, 620–621
AtAHA2 protein, 236, *237*
AtCO gene, *616*
ATG genes. *See* Autophagy-related genes
ATML1 gene, 683
Atmosphere (unit of pressure), *157*
Atmospheric carbon dioxide
  carbon isotope ratio, 340–342
  diffusion to the chloroplast, 334–336
  effect on shoot nitrate assimilation, 440
  effects of elevated global levels on photosynthesis and respiration, 338–340
  effects of elevated levels on plant respiration, 405
  evolution of C_4 plants, 337
  fertilizer production, 190
  fixation in the Calvin–Benson cycle, 282–290
  greenhouse effect, 338–339
  rising levels of, 334, *335*
  supply and demand analysis of photosynthesis, 322
Atmospheric nitrogen fixation, *418,* 419
AtMYB2 protein, 716
AtNAP protein, 707
AtNHX1 antiporter gene, 232
ATP sulfurylase, 436, 439
ATP synthase
  in chloroplasts, 29
  in mitochondria, 29
  mitochondrial electron transport chain, 394–396
  mitochondrial transmembrane transport and, 396, *397*
  oxidative phosphorylation, 381, *393*
  in photosynthesis, *262,* 263
  proton transport in mitochondria and chloroplasts, 223
  structure and function, 271–272
  thylakoid photosynthetic protein complexes, *258,* 259
  See also specific ATPases
ATP synthesis
  in anoxygenic photosynthesis, 259
  fermentation, 385–386
  glycolysis, 382, *383,* 384–385
  lipid oxidation and, 406
  mitochondrial electron transport, 394–396
  overview of plant respiration, 380
  oxidative phosphorylation, 381, 391–392, *393,* 394–396
  phosphate assimilation, 438
  photophosphorylation in the chloroplast, 270–273
  in photosynthesis, 254, *258,* 259, 272–273
  in plant respiration, 382
  proton motive force, 270–271
  substrate-level phosphorylation, *383,* 384–385
  total yield in aerobic respiration, 396, *398*
  tricarboxylic acid cycle, 381, 389, *390,* 391
ATPase, 270, 271–272
  See also ATP synthase
ATP-binding cassette (ABC) membrane transporters
  ABCG transporters, 127–128
  auxin efflux and, 130
  overview, *229,* 231
  See also ABCB proteins
ATP-dependent kinases, 699
ATP-dependent phosphofructokinase, 385, 402
Atrichoblasts, 521, 522
Atriplex, 301
  A. glabriuscula, 332
  A. triangularis, 327, 328
Aureochrome, *495,* 496
Autocrine effectors, 113
Autolysis, 692–693
  See also Programmed cell death
Autonomous flowering pathway, 592, 613
Autophagic body, 694, *695*
Autophagosomes, 27–28, 694, *695,* 698, 699
Autophagy
  definition and description of, 23, 693–694, *695*
  leaf senescence and, 696, 698–699
Autophagy-related (ATG) genes, 695, 696, *699*
Autophosphorylation, of phototropin, 496, *497*
Autopolyploidy, 78–79
Autotetraploidy, 79
Autotoxicity, 729
Autumn crocus, 79
Aux1 mutant, 130
AUX1 protein
  chemiosomotic model of auxin transport, *129,* 130
  fountain model of auxin transport, 527, *528*
  gravitropism, 529
  nutational growth in root seedlings, 523
  regulation of, 131
  root hair development, 522
AUX/IAA repressor protein. *See* AUXIN/INDOLE-3-ACETIC ACID repressor protein
AUXI/LAX auxin symporters, 129
Auxin
  abscission and, 711, *712*
  apical dominance and axillary bud growth, 569–571, 572
  biosynthesis, 119
  canalization model and leaf vein formation, 560–562, 563–564
  cell wall loosening and acid growth, 526
  chemical structure, *115*
  coleoptile bending response, 103, 114, *115*
  discovery of and early studies in, 103, 114, *115*
  embryogenesis and, 679–682
  establishment of adaxial leaf identity, 552–553
  formation of axillary meristems, 548
  forms of, 114
  fruit set and parthenocarpic fruits, 657–658
  gravitropism and, 526–529, 530–532
  homeostatic regulation, 120–121
  hormonal cross talk in abiotic stress responses, 460
  inhibition of fruit ripening in strawberry, 663
  interactions with ethylene in root growth, 524–525
  lag time for auxin-induced elongation, 525–526
  lateral root formation, 574, *575,* 576
  leaf initiation, 547–548
  leaf senescence, 709
  leaflet formation, 554
  maintenance of the root apical meristem, 543, *544,* 545
  methods of measuring plant auxin levels, *131*
  opening of the apical hook, 519
  phototropism and, 535–536, 537, 538
  PIN-FORMED efflux carrier proteins, 108
  plant development and, 114
  plant nastic movements, 523
  radial patterning during embryogenesis and, 684
  regulation of blade outgrowth, 553
  regulation of secondary growth, 584
  root hair development, 522
  root hydrotropism, 535
  root thigmotropism, 533
  seed coat development, 653
  seedling growth, 524–526
  synthetic auxins, 114
  vascular cambium development, 581–582
  See also Indole-3-acetic acid
Auxin clock model of lateral root formation, 574, *575,* 576
Auxin reporters, 128, 131–132
AUXIN RESISTANT 1. *See* AUX1 protein
Auxin response element (AuxRE), 141
Auxin response factors (ARFs)
  auxin maintenance of the root apical meristem, 543
  auxin signaling in embryogenesis, 679–680, 681–682
  auxin signaling pathways, 141, *142,* 144
  fruit set and parthenocarpy in tomato, 657–658
  hormonal cross talk in abiotic stress responses, 460
  leaf senescence, 709
Auxin signaling
  feedback regulation, 143–144
  inactivation of repressor proteins in, *140,* 141–143
  tissue-specific responses, 144
Auxin sink, 560
Auxin source, 560
Auxin transport
  chemiosmotic model of, 128–130
  fountain model of, 527–528
  plant nastic movements and, 523
  polar transport, 128–132 (*see also* Polar auxin transport)
  in roots, 522
Auxin transporters
  amino acid transporters and, 231
  hormonal cross talk in abiotic stress responses, 460
  root hair development, 522
  See also ABCB proteins; PIN-FORMED proteins
AUXIN-BINDING PROTEIN1 (ABP1), 121
AUXIN/INDOLE-3-ACETIC ACID (AUX/IAA) repressor protein
  auxin reporters and, 128
  auxin signaling during embryogenesis, 682
  degradation of in auxin signaling, *140,* 141, *142*
  regulation of, 143–144
  TMK1 and the repression of auxin signaling, 526
AuxRE. *See* Auxin response element
AuxSen reporter, 128
Avena sativa. See Oat
Avicennia, 405
Avocado seed, 654
Avogadro's number, 323
Avoidance, 445–446
Axillary buds
  defined, 10
  factors affecting dormancy in, 572–573
  hormonal regulation of outgrowth, 569–571, *572*
  nutrient deficiency response and, 572
  phyllotaxis, 573
  phytomeres and, 568
  shade avoidance response and, 572
  shoot branching and architecture, 567, 568
  stems, *8*
  suppression during monocarpic senescence, 716
Axillary meristems
  formation of, 548–549

formation of axillary buds, 568
hormonal regulation of outgrowth, 569–571, *572*
AXR4 protein, 131
Azolla, 61, 428, 429, 543
Azorhizobium, 428, *429*
Azospirillum, 428
Azotobacter, 428, 430

B

Bacillus, 428
B. subtilis, 725
B. thuringiensis (Bt), 100
Bacteria
anoxygenic photosynthetic bacteria, 259
bacteriophytochromes, 480
biological nitrogen fixation, 428–434
effects of soil pH on, 204
endosymbiotic theory, 80
pathogenic (*see* Pathogens; Plant pathology)
plant receptors and, 105–106
rhizobacteria, 725
two-component regulatory systems, 132, *133*
Bacteriochlorophylls
absorption characteristics of P870, 264
absorption spectrum of bacteriochlorophyll *a, 251*
molecular structure of bacteriochlorophyll *a, 251*
overview, 250
Bacteriophytochromes (BphPs), 480
Bacteroids, 434
BAK1. *See* BRI1-ASSOCIATED RECEPTOR KINASE1
BAK1/SERK co-receptors, 108, 557
Bakanae, 116
Bananas, 664
Banksia, 204
Bark, 10, *579,* 586
Bark beetles, 729
Bark storage proteins, 586
Barley (*Hordeum vulgare*)
after-ripening treatment of seeds, 512
aleurone layers, 652
gerontoplasts and leaf senescence, *698*
grain structure and germination, *515*
leaf air space volume, 182
lytic vacuoles, *27*
nitrogen compounds in xylem sap, *422*
phytochrome and flowering, 606
root absorption of calcium, 207
SD vernalization, 611
shoot CO_2 levels and nitrate assimilation, *440*
storage proteins, *517*
Barrel clover (*Medicago truncatula*), 654, 655, *724*
Basal angiosperms, 4
Basal cell, 670, 671, *672,* 673, 674
Base editing, 97–98
Basidiomycota, 211
Basipetal flow, 128
BASL protein, 558
BASS6. *See* Bile acid sodium symporter
Bassham, J. A., 282
Basswood, *347*
BDL protein, 682
Beal, W. J., 655–656
Beet armyworm (*Spodoptera exigua*), 733, 734
Beet seeds, 507
Beetles, 733
Beijerinckia, 428
BEL5 transcription factor, 375
Belemnite, 340
Benson, A., 282
Benzoxazinoids, 731
Benzyl cyanide, 739
Bermuda grass, *29*
Berries, 657
Berry, Joe, 321
Bertholletia excelsa (Brazil nut), *506*
BES1. *See* BRI1-EMS SUPPRESSOR1
Beta
B. maritima, 346
B. vulgaris, 346, 352, 374
Beta-conglutin, *517*
Betula, 511
B. pendula, 711
B. verrucosa, 593
Betulaceae, 211, 586
Betulin, 586
Beyer, Peter, 100
BF protein, 661
BFN1 protein, 693
bHLH leucine zipper (bHLH-LZ) proteins
cryptochromes, 493
DELLA degradation, 141
stomata development, 556, 558
Bi gene, 661
Bicarbonate
C_4 photosynthesis, 298, 299
crassulacean acid metabolism, 303, 304, 305
BICs, 492
Bieneertia, 299, 302
B. cycloptera, 300
Biennial plants, 714
BIFUNCTIONAL NUCLEASE 1 (BFN1) protein, 693
Bigtooth aspen (*Populus grandidentata*), *714*
Bile acid sodium symporter (BASS6), 291, *292–293*
BIN2. *See* BRASSINOSTEROID INSENSITIVE 2 protein
Biochemical model of C_3 photosynthesis, 321–322
Biochemical stress sensing, 452
Biofuels, 407
Biogeochemical cycles, nitrogen, 418–420
Biolistics, 94
Biological glasses, 655
Biological membranes, 15–18
See also Membranes; *specific biological membranes*
Biological nitrogen fixation
biotechnology and the future of agriculture, 430
conversion of ammonia to organic forms, 435
energy cost of, 417
free-living and symbiotic bacteria in, 428–429, 430
microanaerobic or anaerobic conditions, 429–430
nitrogen biogeochemical cycle, *418,* 419
nitrogenase enzyme and the energetics of, 434–435
overview, 427–428
See also Symbiotic biological nitrogen fixation
Biomass, cellulosic, 45
Biophysical stress sensing, 452
Biotechnology
Green Revolution, 190, 567
lipids and, 407
relevance of phloem translocation and signaling to, 376
See also Genetic engineering; Transgenes
Biotic interactions
with beneficial microorganisms, 723–725
herbivore interactions that harm plants, 725–732
inducible defenses to insect herbivores, 732–741 (*see also* Inducible defenses)
overview, 721–723
plant defenses against pathogens, 741–750 (*see also* Plant pathology)
Biotic stress
combined with abiotic stress, 451
stress-induce changes in gene expression, *458*
Biotrophic pathogens, 741
Bipinnate leaves, *549*
Birches (*Betula*), 511
1,3-Bisphosphoglycerate, 283, *284–285, 382, 383,* 384, 438
BITTER FRUIT (BF) protein, 661
Bitter (*Bi*) gene, 661
BITTER LEAF (BL) protein, 661
Bivalents, 78
BKI1. *See* BRI1-KINASE INHIBITOR1
BL protein, 661
Black mustard, *80*
Blackgum (*Nyssa sylvatica*), *714*
Blackman, F. F., 321
Bladderwort, 75
Blade
defined, 7, 549
establishment of abaxial–adaxial identity, 551–553
establishment of proximal–distal identity, 553–554
regulation of outgrowth, 553
Blade on Petiole (*BOP*) genes, *553,* 554
Bleaching, of chlorophylls, 264
Blue light
absorption by chlorophyll, 250
See also Blue-light responses
BLUE LIGHT SIGNALING 1 (BLUS1) protein kinase, 499–500, 538
Blueberries (*Vaccinium*), *661,* 739
BLUE-LIGHT INHIBITORS OF CRYPTOCHROMES (BICs), 492
Blue-light photoreceptors
cryptochromes, 491–493 (*see also* Cryptochromes)
overview, 477
phototropins, 477, 478, *480,* 490, 495–500 (*see also* Phototropins)
Blue-light responses
chloroplast movements, 329, 496–497, *498*
entrainment of the circadian clock, 597
flowering response in long-day plants, 606
kinetics and lag time, 490
overview, 490
phototropism, 478, *480,* 535, 536–538 (*see also* Phototropism)
solar tracking, 325
stomatal opening, 186, 239–240, 498–500
BLUS1 protein kinase, 499–500, 538
BODNELOS protein, 682, *688*
Bok choy, *80*
BOP genes, *553,* 554
Bordered pits, *15*
Boric acid, 235, 636
Boron
cellulose microfibrils and, 54
effects of soil pH on availability, *201*
functional roles in plant nutrition, 197
mobility within the plant, *196*
in plant nutrition, 192
plant tissue concentration, *191*
Boron deficiency, 195, 197
Boron transporters, 235, 242
Botanical fruit, 656
Boundary layer resistance, *181,* 182–183, 334, 335, *336*
Bowen ratio, 332
Boysen-Jensen, P., *115*
BR11 ASSOCIATED KINASE (BAK1)/SOMATIC EMBRYOGENESIS RECEPTOR KINASE (SERK) co-receptors, 108
Brace roots, 205, 577
Brachypodium, 559
Brachytic 2 (*BR2*) gene, *130*
Bracken (*Pteridium aquilinum*), *714*
Bracts, 549
Bradyrhizobium, 428, *429*
B. japonicum, 429
Branch meristems, root anatomy, *8*
Branch roots, 573
See also Lateral roots
BRANCHED FLORETLESS1 gene, *616*
BRANCHED (BRC) proteins, 571, 572

Branching
  gravitropic setpoint angle, 568, *569,* 577–578
  overview, 567
  root branching and architecture, 567, 573–578
  shoot branching and architecture, 568–573
Brassica
  B. canola, 517
  B. carinata, 80
  B. juncea, 80
  B. napus, 80, 118, *506,* 517, 659
  B. napus ssp. *napus,* 517
  B. nigra, 80
  B. oleracea, 80
  B. rapa, 80
Brassicaceae (cabbage family)
  absence of mycorrhizas, 211
  allopolyploidy, 79, *80*
  ovule development, 631–632
  root epidermis, 521
  sporophytic self-incompatibility and, 645
  See also Arabidopsis
Brassicales, 731–732
BRASSINAZOLE-RESISTANT 1 (BZR1), 136, *137, 138*
Brassinolide
  brassinosteroid signaling pathways, 136, *137, 138*
  chemical structure, *115*
  discovery of, 118
BRASSINOSTEROID INSENSITIVE 1 (BRI1) protein, 108, 136, *137, 138*
BRASSINOSTEROID INSENSITIVE 2 (BIN2) protein, 136, *137, 138*
Brassinosteroids
  chemical structure, *115*
  clam mutation, *76*
  functions, 118
  inhibition of root hair development, 522
  maize *nana1* mutant, *118,* 127
  mediation of brassinosteroid signaling by receptor-like kinases, 136–138
  movement within the plant, 128
  plant development and, 114
  primary locations of receptors, *106*
  propiconazole as a fungicide, 127
  seed dormancy and, 511
  suppression of photomorphogenesis in darkness, 518, *519*
  synthesis and homeostatic regulation, 126–127
Brassins, 118
Brazil nut (*Bertholletia excelsa*), *506*
BRC proteins, 571, 572
BRE. *See* TFIIB recognition element
Bread wheat. *See* Wheat
BREAKING OF ASYMMETRY IN THE STOMATAL LINEAGE (BASL) protein, 558
Breeding
  "bridge" crossing, 92
  inbreeding depression, 642
  marker-assisted, 91–92
  selective breeding of crop plants, 99
BRI1 protein. *See* BRASSINOSTEROID INSENSITIVE 1 protein
BRI1 SUPPRESSOR1 (BSU1), 136, *138*
BRI1-ASSOCIATED RECEPTOR KINASE1 (BAK1), 136, *137, 138,* 712, *713*
BRI1-EMS SUPPRESSOR1 (BES1), 136, *137, 138*
BRI1-KINASE INHIBITOR1 (BKI1), 136, *137, 138*
"Bridge" crossing, 92
Briggs, Winslow, 495
Bristlecone pine (*Pinus longaeva*), 714, 715
Broad bean (*Vicia faba*)
  amide forms of nitrogen, 435
  fatty acid composition of mitochondria, *465*
  mitochondria, *389*
  nitrogen compounds in xylem sap, *422*
  plastid development, *31*
  stomatal opening, *238*
  transfer cells and phloem loading, 353
Broccoli, *80,* 199
Bromeliaceae, 613
Broomrapes, 118
Broszczowia aralocaspica. See Suaeda aralocaspica
Brown plant hoppers, 739
BR-SIGNALING KINASES (BSKs), 136, *138*
Brucella abortus, 490
Bryophyllum, 599, 607, 612, 650–651
Bryophytes, 4, *5,* 7, *481,* 669
BSAS gene family, 438
BSKs. *See* BR-SIGNALING KINASES
BSU1. *See* BRI1 SUPPRESSOR1
Bt toxin, 100
Bud scales, 549
Bud scars, *572*
Bulbochaete, 24
Bulk flow
  larger-diameter leaf veins and, 559
  pressure-driven bulk flow in xylem, 176–177
  of soil water, 171
Bulliform cells, 330
Bundle sheath parenchyma, *8*
Bundle sheaths
  C_4 photosynthesis, 298–299, *300,* 301–302, 303
  cyclic electron flow and ATP synthesis, 273
  oligomer-trapping model of phloem loading, 354–355
  phloem in, 347
  phloem loading, *352*
Bünning, Erwin, 602
Burclover, 727
Buttercup (*Ranunculus repens*), *48, 347*
Butyryl-ACP, 409
BZR1. *See* BRASSINAZOLE-RESISTANT 1

C

C_3 photosynthesis
  biochemical model of, 321–322
  CO_2 supply and limitations on, 336–337
  evolution of C_4 photosynthesis and, 301
  factors limiting the rates of, 297
  as a function of leaf temperature, 332
  maximum quantum yield of, 327
  optimal temperature for, 303
  partitioning of assimilated carbon, 302–303
  photosynthetic thermal optimum, 333
  temperature sensitivity of photosynthetic efficiency, 333, *334*
  transport processes, 302–303
C_3 plants
  carbon isotope ratio, 340–341, 342
  carbon–nitrogen relations, 439
  effects of increasing atmospheric CO_2 levels on nitrate assimilation, 440
  transpiration ratio, 186
C_4 photosynthesis
  biochemical differences in mesophyll and bundle sheath cells, 302
  biochemical subtypes, 301
  CO_2 supply and limitations on, 337–338
  cyclic electron flow and ATP synthesis, 273
  definition and overview of, 297
  effects of elevated global CO_2 levels on, 339
  evolution of, 301, 337
  as a function of leaf temperature, 332
  in hot, dry climates, 303
  Kranz anatomy, 297–298, *300,* 301–302
  maximum quantum yield of, 327
  photorespiration and, 303
  photosynthetic thermal optimum, 333
  primary carboxylation products of, 297–298
  reactions of, *298,* 299–301
  regulation by light, 302
  single-cell C_4 plants, *300,* 302
  temperature sensitivity of photosynthetic efficiency, 333, *334*
  transport processes, 302–303
C_4 photosynthetic carbon fixation, 297–303, 439
C_4 plants
  carbon isotope ratio, 340–341, 342
  carbon–nitrogen relations, 440
  CO_2 levels and the evolution of, 301, 337
  cyclic electron flow and ATP synthesis, 273
  sodium deficiency, 198
  transpiration ratio, 186
C-14 reductase, 679
CA1P. *See* 2-Carboxy-D-arabintol 1-phosphate
Ca^{2+} exchangers, 110
Ca^{2+} pumps, 110
Ca^{2+} sensors, 109–110
Ca^{2+}-activated anion channels, 466, *468*
Ca^{2+}-activated TPC1/SV channel, 232
Ca^{2+}-ATPases, 233, 236
Ca^{2+}-binding protein kinases, 108
Ca^{2+}–CAM complexes, *453,* 454
Ca^{2+}–H^+ antiporters, 233
Cabbage family. *See* Brassicaceae
Cabbage looper (*Trichoplusia ni*), 740
Cacti (Cactaceae)
  CAM idling, 338
  cell water relations within stems, 164
  crassulacean acid metabolism, 303, 305
  spines, *726*
Cadmium, 449–450, 465–466
Caeliferins, *733,* 734
CAL gene, *616*
Calamagrostis epigeios (reed grass), *714*
Calcineurin-B like proteins (CBLs), 110
Calcium channels
  electrical signaling in systemic defenses, 738
  overview and types of, 225, *231,* 232
  plant R proteins, 744
  PRR-triggered immunity, *742,* 744
  second messenger functioning of calcium ions, 109
  stress-response pathways, 453
  stress-sensing mechanisms, 453
  systemic acquired acclimation, 456, *457*
Calcium deficiency, 195, 198
Calcium pectate, *233*
Calcium/calcium ions
  ABA-induced stomatal closure in response to water stress, 466, *468*
  activation of pollen grains, 635–636
  aerenchyma formation, 461–462
  Ca^{2+}-dependent pH changes, 111
  calcium sensors, 109–110
  carriers, 233
  in double fertilization, 641
  effects of soil pH on availability, *201*
  electrical signaling in systemic defenses, 737, 738
  electrostatic complexes, *233*

glutamate-initiated wound response, 373
gravitropism, 532, 533
hypersensitive response, 745
inducible plant defenses, 734
mechanisms excluding toxic ions, 465
mobility within the plant, *196*
observed and predicted concentrations in pea root tissue, *221,* 222
oxygen-evolving complex in photosynthesis, 265
in phloem sap, *362*
plant action potentials, 146, 147
in plant nutrition, *192,* 198
plant tissue concentration, *191*
pollen tube tip growth, 636, *637,* 638
PRR-triggered immunity, *742,* 744
regulation of NADPH oxidase, 111
root absorption of, 207
root hydrotropism, 534, *535*
root nodule formation, 432
root thigmotropism, 533, *534*
as a second messenger, 198
as second messengers, 109–110
in soils, 204
stomatal closure, *239,* 240
stress-response pathways, 453–454, 455
symbiotic biological nitrogen fixation, 723, *724*
systemic acquired acclimation, 456, *457*
Calcium/calmodulin-dependent protein kinases (CCaMKs), 110, 432
Calcium-dependent protein kinases (CDPKs)
ABA-induced stomatal closure in response to water stress, *468*
inducible plant defenses, 734
PRR-triggered immunity, *742,* 744
regulation of NADPH oxidase, 111
second messenger signaling, 110
stress-response pathways, *453,* 454, *455*
Calendula
C. officinalis, 607
C. vulgaris, 628
Caleosins, 515, 517
Callase, 628
Callose
composition, 49
in growing pollen tubes, 636
microspore cell walls, 627, 628, 629
PRR-triggered immunity, 744
sealing off of damaged sieve elements, 364, 365
Callose-hydrolyzing enzymes, 365
Calluna vulgaris (Scots heather), *714*
Callus, *117*
Calmodulin (CaM), 110, *453,* 454
Calmodulin-like proteins, 110
Calothrix, 428
Calvin, M., 282
Calvin–Benson cycle
C_4 photosynthesis, 298, 300, 301
carbon mobilization in land plants, *306*
crassulacean acid metabolism, 304, 305
definition and overview of, 282
induction period, 285–286
mechanisms regulating, 286–290
phases of, 282–283, *284*
photorespiration and, 291, *294,* 295
in plant respiration, *380*
reactions in, 283–285
CaM. *See* Calmodulin
CAM. *See* Crassulacean acid metabolism
CAM idling, 338
Camalexin, 747
Cambial initials, 579–580, *581*
Cambium, 10, *11*
See also Cork cambium; Vascular cambium
Cambium organizer, *581,* 582
Camellia sinensis, 13
Campanula medium (Canterbury bells), 599
Campestrol, 126
Canalization model, 560–562, 564
Canary grass, 114
Canna compacta (canna lily), 656
Cannabis sativa (hemp), 193
Canola (*Brassica napus* ssp. *napus*), 517
Canola oil, 407
Canopy
leaf angle and light absorption, 325
optimization of light absorption, 324–325
Canopy plant, 73
Canterbury bells (*Campanula medium*), 599
Capillarity
defined, 156
soil water, 170
soil–plant–atmosphere continuum and, 186–187
Capsidiol, *747*
Capsules, *6*
Carbohydrates
conversion of storage lipids into in germinating seeds, 411–413
juvenile-to-adult phase changes and, 593
percent of solar energy converted into, 323
in phloem sap, 361, 362, *363*
See also Photosynthate; Starch; Sugars
Carbon
allocation of fixed carbon, 371
carbon cycle of photorespiration, 294
carbon isotope ratio, 340–342
cell wall as a carbon reservoir, 45
fixation (*see* Carbon fixation reactions)
mobilization in land plants, *306*
oxidation in respiration, 380, 382
oxidative pentose phosphate pathway, 381
plant tissue concentration, *191*
See also Carbon reactions of photosynthesis
Carbon compounds
noncovalent bonds with cations, 233
plant mineral deficiencies and, 196–197
Carbon dioxide
activator and substrate of Rubisco, 287, *288*
bioengineered photorespiratory bypass pathways, 296
C_4 photosynthesis, 297–303
Calvin–Benson cycle, 282–290
CO_2 supply and limitations on photosynthesis, 336–338
conversion of storage lipids into carbohydrates and, *412,* 413
crassulacean acid metabolism, 303–305
diffusion to the chloroplast, 334–336
effect on photosynthesis in the intact leaf, 334–340
effect on plant respiration, 405
effect on stomata development, 558
fatty acid biosynthesis and, 409
overall chemical reaction for photosynthesis, 252, 254
overview of inorganic carbon-concentrating mechanisms, 297
photorespiration, 291, *292–293,* 294–295
production in fermentation, *383,* 385
production in glycolysis, *383*
production in respiration, 380, 382
production in the oxidative pentose phosphate pathway, 381, 386, *387*
production in the tricarboxylic acid cycle, 381, 390
respiratory quotient, 404
soil pH and, 204
specificity factor of Rubisco for, 294–295
stomatal closure, *239,* 240
supply and demand analysis of photosynthesis, 322
transpiration ratio and, 186
See also Atmospheric carbon dioxide
Carbon dioxide compensation point, 336, 337
Carbon fixation reactions
C_4 photosynthetic carbon fixation, 297–303
Calvin–Benson cycle, 282–290
carbon isotope ratio, 340–342
crassulacean acid metabolism, 303–305
defined, 247
location in the stroma, 257
overview, 254–255
overview of inorganic carbon-concentrating mechanisms, 297
photosynthetic light-response curves, 326–328
stomatal coupling of transpiration to photosynthesis and, 183
transpiration ratio and, 186
Carbon isotope ratio, 340–342
Carbon reactions of photosynthesis
accumulation and partitioning of photosynthates, 305–306
C_4 photosynthetic carbon fixation, 297–303
Calvin–Benson cycle, 282–290
crassulacean acid metabolism, 303–305
formation and mobilization of chloroplast starch, 306–312
interrelationship with the light reactions, *282*
overview, 281–282
overview of inorganic carbon-concentrating mechanisms, 297
oxygenation of Rubisco and photorespiration, 290–297
sucrose biosynthesis and signaling, 312–316
Carbonic acid, 234
Carbonic anhydrase, *298,* 299, 303
2-Carboxy-3-ketoarabinitol 1,5-bisphosphate, 283, *285*
2-Carboxy-D-arabintol 1-phosphate (CA1P), 287, *288*
Carboxylation
Calvin–Benson cycle, 283–284
carbon isotope ratio and, 341
Carboxylic acid, 384
Cardenolides, 730, *731*
Cardiac glycosides, 728–729
Cardiolipin, 389, *408, 410*
CArG-box, 619
Cargo domain, 34
Cargo proteins, 24
β-Carotene (vitamin A)
"golden rice," 100
in green algae and land plants, 4
molecular structure and absorption spectrum, *251*
ROS scavenging and, 462, *463*
Carotene desaturase gene, 100
Carotenoids
abscisic acid synthesis, 125
flavor volatiles, 661
fruit ripening, 660, *661*
functions of, 251–252
molecular structure and absorption spectrum, *251*
photoprotection, 273–274
strigolactone synthesis, 127

thylakoid pigment–protein complexes, 257
xanthophyll cycle, 328–329
Carpels
ABC model of floral organ identity, 617, 618
Class D genes and ovule formation, 620
female gametophytes, 626, 630–633
fleshy fruit development, 659
floral organ identity genes, 616–617
fruits and, *657*
initiation of, 614, 615
plant life cycle, 626
Quartet model of floral organ specification, *620*
valves, 631
Carriers
cation carriers, 232–233
definition and overview, *223,* 226
kinetic analyses of, 228
secondary active transport, 226–227
Carrots, 100
Caruncle, *507*
Caryopses, *506*
Cas9 protein, 96, 97–98
See also CRISPR-Cas9 technology
Caseinolytic protease (*Clp*) gene, 699
Casparian strip
defined, 14
formation of, 206–207
lignification, 69
root absorption of mineral ions, 207
transport of ions in roots, 241–242
water movement in roots, 172–173
CASPARIAN STRIP PROTEIN 1 (CASP1), 69
Cassava (*Manihot esculenta*), 732
Castasterone, 118
Castilleja chromosa (desert paintbrush), 599
Castor bean (*Ricinus communis*)
endospermic seeds, 508
gluconeogenesis, 385
phloem sap composition, *362*
protein storage vacuoles, *27*
seed anatomy, *507*
sieve elements and companion cells, *349*
CASTOR cation channel, *432*
Casuarina, 428
Catalase
antioxidative functions, 462, *463*
bioengineered photorespiratory bypass pathways, 296
in peroxisomes, 28
photorespiration, *29–293,* 291, 294
Catechin, 749
Caterpillars, 733
Catharanthus roseus, 109
Cation adsorption, 203
Cation exchange, 203
Cation exchange capacity (CEC), 203
Cation transporters
carriers, 232–233
channels, 231–232
Cation–H^+ antiporters, 232
Cations
diffusion potential, 220
noncovalent bonds with carbon compounds, 233
observed and predicted concentrations in pea root tissue, *221,* 222
Cauliflower, *80,* 199, *465*
CAULIFLOWER (*CAL*) gene, *616*
Cauline leaves, *614*
Cavitation, 157, 180–181
CBC. *See* CONVERGENCE OF BLUE LIGHT AND CO_2 proteins
CBL-interacting protein kinases (CIPKs), 110, 111
CBLs. *See* Calcineurin-B like proteins
CCA1. *See* CIRCADIAN CLOCK-ASSOCIATED 1 protein
CCAAT box, *82,* 83
CCaMKs. *See* Calcium/calmodulin-dependent protein kinases
CCGs. *See* Chlorophyll catabolic genes
CC-NLR proteins, 744–745
CDG1. *See* CONSTITUTIVE DIFFERENTIAL GROWTH1 protein
CDKs. *See* Cyclin-dependent protein kinase family
cDNA. *See* Complementary DNA
CDPKs. *See* Calcium-dependent protein kinases
Ceanothus, 428
CEC. *See* Cation exchange capacity
Celery, 13
Cell autonomous response, 105
Cell cycle
phases and overview of, 36–38
regulation of, *37,* 38
Cell dehydration
from freezing stress, 449
from water stress, 447, *448*
Cell division
anticlinal divisions, 579–580
in meristems, 10
periclinal divisions (*see* Periclinal divisions)
radial patterning during embryogenesis and, 682–686
in zygote polarization, 673–676
See also Meiosis; Mitosis
Cell expansion
acid growth, 63–64
cell wall stress relaxation, 62–64
cellulose microfibril orientation, 59–62
effects of ethylene on microtubule orientation, 523–524
effects of water deficit on, 166
factors influencing the extent and rate of, 62
leaf epidermal pavement cell model of, 63
mediation by expansins, 63–64
molecular models of cell walls and, 64–65
overview, 59
plant nastic movements, 522–523
role of cortical microtubules in, 60–62
structural changes accompanying the cessation of, 65–66
Cell plate, *39,* 40, 47
Cell volume
benefits of maintaining a positive turgor pressure, 166–167
changes in turgor pressure and, 163–164
osmosis and, 159
Cell wall invertases, 384
Cell wall polysaccharides, 26
Cell walls
abscission and, 709–713
acid growth, 63–64
acidification in shoot phototropism, 538
auxin and acid growth, 526
cellularization of coenocytic endosperm, 648–650
cellulose microfibrils, 50–53
changes in pH as second messengers, 110–111
cohesion–tension theory of xylem water transport, 178, *179*
components of primary and secondary walls, 48–50
cortical microtubules and cellulose orientation, 34
effects of ethylene on microtubule orientation and cell expansion, 523–524
factors influencing rate of expansion, 62
guard cells, 183–184, *185*
hemicelluloses, 54, *55*
importance in plant growth, development, and physiology, 46
layering of, *47*
matrix polysaccharides, 53–54
mechanisms of cell expansion, 59–66
of microspores, 627
molecular models of, 64–65
overview and description of, 7, *9,* 45
pectins, 56–58
phytoliths, 727
plasmodesmata, 7, *9,* 10
pollen grains, 629–630
PRR-triggered immunity, 744
reactive oxygen species, 111
receptor-like serine/threonine kinases, 109
remodeling during fruit ripening, 661
stress relaxation, 62–63
variability in structure and function, 46–48
water movement from leaf to atmosphere, 181
water movement in roots, 172, *173*
water status of plants, 163–164
xylem transport of water in trees, 178–179
yielding properties of, 62
See also Primary cell walls; Secondary cell walls
Cell-cell communication, in embryogenesis, 677–678
Cell-content insect feeders, 733
Cellobiose, *48*
Cells
ablation to produced male-sterile plants, 643
origin of new cells, 10, *11*
origin of term, 46
overview of cell structure, 7, *9,* 10
Cellularization, of coenocytic endosperm, 648–650
Cellulase, 711
Cellulose
allomorphs, 50
barrier to enzymatic attack, 51
binding of hemicelluloses to, 54
cellulosic biomass, 45
composition and functions, 49
macrofibrils, 51, *66,* 67
microfibrils (*see* Cellulose microfibrils)
molecular models of cell walls, 65
primary cell walls, 49, 50, *53*
secondary cell walls, 67
Cellulose macrofibrils, 51, *66,* 67
Cellulose microfibrils
boron and the alignment of, 54
cohesion–tension theory of xylem water transport, 178, *179*
effects of ethylene on microtubule orientation and cell expansion, 523–524
guard cells, 184
influence of cortical microtubules on the orientation of, 60–62
macrofibrils and, 51, *66,* 67
microfibril orientation and directionality of cell growth, 59–62
molecular models of cell walls, 65
orientation of cortical microtubules and, 34
secondary cell walls, *66,* 67
structure and allomorphs, 50–51
synthesis, 52–53
variability in width and degree of order, 51
Cellulose synthase, 52–53
Cellulose synthase A (CESA)
cellulose microfibril synthesis, 52, 53
cellulose synthesis in woody tissues, 67

influence of cortical microtubules on the orientation of, 60, *61,* 62
Cellulose synthase complexes, 52–53, 66, 67
Cellulosic biomass, 45
Centaurea maculosa (spotted knapweed), 749
Central cells
Arabidopsis, 631
double fertilization and, 626, 633–634, 641–642
formation of, 632
programic phase of reproduction, 633, 634
Central zone (CZ), 545, 546
Centromeres
chromosome organization in interphase, 76
definition and function of, 74
mitosis, 38, *39,* 40
prophase of meiosis, 78
Century plant (*Agave americana*), 714, *715*
CEP Receptors 1 and 2, 210
CEP1-mediated systemic nitrogen-demand signaling, 423
CEPs. *See* C-terminally Encoded Peptides
Cereals
aleurone layer, 652
caryopses, *506*
cellularization of the coenocytic endosperm, 649–650
embryonic structures, 508
endophytes, 430
grain yield as a function of water use, *154*
mobilization of endosperm starch, 514, 515–516
modification of shoot architecture in, 567
preharvest sprouting, 509–510
seed anatomy, 515
seed structure, *648*
starchy endosperm, 652
storage of starch in endosperm, 514
storage proteins, 516, *517*
Cerling, Thure, 340, 342
CESA. *See* Cellulose synthase A
CESA interactive protein 1 (CSI1), 62
CESA-like (*CSL*) genes, 53
Cestrum nocturnum (night-blooming jasmine), 599
CF_0-CF_1, 271–272
Chailakhyan, Mikhail, 607
Chalaza, 631, 632, *648*
Chalazal endosperm, 648, 649, *650*
Chalcone synthase, 90
Channels
cation channels, 231–232
definition and overview, *223,* 224–226, *229*
in xylem parenchyma, 242
See also specific channels and channel types
Chara, 34, 222
Charge-separated state, 263
Charpentier, Emmanuelle, 96–97
CHASE domain, 132, *134*
Checkpoint, cell cycle, 37
Chelates, 234–235
Chelation, 465–466
Chelators, 195
Chemical bonds, between cations and carbon compounds, 233
Chemical potential, 159, 218–219, 270
Chemiosmosis
chemiosmotic model of polar auxin transport, 128–130
mitochondrial ATP synthesis, 394–396
overview of the chemiosmotic mechanism, 394–395
photophosphorylation and, 270–271
Chemoattractants, 639, 640–641
Chemotaxis, 431, 639, 640–641
Chemotropic hypothesis of pollen tube growth, 639, 640–641
Chenopodiaceae, 211, 302
Chenopodium, 608
C. album, 484
Cherry plum (*Prunus cerasifera*), *211*
Chestnut oak (*Quercus montana*), *714*
Chewing insects, 733
Chiasmata, *77,* 78
Chilling sensitivity/stress
effects of, *448*
membrane lipids and, 411, 463–464, *465*
Chilling treatment, 511, *512*
Chilling-resistant plants, 464, *465*
Chilling-sensitive plants, 464, *465*
Chinese cabbage, *80*
Chitin-oligosaccharide deacetylase, 431
Chitin-oligosaccharide synthase, 431
CHL1 nitrate transporter, 423, *424*
CHL1/NRT1.1 gene, 230
Chlorate, 230
Chlorella pyrenoidosa, 254
Chlorenchyma, 302
Chloride
ABA-induced stomatal closure in response to water stress and, 466
observed and predicted concentrations in pea root tissue, *221,* 222
osmotic adjustment and, 460
oxygen-evolving complex in photosynthesis, 265
in phloem sap, *362*
pollen tube tip growth, 636, *637,* 638
in soils, 203
stomatal closure, *239,* 240
transport into the vacuole, 238
unloading from xylem parenchyma, 242
Chloride transporters, 233–234
Chlorine
mobility within the plant, *196*
in plant nutrition, *192,* 198
plant tissue concentration, *191*
Chlorine deficiency, 198
4-Chloro-IAA, 114
Chlorophyll *a*
absorption spectrum, *251*
abundance of, 250
antenna complexes, 260–261
biosynthesis, *277*
coordination complex with magnesium ions, 233
in green algae and land plants, 4, *5*
leaf senescence, *700*
molecular structure, *251*
Chlorophyll a/b antenna proteins, 260–261
Chlorophyll *b*
absorption spectrum, *251*
abundance of, 250
antenna complexes, 260–261
in green algae and land plants, 4, *5*
leaf senescence, *700*
molecular structure, *251*
Chlorophyll *b* reductase, *700*
Chlorophyll *c,* 250
Chlorophyll catabolic genes (CCGs), 700
Chlorophyll *d,* 250, *251*
Chlorophyll *f,* 250
Chlorophyllase, 276
Chlorophylls
absorption characteristics of PSI and PSII, 264
absorption spectra, 249–250, *251*
antenna complexes, 259–261
biosynthesis and breakdown of, 276, *277*
breakdown during leaf senescence, 698, 699–700
de-etiolation, 477–478
development from protochlorophyllide, 31
electron transfer by excited-state chlorophyll, 263–264
energy transfer between antennas and reaction centers, 253–254
fruit ripening, 660
light absorption and emission, 248–250
lowest excited state, 250
nonphotochemical quenching, 274
PSI reaction center, 268.269
role in photosynthesis, 247
sieve effect, 324
thylakoid pigment–protein complexes, 257
in thylakoids, 256–257
Chlorophytes, *481*
Chloroplast genome
base editing, 98
characteristics of plastid genomes, 80–81
non-Mendelian inheritance, 275
nuclear genes and the assembly of chloroplast proteins, 275–276
Chloroplast movement
overview, 32
phototropin-mediated, 496–497, *498*
phytochrome and, 487
to reduce absorption of excess light energy, 329–330
CHLOROPLAST UNUSUAL POSITIONING1 (CHUP1), 497, *498*
Chloroplastidae, 281
Chloroplasts
abiotic stress perception, 456
aminotransferases, 426
ATP synthase and proton transport, 223
bioengineered photorespiratory bypass pathways, 296
biosynthesis of glycerolipids, 410, 411
breakdown during leaf senescence, 698–699
Calvin–Benson cycle, 282–290
carbon mobilization in land plants, *306*
chlorophylls and photosynthetic pigments, 247, 250–252 (*see also* Chlorophylls)
conversion to chromoplasts in ripening fruit, 660
crassulacean acid metabolism, *304*
development from proplastids, 30–31
diffusion of carbon dioxide to, 334–336
effects of herbicides on, 269
endosymbiosis and the origin of, 276
fission, 31
growth in size, 31–32
guard cells, 11–12
jasmonate biosynthesis, 735
mechanisms of electron transport, 261–269, *270*
membrane lipids, 407, *410*
mesophyll cells, *12*
movement (*see* Chloroplast movement)
organization of antenna complexes, 259–261
organization of photosynthetic apparatus, 256–259
origin of photorespiratory enzymes, 295
oxidative pentose phosphate pathway, 386
phosphate assimilation, 438
photoassimilation, 439
photorespiration, 291, *292–293*
plant cell structure, *16*
proton transport and ATP synthesis, 270–273
quenching of, 273, 274
sieve effect, 324
starch metabolism, 305–312
structure and function, 29, *30,* 256–257
thylakoid reactions, 247–248
Chlorosis, 196, 197, 198, 199
Chlorphyllide *a, 277*
Cholodny-Went model, 526, 535, 536
Chorismate, 740
Chromatids
meiosis, 76–78

mitosis, 38, *39,* 40
structure, *19*
Chromatin, *16*
chromatin-regulated regulation of leaf senescence, *702,* 703, *704*
chromosome structure, *19*
condensation during mitosis, 20
defined, 20, 74
structure and types of, 74
vernalization of the *FLC* gene, 612
Chromatin Conformation Capture (3C), 76
Chromatium, 428
Chromophores
action spectra and, 252
of cryptochrome, 491–492
defined, 476
phytochromobilin, 481–482, 483
Chromoplasts, 30, 31, 660
Chromosome territory, 76
Chromosomes
centromeres, telomeres, and nucleolar organizer regions, 74–75
condensation during mitosis, 20
in diploid and haploid cells, 5
endoreduplication in starchy endosperm, 652
meiosis, 76–78
methods to produce polyploidy, 92
mitosis, 37, 38–40
nucleolus and ribosomal RNA genes, 20
organization in the interphase nucleus, 76
polyploidy, 78–80
structure, 19–20
teleomere shortening, 715
Chronic photoinhibition, 330, *331*
Chrysanthemum morifolium (florist's chrysanthemum), 593, 599, 601
Chrysanthemums, 569, 593, 599, 601
CHUP1, 497, *498*
Chymotrypsin, 736
CIB1, 493
Cicuta (hemlock plant), 728, *729*
Cicutoxin, 728, *729*
Cinchona, 586
trans-Cinnamic acid, 146
CIPKs. *See* CBL-interacting protein kinases
Circadian clock
axillary bud dormancy and, 573
clock hypothesis of photoperiodic timekeeping, 601–602
entrainment, 494
regulation by photoreceptors, 494–495
CIRCADIAN CLOCK-ASSOCIATED 1 (CCA1) protein, 706, *707,* 740
Circadian rhythms
characteristic features, 595–596
clock hypothesis of photoperiodic timekeeping, 601–602
defined, 594
endogenous oscillator, 594–595
entrainment, 595–596, 597
external coincidence model, 602
induction of flowering by far-red light in long-day plants and, 606
leaf senescence and, 705–706, *707*
phase shifting, *596,* 597
regulation of plant inducible defenses, 739–741
Circumnutation, 522–523, 538
Cis cisternae, 24–26
Cis-acting control elements, *82,* 83
Cis-elements, 86
*Cis*genics, 99
Cisternae
endoplasmic reticulum, 23
Golgi apparatus, 24–26
Citrate. *See* Citric acid
Citrate synthase, 389, *390,* 391
Citric acid (citrate), 195
conversion of storage lipids into carbohydrates, *412,* 413
iron chelates, 234–235
malic enzyme reaction, 391
mitochondrial transmembrane transport, 396, *397*
tricarboxylic acid cycle, 389, *390*
Citric acid cycle. *See* Tricarboxylic acid cycle
Citrulline, *363,* 435
Citrus, 593, 683, *726*
Cladodes, 338, 551
Cladogram, of land plants, 4, *5*
Clam mutation, *76*
Class A genes, *616,* 617–620
Class B genes, *616,* 617–620
Class C genes, *616,* 617–620
Class D genes, 617
Class E genes, *616,* 617–618
Class III Homeodomain-Leucine Zipper (HD-ZIP III) proteins
adaxial–abaxial leaf patterning, 552, *553*
formation of the shoot apical meristem, 687, *688*
patterning of the vascular cambium, 581–582
Clathrin, *25,* 26
CLAVATA proteins, 114, 546–547
CLAVATA3/Embryo Surrounding Region-Related (CLE) protein, 114, 547, 582, *583*
Clay soils
characteristics affecting water content and movement, 169, 170
hydraulic conductivity, 171
soil particle size, 203
CLC proton-nitrate antiporter, *420*
CLE protein. *See* CLAVATA3/Embryo Surrounding Region-Related protein
Clear zone, of pollen tubes, 636, *637*
Climacteric, 403, 662, 663
Climate change. *See* Global warming
Clock proteins, 144, *145*
Clonal communities, 714, 715
Clonal reproduction, 647
Clostridium, 428, 430
Clovers (*Trifolium*), *429,* 435, 509
Clp gene, 699
Clusia, 305
Cluster roots, 206
CLV3 locus, 659
CNGCs. *See* Cyclic nucleotide-gated channels
Cnr locus, 663, 664
CO protein. *See* CONSTANS protein
CO_2 compensation point, 336, 337
CO_2 RESPONSE SECRETED PROTEASE, 558
Coarse sand, 203
Coat-imposed dormancy, 508–509, 511
Coatomer I (COPI) protein-coated vesicles, 24, *25*
Coatomer type II (COPII) proteins, 24, 25
Cobalamin, 193
Cobalt/cobalt deficiency, 193
COBRA protein family, *67*
Cochliobolus carbonum, 743
Cocklebur (*Xanthium strumarium*)
grafting studies on the floral stimulus, 607
night length and floral induction, 600
nitrate assimilation, 422
photoreversible responses induced by phytochrome, *481*
phytochrome and flowering, 605
Coco de mer (*Lodoicea maldivica*), 507
Coconut (*Cocos nucifera*), *506*
Coding strand, gene expression, 81, *82*
Coenocytic endosperm
cellularization in *Arabidopsis,* 648–649, *650*
cellularization in cereals, 649–650
Coevolution, 721
Coffee bean (*Coffea*), *506*
Cohesins, 37, *38, 77*
Cohesion, 155, 156
Cohesion–tension mechanism of sap ascent
description of, 178, *179*
physical challenges in trees, 178–180
xylem cavitation and mechanisms to overcome, 180–181
COI1 protein. *See* CORONATINE-INSENSITIVE1 protein
Colchicine, 79, *91,* 92
Colchicum autumnale, 79
Cold stress
alteration of membrane lipids in response to, 463–464, *465*
stress-response regulons and acclimation, *456*
Coleoptile stage embryo, 671
Coleoptiles
auxin and, 524
blue light phototropism in maize, *477*
cereal seed structure, *648*
the Darwin studies of the bending response in, 103, 114, *115*
description and function of, 508
gravitropism, 528
lag time for auxin-induced elongation, 525–526
maize embryogenesis, 671
phototropism, 535, 536
seedling development in light or dark, 517, *518*
in seedling emergence, 517
Coleorhiza, *507,* 508, *648,* 671
Coleus blumei, 24, 354
Collard greens, *80*
Collection phloem, 346
Collenchyma, 13
Colorless non-ripening (*Cnr*) locus, 663, 664
Columella
Arabidopsis embryogenesis, 674
fountain model of auxin transport, 527
gravitropism, 529–533
origin of, 543, *544*
root cap and, 520
root thigmotropism, 533
Columella initials, 543, *544*
Commensalisms, 721
Common bean (*Phaseolus vulgaris*)
a day-neutral plant, 599
nitrogen compounds in xylem sap, *422*
rhizobial symbiont, *429*
root nodules, *428*
seed characteristics, 507
seed storage protein, *517*
uride forms of nitrogen, 435
Common coleus (*Coleus blumei*), 354
Common symbiotic pathway, 723, 725
Companion cells
defined, *14,* 15
phloem loading, 350–351, 351–357
phloem sap composition and, 364
in phloem tissue, 348, *349*
pressure-flow model of phloem translocation, *358*
structure and function, 350
transfer cells, 353–354
unloading and reloading of photosynthates during transport and, 357
Compatible solutes, 460–461
Complementary DNA (cDNA), 230
Complementation, 90
Complex I. *See* NADH dehydrogenase
Complex II. *See* Succinate dehydrogenase
Complex III. *See* Cytochrome bc_1 complex

Complex IV. *See* Cytochrome *c* oxidase
Complex V. *See* F_OF_1-ATP synthase
Compound fertilizers, 201
Compound leaves
  leaflet formation, 554–555
  types of, *549,* 550
Compound perforation plates, *175,* 176
Compression wood, *104*
Concentration, water potential and, 159, 160
Concentration gradients, diffusion and, 158
Concentration potential, 218
Condensed tannins, 652
Cones, *6, 7*
Conglutin, *517*
Conifer resin ducts, 729
Conifers
  bordered pit pairs, *175*
  defined, 4
  megastrobili and microstrobili, *7*
  tracheid pit membranes, *175,* 176, 177
  See also Pinus
Coniferyl alcohol, 67
CONSTANS (CO) protein
  flowering in long-day plants, 602–603
  gibberellin-induced flowering, 612
  mediation by FT protein in flowering, 608
  modulation by cryptochromes in flowering, 606
  molecular mechanisms of flowering in natural environments, 604
  photoperiodic flowering pathway, 613
Constitutive defenses
  defined, 722
  mechanical barriers, 726–728
  secondary metabolites, 728–732
CONSTITUTIVE DIFFERENTIAL GROWTH1 (CDG1) protein, 136, *138*
CONSTITUTIVE PHOTOMORPHOGENESIS 1 (COP1) protein
  inhibition of degradation by nuclear cryptochromes, 493
  phytochrome-induced photomorphogenesis, 489–490, 518
  stomatal formation, 558
  UV responses, 500, *501*
CONSTITUTIVE TRIPLE RESPONSE 1 (CTR1) protein, 133, *135,* 136
Contact angle, 156
CONVERGENCE OF BLUE LIGHT AND CO_2 (CBC) proteins, *499,* 500, *537,* 538
Convicilin, *517*
Coordination bonds, 233
Coordination complexes, 233
COP 9 SIGNALOSOME (CSN) complex, 489
COP1 protein. *See* CONSTITUTIVE PHOTOMORPHOGENESIS 1 protein
COPI protein-coated vesicles, 24, *25*
COPII proteins, 24, 25
Copper
  effects of soil pH on availability, *201*
  mobility within the plant, *196*
  in plant nutrition, *192,* 199
  plant tissue concentration, *191*
Copper deficiency, 199
Core promoter, 81–83
Core promoter elements, 82
Core symbiotic genes, 723, *724*
Cork, *579, 580,* 585–586
Cork cambium
  bark and, 586
  defined, 10
  production of periderm, 585–586
  production of phellem and phelloderm, 580
  secondary growth, 568, 579
Cork cells, 10
Cork oak (*Quercus suber*), 46, 586
Corn earworm (*Helicoverpa zea*), 734
Cornus florida (flowering dogwood), 404, *714*
CORONATINE-INSENSITIVE1 (COI1) protein, 141, 708, 735, *736*
Corpus, 546
Cortex
  bark and, 10
  differentiation of, 684–686
  ground tissue, 10
  root anatomy, *8, 241*
  root nodule formation and, 432–433
  root uptake of nutrients via mycorrhizas and, 211
  roots, 13–14
  secondary growth in roots and stems, *11*
  stem anatomy, *8*
  water movement through, 172, *173*
Cortical division site, 38
Cortical endoplasmic reticulum, 23
Cortical microtubules
  cytokinesis, 40
  mitosis, 38, *39*
  orientation of cell wall cellulose microfibrils and, 34, 60–62
  plant cell structure, *16*
Cortical–endodermal initials, 543, *544*
Cosuppression, 90
Cotton (*Gossypium hirsutum*), *164, 469*
Cottonwood, *180*
Cotyledons
  Arabidopsis embryogenesis, 671, *672,* 675
  food storage and, 647
  modification in cereal grains, 508
  seed anatomy, 506, 507
  in seedling emergence, 517
p-Coumaryl alcohol, 67
Cow pea, 734
CP7 protein, *265, 266*
CP12 protein, 289, *290*
CP43 protein, *265, 266*
Crassulaceae, 305
Crassulacean acid metabolism (CAM)
  carbon isotope ratio, 342
  CO_2 and photosynthesis, 338
  defined, 303
  facultative CAM plants, 304, 305
  pattern of stomatal opening and closing, 183
  reactions and phases in, 303–305
  regulation of PEPCase, 305
  sodium deficiency, 198
  transpiration ratio, 186
  versatility in response to environmental stimuli, 305
Crataegus, 104
Craterostigma plantagineum, 655
CRE1 protein. *See* CYTOKININ RESPONSE 1 protein
Creep, 63–64
Creosote bush (*Larrea tridentata*), *336, 714*
Cress, *476*
CRFs. *See* CYTOKININ RESPONSE FACTORs
CRISPR RNA (crRNA), 96
CRISPR-Cas9 technology
  description of, 95–97
  homology-directed repair and, 97, *98*
  prime editing and, *98,* 99
  production of the *RIN-KO* tomato mutant, 664
  tomato "domestication" and, 660
CRISPR-derived base editing, 98
Cristae, 29, 388, *389*
Critical day length, 598, *599*
Crop plants
  apomixis and future crop improvement, 647
  cytoplasmic male sterility, 642–643
  double fertilization and, 626–627
  effects of combined heat and water deficit stress, 450
  fertilizer application in response to mineral deficiencies, 200–201
  genetic engineering, 99–101
  hydroponics and aeroponics, 193–194
  introgression of wild relative genes, 91–92
  lipids and biotechnology, 407
  membrane lipids and chill sensitivity, 411
  modifying respiration in, 404
  organ abscission, 709
  phloem translocation and biotechnology, 376
  relationship of productivity to total seasonal light, 327
  selective breeding, 99
  uses of synthetic auxins, 121
  See also Agriculture; Cereals
Crop wild relatives (CWRs), 92
Crop Wild Relatives Project, 92
Cross talk, among stress-response pathways, 454–455
Cross-pollination, 633
Cross-protection, 451
Cross-regulation, 147
Crown gall, 93
Crown gall disease, 93
Crown roots, 576–577
CrRLK1 protein, 109, 638
CrRLK1-like RLKs, 109
crRNA. *See* CRISPR RNA
Cruciferins, *517*
Cry-Interacting bHLH1 (CIB1), 493
Cryoprotectants, 466
CRYPTOCHROME1 (CRY1)
  blue-light entrainment of the circadian clock, 597
  blue-light inhibition of stem elongation, 494
  developmental effects of, 492
  discovery of, 491
  flowering response in long-day plants, 606
  inhibition of COP1-induced protein degradation, 493
CRYPTOCHROME2 (CRY2)
  blue-light entrainment of the circadian clock, 597
  blue-light inhibition of stem elongation, 494
  developmental effects of, 492
  flowering response in long-day plants, 606
  inhibition of COP1-induced protein degradation, 493
CRYPTOCHROME3 (CRY3), 492
Cryptochromes
  bacterial proteins and, 106
  blue-light entrainment of the circadian clock, 597
  de-etiolation, 477–478
  developmental effects of cry1 and cry2, 492
  domain structure and conformational changes, 491–492
  flowering response in long-day plants, 606
  functions of, 477
  interactions with other photoreceptors, 493–495
  nuclear cryptochromes and photomorphogenesis, 493
  overview, 491
  photomorphogenic functions, 518
  photoperiodic flowering, 602
CSI1. *See* CESA interactive protein 1
CSN complex, 489
C-terminal extension (CTE) of cryptochrome, *491,* 492, 493

C-terminally Encoded Peptides (CEPs), 114, 210, 423
CTR1 protein. *See* CONSTITUTIVE TRIPLE RESPONSE 1
CUC transcription factors, *553,* 554
Cucumber (*Cucumis sativus*), 193, 490, *561,* 661
Cucumis
  C. melo, 354, 663
  C. sativus, 193, 490, *561,* 661
Cucurbita
  C. maxima, 349
  C. pepo, 172, 354, *365*
Cucurbitacins, 661
Cucurbitadienol synthase, 661
Cullin protein, *140,* 141, *142, 143*
CUP-SHAPED COTYLEDON (CUC) transcription factors, *553,* 554
Curly dock (*Rumex crispus*), 512
Cuscuta (dodder), 749, *750*
Cuticle
  a constitutive defense, 722
  leaf anatomy, *8*
  organ abscission, 712
  plant phenotypic plasticity in response to abiotic stress, 468
  water movement from leaf to atmosphere, *181*
Cyanelles, 281
Cyanide, 222–223, 732
Cyanide-resistant respiration, 393–394, 398–399
Cyanobacteria
  biological nitrogen fixation, 419, 428, 429
  endosymbiosis, 80, 276
  heterocysts, 429
Cyanobacterial phytochrome 1, *482,* 483
Cyanogenic glycosides, 732
Cyanohydrin, *732*
Cycads, 4, 7, 545
CYCLASE HISTIDINE KINASE ASSOCIATED SENSORY EXTRACELLULAR (CHASE) domain, 132, *134*
Cyclic electron flow, 272–273
Cyclic nucleotide-gated channels, 109, *231,* 232, 453
Cyclin-dependent protein kinase family (CDKs), *37,* 38, 107
Cyclins, *37,* 38
β-Cyclocitrical, 118
Cycloheximide, 525
CYCLOIDEA gene, 621
CYCLOPS protein, 432
Cynodon dactylon, 29
CYP. *See* Cytochrome P450 monooxygenase
Cypselae, *506*
Cyst nematodes, 748–749
Cysteine
  biosynthetic pathway, *427*
  methionine biosynthesis, 438
  phytochelatins, 465–466
  protein modification and, 109
  ROS signaling, 111
  sulfate assimilation, 417
  sulfur assimilation, *436,* 437–438
Cysteine linkages, 23
Cysteine protease, 736
Cytidine deaminase, 98
Cytochrome b_6f complex
  cyclic electron flow, 273
  location in the thylakoid membrane, 257, *258*
  mechanisms of electron transport, 266–268
  structure of, *267*
  Z scheme electron transport, 261, *262,* 263
Cytochrome b_{559}, 264
Cytochrome bc_1 complex, 392, *393*
Cytochrome *c,* 392, *393,* 394
Cytochrome *c* oxidase, 392, *393,* 394, *395*
Cytochrome *f,* 266
Cytochrome P450, 127
Cytochrome P450 monooxygenase (CYP), *123,* 126
Cytokinesis, 38, *39,* 40, 78
Cytokinin oxidases, 124
Cytokinin receptors, 132, *134*
CYTOKININ RESPONSE 1 (CRE1) protein, 132, *133, 134,* 684
CYTOKININ RESPONSE FACTORs (CRFs), 708–709
Cytokinins
  abiotic stress responses, 459
  chemical structure, *115*
  compound leaf development, 555
  discovery of, 116
  functions, 116–117
  leaf senescence, 708–709
  maintenance of the root apical meristem, 543, *544,* 545
  maintenance of the shoot apical meristem, 547
  movement within the plant, 128
  plant development and, 114
  plant response to nitrogen deficiency, 210
  primary locations of receptors, *106*
  radial patterning during embryogenesis, 684
  regulation of apical dominance and axillary bud growth, 569, 571, 572
  regulation of secondary growth, 584–585
  root hydrotropism, 534–535
  signal transduction pathway, 132–133, *134*
  symbiotic biological nitrogen fixation, 723, *724*
  synthesis and homeostatic regulation, 123–124
  tissue culture, 116, *117*
Cytoplasm
  cell division, 38, *39,* 40
  defined, 7
  gravitropism and cytoplasmic pH, 532–533
  plasmodesmata, 7, *9,* 10
Cytoplasmic genomes, 80–81
Cytoplasmic male sterility, 398, 629, 642–643
Cytoplasmic streaming, 34, 36
Cytorrhysis, 162
Cytosine base editors, 97–98
Cytosine methylation, 84, *85*
Cytoskeleton
  ABA-induced stomatal closure in response to water stress, 467
  defined, 32
  microtubule and microfilament elements, 32–34, *35*
  motor proteins and cytoplasmic streaming, 34, 36
Cytosol
  ABA-induced stomatal closure in response to water stress, 466–467, *468*
  changes in pH as second messengers, 110–111
  defined, 7
  osmotic adjustment, 460–461
  oxidative pentose phosphate pathway, 386
  phytochrome signaling, 483
  plant cell structure, *16*
  sucrose synthesis, 312–316
Cytosolic invertase, 384
Cytotoxic S-ribonuclease (S-RNase), 646–647
CZ. *See* Central zone

D

D1 protein, 264, 265, *266,* 275
D2 protein, 264, *265, 266*
D6 PROTEIN KINASE (D6PK), 108, 538
D6PK AGC kinase, 131, 132
Dahlia pinnata, 346
Damaged-associated molecular patterns (DAMPS), 742, 743, 744
β-Damascenone, 661
DAMPS. *See* Damaged-associated molecular patterns
Danaus plexippus (monarch butterfly), 730, *731*
Dark reactions. *See* Carbon reactions of photosynthesis
Darnel ryegrass (*Lolium temulentum*), 606
Darwin, Charles, 114, *115,* 522, 535, 641
Darwin, Francis, 114, *115,* 522, 535
Date palm (*Phoenix dactylifera*), 653–654, 656
Datisca, 428
Day length
  critical day length, 598, *599*
  latitudinal gradient in, 597, *598*
  photoperiodism, 597–606 (*see also* Photoperiodism)
Day-neutral plants (DNPs), 599
DCL proteins. *See* DICER-LIKE proteins
DCMU, 269, *270*
Debranching enzymes, *309, 311*
Deciduous trees, seasonal leaf senescence, 697
Decrease in dna methylation (*ddm1*) mutation, *76*
Decussate phyllotaxis, 547
DEEPER ROOTING (DOR) transcription factors, 578
De-etiolation, 477–478, 486, 494
Defensins, 640
DEFH genes, *616*
Deficiency zone, 199–200
DEFICIENS gene, 619
Deforestation, rising levels of atmospheric carbon dioxide and, 334
Dehiscence zone, 658–659
Dehiscent fruits, 657, 658–659
Dehydrins (DHNs), 463, 655
Dehydroascorbate reductase, 462, *463*
Deinococcus radiodurans, 480
DELLA proteins
  gibberellin signaling, *140,* 141, *143,* 144, *145*
  gibberellin-induced flowering, 612
  parthenocarpy, 658
  proteasome-dependent degradation, *140*
Denitrification, *418, 419*
D-enzymes, *309,* 310, *311*
Deoxy sugars, *48*
Deoxyribonucleic acid (DNA)
  basic steps in gene expression, 20, *21*
  chromatin, 74
  chromosome structure, 19–20
  cytoplasmic genomes, 80–81
  editing, 95–99, 97, *98*
  endoreduplication, 37–38, 652
  epigenetic modifications and gene expression, 84, *85*
  genetic engineering and (*see* Genetic engineering)
  meiosis, 76–78
  methylation (*see* DNA methylation)
  mitosis, *37,* 38–40
  Quartet Model of floral organ identity, 619–620
  repair pathways, 97, *98*
  replication in the cell cycle, 36, 37–38
  RNA polymerase II and transcription of protein-coding genes, 81–83
  teleomere shortening, 715
5-Deoxystrigol, *127*
Dephosphorylation, phytochrome signaling and, 488–489
Depolarization. *See* Membrane depolarization
Dermal tissue, *8,* 10, 11–12
Derxia, 428
Desaturase enzymes, 410
Desert paintbrush (*Castilleja chromosa*), 599
Desert sand verbena (*Abronia villosa*), 599
Desiccation tolerance, 653–656
Desmotubules, *9,* 10, 240
Determinate growth, 614
Developmental programmed cell death, 693, 696
"Dewdrops," 174
DHNs. *See* Dehydrins

Dhurrin, *732*
2,4-Diacetylphloroglucinol, 725
Diacylglycerol (DAG), 113, *406,* 410, 411
Diacylglycerol kinases, 113
Diaheliotropism, 325, 467
Diakinesis, *77,* 78
Diarch vascular tissue, 573, *574*
Diazotrophs, 428–434
DIBOA, *731*
Dicamba, 114, 121
Dicarboxylate transporter, 303, 396, *397*
DICER-LIKE (DCL) proteins, 86, *87,* 88, 89
2,4-Dichlorophenoxyacetic acid (2,4-D), 114, 121
Dichlorophenyldimethylurea (DCMU), 269, *270*
Dichogamy, 642, *643*
DICHOTOMA gene, 621
Dichotomous branching, 568
Dieffenbachia, 727
Diel rhythms, 594, 602
Differentiation
  in embryogenesis, 682–683, 684–686 (*see also* Embryogenesis)
  histogenesis and, 670
Diffuse growth, 59–60
Diffusion
  of carbon dioxide to the chloroplast, 334–336
  definition and description of, 157–158
  effectiveness over short distances, 158–159
  of soil mineral nutrients to roots, 208
  transport of ions across membrane barriers, 219–222
  See also Passive transport
Diffusion coefficient (D_s), 158
Diffusion potential, 220, 222
Diffusional resistance, 182–183
Digalactosyldiacylglycerol, *408, 410*
Digitalis (foxglove), 728–729
Digitoxin, 728–729
Dihydroxyacetone phosphate
  Calvin–Benson cycle, *284–285*
  glycolysis, *383,* 384
  interconversion, 302
  structure, *382*
  sucrose biosynthesis, 312, *313,* 314
Dihydrozeatin, 123
DII domain-based reporters, 680
DII-Venus auxin reporter, 128
Dimethylallyl diphosphate (DMAPP), 123
3-Dimethylsulfoniopropionate (DMSP), *461*
Dimorphic sperm cells, 642
2,4-Dinitrophenol, 396
Dioecious plants, *7*
Dionaea muscipula, 104, 146–147
Dioxygenase of auxin, 120
Diphosphatidylglycerol, 389, *408, 410*
Diploids (2N)
  defined, 5
  meiosis, 78
  plant life cycles, 5–7
Diplotene, *77,* 78
Directed organelle movement, 34, 36
Dirigent-domain proteins, 69
Disaccharides, 655
Dispersed repeats, 74
Disproportionating enzymes. *See* D-enzymes
Distal regulatory promoter sequences, 83
Disulfide bonds (disulfide bridges), 111, 435
Dittmer, H. J., 205
Diuron, 269, *270*
DIVARICATA (*DIV*) gene, 620, 621
DMSP, *461*
DNA methylation
  gene expression and, 84, *85*
  regulation of transposons, *75,* 76
  RISC-bound siRNAs, 88
  RNAi pathway and the resetting of epigenetic marks, 89
  stress-induce changes in gene expression, *458*
DNA synthesis phase (S phase), 36, *37,* 38
DNA transposons, 75
DNPs. *See* Day-neutral plants
Dodder (*Cuscuta*), 749, *750*
Dolichol diphosphate, 26
Domains, of genes, 92
DOR transcription factors, 578
Doritaenopsis, 338
Dormancy
  defined, 670
  factors affecting axillary bud dormancy, 572–573
  See also Seed dormancy
Dormancy cycling, *510*
Double fertilization
  defined, 626
  programic phase of reproduction, 633–634
  stages in, 633–634, 641–642
Double-stranded RNA (dsRNA), 86–90
Double-stranded RNA-binding domain protein (dsRBP), 86
Doudna, Jennifer, 96–97
Downstream promoter element (DPE), 82
DR5 promotor-based reporters, 128, 680
Drosophila
  CRY proteins and the circadian clock, 597
  diel rhythms, 594
  homeotic genes, 616
Drought
  CAM photosynthesis, 338
  defined, 447
  physiological processes affected by, 166
  xylem cavitation, 177, 180–181
Drought tolerance, 164
Drupes, 657, 659
dsRBP. *See* Double-stranded RNA-binding domain protein
dsRNA. *See* Double-stranded RNA
Dual–day length plants, 599
Duckweed, 4, *330*
"Dumb cane," 727
Dumbell-shaped guard cells, 184
Dwarf plants, 116
DWARF4 gene, *76*
Dynamic photoinhibition, 330, *331*

E

E1 ubiquitin-activating enzyme, 139, *140*
E2 ubiquitin-activating enzyme, 139, *140,* 141
E3 ubiquitin ligase complexes, 106
Early endosome compartment, 26
EARLY FLOWERING 3 (ELF3), 494–495
EBF1/2 mRNAs, *135,* 136
EC1 protein, 642
ECA1, 534, *535*
Echeveria (*Echeveria harmsii*), 599
Ecosystem productivity, importance of water, 153, *154*
Ectomycorrhizas, 210, 211, 212, 213
Ectopic, 683
o,o EDDHA, 195
EDTA, 195
EEL protein, 705, *706*
Effectors
  definition and description of, 742–743
  effector-triggered immunity, 741, *742,* 744–745
  parasitic nematodes, 748–749
  plant R proteins and, 744–745
Effector-triggered immunity (ETI)
  definition and description of, 741, *742,* 744–745
  hypersensitive response, 745–746
Egg
  plant life cycles, 5, *6*
  uniparental inheritance of cytoplasmic genomes, 81
Egg apparatus, 632–633
Egg cells
  angiosperm life cycle, *626*
  Arabidopsis, 631
  double fertilization, 633, 641–642
  formation of, 626, 632
  programic phase of reproduction, 633, 634
  syngamy, 626
EGTA, 533, 745
Egyptian cotton leafworm (*Spodoptera littoralis*), 737
80S ribosomes, 20
EIL. *See* ETHYLENE-INSENSITIVE LIKE
EIN2. *See* ETHYLENE-INSENSITIVE 2
EIN2 ASSOCIATED PROTEIN 1(ENAP1), *135,* 136
EIN3. *See* ETHYLENE-INSENSITIVE 3
Electrical potential, 218, 220–221
Electrical signaling, 146–147, 737–738
Electrochemical potential, 219
Electrochemical proton gradient
  chemiosmotic mechanism of mitochondrial ATP synthesis, 395–396
  mitochondrial transmembrane transport, 396, *397*
  uncouplers, 395–396
Electrogenic pumps
  membrane potential and proton transport, 222–223
  primary active transport, 226
  vacuolar proton pumps, 237–238
Electrogenic transport, 226
Electromagnetic spectrum, *248*
Electron transport
  artificial electron acceptors, 254
  in photosynthesis (*see* Photosynthetic electron transport)
  in respiration (*see* Mitochondrial electron transport)
  similarity of photosynthetic and respiratory electron flow, *272*
Electronegativity, of water, 154, *155*
Electroneutral transport, 226
Electrostatic bonds, 233
Electrostatic complexes, *233*
ELF3. *See* EARLY FLOWERING 3
Elf18, 744
Elicitors, 733–734
ELONGATED HYPOCOTYLY5 (HY5), 492
Elongation zone
  definition and description of, 206–207, 542, *543*
  fountain model of auxin transport, 527–528
  lateral root formation, 574, *575*
  root hydrotropism, 534
Embolism, 15, 177, 180–181
Embryo dormancy, 509
Embryo lethal mutants, 678
Embryo rescue, 92
Embryo sac
  Arabidopsis, 631
  double fertilization, 641–642
  plant life cycles, *6*
  Polygonum-type development, 632–633
  programic phase of reproduction, 633–634
Embryogenesis
  alternate pathways of, 687–688
  autonomous development of endosperm, 651
  autophagy, 696
  auxin signaling during, 680–682
  establishment of apical–basal polarity, 672–676
  formation of root and shoot apical meristems, 686–687
  introduction and overview, 669–670
  mechanisms guiding, 676–680
  in monocots and eudicots, 670–672
  radial patterning during, 682–686
  somatic embryogenesis, 650–651

Embryophytes, 4, *5,* 669
Embryos
  Arabidopsis seed structure, *648*
  cereal seed structure, *648*
  embryogenesis (*see* Embryogenesis)
  glassy state, 655
  plant life cycles, 6
Emerson, Robert, 254
EMS. *See* Ethylmethanesulfonate
ENAP1. *See* EIN2 ASSOCIATED PROTEIN 1
Endocarp, 659, *660*
Endocrine hormones, 113
Endocytosis, 23, 26
Endodermis
  defined, 14
  formation and differentiation of, 206–207, 683, 684–686
  periderm formation in roots and, *585,* 586
  prevention of gas bubbles from entering xylem, 180
  root anatomy, *8, 241*
  secondary growth in roots, *11*
  transport of ions in roots, 241–242
  water movement in roots, 172–173
Endogenous dormancy, 509
Endogenous oscillator
  clock hypothesis of photoperiodic timekeeping, 601–602
  description of, 594–595
  entrainment, 595–596, 597
  external coincidence model, 602
  phase shifting, *596,* 597
Endoglucanases, 53, 54
Endomembrane system
  endoplasmic reticulum, 23–24
  functions, 15
  Golgi apparatus, 24–26
  oil bodies, 28
  organelles derived from, 15
  overview and functions of, 23
  peroxisomes, 28–29
  plasma membrane recycling, 26
  protein synthesis, 20, *21,* 22
  sequestration of auxin, 121
  vacuoles, 27–28
Endonucleases, 692
Endophytes, 430
Endoplasmic reticulum (ER)
  autophagy, 694, *695*
  biosynthesis of auxin, 119
  biosynthesis of glycerolipids, 410–411
  biosynthesis of triacylglycerols, 407
  cytokinesis, 40
  cytokinin signaling pathway, 132, *134*
  cytoplasmic streaming, 34
  endomembrane system, 15
  ethylene signaling pathway, 133, *135,* 136
  florigen, 608, *609*
  Golgi apparatus, 24
  lipid composition of membranes, *410*
  mitosis, 38, *39*
  oil bodies, 28
  phragmoplast, 40
  plasmodesmata, *9*
  protein glycosylation, 26
  protein synthesis, 20, *21,* 22
  root hydrotropism, 534
  sequestration of auxin, 121
  structure and function, 23–24
  vacuoles, 28
Endoplasmic reticulum Ca^{2+}-ATPase (ECA1), 534, *535*
Endopolyploidy, 78
Endoproteases, 516
Endoreduplication, 37–38, 652
Endosomes
  endomembrane system, 15
  motor proteins and cytoplasmic streaming, 34
  plasma membrane recycling, 26
Endosperm
  Arabidopsis seed structure, *648*
  cereal seed structure, *648*
  description of, 508
  double fertilization and formation of, 626, 633–634 (*see also* Endosperm development)
  mobilization of starch in cereals, 515–516
  protein storage vacuoles, *27*
  regulation of seed coat development, 652–653
  seed anatomy, *507*
  storage of starch in, 514
Endosperm development
  aleurone layer, 652
  cellularization of coenocyctic endosperm in *Arabidopsis,* 648–649, *650*
  cellularization of coenocyctic endosperm in cereals, 649–650
  imprinted gene expression and, 651–652
  independent of embryogenesis, 650–651
  overview, 647–648
  starchy endosperm, 652
Endospermic seeds, 507, 508
Endosymbiosis, 15, 276, 281
Endosymbiotic theory, 80
Endothecium, 627
Endothelium, 652
Enediol, 283, *285,* 287
Energy conversion efficiency, of photosynthesis, 255–256
Energy transfer, by chlorophyll, 250
Engelmann, T. W., 252–253
English ivy (*Hedera helix*), 592, *593, 714*
English oak (*Quercus robur*), *593*
ENHANCED EM LEVEL (EEL), 705, *706*
ENHANCED SUBERIN 1 (ESB1), 69
Enhancers, 83
Enolase, *383*
Enolpyruvalshikimate-3-phosphate synthase (EPSPS), 99–100
Ent-kaurene, 121, *122*
Entrainment
  circadian clock, 494
  circadian rhythms, 595–596, 597
  molecular mechanisms, 597
Entropy
  diffusion and, 157–158
  osmosis and, 159
Envelope membranes, of chloroplasts, *256,* 257
EPF. *See* EPIDERMAL PATTERNING FACTOR
EPF-like peptides, 557, 559
Ephedra, 4
Epicormic buds and branches, 586–587
Epicotyls, 522–523
EPIDERMAL PATTERNING FACTOR (EPF), 108, 557, *558,* 559
Epidermal–lateral root cap initials, 543, *544*
Epidermis
  cell expansion in leaf pavement cells, 63
  defined, 10
  development of root hairs, 521–522
  development of stomata, 555–559
  leaf light absorption, 323–324
  leaves, 11–12
  mechanical barriers to herbivores, 726–727
  of microsporangia, 627
  organ abscission, 712
  origin of, 683
  origin of root hairs, 12
  periderm formation in roots, *585*
  plant nastic movements, 522–523
  roots, *8, 241,* 543, *544*
  secondary growth in roots and stems, *11*
  stem anatomy, *8*
  sun and shade leaves, *322*
  types of cells in, 555
Epigenetic modifications
  acetate and, 386
  adaptations to abiotic stress, 456–459
  in gene expression, 84–86
  imprinted gene expression, 651–652
  RNAi pathway and the resetting of epigenetic marks, 89
  vernalization and, 611–612
Epigenetic stress sensing, 452
Epinasty, 117
EPITHIOSPECIFYING SENESCENCE REGULATOR (ESR), 703, *704*
EPSPS. *See* Enolpyruvalshikimate-3-phosphate synthase
Equilibrium, distinguished from steady state, 221
Equilibrium potential, 222, 225
Equisetaceae, 192, 197
Equisetum, 521
  E. hyemale, 727
ER. *See* Endoplasmic reticulum
ERECTA protein, 557, 559
ERECTA-like protein, 557
ERF1 protein, 136
Erica carnea (spring heath), *714*
ER–plasma membrane contact sites, 23
Eruca (mustard), *518*
Erwinia uredovora, 100
Erythrose 4-phosphate, *284–285, 387,* 388
Escape from photoreversibiltiy, 484
ESCRT proteins, *27*
ESR protein, 703, *704*
Essential elements
  definition and overview of, 191–193
  effects of soil pH on availability, *201*
  heavy metals and the mimicking of, 449–450
  leaching in soils, 201
  mineral deficiencies, 195–202 (*see also* Mineral deficiencies)
  mobility within the plant, *196*
  plant tissue concentrations, *191*
Ethanol
  fermentation, *383,* 385
  structure, *382*
  surface tension, *156*
Ethylation, of nucleotide bases, 90
Ethylene
  abscission, 711, *712*
  aerenchyma formation, 461–462
  chemical structure, *115*
  discovery as a plant hormone, 117
  effect on microtubule orientation and lateral cell expansion, 523–524
  fruit ripening, 662, 663, 664
  functions, 117, *124*
  hormonal cross talk in abiotic stress responses, 460
  inducible plant defenses, 735
  induction of flowering, 613
  leaf senescence, *706,* 707
  movement within the plant, 128
  nutational growth in root seedlings, 523
  opening of the apical hook, 519, 520
  plant development and, 114
  primary locations of receptors, *106*
  regulation of secondary growth, 585
  root growth, 524–525
  root hair development, 521
  root nodule formation, 433
  seed dormancy, 511
  signal transduction pathway, 133, *135,* 136
  starchy endosperm cell death, 652
  synthesis, 124–125
ETHYLENE BINDING FBOX 1 and *2* (*EBF1/2*) mRNAs, *135,* 136

ETHYLENE RECEPTOR 1 (ETR1), *135,* 711
Ethylene receptors, 133, *135,* 136, 711
ETHYLENE RESPONSE FACTOR1 (ERF1), 136
Ethylenediamine-N,N′-bis (o-hydroxyphenylacetic) acid (*o,o* EDDHA), 195
Ethylenediaminetetraacetic acid (EDTA), 195
ETHYLENE-INSENSITIVE 2 (EIN2), 133, *135,* 136, 702–703
ETHYLENE-INSENSITIVE 3 (EIN3), 133, *135,* 136, 705, *706*
ETHYLENE-INSENSITIVE LIKE (EIL) protein, 133, *135*
Ethylene-response factor group VII transcription factors, 453
Ethylmethanesulfonate (EMS), 90
ETI. *See* Effector-triggered immunity
Etiolated shoots, 517, 518, *519*
Etiolation, ethylene and, 117
Etioplasts, 30–31
ETR1. *See* ETHYLENE RECEPTOR 1
Eucalyptus, 587
Eucalyptus regnans, 177–178, 717
Euchromatin, 20, 74
Eudicots
  chelators, 195
  major group among angiosperms, 4
  overview of embryogenesis in, 670, 671–672 (*see also* Embryogenesis)
  in plant evolution, *5*
  reticulate leaf venation, 559
  root system architecture, 205, 206, 573, 577
  seedling photomorphogenesis, 517–518, 519–520
  transition to secondary growth, 579
Eukaryotic pathway, of glycerolipid biosynthesis, 410–411
"Eukaryotic" protein synthesis, 20
Euphorbia, 13
  E. pulcherrima, 601
European ash (*Fraxinus excelsior*), *714*
European beech (*Fagus sylvatica*), *593, 714*
Evaporation
  cohesion–tension theory of xylem water transport, 178, *179*
  evaporative heat loss, 331, 332
Evolution
  of C_4 photosynthesis, 301, 337
  endosymbiosis and the evolution of chloroplasts, 276
  of photosystems, 276
  reciprocal plant–insect evolution, 741
  transposons and, 75
Exclusion, 463
Exine, 629, 630
Exocarp, 659, *660*
Exocyst, 26
Exocytosis, 23, 53
Exodermis, 207, 211, 242
Exogenous dormancy, 508–509, 511
Exogenous RNAs, RNAi pathway and, 87–88, 89
Exons, *82*
Exonucleases, 86
Exoproteases, 516
Expansins, 64, 65, 526, 712
Explosives, 417
Export, in phloem translocation, 351
External coincidence model of flowering, 602–604
External phloem, 347
Extracellular space, 240
  See also Apoplast
Extrafloral nectaries, 739

F

F_1, 395
Fabaceae
  biological nitrogen fixation, 428
  P-proteins, 364
  See also Legumes
FACE experiments. *See* Free Air CO_2 Enrichment experiments
Facilitated diffusion, 226
FACKEL (*FK*) gene, 679
F-actin. *See* Filamentous actin
Facultative CAM plants, 304, 305
Facultative flowering response, 592
FAD. *See* Flavin adenine dinucleotide
Fagaceae, 211
Fagus sylvatica (European beech), *593, 714*
False fruit, 656
Fama mutant, *555,* 556
FAMA transcription factor, 556, *558,* 559
Far upstream element (FUE), *82,* 84
FARINELLI gene, *616*
Farnesyl, *17*
Farnesyl phosphate, 109
Farquhar, Graham, 321, 322
FAR-RED ELONGATED HYPOCOTYL1 (FHY1), 483
Far-red light
  absorption by photosystem I, 255
  molecular mechanisms of flowering in natural environments, 604
  phytochrome as the primary receptor for, 477, 480, *481*
  plant acclimation to light quality, 326
  See also Red:far-red ratio
FASCIATED locus, 659, 660
Fascicular cambium, *11*
FASS gene, *677,* 684
F-ATPases (F-ATP synthase), 237, *258*
Fats
  characteristics of triacylglycerols, 406–407
  defined, 406
  energy storage, 405–406
Fatty acid amides, 733–734, 735
Fatty acid synthase, 407
Fatty acids
  biosynthesis, 407, 409–410
  biosynthesis of glycerolipids, 410–411
  biotechnology and, 407
  common fatty acids in higher plants, *406*
  conversion of storage lipids into carbohydrates, *412,* 413
  flavor volatiles, 661
  membrane fluidity, 18, 463–464, *465*
  membrane lipids and chill sensitivity, 411
  β-oxidation, *412,* 413, 517
  phospholipids, 16, *17,* 18
  polar glycerolipids, 407
  triacylglycerols, 406
  β-oxidation in glyoxysomes, 28
Fatty-acyl-CoA, *412,* 413
Fatty-acyl-CoA synthetase, *412,* 413
F-box proteins
  gametophytic self-incompatibility, 645–647
  KISS ME DEADLY family, 133
  Skp1/SCF complexes, *140,* 141, *142, 143*
F-box receptor/ubiquitin ligase system, 106
FBP7/11, 620
FC1 gene, 571
FCCP, 396
Fd. *See* Ferredoxin
Fe protein, 434
Fe_2S_2 centers, 235
Fe^{3+}-citrate complex, 195
Feedback regulation, of hormone signaling pathways, 143–144, *145*
Female gametophytes
  angiosperm life cycle, *626*
  double fertilization, 626
  formation and development, 78, 626, 630–633
  plant life cycle, 626
Fenugreek seeds, *507*
Fermentation
  efficiency of, 385–386
  overview, 382
  reactions in, *383,* 385
  respiratory quotient, 404
Fern allies, 4, *5*
Ferns, 4, *5, 6*
FERONIA receptor, 109
FERONIA receptor-like kinase, 638, 641
Ferredoxin (Fd)
  ammonium assimilation, 425, 426
  biological nitrogen fixation, 434
  formation of reactive oxygen species in photosynthesis, 275
  nitrate assimilation, *420,* 421, 422
  photorespiration, *293,* 295
  PSI reaction center, 269
  sulfur assimilation, 437, 438
  -thylakoid reactions, *258*
  Z scheme electron transport, *262,* 263
Ferredoxin-$NADP^+$ reductase (FNR), *258, 262,* 269
Ferredoxin–thioredoxin reductase, 288
Ferredoxin–thioredoxin system
  regulation of C_4 photosynthesis, 302
  regulation of the Calvin–Benson cycle, 288–290
  regulation of the oxidative pentose phosphate pathway, 388
Ferric ions, 195, 234, 235
Ferritins, 235
Ferrochelatase, 235
Ferrous ions, 234, 235
Fertilization, 5, 6, 626
  See also Double fertilization
FERTILIZATION-INDEPENDENT SEEDS (*FIS*) genes, 651, 652
Fertilizers
  applying in response to mineral deficiencies, 200–202
  climate change and, 190
  importance of, 189
  industrial nitrogen fixation, 418, 419
  leaching, 189, 191
Ferulate 5-hydroxylase, 69
Fe–S centers, 269
Festuca ovina (sheep fescue), *714*
FHY1 protein, 483
FHY1-LIKE (FHL) protein, 483
Fibers, 13, 15, 348
Fibrous root systems, 205, 573, 576–577
Fick, Adolf, 158
Fick's first law, 158
Filament, 627
Filamentous actin (F-actin)
  cytoplasmic streaming, 34, 36
  defined, 32
  phragmoplast, 40
Filamentous temperature-sensitive H (*FtsH*) gene, 699
Filiform apparatus, 632–633
Fimbrin, 32, *33*
FINE CULM 1 (*FC1*) gene, 571
Fine sand, 203
Fire, epicormic sprouts and, 587
FIS genes, 651, 652
FISH. *See* Fluorescent in situ hybridization
Fission, of plastids and mitochondria, 31
FK gene, 679
FKF1, 602, 606
FL gene, *616*
FLAGELLIN SENSITIVE 2 receptor, 108
Flaveria
  F. bidentis, 440
  F. pringlei, 440

Flavin adenine dinucleotide ($FAD/FADH_2$)
  cryptochrome and, 491–492
  functions of, 382
  mitochondrial electron transport, 392, *393*
  nitrate assimilation, 421
  role in plant respiration, *380*
  structure and reactions of, *381*
  total yield in aerobic respiration, 396, *398*
  tricarboxylic acid cycle, 381, 390, 391
Flavin mononucleotide (FMN)
  LOV2 phototropin domain and, 478
  mitochondrial electron transport, 392, *393*
  structure and reactions of, *381*
FLAVIN-BINDING KELCH REPEAT, F-BOX 1 (FKF1), 602, 606
FLAVIN-DEPENDENT MONOOXYGENASE1 (FMO1), 746
Flavonoids, 131
Flavoprotein:quinone oxidoreductase, 394
Flavoproteins, 106, 518
Flavor volatiles, 661–662
Flax, *8*
FLC gene. *See* FLOWERING LOCUS C gene
Fleshy fruits
  development, 659–660
  ripening and its regulation, 660–664
Flg22 peptide, 108, 744
Flippases, 24
FLM gene, *616*
FLO gene, 615, *616*
Flooded soils. *See* Waterlogged soils
Floral evocation, 591–592
Floral meristem identity genes, 615, *616*
Floral meristems
  defined, 614
  floral organs initiated by, 614–615
  inflorescence meristems, 614
  transition from vegetative development to, 613–614
Floral organ development
  ABC model, 617–618
  ABCE model, 618–620
  asymmetry in flowers, 620–621
  floral meristem identity genes, 615, *616*
  floral organ identity genes, 615, 616–620
  initiation of organs in whorls, 614–615
Floral organ identity genes, 615, 616–620
Floral organs, 549
  See also Flowers
FLORAL-BINDING PROTEIN7/11 (*FBP7/11*), 620
FLORICAULA (*FLO*) gene, 615, *616*
Florigen
  discovery of, 606–608
  identification as the floral stimulus, 608
  phloem translocation, 608, *609*
  regulation of flowering in *Arabidopsis*, 608–610
Flowering
  circadian rhythms, 594–597
  epigenetic regulation in response to abiotic stress, 456–457, *458*
  floral evocation, 591–592
  floral meristems and floral organ development, 613–621
  florigen and, 606–610
  long-distance signaling in, 606–608
  multiple pathways in, 612–613
  phloem signaling and biotechnology, 376
  photoperiodism, 597–606 (*see also* Photoperiodism)
  phytochrome interactions with cryptochrome, 494
  shoot apex and phase changes, 592–594
  vernalization, 610–612
FLOWERING D (*FD*) gene
  characteristics and functions of, *616*
  a floral meristem identity gene, 615, *616*
  florigen-mediated flowering, 608, *609*, 610
  flowering pathways and, 613
  repression by FLC protein, 612
Flowering dogwood (*Cornus florida*), 404, *714*
FLOWERING LOCUS C (*FLC*) gene, 457, 611–612, 613, *616*
FLOWERING LOCUS M (*FLM*) gene, *616*
FLOWERING LOCUS T (FT)
  activation by CRY2 protein, 597
  biotechnology and, 376
  cryptochrome signaling, 493
  epigenetic regulation in response to abiotic stress, 457
  evidence as a strong promoter of flowering, 603
  FT protein as florigen, 608–610
  molecular mechanisms of flowering in natural environments and, 604
  movement through plasmodesmata, 375
  in phloem sap and signaling, 364, 375
  photoperiodic flowering pathway, 613
  repression by FLC protein, 612
Flowering plants, 4
  See also Angiosperms
FLOWERING WAGENIGEN (*FWA*) gene, 652
Flowers
  abscission, 709–713
  angiosperm life cycle, *626*
  monoecious and dioecious plants, 7
  plant life cycles, *6*, 625–627
  selfing versus outcrossing, 642–647
  thermogenic, 399
Fluence
  categories of phytochrome responses, 484–486
  ecological ranges of, *476*
  photoresponses, 478–479
Fluid mosaic model, 16, *17*
Fluorescence, by chlorophyll, *249*, 250
Fluorescence resonance energy transfer (FRET), 128, 259–260
Fluorescent in situ hybridization (FISH), 74
Flux density, 158
Fluxes, 220
FMN. *See* Flavin mononucleotide
FMO1 protein, 746
FNR. *See* Ferredoxin-$NADP^+$ reductase
F_O, 395
F_OF_1-ATP synthase, 394, 395, *397*
Foliage leaves, 549
Foliar application, 202
"Foolish seedling disease," 116, 743
Forest fires, epicormic sprouts and, 587
Forests
  canopy optimization of light absorption, 324–325
  sunflecks, 324–325
Forisomes, 364, 365
Formic acid, 727
Formins, 32, *33*
Fossil fuels
  release of sulfur, 435
  rising levels of atmospheric carbon dioxide, 334, *335*
Fountain model of auxin transport, 527–528
14-3-3 Proteins
  blue light-initiated stomatal opening, *498*, 499
  brassinosteroid signal transduction pathway, *137*, *138*
  fusicoccin, 743
  inactivation of nitrate reductase, 421
  phototropism, 537
  regulation of H^+-ATPases, 236–237
Fox millet (*Panicum italicum*), *470*
Foxglove (*Digitalis*), 728–729
Fragaria. See Strawberry fruit
Frankia, 428
Fraxinus excelsior (European ash), *714*
Free Air CO_2 Enrichment (FACE) experiments, 339–340
Free energy, of water, 159
Free nuclear mitotic divisions, 632
Free-living nitrogen fixation, *428*, 430
Free-running circadian rhythms, 596
Freezing
  cryoprotectants and antifreeze proteins, 466
  effects of, *448*, 449
  formation of gas bubbles in xylem, 180
Frequency
  absorption spectra and, 250
  of light, 248
FRET. *See* Fluorescence resonance energy transfer
Fritillaria assyriaca, 19
Fructose
  carbon mobilization in land plants, *306*
  glycolysis, *383*, 384
  a reducing sugar, 362, *363*
Fructose 1,6-bisphosphatase
  Calvin–Benson cycle reactions, *284–285*
  gluconeogenesis, 385
  inhibition by fructose 2,6-bisphosphate, 402
  regulation of in the Calvin–Benson cycle, 287, 288, 289
  sucrose biosynthesis, *313*, 314
Fructose 1,6-bisphosphate
  Calvin–Benson cycle, *284–285*
  dynamic regulation of respiration and, 401
  glycolysis, *383*, 385
  structure, *382*
  triose phosphates and the cytosolic pool of, 312–314
Fructose 1,6-bisphosphate aldolase, *313*
Fructose 2,6-bisphosphatase, *313*, 314
Fructose 2,6-bisphosphate, *313*, 314, 402
Fructose 6-phosphate
  Calvin–Benson cycle, *284–285*
  dynamic regulation of respiration, 401
  glycolysis, *383*, 385
  oxidative pentose phosphate pathway, 386, *387*
  structure, *382*
  sucrose biosynthesis, *313*, 314, *315*
Fructose 6-phosphate 1-kinase, *313*
Fructose 6-phosphate 2-kinase, *313*, 314
Fruit ripening
  changes in fruit color, 660, *661*
  climacteric, 403, 662, 663
  commercial manipulation of, 664
  definition and overview of, 660
  ethylene, 662–663, 664
  factors affecting fruit taste and flavor, 661–662
  fruit softening, 661
  transcriptional regulation of, 663–664
Fruit set, 656–657
FRUITFUL (*FUL*) gene, *616*, 659
Fruits
  definition and types of, 656
  development of the dehiscence zone, 658–659
  factors affecting taste and flavor, 661–662

fleshy fruit development, 659–660
fruit development and whole plant senescence, 716
phloem import, 367–368
regulation of fruit set and parthenocarpy, 656–658
ripening, 660–664 (*see also* Fruit ripening)
seedlike fruits, *506*
storage temperature, 405
FT. *See* FLOWERING LOCUS T
FT INTERACTING PROTEIN1 (FTIP1), 608, *609*
FtsH gene, 699
Fuchsia, 601
Fucose, *48,* 54, *55*
FUE. *See* Far upstream element
FUL gene, *616,* 659
Fumarate, 389, *390*
Fungi
effects of soil pH on, 204
mycorrhizal, 210–213 (*see also* Mycorrhizas)
pathogenic (*see* Pathogens; Plant pathology)
Fungicides, 127
Funiculus, 631, 632, *634*
Fusarium fujikuroi, 116
Fusicoccin, 63, 236–237, 498, 743
Fusicoccum amygdali, 743
Fusiform cells, *579*
Futile cycles, 404
Fw2 locus, 659, 660
FWA gene, 652

G

G proteins, 106
G_1 phase, 36, 37, 38
G_2 phase, 36, 37, 38
GA 20-OXIDASE (*GA20ox*) gene family, 123, 144, *145,* 547
GA3ox gene family, 123, 144, *145*
GABA shunt, 391
Gaeumannomyces graminis, 725
GAF domain of phytochrome, 482, *483*
GA–GID1 receptor complex, 658
Galactan, 48, 57, 58
Galactinol, 355
Galactolipids, 18, 406
Galactono-gamma-lactone dehydrogenase, 394
Galactose
arabinogalactan proteins, 49
cell wall polysaccharides, *48*
hemicelluloses, 54, *55*
pectins, 56
raffinose-family sugars and, 362, *363*
Galacturonic acid
cell wall polysaccharides, *48,* 49, 53–54
pectins, 56, 57
Galium aparine, 12
Gametes
defined, 5
double fertilization, 641–642 (*see also* Double fertilization)
events of meiosis, 76–78
formation, 626
microgametogenesis, 628–629
plant life cycles, 5, *6*
programic phase of reproduction, 633–634
syngamy, 626
unreduced gametes, 79
Gametophyte generation, *6,* 7, 625–626, 669
Gametophytes
defined, 5
plant life cycles, 5, 6, 7, 625–626
See also Female gametophytes; Male gametophytes
Gametophytic self-incompatibility (GSI), 644–647
Gamma-aminobutyric acid (GABA), 391
γ-Radiation, transfer of "alien" chromosome segments by, 92
GA-MYB transcriptional activator, 516
GAPs. *See* GTPase-activating proteins
Garden bean. *See* Common bean
Garner, Wightman, 597–598
Gas bubbles
mechanisms of formation in xylem, 180
pit membranes and, 177
xylem cavitation, 177, 180–181
Gated channels
cyclic nucleotide-gated channels, 109, *231,* 232, 453
ligand-gated channels, *231,* 232
overview, 224
voltage-gated channels, 224
See also specific gated channels
Gates, 224
GAUT1, 53–54
GAX. *See* Glucoronoarabinoxylan
GC box, *82,* 83
GDH. *See* Glutamate dehydrogenase
GDP. *See* Guanosine diphosphate
GEFs. *See* Guanine nucleotide exchange factors
Gelatin, *156*
Gene editing
base editing, 97–98
gene replacement, 97, *98*
overview, 95
prime editing, *98,* 99
sequence-specific nucleases and targeted mutations, 95–97
Gene expression
abiotic stress and signaling pathways altering gene expression, 453–460
abscisic acid-mediated, 138–139
basic steps in, 20–22
brassinosteroid-mediated, 136, *137, 138*
cryptochrome signaling, 493
cytokinin-mediated, 133, *134*
effects of catechin on, 749
ethylene-mediated, *135,* 136
imprinted gene expression, 651–652
inactivation of repressor proteins in hormone signaling pathways, 141–143
overview of events in, *82*
photorespiratory conditions and, 297
phytochrome signaling, 483–484, 487–488
plant defense responses to pathogens, *742,* 743
posttranscriptional regulation, 86–90
PRR-triggered immunity, 744
retrograde regulation, 399
sugar-dependent, 402
transcriptional regulation, 81–86
transcriptional regulation of leaf senescence, 701–703, *704*
Gene fusions, 92–93
Gene gun, 94
Gene knockout technology, 97
Gene networks, controlling secondary meristems, 582–584
Gene regulatory proteins, 81
Gene silencing
cosuppression, 90
plant antiviral immune response, 747
RNAi pathway and, 86
General transcription factors, 81, 82, 83
Generative cell, *626,* 628, 629
Genes
domains, 92
introgression in crop plants, 91–92
ionomics and, 200
RNA polymerase II and transcription of protein-coding genes, 81–83
tools for studying gene function, 90–93
Genetic engineering
controversies in the use of, 100–101
crop plants, 99–101
editing plant genomes, 95–99
methods of transformation, 93–94
See also Biotechnology; Transgenes
Genetic imprinting, 651–652
Genetic mosaicism, 715
Genetically Engineered Organisms (GEOs), 100–101
Genetically Modified Organisms (GMOs), 100–101
Genomes
cytoplasmic genomes, 80–81
methods of editing, 95–99
methylation and regulation of transposons, 75, *76*
model organisms, 4
nuclear genome, 73–80 (*see also* Nuclear genome)
See also Chloroplast genome; Mitochondrial genome
GEOs. *See* Genetically Engineered Organisms
Geranylgeranyl, *17,* 109
Geranylgeranyl diphosphate (GGPP), 121, *122*
Germination, 512, 670
See also Seed germination
Gerontoplasts, *698*
GFP. *See* Green fluorescent protein
GI protein, 144, *145*
Giant redwood (*Sequoiadendrom giganteum*), 357, *440, 714*
Gibberella fujikuroi, 116, 743
Gibberellic acid, 116, 743
GIBBERELLIN INSENSITIVE DWARF 1 (GID1), *140,* 141, *143, 145,* 658
Gibberellin signaling pathway
inactivation of repressor proteins in, *140,* 141–143
primary locations of receptors, *106*
regulatory mechanisms, 144, *145*
Gibberellins
bioactive forms, 114, 116
biosynthesis, 121, *122*
breaking of seed dormancy, 511, 512
chemical structure, *115*
compound leaf development, 555
discovery of, 116
"foolish seedling disease," 743
fruit set and parthenocarpic fruits, 657, 658
functions of, 114, 116
homeostatic regulation, 123
induction of flowering, 612–613
juvenile-to-adult phase changes, 593–594
maintenance of the shoot apical meristem, 547
mobilization of starch endosperm, 515, 516
mobilization of storage proteins, 516
movement within the plant, 128
plant development and, 114
as plant growth regulators, 123
plant nastic movements, 523
regulation of secondary growth, 584
seed dormancy, 509, 510–511
suppression of photomorphogenesis in darkness, 518
Gibbs free energy, 380
GID1. *See* GIBBERELLIN INSENSITIVE DWARF 1
GIGANTEA (GI), 144, *145*
Ginkgo, 4, 7, *66*
G. biloba, 177, *710,* 715
GIPC. *See* Glycosylinositol phosphoryl ceramide
GK gene, 679
Glandular trichomes, 726, 729
Glassy state, 655
Glaucophytae, 281
Gliadins, *517*
GLK proteins, 705, *706, 707*
Global warming
aerenchyma and methane release, 404
combined effects of heat and water-deficit stress, 450–451

effect on plant respiration, 404, 405
effects of elevated global CO_2 levels on photosynthesis and respiration, 338–340
greenhouse effect, 338–339
nitrogen fertilizers and, 190
GLOBOSA gene, *616*
Globular actin (G-actin), 32
Globular embryo stage
Arabidopsis embryogenesis, 671, *672, 673,* 674–675
formation of root and shoot apical meristems, 686–687, *688*
maize embryogenesis, 670, *671*
radial patterning during embryogenesis, 682–683
Globulins, 516, *517*
Gloeothece, 428, 430
Glomeromycota, 210, 723
Glomus mosseae, 211
GLOSSY15 gene, *616*
GLRs. *See* Glutamate-like receptors
Glucan
cell wall rigidification and, 65
cellulose and cellulose microfibrils, 49, 50, 51
cellulose synthesis, 52–53
defined, 48
hemicelluloses, 54, *55*
starch degradation, 310, *311*
starch synthesis, 308–310
(1,3;1,4)-β-D-Glucan, 54, 65
Glucan phosphatases, 310, *311*
Glucan phosphorylases, 310, *311,* 312
β-1,4-Glucanase, 711
Glucan–water dikinases, 310, *311,* 312
Glucoinsolates, 731–732
Glucomannan, *49,* 54, *55, 66,* 67
Gluconeogenesis, 385, *412,* 413
Glucoronoarabinoxylan (GAX), 54, *55,* 64, 70
Glucose
carbon mobilization in land plants, *306*
cell wall polysaccharides, *48,* 49
cellulose microfibrils, 50, 51
conformational structures, *48*
diffusion in water, 158–159
dynamic regulation of respiration, 402
gluconeogenesis, 385
glycolysis, *383,* 384
hemicelluloses, 54, *55*
overall chemical reaction for photosynthesis, 252
protein glycosylation, 26
a reducing sugar, 362, *363*
starch breakdown, 310, 311
starch synthesis, 307, 308–310
water-soluble sugar conjugates of secondary metabolites, 730–731, 732
Glucose 1-phosphate
glycolysis, *313*
sucrose biosynthesis, 314, *315, 383*
Glucose 6-phosphate
glycolysis, *383,* 384
oxidative pentose phosphate pathway, 381, 386, *387*
starch breakdown, 311
structure, *382*
sucrose biosynthesis, *313,* 314, *315, 316*
Glucose 6-phosphate dehydrogenase, *387,* 388
Glucose oxidase, 734
Glucose transporter, 310, 312
Glucosyl, *48*
Glucosylceramide, *408*
Glucuronic acid, *48,* 54, *55*
β-Glucuronidase (GUS), 93, 128
Glucuronoarabinoxylan, 49
Glucuronoxylan, 54
Glutamate
amino acid biosynthesis, 427
ammonium assimilation, 424, 425, 426
biosynthetic pathway, *427*
C_4 photosynthesis, 299
Ca^{2+}-mediated wound response, 373
nitrate assimilation, *420*
photorespiration, 291, *292–293,* 294, 295
phytochelatins, 465, *466*
Glutamate dehydrogenase (GDH), *425,* 426
Glutamate receptor channels, *231,* 232
Glutamate synthase, *420,* 424–426
Glutamate:glyoxylate aminotransferase, 291, *292–293,* 294, 295
Glutamate-like receptors (GLRs), 109, 373, 737–738
Glutamic acid, *277, 363*
Glutamine
amino acid biosynthesis, 427
ammonium assimilation, 424–425
biosynthetic pathway, *427*
conversion of nitrite to ammonium, 422
linking of carbon and nitrogen metabolism, 426
nitrate assimilation, *420,* 422
phloem sap, *363*
photorespiration, 291, *292–293,* 294
Glutamine synthetase (GS)
ammonium assimilation, 424, 425
nitrate assimilation, *420*
photorespiration, 291, *292–293,* 295
Glutamine:2-oxoglutarate aminotransferase (GOGAT)
ammonium assimilation, 424–426
nitrate assimilation, *420*
photorespiration, *293,* 294, 295
Glutaredoxin, 210
Glutathione
detoxification of hydrogen peroxide, 462
phytochelatins, *466*
sulfur assimilation, 437, 438
Glutathione peroxidase, 462, *463*
Glutathione reductase, 462, *463*
Glutathione S-transferases, 121
Glutelins, 516, *517*
Glycan, 48–49
Glycan synthases, 53
Glyceollin I, *747*
Glyceraldehyde 3-phosphate
C_3 photosynthesis, 302
Calvin–Benson cycle, 283–285
glycolysis, *383,* 384
oxidative pentose phosphate pathway, 386, *387*
structure, *382*
sugar biosynthesis, 312, *313,* 314
Glyceraldehyde 3-phosphate dehydrogenase, 289, 290, *383,* 384
Glycerate, 291, *292–293,* 294
Glycerate kinase, 291, *292–293,* 295
Glyceroglycolipids, 407, *408*
Glycerol
phospholipids, 16
polar glycerolipids, 407
structure, *406*
triacylglycerols, 406
Glycerol 3-phosphate, 410
Glycerolipids
biosynthesis, 410–411
biotechnology and, 407
overview, 405
Glycerophospholipids, 407, *408, 410*
Glycine
biosynthetic pathway, *427*
photorespiration, 291, *292–293*
phytochelatins, 465, *466*
Glycine betaine, 461
Glycine decarboxylase, 291, *292–293,* 295, 296, 297
Glycine max. See Soybean
Glycine-rich protein, *50*
Glycinin, *517*
Glycolate
bioengineered photorespiratory bypass pathways, 296
photorespiration, 291, *292–293,* 294
Glycolate oxidase
bioengineered photorespiratory bypass pathways, 296
cell redox homeostasis, 297
photorespiration, 291, *292–293,* 294
Glycolysis
alternative glycolytic reactions, 385
amino acid biosynthesis, 427
fermentation, *383,* 385–386
metabolic profiling, 386
metabolic redundancy, 384
modifying plant respiration and, 404
overview, 380, 382
Pasteur effect, 386
phosphate assimilation, 438
in plant biosynthetic and redox networks, 400–401
in plant respiration, 380
structures of carbon intermediates, *382*
total ATP yield, 396, *398*
Glycophytes, 446, 449, 465
Glycoproteins, 26, 65
Glycosidases, 54, 58, *732*
Glycoside cytokinins, 124
Glycosides, 730–731, 732
Glycosidic linkages
glycosylated secondary metabolites, 730–731
starch mobilization, 310, *311*
starch synthesis, 307, 308–310
Glycosylases, 84
Glycosylation, 109
Glycosylceramide, 18
Glycosylglycerides, 18
Glycosylinositol phosphoryl ceramide (GIPC), *17,* 18
Glycosylphosphatidylinositol anchor, *17,* 18
Glycosyltransferases, 53–54
Glyoxylate, 28, 291, *292–293,* 296
Glyoxylate cycle, *412,* 413
Glyoxysomes, 15, 28, *412,* 413
Glyphosate, 99–100
Glyphosate resistance, 99–100
GMC. *See* Guard mother cell
GMOs. *See* Genetically Modified Organisms
GmSARK gene, 705
GN protein. *See* GNOM protein
Gnetales, 174
Gnetophytes, 4
GNOM (GN) protein, 679–680, 681, 682
Goethe, Johann Wolfgang von, 617
GOGAT. *See* Glutamine:2-oxoglutarate aminotransferase
Golden rice, 100
GOLDEN2-LIKE (GLK) proteins, 705, *706, 707*
Goldman diffusion potential, 222
Goldman equation, 222
Golgi apparatus
cell cycle, 37–38
endomembrane system and, 15
endoplasmic reticulum and, 24
enzymes localized in, 26
exocytosis, 23
H^+-pyrophosphatase, 226
motor proteins and cytoplasmic streaming, 34
phragmoplast, 40
plant cell structure, *16*
protein glycosylation, 26
synthesis of matrix polysaccharides, 53–54
vesicles and root nodule formation, 432, *433*
vesicular trafficking, 24–26
See also Trans Golgi network
Gossypium hirsutum (cotton), *164, 469*
Grafting studies, discovery of florigen, 607–608
Grain yield, *154*
Grana, 29, *30*
Grana lamellae, *256,* 257

'Grand Rapids' lettuce cultivar, 511
Grapes (*Vitis*), 116, *593,* 727
Grass family. *See* Poaceae
Grasshoppers, 733, 734
Gravel, 203
Gravitational potential, 160, 171
Gravitropic setpoint angle, 568, *569,* 577–578
Gravitropism
  defined, 526
  gravity-independence of polar auxin transport, 526, *527*
  interactions with root thigmotropism, *533,* 534
  lateral redistribution of auxin, 526–529, 530, *531*
  roles of pH and Ca^{2+} gradients in, 532–533
  root cap, 206, 521
  sedimentation of statoliths, 529–532
Gravity
  circumnutation, 522
  water movement in the tallest trees, 178
  water potential, 159, 160
Gravity sensors, 30
Great Irish Famine, 741, 744
Green algae
  cytoplasmic streaming, 34
  ion concentrations in cytosol, 222
  photosynthesis experiments, 254
  photosynthetic pigments, 4
  plant evolution and, *5*
Green fluorescent protein (GFP), 93, 128
Green Revolution, 190, 567
Green sulfur bacteria, 259
Greenhouse effect, 338–339
Greenhouse gases, 190
Green-leaf volatiles, 738–739
Gretchen Hagen 3 (GH3) amido synthetases, 120
gRNA. *See* Guide RNA
Ground pine (*Lycopodium complanatum*), *714*
Ground tissue
  definition and description of, 10, 12–14
  leaf anatomy, *8*
  origin of, 683
  root anatomy, *8*
  stem anatomy, *8*
Groundsel (*Senecio vulgaris*), 592
Growth efficiency, 717
Growth respiration, 403
GS. *See* Glutamine synthetase
GS2 plastid, 426
GSI. *See* Gametophytic self-incompatibility
GTP. *See* Guanosine triphosphate
GTPase-activating proteins (GAPs), 638
GTPases, pollen tube tip growth and, 638
Guanine nucleotide exchange factors (GEFs), 638, 679, 681
Guanosine diphosphate (GDP)
  GTPases and pollen tube tip growth, 638
  tubulin and, 32, 33, 34, *35*
Guanosine triphosphate (GTP)
  GTPases and pollen tube tip growth, 638
  tubulin and, 32, 33, 34, *35*
Guard cells
  ABA-induced stomatal closure in response to water stress, 466–467, *468*
  blue light-induced stomatal opening, 498–500
  cell wall features, 183–184, *185*
  chloroplasts, 11–12
  defined, 555
  development of stomata, 555–559
  effects of fusicoccin on, 743
  factors regulating the osmotic balance of, 185–186
  leaf anatomy, *8*
  transport activities in, 238–240
  turgor pressure changes and stomatal opening, 184–185
  water movement from leaf to atmosphere and, *181*
Guard mother cell (GMC), 556, 557, *558,* 559
Guide RNA (gRNA), 96–97
GUN1 gene, 456
Gunnera, 428, 430
Gunpowder, 417
GURKE (*GK*) gene, 679
GUS. *See* β-Glucuronidase
Guttation, 174
Gymnosperms
  albuminous cells, 15
  compression wood, *104*
  defined, 4
  embryogenesis, 670
  hemicelluloses, 54
  life cycle, *6, 7*
  passive symplasmic phloem loading, 356
  phloem characteristics, 348, 350, *350,* 351
  phloem translocation, 361
  photoreversible responses induced by phytochrome, *481*
  in plant evolution, 4, *5*
  sieve cells, 14
  tracheid pit membranes, *175,* 176, 177
  transition to secondary growth, 579
  xylem cell types, 174, *175,* 176
Gynoecium
  female gametophyte development, 630–633
  initiation of, 615
  plant life cycle, 626
  programic phase of reproduction, 633–634
Gypsum, 204

H

H^+ pumps, *229,* 230
H2A.Z histone subunit, 488
Haber–Bosch process, 418
Haemophilus influenzae, 224
HAESA (HAE) receptor kinase, 712, *713*
HAESA-LIKE2 (HSL2) receptor kinase, 712, *713*
HAIKU gene, 653
Hairs. *See* Trichomes
HAK (HAK/KT/KUP) transporter family, 233
Hakea, 204
  H. prostrata, 206
Half-unit membranes, 28
Halophytes, 166, 204, 449, 460
HAPLESS2 (HAP2) protein, 642
Haploids (1N), 5, 6, 7, 78
Hardening off, 446
Hard-seededness, 509
Hartig net, 212
Harvest index, 376
HASTY protein, 86, *87*
HAT. *See* Histone acetyltransferase
Hatch, M.D., 298
Hatch–Slack cycle. *See* C_4 photosynthesis
H^+-ATPases
  ABA-induced stomatal closure in response to water stress and, 467, *468*
  acid growth and, 63
  auxin-induced cell wall acidification, 526
  blue light-induced stomatal opening, 239–240, 498–500
  exclusion of sodium ions by glycophytes, 465
  functions of, 230
  fusicoccin and, 743
  gravitropism, 533
  membrane potential and proton transport, 222–223
  phototropism, *537,* 538
  plasma membrane H^+-ATPases, 226, 236–237
  polar auxin transport, 128, *129*
  secondary active transport, 226
  stomatal closure, *239,* 240
  structure, function, and regulation of, 236–237
  tonoplast H^+-ATPases, 237–238
  xylem loading, 242
Haustorium, 749, 750
Hawthorns, *104*
HC-toxin, 743
Hd proteins. *See* Heading-date proteins
HDA9 protein, *702,* 703, *704*
HDAC. *See* Histone deacetylase
HD-ZIP III proteins. *See* Class III Homeodomain-Leucine Zipper proteins
Heading-date (Hd) proteins, 603–604, 608, *616*
Heart stage embryo, 671, *672*
Heat
  C_4 photosynthesis and, 303
  dissipation by leaves, 331–332
Heat production
  alternative oxidase and cyanide-resistant respiration, 398–399
  uncoupling protein, 399–400
Heat shock factors, 462
Heat shock proteins (HSPs), 453, 462, *464*
Heat stress
  effects of, 447–448
  effects when combined with water-deficit stress, 450–451
  stress matrix, 451
Heather (*Calendua vulgaris*), 628
Heavy metal stress
  chelation and phytochelatins, 465–466
  combined with heat stress, 451
  effect on plants, 449–450
Hedera helix (English ivy), 592, *593, 714*
Hedge mustard (*Sisymbrium officinale*), 512
Helianthus. See Sunflowers
Helicoverpa zea (corn earworm), 734
Heliobacteria, 259
Heliotropism, 325
Hemibiotrophic pathogens, 741
Hemicelluloses
  binding to cellulose, 54
  cellulose microfibril synthesis, 53
  composition and functions, 49, *50*
  molecular models of cell walls, 64–65
  pectins, 56
  primary cell wall assembly, 58
  primary cell walls, 49, 50, *53*
  secondary cell walls, 67
  structures of, 54, *55*
Hemiparasitic plants, 749
Hemlock plant (*Cicuta*), 728, *729*
Hemlock tree (*Tsuga canadensis*), 511
Hemp (*Cannabis sativa*), 193
Henbane, *486,* 607
Herbaspirillum, 430
Herbicide resistance, 99–100
Herbicides
  blocking of photosynthetic electron flow, 269, *270*
  synthetic auxins, 121
Herbivore-induced volatiles, 738–739
Herbivory/Herbivores
  biotic interactions and, 721
  inducible plant defenses, 732–741 (*see also* Inducible defenses)
  interactions that harm plants, 725–732
Hermaphroditic flowers, 642, *643*
Heterochromatin, 20, 74, 75
Heterochromatization, 86
Heterocysts, 429
Heteroglycans, 311
Heterophylly, 467
Heterosis (hybrid vigor), 79–80, 643, 647
Heterostyly, 642, *643*
HetP protein, 429
HetR transcription factor, 429
Hevea brasiliensis (rubber plant), 730
Hexanals, 661
Hexenols, 661
Hexokinase, 311, *383*

Hexose phosphate isomerase, *313,* 314, *383, 387*
Hexose phosphates
  carbon mobilization in land plants, *306*
  glycolysis, 380, 382, *383,* 384
  starch breakdown, *311*
  triose phosphates and the cytosolic pool of, 312–314
Hexoses
  cell wall polysaccharides, *48*
  reducing sugars, 362, *363*
HG. *See* Homogalacturonan
H^+–HPO_4^{2-} symporter, 438
High light intensity. *See* Light stress
High temperature. *See* Heat; Heat stress
High-irradiance responses (HIRs), 484, 485–486, 606
High-pressure manifold model of phloem transport, 361
High-throughput elemental analysis, 200
Hill, Robert, 254
Hill reaction, 254
HIRs. *See* High-irradiance responses
Histamine, 727
Histidine, *427,* 465
Histidine kinase-related domain (HKRD), 482, 483
Histidine kinases, 107, 132, 133, *134*
Histogenesis, 670
Histone acetylation, gene expression and, 84, *85,* 86
Histone acetyltransferase (HAT)
  ethylene signaling, *135,* 136
  hormone signaling pathways, 141, *142, 143*
  leaf senescence, 703
Histone code, 86
Histone deacetylase (HDAC)
  functions of, 84, *85*
  hormone signaling pathways, 141, *142, 143*
  inhibition by HC toxin, 743
HISTONE DEACETYLASE 9 (HDA9) protein, *702,* 703, *704*
Histone demethylases, 84, *85*
Histone methylation
  gene expression and, 84, *85,* 86
  regulation of transposons, 75
  RNAi pathway and the resetting of epigenetic marks, 89
Histone methyltransferase, *85*
Histones
  chromatin-regulated regulation of leaf senescence, *702,* 703, *704*
  chromosome structure, *19,* 20
  epigenetic modifications and gene expression, 84–86
  gene transcription and, 81, 84–86
  H2A.Z subunit, 488
  modifications in adaptations to abiotic stress, 456–457, *458*
  nucleosomes, 74
H^+–K^+ symporters, 232
H^+/K^+-ATPase, 226
HKRD. *See* Histidine kinase-related domain
HKT transporters, 232
Hoagland, Dennis R., 194
Hoagland solution, 194–195
Hoaryleaf ceanothus, *180*
Holoparasitic plants, 749
Homeotic genes, 616–617
  See also Floral organ identity genes
Homogalacturonan (HG)
  cell wall expansion, 62
  enzyme-mediated primary cell wall assembly, 58
  a pectin, *49*
  structure and properties, 56–57, 58
  synthesis, 53–54
Homologous chromosomes (homologs), 76–78
Homologous recombination (HR) DNA repair pathway, 97, *98*
Hooke, Robert, 46
HOOKLESS 1 (*HSL1*) gene, 703
Hordeins, *517*
Hordeum vulgare. See Barley
Hormonal signaling pathways
  abscisic acid pathway, 138–139
  brassinosteroid signaling, 136–138
  cross-regulation and the integration of pathways, 147
  cytokinin and ethylene signal transduction pathways, 132–136
  modulation by endogenous molecules, 144, 146
  negative regulation, 139, 144
  protein degradation and the ubiquitin-proteasome pathway, 139–142, *143*
  termination or attenuation of signaling, 143–144, *145*
  tissue-specific responses, 144
Hormone balance theory, 510–511
Hormone receptors
  in hormonal regulation, 113, 114
  location and conservation across kingdoms, 105–106
Hormones. *See* Phytohormones
Hornworts, 4, *5*
Horse chestnut (*Aesculus hippocastanum*), *572*
Hos15 gene, 457
"Hot spot" model of cell walls, 65
H^+-pyrophosphatase (H^+-PPase), 226
HRGPs. *See* Hydroxyproline-rich glycoproteins
HSL1 gene, 703
HSL2 receptor kinase, 712, *713*
H^+–SO_4^{2-} symporter, 435
HSPs. *See* Heat shock proteins
Human diet, carbon isotope ratio and, 342
Humus, 169
HY5 transcription factor, 423, *493*
Hybrid sensor histidine kinases, 132
Hybrid vigor (heterosis), 79–80, 643, 647
Hybrids, 79–80
Hydathodes, 174
Hydraulic conductivity, 164–165, 171
Hydraulic resistance, of leaves, 181–182
Hydrogen, plant tissue concentration, *191*
Hydrogen bonds
  properties of water and, 154–157
  structure of water, 154, *155*
Hydrogen cyanide, 732
Hydrogen peroxide
  bioengineered photorespiratory bypass pathways, 296
  cell redox homeostasis, 297
  detoxification, 462, *463*
  leaf senescence, 708
  photodamage, 273, 274
  photorespiration, 291, *292–293,* 294
  PRR-triggered immunity, 744
  a reactive oxygen species, 111, 446
  sources of, *454*
Hydrogen sulfide, 204, 435
13-Hydroperoxy linolenic acid, *735*
2-Hydroperoxy-3-ketonarabinitol 1,5-bisphosphate, *285*
Hydrophilins, 463
Hydroponics, 193, 195
Hydrostatic potential, 218
Hydrostatic pressure
  cohesion–tension theory of xylem water transport, 178, *179*
  defined, 156–157
  metastable state of water in tree xylem, 179–180
  root pressure, 174
  tension, 160
  turgor pressure, 160
Hydrotropism, 526, 534–535, 578
Hydroxyl radical
  free iron and, 235
  photodamage, 274
  PRR-triggered immunity, 744
  a reactive oxygen species, 446
  sources of, *454*
Hydroxynitrile, *732*
Hydroxyproline-rich glycoproteins (HRGPs), 47, *50*
Hydroxypyruvate, 291, *292–293*
Hydroxypyruvate reductase, *293,* 295
Hyoscyamus, 486
  H. niger, 607
Hypanthium, 657
Hyperaccumulation, 465
Hyperacidification, of vacuoles, 238
Hypernutation, 523
Hyperosmolality gated Ca^{2+}-permeable channels, 453
Hypersensitive response
  definition and description of, 741, 745–746
  programmed cell death and, 693, *694,* 695–696
Hyphae, mycorrhizas, 211, 212, 213
Hyphal coils, 211, *212*
Hypocotyl
  Arabidopsis embryogenesis, 675
  blue-light responses, 490, 491
  effects of ethylene on microtubule orientation and cell expansion, 523–524
  gibberellin signaling, 144, *145*
  lag time for auxin-induced elongation, 525–526
  modification in cereal grains, 508
  nastic movements, 522–523
  opening of the apical hook, 519
  phototropism, *536,* 537–538
  phytochromes and elongation, 485, 486
  seed anatomy, 506, *507*
  seedling development in light or dark, 517, 518
  seedling emergence, 517
  vascular differentiation in, 520
Hypohysis, 674
HYPONASTIC LEAVES 1 (HYL1), 86, *87*
Hypoxia
  aerenchyma and, 405, 461–462
  fermentation and, 385

I

IAA. *See* Indole-3-acetic acid
IAAH, 128–129
IBA. *See* Indole-3-butyric acid
Ice crystal formation
  cryoprotectants and antifreeze proteins, 466
  freezing stress, 449
Ice plant (*Mesembryanthemum crystallinum*), 305
IDA protein, 712, *713*
Idioblasts, 727
IGT transcription factors, 578
Illite, 203
Imbibition, 513
Immunodetection, measurement of plant auxin levels, *131*
Impatiens, *422*
Import, into sinks, 366–369
Imprinted gene expression, 651–652
In situ hybridization, 92
INAPERTURATE POLLEN1 gene, 630
Inbreeding depression, 642
Incongruity, 641
Indehiscent fruits, *506,* 657
INDEHISCENT (*IND*) gene, 659
Indeterminate growth
  Arabidopsis inflorescence meristem, 614
  branching and, 567
  meristems and, 541–542
  root apical meristem, 542–545
  shoot apical meristem, 545–549
Indian lotus (*Nelumbo nucifera*), 509, 656
Indian mustard, *80*
Indole acetonitrile, 119
Indole-3-acetate O-methyltransferase1 (IAMT1), 120

Indole-3-acetic acid (IAA)
biosynthesis, 119
coleoptile bending response, 103
discovery of, 114
fountain model of transport in roots, 527–528
gravitropism, 528–529, 530–532
homeostatic regulation, 120–121
inhibition of axillary bud outgrowth, *570*
polar transport, 128–132, 526–527
primary locations of receptors, *106*
structure, *115*
synthetic auxins, 114
zinc deficiency and, 198
See also Auxin
Indole-3-acetic acid–amido synthetase, 460
Indole-3-butyric acid (IBA), 114, 120
Indole-3-pyruvate, 119
Inducible defenses
activation by jasmonate, 734–735, *736*
Ca^{2+} and MAP kinase signaling, 734
defined, 722
elicitors, 733–734
herbivore-induced volatiles, 738–739
hormonal interactions in, 735–736
inhibition of herbivore digestion, 736
overview, 733
reciprocal plant–insect evolution, 741
regulation by circadian rhythms, 739–741
systemic defenses, 736–738
trade-offs with, 732–733
Induction period, Calvin–Benson cycle, 285–286
Inductively coupled plasma mass spectrometry (ICP-MS), 200
Industrial nitrogen fixation, 418, 419, 434
Infection thread, 432, 433
INFLORESCENCE DEFICIENT IN ABSCISSION (IDA) protein, 712, *713*
Inflorescence meristems, 614
Ingenhousz, Jan, 252
Initial cells
cambial initials, 579–580, *581*
definition and description of, 542
formation of axillary meristems, 548
root apical meristem, 543, *544*
shoot apical meristem, 545–547, 548
Initiation complexes, 34
Initiator element (INR), 82–83
Innate immunity
abiotic stress and, 451
effector-triggered immunity, 741, *742*, 744–745
pattern recognition receptor-triggered immunity, 741, 742–743
Inner integument, 631–632, 652
Inner mitochondrial membrane
chemiosmotic mechanism of ATP synthesis, 395
description of, 388, 389
electron transport chain, 392, *393*
supplementary branches of the electron transport chain, 393–394
transmembrane transport, 396, *397*
transport of pyruvate across, 389
uncouplers, 396
INO80 chromatin remodeling complex, 488
Inorganic carbon-concentrating mechanisms
C_4 photosynthetic carbon fixation, 297–303
crassulacean acid metabolism, 303–305
overview, 297
Inorganic fertilizers, 201
Inorganic phosphate (P_i)
C_4 photosynthesis, *299*, 300–301
dynamic regulation of respiration, 401, 402
oxidative phosphorylation, 381, *393*, 394, 395, 396
phosphate assimilation, 438
phosphate transporter, 396, *397*
regulation of glycolysis, 402
starch degradation, 310, *311*
sulfate assimilation, 436
Inositol 1,4,5-trisphosphate (IP_3), 113
Inositol phosphates, 113
Input domain, of sensor proteins, 132, *133*
Insect herbivores
elicitors, 733–734
inducible plant defenses, 732–741 (*see also* Inducible defenses)
reciprocal evolution with plants, 741
transfer of pathogens to plants, 741
types of, 733
Integral membrane proteins
anchoring in the membrane, 22
anoxygenic photosynthesis, 259
desaturase enzymes, 410
description and types of, 18
F_OF_1-ATP synthase, 395
phospholipid bilayers, *17*
synthesis, 20, *21*, 22
of thylakoids, 257
Integuments
angiosperm life cycle, *626*
Arabidopsis, 631–632
progamic phase of reproduction, *634*
seed coat development, 652, *653*
Intercalary meristems, 542
Intercellular air space resistance, 334, 335, *336*
Interface light scattering, 324
Interfascicular cambium, *11*
Intermediary-type companion cells, 354–355, 356
Internal phloem, 347
Internal tolerance, 464–465
Internodes, 7, *8*, 568
Interphase, 36, 76
Interspecies hybrids, 79–80
Interveinal chlorosis, 198, 199
Intine, 629
Intraluminal vesicles, 27
Introgression, 91–92
Introns, *82*
Invertases, 368, *383*, 384
Inwardly rectifying (inward) K^+ channels, 225–226, *238*, 239
Ionome, 200
Ionomics, 200
Ions
electrochemical potential, 219
ion gradients and secondary active transport, 226–227
membrane potential and, 220–221
observed and predicted concentrations in pea root tissue, *221*, 222
passive and active transport, 218–219
transport across membrane barriers, 219–223
Ipomoea nil (morning glory), 360
IPT. *See* Isopentenyl transferase
IQD1 protein, 734
Iron
effects of soil pH on availability, *201*
foliar application, 202
mechanisms of root uptake, 234–235
mobility within the plant, *196*
nutrient solutions and chelators, 195
phosphate availability in soils and, 204
in plant nutrition, 192, 198–199
plant tissue concentration, *191*
root absorption of, 208
Iron deficiency, 199, 200, 235
Iron hydroxide, 195
Iron phosphate, 195
Iron-chelate reductase, 234
Irradiance
defined, 322, 478
high-irradiance phytochrome responses, 485–486
Irrigation, soil salinization and, 204
Isoamylases, *309*, 310
Isochorismate, 740–741
Isochorismate synthase, 741
Isocitrate. *See* Isocitric acid
Isocitrate lyase, *412*, 413
Isocitric acid (isocitrate)
conversion of storage lipids into carbohydrates, *412*, 413
malic enzyme reaction, *391*
mitochondrial transmembrane transport, 396, *397*
tricarboxylic acid cycle, 389, *390*
Isoflavinoids, 747
Isoleucine, *427*
Isomorphic sperm cells, 641–642
Isomorphous substitution, 202
Isopentenyl adenine, 123
Isopentenyl transferase (IPT), 123, 124, 459, 571, 708, *709*
Isoprenoids, 406
Isothiocyanates, 731–732
Isotropic growth, *550*, 551

J

JA. *See* Jasmonate
Jafendorf, André, 270, *271*
JA-Ile. *See* Jasmonic acid-isoleucine
JA-ILE ZIM-DOMAIN (JAZ) protein family, 141, *143*, 735, *736*
Japanese timber bamboo (*Phyllostachys bambusoides*), 714
JAR proteins, 735, *736*
Jasmonate (JA)
activation of plant inducible defenses, 734–735, *736*
biosynthesis of plant defense proteins, 736
biosynthetic pathway, 735
circadian rhythms in the regulation of plant inducible defenses, 740
green-leaf volatiles, 739
linolenic acid, 411
plant development and, 114
plant systemic defenses, 736–737, 738
Jasmonate resistance (JAR) proteins, 735, *736*
Jasmonic acid-isoleucine (JA-Ile)
activation of plant inducible defenses, 7216, 734, 735
biosynthetic pathway, 735
chemical structure, *115*
inactivation of repressor proteins in signaling pathway of, 141–143
plant development and, 114
plant systemic defenses and, 736, 737, 738
primary locations of receptors, *106*
JAZ protein family. *See* JA-ILE ZIM-DOMAIN protein family
JOINTLESS gene, 711
Jorgensen, Richard, 90
Judaean date palm (*Phoenix dactylifera*), 653–654, 656
Jumping genes. *See* Transposons
Juvenile-to-adult phase changes, 592–594
Jα-helix, *495*, 496, *497*

K

K domain, 619
Kalanchoe
crassulacean acid metabolism, 303, *304*, 305
light requirement for seed germination, 511

a long-short-day plant, 599
night break treatments, 601
somatic embryogenesis, 650–651
K. pinnata, 303
Kale, *80*
KANADI transcription factors, 552–553
Kaolinite, 203
Karpilov, Y., 298
Karrikinolide, 512
Karrikins, 118–119
Katanin, 34, *35*
Keeling, C. David, 334
3-Ketoacyl-ACP synthase, 409
Ketone, 362, *363*
K^+–H^+ antiporters, *239,* 240
K^+–H^+ symporters, 232
Kidney bean. *See* Common bean
Kidney-shaped guard cells, 184
Kinases, conservation across kingdoms, 106
Kinesins, 34, 40
Kinetic analyses, of transport mechanisms, 228
Kinetin, *115,* 116
Kinetochore
centromeres and, 74
meiosis, 78
metaphase chromosomes, 37, *38,* 40
King's lomatia (*Lomatia tasmanica*), 714
KISS ME DEADLY (KMD) proteins, 133, 141
Klebsiella, 428
KMD proteins. *See* KISS ME DEADLY proteins
K^+–Na^+ symporters, 232
KNAT1 protein, 712, *713*
KNAT1/BP protein, 712, *713*
Knop, Wilhelm, 194
KNOTTED protein, 547
KNOTTED-LIKE FROM ARABIDOPSIS THALIANA 1/BREVIPEDICELLUS (KNAT1/BP) protein, 712, *713*
KNOTTED-LIKE FROM ARABIDOPSIS THALIANA (KNAT1) protein, 712, *713*
KNOX proteins
compound leaf development and, *554,* 555
establishment of adaxial–abaxial leaf polarity, 552, *553*
inhibition of gibberellin, 123
maintenance of proliferation in the shoot apical meristem, 547
upregulation of cytokinin, 124
KORRIGAN protein family, 67
Kortschack, H. P., 298
Kranz anatomy, 298–299, *300,* 301–302
Krebs, Hans A., 388
Kurosawa, Eiichi, 116

L

L1 layer, 546, 561
L2 layer, 546
L3 layer, 546
Laccases, 68, 69
Lactate, *382, 383,* 385
Lactate dehydrogenase, *383,* 385
Lactic acid fermentation, *383,* 385
Lactuca (lettuce), *481,* 511, *521*
Lactuca sativa (lettuce), 511
Lady's mantle (*Alchemilla vulgaris*), *174*
Lag time, in phytochrome responses, 484
Lamina, 549
See also Blade
Laminar flow, 176–177
Land plants, 4, *5*
Larrea tridentata (creosote bush), *336, 714*
Late Embryogenesis Abundant (LEA) proteins, 460, 463, 655
Late endosome, 26, *27,* 28
Latent heat loss, 332
Latent heat of vaporization, 155, 160
Lateral meristems, 578–579
See also Cork cambium; Vascular cambium
LATERAL ORGAN BOUNDARIES (LBD) protein family, 582, *583*
Lateral root cap, 543, *544*
Lateral root founder cells, 574, *575,* 576
Lateral roots
defined, 10, 573
eudicot root systems, 577
gravitropic setpoint angle, 577–578
origin and development of, 542, *543,* 573–576
plant response to nitrogen deficiency, 210
plant response to phosphorus deficiency, 209
rhizotaxis, 573
root anatomy, *8*
in taproot systems, 205
Lateral shoots
development of, 568
gravitropic setpoint angle, 568, *569,* 577–578
hormonal regulation of growth in, 569–571, *572*
"stool shoots," 587
See also Axillary buds
LATERAL SUPPRESSOR (LS) protein, 548–549, 711
Latex, 13, 730
Laticifers, 13, 348, 729, 730
Lauric acid, *406*
Lavatera, 325
Law of reciprocity, 485
LAZY transcription factors, 578
LBD protein family, 582, *583*
LDPs. *See* Long-day plants
LEA proteins, 460, 463, 655
Leaching
effects of soil pH on, 201
of fertilizers, 189, 191
soil pH and, 204
LEA/DHN/RAB protein family, 463
Leaf anatomy
Kranz anatomy, 298–299, *300,* 301–302
optimization of light absorption, 323–324
sun and shade leaves, *322*
Leaf angle, light absorption and, 325
Leaf development
determination of leaf shape, *550,* 551
development of stomata, 555–559
establishment of polarity, 551–555
formation of axillary meristems and, 548–549
formation of leaf primordia, 545, 547–548
leaf structure and leaf types, 549–551
venation patterns, 559–564
Leaf movement
light absorption and, 325
nyctinasty, 475, 728
photonasty, 475
to reduce excess radiation, 330
solar tracking, 325, 475
Leaf polarity
establishment of adaxial–abaxial polarity, 551–553
establishment of proximal–distal identity, 553–554
regulation of blade outgrowth, 553
Leaf primordia
establishment of polarity, 551–553
formation by the shoot apical meristem, 545, 547–548
formation of axillary meristems and, 548–549
maize embryogenesis, 671
phyllotaxis, 573
shoot apex, *8*
vascular development, 560–562
Leaf primordia stage embryo, 671
Leaf rolling, 467
Leaf scars, *572*
Leaf senescence
autolysis of chloroplast proteins, 698–699
autophagy, 696, 698–699
LHCP II protein recycling and chlorophyll catabolism, 699–700
metabolic pathways up- or down-regulated during, *701*
overview, 696–697
programmed cell death, 693
regulation of, 700–709
structural and biochemical changes during, 698
types of, 697
Leaf temperature
cohesion–tension mechanism of xylem water transport and, 178
heat dissipation, 331–332
impact on transpiration, 182
Leaf trace, 560–562
Leaf veins, *549*
development of, 559–564
hierarchical organization, 559
leaf hydraulic resistance, 182
leaf transition from sink to source, 370
types of venation patterns, 559
Leaf wilting, 467
Leaflets
compound leaves, *549,* 550
formation of, 554–555
LEAFY (*LFY*) gene
activation in flowering, *609,* 610, 613
characteristics and functions of, *616*
a floral meristem identity gene, 615, *616*
gibberellin-induced flowering, 612
Leaves
ABA-induced stomatal closure in response to water stress, 466–467, *468*
abscission, 709–712
acclimation to sun and shade environments, 325–326
adaxial and abaxial surfaces, 7, *8*
air space volume, 182
CAM plants, 303
carbon isotope ratio, 341–342
carbon metabolism, 305–306
cell expansion in epidermal pavement cells, 63
chloroplast movements, 329–330, 496–497, *498*
chlorosis from mineral deficiencies, 196, 197, 198, 199
cohesion–tension theory of xylem water transport, 178, *179*
diffusion of carbon dioxide to the chloroplast, 334–336
effects of angle and movement on light absorption, 325
effects of carbon dioxide on photosynthesis, 334–340
effects of light on photosynthesis in the intact leaf, 326–330, *331*
effects of temperature on photosynthesis, 331–333, *334*
epidermis, 11–12
excess light energy dissipation, 328–330
foliar application of nutrients, 202
as "ground state" organs, 617
growth efficiency of tall trees and, 717
guttation, 174
heat dissipation, 331–332
hydraulic resistance, 181–182
Kranz anatomy and C_4 photosynthesis, 298–299, *300,* 301–302, 303
mesophyll cells, 12–13
necrosis from mineral deficiencies, 197, 198, 199
nitrogen assimilation, *439*

optical properties, *323*
ozone injury lesions, 450
percent of solar energy converted into carbohydrates, 323
phenotypic plasticity in response to abiotic stress, 467–468, *469*
photoperiodic induction and, 599
photorespiration and cell redox homeostasis, 297
phytomeres and, 568
properties influencing photosynthesis, 322–326
seedling development in light or dark, 517, 518
senescence regulation, 700–709
senescence syndrome, 696–700
sink-to-source transition, 369–371
soil–plant–atmosphere continuum of water transport, *170*
solar tracking and heliotropism, 325
starch metabolism in chloroplasts, 305–312
structure, function, and types of, 7, *8,* 549–551
sucrose synthesis, 312–316
sulfur assimilation, 438
variegation, 81
venation patterns, 559–564
water movement to the atmosphere, 181–186
Lectins, 736
Leghemoglobins, 431
Legumes
amide or ureide exporters, 435
biological nitrogen fixation, 428, 430–435
exogenous seed dormancy, 509
nitrogen-use efficiency of agriculture, 190
nodules, 430–431
phytoalexins, 747
pod shattering resistance, 659
protein mobilization in seeds, 516, *517*
seeds, 507
solar tracking, 325
Legumins, 516, *517*
Lemna, 4, *330*
Lemon tree, *726*
Lentil (*Lens*), 435
Leptotene, *77,* 78
Lettuce, *481,* 511, *521*
Leucine, *427*
Leucine rich repeat ligand-binding domain, 108
Leucine rich repeats (LRRs), 744
Leucoplasts, 30
LFRs. *See* Low-fluence responses
LFY gene. *See* LEAFY gene
LHCB gene, 456
LHCI. *See* Light-harvesting complex I
LHCII. *See* Light-harvesting complex II
LHCP II protein, 698, 699–700
LHW protein, 684, *685*
Life cycles, 5–7, 625–627
Ligand-gated channels, *231,* 232
Light
absorption and emission by chlorophylls, 248–250
action and absorption spectra of photoreceptors, 477–478, *479, 480*
action spectra of photosynthesis, 252–253
amount required to induce photoresponses, 478–479
breaking of seed dormancy, 511
canopy and light absorption, 324–325
circadian rhythms, 594–597
driver of the photosynthesis, 254–255
ecologically important parameters, *476*
effect on photosynthesis in the intact leaf, 326–330, *331*
irradiance and quantum flux, 322–323
juvenile-to-adult phase changes and, 593
leaf anatomy and light absorption, 323–324
leaf dissipation of excess light energy, 328–330
light deprivation-induced leaf senescence, 705, *706*
photoinhibition, 330, *331*
photosynthetic light-response curves, 326–328
physical properties of, 248
plant photoresponses, 475–476, *477* (*see also* Photoresponses)
quantum efficiency of photosynthesis, 256
quantum yield of photosynthesis, 252
regulation of C_4 photosynthesis, 302
regulation of the Calvin–Benson cycle, 287, 288–290
seedling photomorphogenesis, 517–518, 519–520
Light channeling, 324
Light compensation point, 327
Light reactions of photosynthesis. *See* Thylakoid reactions
Light stress
chloroplasts and the perception of, 456
effects of, *448*
Light-harvesting chlorophyll-binding protein II (LHCP II), 698, 699–700
Light-harvesting complex I (LHCI), 260–261, 268, *269*
Light-harvesting complex II (LHCII), 260–261, 275, 456
Lightning, atmospheric nitrogen fixation, *418,* 419
LIGHT-OXYGEN-VOLTAGE (LOV) phototropin domains, 478, *480, 495,* 496, *497*
Lignin
Casparian strip, 172
organ abscission, 712
PRR-triggered immunity, 744
secondary cell walls, 7, 48, 49, 67–70
synthesis, 67–68
xylem transport cells, 174
Lilium longiflorum, 633
Lima bean (*Phaseolus lunatus*), 739
Lime, 201
Limit dextrinase, 310, 312
Limiting factor hypothesis of photosynthesis, 321
Limiting nutrients
defined, 189
fertilizers, 189, 190, 191
Linamarin, *732*
Linaria vulgaris (toadflax), 620, *621*
Linnaeus, Carl, 620
Linoleic acid, 406, *465,* 661
Linolenic acid, 406, 411, *465,* 661, *735*
Linum usitatissimum, 8
Lipases, *412,* 413, 517
Lipid droplets. *See* Oil bodies
Lipids
biosynthesis of fatty acids, 407, 409–410
biosynthesis of glycerolipids, 410–411
biotechnology and, 407
breakdown during leaf senescence, 698
conversion of storage lipids into carbohydrates, 411–413
defined, 405–406
energy storage and, 405–406
lipid signaling molecules as second messengers, 111–113
mobilization of stored reserves in seeds, 514, 515, 517
overview and significance of, 405
oxidation by ROS, 111
pollen hydration, 635
storage in oil bodies, 514, 515, 517
See also Membrane lipids; Phospholipids
Lipochitin oligosaccharides, 431–432
Lipoxygenase, 661, 698, *735*
LIPOXYGENASE 1 (*LOX1*) gene, 707–708
Liverworts, 4, *5*
Loblolly pine, *440*
Locule, 627, 628, 629
LOCULE NUMBER locus, 659
Lodoicea maldivica (coco de mer), 507
Lolium temulentum (darnel ryegrass), 606
Lomatia tasmanica (King's lomatia), 714
LONELY GUY family of enzymes, *123*
LONESOME HIGHWAY (LHW) protein, 684, *685*
Long-day plants (LDPs)
CONSTANS expression and flowering, 602–603
definition and description of, 598, 599
external coincidence model, 602
induction of flowering by gibberellin, 612, 613
night length and floral induction, *600*
photoperiodic flowering pathway, 613
phytochrome and flowering, 605–606
regulation of flowering by blue-light photoreceptors, 606
response to night breaks, 600–601, 605–606
Long-distance transport
mass transfer rate, 357
in phloem translocation, 351
pressure-flow model, 357–361
unloading and reloading of photosynthates during, 357
Long–short-day plants (LSDPs), 599
LORELEI co-receptors, 109
Lorimer, George, 287
LOV1 domain of phototropin, 496, *497*
LOV2 domain of phototropin, 478, *480, 495,* 496, *497*
Lowest excited state of chlorophyll, 250
Low-fluence responses (LFRs), 484–485, 486
LOX1 gene, 707–708
LS protein. *See* LATERAL SUPPRESSOR protein
LSDPs. *See* Long–short-day plants
Luciferase reporter gene, 494, 606
Lumen. *See* Thylakoid lumen
Lupines, 204, 325, 330
Lupinus, 362
L. albus, 204, 422, *517*
L. succulentus, 325
LURE pollen guidance peptides, 109, 640–641
LURE-like proteins, 641
Lutein, *261*
Lycopene, *100,* 660, *661*
Lycopene crystals, *31*
Lycopodium, 521
L. complanatum, 714
Lysine, *427*
Lysine methylation, 84, *85*
Lysophospholipid, 111, *112,* 113
Lytic vacuoles, 27–28

M

Macadamia, 204
MACROCALYX (MC) protein, 664, 711
Macrofibrils, of cellulose, 51, *66, 67*
Macronutrients
inorganic fertilizers, 201
modified Hoagland solution, *194*
plant tissue concentrations, *191*
See also Essential elements
MADS box, 619
MADS box genes, 619–620
MADS domain, 619–620

MADS-RIN protein, 663, 664
Magnesium
  activation of Rubisco, 287, *288*
  chlorophyll biosynthesis, *277*
  chlorophyll breakdown, 276
  coordination complex with chlorophyll *a*, 233
  effects of soil pH on availability, *201*
  metabolic regulation of pyruvate dehydrogenase, *402*
  mobility within the plant, *196*
  observed and predicted concentrations in pea root tissue, *221*, 222
  in phloem sap, *362*
  in plant nutrition, *192*, 198
  plant tissue concentration, *191*
  regulation of the Calvin–Benson cycle, 289
Magnesium de-chelatase, 276
Magnesium deficiency, 198
Magnolia relatives, *5*
Maidenhair tree (*Ginkgo biloba*), 177, *710*, 715
Maintenance respiration, 403
Maize (*Zea mays*)
  aleurone layer, 652
  apomixis and future crop improvement, 647
  asparagine synthesis, 426
  biological nitrogen fixation, 430
  brassinosteroid and the *nana1* mutant, *118*, 127
  C_4 photosynthesis, *301*
  chromosomal landmarks, *74*
  coleoptile phototropism, *477*, 536
  effects of water stress on, 444, *445*
  embryogenesis, 670–672
  endoreduplication in starchy endosperm, 652
  fatty acid composition of mitochondria, *465*
  fermentation in waterlogged soils, 385
  herbivore-induced volatiles, 739
  imprinted gene expression, 651
  induced aerenchyma, 461
  insect elicitors and, 734
  KNOTTED protein, 547
  leaf air space volume, 182
  light- and dark-grown seedlings, *518*
  nitrogen compounds in xylem sap, *422*
  northern leaf blight disease, 743
  pollen, 630
  preharvest sprouting, 510
  root absorption of ammonium, 208
  root system architecture, 576–577
  selective breeding, 99
  shoot CO_2 levels and nitrate assimilation, *440*
  shrunken2 mutant and starchy endosperm cell death, 652
  stem pectins, 58
  stomata, *184*
  TEOSINTE BRANCHED 1 gene and branching in, 571, *572*
Major histocompatibility complex (MHC), 643
Malaria, 642
Malate
  ABA-induced stomatal closure in response to water stress, 466
  C_4 photosynthesis, 298, *299*, 301
  CAM photosynthesis, 338
  carbon–nitrogen relations and, 439–440
  conversion of storage lipids into carbohydrates, *412*, 413
  crassulacean acid metabolism, 303, *304*, 305
  glycolysis, *383*, 384
  mitochondrial transmembrane transport, 396, *397*
  oxidative decarboxylation by malic enzyme, 391
  PEP metabolism, *383*, 385
  stomatal closure, *239*, 240
  transport into the vacuole, 238
  tricarboxylic acid cycle, 390, 391
Malate dehydrogenase
  conversion of storage lipids into carbohydrates, *412*, 413
  PEP metabolism, *383*, 385
  tricarboxylic acid cycle, 390, 391
Malate synthase, 296, *412*, 413
Male competition, pollen tube growth and, 634
Male gametes
  microgametogenesis, 628–629
  See also Sperm
Male gametophytes
  angiosperm life cycle, *626*
  formation of, 78, 626, 627–630
  plant life cycle, 626
Male sterility, 629, 642–643
Malic acid, *233*, 234–235, 338
Malic enzyme, 391
Malonyl-ACP, 409
Malonyl-CoA, 409
Malto-oligosaccharides, 310
Maltopentaose, 310
Maltose, *306*, 310–311, 351
Maltose transporter, 312
Maltotriose, 310
Malus domestica. See Apple
Malvaceae, 325
MAMPs. *See* Microbe-associated molecular patterns
Manduca sexta (tobacco hornworm), 734
Manganese
  effects of soil pH on availability, *201*
  foliar application, 202
  metabolic regulation of pyruvate dehydrogenase, *402*
  oxygen-evolving complex in photosynthesis, 265
  in plant nutrition, *192*, 193, 199
  plant tissue concentration, *191*
Manganese deficiency, 199
Mango seed, 654
Manihot esculenta (cassava), 732
Mannan, 48
Mannitol, 353, 362, *363*
Mannose
  cell wall polysaccharides, *48*
  glucomannan, 54, *55*
  protein glycosylation, 26
  reducing sugars, *363*
Manometers, 174
Mantle, of mycelium, 212
MAP kinase kinase (MAP2K), 107
MAP kinase kinase kinase (MAP3K), 107
MAP kinase phosphatases, 143
Map-based cloning, 90
MAPK modules, 455
MAPKs. *See* Mitogen-activated protein kinases
Maples (*Acer*), *506*
Marginal veins, *559*
Margo, *175*, 177
Marker-assisted breeding, 91–92
'Maryland Mammoth' tobacco, 598, 607
Mask flower (*Alonsoa warscewiczii*), *354*
Mass flow
  pressure-flow model of phloem translocation, 358
  of soil mineral nutrients to roots, 208
Mass spectrometers, 340
Mass spectroscopy, measurement of plant auxin levels, *131*
Mass transfer rate, 357
Massulae, 628
Maternal inheritance, of chloroplast genes, 275
Maternally expressed genes (MEGs), 652
Matric potential, 160–161, 513
Matrix, mitochondrial. *See* Mitochondrial matrix
Matrix polysaccharides
  cell wall rigidification, 65
  defined, 49
  guard cells, 184
  hemicelluloses, 54, *55*
  lignification, 70
  pectins, 56–58
  primary cell wall assembly, 58–59
  synthesis and delivery to the cell wall, 53–54
Maturation. *See* Seed maturation
Maturation zone, 207, 574, *575*, 576
Mature stage embryo, 671, *672*
Maximum quantum yield of photosynthesis, 327
MC protein. *See* MACROCALYX protein
MC9 protein, 693
MDIS1-MIK receptor-like kinases, 641
Mechanical hypothesis of pollen tube growth, 639
Mechanosensitive channel of small conductance (MscS), 105
Mechanosensitive channels, 105, *106*
Medicago sativa. See Alfalfa
Medicago truncatula (barrel clover), 654, 655, *724*
Medicarpin, *747*
Medick, 727
Megagametophytes. *See* Female gametophytes
Megapascals (MPa), 156, *157*
Megaspore mother cell, 631, 632
Megaspores
  angiosperm life cycle, *626*
  defined, 7
  formation of, 78, 626
  plant life cycles, *6*, *7*
  Polygonum-type embryo sac development, 632–633
Megasporocytes, *626*
Megastrobili, 7
Megathyrsus maximus, *301*
MEGs. *See* Maternally expressed genes
Meiosis
  angiosperm life cycle, *626*
  defined, 5
  description of, 76–78
  in microsporogenesis, 627, *628*
  plant life cycles, 5, 6, 626
  polyploidy and, 78–79
Meiotic reduction, 78
MeJA. *See* Methyl jasmonate
MEKK1, *704*
Melon (*Cucumis melo*), 354, 663
Membrane depolarization
  ABA-induced stomatal closure, 466, *468*
  blue-light inhibition of stem elongation, 494
Membrane fluidity
  factors affecting, 18
  temperature stress and, 463–464, *465*
Membrane lipids
  alteration in response to abiotic stress, 463–464, *465*
  breakdown during leaf senescence, 698
  effect on membrane function, 411
  influence on membrane function, 411
  mitochondrial membranes, 389, *410*
  overview and description of, 16–18
  polar glycerolipids, 407, *408*, *410*
  as precursors of signaling compounds, 411
Membrane permeability
  channels, 224–226
  comparing artificial to biological membranes, 223
  defined, 219
  diffusion potential, 220
  transport proteins, 223–224
Membrane potential
  distribution of ions across a membrane, 220–221
  methods of measuring, 221
  phytochrome regulation of, 487
  proton transport, 222–223

Membrane proteins
  description of, 18
  in phospholipid bilayers, *17*
  polarized localization, 18
  See also Transport proteins
Membrane transport processes
  carriers, *223,* 226
  channels, *223,* 224–226
  kinetic analyses of, 228
  primary active transport, 226
  secondary active transport, 226–227
  transport proteins and, 223–224
Membrane transport proteins. *See* Transport proteins
Membranes
  alteration of membrane lipids in response to abiotic stress, 463–464, *465*
  aquaporins and water movement, 165–166
  oil-body membrane, 407
  plasma membrane hydraulic conductivity, 164–165
  selective permeability and osmosis, 159
  transport of ions across, 219–223
  See also Plasma membrane
Memory, plant recovery from abiotic stress and, 470
Meristematic zone, 206, *207,* 542, *543*
Meristemoid mother cells (MMCs), 556, 557, 558
Meristemoids, 542, 556, 557–558
Meristems
  defined, 10, 541
  indeterminate growth and, 541–542
  proplastids, 30
  secondary growth and, 10, *11*
  types of, 10, 542
  See also specific meristems
Mesembryanthemum crystallinum (ice plant), 305
Mesocarp, 659, *660*
Mesocotyl, 508
Mesophyll
  ABA-induced stomatal closure, 186
  C_4 photosynthesis, 298
  functions, 12
  ground tissue, 10
  Kranz anatomy and C_4 photosynthesis, 298–299, *300,* 301–302, 303
  leaf hydraulic resistance, 182
  oligomer-trapping model of phloem loading, 354–355
  parenchyma, 12–13
  passive symplasmic phloem loading, 355–356
  in photosynthesis, 247–248
  stomata development, 557
  transport of photosynthate to sieve elements, 351
  water movement from leaf to atmosphere, 181
  See also Spongy mesophyll
Mesophyll resistance, 335–336
Mesorhizobium, 428
Mesquite, 205, *750*
Messenger RNA (mRNA)
  basic steps in gene expression, 20, *21,* 22
  degradation, 86
  mobile RNAs in phloem signaling, 374–375
  in phloem sap, 364
  posttranscriptional modification and the RNAi pathway, 86–90
  transcription and the formation of, 81–83
  transcription termination and polyadenylation, *82,* 84
  transcriptional analysis, 92
Metabolic profiling, 386
Metabolic redundancy, 384
Metabolic stress sensing, 452
Metabolons, 388
METACASPASE 9 (MC9) protein, 693
Metal transporters, 234–235
Metalloid transporters, 235
Metalloproteases, 516
Metaphase
  meiosis, *77,* 78
  mitosis, 37, 38, *39,* 40
Metaphase plate, 40, *77,* 78
Metaphloem, 520
Metaxylem, 520
Methane, 338, 404
Methanococcus, 428
Methionine, 124, *427,* 438
2-Methoxy-3,6-dichlorobenzoic acid (dicamba), 114, 121
Methyl jasmonate (MeJA)
  adventitious resin ducts and, 730
  leaf senescence and, 707–708
  root hair development and, 522
Methyl salicylate, 661
Methylation
  of DNA, 84, *85*
  of histones, 84–86
Methylbutanals, 661
Methylbutanols, 661
Methylenetetrahydrofolate (MTHF), 291, *292–293,* 297, 491–492
Methyl-IAA, 120
Methyltransferases, 84
MHC. *See* Major histocompatibility complex
Microbe-associated molecular patterns (MAMPs), *742,* 743, 744
Microelectrodes, 221
Microfilaments. *See* Actin microfilaments
Microgametogenesis, 627, 628–629
Microgametophytes. *See* Male gametophytes
Micrographia (Hooke), 46
Micronutrients
  in fertilizers, 201
  modified Hoagland solution, *194*
  plant tissue concentrations, *191*
  See also Essential elements
Microorganisms
  beneficial interactions, 723–725
  pathogenic interactions, 721 (*see also* Plant pathology)
  plant tolerance to abiotic stress and, 451–452
Microplitis croceipes, 739
Micropylar endosperm, 648, 649, *650*
Micropyle
  Arabidopsis, 631, 632, *648*
  in double fertilization, 641
  guided growth of the pollen tube toward, 639, 640–641
  programic phase of reproduction, *634*
MicroRNAs (miRNAs)
  abiotic stress responses, 458–459
  double-stranded RNA and, 86
  establishment of adaxial leaf identity, 552, *553*
  mobile RNAs in phloem signaling, 374
  phase transitions in plants, 594
  in phosphate and sulfate signaling, 438–439
  regulation of leaf senescence, 702–703, *704,* 705
  RNAi pathway and posttranscriptional gene regulation, 86, 87, 88, 90
  shoot apical meristem formation, *688*
Microsatellites, 74
Microsporangia, 627–629
Microspores
  angiosperm life cycle, *626*
  defined, 7
  formation of, 78, 626, 627–628
  microgametogenesis, 628–629
  plant life cycles, *6,* 7
Microsporocytes, *626,* 627–628
Microsporogenesis, 627–628
Microstrobili, 7
Microtubule organizing centers (MTOCs), 34
Microtubules
  cell wall rigidification, 66
  defined, 32
  kinesins and cytoplasmic streaming, 34
  mitosis, 38, *39,* 40
  plant cell structure, *16*
  polarity, dynamic instability, and treadmilling, 34, *35*
Middle lamella
  abscission, 709, 712
  composition, 47
  definition and description of, 7, *9*
  lignification, 69
  plant cell structure, *16*
Midrib, *549*
Midvein, *559,* 561–562
  See also Primary vein
Milkweed (*Asclepia curassavica*), 730
Milkweed aphid (*Aphis nerii*), 730, *731*
Milkweed bug (*Oncopeltus fasciatus*), 730, *731*
Mimosa pudica, 104, 146, *728*
Mimulus guttatus (yellow monkey flower), 468
Mineral deficiencies
  causes of and difficulties in diagnosing, 195
  disruption of plant metabolism and function, 195–196
  fertilizer applications, 200–202
  methods of analyzing, 199–201
  mobility of elements within the plant, 196
  in nutrients important for structural integrity, 197
  in nutrients in ionic form, 197–198
  in nutrients involved in redox reactions, 198–199
  in nutrients part of carbon compounds, 196–197
  shoot branching and the nutrient deficiency response, 572
Mineral nutrition
  assimilation of nutrients (*see* Nutrient assimilation)
  deficiency zone, 199–200
  defined, 189
  effects of soil pH on nutrient availability, *201*
  essential elements, 191–193
  fertilizers, 189, 190, 191, 200–202
  foliar application of nutrients, 202
  methods of analyzing plant nutritional status, 199–201
  mineral deficiencies, 195–202 (*see also* Mineral deficiencies)
  nutrient distribution and monocarpic senescence, 716
  nutrient solutions, 194–195
  recycling during leaf senescence, 696, 699–700
  root systems and mycorrhizas, 205–213
  soils and, 202–205
  techniques in nutritional studies, 193–194
Mineralization, 201–202, *418*
Minimum promoter, 81–83
Mini-phragmoplasts, 649, *650*
miRNAs. *See* MicroRNAs
Miscanthus, 303, 333, *428*
Mistletoe (*Viscum*), 749, *750*
Mitchell, Peter, 267, 270, 394
Mites, 733
Mitochondria
  abiotic stress perception, 456
  ATP synthase and proton transport, 223
  bioengineered photorespiratory bypass pathways, 296
  companions cells, 350
  conversion of storage lipids into carbohydrates, *412,* 413
  crassulacean acid metabolism, *304*
  defined, 388

endosymbiosis and the origin of, 276
fatty acid composition, *465*
fission, 31
growth in size, 31–32
lipid composition of membranes, *410*
motor proteins and cytoplasmic streaming, 34
movement in the cell, 32
NADPH dehydrogenase, 386
oxidative phosphorylation, 391–400
phosphate assimilation, 438
photorespiration, 291, *292–293*
in plant biosynthetic and redox networks, 400–401
plant cell structure, *16*
in plant respiration, *380*
sieve elements, 348, *349*
significance of respiration in photosynthesis, 403
structure and function, 29, 388–389
transmembrane transport and, 396, *397*
tricarboxylic acid cycle, 388–391
Mitochondrial DNA (mtDNA), 398
Mitochondrial electron transport
ATP synthesis, 394–396
description of, 392, *393*
location of, 29
non-energy conserving electron transport, 393–394, 398–400, 404
overview, 381
similarity to photosynthetic electron flow, *272*
supplementary branches, 393–394
See also Oxidative phosphorylation
Mitochondrial genome
base editing, 98
cytoplasmic male sterility, 398, 642–643
description of, 80–81
encoding of subunits of the respiratory complexes, 398
RNA processing and, 396
size of, 398
Mitochondrial matrix
description of, 388, *389*
electron transport chain, 392, *393*
malic enzyme, 391
mitochondrial transmembrane transport, 396, *397*
tricarboxylic acid cycle, 29, 389–391
MITOGEN-ACTIVATED PROTEIN KINASE KINASE KINASE 1 (MEKK1), *704*
Mitogen-activated protein kinases (MAPKs)
abscission, 712, *713*
inducible plant defenses, 734
leaf senescence, 705, 708
PRR-triggered immunity, *742,* 744
regulation of MAP kinase pathway, 143
signal amplification, 107
stress-response pathways, 454–455
Mitosis
angiosperm life cycle, *626*
condensation of chromatin, 20
defined, 5
events of, 38–40
formation of gametes, 626
formation of gametophytes, 626
free nuclear mitotic divisions in embryo sac development, 632
in microgametogenesis, 628, 629
mitotic phase of the cell cycle, 36, *37,* 38
in nuclear-type endosperm development, 648, 649–650
overview, 37
plant life cycles, 5–7
vegetative segregation of plastids and mitochondria, 81
Mitotic phase (M phase), 36, *37,* 38
See also Mitosis
Mitotic spindle, 38, *39,* 40
Mixed fertilizers, 201
MIZU-KUSSEI 1 (MIZ1), 534
MKK4/5, 712, *713*
MKK9-MAPK6 (MPK6), *702,* 705
MMCs. *See* Meristemoid mother cells
Model organisms, 4
Modified Hoagland solution, 194–195
MoFe protein, 434
Molecular chaperones, 462–463, *464*
Molecular shielding, 463
Molybdenum
effects of soil pH on availability, *201*
mobility within the plant, *196*
nitrate assimilation, 421
in plant nutrition, *192,* 199
plant tissue concentration, *191*
Molybdenum deficiency, 199, 421
Monarch butterfly (*Danaus plexippus*), 730, *731*
Monocarpic plants
definition and examples of, 714, *715*
senescence and, 715–716
Monocots
chelators, 195
major group among angiosperms, 4
overview of embryogenesis in, 670–671, 672 (*see also* Embryogenesis)
parallel leaf venation, 559
in plant evolution, *5*
potassium deficiency, 197
root system architecture, 205, 206, 573, 576–577
secondary growth in, 568
seedling photomorphogenesis, 517, *518*
stomata development, 558–559
Monodehydroascorbate reductase, 462, *463*
Monoecious flowers, 642, *643*
Monoecious plants, 7
Monogalactosyldiacylglycerol, *408, 410*
Monolignols, 67–68, 69
MONOPTEROS (*MP*) gene, 679–680, 681–682, 684, 686, *687*
Monovinyl protochlorophyllide *a, 277*
Montmorillonite, 203
Morning glory (*Ipomoea nil*), 360
Morphogenesis, 669
Morphogens, 127–132
Morphs, 642, *643*
Morus (mulberry), *730*
Mosses, 4, *5, 6,* 669
Moth mullein (*Verbascum blattaria*), 656
Moths, 739
Motor proteins, 34, 36
Mougeotia, 481, 487
Mountain ash, 177–178
MP gene. *See* MONOPTEROS gene
MPK3/6, 712, *713*
MPK6, *702,* 705
MscS. *See* Mechanosensitive channel of small conductance
mtDNA. *See* Mitochondrial DNA
MTHF. *See* Methylenetetrahydrofolate
MTOCs. *See* Microtubule organizing centers
Mucigel, 206, *207*
Mucilage, 521
Mulberry (*Morus*), *730*
Muller, H. J., 90
Multinet growth hypothesis, 60
Multiple fruits, 657
Multivesicular bodies, 26, *27*
Münch, Ernst, 357
Muriate of potash, 201
Mustard (*Eruca*), *518*
Mustard family. *See* Brassicaceae
Mutagenesis
methods in, 90–91
sequence-specific nucleases and targeted mutations, 95–*97*
Mutants/mutations
defined, 90
transposons, 75, *76*
using to study gene function, 90–91
whole-plant senescence, 715
Mutational load, 715
Mute mutant, *555,* 556
MUTE transcription factor, 556, *558,* 559
Mutualisms
common symbiotic pathway and, 723, 725
defined, 721
mycorrhizas (*See* Mycorrhizas)
overview, 723
symbiotic nitrogen fixation, 723, *724* (*see also* Symbiotic biological nitrogen fixation)
MYB transcription factor, 552, *553*
Myc factor signaling, 723
MYC transcription factors, 141, *143,* 735, *736*
Mycelium, 211, 212, 213
Mycorrhizal fungi, 210–213
Mycorrhizas (mycorrhizae)
arbuscular mycorrhizal associations, 210–212, 723, 725
common symbiotic pathway, 723, 725
defined, 210
ectomycorrhizas, 210, 211, 212, 213
movement of nutrients from soils to roots, 213
nutrient deficiency response and, 572
nutrient uptake by roots, 210–213, 578
phosphate availability in soils and, 204
transfer of nutrients between plants, 213
Myelobastosis (MYB) transcription factor, 552, *553*
Myosins, 34, 36
Myristic acid, *17, 406*
Myrosinase, 731
Myrtaceae, 211

N

NAC SECONDARY WALL THICKENING PROMOTING FACTORS (NSTs), 659
NAC transcription factor family, 693, 702, 707
NAC-NOR protein, 663
Na^+-dependent pyruvate transporter, 303
NADH. *See* Nicotinamide adenine dinucleotide
NADH dehydrogenase
ADP:O ratio and, 394, *395*
mitochondrial electron transport, 392, *393*
non-energy conserving electron transport, 393, *394*
NADH-dependent reductase, 291, *292–293*
NADP. *See* Nicotinamide adenine dinucleotide phosphate
NADP–glyceraldehyde-3-phosphate dehydrogenase
Calvin–Benson cycle reactions, 283, *284–285*
regulation of in the Calvin–Benson cycle, 287, 288, 289
NAD(P)H dehydrogenases, 386, 393
NADPH oxidase
ABA-induced stomatal closure in response to water stress, *468*
lignification of the Casparian strip an, 69
reactive oxygen species and, 111
stress-response pathways, 454, *455*
systemic acquired acclimation, 456, *457*
See also Respiratory burst oxidase homologs

NAD(P)–malate dehydrogenase
  C_4 photosynthesis, *299,* 301, 302
  crassulacean acid metabolism, 303, *304,* 305
NADP–malic enzyme
  bioengineered photorespiratory bypass pathways, 296
  C_4 photosynthesis, *298,* 299, 301, 302, 303
Nagaharu U, *80*
Na^+–H^+ antiporter, 230, 232, 465
Na^+/K^+-ATPase, 226, 728–729
Nana1 mutant, *118,* 127
1-Naphthoxyacetic acid, 130
N-1-Naphthylphthalamic acid (NPA), 130, 519, 547
Napin, *517*
1-Napthalene acetic acid (NAA), 114
Nastic movements, 522–523
NCED enzyme, 125
ncRNAs. *See* Noncoding RNAs
ND_{in}(NADH), 393, 400
ND_{in}(NADPH), 393
Necrosis, 691
Necrotic spots, 197, 198, 199
Necrotrophic pathogens, 741
Negative regulation
  ethylene receptors and, 133, 136
  hormone signaling pathways, 139, 144
Neljubov, Dimitry, 117
Nelumbo nucifera (Indian or Asian lotus), 509, 656
Nematodes, 748–749
Neochrome, 487, *495,* 496
Neoxanthin, *261*
Nepenthes alata, 230
Nerium oleander (oleander), 730, *731*
Nernst equation, 221–222
Nernst potential, 221
Neurospora, 594
Neutral pectic polysaccharides, 57
Never-ripe tomato mutation, 662
Nexine, 629
NH_3–H^+ symporters, 230
NHEJ pathway. *See* Non-homologus end-joining DNA repair pathway
N-hydroxy-pipecolic acid (NHP), 746, 747
Nickel, *191, 192,* 199
Nickel deficiency, 199
Nicotiana
  grafting studies on the floral stimulus, 607
  juvenile-to-adult phase changes, 593
  leaf transition from sink to source, 369–370
  N. attenuata, 734, 739
  N. plumbaginifolia, 512
  N. sylvestris, 607
  See also Tobacco
Nicotianamine, 465
Nicotinamide adenine dinucleotide ($NAD^+/NADH_2$)
  ammonium assimilation, 425–426
  bioengineered photorespiratory bypass pathways, 296
  carbon–nitrogen relations and, 440
  conversion of storage lipids into carbohydrates, *412,* 413
  dynamic regulation of respiration, 401
  fermentation, *383,* 385
  glycolysis, 380, 382, *383,* 384, 385
  iron-chelate reductase and, 234
  metabolic regulation of pyruvate dehydrogenase, *402*
  mitochondrial respiration in photosynthesis, 403
  nitrate assimilation, *420,* 421, 440
  nitrogen assimilation, *439*
  oxidative phosphorylation, 381
  photorespiration, 291, *292–293*
  role in plant respiration, *380*
  role in redox reactions, 381–382
  ROS scavenging and, 462, *463*
  rotenon-insensitive dehydrogenases and, 393, 400
  structure and reactions of, *381*
  sulfur assimilation, 438
  TIR-NLR proteins and, 744
  total yield in aerobic respiration, 396, *398*
  tricarboxylic acid cycle, 381, 389, 390, 391
Nicotinamide adenine dinucleotide phosphate ($NADP^+$/NADPH)
  ammonium assimilation, *425,* 426
  bioengineered photorespiratory bypass pathways, 296
  C_4 photosynthesis, *299*
  Calvin–Benson cycle, 282, 283, *284–285,* 285
  dynamic regulation of respiration, 401
  fatty acid biosynthesis, 409
  functions of, 382
  iron-chelate reductase and, 234
  nitrate assimilation, *420,* 421
  oxidative pentose phosphate pathway, 381, 386, *387,* 388
  in photosynthesis, 247, 248, 254, 255, *258,* 259
  photosynthetic electron transport, *255,* 261, *262,* 263
  ROS scavenging and, 462, *463*
  rotenone-insensitive dehydrogenases and, 393, 400
  structure and reactions of, *381*
  sulfur assimilation, 438
Nicotine, 739
Niel, C. B. van, 252
Night breaks, 600–601, 605–606
Night length, floral induction and, 599–600
Night-blooming jasmine (*Cestrum nocturnum*), 599
NIN protein, 432
NINJA protein, 141, *143*
Nitella, 34, 59, 222
Nitrate
  assimilation, 417, 420–423, *424,* 439–440
  bioengineering of plant respiration and, 404
  breaking of seed dormancy, 512
  fertilizer leaching, 191
  modified Hoagland solution, 195
  nitrogen biochemical cycle, 419
  nitrogen fixation, 418
  observed and predicted concentrations in pea root tissue, *221,* 222
  in phloem sap, *362*
  root absorption of, 208
  in soils, 203, 204
  stomatal closure and, *239,* 240
  toxicity and plant responses to, 419–420
  unloading from xylem parenchyma, 242
  whole plant responses to nitrogen deficiency, 210
Nitrate leaching, 201, *418, 419*
Nitrate reductase, 199, *420,* 421, 423, *424*
Nitrate transceptor, 423, *424*
Nitrate transporters
  auxin transport, 130
  description of, 230, 233–234
  nitrate signaling, 423, *424*
  nitrate transport, 422, 423
  nitrate uptake, 420
  response to nitrogen deficiency in roots, 210
Nitric acid, 204, 419
Nitric oxide, *454,* 512
Nitrification, *418, 419*
Nitrile, *732*
Nitrite
  nitrate assimilation, 417, 420, 421–422
  nitrogen biogeochemical cycle, *419*
Nitrite reductase, 421–422, 423, *424*
Nitrogen
  assimilation (*see* Nitrogen assimilation)
  availability in soils, 196
  bark storage proteins, 586
  biogeochemical cycle, 418–420
  effects of soil pH on availability, *201*
  fixation (*see* Biological nitrogen fixation; Nitrogen fixation)
  foliar application, 202
  inorganic fertilizers, 201
  mobility within the plant, *196*
  modified Hoagland solution, 195
  photorespiration and, 294, 295, 297
  in plant nutrition, 191–192, 196
  plant tissue concentration, *191*
  root uptake via mycorrhizas, 213
  transport proteins for nitrogen-containing compounds, 230–231
Nitrogen assimilation
  amino acid biosynthesis, 426–427
  ammonium assimilation, 424–426
  biological nitrogen fixation, 427–435 (*see also* Biological nitrogen fixation)
  energetics of, 439, 440
  nitrate assimilation, 417, 420–423, *424*
  nitrogen biogeochemical cycle, *418,* 419
  photoassimilation, 439
  photorespiration and, 439–440
Nitrogen deficiency
  description of, 196
  molybdenum and, 199
  nutrient mobility within the plant and, 195
  root system responses to, 210
Nitrogen fertilizers
  climate change, 190
  energy expenditure on, 189
  leaching, 189, 191
Nitrogen fixation
  biological (*see* Biological nitrogen fixation)
  industrial, 418, 419
  molybdenum deficiency and, 199
  nitrogen biogeochemical cycle, 418–419
Nitrogen oxides (NOx), 190
Nitrogenase
  anaerobic conditions, 429, 431
  molybdenum and, 199
  reactions catalyzed by, *435*
Nitrogenase enzyme complex, 434–435
Nitrogen-use efficiency (NUE), 190
Nitroglycerin, 417
p-Nitrophenyl β-D-glucuronide, 128
Nitrosylation, 109
Nitrous oxide, 190, 422
N-linked glycan, 26
N-linked glycoproteins, 26
NLP7 transcription factor, 423, *424*
NLRs. *See* Nucleotide-binding site–leucine rich repeat proteins
NLS. *See* Nuclear localization signal
N-myristoylation, 109
Nod box, 431
Nod factor receptors (NFRs), 432, 723, *724*
Nodal roots, 205
Nodes, 7, *8,* 568
Nodulation (Nod) factors, 431–432, 723, *724*
Nodulation (nod) genes, 431–432
Nodule inception (NIN) protein, 432
Nodule meristem, 434
Nodule primordium, 432–433
Nodules
  conversion of ammonia to organic forms, 435
  description of, 430–431
  formation of, 432–434
  signaling molecules in the formation of, 431–432
Nodulin genes, 431–432

N-OGlc-pipecolic acid, 746
Non-articulated laticifers, 730
Non-cell autonomous response, 105
Nonclimacteric fruit, 662, 663
Noncoding RNAs (ncRNAs)
  nuclear genome, 73–74
  RNAi pathway and the regulation of mRNA activity, 86–90
Non-endospermic seeds, 507
Non-energy conserving electron transport, 393–394, 398–400, 404
Nonenzymatic proteins, in cell walls, 49, *50*
NONEXPRESSOR OF PR GENES (NPR) proteins, 705, 746–747
Non-homologus end-joining (NHEJ) DNA repair pathway, 97
Non-Mendelian inheritance, 275
Nonphotochemical quenching, 274, 328–330
NONPHOTOTROPIC HYPOCOTYL (NPH) proteins, 495, 537, 538, *687*
Nonreducing sugars, 362, *363*
Non-ripening (*nor*) locus, 663, 664
Non-seed plants, 4
Nonvascular plants, 4, *5*
NON-YELLOW COLORING 1 (NYC1) protein, *706*
Nor locus, 663, 664
NORs. *See* Nucleolar organizer regions
Northern blotting, 92
Northern leaf blight disease, 743
Norway spruce, 75, 696
Nostoc, 428
NPA. *See N*-1-Naphthylphthalamic acid
NPF3 nitrate/peptide transporter, 128
NPH proteins. *See* NONPHOTOTROPIC HYPOCOTYL proteins
NPH3/RPT2 LIKE (NRL) proteins, 537
NPH4 gene, *687*
NPPB anion channel blocker, 494
NPR proteins. *See* NONEXPRESSOR OF PR GENES proteins
NRL proteins, 537
NRT nitrate transporters, 130, 210, 420, 422, 423, *424*
NSTs. *See* NAC SECONDARY WALL THICKENING PROMOTING FACTORS
NtcA transcription factor, 429
Nucellus, 507, 631, 632
Nuclear envelope
  endomembrane system, 15
  meiosis, 78
  mitosis, 38, *39*
  plant cell structure, *16*
  structure, 19
Nuclear genome
  defined, 18–19
  interphase chromosomes, 76
  meiosis, 76–78
  overview, 73–74
  polyploidy, 78–80
  posttranscriptional regulation of gene expression, 86–90
  structural landmarks of chromosomes, 74–75
  transcriptional regulation of gene expression, 81–86
  transposons, 75–76
  types and structure of chromatin, 74
Nuclear localization signal (NLS), 19, 482, 483
Nuclear pores
  export of miRNA, 86, *87*
  protein synthesis, 20, *21*
  structure, 19
Nuclear-type endosperm development, 647, 648–650
Nucleation sites, 180
Nucleolar organizer regions (NORs), 20, 74–75
Nucleolus, *16,* 20, 38, 75
Nucleoplasm, 19
Nucleoporins, 19
Nucleosomes, 20, 74, 81, 84–86
Nucleotide-binding domain (NBD), 744
Nucleotide-binding site–leucine rich repeat proteins (NLRs), *742,* 744–745, 749
Nucleus
  chromosomes, 19–20
  defined, 18
  gene expression, 20, *21*
  interphase, 76
  nuclear genome, 18–19
  nucleolus, 20
  phytochrome signaling, 483–484
  plant cell structure, *16*
  structure, 19
NUE. *See* Nitrogen-use efficiency
Nutation, 522, 523
Nutational growth, 551
Nutrient assimilation
  amino acid biosynthesis, 426–427
  ammonium assimilation, 424–426
  biological nitrogen fixation, 427–435
  definition and overview of, 417–418
  energetics of, 417, 439–440
  nitrate assimilation, 420–423, *424*
  oxygen assimilation, 439
  phosphate assimilation, 438–439
  root system plasticity and, 578
  sulfur assimilation, 435–438
Nutrient deficiency response, 572
  See also Mineral deficiencies
Nutrient depletion zone, 208
Nutrient recycling, during leaf senescence, 696, 699–700
Nutrient solutions
  foliar applications, 202
  formulations for rapid plant growth, 194–195
  in nutritional studies, 193–194
Nutrients. *See* Macronutrients; Micronutrients; Mineral nutrition
Nuts, *506*
NXH transporter family, 232
NYC1 protein, *706*
Nyctinasty, 475, 728
Nymphaeaceae, 521
Nymphaeales, 632
Nyssa sylvatica (blackgum), *714*

O

Oaks (*Quercus*)
  bark, 586
  cell walls, 46
  length of juvenile period, *593*
  longevity, *714*
  phellogen and phellem, 586
  phenotypic plasticity of leaves, *469*
  pollen, 630
  seeds, *506*
OAS. *See O*-Acetylserine
Oat (*Avena sativa*)
  lag time for auxin-induced elongation, 525
  nitrogen compounds in xylem sap, *422*
  photoreversible responses induced by phytochrome, *481*
  proplastid development, *31*
  very low fluence phytochrome responses, 485
Obligate flowering response, 592
Octant embryo, 671, *672, 673,* 674–675
OEC. *See* Oxygen-evolving complex
Oenothera, 633
Oil bodies
  endomembrane system, 15
  mobilization of stored reserves in seeds, 514, 515, 517
  plant cell structure, *16*
  storage of lipids in, 514, 515, 517
  storage of proteins in, 515
  storage of triacylglycerols in, 406–407, 411
  structure and function, 28
Oils
  biotechnology and, 407
  characteristics of triacylglycerols, 406–407
  defined, 406
  energy storage, 405–406
Oilseed plants, 515
Oilseeds, 411, 413
Oleander (*Nerium oleander*), 730, *731*
Oleic acid, 406, 407, *465*
Oleosins, 407, 515, 517
Oleosomes, 28
  See also Oil bodies
Oligomer-trapping model of phloem loading, 354–355, 356, 357
Oligosaccharides
  LEA proteins and seed dessication tolerance, 655
  oligomer-trapping model of phloem loading, 354–355, 356, 357
O-linked oligosaccharides, 26
Omega-3 fatty acid desaturase, 463
Onagraceae, 632
Oncopeltus fasciatus (milkweed bug), 730, *731*
Onions, *47,* 185, *507*
Onoclea, 481
ONSEN retrotransposon, 76, 459
Oomycetes, 741, 743
Open Stomata 1 (OST1) kinase, 453, *468*
Opines, 93
Opuntia, 551, *726*
  O. ficus-indica, 164
  O. stricta, 305
Orchids
  crassulacean acid metabolism, 303
  hollow styles, 633
  pollinia, 628
  seed size, 506–507
ORESARA1 (ORE1) protein, 702–703, 705, 706, *707*
Organ abscission, 709–713
Organ senescence, 691
Organelles
  base editing of genomes, 98
  cell cycle and, 37–38
  directed organelle movement, 34, 36
  endomembrane system, 23–29
  independently dividing semi-autonomous organelles, 29–32
  main categories of, 15
  nucleus, 18–22
Organic acids, in phloem sap, 362
Organic fertilizers, 201–202
Organic matter, cation exchange capacity, 203
Organic residues, mineralization, 201–202
Organogenesis, 669–670
Organosilicon surfactants, 202
Orobanche, 118
Orthodox seed, 653–656
Oryza sativa. See Rice
Oryza sativa NAC2 (OsNAC2) protein, 707
Oryzalin, 60, *61*
OsFD1 gene, *616*
Osmolarity, 160
Osmoprotectants, 461
Osmosis, 157, 159, 162
Osmotic adjustment, 460–461
Osmotic potential
  blue light-induced stomatal opening, 240
  defined, 160
  osmotic adjustment, 460–461
  phloem loading, 352–353
  root pressure, 174
  of soil water, 170
  stomatal opening, 185
  See also Solute potential
Osmotic stress, 449
OsNAC protein, 707
OST1 kinase, 453, *468*
Outcrossing, 633, 642
  See also Cross-pollination

Outer integument, *631,* 632, 652
Outer mitochondrial membrane, 388, 389, 396, *397*
Output domain of response regulators, 132, *133*
Outwardly rectifying (outward) K^+ channels, 225, 226, *239,* 240, 242
Ovaries
  female gametophytes, 626
  fruits and, *657*
  ovule development, 631–632
  placenta, 631
  programic phase of reproduction, 633–634
  strawberry achenes, 656, 657
OVATE locus, 660
Ovules
  Class D genes and formation of, 620
  endosperm development, 647–652
  female gametophytes, 626, 630–633
  fruits and, *657*
  guided growth of the pollen tube growth, 638–640
  programic phase of reproduction, 633–634
Oxalic acid, 727
Oxaloacetate
  amino acid biosynthesis, 427
  ammonium assimilation, *425,* 426
  C_4 photosynthesis, *299,* 300, 301
  CAM photosynthesis, 338
  conversion of storage lipids into carbohydrates, *412,* 413
  crassulacean acid metabolism, 303, *304*
  PEP metabolism, *383,* 385
  tricarboxylic acid cycle, 389, 390, 391
Oxidases, primary cell wall assembly, 58–59
β-Oxidation of fatty acids, 28, *412,* 413, 517
Oxidative pentose phosphate pathway
  overview, 380–381, 386
  in plant biosynthetic and redox networks, 400–401
  in plant respiration, *380*
  reactions in, 386, *387*
  regulation of, 388
  roles in plant metabolism, 386, 388
Oxidative phosphorylation
  ATP synthesis, 394–396
  electron transport chain, 392–394
  encoding of complexes by nuclear and mitochondrial genomes, 398
  mitochondrial transmembrane transport, 396, *397*
  non-energy-conserving pathways and their functions, 393–394, 398–400
  overview, 381, 391–392
  in plant respiration, *380*
2-Oxoglutarate
  amino acid biosynthesis, 427
  ammonium assimilation, 425, 426
  biological nitrogen fixation, 429
  mitochondrial respiration in photosynthesis, 403
  photorespiration, 291, *292–293,* 294
  tricarboxylic acid cycle, *390,* 391
Oxygen
  action spectra for photosynthesis and, 252–253
  ADP:O ratio, 394, *395*
  affinity of leghemoglobins for, 431
  assimilation of, 439
  concentration in nodules, 430–431
  effect on plant respiration, 404–405
  exogenous seed dormancy, 509
  hydroponics, 193
  oxidative phosphorylation, 392–400
  photorespiration, 291, *292–293,* 294
  plant tissue concentration, *191*
  production in photosynthesis, 254, 255, 264–265
  reduction in respiration, 380, 382
  respiratory quotient, 404
  specificity factor of Rubisco for, 294–295
  triplet chlorophyll and, 250
Oxygen deficiency. *See* Hypoxia
Oxygen fixation, 439
Oxygenases, 439
Oxygen-evolving complex (OEC), 264–265
Ozone, 190, *454*
Ozone stress, 450

P

P680
  absorption characteristics, 264
  oxygen-evolving complex in photosynthesis, 265
  photosystem II, *255* (*see also* Photosystem II)
  Z scheme electron transport, *255,* 261, *262*
P700
  absorption characteristics, 264
  cyclic electron flow, 273
  photosystem I, *255* (*see also* Photosystem I)
  PSI and, 268, *269*
  Q cycle, 267, *268*
  Z scheme electron transport, *255,* 261, *262*
P870, 264
PA. *See* Phosphatidic acid
Pachytene, *77,* 78
Pacific yew, 586
Paclitaxel, 586
Paclobutrazol, 123
Palisade cells
  defined, 324
  leaf light absorption, 324
  parenchyma, *8*
  phototropin-mediated chloroplast movement, 496–497, *498*
  sun and shade leaves, *322*
Palisade mesophyll, 12
Palmate leaves, *549*
Palmitic acid, *17,* 406, *465*
PANGLOSS (PAN) proteins, *558,* 559
Panicum italicum (fox millet), *470*
Papaver rhoeas, 647
Papillae cells, 634, 635, 636, 645
PAPS. *See* 3′-Phosphoadenosine-5′-phosphosulfate
PAR. *See* Photosynthetically active radiation
Paracrine hormones, 113
Paraheliotropism, 325, 330, 467
Parallel venation, 559
Paraquat, 269, *270*
Parasites
  defined, 721
  parasitic nematodes, 748–749
  parasitic plants, 749–750
Parasitoid wasps, 739
Parasponia, 428, 429
Parenchyma
  bundle sheath and palisade parenchyma, *8*
  description of, 12–13
  phloem parenchyma, 348, *351,* 352, 586
  primary cell wall components, 50
  xylem parenchyma, *241,* 242
Parent-of-origin effects, 651–652
Paripinnate leaves, *549*
Paris japonica, 73
Parthenocarpy, 657–658
Partitioning, 371, 372, 376
PAS domain of phytochrome, 482, *483*
Pascals (Pa), 156, *157*
PAS-related domain (PRD) repeats, 482, 483
Passive flux, 220
Passive symplasmic phloem loading, 355–356, 357
Passive transport, 218–219, 226 *See also* Diffusion
Pasteur, Louis, 386
Pasteur effect, 386
Patch clamping, 224
Paternally expressed genes (PEGs), 652
Pathogenesis-related (PR) genes, 746
Pathogens
  effectors, 742–743
  hypersensitive response-type programmed cell death, 693, *694,* 695–696
  plant defenses against, 741–750 (*see also* Plant pathology)
  strategies to invade plants, 741–742
Pattern recognition receptors (PRRs), 742, 743–744
Pattern recognition receptor-triggered immunity (PTI), 741, 742–743
Pavement cells
  cell expansion in leaf epidermis, 63
  definition and description of, 11, *12,* 555
  leaf anatomy, *8*
  patterning of stomata, 557
PAX protein kinase, 108, 538
PC. *See* Phosphatidylcholine; Plastocyanin
PCD. *See* Programmed cell death
PC:DAG acyltransferase, 411
PC:DAG cholinephosphotransferase, 411
PDF2 gene, 683
PDK1 protein, 108
Pea (*Pisum sativum*)
  amide forms of nitrogen, 435
  axillary bud dormancy, 573
  chloroplast, *256*
  ethylene and etiolation, 117
  fatty acid composition of mitochondria, *465*
  flower and fruit, *657*
  green cotyledon phenotype, 700
  nitrogen compounds in xylem sap, *422*
  observed and predicted ion concentrations in root tissue, *221,* 222
  phloem callose, *365*
  photoreversible responses induced by phytochrome, *481*
  rhizobial symbiont, *429*
  shoot apical meristem senescence, 715–716
  stem pectins, 58
  storage proteins, *517*
  transfer cell and phloem loading, *354*
Peanut (*Arachis*), 435
Peanut oil, *406*
PEAR proteins, 581, 582
Pears, *657*
Pectin acetyltransferases, 58
Pectin methyl esterases, 57, 58
Pectins
  cell plate, 47
  cell wall expansion, 62
  cell wall rigidification, 65
  composition and functions, 49
  grass cell walls, 54
  molecular models of cell walls, 64–65
  primary cell walls, 49, 50, *53*
  realignment in the cell wall, 54
  secondary cell walls, 67
  structures and properties of, 56–58
  synthesis and delivery to the cell wall, 53–54
Pee Dee limestone formation, 340
pegRNA. *See* Prime editing guide RNA
PEGs. *See* Paternally expressed genes
Peloria mutant, 620, *621*
Pentatricopeptide repeat (PRR) proteins, 287
Pentose phosphate epimerase, *387*
Pentose phosphate isomerase, *387*

Pentose phosphates, *380,* 381
Pentoses, *48*
PEP. *See* Phosphoenolpyruvate
PEP carboxykinase (PEPCK)
  C_4 photosynthesis, *299,* 301, 302
  conversion of storage lipids into carbohydrates and, *412,* 413
Pep-13, 744
PEPcase. *See* Phosphoenolpyruvate carboxylase
PEPCase kinase, 302
PEPCK. *See* PEP carboxykinase
Peperomia, 633
Peptide hormones, 114
Peptide transporters, 230–231
Peptides, protein modification and, 109
Perennial plants
  defined, 714
  somatic mutations and, 715
  trade-offs between reproductive and vegetative growth in responses to stress, 445
"Perfect" flowers, 7
Perforation plates, *175,* 176
Perhydroxyl radical, *454*
Peribacteroid membrane, 434
Pericarp
  cereal seed structure, *648*
  defined, 506, *507*
  fleshy fruit development, 659–660
Periclinal divisions
  cambial initials, 579, *580*
  radial patterning in embryogenesis and, 683–684
Pericycle
  bark and, 10
  defined, 10, *11*
  nodule formation, 432–433
  origin of, 543, *544*
  origin of lateral root primordia, 573, 574, *575*
  periderm formation, *585,* 586
  phloem import in growing roots, 367
  root anatomy, *8*
Periderm
  a constitutive defense, 722
  cork cambium and the formation of, 585–586
  defined, 10, *11,* 579
Perilla
  P. crispa, 599, 607, 608
  P. fruticosa, 422
Period, of circadian rhythms, 595, *596*
Peripheral endosperm, 648, *649, 650*
Peripheral membrane proteins, *17,* 18, 395
Peripheral zone (PZ), 545, 546
Perisperm, 507
Permanent charge, 202
Peroxidases, 66, 68
Peroxiredoxins (Prx), 462, *463*
Peroxisomes, *12*
  bioengineered photorespiratory bypass pathways, 296
  endomembrane system, 15
  functions of, 28–29
  jasmonate biosynthesis, 735
  leaf senescence, 698
  motor proteins and cytoplasmic streaming, 34
  β-oxidation of fatty acids, 413
  photorespiration, 291, *292–293,* 295
  plant cell structure, *16*
PETAL LOSS (PTL) protein, 582, *583*
Petals
  ABC model of floral organ identity, 617, 618
  asymmetrical floral development, 620–621
  floral organ identity genes, 616, 617
  hypanthium, 657
  initiation of, 614, 615
  Quartet model of floral organ specification, *620*
Petioles, *549,* 550
Petunia, 90, 607, 620
Petunia hybrida, 607
Pfr
  action and absorption spectra for seed germination, 478, *479*
  escape from photoreversibility, 484
  flowering response in short-day plants, 605
  interconversion with Pr, 478, *479,* 480–481
  physiologically active from of phytochrome, 481
  phytochrome interacting factors, 488
  phytochrome signaling, 483
  seedling photomorphogenesis, 518
  very low fluence responses, 485
PGPR. *See* Plant growth-promoting rhizobacteria
pH
  ammonium toxicity and pH gradients, *420*
  cell wall acidification and acid growth, 63–64
  changes in cytosolic or cell wall pH as second messengers, 110–111
  chloroplast pH gradient, 271
  effect on Fe^{3+}-citrate complexes, *195*
  gravitropism, 532–533
  pollen tube tip growth, 636, *637,* 638
  root thigmotropism, 533, *534*
  shoot phototropism, 538
  of vacuolar sap, 238
PHABULOSA (PHB) protein, 687
Phagophores, 694, *695*
Phalaris canariensis, 114
PHAN gene, 552, *553*
Pharbitis, 600
  P. nil, 605
Phase, of circadian rhythms, 595, *596*
Phaseolin, *517*
Phaseolus
  P. lunatus, 739
  P. vulgaris (*see* Common bean)
PHB protein, 687
Phelipanche, 118
Phellem, 580, 585–586
Phelloderm, *579,* 580, 585, 586
Phellogen, 10, 579, 585, 586
  See also Cork cambium
Phenocopying, 681
Phenol, *156*
Phenolic groups, 66
Phenolics, 235, 726, 738
Phenotype
  factors determining, 73
  rescue of, 684
Phenotypic plasticity
  defined, 467
  responses to abiotic stress, 467–469, *470*
Phenylacetaldehyde, 661
Phenylacetic acid, 114
Phenylalanine, 67, *427*
2-Phenyl-ethanol, 661
Phenylpropanoids, 67, 146, 660
Pheophorbide *a, 700*
Pheophorbide *a* oxygenase, *700*
Pheophytin, *262,* 265–266
Pheophytin *a, 700*
Pheophytinase, *700*
PHERES1 (*PHE1*) gene, 652
Phleum pratense, 30, 185
Phloem
  cell types and function, 14–15
  defined, 11, 345
  differentiation in seedlings, 520
  leaves, *8*
  location in vascular tissue, 347
  members of phloem tissue, 348
  nitrate transport, 422–423
  radial patterning in embryogenesis and, 683–684, *685*
  roots, *8,* 207, *241,* 573, *574*
  secondary growth, 10, *11*
  stem anatomy, *8*
  translocation in (*see* Phloem translocation)
  transport of hormones in, 364
  transport of signaling molecules, 373–375
  types of, 346
PHLOEM EARLY DOF (PEAR) proteins, 581, 582
Phloem feeders, 733, 741
Phloem fibers, 10, *11*
PHLOEM INTERCALATING WITH XYLEM (PXY) protein, 582, *583,* 584
Phloem loading
  apoplastic pathway, 352–354
  companions cells, 350–351
  defined, 351
  overview of pathways in, 351–352
  patterns in apoplastic and symplasmic loading, 356
  presence of multiple loading mechanisms, 357
  pressure-flow model of phloem translocation, 357, 358
  regulation by turgor pressure and chemical signals, 374
  smaller-diameter leaf veins and, 559
  transport of photosynthate from mesophyll to sieve elements, 351
Phloem parenchyma, 348, *351,* 352, 361, 586
Phloem pole pericycle, 573, *574,* 586
Phloem rays, *579*
Phloem sap
  defined, 345
  materials in, 361–364
  translocation (*see* Phloem translocation)
  using aphids to sample, 362
Phloem signaling
  interaction of turgor pressure and chemical signals, 374
  mobile proteins, 375
  mobile RNAs, 374–375
  overview, 373–374
  plasmodesmata and, 375
  relevance for biotechnology and climate change, 376
Phloem translocation
  early experiments on, 347
  of florigen, 608, *609*
  gymnosperms, 361
  introduction, 345
  mass transfer rate, 357
  materials translocated, 361–365
  pathways of, 347–351
  phloem loading, 351–357
  phloem unloading, 365–369
  pressure-flow model, 357–361
  relevance for biotechnology and climate change, 376
  in roots, 207
  sink-to-source transition, 369–371
  source-to-sink pattern, 346–347
  of sulfur compounds, 438
  transport of signaling molecules, 373–375
  unloading and reloading of photosynthates, 357
Phloem unloading
  apoplastic pathways, 366, 367–368
  energy requirement of apoplastic import, 368–369
  overview, 369–370
  pressure-flow model of phloem translocation, 357, 358
  regulation by turgor pressure and chemical signals, 374
  symplasmic pathway, 366–367
Phoenix dactylifera (date palm), 653–654, 656
Phosphatases, 109
Phosphate
  assimilation of, 438–439
  observed and predicted concentrations in pea root tissue, *221,* 222
  in phloem sap, *362*
  phosphate-limited photosynthesis, 333
  root absorption of, 208
  root uptake via arbuscular mycorrhizas, 211–212

in soils, 204
storage in seeds, 515
sucrose biosynthesis, *313,* 314, 315
topsoil foraging by roots, 209–210
See also Inorganic phosphate; Pyrophosphate
Phosphate deficiency, 200, 438
PHOSPHATE (*PHO*) genes, 438
PHOSPHATE TRANSPORTER 1 (PHT1) protein, 438
Phosphate transporters, 211–212, 233–234, 396, *397*
Phosphate/triose phosphate translocator, *313*
Phosphatidic acid (PA), *112,* 113, *406,* 410
Phosphatidylcholine (PC)
biosynthesis, 410, 411
in cellular membranes, *410*
lipid signaling, *112,* 113
structure, *17, 406, 408*
Phosphatidylethanolamine, *406, 408,* 410
Phosphatidylglycerol, *408,* 410, 411
Phosphatidylinositol, 113, *408,* 410
Phosphatidylinositol 4,5-bisphosphate (PIP_2), 411
Phosphatidylserine, *408*
3′-Phosphoadenosine-5′-phosphosulfate (PAPs), *436,* 438
3′-Phosphoadenylate, *436*
Phosphoenolpyruvate (PEP)
alternative pathways of metabolism, 391
amino acid biosynthesis, 427
C_4 photosynthesis, *298,* 299, 300–301, 303
CAM photosynthesis, 338
conversion of storage lipids into carbohydrates, *412,* 413
crassulacean acid metabolism, 303, *304*
dynamic regulation of respiration, 401–402
glycolysis and metabolism to pyruvate or malate, *383,* 384, 385
shikimic acid pathway, 388
sodium deficiency and, 198
structure, *382*
Phosphoenolpyruvate carboxykinase (PEPCK)
C_4 photosynthesis, *299,* 301, 302
crassulacean acid metabolism, 303, *304,* 305
Phosphoenolpyruvate carboxylase (PEPcase)
C_4 photosynthesis, 298, 299, 302, 303
carbon isotope ratio and, 341, 342
crassulacean acid metabolism, 303, 304, 305
dynamic regulation of, 402
dynamic regulation of respiration and, 401
PEP metabolism and, *383,* 385, 391
regulation in CAM plants versus C_4 plants, 305
Phosphoenolpyruvate dikinase, *298*
Phosphoenolpyruvate phosphate translocator, 303
Phosphofructokinase, 290, *313,* 314
Phosphoglucan phosphatase, 312
Phosphoglucoisomerase, 312
Phosphoglucomutase, 312, *313,* 314, *383*
6-Phosphogluconate, *387*
2-Phosphoglycerate, *382, 383*
3-Phosphoglycerate
amino acid biosynthesis, 427
C_4 photosynthesis, 298
Calvin–Benson cycle, 283, *284–285, 286*
glycolysis, *383,* 384
photorespiration, 291, *292–293,* 295
product of Rubisco activity, 290
structure, *382*
Phosphoglycerate kinase, *383,* 384
3-Phosphoglycerate kinase, 283, *284–285*
Phosphoglycerate mutase, *383*
Phosphoglycerolipids, 111
2-Phosphoglycolate
Calvin–Benson cycle, *285*
oxygenation of ribulose 1,5-bisphosphate, 290–291
photorespiration, 291, *292–293,* 295
2-Phosphoglycolate phosphatase, 291, *292–293*
PHOSPHOINOSITIDE DEPENDENT KINASE 1 (PDK1), 108
Phosphoinositides, 411
Phospholipase A (PLA), *112,* 113
Phospholipase C (PLC), *112,* 113
Phospholipase D (PLD), *112,* 113, 698
Phospholipases, 111, *112,* 113
Phospholipid monolayers, 28
Phospholipids
functions of, 406
membrane fluidity, 18
oil-body membrane and, 407
overview and description of, 16–18
synthesis in smooth ER, 24
Phosphoribulokinase, *284–285,* 287, 288, 289–290
Phosphorite, 201
Phosphorus
availability in soils, 196, 204
effects of soil pH on availability, *201*
inorganic fertilizers, 201
mobility within the plant, *196*
in plant nutrition, 191–192, 197
plant tissue concentration, *191*
topsoil foraging by roots, 209–210
Phosphorus deficiency, 195, 197, 209–210
Phosphorus fertilizers, 189, 191
Phosphorylases, *309,* 310
Phosphorylation, phytochrome signaling and, 488–489
Phosphorylation relay system, 132–133, *134*
Phosphotidylinositol, 411
Phosphotidylinositol 4,5-bisphosphate (PIP_2), 411
Phosphotransfer proteins, 132, *133, 134*
PHOT1. *See* Phototropin 1
PHOT2. *See* Phototropin 2
Photoassimilation, 439
Photoblasty, 475, 511
Photochemistry, 250
Photochromism, 480
See also Photoreversibility
Photodamage, 256
Photoinhibition, 330, *331*
Photolyase, 491
Photolyase-homology region (PHR) of cryptochrome, *491,* 492, 493
Photomorphogenesis
blue light responses and photoreceptors, 490
cryptochromes, 491–493
definition and overview, 475–476
interactions of cryptochromes with other photoreceptors, 493–495
photoreceptors, 476–479, *480*
phototropins, 495–500
phytochrome responses, 484–487
phytochrome signaling pathways, 487–490
phytochromes, 480–484
responses to UV radiation, 500–501
Photon flux density, 322–323
Photonasty, 475
Photons
absorption and emission by chlorophylls, 248–250
photodamage and, 273
physical properties of, 248
Photoperiodic induction, 599
Photoperiodism
axillary bud dormancy, 573
blue-light photoreceptors and flowering in long-day plants, 606
clock hypothesis of photoperiodic timekeeping, 601–602
CONSTANS and flowering in long-day plants, 602–603
defined, 475, 592, 597
external coincidence models, 602–604
latitudinal gradient in day length, 597, *598*
leaves and photoperiodic induction, 599
linked to vernalization, 610–611
molecular mechanisms of flowering in natural environments, 604
night breaks, 600–601, 605–606
night length and floral induction, 599–600
photoperiodic flowering pathway, 613
phytochrome as the primary photoreceptor in, 605–606
types of photoperiodic responses, 597–599
Photophosphorylation, 270–273
Photoprotection, 273–274
Photoreceptors
absorption and action spectra, 477–478, *479, 480*
amount of light required to induce activity, 478–479
bacterial proteins and, 105–106
characteristics and overview of, 476–477
conventions for abbreviating, 477
cryptochromes, 491–495
phototropins (*see* Phototropins)
phytochromes, 480–490 (*see also* Phytochromes)
promoting photomorphogenic responses, 518
Photorespiration
C_4 photosynthesis and, 302, 303
carbon–nitrogen relations and, 439–440
CO_2 compensation point and, 336, 337
crassulacean acid metabolism and, 304, 305
enhancing biomass by the bioengineering of, 296
enzymes of derive from different ancestors, 295–296
interactions with metabolic pathways, 296–297
linkage to photosynthetic electron transport, 295
overview and reactions in, 290–295
photosynthetic efficiency and, 333
temperature-response curves of photosynthesis and, 333
Photorespiratory phenotype, 296, 297
Photoresponses
amount of light required to induce, 478–479
blue-light responses, 478, *480,* 490, 496–500 (*see also* Blue-light responses)
electromagnetic spectrum of signals, *477*
influence of light quality or spectral energy on, 477–478, *479, 480*
overview, 475–476, *477*
photoreceptors, 476–479, *480*
red and far-red light responses, 480–490 (*see also* Phytochromes)
to UV radiation, 500–501
Photoreversibility
escape from, 484
mediation by phyB, 486
of phytochromes, 478, *479,* 480–481
Photostationary state, 481
Photosynthate
accumulation and partitioning of, 305–306

allocation and partitioning, 371–373
defined, 346
phloem loading, 351–357
phloem unloading, 365–369
sink-to-source transition, 369–371
source-to-sink pattern of phloem translocation, 346–347
transport from mesophyll to sieve elements, 351
unloading and reloading during transport, 357
Photosynthesis
action spectra, 252–253
anoxygenic, 259
biochemical model of, 321–322
carbon isotope ratio, 340–342
carbon reactions of (*see* Carbon reactions of photosynthesis)
coupling of transpiration to by stomata, 183
effects of carbon dioxide on in the intact leaf, 334–340
effects of elevated global CO_2 levels on, 338–340
effects of leaf properties on, 322–326
effects of light on in the intact leaf, 326–330, *331*
effects of temperature on in the intact leaf, 331–333, *334*
electron transport (*see* Photosynthetic electron transport)
energy conversion efficiency, 255–256
energy transfer between antennas and reaction centers, 253–254
interrelationship of the light and carbon reactions, *282*
key experiments in understanding, 252–256
light as the driver of, 254–255
light-response curves, 326–328
limitations on, 256
limiting factor hypothesis of, 321
manganese deficiency and, 199
meaning of term, 247
mechanisms of repair and regulation, 273–275
optimal temperature, 332
organization of antenna complexes, 259–261
organization of photosynthetic apparatus, 256–259
overall chemical reaction, 252, 254
overview, 247–248
photoinhibition, 274–275
photosynthetic yield consumed by respiration, 403
photosystems (*see* Photosystem I; Photosystem II)
physical properties of light, 248
proton transport and ATP synthesis, 270–273
quantum yield (*See* Quantum yield of photosynthesis)
temperature sensitivity of photosynthetic efficiency, 333, *334*
temperature-response curves, 332–333
Photosynthetic carbon reduction cycle. *See* Calvin–Benson cycle
Photosynthetic electron transport
absorption characteristics of PSI and PSII, 264
in anoxygenic photosynthesis, 259
artificial electron acceptors and the discovery of, 254
blocking by herbicides, 269, *270*
cyclic electron flow and ATP synthesis, 272–273
electron transfer by excited-state chlorophyll, 263–264
mechanisms of, 261–269, *270*
organization and structure of PSII, 264, *265, 266*
organization in the thylakoid membrane, 257–259
overview, *253,* 254, 255
oxidation of water by PSII, 264–265, *266*
photorespiration and, 295
proton translocation and, *258,* 259, 265, 270
role of cytochrome b_6f complex, 266–268
role of pheophytin and quinones, 265–266
role of plastocyanin, 268
role of PSI reaction center, 268–269
similarity to respiratory electron flow, *272*
thylakoid integral membrane proteins and, 257
uncoupled, 270
Z scheme, 255, 261–263
Photosynthetic photon flux density (PPFD)
defined, 323
photoinhibition and, 330, *331*
photosynthetic light-response curves, 326–328
xanthophyll cycle and, 329
Photosynthetic pigments
absorption spectra, 249–250, *251*
molecular structure of, 250–251
See also Chlorophylls
Photosynthetic rate
limiting factor hypothesis, 321
optimal temperature, 332
photoinhibition and, 330, *331*
Photosynthetic thermal optimum, 332, 333
Photosynthetically active radiation (PAR), 186, 323, 324
Photosystem I (PSI)
absorption characteristics, 264
C_4 photosynthesis, 302
cyclic electron flow and, 273
electron transfer by excited-state chlorophyll, 263–264
electron transfer to by plastocyanin, 268
light-harvesting complex I proteins, 260–261
organization and structure, 257–259, 268–269
overview, 255
Q cycle, 267, 268
superoxide and photodamage, 273–274
thylakoid stacking and energy partitioning between photosystems, 275
Z scheme electron transport, 255, 261–263
Photosystem II (PSII)
absorption characteristics, 264
C_4 photosynthesis, 302
effects of herbicides on, 269, *270*
electron transfer by excited-state chlorophyll, 263–264
light-harvesting complex II proteins, 260–261
organization and structure of, 264, *265, 266*
organization in the thylakoid membrane, 257–259
overview, 255
oxidation of water by, 264–265, *266*
pheophytin and electron transfer to plastoquinone, 265–266, *266*
photoinhibition and, 330, *331*
photoinhibition and protection from, 273–275
plant acclimation to shade and, 326
PsbS protein and, 274
purple bacteria reaction centers and, 259
Q cycle and, 267, *268*
thylakoid stacking and energy partitioning between photosystems, 275
Z scheme electron transport, 255, 261–263
Photosystems
assembly of, 275–276
biosynthesis and breakdown of chlorophyll, 276, *277*
evolution, 276
genetics of, 275
mechanisms of repair and regulation, 273–275
overview, 248, 255
plant acclimation to light quality and, 326
spatial separation in the thylakoid membrane, 257–259
thylakoid stacking and energy partitioning between, 275
Z scheme of photosynthesis, 255
See also Photosystem I; Photosystem II
Phototaxis, 490
Phototropin 1 (PHOT1)
functions of, 495, 535
phosphorylation of BLUS1 kinase, 499
phot1 mutant, 494, 497
phot1/phot2 double mutant, 497, 498
shoot phototropism, 537, 538
Phototropin 1 photoreceptor kinase, 131
Phototropin 2 (PHOT2)
functions of, 495, 535
phosphorylation of BLUS1 kinase, 499
phot1/phot2 double mutant, 497, 498
phot2 mutant, 497
Phototropins
action and absorption spectra for phototropism, 478, *480*
autophosphorylation, 496, *497*
blue light-induced stomatal opening and, 186, 239–240
discovery of, 495
domain structure and conformational changes, 495–496
functions of, 477
kinetics of blue-light responses and, 490
LOV2 domain, 478, *480, 495,* 496, *497*
overview, 495
in phototropism, 535, 537, 538
plant movements to enhance light use, 496–497, *498*
stomatal opening and, 498–500
See also Phototropin 1; Phototropin 2
Phototropism
action and absorption spectra of phototropin, 479, *480*
defined, 475, *477,* 526
lateral redistribution of auxin, 535–536, 537
phototropins and, 535, 537, 538
steps in shoot phototropism, 536–538
PHR1 transcription factor, 438
Phragmoplast, *39,* 40
PHT1 protein, 438
PHY apoprotein, 482
PHY domain of phytochrome, 482, *483*
Phycoerythorbilin, *251*
Phyllodes, 551
Phyllome, 549
Phyllostachys bambusoides (Japanese timber bamboo), 714
Phyllotaxis, 7, 547, 573
Physical stress sensing, 452
Phytase, 515
Phytic acid, 515
Phytin, 515
Phytochelatins, 446, 465–466
Phytochrome A (phyA)
axillary bud dormancy, 573
flowering response, 606
inhibition of stem elongation, 494
interaction with phytochrome kinase substrate proteins, 489
interactions with CONSTANS in flowering, 602
mediation of responses to continuous far-red light, 486

molecular mechanisms of flowering in natural environments and, 604
nuclear import and regulation of gene expression, 487–488
regulation of the circadian clock, 494
Phytochrome B (phyB)
flowering response, 606
interaction with phytochrome kinase substrate proteins, 489
interactions with CONSTANS in flowering, 602
light deprivation-induced leaf senescence, 705, *706*
mediation of responses to continuous red or white light, 486
nuclear import and regulation of gene expression, 487–488
regulation of the circadian clock, 494
shade avoidance response, 572
water deficit-mediated stomata development, 558
Phytochrome Cph1, *482,* 483
Phytochrome interacting factors (PIFs)
definition and functions of, 488
gibberellin signaling and, 141, *143*
induction of flowering and, 612, *616*
light deprivation-induced leaf senescence and, 705, *706*
phytochrome signaling and, 486, 488, 489
PIF4, 558, 612, *616*
regulation of stomatal density and, 558
Phytochrome kinase substrate (PKS) protein, 489, 537–538
Phytochromes
action and absorption spectra for seed germination, 478, *479*
characteristics as a photoreceptor, 518
chloroplast movements in response to light in algae, 329
de-etiolation, 477–478
defined, 477
diversity of, 480
entrainment of the circadian clock, 597
functions of, 477
interactions with cryptochromes, 493, 494
light deprivation-induced leaf senescence, 705, *706*
light-regulated seed germination, 511
opening of the apical hook, 519–520
photoperiodic flowering, 602
photoreversibility, 478, *479,* 480–481
photostationary state, 481
phyA (*see* Phytochrome A)
phyB (*see* Phytochrome B)
phyC, phyD, phyE, 486–487
physiologically active form, 481
phytochrome responses, 484–487
primary photoreceptor for red and far-red light, 480, *481*
primary photoreceptor in photoperiodism, 605–606
seed germination, 478, *479,* 485, 486
seedling photomorphogenesis, 518
signaling pathways, 487–490
steps in activation and signal transduction, 483–484
structure, domains, and changes in response to red light, 481–483
Phytochromobilin, 481–482, 483
12-*oxo*-Phytodienoic acid, *735*
Phytoene, 660
Phytoene synthase, 100, 660, *661*
Phytohormones
biosynthesis and homeostatic regulation, 119–127
general scheme of hormonal regulation, *114*
hormone balance theory of seed dormancy, 510–511
inducible plant defenses and, 735–736
movement within the plant, 127–132
overview and importance of, 113
plant development and, 113–119
regulation of abiotic stress responses, 459–460
regulation of apical dominance and axillary bud growth, 569–571, *572*
regulation of leaf senescence, 706–709
regulation of secondary growth, 584–585
regulation of source–sink relationships, 374
signaling pathways, 132–147 (*see also* Hormonal signaling pathways)
structures of, *115*
transport in phloem, 364
vacuolar-type programmed cell death and, 693, *694*
See also individual phytohormones
Phytol, *700*
Phytoliths, 727
Phytomeres, 568
Phytophthora, 741, 744
P. infestans, 743
Phytosiderophores, 195
Phytotoxins, 749
PI gene, 616, 617, 619, 620
Picea
P. abies, 75, *350*
P. sitchensis, 328
Piercing-and-sucking insects, 733
Piericidin, 393
PIF-like proteins (PILs), 488
PIFs. *See* Phytochrome interacting factors
Pigments
accessory pigments, 251–252
fruit ripening and, 660, *661*
See also Photosynthetic pigments
Pigweed (*Chenopodium album*), 484
Pilobolus, 594
PILs. *See* PIF-like proteins
PIN auxin efflux carriers. *See* PIN-FORMED proteins
PIN proteins. *See* PIN-FORMED proteins
Pinaceae, 211, *213*
Pineapple (*Ananas comosus*), 303, 613
Pinene, *729*
Pines
ectomycorrhiza, 211, *213*
needle air space volume, 182
photoreversible responses induced by phytochrome, *481*
PIN-FORMED proteins (PIN auxin efflux carriers)
AGC kinases and the activation of, 108
auxin regulation of axillary bud outgrowth, 569
auxin sequestration in the endoplasmic reticulum, 121
auxin signaling in embryogenesis, 679, 680–681
auxin-mediated leaf initiation, 547–548
auxin-mediated leaf vein development, 561–562, 564
fountain model of auxin transport, 527–528
gravitropism, 529, 530–532, *531*
leaflet formation, 554
polar auxin transport, *129,* 130, 131–132
root hair development, 522
shoot phototropism, *537,* 538
PIN-LIKE (PIL) proteins, 121
Pinnately trifoliate leaves, *549*
PINOID kinase, 108, 132
Pinus
ectomycorrhiza, 211, *213*
needle air space volume, 182
photoreversible responses induced by phytochrome, *481*
P. cembra, 714
P. longaeva, 714, 715
P. silvestris, 714
PIP_2, 411
Pipecolates, 114
Piscidic acid, 235
PISTILLATA (*PI*) gene, 616, 617, 619, 620
Pistillate flowers, 7
Pistils
dichogamy, 642, *643*
floral organ identity genes and, 617
guided growth of pollen tubes in, 638–639
heterostyly, 642, *643*
initiation of, 615
programic phase of reproduction, 633–634
S locus and mechanisms of self-incompatibility, 644–647
Pisum sativum. See Pea
Pit (stone), 659
Pit fields, 48
Pit membranes
gas bubbles, 180
pressure-driven bulk flow, 177
types of, *175,* 176
Pit pairs, *175,* 176
Pitcher plants, 230
Pith, *8,* 10, 13, *579*
Pith rays, *11*
Pits
defined, 48
description of, 15
structure and function in tracheids, 174, *175,* 176
structure and function in vessel elements, *175,* 176
PKS protein, 489, 537–538
PLA. *See* Phospholipase A
Placenta, 631
Planck's constant, 248, 323
Plant cells
basic organization, 15, *16*
cell cycle regulation, 36–40
cytoskeleton, 32–36
endomembrane system, 23–29
independently dividing semiautonomous organelles, 29–32
mechanisms of cell expansion, 59–66
nucleus, 18–22
plasma membrane, 15–18
plasmodesmata, 7, *9,* 10
structure and cell walls, 7, *9*
Plant defenses
inducible defenses to insect herbivores, 732–741
mechanical barriers, 726–728
against pathogens, 741–750
secondary metabolites, 728–732
types of, 722
Plant growth. *See* Embryogenesis; Primary growth; Secondary growth; Seedlings; Vegetative growth
Plant growth regulators
gibberellins and gibberellin antagonists, 123
synthetic auxins, 121
Plant growth-promoting rhizobacteria (PGPR), 725
Plant pathology
allelopathic secondary metabolites, 749
definition and overview of, 741
hypersensitive response, 745–746
overview of plant defense responses, *742*
parasitic nematodes, 748–749
parasitic plants, 749–750
pathogen effector molecules and PRR-triggered immunity, 742–743
pathogen strategies to invade plants, 741–742
phytoalexins, 747

plant perception of pathogen-derived "danger signals," 743–744
plant resistance proteins and resistosomes, 744–745
RNA interference, 747
systemic acquired resistance and salicylic acid signaling, 746–747
Plant physiology, 3
Plant tissue analysis, 199–200
Plants
hormonal regulators of development, 113–119
life cycles, 5–7
overview of plant structure, 7–10, *11*
tissue types, 10–15
unifying principles, 4–7
Plasma membrane (plasmalemma)
ABA-induced stomatal closure in response to water stress, 466, 467, *468*
attachment of cortical ER to, 23
blue light-induced stomatal opening, 498–500
cytokinesis, 40
cytoplasmic streaming, 34
definition and function, 7
freezing stress, 449
functions of, 15–16
H^+-ATPases, 236–237
hydraulic conductivity, 164–165
lipids, 16–18
membrane proteins, 15–16, *17,* 18
phototropin receptors, 495–496
phytochrome regulation of ion fluxes, 487
plant cell structure, *16*
plasmodesmata, *9*
polar auxin transport, 128–130, 131
recycling of, 26
transport proteins, 228–238
of xylem parenchyma, 242
Plasma membrane H^+-ATPase, 226
Plasmodesmata
apoplastic phloem loading, 353–354
C_4 photosynthesis, 299
cell-cell communication in embryogenesis, 677–678
cytokinesis, 40
function in phloem signaling, 375
high-pressure manifold model of phloem transport, 361
leaf transition from sink to source, 370
oligomer-trapping model of phloem loading, 354–355
passive symplasmic phloem loading, 355, 356, 357
phloem, 14–15
plant cell structure, *16*
plant nastic movements, 523
pore-plasmodesma contacts, *349,* 350
shoot phototropism, 538
size exclusion limit, 375
structure and function, 7, *9,* 10
symplasmic phloem unloading, 366
symplasmic transport of viruses, 10
transport of ions in roots, 240–241
water movement in roots, 172, *173*
Plasmodium, 642
Plasmolysis, 162
Plastic deformation, 62
Plasticity, 326
See also Phenotypic plasticity
Plastid genomes
base editing, 98
description of, 80–81
PLASTID RIBOSOMAL SMALL UNIT PROTEIN 17 (PRPS17), *702,* 705
Plastidial glycolate/glycerate transporter (PLGG1), 291, *292–293,* 296
Plastids
abscisic acid synthesis, 125
amyloplasts, 514, 515 (*see also* Amyloplasts)
biosynthesis of glycerolipids, 410, 411
cytokinin synthesis, 123
fatty acid biosynthesis, 407
fission, 31
gibberellin synthesis, 121, *122*
growth in size, 31–32
membranes of, 18
movement in the cell, 32
oxidative pentose phosphate pathway, 386, 388
role in plant respiration, *380*
sieve elements, 348
strigolactone synthesis, 127
types and functions of, 29–30
Plastocyanin (PC)
copper and, 199
electron transfer between cytochrome b_6f and PSI, 268
organization of the photosynthetic electron transport chain, 257, *258,* 259
transit peptide, 276
Z scheme electron transport, 261, *262,* 263
Plastohydroquinone
cyclic electron flow, 273
photosynthetic electron transport, *258,* 266
Q cycle, 267, 268
structure of, *267*
Z scheme electron transport, 261, *262,* 263
Plastoquinone (PQ)
effects of herbicides on, 269, *270*
electron transfer from pheophytin, 265–266
energy partitioning between photosystems, 275
organization of the photosynthetic electron transport chain, 257, *258,* 259
redox reactions, *267*
structure of, *267*
Z scheme electron transport, 261, *262,* 263
Plastosemiquinone, 266, *267*
Plateau phase, of lateral root growth, 577
PLC. *See* Phospholipase C
PLD. *See* Phospholipase D
PLENA gene, *616*
PLETHORA (PLT) proteins
maintenance of the root apical meristem, 543, *544,* 545
root formation, 576, 686–687, *688*
PLGG1. *See* Plastidial glycolate/glycerate transporter
PLT proteins. *See* PLETHORA proteins
Plumbagella, 633
Plumbago, 633
P. zeylanica, 642
Plumule, 506, *507*
Pneumatophores, 405
Poaceae (grass family)
aleurone layers, 508
antipodal cells, 632
chilling-tolerant C_4 plants, 303
coleoptile bending response, 103, 114, *115*
composition of lignin, 68
glycosylated chemical defenses, 731
guard cells, 184, *185*
lignification and, 70
mechanisms of root uptake of iron, 234, 235
pollen, 630
primary cell wall hemicelluloses, 54
stomata development, 558–559
See also Maize
Pod shattering resistance, 659
Podocarpus, 66
Poinsettia (*Euphorbia pulcherrima*), 601
Poiseuille, Jean Léonard Marie, 176
Poiseuille equation, 176–177, 360
Polar auxin transport
auxin regulation of axillary bud outgrowth, 569
auxin reporters, 128
fountain model of in roots, 527–528
gravitropism, 529
gravity-independence of, 526, *527*
overview and chemiosmotic model of, 128–130
PIN proteins, 108
regulation of, 131–132
root hydrotropism, 535
in seedlings, 526–528
suppression in root nodule formation, 433
terms describing the direction of movement, 526, *527*
Polar glycerolipids
in cellular membranes, *410*
description and functions of, 407
overview, 405
structure of, *406, 408*
Polar microtubules, *39*
Polar molecules, water, 154, *155*
Polar nuclei, *626,* 632, 633
Polarity
in embryogenesis, 672–676
in leaf development, 551–554
Polarized microspores, 628
Pollen
cytoplasmic male sterility, 398
mutational load, 715
plant life cycles, *6*
self-incompatibility, 642, 643–647
uniparental inheritance of cytoplasmic genomes, 81
Pollen grains
adhesion and hydration on stigma surfaces, 634–635
angiosperm life cycle, *626*
Ca^{2+}-triggered activation, 635–636
cell walls and apertures, 629–630
effects of high temperature on, 633
formation, 627–629
pollination, 633, 634–641
programic phase of reproduction, 633, *634*
S locus and mechanisms of self-incompatibility, 644–647
Pollen mother cells, 627–628
Pollen tube growth
guided growth in the pistil, 638–639
mechanisms of tip growth, 636–638
molecular motors, 34
rates of and male competition, 634
style tissue and the conditioning of pollen tubes, 639–640
synergid cells and chemoattractants, 640–641
Pollen tubes
angiosperm life cycle, *626*
clear zone, 636, *637*
cytoplasmic streaming, 34
in double fertilization, 641
gametophytic self-incompatibility, 644, 646–647
pollen grain activation and the formation of, 635–636
primary cell wall components, 50
programic phase of reproduction, 633, 634
Pollination
adhesion and hydration of pollen grains on stigma surfaces, 634–635
defined, 633
pollen tube formation, 635–636
pollen tube growth, 636–641 (*see also* Pollen tube growth)
programic phase of reproduction, 633, *634*
self-pollination and cross-pollination, 633
Pollinia, 628
POLLUX cation channel, *432*
Poly-A signals, *82,* 84
Poly-A tail, *82,* 84, 86
Polyadenylation, *82,* 84

Polyads, 628
Polyamines, 111
Polycarpic plants, 714, 715
POLYCOMB REPRESSIVE COMPLEX 2 (PRC2), 653
Polygalacturonase, 712
Polygonum-type embryo sac development, 632–633
Polyploidy
  artificial induction of, 79, 92
  endopolyploidy, 78
  endoreduplication, 37–38
  hybrid vigor, 79–80
  pathways to, 78–79, *80*
  subfunctionalization and, 80
Polyribosomes (polysomes), 20, *24,* 698
Polysaccharides
  cell plate, 47
  cell walls, 48–50 (*see also* Matrix polysaccharides)
  lignification, 70
Polytrichum, 481
Pome fruits, 657
Poplar
  genetic control of secondary meristems, 582
  lignin, *68,* 69
  phytohormones and secondary growth, 584–585
  transition to secondary growth, 579
Poppies, 647
Populus
  P. grandidentata, 714
  P. tremula, 739
  P. tremuloides, 715
  See also Poplar
Pore–plasmodesmata contacts, *349,* 350, 364
Pores
  phloem translocation in gymnosperms, 361
  in pollen cell walls, 629–630
  pore-plasmodesma contacts, *349,* 350
  sieve elements, 348, *349,* 350
Porphobilinogen, *277*
Position-dependent development, 677
Posttranscriptional regulation
  of leaf senescence, *702,* 703, 705
  of nuclear gene expression, 86–90
Posttranslational regulation of leaf senescence, *702, 704,* 705
Potassium channels
  ABA-induced stomatal closure in response to water stress, 466, 467, *468*
  blue light-induced stomatal opening, 239, 240
  inwardly or outwardly rectifying, 225–226
  models of, *224*
  stomatal closure, *239,* 240
  types of, *231,* 232
Potassium chloride, 201
Potassium deficiency, 195, 197
Potassium malate, *233*
Potassium transporters, 224, 465
Potassium/potassium ions
  ABA-induced stomatal closure in response to water stress, 466, *468*
  adsorption by soil particles, 203
  blue light-induced stomatal opening, 239, 240, 498
  carriers, 232
  effects of soil pH on availability, *201*
  electrostatic complexes, 233
  inorganic fertilizers, 201
  membrane potential and, 222
  membrane transport proteins, *229,* 230
  mobility within the plant, *196*
  observed and predicted concentrations in pea root tissue, *221,* 222
  osmotic adjustment and, 460
  osmotic potential and guard cells, 185
  in phloem sap, 361, *362,* 364
  plant action potentials, 146
  in plant nutrition, *192,* 197
  plant tissue concentration, *191*
  root absorption of, 208
  salinity stress, 449
Potato (*Solanum tuberosum*)
  mobile mRNAs in phloem signaling, 375
  phloem, *349, 351*
  phytoalexins, *747*
  shoot apical meristem and leaf primordium development, *551*
  storage temperature for tubers, 405
Potato late blight, 741, 744
Potrykus, Ingo, 100
Power of Movement in Plants, The (Darwin & Darwin), 114, 522
POWERDRESS (PWR) protein, 703, *704*
PP complex, 500
PP2A. *See* Protein phosphatase 2A
PP2C. *See* Protein phosphatase 2C
PPFD. *See* Photosynthetic photon flux density
PP_i-dependent phosphofructokinase, *313,* 314, *383,* 384, 385, 402
P-proteins
  distribution in the sieve tube lumen, 360
  location and functions of, 14, 348, *349*
  obstruction of sieve plate pores in damaged sieve elements, 359, 364–365
  in phloem sap, 364
  presence in angiosperms, 348, *350*
PQ. *See* Plastoquinone
Pr
  action and absorption spectra for seed germination, 478, *479*
  flowering response in short-day plants, 605
  interconversion with Pfr, 478, *479,* 480–481
  phytochrome signaling, 483
  very low fluence responses, 485
PR genes. *See* Pathogenesis-related genes
PRD repeats, 482, 483
Prebranch site, 574, *575, 576*
Precipitation
  ecosystem productivity and, *154*
  plant carbon isotope ratio and, 342
Preharvest sprouting, 509–510
Prenylation, 109
Pre-phloem pathway/transport, *346,* 351, 355–356
Pre-procambium, 562–563, 564
Preprophase, 38, *39*
Preprophase band, 38, *39*
Pressure
  hydrostatic pressure, 156–157
  units of, 156, *157*
  water potential and, 159, 160
Pressure chambers, 160
Pressure gradients
  pressure-driven bulk flow in xylem, 176–177
  pressure-flow model of phloem translocation, 357–358
  water movement in the tallest trees, 177–178
  water movement through soil, 171
Pressure potential
  defined, 160
  measuring, 160
  reverse osmosis and, 162
  of soil water, 170–171
  variability within the plant, 163
Pressure-driven bulk flow, 176–177
Pressure-flow model
  modifications of, 361
  osmotically generated pressure gradient, 357–358
  overview, 357
  phloem transport in trees, 360–361
  predictions from, 359
  sieve plate pores and, 359–360
Pressure–volume curve, 164
Prevacuolar compartments, 26, 27, 28
Preventitious buds, 587
Prickles, 726
Priestly, Joseph, 252
Primary active transport, 227
Primary cell walls
  components of, 48–50
  defined, *7*
  diffuse growth and the orientation of cellulose microfibrils, 59–60
  hemicelluloses, 54
  lignification, 68–69
  major structural components, *53*
  mechanisms of assembly, 58–59
  molecular models of, 64–65
  morphological diversity, 47
  parenchyma, 13
  pectins, 56–58
  plant cell structure, *16*
  plasmodesmata, *9*
Primary cross-regulation, 147
Primary dormancy, 508
Primary endosperm cell, 626, 633
Primary growth
  defined, 10
  differentiation of epidermal cell types, 555–559
  leaf development, 549–551
  leaf venation patterns, 559–564
  limits on plant growth and, 567
  overview, 541
  root apical meristem, 542–545
  shoot apical meristem, 545–549
  transition to secondary growth, 579, *580*
  types of meristems, 541–542
Primary inflorescence meristems, 614
Primary meristems, gene networks controlling, 582–584
Primary metabolites, 728
Primary nitrate response, 423, *424*
Primary phloem, *11,* 562, *579, 580*
Primary plant axis, *7*
Primary plant body, 10
Primary plasmodesmata, *9,* 10
Primary response genes, 488
Primary roots, 205, 576–577
Primary vein, *559,* 560, 561–562, 564
Primary xylem, *11,* 562, *579, 580*
Prime editing guide RNA (pegRNA), *98,* 99
Prime editor, *98,* 99
Primexine, 629
Priming, 574, *575*
Primrose family, 632
Primula kewensis, 24
PRK6 receptor kinase, 641
Proanthocyanidin, 652, 653
Procambium
  in embryogenesis, 683
  leaf vein development, 560, 561–562, 563
  roots, 581–582
Processing bodies (P-bodies), 86
Profilin, 32, *33*
Programic phase of reproduction, 633–642
Programmed cell death (PCD)
  of the aleurone layer, 516
  autophagy, 693–695
  cytoplasmic male sterility, 398
  defined, 691
  examples of, *692*
  heavy metal stress, 449
  leaf senescence, 696 (*see also* Leaf senescence)
  of megaspore cells, *626,* 632
  overview, 692–693
  ozone stress, 450
  of starchy endosperm, 652
  of synergid cells, 641
  of tapetal cells, 629

tracheids and vessels, 15
types of and processes in, 693, *694*
Prokaryotic pathway of glycerolipid biosynthesis, 410, 411
"Prokaryotic" protein synthesis, 20
Prolamellar bodies, 30–31
Prolamins, 516, *517*
Proline, 231, 394, *427,* 461
Proline dehydrogenase, 394
Proline-rich protein, *50*
Promoters
light-regulated, 487
in mitochondrial DNA, 398
structure and function, 81–83
Propagules, *651*
Prophase
meiosis, *77,* 78
mitosis, 38, *39*
Propiconazole, 127
Proplastids, 30–31
Prosopis, 205, *750*
Protea, 204
Proteaceae, 204, 206, 211
Protease inhibitors, 516
Proteases, 516, 517, 692–693, 698
Proteasomes, 22
PROTEIN KINASE ASSOCIATED WITH BREVIX RADIX (PAX), 108, 538
Protein kinases
ABA-induced stomatal closure in response to water stress, 467, *468*
conservation across kingdoms, 106
protein phosphorylation, 107
regulation of starch metabolism, 312
signal amplification, 107
stress-response pathways, *453,* 454
types and functions of, 107–108
Protein phosphatase 2A (PP2A), 136, *138,* 302, 305
Protein phosphatase 2C (PP2C)
abscisic acid signaling, 138, 139, 707
auxin-induced cell expansion, 526
PP2C.D1, 526
stomatal closure, 113, *468*
PROTEIN PHOSPHATASE1 (PP1) complex, 500
Protein phosphatases
ABA-induced stomatal closure in response to water stress, 467, *468*
abscisic acid signaling pathway, 138–139
stress-response pathways, *453*
Protein phosphorylation
phosphatases, 109
phytochrome signaling, 488–489
Protein storage vacuoles (PSVs)
definition and functions of, 27, 508, 514
in endosperm, 508
formation in seeds, 28
mobilization of stored reserves in seeds, 514–515, 516, *517*
in starchy endosperm, 652
Protein synthesis
basic steps in gene expression, 20–22
functions of rough ER, 23–24
posttranslational modifications, 22
ribosomes, 20
Proteinase inhibitors, 736
Proteins
acid growth and, 64
breakdown during leaf senescence, 698–700
in cell walls, 49, *50*
folding in the ER, 23–24
glycosylation, 26
inactivation of repressor proteins in hormone signaling pathways, 139–142, *143*
membrane transport proteins, 15–16
mobile proteins in phloem signaling, 375
mobilization of stored reserves in seeds, 514–515, 516, *517*
molecular chaperones and molecular shields, 462–463, *464*
in phloem sap, *362*
phytochrome signaling and, 488–490
protein modifications and the reconfiguring of cellular processes, 109
turnover, 22
See also Storage proteins; Transport proteins
Proteoid roots, 206
Proteomics, 92
Protochlorophyllide, 31, 477–478
Protochlorophyllide oxidoreductase, *277*
Protoderm, 555, 671, *672,* 675, 683
PROTODERMAL FACTOR 2 (*PDF2*) gene, 683
Protofilaments, 32
Protogyny, 642, *643*
Protolignin, 69
Proton motive force
in anoxygenic photosynthesis, 259
chemiosmotic mechanism of mitochondrial ATP synthesis, 395–396
defined, 226, 270–271
functions of, 110–111
photophosphorylation, 270–271
secondary active transport, 226
uncouplers and, 395–396
vacuolar proton pumps, 237–238
Proton pumps
H^+ pumps, *229,* 230
vacuolar, 237–238
See also H^+-ATPases
Proton transport
ATP synthesis in photosynthesis, *258,* 259
ATP synthesis in the chloroplast, 270–273
chemiosmotic mechanism of mitochondrial ATP synthesis, 395–396
mitochondrial electron transport, 392, *393*
oxidation of water in photosynthesis, 265
Q cycle, 268
Z scheme electron transport, 261, *262,* 263
Protons
acidification of the thylakoid lumen in nonphotochemical quenching, 274
chemiosmotic mechanism of mitochondrial ATP synthesis, 395–396
membrane potential, 222–223
mitochondrial transmembrane transport, 396, *397*
as second messengers, 110–111
secondary active transport, 226–227
Protophloem, 367, 520, 562, 581, 582
Protophloem sieve element precursors, 581, 582
Protoplast fusion, 92, 94
Protoporphyrin IX, *277*
Protospacers, 96
Protoxylem, 520, 581, 582
Protrandry, 642, *643*
Proximal promoter, 83
Proximal–distal polarity, establishment in leaves, 553–554
PRPS17 protein, *702,* 705
PRR proteins. *See* Pentatricopeptide repeat proteins
PRRs. *See* Pattern recognition receptors
PRR-triggered immunity. *See* Pattern recognition receptor-triggered immunity
PRSL1 subunit, 500
Prunus cerasifera (cherry plum), *211*
Prx. *See* Peroxiredoxins
PsaA protein, 268, *269*
PsaB protein, 268, *269*
P_{SARK}, *459*
PsbS protein, 274
Pseudogenes, 73, 74
Pseudomonas, 725
P. aeruginosa, 725
P. syringae, 695
P. syringae pathovar *tomato,* 743
PSI. *See* Photosystem I
PSII. *See* Photosystem II
PSVs. *See* Protein storage vacuoles
Psychrometers, 160
Pteridium aquilinum (bracken), *714*
Pteridophytes, *481*
Pterin, 421, 491–492
PTI. *See* Pattern recognition receptor-triggered immunity
PTL protein, 582, *583*
P-type ATPases, 236–237
Pullulanases, *309,* 310, 312
Pulse-chase labeling, 298
Pulvinus, 325, 728
Pumpkin (*Cucurbita pepo*), *172,* 354, *365*
Pumps
Ca^{2+} pumps, 110
definition and overview, *223,* 226
primary active transport, 226
secondary active transport, 226
See also Electrogenic pumps; H^+-ATPases; Proton pumps
Purple photosynthetic bacteria, 259, *272*
Purple witchweed, *119*
PWR protein, 703, *704*
PXY protein. *See* PHLOEM INTERCALATING WITH XYLEM protein
PYL protein. *See* PYR1-LIKE protein
PYR1 protein. *See* PYRABACTIN RESISTANCE1 protein
PYR1-LIKE (PYL) protein, 139, 707
Pyrabactin, 138
PYRABACTIN RESISTANCE1 (PYR1) protein, 138, 707
Pyridoxal phosphate, 426
Pyrophosphatase, *299,* 436–437
Pyrophosphate (PP_i)
C_4 photosynthesis, *299,* 301
glycolysis, *383,* 384, 385
sucrose biosynthesis, 314, *315*
sulfate activation, 436
Pyrophosphate-dependent phosphofructokinase, *313,* 314
PYR/PYL/RCAR protein subfamily, 138–139
Pyruvate
amino acid biosynthesis, 427
bioengineered photorespiratory bypass pathways, 296
C_4 photosynthesis, *298, 299,* 300, 301, 303
fermentation, *383,* 385
glycolysis, 382, *383,* 384
malic enzyme reaction, *391*
metabolic regulation of pyruvate dehydrogenase, *402*
mitochondrial transmembrane transport, *397*
structure, *382*
tricarboxylic acid cycle, 381, 389–391
Pyruvate decarboxylase, *383,* 385
Pyruvate dehydrogenase
bioengineered photorespiratory bypass pathways, 296
dynamic regulation of respiration, 401, 402
metabolic regulation of, 402
mitochondrial respiration in photosynthesis, 403
Pyruvate kinase
dynamic regulation of, 402
dynamic regulation of respiration, 401
glycolysis, *383,* 384, 385
Pyruvate transporter, *397*
Pyruvate–phosphate dikinase, *299,* 301, 302
PZ. *See* Peripheral zone

Q

Q cycle, 261, *262,* 263, 267–268
Q_{10}, 405
QC. *See* Quiescent center
qRT-PCR. *See* Quantitative reverse transcription polymerase chain reaction
Qualisoy, 407
Qualitative flowering response, 592
Qualitative long-day plants, 598
Qualitative short-day plants, 598
Quanta, 248, 322–323
Quantitative flowering response, 592
Quantitative long-day plants, 598
Quantitative reverse transcription polymerase chain reaction (qRT-PCR), 92
Quantitative short-day plants, 598
Quantum flux, 322–323
Quantum yield of photosynthesis
  defined, 253, 327
  efficiency of photosynthesis and, 255, 256, 333, *334*
  photoinhibition and, 330
Quartet Model, 619–620
Quaternary veins, *559*
Quenching of chlorophylls, 273, 274
Quercus, 506
  Q, robur, 593
  Q. montana, 714
  Q. rubra, 714
  Q. suber, 46, 586
  See also Oaks
Quiescent center (QC)
  Arabidopsis embryogenesis, 674
  definition and description of, 206, *207,* 543, *544*
  expression of WOX5 in, 544, 545
Quinine, 586
Quorum sensing, 725

R

R proteins, *742,* 744–745
RabG3b protein, 695–696
Rabl, Carl, 76
Rabl configuration, 76
Rachis, *549,* 550
RAD gene, 620–621
Radial axis, in embryogenesis, 672, 682–686
RADIALIS (*RAD*) gene, 620–621
Radiative heat loss, 331
Radicle
  emergence at the end of germination, 513–514
  light-regulated seed germination, 511
  maize embryogenesis, 671
  seed anatomy, 506, *507*
  thigmotropism, 533
  vascular differentiation in, 520
Radicula, *648*
Radish, *422*
Raffinose, 354, 355, 356, 362, *363*
RALFs. *See* RAPID ALKALINIZATION FACTORS
RAM. *See* Root apical meristem
Ramie, 13
Ranunculus
  R. occidentalis, 48
  R. repens, 48, 347
Rape plant, 118
Rapeseed (*Brassica napus*), *80,* 118, *506,* 517, 659
Raphides, 727
RAPID ALKALINIZATION FACTORS (RALFs), 109, 638
Ras GTPase, 24
ra-siRNAs. *See* Repeat-associated silencing RNAs
Raspberry fruit, *657, 659*
Ray cells, *579,* 580
Rays, 10, *11, 579,* 580
RBOHs. *See* Respiratory burst oxidase homologs
RCAR/PYR/PYL ABA receptors, *468*
RCARs, 139, 707
RCBs. *See* Rubisco-containing bodies
RCC reductase, *700*
RdRP. *See* RNA-dependent RNA polymerases
Reaction center complexes
  absorption characteristics of PSI and PSII, 264
  electron transfer by excited-state chlorophyll, 263–264
  energy transfer in photosynthesis, 253–254
  funneling of energy to by antenna complexes, 260
  photodamage and protection from, 273–275
  thylakoid integral membrane proteins and, 257
  See also Photosystem I; Photosystem II
Reactive nitrogen species (RNS), 190
Reactive oxygen species (ROS)
  alternative oxidase expression, 399
  antioxidants and ROS scavenging, 462, *463*
  conversion of ozone into, 450
  cytoplasmic male sterility, 643
  definition and forms of, 446
  electrical signaling in systemic defenses, 737
  leaf senescence, 708
  photodamage and protection from, 273–274, 275
  plant recovery from abiotic stress, 470
  PRR-triggered immunity, 744
  released by cell dehydration, 447
  roles in abiotic stress, 446–447
  root thigmotropism, 533
  as second messengers, 111
  sources of, *455*
  stress-response pathways, 453–454, 455
  systemic acquired acclimation, 456, *457*
  thioredoxin and protection against, 289
  uncoupling protein, 399, 400
  uptake of heavy metals, 449
Recalcitrant seeds, 654
Receiver domain of response regulators, 132, *133*
Receptacles, *657*
Receptor kinases, 106
RECEPTOR PROTEIN KINASE 1 (*RPK1*) gene, 705
Receptor-like cytoplasmic kinases (RLCKs), *742,* 744
Receptor-like kinases (RLKs)
  leaf senescence, 705
  plant detection of pathogens, 743, 744
  pollen tube growth, 638
Receptor-like serine/threonine kinases
  mediation of brassinosteroid signaling pathway, 136–138
  poor representation in other kingdoms, 106
  types and functions of, 108–109
Receptor-mediated endocytosis, 26
Receptors
  conservation across kingdoms, 105–106
  defined, 103
  location of, 105, *106*
  receptor kinases, 106
  receptor-like serine/threonine kinases, 108–109
Red algae, *5*
Red light
  absorption by chlorophyll, 250
  absorption by photosystem II, 255
  entrainment of the circadian clock, 597
  molecular mechanisms of flowering in natural environments and, 604
  phytochrome and seed germination, 478, *479*
  phytochrome as the primary receptor for, 477, 480, *481*
  seedling photomorphogenesis, 518, 519–520
  See also Red:far-red ratio
Red mangrove (*Rhizophora mangle*), 509
Red oak (*Quercus rubra*), *714*
Red:far-red (R:FR) ratio
  ecological ranges of, *476*
  light deprivation-induced leaf senescence, 705, *706*
  molecular mechanisms of flowering in natural environments and, 604
  phytochrome and, 481
  phytochrome interacting factors and, 488
  shade avoidance response, 572
Redox homeostasis, 297
Redox reactions
  photosynthesis as, 254, 255
  plant mineral deficiencies and, 198–199
  regulation of starch breakdown, 311–312
Reducing sugars, 362, *363*
Reductive pentose phosphate pathway. *See* Calvin–Benson cycle
Redwood (*Sequoia sempervirens*), 177–178, *593,* 717
Redwood burls, 587
Reed grass (*Calamagrostis epigeios*), *714*
REGULATORY COMPONENTS OF ABA RECEPTORS (RCARs), 139, 707
Regulatory promoters, 81–82, 83
Relay model of phloem transport, 361
Release phloem, 346
Repeat-associated silencing RNAs (ra-siRNAs), 87
Repetitive DNA sequences
  short-interfering RNAS, 86–88
  tandem repeats and dispersed repeats, 74
  transposons, 75–76
Replum, 631, 658, 659
REPLUMLESS (*RPL*) gene, 659
Reporter genes, 92–93
REPRESSOR OF UVR8 proteins, 500, *501*
Repressors
  inactivation in hormone signaling pathways, 139–142, *143*
  inhibition of transcription, 83
Rescue of phenotype, 684
Residuum cells, 709, *710,* 712–713
Resin ducts, 729–730
Resistance (R) proteins, *742,* 744–745
Resistosomes, *742,* 744–745
Respirasomes, 392
Respiration
  CO_2 compensation point and, 336
  effects of elevated global CO_2 levels on, 338–340
  global warming and, 404
  glycolysis, 382–386
  in intact plants and tissues, 402–405
  modifying in crop plants, 404
  overview and overall equation for, 379–382, 380, 382
  oxidative pentose phosphate pathway, 386–388
  oxidative phosphorylation, 391–402 (*see also* Oxidative phosphorylation)
  photosynthetic yield consumed by, 403
  plant biosynthetic and redox networks and, 400–401
  regulation at multiple levels, 401–402
  total ATP yield, 396, *398*
  tricarboxylic acid cycle, 388–391
Respiration rates
  environmental factors affecting, 404–405
  overview of factors affecting, 402–403
  of plants and animals compared, 403
  variability in different tissues and organs, 403–404

Respiratory burst oxidase homologs (RBOHs), *455,* 456, *457, 468, 742,* 744
  See also NADPH oxidase
Respiratory quotient (RQ), 404
Response regulator, 132, *133,* 481
"Resurrection plants," 655
Reticulate venation, 559
Reticuloplasmins, 24
Retrograde regulation, 399
Retrotransposons, 75, 459
Reverse osmosis, 162
Reverse transcriptase, *75, 98,* 99
R:FR ratio. *See* Red:far-red ratio
Rhamnogalacturonan I (RGI)
  plant cell walls, 49
  primary cell walls, 56, 57, 58
  secondary cell walls, 67
Rhamnogalacturonan II (RGII)
  boron and, 197, 636
  plant cell walls, *49*
  primary cell walls, *53,* 56, 57, 58
  secondary cell walls, 67
Rhamnose, *48,* 49, 56, 57
Rheological properties, 62
Rhizobacteria, 725
Rhizobia
  nitrogenase enzyme complex, 434–435
  nodules and nodule formation, 430–431, 432–434
  signaling molecules in symbiotic nitrogen fixation, 431–432, 723, *724*
  in symbiotic nitrogen fixation, 428, *429*
Rhizobium, 428
  R. etli, 429
  R. leguminosarum bv. *phaseoli, 429*
  R. leguminosarum bv. *trifolii, 429*
  R. leguminosarum bv. *viciae, 429,* 431–432
  R. meliloti, 431–432
  R. tropici, 429
Rhizophora, 405
  R. mangle, 509
Rhizosphere
  defined, 205
  nutrient depletion zone, 208
  root absorption of nutrients, 207–208
Rhizotaxis, 573
Rho GTPases (ROPs), 63, 467, 638
Rhodophyceae, 281
Rhodopseudomonas palustris, 480
Rhodospirillum, 428, 430
  R. centenum, 480
Rib zone (RZ), 545, *546*
Ribonucleic acid (RNA)
  mobile RNAs in phloem signaling, 374–375
  in phloem sap, 364
  processing in mitochondria, 396
  retrotransposons, 75
Ribose 5-phosphate, *284–285, 387,* 388
Riboside cytokinins, *123,* 124
Ribosomal RNA (rRNA)
  leaf senescence, 698
  mobile RNAs in phloem signaling, 374
  nucleolar organizer regions and, 20, 74–75
  translation, 20, *21*
Ribosomes
  leaf senescence and, 698
  nucleolar organizer regions and, 74–75
  plant cell structure, *16*
  protein synthesis, 20, *21,* 22
  rough ER and, 23
  synthesis in the nucleolus, 20
  types of, 20
Ribotide cytokinins, *123,* 124
Ribulose 1,5-bisphosphate (RuBP)
  biochemical model of C_3 photosynthesis, 322
  Calvin–Benson cycle, 283, 284, 285, *286*
  carboxylation and oxygenation by Rubisco, 290–291
  CO_2-limited photosynthesis and, 337
  crassulacean acid metabolism, 305
  photorespiration, 291, *292–293,* 294, 295
  regulation of Rubisco, 287, *288*
Ribulose 5-phosphate, 381, 386, *387,* 388
Ribulose 5-phosphate epimerase, *284–285*
Ribulose 5-phosphate isomerase, *284–285*
Ribulose 5-phosphate kinase, *284–285*
Ribulose-1,5-bisphosphate carboxylase/oxygenase (rubisco)
  assembly of, 275
  biochemical model of C_3 photosynthesis, 322
  bioengineered photorespiratory bypass pathways, 296
  breakdown during leaf senescence, 698–699
  C_4 photosynthesis, 297, 298, 299, 300, 301, 302, 303, 337
  Calvin–Benson cycle, 283, *284–285*
  carbon isotope ratio and, 341
  carboxylation and oxygenation of ribulose 1,5-bisphosphate, 290–291
  CO_2 concentration and limitations on photosynthesis, 336
  crassulacean acid metabolism, 304, 305
  localized in chloroplast stroma, 29
  oxygen fixation and, 439
  oxygenation and photorespiration, 290–295 (*see also* Photorespiration)
  photosynthetic thermal optimum and, 333
  regulation of catalytic activity by Rubisco activase, 287–288
  specificity factors for oxygen and carbon dioxide, 294–295
Rice (*Oryza sativa*)
  aerenchyma, 461, 462
  aleurone layer, 652
  arsenic poisoning and, 235
  FINE CULM 1 gene and branching in, 571
  gene replacement technology, 97, *98*
  gibberellin and "foolish seedling disease," 116, 743
  global warming and methane emission, 404
  herbivore-induced volatiles, 739
  phloem callose, 365
  regulation of shoot gravitropic setpoint angles, 578
  root absorption of ammonium, 208
  root parasites, *119*
  self-pollination, 633
  storage proteins, *517*
  strigolactones, 118
  transgenic golden rice, 100
Ricinus communis. See Castor bean
RICs. *See* ROP-interactive CROB motif-containing proteins
Rieske iron-sulfur protein, 266, 267
Ripening inhibitor (*rin*) locus, 663, 664
RISC. *See* RNA-induced silencing complex
Rishitin, *747*
RITS. *See* RNA-induced transcriptional silencing
RLCKs. *See* Receptor-like cytoplasmic kinases
RLF gene, *616*
RLKs. *See* Receptor-like kinases
RNA interference (RNAi), 86–90, 747
RNA polymerase, gene transcription and, 81, 82, *83*
RNA polymerase II
  gene transcription and, 81, 82, *83*
  transcription of miRNA-coding sequences, 87
  transcription termination, *82,* 84
RNA polymerase IV, 87
RNA polymerase V, 87
RNA viruses, 747
RNA-dependent RNA polymerases (RdRP), 87, 90
RNAi. *See* RNA interference
RNA-induced silencing complex (RISC), *87,* 88, 89, 458
RNA-induced transcriptional silencing (RITS), 458
RNases, 698
RNS. *See* Reactive nitrogen species
Rock phosphate, 201
Root apex, *8*
Root apical meristem (RAM)
  Arabidopsis embryogenesis, 671, *672,* 674, 675
  definition and description of, 206, *207,* 542
  developmental zones, 542, *543*
  formation of, 686–687, 688
  gene networks controlling, 582–584
  indeterminate growth, 542
  initial cells and origin of root tissues, 543, *544*
  of lateral roots, 576
  maize embryogenesis, 671
  roles of auxin and cytokinin in the maintenance of, 543, *544,* 545
  root anatomy, *8*
Root branch meristem, 10
Root cap
  amyloplast gravity sensors, 30
  Arabidopsis embryogenesis, 674
  definition and description of, 206, *207,* 542, *543*
  development in seedlings, 520–521
  fountain model of auxin transport, 527–528
  gravitropism, 521, 529–533
  root anatomy, *8*
Root exudates, 749
Root hairs
  absorption of ions, 241
  absorption of phosphate, 208
  absorption of water, 171
  acid growth, 63
  appearance in the maturation zone, 207
  contact with soil particles, 171
  development in seedlings, 521–522
  epidermal origin, 12
  nodule formation and, 432–434
  origin in the elongation zone, 542, *543*
  root anatomy, *8*
  rye root systems, 205
  symbiotic biological nitrogen fixation, 723, *724*
Root knot nematodes, 748, 749
Root parasites, *119*
ROOT PHOTOTROPISM 2 (RPT2), 537
Root pressure, 174, 181
Root system architecture
  definition and description of, 205–206, 573
  gravitropic setpoint angle, 577–578
  modifications to optimize water and nutrient uptake, 578
  of monocots and eudicots, 573, 576–577
  origin and development of lateral roots, 573–576
Roots
  absorption of mineral ions, 207–208
  absorption of water, 171–174
  aerenchyma, 461–462
  ammonium assimilation, 426
  anaerobic stress from flooding, 448–449
  anatomy of, *520*
  apical growth regions, 206–207
  apical meristems, 10
  auxin-regulated ABA signaling, 526
  branching and architecture, 567, 573–578
  calcium deficiency, 198
  Casparian strip, 14

chemoattraction of nitrogen-fixing bacteria, 431
cortex, 13–14
development in seedlings, 520–522
development of vascular cambium, 581–582
developmental zones, 542, *543*
dimensions and diversity of, 205
effects of fertilization and irrigation on, 205
effects of nutrient availability on growth and development, 208–210
effects of pH on growth, 204
effects of water deficit on, 166
endodermis, 14
fountain model of auxin transport, 527–528
gravitropism, 528–533
gravity-independent auxin transport, 526, *527*
hydrotropism, 534–535
interactions of auxin and ethylene in growth, 524–525
mechanisms of iron uptake, 234–235
mycorrhizal symbioses and nutrient uptake, 210–213
nitrate assimilation, 422
nodule formation, 432–434
nutational growth in seedlings, 523
nutrient depletion zone, 208
observed and predicted ion concentrations in pea root tissue, *221,* 222
parasitic nematodes, 748–749
parasitic plants and, 750
pathways of water transport, 172–173
periderm formation, *585,* 586
phloem import in growing regions, 367
potassium deficiency, 197
radial patterning during embryogenesis and, 684–686
rhizotaxis, 573
root pressure, 174, 181
root system architectures, 205–206
root-to-shoot ratio, 205, 468–469, *470*
secondary growth, 10, *11*
structure and function, *7*, *8*
symbiotic biological nitrogen fixation, 428, 429, 430–434, 723, *724*
thigmotropism, 533–534
tissue organization in, *241*
transport of ions in, 240–242
triple response, 519
variability in respiration rates, 403
Root-to-shoot ratio, 205, 468–469, *470*
Rootward transport, 128
ROP-interactive CROB motif-containing proteins (RICs), 638
ROPs. *See* Rho GTPases
ROS scavenging, 462, *463*
Rosaceae, 645–647
ROS-activated Ca^{2+} channels, 454, *455*
Roses (*Rosa*), *593, 726*
Rosette configuration, *76*
Rosette leaves, *614*
Rotenone, 393
Rotenone-insensitive NAD(P)H dehydrogenases, 393, 400
Rough endoplasmic reticulum
functions of, 23–24
plant cell structure, *16*
protein synthesis, *21*
vesicular trafficking, *25*
Roundup herbicide, 99–100
Roundworms, 748–749
RPK1 gene, 705
RPL gene, 659
RPT2, 537
RQ. *See* Respiratory quotient
Rubber plant (*Hevea brasiliensis*), 730
Rubisco. *See* Ribulose-1,5-bisphosphate carboxylase/oxygenase
Rubisco activase, 287–288
Rubisco-containing bodies (RCBs), 698, 699
RuBP. *See* Ribulose 1,5-bisphosphate
Rumex crispus (curly dock), 512
Runner beans, *507*
Rye (*Secale cereale*), 205, *611*
RZ. *See* Rib zone

S

S haplotypes, 644, 645
S locus, 643–644, 645–647
S phase, 36, *37,* 38
S states, 265
SA. *See* Salicylic acid
SAA. *See* Systemic acquired acclimation
Sachs, Julius von, 113
S-acylation, 109
Sagebrush (*Artemisia tridentata*), 739
SAGs. *See* Senescence-associated genes
Salicaceae, 211
Salicylic acid (SA)
chemical structure, *115*
circadian rhythms in the regulation of plant inducible defenses, 740
human uses and plant sources of, 586
leaf senescence, 705, 708
plant development and, 114
systemic acquired resistance, 746–747
SALICYLIC ACID INDUCTION-DEFICIENT 2 (*SID2*) protein, 708
Saline soils, 166, 204
Salix babylonica, 355–356
Salt Overly Sensitive (SOS1. SOS1-type) antiporters, 232
Salt stress, 204, *448,* 449, 451
Salt-tolerant plants, 204, 449
SAM. *See* Shoot apical meristem
Samaras, *506,* 656
Sand verbena (*Abronia umbellata*), *750*
Sandy soils, 169, 170, 171
Sap
cohesion–tension mechanism of sap ascent, 178–181
defined, 345
nitrogen compounds in xylem sap, *422*
See also Phloem sap
SAR. *See* Systemic acquired resistance
SARK protein, 705
Saturated fatty acids, 18, *406,* 411
SAUR protein family, 526, 529, 538
Sauromatum guttatum (voodoo lily), 399
SAVs. *See* Senescence-associated vacuoles
SCA. *See* Stigma/style cysteine-rich adhesin
Scalariform perforation plates, *175,* 176
Scandinavian thyme (*Thymus chamaedrys*), *714*
SCARECROW (*SCR*) gene, 684, *685,* 686, *687*
SCF complexes. *See* S-phase kinase associated protein 1 (Skp1)/Cullin/F-box complexes
Schistocerca americana, 733, 734
Schlerenchyma, 13
Sclereids, 13, *66,* 348
Scots heather (*Calluna vulgaris*), *714*
Scots pine (*Pinus silvestris*), *714*
Scouring rushes, 197
SCR gene. *See SCARECROW* gene
SCREAM (SCRM) proteins, 556
Scrm mutant, *555,* 556
Scrophulariaceae, 645–647
SCRs. *See* S-locus cysteine-rich proteins
Scutellum
cereal seed structure, *507, 648*
defined, 508
maize embryogenesis, 670, 671
starch mobilization in cereals and, 516
SD vernalization, 611
SDGs. *See* Senescence down-regulated genes
SDPs. *See* Short-day plants
Seasonal leaf senescence, 697
Secale cereale (rye), 205, *611*
Secession cells, 709, *710,* 712–713
Second law of thermodynamics
diffusion and, 157–158
osmosis and, 159
Second messengers
calcium ions, 109–110, 198
changes in cytosolic or cell wall pH as, 110–111
defined, 103
lipid signaling molecules, 111–113
reactive oxygen species, 111
vacuolar-type programmed cell death and, 693, *694*
Secondary accessory buds, *572*
Secondary active transport, 129–130, 226–227
Secondary cell walls
components of and hierarchical organization, 48–49, *50, 66,* 67
defined, 7
fibers, 13
hemicelluloses, 54
morphological diversity, 47–48
overview and functions of, 66–67
plasmodesmata, *9*
schlerenchyma, 13
xylem cells, 15, 174
Secondary cross-regulation, 147
Secondary dormancy, 508
Secondary growth
bark and its functions, 586
cork cambium and periderm, 585–586
definition and overview, 10, 568, 587
development of vascular cambium, 580–582
epicormic buds and branches, 586–587
gene networks controlling secondary meristems, 582–584
lateral meristems involved in, 578–579
regulation by phytohormones, 584–585
in roots and stems, 10, *11*
secondary xylem and phloem produced by the vascular cambium, 579–580
transition to from primary growth, 579, *580*
Secondary inflorescence meristem, 614
Secondary metabolites
allelopathic, 749
in bark, 586
as a constitutive defense, 722
defined, 728
examples of, 728–729
in glandular trichomes, 726
plant storage of, 729–732
water-soluble sugar conjugates, 730–732
Secondary nucleus, 632
Secondary phloem
defined, 10
early experiments on phloem translocation, 347
functions of, 579
production by the vascular cambium, 579–580
regulation of differentiation by phytohormones, 584–585
in roots and stems, *11*
secondary growth and, 568
woody stems, *579, 580*
Secondary plasmodesmata, *9,* 10
Secondary response genes, 488
Secondary signals, 103
Secondary veins, *559,* 562, *563,* 564
Secondary xylem
defined, 10
functions of, 579

production by the vascular cambium, 579–580
regulation of differentiation by phytohormones, 584–585
in roots and stems, *11*
secondary growth and, 568
woody stems, *579, 580*
Secretory proteins
synthesis, 20, *21,* 22, 23–24
vesicular trafficking, 24–26
Sedoheptulose 1,7-bisphosphatase, *284–285,* 287, 288, 289
Sedoheptulose 1,7-bisphosphate, *284–285*
Sedoheptulose 7-phosphate, *284–285, 387*
Seed banks, 508
Seed coat
Arabidopsis seed structure, *648*
coat-imposed seed dormancy, 655–656
development of, 652–653
exogenous dormancy, 508–509
functions of, 652
seed anatomy, 506, *507*
Seed dormancy
definition and overview, 505, 508
endogenous dormancy, 509
exogenous dormancy, 508–509
release from, 511–512
seed coat-imposed, 655–656
types of, 508
vivipary and precocious germination, 509–510
Seed filling, 654
Seed germination
breaking of dormancy, 511–512
conversion of storage lipids into carbohydrates, 411–413
definition and overview, 505, 508, 512–513
mobilization of stored reserves, 514–516
phases of, 513–514
phytochrome and, 478, *479,* 485, 486
vivipary and preharvest sprouting, 509–510
water uptake and, 512–514
Seed longevity, 653–654, 655–656
Seed maturation, 505, 653–656
Seed plants, 4, 505, 669
Seed quiescence, 505, 508
Seed storage proteins, 516, *517*
Seedling defective mutants, 678
Seedlings
apical–basal polarity, *673, 674*
development in light or dark, 517–518, *519*
mechanisms of differential growth, 522–526
principle axes of, 672
regulation of apical hook opening, 519–520
root tip and root hair development, 520–522
seedling establishment defined, 517
tropisms, 526–538 (*see also* Tropisms)
vascular differentiation, 520
Seeds
agriculture and wheat seeds, 626–627
alternative embryogenesis and suspensor cells, 688
apomixis, 647
breaking of dormancy, 511–512
dormancy, 508–511 (*see also* Seed dormancy)
effects of seed size on seedling establishment, 517
endosperm development, 647–652
examples of, *506*
germination, 512–514 (*see also* Seed germination)
longevity, 653–654, 655–656
maturation and dessication tolerance, 653–656
mobilization of stored reserves, 514–516
overview of development, 505–506
phloem import, 367–368
proplastids, 30–31
seed coat development, 652–653
seed development and whole plant senescence, 716
structure of, 506–508, 515, *648*
vivipary and precocious germination, 509–510
SEEDSTICK (*STK*) gene, 620
Selaginella, 521
Selective breeding, 99
Selectively permeable membranes, 159
Selenium, 193
Self-incompatibility (SI)
gametophytic self-incompatibility, 644–647
overview, 643–644
sporophytic self-incompatibility, 644–645
Selfing (self-pollination)
defined, 633, 642
inbreeding depression, 642
mechanisms to prevent, 642–647
SELF-PRUNING locus, 660
Semiautonomous organelles
division of mitochondria and plastids, 31–32
overview and key features of, 29–30
proplastids, 30–31
Seminal roots, 205, 576–577
Senecio vulgaris (groundsel), 592
Senescence
abscission, 709–713
autophagy and nutrient recycling, 696
climacteric, 403
defined, 691
leaf senescence regulation, 700–709
leaf senescence syndrome, 696–700
programmed cell death, 692–696
whole-plant senescence, 713–717
Senescence down-regulated genes (SDGs), 701
Senescence-associated cell death, 693
Senescence-associated genes (SAGs), 700–701, 703, *706,* 709
SENESCENCE-ASSOCIATED RECEPTOR-LIKE KINASE (SARK) protein, 705
Senescence-associated vacuoles (SAVs), 698–699
SENESCENCE-SUPPRESSED PROTEIN PHOSPHATASE (SSPP), 705
Sensible heat loss, 331–332
Sensitive fern, *481*
Sensitive plant, 104, 146, 728
Sensor proteins, 132, *133, 134,* 481
SEO gene family, 364
SEOR proteins, *359,* 360, 364
SEPALLATA (SEP) protein, *616,* 618–619, 620, 663, *664*
Sepals
ABC model of floral organ identity, 617, *618*
floral organ identity genes and, 616, 617
hypanthium and, 657
initiation of, 614, 615
Quartet model of floral organ specification, *620*
Separase, 37
Separation layer, *658,* 659
Septum, 631, 632, 658
Sequence-specific nucleases (SSNs), 95–97
Sequential branches, *572*
Sequential buds, *572,* 573
Sequential leaf senescence, 697
Sequoia sempervirens (redwood), 177–178, *593,* 717
Sequoiadendrom giganteum (giant redwood), 357, *440, 714*
SERAT gene family, 438
Serine
biosynthetic pathway, *427*
photorespiration, 291, *292–293*
sulfur assimilation, *436*
Serine acetyltransferase, *436,* 437–438
Serine hydroxymethyltransferase, 291, *292–293,* 295, 297
Serine proteases, 516
Serine:2-oxoglutarate aminotransferase, 291, *292–293,* 295
Serine/threonine-specific protein phosphatases, 109
SERK 1/2 receptor kinases, 712, *713*
Serotonin, 727
Serpentine soils, 445
Sesbania, 429
Sesquiterpenes, 747
Sesquiterpenoids, 125
Sessile leaves, *549,* 550
70S ribosomes, 20
Sexine, 629
Sexual reproduction
apomixis, 647
development of the gametophyte generations, 625–627
endosperm development, 647–652
female gametophyte development, 630–633
formation of male gametophytes, 627–630
fruit development and ripening, 656–664
introduction, 625
pollination and fertilization in angiosperms, 633–642 (*see also* Double fertilization; Pollination)
seed coat development, 652–653
seed maturation and dessication tolerance, 653–656
selfing versus outcrossing, 642–647
Sexual selection, 625
SFA-8, *517*
SGR protein, 699–700, *706*
Shade avoidance response, 572
Shade leaves
acclimation to light quality, 326
anatomy of, *322*
biochemical and morphological characteristics, 326
excess light energy and, *329*
Shade plants
acclimation to light quality, 326
photosynthetic light-response curves, 327
Sharkey, Tom, 322
Shattering resistance, 659
SHATTERING1-5 (SHAT1-5) proteins, 659
SHATTERPROOF (*SHP*) genes, 620, 659
Sheep fescue (*Festuca ovina*), *714*
Shikimic acid pathway, 99–100, 388
Shoot apex
anatomy, *8*
apical dominance, 569
defined, 545
seed anatomy, 506, *507*
Shoot apical meristem (SAM), *8*
Arabidopsis embryogenesis, 671, *672,* 675
definition and description of, 542, 545
developmental regulation of determinacy in, 715–716
dichotomous branching and, 568
establishment of leaf polarity, 551–552, 553–554
floral evocation, 591–592
formation of, 687, *688*
formation of axillary buds, 548–549
gene networks controlling, 582–584
indeterminate growth, 542
leaf initiation, 547–548
maintenance of meristem size, 546–547
maize embryogenesis, 670, 671
organization of, 545–546
seed anatomy, *507*
in seedling emergence, 517

transition from vegetative to reproductive development, 613–614
vernalization and the competence to flower, 610–611
SHOOT MERISTEMLESS (*STM*) gene, 687
Shoots
apical meristems, 10
branching and architecture, 567, 568–573
defined, 7
etiolated, 517, 518, *519*
gravity-independent auxin transport, 526, *527*
nitrate assimilation, 422
phototropism, 535–538
phyllotaxis, 573
root-to-shoot ratio, 205, 468–469, *470*
shoot apex and phase changes, 592–594
Shootward transport, 128
Short interfering RNAs (siRNAs), 86–88, 89, 90, 458–459, 747
SHORT ROOT (*SHR*) gene, 684–686, *687*
SHORT VEGETATIVE PHASE (SVP) protein, 582, *616*
Short-day plants (SDPs)
clock hypothesis of photoperiodic timekeeping, 601–602
definition and description of, 598, 599
external coincidence model of flowering, 602, 603–604
induction of flowering by gibberellin, 612
night length and floral induction, 600
phytochrome and flowering, 605
response to night breaks, 600–601, 605
Short–long-day plants (SLDPs), 599
SHP genes, 620, 659
SHR gene, 684–686, *687*
SI. *See* Self-incompatibility
SID2 protein, 708
Siderophores, 234, 235, 725
Sieve areas, 350
Sieve cells, 14, 15, 348, 361
See also Sieve elements
Sieve effect, 324
Sieve element occlusion (SEO) gene family, 364
Sieve element occlusion related (SEOR) proteins, *359,* 360, 364
Sieve element precursors, 581
Sieve element–companion cell complex, 351–357
Sieve elements
characteristics in angiosperms and gymnosperms, *350*
companion cells, *349*
defined, 347
early experiments on phloem translocation, 347
mass transfer rate, 357
phloem import in growing roots and, 367
phloem loading, 351–357
pore-plasmodesma contacts, *349*
pressure-flow model of phloem translocation, 357–361
sealing of in response to damage, 359, 364–365
sieve area pores, 348, *349,* 350
specializations for phloem translocation, 347–348, *349*
transport of photosynthate to from mesophyll cells, 351
Sieve plate pores
description of, 348, *349,* 350
pressure-flow model of phloem translocation, 359–360
sealing of in response to damage, 359, 364–365
Sieve plates, 14–15
Sieve tube elements
companion cells, 15, *349,* 350–351
defined, 14, 347–348
See also Sieve elements
Sieve tubes, 14, 348
Signal peptides, 20, *21,* 22
Signal recognition particle (SRP), 20, *21,* 22
Signal transduction pathways
abscisic acid signaling, 138–139
activated in response to abiotic stress, 453–460
brassinosteroid signaling, 136–138
cytokinin signaling, 132–133, *134*
the Darwin studies of the coleoptile bending response, 103
defined, 103
ethylene signaling, 133, *135,* 136
general scheme for signal transduction, *105*
negative regulation of hormone pathways, 139, 144
phosphatases and protein phosphorylation, 109
phytochrome signaling, 487–490
phytochrome signaling and, 483–484
protein modifications and, 109
receptors, 105–106
regulation of polar auxin transport, 131
second messengers, 109–113
signal amplification, 106–107
stress response pathways and, *452*
temporal and spatial aspects of signaling, 104–105
types and functions of protein kinases, 107–108
Signals
definition and overview of, 103–104
general scheme for signal transduction, *105*
hormones and, 113 (*see also* Phytohormones)
lipids as signaling compounds, 411
phloem transport of signaling molecules, 373–375
receptors, 105–106
signal amplification, 106–107
temporal and spatial aspects of signaling, 104–105
Silene, 607
Silica, 197, 727
Silicates, 202, 727
Silicic acid, 192, 235
Silicon
in plant nutrition, 192, 197
plant tissue concentration, *191*
in soils, 202
Silicon deficiency, 197
Silicon transporters, 235
Siliques, 657
Silt, 203
Silver birch (*Betula verrucosa*), 593
Simple fruits, 657
Simple leaves, *549,* 550
Simple perforation plates, *175,* 176
Simple pits, *15*
Simple sequence repeats (SSRs), 74
Sinapis, 608
S. alba, 486
S. arvensis, 509w
Sinapyl alcohol, 67
Single nucleotide polymorphisms (SNPs), 98
Single-cell C_4 photosynthesis, *300,* 302
Singlet oxygen, 273, 446, *454*
Sinigrin, *732*
Sink activity, 366, 372–373
Sink size, 372
Sink strength, 372–373
Sinks
allocation of photosynthate, 371
biotechnology and, 376
competition for translocated photosynthate, 372
defined, 346
partitioning of photosynthate, 372
phloem unloading, 365–369
pressure-flow model of phloem translocation, *358*
regulation by turgor pressure and chemical signals, 374
sink strength, 372–373
sink-to-source transition, 369–371
source-to-sink pattern of phloem translocation, 346–347
Sinorhizobium, 428
S. fredii, 429
S. meliloti, 429
SIPK protein kinase, 734
siRNAs. *See* Short interfering RNAs
Sisymbrium officinale (hedge mustard), 512
Sitka spruce, *328*
Sitosterol, 18
Size exclusion limit (SEL), 10, 375
SKOR channels, 242
Skotomorphogenesis, 488, 517–518, *519*
SKP1-CULLIN-F-BOX protein complexes. *See* S-phase kinase associated protein 1 (Skp1)/Cullin/F-box complexes
Skp1/SCF complexes, *140,* 141, *142, 143*
Slack, S. R., 298
SLDPs. *See* Short–long-day plants
SLF/SFB protein, 645–646, 647
SLGC. *See* Stomatal lineage ground cell
SLIM1 transcription factor, 438–439
S-locus cysteine-rich proteins (SCRs), 645
S-locus receptor kinase (SRK), 645
SLY1 protein, 141, *143, 145*
Small Auxin Up RNAs (SAUR) proteins, 526
Small RNAs (sRNAs), 458–459
See also Noncoding RNAs
Small-interfering RNAs. *See* Short interfering RNAs
Smoke, breaking of seed dormancy and, 512
Smooth endoplasmic reticulum
functions of, 24
gymnosperm sieve areas, 350
phloem translocation in gymnosperms, 361
plant cell structure, *16*
sieve elements, 348
Snapdragon (*Antirrhinum majus*), 552, 620
SNAREs, 26
SNF1-RELATED PROTEIN KINASES. *See* Sucrose non-Fermenting (SNF) Related Kinases
SnRKs. *See* Sucrose non-Fermenting (SNF) Related Kinases
SOC1 gene. *See* SUPPRESSOR OF OVEREXPRESSION OF CONSTANS1 gene
Sodium chloride
saline soils and, 166, 204
salt stress, 204, *448,* 449, 451
Sodium deficiency, 198
Sodium nitrate, 201
Sodium sulfate, 204
Sodium/sodium ions
carriers, 232
glycophytes and exclusion of, 465
halophytes and tolerance of, 465
membrane transport proteins and, *229,* 230
mobility within the plant, *196*
observed and predicted concentrations in pea root tissue, *221,* 222
osmotic adjustment and, 460
in phloem sap, *362*
in plant nutrition, *192,* 198
plant tissue concentration, *191*
saline soils, 204
salinity stress, 449
Soil analysis, 199
Soil hydraulic conductivity, 171
Soil particles
adsorption of mineral nutrients, 202–204
categorization by size, 203

contact of root hairs with, 171
impact of mycorrhizas on, 211
Soil pH
adsorption of mineral nutrients by soil particles, 203, 204
effect on nutrient availability, microbes, and root growth, *201,* 204
leaching and, 201
methods of modifying, 201
Soil water
absorption by roots, 171–174
movement by bulk flow, 171
movement of nutrients to roots by mass flow or diffusion, 208
soil characteristics and, 169–170
soil–plant–atmosphere continuum, *170,* 186–187
Soil water potential, 170–171
Soils
characteristics affecting water content and movement, 169–170
as ecosystems, 202
effects of salinity stress on plants, *448,* 449
impact of mycorrhizas on, 211
mechanisms of iron uptake by roots, 234–235
movement of nutrients to roots by mass flow or diffusion, 208
nitrogen and phosphorus availability, 196
oxygen availability and plant respiration, 404, 405
phosphate in, 438
physical features, 202
plant mineral nutrition and, 202–205
rhizobacteria, 725
root hydrotropism, 534–535
root thigmotropism, 533–534
salinization, 204
serpentine soils, 445
soil–plant–atmosphere continuum, *170,* 186–187
sulfate in, 435
sulfur availability, 196
See also Clay soils; Waterlogged soils
Solanaceae (potato family), 54, 645–647, 660, 747
Solanum
S. lycopersicum (*see* Tomato)
S. pimpinellifolium, 660
S. tuberosum (*see* Potato)
Solar energy
percent converted into carbohydrates, 323
See also Light
Solar tracking, 325, 475
Solute potential
defined, 160
halophytes, 166
maintenance of turgor pressure and cell volume, 166–167
measuring, 160
movement of water into and out of cells, 161–162, *163*
pressure-flow model of phloem translocation, 358
variability within the plant, 163
Solute transport. *See* Transport
Solutes
maintenance of turgor pressure and cell volume, 166–167
osmotic adjustment, 460–461
water potential and, 160
Solution culture, 193
Solvents, water as, 154–155
Somatic embryogenesis, 650–651
SOMATIC EMBRYOGENESIS RECEPTOR KINASES 1 and 2 (SERK1/2), 712, *713*
Somatic hybridization, 92
Sorbitol, 353, 362, 461
Sorghum (*Sorghum bicolor*), 732
Sorting-out, 81
Sorus, *6*
SOS pathway, 446
SOS1.SOS1-type antiporters, 232
Sources
adjustment to long term changes in source-to-sink ratio, 373
allocation of photosynthate, 371–372
biotechnology and, 376
defined, 346
phloem loading, 351–357
pressure-flow model of phloem translocation, *358*
regulation by turgor pressure and chemical signals, 374
sink-to-source transition, 369–371
source-to-sink pattern of phloem translocation, 346–347
Southern pea (*Vigna*), 435
Soybean (*Glycine max*)
allocation of photosynthate, 372
C_4 photosynthesis, *301*
effects of depodding, 716
flowering response to night breaks, *601*
grafting studies on the floral stimulus, 607
lag time for auxin-induced elongation, 525
leaf adjustment to long term changes in source-to-sink ratio, 373
leaf movements in response to osmotic stress, *469*
monocarpic senescence, *714*
night length and floral induction, 600
phytoalexins, *747*
rhizobial symbiont, *429*
root system architecture, 577
shattering resistance, 659
storage proteins, *517*
ureide forms of nitrogen, 435
Soybean oil, 406, 407
SPA1. *See* SUPPRESSOR OF PHYTOCHROME A1 protein kinase
Spacing divisions, 556
Spartina, 303
Spch mutant, *555,* 556
SPCH transcription factor, 556, *557,* 558, 559
Specialized metabolites. *See* Secondary metabolites
Specific heat capacity, 155
Specific transcription factors, 81, *83*
Spectrophotometry, 250
SPEECHLESS (SPCH) transcription factor, 556, *557,* 558, 559
Sperm (sperm cells)
angiosperm life cycle, *626*
double fertilization, 626, 633–634, 641–642
formation of, 626, 628, 629
in growing pollen tubes, 636
isomorphic or dimorphic, 641–642
migration into the pollen tube, 636
plant life cycles, 5, *6*
pollen grains as vehicles for transporting, 633
programic phase of reproduction, 633–634
syngamy, 626
Spermatophytes, 505, 669
S-phase kinase associated protein 1 (Skp1)/Cullin/F-box (SCF) complexes
an E3 ubiquitin ligase complex, 106, 141, *142*
jasmonic acid signaling and, *143,* 735, *736*
proteasome degradation of DELLA proteins and, *140*
SCF^{SLF} proteins and gametophytic self-incompatibility, *646,* 647
Sphingolipids, 18, 111, 406, 407
Spinach (*Spinacea oleracea*), 411, 613, 716
Spines, 726
Spiral phyllotaxis, 547
Spirogyra, 253
Spodoptera
S. exigua, 733, 734
S. littoralis, 737
Spoke proteins, *9,* 10
Spongy mesophyll
definition and description of, 12, 324
leaf anatomy, *8*
leaf light absorption, 324
sun and shade leaves, *322*
See also Mesophyll
Spores
defined, 5
plant life cycles, 5, 6–7, 626
Sporophyte generation
angiosperm life cycle, *626*
defined, 6–7, 625
plant life cycles, 669
Sporophytes, 5–7
Sporophytic self-incompatibility (SSI), 644–645
Sporopollenin, 629, 630
Spotted knapweed (*Centaurea maculosa*), 749
Spring heath (*Erica carnea*), *714*
SQUAMOSA PROMOTER BINDING PROTEIN-LIKE proteins, *594*
SQUAMOSA protein, *616,* 663
S-ribonuclease (S-RNase), 646–647
SRK. *See* S-locus receptor kinase
S-RNase. *See* Cytotoxic S-ribonuclease
SRP. *See* Signal recognition particle
SRP receptors, 20, *21,* 22
SSI. *See* Sporophytic self-incompatibility
SSPP protein, 705
SSRs. *See* Simple sequence repeats
Stachyose, 354, 355, 362, *363*
Stadler, L. J., 90
Stamens
ABC model of floral organ identity, 617, 618
dichogamy, 642, *643*
floral organ identity genes and, 616–617
formation of male gametophytes, 627–630
fruits and, *657*
heterostyly, 642, *643*
hypanthium and, 657
initiation of, 614, 615
plant life cycle, 626
Quartet model of floral organ specification, *620*
Staminate flowers, 7
Stanleya, 193
Starch
accumulation and partitioning of, 305–306
carbon mobilization in land plants, *306*
chemical structure, 307
conversion to sugars in ripening fruit, 661
defined, 282
formation of starch granules, 307–310
metabolism in chloroplasts, 305–312
mobilization of stored reserves in seeds, 514, 515–516
storage in amyloplasts, 514
storage in endosperm, 514
transitory, 305–306 (*see also* Transitory starch)
Starch granules
composition and structure of, *307*
formation of, 307–310
regulation of synthesis and degradation, 311–312
starch mobilization, 310–312
starchy endosperm, 515
Starch sheath, 529–532
Starch storers, 371
Starch synthases, 308, *309,* 310, 312
Starch synthesis
allocation of photosynthate and, 371–372
key enzymes in, 372
synthesis of chloroplast starch, 307–310

Starch-branching enzymes, *309,* 310, 312
Starchy endosperm, 515–516, *648,* 650, 652
START domain protein superfamily, 138
Statocytes, 529–532
Statoliths, 529–532
STAY-GREEN (SGR) protein, 699–700
Steady state, 221
Stearic acid, *406, 465*
Stele
  definition and description of, 207
  radial patterning in embryogenesis and, 683–684, *685*
Stele initials, 543, *544*
Stellar outwardly rectifying (SKOR) potassium channels, 242
Stellaria media, 422
Stem elongation
  blue-light inhibition, 490, 493–494
  inhibition by phytochromes, 484, 485, 486, 493–494
Stems
  apical meristems, 10
  auxin and stem growth in seedlings, 524
  de-etiolation, 477–478, 486, 494
  effects of mineral deficiencies on, 196, 197, 198
  secondary growth, 10, *11*
  structure and function, *7*, *8*
Steroleosins, 515, 517
Sterols, 18, 407
Stigma
  adhesion and hydration of pollen grains, 634–635
  fruits and, *657*
  pollen germination, 636
  pollen tube growth, 636, 639 (*see also* Pollen tube growth)
  programic phase of reproduction, 633
  S locus and mechanisms of self-incompatibility, 644–647
  transmitting tract, 632, *634,* 639, 645–647
Stigmasterol, 18
Stigma/style cysteine-rich adhesin (SCA), 639
"Stinging hairs," 727
Stinging nettle (*Urtica dioica*), 727
Stipules, *549,* 550
STK gene, 620
STM gene, 687
Stomata
  CAM photosynthesis, 183, 338
  coupling of transpiration to photosynthesis, 183
  crassulacean acid metabolism, 303, 304, 305
  defined, 555
  development of, 555–559
  developmental mutants, 555
  diffusion of carbon dioxide to the chloroplast, 334, 335, 336
  effects of fusicoccin on, 743
  guard cells, 11–12, 183–186
  leaf anatomy, *8*
  leaf boundary layer resistance and, 183
  opening and closure (*see* Stomatal movement)
  water movement from leaf to atmosphere and, 181, 182–186
Stomatal complex, 184
Stomatal lineage ground cell (SLGC), 556, 557–558
Stomatal movement
  ABA-induced closure, 113, *118,* 186, *239,* 240, 466–467, *468*
  blue light-induced opening, 186, 239–240, 498–500
  closure in response to water stress, 186, 466–467, *468*
  sucrose and, 316
  transport activities in guard cells and, 238–240
Stomatal resistance
  carbon dioxide diffusion into the leaf and, 334, 335, 336
  defined, 182
  leaf transpiration and, *181,* 182, 183
Stone (pit), 659
Stone pine (*Pinus cembra*), *714*
"Stool shoots," 587
Stop codons, *82,* 84, 98
Storage organs
  phloem import, 367–368
  source-to-sink pattern of phloem translocation, 346
Storage proteins
  bark storage proteins, 586
  major families of seed storage proteins, 516, *517*
  in oil bodies, 515
  in protein storage vacuoles, 514 (*see also* Protein storage vacuoles)
  in starchy endosperm, 652
Straight fertilizers, 201
Strasburger cells, *350,* 357
Stratification, 511, *512*
Strawberry fruit (*Fragaria*)
  achenes, *506*
  an accessory fruit, 656
  anthocyanins, *661*
  fruit set, 657
  ripening, 660, *661*
Streptococcus thermophilus, 96
Stress
  defined, 444
  leaf senescence and, 697, 701
  stress-sensing mechanisms, 452–453
  See also Abiotic stress; Abiotic stress response
Stress matrix, 451
Stress relaxation, 62–63
Stress-induced leaf senescence, 697
Stress-induced protein kinase (SIPK), 734
Stress-related leaf senescence, 701
Stress-response regulons, 455, *456*
Striga, 118, 750
  S. hermonthica, 119
Strigolactones
  chemical structure, *115*
  functions, 118–119
  movement within the plant, 127–128
  plant development and, 114
  regulation of apical dominance and axillary bud growth, 569, *570,* 571, 572
  synthesis, 127
Stroma
  Calvin–Benson cycle, 282–290
  carbon reactions of photosynthesis, 247, 281–282
  chloroplast structure, 29, *30*
  description of, *256,* 257
  photoassimilation, 439
  starch metabolism, 305–313
  thylakoid reactions and, *258,* 259
Stroma lamellae
  ATP synthase and, 259
  chloroplast structure, 29, *30*
  defined, 257
  development from prolamellar bodies, 31
  pea chloroplast, *256*
Stroma reactions, 255
  See also Carbon fixation reactions
Stylar canals, 633
Style
  gametophytic self-incompatibility, 646–647
  pollen tube growth and, 639–640
  programic phase of reproduction, 633
  stylar canals, 633
Stylets
  aphids, 733
  nematodes, 748
Suaeda aralocaspica, 299, *300,* 302
Suberin, *172,* 206–207
Subfunctionalization, 80
Subsidiary cells, 184, *185,* 558, 559
Substrate-level phosphorylation
  glycolysis, *383,* 384–385
  total yield in aerobic respiration, 396, *398*
  tricarboxylic acid cycle, 389, *390,* 391
Subtelomeric regions, 74
SUC2 sucrose–H^+ symporter, 353, 370, 371
Succinate
  conversion of storage lipids into carbohydrates and, *412,* 413
  GABA shunt, 391
  mitochondrial electron transport, 392, *393,* 394
  mitochondrial transmembrane transport, 396, *397*
  tricarboxylic acid cycle, 390
Succinate dehydrogenase
  ADP:O ratio and, 394, *395*
  mitochondrial electron transport, 392, *393*
  tricarboxylic acid cycle, 389, 390
Succinyl-CoA, 389, *390*
Succinyl-CoA synthetase, 389, *390,* 391
Sucrose
  accumulation and partitioning of, 305–306
  carbon mobilization in land plants, *306*
  conversion of storage lipids into in germinating seeds, 411–413
  defined, 282
  diffusion across a plasma membrane, 219
  dynamic regulation of respiration, 402
  fruit ripening in strawberry, 663
  gluconeogenesis, 385
  glycolysis, 380, 384
  kinetic analyses of sucrose uptake, 228
  LEA proteins and seed dessication tolerance, 655
  phloem import into sink tissues, 368
  phloem loading, 351–357
  in phloem sap, 361, 362, *363*
  stomatal regulation, 316
  structure, *382*
  synthesis (*See* Sucrose synthesis)
  transport from mesophyll to sieve elements, 351
Sucrose 6^F-phosphate, 314, *315*
Sucrose 6^F-phosphate phosphatase, 314, *315*
Sucrose 6^F-phosphate synthase, 314, 315, *316*
Sucrose 6^F-phosphate synthase phosphatase, *315, 316*
Sucrose non-Fermenting (SNF) Related Kinases (SnRKs)
  SNF1-related kinase and stress sensing, 452
  SnRK1 and sucrose synthesis, 315, *316*
  SnRK1 and sugar-dependent gene expression, 402
  SnRK2 and ABA signaling, 138, 139, 707
Sucrose phosphate synthase, 372
Sucrose synthase, *383,* 384, 386
Sucrose synthesis
  allocation of photosynthate and, 371, 372
  description of, 312–316
  key enzymes in, 372
Sucrose transporters, 316
Sucrose–H^+ symporter
  apoplastic phloem import and, 368–369
  apoplastic phloem loading, 353
  leaf transition from sink to source, 370, 371
  regulation by sugar levels in source leaves, 374
Sugar alcohols, 353, 362, *363,* 461
Sugar beet (*Beta vulgaris*), *346,* 352, 374
Sugar glasses, 655
Sugar maples, *440*
Sugar phosphates, 380, 381
Sugarcane, *428,* 430

Sugar-nucleotide polysaccharide glycosyltransferases, 52
Sugars
in cell wall polysaccharides, 48–49
conversion of storage lipids into in germinating seeds, 411–413
early experiments on phloem translocation, 347
gluconeogenesis, 385
overall chemical reaction for photosynthesis, 252
partitioning in sinks, 372
phloem loading, 351–357
in phloem sap, 361, 362, *363*
phloem unloading, 365–369
pressure-flow model of phloem translocation, 357–361
reducing or nonreducing sugars, 362, *363*
in ripening fruit, 661
sugar-induced leaf senescence, 708
water-soluble sugar conjugates of secondary metabolites, 730–732
See also Fructose; Photosynthate; Sucrose
Sulfate
assimilation of, 417, 436–438
miRNAs and sulfate signaling, 438–439
observed and predicted concentrations in pea root tissue, *221,* 222
in phloem sap, *362*
in soils, 204
transport in plants, 435
Sulfate deficiency, 438–439
SULFATE TRANSPORTER 2;1 (*SULTR2;1*), 439
Sulfate transporters, 233–234, 439
Sulfide, *436,* 437
Sulfite, *436,* 437
Sulfite reductase, *436,* 437
S-Sulfoglutathione, *436*
Sulfolipid, *408, 410*
Sulfoquinovosyldiacylglycerol, *408*
Sulfotransferases, *436,* 438
Sulfur
assimilation of, 435–438
availability in soils, 196, 204
effects of soil pH on availability, *201*
functions of, 435
mobility within the plant, *196*
modification of soil pH with, 201
in plant nutrition, 191–192, 196
plant tissue concentration, *191*
Sulfur deficiency, 196–197
Sulfur dioxide, 435
SULFUR LIMITATION 1 (SLIM1) transcription factor, 438–439
Sulfur trioxide, 435
Sulfuric acid, 204, 435
Sumuki, Yusuke, 116
Sun leaves, *322,* 326
Sun plants, photosynthetic light-response curves, 327, *328*
Sunflecks, 324–325
Sunflowers (*Helianthus*)
cell walls, *48*
cypselae, *506*
diurnal changes in xanthophyll content, *329*
effects of water stress on photosynthesis and leaf expansion, *447*
grafting studies on the floral stimulus, 607
leaf wilting, 330
nitrogen compounds in xylem sap, *422*
storage proteins, *517*
Supercooling, 466
Superoxide
detoxification, 462, *463*
effects of herbicides on chloroplasts and, 269
photodamage and protection from, 273–274, 275
PRR-triggered immunity, 744
a reactive oxygen species, 446
ROS signaling, 111
sources of, *454*
Superoxide dismutase, 273, 462, *463*
Superphosphate, 201
SUPPRESSOR OF OVEREXPRESSION OF CONSTANS1 (*SOC1*) gene
characteristics and functions of, *616*
in diverse flowering pathways, 613
epigenetic regulation of flowering, 457
a floral meristem identity gene, 615, *616*
florigen-mediated flowering response, *609,* 610
repression by FLC protein, 612
SUPPRESSOR OF PHYTOCHROME A1 (SPA1) protein kinase, 489, 493, 500, *501*
SUPPRESSOR OF VARIEGATION 3-9 HOMOLOG 2 (SUVH2), *702,* 703, *704*
Surface tension, 155–156, 170–171
Surfactants, 202
Suspensor
alternative embryogenesis and, 688
Arabidopsis embryogenesis, 674, 675
Arabidopsis seed structure, *648*
maize embryogenesis, 670, *671*
Sustainable, Ecological, Consistent, Uniform, Responsible, Efficient (SECURE) rule, 100
SUT1 sucrose–H^+ symporter, 353, 368–369
SUVH2 protein, *702,* 703, *704*
SVP protein, 582, *616*
Sweet gum, *440*
Sweet potato, *465*
SWIch2/Sucrose Non-Fermentable 2 (SWI2/SNF2) proteins, 703
Sycamore maple (*Acer pseudoplatanus*), *593*
Symbioses
biological nitrogen fixation, 428–435, 723, *724,* 725
defined, 202
mycorrhizal, 210–213
with soil organisms, 202
Symbiosis receptor-like kinase (SYMRK), 723, *724*
Symbiosomes, 433–434
Symbiotic biological nitrogen fixation
bacteria in, 428–429
common symbiotic pathway, 723, 725
microaanaerobic or anaerobic conditions, 429–430
nitrogenase enzyme complex, 434–435
nodules and nodule formation, 430–431, 432–434
signaling molecules in, 431–432, 723, *724*
Symplasm
defined, 10, 240
size exclusion limit, 10
Symplasmic transport
defined, 10
of ions in roots, 240–242
phloem loading, 351–352
phloem unloading, 366–368
pre-phloem transport, 351
size exclusion limit, 10
of viruses, 10
water movement in roots, 172–173
Symplast, 10n2
Symport, 226, 227
Symporters, 227, *229*
SYMRK, 723, *724*
Synaptonemal complexes, *77,* 78
Syncytium, 632, 748
Synergid cells (synergids)
angiosperm life cycle, *626*
Arabidopsis, 631
in double fertilization, 641
embryo sac development, 632
functions of, 633
guided pollen tube growth, 640–641
programic phase of reproduction, *634*
Syngamy, 626
Synthetic auxins, 114, 121
Systemic acquired acclimation (SAA), 456, *457*
Systemic acquired resistance (SAR), 725, 741, 746
Systemic defenses
defined, 722
electrical signaling in, 737–738
induced by herbivore damage, 736–737
systemic acquired resistance, 741
Systemin, 736–737, 744
Systems biology, 147

T

TAC transcription factors, 578
TAL effectors. *See* Transcription activator-like effectors
TALENs. *See* Transcription activator-like effector nucleases
Tandem repeats, 74
Tapetum
boron and, 636
defined, 627–628
pollen grain formation, 627–628, 629
sporophytic self-incompatibility, 644, 645
tryphine and, 630
Taproots, *8,* 205, 573, 577
TARGET OF MONOPTEROS 5 (*TMO5*) gene, 684, *685,* 686
TARGET OF MONOPTEROS 6 (TMO6) protein, 582
TARGET OF MONOPTEROS7 (TMO7) protein, 682, 686
Tartaric acid, 195, 727
TATA box, 82, 83
TB1 gene, 571, *572*
TDIF RECEPTOR (TDR) protein, 582, *583*
T-DNA, 93–94
TDR protein, 582, *583*
Tectum, *629*
Telomerase, 715
Telomere shortening, 715
Telomeres, 38, 74, *76*
Telophase
meiosis, *77,* 78
mitosis, *39,* 40
Temperature
C_4 photosynthesis and, 303
defined, 155
effect on photosynthesis in the intact leaf, 331–333, *334*
effect on plant respiration, 405
effect on stomata development, 558
optimal temperature for C_3 photosynthesis, 303
temperature-response curves of photosynthesis, 332–333
thermal properties of water, 155
See also Temperature stress
Temperature coefficient (Q_{10}), 405
Temperature compensation, 596
Temperature stress
alteration of membrane lipids in response to, 463–464, *465*
effects of, 447–448
effects of combined heat stress and water-deficit stress, 450–451
stress matrix, 451
Template strand, 81, *82*
Tensile strength, of water, 156–157
Tension, negative hydrostatic pressure, 160
Tension wood, *104,* 585
Teosinte (*Zea mays* ssp. *parviglumis*), 99, 571, *572*
TEOSINTE BRANCHED 1 (*TB1*) gene, 571, *572*

TEOSINTE BRANCHED/CYCLOIDEA/PCF (TCP), 705
Terpenes, 739
Terpenoids
  abscisic acid synthesis, 125
  conifer resin ducts, 729
  functions of, 406
  glandular trichomes, 726
  herbivore-induced volatiles, 738, 739
Tertiary cross-regulation, 147
Tertiary veins, *559,* 562–563
Testa, 506, *507, 648*
  See also Seed coat
"Tethered-network" model of cell walls, 64–65
Tetrarch vascular tissue, 573, *574*
Tetrads, 78, 628
Tetrapyrrole, 276
Tetrasaccharides, 354, 355
Teucrium scorondonia (wood sage), *714*
TFIIB recognition element (BRE), *82,* 83
TGN. *See* Trans Golgi network
Thermal reversion, 481
Thermogenic flowers, 399
Thermopsis montana, 322
Thigmotropism, 526, 533–534
Thioether linkages, 482
Thioglucosidase, *732*
Thiols, 465–466
Thioredoxin, 289, 310, 462, *463*
  See also Ferredoxin–thioredoxin system
"Thompson seedless" grapes, 116
Thorns, 726
Threonine, *427*
Threonine kinase–phosphatase, 302
Thrips, 733
Thylakoid lumen, 257, *258,* 259, 274
Thylakoid reactions
  cyclic electron flow and ATP synthesis, 272–273
  general concepts underlying, 248–252
  key experiments in understanding, 252–256
  light as the driver of, 254
  mechanisms of electron transport, 261–269, *270* (*see also* Photosynthetic electron transport)
  organization and function of antenna complexes, 259–261
  organization of the photosynthetic apparatus, 256–259
  overview, 247–248, 254
  photosystems I and II, 255 (*see also* Photosystem I; Photosystem II)
  proton transport and ATP synthesis, 270–273
  Z scheme, 255, 261–263
Thylakoids
  chloroplast structure, 29, *30*
  development from prolamellar bodies, 31
  integral membrane proteins, 257
  organization and function of antenna complexes, 259–261
  photosystems I and II, 257–259
  structure of, 256–257
  thylakoid stacking and energy partitioning between photosystems, 275
Thymus chamaedrys (Scandinavian thyme), *714*
Ti plasmid, 93–94
TIBA auxin transport inhibitor, 571
TIC gene, 494–495
Tidestromia oblongifolia, 332, *336*
Tilia, 347
  T. platyphyllos, 587
TILLER ANGLE CONTROL (TAC) transcription factors, 578
TIME FOR COFFEE (*TIC*) gene, 494–495
TIMING OF CAB EXPRESSION 1 (TOC1) protein, 705–706, *707*
Timothy grass, *30*
Tip growth
  cell wall expansion and, 62
  defined, 59
  pollen tubes, 34, 636–638 (*see also* Pollen tube growth)
  root hair development, 521, 522
TIR1/AFB receptors, *140,* 141, 144
TIR-NLR proteins, 744, 745
TIRs. *See* Toll-like receptors and Interleukin receptors
Tissue culture
  cytokinins and, 116, *117*
  somatic embryos, 651
Tissue systems, 10–15
TLD1 gene, 460
TMK1, 526, 538
TMK4, 538
TMO5 gene, 684, *685,* 686
TMO6 protein, 582
TMO7 protein, 682, 686
TNT (trinitrotoluene), 417
Toadflax (*Linaria vulgaris*), 620, *621*
Tobacco (*Nicotiana tabacum*)
  cytokinin and leaf senescence, *709*
  effects of water deficit on cytokinin, *459*
  Golgi apparatus, *24*
  grafting studies on the floral stimulus, 607
  guard cells, *185*
  leaf air space volume, 182
  leaf transition from sink to source, 369–370
  'Maryland Mammoth,' 598
  photoperiodic responses, 598
  phytoalexins, 747
  pollen hydration on stigmas, 635
  pollen tube tip growth, *637*
  P-protein, 364
Tobacco hornworm (*Manduca sexta*), 734
TOC1 protein, 705–706, *707*
α-Tocopherol (vitamin E), 462, *463*
Toll-like receptors and Interleukin receptors (TIRs), 657, 744
Tomato (*Solanum lycopersicum*)
  auxin-mediated leaf initiation, 547, *548*
  axillary meristem formation, *548*
  chromoplast, *31*
  commercial manipulation of ripening, 664
  ethylene and leaf epinasty, *117*
  flower abscission, 711
  fruit development, 659–660
  fruit ripening and its regulation, 660, 661, 662, 663–664
  hydroponic production, 193
  Never-ripe mutation, 662
  parthenocarpic fruits, 657–658
  phytoalexins, *747*
  root biomass as a function of soil nitrate and ammonium, *209*
  selective breeding, 99
  shoot apex, *545*
  shoot CO_2 levels and nitrate assimilation, *440*
  systemin, 744
  trichomes, *726*
  water uptake and seed germination, 513
Tonoplast
  cation carriers, 232
  channels, 232
  defined, 27
  expansion of, 28
  H^+-ATPases, 237–238
  membrane transporters, 121
  plant cell structure, *16*
  transport proteins, 228–230
  water movement in roots, 172
TOO MANY MOUTHS protein, 108, 557, 559
TOPLESS (TPL) protein, 141, *142, 143, 688*
Topsoil foraging, 209–210
TOR (TARGET OF RAPAMYCIN) complex, 370
Torenia fournieri, 639–641
Torpedo stage embryo, 671, *672*
Torus, *175,* 177, 180
Toxic ions
  chelation and phytochelatins, 465–466
  exclusion and internal tolerance, 464–465
Toxins, secreted by pathogens, 743
Toxoplasma, 642
TPC1/SV channel, 232
TPK/VK channel, *231,* 232
TPL protein. *See* TOPLESS protein
Trace elements
  hyperaccumulation, 465
  toxicity, *448*
Tracheary elements, 15
Tracheids
  defined, 15
  freezing stress and, 449
  pressure-driven bulk flow and, 177
  secondary cell walls, *66*
  structure and function, 174, *175,* 176
Tracheophytes, 4, *5,* 669
tracrRNA. *See* Trans-activating CRISPR RNA
Trade-offs, between reproductive and vegetative growth in responses to stress, 445
Tradescantia, 12
  T. zebrina, 184
Traits, introgression of wild traits into crop plants, 91–92
Trans cisternae, 24–26
Trans Golgi network (TGN), *24*
  endomembrane system, 15
  exocytosis, 23
  phragmoplast, 40
  plasma membrane recycling, 26
  vesicular trafficking, 25–26
Trans-acting factors, 83
Trans-activating CRISPR RNA (tracrRNA), 96–97
Transaldolase, *387*
Transamination reactions, *425,* 426
Transcription
  epigenetic modifications, 84–86
  methods of evaluating, 92
  overview, 20, *21*
  overview of gene expression, *82*
  phytochrome signaling, 483–484, 487–488
  RNA polymerase II and the mechanisms of, 81–83
  termination and polyadenylation, *82,* 84
Transcription activator-like effector nucleases (TALENs), 95
Transcription activator-like (TAL) effectors, 95, 98, 743
Transcription factors
  gene transcription, 81, 82, 83
  heat shock factors, 462
  photorespiratory conditions, 297
  stress-response pathways, 453–454
  stress-response regulons, 455, *456*
  transcriptional regulation of leaf senescence, 701–703, *704*
Transcription initiation complex, 81, *82,* 83
Transcriptional regulation
  defined, 81
  epigenetic modifications, 84–86
  of leaf senescence, 701–703, *704*
  RNA polymerase II and the mechanisms of transcription, 81–83
  transcription termination and polyadenylation, *82,* 84
Transcriptomics, 92
Transdifferentiation, 712
Transfer cells, 353–354, 356
Transfer DNA (T-DNA), 93–94
Transfer RNA (tRNA)
  leaf senescence, 698
  mobile RNAs in phloem signaling, 374
  translation, 20, *21*
Transformation, 93–94

Transgenes
  controversies in the use of, 100–101
  genetic engineering of crop plants, 99–101
  methods of plant transformation, 93–94
  RNAi pathway and cosuppression, 90
Transgenics, 99–100
Transglucosidase, 311, 312
Transglycosylases, 58
Transit peptides, 276
Transition stage
  Arabidopsis embryogenesis, *673*
  maize embryogenesis, 670, *671*
Transitory starch
  definition and functions of, 305–306
  degradation at night, 310–311
  regulation of, 311–312
  synthesis of, 307–310
Transketolase, *284–285, 387*
Translation, 20, *21,* 22, *82*
Translational regulation, of leaf senescence, *702,* 705
Translocation
  defined, 217
  xylem loading, 242
  See also Phloem translocation
Translocons, 20, *21,* 22
TRANSMEMBRANE KINASE 1 (TMK1), 526, 538
TRANSMEMBRANE KINASE 4 (TMK4), 538
Transmembrane pathway, of water movement in roots, 172, *173*
Transmembrane proteins, 22
Transmitter domain of sensor proteins, 132, *133*
Transmitting tract
  defined, 632, 639
  gametophytic self-incompatibility, 646–647
  ovule development, 632
  pollen tube growth, *634,* 639
TRANSPARENT TESTA GLABRA2 (*TTG2*) gene, 653
Transpiration
  cohesion–tension theory of xylem water transport, 178, *179*
  coupling to photosynthesis by stomata, 183
  defined, 153
  evaporative heat loss, 331, 332
  major factors affecting, 182
  stomatal control of, 183–186
  water loss, 153–154
Transpiration ratio, 186
Transport
  definition and overview, 217
  ion transport in roots, 240–242
  of ions across membrane barriers, 219–223
  membrane transport processes, 223–228
  membrane transport proteins, 228–238 (*see also* Transport proteins)
  passive and active, 218–219 (*see also* Active transport; Passive transport)
  in stomatal guard cells, 238–240
  See also Translocation
Transport Inhibitor of Auxin Resistant 1 (*TIR1*) gene, 657
Transport phloem, 346
Transport proteins
  anion transporters, 233–234
  aquaporins (*see* Aquaporins)
  carriers, *223,* 226–227
  cation transporters, 231–233
  channels, *223,* 224–226
  definition and overview, 223–224
  functions of, 15–16
  genes encoding, 230
  H^+-pyrophosphatases and P-type H^+-ATPases, 238
  kinetic analyses of, 228
  for nitrogen-containing compounds, 230–231
  overview of plasma membrane and vacuole transporters, 228–230
  plasma membrane H^+-ATPases, 236–237
  tonoplast H^+-ATPase, 236–237
  tonoplast transporters and auxin, 121
  transporters for metal and metalloid ions, 234–235
TRANSPORTER OF IBA1 (TOB1), 121
Transposon tagging, 90
Transposons (transposable elements)
  abiotic stress responses, 459
  definition and classes of, 75
  dispersed repeats, 74
  mutations and, 75, *76*
  regulation of, 75–76
  transposon tagging, 90
Transvacuolar strands, *16,* 23, 36, *37*
Traumatic resin ducts, 729–730
Treadmilling
  microfilaments, 32–33
  microtubules, 34, *35*
Trees
  ectomycorrhiza, 211, 213
  extent of root systems, 205
  passive symplasmic phloem loading, 355–356
  pressure gradient and water movement, 177–178
  pressure-flow model of phloem translocation, 360–361
  productivity and senescence in tall trees, 716–717
  seasonal leaf senescence, 697
  unloading and reloading of photosynthates during phloem transport, 357
Trehalose, 312
Trehalose 6-phosphate, 312, 402, 593, 708
Triacylglycerols
  biosynthesis, 407, 411
  conversion into carbohydrates in germinating seeds, 411–413
  oil bodies, 28, 406–407, 517
  overview, 405
  proportions of fatty acids in, 406
  structural features, 406
Triangle of U, *80*
Triangle orache, *327, 328*
Triarch vascular tissue, 573, *574*
Tricarboxylate transporter, 396, *397*
Tricarboxylic acid (TCA) cycle
  amino acid biosynthesis, 427
  discovery of, 388
  dynamic regulation of respiration, 401
  encoding by proteins in by nuclear genes, 398
  location in mitochondria, 29
  metabolic regulation of pyruvate dehydrogenase, 402
  mitochondrial respiration in photosynthesis and, 403
  mitochondrial structure and function, 388–389
  overview, 381
  in plant biosynthetic and redox networks, 400–401
  in plant respiration, *380*
  reactions in, 389–391
  total ATP yield, 396, *398*
  unique features in plants, 391
Trichoblasts, 521–522
  See also Root hairs
Trichomes
  Arabidopsis, 11, *12*
  defined, 555, 726
  in plant defenses, 726–727
  plant phenotypic plasticity in response to abiotic stress, 467–468
Trichoplusia ni (cabbage looper), 740
p-Trifluoromethoxycarbonylcyanide phenylhydrazone (FCCP), 396
Trifolium, 429, 435, 509
  T. repens, 422, 599
2,3,5-Triiodobenzoic acid (TIBA), 571
Trinitrotoluene (TNT), 417
Triose phosphate isomerase
  Calvin–Benson cycle, *284–285*
  glycolysis, *383,* 384
  inhibition by 2-phosphoglycolate, 290
  interconversion of triose phosphates, 302
  sucrose synthesis, *313*
Triose phosphate translocator, 302
Triose phosphates
  allocation, 371
  biochemical model of C_3 photosynthesis, 322
  Calvin–Benson cycle, 283–286
  carbon mobilization in land plants, *306*
  conversion to sucrose in the cytosol, 351
  crassulacean acid metabolism, 303, 304
  glycolysis, 380, 382, *383,* 384
  phosphate-limited photosynthesis, 333
  starch breakdown, *311*
  sucrose biosynthesis, 312–314
  transport in C_3 and C_4 plants, 302–303
Tripinnate leaves, *549*
Triple response, *117,* 519–520
Triplet chlorophylls, 250, 252
Triplet oxygen, *454*
Trisaccharides, 354, 355
Triticum, 506, 517
  T. aestivum (*see* Wheat)
Trk/HKT transporters, 232
Tropisms
  definition and overview of, 526
  gravitropism, 526–533
  hydrotropism, 534–535
  phototropism, 535–538 (*see also* Phototropism)
  thigmotropism, 533–534
True seeds, *506*
Tryphine, 630
Trypsin, 736
Tryptophan, 119, *427*
Tryptophan aminotransferase, 119
Tsuga canadensis (hemlock), 511
TTG2 gene, 653
Tubulin
  defined, 32
  dynamic equilibrium in the cell, 32, 33, 34, *35*
  α-tubulin, 33
  β-tubulin, 33, 34, *35*
  γ-tubulin, 34, *35*
Tumor-inducing (Ti) plasmid, 93–94
Turgor pressure
  ABA-induced stomatal closure in response to water stress, 186, 466
  benefits of maintaining a positive pressure, 166–167
  cell wall expansion, 62–63
  changes in cell volume, 163–164
  defined, 153, 160
  flaccid cells, 161
  impact of water deficit on, 447, *448*
  plasma membrane recycling, 26
  pressure-flow model of phloem translocation, 358, 360–361
  role in coordinating source and sink activities, 374
  stomatal movements, 184–185
  wilting, 163
Turnips, *465*
Turnover, 22
Tween 80®, 202
26S proteasomes, 22, *140,* 141
TWISTED DWARF1 protein, 131
Two-component regulatory systems
  in bacteria, 132, *133*
  cytokinin and ethylene signaling pathways, 132–136
Type 2 proteins, 26

Type 2A protein phosphatases, 496
Type-1 arabinogalactan, *56,* 57
Type-A ARR genes, 132, 133
Type-B ARR genes, 132–133, 141
Tyrosine, *427*

U

Ubiquinone (ubiquinol)
  alternative oxidase pathway, 393–394
  mitochondrial electron transport, 392, *393*
Ubiquitin ligase, 22, 735, *736*
Ubiquitin-activating enzyme, 22
Ubiquitin-conjugating enzyme, 22
Ubiquitine-protein ligase (UPL), *704,* 705
Ubiquitin-proteasome pathway
  gametophytic self-incompatibility, *646,* 647
  inactivation of repressor proteins in hormone signaling pathways, 139–142, *143*
Ubiquitin/ubiquitination
  leaf senescence and, *704,* 705
  protein turnover, 22
  ubiquitin-proteasome pathway and, 139, *140*
UDP. *See* Uridine diphosphate
UDP-glucose. *See* Uridine diphosphate glucose
UDP-glucose pyrophosphorylase, 314, *315, 383,* 384
Ultraviolet (UV) radiation
  effects of, 450
  fluence and photoresponses, 479
  plant defenses against, 475
  plant responses to, 500–501
  UV-A photoreceptor, 477
  UV-B, 500, *501*
Uncouplers, 395–396, *397*
Uncoupling protein (UCP), *393,* 396, *397,* 399–400
Unfolded protein response, 23–24
Uniconazole, 123
Uniparental inheritance, 81
United States Department of Agriculture, 100
Unreduced gametes, 79
Unsaturated fatty acids, 18, *406,* 411
Uracil glycosylase inhibitor, 98
Urea, 199
Urease, 199
Ureide exporters, 435
Ureides, *363*
Uridine diphosphate (UDP), *383,* 384
Uridine diphosphate glucose (UDP-glucose), 52, 314, *315, 383,* 384
Uridine triphosphate (UTP), 314, *315, 383,* 384
Uronic acids, *48*
Urtica dioica (stinging nettle), 727
UTP. *See* Uridine triphosphate
Utricularia gibba, 75
UV RESISTANCE LOCUS 8 (UVR8) photoreceptor, 477, 500, *501*

V

Vaccines, transgenic plants and, 100
Vaccinium (blueberries), *661,* 739
Vacuolar H^+-ATPase (V-ATPase), 226, 237–238
Vacuolar-type programmed cell death, 693, *694,* 696
Vacuoles
  autophagy, 694, *695*
  auxin transport from, 121
  cation carriers, 232
  cell cycle and, 36
  crassulacean acid metabolism, 303, *304*
  defined, 7
  endomembrane system, 15
  hyperacidification, 238
  nitrate storage, 422–423
  osmotic adjustment, 460–461
  pH of vacuolar sap, 238
  plant cell structure, *16*
  plasma membrane recycling, 26
  senescence-associated vacuoles, 698–699
  sequestration of mineral ions in, 204–205
  stomatal movements, *239,* 240
  storage of secondary metabolites in, 729, 730–732
  tonoplast channels, 232
  tonoplast transport proteins, 228–230
  types and functions of, 27–28
  vacuolar-type programmed cell death, 693, *694,* 696
  V-ATPase, 226, 237–238
Valine, *427*
Valves, 631, 658–659
van Niel, C. B., 252
Variegation, 81
Vascular bundles, 568
Vascular cambium
  bark and, 586
  defined, 10, 542
  development of, 580–582
  gene networks controlling, 582–584
  growth–dormancy cycles, 580
  production of secondary xylem and phloem, 579–580
  regulation by phytohormones, 584–585
  role in secondary growth, 578–579
  root anatomy, *8*
  secondary growth, 10, *11,* 568
  stem anatomy, *8*
Vascular plants, 4, *5,* 669
Vascular tissue
  arrangement in roots, 573, *574*
  defined, 10–11
  differentiation in seedlings, 520
  leaf anatomy, *8*
  leaf venation patterns, 559–564
  origin in roots, 543
  radial patterning in embryogenesis, 683–684, *685*
  root anatomy, *8*
  secondary growth (*see* Secondary growth)
  stem anatomy, *8*
  types and functions of, 14–15
V-ATPase, 226, 237–238
Vegetative cell, 628, 635, 647
Vegetative growth
  circadian rhythms, 594–597
  differentiation of epidermal cell types, 555–559
  effects of abiotic stress on, 444–445 (*see also* Abiotic stress)
  effects of excess soil mineral ions on, 204–205
  effects of mineral deficiencies on, 196–197, 198, 199
  effects of nutrient availability on root growth, 208–210
  establishment of leaf polarity, 551–555
  introduction, 567–568
  leaf development, 549–551
  leaf venation patterns, 559–564
  phloem signaling, 374–375
  photoperiodism, 597–606 (*see also* Photoperiodism)
  root apical meristem, 542–545
  root branching and architecture, 573–578
  secondary growth, 578–587 (*see also* Secondary growth)
  shoot apex and phase changes, 592–594
  shoot apical meristem, 545–549
  shoot branching and architecture, 568–573
  trade-offs in physiological adjustments to abiotic stress, 445
  tropisms, 526–538 (*see also* Tropisms)
  See also Primary growth; Seedlings
Vegetative nucleus
  in double fertilization, *641*
  in growing pollen tubes, 636
  migration into the pollen tube, 636
Vegetative segregation, 81
Velocity, of materials in sieve elements, 357
Venation patterns, 559–564
Venus flytrap, 104, 146–147
Verbascoe, 362, *363*
Verbascum blattaria (moth mullein), 656
Vernalization
  competence to flower at the shoot apical meristem, 610–611
  defined, 105, 592, 610
  diversity of pathways in, 612
  effective temperature range for, 610
  vernalization flowering pathway, 613
Very low fluence responses (VLFRs), 484–485, 486
Very-long-chain fatty acids (VLCFAs), 679
Vesicles
  Golgi apparatus and vesicular trafficking, 24–26
  plasma membrane recycling, 26
Vessel elements
  defined, 15
  increase in volume during growth, 62
  pressure-driven bulk flow, 177
  structure and function, 174, *175,* 176
Vessels
  defined, 15, 176
  freezing stress, 449
  structure and function of vessel elements, *175,* 176
Vicia faba. See Broad bean
Vicilins, 516, *517*
Vigna (southern pea), 435
Villin, 32, *33*
Violaxanthin, *261,* 328, 329
Violaxanthin de-epoxidase, 274
Viral movement proteins, 10
Viridiplantae, 281
Virulence (*vir*) genes, 93, *94*
Viruses
  HAP2 protein and, 642
  plant RNA interference response, 89, 747
  symplasmic transport, 10
  transfer to plants by insect herbivores, 741
  See also Pathogens; Plant pathology
Virus-induced gene silencing, 747
Viscoelastic properties, 62
Viscosity, pressure-driven bulk flow in xylem and, 176
Viscum (mistletoe), 749, *750*
Vitamin A. *See* β-Carotene
Vitamin A deficiency, 100
Vitamin B_6, 426
Vitamin B_{12}, 193
Vitamin C. *See* Ascorbic acid
Vitamin E, 462, *463*
Vitis (grapes), 116, *593,* 727
Vivipary, 509
VLFRs. *See* Very low fluence responses
V_{max}, 228
Volatile organic compounds (VOCs; volatiles)
  growth-promoting rhizobacteria and, 725
  herbivore-induced volatiles, 738–739
  isothiocyanates, 731–732
Volatilization, *418*
Volicitin, 733
Voltage-gated channels, 224
Voltage-gated potassium channels
  ABA-induced stomatal closure in response to water stress, 466
  blue light-induced stomatal opening, 498
  functions of, 232
Volumetric elastic modulus, 164
von Caemmerer, Susanne, 321

Voodoo lily (*Sauromatum guttatum*), 399
Vulnerability curves, 180

W

WALLS ARE THIN1 (WAT1) tonoplast transporter, 121
Water
  blue light-induced stomatal opening and, 239, 240
  Calvin–Benson cycle, 283, *284–285,* 285
  diffusion and osmosis, 157–159
  exogenous seed dormancy, 509
  free energy of, 159
  importance in plant life, 153–154
  metastable state in tree xylem, 179–180
  overall chemical reaction for photosynthesis, 252, 254
  oxidation in photosynthesis, 264–265, *266*
  pressure-flow model of phloem translocation, 357–361
  production in glycolysis, *383*
  production in respiration, 380
  seed germination and, 512–514
  structure and properties, 154–157
Water lily family, 521
Water loss
  CAM plants, 338
  diffusion of carbon dioxide to the chloroplast and, 334
  transpiration, 153–154
Water potential
  blue light-induced stomatal opening, 239
  cell volume and turgor pressure relationship, 163–164
  defined, 159
  impact of water deficit on, 447, *448*
  major factors influencing, 159–160
  matric potential, 160–161
  measuring, 160
  movement of water along water potential gradients, 161–162, *163*
  osmotic adjustment, 460–461
  plant water status, 166–167
  pressure-flow model of phloem translocation, 358
  root hydrotropism, 534–535
  root pressure, 174
  seed germination, 513, 514
  soil water potential, 170–171
  variability within the plant, 163
  water movement from leaf to atmosphere and, 181
Water status
  influence of cell walls on, 163–164
  physiological processes affected by, 166
  plasma membrane hydraulic conductivity and, 164–165
  water potential and, 166–167
Water storage cells, 164
Water transport
  along water potential gradients, 161–162, *163*
  aquaporins, 165–166
  introduction, 169
  from leaf to atmosphere, 181–186
  osmosis, 158–159
  plasma membrane hydraulic conductivity, 164–165
  properties of soil water, 169–171
  root system plasticity and, 578
  soil–plant–atmosphere continuum, *170,* 186–187
  through roots, 172–174
  through xylem, 174–181 (*see also* Xylem water transport)
  transpiration, 153–154
  water absorption by roots, 171–174
Water vapor
  cohesion–tension theory of xylem water transport, 178, *179*
  soil–plant–atmosphere continuum of water transport, *170*
  transpiration, 181, 182
  transpiration ratio, 186
Water-deficit stress
  ABA-induced stomatal closure, 186, 466–467, *468*
  carbon isotope ratio and, 341, 342
  effect on stomata development, 558
  effects when combined with heat stress, 450–451
  hormonal responses, 459
  impact on plants, 444, *445,* 447, *448*
  physiological processes affected by, 166
  root-to-shoot ratio and, 468–469
  stress-response regulons and acclimation, *456*
Waterlogged soils
  aerenchyma, 461–462
  anaerobic stress in roots, 448–449
  fermentation, 385
  oxygen availability and plant respiration, 405
Water-use efficiency, 186, 303, 305
Wavelength
  absorption spectra and, 250
  of light, 248
Weathering of rock, 204
Wetland plants, 461–462
Wheat (*Triticum aestivum*)
  agriculture and, 626–627
  aleurone layer, 652
  atmospheric CO_2 levels and nitrate assimilation, 440
  foliar application of nitrogen, 202
  introgression of genetic traits, 91, 92
  leaf senescence, *697*
  a long-day plant, 599
  preharvest sprouting, *510*
  root system, *205*
  SD vernalization, 611
  seed anatomy, *507*
  seed structure, *648*
  selective breeding, 99
Whiptail disease, 199
WHIRLY 1 (WHY1) transcription factor, *702,* 703, *704*
White clover (*Trifolium repens*), *422,* 599
White lupine (*Lupinus albus*), 204, 422, *517*
White mustard (*Sinapis alba*), 486
Whiteflies, 733, 741
Whole-plant senescence, 692, 713–717
Whorls, 614–615
  See also Floral organ development
WHY1 transcription factor, *702,* 703, *704*
Wild beet (*Beta maritima*), 346
Wild ginger, *327*
Wild mustard (*Sinapis arvensis*), 509
Willows, 355–356, 586
Wilting
  defined, 163
  effect on leaf orientation, 467
  effect on transpiration, 183
  to reduce absorption of excess light energy, 330
Wilty mutants, 459
Winter squash (*Cucurbita maxima*), *349*
Winter wheat, 599
WIPK protein kinase, 734
Witchweeds, 118, *119*
WOL gene, 684, *685*
Wood
  functions of, 578
  hemicelluloses, 54
  secondary growth, 578 (*see also* Secondary growth)
  tension and compression wood, *104,* 585
Wood sage (*Teucrium scorodonia*), *714*
WOODEN LEG (*WOL*) gene, 684, *685*
Woody plants, juvenile-to-adult phase changes, 593
Wound callose, 365
Wound response, 373
Wound-induced protein kinase (WIPK), 734
WOX (WUSCHEL homeobox family) proteins
  control of secondary meristems, 582, *583*
  establishment of adaxial leaf identity, 552, *553*
  formation of the root apical meristem, *687*
  maintenance of the root apical meristem, 543, 545
  regulation of blade outgrowth, 553
WRKY proteins, *702,* 703, *704,* 705
WUSCHEL (WUS) protein, 546, 547, 582, *583,* 659
Wyoming sagebrush, *180*

X

Xanthium, 600, *601,* 607
  X. strumarium (*see* Cocklebur)
Xanthomonas, 95, 743
Xanthophyll cycle, 328–329
Xanthophylls, 274
Xanthoxin, 125–126
XCP proteins, 693
Xenopus, 230
XET. *See* Xyloglucan endotransglucosylase
XIUQUI polypeptides, 641
XTHs. *See* Xyloglucan endotransglucosylase/hydrolases
Xylan, 48, 54, *66, 67*
Xylem
  arrangement in roots, 573, *574*
  cambium organizer, 582
  cell types and functions, 15
  defined, 11
  differentiation in seedlings, 520
  freezing stress, 449
  leaf anatomy, *8*
  leaf hydraulic resistance, 181–182
  mechanisms of gas bubble formation in, 180
  nitrate transport, 422–423
  pressure-flow model of phloem translocation, 358
  radial patterning in embryogenesis, 683–684, *685*
  roots, *8,* 207, *241*
  secondary growth, 10, *11*
  stems, *8*
  transport of ions in roots, 241, 242
  water transport in, 174–181 (*see also* Xylem water transport)
XYLEM CYSTEINE PEPTIDASES (XCPs), 693
Xylem loading, 242
Xylem parenchyma, *241,* 242
Xylem pole pericycle
  cambium organizer and, 582
  formation of lateral root primordia and, 573, 574, *575*
  periderm formation and, 586
  plasticity of, 586
Xylem rays, *579*
Xylem sap
  cohesion–tension mechanism of sap ascent, 178–181
  nitrogen compounds in, *422*
Xylem water transport
  of amides and ureides, 435
  cohesion–tension mechanism of sap ascent, 178–180
  efficiency of, 177
  gas bubbles and cavitation, 177, 180–181
  physical challenges in trees, 178–180
  pressure-driven bulk flow, 176–177
  in roots, 172–173, 174
  soil–plant–atmosphere continuum, *170,* 186–187
  in the tallest trees, 177–178
  water-transporting xylem cells, 174–176

Xyloglucan
enzyme-mediated primary cell wall assembly, 58, *59*
expansins and acid growth, 64
molecular models of cell walls, 64–65
primary cell walls, *53*
structure, 49, 54, *55*
Xyloglucan endotransglucosylase (XET), 58, *59*
Xyloglucan endotransglucosylase/hydrolases (XTHs), 58, 712
Xylorhiza, 193
Xylose, *48*, *55*
Xylosyl, 54
Xylulose 1,5-bisphosphate, 287, *288*
Xylulose 5-phosphate, *284–285*, *387*

Y

YABBY transcription factors, 552–553
Yabuta, Teijiro, 116
Yang cycle, 124
Yellow fluorescent protein (YFP), *359*, 360
Yellow monkey flower (*Mimulus guttatus*), 468
YFP. *See* Yellow fluorescent protein
Young–Laplace equation, 170–171
YUCCA family proteins, 119, *120*, 709

Z

Z scheme, 255, 261–263
ZAG1 gene, *616*
ZAP1 gene, *616*
Zaxinone, 118
Zea, 99
Z. mays (*see* Maize)
Z. mays ssp. *parviglumis*, 99, 571, *572*
Zeatin, *115*, 123
Zeaxanthin, 274, 328–329
Zeitgebers, 596
ZEITLUPE (ZTL) photoreceptors, 477, *495*, 496, 602, 606
Zenillia adamsoni, 730
Zinc
effects of soil pH on availability, *201*
mobility within the plant, *196*
in plant nutrition, *192*, 198
plant tissue concentration, *191*
Zinc deficiency, 198
Zinnia, *61*
ZIP transporters, 234
ZMM genes, *616*
ZTL photoreceptors. *See* ZEITLUPE photoreceptors
Zygote
formation of, 626, 633
plant life cycles, 5–6
polarization, 673–676
See also Embryogenesis
Zygote stage embryo
Arabidopsis embryogenesis, 671, *672*
maize embryogenesis, 670, *671*
Zygotene, *77*, 78